Site AZ.PFO

Location: Cecil and Ida Green Pinon Flat Observatory, Riverside County, California

Latitude: 33.61167 **Longitude:** -116.45943
(Station coordinates from site GPS survey, WGS84 coordinate system)

V_{S30} (measured): 763 m/s (±10% beneath seismic line)

V_{S30} (adjusted to more accurately reflect seismic station conditions): 848 (average S-wave velocity between 1 and 31 m adjusting for assumed sensor depth).

NEHRP Site Class: B/C (significant lateral velocity variation in the immediate site vicinity will result site class ranging from C to B. Adjusting V_{S30} for seismic station conditions will result in site class ranging from C/B to B).

Geomatrix Code: IGA

Geologic Conditions/Observations: Seismic station located on Mesozoic (Cretaceous) granitic rock (quartz diorite, granodiorite).

Site Conditions: Rural site. Relatively flat terrain in site vicinity with gradual topographic decline to south.

Geophysical Methods Utilized: HVSR, Seismic Refraction (P- and S-wave), MASW (Rayleigh wave), MALW (Love wave)

Geophysical Testing Arrays:

1. Array PFO-1 (48 channel MASW array utilizing 4.5 Hz vertical geophones spaced 1.5 m apart for a length of 70.5 m, forward and reverse shot locations with multiple source offsets and source types and center shot location).
2. Array PFO-1 (48 channel MALW and S-wave seismic refraction array utilizing 4.5 Hz horizontal geophones spaced 1.5 m apart for a length of 70.5 m, forward and reverse shot locations with multiple source offsets and multiple interior shot locations). Coincident with MASW array of same name.
3. Array PFO-2 (48 channel P-wave seismic refraction array utilizing 4.5 Hz vertical geophones spaced 3 m apart for a length of 141 m, forward and reverse shot locations with multiple source offsets and multiple interior shot locations using accelerated weight drop energy source). Arrays PFO-1 and PFO-2 have a common center and orientation.
4. Three HVSR measurement locations: two distributed along array PFO-2 and the other adjacent to the seismic station.

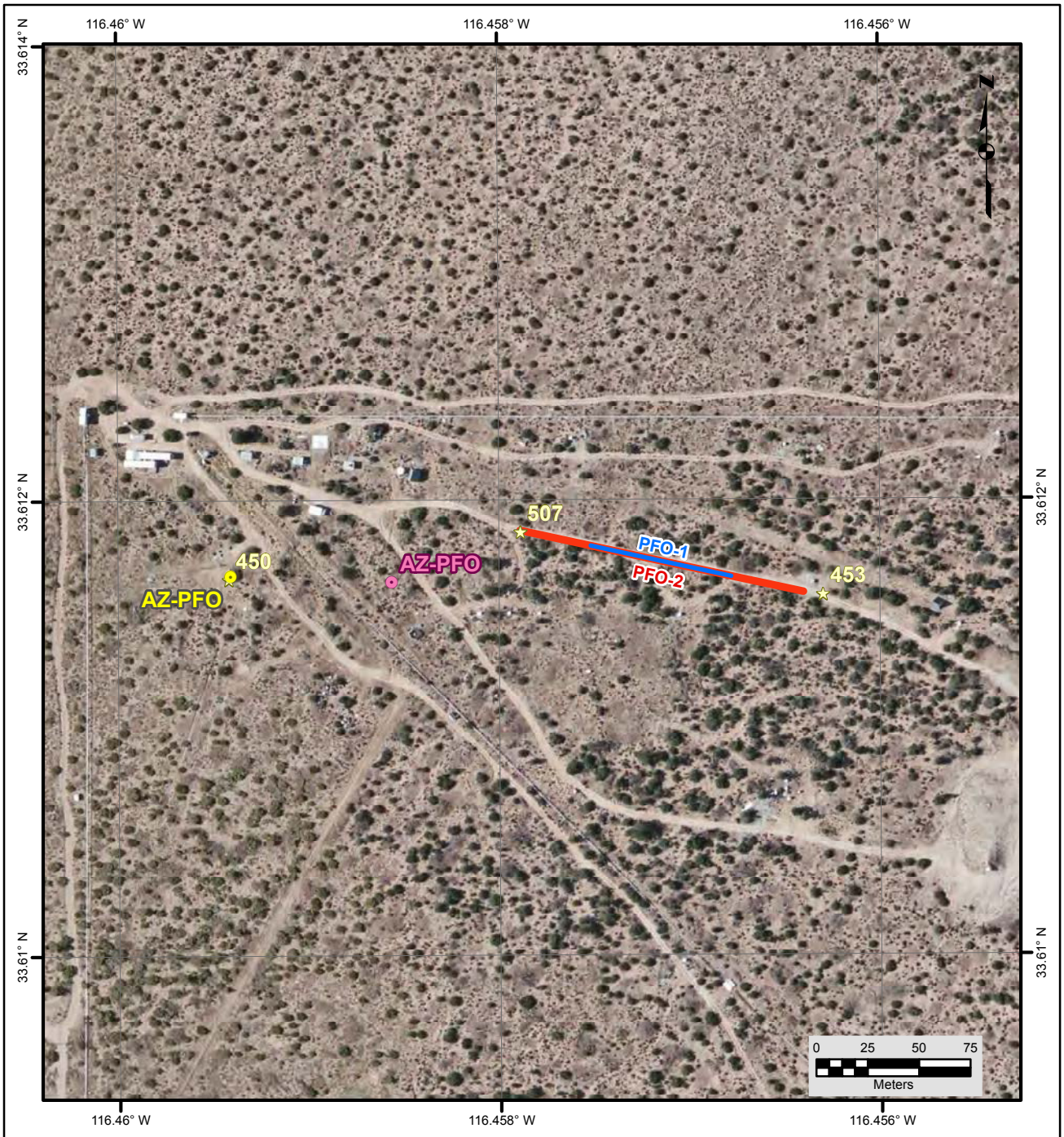

Legend

- Seismic Station - Approximate Surveyed Location
- Seismic Station - Approximate Location of Record
- H/V Spectral Ratio Location
- MASW Array
- MASW and Seismic Refraction Array

NOTES:
1. WGS 1984 COORDINATE SYSTEM
2. Image Source: ESRI, i-cubed, USDA FSA, USGS, AEX, GeoEye, Getmapping, Aerogrid, IGP

File Name: AZ-PFO-I

Date: 2/2/2012

USGS science for a changing world

GEOVision geophysical services

RECOVERY.GOV

SITE MAP
AZ•PFO

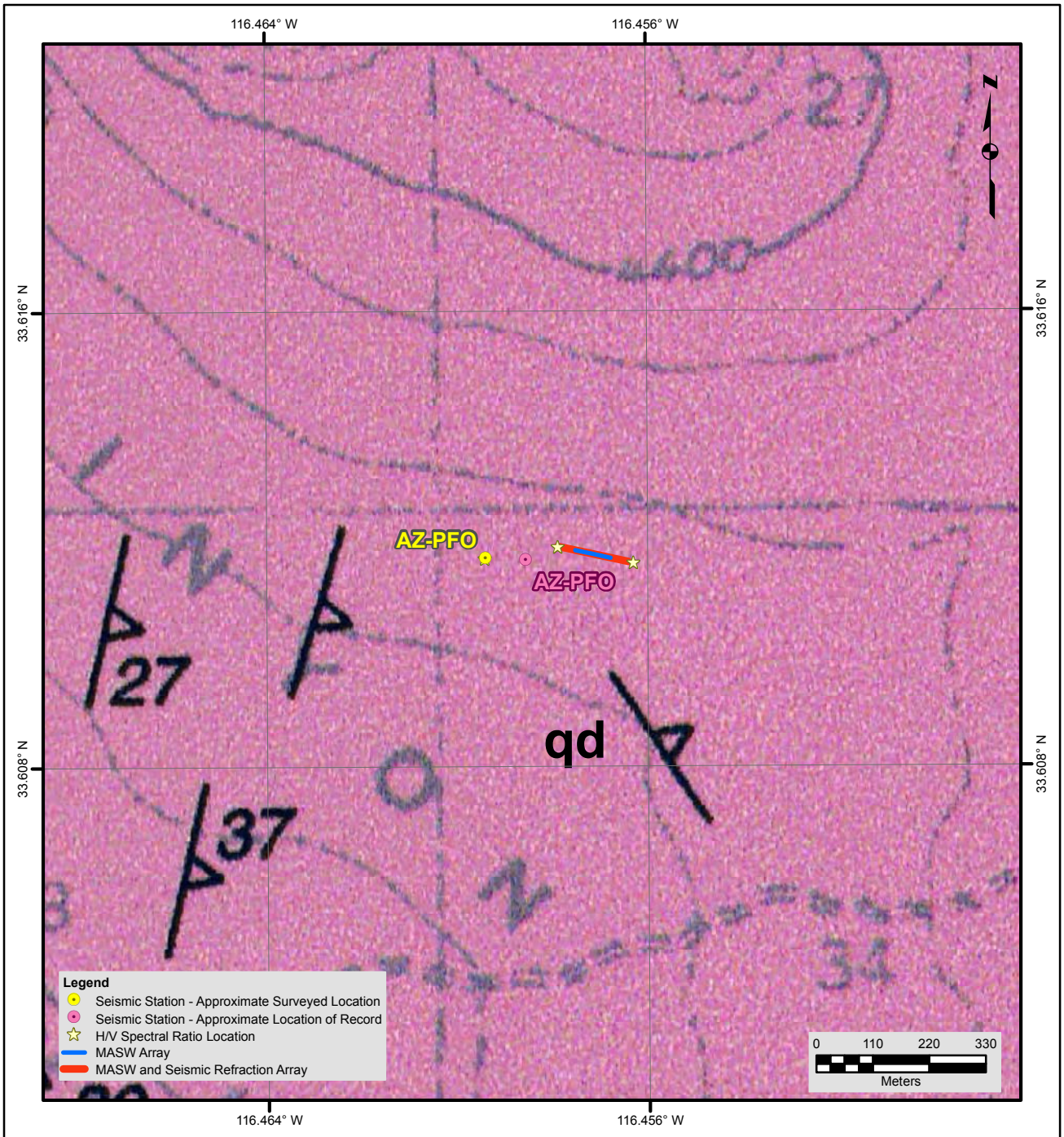

Description of Geologic Map Units

qd = Cretaceous (Mesozoic) quartz diorite, massive to gneissoid

NOTES:
1. WGS 1984 COORDINATE SYSTEM
2. Geologic Map of the Palm Desert & Coachella 15 Minute Quadrangles, Riverside County, California By Thomas W. Dibblee, Jr., 2008
3. See site map for details of geophysical survey

File Name: AZ-PFO

Date: 2/2/2012

USGS science for a changing world

GEOVision geophysical services

RECOVERY.GOV

GEOLOGIC MAP
AZ•PFO

AZ.PFO seismic station

HVSR measurements next to seismic station using both a Nanometrics Trillium Compact and Tromino ENGR

Looking towards seismic station from array PFO-2

Looking northwest along arrays PFO-1/2

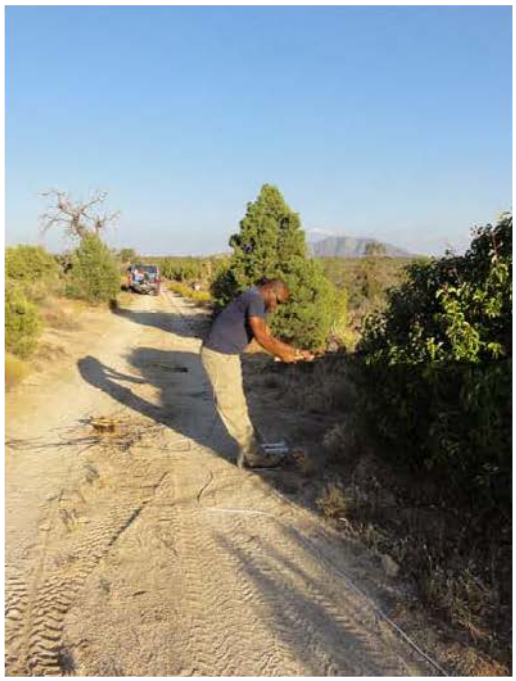

S-wave seismic refraction and MALW (Love wave) data acquisition along array PFO-1

Location of Geophysical Testing Arrays:

Location	Latitude	Longitude
PFO-1, Northwest End of MASW/Refraction Array	33.61180	-116.45753
PFO-1, Center of MASW/Refraction Array	33.61173	-116.45716
PFO-1, Southeast End of MASW/Refraction Array	33.61166	-116.45680
PFO-2, Northwest End of MASW/Refraction Array	33.61186	-116.45791
PFO-2, Center of MASW/Refraction Array	33.61173	-116.45716
PFO-2, Southeast End of MASW/Refraction Array	33.61159	-116.45642
HVSR Sensor 507	33.61186	-116.45790
HVSR Sensor 453	33.61158	-116.45631
HVSR Sensor 450	33.61165	-116.45943
AZ.PFO Seismic Station	33.61167	-116.45943

Notes: 1) WGS84 Coordinate System (decimal degrees)
2) Survey accuracy is estimated at 1 to 2 m.

Results:

V_S Model from MASW (Rayleigh Wave) Sounding, Assumed Poisson's Ratio = 0.2 (MASW Model 1)

Depth to Top of Layer (m)	Layer Thickness (m)	S-Wave Velocity (m/s)	Inferred P-Wave Velocity (m/s)	Assumed Poisson's Ratio	Assumed Density (g/cm^3)
0	1	196	320	0.2	1.70
1	1.5	426	695	0.2	1.80
2.5	2.5	440	718	0.2	1.90
5	4	608	994	0.2	2.00
9	14	948	1547	0.2	2.10
23	10	1508	2462	0.2	2.30
33	>12	2231	3643	0.2	2.50

Notes: 1) Depth of investigation is about 45 m.
2) Bottom layer is a half space.
3) V_{S30} = 744 m/s.

V_S Model from MASW (Rayleigh Wave) Sounding, Assumed Poisson's Ratio = 0.25 (MASW Model 2)

Depth to Top of Layer (m)	Layer Thickness (m)	S-Wave Velocity (m/s)	Inferred P-Wave Velocity (m/s)	Assumed Poisson's Ratio	Assumed Density (g/cm^3)
0	1	191	331	0.25	1.70
1	1.5	398	690	0.25	1.80
2.5	2.5	433	749	0.25	1.90
5	4	575	996	0.25	2.00
9	15	911	1578	0.25	2.10
24	9	1467	2541	0.25	2.30
33	>12	2093	3625	0.25	2.50

Notes: 1) Depth of investigation is about 45 m.
2) Bottom layer is a half space.
3) V_{S30} = 709 m/s.

V_S Model from MASW (Rayleigh Wave) Sounding, Assumed Poisson's Ratio = 0.3 (MASW Model 3)

Depth to Top of Layer (m)	Layer Thickness (m)	S-Wave Velocity (m/s)	Inferred P-Wave Velocity (m/s)	Assumed Poisson's Ratio	Assumed Density (g/cm^3)
0	1	183	342	0.3	1.70
1	1.5	388	727	0.3	1.80
2.5	2.5	415	777	0.3	1.90
5	4	548	1026	0.3	2.00
9	15	862	1613	0.3	2.10
24	9	1318	2466	0.3	2.30
33	>12	1959	3666	0.3	2.50

Notes: 1) Depth of investigation is about 45 m.
2) Bottom layer is a half space.
3) V_{S30} = 673 m/s.

V_S Model from MALW (Love Wave) Sounding, Northwest Off-End and Interior Shot Locations (MALW Model 1)

Depth to Top of Layer (m)	Layer Thickness (m)	S-Wave Velocity (m/s)	Inferred P-Wave Velocity (m/s)	Assumed Poisson's Ratio	Assumed Density (g/cm^3)
0	0.75	208	389	0.3	1.70
0.75	1.75	459	859	0.3	1.90
2.5	2.5	538	1006	0.3	2.00
5	4	783	1465	0.3	2.10
9	6	875	1637	0.3	2.10
15	8	919	1720	0.3	2.15
23	10	1207	2259	0.3	2.20
33	>2	1714	3207	0.3	2.30

Notes: 1) Depth of investigation is about 35 m.
2) Bottom layer is a half space.
3) V_{S30} = 779 m/s.

V_S Model from MALW (Love Wave) Sounding, Southeast Off-End and Interior Shot Locations (MALW Model 2)

Depth to Top of Layer (m)	Layer Thickness (m)	S-Wave Velocity (m/s)	Inferred P-Wave Velocity (m/s)	Assumed Poisson's Ratio	Assumed Density (g/cm^3)
0	0.75	207	388	0.3	1.70
0.75	1.75	465	869	0.3	1.90
2.5	2.5	549	1027	0.3	2.00
5	4	761	1424	0.3	2.10
9	6	951	1779	0.3	2.10
15	8	1145	2143	0.3	2.15
23	10	1512	2829	0.3	2.30
33	>2	2025	3789	0.3	2.40

Notes: 1) Depth of investigation is about 35 m.
2) Bottom layer is a half space.
3) V_{S30} = 854 m/s.

Average V_S Model from Central Portion of S-wave Refraction Line (Layered Starting Model)

Depth to Top of Layer (m)	Layer Thickness (m)	S-Wave Velocity (m/s)
0.00	0.51	244
0.51	1.02	327
1.52	1.02	661
2.54	1.02	669
3.56	1.02	694
4.57	1.02	744
5.59	1.02	761
6.60	2.13	765
8.74	2.13	770
10.87	2.13	799
13.00	2.13	1275
15.13	2.13	1306
17.27	2.13	1312
19.40	2.13	1327
21.53	2.13	1395
23.67	Half Space	1663

Average V_S Model from Central Portion of S-wave Refraction Line (Smooth Starting Model)

Depth to Top of Layer (m)	Layer Thickness (m)	S-Wave Velocity (m/s)
0.00	0.70	235
0.70	1.40	456
2.10	1.40	671
3.49	1.40	692
4.89	1.40	735
6.29	1.40	766
7.68	1.40	825
9.08	2.93	936
12.01	2.93	1062
14.95	2.93	1200
17.88	2.93	1263
20.81	2.93	1392
23.75	2.93	1543
26.68	2.93	1653
29.61	2.93	1869
32.55	Half Space	1915

Average V_P and Estimated V_S Models from Central Portion of P-wave Seismic Refraction Line (Layered Starting Model)

Depth to Top of Layer (m)	Layer Thickness (m)	P-Wave Velocity (m/s)	Estimated S-Wave Velocity (m/s)			
			Poisson's Ratio = 0.2	Poisson's Ratio = 0.25	Poisson's Ratio = 0.30	Poisson's Ratio = 0.35
0.00	0.68	411	252	237	220	197
0.68	1.36	789	483	456	422	379
2.04	1.36	1079	661	623	577	519
3.40	1.36	1128	691	651	603	542
4.77	1.36	1199	734	692	641	576
6.13	1.36	1306	800	754	698	628
7.49	1.36	1410	864	814	754	678
8.85	2.86	1451	889	838	776	697
11.71	2.86	1456	892	841	778	700
14.57	2.86	1462	895	844	782	702
17.43	2.86	1752	1073	1011	936	842
20.29	2.86	1999	1224	1154	1068	960
23.15	2.86	2760	1690	1593	1475	1326
26.01	2.86	2994	1833	1728	1600	1438
28.86	2.86	3101	1899	1790	1657	1490
31.72	2.86	3815	2336	2203	2039	1833
34.58	Half Space	4074	2495	2352	2178	1957

Average V_P and Estimated V_S Models from Central Portion of P-wave Seismic Refraction Line (Smooth Velocity Gradient Starting Model)

Depth to Top of Layer (m)	Layer Thickness (m)	P-Wave Velocity (m/s)	Estimated S-Wave Velocity (m/s)			
			Poisson's Ratio = 0.20	Poisson's Ratio = 0.25	Poisson's Ratio = 0.30	Poisson's Ratio = 0.35
0.00	0.89	434	266	251	232	208
0.89	1.77	898	550	518	480	431
2.66	1.77	1122	687	648	600	539
4.44	1.77	1236	757	714	661	594
6.21	1.77	1296	794	748	693	623
7.99	1.77	1400	857	808	748	672
9.76	1.77	1456	892	841	778	700
11.54	3.73	1647	1009	951	881	791
15.26	3.73	1856	1136	1071	992	892
18.99	3.73	2158	1321	1246	1153	1036
22.72	3.73	2346	1437	1355	1254	1127
26.45	3.73	2676	1639	1545	1430	1286
30.17	3.73	3025	1852	1746	1617	1453
33.90	3.73	3555	2177	2052	1900	1708
37.63	3.73	4044	2476	2335	2162	1943
41.36	Half Space	4185	2563	2416	2237	2010

Observations/Discussion:

- The center of the seismic line was located about 225 m from the seismic station, based on direction from the site representative.
- There are no low frequency peaks in the HVSR data, as expected for a rock site. HVSR sensor 507 has a clear peak at 7 Hz and a trough at about 18 Hz. HVSR sensor 453 has a broad, very low amplitude peak in the 6 to 11.5 Hz range (possible separate peaks at 6.5 and 11 Hz) and a trough at 15 Hz. HVSR sensor 450 does not have a distinct HVSR peak, but has a trough at about 18.5 Hz. The differences in high frequency HVSR response may be indicative of near surface lateral velocity variation, although the source of high frequency microtremor energy is not clear.
- Several geophysical techniques including P- and S-wave seismic refraction, MASW (Rayleigh wave) and MALW (Love wave) techniques were evaluated at this site. MASW data were acquired along the 70.5 m long array PFO-1. P-wave seismic refraction data were acquired along the 141 m long array PFO-2. S-wave seismic refraction and MALW data were acquired along the 70.5 m long array PFO-1. MASW data were acquired along the 70.5 m long array PFO-1.
- The P-wave seismic refraction data for array PFO-1 and S-wave seismic refraction data for array PFO-1 were modeled using a tomographic inversion routine with both layer-based and smooth velocity gradient starting models. The seismic refraction models were extended to far offset shot locations to extend depth of investigation. A longer line would have been preferred for the S-wave seismic refraction survey, but the data were acquired in combination with MALW data.
- The P- and S-wave seismic refraction data sets are of excellent and good quality, respectively. The P-wave first arrival data were picked to a greater degree of accuracy than the S-wave first arrival data because the S-wave is not typically the first energy on a seismic record, even when using a horizontal traction plank as an energy source. It is preferred to acquire both P- and S-wave refraction data and reconcile the models; as converted waves are always a possibility in S-wave refraction data collected at heterogeneous sites.
- Tomographic inversion of the P-wave first arrival data utilizing layered and smooth starting models yielded quite different V_P models. As with all inversion of surface geophysical data, the starting model affects the final model. The P-wave seismic refraction survey design allowed P-wave velocity to be imaged to a maximum depth of about 35 to 45 m. The seismic refraction model, developed using a layered starting model, indicates that P-wave velocity is about 450 to 550 m/s at the surface and increases to 1,000 m/s at a nominal depth of 2 m, gradually increases to 1,500 m/s at a depth of 15 to 20 m, abruptly increases to over 2,500 m/s, and exceeds 3,500 m/s at depths below 25 to 30 m. The maximum P-wave velocity in the model is about 4,250 m/s at a minimum depth of about 35 m. The seismic refraction model, developed using a smooth velocity gradient starting model, shows P-wave velocity gradually increasing with depth from 450 to 550 m/s at the surface to over 4,000 m/s at a depth below 35 m.
- The P-wave seismic refraction first arrival data warrants closer inspection to determine if layered structure is realistic in this environment. Previous experience has indicated that weathering of rock is highly variable and both layered (abrupt velocity increases) and smooth velocity gradients can occur. Additionally, all layer based starting models are generated with the relatively simple time-term inversion technique. It would be

interesting to explore the use of more accurate layer based models developed using techniques such as the generalized reciprocal method, as starting models.

- Although the P-wave refraction models do not appear to show significant lateral velocity variation, there is a distinct thickening of the weathered zone to the southeast between a position of about 40 and 100 m, which is coincident with the location of the MASW/MALW array. This thickening of the weathered zone amounts to an effective 5 degree dip to the southeast of the top of more competent rock beneath the MASW and MALW arrays.
- Tomographic inversion of the S-wave first arrival data utilizing layered and smooth starting models also yielded differing V_S models. The S-wave seismic refraction survey design allowed S-wave velocity to be imaged to a maximum depth of about 25 to 30 m, although a longer line would have been preferred to image to this depth. The seismic refraction model, developed using a layered starting model, indicates that S-wave velocity is about 250 to 300 m/s at the surface and increases to 600 m/s at a nominal depth of 2 m, gradually increases to 800 m/s at a depth of 7 to 10 m, abruptly increases to over 1,200 m/s, and exceeds 1,600 m/s at depths below 20 to 24 m. The maximum S-wave velocity in the model is about 1,700 m/s at a minimum depth of about 25 m. The seismic refraction model, developed using a smooth velocity gradient starting model, shows S-wave velocity gradually increasing with depth from 250 to 300 m/s at the surface to over 1,800 m/s at a depth below 30 m.
- The P- and S-wave seismic refraction models are in poor agreement over the 13 to 24 m depth range, where V_S in the S-wave refraction model is much higher than that estimated from the P-wave refraction model using assumed constant values for Poisson's ratio. The difference in the models results in a significantly higher estimated V_{S30} from the S-wave refraction model. Additionally, the difference in the models is too large to be explained by increased first arrival error in the S-wave refraction data and may indicate that some type of mode conversion is occurring in the S-wave refraction data. For this reason, it is always prudent to also acquire P-wave refraction data when acquiring S-wave refraction data, except in cases of shallow groundwater, and compare resulting models. The surface wave soundings will be used to determine the more reliable set of models.
- V_{S30} was estimated between 27 and 49.5 m on the S-wave refraction model for array PFO-1, developed using a layered starting model, by projecting the velocity at 24 m depth to 30 m depth. Over this interval, V_{S30} ranges from about 883 to 969 m/s, about a 9% variation over a 22 m distance on the array. An average V_S model was developed over the 27 to 49.5 m distance interval by averaging the travel time though each model cell at a particular depth and average V_{S30} was determined to be 923 m/s. Average V_S between 1 and 31 m is 1,016 m/s.
- V_{S30} was estimated between 27 and 49.5 m on the S-wave refraction model for array PFO-1 that was developed using a smooth velocity gradient starting model. Over this interval, V_{S30} ranges from about 890 to 971 m/s, about a 9% variation over a 22 m distance. An average V_S model was developed over the 27 to 49.5 m distance interval by averaging the travel time though each model cell at a particular depth and average V_{S30} was determined to be 932 m/s. Average V_S between 1 and 31 m is 1,031 m/s.
- On the P-wave velocity model for array PFO-2, developed using a layered starting model, V_{P30} between 30 and 111 m (equivalent position of -5.25 to 75.75 m on array PFO-1) varies from about 1,315 to 1,640 m/s, a 22% variation, and averages 1,478 m/s.

Estimating V_{S30} from V_{P30} assuming constant Poisson's ratio in the range of 0.2 to 0.35 results in V_{S30} in the 905 to 710 m/s range, respectively. This large variation in potential V_{S30} demonstrates the risks in attempting to estimate V_{S30} from P-wave velocity data, even with a realistic estimate of Poisson's ratio and this approach should only be used as a last resort.

- On the P-wave velocity model for array PFO-2, developed using a smooth velocity gradient starting model, V_{P30} between 30 and 111 m (equivalent position of -5.25 to 75.75 m on array PFO-1) varies from about 1,387 to 1,651 m/s, a 17% variation, and averages 1,514 m/s. Estimating V_{S30} from V_{P30} assuming constant Poisson's ratio in the range of 0.20 to 0.35 results in V_{S30} in the 927 to 727 m/s range.
- Noise conditions at the site were not sufficient for application of passive surface wave techniques.
- Both MASW (Rayleigh wave) and MALW (Love wave) data collected along array PFO-1 were reduced and modeled. MASW data extracted from the array PFO-2 seismic refraction data set were combined with that from array PFO-1 for modeling. It is difficult to predict the effect of the significant lateral velocity variation (20% or larger variation in V_{S30} beneath the array) on the resulting surface wave models.
- The minimum wavelength surface wave phase velocity data extracted from the 48-channel MASW and MALW arrays is about 14 an 10 m, respectively. MASW and MALW data reduction using seismic records from smaller hammer sources and a limited offset receiver array (i.e. less active geophones) allowed extraction of surface wave dispersion data to a minimum wavelength of about 3 and 2 m, respectively.
- There is nominally about 100 to 150 m/s scatter in MASW and MALW dispersion data, likely due to the effects of lateral velocity variation.
- Both MASW and MALW dispersion curves derived from source locations offset from the northwest and southeast ends of the array diverge at long wavelengths (small frequencies) due to the lateral velocity variation. MASW dispersion data from northwest and southeast source locations on the longer MASW array PFO-2 diverged less at long wavelengths.
- A single, average representative dispersion curve was generated for the combined arrays PFO-1 and PFO-2 MASW data sets using a moving average, polynomial curve fitting routine and used for modeling. Separate representative dispersion curves were generated for the northwest and southeast MALW source locations, both combined with dispersion data from interior shot locations.
- The maximum wavelength Rayleigh wave phase velocity data extracted from MASW array PFO-1 was fixed at 25% greater than the source to center of the receiver array distance. The maximum wavelength Rayleigh wave phase velocity data extracted from MASW array PFO-2 was fixed at 15% greater than the source to center of the receiver array distance. The maximum wavelength Rayleigh wave phase velocity used for modeling was about 105 m, resulting in a maximum depth of investigation of about 45 to 50 m.
- Because Love waves require longer wavelengths than Rayleigh waves to image to a particular depth, Love wave phase velocity data to wavelengths of 110 to 120 m were extracted from the dataset, even though the receiver array only had a length of 70.5 m with a maximum source offset of 30 m. There does appear to be evidence of significant near field effects in the data; however, a longer array would definitely have been

preferred. Maximum Love wave depth of investigation appears to be on the order of one-third the maximum wavelength, which is 35 m at this site.

- Three models were developed for the MASW data set using assumed Poisson's ratios of 0.2, 0.25 and 0.3 and the fundamental mode assumption (Models 1 to 3). Separate models were developed for the MALW dispersion curves derived from northwest off-end and interior and southeast off-end and interior sources, respectively (Models 1 and 2). A similar process would have been conducted for the MASW data set, had long wavelength phase velocity data not been available from the longer array PFO-2.
- V_{S30} from the MASW V_S models with assumed Poisson's ratios of 0.2, 0.25 and 0.3 are 744, 709, and 673 m/s, respectively (Site Class C/B).
- Average S-wave velocity between 1 and 31 m, to account for assumed sensor depth and the fact that the sensor would be placed below the thin residual soil layer, from the MASW V_S models with assumed Poisson's ratio of 0.2, 0.25 and 0.3 are 837, 795, and 752 m/s, respectively (Site Class B/C).
- V_{S30} from the MALW V_S Models 1 (northwest and interior sources) and 2 (southeast and interior sources) are 779 and 854 m/s, respectively (Site Class B/C).
- Average S-wave velocity between 1 and 31 m for MALW V_S Models 1 and 2 is 852 and 949 m/s, respectively (Site Class B).
- The average V_{S30} estimated from the MALW dispersion data is over 12% higher than V_{S30} estimated from the MASW dispersion data, primarily due to significantly lower VS between a depth of about 2.5 and 9 m in the MASW model. All of the MASW phase velocity data at wavelengths smaller than 15 m were derived from the array PFO-1 center shot location, off-end shot locations at the lower velocity southeast end of array PFO-1 and selected interior shot locations from array PFO-2. Therefore, velocities in the upper several meters in the MASW model may be biased towards some of the lower velocities at the site, although this does not explain the difference in velocity structure at depths approaching 9 m. Shear wave anisotropy in near surface weathered rock may also play a role in the difference in velocity. The MASW and MALW models are very similar at depths below 9 m. The MALW model is the most consistent with S-wave velocity structure in the upper 9 m estimated from the P-wave velocity model using assumed constant Poisson's ratios.
- The S-wave refraction V_S model generally overestimates Vs over the 13 to 23 m depth range, relative to other methods, and the possibility cannot be discounted that the S-wave refraction data has been compromised by converted waves, due to the irregular velocity structure. The S-wave refraction data needs to be more carefully reviewed to determine if a consistent bias in first arrival picking may be influencing the results. The higher V_S in the 13 to 23 m depth range results in the S-wave refraction survey providing the highest estimates of V_{S30}, which are 923 and 932 m/s for the models derived using layered and smooth velocity gradient starting models, respectively. At this time, the S-wave refraction V_S model should not be used for site characterization.
- The V_S models developed from the MASW, MALW and P-wave refraction models are generally in good agreement at depths below 9 m with the P-wave refraction model derived using a smooth velocity gradient starting model comparing best. V_{S30} estimated from the average P-wave refraction model and assumed constant Poisson's ratio of 0.25 and 0.3, which are realistic for competent to weathered granitic rocks, are 853 and 790 m/s, respectively, for the layered starting model and 874 and 809 m/s, respectively, for

the smooth starting model. These V_{S30} estimates are consistent with those derived from the MALW dispersion data, but higher than those developed from the MASW dispersion data. The V_S models developed from the MASW and MALW data are generally in acceptable agreement, except over the 2 to 9 m depth range where V_S developed from the MALW data is much higher, potentially more so than can be explained by anisotropy. Additional research is necessary to completely understand the conditions, other than anisotropy, under which the MASW and MALW techniques may yield different V_S models.

- Further review of the MASW V_S models indicates that superposition of the fundamental and first higher modes would be expected at frequencies lower than 20 to 25 Hz. Average/effective mode modeling was not conducted in an attempt to account for potential modal superposition as V_S at depth in the fundamental mode models was consistent with that derived from the MALW data. Effective mode modeling of the Rayleigh wave dispersion data would lower V_{S30}, thereby increasing the difference in V_{S30} between the MASW and MALW techniques.
- For site characterization purposes, we recommend averaging the MASW V_S model, with an assumed Poisson's ratio of 0.25 and the average V_S structure derived from the two MALW models.
- V_{S30} from the MASW model with Poisson's ratio of 0.25 is 709 m/s and the average V_{S30} of the MALW models is 816 m/s. The average V_{S30} between the MASW and MALW V_S models is 763 m/s (NEHRP Site Class C/B). Considering that the P-wave refraction model shows V_{P30} varying by about 20% beneath the array, V_{S30} may vary from about 685 to 840 m/s beneath the array and there may be much more variation in the immediate site vicinity.
- The average V_S between 1 and 31 m is 795 m/s from the MASW model with Poisson's ratio of 0.25 and 900 m/s from the MALW models, averaging 848 m/s (NEHRP Site Class B). Considering that the P-wave refraction model shows V_{P30} varying by about 20% beneath the array, average V_S between 1 and 31 m may vary from about 763 to 933 m/s beneath the array and there may be much more variation in the immediate site vicinity.
- Given the significant lateral velocity variation at this site, it would be desirable to have conducted geophysical testing in closer proximity to the seismic station. There is, however, sensitive equipment in close proximity to the seismic station. Even a simple surface wave measurement focused on determining the phase velocity of a 40 m wavelength Raleigh wave, which could be determined with a single SASW receiver spacing, would facilitate correlation of V_{S30} measured along the seismic line to that expected at the seismic station.

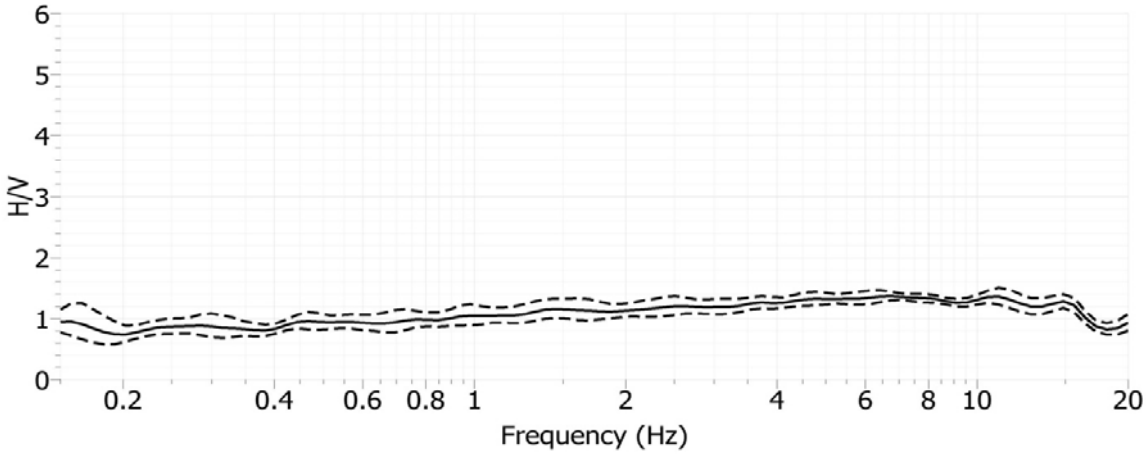

Site AZ.PFO, H/V Spectral Ratio, Near Seismic Station, Sensor 450

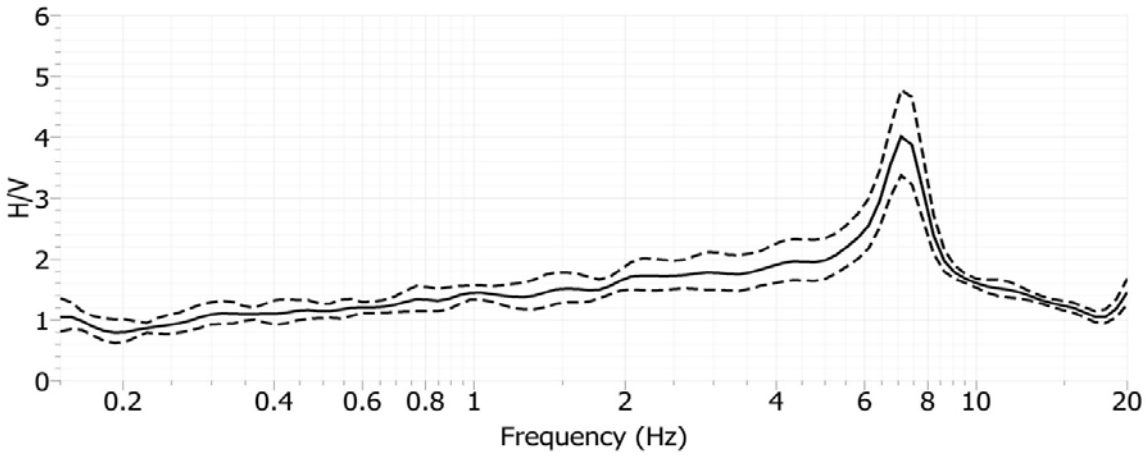

Site AZ.PFO, H/V Spectral Ratio, Array PFO-2, Sensor 507

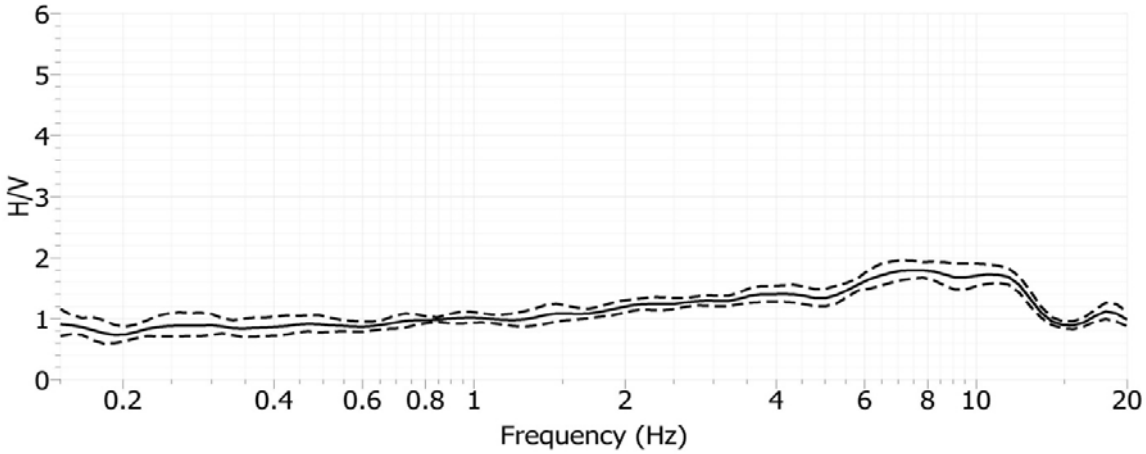

Site AZ.PFO, H/V Spectral Ratio, Array PFO-2, Sensor 453

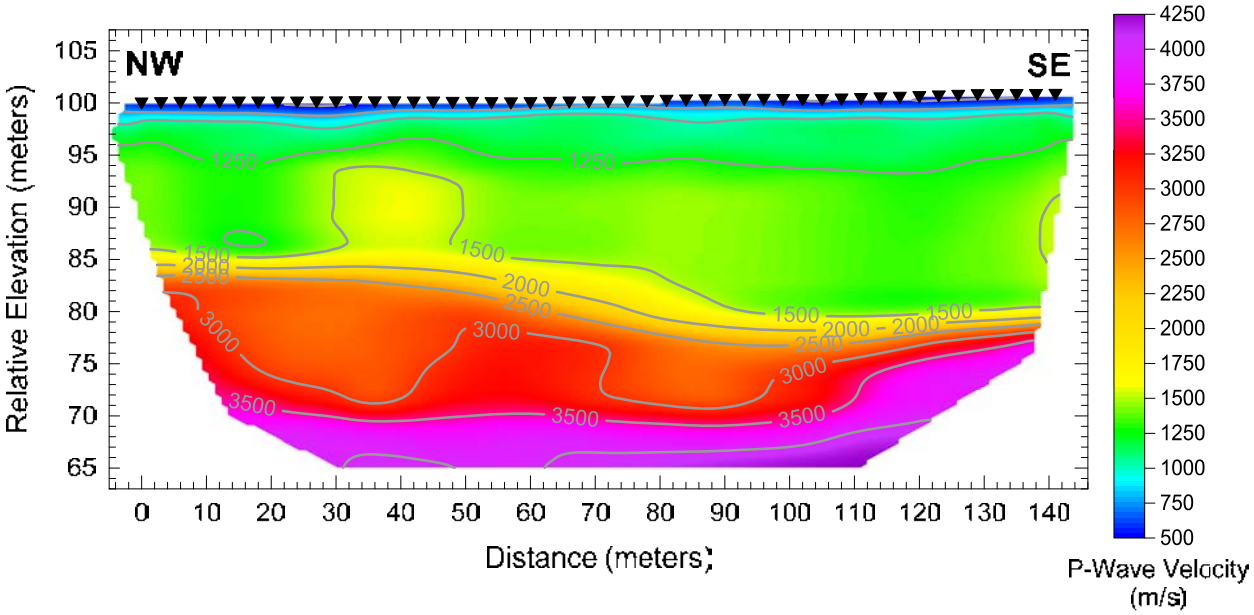

Array PFO-2 – P-wave Tomographic Seismic Refraction Model utilizing Layer Based Starting Model

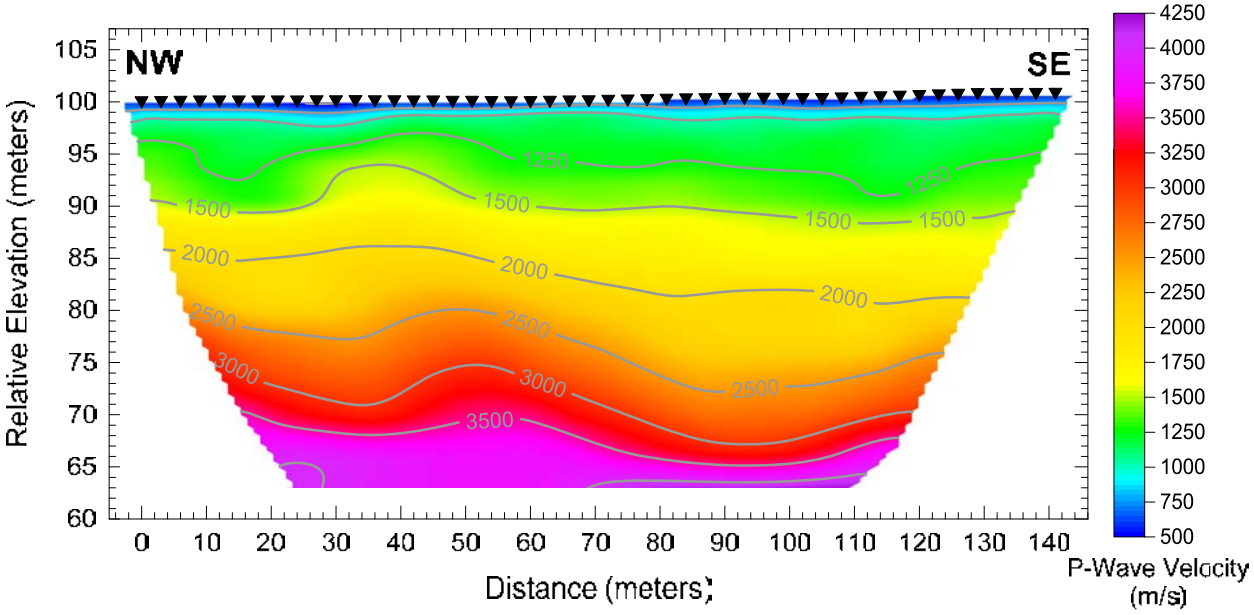

Array PFO-2 – P-wave Tomographic Seismic Refraction Model utilizing Smooth Velocity Gradient Starting Model

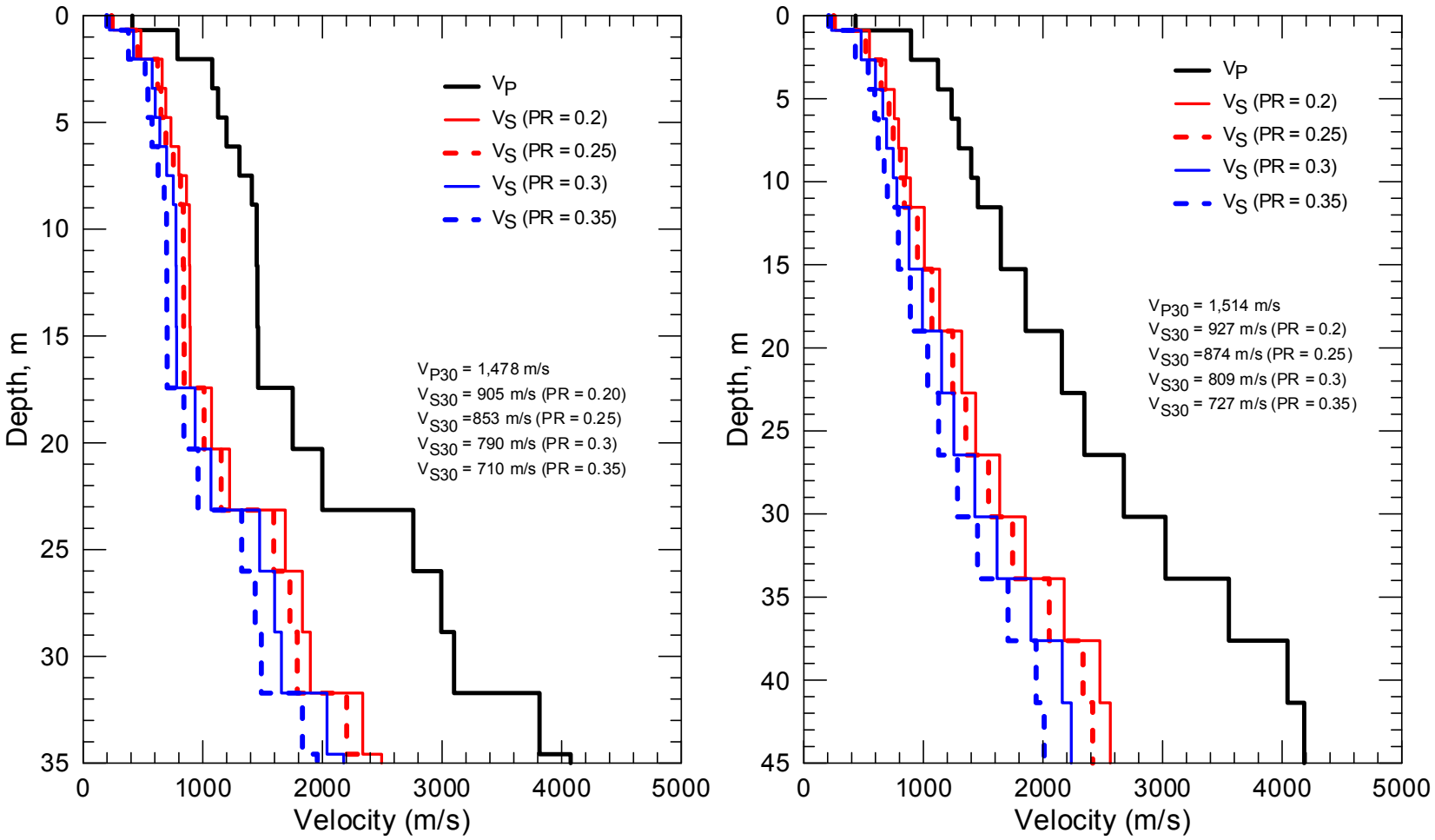

AZ.PFO – Average P-wave velocity structure and estimated S-wave velocity structure between a position of 30 and 111 m on the array PFO-2 P-wave seismic refraction models that utilized both layered (left) and smooth velocity gradient (right) starting models. Array PFO-1, utilized to collect MASW, MALW and S-wave refraction data, is located between 35.25 and 105.75 m on array PFO-2, which is approximately coincident with the region used to develop the estimated S-wave velocity model from the P-wave refraction data.

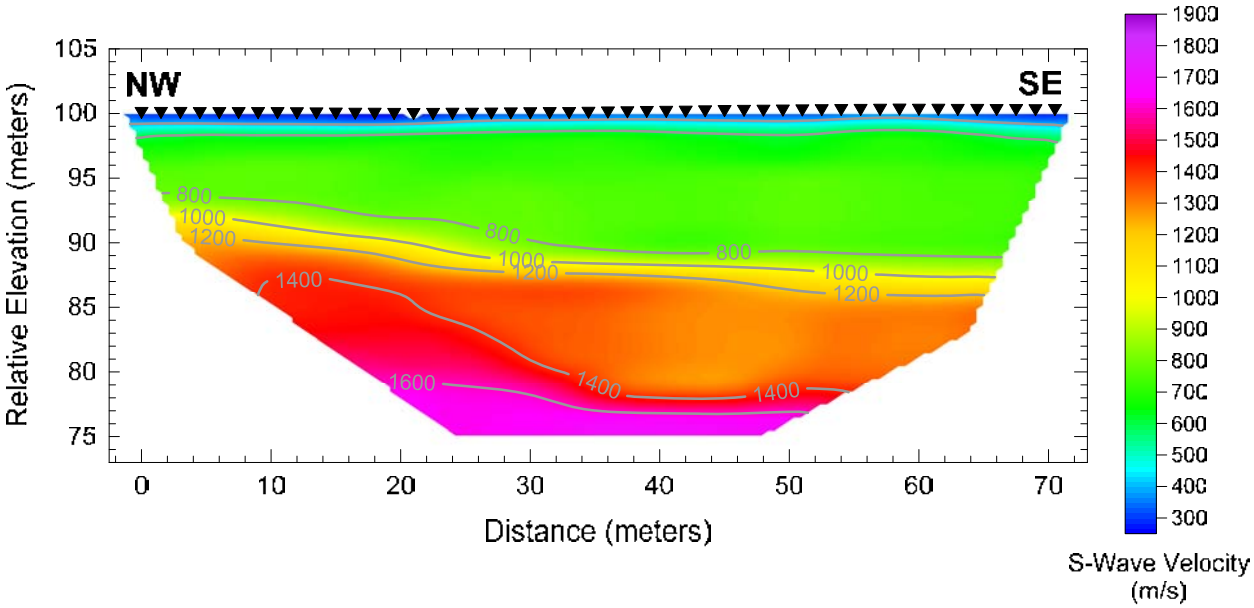

Array PFO-1 – S-wave Tomographic Seismic Refraction Model utilizing Layer Based Starting Model

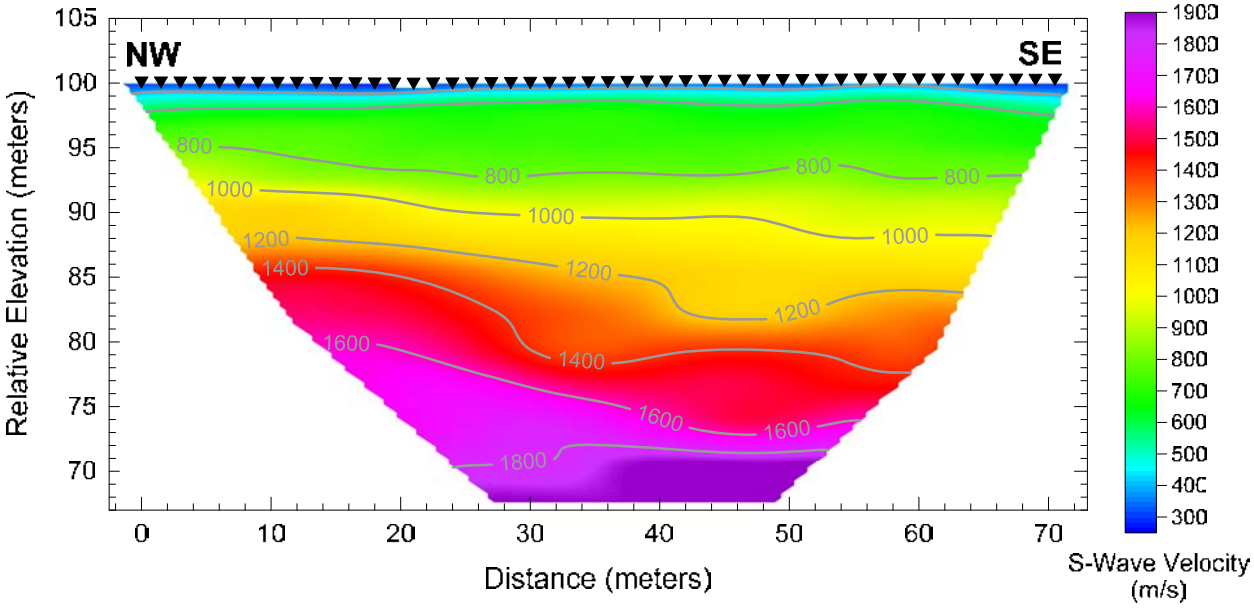

Array PFO-1 – S-wave Tomographic Seismic Refraction Model utilizing Smooth Velocity Gradient Starting Model

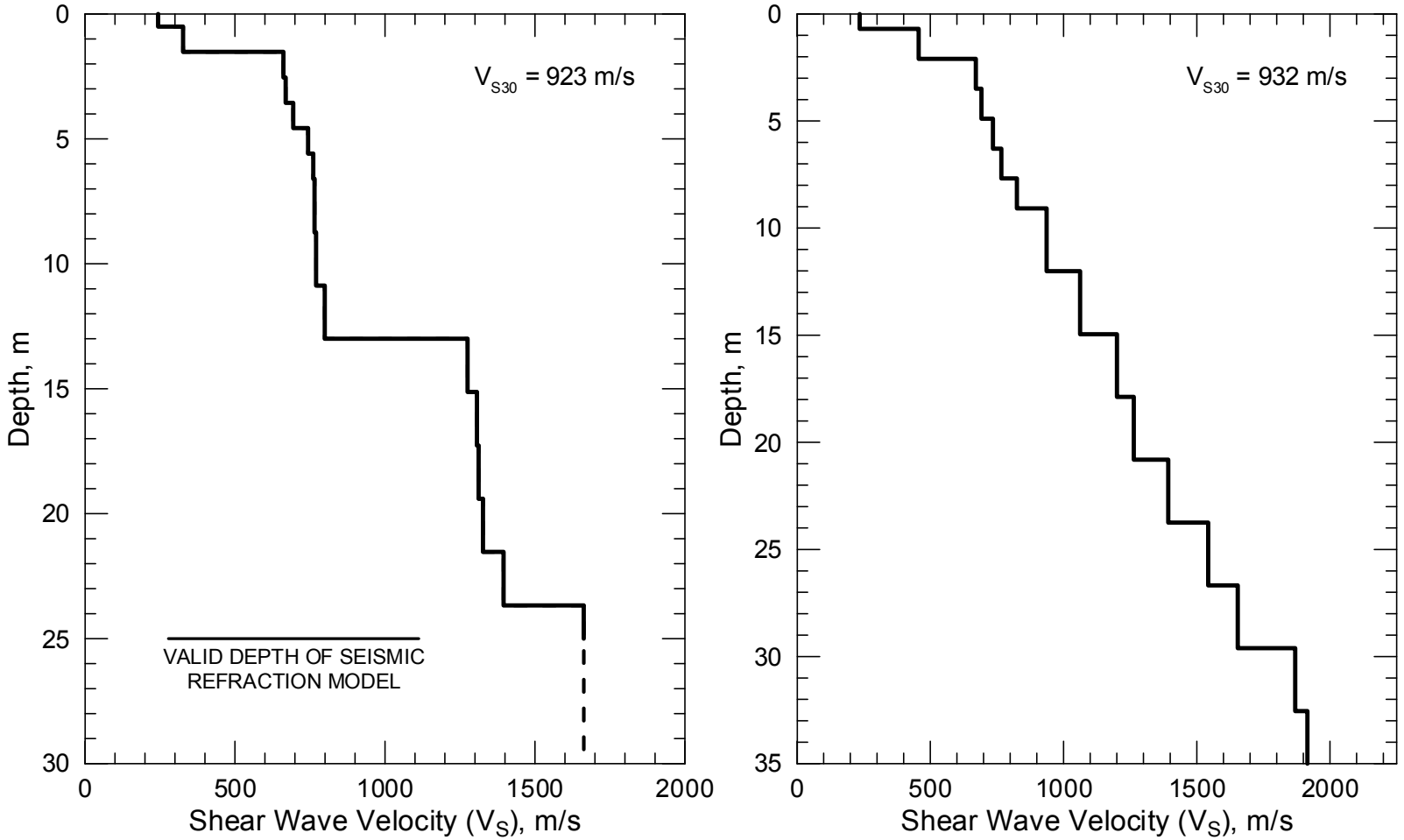

AZ.PFO – Average S-wave velocity structure between a position of 7 and 47.5 m on the S-wave seismic refraction models for array PFO-1 resulting from tomographic inversions that utilized a layered starting model (left) and smooth velocity gradient starting model (right). V_S over the 13 to 23 m depth range is high relative to the P-wave refraction models and surface wave models. The possibility cannot be discounted that converted waves are present as first arrivals in segments of the S-wave refraction data. Therefore, the S-wave refraction model should not be used for the purpose of site characterization until further investigation. A longer seismic line would be preferred to more accurately image to 30 m depth and for more direct correlation to the P-wave refraction model.

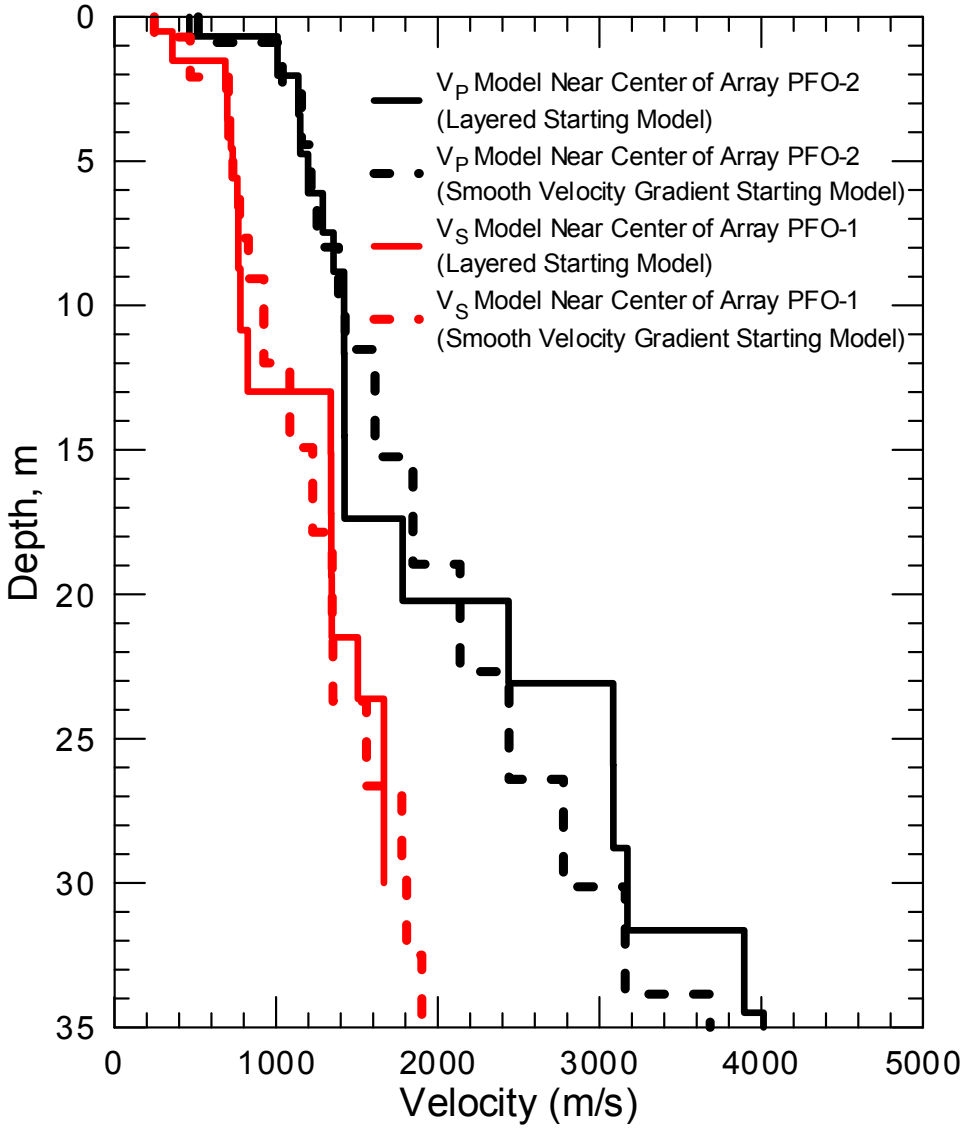

V_S model from near the center of S_H-wave refraction array PFO-1 (70.5 m long array) and V_P model from near the center of P-wave refraction array PFO-2 (141 m long array with common center and orientation as array PFO-1). There is no conclusive evidence of a converted wave (S_H to P) generated along an irregular interface (e.g. dipping interface not orthogonal to seismic line), with the possible exception of nearly equivalent V_S and V_P over the 13 to 18 m depth range in the refraction models developed using layered starting models. Error in the layered starting models may result in the similarity between V_S and V_P over this depth interval. The velocity models developed utilizing a smooth velocity gradient starting model probably provide a better mechanism by which to evaluate the presence of converted waves in the S-wave refraction models. If converted waves are not present in the S-wave refraction and first arrival errors do not significantly impact the model, then Poisson's ratio may be very low at intermediate depths. The surface wave V_S models, however, are more consistent with the P-wave refraction models. S-wave refraction data could be acquired along the longer array PFO-2 for a better comparison.

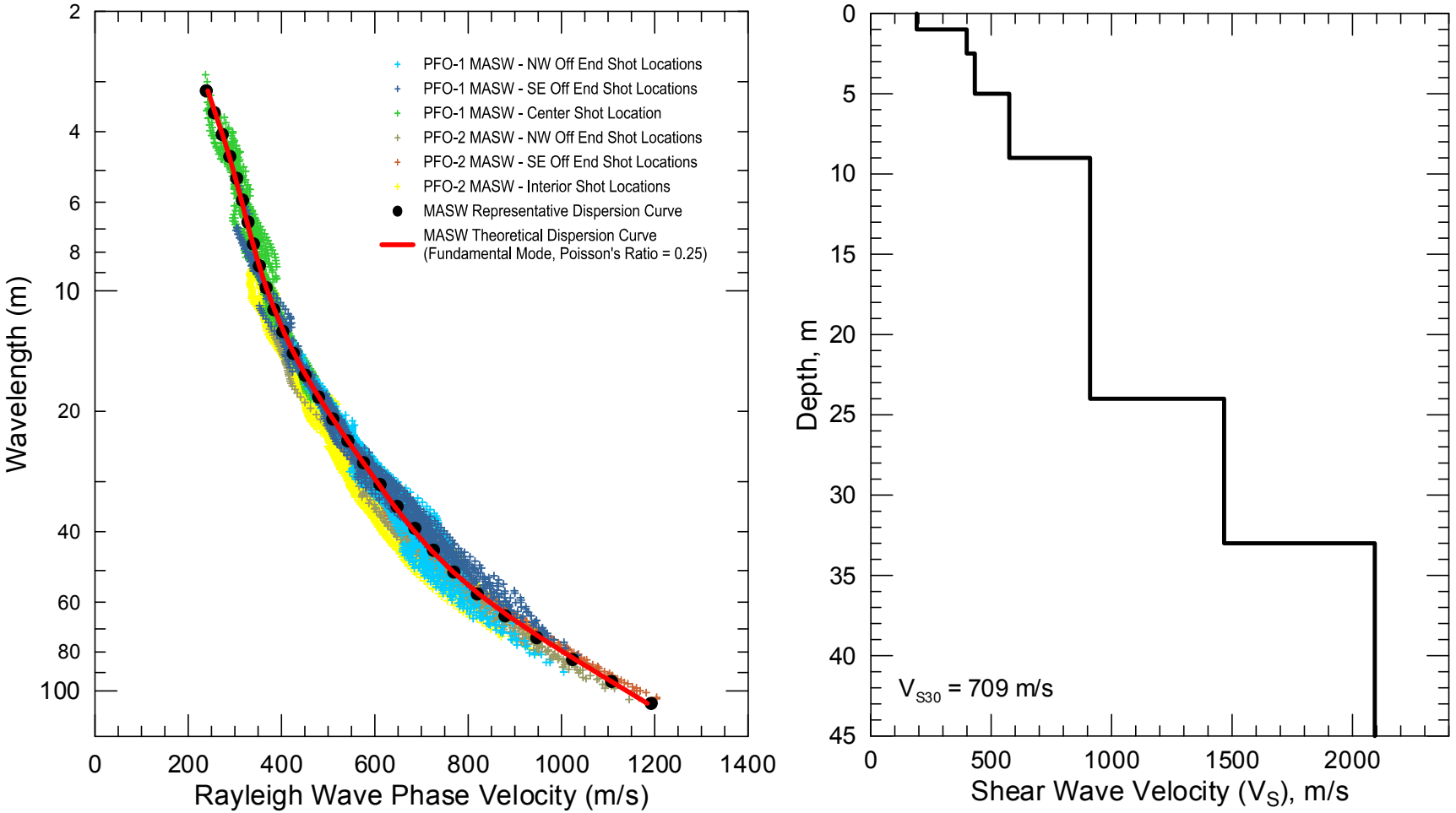

AZ.PFO - Field, representative and inverted theoretical surface wave dispersion data (left) and associated V_S model (right) for Rayleigh wave data (fundamental mode assumption, Poisson's ratio = 0.25). Surface wave dispersion data from the 70.5 m long array PFO-1 and 141 m long array PFO-2 are combined for modeling. Seismic refraction models indicate that there is lateral velocity variation beneath the array, which causes surface wave dispersion data from shot locations at each end of the array to diverge at long wavelengths. Much of the lateral velocity variation occurs beneath array PFO-1, which exhibits the largest divergence of phase velocity at long wavelengths.

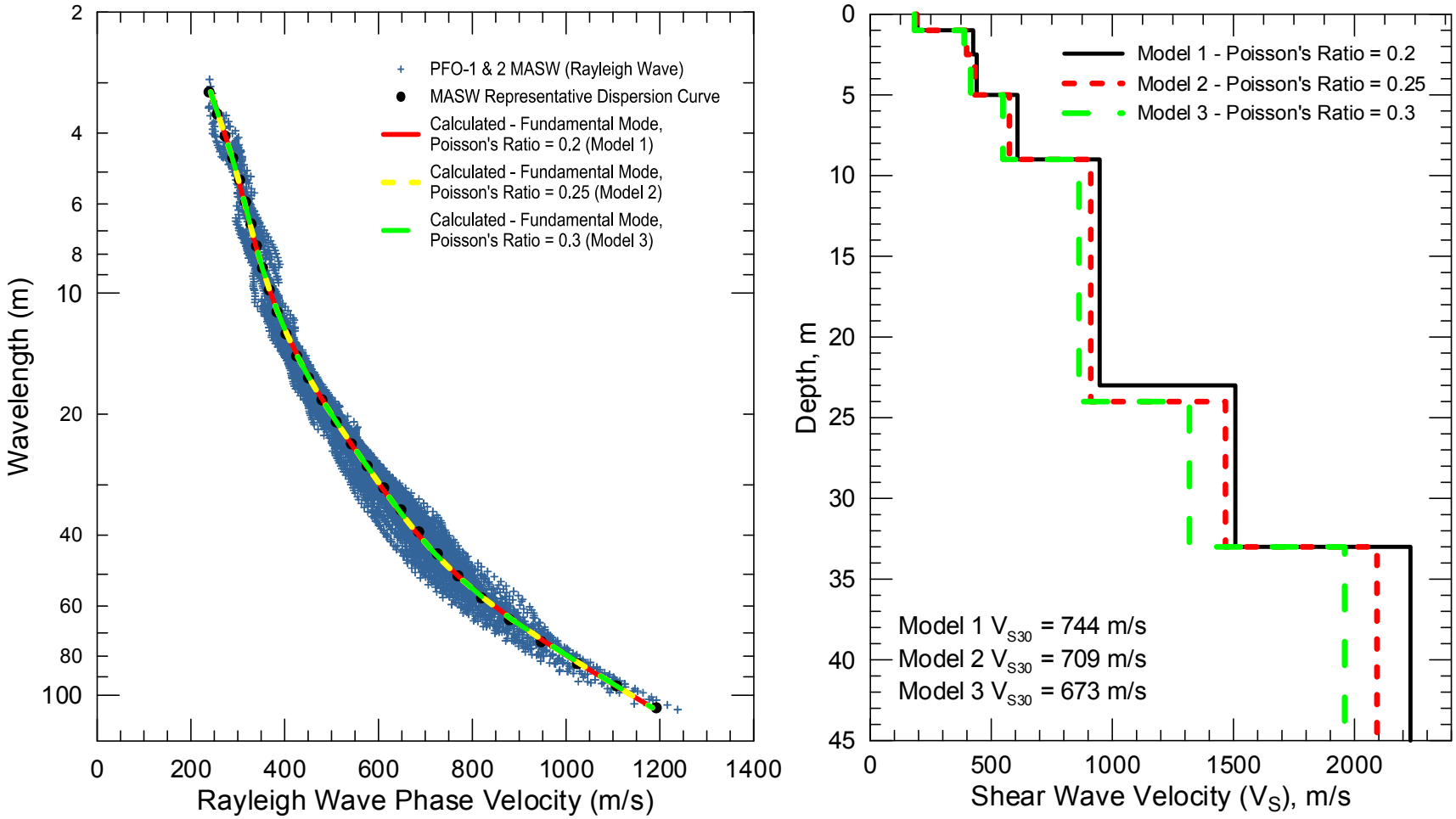

AZ.PFO - Field, representative and inverted theoretical surface wave dispersion data (left) and V_S models utilizing different values of Poisson's ratio (right) for Rayleigh wave data.

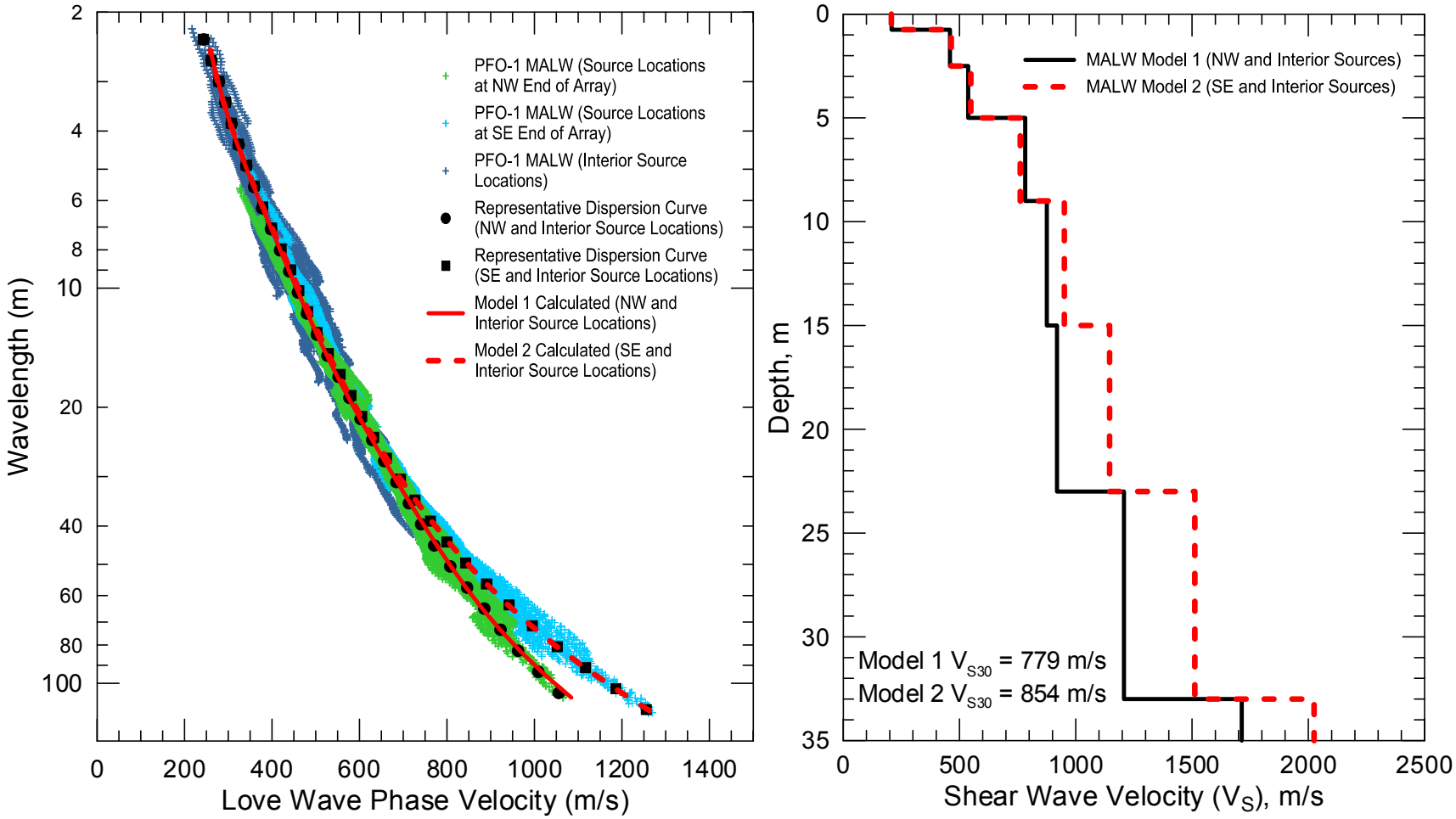

AZ.PFO - Field, representative and inverted theoretical surface wave dispersion data (left) and associated V_S model (right) for Love wave data. Similar to the Rayleigh wave data, Love wave dispersion curves from source locations at the NW and SE ends of array PFO-1 diverge at long wavelengths/low frequencies. Love wave phase velocity data from the NW and SE off-end source locations were combined with dispersion data from interior source locations and modeled separately. It would have been beneficial to have acquired Love wave data on the longer array PFO-2.

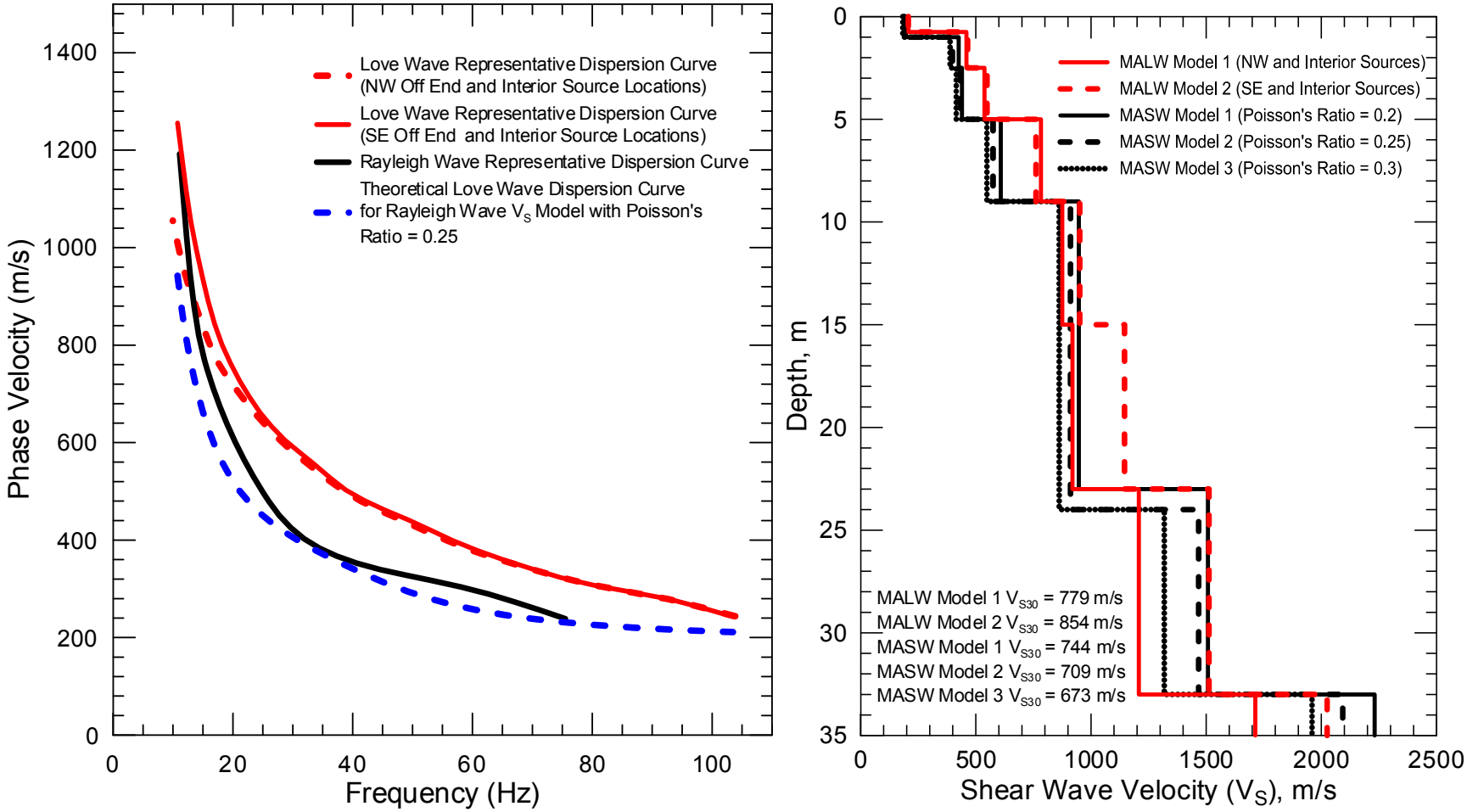

AZ.PFO - Comparison of V_S models resulting from inversion of Rayleigh and Love wave dispersion curves. The V_S models developed from the Rayleigh and Love wave dispersion data are in reasonable agreement except for the 2.5 to 9 m depth range where the Love wave V_S model has significantly higher velocities. The velocity difference over this depth interval is what gives rise to the greater than 100 m/s difference in V_{S30}. The observed Love wave dispersion curves are significantly different than the theoretical Love wave dispersion curve for the V_S model developed from the Rayleigh wave dispersion curve and assumed Poisson's ratio of 0.25. The higher phase velocities in the observed Love wave dispersion curves give rise to the higher V_S in the 2.5 to 9 m depth range. S-wave anisotropy and lateral velocity variation (~20% variation in V_{P30} beneath array) may contribute to some difference in the models.

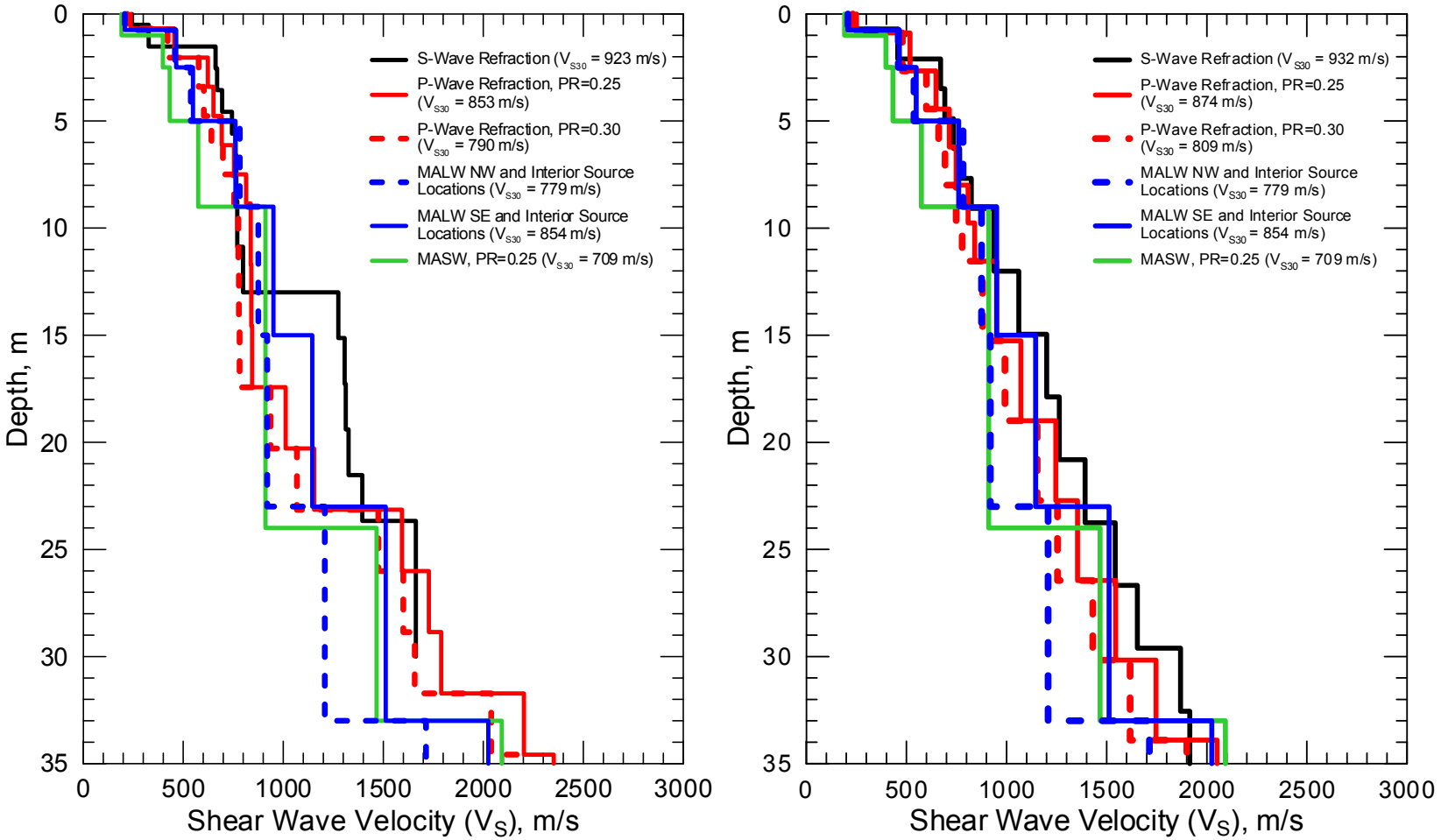

AZ.PFO – Comparison of S-wave velocity models derived from the MASW (Rayleigh wave), MALW (Love wave), S-wave seismic refraction and P-wave seismic refraction surveys. The plots on the left and right present seismic refraction models that were developed using utilized layered and smooth velocity gradient starting models, respectively. The S-wave refraction V_S model generally overestimates Vs over the 13 to 23 m depth range, relative to other methods. The MASW V_S model underestimates V_S over the 2.5 to 9 m depth range, relative to other methods, resulting in lower estimated V_{S30}. The V_S models developed from the MASW, MALW and P-wave refraction models are generally in good agreement at depths below 9 m.

Site BK.KCC

Location: Kaiser Creek, Fresno County, California

Latitude: 37.32363 **Longitude:** -119.31870
(Station coordinates provided by USGS, WGS84 coordinate system)

V_{S30} (measured): 1,252 m/s (not reflective of seismic station conditions)

V_{S30} (adjusted to more accurately reflect seismic station conditions): 2,000 to 2,500 m/s (seismic station located in a tunnel at least 30 m lower in elevation than test area, velocity estimate based on velocity below 15 m depth in the surface wave models).

NEHRP Site Class: B (based on V_{S30}), A (based on adjusted V_{S30})

Geomatrix Code: FGA

Geologic Conditions/Observations: Seismic station located in a tunnel cut into the Mesozoic (Cretaceous) Mount Givens Granodiorite.

Site Conditions: Rural site. Steep mountainous terrain in the site vicinity.

Geophysical Methods Utilized: HVSR, Seismic Refraction, MASW

Geophysical Testing Arrays:

1. Array KCC-1 (48 channel MASW and seismic refraction array utilizing 4.5 Hz vertical geophones spaced 1 m apart for a length of 47 m, forward and reverse shot locations with multiple source offsets and source types (hammers only) and multiple interior shot locations).
2. Array KCC-2 (48 channel MASW and seismic refraction array utilizing 4.5 Hz vertical geophones spaced 1.5 m apart for a length of 70.5 m, forward and reverse shot locations with multiple source offsets and source types and multiple interior shot locations).
3. Three HVSR measurement locations distributed along array KCC-2.

Legend

- Seismic Station - Approximate Location of Record
- H/V Spectral Ratio Location
- MASW and Seismic Refraction Array

NOTES:
1. WGS 1984 COORDINATE SYSTEM
2. Image Source: ESRI, i-cubed, USDA FSA, USGS, AEX, GeoEye, Getmapping, Aerogrid, IGP

File Name: BK-KCC-I

Date: 10/4/2012

USGS science for a changing world

GEOVision geophysical services

RECOVERY.GOV

SITE MAP
BK•KCC

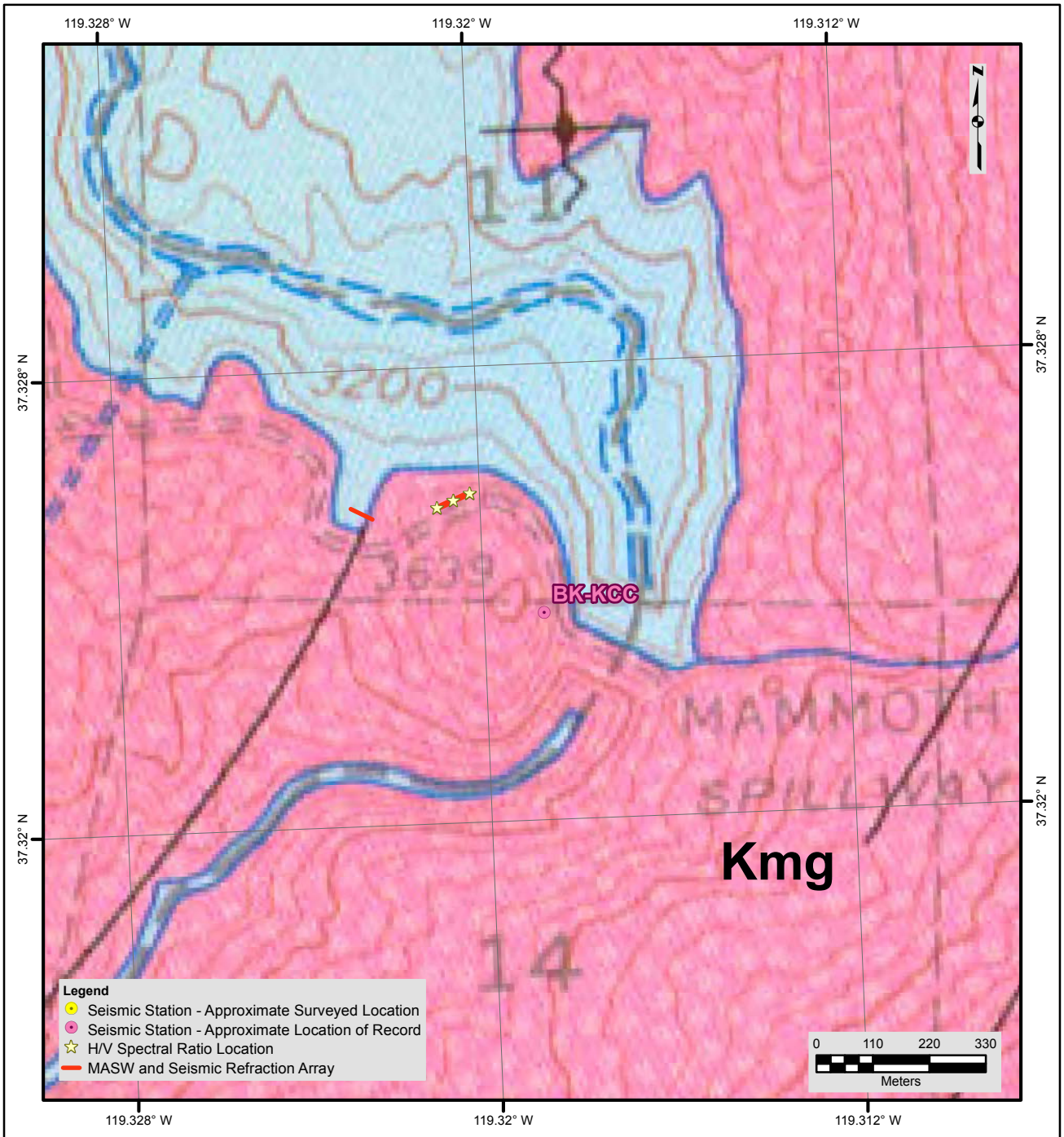

Description of Geologic Map Units

Kmg = Mesozoic (Cretaceous) Mount Givens Granodiorite, porphyritic phase

NOTES:
1. WGS 1984 COORDINATE SYSTEM
2. Geologic Map of the Shuteye Peak Quadrangle, Sierra Nevada, California by N. King Huber, 1968
3. See site map for details of geophysical survey

File Name: BK-KCC

Date: 10/4/2012

USGS science for a changing world

GEOVision geophysical services

GEOLOGIC MAP
BK•KCC

RECOVERY.GOV

Looking southeast along MASW array KCC-1

Looking southeast towards center of MASW array KCC-1

Looking at HVSR sensor 507

Looking northwest along array KCC-2 and at HVSR sensor 453

Looking southwest along array KCC-2 and at HVSR sensor 507

Location of Geophysical Testing Arrays:

Location	Latitude	Longitude
KCC-1, Northwest End of MASW/Refraction Array	37.32558	-119.32286
KCC-1, Southeast of MASW/Refraction Array	37.32538	-119.32239
KCC-2, Southwest End of MASW/Refraction Array	37.32554	-119.32096
KCC-2, Center of MASW/Refraction Array	37.32566	-119.32060
KCC-2, Northeast End of MASW/Refraction Array	37.32578	-119.32023
HVSR Sensor 450	37.32566	-119.32059
HVSR Sensor 453	37.32554	-119.32096
HVSR Sensor 507	37.32578	-119.32023

Notes: 1) WGS84 Coordinate System (decimal degrees)

2) Survey accuracy is estimated at 1 to 2 m.

Results:

Average V_P and Estimated V_S Models from Central Portion of P-wave Seismic Refraction Array KCC-2

Depth to Top of Layer (m)	Layer Thickness (m)	P-Wave Velocity (m/s)	Estimated S-Wave Velocity (m/s)			
			Poisson's Ratio = 0.25	Poisson's Ratio = 0.3	Poisson's Ratio = 0.3333	Poisson's Ratio = 0.35
0.00	0.42	687	397	367	343	330
0.42	0.85	696	402	372	348	334
1.27	0.85	717	414	383	359	345
2.12	0.85	1406	812	752	703	675
2.97	0.85	2538	1465	1357	1269	1219
3.81	0.85	2709	1564	1448	1355	1301
4.66	0.85	2830	1634	1513	1415	1360
5.51	1.78	3284	1896	1755	1642	1577
7.29	1.78	3540	2044	1892	1770	1700
9.07	1.78	3922	2265	2097	1961	1884
10.85	1.78	3936	2272	2104	1968	1891
12.63	1.78	3982	2299	2128	1991	1913
14.41	1.78	4329	2499	2314	2165	2080
16.19	Half Space	4331	2500	2315	2166	2080

Notes: 1) V_{S30} = 1639, 1518, 1420 and 1364 m/s for constant Poisson's ratio = 0.25, 0.3, 0.3333 and 0.35, respectively.

V_S Model 1 from MASW Data with Fundamental Mode Assumption

Depth to Top of Layer (m)	Layer Thickness (m)	S-Wave Velocity (m/s)	Inferred P-Wave Velocity (m/s)	Assumed Poisson's Ratio	Assumed Density (g/cm^3)
0	0.75	133	248	0.3	1.80
0.75	1.75	364	681	0.3	1.90
2.5	6	1072	2006	0.3	2.30
8.5	6	1865	3490	0.3	2.40
14.5	>15.5	2445	4575	0.3	2.50

Notes: 1) Fundamental mode assumption should not be valid given the velocity structure.
2) Depth of investigation is about 30 m.
3) Bottom layer is a half space.
4) V_{S30} = 1,172 m/s.

V_S Model 2 from MASW Data with Fundamental Mode Assumption

Depth to Top of Layer (m)	Layer Thickness (m)	S-Wave Velocity (m/s)	Inferred P-Wave Velocity (m/s)	Assumed Poisson's Ratio	Assumed Density (g/cm^3)
0	2	226	423	0.3	1.80
2	>28	2059	3852	0.3	2.50

Notes: 1) Fundamental mode assumption should not be valid given the velocity structure.
2) Depth of investigation is about 30 m.
3) Bottom layer is a half space.
4) V_{S30} = 1,332 m/s.

V_S Model from MASW Data with Average Mode Assumption

Depth to Top of Layer (m)	Layer Thickness (m)	S-Wave Velocity (m/s)	Inferred P-Wave Velocity (m/s)	Assumed Poisson's Ratio	Assumed Density (g/cm^3)
0	0.75	200	375	0.3	1.80
0.75	2.25	326	609	0.3	1.90
3	4	585	1095	0.3	2.10
7	9	1491	2788	0.3	2.30
16	>14	2190	4097	0.3	2.50

Notes: 1) Depth of investigation is about 30 m.
2) Bottom layer is a half space.
3) V_{S30} = 1,003 m/s.

V_S Model from MASW Data using 3-D Global Inversion in WinSASW Software Package

Depth to Top of Layer (m)	Layer Thickness (m)	S-Wave Velocity (m/s)	Inferred P-Wave Velocity (m/s)	Assumed Poisson's Ratio	Assumed Density (g/cm^3)
0	0.75	197	369	0.3	1.80
0.75	2.25	319	596	0.3	1.90
3	4	562	1051	0.3	2.10
7	9	1485	2779	0.3	2.30
16	>14	2142	4006	0.3	2.50

Notes: 1) 3-D global inversion is not expected to be valid for MASW data.
2) Depth of investigation is about 30 m.
3) Bottom layer is a half space.
4) V_{S30} = 981 m/s.

Observations/Discussion:

- The seismic station is located in a tunnel. There was not sufficient space near the entrance to the tunnel for surface wave testing. Therefore, surface wave and seismic refraction testing were conducted near the top of a mountain, at least 30 m higher in elevation than the seismic station. Initially, geophysical data were acquired in the dam spillway (array KCC-1) where surficial bedrock appeared relatively unweathered. Data quality was very poor and it appears that the granitic rock beneath part of the array had separated along a horizontal joint and was, therefore, not well coupled to underlying rock. Therefore, in the limited time left in the field day, P-wave seismic refraction and MASW data were acquired along array KCC-2. Array KCC-2 was located along a dirt road in an area where surficial rock appeared more weathered.
- There are no distinct HVSR peaks as expected for a rock site. The HVSR data for sensor 450 is very noisy due to poor coupling or cable not deployed correctly (i.e. touching side of bucket covering sensor). There was not sufficient time to repeat this measurement. The site was not revisited as Southern California Edison escorts are required.
- The seismic data acquired along array KCC-1 were not useable due to possible decoupling of a section of rock beneath the line along a horizontal joint. This conclusion is based on strong ringing in some of the seismic data.
- The P-wave seismic refraction and MASW data collected along array KCC-2 are of marginal quality due to site conditions. The P-wave first arrival from the high velocity, fractured rock is very weak, possibly due to significant scattering in the fractured rock. It is difficult to predict how seismic refraction is going to perform at crystalline rock sites as some sites yield excellent quality data and others poor quality data, independent of environmental conditions.
- The P-wave seismic refraction data for array KCC-2 were modeled using a tomographic inversion routine with a layer based starting model. The model was extended to far offset

source locations to extend depth of investigation. A longer array, rather than the utilization of far offset shot locations, is preferred for extending depth of investigation, when applying tomographic inversion routines and also for better constraining high seismic velocities. However, the seismic refraction data were acquired in conjunction with surface wave data, where a shorter array length is preferred.

- The P-wave seismic refraction survey design allowed P-wave velocity to be imaged to a maximum depth of about 16 m. The seismic refraction model indicates that P-wave velocity is about 350 to 600 m/s at the surface and increases to 1,500 m/s at a depth of 1 to 4 m, 3,000 m/s at a depth of 3 to 8 m and over 4,000 m/s at a depth of 4 to 14 m.
- The seismic refraction survey indicates that there is some lateral velocity variation beneath the array associated with variable thickness of the sediments overlying bedrock and differential weathering within bedrock.
- The average P-wave velocity of the upper 30 m (V_{P30}) was estimated between 30 and 51 m on the P-wave refraction model, where depth of investigation is greatest, by projecting the velocity at 16 m depth to 30 m depth. The average V_P at a depth of 16 m is very high and only expected to gradually increase with depth. Additionally, even a significant increase in the velocity below 16 m will only have a small effect of V_{P30}. V_{P30} ranges from about 2,625 to 3,091 m/s between a position of 30 to 51 m, a 16% variation.
- An average V_P model was developed over the 30 to 51 m distance interval by horizontally averaging the cell thickness and travel time of each model cell or slowness, if cells have uniform thickness, and average V_{P30} was determined to be 2,840 m/s. Assuming a constant Poisson's ratio of 0.25, 0.3, 0.3333 and 0.35 would result in an estimated V_{S30} of 1639, 1518, 1420 and 1364 m/s, respectively. Bedrock is not expected to be saturated in the upper 30 m and, therefore, Poisson's ratio in the 0.25 to 0.35 range is probable.
- Noise conditions at the site were not sufficient for application of passive surface wave techniques.
- It was difficult to construct a coherent dispersion curve from the MASW (Rayleigh wave) data. A dominant first higher mode was expected to be problematic due to a thin low velocity zone overlying high velocity rock. High velocity rock sites can be poorly suited for application of surface wave techniques, especially if there is soil cover. It was especially difficult to extract Rayleigh wave phase velocity data at intermediate wavelengths and the near field wavelength restriction applied during this investigation had to be significantly relaxed to obtain a continuous dispersion curve. Lateral velocity variation at the site (variable sediment cover and differential weathering of rock) was such that the overtone images from various source locations and receiver gathers appeared to excite higher modes differently. Attempts were made to pick the fundamental mode, although synthetic modeling indicates that the first higher mode should be dominant at low frequencies and that there may not be sufficient resolution in v-f space to identify the fundamental mode.
- The minimum wavelength surface wave phase velocity data extracted from the 48-channel MASW array is about 55 m, which attests to the difficulty developing a dispersion curve at this site. A maximum Rayleigh wave wavelength of 90 m was extracted from the MASW data set, which required relaxing of the near field criteria typically applied during this investigation. Data reduction using seismic records from smaller hammer sources and a limited offset receiver array (i.e. less active geophones)

allowed extraction of surface wave dispersion data to a minimum wavelength of about 2 m.

- There is nominally a significant 200 m/s scatter in MASW dispersion data, likely due to the effects of lateral velocity variation.
- A representative dispersion curve was generated for the MASW data set using a moving average, polynomial curve fitting routine and used for modeling.
- The velocity structure at this site is such that the first higher mode may dominate over a wide frequency range. The fundamental mode appears to be recovered at high frequencies using limited offset receiver gathers and small offset source locations. The fundamental mode may also be recovered at low frequencies, but the possibility must be considered that the fundamental mode jumps to the first higher mode at intermediate to low frequencies and that there is insufficient resolution to resolve the fundamental mode. Alternatively, the fundamental and first higher modes may become superimposed at low frequencies. Because of the distinct possibility of a dominant first higher mode, V_S models were developed using several approaches. Attempts were first made to model the data using the fundamental mode assumption and two models presented, the second being a simple two layer model. The calculated dispersion curves for both models do not fit the dispersion data particularly well, especially at small wavelengths. This alone does not require that the models be discounted due to the difficulty in constructing the dispersion curve. However, both of these velocity models should excite a dominant first higher mode at intermediate to low frequencies. Multi-mode modeling was considered, where the dispersion curve below a frequency of 35 Hz would have been assigned to the first higher mode, dispersion data above 40 Hz assigned to the fundamental mode and dispersion data between 35 and 40 Hz dropped. However, it became apparent during modeling that the average mode (based on relative amplitude of all modes) cleanly transitioned from the fundamental to first higher modes over the 40 to 35 Hz range. Therefore, the average mode assumption was used to develop a V_S model; which, in this case, should be almost identical to a model developed using the multi-mode approach. Finally, the 3-D global inversion in the WinSASW software package was applied to the MASW dispersion data. This effective mode modeling routine was developed for SASW data and is not considered applicable to MASW data. However, this modeling routine was utilized as part of the exploration of possible approaches to deal with modal superposition, which may occur at low frequencies when there is an abrupt increase in velocity at depth. The 3-D global inversion yields a V_S model almost identical to that resulting from average mode inversion. There is no MASW equivalent to the 3-D global and array based effective mode inversion routines that account for the effects of body waves and higher modes and source location as available for the SASW technique. Average (effective) mode and multi-mode inversion are the most similar MASW modeling techniques, but do not consider the effects of body waves and typically do not consider source-receiver geometry and assume plane wave propagation. Although there are MASW inversion schemes that consider source and receiver geometry, they effectively require that a wide bandwidth dispersion curve is generated from a single source location, which is seldom the case, especially when imaging to greater depths.
- V_{R40} is in the 1,100 to 1,275 m/s range which would result in an estimated V_{S30} of 1,150 to 1,332 m/s, based on the Brown, et al., 2000 relationship, assuming that the dispersion curve at 40 m wavelength is the fundamental mode. V_{S30} would be lower if the

dispersion curve were associated with the first higher mode or if modal superposition occurs at low frequencies. V_{S30} from the average seismic refraction V_P model using a Poisson's ratio of 0.3 is 1,518 m/s, which is significantly higher than the values above. As noted above, P-wave seismic refraction data quality is not particularly good, although the seismic refraction data clearly indicate that V_P exceeds 4,000 m/s in the upper 15 m. It should be noted that an out of plane refractor or first arrival occurring from a localized zone of rock with high velocity, not representative of the rock volume as a whole (e.g. dike), would result in the seismic refraction model overestimating subsurface velocity structure. With the very weak first arrival data observed in the seismic records, such a possibility cannot be discounted.

- Surface wave depth of investigation is about 30 m based on the one third of the maximum wavelength, which is more appropriate that one-half the maximum wavelength at sites with large impedance contrasts.
- The MASW V_S models developed using the fundamental mode assumption are most consistent with the estimated V_S models developed from the P-wave refraction model and assumed constant Poisson's ratio in the 0.25 to 0.35 range. As discussed above, analysis of both data sets was problematic. The fundamental mode assumption should not be considered valid at this site. However, if the refraction model is indeed correct then it would appear that the dispersion curve picked for analysis closely reflects the fundamental mode. The average mode and 3-D global inversion V_S models are almost identical and both significantly underestimate V_S over the 2 to 16 m depth range, relative to the seismic refraction and fundamental mode V_S models. Both of these models model the dispersion curve with the fundamental mode jumping to the first higher mode at a frequency below 40 to 35 Hz, which is expected for the modeled velocity structure, at least for a 1-D earth and plane wave propagation. These models should be considered conservative with both models likely presenting the lower bound of possible near surface V_S. The possibility that the 2-D velocity structure at the site (i.e. some source locations may be on rock), use of limited offset receiver gathers for much of the dispersion curve below wavelengths of 55m, effect of source location (i.e. cylindrical rather than planar wavefront), etc. combine to give rise to an identifiable fundamental mode on some seismic records.
- V_{S30} is 1,172 and 1,332 m/s for fundamental mode models 1 and 2, respectively (NEHRP Site Class B). The 10% difference between the two models is associated with neither model fitting the dispersion data very well at small wavelengths. These models are most consistent with the V_S models estimated from the P-wave refraction model. Consistency with the seismic refraction model should not be used to confirm that these models are representative of subsurface velocity structure because of issues with both data sets as discussed above, particularly in that the fundamental mode should not have dominant energy at low frequencies.
- V_{S30} is 1,003 and 981 m/s for the average mode and 3-D global inversion surface wave models, respectively (NEHRP Site Class B).
- V_{S30} presented above is not representative of the seismic station, which is located in a tunnel at least 30 m lower in elevation than the test area. V_S at a depth below 15 m is assumed to be representative of V_{S30} at the seismic station. Fortunately, even given the difficulties with data analysis of the MASW and seismic refraction models, all V_S models developed have V_S in the 2,000 to 2,500 m/s range below a depth of about 15m. We,

therefore, conclude that V_{S30} is in the 2,000 to 2, 500 m/s range at the seismic station (NEHRP Site Class A).

- There is uncertainty in the V_S models at this site, related to uncertainty in which Rayleigh wave modes are dominant. Acquisition of S-wave seismic refraction and MALW (Love wave) data could better constrain subsurface velocity structure. Considering that the fundamental mode MASW models are relatively consistent with the P-wave refraction model, these models should be considered representative of subsurface velocity structure, regardless of potential dominant higher mode issues. The average velocity structure between the two fundamental mode models closely tracks the seismic refraction model. Regardless of the uncertainly with data modeling at this site, all presented models indicate that once V_{S30} is adjusted for seismic station conditions that the site falls into NEHRP Site Class A.

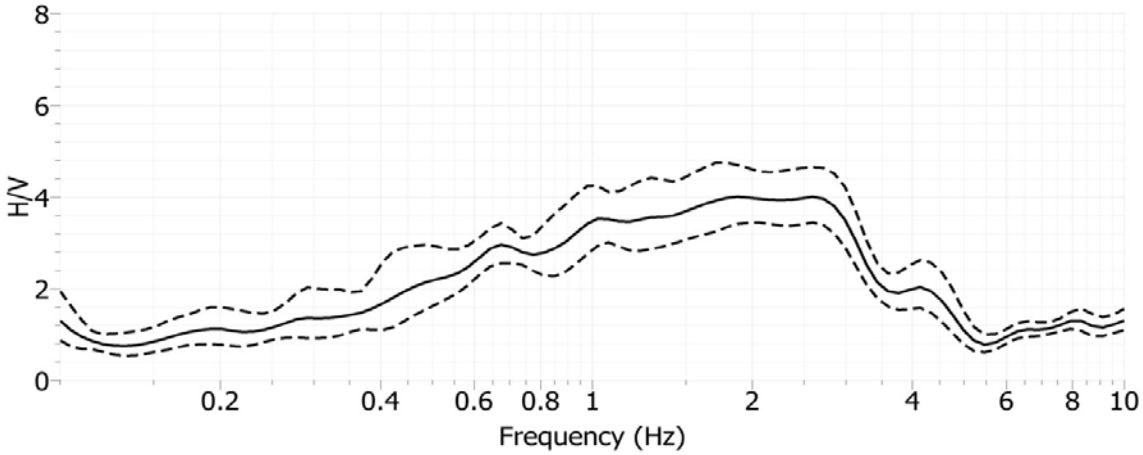

Site BK.KCC, H/V Spectral Ratio, Array KCC-2, Sensor 453

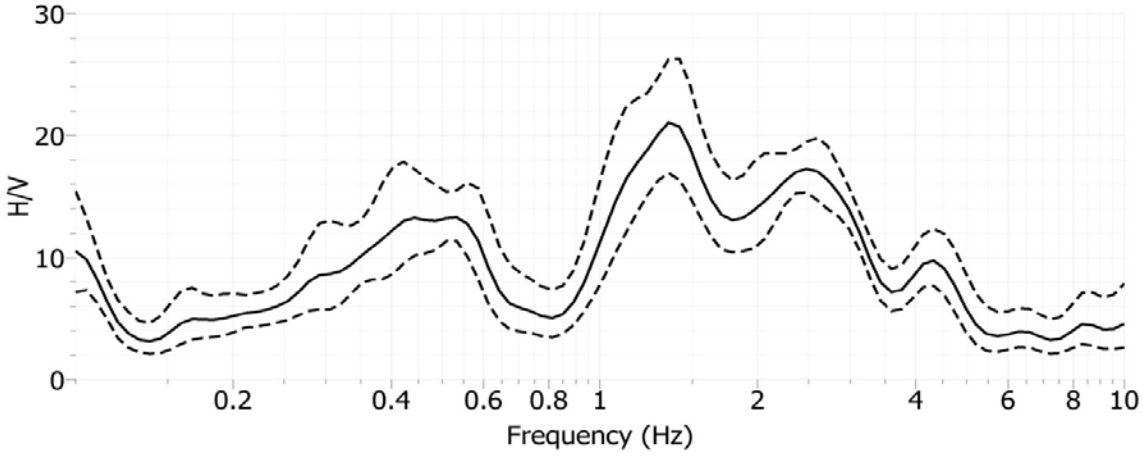

Site BK.KCC, H/V Spectral Ratio, Array KCC-2, Sensor 450 (not valid)

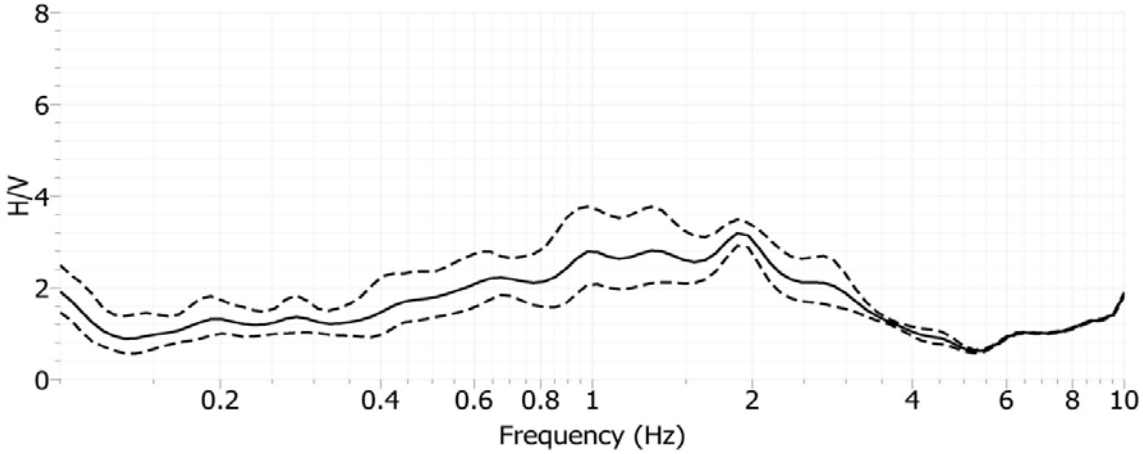

Site CI.BK-KCC, H/V Spectral Ratio, Array KCC-2, Sensor 507

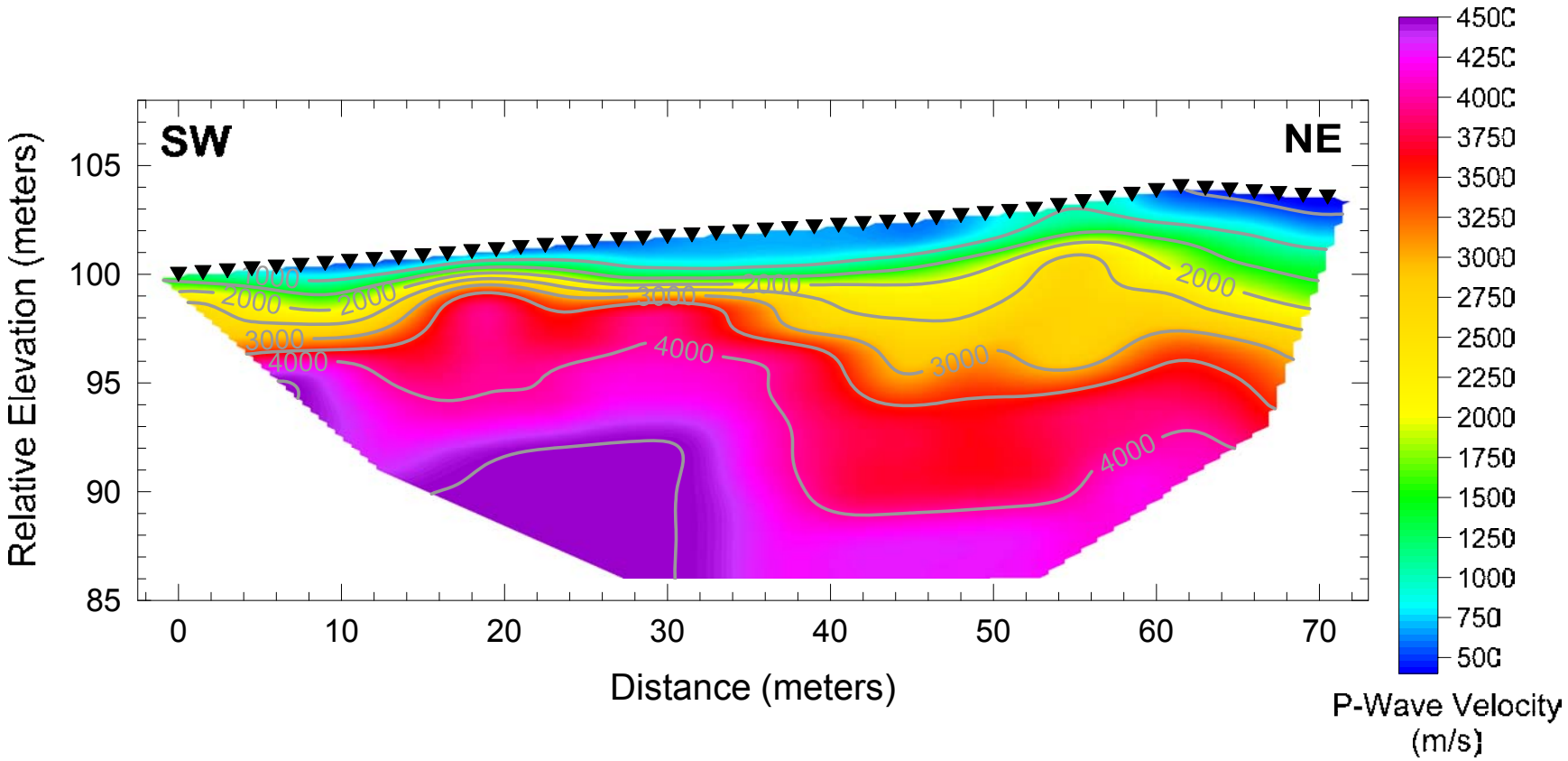

Array KCC-2 – P-wave tomographic seismic refraction model developed utilizing a layered starting model

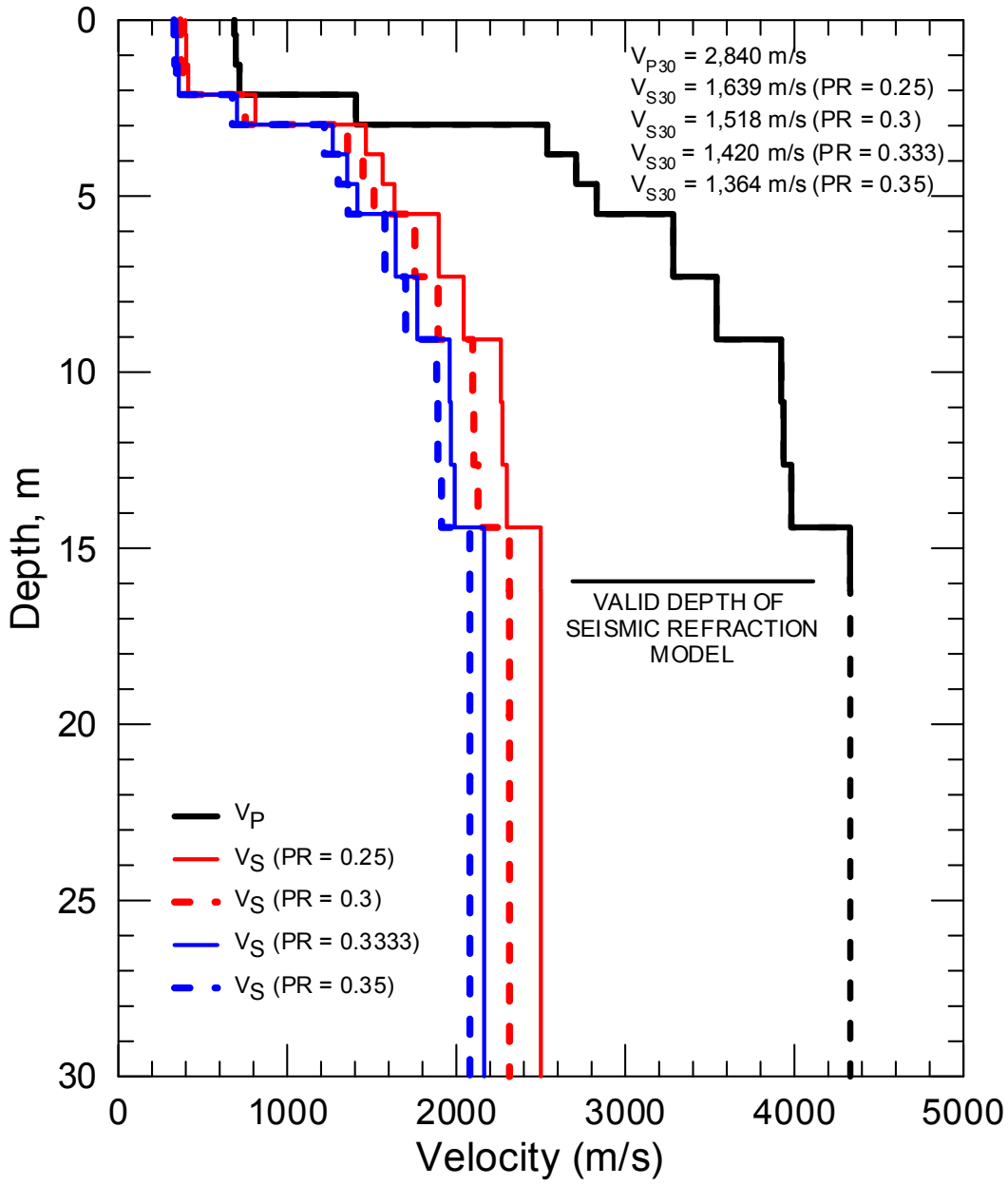

BK.KCC – Average P-wave velocity structure and estimated S-wave velocity structure between a position of 30 and 51 m on the P-wave seismic refraction model for array KCC-2 developed using a layered starting model. Although the maximum seismic refraction depth of investigation is limited to about 16 m, P-wave velocity is only expected to gradually increase with depth between 16 and 30 m.

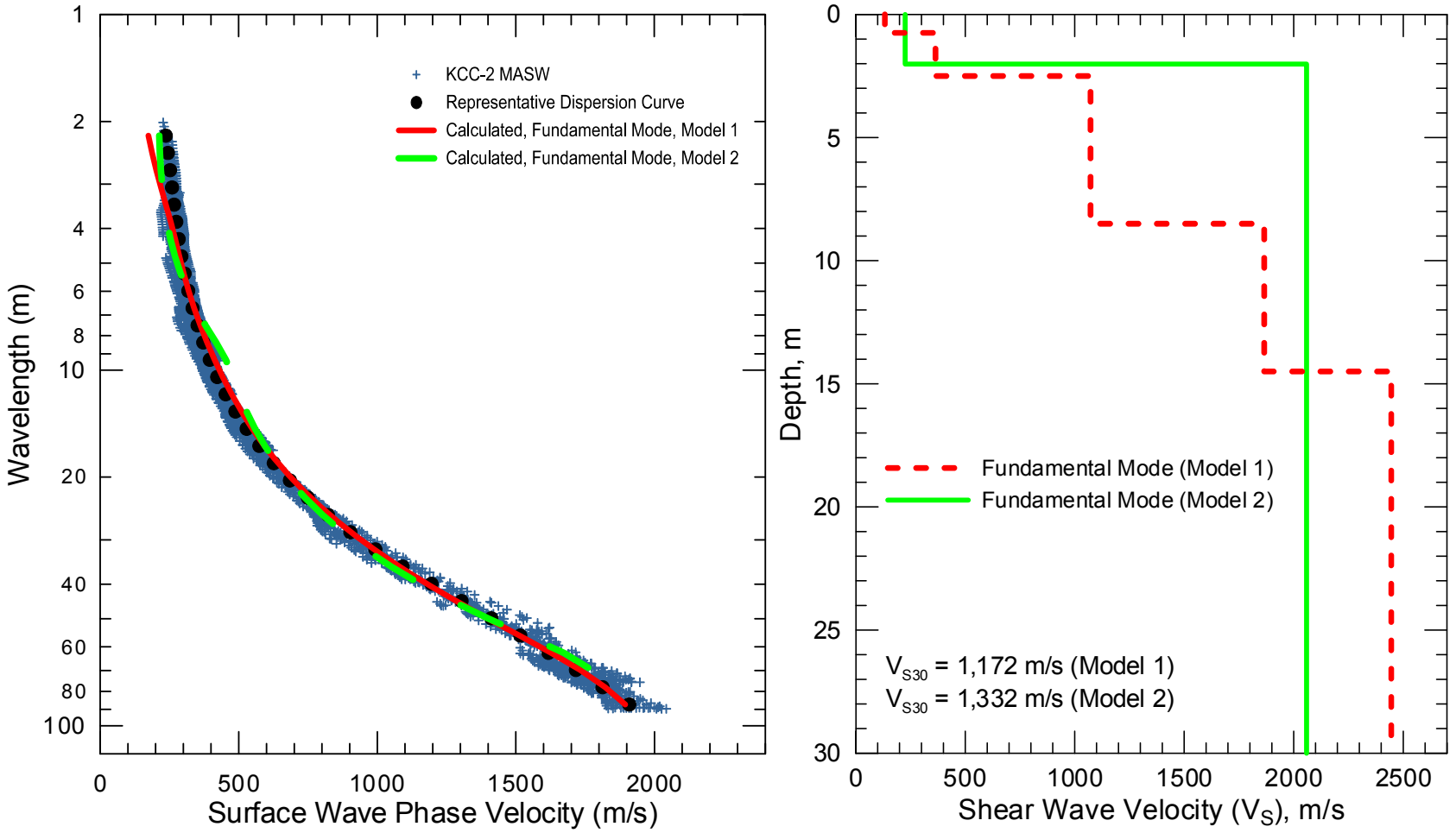

BK.KCC - Field, representative and inverted theoretical surface wave dispersion data (left) and associated V_S models (right) for fundamental mode assumption. Neither V_S model yields a calculated dispersion curve that fits the data well at small wavelengths/high frequencies. Both V_S models should excite a dominant first higher mode and it is unlikely that the fundamental mode models are valid. It is unclear what effects lateral velocity variation due to variable thickness of a thin sediment layer and differential weathering of bedrock will have on predicted Rayleigh wave modes.

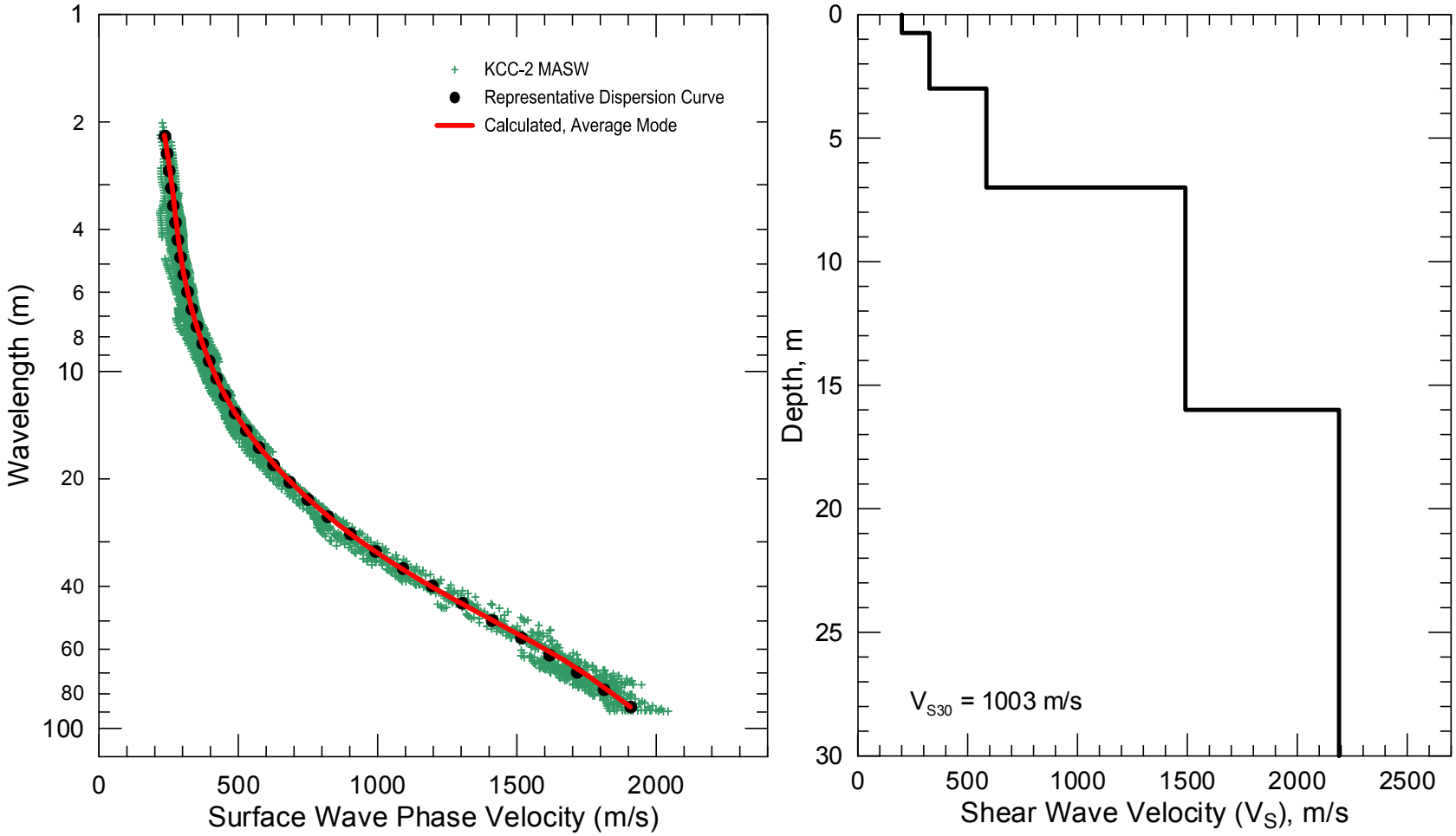

BK.KCC - Field, representative and inverted theoretical surface wave dispersion data (left) and associated V_S model (right) for average mode assumption

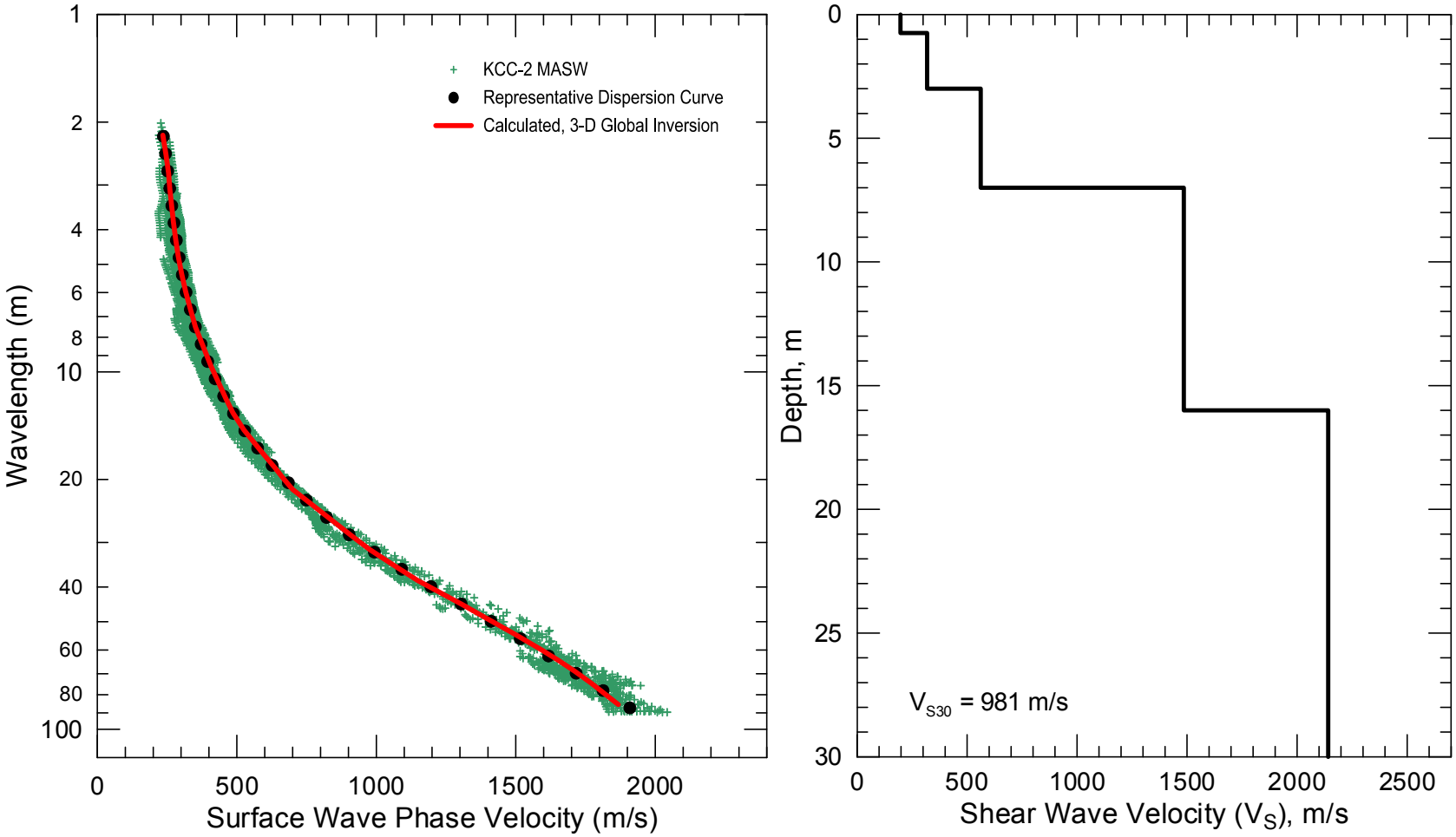

BK.KCC - Field, representative and inverted theoretical surface wave dispersion data (left) and associated V_S model (right) utilizing 3-D global inversion routine in WinSASW software package (use of this modeling approach is not defensible)

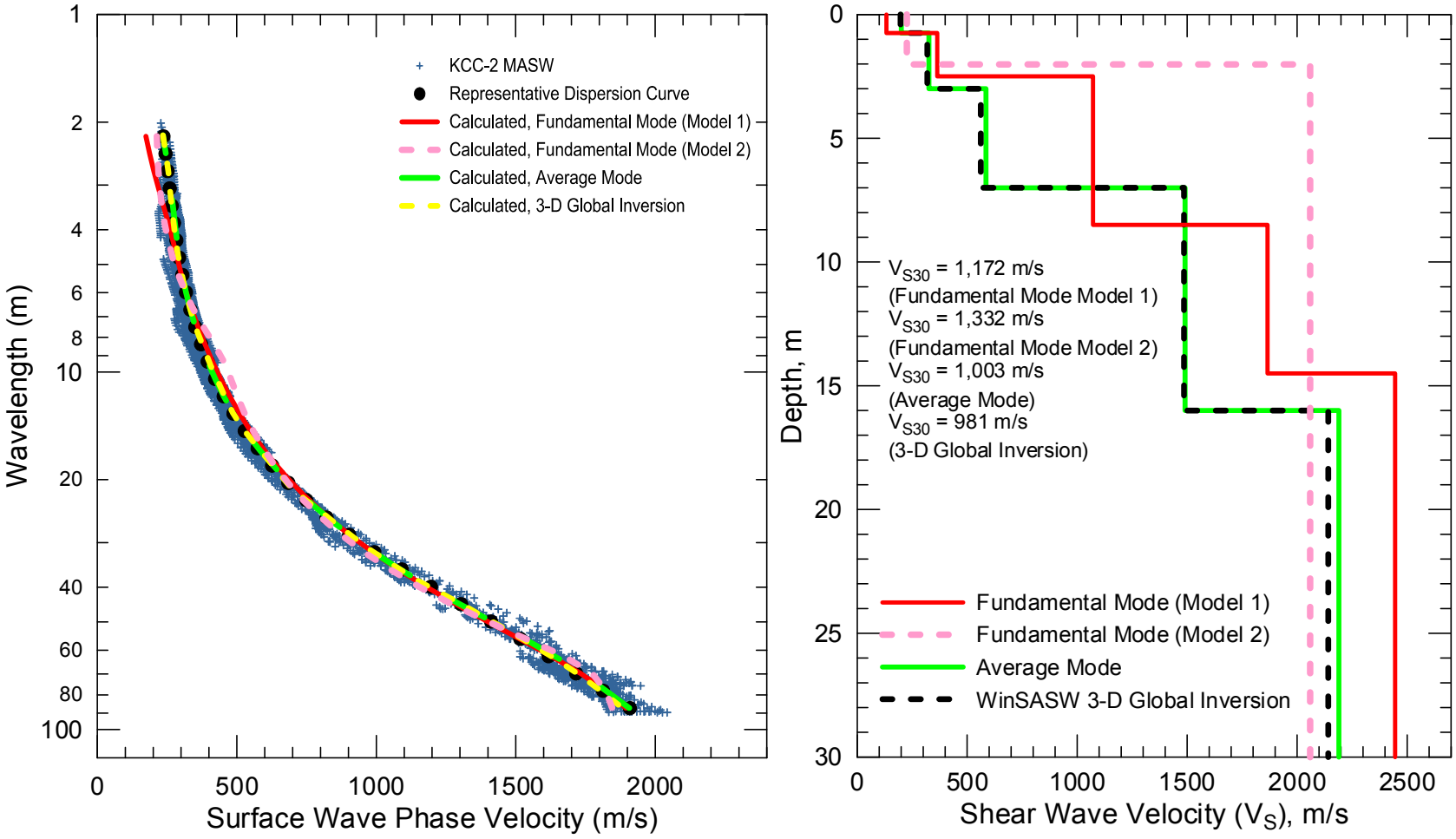

BK.KCC - Field, representative and inverted theoretical surface wave dispersion data (left) and associated V_S models (right) for fundamental and average mode assumption and 3-D global inversion

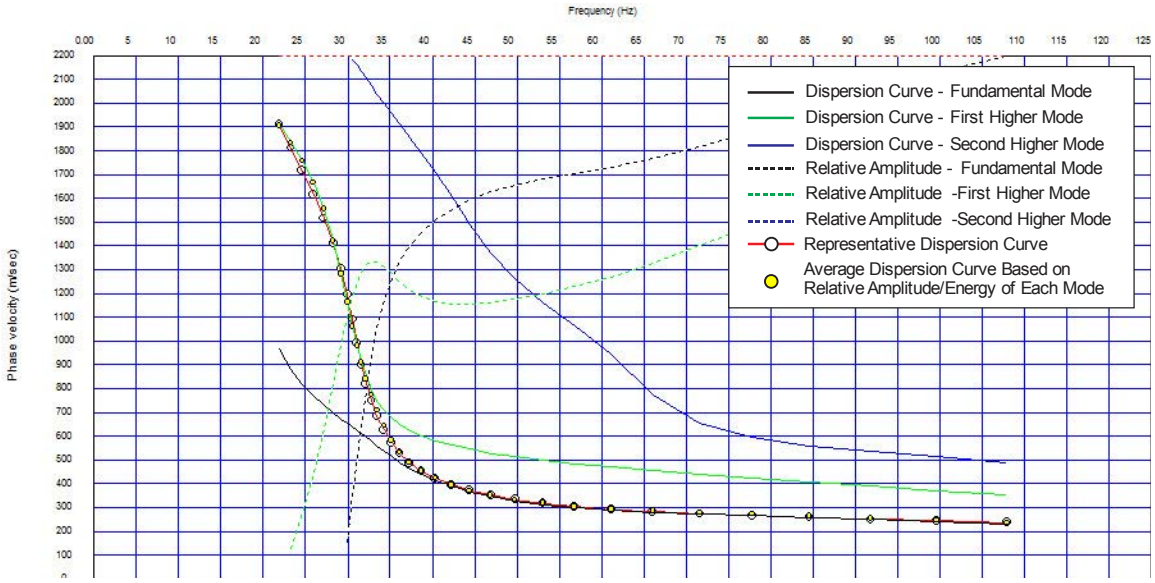

Calculated Rayleigh wave phase velocity modes for V_S model developed using the average mode assumption in an attempt to account for possible modal superposition and jump to first higher mode at low frequencies. Alternatively, Rayleigh wave phase velocities below 35 Hz and above 40 Hz could have been assigned to the first higher mode and fundamental mode, respectively and a multi-mode inversion routine used. In this case, inversion of the average mode is expected to yield similar results because it closely tracks the first higher mode at frequencies below 35 Hz.

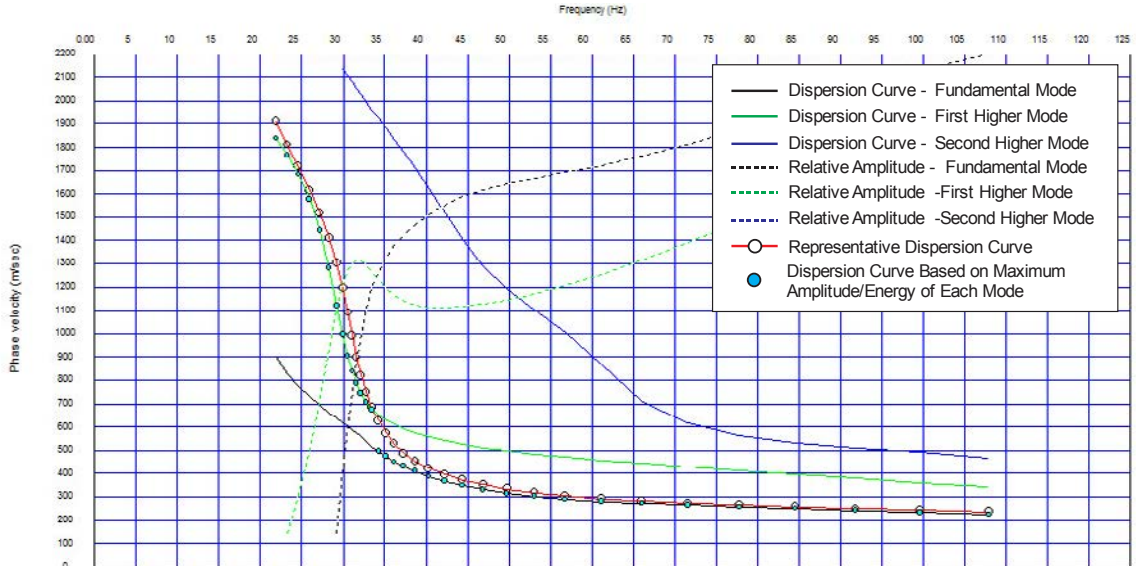

Calculated Rayleigh wave phase velocity modes for V_S model developed using the 3-D global inversion routine in the WinSASW software package. This routine is not designed for MASW data, but in this case the representative dispersion curve closely tracks the fundamental mode at frequencies higher than 40 Hz and jumps to near the first higher mode at frequencies less than 35 Hz. The resulting V_S model is therefore expected to be similar to that resulting from average mode inversion or multi-mode inversion.

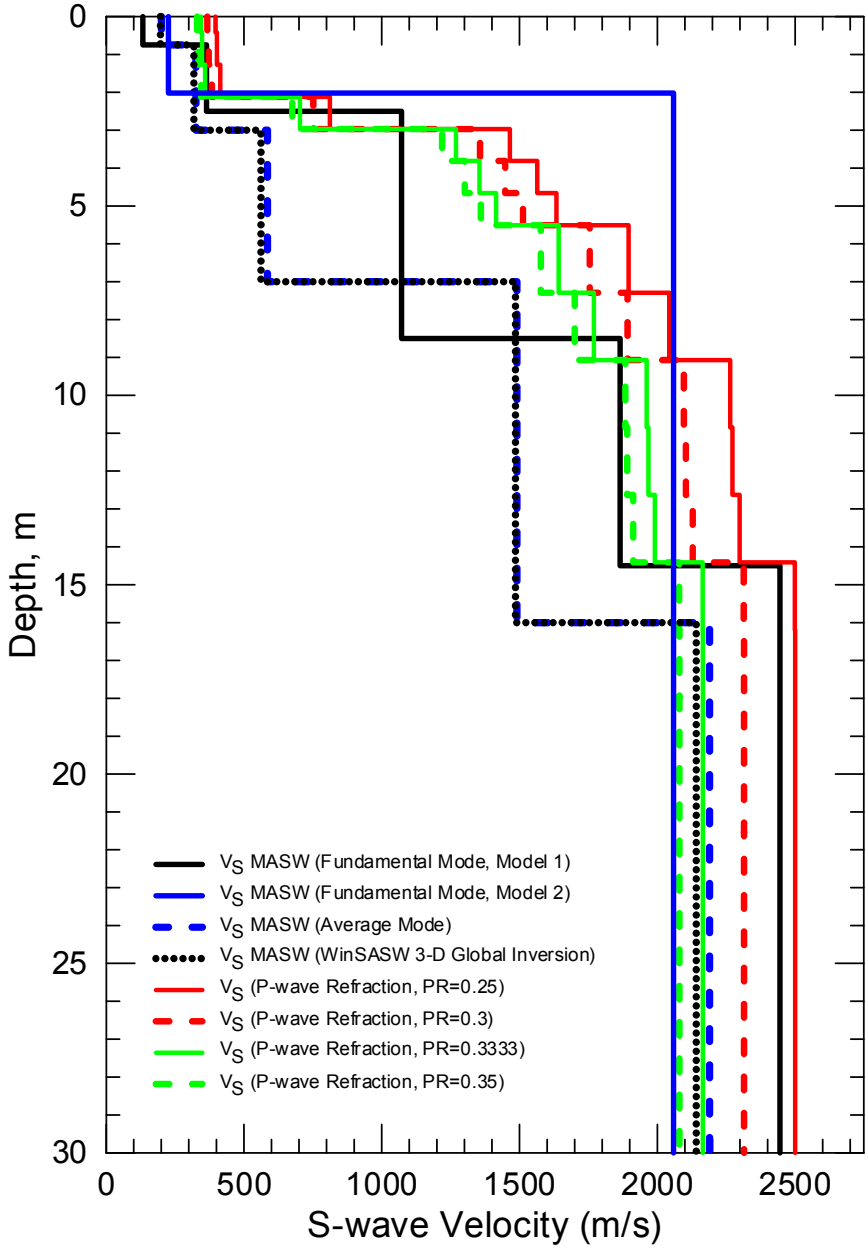

BK.KCC – Comparison of S-wave velocity models derived from the MASW and P-wave seismic refraction surveys. Although the velocity structure at this site should excite a dominant first higher mode Rayleigh waves at lower frequencies, the average of the two V_S models developed using the fundamental mode assumption agrees best with the seismic refraction models. The surface wave models developed using the average mode assumption and 3-D global inversion (an SASW inversion strategy not generally considered valid for MASW data) are almost identical at this site and both effectively model the fundamental mode at high frequencies and first higher mode at lower frequencies. These models should be most representative of subsurface velocity structure based on expected dominance of the first higher mode at frequencies below 35 Hz, but are not in good agreement with the seismic refraction model. The seismic refraction first arrivals are very weak and the possibility of out of plane refractors, which would incorrectly increase near surface velocities, cannot be discounted. Additionally, the effects of lateral velocity variation, source location and utilization of limited offset range receiver gathers to extract high frequency Rayleigh wave phase velocity data on the relative amplitude of higher modes cannot be predicted.

Site BK.RAMR

Location: Ramage Ranch, San Luis Obispo County, California

Latitude: 35.63604 **Longitude:** -120.86978
(Coordinates from Site GPS Survey, WGS84 Coordinate System)

V_{S30} (measured): 300 m/s

V_{S30} (adjusted to more accurately reflect seismic station conditions): 328 m/s (average S-wave velocity between 1 and 31 m adjusting for 1 m nominal sensor depth and with V_S of the upper two layers replaced with that of the underlying layer to account for V_P of the surficial sediments being about 500 m/s in the vicinity of the seismic station).

NEHRP Site Class: D

Geomatrix Code: IMD

Geologic Conditions/Observations: Seismic station located on Tertiary (Miocene) Monterey Shale; a thin-bedded, platy shale unit.

Site Conditions: Rural site. Rolling topography in site vicinity. Seismic station located on a small hilltop. There is about 9 m of elevation variation along the seismic lines.

Geophysical Methods Utilized: HVSR, Seismic Refraction, MASW

Geophysical Testing Arrays:

1. Array RAMR-1 (48 channel MASW and P-wave seismic refraction array utilizing 4.5 Hz vertical geophones spaced 1.5 m apart for a length of 70.5 m, forward and reverse shot locations with multiple source offsets and source types and multiple interior shot locations).
2. Array RAMR-2 (48 channel MASW array utilizing 4.5 Hz vertical geophones spaced 1.5 m apart for a length of 70.5 m, forward and reverse shot locations with multiple source offsets and source types and a center shot locations).
3. Array RAMR-3 (48 channel P-wave seismic refraction array utilizing 4.5 Hz vertical geophones spaced 3 m apart for a length of 141 m, forward, reverse and multiple interior shot locations). Array RAMR-2 lies along a segment of this array.
4. Five HVSR measurement locations: two distributed along array RAMR-1, two distributed along array RAMR-2 and the other adjacent to the seismic station.

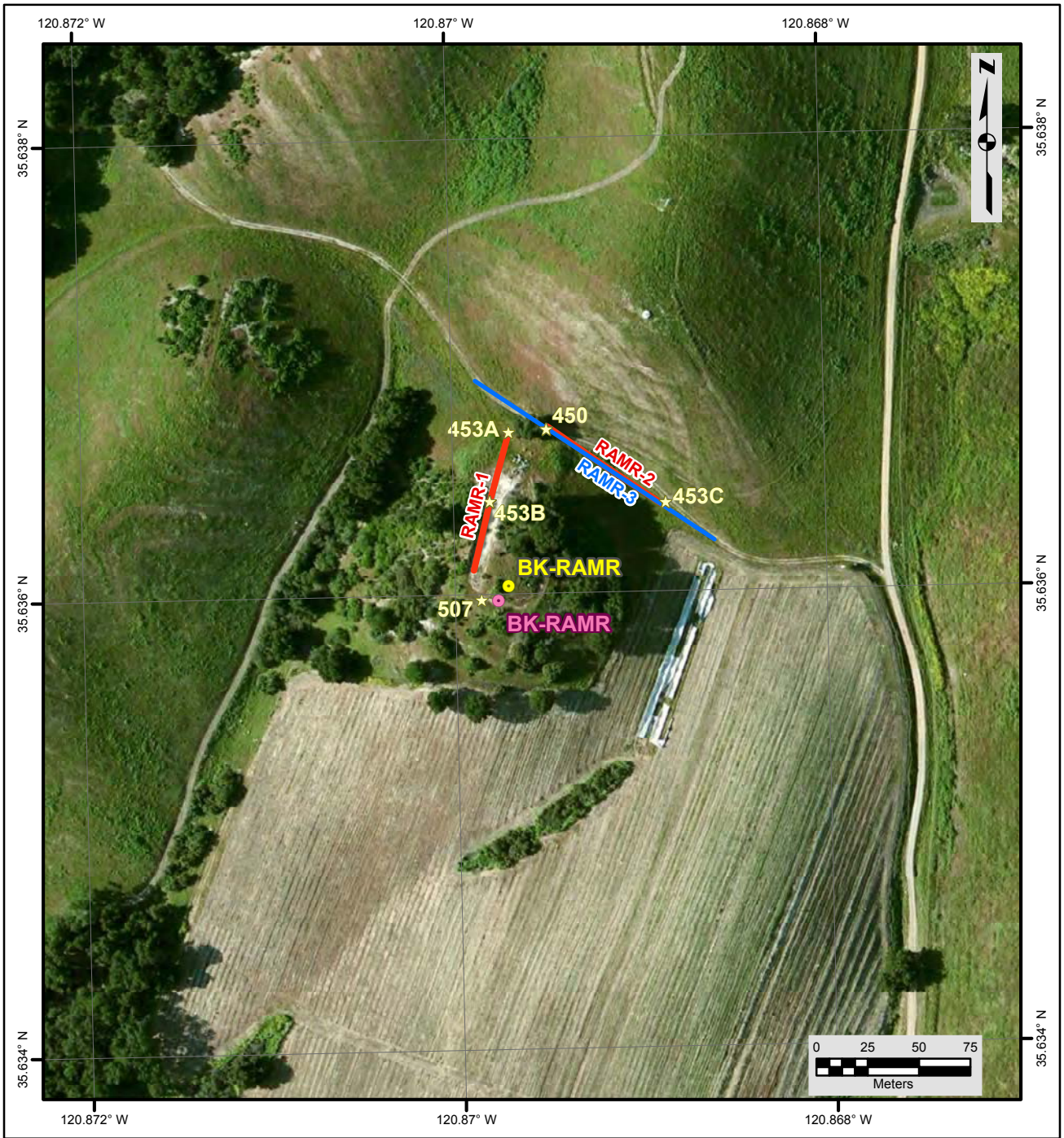

Legend

- Seismic Station - Approximate Surveyed Location
- Seismic Station - Approximate Location of Record
- H/V Spectral Ratio Location
- Seismic Refraction Array
- MASW and Seismic Refraction Array

NOTES:
1. WGS 1984 COORDINATE SYSTEM
2. Image Source: ESRI, i-cubed, USDA FSA, USGS, AEX, GeoEye, Getmapping, Aerogrid, IGP

File Name: BK-RAMR-I

Date: 2/7/2013

USGS science for a changing world

GEOVision geophysical services

RECOVERY.GOV

SITE MAP
BK•RAMR

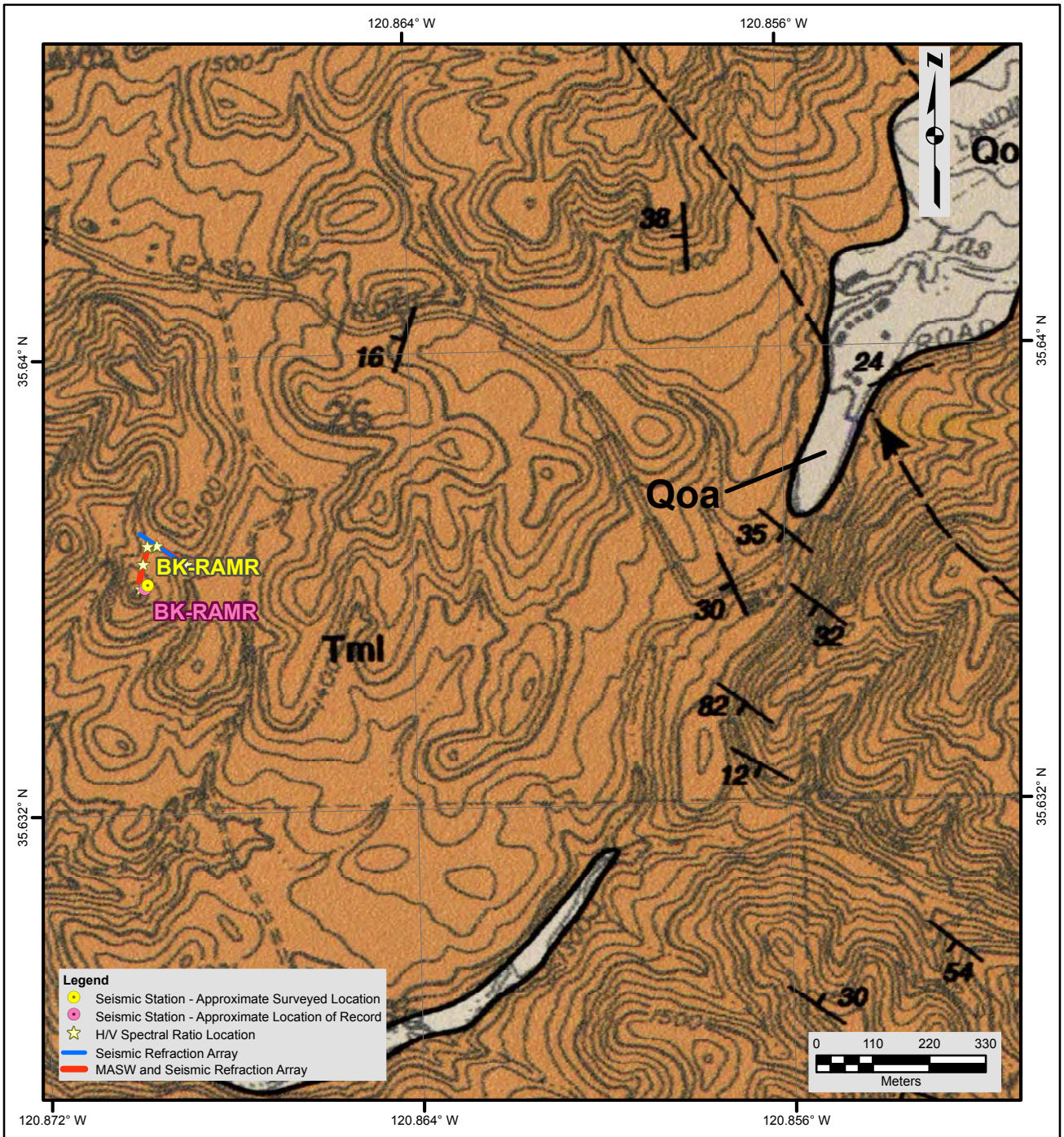

Description of Geologic Map Units

Qa = Quaternary (Holocene) alluvial gravel, sand and clay
Qoa = Quaternary (Pleistocene) dissected alluvial gravel sand and clay, weakly indurated
Tml = Tertiary (Middle Miocene) Monterey Shale, lower part; thin-bedded, semi-siliceous, platy, fissile, includes thin layers and nodules of dolomite

NOTES:
1. WGS 1984 COORDINATE SYSTEM
2. Geologic Map of the Adelaida Quadrangle, San Luis Obispo County, California by Thomas W. Dibblee, Jr., 2006
3. See site map for details of geophysical survey

File Name: BK-RAMR

Date: 2/7/2013

USGS science for a changing world

GEOVision geophysical services

GEOLOGIC MAP
BK•RAMR

RECOVERY.GOV

Looking southwest along array RAMR-1 towards HVSR sensor 453A

BK.RAMR seismic station

Looking northeast along array RAMR-1

Looking northwest towards end of array RAMR-3

Looking northwest along array RAMR-2 towards HVSR sensor 453C

Location of Geophysical Testing Arrays:

Location	Latitude	Longitude
RAMR-1, South End of MASW/Refraction Array	35.63611	-120.86997
RAMR-1, Center of MASW/Refraction Array	35.63641	-120.86988
RAMR-1, North End of MASW/Refraction	35.63671	-120.86977
RAMR-2, Northwest End of MASW/Refraction Array	35.63673	-120.86956
RAMR-2, Center of MASW/Refraction array	35.63655	-120.86926
RAMR-2, Southeast End of MASW/Refraction Array	35.63638	-120.86894
RAMR-3, Northwest End of Refraction Array	35.63694	-120.86994
RAMR-3, Southeast End of Refraction Array	35.63622	-120.86867
HVSR Sensor 507	35.63598	-120.86993
HVSR Sensor 453A	35.63671	-120.86977
HVSR Sensor 453B	35.63641	-120.86988
HVSR Sensor 450	35.63672	-120.86956
HVSR Sensor 453C	35.63639	-120.86893
BK.RAMR Seismic Station	35.63604	-120.86978

Notes: 1) WGS84 Coordinate System (decimal degrees)
2) Survey accuracy is estimated at 1 to 2 m.

Results:

V_S Model

Depth to Top of Layer (m)	Layer Thickness (m)	S-Wave Velocity (m/s)	Inferred P-Wave Velocity (m/s)	Inferred Poisson's Ratio	Inferred Density (g/cm^3)
0	1.5	146	272	0.300	1.7
1.5	2	186	348	0.300	1.7
3.5	4	256	480	0.300	1.8
7.5	6.5	333	624	0.300	1.8
14	8	347	1800	0.481	1.9
22	10	384	1900	0.479	1.9
32	>3	468	2000	0.471	2.0

Notes: 1) Saturated zone, with V_P of about 1,800 to 2,000 m/s, constrained at a depth of about 14 m based on seismic refraction survey.
2) Depth of investigation is about 35 m.
2) Bottom layer is a half space.

Observations/Discussion:

- Geologic maps indicate that the Monterey Formation is folded in the site vicinity with highly variable dips. Attitude measurements of bedding were not made at this site. The Monterey Formation is highly weathered in the site vicinity.
- The HVSR curves at the five measurement locations are very similar at lower frequencies with a distinct peak at about 0.7 Hz. A 0.7 Hz HVSR peak could be associated with a geologic structure at a depth of 150 m, or more, depending upon velocity structure. HVSR measurements at stations 450 and 453C were made about 5 months after those at stations 453A, 453B and 507. At high frequencies, there are subtle differences between the HVSR data, but no distinct peaks by which to assess lateral velocity variation.
- Preliminary review of seismic refraction and MASW data for array RAMR-1 indicated that there was significant near surface lateral velocity variation that was expected to complicate surface wave modeling. Therefore, MASW and P-wave seismic refraction data were acquired along arrays RAMR-2 and RAMR-3, respectively, which were located at the north end and approximately perpendicular to array RAMR-1.
- The P-wave refraction data for arrays RAMR-1 and RAMR-3 were modeled using a tomographic inversion routine with layer-based starting models. The seismic refraction model for array RAMR-1 was extended to far offset shot locations to extend depth of investigation.
- The P-wave seismic refraction survey design for array RAMR-1 allowed P-wave velocity to be imaged to a maximum depth of about 20 to 25 m. The seismic refraction model shows that P-wave velocity is about 300 to 500 m/s at the surface and increases with depth to about 600 m/s at a depth of 1 to 5 m, 800 m/s at a depth of 7 to 18 m and over 1,400 m/s at a depth of 19 to 26 m. Depth of investigation was not great enough to determine if the high velocity unit at the base of the model is associated with saturated sediments. This seismic line is placed along a small cut in a hill. At the south end of the seismic line located at the top of the hill near the seismic station, P-wave velocity at the surface is about 450 to 500 m/s. At the north end of the line located at the bottom of the hill there is an additional meter of soil cover with surface velocities being under 300 m/s. This very slight thickening of lower velocity sediments will give rise to large differences in small wavelength/high frequency Rayleigh wave phase velocity data reduced from source locations at each end of the line.
- The P-wave seismic refraction survey design for array RAMR-3 allowed P-wave velocity to be imaged to a maximum depth of about 25 to 30 m. The seismic refraction model shows that P-wave velocity is about 250 to 300 m/s at the surface and increases with depth to about 600 m/s at a depth of 2 to 3 m, 800 m/s at a depth of 2 to 14 m and over 1,600 m/s at a depth of about 13 to 19 m. The maximum P-wave velocity in the model is about 1,950 m/s. This line has similar near surface velocity structure to the north end of array RAMR-1.
- The site conditions were not conducive to application of passive surface wave techniques.
- Array RAMR-2 yielded better quality surface wave data than array RAMR-1 and was, therefore, used for site characterization. The Rayleigh wave phase velocity at 40 m wavelength (V_R40) is similar in both data sets.
- There is some scatter in the MASW surface wave dispersion data, about 25 to 40 m/s, possibly in part due to minor lateral velocity variation.

- The minimum wavelength surface wave phase velocity data extracted from the 48-channel MASW array was about 6 m. Data reduction using seismic records from smaller hammer sources and a limited offset receiver array (i.e. less active geophones) allowed extraction of surface wave dispersion data to a minimum wavelength of about 4.5 m. It was not possible to extract reliable Rayleigh wave phase velocity data at smaller wavelengths/higher frequencies due to dominant higher modes.
- A representative dispersion curve was generated for the MASW data set using a moving average, polynomial curve fitting routine and used for modeling.
- The saturated zone with V_P between 1,800 and 2,000 m/s was constrained at nominal depth of 14 m based on the seismic refraction model for array RAMR-3.
- P-wave velocities above the saturated zone in the seismic refraction models are generally slightly higher than in the surface wave models (based on assumed Poisson's ratio of 0.3).
- Surface wave depth of investigation is about 35 m based on half of maximum wavelength criteria.
- V_{S30} is 300 m/s (Site Class D).
- The seismic refraction model for array RAMR-1 indicates that P-wave velocity is slightly higher at the surface (450 to 500 m/s) near the seismic station than at the location of array RAMR-2. Therefore, to adjust for an assumed 1 m seismic sensor depth and surficial conditions, the average S-wave velocity is estimated between 1 m and 31 m after replacing the V_S of the upper 3.5 m with that of the underlying layer and is 328 m/s.

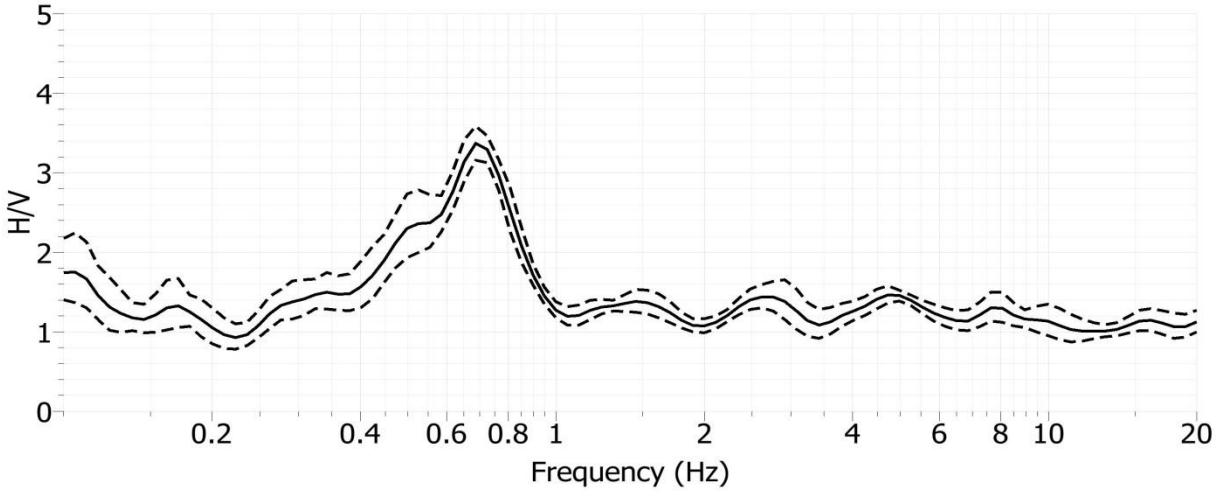

Site BK.RAMR, H/V Spectral Ratio, Array RAMR-1, Sensor 453A

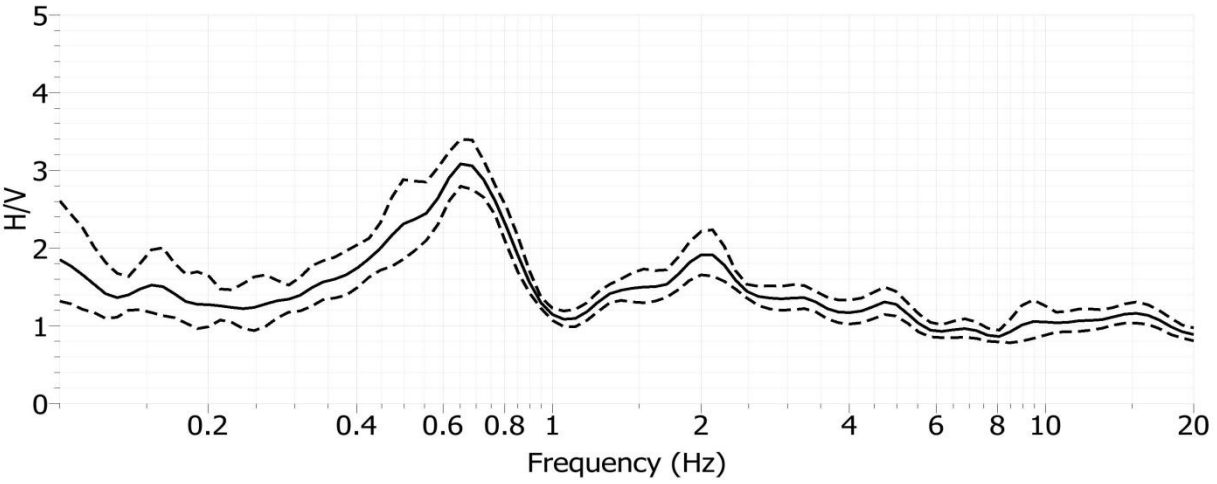

Site BK.RAMR, H/V Spectral Ratio, Array RAMR-1, Sensor 453B

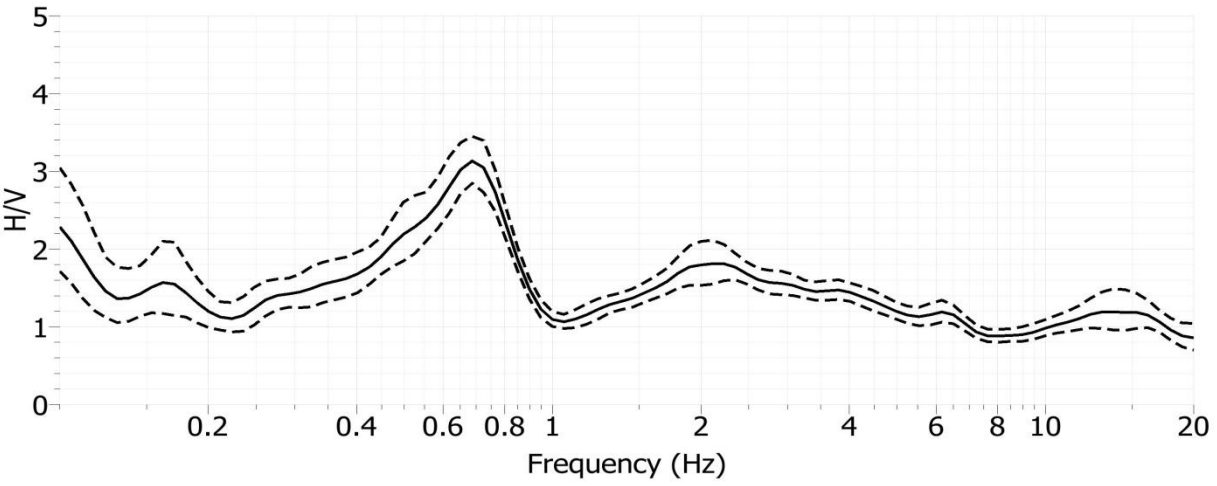

Site BK.RAMR, H/V Spectral Ratio, Near Seismic Station, Sensor 507

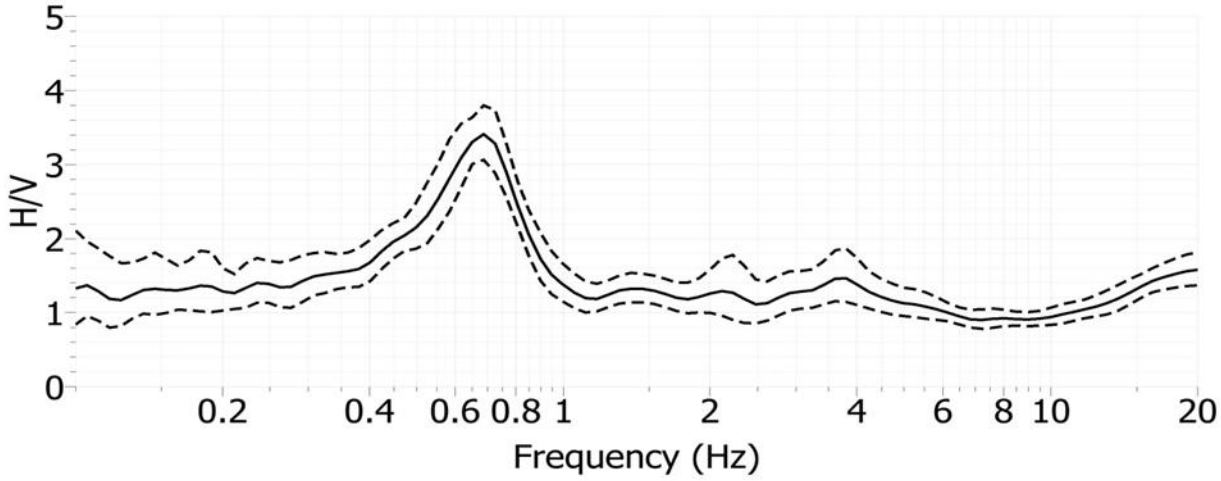

Site BK.RAMR, H/V Spectral Ratio, Array RAMR-1, Sensor 450

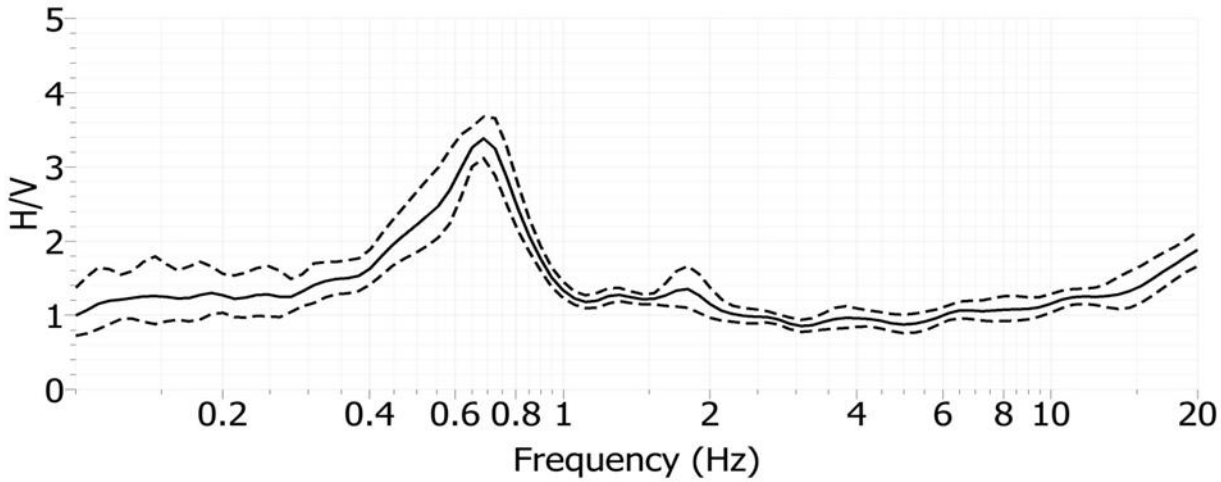

Site BK.RAMR, H/V Spectral Ratio, Array RAMR-1, Sensor 453C

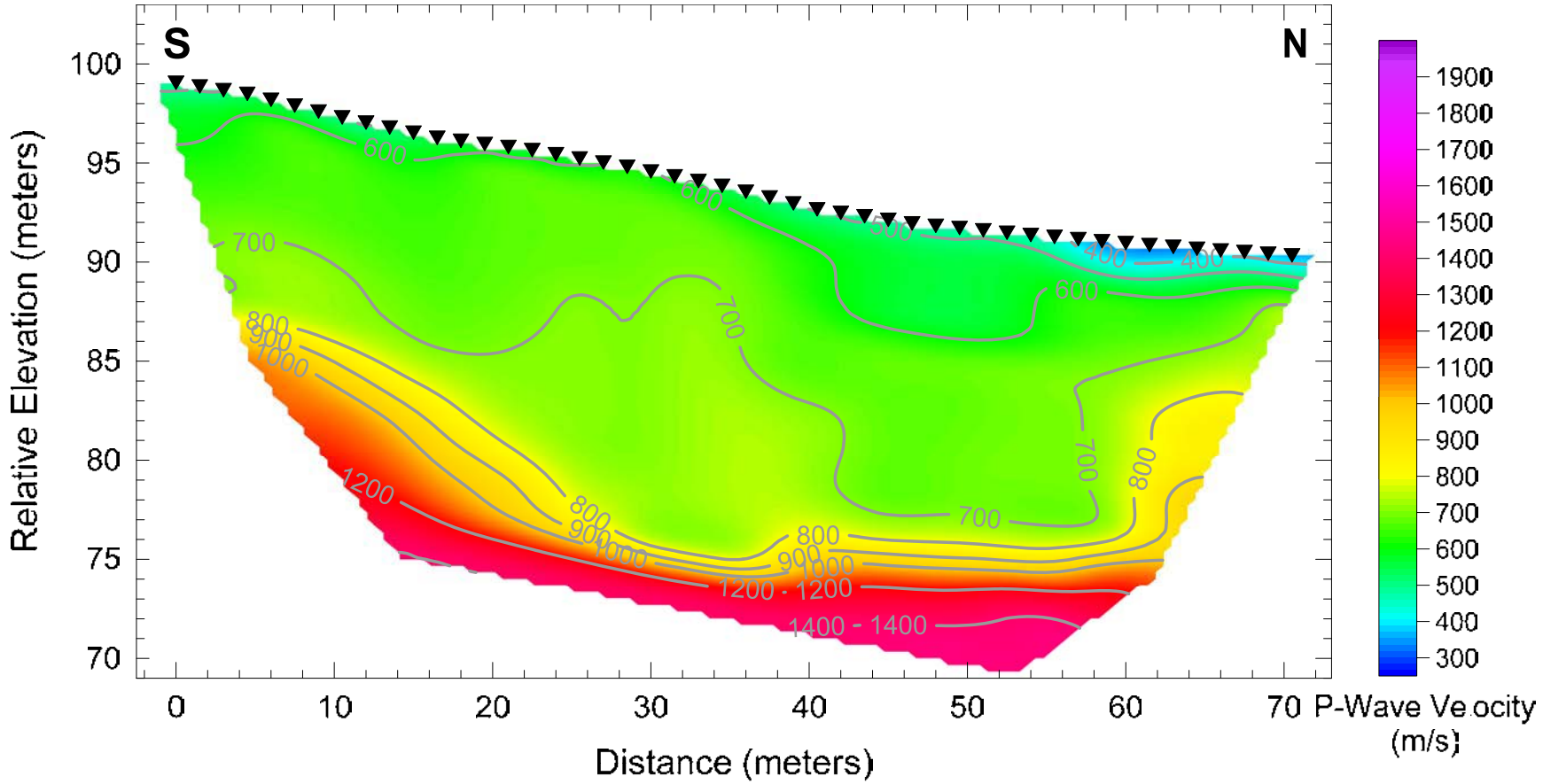

Array RAMR-1 – Tomographic Seismic Refraction Model utilizing Layer Based Starting Model

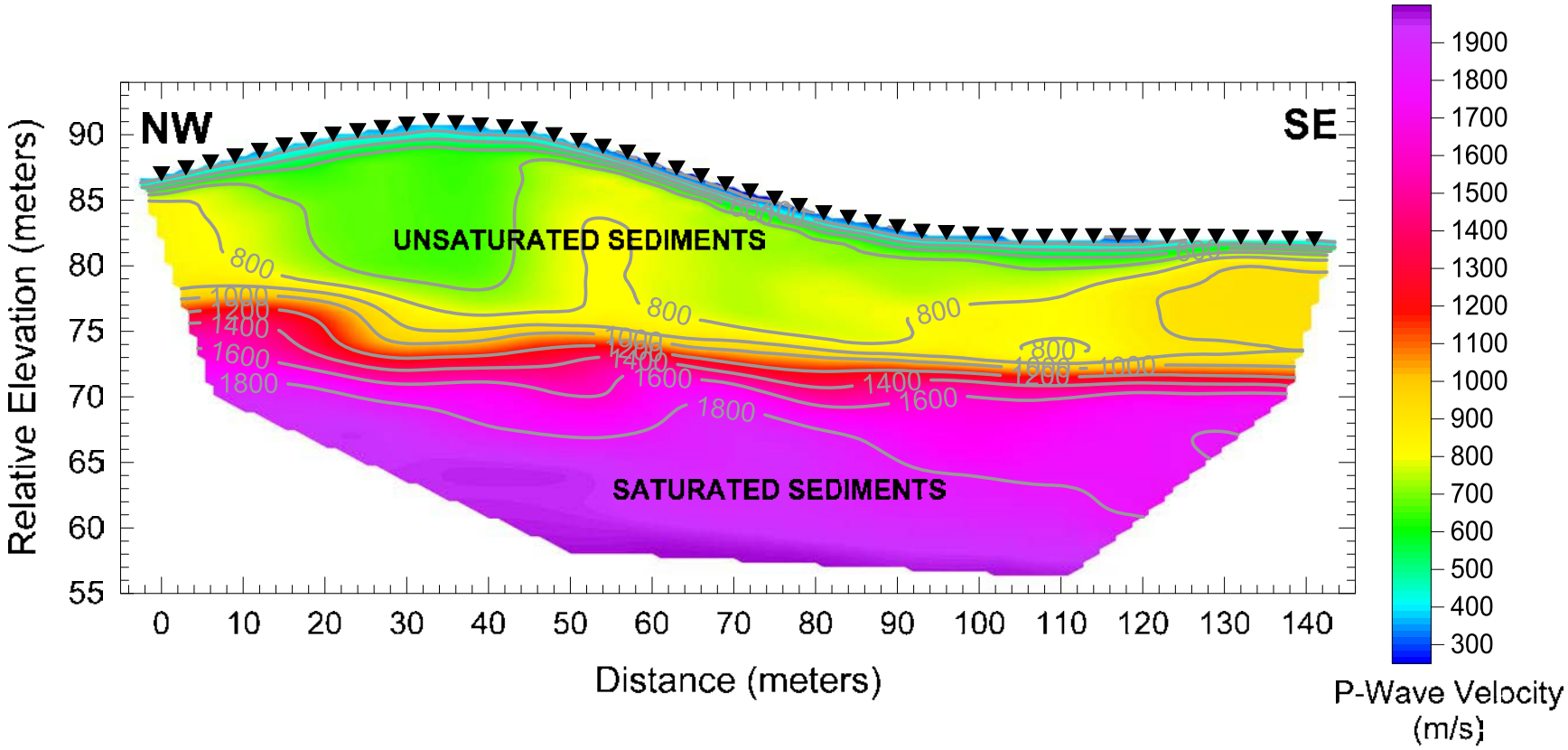

Array RAMR-3 – Tomographic Seismic Refraction Model utilizing Layer Based Starting Model

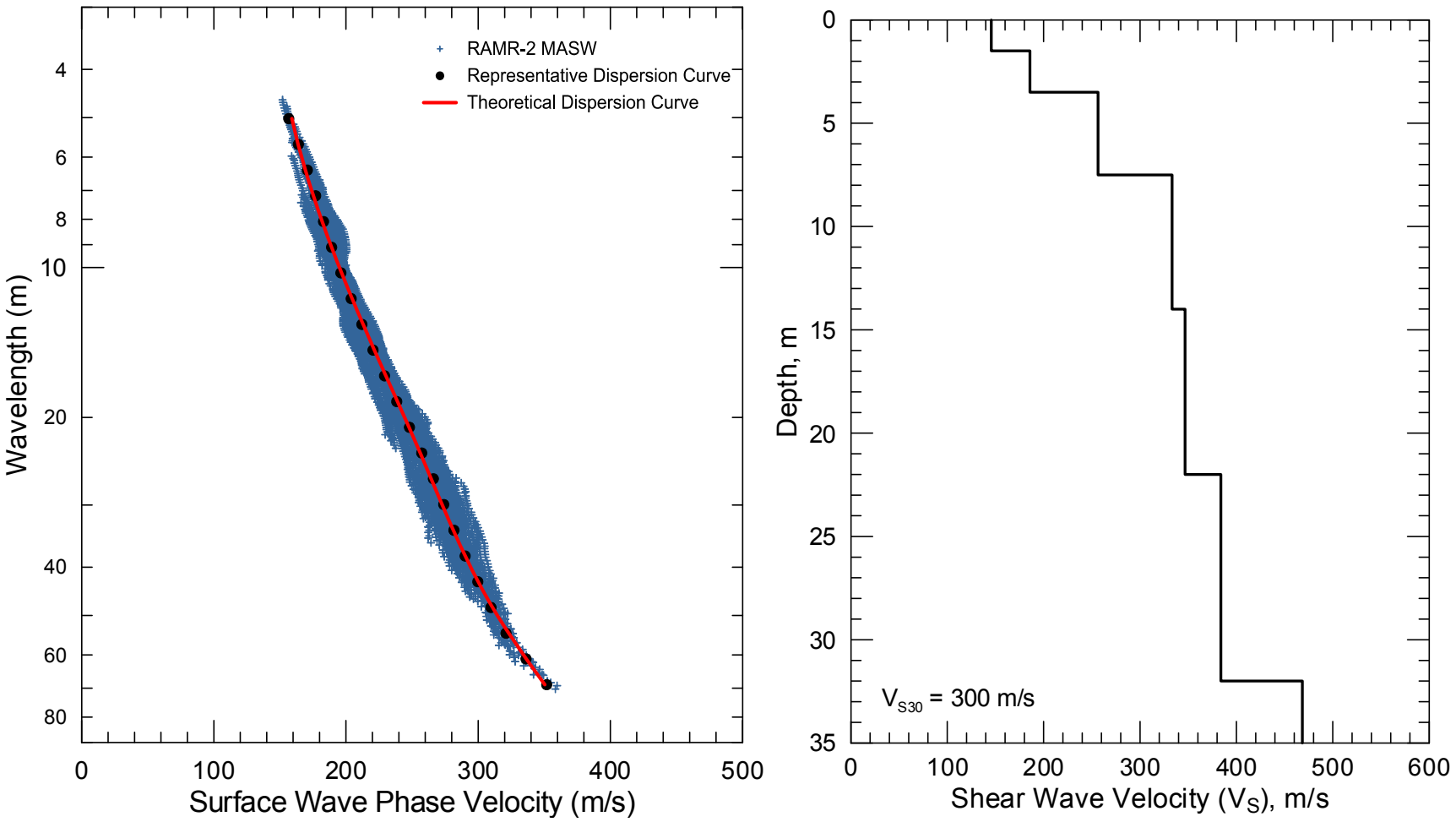

BK.RAMR - Field, representative and inverted theoretical surface wave dispersion data (left) and associated V_S model (right)

Site CE.11023

Location: Niland Fire District, 8071 Luxor Avenue, Niland, California

Latitude: 33.23890 **Longitude:** -115.51300
(Station coordinates modified using published coordinates from http://www.strongmotioncenter.org, which were visually confirmed to be on subject property, WGS84 coordinate system)

V_{S30} (measured): 212 m/s

V_{S30} (adjusted to more accurately reflect seismic station conditions): 212 m/s (no adjustment necessary).

NEHRP Site Class: D

Geomatrix Code: AHD

Geologic Conditions/Observations: Quaternary (Holocene) lake deposits, deep soil site.

Site Conditions: Rural site with some noise sources from sporadic traffic in site vicinity. Relatively flat terrain in test area. Ground surface elevation gently decreases to southwest in site vicinity.

Geophysical Methods Utilized: HVSR, MASW, array microtremor, ReMi™

Geophysical Testing Arrays:

1. Array 11023-1 (48 channel MASW array utilizing 4.5 Hz vertical geophones spaced 1.5 m apart for a length of 70.5 m, forward and reverse shot locations with multiple source offsets and source types and center shot location).
2. Array 11023-2 (24 channel, linear passive surface wave array utilizing 4.5 Hz vertical geophones spaced 4.5 m apart for a length of 103.5 m) and orientated along 11023-1.
3. Array 11023-3 (10 channel, triangle passive surface wave array utilizing 1 Hz geophones and a 40 m length for outer side of array).
4. Three HVSR measurement locations distributed along 11023-1.

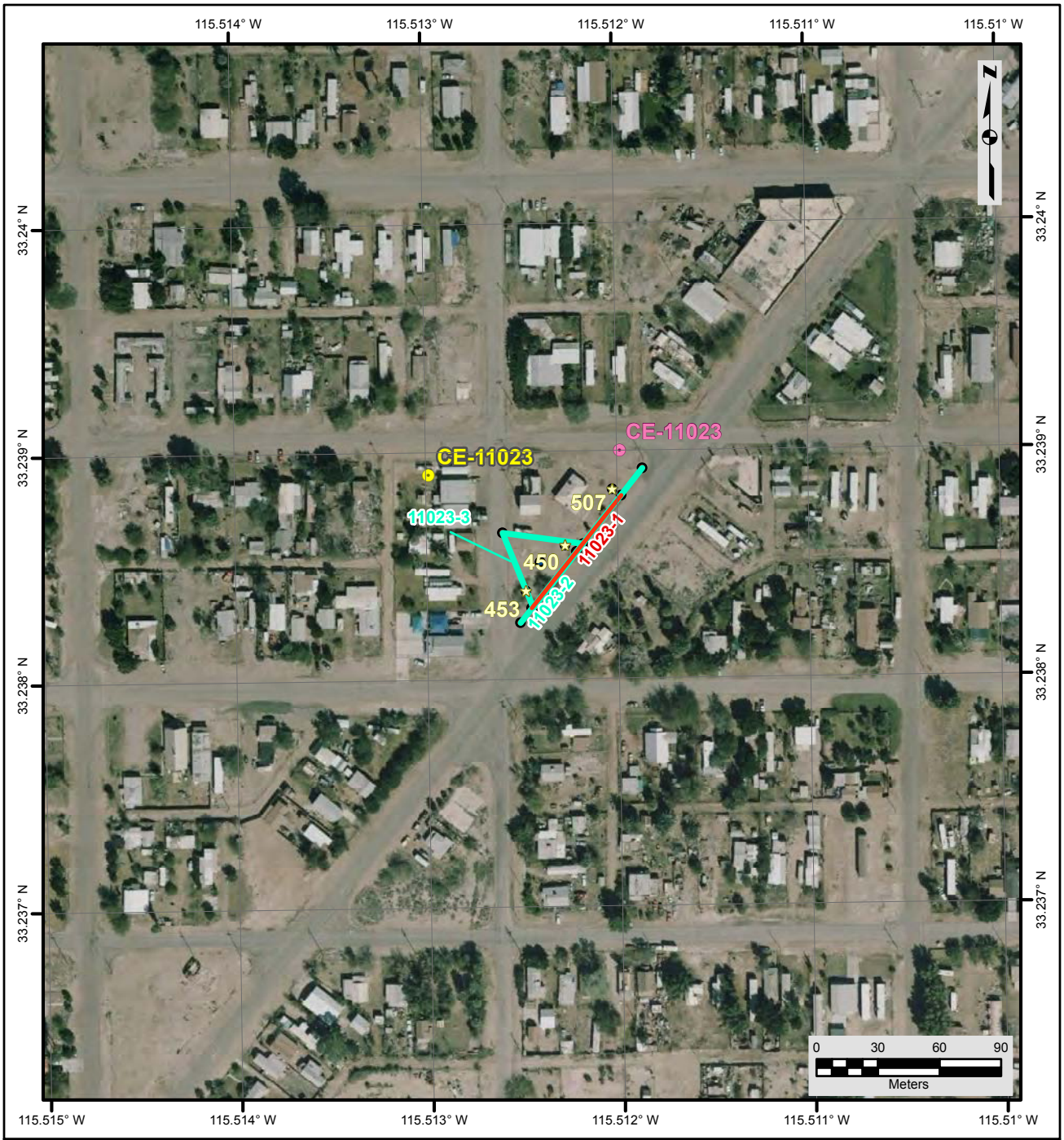

Legend

- Seismic Station - Approximate Location of Record
- Seismic Station - Approximate Improved Location
- H/V Spectral Ratio Measurement Location
- MASW Array
- Passive Surface Wave Array

NOTES:
1. WGS 1984 COORDINATE SYSTEM
2. Image Source: ESRI, i-cubed, USDA FSA, USGS, AEX, GeoEye, Getmapping, Aerogrid, IGP

File Name: CE-11023-I

Date: 4/7/2011

USGS science for a changing world

GEOVision geophysical services

RECOVERY.GOV

SITE MAP
CE•11023

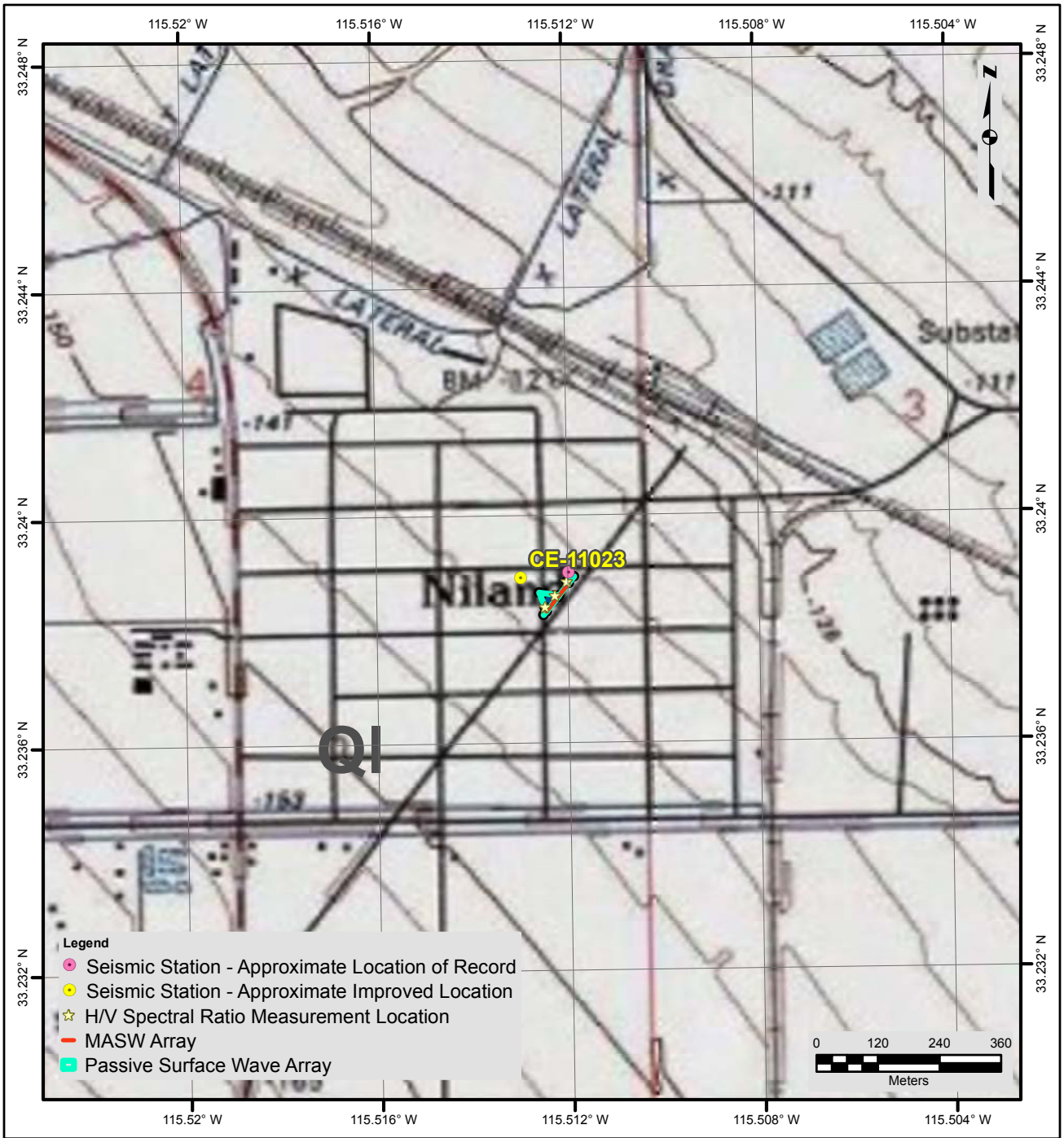

Description of Geologic Map Units

Qls = Quaternary (Holocene) lake deposits

NOTES:
1. WGS 1984 COORDINATE SYSTEM
2. Topo Image Sources: USGS, FAO, NPS, EPA, NRCAN, GeoBase, Esri, DeLorme, TANA, Intermap, AND, other suppliers, and the GIS community
3. Geologic Map of California, Salton Sea Sheet, Olaf P Jenkins Edition by Charles W. Jennings, 1967
4. See site map for details of geophysical survey

File Name: CE-11023

Date: 4/7/2011

USGS science for a changing world

GEOVision geophysical services

GEOLOGIC MAP
CE•11023

RECOVERY.GOV

Looking northwest towards Niland Fire Station from near the center of MASW array 11023-1

MASW Array 11023-1

Looking northwest towards central portion of passive surface wave array 11023-3

Looking northeast along passive surface wave arrays 11023-2 and 11023-3

Looking towards fire station from HVSR sensor 507

Location of Geophysical Testing Arrays:

Location	Latitude	Longitude
11023-1, Southwest End of Array	33.23831	-115.51247
11023-1, Center of Array	33.23856	-115.51223
11023-1, Northeast End of Array	33.23880	-115.51199
11023-2, Southwest End of Array	33.23825	-115.51253
11023-2, Northeast End of Array	33.23892	-115.51188
11023-3, Corner of Array, Sensor Location 1	33.23831	-115.51246
11023-3, Corner of Array, Sensor Location 3	33.23859	-115.51220
11023-3, Corner of Array, Sensor Location 5	33.23864	-115.51262
11023-3, Center of Array, Sensor Location 10	33.23851	-115.51242
HVSR Sensor 507	33.23883	-115.51204
HVSR Sensor 453	33.23839	-115.51250
HVSR Sensor 450	33.23859	-115.51229

Notes: 1) WGS84 Coordinate System (decimal degrees)
2) Survey accuracy is estimated at 1 to 2 m

Results:

V_S Model

Depth to Top of Layer (m)	Layer Thickness (m)	S-Wave Velocity (m/s)	Inferred P-Wave Velocity (m/s)	Inferred Poisson's Ratio	Inferred Density (g/cm^3)
0	2	151	282	0.300	1.9
2	2	146	274	0.300	1.9
4	2	162	303	0.300	1.9
6	5	214	1500	0.490	2.0
11	8	223	1500	0.489	2.0
19	12	255	1500	0.485	2.0
31	>14	301	1500	0.479	2.0

Observations/Discussion:

- Best quality HVSR data at the locations of sensors 453 and 507 where HVSR curves are almost identical, validating the 1-D velocity assumption. Data quality form sensor 450 not as good, likely the result of poorer sensor coupling to the ground.
- Broad low frequency or double HVSR peak in the 0.17 to 0.24 Hz range, which is consistent for a deep soil site.
- Low amplitude secondary HVSR peak at about 0.85 Hz.
- Surface wave dispersion data from active and passive surface wave datasets are in acceptable agreement at this site.
- About 25 m/s scatter in MASW dispersion data over the 20 to 45 m wavelength range (5 to 8.5 Hz frequency range) possibly resulting from a combination of lateral velocity variation and traffic noise. The higher phase velocities over this wavelength range are in the best agreement with passive surface wave data.
- Passive surface wave data acquired in early evening after MASW data acquisition as there was very little vehicle traffic in site vicinity in the morning. Passive surface wave data acquisition in the early afternoon may have been more appropriate. Nevertheless, noise conditions at site appeared sufficient for successful application of passive surface wave techniques and passive surface wave data successfully extended depth of investigation.
- Both the time and frequency domain ESAC techniques used to extract surface wave dispersion data from passive triangle array data. The ReMi™ technique appeared to yield better dispersion data from the linear array than the ESAC technique.
- Representative dispersion curves were generated for each surface wave data set using a moving average, polynomial curve fitting routine. These individual representative dispersion curves were combined and a representative dispersion curve generated for the combined data set for data modeling.
- Water table depth constrained to about 6 m based on a simple, 2-layer interactive analysis of seismic refraction data from MASW shot records. V_P of saturated sediments was estimated to be about 1,500 m/s.
- Surface wave depth of investigation is about 45 m based on half of maximum wavelength criteria.
- V_{S30} is 212 m/s (NEHRP Site Class D).
- Average S-wave velocity of the upper 45 m (V_{S45}) is 234 m/s.

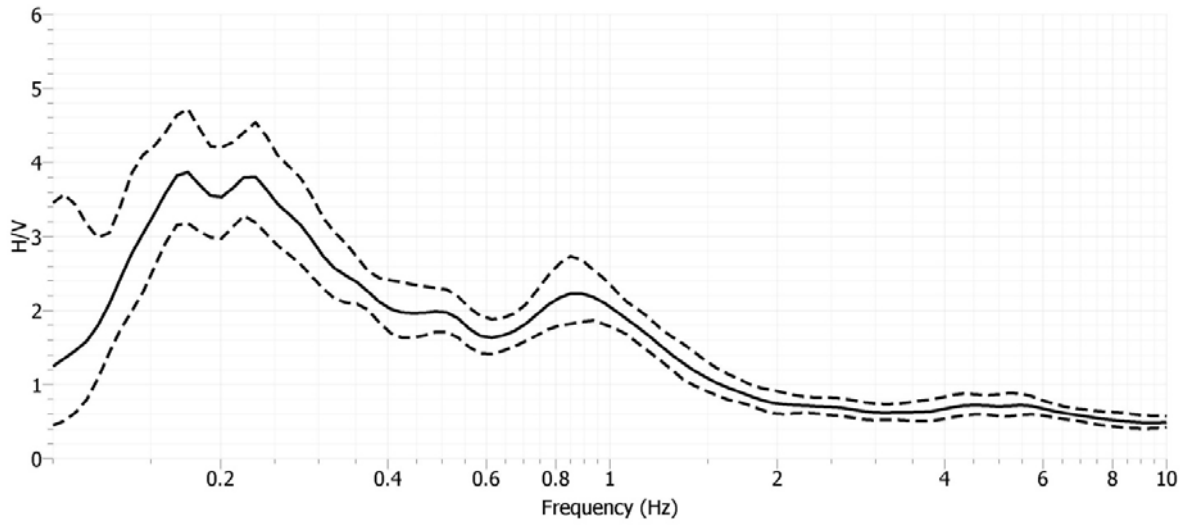

Site CE.11023, H/V Spectral Ratio, Array 11023-1, Sensor 507

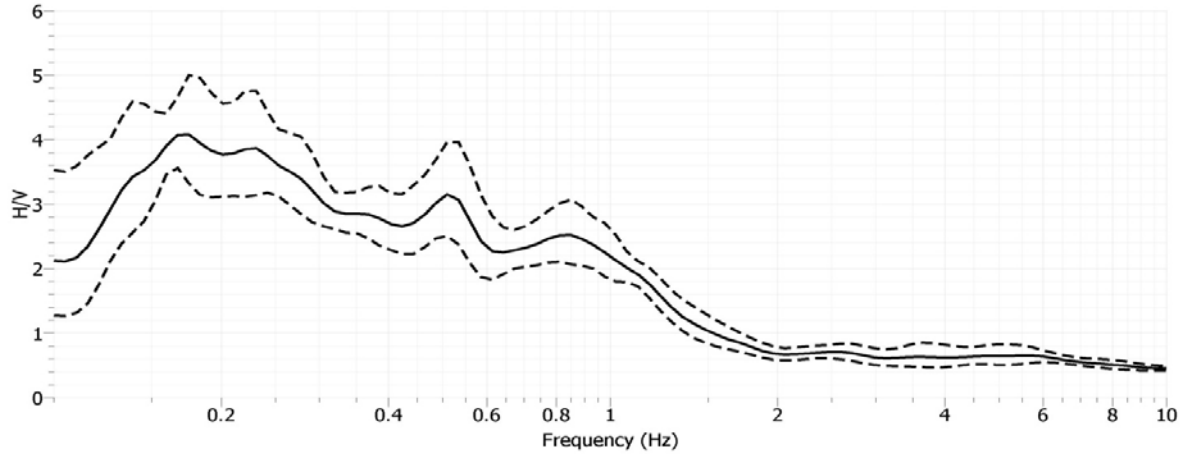

Site CE.11023, H/V Spectral Ratio, Array 11023-1, Sensor 450

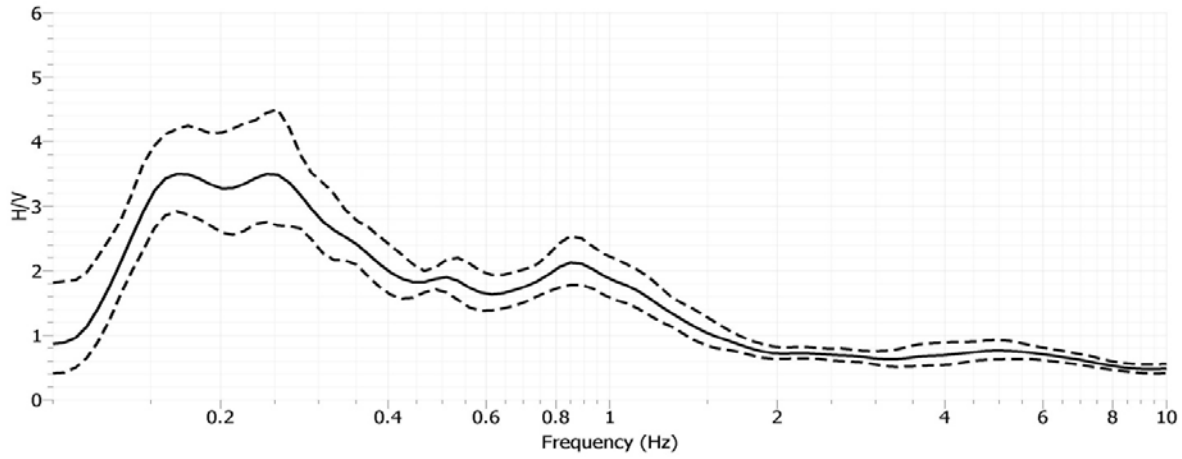

Site CE.11023, H/V Spectral Ratio, Array 11023-1, Sensor 453

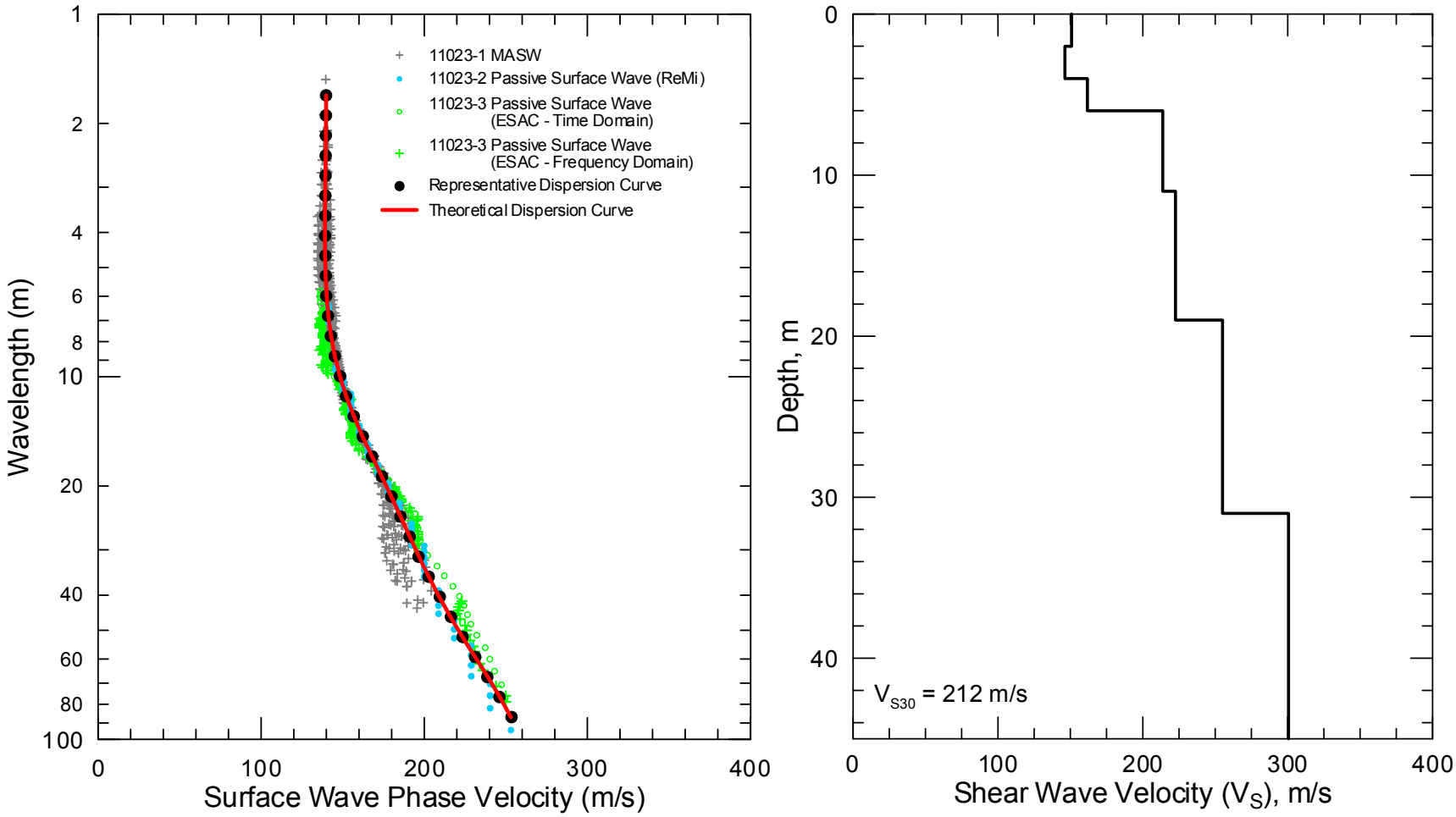

CE.11023 - Field, representative and inverted theoretical surface wave dispersion data (left) and associated V_S model (right)

Site CE.11625

Location: Coachella Valley Water District, Mecca Yard, Riverside County, California

Latitude: 33.56409 **Longitude:** -115.98763
(Station coordinates modified based on visual observation of station location in field and identification of approximate station location on Google Earth – no access to fenced compound to survey station location, WGS84 coordinate system.)

V_{S30} (measured): 318 m/s

V_{S30} (adjusted to more accurately reflect seismic station conditions): 318 m/s (no adjustment necessary).

NEHRP Site Class: D

Geomatrix Code: IHD

Geologic Conditions/Observations: Quaternary (Holocene) alluvium.

Site Conditions: Rural site. Coachella canal located immediately north of test area. Relatively flat terrain in test area.

Geophysical Methods Utilized: HVSR, SASW, MASW

Geophysical Testing Arrays:

1. Array 11625-1 (MASW array utilizing 48 4.5 Hz vertical geophones spaced 1.5 m apart for an array length of 70.5 m, forward and reverse shot locations with multiple source offsets and source types and center shot location).
2. Array 11625-1 (SASW array centered at the midpoint of and aligned along the MASW array with the same name. SASW data acquired using 1 Hz geophones, common center point and forward and reversed shot locations).
3. Three HVSR measurement locations distributed along 11625-1.

Legend

- Seismic Station - Approximate Location of Record
- Seismic Station - Approximate Improved Location
- H/V Spectral Ratio Measurement Location
- SASW Array
- MASW Array

NOTES:
1. WGS 1984 COORDINATE SYSTEM
2. Image Source: ESRI, i-cubed, USDA FSA, USGS, AEX, GeoEye, Getmapping, Aerogrid, IGP

File Name: CE-11625-I

Date: 3/31/2011

USGS science for a changing world

GEOVision geophysical services

RECOVERY.GOV

SITE MAP
CE•11625

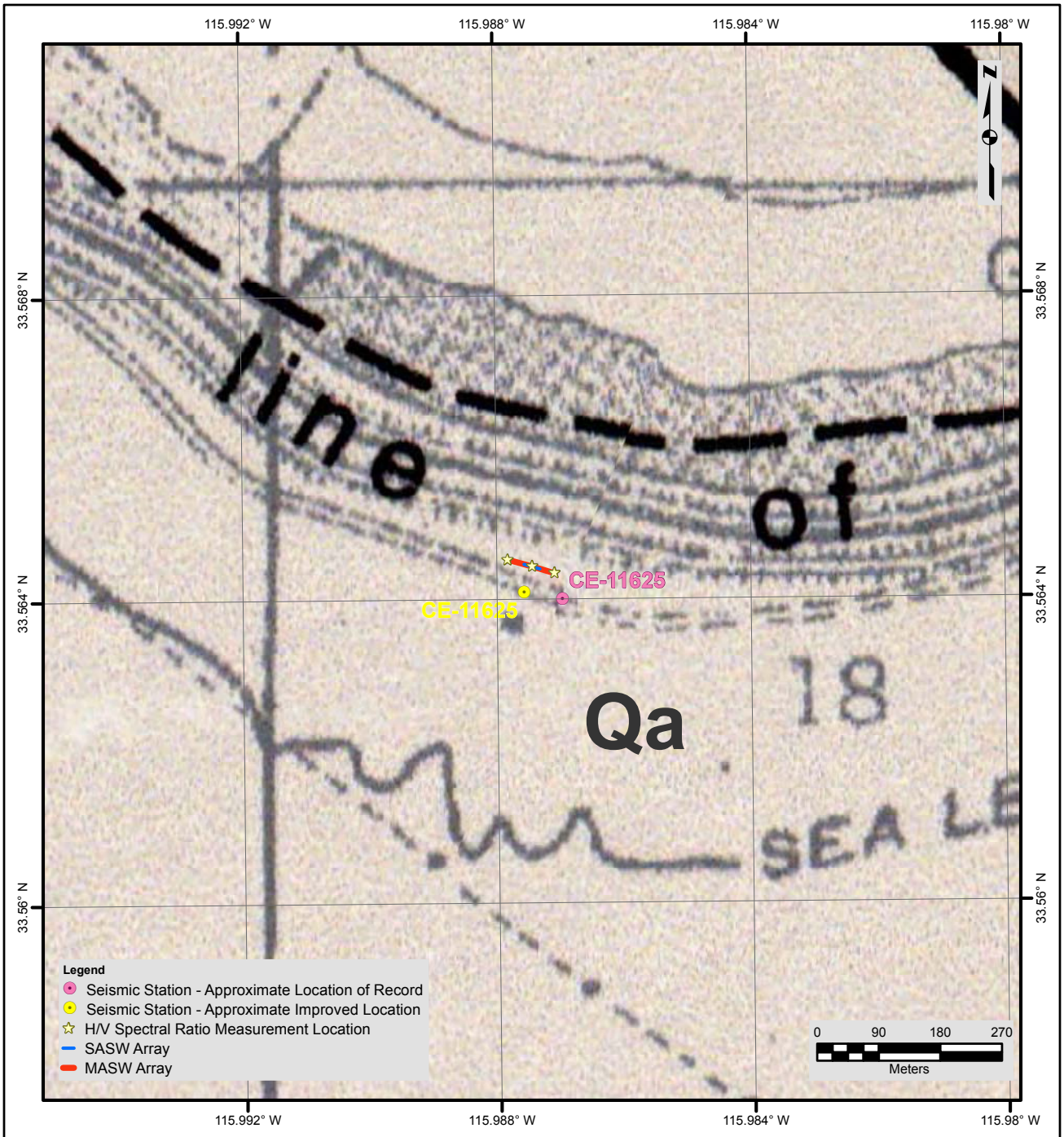

Description of Geologic Map Units

Qa = Quaternary (Holocene) alluvial sand, gravel, silt and clay of valley areas

NOTES:
1. WGS 1984 COORDINATE SYSTEM
2. Geologic Map of the Cottonwood Spring & Canyon Spring 15 Minute Quadrangles, Riverside County, California by Thomas W. Dibblee, Jr., 2008

File Name: CE-11625

Date: 4/1/2011

USGS science for a changing world

GEOVision geophysical services

RECOVERY.GOV

GEOLOGIC MAP
CE•11625

CE.11625 seismograph station

Looking towards seismograph station from HVSR sensor 507

Looking east along MASW array 11625-1

SASW data acquisition

Looking west along SASW array 11625-1

Location of Geophysical Testing Arrays:

Location	Latitude	Longitude
11625-1, West end of MASW array	33.56453	-115.98786
11625-1, Center of MASW and SASW array	33.56443	-115.98748
11625-1, East end of MASW array	33.56434	-115.98713
HVSR Sensor 507	33.56452	-115.98786
HVSR Sensor 453	33.56444	-115.98748
HVSR Sensor 450	33.56435	-115.98712

Notes: 1) WGS84 Coordinate System (decimal degrees)
2) Survey accuracy is estimated at 1 to 2 m

Results:

V_S Model

Depth to Top of Layer (m)	Layer Thickness (m)	S-Wave Velocity (m/s)	Inferred P-Wave Velocity (m/s)	Inferred Poisson's Ratio	Inferred Density (g/cm^3)
0	0.5	195	365	0.3	1.9
0.5	1	197	368	0.3	1.9
1.5	3	246	460	0.3	1.9
4.5	6	270	506	0.3	1.9
10.5	10	337	630	0.3	2.0
20.5	>9.5	419	784	0.3	2.0

Observations/Discussion:

- HVSR curves almost identical, validating the 1-D velocity assumption.
- Low frequency HVSR peak at about 0.11 Hz, which is consistent for a deep soil site.
- Scatter in MASW dispersion data (40-50 m/s) over the 35 to 60 m wavelength range (5 to 8 Hz frequency range), primarily between forward and reverse direction sources, and possibly resulting from lateral velocity variation at depth (e.g. dipping geologic layer).
- Surface wave dispersion data from MASW and SASW datasets are in acceptable agreement at this site with averaged representative dispersion curves from each data set being similar. The largest differences between the MASW and SASW data occur at small wavelengths (high frequencies) and associated with lateral velocity variation (i.e. the SASW dispersion data at small wavelengths are sampled over a short segment of the MASW array). At long wavelengths the SASW dispersion data bisects the differing MASW dispersion data from forward and reverse shots.
- MASW and SASW representative dispersion curves were combined with equal weighting and a representative dispersion curve generated from the combined data set for data modeling.
- Water table located at a depth greater than 30 m based on review of seismic refraction data.
- Based on review of first arrival data, P-wave velocity in upper 20 m ranges from about 350 m/s near surface to about 500 m/s at a depth of 10 to 11 m. Far offset, MASW seismic records indicate that P-wave velocity may exceed 700 m/s at a depth of 20 to 30 m.
- A longer seismic refraction line may help determine if deeper geologic units have shallow dip although refractors with velocity greater than 700 m/s may be hidden layers due to water table refractor. In this case, a more costly seismic reflection line would be required to determine the structure of subsurface geologic units.
- Surface wave depth of investigation is about 30 m based on half of maximum wavelength criteria.
- S-wave velocities at intermediate depths (4.5 to 20.5) in the surface wave model do not appear to be consistent with observed P-wave velocities in seismic refraction first arrival data. A Poisson's ratio of lower than 0.3 or unknown geologic structure could explain the difference. Of course, it is always difficult to reconcile S-wave velocities from surface wave surveys with P-wave seismic refraction models because Poisson's Ratio is not known and both methods suffer from nonuniqueness. A more comprehensive P- and S-wave seismic refraction survey could help resolve the differences in the models and source of scatter in the surface wave dispersion data.
- V_{S30} is 318 m/s (Site Class D).
- Modeling upper and lower envelopes of SASW and MASW dispersion data would only result in about a 10 % variation in the velocities of the lower three layers and a ±5 % change in V_{S30}.

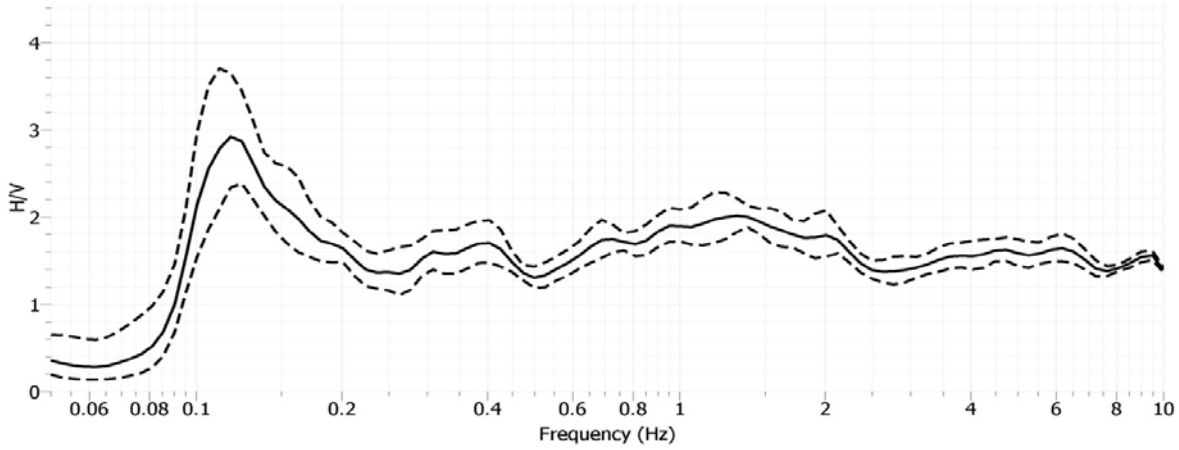

Site CE.11625, H/V Spectral Ratio, Array 11625-1, Sensor 507

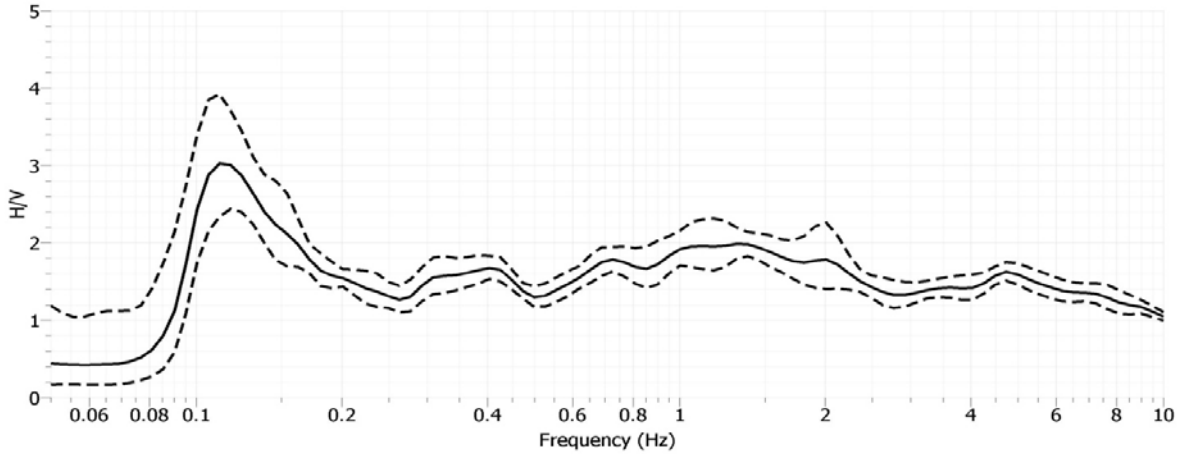

Site CE.11625, H/V Spectral Ratio, Array 11625-1, Sensor 453

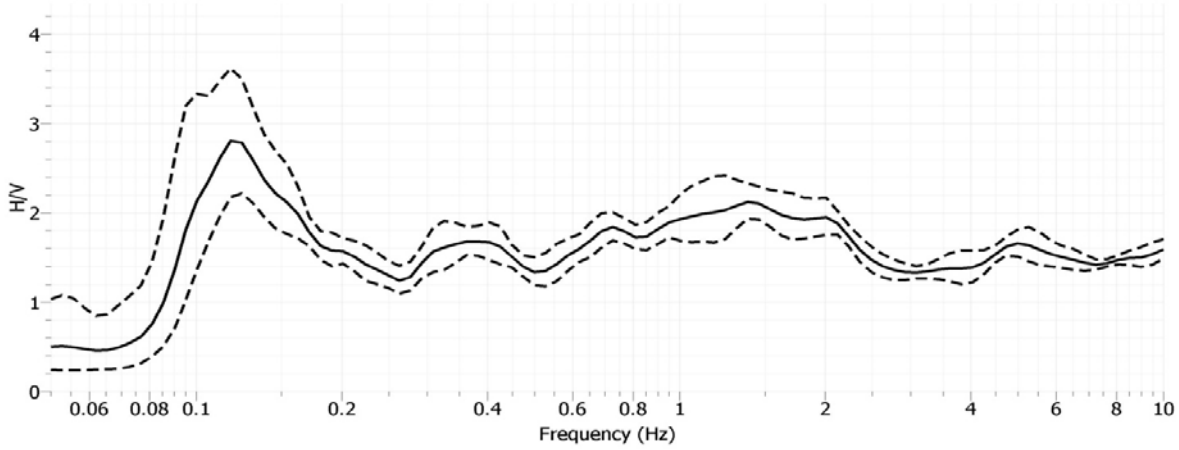

Site CE.11625, H/V Spectral Ratio, Array 11625-1, Sensor 450

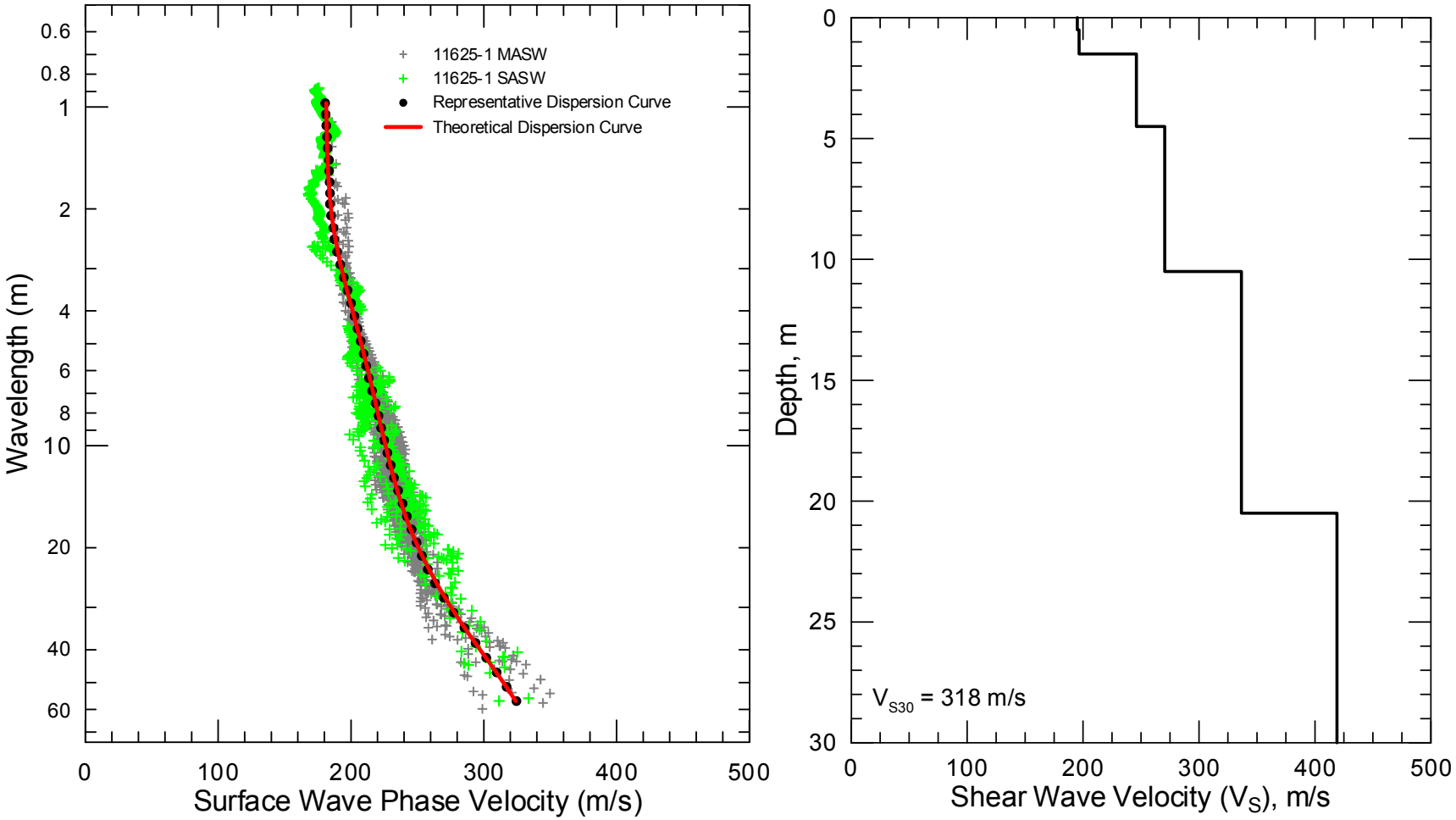

CE.11625 - Field, representative and inverted theoretical surface wave dispersion data (left) and associated V_S model (right)

Site CE.11684

Location: Spa Road and S. Sunshine Drive, near Frink, California

Latitude: 33.39799 **Longitude:** -115.65859
(Station coordinates modified based on field GPS survey, WGS84 coordinate system)

V_{S30} (measured): 202 m/s

V_{S30} (adjusted to more accurately reflect seismic station conditions): 202 m/s (no adjustment necessary).

NEHRP Site Class: D

Geomatrix Code: IHD

Geologic Conditions/Observations: Site located on mapped Quaternary (Holocene) lake deposits near the mapped intersection of Quaternary alluvium, lake deposits and older continental deposits. Surficial gravelly soils indicate that a thin layer of alluvium likely overlies lake deposits at the site.

Site Conditions: Rural site with almost constant traffic into adjacent RV Park. Relatively flat terrain in test area. Ground surface elevation decreases gradually to southwest.

Geophysical Methods Utilized: HVSR, SASW, MASW

Geophysical Testing Arrays:

1. Array 11684-1 (MASW array utilizing 48 4.5 Hz vertical geophones spaced 1.5 m apart for an array length of 70.5 m, forward and reverse shot locations with multiple source offsets and source types and center shot location).
2. Array 11684-2 (SASW array using 1 Hz geophones, common center point, receiver spacing of 2 to 32 m and forward and reversed shot locations).
3. Array 11684-3 (SASW array using 1 Hz geophones, common center point, receiver spacing of 2 to 32 m and forward and reversed shot locations).
4. Array 11684-4 (MASW array utilizing 24 4.5 Hz vertical geophones spaced 5 m apart for an array length of 115 m, forward and reverse shot locations with multiple source offsets and center shot location). SASW array 11684-3 located at west end of this MASW array.
5. Arrays 11684-2 to 11684-4 were all added after observing lateral velocity variation or a velocity discontinuity on array 11684-1.
6. Three HVSR measurement locations distributed along 11684-1.

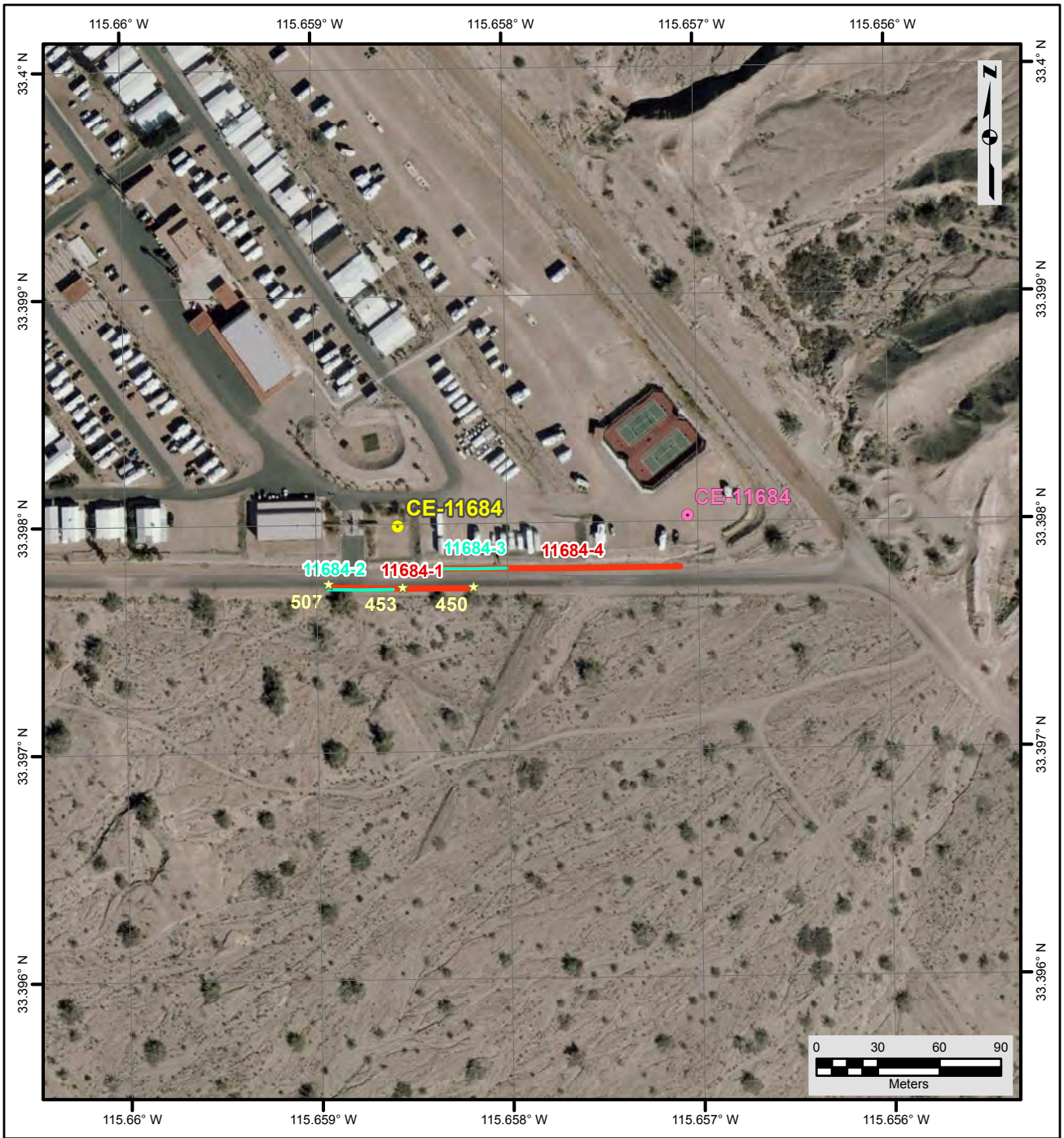

Legend

- Seismic Station - Approximate Location of Record
- Seismic Station - Approximate Surveyed Location
- H/V Spectral Ratio Location
- SASW Array
- MASW Array

NOTES:
1. WGS 1984 COORDINATE SYSTEM
2. Image Source: ESRI, i-cubed, USDA FSA, USGS, AEX, GeoEye, Getmapping, Aerogrid, IGP

File Name: CE-11684-I

Date: 4/7/2011

USGS science for a changing world

GEOVision geophysical services

RECOVERY.GOV

SITE MAP
CE•11684

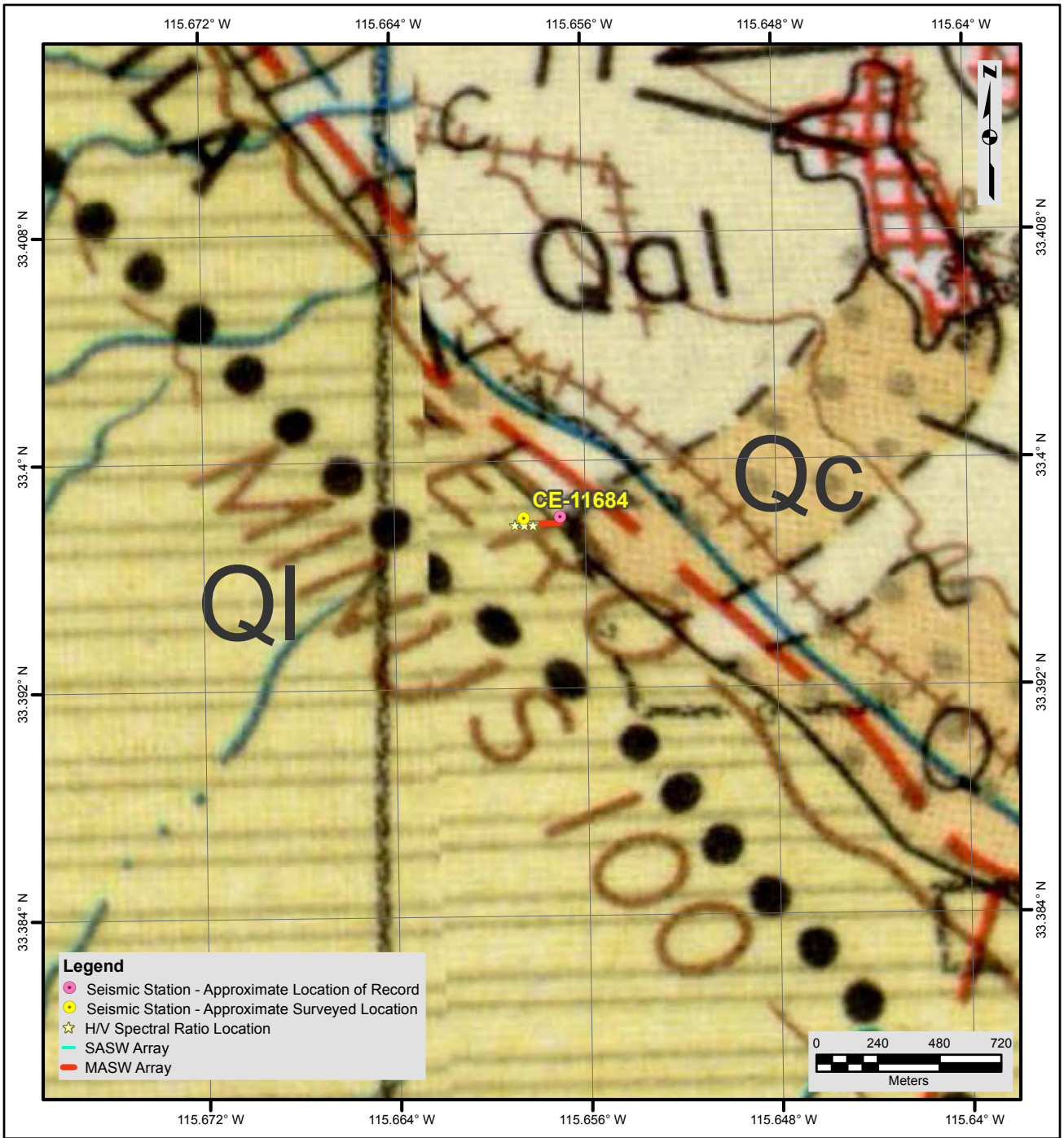

Description of Geologic Map Units

Qal = Quaternary (Holocene) alluvium
Ql = Quaternary (Holocene) lake deposits
Qc = Quaternary (Pleistocene) nonmarine

NOTES:
1. WGS 1984 COORDINATE SYSTEM
2. Geologic Map of California, Salton Sea Sheet, Olaf P Jenkins Edition by Charles W. Jennings, 1967
3. See site map for details of geophysical survey

File Name: CE-11684

Date: 4/7/2011

USGS science for a changing world

GEOVision geophysical services

RECOVERY.GOV

GEOLOGIC MAP
CE•11684

Looking north towards CE.12684 seismograph station from near center of MASW array 11684-1

SASW data acquisition along array 11684-3

Looking northeast towards seismic station from HVSR sensor 507

MASW array 11684-4

SASW data acquisition along array 11684-2

Location of Geophysical Testing Arrays:

Location	Latitude	Longitude
11684-1, West End of MASW Array	33.39773	-115.65895
11684-1, Center of MASW Array	33.39772	-115.65857
11684-1, East End of MASW Array	33.39772	-115.65819
11684-2, West End of SASW Receiver Array	33.39772	-115.65896
11684-2, Center of SASW Receiver Array	33.39772	-115.65879
11684-2, East End of SASW Receiver Array	33.39772	-115.65861
11684-3, West End of SASW Receiver Array	33.39780	-115.65836
11684-3, Center of SASW Receiver Array	33.39780	-115.65819
11684-3, East End of SASW Receiver Array	33.39780	-115.65802
11684-4, West End of MASW Array	33.39780	-115.65835
11684-4, Center of MASW Array	33.39780	-115.65773
11684-4, East End of MASW Array	33.39780	-115.65711
HVSR Sensor 507	33.39774	-115.65895
HVSR Sensor 453	33.39772	-115.65856
HVSR Sensor 450	33.39772	-115.65819
CE.11684 seismograph station	33.39799	-115.65859

Notes: 1) WGS84 Coordinate System (decimal degrees)
2) Survey accuracy is estimated at 1 to 2 m

Results:

V_S Model – Array 11684-1

Depth to Top of Layer (m)	Layer Thickness (m)	S-Wave Velocity (m/s)	Inferred P-Wave Velocity (m/s)	Inferred Poisson's Ratio	Inferred Density (g/cm^3)
0	0.75	145	271	0.300	1.9
0.75	1.25	136	254	0.300	1.9
2	1	170	318	0.300	1.9
3	6	168	1500	0.494	2.0
9	7	210	1500	0.490	2.0
16	8	214	1500	0.490	2.0
24	>6	299	1500	0.479	2.0

Note: Model valid to 25 m.

V_S Model – Array 11684-2

Depth to Top of Layer (m)	Layer Thickness (m)	S-Wave Velocity (m/s)	Inferred P-Wave Velocity (m/s)	Inferred Poisson's Ratio	Inferred Density (g/cm^3)
0	0.75	131	245	0.300	1.9
0.75	0.75	124	232	0.300	1.9
1.5	1.5	160	299	0.300	1.9
3	5	163	1500	0.494	2.0
8	6	189	1500	0.492	2.0
14	9	208	1500	0.490	2.0
23	>7	347	1500	0.472	2.0

Note: Model valid to 30 m.

V_S Model – Arrays 11684-3 and 11684-4

Depth to Top of Layer (m)	Layer Thickness (m)	S-Wave Velocity (m/s)	Inferred P-Wave Velocity (m/s)	Inferred Poisson's Ratio	Inferred Density (g/cm^3)
0	0.75	105	197	0.300	1.9
0.75	0.75	108	202	0.300	1.9
1.5	1.5	156	292	0.300	1.9
3	5	151	1500	0.495	2.0
8	6	187	1500	0.492	2.0
14	9	220	1500	0.489	2.0
23	>7	352	1500	0.471	2.0

Note: Model valid to 30 m.

Observations/Discussion:

- HVSR analysis very difficult due to almost constant transients from traffic into adjacent RV Park. Sensor coupling also not very good in gravelly soils. Data quality would likely be improved with measurements made at night when traffic is reduced.
- Some variation of HVSR data, particularly amplitude, due to difficulty working around transients and sensor coupling issues.
- No clear narrow HVSR peak. Very broad, low frequency HVSR peak in 0.3 to 0.9 Hz range, indicative of a deep soil site. As mentioned above, HVSR data should be reacquired at a time when there is no traffic.
- Clear shallow lateral velocity variation or geologic discontinuity observed in MASW array 11684-1 seismic records, which affects surface wave propagation, the water table refractor and seismic reflections as shown on attached figures. Therefore, separate SASW arrays (11684-2 and 11684-3) placed on each side of the feature. Additionally, a long MASW array (11684-4) placed coincident with SASW array 11684-3 to demonstrate that obvious lateral velocity variations were not present beneath the SASW array.
- Surface wave dispersion data from forward and reverse shots on MASW array 11684-1 are slightly different at wavelengths smaller than about 10 m, indicating that lateral S-wave velocity variation is limited to the shallow sediments.
- Even with the lateral velocity variation, the surface wave dispersion data from MASW array 11684-1 is not significantly different from that from SASW array 11684-2, which is located at the west end of the MASW array.
- Surface wave dispersion curves from SASW array 11684-3 and MASW array 11684-4 are similar and data combined for modeling.
- The lateral velocity variation observed on array 11684-1 does not seem to have a significant impact on S-wave velocity structure at the site but could be characterized in more detail utilizing seismic refraction, seismic reflection or 2-D MASW techniques.
- Water table located at a nominal depth of 3 m based on review of seismic refraction data from Array 11684-4.
- Surface wave depth of investigation is about 25 m for array 11684-1 and 30 m for arrays 11684-2 to 11684-4 based on half of maximum wavelength criteria.
- V_{S30} is 204 m/s for SASW array 11684-2 and 200 m/s for combined SASW array 11684-3 and MASW array 11684-4.
- Although the valid depth of investigation for array 11684-1 is only 25 m, V_{S30} is estimated at 204 m/s. This is almost identical to array 11684-2, indicating that the lateral velocity variation discussed above has little impact on the estimated value of V_{S30}.
- The average V_{S30} of arrays 11684-2 and 11684-3/4 is 202 m/s (Site Class D).

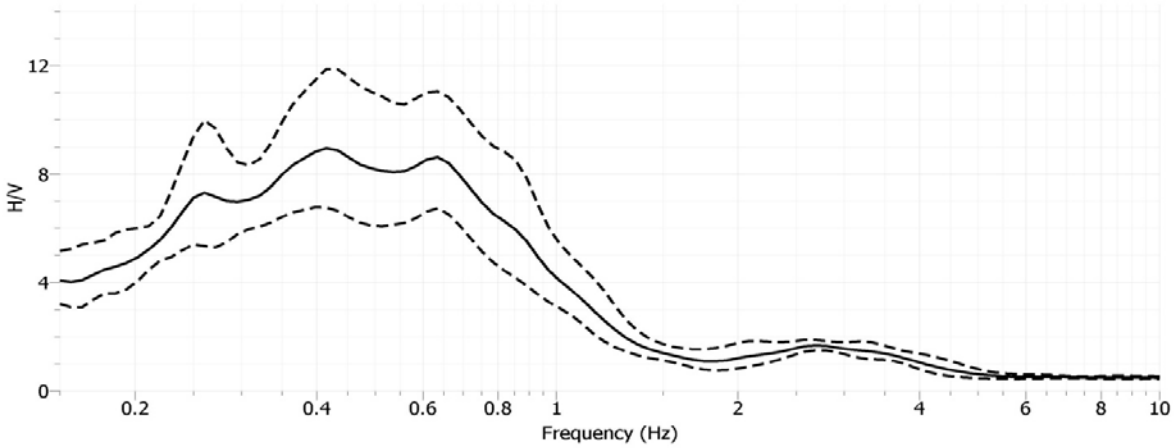

Site CE.11684, H/V Spectral Ratio, Array 11684-1, Sensor 507

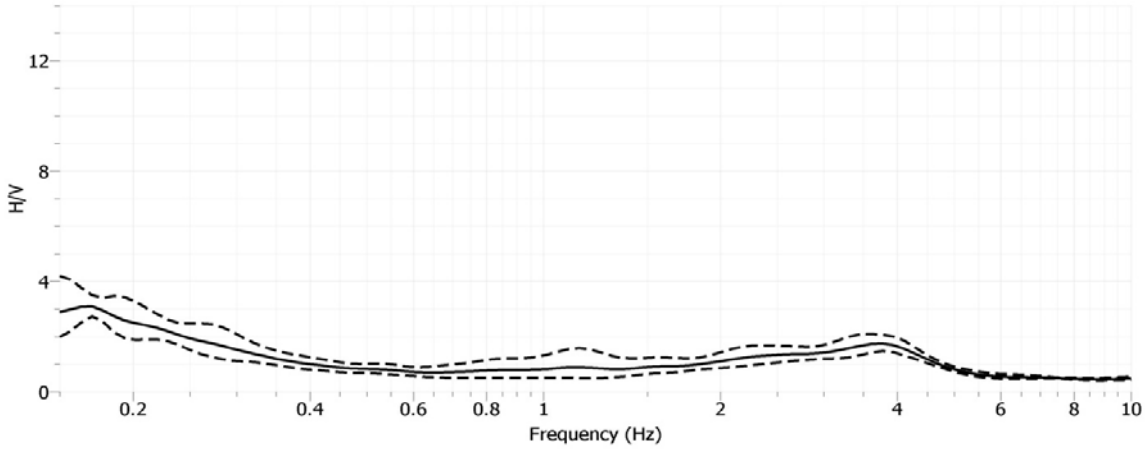

Site CE.11684, H/V Spectral Ratio, Array 11684-1, Sensor 453

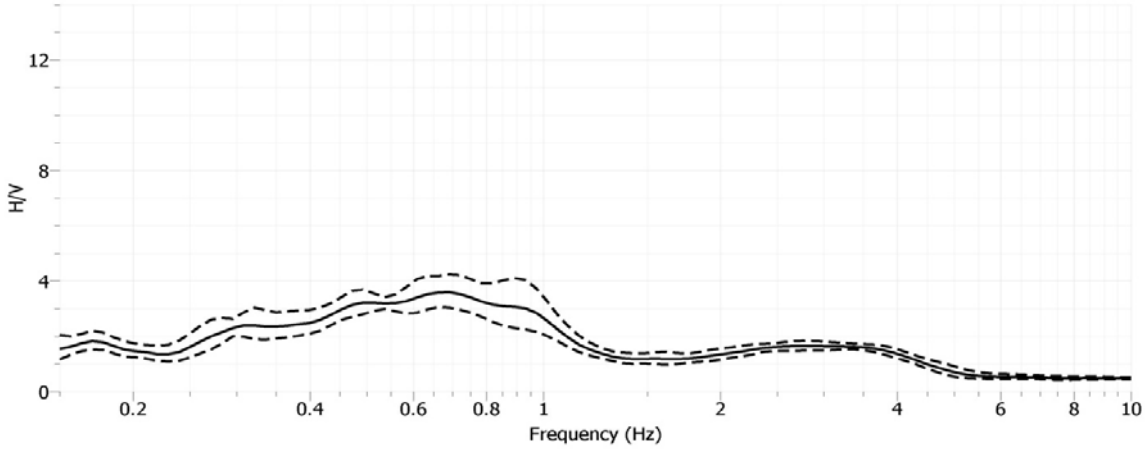

Site CE.11684, H/V Spectral Ratio, Array 11684-1, Sensor 450

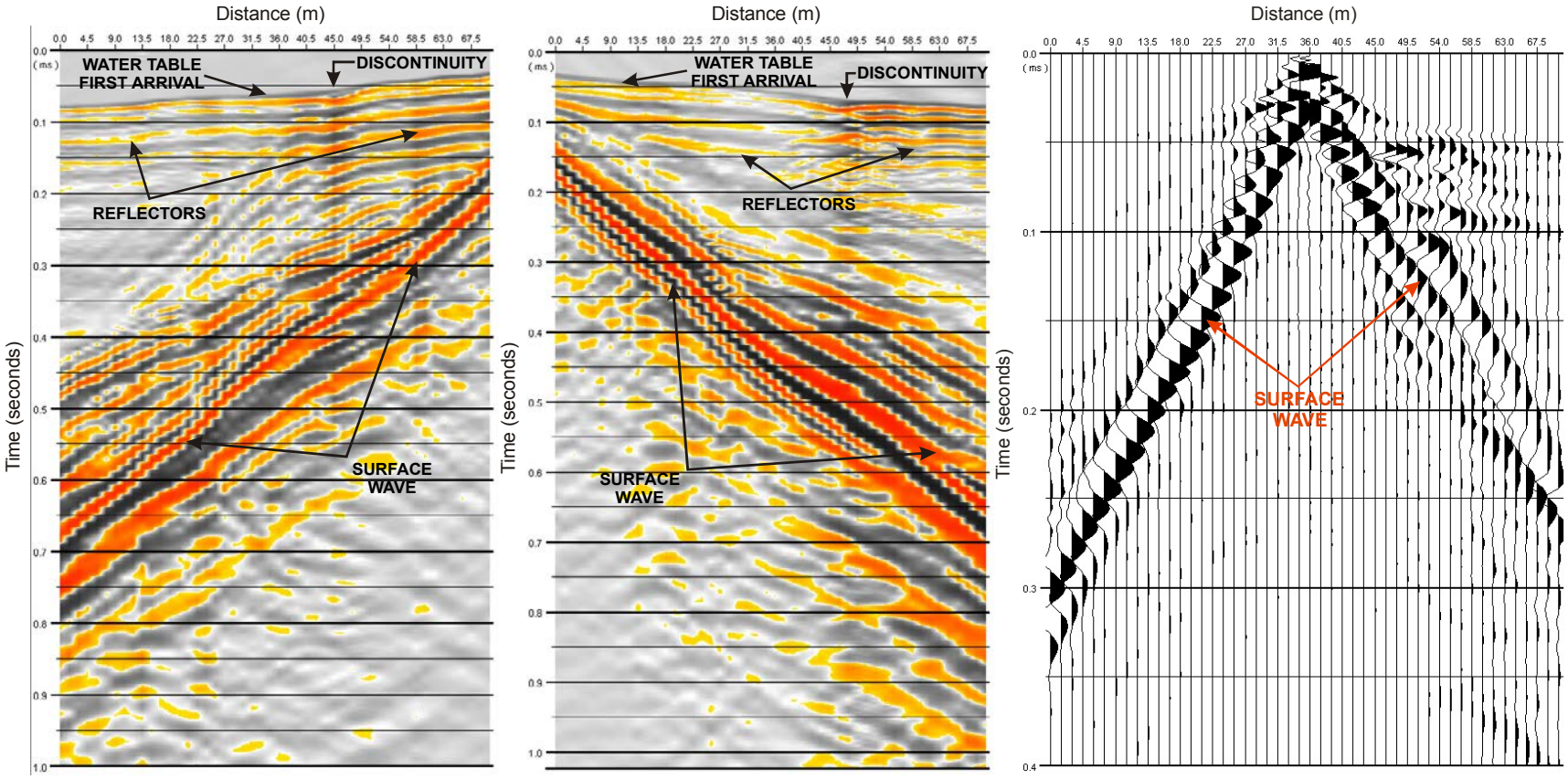

Forward (center) and reverse (left) off-end and center (right) shot locations for MASW array 11684-1 illustrating the presence of a velocity discontinuity affecting the water table refracted arrival, reflections and surface wave propagation between a position of 45 and 49.5 m.

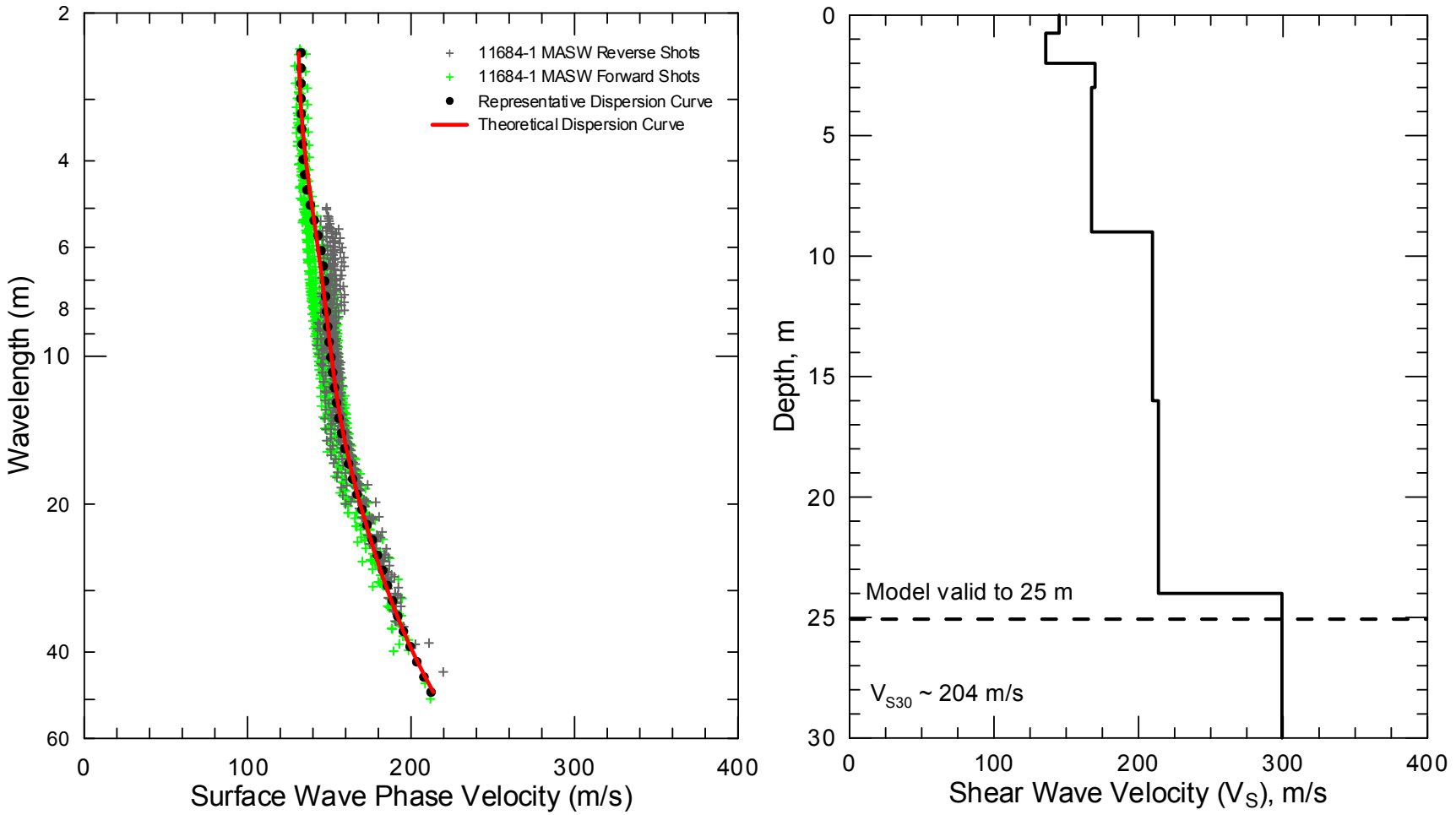

CE.11684, Array 11684-1 - Field, representative and inverted theoretical surface wave dispersion data (left) and associated V_S model (right)

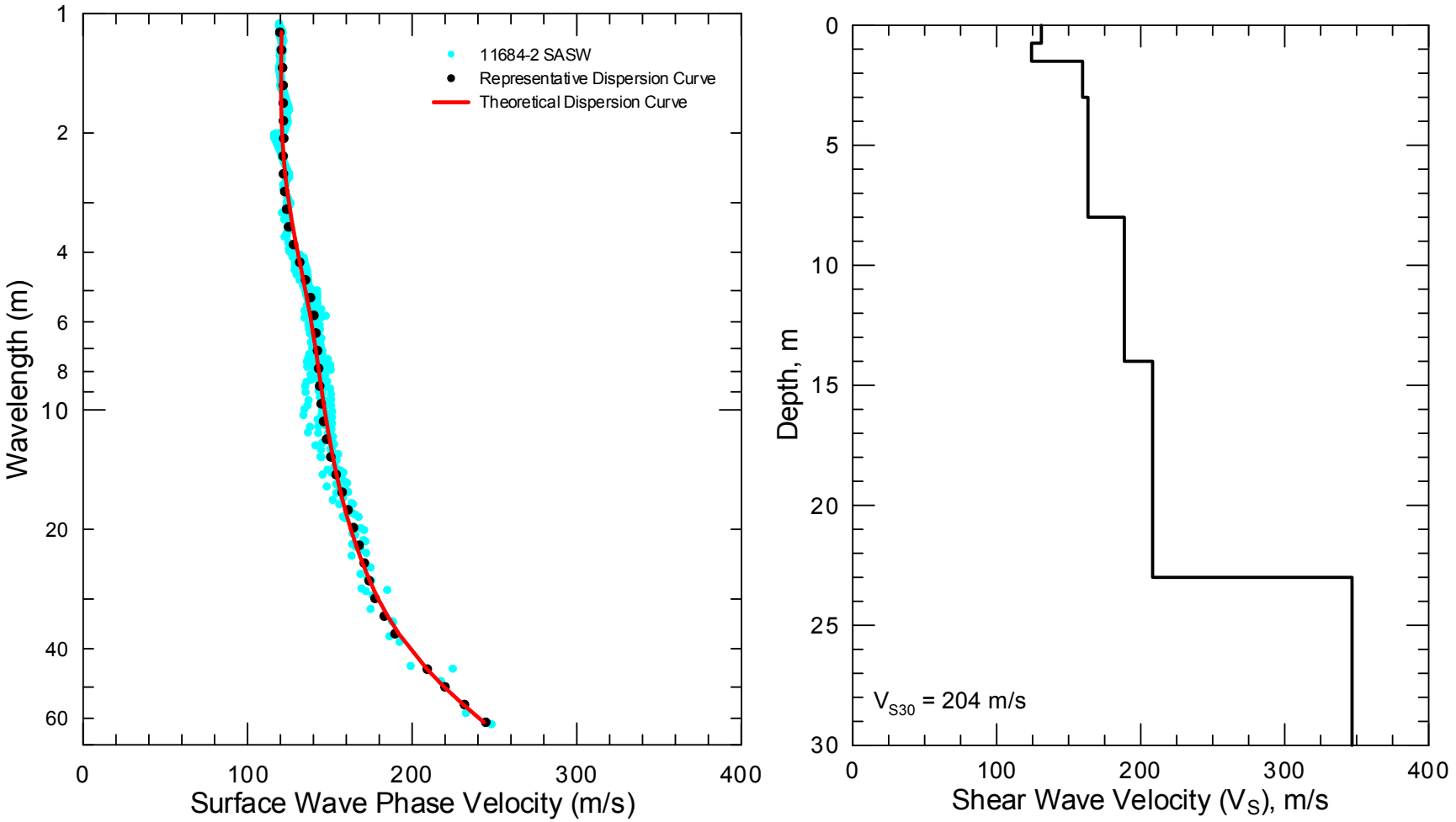

CE.11684, Array 11684-2 - Field, representative and inverted theoretical surface wave dispersion data (left) and associated V_S model (right)

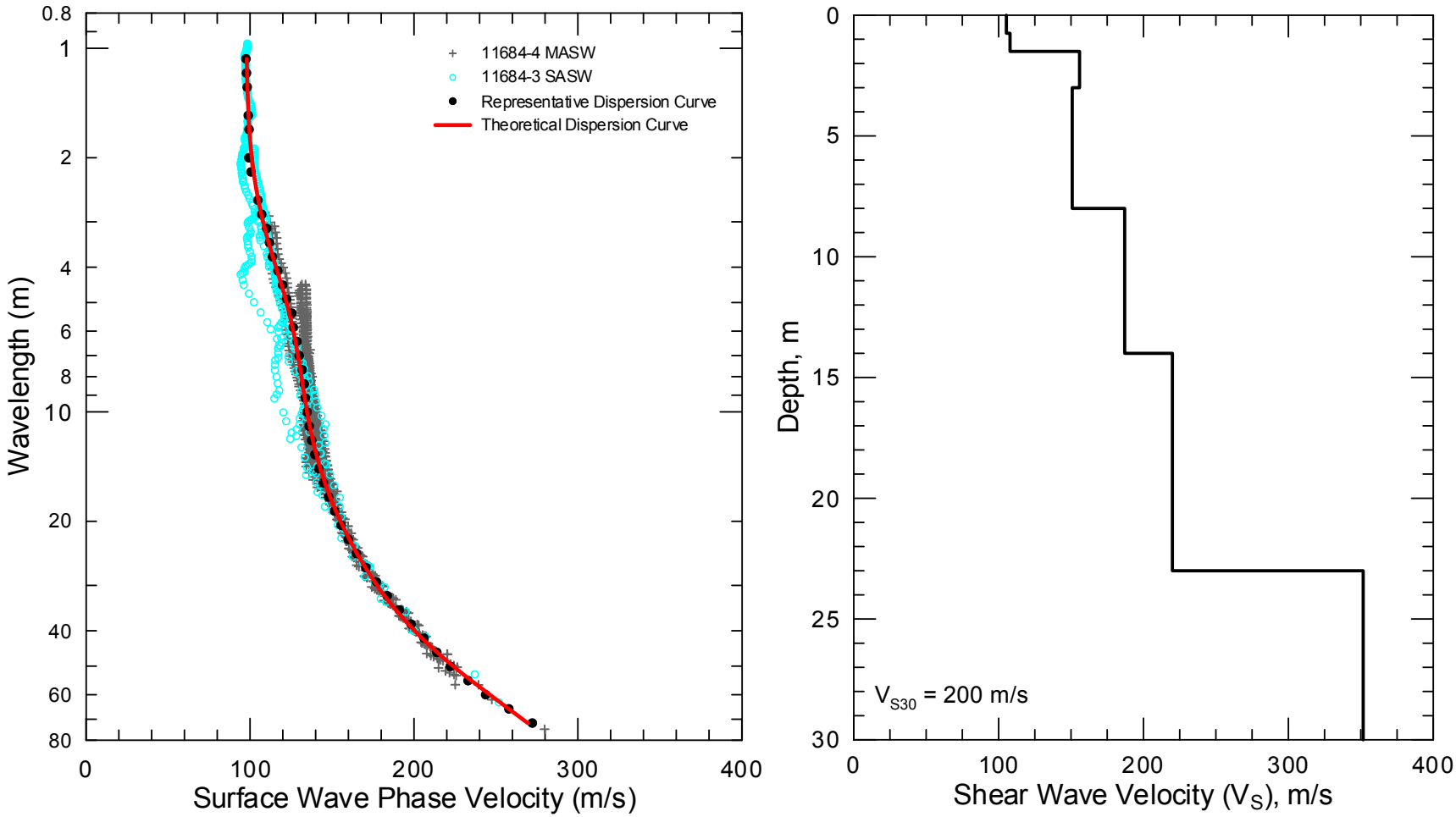

CE.11684, Arrays 11684-3 and 4 - Field, representative and inverted theoretical surface wave dispersion data (left) and associated V_S model (right)

Site CE.12076

Location: City of Coachella Fire Station #79, Riverside County, California

Latitude: 33.6781 **Longitude:** -116.178
(Station coordinates from www.strongmotioncenter.org, WGS84 coordinate system)

V_{S30} (measured): 263 m/s

V_{S30} (adjusted to more accurately reflect seismic station conditions): 263 m/s (no adjustment necessary).

NEHRP Site Class: D

Geomatrix Code: AHD

Geologic Conditions/Observations: Quaternary alluvial and playa lake deposits, deep soil site.

Site Conditions: Urban site with significant noise sources from traffic in site vicinity. Relatively flat topography in the site vicinity. High traffic road immediately west of survey area.

Geophysical Methods Utilized: HVSR, MASW, array microtremor, ReMi™

Geophysical Testing Arrays:

1. Array 12076-1 (24 channel, linear passive surface wave array utilizing 4.5 Hz vertical geophones spaced 6 m apart for a length of 138 m).
2. Array 12076-2 (10 channel, triangle passive surface wave array utilizing 1 Hz geophones and an 60 m length for outer side of array).
3. Array 12076-1 was also used to acquire limited MASW and seismic refraction data (off-end shots with accelerated weight drop energy source).
4. Array 12076-3 (48 channel MASW array utilizing 4.5 Hz vertical geophones spaced 1.5 m apart for a length of 70.5 m). Array 12076-3 was aligned along array 12076-1.
5. Three HVSR measurement locations, two located near ends of 12076-3 and one located in a small open lot closer to the seismic station.

Legend

- Seismic Station - Approximate Location of Record
- Seismic Station - Approximate Improved Location
- H/V Spectral Ratio Measurement Location
- MASW Array
- Passive Surface Wave Array

NOTES:
1. WGS 1984 COORDINATE SYSTEM
2. Image Source: ESRI, i-cubed, USDA FSA, USGS, AEX, GeoEye, Getmapping, Aerogrid, IGP

File Name: CE-12076-I

Date: 3/31/2011

USGS science for a changing world

GEOVision geophysical services

RECOVERY.GOV

SITE MAP
CE•12076

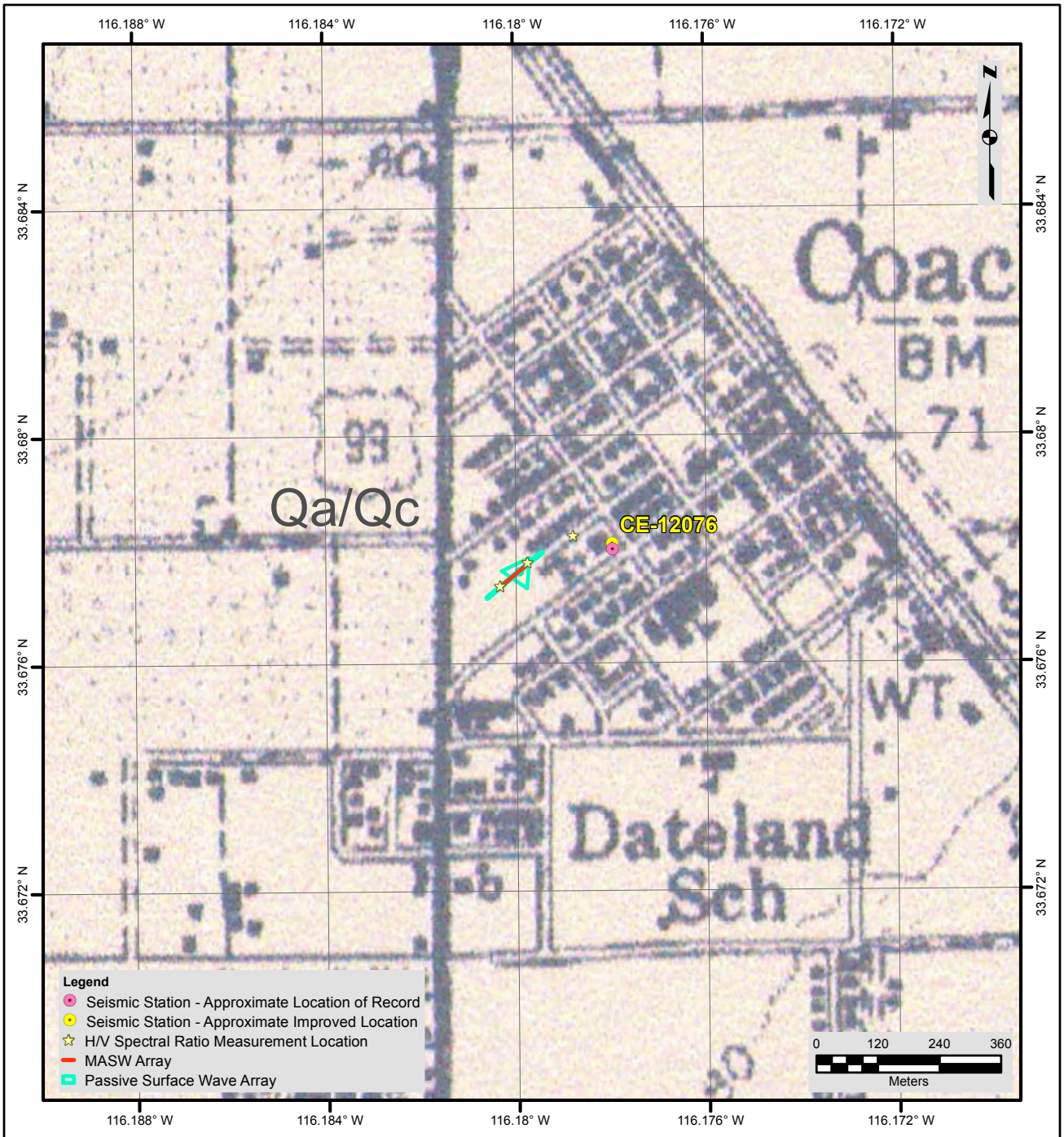

Description of Geologic Map Units

Qa = Quaternary (Holocene) alluvial sand and clay of valleys
Qc = Quaternary (Holocene) clay of playa lakes

NOTES:
1. WGS 1984 COORDINATE SYSTEM
2. Geologic Map of the Palm Desert & Coachella 15 Minute Quadrangles, Riverside County, California By Thomas W. Dibblee, Jr., 2008
3. See site map for details of geophysical survey

File Name: CE-12076

Date: 4/1/2011

USGS science for a changing world

GEOVision geophysical services

RECOVERY.GOV

GEOLOGIC MAP
CE•12076

Looking east from HVSR sensor 453 towards fire station housing CE.12076 seismograph

Looking east from center of passive surface wave array 12076-2 towards fire station

Looking northeast along MASW array 12076-3

Looking northeast along passive surface wave and MASW array 12076-1

1 Hz geophone utilized on passive surface wave array 12076-2

Location of Geophysical Testing Arrays:

Location	Latitude	Longitude
12076-1, Southwest End of Array	33.67716	-116.18063
12076-1, Northeast End of Array	33.67795	-116.17948
12076-2, Corner of Array, Sensor Location 1	33.67732	-116.17980
12076-2, Corner of Array, Sensor Location 3	33.67786	-116.17974
12076-2, Corner of Array, Sensor Location 5	33.67762	-116.18033
12076-2, Center of Array, Sensor Location 10	33.67760	-116.17996
12076-3, Southwest End of Array	33.67735	-116.18036
12076-3, Center of Array	33.67756	-116.18006
12076-3, Northeast of Array	33.67776	-116.17977
HVSR Sensor 507	33.67777	-116.17979
HVSR Sensor 453	33.67823	-116.17883
HVSR Sensor 450	33.67736	-116.18037

Notes: 1) WGS84 Coordinate System (decimal degrees)
2) 12076-3 aligned along 12076-1
3) Typical survey accuracy is estimated at 1 to 2 m

Results:

V_S Model

Depth to Top of Layer (m)	Layer Thickness (m)	S-Wave Velocity (m/s)	Inferred P-Wave Velocity (m/s)	Assumed Poisson's Ratio	Assumed Density (g/cm^3)
0	1	136	254	0.300	1.9
1	2	211	394	0.300	1.9
3	3	231	433	0.300	1.9
6	6	265	496	0.300	1.9
12	6	265	1600	0.486	2.0
18	8	295	1600	0.482	2.0
26	10	340	1600	0.476	2.0
36	12	402	1600	0.466	2.0
48	>12	450	1600	0.457	2.0

Observations/Discussion:

- CE.12076 geophysical survey area located about 200 m from seismograph station where there was more available space for passive surface wave testing and vehicle induced transients could be avoided in HVSR data. The geologic conditions at the test location are the same as those at the seismograph station.
- HVSR curves almost identical at all stations validating the 1-D velocity assumption.
- HVSR peak at about 0.16 Hz, which is consistent with a deep soil site.
- Noise conditions at site are reasonable for successful application of passive surface wave techniques.
- ESAC technique used to extract surface wave dispersion data from passive "L" array data. Both the ReMi™ and ESAC techniques used to extract surface wave dispersion data from the linear arrays. All passive surface wave data used for analysis.
- Surface wave dispersion data from all active and passive surface wave datasets are in excellent agreement at this site.
- As is typical, MASW data provides surface wave dispersion data at smaller wavelengths (higher frequencies) than the passive surface wave data and vice versa.
- MASW data was also acquired along the long, linear passive surface wave arrays to obtain long wavelength surface wave data without concern of near field effects in the frequency range of interest.
- Representative dispersion curves were generated for each surface wave data set using a moving average, polynomial curve fitting routine. These individual representative dispersion curves were combined and a representative dispersion curve generated for the combined data set for data modeling.
- Water table depth constrained at about 12 m based on a simple, 2-layer interactive analysis of seismic refraction data from MASW shot records (400 m/s V_P for unsaturated sediments, 1,600 m/s V_P for saturated sediments).
- Surface wave depth of investigation is about 60 m, based on half of maximum wavelength criteria.
- V_{S30} is 263 m/s (Site Class D).
- Average S-wave velocity of the upper 60 m (V_{S60}) is 319 m/s.

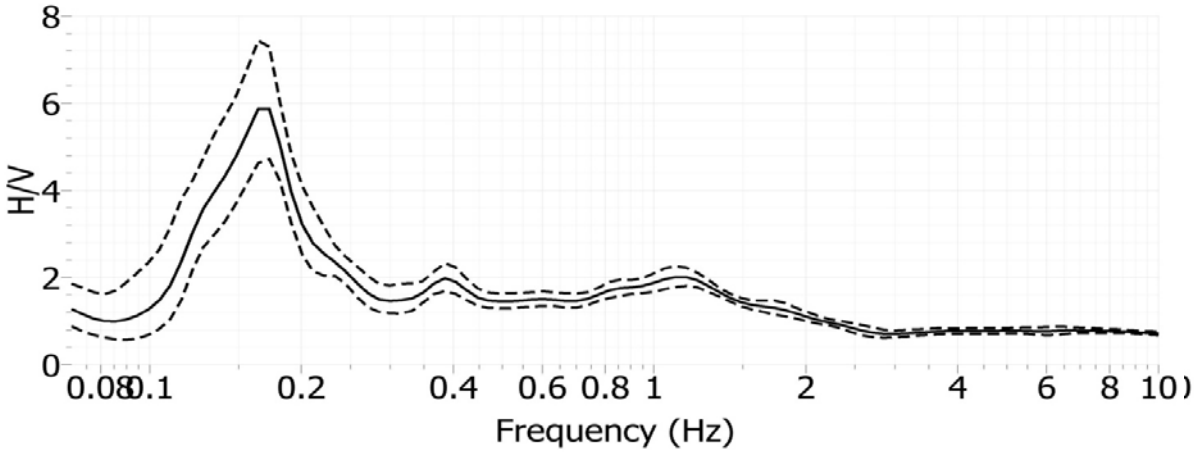

Site CE. 12076, H/V Spectral Ratio, Near Seismic Station, Sensor 453

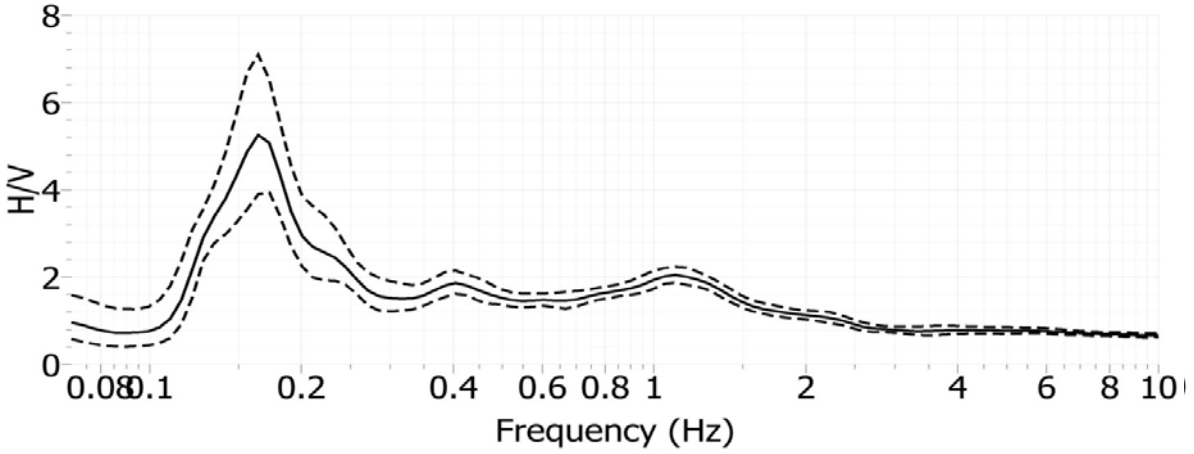

Site CE.12076, H/V Spectral Ratio, Array 12076-3, Sensor 507

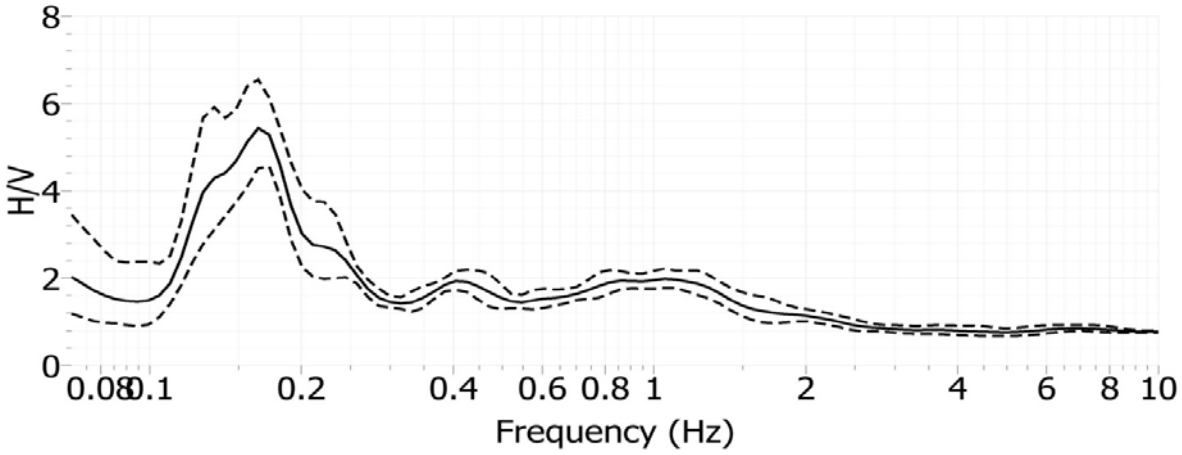

Site CE.12076, H/V Spectral Ratio, Array 12076-3, Sensor 450

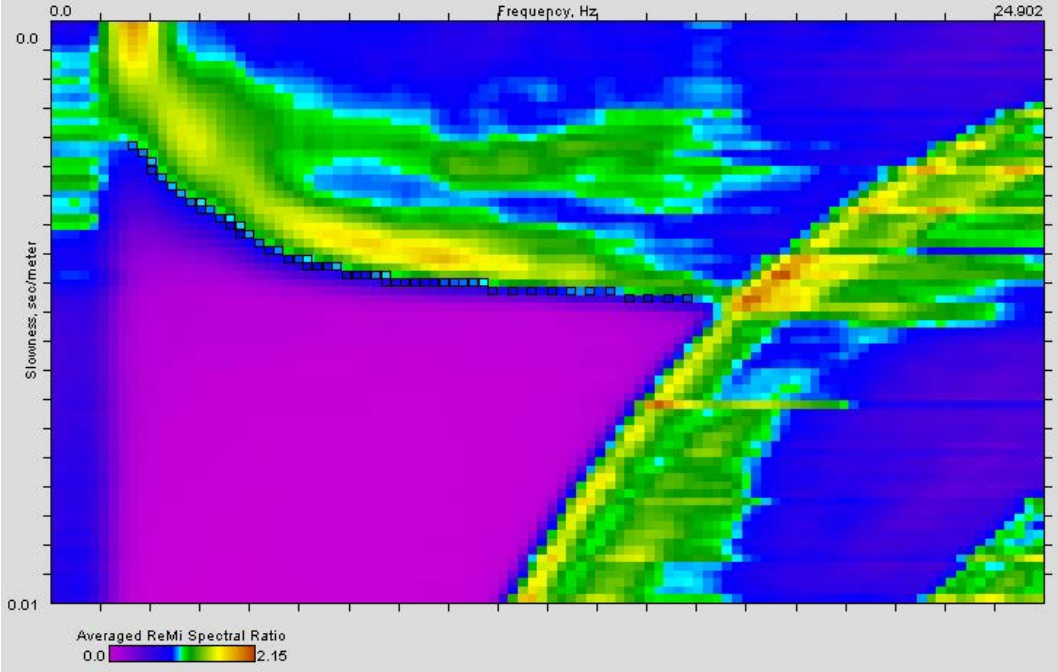

Analysis of passive linear array 12076-1 using ReMi™ technique. Note that dispersion curve picked along lower envelope of surface wave energy in p-f panel.

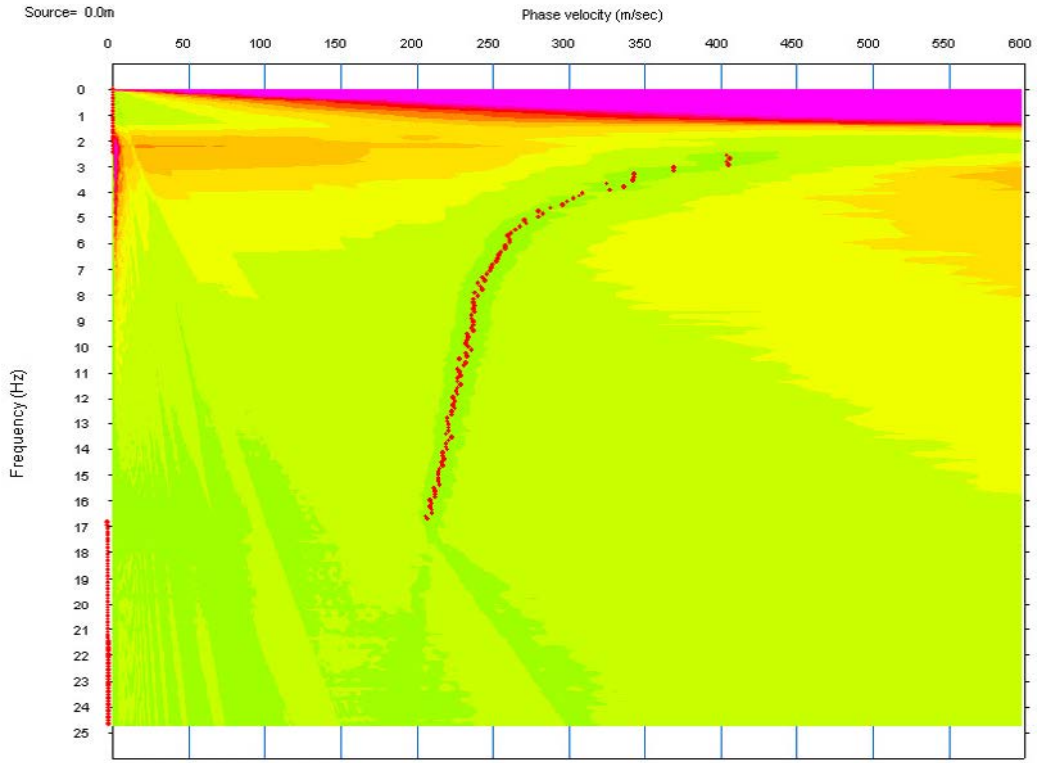

Analysis of passive linear array 12076-1 using ESAC technique. Dispersion curve is best fit of a Bessel function of the first kind and zero order to the SPAC coefficients.

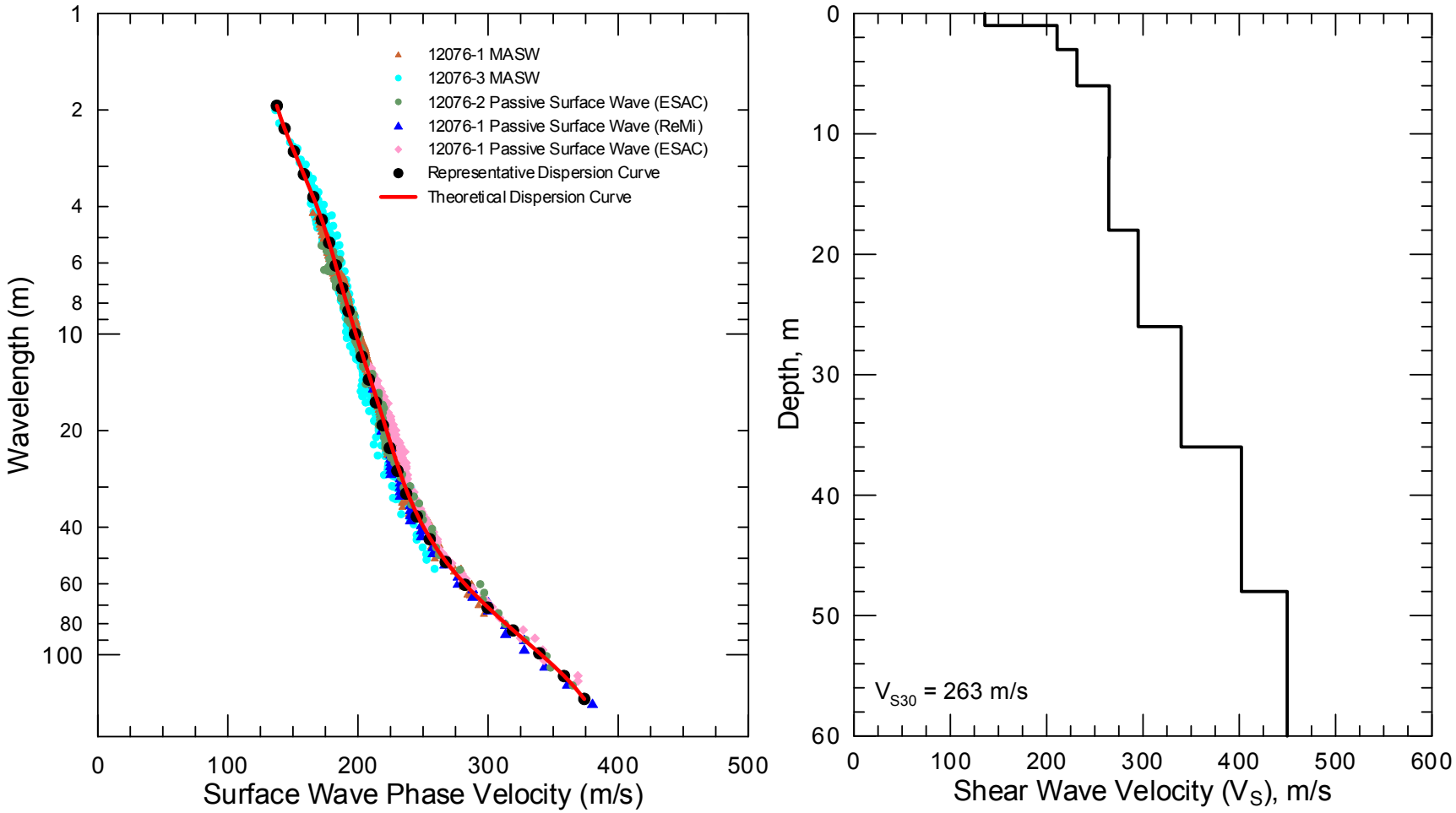

CE.12076 - Field, representative and inverted theoretical surface wave dispersion data (left) and associated V_S model (right)

Site CE.12108

Location: Cathedral City Fire Station 412, 32-100 Desert Vista Road, Cathedral City, California

Latitude: 33.81490 **Longitude:** -116.46120
(Station coordinates modified using published coordinates from http://www.strongmotioncenter.org with an additional adjustment using Google Earth, WGS84 coordinate system)

V_{S30} (measured): 301 m/s

V_{S30} (adjusted to more accurately reflect seismic station conditions): 301 m/s (no adjustment necessary).

NEHRP Site Class: D

Geomatrix Code: AHD

Geologic Conditions/Observations: Quaternary (Holocene) surficial sediments (e.g. wind blown sands) overlying alluvium. Expected deep soil site.

Site Conditions: Urban site with significant traffic noise from nearby roads, particularly the adjacent Ramon Road. Relatively flat terrain in site vicinity.

Geophysical Methods Utilized: HVSR, MASW, array microtremor, ReMi™

Geophysical Testing Arrays:

1. Array 12108-1 (24 channel, linear passive surface wave array utilizing 4.5 Hz vertical geophones spaced 4 m apart for a length of 92 m). Limited MASW data also acquired along array 12108-1.
2. Array 12108-2 (10 channel, triangle passive surface wave array utilizing 1 Hz geophones and a 60 m length for outer side of array).
3. Array 12108-3 (48 channel MASW array utilizing 4.5 Hz vertical geophones spaced 1 m apart for a length of 47 m, forward and reverse shot locations with multiple source offsets and source types and center shot location).
4. Three HVSR measurement stations located near the corners of array 12108-2.

Legend

- Seismic Station - Approximate Improved Location
- Seismic Station - Approximate Location of Record
- H/V Spectral Ratio Measurement Location
- MASW Array
- SASW Array
- Passive Surface Wave Array
- Center of SASW Array

NOTES:
1. WGS 1984 COORDINATE SYSTEM
2. Image Source: ESRI, i-cubed, USDA FSA, USGS, AEX, GeoEye, Getmapping, Aerogrid, IGP

File Name: CE-12108-I

Date: 7/21/2011

USGS science for a changing world

GEOVision geophysical services

RECOVERY.GOV

SITE MAP
CE•12108

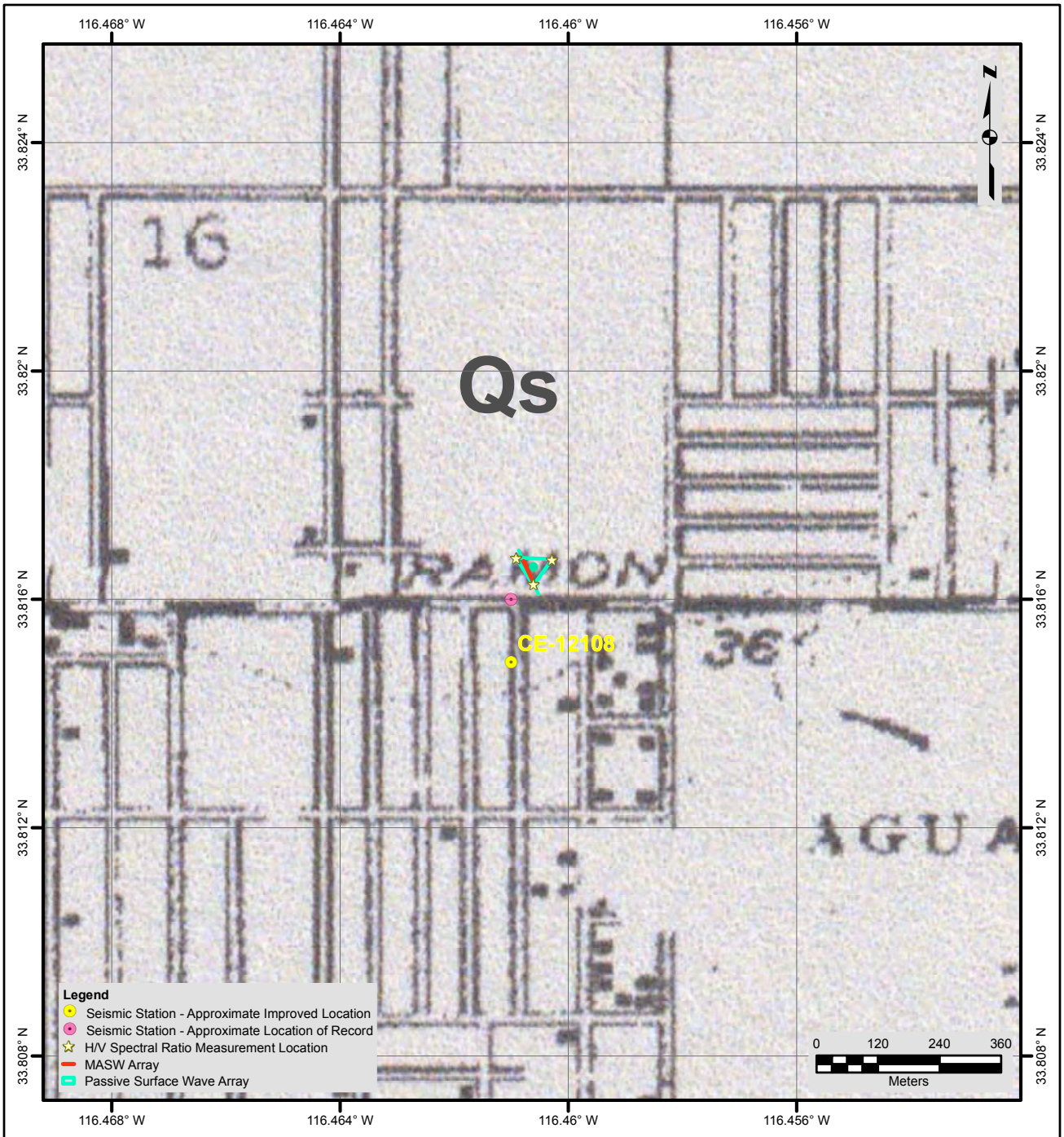

Description of Geologic Map Units

Qs = Quaternary (Holocene) surficial sediments, loose fine sand deposited by prevailing winds as dunes or thin cover over alluvial sand and gravel

NOTES:
1. WGS 1984 COORDINATE SYSTEM
2. Geologic Map of the Thousand Palms & Lost Horse Mountains, Riverside County, California by Thomas W. Dibblee, Jr., 2008
3. See site map for details of geophysical survey

File Name: CE-12108

Date: 4/1/2011

USGS science for a changing world

GEOVision geophysical services

GEOLOGIC MAP
CE•12108

RECOVERY.GOV

Looking south from survey area towards Cathedral City Fire Station 412 and seismic station CE-12108

Passive surface wave testing along arrays 12108-1 and 12108-2

Accelerated weight drop source utilized during MASW testing along array 12108-3

HVSR testing and 1 Hz geophone forming part of passive surface wave array 12108-2

Looking northwest along passive surface wave array 12108-1

Location of Geophysical Testing Arrays:

Location	Latitude	Longitude
12108-1, Southeast End of Array	33.81609	-116.46052
12108-1, Center of Array	33.81648	-116.46070
12108-1, Northwest End of Array	33.81686	-116.46087
12108-2, Corner of Array, Sensor Location 1	33.81671	-116.46028
12108-2, Corner of Array, Sensor Location 3	33.81673	-116.46092
12108-2, Corner of Array, Sensor Location 5	33.81625	-116.46061
12108-2, Center of Array, Sensor Location 10	33.81656	-116.46061
12108-3, Southeast End of Array	33.81628	-116.46061
12108-3, Center of Array	33.81648	-116.46070
12108-3, Northwest End of Array	33.81667	-116.46079
HVSR Sensor 507	33.81669	-116.46029
HVSR Sensor 453	33.81626	-116.46061
HVSR Sensor 450	33.81672	-116.46092

Notes: 1) WGS84 Coordinate System (decimal degrees)
2) Survey accuracy is estimated at 1 to 2 m

Results:

V_S Model

Depth to Top of Layer (m)	Layer Thickness (m)	S-Wave Velocity (m/s)	Inferred P-Wave Velocity (m/s)	Assumed Poisson's Ratio	Assumed Density (g/cm^3)
0	1	146	273	0.300	1.9
1	2	210	394	0.300	1.9
3	3	242	453	0.300	1.9
6	4	274	513	0.300	1.9
10	6	298	558	0.300	1.9
16	8	359	671	0.300	1.9
24	10	436	815	0.300	1.9
34	15	467	1600	0.453	2.0
49	>11	483	1600	0.450	2.0

Observations/Discussion:

- HVSR curves almost identical, validating the 1-D velocity assumption.
- Low frequency HVSR peak in the 0.3 to 0.32 Hz range, which is consistent for a deep soil site.
- Noise conditions at site (multi-directional or omni-directional noise sources) appeared sufficient for successful application of passive surface wave techniques.
- ESAC technique used to extract surface wave dispersion data from passive triangle array data. Both the ReMi™ and ESAC techniques used to extract surface wave dispersion data from the linear array.
- Surface wave dispersion data from active and passive surface wave datasets are in good agreement at this site. MASW phase velocities are slightly lower than those from the passive surface wave arrays over the 25 to 40 m wavelength range.
- Representative dispersion curves were generated for each surface wave data set using a moving average, polynomial curve fitting routine. These individual representative dispersion curves were combined and a representative dispersion curve generated for the combined data set for data modeling.
- Water table located at a depth greater than 30 m based on review of seismic refraction data and probable water table reflection. Simple, interactive layer based modeling indicates that water table reflector may be in the 30 to 35 m depth range with the P-wave RMS velocity of about 575 m/s for sediments overlying the saturated zone.
- Based on simple layer-based analysis of seismic refraction first arrival data, P-wave velocity in upper 20 m ranges from about 275 m/s near the surface to about 650 m/s at a depth on the order of 10 m.
- Surface wave depth of investigation is about 60 m based on half of maximum wavelength criteria.
- Average inferred P-wave velocity in sediments above approximate water table from the surface wave model is consistent with the approximate RMS velocity required to fit the potential water table reflector.
- V_{S30} is 301 m/s (Site Class D).
- Average S-wave velocity of the upper 60 m (V_{S60}) is 367 m/s.

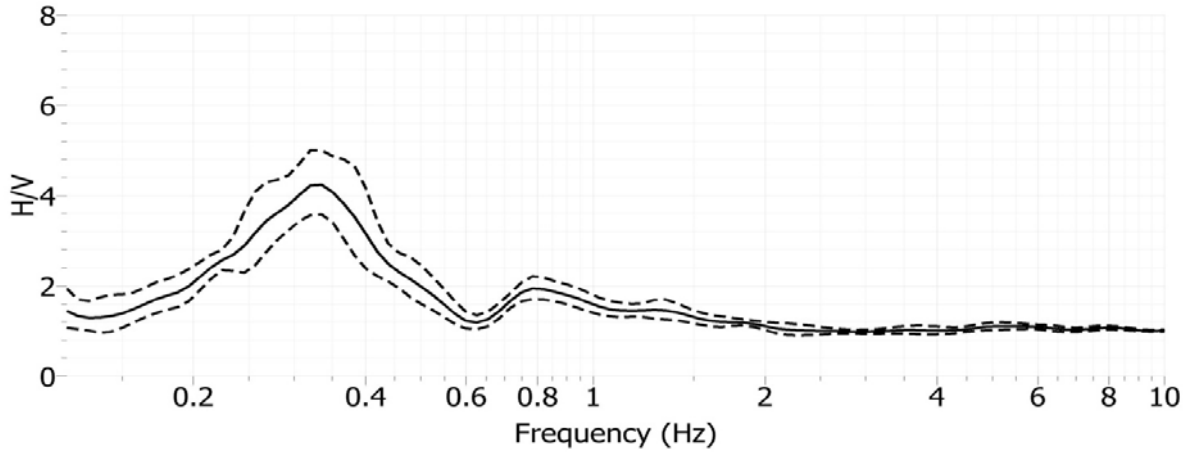

Site CE.12108, H/V Spectral Ratio, Array 12108-2, Sensor 450

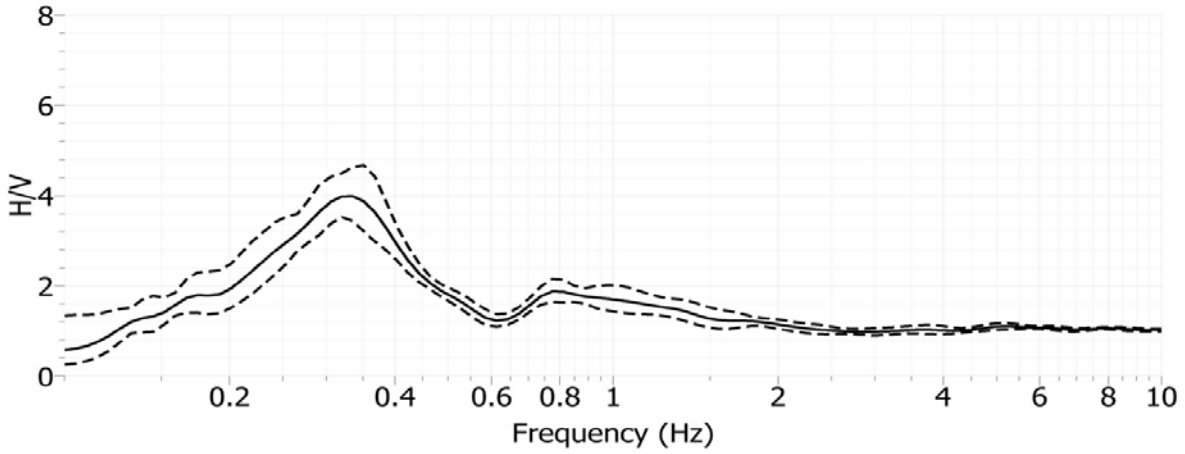

Site CE.12108, H/V Spectral Ratio, Array 12108-2, Sensor 453

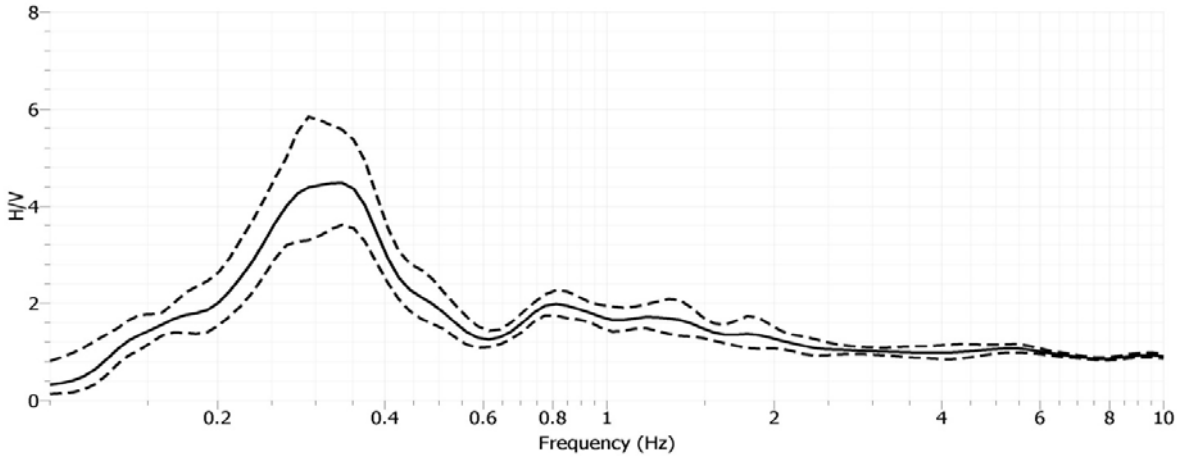

Site CE.12108, H/V Spectral Ratio, Array 12108-2, Sensor 507

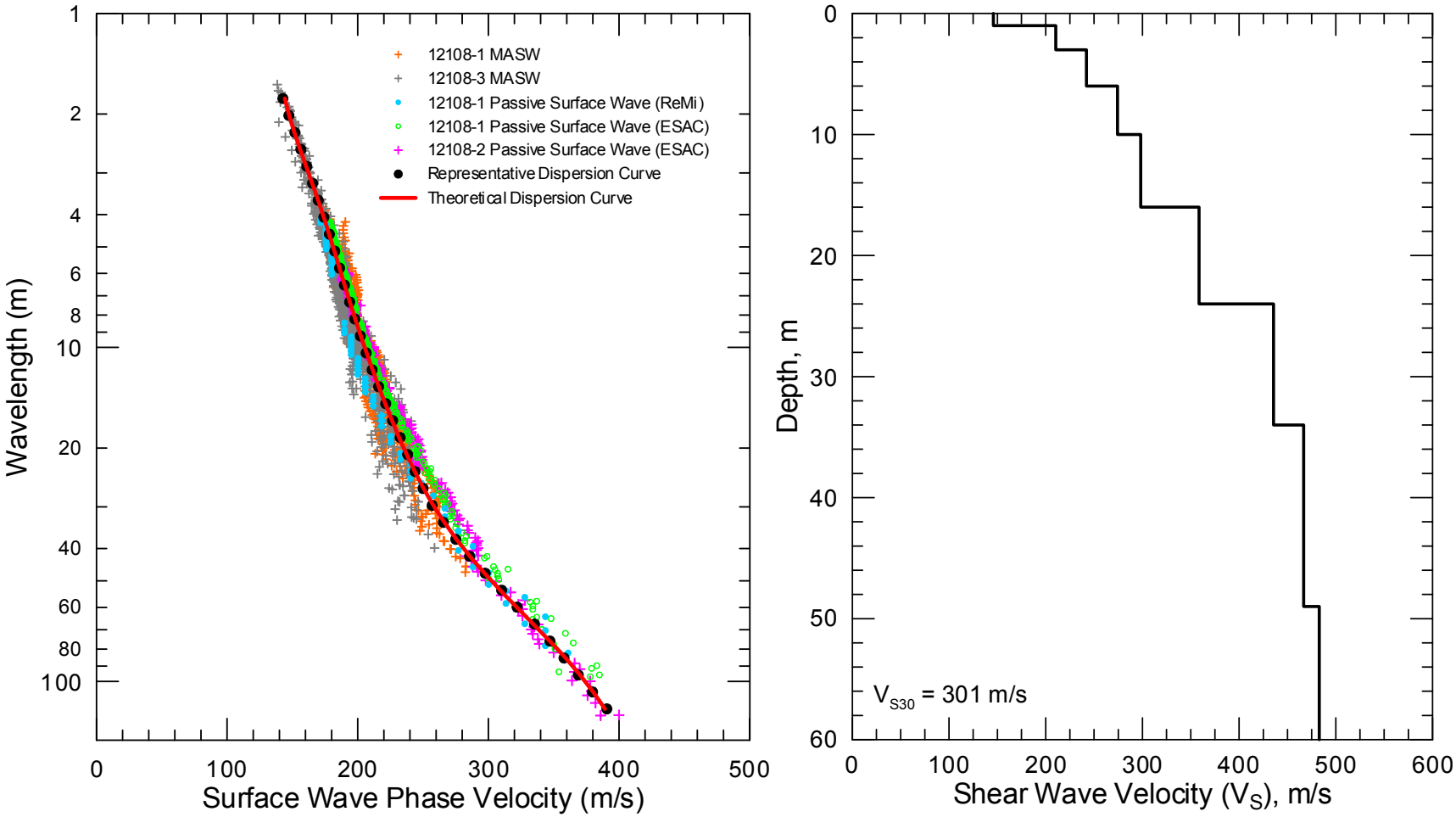

CE.12108 - Field, representative and inverted theoretical surface wave dispersion data (left) and associated V_S model (right)

Site CE.12149

Location: Desert Hot Springs Fire Station 37, 65958 Pierson Blvd., Desert Hot Springs, California

Latitude: 33.96170 **Longitude:** -116.51050
(Station coordinates modified using published coordinates from http://www.strongmotioncenter.org with further adjustment made by identifying the fire station on Google Earth)

V_{S30} (measured): 359 m/s

V_{S30} (adjusted to more accurately reflect seismic station conditions): 385 m/s (based on Oyo PS suspension log, closer to the seismograph station than the surface wave test area).

NEHRP Site Class: D/C

Geomatrix Code: AHD

Geologic Conditions/Observations: Site located in area mapped as Quaternary (Holocene) alluvial sand and gravelly sand deposits. The inferred location of the Mission Creek strand of the San Andreas Fault is located about 0.5 km northeast of the site. Deep soil site.

Site Conditions: Urban site with significant traffic noise from nearby Pierson Blvd. and other nearby roads. Relatively flat terrain in site vicinity with ground surface elevation gently decreasing to south-southeast.

Geophysical Methods Utilized: HVSR, MASW, array microtremor, ReMi™

Geophysical Testing Arrays:

1. Array 12952-1 (48 channel MASW array utilizing 4.5 Hz vertical geophones spaced 1 m apart for a length of 47 m, forward and reverse shot locations with multiple source offsets and source types and center shot location).
2. Array 12952-2 (48 channel, "L" shaped passive surface wave array utilizing 4.5 Hz vertical geophones spaced 3 m apart resulting in lengths of the linear segments of the array of 69 and 72 m). The SPAC technique was used to analyze the "L" array data. Both SPAC and ReMi™ techniques were used to analyze each linear segment of the passive surface wave data.
3. Three HVSR measurement locations distributed in test area. The HVSR measurement locations were offset from array 12149-1 to increase distance from the adjacent street.

Legend

- Seismic Station - Approximate Improved Location
- Seismic Station - Approximate Location of Record
- H/V Spectral Ratio Measurement Location
- MASW Array
- Passive Surface Wave Array

NOTES:
1. WGS 1984 COORDINATE SYSTEM
2. Image Source: ESRI, i-cubed, USDA FSA, USGS, AEX, GeoEye, Getmapping, Aerogrid, IGP

File Name: CE-12149-I

Date: 4/1/2011

USGS science for a changing world

GEOVision geophysical services

RECOVERY.GOV

SITE MAP
CE•12149

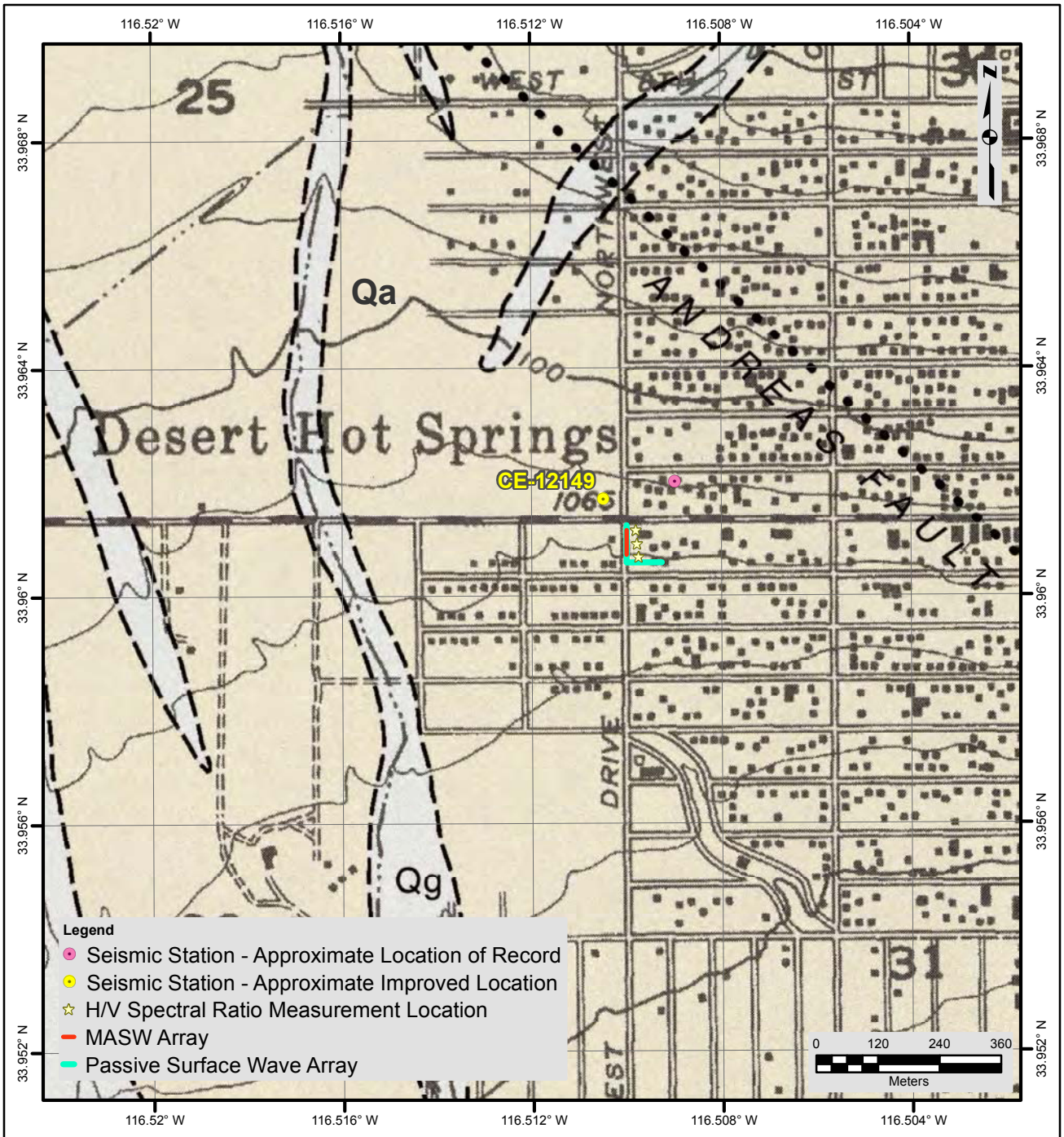

Description of Geologic Map Units

Qg = Quaternary (Holocene) alluvial sand and gravelly sand of stream channel washes
Qa = Quaternary (Holocene) alluvial sand and gravel of valley areas

NOTES:
1. WGS 1984 COORDINATE SYSTEM
2. Geologic Map and Sections of the Desert Hot Springs Area, Riverside County, California by Richard J. Proctor, 1968
3. See site map for details of geophysical survey

File Name: CE-12149

Date: 7/21/2011

USGS science for a changing world

GEOVision geophysical services

GEOLOGIC MAP
CE•12149

RECOVERY.GOV

Looking northwest towards HVSR sensor 450 and Desert Hot Springs Fire Station 37

Looking northwest towards HVSR test locations

Looking northwest towards center of MASW array 12149-1 and Desert Hot Springs Fire Station 37

Looking northwest from corner of array 12149-2 towards fire station housing seismic station CE-12149

Various hammers used for MASW testing on array 12149-1

Location of Geophysical Testing Arrays:

Location	Latitude	Longitude
12149-1, South End of Array	33.96072	-116.51002
12149-1, Center of Array	33.96094	-116.51002
12149-1, North End of Array	33.96115	-116.51001
12149-2, Northwest End of Array, Channel 1	33.96124	-116.51001
12149-2, Southwest Corner of Array, Channel 25	33.96058	-116.51002
12149-2, Southeast End of Array, Channel 48	33.96058	-116.50927
HVSR Sensor 507	33.96068	-116.50977
HVSR Sensor 453	33.96091	-116.50980
HVSR Sensor 450	33.96115	-116.50982

Notes: 1) WGS84 Coordinate System (decimal degrees)
2) Survey accuracy is estimated at 1 to 2 m

Results:

V_S Model

Depth to Top of Layer (m)	Layer Thickness (m)	S-Wave Velocity (m/s)	Inferred P-Wave Velocity (m/s)	Inferred Poisson's Ratio	Inferred Density (g/cm^3)
0	1.25	183	343	0.3	1.9
1.25	1.75	294	549	0.3	1.9
3	7	307	575	0.3	1.9
10	12	389	728	0.3	1.9
22	12	468	876	0.3	2.0
34	20	524	981	0.3	2.0
54	>1	604	1131	0.3	2.0

Observations/Discussion:

- HVSR curves are similar although there is no clear peak. HVSR data quality map be negatively impacted by transients (constant vehicle traffic within 15 m of sensors) and possibly sensor coupling and moderate winds. Making the HVSR measurements when there is less traffic may improve results.
- HVSR data quality appears to be best at sensor location 453 although there is still noise at very low frequencies possibly associated with sensor coupling.
- HVSR sensor 453 and to a lesser degree 450 reveals a low amplitude HVSR peak at about 0.4, which is consistent for a deep soil site.

- Noise conditions at site (multi-directional or omni-directional noise sources) appeared sufficient for successful application of passive surface wave techniques.
- Surface wave dispersion data from active and passive surface wave datasets are in good agreement at this site.
- SPAC technique used to extract surface wave dispersion data from passive "L" array data. Both the ReMi™ and SPAC techniques used to extract surface wave dispersion data from the linear array with the SPAC technique providing dispersion data in better agreement with that from the "L" array. Only passive surface wave dispersion data obtained using SPAC technique used for data modeling.
- Representative dispersion curves were generated for each surface wave data set using a moving average, polynomial curve fitting routine. These individual representative dispersion curves were combined and a representative dispersion curve generated for the combined data set for data modeling.
- Water table located at a depth greater than 30 m based on review of seismic refraction data. No obvious water table reflector by which to identify approximate water table depth. The Mission Creek Fault, located about 0.5 km northeast of the site, is documented in other areas as forming a groundwater barrier and, therefore, the water table could be quite deep at the site.
- Based on simple layer-based analysis of seismic refraction first arrival data, P-wave velocity in the upper 15 m ranges from about 375 m/s at the surface to over 575 m/s at a depth on the order of 7 m.
- Surface wave depth of investigation is about 55 m based on half of maximum wavelength criteria.
- V_{S30} is 359 m/s (Site Class D/C).
- Average S-wave velocity of the upper 55 m (V_{S55}) is 417 m/s.
- Oyo PS suspension log previously acquired in 100 m borehole in Desert Hot Springs Fire Station, about 150 m north of geophysical test area. V_{S30} developed from the PS log higher resolution receiver to receiver analysis is 385 m/s (Site Class C), about 7% higher than surface wave sounding. V_{S30} developed from the PS log lower resolution receiver to receiver analysis is 372 m/s (Site Class C), about 4% higher than surface wave sounding. These differences may be due to relative error/scatter between the two methods although the possibility cannot be discounted that V_{S30} gradually decreases to the south or that geologic layers deepen the south.
- Surface wave Vs model is similar to Oyo PS suspension log Vs, particularly source to receiver analysis, in upper 30 m but has lower Vs below a 30 m depth. Shallow dip to the south of the deeper geologic units is a possible explanation for the difference as the surface wave testing was conducted about 150 m south of the borehole.
- Increasing the velocity of the upper layer from 183 to 240 m/s, which is likely on the engineered pad for the Desert Hot Springs Fire Station and supported by PS suspension log, would increase V_{S30} to 366 m/s.
- A surface wave sounding north of Pierson Blvd. would determine if V_{S30} increases to north. A shallow MASW or SASW sounding in the fire station parking lot would determine if shallow soils have higher velocities than in the test area.

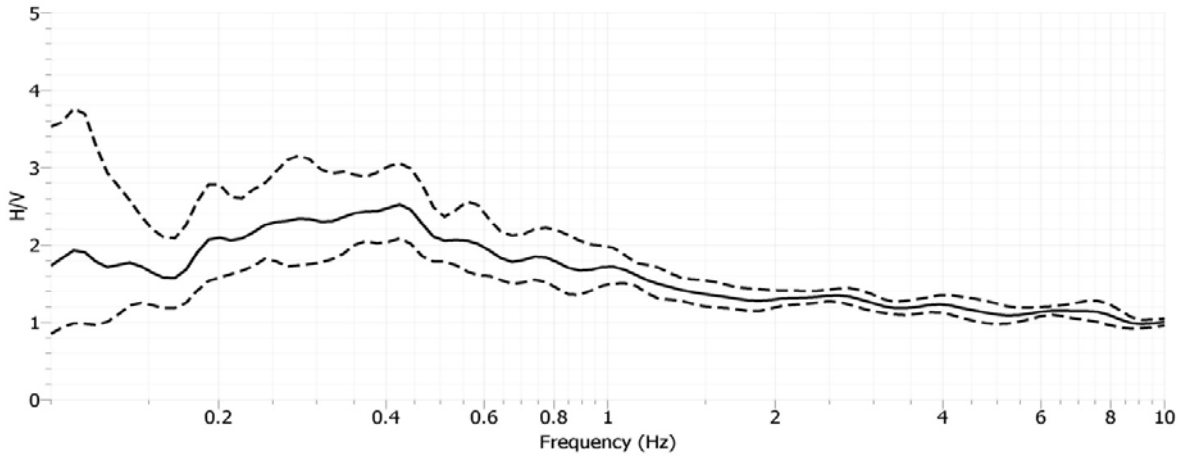

Site CE.12149, H/V Spectral Ratio, Array 12149-1, Sensor 450

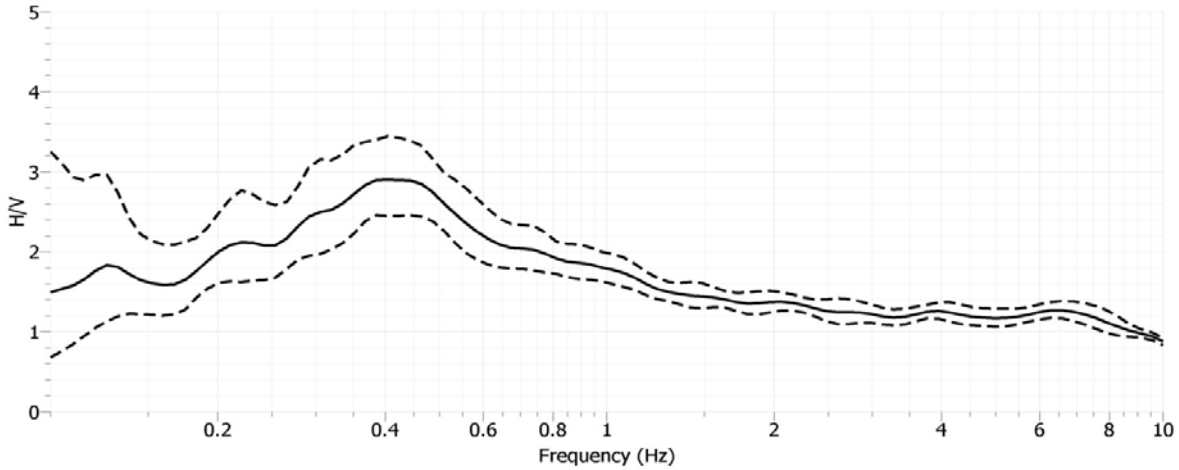

Site CE.12149, H/V Spectral Ratio, Array 12149-1, Sensor 453

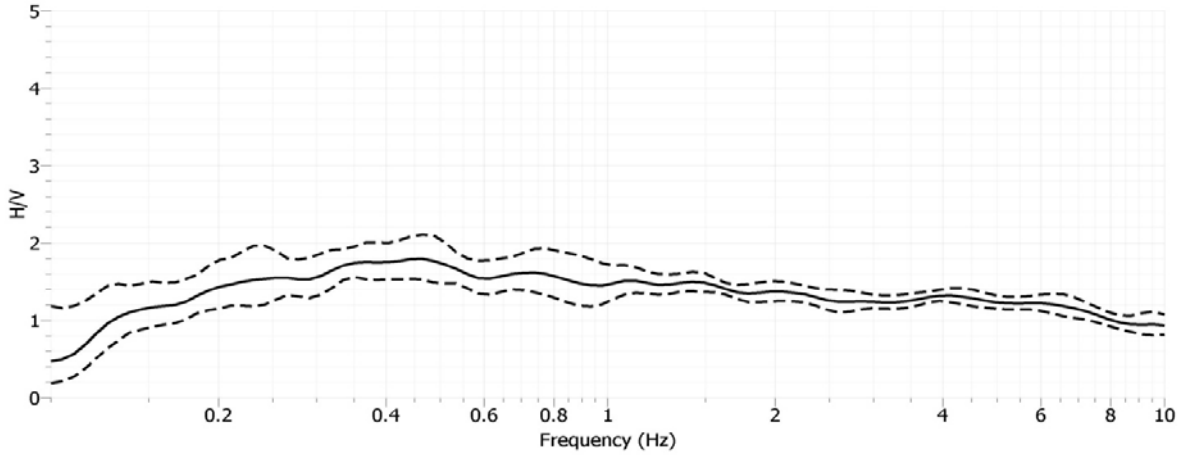

Site CE.12149, H/V Spectral Ratio, Array 12149-1, Sensor 507

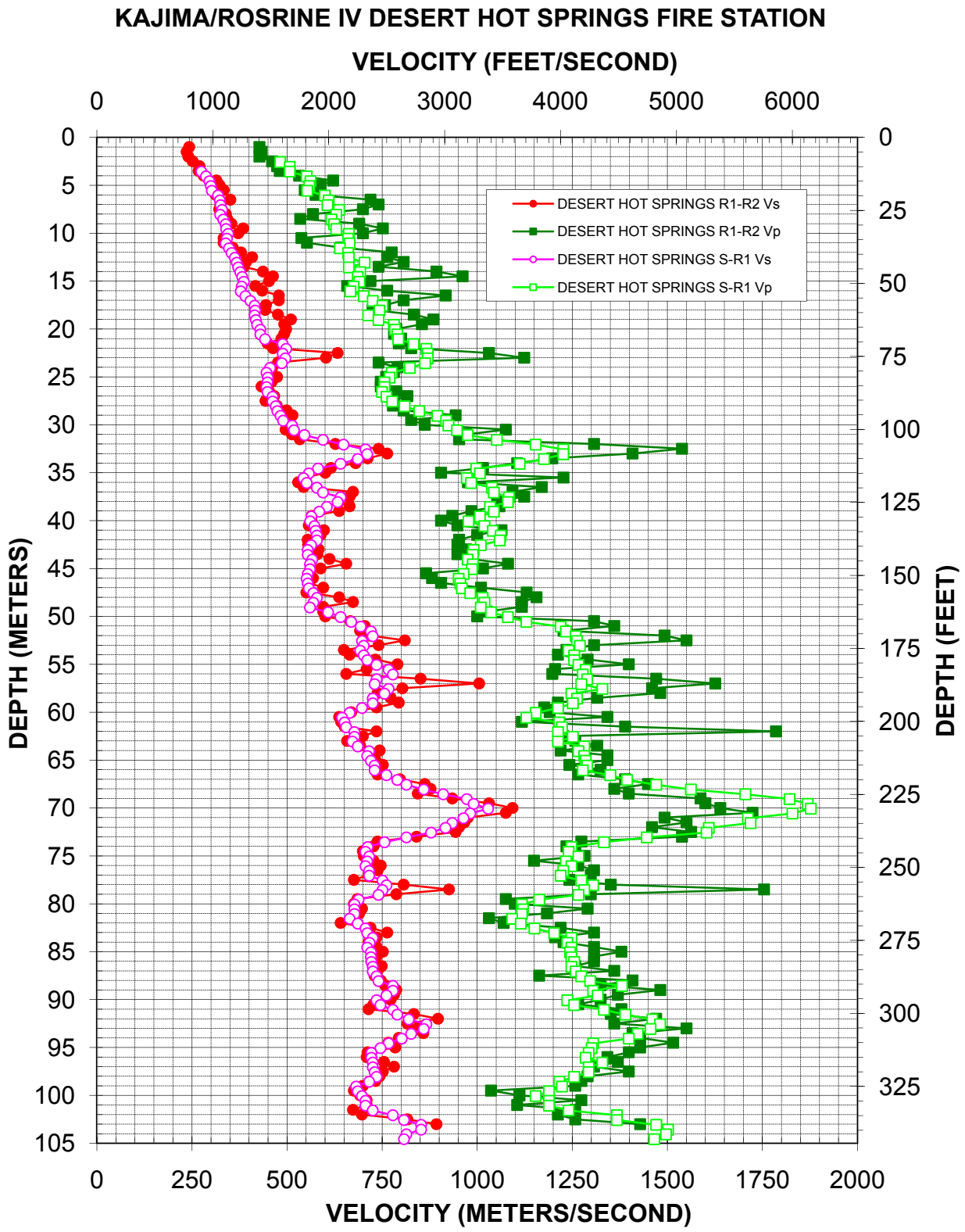

CE.12149- Oyo PS suspension log conducted as part of the Kajima/Rosrine Project. Source to receiver (S-R1) and receiver to receiver (R1-R2) analysis.

CE.12149- Oyo PS suspension log conducted as part of the Kajima/Rosrine Project. Receiver to Receiver (R1-R2) analysis.

DEPTH (M)	Vs (M/SEC)	Vp (M/SEC)	DEPTH (M)	Vs (M/SEC)	Vp (M/SEC)	DEPTH (M)	Vs (M/SEC)	Vp (M/SEC)
1	243	427	20	498	787	39	637	985
1.5	236	433	20.5	493	781	39.5	565	935
2	240	427	21	485	800	40	563	905
2.5	252	461	21.5	448	794	40.5	557	948
3	270	474	22	463	826	41	597	1064
3.5	267	481	22.5	633	1031	41.5	588	1000
4	281	532	23	602	1124	42	554	952
4.5	314	621	23.5	476	741	42.5	556	948
5	323	588	24	461	791	43	583	971
5.5	333	546	24.5	456	781	43.5	580	948
6	313	575	25	474	760	44	612	980
6.5	351	719	25.5	460	746	44.5	656	1081
7	325	741	26	433	746	45	588	1015
7.5	322	699	26.5	452	787	45.5	560	866
8	339	568	27	466	816	46	568	881
8.5	342	535	27.5	443	781	46.5	557	905
9	353	690	28	473	778	47	595	1010
9.5	385	752	28.5	499	806	47.5	551	1130
10	372	699	29	514	943	48	637	1156
10.5	333	538	29.5	496	826	48.5	673	1117
11	333	552	30	506	862	49	595	1117
11.5	357	641	30.5	496	1075	49.5	595	1026
12	379	775	31	513	971	50	601	1000
12.5	408	763	31.5	533	952	50.5	667	1307
13	392	806	32	627	1307	51	704	1361
13.5	386	741	32.5	741	1538	51.5	692	1227
14	437	893	33	763	1408	52	717	1493
14.5	463	962	33.5	712	1198	52.5	810	1550
15	452	719	34	680	1105	53	741	1307
15.5	417	658	34.5	615	1015	53.5	649	1235
16	435	763	35	601	905	54	664	1212
16.5	478	917	35.5	549	1227	54.5	733	1290
17	478	806	36	529	976	55	791	1399
17.5	444	758	36.5	543	1170	55.5	709	1205
18	442	725	37	673	1093	56	656	1198
18.5	476	833	37.5	664	1124	56.5	851	1471
19	510	885	38	637	1053	57	1005	1626
19.5	493	855	38.5	664	1058	57.5	803	1460

CE.12149- Oyo PS suspension log conducted as part of the Kajima/Rosrine Project.
Receiver to receiver (R1-R2) analysis (cont.)

DEPTH (M)	Vs (M/SEC)	Vp (M/SEC)	DEPTH (M)	Vs (M/SEC)	Vp (M/SEC)	DEPTH (M)	Vs (M/SEC)	Vp (M/SEC)
58	738	1481	77	714	1299	96	709	1342
58.5	772	1316	77.5	676	1242	96.5	755	1370
59	794	1212	78	806	1351	97	781	1307
59.5	735	1176	78.5	926	1754	97.5	752	1399
60	669	1190	79	787	1299	98	743	1290
60.5	637	1342	79.5	685	1075	98.5	733	1274
61	642	1117	80	676	1099	99	699	1258
61.5	651	1389	80.5	697	1290	99.5	676	1036
62	735	1786	81	690	1183	100	692	1111
62.5	699	1227	81.5	671	1031	100.5	709	1274
63	658	1258	82	641	1070	101	709	1105
63.5	692	1316	82.5	719	1220	101.5	673	1258
64	743	1220	83	763	1307	102	697	1212
64.5	727	1342	83.5	735	1205	102.5	816	1258
65	733	1342	84	714	1227	103	893	1429
65.5	752	1242	84.5	735	1307			
66	738	1325	85	752	1379			
66.5	738	1266	85.5	735	1307			
67	797	1389	86	722	1307			
67.5	862	1449	86.5	749	1258			
68	877	1361	87	738	1361			
68.5	844	1399	87.5	730	1163			
69	935	1587	88	746	1408			
69.5	1031	1600	88.5	758	1325			
70	1093	1639	89	787	1481			
70.5	1075	1724	89.5	781	1370			
71	976	1493	90	772	1325			
71.5	966	1550	90.5	727	1266			
72	952	1460	91	714	1379			
72.5	943	1563	91.5	833	1351			
73	840	1538	92	897	1471			
73.5	738	1274	92.5	816	1361			
74	727	1235	93	844	1550			
74.5	699	1258	93.5	858	1408			
75	702	1282	94	794	1429			
75.5	727	1149	94.5	766	1515			
76	746	1266	95	784	1429			
76.5	738	1307	95.5	712	1399			

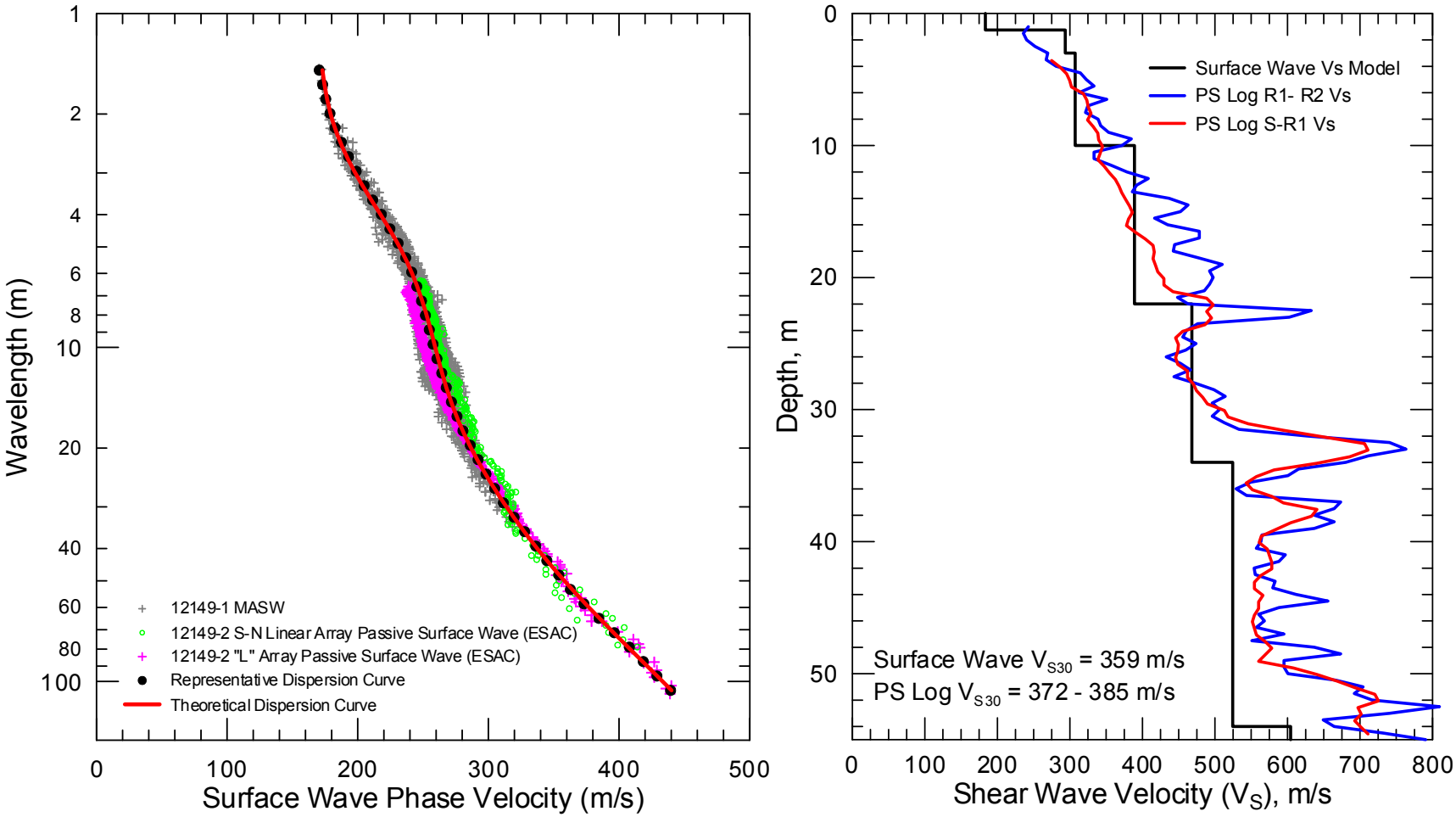

CE.12149 - Field, representative and inverted theoretical surface wave dispersion data (left) and associated V_S model (right)

Site CE.12952

Location: North Palm Desert Fire Station 37, 73995 Country Club Drive, Palm Desert, California

Latitude: 33.75770 **Longitude:** -116.37400
(Station coordinates modified using published coordinates from http://www.strongmotioncenter.org, WGS84 coordinate system.)

V_{S30} (measured): 274 m/s

V_{S30} (adjusted to more accurately reflect seismic station conditions): 274 m/s (no adjustment necessary).

NEHRP Site Class: D

Geomatrix Code: AHD

Geologic Conditions/Observations: Quaternary (Holocene) surficial sediments overlying alluvium, deep soil site.

Site Conditions: Urban site with significant traffic noise from nearby Country Club Road and Portola Avenue. Relatively flat terrain in site vicinity.

Geophysical Methods Utilized: HVSR, MASW, array microtremor, ReMi™

Geophysical Testing Arrays:

1. Array 12952-1 (24 channel, linear passive surface wave array utilizing 4.5 Hz vertical geophones spaced 4 m apart for a length of 92 m).
2. Array 12952-2 (10 channel, triangle passive surface wave array utilizing 1 Hz geophones and a 60 m length for outer side of array).
3. Array 12952-3 (48 channel MASW array utilizing 4.5 Hz vertical geophones spaced 1.5 m apart for a length of 70.5 m, forward and reverse shot locations with multiple source offsets and source types and center shot location).
4. Three HVSR measurement locations distributed along arrays 12952-1, 12952-2 and 12952-3.

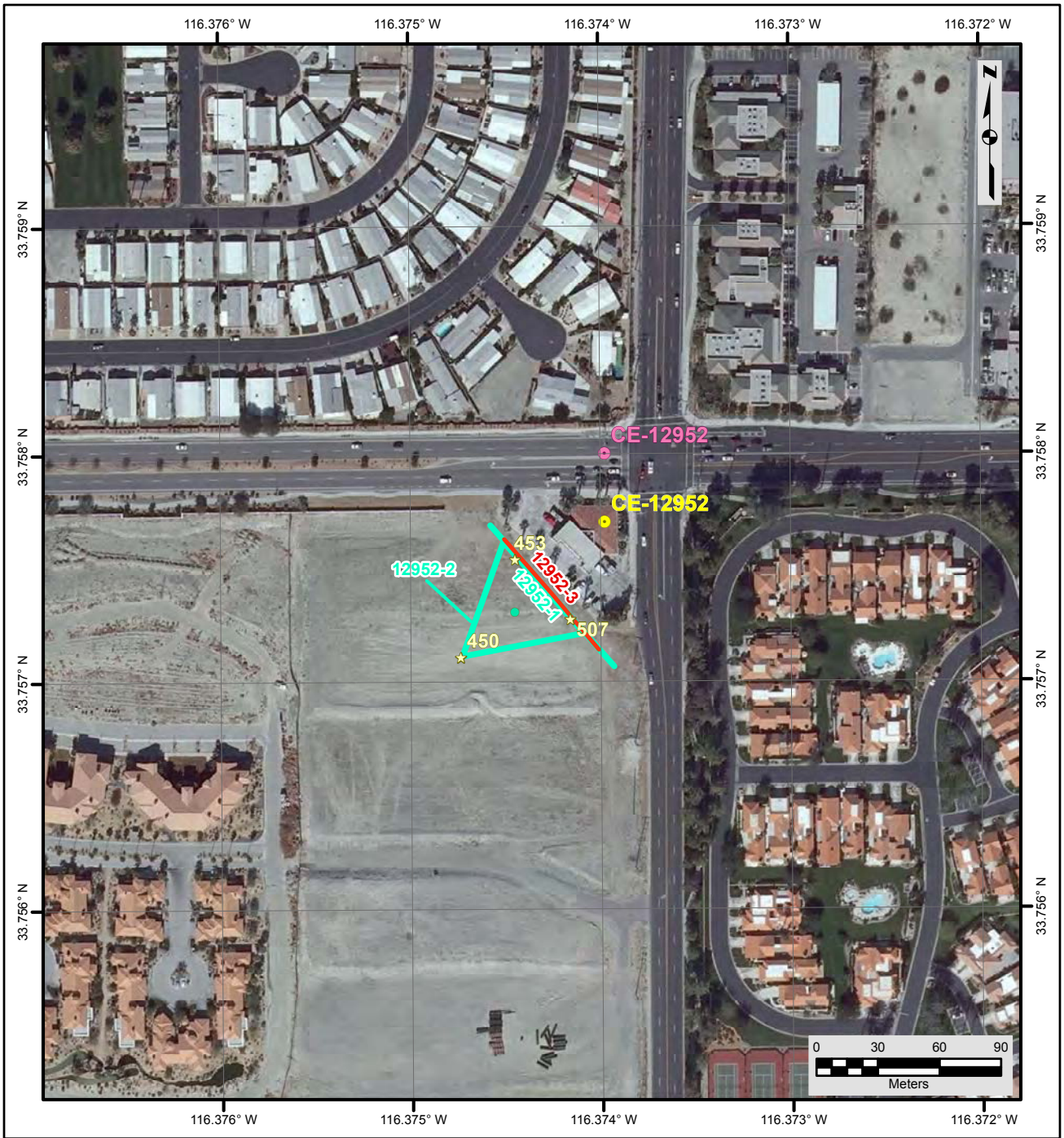

Legend

- Seismic Station - Approximate Location of Record
- Seismic Station - Approximate Improved Location
- H/V Spectral Ratio Measurement Location
- MASW Array
- Passive Surface Wave Array

NOTES:
1. WGS 1984 COORDINATE SYSTEM
2. Image Source: ESRI, i-cubed, USDA FSA, USGS, AEX, GeoEye, Getmapping, Aerogrid, IGP

USGS science for a changing world
GEOVision geophysical services

RECOVERY.GOV

SITE MAP
CE•12952

File Name: CE-12952-I

Date: 4/7/2011

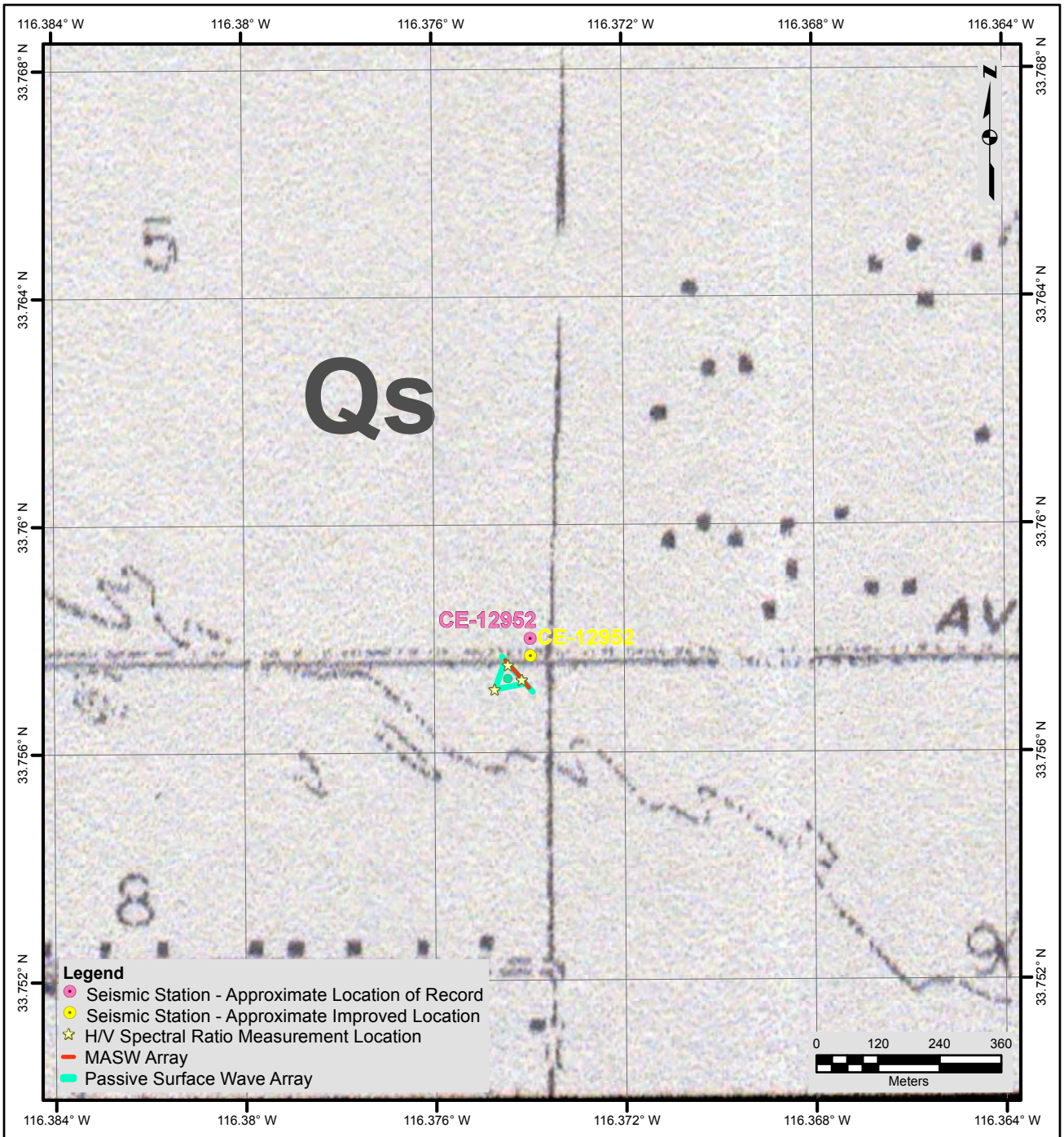

Description of Geologic Map Units

Qs = Quaternary (Holocene) surficial sediments, loose fine sand deposited by prevailing winds as dunes or thin cover over alluvial sand and gravel

NOTES:
1. WGS 1984 COORDINATE SYSTEM
2. Geologic Map of the Thousand Palms & Lost Horse Mountains, Riverside County, California by Thomas W. Dibblee, Jr., 2008
3. See site map for details of geophysical survey

File Name: CE-12952

Date: 4/1/2011

USGS science for a changing world

GEOVision geophysical services

GEOLOGIC MAP
CE•12952

RECOVERY.GOV

Looking northeast from survey area towards North Palm Desert Fire Station 71 housing seismograph station CE-12952

Looking northwest along passive surface wave array 12952-1 and one site of passive surface wave array 12952-2

MASW array 12952-3

Looking northeast towards fire station from HVSR sensor 450 and corner of array 12952-2

Data acquisition along MASW array 12952-3

Location of Geophysical Testing Arrays:

Location	Latitude	Longitude
12952-1, Northwest End of Array	33.75769	-116.37460
12952-1, Southeast End of Array	33.75707	-116.37395
12952-2, Corner of Array, Sensor Location 1	33.75721	-116.37411
12952-2, Corner of Array, Sensor Location 3	33.75761	-116.37453
12952-2, Corner of Array, Sensor Location 5	33.75711	-116.37475
12952-2, Center of Array, Sensor Location 10	33.75731	-116.37448
12952-3, Northwest End of Array	33.75763	-116.37453
12952-3, Center of Array	33.75739	-116.37428
12952-3, Southeast End of Array	33.75714	-116.37403
HVSR Sensor 507	33.75727	-116.37418
HVSR Sensor 453	33.75754	-116.37447
HVSR Sensor 450	33.75711	-116.37476

Notes: 1) WGS84 Coordinate System (decimal degrees)
2) Survey accuracy is estimated at 1 to 2 m

Results:

V_S Model

Depth to Top of Layer (m)	Layer Thickness (m)	S-Wave Velocity (m/s)	Inferred P-Wave Velocity (m/s)	Assumed Poisson's Ratio	Assumed Density (g/cm^3)
0	0.75	189	353	0.3	1.9
0.75	1	219	409	0.3	1.9
1.75	2.25	194	363	0.3	1.9
4	5	258	482	0.3	1.9
9	8	283	530	0.3	1.9
17	12	307	573	0.3	1.9
29	15	399	747	0.3	2.0
44	>16	468	875	0.3	2.0

Observations/Discussion:

- HVSR curves almost identical, validating the 1-D velocity assumption.
- Low frequency HVSR peak in the 0.38 to 0.4 Hz range, which is consistent for a deep soil site.
- Surface wave dispersion data from active and passive surface wave datasets are in good agreement at this site.
- Noise conditions at site (multi-directional or omni-directional noise sources) appeared sufficient for successful application of passive surface wave techniques.
- ESAC technique used to extract surface wave dispersion data from passive triangle array data. Both the ReMi™ and ESAC techniques used to extract surface wave dispersion data from the linear array with the ESAC technique providing dispersion data in better agreement with that from the triangle array and MASW data, particularly at small wavelengths. Therefore, ReMi™ surface wave dispersion data not used for data analysis.
- Representative dispersion curves were generated for each surface wave data set using a moving average, polynomial curve fitting routine. These individual representative dispersion curves were combined and a representative dispersion curve generated for the combined data set for data modeling.
- Water table located at a depth greater than 30 m based on review of seismic refraction data and possible water table reflection. Simple, interactive layer based modeling indicates that the possible water table reflector may be as deep as 80 m with an approximate 625 m/s P-wave RMS velocity for the 80 m of sediments overlying the saturated zone.
- Based on simple layer-based analysis of seismic refraction first arrival data, P-wave velocity in upper 20 m ranges from about 315 m/s near the surface to about 475 m/s at a depth on the order of 10 m. P-wave velocity may exceed 600 m/s at a depth greater than 20 m.
- Surface wave depth of investigation is about 60 m based on half of maximum wavelength criteria.
- V_{S30} is 274 m/s (Site Class D).
- Average S-wave velocity of the upper 60 m (V_{S60}) is 336 m/s.

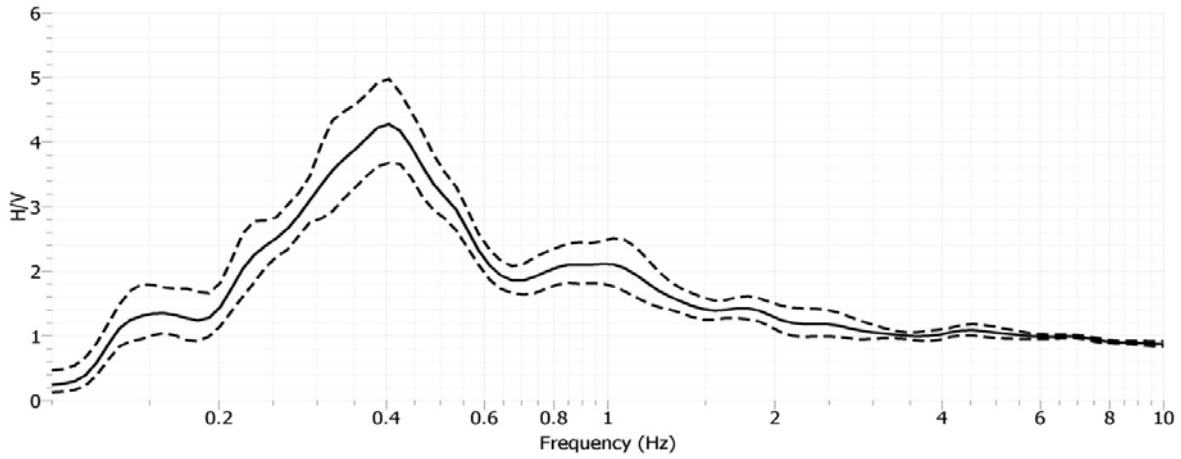

Site CE.12952, H/V Spectral Ratio, Array 12952-2, Sensor 450

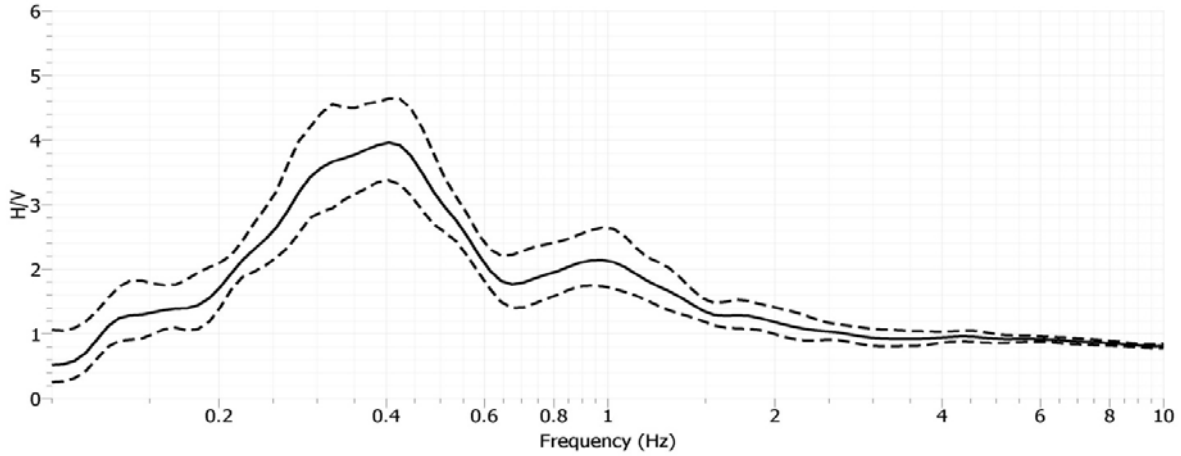

Site CE.12952, H/V Spectral Ratio, Array 12952-1, Sensor 453

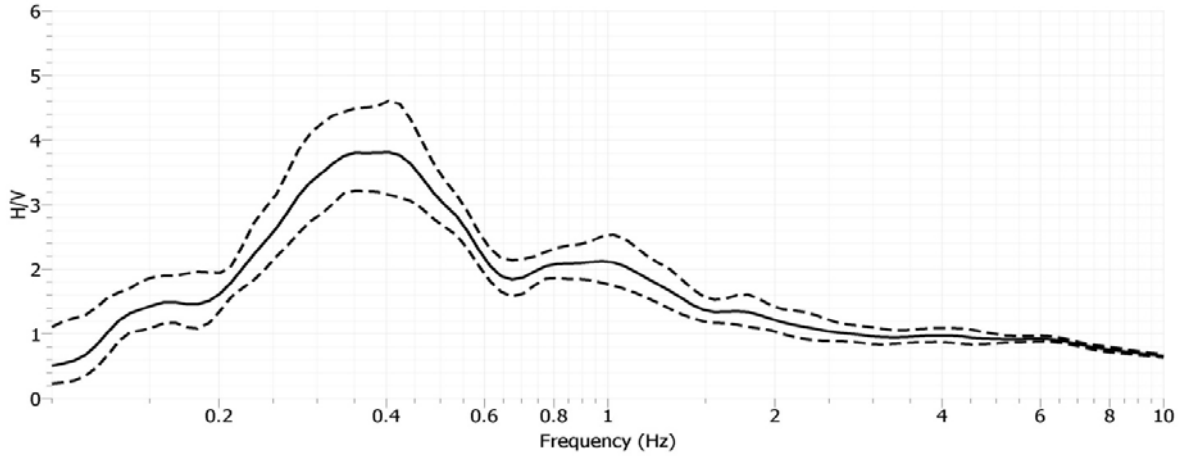

Site CE.12952, H/V Spectral Ratio, Array 12952-1, Sensor 507

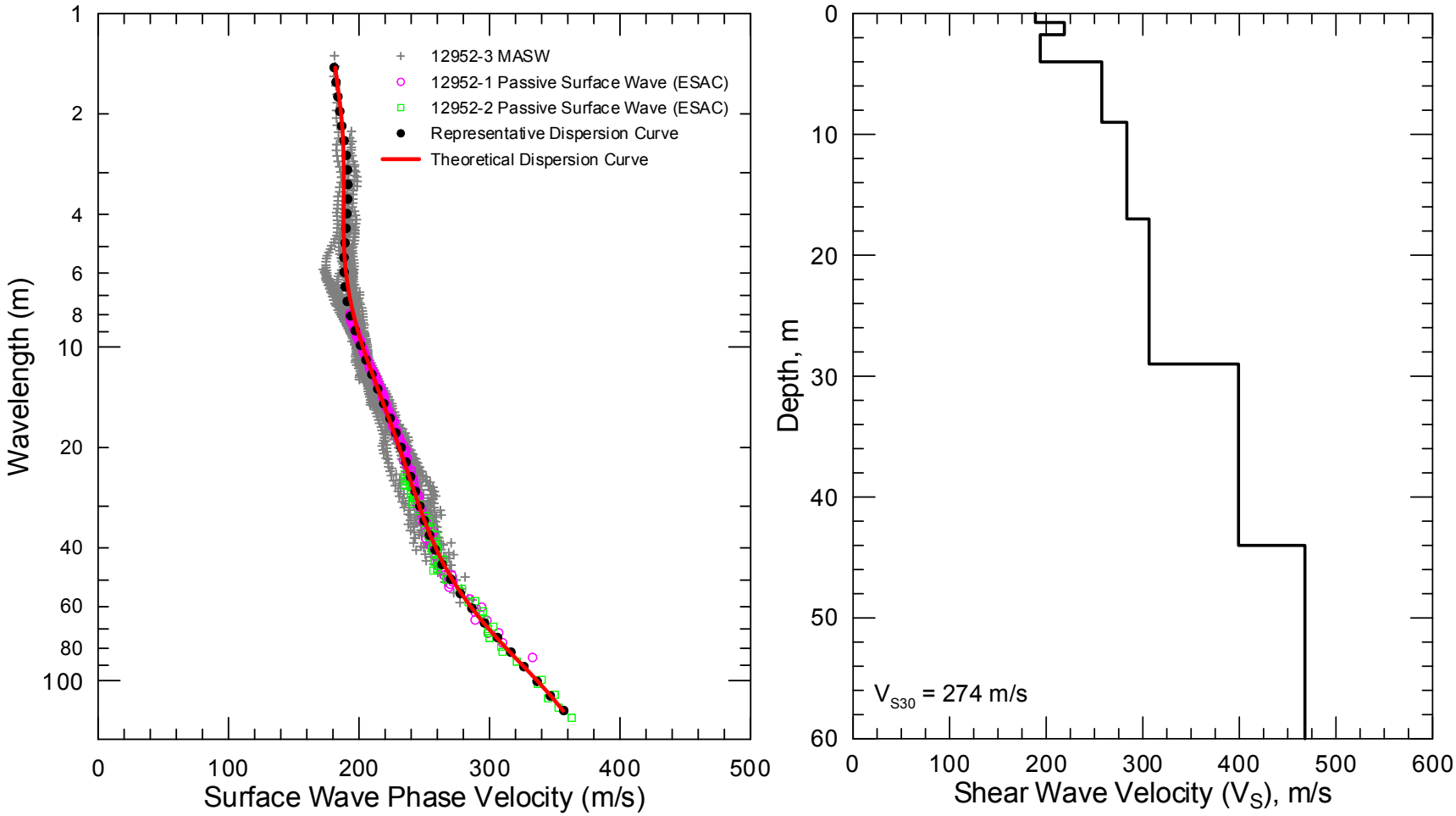

CE.12952 - Field, representative and inverted theoretical surface wave dispersion data (left) and associated V_S model (right)

Site CE.13096

Location: Canyon Lake Fire Station, 28730 Vacation Drive, Canyon Lake, California

Latitude: 33.69884 **Longitude:** -117.26640
(Station coordinates modified using published coordinates from http://www.strongmotioncenter.org with further adjustment made after field inspection by identifying the structure housing the seismic sensor on Google Earth or ESRI Imagery, WGS84 coordinate system.)

V_{S30} (measured): 646 m/s

V_{S30} (adjusted to more accurately reflect seismic station conditions): 699 m/s (replace V_S of upper layer with that of lower layer to account for seismic station sitting on an engineered pad for the fire station).

NEHRP Site Class: C

Geomatrix Code: ATA

Geologic Conditions/Observations: Seismic station located on geologic unit mapped as Triassic phyllite whereas the testing was conducted on a geologic unit mapped as Triassic quartzite and metasandstone. These geologic units could not be differentiated in the field and it appears that the testing was conducted on similar material to the seismic station and, if not, the physical properties of the two geologic units should be similar.

Site Conditions: Rural site. Relatively flat terrain in the vicinity of the seismic array, but relatively steep, undulating topography in site vicinity.

Geophysical Methods Utilized: HVSR, Seismic Refraction, MASW

Geophysical Testing Arrays:

1. Array 13096-1 (48 channel MASW and P-wave seismic refraction array utilizing 4.5 Hz vertical geophones spaced 1.5 m apart for a length of 70.5 m, forward and reverse shot locations with multiple source offsets and source types and multiple interior shot locations).
2. Three HVSR measurement locations; two distributed along array 13096-1 and the other adjacent to the fire station.

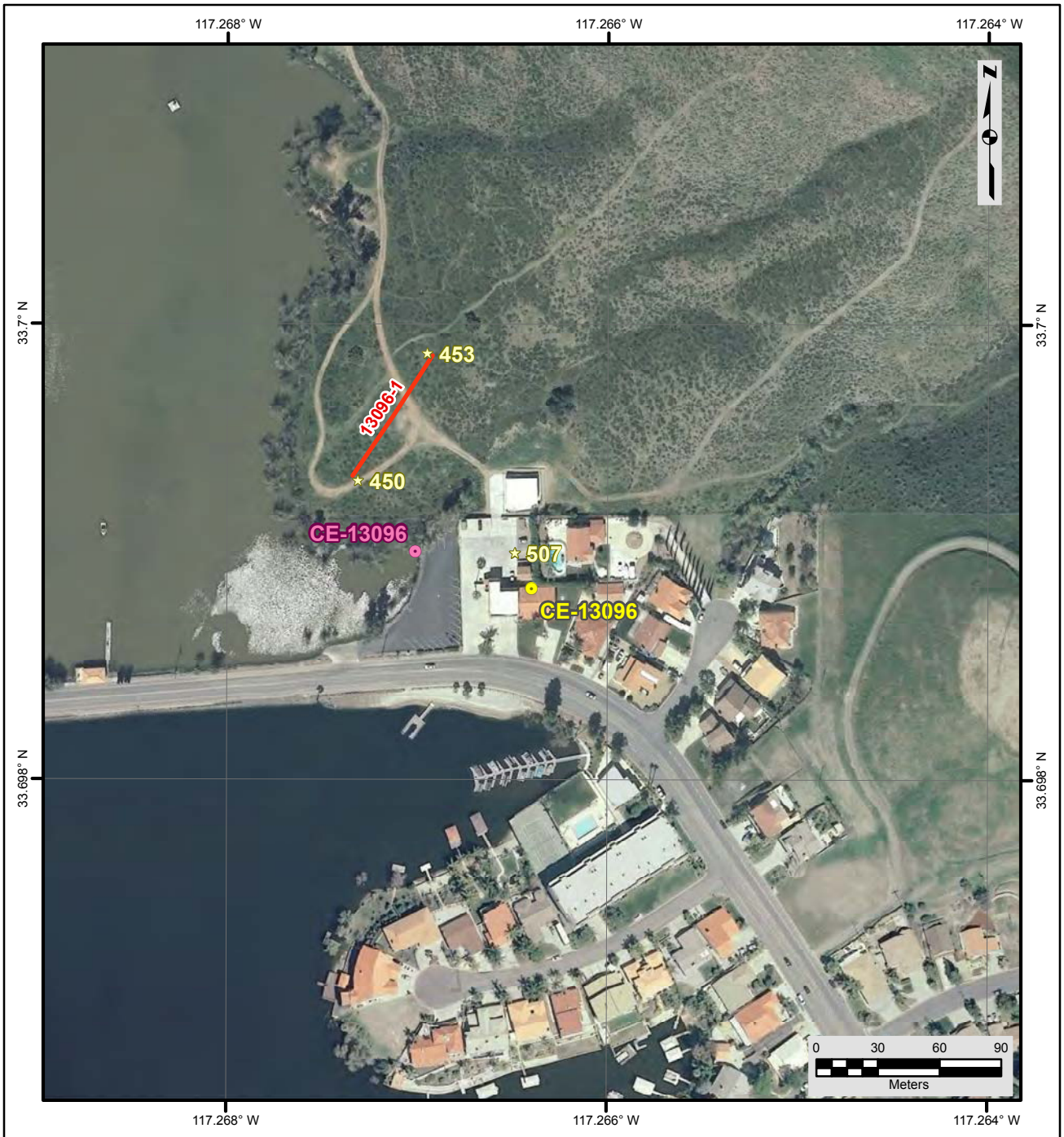

Legend

- Seismic Station - Approximate Improved Location
- Seismic Station - Approximate Location of Record
- H/V Spectral Ratio Measurement Location
- MASW and Seismic Refraction Array

NOTES:
1. WGS 1984 COORDINATE SYSTEM
2. Image Source: ESRI, i-cubed, USDA FSA, USGS, AEX, GeoEye, Getmapping, Aerogrid, IGP

File Name: CE-13096-I

Date: 8/18/2011

USGS science for a changing world

GEOVision geophysical services

RECOVERY.GOV

SITE MAP
CE•13096

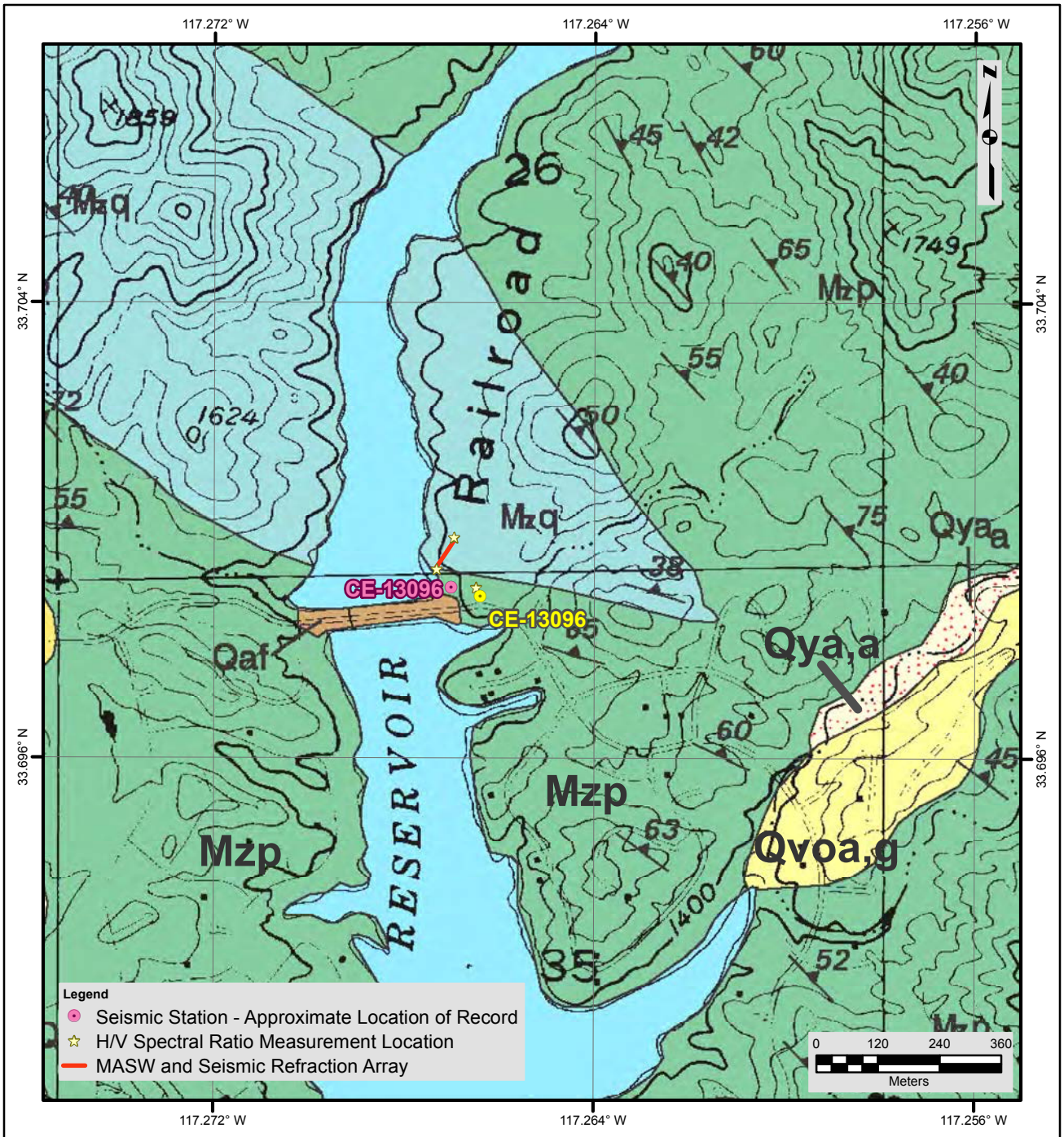

Description of Geologic Map Units

Qaf = Quaternary (Holocene) artificial fill resulting from construction, mining or quarrying
Qya,a = Quaternary (Holocene) young alluvial-channel deposits, fluvial, unconsolidated sand, silt and clay-bearing alluvium
Qvoa,g = Quaternary (Pleistocene) very old alluvial-channel deposits, fluvial sediments, undissected gravel, sand, silt and clay-bearing alluvium
Mzq = Mesozoic (Triassic) quartzite and quartz-rich metasandstone
Mzp = Mesozoic (Triassic) fissile black phyllite

NOTES:
1. WGS 1984 COORDINATE SYSTEM
2. Preliminary Geologic Map of the Elsinore 7.5' Quadrangle, Riverside County, California, Version 1.0 by Douglas M. Morton and F. Harold Weber, Jr. 1973-77, 1978, 1998
3. See site map for details of geophysical survey

File Name: CE-13096

Date: 8/19/2011

USGS science for a changing world

GEOVision geophysical services

GEOLOGIC MAP
CE•13096

RECOVERY.GOV

Looking southeast towards the fire station housing CE.13096 and HVSR sensor 507

Looking northeast along array 13096-1 and at HVSR sensor 450

Looking southeast towards the fire station housing CE.13096 from the center of MASW array 13096-1

MASW data acquisition

Seismic refraction data acquisition along array 13096-1

Location of Geophysical Testing Arrays:

Location	Latitude	Longitude
13096-1, North end of Array	33.69986	-117.26691
13096-1, Center of Array	33.69960	-117.26712
13096-1, South end of Array	33.69933	-117.26733
HVSR Sensor 507	33.69900	-117.26648
HVSR Sensor 450	33.69931	-117.26730
HVSR Sensor 453	33.69987	-117.26694

Notes: 1) WGS84 Coordinate System (decimal degrees)
2) Survey accuracy is estimated at 1 to 2 m.

Results:

V_S Model

Depth to Top of Layer (m)	Layer Thickness (m)	S-Wave Velocity (m/s)	Inferred P-Wave Velocity (m/s)	Assumed Poisson's Ratio	Assumed Density (g/cm^3)
0	1.5	204	382	0.3	1.9
1.5	2.5	394	737	0.3	2.0
4	4	525	981	0.3	2.0
8	8	639	1195	0.3	2.1
16	10	984	1840	0.3	2.2
26	>9	1638	3065	0.3	2.3

Notes: 1) Depth of investigation is about 35 m.
2) Bottom layer is a half space.

Observations/Discussion:

- The HVSR curves are very similar validating the 1-D velocity structure assumption. The HVSR amplitudes are, however, slightly different.
- There is a clear HVSR peak in the 6 to 6.5 Hz range and a possible small secondary peak in the 13 to 15 Hz range.
- Seismic refraction data were modeled using a tomographic inversion routine and a smooth velocity gradient starting model. The starting model was extended to off-end shot locations to increase depth of investigation. To maximize performance of tomographic inversion routines, it would have been preferable to acquire the seismic refraction data using a longer receiver array without far-offset shot locations.
- The seismic refraction model indicates that P-wave velocity increases with depth from about 450 m/s near the surface to over 750 m/s at a depth of 1 to 1.5 m, over 1,250 m/s at a depth of 3 to 8.5 m and over 2,000 m/s at a depth of 12 to 15 m.
- Seismic refraction depth of investigation is about 15 to 20 m.
- The seismic refraction model indicates that there is not significant lateral velocity variation beneath the array.
- Noise conditions at the site were not sufficient for application of passive surface wave techniques.
- The minimum wavelength surface wave phase velocity data extracted from the 48-channel MASW array was about 12 m. Reducing data from smaller hammer sources using a limited offset receiver array (i.e. less active geophones) allowed extraction of surface wave dispersion data to a minimum wavelength of about 4 m.
- There is only minor scatter in MASW dispersion data, which is likely due to lateral velocity variation caused by differential weathering of near surface rock.
- A representative dispersion curve was generated for the MASW data set using a moving average, polynomial curve fitting routine and used for modeling.
- Surface wave depth of investigation is about 35 m based on half of maximum wavelength criteria.
- Inferred P-wave velocities in the surface wave model in the upper 15 to 20 m are consistent with those in the seismic refraction model, especially considering the unknown Poisson's ratio.
- Synthetic HVSR data for the S-wave velocity model, derived from the surface wave data, is not consistent with that measured in the field. It may not be possible to reconcile HVSR and surface wave data at this site, at least under the assumption that the microtremor noise field is dominated by Rayleigh and Love waves.
- V_{S30} is 646 m/s (Site Class C).
- If the V_S of the upper layer of low velocity soil was replaced with that of the underlying layer, to account for the seismic station being located on an engineered pad constructed for the fire station, then V_{S30} would be 699 m/s.

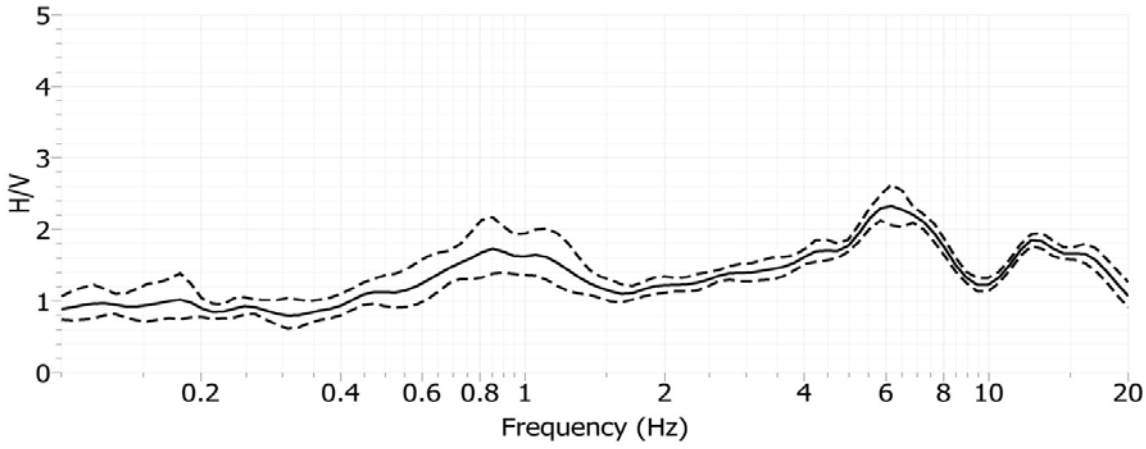

Site CE.13096, H/V Spectral Ratio, Array 13096-1, Sensor 453

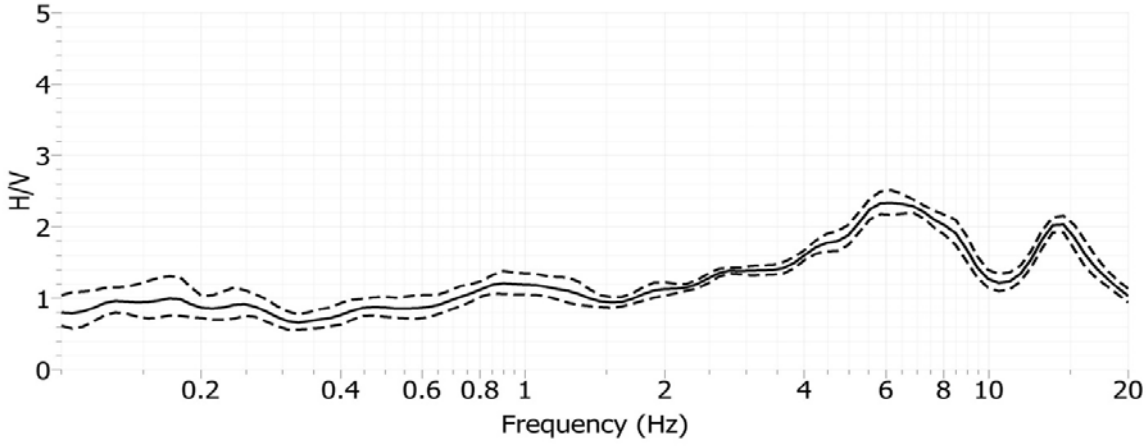

Site CE.13096, H/V Spectral Ratio, Array 13096-1, Sensor 450

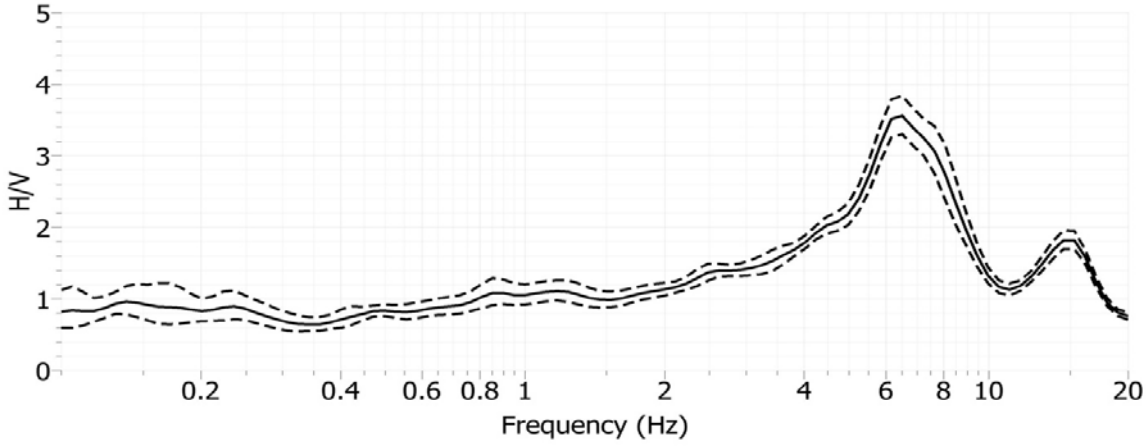

Site CE.13096, H/V Spectral Ratio, Near Seismic Station, Sensor 507

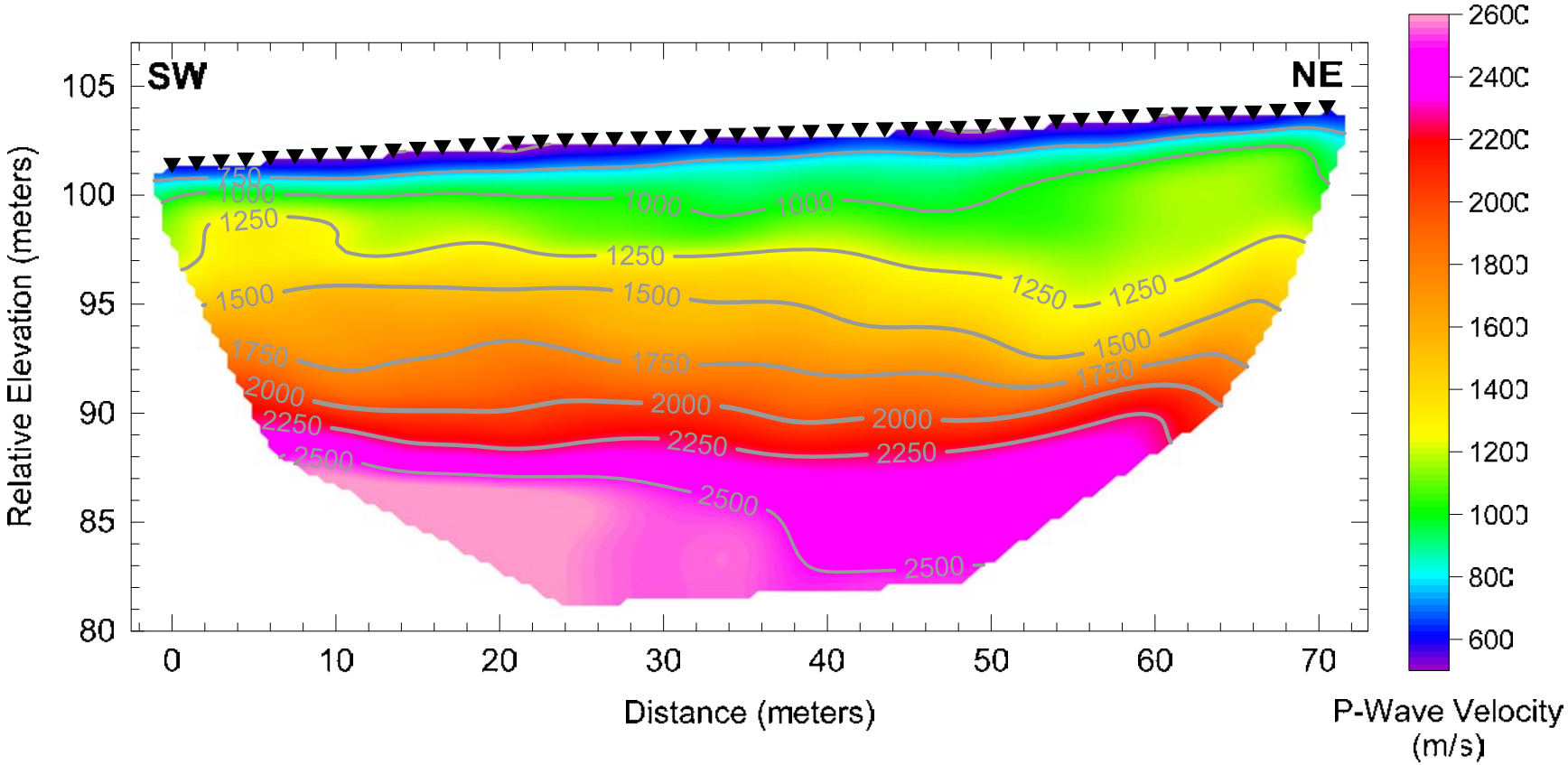

Array 13096-1 – Tomographic Seismic Refraction Model utilizing Smooth Velocity Gradient Starting Model

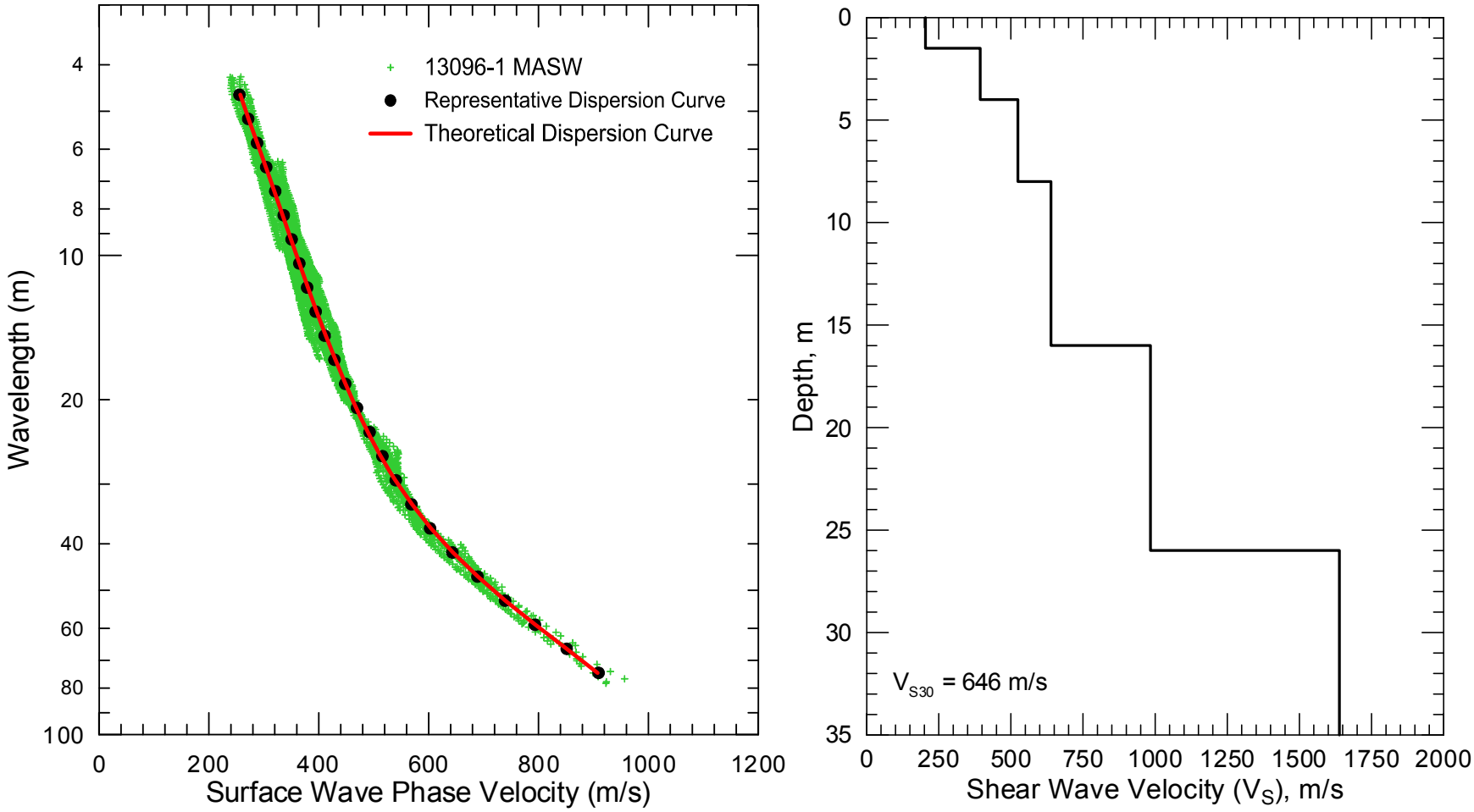

CE.13096 - Field, representative and inverted theoretical surface wave dispersion data (left) and associated V_S model

Site CE.13099

Location: Corona Fire Station No. 3, 790 S. Smith Avenue, Corona, California

Latitude: 33.87590 **Longitude:** -117.59280
(Station coordinates modified using published coordinates from http://www.strongmotioncenter.org with further adjustment made by identifying the fire station on Google Earth, WGS84 coordinate system.)

V_{S30} (measured): 420 m/s

V_{S30} (adjusted to more accurately reflect seismic station conditions): 420 m/s (no adjustment necessary).

NEHRP Site Class: C

Geomatrix Code: AHD

Geologic Conditions/Observations: Site located in area mapped as Quaternary (Holocene) young alluvial fan deposits. Areas mapped as Old Quaternary (Pleistocene) alluvial fan deposits within 200 m of site. Geologic conditions cannot be confirmed due to development in site vicinity. Deep soil site.

Site Conditions: Urban site with significant traffic noise from nearby Smith Avenue, 6th Street and other nearby roads and freeways. Relatively flat terrain in site vicinity with surface elevation gently decreasing to north.

Geophysical Methods Utilized: HVSR, MASW, array microtremor, ReMi™

Geophysical Testing Arrays:

1. Array 13099-1 (24 channel, linear passive surface wave array utilizing 4.5 Hz vertical geophones spaced 4 m apart for a length of 92 m).
2. Array 13099-2 (10 channel, triangle passive surface wave array utilizing 1 Hz geophones and a 45 m length for outer side of array).
3. Array 13099-3 (48 channel MASW array utilizing 4.5 Hz vertical geophones spaced 1.5 m apart for a length of 70.5 m, forward and reverse shot locations with multiple source offsets and source types and center shot location).
4. Three HVSR measurement locations distributed along arrays 13099-1, 13099-2 and 13099-3.

Legend

- Seismic Station - Approximate Location of Record
- Seismic Station - Approximate Improved Location
- H/V Spectral Ratio Measurement Location
- MASW Array
- Passive Surface Wave Array

NOTES:
1. WGS 1984 COORDINATE SYSTEM
2. Image Source: ESRI, i-cubed, USDA FSA, USGS, AEX, GeoEye, Getmapping, Aerogrid, IGP

File Name: CE-13099-I

Date: 4/7/2011

USGS science for a changing world

GEOVision geophysical services

RECOVERY.GOV

SITE MAP
CE•13099

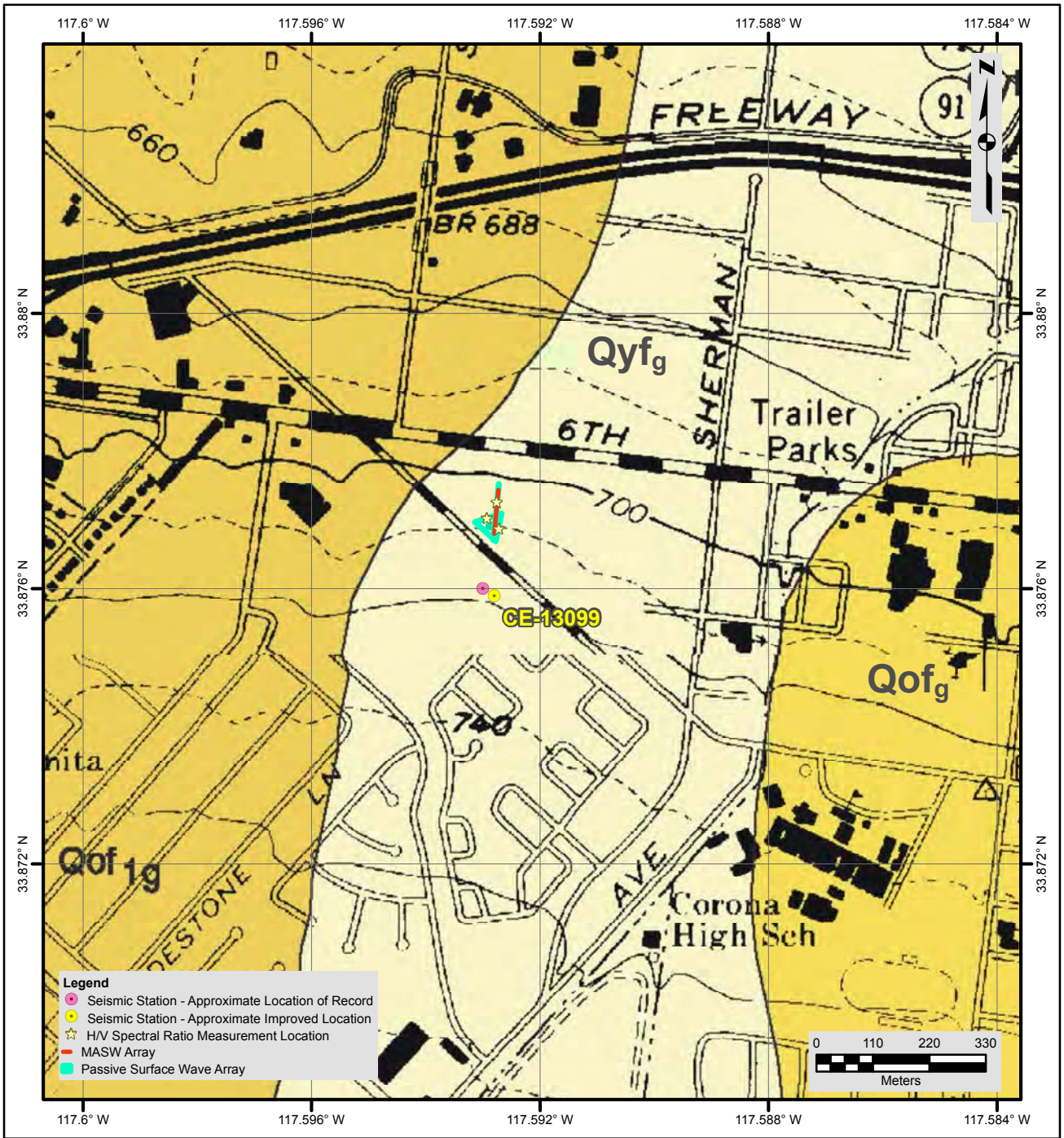

Description of Geologic Map Units

Qyf$_g$ = Quaternary (Holocene and Late Pleistocene) young alluvial fan deposits - sand, cobble-sand and gravel-sand deposits, gravelly
Qof$_g$ = Quaternary (Late Pleistocene) old alluvial fan deposits - gravelly
Qof $_{1g}$ = Quaternary (Middle Pleistocene) old alluvial fan deposits Unit 1 - indurated, gravelly

NOTES:
1. WGS 1984 COORDINATE SYSTEM
2. Geologic Map of the Corona North 7.5' Quadrangle V1.0 and Corona South 7.5' Quadrangle Version 1.0 , Orange, Riverside and San Bernardino Counties, California by C.H. Gray, Jr., Douglas M. Morton, and F.H. Weber, Jr., 1975, 1961, 1976, 1995-1997
3. See site map for details of geophysical survey

File Name: CE-13099

Date: 2/7/2013

USGS science for a changing world

GEOVision geophysical services

GEOLOGIC MAP
CE•13099

Looking southeast from center of array 13099-2 towards Corona Fire Station No. 3 housing seismic station CE-13099

Passive surface wave array 13099-2

HVSR measurement station and a 1 Hz geophone forming part of array 13099-2

Hammer energy source utilized on MASW array 13099-3

Accelerated weight drop energy source utilized on MASW array 13099-3

Location of Geophysical Testing Arrays:

Location	Latitude	Longitude
13099-1, South End of Array	33.87671	-117.59282
13099-1, Center of Array	33.87711	-117.59277
13099-1, North End of Array	33.87752	-117.59272
13099-2, Corner of Array, Sensor Location 1	33.87697	-117.59314
13099-2, Corner of Array, Sensor Location 3	33.87669	-117.59278
13099-2, Corner of Array, Sensor Location 5	33.87709	-117.59268
13099-2, Center of Array, Sensor Location 10	33.87691	-117.59287
13099-3, South End of Array	33.87680	-117.59281
13099-3, North End of Array	33.87744	-117.59273
HVSR Sensor 507	33.87702	-117.59293
HVSR Sensor 453	33.87687	-117.59272
HVSR Sensor 450	33.87726	-117.59276

Notes: 1) WGS84 Coordinate System (decimal degrees)
2) Survey accuracy is estimated at 1 to 2 m

Results:

V_S Model

Depth to Top of Layer (m)	Layer Thickness (m)	S-Wave Velocity (m/s)	Inferred P-Wave Velocity (m/s)	Assumed Poisson's Ratio	Assumed Density (g/cm^3)
0	1	278	521	0.3	1.9
1	2	336	628	0.3	1.9
3	4	345	646	0.3	1.9
7	5	429	802	0.3	2.0
12	8	460	860	0.3	2.0
20	12	470	880	0.3	2.0
32	15	541	1011	0.3	2.0
47	>13	665	1245	0.3	2.0

Observations/Discussion:

- HVSR curves are very similar, validating the 1-D velocity assumption.
- HVSR data quality from sensor 453 is not as good as the other sensors, particularly at low frequencies, possibly due to worse sensor coupling, although this sensor was also placed relatively close to a building and busy street.
- Low frequency HVSR peak in the 0.38 to 0.4 Hz range, which is consistent for a deep soil site.
- Noise conditions at site (multi-directional or omni-directional noise sources) appeared sufficient for successful application of passive surface wave techniques.
- Surface wave dispersion data from active and passive surface wave datasets are in good agreement at this site.
- ESAC technique used to extract surface wave dispersion data from passive triangle array data. Both the ReMi™ and ESAC techniques used to extract surface wave dispersion data from the linear array with the ESAC technique providing dispersion data in better agreement with that from the triangle array.
- Significant scatter (30 to 50 m/s) in MASW dispersion data at wavelengths less than about 15 m, which is likely due to lateral velocity variation.
- The possibility cannot be discounted that Raleigh wave phase velocity data at wavelengths less than 10 m are associated with a higher mode or superimposed modes. Alternatively, lateral velocity variation may explain the discontinuity in the dispersion data near a 10 m wavelength. If the dispersion curve at wavelengths less than 10 m is not associated with the fundamental mode then there will some error in the velocity model in the upper 5 m; however, V_{S30} should still be relatively accurate.
- Representative dispersion curves were generated for each surface wave data set using a moving average, polynomial curve fitting routine. These individual representative dispersion curves were combined and a representative dispersion curve generated for the combined data set for data modeling.
- Water table located at a depth greater than 30 m based on review of seismic refraction data. No obvious water table reflector by which to estimate possible water table depth.
- Based on simple layer-based analysis of seismic refraction first arrival data, P-wave velocity of surficial sediments is about 575 m/s. There is a 900 m/s refractor at a depth of 1 to 2 m, which may be a relatively thin high velocity layer because first arrivals appear to attenuate rapidly towards the end of the line. Not possible to accurately identify higher mode surface waves to implement a multi mode inversion.
- Surface wave depth of investigation is about 60 m based on half of maximum wavelength criteria.
- V_{S30} is 420 m/s (Site Class C).
- Average S-wave velocity of the upper 60 m (V_{S60}) is 488 m/s.

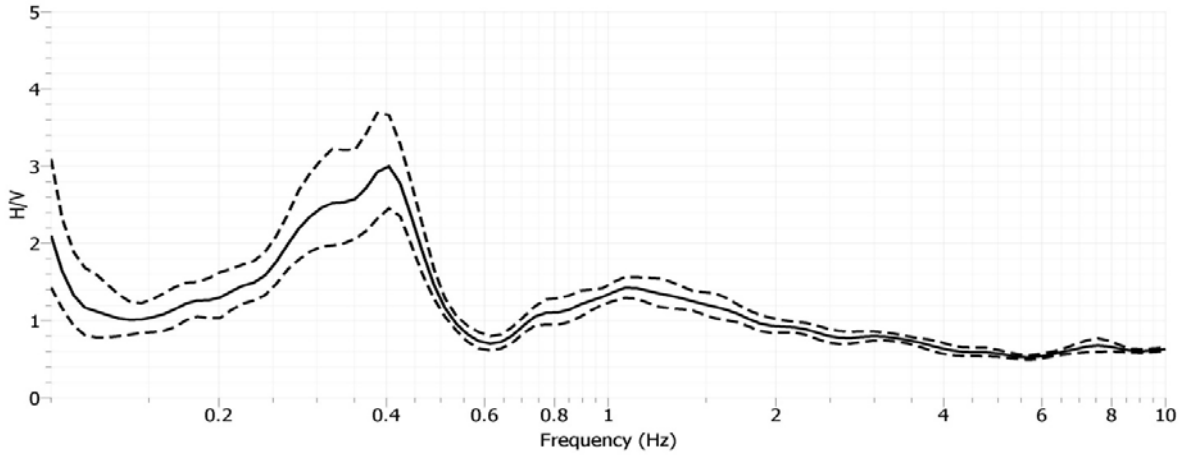

Site CE.13099, H/V Spectral Ratio, Array 13099-3, Sensor 450

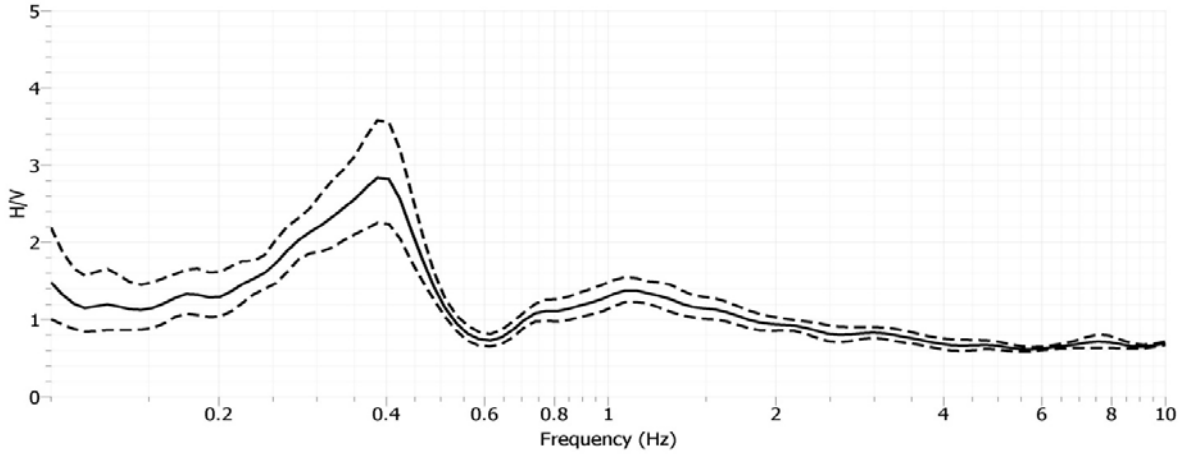

Site CE.13099, H/V Spectral Ratio, Array 13099-2, Sensor 507

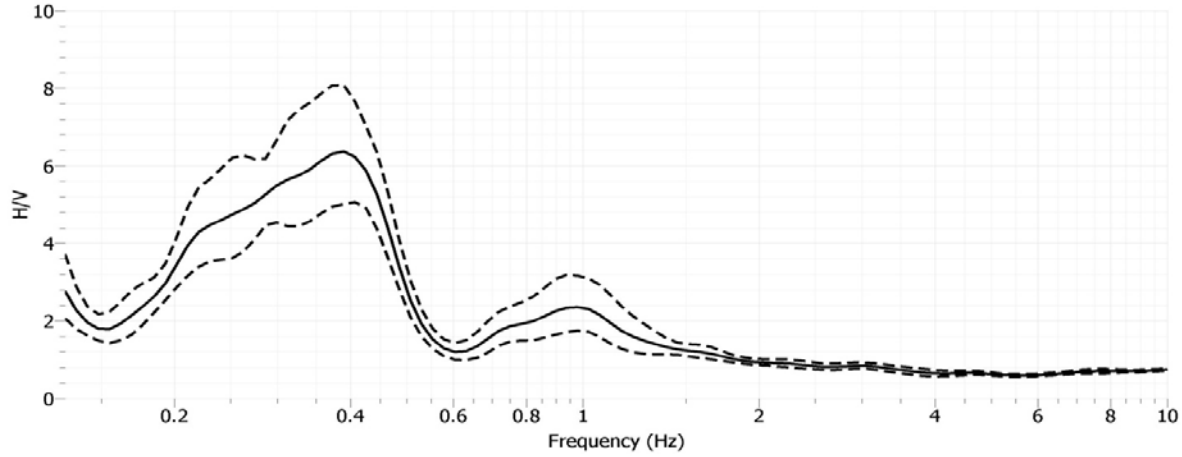

Site CE.13099, H/V Spectral Ratio, Array 13099-2, Sensor 453

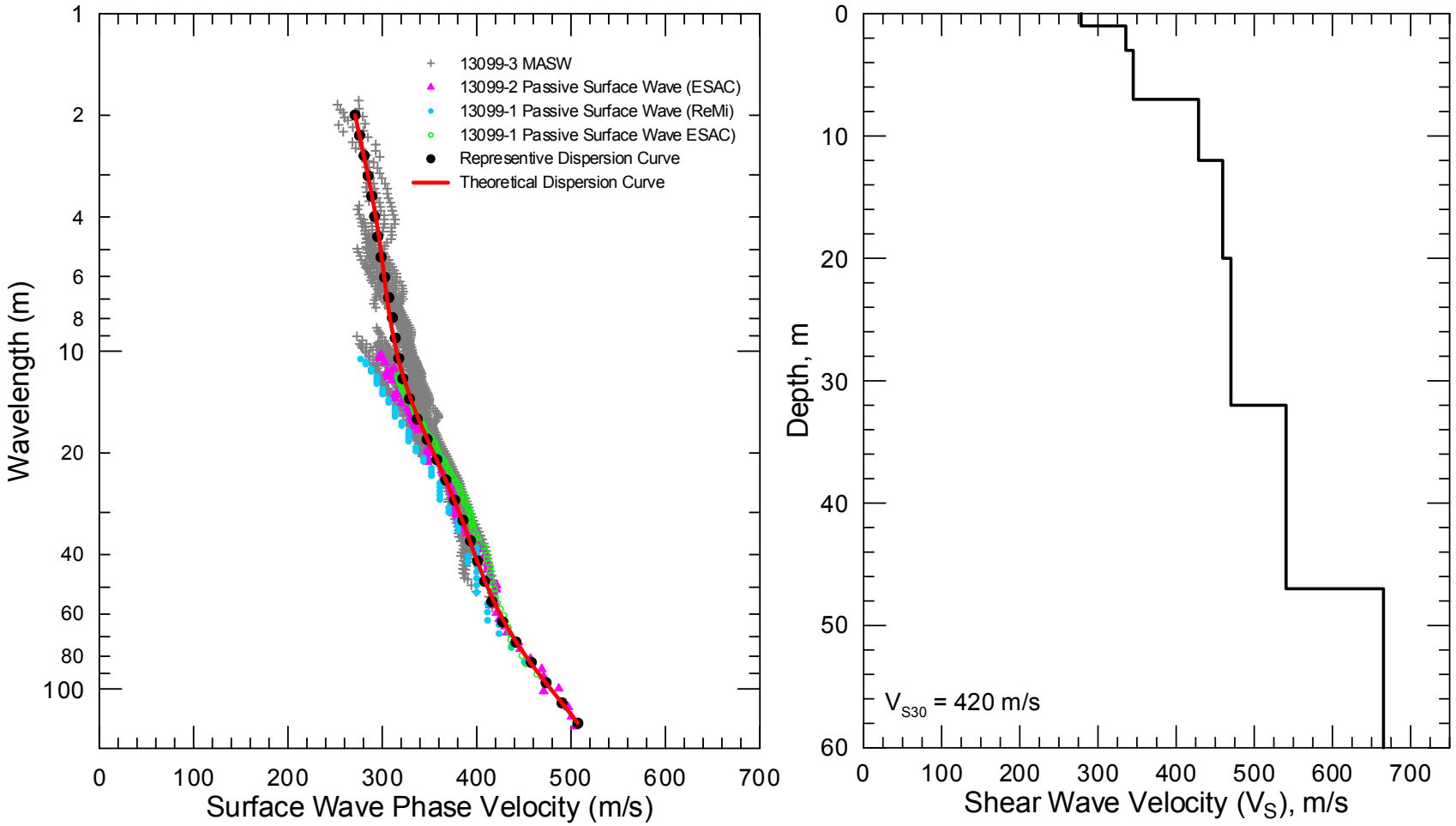

CE.13099 - Field, representative and inverted theoretical surface wave dispersion data (left) and associated V_S model (right)

Site CE.13100

Location: City of Corona Fire Station #5, 1200 Canyon Crest, Corona, California

Latitude: 33.87559 **Longitude:** -117.63549

(Station coordinates modified based on field observation of station location and identification of approximate station location on Google Earth/ESRI Imagery – could not survey the seismic station as located inside a building, WGS84 coordinate system)

V_{S30} (measured): 341 m/s

V_{S30} (adjusted to more accurately reflect seismic station conditions): 357 m/s (replacement of velocity of upper layer with that of underlying layer to compensate for seismic station being located on concrete pad of structure sitting on engineered fill).

NEHRP Site Class: D/C

Geomatrix Code: AQD

Geologic Conditions/Observations: Site located in area mapped as Quaternary (Pleistocene) older alluvium. Tertiary sedimentary rocks underlay Quaternary alluvium in the site vicinity.

Site Conditions: Suburban site with some traffic noise from nearby roads. Rolling (hilly) topography in site vicinity. Geophysical arrays located on horizontal or slightly sloping surfaces.

Geophysical Methods Utilized: HVSR, MASW, array microtremor, ReMi™

Geophysical Testing Arrays:

1. Array 13100-1 (48 channel "L" shaped array utilizing 4.5 Hz vertical geophones spaced 2.5 m apart on one 24 channel leg and 3 m apart on the other leg and a 77.25 degree angle between legs) used to acquire passive surface wave data.
2. Array 13100-2 (48 channel MASW array utilizing 4.5 Hz vertical geophones spaced 1 m apart for a length of 47 m, forward and reverse shot locations with multiple source offsets and source types and center shot location). Array located along the northwest to southeast leg of array 13100-1.
3. Array 13100-3 (48 channel MASW array utilizing 4.5 Hz vertical geophones spaced 1 m apart for a length of 47 m, forward and reverse shot locations with multiple source offsets and source types (hammers only) and center shot location). Array located along the southwest to northeast leg of array 13100-1.
4. Array 13100-4 (48 channel "L" shaped array utilizing 4.5 Hz vertical geophones spaced 3 m apart on each 24 channel leg and a 99 degree angle between legs) used to acquire passive surface wave data.
5. Array 13100-5 (48 channel MASW array utilizing 4.5 Hz vertical geophones spaced 1 m apart for a length of 47 m, forward and reverse shot locations with multiple

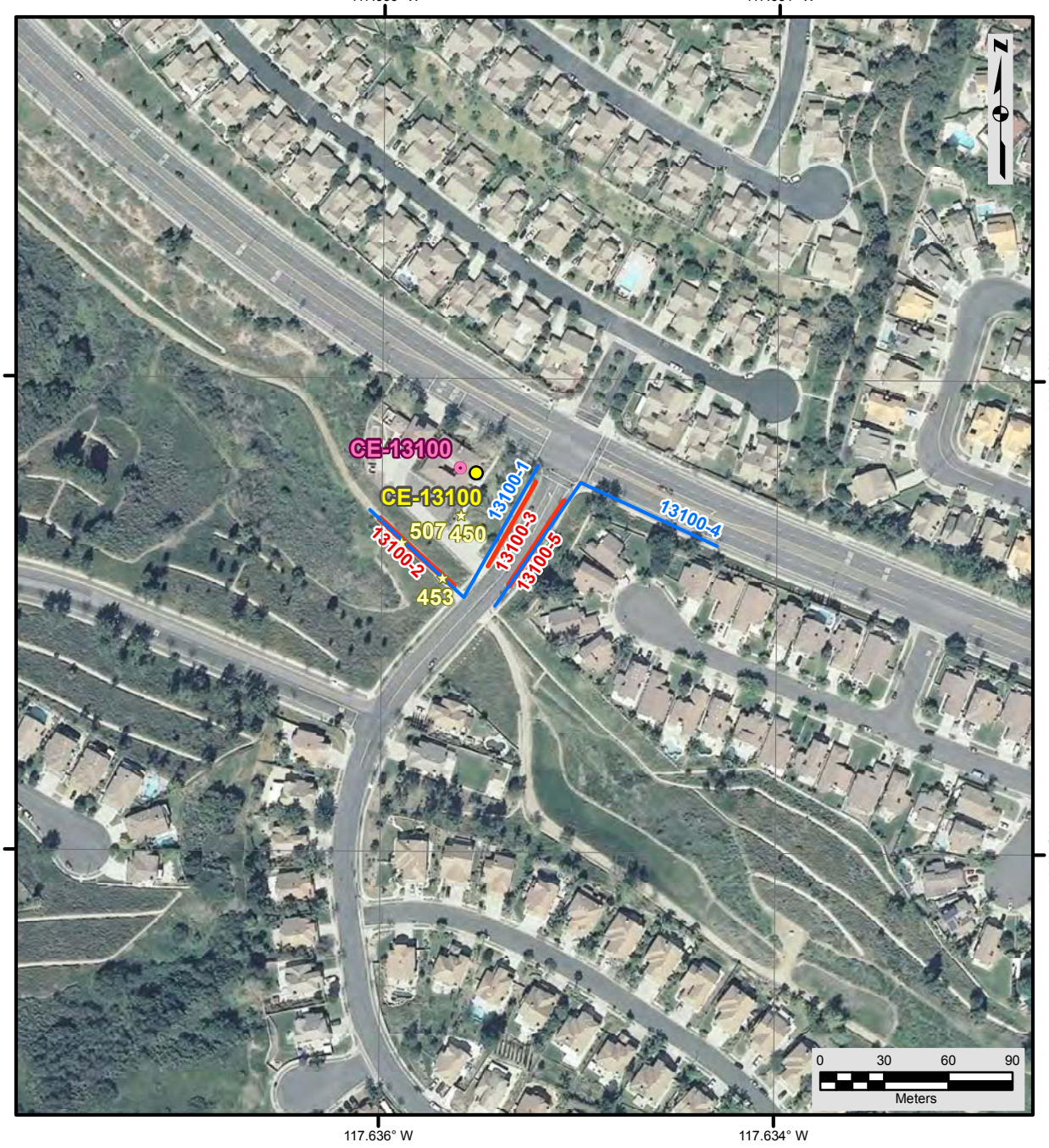

Legend

- Seismic Station - Approximate Improved Location
- Seismic Station - Approximate Location of Record
- H/V Spectral Ratio Measurement Location
- Passive Surface Wave Array
- MASW Array

NOTES:
1. WGS 1984 COORDINATE SYSTEM
2. Image Source: ESRI, i-cubed, USDA FSA, USGS, AEX, GeoEye, Getmapping, Aerogrid, IGP

File Name: CE-13100-I

Date: 9/29/2011

USGS science for a changing world

GEOVision geophysical services

RECOVERY.GOV

SITE MAP
CE•13100

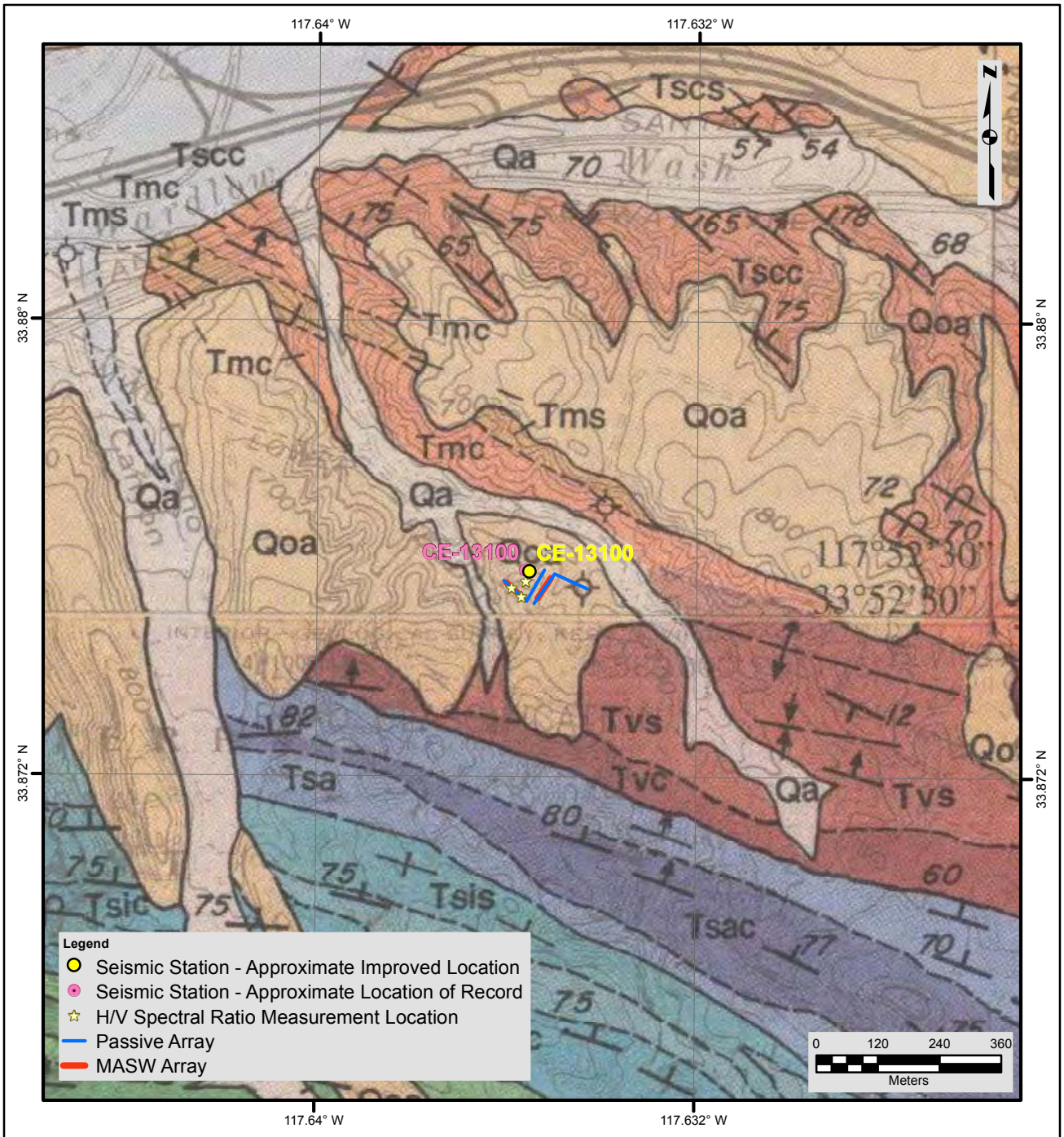

Description of Geologic Map Units

Qa = Quaternary (Holocene) alluvial gravel, sand and silt of valleys and floodplains
Qoa = Quaternary (Pleistocene) elevated, dissected remnants of alluvial gravel, sand and silt
Tscc = Tertiary (Miocene) Sycamore Canyon Formation - conglomerate or eastern facies
Tmc, Tms = Tertiary (Miocene) Monterey Formation - clay shale facies, unassigned sandstone
Tvc, Tvs = Tertiary (Oligocene) Vaqueros Formation - mostly sandstone
Tsa, Tsac = Tertiary (Eocene) Santiago Formation - silty to sandy claystone, cobble conglomerate
Tsia, Tsic, Tsis = Tertiary (Paleocene) Silverado Formation - argillaceous sediments, sandy sediments, conglomerate

NOTES:
1. WGS 1984 COORDINATE SYSTEM
2. Geologic Map of the Yorba Linda and Prado Dam Quadrangles (Eastern Puente Hills), Los Angeles, Orange, San Bernardino and Riverside Counties, California, by Thomas W. Dibblee, Jr, 2001
3. See site map for details of geophysical survey

USGS science for a changing world
GEOVision geophysical services

GEOLOGIC MAP
CE•13100

RECOVERY.GOV

File Name: CE-13100
Date: 9/29/2011

Looking northwest towards fire station housing seismic station CE.13100 and HVSR sensor 450

Looking northwest along MASW array 13100-2

Looking northwest towards corner of passive surface wave array 13100-1 and fire station

Looking west towards corner of passive surface wave array 13100-4 and fire station

Looking northeast along MASW array 13100-5

source offsets and source types and center shot location). Array located along the southwest to northeast leg of array 13100-4.

6. Three HVSR measurement locations; two distributed along array 13100-2 and the other near building housing the seismic station.

Location of Geophysical Testing Arrays:

Location	Latitude	Longitude
13100-1, Northwest End of Array	33.87544	-117.63604
13100-1, Corner of Array	33.87508	-117.63556
13100-1, Northeast End of Array	33.87563	-117.63519
13100-2, Northwest End of Array	33.87541	-117.63599
13100-2, Center of Array	33.87526	-117.63580
13100-2, Southeast End of Array	33.87512	-117.63561
13100-3, Southwest End of Array	33.87521	-117.63544
13100-3, Northeast End of Array	33.87556	-117.63520
13100-4, Southwest End of Array	33.87504	-117.63540
13100-4, Corner of Array	33.87556	-117.63497
13100-4, Northeast End of Array	33.87530	-117.63428
13100-5, Southwest end of Array	33.87513	-117.63533
13100-5, Northeast end of Array	33.87548	-117.63505
HVSR Sensor 450	33.87542	-117.63558
HVSR Sensor 453	33.87515	-117.63567
HVSR Sensor 507	33.87530	-117.63587

Notes: 1) WGS84 Coordinate System (decimal degrees)

2) Survey accuracy is estimated at 1 to 2 m.

Results:

V_S Model

Depth to Top of Layer (m)	Layer Thickness (m)	S-Wave Velocity (m/s)	Inferred P-Wave Velocity (m/s)	Assumed Poisson's Ratio	Assumed Density (g/cm^3)
0	1	120	224	0.3	1.8
1	1.5	224	420	0.3	1.8
2.5	2.5	288	538	0.3	1.9
5	4	314	588	0.3	1.9
9	5	328	613	0.3	1.9
14	6	388	725	0.3	1.9
20	8	466	873	0.3	2.0
28	>12	547	1024	0.3	2.0

Notes: 1) Depth of investigation is about 40 m.
2) Bottom layer is a half space.

Observations/Discussion:

- Passive surface wave array 13100-1 and MASW array 13100-2 were not effective due to significant lateral velocity variation along the arrays. Therefore, passive surface array 13100-4 and MASW array 13100-5 were acquired and used for site characterization.
- The HVSR curves are similar at frequencies below 4 Hz, but differ at higher frequencies; particularly sensor 507 which does not have the peak at 5.3 Hz that is observed on the HVSR plots for sensors 450 and 453. This implies that shallow velocity structure may be different in the vicinity of sensor 507 than that near sensors 450 and 453.
- Noise conditions at site (multi-directional or omni-directional noise sources) appeared sufficient enough to attempt the use of passive surface wave techniques. There may, however, be some directional noise bias and topography may have some influence of Rayleigh wave propagation in the site vicinity.
- Only passive surface wave array 13100-4 was used for data analysis. ESAC technique used to extract surface wave dispersion data from passive "L" array data. Both the ReMi™ and ESAC techniques used to extract surface wave dispersion data from the linear arrays.
- Surface wave dispersion data from MASW array 13100-5 and "L" array passive surface wave array 13100-4 are offset by about 20 to 25 m/s over the 20 to 40 m wavelength range, likely the result of lateral velocity variation. The passive surface wave data from the southwest to northeast leg of the "L" array, extracted using both the ReMi™ and ESAC techniques, is in excellent agreement with the MASW data. The passive surface wave data from the northwest to southeast leg of the "L" array, extracted using the ESAC technique, is also in excellent agreement with the MASW data. Passive surface wave

data extracted from this array using the ReMi™ underestimates phase velocity relative to the MASW data, possibly due to a strong in-line noise component.

- Each leg of passive surface array 13100-4 was only 69 m long and, therefore, surface wave dispersion data extracted from the linear arrays is only valid to a wavelength of about 70 to 80 m.
- There is some scatter in the passive surface wave dispersion data extracted from the linear arrays at wavelengths greater than 60 m, likely the result of both ambient noise conditions and relatively short length of the arrays. Data quality is significantly better on the "L" array where surface wave dispersion data is valid to wavelengths of about 140 m. However, surface wave phase velocity data from this array was not utilized due to a small offset from the MASW data.
- Representative dispersion curves were generated for each surface wave data set using a moving average, polynomial curve fitting routine. These individual representative dispersion curves were combined and a representative dispersion curve generated for the combined data set for data modeling.
- Saturated sediments are not expected to be located within 40 m of the surface at this site.
- Surface wave depth of investigation is about 40 m based on half of maximum wavelength criteria.
- V_{S30} is 341 m/s (Site Class D).
- If the upper layer velocity was replaced with that of the underlying layer to compensate for the seismic station being located on the concrete pad of structure sitting on engineered fill then V_{S30} would be 357 m/s (Site Class D/C).

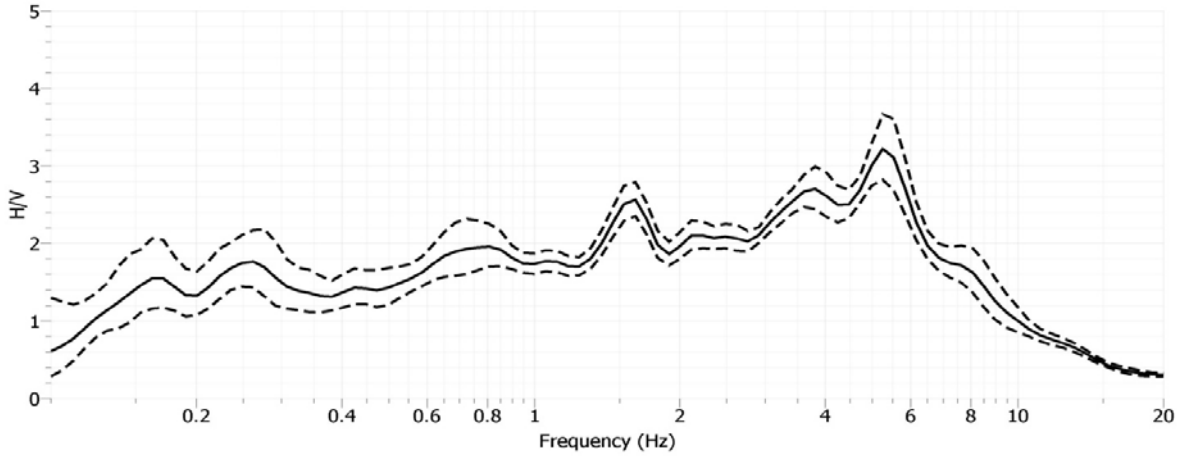

Site CE.13100, H/V Spectral Ratio, Near Fire Station, Sensor 450

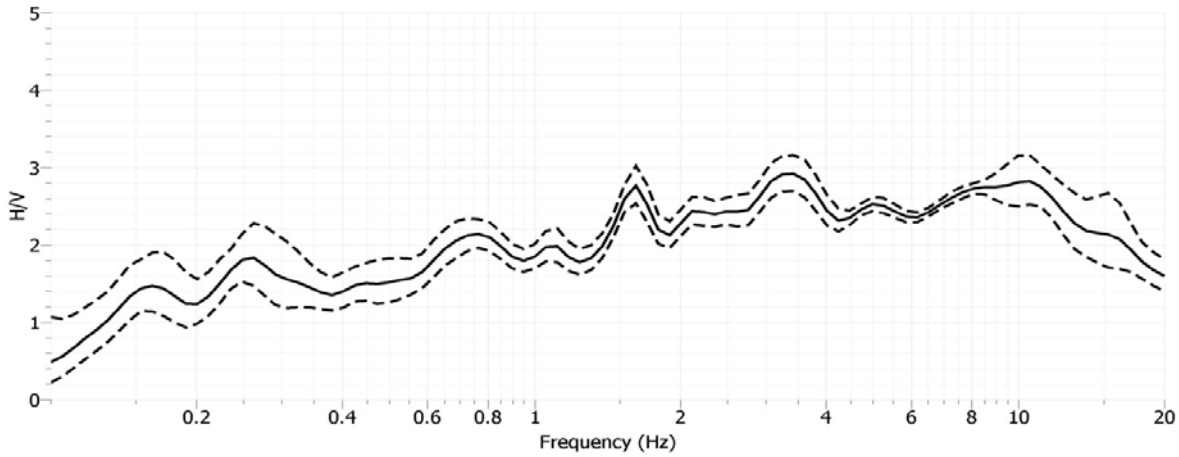

Site CE.13100, H/V Spectral Ratio, Array 13100-2, Sensor 507

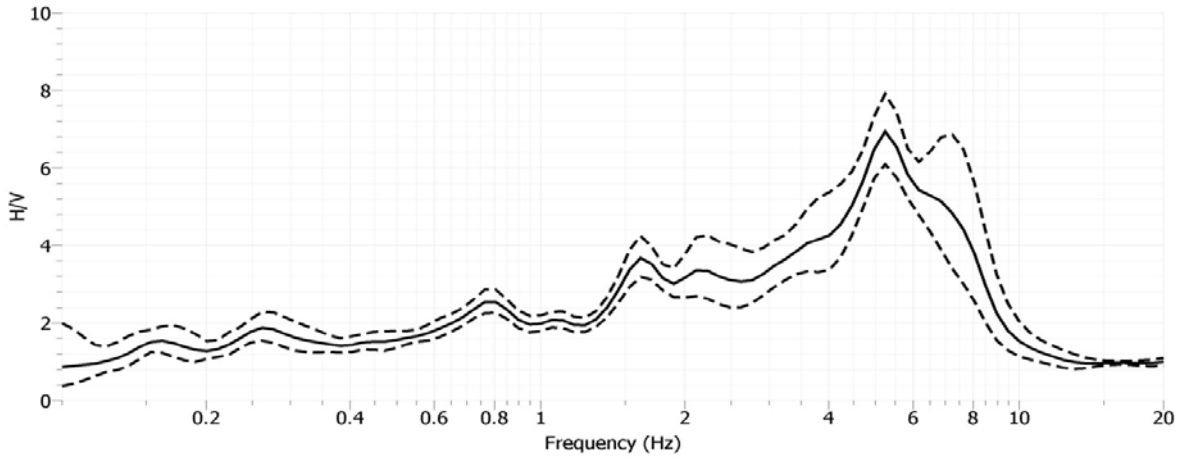

Site CE.13100, H/V Spectral Ratio, Array 13100-2, Sensor 453

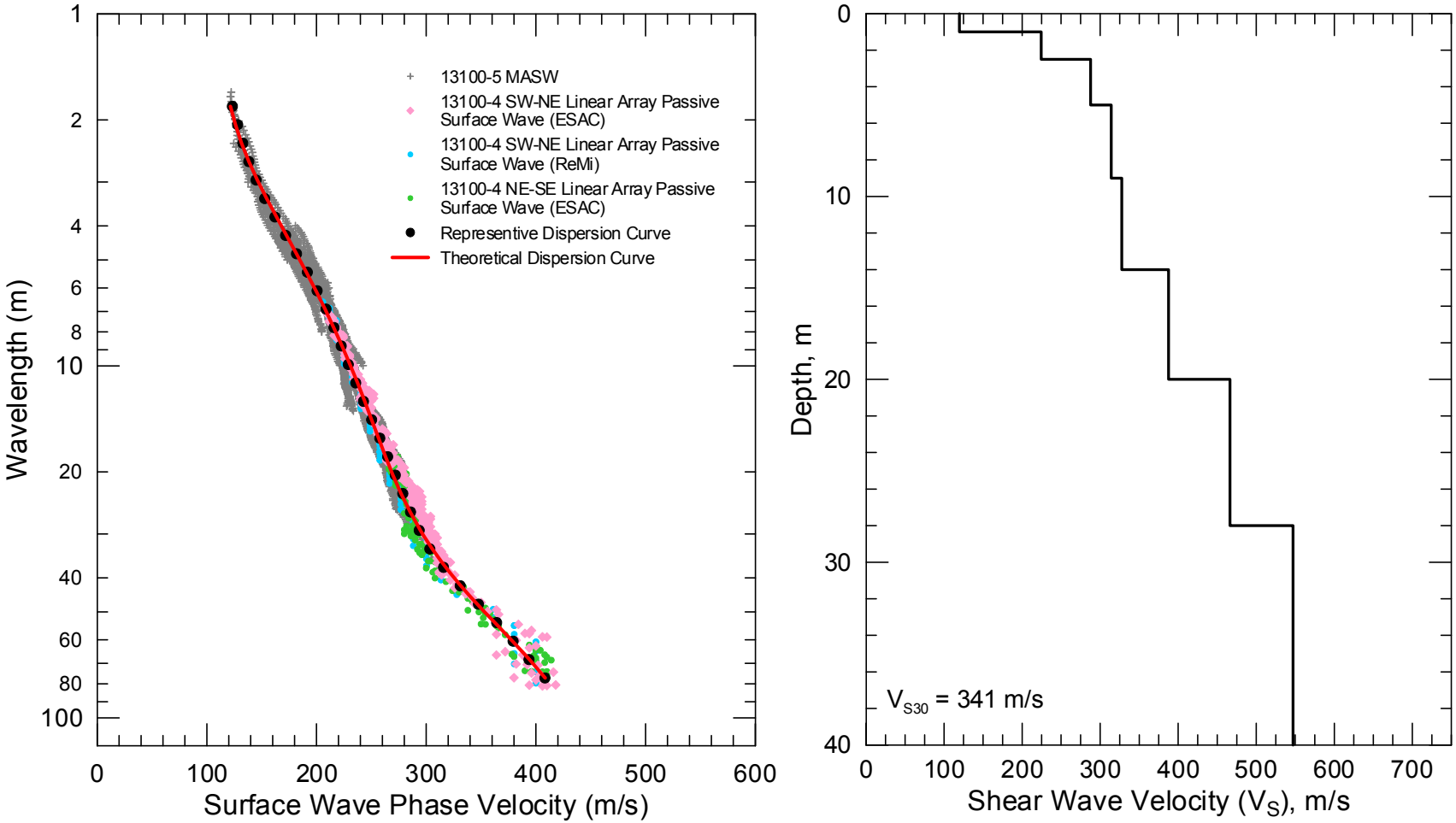

CE.13100 - Field, representative and inverted theoretical surface wave dispersion data (left) and associated V_S model (right)

Site CE.13922

Location: Elsinore Fire Station #10, 410 W Graham Avenue, Lake Elsinore, California

Latitude: 33.66910 **Longitude:** -117.33225
(Station coordinates modified using published coordinates from http://www.strongmotioncenter.org with further adjustment made by identifying the structure housing the seismic sensor on Google Earth, WGS84 coordinate system.)

V_{S30} (measured): 581 m/s

V_{S30} (adjusted to more accurately reflect seismic station conditions): 675 m/s (V_{S30} from test area adjusted to higher frequency HVSR peak observed near the seismic station).

NEHRP Site Class: C

Geomatrix Code: AHB/AQB

Geologic Conditions/Observations: Site located on Quaternary (Late Pleistocene to Holocene) alluvium overlying Mesozoic (Cretaceous) granitic rock or Mesozoic (Pre-Cretaceous) metasediments.

Site Conditions: Suburban site with significant traffic noise from adjacent roads. Relatively flat terrain in site vicinity with gradual elevation decline to south.

Geophysical Methods Utilized: HVSR, Seismic Refraction, MASW (Rayleigh and Love Wave)

Geophysical Testing Arrays:

1. Array 13922-1 (48 channel MASW and P-wave seismic refraction array utilizing 4.5 Hz vertical geophones spaced 1.5 m apart for a length of 70.5 m, forward and reverse shot locations with multiple source offsets and source types and multiple interior shot locations).
2. Array 13922-1 (24 channel S-wave seismic refraction array utilizing 28 Hz horizontal geophones spaced 3 m apart for a length of 69 m, forward and reverse shot locations with multiple source offsets and multiple interior shot locations). Same origin and orientation as MASW and P-wave refraction line of same name.
3. Array 13922-2 (48 channel "T" shaped array utilizing 4.5 Hz vertical geophones, 24 geophones spaced 4 m apart along the southwest to northeast segment and 24 geophones spaced 3 m apart along the northwest to southeast segment).
4. Array 13922-4 (48 channel MASW and P-wave seismic refraction array utilizing 4.5 Hz vertical geophones spaced 1.5 m apart for a length of 70.5 m, forward and reverse shot locations with multiple source offsets and source types and multiple interior shot locations).

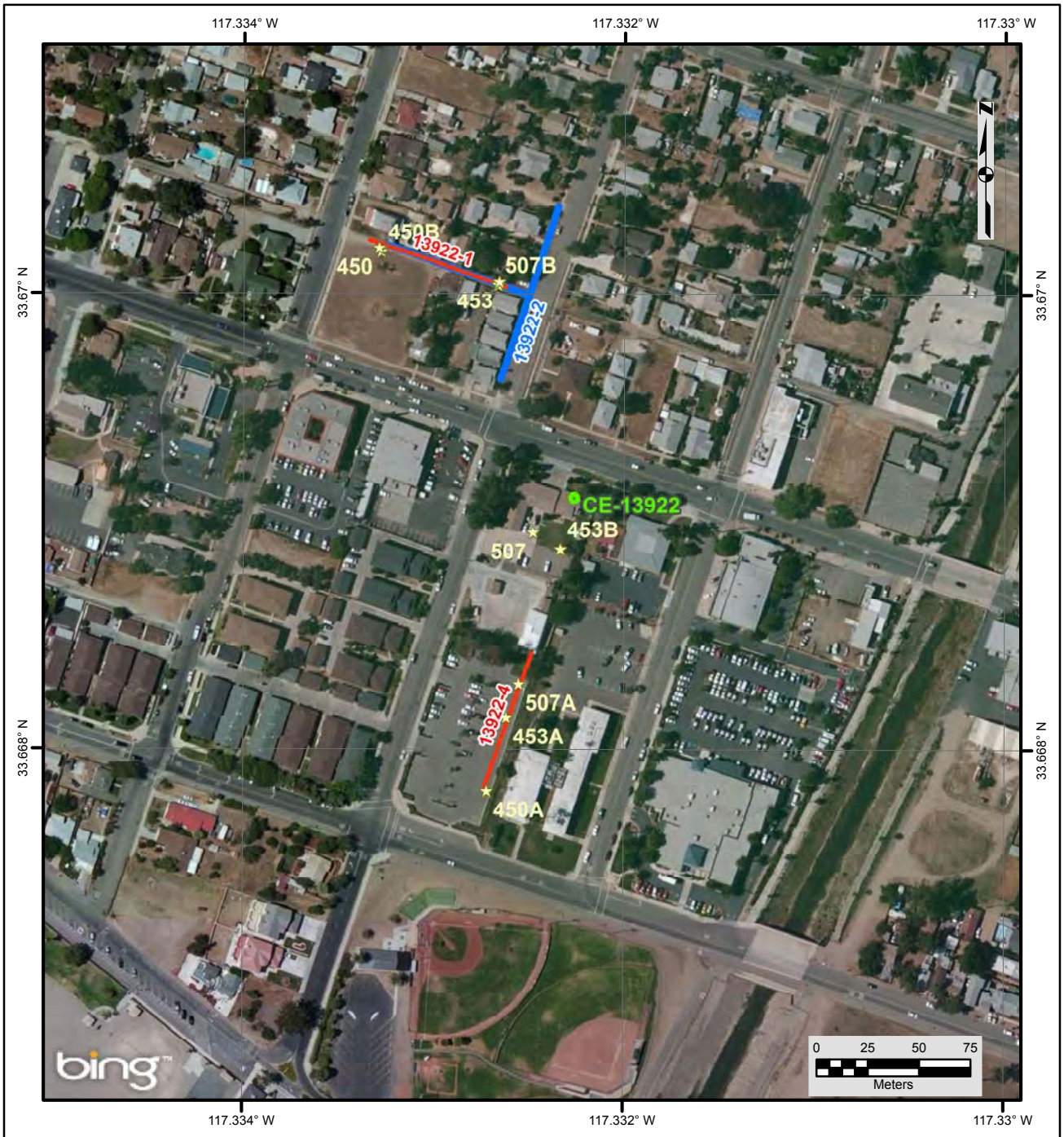

Legend

- Seismic Station - Approximate Improved Location
- H/V Spectral Ratio Location
- MASW and Seismic Refraction Array
- Passive Surface Wave Array

NOTES:
1. WGS 1984 COORDINATE SYSTEM
2. Image Source: (c) Microsoft Corporation and its data suppliers

File Name: CE-13922-IALL

Date: 10/25/2012

USGS science for a changing world

GEOVision geophysical services

RECOVERY.GOV

SITE MAP
CE•13922

Description of Geologic Map Units

Qw = Quaternary (Holocene) very young wash deposits, bouldery to sandy alluvium
Ql = Quaternary (Holocene) very young lacustrine deposits, clayey/silty/fine sand
Qya_a = Quaternary (Late Pleistocene to Holocene) young alluvial channel deposits, fluvial, unconsolidated clay, sand and silt, sandy
Qyf1 a = Quaternary (Late Pleistocene to Early Holocene) young unconsolidated alluvial fan deposits, unit 1, gravel, sand, and silt, sandy
Qyv_a= Quaternary (Late Pleistocene to Holocene) young alluvial-valley deposits, unconsolidated sand, silt and clay, sandy

Kgd = Mesozoic (Cretaceous) undifferentiated granodiorite, massive
Khg = Mesozoic (Cretaceous) heterogeneous granitic rocks, mostly tonalite
Mzu = Mesozoic (Pre-Cretaceous) undifferentiated low to high grade metasedimentary rocks
Mzq = Mesozoic (Pre-Cretaceous) quartz-rich rocks; quartzite and quartz-rich metasandstone
Mzp = Mesozoic (Pre-Cretaceous) phyllite, fissile and black

NOTES:
1. WGS 1984 COORDINATE SYSTEM
2. Preliminary Geologic Map of the Elsinore 7.5' Quadrangle, Riverside County, California, Version 1.0 by Douglas M. Morton and F. Harold Weber, Jr. 1973-77, 1978, 1998
3. See site map for details of geophysical survey

USGS science for a changing world
GEOVision geophysical services

GEOLOGIC MAP
CE•13922

File Name: CE-13922ALL
Date: 11/15/2012

Looking northeast towards fire station housing seismic station CE.13922 and at HVSR sensor 507

Looking southeast along S-wave refraction array 13922-1

Looking south along array 13922-4

Looking northwest along northwest-southeast segment of passive surface wave array 13922-2

Looking northeast along MASW and MALW array 13922-4 and at HVSR sensor 450A

5. Array 13922-4 (48 channel MALW and S-wave seismic refraction array utilizing 4.5 Hz horizontal geophones spaced 1.5 m apart for a length of 70.5 m, forward and reverse shot locations with multiple source offsets and multiple interior shot locations).
6. Seven HVSR measurement locations: two near the seismic station, two distributed along array 13922-1 and three distributed along array 13922-4.

Location of Geophysical Testing Arrays:

Location	Latitude	Longitude
13922-1, Northwest End of MASW/Refraction Array	33.67024	-117.33333
13922-1, Center of MASW/Refraction Array	33.67014	-117.33297
13922-1, Southeast End of MASW/Refraction Array	33.67003	-117.33261
13922-2, Northwest End of Passive "T" array (Geophone 48)	33.67021	-117.33323
13922-2, Intersection of SW-NE and NW-SE Segments of Passive "T" Array (Geophone 12)	33.66999	-117.33249
13922-2, Northeast End of Passive "T" Array (Geophone 24)	33.67039	-117.33234
13922-2, Southwest End of Passive "T" array (Geophone 1)	33.66963	-117.33264
13922-4, Southwest End of MASW/Refraction Array	33.66783	-117.33272
13922-4, Center of MASW/Refraction Array	33.66812	-117.33260
13922-4, Northeast End of MASW/Refraction Array	33.66842	-117.33247
HVSR Sensor 507	33.66895	-117.33247
HVSR Sensor 450	33.67020	-117.33328
HVSR Sensor 453	33.67005	-117.33265
HVSR Sensor 450A	33.66782	-117.33271
HVSR Sensor 507A	33.66875	-117.33234
HVSR Sensor 453A	33.66814	-117.33261
HVSR Sensor 507B	33.67004	-117.33265
HVSR Sensor 450B	33.67018	-117.33327
HVSR Sensor 453B	33.66888	-117.33232

Notes: 1) WGS84 Coordinate System (decimal degrees)

2) Survey accuracy is estimated at 1 to 2 m.

Results:

V_S Model 1

Depth to Top of Layer (m)	Layer Thickness (m)	S-Wave Velocity (m/s)	Inferred P-Wave Velocity (m/s)	Assumed Poisson's Ratio	Assumed Density (g/cm^3)
0	1.5	225	420	0.3	1.80
1.5	3.5	317	593	0.3	1.85
5	8	357	668	0.3	1.90
13	>17	1261	2361	0.3	2.30

Notes: 1) Depth of investigation is about 30 m.
2) Half space depth only accurate to about 20% of depth.
3) Bottom layer is a half space.
4) Half space V_S not well resolved.

V_S Model 2

Depth to Top of Layer (m)	Layer Thickness (m)	S-Wave Velocity (m/s)	Inferred P-Wave Velocity (m/s)	Assumed Poisson's Ratio	Assumed Density (g/cm^3)
0	1.5	209	390	0.3	1.80
1.5	11.5	340	636	0.3	1.90
13	>17	1600	2993	0.3	2.30

Notes: 1) Depth of investigation is about 30 m.
2) Half space depth only accurate to about 20% of depth.
3) Bottom layer is a half space.
4) Half space V_S constrained at 1,600 m/s and not well resolved.

Observations/Discussion:

- Because the seismic station is located in a developed area, geophysical data acquisition was limited to arrays placed on roads or parking lots in relatively close proximity to the seismic station. Because bedrock was found to be relatively shallow, it was very important acquire the geophysical data as close as possible to the seismic station due to the strong influence of bedrock depth on V_{S30}.
- Seismic refraction and surface wave data were acquired at this site during two site visits on 1/19/11 and 8/29/11. During the first site visit, P-wave seismic refraction and MASW data (array 13922-1) and passive surface wave data (array 13922-2) were acquired along an alley and Poe Avenue. Two HVSR measurements were made along array 13922-1 and an HVSR measurement was made in the fire station parking lot. After field review of the data, it became clear that high velocity bedrock was quite shallow and Rayleigh wave data were degraded by a dominant higher first mode and/or modal superposition.

Therefore, S-wave seismic refraction data were acquired along a 24 channel array coincident with array 13922-1. This is about the time in the investigation that the need for Love wave (MALW) testing at some sites was recognized; however, low frequency geophones were not available during field testing. Preliminary data analysis revealed that Rayleigh wave techniques (passive and active) were generally not applicable at the site because the low frequency portion of the dispersion associated with bedrock could not be clearly identified. Review of Love wave data from the S-wave refraction line, however, looked promising. Additionally, the HVSR peak near the fire station had higher amplitude and slightly higher frequency than that along array 13922-1. Therefore, during the second site visit a decision was made to acquire MASW and MALW data in a parking lot south of the seismic station.

- Initial HVSR measurements were made at sensor locations 507 (near seismic station), 450 and 453 (both along array 13922-1). At sensor locations 450 and 453 there is a low amplitude HVSR peak in the 8 to 8.25 Hz range. Sensor 453 has a problem with the sensor deployment (sensor coupling, poor sensor cable deployment, etc.) resulting in the elevated HVSR response between 0.4 and 2 Hz. This demonstrates the importance of multiple measurements at a site to avoid potential misinterpretation. HVSR sensor 507, located near the seismic station, has a higher frequency HVSR peak (9.2 Hz) with higher amplitude. Assuming that the S-wave velocity of bedrock in the site vicinity is constant, the higher frequency HVSR peak at sensor 507 indicates that bedrock is shallower and/or the V_S of the sediments higher in the vicinity of the seismic station than in the vicinity of array 13922-1. The higher amplitude HVSR peak presents the possibility that the V_S of the sediments may be lower in the vicinity of the seismic station. Therefore, it is possible that bedrock is slightly shallower and that the overlying sediments have slightly lower V_S near the seismic station than in the vicinity of array 13922-1. Of course, possible effects of ground surface conditions on HVSR peak cannot be discounted.
- During the second site visit, HVSR measurements were made along array 13922-4 (sensors 450A, 453A and 507A), a new measurement made near the seismic station (sensor 453B), and measurements repeated along array 13922-1 (sensors 450B and 507B). The measurements repeated along array 13922-1 are almost identical to the original measurements, minus the sensor coupling artifact, demonstrating the repeatability of HVSR measurements, at least for high frequency peaks. The HVSR peak is in the 8 to 8.5 Hz range and amplitude is very low, as with the original measurements. The new measurement location near the seismic station (sensor 453B) yielded a similar amplitude, but much broader peak (7.5 to 10 Hz) than the original measurement. Undulating bedrock topography or influence of the nearby structure are possible explanations to the more complicated HVSR response near the seismic station. Finally, the HVSR measurements made along array 13922-4 have much higher amplitude and lower frequency (6.5 to 7 Hz) than the measurements made near the seismic station or along array 13922-1.
- The lower frequency HVSR peak along that array 13922-4 indicates that either bedrock is deeper or the sediments have lower V_S in the vicinity of the array than at the seismic station, while the higher amplitude HVSR response may indicate that sediments have a lower velocity beneath array 13922-4. In fact the increasing amplitude in HVSR response to the south from array 13922-1, may indicate that the sediment velocity is decreasing towards the south, assuming that bedrock properties are constant.

- Noise conditions at the site appeared adequate for application of passive surface wave techniques. However, passive surface wave (Rayleigh wave) techniques were not effective at this site because shallow high velocity bedrock excited dominant higher modes, which could not be accurately defined. This would be an excellent site to evaluate Love wave passive surface wave techniques, a technique which we did not have available during this investigation.
- P- and S-wave seismic refraction data collected along array 13922-1 were modeled using a tomographic inversion routine with a layer based starting model to determine the approximate velocity structure of bedrock. Bedrock depths are not considered valid in these models because the sediment velocities could not be accurately determined. It appears that compacted soils in the alley or a covered asphalt layer caused velocity of the sediments to be overestimated which resulted in overestimated depth to bedrock. It should be noted that there is significant traffic noise in the site vicinity, which severely degraded S-wave refraction data and the S-wave refraction models should only be used to determine the approximate V_S of bedrock in the site vicinity to guide surface wave modeling. P-wave refraction data quality is much better; however, a longer profile would have been preferred to more accurately characterize the high velocity of bedrock.
- The P-wave seismic refraction model for array 13922-1 indicates that V_P of bedrock is likely in the 4,000 to 4,500 m/s range. The S-wave seismic refraction model for array 13922-1 indicates that V_S of bedrock is likely in the 1,600 to 1,800 m/s range, although data quality was not adequate to accurately resolve the velocity. A longer seismic line in a more open area with less traffic noise may allow V_P and V_S of the bedrock unit to be more accurately resolved. This would involve testing further away from the seismic station. A ball park located about 250 m south of the seismic station is the closest area with enough open space for a longer seismic profile.
- P-wave and S-wave refraction data collected along array 13922-4 were not modeled due to strong interference from the asphalt layer in many areas. Not all seismic records were significantly degraded by the asphalt and it was possible to inspect the data to determine generalized velocity structure. The P-wave first arrival data could be fit with bedrock at a depth of about 11 m and V_P of the sediments and bedrock on the order of 600 m/s and 4,000 to 4,500 m/s, respectively. The P-wave velocity of bedrock is consistent with that observed beneath array 13922-1. Shallow groundwater is possible at this site due to the proximity to Lake Elsinore. As an example, a 1 m thick zone of saturated sediments, which would not give rise to a first arrival, would drop bedrock depth by about 2 m. The S-wave seismic refraction data could be fit with bedrock at a depth of about 12 to 13 m and V_S of the sediments in the 350 and 2,000± m/s ranges, respectively.
- Assuming that P-wave velocity of weathered bedrock averages 4,250 m/s and that the bedrock is saturated, in which case Poisson's ratio in the 0.35 to 0.4 range is plausible, estimated V_S would be in the 1,735 to 2,040 m/s range.
- Rayleigh wave MASW data were not useful at this site due to dominant higher mode energy associated with the large impedance contrast at shallow depth. Because of issues with S-wave seismic refraction data in this high noise environment, MALW (Love wave) data acquired along array 13922-4 was the primary data set used for site characterization. The Love wave fundamental mode is dominant at sites with shallow bedrock and, therefore, interpretation is less complicated than attempting multi-mode inversion of Rayleigh wave dispersion data. When utilizing surface wave methods to characterize

velocity structure at shallow rock sites, S-wave seismic refraction is important to constrain bedrock velocity, because surface wave techniques are not generally capable of accurately modeling the bedrock velocity, even when relatively shallow.

- Although Rayleigh wave methods were not successful at this site due to inability to reliably pick the low frequency portion of the dispersion curve associated with rock, possible modifications to survey design may have allowed the dispersion curve to be more reliably interpreted, in which case multi-mode inversion could have been attempted. A shorter array may have been more successful; however the cylindrical beamformer (Zywicki, 2005) would need to be utilized for the wavefield transform to mitigate near field effects. Additionally, SASW testing could be attempted and, if successful at obtaining a dispersion curve, 3-D array based inversion, which can account for modal superposition and body waves, could be applied to model the dispersion curve.
- The smallest wavelength extracted from the MALW data is 8 m, possibly due to the presence of a stiff surface asphalt and subgrade layer.
- There is about 50 m/s scatter in the Love wave dispersion data, likely the result of lateral velocity variation.
- A representative dispersion curve was generated for the Love wave MASW data set using a moving average, polynomial curve fitting routine and used for modeling.
- There is no published guideline on maximum wavelength Love waves that can be extracted as a function of survey design and near field effects need to be evaluated. Near field criteria typically applied to Rayleigh wave data are not necessarily applicable to Love waves. In fact, near field effects may not be as restrictive for Love waves as the particle motion is orthogonal to direction of propagation. The maximum wavelength Love wave data extracted from the seismic records was, therefore, arbitrarily set to 1.75 times the distance from the source to midpoint of the receiver array, allowing extraction of Love wave dispersion data to a maximum wavelength of 115 m. The possibility that there are near field effects in the longest wavelength Love wave data cannot be discounted.
- Inversion of surface wave data can only determine the depth to bedrock to an accuracy of about 20% of depth, unless the maximum velocity of the sediments can be constrained. However, the nonuniqueness is such that V_{S30} can be reliably estimated (i.e. average velocity of sediments increases for deeper bedrock interpretation and vice versa). We believe that HVSR suffers from similar nonuniqueness issues and at best would only slightly narrow the range of potential V_S models. Possibly, multi-mode inversion, assuming multiple modes can accurately be picked and identified, could more accurately model depth to bedrock.
- The V_S model (Model 1) provided to represent subsurface velocity structure has bedrock interpreted at an intermediate depth of 13 m with alternate interpretations having bedrock in the 11 to 16 m depth range being viable. Inversion of the Love wave dispersion data (or for that matter Rayleigh wave data) is unable to accurately model the V_S of the half space (i.e. bedrock) and, in this case, appears to significantly underestimate bedrock velocity relative to P- and S-wave refraction data. Therefore, an alternate model (Model 2) is presented with bedrock V_S fixed at 1,600 m/s, which is still expected to be conservative. This model has higher RMS error, but still falls within the scatter in the dispersion data, expect at longest wavelengths, which may have underestimated phase velocity due to near field effects.

- Surface wave depth of investigation is difficult to quantify at sites with an abrupt increase in velocity at shallow depth, but is assumed to be about 30 m.
- V_{S30} beneath array 13922-4 is 560 and 581 m/s for Models 1 and 2, respectively (NEHRP Site Class C).
- Based on HVSR measurements, V_{S30} beneath array 13922-4 may not be representative of conditions beneath the nearby seismic station as it appears that both bedrock depth and sediment velocity is slightly variable in the site vicinity. At shallow rock sites, V_S of near surface sediments and bedrock depth have the most significant influence on V_{S30} with the V_S of bedrock having only secondary influence. For example, a 10% change in the depth to bedrock increases/decreases V_{S30} by about 8%. Likewise increasing or decreasing average V_S of the sediments by 10% changes V_{S30} by about 8%. On the other hand, the V_S of the bedrock unit must increase by 56% to increase V_{S30} by 8%. Therefore, although it is not possible to accurately constrain bedrock V_S without additional testing at an alternate location, the effect on observed V_{S30} is minimal.
- Synthetic HVSR models were generated for V_S Model 2 using both the Micromed Grilla and Geometrics WaveEq software packages. The calculated HVSR peak is about 7 Hz, which is at the high end of the observed HVSR peaks along array 13922-4. HVSR amplitude cannot be matched as theoretical amplitudes are always significantly higher than observed amplitudes at sites with large increases in V_S.
- The HVSR peak can also be predicted using the simple quarter wavelength approximation, which states that $D = V_{Save}/4f_0$ where D = depth to bedrock, V_{Save} = average V_S of sediments overlying bedrock and f_0 = fundamental frequency, assumed to be approximated by the HVSR peak frequency. The predicted HVSR peak for Model 2 using the quarter wavelength approximation is 6.1 Hz, slightly lower than that observed.
- At this site, HVSR modeling performs better than the quarter wavelength approximation at predicting the HVSR peak, although this is not always the case.
- To adjust V_{S30} beneath array 13922-4 to that at the seismic station, Model 2 was adjusted using HVSR modeling software. The highest frequency HVSR peak along array 13922-4 is 7 Hz and the average HVSR peak near the seismic station is about 9 Hz, although adjustments are made from 7 Hz to both 8 and 9 Hz. Adjustments to V_{S30} are made two ways, first by keeping bedrock depth constant and adjusting the V_S of the overlying sediment layer and secondly by keeping the average V_S of the sediments constant and adjusting thickness of the sediment layer overlying bedrock.
- Adjusted V_{S30} keeping bedrock depth constant for 8 and 9 Hz HVSR peaks is about 619 and 654 m/s, respectively.
- Adjusted V_{S30} keeping the average V_S of the sediments constant for 8 and 9 Hz HVSR peaks is about 639 and 696 m/s, respectively.
- Although more HVSR measurements are needed for confirmation, we believe a 9 Hz HVSR peak best characterizes the seismic station and that both sediment velocity and bedrock depth may be different at seismic station CE.13922 than beneath array 13922-2. Therefore, we recommend using the average of the two adjusted V_{S30} values for a 9 Hz peak, which is 675 m/s. The accuracy of adjusted V_{S30} shouldn't be considered more accurate than about 10%.

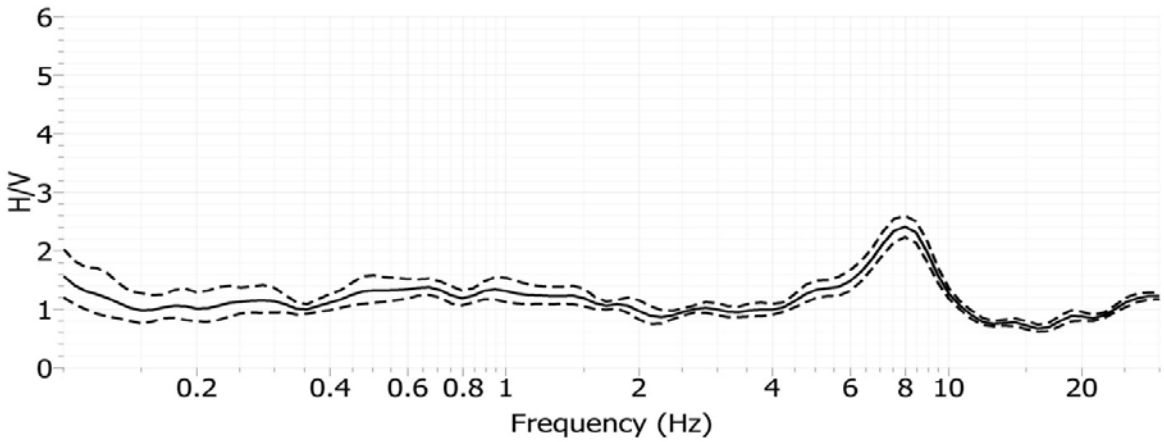

Site CE.13922, H/V Spectral Ratio, Array 13922-1, Sensor 450B

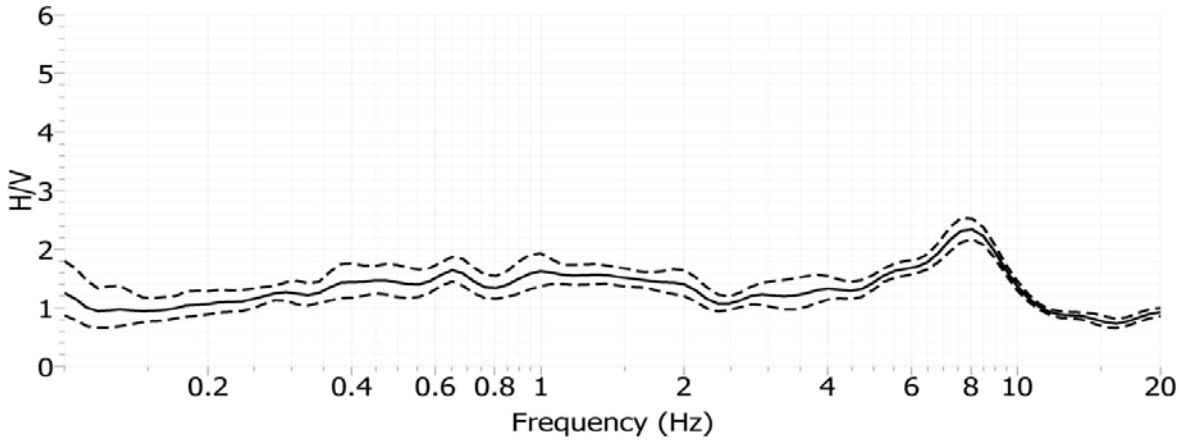

Site CE.13922, H/V Spectral Ratio, Array 13922-1, Sensor 450

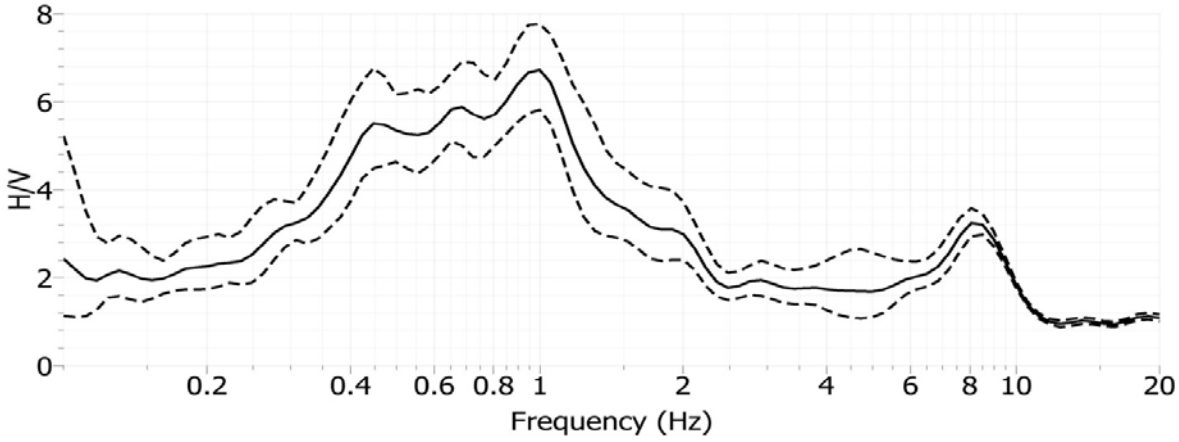

Site CE.13922, H/V Spectral Ratio, Array 13922-1, Sensor 453 (elevated HVSR response between 0.3 and 2 Hz associated with poor sensor coupling)

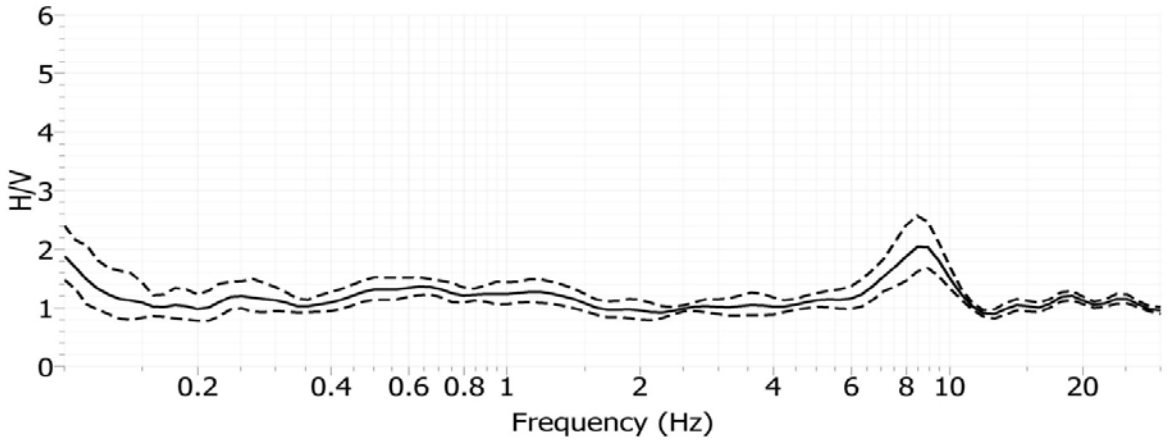

Site CE.13922, H/V Spectral Ratio, Array 13922-1, Sensor 507B

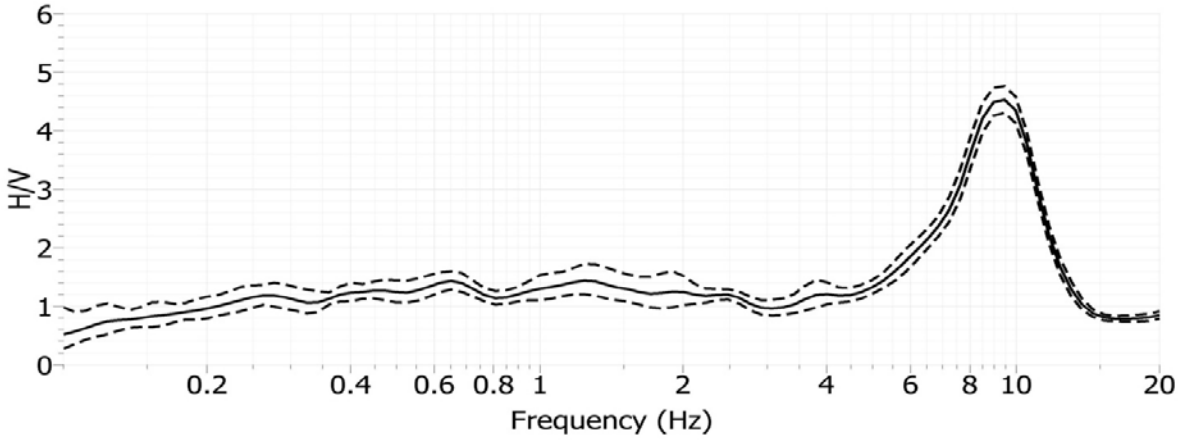

Site CE.13922, H/V Spectral Ratio, Near Seismic Station, Sensor 507

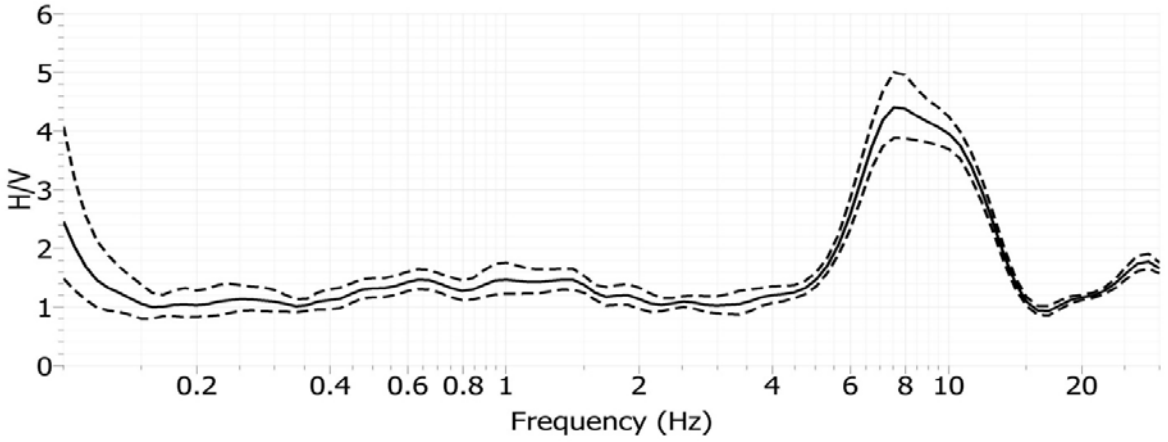

Site CE.13922, H/V Spectral Ratio, Near Seismic Station, Sensor 453B

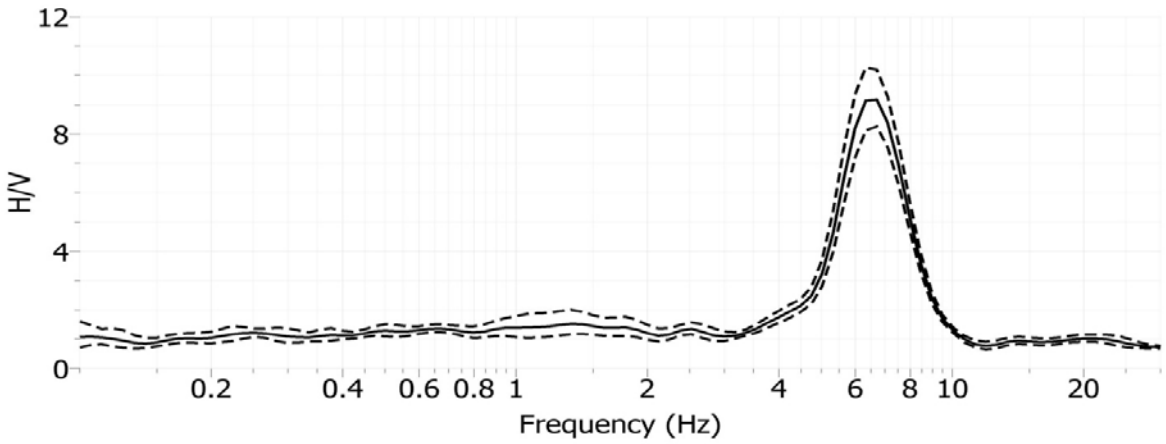

Site CE.13922, H/V Spectral Ratio, Array 13922-4, Sensor 507A

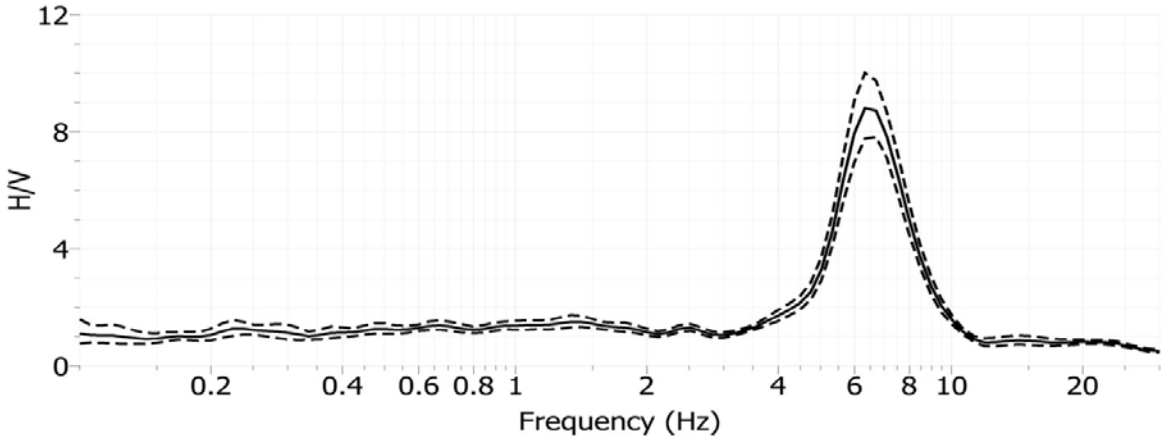

Site CE.13922, H/V Spectral Ratio, Array 13922-4, Sensor 453A

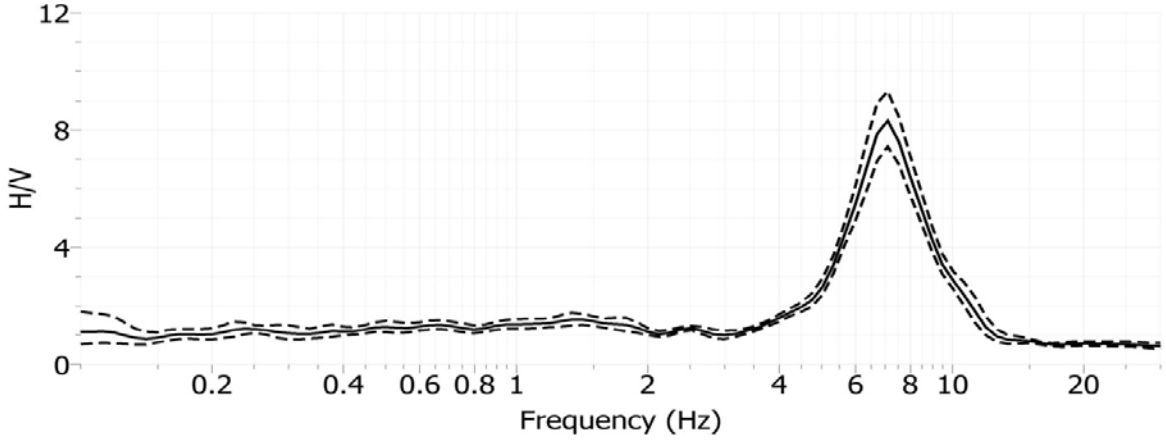

Site CE.13922, H/V Spectral Ratio, Array 13922-4, Sensor 450A

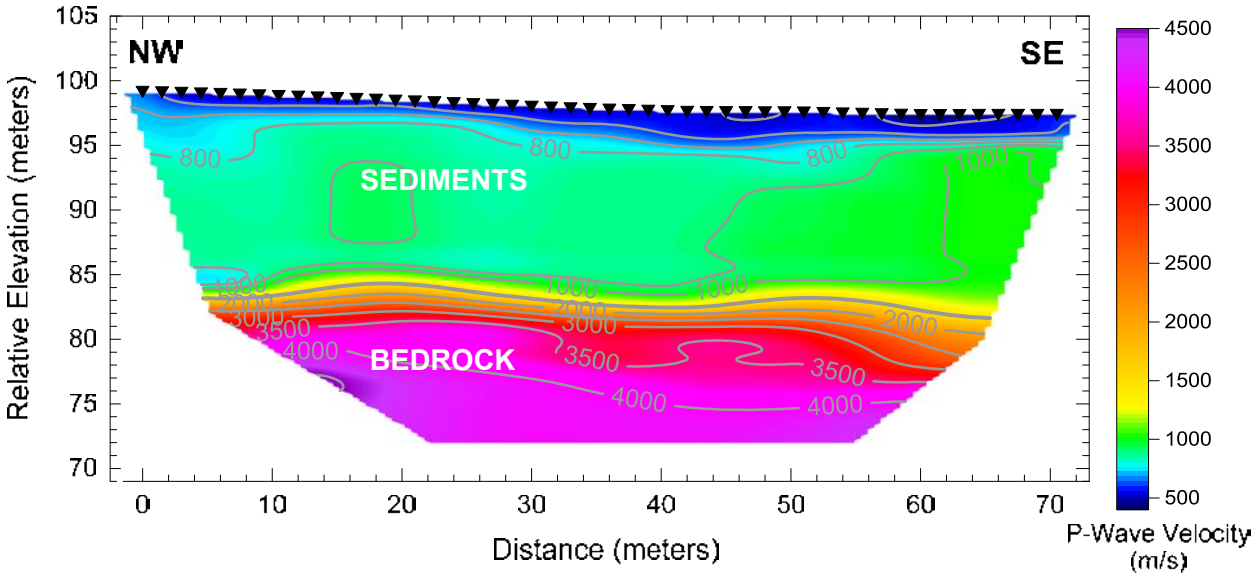

Array 13922-1 – Tomographic P-wave seismic refraction model utilizing layer based starting model. Bedrock depth is not reliable due to difficulty accurately determining sediment velocity; however, bedrock depth should be reliable.

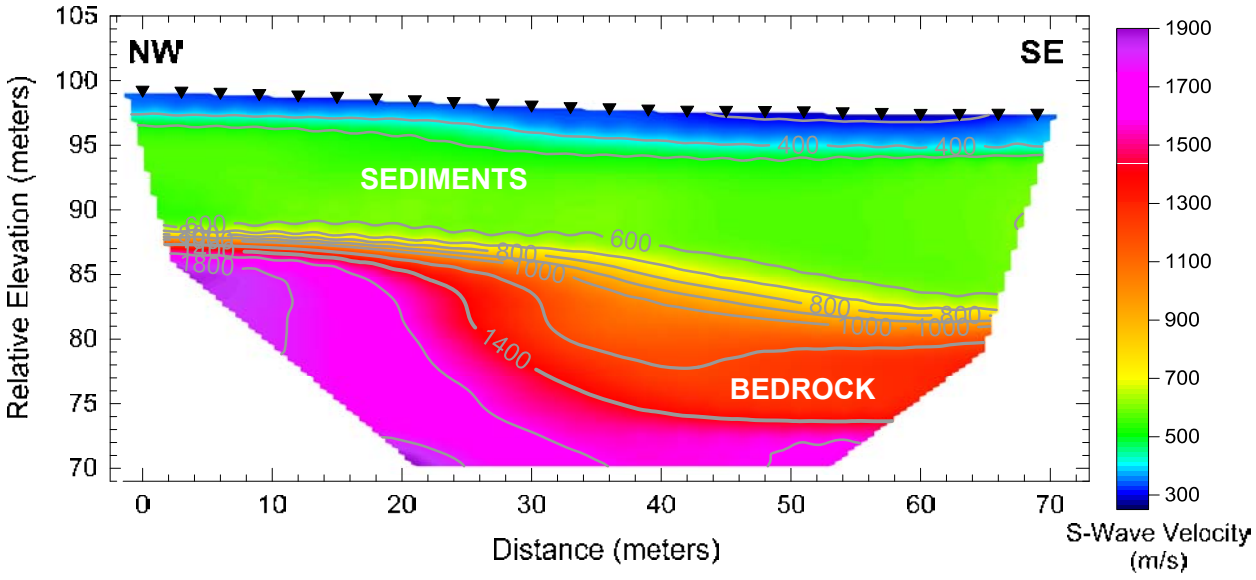

Array 13922-1 – Tomographic S-wave seismic refraction model utilizing layer based starting model. Bedrock depth is not reliable due to difficulty accurately determining sediment velocity. Additionally, S-wave seismic refraction data are quite noisy due to vehicular traffic and should only be used as an approximate guide as to bedrock velocity.

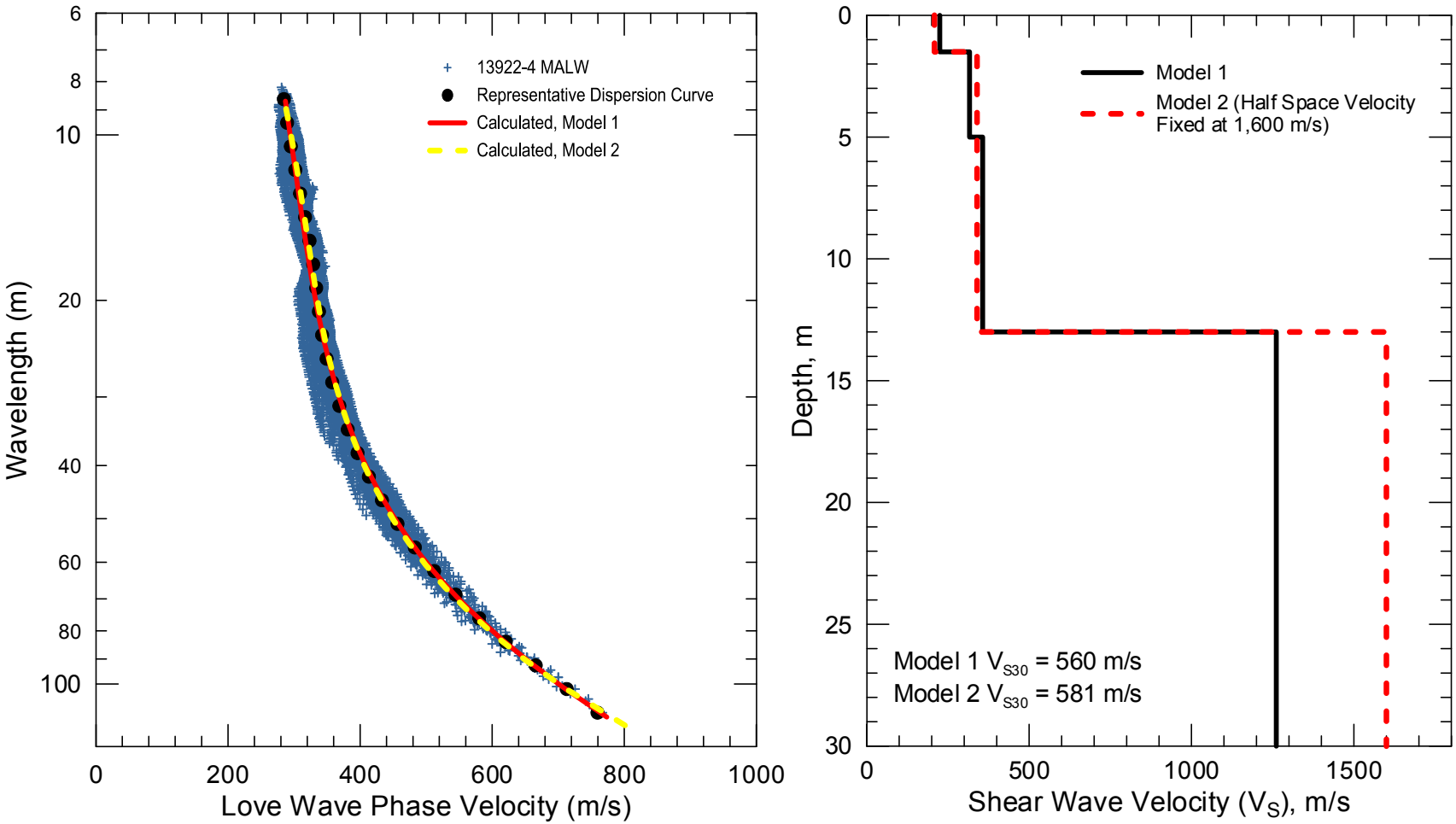

CE.13922 - Field, representative and inverted theoretical surface wave dispersion data (left) and associated V_S model (right)

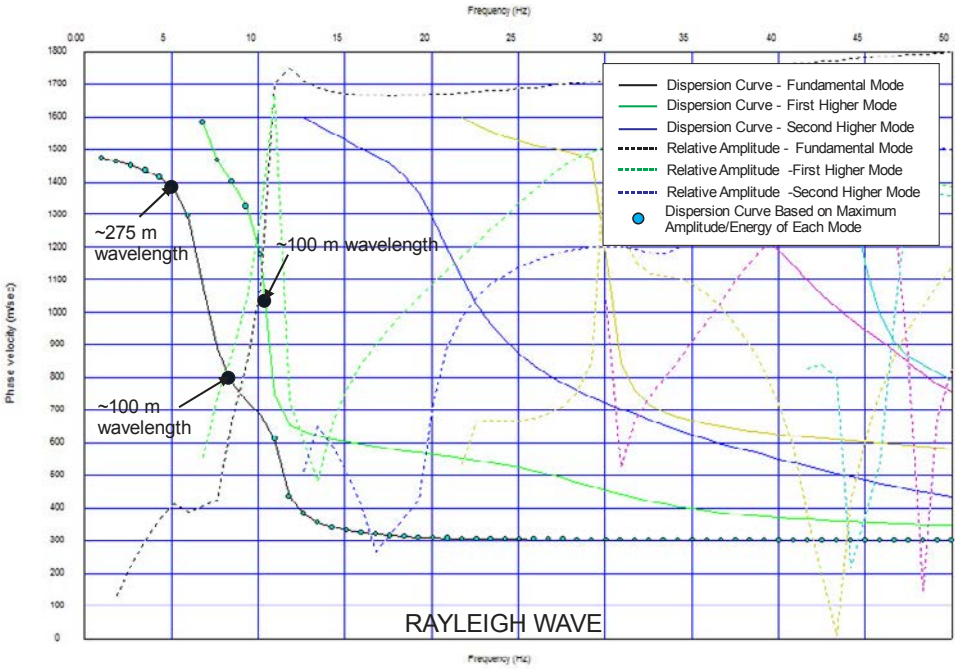

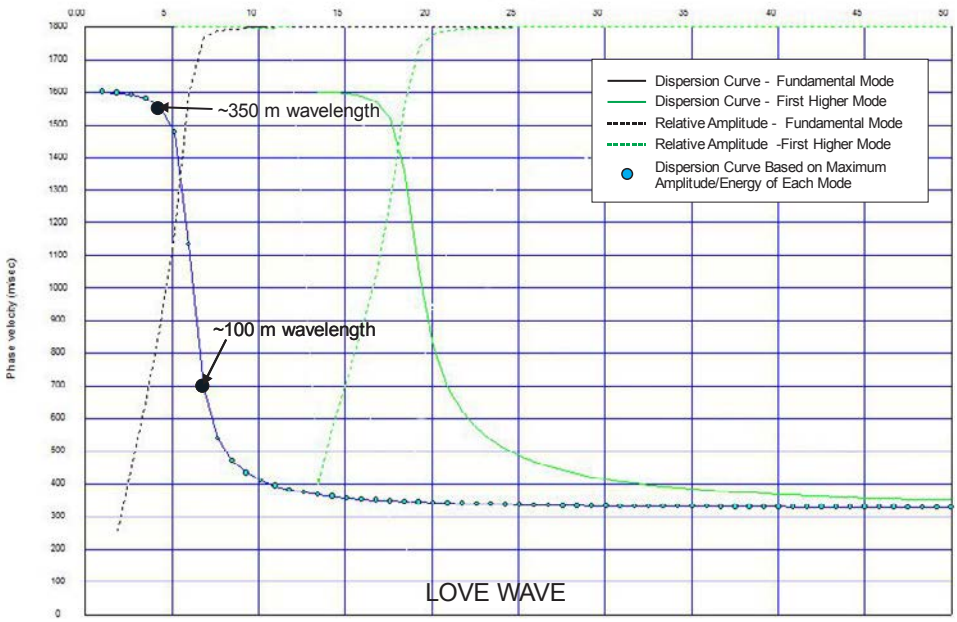

Multi-mode Rayleigh and Love wave response to a simple geologic model representative of subsurface velocity structure at CE.13922 (13 m of sediments with V_S=325 m/s over bedrock with V_S=1,600 m/s). Rayleigh wave response is complicated with the fundamental mode jumping to the first higher mode at about 11 Hz and back to the fundamental mode at 6 Hz, where the first higher mode terminates. The fundamental mode is dominant at all frequencies for the Love wave response. This figure also demonstrates one reason why surface wave techniques cannot accurately constrain the bedrock velocity, even in cases of relatively shallow bedrock. Typically, it is difficult to extend Rayleigh and Love waves wavelengths to greater than 100 m, assuming some type of near field wavelength restriction is applied. However, the Rayleigh and Love wave dispersion curves do not start to bend towards the half space velocity until wavelengths of about 275 and 350 m, respectively.

Site CE.13929

Location: Menifee Valley, Riverside County Fire Station #68, Murrieta Road and Wickerd Road, Menifee, California

Latitude: 33.64911 **Longitude:** -117.20525
(Station coordinates modified using published coordinates from http://www.strongmotioncenter.org with further adjustment made by identifying the structure housing the seismic sensor on Google Earth, WGS84 coordinate system.)

V_{S30} (measured): 565 m/s

V_{S30} (adjusted to more accurately reflect seismic station conditions): 565 m/s (no adjustment necessary.)

NEHRP Site Class: C

Geomatrix Code: AQB

Geologic Conditions/Observations: Site located on thin layer of Quaternary (Pleistocene) alluvium over Cretaceous granitic rock.

Site Conditions: Suburban site with significant traffic noise from adjacent road. Relatively flat terrain in the immediate site vicinity. Crystalline basement mapped as gabbro outcrops in a small hill about 60 m southeast of the seismic station and granodiorite/tonalite outcrops about 150 m west of the seismic station. Based on topography in the site vicinity, the more prevalent granodiorite and tonalite outcrops may be significantly more weathered than the localized gabbro outcrop. Test area located about 2 m lower in elevation than the seismic station and further away from bedrock outcrop.

Geophysical Methods Utilized: HVSR, Seismic Refraction, MASW (Rayleigh Wave), MALW (Love Wave)

Geophysical Testing Arrays:

1. Array 13929-1 (48 channel MASW and P-wave seismic refraction array utilizing 4.5 Hz vertical geophones spaced 1.5 m apart for a length of 70.5 m, forward and reverse shot locations with multiple source offsets and source types and multiple interior shot locations). Passive surface wave data were also recorded on this array.
2. Array 13929-1 (48 channel MASW and S-wave seismic refraction array utilizing 10 Hz horizontal geophones spaced 1.5 m apart for a length of 70.5 m, forward and reverse shot locations with multiple source offsets and source types (hammers only) and multiple interior shot locations).
3. Three HVSR measurement locations: two distributed along array 13929-1 and the other adjacent to the fire station housing the seismic station.

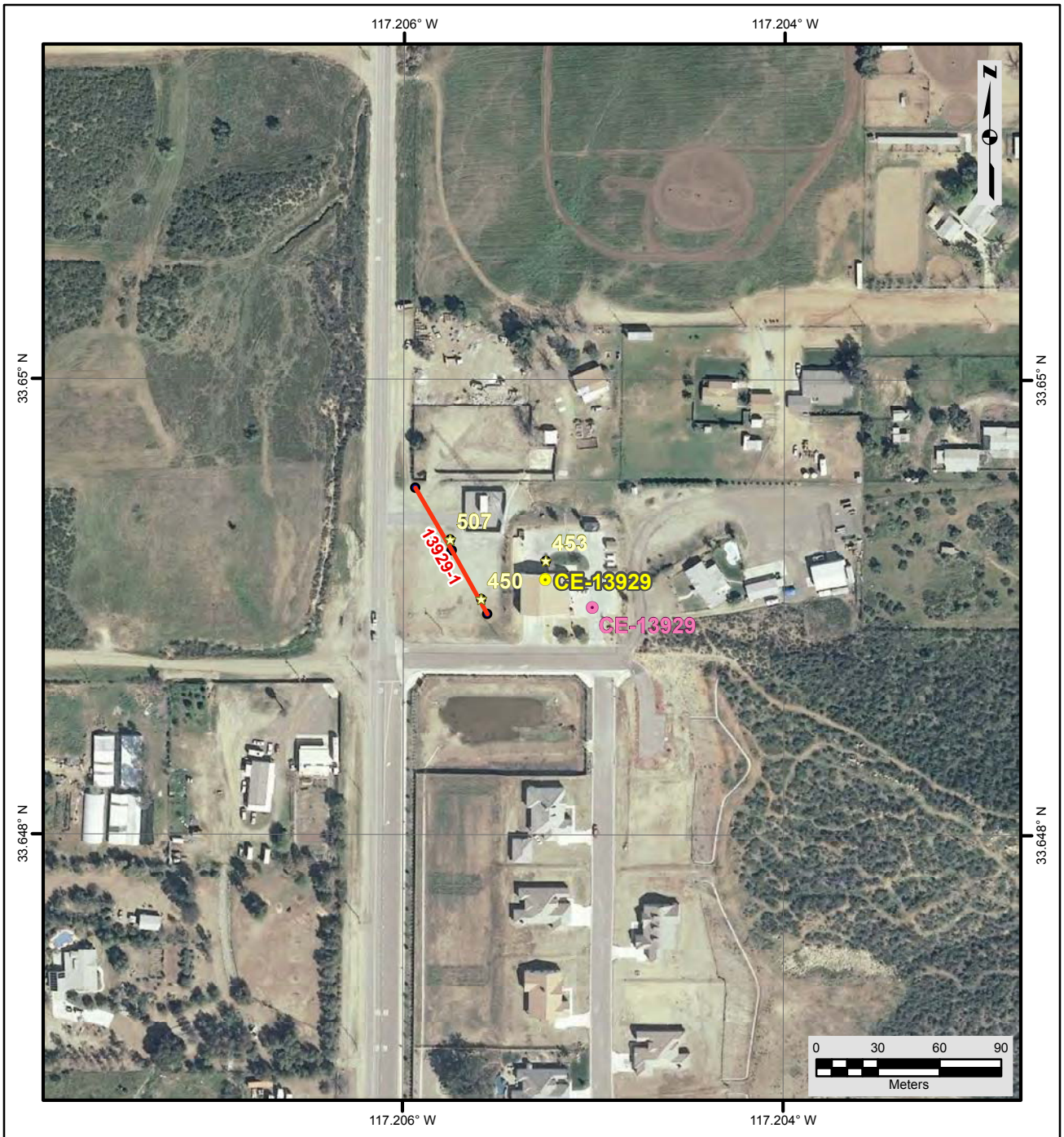

Legend

- Seismic Station - Approximate Improved Location
- Seismic Station - Approximate Location of Record
- H/V Spectral Ratio Location
- MASW and Seismic Refraction Array

NOTES:
1. WGS 1984 COORDINATE SYSTEM
2. Image Source: ESRI, i-cubed, USDA FSA, USGS, AEX, GeoEye, Getmapping, Aerogrid, IGP

File Name: CE-13929-I

Date: 8/19/2011

USGS science for a changing world

GEOVision geophysical services

RECOVERY.GOV

SITE MAP
CE•13929

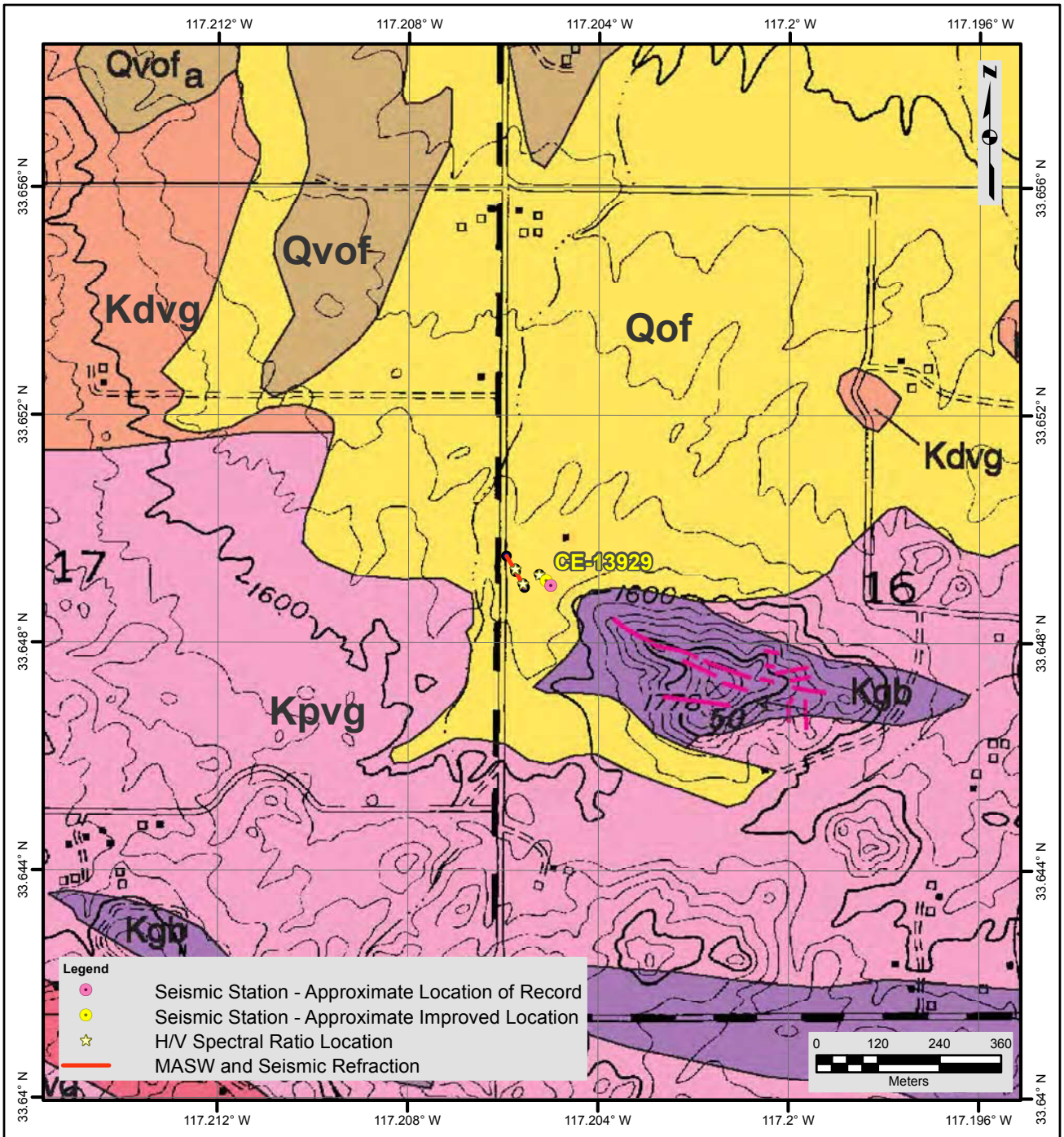

Description of Geologic Map Units

Qof = Quaternary (Pleistocene) old alluvial fan deposits, gravel and sand
Qvof = Quaternary (Pleistocene) very old alluvial fan deposits, sandy
Qvofa = Quaternary (Pleistocene) very old alluvial fan deposits, sand and gravel
Kdvg = Mesozoic (Cretaceous) granodiorite to tonalite, Domenigoni Valley pluton, some mafic rich rocks
Kpvg = Mesozoic (Cretaceous) monzogranite to granodiorite, contains inclusions of blocks of gabbro
Kgb = Mesozoic (Cretaceous) hornblende gabbro, includes noritic and dioritic composition rocks

NOTES:
1. WGS 1984 COORDINATE SYSTEM
2. Geologic Map of the Romoland 7.5' Quadrangle, Riverside County, California, Version 1.0 by Douglas M. Morton, 1991, 1995 and 1996
3. See site map for details of geophysical survey

File Name: CE-13929

Date: 4/7/2011

USGS science for a changing world

GEOVision geophysical services

RECOVERY.GOV

GEOLOGIC MAP
CE•13929

Looking east towards location of CE.13929 seismograph station and HVSR sensor 453

Looking southeast along MASW array 13929-1

Looking southeast towards fire station housing CE.13929 and center of S-wave array 13929-1

S-wave refraction/MASW data acquisition

S-wave seismic sources

Location of Geophysical Testing Arrays:

Location	Latitude	Longitude
13929-1, Southeast end of Array	33.64897	-117.20555
13929-1, Center of Array	33.64925	-117.20574
13929-1, Northwest end of Array	33.64952	-117.20593
HVSR Sensor 507	33.64930	-117.20575
HVSR Sensor 450	33.64903	-117.20558
HVSR Sensor 453	33.64920	-117.20524

Notes: 1) WGS84 Coordinate System (decimal degrees)
2) Survey accuracy is estimated at 1 to 2 m.

Results:

V_S Model

Depth to Top of Layer (m)	Layer Thickness (m)	S-Wave Velocity (m/s)	Inferred P-Wave Velocity (m/s)	Inferred Poisson's Ratio	Inferred Density (g/cm^3)
0	1	169	316	0.3	1.7
1	6	238	445	0.3	1.8
7	8	850	1591	0.3	2.1
15	9	1086	2032	0.3	2.2
24	>6	1427	2670	0.3	2.3

Observations/Discussion:

- The HVSR plots for sensor location 453, located near the seismic station, and 450, located on the seismic test array, have identical 7.5 Hz peaks. This confirms that the test area is representative of conditions beneath the seismograph station (i.e. bedrock depth may be similar at the seismic station and test array). There is, however, an amplitude difference at the two sensor locations possibly due to sensor 453 being located on concrete.
- The HVSR plot for sensor 507 has a slightly lower frequency 6.7 Hz peak, indicating that bedrock may be slightly deeper, overlying sediments slightly softer or a different weathering profile present in bedrock.
- There was not sufficient space for passive surface wave testing; however, passive surface wave data were recorded into the MASW array. The passive surface wave data, however, were not useful due to dominant higher mode surface waves.
- A tomographic inversion of P-wave seismic refraction data was conducted using a layer based starting model and indicates that high velocity bedrock is located at depths in the 5 to 8 m range. P-wave velocity of the bedrock appears to exceed 3,000 m/s at depths between 7 and 15 m indicating that S-wave velocity may exceed 1,500 m/s at similar depths (assuming a Poisson's ratio of 0.333). The P-wave refraction data also indicates

that there is some weathering in the uppermost bedrock unit. A longer line would be beneficial to better constrain the higher P-wave velocities, although there was limited space to work at the site. It should be noted that the relatively high velocities could be associated with the gabbro outcropping adjacent to the site. Most bedrock in the site vicinity consists of granodiorite and tonalite, which may have a thicker weathering profile and, therefore, lower P-wave velocities.

- Rayleigh wave MASW data were not useful at this site due to dominant higher mode energy associated with the large impedance contrast at shallow depth. Therefore, S-wave seismic refraction and Love wave MALW data were acquired in an attempt to characterize S-wave velocity structure at the site.
- S-wave seismic refraction data, considered important to constrain the S-wave velocity of bedrock, were not useful at this site due to heavy traffic on the adjacent Murrieta Road and weak S-wave energy.
- Love wave MALW data did not suffer from dominant higher modes and was used to generate an S-wave velocity model.
- A representative dispersion curve was generated for the Love wave MALW data set using a moving average, polynomial curve fitting routine and used for modeling.
- The V_S for bedrock is not well constrained in the surface wave model and there are a multitude of bedrock V_S structures that can fit the dispersion curve equally well. Bedrock V_S in the Love wave V_S model is generally underestimated relative to the seismic refraction V_P model. Based on P-wave refraction data, V_S is expected to exceed 1,500 m/s at relatively shallow depth unless either the weathering and/or saturation of weathered rock results in a Poisson's ratio of greater than 0.35.
- Surface wave depth of investigation is about 30 m based on one third of maximum wavelength criteria. Longer wavelength Love wave dispersion data may be required than Rayleigh wave dispersion data to image velocity structure to a specific depth.
- The predicted HVSR peak for the V_S model using the quarter wavelength approximation is about 8 Hz, 0.5 Hz higher than the measured peak. The predicted HVSR peak for the V_S model using HVSR modeling software is about 8.5 Hz, 1 Hz higher than the measured peak. Joint inversion of the HVSR and Love wave dispersion data may yield a better fit between the observed and calculated HVSR response.
- V_{S30} is 565 m/s (Site Class C).
- V_{S30} is highly dependent upon depth to bedrock and the probable variable weathering profile within bedrock and, therefore, may vary by 10%, or more, in the immediate site vicinity.

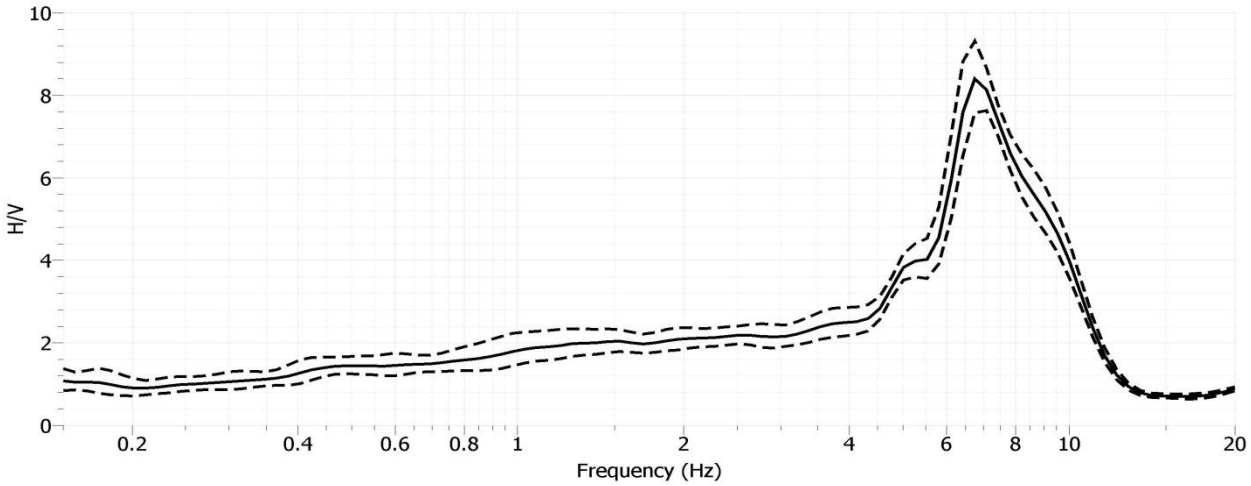

Site CE.13929, H/V Spectral Ratio, Array 13929-1, Sensor 507

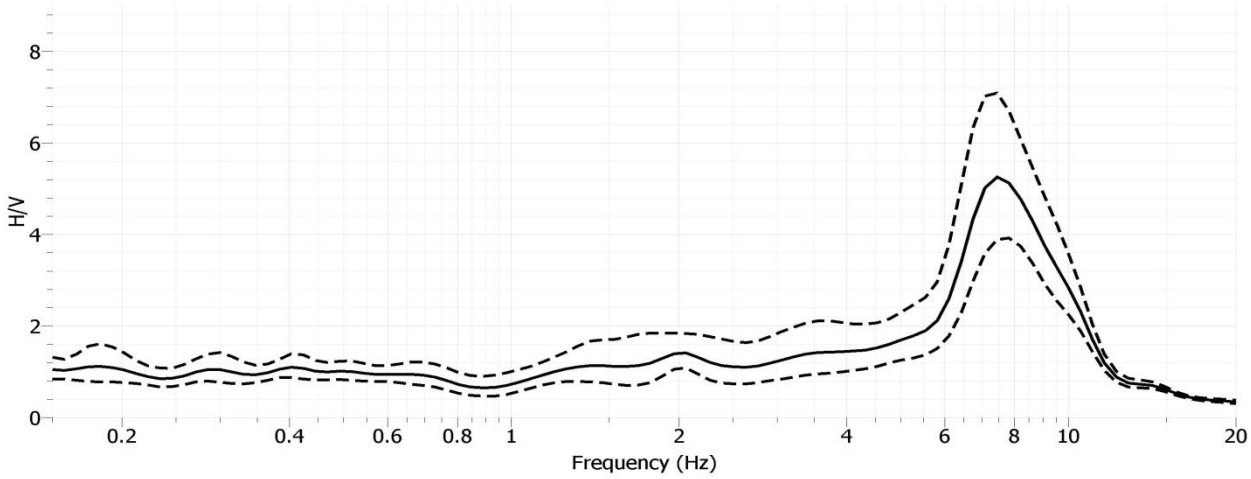

Site CE.13929, H/V Spectral Ratio, Near Seismic Station, Sensor 453

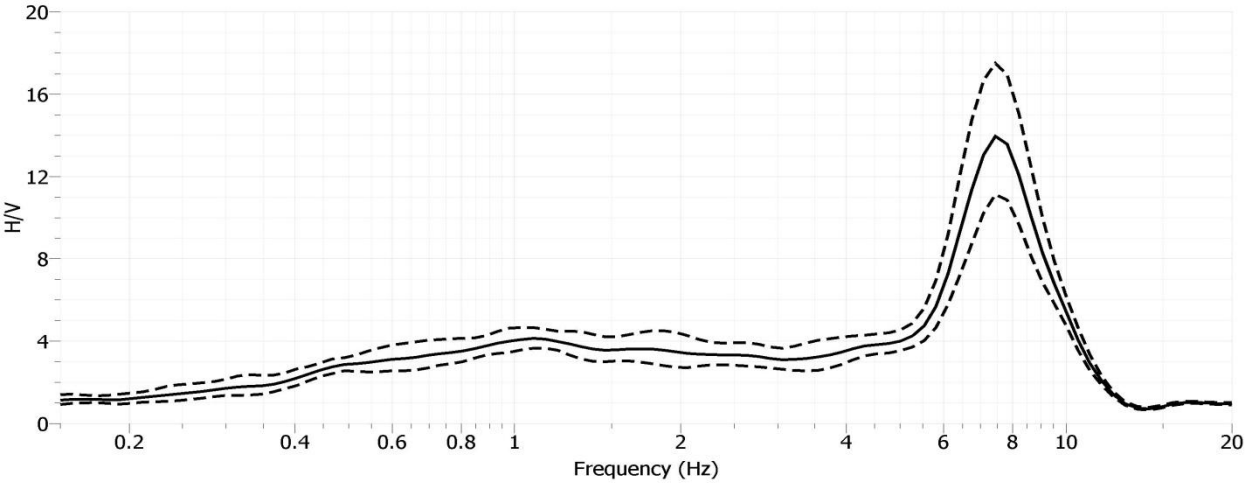

Site CE.13929, H/V Spectral Ratio, Array 13929-1, Sensor 450

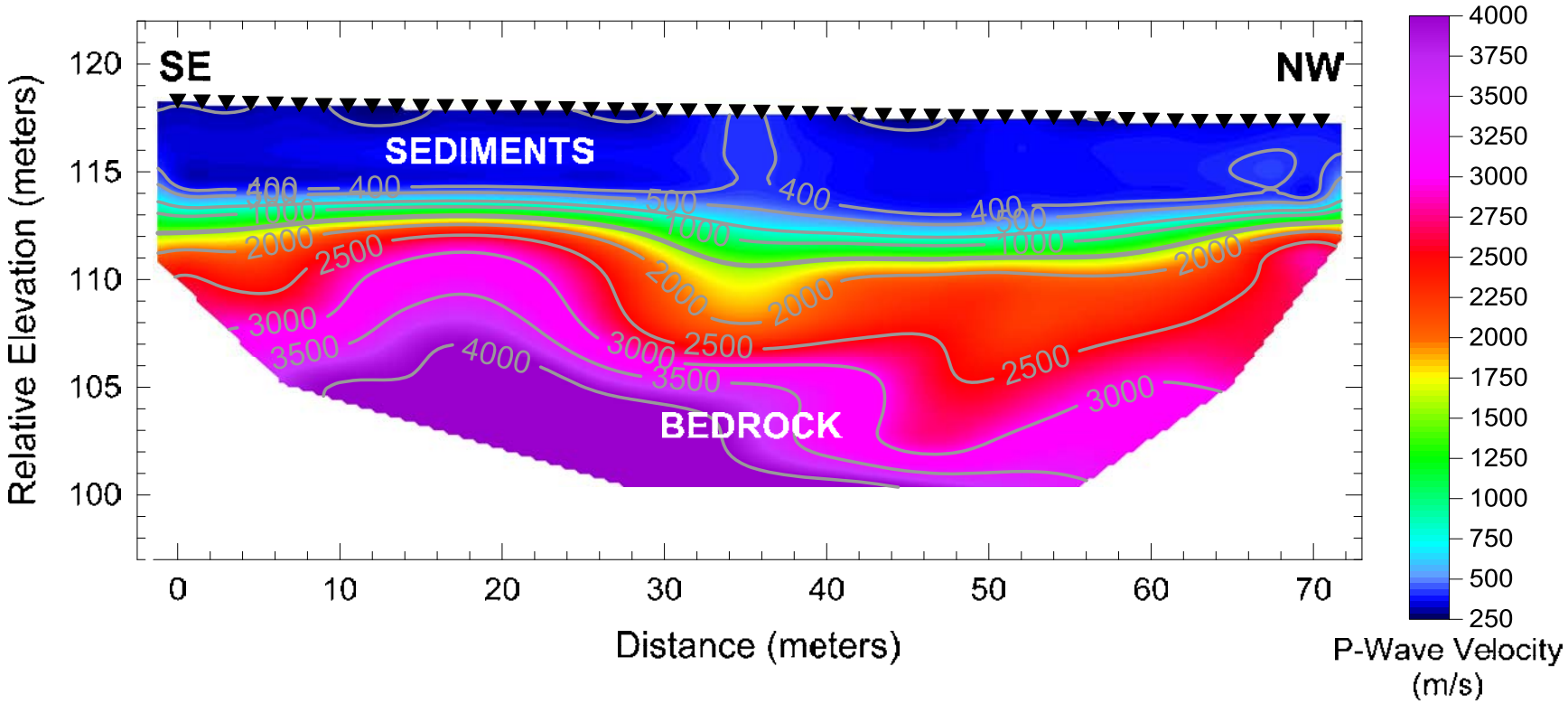

Array 13929-1 – Tomographic seismic refraction model developed using a layer based starting model

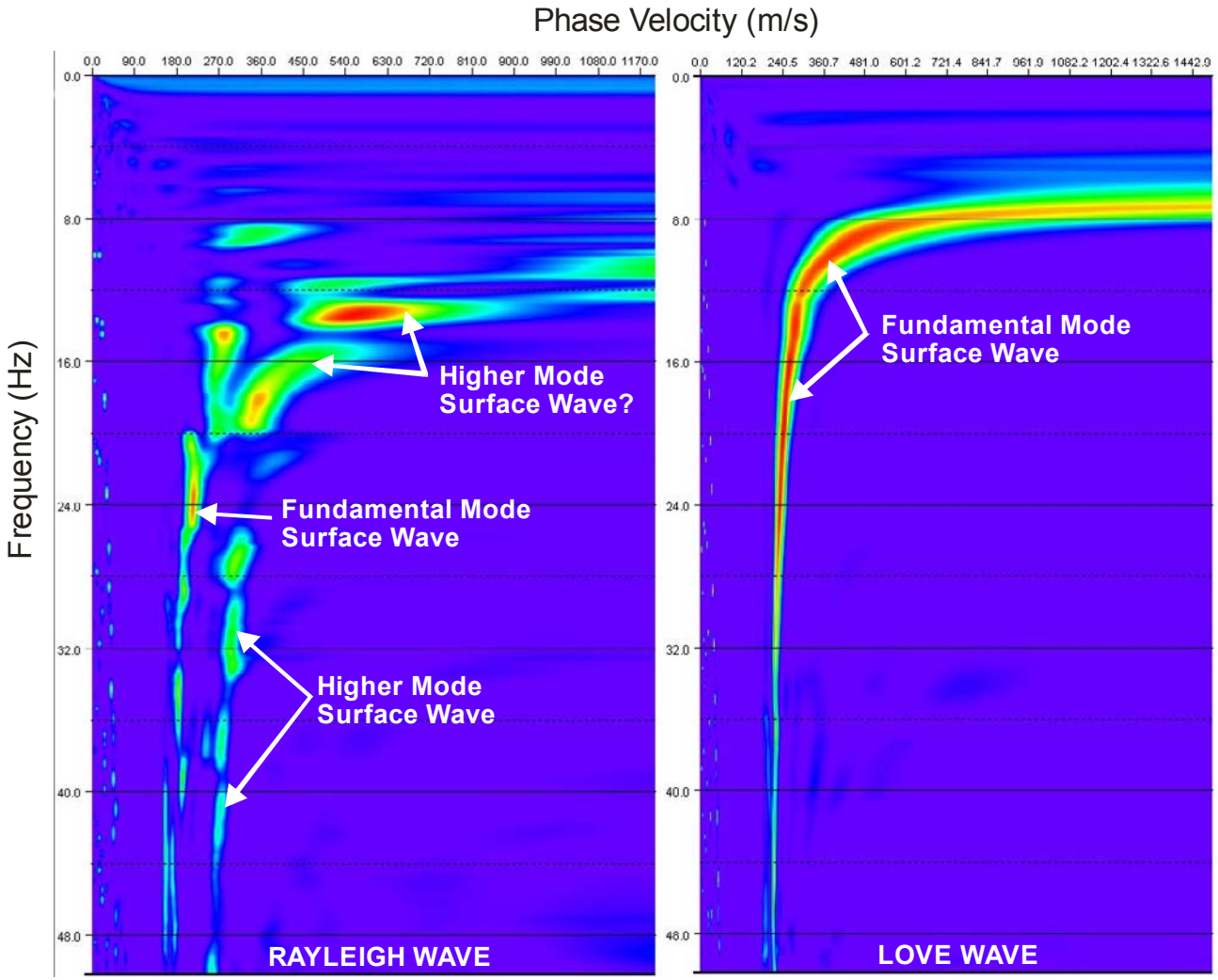

Array 13929-1 – Comparison of Rayleigh and Love wave overtone images demonstrating the higher mode contamination in the Rayleigh wave data.

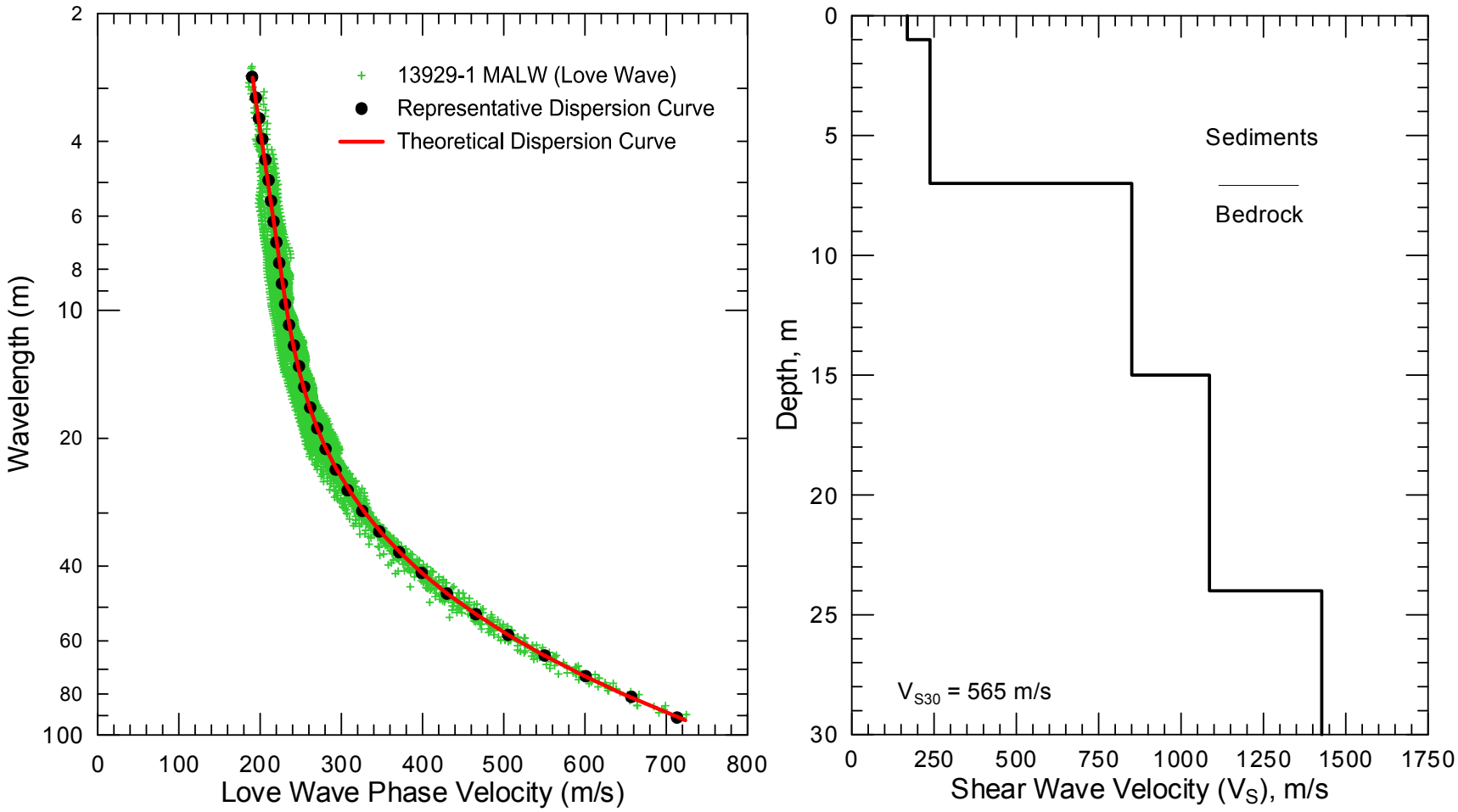

CE.13929 - Field, representative and inverted theoretical surface wave dispersion data (left) and associated V_S model (right)

Site CE.14241

Location: Long Beach Recreation Park, 4900 East 7th Street, Long Beach, California

Latitude: 33.77725 **Longitude:** -118.13308
(Station coordinates consist of published coordinates from http://www.strongmotioncenter.org with modification using Google Earth. Station location confirmed in field, but could not be surveyed as located under tree cover, WGS84 coordinate system.)

V_{S30} (measured): 282 m/s

V_{S30} (adjusted to more accurately reflect seismic station conditions): 282 m/s (no adjustment necessary)

NEHRP Site Class: D

Geomatrix Code: IQD

Geologic Conditions/Observations: Site located in area mapped as Quaternary (Pleistocene) old paralic deposits. Site located in the Newport-Inglewood Fault Zone. Expected deep soil site.

Site Conditions: Urban site with significant noise from nearby roads. Relatively flat terrain in site vicinity.

Geophysical Methods Utilized: HVSR, MASW, array microtremor, ReMi™

Geophysical Testing Arrays:

1. Arrays 14241-1 (24 channel linear array utilizing 4.5 Hz vertical geophones spaced 5 m apart for an array length of 115 m) and 14241-2 (24 channel linear array utilizing 4.5 Hz vertical geophones spaced 4 m apart for an array length of 92 m) used to acquire passive surface wave data. Arrays combined to form an "L" shaped array.
2. Array 14241-3 (48 channel MASW array utilizing 4.5 Hz vertical geophones spaced 1 m apart for a length of 47 m, forward and reverse shot locations with multiple source offsets and source types (hammers only) and center shot location).
3. Three HVSR measurement locations distributed along arrays 14241-2 and 14241-3.

Legend

- Seismic Station - Approximate Surveyed Location
- Seismic Station - Approximate Location of Record
- H/V Spectral Ratio Location
- MASW Array
- Passive Array

NOTES:
1. WGS 1984 COORDINATE SYSTEM
2. Image Source: ESRI, i-cubed, USDA FSA, USGS, AEX, GeoEye, Getmapping, Aerogrid, IGP

File Name: CE-14241-I

Date: 7/10/2011

USGS science for a changing world

GEOVision geophysical services

RECOVERY.GOV

SITE MAP
CE•14241

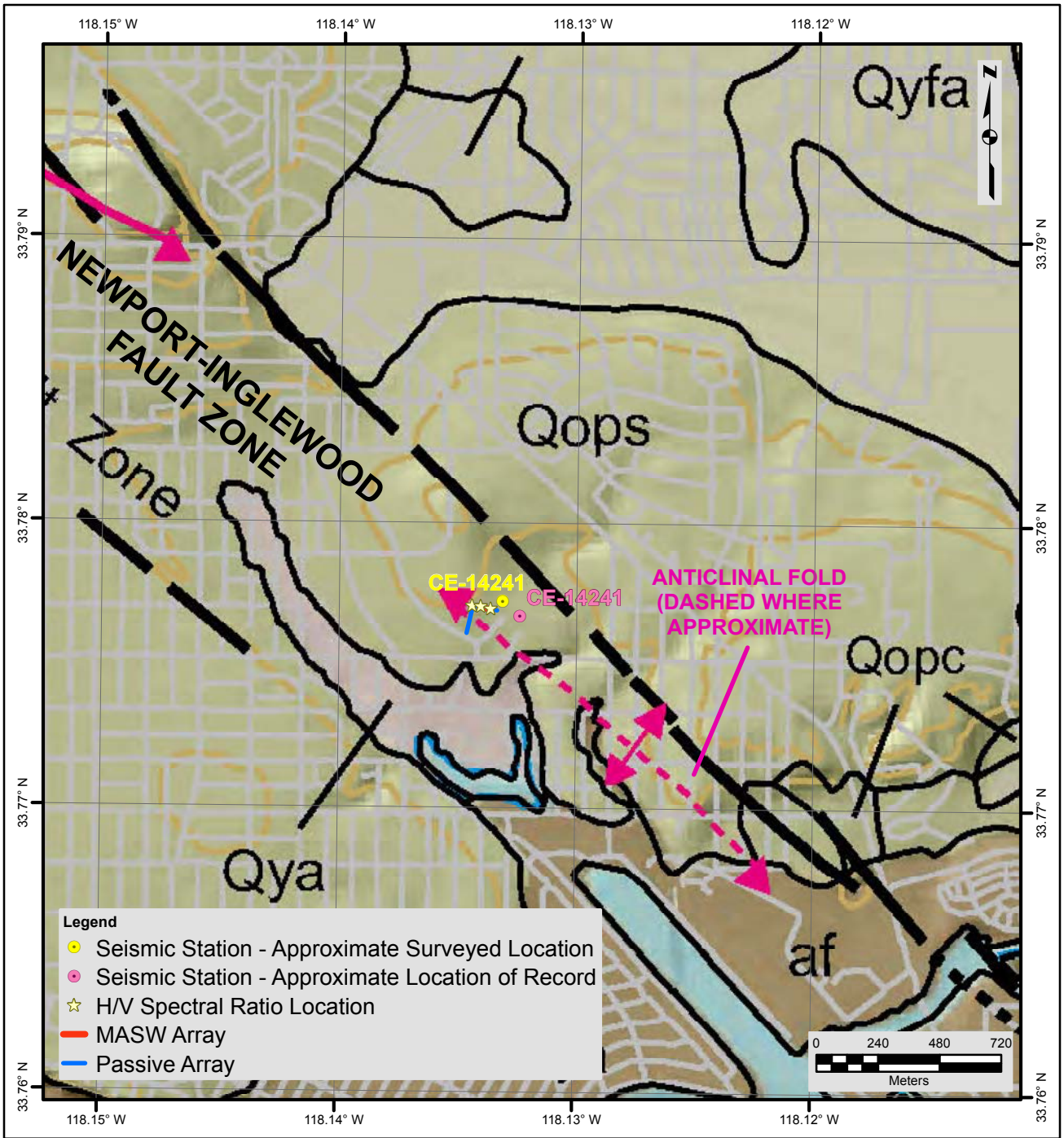

Description of Geologic Map Units

af = Quaternary (Holocene) artificial fill
Qyfa = Quaternary (Holocene) young alluvial fan and valley deposits, sand
Qya = Quaternary (Holocene) young alluvial flood plain deposits, unit 1
Qops = Quaternary (Pleistocene) old paralic deposits, silt
Qopc = Quaternary (Pleistocene) old paralic deposits, clay

NOTES:
1. WGS 1984 COORDINATE SYSTEM
2. Geologic Map of the California, Long Beach Sheet,
Olaf P. Jenkins Edition
Compilation by Charles W. Jennings, 1962 (Third Printing, 1978)
3. See site map for details of geophysical survey

File Name: CE-14241

Date: 7/15/2011

USGS science for a changing world

GEOVision geophysical services

GEOLOGIC MAP
CE•14241

RECOVERY.GOV

CE.14241 Seismic Station

Looking south along passive surface wave array 14241-1

Looking northeast towards passive surface wave array 14241-2 and seismic station

Shallow hole excavated for HVSR sensor

Looking northeast towards MASW array 14241-3 and seismic station

Location of Geophysical Testing Arrays:

Location	Latitude	Longitude
14241-1, South End of Passive SW Array	33.776124	-118.134583
14241-1 and 2, North and West End of Passive SW Arrays, respectively.	33.777094	-118.134328
14241-2, East End of Passive SW Array	33.776921	-118.133315
14241-3, West End of MASW Array	33.777052	-118.134042
14241-3, East End of MASW Array	33.77697	-118.133629
HVSR Sensor 450	33.77710	-118.13436
HVSR Sensor 453	33.77708	-118.13400
HVSR Sensor 507	33.77700	-118.13357

Notes: 1) WGS84 Coordinate System (decimal degrees)
2) Survey accuracy is estimated at 3 to 4 m
3) GPS data quality degraded due to tree cover and some coordinates moved several meters based on field observations.

Results:

V_S Model

Depth to Top of Layer (m)	Layer Thickness (m)	S-Wave Velocity (m/s)	Inferred P-Wave Velocity (m/s)	Assumed Poisson's Ratio	Assumed Density (g/cm^3)
0	1	215	402	0.300	1.9
1	2.5	172	321	0.300	1.9
3.5	3.5	232	433	0.300	1.9
7	4	273	1900	0.489	2.0
11	6	317	1900	0.486	2.0
17	9	331	1900	0.484	2.0
26	15	350	1900	0.482	2.0
41	15	426	2000	0.476	2.0
56	18	503	2000	0.466	2.1
74	>6	574	2000	0.455	2.1

Observations/Discussion:

- The HVSR curves are almost identical below a frequency of 2 Hz, validating the 1-D velocity structure assumption. There are, however, no high frequency HVSR peaks to characterize variability of shallow velocity structure.
- High amplitude HVSR peak at 0.14 Hz, which is consistent for a very deep sedimentary basin.
- Noise conditions at site (multi-directional or omni-directional noise sources) appeared sufficient for successful application of passive surface wave techniques.
- ESAC technique used to extract surface wave dispersion data from passive "L" array data. Both the ReMi™ and ESAC techniques used to extract surface wave dispersion data from the linear arrays. Only the higher quality passive surface wave data from the "L" array was used for analysis. Linear passive surface wave array 14241-1 yielded slightly higher phase velocities that the "L" array at wavelengths greater than 40 m. Linear passive surface wave array 14241-2 yielded similar phase velocities to the "L" array at wavelengths less than 100 m.
- Surface wave dispersion data from active and passive surface wave data sets are in acceptable agreement over the 15 to 30 m overlapping wavelength range. The passive surface wave dispersion data is consistent with the higher velocity MASW dispersion data over this wavelength range. The MASW data were acquired along a 47 m long array, whereas the passive surface wave data were acquired along a much larger 96 by 115 m array and slight differences in the surface wave dispersion data are attributed to near surface lateral velocity variation.
- Representative dispersion curves were generated for each surface wave data set using a moving average, polynomial curve fitting routine. These individual representative dispersion curves were combined and a representative dispersion curve generated for the combined data set for modeling purposes.
- Water table located at a depth of about 7 m based on interactive layer-based analysis of seismic refraction first arrival data. P-wave velocity of about 350 m/s modeled for unsaturated sediments and 1,900 to 2,000 m/s modeled for upper portion of saturated zone.
- Multiple reflectors are clearly evident on the seismic records in the upper 35 to 75 m indicating that the P-wave seismic reflection technique could be successfully applied in the site vicinity to mapping the Newport-Inglewood fault zone.
- Surface wave depth of investigation is about 80 m based on half of maximum wavelength criteria and assuming that surface wave dispersion data at frequencies as low as 2.6 Hz are valid utilizing 4.5 Hz geophones (low frequency geophone phase response differences will cancel out if noise is omni-directional and/or the phase response differences are random in nature).
- V_{S30} is 282 m/s (Site Class D).
- Average S-wave velocity of the upper 80 m (V_{S80}) is 365 m/s.

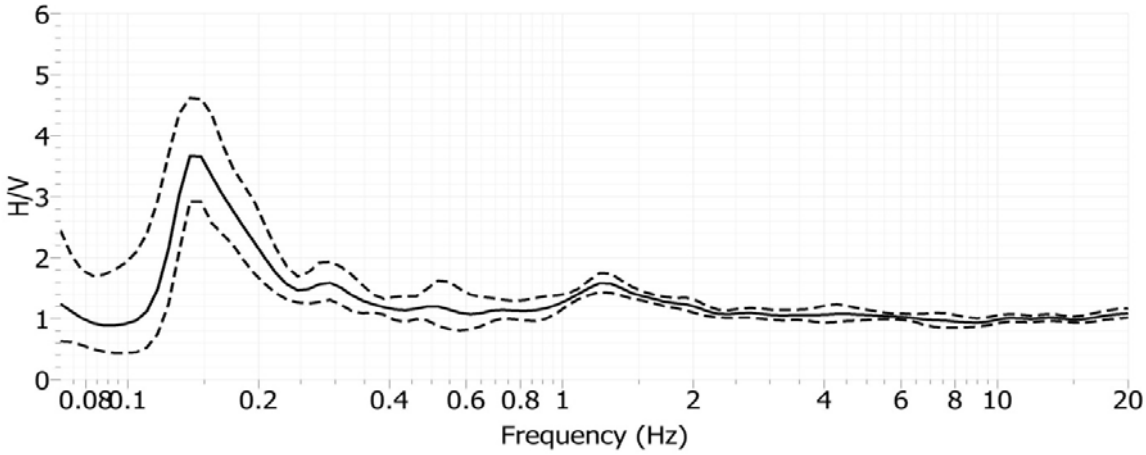

Site CE.14241, H/V Spectral Ratio, Array 14241-1, Sensor 450

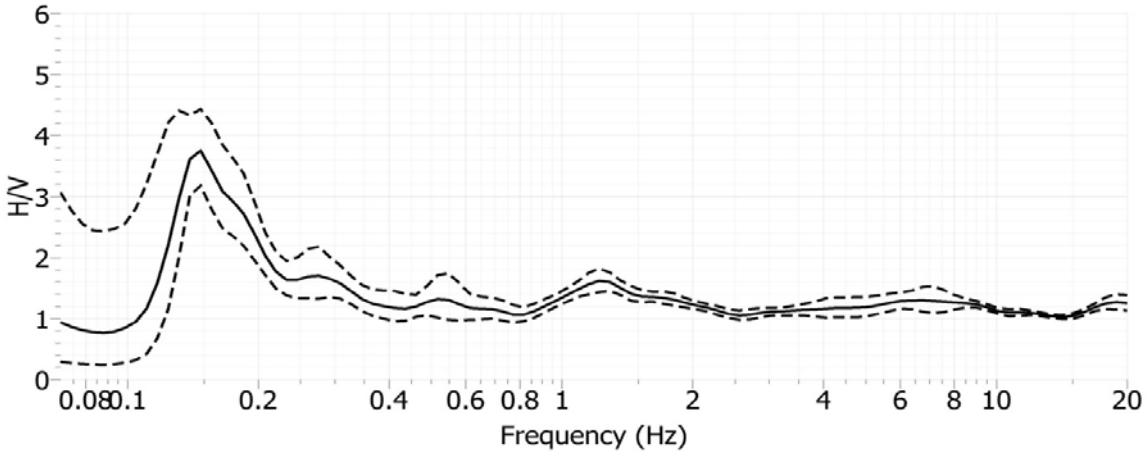

Site CE.14241, H/V Spectral Ratio, Array 14241-3, Sensor 453

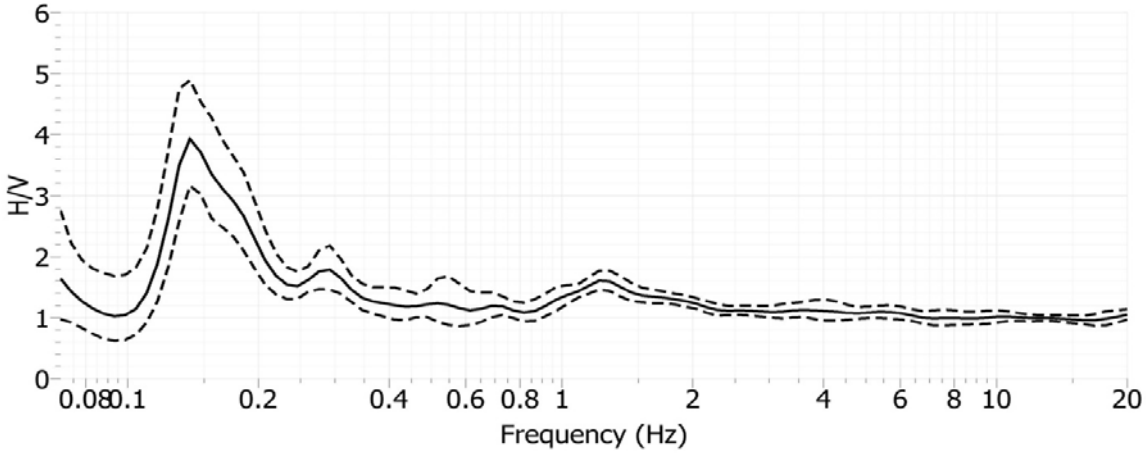

Site CE.14241, H/V Spectral Ratio, Array 14241-3, Sensor 507

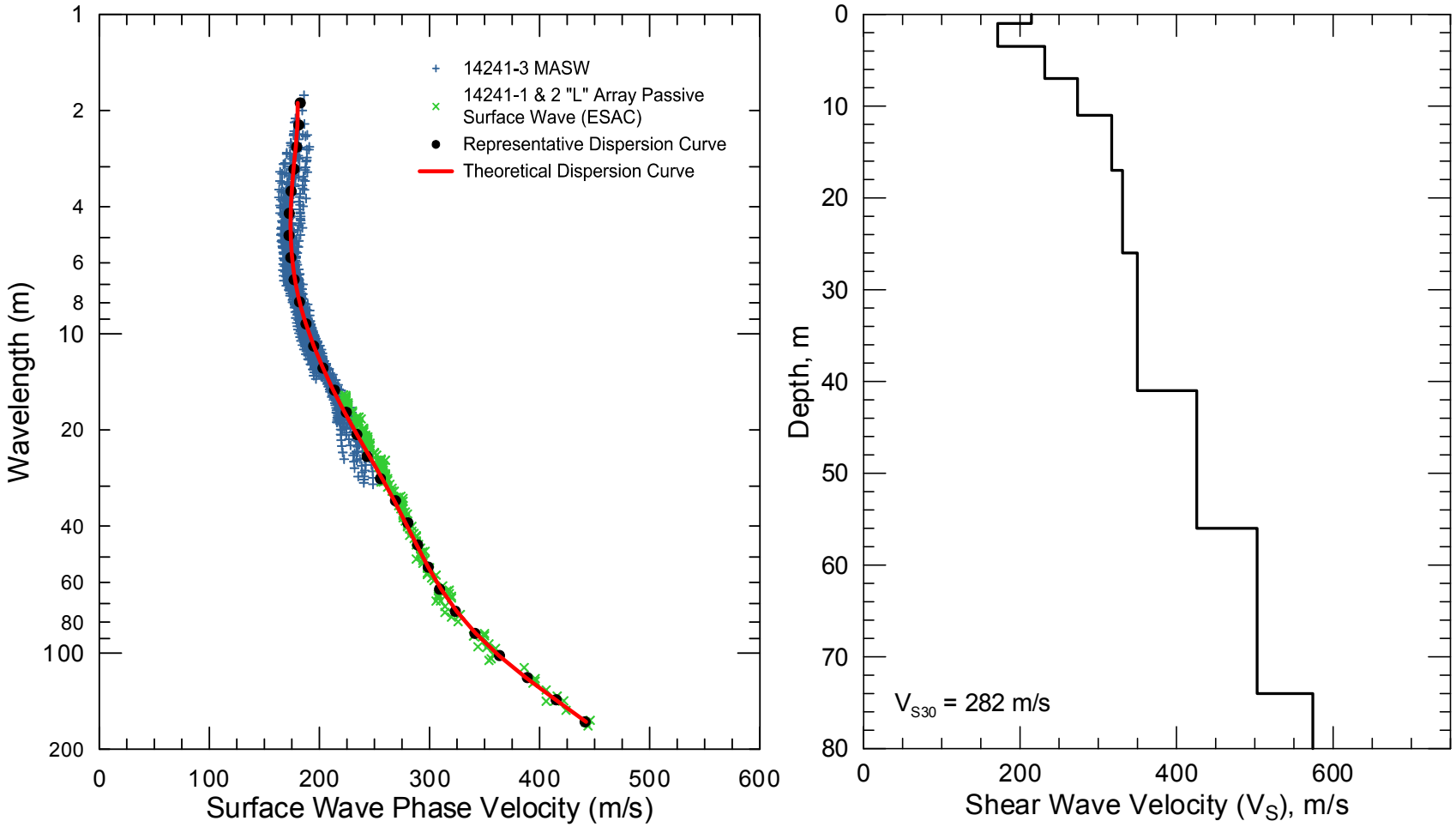

CE.14241 - Field, representative and inverted theoretical surface wave dispersion data (left) and associated V_S model (right)

Site CE.14395

Location: Long Beach Harbor Plaza, 1012 Harbor Plaza, Long Beach, California

Latitude: 33.75513 **Longitude:** -118.20115
(Station coordinates modified based on field GPS survey, WGS84 coordinate system)

V_{S30} (measured): 230 m/s

V_{S30} (adjusted to more accurately reflect seismic station conditions): 230 m/s (no adjustment necessary)

NEHRP Site Class: D

Geomatrix Code: IHD

Geologic Conditions/Observations: Site located in area mapped as Quaternary (Holocene) alluvium, although there may be some artificial fill overlying alluvium. Expected deep soil site.

Site Conditions: Urban site with significant noise from nearby roads and freeways and some pedestrian activity. Relatively flat terrain in site vicinity.

Geophysical Methods Utilized: HVSR, MASW, array microtremor, ReMi™

Geophysical Testing Arrays:

1. Arrays 14395-1 (24 channel linear array utilizing 4.5 Hz vertical geophones spaced 3 m apart for an array length of 69 m) and 14395-2 (24 channel linear array utilizing 4.5 Hz vertical geophones spaced 4 m apart for an array length of 92 m) used to acquire passive surface wave data. Arrays combined to form an "L" shaped array.
2. Array 14395-3 (9 channel "L" Array utilizing 1 Hz vertical geophones with a variable 10 to 30 m spacing for an array length of 75 m on each side) used to acquire passive surface wave data. The location of array 14395-3 is coincident with arrays 14395-1 and 2.
3. Array 14395-4 (48 channel MASW array utilizing 4.5 Hz vertical geophones spaced 1 m apart for a length of 47 m, forward and reverse shot locations with multiple source offsets and source types (hammers only) and center shot location).
4. Three HVSR measurement locations; two distributed along array 14395-2, one near the seismic station.

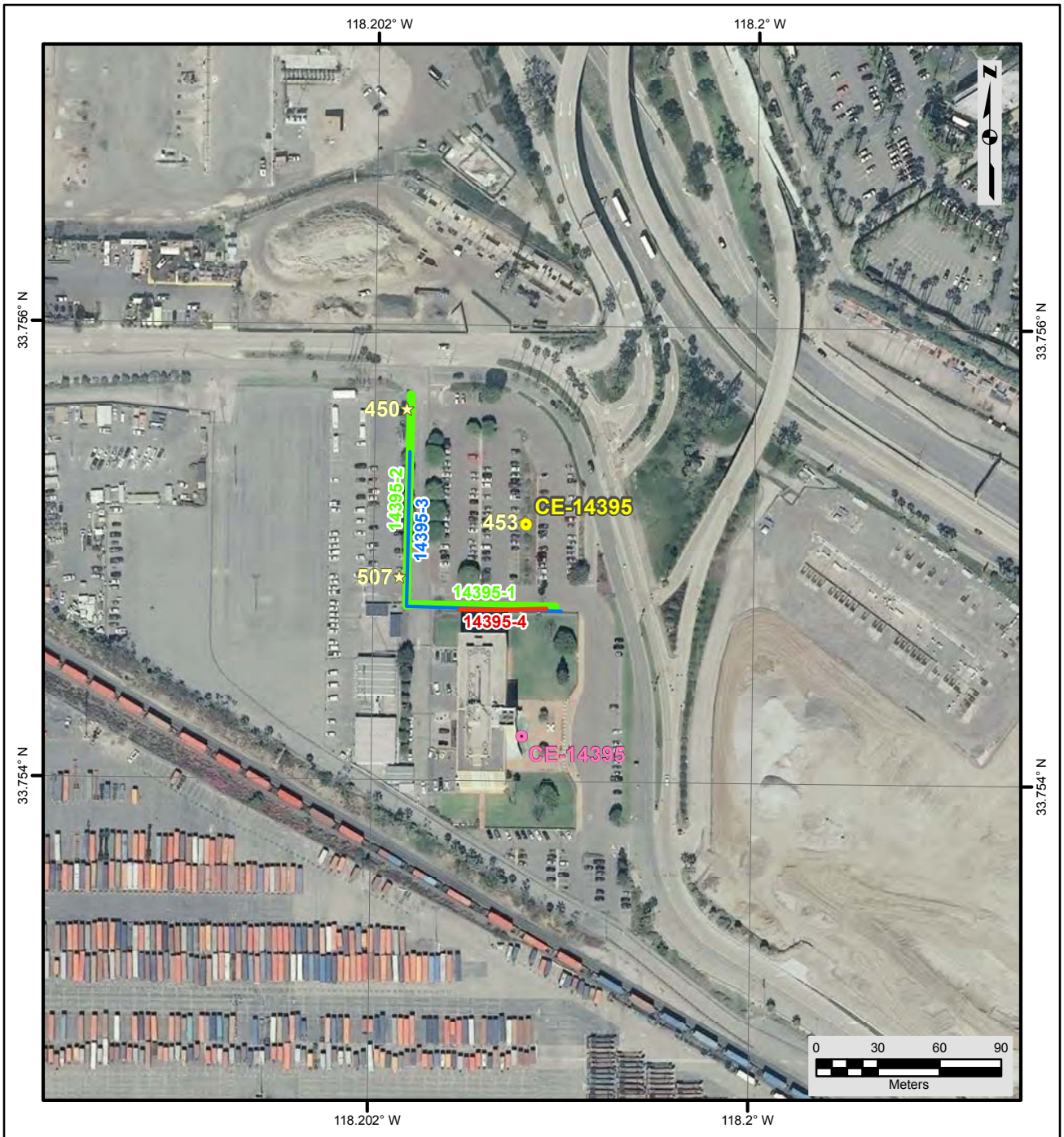

Legend

- Seismic Station - Approximate Surveyed Location
- Seismic Station - Approximate Location of Record
- H/V Spectral Ratio Location
- MASW Array
- Passive Array
- Passive Array

NOTES:
1. WGS 1984 COORDINATE SYSTEM
2. Image Source: ESRI, i-cubed, USDA FSA, USGS, AEX, GeoEye, Getmapping, Aerogrid, IGP

USGS science for a changing world
GEOVision geophysical services

RECOVERY.GOV

SITE MAP
CE•14395

File Name: CE-14395-I

Date: 7/21/2011

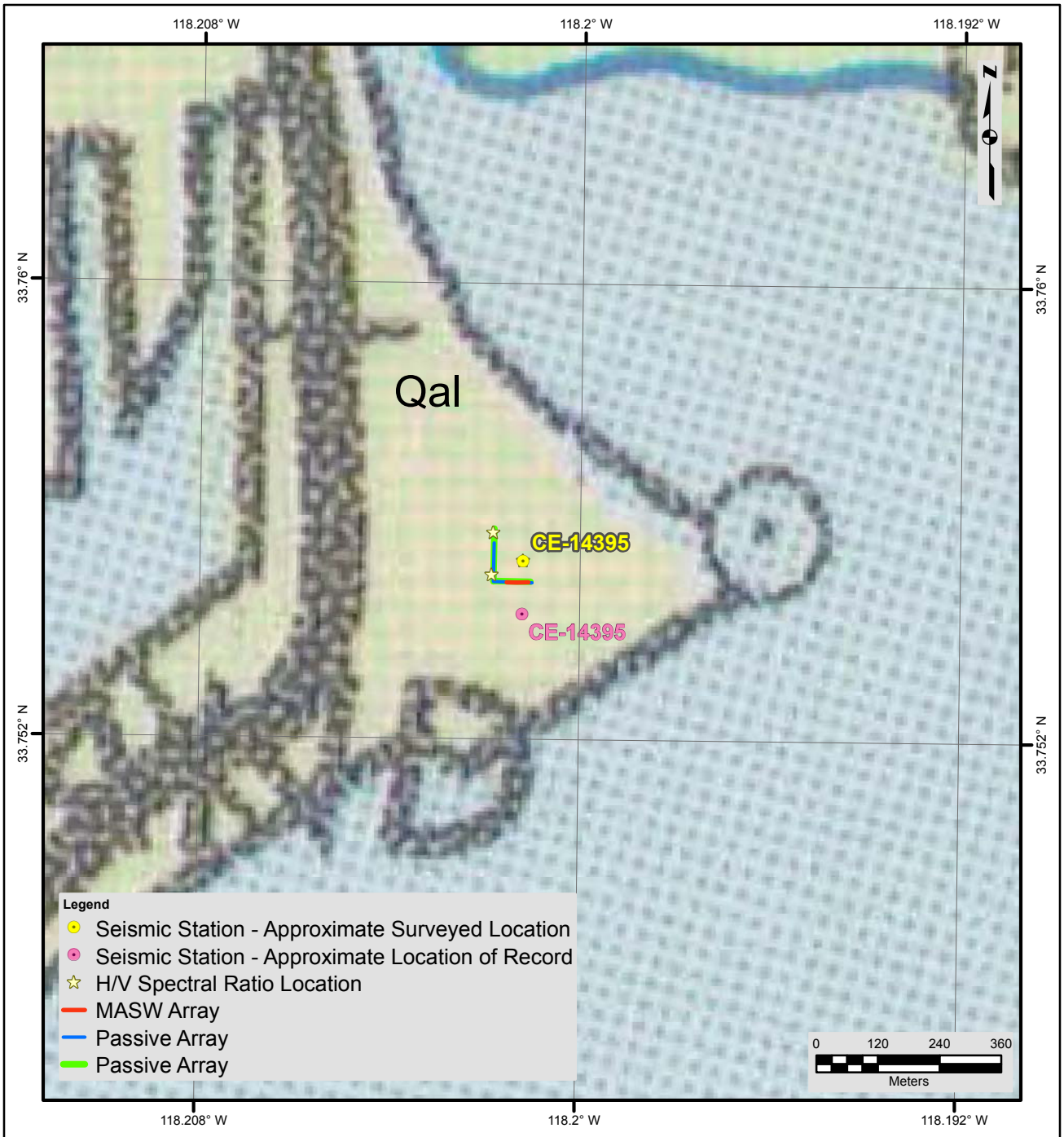

Description of Geologic Map Units

Qal = Quaternary (Holocene) alluvium

NOTES:
1. WGS 1984 COORDINATE SYSTEM
2. Geologic Map of California, Long Beach Sheet, Olaf P. Jenkins Edition
Compilation by Charles W. Jennings, 1962 (Third Printing, 1978)
3. See site map for details of geophysical survey

File Name: CE-14395

Date: 7/21/2011

USGS science for a changing world

GEOVision geophysical services

RECOVERY.GOV

GEOLOGIC MAP
CE•14395

CE.14395 Seismic Station

Looking northeast towards HVSR sensor 507 and seismic station

Looking northeast towards seismic station from near corner of arrays 14395-1/2 and 14395-3

Looking north along passive surface wave array 14395-2 and 14395-3

Looking east along MASW array 14395-4

Location of Geophysical Testing Arrays:

Location	Latitude	Longitude
14395-1, East End of Array	33.75477	-118.20100
14395-1, West End of Array	33.75477	-118.20174
14395-2, South End of Array	33.75477	-118.20178
14395-2, North End of Array	33.75569	-118.20177
14395-3, East End of Array	33.75475	-118.20097
14395-3, Corner of "L" Array	33.75476	-118.20178
14395-3, North End of Array	33.75544	-118.20177
14395-4, East End of MASW Array	33.75476	-118.20104
14395-4, Center of MASW Array	33.75475	-118.20129
14395-4, West End of MASW Array	33.75475	-118.20150
HVSR Sensor 450	33.75563	-118.20179
HVSR Sensor 453	33.75514	-118.20116
HVSR Sensor 507	33.75489	-118.20182
CE.14395 Seismic Station	33.75513	-118.20115

Notes: 1) WGS84 Coordinate System (decimal degrees)

2) Survey accuracy is estimated at 1 to 2 m

Results:

V_S Model

Depth to Top of Layer (m)	Layer Thickness (m)	S-Wave Velocity (m/s)	Inferred P-Wave Velocity (m/s)	Inferred Poisson's Ratio	Inferred Density (g/cm^3)
0	2	228	427	0.300	1.9
2	3	203	379	0.300	1.9
5	4	175	328	0.300	1.9
9	6	222	1750	0.492	2.0
15	9	238	1750	0.491	2.0
24	12	312	1750	0.484	2.0
36	15	386	1850	0.477	2.0
51	20	421	1850	0.473	2.0
71	>4	499	1850	0.461	2.0

Observations/Discussion:

- The HVSR curves are almost identical, validating the 1-D velocity structure assumption; although there are no significant high frequency HVSR peaks to characterize variability of shallow velocity structure.
- High amplitude HVSR peak at 0.15 Hz, which is consistent for a very deep sedimentary basin. Possible weak HVSR peak in the 1.4 Hz range, which may be associated with a subtle impedance contrast at intermediate depth.
- Noise conditions at site (multi-directional or omni-directional noise sources) appeared sufficient for successful application of passive surface wave techniques.
- ESAC technique used to extract surface wave dispersion data from passive "L" array data. Both the ReMi™ and ESAC techniques used to extract surface wave dispersion data from the linear arrays. Only the higher quality passive surface wave data from the "L" arrays (14395-1/2 and 14395-3) were used for analysis. Linear passive surface wave arrays 14395-1 and 14395-2 yielded similar phase velocities to the "L" arrays over the useable wavelength ranges, but data quality was not as good.
- The coincident "L" arrays 14395-1/2 (4.5 Hz geophones) and 14395-3 (1 Hz geophones) yielded identical dispersion curves to a frequency of about 2.5 Hz.
- Surface wave dispersion data from active and passive surface wave data sets are in good agreement at this site.
- Representative dispersion curves were generated for each surface wave data set using a moving average, polynomial curve fitting routine. These individual representative dispersion curves were combined and a representative dispersion curve generated for the combined data set for data modeling.
- The water table is located at a depth of about 9 m based on interactive layer-based analysis of seismic refraction first arrival data, which was very noisy due to heavy vehicle traffic in site vicinity. P-wave velocities of about 350 and 1,750 m/s were modeled for unsaturated and saturated sediments, respectively.
- Surface wave depth of investigation is about 75 m based on half of maximum wavelength criteria. The "L" arrays utilizing 1 Hz and 4.5 Hz geophones yield identical low frequency surface wave dispersion data to frequencies of about 2.5 Hz.
- V_{S30} is 230 m/s (Site Class D).
- Average S-wave velocity of the upper 75 m (V_{S75}) is 307 m/s.

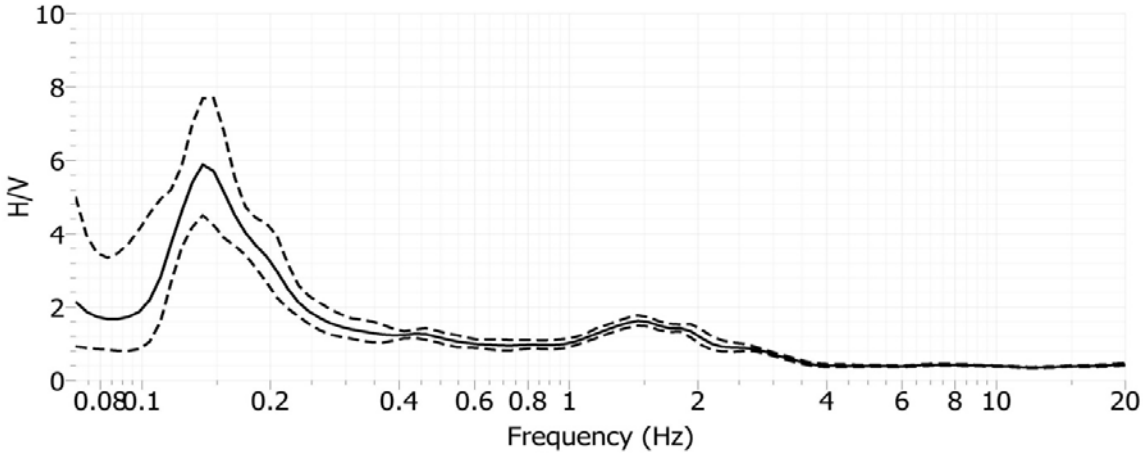

Site CE.14395, H/V Spectral Ratio, Array 14395-2, Sensor 450

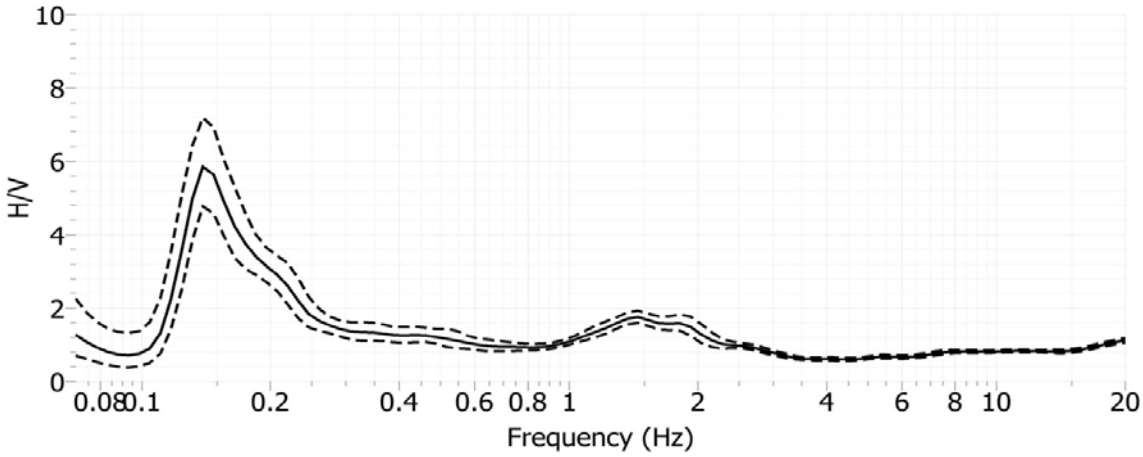

Site CE.14395, H/V Spectral Ratio, Adjacent to Seismic Station, Sensor 453

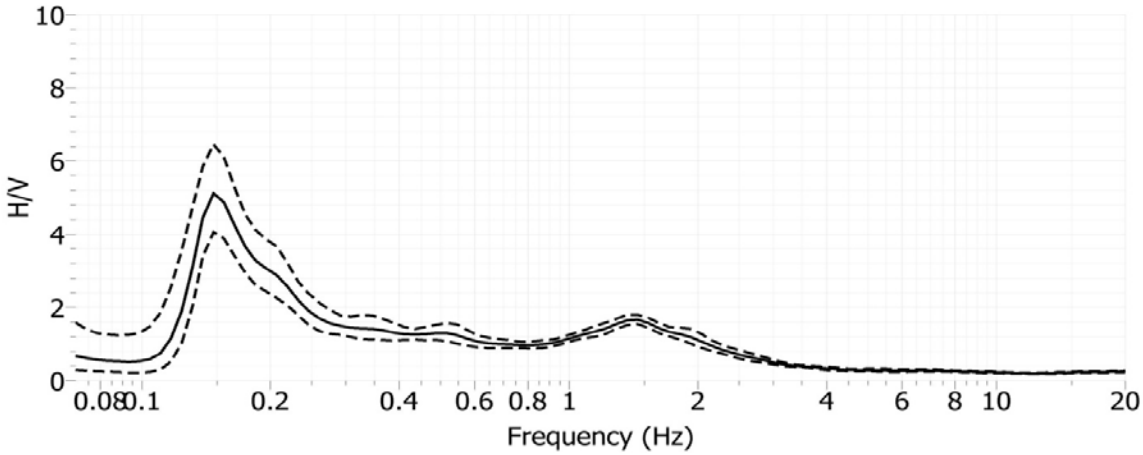

Site CE.14395, H/V Spectral Ratio, Array 14395-2, Sensor 507

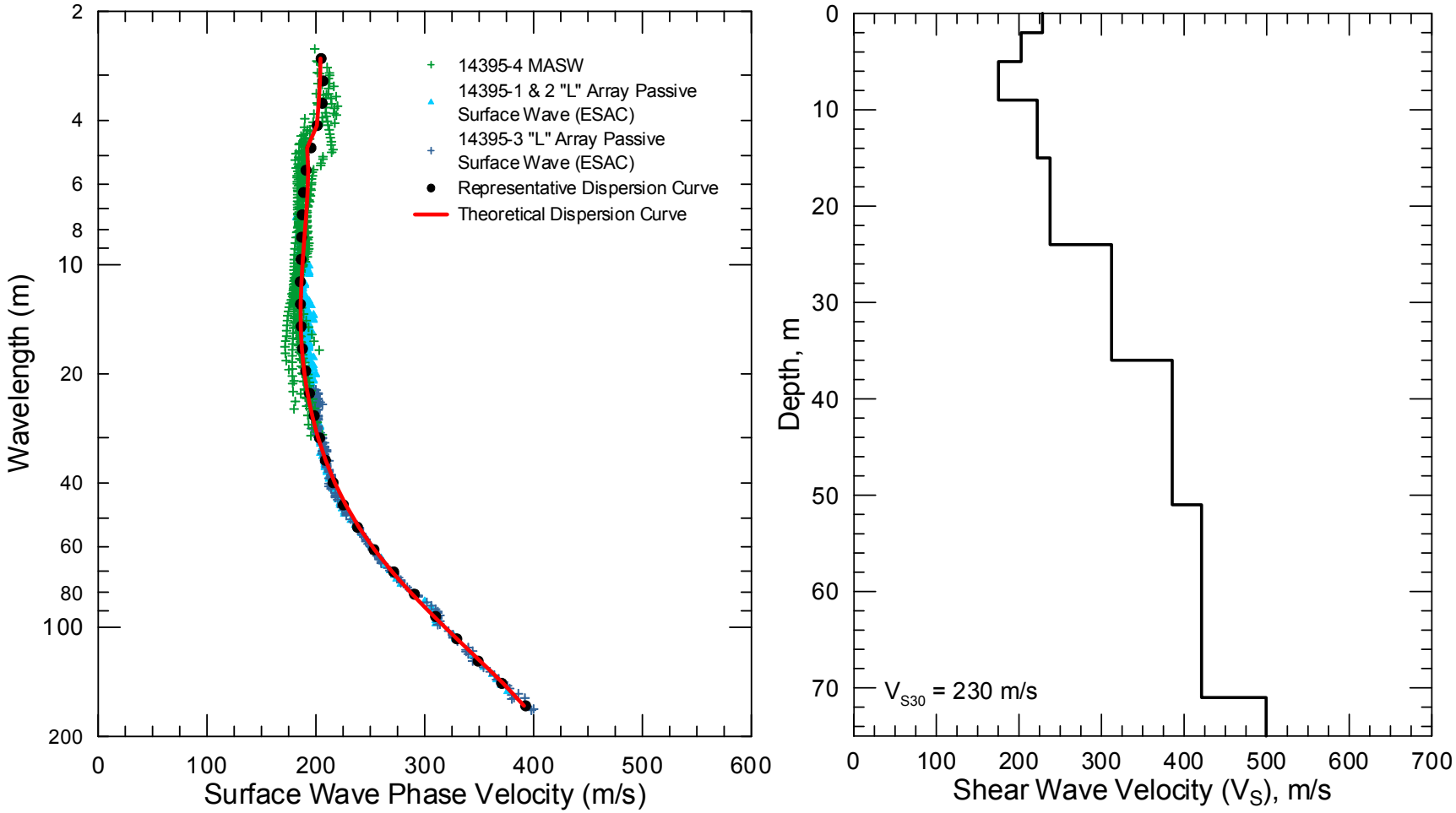

CE.14395 - Field, representative and inverted theoretical surface wave dispersion data (left) and associated V_S model (right)

Site CE.14560

Location: Long Beach City Hall Grounds, Long Beach, California

Latitude: 33.76856 **Longitude:** -118.19654
(Station coordinates modified based on field GPS survey, WGS84 coordinate system)

V_{S30} (measured): 322 m/s

V_{S30} (adjusted to more accurately reflect seismic station conditions): 322 m/s (no adjustment necessary).

NEHRP Site Class: D

Geomatrix Code: IQD/IHD

Geologic Conditions/Observations: Site located in area mapped as Quaternary (Holocene to Pleistocene) nonmarine terrace deposits.

Site Conditions: Urban site with significant traffic noise from nearby Broadway Avenue, Ocean Boulevard and Magnolia Avenue. Flat terrain in site vicinity. Test area located about 350 m from seismic station due to subsurface utilities and underground structures.

Geophysical Methods Utilized: HVSR, MASW, array microtremor, ReMi™

Geophysical Testing Arrays:

1. Array 14560-1 (24 channel, linear passive surface wave array utilizing 4.5 Hz vertical geophones spaced 4.5 m apart for a length of 103.5 m).
2. Array 14560-2 (10 channel, triangle passive surface wave array utilizing 1 Hz geophones and a 60 m length for outer side of array). Passive surface wave data also acquired on this array using 4.5 Hz vertical geophones.
3. Array 14560-3 (48 channel MASW array utilizing 4.5 Hz vertical geophones spaced 1 m apart for a length of 47 m, forward and reverse shot locations with multiple source offsets and source types and center shot location).
4. Three HVSR measurement locations distributed in the survey area.

Legend

- Seismic Station - Approximate Location of Record
- Seismic Station - Approximate Surveyed Location
- H/V Spectral Ratio Location
- MASW and Seismic Refraction Array
- Passive Surface Wave Array

NOTES:
1. WGS 1984 COORDINATE SYSTEM
2. Image Source: ESRI, i-cubed, USDA FSA, USGS, AEX, GeoEye, Getmapping, Aerogrid, IGP

File Name: CE-14560-I

Date: 2/7/2013

USGS science for a changing world

GEOVision geophysical services

RECOVERY.GOV

SITE MAP
CE•14560

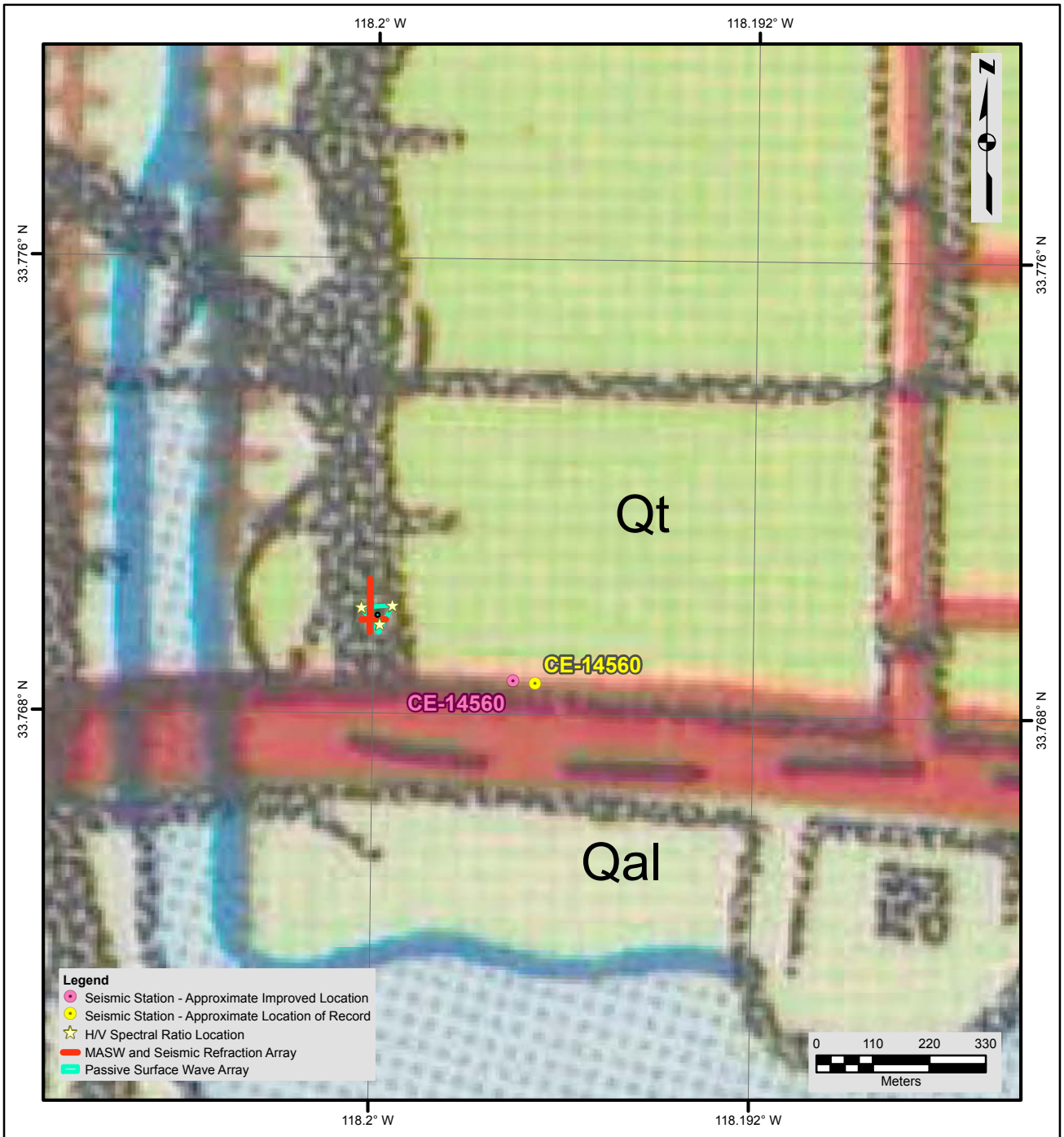

Description of Geologic Map Units

Qal = Quaternary (Holocene) alluvium
Qt = Quaternary (Holocene to Pleistocene) nonmarine terrace deposits

NOTES:
1. WGS 1984 COORDINATE SYSTEM
2. Geologic Map of the California, Long Beach Sheet, Olaf P. Jenkins Edition
Compilation by Charles W. Jennings, 1962 (Third Printing, 1978)
3. See site map for details of geophysical survey

File Name: CE-14560

Date: 2/7/2013

USGS science for a changing world

GEOVision geophysical services

GEOLOGIC MAP
CE•14560

RECOVERY.GOV

CE.14560 Seismic Station

Looking southeast at triangle passive surface wave array 14560-2

Looking southeast at HVSR station 450

Looking north along linear passive surface wave array 14560-1

Looking east along MASW array 14560-3. Seismic station located behind building in background

Location of Geophysical Testing Arrays:

Location	Latitude	Longitude
14560-1, South End of Array	33.76942	-118.20003
14560-1, North End of Array	33.77036	-118.20004
14560-2, Corner of Array, Sensor Location 1	33.76990	-118.19956
14560-2, Corner of Array, Sensor Location 3	33.76985	-118.20022
14560-2, Corner of Array, Sensor Location 5	33.76941	-118.19984
14560-2, Center of Array, Sensor Location 10	33.76972	-118.19987
14560-3, West End of Array	33.76964	-118.20021
14560-3, Center of Array	33.76965	-118.19996
14560-3, East End of Array	33.76964	-118.19970
HVSR Sensor 450	33.76957	-118.19982
HVSR Sensor 453	33.76986	-118.20021
HVSR Sensor 507	33.76989	-118.19956
CE.14560 Seismic Station	33.76856	-118.19654

Notes: 1) WGS84 Coordinate System (decimal degrees)
2) Survey accuracy is estimated at 1 to 2 m.

Results:

V_S Model

Depth to Top of Layer (m)	Layer Thickness (m)	S-Wave Velocity (m/s)	Inferred P-Wave Velocity (m/s)	Assumed Poisson's Ratio	Assumed Density (g/cm^3)
0	1.5	241	451	0.300	1.8
1.5	4.5	245	458	0.300	1.8
6	4	271	506	0.300	1.8
10	5	327	1750	0.483	1.9
15	6	363	1750	0.478	2.0
21	8	408	1750	0.472	2.0
29	>6	434	1750	0.467	2.0

Notes: 1) Saturated zone, with V_P of about 1,750 m/s, constrained at a depth of about 10 m based on analysis of seismic refraction data.
2) Depth of investigation is about 35 m.
2) Bottom layer is a half space.

Observations/Discussion:

- Surface wave testing was conducted in a parking lot about 350 m northwest of the seismic station. All structures in the immediate vicinity of the seismic station had subterranean levels and passive surface wave testing was not feasible. Due to construction activities, there was also a shallow excavation in the lot immediately east of the test area. Although the test area is not immediately adjacent to a structure with underground levels, underground levels in the majority of the buildings in the site vicinity could impact passive surface wave data.
- There is not much high frequency character in the HVSR curves, by which to validate the 1-D velocity assumption.
- There is a very low frequency HVSR peak at about 0.14 Hz range, which is consistent for a deep soil site. Longer duration measurements at night would improve quality of low frequency HVSR data.
- Noise conditions at site (multi-directional or omni-directional noise sources) appeared sufficient for successful application of passive surface wave techniques, with the exception discussed above.
- ESAC technique used to extract surface wave dispersion data from passive triangle array data. Both the ReMi™ and ESAC techniques used to extract surface wave dispersion data from the linear array. Passive surface wave data from the linear and triangle arrays are in good agreement at wavelengths below 65 m, but diverge significantly at larger wavelengths. Passive surface wave dispersion data were not extracted from ESAC analysis of the linear array data at wavelengths greater than 65 m, which indicates that data extracted using the ReMi technique at longer wavelengths may be unreliable. Passive surface wave data extracted from the triangle array may also be unreliable at long wavelengths, unless there is a velocity inversion below 30 m depth causing the observed signature. Due to uncertainly, passive Rayleigh wave phase velocity data were not used at wavelengths greater than 70 m.
- Surface wave dispersion data from active and passive surface wave datasets are not in particularly good agreement at wavelengths between 20 and 40 m, the maximum wavelength extracted from the MASW data. The MASW Rayleigh wave phase velocities are about 30 m/s lower than the passive phase velocity data at a wavelength of 40 m. This is not much higher than the scatter in the MASW at small wavelengths less than 6 m due to near surface lateral velocity variation. The MASW array was not orientated along the linear passive surface wave array, as is normally the case, due to utility lines in the vicinity of the passive surface wave array. Lateral velocity variation may explain the difference between the active and passive data sets, although Rayleigh wave phase velocity data from the two passive surface wave arrays are similar.
- Representative dispersion curves were generated for each surface wave data set using a moving average, polynomial curve fitting routine. These individual representative dispersion curves were combined (MASW data were given a weight equal to the combined weight passive surface wave data) and a representative dispersion curve generated for the combined data set for data modeling.
- The saturated zone was constrained at depth of about 10 m, based on review of seismic refraction data, with P-wave velocity of saturated sediments fixed at 1,750 m/s.

- Surface wave depth of investigation is about 35 m based on half of maximum wavelength criteria.
- V_{S30} is 322 m/s (Site Class D).
- The difference in the MASW and passive surface wave data at intermediate wavelengths indicates thatV_{S30} could vary by as much as 5% in the immediate site vicinity or have an error on the order of 5%.
- The triangle array passive surface wave data indicates that there is a possibility of a velocity inversion at depth below 30 m; however, there is not sufficient confidence in data quality, as discussed above, to conclusively make this statement.
- More work is necessary in this type of environment to fully understand the impact of multiple subterranean structures, if any, on passive surface wave measurements.

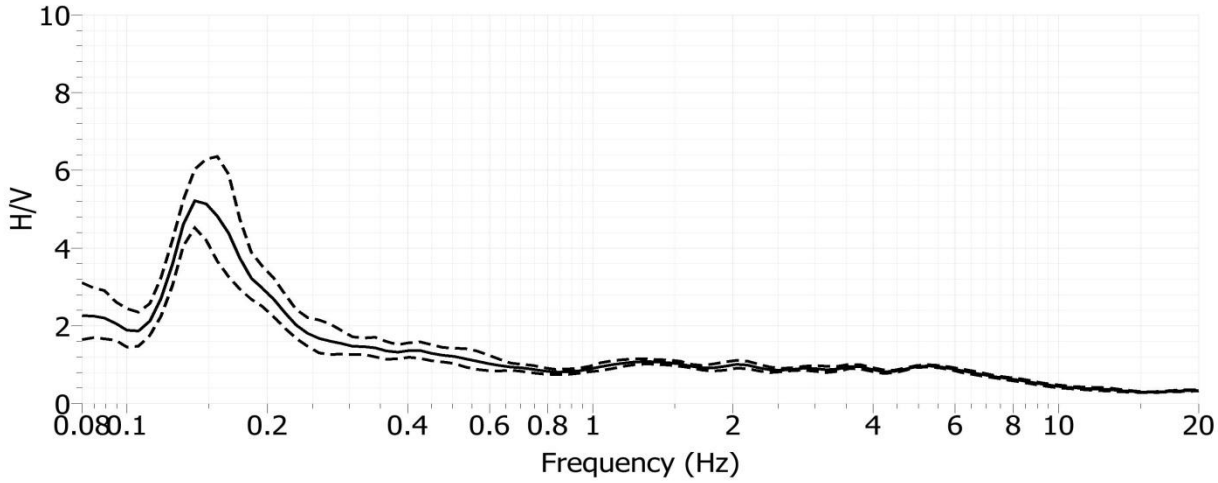

Site CE.14560, H/V Spectral Ratio, Array 14560-2, Sensor 453

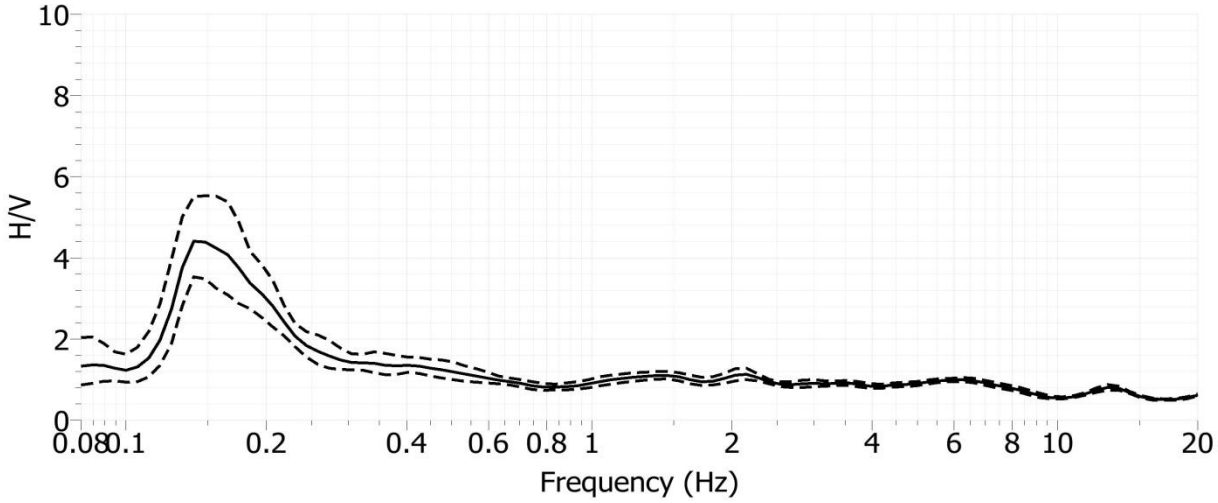

Site CE.14560, H/V Spectral Ratio, Array 14560-2, Sensor 507

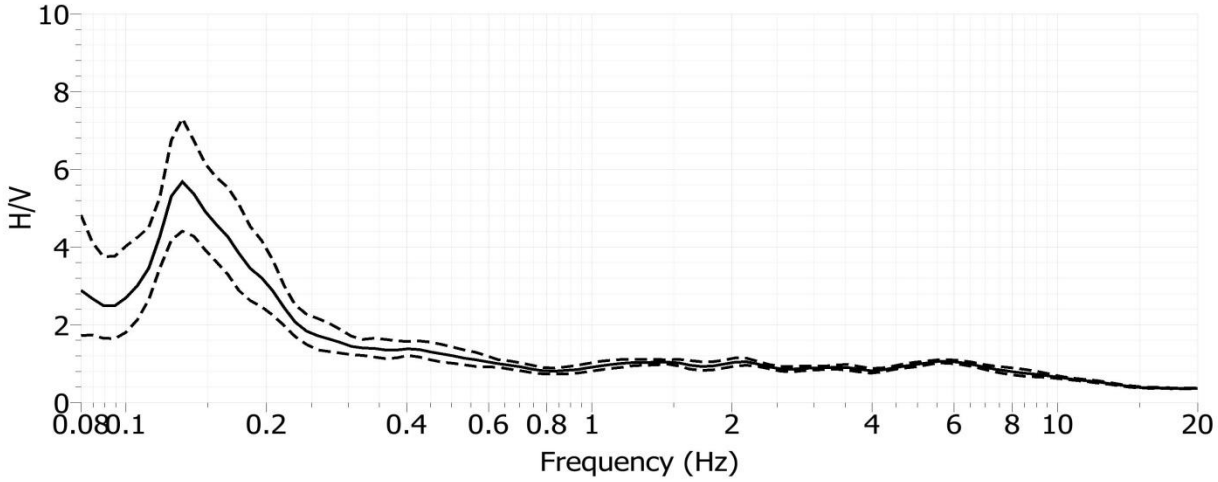

Site CE.14560, H/V Spectral Ratio, Sensor 450

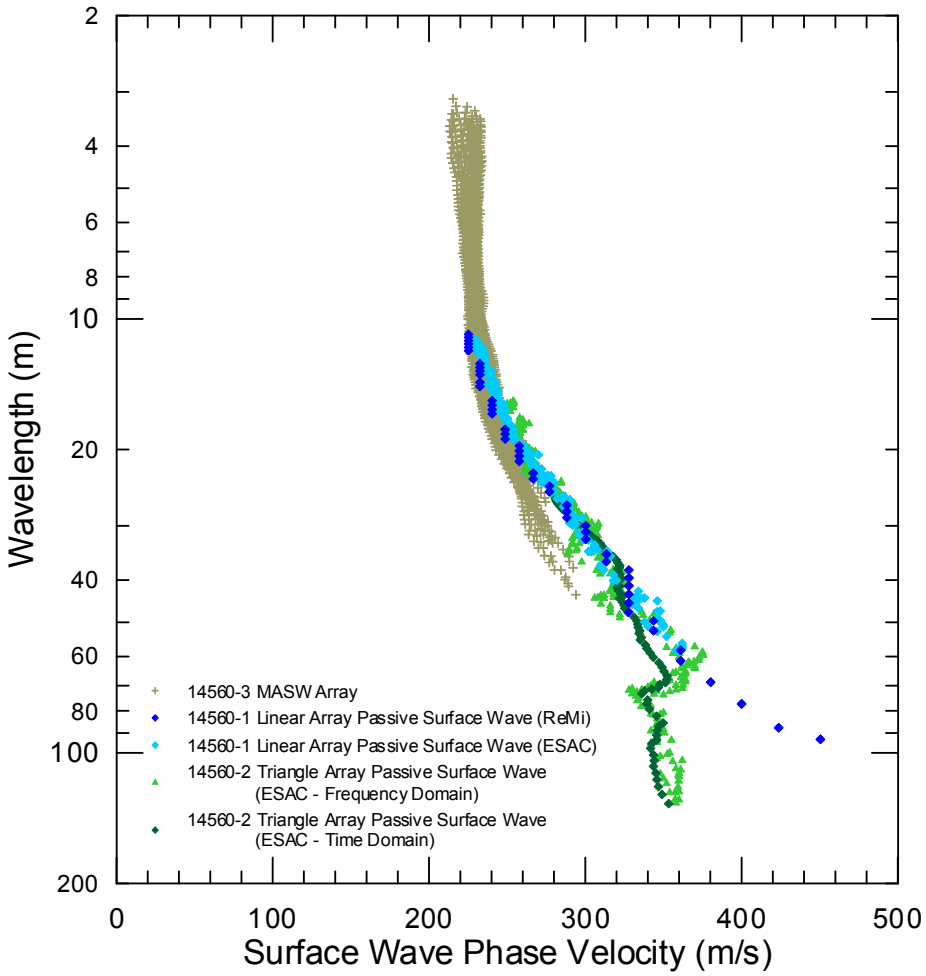

CE.14560 – Observed active and passive Rayleigh wave phase velocity data. MASW Rayleigh wave phase velocity data are slightly lower than the passive surface wave data at wavelengths between 20 and 40 m. None of the surface wave arrays are coincident and, therefore, lateral velocity variation could explain the difference in phase velocity over the 20 to 40 m wavelength range. The two passive surface waves yield similar surface wave data at wavelengths less than about 66 m. The linear array passive surface wave data (14560-1), analyzed using the ReMi™ technique, diverge from the triangle array passive surface wave data (14560-2), analyzed using the ESAC technique, at wavelengths greater than 70 m. The linear array passive surface wave data were also analyzed using the ESAC technique and reliable Rayleigh wave phase velocity data could not be extracted at wavelengths greater than 60 m. This would tend to indicate that the dispersion data extracted using the ReMi™ technique are also suspect at wavelengths greater than 60 m. Rayleigh wave phase velocity data from the triangle array decrease slightly at wavelengths greater than 70 m. A velocity inversion at depth below 30 m would be required to model a surface wave dispersion curve with these characteristics. There are many high rise buildings with subterranean levels in the site vicinity, which could scatter long wavelength passive surface wave data and it is unclear if the long wavelength passive surface wave data from the triangle array is representative of subsurface geologic conditions. Therefore, a maximum wavelength of 70 m from the passive surface wave data was utilized for modeling. Additional testing was considered; however, the test area, a former parking lot, is no longer accessible due to construction of a building.

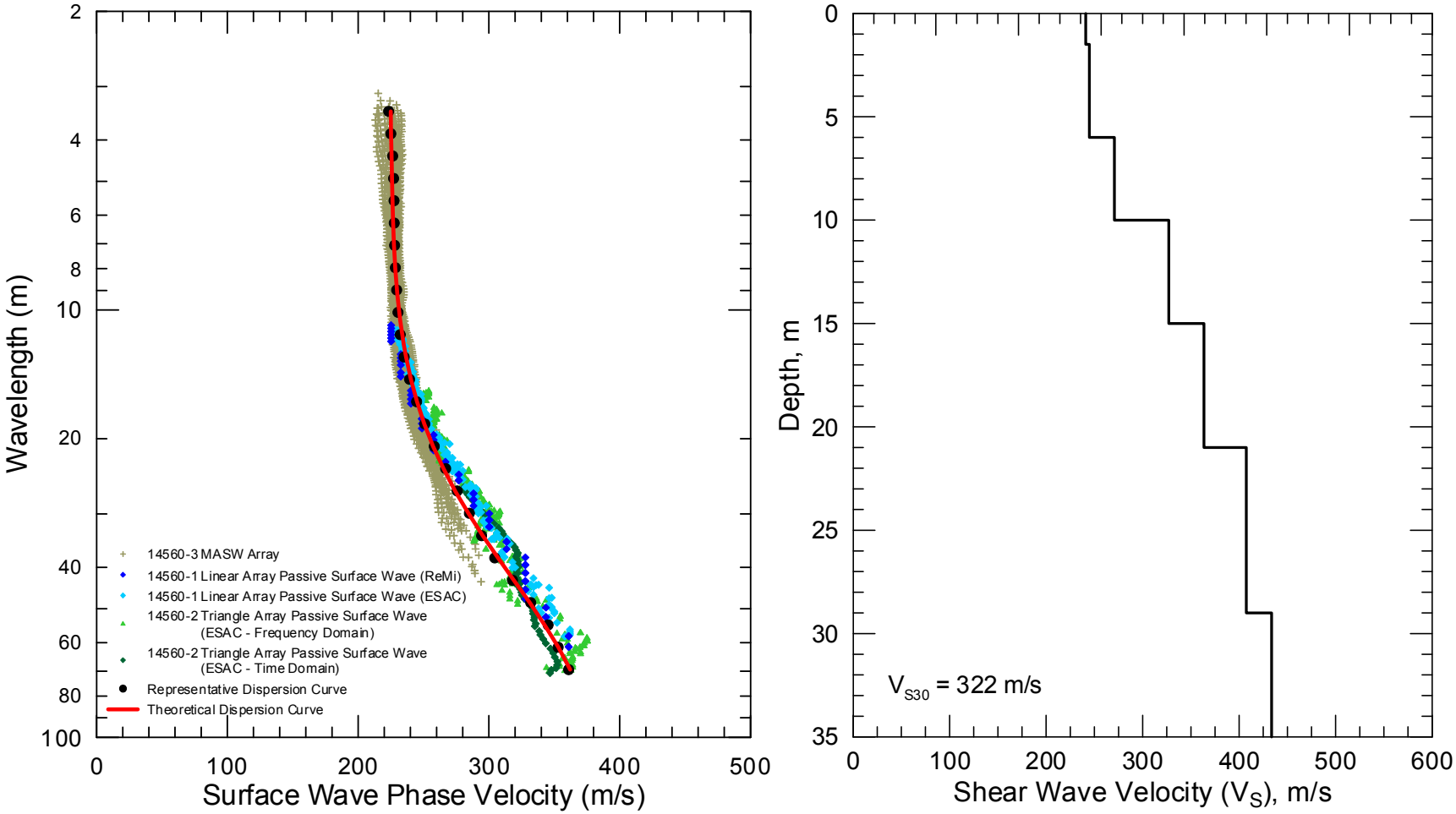

CE.14560 - Field, representative and inverted theoretical surface wave dispersion data (left) and associated V_S model (right)

Site CE.23063

Location: Los Angeles County Fire Station 79, 33957 Longview Road, Pearblossom, California

Latitude: 34.50250 **Longitude:** -117.89700

(Station coordinates consist of published coordinates from http://www.strongmotioncenter.org. Station location confirmed in field, WGS84 coordinate system.)

V_{S30} (measured): 506 m/s

V_{S30} (adjusted to more accurately reflect seismic station conditions): 506 m/s (no adjustment necessary)

NEHRP Site Class: C

Geomatrix Code: AQD

Geologic Conditions/Observations: Site located in area mapped as Quaternary (Pleistocene) old alluvial fan deposits. Bedrock may be as shallow as 20 to 24 m deep based on seismic refraction data.

Site Conditions: Rural site with some traffic noise from Pearblossom Highway (Hwy 138), located about 400 m north of the site, and nearby roads. Relatively flat terrain in site vicinity.

Geophysical Methods Utilized: HVSR, MASW, array microtremor, ReMi™, seismic refraction

Geophysical Testing Arrays:

1. Arrays 23063-1 (24 channel linear array utilizing 4.5 Hz vertical geophones spaced 6 m apart for an array length of 138 m) and 23063-2 (24 channel linear array utilizing 4.5 Hz vertical geophones spaced 4.5 m apart for an array length of 103.5 m) used to acquire passive surface wave data. Arrays combined to form an "L" shaped array. Limited MASW data also acquired on array 23063-1.
2. Array 23063-3 (48 channel MASW array utilizing 4.5 Hz vertical geophones spaced 1.5 m apart for a length of 70.5 m, forward and reverse shot locations with multiple source offsets and source types and center shot location).
3. Array 23063-4 (48 channel seismic refraction and MASW array utilizing 4.5 Hz vertical geophones spaced 3 m apart for a length of 141 m, forward and reverse shot locations with multiple source offsets and source types and multiple interior shot locations).
4. Three HVSR measurement locations, distributed along array 23063-3 and one near the seismic station.

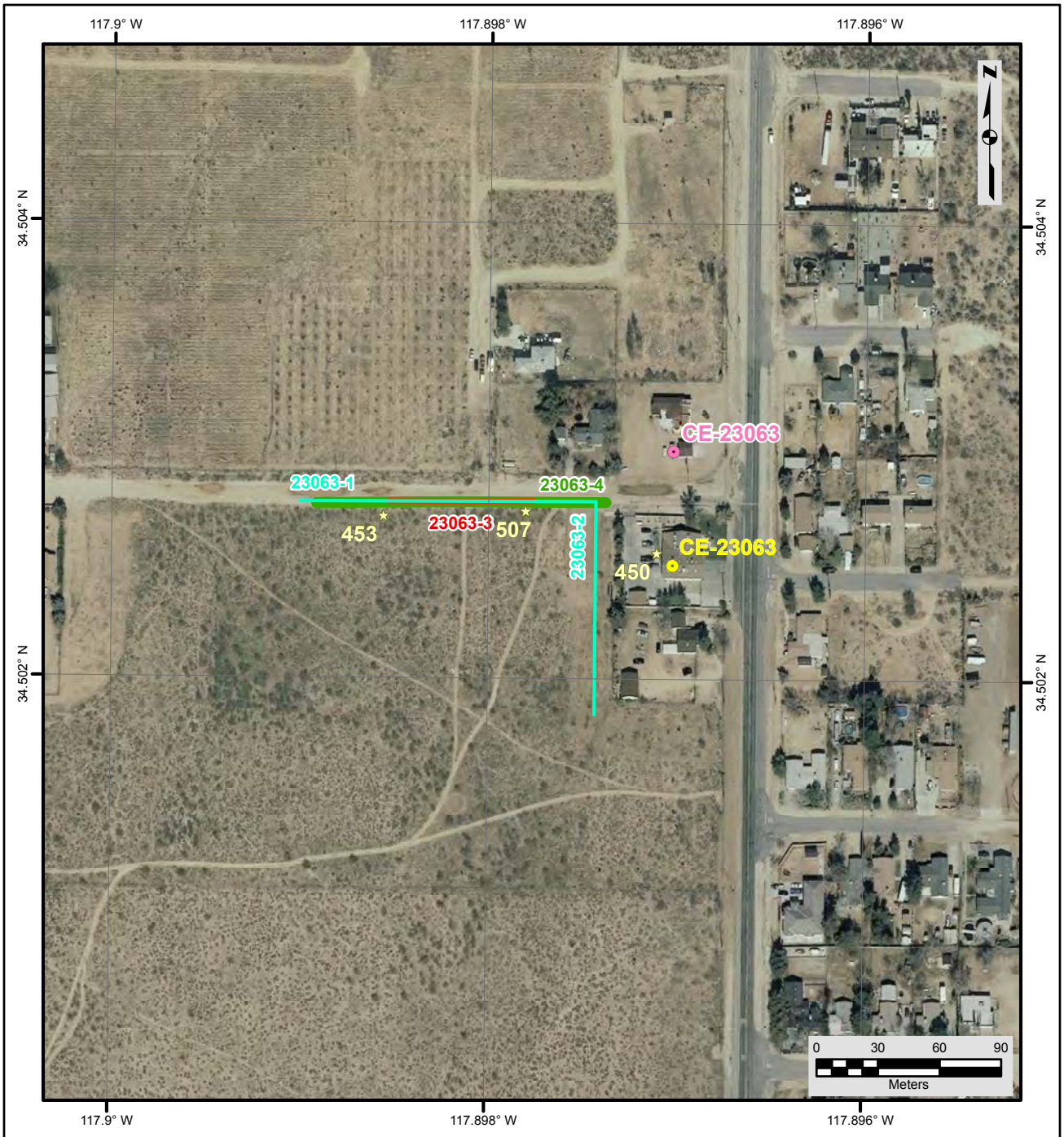

Legend

- Seismic Station - Approximate Improved Location
- Seismic Station - Approximate Location of Record
- H/V Spectral Ratio Measurement Location
- Passive Surface Wave Array
- MASW Array
- MASW Array

NOTES:
1. WGS 1984 COORDINATE SYSTEM
2. Image Source: ESRI, i-cubed, USDA FSA, USGS, AEX, GeoEye, Getmapping, Aerogrid, IGP

File Name: CE-23063-I

Date: 6/15/2011

USGS science for a changing world

GEOVision geophysical services

RECOVERY.GOV

SITE MAP
CE•23063

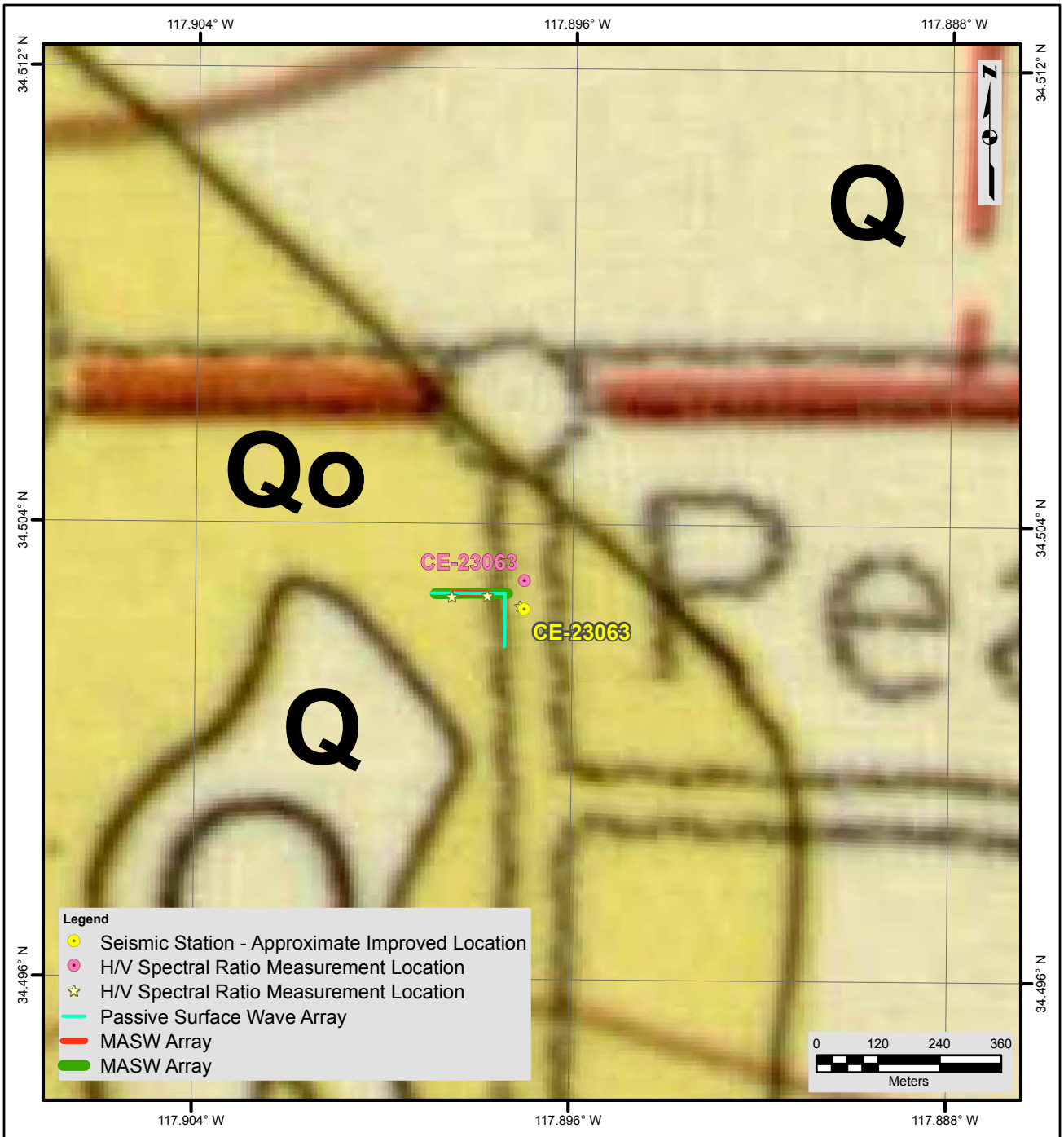

Description of Geologic Map Units

Q = Quaternary (Holocene) alluvium, undifferentiated
Qo = Quaternary (Pleistocene) older alluvium, undifferentiated

NOTES:
1. WGS 1984 COORDINATE SYSTEM
2. Geologic Map of the San Bernardino Quadrangle, California Compilation by E.J. Bortugno and T.E. Spittler, 1986 (Rev 1998)
3. See site map for details of geophysical survey

File Name: CE-23063

Date: 6/15/2011

USGS science for a changing world

GEOVision geophysical services

RECOVERY.GOV

GEOLOGIC MAP
CE•23063

CE.23063 Seismic Station

HVSR sensor 450 outside fire station housing CE.23063

Looking east along passive surface wave array 23063-1

Deep hole excavated for HVSR sensor 453

Looking east along MASW and seismic refraction array 23063-4

Location of Geophysical Testing Arrays:

Location	Latitude	Longitude
23063-1, West End of Array, Channel 1	34.50277	-117.89898
23063-1, East End of Array, Channel 24	34.50278	-117.89748
23063-2, North End of Array, Channel 25	34.50278	-117.89741
23063-2, South End of Array, Channel 48	34.50184	-117.89741
23063-3, West End of Array	34.50277	-117.89851
23063-3 and 23063-4, Center of Array	34.50277	-117.89813
23063-3, East End of Array	34.50278	-117.89774
HVSR Sensor 507	34.50273	-117.89778
HVSR Sensor 453	34.50271	-117.89854
HVSR Sensor 450	34.50255	-117.89715

Notes: 1) WGS84 Coordinate System (decimal degrees)
2) Survey accuracy is estimated at 1 to 2 m

Results:

V_S Model 1 from MASW Data

Depth to Top of Layer (m)	Layer Thickness (m)	S-Wave Velocity (m/s)	Inferred P-Wave Velocity (m/s)	Inferred Poisson's Ratio	Inferred Density (g/cm^3)
0	4	349	654	0.3	1.9
4	6	421	788	0.3	2.0
10	14	533	997	0.3	2.0
24	>6	751	1405	0.3	2.2

V_S Model 2 from MASW and Passive Surface Wave Data (maximum wavelength of 120 m)

Depth to Top of Layer (m)	Layer Thickness (m)	S-Wave Velocity (m/s)	Inferred P-Wave Velocity (m/s)	Inferred Poisson's Ratio	Inferred Density (g/cm^3)
0	4	348	652	0.3	1.9
4	6	421	787	0.3	2.0
10	14	536	1003	0.3	2.0
24	20	859	1607	0.3	2.2
44	>6	1186	2219	0.3	2.2

V_S Model 3 from MASW and Passive Surface Wave Data (maximum wavelength of 300 m)

Depth to Top of Layer (m)	Layer Thickness (m)	S-Wave Velocity (m/s)	Inferred P-Wave Velocity (m/s)	Inferred Poisson's Ratio	Inferred Density (g/cm^3)
0	4	348	652	0.3	1.9
4	6	420	787	0.3	2.0
10	14	538	1006	0.3	2.0
24	20	832	1556	0.3	2.2
44	70	1212	2267	0.3	2.2
114	>11	1890	3536	0.3	2.4

Observations/Discussion:

- The HVSR curves are very similar at frequencies below 5 Hz validating the 1-D velocity structure assumption.
- Two HVSR peaks at all test locations: a weak, narrow peak at 4.9 Hz and broad or double peak in the 1 to 2 Hz range. This indicates that there may be two significant S-wave impedance contrasts in the subsurface velocity structure.
- Noise conditions at site may not have been sufficient for successful application of passive surface wave techniques due to possible directional noise bias from Hwy 138 and limited traffic on roads in immediate site vicinity.
- Surface wave dispersion data from active and passive surface wave datasets are in good agreement at this site, except for longer wavelengths where the passive surface wave dispersion data has slightly higher phase velocities.
- ESAC technique used to extract surface wave dispersion data from passive "L" array data. Both the ReMi™ and ESAC techniques used in an attempt to extract surface wave dispersion data from the linear arrays. Passive surface wave data collected along linear arrays were not useful at this site. Passive "L" array data were also somewhat noisy with a gap in the dispersion data over the 110 to 150 m wavelength range.
- It was very difficult extracting surface wave dispersion data from the MASW seismic records at wavelengths of less than 8 m due to a dominant higher mode at high frequencies. MASW data were acquired along a dirt road and the apparent dominant higher mode may be related to a high velocity surface layer, subsurface utilities or some other feature. Additional surface wave data (SASW or MASW) acquired off the road may improve the higher frequency dispersion data, unless there is a geologic high velocity layer in the near surface (i.e. upper 4 m).
- Representative dispersion curves were generated for each surface wave data set using a moving average, polynomial curve fitting routine. These individual representative dispersion curves were combined and a representative dispersion curve generated for the combined data set for data modeling.

- The generalized reciprocal method (GRM) was used to generate a 3 layer model of the seismic refraction data collected along array 23063-4. This model consists of a 1 to 4 m thick layer of sediments with a P-wave velocity of 625 m/s, intermediate sediment layer with P-wave velocity of about 925 m/s underlain by possible bedrock at a depth of about 21 to 24 m and with P-wave velocity of about 3,075 m/s. There is no conclusive evidence of the water table in the seismic refraction data.
- Three models were generated for the surface wave data: Model 1 using only MASW dispersion data, Model 2 using MASW dispersion data and "L" array passive surface wave data at wavelengths of less than 120 m (before gap in passive surface wave dispersion data) and Model 3 using MASW and all "L" array passive surface wave data.
- HVSR and seismic refraction data were used to guide the surface wave modeling although the multiple data sets have not been jointly modeled at this point. HVSR data indicate that there may be two significant impedance contrasts in the subsurface, a shallow impedance contrast associated with the 4.9 Hz peak and a deep impedance contrast associated with the 1 to 2 Hz peak.
- A minimal number of layers were utilized to model the surface wave data. Specifically, one layer was used to represent the upper 4 m where there may be significant uncertainty in the model due to difficulty extracting consistent dispersion data at wavelengths less than 8 m. A layer contact was also placed at 24 m depth based on the seismic refraction model.
- The impedance contrast at a depth of 24 m on models 1 to 3 is consistent with the 4.9 Hz HVSR peak. However, the S-wave velocity of this layer (751 m/s on Model 1, 859 m/s on Model 2 and 833 m/s on Model 3) is not consistent with the approximate 3,075 m/s P-wave velocity on the seismic refraction model. It is, therefore, possible that this layer is associated with a saturated, high velocity sedimentary unit rather than weathered crystalline basement. It is not certain if saturation would strongly influence the P-wave velocity of decomposed or intensely weathered crystalline rock.
- Although not considered particularly reliable at this site, long wavelength passive surface wave data were modeled in an attempt to determine if there was possible geologic structure associated with the 1 to 2 Hz HVSR peak. A large impedance contrast, likely associated with the top of competent crystalline basement, is modeled at a depth on the order of 114 m. The depth of this layer is not particularly accurate, but the S-wave velocity model would result in an associated HVSR peak at about 1.9 Hz. The measured HVSR peak in this frequency range indicates that geologic structure is more complicated than represented in the S-wave velocity model. Joint modeling of HVSR and surface wave data is recommended, but not until an attempt is made to acquire better high and low frequency surface wave data, if possible.
- Surface wave depth of investigation of Models 1, 2 and 3 is estimated at 40, 50 and greater than 125 m, respectively.
- V_{S30} is 500, 510 and 508 m/s for Models 1 to 3, respectively and averages 506 m/s (Site Class C).

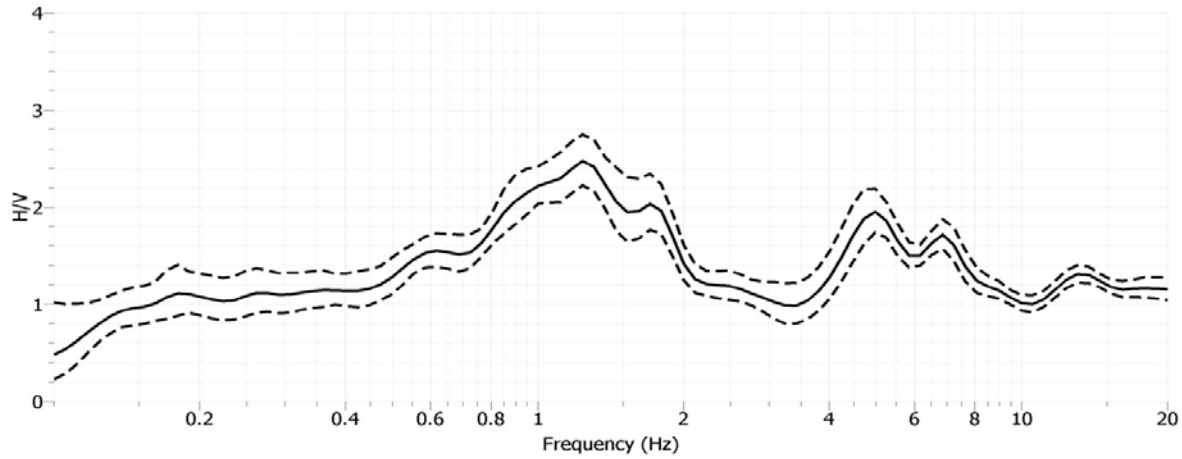

Site CE.23063, H/V Spectral Ratio, Array 23063-3, Sensor 453

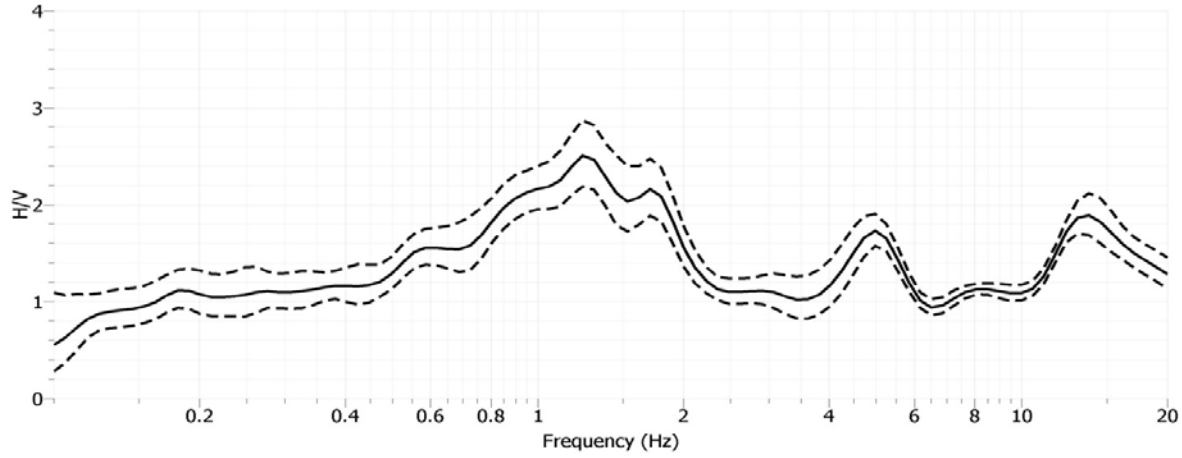

Site CE.23063, H/V Spectral Ratio, Array 23063-3, Sensor 507

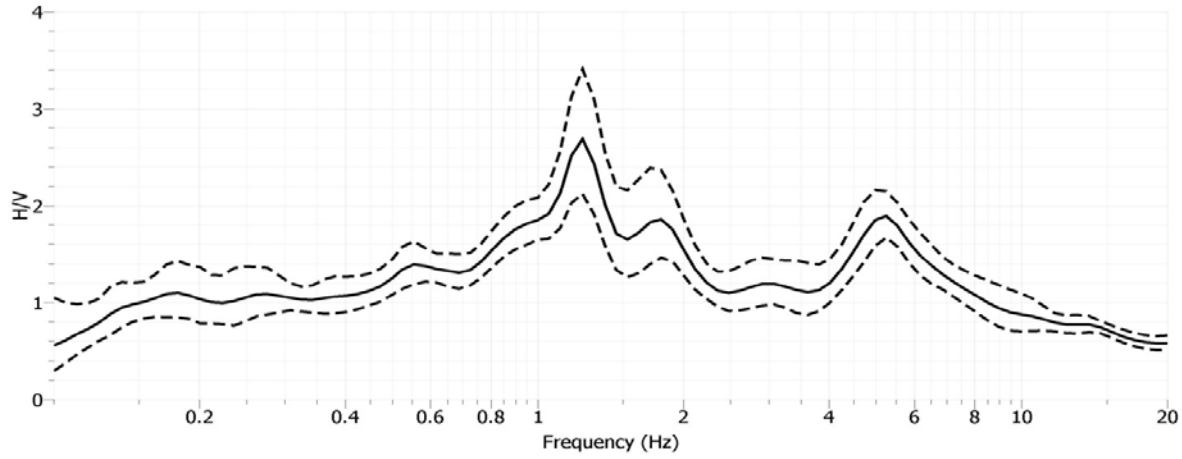

Site CE.23063, H/V Spectral Ratio, Array 23063-3, Sensor 450

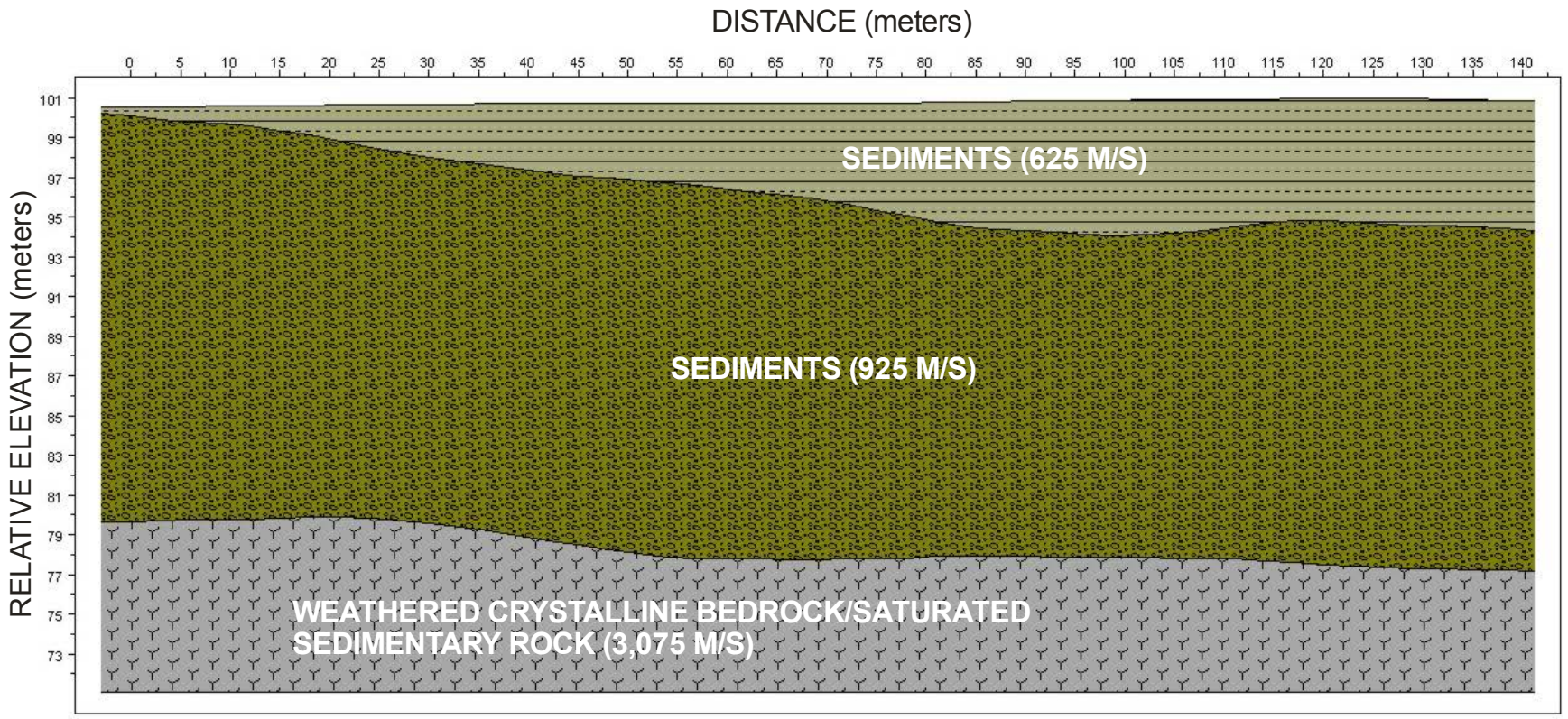

Array 23063-4 – Layer based seismic refraction model

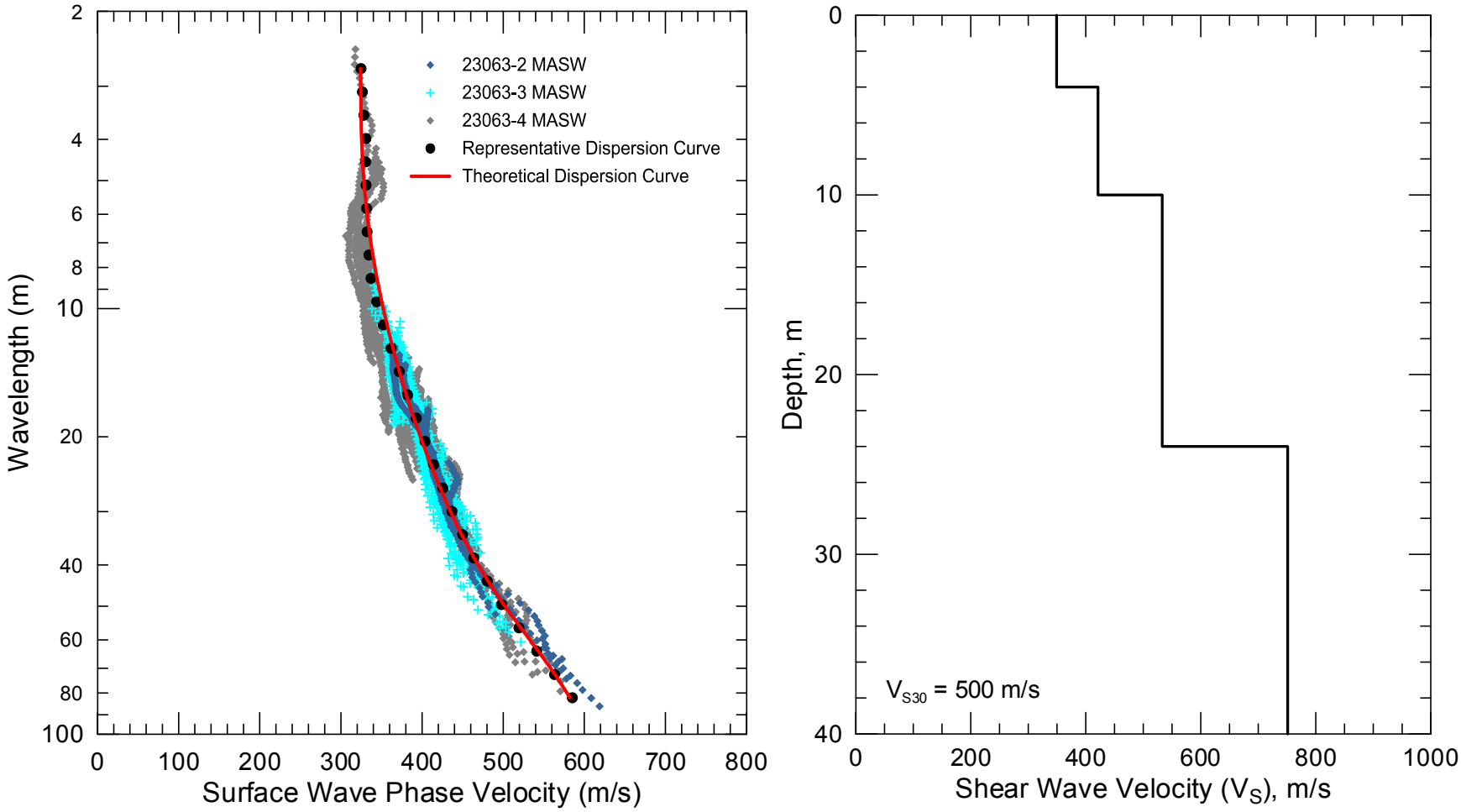

CE.23063 - Field, representative and inverted theoretical surface wave dispersion data (left) and associated V_S model (right) for analysis of MASW data only

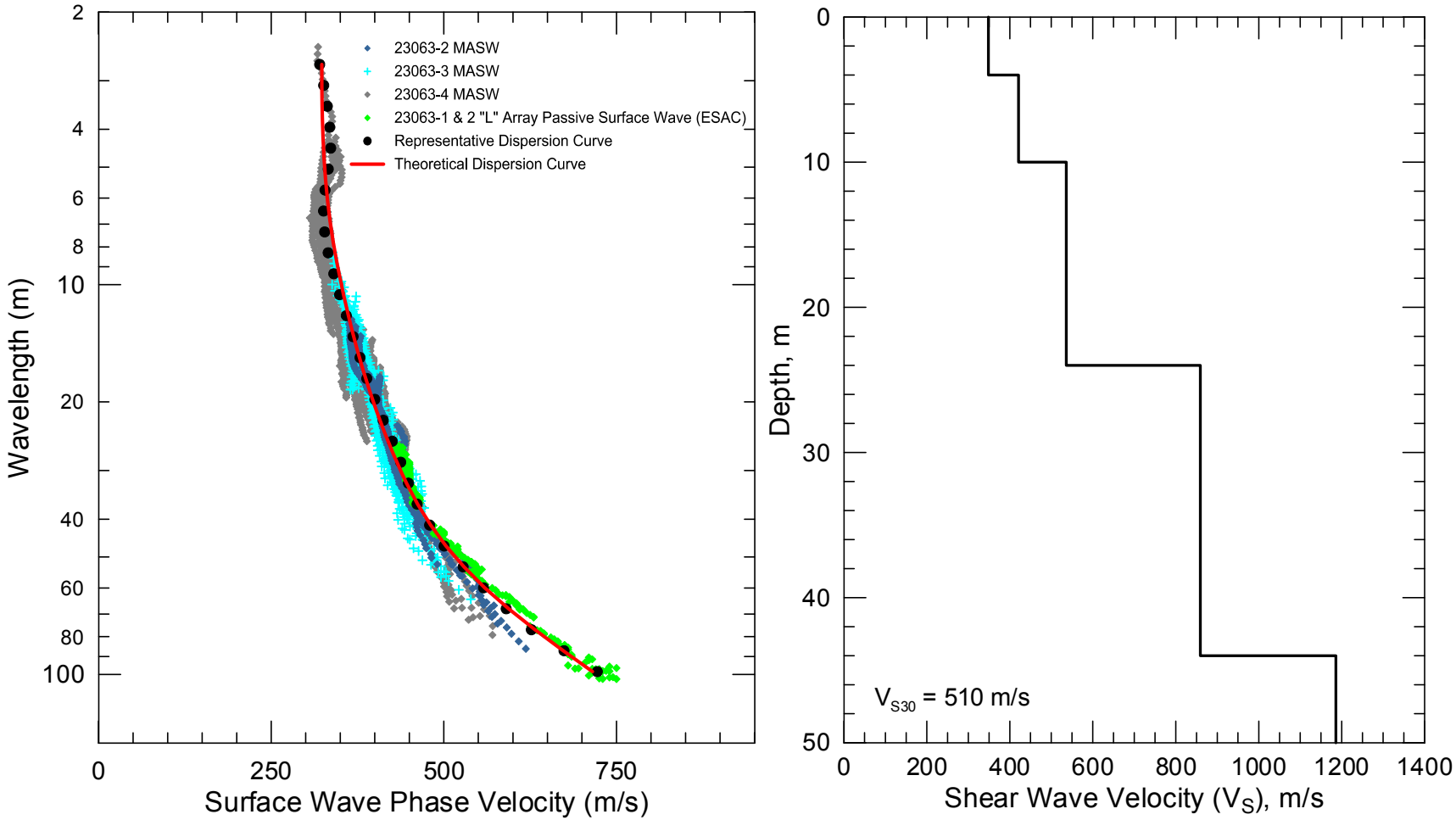

CE.23063 - Field, representative and inverted theoretical surface wave dispersion data (left) and associated V_S model (right) for analysis of MASW data and passive surface wave data to a maximum wavelength of 120 m

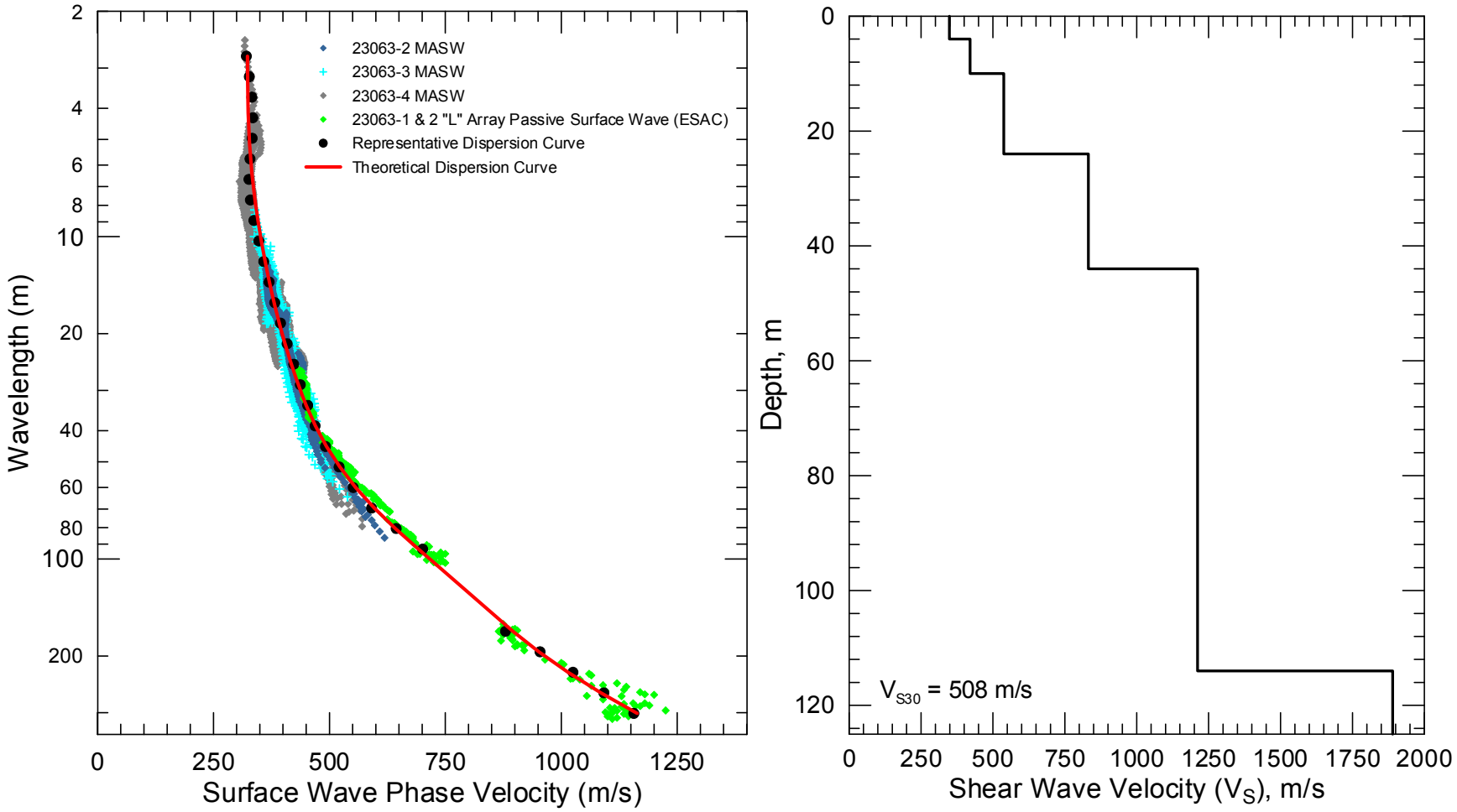

CE.23063 - Field, representative and inverted theoretical surface wave dispersion data (left) and associated V_S model (right) for analysis of MASW data and passive surface wave data to a maximum wavelength of 300 m

Site CE.23897

Location: San Bernardino City Fire Station 226, 1920 N. Del Rosa Avenue, San Bernardino, California

Latitude: 34.13322 **Longitude:** -117.25281
(Station coordinates modified using published coordinates from http://www.strongmotioncenter.org with further adjustment made by identifying the structure housing the seismic sensor on Google Earth or ESRI Imagery, WGS84 coordinate system.)

V_{S30} (measured): 584 m/s

V_{S30} (adjusted to more accurately reflect seismic station conditions): 584 m/s (no adjustment necessary).

NEHRP Site Class: C

Geomatrix Code: AHB/AKB

Geologic Conditions/Observations: Seismic station sitting on a thin layer of Quaternary (Holocene) alluvium overlying Mesozoic (Late Cretaceous) Pelona Schist. There are probably no more than several meters of alluvium overlying schist in the immediate site vicinity.

Site Conditions: Suburban site. Relatively flat topography in test area although a hill comprised of Pelona Schist outcrops immediately northwest of the test area and seismic station.

Geophysical Methods Utilized: HVSR, Seismic Refraction (P- and S-wave), MASW (Rayleigh wave), MALW (Love Wave)

Geophysical Testing Arrays:

1. Array 23897-1 (48 channel MASW and P-wave seismic refraction array utilizing 4.5 Hz vertical geophones spaced 1.5 m apart for a length of 70.5 m, forward and reverse shot locations with multiple source offsets and source types and multiple interior shot locations).
2. Array 23897-1 (48 channel S-wave seismic refraction array utilizing 10 Hz horizontal geophones spaced 1.5 m apart for a length of 70.5 m, forward and reverse shot locations with multiple source offsets and multiple interior shot locations). Coincident with P-wave array of same name.
3. Three HVSR measurement locations distributed along array 23897-1.

Legend

- Seismic Station - Approximate Improved Location
- Seismic Station - Approximate Location of Record
- H/V Spectral Ratio Location
- MASW Array

NOTES:
1. WGS 1984 COORDINATE SYSTEM
2. Image Source: ESRI, i-cubed, USDA FSA, USGS, AEX, GeoEye, Getmapping, Aerogrid, IGP

File Name: CE-23897-I

Date: 2/7/2013

USGS science for a changing world

GEOVision geophysical services

RECOVERY.GOV

SITE MAP
CE•23897

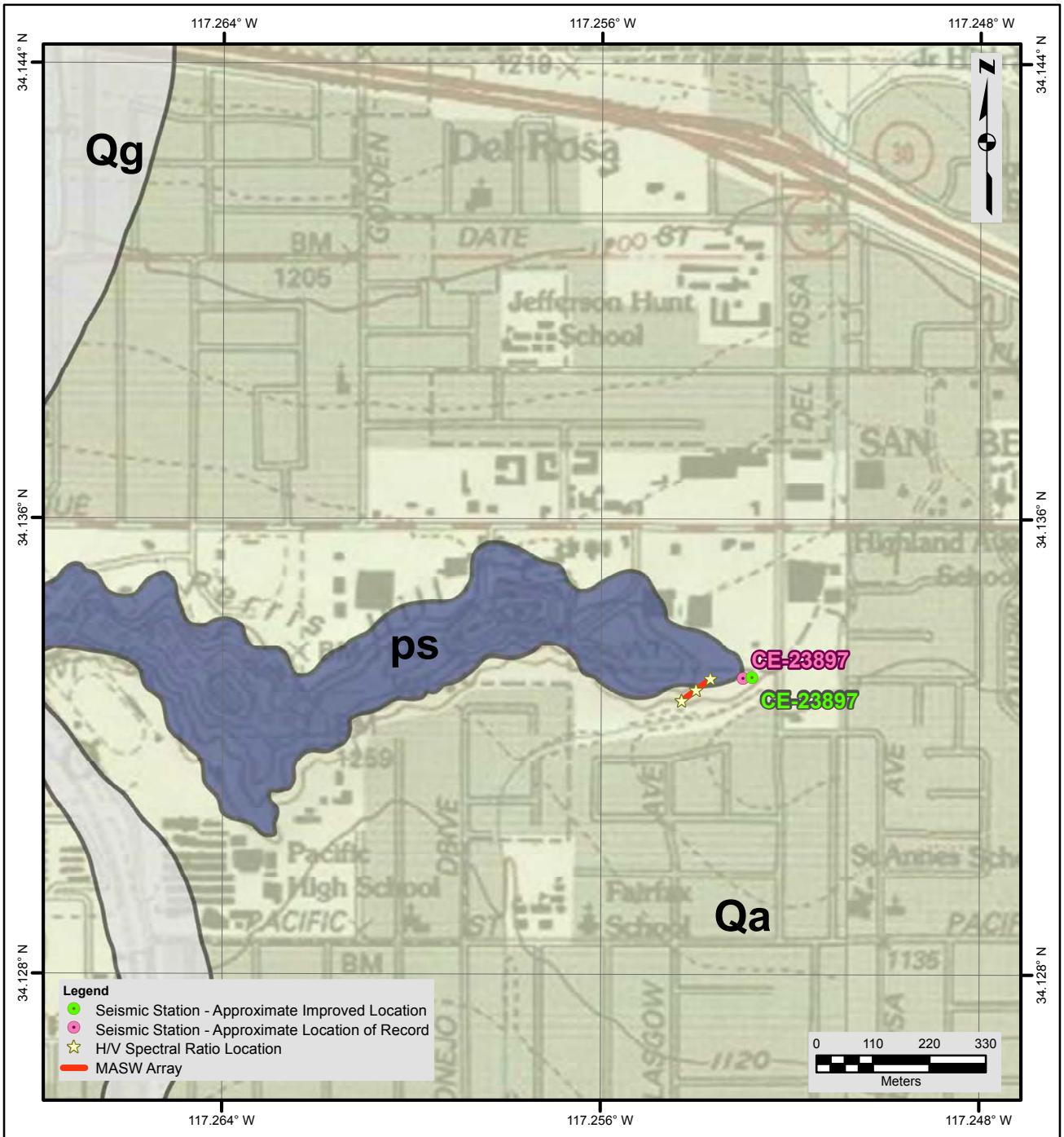

Description of Geologic Map Units

Qg = Quaternary (Holocene) alluvial gravel and sand of stream channels
Qa = Quaternary (Holocene) alluvial fan gravel and sand of valley areas
ps = Mesozoic (Late Cretaceous) Pelona Schist, mica schist, muscovite and biotite micas, albite feldspar and quartz, locally chlorite

NOTES:
1. WGS 1984 COORDINATE SYSTEM
2. Modified From Geologic Map of the San Bernardino North / North ½ of San Bernardino South Quadrangles, San Bernardino and Riverside Counties, California by Thomas W. Dibblee, Jr., 2004
3. See site map for details of geophysical survey

File Name: CE-23897

Date: 2/7/2013

USGS science for a changing world

GEOVision geophysical services

GEOLOGIC MAP
CE•23897

RECOVERY.GOV

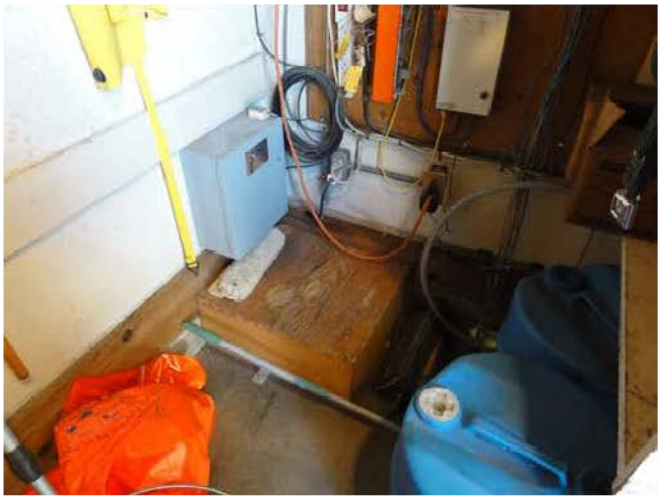

CE.23897 seismic station

Looking east at HVSR sensor 507 and the fire station housing the seismic sensor

Looking northeast from center of array 23897-1

Looking southwest along array 23897-1

Pelona Schist outcrops in drainage channel south of test area indicated that bedrock is only several meters deep in the vicinity of the seismic station

Location of Geophysical Testing Arrays:

Location	Latitude	Longitude
23897-1, Southwest End of MASW/Refraction Array	34.13281	-117.25429
23897-1, Center of MASW/Refraction Array	34.13300	-117.25399
23897-1, Northeast End of MASW/Refraction Array	34.13319	-117.25368
HVSR Sensor 450	34.13281	-117.25429
HVSR Sensor 453	34.13300	-117.25399
HVSR Sensor 507	34.13319	-117.25368
CE.23897 Seismic Station	34.13322	-117.25281

Notes: 1) WGS84 Coordinate System (decimal degrees)
2) Survey accuracy is estimated at 1 to 2 m.
3) Seismic station not surveyed as located inside building.

Results:

V_S Model (MASW Array)

Depth to Top of Layer (m)	Layer Thickness (m)	S-Wave Velocity (m/s)	Inferred P-Wave Velocity (m/s)	Assumed Poisson's Ratio	Assumed Density (g/cm^3)
0	1	207	387	0.3	1.70
1	2	335	627	0.3	1.80
3	3	414	774	0.3	1.90
6	5	531	994	0.3	2.00
11	6	612	1145	0.3	2.05
17	7	821	1537	0.3	2.10
24	>6	1074	2009	0.3	2.15

Notes: 1) Depth of investigation is about 30 m.
2) Bottom layer is a half space.
3) Half space S-wave velocity not well resolved.

Average V_P and Estimated V_S Models from Central Portion of P-wave Seismic Refraction Line

Depth to Top of Layer (m)	Layer Thickness (m)	P-Wave Velocity (m/s)	Estimated S-Wave Velocity (m/s)			
			Poisson's Ratio = 0.25	Poisson's Ratio = 0.30	Poisson's Ratio = 0.3333	Poisson's Ratio = 0.35
0.00	0.63	306	176	163	153	147
0.63	1.25	687	396	367	343	330
1.88	1.25	866	500	463	433	416
3.13	1.25	920	531	492	460	442
4.38	1.25	978	565	523	489	470
5.63	1.25	994	574	531	497	478
6.88	1.25	1013	585	542	507	487
8.13	2.63	1137	656	608	568	546
10.75	2.63	1160	670	620	580	557
13.38	2.63	1194	689	638	597	574
16.00	2.63	1269	732	678	634	609
18.63	2.63	1572	908	840	786	755
21.25	2.63	1682	971	899	841	808
23.88	Half Space	1862	1075	995	931	894

Note: P-wave velocity not well constrained below 25 m and V_{P30} and V_{S30} are estimated assuming that velocity is constant between 25 and 30 m depth.

Observations/Discussion:

- The HVSR plots are almost identical validating the 1-D velocity assumption. There are, however, no distinct, high amplitude HVSR peaks.
- Surface wave techniques did not appear to be very effective in the field due to shallow bedrock. Therefore, P- and S-wave seismic refraction data were acquired at the site along with MASW (Rayleigh wave) and MALW (Love wave) data. Accurate picking of S-wave first arrival date appeared quite difficult with this data set and MASW data quality was significantly better than MALW data quality. Therefore, interpretation was based on analysis of MASW and P-wave seismic refraction data.
- The P-wave seismic refraction data for array 23897-1 were modeled using a tomographic inversion routine with a smooth velocity gradient starting model. The P-wave seismic refraction model was extended to far offset shot locations to extend depth of investigation. It should be noted that a larger geophone spacing, rather than the utilization of far offset shot locations, is preferred for extending depth of investigation, when applying tomographic inversion routines. However, the seismic refraction data were acquired in conjunction with surface wave data, where a shorter array length is preferred.
- The P-wave seismic refraction survey design allowed P-wave velocity to be imaged to a maximum depth of about 24 m. The seismic refraction model indicates that P-wave velocity is about 250 to 400 m/s at the surface and increases to over 800 m/s at a depth of 1 to 2 m, 1,000 m/s at a depth of 2.5 to 8.5 m, 1,400 m/s at a depth of 15 to 18 m and over 1,800 m/s at a nominal depth of 19 to 23 m. The maximum P-wave velocity in the central portion of the model, where depth of investigation is greatest is slightly less than 1,900 m/s.
- The seismic refraction survey indicates that there is some lateral velocity variation at the site, primarily in the upper 10 m where there is a thickening of lower velocity, weathered rock to the southwest.
- The average P-wave velocity of the upper 30 m (V_{P30}) was estimated between 19.5 and 48 m on the P-wave refraction model, where depth of investigation is greatest. To estimate V_{P30} the P-wave velocity at a depth of 24 m, maximum depth of investigation, was projected to 30 m depth. V_{P30} ranges from about 1,105 to 1,202 m/s over the 19.5 to 48 m position interval, an 8% variation.
- An average V_P model was developed over the 19.5 to 48 m distance interval by averaging the slowness of each model cell and average V_{P30} was determined to be 1,163 m/s. Assuming constant Poisson's ratios of 0.25, 0.3, 0.3333 and 0.35 would result in an estimated V_{S30} of 671, 622, 581 and 559 m/s, respectively.
- Passive surface wave testing was not conducted at this site because the site is located only a few meters above rock and there was concern about variable bedrock topography as distance increased from the outcrop.
- MASW (Rayleigh wave) data were not easy to reduce, possibly because of either a thin soil layer over weathered rock, dipping rock beneath the array, or lateral velocity variation. No attempt was made to reduce the MALW (Love wave) data, which was of poorer quality than the MASW data. Although difficult, a coherent Rayleigh wave phase velocity dispersion curve was developed, which is considered representative of site

conditions. No attempt was made to extract Rayleigh wave phase velocity data at wavelengths greater than 65 m.

- The minimum wavelength surface wave phase velocity data extracted from the 48-channel MASW array is about 24 m. Data reduction using seismic records from smaller hammer sources and a limited offset receiver array (i.e. less active geophones) allowed extraction of surface wave dispersion data to a minimum wavelength of about 3 m.
- There is nominally about 50 m/s scatter in MASW dispersion data likely due to the effects of lateral velocity variation.
- A representative dispersion curve was generated for the MASW data set using a moving average, polynomial curve fitting routine and used for modeling.
- Surface wave depth of investigation is about 30 m based on half of maximum wavelength criteria.
- There is good agreement between the average V_S models calculated from the P-wave seismic refraction model assuming constant values of Poisson's ratio and the V_S model resulting from inversion of the Rayleigh wave phase velocity data.
- V_{S30} from the MASW V_S model is 584 m/s (Site Class C).
- V_{S30} from the P-wave seismic refraction model and assumed constant Poisson's ratio of 0.3333 is 581 m/s (Site Class C), almost identical to that measured using the MASW technique.
- For site characterization purposes, the use of the MASW V_S model is recommended. Modeling the MASW data using the average mode assumption (not presented), only resulted in a reduction in the half space V_S by about 10%, which agrees better with the seismic refraction models. At this site V_S models were estimated from the P-wave refraction data to check results and to evaluate the possible use of P-wave data at sites where saturated sediments/rock are not present and acceptable surface wave and S-wave seismic refraction data cannot be obtained or is not available.

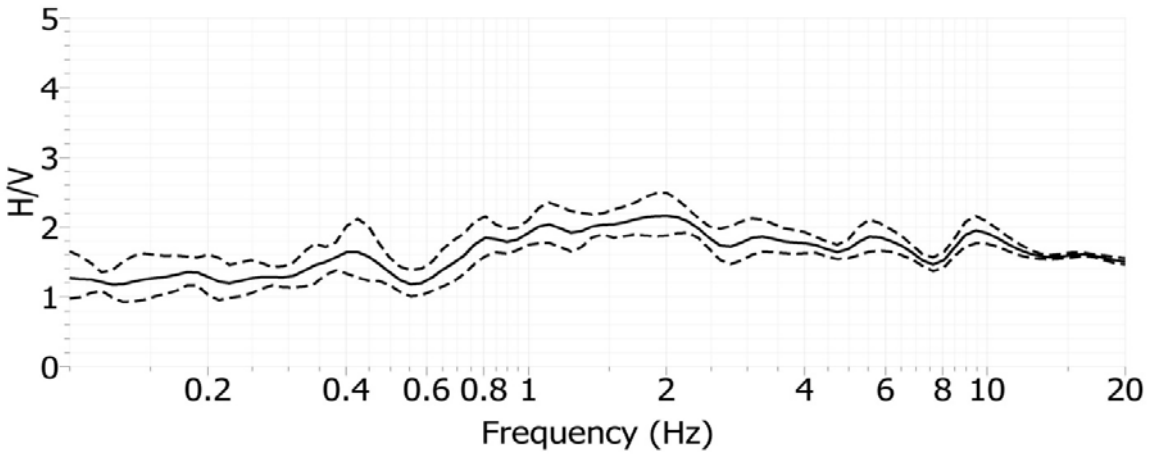

Site CE.23897, H/V Spectral Ratio, Array 23897-1, Sensor 507

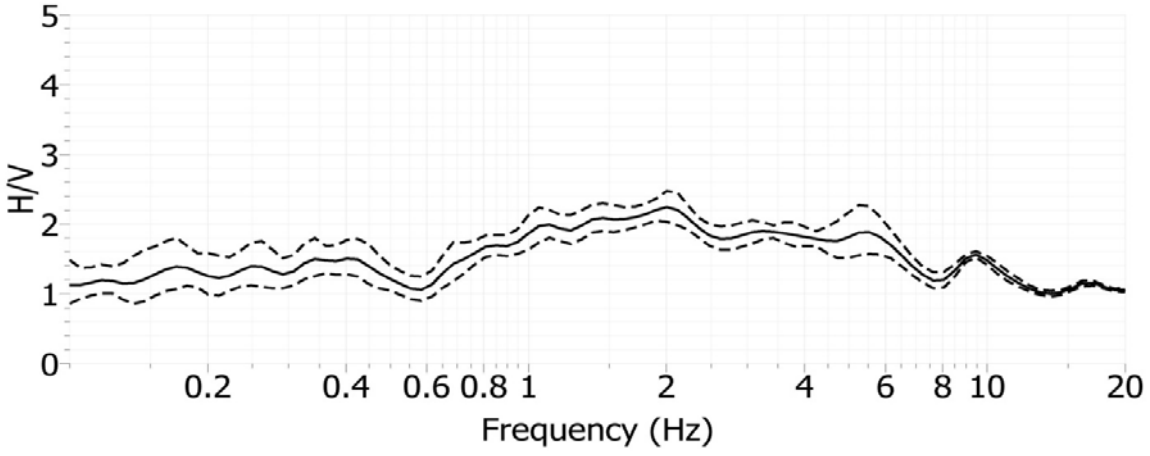

Site CE.23897, H/V Spectral Ratio, Array 23897-1, Sensor 453

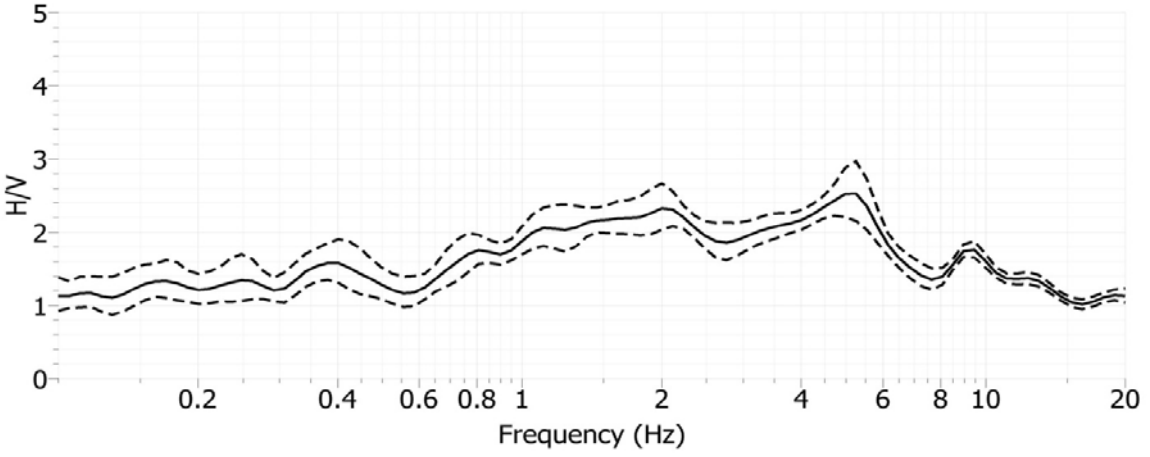

Site CE.23897, H/V Spectral Ratio, Array 23897-1, Sensor 450

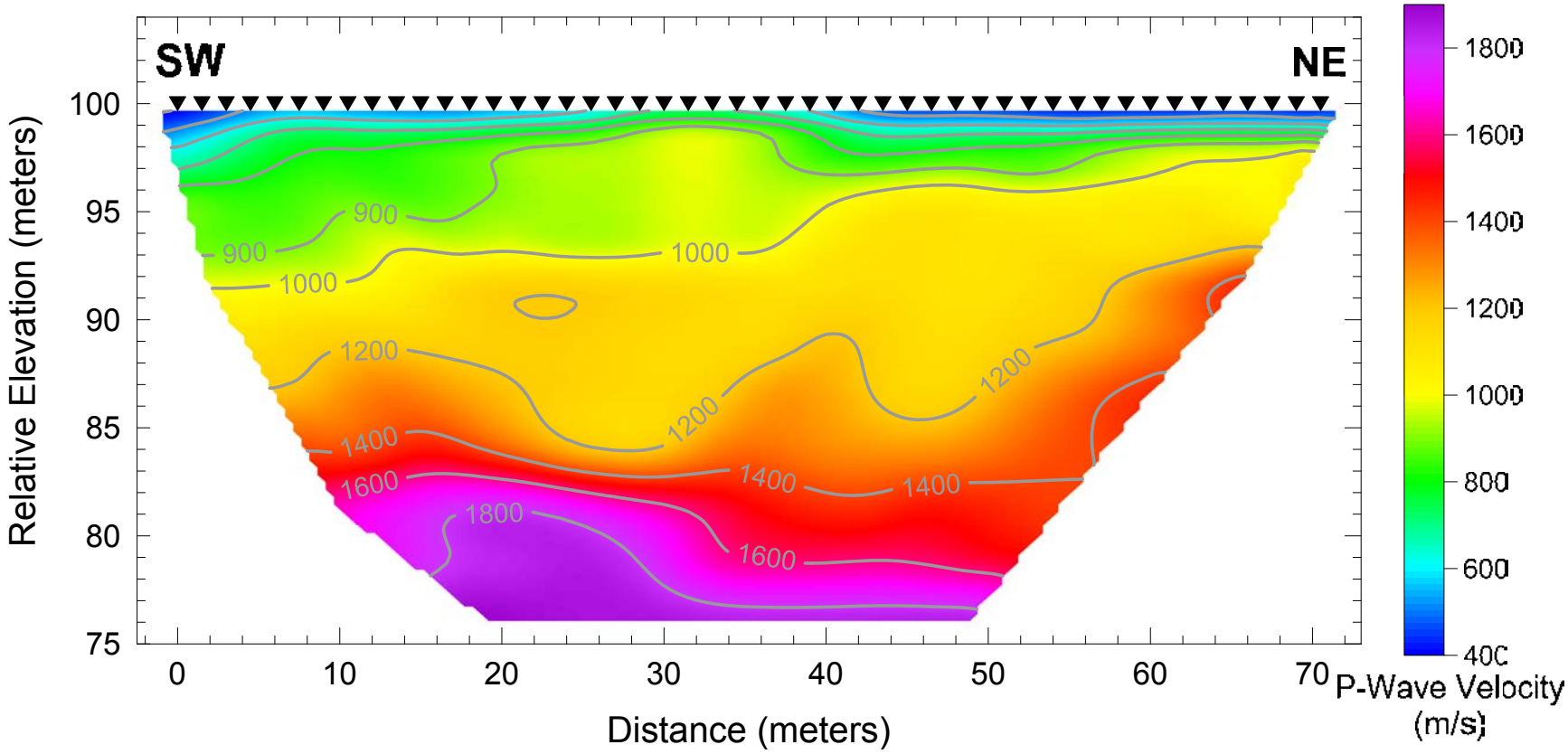

Array 23897-1 – Tomographic Seismic Refraction Model utilizing Smooth Velocity Gradient Starting Model

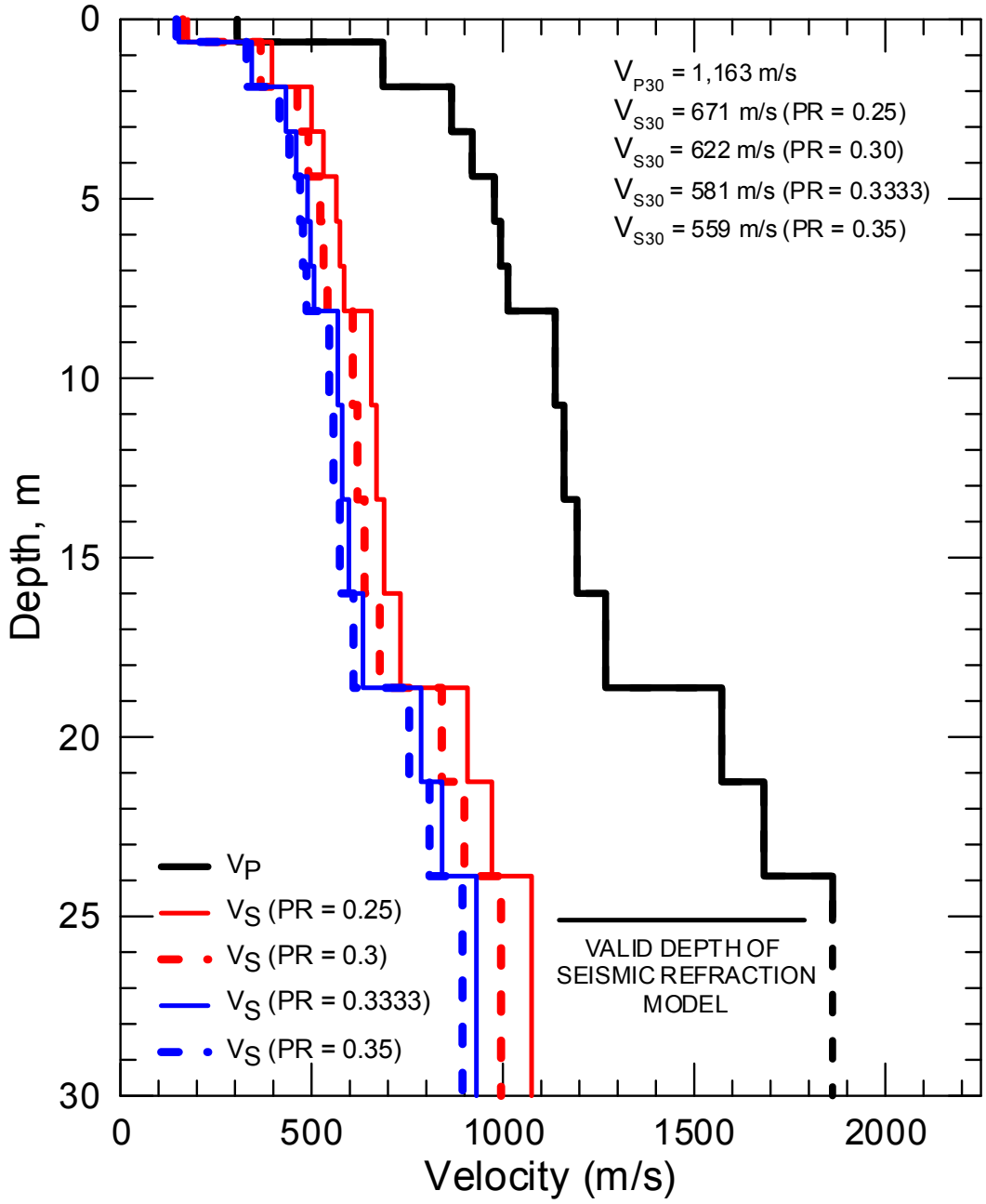

CE.23897 – Average P-wave velocity structure and estimated S-wave velocity structure between 19.5 and 48 m on P-wave seismic refraction array 23897-1. P-wave velocity is not well constrained below a depth of 25 m and computations are made assuming that velocity is constant below this depth. A longer seismic line would be preferred to both more accurately model the high P-wave velocities and to image to 30 m depth.

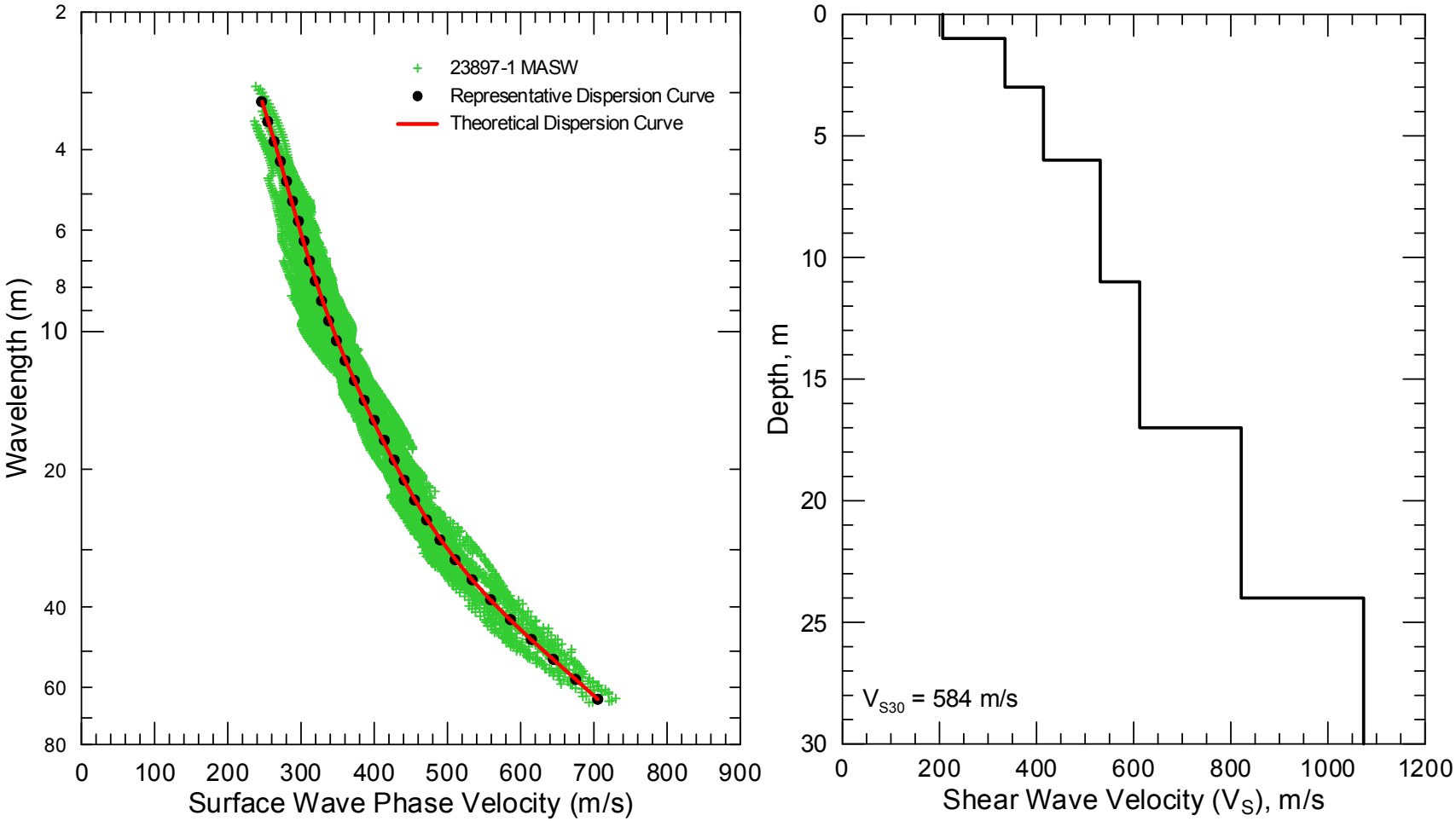

CE.23897 - Field, representative and inverted theoretical surface wave dispersion data (left) and associated V_S model (right)

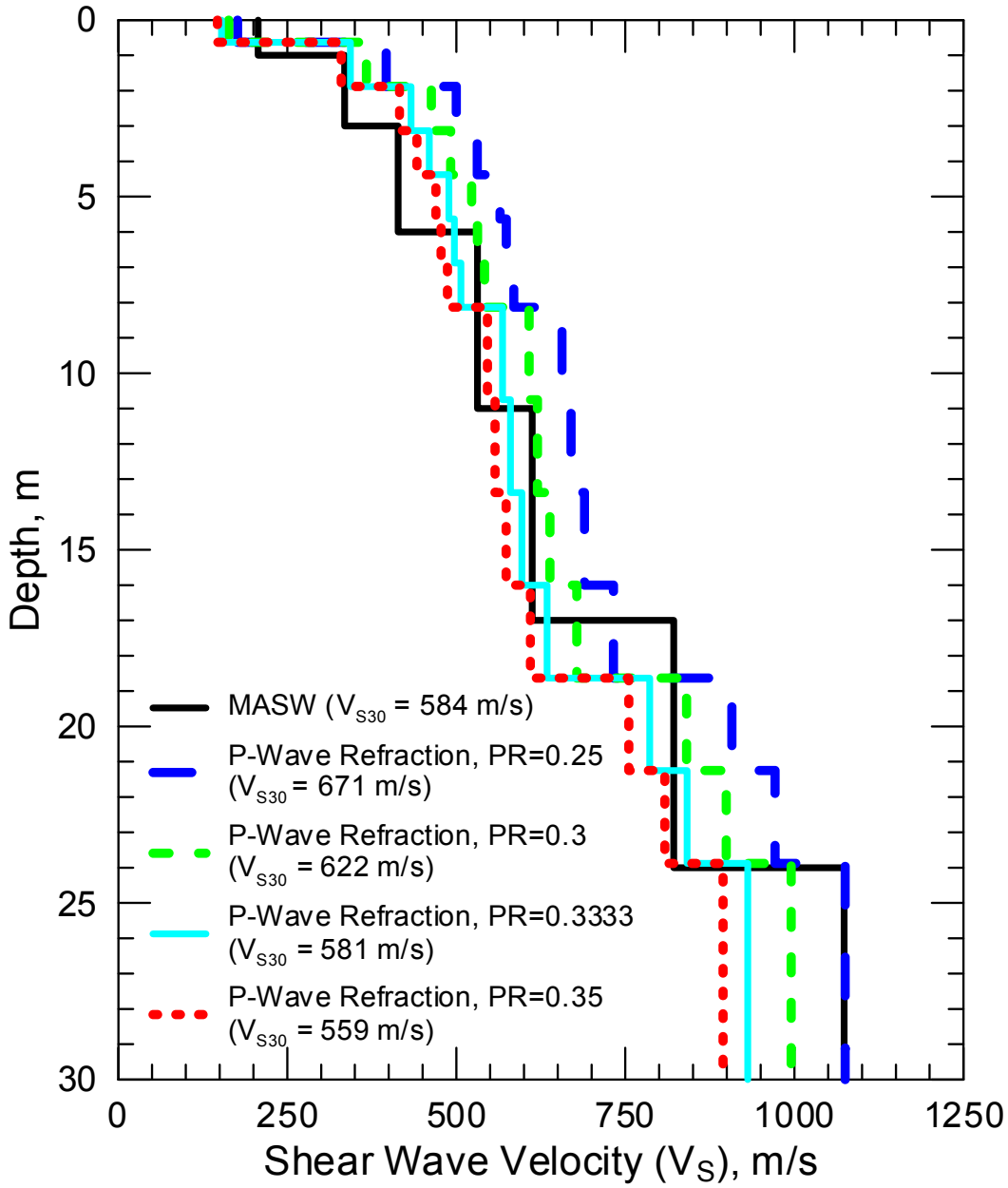

CE.23897 – Summary of S-wave velocity models derived from the MASW (Rayleigh wave) and P-wave seismic refraction surveys. The V_S model developed from the MASW sounding is generally in good agreement with estimated V_S from the P-wave seismic refraction model assuming Poisson's ratio in the 0.3 to 0.35 range. V_{S30} calculated from the MASW V_S model is almost identical to that estimated from the P-wave refraction model assuming a constant Poisson's ratio of 0.3333. The P-wave seismic refraction model indicates that V_{P30} varies by about 10% beneath the seismic line, which is consistent with the variability in V_{S30} based on scatter in the Rayleigh wave dispersion data.

Site CE.23958

Location: Pinon Hills Fire Station 102, 10433 Mountain Road, Pinon Hills, California

Latitude: 34.43942 **Longitude:** -117.64644
(Station coordinates modified using published coordinates from http://www.strongmotioncenter.org with further adjustment made by identifying the structure housing the seismic sensor on Google Earth or ESRI Imagery, WGS84 coordinate system)

V_{S30} (measured): 423 m/s

V_{S30} (adjusted to more accurately reflect seismic station conditions): 443 m/s (S-wave velocity of upper 1 m thick layer replaced with that of underlying layer to reflect fact that seismic station located in building on engineered fill).

NEHRP Site Class: C

Geomatrix Code: AHD

Geologic Conditions/Observations: Site located in area mapped as Quaternary (Holocene) alluvium.

Site Conditions: Rural site with some traffic noise from nearby roads, particularly Hwy 138. Relatively flat terrain in site vicinity. Ground surface elevation decreases gradually to the north.

Geophysical Methods Utilized: HVSR, MASW, array microtremor, ReMi™

Geophysical Testing Arrays:

1. Arrays 23958-1 (24 channel linear array utilizing 4.5 Hz vertical geophones spaced 6 m apart for an array length of 138 m) and 23958-2 (24 channel linear array utilizing 4.5 Hz vertical geophones spaced 4.5 m apart for an array length of 103.5 m) used to acquire passive surface wave data. Arrays combined to form an "L" shaped array.
2. Array 23958-3 (48 channel MASW array utilizing 4.5 Hz vertical geophones spaced 1.5 m apart for a length of 70.5 m, forward and reverse shot locations with multiple source offsets and source types and center shot location).
3. Three HVSR measurement locations; two along arrays 23958-1 and 23958-3 and the other near the seismic station.

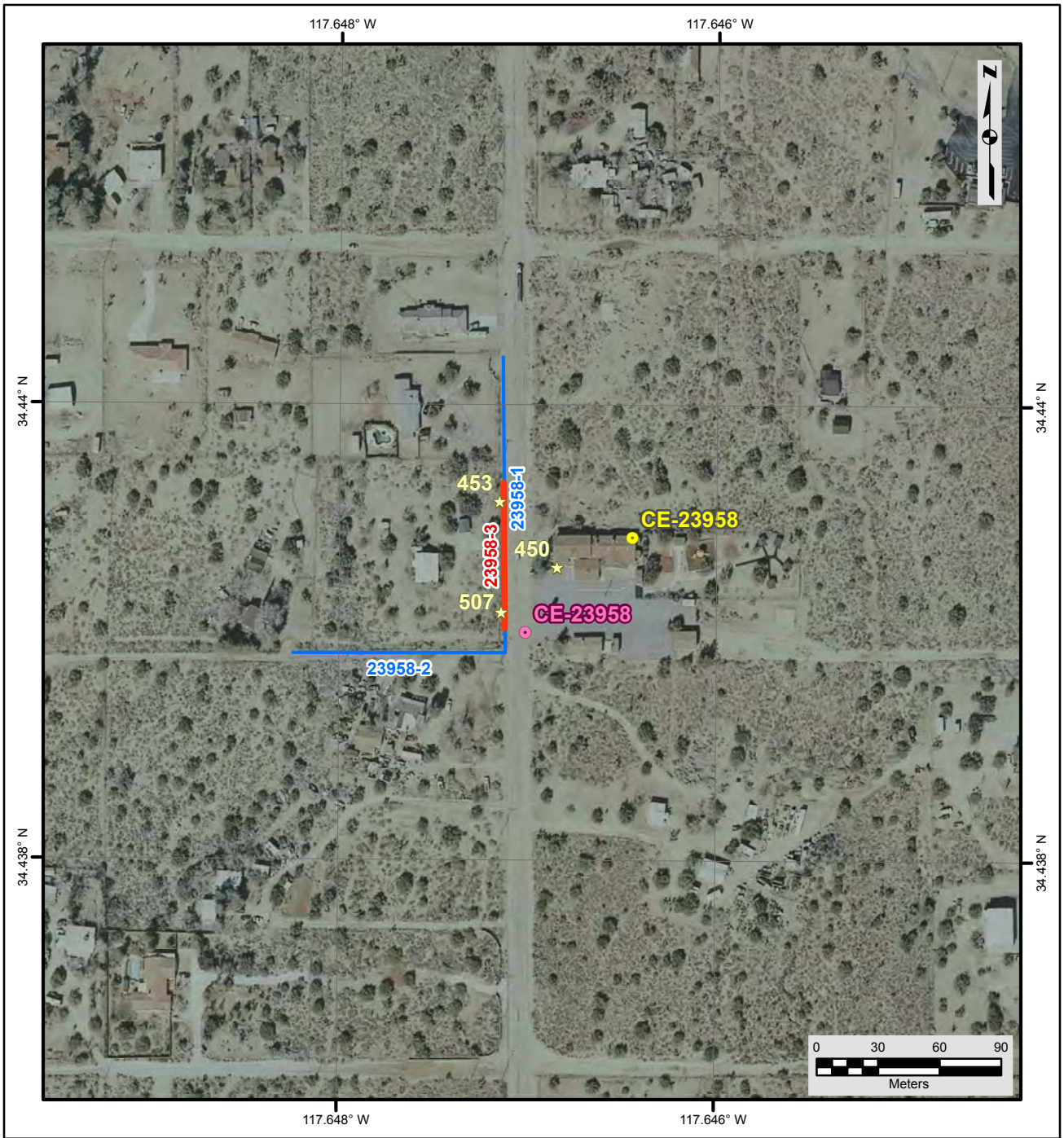

Legend

- Seismic Station - Approximate Location of Record
- H/V Spectral Ratio Location
- MASW Array
- Passive Surface Wave Array

NOTES:
1. WGS 1984 COORDINATE SYSTEM
2. Image Source: ESRI, i-cubed, USDA FSA, USGS, AEX, GeoEye, Getmapping, Aerogrid, IGP

File Name: CE-23958-1

Date: 10/14/2011

USGS science for a changing world

GEOVision geophysical services

RECOVERY.GOV

SITE MAP
CE•23958

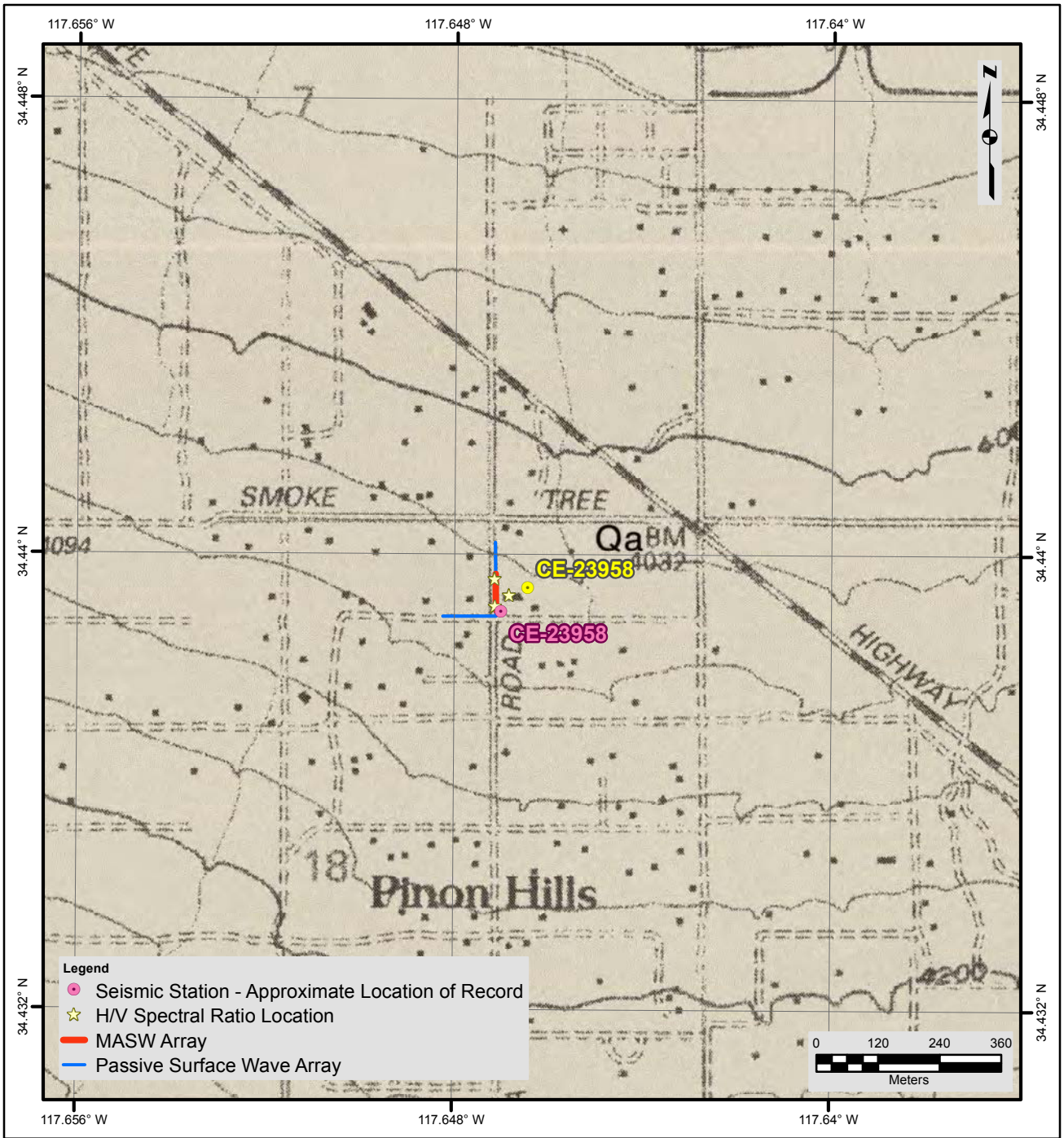

Description of Geologic Map Units

Qa = Quaternary (Holocene) alluvial gravel, sand and silt/clay of valleys and canyon flood plains

NOTES:
1. WGS 1984 COORDINATE SYSTEM
2. Geologic Map of the Mescal Creek Quadrangle, Los Angeles and San Bernardino Counties, California by Thomas W. Dibblee, Jr., 2002
3. See site map for details of geophysical survey

File Name: CE-23958

Date: 10/14/2011

USGS science for a changing world

GEOVision geophysical services

RECOVERY.GOV

GEOLOGIC MAP
CE•23958

Looking southeast towards fire station housing CE.23958 seismic station from center of array 23958-3

MASW/seismic refraction array 23958-3

Looking north along passive surface wave array 23958-1

Looking northeast towards fire station housing CE.23958 seismic station from HVSR Sensor 507

Nanometrics Trillium Compact seismic sensor in shallow hole used for HVSR measurements

Location of Geophysical Testing Arrays:

Location	Latitude	Longitude
23958-1, North End of Array, Channel 1	34.44021	-117.64713
23958-1, South End of Array, Channel 24	34.43897	-117.64711
23958-2, East End of Array, Channel 25	34.43892	-117.64711
23958-2, West End of Array, Channel 48	34.43891	-117.64823
23958-3, South End of Array	34.43902	-117.64711
23958-3, Center of Array	34.43935	-117.64712
23958 3, North End of Array	34.43966	-117.64712
HVSR Sensor 507	34.43909	-117.64713
HVSR Sensor 453	34.43957	-117.64714
HVSR Sensor 450	34.43928	-117.64683

Notes: 1) WGS84 Coordinate System (decimal degrees)
2) Survey accuracy is estimated at 1 to 2 m.

Results:

V_S Model

Depth to Top of Layer (m)	Layer Thickness (m)	S-Wave Velocity (m/s)	Inferred P-Wave Velocity (m/s)	Inferred Poisson's Ratio	Inferred Density (g/cm^3)
0	1	147	275	0.3	1.7
1	2	280	524	0.3	1.8
3	3	364	681	0.3	1.9
6	5	399	746	0.3	1.9
11	9	498	931	0.3	2.0
20	12	552	1032	0.3	2.0
32	15	593	1109	0.3	2.0
47	20	643	1202	0.3	2.1
67	>13	719	1344	0.3	2.1

Notes: 1) Depth of investigation is about 80 m.
2) Bottom layer is a half space.

Observations/Discussion:

- There are no high frequency HVSR peaks by which to assess lateral velocity variation.
- HVSR sensor 450 yields the highest quality data as it is located furthest from a nearby road. There is a broad, low amplitude HVSR peak in the 0.3 to 0.5 Hz range for sensor 450, which would be indicative of deep basement. Processing of HVSR data from sensors 453 and 507 was complicated by numerous transients from nearby vehicular

traffic. Acquisition of HVSR data at these locations at night or acquisition of HVSR data at alternate locations further from Mountain Road would be necessary to validate the peak observed in the sensor 450 data.

- Based on simple layer-based analysis of seismic refraction first arrival data, P-wave velocity in the upper 15 m ranges from about 350 to 450 m/s near the surface to about 750 to 850 m/s below a depth of 2 to 3 m and 1,000 to 1,100 m/s below a depth of 8 m. There is no evidence of shallow groundwater in the seismic refraction data.
- Noise conditions at site (multi-directional or omni-directional noise sources) appeared sufficient for successful application of passive surface wave techniques.
- ESAC technique used to extract surface wave dispersion data from passive "L" array data. Both the ReMi™ and ESAC techniques used to extract surface wave dispersion data from the linear arrays. The passive "L" shaped array yields the best quality passive surface wave data. Linear array 23958-1 yields better quality passive surface wave dispersion data than array 23958-2, possibly because the latter has more broadside noise from Hwy 138. Neither linear array yields reliable passive surface wave data below about 5 Hz. The linear passive surface wave data reduced using the ReMi™ technique has very large potential error at wavelengths greater than 100 m, due to subjective nature of dispersion curve picking, and was not used for modeling.
- The minimum wavelength surface wave phase velocity data extracted from the 48-channel MASW array was about 15 m. It was difficult extracting surface wave dispersion data at wavelengths below 10 m due to the effects of potential near surface lateral velocity variation and/or nearby subsurface utilities. Data reduction using seismic records from the smaller hammer sources at the south side of the array and a limited offset receiver array (i.e. less active geophones) allowed extraction of surface wave dispersion data to a minimum wavelength of about 1.5 m.
- Surface wave dispersion data from active and passive surface wave data sets are in good agreement over the approximate 11 to 60 m overlapping wavelength range.
- Representative dispersion curves were generated for each surface wave data set using a moving average, polynomial curve fitting routine. These individual representative dispersion curves were combined and a representative dispersion curve generated for the combined data set for data modeling.
- Surface wave depth of investigation is about 80 m based on half of maximum wavelength criteria and assuming that surface wave dispersion data at frequencies as low as 3.5 Hz are valid utilizing 4.5 Hz geophones (low frequency geophone phase response differences will cancel out if noise is omni-directional and/or the phase response differences are random in nature).
- V_{S30} is 423 m/s (NEHRP Site Class C).
- V_{S30} is 443 m/s, if the upper 1 m layer is replaced with the velocity of the underlying layer, to reflect the fact the seismic station is located in a building on engineered fill (NEHRP Site Class C).
- Average S-wave velocity of the upper 75 m (V_{S75}) is 528 m/s.

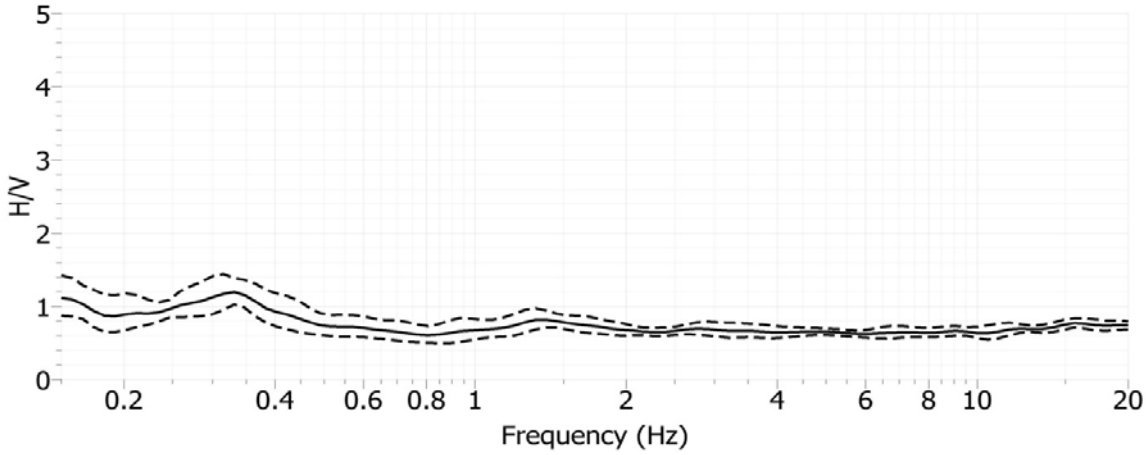

Site CE.23958, H/V Spectral Ratio, Array 23958-1/3, Sensor 453

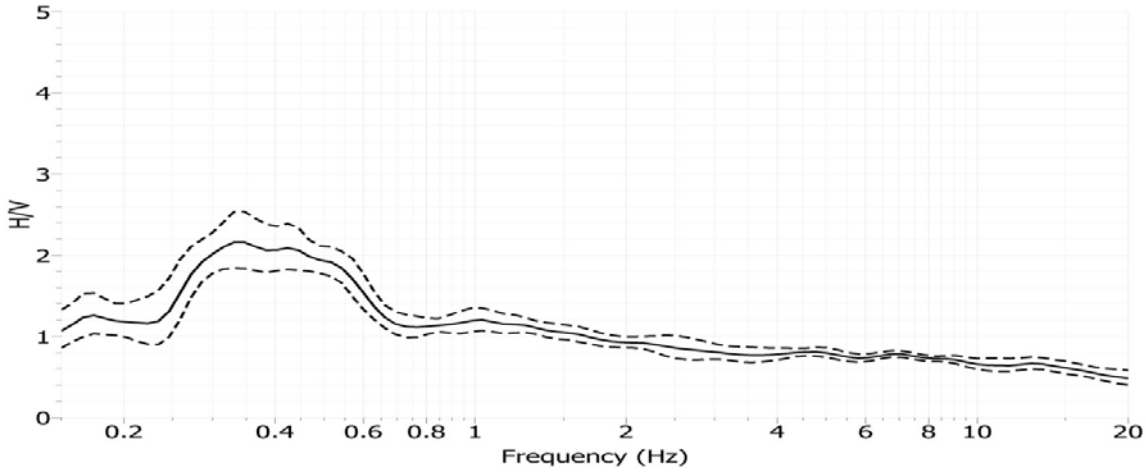

Site CE.23958, H/V Spectral Ratio, Near Seismic Station, Sensor 450

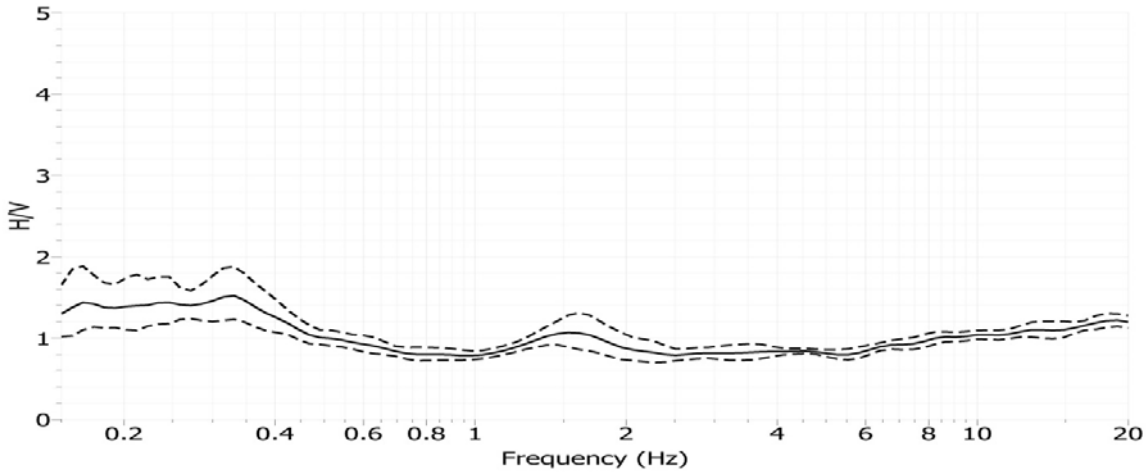

Site CE.23958, H/V Spectral Ratio, Array 23958-1/3, Sensor 507

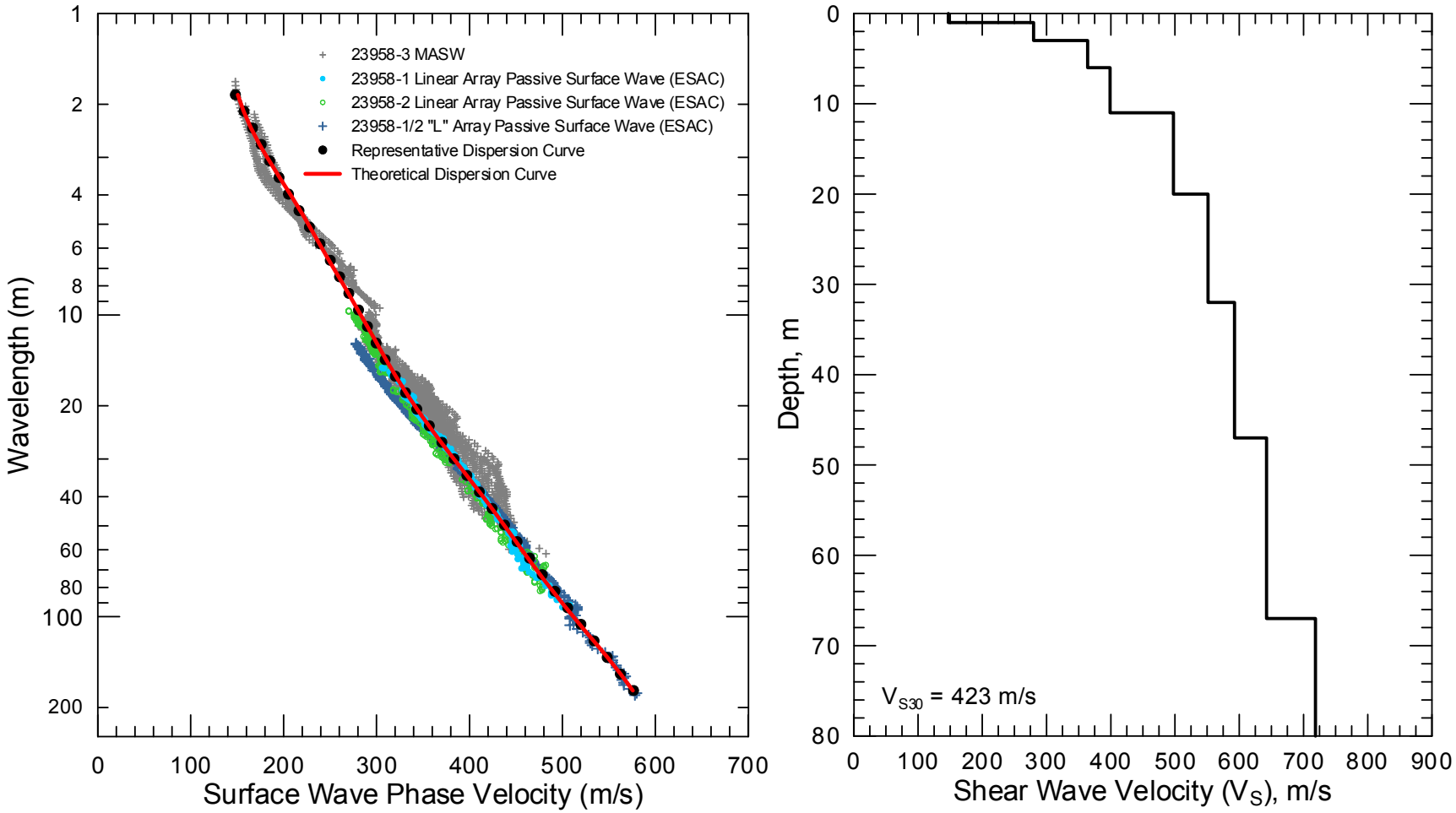

CE.23958 - Field, representative and inverted theoretical surface wave dispersion data (left) and associated V_S model (right)

Site CE.24029

Location: San Gabriel Fire Department Station 52, 115 N. Del Mar Avenue, San Gabriel, California

Latitude: 34.10353 **Longitude:** -118.10011
(Station coordinates modified using published coordinates from http://www.strongmotioncenter.org with further adjustment made by identifying the structure housing the seismic sensor on Google Earth, WGS84 coordinate system.)

V_{S30} (measured): 369 m/s

V_{S30} (adjusted to more accurately reflect seismic station conditions): 377 m/s (upper 0.75 m thick low velocity layer replaced with velocity of underlying layer to better reflect higher velocities expected beneath the fire station.)

NEHRP Site Class: C/D

Geomatrix Code: AQD

Geologic Conditions/Observations: Site located in area mapped as Quaternary (Pleistocene) slightly elevated and locally dissected alluvial gravel and sand.

Site Conditions: Urban site with significant traffic noise from nearby busy roads and railroad. Relatively flat terrain in site vicinity with gradual decrease in surface elevation to south. Seismic station located inside fire station building.

Geophysical Methods Utilized: HVSR, MASW, array microtremor, ReMi™

Geophysical Testing Arrays:

1. Arrays 24029-1 (24 channel linear array utilizing 4.5 Hz vertical geophones spaced 3 m apart for an array length of 69 m) and 24029-2 (24 channel linear array utilizing 4.5 Hz vertical geophones spaced 5 m apart for an array length of 115 m) used to acquire passive surface wave data. Arrays combined to form an "L" shaped array.
2. Array 24029-3 (48 channel MASW array utilizing 4.5 Hz vertical geophones spaced 1 m apart for a length of 47 m, forward and reverse shot locations with multiple source offsets and source types (hammers only) and center shot location).
3. Three HVSR measurement locations; two distributed along arrays 24029-1 and 24029-2 and one near the seismic station.

Legend

- Seismic Station - Approximate Improved Location
- Seismic Station - Approximate Location of Record
- H/V Spectral Ratio Location
- MASW Array
- Passive Array

NOTES:
1. WGS 1984 COORDINATE SYSTEM
2. Image Source: ESRI, i-cubed, USDA FSA, USGS, AEX, GeoEye, Getmapping, Aerogrid, IGP

File Name: CE-24029-I

Date: 2/7/2013

USGS science for a changing world

GEOVision geophysical services

RECOVERY.GOV

SITE MAP
CE•24029

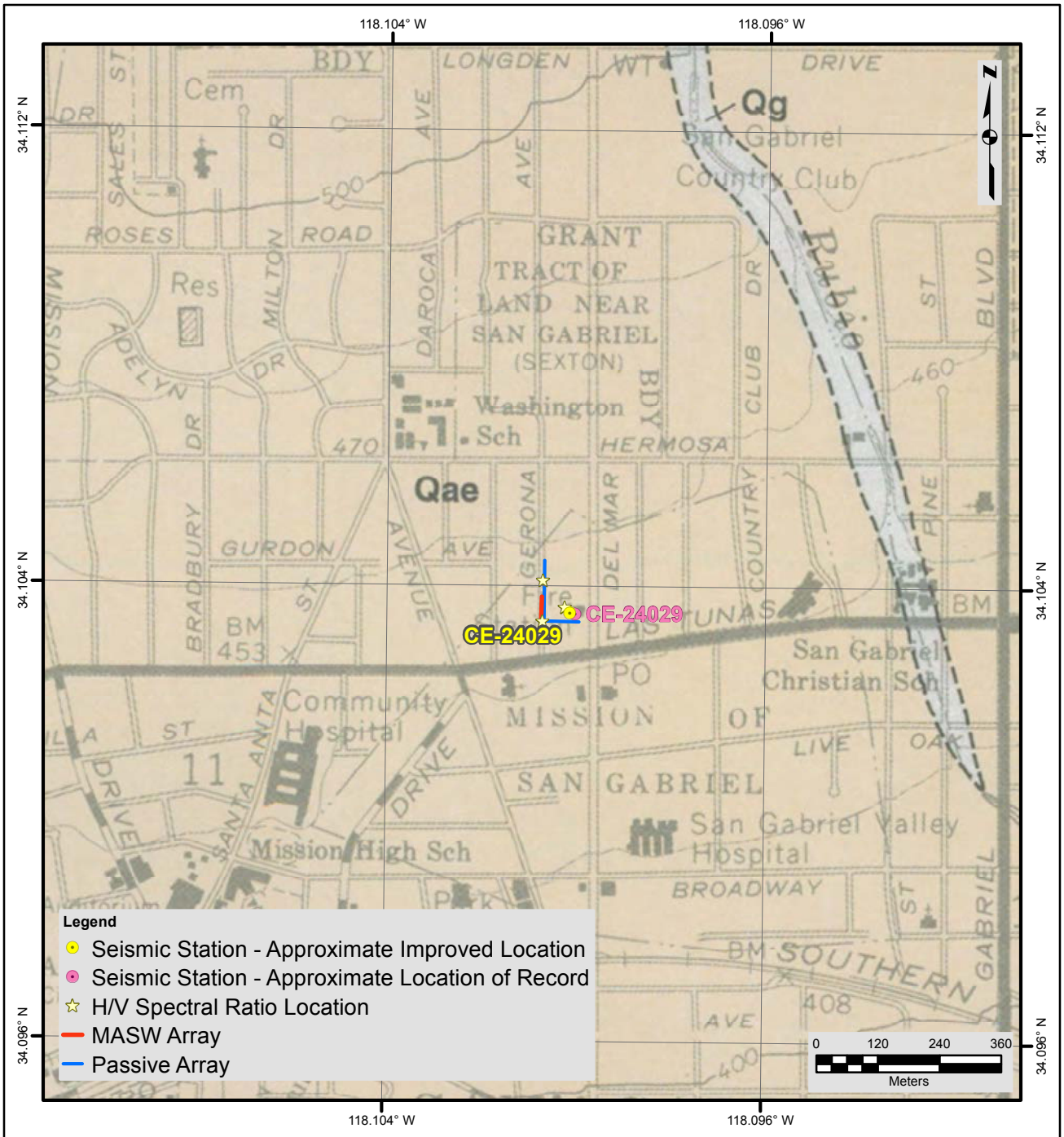

Description of Geologic Map Units

Qg = Quaternary (Holocene) gravel and sand of major streams, and alluvial fan detritus from San Gabriel Mountains
Qae = Quaternary (Pleistocene) alluvial gravel and sand

NOTES:
1. WGS 1984 COORDINATE SYSTEM
2. Geologic Map of the El Monte and Baldwin Park Quadrangles, Los Angeles County, California By Thomas W. Dibblee, Jr., 1999
3. See site map for details of geophysical survey

File Name: CE-24029

Date: 7/15/2011

USGS science for a changing world

GEOVision geophysical services

GEOLOGIC MAP
CE•24029

Looking northeast towards San Gabriel Fire Department Station 52 housing seismic station CE.24029 and passive surface wave array 24029-1

CE.24029 seismic station

Looking north along passive surface wave array 24029-2

HVSR Sensor 507 located in fire station parking lot

Looking north towards MASW array 24029-3

Location of Geophysical Testing Arrays:

Location	Latitude	Longitude
24029-1, East End of Array, Channel 1	34.10337	-118.09992
24029-1 and 24029-2, West and South End of Arrays, respectively, Channel 24	34.10338	-118.10066
24029-2, North End of Array, Channel 48	34.10445	-118.10065
24029-3, South End of Array	34.10340	-118.10071
24029-3, North End of Array	34.10381	-118.10071
HVSR Sensor 507	34.10363	-118.10021
HVSR Sensor 453	34.10338	-118.10069
HVSR Sensor 450	34.10410	-118.10068

Notes: 1) WGS84 Coordinate System (decimal degrees)
2) Survey accuracy is estimated at 2 m.

Results:

V_S Model

Depth to Top of Layer (m)	Layer Thickness (m)	S-Wave Velocity (m/s)	Inferred P-Wave Velocity (m/s)	Inferred Poisson's Ratio	Inferred Density (g/cm^3)
0	0.75	172	321	0.3	1.9
0.75	1.75	289	540	0.3	1.9
2.5	3.5	296	553	0.3	1.9
6	6	359	672	0.3	1.9
12	10	403	753	0.3	1.9
22	15	457	854	0.3	1.9
37	20	530	991	0.3	2.0
57	>13	615	1151	0.3	2.0

Observations/Discussion:

- The HVSR curves are almost identical at frequencies below 4 Hz, validating the 1-D velocity structure assumption. There are, however, no significant high frequency HVSR peaks to characterize variability of shallow velocity structure.
- HVSR sensor 507, located on asphalt in the fire station parking lot, yielded the best quality data at the site. HVSR sensors 450 and 453 were located on concrete sidewalks near busy roads. Although setting the HVSR sensors on soil is preferred, permission was not obtained to dig shallow holes in the grass on nearby private residences. Better quality

data may be obtained if the measurements were made at night, when vehicle traffic is at a minimum.

- There is no distinct high amplitude HVSR peak at the site. The maximum HVSR response is at about 0.24 Hz, which could be indicative of very deep bedrock.
- Noise conditions at site (multi-directional or omni-directional noise sources) appeared sufficient for successful application of passive surface wave techniques.
- ESAC technique used to extract surface wave dispersion data from passive "L" array data. Both the ReMi™ and ESAC techniques used to extract surface wave dispersion data from the linear arrays. Only the higher quality passive surface wave data from the "L" array (24029-1/2) were used for analysis. Linear passive surface wave array 24029-1 did not yield useful data, as expected because the array was parallel to a busy street. Passive surface wave array 24029-2 yielded similar phase velocities to the "L" array, but data quality were not as good.
- It was very difficult to obtain surface wave dispersion data at wavelengths less than 4 m from the MASW array due to probable near-surface lateral velocity variation, subsurface utilities, etc. Therefore, an attempt was made to extract SASW dispersion data from selected receiver pairs on the MASW seismic records to supplement the MASW dispersion data at small wavelengths/high frequencies.
- Surface wave dispersion data from the active and passive surface wave data sets are in good agreement at this site.
- Representative dispersion curves were generated for each surface wave data set using a moving average, polynomial curve fitting routine. These individual representative dispersion curves were combined and a representative dispersion curve generated for the combined data set for data modeling.
- Based on interactive layer-based analysis of seismic refraction first arrival data, P-wave velocity in the upper 15 m ranges from about 350 to 450 m/s near the surface to about 700 m/s at a depth on the order of 4 m and 850 m/s at a depth of about 8 to 9 m. There is no evidence of a shallow saturated zone at the site.
- Surface wave model is relatively consistent with simplified P-wave refraction model considering uncertainty in Poisson's ratio. The inferred P-wave velocities in the surface wave model would better fit the refraction data if Poisson's ratio was slightly higher than the assumed 0.3.
- Surface wave depth of investigation is about 70 m based on half of maximum wavelength criteria and assuming that surface wave dispersion data at frequencies as low as 3.2 Hz are valid utilizing 4.5 Hz geophones (low frequency geophone phase response differences will cancel out if noise is omni-directional and/or the phase response differences are random in nature).
- V_{S30} is 369 m/s (Site Class C/D).
- V_{S30} would be 377 m/s (Site Class C/D) if the 0.75 m thick low velocity layer at the surface were replaced with the velocity of the underlying layer to more accurately reflect probable velocity structure beneath the fire station.
- Average S-wave velocity of the upper 70 m (V_{S70}) is 450 m/s.

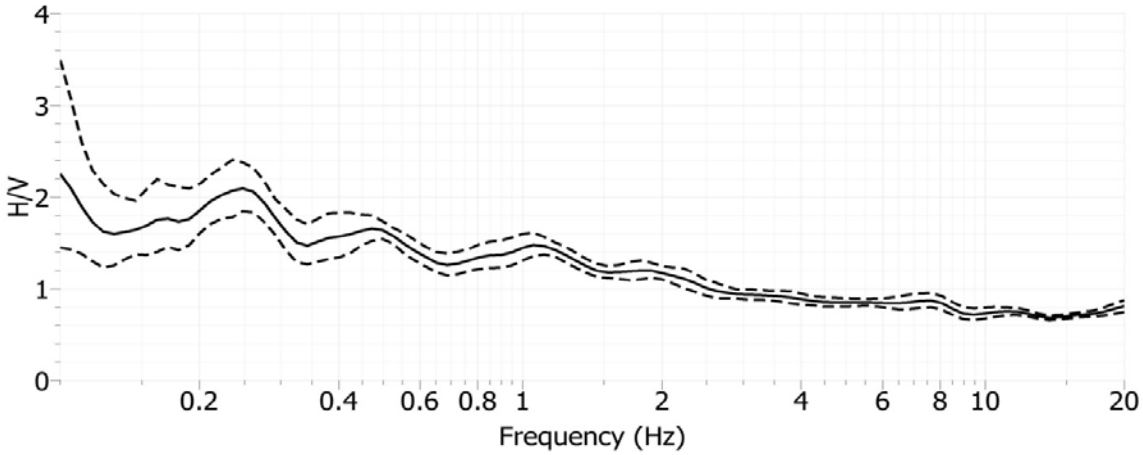

Site CE.24029, H/V Spectral Ratio, Array 24029-2, Sensor 450

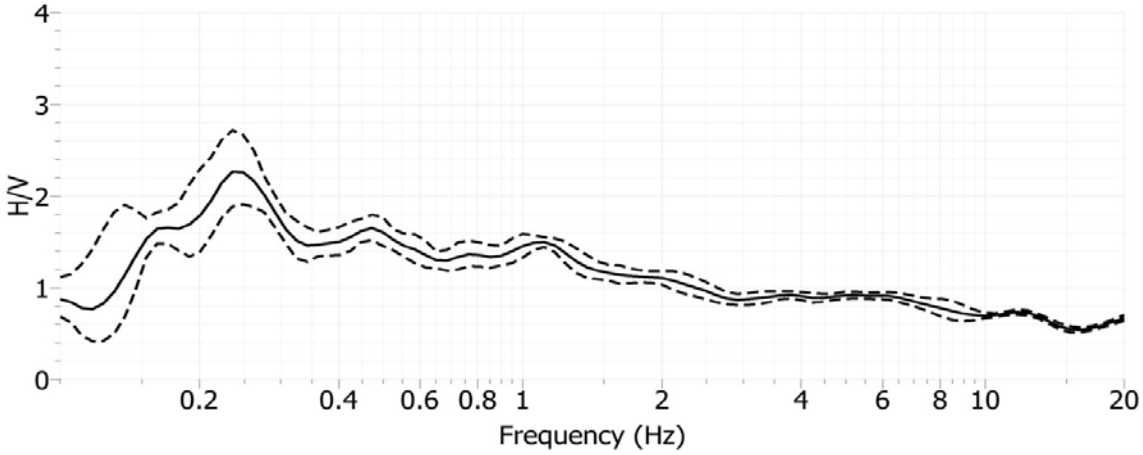

Site CE. 24029, H/V Spectral Ratio, Near Seismic Station, Sensor 507

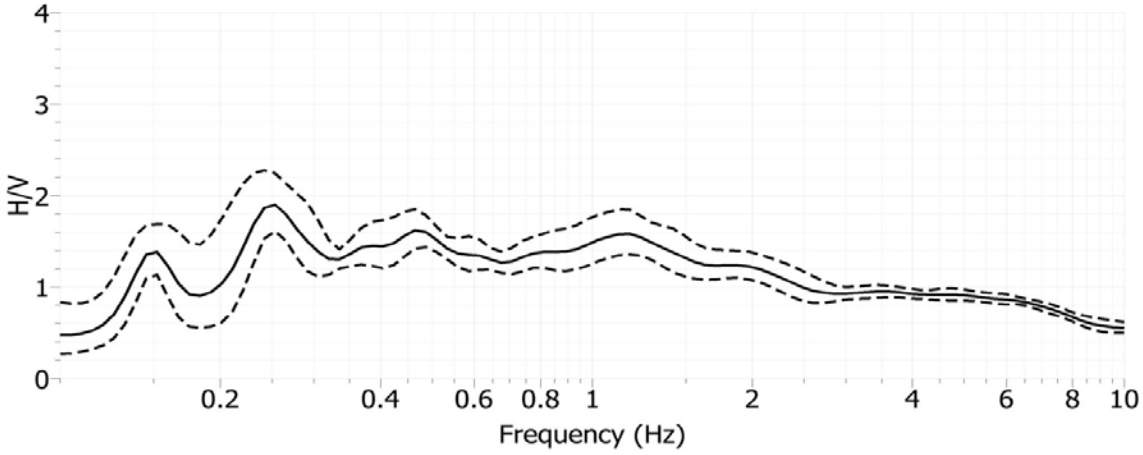

Site CE. 24029, H/V Spectral Ratio, Array 24029-1/2, Sensor 453

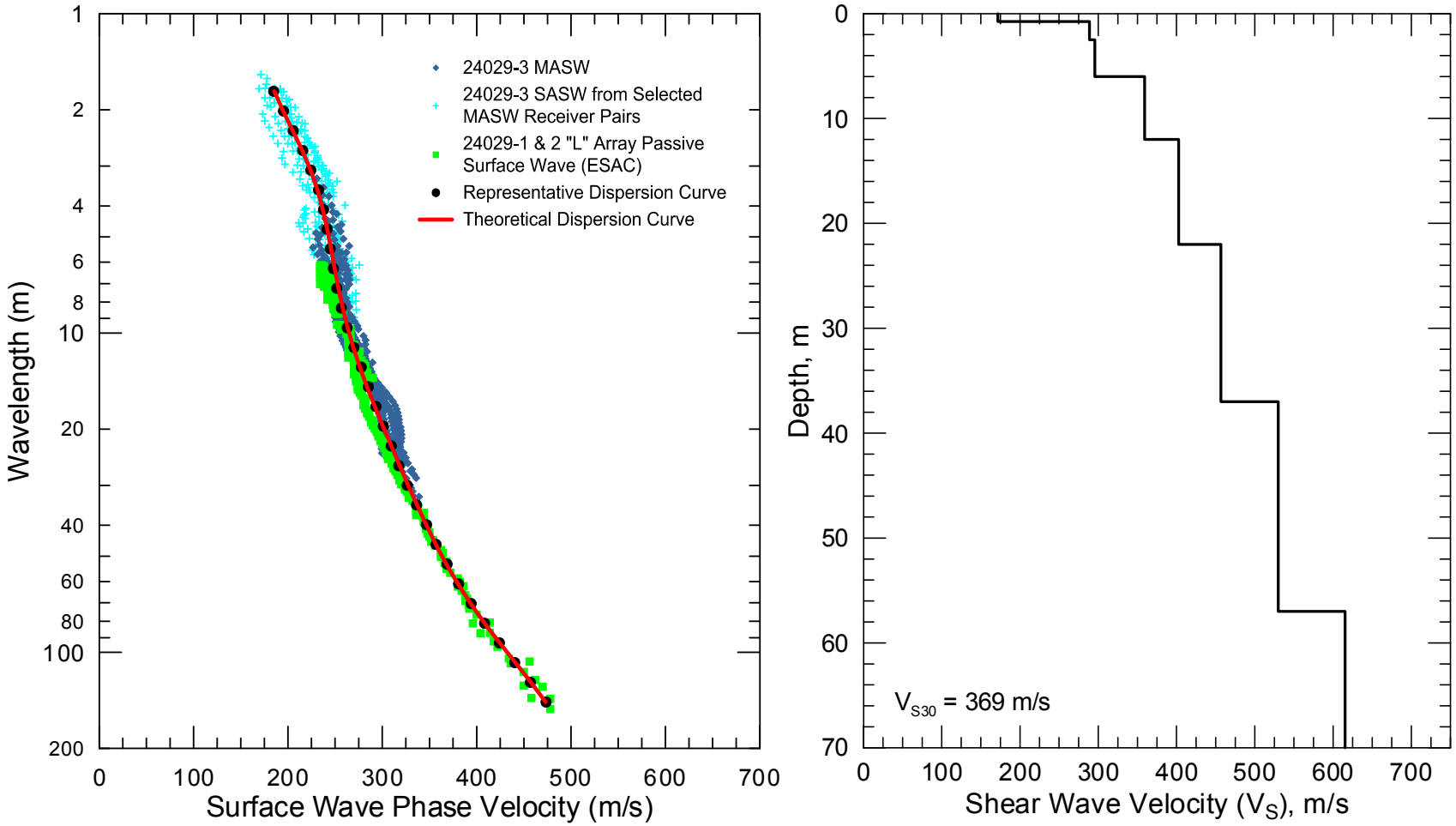

CE.24029 - Field, representative and inverted theoretical surface wave dispersion data (left) and associated V_S model (right)

Site CE.24644

Location: Sandberg – Bald Mountain, Los Angeles County, California

Latitude: 34.74335 **Longitude:** -118.72493
(Station coordinates modified based on site GPS survey and are in WGS84 coordinate system).

V_{S30} (measured): 421 m/s

V_{S30} (adjusted to more accurately reflect seismic station conditions): 421 m/s (no adjustment necessary)

NEHRP Site Class: C

Geomatrix Code: IGB

Geologic Conditions/Observations: Seismic station located on Mesozoic granitic rocks mapped as granodiorite, quartz monzonite and quartz diorite. The Liebre Fault Zone is located about 1.5 km to the south. Mesozoic granitic rocks have been thrust over Tertiary sedimentary rock along this fault zone. Field observations indicate that there is a thin layer of residual soil overlying weathered rock.

Site Conditions: Rural site. Seismic station and test area located on top of Bald Mountain. Relatively flat to rolling terrain in immediate site vicinity, but steep mountainous terrain nearby site.

Geophysical Methods Utilized: HVSR, Seismic Refraction, MASW

Geophysical Testing Arrays:

1. Array 24644-1 (48 channel MASW and P-wave seismic refraction array utilizing 4.5 Hz vertical geophones spaced 1.5 m apart for a length of 70.5 m, forward and reverse shot locations with multiple source offsets and source types and multiple interior shot locations).
2. Five HVSR measurement locations distributed along array 24644-1.

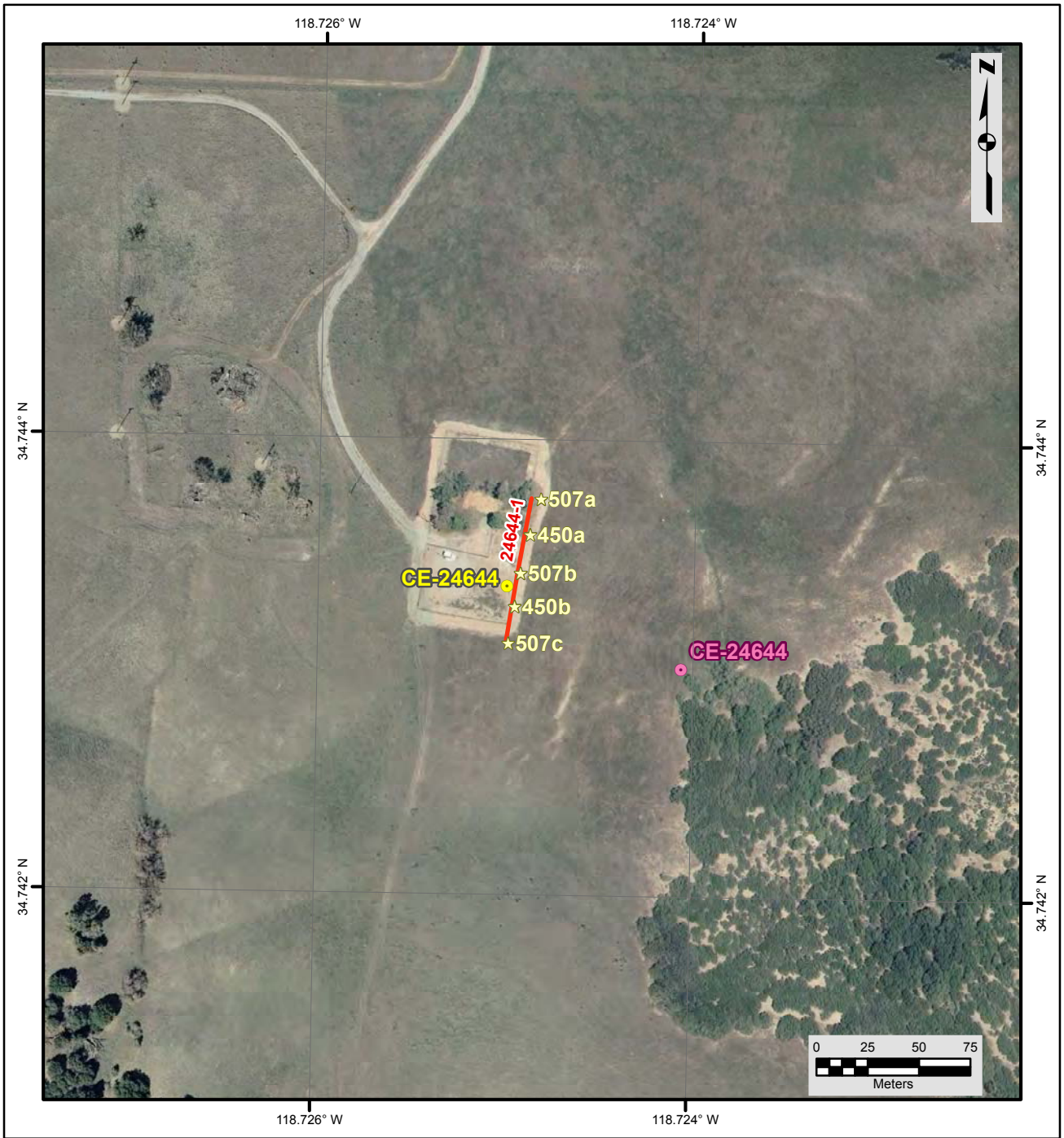

Legend

- Seismic Station - Approximate Surveyed Location
- Seismic Station - Approximate Location of Record
- H/V Spectral Ratio Location
- MASW and Seismic Refraction Array

NOTES:
1. WGS 1984 COORDINATE SYSTEM
2. Image Source: ESRI, i-cubed, USDA FSA, USGS, AEX, GeoEye, Getmapping, Aerogrid, IGP

File Name: CE-24644-I

Date: 2/7/2013

USGS science for a changing world

GEOVision geophysical services

RECOVERY.GOV

SITE MAP
CE•24644

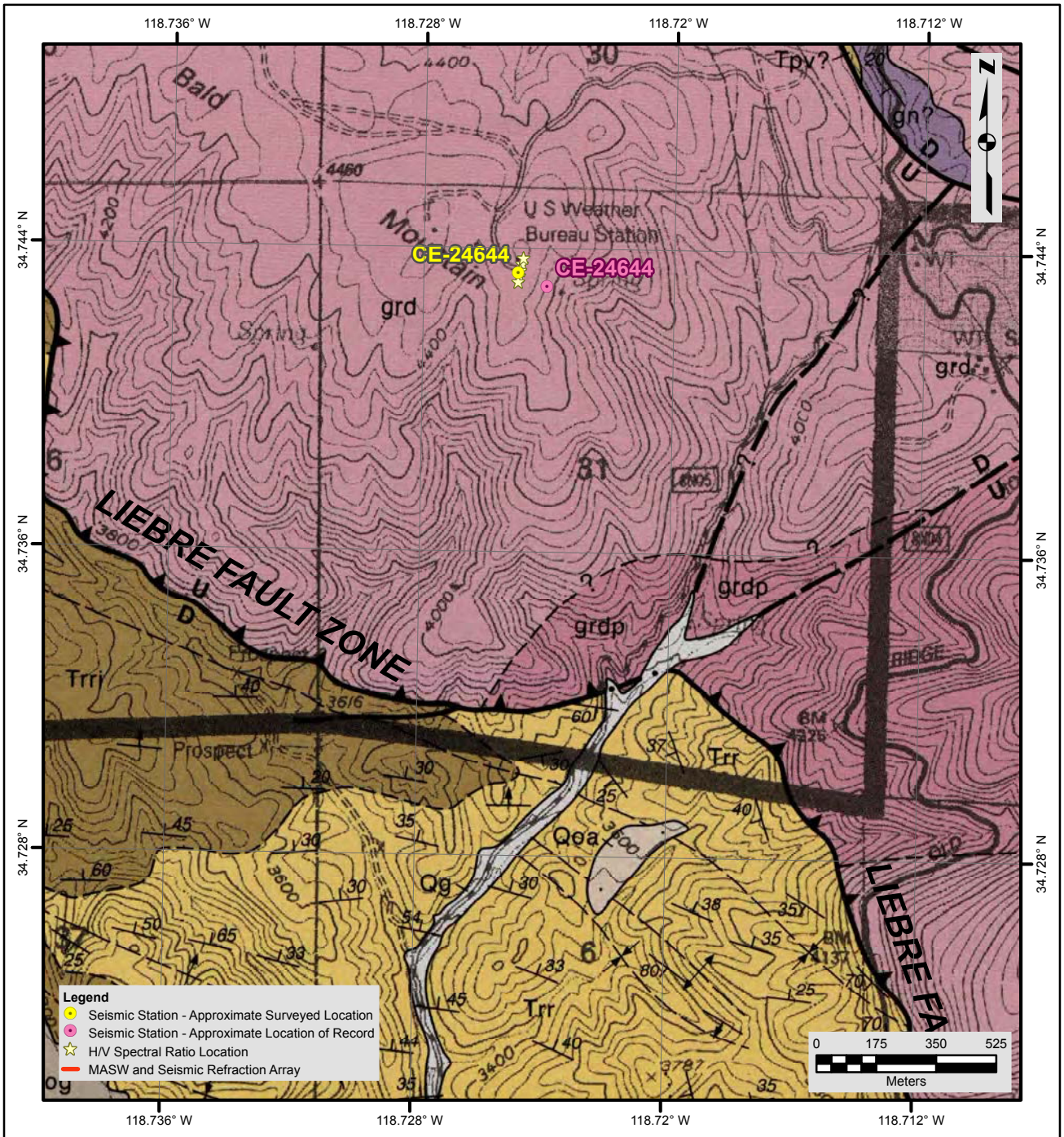

Description of Geologic Map Units

Qg = Quaternary (Holocene) alluvial gravel and sand of stream channels
Qoa = Quaternary (Pleistocene) remnants of alluvial gravel and sand
Trr = Tertiary (Miocene) Ridge Basin Group; sandstone facies, bedded, arkosic, minor pebbly sandstone, minor thin clayshale layers
Trri = Tertiary (Miocene) Ridge Basin Group; interbedded facies, shale and sandstone
grd = Mesozoic (Cretaceous) granodiorite, quartz monzonite and quartz diorite; sodic plagioclase feldspar
grdp = Mesozoic (Triassic) megaporphyritic monzogranite-quartz monzonite, massive

NOTES:
1. WGS 1984 COORDINATE SYSTEM
2. Geologic Map of the Liebre Mountain Quadrangle, Los Angeles County, California by Thomas W. Dibblee, Jr., 2002
3. See site map for details of geophysical survey

File Name: CE-24644

Date: 2/7/2013

USGS science for a changing world

GEOVision geophysical services

RECOVERY.GOV

GEOLOGIC MAP
CE•24644

Seismic station CE.24644

Looking north along array 24644-1 and at an HVSR measurement location and the seismic station

P-wave seismic refraction data acquisition

HVSR sensors placed in shallow holes

MASW and seismic refraction data acquisition using accelerated weight drop energy source

Location of Geophysical Testing Arrays:

Location	Latitude	Longitude
24644-1, South End of MASW Array	34.74311	-118.72493
24644-1, Center of MASW Array	34.74342	-118.72488
24644-1, North End of MASW Array	34.74374	-118.72481
HVSR Sensor 507a	34.74374	-118.72476
HVSR Sensor 450a	34.74358	-118.72481
HVSR Sensor 507b	34.74341	-118.72486
HVSR Sensor 450b	34.74327	-118.72489
HVSR Sensor 507c	34.74310	-118.72492
CE.24644 Seismic Station	34.74335	-118.72493

Notes: 1) WGS84 Coordinate System (decimal degrees).
2) Survey accuracy is estimated at 1 to 2 m.

Results:

V_S Model 1

Depth to Top of Layer (m)	Layer Thickness (m)	S-Wave Velocity (m/s)	Inferred P-Wave Velocity (m/s)	Assumed Poisson's Ratio	Assumed Density (g/cm^3)
0	1.5	194	364	0.3	1.8
1.5	2.5	244	456	0.3	1.8
4	3	312	584	0.3	1.9
7	4	338	632	0.3	1.9
11	6	354	663	0.3	1.9
17	>18	953	1782	0.3	2.1

Notes: 1) Depth of investigation is about 35 m.
2) Bottom layer is a half space.

V_S Model 2

Depth to Top of Layer (m)	Layer Thickness (m)	S-Wave Velocity (m/s)	Inferred P-Wave Velocity (m/s)	Assumed Poisson's Ratio	Assumed Density (g/cm^3)
0	1.5	196	366	0.3	1.8
1.5	2.5	241	452	0.3	1.8
4	9	321	600	0.3	1.9
13	5	464	867	0.3	2
18	7	700	1310	0.3	2.1
25	8	876	1639	0.3	2.1
33	>2	1109	2074	0.3	2.2

Notes: 1) Depth of investigation is about 35 m.
2) Bottom layer is a half space.

Observations/Discussion:

- HVSR plots are not similar at this site. The source of microtremor energy at this rural mountain top site is unclear. Measurements were made in heavy winds with the sensors covered. Generally, the HVSR response is elevated over the 1.5 to 8 Hz range at all sensor locations, although the frequency and amplitude of the maximum response varies along the line. It would be interesting to repeat the HVSR measurements at another time in the absence of heavy wind. The HVSR data may indicate that the 1-D velocity structure assumption is not met at this site.
- Two models were generated for the seismic refraction data using tomographic inversion; one using a layer based starting model and the other using a smooth velocity gradient starting model. The seismic refraction models were extended to far offset shot locations. Extending the model to far offset shot locations allowed depth of investigation to be increased to validate the surface wave model at depth. Both seismic refraction models have similar RMS errors. A longer receiver array is preferred for extending depth of investigation, but at the expense of the efficiency in combining seismic refraction and MASW data acquisition along the shorter array.
- Both seismic refraction models show similar P-wave velocity structure in the upper 9 m. P-wave velocity is about 400 to 500 m/s at the surface and increases to 600 m/s at a nominal depth of 6 to 9 m. Below a depth of 9 m the models are significantly different. The velocity model that used a layer based starting model, has a thick zone with P-wave velocity between 700 and 800 m/s to a depth of about 19 to 21 m, below which velocity abruptly increases to over 2,000 m/s. The velocity model that used a smooth velocity gradient starting model shows a gradual increase in velocity with depth below 9 m with P-wave velocity reaching 800 m/s at 10 to 14 m depth, 1,250 m/s at 17 to 22 m depth, 1,600 m/s at 22 to 27 m depth. In this model P-wave velocity exceeds 2,000 m/s at depths greater than about 30 m. The high P-wave velocities at depth in the seismic refraction models are required to fit the travel time data from far offset shot locations, but would have been much better constrained with a longer refraction profile.

- Noise conditions at the site were not sufficient for application of passive surface wave techniques.
- The minimum wavelength surface wave phase velocity data extracted from the 48-channel MASW array was about 10 m. Reducing data from smaller hammer sources using a limited offset receiver array (i.e. less active geophones) allowed extraction of surface wave dispersion data to a minimum wavelength of about 3 m.
- There is some scatter in the MASW dispersion data, particularly at wavelengths below 35 m, which is in part due to lateral velocity variation caused by differential weathering of near surface rock and possible variable thickness of the residual soil layer.
- A representative dispersion curve was generated for the MASW data set using a moving average, polynomial curve fitting routine and used for modeling.
- Two V_S models were generated for the surface wave dispersion data: a model with a minimal number of layers resulting in a large impedance contrast at 17 m depth (Model 1) and a model with gradual increase in velocity with depth after a large velocity increase at 13 m (Model 2). It should be noted that there is significant non-uniqueness in the velocity structure of the more competent bedrock.
- Surface wave depth of investigation is about 35 m based on half of maximum wavelength criteria.
- The inferred P-wave velocities in surface wave model 1, based on an assumed Poisson's ratio of 0.3 and modeled S-wave velocity, appear to underestimate the depth to the large impedance contrast in the seismic refraction model that utilized a layer based starting model. The abrupt increase in velocity in the surface wave model occurs at a depth of about 17 m, whereas the abrupt velocity increase in the seismic refraction model occurs at a depth several meters deeper that the 900 m/s velocity contour at 19 to 21 m depth.
- The inferred P-wave velocities in surface wave model 2, based on an assumed Poisson's ratio of 0.3 and modeled S-wave velocity, are relatively consistent with the P-wave refraction models that utilized a smooth velocity gradient starting model. Therefore, surface wave model 2, or a similar model that shows increase in bedrock velocity with depth, is expected to be more representative of subsurface V_S structure at the site.
- Both V_S models generate a synthetic HVSR peak at a frequency in the 6 to 7 Hz range. There is no clear HVSR peak at 6 to 7 Hz in the field measurements, although there may not be a local noise source generating high frequency energy. Additionally, there is significant topographic variation in the site vicinity and the weathering profile in the crystalline bedrock may be quite complex. There is, however, slightly elevated HVSR response in the 6 to 7 Hz frequency range in the field measurements, but the elevated HVSR response extends to frequencies lower than 2 Hz, which may indicate that velocity increases with depth.
- V_{S30} is 429 m/s for Model 1 and 413 m/s for Model 2, averaging 421 m/s (Site Class C).
- The seismic refraction data indicates that Model 2, or at least a similar model that shows a smooth transition to competent bedrock (i.e. decrease in weathering with depth) rather than an abrupt transition to more competent rock, may be most representative of site conditions. The absence of a sharp HVSR peak may also indicate that velocity of the bedrock increases smoothly with depth, although site conditions (mountain top, absence of local noise sources, possible complex bedrock velocity structure) are not conducive to effective use of the HVSR technique.

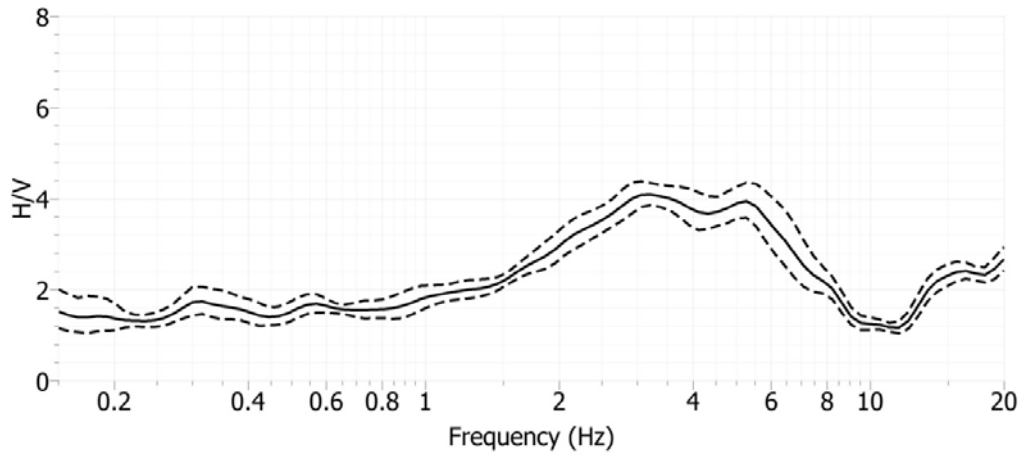

Site CE.24644, H/V Spectral Ratio, Array 24644-1, Sensor 507a

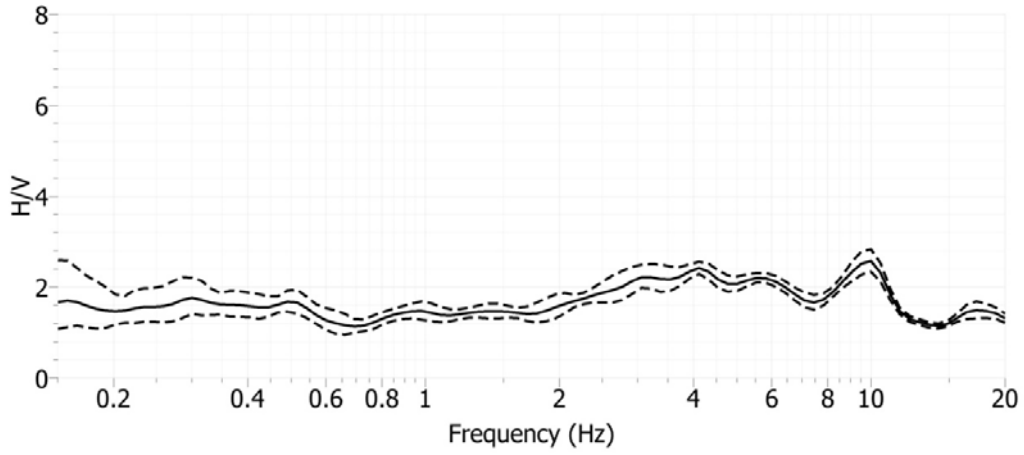

Site CE.24644, H/V Spectral Ratio, Array 24644-1, Sensor 450a

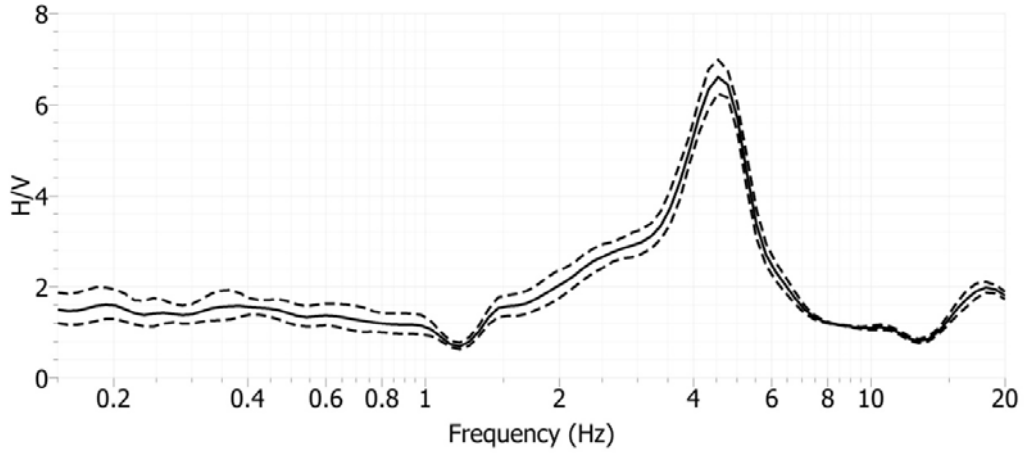

Site CE.24644, H/V Spectral Ratio, Array 24644-1, Sensor 507b

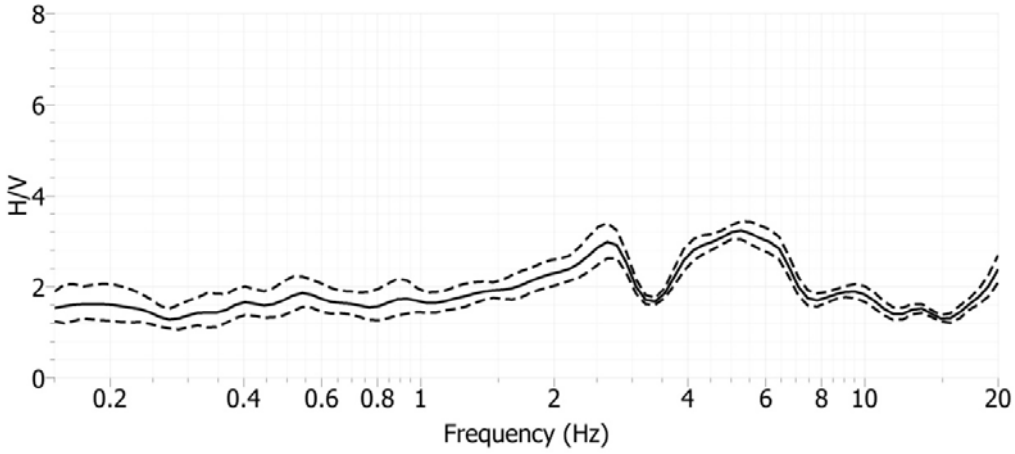

Site CE.24644, H/V Spectral Ratio, Array 24644-1, Sensor 450b

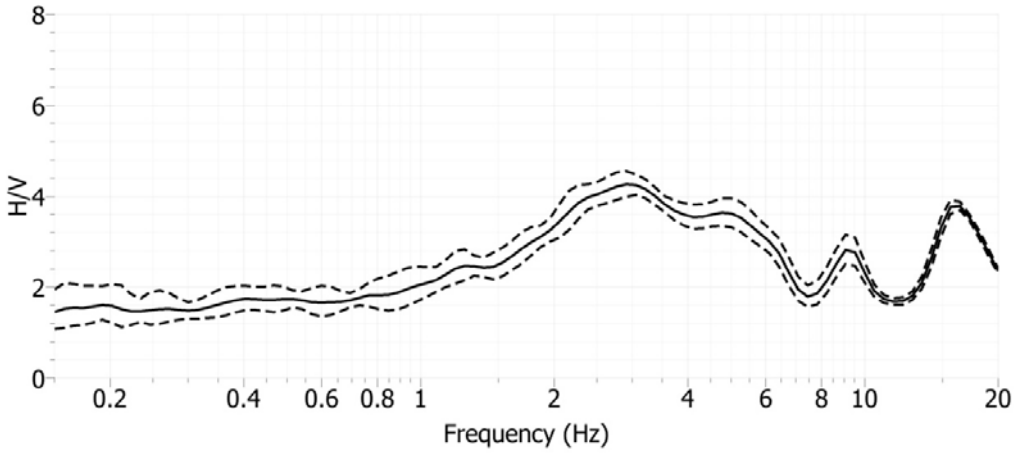

Site CE.24644, H/V Spectral Ratio, Array 24644-1, Sensor 507c

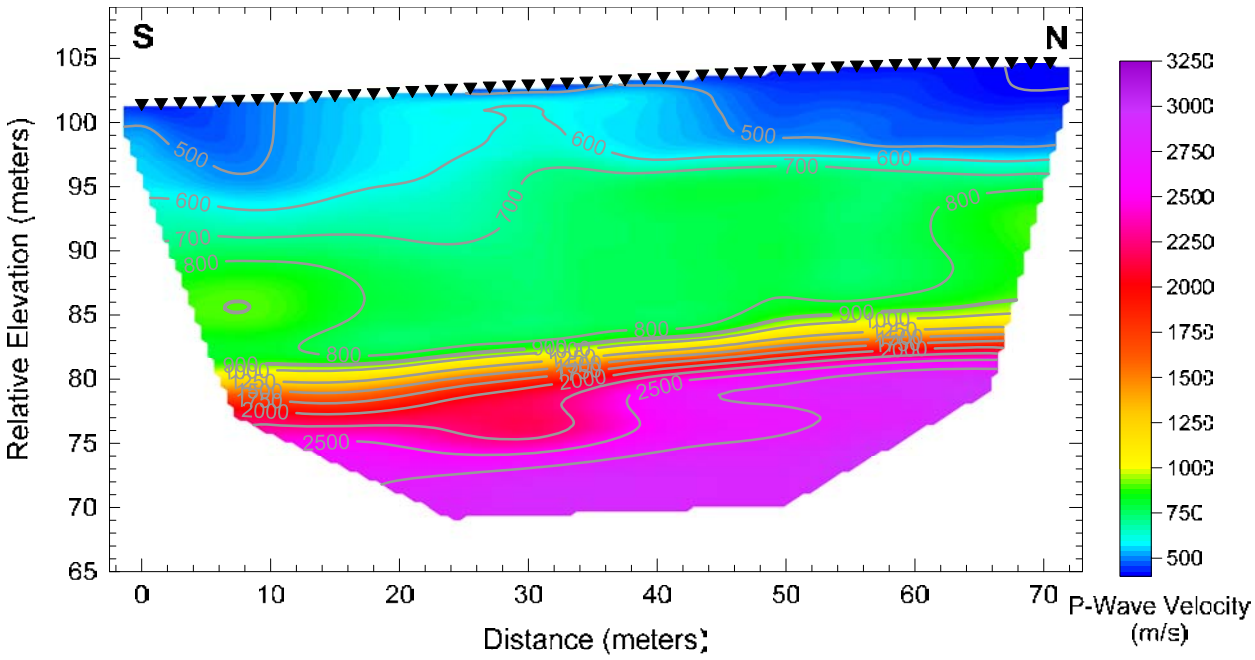

Array 24644-1 – Tomographic Seismic Refraction Model utilizing Layer Based Starting Model

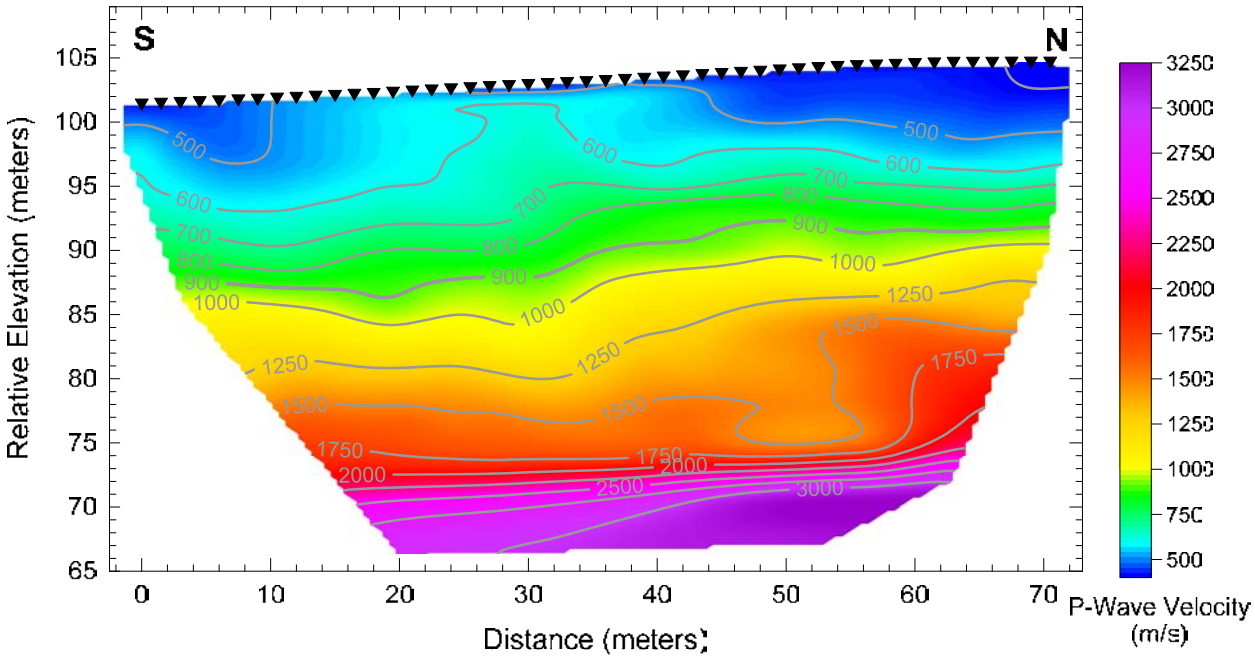

Array 24644-1 – Tomographic Seismic Refraction Model utilizing Smooth Velocity Gradient Starting Model

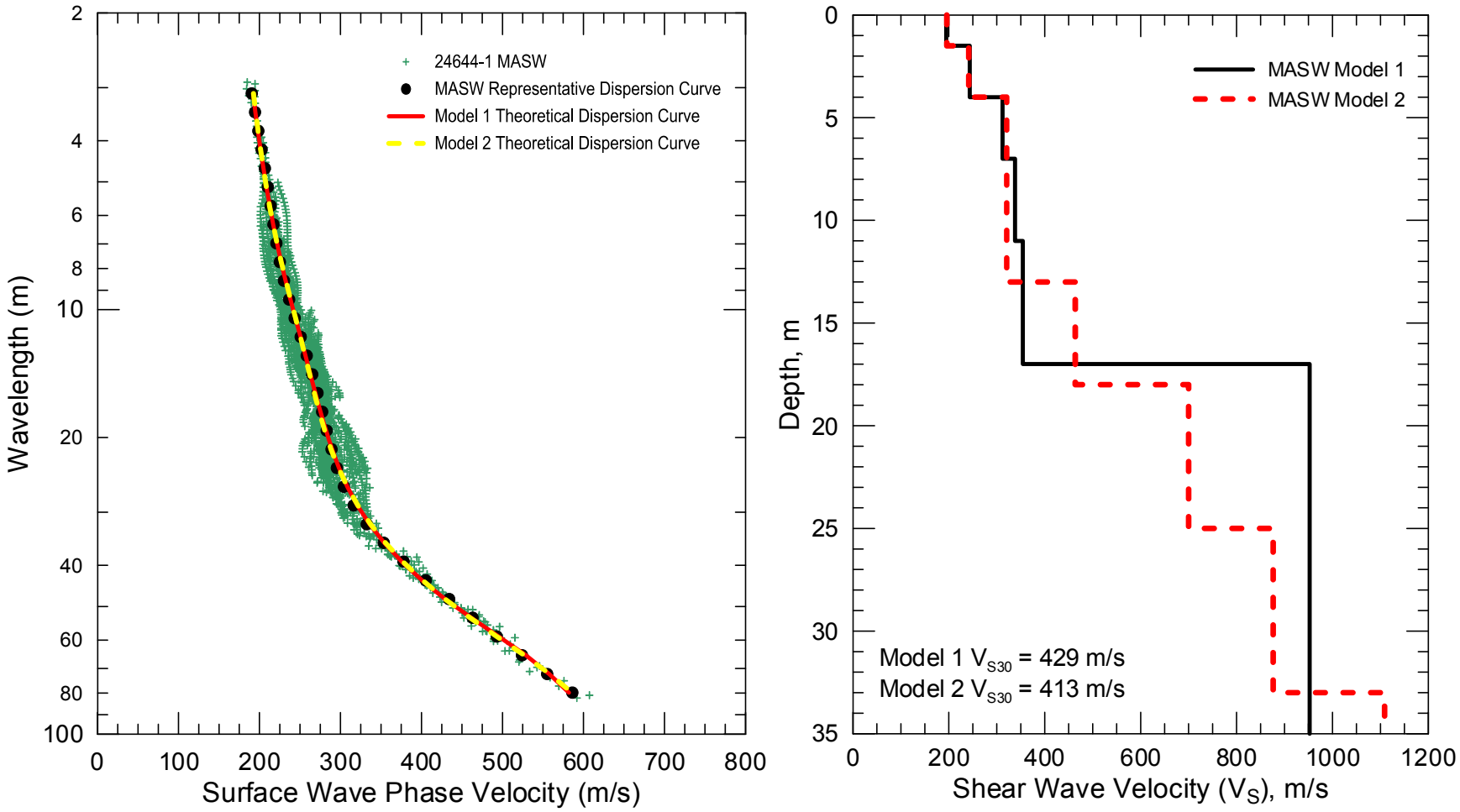

CE.24644 - Field, representative and inverted theoretical surface wave dispersion data (left) and associated V_S model (right)

Site CE.24706

Location: Barrel Springs Bridge and Highway 14, Palmdale, California

Instrumented Bridge

Latitude: 34.546507 **Longitude:** -118.129614
(Station coordinates estimated from Google Earth or ESRI Imagery and are in WGS84 coordinate system)

Free Field Seismic Station

Latitude: 34.54726 **Longitude:** -118.12992
(Station coordinates modified based on site GPS survey and are in WGS84 coordinate system)

V_{S30} (measured): 468 m/s

V_{S30} (adjusted to more accurately reflect seismic station conditions): 501 m/s (bedrock depth decreased by 3 m to approximately account for higher frequency HVSR peak near the seismic station).

NEHRP Site Class: C

Geomatrix Code: GHB (CE.24706 – Instrumented Bridge), IHB (CE.24706 – Free Field)

Geologic Conditions/Observations: Site located in area mapped as Quaternary (Holocene) alluvial gravel, sand and silt. The mapped inferred location of the Nadeau Fault is located about 150 m northeast of the site and the San Andreas Fault is located about 1 km northeast of the site. Lake Palmdale sits between the Nadeau and San Andreas Faults. Quartz monzonite units outcrop about 350 m southwest of test area.

Site Conditions: Rural site with significant traffic noise from adjacent highway and nearby roads. Windy conditions during testing. Relatively flat terrain in site vicinity with ground surface elevation gently decreasing to the northeast.

Geophysical Methods Utilized: HVSR, MASW, Seismic Refraction, Array Microtremor, ReMi™

Geophysical Testing Arrays:

1. Arrays 24706-1 (24 channel linear array utilizing 4.5 Hz vertical geophones spaced 5 m apart for an array length of 115 m) and 24706-2 (24 channel linear array utilizing 4.5 Hz vertical geophones spaced 4.5 m apart for an array length of 103.5 m) used to acquire passive surface wave data. Arrays combined to form an "L" shaped array.
2. Array 24706-3 (48 channel MASW array utilizing 4.5 Hz vertical geophones spaced 1 m apart for a length of 47 m, forward and reverse shot locations with multiple source offsets and source types and center shot location).
3. Three HVSR measurement locations; one at the corner of arrays 24706-1 and 2, one in the center of array 24706-3 and one near the free field seismic station CE.24706.

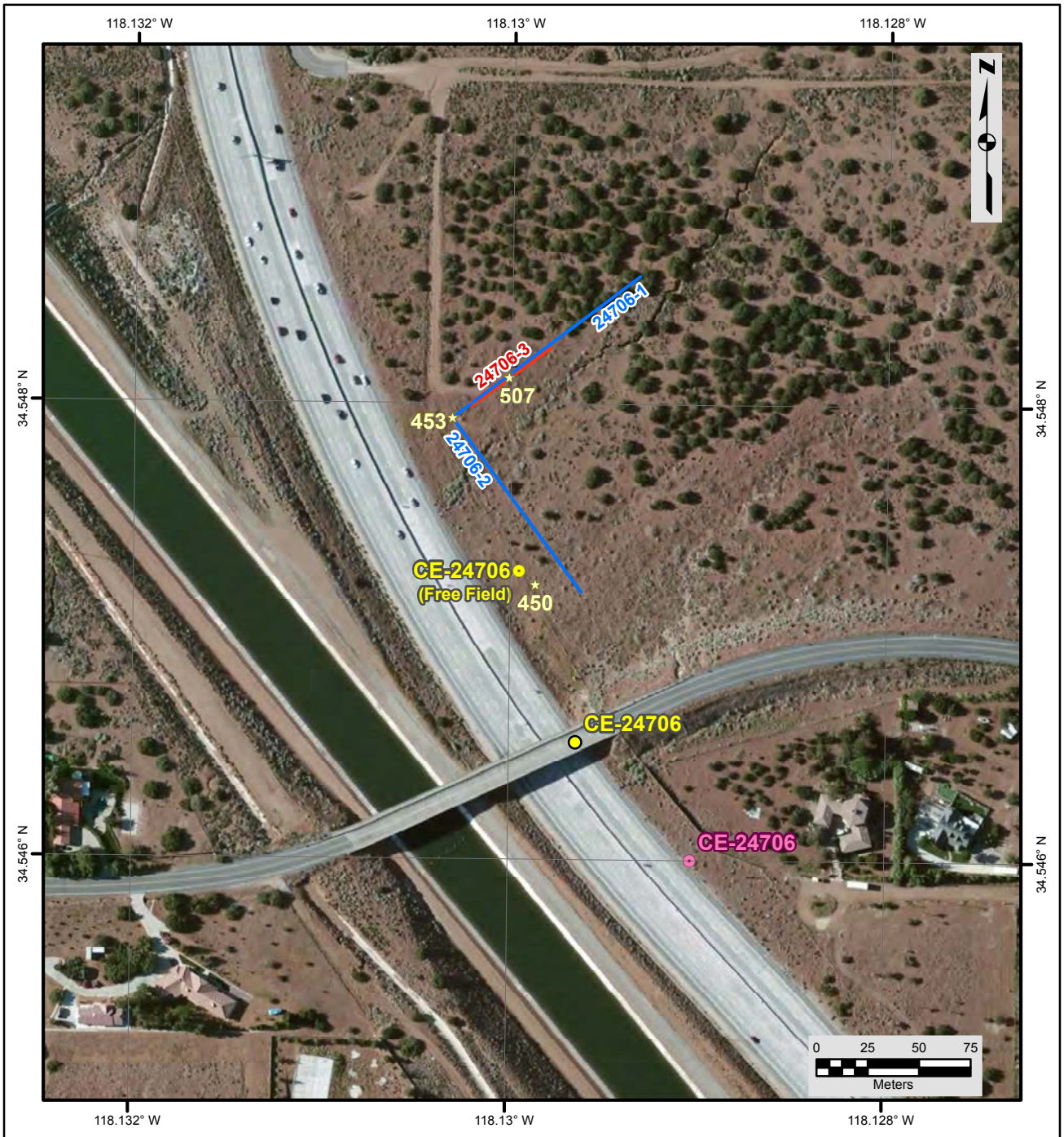

Legend

- Seismic Station - Approximate Surveyed Location
- Seismic Station - Approximate Improved Location
- Seismic Station - Approximate Location of Record
- H/V Spectral Ratio Location
- Passive Surface Wave Array
- MASW and Seismic Refraction Array

NOTES:
1. WGS 1984 COORDINATE SYSTEM
2. Image Source: ESRI, i-cubed, USDA FSA, USGS, AEX, GeoEye, Getmapping, Aerogrid, IGP

File Name: CE-24706-I

Date: 2/7/2013

USGS science for a changing world

GEOVision geophysical services

RECOVERY.GOV

SITE MAP
CE•24706

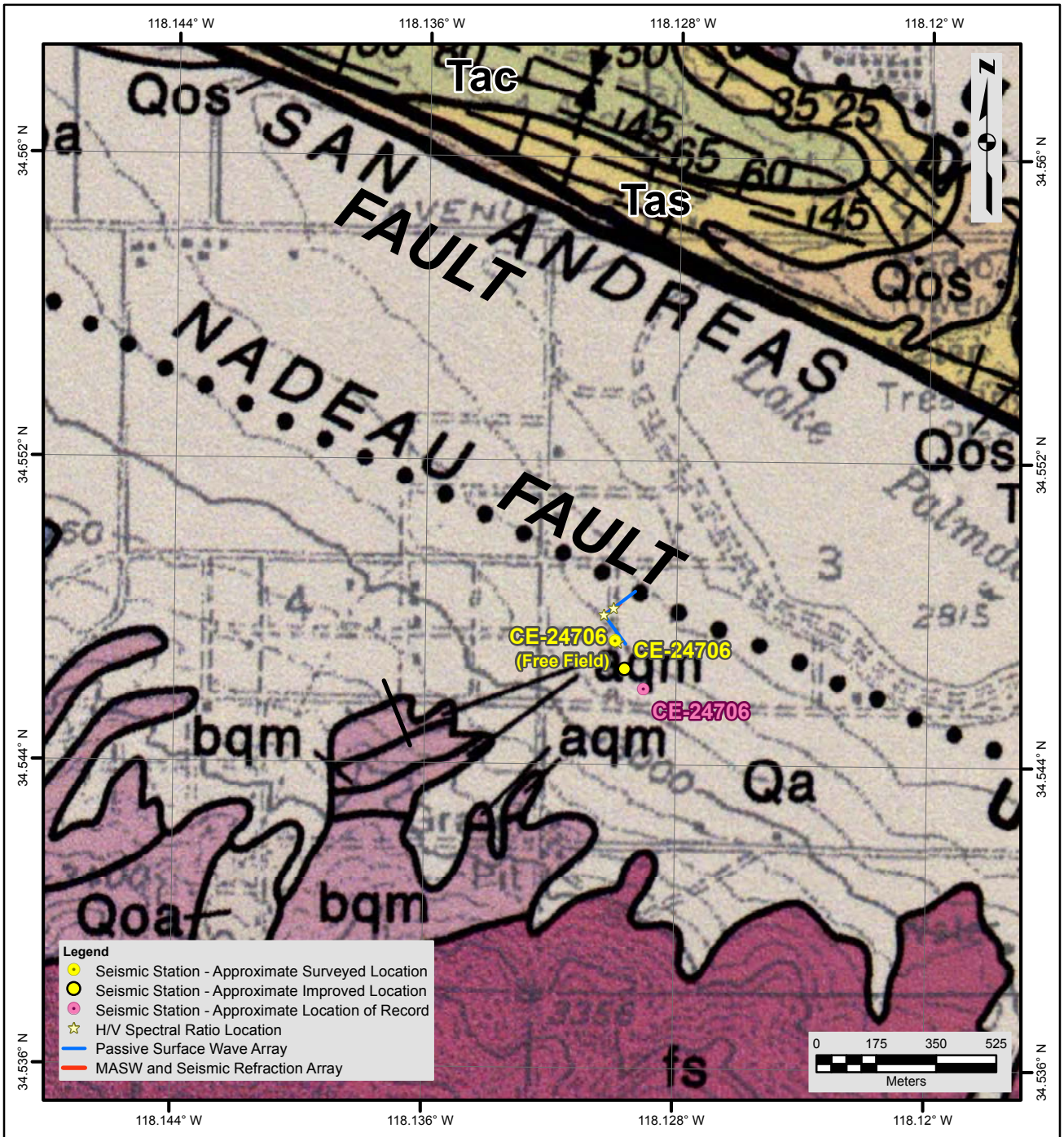

Description of Geologic Map Units

Qa = Quaternary (Holocene) alluvial gravel, sand and silt
Qoa = Quaternary (Pleistocene) weakly consolidated alluvial sediments
fanglomerate of boulders, cobble-pebble gravel, and sand, poorly bedded
Qos = Quaternary (Pleistocene) weakly consolidated alluvial sediments,
schist-cobble gravel, poorly bedded
aqm = Mesozoic aplitic quartz monzonite, massive to gneissoid, fine-grained
bqm = Mesozoic biotite quartz monzonite, indistinctly gneissoid, fine- to medium grained
fs = Mesozoic ferruginous syenite, massive, medium-grained

NOTES:
1. WGS 1984 COORDINATE SYSTEM
2. Geologic Map of the Lancaster & Alpine Butte 15 Minute Quadrangles, Los Angeles County, California by Thomas W. Dibblee, Jr., 2008
3. See site map for details of geophysical survey

USGS science for a changing world

GEOVision geophysical services

GEOLOGIC MAP
CE•24706

File Name: CE-24706

Date: 2/7/2013

Looking south towards instrumented bridge (seismic station CE.24706) and HVSR sensor 450

Looking south at seismic stations CE.24706 free field (in foreground) and CE.24706 instrumented bridge

Looking southeast along array 24706-2 towards Barrel Springs Bridge

Looking northeast along array 24706-1

MASW and seismic refraction data acquisition along array 24706-3

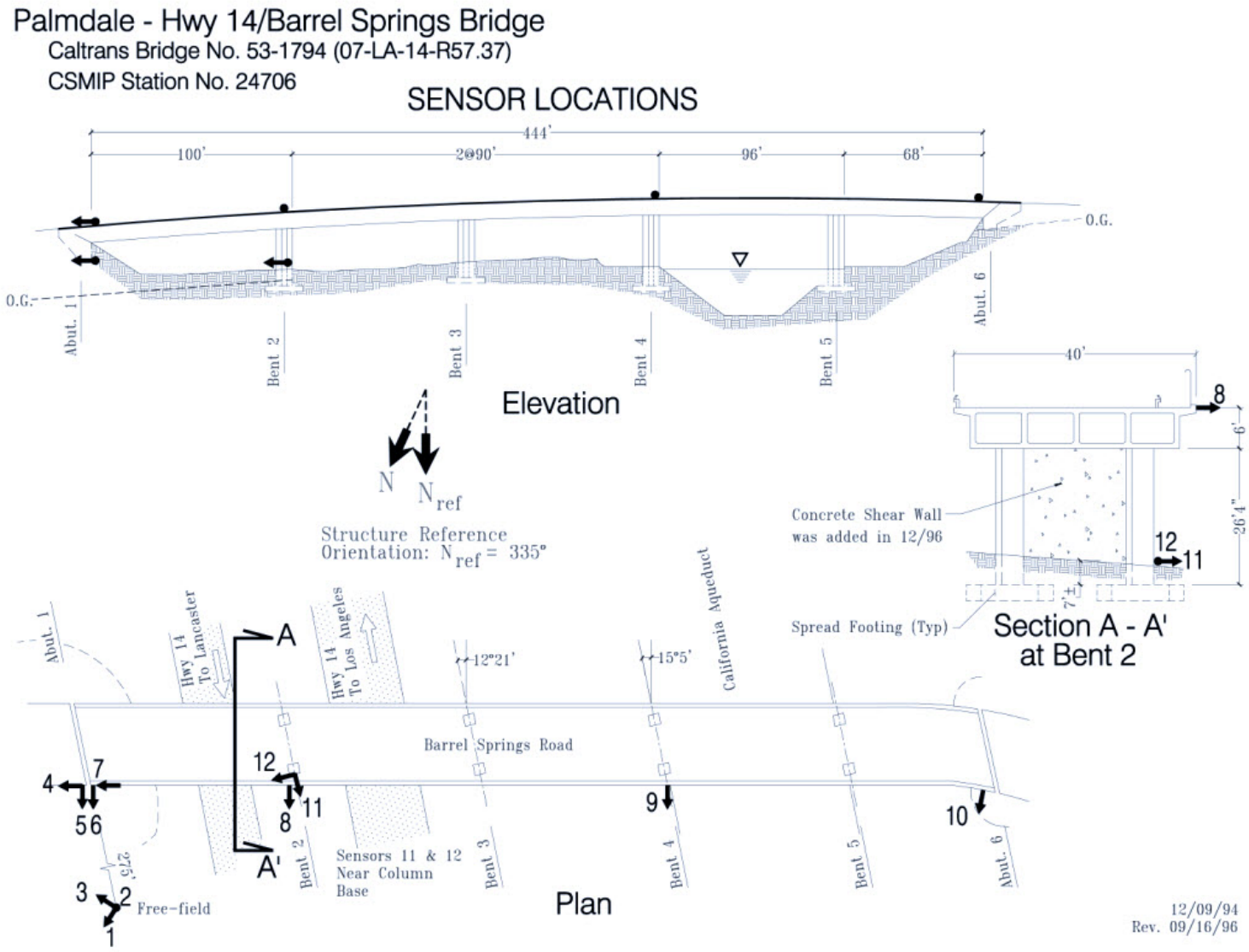

CE.24706 Seismic Sensor Locations (source: www.strongmotioncenter.org)

Location of Geophysical Testing Arrays:

Location	Latitude	Longitude
24706-1, Northeast End of Passive Array	34.54856	-118.12929
24706-1, Southwest End of Passive Array	34.54793	-118.13028
24706-2, Northwest End of Passive Array	34.54790	-118.13026
24706-2, Southeast End of Passive Array	34.54717	-118.12959
24706-3, Southwest End of MASW/Refraction Array	34.54799	-118.13018
24706-3, Center of MASW/Refraction Array	34.54812	-118.12999
24706-3, Northeast End of MASW/Refraction Array	34.54824	-118.12978
HVSR Sensor 450	34.54720	-118.12983
HVSR Sensor 453	34.54794	-118.13028
HVSR Sensor 507	34.54811	-118.12998
CE.24706 Seismic Station (Free Field Station)	34.54726	-118.12992

Notes: 1) WGS84 Coordinate System (decimal degrees)
2) Survey accuracy is estimated at 1 to 2 m.

Results:

V_S Model 1A (Combined Passive Array 24706-1 and MASW array 24706-3, Average Mode Assumption, Assumed Poisson's Ratio of 0.25)

Depth to Top of Layer (m)	Layer Thickness (m)	S-Wave Velocity (m/s)	Inferred P-Wave Velocity (m/s)	Assumed Poisson's Ratio	Assumed Density (g/cm^3)
0	2	219	382	0.25	1.7
2	3	303	525	0.25	1.8
5	5	387	668	0.25	1.9
10	9	416	720	0.25	1.9
19	>11	1113	1924	0.25	2.2

Notes: 1) Depth of investigation is greater than 30 m.
2) Bottom layer is a half space.

V_S Model 1B (Combined Passive Array 24706-1 and MASW array 24706-3, Average Mode Assumption, Assumed Poisson's Ratio of 0.3)

Depth to Top of Layer (m)	Layer Thickness (m)	S-Wave Velocity (m/s)	Inferred P-Wave Velocity (m/s)	Assumed Poisson's Ratio	Assumed Density (g/cm^3)
0	2	229	428	0.30	1.7
2	3	283	530	0.30	1.8
5	5	379	708	0.30	1.9
10	9	401	751	0.30	1.9
19	>11	983	1838	0.30	2.2

Notes: 1) Depth of investigation is greater than 30 m.
2) Bottom layer is a half space.

V_S Model 2A (L-Shaped Passive Array 24706-1/2, Average Mode Assumption, Assumed Poisson's Ratio of 0.25)

Depth to Top of Layer (m)	Layer Thickness (m)	S-Wave Velocity (m/s)	Inferred P-Wave Velocity (m/s)	Assumed Poisson's Ratio	Assumed Density (g/cm^3)
0	2	214	371	0.25	1.7
2	3	305	528	0.25	1.8
5	5	371	641	0.25	1.9
10	7	425	736	0.25	1.9
17	>13	1112	1925	0.25	2.2

Notes: 1) Depth of investigation is greater than 30 m.
2) Bottom layer is a half space.

V_S Model 2B (L-Shaped Passive Array 24706-1/2, Average Mode Assumption, Assumed Poisson's Ratio of 0.3)

Depth to Top of Layer (m)	Layer Thickness (m)	S-Wave Velocity (m/s)	Inferred P-Wave Velocity (m/s)	Assumed Poisson's Ratio	Assumed Density (g/cm^3)
0	2	212	395	0.30	1.7
2	3	298	559	0.30	1.8
5	5	344	644	0.30	1.9
10	7	418	781	0.30	1.9
17	>13	979	1829	0.30	2.2

Notes: 1) Depth of investigation is greater than 30 m.
2) Bottom layer is a half space.

Observations/Discussion:

- The HVSR curves have slightly different peaks in the 4.7 to 6 Hz range indicating that shallow bedrock depth is slightly variable. The highest frequency HVSR peak occurs near the free field seismic station (sensor 450 – 6 Hz). HVSR peaks of about 4.7 Hz (sensor 507) and 5.5 Hz (sensor 453) occur in the vicinity of the active and passive surface wave arrays. The HVSR data indicates that bedrock is gradually deepening in a north or northeast direction. Based on HVSR peaks and the quarter wavelength approximation, bedrock could be 10 to 20% shallower in the vicinity of the seismic station, assuming constant shear wave velocity of the overburden.
- P-wave seismic refraction data were acquired along array 24706-3. First arrival data were quite noisy due to the proximity of the array to Highway 14, but data analysis was possible.
- Tomographic inversion of the P-wave first arrival data was conducted utilizing a layered starting model. The P-wave seismic refraction survey design allowed P-wave velocity to be imaged to a maximum depth of about 15 m. The seismic refraction model indicates that P-wave velocity is about 350 m/s at the surface and increases to over 600 m/s at a depth of about 2.5 m then remains below about 725 m/s until an abrupt increase in velocity to over 2,250 m/s at a depth of about 12 to 13 m. The maximum P-wave velocity in the model is less than 2,500 m/s.
- A P-wave velocity of 2,250 m/s could be associated with saturated sediments and/or weathered bedrock. If shallow groundwater occurs in the site vicinity, then bedrock may be deeper than the layer at 12 to 13 m depth in the seismic refraction model. In this case, an S-wave seismic refraction survey would be required to map depth to bedrock. Such a survey would have to be conducted at night when traffic on Highway 14 is at a minimum.
- Noise conditions at the site (multi-directional or omni-directional noise sources) appeared sufficient for successful application of passive surface wave techniques.
- The ESAC technique was used to extract surface wave dispersion data from passive "L" array data. Both the ReMi™ and ESAC techniques were used to extract surface wave dispersion data from the linear arrays.
- MASW data reduction was complicated by dominant higher modes at high frequencies and did not provide surface wave dispersion data at smaller wavelengths/higher frequencies than the passive surface wave soundings.
- Surface wave dispersion data from the MASW and passive surface wave data set collected along linear array 24706-1 are in good agreement. Passive surface wave data collected along the L-shaped array (combined arrays 24706-1 and 24706-2) does not tie in well with the MASW data and indicates that bedrock is on average shallower beneath the array; which is consistent with the array location relative to the HVSR measurement stations.
- Separate models were generated for the combined MASW array 24706-3, linear passive array 24706-1 and for the L shaped passive surface wave array (24706-1 and 24706-2).
- Representative dispersion curves were generated for each surface wave data set using a moving average, polynomial curve fitting routine. These individual representative dispersion curves were combined and a representative dispersion curve generated for the combined data sets for data modeling, as appropriate.
- It was not possible to model the dispersion curve with the fundamental mode Rayleigh wave assumption. High velocity bedrock is expected to underlie low velocity sediments

at this site and with this type of velocity structure, the fundamental and first higher modes may become superimposed at long wavelengths (low frequencies). In this case, the only approaches to model the data are to assume a mode jump at some frequency and use multi-mode inversion routines or assume that the dispersion curve represents the average (effective) mode based on the relative amplitude of the fundamental mode and higher modes. Data was modeled using the average mode assumption (far-field, plane wave, no body wave effects) and assumed Poisson's ratios of 0.25 and 0.3. Attempting to model the dispersion curve as fundamental mode would lead to unrealistically high S-wave velocity of bedrock and poor fit of observed and calculated dispersion curves. Modeling the low frequency portion of the dispersion curve (assuming a jump from fundamental mode to first higher mode) would generally result in a lower S-wave bedrock velocity. Interestingly, the average mode models with an assumed Poisson's ratio of 0.3 are very similar as the models that would have been obtained with multi-mode modeling (i.e. the average mode is approximately representative of the fundamental mode at high frequencies and first higher mode at low frequencies). The possibility must be considered that the modeled S-wave velocity of the half space (bedrock) is not well constrained.

- Surface wave depth of investigation is greater than 30 m.
- A large velocity increase associated with weathered bedrock is modeled at a depth of 19 m in Models 1A and 1B (Arrays 24706-1 and 3) and 17 m in Models 2A and 2B (Arrays 24706-1 and 2). This is slightly deeper than the 12 to 13 m depth to the high velocity unit imaged in the P-wave refraction data. This raises the possibility that the saturated sediments are present above the bedrock surface or that hidden layers are present in the seismic refraction data, in which case the seismic refraction model would underestimate bedrock depth.
- Inferred P-wave velocity of the bedrock unit in the surface wave models is lower than that in the seismic refraction models, indicating that either highly fractured/weathered bedrock is saturated or that the average mode assumption results in underestimated S-wave velocity of the bedrock.
- Joint modeling/inversion of the surface wave and HVSR data may improve the accuracy of the S-wave velocity model. The predicted fundamental frequency of the soil column, using the quarter wavelength approximation, is about 5 Hz for Model 2B, which is consistent with the field measurements. Generating synthetic HVSR data for the S-wave velocity model yields a higher frequency peak than measured in the field.
- V_{S30} is 472 and 453 for Models 1A (assumed Poisson's ratio of 0.25) and 1B (assumed Poisson's ratio of 0.3), respectively (Site Class C).
- V_{S30} is 493 and 468 for Models 2A (assumed Poisson's ratio of 0.25) and 2B (assumed Poisson's ratio of 0.3), respectively (Site Class C).
- It is assumed that Model 2 (A and B) generated from the passive L-shaped array, which is closer to the free field seismic station, is most representative of seismic station conditions. A Poisson's ratio of 0.3 is more realistic than 0.25, especially if fractured rock is saturated and, therefore, Model 2B, with V_{S30} of 468 m/s, is considered most representative of site conditions.
- The possibility must be considered that the surface wave models underestimate S-wave velocity of bedrock. An increase in bedrock velocity by 25% in Model 2B only increases V_{S30} to 489 m/s, a 4% increase.

- The HVSR data indicates that bedrock may be shallower at the seismic station than reflected in Models 1 and 2. A reduction in the Model 2B depth to bedrock by 2 m increases V_{S30} to 489 m/s, a 4% increase. A reduction in the Model 2B depth to bedrock by 3 m increases V_{S30} to 501 m/s, a 7% increase.
- Both a 25% increase in bedrock velocity and a 2 m decrease in depth to bedrock increases Model 2B V_{S30} to 515 m/s, a 10% increase.
- This would be an excellent site to evaluate Love wave passive surface wave techniques because the Love wave dispersion data is expected to be dominated by the fundamental mode at all frequencies. An S-wave seismic refraction survey is also recommended to better constrain the S-wave velocity of the bedrock. However, given the proximity of the site to Highway 14, an S-wave refraction survey would have to be conducted at night or at a larger distance from the seismic station.

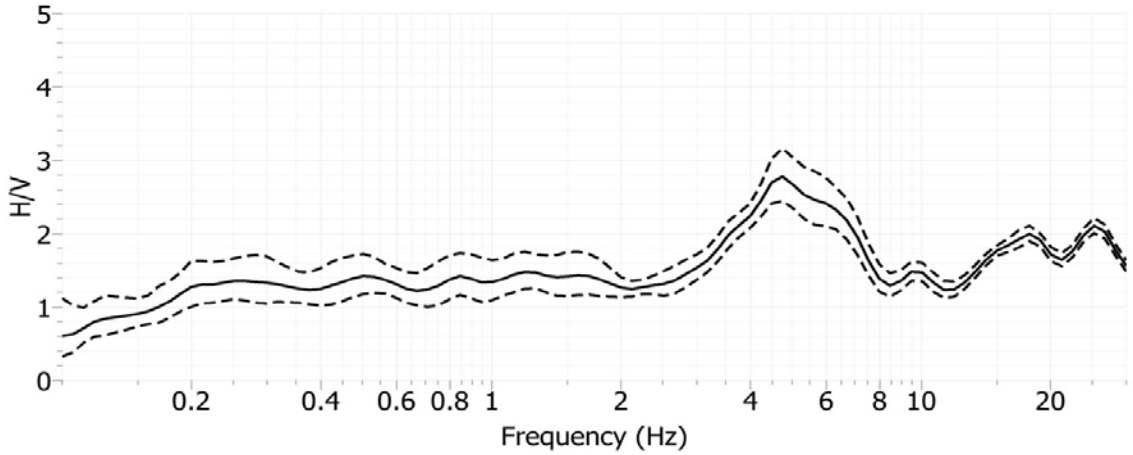

Site CE.24706, H/V Spectral Ratio, Array 24706-3, Sensor 507

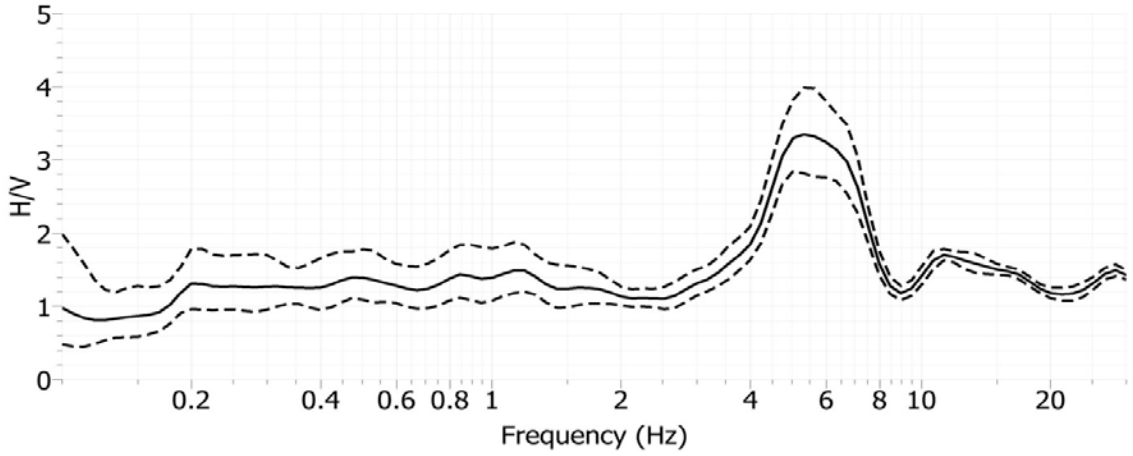

Site CE.24706, H/V Spectral Ratio, Array 24706-1/2, Sensor 453

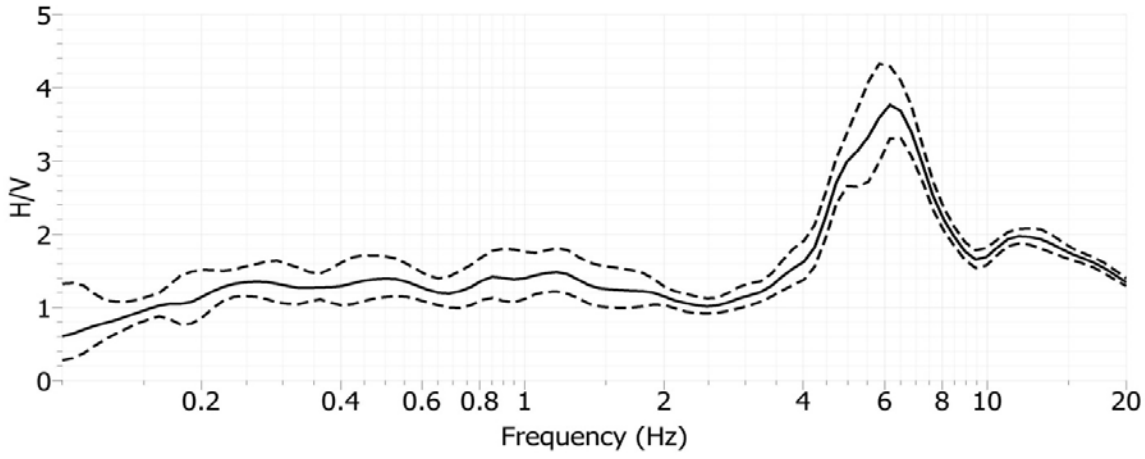

Site CE.24706, H/V Spectral Ratio, Near Seismic Station, Sensor 450

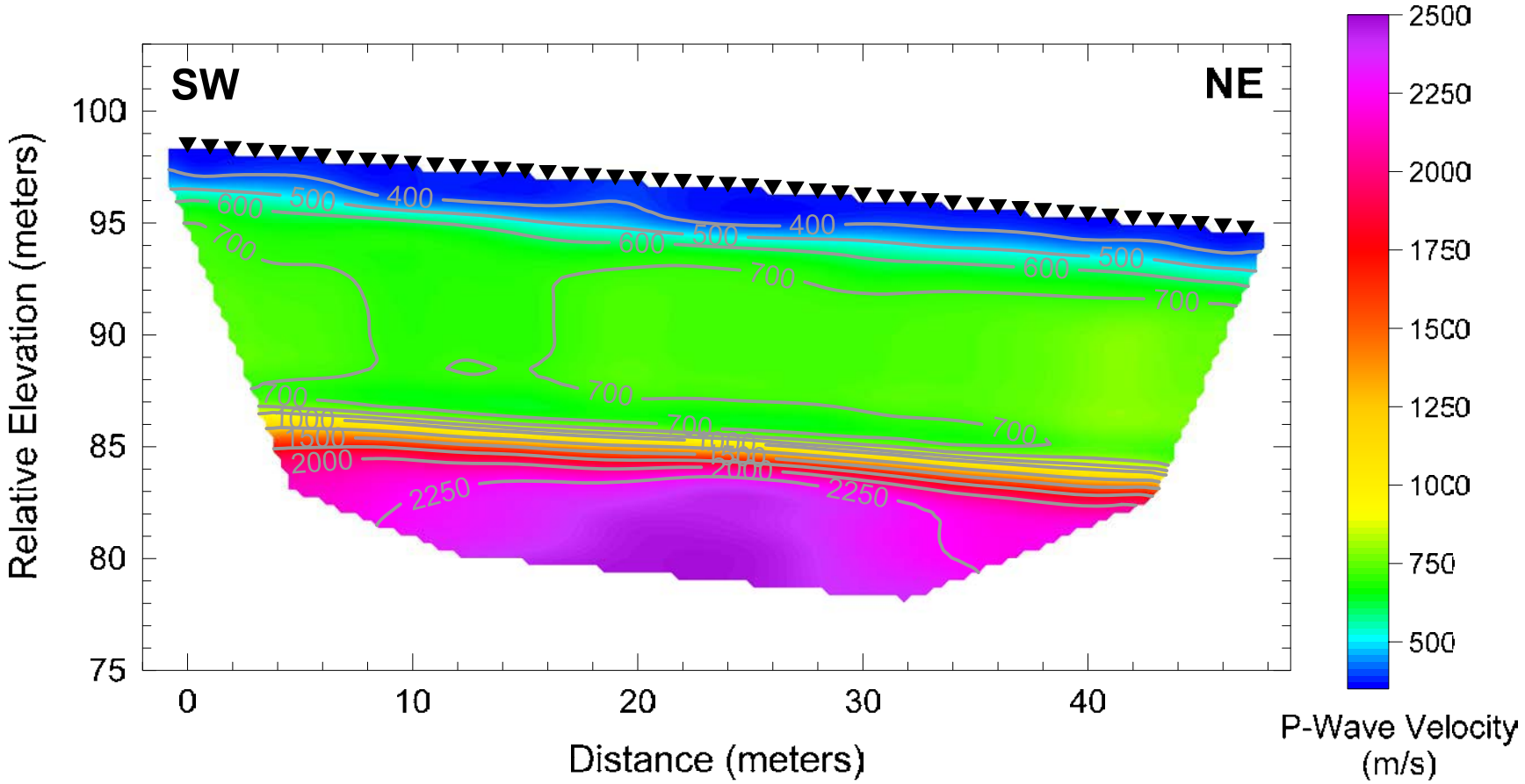

Array 24706-3 – Tomographic seismic refraction model utilizing layer based starting model

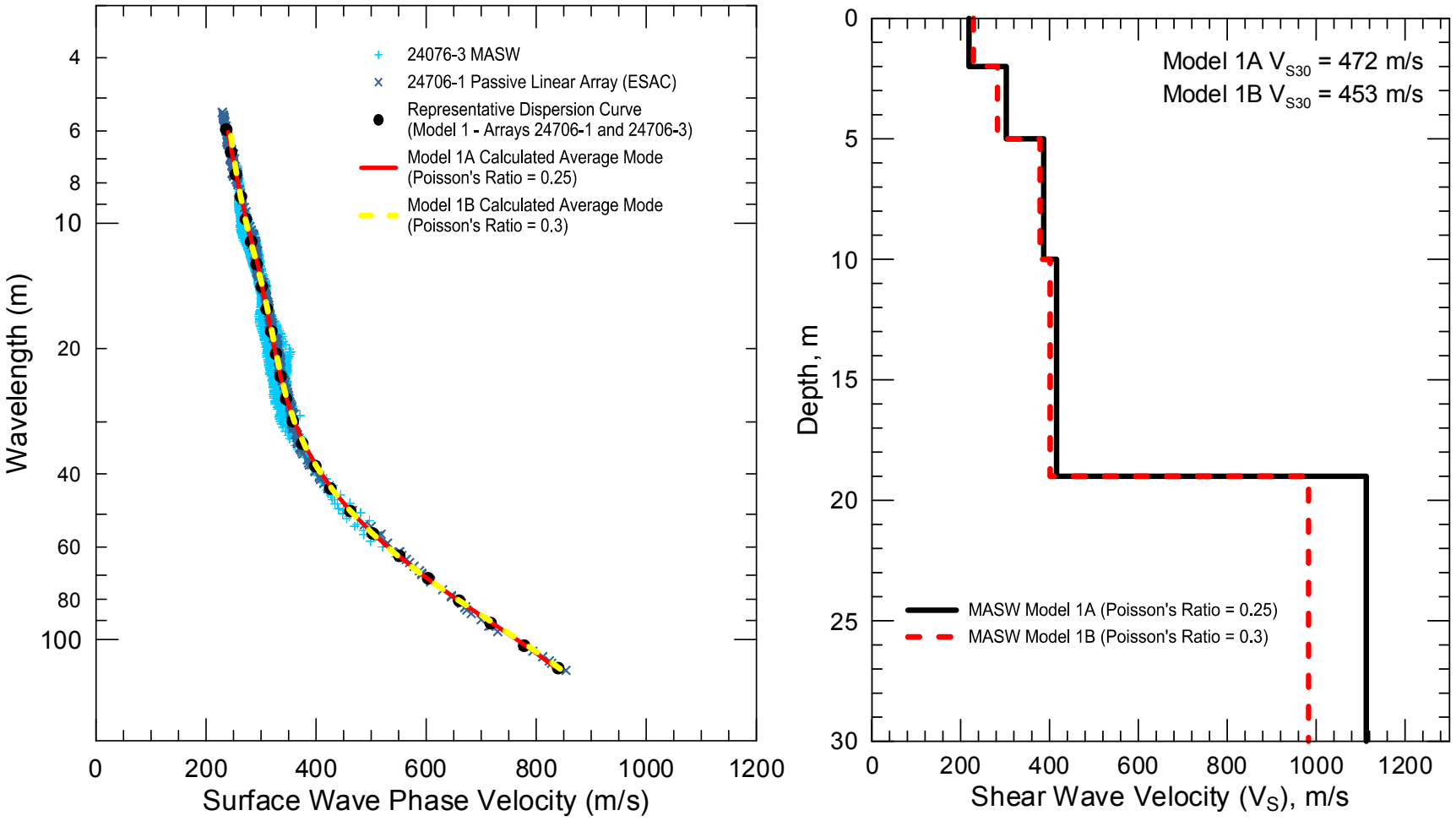

CE.24706 - Field, representative and inverted theoretical surface wave dispersion data (left) and associated V_S models (right) for combined MASW array 24706-3 and linear passive surface wave array 24706-1. Data modeled using average (effective) mode assumption with Poisson's ratio of 0.25 (Model 1A) and 0.3 (Model 1B).

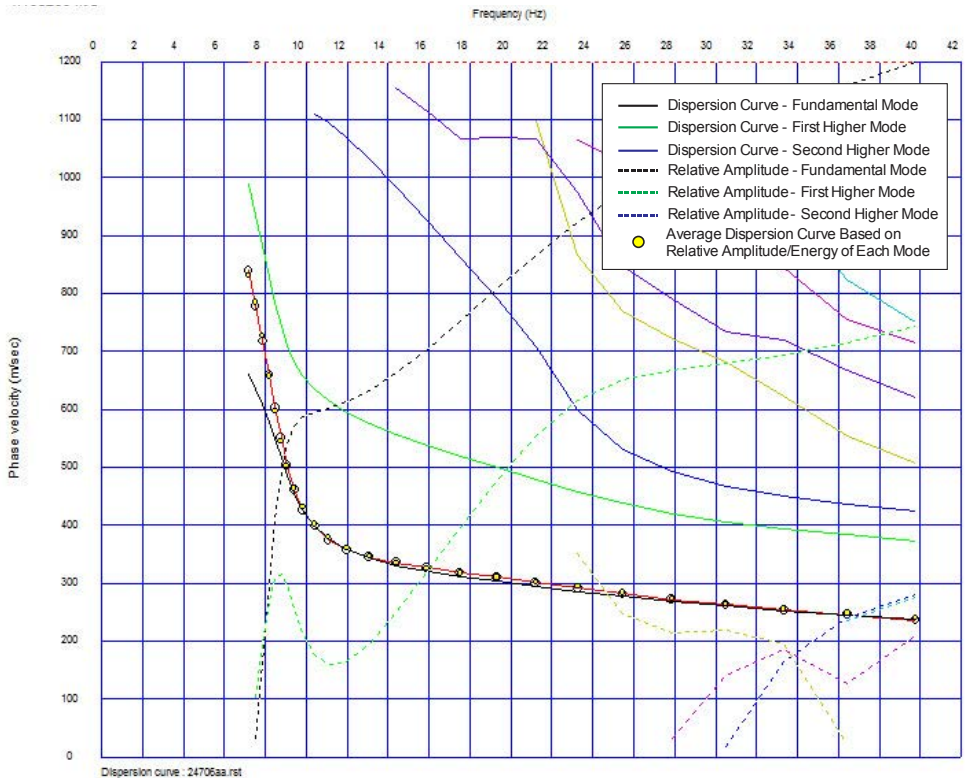

Calculated Rayleigh Wave Modes for Model 1 (Passive Array 24706-1 and MASW Array 24706-3) – data modeled using average mode assumption and Poisson's ratio = 0.25

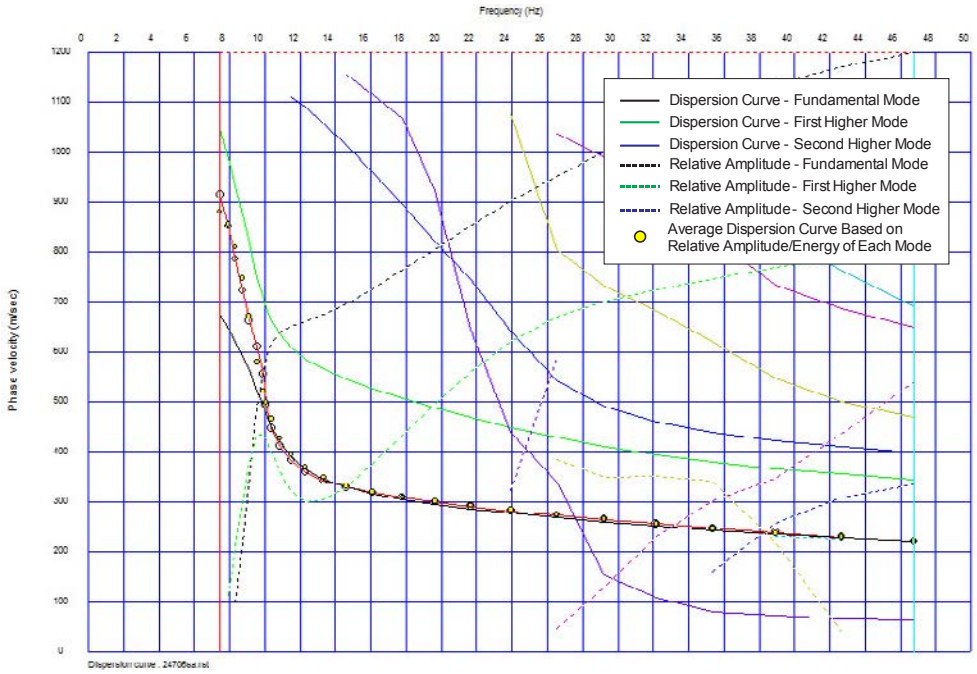

Calculated Rayleigh Wave Modes for Model 2 (Passive L-shaped Array 24706-1/2) – data modeled using average mode assumption and Poisson's ratio = 0.25

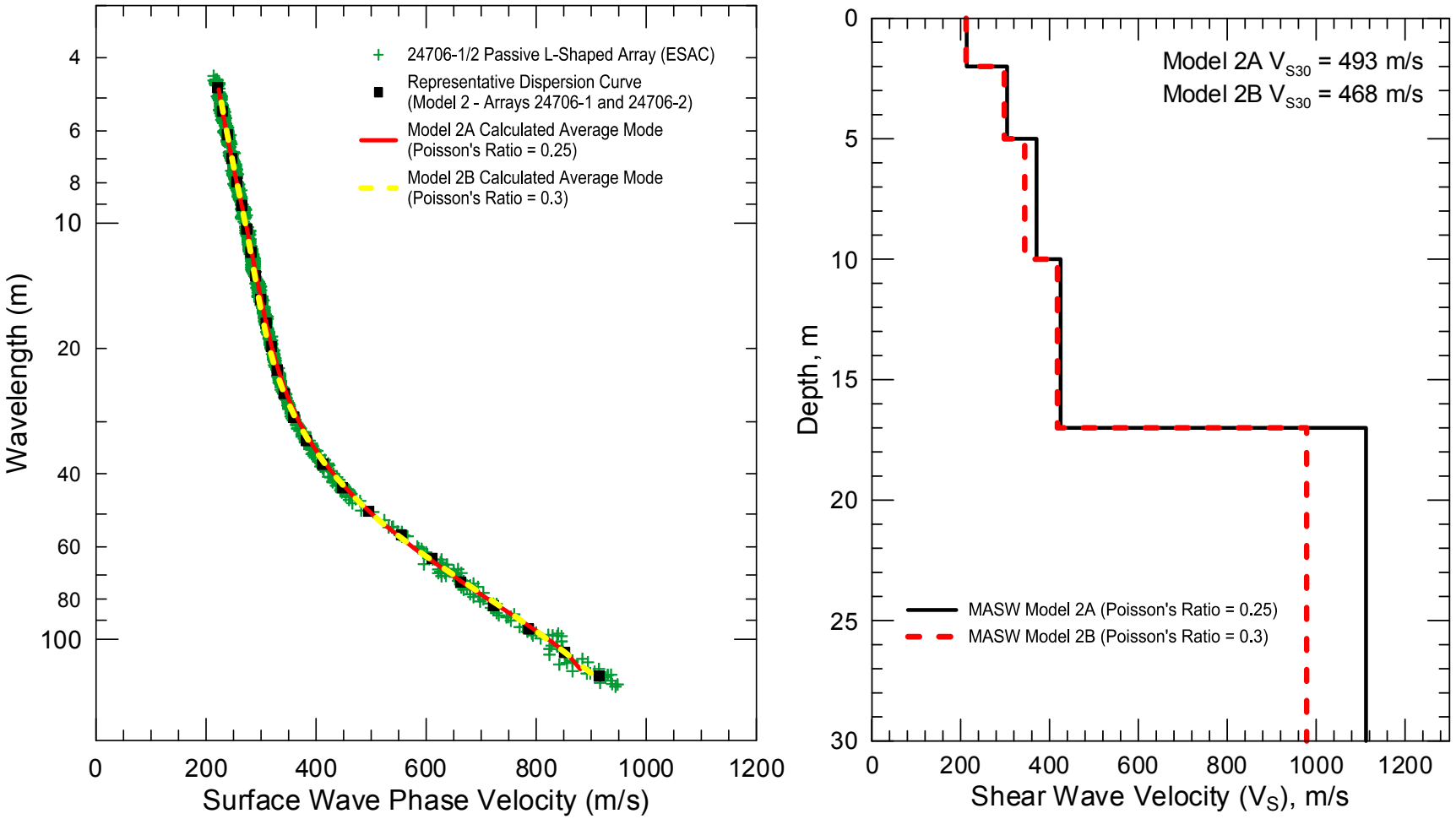

CE.24706 - Field, representative and inverted theoretical surface wave dispersion data (left) and associated V_S models (right) for L-shaped passive surface wave array 24706-1/2. Data modeled using average (effective) mode assumption with Poisson's ratio of 0.25 (Model 2A) and 0.3 (Model 2B).

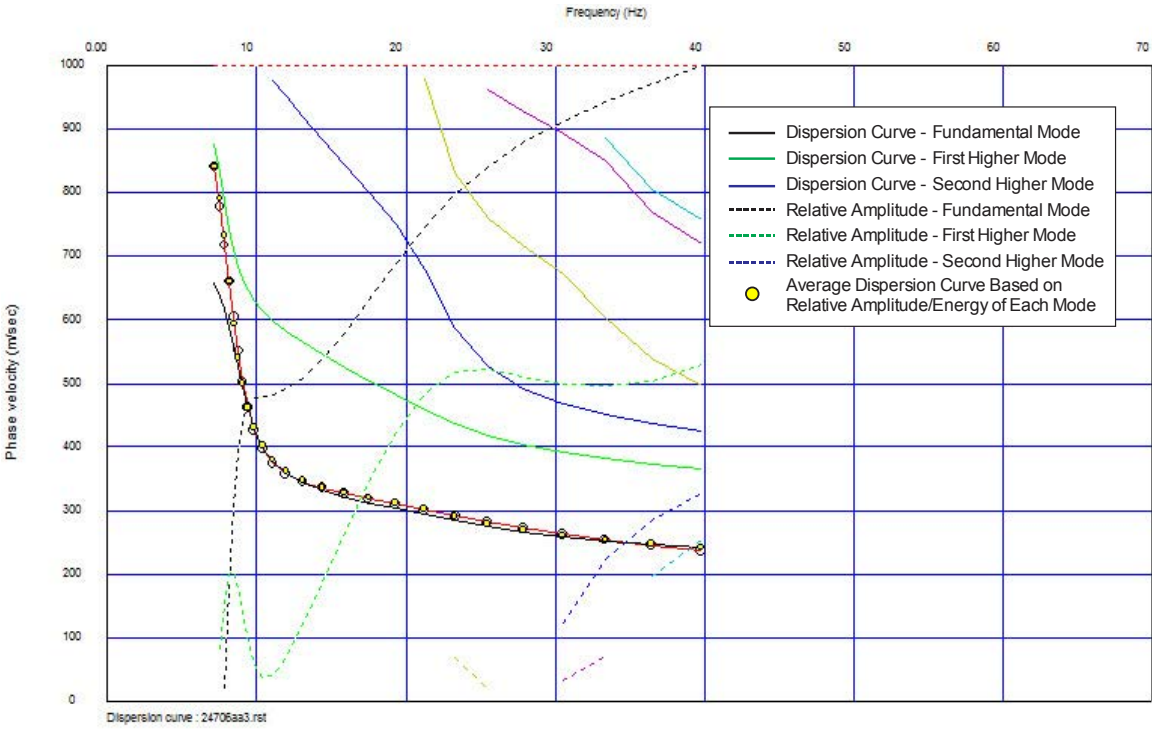

Calculated Rayleigh Wave Modes for Model 1 (Passive Array 24706-1 and MASW Array 24706-3) – data modeled using average mode assumption and Poisson's ratio = 0.3

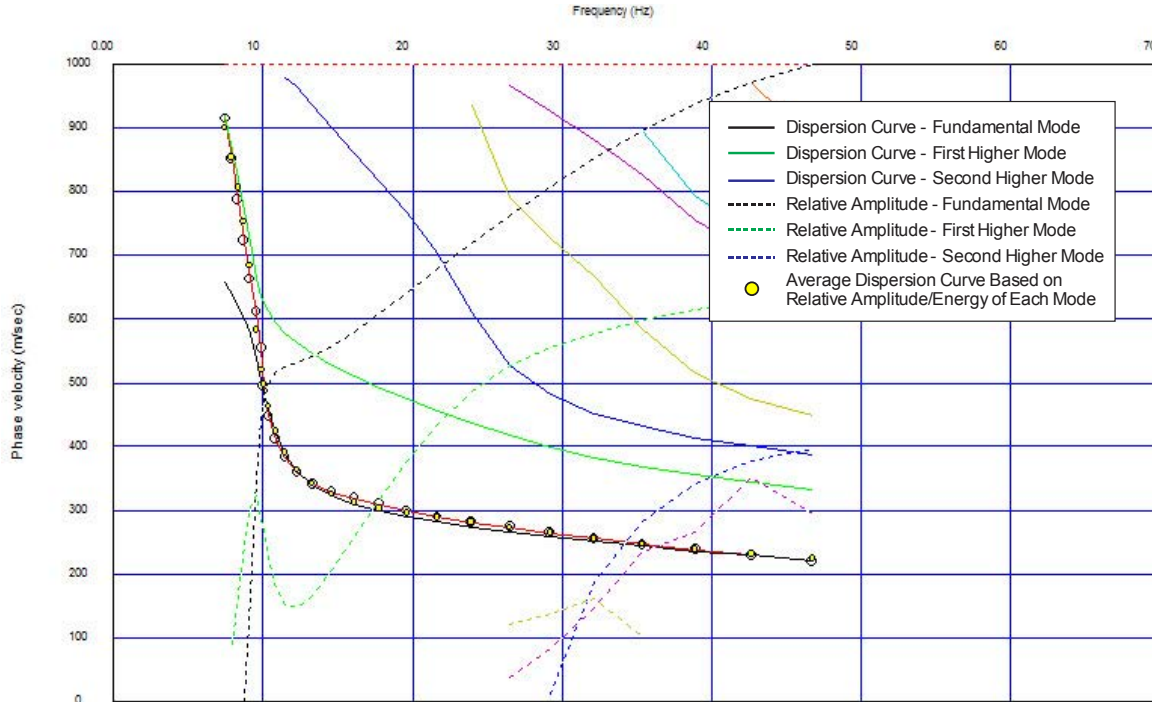

Calculated Rayleigh Wave Modes for Model 2 (Passive L-shaped Array 24706-1/2) – data modeled using average mode assumption and Poisson's ratio = 0.3

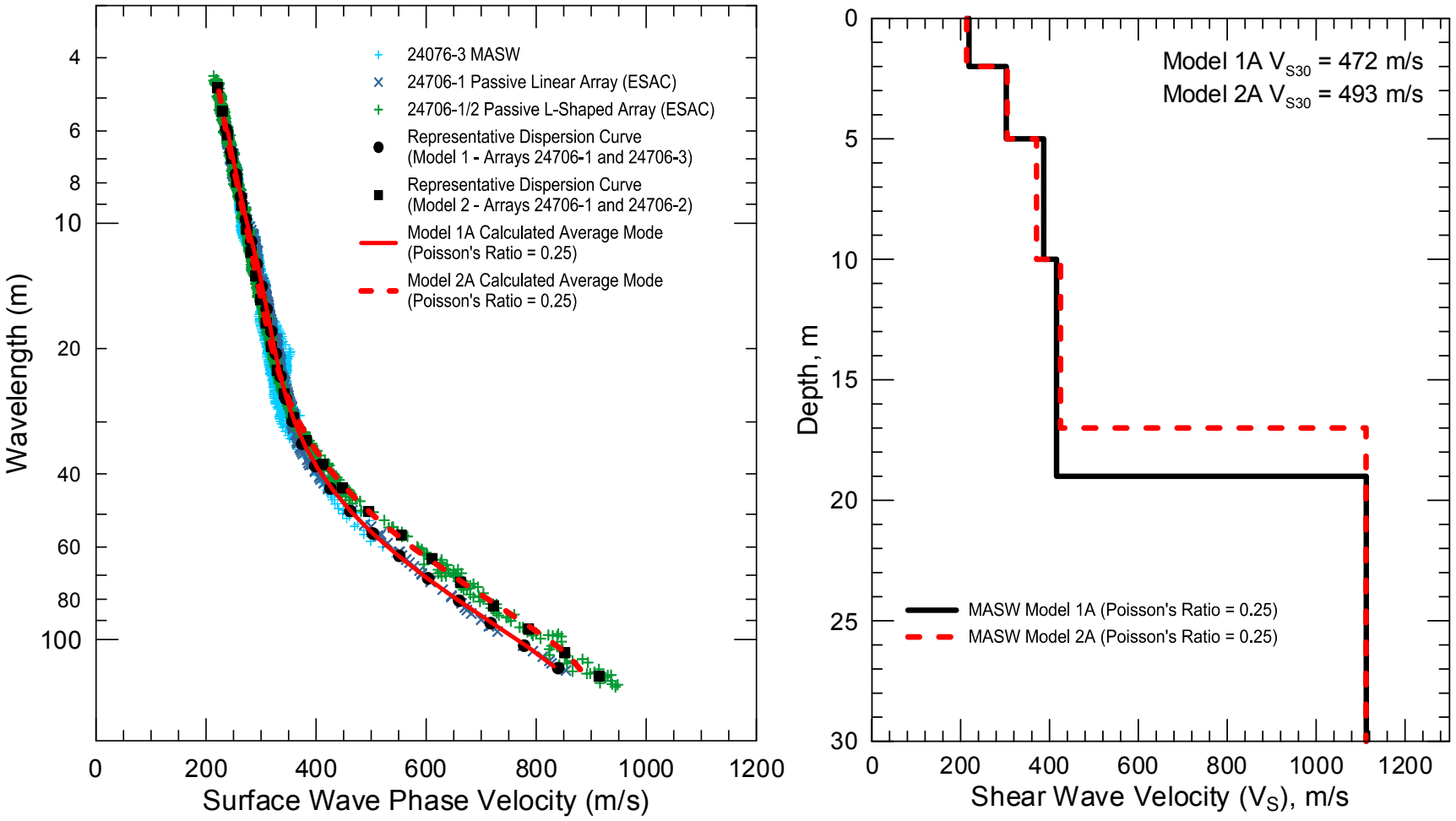

CE.24706 - Field, representative and inverted theoretical surface wave dispersion data (left) and associated V_S models (right) for combined MASW array 24706-3 and linear passive surface wave array 24706-1 (Model 1A) and L-shaped passive surface wave array 24706-1/2 (Model 2A). Data modeled using average (effective) mode assumption with Poisson's ratio of 0.25.

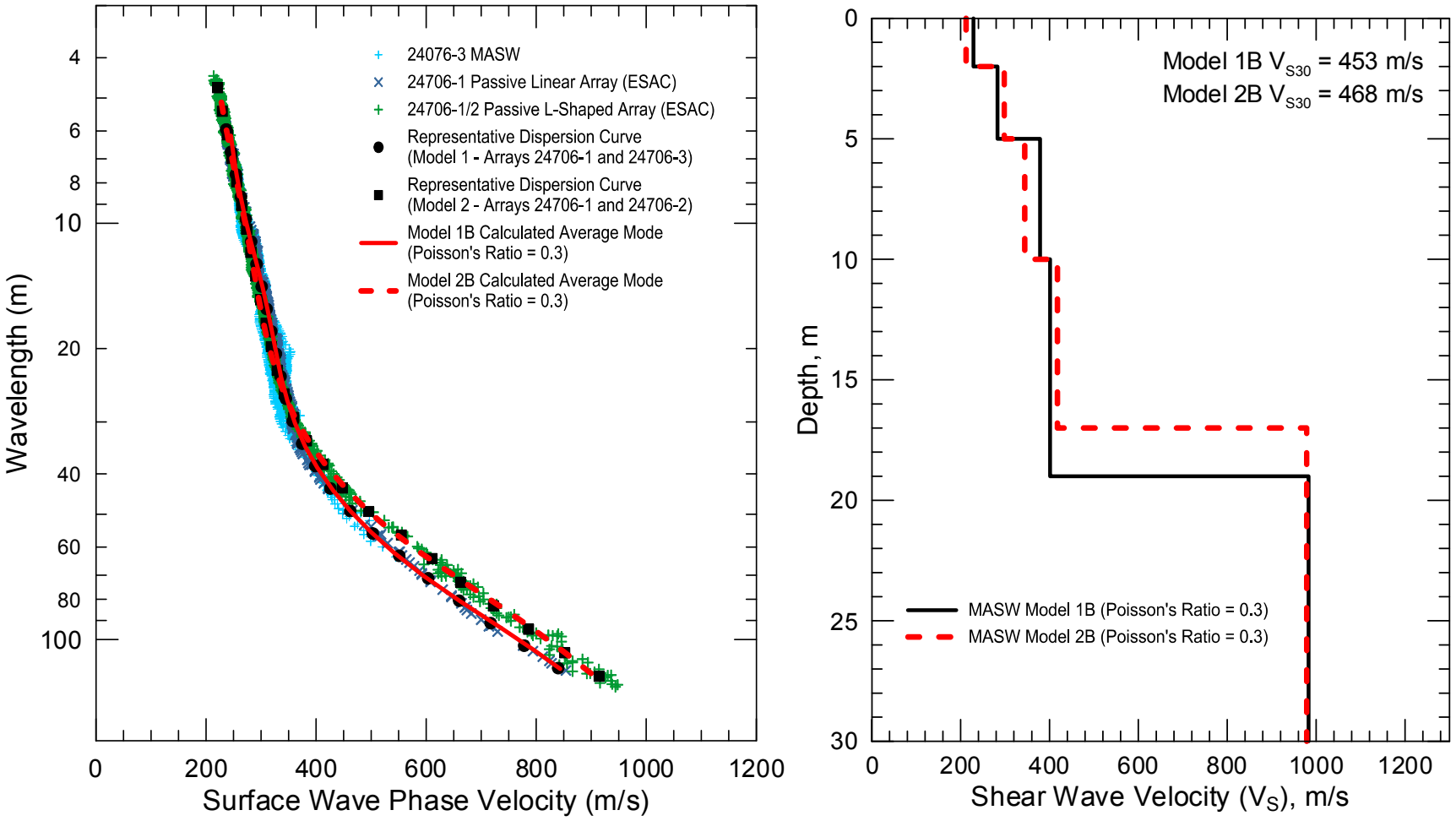

CE.24706 - Field, representative and inverted theoretical surface wave dispersion data (left) and associated V_S models (right) for combined MASW array 24706-3 and linear passive surface wave array 24706-1 (Model 1B) and L-shaped passive surface wave array 24706-1/2 (Model 2B). Data modeled using average (effective) mode assumption with Poisson's ratio of 0.3.

Site CE.24775

Location: Lebec Road Bridge/Interstate 5, Kern County, California

Instrumented Bridge

Latitude: 34.86637 **Longitude:** -118.88359
(Station coordinates estimated from Google Earth or ESRI Imagery and are in WGS84 coordinate system)

Free Field Seismic Station

Latitude: **Longitude:**
(Station could not be located in the field and may be buried)

V_{S30} (measured): 437 m/s

V_{S30} (adjusted to more accurately reflect seismic station conditions): 437 m/s (no adjustment necessary).

NEHRP Site Class: C

Geomatrix Code: GHB/GHC (CE.24706 – Instrumented Bridge), IHC (CE.24706 – Free Field)

Geologic Conditions/Observations: Site located on geologic unit mapped as Quaternary (Holocene) alluvium. Granitic bedrock may be very shallow beneath the northern bridge abutment and is significantly deeper beneath the southern abutment.

Site Conditions: Rural site next to high traffic freeway. Relative flat topography in immediate site vicinity with mountains/hills to west and east.

Geophysical Methods Utilized: HVSR, MASW

Geophysical Testing Arrays:

1. Array 24775-1 (48 channel MASW array utilizing 4.5 Hz vertical geophones spaced 1.5 m apart for a length of 70.5 m, forward and reverse shot locations with multiple source offsets and source types and multiple interior shots).
2. Three HVSR measurement locations: one on each side of the bridge and one on array 24775-1.

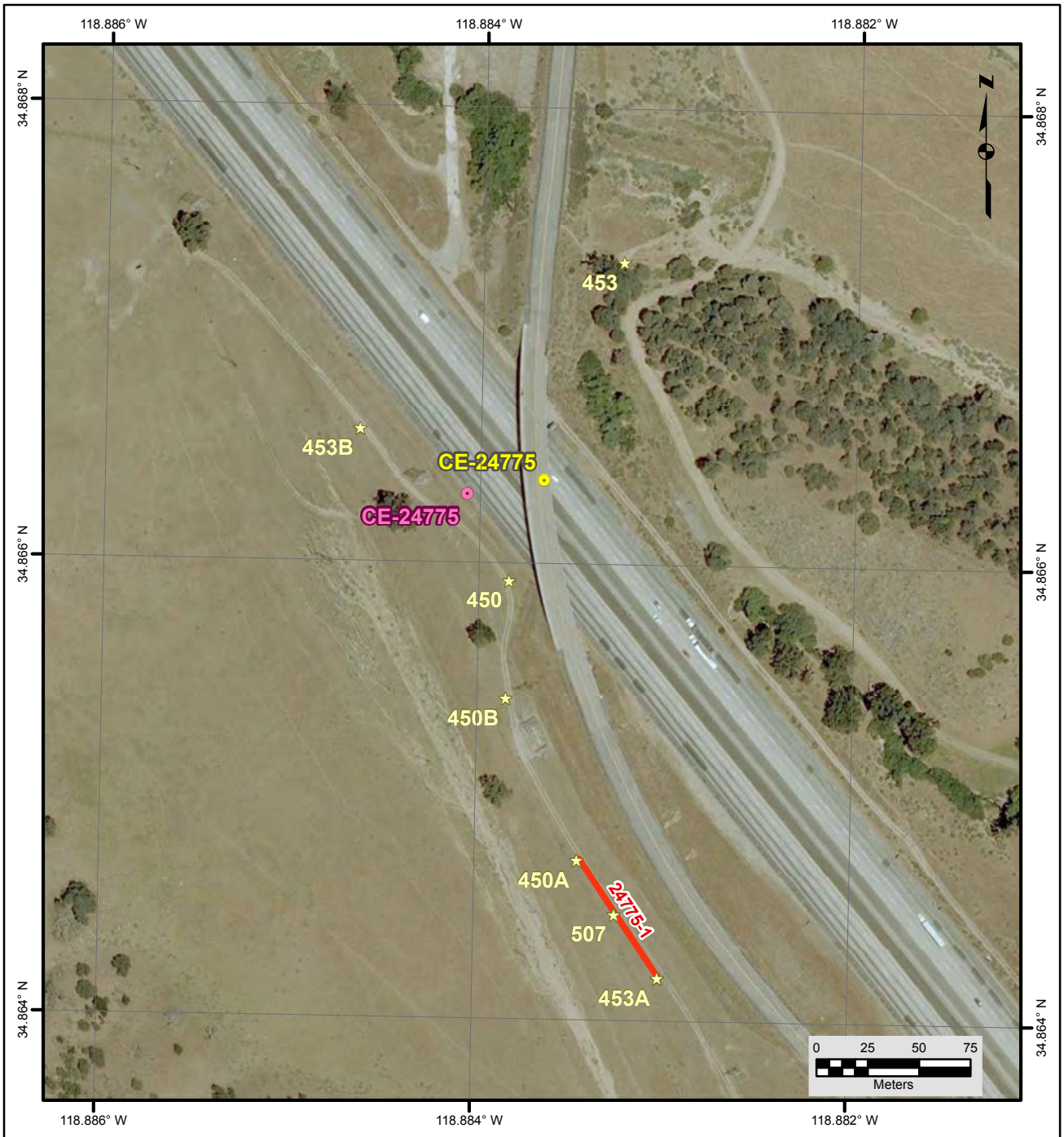

Legend

- Seismic Station - Approximate Improved Location of Record
- Seismic Station - Approximate Location of Record
- H/V Spectral Ratio Location
- MASW and Seismic Refraction Array

NOTES:
1. WGS 1984 COORDINATE SYSTEM
2. Image Source: ESRI, i-cubed, USDA FSA, USGS, AEX, GeoEye, Getmapping, Aerogrid, IGP

File Name: CE-24775-I

Date: 2/24/2012

USGS science for a changing world

GEOVision geophysical services

RECOVERY.GOV

SITE MAP
CE•24775

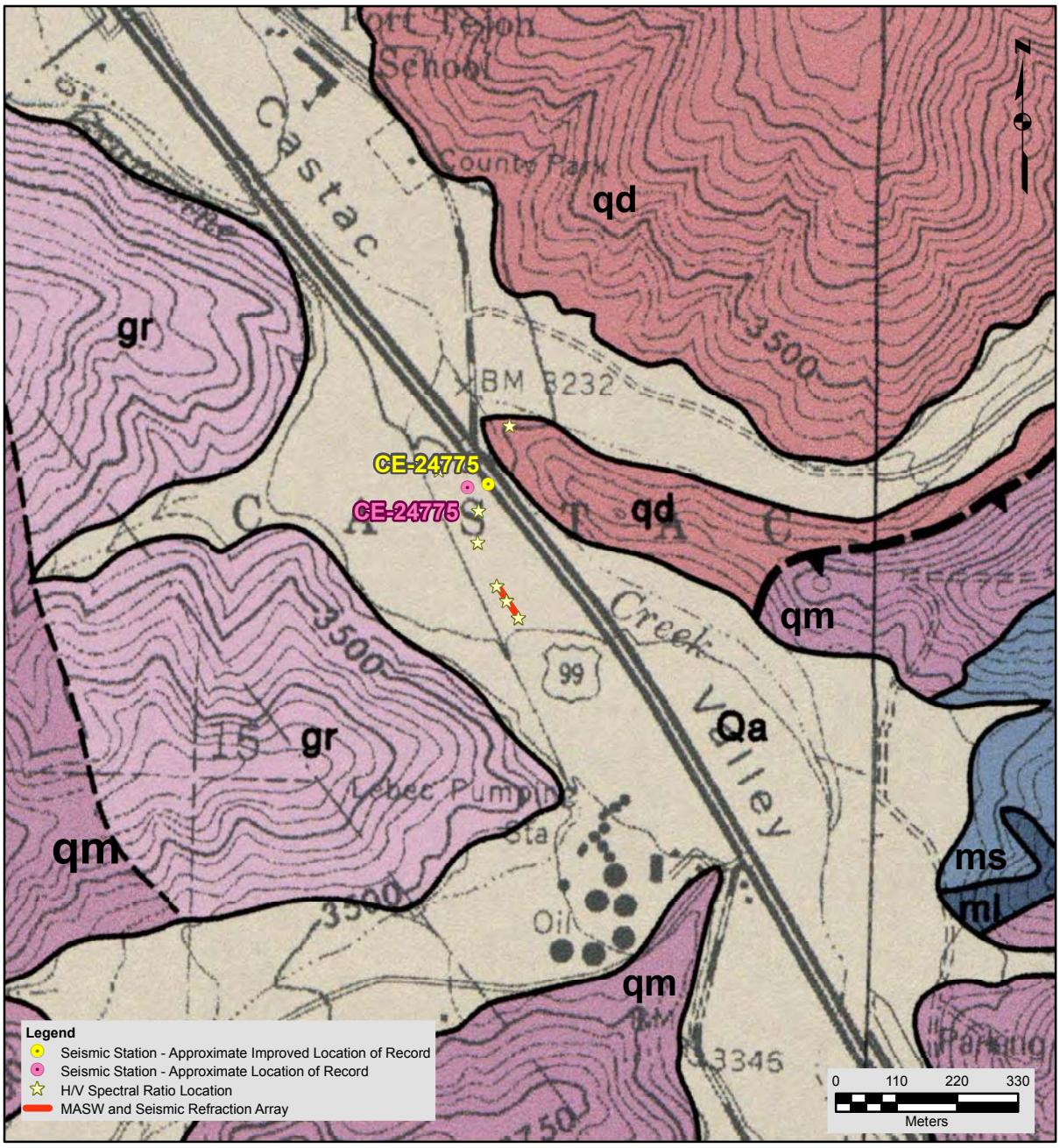

Description of Geologic Map Units

Qa = Quaternary (Holocene) alluvial gravel, sand and clay of valley areas
gr = Mesozoic (Cretaceous) medium-grained holocrystalline granite to quartz monzonite, massive, some biotite
qd = Mesozoic (Cretaceous) medium-grained holocrystalline quartz diorite, massive, biotite rich
qm = Mesozoic (Cretaceous) medium-grained holocrystalline quartz monzonite-granite
ms = Paleozoic to Mesozoic schist-phyllite, in part gneissic
ml = Paleozoic to Mesozoic marble, white (Limestone/dolomite), medium-coarse grained

NOTES:
1. WGS 1984 COORDINATE SYSTEM
2. Geologic Map of the Frazier Mountain & Lebec Quadrangles, Los Angeles, Ventura & Kern Counties, California by Thomas W. Dibblee, Jr., 2006
3. See site map for details of geophysical survey

USGS science for a changing world

GEOVision geophysical services

GEOLOGIC MAP
CE•24775

File Name: CE-24775

Date: 2/24/2012

Looking northwest towards instrumented Lebec Road Bridge/Interstate 5

Looking east towards HVSR sensor 453 and west end of bridge

Looking southwest towards HVSR sensor 453 and east end of bridge. HVSR sensor 453 located at edge of outcrop of Mesozoic quartz diorite.

Looking northwest along array 24775-1 and at HVSR sensor 507

Looking northwest along array 24775-1

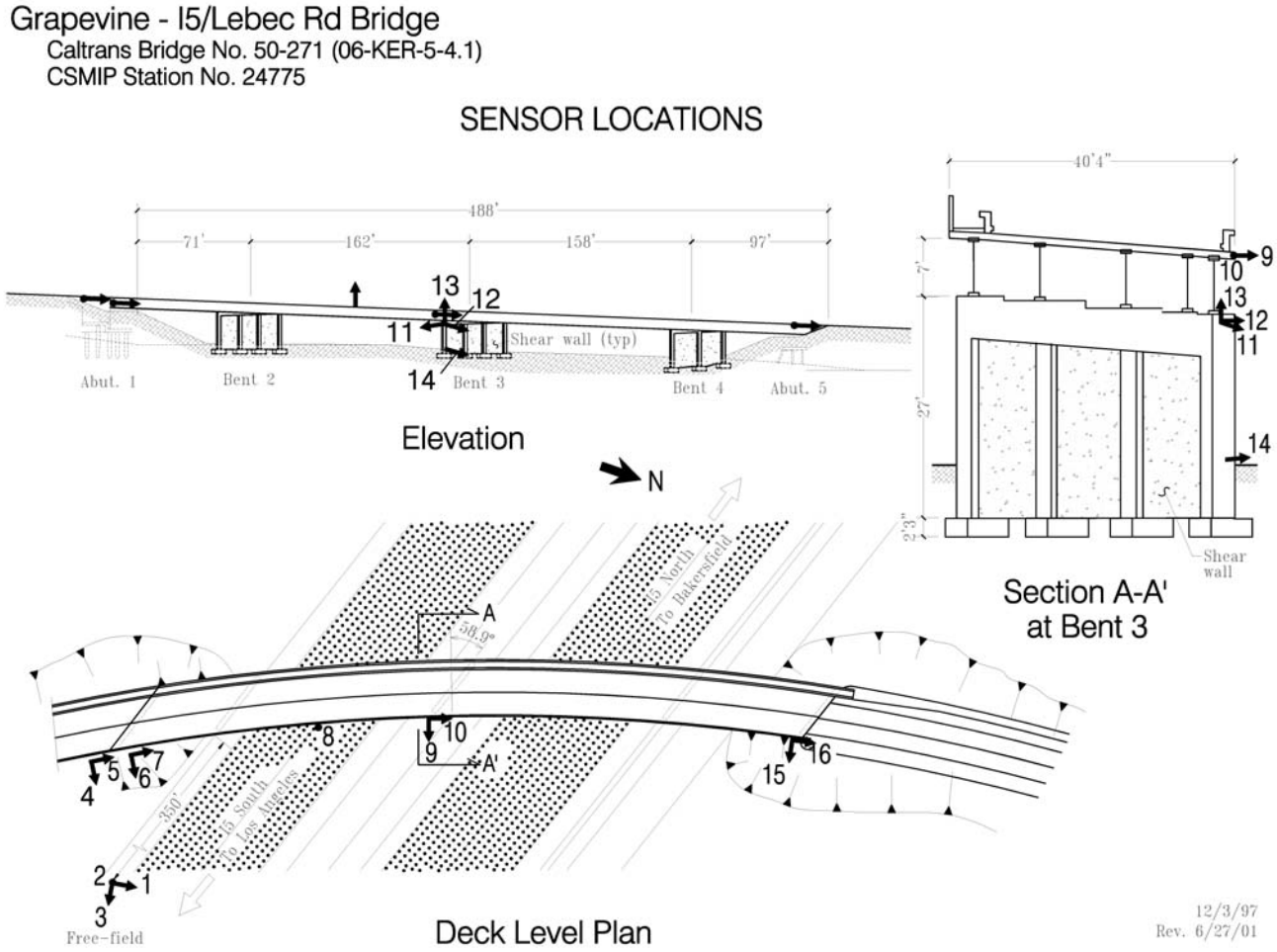

CE.24775 Seismic Sensor Locations (source: www.strongmotioncenter.org)

Location of Geophysical Testing Arrays:

Location	Latitude	Longitude
24775-1, Northwest End of MASW Array	34.86471	-118.88337
24775-1, Center of MASW Array	34.86445	-118.88315
24775-1, Southeast End of MASW Array	34.86419	-118.88294
HVSR Sensor 450	34.86592	-118.88377
HVSR Sensor 453	34.86732	-118.88318
HVSR Sensor 507	34.86446	-118.88318
HVSR Sensor 450A	34.86470	-118.88338
HVSR Sensor 453A	34.86419	-118.88294
HVSR Sensor 450B	34.86541	-118.88378
HVSR Sensor 453B	34.86658	-118.88458

Notes: 1) WGS84 Coordinate System (decimal degrees)
2) Survey accuracy is estimated at 1 to 2 m

Results:

V_S Model

Depth to Top of Layer (m)	Layer Thickness (m)	S-Wave Velocity (m/s)	Inferred P-Wave Velocity (m/s)	Assumed Poisson's Ratio	Assumed Density (g/cm^3)
0	1	251	470	0.300	1.7
1	2	262	491	0.300	1.7
3	3	322	602	0.300	1.8
6	5	395	740	0.300	1.8
11	6	474	887	0.300	1.9
17	8	550	1029	0.300	2.0
25	>5	632	1800	0.430	2.1

Notes: 1) Although inconclusive, saturated sediments may be as shallow as 25 m based on seismic refraction first arrival data.
2) Depth of investigation is about 30 m.
3) Bottom layer is a half space.

Observations/Discussion:

- Seismic station CE.24775 consists of 13 accelerometers on the bridge and 3 accelerometers at a free-field site. The free-field site is documented as being located about 350 ft southeast of the southern abutment (Abutment 1), but could not be located in the field. Weathered granitic bedrock may be very shallow beneath the northern bridge abutment and much deeper beneath the southern abutment. Due to expected highly variable bedrock depths in the vicinity of the bridge, the seismic testing was conducted as close as possible to the documented free-field station, while maintaining sufficient distance from the freeway to obtain useable data.
- HVSR measurements were originally made on each side of the bridge and in the center of the MASW array. As expected, measurements on each side of the bridge are different due to variable bedrock depth. HVSR data at sensor location 450, located at the southern end of the bridge, is also significantly different than HVSR data at sensor 507, located at the center of array 24775-1. It is possible that the HVSR measurements at sensor locations 450 and 453 are impacted by the proximity of the sensors to the bridge. The HVSR plot for sensor 507 has a distinct peak at about 2 Hz, likely associated with bedrock at a depth greater than the 30 m depth of investigation.
- Due to differences in HVSR data the site was revisited and four additional HVSR measurements were made on the west side of the freeway; one at each end of array 24775-1 and one south and one north of the bridge. The measurements at each end or array 24775-1 are very similar to the original measurement made in the center of the array with an HVSR peak at about 2 Hz, validating the 1-D velocity structure assumption. The HVSR measurements made south and north of the bridge are also relatively similar to those made along array 24775-1.
- P-wave seismic refraction data were not acquired at this site; however, MASW seismic records were reviewed to determine general P-wave velocity structure. Surficial sediments have a P-wave velocity on the order of 400 m/s. P-wave velocity increases to about 700 to 750 m/s at a depth on the order of 2.5 to 3.5 m and to about 900 to 1,000 m/s at a depth of about 10 to 13 m. There is a higher velocity refractor at greater depth, which could not be accurately resolved due to survey design and proximity of the array to the freeway. This refractor occurs at a depth on the order of 25 m and could have a P-wave velocity of 1,800 m/s, or greater. HVSR data indicate that this refractor is too shallow to be associated with bedrock and we assume that it is associated with saturated sediments for the purpose of surface wave modeling. Saturated sediments at this depth will have a minimal effect of the S-wave velocity model derived from Rayleigh wave phase velocity data.
- Given the proximity of the site to the I-5 freeway, it would have been desirable to acquire passive surface wave data. However, low lying vegetation was very dense near the roads and passive surface wave data were not acquired.
- MASW data quality was degraded by the proximity of the site to the freeway and no attempt was made to image to a depth greater than 30 m.
- The minimum wavelength surface wave phase velocity data extracted from the 48-channel MASW array is about 5.5 m. Data reduction using seismic records from smaller hammer sources and a limited offset receiver array (i.e. less active geophones) allowed extraction of surface wave dispersion data to a minimum wavelength of about 3 m.

- There is nominally about 25 to 40 m/s scatter in the MASW dispersion data likely due to lateral velocity variation.
- A representative dispersion curve was generated for the MASW data set using a moving average, polynomial curve fitting routine and used for modeling.
- The saturated zone with an estimated P-wave velocity of 1,800 m/s was fixed at a depth of 25 m during data modeling.
- Surface wave depth of investigation is about 30 m based on half of maximum wavelength criteria.
- V_{S30} is 437 m/s (Site Class C).

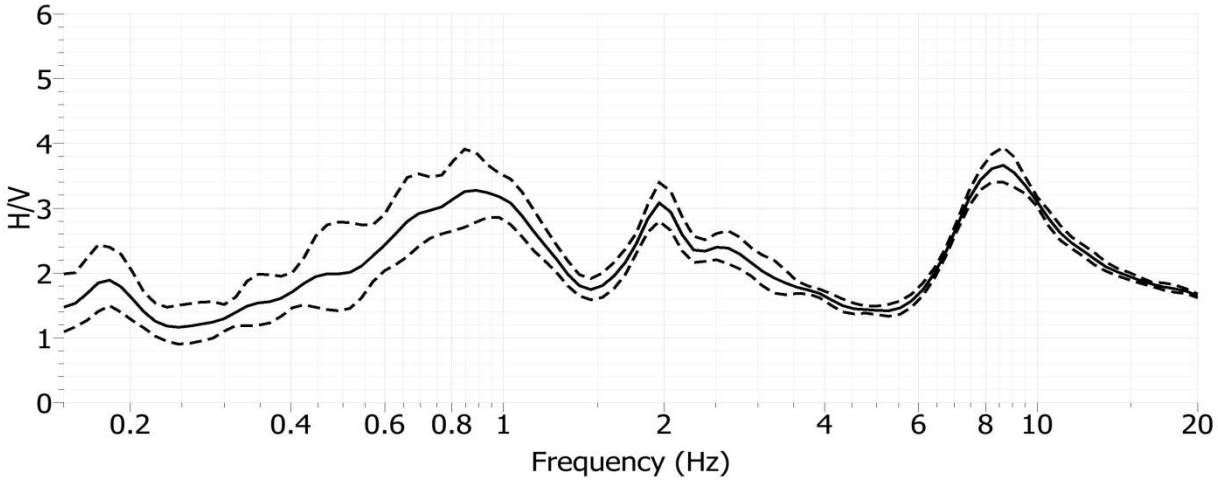

Site CE.24775, H/V Spectral Ratio, East Side of Bridge, Sensor 453

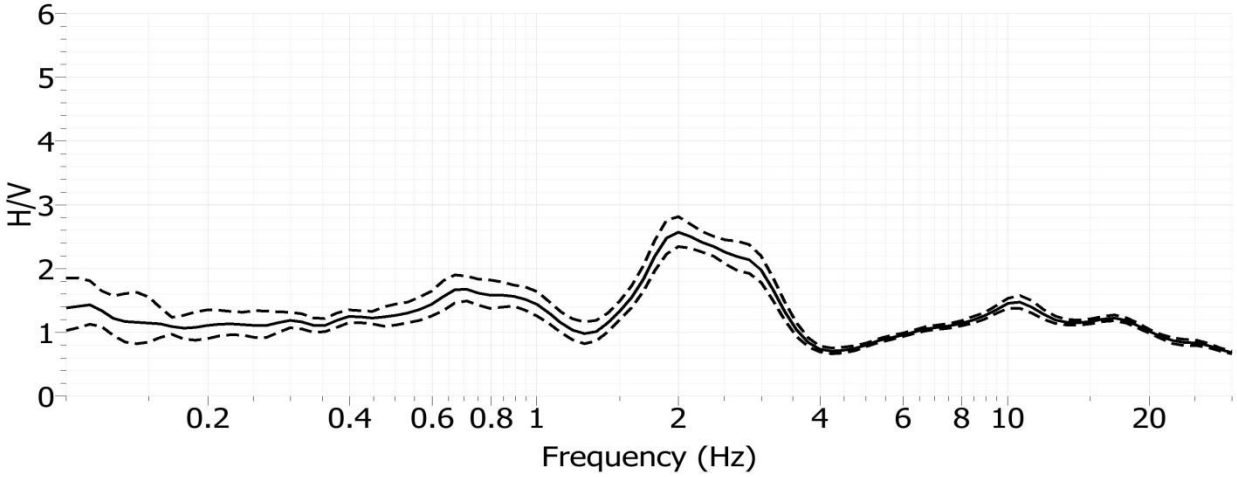

Site CE.24775, H/V Spectral Ratio, Sensor 453B

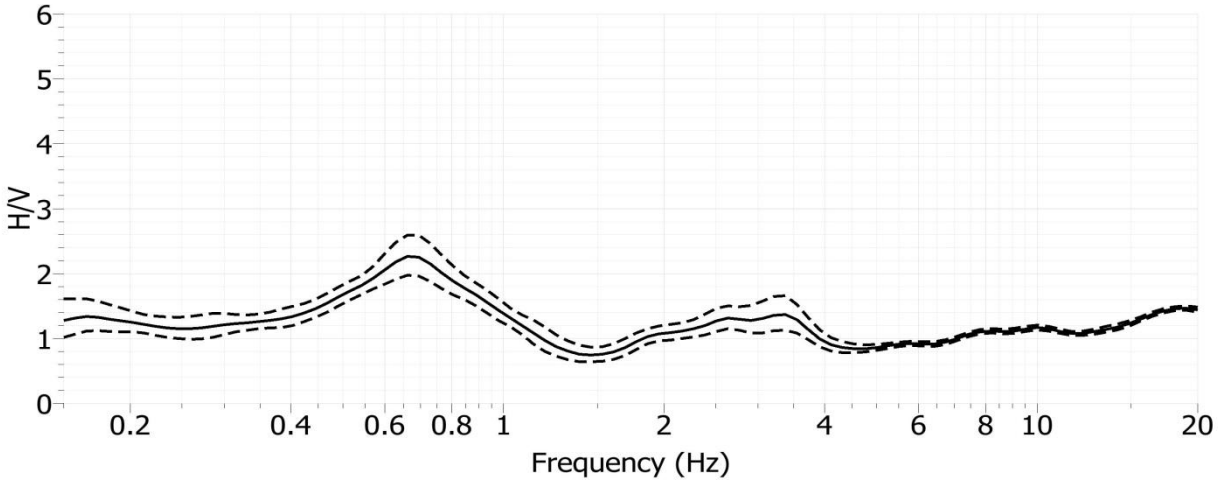

Site CE.24775, H/V Spectral Ratio, West Side of Bridge, Sensor 450

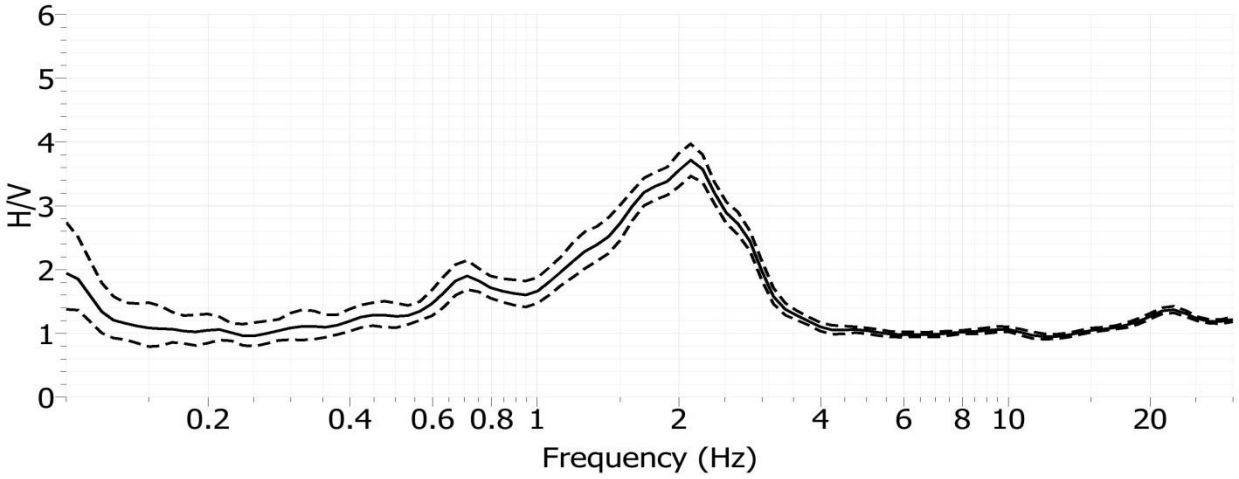

Site CE.24775, H/V Spectral Ratio, Sensor 450B

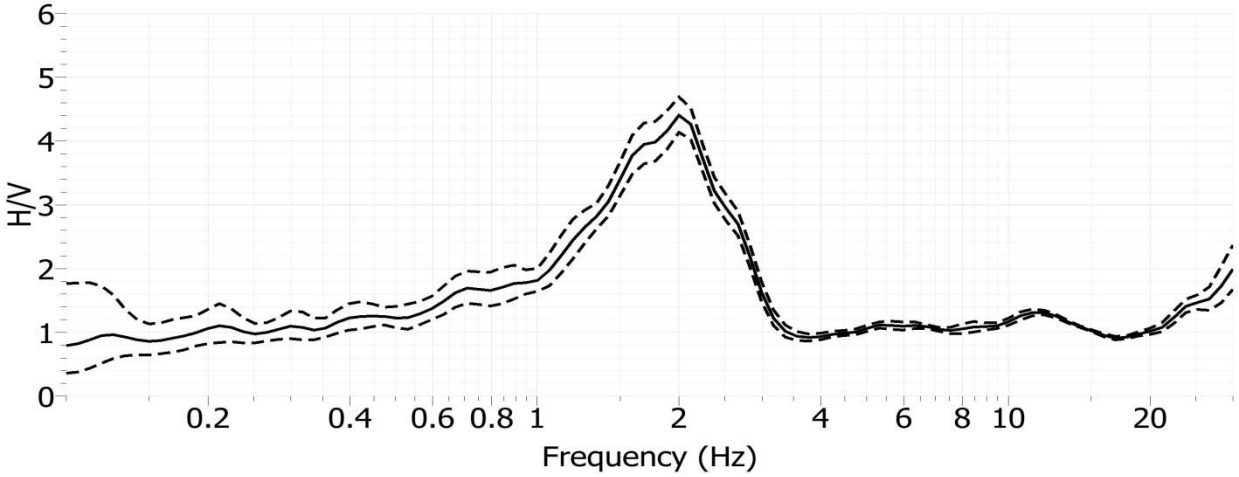

Site CE.24775, H/V Spectral Ratio, Array 24775-1, Sensor 450A

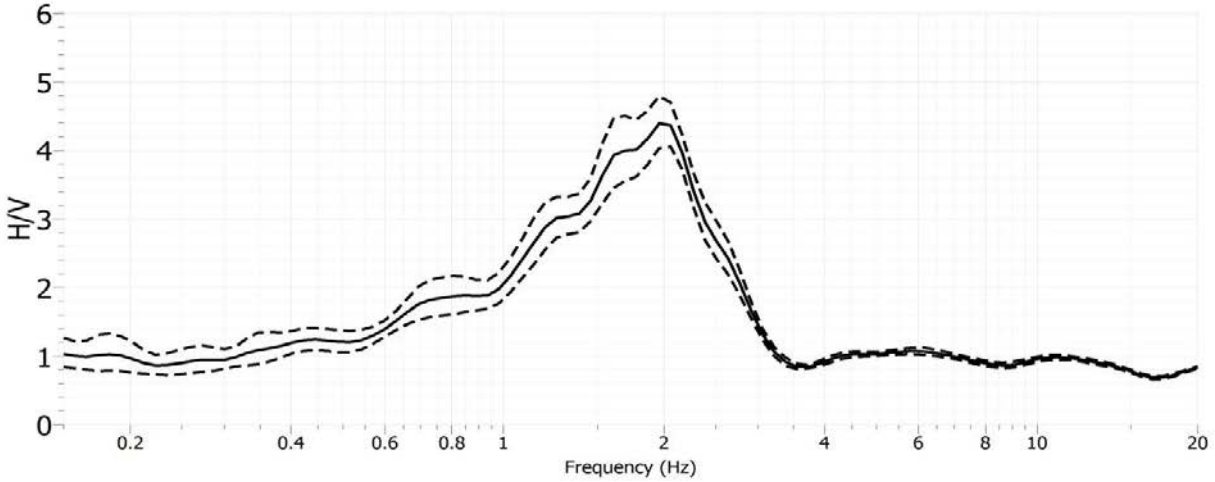

Site CE.24775, H/V Spectral Ratio, Array 24775-1, Sensor 507

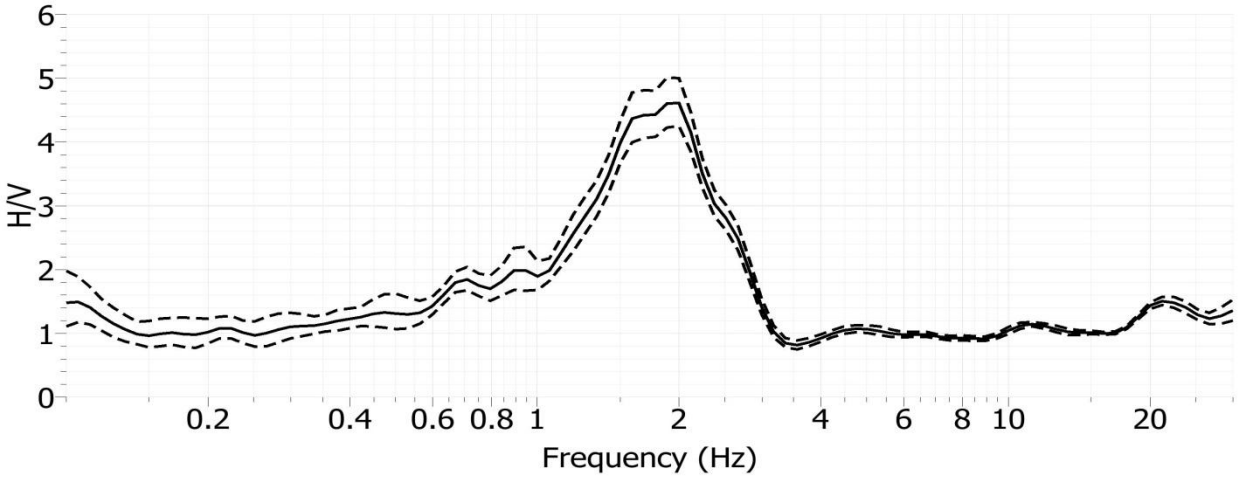

Site CE.24775, H/V Spectral Ratio, Array 24775-1, Sensor 453A

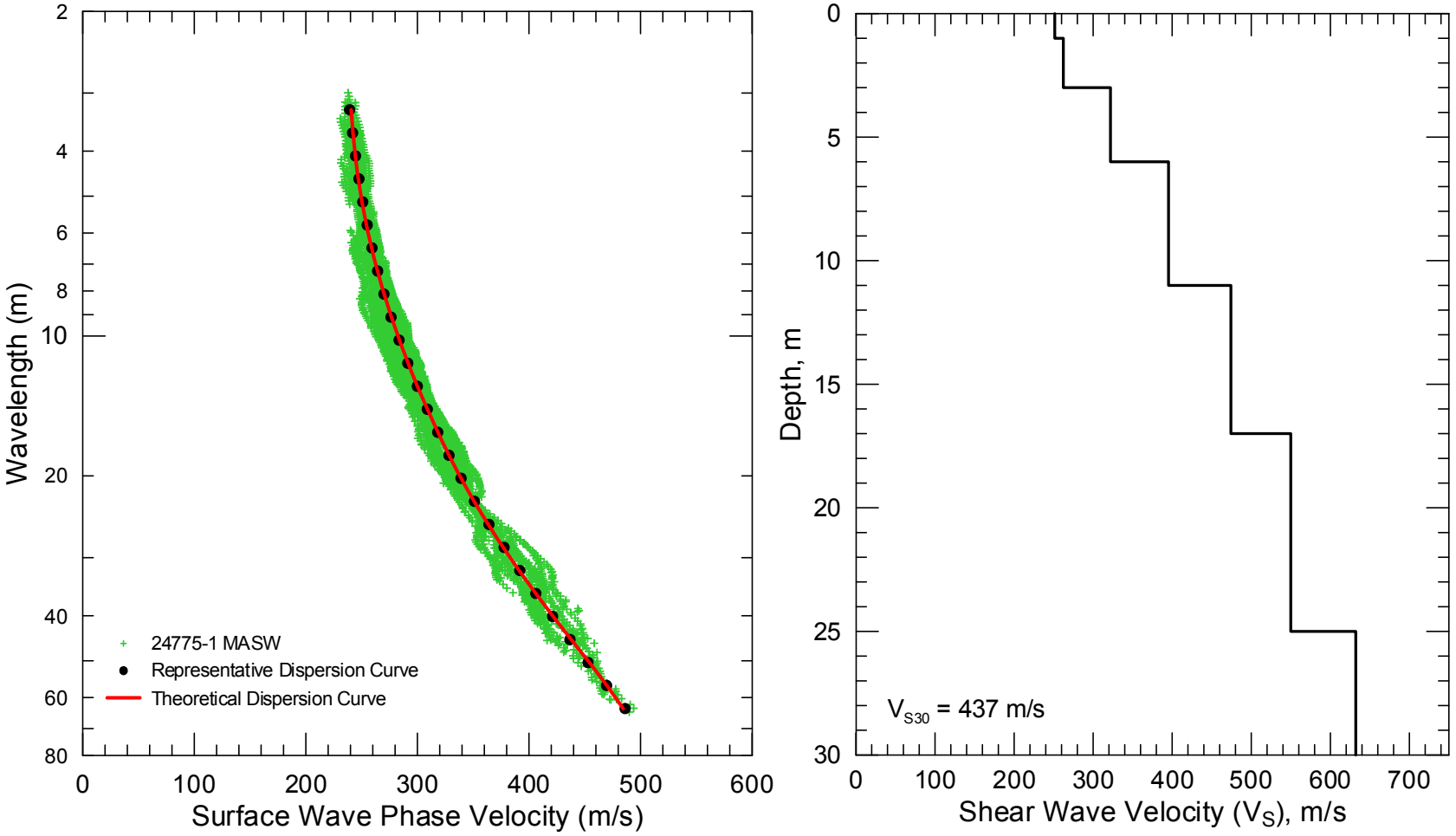

CE.24775 - Field, representative and inverted theoretical surface wave dispersion data (left) and associated V_S model (right)

Site CE.24965

Location: Domenic Massari Park, 37716 55th Street East, Palmdale, California

Latitude: 34.57020 **Longitude:** -118.02999

(Station coordinates modified using published coordinates from http://www.strongmotioncenter.org with further adjustment made by identifying the structure housing the seismic sensor on Google Earth)

V_{S30} (measured): 326 m/s

V_{S30} (adjusted to more accurately reflect seismic station conditions): 326 m/s (no adjustment necessary)

NEHRP Site Class: D

Geomatrix Code: AHD

Geologic Conditions/Observations: Site located in area mapped as Quaternary (Holocene) young alluvial fan deposits. Bedrock is about 55 m deep based on HVSR and surface wave data.

Site Conditions: Urban site with significant traffic noise from nearby roads. Relatively flat terrain in site vicinity.

Geophysical Methods Utilized: HVSR, MASW, array microtremor, ReMi™

Geophysical Testing Arrays:

1. Arrays 24965-1 (24 channel linear array utilizing 4.5 Hz vertical geophones spaced 5 m apart for an array length of 115 m) and 24965-2 (24 channel linear array utilizing 4.5 Hz vertical geophones spaced 4 m apart for an array length of 92 m) used to acquire passive surface wave data. Arrays combined to form an "L" shaped array.
2. Array 24965-3 (48 channel MASW array utilizing 4.5 Hz vertical geophones spaced 1.5 m apart for a length of 70.5 m, forward and reverse shot locations with multiple source offsets and source types (hammers only) and center shot location).
3. Three HVSR measurement locations distributed along array 24965-3.

Legend

- Seismic Station - Approximate Improved Location
- Seismic Station - Approximate Location of Record
- H/V Spectral Ratio Measurement Location
- MASW Array
- Passive Surface Wave Array

NOTES:
1. WGS 1984 COORDINATE SYSTEM
2. Image Source: ESRI, i-cubed, USDA FSA, USGS, AEX, GeoEye, Getmapping, Aerogrid, IGP

File Name: CE-24965-I

Date: 2/7/2013

USGS science for a changing world

GEOVision geophysical services

RECOVERY.GOV

SITE MAP
CE•24965

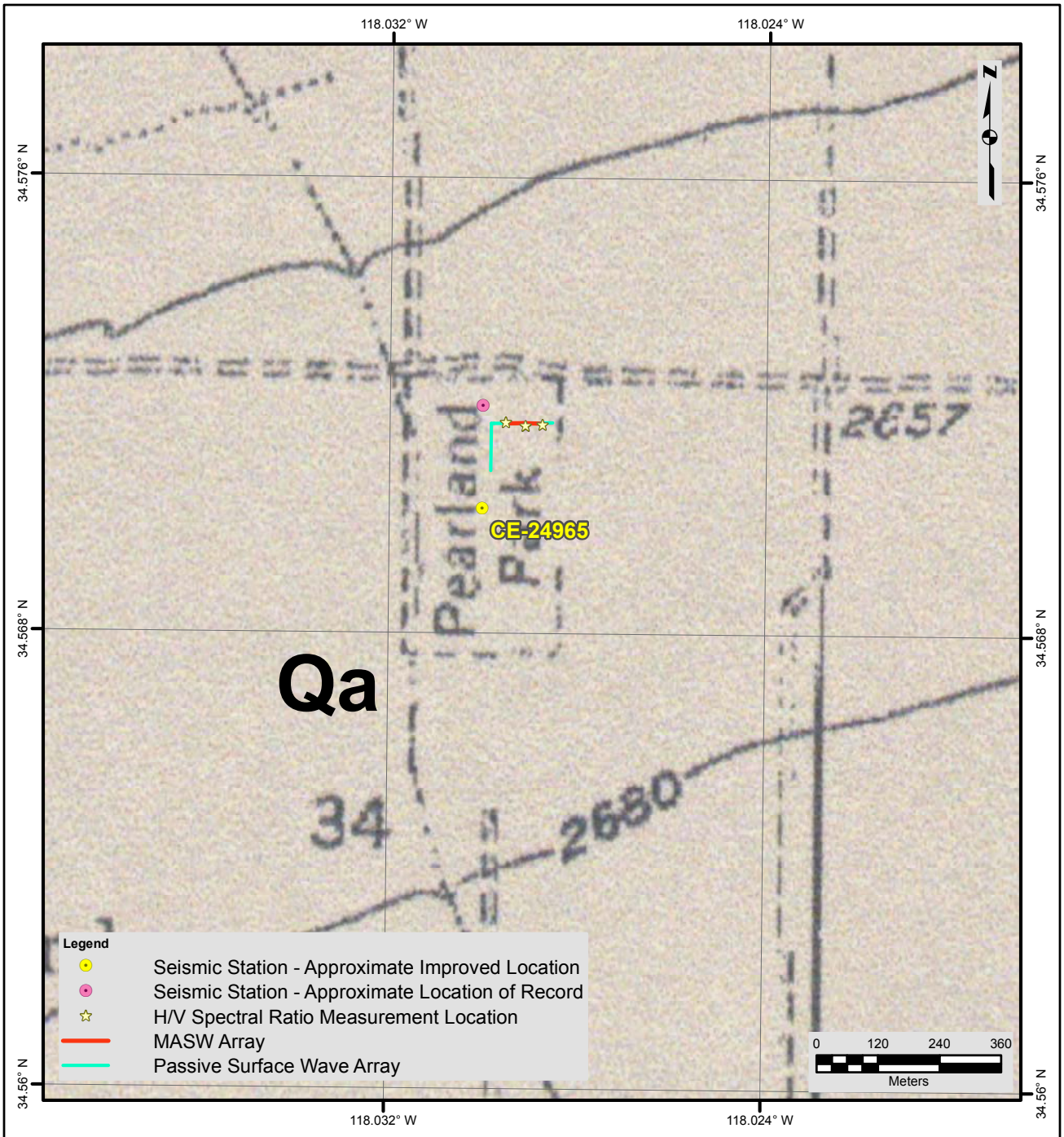

Description of Geologic Map Units

Qa = Quaternary (Holocene) alluvial gravel, sand and silt

NOTES:
1. WGS 1984 COORDINATE SYSTEM
2. Geologic Map of the Lancaster & Alpine Butte 15 Minute Quadrangles, Los Angeles County, California by Thomas W. Dibblee, Jr., 2008
3. See site map for details of geophysical survey

File Name: CE-24965

Date: 5/26/2011

USGS science for a changing world

GEOVision geophysical services

RECOVERY.GOV

GEOLOGIC MAP
CE•24965

Looking west at HVSR sensor 450 and passive surface wave array 24965-1

Looking northeast at HVSR sensor 453

Looking east towards HVSR sensor 507 and passive surface wave array 24965-1

MASW data acquisition along array 24965-3

Looking east along MASW array 24965-3

Location of Geophysical Testing Arrays:

Location	Latitude	Longitude
24965-1, East End of Array, Channel 1	34.57170	-118.02852
24965-1, West End of Array, Channel 24	34.57168	-118.02976
24965-2, North End of Array, Channel 25	34.57169	-118.02982
24965-2, South End of Array, Channel 48	34.57086	-118.02982
24965-3, West End of Array	34.57169	-118.02950
24965-3, Center of Array	34.57170	-118.02911
24965-3, East End of Array	34.57169	-118.02873
HVSR Sensor 507	34.57171	-118.02951
HVSR Sensor 453	34.57165	-118.02909
HVSR Sensor 450	34.57167	-118.02873

Notes: 1) WGS84 Coordinate System (decimal degrees)
2) Survey accuracy is estimated at 1 to 2 m

Results:

V_S Model

Depth to Top of Layer (m)	Layer Thickness (m)	S-Wave Velocity (m/s)	Inferred P-Wave Velocity (m/s)	Inferred Poisson's Ratio	Inferred Density (g/cm^3)
0	1	145	271	0.30	1.90
1	2	182	341	0.30	1.90
3	3	243	454	0.30	1.90
6	4	357	668	0.30	1.90
10	6	388	726	0.30	1.95
16	9	393	735	0.30	2.00
25	12	413	772	0.30	2.00
37	18	434	812	0.30	2.00
55	>20	1342	2510	0.30	2.50

Notes: 1) Depth of investigation is about 75 m.
2) Bottom layer is a half space.
3) Half space velocity not well resolved.

Observations/Discussion:

- The HVSR curves are almost identical, validating the 1-D velocity structure assumption.
- High amplitude HVSR peak at 1.6 Hz indicative of significant impedance contrast (i.e. bedrock) at depth of less than about 100 m.
- Noise conditions at site (multi-directional or omni-directional noise sources) appeared sufficient for successful application of passive surface wave techniques.
- Surface wave dispersion data from active and passive surface wave data sets are in good agreement at this site.
- ESAC technique used to extract surface wave dispersion data from passive "L" array data. Both the ReMi™ and ESAC techniques used to extract surface wave dispersion data from the linear arrays.
- Representative dispersion curves were generated for each surface wave data set using a moving average, polynomial curve fitting routine. These individual representative dispersion curves were combined and a representative dispersion curve generated for the combined data set for data modeling.
- Based on simple layer-based analysis of seismic refraction first arrival data, P-wave velocity in the upper 15 m ranges from about 275 m/s near the surface to 750 m/s at a depth on the order of 5 m. Possible reflector at a depth of 25 to 30 m, but not conclusively associated with water table.
- Surface wave depth of investigation is about 75 m based on half of maximum wavelength criteria and assuming that surface wave dispersion data at frequencies as low as 3.5 Hz are valid utilizing 4.5 Hz geophones (low frequency geophone phase response differences may cancel out, to a certain degree, if noise is omni-directional and/or the phase response differences are random in nature).
- A large impedance contrast, likely associated with bedrock, is modeled at a depth of about 55 m and is consistent with the 1.6 Hz HVSR peak. Predicted HVSR peak from surface wave V_S model using the quarter wavelength approximation (predicted fundamental frequency equal to average V_S of the sediments divided by 4 times the bedrock depth) is about 1.66 Hz. The modeled HVSR peak, however, is at a much higher frequency of about 2.6 Hz.
- Joint modeling/inversion of the surface wave and HVSR data may improve the accuracy of the S-wave velocity model.
- Nonuniqueness of the V_S model is such that the modeled depth to the bedrock unit (half space) is only accurate to about 20% of depth. Additionally, the modeled S-wave velocity of the bedrock unit is not well constrained and may be much higher than modeled.
- V_{S30} is 326 m/s (NEHRP Site Class D).
- Average S-wave velocity of the upper 50 m (V_{S50}) is 360 m/s.

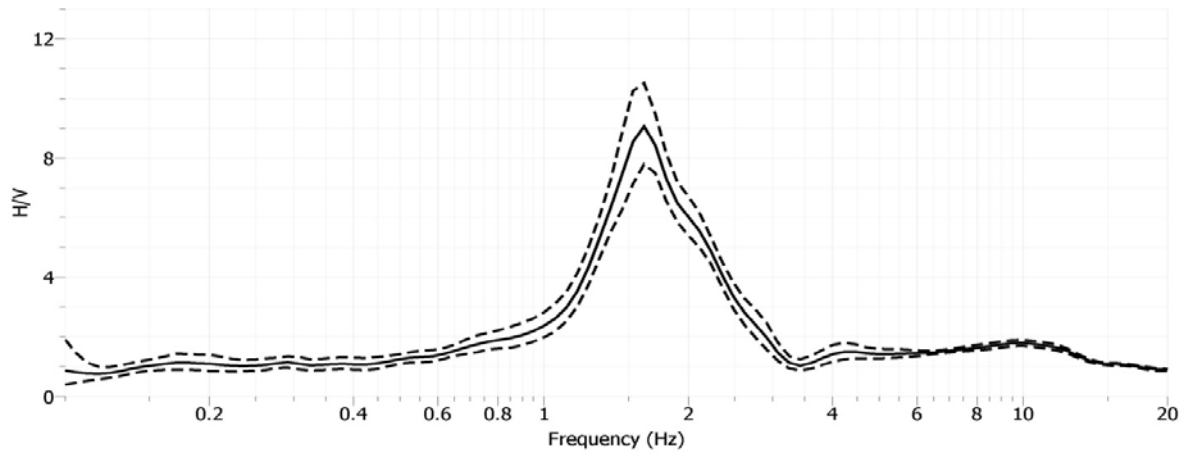

Site CE.24965, H/V Spectral Ratio, Array 24965-3, Sensor 507

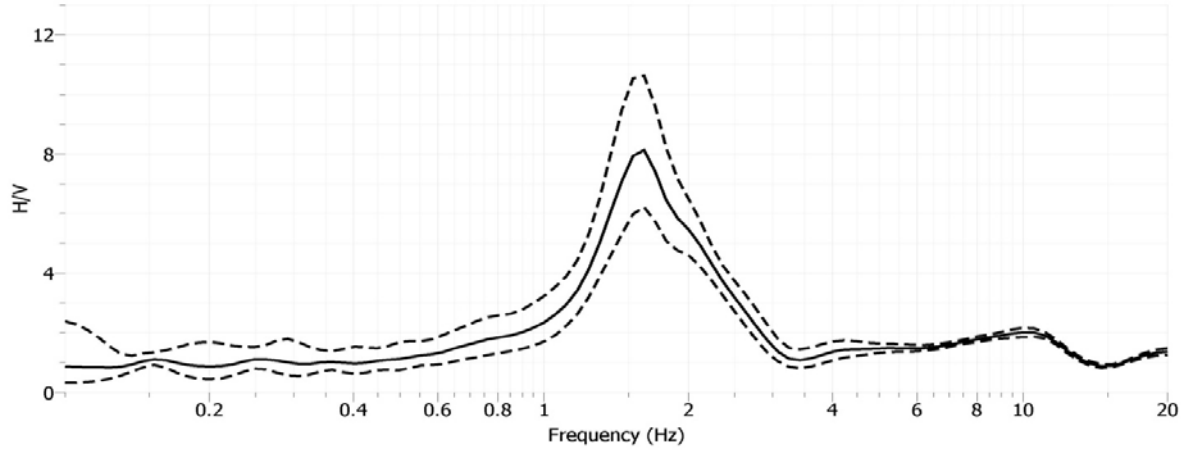

Site CE.24965, H/V Spectral Ratio, Array 24965-3, Sensor 453

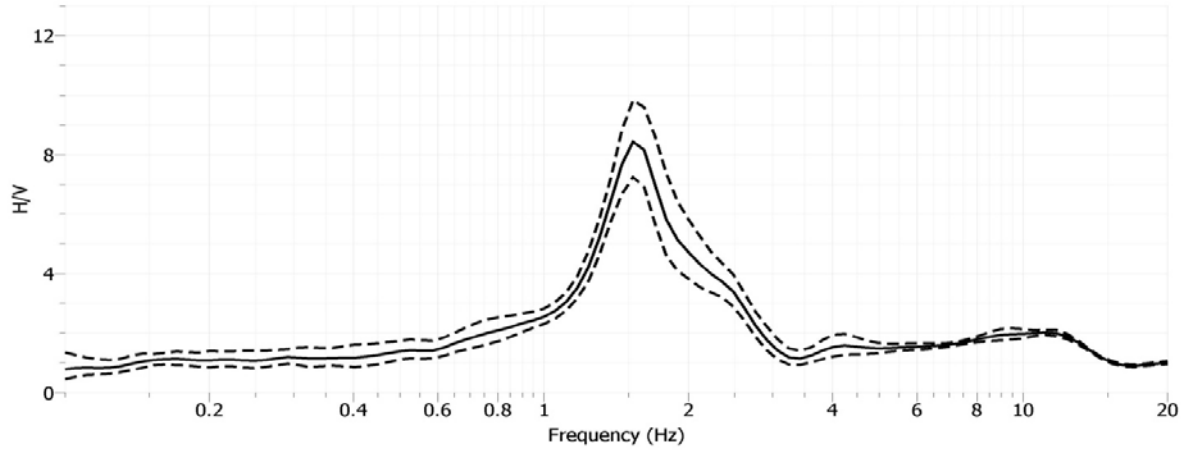

Site CE.24965, H/V Spectral Ratio, Array 24965-3, Sensor 450

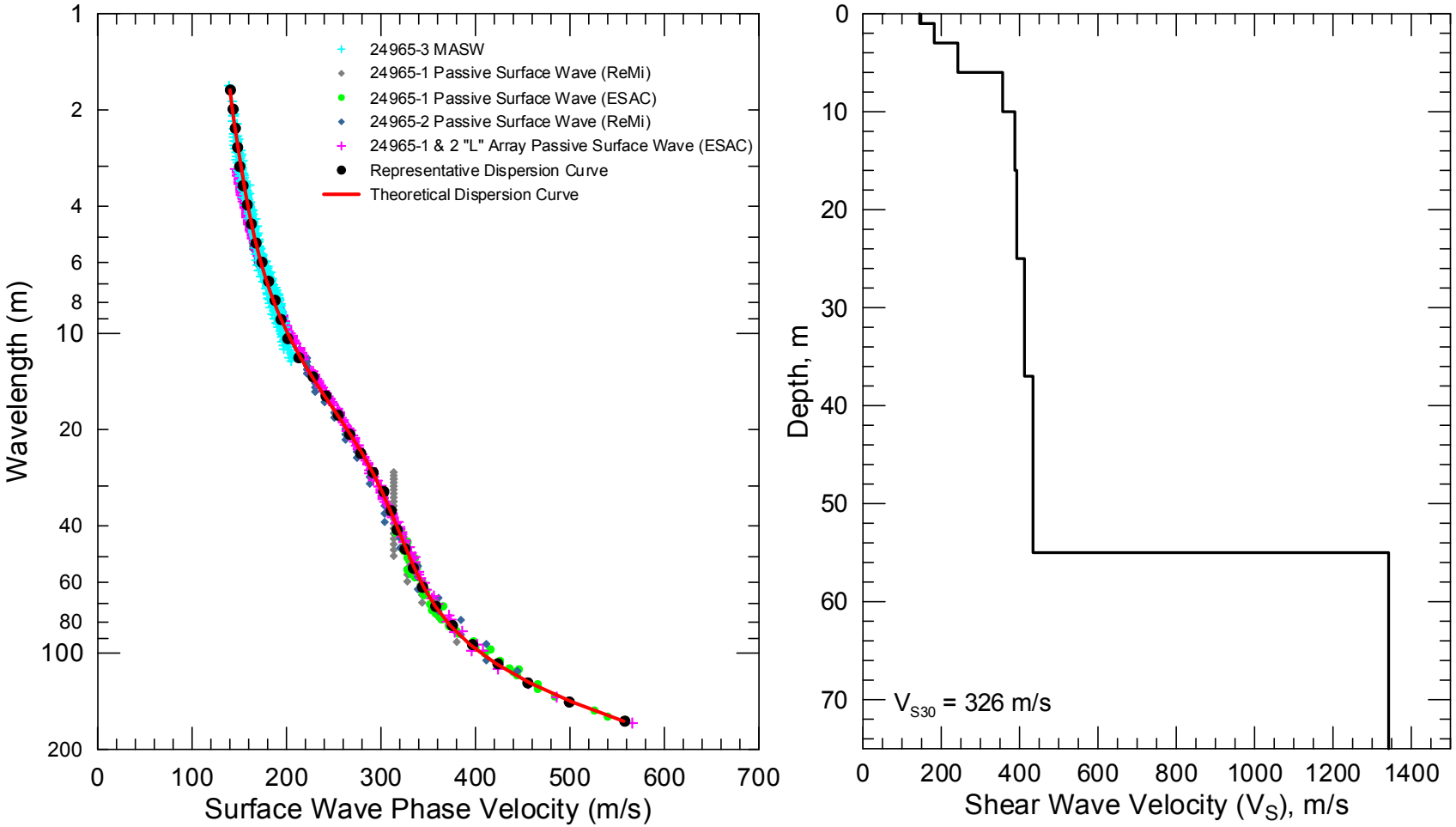

CE.24965 - Field, representative and inverted theoretical surface wave dispersion data (left) and associated V_S model (right)

Site CE.24967

Location: Marie Kerr Park, 39700 30th Street West, Palmdale, California

Latitude: 34.60335 **Longitude:** -118.18212

(Station coordinates modified using published coordinates from http://www.strongmotioncenter.org with further adjustment made by identifying the structure housing the seismic sensor on Google Earth or ESRI Imagery, WGS84 coordinate system)

V_{S30} (measured): 330 m/s

V_{S30} (adjusted to more accurately reflect seismic station conditions): 330 m/s (no adjustment necessary)

NEHRP Site Class: D

Geomatrix Code: AHD

Geologic Conditions/Observations: Site located in area mapped as Quaternary (Holocene) alluvium. Bedrock is about 60 m deep (± 20%) based on surface wave data.

Site Conditions: Urban site with significant traffic noise from nearby roads. Relatively flat terrain in site vicinity.

Geophysical Methods Utilized: HVSR, MASW, array microtremor, ReMi™

Geophysical Testing Arrays:

1. Arrays 24967-1 (24 channel linear array utilizing 4.5 Hz vertical geophones spaced 5 m apart for an array length of 115 m) and 24967-2 (24 channel linear array utilizing 4.5 Hz vertical geophones spaced 3.5 m apart for an array length of 80.5 m) used to acquire passive surface wave data. Arrays combined to form an "L" shaped array.
2. Array 24967-3 (48 channel MASW array utilizing 4.5 Hz vertical geophones spaced 1.5 m apart for a length of 70.5 m, forward and reverse shot locations with multiple source offsets and source types (hammers only) and center shot location).
3. Three HVSR measurement locations; two in the vicinity of arrays 24967-1 and 24967-2 and one near the seismic station.

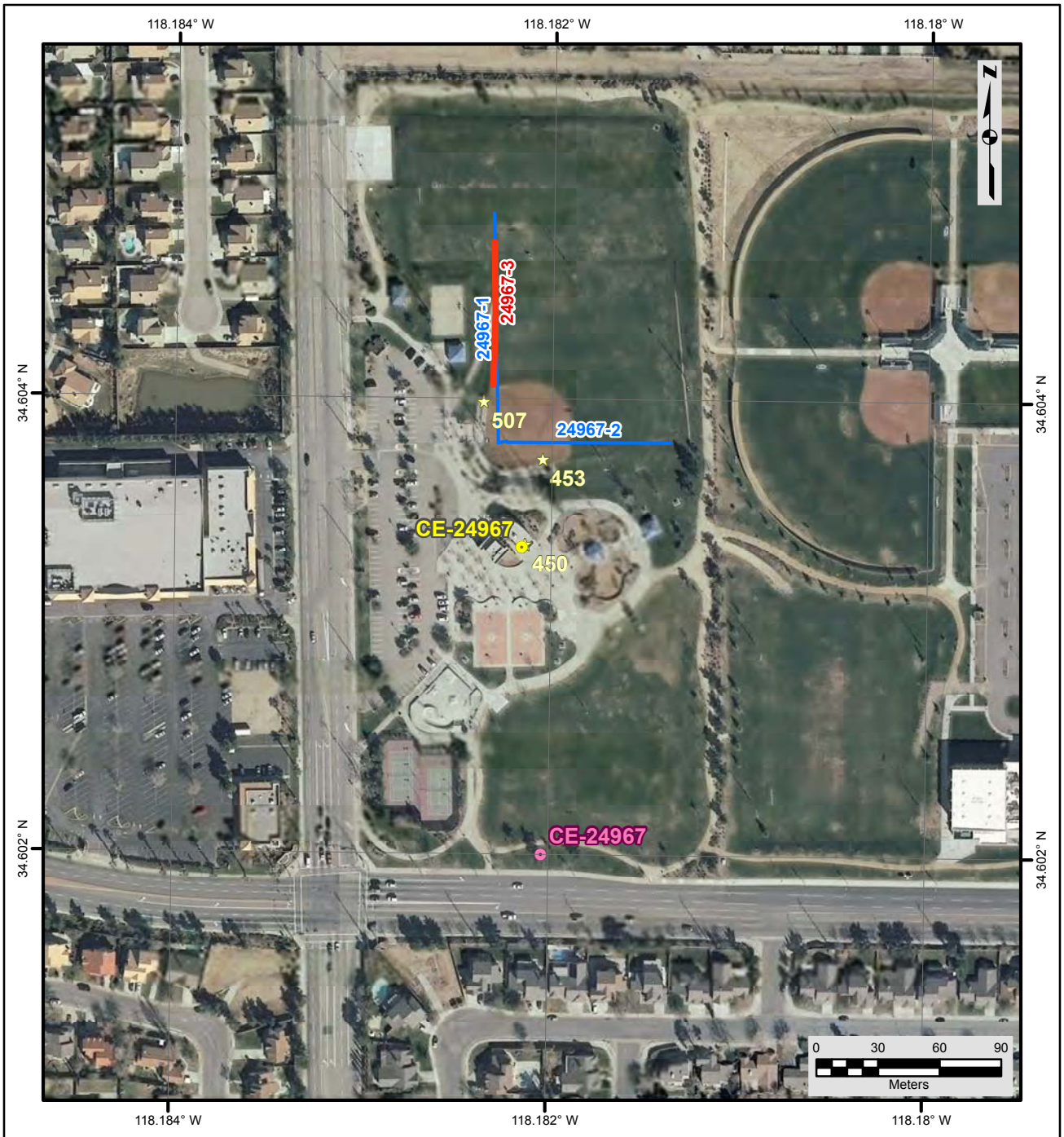

Legend

- Seismic Station - Approximate Improved Location
- Seismic Station - Approximate Location of Record
- H/V Spectral Ratio Location
- MASW Array
- Passive Surface Wave Array

NOTES:
1. WGS 1984 COORDINATE SYSTEM
2. Image Source: ESRI, i-cubed, USDA FSA, USGS, AEX, GeoEye, Getmapping, Aerogrid, IGP

File Name: CE-24967-I

Date: 10/14/2011

USGS science for a changing world

GEOVision geophysical services

RECOVERY.GOV

SITE MAP
CE•24967

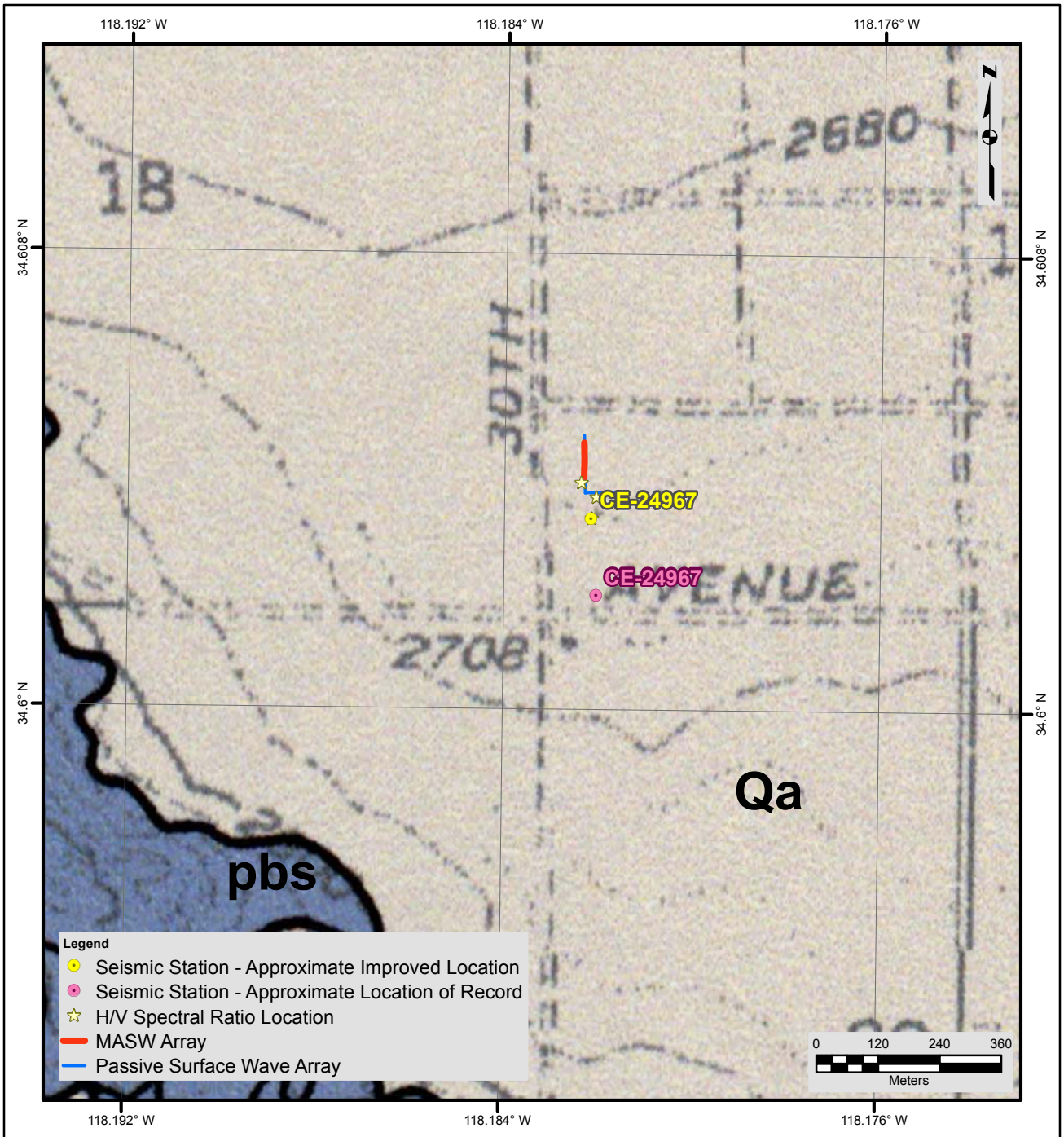

Description of Geologic Map Units

Qa = Quaternary (Holocene) alluvial gravel, sand and silt
pbs = Precambrian (?) biotite schist, fine- to medium-grained

NOTES:
1. WGS 1984 COORDINATE SYSTEM
2. Geologic Map of the Lancaster & Alpine Butte 15 Minute Quadrangles, Los Angeles County, California by Thomas W. Dibblee, Jr., 2008
3. See site map for details of geophysical survey

File Name: CE-24967

Date: 10/14/2011

USGS science for a changing world

GEOVision geophysical services

RECOVERY.GOV

GEOLOGIC MAP
CE•24967

CE.24967 seismograph station and HVSR Sensor 450

MASW data acquisition along 24967-3 array

Looking north at HVSR Sensor 507

Looking north along passive surface wave array 24967-1

Looking south along the MASW array 24967-3

Location of Geophysical Testing Arrays:

Location	Latitude	Longitude
24967-1, North End of Array, Channel 1	34.60481	-118.18229
24967-1, South End Array, Channel 24	34.60381	-118.18225
24967-2, West End of Array, Channel 25	34.60381	-118.18221
24967-2, East End of Array, Channel 48	34.60381	-118.18133
24967-3, South End of Array	34.60406	-118.18228
24967-3, Center of Array	34.60437	-118.18227
24967-3, North End of Array	34.60468	-118.18228
HVSR Sensor 507	34.60399	-118.18233
HVSR Sensor 453	34.60373	-118.18201
HVSR Sensor 450[3]	34.60336	-118.18210
CE.24967 Seismic Station[3]	34.60335	-118.18212

Notes: 1) WGS84 Coordinate System (decimal degrees)
2) Survey accuracy is estimated at 2 to 3 m.
3) CE.24967 seismic station and HVSR sensor were not surveyed with GPS (inside a structure) and locations were estimated based on field observations and ESRI Imagery or Google Earth.

Results:

V_S Model (Bedrock at 60 m depth)

Depth to Top of Layer (m)	Layer Thickness (m)	S-Wave Velocity (m/s)	Inferred P-Wave Velocity (m/s)	Assumed Poisson's Ratio	Assumed Density (g/cm^3)
0	3	215	403	0.3	1.7
3	3	248	464	0.3	1.8
6	10	332	622	0.3	1.8
16	12	390	730	0.3	1.9
28	15	489	915	0.3	2
43	17	614	1149	0.3	2.1
60	>20	2233	4178	0.3	2.5

Notes: 1) Depth of investigation is about 80 m.
2) Bottom layer is a half space.
3) Bedrock depth and velocity not well constrained and may vary by 20%, or more.

Observations/Discussion:

- HVSR measurements were made in a relatively small area as permission was not obtained to dig small holes in the playing fields at Marie Kerr Park. In retrospect, it would have been better to have covered a larger area with the HVSR measurements by placing them around the perimeter of the park.
- The HVSR curves are almost identical, validating the 1-D velocity structure assumption.
- All HVSR plots show a well defined peak at 2 Hz indicative of significant impedance contrast (i.e. bedrock) within the expected depth of investigation of the active and passive surface wave sounding. HVSR data quality is best for sensor 453.
- Based on simple layer-based analysis of seismic refraction first arrival data, P-wave velocity in the upper 15 m ranges from about 450 m/s near the surface to about 600 to 650 m/s below a depth of 6 to 8 m. There is a probable reflector at a depth on the order of 40 m. This reflector could be associated with bedrock, water table or some other geologic unit.
- Noise conditions at site (multi-directional or omni-directional noise sources) appeared sufficient for successful application of passive surface wave techniques.
- ESAC technique used to extract surface wave dispersion data from passive "L" array data. Both the ReMi™ and ESAC techniques used to extract surface wave dispersion data from the linear arrays. All passive surface wave dispersion data are in good agreement and were used for analysis.
- MASW data acquisition was limited to hammer sources and, given the noise levels at the site and type of energy source, surface wave phase velocities are likely only accurate to a wavelength of about 40 m, corresponding to a frequency of about 7.5 Hz. MASW surface wave dispersion data were, however, extracted to a maximum wavelength of about 52 m, corresponding to a frequency of about 6.5 Hz, because the data were in acceptable agreement with the passive surface wave data.
- Surface wave dispersion data from active and passive surface wave data sets are in good agreement over the approximate 8 to 52 m overlapping wavelength range.
- Representative dispersion curves were generated for each surface wave data set using a moving average, polynomial curve fitting routine. These individual representative dispersion curves were combined and a representative dispersion curve generated for the combined data set for data modeling.
- A saturated sediment layer was not used for modeling, although a possible seismic reflector indicates that the saturated zone, or alternatively bedrock, may be located at a depth on the order of 40 m.
- Surface wave depth of investigation is about 75 m based on half of maximum wavelength criteria and assuming that surface wave dispersion data at frequencies as low as 3.5 Hz are valid utilizing 4.5 Hz geophones (low frequency geophone phase response differences will cancel out if noise is omni-directional and/or the phase response differences are random in nature).
- The S-wave velocity and depth of the bedrock unit is not well constrained. Sites with large impedance contrasts can exhibit some of the most severe non-uniqueness in surface wave modeling. Equivalent models with bedrock depth varying from 45 to 70 m and similar RMS error are presented. The lowest RMS errors occur for modeled bedrock

depths in the 55 to 65 m range. The V_S models indicate that bedrock depth may vary by as much as 20%, while still yielding realistic velocities for the overlying sediments and bedrock units. It is expected that crystalline bedrock at a depth of greater than 50 m would be relatively unweathered with P-wave velocities in the 3,000 to 4,500 m/s range being realistic.

- A large increase in V_S associated with bedrock is modeled at a depth of about 45 to 70 m. Predicted HVSR peaks from these models are between 1.6 Hz (70 m depth to bedrock) and 2 Hz (45 m depth to bedrock) using the quarter wavelength approximate relationship between fundamental soil resonance frequency, bedrock depth and average S-wave velocity for a simple two layer model. HVSR modeling using the S-wave velocity models predicts higher frequency HVSR peaks in the 2.5 to 3 Hz range. The measured HVSR peak of 2 Hz is intermediate to that based on the quarter wavelength approximate and HVSR modeling.
- The V_S model presented herein has bedrock at an intermediate depth of 60 m, the average depth of the effectively equivalent V_S models.
- V_{S30} is 330 m/s for the model presented (NEHRP Site Class D).
- V_{S30} is between 324 and 335 for the equivalent V_S models.
- Average S-wave velocity of the upper 80 m for the model presented (V_{S80}) is 519 m/s.
- V_{S80} is between 505 and 537 m/s for the equivalent models.

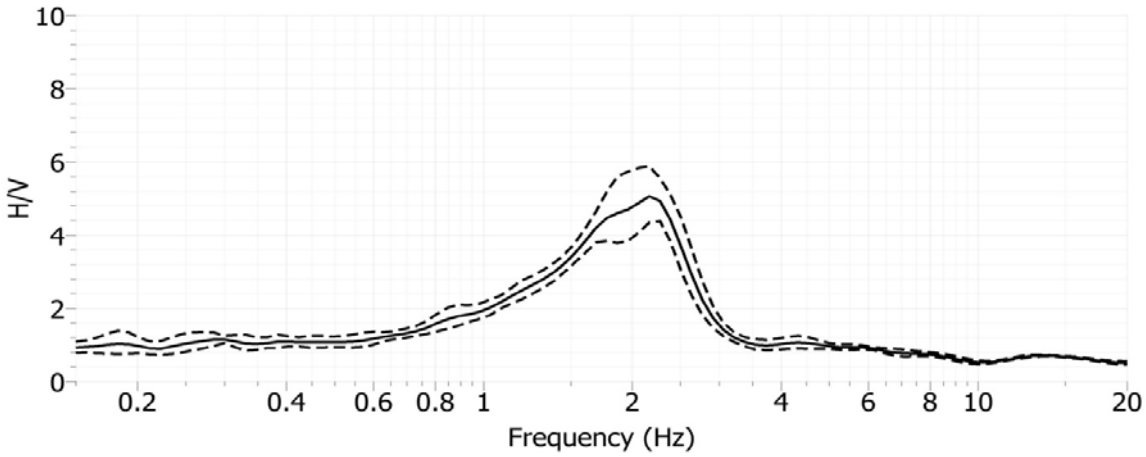

Site CE.24967, H/V Spectral Ratio, Array 24967-1, Sensor 507

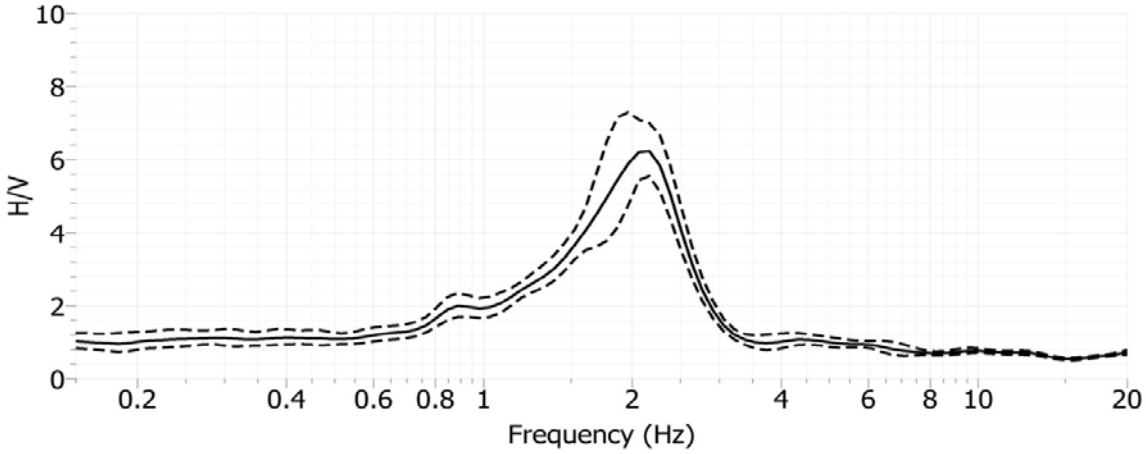

Site CE.24967, H/V Spectral Ratio, Array 24967-2, Sensor 453

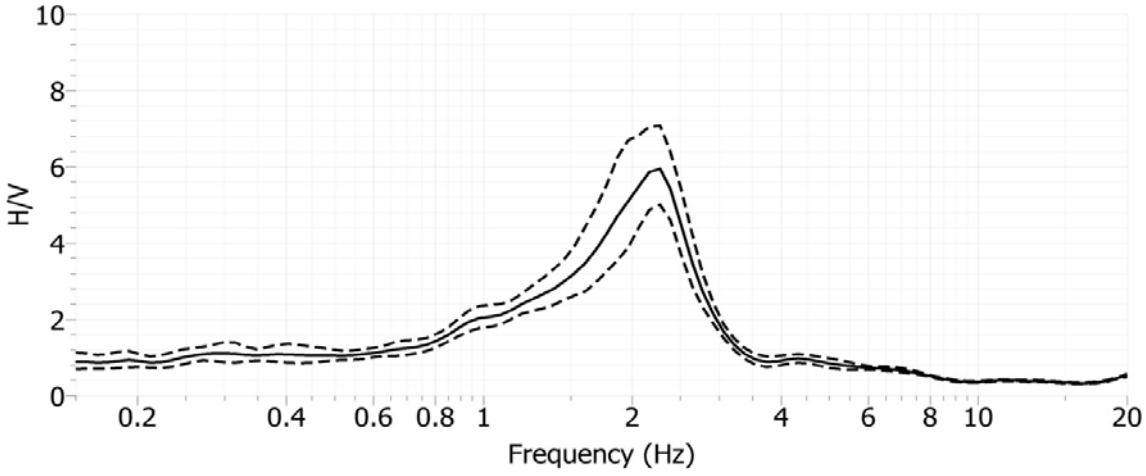

Site CE.24967, H/V Spectral Ratio, Near Seismic Station, Sensor 450

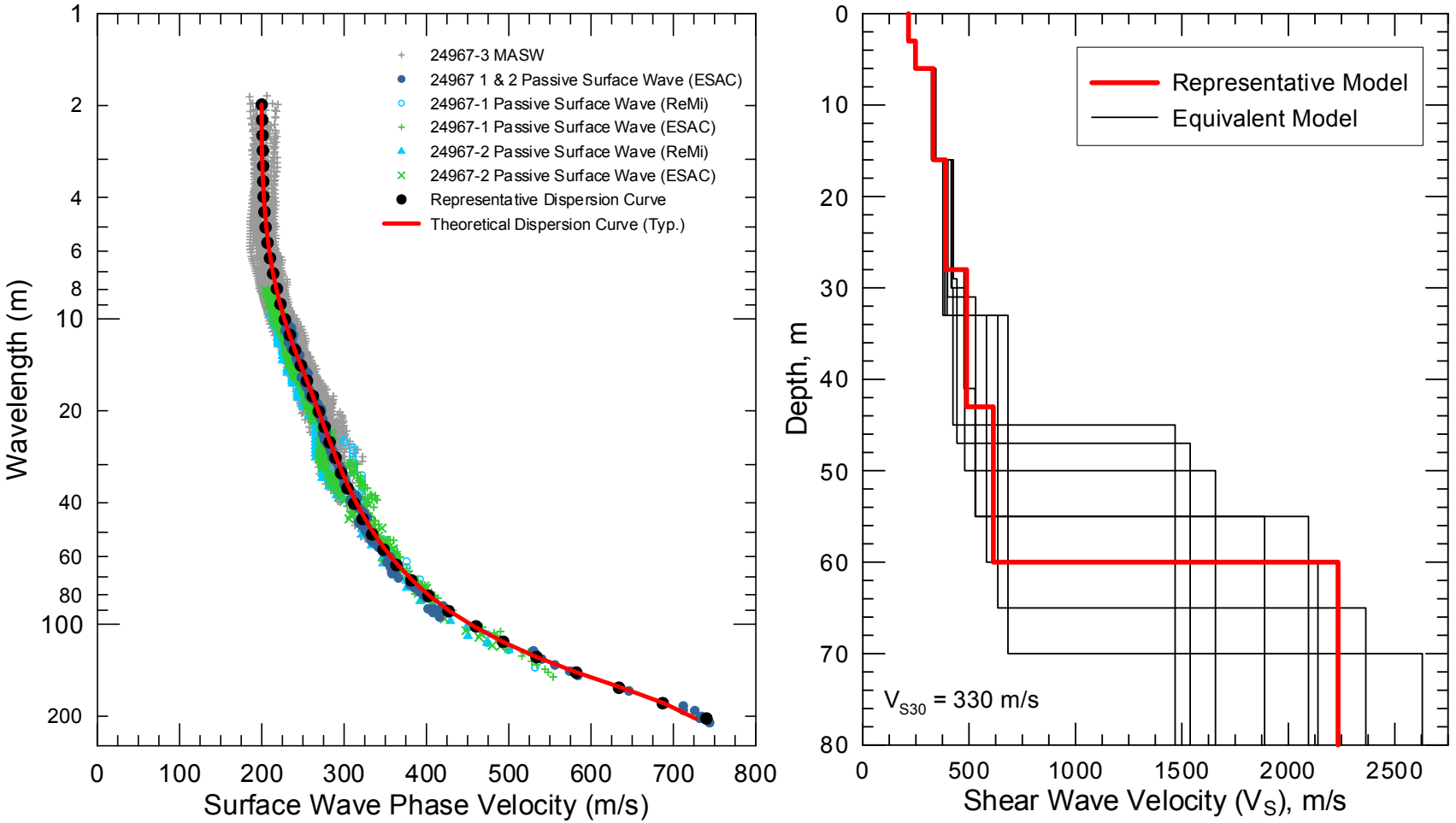

CE.24967 - Field, representative and inverted theoretical surface wave dispersion data (left) and associated V_S model (right)

Site CE.65097

Location: Antelope Valley Fire Department, Walker, Mono County, California

Latitude: 38.51455 **Longitude:** -119.47973
(Station coordinates modified using published coordinates from http://www.strongmotioncenter.org with further adjustment made by identifying the structure housing the seismic sensor on Google Earth, WGS84 coordinate system)

V_{S30} (measured): 415 m/s

V_{S30} (adjusted to more accurately reflect seismic station conditions): 415 m/s (no adjustment necessary).

NEHRP Site Class: C

Geomatrix Code: AHD/AQD

Geologic Conditions/Observations: Quaternary (Holocene and Pleistocene) alluvial fan deposits. Mountain range composed of Cretaceous granodiorite located about 275 m southwest of site. The Antelope Valley Fault is located along the base of the mountain range and it is, therefore, difficult to predict bedrock depth at the site.

Site Conditions: Rural site with some traffic noise from SR-395, located about 200 m east of site. Relatively flat terrain in immediate site vicinity.

Geophysical Methods Utilized: HVSR, MASW, SASW, array microtremor, ReMi™

Geophysical Testing Arrays:

1. Array 65097-1 (24 channel, linear array utilizing 4.5 Hz vertical geophones spaced 2.75 m apart for a length of 63.25 m) utilized to acquire passive and limited MASW data.
2. Array 65097-1 (SASW array with same midpoint and orientation as passive surface wave and MASW array of same name utilizing 1 Hz vertical geophones and maximum receiver spacing of 30 m).
3. Array 65097-2 (7 channel, triangle passive surface wave array utilizing 1 Hz geophones and a 50 m length for outer side of array).
4. Array 65097-3 (48 channel MASW array utilizing 4.5 Hz vertical geophones spaced 1 m apart for a length of 47 m, forward and reverse shot locations with multiple source offsets and source types and center shot location).
5. Arrays 65097-4 (24 channel linear array utilizing 4.5 Hz vertical geophones spaced 5 m apart for an array length of 115 m) and 65097-5 (24 channel linear array utilizing 4.5 Hz vertical geophones spaced 3 m apart for an array length of 69 m) used to acquire passive surface wave data. Arrays combined to form an “L” shaped array.
6. Eight (8) HVSR measurement locations distributed around the site and made on multiple site visits.

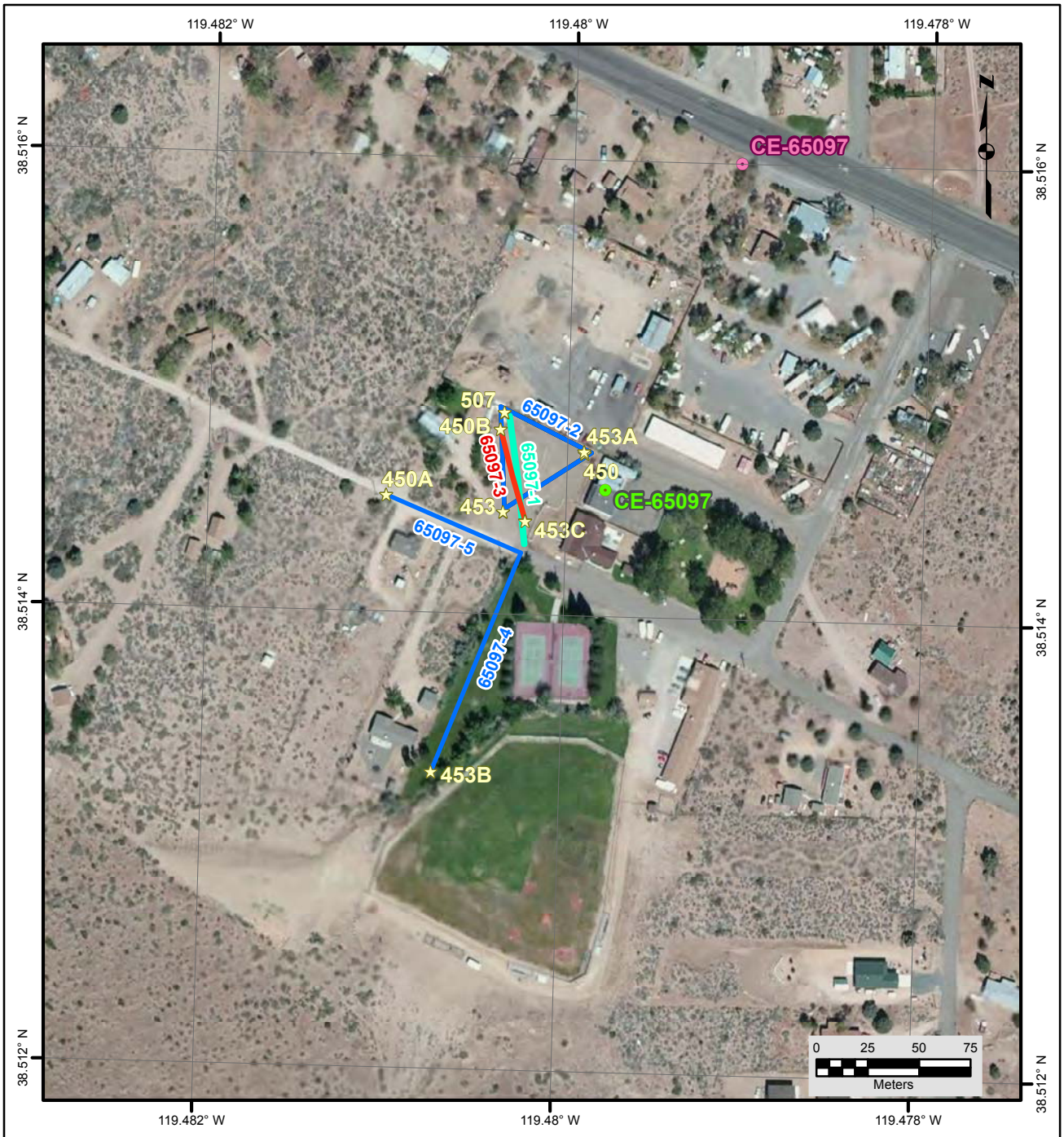

Legend

- Seismic Station - Approximate Improved Location
- Seismic Station - Approximate Location of Record
- H/V Spectral Ratio Location
- Passive Surface Wave Array
- MASW Array
- MASW, SASW and Passive Surface Wave Array

NOTES:
1. WGS 1984 COORDINATE SYSTEM
2. Image Source: ESRI, i-cubed, USDA FSA, USGS, AEX, GeoEye, Getmapping, Aerogrid, IGP

File Name: CE-65097-I

Date: 3/8/2012

USGS science for a changing world

GEOVision geophysical services

RECOVERY.GOV

SITE MAP
CE•65097

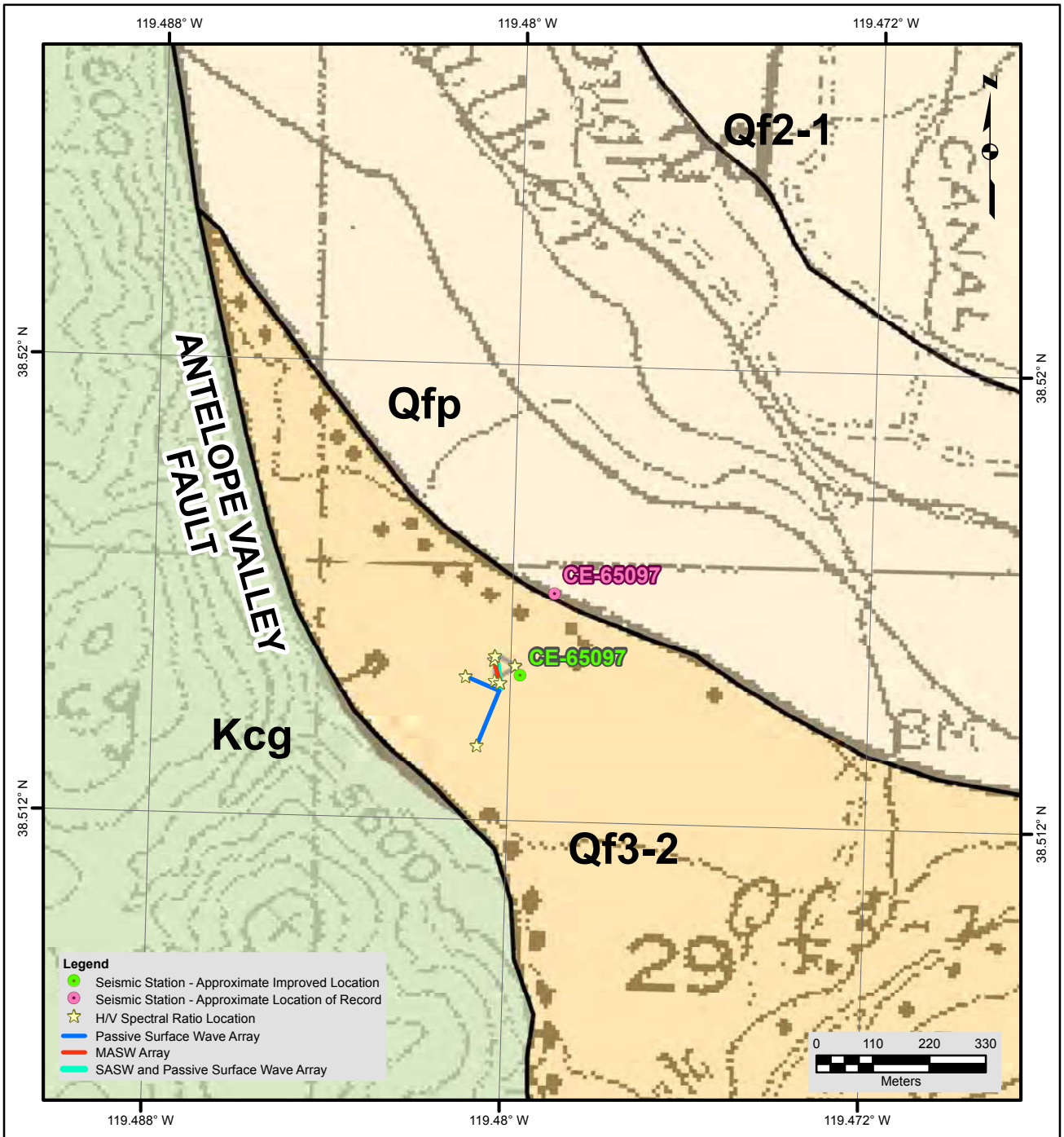

Description of Geologic Map Units

Qfp = Quaternary (Holocene) flood-plain alluvial deposits, moderately to poorly sorted ravel, gravelly sand, sand, and sandy silt
Qf3-2 = Quaternary (Holocene and Pleistocene) young and intermediate alluvial fan deposits; poorly sorted boulders, cobbles, gravel, sand and silt
Qf2-1 = Quaternary (Pleistocene) intermediate and old alluvial fan deposits, similar to Qf3
Kcg = Late Cretaceous granodiorite of China Garden

NOTES:
1. WGS 1984 COORDINATE SYSTEM
2. Geologic Map of Desert Creek Peak Quadrangle, Lyon and Douglas Counties, Nevada, and Mono County, California by John H. Stewart, Gerald F. Brem and John C. Dohrenwend, 1989
3. See site map for details of geophysical survey

File Name: CE-65097

Date: 10/4/2012

USGS science for a changing world

GEOVision geophysical services

GEOLOGIC MAP
CE•65097

Looking southeast at fire station housing seismic station CE.65097 and at HVSR sensor 453A

Looking south along SASW array 65097-1

Looking northwest and HVSR sensor 453, a 1 Hz geophone forming part of triangle array 65097-2 and passive linear and MASW array 65097-1

Looking north at MASW array 65097-3

Looking northwest along array 65097-5 and at corner of array 65097-4

Location of Geophysical Testing Arrays:

Location	Latitude	Longitude
65097-1, Southeast End of Passive/MASW Array	38.51431	-119.48016
65097-1, Center of Passive/MASW/SASW Array	38.51459	-119.48021
65097-1, Northwest End of Passive/MASW Array	38.51487	-119.48026
65097-2, Corner of Passive Array, Sensor Location 1	38.51472	-119.47980
65097-2, Corner of Passive Array, Sensor Location 3	38.51491	-119.48031
65097-2, Corner of Passive Array, Sensor Location 5	38.51446	-119.48028
65097-2, Center of Passive Array, Sensor Location 7	38.51469	-119.48013
65097-3, Southeast End of MASW Array	38.51441	-119.48016
65097-3, Center of MASW Array	38.51461	-119.48024
65097-3, Northwest End of MASW Array	38.51481	-119.48031
65097-4, Southwest End of L-Shaped Array, Geophone 1	38.51330	-119.48065
65097-4, Southeast Corner of L-Shaped Array, Geophone 24	38.51427	-119.48018
65097-5, Southeast End of L-Shaped Array, Geophone 25	38.51426	-119.48022
65097-5, Northwest End of L-Shaped Array, Geophone 48	38.51451	-119.48094
HVSR Sensor 450	38.51471	-119.47984
HVSR Sensor 453	38.51445	-119.48029
HVSR Sensor 507	38.51488	-119.48029
HVSR Sensor 453A	38.51472	-119.47984
HVSR Sensor 450A	38.51451	-119.48094
HVSR Sensor 453B	38.51330	-119.48065
HVSR Sensor 450B	38.51481	-119.48031
HVSR Sensor 453C	38.51441	-119.48016

Notes: 1) WGS84 Coordinate System (decimal degrees)
2) Survey accuracy is estimated at 1 to 2 m.

Results:

V_S Model

Depth to Top of Layer (m)	Layer Thickness (m)	S-Wave Velocity (m/s)	Inferred P-Wave Velocity (m/s)	Assumed Poisson's Ratio	Assumed Density (g/cm^3)
0	0.75	187	349	0.3	1.8
0.75	1.5	217	406	0.3	1.8
2.25	1.75	304	569	0.3	1.9
4	6	388	726	0.3	1.9
10	9	474	886	0.3	2.0
19	27	519	972	0.3	2.0
46	>14	675	1264	0.3	2.1

Notes: 1) Depth of investigation is about 60 m.
2) Bottom layer is a half space.

Observations/Discussion:

- Geophysical testing was conducted at this site on multiple site visits on 8/24/10, 10/25/11 and 11/09/11. During the site visit on 8/24/10 linear passive surface wave, limited MASW and SASW data were acquired along array 65097-1 and passive surface wave data were acquired along the triangle array 65097-2. Additionally, HVSR data were acquired near the corners of array 65097-2 (sensor locations 450, 453 and 507). This testing was conducted in a dirt covered parking area adjacent to the fire station housing the seismic station. On 10/25/11 the site was revisited to further investigate potential dominant higher mode and/or lateral velocity variation issues with the previously acquired data. Additional HVSR data were also acquired using modified field procedures (improved sensor coupling, deeper holes for sensors and covering of sensors) developed after the initial site visit. During this site visit, MASW data were acquired along array 65097-3, located near and subparallel to array 65097-1, using a smaller geophone interval, larger number of geophones, and larger number of shot locations. Passive surface wave data were also acquired along an "L" shaped array south of the original test area (linear arrays 65097-4 and 65097-5). On 11/09/11, two additional HVSR measurements were made while in route to another site.
- All presented HVSR data were collected with Nanometrics Trillium Compact 120 second seismometers. The HVSR data at sensor locations 450, 453 and 507 were collected on 8/24/10. Two of the sensors were placed on small ceramic plates and the other was placed directly on the ground. The sensors were not placed in shallow holes. Additionally, the sensors were not covered; however, there were only light winds during data acquisition. HVSR plots for all sensors are similar with a broad peak in the 0.5 to 1.5 Hz range. HVSR data for sensor 453A, located near sensor location 450, were acquired on 10/25/11. The sensor was placed in a shallow hole, coupled to the ground using a manufacturer provided aluminum cradle with no legs and covered with a bucket to keep wind from moving the sensor cable. A more distinct HVSR peak(s) was observed during this measurement sequence with double peaks at about 1.3 and 2.1 Hz. Although the HVSR signature is somewhat different from that recorded on 8/24/10, both data sets have HVSR peaks in the 1 to 1.5 Hz range. The differences may be associated with improved field procedures or some change in the noise (microtremor) field. The newer measurement is definitely expected to be more reliable. HVSR data for sensor locations 453B, 453C, 450A and 450B were made on 11/9/11. Sensors were placed in small holes, except for sensor 450A, and coupled to the ground using a small aluminum tripod, with or without legs, and covered with a bucket. Interestingly, sensor 450A, which was placed directly on the ground, has similar HVSR response to measurements made on 8/24/10 with a broad HVSR peak in the 0.8 to 1.5 Hz range. Sensors 450B, 453B and 453C, which were all placed in shallow holes, have more distinct single or double peaks in the 1.3 to 2.1 Hz range. These data may demonstrate the importance of sensor coupling in achieving reliable results, especially at sites with expected low ambient noise levels. It should be noted that HVSR measurements made with a Tromino ENGY, a higher frequency sensor did not yield an HVSR peak in the 1 Hz range. Due to very low ambient noise levels at the site, the HVSR data should not be considered reliable. Additional investigation into HVSR response as a function of sensor coupling and sensor type in low noise environments such as this is recommended.

- Based on simple, interactive horizontal layer-based analysis of seismic refraction first arrival data, P-wave velocity in the upper 15 m ranges from about 400 m/s at the surface, about 650 to 750 m/s at a depth of 2 to 3 m and 900 to 950 m/s at a depth of 7 to 8 m. There is no evidence of a saturated zone in the upper 20 m in the first arrival data. There is, however, a clear reflector at a depth on the order of 40 to 45 m that could be associated with the water table.
- Noise conditions at site (multi-directional noise sources) appeared sufficient for possible successful application of passive surface wave techniques. The primary noise source was traffic on SR-395 located about 200 m from the site. With a single road as a dominant noise source, it was important to orient linear passive arrays orthogonal to the highway, with 2-D passive surface wave arrays definitely preferable.
- Active surface wave data (SASW and MASW) were difficult to reduce due to possible higher modes, modal superposition and/or lateral velocity variation. SASW dispersion data from receiver spacings of 8 to 20 m appeared to be associated with a higher mode and, therefore, only limited use was made of this data. 3-D array based inversion of the full SASW dataset could be considered to model the higher mode influence, but in this case the data cannot be combined with MASW and passive surface wave data. There was also significant scatter in the MASW dispersion data at wavelengths greater than 20 m, likely the result of modal superposition (mode mixing) and/or lateral velocity variation. Rayleigh wave phase velocities at wavelengths greater than 20 m varied with source offset, source type and source location (forward versus reverse direction). Variation in Rayleigh wave phase velocity data at long wavelengths (i.e. no clearly identifiable higher mode) limited application of multi-mode modeling techniques.
- The ESAC technique was used to extract surface wave dispersion data from the passive triangle and "L" array data. Both the ReMi™ and ESAC techniques were used to extract surface wave dispersion data from the linear arrays. Linear array passive surface wave data reduced using the ESAC and ReMi™ techniques yielded similar dispersion curves. Only linear array passive surface wave data from array 65097-1 were used for modeling as this array is in close proximity to the other surface wave arrays. Surface wave dispersion data from array 65097-1 tracks the upper envelope of the MASW dispersion data, but has lower phase velocity than the higher mode SASW dispersion data that were not utilized for analysis. Surface wave dispersion data from the triangle passive array 65097-2 tracks the lower envelope of the MASW and SASW dispersion data and has lower phase velocity than the other passive surface wave arrays at overlapping wavelengths in the 55 to 80 m range. Therefore, surface wave dispersion data from this array is associated with the fundamental mode or provides evidence of lateral velocity variation at the site. Surface wave dispersion data from the "L" array 65097-4/5 lies between that from arrays 65097-1 and 2 and was, therefore, also used for analysis. Reduction of passive surface wave data from linear array 65097-4 and "L" array 65097-4/5 leads us to believe that the area in the vicinity of array 65097-4 may be less problematic for MASW and SASW acquisition. Unfortunately, MASW data were not acquired along a segment of array 65097-4 because permission had not been obtained to use hammer and weight drop energy sources in the park.
- The minimum wavelength Rayleigh wave extracted from linear passive array 65097-1 using the ESAC and ReMi™ techniques was 6.5 and 12 m, respectively. The maximum wavelength Rayleigh wave extracted from this array was 70 m. The minimum

wavelength Rayleigh wave extracted from the triangle passive array 65097-2 was 56 m. The maximum allowed wavelength for this array was about 130 m. The minimum and maximum wavelength Rayleigh wave extracted from the passive L-shaped array 65097-4/5 were 23 and 77 m, respectively. The minimum wavelength Rayleigh wave data extracted from SASW array 65097-1, MASW array 65097-1 and MASW array 65097-3 were about 1, 2.5 and 1.3 m, respectively.

- There is excellent agreement in SASW and MASW phase velocity data at wavelengths smaller than 20 m. At longer wavelengths there is significant scatter in the MASW dispersion data due to lateral velocity variation and/or influence of higher mode surface waves.
- Representative dispersion curves were generated for each surface wave data set using a moving average, polynomial curve fitting routine. These individual representative dispersion curves were assigned a weight and combined and a representative dispersion curve generated for the combined data set for data modeling.
- The saturated zone was not fixed for surface wave modeling as it is expected to occur at a depth greater than 40 m and will not have a significant impact of the V_S model.
- Surface wave depth of investigation is about 60 m, based on half of maximum wavelength criteria.
- V_{S30} is 415 m/s (NEHRP Site Class C).
- Based on the scatter in the surface wave dispersion data, V_{S30} may vary by as much as 10% in the immediate site vicinity. The site, however, should remain NEHRP Site Class C.
- Average S-wave velocity of the upper 60 m (V_{S60}) is 484 m/s.
- Based on the quarter wavelength approximation, an HVSR peak in the 1.3 Hz range would be associated with a large increase in V_S at a depth on the order of 100 m, possibly the bedrock surface. An HVSR peak in the 2 Hz range would likely be associated with a velocity increase at a depth on the order of 50 to 60 m. The HVSR data should, however, be used with caution at this site due to low ambient noise levels.

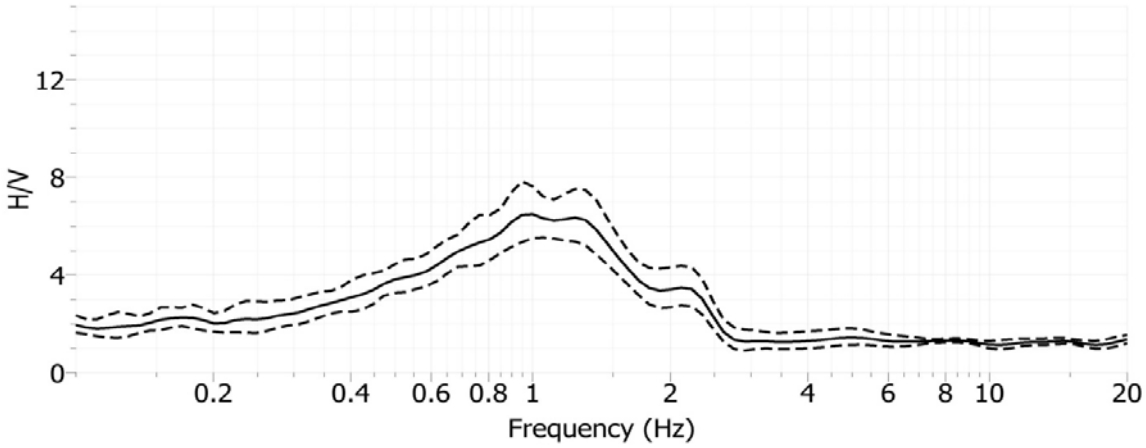

Site CE.65097, H/V Spectral Ratio, Array 65097-2, Sensor 507

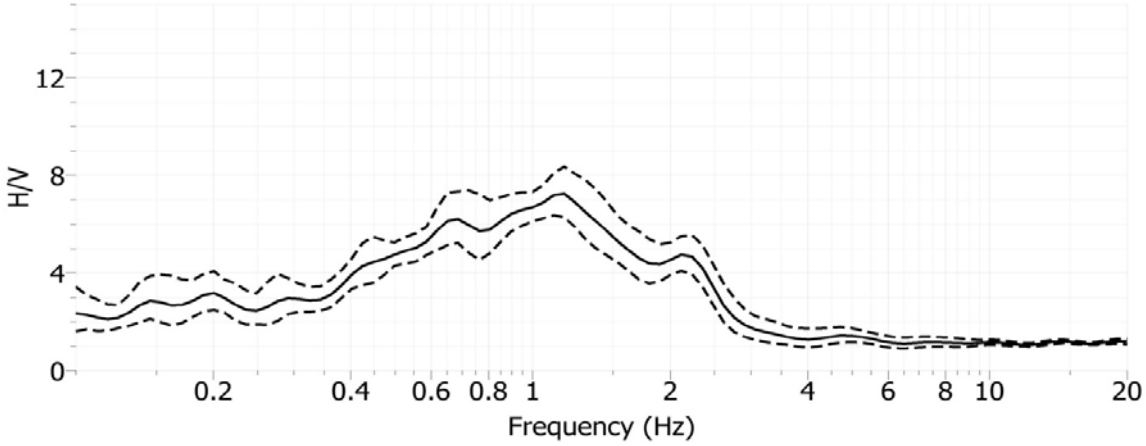

Site CE.65097, H/V Spectral Ratio, Array 65097-2, Sensor 450

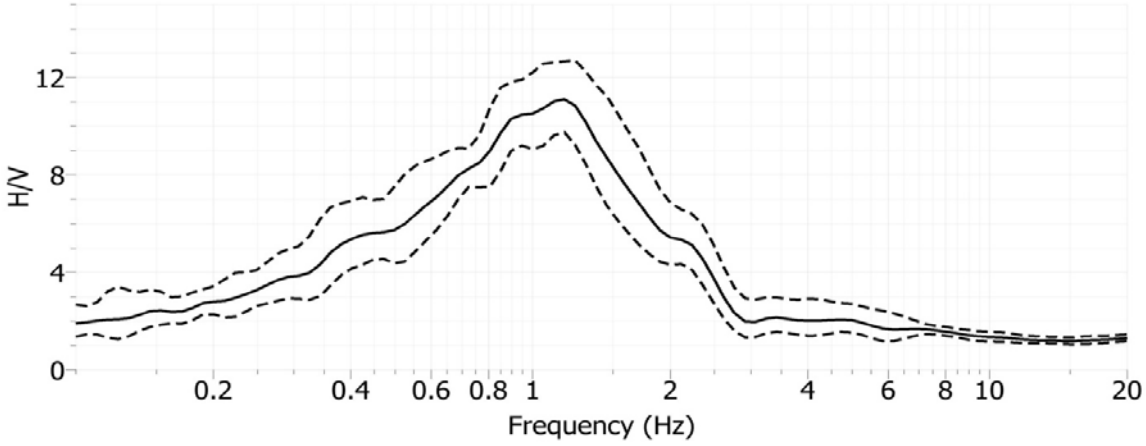

Site CE.65097, H/V Spectral Ratio, Array 65097-2, Sensor 453

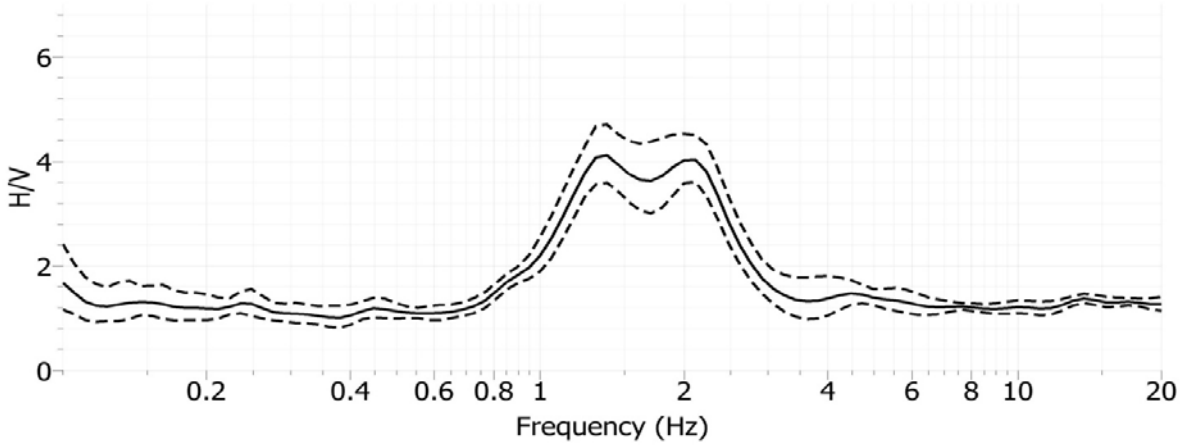

Site CE.65097, H/V Spectral Ratio, Array 65097-2, Sensor 453A

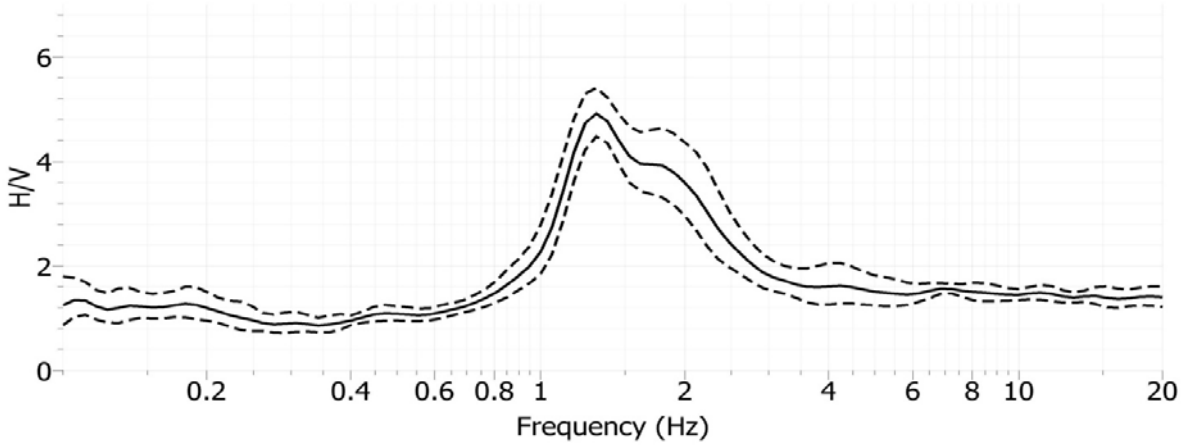

Site CE.65097, H/V Spectral Ratio, Array 65097-3, Sensor 453C

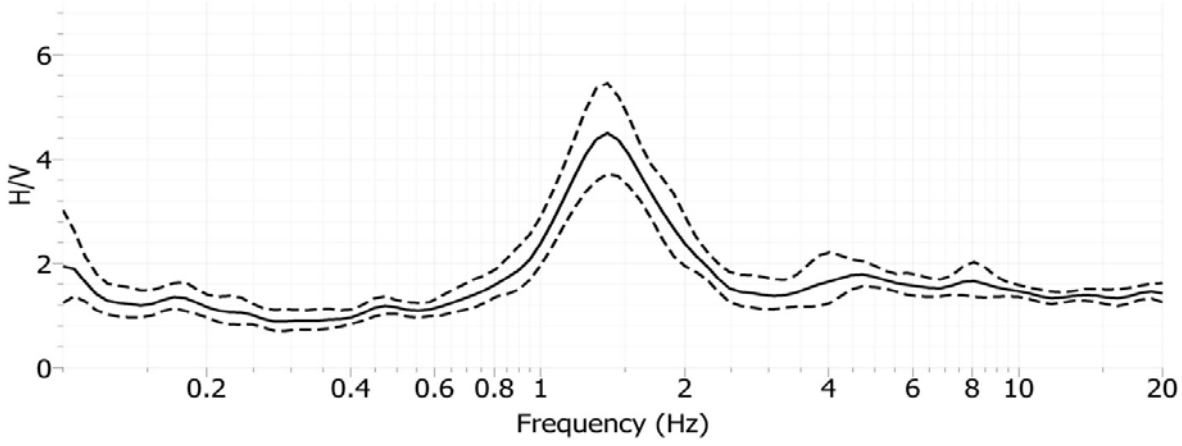

Site CE.65097, H/V Spectral Ratio, Array 65097-4, Sensor 453B

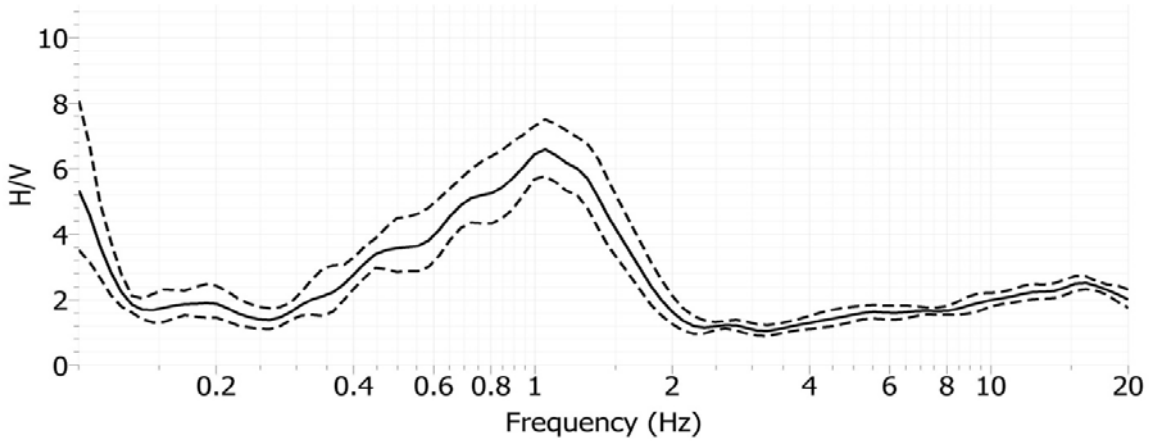

Site CE.65097, H/V Spectral Ratio, Array 65097-5, Sensor 450A

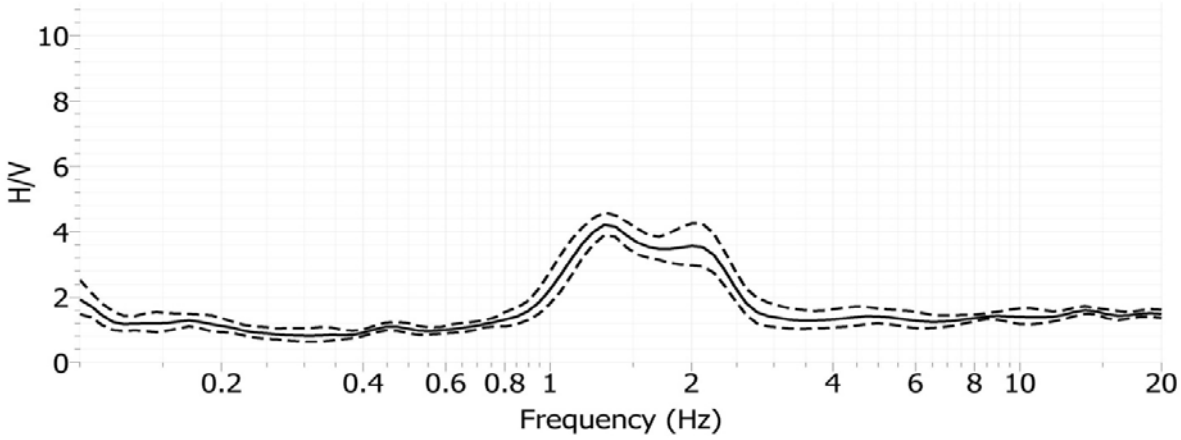

Site CE.65097, H/V Spectral Ratio, Array 65097-3, Sensor 450B

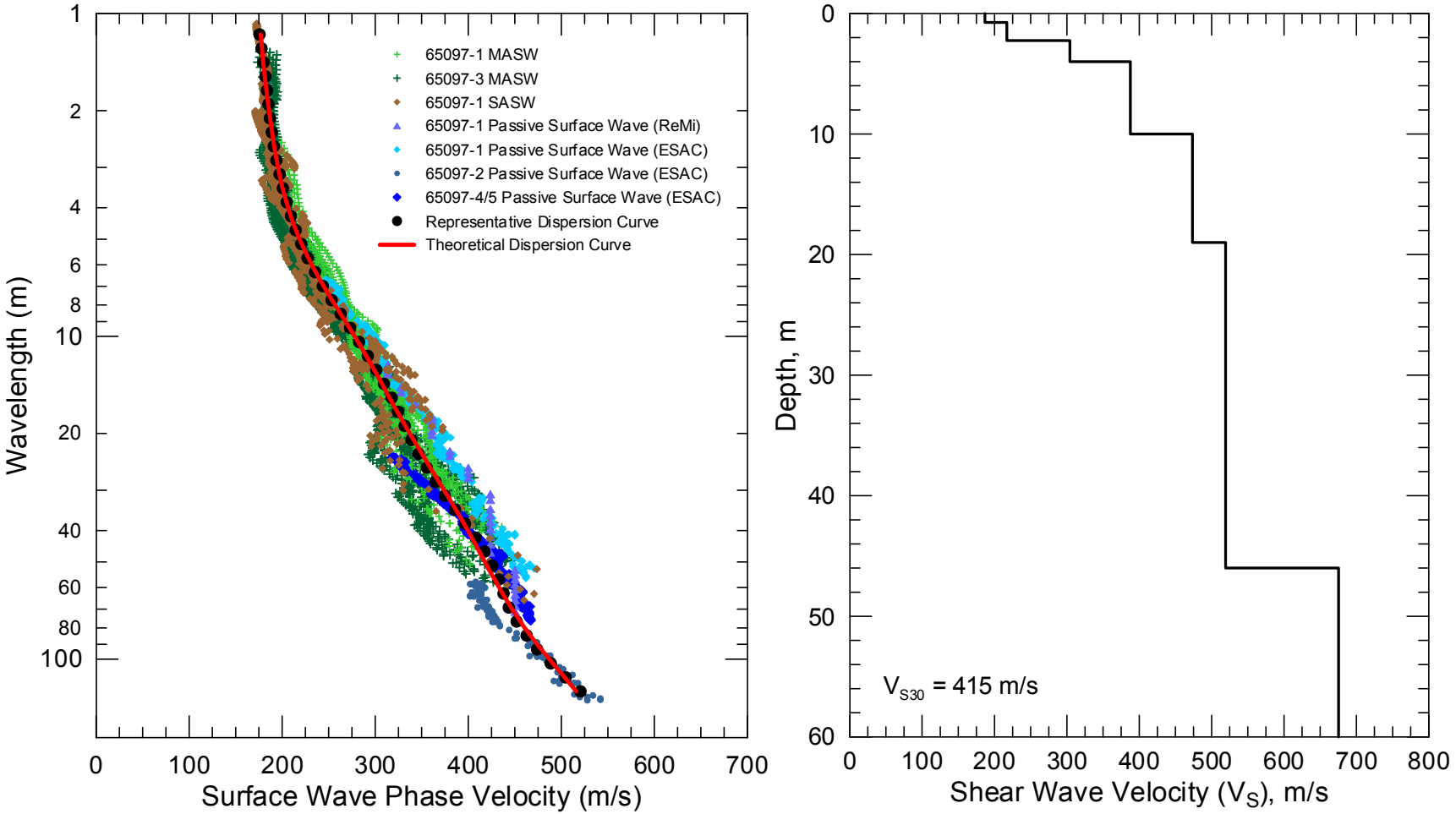

CE.65097 - Field, representative and inverted theoretical surface wave dispersion data (left) and associated V_S model (right)

Site CI.ADO

Location: LADWP Adelanto Converter Station, Adelanto, California

Latitude: 34.55048 **Longitude:** -117.43399

(Station coordinates modified based on field GPS survey, WGS84 coordinate system)

V_{S30} (measured): 375 m/s

V_{S30} (adjusted to more accurately reflect seismic station conditions): 400 m/s (average S-wave velocity between 2 and 32 m adjusting for nominal sensor depth)

NEHRP Site Class: C

Geomatrix Code: IHD

Geologic Conditions/Observations: Site located on geologic unit mapped as Quaternary (Holocene) alluvium. Crystalline basement expected to be deep at this site.

Site Conditions: Rural site with sporadic traffic on nearby streets. Relatively flat terrain in test area.

Geophysical Methods Utilized: HVSR, MASW, SASW

Geophysical Testing Arrays:

1. Array ADO-1 (48 channel MASW array utilizing 4.5 Hz vertical geophones spaced 1.5 m apart for a length of 70.5 m, forward and reverse shot locations with multiple source offsets and source types and center shot location).
2. Array ADO-1 (SASW array with common midpoint and orientation as MASW array of same name utilizing 4.5 and 1 Hz vertical geophones and maximum receiver spacing of 32 m).
3. Three HVSR measurement locations distributed along array ADO-1.

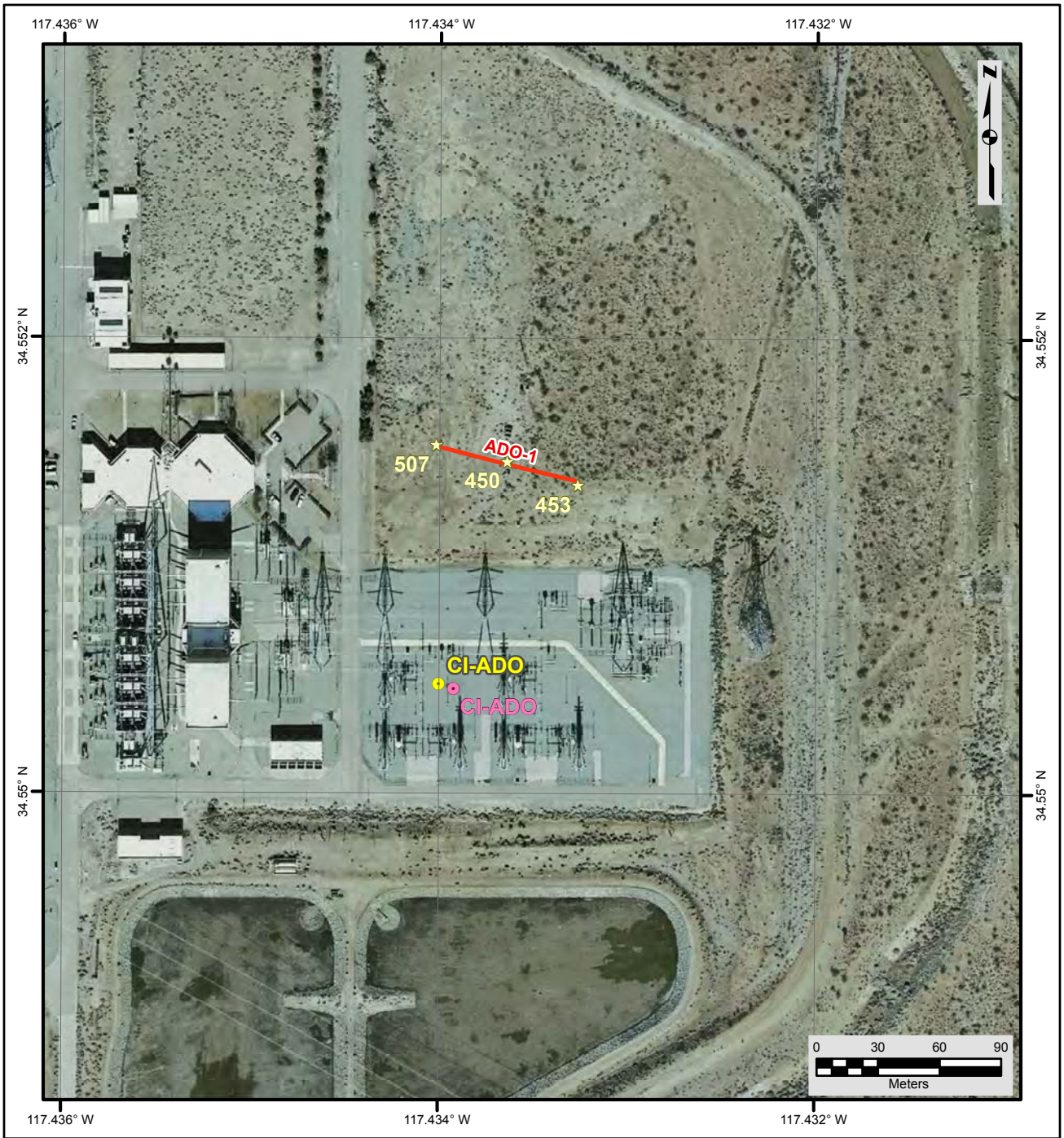

Legend

- Seismic Station - Approximate Surveyed Location
- Seismic Station - Approximate Location of Record
- H/V Spectral Ratio Location
- MASW and Refraction Array

NOTES:
1. WGS 1984 COORDINATE SYSTEM
2. Image Source: ESRI, i-cubed, USDA FSA, USGS, AEX, GeoEye, Getmapping, Aerogrid, IGP

File Name: CI-ADO-I

Date: 7/7/2011

USGS science for a changing world

GEOVision geophysical services

RECOVERY.GOV

SITE MAP
CI•ADO

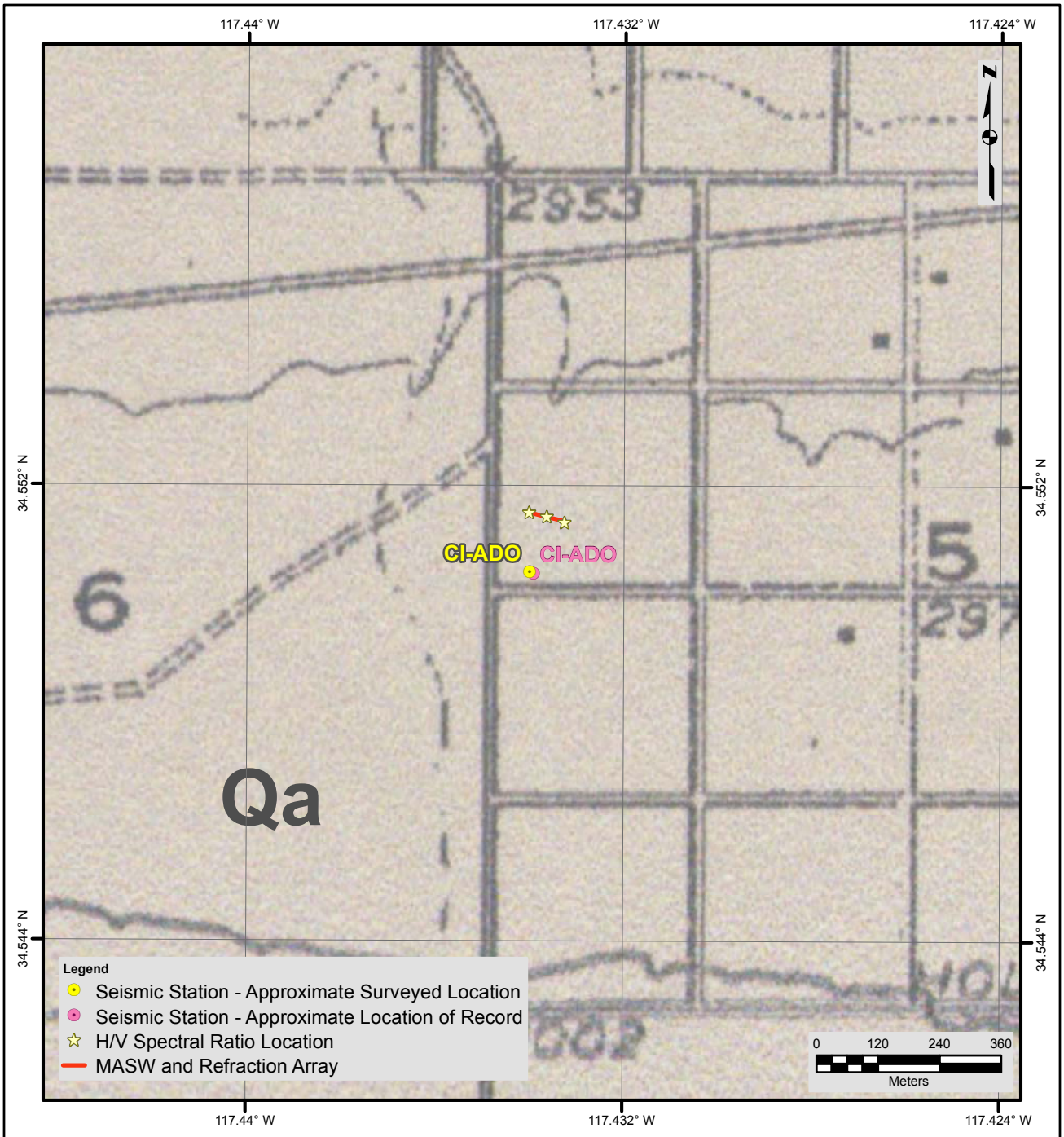

Description of Geologic Map Units

Qa = Quaternary (Holocene) alluvial silt, sand and gravel of valley areas

NOTES:
1. WGS 1984 COORDINATE SYSTEM
2. Geologic Map of the Shadow Mountains & Victorville 15 Minute Quadrangles, San Bernardino & Los Angeles Counties, California by Thomas W. Dibblee, Jr., 2008
3. See site map for details of geophysical survey

File Name: CI-ADO

Date: 7/7/2011

USGS science for a changing world

GEOVision geophysical services

GEOLOGIC MAP
CI•ADO

RECOVERY.GOV

Looking north towards seismic station CI.ADO and test area

Looking south towards seismic station from HVSR sensor 507

Looking south towards MASW array ADO-1 and seismic station

Looking east along MASW array ADO-1

Looking east along SASW array ADO-1

Location of Geophysical Testing Arrays:

Location	Latitude	Longitude
ADO-1, West End of MASW Array	34.55152	-117.43400
ADO-1, Center of MASW and SASW Arrays	34.55144	-117.43363
ADO-1, East End of MASW Array	34.55137	-117.43325
CI-ADO Seismic Station	34.55048	-117.43399
HVSR Sensor 507	34.55153	-117.43401
HVSR Sensor 450	34.55146	-117.43363
HVSR Sensor 453	34.55135	-117.43325

Notes: 1) WGS84 Coordinate System (decimal degrees)
2) Survey accuracy is estimated at 1 to 2 m

Results:

V_S Model

Depth to Top of Layer (m)	Layer Thickness (m)	S-Wave Velocity (m/s)	Inferred P-Wave Velocity (m/s)	Inferred Poisson's Ratio	Inferred Density (g/cm^3)
0	1	187	350	0.300	1.9
1	2	230	431	0.300	1.9
3	2	326	610	0.300	1.9
5	>25	419	783	0.300	1.9

Observations/Discussion:

- HVSR plots are almost identical at all measurement locations validating the 1-D velocity structure assumption, although there are no high frequency peaks indicative of shallow, large impedance contrasts.
- There is high amplitude HVSR peak at 0.29 Hz, indicative of deep bedrock, and a possible low amplitude secondary peak at 0.9 Hz.
- Noise conditions at site were not sufficient to apply passive surface wave techniques.
- SASW and MASW data reduction was difficult due to probably near surface lateral velocity variation, possible strong near field effects, complex subsurface velocity structure, subsurface scatterers, etc. SASW dispersion data did not appear reliable at wavelengths greater than 40 m and was, therefore, not utilized for analysis.
- For data modeling, a representative dispersion curve was generated for the MASW data set using a moving average, polynomial curve fitting routine.
- Water table located at a depth of greater than 30 m based on seismic refraction survey design and absence of a water table refractor.
- Based on simple horizontal layer-based analysis of seismic refraction first arrival data, P-wave velocity in the upper 15 to 20 m ranges from about 450 to 725 m/s (about 3 to 4 m of sediments with velocity less than 475 m/s overlying about 2 m of sediments with P-wave velocity of about 650 m/s, underlain by sediments with velocity in the 700 to 725 m/s range).
- Surface wave depth of investigation is about 30 m based on half of maximum wavelength criteria.
- Inferred P-wave velocities in the surface wave model are relatively consistent with simplified P-wave refraction model considering unknown Poisson's ratio. Lowering Poisson's ratio to about 0.25 would make the inferred P-wave velocity below 5 m depth consistent between the P-wave refraction data and surface wave model.
- V_{S30} is 375 m/s (Site Class C).
- The possibility cannot be discounted that V_{S30} is slightly lower (about 5%) based on SASW dispersion data.
- Average S-wave velocity between 2 m (nominal sensor depth) and 32 m is 400 m/s.

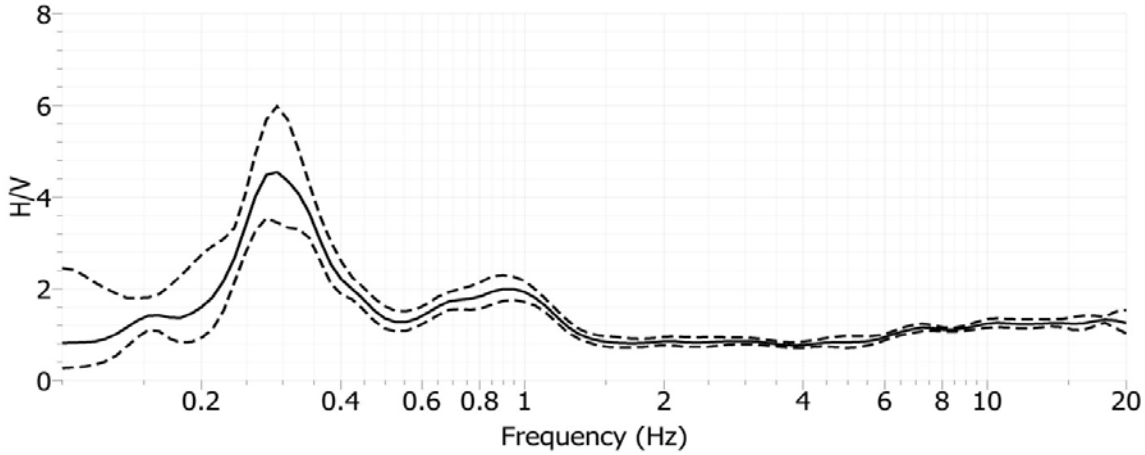

Site CI.ADO, H/V Spectral Ratio, Array ADO-1, Sensor 507

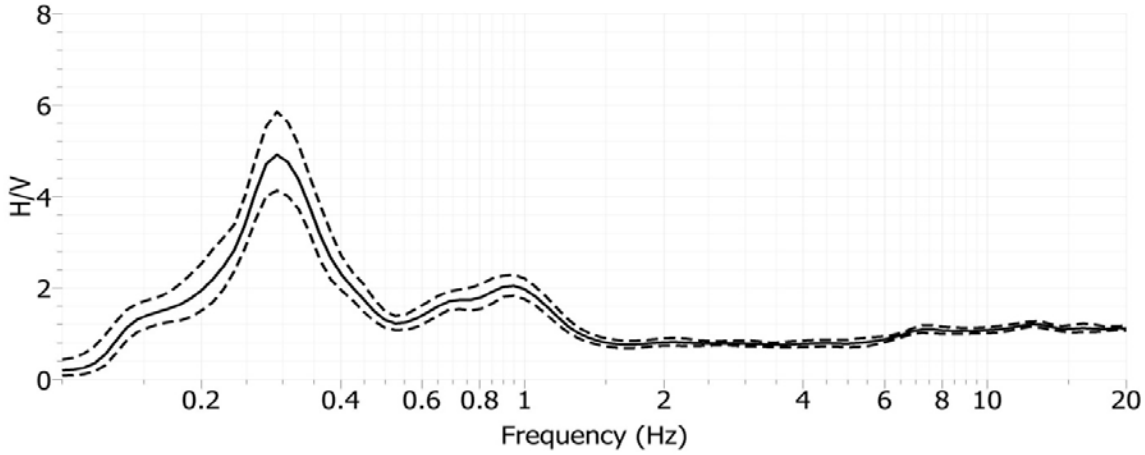

Site CI.ADO, H/V Spectral Ratio, Array ADO-1, Sensor 450

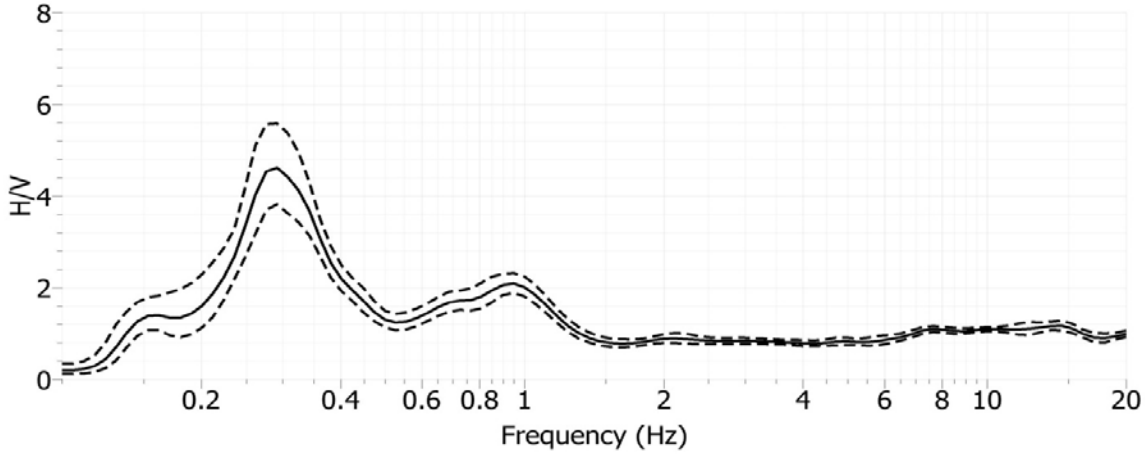

Site CI.ADO, H/V Spectral Ratio, Array ADO-1, Sensor 453

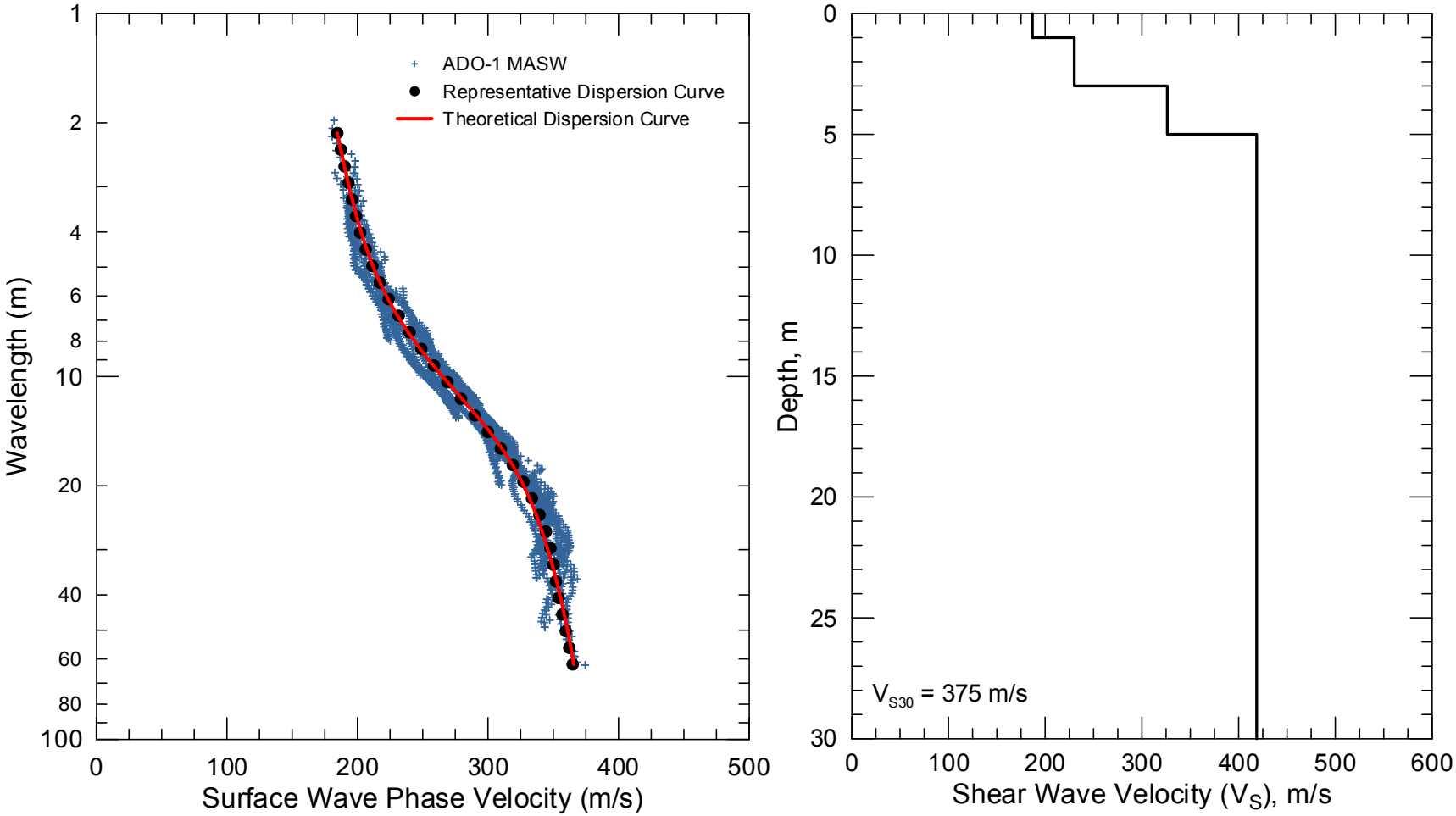

CI.ADO - Field, representative and inverted theoretical surface wave dispersion data (left) and associated V_S model (right)

Site CI.ALP

Location: Antelope Southern California Edison Substation, 9634 West Avenue J, Lancaster, California

Latitude: 34.68702 **Longitude:** -118.29947
(Station coordinates modified based on site GPS survey and are in WGS84 coordinate system)

V_{S30} (measured): 347 m/s

V_{S30} (adjusted to more accurately reflect seismic station conditions): 362 m/s (average S-wave velocity between 2 and 32 m adjusting for 2 m nominal sensor depth).

NEHRP Site Class: D/C

Geomatrix Code: IHD

Geologic Conditions/Observations: Quaternary (Holocene) alluvium.

Site Conditions: Rural site. Relative planar topography in site vicinity. Very gentle topographic decline to the northeast.

Geophysical Methods Utilized: HVSR, MASW

Geophysical Testing Arrays:

1. Array ALP-1 (48 channel MASW array utilizing 4.5 Hz vertical geophones spaced 1.5 m apart for a length of 70.5 m, forward and reverse shot locations with multiple source offsets and source types and multiple interior shot locations).
2. Three HVSR measurement locations; two distributed along array ALP-1 and the other adjacent to the seismic station.

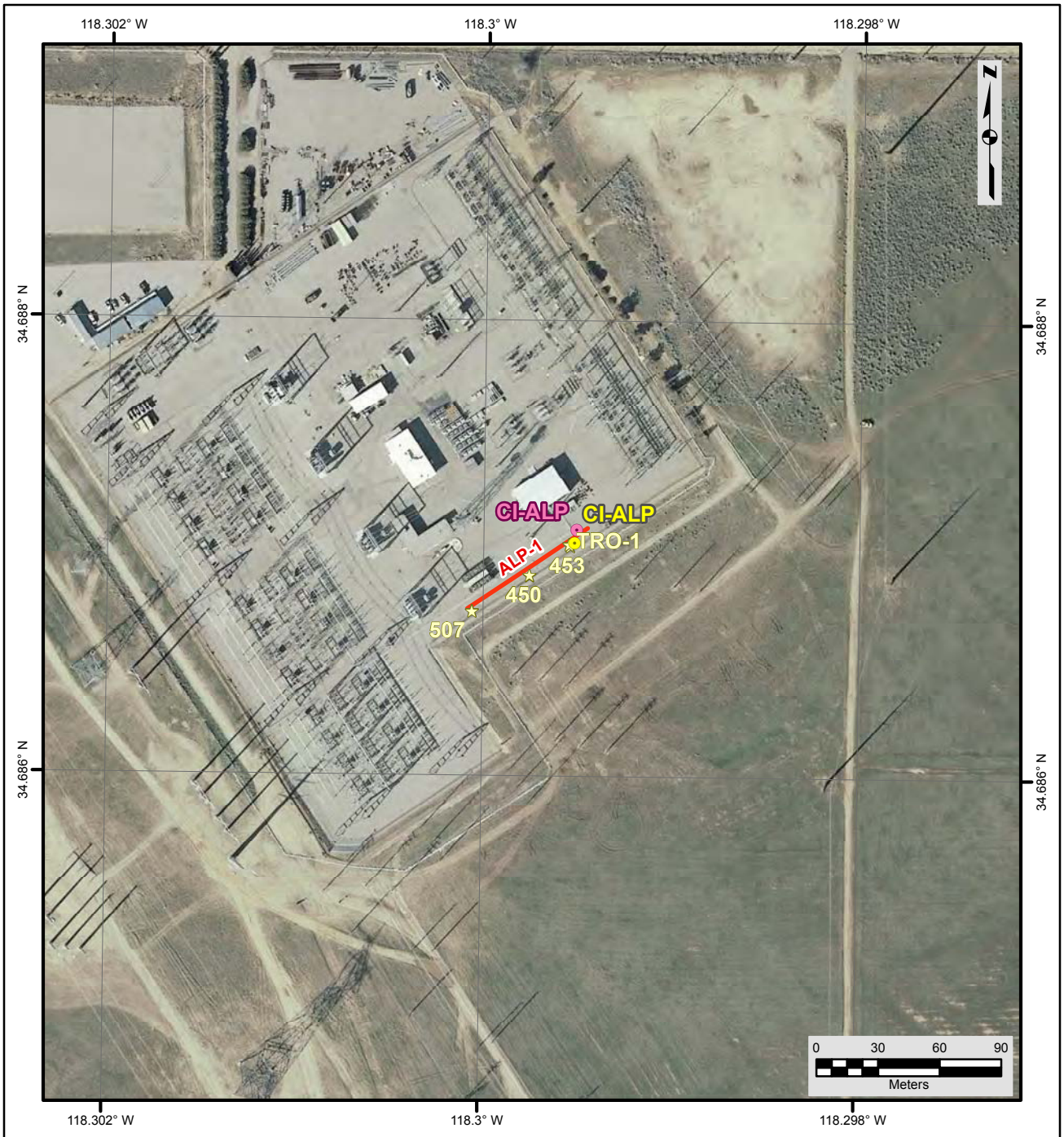

Legend

- Seismic Station - Approximate Surveyed Location
- Seismic Station - Approximate Location of Record
- H/V Spectral Ratio Location
- MASW Array

NOTES:
1. WGS 1984 COORDINATE SYSTEM
2. Image Source: ESRI, i-cubed, USDA FSA, USGS, AEX, GeoEye, Getmapping, Aerogrid, IGP

File Name: CI-ALP-I

Date: 9/22/2011

USGS science for a changing world

GEOVision geophysical services

RECOVERY.GOV

SITE MAP
CI•ALP

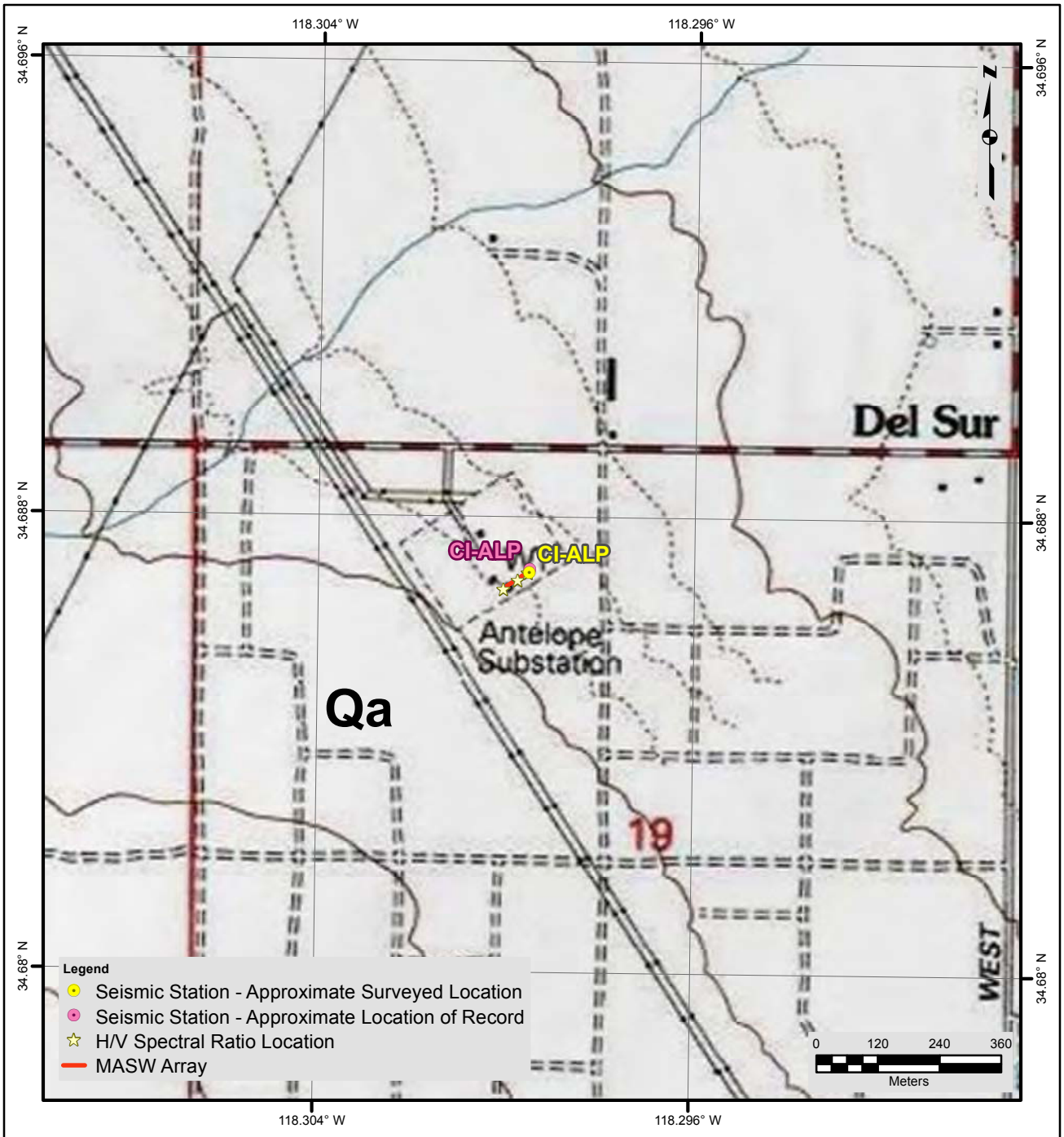

Description of Geologic Map Units

Qa = Quaternary (Holocene) alluvial gravel, sand and clay of valley areas

NOTES:
1. WGS 1984 COORDINATE SYSTEM
2. Geologic units from Geologic Map of the Lake Hughes and Del Sur Quadrangles, Los Angeles County, California by Thomas W. Dibblee, Jr., 2002; Topographic imagery from ESRI ArcGIS Online and data partners including USGS and © 2007 National Geographic Society
3. See site map for details of geophysical survey

File Name: CI-ALP

Date: 9/22/2011

USGS science for a changing world

GEOVision geophysical services

GEOLOGIC MAP
CI•ALP

RECOVERY.GOV

Looking southwest towards Seismic Station, HVSR sensor 453, and Tromino ENGR sensor

MASW data acquisition

Looking southwest at HVSR sensor 450 and MASW array ALP-1

GPS data acquisition on northeast end of array ALP-1

MASW data acquisition using weight drop off southeastern end of array

Location of Geophysical Testing Arrays:

Location	Latitude	Longitude
ALP-1, Southwest End of MASW Array	34.68673	-118.30004
ALP-1, Center of MASW Array	34.68691	-118.29972
ALP-1, Northeast End of MASW Array	34.68709	-118.29940
Tromino ENGY Sensor (TRO-1)	34.68702	-118.29950
HVSR Sensor 450	34.68688	-118.29971
HVSR Sensor 453	34.68701	-118.29949
HVSR Sensor 507	34.68672	-118.30001
CI.ALP Seismic Station	34.68702	-118.29947

Notes: 1) WGS84 Coordinate System (decimal degrees)
2) Survey accuracy is estimated at 1 to 2 m

Results:

V_S Model

Depth to Top of Layer (m)	Layer Thickness (m)	S-Wave Velocity (m/s)	Inferred P-Wave Velocity (m/s)	Assumed Poisson's Ratio	Assumed Density (g/cm^3)
0	1.5	229	429	0.3	1.8
1.5	2.5	282	528	0.3	1.8
4	4	337	631	0.3	1.9
8	8	350	654	0.3	1.9
16	8	356	666	0.3	1.9
24	>6	434	811	0.3	2.0

Notes: 1) Model valid to a depth of 30 m.
2) Lowest layer is a half space.

Observations/Discussion:

- The HVSR curves are very similar at a frequency below 10 Hz validating the 1-D velocity structure assumption. HVSR sensor 453 may be impacted by low frequency noise.
- There may be a broad low amplitude HVSR peak in the 0.35 to 0.6 Hz range. It is unclear whether this HVSR response is geologic in nature or associated with sensor noise/coupling, especially sensor 453 which has a much higher amplitude response over this frequency range. All three Trillium sensors do, however, have slightly elevated HVSR amplitude in this frequency range. A Tromino ENGY sensor, located adjacent to Trillium sensor 453, does not yield elevated HVSR response in this frequency range. The Tromino does, however, yield very similar HVSR response over the 1.5 to 4 Hz range.
- Noise conditions at the site were not sufficient for application of passive surface wave techniques.
- There is 60 Hz noise in some of the seismic records, but it is not expected to impact analysis of the surface wave data. It does, however, limit the depth to which seismic refraction first arrival data can be used to characterize.
- Based on interactive, horizontal layer-based analysis of seismic refraction first arrival data, P-wave velocity structure in the upper 15 to 20 m ranges from about 400 to 450 m/s in the upper 2.5 to 5 m, 525 to 600 m/s below a depth of 2.5 to 5 m, and is about 650 m/s below a depth of 8 to 10 m.
- A representative dispersion curve was generated for the MASW data set using a moving average, polynomial curve fitting routine and used for modeling.
- There is some scatter in the MASW dispersion data, which may be partially associated with lateral velocity variation.
- A representative dispersion curve was generated for the combined MASW data set using a moving average, polynomial curve fitting routine and used for modeling.
- Water table depth expected to be greater than 30 m based on survey design and absence of a clear water table refractor. Far offset shot records are, however, affected by 60 Hz noise from the nearby substation.
- P-wave velocities in the surface wave model, based on an inferred Poisson's ratio of 0.3, are relatively consistent with simplified P-wave refraction model, especially near the surface and below a depth of 8 m.
- Surface wave depth of investigation is about 30 m based on half of maximum wavelength criteria.
- V_{S30} is 347 m/s (Site Class D/C).
- Average S-wave velocity between 2 m (nominal sensor depth) and 32 m is 362 m/s (Site Class D/C).

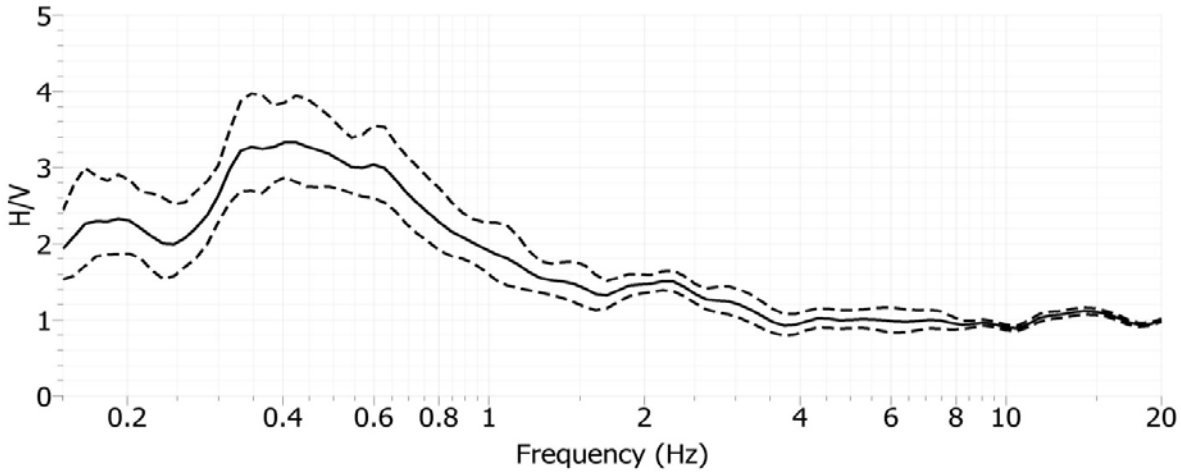

Site CI.ALP, H/V Spectral Ratio, Array ALP-1 Near Seismic Station, Sensor 453

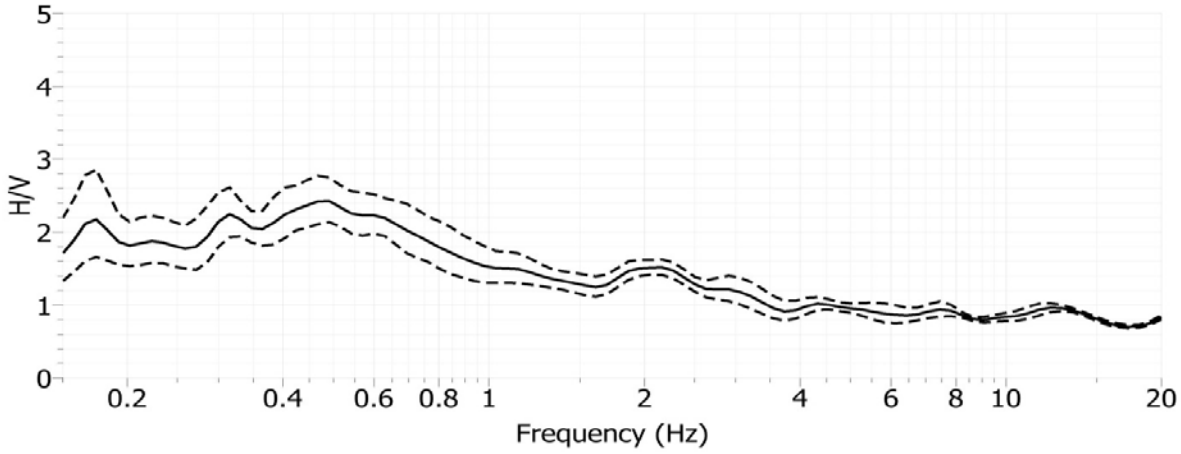

Site CI.ALP, H/V Spectral Ratio, Array ALP-1, Sensor 450

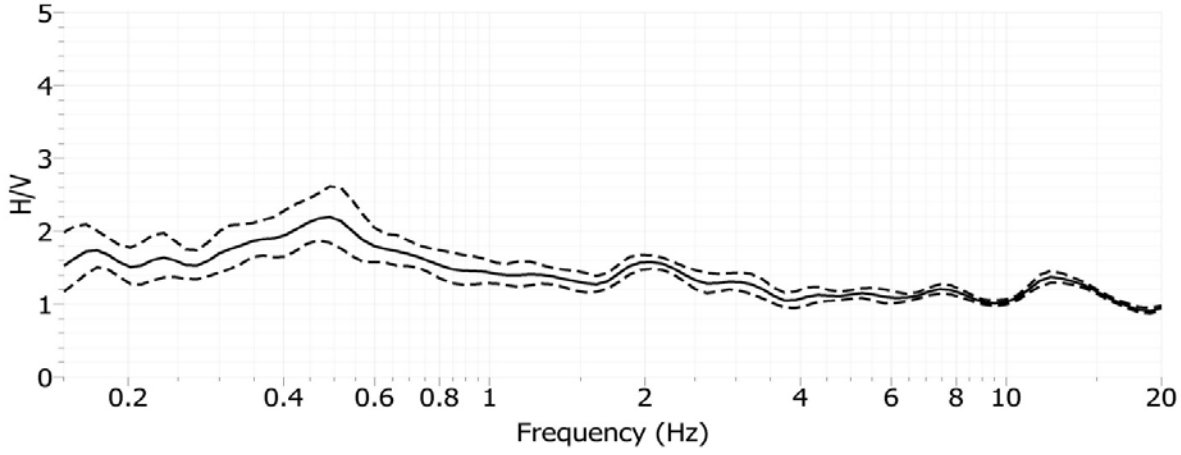

Site CI.ALP, H/V Spectral Ratio, Array ALP-1, Sensor 507

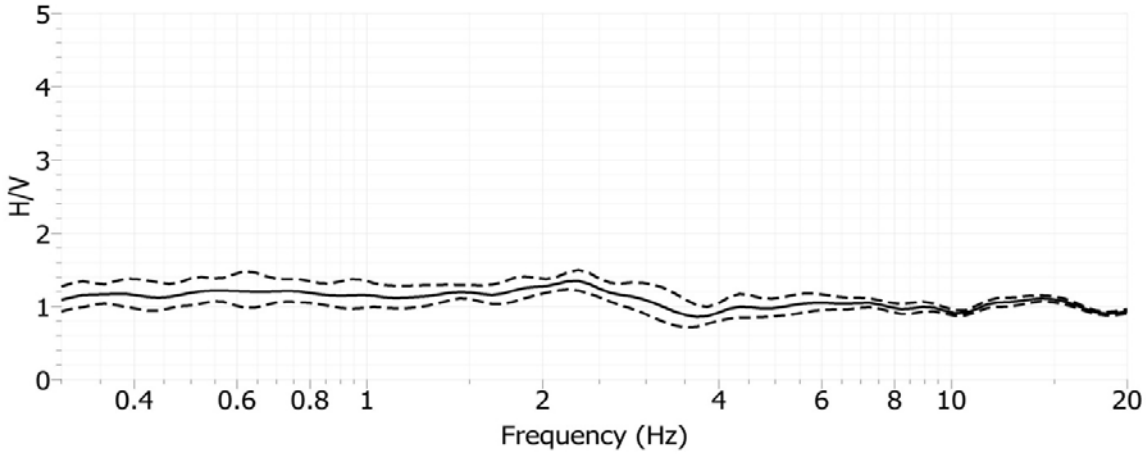

Site CI.ALP, H/V Spectral Ratio, Array ALP-1 Near Seismic Station, Tromino ENGY Sensor (TRO-1)

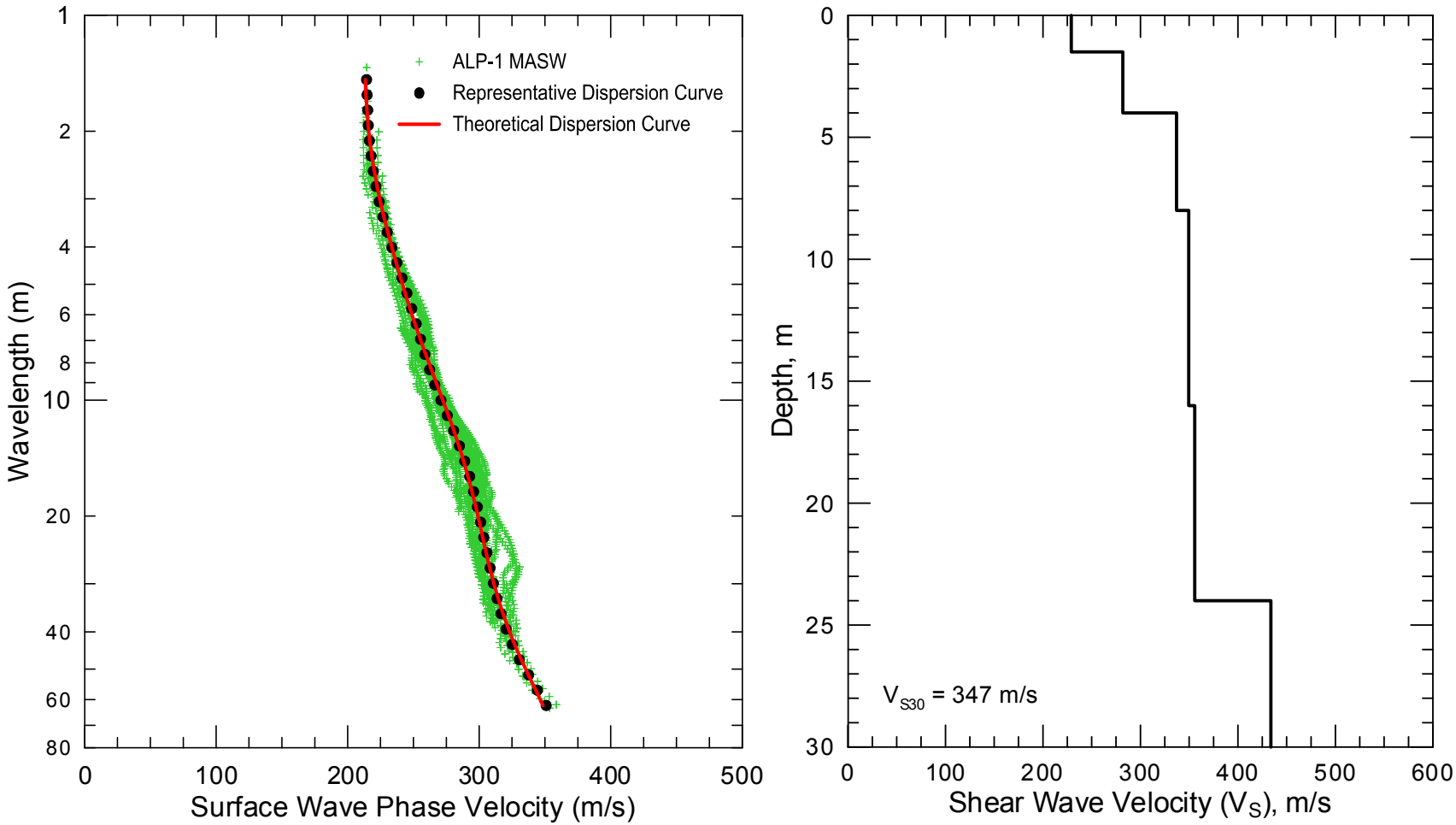

CI.ALP - Field, representative and inverted theoretical surface wave dispersion data (left) and associated V_S model (right)

Site CI.ARV

Location: Arvin, Tejon Ranch, Kern County, California

Latitude: 35.12690 **Longitude:** -118.83009
(Coordinates provided by USGS – WGS84 coordinate system)

V_{S30} (measured): 348 m/s

V_{S30} (adjusted to more accurately reflect seismic station conditions): 395 m/s (average S-wave velocity between 2 and 32 m adjusting for 2 m nominal sensor depth).

NEHRP Site Class: D/C

Geomatrix Code: IMD

Geologic Conditions/Observations: Seismic station located near the mapped contact of the Tertiary (Miocene) Santa Margarita Formation and Bena Gravels. The Santa Margarita Formation is described as a sandstone with conglomerate and siltstone layers. The Bena Gravel is described as pebbly clays and silts, sands and conglomerate. Regional dip of the geologic bedding in the site vicinity is generally about 10 to 20 degrees to the southeast.

Site Conditions: Rural site. Hilly terrain in site vicinity. Seismic lines placed along ridges with minimal topographic variation; however, there are relatively steep slopes near the sides of the lines. Seismic data acquired along two arrays due to differing mapped geologic units.

Geophysical Methods Utilized: HVSR, Seismic Refraction, MASW

Geophysical Testing Arrays:

1. Array ARV-1 (48 channel MASW and P-wave seismic refraction array utilizing 4.5 Hz vertical geophones spaced 1.5 m apart for a length of 70.5 m, forward and reverse shot locations with multiple source offsets and source types and center shot location).
2. Array ARV-2 (48 channel MASW and P-wave seismic refraction array utilizing 4.5 Hz vertical geophones spaced 1.5 m apart for a length of 70.5 m, forward and reverse shot locations with multiple source offsets and source types and multiple interior shot locations).
3. Three HVSR measurement locations distributed evenly along array ARV-1.

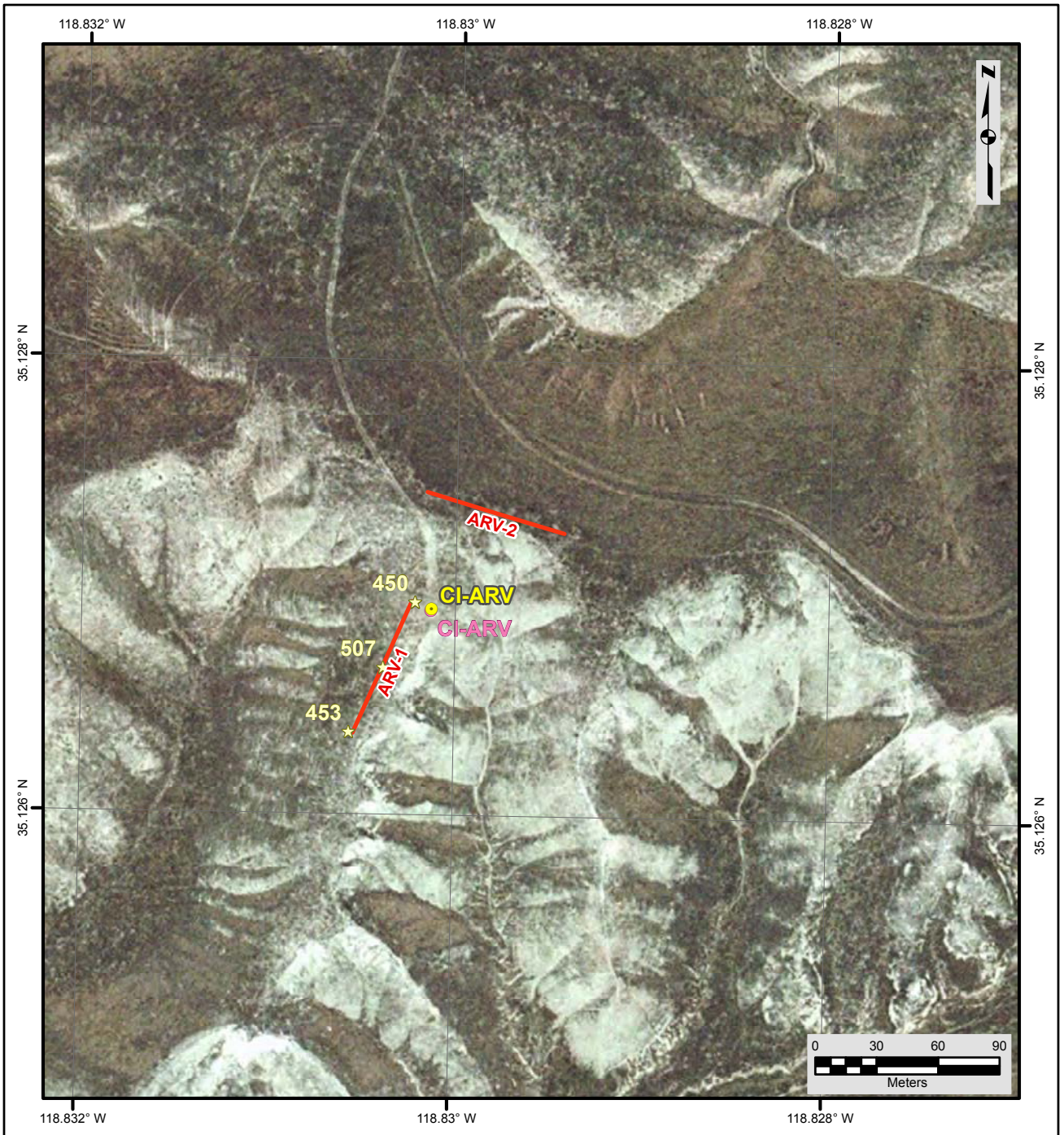

Legend

- Seismic Station - Approximate Surveyed Location
- Seismic Station - Approximate Location of Record
- H/V Spectral Ratio Location
- MASW Array

NOTES:
1. WGS 1984 COORDINATE SYSTEM
2. Image Source: ESRI, i-cubed, USDA FSA, USGS, AEX, GeoEye, Getmapping, Aerogrid, IGP

File Name: CI-ARV-I

Date: 7/7/2011

USGS science for a changing world

GEOVision geophysical services

RECOVERY.GOV

SITE MAP
CI•ARV

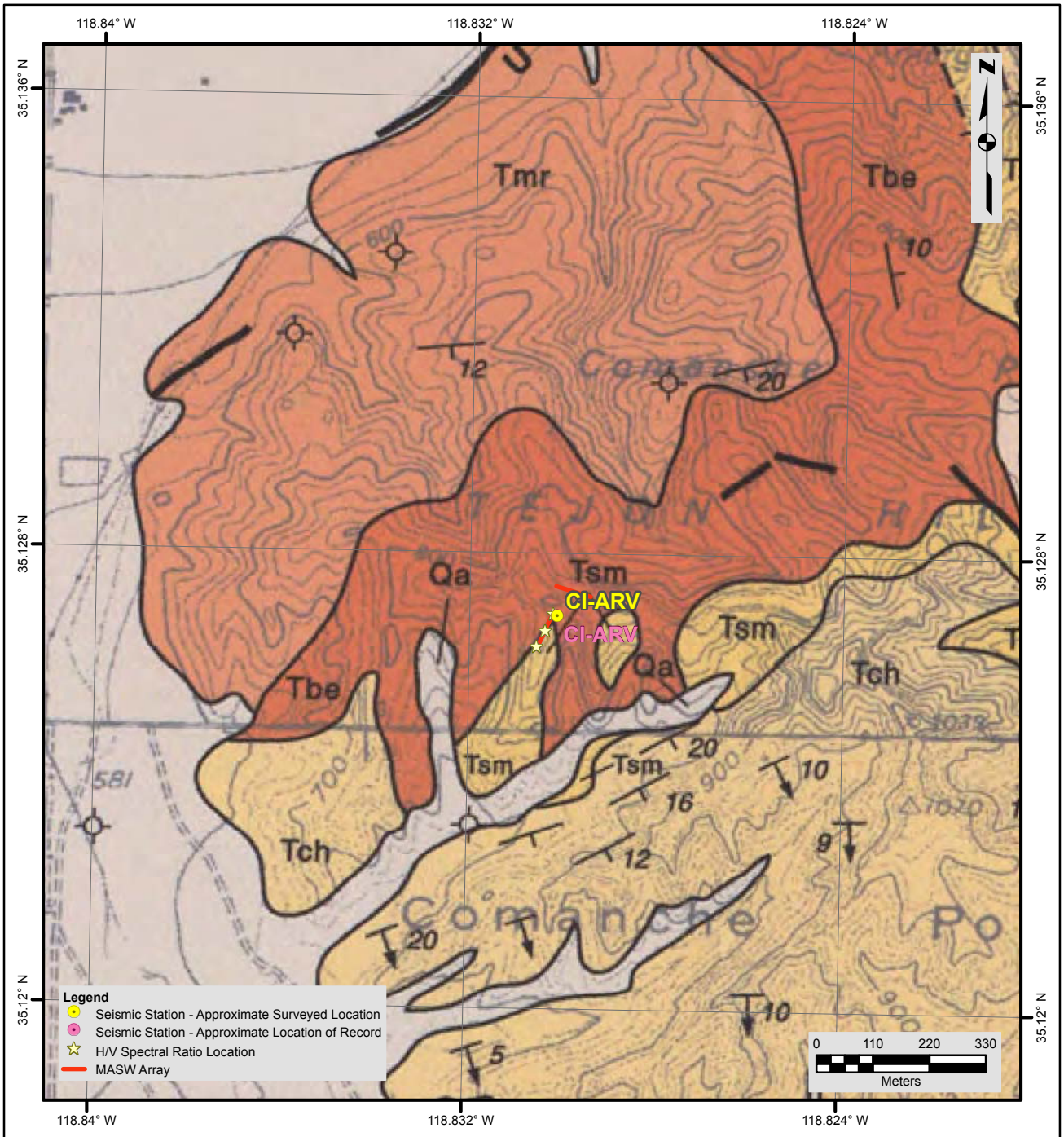

Description of Geologic Map Units

Qa = Quaternary (Holocene) alluvial cobble-pebble gravel and sand near hills, grades outward into sand and silt in level valley areas
Tch = Tertiary (Miocene) Chanac Formation;conglomerate, minor silt, clay and pebbly sand
Tsm = Tertiary (Miocene) Santa Margarita Formation; fine to coarse grained sandstone with pebble conglomerate and green siltstone, fossiliferous
Tbe = Tertiary (Miocene) Bena Gravels; greenish-gray pebbly clays and silts, green to gray-white pebbly arkosic sands, and pebble conglomerate, with lenses of boulder conglomerate
Tmr = Tertiary (Miocene) Reserve Sandstone, massive, and pebbly conglomerate

NOTES:
1. WGS 1984 COORDINATE SYSTEM
2. Geologic Map of the Arvin & Tejon Hills Quadrangles, Kern County, California by Thomas W. Dibblee, Jr., 2008
3. See site map for details of geophysical survey

USGS science for a changing world

GEOVision geophysical services

RECOVERY.GOV

GEOLOGIC MAP
CI•ARV

File Name: CI-ARV

Date: 2/7/2013

Looking southwest towards CI.ARV seismic station and location of array ARV-1

Looking southwest along array ARV-1

Looking northeast at center of array ARV-1 and towards seismic station

Looking from seismic station towards location of array ARV-2 (top of truck over hill)

Looking southeast along array ARV-2

Location of Geophysical Testing Arrays:

Location	Latitude	Longitude
ARV-1, Southwest End of MASW/Refraction Array	35.12636	-118.83050
ARV-1, Center of MASW/Refraction Array	35.12665	-118.83035
ARV-1, Northeast End of MASW/Refraction Array	35.12694	-118.83019
ARV-2, Northwest End of MASW/Refraction Array	35.12742	-118.83012
ARV-2, Center of MASW/Refraction Array	35.12733	-118.82975
ARV-2, Southeast End of MASW/Refraction Array	35.12725	-118.82938
HVSR Sensor 450	35.12694	-118.83018
HVSR Sensor 507	35.12665	-118.83034
HVSR Sensor 453	35.12636	-118.83052
CI.ARV Seismic Station	35.12691	-118.83009

Notes: 1) WGS84 Coordinate System (decimal degrees)
2) Survey accuracy is estimated at 1 to 2 m.

Results:

V_S Model 1 - Array ARV-1

Depth to Top of Layer (m)	Layer Thickness (m)	S-Wave Velocity (m/s)	Inferred P-Wave Velocity (m/s)	Inferred Poisson's Ratio	Inferred Density (g/cm^3)
0	1	128	240	0.3	1.7
1	1.25	168	314	0.3	1.7
2.25	14.75	359	672	0.3	1.8
17	15	456	853	0.3	1.9
32	>3	517	967	0.3	1.9

Notes: 1) Depth of investigation is about 35 m.
2) Bottom layer is a half space.

V_S Model 2 - Array ARV-1

Depth to Top of Layer (m)	Layer Thickness (m)	S-Wave Velocity (m/s)	Inferred P-Wave Velocity (m/s)	Inferred Poisson's Ratio	Inferred Density (g/cm^3)
0	1	129	241	0.3	1.7
1	1.25	165	309	0.3	1.7
2.25	6.75	368	688	0.3	1.8
9	8	346	647	0.3	1.8
17	15	471	881	0.3	1.9
32	>3	508	950	0.3	1.9

Notes: 1) Depth of investigation is about 35 m.
2) Bottom layer is a half space.

V_S Model – Array ARV-2

Depth to Top of Layer (m)	Layer Thickness (m)	S-Wave Velocity (m/s)	Inferred P-Wave Velocity (m/s)	Inferred Poisson's Ratio	Inferred Density (g/cm^3)
0	1.75	135	252	0.3	1.7
1.75	3	232	434	0.3	1.7
4.75	11.25	371	694	0.3	1.8
16	12	423	791	0.3	1.9
28	>7	658	1232	0.3	2.0

Notes: 1) Depth of investigation is about 35 m.
2) Bottom layer is a half space.

Observations/Discussion:

- Seismic refraction and MASW data were acquired along two arrays at this site because the seismic station is located in close proximity to the mapped contact of two geologic units. The two arrays are approximately orthogonal due to orientation of ridges in the site vicinity, which is probably beneficial as the geologic bedding has shallow dip in the site vicinity.
- HVSR plots are similar at frequencies lower than 10 Hz at every station. There are no distinct HVSR peaks below 10 Hz. There are potential weak HVSR peaks at frequencies between 15 and 20 Hz, which would normally be associated with very shallow structure in the upper several meters. It should be noted, however, that these peaks are not normally associated with both horizontal components. The source of energy in this frequency range is unclear given the remote site location.
- The P-wave refraction data for arrays ARV-1 and ARV-2 were modeled using a tomographic inversion routine with a smooth velocity gradient starting model. The seismic refraction models were extended to far offset shot locations to extend depth of investigation.
- The seismic refraction survey design allowed P-wave velocity to be imaged to a maximum depth of about 20 m.
- The seismic refraction model for array ARV-1 shows that P-wave velocity is about 250 to 350 m/s at the surface, increasing to 400 m/s at a depth of about 1 m, 600 m/s at a depth of 2 to 5 m, 800 m/s at a depth of 3 to 15 m and 1,000 m/s at a depth of 12 to 18 m.
- The seismic refraction model for array ARV-2 shows that P-wave velocity is about 250 to 350 m/s at the surface, increasing to 400 m/s at a depth of 1 to 2 m, 600 m/s at a depth of 2 to 7 m, 800 m/s at a depth of 4 to 14 m, 1,000 m/s at a depth of 5 to 18 m and 1,200 m/s at a depth of 6 to greater than 20 m.
- The seismic refraction models indicate that there is lateral velocity variation at the site, which is not unexpected due to dipping bedding. Near surface sediments have slightly higher velocity beneath the northeast end of array ARV-1 and deeper sediments/soft rock have higher velocity beneath the southwest end of the array. There is a distinct shallowing of higher velocity soft rock to the southeast beneath array ARV-2.
- Noise conditions at the site were not sufficient for application of passive surface wave techniques.
- MASW data reduction was quite difficult and dominant higher mode energy was common at frequencies above 25 Hz. Significant effort utilizing limited offset receiver arrays was required to extract small wavelength, fundamental mode Rayleigh wave phase velocity data. Lateral velocity variation probably contributes to the difficulty reducing the MASW data.
- The minimum wavelength surface wave phase velocity data extracted from the 48-channel MASW array was about 13 and 15 m, for arrays ARV-1 and ARV-2, respectively. Reducing data from smaller hammer sources using a limited offset receiver array (i.e. less active geophones) allowed for extraction of surface wave dispersion data to a minimum wavelength of about 3 and 5.5 m for arrays ARV-1 and ARV-2, respectively.

- There is about 40 m/s of scatter in the MASW dispersion data, which is likely the result of lateral velocity variation. The lateral velocity variation is such that it was not possible to extract Rayleigh wave phase velocity data at wavelengths less than 13 to 15 m from the 48 channel MASW receiver array. Dominant higher modes were also an issue at smaller wavelengths/higher frequencies.
- A representative dispersion curve was generated for each MASW data set using a moving average, polynomial curve fitting routine and used for modeling.
- Two V_S models are presented for array ARV-1. Model 1 utilized thicker layers to avoid velocity inversions in the model. Model 2 allowed a minor velocity inversion to occur. The calculated dispersion curve for Model 2 has slightly lower RMS error than Model 1. A velocity inversion does probably not have much significance, given the lateral velocity variation at the site and the fact that the velocity model is only representative of generalized or averaged velocity structure. V_{S30} is almost identical for each of the models. Only a single model was developed for Array ARV-2. The models are not unique and multiple models could be developed to fit the observed dispersion curve with similar RMS errors. V_{S30}, however, is not particularly sensitive to the nonuniqueness in the models.
- Surface wave depth of investigation is about 35 m based on half of maximum wavelength criteria.
- V_{S30} for array ARV-1 Models 1 and 2 is 354 and 355 m/s, respectively, and averages 354 m/s (Site Class D/C).
- V_{S30} is 342 m/s for array ARV-2 (Site Class D/C).
- The average V_{S30} for the two arrays is 348 m/s (Site Class D/C).
- Average S-wave velocity between 2 m (assumed sensor depth) and 32 m for array ARV-1 Models 1 and 2 is 398 and 401 m/s, respectively, and averages 399 m/s (Site Class C).
- Average S-wave velocity between 2 and 32 m for array ARV-2 is 392 m/s (Site Class C).
- The average S-wave velocity between 2 and 32 m for the two arrays is 395 m/s (Site Class C).
- More research is needed on the effects of varying degrees of lateral velocity variation on S-wave velocity modes developed from surface wave testing. We believe that if a coherent dispersion curve can be developed that utilizes most data from multiple source locations at each end of the array and interior source locations then the resulting V_S model may be representative of average velocity structure. However, synthetic modeling is required to test this hypothesis.

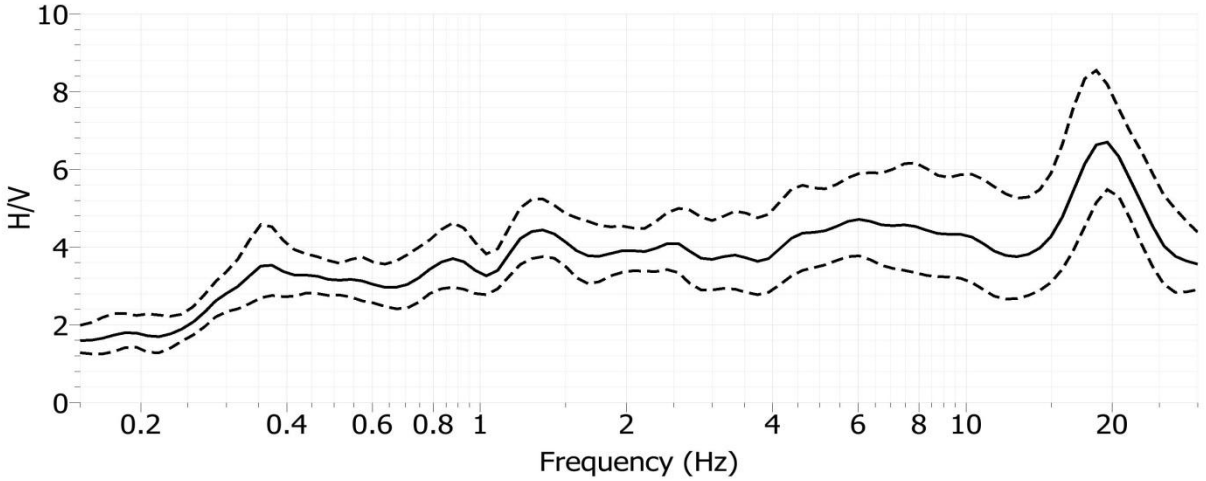

Site CI.ARV, H/V Spectral Ratio, Array ARV-1, Sensor 450

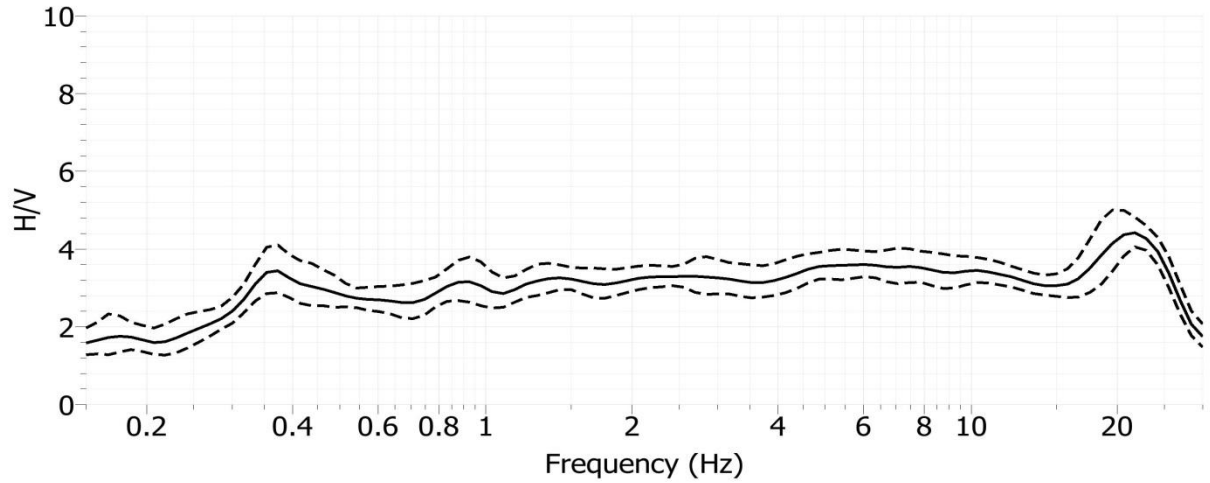

Site CI.ARV, H/V Spectral Ratio, Array ARV-1, Sensor 507

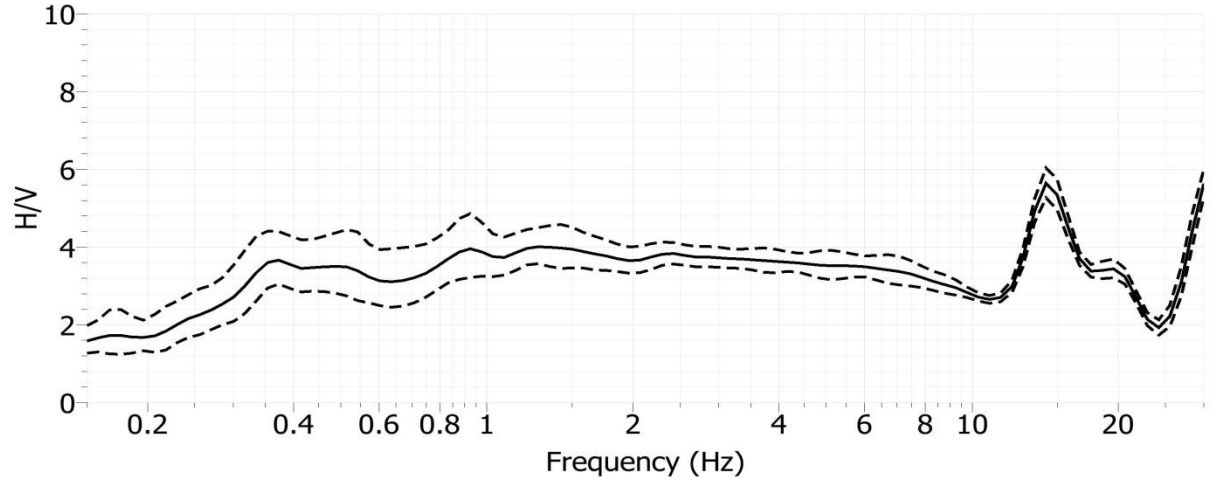

Site CI.ARV, H/V Spectral Ratio, Array ARV-1, Sensor 453

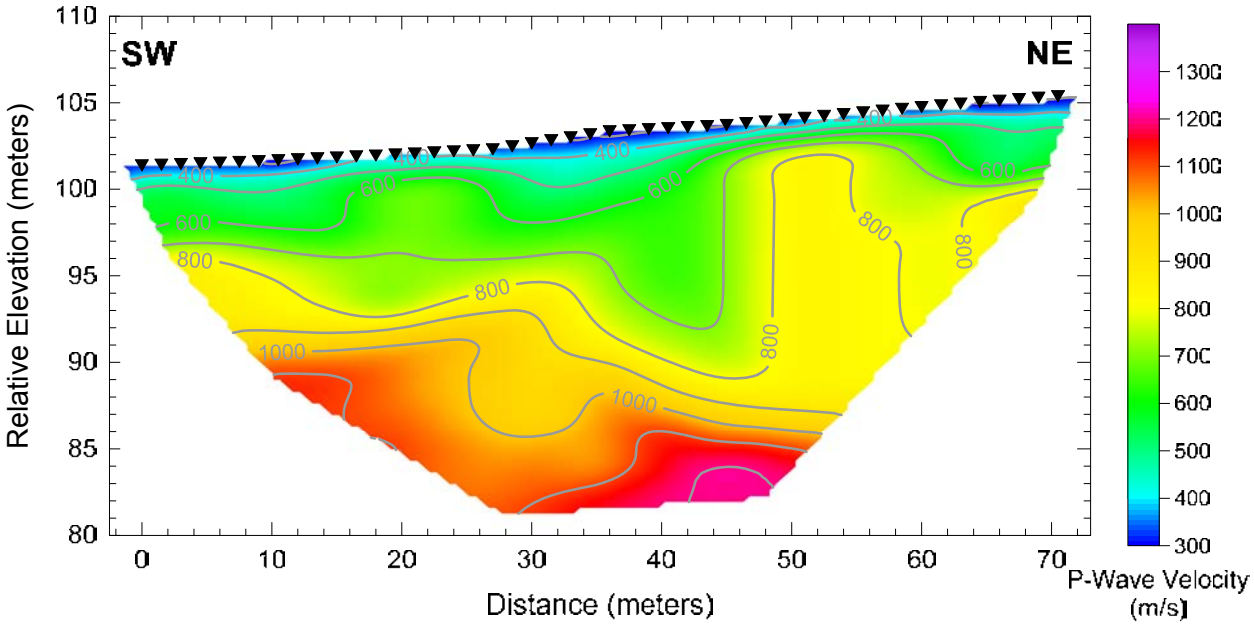

Array ARV-1 – P-wave Tomographic Seismic Refraction Model utilizing Smooth Velocity Gradient Starting Mode

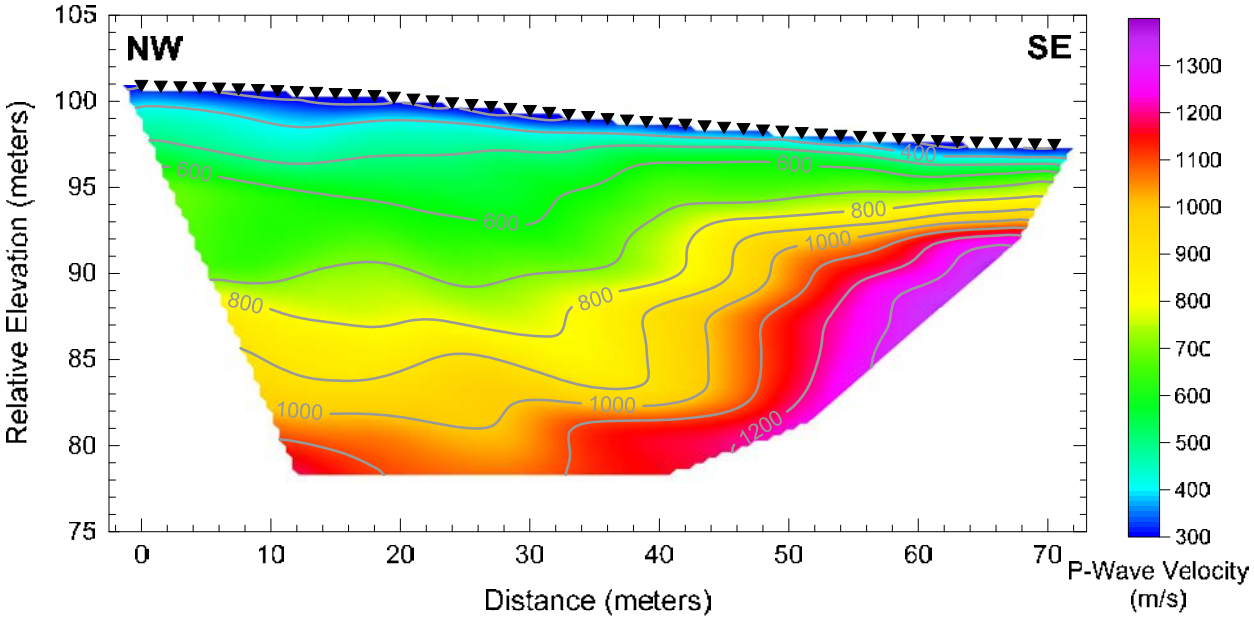

Array ARV-2 – P-wave Tomographic Seismic Refraction Model utilizing Smooth Velocity Gradient Starting Model

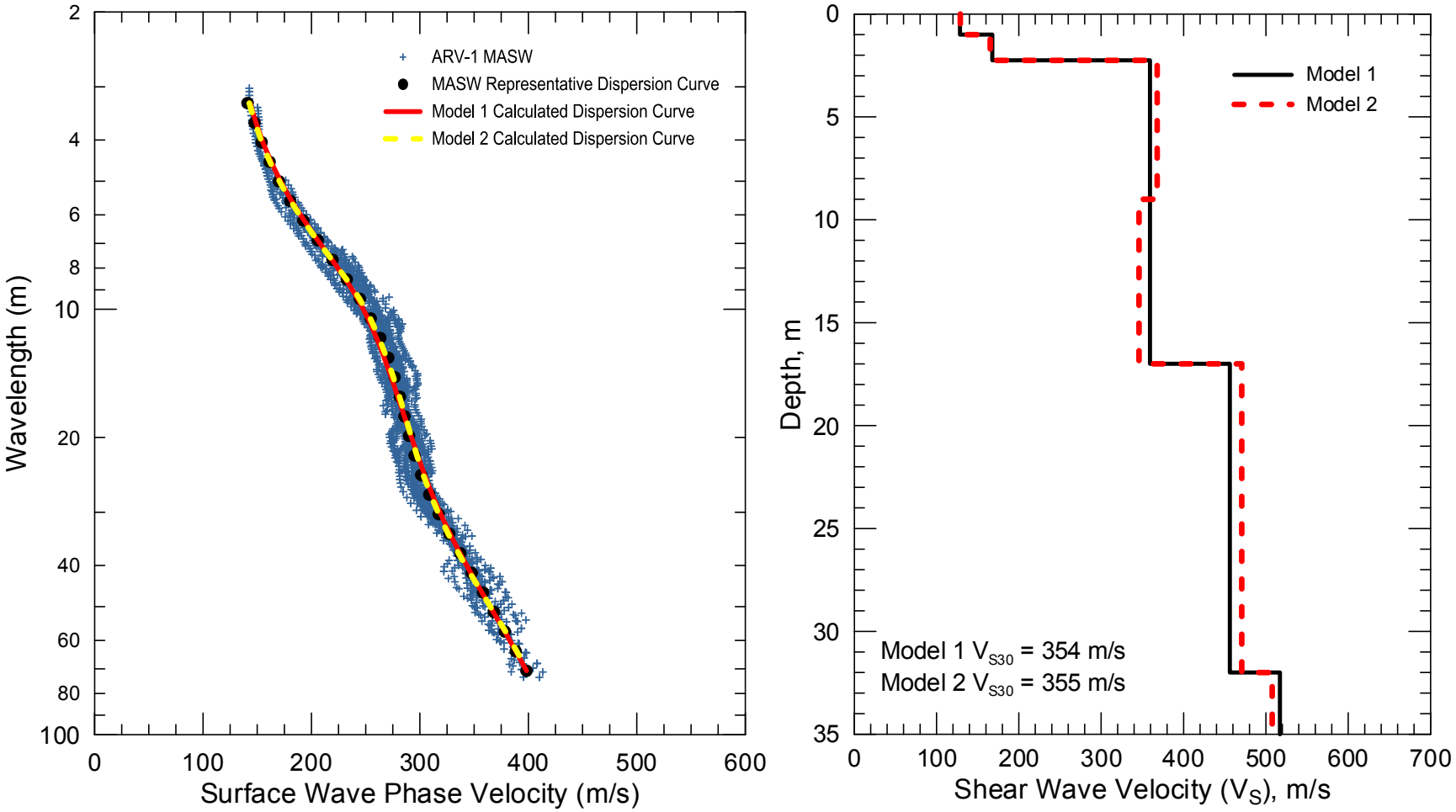

CI.ARV - Field, representative and inverted theoretical surface wave dispersion data (left) and associated V_S model (right) for Array ARV-1

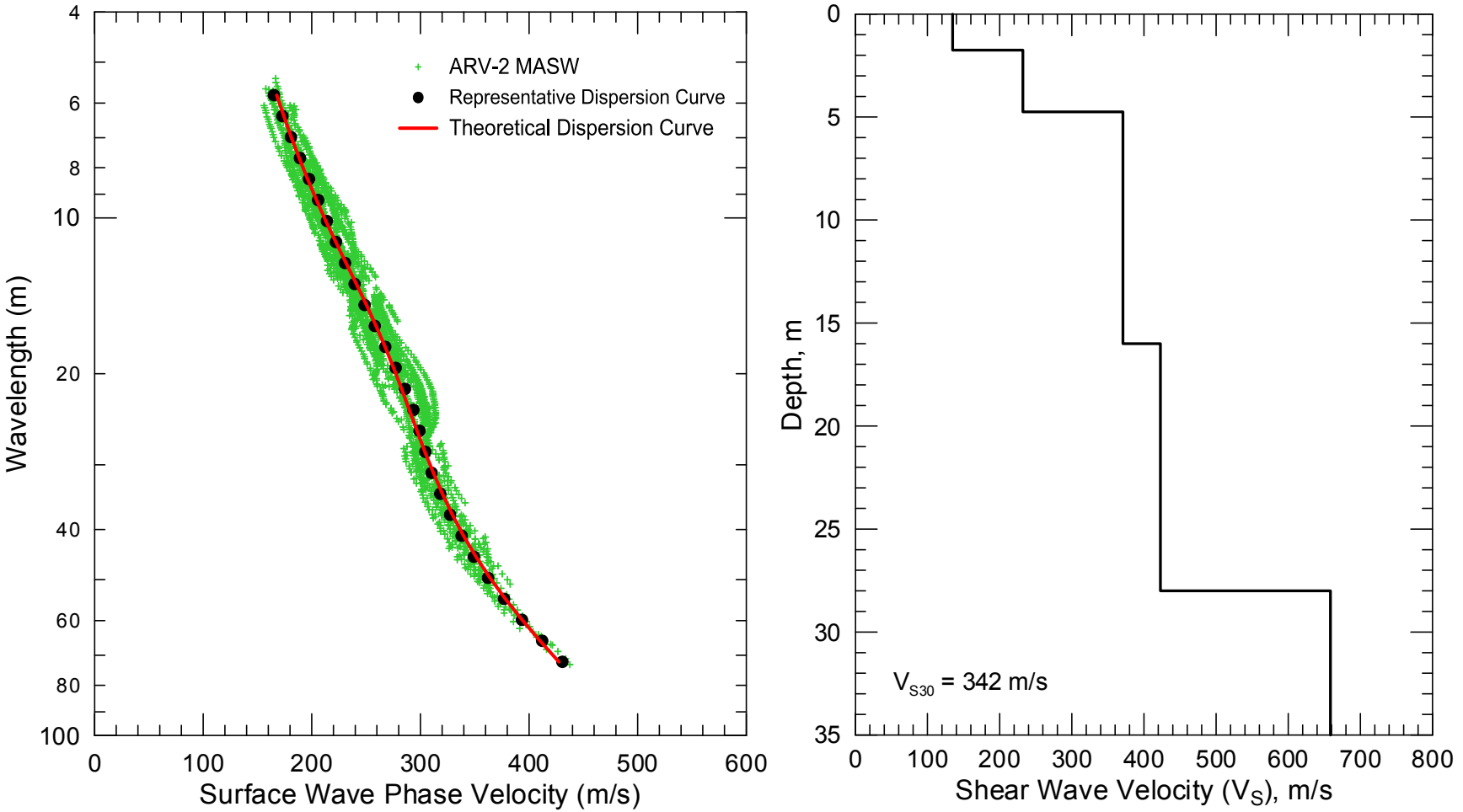

CI.ARV - Field, representative and inverted theoretical surface wave dispersion data (left) and associated V_S model (right) for Array ARV-2

Site CI.BAK

Location: California State University, Bakersfield, California

Latitude: 35.34444 **Longitude:** -119.10445
(Station coordinates provided by USGS, WGS84 coordinate system)

V_{S30} (measured): 275 m/s

V_{S30} (adjusted to more accurately reflect seismic station conditions): 299 m/s (average S-wave velocity between 2 and 32 m adjusting for inferred 2 m seismic sensor depth).

NEHRP Site Class: D

Geomatrix Code: IHD

Geologic Conditions/Observations: Quaternary (Holocene) alluvial fan deposits, deep soil site.

Site Conditions: Urban site with significant noise sources from traffic in site vicinity. Relatively flat topography in site vicinity. High traffic road located immediately south of survey area.

Geophysical Methods Utilized: HVSR, MASW, SASW, array microtremor, ReMi™

Geophysical Testing Arrays:

1. Array BAK-1 (24 channel, linear passive surface wave array utilizing 4.5 Hz vertical geophones spaced 5 m apart for a length of 115 m) and orientated perpendicular to road south of survey area. Limited MASW and seismic refraction data (off-end shots with accelerated weight drop energy source) acquired along array BAK-1.
2. Array BAK-2 (10 channel, triangle passive surface wave array utilizing 1 Hz geophones and an 80 m length for outer side of array).
3. Array BAK-3 (48 channel MASW array utilizing 4.5 Hz vertical geophones spaced 1 m apart for a length of 47 m and a common midpoint SASW array utilizing 1 Hz geophones with maximum receiver spacing of 32 m). Array BAK-3 was aligned along array BAK-1 and centered at midpoint of array BAK-1.
4. Three HVSR measurement locations located near the outer corners of BAK-2.

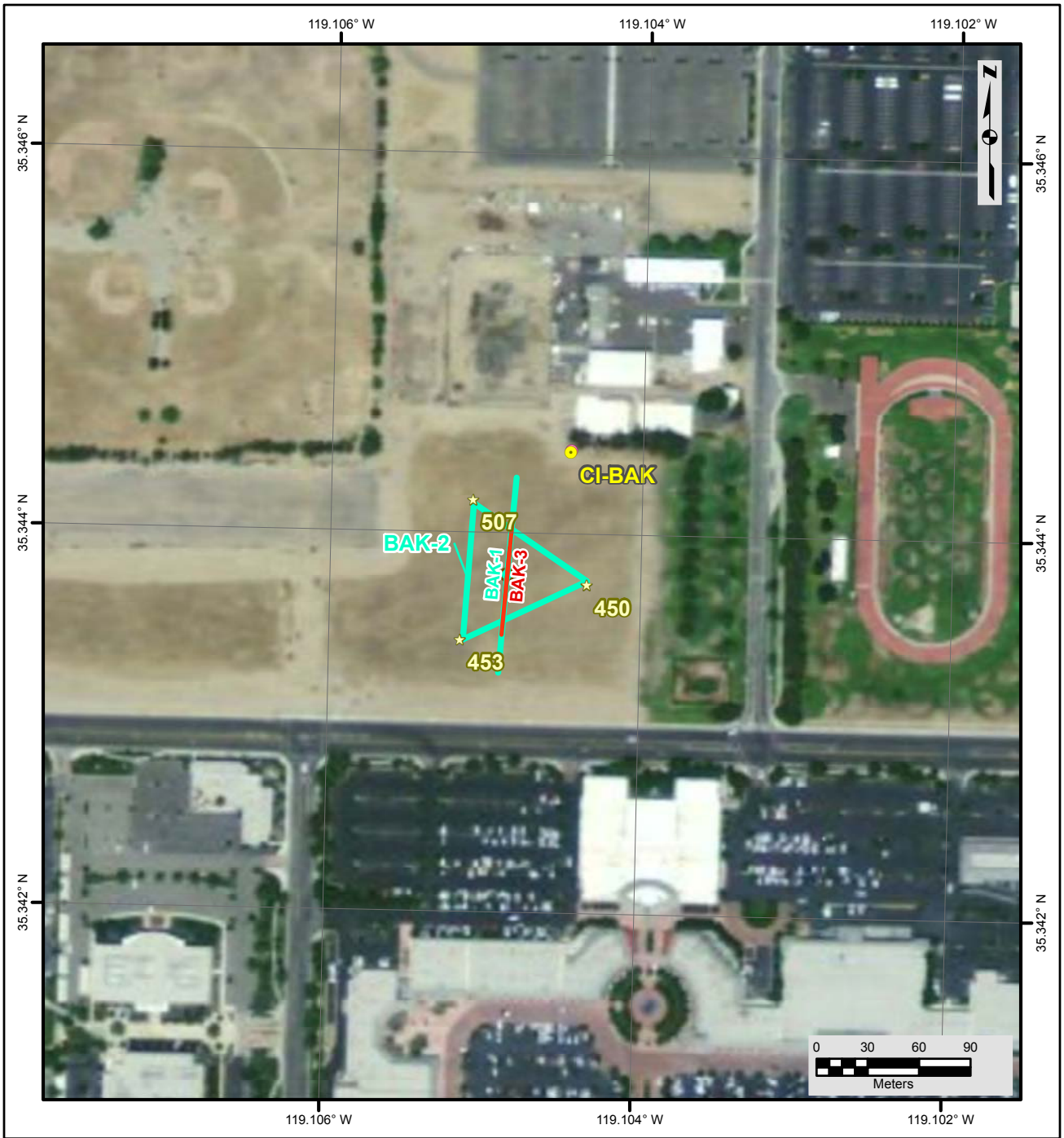

Legend

- Seismic Station - Approximate Surveyed Location
- Seismic Station - Approximate Location of Record
- H/V Spectral Ratio Measurement Location
- MASW and SASW Array
- Passive Surface Wave Array

NOTES:
1. WGS 1984 COORDINATE SYSTEM
2. Image Source: ESRI, i-cubed, USDA FSA, USGS, AEX, GeoEye, Getmapping, Aerogrid, IGP

File Name: CI-BAK-I

Date: 4/7/2011

USGS science for a changing world

GEOVision geophysical services

RECOVERY.GOV

SITE MAP
CI•BAK

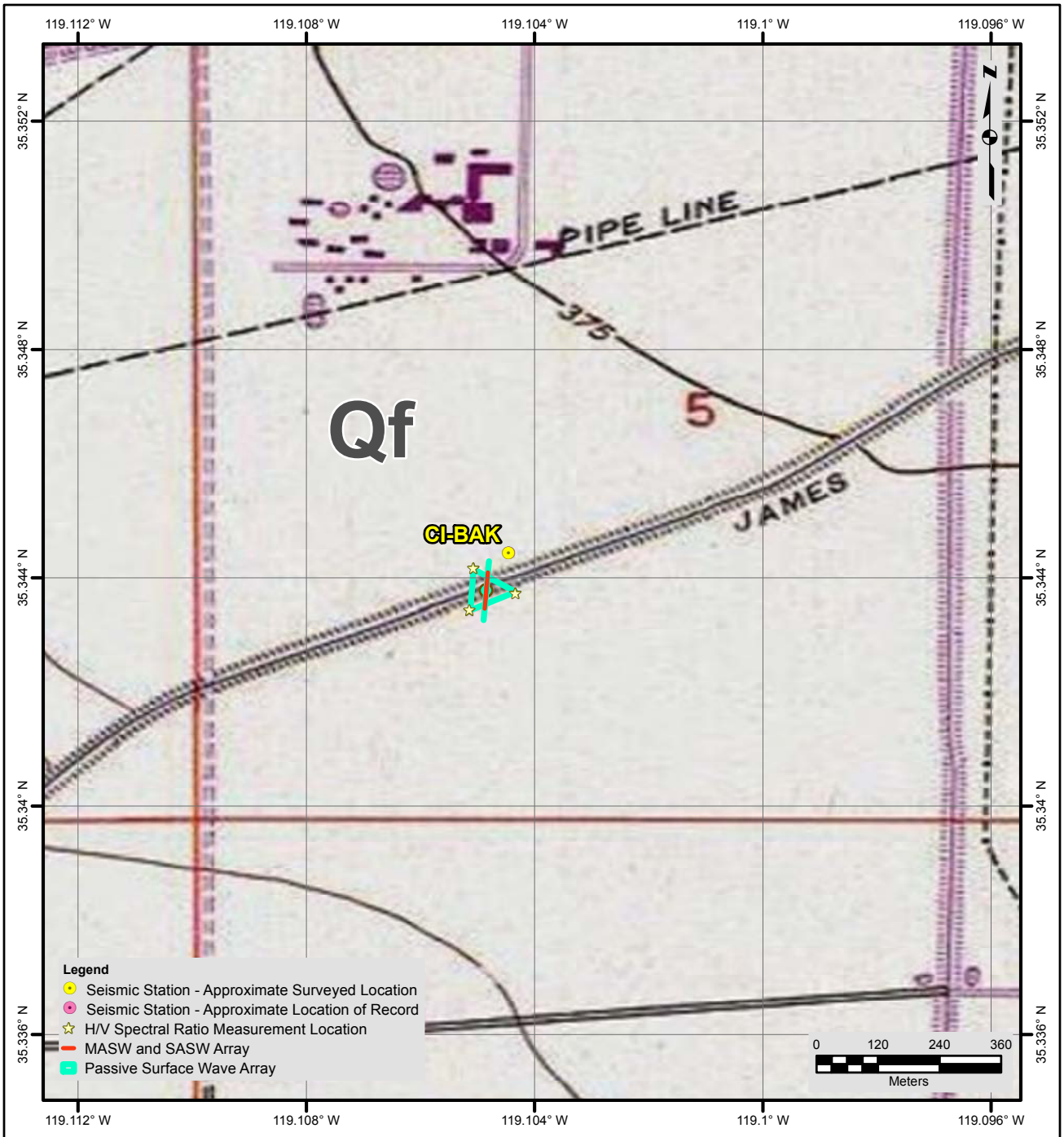

Description of Geologic Map Units

Qf = Quaternary (Holocene) Great Valley recent fan deposits

NOTES:
1. WGS 1984 COORDINATE SYSTEM
2. Topo Image Sources: USGS, FAO, NPS, EPA, NRCAN, GeoBase, Esri, DeLorme, TANA, Intermap, AND, other suppliers, and the GIS community
3. Geologic Map Units from:
Geologic Map of California (Olaf P. Jenkins edition), Fresno Sheet compiled by Robert A Matthews and John L. Burnett, 1965
4. See site map for details of geophysical survey

File Name: CI-BAK

Date: 4/1/2011

USGS science for a changing world

GEOVision geophysical services

RECOVERY.GOV

GEOLOGIC MAP
CI•BAK

Looking northeast from survey area towards CI.BAK seismograph station

Looking east towards seismograph station from off-end shot point on array BAK-1

SASW array BAK-3

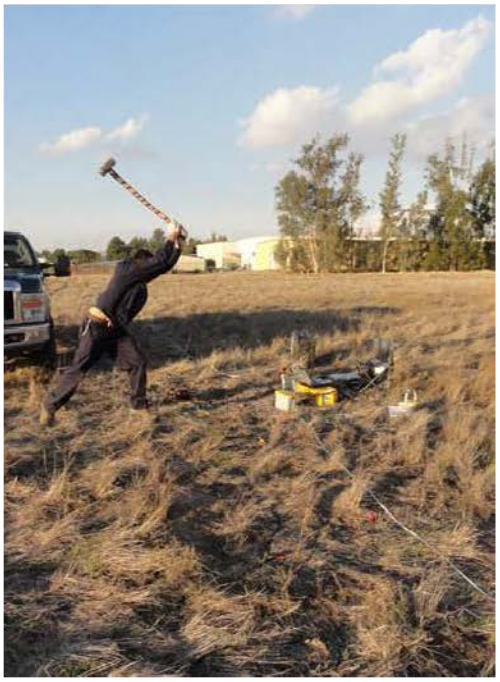

MASW array BAK-3

Looking northeast towards seismograph station from HVSR sensor 453 and corner of triangle array BAK -2

Location of Geophysical Testing Arrays:

Location	Latitude	Longitude
BAK-1, South End of Array	35.34326	-119.10489
BAK-1, North End of Array	35.34429	-119.10480
BAK-2, Corner of Array, Sensor Location 1	35.34415	-119.10507
BAK-2, Corner of Array, Sensor Location 3	35.34343	-119.10512
BAK-2, Corner of Array, Sensor Location 5	35.34375	-119.10433
BAK-2, Center of Array, Sensor Location 10	35.34378	-119.10485
BAK-3, Center of Array	35.34378	-119.10485
HVSR Sensor 507	35.34417	-119.10508
HVSR Sensor 453	35.34343	-119.10514
HVSR Sensor 450	35.34373	-119.10434
CI.BAK Seismometer Location (approximate)	35.34443	-119.10445

Notes: 1) WGS84 Coordinate System (decimal degrees)
2) BAK-3 aligned along BAK-1
3) Typical survey accuracy is estimated at 1 to 2 m.

Results:

V_S Model

Depth to Top of Layer (m)	Layer Thickness (m)	S-Wave Velocity (m/s)	Inferred P-Wave Velocity (m/s)	Assumed Poisson's Ratio	Assumed Density (g/cm^3)
0	0.5	77	145	0.3	1.9
0.5	1	220	411	0.3	1.9
1.5	2	221	414	0.3	1.9
3.5	3	202	378	0.3	1.9
6.5	5	274	513	0.3	1.9
11.5	7.5	296	553	0.3	1.9
19	10	353	660	0.3	2.0
29	13	454	849	0.3	2.0
42	16	500	936	0.3	2.0
58	>22	613	1148	0.3	2.0

Observations/Discussion:

- Test area inadvertently centered on a backfilled channel, which is evident on topographic maps and older aerial photographs of the site. Review of seismic waveforms from arrays BAK-1 and BAK-3 show no evidence of significant lateral velocity variation or artifacts associated with the backfilled channel.
- HVSR curves generally similar at all stations validating the 1-D velocity assumption.
- HVSR peak at about 0.13 Hz, which is consistent for a deep soil site.
- Noise conditions at site appeared sufficient for successful application of passive surface wave techniques and passive surface wave data successfully extended depth of investigation.
- The ESAC technique was used to extract surface wave dispersion data from the passive triangle array data. Both the ReMi™ and ESAC techniques were used to extract surface wave dispersion data from the linear arrays.
- Surface wave dispersion data from all active and passive surface wave datasets are in good agreement at this site with minor differences likely associated with lateral velocity variation.
- SASW data provides Rayleigh wave dispersion data to slightly smaller wavelengths (higher frequencies) than the MASW data and passive surface wave data.
- MASW data was also acquired on the linear passive surface wave array (BAK-1) to obtain long wavelength surface wave data without concern of near field effects over the frequency range of interest.
- Representative dispersion curves were generated for each surface wave data set using a moving average, polynomial curve fitting routine. These individual representative dispersion curves were assigned a weight and combined and a representative dispersion curve generated for the combined data set for data modeling.
- No evidence of a shallow water table on MASW seismic records.
- Surface wave depth of investigation is about 75 to 80 m based on one half of maximum wavelength criteria.
- V_{S30} is 275 m/s (NEHRP Site Class D).
- The upper 0.5 m thick low velocity layer in S-wave velocity model results from high frequency SASW dispersion data only and is likely associated with disturbed surficial soils, which may have highly variable velocity across the site. Removal of this layer increases V_{S30} to 288 m/s.
- Average S-wave velocity between 2 m (nominal sensor depth) and 32 m is 299 m/s.
- Average S-wave velocity of the upper 75 m (V_{S75}) is 384 m/s.

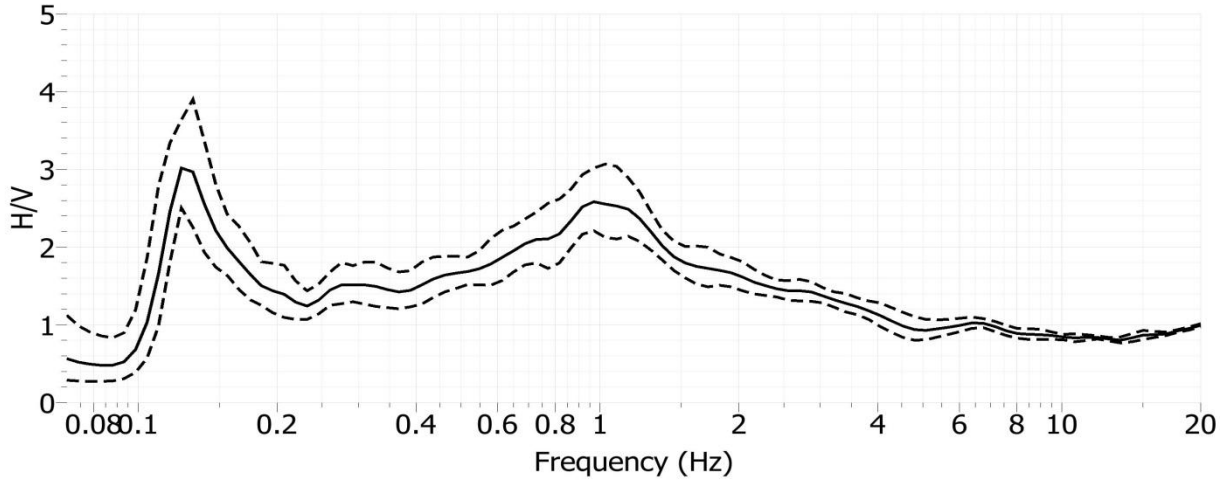

Site CI.BAK, H/V Spectral Ratio, Array BAK-2, Sensor 507

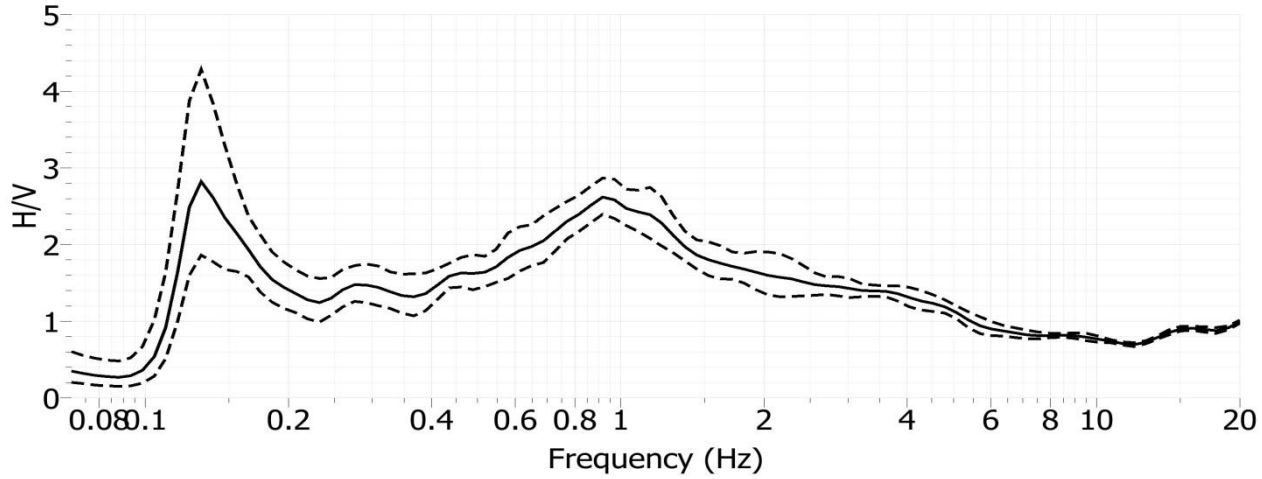

Site CI.BAK, H/V Spectral Ratio, Array BAK-2, Sensor 450

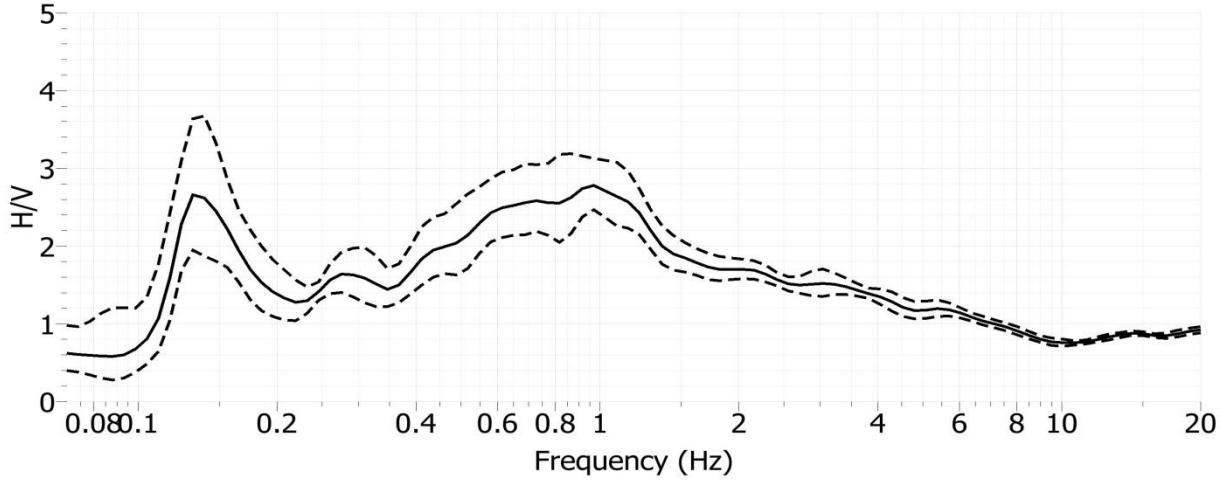

Site CI.BAK, H/V Spectral Ratio, Array BAK-2, Sensor 453

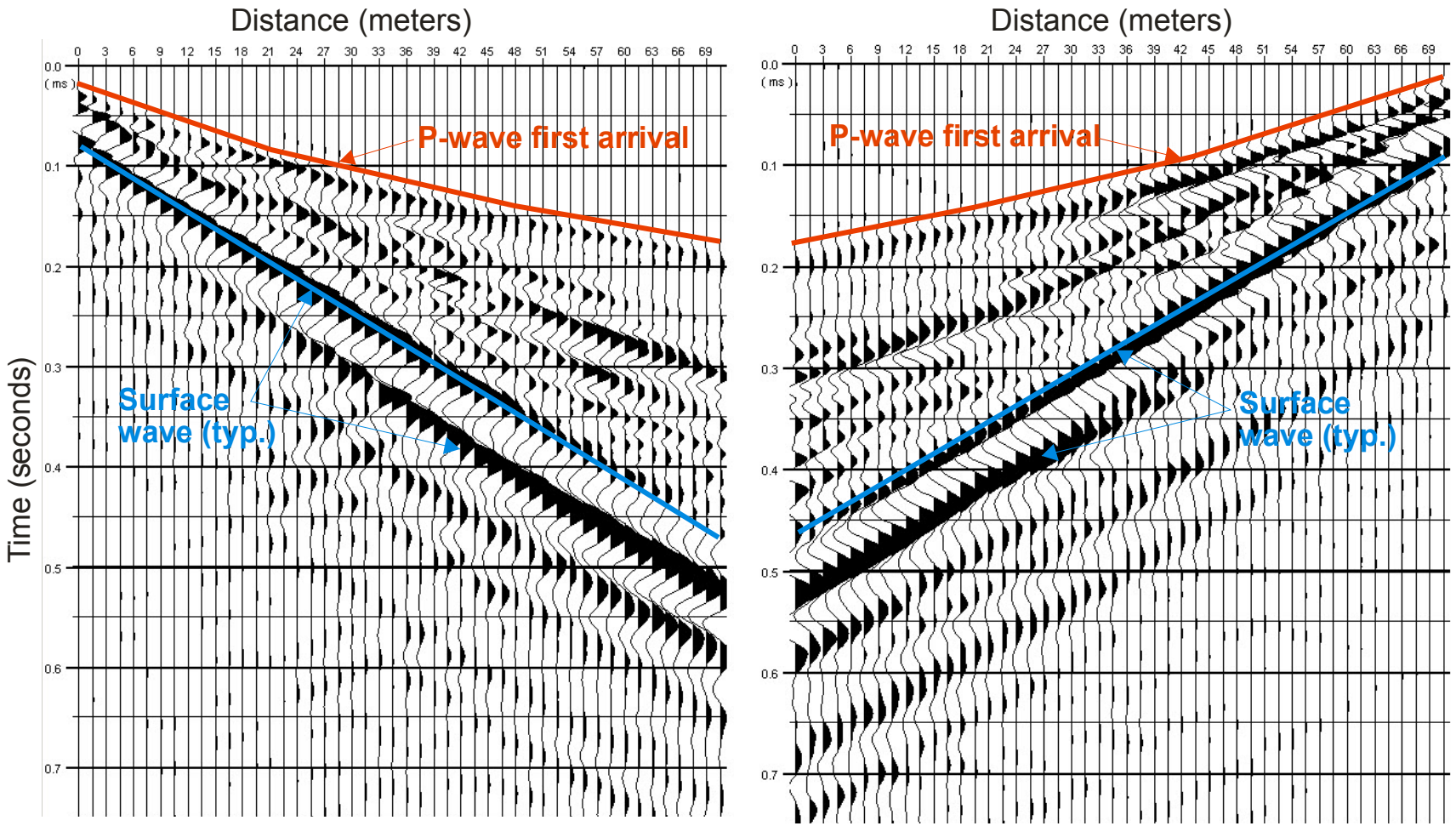

Example forward and reverse seismic records from Array BAK-3 illustrating that there is no clear lateral velocity variation or artifacts associated with seismic line bisecting a backfilled channel

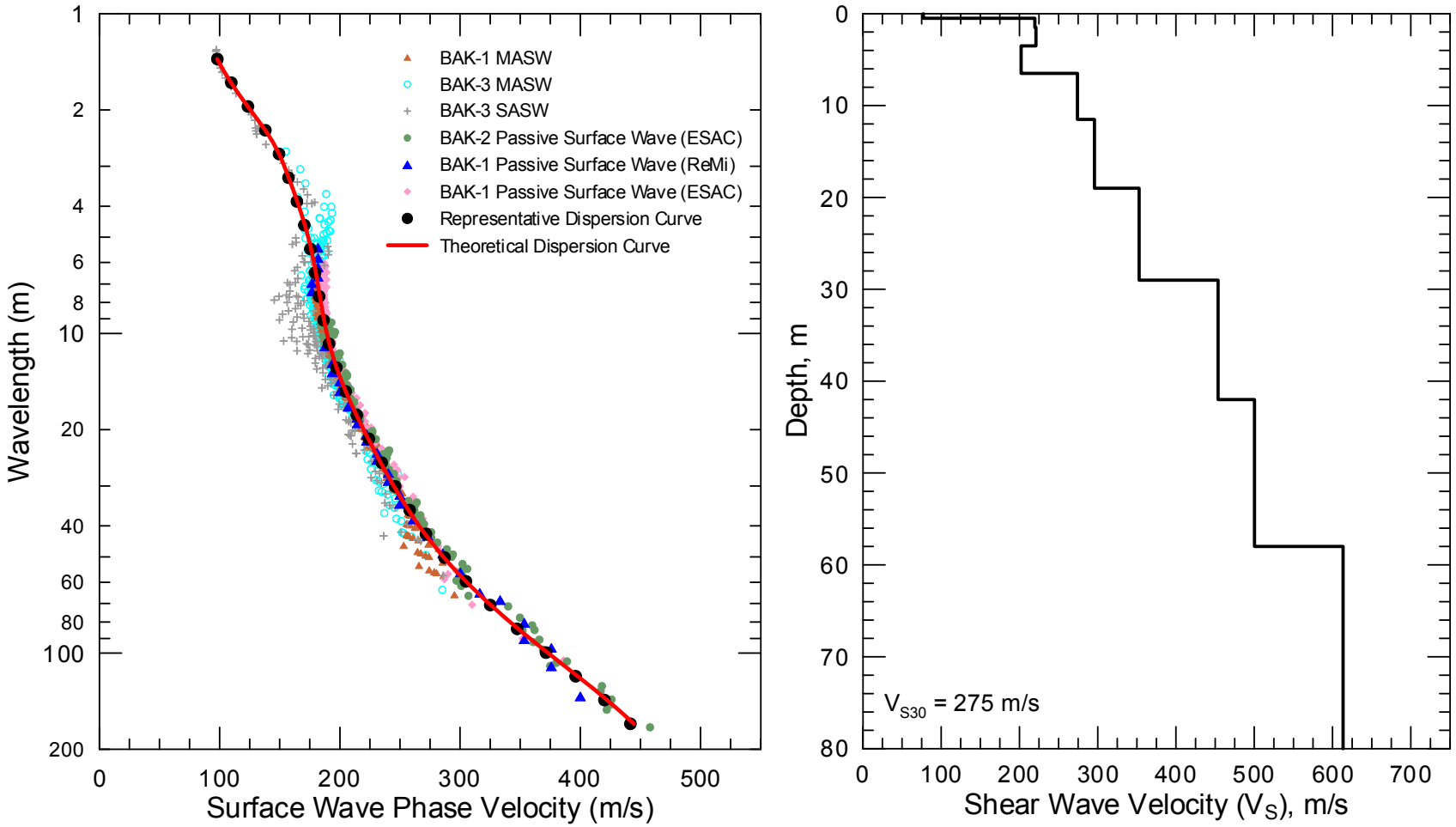

CI.BAK - Field, representative and inverted theoretical surface wave dispersion data (left) and associated V_S model (right)

Site CI.BAR

Location: Barrett Dam, San Diego County, California

Latitude: 32.68005 **Longitude:** -116.67215
(Station coordinates provided by USGS, WGS84 coordinate system)

V_{S30} (measured): 511 m/s

V_{S30} (adjusted to more accurately reflect seismic station conditions): 559 m/s (average S-wave velocity between 1 and 31 m adjusting for sensor being located on weathered rock rather than fill).

NEHRP Site Class: C (less weathered granitic rock that is possibly Site Class B is located within about 20 m of the seismic station).

Geomatrix Code: AGB/AGA

Geologic Conditions/Observations: Site located on geologic unit mapped as Mesozoic granitic rock. Field observations indicate that the near surface rock is decomposed to very intensely weathered and that the rock may be much more competent at the southern end of the survey area and north of the survey area. Laterally variable weathering of granitic rocks is typical in the site vicinity.

Site Conditions: Rural site located adjacent to a dirt road cut into the side of a mountain. Steep topography in site vicinity.

Geophysical Methods Utilized: HVSR, Seismic Refraction, MASW

Geophysical Testing Arrays:

1. Array BAR-1 (48 channel MASW array utilizing 4.5 Hz vertical geophones spaced 1.5 m apart for a length of 70.5 m, forward and reverse shot locations with multiple source offsets and source types and center shot location).
2. Array BAR-2 (48 channel MASW array utilizing 4.5 Hz vertical geophones spaced 3 m apart for a length of 141 m, forward and reverse shot locations with multiple source offsets and source types and multiple interior shot locations).
3. S-wave seismic refraction data also acquired along array BAR-2 (48 channel array utilizing 10 Hz horizontal geophones spaced 3 m apart for a length of 141 m, several forward and reverse shot locations and a center shot).
4. Three HVSR measurement locations distributed along array BAR-1.

Legend

- Seismic Station - Approximate Surveyed Location
- Seismic Station - Approximate Location of Record
- H/V Spectral Ratio Location
- Seismic Refraction Array
- MASW and Seismic Refraction Array

NOTES:
1. WGS 1984 COORDINATE SYSTEM
2. Image Source: ESRI, i-cubed, USDA FSA, USGS, AEX, GeoEye, Getmapping, Aerogrid, IGP

File Name: CI-BAR-I

Date: 2/7/2013

USGS science for a changing world

GEOVision geophysical services

RECOVERY.GOV

SITE MAP
CI•BAR

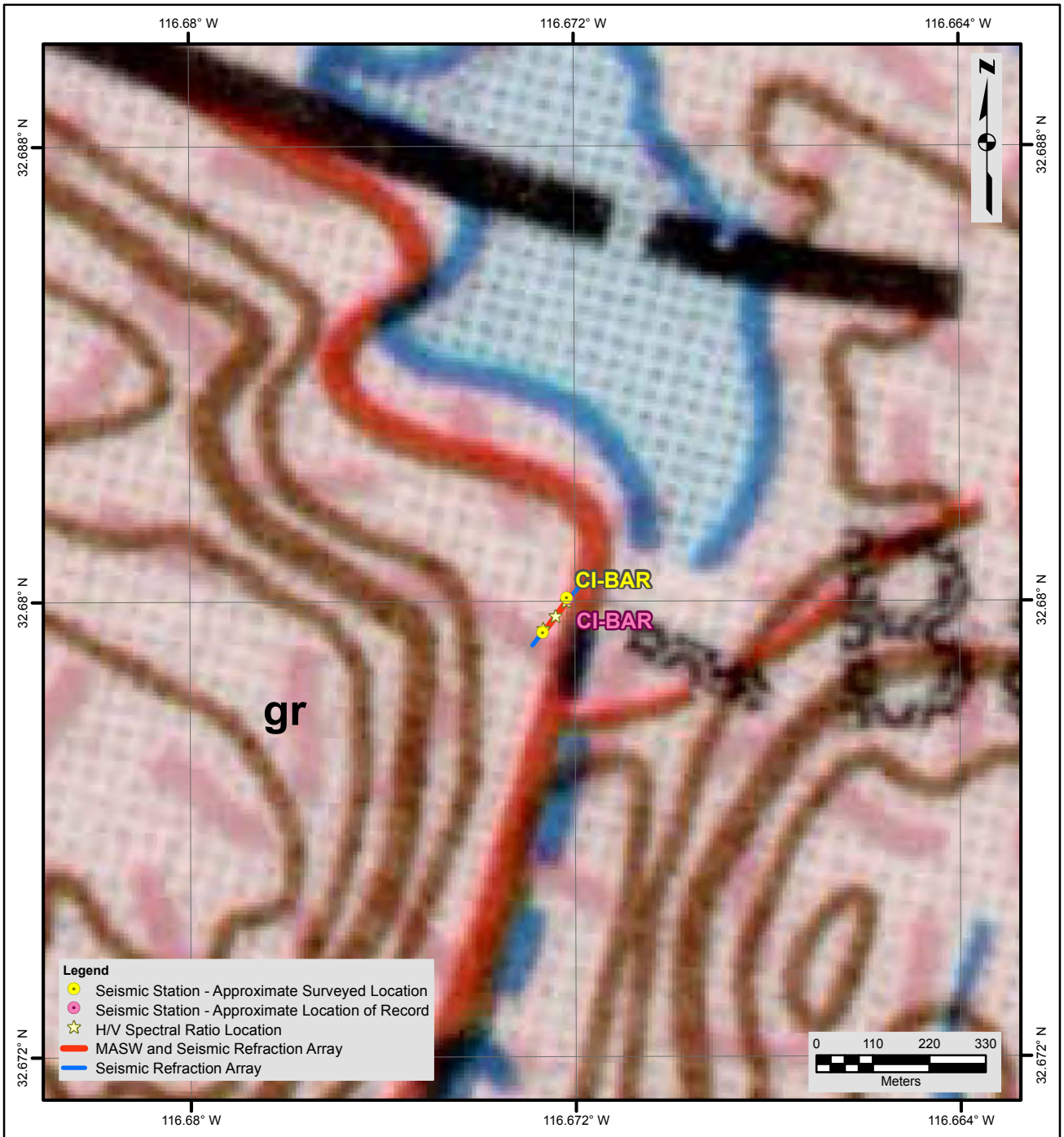

Description of Geologic Map Units

gr = Mesozoic granitic rocks

NOTES:
1. WGS 1984 COORDINATE SYSTEM
2. Geologic Map of California, San Diego-El Centro Sheet, Olaf P Jenkins Edition
by Rudolph G. Strand, 1962
3. See site map for details of geophysical survey

File Name: CI-BAR

Date: 2/7/2013

USGS science for a changing world

GEOVision geophysical services

RECOVERY.GOV

GEOLOGIC MAP
CI•BAR

Looking southwest towards structure housing CI.BAR seismic station and array BAR-1

Looking north at northeast end of array BAR-1, seismic station and weight drop energy source

Looking northeast along array BAR-2

Looking at outcrop of decomposed granitic rock near the seismic station

Looking southwest along array BAR-1. Bedrock outcrop in background appears more competent than that adjacent to the array

Location of Geophysical Testing Arrays:

Location	Latitude	Longitude
BAR-1, Southwest End of MASW/Refraction Array	32.67949	-116.67264
BAR-1, Center of MASW/Refraction Array	32.67974	-116.67241
BAR-1, Northeast End of MASW/Refraction Array	32.68000	-116.67218
BAR-2, Southwest End of Refraction Array	32.67923	-116.67290
BAR-2, Center of Refraction Array	32.67973	-116.67242
BAR-2, Northeast End of Refraction Array	32.68022	-116.67196
HVSR Sensor 450	32.67952	-116.67266
HVSR Sensor 453	32.67974	-116.67241
HVSR Sensor 507	32.67999	-116.67218
CI.BAR Seismic Station (Approximate)	32.68006	-116.67218

Notes: 1) WGS84 Coordinate System (decimal degrees)

2) Survey accuracy is estimated at 2 to 3 m.

Results:

Average V_P and Estimated V_S Models from Central Portion of P-wave Seismic Refraction Array BAR-2

Depth to Top of Layer (m)	Layer Thickness (m)	P-Wave Velocity (m/s)	Estimated S-Wave Velocity (m/s)			
			Poisson's Ratio = 0.25	Poisson's Ratio = 0.30	Poisson's Ratio = 0.3333	Poisson's Ratio = 0.35
0.00	0.51	429	248	229	214	206
0.51	1.02	576	333	308	288	277
1.53	1.02	649	375	347	325	312
2.56	1.02	766	442	410	383	368
3.58	1.02	867	501	463	434	417
4.60	1.02	982	567	525	491	472
5.62	1.02	1006	581	538	503	483
6.65	2.15	1100	635	588	550	528
8.79	2.15	1118	646	598	559	537
10.94	2.15	1146	662	613	573	550
13.09	2.15	1203	695	643	602	578
15.24	2.15	1253	723	670	626	602
17.38	2.15	1313	758	702	656	631
19.53	2.15	1374	793	734	687	660
21.68	2.15	1426	823	762	713	685
23.82	2.15	1502	867	803	751	722
25.97	2.15	1583	914	846	792	760
28.12	Half Space	1664	960	889	832	799

V_S Model (MASW)

Depth to Top of Layer (m)	Layer Thickness (m)	S-Wave Velocity (m/s)	Inferred P-Wave Velocity (m/s)	Assumed Poisson's Ratio	Assumed Density (g/cm^3)
0	1	169	315	0.3	1.8
1	6	301	563	0.3	1.8
7	8	509	953	0.3	2.0
15	10	799	1495	0.3	2.1
25	>5	1088	2036	0.3	2.2

Notes: 1) Depth of investigation is about 30 m.
2) Bottom layer is a half space.
3) Half space velocity not well resolved.

Observations/Discussion:

- The HVSR curves are very similar at frequencies lower than 7 Hz. There is a possible weak HVSR peak at about 4 Hz and a trough at 6 Hz at all sensor locations. This possible HVSR peak could be associated with the base of the uppermost zone of weathered rock.
- Both P-wave seismic refraction and MASW data reduction was difficult at this site. The only location to conduct seismic testing was on a dirt road cut into the slope near the seismic station. There is a distinct possibility that the thickness of fill in the road increases moving away from the toe of slope. There is possible evidence of out of plane refractors in the seismic refraction data and most definitely variable weathering of bedrock in the site vicinity. The S-wave seismic refraction and MALW data collected along array BAR-2 was not useable.
- The P-wave seismic refraction data for the 141 m long array BAR-2 were modeled using a tomographic inversion routine with a smooth velocity gradient starting model.
- The P-wave seismic refraction survey design allowed P-wave velocity to be imaged to a maximum depth of about 28 m. The seismic refraction model indicates that P-wave velocity is about 350 to 500 m/s at the surface and increases to 1,000 m/s at a depth of 2 to 7 m and over 1,500 m/s at a depth of 5 to 25 m. P-wave velocity appears to exceed 1,750 m/s at relatively shallow depth between positions of 20 and 50 m and 110 and 141 m.
- The seismic refraction survey indicates that there is significant lateral velocity variation at the site with shallow zones of high velocity rock between 20 and 50 m and 110 and 141 m on the seismic line. These zones of higher velocity rock are consistent with field observations, which indicate that there are zones of decomposed rock adjacent to zones of less weathered rock.
- The average P-wave velocity of the upper 30 m (V_{P30}) was estimated between 51 and 99 m on the P-wave refraction model, where depth of investigation is greatest. V_{P30} ranges from about 1,039 to 1,313 m/s between a position of 51 to 99 m, a 25% variation, and is

expected to be much higher on both sides of this interval. The lowest and highest estimated V_{P30} over this distance interval occurs at a position of 93 and 51 m, respectively. MASW array BAR-1 is located between 39 and 109.5 m on array BAR-2, primarily covering the segment of array BAR-2 with lower velocities.

- An average V_P model was developed over the 51 to 99 m distance interval by horizontally averaging the travel time of each model cell and cell thickness and average V_{P30} was determined to be 1,112 m/s. Assuming constant Poisson's ratios of 0.25, 0.3, 0.3333 and 0.35 would result in an estimated V_{S30} of 642, 594, 556 and 534 m/s, respectively. Bedrock is not expected to be saturated in the upper 30 m, therefore, Poisson's ratios in the 0.25 to 0.35 range is probable.
- The lowest value of V_{P30} over the 51 to 99 m distance interval, 1,039 m/s, occurs at a position of 93 m. Assuming constant Poisson's ratios of 0.25, 0.3, 0.3333 and 0.35 would result in an estimated V_{S30} of 600, 555, 519 and 499 m/s, respectively.
- The highest value of V_{P30} over the 51 to 99 m distance interval, 1,313 m/s, occurs at a position of 51 m. Assuming constant Poisson's ratios of 0.25, 0.3, 0.3333 and 0.35 would result in an estimated V_{S30} of 758, 702, 657 and 631 m/s, respectively. V_{P30} is expected to be higher than that presented above between a position of 20 and 50 m and 110 and 140 m.
- Noise conditions at the site were not sufficient for application of passive surface wave techniques.
- MASW (Rayleigh wave) data were difficult to reduce due to lateral velocity variation, a possible dipping bedrock surface beneath the seismic line and probable variable thickness fill layer beneath the array. It was very difficult to construct a coherent dispersion curve at wavelengths less than 10 m and alternate interpretations are possible. Because seismic refraction data were not acquired along array BAR-1, interior shot locations were not available to reduce MASW data. Generally, at difficult sites, a large number of source locations provides more opportunity to extract small wavelength/high frequency surface wave dispersion data.
- The minimum wavelength surface wave phase velocity data extracted from the 48-channel MASW array is about 18 m. Data reduction using seismic records from smaller hammer sources and a limited offset receiver array (i.e. less active geophones) allowed extraction of surface wave dispersion data to a minimum wavelength of about 2 m.
- There is nominally about 40 to 80 m/s scatter in MASW dispersion data selected for modeling, likely due to the effects of lateral velocity variation.
- A representative dispersion curve was generated for the MASW data set using a moving average, polynomial curve fitting routine and used for modeling.
- Surface wave depth of investigation is about 30 m based on half of maximum wavelength criteria.
- There is acceptable agreement between the average V_S models calculated from the P-wave seismic refraction model assuming constant values of Poisson's ratio and the V_S model resulting from inversion of the Rayleigh wave phase velocity data. The primary difference in the models is that the MASW V_S model has lower velocity over the 3 to 7 m depth range, which could be associated with the fact that the bedrock surface may be dipping beneath the array.
- V_{S30} from the MASW V_S model is 511 m/s (NEHRP Site Class C).

- Average S-wave velocity between a depth of 1 and 31 m, to account for the seismic sensor being placed on weathered rock, is 559 m/s (NEHRP Site Class C).
- V_{S30} from the average P-wave seismic refraction model and assumed constant Poisson's ratio of 0.3333 is 556 m/s (Site Class C), about 9% higher than that measured using the MASW technique. The lowest V_{S30} from the central portion of the P-wave seismic refraction model and assumed constant Poisson's ratio of 0.3333 is 519 m/s, about 2% higher than that measured using the MASW technique.
- V_{R40} is 503 m/s (±5%) which, using the Brown, et al., 2000 relationship, would result in an estimated V_{S30} of 526 m/s (±5%), assuming that the dispersion curve at 40 m wavelength is the fundamental mode. This is consistent with that modeled from the MASW data and estimated from the P-wave seismic refraction models.
- Although P-wave seismic refraction and MASW data quality is not particularly good at this site, both methods result in reasonably similar estimates of V_{S30} and, therefore, the results can be considered valid.
- For site characterization purposes, the use of the MASW V_S model, which may be slightly conservative, is recommended. This model likely reflects the lower bound of V_{S30} in the site vicinity. The seismic refraction model and field observations indicate that there are zones of much higher velocity rock in the site vicinity. Although the seismic station appears to be located on decomposed rock, similar to that beneath the MASW array BAR-1 and central portion of the seismic refraction array BAR-2, there is a localized zone of much higher velocity rock, possibly at the low end of NEHRP Site Class B, less than 20 m to the northeast.
- This would be an interesting site to determine if a carefully placed SASW sounding, which requires a smaller maximum receiver spacing, would be less impacted by the lateral velocity variation. There are no reasonable alternate test locations at this site and, given the lateral velocity variation in the site vicinity, testing had to be conducted as close as possible to the seismic station.

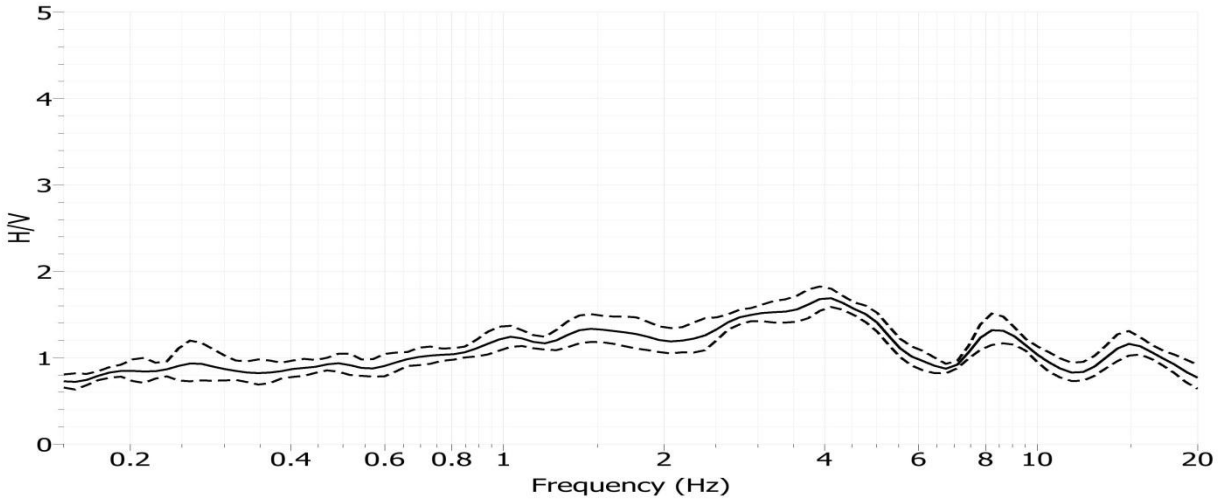

Site CI.BAR, H/V Spectral Ratio, Array BAR-1, Sensor 507

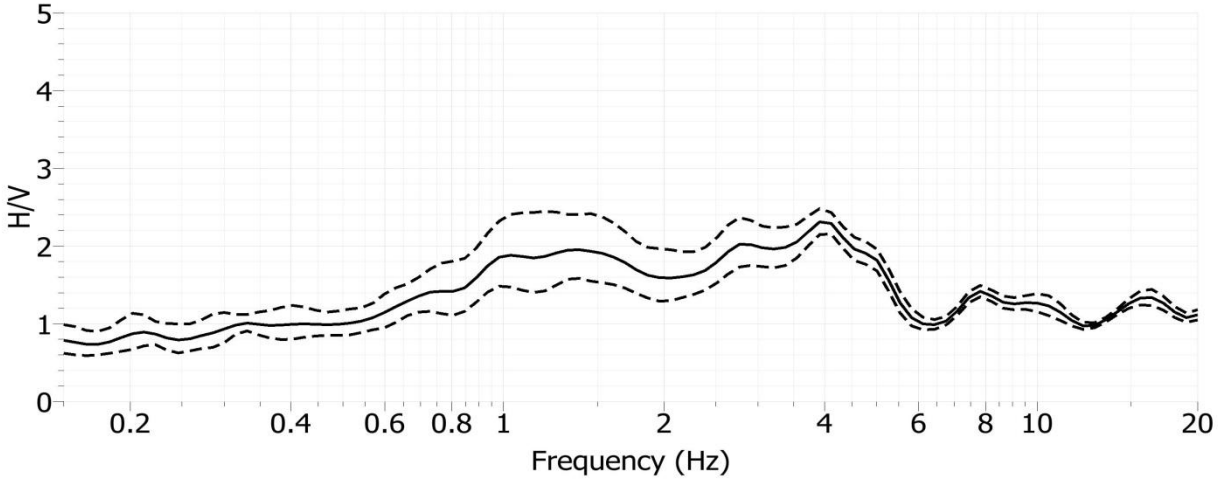

Site CI.BAR, H/V Spectral Ratio, Array BAR-1, Sensor 453

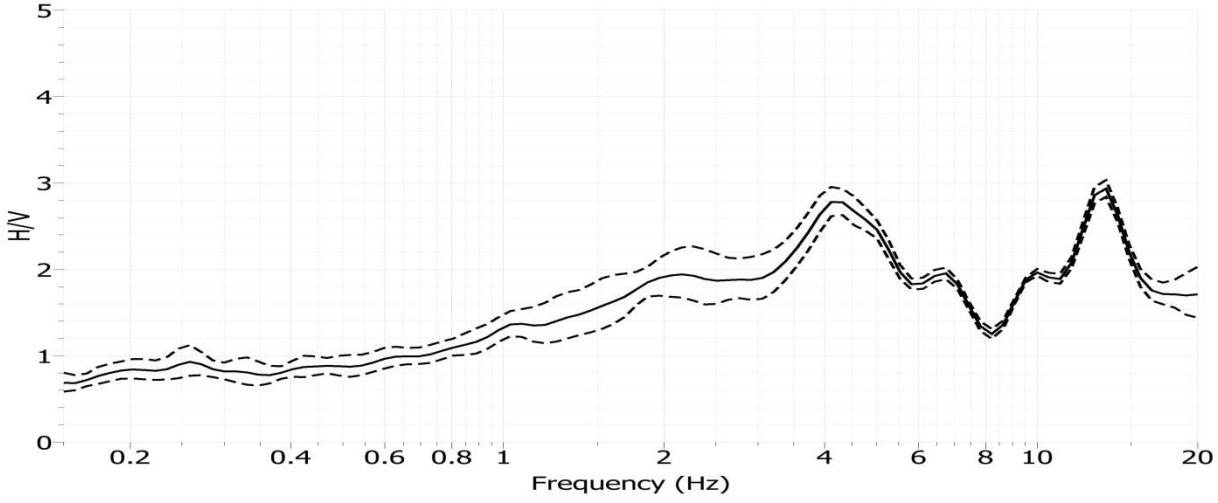

Site CI.BAR, H/V Spectral Ratio, Array BAR-1, Sensor 450

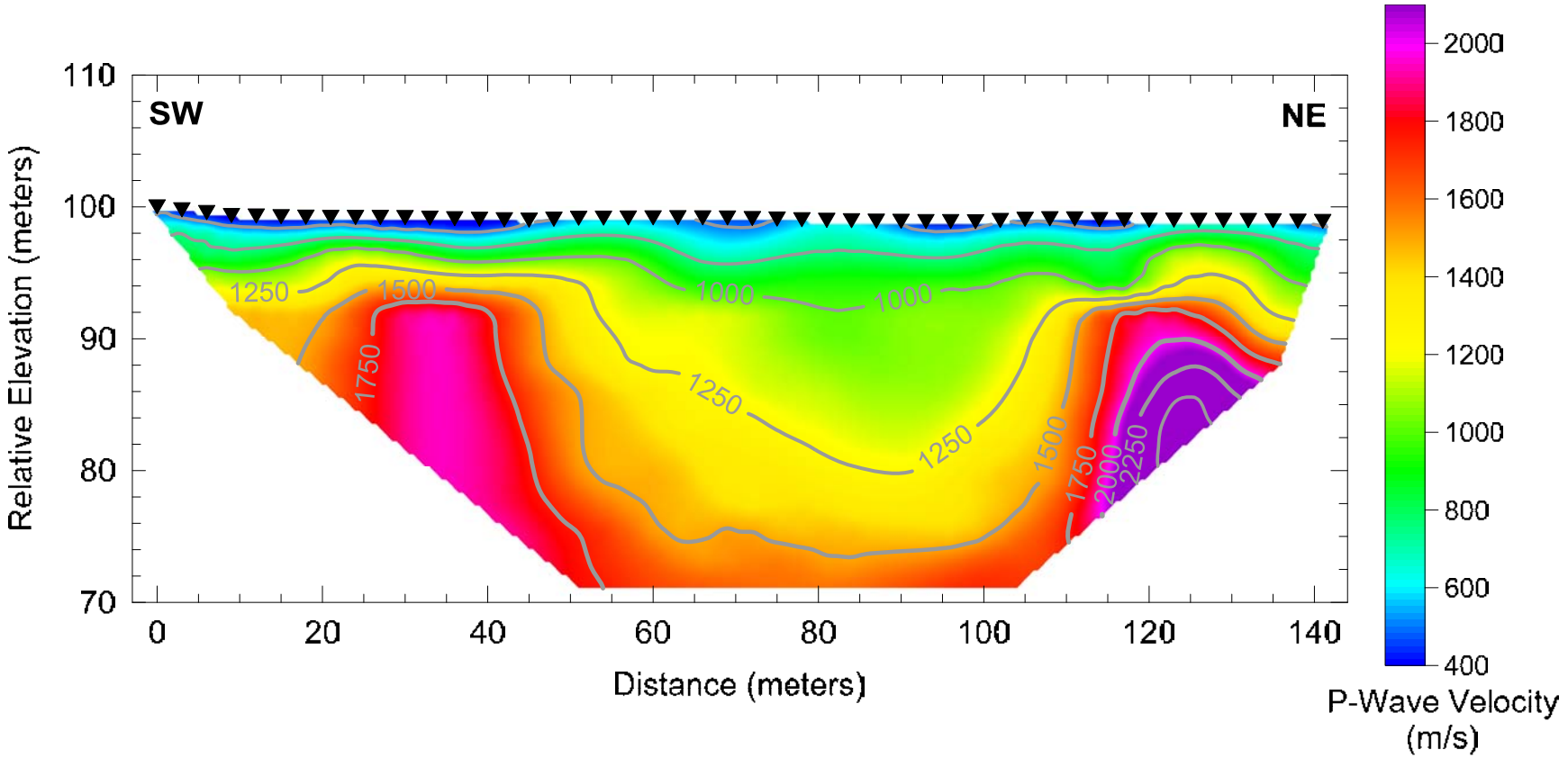

Array BAR-2 – Tomographic Seismic Refraction Model developed utilizing Smooth Velocity Gradient Starting Model

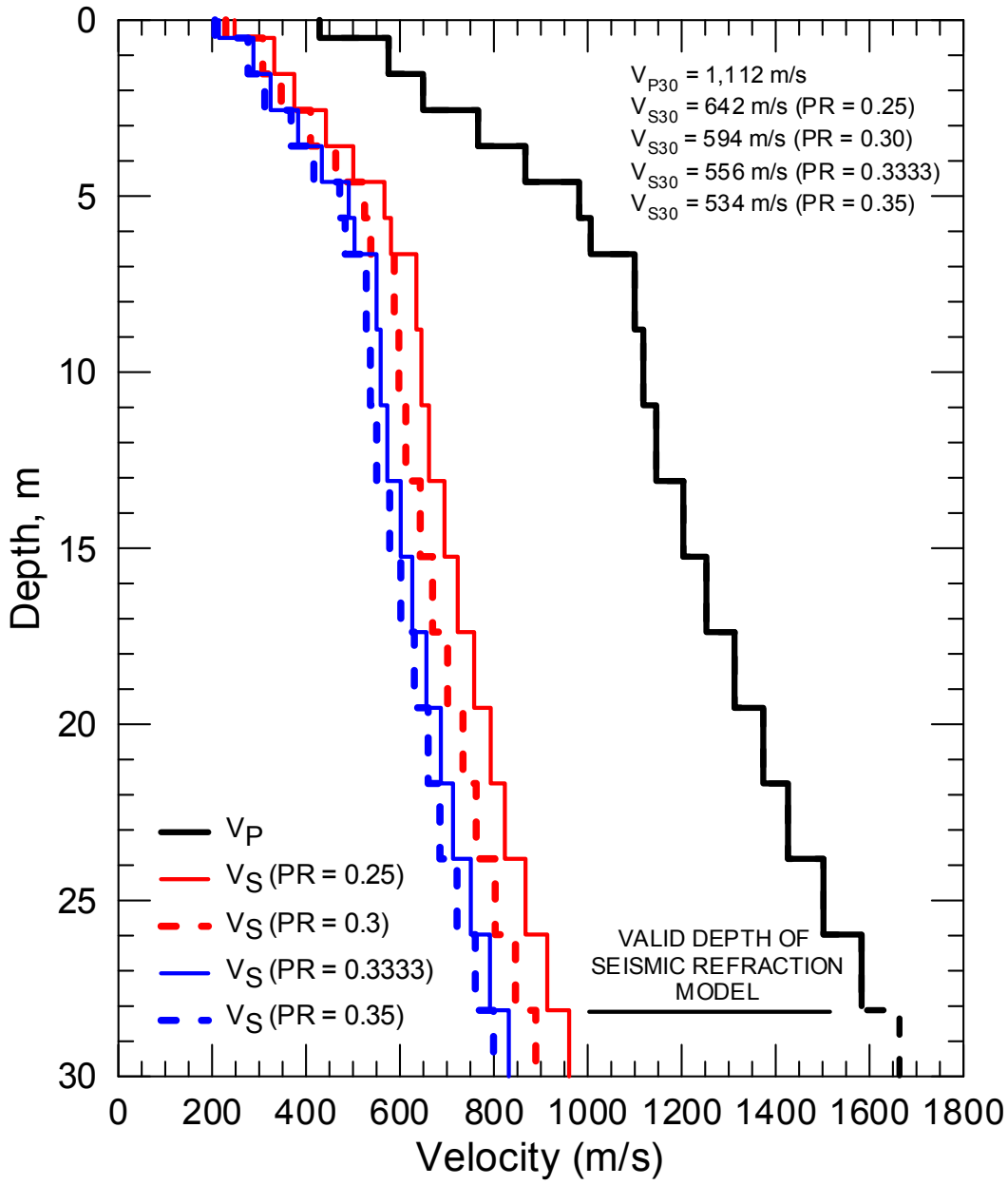

CI.BAR – Average P-wave velocity structure and estimated S-wave velocity structure between a position of 51 and 99 m on the P-wave seismic refraction model for array BAR-2 developed by tomographic inversion with a smooth velocity gradient starting model.

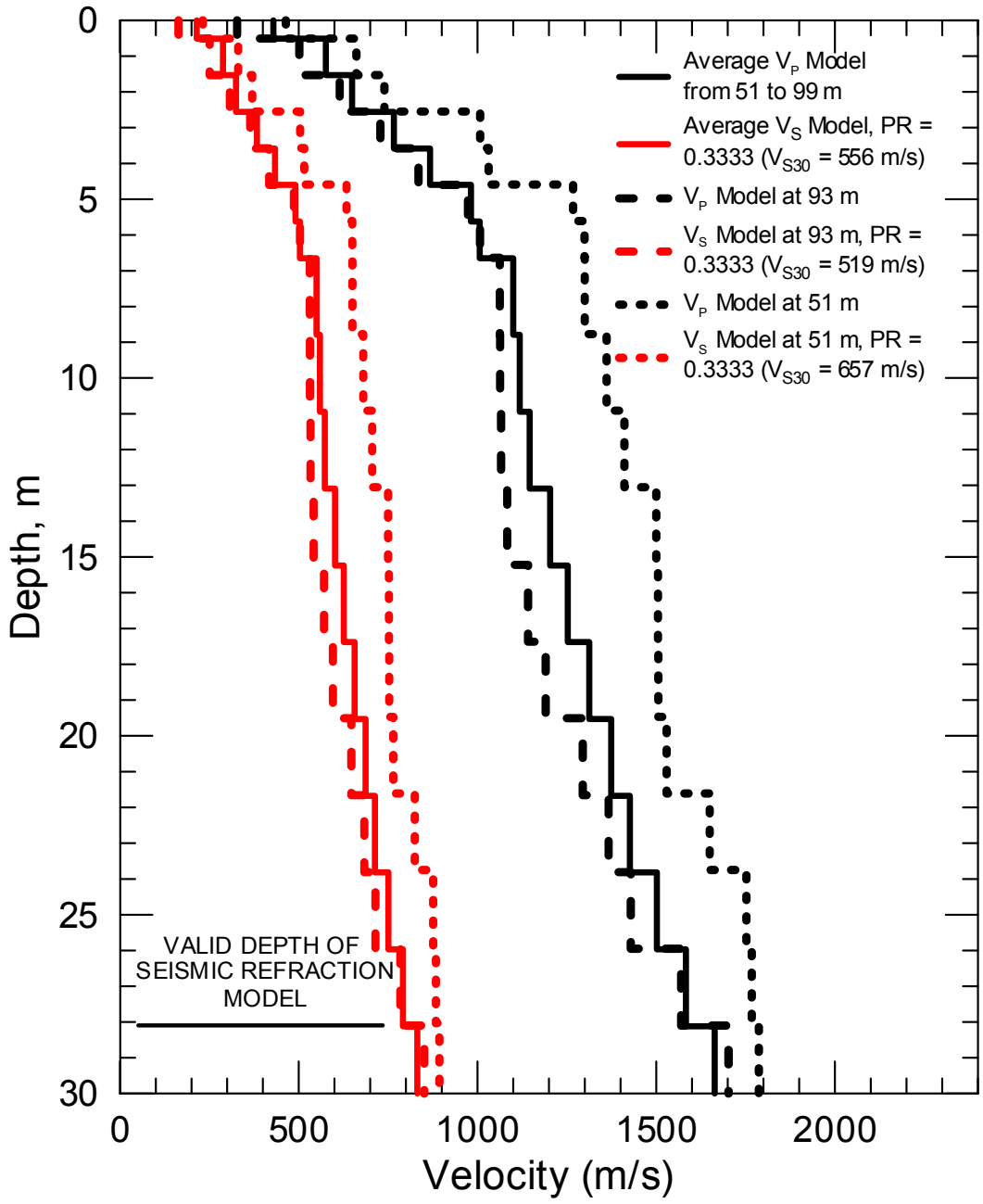

CI.BAR – Comparison of P-wave and estimated S-wave velocity structure between the average P-wave velocity model and models with minimum (position of 93 m) and maximum (position of 51 m) V_{P30} between 51 to 99 m on array BAR-2. There is about 25% variation in V_{P30} between a position of 51 and 99 m on array BAR-2, more if the higher velocity zones to the southwest and northeast were included. The minimum V_{P30} appears to be located within the 51 to 99 m interval on the seismic line. The highest V_{P30}, however, is located outside of the 51 to 99 m position range.

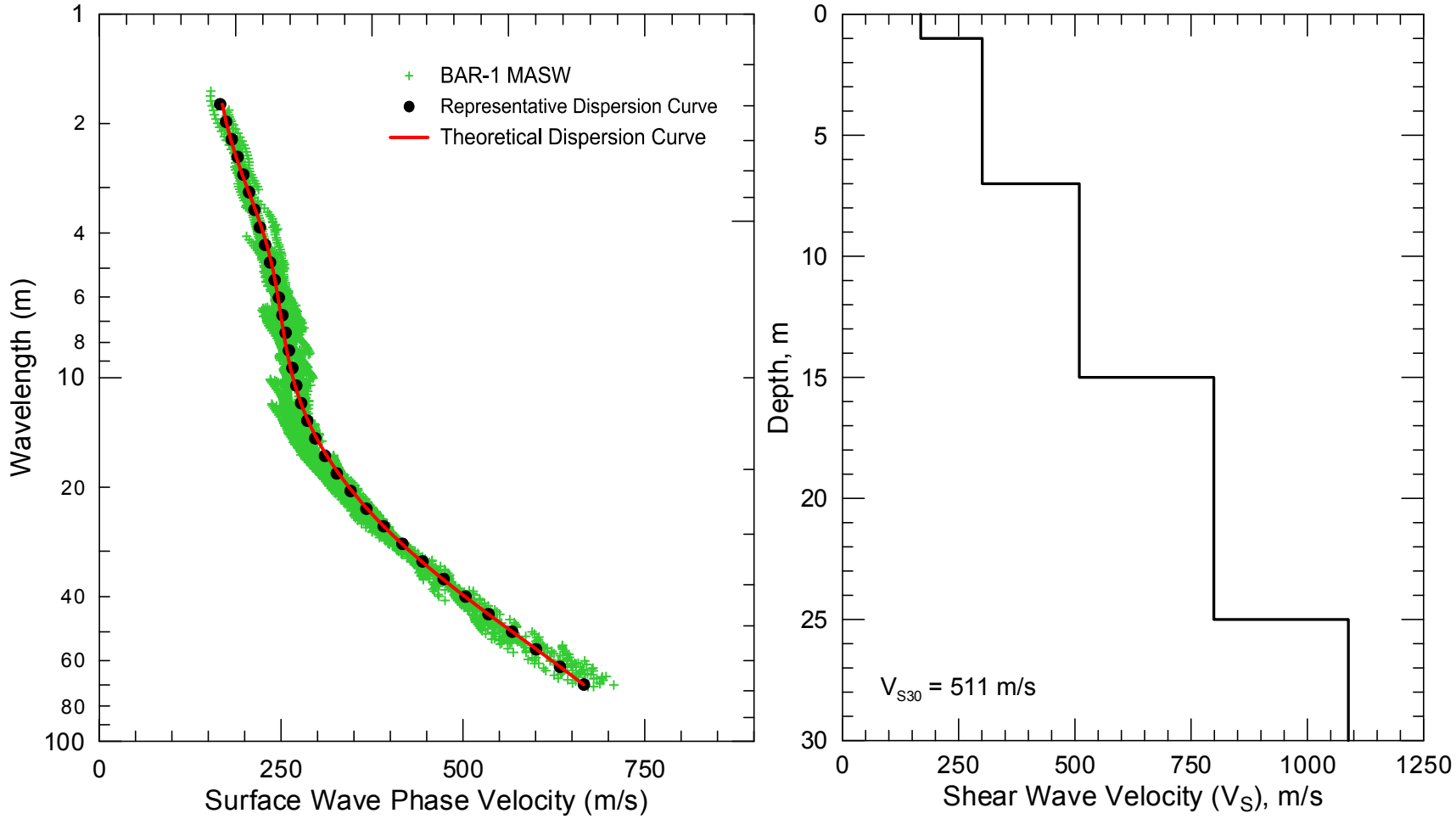

CI.BAR - Field, representative and inverted theoretical surface wave dispersion data (left) and associated V_S model (right)

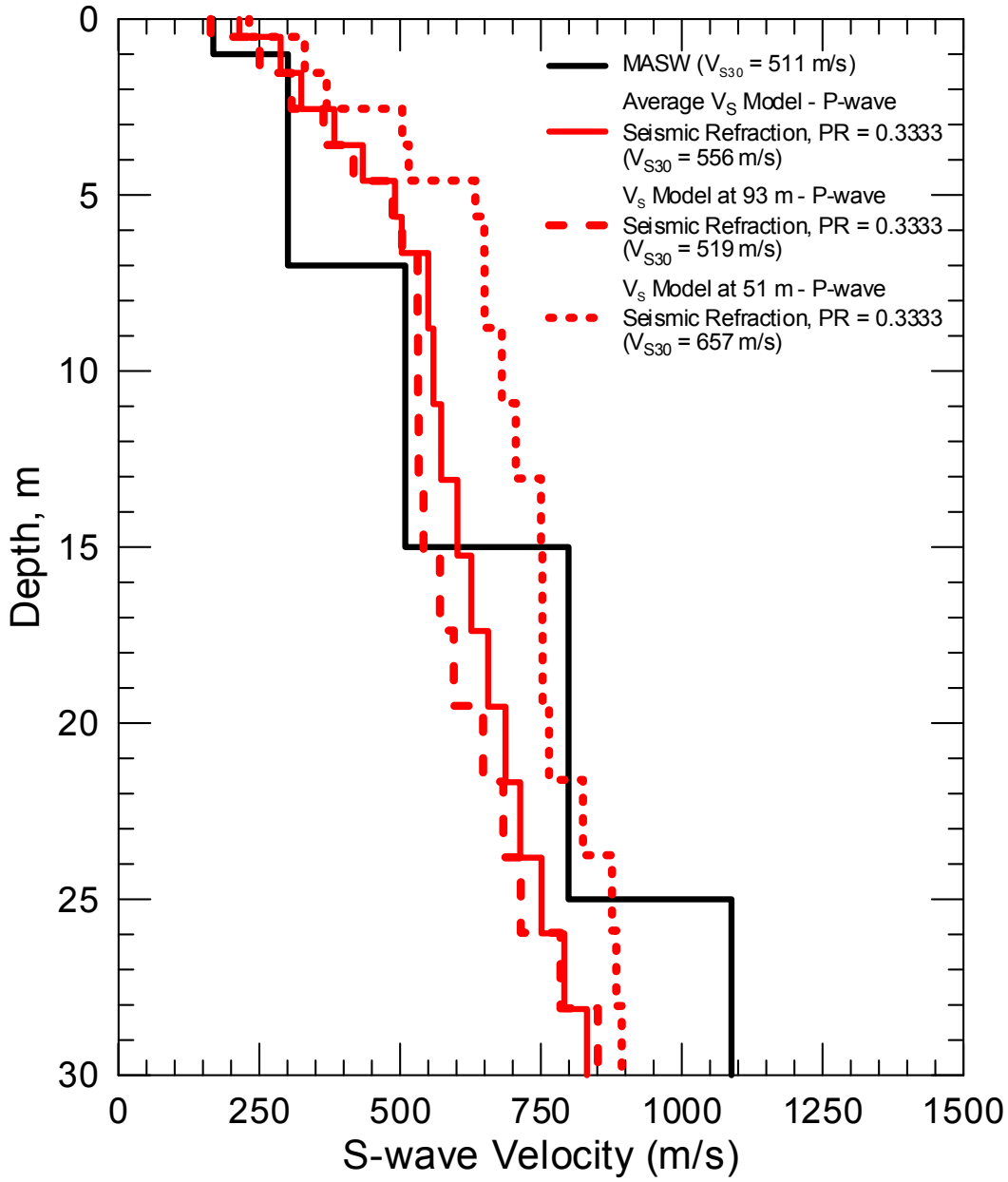

CI.BAR – Comparison of S-wave velocity models derived from the MASW and P-wave seismic refraction surveys (constant Poisson's ratio of 0.3333).

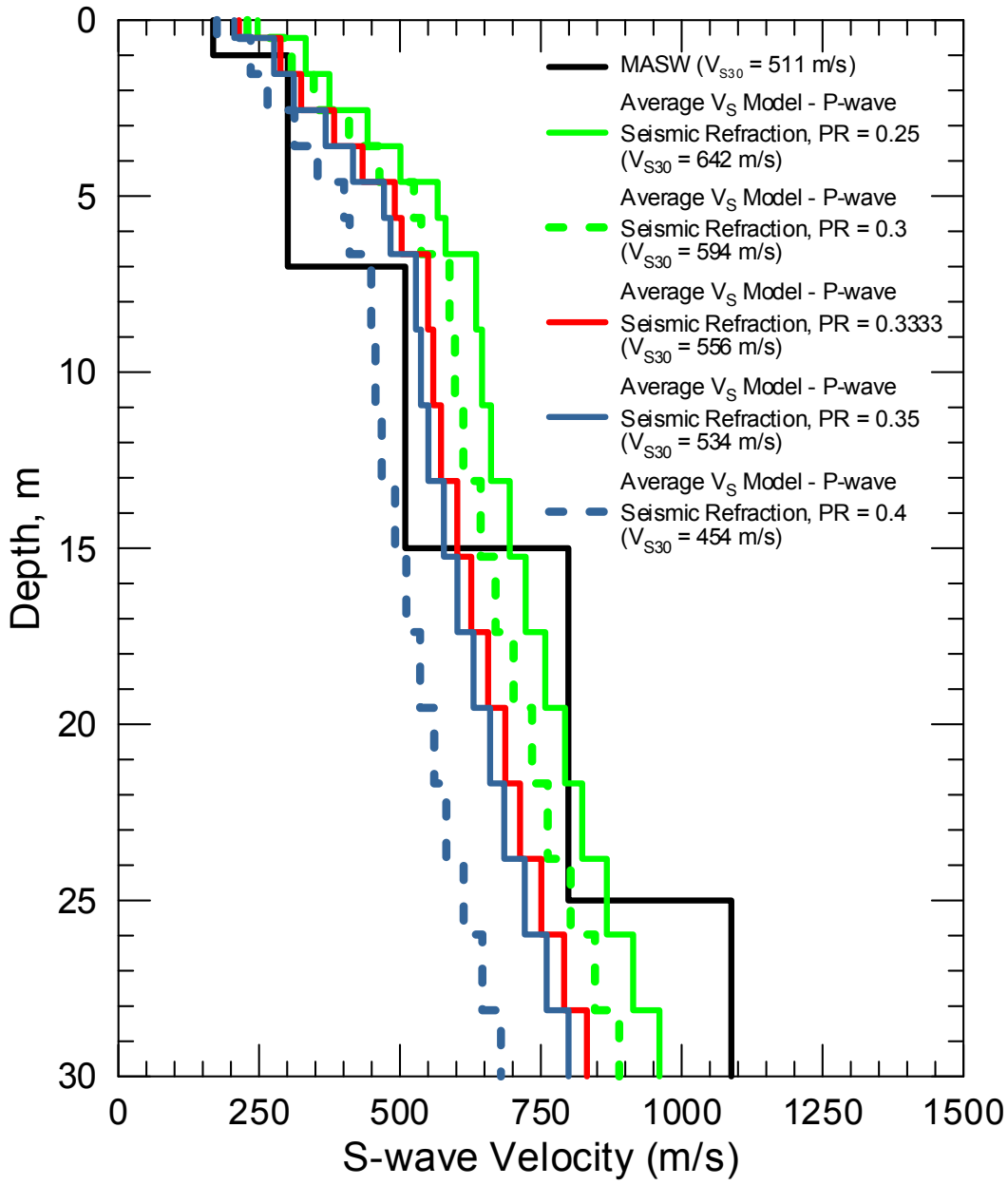

CI.BAR – Comparison of S-wave velocity models derived from the MASW and Average P-wave velocity model using constant Poisson's ratio in the 0.25 to 0.4 range.

Site CI.BBR

Location: Big Bear Solar Observatory, Big Bear, California

Latitude: 34.26215 **Longitude:** -116.92084

(Station coordinates modified based on field GPS survey, WGS84 coordinate system)

V_{S30} (measured): 356 m/s

V_{S30} (adjusted to more accurately reflect seismic station conditions): 380 m/s (average S-wave velocity between 1 and 31 m adjusting for inferred sensor depth)

NEHRP Site Class: D/C

Geomatrix Code: IHD

Geologic Conditions/Observations: Site located on geologic unit mapped as Quaternary (Holocene) young alluvial fan deposits. Seismic station located about 500 meters north of Big Bear Lake.

Site Conditions: Rural site. Site located on relatively flat topography. Slight decrease in ground surface elevation to south.

Geophysical Methods Utilized: HVSR, MASW

Geophysical Testing Arrays:

1. Array BBR-1 (48 channel MASW array utilizing 4.5 Hz vertical geophones spaced 1.5 m apart for a length of 70.5 m, forward and reverse shot locations with multiple source offsets and source types and multiple interior shots).
2. Three HVSR measurement locations, two distributed along array BBR-1 and the other near the seismic station.

Legend

- Seismic Station - Approximate Surveyed Location
- Seismic Station - Approximate Location of Record
- H/V Spectral Ratio Location
- MASW Array

NOTES:
1. WGS 1984 COORDINATE SYSTEM
2. Image Source: ESRI, i-cubed, USDA FSA, USGS, AEX, GeoEye, Getmapping, Aerogrid, IGP

File Name: CI-BBR-I

Date: 2/7/2013

USGS science for a changing world

GEOVision geophysical services

RECOVERY.GOV

SITE MAP
CI•BBR

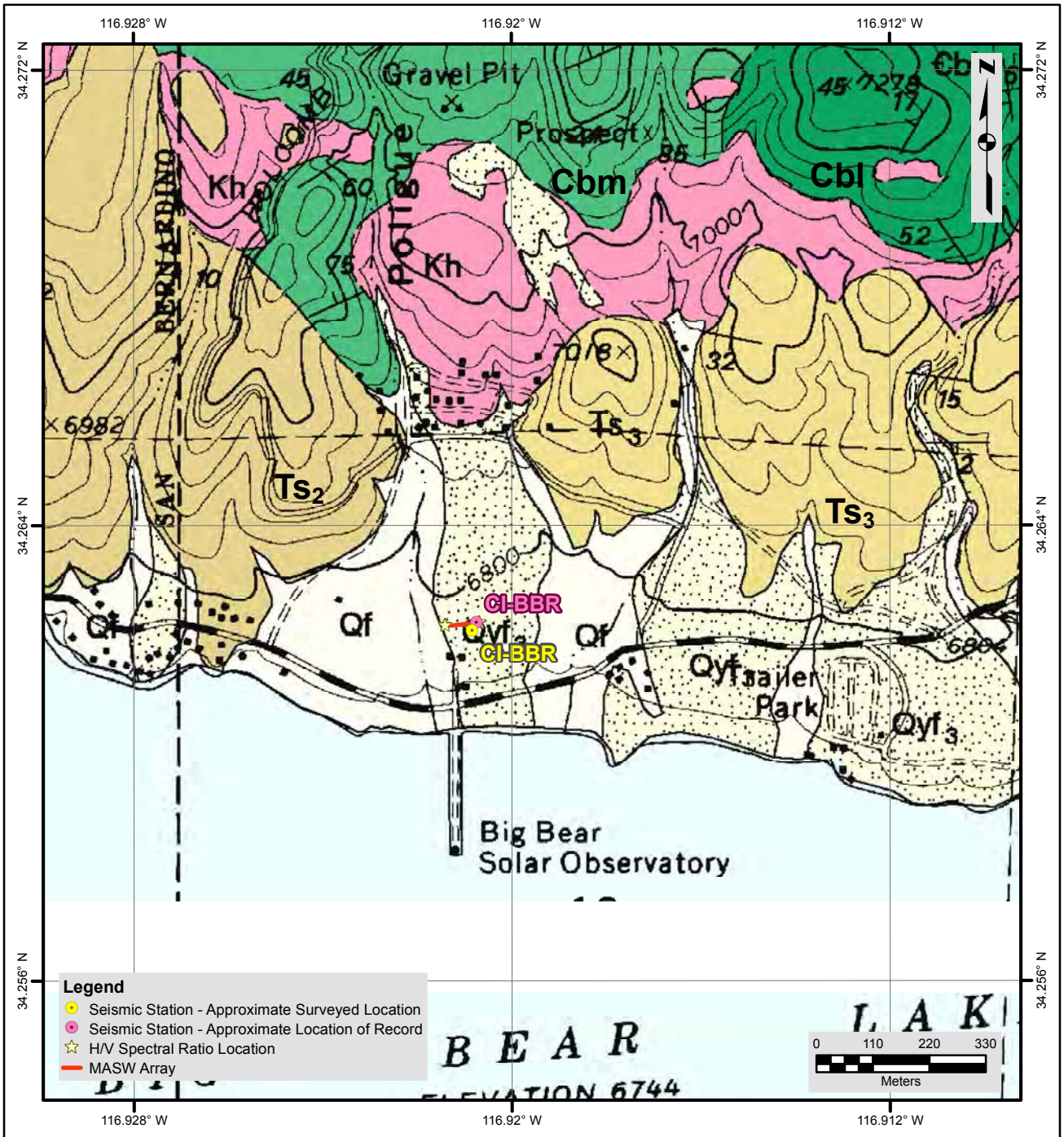

Description of Geologic Map Units

Qf = Quaternary (Holocene) unconsolidated alluvial deposits
Qyf_3 = Quaternary (Holocene) young alluvial fan deposits; sand and pebble-boulder gravel
Ts_3 = Tertiary (Pliocene) sedimentary rocks south of Bertha Ridge John Bull Mountain; limestone conglomerate and siltstone to sandstone
Ts_2 = Tertiary (Pliocene) sedimentary rocks of Poligue Canyon; pebbly and cobbly sand and sandy pebble-cobble conglomerate
Kh = Mesozoic (Cretaceous) coarse-grained hornblende-biotite granodiorite
Cbm = Paleozoic (Cambrian) thin- to thick-bedded, laminated to texturally massive to mottled dolomite marble and calcareous metadolomite
Cbl = Paleozoic (Cambrian) thick- to thick-bedded limestone and calcite marble

NOTES:
1. WGS 1984 COORDINATE SYSTEM
2. Geologic Map of the Fawnskin 7.5' Quadrangle, San Bernardino County, California, Version 1.1 by Fred K. Miller, Jonathan C. Mati, Howard J. Brown, and Robert E. Powell
3. See site map for details of geophysical survey

USGS science for a changing world

GEOVision geophysical services

GEOLOGIC MAP
CI•BBR

File Name: CI-BBR
Date: 2/7/2013

Looking southwest towards seismic station CI.BBR and HVSR sensor 507

Looking south towards seismic station CI.BBR from MASW array BBR-1

Looking southwest towards MASW array BBR-1 and HVSR sensor 453

MASW data acquisition

Looking west along MASW array BBR-1

Location of Geophysical Testing Arrays:

Location	Latitude	Longitude
BBR-1 West End of MASW Array	34.26223	-116.92141
BBR-1 Center of MASW Array	34.26226	-116.92104
BBR-1 East End of MASW Array	34.26229	-116.92067
HVSR Sensor 450	34.26226	-116.92141
HVSR Sensor 453	34.26230	-116.92070
HVSR Sensor 507	34.26219	-116.92085
CI.BBR Seismic Station	34.26215	-116.92084

Notes: 1) WGS84 Coordinate System (decimal degrees)

2) Survey accuracy is estimated at 2 to 3 m

Results:

V_S Model

Depth to Top of Layer (m)	Layer Thickness (m)	S-Wave Velocity (m/s)	Inferred P-Wave Velocity (m/s)	Inferred Poisson's Ratio	Inferred Density (g/cm^3)
0	1	142	265	0.300	1.9
1	2	204	382	0.300	1.9
3	3	266	498	0.300	1.9
6	5	380	1650	0.472	2.0
11	12	394	1650	0.470	2.0
23	>7	562	1650	0.434	2.0

Observations/Discussion:

- HVSR plots are generally similar at all measurement locations validating the 1-D velocity structure assumption.
- There is a distinct HVSR peak at 1 Hz indicating that bedrock is at least 100 m deep at the site. The irregular shape of the peak (i.e. broadening to lower frequencies) may indicate complex basement geometry, a weathering profile in bedrock or that the 1 Hz HVSR peak is associated with an impedance contrast above a deeper basement complex.
- Noise conditions at the site were not sufficient to apply passive surface wave techniques.
- Only hammer energy sources were utilized at the site due to vehicle access limitations. A 30 m depth of investigation is generally the maximum depth of investigation for a 20 lb sledge hammer at a very stiff soil site with low noise. At this site surface wave phase velocity with 60 m wavelength occurred at a frequency of 7 Hz.
- Scatter in the surface wave dispersion data likely results from lateral velocity variation.
- A representative dispersion curve was generated for the surface wave data set using a moving average, polynomial curve fitting routine. This representative dispersion curve was used for data modeling.
- The water table was modeled at a depth of about 6 m based on interactive layer-based analysis of seismic refraction first arrival data. P-wave velocities of about 350 and 1,650 m/s were modeled for unsaturated and saturated sediments, respectively.
- Surface wave depth of investigation is about 30 m based on half of maximum wavelength criteria.
- V_{S30} is 356 m/s (Site Class D/C).
- Average S-wave velocity between 1 m (inferred sensor depth) and 31 m is 380 m/s.

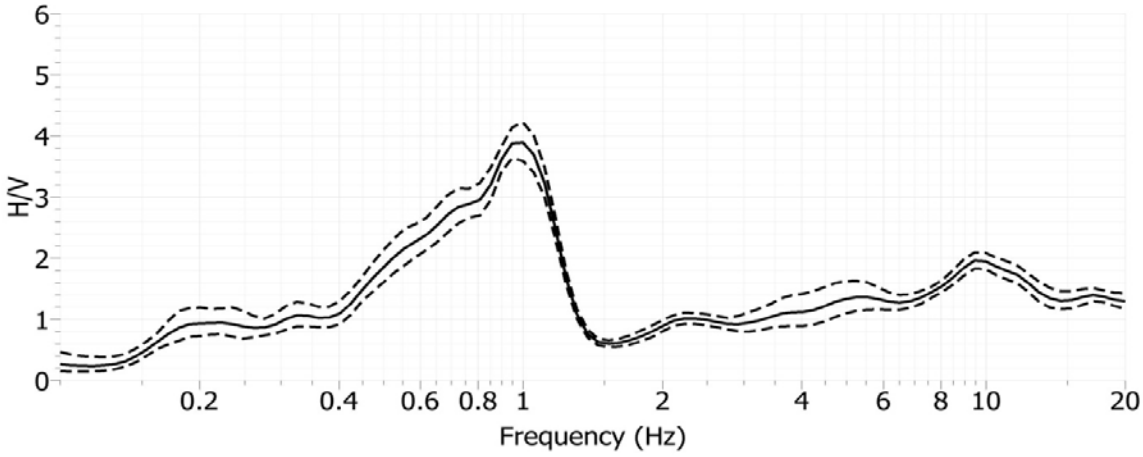

Site CI. BBR, H/V Spectral Ratio, Array BBR-1, Sensor 450

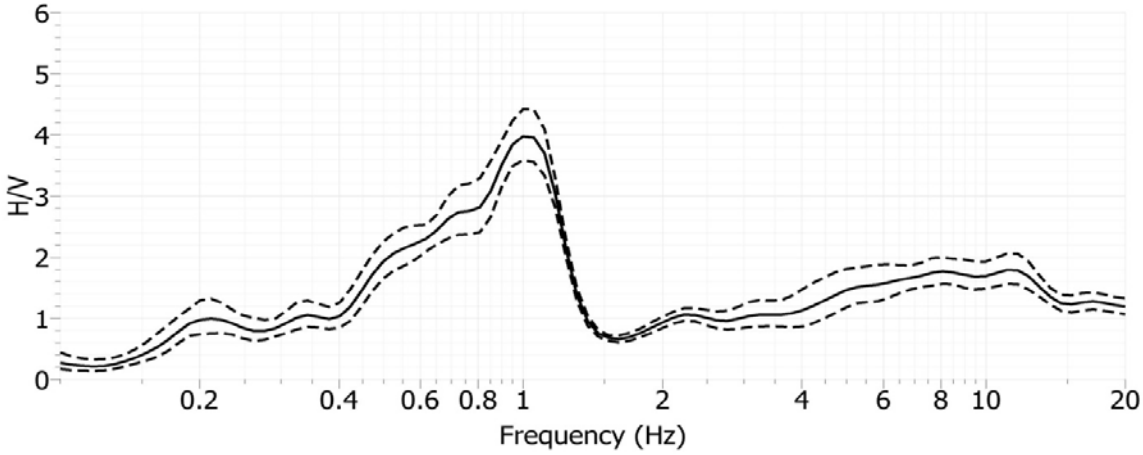

Site CI.BBR, H/V Spectral Ratio, Adjacent to Seismic Station, Sensor 507

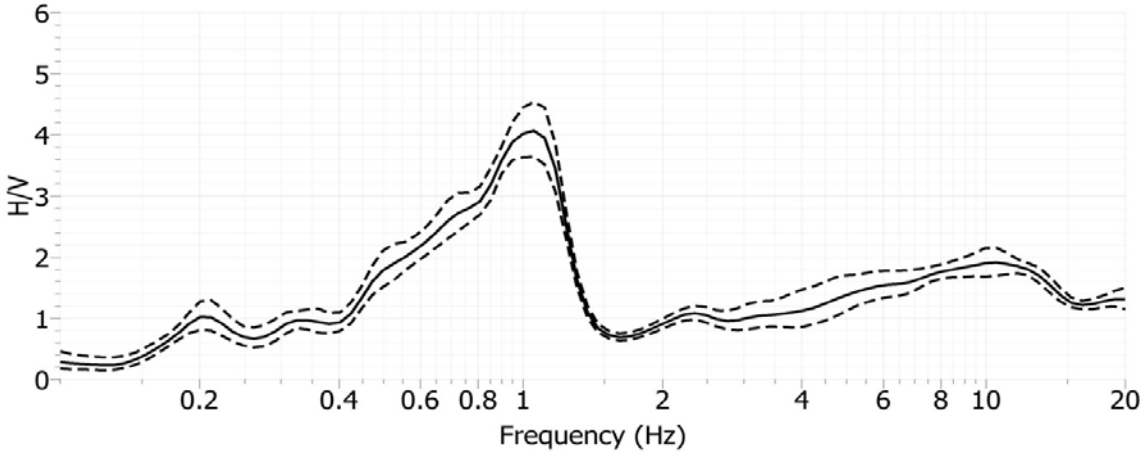

Site CI. BBR, H/V Spectral Ratio, Array BBR-1, Sensor 453

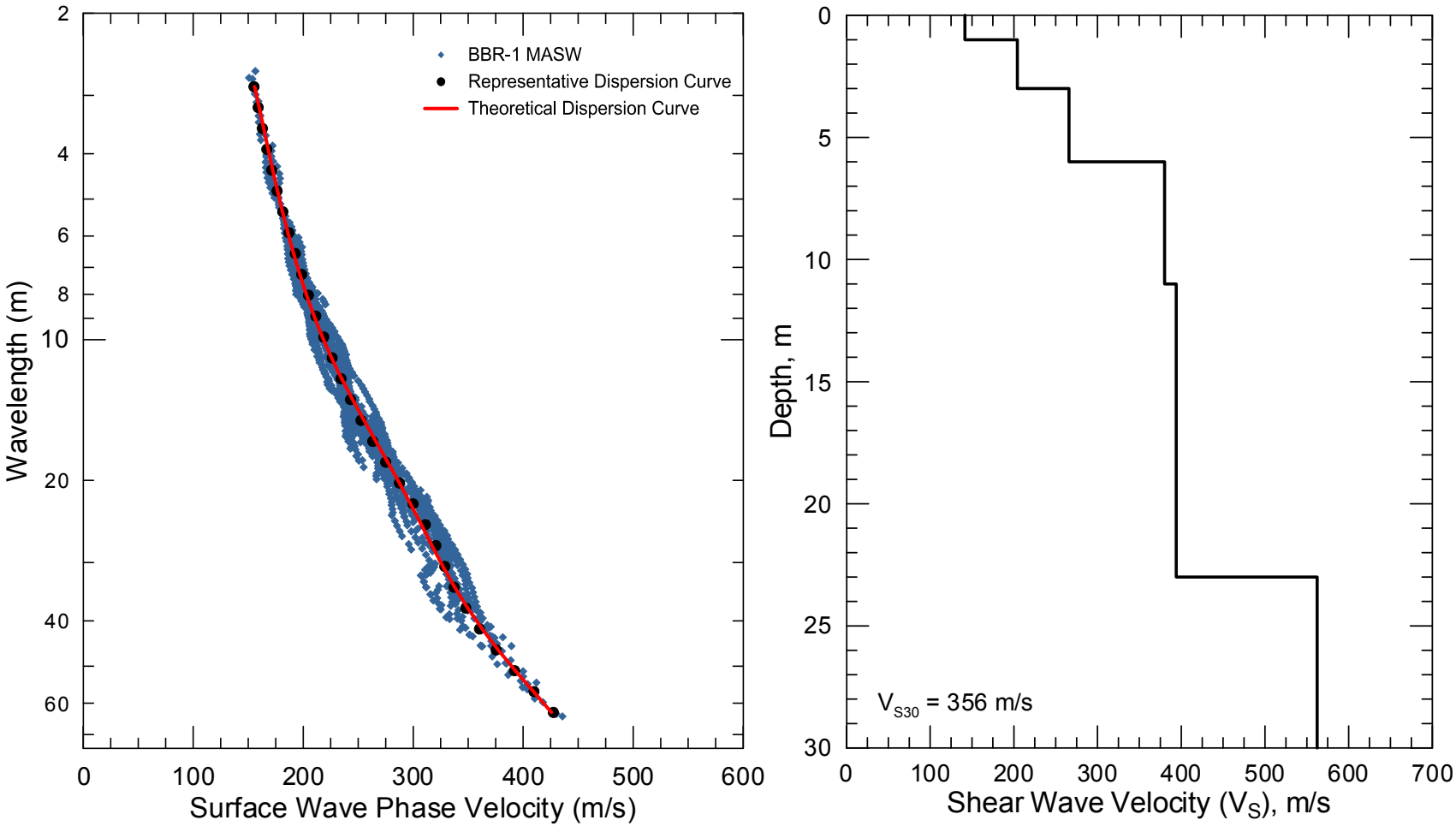

CI.BBR - Field, representative and inverted theoretical surface wave dispersion data (left) and associated V_S model (right)

Site CI.BBS

Location: Southern California Gas Company, 251 East 1st Street, Beaumont, California

Latitude: 33.92139 **Longitude:** -116.98058
(Station coordinates provided by USGS, WGS84 coordinate system)

V_{S30} (measured): 341 m/s

V_{S30} (adjusted to more accurately reflect seismic station conditions): 352 m/s (average S-wave velocity between 2 and 32 m adjusting for nominal 2 m seismic sensor depth).

NEHRP Site Class: D

Geomatrix Code: IQD

Geologic Conditions/Observations: Site located in area mapped as Quaternary (Pleistocene) old alluvial fan deposits. Probable deep soil site.

Site Conditions: Urban site with significant traffic noise from nearby 1st Street and other nearby roads. Most noise sources are located north of site. Relatively flat terrain in site vicinity.

Geophysical Methods Utilized: HVSR, MASW, array microtremor, ReMi™

Geophysical Testing Arrays:

1. Array BBS-1 (48 channel MASW array utilizing 4.5 Hz vertical geophones spaced 1.5 m apart for a length of 70.5 m, forward and reverse shot locations with multiple source offsets and source types and center shot location).
2. Array BBS-2 (48 channel, "T" shaped passive surface wave array utilizing 4.5 Hz vertical geophones spaced 5 m apart (S-N segment) and 3 m apart (W-E segment). Two linear arrays with lengths of 115 and 69 m, respectively, were extracted from the "T" array.
3. Three HVSR measurement locations distributed in test area, one near the seismograph station and two distributed along MASW array BBS-1.

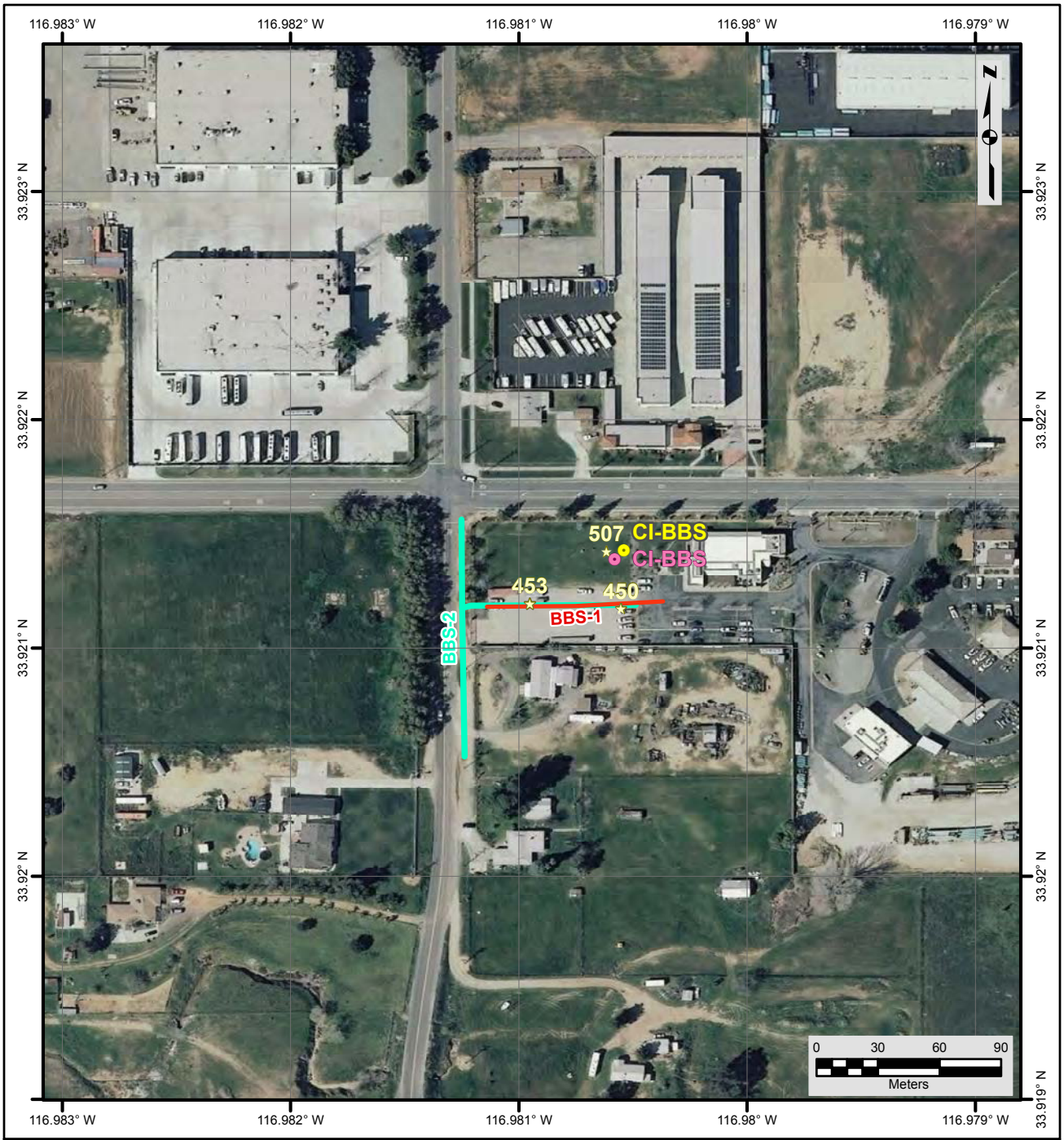

Legend

- Seismic Station - Approximate Surveyed Location
- Seismic Station - Approximate Location of Record
- H/V Spectral Ratio Measurement Location
- MASW Array
- Passive Surface Wave Array

NOTES:
1. WGS 1984 COORDINATE SYSTEM
2. Image Source: ESRI, i-cubed, USDA FSA, USGS, AEX, GeoEye, Getmapping, Aerogrid, IGP

USGS science for a changing world
GEOVision geophysical services

RECOVERY.GOV

SITE MAP
CI•BBS

File Name: CI-BBS-I

Date: 4/7/2011

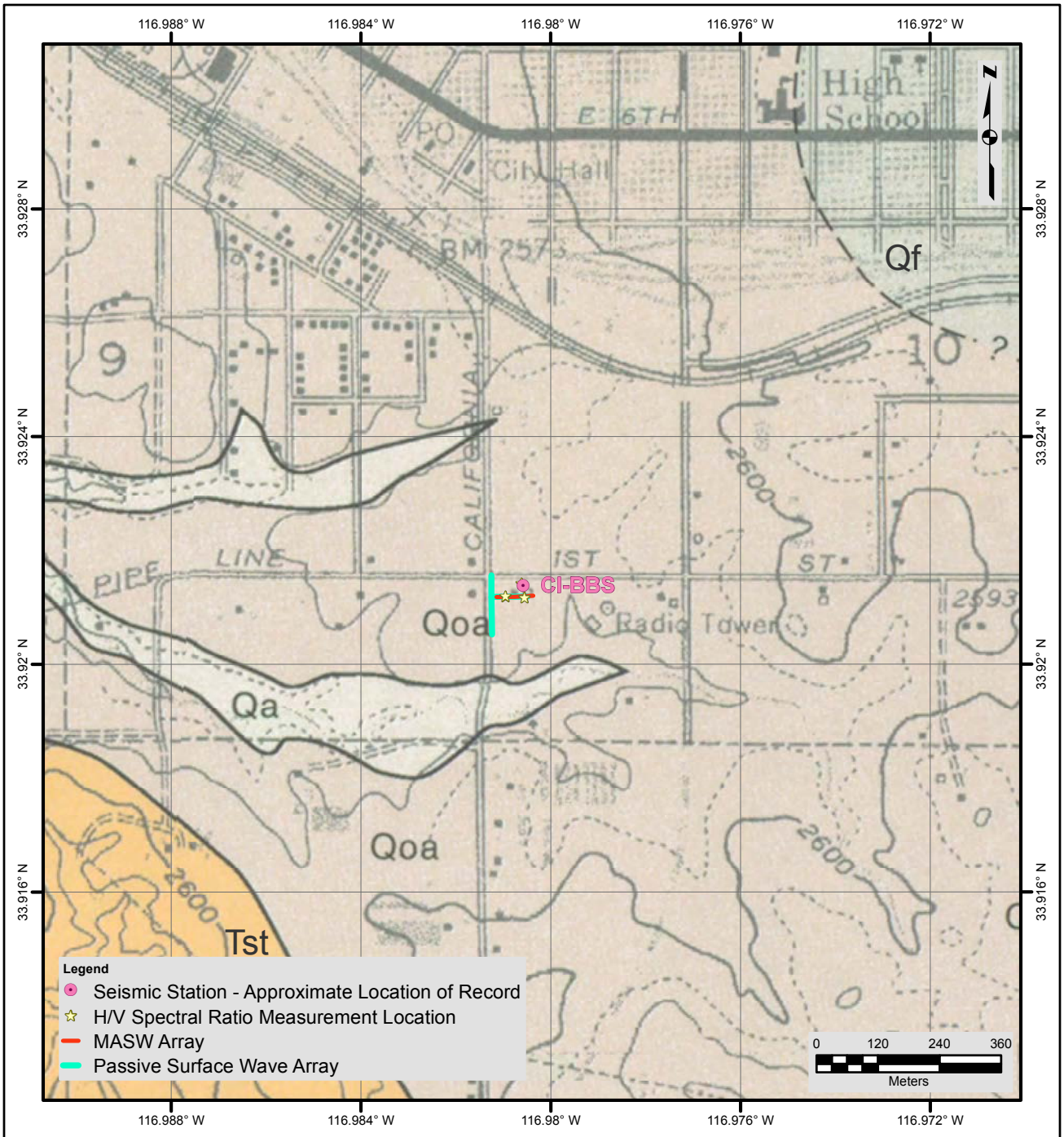

Description of Geologic Map Units

Qa = Quaternary (Holocene) alluvial sand, gravel and clay of flat flood plains of stream channels
Qf = Quaternary (Pleistocene) alluvial fan sand and gravel of plutonic and gneissic detritus
Qoa = Quaternary (Pleistocene) dissected alluvial fan sand and gravel, light reddish, crudely bedded
Tst = Tertiary (Pliocene) San Timoteo Formation; sandstone, light grey, friable, arkosic; includes some interbedded pebble-cobble conglomerate and greenish to reddish claystone

NOTES:
1. WGS 1984 COORDINATE SYSTEM
2. Geologic Map of the Beaumont Quadrangle, Riverside County, California
By Thomas W. Dibblee, Jr., 2003
3. See site map for details of geophysical survey

File Name: CI-BBS

Date: 4/1/2011

USGS science for a changing world

GEOVision geophysical services

GEOLOGIC MAP
CI•BBS

RECOVERY.GOV

Looking northeast towards seismograph station CI-BBS from near HVSR sensor 453

Looking east towards seismograph station and HVSR sensor 507

Looking east along W-E segment of passive surface wave array BBS-2

Looking north along S-N segment of passive surface wave array BBS-2

Looking northeast towards seismograph station and MASW array BBS-1

Location of Geophysical Testing Arrays:

Location	Latitude	Longitude
BBS-1, West End of Array	33.92118	-116.98114
BBS-1, Center of Array	33.92118	-116.98075
BBS-1, East End of Array	33.92120	-116.98037
BBS-2, South End of S-N Array Segment, Channel 1	33.92053	-116.98124
BBS-2, North End of S-N Array Segment, Channel 24	33.92156	-116.98125
BBS-2, Intersection of W-E and S-N Array Segments	33.92118	-116.98125
BBS-2, West End of W-E Array Segment, Channel 25	33.92119	-116.98121
BBS-2, East End of W-E Array Segment, Channel 48	33.92119	-116.98049
HVSR Sensor 507	33.92142	-116.98062
HVSR Sensor 453	33.92119	-116.98095
HVSR Sensor 450	33.92117	-116.98055
CI.BBS Seismograph Station	33.92143	-116.98054

Notes: 1) WGS84 Coordinate System (decimal degrees)
2) Survey accuracy is estimated at 1 to 2 m.

Results:

V_S Model

Depth to Top of Layer (m)	Layer Thickness (m)	S-Wave Velocity (m/s)	Inferred P-Wave Velocity (m/s)	Inferred Poisson's Ratio	Inferred Density (g/cm^3)
0	1	233	436	0.300	1.9
1	4	286	536	0.300	1.9
5	7	297	555	0.300	1.9
12	9	374	1743	0.476	2.0
21	11	407	1760	0.472	2.0
32	>28	900	1850	0.345	2.1

Observations/Discussion:

- HVSR curves are similar, validating the 1-D velocity structure assumption.
- Broad low amplitude HVSR peak in the 0.15 to 0.4 Hz range or double HVSR peaks at about 0.16 and 0.4 Hz. Low frequency HVSR peaks such as these are consistent for a deep soil site.

- Noise conditions at site (multi-directional or omni-directional noise sources) appeared sufficient for successful application of passive surface wave techniques although most noise sources were expected to occur north of the site.
- ESAC technique used to extract surface wave dispersion data from passive "L" array data. Both the ReMi™ and ESAC techniques used to extract surface wave dispersion data from the linear arrays.
- The W-E orientated linear array did not yield useful surface wave dispersion data, which was expected based on expected azimuth of noise sources. The ESAC and ReMi™ techniques generated different dispersion curves for the S-N orientated linear array with both techniques generating higher phase velocities than the MASW data and passive "L" array data at wavelengths less that 30 m. The linear array, passive surface wave data is, therefore, not considered reliable at this site, although wavelengths greater than 30 m from the S-N array were utilized for modeling.
- Surface wave dispersion data from MASW and passive "L" array datasets are in excellent agreement at this site. Surface wave dispersion data from the passive "L" array is sparse and may not be reliable over the 70 to 115 m wavelength range. The possibility cannot be discounted that there is a large impedance contrast below a depth of 30 m and interference from higher mode surface waves.
- Representative dispersion curves were generated for each surface wave data set using a moving average, polynomial curve fitting routine. These individual representative dispersion curves were combined and a representative dispersion curve generated for the combined data set for data modeling.
- Possible water table refractor located at a depth of about 12 m based on interactive layer-based analysis of seismic refraction first arrival data (approximately 12 m of unsaturated sediments with a P-wave velocity of about 450 m/s over saturated sediments with a P-wave velocity of about 1,750 m/s). However, review of groundwater documents for the Beaumont area indicates that groundwater is nominally on the order of 45 m deep in the site vicinity. It is therefore possible that the interpreted water table is associated with perched water; however, the top of the saturated zone is assumed to be 12 m for modeling.
- The velocity structure is such that the fundamental mode should be dominant at all frequencies.
- Surface wave depth of investigation is about 75 m assuming a valid wavelength up to 150 m; however the S-wave velocity model is most accurate in the upper 30 m. Wavelengths up to 200 m used for modeling to better characterize the velocity of a possible high velocity layer modeled at about 32 m. This large impedance contrast may limit effective depth of investigation to about 60 m (i.e. one third of the maximum wavelength).
- There is no HVSR peak, expected at about 2.5 to 3 Hz, to validate the large impedance contrast at 32 m mentioned above.
- V_{S30} is 341 m/s (Site Class D).
- Average S-wave velocity between 2 m (nominal sensor depth) and 32 m is 352 m/s.
- Average S-wave velocity of the upper 60 m (V_{S60}) is 484 m/s.

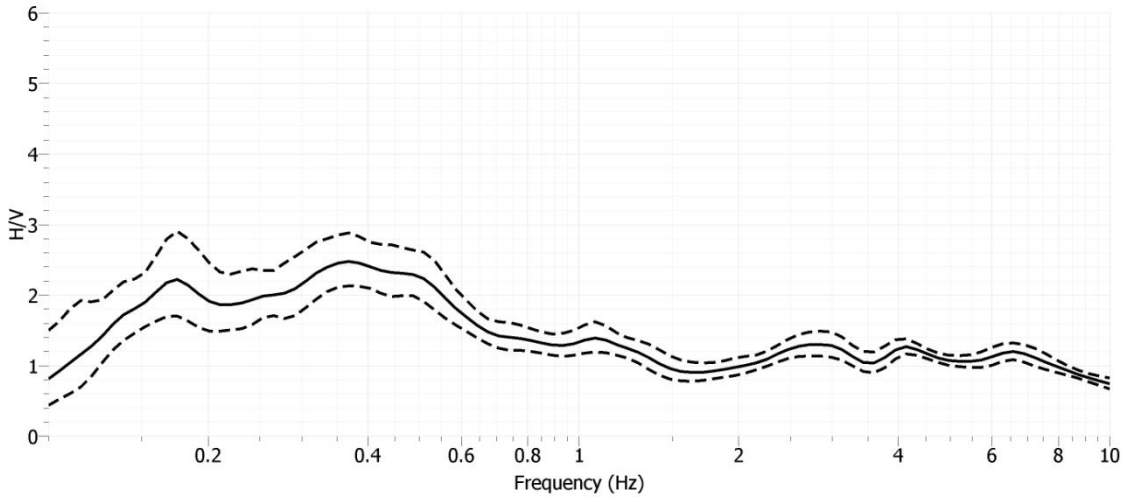

Site CI.BBS, H/V Spectral Ratio, Array BBS-1, Sensor453

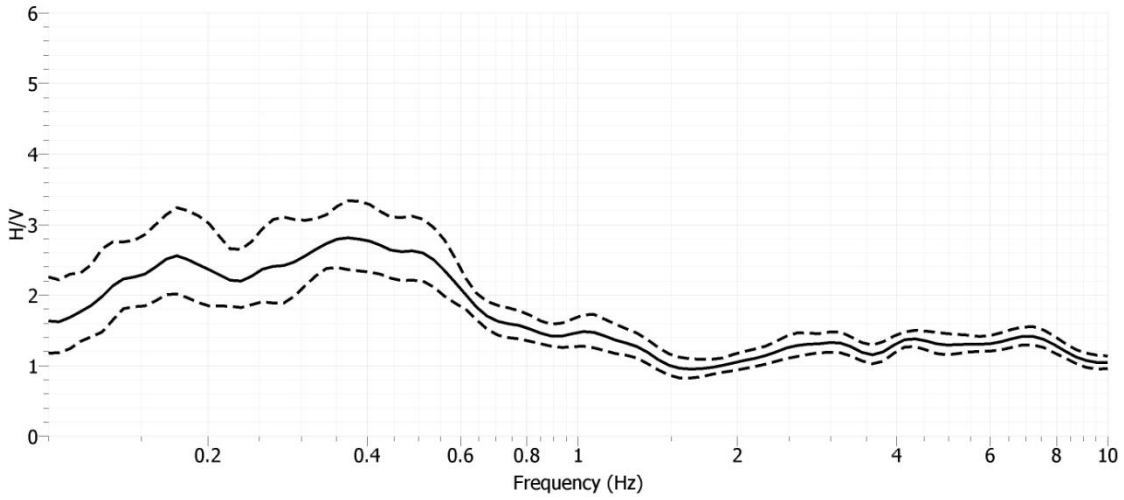

Site CI.BBS, H/V Spectral Ratio, Near Seismic Station, Sensor 507

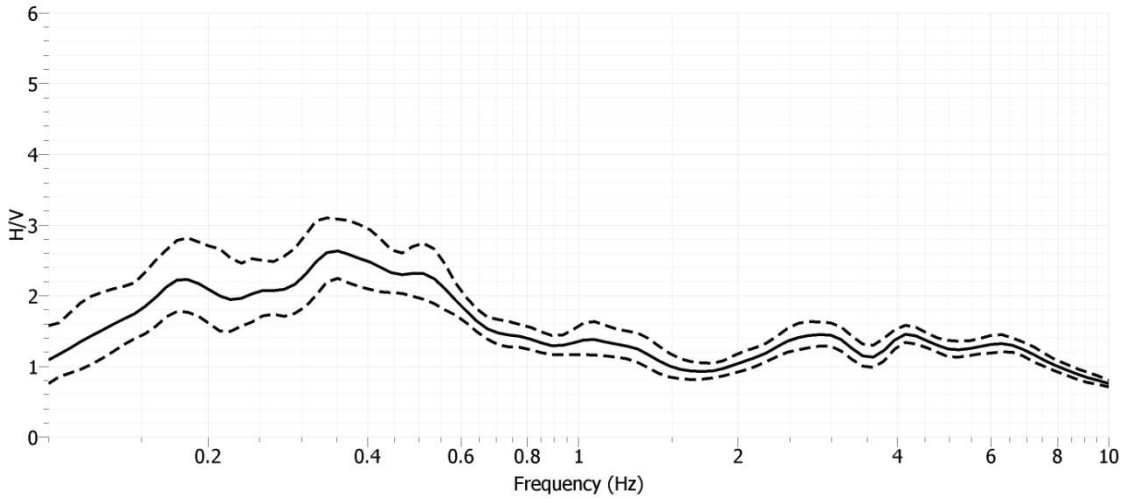

Site CI.BBS, H/V Spectral Ratio, Array BBS -1, Sensor 450

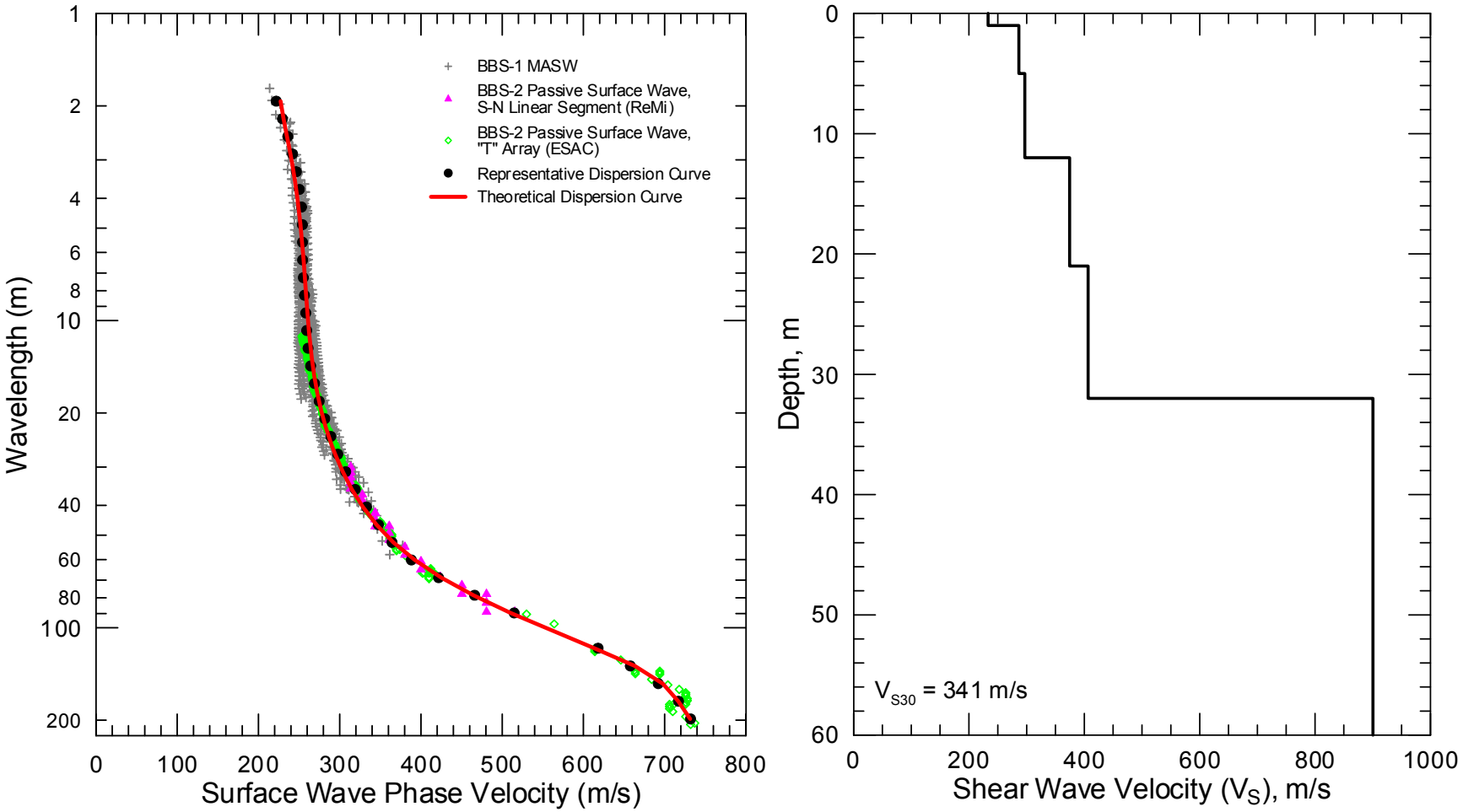

CI.BBS - Field, representative and inverted theoretical surface wave dispersion data (left) and associated V_S model (right)

Site CI.BC3

Location: Big Chuckwalla Mountains, Riverside County, California

Latitude: 33.65513 **Longitude:** -115.45364
(Station coordinates modified based on field GPS survey, WGS84 coordinate system)

V_{S30} (measured): 763 m/s

V_{S30} (adjusted to more accurately reflect seismic station conditions): 862 m/s (average S-wave velocity between 1 and 31 m adjusting for 1 m estimated sensor depth).

NEHRP Site Class: B

Geomatrix Code: IGA

Geologic Conditions/Observations: Seismic station located on geologic unit mapped as Mesozoic (Cretaceous) granitic rocks. Field observations indicate that a thin layer of soil and gravel overly bedrock at the surface in the test area although the seismic station may sit on rock.

Site Conditions: Rural site located on a mountain top. Steep terrain in site vicinity. Geophysical test line placed in only feasible location Testing was conducted along a dirt road and the ground surface elevation was relatively flat along the 70.5 m long MASW and seismic refraction array.

Geophysical Methods Utilized: HVSR, Seismic Refraction, MASW.

Geophysical Testing Arrays:

1. Array BC3-1 (48 channel MASW and P-wave seismic refraction array utilizing 4.5 Hz vertical geophones spaced 1.5 m apart for a length of 70.5 m, forward and reverse shot locations with multiple source offsets and source types (hammers only) and multiple interior shot locations).
2. Three HVSR measurement locations distributed along array BC3-1.

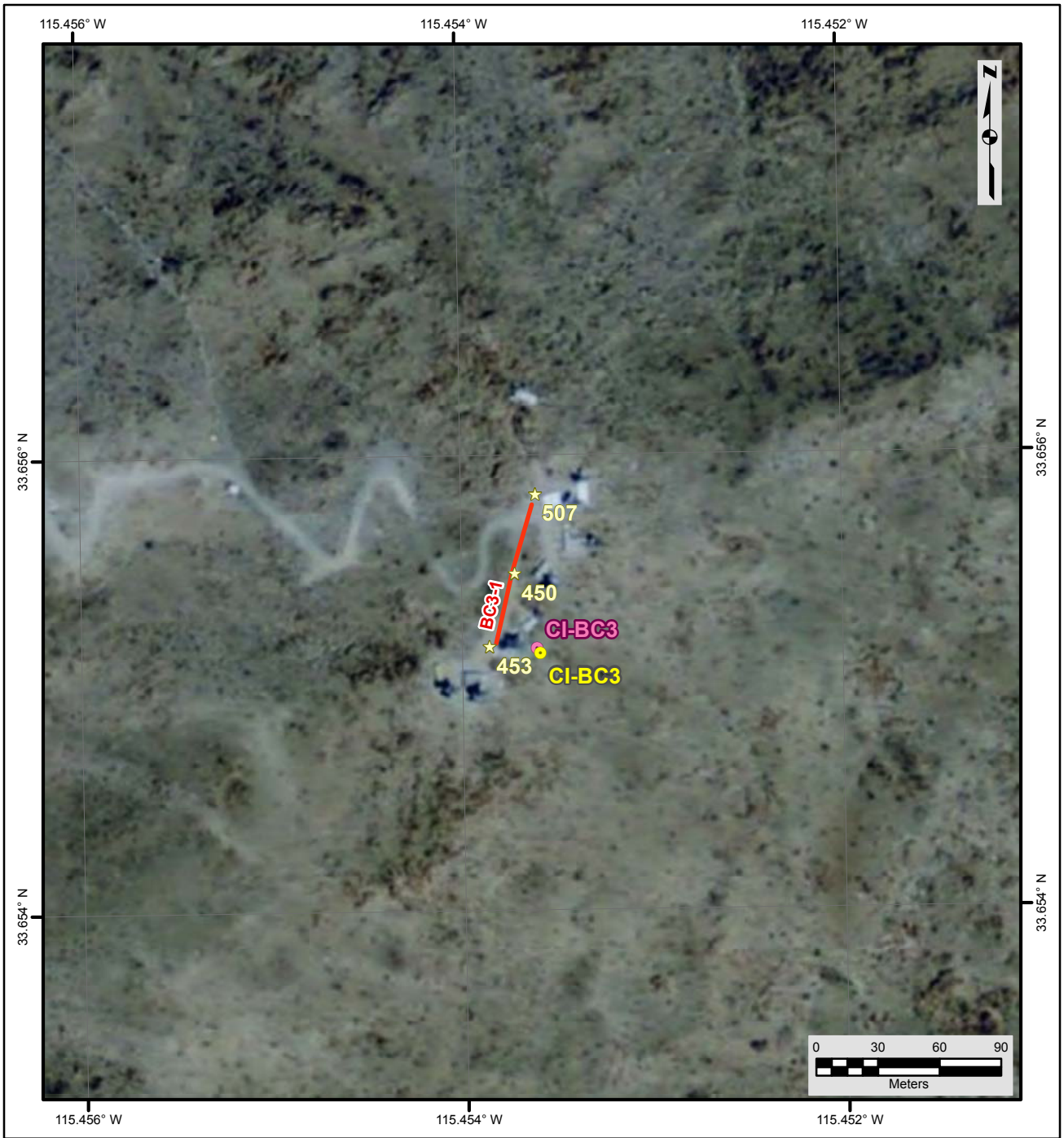

Legend

- Seismic Station - Approximate Surveyed Location
- Seismic Station - Approximate Location of Record
- H/V Spectral Ratio Location
- MASW and Seismic Refraction Array

NOTES:
1. WGS 1984 COORDINATE SYSTEM
2. Image Source: ESRI, i-cubed, USDA FSA, USGS, AEX, GeoEye, Getmapping, Aerogrid, IGP

File Name: CI-BC3-I

Date: 10/13/2011

USGS science for a changing world

GEOVision geophysical services

RECOVERY.GOV

SITE MAP
CI•BC3

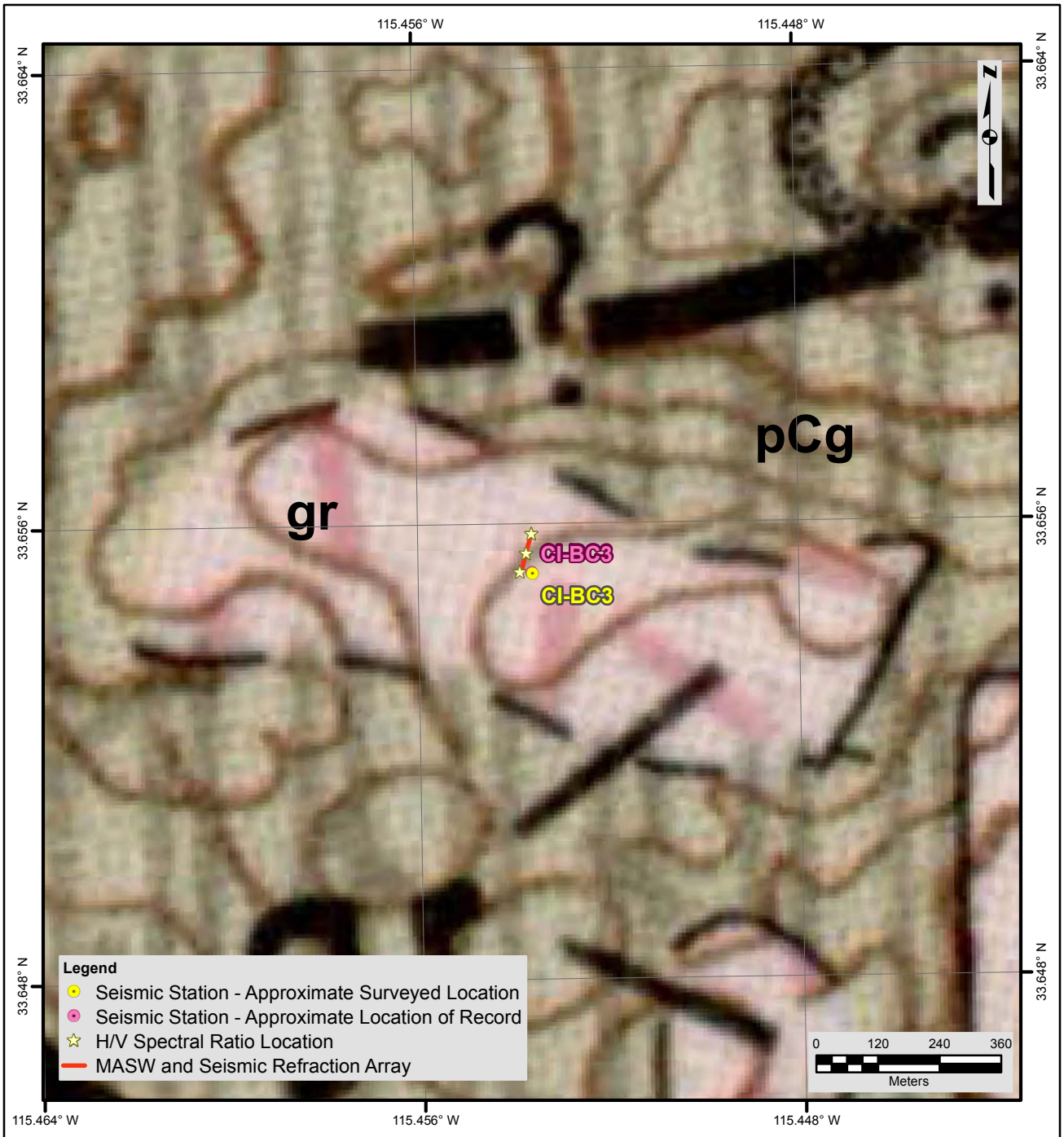

Description of Geologic Map Units

gr = Mesozoic (Cretaceous) granitic rocks
pCg = Precambrian undivided granitic rocks

NOTES:
1. WGS 1984 COORDINATE SYSTEM
2. Geologic Map of California Salton Sea Sheet, Olaf P. Jenkins Edition
Compilation by Charles W. Jennings, 1967
3. See site map for details of geophysical survey

File Name: CI-BC3

Date: 10/13/2011

USGS science for a changing world

GEOVision geophysical services

GEOLOGIC MAP
CI•BC3

RECOVERY.GOV

CI.BC3 seismic station

Looking east towards seismic station from about 10 m east of the southern end of array BC3-1

Looking northwest at HVSR sensor 450 and center of array BC3-1

Looking south along array BC3-1

Looking north from the center of array BC3-1

Location of Geophysical Testing Arrays:

Location	Latitude	Longitude
BC3-1, Southwest End of MASW/Seismic Refraction Array	33.65517	-115.45387
BC3-1, Center of MASW/Seismic Refraction Array	33.65549	-115.45379
BC3-1, Northeast End of MASW/Seismic Refraction Array	33.65578	-115.45368
HVSR Sensor 450	33.65548	-115.45377
HVSR Sensor 453	33.65516	-115.45391
HVSR Sensor 507	33.65583	-115.45366
CI.BC3 Seismic Station	33.65513	-115.45364

Notes: 1) WGS84 Coordinate System (decimal degrees)
2) Survey accuracy is estimated at 1 to 2 m.

Results:

V_S Model 1 (Fundamental Mode Assumption)

Depth to Top of Layer (m)	Layer Thickness (m)	S-Wave Velocity (m/s)	Inferred P-Wave Velocity (m/s)	Assumed Poisson's Ratio	Assumed Density (g/cm^3)
0	1	195	364	0.3	1.8
1	1.5	441	826	0.3	2.0
2.5	3.5	655	1226	0.3	2.1
6	4	685	1282	0.3	2.1
10	6	696	1302	0.3	2.1
16	8	1105	2067	0.3	2.2
24	>6	1605	3004	0.3	2.3

Notes: 1) Depth of investigation is about 30 m.
2) Bottom layer is a half space.

V_S Model 2 (Average Mode Assumption)

Depth to Top of Layer (m)	Layer Thickness (m)	S-Wave Velocity (m/s)	Inferred P-Wave Velocity (m/s)	Assumed Poisson's Ratio	Assumed Density (g/cm^3)
0	1	201	376	0.3	1.8
1	1.5	434	811	0.3	1.9
2.5	2.5	516	965	0.3	2.0
5	5	684	1280	0.3	2.1
10	6	707	1322	0.3	2.1
16	6	1071	2005	0.3	2.2
22	>8	1428	2671	0.3	2.3

Notes: 1) Depth of investigation is about 30 m.
2) Bottom layer is a half space.

Observations/Discussion:

- The HVSR data quality may be suspect due to large antennas in the site vicinity and gusting winds during data acquisition. All HVSR plots have slightly elevated response over the 0.4 to 10 Hz range, but no distinct peaks. The absence of a distinct HVSR peak is not unexpected for a mountaintop rock site, such as this site.
- Picking of seismic refraction first arrival data was complicated by noise, weak first arrivals, possible out of plane refractors, etc.
- The P-wave refraction data for array BC3-1 were modeled using a tomographic inversion routine with a smooth velocity gradient starting model. The seismic refraction model was extended to far offset shot locations to extend depth of investigation. A longer receiver array is preferred for extending depth of investigation, but at the expense of the efficiency in combining seismic refraction and MASW data acquisition along the shorter array. However, limited space at the site did not allow for a longer array and also limited the number of far offset shot locations.
- The seismic refraction survey design allowed P-wave velocity to be imaged to a maximum depth of about 10 to 13 m. Without extension of the model to far offset shot locations, the effective depth of investigation is less than 10 m. The seismic refraction model shows that P-wave velocity is about 600 to 800 m/s at the surface, increasing to 1,000 m/s at a depth of 1 to 3 m, 1,200 m/s at a depth of 2 to 7 m and greater than 1,400 m/s at a depth below 4 to 9 m.
- The seismic refraction model indicates that there is lateral velocity variation at this site, with lower P-wave velocities to deeper depths near the northern half of the line. Field inspection revealed highly variable weathering of the rock in the site vicinity with the more mafic rocks being significantly less weathered than the felsic rocks.
- Noise conditions at the site were not sufficient for application of passive surface wave techniques.

- The minimum wavelength surface wave phase velocity data extracted from the 48-channel MASW array was about 10 m. Reducing data from smaller hammer sources using a limited offset receiver array (i.e. less active geophones) allowed extraction of surface wave dispersion data to a minimum wavelength of about 3 m. Small wavelength Rayleigh wave phase velocity data were only utilized from the shot locations near the center and north end of the array.
- There is about 80 m/s scatter in the MASW dispersion data, likely due to lateral velocity variation.
- A representative dispersion curve was generated for the MASW data set using a moving average, polynomial curve fitting routine and used for modeling.
- Two V_S models were generated from the surface wave data. The first (Model 1) assumes that the dispersion curve consists of only the fundamental mode Rayleigh wave. Forward modeling reveals that this velocity structure would excite a dominant first higher mode over the 40 to 65 Hz frequency range, but not at low frequencies (long wavelengths). Sufficient resolution is expected in the v-f transform (overtone image) over this frequency range to isolate the fundamental mode and, therefore, the fundamental mode model is likely valid. An alternate V_S model (Model 2) was developed assuming the observed dispersion curve consists of the average/effective mode (average of all modes based on relative amplitude each mode for a far-field plane wave with no body wave effects) to demonstrate the effect of possibly incorrectly assuming that the measured dispersion curve reflects the average/effective mode.
- There is only a 2% difference inV_{S30} between the fundamental and average/effective mode models. The two models are very similar except that Model 2 has lower velocity over the 2.5 to 5 m depth interval, which is associated with the first higher mode having significant energy over a wide intermediate frequency range. The lower velocity in Model 2 between 2.5 and 5 m is the cause of the slightly lower estimate of V_{S30}. The models also have slightly difference velocity structure at depth, primarily because the layering is different. At this site, the fundamental mode model (Model 1) is likely most representative of subsurface velocity structure.
- The surface wave model is generally consistent with the P-wave refraction model, especially considering unknown Poisson's ratio.
- Surface wave depth of investigation is about 30 m based on half of maximum wavelength criteria.
- Modeling of the upper and lower envelopes of the MASW dispersion data was not conducted, but would be expected to result in an approximate 5% variation in V_{S30}.
- V_{S30} is 763 for Model 1 (fundamental mode assumption) and 745 m/s Model 2 (average/effective mode assumption), averaging 754 m/s (Site Class C/B).
- Average S-wave velocity between 1 m (assumed sensor depth) and 31 m is 862 m/s for Model 1 and 833 m/s for Model 2, averaging 848 m/s (Site Class B).
- As discussed above, the fundamental mode model (Model 1) is probably most representative of subsurface velocity structure. However, the possibility cannot be discounted that Model 2 (average/effective mode assumption) more accurately reflects velocity structure below a depth of 20 m.

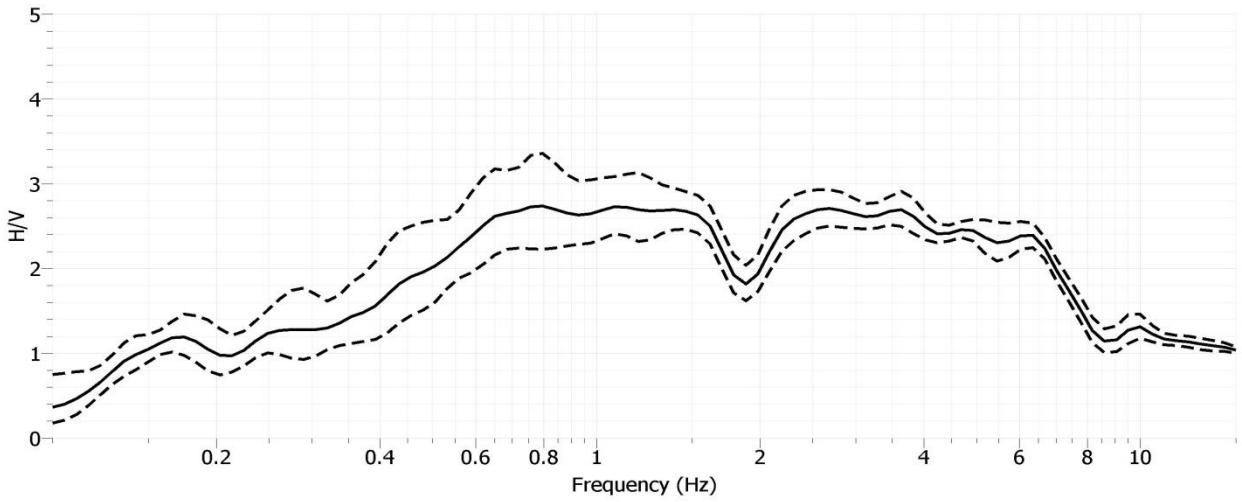

Site CI.BC3, H/V Spectral Ratio, Array BC3-1, Sensor 507

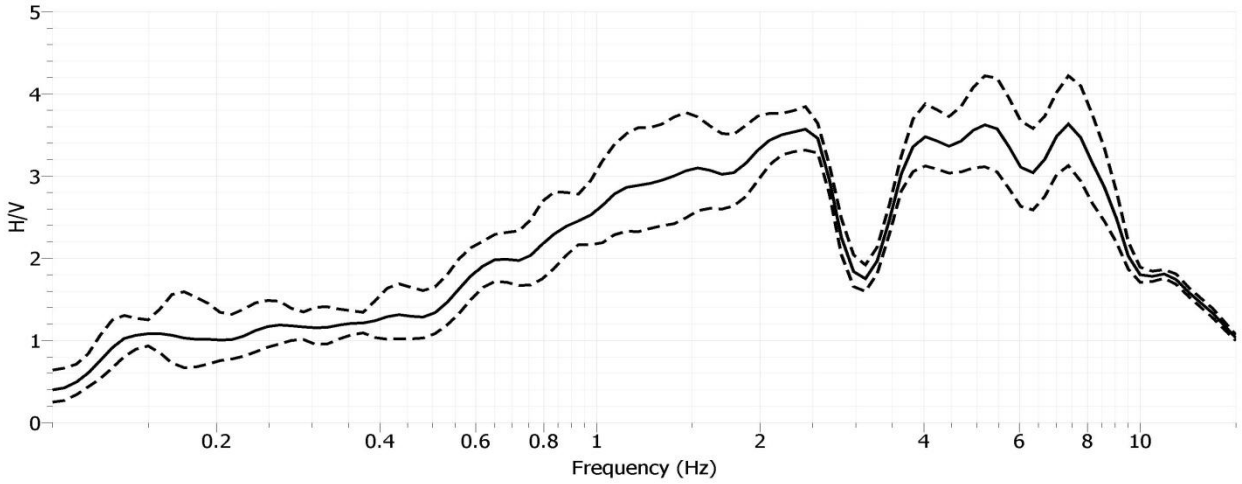

Site CI.BC3, H/V Spectral Ratio, Array BC3-1, Sensor 450

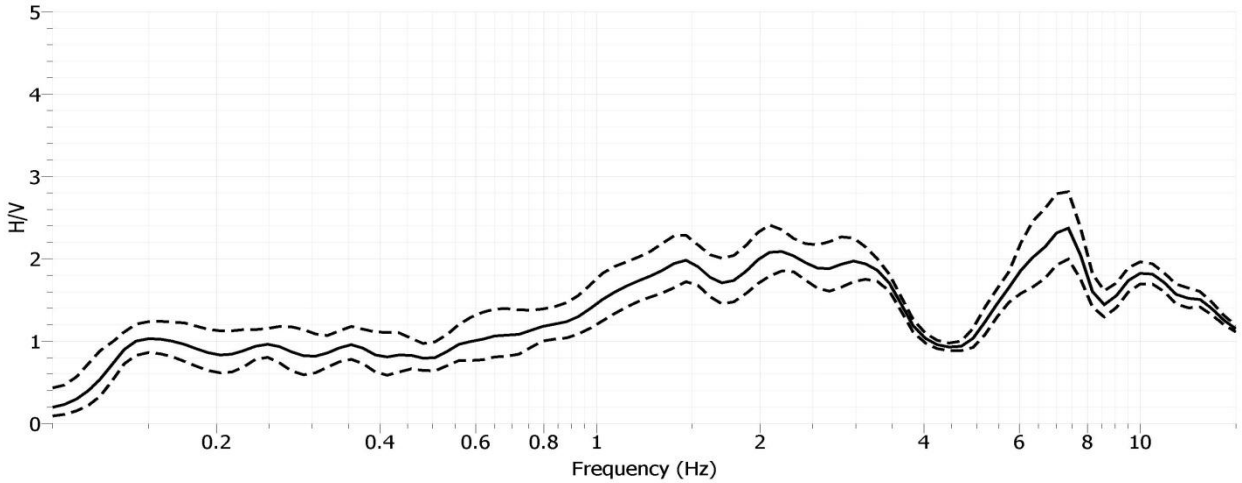

Site CI.BC3, H/V Spectral Ratio, Array BC3-1, Sensor 453

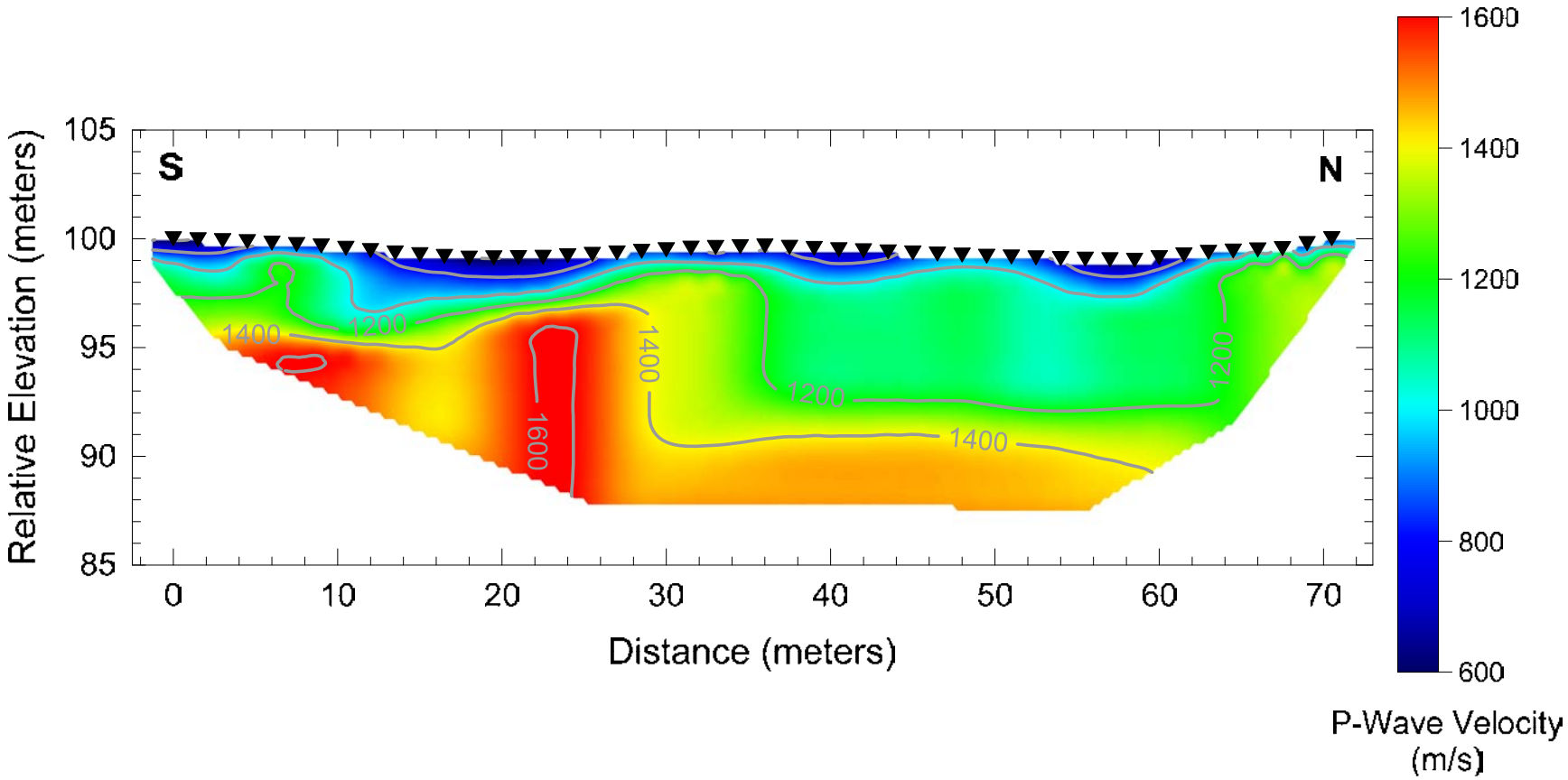

Array BC3-1 – Tomographic Seismic Refraction Model utilizing Layer Based Starting Model

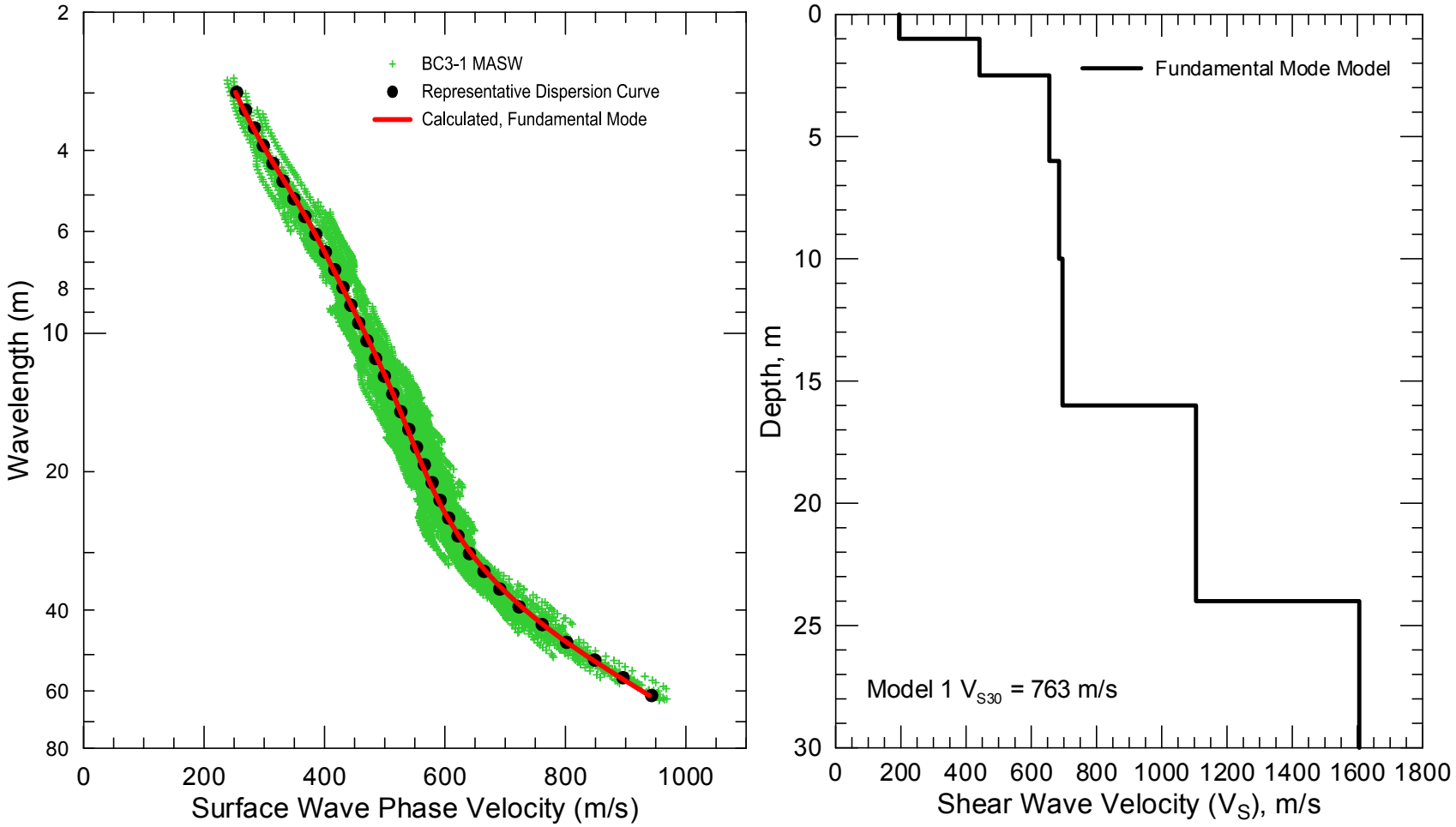

CI.BC3 - Field, representative and inverted theoretical surface wave dispersion data (left) and associated V_S model (right).

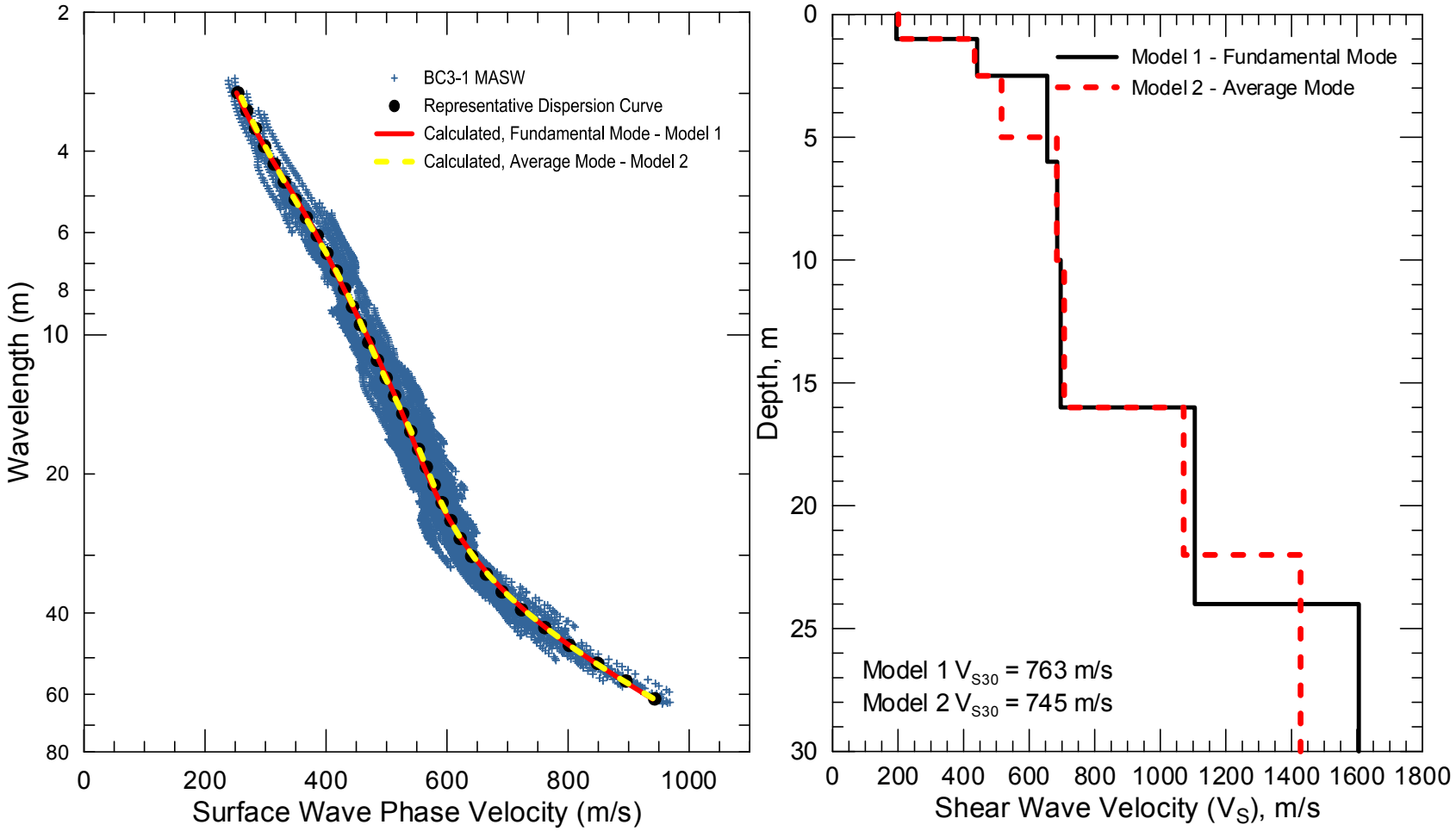

CI.BC3 - Field, representative and inverted theoretical surface wave dispersion data (left) and associated V_S models (right). Model 1, based on the fundamental mode assumption, is probably most representative of subsurface velocity structure although the possibility cannot be discounted that Model 2, based on the average/effective mode assumption, more accurately reflects velocity structure at depths below 20 m.

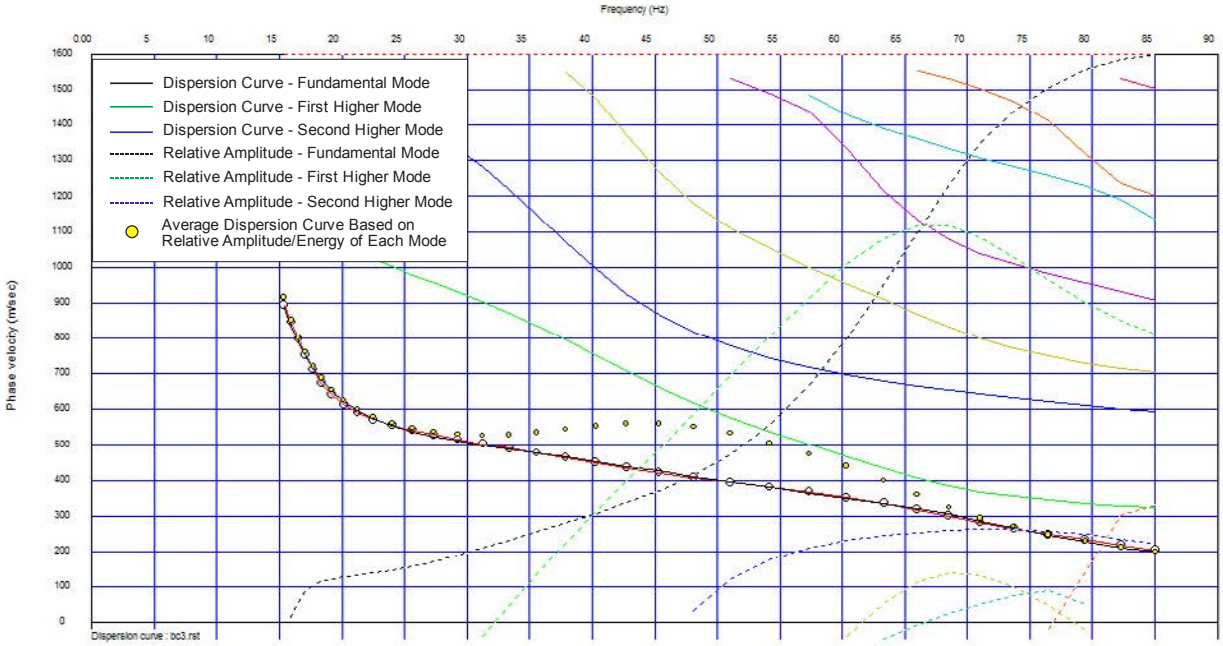

CI.BC3 – Model 1 (fundamental mode assumption) expected to have a dominant first higher mode over the 40 to 65 Hz frequency range. The fundamental mode assumption may, however, be valid at greater depths. We would expect there for be sufficient resolution over the 40 to 65 Hz range to be able to pick fundamental mode. Average/effective mode modeling may, therefore, not be applicable to this site.

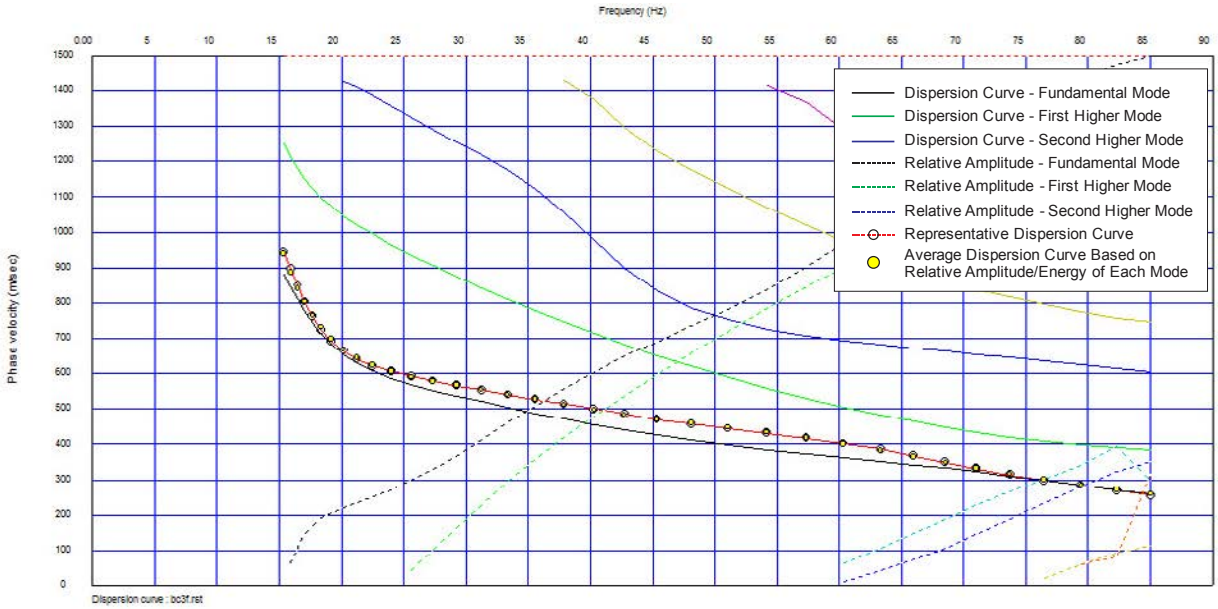

CI.BC3 – Model 2 (average/effective mode assumption) is only expected to be applicable if there is insufficient resolution in the v-f transform to isolate separate modes at low frequencies. Modal superposition at low frequencies is assumed to be represented by the average mode. However, if the fundamental mode is successfully identified at intermediate to high frequencies then V_S may be underestimated at shallow depth.

Site CI.BCW

Location: Bitter Creek Wildlife, Kern County, California

Latitude: 34.94010 **Longitude:** -119.41314
(Station coordinates modified based on field GPS survey, WGS84 coordinate system)

V_{S30} (measured): 305 m/s

V_{S30} (adjusted to more accurately reflect seismic station conditions): 335 m/s (average S-wave velocity between 2 and 32 m adjusting for 2 m estimated sensor depth).

NEHRP Site Class: D

Geomatrix Code: IOC

Geologic Conditions/Observations: Seismic station located on geologic unit mapped as Tertiary (Oligocene) Simmler Formation consisting of an arkosic, lithified sandstone. The San Andreas Fault Zone is located about 270 m northeast of site. Geologic layers are folded and have steep dip in the site vicinity.

Site Conditions: Rural site located on gently rolling hills. Ground surface elevation decreases about 6 m to the east along the 70.5 m long MASW and seismic refraction array. The seismic line is oriented subparallel to geologic strike.

Geophysical Methods Utilized: HVSR, Seismic Refraction, MASW

Geophysical Testing Arrays:

1. Array BCW-1 (48 channel MASW and P-wave seismic refraction array utilizing 4.5 Hz vertical geophones spaced 1.5 m apart for a length of 70.5 m, forward and reverse shot locations with multiple source offsets and source types and multiple interior shot locations).
2. Three HVSR measurement locations: two distributed along array BCW-1 and one adjacent to the seismic station.

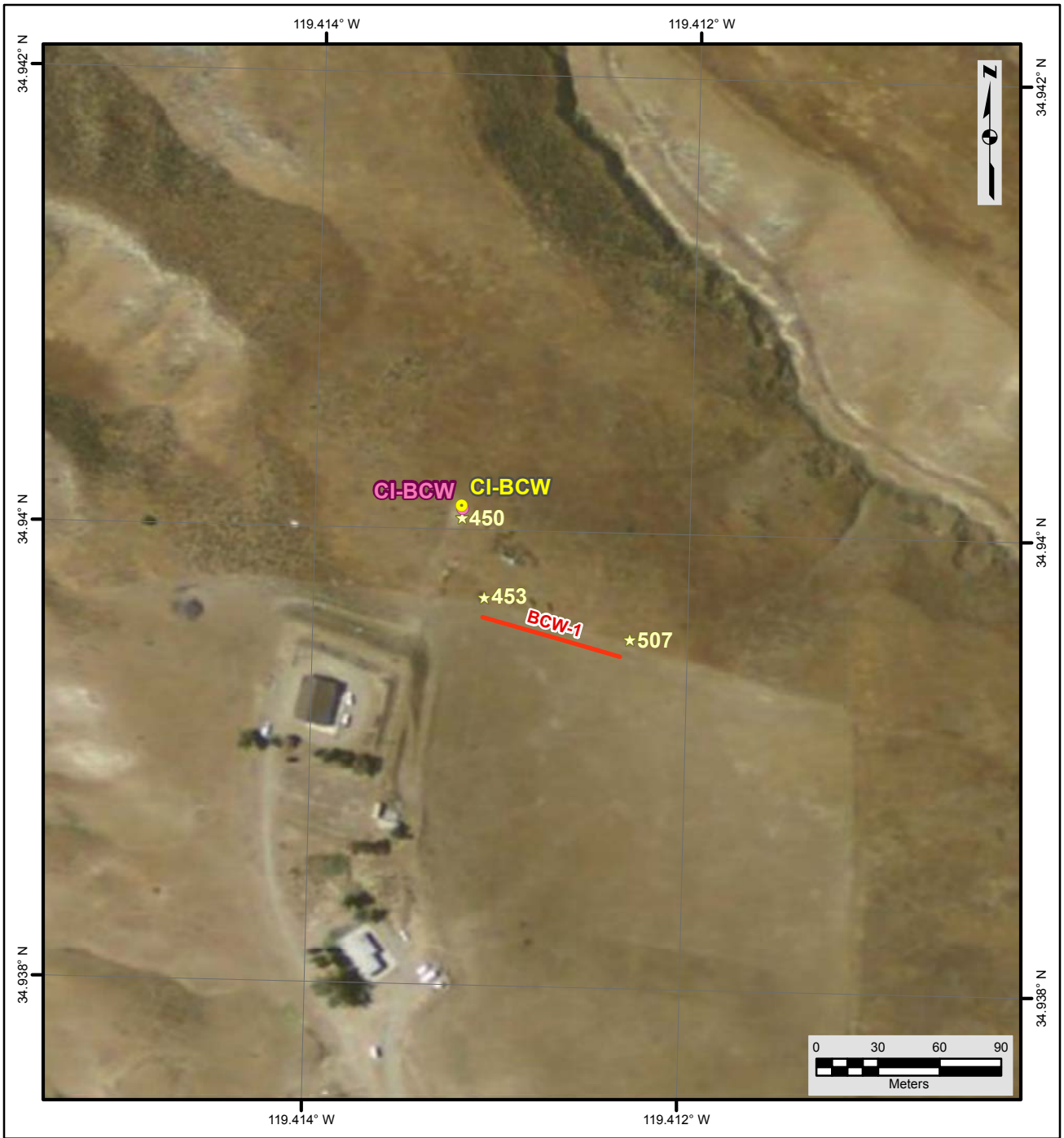

Legend

- Seismic Station - Approximate Surveyed Location
- Seismic Station - Approximate Location of Record
- H/V Spectral Ratio Measurement Location
- MASW and Seismic Refraction Array

NOTES:
1. WGS 1984 COORDINATE SYSTEM
2. Image Source: ESRI, i-cubed, USDA FSA, USGS, AEX, GeoEye, Getmapping, Aerogrid, IGP

File Name: CI-BCW-I

Date: 10/13/2011

USGS science for a changing world

GEOVision geophysical services

RECOVERY.GOV

SITE MAP
CI•BCW

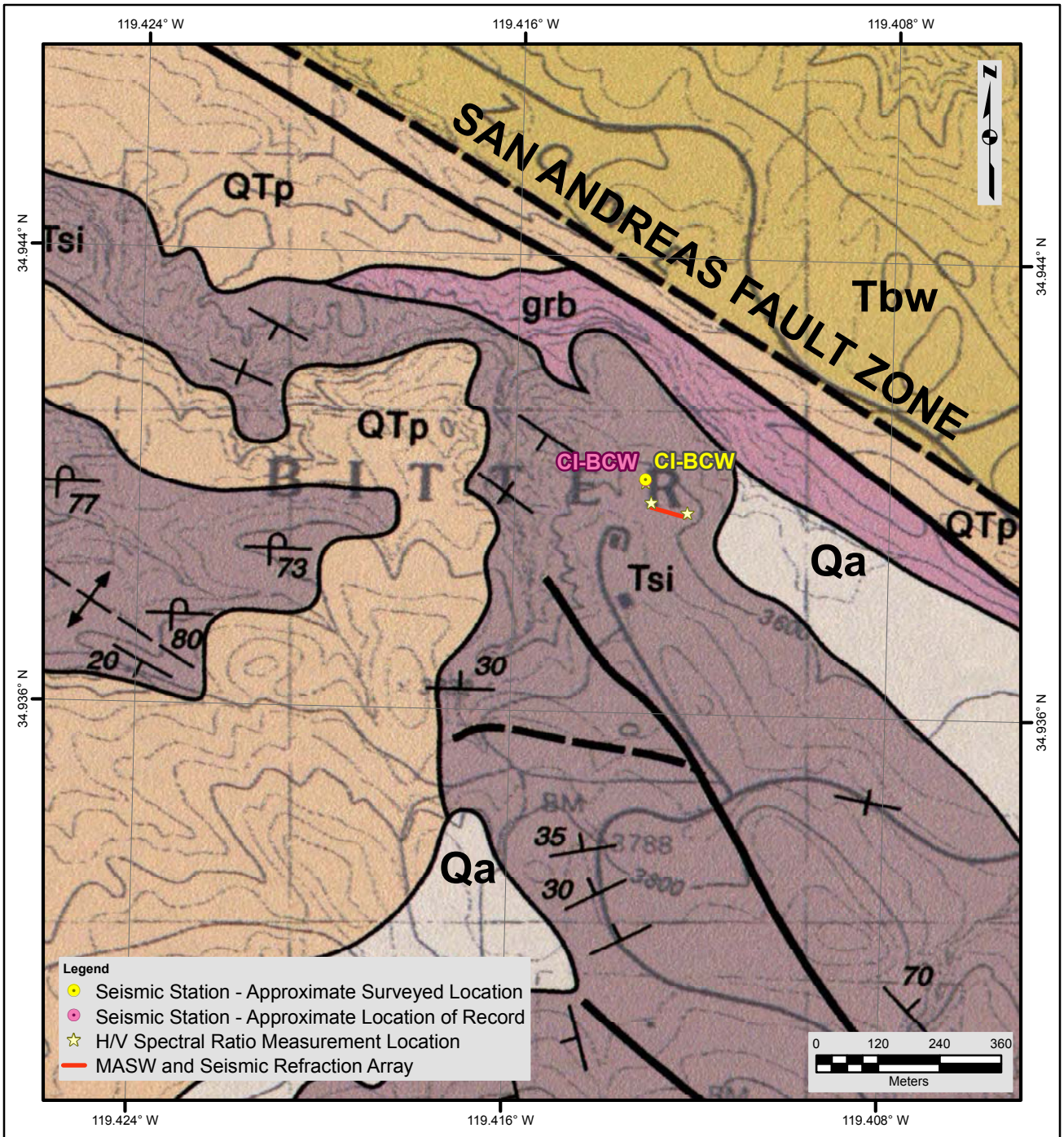

Description of Geologic Map Units

Qa = Quaternary (Holocene) alluvial gravel, sand and clay of stream channels
QTp = Quaternary (Pleistocene) Paso Robles Formation; alluvial conglomerate, pebble to cobble conglomerate, sand and clay
Tbw = Tertiary (Upper Miocene) Bitterwater Creek Shale; marine biogenic, lithified, diatomaceous mudstone, massive to vaguely bedded
grb = Tertiary (Miocene) Caliente Formation; weakly lithified, granitic breccia
Tsi = Tertiary (Oligocene) Simmler Formation; lithified, sandstone, arkosic, locally pebbly

NOTES:
1. WGS 1984 COORDINATE SYSTEM
2. Geologic Map of the Ballinger Canyon Quadrangle, San Luis Obispo, Santa Barbara, Ventura & Kern Counties, California by Thomas W. Dibblee, Jr., 2005
3. See site map for details of geophysical survey

USGS science for a changing world
GEOVision geophysical services

GEOLOGIC MAP
CI•BCW

File Name: CI-BCW
Date: 10/13/2011

CI.BCW seismic station

Looking east along MASW and seismic refraction array BCW-1

Looking north towards seismic station CI.BCW and HVSR Sensor 450

MASW data acquisition using accelerated weight drop energy source

Looking west along MASW and seismic refraction array BCW-1

Location of Geophysical Testing Arrays:

Location	Latitude	Longitude
BCW-1, Northwest End of MASW/Refraction Array	34.93962	-119.41301
BCW-1, Center of MASW/Refraction Array	34.93954	-119.41264
BCW-1, Southeast End of MASW/Refraction Array	34.93946	-119.41227
HVSR Sensor 450	34.94005	-119.41313
HVSR Sensor 453	34.93970	-119.41300
HVSR Sensor 507	34.93953	-119.41222
CI.BCW Seismic Station	34.94010	-119.41314

Notes: 1) WGS84 Coordinate System (decimal degrees)
2) Survey accuracy is estimated at 1 to 2 m.

Results:

V_S Model

Depth to Top of Layer (m)	Layer Thickness (m)	S-Wave Velocity (m/s)	Inferred P-Wave Velocity (m/s)	Assumed Poisson's Ratio	Assumed Density (g/cm^3)
0	1	138	258	0.300	1.7
1	1.5	197	368	0.300	1.7
2.5	3.5	281	525	0.300	1.8
6	15	301	2000	0.488	1.9
21	8	411	2000	0.478	2.0
29	>6	579	2000	0.454	2.0

Notes: 1) Saturated zone, with V_P of about 2,000 m/s, constrained at a depth of about 6 m based on seismic refraction survey.
2) Depth of investigation is about 35 m.
2) Bottom layer is a half space.

Observations/Discussion:

- There are some differences between the HVSR plots and no clear HVSR peaks.
- The P-wave refraction data for array BCW-1 were modeled using a tomographic inversion routine with a layer based starting model. The seismic refraction models were extended to far offset shot locations. Extending the model to far offset shot locations allowed depth of investigation to be increased to validate the surface wave model at depth. A longer receiver array is preferred for extending depth of investigation, but at the expense of the efficiency in combining seismic refraction and MASW data acquisition along the shorter array.
- The seismic refraction survey design allowed P-wave velocity to be imaged to a maximum depth of about 15 m. Without extension of the model to far offset shot locations, the effective depth of investigation is about 10 m. The seismic refraction model shows that P-wave velocity is about 400 m/s at the surface, increasing to 500 m/s at a depth of 3 to 4 m, 1,500 m/s at a depth of 5 to 7 m and greater than 2,000 m/s at a depth below 6 to 10 m. The increase in P-wave velocity from 500 to 2,000 m/s generally occurs over a 2 to 3 m depth interval and is a associated with saturated sediments located at a depth on the order of 6 to 7 m.
- Noise conditions at the site were not sufficient for application of passive surface wave techniques.
- There is about 20 to 40 m/s scatter in the MASW dispersion data, which is likely due to minor lateral velocity variation.
- The minimum wavelength surface wave phase velocity data extracted from the 48-channel MASW array was about 10 m. Data reduction using seismic records from smaller hammer sources and a limited offset receiver array (i.e. less active geophones) allowed extraction of surface wave dispersion data to a minimum wavelength of about 3 m. The smallest wavelength Rayleigh wave phase velocity data originated from small hammer source locations at the southeast end of the surface wave array.
- A representative dispersion curve was generated for the MASW data set using a moving average, polynomial curve fitting routine and used for modeling.
- The saturated zone with P-wave velocity of 2,000 m/s was anchored at a depth of 6 m for surface wave modeling.
- Surface wave depth of investigation is about 35 m based on half of maximum wavelength criteria.
- V_{S30} is 305 m/s (Site Class D).
- Average S-wave velocity between 2 m (assumed sensor depth) and 32 m is 335 m/s (Site Class D).

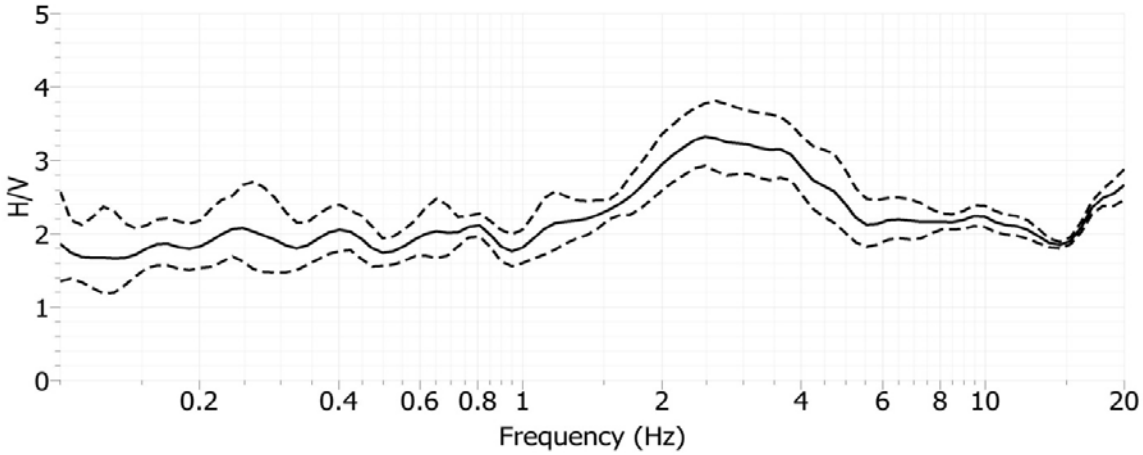

Site CI.BCW, H/V Spectral Ratio, Array BCW-1, Sensor 450

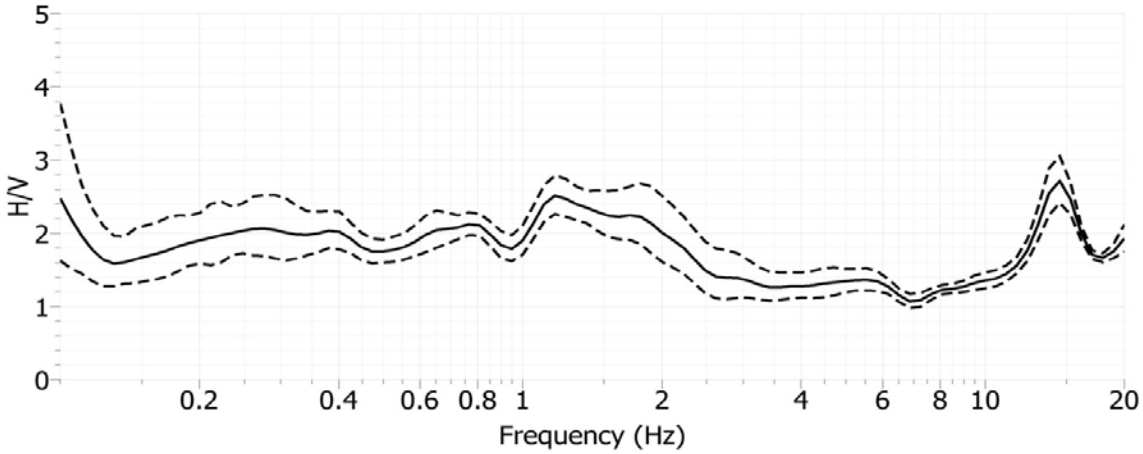

Site CI.BCW, H/V Spectral Ratio, Array BCW-1, Sensor 453

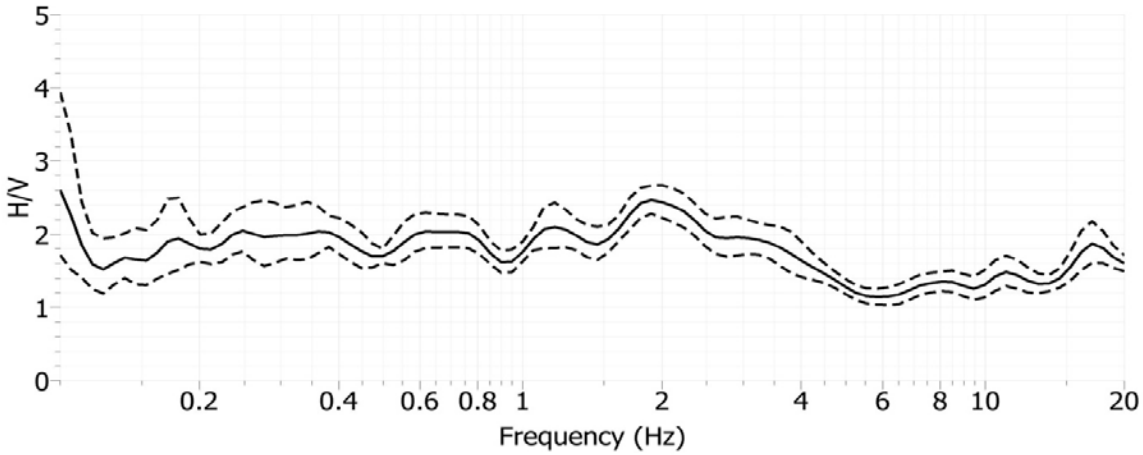

Site CI.BCW, H/V Spectral Ratio, Array BCW-1, Sensor 507

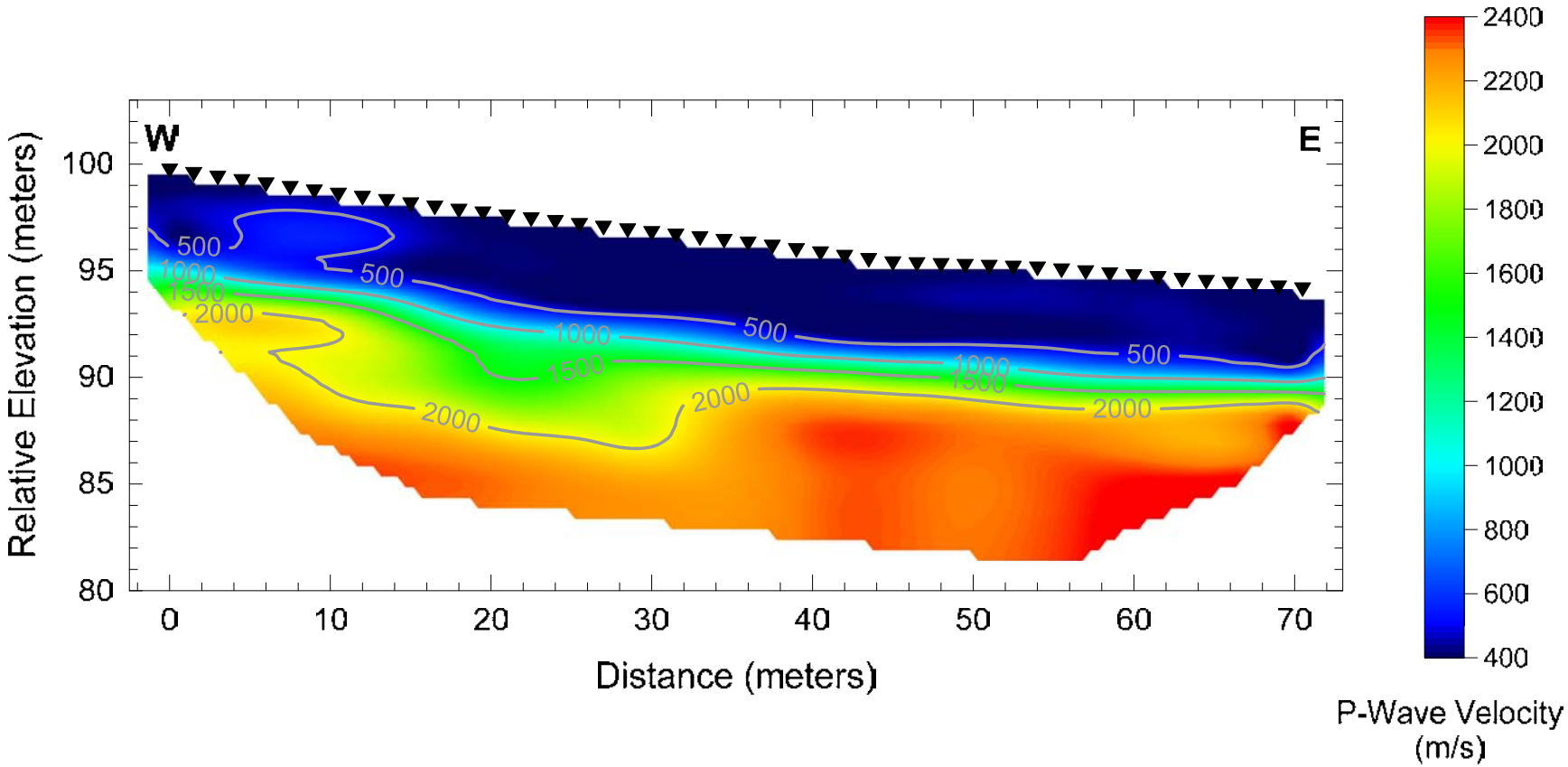

Array BCW-1 – Tomographic Seismic Refraction Model utilizing Layer Based Starting Model

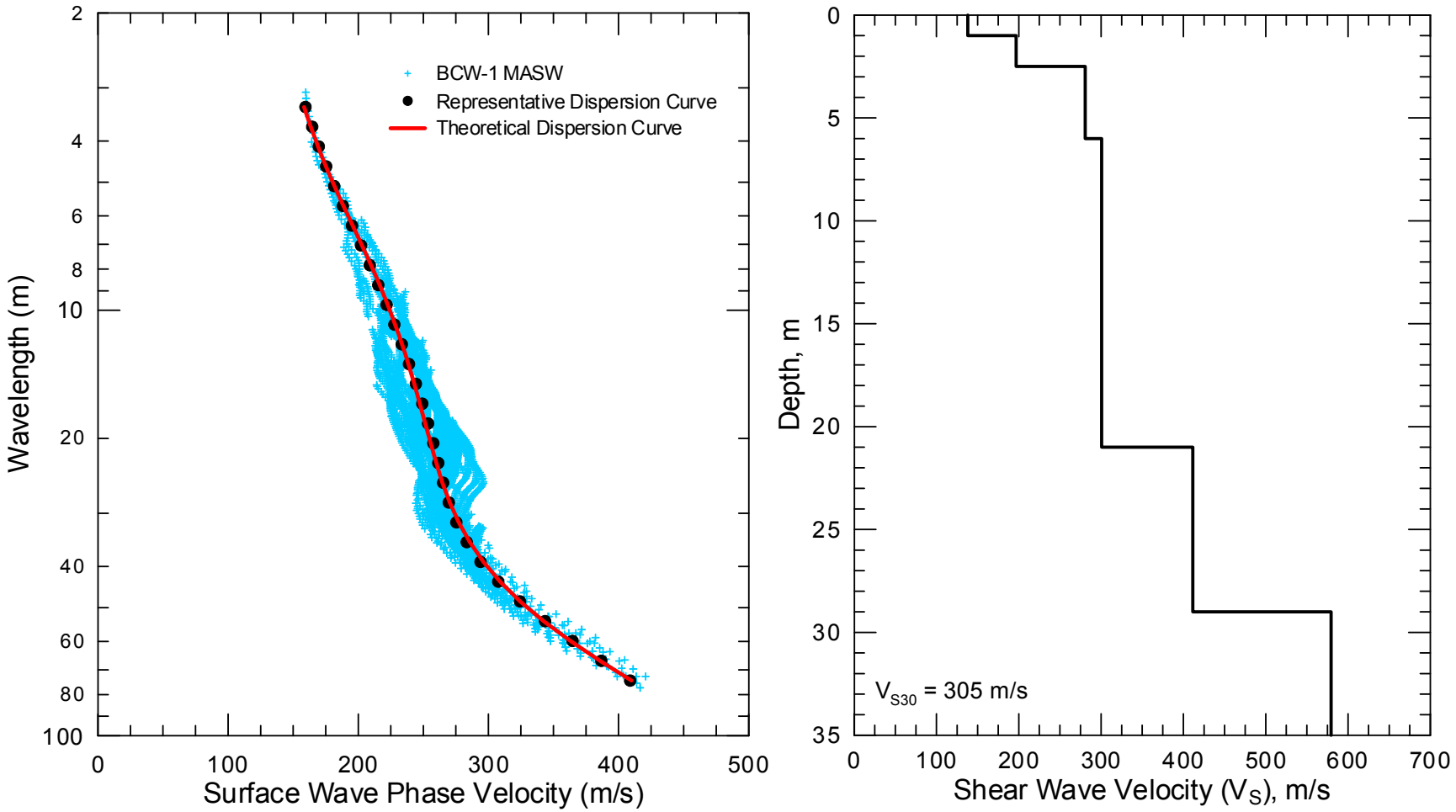

CI.BCW - Field, representative and inverted theoretical surface wave dispersion data (left) and associated V_S model (right)

Site CI.BEL

Location: Belle Mountain, Joshua Tree National Park, San Bernardino County, California

Latitude: 34.00057 **Longitude:** -115.99816
(Station coordinates modified based on site GPS survey and are in WGS84 coordinate system)

V_{S30} (measured): 796 m/s

V_{S30} (adjusted to more accurately reflect seismic station conditions): 796 m/s (no adjustment necessary).

NEHRP Site Class: B

Geomatrix Code: INA

Geologic Conditions/Observations: Seismic station located on Precambrian Pinto gneiss. Seismic station located on rock outcrop.

Site Conditions: Rural site. Windy conditions during geophysical testing. Steep, undulating topography in site vicinity.

Geophysical Methods Utilized: HVSR, Seismic Refraction, MASW

Geophysical Testing Arrays:

1. Array BEL-1 (48 channel MASW and P-wave seismic refraction array utilizing 4.5 Hz vertical geophones spaced 1.5 m apart for a length of 70.5 m, forward and reverse shot locations with multiple source offsets and source types (hammers only) and multiple interior shot locations).
2. Array BEL-2 (48 channel MASW and P-wave seismic refraction array utilizing 4.5 Hz vertical geophones spaced 1.5 m apart for a length of 70.5 m, forward and reverse shot locations with multiple source offsets and source types (hammers only) and multiple interior shot locations).
3. Three HVSR measurement locations distributed evenly along array BEL-1.

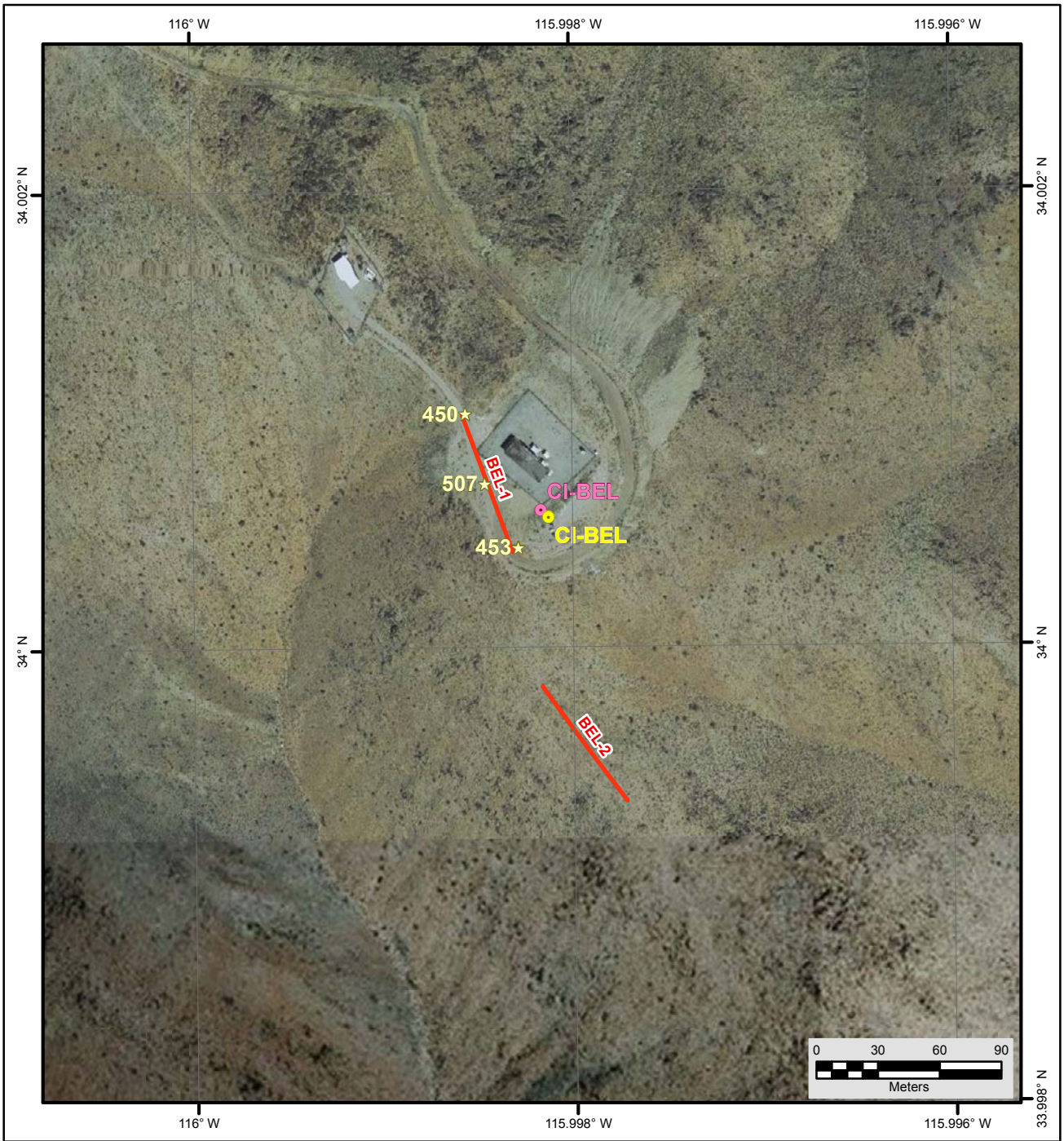

Legend

- Seismic Station - Approximate Surveyed Location
- Seismic Station - Approximate Location of Record
- H/V Spectral Ratio Location
- MASW and Seismic Refraction Array

NOTES:
1. WGS 1984 COORDINATE SYSTEM
2. Image Source: ESRI, i-cubed, USDA FSA, USGS, AEX, GeoEye, Getmapping, Aerogrid, IGP

File Name: CI-BEL-I

Date: 6/17/2012

USGS science for a changing world

GEOVision geophysical services

RECOVERY.GOV

SITE MAP
CI•BEL

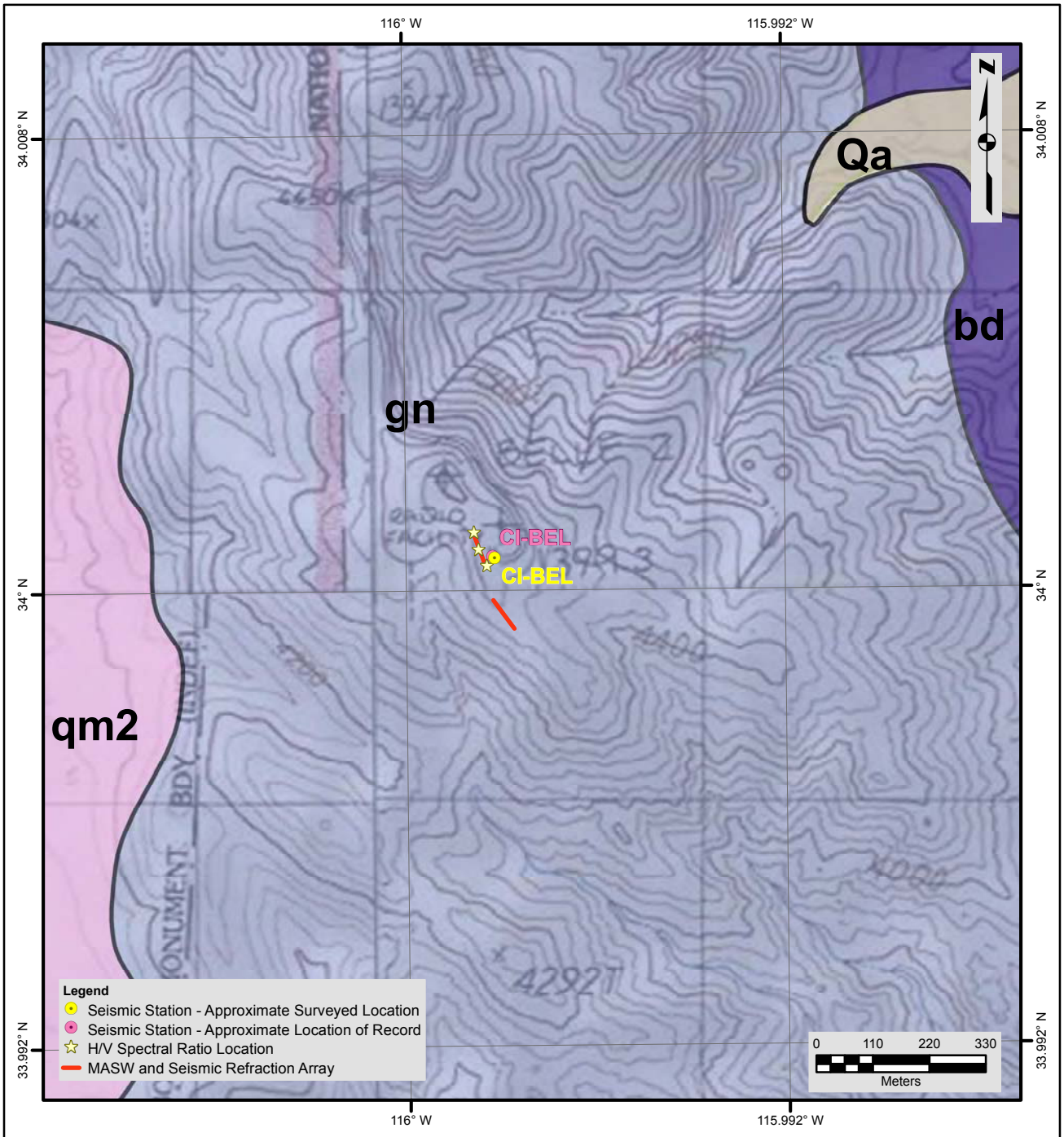

Description of Geologic Map Units

Qa = Quaternary (Holocene) alluvial sand and gravel of valley areas
qm2 = Mesozoic (Cretaceous) quartz monzonite, coarse-grained
bd = Mesozoic (?) biotite diorite, massive to faintly gneissoid, medium-grained, composed mainly of plagioclase and biotite
gn = Precambrian (?) gneissic rocks ranging from quartz monzonite to quartz diorite

NOTES:
1. WGS 1984 COORDINATE SYSTEM
2. Modified from Geologic Map of the Joshua Tree & Twentynine Palms, Hexie Mountains & Pinto Basin, Thousand Palms & Lost Horse and Valley Mountain & Dale Lake Mountains 15 Minute Quadrangles, Riverside & San Bernardino Counties, California by Thomas W. Dibblee, Jr., 2008
3. See site map for details of geophysical survey
4. Topo Image Sources: USGS, FAO, NPS, EPA, NRCAN, GeoBase, Esri, DeLorme, TANA, Intermap and other suppliers and the GIS community

USGS science for a changing world

GEOVision geophysical services

GEOLOGIC MAP
CI•BEL

File Name: CI-BEL

Date: 2/7/2013

Looking north towards seismic station on top of hill and HVSR Sensor 453

Looking north along Array BEL-2

Looking southeast along array BEL-1 towards seismic station

Looking south along array BEL-2

Looking north towards seismic station from array BEL-2

Location of Geophysical Testing Arrays:

Location	Latitude	Longitude
BEL-1, Southeast End of MASW/Refraction Array	34.00042	-115.99835
BEL-1, Center of MASW/Refraction Array	34.00072	-115.99848
BEL-1, Northwest End of MASW/Refraction Array	34.00102	-115.99861
BEL-2, South End of MASW/Refraction Array	33.99932	-115.99776
BEL-2, Center of MASW/Refraction Array	33.99957	-115.99798
BEL-2, North End of MASW/Refraction Array	33.99983	-115.99820
CI.BEL Seismic Station	34.00057	-115.99816
HVSR Sensor 450	34.00102	-115.99859
HVSR Sensor 453	34.00044	-115.99832
HVSR Sensor 507	34.00072	-115.99849

Notes: 1) WGS84 Coordinate System (decimal degrees)
2) Survey accuracy is estimated at 1 to 2 m

Results:

V_S Model

Depth to Top of Layer (m)	Layer Thickness (m)	S-Wave Velocity (m/s)	Inferred P-Wave Velocity (m/s)	Assumed Poisson's Ratio	Assumed Density (g/cm^3)
0	2	505	945	0.3	2.0
2	3	697	1304	0.3	2.0
5	5	802	1500	0.3	2.1
10	7	840	1572	0.3	2.1
17	9	851	1591	0.3	2.1
26	>9	933	1746	0.3	2.1

Notes: 1) Depth of investigation is about 35 m.
2) Bottom layer is a half space.

Observations/Discussion:

- Seismic station located on an outcrop of relatively hard bedrock.
- Array BEL-1 located along a gravel road near the seismic station. During testing it became clear that there was a significant lateral velocity variation along the array due to thickening of a fill pad to the north. Therefore, array BEL-2 was established along a sloping bedrock ridge north of the seismic station.
- No attempt was made to process MASW data from array BEL-1 due to the significant lateral velocity variation, which was not indicative of the seismic station conditions. Additionally, seismic refraction first arrival data is extremely noisy due to high wind, possible out of plane refractors, etc. and the seismic refraction data were not analyzed. Inspection of the seismic refraction data, however, indicates that the rock velocities are similar to those on array BEL-2.
- There are no clear peaks in the HVSR data, as expected for a rock site.
- HVSR sensor 453 appears to have the best quality data. Sensors 450 and 453 have higher than expected HVSR response over a wide frequency range due to elevated response on one or both horizontal channels. It is unclear if this is related to sensor coupling, heavy winds during testing, or the steep terrain in the site vicinity.
- Seismic refraction data were modeled using a tomographic inversion routine and a smooth velocity gradient starting model. The seismic refraction model indicates that P-wave velocity increases with depth from about 600 to 1,000 m/s near the surface to over 1,250 m/s at a depth of 1 to 4 m and over 1,500 m/s at a depth of 2 to 10 m.
- Seismic refraction depth of investigation is only about 10 m because rock velocities only appear to be increasing gradually with depth. The seismic refraction survey would have detected a bedrock unit with P-wave velocity of 2,000 m/s if located within about 15 m of the surface.
- The seismic refraction model indicates that there is a significant thickening of the weathered zone at the southern end of the line.
- Noise conditions at the site were not sufficient for application of passive surface wave techniques.
- The minimum wavelength surface wave phase velocity data extracted from the 48-channel MASW array was about 15 m. Reducing data from smaller hammer sources using a limited offset receiver array (i.e. less active geophones) allowed extraction of surface wave dispersion data to a minimum wavelength of about 6 m.
- No attempt was made to extract small wavelength/high frequency surface wave phase velocity data from shot locations at the south end of the array because the seismic refraction model indicates that there is a thicker zone of residual soil and highly weathered rock in this area. This thicker weathered zone is probably not characteristic of the seismic station, which is located on a relatively hard rock outcrop.
- There is significant scatter in MASW dispersion data (about 5% of velocity), which is likely due to lateral velocity variation caused by differential weathering of near surface rock.
- A representative dispersion curve was generated for the MASW data set using a moving average, polynomial curve fitting routine and used for modeling.

- Surface wave depth of investigation is about 35 m based on half of maximum wavelength criteria.
- Inferred P-wave velocities in the surface wave model in the upper 10 m are consistent with those in the seismic refraction model, especially considering the unknown Poisson's ratio.
- V_{S30} is 796 m/s (Site Class B).
- The scatter in MASW dispersion data indicates that V_{S30} may vary by as much as 5% in the vicinity of array BEL-2. The seismic station appears to have a slightly thinner weathering zone and, therefore, the seismic station likely resides on rock with V_{S30} in the higher range.

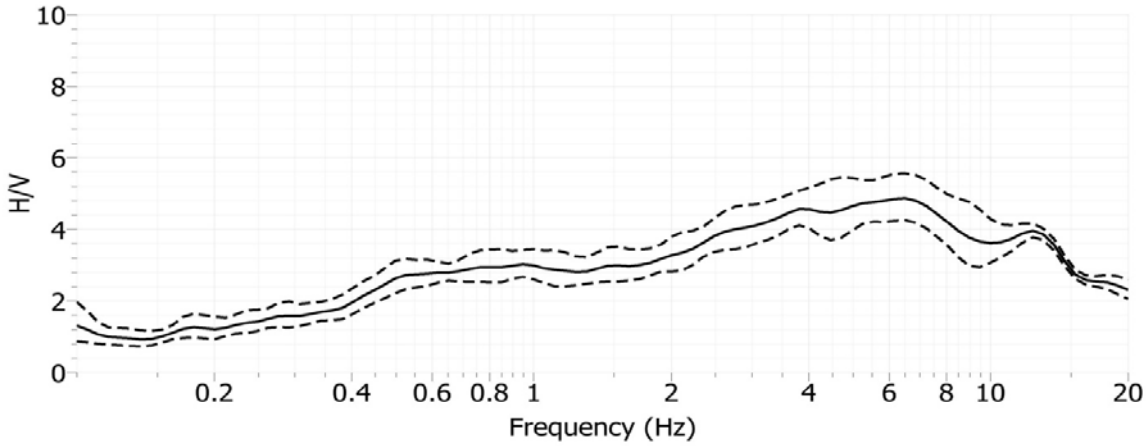

Site CI-BEL, H/V Spectral Ratio, Array BEL-1, Sensor 450

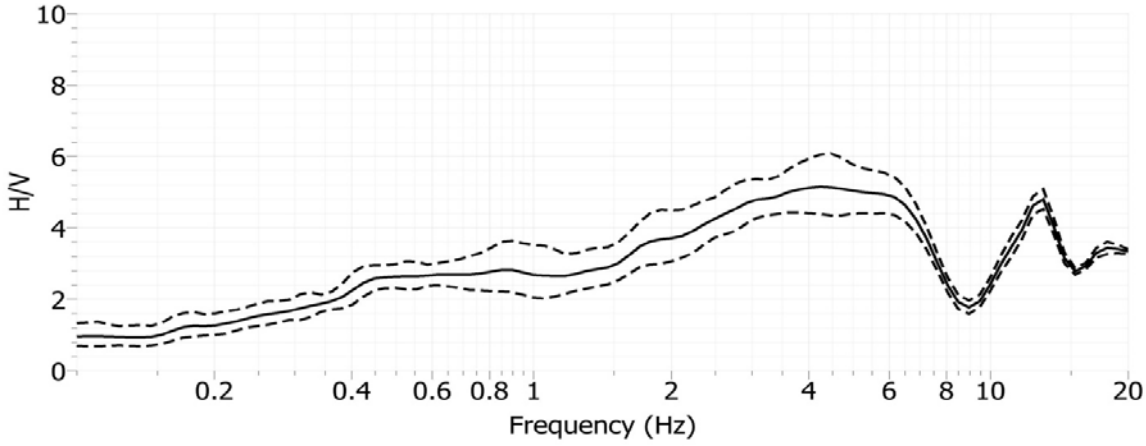

Site CI-BEL, H/V Spectral Ratio, Array BEL-1, Sensor 507

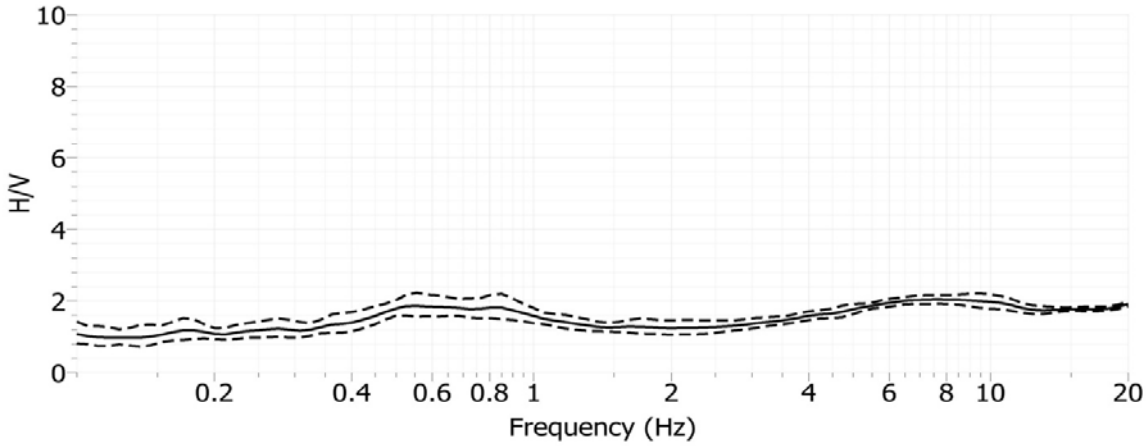

Site CI-BEL, H/V Spectral Ratio, Array BEL-1, Sensor 453

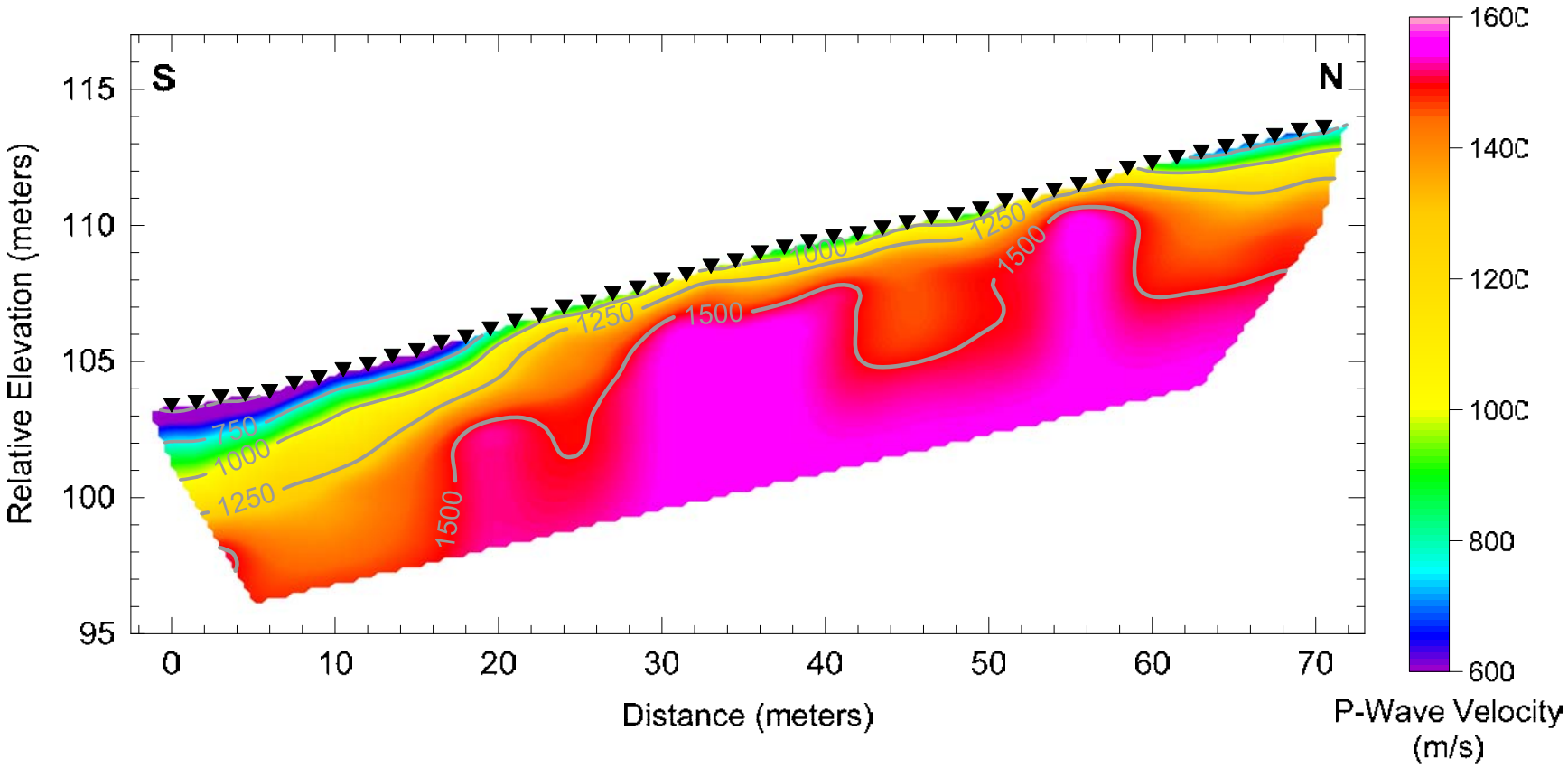

Array BEL-2 – Tomographic seismic refraction model utilizing smooth velocity gradient starting model

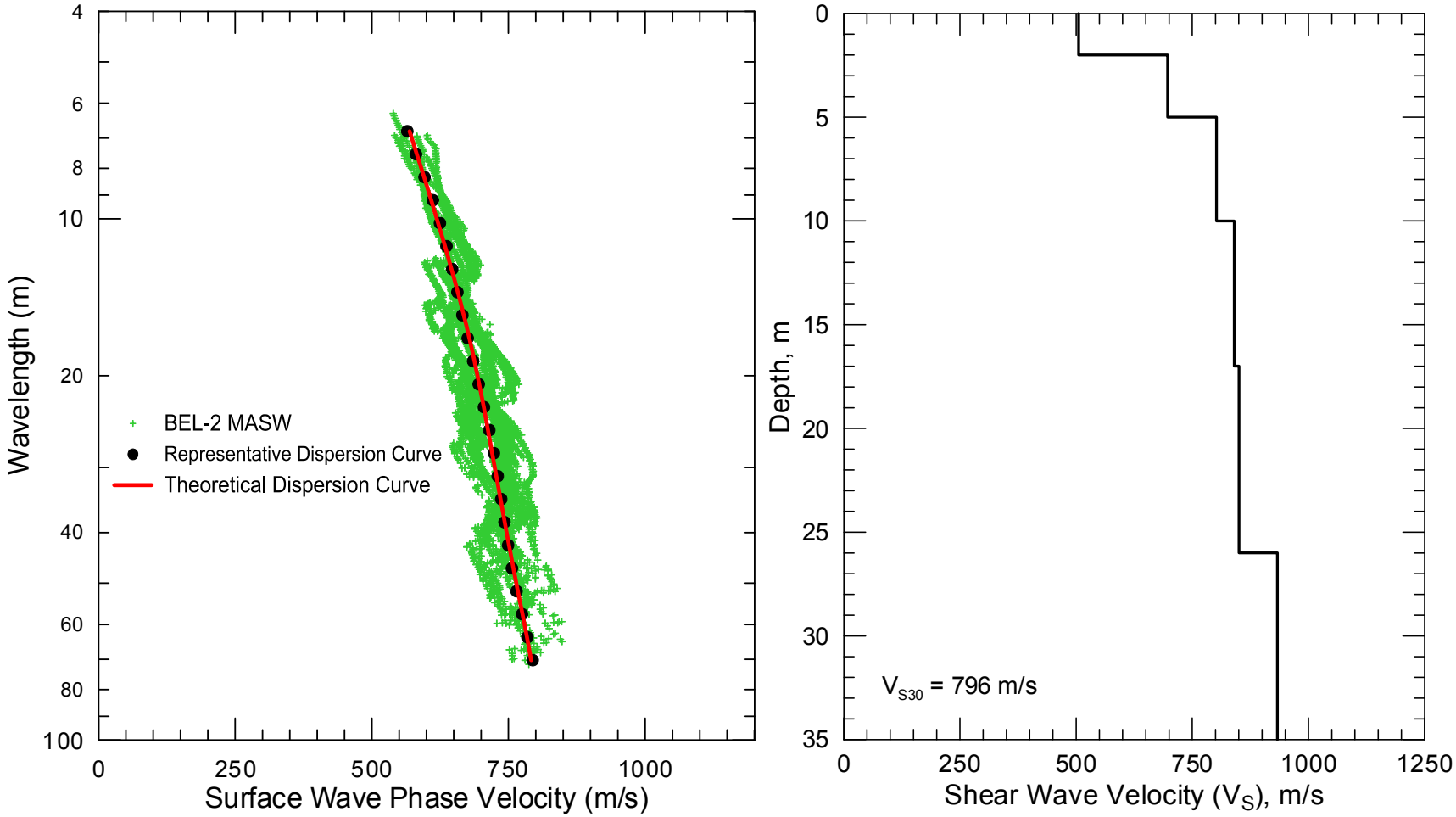

CI.BEL - Field, representative and inverted theoretical surface wave dispersion data (left) and associated V_S model (right)

Site CI.BFS

Location: Mt. Baldy Ranger Station, Angeles National Forest, California

Latitude: 34.23883 **Longitude:** -117.65853
(Station coordinates provided by USGS, WGS84 coordinate system)

V_{S30} (measured): 500 m/s

V_{S30} (adjusted to more accurately reflect seismic station conditions): 731 m/s (see discussion, estimated accuracy of about 10%).

NEHRP Site Class: C

Geomatrix Code: IHB/IHA

Geologic Conditions/Observations: Seismic station located on Quaternary (Holocene) alluvial sands and gravel. Precambrian metamorphic rocks (gneiss) and Mesozoic granitic rocks expected at very shallow depth. The San Gabriel Fault Zone is located in close proximity to the site.

Site Conditions: Rural site located near mountain top. Relatively flat topography in immediate site vicinity, but steep mountainous topography within 100 m of site.

Geophysical Methods Utilized: HVSR, Seismic Refraction (P- and limited S-wave), MASW (Rayleigh Wave) and limited MALW (Love wave)

Geophysical Testing Arrays:

1. Array BFS-1 (48 channel MASW and P-wave seismic refraction array utilizing 4.5 Hz vertical geophones spaced 1.5 m apart for a length of 70.5 m, forward and reverse shot locations with multiple source offsets and source types and three interior shot locations).
2. Array BFS-3 (48 channel MASW/P-wave refraction and limited MALW/S-wave seismic refraction arrays utilizing 4.5 Hz vertical geophones and 10 Hz horizontal geophones spaced 1 m apart for a length of 47 m, forward and reverse shot locations with multiple source types (hammers only) and multiple interior shot locations).
3. Array BFS-5 (48 channel MASW and P-wave seismic refraction array utilizing 4.5 Hz vertical geophones spaced 1.5 m apart for a length of 70.5 m, forward and reverse shot locations with multiple source offsets and source types and multiple interior shot locations).
4. Six HVSR measurement locations: two along array BFS-1, two along array BFS-3 (one near the seismic station) and two along array BFS-5.

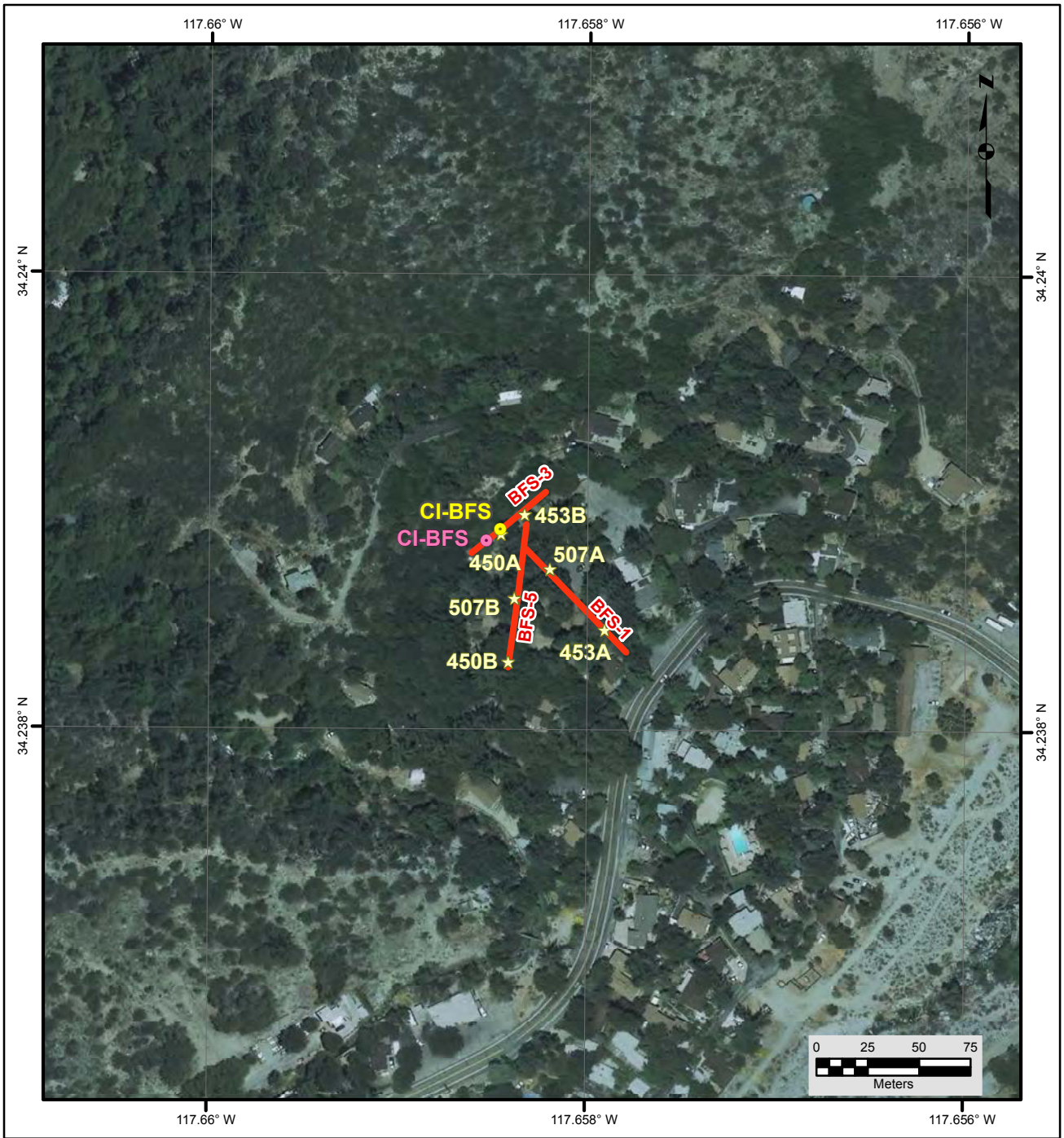

Legend

- Seismic Station - Approximate Surveyed Location
- Seismic Station - Approximate Location of Record
- H/V Spectral Ratio Location
- MASW Array

NOTES:
1. WGS 1984 COORDINATE SYSTEM
2. Image Source: ESRI, i-cubed, USDA FSA, USGS, AEX, GeoEye, Getmapping, Aerogrid, IGP

File Name: CI-BFS-I

Date: 5/11/2012

USGS science for a changing world

GEOVision geophysical services

RECOVERY.GOV

SITE MAP
CI•BFS

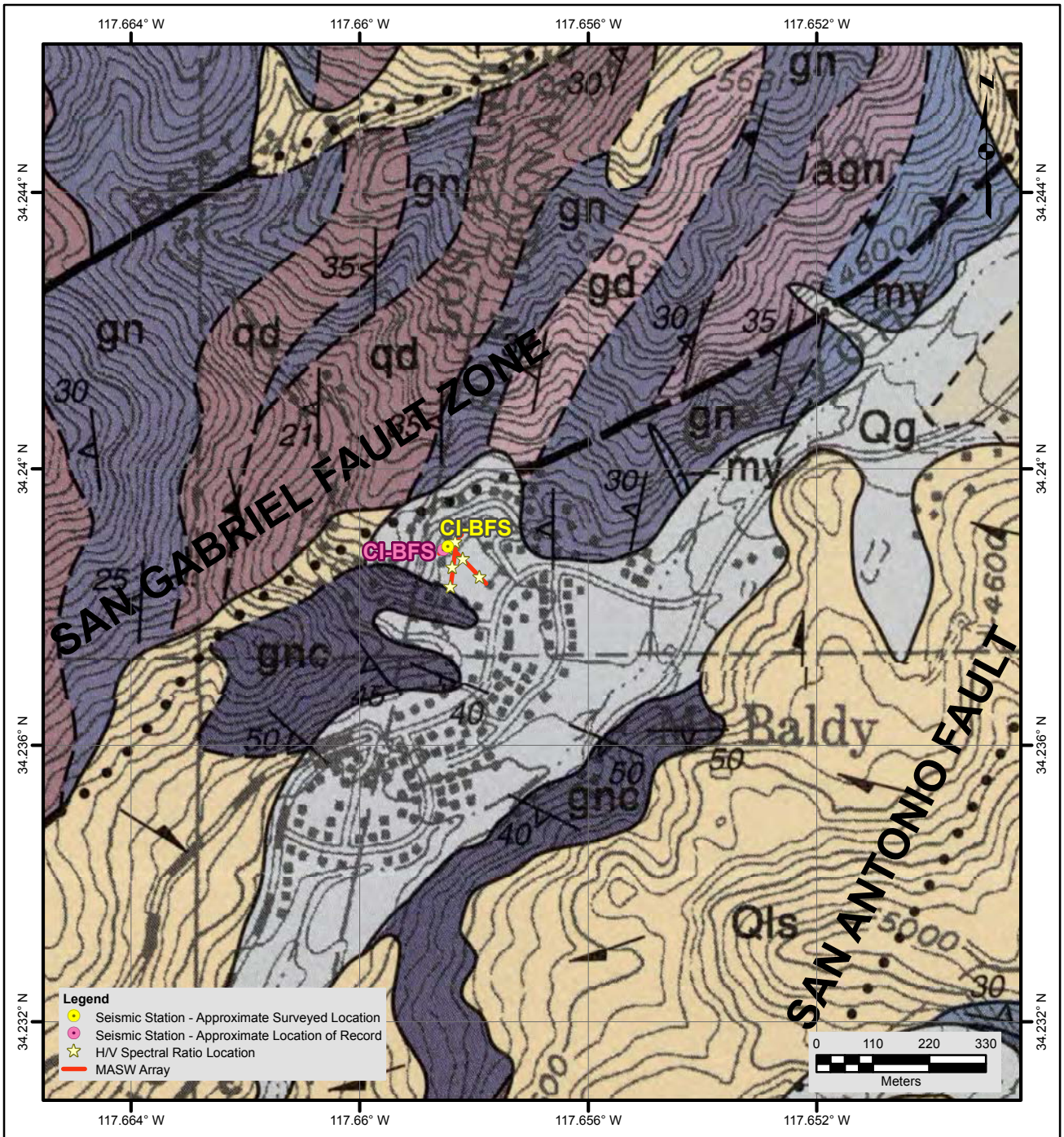

Description of Geologic Map Units

Qg = Quaternary (Holocene) alluvial gravel and sand of stream channels
Qls = Quaternary (Holocene) landslide and talus rubble
qd = Mesozoic (Cretaceous) quartz diorite, tonalite, massive to gneissoid
gd = Mesozoic (Cretaceous) granodiorite, similar to qd
gn = Precambrian gneiss, hard but brittle, closely fractured
gnc = Precambrian cataclastic gneiss, sheared laminae, mylonite laminae
agn = Precambrian augen gneiss, gneissoid quartz monzonite to granodiorite
my = Precambrian mylonite gneissoid rocks

NOTES:
1. WGS 1984 COORDINATE SYSTEM
2. Geologic Map of the Mount Baldy Quadrangle, Los Angeles and San Bernardino Counties, California by Thomas W. Dibblee, Jr., 2002
3. See site map for details of geophysical survey

File Name: CI-BFS

Date: 5/10/2012

USGS science for a changing world

GEOVision geophysical services

RECOVERY.GOV

GEOLOGIC MAP
CI•BFS

CI.BFS seismic station

Looking northeast along array BFS-3

Looking southeast along array BFS-1

HVSR measurements at sensor location 450 near seismic station

Looking north towards center of array BFS-5 and seismic station

Location of Geophysical Testing Arrays:

Location	Latitude	Longitude
BFS-1, Northwest End of MASW/Refraction Array	34.23879	-117.65832
BFS-1, Center of MASW/Refraction Array	34.23857	-117.65805
BFS-1, Southeast End of MASW/Refraction Array	34.23834	-117.65779
BFS-3, Southwest End of MASW/Refraction Arrays	34.23877	-117.65861
BFS-3, Center of MASW/Refraction Arrays	34.23890	-117.65841
BFS-3, Northeast End of MASW/Refraction Arrays	34.23904	-117.65822
BFS-5, South End of MASW/Refraction Array	34.23827	-117.65841
BFS-5, Center of MASW/Refraction Array	34.23859	-117.65836
BFS-5, North End of MASW/Refraction Array	34.23890	-117.65832
HVSR Sensor 450A	34.23886	-117.65845
HVSR Sensor 453A	34.23844	-117.65790
HVSR Sensor 507A	34.23870	-117.65819
HVSR Sensor 450B	34.23894	-117.65833
HVSR Sensor 453B	34.23830	-117.65841
HVSR Sensor 507B	34.23858	-117.65838
CI.BFS Seismic Station	34.23888	-117.65846

Notes: 1) WGS84 Coordinate System (decimal degrees)
2) Survey accuracy is estimated at 2 to 4 m

Results:

V_S Model for MASW Array BFS-5

Depth to Top of Layer (m)	Layer Thickness (m)	S-Wave Velocity (m/s)	Inferred P-Wave Velocity (m/s)	Assumed Poisson's Ratio	Assumed Density (g/cm^3)
0	1	164	306	0.3	1.60
1	1.5	288	539	0.3	1.70
2.5	5.5	344	644	0.3	1.80
8	7	401	751	0.3	1.90
15	6	748	1398	0.3	2.10
21	>9	1253	2344	0.3	2.20

Notes: 1) Depth of investigation is about 30 m.
2) Bottom layer is a half space.

Average V_P Model and Estimated V_S Models from Central Portion of P-wave Seismic Refraction Array BFS-3

Depth to Top of Layer (m)	Layer Thickness (m)	P-Wave Velocity (m/s)	Estimated S-Wave Velocity (m/s)			
			Poisson's Ratio = 0.25	Poisson's Ratio = 0.3	Poisson's Ratio = 0.35	Poisson's Ratio = 0.4
0.00	0.45	378	218	202	181	154
0.45	0.91	404	233	216	194	165
1.36	0.91	508	293	271	244	207
2.27	0.91	634	366	339	305	259
3.18	0.91	833	481	445	400	340
4.08	0.91	960	554	513	461	392
4.99	0.91	1034	597	553	497	422
5.90	1.91	1332	769	712	640	544
7.80	1.91	1448	836	774	695	591
9.71	1.91	1675	967	895	805	684
11.61	1.91	1909	1102	1020	917	779
13.52	Half Space	2095	1210	1120	1006	855

Observations/Discussion:

- Geologic conditions at the site, based on field observations, likely consist of a relatively thin layer of alluvium overlying weathered granitic and metamorphic bedrock. Characterization of this site were complicated by limited space for arrays and irregular bedrock topography.
- P-wave refraction and MASW data were acquired along three arrays (BFS-1, BFS-3 and BFS-5) in an attempt to characterize subsurface velocity structure. Limited S-wave refraction and MALW data was also acquired along array BFS-3.
- Limited P-wave refraction data and MASW data were collected along the 70.5 m long array BFS-1. It was clearly evident in the seismic records that there is significant variation in bedrock depth beneath the array. The seismic refraction data were not modeled because shot density was not high enough to apply tomographic inversion techniques and there was not enough space for far offset shot locations to effectively use layer based modeling techniques to map bedrock topography. MASW data quality was also not particularly good along this array.
- Array BFS-3, limited to a length of 47 m by space restrictions, was considered the most practical array to characterize the seismic station as it was aligned along the toe of a small hill at which the seismic station is located. Interpretation of P-wave refraction data was complicated by a possible out of plane refractor in the central portion of the line on some seismic records. Complex subsurface velocity structure increased the likelihood of converted waves occurring as first arrivals in S-wave refraction data. Although there is

no distinct evidence of converted waves in the S-wave seismic refraction data, P-wave arrivals were very high amplitude and there was not sufficient polarity reversal on reversed S-wave shot records to unambiguously interpret the S-wave seismic refraction data. Regardless of data quality, a 47 m long array without offend shot locations can typically only image velocity structure to a maximum depth to 10 to 15 m.

- P-wave refraction and MASW data were also collected along the 70.5 m long array BFS-5. It was clearly evident in the seismic records that there is significant variation in bedrock depth beneath the array. Both seismic refraction data and MASW data were modeled for this array, although the effects of variation in bedrock topography on MASW data are uncertain.
- Six HVSR measurements were made at the site. HVSR peaks vary between about 5.5 and 9.5 Hz due to variable depth to bedrock in the site vicinity. The highest frequency HVSR peak of 9.5 Hz occurs at sensor location 453B, located at the south end of array BLS-5 near a mapped bedrock outcrop. HVSR sensors 450A and 450B, located adjacent to the seismic station and near the projected intersection of arrays BFS-3 and BFS-5, respectively, have primary HVSR peaks in the 8 to 8.5 Hz range. HVSR sensors 507A, 507B and 453, located in areas where bedrock is expected to occur at greater depth, have HVSR peaks in the 5.5 to 7 Hz range. It should be noted that the low frequency peak at sensor location 507B does not have a geologic source and appears to be associated with a sensor coupling issue.
- The P-wave refraction data for arrays BFS-3 and BFS-5 were modeled using a tomographic inversion routine with a smooth velocity starting model. The seismic refraction models were extended to limited far offset shot locations on array BFS-5 to extend depth of investigation. There was insufficient space for far offset shot locations on array BFS-3.
- The maximum depth of investigation for array BFS-3 is about 15 m. The velocity model may have some error due to the influence of a possible out of plane refractor in the central portion of the array. The seismic refraction model indicates that P-wave velocity is about 300 to 400 m/s at the surface and increases to 750 m/s at a depth of 2.5 to 4.5 m, 1,000 m/s at a depth of 4 to 6 m, 1,500 m/s at a depth of 8 to 10 m and over 2,000 m/s at a depth of 11 m, or greater. The uppermost zone of weathered bedrock is probably located between the 750 and 1,000 m/s contours at a depth of 3 to 6 m. A longer array would be required to better constrain the higher seismic velocities at depth. Assuming a bedrock depth of 6 m and average S-wave velocity of 200 m/s for the overlying sediments would result in an HVSR peak of 8.3 Hz, based on the quarter wavelength approximation. However, the seismic refraction model appears to indicate that S-wave velocity of the upper 6 m may be higher than 200 m/s.
- The average P-wave velocity of the upper 30 m (V_{P30}) was estimated between 17 and 34 m on the array BFS-3 refraction model, where depth of investigation is greatest. The P-wave velocity at a depth of 15 m was extrapolated to 30 m depth. P-wave velocity is expected to gradually increase with depth below 15 m and, therefore, V_{P30} may be underestimated. On the other hand, the influence of a possible out of plane refractor may result in shallow velocity structure being overestimated, resulting in V_{P30} being overestimated. At best, one can hope that the errors between the two features mentioned above cancel to a certain degree and that resulting estimates of V_{P30} are in a realistic range for the site. V_{P30} ranges from about 1,287 to 1,384 m/s over the 17 to 34 m

position interval; a 7% variation. The small amount of apparent lateral velocity variation does not adequately depict the complex wave propagation beneath the array due to heterogeneities in the bedrock unit that are evident in seismic records. An average V_P model was developed over the 17 to 34 m distance interval by horizontally averaging the travel time of each model cell and cell thickness and average V_{P30} was determined to be 1,344 m/s. Assuming constant Poisson's ratios of 0.25, 0.3, 0.35 and 0.4 would result in an estimated V_{S30} of 776, 718, 645 and 549 m/s, respectively. The average V_P between 1 and 31 m (adjusted V_{P30}) to account for assumed seismic sensor depth, was determined to be 1,481 m/s. Assuming constant Poisson's ratios of 0.25, 0.3, 0.35 and 0.4 would result in an estimated adjusted V_{S30} of 855, 792, 712 and 605 m/s, respectively. It is unlikely that Poisson's ratio of the weathered granitic rocks is lower than 0.3 or higher than 0.35, unless the rock is saturated which is not expected. Therefore the P-wave refraction model indicates that V_{S30} could be in the 645 to 718 m/s range (NEHRP Site Class C) and that adjusted V_{S30} (average V_S between 1 and 31 m) is in the 712 to 792 m/s range (NEHRP Site Class C/B). These estimates of V_{S30} and adjusted V_{S30} should be used with caution due to both limited depth of investigation and possible errors in the seismic refraction model caused by out of plane refractors. It would be worthwhile to determine if there are any areas in the immediate site vicinity where seismic refraction surveys can be conducted on rock to characterize the bedrock velocity structure more accurately, although space limitations may make this difficult.

- The maximum depth of investigation for array BFS-5 is about 23 m. The velocity model indicates that there are three geologic units beneath the array: a surficial layer of low velocity sediments with V_P between 300 and 600 m/s and thickness of 1.5 to 3.5 m; an intermediate layer with V_P between 700 and 900 m/s that is likely associated with higher velocity alluvium, although the possibility of decomposed rock cannot be discounted, and a lower layer of weathered rock with $V_P > 1{,}000$ m/s. The top of bedrock likely tracks the 1,000 to 1,250 m/s contours and varies in depth from about 5 m at the south and north ends of the array to 15 m in the center of the array. Bedrock velocity is not expected to be well resolved in the model due to the steeply dipping bedrock surface at each end of the array and limited space for offend shot location.
- Noise conditions at the site were not sufficient for application of passive surface wave techniques.
- Due to probable complex velocity structure, Arrays BFS-1 and BFS-3 did not yield surface wave dispersion data of sufficient reliability to use for site characterization. Array BFS-3 is the only array located on the same geologic structure as the seismic station. Careful review of the MASW data collected along array BFS-3 indicates that the phase velocity of a Rayleigh wave at a 40 m wavelength (V_{R40}) averages about 680 m/s. Using the Brown, et al. (2000) relationship between V_{R40} of the fundamental mode Rayleigh wave and V_{S30} ($V_{S30} = 1.045*V_{R40}$) indicates that V_{S30} may be about 736 m/s beneath array BFS-3. The possibility cannot be discounted that V_{R40} is influenced by higher mode Rayleigh waves, in which case V_{S30} would be overestimated. Additionally, surface wave dispersion data were very difficult to extract from this array and there is likely significant error in the estimated V_{R40}.
- There was much less uncertainly in reduction of MASW data collected along array BFS-5 and, therefore, this array was used for site characterization. However, the seismic refraction and HVSR data indicate that bedrock is deeper in the central portion of array

BFS-5 than at the seismic station, which will complicate correlation of the V_S model developed for array BFS-5 to the seismic station.

- The maximum wavelength Rayleigh wave phase velocity data extracted from the array BFS-5 data set was typically set equal to the lesser of 70 m or 1.5 times the distance from the source to midpoint of the active receiver array.
- The minimum wavelength surface wave phase velocity data extracted from the 48-channel MASW array was about 13 m. Reducing data from smaller hammer sources using a limited offset receiver array (i.e. less active geophones) allowed for extraction of Rayleigh wave dispersion data to a minimum wavelength of about 2 m.
- There is nominally about 80 m/s scatter in Rayleigh wave dispersion data for array BFS-5, likely the result of lateral velocity variation.
- A representative dispersion curve was generated for the array BFS-5 MASW data set using a moving average, polynomial curve fitting routine and used for modeling.
- Surface wave depth of investigation for array BFS-5 is about 30 m based on half of maximum wavelength criteria.
- The inferred P-wave velocities in the surface wave model, assuming a Poisson's ratio of 0.3, are generally consistent with the central portion of the seismic refraction model, where bedrock is deepest.
- An HVSR peak of about 5.6 Hz is expected for the array BFS-5 V_S model based on the quarter wavelength approximation. Modeling HVSR response for the V_S model results in a predicted HVSR peak of about 8 Hz. The measured HVSR peak is between that predicted by modeling and that predicted by the quarter wavelength approximation.
- V_{S30} is 500 m/s for the array BFS-5 V_S model (NEHRP Site Class C).
- Bedrock is about 4 to 6 m deep beneath array BFS-3 and the seismic station based on the seismic refraction model and HVSR data, much shallower than the 15 m depth to bedrock in the array BFS-5 V_S and seismic refraction models. Therefore, adjusted V_{S30} at the seismic station is calculated between 1 m (assumed sensor depth) and 31 m after replacing the velocity of the sediments below 4 and 5 m, respectively, with the velocity of the rock at 15 m depth. Adjusted V_{S30} assuming a 4 and 5 m bedrock depth is 745 and 717 m/s, respectively (NEHRP Site Class C). Estimated adjusted V_{S30} (average V_S between 1 and 31 m) from the P-wave refraction model for array BFS-3, which is not considered particularly reliable, is in the 712 to 792 m/s range (constant Poisson's ratio of 0.3 to 0.35), which is consistent with that determined from the V_S model for array BFS-5. Estimated V_{S30} for array BFS-3, based on review of V_{R40}, is about 736 m/s, also consistent with adjusted V_{S30} based on the V_S model for array BFS-5. Adjusted V_{S30} for array BFS-3 would be higher than 736 m/s.
- In conclusion, V_{S30} adjusted to seismic station conditions is most likely between 712 and 792 m/s (NEHRP Site Class C/B). For the purpose of site characterization we use the average adjusted V_{S30} for the MASW array BFS-5 V_S model (bedrock depths of 4 and 5 m from array BFS-3 seismic refraction model and HVSR data), which is 731 m/s (NEHRP Site Class C/B). This estimate of adjusted V_{S30} should not be considered any more accurate than about 10 %.

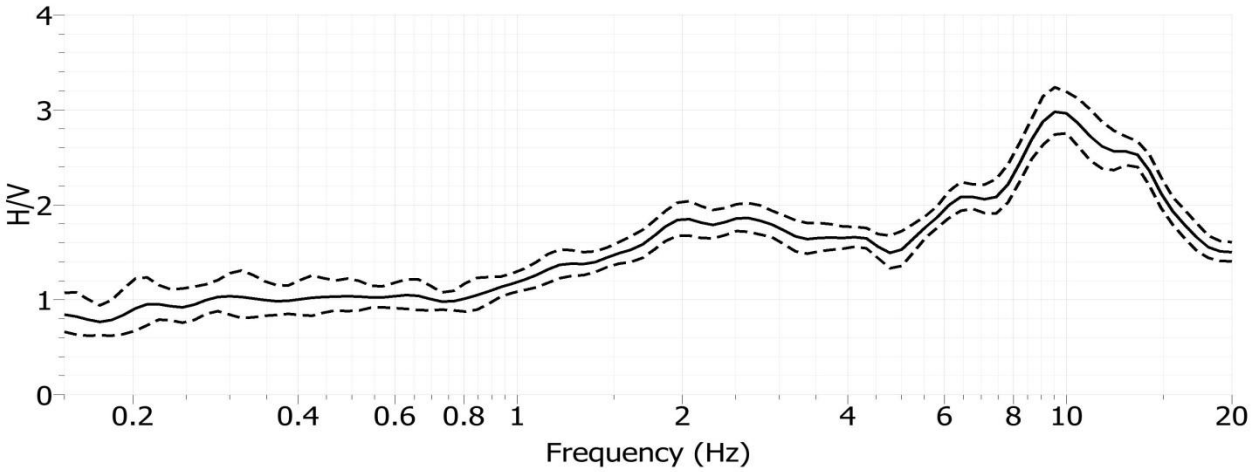

Site CI. BFS, H/V Spectral Ratio, Array BFS -5, Sensor 453B

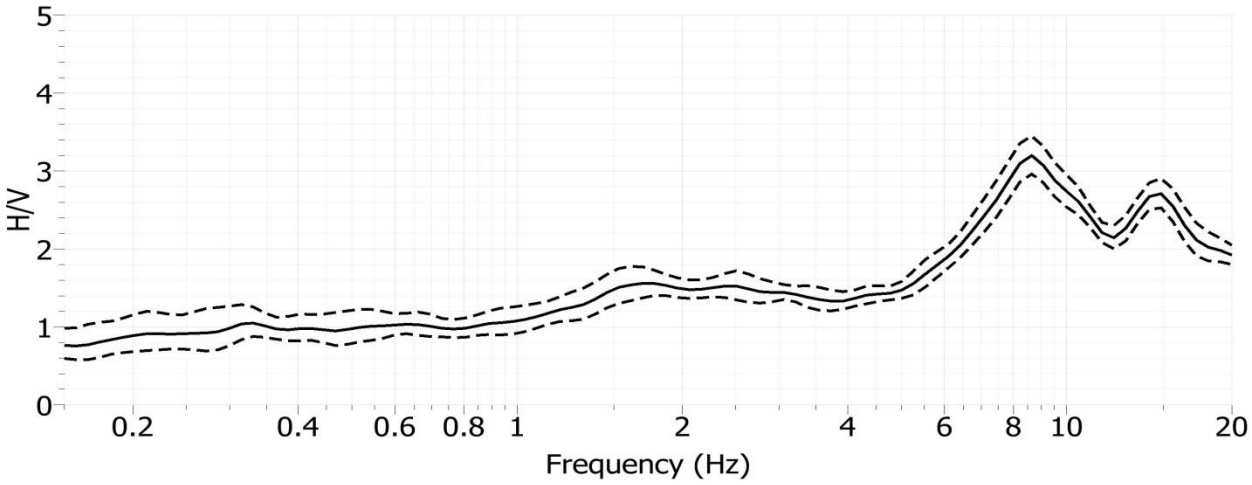

Site CI.BFS, H/V Spectral Ratio, Near Seismic Station, Sensor 450A

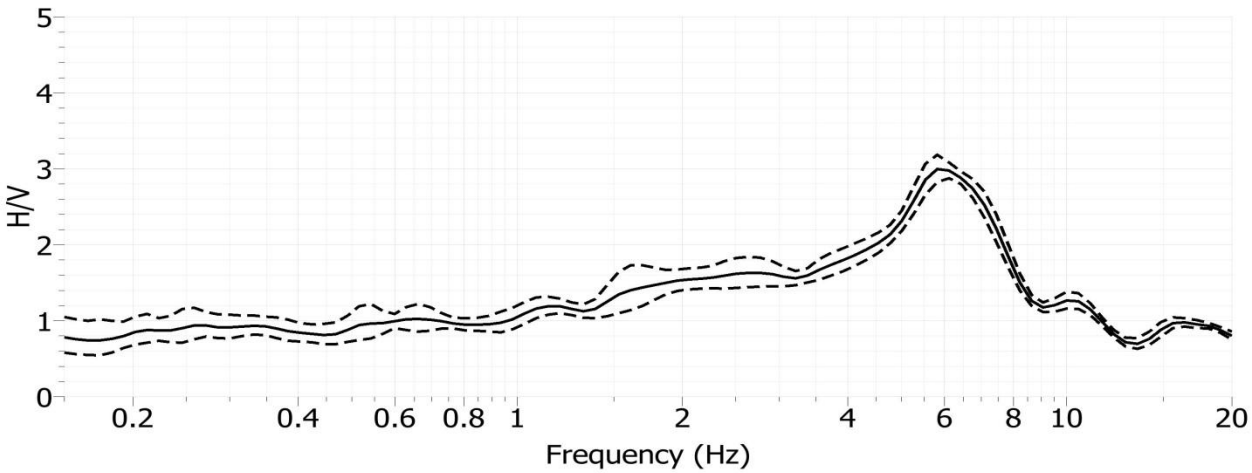

Site CI. BFS, H/V Spectral Ratio, Array BFS -1, Sensor 507A

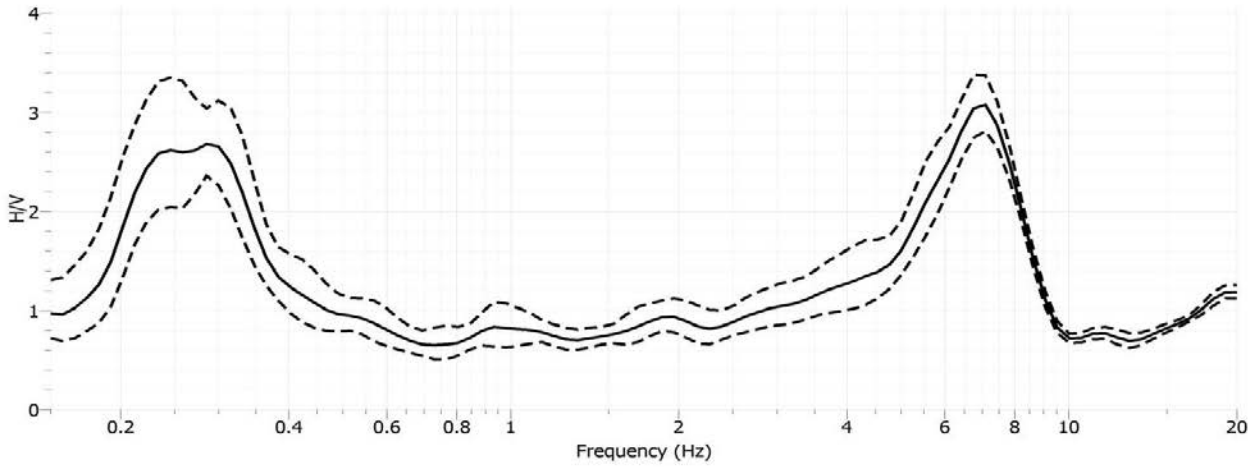

Site CI. BFS, H/V Spectral Ratio, Array BFS -5, Sensor 507B

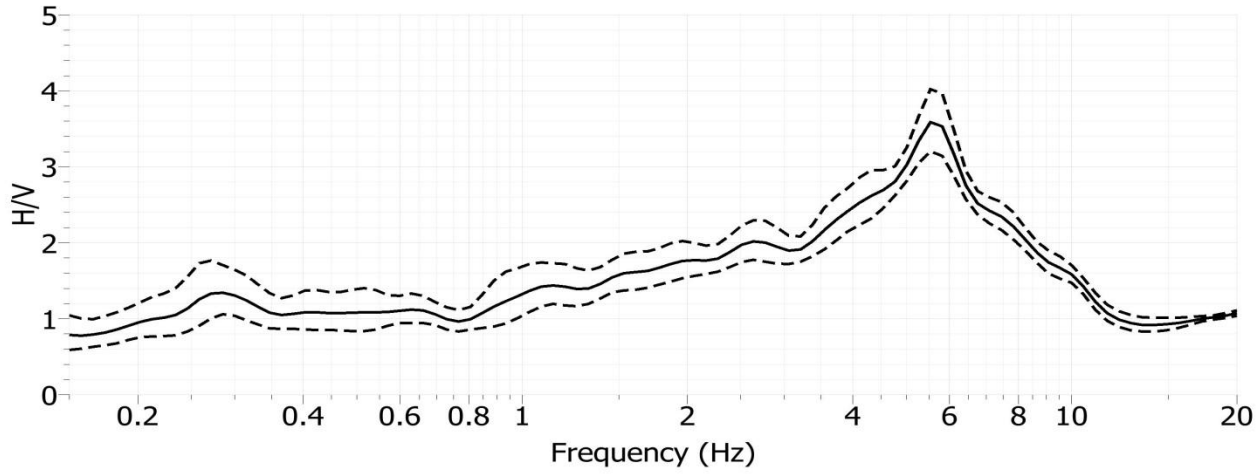

Site CI. BFS, H/V Spectral Ratio, Array BFS -1, Sensor 453A

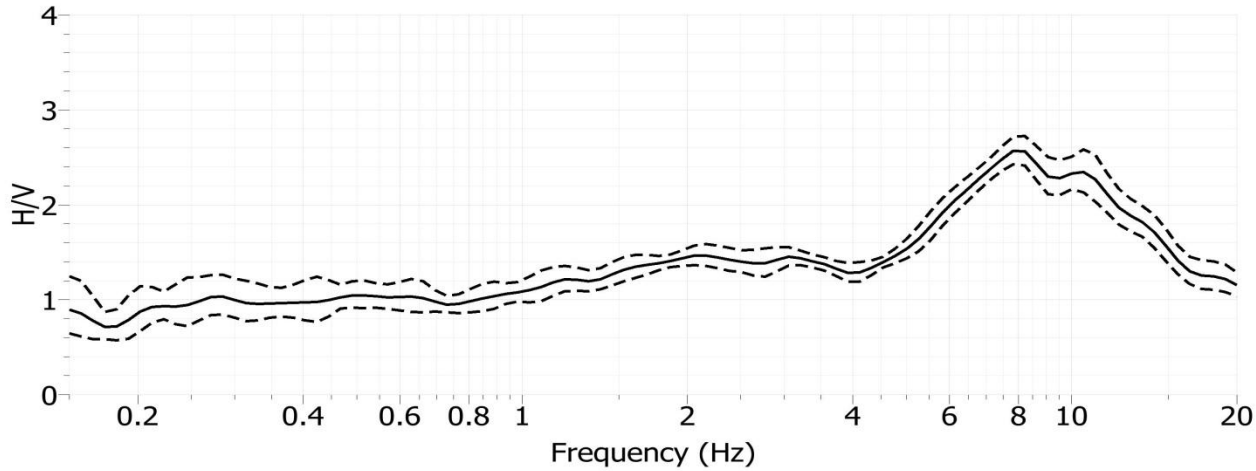

Site CI. BFS, H/V Spectral Ratio, Array BFS -5, Sensor 450B

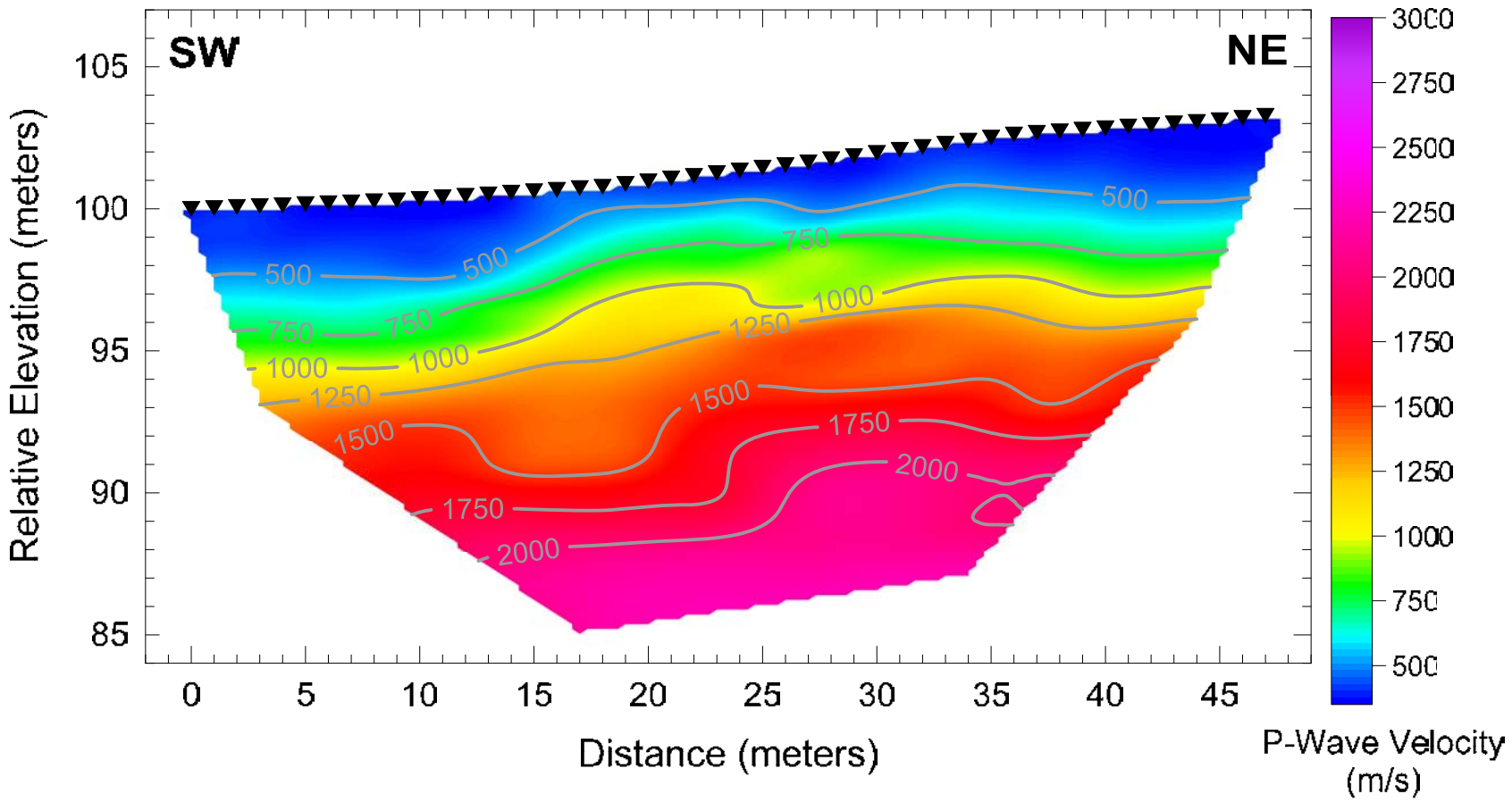

Array BFS-3 – P-wave tomographic seismic refraction model developed using a smooth velocity gradient starting model

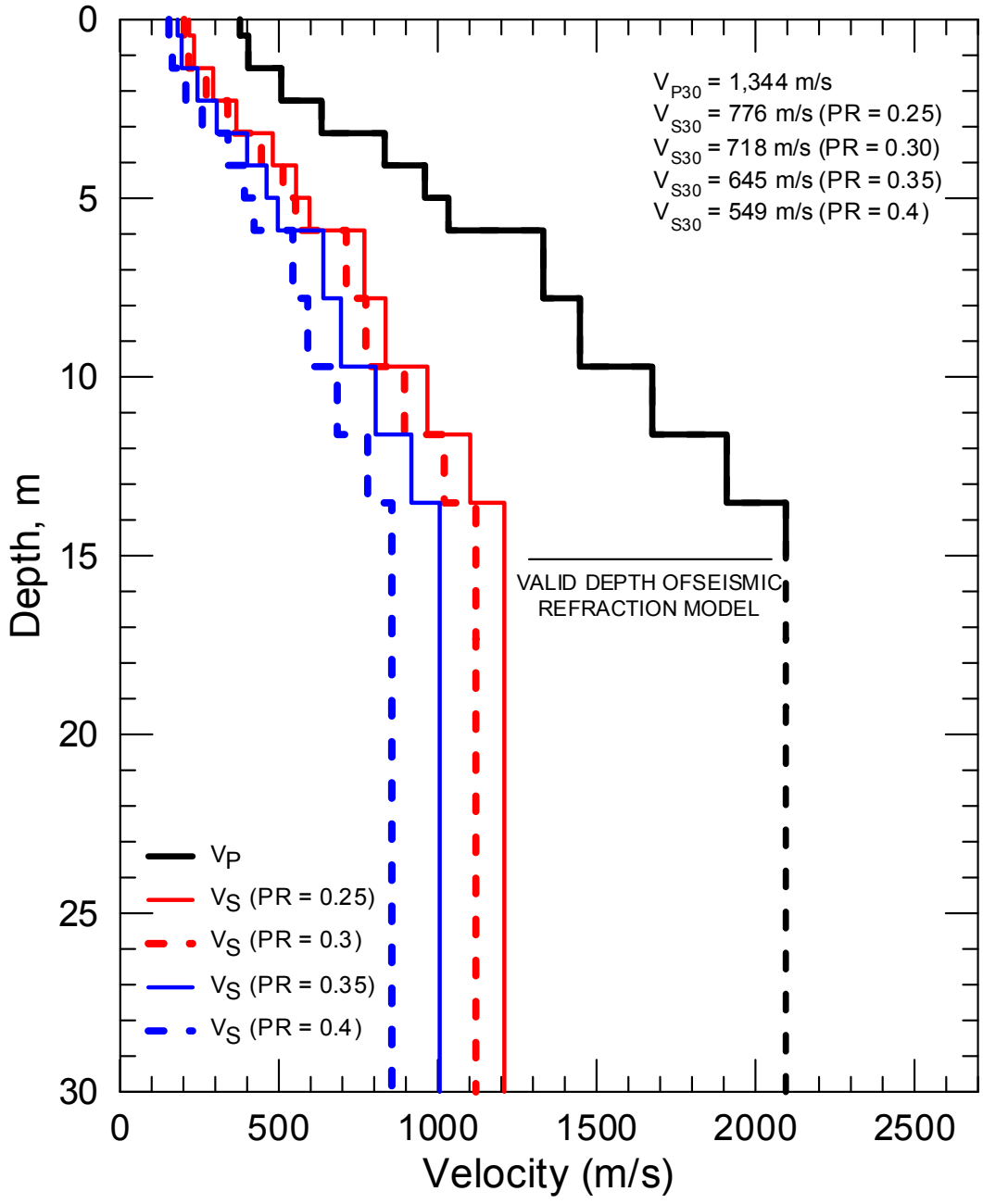

CI.BFS – Average P-wave velocity structure and estimated S-wave velocity structure between a position of 17 and 34 m on the P-wave seismic refraction model for array BFS-3 developed using a smooth velocity gradient starting model. The seismic refraction model is not considered accurate enough and depth of investigation is not sufficient for the model to be used to characterize velocity structure in the upper 30 m.

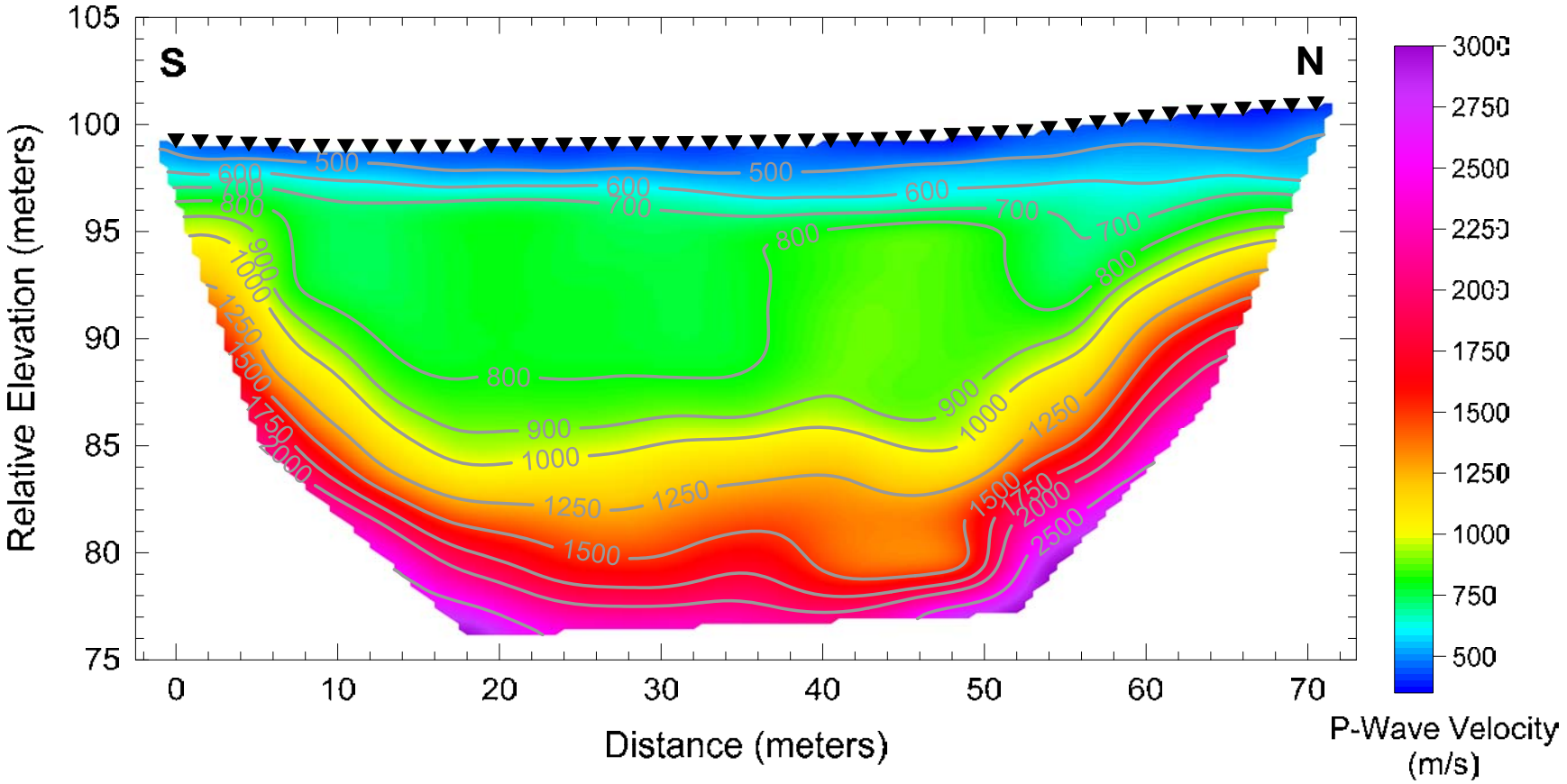

Array BFS-5 – Tomographic seismic refraction model developed utilizing a smooth velocity gradient starting model

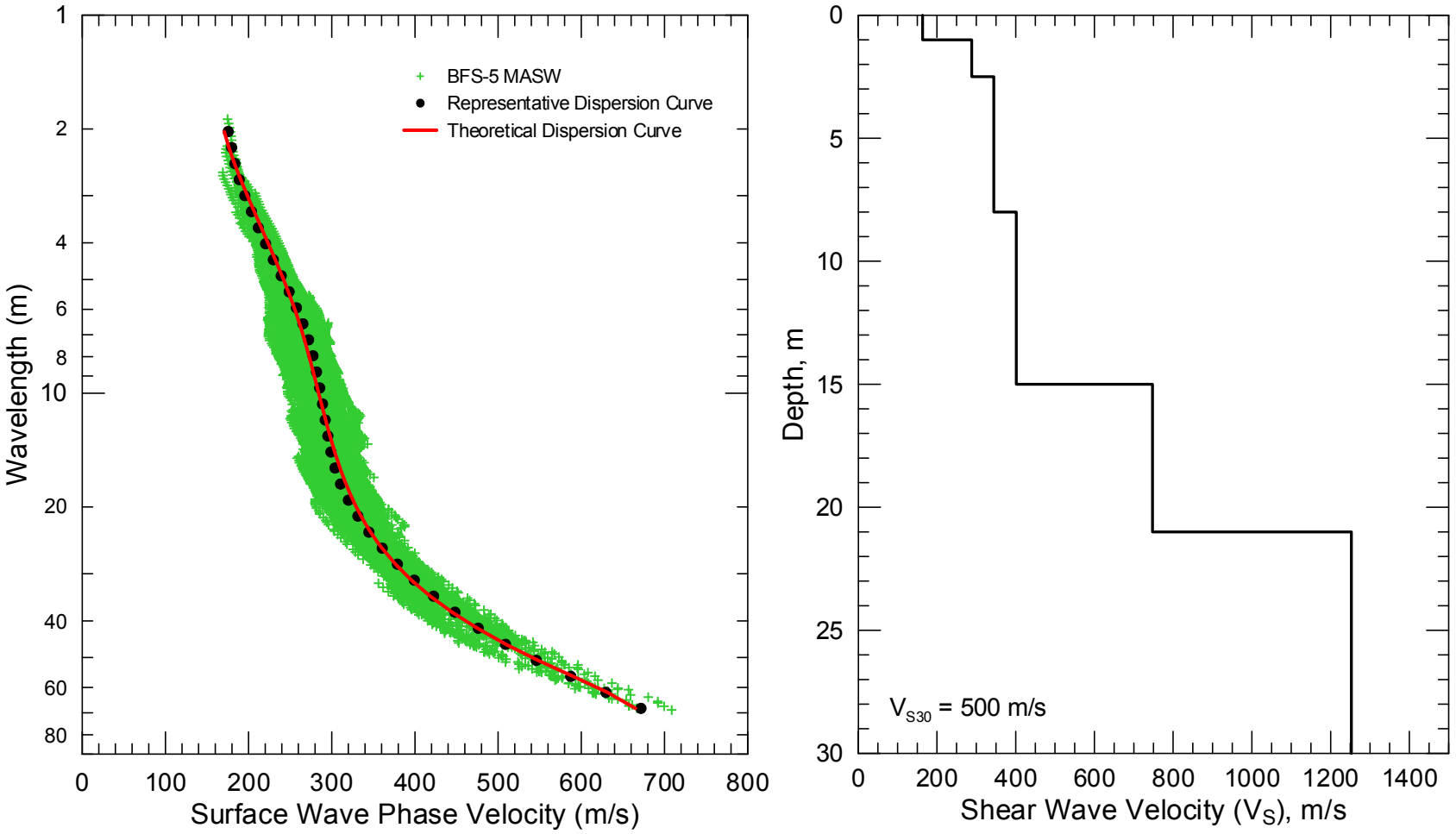

CI.BFS - Field, representative and inverted theoretical surface wave dispersion data (left) and associated V_S model (right) for MASW array BFS-5

Site CI.BHP

Location: Baldwin Hills Oil Field, 5640 South Fairfax Avenue, Los Angeles, California

Latitude: 33.99053 **Longitude:** -118.36171
(Station coordinates provided by USGS, WGS84 coordinate system)

V_{S30} (measured): 300 m/s

V_{S30} (adjusted to more accurately reflect seismic station conditions): 323 m/s (average S-wave velocity between 2 and 32 m adjusting for nominal sensor depth)

NEHRP Site Class: D

Geomatrix Code: IQD

Geologic Conditions/Observations: Seismic station located in area mapped as older Quaternary (Late Pleistocene) alluvium. Portions of the surface wave arrays are located on area mapped as artificial fill. The artificial fill in the test area does not appear to be very thick and should not significantly affect results. Inglewood fault zone located approximately 300 meters east of the test area.

Site Conditions: Urban site with significant traffic noise from nearby roads. Undulating terrain in site vicinity. Relatively planar ground surface in test area with elevations decreasing gradually to southeast.

Geophysical Methods Utilized: HVSR, MASW, array microtremor, ReMi™

Geophysical Testing Arrays:

1. Arrays BHP-1 (24 channel linear array utilizing 4.5 Hz vertical geophones spaced 5 m apart for an array length of 115 m) and BHP-2 (24 channel linear array utilizing 4.5 Hz vertical geophones spaced 3 m apart for an array length of 69 m) used to acquire passive surface wave data. Arrays combined to form an "L" shaped array.
2. Array BHP-3 (48 channel MASW array utilizing 4.5 Hz vertical geophones spaced 1 m apart for a length of 47 m, forward and reverse shot locations with multiple source off-sets and source types (hammers only) and center shot location).
3. Three HVSR measurement locations; two distributed along arrays BHP-2 and BHP-3 and one near the seismic station.

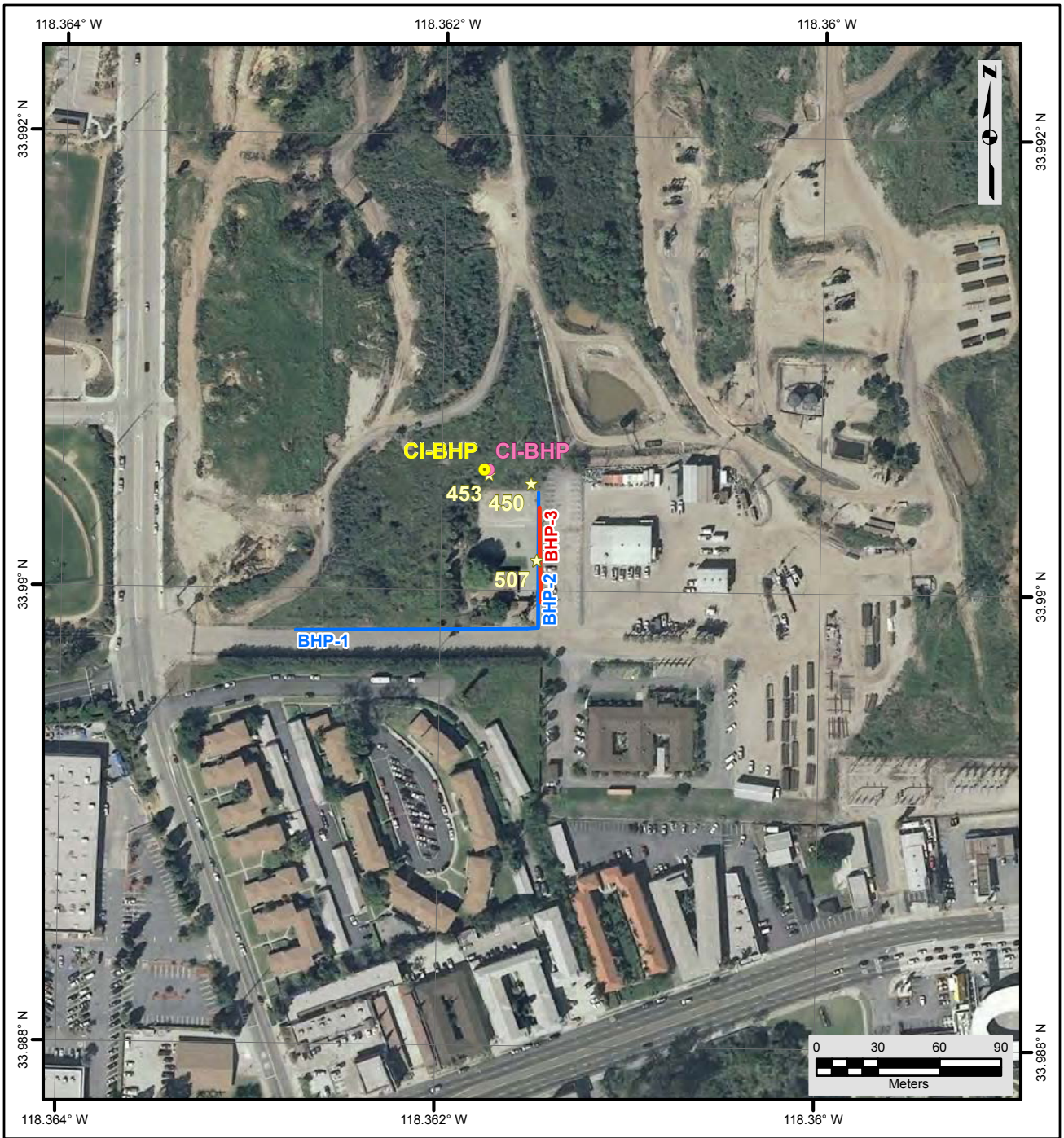

Legend

- Seismic Station - Approximate Surveyed Location
- Seismic Station - Approximate Location of Record
- H/V Spectral Ratio Location
- MASW Array
- Passive Array

NOTES:
1. WGS 1984 COORDINATE SYSTEM
2. Image Source: ESRI, i-cubed, USDA FSA, USGS, AEX, GeoEye, Getmapping, Aerogrid, IGP

File Name: CI-BHP-I

Date: 6/29/2011

USGS science for a changing world

GEOVision geophysical services

RECOVERY.GOV

SITE MAP
CI•BHP

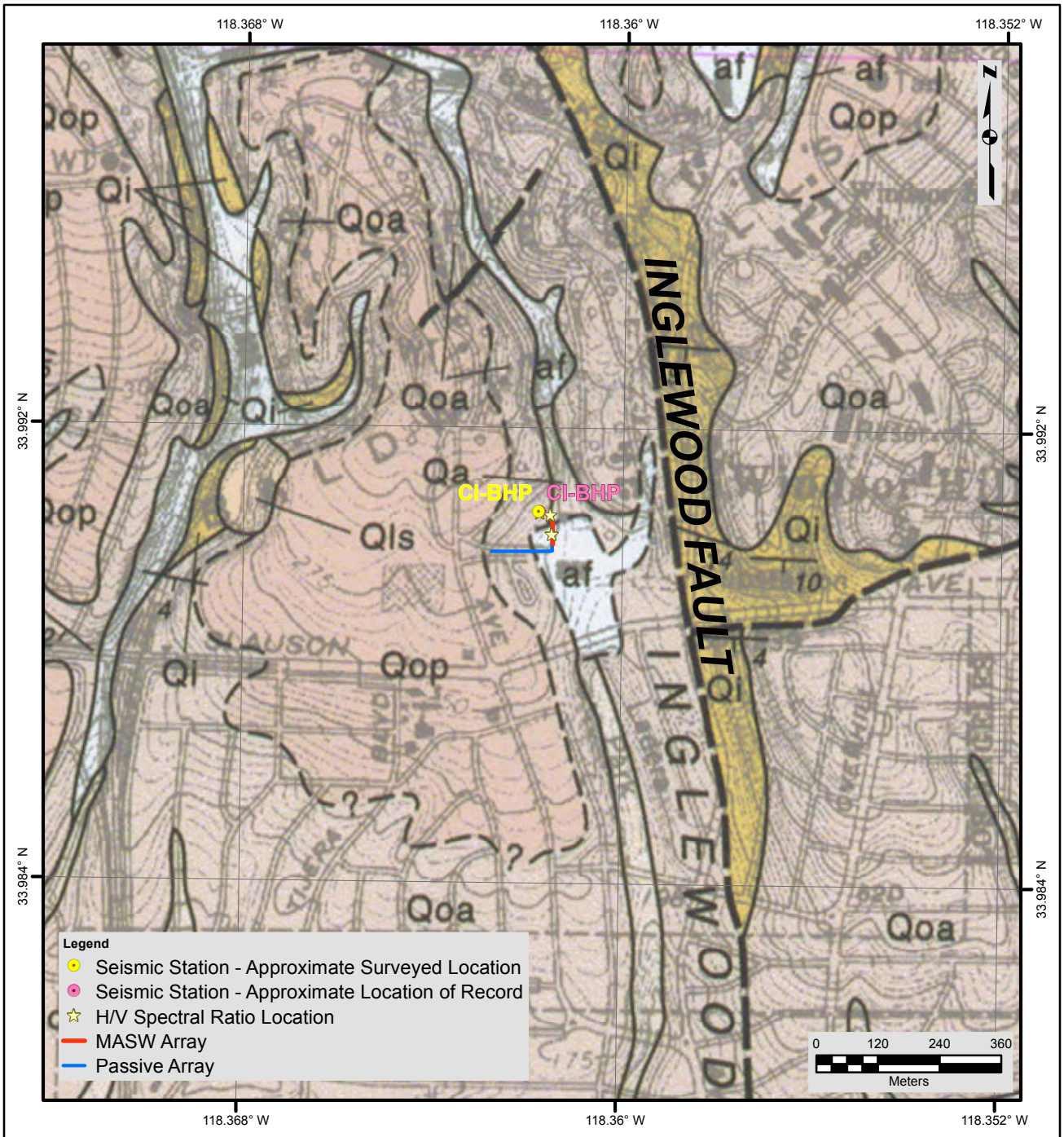

Description of Geologic Map Units

af = Quaternary (Holocene) artificial cut and fill
Qoa = Quaternary (Pleistocene) older alluvium of gray to light brown pebble-gravel, sand, and silt-clay, elevated and dissected
Qop = Quaternary (Pleistocene) paleosol in Baldwin Hills; sandy, locally pebbly, moderately indurated "hardpan" on Qoa
Qi = Quaternary (Pleistocene) Inglewood Formation; light gray, soft, firable, fine-grained sandstone, and interbedded soft gray siltstone

NOTES:
1. WGS 1984 COORDINATE SYSTEM
2. Geologic Map of the Venice and Inglewood Quadrangles, Los Angeles County, California By Thomas W. Dibblee, Jr., 2007
3. See site map for details of geophysical survey

File Name: CI-BHP

Date: 7/18/2011

USGS science for a changing world

GEOVision geophysical services

GEOLOGIC MAP
CI•BHP

RECOVERY.GOV

Looking east along passive surface wave array BHP-1

Looking south along passive surface wave array BHP-2

Looking northwest towards MASW array BHP-3 and seismic station

Looking southeast towards seismic station CI.BHP

Plaster used to couple HVSR sensor 507 to gravelly soil

Location of Geophysical Testing Arrays:

Location	Latitude	Longitude
BHP-1, West End of Passive SW Array	33.98982	-118.36272
BHP-1, East End of Passive SW Array	33.98983	-118.36150
BHP-2, South End of Passive SW Array	33.98984	-118.36144
BHP-2, North End of Passive SW Array	33.99043	-118.36145
BHP-3, South End of MASW Array	33.98995	-118.36143
BHP-3, Center of MASW Array	33.99014	-118.36143
BHP-3, North End of MASW Array	33.99036	-118.36144
HVSR Sensor 450	33.99047	-118.36148
HVSR Sensor 453	33.99051	-118.36171
HVSR Sensor 507	33.99013	-118.36145
CI.BHP Seismic Station	33.99053	-118.36173

Notes: 1) WGS84 Coordinate System (decimal degrees)

2) Survey accuracy is estimated at 1 to 2 m

Results:

V_S Model 1 (Passive surface wave data and northern half of MASW array BHP-3)

Depth to Top of Layer (m)	Layer Thickness (m)	S-Wave Velocity (m/s)	Inferred P-Wave Velocity (m/s)	Inferred Poisson's Ratio	Inferred Density (g/cm^3)
0	1	142	266	0.3	1.9
1	2	165	309	0.3	1.9
3	3	249	465	0.3	1.9
6	4	322	602	0.3	1.9
10	6	327	612	0.3	1.9
16	9	343	642	0.3	1.9
25	12	409	765	0.3	2.0
37	15	455	851	0.3	2.0
52	>13	479	896	0.3	2.0

V_S Model 2 (Passive surface wave data and southern half of MASW array BHP-3)

Depth to Top of Layer (m)	Layer Thickness (m)	S-Wave Velocity (m/s)	Inferred P-Wave Velocity (m/s)	Inferred Poisson's Ratio	Inferred Density (g/cm^3)
0	1	156	291	0.3	1.9
1	2	223	418	0.3	1.9
3	8	272	508	0.3	1.9
11	8	326	610	0.3	1.9
19	8	349	652	0.3	1.9
27	12	421	787	0.3	2.0
39	15	462	865	0.3	2.0
54	>11	472	884	0.3	2.0

Observations/Discussion:

- The HVSR curves are almost identical at frequencies below 10 Hz, validating the 1-D velocity structure assumption. There are, however, no significant high frequency HVSR peaks by which to characterize shallow velocity structure.
- High amplitude HVSR peak at 0.16 Hz, which is consistent with deep sedimentary basin. There may be a weaker, but inconclusive, secondary peak in the 0.26 Hz range. The HVSR data from all measurement locations have similar characteristics at 1.1 and 2.2 Hz.
- Noise conditions at site (multi-directional or omni-directional noise sources) appeared sufficient for successful application of passive surface wave techniques.
- SPAC technique used to extract surface wave dispersion data from passive "L" array data. Both the ReMi™ and SPAC techniques used to extract surface wave dispersion data from the linear arrays. Only the higher quality "L" array dispersion data used for analysis. The linear arrays yielded similar dispersion curves that were within 25 m/s of the "L" array dispersion data at a wide frequency range. Scatter in the passive dispersion data at wavelengths above 60 m, which may result in larger model error at depths below 30 m.
- Lateral velocity variation observed in the MASW data, possibly related to a thin layer of artificial fill that may be present beneath the MASW array. Therefore, separate surface wave dispersion data were generated for the northern and southern portions of the MASW seismic records.
- Surface wave dispersion data from active and passive surface wave data sets are in acceptable agreement at this site, especially the passive surface wave data and MASW dispersion data from the southern half of the MASW array.
- Representative dispersion curves were generated for each surface wave data set using a moving average, polynomial curve fitting routine. These individual representative dispersion curves were combined and a representative dispersion curve generated for the combined data set for data modeling. Two representative dispersion curves were generated: one from the passive surface array and northern half of the MASW array

(Model 1) and the other from the passive surface wave array and southern half of the MASW array (Model 2). Separate S-wave velocity versus depth models were developed for each representative dispersion curve.

- Based on simple layer-based analysis of seismic refraction first arrival data, P-wave velocity in the upper 15 m ranges from about 350 to 425 m/s in the upper 3 m, 475 to 500 m/s between about 3 and 10 m, and 625 m/s, or higher, below a depth on the order of 10 m. There is no evidence of saturated sediments in the upper 20 m.
- Surface wave models are generally consistent with simplified P-wave refraction model considering unknown Poisson's ratio.
- Surface wave depth of investigation is about 65 m based on half of maximum wavelength criteria and assuming that surface wave dispersion data at frequencies as low as 3.0 Hz are valid utilizing 4.5 Hz geophones (low frequency geophone phase response differences may cancel out if noise is omni-directional and/or the phase response differences are random in nature).
- V_{S30} is 299 m/s for Model 1 and 302 m/s for Model 2 and averages 300 m/s (Site Class D).
- Average S-wave velocity between 2 m (nominal sensor depth) and 32 m is 325 m/s for Model 1 and 322 m/s for Model 2, averaging 323 m/s.
- Average S-wave velocity of the upper 65 m (V_{S65}) is 366 m/s for Model 1 and 368 m/s for Model 2, averaging 367 m/s.

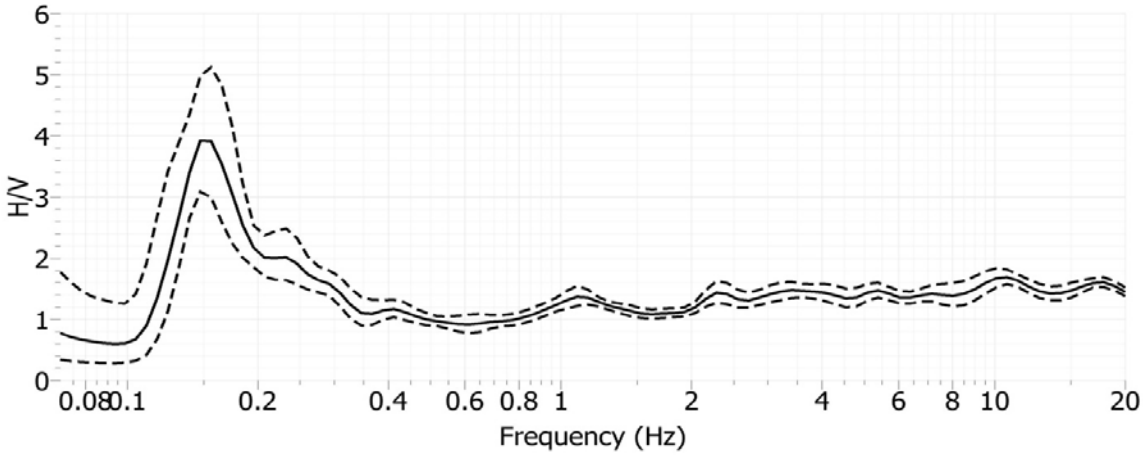

Site CI. BHP, H/V Spectral Ratio, Adjacent to Seismic Station, Sensor 453

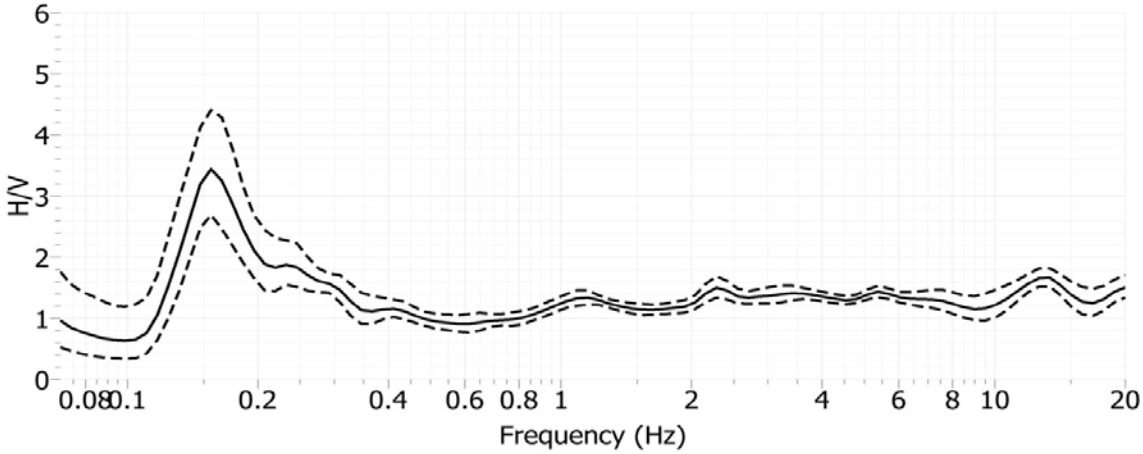

Site CI. BHP, H/V Spectral Ratio, Array BHP-3, Sensor 450

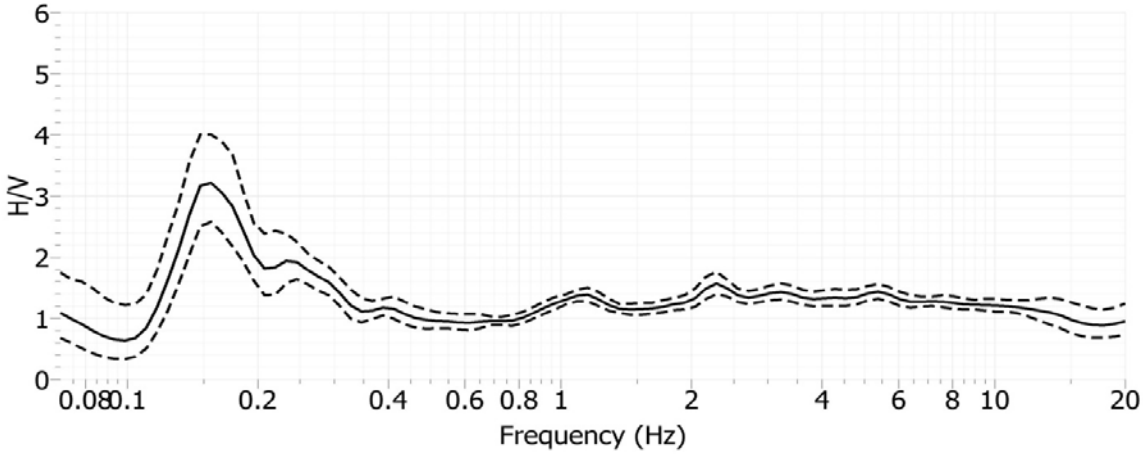

Site CI.BHP, H/V Spectral Ratio, Array BHP-3, Sensor 507

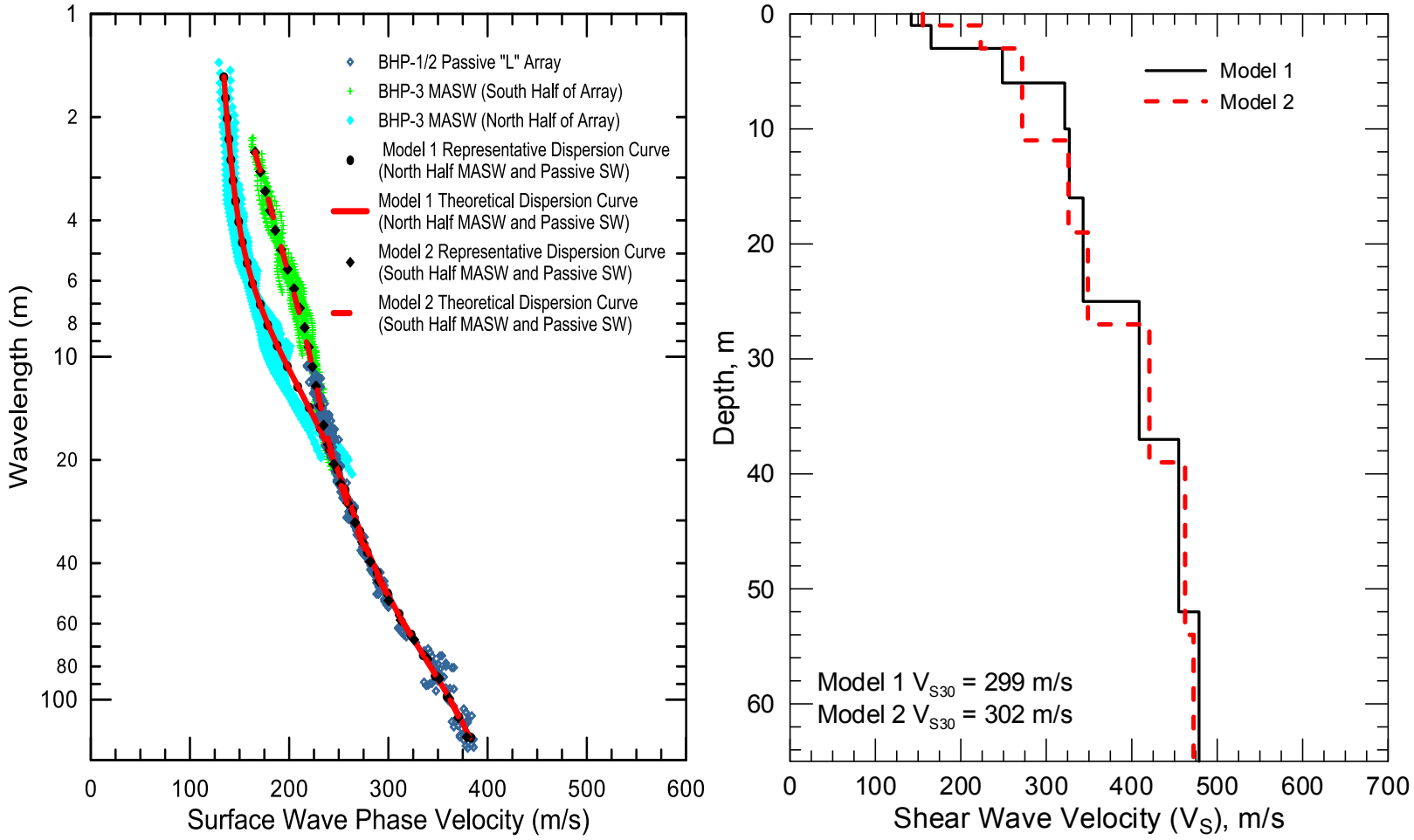

CI.BHP - Field, representative and inverted theoretical surface wave dispersion data (left) and associated V_S model (right)

Site CI.BLA and CI.BLA2

Location: Black Rock Canyon Campground, Joshua Tree National Park, Yucca Valley, California

CI.BLA Latitude: 34.06948 **CI. BLA Longitude:** -116.38896
(Station coordinates provided by USGS, WGS84 coordinate system)

CI.BLA2 Latitude: 34.06931 **CI. BLA2 Longitude:** -116.38993
(Station coordinates provided by USGS, WGS84 coordinate system)

V_{S30} (measured): 524 m/s

V_{S30} (adjusted to more accurately reflect seismic station conditions): 613 m/s (average S-wave velocity between 2 and 32 m adjusting for 2 m nominal sensor depth).

NEHRP Site Class: C

Geomatrix Code: IQB

Geologic Conditions/Observations: Seismic station and test area located on unit mapped as Quaternary (Pleistocene) older alluvial silt, sand and gravel, but many small, several meter high outcrops of weathered gneissic bedrock nearby. Weathered rock expected to be very shallow in site vicinity.

Site Conditions: Rural site. Hummocky topography in site vicinity. Seismic station and test area located on dirt road.

Geophysical Methods Utilized: HVSR, Seismic Refraction, MASW

Geophysical Testing Arrays:

1. Array BLA-1 (48 channel MASW and P-wave seismic refraction array utilizing 4.5 Hz vertical geophones spaced 1.5 m apart for a length of 70.5 m, forward and reverse shot locations with multiple source offsets and source types and multiple interior shot locations).
2. Three HVSR measurement locations evenly distributed along array BLA-1.

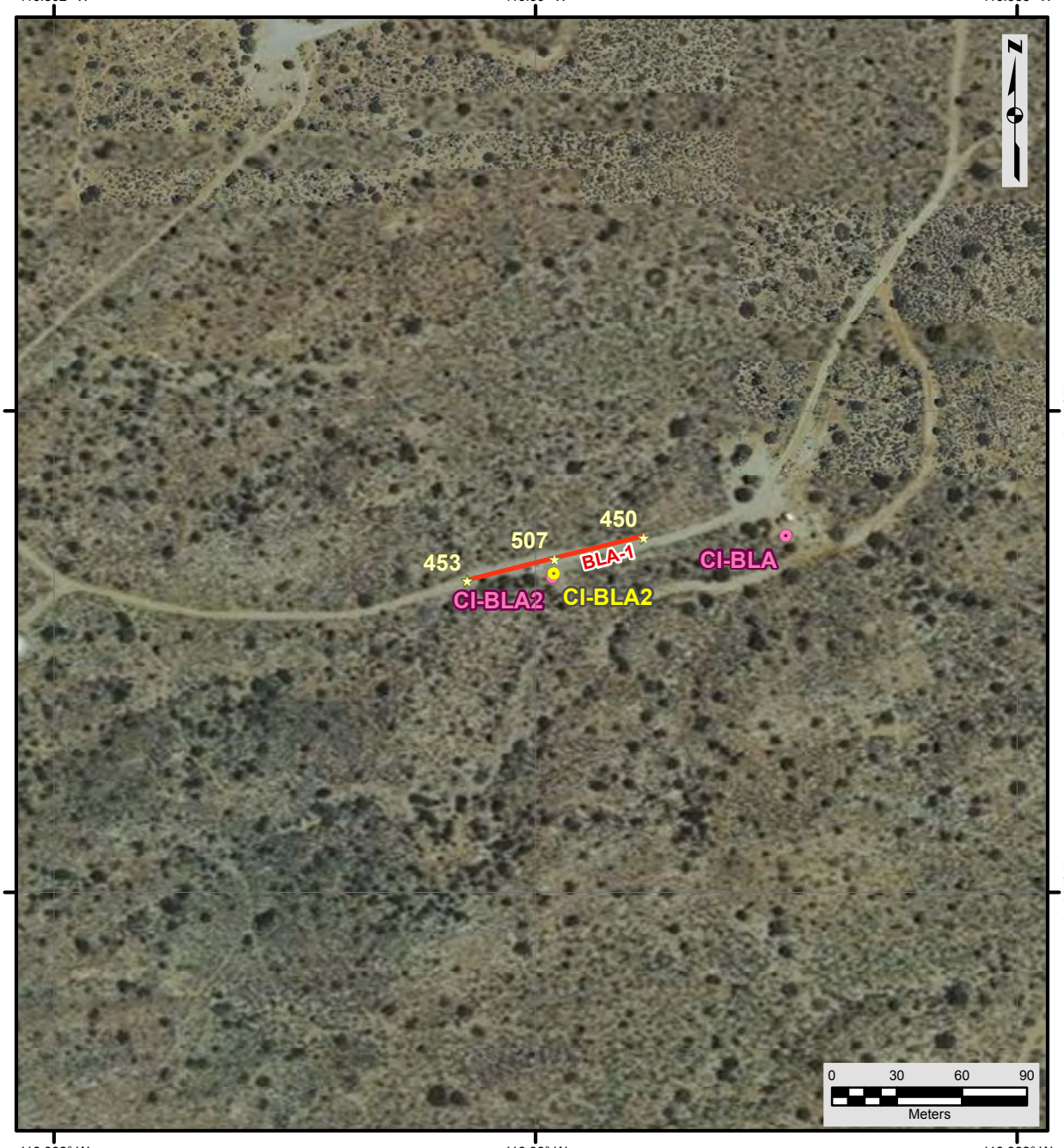

Legend

- Seismic Station - Approximate Surveyed Location
- Seismic Station - Approximate Location of Record
- H/V Spectral Ratio Location
- MASW and Seismic Refraction Array

NOTES:
1. WGS 1984 COORDINATE SYSTEM
2. Image Source: ESRI, i-cubed, USDA FSA, USGS, AEX, GeoEye, Getmapping, Aerogrid, IGP

File Name: CI-BLA-I

Date: 10/6/2011

USGS science for a changing world

GEOVision geophysical services

RECOVERY.GOV

SITE MAP
CI•BLA

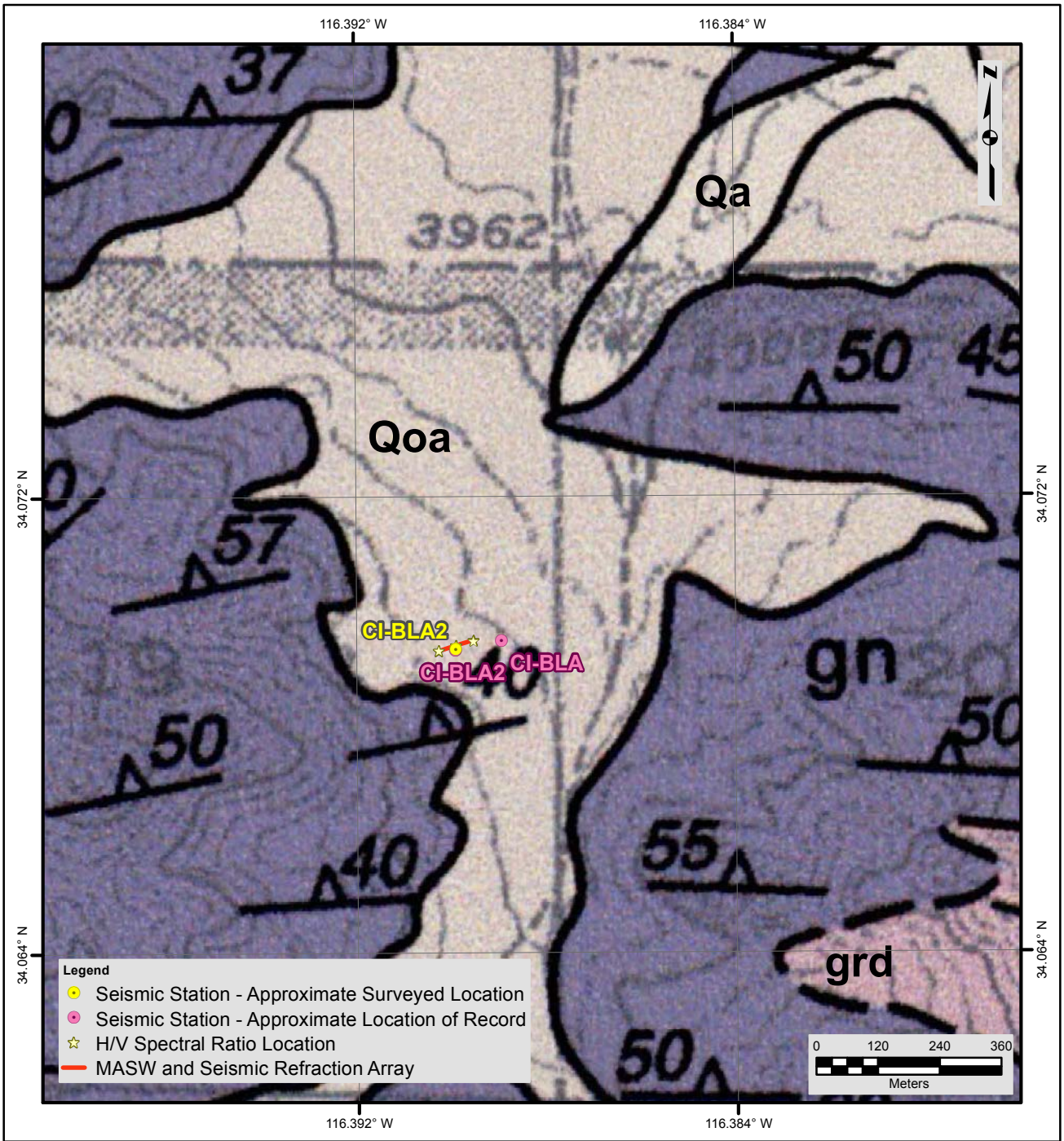

Description of Geologic Map Units

Qa = Quaternary (Holocene) alluvial sand and gravel of valley areas
Qoa = Quaternary (Pleistocene) older surficial sediments, granitic cobble-pebble gravel and sand
gn = Precambrian (?) gneissic rocks ranging from quartz monzonite to quartz diorite

NOTES:
1. WGS 1984 COORDINATE SYSTEM
2. Geologic Map of the Joshua Tree & Twentynine Palms 15 Minute Quadrangles, Riverside & San Bernardino Counties, California by Thomas W. Dibblee, Jr., 2008
3. See site map for details of geophysical survey

File Name: CI-BLA

Date: 10/17/2011

USGS science for a changing world

GEOVision geophysical services

GEOLOGIC MAP
CI•BLA

Looking south towards CI.BLA2 seismic station, HVSR Sensor 507 and center of Array BLA-1

Looking east towards former location of CI.BLA seismic station, HVSR sensor 450 and northeast end of array BLA-1

Looking southwest along array BLA-1

Looking northeast from center of array BLA-1

Seismic refraction and MASW data acquisition along array BLA-1

Location of Geophysical Testing Arrays:

Location	Latitude	Longitude
BLA-1, Southwest End of MASW/Refraction Array	34.06930	-116.39028
BLA-1, Center of MASW/Refraction Array	34.06939	-116.38992
BLA-1, Northeast End of MASW/Refraction Array	34.06948	-116.38956
HVSR Sensor 450	34.06947	-116.38955
HVSR Sensor 453	34.06929	-116.39028
HVSR Sensor 507	34.06938	-116.38992
CI.BLA2 Seismic Station	34.06933	-116.38992

Notes: 1) WGS84 Coordinate System (decimal degrees)
2) Survey accuracy is estimated at 1 to 2 m.

Results:

V_S Model

Depth to Top of Layer (m)	Layer Thickness (m)	S-Wave Velocity (m/s)	Inferred P-Wave Velocity (m/s)	Assumed Poisson's Ratio	Assumed Density (g/cm^3)
0	1.5	167	313	0.3	1.8
1.5	2	320	599	0.3	1.9
3.5	4.5	404	757	0.3	1.9
8	6	523	979	0.3	2.0
14	8	745	1394	0.3	2.1
22	10	914	1711	0.3	2.1
32	>8	1081	2023	0.3	2.2

Notes: 1) Depth of investigation is about 40 m.
2) Bottom layer is a half space.

Observations/Discussion:

- Geologic conditions at the site, based on field observations, consist of a thin layer of sediments over weathered gneiss.
- There are not peaks in the HVSR data. HVSR sensor 507 appears to have the best data quality. HVSR sensors 450 and 453 have slightly elevated HVSR response over a wide frequency range.
- The P-wave refraction data for array BLA-1 were modeled using a tomographic inversion routine with a smooth velocity gradient starting model. The seismic refraction data were modeled with and without extending the model to far offset shot locations. Extending the model to far offset shot locations allowed depth of investigation to be increased to validate the surface wave model at depth. A longer receiver array is preferred for extending depth of investigation, but at the expense of the efficiency in combining seismic refraction and MASW data acquisition along the shorter array.
- Both seismic refraction models show similar P-wave velocity structure in the upper 15 m. P-wave velocity is about 375 to 400 m/s at the surface increasing to 600 m/s at a depth of 1 to 2 m, 800 m/s at a depth of 2 to 3.5 m, 1,000 m/s at a depth of 2 to 5 m and 1,400 m/s at a depth of 4 to 15 m. Without extension of the model to far offset shot locations the effective depth of investigation is about 15 m. Extending the model to far offset shot locations allowed the model to be extended to greater depth revealing the possible presence of bedrock with P-wave velocity on the order of 1,800 to 2,000 m/s at nominal depths of 24 m to 30 m. It should be noted that a longer receiver array would be required to accurately image velocity structure at these depths; however, the far offset shot locations do support P-wave velocity continuing to increase with depth below 15 m.
- The seismic models show that less weathered (higher velocity) bedrock is located at shallower depth at the southwest end of array BLA-1. Seismic station CI.BLA2 is located adjacent to the center of the seismic refraction/MASW array. Seismic station CI.BLA was located about 65 m east of the northeast end of the array.
- Noise conditions at the site were not sufficient for application of passive surface wave techniques.
- Scatter in MASW dispersion data is likely due to lateral velocity variation associated with both variable thickness of the sediment layer and differential weathering of near surface gneissic bedrock.
- The minimum wavelength surface wave phase velocity data extracted from the 48-channel MASW array was about 24 m. Data reduction using seismic records from smaller hammer sources and a limited offset receiver array (i.e. less active geophones) allowed extraction of surface wave dispersion data to a minimum wavelength of about 4 m.
- A representative dispersion curve was generated for the MASW data set using a moving average, polynomial curve fitting routine and used for modeling.
- Surface wave depth of investigation is about 40 m based on half of maximum wavelength criteria.
- The inferred P-wave velocities in the surface wave model, assuming a Poisson's ratio of 0.3, are generally consistent with the central portion of the seismic refraction models, where there is the thickest sequence of lower velocity, weathered bedrock.

- The seismic refraction model that utilized far offset source locations supports the S-wave velocities greater than 900 m/s at depths below about 22 m. Although not well constrained, the seismic refraction model supports P-wave velocities of greater than 1,800 m/s below this depth.
- V_{S30} is 524 m/s (Site Class C).
- Average S-wave velocity between 2 m (nominal sensor depth) and 32 m is 613 m/s.
- Replacing the S-wave velocity of the third and fourth layers to 745 m/s to better reflect the shallow higher bedrock velocities at the southwest end of the array raises V_{S30} to 615 m/s and the average S-wave velocity between 2 and 32 m to 742 m/s, still Class C.

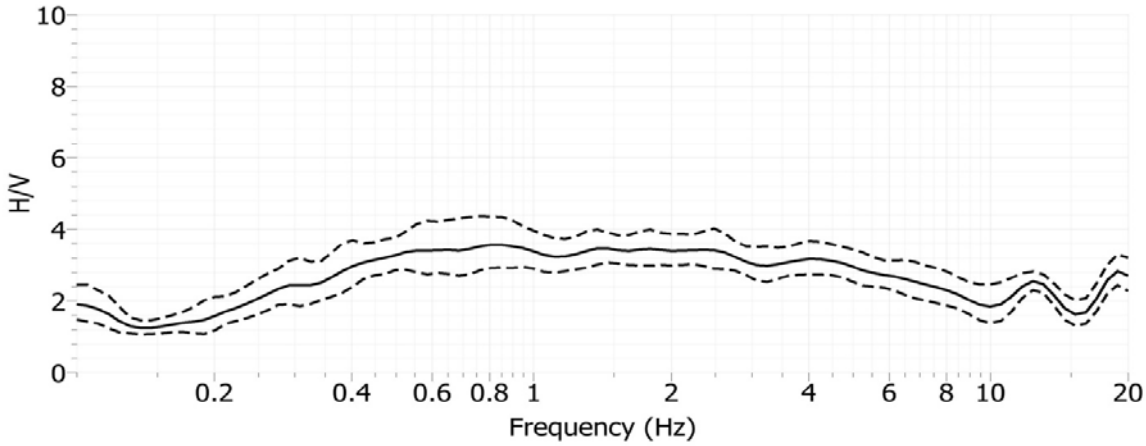

Site CI.BLA, H/V Spectral Ratio, Array BL -1, Sensor 453

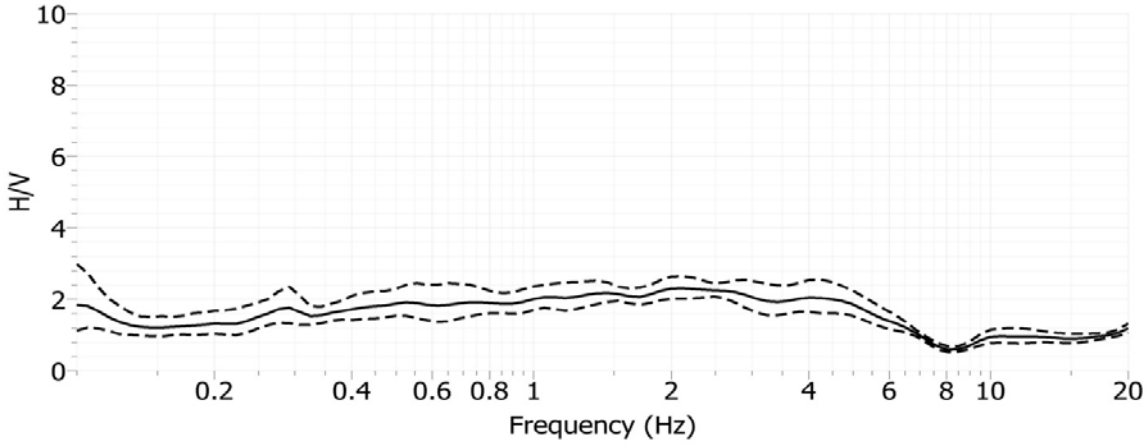

Site CI.BLA, H/V Spectral Ratio, Array BLA-1, Sensor 507

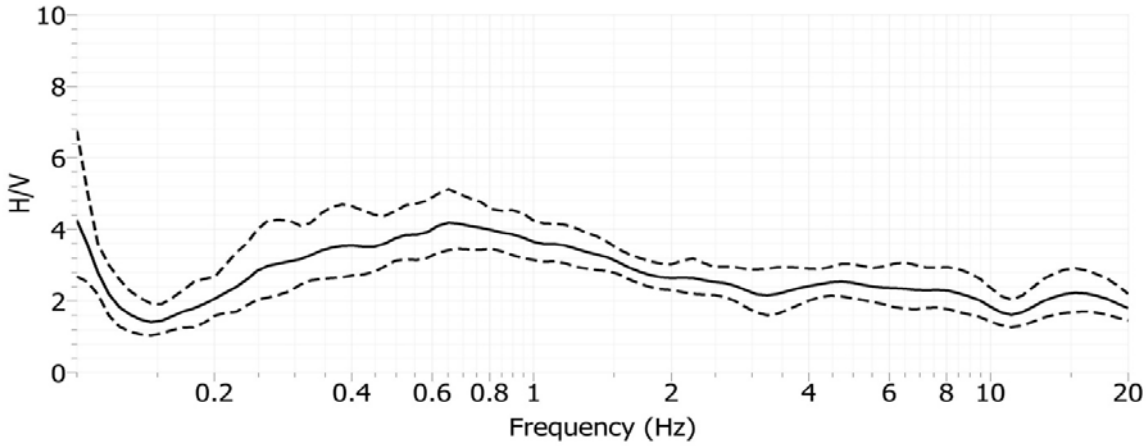

Site CI.BLA, H/V Spectral Ratio, Array BLA-1, Sensor 450

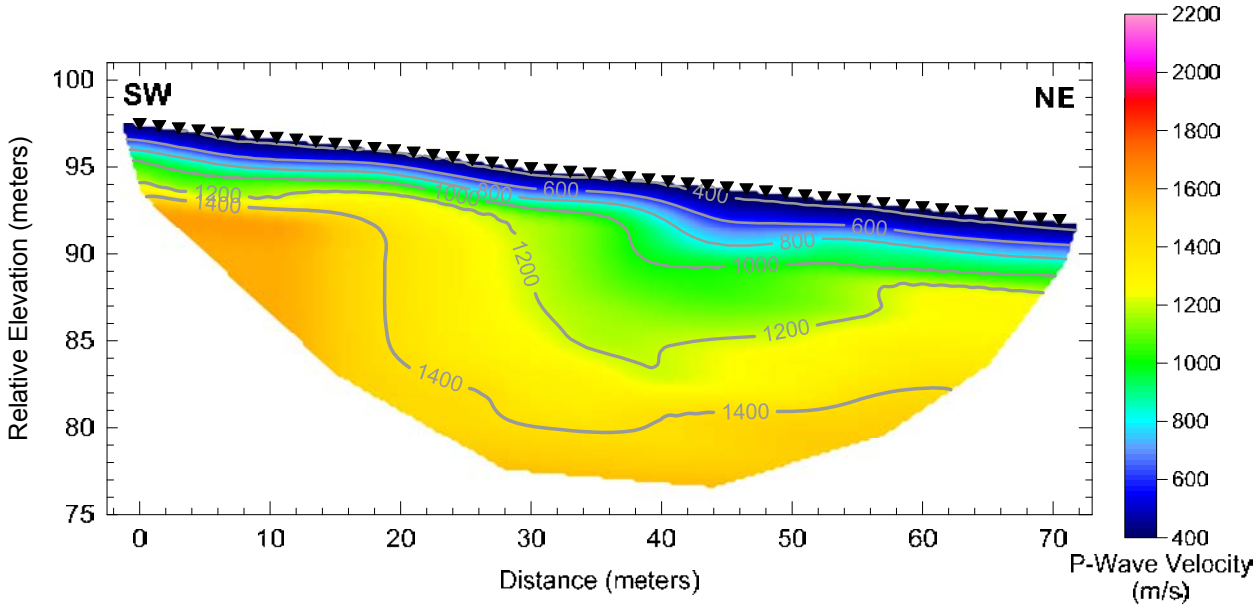

Array BLA-1 – Tomographic Seismic Refraction Model utilizing Smooth Velocity Gradient Starting Model Not Extended to Far Offset Shot Locations

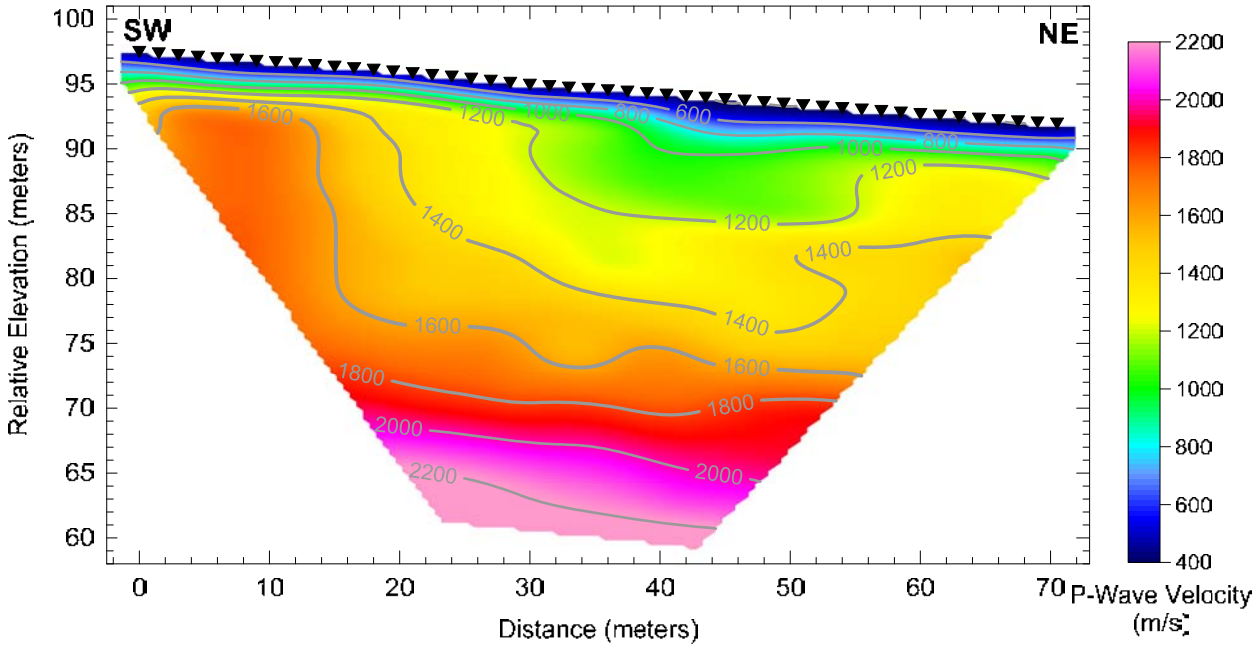

Note: High velocity unit at base of model exists but is poorly constrained (both velocity and geometry) due to inadequate line length and shot offsets. Increasing velocity at depths below 15 m is required to fit travel time curves from far offset shot locations

Array BLA-1 – Tomographic Seismic Refraction Model utilizing Smooth Velocity Gradient Starting Model Extended to Off-End Shot Locations

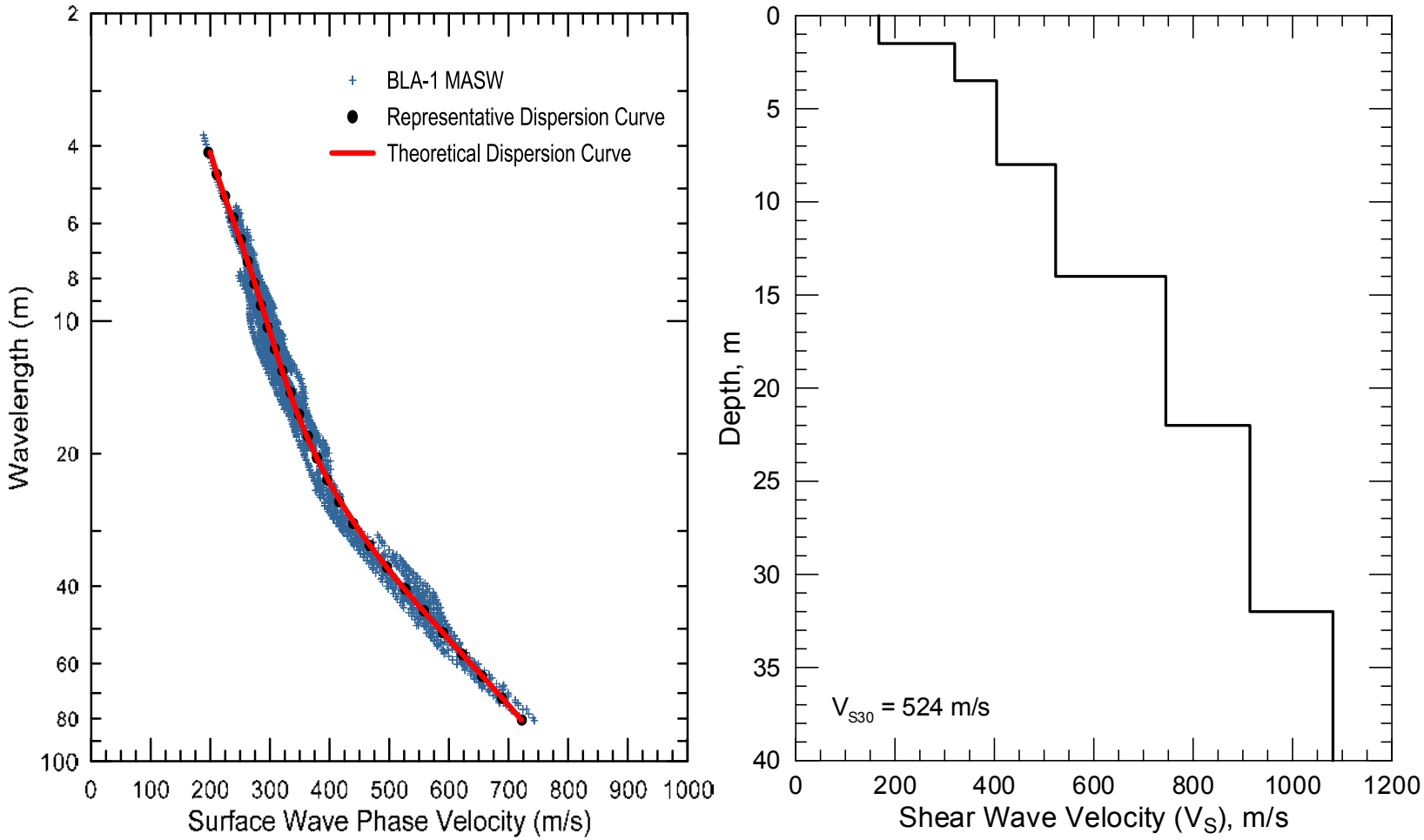

CI.BLA - Field, representative and inverted theoretical surface wave dispersion data (left) and associated V_S model (right)

Site CI.BLY

Location: Big Maria Mountains, Near Blythe, Riverside County, California

Latitude: 33.75030 **Longitude:** -114.52373
(Station coordinates modified based on field GPS survey, WGS84 coordinate system)

V_{S30} (measured): 1,029 m/s

V_{S30} (adjusted to more accurately reflect seismic station conditions): 1,197 m/s (average S-wave velocity between 1.5 and 31.5 m adjusting for both the expected sensor depth and sensor being placed on rock).

NEHRP Site Class: B

Geomatrix Code: IZA

Geologic Conditions/Observations: Seismic station located on geologic unit mapped as Permian and Pennsylvanian sedimentary rocks. Field observations indicate that the rock is locally quite hard, but highly fractured, being easily broken along fractures.

Site Conditions: Rural site. Test site located along a ridge with steep slopes to the sides. Surface topography drops abruptly and steeply immediately west of the seismic station. Air conditioning unit in nearby structure and generator running during HVSR testing. Some construction noise at site, but no vehicle traffic.

Geophysical Methods Utilized: HVSR, Seismic Refraction, MASW

Geophysical Testing Arrays:

1. Array BLY-1 (48 channel MASW and P-wave seismic refraction array utilizing 4.5 Hz vertical geophones spaced 1.5 m apart for a length of 70.5 m, forward and reverse shot locations with multiple source offsets and source types and center shot location).
2. Three HVSR measurement locations distributed evenly along array BLY-1.

Legend

- Seismic Station - Approximate Surveyed Location
- Seismic Station - Approximate Location of Record
- H/V Spectral Ratio Measurement Location
- MASW and Seismic Refraction Array

NOTES:
1. WGS 1984 COORDINATE SYSTEM
2. Image Source: ESRI, i-cubed, USDA FSA, USGS, AEX, GeoEye, Getmapping, Aerogrid, IGP

File Name: CI-BLY-I

Date: 10/13/2011

USGS science for a changing world

GEOVision geophysical services

RECOVERY.GOV

SITE MAP
CI•BLY

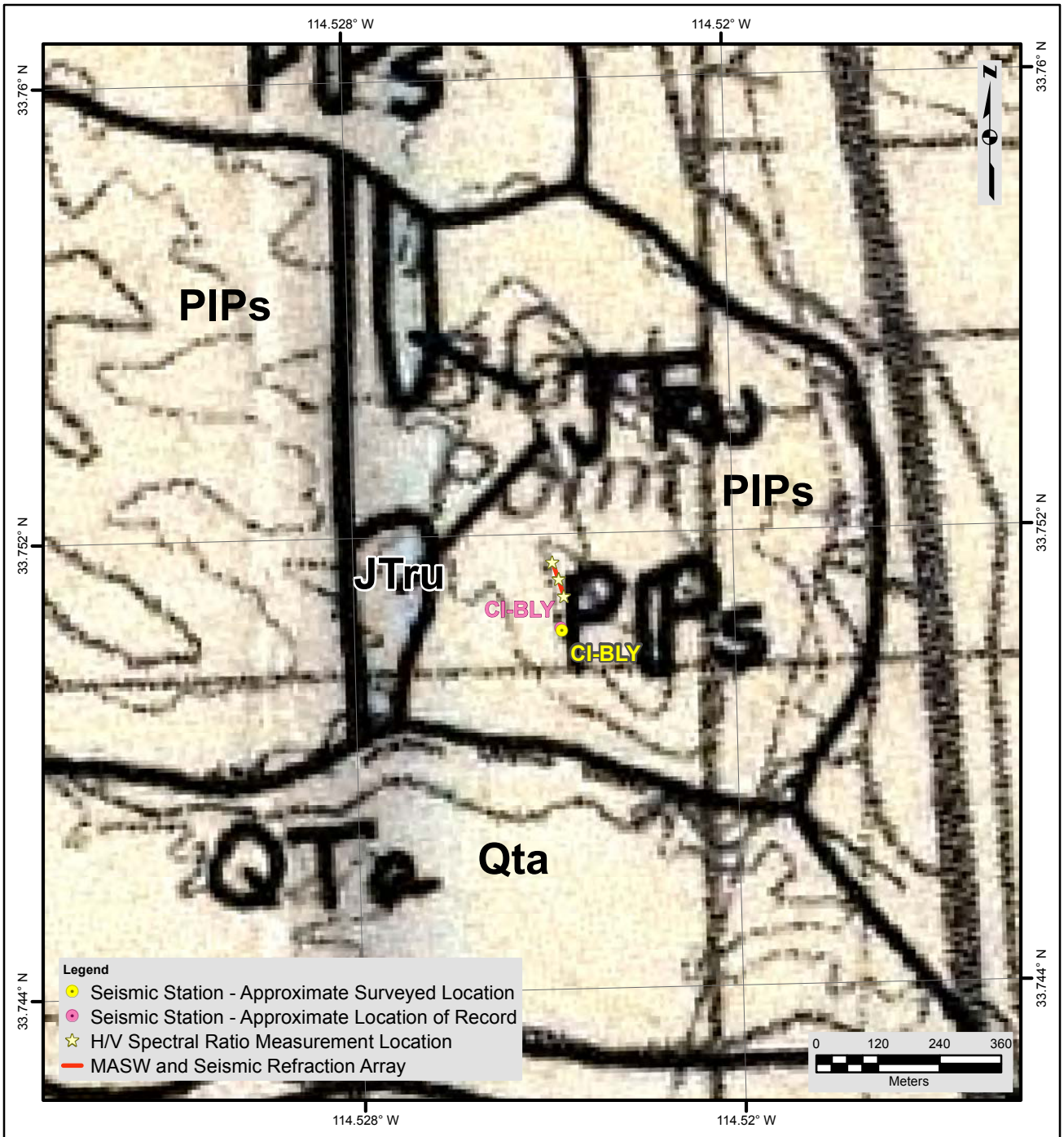

Description of Geologic Map Units

Qta = Quaternary and Tertiary alluvial fan and fluvial deposits
JTru = Jurassic and Triassic volcanic and sedimentary rocks
PIPs = Permian and Pennsylvanian sedimentary rocks

NOTES:
1. WGS 1984 COORDINATE SYSTEM
2. Geologic Map of the Blythe 30' by 60' Quadrangle, California and Arizona by Paul Stone, 1990
3. See site map for details of geophysical survey

File Name: CI-BLY

Date: 10/13/2011

USGS science for a changing world

GEOVision geophysical services

RECOVERY.GOV

GEOLOGIC MAP
CI•BLY

Seismic Station CI-BLY

Looking northwest along array BLY-1 at HVSR sensors 450 and 507

Accelerated weight drop energy source utilized during MASW and seismic refraction testing along array BLY-1

Looking north at seismic station and relatively hard but intensely fractured sedimentary or metasedimentary rocks near the seismic station

Looking southeast along array BLY-1. Seismic station located behind building in upper right corner of photo.

Location of Geophysical Testing Arrays:

Location	Latitude	Longitude
BLY-1, Southeast End of MASW/Seismic Refraction Array	33.75090	-114.52367
BLY-1, Center of MASW/Seismic Refraction Array	33.75120	-114.52378
BLY-1, Northwest End of MASW/Seismic Refraction Array	33.75150	-114.52389
HVSR Sensor 450	33.75120	-114.52377
HVSR Sensor 453	33.75090	-114.52367
HVSR Sensor 507	33.75150	-114.52390
CI.BLY Seismic Station	33.75030	-114.52373

Notes: 1) WGS84 Coordinate System (decimal degrees)
2) Survey accuracy is estimated at 1 to 2 m.

Results:

V_S Model 1 (Energy sources at SE end of array)

Depth to Top of Layer (m)	Layer Thickness (m)	S-Wave Velocity (m/s)	Inferred P-Wave Velocity (m/s)	Assumed Poisson's Ratio	Assumed Density (g/cm^3)
0	1.5	292	546	0.3	1.8
1.5	28.5	1208	2260	0.3	2.2
30	>5	2083	3898	0.3	2.4

Notes: 1) Depth of investigation is about 35 m.
2) Bottom layer is a half space.
3) Thin surficial layer permitted in model based on seismic refraction data.

V_S Model 2 (Energy sources at NW end of array)

Depth to Top of Layer (m)	Layer Thickness (m)	S-Wave Velocity (m/s)	Inferred P-Wave Velocity (m/s)	Assumed Poisson's Ratio	Assumed Density (g/cm^3)
0	1.1	242	452	0.3	1.8
1.1	29.9	1154	2159	0.3	2.2
31	>4	1747	3268	0.3	2.4

Notes: 1) Depth of investigation is about 35 m.
2) Bottom layer is a half space.
3) Thin surficial layer permitted in model based on seismic refraction data.

Observations/Discussion:

- The HVSR plots are very similar validating the 1-D velocity structure assumption.
- There is a weak HVSR peak between 1 and 1.5 Hz. The significance of this peak is not clear given the topographic variation in the site vicinity and the fact that the site is located on sedimentary or metasedimentary rock.
- Seismic refraction data were modeled using a tomographic inversion routine and a smooth velocity gradient starting model. The seismic refraction model was extended to far-offset shot locations to extend depth of investigation.
- The seismic refraction model indicates that P-wave velocity increases with depth from about 600 to 1,500 m/s near the surface to over 2,000 m/s at a depth of 1 to 2 m and over 3,000 m/s at a depth of 2 to 5 m.
- Seismic refraction depth of investigation is about 12 m.
- Noise conditions at the site were not sufficient for application of passive surface wave techniques.
- The minimum wavelength surface wave phase velocity data extracted from the 48-channel MASW array was about 12 m. Reduction of MASW data from seismic records acquired using smaller hammer sources did not extract surface wave dispersion data at smaller wavelengths. Therefore, interior seismic refraction shot locations and smaller hammer source seismic data were not utilized for surface wave analysis. This is one of the few sites were there was not significant benefit utilizing smaller hammer sources.
- Surface wave dispersion curves developed from source locations at the southern and northern ends of the line are slightly different and were, therefore, modeled separately.
- There is about a 50 to 125 m/s scatter in the surface wave dispersion data, likely the result of lateral velocity variation.
- Representative dispersion curves were generated for each surface wave data set using a moving average, polynomial curve fitting routine.
- Although the minimum Rayleigh wave phase velocity is about 12 m, a 1 to 1.5 m low velocity layer was permitted in the surface wave V_S models based on the seismic refraction data.
- Surface wave depth of investigation is about 35 m based on half of maximum wavelength criteria
- The inferred P-wave velocities in the surface wave model, assuming a Poisson's ratio of 0.3, are somewhat lower below a depth of 5 m than the P-wave velocity structure in the seismic refraction model.
- V_{S30} is 1,044 and 1,014 m/s for Model 1 (SE sources) and Model 2 (NW sources), respectively, averaging 1,029 m/s (Site Class B).
- Average S-wave velocity between 1.5 and 31.5 m, to adjust for the expected seismic station depth and fact that the seismic station is placed on rock, is 1,234 m/s for Model 1 and 1,161 m/s for Model 2, averaging 1,197 m/s.

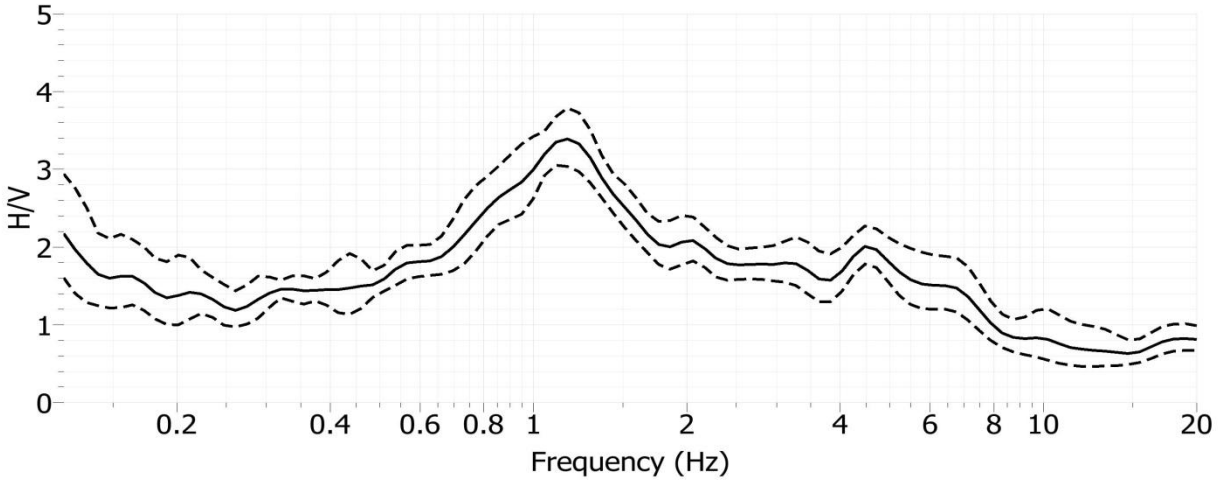

Site CI.BLY, H/V Spectral Ratio, Array BLY -1, Sensor 507

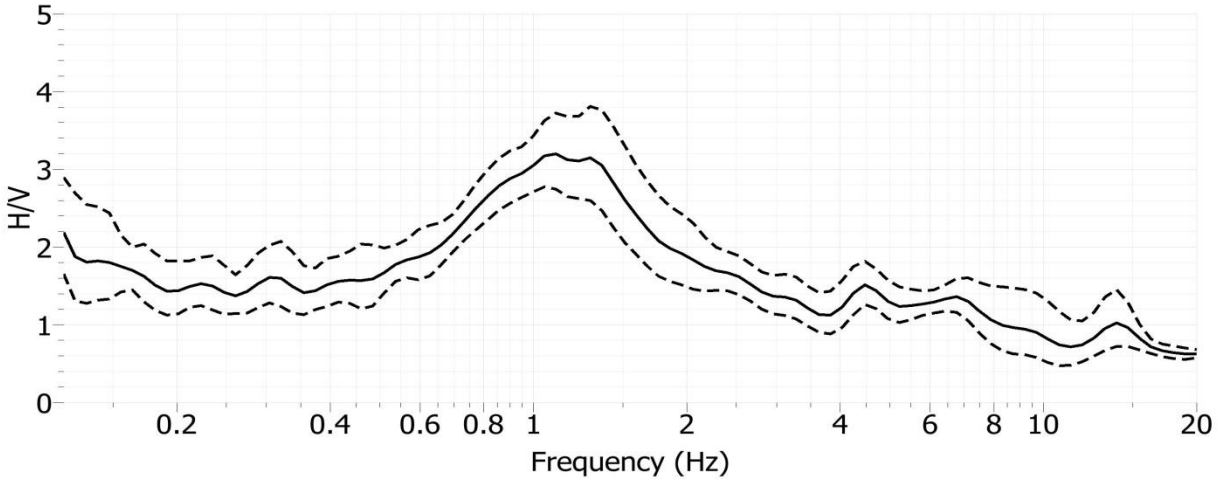

Site CI.BLY, H/V Spectral Ratio, Array BLY -1, Sensor 450

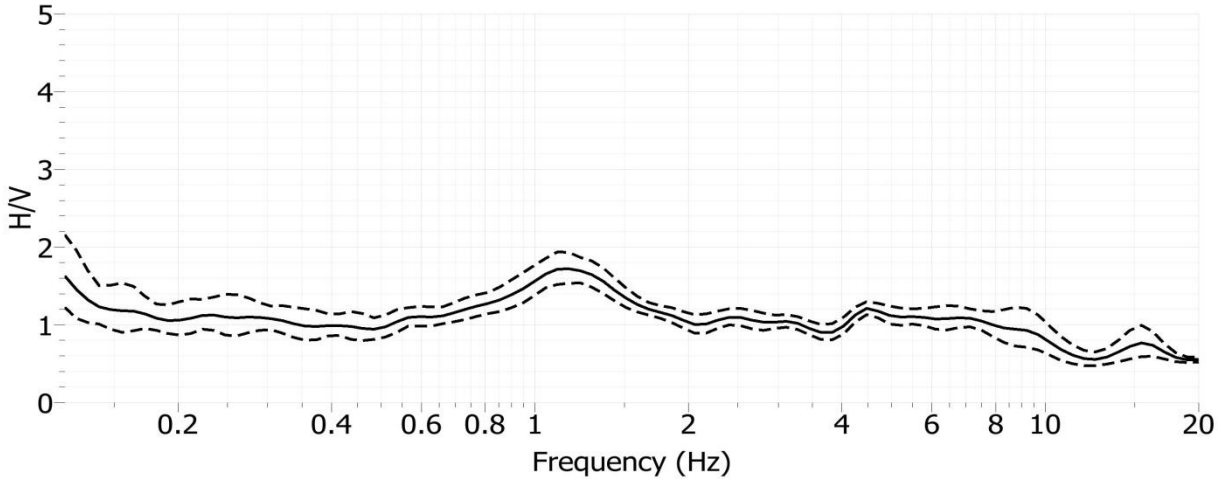

Site CI.BLY, H/V Spectral Ratio, Array BLY -1, Sensor 453

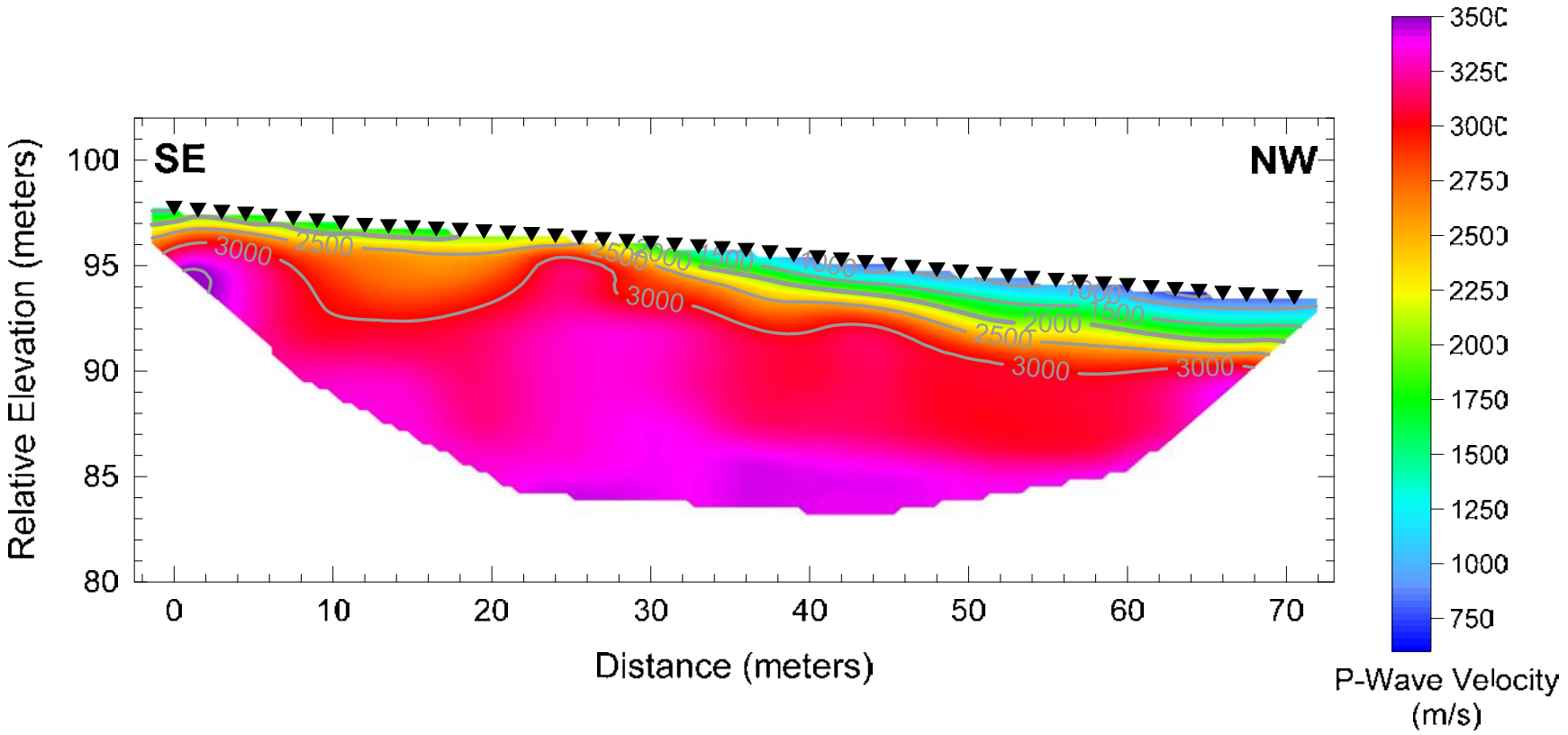

Array BLY-1 – Tomographic seismic refraction model utilizing smooth velocity gradient starting model

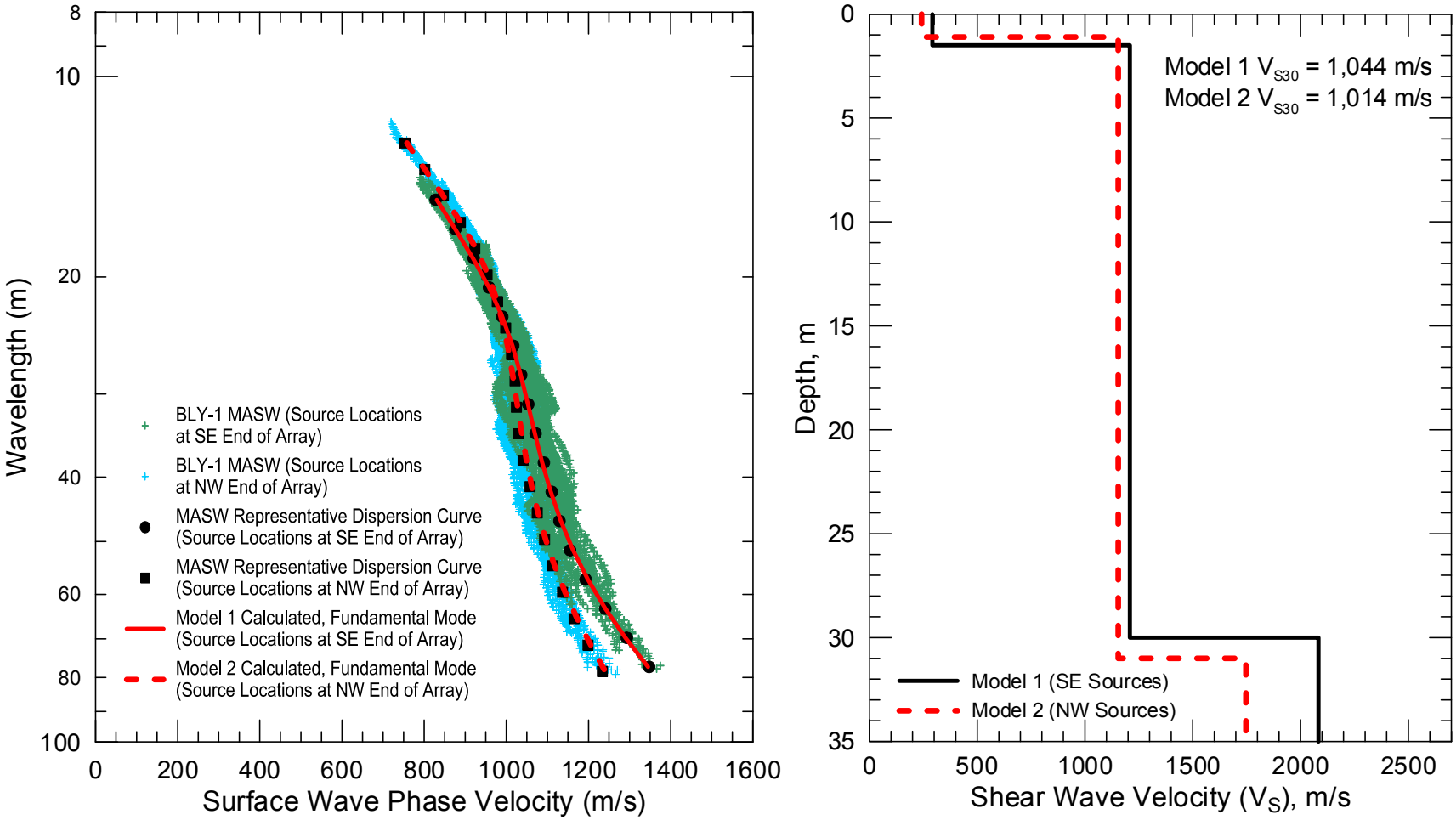

CI.BLY - Field, representative and inverted theoretical surface wave dispersion data (left) and associated V_S model (right)

Site CI.BOM

Location: Coachella Valley Water District Property, Bombay Beach, Imperial County, California

Latitude: 33.36465 **Longitude:** -115.72963
(Station coordinates provided by USGS, WGS84 coordinate system)

V_{S30} (measured): 202 m/s

V_{S30} (adjusted to more accurately reflect seismic station conditions): 214 m/s (average S-wave velocity between 2 and 32 m adjusting for 2 m assumed sensor depth).

NEHRP Site Class: D

Geomatrix Code: IHD/IQD

Geologic Conditions/Observations: Seismic station located on thin layer of fill over Quaternary (Holocene) to Tertiary (undivided) lake deposits. The site is not located on Holocene dune sands, as mapped. The site is located between mapped strands of the San Andreas Fault Zone. Bedrock expected to be deep at this site.

Site Conditions: Rural site with some noise sources in site vicinity (pond pumps, trains). Relatively flat terrain in test area. Testing conducted after a period of heavy rain and, therefore, near surface soils were very moist.

Geophysical Methods Utilized: HVSR, MASW, SASW

Geophysical Testing Arrays:

1. Array BOM-1 (48 channel MASW array utilizing 4.5 Hz vertical geophones spaced 1.5 m apart for a length of 70.5 m, forward and reverse shot locations with multiple source offsets and source types and center shot location).
2. Array BOM-1 (SASW array with common midpoint and orientation as BOM-1. SASW data acquired using 4.5 and 1 Hz geophones, common source and common center point geometry, forward and reverse shot locations).
3. Three HVSR measurement locations distributed along BOM-1.

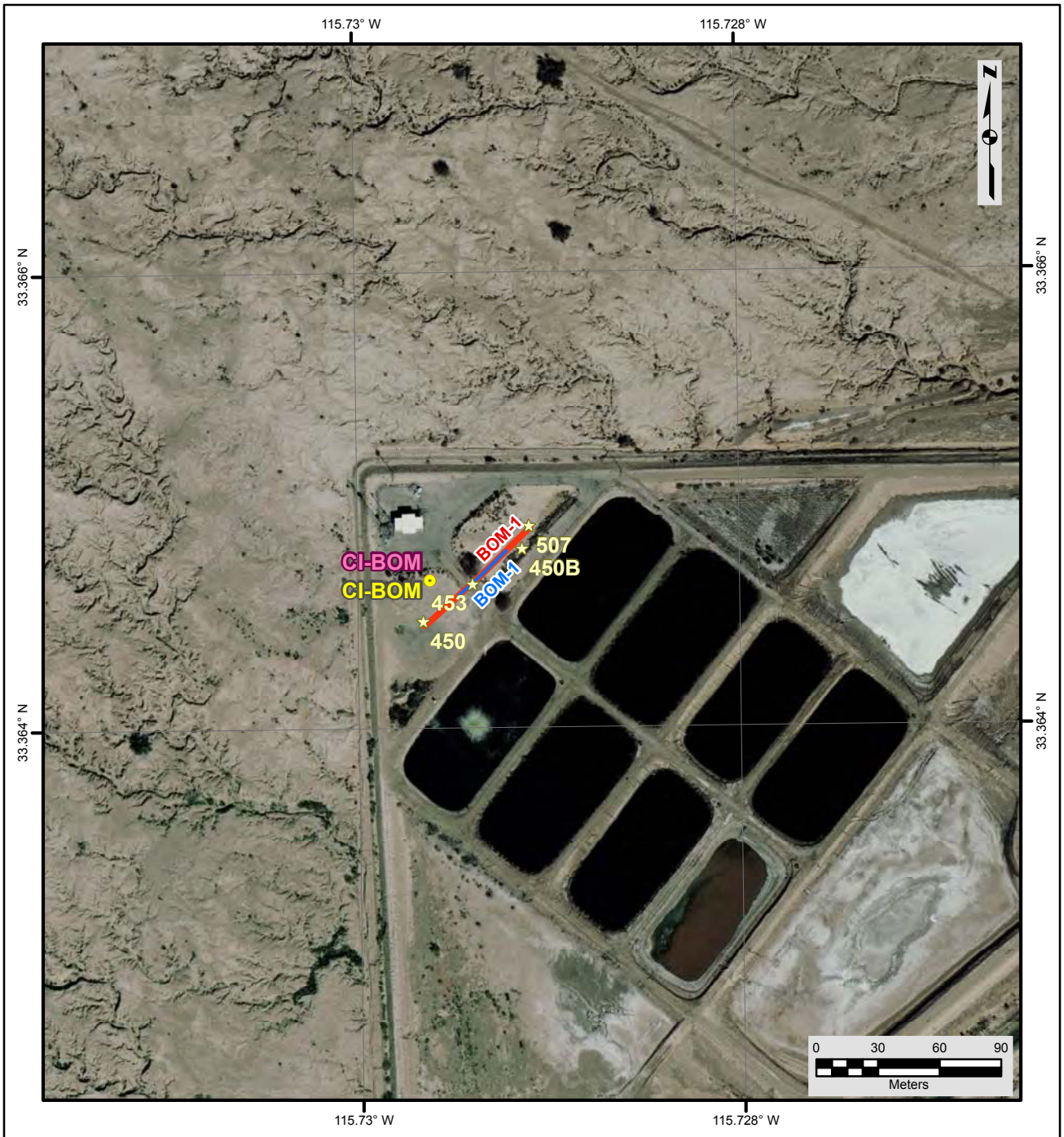

Legend

- Seismic Station - Approximate Surveyed Location
- Seismic Station - Approximate Location of Record
- H/V Spectral Ratio Location
- SASW Array
- MASW Array

NOTES:
1. WGS 1984 COORDINATE SYSTEM
2. Image Source: ESRI, i-cubed, USDA FSA, USGS, AEX, GeoEye, Getmapping, Aerogrid, IGP

File Name: CI-BOM-I

Date: 9/29/2011

USGS science for a changing world

GEOVision geophysical services

RECOVERY.GOV

SITE MAP
CI•BOM

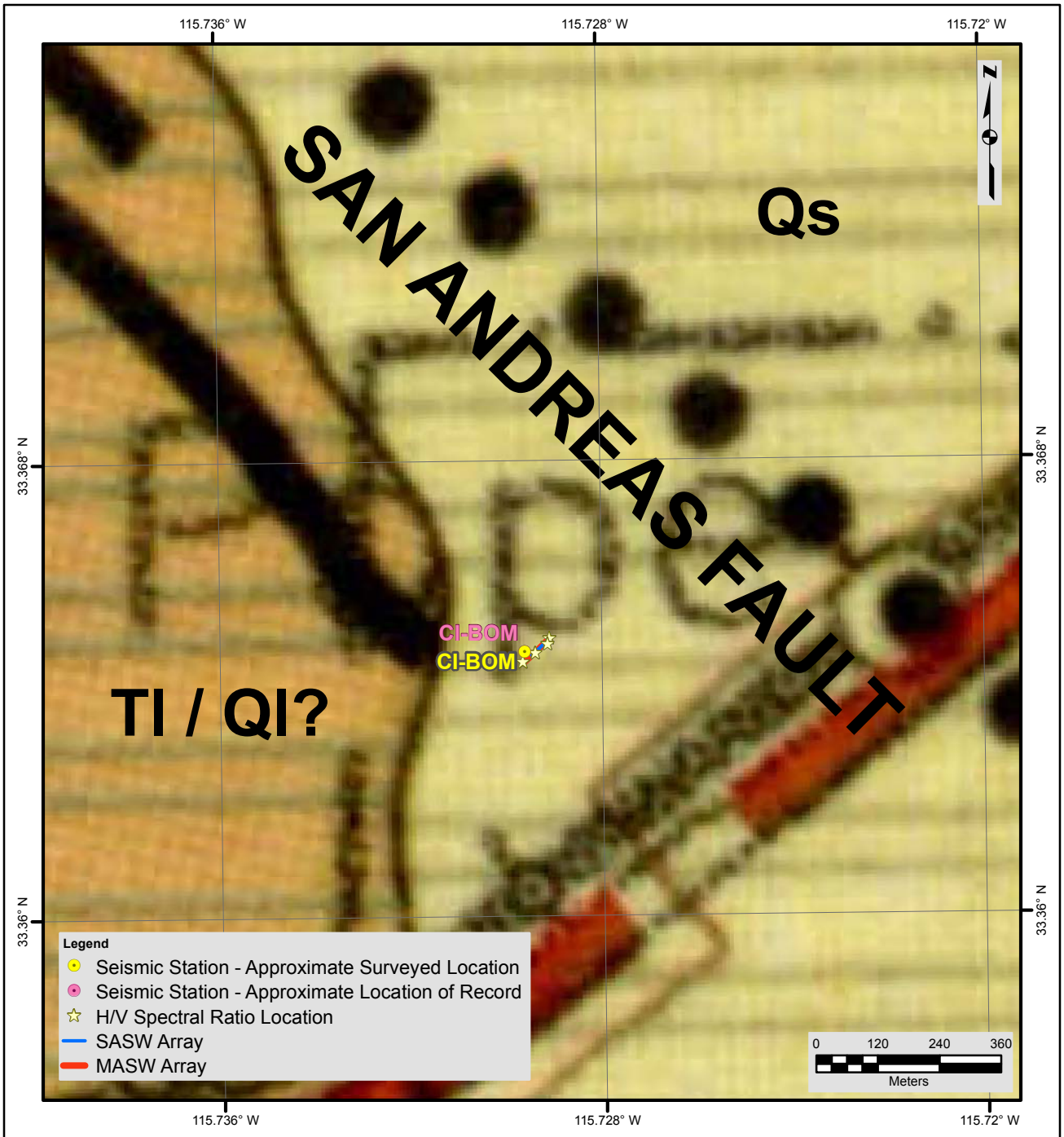

Description of Geologic Map Units

Qs = Quaternary (Holocene) dune sand
Tl / Ql = Tertiary (Undivided) to Quaternary (Pleistocene to Holocene) lake deposits

NOTES:
1. WGS 1984 COORDINATE SYSTEM
2. Geologic Map of California, Salton Sea Sheet, Olaf P Jenkins Edition by Charles W. Jennings, 1967
3. See site map for details of geophysical survey

File Name: CI-BOM

Date: 9/29/2011

USGS science for a changing world

GEOVision geophysical services

RECOVERY.GOV

GEOLOGIC MAP
CI•BOM

CI.BOM seismic station

Looking northeast along MASW array BOM-1

Looking north towards CI.BOM from HVSR sensor 450 and southwest end of MASW array BOM-1

Looking northeast along SASW array BOM-1

Looking northwest towards seismic station from center of SASW array BOM-1

Location of Geophysical Testing Arrays:

Location	Latitude	Longitude
BOM-1, Southwest End of MASW Array	33.36445	-115.72966
BOM-1, Center of MASW and SASW Arrays	33.36468	-115.72935
BOM-1, Northeast End of MASW Array	33.36488	-115.72910
HVSR Sensor 450	33.36447	-115.72967
HVSR Sensor 453	33.36463	-115.72941
HVSR Sensor 507	33.36489	-115.72911
HVSR Sensor 450b	33.36479	-115.72915
HVSR Sensor 453b	33.36479	-115.72915
HVSR Sensor 507b	33.36477	-115.72913
CI.BOM Seismic Station	33.36465	-115.72963

Notes: 1) WGS84 Coordinate System (decimal degrees).
2) Survey accuracy is estimated at 1 to 2 m.

Results:

V_S Model – MASW Array BOM-1

Depth to Top of Layer (m)	Layer Thickness (m)	S-Wave Velocity (m/s)	Inferred P-Wave Velocity (m/s)	Assumed Poisson's Ratio	Assumed Density (g/cm^3)
0	1	146	273	0.300	1.8
1	2	170	317	0.300	1.8
3	3	190	356	0.300	1.8
6	8	212	1600	0.491	1.9
14	15	215	1600	0.491	1.9
29	>1	301	1600	0.482	2.0

Notes: 1) Saturated sediments estimated at 6 m depth from seismic refraction first arrival data. The P-wave velocity of saturated sediments is about 1,600 m/s.
2) Depth of investigation is about 30 m.
3) Bottom layer is a half space.

V_S Model – SASW Array BOM-1 (Model 1 - Lower Envelope of Surface Wave Dispersion Data)

Depth to Top of Layer (m)	Layer Thickness (m)	S-Wave Velocity (m/s)	Inferred P-Wave Velocity (m/s)	Assumed Poisson's Ratio	Assumed Density (g/cm^3)
0	1	110	205	0.300	1.8
1	5	166	311	0.300	1.8
6	5	182	1600	0.493	1.9
11	7	206	1600	0.492	1.9
18	9	214	1600	0.491	1.9
27	>3	314	1600	0.480	2.0

Notes: 1) Saturated sediments estimated at 6 m depth from seismic refraction first arrival data. The P-wave velocity of saturated sediments is about 1,600 m/s.
2) Depth of investigation is about 30 m.
3) Bottom layer is a half space.

V_S Model – SASW Array BOM-1 (Model 2 - Average of Surface Wave Dispersion Data)

Depth to Top of Layer (m)	Layer Thickness (m)	S-Wave Velocity (m/s)	Inferred P-Wave Velocity (m/s)	Assumed Poisson's Ratio	Assumed Density (g/cm^3)
0	0.75	100	187	0.300	1.8
0.75	2.25	160	299	0.300	1.8
3	3	196	366	0.300	1.8
6	8	205	1600	0.492	1.9
14	13	207	1600	0.491	1.9
27	>3	322	1600	0.479	2.0

Notes: 1) Saturated sediments estimated at 6 m depth from seismic refraction first arrival data. The P-wave velocity of saturated sediments is about 1,600 m/s.
2) Depth of investigation is about 30 m.
3) Bottom layer is a half space.

Observations/Discussion:

- The HVSR curves are similar validating the 1-D velocity structure assumption.
- HVSR sensor 507 has significant low frequency noise, likely associated with poor coupling and is replaced by HVSR station 450B. HVSR station 450B was acquired one week later, along with stations 453B and 507B (not presented), as part of an evaluation of sensor coupling techniques. HVSR results are very similar between measurements taken one week apart (sensors 450 and 453 compared to sensor 450B).
- There is a high amplitude HVSR peak at about 0.16 Hz, likely associated with the deep basement complex, and a secondary HVSR peak at about 0.8 Hz, which is associated with a structure at greater depth than imaged with the surface wave sounding.
- The water table, with P-wave velocity of about 1,600 m/s was modeled at a depth of about 6 m based on interactive layer-based analysis of seismic refraction first arrival data. P-wave velocities of the unsaturated sediments range from about 250 to 350 m/s to a depth of about 1.5 m, below which velocities are in the 400 to 500 m/s range to the water table.
- There is some reflectivity in the MASW seismic records with multiple reflectors in the approximate 40 to 100 m depth range.
- Noise conditions at the site were not sufficient to apply passive surface wave techniques.
- The SASW and MASW surface wave dispersion data are sufficiently different to require separate modeling.
- SASW dispersion data are interesting and we don't have an explanation of the signature of the dispersion data, which almost forms two separate dispersion curves. Both the lower envelope (Model 1) and average (Model 2) of the SASW dispersion data were modeled for comparison.
- The MASW dispersion data more closely tracks the higher phase velocity segment of the SASW dispersion curve and, therefore, should more closely resemble SASW Model 2.
- There is significant scatter in the MASW dispersion data over the 20 to 45 m wavelength range.
- Small wavelength/high frequency MASW dispersion data were only extracted from data acquired with small hammers on the southwest end of the line, where surface soils consisted of compacted fill and weathered asphalt. The center and northeast shot locations were located on a very moist, spongy fill that had not been compacted. The SASW sounding effectively characterized the low velocity of this material.
- A representative dispersion curve was generated for the MASW and SASW data sets using a moving average, polynomial curve fitting routine for data modeling.
- During data modeling, layer thicknesses were adjusted to avoid velocity inversions occurring in the models. We believe that the characteristics of the representative dispersion curves that would lead to velocity inversions are associated with scatter in the dispersion data or artifacts in the dispersion data rather than velocity structures.
- The S-wave velocity of the lowest layer in the models is not well constrained due to its depth relative to the depth of investigation.
- The MASW model is very similar to the SASW Model 2 (average of SASW dispersion curve) except for the upper meter where the two techniques are sampling different areas on site. The SASW Model 1 (lower envelope of SASW dispersion data) has about 10 to 15% lower velocities over the 3 to 11 m depth range than the MASW model and SASW Model 2.

- Surface wave depth of investigation is about 30 m based on half of maximum wavelength criteria.
- V_{S30} is 207 m/s for MASW array BOM-1, 197 m/s for the lower envelope of the surface wave dispersion data for SASW array BOM-1 and 203 m/s for the average of the surface wave dispersion data for SASW array BOM-1.
- The average V_{S30} between the three models is 202 m/s (Site Class D).
- Average S-wave velocity between 2 m (nominal sensor depth) and 32 m is 216 m/s for MASW array BOM-1, 209 m/s for the lower envelope of the surface wave dispersion data for SASW array BOM-1 and 216 m/s for the average of the surface wave dispersion data for SASW array BOM-1.
- Average S-wave velocity between 2 m (nominal sensor depth) and 32 m for the three models is 214 m/s.
- Interestingly, V_{S30} from the three distinct surface wave dispersions curves is very similar, varying by about 5%.

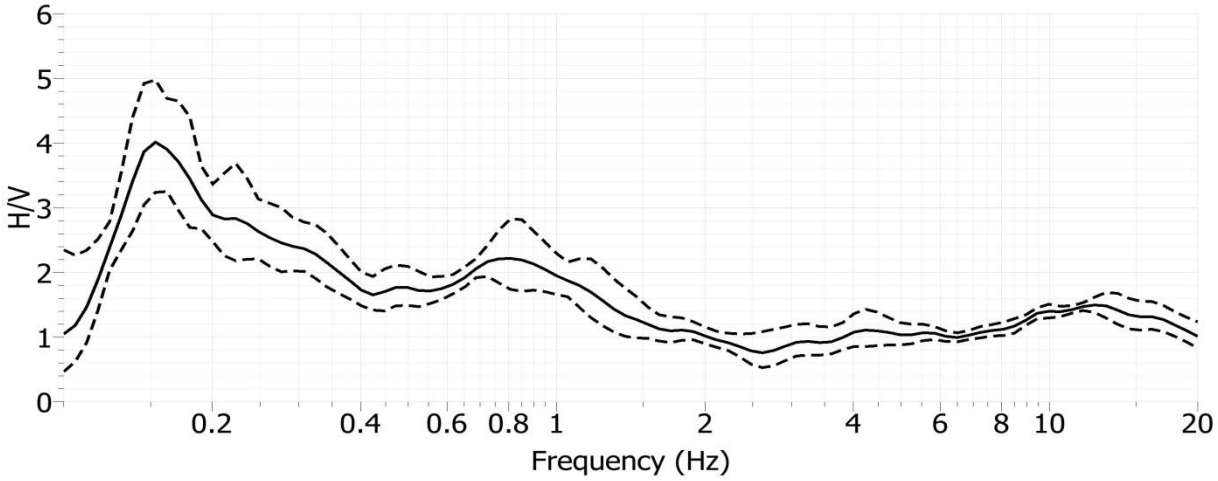

Site CI.BOM, H/V Spectral Ratio, Line BOM-1, Sensor 450B

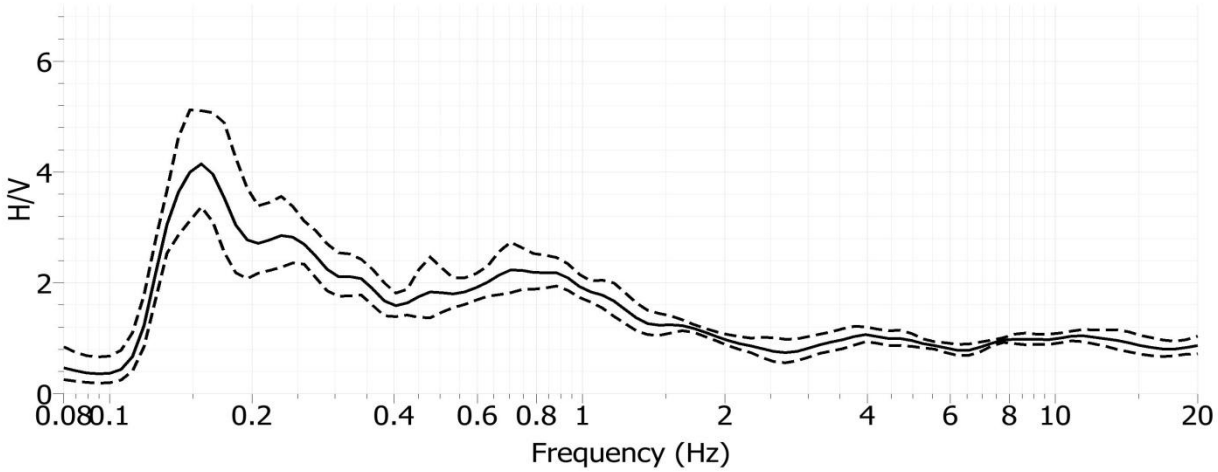

Site CI.BOM, H/V Spectral Ratio, Line BOM-1, Sensor 453

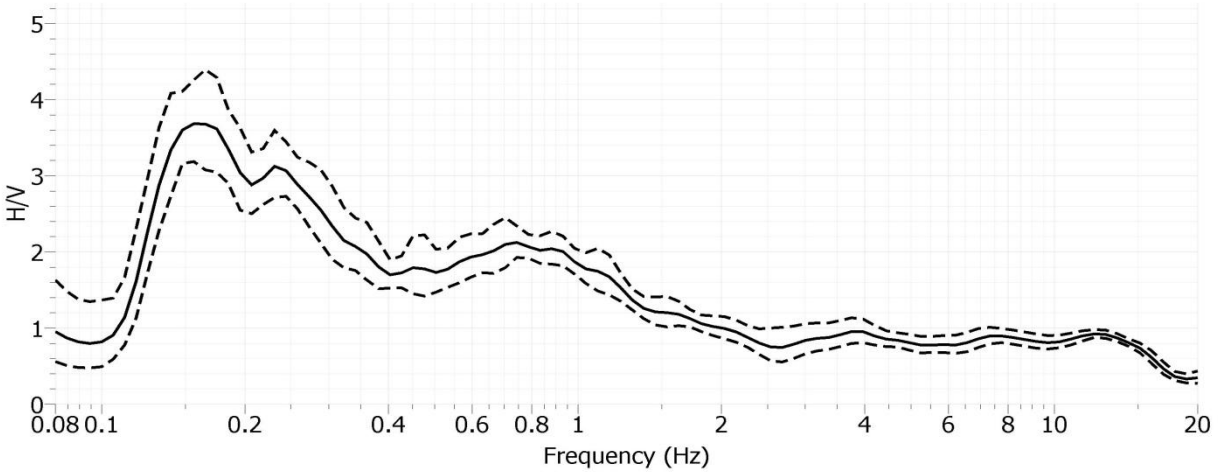

Site CI.BOM, H/V Spectral Ratio, Line BOM-1, Sensor 450

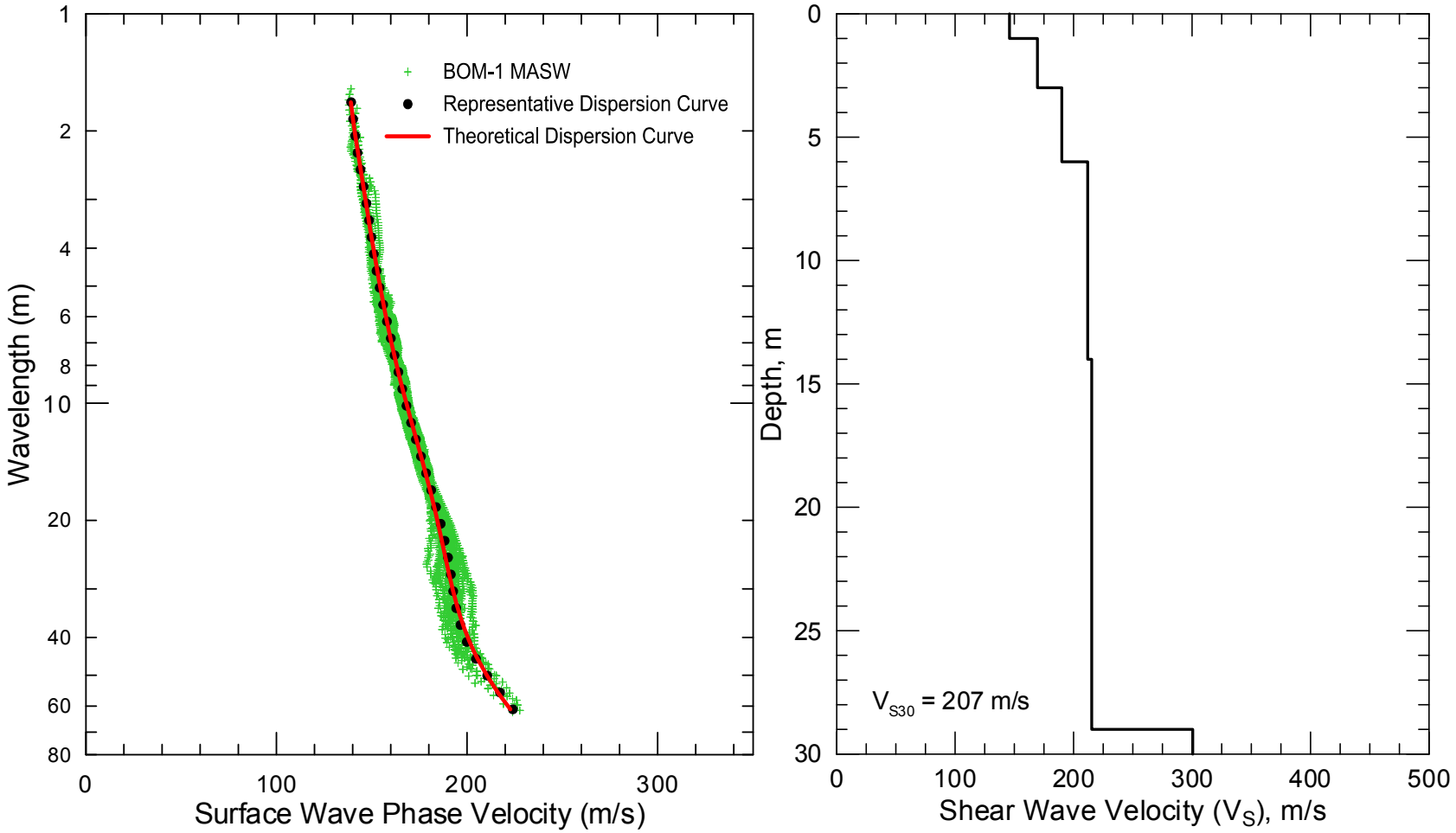

CI.BOM - Field, representative and inverted theoretical surface wave dispersion data (left) and associated V_S model (right) for MASW array BOM-1

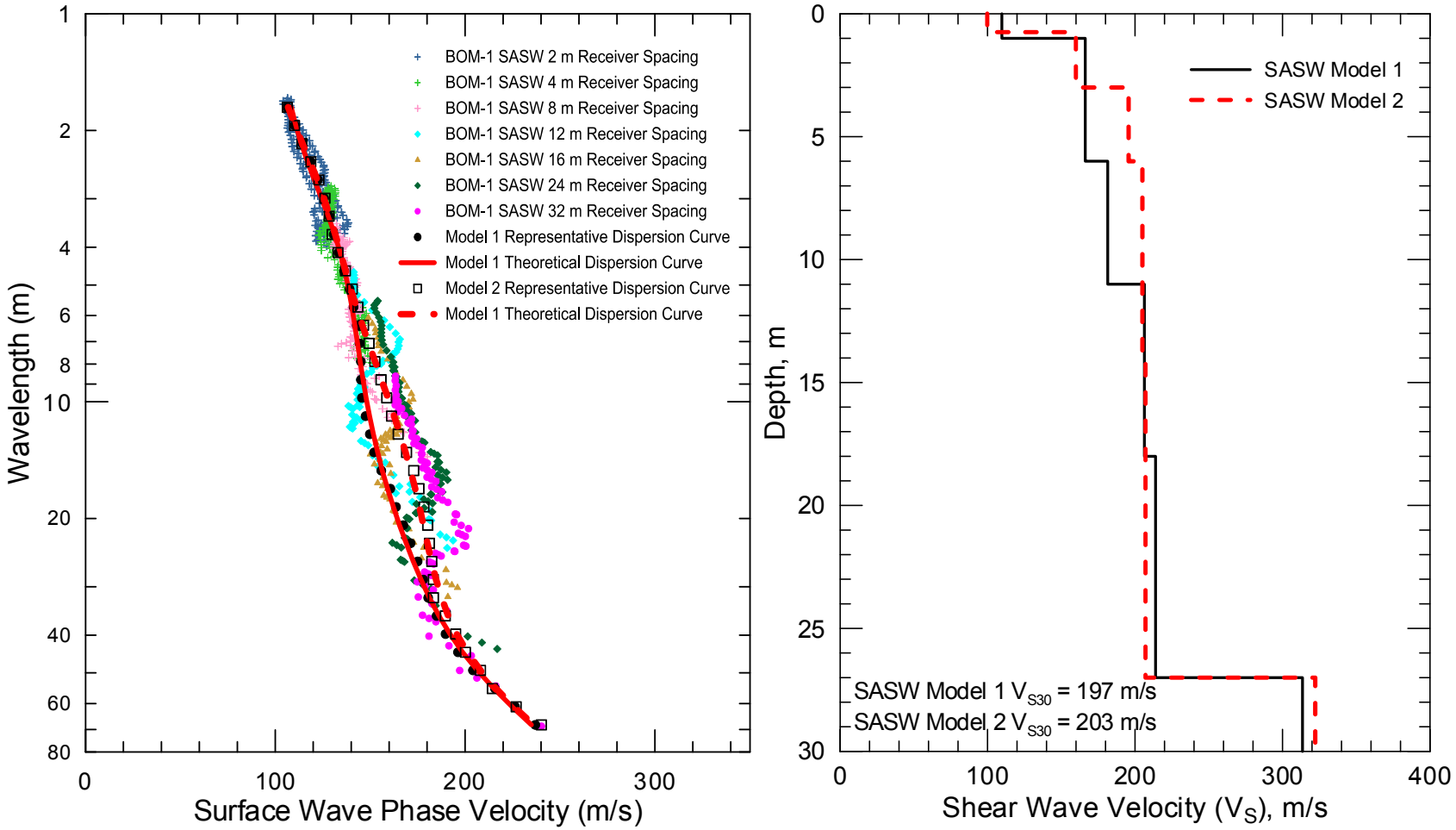

CI.BOM - Field, representative and inverted theoretical surface wave dispersion data (left) and associated V_S models (right) for SASW array BOM-1

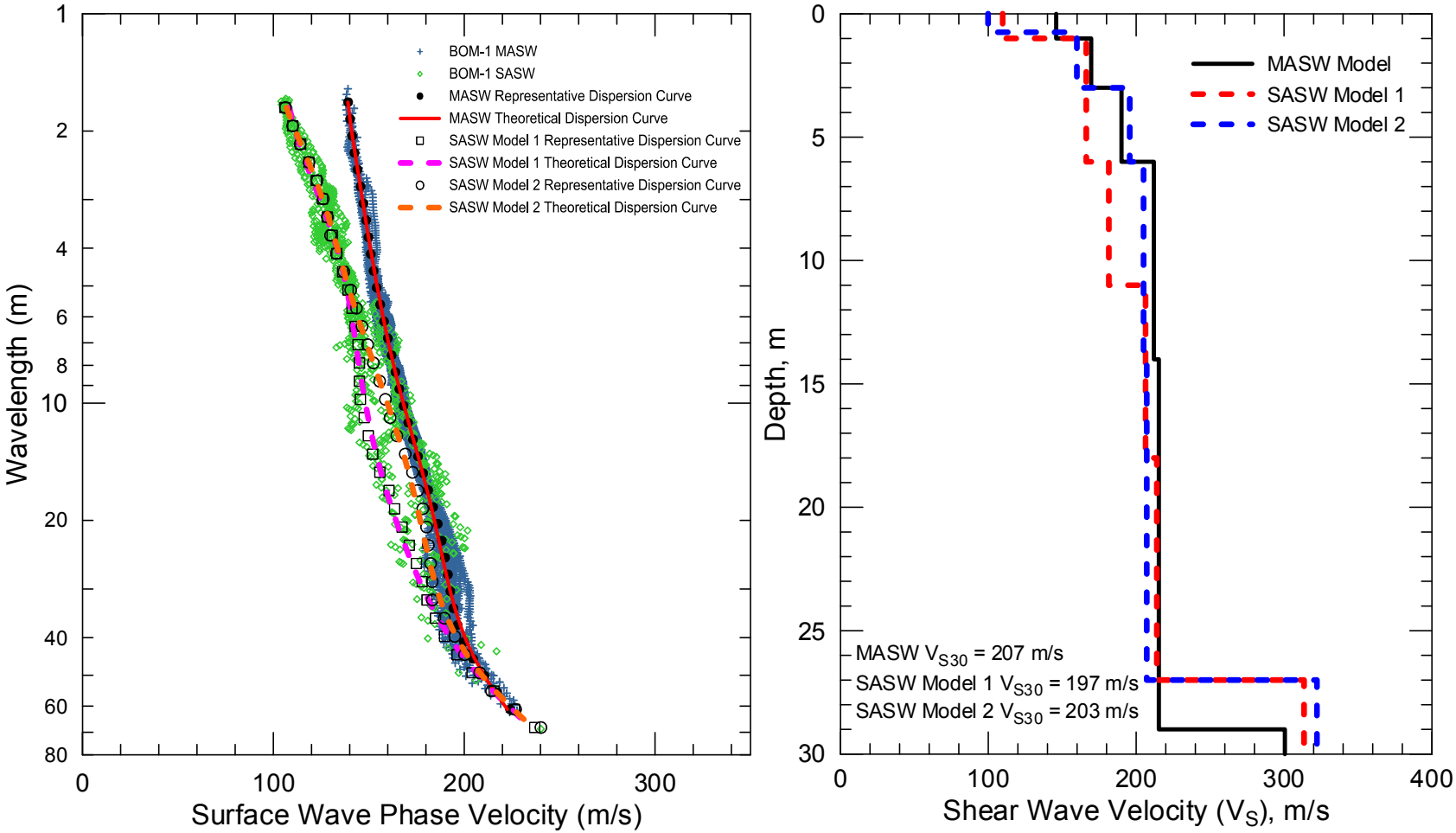

CI.BOM - Field, representative and inverted theoretical surface wave dispersion data (left) and associated V_S models (right) for MASW and SASW arrays BOM-1

Site CI.BOR

Location: Borrego Palm Canyon Campground, Borrego Springs, California

Latitude: 33.2682 **Longitude:** -116.41716
(Station coordinates provided by USGS, WGS84 coordinate system)

V_{S30} (measured): 619 m/s (from MASW array BOR-2 and not representative of seismic station conditions due to bedrock depth). Estimated V_{S30} from the average P-wave seismic refraction models and assumed constant Poisson's ratio of 0.3 is 694 m/s, likely at the lower range at the seismic station based on bedrock depth in the seismic refraction model. Adjusting the V_S model from MASW array BOR-2 for estimated bedrock depths in the 4 to 7 m range results in an adjusted V_{S30} in the 720 to 786 m/s range.

V_{S30} (adjusted to more accurately reflect seismic station conditions): 909 to 1,016 m/s (average S-wave velocity between 2 and 32 m, adjusting for 2 m nominal sensor depth, after placing bedrock V_S from MASW array BOR-2 at a depth of 7 and 4 m, respectively). The P-wave refraction models yield consistent results for an assumed Poisson's ratio of about 0.3.

NEHRP Site Class: C (based on V_{S30}), B (based on adjusted V_{S30})

Geomatrix Code: IHA/IHB

Geologic Conditions/Observations: Seismic station located on geologic unit mapped as Quaternary (Holocene) alluvial fan gravels and about 7 m from an outcrop of Mesozoic, or older, gneiss and mylonite schist.

Site Conditions: Rural site. Test area located on a sloping but relatively planar alluvial fan surface with steep mountainous topography immediately to the southwest.

Geophysical Methods Utilized: HVSR, Seismic Refraction, MASW

Geophysical Testing Arrays:

1. Array BOR-1 (48 channel P-wave seismic refraction array utilizing 4.5 Hz vertical geophones spaced 2.5 m apart for a length of 117.5 m, forward and reverse shot locations with multiple source offsets and source types (hammers only) and multiple interior shot locations).
2. Array BOR-2 (48 channel MASW array utilizing 4.5 Hz vertical geophones spaced 1 m apart for a length of 47 m, forward and reverse shot locations with multiple source offsets and source types (hammers only) and center shot location).
3. Three HVSR measurement locations: two distributed along array BOR-1 and one near the seismic station.

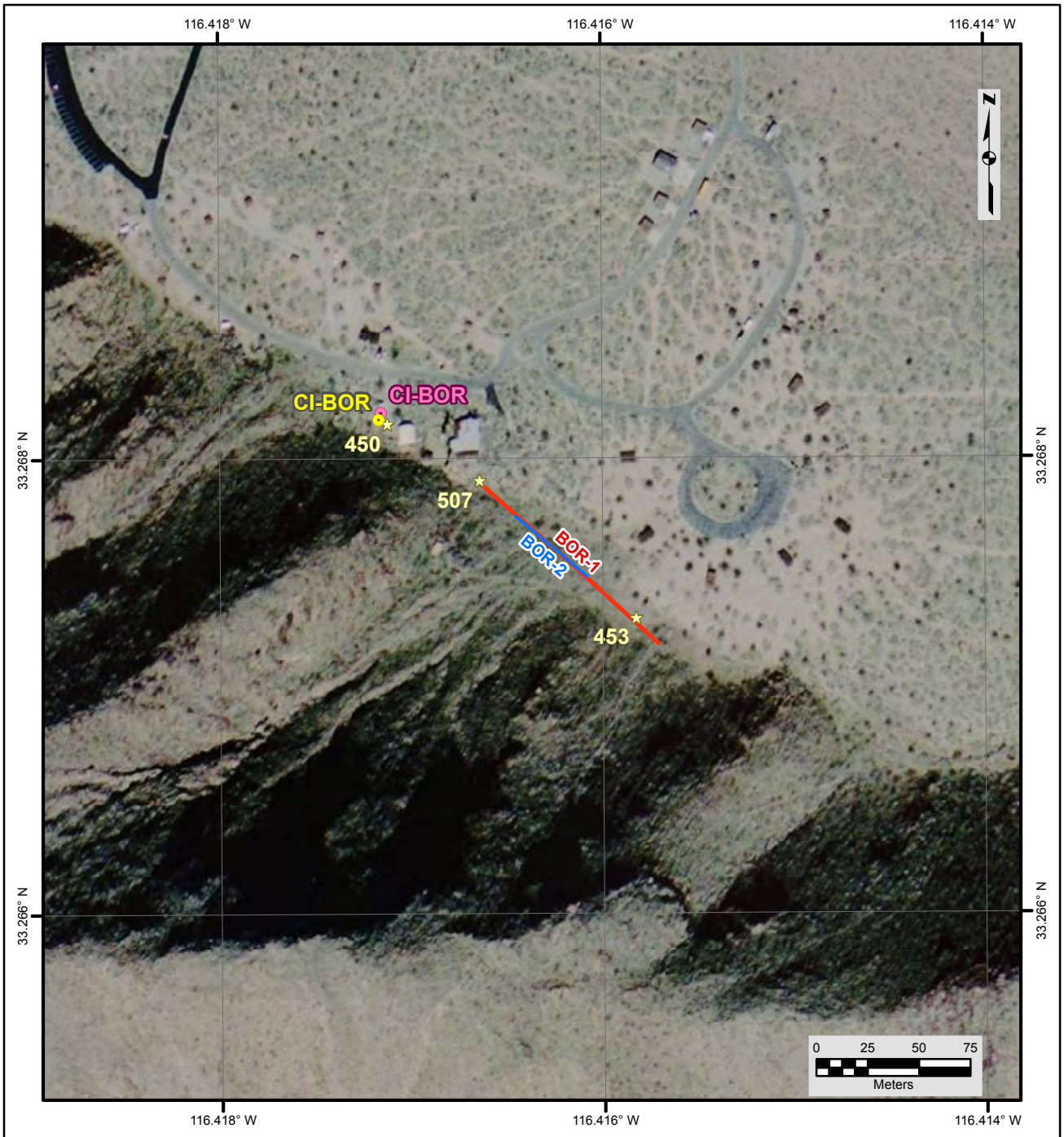

Legend

- Seismic Station - Approximate Surveyed Location
- Seismic Station - Approximate Location of Record
- H/V Spectral Ratio Location
- MASW Array
- MASW and Seismic Refraction Array

NOTES:
1. WGS 1984 COORDINATE SYSTEM
2. Image Source: ESRI, i-cubed, USDA FSA, USGS, AEX, GeoEye, Getmapping, Aerogrid, IGP

File Name: CI-BOR-I

Date: 3/29/2012

USGS science for a changing world

GEOVision geophysical services

SITE MAP
CI•BOR

RECOVERY.GOV

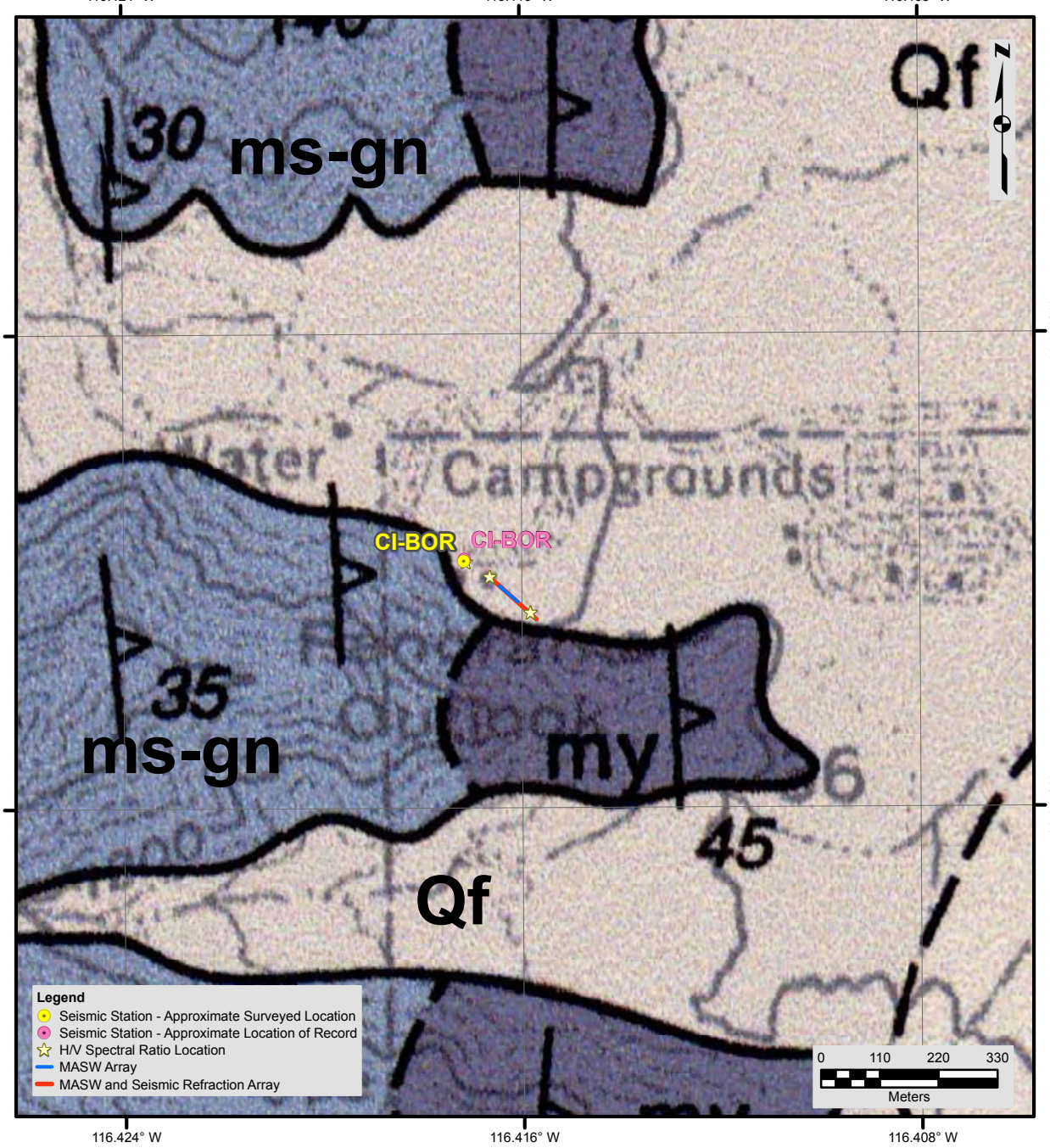

Description of Geologic Map Units

Qf = Quaternary (Holocene) alluvial fan gravel
ms-gn = Mesozoic or Older mica schist to phyllite and gneiss, foliated, locally includes hornfels, tactite
my = Mesozoic or Older mylonitic cataclastic schist and gneiss, includes some marble

NOTES:
1. WGS 1984 COORDINATE SYSTEM
2. Geologic Map of the Clark Lake & Rabbit Peak 15 Minute Quadrangles, Riverside, San Diego, and Imperial Counties, California
By Thomas W. Dibblee, Jr., 2008
3. See site map for details of geophysical survey

File Name: CI-BOR

Date: 3/29/2012

USGS science for a changing world

GEOVision geophysical services

GEOLOGIC MAP
CI•BOR

RECOVERY.GOV

Seismic station CI.BOR and HVSR sensor 450

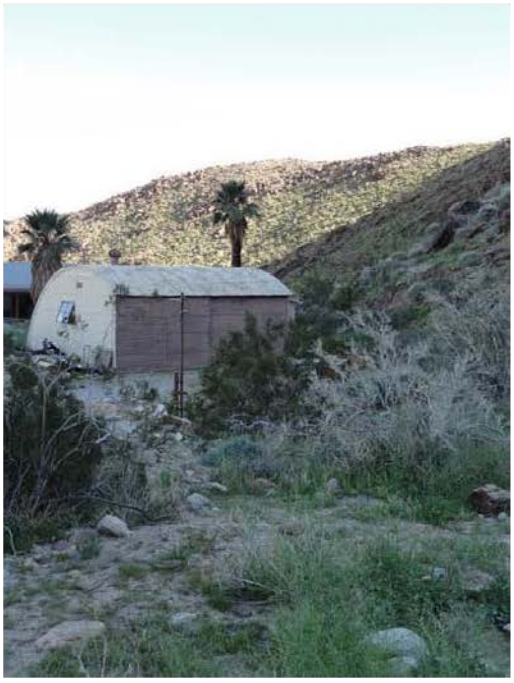

Looking southeast towards seismic station and test area located on other side of buildings

Looking northwest along array BOR-1

Looking northwest towards HVSR sensor 507 and northwest end of array BOR-1

Looking northwest towards center of array BOR-2

Location of Geophysical Testing Arrays:

Location	Latitude	Longitude
BOR-1, Southeast End of Seismic Refraction Array	33.26718	-116.41571
BOR-1, Center of Seismic Refraction Array	33.26754	-116.41617
BOR-1, Northwest End of Seismic Refraction Array	33.26790	-116.41665
BOR-2, Southeast End of MASW Array	33.26748	-116.41608
BOR-2, Center of MASW Array	33.26761	-116.41627
BOR-2, Northwest End of MASW Array	33.26774	-116.41646
HVSR Sensor 450	33.26815	-116.41712
HVSR Sensor 453	33.26730	-116.41583
HVSR Sensor 507	33.26790	-116.41664
CI.BOR Seismic Station	33.26817	-116.41717

Notes: 1) WGS84 Coordinate System (decimal degrees)
2) Survey accuracy is estimated at 1 to 2 m.

Results:

V_S Model (MASW Array BOR-2)

Depth to Top of Layer (m)	Layer Thickness (m)	S-Wave Velocity (m/s)	Inferred P-Wave Velocity (m/s)	Assumed Poisson's Ratio	Assumed Density (g/cm^3)
0	1	172	323	0.300	1.70
1	1.5	233	437	0.300	1.80
2.5	2.5	376	704	0.300	1.90
5	4	561	1049	0.300	2.00
9	6	566	1059	0.300	2.00
15	6	1088	2036	0.300	2.15
21	>9	1417	2650	0.300	2.30

Notes: 1) Depth of investigation is about 30 m.
2) Bottom layer is a half space.
3) Based on surface wave and seismic refraction model, bedrock is likely about 7 m, or more, deeper than at seismic station.

Average V_P and Estimated V_S Models between 20 and 55 m on the P-wave Seismic Refraction Model Developed using a Layer-Based Starting Model

Depth to Top of Layer (m)	Layer Thickness (m)	P-Wave Velocity (m/s)	Estimated S-Wave Velocity (m/s)			
			Poisson's Ratio = 0.25	Poisson's Ratio = 0.3	Poisson's Ratio = 0.35	Poisson's Ratio = 0.4
0.00	0.49	265	153	142	127	108
0.49	0.97	282	163	151	136	115
1.46	0.97	399	231	213	192	163
2.43	0.97	954	551	510	458	389
3.40	0.97	1075	621	575	517	439
4.38	0.97	1157	668	618	556	472
5.35	0.97	1182	683	632	568	483
6.32	2.04	1228	709	657	590	501
8.36	2.04	1459	843	780	701	596
10.40	2.04	1933	1116	1033	929	789
12.45	2.04	1973	1139	1054	948	805
14.49	2.04	2079	1200	1111	999	849
16.53	2.04	2130	1230	1138	1023	869
18.57	2.04	2301	1328	1230	1105	939
20.61	Half Space	2425	1400	1296	1165	990

Average V_P and Estimated V_S Models between 20 and 55 m on the P-wave Seismic Refraction Model Developed using a Smooth Velocity Gradient Starting Model

Depth to Top of Layer (m)	Layer Thickness (m)	P-Wave Velocity (m/s)	Estimated S-Wave Velocity (m/s)			
			Poisson's Ratio = 0.25	Poisson's Ratio = 0.3	Poisson's Ratio = 0.35	Poisson's Ratio = 0.4
0.00	0.53	242	140	130	116	99
0.53	1.06	332	192	177	159	135
1.59	1.06	568	328	304	273	232
2.65	1.06	724	418	387	348	296
3.71	1.06	921	532	492	442	376
4.78	1.06	1066	615	570	512	435
5.84	1.06	1237	714	661	594	505
6.90	2.23	1532	885	819	736	626
9.13	2.23	1616	933	864	776	660
11.35	2.23	1789	1033	956	860	731
13.58	2.23	1991	1150	1064	957	813
15.81	2.23	2095	1209	1120	1006	855
18.04	2.23	2169	1252	1159	1042	885
20.27	2.23	2310	1334	1235	1110	943
22.50	2.23	2420	1397	1294	1163	988
24.72	Half Space	2478	1431	1325	1191	1012

Observations/Discussion:

- The seismic station is located about 7 m from an outcrop of Mesozoic, or older, mica schist to gneiss. Assuming that the bedrock surface dips at 30 to 45 degrees, bedrock would be expected at 4 to 7 m depth beneath the seismic station. Seismic stations located at the toe of slope of a bedrock outcrop have proven the most difficult to characterize. Surface wave techniques are not applicable as the bedrock surface will be steeply dipping beneath an array orientated parallel to slope. Generally, these types of sites have been characterized with P- and/or S-wave seismic refraction surveys. This site was characterized with a P-wave seismic refraction survey along a profile parallel to the bedrock outcrop and an MASW sounding in an area with expected deeper bedrock. The preferred location for an S-wave refraction array was not available due to the presence of campers.
- There was not enough space immediately adjacent to the seismic station for geophysical testing. The best location for acquisition of seismic refraction data would be along the toe of slope of the bedrock outcrop northwest of the seismic station. However, campers occupied this area at the time of the field investigation and, therefore, geophysical testing was conducted southeast of the seismic station in an area where a larger variation of bedrock depth was expected. P-wave seismic refraction data were acquired along the 117.5 m long array BOR-1. The bedrock outcrop is located 5 and 8 m from the southeast and northwest ends of the array, respectively. However, the northwestern half of the array crosses a small alluvial fan where the bedrock outcrop is as much as 40 m from the array. P-wave seismic refraction data were acquired to determine the P-wave velocity structure of the bedrock unit, by which S-wave velocity could be inferred. The southeastern 55 m of array BOR-1 is located at a similar distance from the bedrock outcrop as the seismic station and is, therefore, considered representative of seismic station conditions. The southeast end of the seismic line is, however, located near a different mapped bedrock unit consisting of mylonitic cataclastic schist and gneiss. MASW data were acquired along the 47 m long array BOR-2, located along the segment of array BOR-1 where bedrock was expected to be deepest. MASW data were acquired to primarily determine the S-wave velocity of the sediments overlying bedrock.
- There are no distinct, high amplitude HVSR peaks at the site. HVSR data may have little use at this site, given the 3-D nature of the bedrock surface near the mountain range.
- The P-wave seismic refraction data for array BOR-1 were modeled using a tomographic inversion routine with both a layer based and smooth velocity gradient starting model. The P-wave seismic refraction model was extended to far offset shot locations to extend depth of investigation.
- The P-wave seismic refraction survey design allowed P-wave velocity to be imaged to a maximum depth of about 25 m. The seismic refraction models developed using a layer based and smooth velocity gradient starting model are generally similar and indicate that P-wave velocity is about 250 to 400 m/s at the surface and increases to over 750 m/s at a depth of 2 to 3 m, 1,500 m/s at a depth of 7 to 16 m and over 2,500 m/s at a depth of 15 to greater than 25 m. The P-wave velocity of bedrock may exceed 3,000 m/s at depth beneath the northwestern portion of the seismic line. P-wave velocities greater than 1,250 m/s are likely associated with weathered bedrock.

- The seismic refraction survey indicates that there is lateral velocity variation at the site, primarily the expected deepening of bedrock between a position of 60 an 100 m.
- The average P-wave velocity of the upper 30 m (V_{P30}) was estimated between 20 and 55 m on the P-wave refraction models, where depth of investigation is greatest and the bedrock depth is expected to be similar to that at the seismic station. To estimate V_{P30}, the P-wave velocity at a depth of 25 m, nominal depth of investigation, was projected to 30 m depth. On the seismic refraction model developed using a layer based starting model, V_{P30} ranges from about 1,227 to 1,335 m/s over the 20 to 55 m position interval, an 8% variation. On the seismic refraction model developed using a smooth velocity gradient starting model, V_{P30} ranges from about 1,227 to 1,348 m/s over the 20 to 55 m position interval, a 9% variation. The V_{P30} estimates are very similar for both models, demonstrating that equivalence in seismic refraction models has minimal effect on depth averaged slowness.
- An average V_P model was developed over the 20 to 55 m distance interval by horizontally averaging the travel time of each model cell and cell thickness and average V_{P30} were determined to be 1,296 and 1,303 m/s for the seismic refraction models developed using layer based and smooth velocity gradient starting models, respectively. Assuming constant Poisson's ratios of 0.25, 0.3, 0.35 and 0.4 would result in an estimated V_{S30} of 748, 693, 622 and 529 m/s, respectively for the average V_P model developed using a layer based starting model. Assuming constant Poisson's ratios of 0.25, 0.3, 0.35 and 0.4 would result in an estimated V_{S30} of 752, 696, 626 and 532 m/s, respectively for the average V_P model developed using a smooth velocity gradient starting model. Saturation is not expected in the upper 30 m and, therefore, Poisson's ratio of the weathered rock may be close to 0.3. The average estimated V_{S30} between the two models for an assumed Poisson's ratio of 0.3 is 694 m/s. Assuming an average Poisson's ratio of 0.3, the average S-wave velocity between 2 and 32 m (adjusted V_{S30}), to account for the assumed 2 m seismometer depth, is 925 and 904 m/s for the average V_P models developed using layer based and smooth velocity gradient starting models, respectively, and average 915 m/s. A very conservative Poisson's ratio of 0.35 yields adjusted V_{S30} of 831 and 813 m/s for the two models. The P-wave seismic refraction models indicate that V_{S30} is likely in the upper range of NEHRP Site Class C, but adjusted V_{S30} is clearly NEHRP Site Class B. Based on P-wave velocity, bedrock is likely in the 6 to 8 m depth range on the seismic refraction models and, therefore, the V_{S30} and adjusted V_{S30} estimates made above are likely at the low range expected for the seismic station.
- An MASW sounding was conducted along the segment of array BOR-1 where bedrock was expected to be deepest to accurately characterize S-wave velocity of the sediments in the site vicinity. Noise conditions at the site were not sufficient for application of passive surface wave techniques.
- The near field criteria typically applied during this investigation was relaxed in order to obtain a dispersion curve to 60 m wavelength.
- The minimum wavelength surface wave phase velocity data extracted from the 48-channel MASW array is about 10.5 m. Data reduction using seismic records from smaller hammer sources and a limited offset receiver array (i.e. less active geophones) allowed extraction of surface wave dispersion data to a minimum wavelength of about 2 m.

- There is nominally about 70 m/s scatter in MASW dispersion data selected for modeling, likely due to the effects of lateral velocity variation.
- A representative dispersion curve was generated for the MASW data set using a moving average, polynomial curve fitting routine and used for modeling.
- Surface wave depth of investigation is 30 m based on the one half of maximum wavelength criteria.
- There is generally good agreement between the sediment velocities in the surface wave V_S model and the P-wave refraction models, especially considering unknown Poisson's ratio. The bedrock velocities are not well constrained in the surface wave V_S model, but are consistent enough with the P-wave velocities in the seismic refraction model to be used for estimating V_{S30}.
- V_{S30} from the MASW V_S model is 619 m/s (NEHRP Site Class C).
- Adjusting V_{S30} for the expected bedrock depth of 4 to 7 m at the seismic station, by replacing the V_S of the sediments between 4 or 7 m and 15 m with that of the underlying bedrock unit, results in an estimated V_{S30} at the seismic station of 720 to 786 m/s (NEHRP Site Class C/B).
- Further adjusting V_{S30} for seismic station conditions by estimating the average V_S between 2 and 32 m, to account for assumed sensor depth, with bedrock in the 4 to 7 m depth range, results in adjusted V_{S30} of 909 to 1,016 m/s (NEHRP Site Class B).
- The average P-wave seismic refraction models between 20 and 55 m on array BOR-1, where bedrock depth is interpreted in the 6 to 9 m depth range, provides results consistent with the surface wave sounding. The average estimated V_{S30} using a Poisson's ratio of 0.3 is 694 m/s, which is consistent with the lower estimate of adjusted V_{S30} from the MASW V_S model. The average estimated V_S between 2 and 32 m from the seismic refraction models is 915 m/s, also consistent with the lower range estimated from the surface wave V_S model. The seismic refraction models are expected to yield estimated V_{S30} and adjusted V_{S30} values at the low range of estimates from the MASW V_S model because bedrock beneath the 20 to 55 m segment of the P-wave refraction models are at the lower range of expected bedrock depth at the seismic station.
- Although there were challenges in characterizing this site, V_{S30} at the seismic station is expected to be NEHRP Site Class C/B and adjusted V_{S30} to account for the estimated 2 m seismic sensor depth is clearly NEHRP Site Class B.
- The above estimates can be improved by acquiring a short refraction array at the seismic station to determine actual bedrock depth. Additionally, an S-wave refraction survey conducted along the toe of slope northwest of the slope should confirm results presented above.

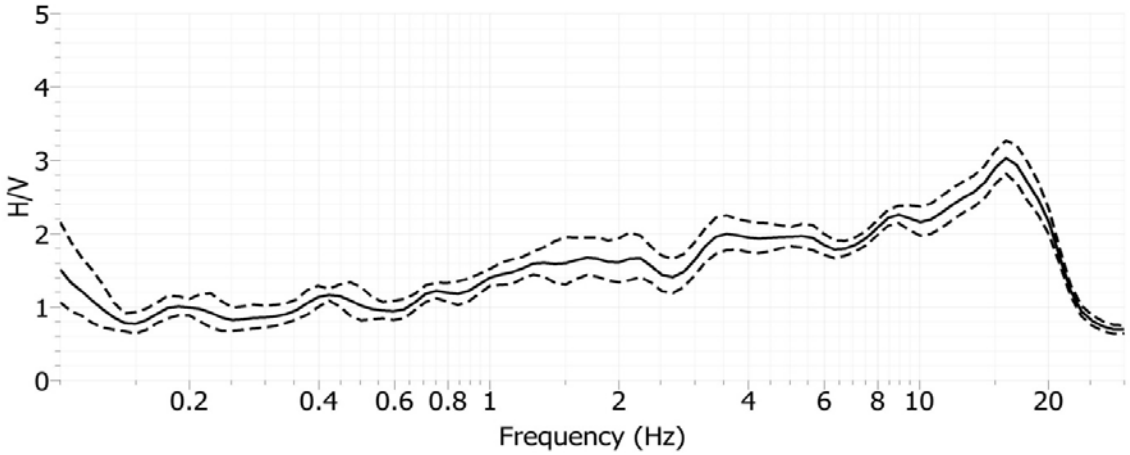

Site CI.BOR, H/V Spectral Ratio, Near Seismic Station, Sensor 450

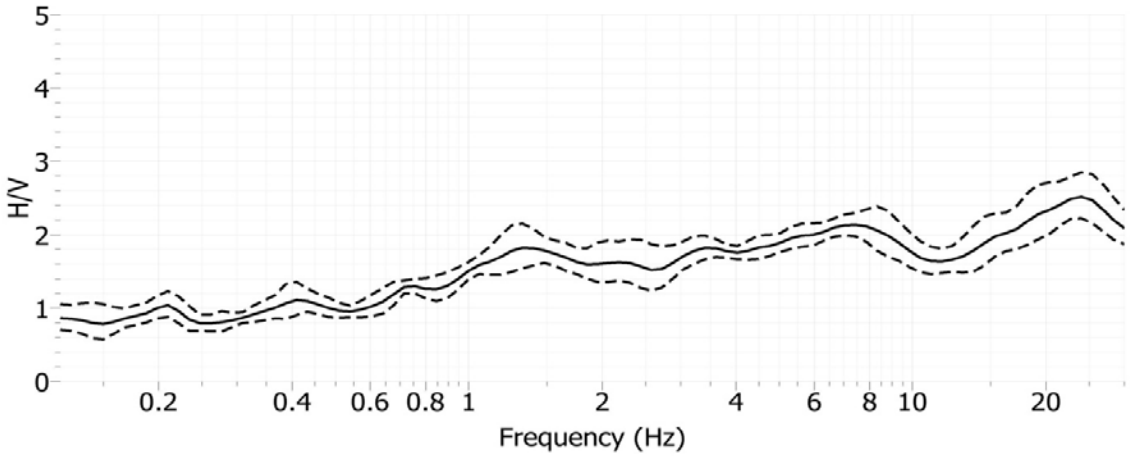

Site CI.BOR, H/V Spectral Ratio, Array BOR-1, Sensor 507

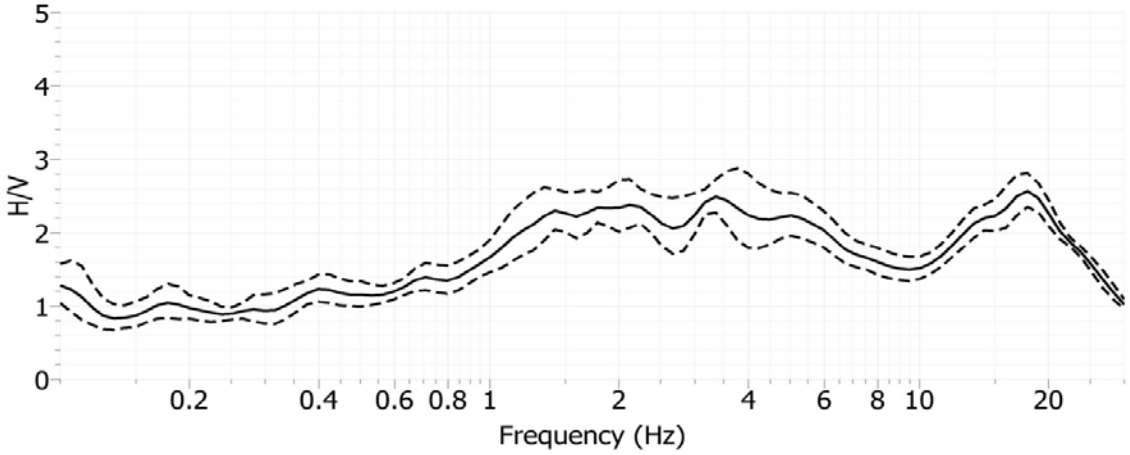

Site CI.BOR, H/V Spectral Ratio, Array BOR-1, Sensor 453

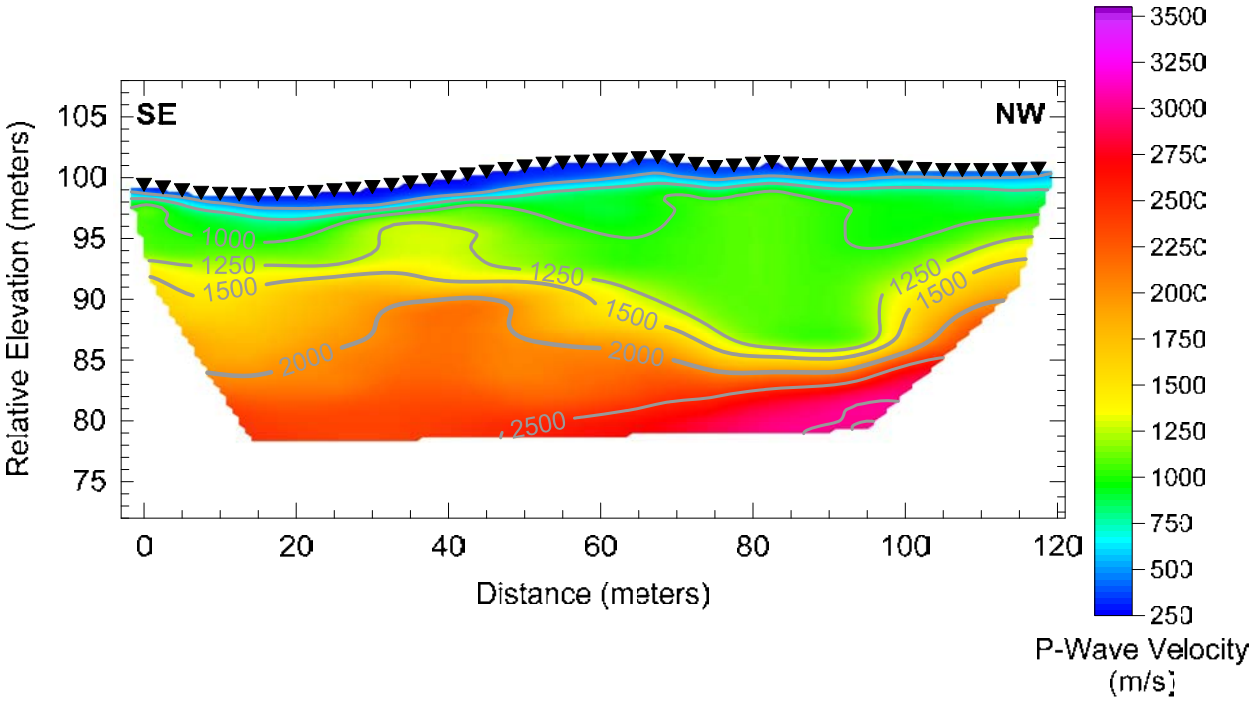

Array BOR-1 – P-wave Tomographic Seismic Refraction Model utilizing Layer Based Starting Model

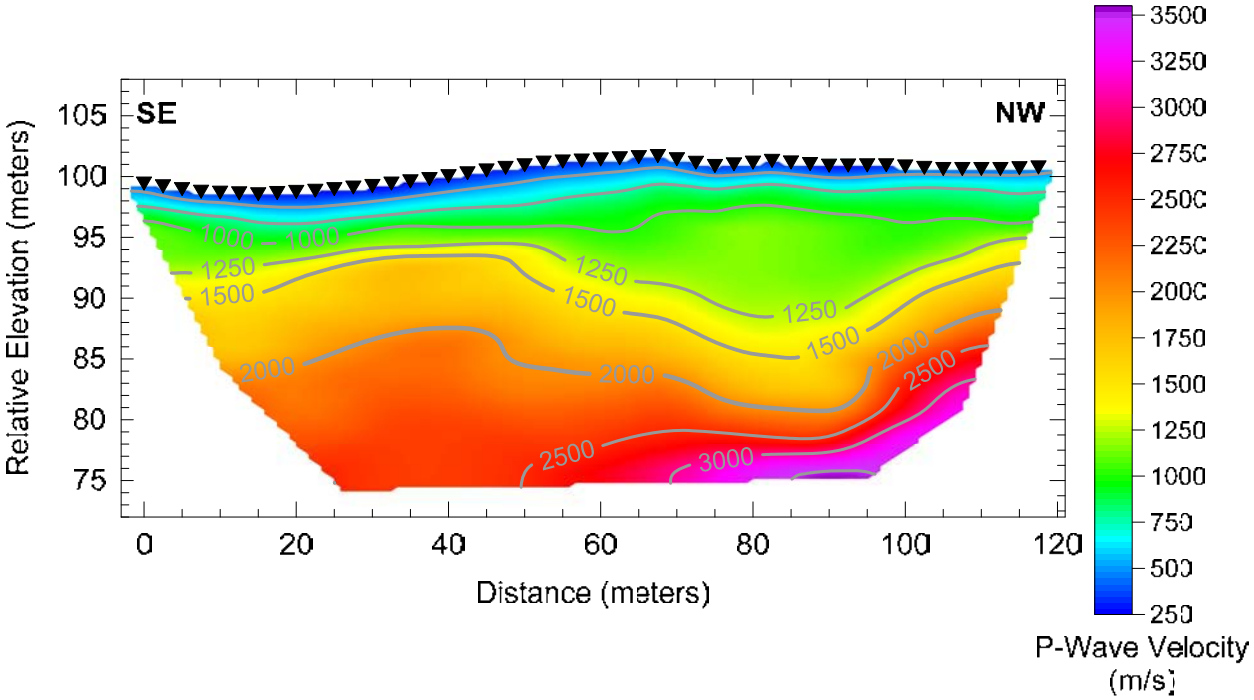

Array BOR-1 – P-wave Tomographic Seismic Refraction Model utilizing Smooth Velocity Gradient Starting Model

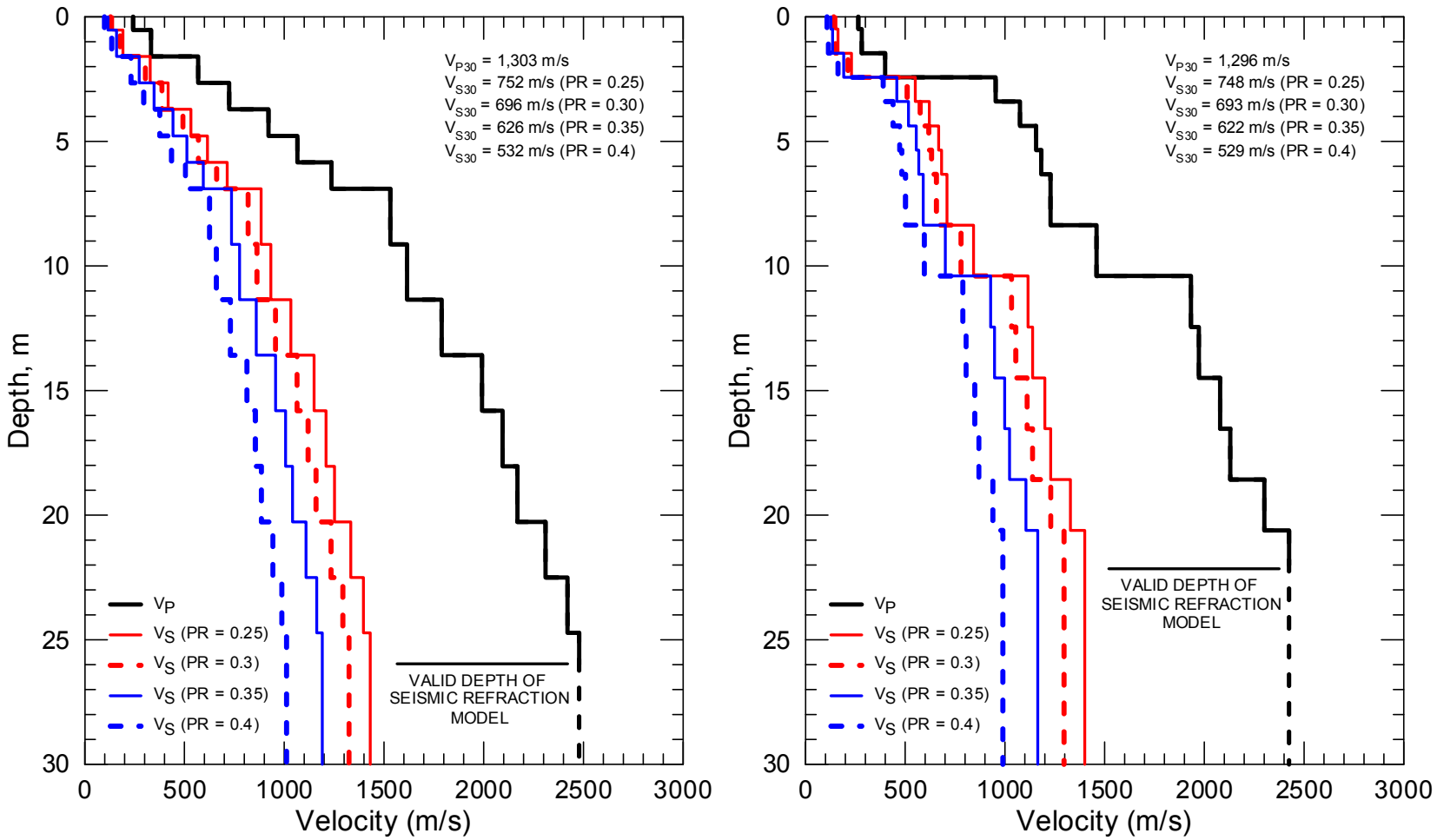

CI.BOR – Average P-wave velocity structure and estimated S-wave velocity structure between a position of 20 and 55 m on the P-wave seismic refraction model for array BOR-1 developed using both smooth velocity gradient (left) and layer-based (right) starting models. Although there are slight differences between the two average velocity models, V_{P30} is almost identical.

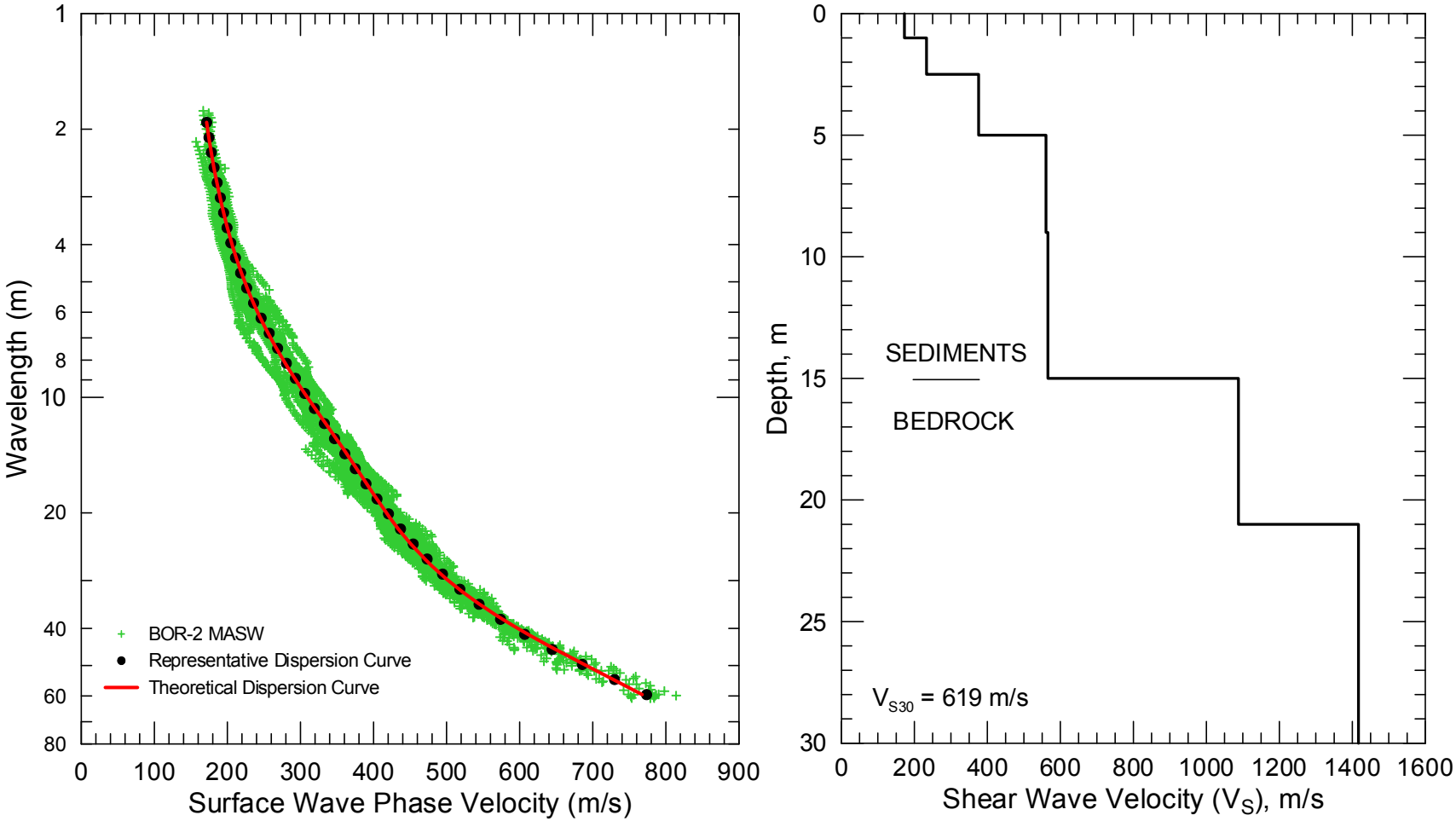

CI.BOR - Field, representative and inverted theoretical surface wave dispersion data (left) and associated V_S model (right)

Site CI.BTP

Location: Burnt Peak, Angeles National Forest, Los Angeles County, California

Latitude: 34.68218 **Longitude:** -118.57406
(Station coordinates modified based on field GPS survey, WGS84 coordinate system)

V_{S30} (measured): 461 m/s

V_{S30} (adjusted to more accurately reflect seismic station conditions): 526 m/s (average S-wave velocity between 2 and 32 m adjusting for inferred 2 m sensor depth).

NEHRP Site Class: C

Geomatrix Code: INB

Geologic Conditions/Observations: Seismic station located on a Precambrian to Mesozoic gneissic rock complex.

Site Conditions: Rural site. Seismic station located on top of a steep mountain peak with high winds and a large communications antenna. Steep topography in site vicinity. Test areas located on hillsides with significant topographic variation.

Geophysical Methods Utilized: HVSR, Seismic Refraction, MASW

Geophysical Testing Arrays:

1. Array BTP-1 - 48 channel MASW and P-wave seismic refraction array utilizing 4.5 Hz vertical geophones spaced 1.5 m apart for a length of 70.5 m, forward and reverse shot locations with limited source offsets and source types (20 lb hammer and accelerated weight drop only) and interior shot locations.
2. Array BTP-2 - 48 channel MASW and P-wave seismic refraction array utilizing 4.5 Hz vertical geophones spaced 1.5 m apart for a length of 70.5 m, forward and reverse shot locations with multiple source offsets and source types and multiple interior shot locations.
3. Three HVSR measurement locations distributed along array BTP-2.

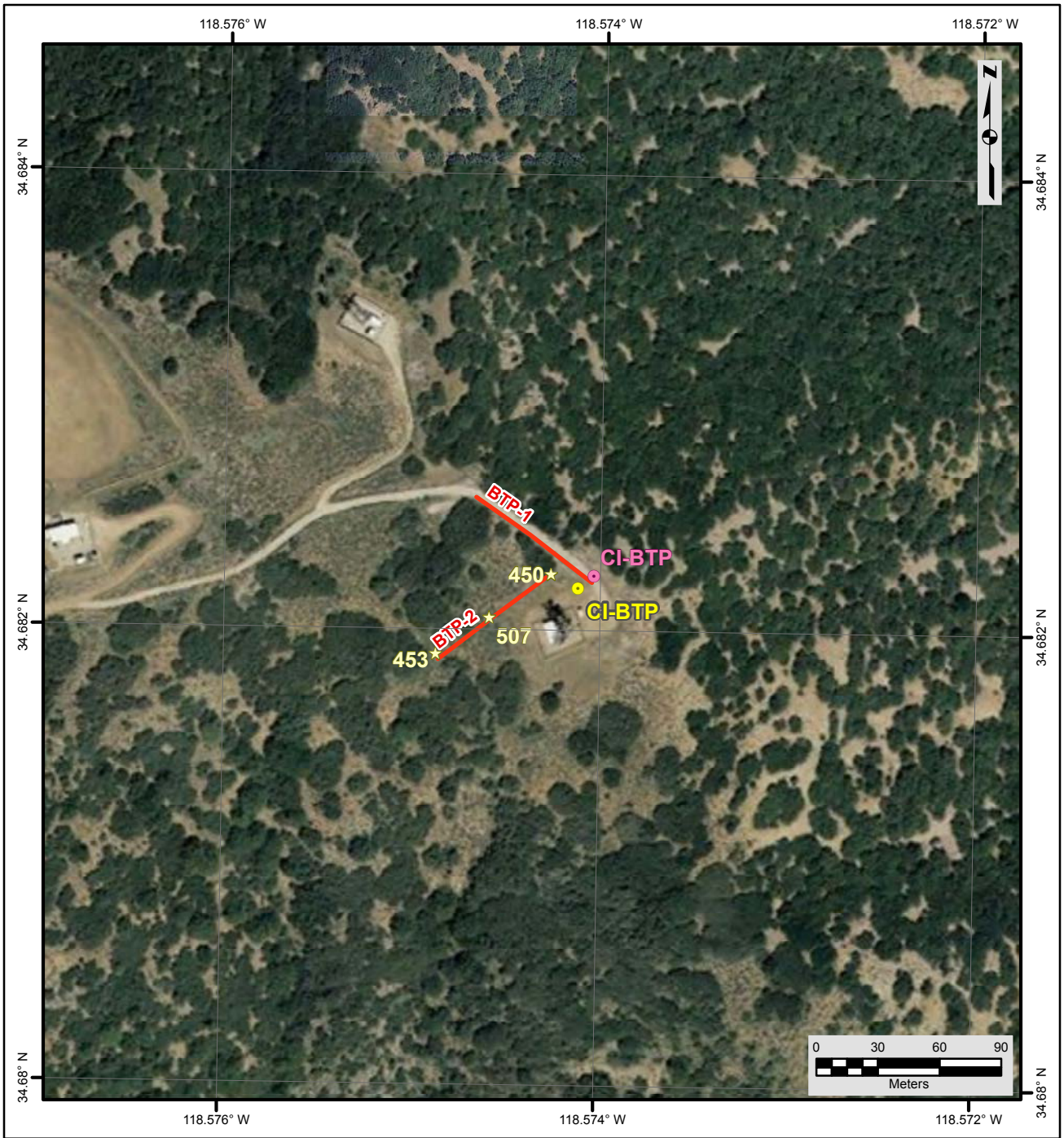

Legend

- Seismic Station - Approximate Surveyed Location
- Seismic Station - Approximate Location of Record
- H/V Spectral Ratio Location
- MASW and Seismic Refraction Array

NOTES:
1. WGS 1984 COORDINATE SYSTEM
2. Image Source: ESRI, i-cubed, USDA FSA, USGS, AEX, GeoEye, Getmapping, Aerogrid, IGP

File Name: CI-BTP-I

Date: 10/13/2011

USGS science for a changing world

GEOVision geophysical services

RECOVERY.GOV

SITE MAP
CI•BTP

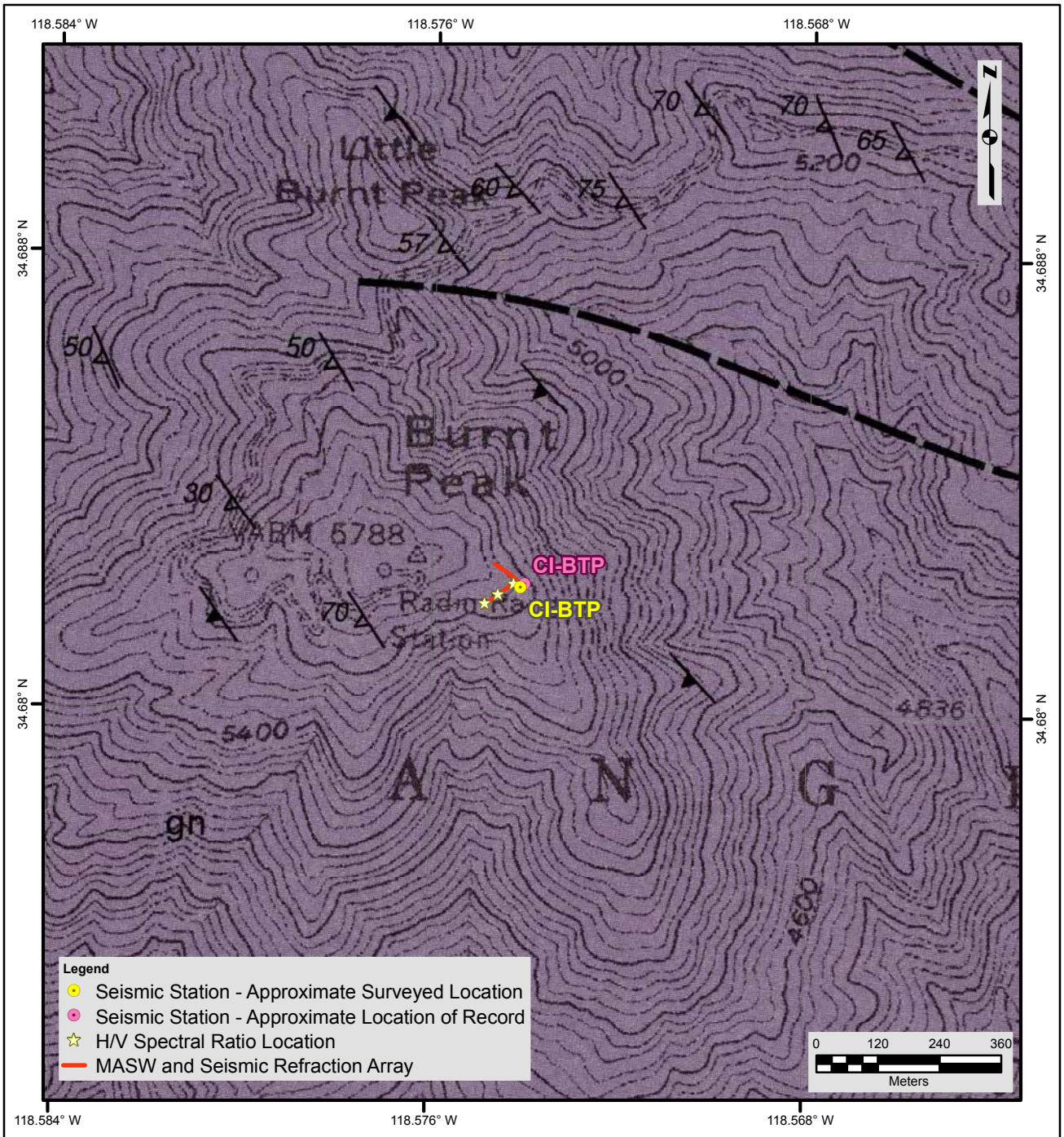

Description of Geologic Map Units

gn = Precambrian (?) gneiss; hard, closely fractured and brittle

NOTES:
1. WGS 1984 COORDINATE SYSTEM
2. Geologic Map of the Burnt Peak Quadrangle, Los Angeles County, California by Thomas W. Dibblee, Jr., 2002
3. See site map for details of geophysical survey

File Name: CI-BTP

Date: 10/13/2011

USGS science for a changing world

GEOVision geophysical services

GEOLOGIC MAP
CI•BTP

RECOVERY.GOV

CI.BTP Seismic Station

Looking northeast and seismic station and southeast end of array BTP-1

Looking southwest along array BTP-2

Looking southeast along array BTP-1

HVSR sensors placed in deep holes and couple to ground using plaster in the very loose surficial sediments

Location of Geophysical Testing Arrays:

Location	Latitude	Longitude
BTP-1, Northwest End of MASW/Refraction Array	34.68258	-118.57461
BTP-1, Center of MASW/Refraction Array	34.68242	-118.57432
BTP-1, Southeast End of MASW/Refraction Array	34.68221	-118.57399
BTP-2, Southwest End of MASW/Refraction Array	34.68187	-118.57480
BTP-2, Center of MASW/Refraction Array	34.68206	-118.57451
BTP-2, Northeast End of MASW/Refraction Array	34.68225	-118.57421
HVSR Sensor 450	34.68225	-118.57421
HVSR Sensor 453	34.68189	-118.57482
HVSR Sensor 507	34.68205	-118.57453
CI.BTP Seismic Station	34.68218	-118.57406

Notes: 1) WGS84 Coordinate System (decimal degrees)
2) Survey accuracy is estimated at 1 to 2 m.

Results:

V_S Model

Depth to Top of Layer (m)	Layer Thickness (m)	S-Wave Velocity (m/s)	Inferred P-Wave Velocity (m/s)	Assumed Poisson's Ratio	Assumed Density (g/cm^3)
0	1	175	328	0.300	1.70
1	2	214	401	0.300	1.75
3	3	340	636	0.300	1.80
6	4	433	810	0.300	1.90
10	6	492	921	0.300	2.00
16	7	612	1144	0.300	2.10
23	>7	847	1584	0.300	2.15

Notes: 1) Depth of investigation is about 30 m.
2) Bottom layer is a half space.
3) Half space velocity not well constrained.

Observations/Discussion:

- Seismic refraction and MASW data were acquired along two arrays at this site. Data acquisition was started on array BTP-1, which is located on a slope with a 14 m elevation decline to the southeast. Lateral velocity variation was observed on seismic records while acquiring data along this array and, therefore, only minimal data acquisition was conducted along this array (3 interior shot locations, 3 offend shots at one end of the array and 4 offend shots at the other end of the array, acquired using a 20 lb sledge hammer or accelerated weight drop) before moving to array BTP-2. This field decision was unfortunate because array BTP-1 provided the better data set for site characterization and data acquisition did not include the high density of interior shot locations preferred for tomographic inversion of seismic refraction data or the small hammer shot locations desired for MASW analysis. Because significant lateral velocity variation has been observed at so many weathered rock sites, we believe that it is important to acquire a complete seismic refraction data set as close as possible to the seismic station before moving to a more suitable test location. At a minimum, this will allow correlation of the models generated at the more suitable test location to the seismic station.
- The HVSR curves are generally similar although there are no distinct high amplitude HVSR peaks. There is, however, a broad, low amplitude HVSR peak over the 1.5 to 5 Hz range with maximum response at about 2.5 Hz. A 2.5 Hz HVSR peak is expected to be associated with a geologic structure at greater depth than imaged by the surface wave sounding.
- The P-wave refraction data collected along array BTP-1 were modeled using a tomographic inversion routine with a smooth gradient starting model. The seismic model was extended to far offset source locations to extend depth of investigation. The interior shot density (3 interior shots) is not ideal for tomographic inversion and likely results in a significantly smoothed velocity model.
- The seismic refraction survey design allowed P-wave velocity to be imaged to a maximum depth of about 10 to15 m. The seismic refraction model shows that P-wave velocity is about 300 to 400 m/s at the surface increasing to 1,000 m/s at a depth of 2 to 11 m. The maximum P-wave velocity in the model is 1,200 m/s.
- The seismic refraction model indicates that there is significant lateral velocity variation beneath array BTP-1 with a much thicker sequence of lower velocity residual soil and decomposed rock beneath the southeast end of the array near the seismic station.
- The P-wave seismic refraction and MASW data collected along array BTP-2 were not suitable for modeling. Seismic refraction first arrival data were very weak and noisy, in part due to a very low velocity residual soil layer. Surface wave data were strongly impacted by significant lateral velocity variation and/or topographic variation and a coherent dispersion curve could not be generated for modeling. Review of the seismic refraction data indicates that average subsurface velocities are lower than those for array BTP-1, likely similar to the lower velocities at the southeast end of array BTP-1.
- Noise conditions at the site were not sufficient for application of passive surface wave techniques.
- MASW data reduction was complicated by lateral velocity variation and the limited number of shot locations (10) and energy sources (20 lb hammer and accelerated weight drop only). The lateral velocity variation caused Rayleigh wave phase velocity data from

source locations at each end of the array to diverge slightly at long wavelengths. There was also significant scatter in small wavelength dispersion data and only source locations at the southeast end of the array, near the seismic station, were used to extract Rayleigh wave phase velocity data at small wavelengths. The final dispersion curve combined long wavelength surface wave dispersion data files from shot locations at both ends of the array and small wavelength surface wave dispersion data from shot locations at the southeast end of the array, near the seismic station.

- The minimum wavelength surface wave phase velocity data extracted from the 48-channel MASW array was about 24 m. Data reduction using seismic records from source locations at the southeast end of the array and a limited offset receiver array (i.e. less active geophones) allowed extraction of surface wave dispersion data to a minimum wavelength of about 2.5 m.
- There is about 60 m/s scatter in the final MASW dispersion data, likely due to lateral velocity variation observed in the seismic refraction model. Note that long wavelength dispersion data are representative of the entire array, whereas, small wavelength dispersion data represents velocity structure at the southeast end of the array, near the seismic station.
- A representative dispersion curve was generated for the MASW data set using a moving average, polynomial curve fitting routine and used for modeling.
- Surface wave depth of investigation is about 30 m based on half of maximum wavelength criteria.
- In the upper 15 m, the seismic refraction depth of investigation, the inferred P-wave velocities in the surface wave model, assuming a Poisson's ratio of 0.3, are generally consistent with the average velocity structure at the southeast end of the seismic refraction model.
- V_{S30} is 461 m/s (NEHRP Site Class C).
- Average S-wave velocity between 2 m (assumed sensor depth) and 32 m is 526 m/s (NEHRP Site Class C).
- The V_{S30} estimate made above is considered representative of the seismic station; however, V_{S30} is likely as much as 20% higher towards the northwest end of array BPT-1. Although there is significant lateral velocity variation in the site vicinity, it does not appear sufficient to change the NEHRP Site Class.
- More suitable test locations (i.e. minimal topographic variation) may be found for surface wave testing at distances of 300 m, or more, from the seismic station. However, it is very likely that the weathering profile in the rock would be much different than at the seismic station. Lateral velocity variation at rock sites almost forces geophysical testing to be conducted as close as possible to the seismic station, even if field conditions are not ideal.

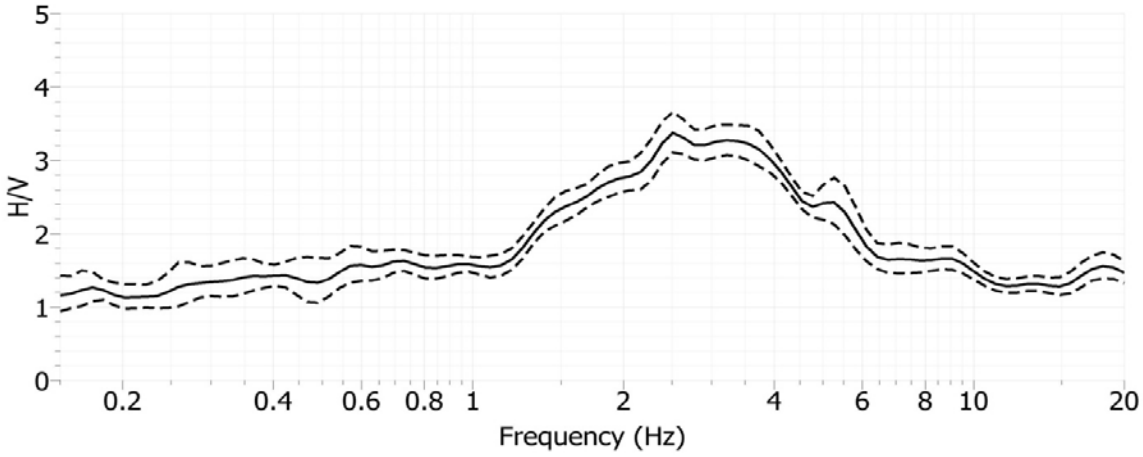

Site CI.BTP, H/V Spectral Ratio, Array BTP-2, Sensor 450

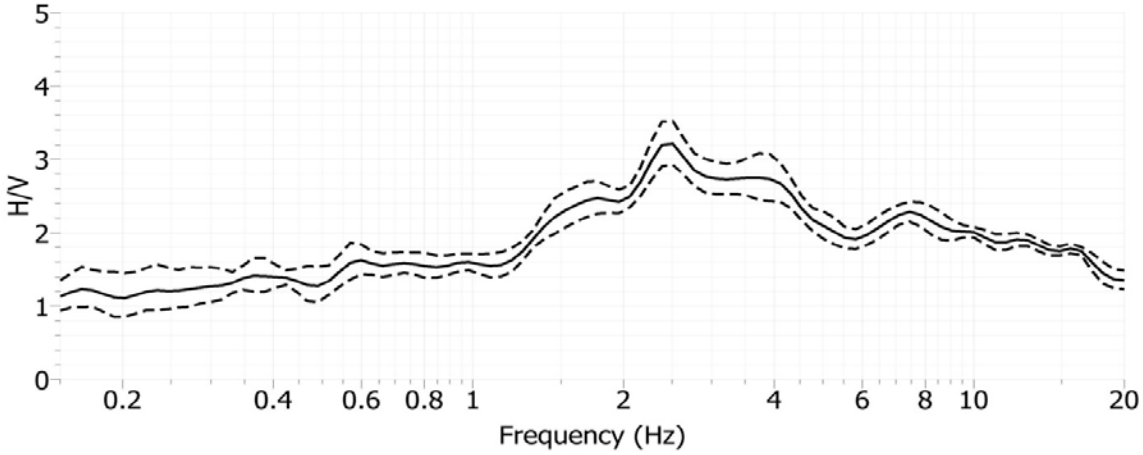

Site CI.BTP, H/V Spectral Ratio, Array BTP-2, Sensor 507

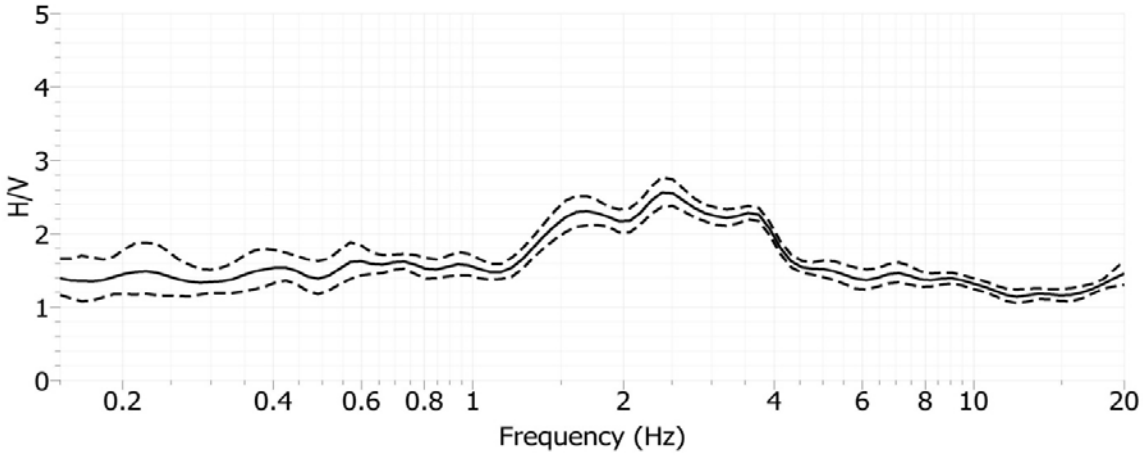

Site CI.BTP, H/V Spectral Ratio, Array BTP-2, Sensor 453

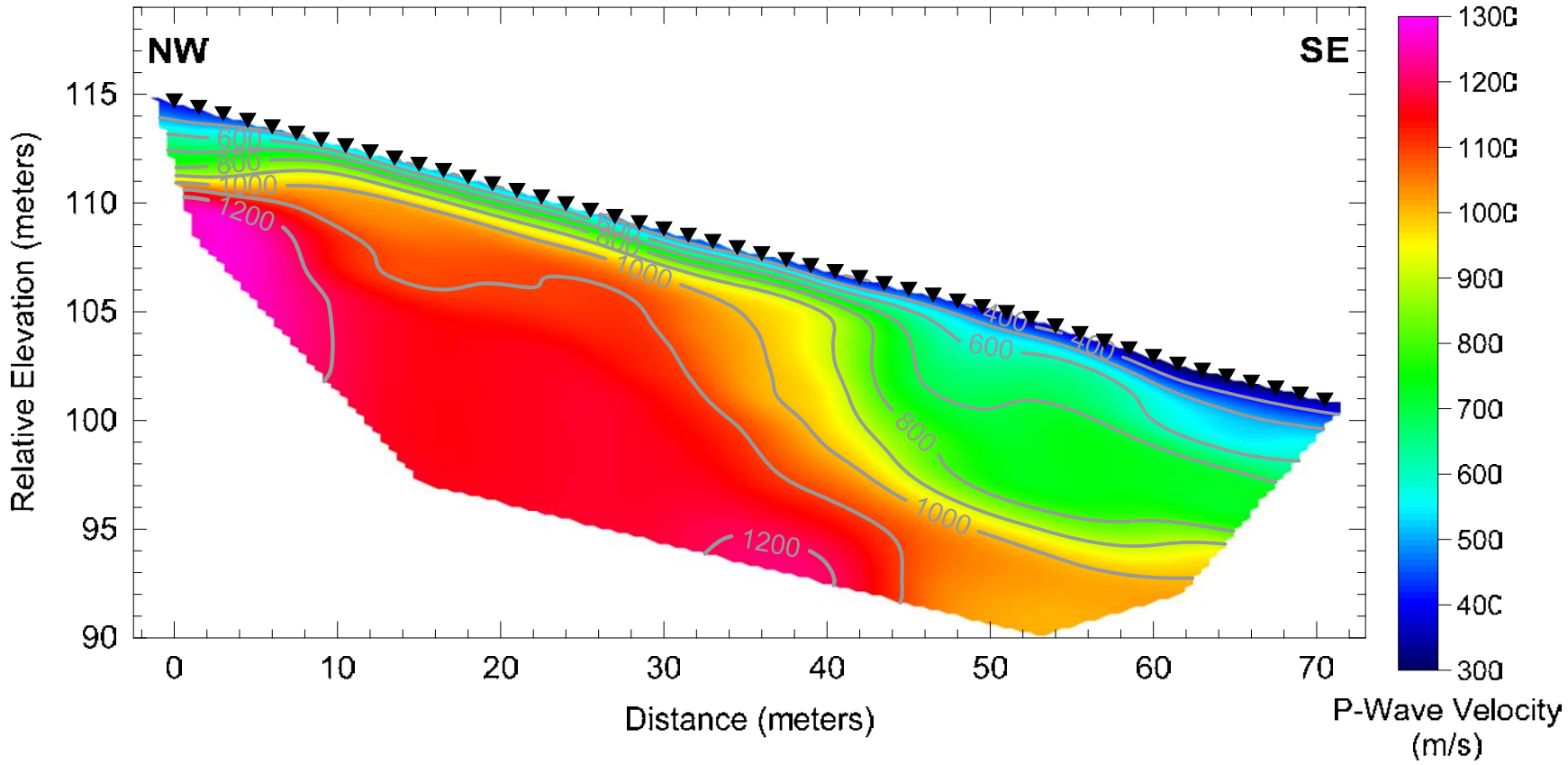

Array BTP-1 – Tomographic seismic refraction model utilizing smooth velocity gradient starting model

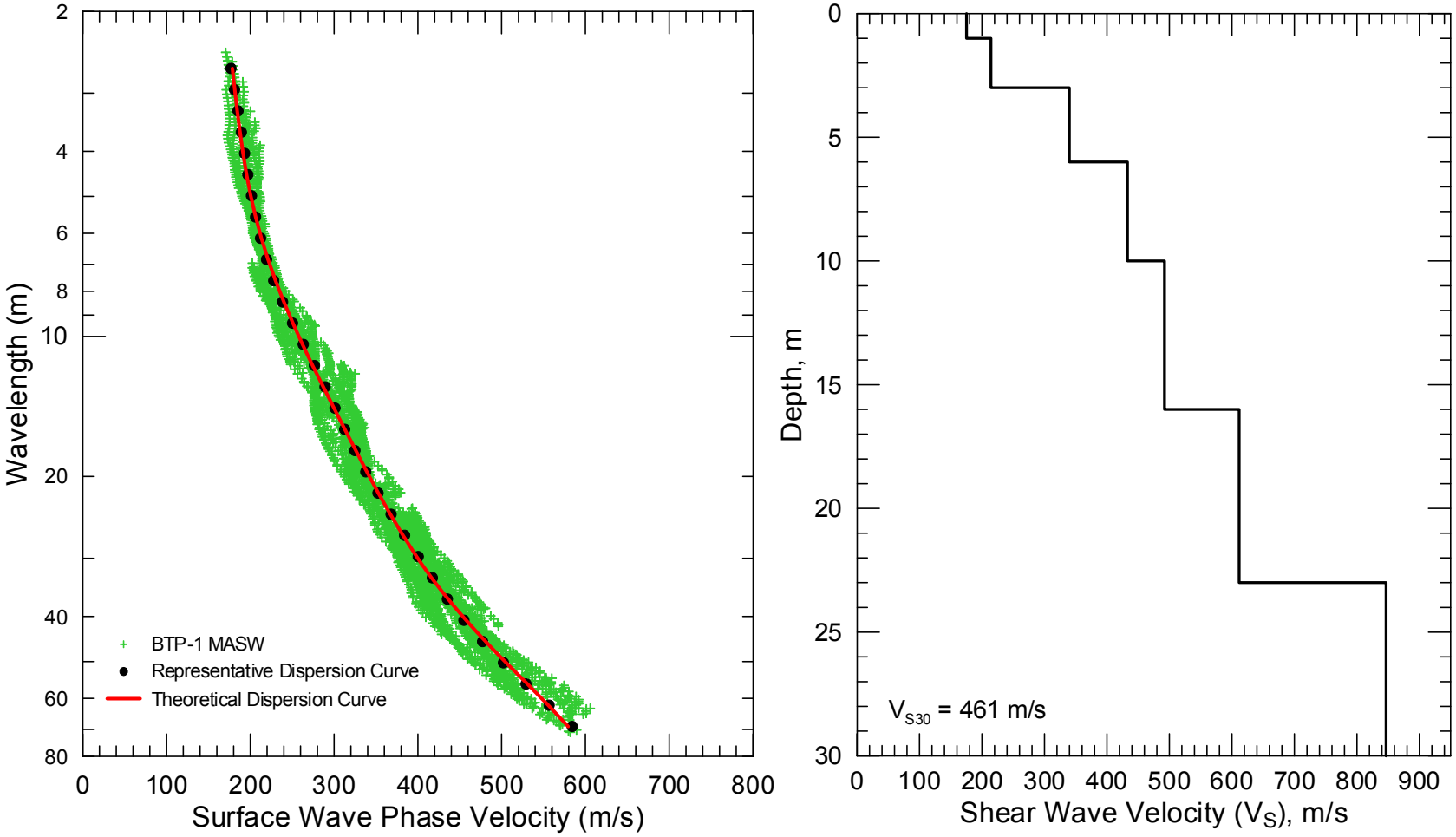

CI.BTP - Field, representative and inverted theoretical surface wave dispersion data (left) and associated V_S model (right) for Array BTP-1

Site CI.CAC

Location: California Institute of Technology, Athenaeum Cellar, Pasadena, California

Latitude: 34.13678 **Longitude:** -118.12199

(Station coordinates provided by USGS – WGS84 coordinate system)

V_{S30} (measured): 399 m/s

V_{S30} (adjusted to more accurately reflect seismic station conditions): 433 m/s (average S-wave velocity between 3 and 33 m adjusting for approximate depth of cellar)

NEHRP Site Class: C

Geomatrix Code: CQD

Geologic Conditions/Observations: Site located in area mapped as Quaternary (Pleistocene) old alluvial fan deposits. Deep soil site.

Site Conditions: Urban site with significant traffic noise from nearby roads. Relatively flat terrain in site vicinity with ground surface elevation gently decreasing to south.

Geophysical Methods Utilized: HVSR, MASW, array microtremor, ReMi™

Geophysical Testing Arrays:

1. Array CAC-1 (48 channel "L" shaped passive surface wave array utilizing 4.5 Hz vertical geophones spaced 3 m apart on the W-E leg along E. California Blvd. and 5 m apart on the S-N leg along S. Hill Ave., resulting in 72 and 115 m lengths of the linear segments).
2. Array CAC-2 (48 channel MASW array, located along the S-N segment of array CAC-1, utilizing 4.5 Hz vertical geophones spaced 0.75 m apart for a length of 35.25 m, forward and reverse shot locations with multiple source offsets and source types and center shot location).
3. Three HVSR measurement locations, one on array CAC-1 and the others on nearby arrays MIK-1 and CRP-1.

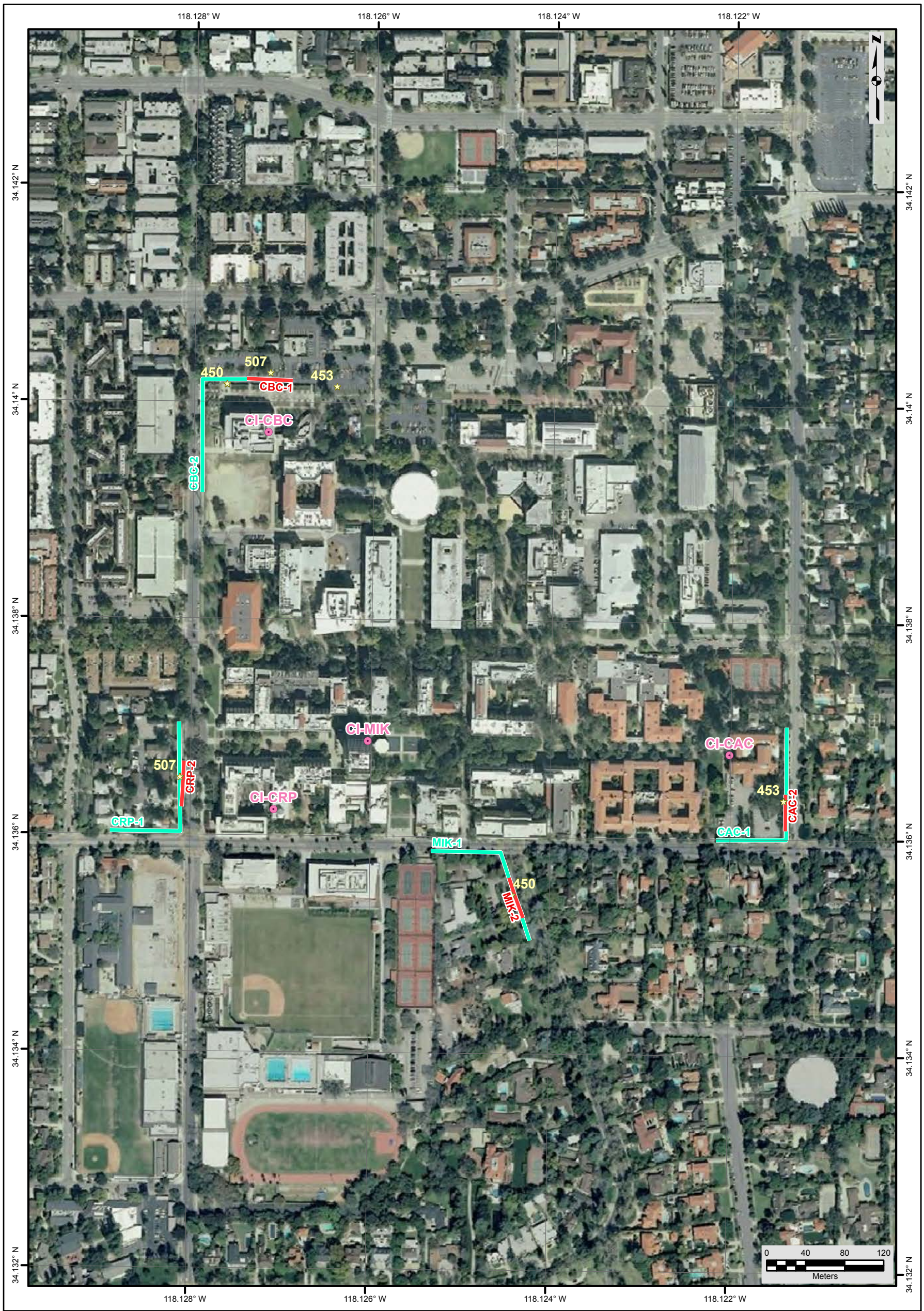

Legend

- Seismic Station - Approximate Location of Record
- H/V Spectral Ratio Measurement Location
- MASW Array
- Passive SASW Array

NOTES:
1. WGS 1984 COORDINATE SYSTEM
2. Image Source: ESRI, i-cubed, USDA FSA, USGS, AEX, GeoEye, Getmapping, Aerogrid, IGP

File Name: Caltech-I

Date: 5/16/2011

GEOVision geophysical services

SITE MAP
CI•CAC, CI•CBC, CI•CRP, CI•MIK

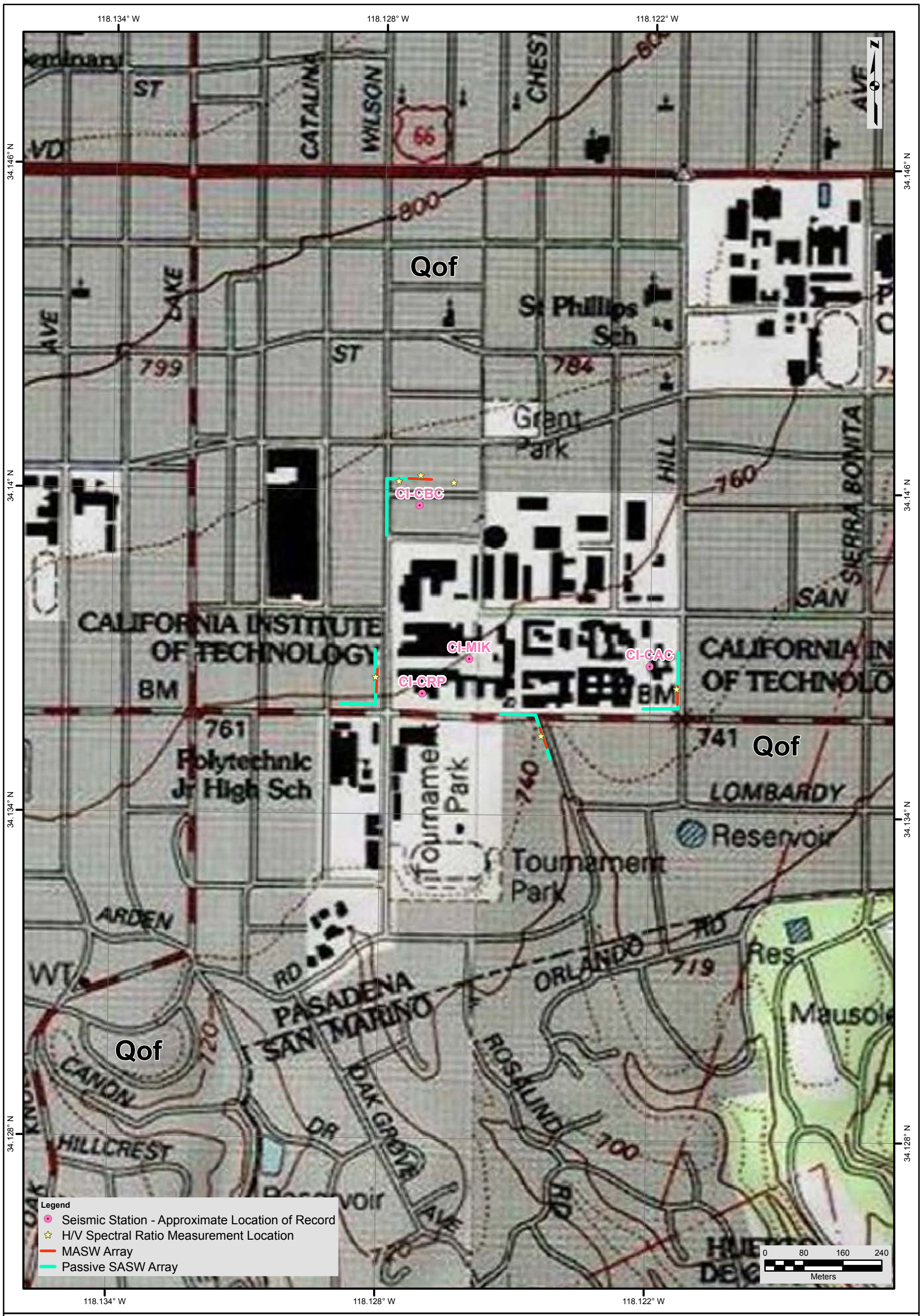

Description of Geologic Map Units

Qof = Quaternary (Holocene) alluvial fan gravel and sand

NOTES:
1. WGS 1984 COORDINATE SYSTEM
2. Topo Image Sources: USGS, FAO, NPS, EPA, NRCAN, GeoBase, Esri, DeLorme, TANA, Intermap and other suppliers and the GIS community
3. Geologic Map Units from:
Geologic Map of the Mt Wilson and Azusa Quadrangles, Los Angeles County, California by Thomas W. Dibblee, Jr., 1998 and
Geologic Map of the Pasadena Quadrangle, Los Angeles County, California by Thomas W. Dibblee, Jr., 1999
4. See site map for details of geophysical survey

File Name: Caltech

Date: 5/26/2011

GEOVision geophysical services

GEOLOGIC MAP
CI•CAC, CI•CBC, CI•CRP, CI•MIK

Looking west along the east-west segment of array CAC-1

Looking north along the south-north segment of array CAC-1

Looking northwest towards location of arrays CAC-1 and CAC-2 and the California Institute of Technology Athenaeum

Location of Geophysical Testing Arrays:

Location	Latitude	Longitude
CAC-1, West End of Array, Channel 1	34.13603	-118.12213
CAC-1, Corner of Array, Channel 25	34.13600	-118.12135
CAC-1, North End of Array, Channel 48	34.13704	-118.12136
CAC-2, South End of Array	34.13608	-118.12136
CAC-2, Center of Array	34.13642	-118.12137
CAC-2, North End of Array	34.13608	-118.12136
HVSR Sensor 507 (on array CRP-1)	34.13653	-118.12809
HVSR Sensor 453 (on array CAC-1)	34.13636	-118.12138
HVSR Sensor 450 (on array MIK-1)	34.13547	-118.12439

Notes: 1) WGS84 Coordinate System (decimal degrees)
2) Survey accuracy is estimated at 1 to 3 m

Results:

V_S Model

Depth to Top of Layer (m)	Layer Thickness (m)	S-Wave Velocity (m/s)	Inferred P-Wave Velocity (m/s)	Inferred Poisson's Ratio	Inferred Density (g/cm^3)
0	1.5	186	349	0.300	1.9
1.5	4	379	708	0.300	1.9
5.5	8	416	779	0.300	1.9
13.5	12	426	797	0.300	1.9
25.5	15	492	921	0.300	2.0
40.5	20	556	1600	0.431	2.0
60.5	25	623	1600	0.410	2.0
85.5	>4.5	679	1600	0.390	2.0

Note: Estimated depth of investigation is 75 m.

Observations/Discussion:

- Surface wave testing conducted on the perimeter of the Caltech campus due to basements on most buildings, dense utilities and possible tunnels connecting buildings on campus.
- Limited photographs taken during field testing as much of the field work was conducted at night. Passive surface wave measurements were typically made in the late afternoon to early evening when there was sufficient traffic noise. MASW data were generally acquired in the early evening when there was less traffic, but not too late so as to disturb

residences. HVSR data were acquired between 11 pm and 2 am when there was minimal traffic noise.

- The HVSR curves are almost identical validating the 1-D velocity structure assumption with respect to deep geologic structure. There are no high frequency peaks by which to determine if shallow velocity structure is uniform.
- There is a clear HVSR peak in the 0.54 to 0.55 Hz range on all the HVSR plots, even though the test locations are about 300 m apart. An HVSR peak in the 0.55 Hz range is consistent with an expected basement depth on the order of 300 m in the site vicinity.
- Noise conditions at site (multi-directional or omni-directional noise sources) appeared sufficient for successful application of passive surface wave techniques with the closest noise source being the west to east trending E. California Blvd.
- ESAC technique used to extract surface wave dispersion data from passive "L" array data. Both the ReMi™ and ESAC techniques used to extract surface wave dispersion data from the linear arrays.
- Only the "L" array passive surface wave data used for analysis. As expected, the E-W linear array segment did not provide useful surface wave dispersion data as it was located along E. California Blvd (i.e. parallel to the oncoming traffic). The S-N linear yielded better agreement with the "L" array.
- Large diffraction observed in MASW seismic records, possibly due to a large diameter utility or other subsurface structure. Such features are expected in an urban environment.
- Surface wave dispersion data from active and passive surface wave data sets are in good agreement at this site although the surface wave dispersion data from the two techniques only overlap over the 17 to 26 m wavelength range. Slight differences in the surface wave dispersion data are attributed to near surface lateral velocity variation and the fact that the MASW data were acquired along a 35.25 m long array, whereas the passive surface wave data were acquired along a much larger 72 by 115 m array. Near surface lateral velocity variation is expected for this site due to all of the construction that has occurred over a long period of time.
- Representative dispersion curves were generated for each surface wave data set using a moving average, polynomial curve fitting routine. These individual representative dispersion curves were combined and a representative dispersion curve generated for the combined data set for data modeling.
- No evidence of a water table refractor or reflector in the MASW seismic records due to both high noise levels and short array length. Water table assumed at a depth of 40 m for modeling and a P-wave velocity of 1,600 m/s utilized for assumed saturated zone.
- Surface wave depth of investigation is about 75 m based on half of maximum wavelength criteria and assuming that surface wave dispersion data at frequencies as low as 3.3 Hz are valid utilizing 4.5 Hz geophones (low frequency geophone phase response differences will cancel out if noise is omni-directional and/or the phase response differences are random in nature).
- V_{S30} is 399 m/s (Site Class C).
- Average S-wave velocity between 3 m (estimated depth of cellar) and 33 m is 433 m/s.
- Average S-wave velocity of the upper 75 m (V_{S75}) is 482 m/s.

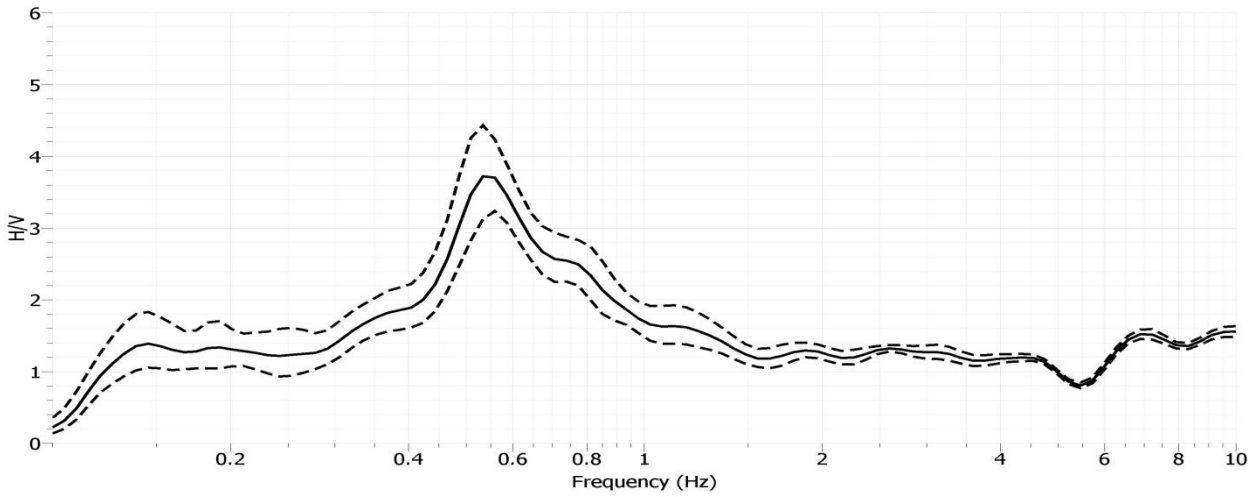

Site CI.CRP, H/V Spectral Ratio, Array CRP-1/2, Sensor 507

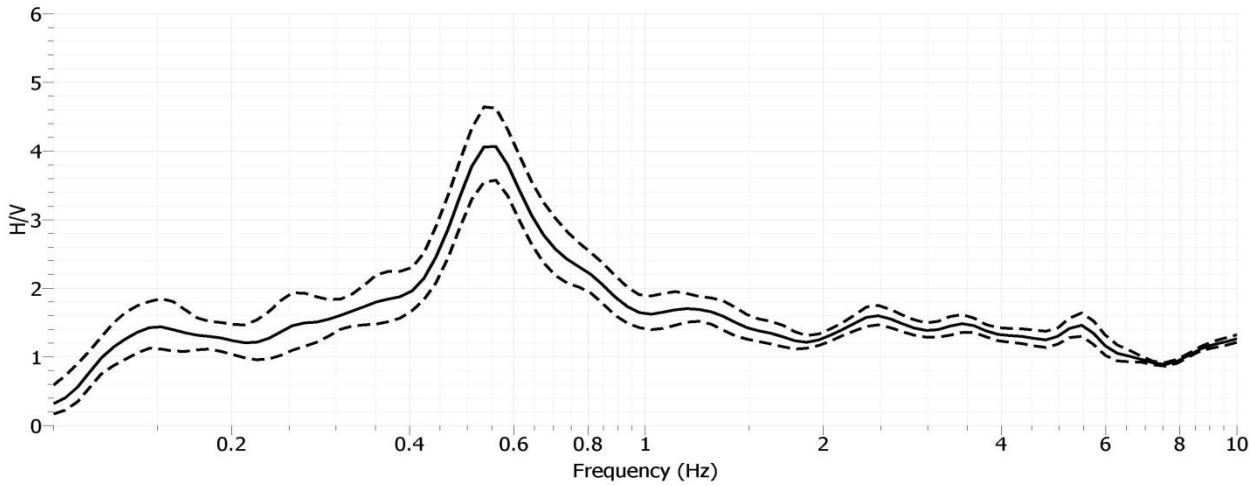

Site CI.MIK, H/V Spectral Ratio, Array MIK-1/2, Sensor 450

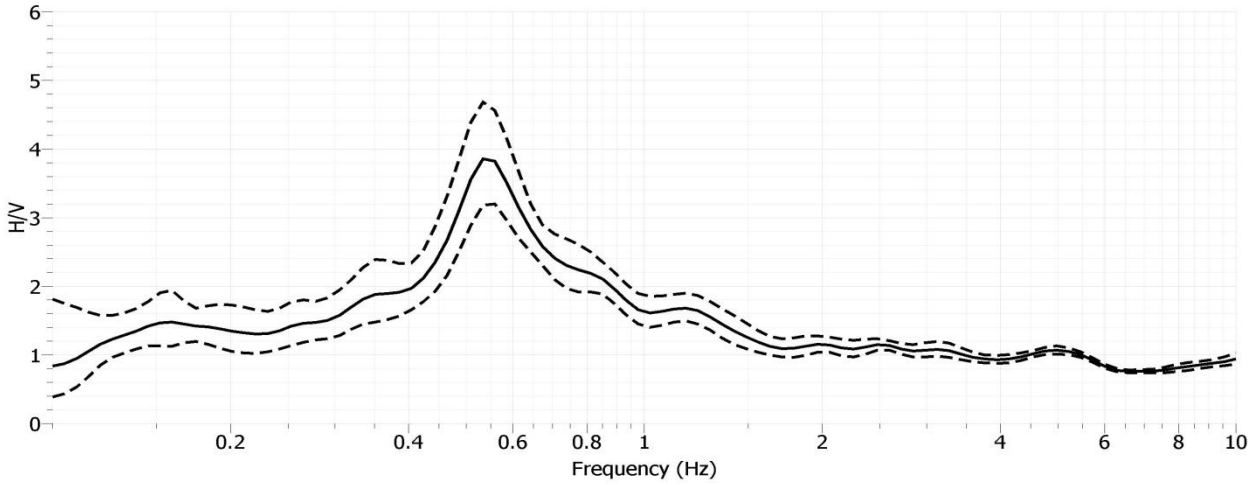

Site CI.CAC, H/V Spectral Ratio, Array CAC-1/2, Sensor 453

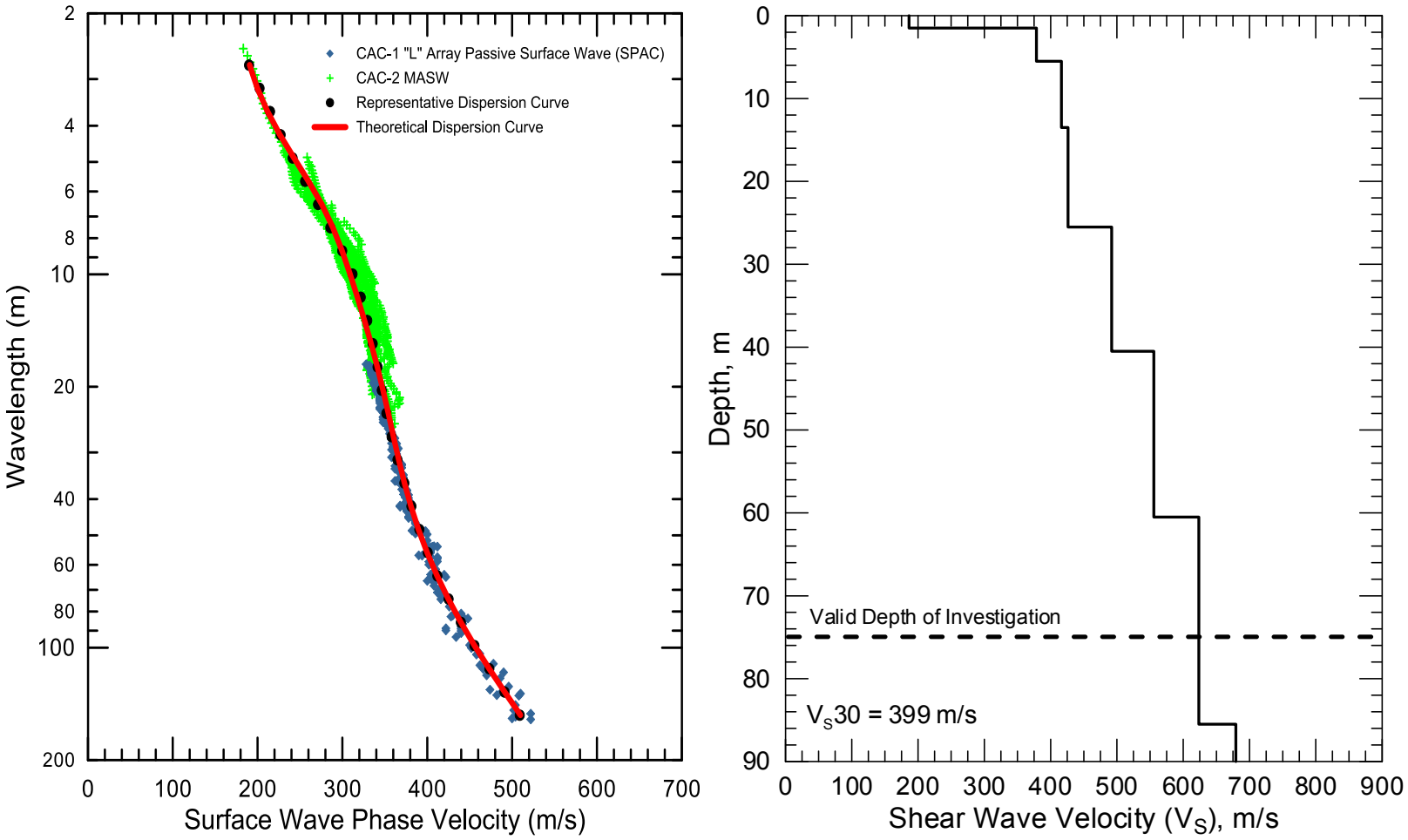

CI.CAC - Field, representative and inverted theoretical surface wave dispersion data (left) and associated V_S model (right)

Site CI.CAR

Location: Carrizo Plain, Anwannee Trail and Armona Road, California Valley, California

Latitude: 35.30819 **Longitude:** -119.84583

(Station coordinates provided by USGS, WGS84 coordinate system)

V_{S30} (measured): 310 m/s

V_{S30} (adjusted to more accurately reflect seismic station conditions): 339 m/s (average S-wave velocity between 2 and 32 m adjusting for nominal sensor depth)

NEHRP Site Class: D

Geomatrix Code: IHD

Geologic Conditions/Observations: Seismic station located on geologic unit mapped as Holocene alluvium and within about 50 m of the contact between Holocene alluvium and Pleistocene Paso Robles Formation (alluvial gravel, sand and clay). Tertiary sedimentary rock units outcrop within 500 m of site. It is possible that the seismic sensor, located 1.5 to 2 m below ground surface, sits on Pleistocene rather than Holocene sediments.

Site Conditions: Rural site with no traffic noise. Relatively flat terrain in test area. Surface topography gradually declines to the southwest. Hilly terrain to the northeast.

Geophysical Methods Utilized: HVSR, Seismic Refraction, MASW, SASW

Geophysical Testing Arrays:

1. Array CAR-1 (48 channel MASW array utilizing 4.5 Hz vertical geophones spaced 1.5 m apart for a length of 70.5 m, forward and reverse shot locations with multiple source offsets and source types and center shot location).
2. Array CAR-2 (48 channel MASW and P-wave seismic refraction array utilizing 4.5 Hz vertical geophones spaced 3 m apart for a length of 141 m, forward and reverse shot locations with multiple offsets with weight drop only and interior shot locations at six station intervals).
3. Array CAR-3 (48 channel P-wave seismic refraction array utilizing 4.5 Hz vertical geophones spaced 3 m apart for a length of 141 m, forward and reverse shot locations with multiple source offsets and source types and interior shot locations at six station intervals).
4. Array CAR-4 (SASW array with common orientation to MASW arrays CAR-1 and CAR-2 utilizing 4.5 and 1 Hz vertical geophones and maximum receiver spacing of 40 m).
5. Three HVSR measurement locations; two at endpoints of array CAR-1 and one near the seismic station.

Legend

- Seismic Station - Approximate Surveyed Location
- Seismic Station - Approximate Location of Record
- H/V Spectral Ratio Location
- SASW Array
- MASW Array
- MASW and Refraction Array

NOTES:
1. WGS 1984 COORDINATE SYSTEM
2. Image Source: ESRI, i-cubed, USDA FSA, USGS, AEX, GeoEye, Getmapping, Aerogrid, IGP

File Name: CI-CAR-I

Date: 6/24/2011

USGS science for a changing world

GEOVision geophysical services

RECOVERY.GOV

SITE MAP
CI•CAR

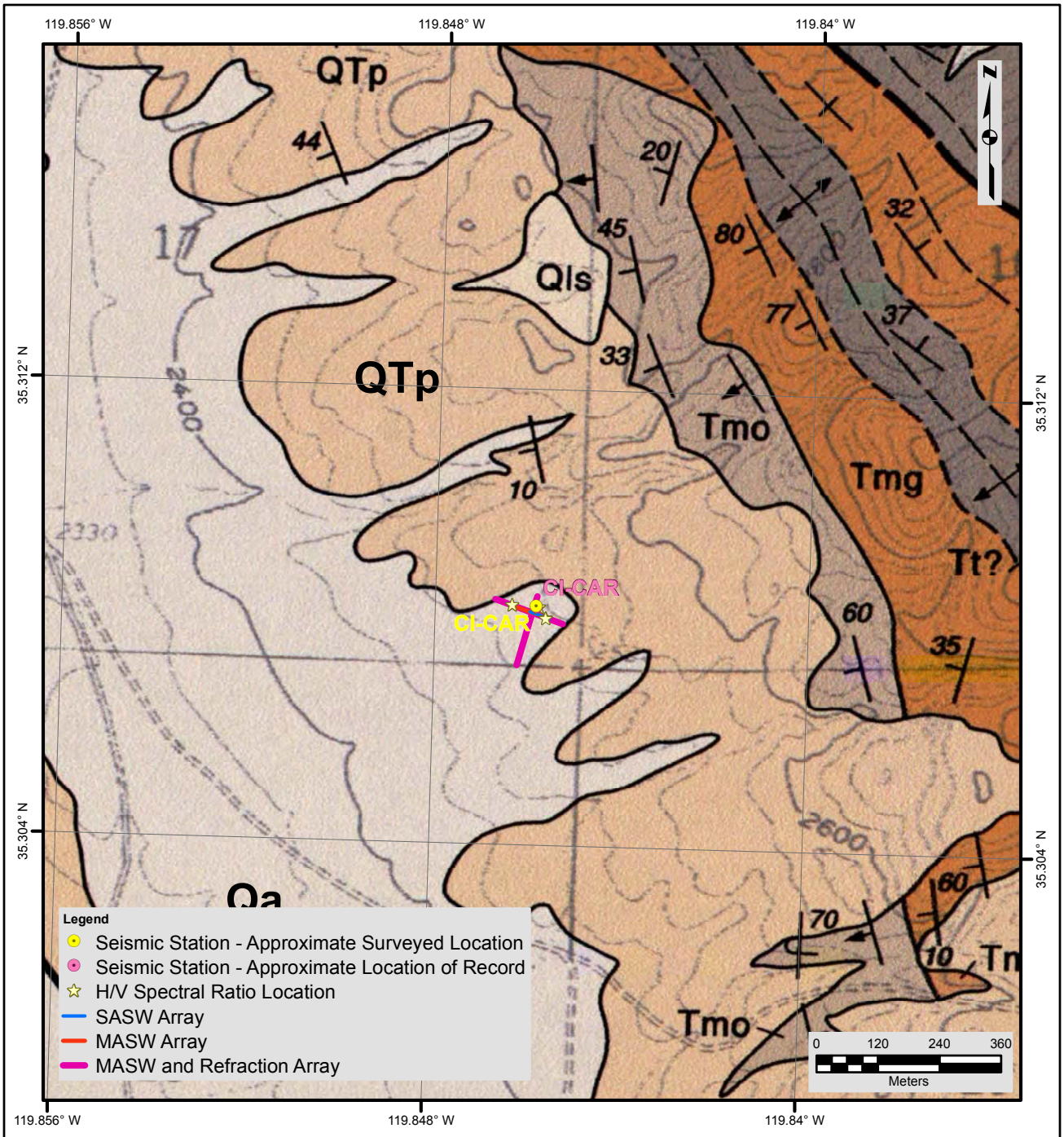

Description of Geologic Map Units

Qa = Quaternary (Holocene) alluvial gravel and sand of valley areas
QTp = Quaternary (Pleistocene) Paso Robles Formation; alluvial gravel, sand and clay
Tmo = Quaternary (Pliocene) Morales Formation; non-marine pebble conglomerate, sandstone and claystone, weakly indurated
Tmg = Tertiary (Middle Miocene) Monterey Shale; Gould Shale Member, silicious, semi-siliceous, and clay shale
Tt = Tertiary (Lower Miocene-Oligocene) Temblor Formation; lithified clay shale, micaceous

NOTES:
1. WGS 1984 COORDINATE SYSTEM
2. Geologic Map of the McKittrick Summit Quadrangle, San Luis Obispo and Kern Counties, California by Thomas W. Dibblee, Jr., 2005
3. See site map for details of geophysical survey

USGS science for a changing world

GEOVision geophysical services

GEOLOGIC MAP
CI•CAR

RECOVERY.GOV

File Name: CI-CAR

Date: 6/24/2011

Looking north towards CI.CAR seismic station and HVSR sensor 450

Looking east towards MASW array CAR-2 and seismic station

Looking northeast along seismic refraction array CAR-3 and towards seismic station

Looking northeast towards center of MASW array CAR-1 and seismic station

Looking northwest along SASW array CAR-4

Location of Geophysical Testing Arrays:

Location	Latitude	Longitude
CAR-1, Northwest End of MASW Array	35.30820	-119.84636
CAR-1, Center of MASW Array	35.30810	-119.84599
CAR-1, Southeast End of MASW Array	35.30800	-119.84562
CAR-2, Northwest End of MASW/Refraction Array	35.30830	-119.84672
CAR-2, Center of MASW/Refraction Array	35.30810	-119.84598
CAR-2, Southeast End of MASW/Refraction Array	35.30789	-119.84526
CAR-3, Southwest End of Seismic Refraction Array	35.30715	-119.84622
CAR-3, Center of Seismic Refraction Array	35.30777	-119.84602
CAR-3, Northwest End of Seismic Refraction Array	35.30837	-119.84582
CAR-4, Northwest End of SASW Receiver Array	35.30809	-119.84597
CAR-4, Center of SASW Array	35.30803	-119.84575
CAR-4, Southeast End of SASW Receiver Array	35.30798	-119.84555
HVSR Sensor 450	35.30818	-119.84578
HVSR Sensor 453	35.30799	-119.84563
HVSR Sensor 507	35.30821	-119.84635
CI.CAR Seismic Station	35.30820	-119.84584

Notes: 1) WGS84 Coordinate System (decimal degrees)
2) Survey accuracy is estimated at 1 to 2 m

Results:

V_S Model

Depth to Top of Layer (m)	Layer Thickness (m)	S-Wave Velocity (m/s)	Inferred P-Wave Velocity (m/s)	Inferred Poisson's Ratio	Inferred Density (g/cm^3)
0	1	123	247	0.333	1.9
1	2	187	374	0.333	1.9
3	3	258	516	0.333	1.9
6	4	303	605	0.333	1.9
10	8	373	745	0.333	1.9
18	12	378	755	0.333	1.9
30	12	388	1500	0.464	2.0
42	>3	402	1500	0.461	2.0

Notes: 1) Approximate depth of saturated zone and P-wave velocity of saturated sediments constrained by seismic refraction survey.
2) Model valid to a depth of 45 m.
3) Lowest layer is half space.

Observations/Discussion:

- HVSR plots are similar at frequencies below 6 Hz at all measurement locations validating the 1-D velocity structure assumption.
- There are no high amplitude HVSR peaks.
- Noise conditions at site were not sufficient to apply passive surface wave techniques.
- Surface wave dispersion data from SASW and MASW data sets are in acceptable agreement at the site. The MASW dispersion curves appear to be less complex than the SASW dispersion curves and were used for modeling.
- Representative dispersion curves were generated for each MASW data set using a moving average, polynomial curve fitting routine. These individual representative dispersion curves were combined and a representative dispersion curve generated for the combined data set for data modeling.
- Top of saturated zone estimated at a depth of about 30 m based on seismic refraction models. A possible refractor associated with the top of the saturated zone was observed on far-offset shot MASW seismic records from array CAR-1. Because of the geologic environment (i.e. higher velocity sedimentary rock units at unknown depth) this refractor could not be conclusively associated with the saturated zone and seismic refraction data were acquired along two longer arrays (CAR-2 and CAR-3) to further investigate. The lack of accessible space for far-offset shot locations still made it difficult to confirm that the refractor is associated with the top of the saturated zone because P-wave velocities of greater than 1,450 to 1,500 m/s are not required to model the data. However, the absence of a high velocity layer at 30 m depth in the surface wave models indicates that the refractor is likely associated with the saturated zone.
- Based on tomographic inversion of seismic refraction first arrival data from arrays CAR-2 and CAR-3 utilizing layer-based starting models, P-wave velocity in the upper 30 m ranges from about 300 m/s near the surface and increases with depth to 700 m/s at a depth generally in the 5 to 10 m range. Below 10 m P-wave velocity is typically in the 700 to 850 m/s range until the saturated zone at a depth on the order of 30 m.
- Surface wave model is consistent with simplified P-wave refraction model considering unknown Poisson's ratio. A Poisson's ratio of 0.333 was used for surface wave modeling and yielded reasonable agreement between inferred P-wave velocities in the surface wave model and seismic refraction models.
- Surface wave depth of investigation is about 45 m based on half of maximum wavelength criteria.
- V_{S30} is 310 m/s (Site Class D).
- Average S-wave velocity between 2 m (nominal sensor depth) and 32 m is 339 m/s.
- Average S-wave velocity of the upper 45 m (V_{S45}) is 333 m/s.

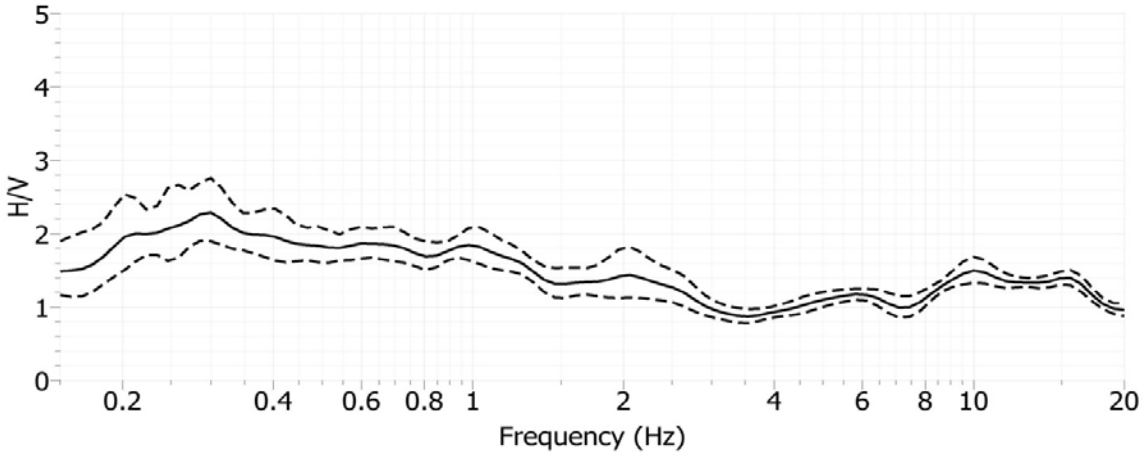

Site CI.CAR, H/V Spectral Ratio, Array CAR -1, Sensor 507

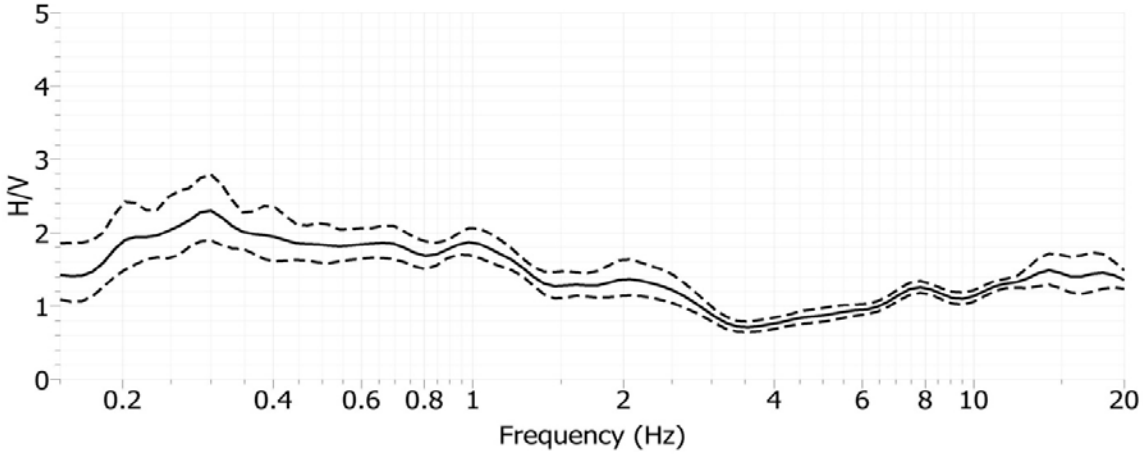

Site CI.CAR, H/V Spectral Ratio, Near Seismic Station, Sensor 450

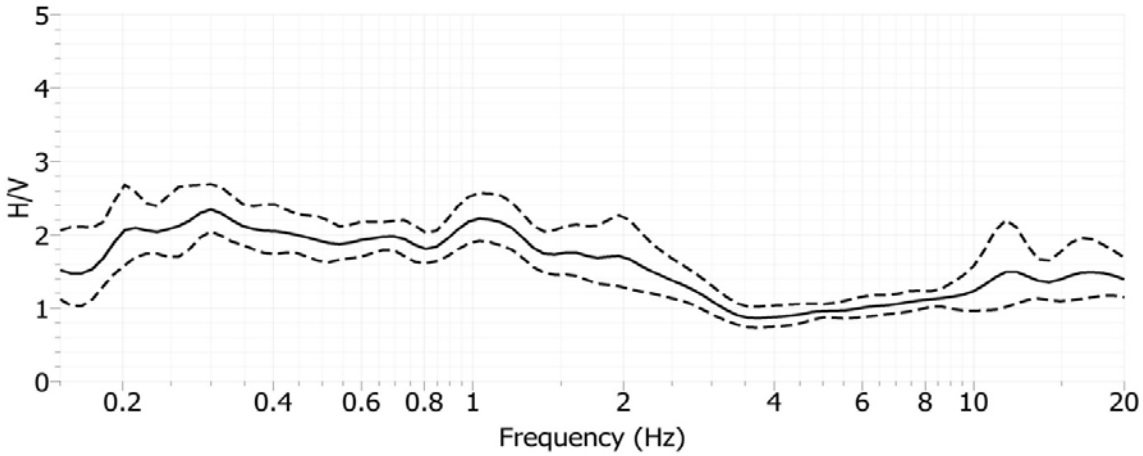

Site CI.CAR, H/V Spectral Ratio, Array CAR -1, Sensor 453

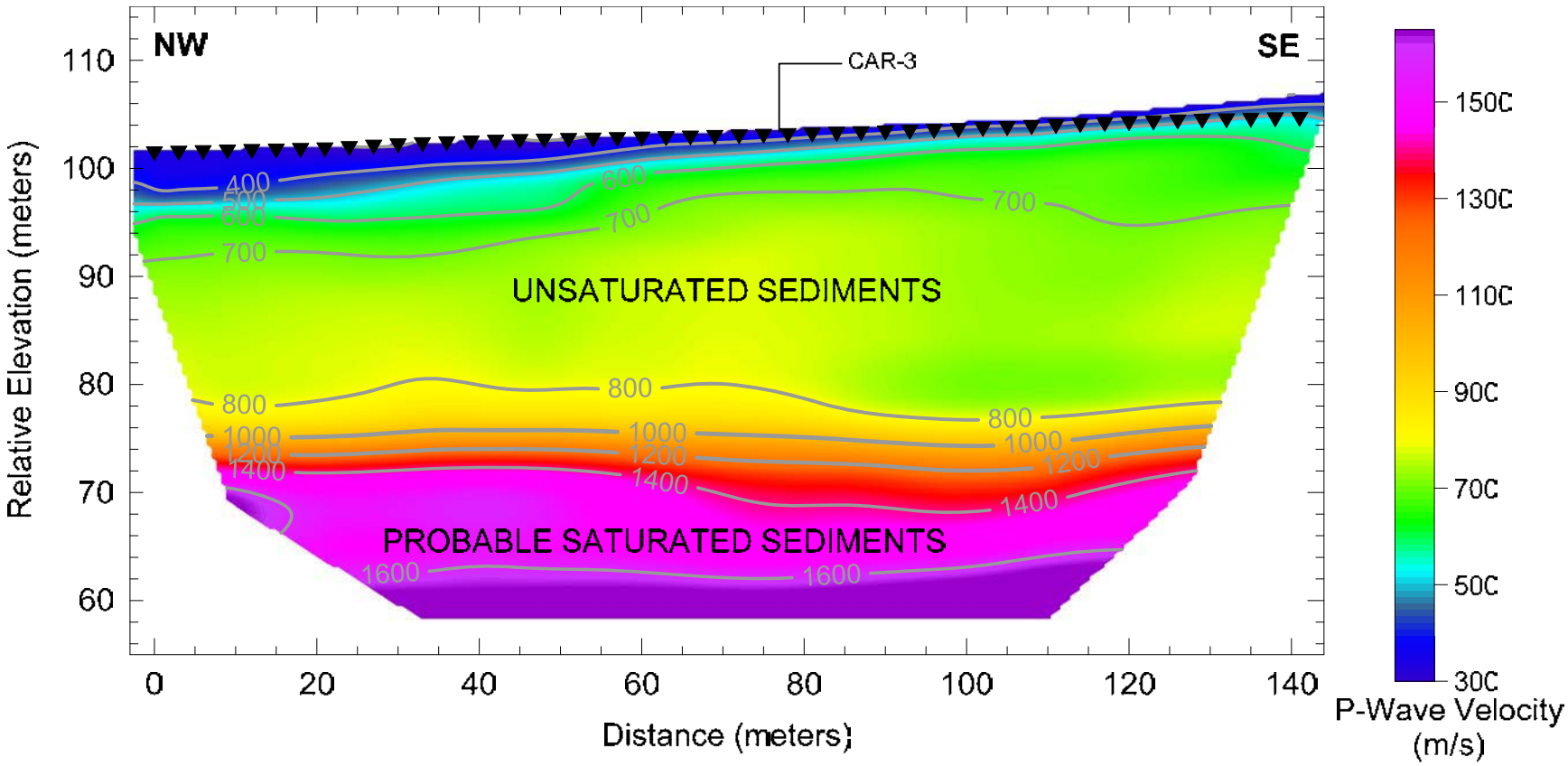

Array CAR-2 – Tomographic seismic refraction model developed using a layer based starting model

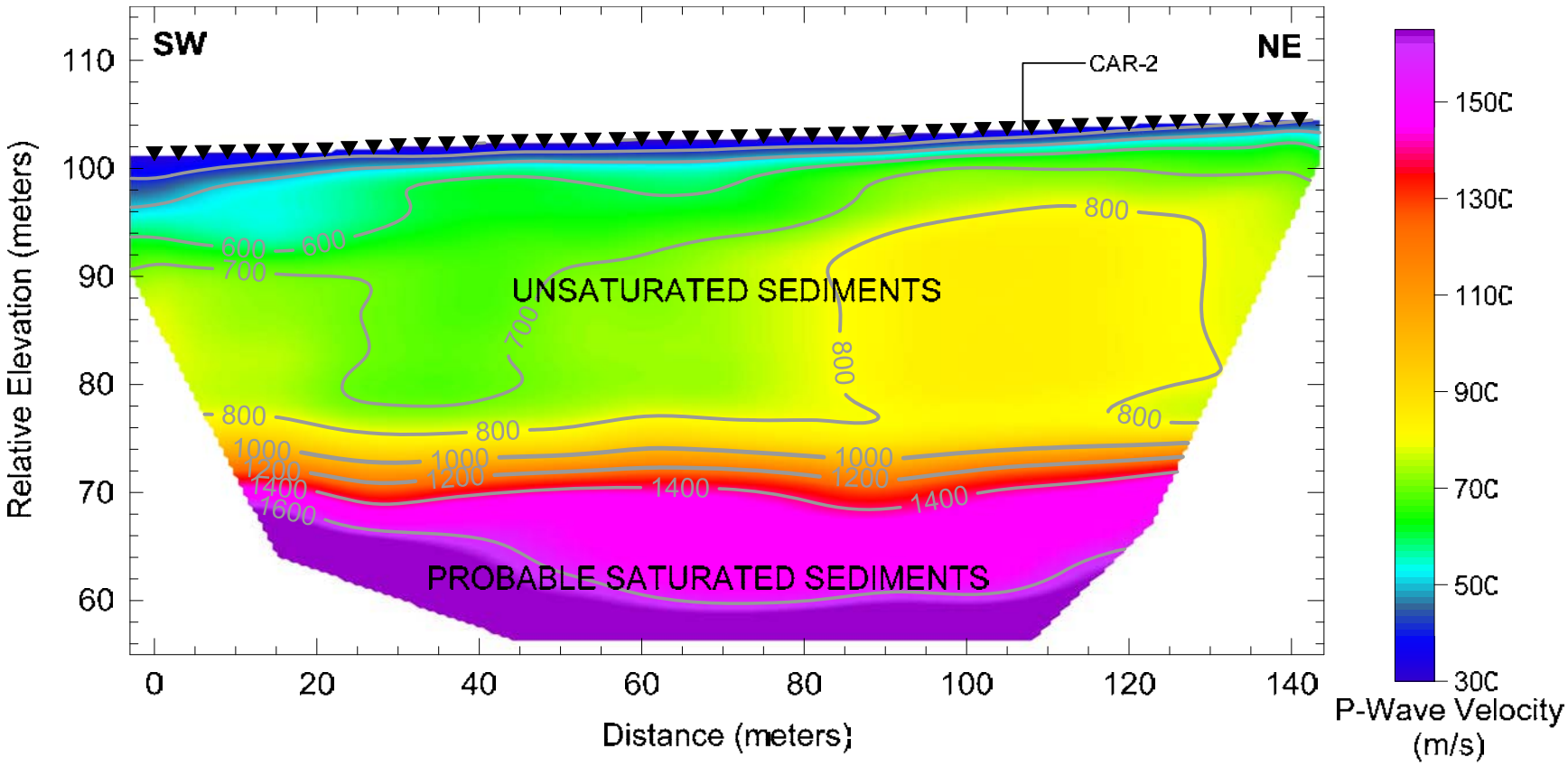

Array CAR-3 – Tomographic seismic refraction model developed using a layer lased starting model

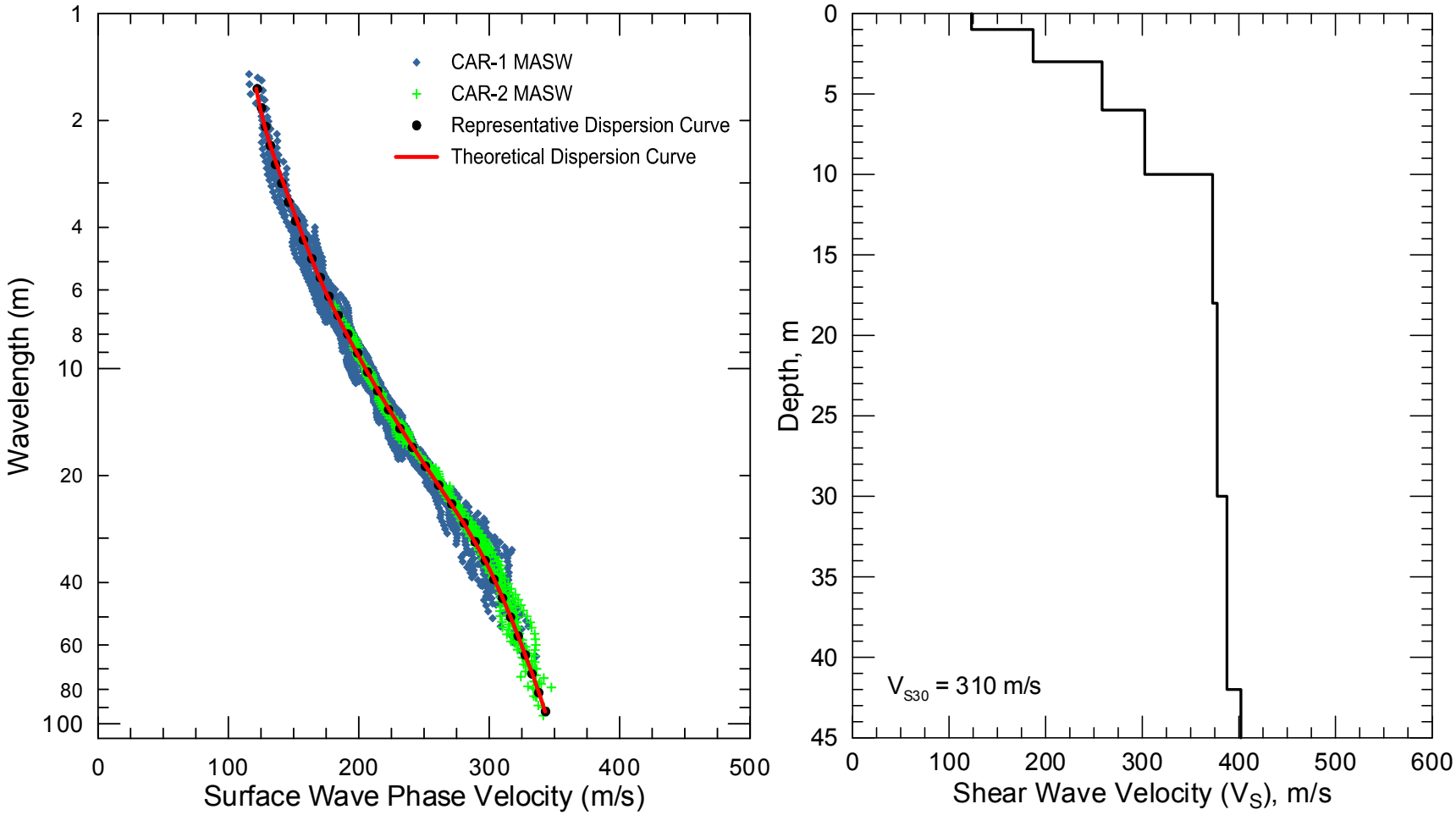

CI.CAR - Field, representative and inverted theoretical surface wave dispersion data (left) and associated V_S model (right)

Site CI.CBC

Location: California Institute of Technology, Broad Center, California

Latitude: 34.13972 **Longitude:** -118.12715

(Station coordinates provided by USGS – WGS84 coordinate system)

V_{S30} (measured): 361 m/s

V_{S30} (adjusted to more accurately reflect seismic station conditions): 437 m/s (average S-wave velocity between 8 and 38 m accounting for fact that building has two basement levels.)

NEHRP Site Class: C/D

Geomatrix Code: GQD

Geologic Conditions/Observations: Site located in area mapped as Quaternary (Pleistocene) old alluvial fan deposits. Deep soil site.

Site Conditions: Urban site with significant traffic noise from nearby roads. Relatively flat terrain in site vicinity with ground surface elevation gently decreasing to south.

Geophysical Methods Utilized: HVSR, MASW, array microtremor, ReMi™

Geophysical Testing Arrays:

1. Array CBC-1 (48 channel MASW array, located at the eastern end of the E-W segment of array CBC-2, utilizing 4.5 Hz vertical geophones spaced 1 m apart for a length of 47 m, forward and reverse shot locations with multiple source offsets and source types and center shot location).
2. Array CBC-2 (48 channel "L" shaped passive surface wave array utilizing 4.5 Hz vertical geophones spaced 4 m apart on the W-E leg and 5 m apart on the S-N leg along S. Wilson Ave., resulting in 92 and 115 m lengths of the linear segments).
3. Array CBC-3 (48 channel MASW array, located at the southern end of the S-N segment of array CBC-2, utilizing 4.5 Hz vertical geophones spaced 1 m apart for a length of 47 m, forward and reverse shot locations with multiple source offsets and source types (hammers only)and center shot location).
4. Three HVSR measurement locations distributed along the E-W leg of array CBC-2.

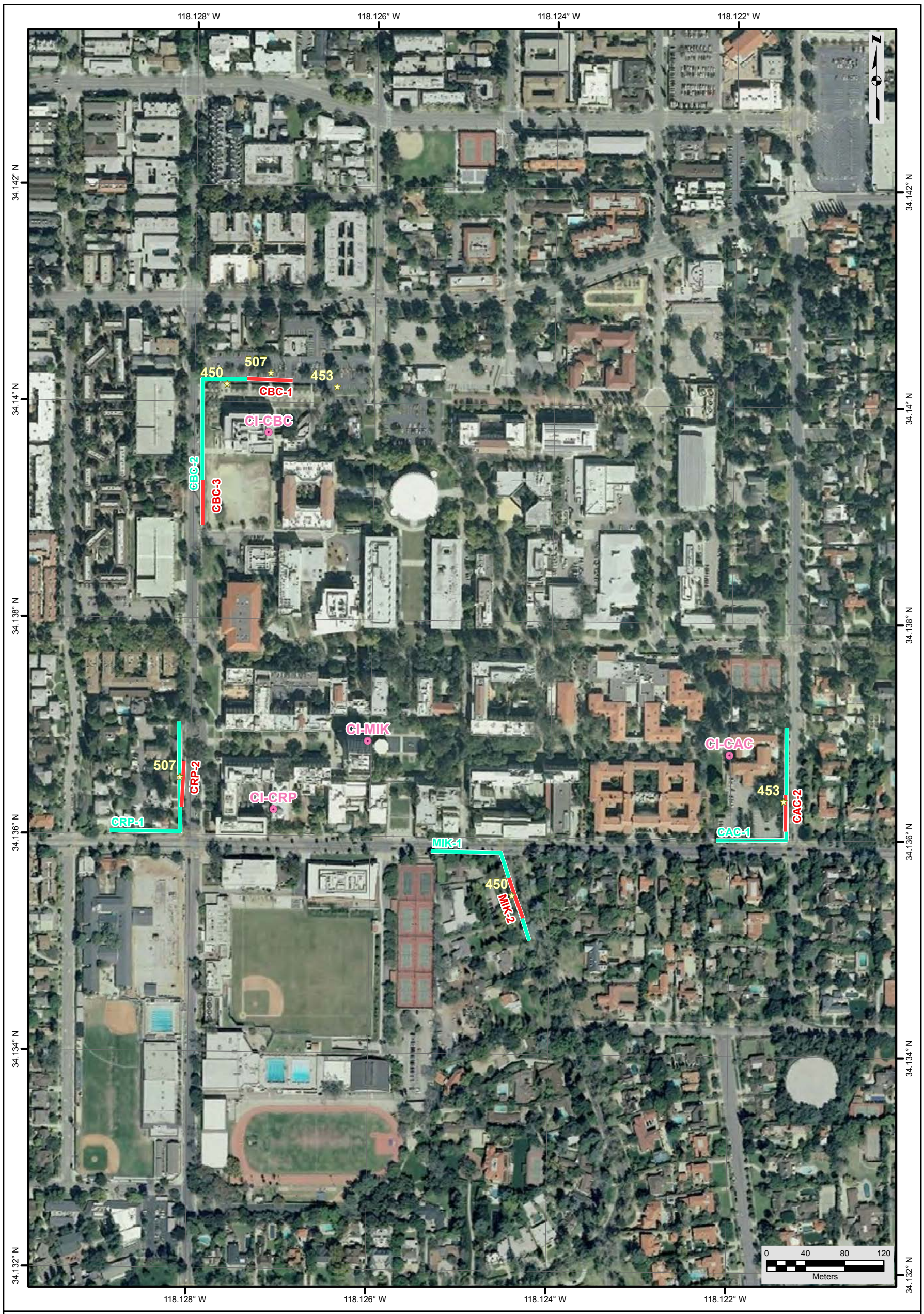

Legend

- Seismic Station - Approximate Location of Record
- H/V Spectral Ratio Measurement Location
- MASW Array
- Passive SASW Array

NOTES:
1. WGS 1984 COORDINATE SYSTEM
2. Image Source: ESRI, i-cubed, USDA FSA, USGS, AEX, GeoEye, Getmapping, Aerogrid, IGP

File Name: Caltech-I

Date: 10/13/2011

GEOVision geophysical services

SITE MAP
CI•CAC, CI•CBC, CI•CRP, CI•MIK

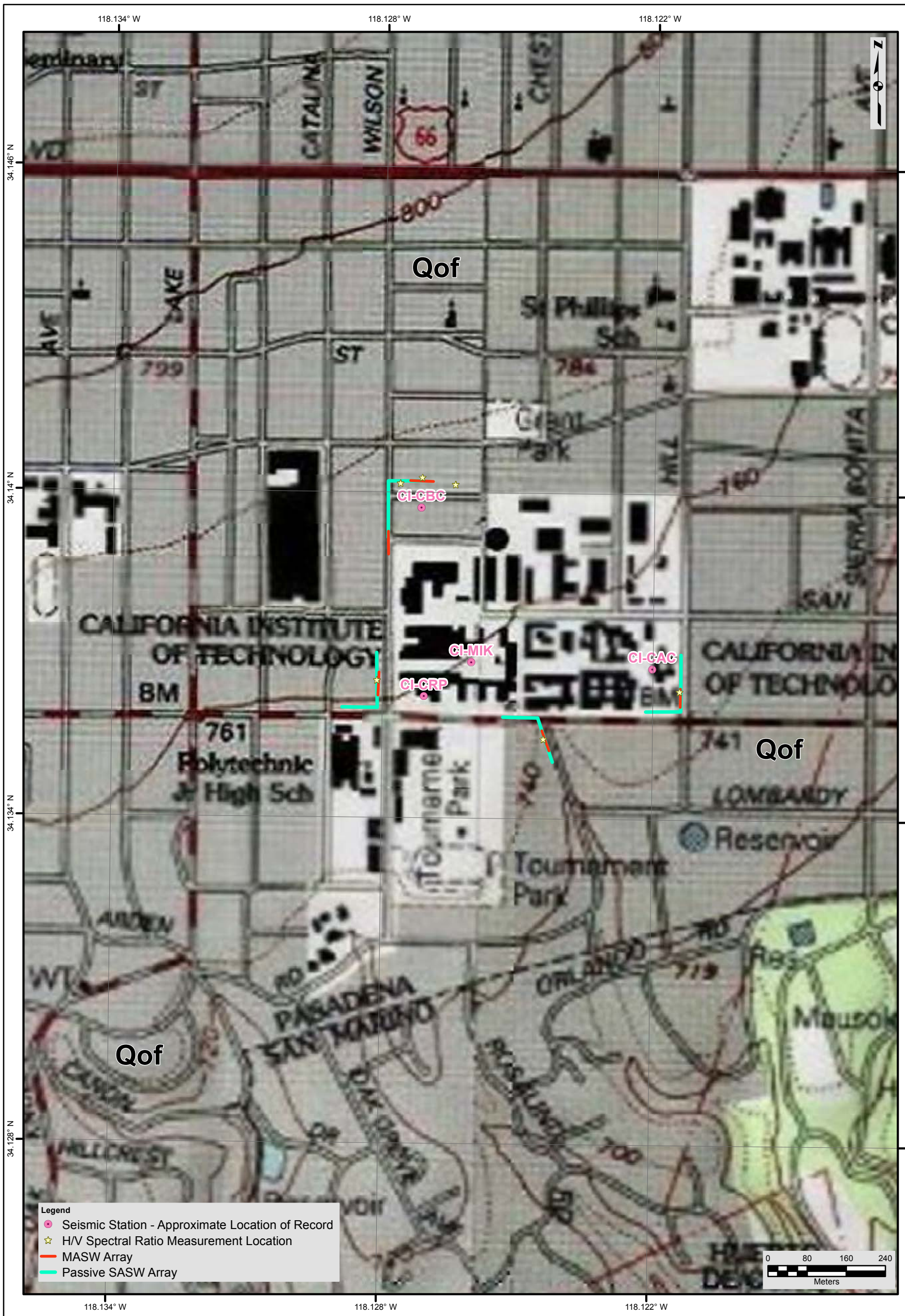

Description of Geologic Map Units

Qof = Quaternary (Holocene) alluvial fan gravel and sand

NOTES:
1. WGS 1984 COORDINATE SYSTEM
2. Topo Image Sources: USGS, FAO, NPS, EPA, NRCAN, GeoBase, Esri, DeLorme, TANA, Intermap and other suppliers and the GIS community
3. Geologic Map Units from:
Geologic Map of the Mt Wilson and Azusa Quadrangles, Los Angeles County, California by Thomas W. Dibblee, Jr., 1998 and
Geologic Map of the Pasadena Quadrangle, Los Angeles County, California by Thomas W. Dibblee, Jr., 1999
4. See site map for details of geophysical survey

File Name: Caltech

Date: 10/13/2011

GEOVision geophysical services

GEOLOGIC MAP
CI•CAC, CI•CBC, CI•CRP, CI•MIK

Looking north along MASW array CBC-3

Looking south along MASW array CBC-3

Looking east at the location of the east-west leg of passive surface wave array CBC-2

Looking southeast from corner of passive surface wave array CBC-2 towards building housing seismic station CI.CBC

Looking south at the location of the south-north leg of passive surface wave array CBC-2

Location of Geophysical Testing Arrays:

Location	Latitude	Longitude
CBC-1, West End of Array	34.14020	-118.12739
CBC-1, Center of Array	34.14021	-118.12714
CBC-1, East End of Array	34.14020	-118.12689
CBC-2, South End of Array, Channel 1	34.13916	-118.12788
CBC-2, Corner of Array, Channel 24	34.14019	-118.12787
CBC-2, East End of Array, Channel 48	34.14021	-118.12712
CBC-3, South End of Array	34.13885	-118.12787
CBC-3, Center of Array	34.13907	-118.12787
CBC-3, North End of Array	34.13928	-118.12788
HVSR Sensor 507	34.14027	-118.12713
HVSR Sensor 453	34.14015	-118.12639
HVSR Sensor 450	34.14016	-118.12762

Notes: 1) WGS84 Coordinate System (decimal degrees).
2) Survey accuracy is estimated at 1 to 3 m.

Results:

V_S Model

Depth to Top of Layer (m)	Layer Thickness (m)	S-Wave Velocity (m/s)	Inferred P-Wave Velocity (m/s)	Inferred Poisson's Ratio	Inferred Density (g/cm^3)
0	0.75	140	261	0.300	1.8
0.75	1.25	207	388	0.300	1.8
2	2	246	461	0.300	1.9
4	4	337	630	0.300	1.9
8	6	392	733	0.300	1.9
14	10	419	784	0.300	1.9
24	16	475	889	0.300	2.0
40	20	514	1600	0.442	2.0
60	>10	570	1600	0.427	2.0

Notes: 1) For modeling, saturated sediments assumed at 40 m depth with P-wave velocity of 1,600 m/s.
2) Depth of investigation is about 70 m.
3) Bottom layer is a half space.

Observations/Discussion:

- Surface wave testing conducted on the perimeter of the Caltech campus due to basements on most buildings, dense utilities and possible tunnels connecting buildings on campus.
- Limited photographs taken during field testing as much of the field work was conducted at night. Passive surface wave measurements were typically made in the late afternoon to early evening when there was sufficient traffic noise. MASW data were generally acquired in the early evening when there was less traffic, but not too late so as to disturb residences. HVSR data were acquired at night when there was minimal traffic noise.
- The HVSR curves are almost identical validating the 1-D velocity structure assumption with respect to deep geologic structure. There are no high frequency peaks by which to determine if shallow velocity structure is uniform.
- There is a clear HVSR peak at about 0.55 Hz on all the HVSR plots, which is consistent with an expected basement depth on the order of 300 m in the site vicinity.
- Noise conditions at the site (multi-directional or omni-directional noise sources) appeared sufficient for successful application of passive surface wave techniques.
- ESAC technique used to extract surface wave dispersion data from passive "L" array data. Both the ReMi™ and ESAC techniques used to extract surface wave dispersion data from the linear arrays.
- The passive surface wave measurements were made at two different times. The first data set was acquired too late in the evening and there was limited local traffic noise. Therefore, the passive surface wave measurements were repeated earlier in the evening at another time. Both data sets yielded similar results, although the second data set, acquired at a time with more local noise sources, was of better quality and used for analysis.
- The E-W passive linear array segment did not provide useful surface wave dispersion data and was not used for modeling. Both the "L" array passive surface wave data and S-N linear array (both ESAC and ReMi™ analysis) yielded comparable surface wave dispersion curves and were used for data analysis. The "L" array data was, however, better quality and given a higher weight.
- MASW dispersion data were also acquired along two arrays, neither of which were near the center of the "L" array due to accessibility. The first MASW array was located at the east end of the E-W passive linear array. Surface wave dispersion data from this array was not in good agreement with the passive surface wave array due to lateral velocity variation. Therefore, a second MASW array was acquired at the southern end of the S-N passive linear array segment. The array yielded surface wave dispersion data in better agreement with the passive data and was used for analysis.
- Surface wave dispersion data from active and passive surface wave data sets are in acceptable agreement and overlap over the 10 to 34 m wavelength range. Slight differences in the surface wave dispersion data occur with the MASW phase velocity data slightly lower than the passive surface wave data. These differences are attributed to near surface lateral velocity variation as the MASW data were acquired along a 47 m long array, whereas the passive surface wave data were acquired along a much larger 95 by 115 m array. Near surface lateral velocity variation is expected for this site due to all of the construction that has occurred over a long period of time.

- Representative dispersion curves were generated for each surface wave data set using a moving average, polynomial curve fitting routine. These individual representative dispersion curves were weighted, combined and a representative dispersion curve generated for the combined data set for data modeling.
- No evidence of a water table refractor or reflector in the MASW seismic records due to both high noise levels and short array length. Water table was assumed at a depth of 40 m for modeling and a P-wave velocity of 1,600 m/s utilized for assumed saturated zone.
- Surface wave depth of investigation is about 70 m based on half of maximum wavelength criteria and assuming that surface wave dispersion data at frequencies as low as 3.25 Hz are valid utilizing 4.5 Hz geophones (low frequency geophone phase response differences will cancel out if noise is omni-directional and/or the phase response differences are random in nature).
- V_{S30} is 361 m/s (Site Class C/D).
- Average S-wave velocity between 8 m (estimated depth of the base of the two basement levels) and 38 m is 437 m/s (Site Class C).
- Average S-wave velocity of the upper 70 m (V_{S70}) is 436 m/s.

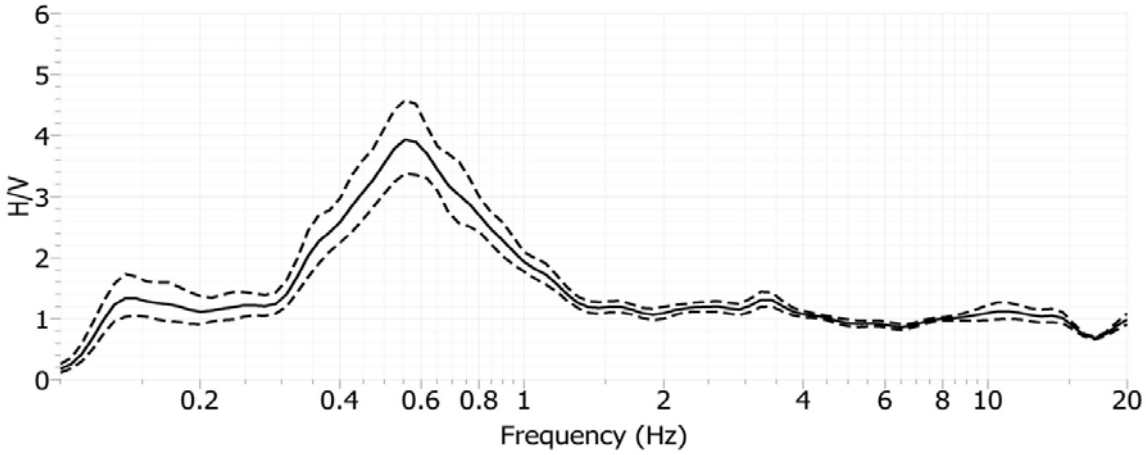

Site CI.CBC, H/V Spectral Ratio, Array CBC-2, Sensor 450

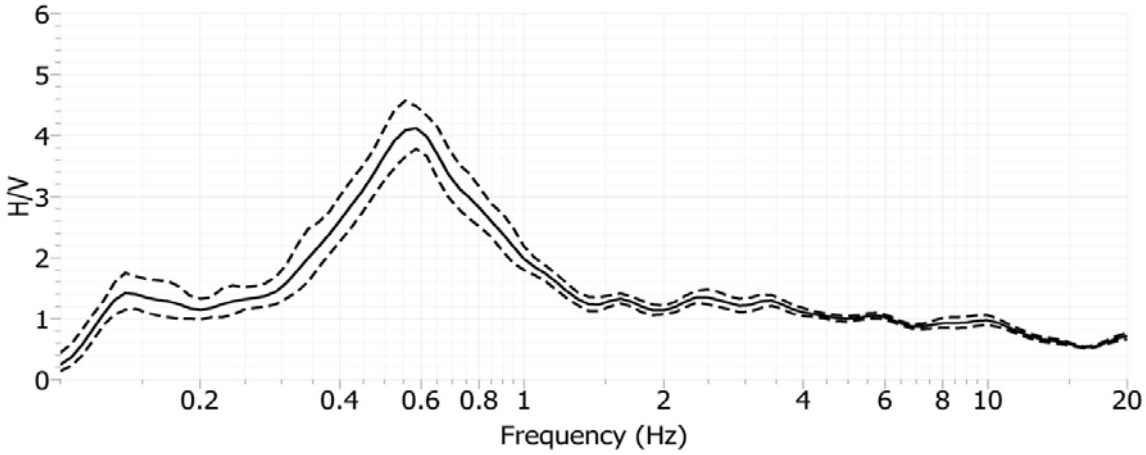

Site CI.CBC, H/V Spectral Ratio, Array CBC-1/2, Sensor 507

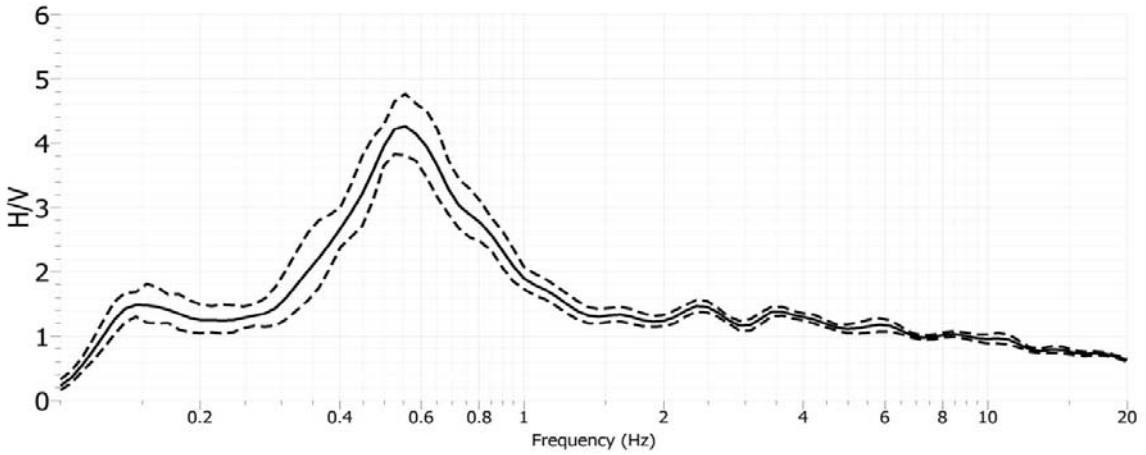

Site CI.CBC, H/V Spectral Ratio, Array CBC-2, Sensor 453

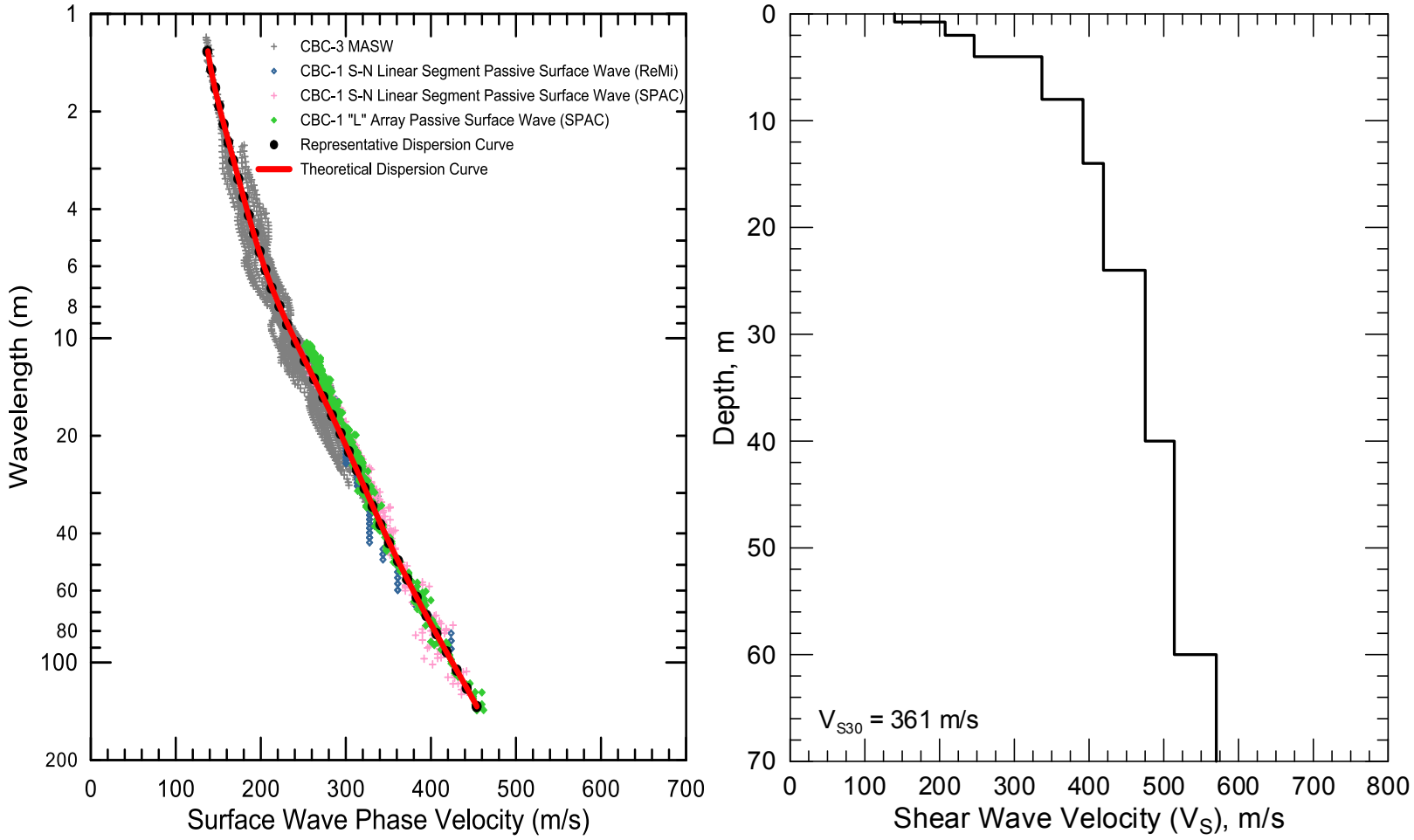

CI.CBC - Field, representative and inverted theoretical surface wave dispersion data (left) and associated V_S model (right)

Site CI.CCC

Location: Christmas Canyon, China Lake NWC, Kern County, California

Latitude: 35.52475 **Longitude:** -117.36459

(Station coordinates modified based on field GPS survey, WGS84 coordinate system)

V_{S30} (measured): 432 m/s

V_{S30} (adjusted to more accurately reflect seismic station conditions): 461 m/s (average S-wave velocity between 2 and 32 m adjusting for nominal sensor depth)

NEHRP Site Class: C

Geomatrix Code: IQD

Geologic Conditions/Observations: Site located near the mapped geologic contact between Quaternary (Upper Holocene) alluvium and Quaternary (Pleistocene) lacustrine silt, sand and gravel. Site inspection revealed that the seismic station is located on the Quaternary (Pleistocene) lucustrine silt, sand and gravel unit. The Garlock Fault is mapped about 60 m south of the seismic station.

Site Conditions: Rural site. Test area located on relatively flat terrain. Hilly topography adjacent to seismic line and seismic station.

Geophysical Methods Utilized: HVSR, MASW

Geophysical Testing Arrays:

1. Array CCC-1 (48 channel MASW array utilizing 4.5 Hz vertical geophones spaced 1.5 m apart for a length of 70.5 m, forward and reverse shot locations with multiple source offsets and source types and multiple interior shots).
2. Three HVSR measurement locations; two distributed along array CCC-1 and one near the seismic station.

Legend

- Seismic Station - Approximate Surveyed Location
- Seismic Station - Approximate Location of Record
- H/V Spectral Ratio Location
- MASW Array

NOTES:
1. WGS 1984 COORDINATE SYSTEM
2. Image Source: ESRI, i-cubed, USDA FSA, USGS, AEX, GeoEye, Getmapping, Aerogrid, IGP

File Name: CI-CCC-I

Date: 7/15/2011

USGS science for a changing world

GEOVision geophysical services

RECOVERY.GOV

SITE MAP
CI•CCC

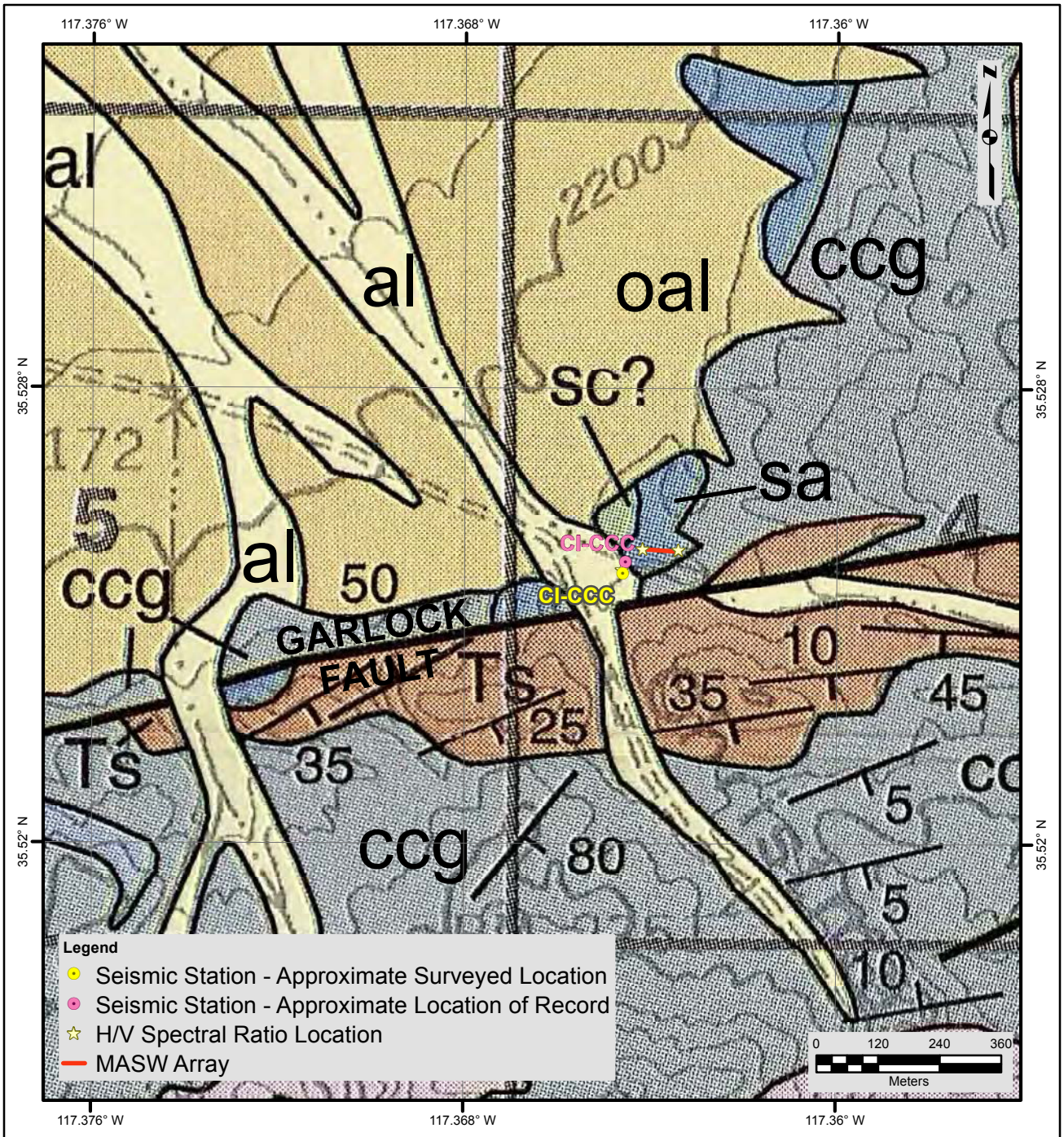

Description of Geologic Map Units

al = Quaternary (Upper Holocene) alluvium; gravel and sand deposited in active channels
oal = Quaternary (Upper and Middle Holocene) older alluvium; medium to coarse sand, some pebbles
sc = Quaternary (Upper Pleistocene) gravel, sand, silt and clay lacustrine deposits
sa = Quaternary (Pleistocene) silt, sand and gravel lacustrine, well indurated
ccg = Quaternary (Pleistocene) gravel and sand alluvial deposits
Ts = Tertiary (Miocene) siltstone and sandstone lacustrine, deformed, well-bedded

NOTES:
1. WGS 1984 COORDINATE SYSTEM
2. Geologic Map of the Searles Valley, Inyo and San Bernardino Counties, California by George I. Smith, 2009
3. See site map for details of geophysical survey

USGS science for a changing world
GEOVision geophysical services

RECOVERY.GOV

GEOLOGIC MAP
CI•CCC

File Name: CI-CCC
Date: 7/18/2011

Looking northeast towards seismic station CI.CCC and test area

Looking north towards HVSR sensor 507 and seismic station CI.CCC

Looking east along MASW array CCC-1

HCSR sensor preparation

Note: Photography restrictions on NWC China Lake

Location of Geophysical Testing Arrays:

Location	Latitude	Longitude
CCC-1, West End of MASW Array	35.52517	-117.36417
CCC-1, Center of MASW Array	35.52515	-117.36378
CCC-1, East End of MASW Array	35.52513	-117.36339
HVSR Sensor 450	35.52516	-117.36339
HVSR Sensor 453	35.52518	-117.36416
HVSR Sensor 507	35.52481	-117.36461
CI.CCC Seismic Station	35.52475	-117.36459

Notes: 1) WGS84 Coordinate System (decimal degrees)
2) Survey accuracy is estimated at 1 to 2 m

Results:

V_S Model

Depth to Top of Layer (m)	Layer Thickness (m)	S-Wave Velocity (m/s)	Inferred P-Wave Velocity (m/s)	Inferred Poisson's Ratio	Inferred Density (g/cm^3)
0	1	164	307	0.3	1.8
1	28	456	854	0.3	1.9
29	>1	509	953	0.3	2.0

Observations/Discussion:

- The site is located near the Garlock Fault and geologic conditions are complex with dipping and folded beds, etc.
- There were limited feasible options for geophysical test locations at this site.
- There are no distinct HVSR peaks at the site.
- Noise conditions at the site were not sufficient to apply passive surface wave techniques.
- There is significant scatter in the surface wave dispersion data likely resulting from lateral velocity variation associated with variable thickness of low velocity surface layers, dipping geologic layers of variable velocity, etc.
- Even with selective use of surface wave dispersion data from MASW seismic records, there is about a 50 to 70 m/s variation in surface wave phase velocity data.
- For the purpose of data modeling, a representative dispersion curve was generated from an ensemble of MASW dispersion curves using a moving average, polynomial curve fitting routine.
- Based on interactive layer-based analysis of seismic refraction first arrival data, P-wave velocity in the upper 15 m ranges from about 350 to 425 m/s in the upper 1 to 2.5 m, 800 to 900 m/s to a depth of 7 to 10+ m, below which P-wave velocity is in the 1,100 to 1,200 m/s range.

- Water table located at a depth of greater than 20 m based on seismic refraction survey design and absence of a water table refractor.
- Surface wave depth of investigation is about 30 m based on half of maximum wavelength criteria.
- Due to significant lateral velocity variation, an S-wave velocity model with minimal number of layers was developed to represent subsurface velocity structure.
- The inferred P-wave velocities in the surface wave model (assumed Poisson's ratio of 0.3) are in reasonable agreement with seismic refraction data at shallow depths, but are lower than refraction velocities at depths greater than 10 m. An increase in Poisson's ratio at depth to 0.35 to 0.4 would yield better agreement between inferred P-wave velocity in the surface wave models and P-wave seismic refraction data.
- V_{S30} is 432 m/s (Site Class C).
- There may be as much as 10% variability of V_{S30} in the site vicinity due to lateral velocity variation, dipping geologic layers, etc.; however, the velocity variability should not affect site class.
- Average S-wave velocity between 2 m (nominal sensor depth) and 32 m is 461 m/s.

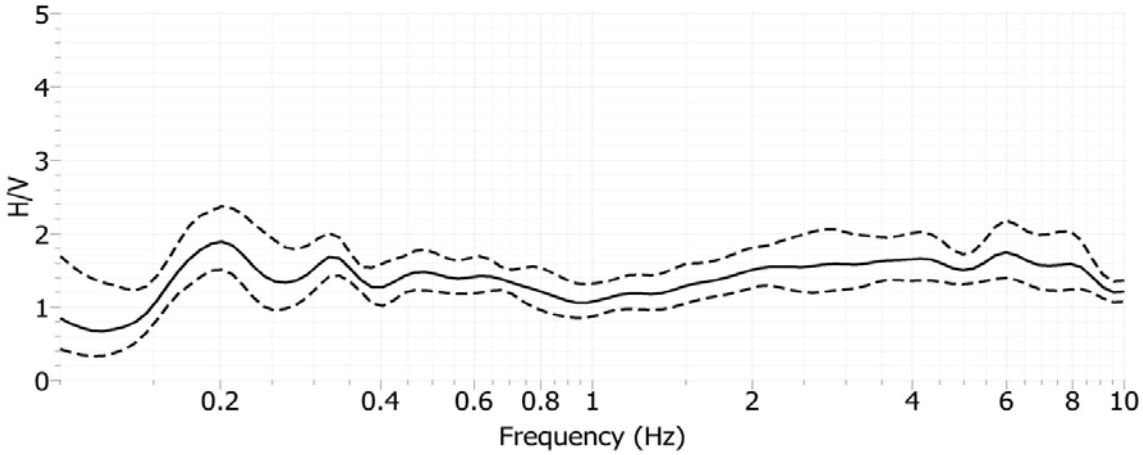

Site CI. CCC, H/V Spectral Ratio, Adjacent to Seismic Station, Sensor 507

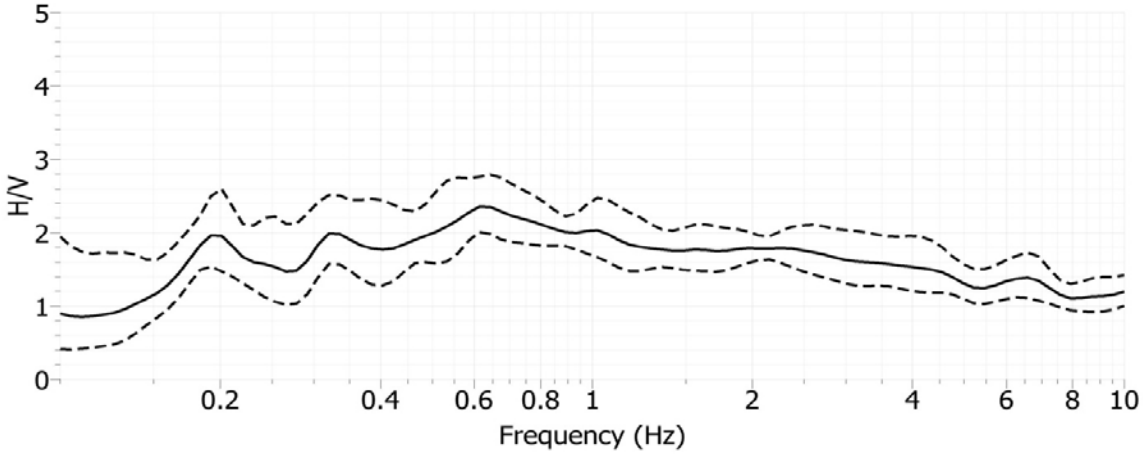

Site CI.CCC, H/V Spectral Ratio, Array CCC-1, Sensor 453

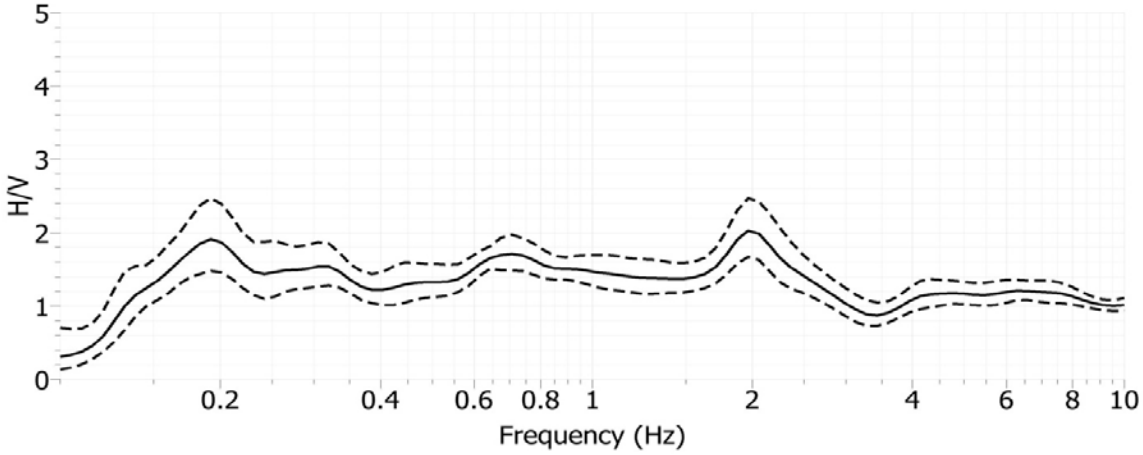

Site CI. CCC, H/V Spectral Ratio, Array CCC-1, Sensor 450

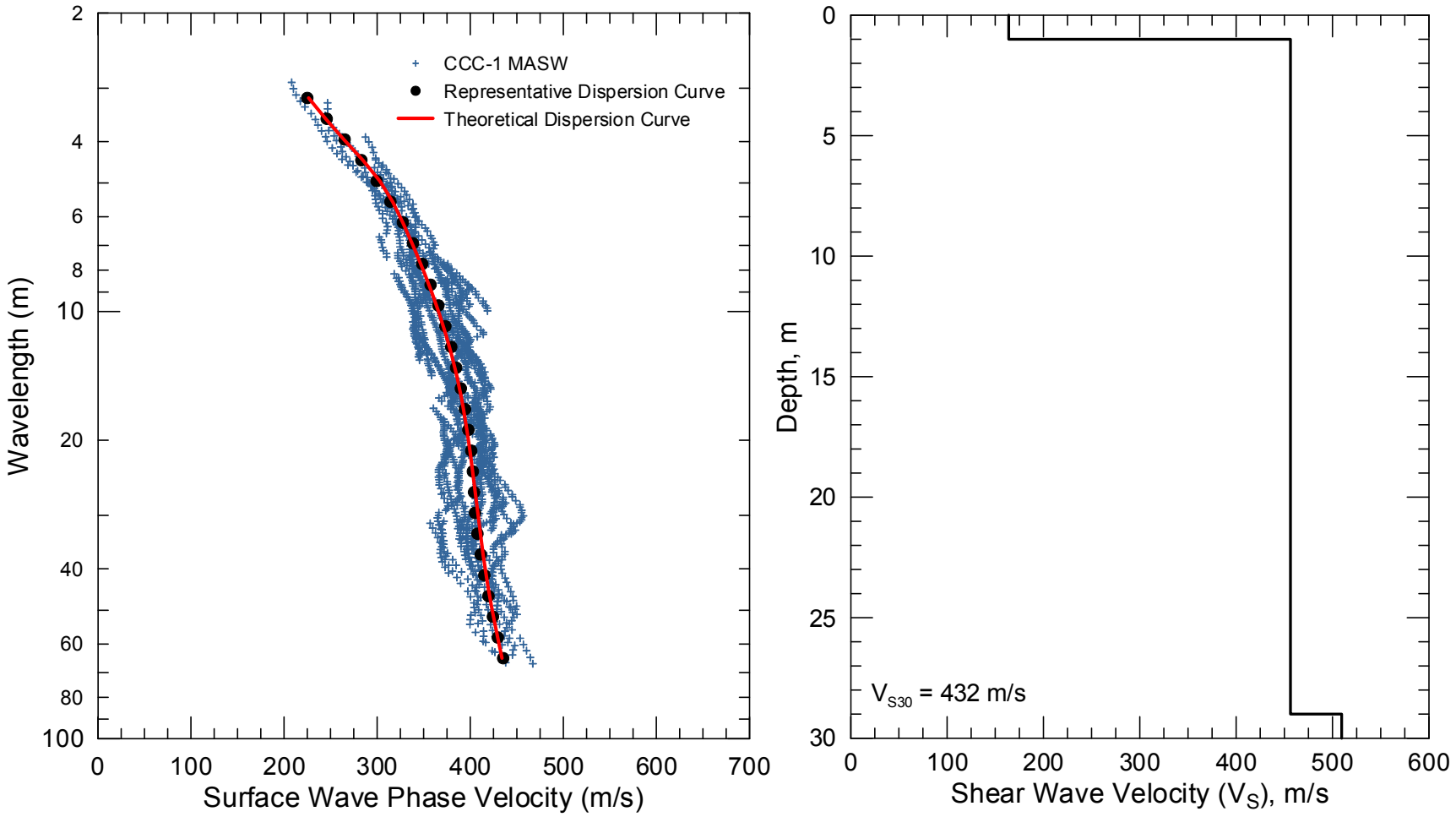

CI.CCC - Field, representative and inverted theoretical surface wave dispersion data (left) and associated V_S model (right)

Site CI.CGO

Location: Cerro Gordo, Keeler, California

Latitude: 36.54998 **Longitude:** -117.80294
(Station coordinates modified based on field GPS survey, WGS84 coordinate system)

V_{S30} (measured): 715 m/s

V_{S30} (adjusted to more accurately reflect seismic station conditions): 739 (average S-wave velocity between 1 and 31 m adjusting for inferred 1 m sensor depth)

NEHRP Site Class: C

Geomatrix Code: IZA

Geologic Conditions/Observations: Seismic station located on weathered and fractured Mississippian Rest Spring Shale unit, which dips about 35 to 45 degrees to the southwest in the site vicinity. Test area located on a sloping ridge of weathered rock.

Site Conditions: Rural site. Steep mountainous terrain in site vicinity. Government communications antennas adjacent to test area. Ground surface elevation decreases about 12 m to the southeast along the 70.5 m long MASW and seismic refraction array CGO-1.

Geophysical Methods Utilized: HVSR, Seismic Refraction, MASW

Geophysical Testing Arrays:

1. Array CGO-1 (48 channel MASW and P-wave seismic refraction array utilizing 4.5 Hz vertical geophones spaced 1.5 m apart for a length of 70.5 m, forward and reverse shot locations with multiple source offsets and source types (hammers only) and center shot location).
2. Three HVSR measurement locations; two distributed along array CGO-1 and one near the seismic station.

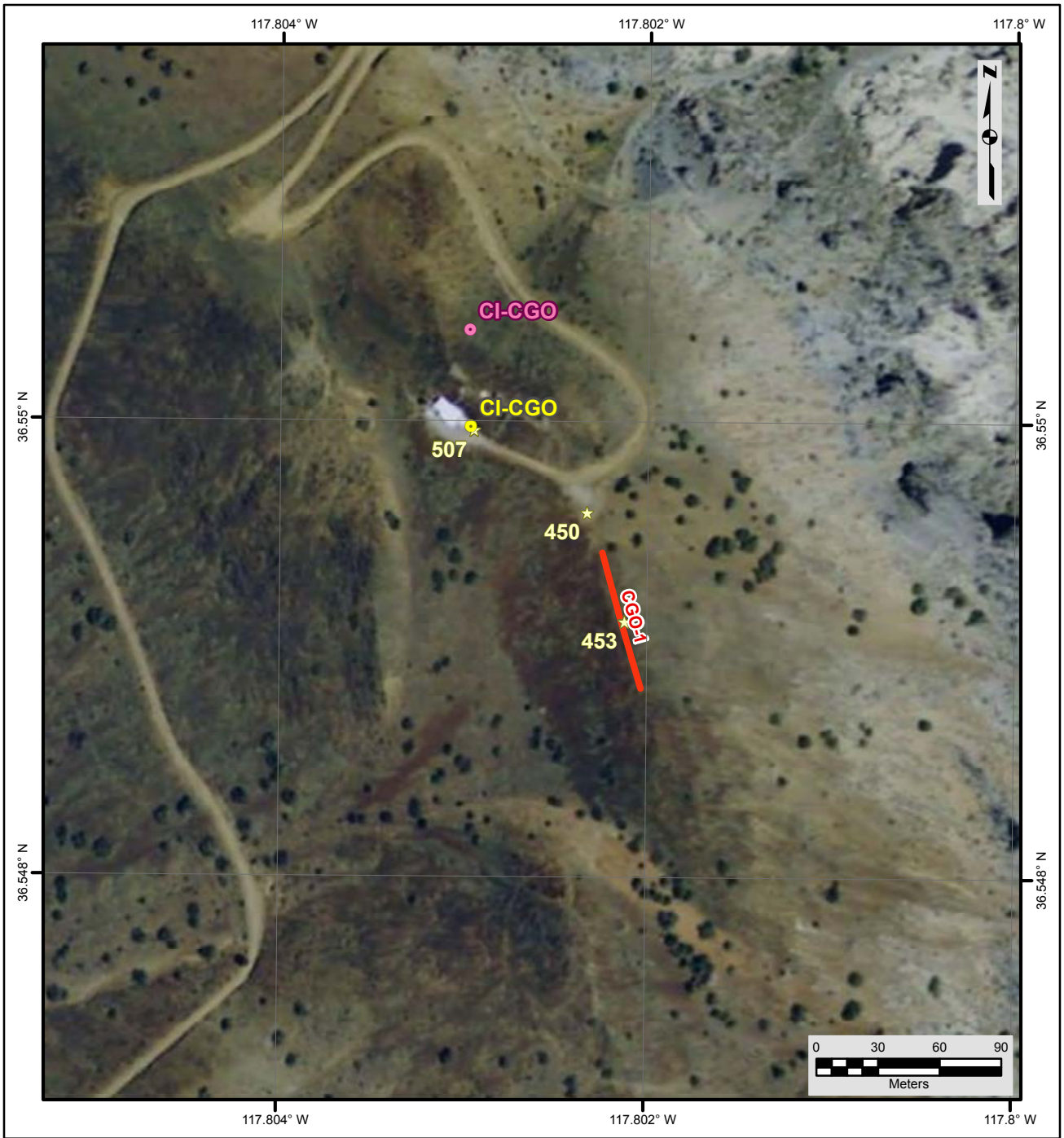

Legend

- Seismic Station - Approximate Surveyed Location
- Seismic Station - Approximate Location of Record
- H/V Spectral Ratio Location
- MASW and Refraction Array

NOTES:
1. WGS 1984 COORDINATE SYSTEM
2. Image Source: ESRI, i-cubed, USDA FSA, USGS, AEX, GeoEye, Getmapping, Aerogrid, IGP

File Name: CI-CGO-I

Date: 10/6/2011

USGS science for a changing world

GEOVision geophysical services

RECOVERY.GOV

SITE MAP
CI•CGO

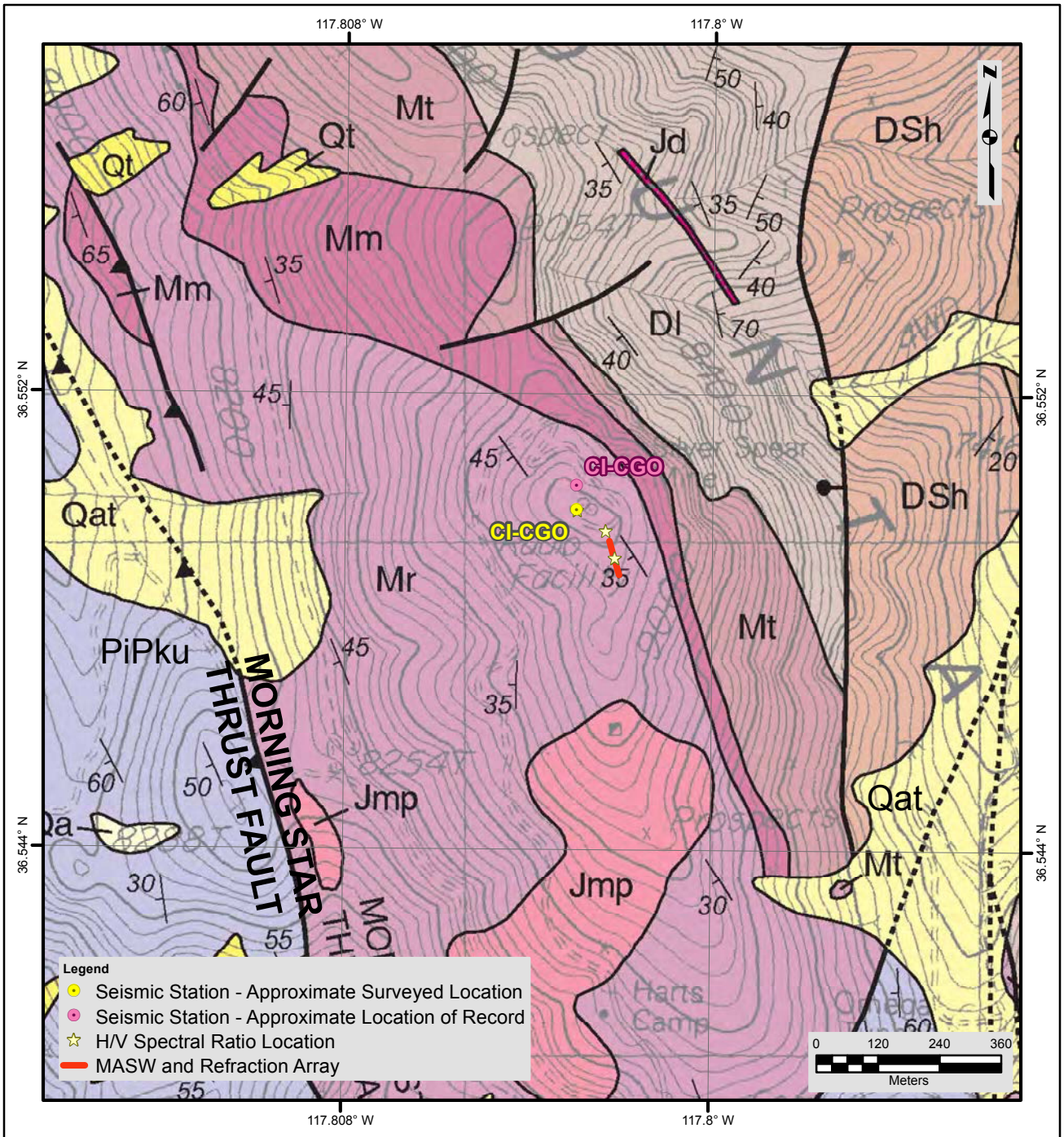

Description of Geologic Map Units

Qt = Quaternary (Holocene) talus
Qat = Quaternary (Holocene) alluvium and talus, undivided
Jmp = Jurassic (?) hornblende monzodiorite to monzonite porphyry
Mr = Paleozoic (Late Mississippian) Rest Spring Shale
Mm = Paleozoic (Late Mississippian) Mexican Spring Formation
Mt = Paleozoic (Early Mississippian) Tin Mountain Limestone
Pipku = Paleozoic (Cisuralian to Middle Pennsylvanian) Upper part of Keeler Canyon Formation
Dl = Paleozoic (Late and Middle Devonian) Lost Burro Formation
DSh = Paleozoic (Middle Devonian to early Silurian) Hidden Valley Dolomite

NOTES:
1. WGS 1984 COORDINATE SYSTEM
2. Geologic Map of the Southern Inyo Mountains and Vicinity Inyo County, California
by Paul Stone, Brian J. Swanson, Calvin H. Stevens, George C. Dunne, and susan S. Priest, 2009
3. See site map for details of geophysical survey

USGS science for a changing world
GEOVision geophysical services

GEOLOGIC MAP
CI•CGO

File Name: CI-CGO
Date: 10/6/2011

Looking north at seismic station CI.CGO

Looking northwest at seismic station CI.CGO and HVSR Sensor 507

P-wave refraction data acquisition along array CGO-1

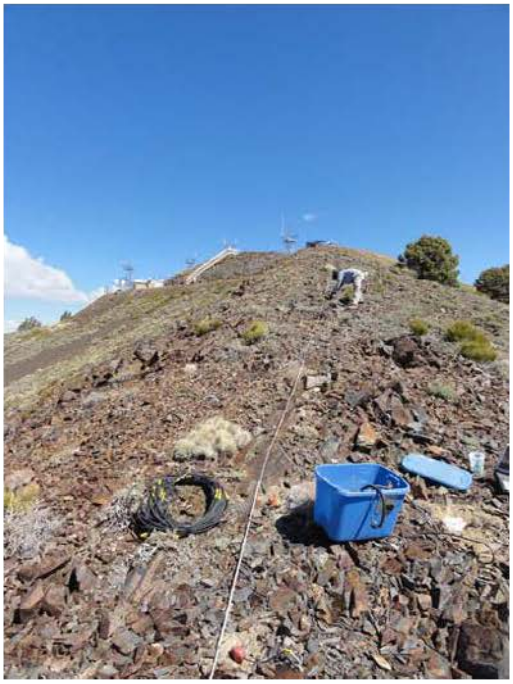

Looking northwest along array CGO-1 toward HVSR sensor 453

MASW data acquisition looking southeast along array CGO-1

Location of Geophysical Testing Arrays:

Location	Latitude	Longitude
CGO-1, Northwest End of MASW/Refraction Array	36.54942	-117.80222
CGO-1, Center of MASW/Refraction Array	36.54912	-117.80212
CGO-1, Southeast End of MASW/Refraction Array	36.54883	-117.80201
HVSR Sensor 450	36.54960	-117.80231
HVSR Sensor 453	36.54912	-117.80210
HVSR Sensor 507	36.54996	-117.80292
CI.CGO Seismic Station	36.54998	-117.80294

Notes: 1) WGS84 Coordinate System (decimal degrees)
2) Survey accuracy is estimated at 1 to 2 m.

Results:

V_S Model

Depth to Top of Layer (m)	Layer Thickness (m)	S-Wave Velocity (m/s)	Inferred P-Wave Velocity (m/s)	Assumed Poisson's Ratio	Assumed Density (g/cm^3)
0	1.5	427	798	0.3	2.1
1.5	2.5	606	1133	0.3	2.1
4	4	659	1233	0.3	2.1
8	6	680	1272	0.3	2.1
14	9	734	1373	0.3	2.1
23	>7	981	1836	0.3	2.2

Notes: 1) Depth of investigation is about 30 m.
2) Bottom layer is a half space.

Observations/Discussion:

- The seismic station in located on a mountain top fill pad for communications antennas. Rock is exposed at the surface in the vicinity of the seismic station.
- Array CGO-1 was located along a ridge to the southeast of the seismic station. There are no other areas in which to attempt site characterization in close proximity to the seismic station. Array CGO-1 is aligned within 15 to 20 degrees of the mapped strike of the geologic bedding in the site vicinity.
- HVSR curves are similar at all sensor locations, particularly sensors 507 and 450. There is no clear HVSR peak, as expected for a rock site. There is slightly elevated HVSR response over the 0.6 to 5 Hz range, which may be related to topography rather than subsurface velocity structure. Data quality is not as good at sensor location 453, possible due to poorer sensor coupling.
- The P-wave refraction data for array CGO-1 were modeled using a tomographic inversion routine with a smooth velocity gradient starting model. The seismic refraction model was extended to far offset shot locations to extend depth of investigation.
- There is some noise in the seismic refraction first arrival data from site facilities, particularly electrical noise from the antennas. Possible out of plane refractions from localized high velocity zones, scattering from heterogeneities and fractures in the rock, may also contribute to minor error in picking of seismic refraction first arrival data.
- The seismic refraction survey design allowed P-wave velocity to be imaged to a maximum depth of about 15 m. Without extension of the model to far offset shot locations, the effective depth of investigation is about 10 m. The seismic refraction model indicates that P-wave velocity increases with depth from about 800 m/s at the surface, 1,100 to 1,200 m/s at a depth of 1 to 5 m, 1,300 to 1,400 m/s at a depth of 5 to 10 m and 1,600 m/s at a depth greater than 15 m.
- Extending the model to far offset shot locations allowed the model to be extended to a greater depth, revealing layers with P-wave velocity on the order of 1,400 to 1,600 m/s at nominal depths of 12 m to 15 m. It should be noted that a longer receiver array would be required to accurately image velocity structure at these depths; however, the far offset shot locations do support P-wave velocity continuing to increase with depth below 15 m.
- The seismic refraction model indicates that there is some lateral velocity variation beneath the line in the upper 10 m, particularly a thicker sequence of lower velocity rock at the southeast end of the line.
- Lateral velocity variation and topography are expected to have some effect on MASW data collected at this site and there were no alternate areas to acquire data in reasonably close proximity to the seismic station. This is a very common problem with mountain top sites.
- Noise conditions at the site were not sufficient for application of passive surface wave techniques.
- The minimum wavelength surface wave phase velocity data extracted from the 48-channel MASW array was about 9 m. Reducing data from smaller hammer sources using a limited offset receiver array (i.e. less active geophones) generally allowed extraction of surface wave dispersion data to a minimum wavelength of about 3.5 m.
- There is significant scatter in the surface wave dispersion data due to lateral velocity variation caused by differential weathering, dipping bedding, topography, etc.

- A representative dispersion curve was generated for the MASW data set using a moving average, polynomial curve fitting routine and used for modeling.
- Surface wave depth of investigation is about 30 m based on half of maximum wavelength criteria.
- The inferred P-wave velocities in the surface wave model, based on an assumed Poisson's ratio of 0.3 and modeled S-wave velocity, are generally consistent with the P-wave refraction model.
- The S-wave velocity model derived from the surface wave testing is believed to be representative of average subsurface velocity structure. However, geology at the site is complex, with dipping bedding and it is difficult to predict the effect of dipping beds on surface wave dispersion data.
- V_{S30} is 715 m/s (Site Class C).
- Average S-wave velocity between 1 m (assumed sensor depth) and 31 m is 739 m/s (Site Class C/B).

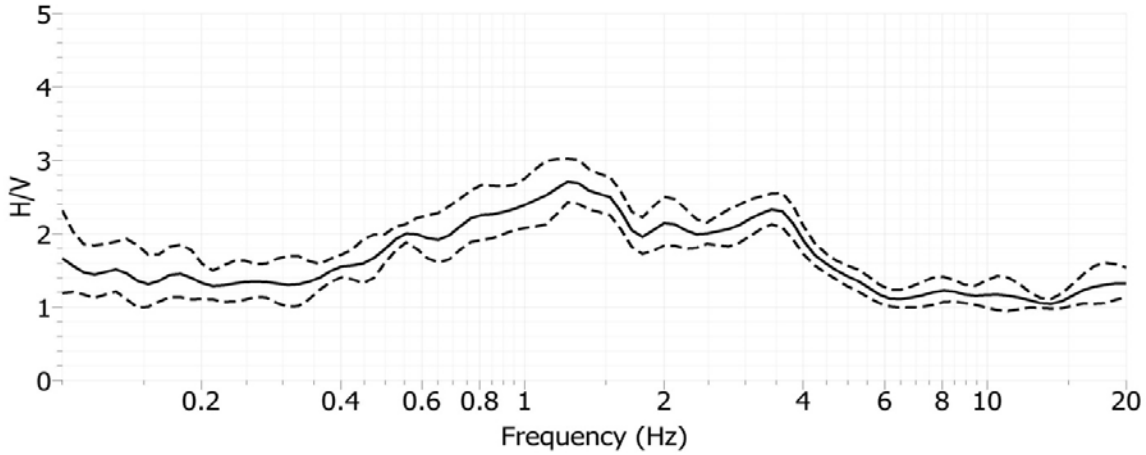

Site CI.CGO, H/V Spectral Ratio, Near Seismic Station, Sensor 507

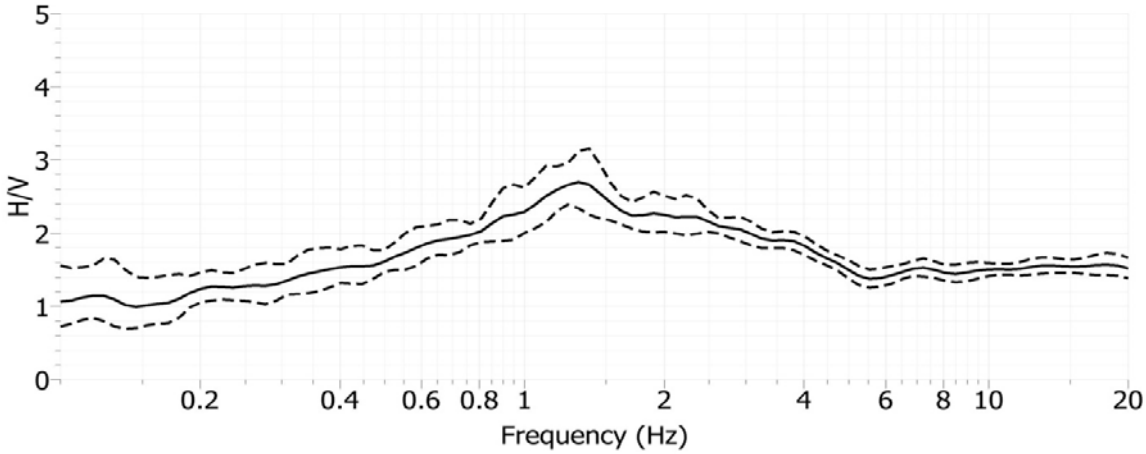

Site CI.CGO, H/V Spectral Ratio, Array CGO-1, Sensor 450

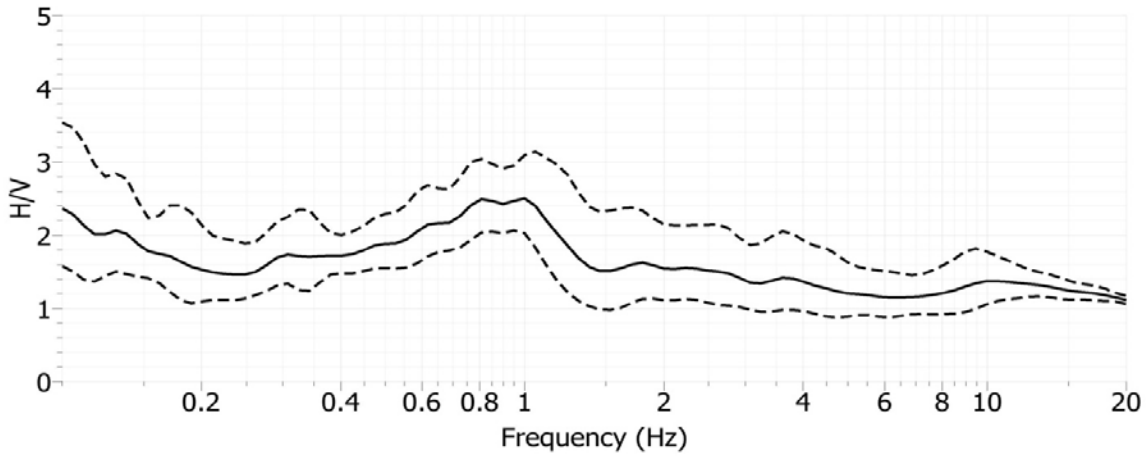

Site CI.CGO, H/V Spectral Ratio, Array CGO-1, Sensor 453

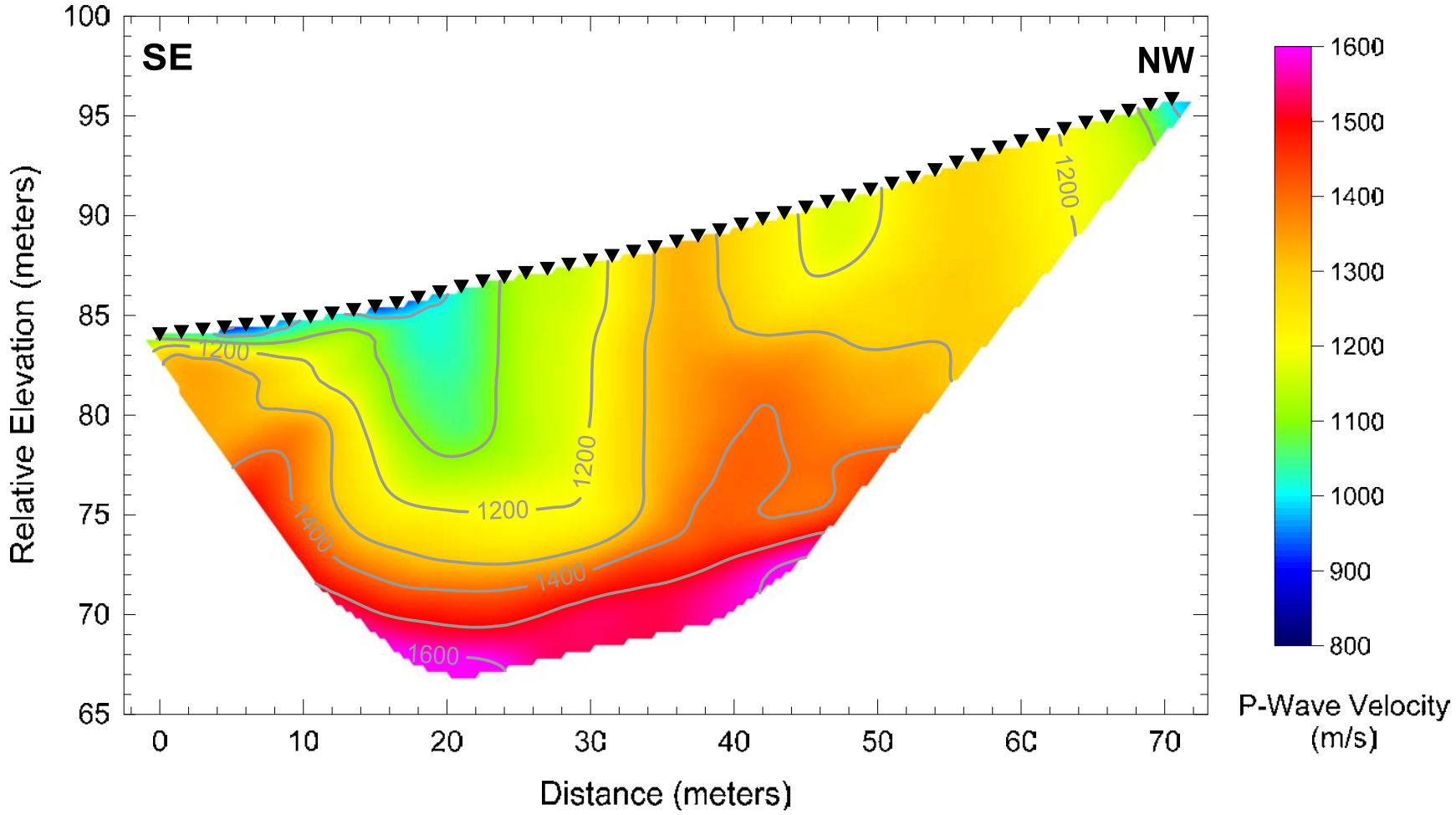

Array CGO-1 – Tomographic seismic refraction model utilizing smooth velocity gradient starting model

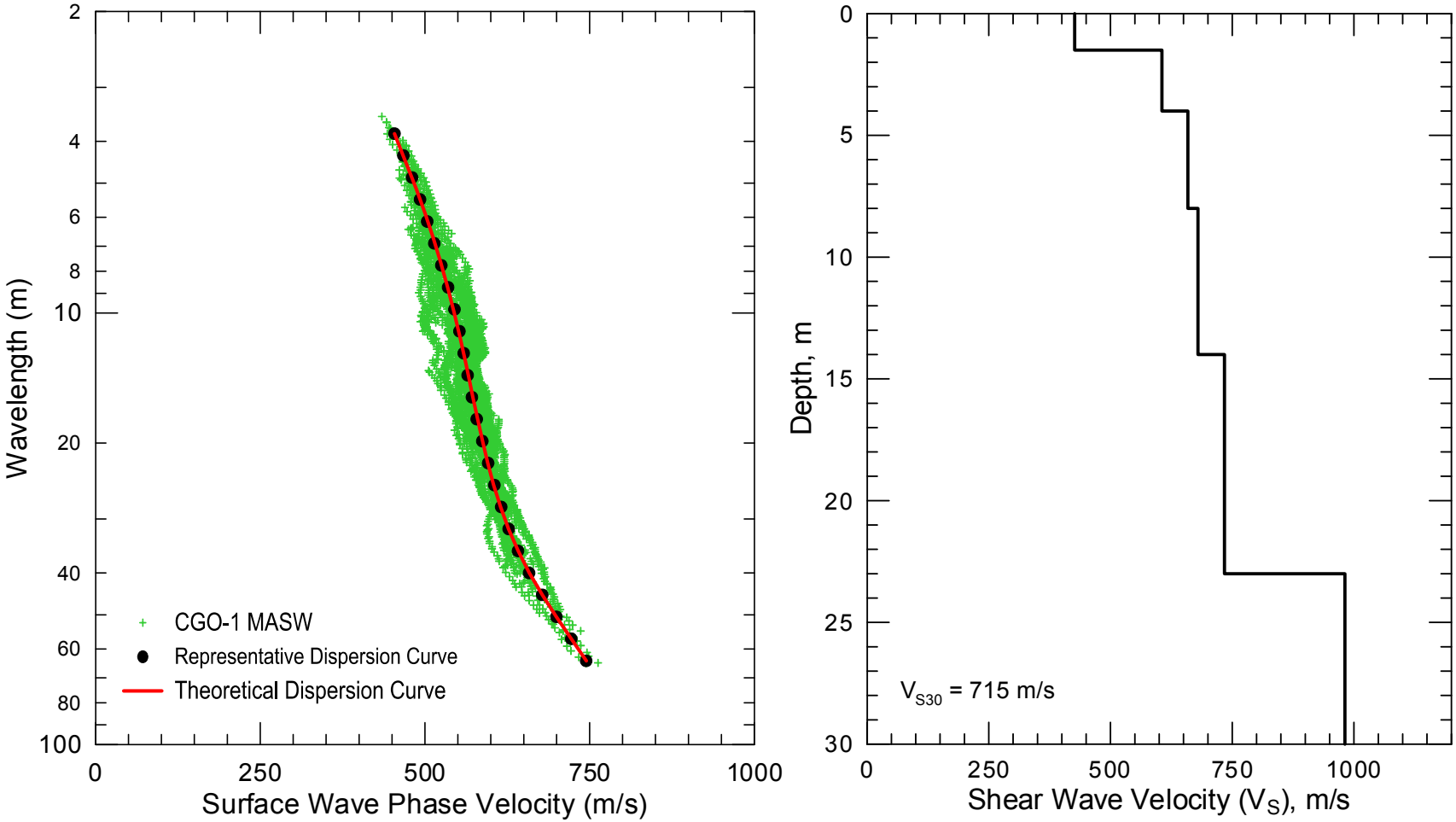

CI.CGO - Field, representative and inverted theoretical surface wave dispersion data (left) and associated V_S model (right)

Site CI.CHF

Location: Chilao Flat Ranger Station, Los Angeles County, California

Latitude: 34.33338 **Longitude:** -118.02588
(Station coordinates modified based on field GPS survey, WGS84 coordinate system)

V_{S30} (measured): 927 m/s

V_{S30} (adjusted to more accurately reflect seismic station conditions): 1,032 m/s (average S-wave velocity between 1.5 and 31.5 m adjusting for 1.5 m assumed sensor depth).

NEHRP Site Class: B

Geomatrix Code: IGA

Geologic Conditions/Observations: Seismic station located on geologic unit mapped as Messozoic (Triassic) Lowe granodiorite. Field observations indicate that a thin layer of sand (residual soil) overlies weathered rock.

Site Conditions: Rural site located in a flat, open mountain meadow with gently sloping hills near a ranger station. Steeper mountainous terrain within about 300 m of the site. Ground surface elevation decreases by about 5 m to the northeast along the 70.5 m long MASW and seismic refraction array.

Geophysical Methods Utilized: HVSR, Seismic Refraction, MASW.

Geophysical Testing Arrays:

1. Array CHF-1 (48 channel MASW and P-wave seismic refraction array utilizing 4.5 Hz vertical geophones spaced 1.5 m apart for a length of 70.5 m, forward and reverse shot locations with multiple source offsets and source types (hammers only) and multiple interior shot locations).
2. Three HVSR measurement locations: two distributed along array CHF-1 and one adjacent to the seismic station.

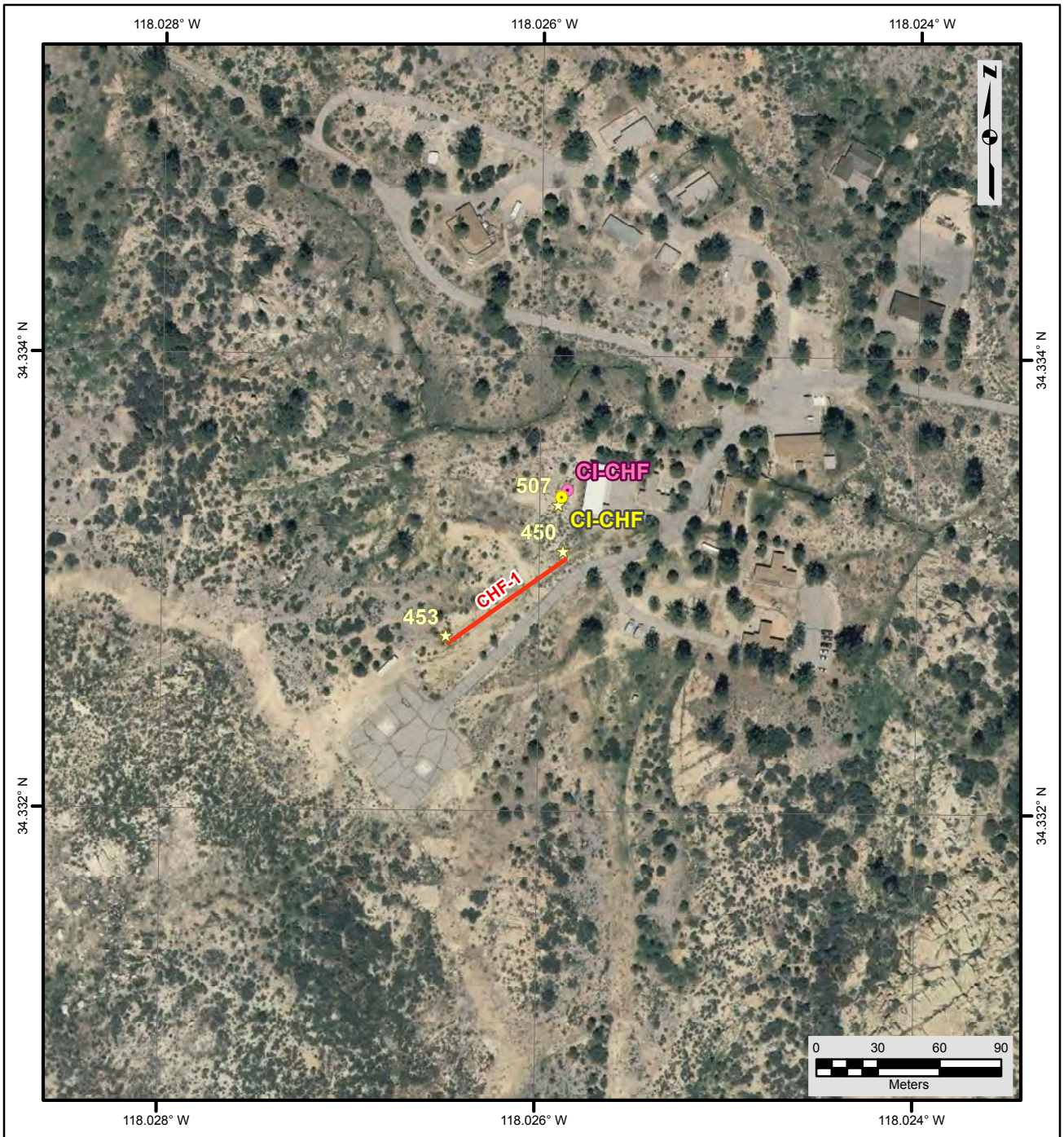

Legend

- Seismic Station - Approximate Surveyed Location
- Seismic Station - Approximate Location of Record
- H/V Spectral Ratio Location
- MASW and Seismic Refraction Array

NOTES:
1. WGS 1984 COORDINATE SYSTEM
2. Image Source: ESRI, i-cubed, USDA FSA, USGS, AEX, GeoEye, Getmapping, Aerogrid, IGP

File Name: CI-CHF-I

Date: 9/16/2011

USGS science for a changing world

GEOVision geophysical services

RECOVERY.GOV

SITE MAP
CI•CHF

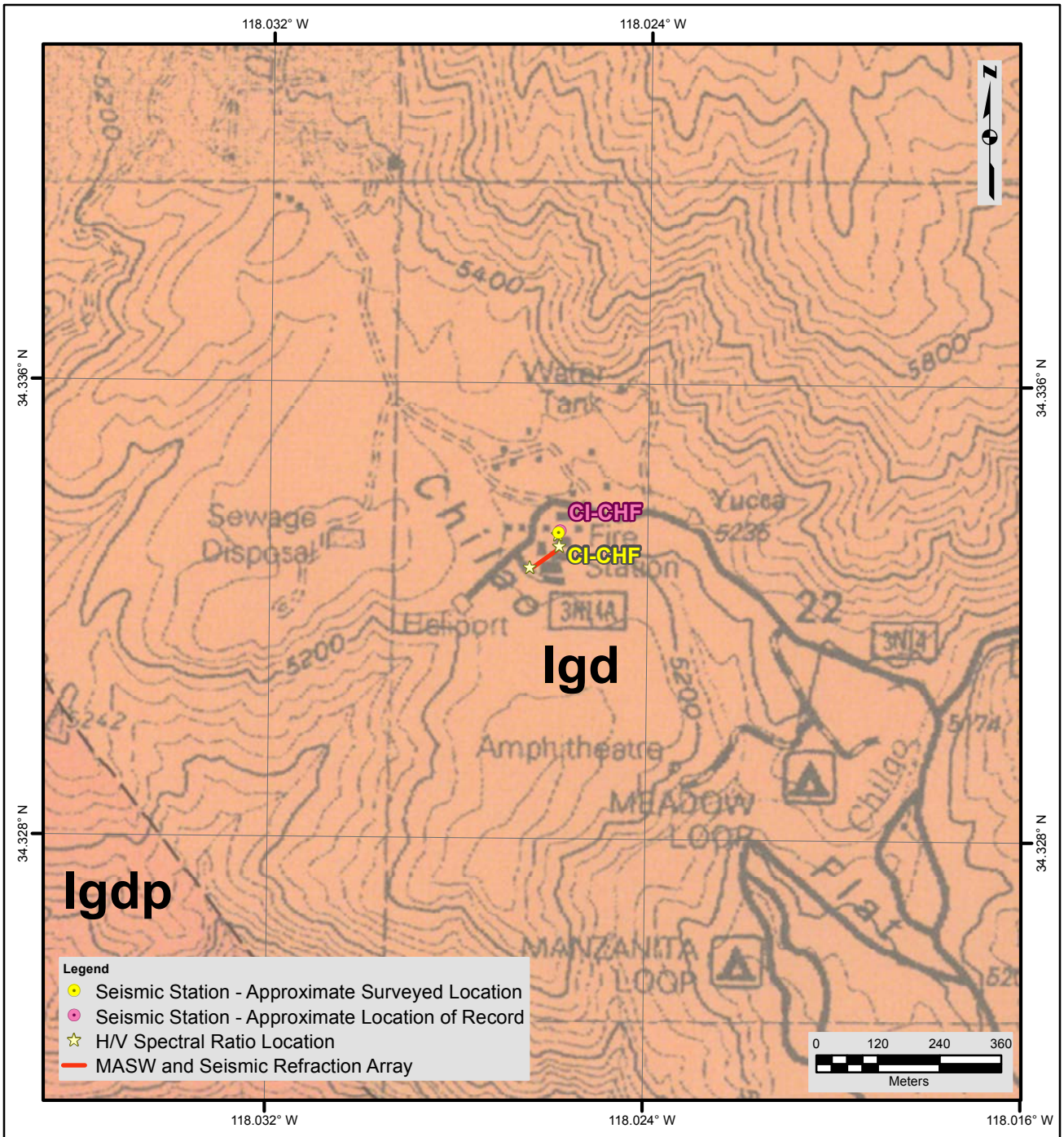

Description of Geologic Map Units

lgd = Mesozoic (Triassic) Lowe granodiorite, undivided, nearly white massive to vaguely gneissoid; contains sparse biotite as minute black flakes; sparse orthoclase phenocrysts; little or no hornblende

lgdp = Mesozoic (Triassic) Lowe granodiorite, porphorytic, with scattered to abundant large orthoclase phenocrysts mostly in lower (SW) part; minor hornblende and scattered crystals of crumbly reddish garnet; slightly gneissoid

NOTES:
1. WGS 1984 COORDINATE SYSTEM
2. Geologic Map of the Chilao Flat Quadrangle, Los Angeles County, California by Thomas W. Dibblee, Jr., 2002
3. See site map for details of geophysical survey

File Name: CI-CHF

Date: 9/16/2011

USGS science for a changing world

GEOVision geophysical services

RECOVERY.GOV

GEOLOGIC MAP
CI•CHF

Looking south and seismic station CI.CHF and HVSR sensor 507

Looking north towards northeastern end of array CHF-1

Looking northeast at HVSR sensors 507 (Nanometrics Trillium Compact) and Tromino ENGR and seismic station

P-wave seismic refraction and MASW data acquisition

Looking southwest along array CHF-1 and at small hammer used for acquisition of high frequency MASW data

Location of Geophysical Testing Arrays:

Location	Latitude	Longitude
CHF-1, Southwest End of MASW/Refraction Array	34.33273	-118.02647
CHF-1, Center of MASW/Refraction Array	34.33292	-118.02617
CHF-1, Northeast End of MASW/Refraction Array	34.33311	-118.02586
HVSR Sensor 450	34.33314	-118.02587
HVSR Sensor 453	34.33277	-118.02649
HVSR Sensor 507	34.33334	-118.02590
CI.CHF Seismic Station	34.33338	-118.02588

Notes: 1) WGS84 Coordinate System (decimal degrees)
2) Survey accuracy is estimated at 1 to 2 m.

Results:

V_S Model 1FM (Not Valid)

Depth to Top of Layer (m)	Layer Thickness (m)	S-Wave Velocity (m/s)	Inferred P-Wave Velocity (m/s)	Assumed Poisson's Ratio	Assumed Density (g/cm^3)
0	1.5	373	646	0.25	1.90
1.5	4.5	658	1139	0.25	2.10
6	4.5	835	1447	0.25	2.10
10.5	7	1223	2118	0.25	2.15
17.5	8	1500	2598	0.25	2.25
25.5	>9.5	3318	5747	0.25	2.60

Notes: 1) Data modeled assuming dispersion curve represents the fundamental mode.
2) Depth of investigation is about 35 m.
3) Bottom layer is a half space.
4) Velocity of half-space not well constrained.

V_S Model 1AM

Depth to Top of Layer (m)	Layer Thickness (m)	S-Wave Velocity (m/s)	Inferred P-Wave Velocity (m/s)	Assumed Poisson's Ratio	Assumed Density (g/cm^3)
0.0	1.5	372	644	0.25	1.90
1.5	4.5	648	1123	0.25	2.10
6.0	4.5	841	1456	0.25	2.10
10.5	7.0	1201	2079	0.25	2.15
17.5	8.0	1500	2598	0.25	2.20
25.5	>9.5	2200	3810	0.25	2.40

Notes: 1) Data modeled assuming dispersion curve represents the average/effective mode (based on relative amplitude of the fundamental and higher surface wave modes).
2) Depth of investigation is about 35 m.
3) Bottom layer is a half space.

V_S Model 2FM

Depth to Top of Layer (m)	Layer Thickness (m)	S-Wave Velocity (m/s)	Inferred P-Wave Velocity (m/s)	Assumed Poisson's Ratio	Assumed Density (g/cm^3)
0	1.5	365	683	0.30	1.90
1.5	4.5	637	1192	0.30	2.10
6	4.5	794	2267	0.43	2.15
10.5	7	1061	2857	0.42	2.25
17.5	8	1215	3112	0.41	2.35
25.5	>9.5	2018	4007	0.33	2.50

Notes: 1) Data modeled assuming dispersion curve represents the fundamental mode.
2) Depth of investigation is about 35 m.
3) Bottom layer is a half space.

V_S Model 2AM

Depth to Top of Layer (m)	Layer Thickness (m)	S-Wave Velocity (m/s)	Inferred P-Wave Velocity (m/s)	Assumed Poisson's Ratio	Assumed Density (g/cm^3)
0.0	1.5	364	680	0.30	1.90
1.5	4.5	621	1150	0.29	2.10
6.0	4.5	797	2275	0.43	2.15
10.5	7.0	1073	2850	0.42	2.25
17.5	8.0	1250	3150	0.41	2.35
25.5	>9.5	1749	3950	0.38	2.45

Notes: 1) Data modeled assuming dispersion curve represents the average/effective mode (based on relative amplitude of the fundamental and higher surface wave modes).
2) Depth of investigation is about 35 m.
3) Bottom layer is a half space.

Observations/Discussion:

- There is no clear HVSR peak at this site, as expected for a rock site.
- The P-wave refraction data for array CHF-1 were modeled using a tomographic inversion routine with a smooth velocity gradient starting model. The seismic refraction model was extended to far offset shot locations to extend depth of investigation. Seismic refraction data quality was very good.
- The seismic refraction survey design allowed P-wave velocity to be imaged to a maximum depth of about 25 m. Without extension of the model to far offset shot locations, the effective depth of investigation would have been limited to about 10 to 15 m.
- The seismic refraction model shows that P-wave velocity is about 500 to 800 m/s at the surface, increasing to 2,000 m/s at a depth of 1 to 4 m, 3,000 m/s at a depth of 6 to 8 m and possibly greater than 4,000 m/s at depths below 12 to 19 m.
- Extending the model to far offset shot locations allowed the model to be extended to a greater depth, revealing layers with P-wave velocity on the order of 4,000 m/s at nominal depths of 12 m to 19 m. It should be noted that a longer receiver array would be required to accurately image velocity structure at these depths; however, the far offset shot locations do support P-wave velocity continuing to increase with depth below 10 m.
- The seismic refraction model indicates that there is lateral velocity variation at this site, with higher P-wave velocities at shallower depth near the southwest end of the line.
- Noise conditions at the site were not sufficient for application of passive surface wave techniques.
- The minimum wavelength surface wave phase velocity data extracted from the 48-channel MASW array was about 21 m. Data reduction using seismic records from smaller hammer sources and a limited offset receiver array (i.e. less active geophones), primarily from source locations in the southern portion of the line, allowed extraction of surface wave dispersion data to a minimum wavelength of about 3.5 m.
- Modeling was conducted using small wavelength (high frequency) Rayleigh wave phase velocity data from limited offset receiver gathers at the northeast end of the line, which is closest to the seismic station. Near surface velocities are slightly higher at the southwest end of the line, as shown in the seismic refraction model.
- There is about a 100 m/s scatter in the MASW dispersion data used for modeling, which is likely due to lateral velocity variation associated with differential weathering of near surface rock.
- A representative dispersion curve was generated for the MASW data set using a moving average, polynomial curve fitting routine and used for modeling.
- Several V_S models were generated from the surface wave data. Model 1FM was developed assuming the dispersion curve consists of only the fundamental mode Rayleigh wave and an assumed Poisson's ratio of 0.25. The velocity of the half space in the model appears unrealistically high, although the P-wave seismic refraction survey did not image to great enough depth to confirm. Additionally, multi-mode modeling reveals that the V_S model should excite a dominant first higher mode at low frequencies. There is expected to be insufficient resolution in the v-f transform (overtone image) to isolate the fundamental mode and first higher mode at low frequencies and, therefore, the fundamental and first higher modes may be superposed (modal superposition/mode mixing). Given the high velocities at the site, a significantly longer receiver array

(several hundred meters) would likely be required to obtain sufficient resolution in v-f space to separately identify the fundamental and first higher modes. This type of space is generally not available at rock sites and longer arrays invariably introduce more lateral velocity variation. Because of possible modal superposition, an alternate V_S model (Model 1AM) was developed assuming the observed dispersion curve consists of the average/effective mode (average of all modes based on relative amplitude of each mode for a far-field source and plane wave). We cannot state with certainty that the observed dispersion data consists of the average mode, but this is a better option than incorrectly assuming that the dispersion data is the fundamental mode. Model 1AM is very similar to Model 1FM, but yields a significantly lower and more realistic velocity for the half space.

- Models 1FM and 1AM, developed using an assumed Poisson's ratio of 0.25, result in P-wave velocities significantly lower that the seismic refraction model. Seismic refraction data quality is very good and there is no evidence that the refraction model is affected by out of plane refractors from local high velocity zones, such as dikes, although the occurrence of out of plane refractors cannot be completely discounted. Therefore, alternate models were developed, assuming both fundamental and average mode (Models 2FM and 2AM), using variable Poisson's ratio in the 0.3 to 0.43 range to better reflect, but still underestimate, the P-wave velocity in seismic refraction model. Even if highly fractured, weathered and saturated, Poisson's ratio as high as 0.43 may not be realistic for granitic rocks. An S-wave refraction survey would be required to confirm Poisson's ratio. The higher Poisson's ratio results in models that excite the first higher model to a lesser degree over the frequency range of interest and, therefore, the fundamental and average mode models are more similar.
- Interestingly, V_{S30} is quite similar between the fundamental and average mode models, but only because there is not significant energy in the first higher mode until wavelengths greater than 40 m. V_{S30} is about 10% lower for the models with a variable Poisson's ratio between 0.3 and 0.43 as compared to those with a Poisson's ratio of 0.25. Only about half of this difference can be attributed to the change in Poisson's ratio, although more testing is required, and the remaining difference appears to be associated with the effect of Poisson's ratio on higher mode amplitudes and resulting influence of modal superposition.
- Love wave MASW (MALW) data was not applied at this site because data quality appeared to be quite good in the field. Love wave MASW may be better suited to characterizing sites with the observed velocity structure because variations in Poisson's ratio do not affect the dispersion curve and higher mode Loves waves should not be an issue at long wavelengths.
- Surface wave depth of investigation is about 35 m based on half of maximum wavelength criteria.
- V_{S30} is 1,047 and 1,016 m/s for Models 1FM and 1AM (Poisson's ratio of 0.25), respectively (Site Class B). We don't believe that model 1FM is valid.
- Average S-wave velocity between 1.5 m (compensating for assumed sensor depth) and 31.5 m is 1,195 and 1,146 m/s for Models 1FM and 1AM, respectively.
- V_{S30} is 930 and 923 m/s for Models 2FM and 2AM (variable Poisson's ratio between 0.29 and 0.43), respectively, and averages 927 m/s (Site Class B).

Average S-wave velocity between 1.5 m (compensating for assumed sensor depth) and 31.5 m is 1,039 and 1,025 m/s for Models 2FM and 2AM, respectively, and averages 1,032 m/s.

- Modeling of the upper and lower envelopes of the MASW dispersion curves was not conducted, but would result in about a 5% variation of V_{S30}.
- Until further data on Poisson's ratio becomes available, V_{S30} should be considered to be about 927 m/s (average V_{S30} between models 2FM and 2AM) because inferred P-wave velocities in Model 2 better agree, although are still somewhat low, with the seismic refraction model.
- Further investigation is warranted at this site. The velocity structure at this site is not expected to excite dominant higher mode Love waves, therefore, the Love wave MASW (MALW) technique would be practical. S-wave refraction could be used to better constrain Poisson's ratio in the Rayleigh wave models. A longer P-wave refraction line would allow the P-wave velocity to be better constrained in the 15 to 30 m depth range. It would also be interesting to evaluate the effectiveness of array based modeling of SASW data at accounting for the influence of higher modes in the dispersion data.

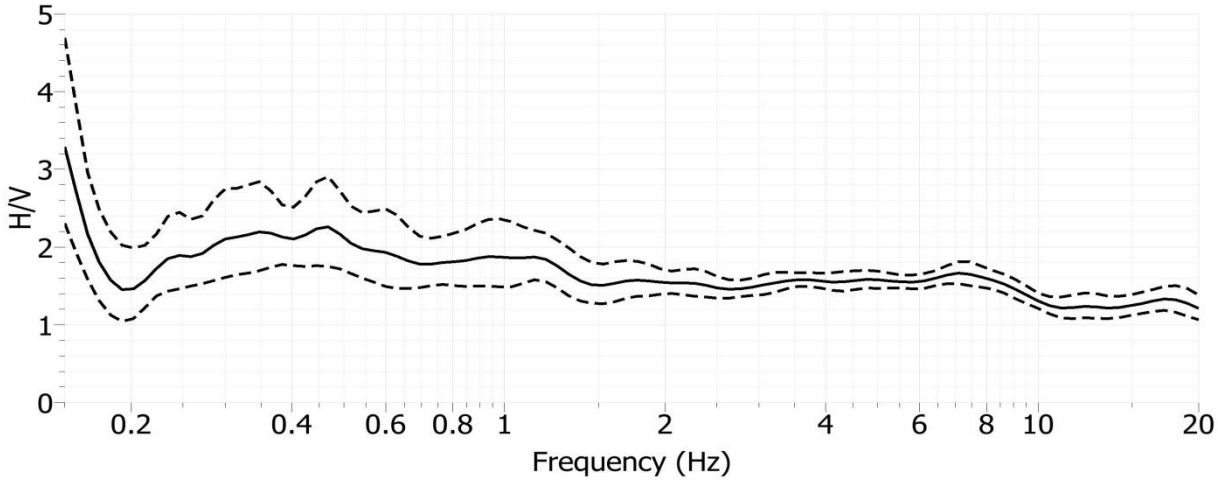

Site CI.CHF, H/V Spectral Ratio, Near Seismic Station, Sensor 507

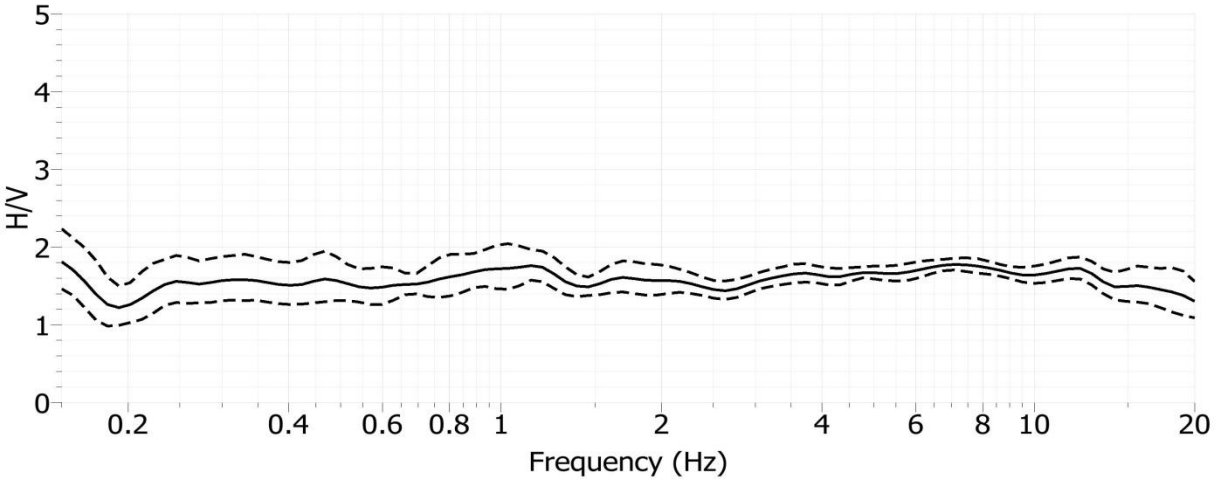

Site CI.CHF, H/V Spectral Ratio, Array CHF-1, Sensor 450

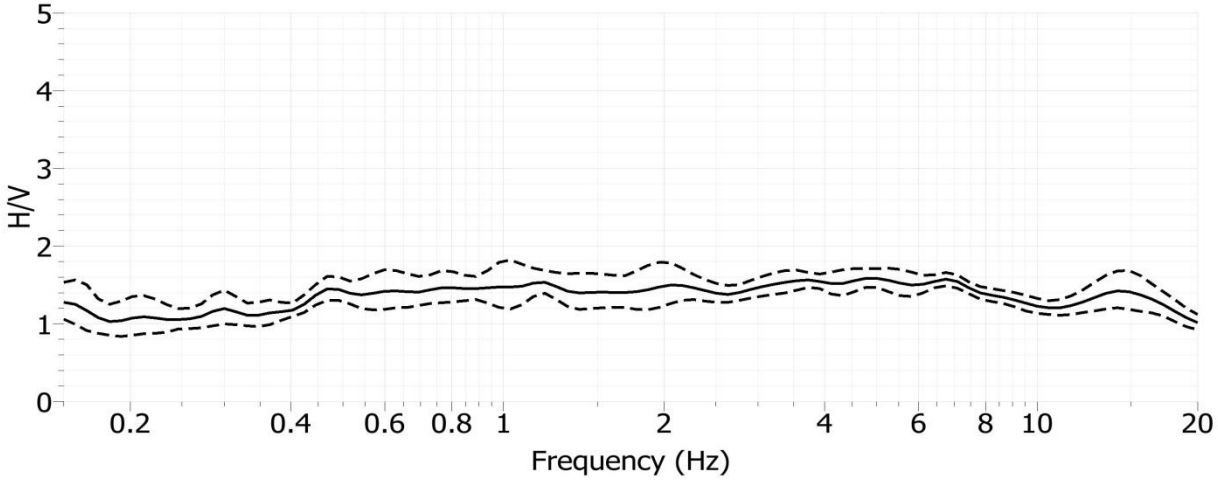

Site CI.CHF, H/V Spectral Ratio, Array CHF-1, Sensor 453

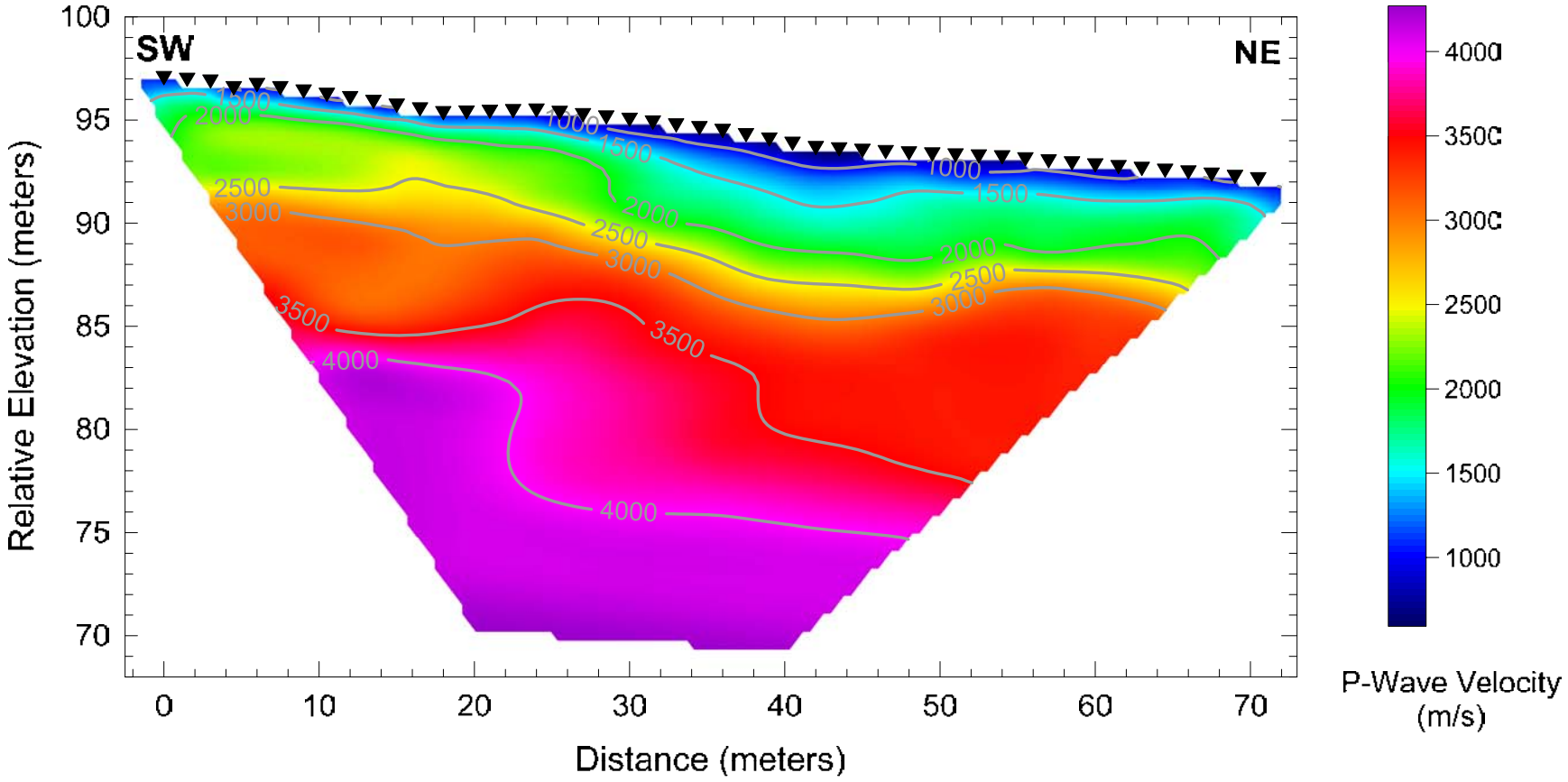

Array CHF-1 – Tomographic seismic refraction model utilizing smooth velocity gradient starting model

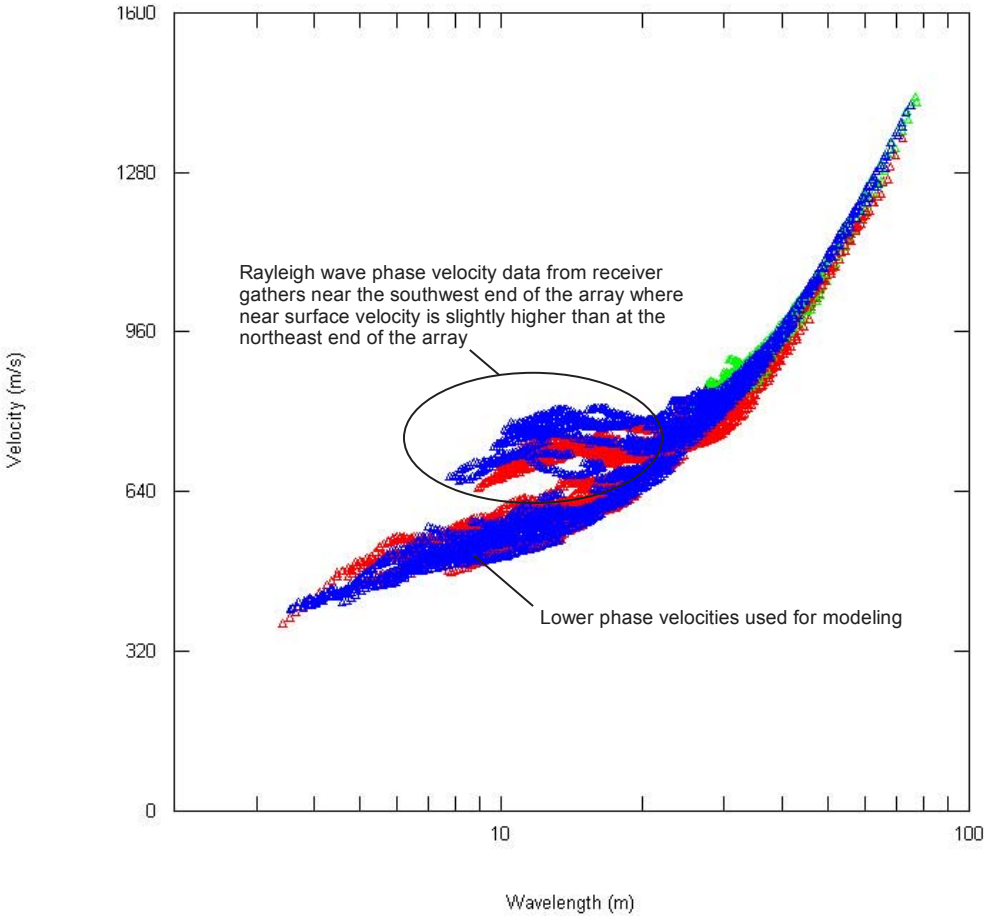

CI.CHF – MASW dispersion data illustrating the effects of near surface lateral velocity variation. Rayleigh wave phase velocities from shot locations at the southwestern end of the array are higher at small wavelengths than those from the northeastern end of the array. The seismic refraction model clearly shows a slightly thinner residual soil layer and less near surface weathering at the southwestern end of the array. The dispersion curves merge at long wavelengths so no significant impact on V_{S30} is expected. This is a common problem at weathered rock sites where lateral velocity variation occurs to varying degrees. At this site, the lower phase velocity data were selected for modeling because the northeast end of the array is closer to the seismic station. Because the minimum wavelength extracted from the 48 channel receiver gathers at this site was about 21 m, the small wavelength phase velocity were only extracted from limited offset receiver gathers, thereby, revealing the extent of near surface lateral velocity variation. Generally, a group of small wavelength dispersion data (e.g. source locations and receiver gathers from a specific segment of the array) is most consistent with the long wavelength dispersion data and selected for modeling. At some sites, modeling of multiple dispersion curves is conducted to assess the effect of lateral velocity variation. In cases of significant lateral velocity variation over a large depth range, dispersion curves from forward and reverse shots can completely diverge over a wide wavelength/frequency range, whereby surface wave techniques are not viable for site characterization.

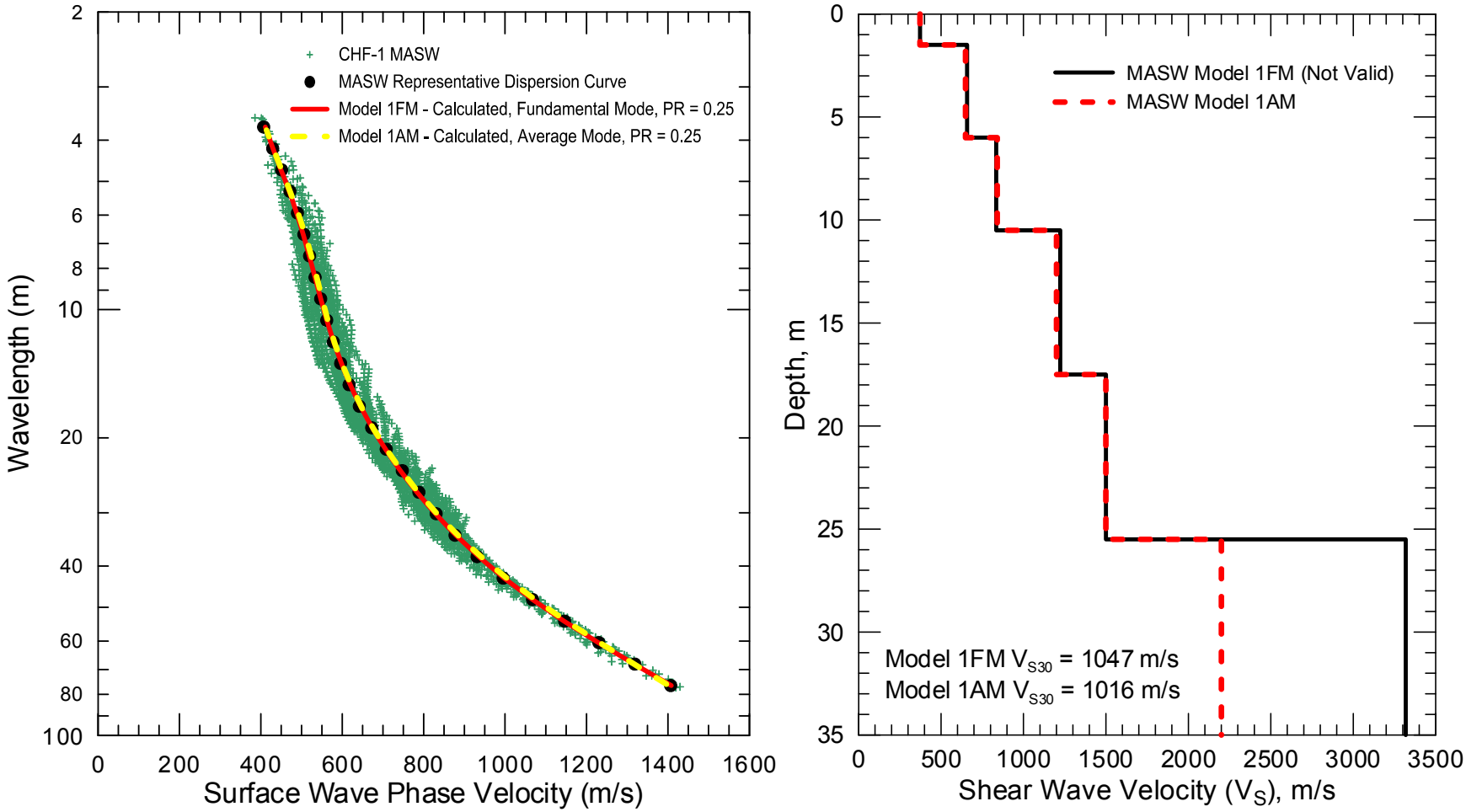

CI.CHF - Field, representative and inverted theoretical surface wave dispersion data (left) and associated V_S models (right) for Model 1, modeled using both fundamental mode and average/effective mode assumptions and an assumed Poisson's ratio of 0.25. The half space velocity in the V_S model developed using the fundamental mode assumption appears to be overestimated due to probable modal superposition at long wavelengths. V_{S30} is similar between the two models because the first higher mode does not significantly affect the dispersion curve until wavelengths greater than about 40 m.

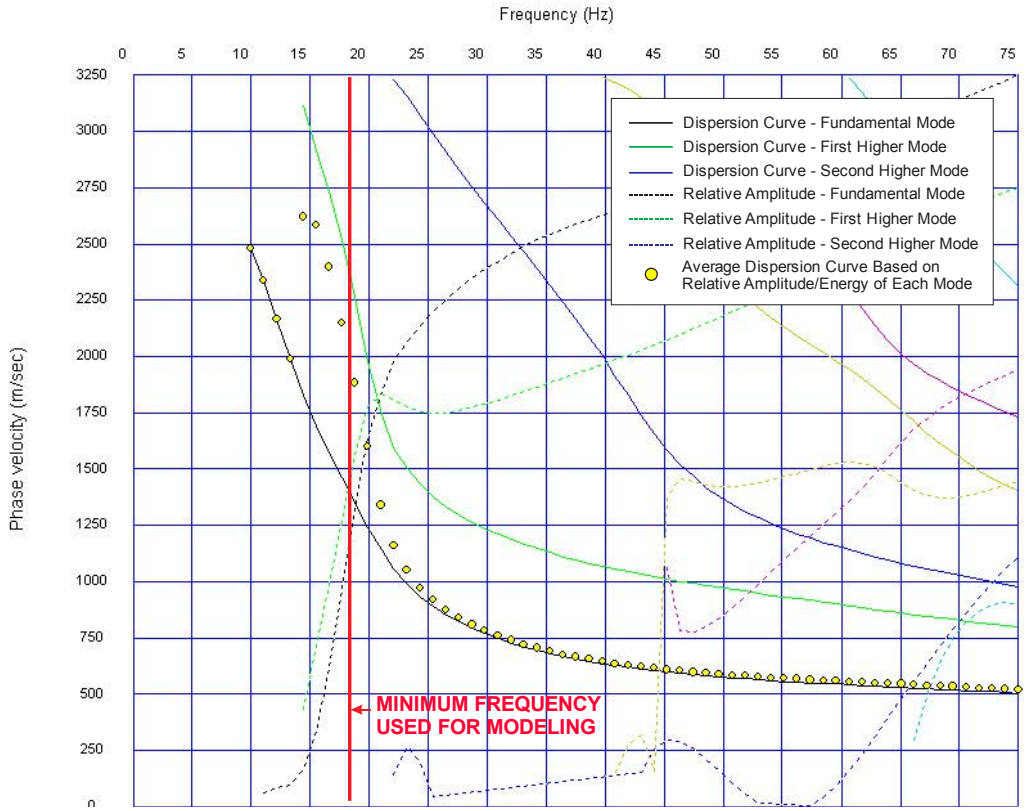

CI.CHF – Model 1FM (fundamental mode, Poisson's Ratio = 0.25) not valid as first higher mode expected to be dominant between a frequency of 14 and 20 Hz.

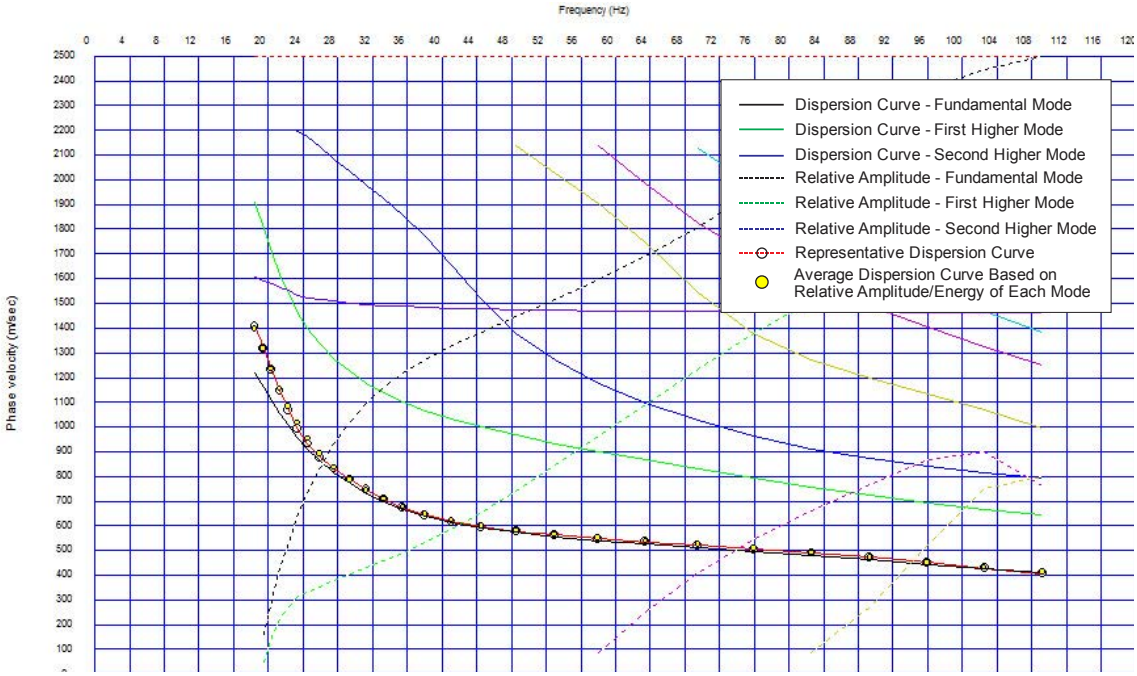

CI.CHF – Model 1AM (average mode, Poisson's Ratio = 0.25). There is insufficient resolution in the v-f transform to isolate separate modes at low frequencies. Modal superposition at low frequencies is <u>assumed</u> to be represented by the average mode.

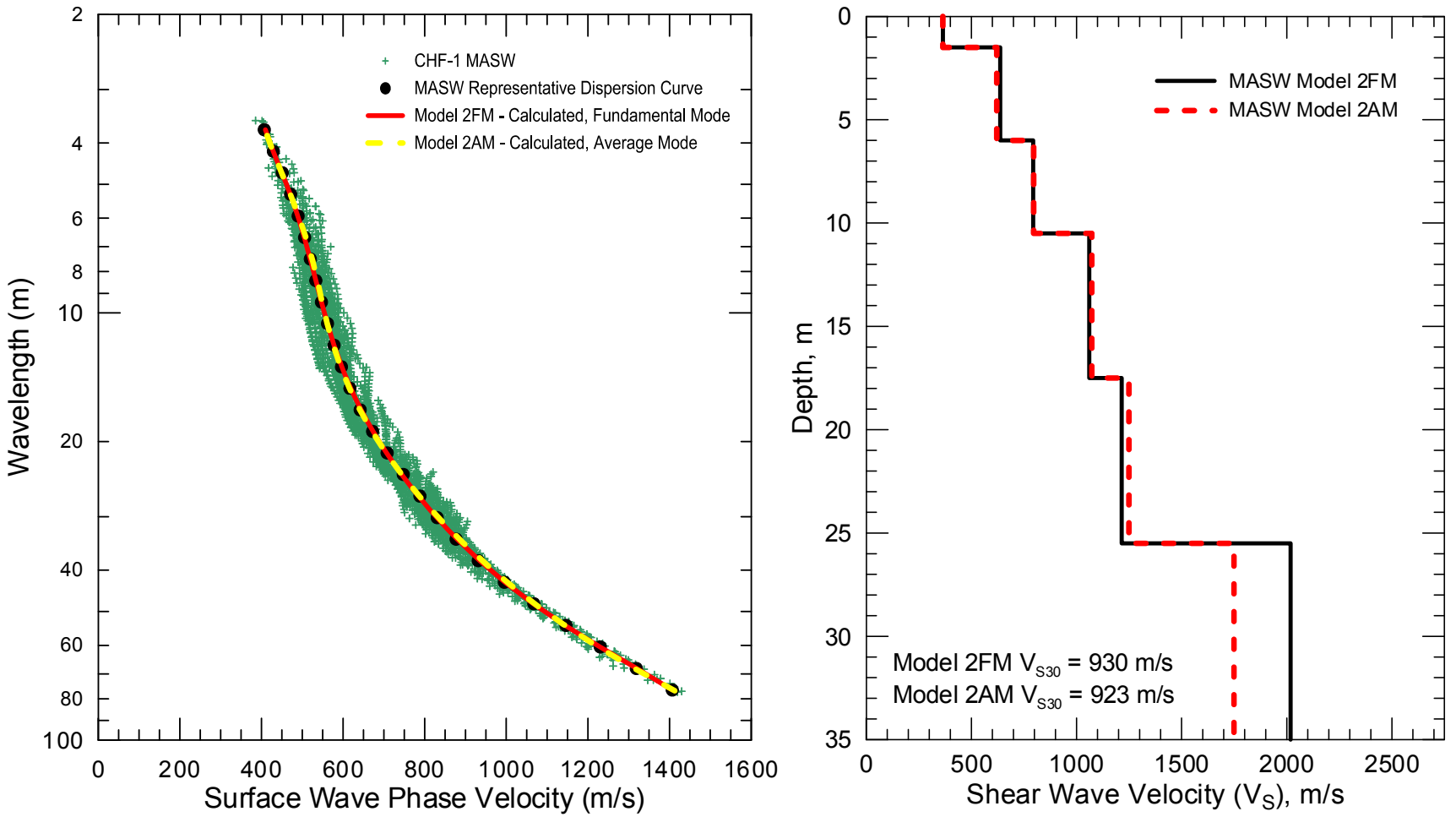

CI.CHF - Field, representative and inverted theoretical surface wave dispersion data (left) and associated V_S models (right) for Model 2, modeled using both fundamental mode and average/effective mode assumptions and a variable Poisson's ratio to better reflect the seismic refraction model. The first higher mode does not have significant influence on wavelengths less than about 60 m and, therefore, both models are realistic.

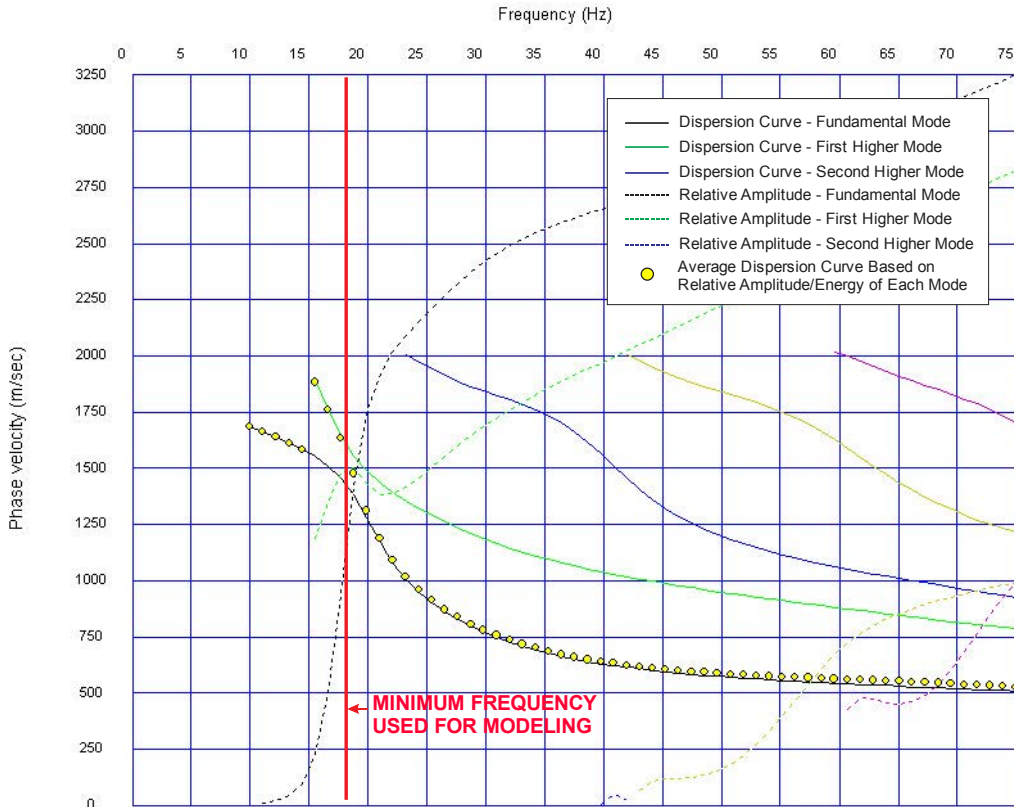

CI.CHF – Model 2FM (fundamental mode, Poisson's Ratio adjusted so P-wave velocity better reflects refraction model). The first higher mode has only a small affect at frequencies higher than used for modeling (higher than 18 Hz), therefore model is valid.

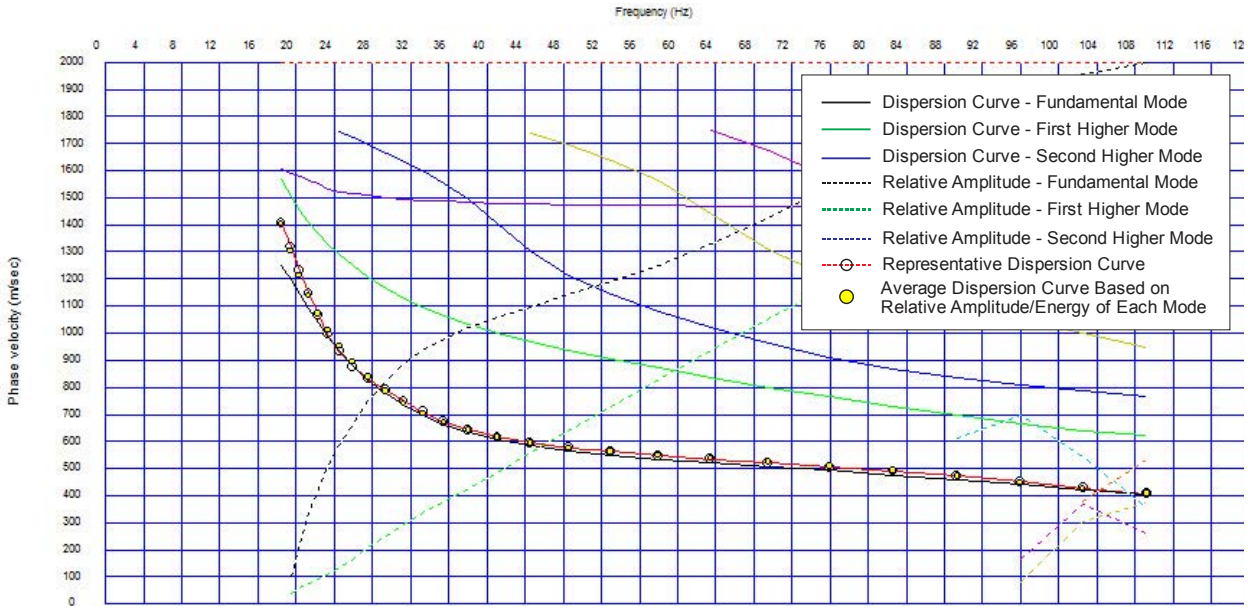

CI.CHF – Model 2AM (average mode, P-wave velocity adjusted as mentioned above). There is insufficient resolution in the v-f transform to isolate separate modes at low frequencies. Modal superposition at low frequencies is <u>assumed</u> to be represented by the average/effective mode.

Site CI.CHN

Location: Southern California Edison Chino Substation, Chino, California

Latitude: 33.99880 **Longitude:** -117.68026
(Station coordinates modified based on field survey, WGS84 coordinate system)

V_{S30} (measured): 292 m/s

V_{S30} (adjusted to more accurately reflect seismic station conditions): 307 m/s (average S-wave velocity between 2 and 32 m adjusting for nominal sensor depth)

NEHRP Site Class: D

Geomatrix Code: IHD

Geologic Conditions/Observations: Site located in area mapped as Quaternary (Holocene) young alluvial fan deposits. Deep soil site.

Site Conditions: Urban site with significant traffic noise from nearby Edison Ave. and other nearby roads. Relatively flat terrain in site vicinity with ground surface elevation gently decreasing to south.

Geophysical Methods Utilized: HVSR, MASW, array microtremor, ReMi™

Geophysical Testing Arrays:

1. Arrays CHN-1 (24 channel linear array utilizing 4.5 Hz vertical geophones spaced 5 m apart for an array length of 115 m) and CHN-2 (24 channel linear array utilizing 4.5 Hz vertical geophones spaced 3 m apart for an array length of 69 m) used to acquire passive surface wave data. Arrays combined to form an "L" shaped array.
2. Array CHN-2 was also used to acquire limited MASW and seismic refraction data (reversed off-end shots with accelerated weight drop energy source).
3. Array CHN-3 (48 channel MASW array utilizing 4.5 Hz vertical geophones spaced 1 m apart for a length of 47 m, forward and reverse shot locations with multiple source offsets and source types and center shot location).
4. Three HVSR measurement locations distributed along arrays CHN-1 and CHN-2.

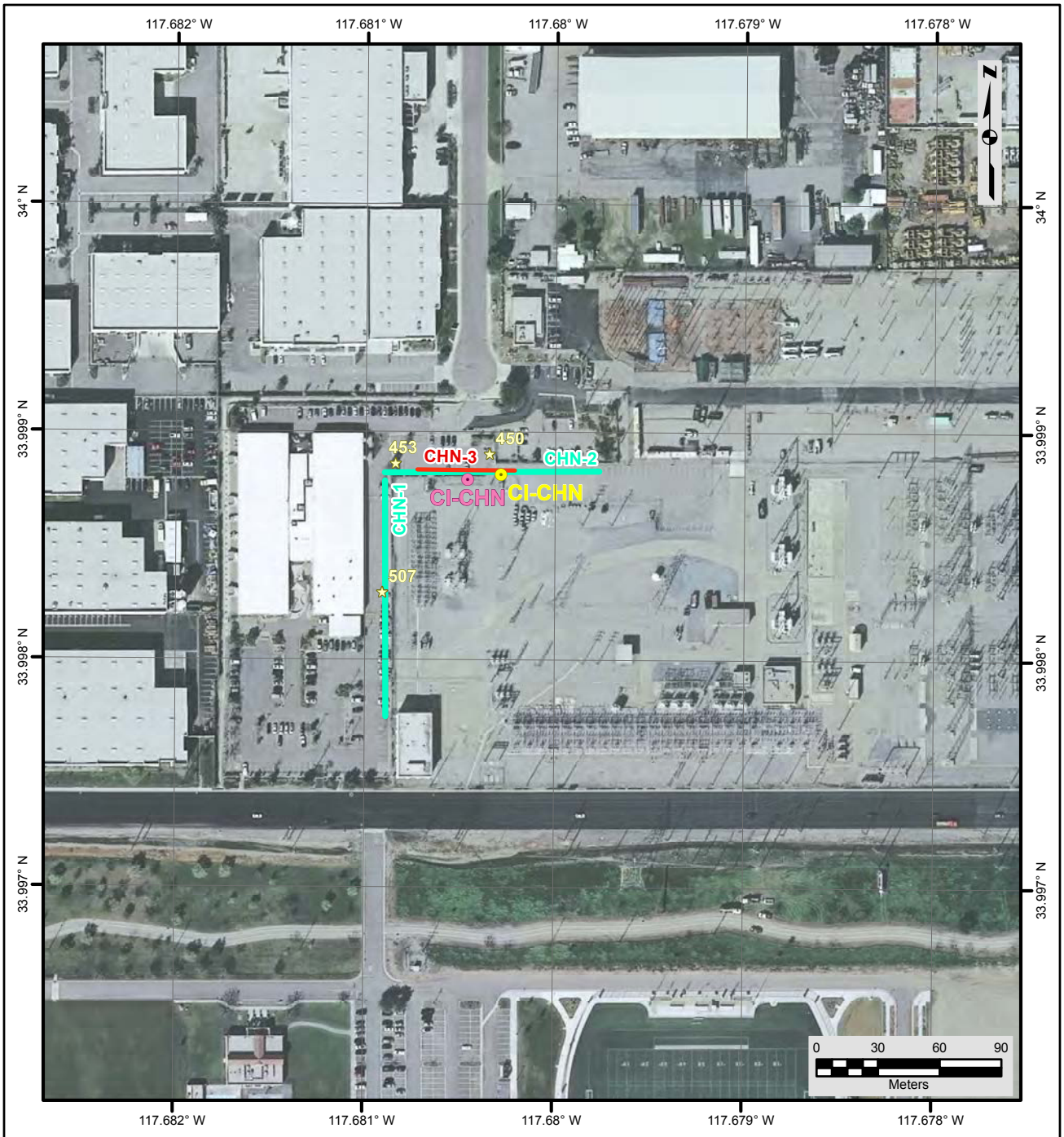

Legend

- Seismic Station - Approximate Location of Record
- Seismic Station - Approximate Surveyed Location
- H/V Spectral Ratio Measurement Location
- MASW Array
- Passive Surface Wave Array

NOTES:
1. WGS 1984 COORDINATE SYSTEM
2. Image Source: ESRI, i-cubed, USDA FSA, USGS, AEX, GeoEye, Getmapping, Aerogrid, IGP

File Name: CI-CHN-I

Date: 4/7/2011

USGS science for a changing world

GEOVision geophysical services

RECOVERY.GOV

SITE MAP
CI•CHN

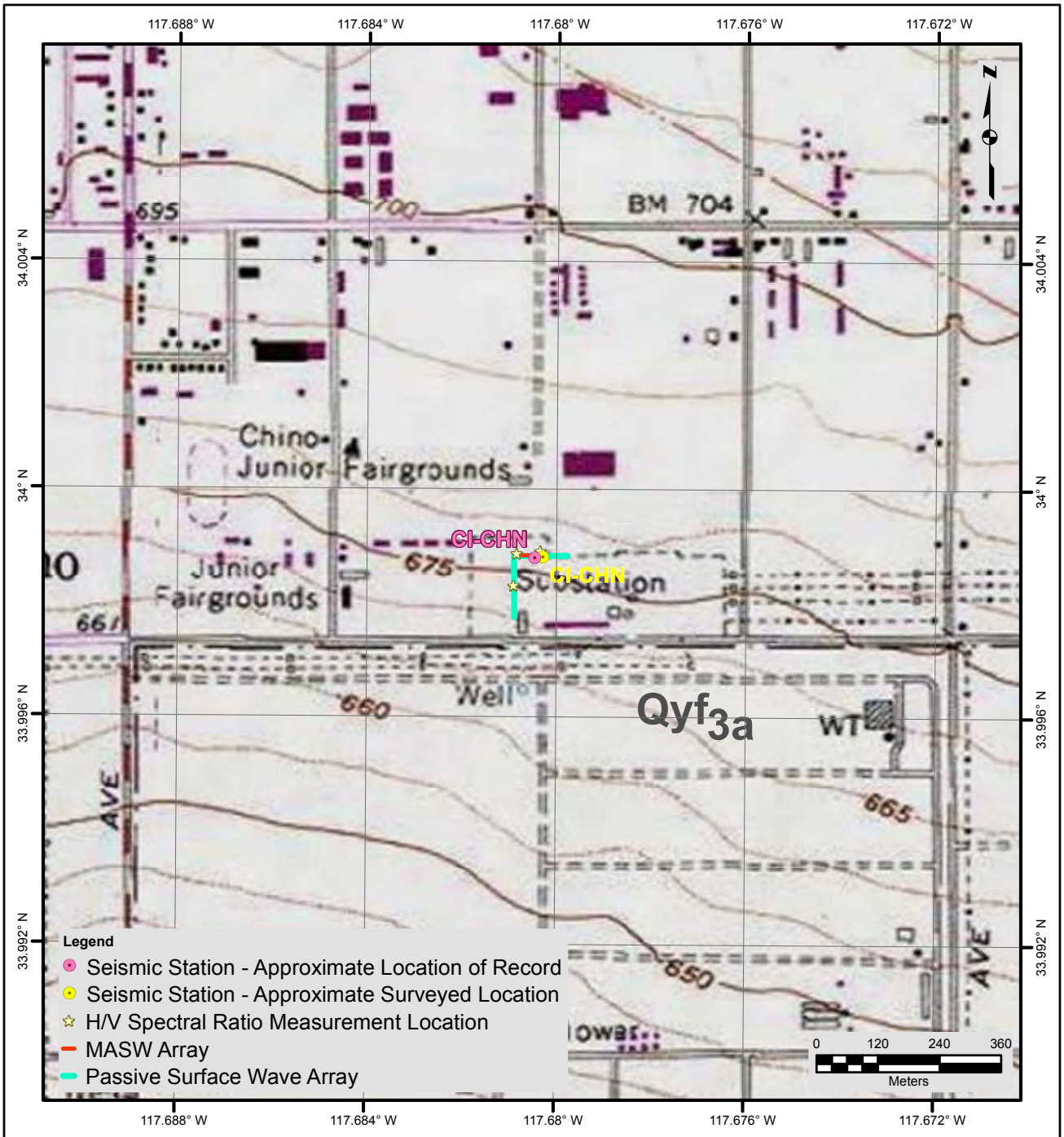

Description of Geologic Map Units

Qyf 3a = Quaternary (Middle Holocene) young alluvial fan deposits
Unit 3; gravel, sand, and silt, mixtures, some contain boulders; Unconsolidiated

NOTES:
1. WGS 1984 COORDINATE SYSTEM
2. Topo Image Sources: USGS, FAO, NPS, EPA, NRCAN, GeoBase, Esri, DeLorme, TANA, Intermap, AND, other suppliers, and the GIS community
3. Geologic Map Units from:
Preliminary Digital Geologic Map of the Santa Ana 30' x 60' Quadrangle, Southern California, Version 2.0 by Kelly R. Bovard and Rachel M. Alvarez, 2004
3. See site map for details of geophysical survey

File Name: CI-CHN

Date: 4/7/2011

USGS science for a changing world

GEOVision geophysical services

RECOVERY.GOV

GEOLOGIC MAP
CI•CHN

CI.CHN seismograph station

Looking west along passive surface wave array CHN-1

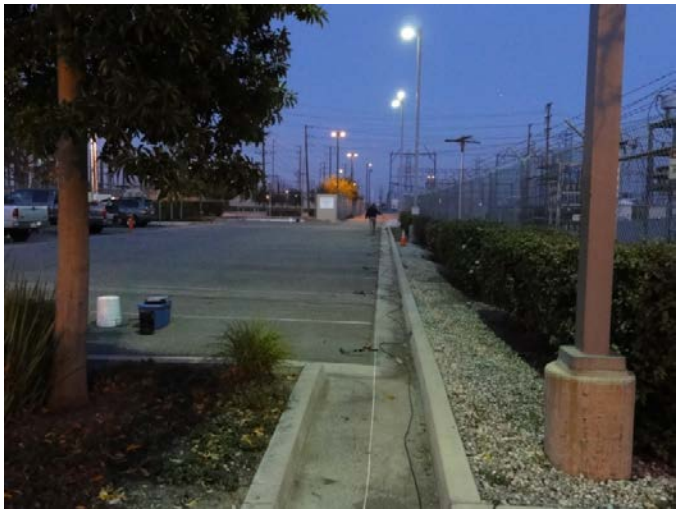

Looking north along passive surface wave array CHN-2

Looking southeast from HVSR sensor 450 towards seismic station

Looking south at MASW array CHN-3 and seismic station

Location of Geophysical Testing Arrays:

Location	Latitude	Longitude
CHN-1, South End of Array, Channel 1	33.99775	-117.68087
CHN-1, North End of Array, Channel 24	33.99878	-117.68088
CHN-2, West End of Array, Channel 25	33.99882	-117.68088
CHN-2, East End of Array, Channel 48	33.99883	-117.67975
CHN-3, West End of Array	33.99883	-117.68071
CHN-3, Center of Array	33.99883	-117.68045
CHN-3, East End of Array	33.99883	-117.68019
HVSR Sensor 507	33.99830	-117.68089
HVSR Sensor 453	33.99886	-117.68082
HVSR Sensor 450	33.99890	-117.68032
CI.CHN Seismograph Station	33.99880	-117.68026

Notes: 1) WGS84 Coordinate System (decimal degrees)
2) Survey accuracy is estimated at 1 to 2 m.

Results:

V_S Model

Depth to Top of Layer (m)	Layer Thickness (m)	S-Wave Velocity (m/s)	Inferred P-Wave Velocity (m/s)	Inferred Poisson's Ratio	Inferred Density (g/cm^3)
0	2	220	411	0.300	1.9
2	6	226	424	0.300	1.9
8	6	261	488	0.300	1.9
14	8	351	657	0.300	1.9
22	8	375	1600	0.471	2.0
30	12	501	1600	0.446	2.0
42	15	601	1600	0.418	2.0
57	20	699	1700	0.398	2.0
77	>23	804	1800	0.375	2.0

Observations/Discussion:

- The HVSR curves are almost identical, validating the 1-D velocity structure assumption.
- There is no clear dominant HVSR peak. Instead there are multiple low amplitude peaks in the 0.33 to 2.3 Hz range, which may be indicative of complex subsurface velocity structure. The highest amplitude HVSR peak occurs at a frequency of about 0.33 to 0.35 Hz.
- Noise conditions at site (multi-directional or omni-directional noise sources) appeared sufficient for successful application of passive surface wave techniques with the closest noise source being the west to east trending Edison Avenue immediately south of the site.
- Surface wave dispersion data from active and passive surface wave datasets are in good agreement at this site.
- ESAC technique used to extract surface wave dispersion data from passive "L" array data. Both the ReMi™ and ESAC techniques used to extract surface wave dispersion data from the linear arrays.
- Useful dispersion data not obtained from linear passive surface wave array CHN-2 due to the parallel Edison Ave. and relatively short length of the array. Therefore, passive surface wave data acquired with array was not used for data analysis. This array did, however, provide good quality MASW data.
- Representative dispersion curves were generated for each surface wave data set using a moving average, polynomial curve fitting routine. These individual representative dispersion curves were combined and a representative dispersion curve generated for the combined data set for data modeling.
- Water table located at a depth of about 22 m based on interactive layer-based analysis of seismic refraction first arrival data. P-wave velocity of about 1,600 m/s modeled for upper portion of saturated zone.
- Based on simple layer-based analysis of seismic refraction first arrival data, P-wave velocity in the upper 22 m (above water table) ranges from about 400 to 600 m/s.
- Surface wave depth of investigation is about 100 m based on half of maximum wavelength criteria and assuming that surface wave dispersion data at frequencies as low as 3 Hz are valid utilizing 4.5 Hz geophones (low frequency geophone phase response differences will cancel out if noise is omni-directional and/or the phase response differences are random in nature).
- V_{S30} is 292 m/s (Site Class D).
- Average S-wave velocity between 2 m (nominal sensor depth) and 32 m is 307 m/s.
- Average S-wave velocity of the upper 100 m (V_{S100}) is 479 m/s.

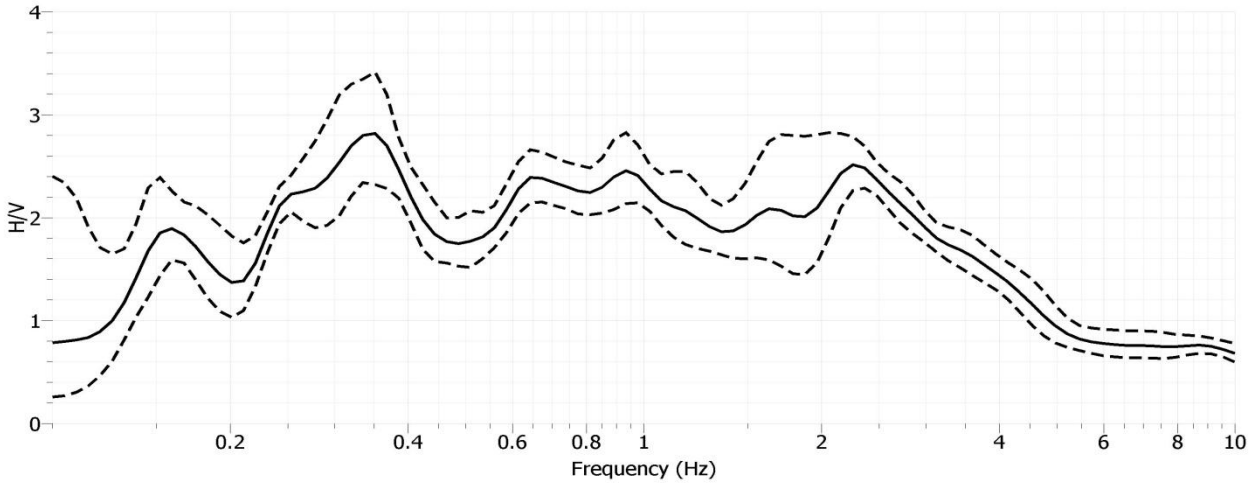

Site CI.CHN, H/V Spectral Ratio, Array CHN -2, Sensor 453

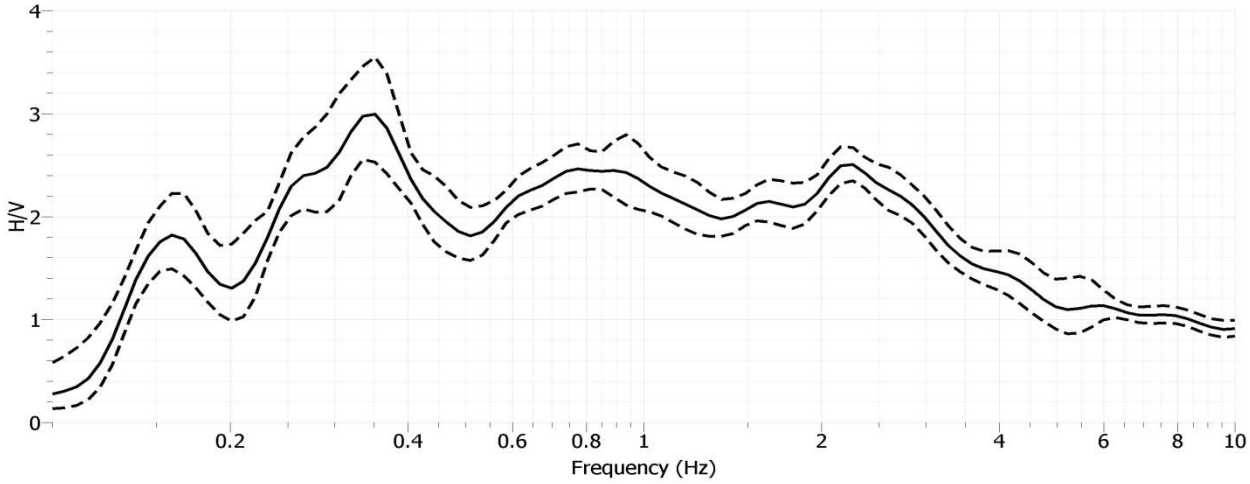

Site CI.CHN, H/V Spectral Ratio, Array CHN -2, Sensor 450

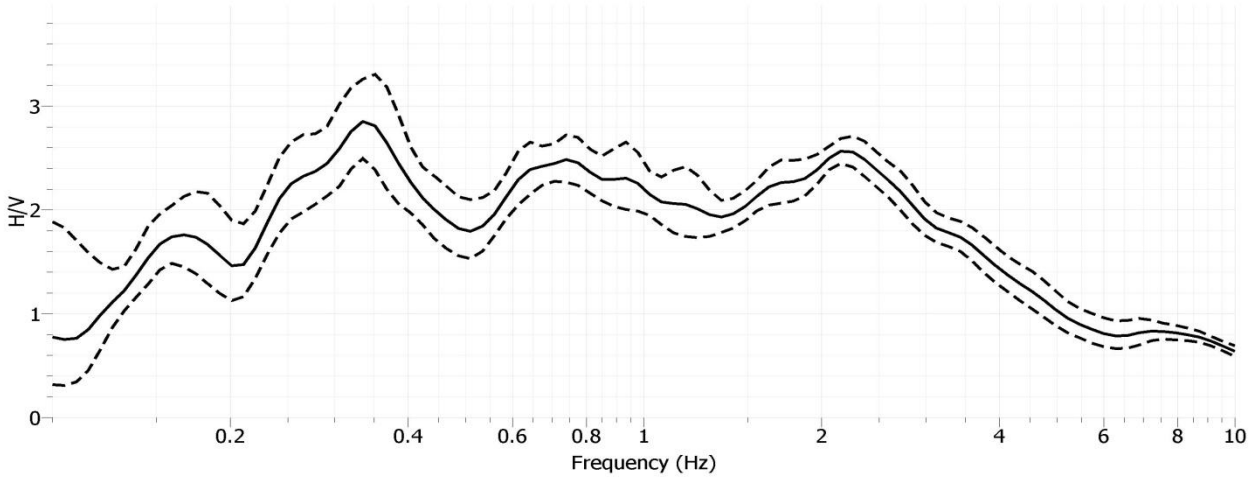

Site CI.CHN, H/V Spectral Ratio, Array CHN -1, Sensor 507

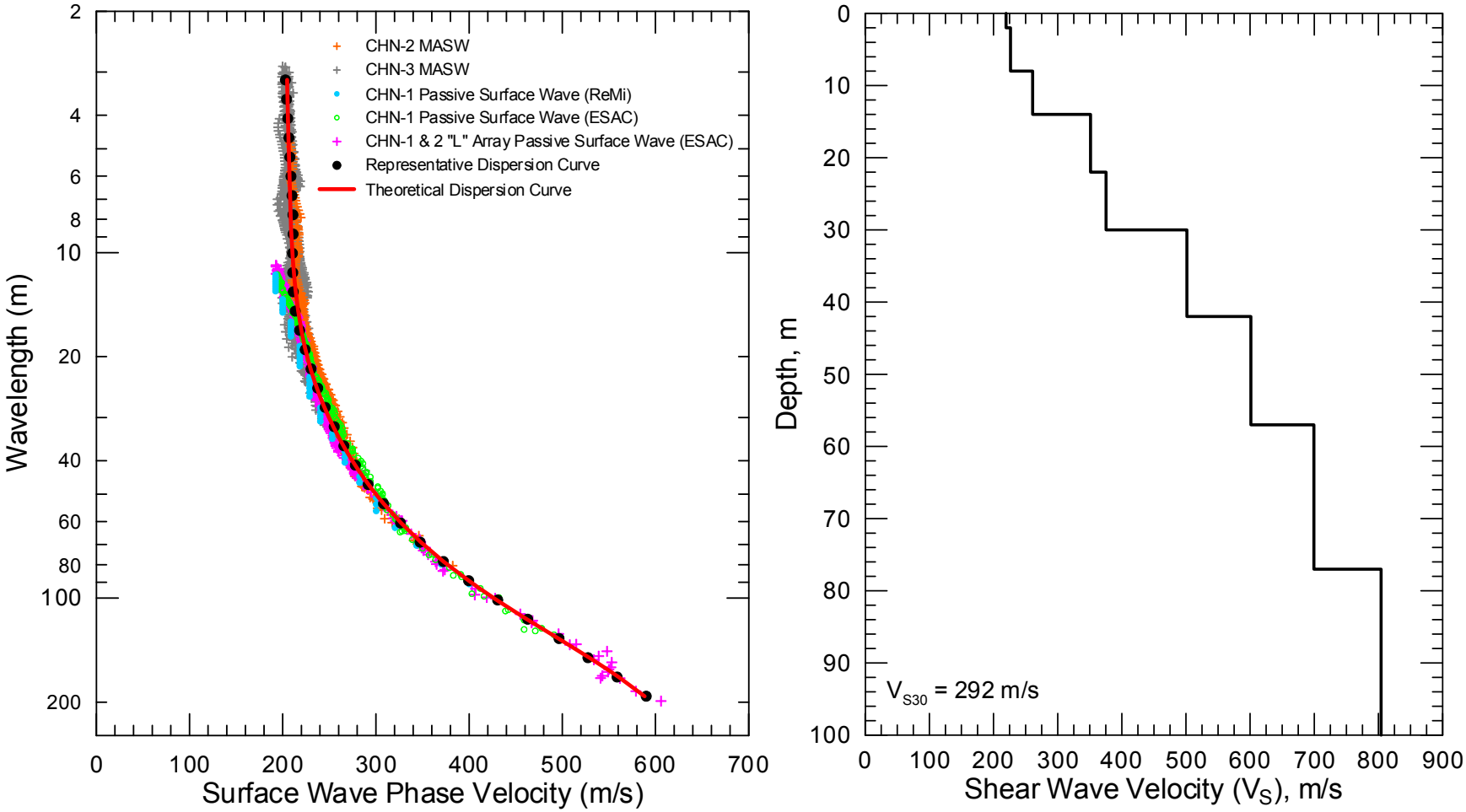

CI.CHN - Field, representative and inverted theoretical surface wave dispersion data (left) and associated V_S model (right)

Site CI.CIA

Location: Catalina Island Airport, Avalon, California

Latitude: 33.40184 **Longitude:** -118.41496
(Station coordinates based on site GPS survey, WGS84 coordinate system)

V_{S30} (measured): 505 m/s

V_{S30} (adjusted to more accurately reflect seismic station conditions): 526 m/s (average S-wave velocity between 1 and 31 m adjusting for inferred 1 m sensor depth).

NEHRP Site Class: C

Geomatrix Code: INB

Geologic Conditions/Observations: Seismic station located on undivided Mesozoic metasedimentary and metavolcanic rocks. The geologic map indicates that the MASW array crosses the contact of Mesozoic undivided metamorphic rocks and Mesozoic ultrabasic intrusive rocks. This potential geologic contact could not be confirmed in the field.

Site Conditions: Rural site. Seismic station located at the Catalina Island Airport on top of a mountain peak. Steep topography in site vicinity. Test area located on a hilltop that has been graded relatively flat.

Geophysical Methods Utilized: HVSR, Seismic Refraction, MASW

Geophysical Testing Arrays:

1. Array CIA-1 (48 channel MASW and P-wave seismic refraction array utilizing 4.5 Hz vertical geophones spaced 1.5 m apart for a length of 70.5 m, forward and reverse shot locations with multiple source offsets and source types (hammers only) and multiple interior shot locations).
2. Three HVSR measurement locations: two distributed along array CIA-1 and one near the seismic station.

Legend

- Seismic Station - Approximate Surveyed Location
- Seismic Station - Approximate Location of Record
- H/V Spectral Ratio Location
- MASW and Seismic Refraction Array

NOTES:
1. WGS 1984 COORDINATE SYSTEM
2. Image Source: ESRI, i-cubed, USDA FSA, USGS, AEX, GeoEye, Getmapping, Aerogrid, IGP

File Name: CI-CIA-I

Date: 10/6/2011

USGS science for a changing world

GEOVision geophysical services

RECOVERY.GOV

SITE MAP
CI•CIA

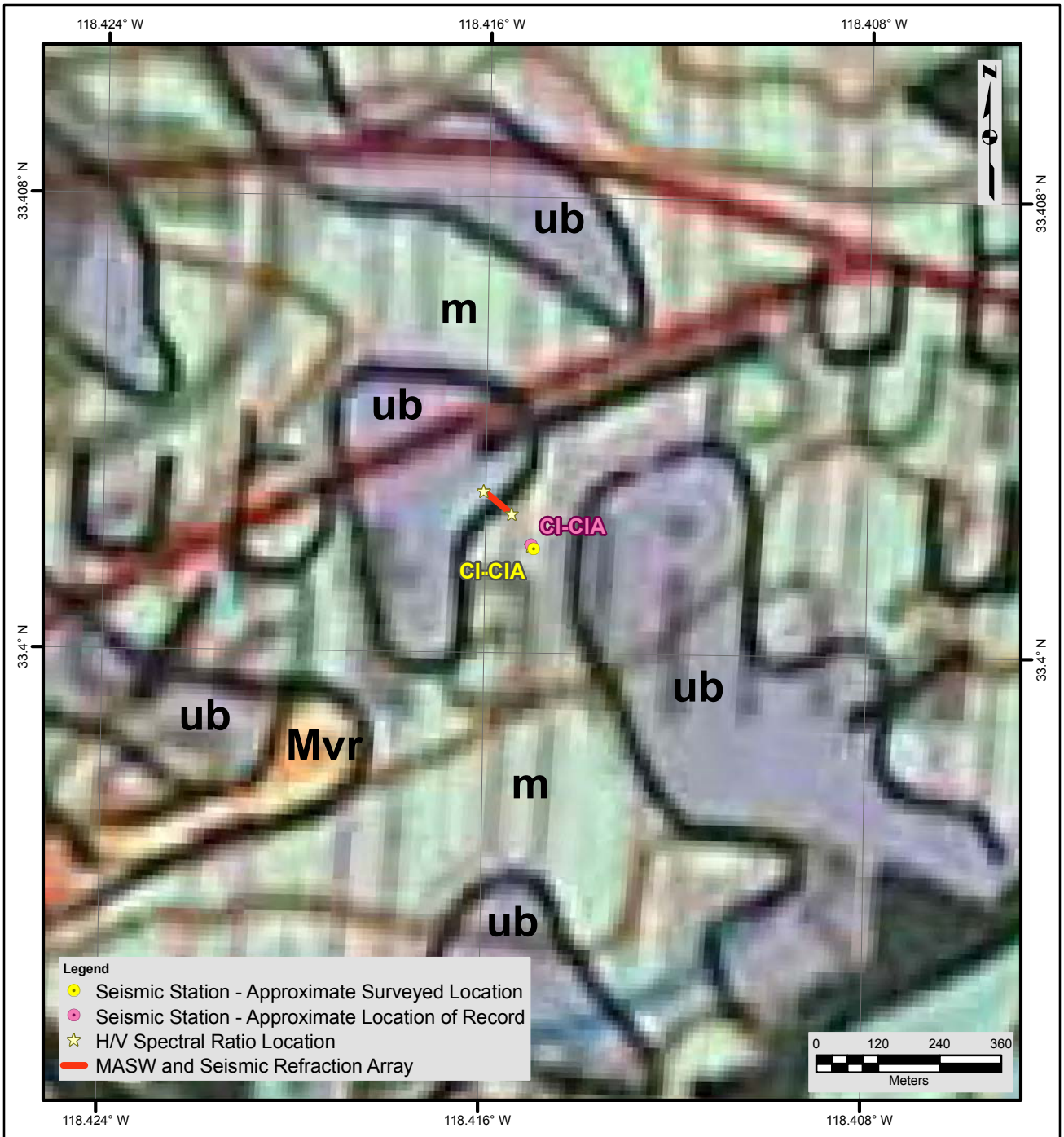

Description of Geologic Map Units

Mvr = Tertiary (Miocene) volcanics, rhyolite
m = Mesozoic (Pre-Cretaceous) undivided metamorphic rocks
ub = Mesozoic (Jurassic) ultrabasic intrusive rocks

NOTES:
1. WGS 1984 COORDINATE SYSTEM
2. Geologic Map of California,
Long Beach Sheet (Olaf P. Jenkins edition)
Compiled by Charles W. Jennings, 1962
3. See site map for details of geophysical survey

File Name: CI-CIA

Date: 10/6/2011

USGS science for a changing world

GEOVision geophysical services

GEOLOGIC MAP
CI•CIA

RECOVERY.GOV

CI.CIA seismic station

Looking southeast along array CIA-1

HVSR data acquired using a Tromino ENGR

MASW data acquisition on array CIA-1

Looking north past array CIA-1 towards runway

Location of Geophysical Testing Array(s):

Location	Latitude	Longitude
CIA-1, Northwest End of MASW/Seismic Refraction Array	33.40283	-118.41602
CIA-1, Center of MASW/Seismic Refraction Array	33.40264	-118.41573
CIA-1, Southeast End of MASW/Seismic Refraction Array	33.40244	-118.41544
HVSR Sensor Tromino 1 (TRO-1)	33.40244	-118.41544
HVSR Sensor Tromino 2 (TRO-2)	33.40283	-118.41603
HVSR Sensor Tromino 3 (TRO-3)	33.40188	-118.41502
CI.CIA Seismic Station	33.40184	-118.41496

Notes: 1) WGS84 Coordinate System (decimal degrees)
2) Survey accuracy is estimated at 1 to 2 m.

Results:

V_S Model

Depth to Top of Layer (m)	Layer Thickness (m)	S-Wave Velocity (m/s)	Inferred P-Wave Velocity (m/s)	Assumed Poisson's Ratio	Assumed Density (g/cm^3)
0	1.5	299	559	0.3	1.80
1.5	2.5	342	640	0.3	1.80
4	3	383	717	0.3	1.90
7	3	403	755	0.3	1.90
10	5	496	927	0.3	2.00
15	6	593	1109	0.3	2.05
21	8	757	1417	0.3	2.10
29	>6	976	1826	0.3	2.10

Notes: 1) Depth of investigation is about 35m.
2) Bottom layer is a half space.

Observations/Discussion:

- There are no peaks in the HVSR data by which to access lateral velocity variation.
- The P-wave refraction data collected along array CIA-1 were modeled using a tomographic inversion routine with a smooth velocity gradient starting model. The seismic refraction model was extended to limited far offset shot locations to extend depth of investigation.
- The seismic refraction survey design allowed P-wave velocity to be imaged to a maximum depth of about 20 to 25 m. The seismic refraction model shows that P-wave velocity is about 600 to 700 m/s at the surface, increasing to 1,000 m/s at a depth of 1 to 13 m and 1,500 m/s at a depth of 12 to 24 m.
- The seismic refraction model indicates that there is significant lateral velocity variation at this site with lower P-wave velocities at the surface and higher P-wave velocities at shallower depth at the southeast end of the line. There were no reasonable alternate test locations at the site in close proximity to the seismic station.
- Noise conditions at the site were not sufficient for application of passive surface wave techniques.
- The minimum wavelength surface wave phase velocity data extracted from the 48-channel MASW array was about 17 m. Data reduction using seismic records from smaller hammer sources and a limited offset receiver array (i.e. less active geophones) allowed extraction of surface wave dispersion data to a minimum wavelength of about 4 m.
- There is about 60 to 80 m/s scatter in the edited MASW dispersion data likely due, in part, to lateral velocity variation. Selective use was made of lower velocity Rayleigh wave phase velocity data at small wavelengths (high frequency) from center and reverse (southeast) shot locations. Small wavelength phase velocity data from forward (northwest) shot locations was higher, as expected based on the seismic refraction model. Rayleigh wave phase velocity data from the forward (northwest) and reverse (southeast) offset shot locations slightly diverge at long wavelengths (low frequency).
- A representative dispersion curve was generated for the MASW data set using a moving average, polynomial curve fitting routine and used for modeling.
- Surface wave depth of investigation is about 35 m based on half of maximum wavelength criteria.
- The inferred P-wave velocities in the surface wave model, assuming a Poisson's ratio of 0.3, are generally consistent with the average velocity structure in the central portion of the seismic refraction model where P-wave velocity is the lowest at intermediate depths.
- V_{S30} is 505 m/s (Site Class C).
- Average S-wave velocity between 1 m (assumed sensor depth) and 31 m is 526 m/s.

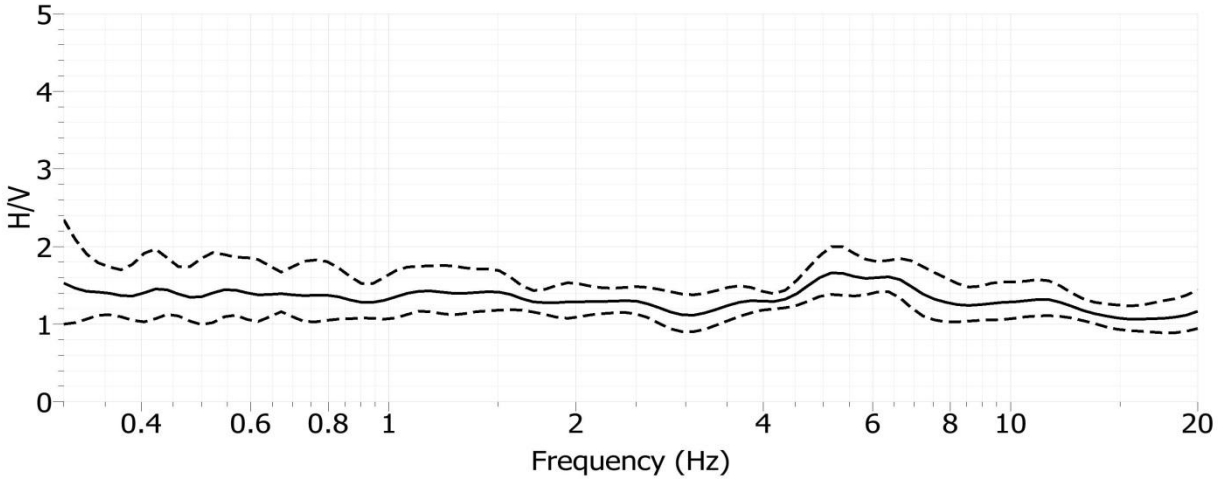

Site CI.CIA, H/V Spectral Ratio, Array CIA-1, TRO-2

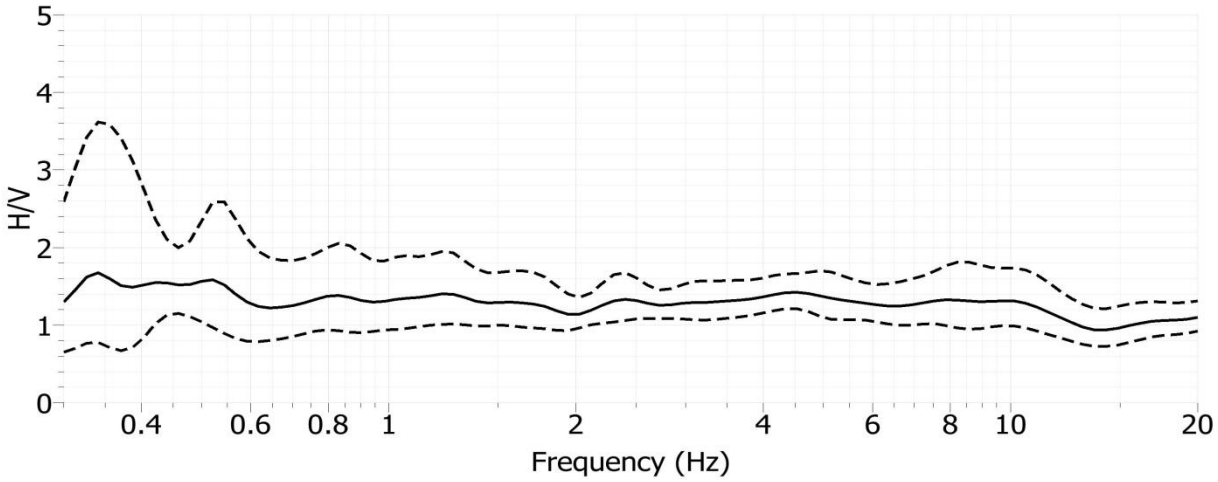

Site CI.CIA, H/V Spectral Ratio, Array CIA-1, TRO-1

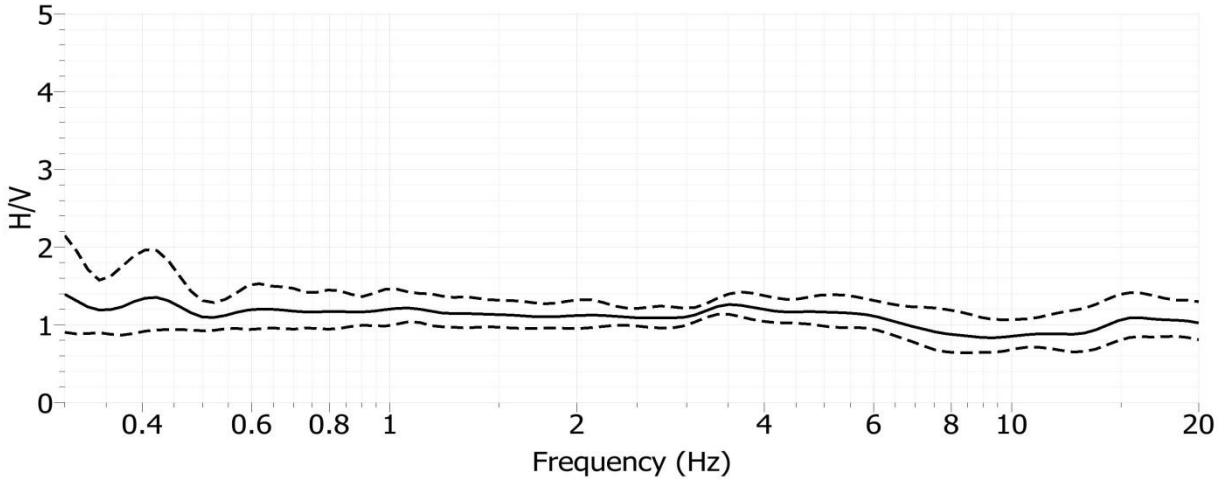

Site CI.CIA, H/V Spectral Ratio, Near Seismic Station, TRO-3

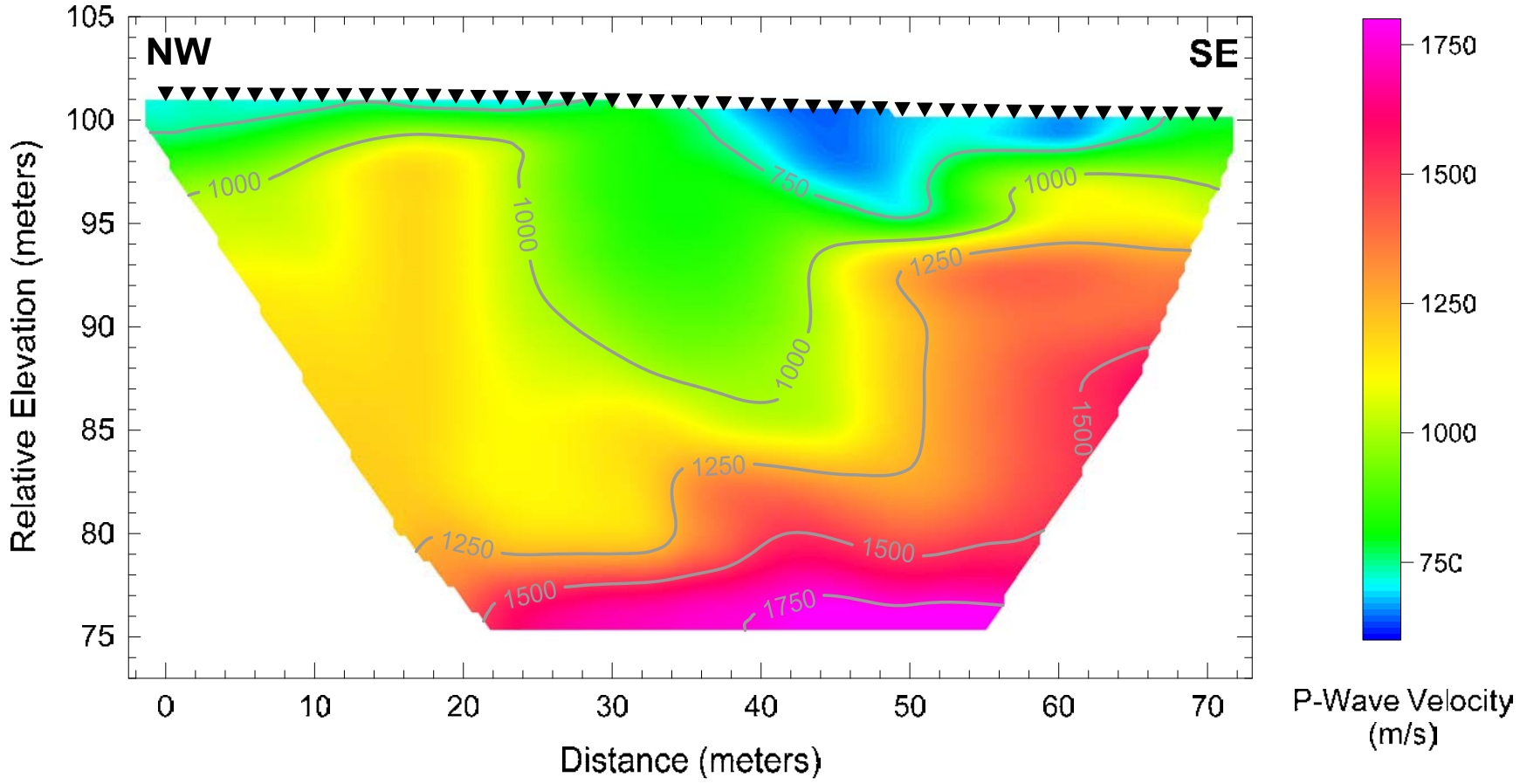

Array CIA-1 – Tomographic seismic refraction model utilizing smooth velocity gradient starting model

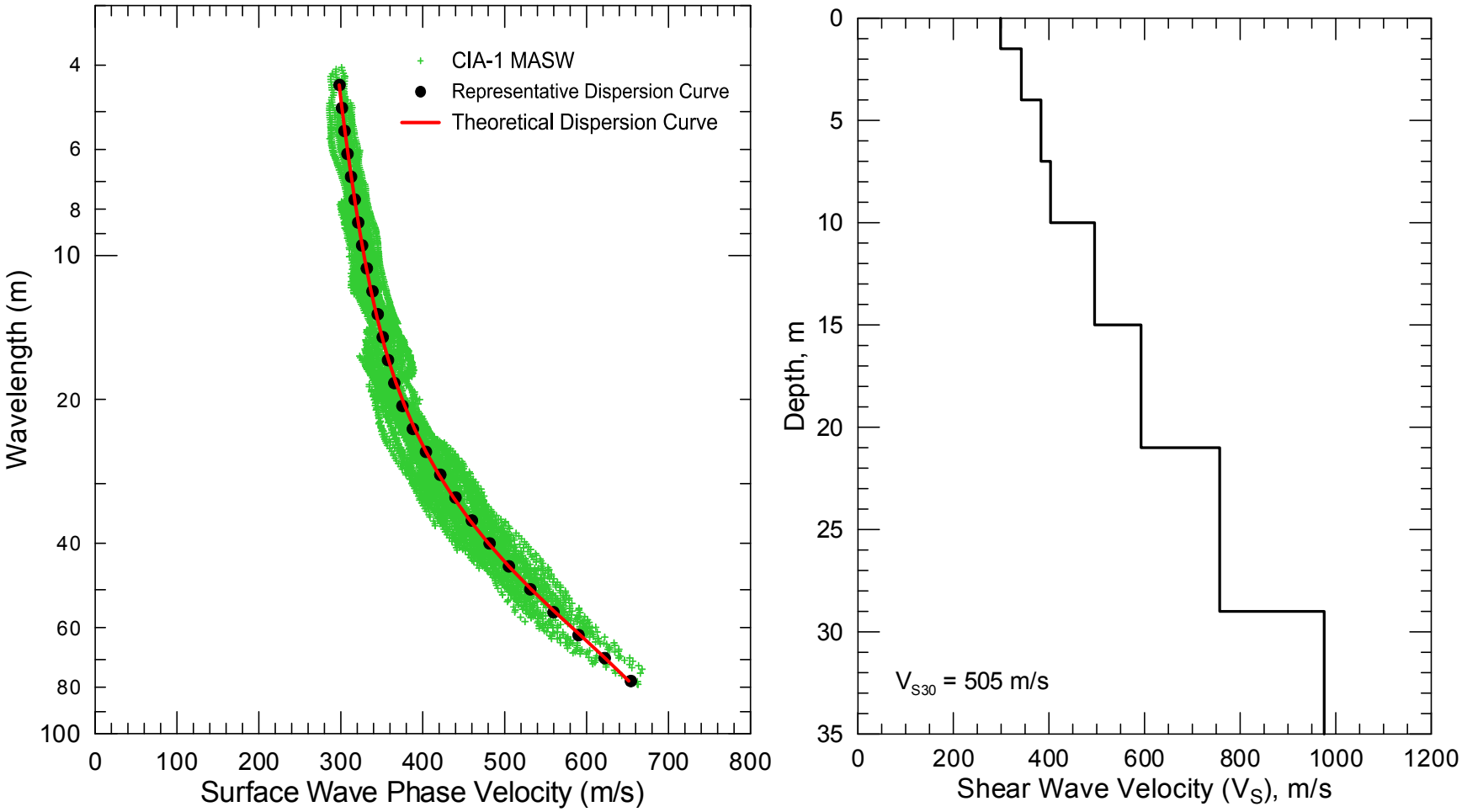

CI.CIA- Field, representative and inverted theoretical surface wave dispersion data (left) and associated V_S model (right)

Site CI.CLC

Location: China Lake South Range Building J-52, China Lake Naval Weapons Center, Ridgecrest, California

Latitude: 35.81574 **Longitude:** -117.59751
(Station coordinates provided by USGS, WGS84 coordinate system)

V_{S30} (measured): 1,464 m/s (based on P-wave seismic refraction model with assumed Poisson's ratio of 0.3 rather than surface wave model).

V_{S30} (adjusted to more accurately reflect seismic station conditions): 1,792 m/s (average S-wave velocity between 2 and 32 m adjusting for seismic sensor depth and sensor being located on rock).

NEHRP Site Class: A/B

Geomatrix Code: IGA

Geologic Conditions/Observations: Seismic station located on an outcrop of Mesozoic (Cretaceous) granitic rocks.

Site Conditions: Rural site. Seismic station located on granitic rock. Test area located along a road cut into the base of a hill with gentle topographic decline to southeast. Bedrock outcrops north and east of the test area.

Geophysical Methods Utilized: HVSR, Seismic Refraction (P- and S-wave), MASW (Rayleigh wave), MALW (Love Wave)

Geophysical Testing Arrays:

1. Array CLC-1 (48 channel MASW and P-wave seismic refraction array utilizing 4.5 Hz vertical geophones spaced 1.5 m apart for a length of 70.5 m, forward and reverse shot locations with multiple source offsets and source types and multiple interior shot locations).
2. Array CLC-1 (48 channel MALW and S-wave seismic refraction array utilizing 10 Hz horizontal geophones spaced 1.5 m apart for a length of 70.5 m, forward and reverse shot locations with multiple source offsets and source types (hammers only) and multiple interior shot locations). Coincident with P-wave array of same name.
3. Three HVSR measurement locations distributed along array CLC-1.

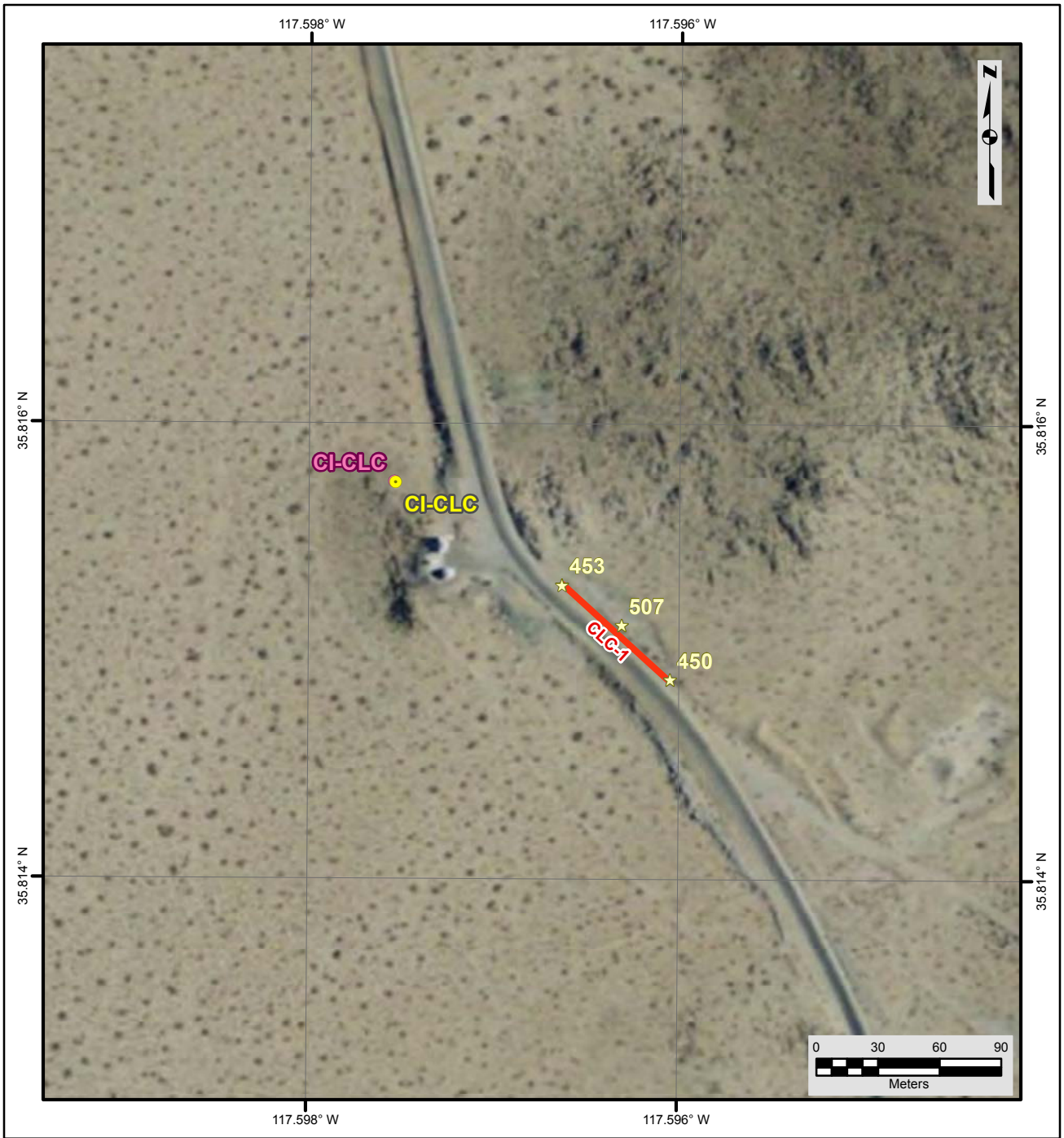

Legend

- Seismic Station - Approximate Surveyed Location
- Seismic Station - Approximate Location of Record
- H/V Spectral Ratio Location
- MASW and Seismic Refraction Array (P- and S-wave)

NOTES:
1. WGS 1984 COORDINATE SYSTEM
2. Image Source: ESRI, i-cubed, USDA FSA, USGS, AEX, GeoEye, Getmapping, Aerogrid, IGP

File Name: CI-CLC-I

Date: 10/13/2011

USGS science for a changing world

GEOVision geophysical services

RECOVERY.GOV

SITE MAP
CI•CLC

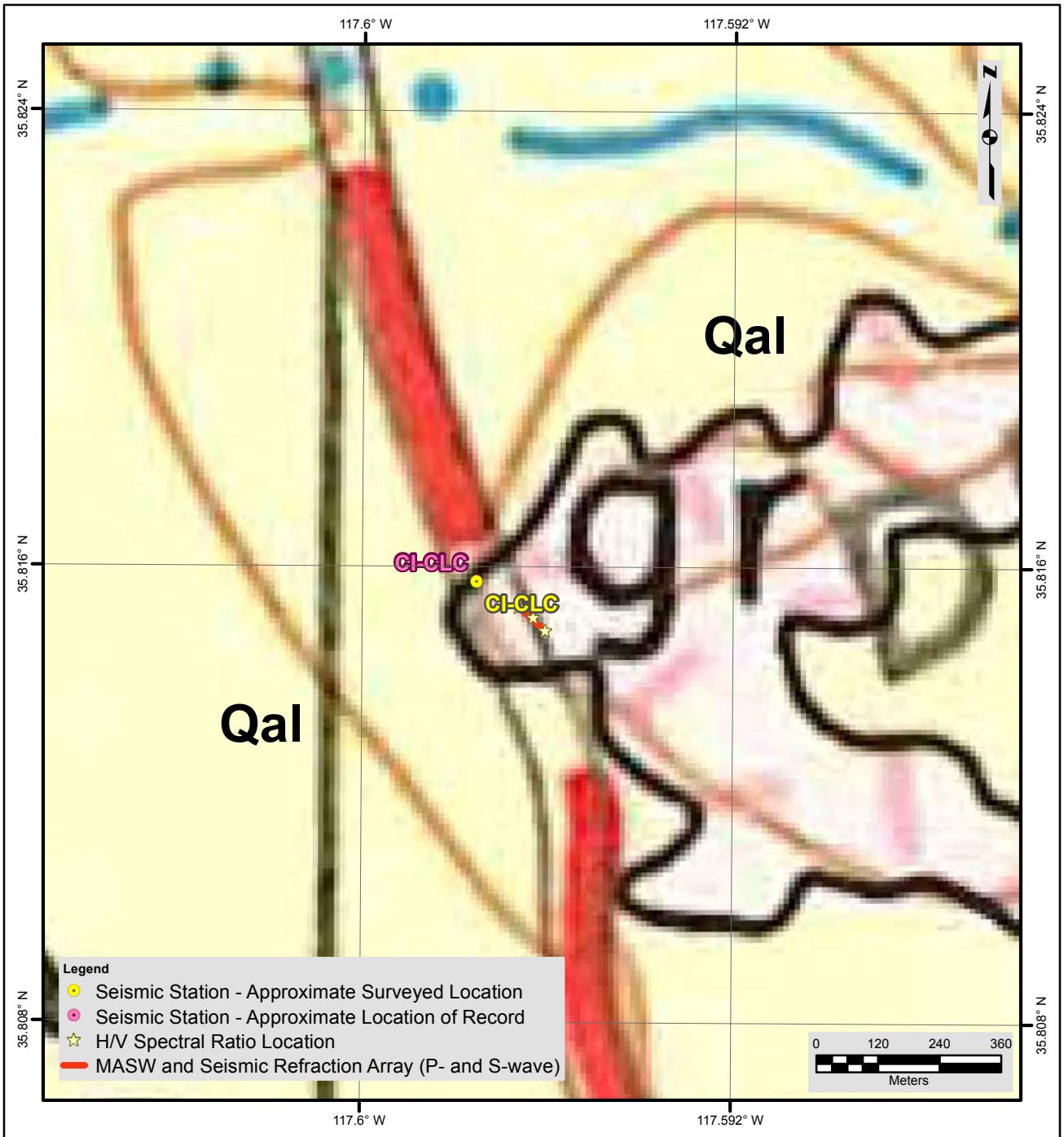

Description of Geologic Map Units

Qal = Quaternary (Holocene) alluvium
gr = Mesozoic (Cretaceous) granitic rocks

NOTES:
1. WGS 1984 COORDINATE SYSTEM
2. Geologic Map California, Trona Sheet by Charles W. Jennings, John L. Burnett & Bennie W. Troxel, 1962
3. See site map for details of geophysical survey

File Name: CI-CLC

Date: 10/13/2011

USGS science for a changing world

GEOVision geophysical services

RECOVERY.GOV

GEOLOGIC MAP
CI•CLC

Seismic station CI.CLC

Seismic station CI.CLC

Looking southeast at HVSR sensor 453 and northwest end of array CLC-1

Looking southeast along array CLC-1

Location of Geophysical Testing Arrays:

Location	Latitude	Longitude
CLC-1, Southeast End of MASW/Refraction Array	35.81487	-117.59603
CLC-1, Center of MASW/Refraction Array	35.81508	-117.59632
CLC-1, Northwest End of MASW/Refraction Array	35.81530	-117.59661
HVSR Sensor 450	35.81488	-117.59603
HVSR Sensor 507	35.81512	-117.59629
HVSR Sensor 453	35.81529	-117.59661
CI.CLC Seismic Station	35.81574	-117.59752

Notes: 1) WGS84 Coordinate System (decimal degrees)
2) Survey accuracy is estimated at 1 to 2 m.

Results:

V_S Model (MASW Array)

Depth to Top of Layer (m)	Layer Thickness (m)	S-Wave Velocity (m/s)	Inferred P-Wave Velocity (m/s)	Inferred Poisson's Ratio	Inferred Density (g/cm^3)
0	0.6	143	248	0.25	1.80
0.6	1.4	569	986	0.25	2.00
2	10	1390	2407	0.25	2.25
12	17	1674	2899	0.25	2.40
29	>6	2229	3860	0.25	2.50

Notes: 1) Depth of investigation is about 35 m.
2) Bottom layer is a half space.

Average V_P and Estimated V_S Models from Northwestern Portion of P-wave Seismic Refraction Line

Depth to Top of Layer (m)	Layer Thickness (m)	P-Wave Velocity (m/s)	Estimated S-Wave Velocity (m/s)			
			Poisson's Ratio = 0.25	Poisson's Ratio = 0.30	Poisson's Ratio = 0.3333	Poisson's Ratio = 0.35
0.00	0.42	542	313	290	271	260
0.42	0.84	894	516	478	447	429
1.26	0.84	944	545	505	472	454
2.11	0.84	1025	592	548	513	493
2.95	0.84	2417	1395	1292	1209	1161
3.79	0.84	2725	1573	1457	1363	1309
4.64	0.84	2786	1608	1489	1393	1338
5.48	1.77	2847	1644	1522	1424	1368
7.25	1.77	2997	1731	1602	1499	1440
9.02	1.77	3217	1858	1720	1609	1546
10.79	1.77	3851	2223	2058	1925	1850
12.56	1.77	3889	2245	2079	1944	1868
14.33	1.77	3963	2288	2118	1981	1904
16.10	1.77	4047	2337	2163	2024	1944
17.87	1.77	4091	2362	2187	2046	1965
19.64	1.77	4205	2428	2248	2103	2020
21.41	1.77	4404	2543	2354	2202	2116
23.18	Half Space	4611	2662	2465	2305	2215

Note: P-wave velocity not well constrained below 17 m and a conservative estimate of V_{P30} and V_{S30} is made assuming that the layer at a depth of 16.1 m is a half space.

Average V_S Model from Northwestern Portion of S-wave Seismic Refraction Line

Depth to Top of Layer (m)	Layer Thickness (m)	S-Wave Velocity (m/s)
0.00	0.42	260
0.42	0.84	355
1.26	0.84	519
2.11	0.84	1504
2.95	0.84	1600
3.79	0.84	1777
4.64	0.84	1900
5.48	1.77	2135
7.25	1.77	2215
9.02	1.77	2382
10.79	1.77	2494
12.56	1.77	2546
14.33	Half Space	2580

Observations/Discussion:

- Only limited photography was permitted at this site.
- The HVSR plots are similar, but there are no distinct peaks by which to assess lateral velocity variation.
- Surface wave techniques did not appear to be very effective in the field due to an apparent deepening of bedrock to the southeast beneath the test array. There was not an alternate test location that would allow the seismic line to be on rock. Therefore, P- and S-wave seismic refraction data were acquired at the site.
- The P-wave first arrival data were picked to a much greater degree of accuracy than the S-wave first arrival data because the S-wave is not typically the first energy on a seismic record. Better data quality also allowed the use of far offset shot locations to image to greater depth when modeling the P-wave data. Therefore, P-wave seismic refraction data should be used for site characterization with S-wave refraction data used to help constrain Poisson's ratio. As discussed below, MASW (Rayleigh wave) data were also modeled, but should be used cautiously due to apparent deepening of bedrock to the southeast beneath the array.
- The P- and S-wave seismic refraction data for array CLC-1 were modeled using a tomographic inversion routine with layer-based starting models. The P-wave seismic refraction model was extended to far offset shot locations to extend depth of investigation. It should be noted that a larger geophone spacing, rather than the

utilization of far offset shot locations, is preferred for extending depth of investigation when applying tomographic inversion routines. However, the seismic refraction data were acquired in conjunction with surface wave data, where a shorter array length is preferred. The S-wave refraction model was not extended to far offset shot locations due to poorer data quality.

- The P-wave seismic refraction survey design allowed P-wave velocity to be imaged to a maximum depth of about 23 m. The seismic refraction model indicates that P-wave velocity is about 550 to 750 m/s at the surface and increases to over 1,000 m/s at a depth of 1 to 6 m, 2,500 m/s at a depth of 3 to 10 m and over 3,500 m/s at a nominal depth of 8 to 11 m. The maximum P-wave velocity in the central portion of the model, where depth of investigation is greatest is about 4,500 m/s. A P-wave velocity this high is indicative of slightly weathered rock and, therefore, we would expect velocity to only increase very gradually with depth below 23 m.
- The S-wave seismic refraction survey design allowed S-wave velocity to be imaged to a maximum depth of about 15 m. The seismic refraction model indicates that S-wave velocity is about 250 to 500 m/s at the surface and increases to over 750 m/s at a depth of 1 to 5 m, 1,500 m/s at a depth of 3 to 8 m and over 2,000 m/s at a depth of 5 to 13 m. The maximum S-wave velocity in the central portion of the model, where depth of investigation is greatest is about 2,500 m/s. An S-wave velocity this high is indicative of slightly weathered rock and, therefore, we would expect velocity to only increase very gradually with depth below 15 m. The S-wave refraction model is not as reliable as the P-wave model due to larger error in the S-wave first arrival data.
- The average P-wave velocity of the upper 30 m (V_{P30}) was estimated between 36 and 54 m on the P-wave refraction model, where bedrock appears to have relatively uniform depth and depth of investigation is greatest. To estimate V_{P30} the P-wave velocity at a depth of 23 m, maximum depth of investigation, was projected to 30 m depth. Over this interval V_{P30} ranges from about 2,689 to 2,880, a 7 % variation, and generally increases to the northwest as bedrock shallows. V_{P30} is expected to continually increase towards the seismic station to the northwest as the sediment cover thins.
- An average V_P model was developed over the 36 to 54 m distance interval by averaging the slowness of each model cell. Average V_{P30} was determined to be 2,806 m/s. Assuming constant Poisson's ratios of 0.25, 0.3, 0.3333 and 0.35 would result in an estimated V_{S30} of 1,620, 1,500, 1,403 and 1,348 m/s, respectively.
- P-wave velocity is not well constrained at depths below 17m. Therefore, the computations made above were repeated by fixing P-wave velocity below 17 m to that occurring at 17 m depth in the model. In this case, V_{P30} ranges from about 2,638 to 2,806 m/s, and averages 2,739 m/s, only about a 2% decrease. Assuming constant Poisson's ratios of 0.25, 0.3, 0.3333 and 0.35 would result in an estimated V_{S30} of 1,581, 1,464, 1,369 and 1,316 m/s, respectively.
- The average S-wave velocity of the upper 30 m (V_{S30}) was also estimated between 36 and 54 m on the S-wave seismic refraction model. The S-wave seismic refraction model is not expected to be as reliable as the P-wave model and should be used cautiously. To estimate V_{S30} the S-wave velocity at a depth of 15 m, maximum depth of investigation, was projected to 30 m depth. Over this interval V_{S30} ranges from about 1,653 to 1,769, a 7 % variation. V_{S30} is expected to continually increase towards the seismic station to the northwest as the sediment cover thins.

- An average V_S model was developed over the 36 to 54 m distance interval by averaging the slowness of each model cell and average V_{S30} was determined to be 1,717 m/s. Based on the more accurate P-wave refraction model, a V_{S30} of 1,717 m/s would indicate that Poisson's ratio is as low as 0.2. Although not implausible, a slightly higher Poisson's ratio in the 0.25 to 0.3 range is a little more conservative and will be used to assess the P-wave seismic refraction model.
- Noise conditions at the site were not sufficient for application of passive surface wave techniques.
- MASW (Rayleigh wave) data were very difficult to reduce because bedrock deepens to the southeast beneath the array as shown in the seismic refraction models, which results in significant lateral velocity variation. No attempt was made to reduce the MALW (Love wave) data, which was of a poorer quality than the MASW data. Although difficult, a coherent Rayleigh wave phase velocity dispersion curve was developed using offend source locations at the northwest end of the array and interior shot locations in the northwestern half of the array. It was most difficult extracting phase velocity data at wavelengths less than 25 m, which may be highly variable beneath the array. Because bedrock deepens to the southeast, if would appear logical that the V_S model derived from the MASW data may underestimate S-wave velocity structure, especially relative to the seismic station which is located on rock.
- The minimum wavelength surface wave phase velocity data extracted from the 48-channel MASW array is about 25 m. Data reduction using seismic records from smaller hammer sources and a limited offset receiver array (i.e. less active geophones) allowed extraction of surface wave dispersion data to a minimum wavelength of about 5 m.
- There is about 100 to 150 m/s scatter in MASW dispersion data, even after selective use of dispersion data, likely due to the effects of lateral velocity variation.
- A representative dispersion curve was generated for the MASW data set using a moving average, polynomial curve fitting routine and used for modeling.
- Surface wave depth of investigation is about 35 m based on half of maximum wavelength criteria.
- V_{S30} from the MASW V_S model is 1,227 m/s (Site Class B). As discussed previously, the possibility cannot be discounted that the surface wave model slightly underestimates S-wave velocity.
- Average S-wave velocity between 2 m and 32 m from the MASW V_S model, to account for seismic sensor depth and the fact than the seismic station is located on rock, is 1,604 m/s (Site Class A).
- V_{S30} from the northwestern portion of the P-wave seismic refraction model and assumed constant Poisson's ratio of 0.25 and 0.3 is 1,620 and 1,500 m/s, respectively (Site Class A/B).
- V_{S30} from the conservative (half space below a depth of 17 m) P-wave seismic refraction model and assumed constant Poisson's ratio of 0.25 and 0.3 is 1,581 and 1,464 m/s, respectively (Site Class A/B).
- Average S-wave velocity between 2 m and 32 m from the P-wave seismic refraction model and assumed constant Poisson's ratio of 0.25 and 0.3, is 2,008 and 1,859 m/s, respectively (Site Class A). Average S-wave velocity between 2 m and 32 m from the conservative P-wave seismic refraction model and assumed constant Poisson's ratio of 0.25 and 0.3, is 1,936 and 1,792 m/s, respectively (Site Class A). It should be noted that

a longer seismic line would be preferred to accurately constrain such high seismic velocities.

- The S-wave seismic refraction model has even higher S-wave velocity than the models discussed above and is not considered reliable.
- For site characterization purposes, we recommend using the S-wave velocity structure derived from the conservative P-wave seismic refraction model with an assumed constant Poisson's ratio of 0.3 (V_{S30} equal to 1,464 m/s and V_S between 2 and 32 m equal to 1,792 m/s). Error is estimated at about 10% of velocity.
- The seismic station is located on a rock outcrop at the bend in a road. Testing was conducted on the south side of the bend rather than the north side so as to be visible to oncoming traffic. It is unclear how bedrock depth varies on the north side of the bend in the road, although minimal traffic control would be required to safely test in this area. The only possible approach to get a more definitive estimate of V_{S30} would be to attempt an SASW sounding, which only requires a maximum 30 to 40 m receiver spacing with equal source offset. If might be possible to center such a sounding on the bedrock outcrop at the bend in the road, providing traffic control was available. However, arranging traffic control at China Lake Naval Weapons Center at a location with limited access due to range control could be difficult.

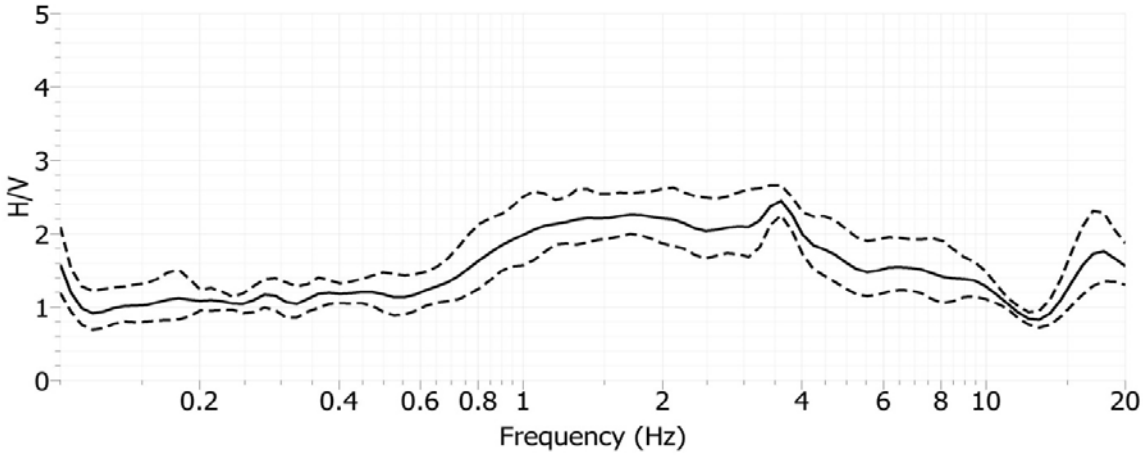

Site CI.CLC, H/V Spectral Ratio, Array CLC-1, Sensor 453

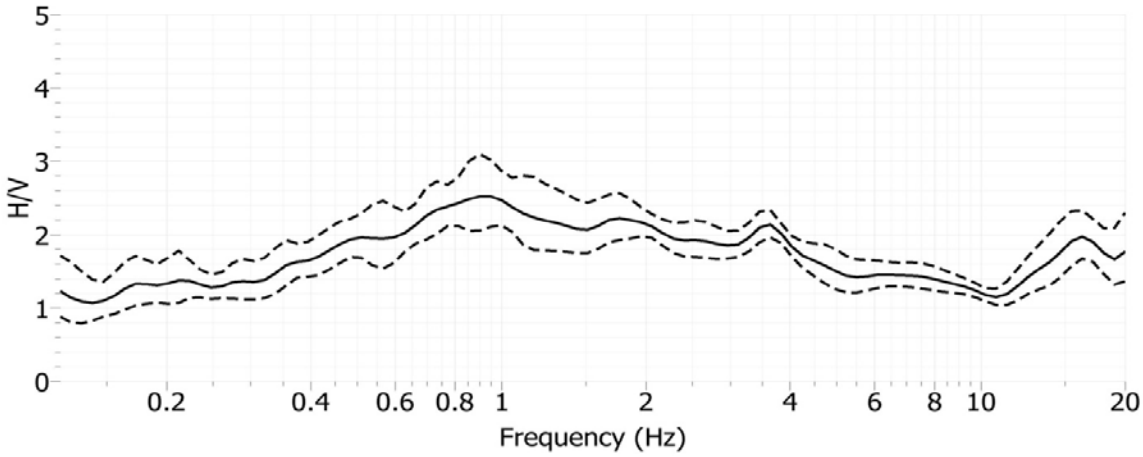

Site CI.CLC, H/V Spectral Ratio, Array CLC-1, Sensor 507

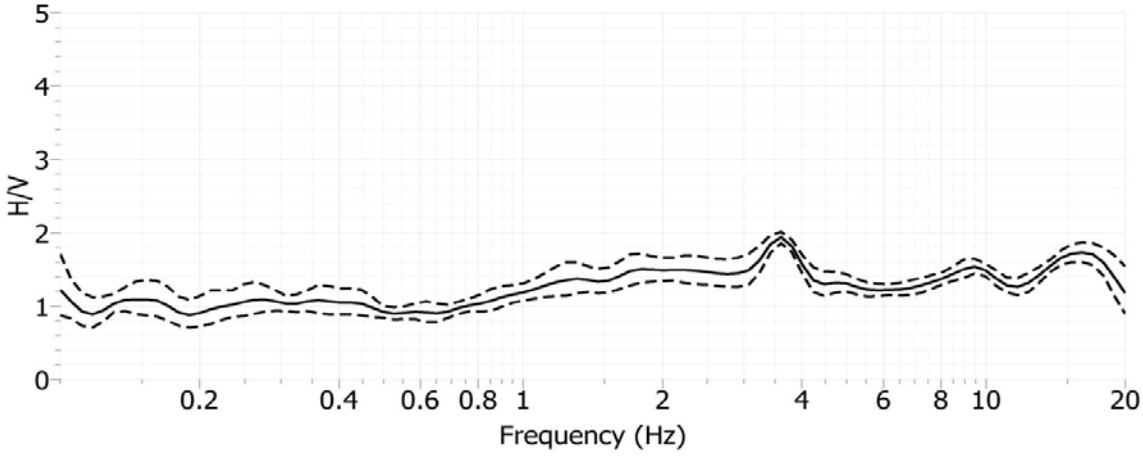

Site CI.CLC, H/V Spectral Ratio, Array CLC-1, Sensor 450

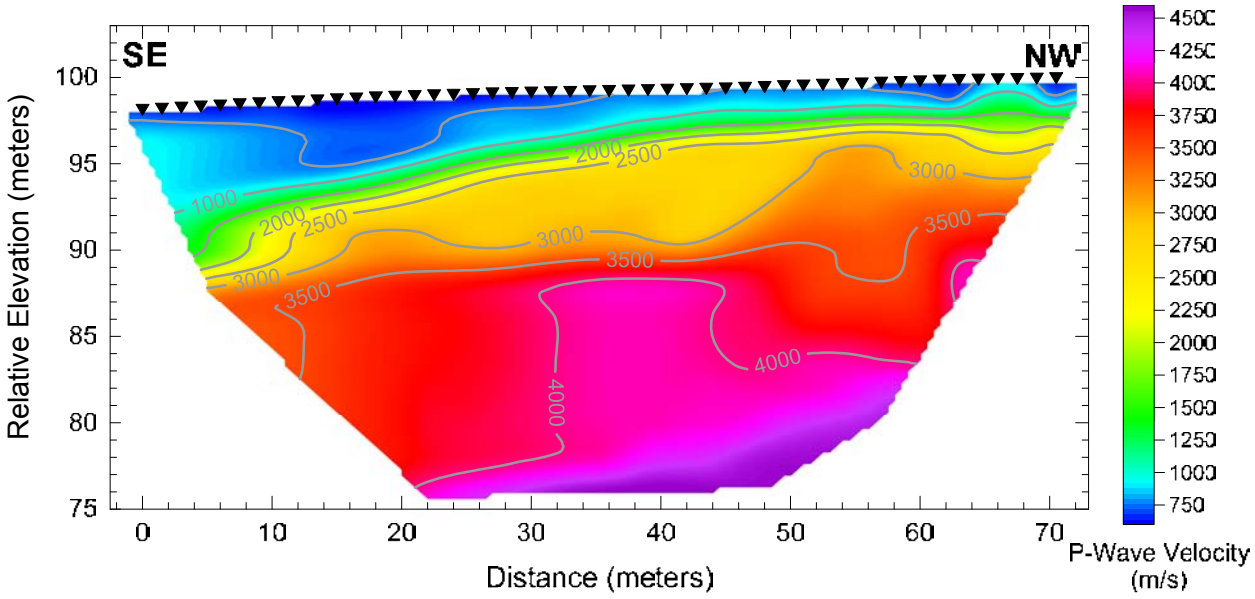

Array CLC-1 – P-wave Tomographic Seismic Refraction Model utilizing Layer Based Starting Model

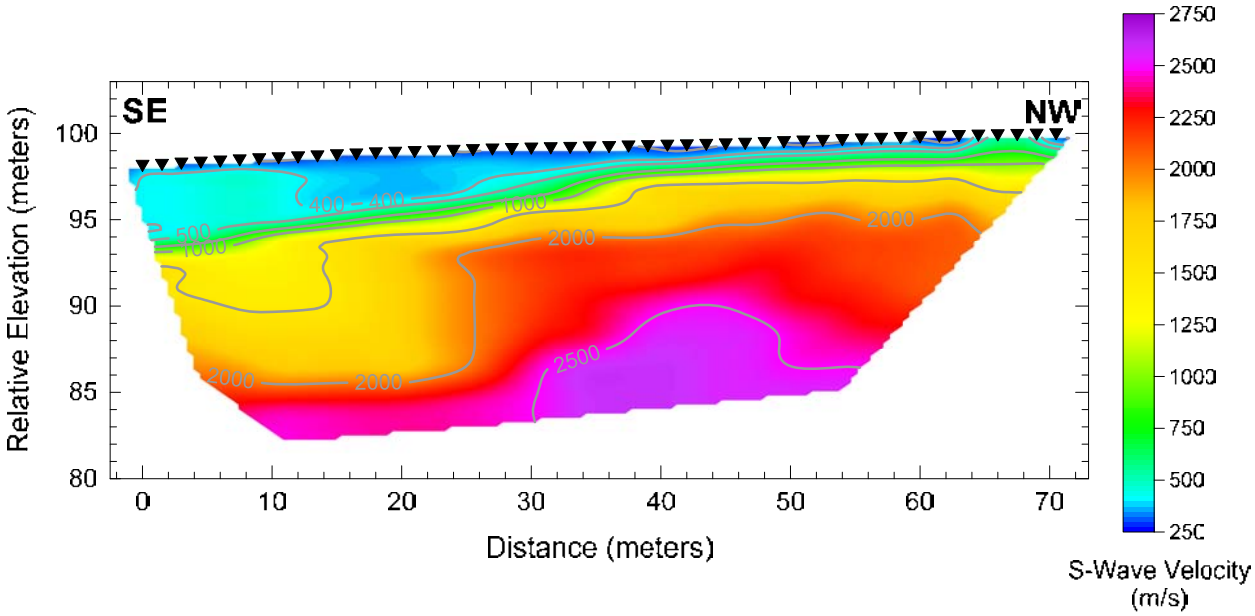

Array CLC-1 – S-wave Tomographic Seismic Refraction Model utilizing Layer Based Starting Model

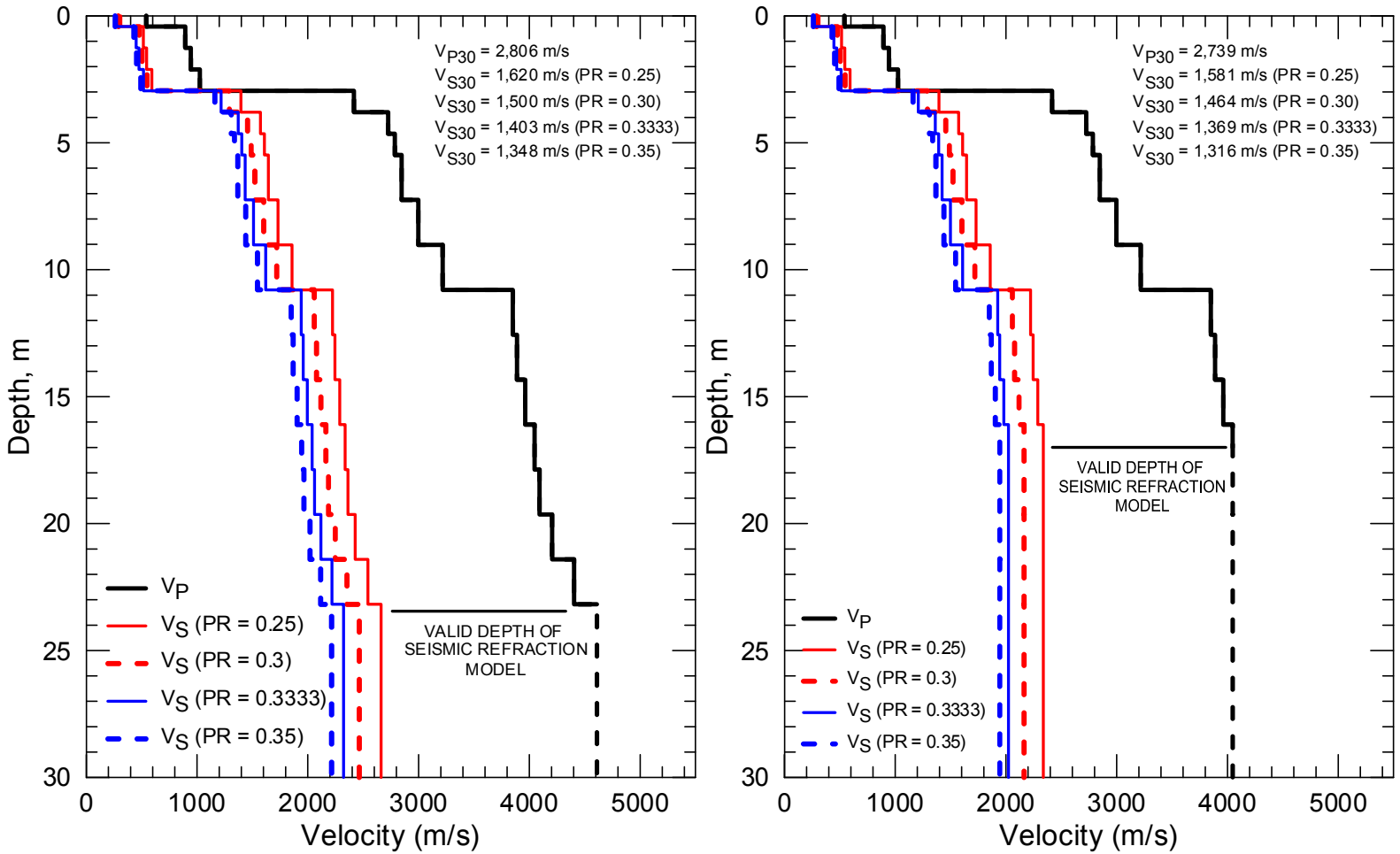

CI.CLC – Average P-wave velocity structure and estimated S-wave velocity structure between 36 and 54 m on P-wave seismic refraction array CLC-1. Although the maximum seismic refraction depth of investigation is limited to about 23 m, P-wave velocity is very high at the bottom of the model and is not expected to increase significantly between 23 and 30 m. P-wave velocity is not well constrained below a depth of 17 m and computations were also made assuming that velocity is constant below this depth. The models on the left and right assume that the model is valid to a depth of 23 and 17 m, respectively. A longer seismic line would be preferred to both more accurately model the high P-wave velocities and to image to 30 m depth.

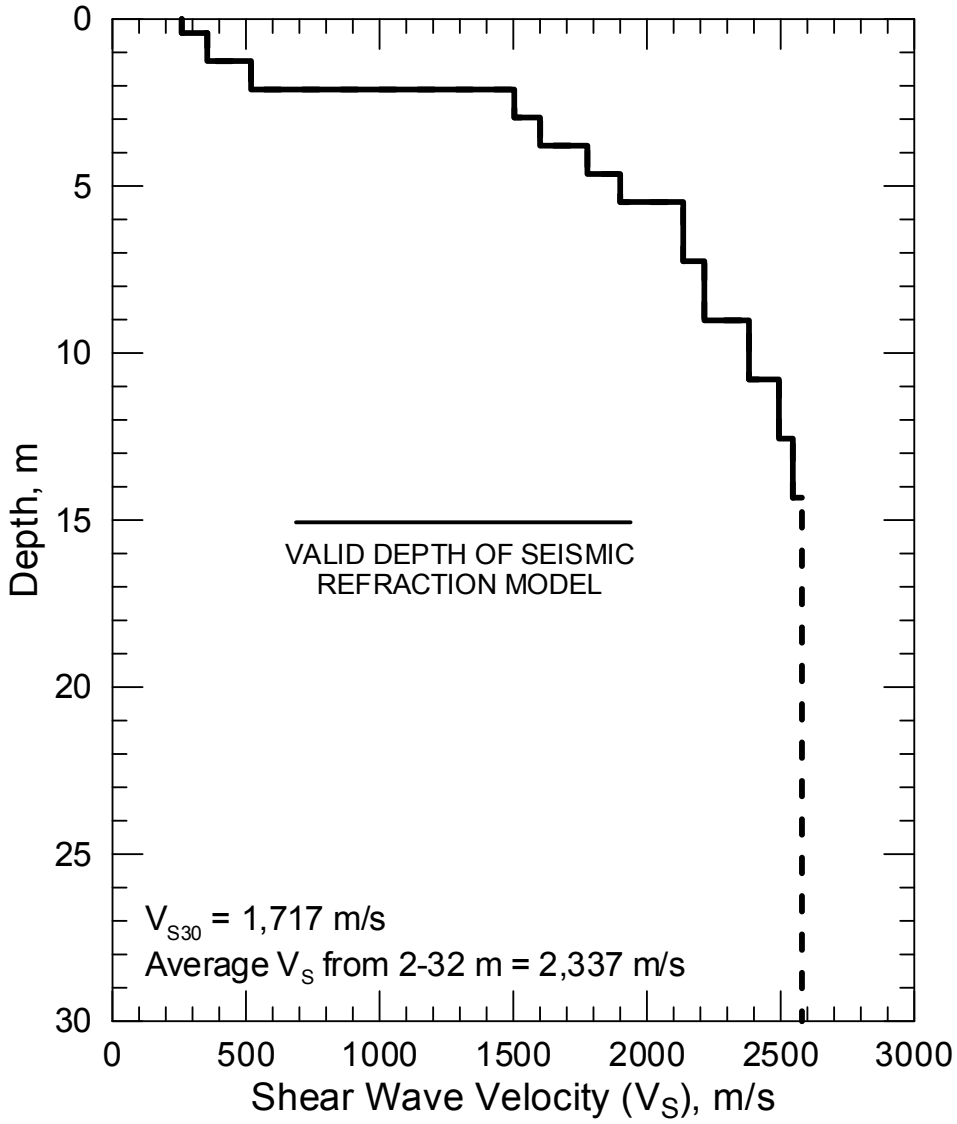

CI.CLC – Average S-wave velocity structure between 36 and 54 m on S-wave seismic refraction array CLC-1. Although seismic refraction depth of investigation limited to about 15 m, S-wave velocity is very high at the bottom of the model and not expected to increase significantly between 15 and 30 m. S-wave velocity model is not as reliable as P-wave model due to difficulty in accurately picking S-wave first arrival data.

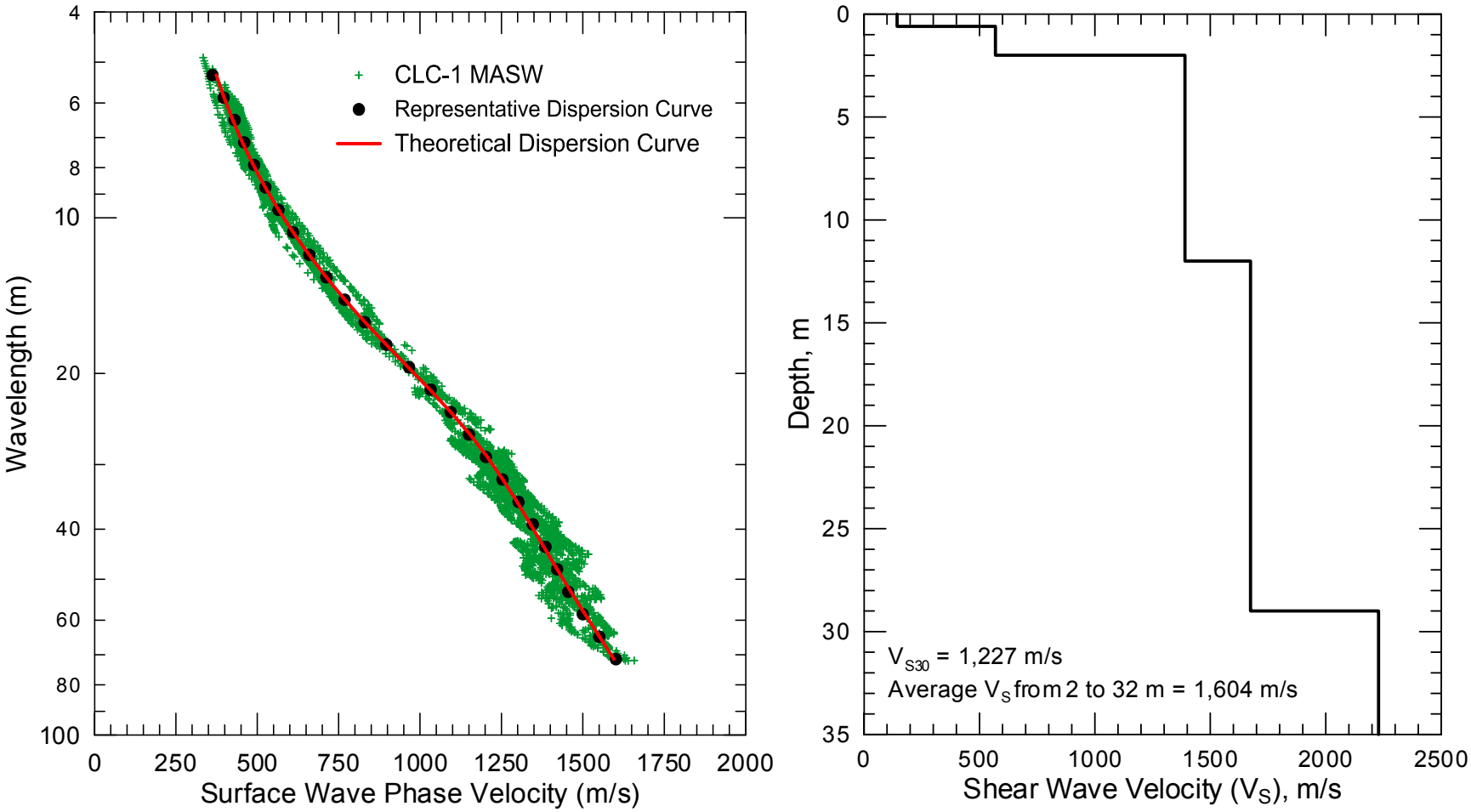

CI.CLC - Field, representative and inverted theoretical surface wave dispersion data (left) and associated V_S model (right)

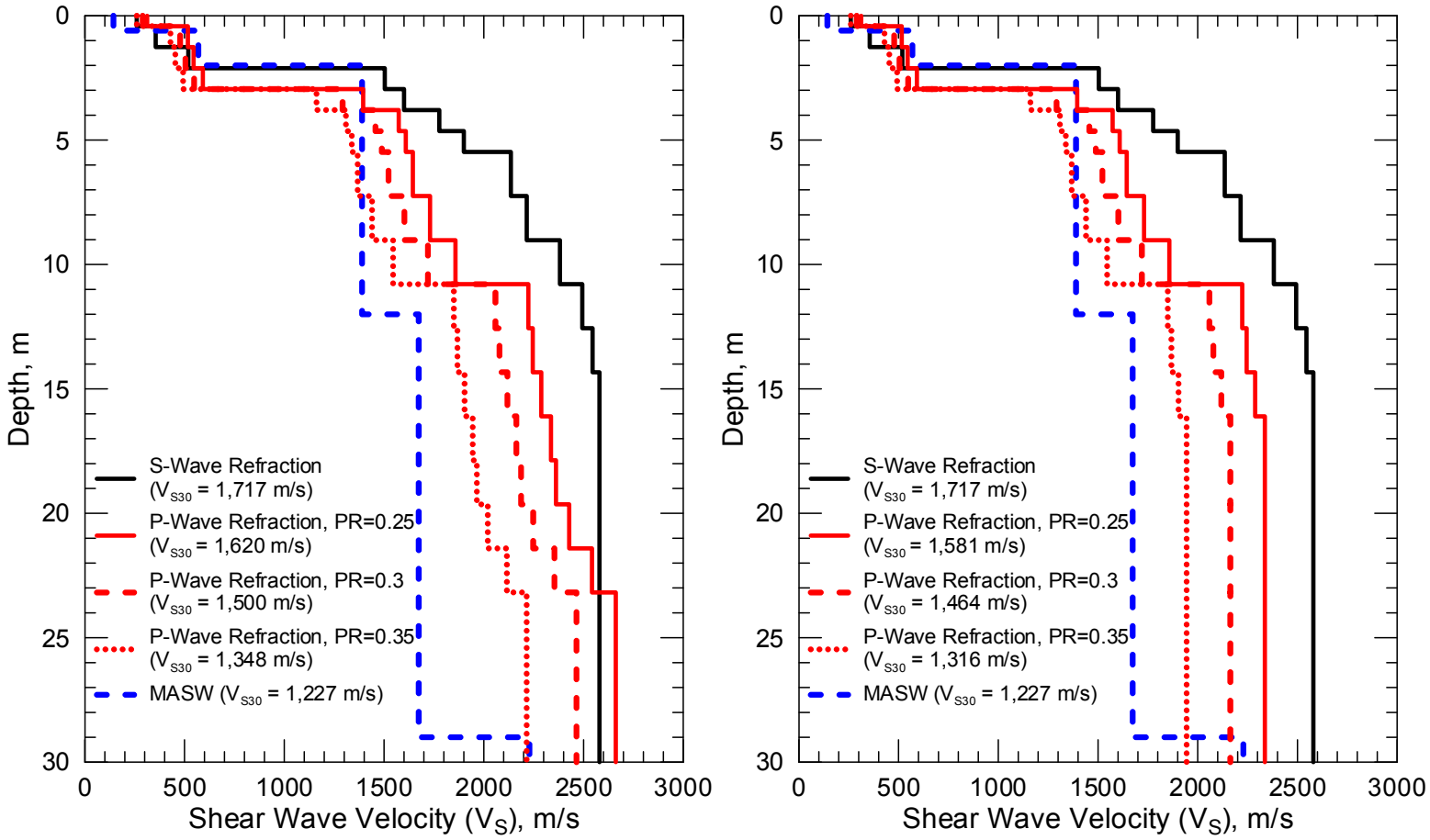

CI.CLC – Summary of S-wave velocity models derived from the S-wave and P-wave seismic refraction and MASW (Rayleigh wave) surveys. The models on the right and left assume that the P-wave refraction model is valid to depths of 17 and 23 m, respectively. The S-wave refraction model is not considered particularly reliable due to some difficulty in accurately picking the S-wave first arrival. The MASW model may underestimate S-wave velocity structure due to deepening bedrock to the southeast beneath the seismic line. We use the S-wave velocity model derived from the P-wave seismic refraction model (17 m depth of investigation) and an assumed Poisson's ratio of 0.3, which is relatively conservative for competent granitic rocks, to represent subsurface velocity structure.

Site CI.CRP

Location: California Institute of Technology, Robinsons Pit Site, Pasadena, California

Latitude: 34.13624 **Longitude:** -118.12705

(Station coordinates provided by USGS – WGS84 coordinate system)

V_{S30} (measured): 340 m/s

V_{S30} (adjusted to more accurately reflect seismic station conditions): 474 m/s (average S-wave velocity between 18 and 48 m adjusting for approximate depth of sensor)

NEHRP Site Class: D/C

Geomatrix Code: FQD

Geologic Conditions/Observations: Site located in area mapped as Quaternary (Pleistocene) old alluvial fan deposits. Deep soil site.

Site Conditions: Urban site with significant traffic noise from nearby roads. Relatively flat terrain in site vicinity with ground surface elevation gently decreasing to south.

Geophysical Methods Utilized: HVSR, MASW, array microtremor, ReMi™

Geophysical Testing Arrays:

1. Array CRP-1 (48 channel "L" shaped passive surface wave array utilizing 4.5 Hz vertical geophones spaced 3 m apart on the W-E leg along E. California Blvd. and 5 m apart on the S-N leg along S. Wilson Ave., resulting in 72 and 115 m lengths of the linear segments). The ESAC technique was used to analyze the "L" shaped array. Both the ESAC and ReMi™ techniques were used to analyze each linear segment of the passive surface wave data.
2. Array CRP-2 (48 channel MASW array, located along the S-N segment of array CRP-1, utilizing 4.5 Hz vertical geophones spaced 1 m apart for a length of 47 m, forward and reverse shot locations with multiple source offsets and source types and center shot location).
3. Three HVSR measurement locations, one on array CRP-1 and the others on nearby arrays MIK-1 and CAC-1.

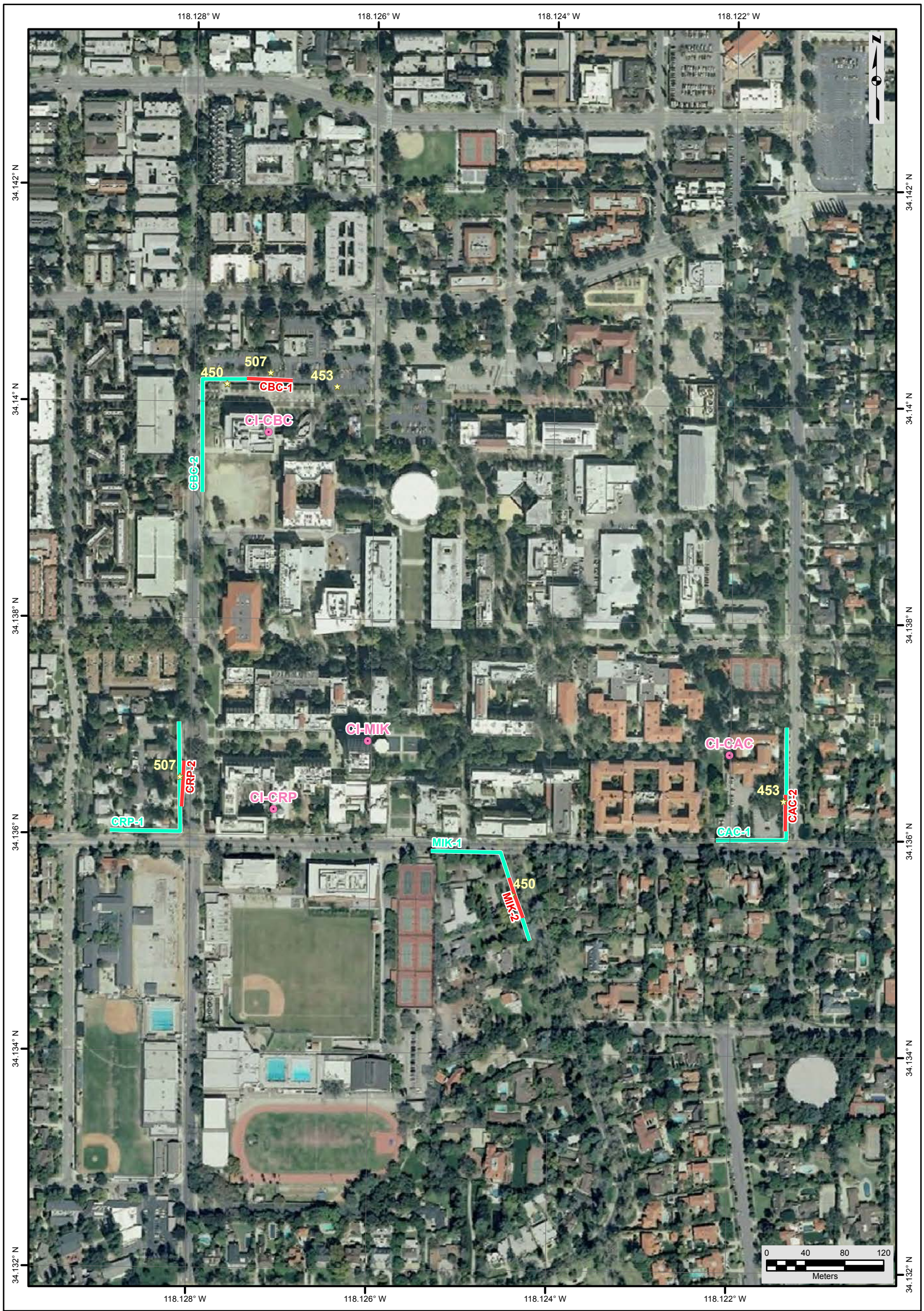

Legend

- Seismic Station - Approximate Location of Record
- H/V Spectral Ratio Measurement Location
- MASW Array
- Passive SASW Array

NOTES:
1. WGS 1984 COORDINATE SYSTEM
2. Image Source: ESRI, i-cubed, USDA FSA, USGS, AEX, GeoEye, Getmapping, Aerogrid, IGP

File Name: Caltech-I

Date: 5/16/2011

GEOVision geophysical services

SITE MAP
CI•CAC, CI•CBC, CI•CRP, CI•MIK

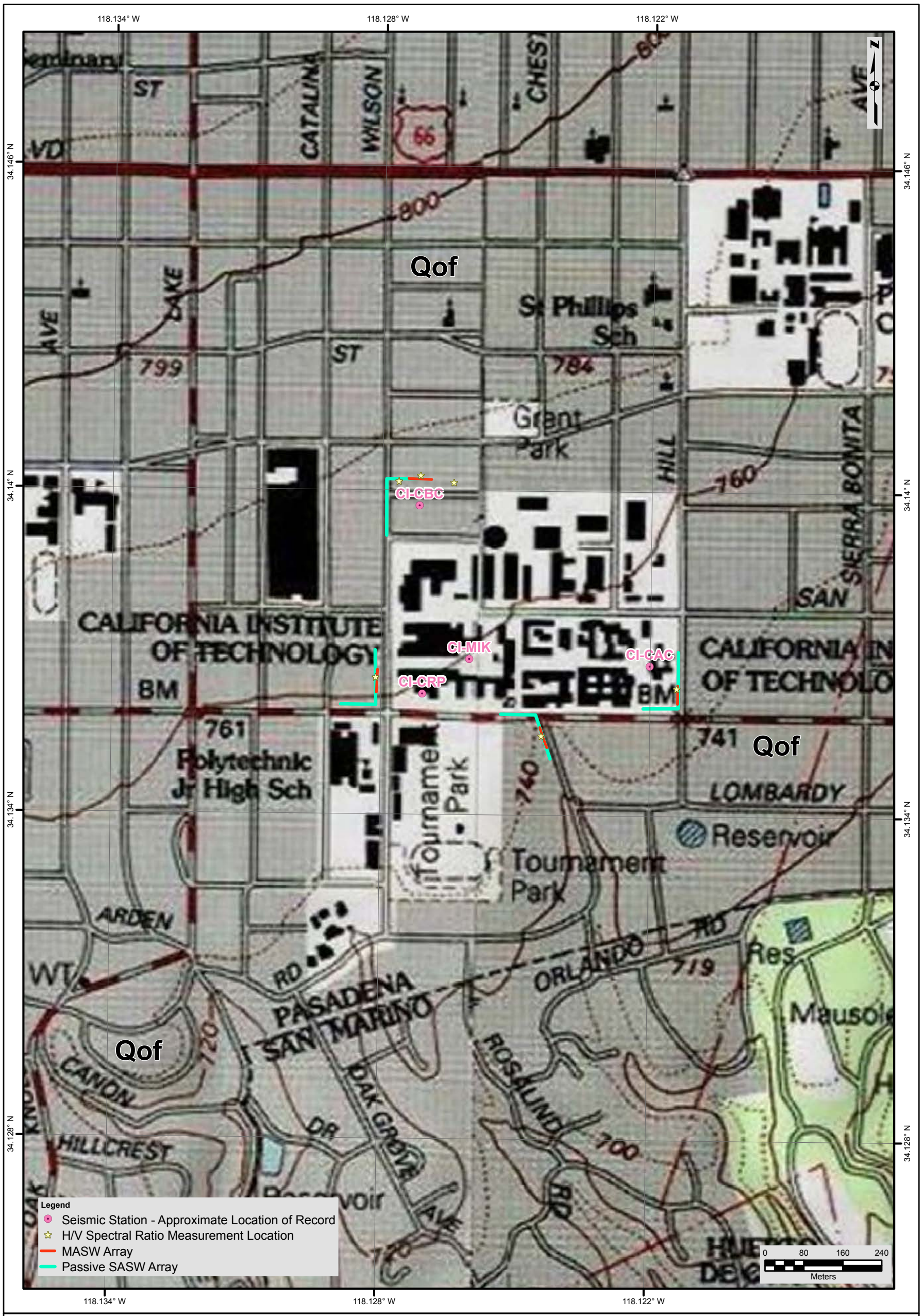

Description of Geologic Map Units

Qof = Quaternary (Holocene) alluvial fan gravel and sand

NOTES:
1. WGS 1984 COORDINATE SYSTEM
2. Topo Image Sources: USGS, FAO, NPS, EPA, NRCAN, GeoBase, Esri, DeLorme, TANA, Intermap and other suppliers and the GIS community
3. Geologic Map Units from:
Geologic Map of the Mt Wilson and Azusa Quadrangles, Los Angeles County, California by Thomas W. Dibblee, Jr., 1998 and
Geologic Map of the Pasadena Quadrangle, Los Angeles County, California by Thomas W. Dibblee, Jr., 1999
4. See site map for details of geophysical survey

File Name: Caltech

Date: 5/26/2011

GEOVision geophysical services

GEOLOGIC MAP
CI•CAC, CI•CBC, CI•CRP, CI•MIK

Looking east from corner of passive surface wave array CRP-1 towards building behind which sits seismic station CI.CRP

Looking south along passive surface wave array CRP-1

Looking south along MASW array CRP-2

Location of Geophysical Testing Arrays:

Location	Latitude	Longitude
CRP-1, West End of Array, Channel 1	34.13603	-118.12887
CRP-1, Corner of Array, Channel 25	34.13603	-118.12809
CRP-1, North End of Array, Channel 48	34.13704	-118.12811
CRP-2, South End of Array	34.13625	-118.12807
CRP-2, Center of Array	34.13643	-118.12806
CRP-2, North End of Array	34.13668	-118.12806
HVSR Sensor 507 (on array CRP-1)	34.13653	-118.12809
HVSR Sensor 453 (on array CAC-1)	34.13636	-118.12138
HVSR Sensor 450 (on array MIK-1)	34.13547	-118.12439

Notes: 1) WGS84 Coordinate System (decimal degrees)
2) Survey accuracy is estimated at 1 to 3 m

Results:

V_S Model

Depth to Top of Layer (m)	Layer Thickness (m)	S-Wave Velocity (m/s)	Inferred P-Wave Velocity (m/s)	Inferred Poisson's Ratio	Inferred Density (g/cm^3)
0	1	139	260	0.300	1.9
1	2	211	395	0.300	1.9
3	3	304	569	0.300	1.9
6	4	324	607	0.300	1.9
10	6	352	658	0.300	1.9
16	9	411	770	0.300	1.9
25	15	478	894	0.300	1.9
40	20	535	1600	0.437	2.0
60	>15	599	1600	0.418	2.0

Observations/Discussion:

- Surface wave testing conducted on the perimeter of the Caltech campus due to basements on most buildings, dense utilities and possible tunnels connecting buildings on campus.
- Limited photographs taken during field testing as much of the field work was conducted at night. Passive surface wave measurements were typically made in the late afternoon to early evening when there was sufficient traffic noise. MASW data were generally acquired in the early evening when there was less traffic, but not too late so as to disturb

residences. HVSR data were acquired between 11 pm and 2 am when there was minimal traffic noise.

- The HVSR curves are almost identical validating the 1-D velocity structure assumption with respect to deep geologic structure. There are no high frequency peaks by which to determine if shallow velocity structure is uniform.
- There is a clear HVSR peak in the 0.54 to 0.55 Hz range on all the HVSR plots, even though the test locations are about 300 m apart. An HVSR peak in the 0.55 Hz range is consistent with an expected basement depth on the order of 300 m in the site vicinity.
- Noise conditions at site (multi-directional or omni-directional noise sources) appeared sufficient for successful application of passive surface wave techniques with the closest noise source being the west to east trending E. California Blvd.
- ESAC technique used to extract surface wave dispersion data from passive "L" array data. Both the ReMi™ and ESAC techniques used to extract surface wave dispersion data from the linear arrays.
- As expected, the E-W linear array segment did not provide useful surface wave dispersion data as it was located along E. California Blvd (i.e. parallel to the oncoming traffic). Both the "L" array passive surface wave data and S-N linear array (both ESAC and ReMi™ analysis) yielded comparable surface wave dispersion curves and were used for data analysis.
- Surface wave dispersion data from active and passive surface wave data sets are in good agreement at this site although the surface wave dispersion data from the two techniques only overlap over the 16 to 40 m wavelength range. Slight differences in the surface wave dispersion data are attributed to near surface lateral velocity variation and the fact that the MASW data were acquired along a 47 m long array, whereas the passive surface wave data were acquired along a much larger 72 by 115 m array. Near surface lateral velocity variation is expected for this site due to all of the construction that has occurred over a long period of time.
- Representative dispersion curves were generated for each surface wave data set using a moving average, polynomial curve fitting routine. These individual representative dispersion curves were combined and a representative dispersion curve generated for the combined data set for data modeling.
- No evidence of a water table refractor or reflector in the MASW seismic records due to both high noise levels and short array length. Water table was assumed at a depth of 40 m for modeling and a P-wave velocity of 1,600 m/s utilized for assumed saturated zone.
- Surface wave depth of investigation is about 75 m based on half of maximum wavelength criteria and assuming that surface wave dispersion data at frequencies as low as 3 Hz are valid utilizing 4.5 Hz geophones (low frequency geophone phase response differences will cancel out if noise is omni-directional and/or the phase response differences are random in nature).
- V_{S30} is 340 m/s (Site Class D).
- Average S-wave velocity between 18 m (estimated depth of Robinsons Pit) and 48 m is 474 m/s.
- Average S-wave velocity of the upper 75 m (V_{S75}) is 437 m/s.

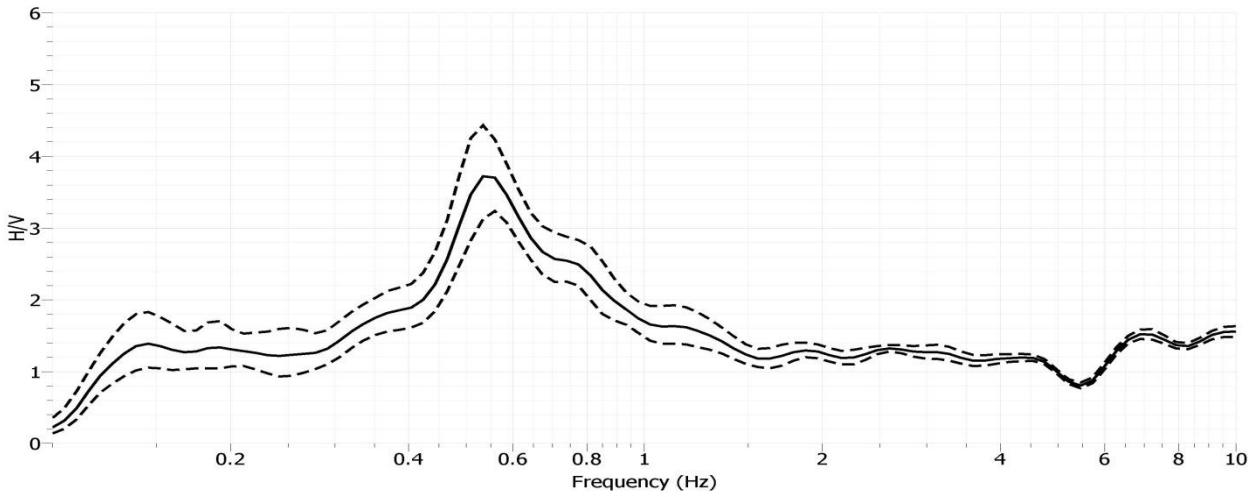

Site CI.CRP, H/V Spectral Ratio, Array CRP-1/2, Sensor 507

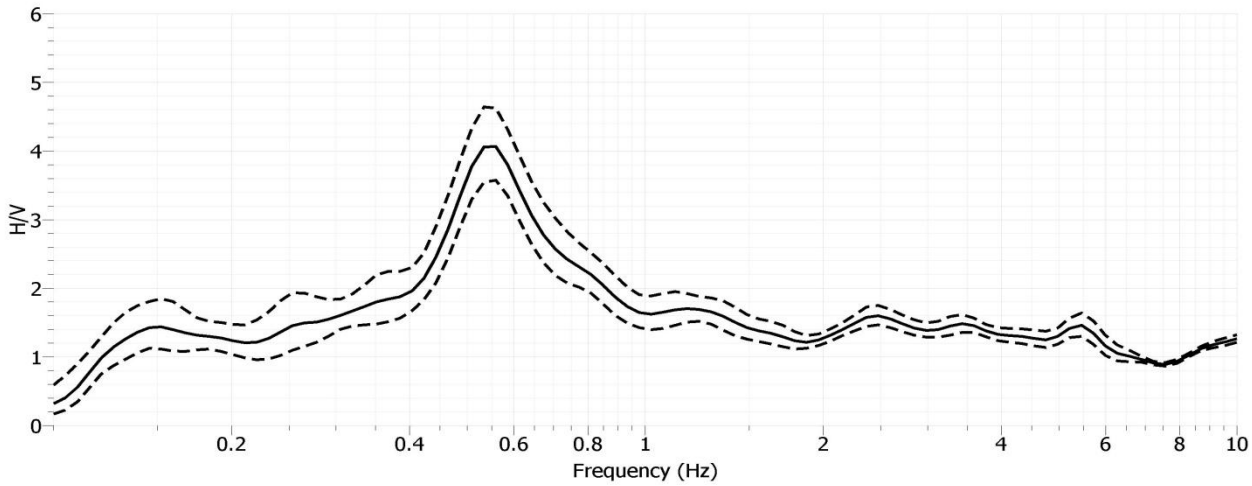

Site CI.MIK, H/V Spectral Ratio, Array MIK-1/2, Sensor 450

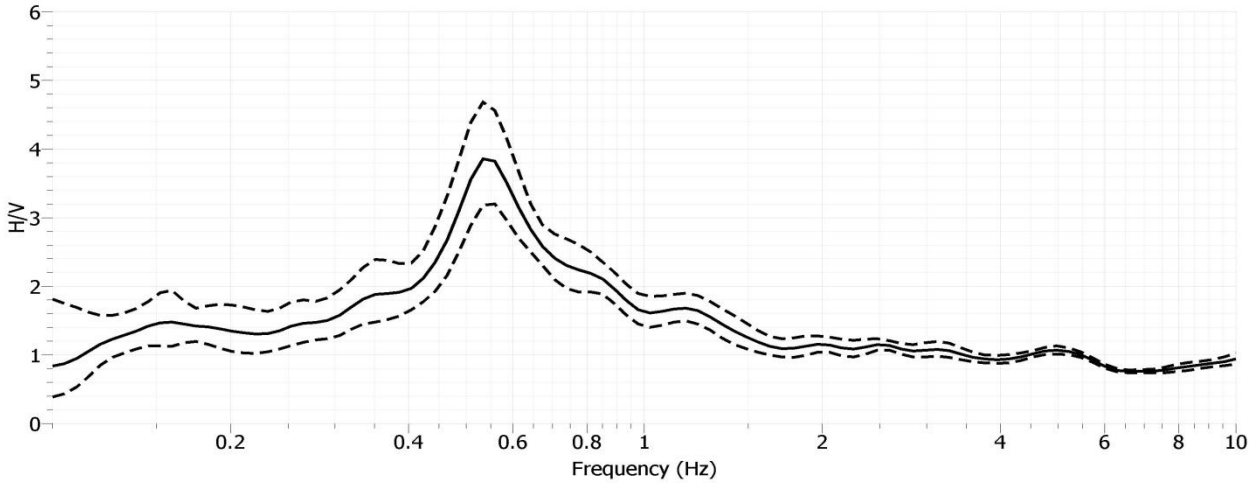

Site CI.CAC, H/V Spectral Ratio, Array CAC-1/2, Sensor 453

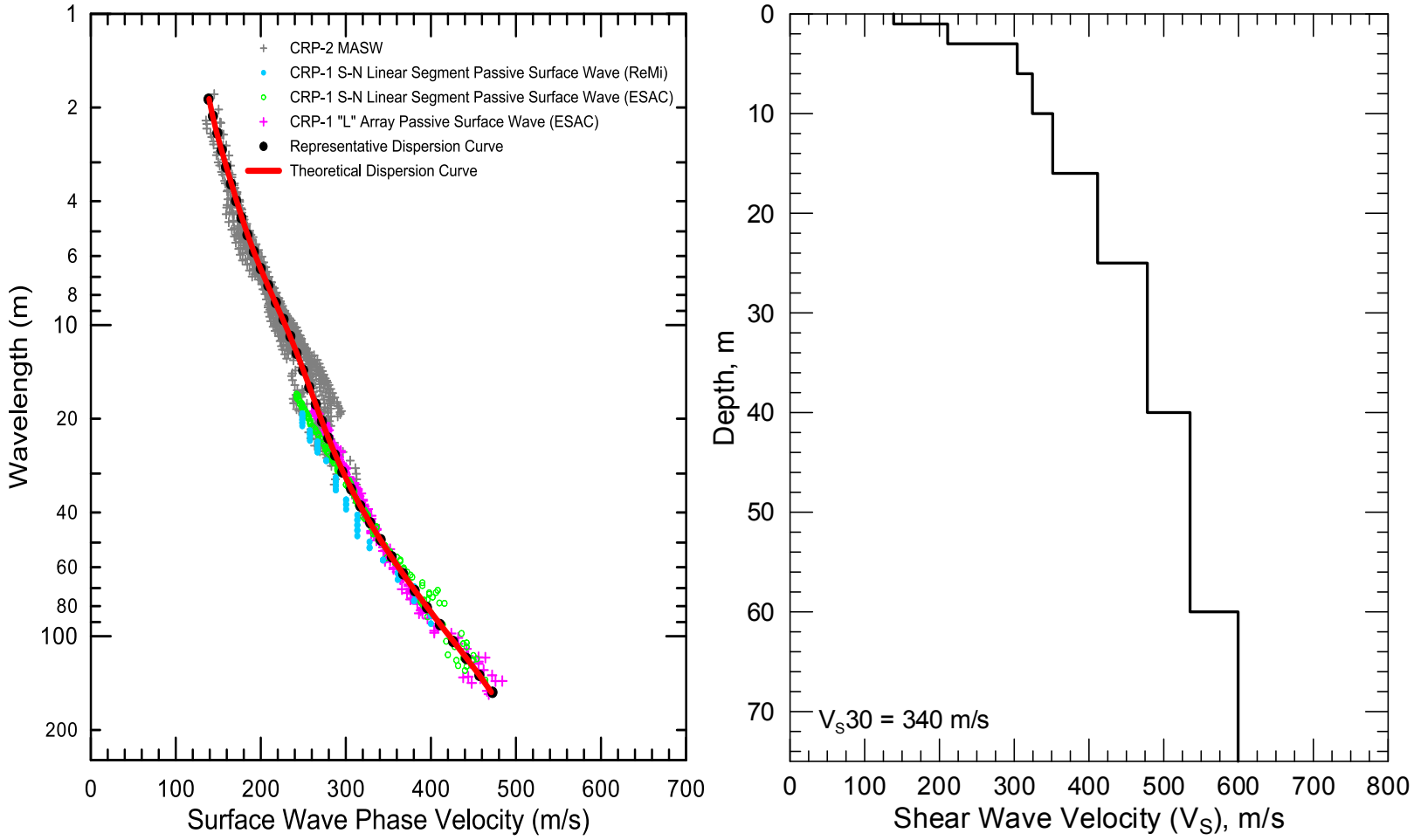

CI.CRP - Field, representative and inverted theoretical surface wave dispersion data (left) and associated V_S model (right)

Site CI.CTC

Location: Cactus City Microwave, approx. 5 km southwest of Cactus City Rest Area on I-10, Riverside County, California

Latitude: 33.65511 **Longitude:** -115.99004

(Station coordinates modified based on field GPS survey, WGS84 coordinate system)

V_{S30} (measured): 370 m/s

V_{S30} (adjusted to more accurately reflect seismic station conditions): 396 m/s (average S-wave velocity between 2 and 32 m adjusting for nominal sensor depth)

NEHRP Site Class: C

Geomatrix Code: IQD

Geologic Conditions/Observations: Site located on geologic unit mapped as Quaternary (Pleistocene) Ocotillo Formation. Crystalline basement expected to be deep at this site.

Site Conditions: Rural site. Site located on top of a hill with moderately steep topography on the sides. Slightly undulating topography along test area with about 3 m of elevation variation.

Geophysical Methods Utilized: HVSR, MASW

Geophysical Testing Arrays:

1. Array CTC-1 (24 channel MASW array utilizing 4.5 Hz vertical geophones spaced 3 m apart for a length of 69 m, forward and reverse shot locations with multiple source offsets and source types and multiple interior shots).
2. Array CTC-1 (24 channel MASW array utilizing 4.5 Hz vertical geophones spaced 1 m apart for a length of 23 m, forward and reverse shot locations with multiple source offsets and source types and center shot).
3. Three HVSR measurement locations, two distributed along array CTC-1 and the other near the seismic station.

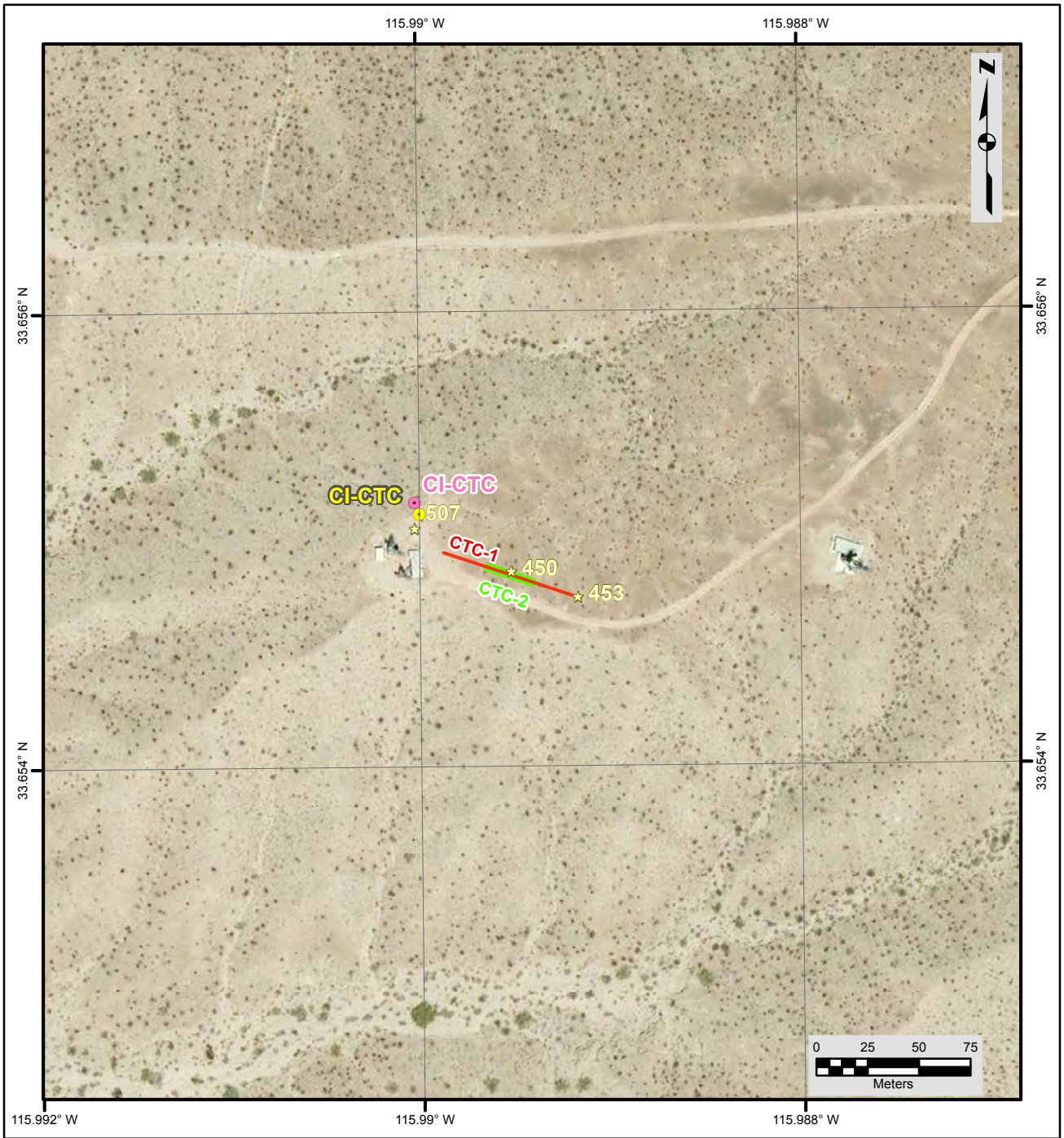

Legend

- Seismic Station - Approximate Surveyed Location
- Seismic Station - Approximate Location of Record
- H/V Spectral Ratio Measurement Location
- MASW Array
- MASW Array

NOTES:
1. WGS 1984 COORDINATE SYSTEM
2. Image Source: ESRI, i-cubed, USDA FSA, USGS, AEX, GeoEye, Getmapping, Aerogrid, IGP

File Name: CI-CTC-I

Date: 2/7/2013

USGS science for a changing world

GEOVision geophysical services

RECOVERY.GOV

SITE MAP
CI•CTC

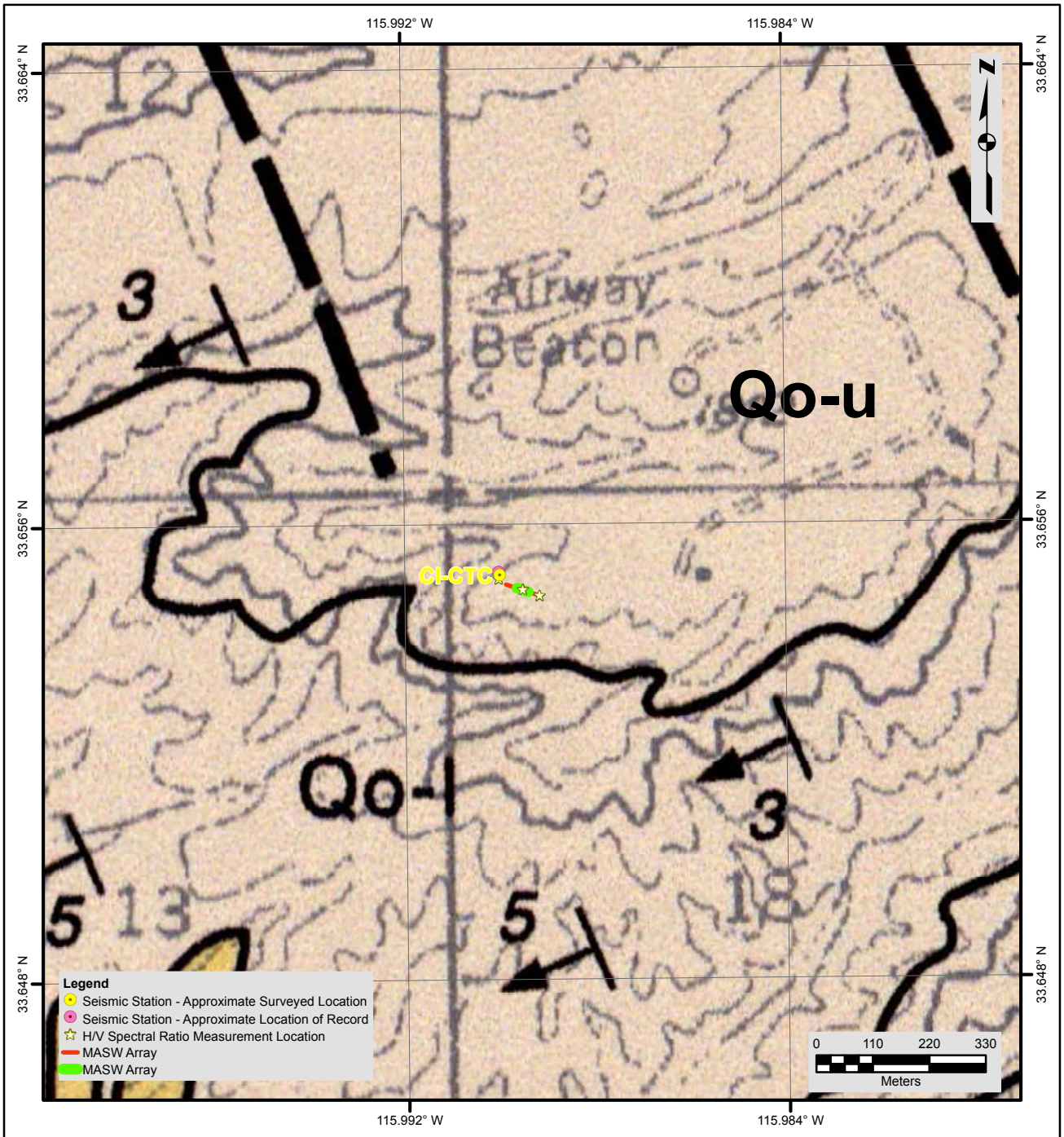

Description of Geologic Map Units

Qo-u = Quaternary (Pleistocene) Ocotillo Formation; upper unit, boulder conglomerate
Qo-l = Quaternary (Pleistocene) Ocotillo Formation; lower member, pebble-cobble conglomerate

NOTES:
1. WGS 1984 COORDINATE SYSTEM
2. Geologic Map of the Cottonwood Spring & Canyon Spring 15 Minute Quadrangles, Riverside County, California by Thomas W. Dibblee, Jr., 2008
3. See site map for details of geophysical survey

File Name: CI-CTC

Date: 2/7/2013

USGS science for a changing world

GEOVision geophysical services

GEOLOGIC MAP
CI•CTC

RECOVERY.GOV

Looking north towards HVSR sensor 507 and CI.CTC seismic station

MASW data acquisition along array CTC-1 using accelerated weight drop

Looking northwest towards center of MASW array CTC-1 and CI.CTC seismic station

MASW and seismic refraction data acquisition along array CTC-1 using sledge hammer

Looking southeast along MASW array CTC-1

Location of Geophysical Testing Arrays:

Location	Latitude	Longitude
CTC-1, Northwest End of MASW Array	33.65494	-115.98991
CTC-1 and CTC-2, Center of MASW Arrays	33.65484	-115.98956
CTC-1, Southeast End of MASW Array	33.65474	-115.98920
HVSR Sensor 507	33.65505	-115.99006
HVSR Sensor 453	33.65474	-115.98921
HVSR Sensor 450	33.65486	-115.98955
CI.CTC Seismic Station	33.65511	-115.99004

Notes: 1) WGS84 Coordinate System (decimal degrees)

2) Survey accuracy is estimated at 1 to 2 m.

Results:

V_S Model

Depth to Top of Layer (m)	Layer Thickness (m)	S-Wave Velocity (m/s)	Inferred P-Wave Velocity (m/s)	Inferred Poisson's Ratio	Inferred Density (g/cm^3)
0	1	185	345	0.3	1.8
1	2	276	517	0.3	1.9
3	3	310	580	0.3	1.9
6	4	356	666	0.3	1.9
10	6	372	696	0.3	1.9
16	8	406	759	0.3	1.9
24	>6	519	971	0.3	2.0

Observations/Discussion:

- HVSR plots are generally similar at all measurement locations validating the 1-D velocity structure assumption. There are some differences in the measurements. The site is located on top of a hill so there may be topographic effects. It was also difficult to couple the sensors in gravelly soils, so sensor coupling may play a role in slight differences between measurements.
- There is no distinct high amplitude HVSR peak at the site. There are, however, broad low amplitude peaks in the 0.4 to 0.6 and 1 to 2 Hz ranges.
- Noise conditions at the site were not sufficient to apply passive surface wave techniques.
- Surface wave dispersion data from the two MASW data sets are in good agreement at the site.
- Scatter in the surface wave dispersion data likely results from lateral velocity variation.
- Representative dispersion curves were generated for each surface wave data set using a moving average, polynomial curve fitting routine. These individual representative dispersion curves were combined and a representative dispersion curve generated for the combined data set for data modeling.
- Water table located at a depth of greater than 30 m based on seismic refraction survey design, absence of a water table refractor and no clear water table reflector.
- Based on analysis of seismic refraction data, P-wave velocity in the upper 15 m ranges from about 400 m/s near the surface to over 600 m/s at a depth of 12 to 15 m.
- Surface wave depth of investigation is about 30 m based on half of maximum wavelength criteria.
- The inferred P-wave velocities in the surface wave model (assumed Poisson's ratio of 0.3) are about 10% higher than the seismic refraction data indicates below depths of about 3 m. A Poisson's ratio of about 0.25 may yield better agreement between the surface wave model and seismic refraction data.
- V_{S30} is 370 m/s (Site Class C).
- Average S-wave velocity between 2 m (nominal sensor depth) and 32 m is 396 m/s.

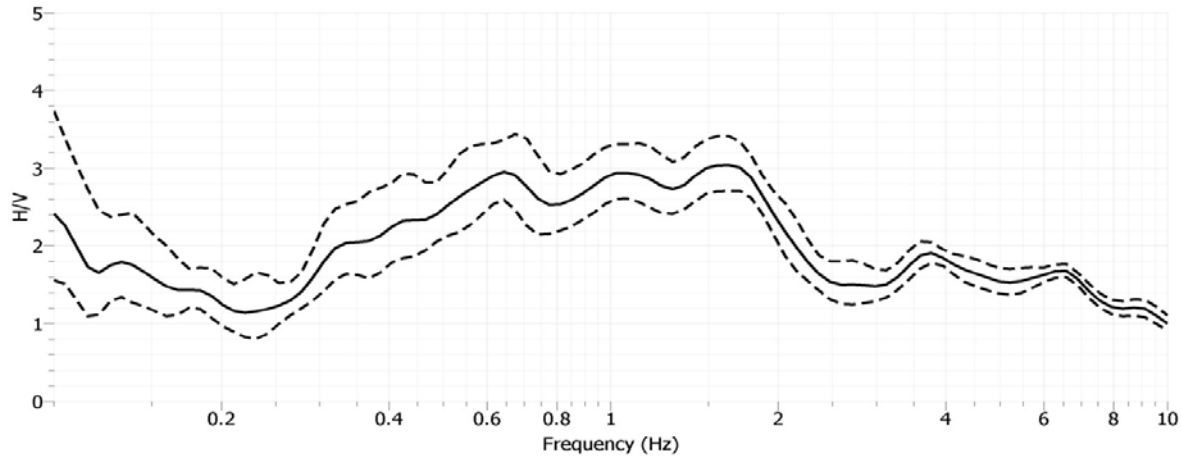

Site CI.CTC, H/V Spectral Ratio, Near Seismic Station, Sensor 507

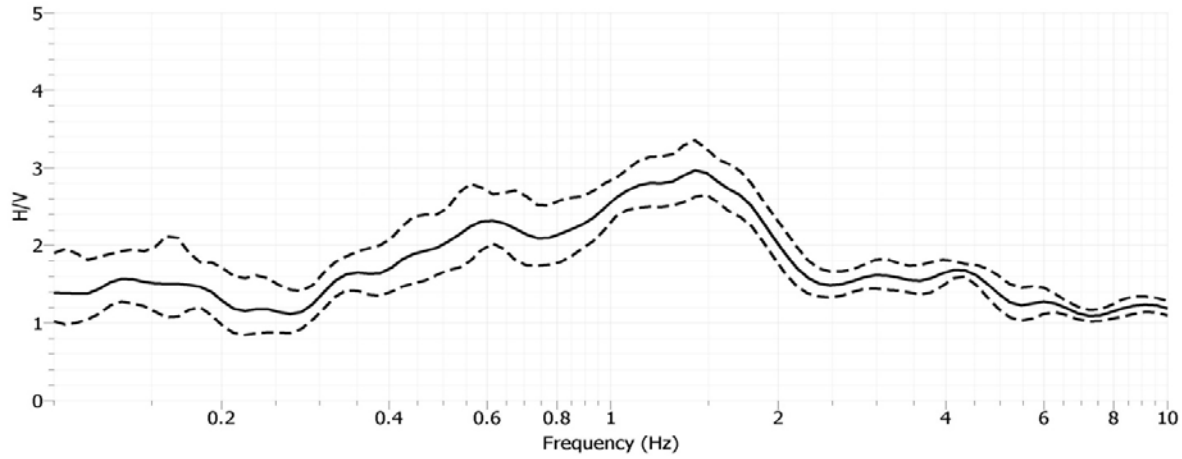

Site CI.CTC, H/V Spectral Ratio, Array CTC-1, Sensor 450

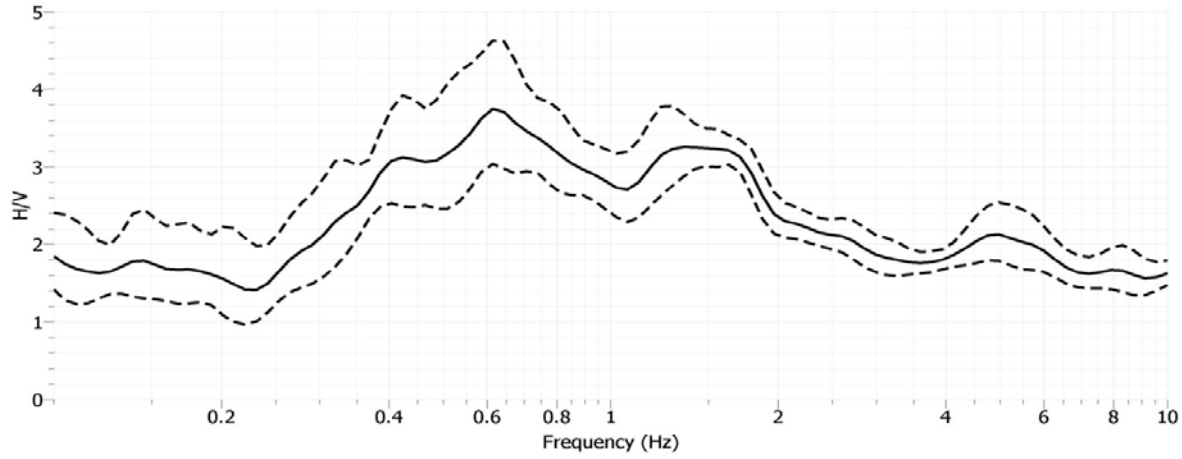

Site CI.CTC, H/V Spectral Ratio, Array CTC-1, Sensor 453

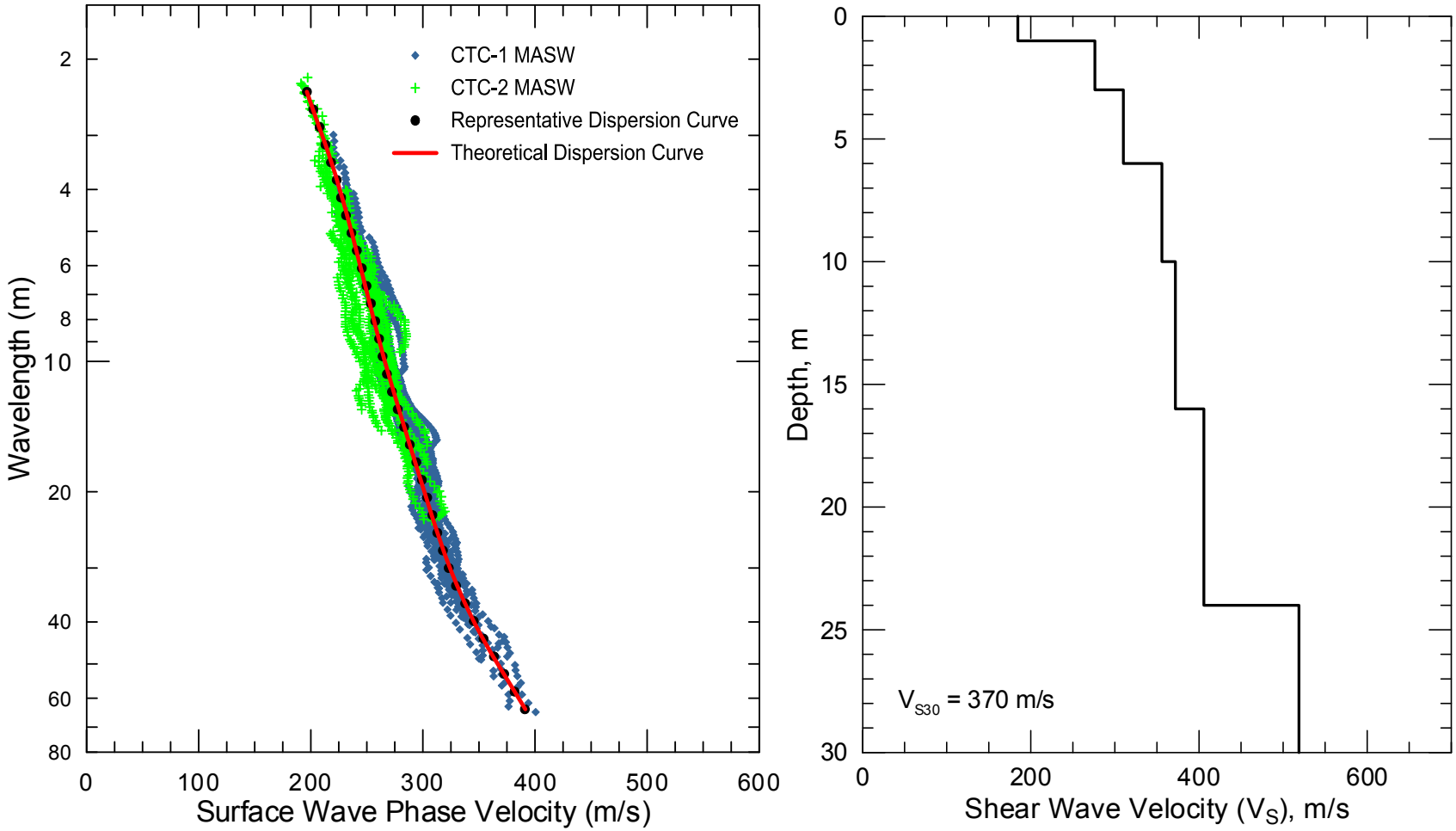

CI.CTC - Field, representative and inverted theoretical surface wave dispersion data (left) and associated V_S model (right)

Site CI.CTD

Location: Catalina Thompson Dam, Catalina Island, California

Latitude: 33.35486 **Longitude:** -118.44436
(Station coordinates provided by USGS, WGS84 coordinate system)

V_{S30} (measured): 756 m/s

V_{S30} (adjusted to more accurately reflect seismic station conditions): 881 to 1,016 m/s. Seismic station is located on a rock outcrop, whereas a thin layer of fill or sediments overlies rock beneath the seismic line. Average V_S between 1 and 31 m is 881 m/s. Average V_S between 3 and 33 m is 1,016 m/s. Replacing the V_S of the upper two probable sediment layers with that of the underlying layer results in V_{S30} of 897 m/s.

NEHRP Site Class: C/B (recommend using Site Class B based on adjustments discussed above).

Geomatrix Code: IFA

Geologic Conditions/Observations: Seismic station located on outcrop of Mesozoic (Jurassic and Cretaceous) Franciscan Formation.

Site Conditions: Rural island site. Seismic station located on a rock outcrop near the top of the dam. Test area located at the toe of the dam as close as possible to the seismic station. Limited locations/space to place MASW and seismic refraction array. Steep topography in site vicinity. The ground surface elevation along seismic refraction line steadily increases to the northeast.

Geophysical Methods Utilized: HVSR, MASW, Seismic Refraction

Geophysical Testing Arrays:

1. Array CTD-1 - 48 channel MASW array utilizing 4.5 Hz vertical geophones spaced 1.5 m apart for a length of 70.5 m, forward and reverse shot locations with multiple source offsets (northeast end of array only) and source types (hammers only) and a center shot location.
2. Array CTD-2 - 48 channel MASW and P-wave seismic refraction array utilizing 4.5 Hz vertical geophones spaced 1.5 m apart for a length of 70.5 m, forward and reverse shot locations with multiple source offsets (southwest end of array only) and source types (hammers only) and multiple interior shot locations. Array CTD-2 coincindent with array CTD-1, but shifted about 20 m to northeast to allow source locations offset from southwest end of the array.
3. Three HVSR measurement locations; two distributed along array CTD-1, one adjacent the seismic station.

Legend

- Seismic Station - Approximate Surveyed Location
- Seismic Station - Approximate Location of Record
- H/V Spectral Ratio Measurement Location
- MASW Array
- MASW and Seismic Refraction Array

NOTES:
1. WGS 1984 COORDINATE SYSTEM
2. Image Source: (c) Microsoft Corporation and its data suppliers

File Name: CI-CTD-I

Date: 2/7/2013

USGS science for a changing world

GEOVision geophysical services

RECOVERY.GOV

SITE MAP
CI•CTD

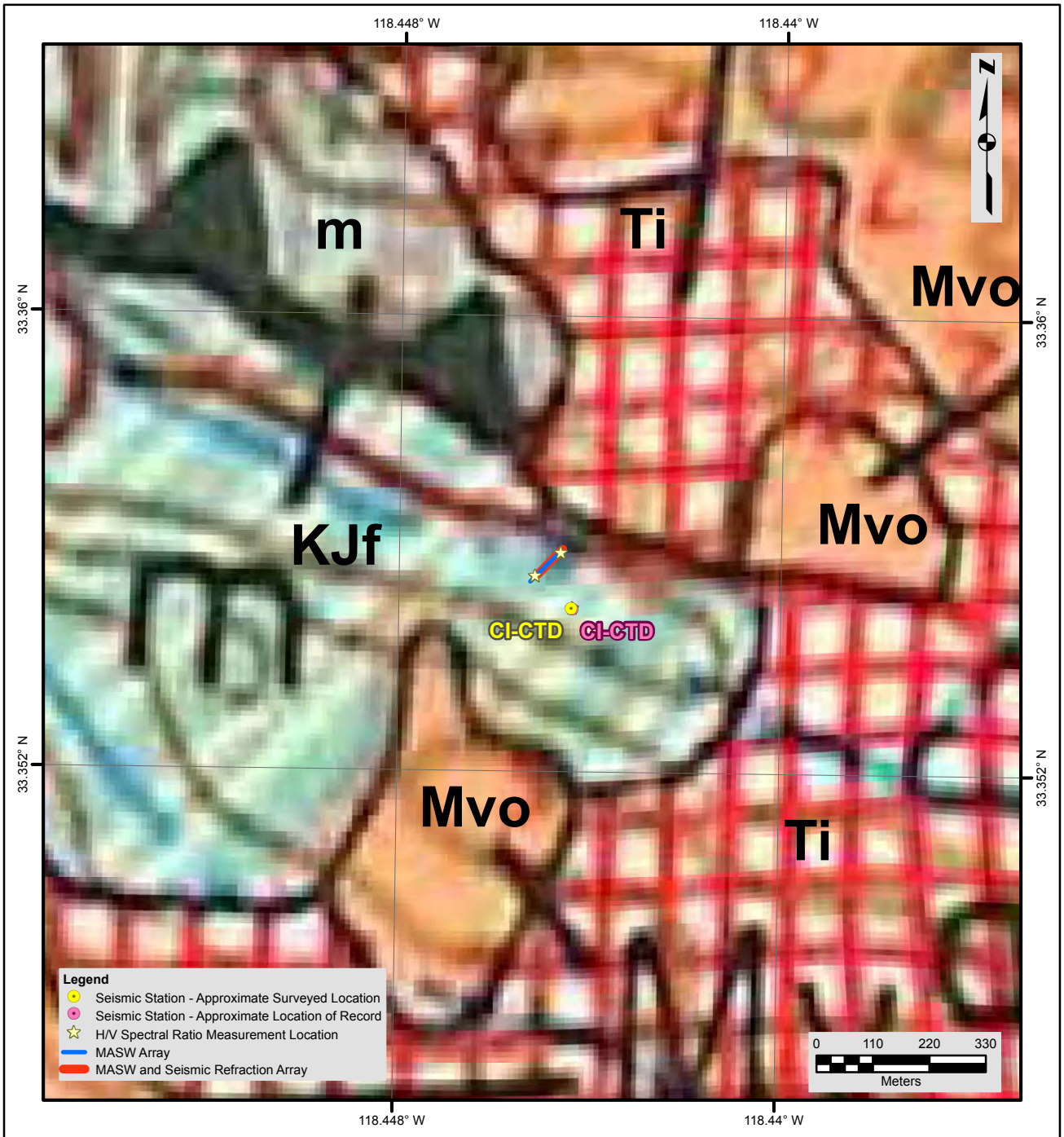

Description of Geologic Map Units

Mvo = Tertiary (Miocene) volcanic deposits; andesite
Ti = Tertiary (Undivided) lake deposits
KJf = Mesozoic (Jurassic and Cretaceous) Franciscan Formation
m = Mesozoic (Precretaceous) undivided metamorphic rocks

NOTES:
1. WGS 1984 COORDINATE SYSTEM
2. Geologic Map of California,
Long Beach Sheet (Olaf P. Jenkins edition)
Compiled by Charles W. Jennings, 1962
3. See site map for details of geophysical survey

File Name: CI-CTD

Date: 2/7/2013

USGS science for a changing world

GEOVision geophysical services

GEOLOGIC MAP
CI•CTD

RECOVERY.GOV

CI.CTD seismic station located on outcrop of Franciscan formation

Looking northeast along arrays CTD-1 and CTD-2

HVSR sensor TRO-1 adjacent the seismic station

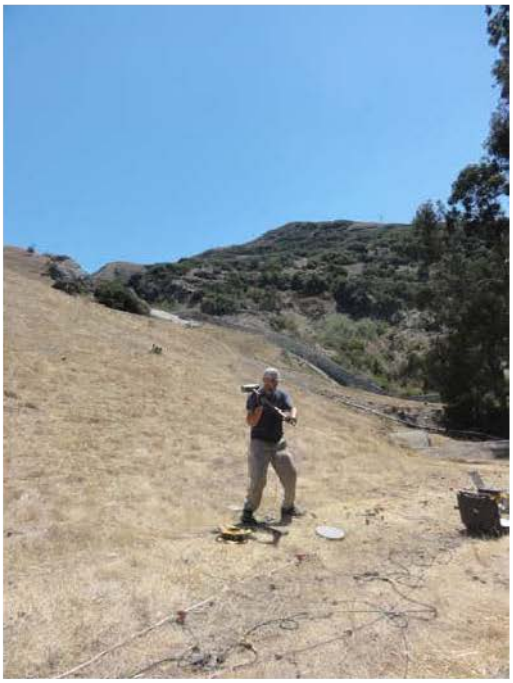

MASW data acquisition on array CTD-1

Bedrock outcrop adjacent to arrays CTD-1 and 2

Location of Geophysical Testing Arrays:

Location	Latitude	Longitude
CTD-1, Southwest End of MASW Array	33.35533	-118.44524
CTD-1, Center of MASW Array	33.35557	-118.44497
CTD-1, Northeast End of MASW Array	33.35579	-118.44470
CTD-2, Southwest End of MASW/Refraction Array	33.35546	-118.44509
CTD-2, Center of MASW/Refraction Array	33.35568	-118.44484
CTD-2, Northeast End of MASW/Refraction Array	33.35590	-118.44457
HVSR Sensor Tromino 1 (TRO-1)	33.35488	-118.44436
HVSR Sensor Tromino 2 (TRO-2)	33.35585	-118.44461
HVSR Sensor Tromino 3 (TRO-3)	33.35543	-118.44515
CI.CTD Seismic Station	33.35487	-118.44438

Notes: 1) WGS84 Coordinate System (decimal degrees)
2) Survey accuracy is estimated at 2 to 4 m

Results:

V_S Model

Depth to Top of Layer (m)	Layer Thickness (m)	S-Wave Velocity (m/s)	Inferred P-Wave Velocity (m/s)	Assumed Poisson's Ratio	Assumed Density (g/cm^3)
0	1	157	294	0.3	1.7
1	2.25	332	621	0.3	1.8
3.25	2.25	469	877	0.3	2.0
5.5	3.5	1028	1923	0.3	2.1
9	7	1091	2041	0.3	2.1
16	9	1106	2070	0.3	2.1
25	>10	1326	2480	0.3	2.2

Notes: 1) Depth of investigation is about 35 m.
2) Bottom layer is a half space.
3) Upper two layers are probably not representative of seismic station conditions.

Observations/Discussion:

- The seismic station is located on a bedrock outcrop at the top of the Thompson Dam. The nearest location to conduct seismic testing was at the toe of the dam where rock is located at or near the surface. We cannot discount the possibility that the weathering profile is slightly different at the location of the seismic station and MASW array due to significant elevation difference.
- There are no peaks in the HVSR data, as expected for a rock site.
- Due to limited space, MASW data were acquired along two arrays (CTD-1 and CTD-2) in order to obtain offset shot locations on each end of the arrays. Array CTD-1 allowed offset source locations at the northeast end of the array. Array CTD-2, shifted about 20 m along array CTD-1, allowed offset source locations at the southwest end of the array. There were no feasible alternate test locations in the vicinity of the seismic station.
- The P-wave refraction data collected along array CTD-2 were modeled using a tomographic inversion routine with a smooth velocity gradient starting model. The seismic refraction model was extended to limited far offset shot locations (southwest end of array only) to extend depth of investigation.
- The seismic refraction survey design allowed P-wave velocity to be imaged to a maximum depth of about 15 m. The seismic refraction model shows that P-wave velocity is about 400 to 600 m/s at the surface, increasing to 800 m/s at a depth of 1 to 3 m, 1,200 m/s at a depth of 1.5 to 4 m, 2,000 m/s at a depth of about 4 to 9 m and 2,800 m/s at a depth of about 6 to 15 m. P-wave velocity may be as high as 4,000 m/s at a depth of 12 m, or more, beneath the southwest end of the array.
- The seismic refraction model indicates that there is significant lateral velocity variation at this site with higher P-wave velocities at shallower depth at the southwest end of the line. There were no reasonable alternate test locations at the site due to limited space and steep topography.
- Noise conditions at the site were not sufficient for application of passive surface wave techniques.
- MASW data reduction at this site was very difficult, especially at intermediate wavelength ranges, due to significant lateral velocity variation and the presence of a thin fill/sediment layer over relatively high velocity rock.
- The minimum wavelength surface wave phase velocity data extracted from the 48-channel MASW array was about 32 m, although data with wavelengths this small were only extracted from seismic records associated with two of the offend source locations. Data reduction using seismic records from smaller hammer sources and a limited offset receiver array (i.e. less active geophones) allowed extraction of surface wave dispersion data to a minimum wavelength of about 3 m. Significant effort was also made reducing data from limited offset receiver arrays with larger hammer sources to obtain surface wave dispersion data over intermediate wavelength ranges.
- There is about 80 to 120 m/s scatter in MASW dispersion data likely due, in part, to lateral velocity variation associated with both a very thin sediment/fill layer of variable thickness, differential weathering of near surface sedimentary rock and dip of the rock.
- A representative dispersion curve was generated for the MASW data set using a moving average, polynomial curve fitting routine and used for modeling.

- Surface wave depth of investigation is about 35 m based on half of maximum wavelength criteria.
- The inferred P-wave velocities in the upper 15 m of the surface wave model, assuming a Poisson's ratio of 0.3, are generally consistent with the average velocity structure at the northeast end of the seismic refraction model.
- Although there is significant lateral velocity variation beneath the MASW array, the V_S model is thought to be representative of average velocity structure.
- V_{S30} is 756 m/s (Site Class C/B).
- The seismic station is located on a rock outcrop on top of the dam, whereas the MASW and seismic refraction array are located at the toe of the dam in an area with a very thin fill/sediment layer over rock. To account for the differences in expected near surface velocity structure at the seismic station and the MASW array, the average S-wave velocity between 1 and 31 m and 3 and 33 m are calculated. Additionally, V_{S30} is calculated after replacing the velocity of the upper two layers in the V_S model (upper 3.25 m) with that of the underlying layer.
- The average S-wave velocity between 1 and 31 m and 3 and 33 m is 881 and 1,016 m/s, respectively (Site Class B). The estimated V_{S30}, after replacing V_S of the upper two layers with that of the underlying layer is 897 m/s (Site Class B).

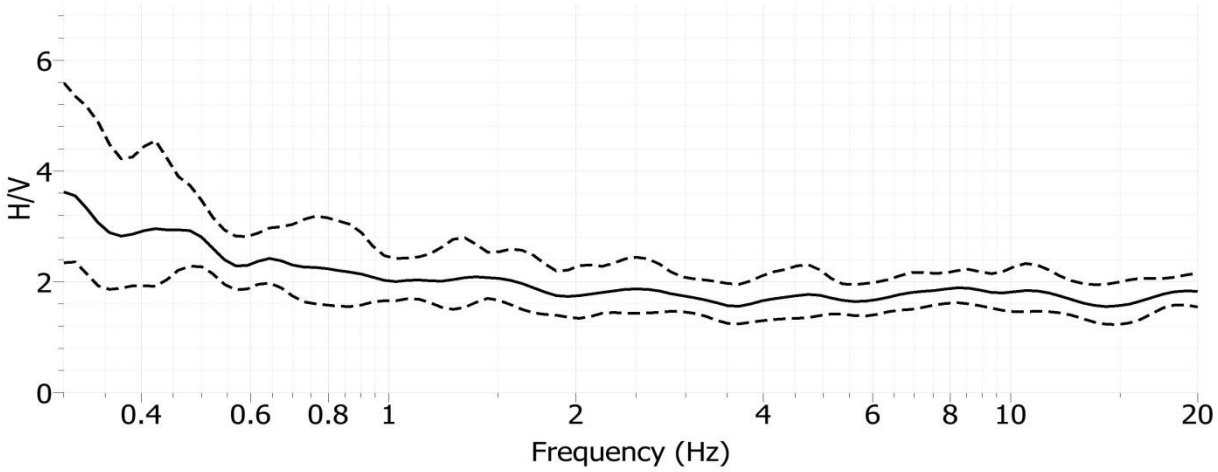

Site CI.CTD, H/V Spectral Ratio, Array CTD-1, TRO-2

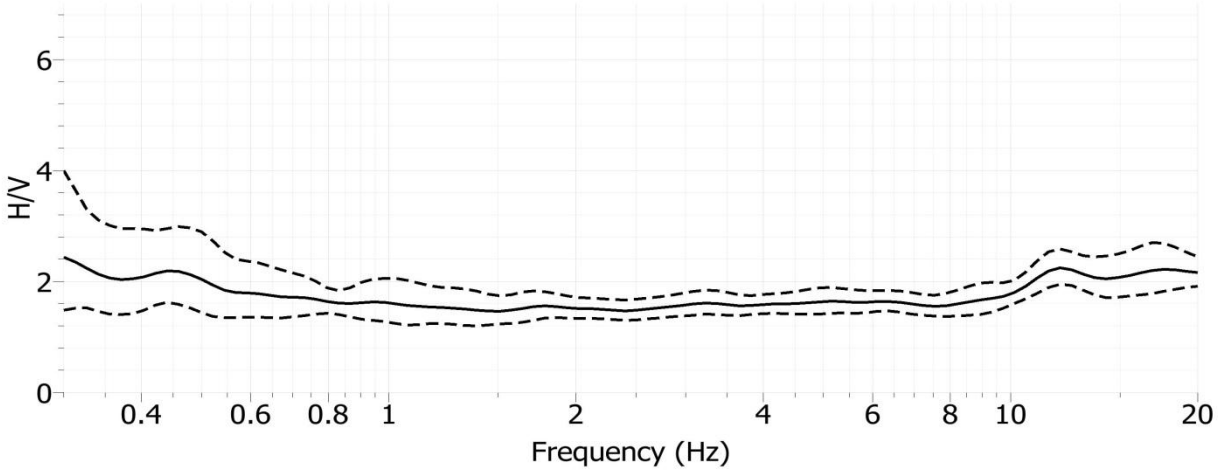

Site CI.CTD, H/V Spectral Ratio, Array CTD-1, TRO-3

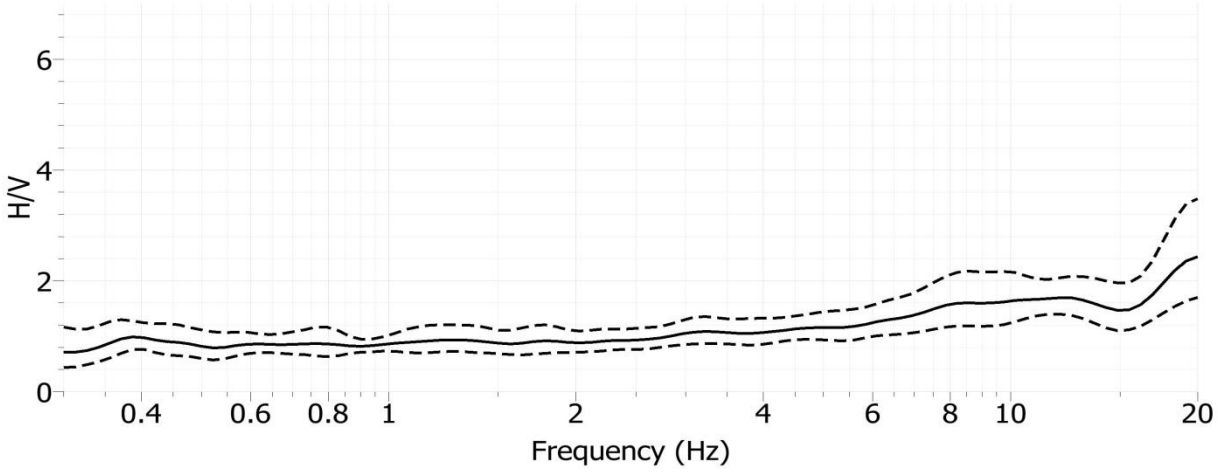

Site CI.CTD, H/V Spectral Ratio, Near Seismic Station, TRO-1

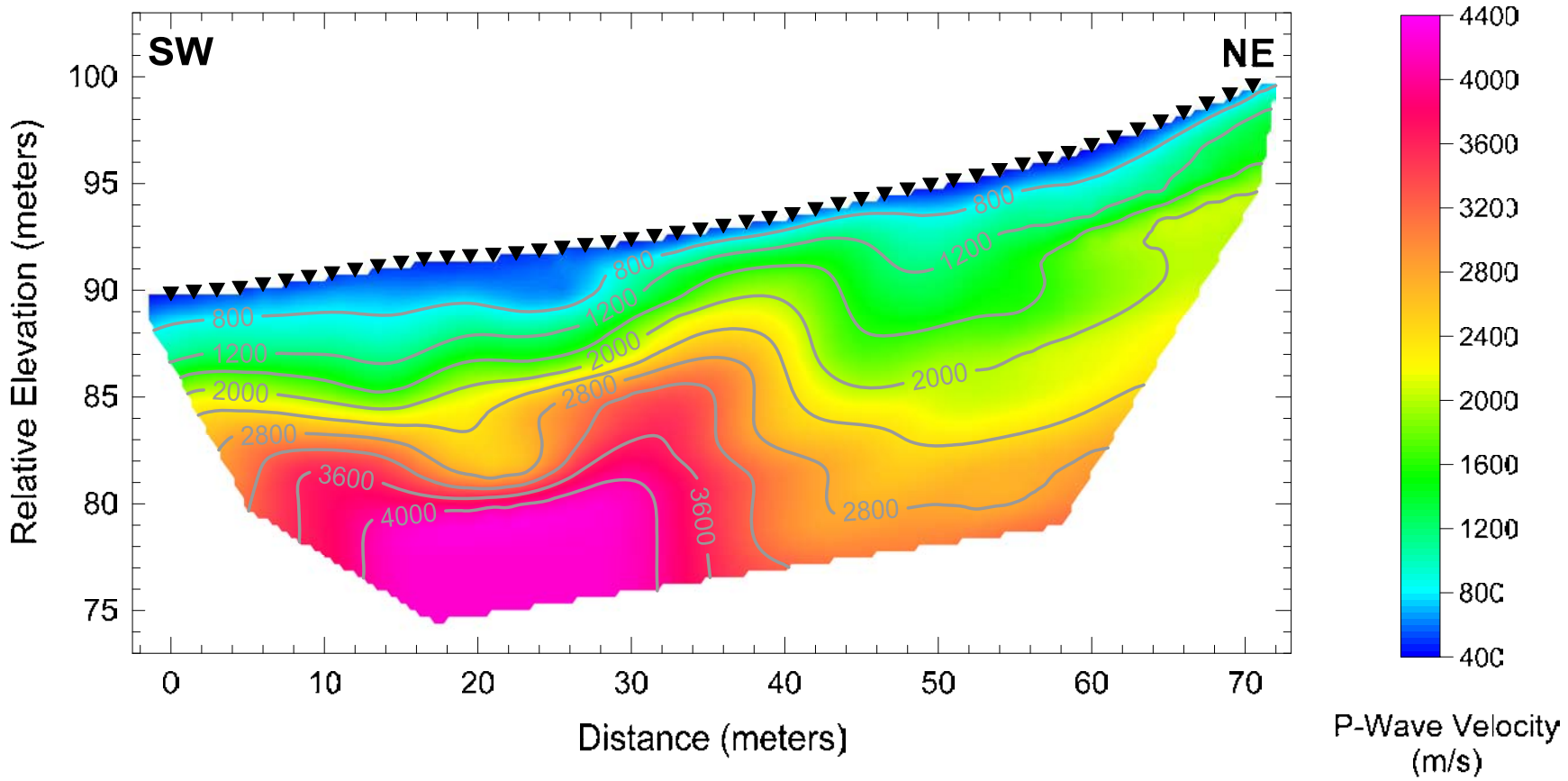

Array CTD-2 – Tomographic seismic refraction model utilizing smooth velocity gradient starting model

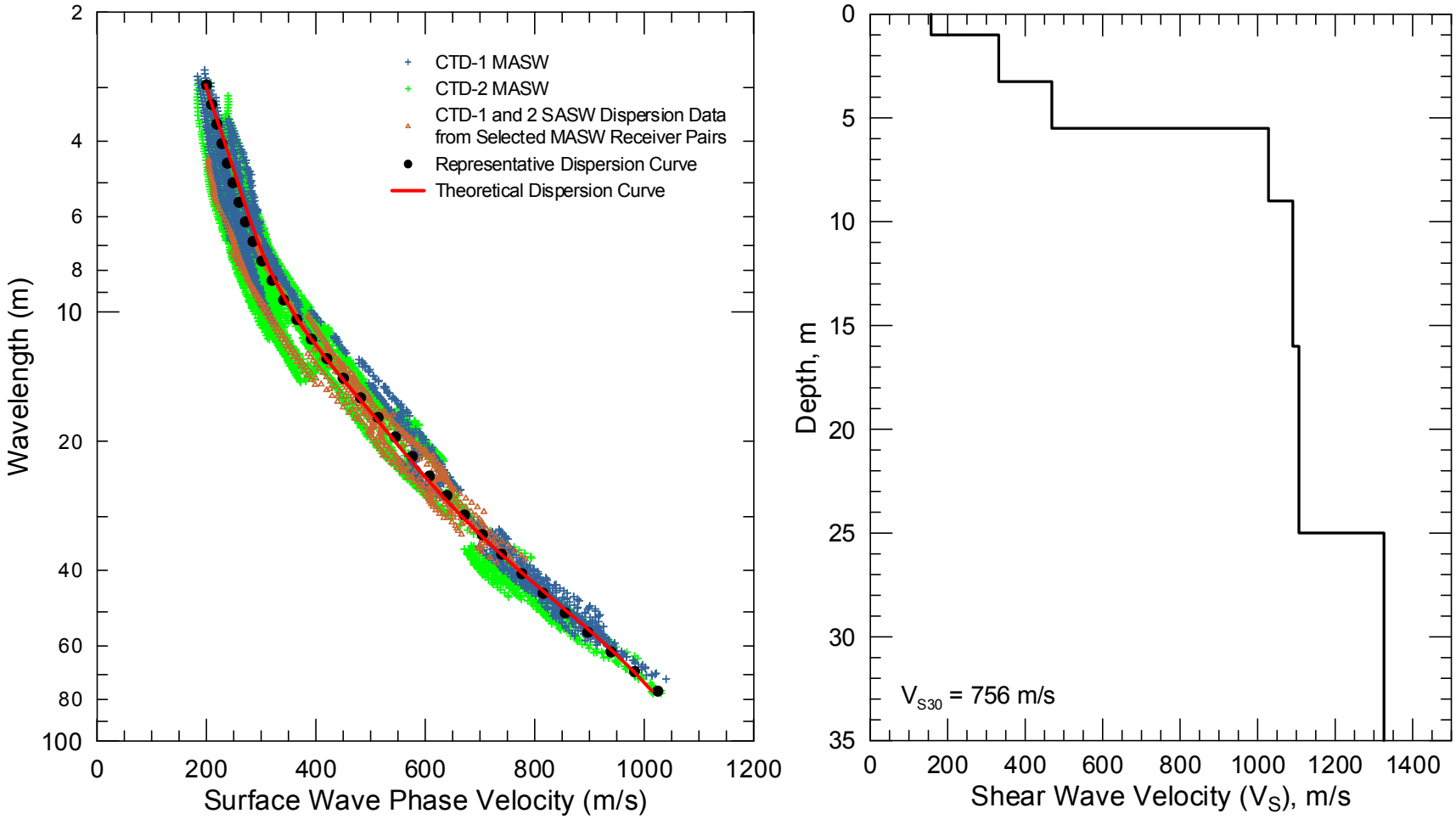

CI.CTD - Field, representative and inverted theoretical surface wave dispersion data (left) and associated V_S model (right)

Site CI.CWC

Location: Cottonwood Canyon, Inyo County, California

Latitude: 36.43907 **Longitude:** -118.08048

(Station coordinates modified based on field GPS survey of small building housing seismic sensor, WGS84 coordinate system)

V_{S30} (measured): 580 m/s

V_{S30} (adjusted to more accurately reflect seismic station conditions): 580 m/s (no adjustment necessary).

NEHRP Site Class: C

Geomatrix Code: AHB

Geologic Conditions/Observations: Seismic station located on geologic unit mapped as Cretaceous mafic plutonic rock. Geologic map was modified based on field inspection, which indicates that the seismic station is located in the middle of a narrow canyon on what appears to be Holocene alluvial stream deposits with an abundance of cobbles and boulders. The current path of the stream is on the north side of the canyon against a steep mountain slope and the stream is about 15 m lower in elevation than the seismic station. Ground surface elevations also decrease to the south before abruptly increasing at the edge of the mountains.

Site Conditions: Rural site. Seismic station located in a narrow canyon with steep slopes to the north and west. Ground surface elevations decrease gradually to the east along the test area.

Geophysical Methods Utilized: HVSR, Seismic Refraction, MASW

Geophysical Testing Arrays:

1. Array CWC-1 (48 channel MASW and P-wave seismic refraction array utilizing 4.5 Hz vertical geophones spaced 1.5 m apart for a length of 70.5 m, forward and reverse shot locations with multiple source offsets and source types and multiple interior shot locations).
2. Three HVSR measurement locations distributed along array CWC-1.

Legend

- Seismic Station - Approximate Surveyed Location
- Seismic Station - Approximate Location of Record
- H/V Spectral Ratio Measurement Location
- MASW Array

NOTES:
1. WGS 1984 COORDINATE SYSTEM
2. Image Source: ESRI, i-cubed, USDA FSA, USGS, AEX, GeoEye, Getmapping, Aerogrid, IGP

File Name: CI-CWC-I

Date: 6/15/2011

USGS science for a changing world

GEOVision geophysical services

RECOVERY.GOV

SITE MAP
CI•CWC

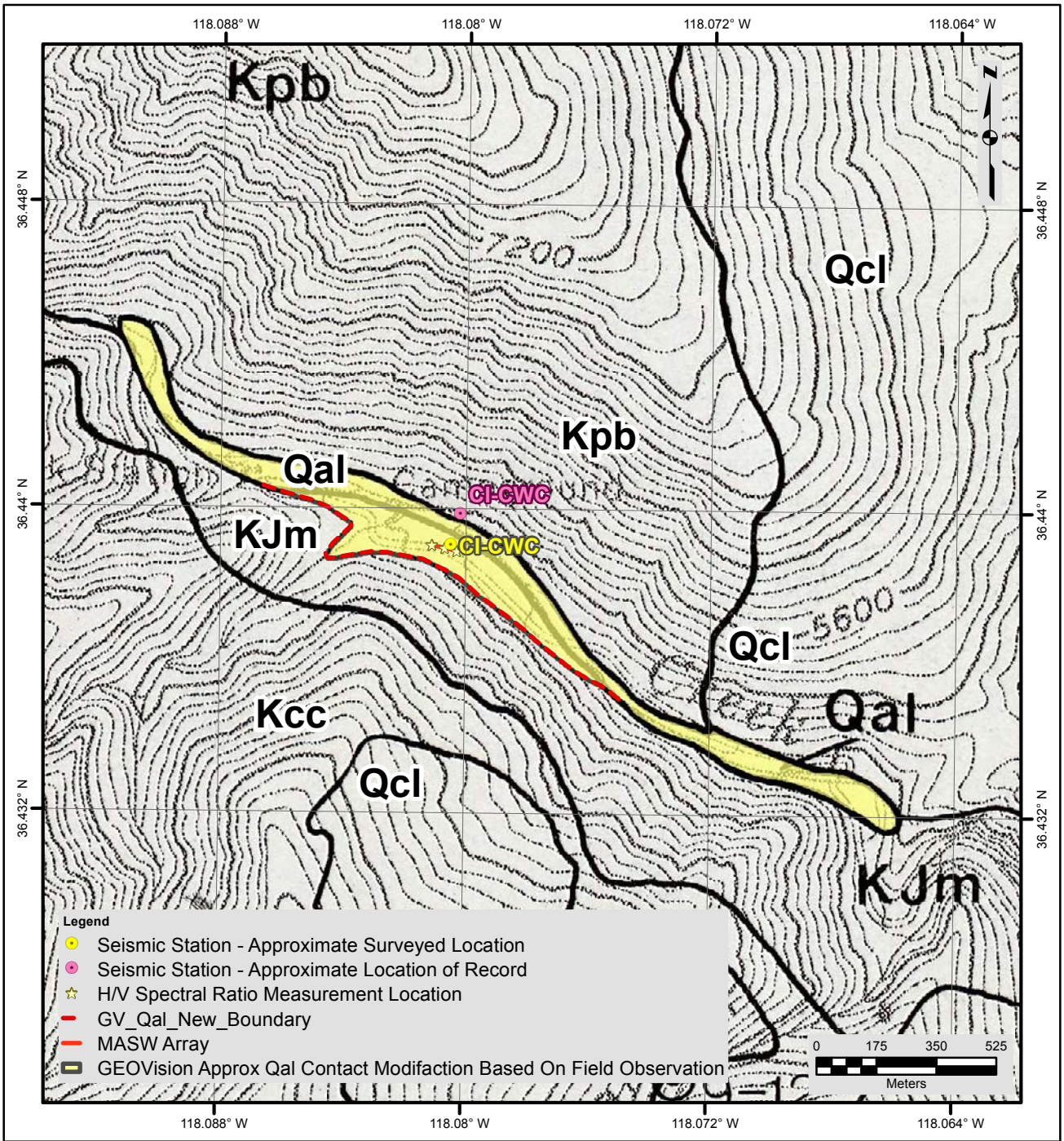

Description of Geologic Map Units

Qal = Quaternary (Holocene) stream deposits
Qcl = Quaternary (Holocene) colluvium
Kpb = Mesozoic (Cretaceous) plutonic Breccia of Timosea Peak, complex intrusion including mafic plutonic rock, aplite, and granodiorite
Kcc = Mesozoic (Cretaceous) granite of Carroll Creek, coarse-grained granite, locally porphyritic
KJm = Mesozoic (Cretaceous or Jurassic) mafic Plutonic Rock, includes fine-grained diorite and tonalite, poikilitic hornblende gabbro, and hybridized mafic granodiorites

NOTES:
1. WGS 1984 COORDINATE SYSTEM
2. Modified from Geologic Map of the Olancha Quadrangle, Southern Sierra Nevada, California by Edward A. du Bray and James G. Moore, 1985
3. See site map for details of geophysical survey

USGS science for a changing world
GEOVision geophysical services

GEOLOGIC MAP
CI•CWC

File Name: CI-CWC
Date: 10/19/2011

Looking north at building housing the seismic station CI.CWC

Seismic sensor placed in shallow hole for HVSR measurements. Sensor was covered and successful measurements made even in windy conditions

Seismic data acquisition system

Looking northeast at HVSR sensor 450 and building housing seismic station

Looking east along array CWC-1. HVSR measurements with uncovered sensors set on the surface in windy conditions were not successful

Location of Geophysical Testing Arrays:

Location	Latitude	Longitude
CWC-1, West End of Array	36.43903	-118.08106
CWC-1, Center of Array	36.43896	-118.08068
CWC-1, East End of Array	36.43889	-118.08029
HVSR Sensor 453	36.43904	-118.08108
HVSR Sensor 450	36.43896	-118.08067
HVSR Sensor 507	36.43888	-118.08028
CI.CWC Seismic Station (approximate)	36.43907	-118.08048

Notes: 1) WGS84 Coordinate System (decimal degrees)
2) Survey accuracy is estimated at 2 to 3 m.

Results:

V_S Model

Depth to Top of Layer (m)	Layer Thickness (m)	S-Wave Velocity (m/s)	Inferred P-Wave Velocity (m/s)	Assumed Poisson's Ratio	Assumed Density (g/cm^3)
0	1.5	361	675	0.300	1.9
1.5	9.5	480	899	0.300	1.9
11	11	539	1600	0.436	2.0
22	>13	1081	2023	0.300	2.2

Notes: 1) Saturated sediments estimated at 11 m depth from seismic refraction model and stream about 15 m lower in elevation than seismic line. The P-wave velocity of saturated sediments is assumed to be 1,600 m/s.
2) Depth of investigation is about 35 m.
3) Bottom layer is a half space.

Observations/Discussion:

- HVSR plots for the three sensor locations are similar. HVSR sensor 507 has a clear peak at about 4.4 Hz. HVSR sensors 450 and 453 have more complex HVSR response with a wider peak or double peaks at about 4.2 and 5.1 Hz. The complex HVSR response may be related to complex basement geometry in the site vicinity.
- There are typically heavy winds in the site vicinity and the first attempt to make HVSR measurements failed because the sensors were not covered. Repeat measurements were made at a time of very heavy water flow in the nearby stream. Due to the remote location of the site, we expect that the only source of 4 Hz energy would be water flow in the stream and indirect effect of wind (i.e. tree motion), neither of which are considered reliable noise sources.
- The P-wave refraction data for array CWC-1 were modeled using a tomographic inversion routine with a layer based starting model. The seismic refraction model was extended to far offset shot locations to extend depth of investigation.
- The seismic refraction survey design allowed P-wave velocity to be imaged to a maximum depth of about 15 m. The seismic refraction model shows that P-wave velocity is about 800 to 900 m/s at the surface and in the 1,000 to 1,200 m/s range between a depth of 1 to 4 m and 7 and 11 m. Below a depth of 8 to 12 m, P-wave velocity rapidly increases with depth from about 1,300 to over 2,400 m/s at a depth of 11 to 14 m. The high velocity zone may be associated with either saturated sediments and/or bedrock. If the higher velocities are associated with bedrock, then the saturated zone could be a hidden layer, in which case bedrock depths would be underestimated. Based on the stream, at the northern edge of the canyon, flowing on bedrock about 15 m lower in elevation, it is plausible that bedrock is deeper than 15 m beneath the seismic line.
- Noise conditions at the site were not sufficient for application of passive surface wave techniques.
- The minimum wavelength surface wave phase velocity data extracted from the 48-channel MASW array was about 6 m. Reducing data from smaller hammer sources using a limited offset receiver array (i.e. less active geophones) allowed extraction of surface wave dispersion data to a minimum wavelength of about 4 m.
- There is some minor scatter in the MASW surface wave dispersion data, partly the result of near surface lateral velocity variation.
- A representative dispersion curve was generated for the MASW data set using a moving average, polynomial curve fitting routine and used for modeling.
- Scatter in the MASW surface wave dispersion data is likely the result of near surface lateral velocity variation.
- Saturated sediments, with P-wave velocity of 1,600 m/s were set at a depth of 11 m in the surface wave model, based on the assumption that the higher velocity zone in the seismic refraction model is associated with saturated sediments rather than bedrock.
- A single V_S model is presented for the MASW data with high velocity bedrock modeled at a depth of 22 m. This type of velocity structure gives rise to significant non-uniqueness in the surface wave models, both with respect to bedrock depth and velocity, which may vary by 20%, or more. The non-uniqueness is not expected to significantly affect V_{S30}.

- P-wave velocities in the surface wave model, estimated from modeled S-wave velocity using an assumed Poisson's ratio of 0.3 for unsaturated sediments and rock, are slightly lower than those in the seismic refraction model. Higher Poisson's ratio in the sediments would result in higher P-wave velocity in the surface wave model. A slight deepening of bedrock would increase the modeled S- and P-wave velocities of the bedrock.
- The estimated/modeled fundamental soil resonant frequency from the V_S model is in the 6 to 7 Hz range, significantly higher than the measured 4 to 5 Hz HVSR peak. The bedrock geometry is very complex in the site vicinity (i.e. narrow canyon) and there may not be reliable high frequency noise sources. Potential noise sources at this remote canyon site are water flow in the nearby stream and indirect effect of wind. Both of these noise sources are not considered reliable. Regardless, the discrepancy between measured and predicted HVSR response should be investigated further.
- Surface wave depth of investigation is about 35 m based on half of maximum wavelength criteria.
- V_{S30} is 580 m/s (Site Class C).
- V_{S30} only varies by about 3% for a large variety of models that equally well fit the surface wave dispersion curve. The presence or absence of the saturated sediment layer has a larger impact on V_{S30} than the non-uniqueness of these models with a saturated layer.

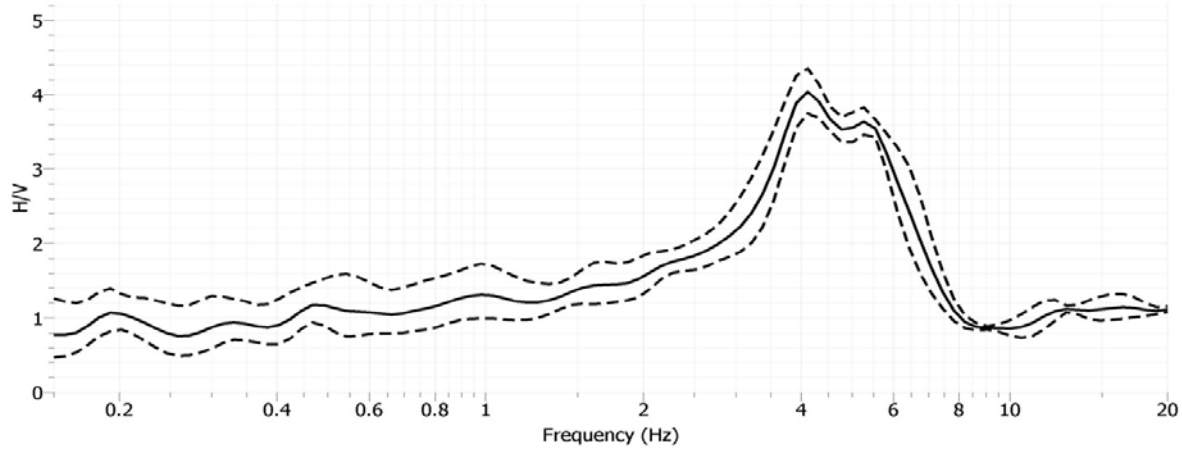

Site CI.CWC, H/V Spectral Ratio, Array CWC-1, Sensor 453

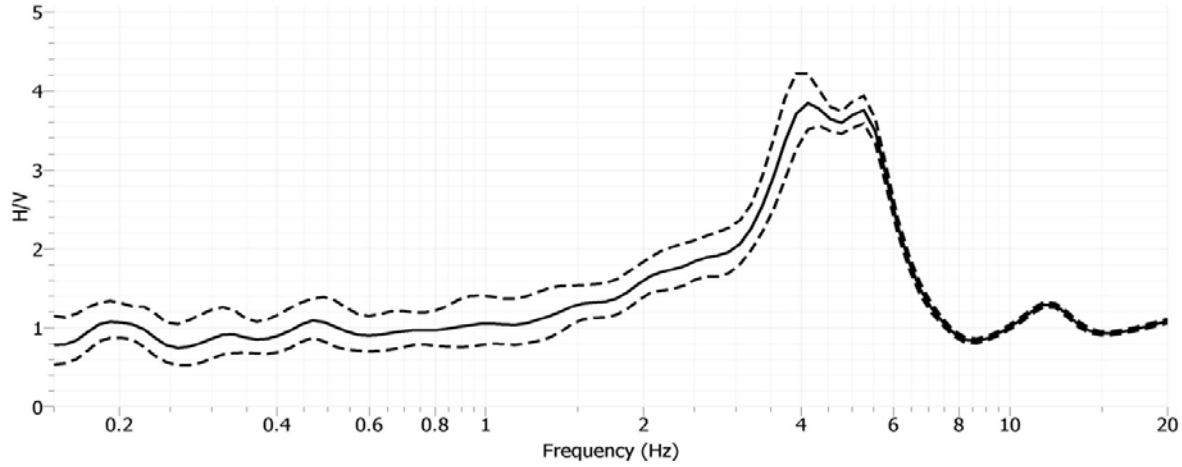

Site CI.CWC, H/V Spectral Ratio, Array CWC-1, Sensor 450

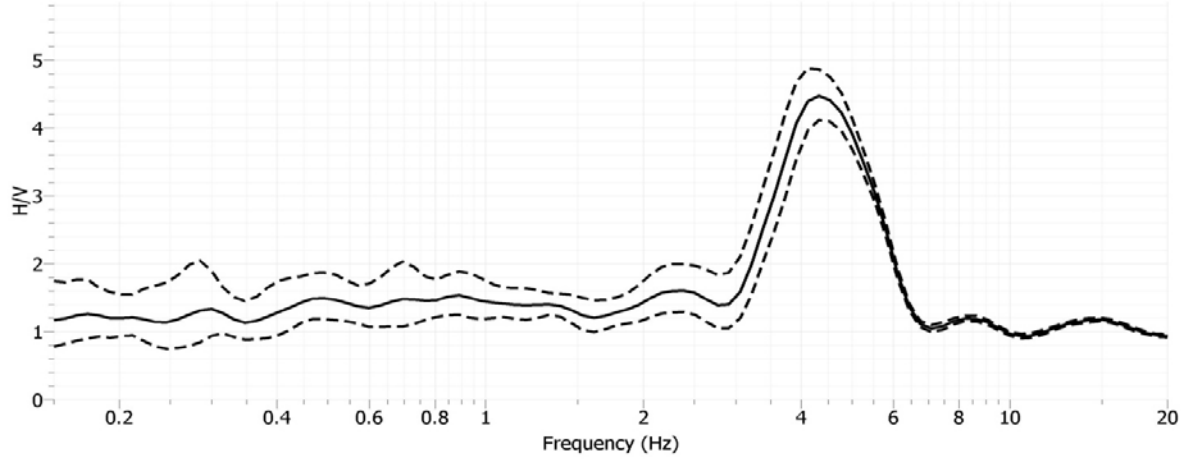

Site CI.CWC, H/V Spectral Ratio, Array CWC-1, Sensor 507

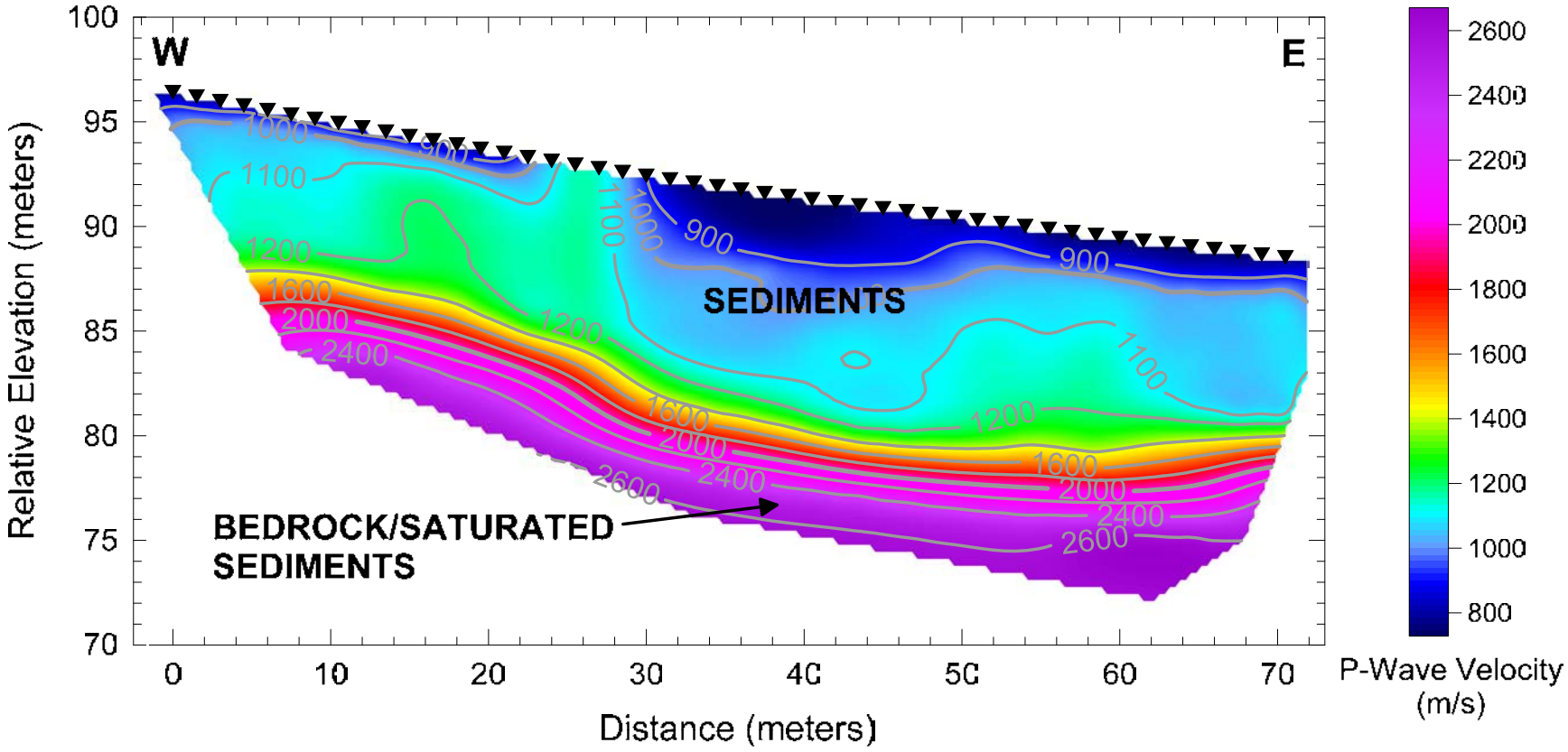

Array CWC-1 – Tomographic seismic refraction model utilizing layer based starting model

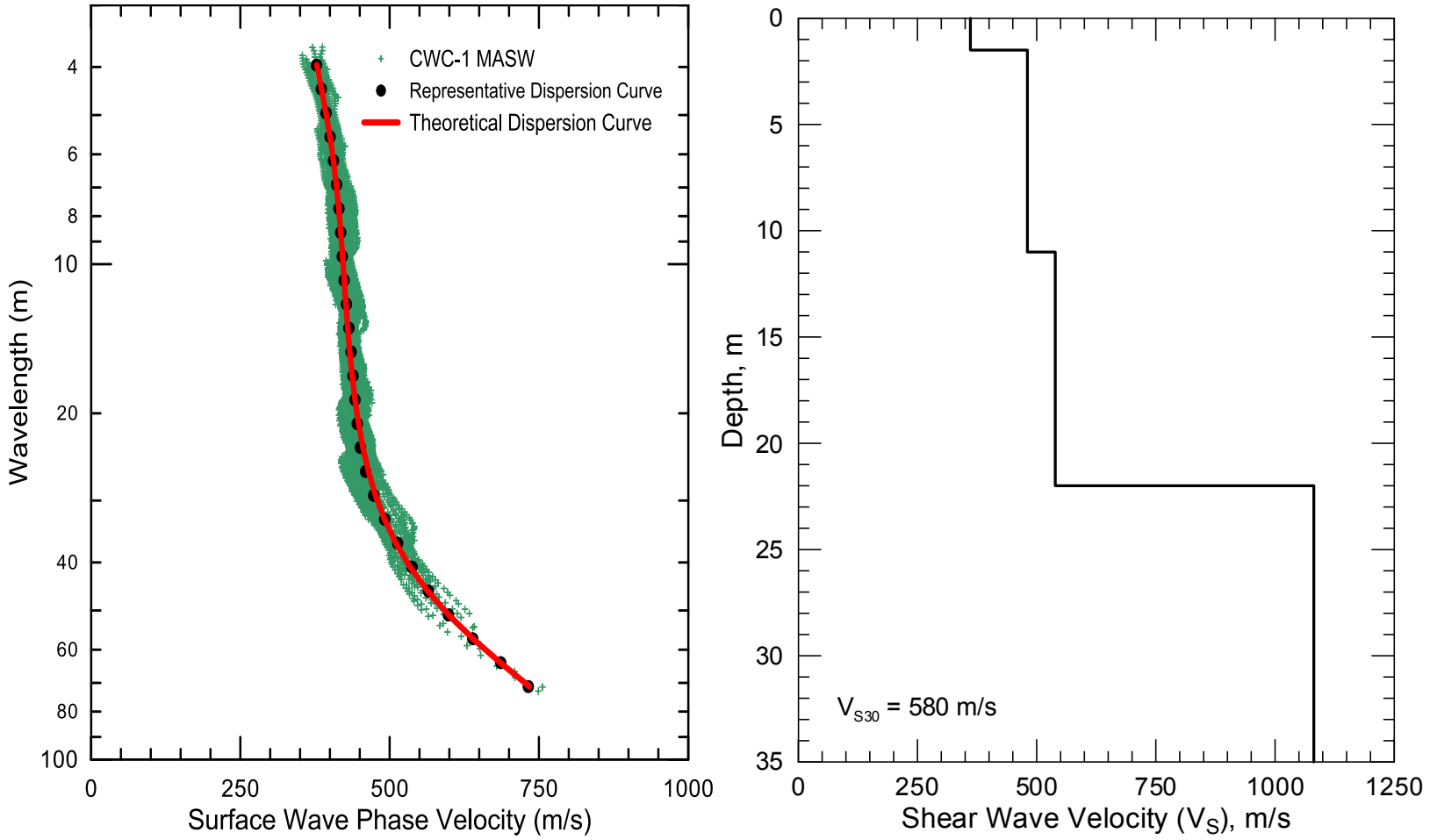

CI.CWC - Field, representative and inverted theoretical surface wave dispersion data (left) and associated V_S model (right)

Site CI.DAN

Location: AT&T facility, south of National Trails Highway, near Danby, California

Latitude: 34.63725 **Longitude:** -115.38010
(Station coordinates modified based on field observation of station location and identification of approximate station location on Google Earth – no access to fenced compound to survey station location, WGS84 coordinate system)

V_{S30} (measured): 477 m/s

V_{S30} (adjusted to more accurately reflect seismic station conditions): 528 m/s (average S-wave velocity between 2 and 32 m adjusting for nominal sensor depth)

NEHRP Site Class: C

Geomatrix Code: IHD

Geologic Conditions/Observations: Site located near mapped contact of Quaternary (Holocene) young alluvial fan deposits and Quaternary (Holocene) young alluvial fan/Quaternary (Pleistocene) intermediate alluvial fan deposits. Unclear how deep bedrock is at the site, but greater than 35 m based on limited seismic refraction data.

Site Conditions: Rural site with sporadic traffic on nearby National Trails Highway. Relatively flat terrain in site vicinity with ground surface elevation gently decreasing to south.

Geophysical Methods Utilized: HVSR, MASW, SASW

Geophysical Testing Arrays:

1. Array DAN-1 (48 channel MASW array utilizing 4.5 Hz vertical geophones spaced 1.5 m apart for a length of 70.5 m, forward and reverse shot locations with multiple source offsets and source types and center shot location).
2. Array DAN-1 (SASW array with common midpoint and orientation as MASW array of same name utilizing 4.5 and 1 Hz vertical geophones and maximum receiver spacing of 48 m).
3. Three HVSR measurement locations distributed along array DAN-1.

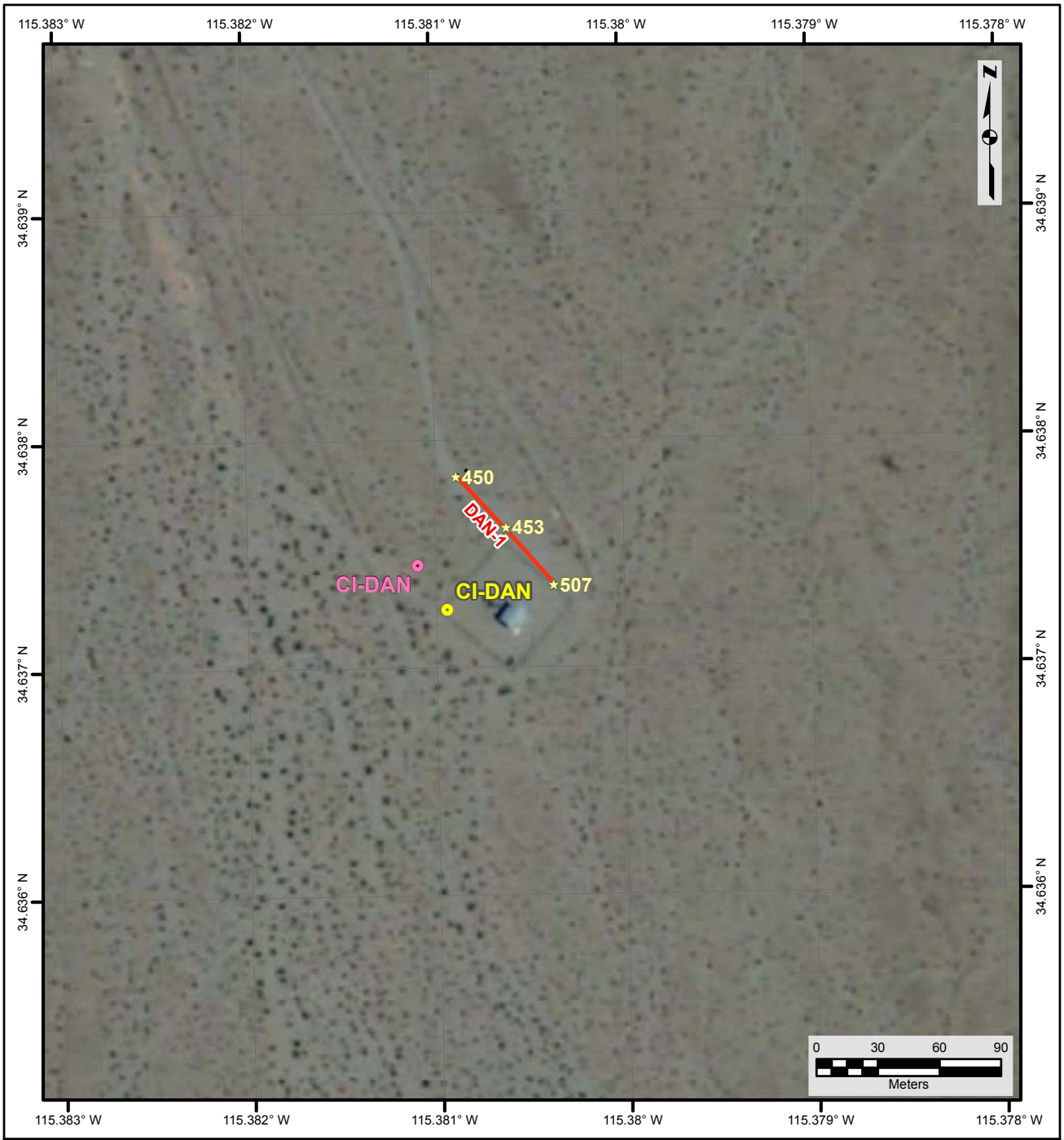

Legend

- Seismic Station - Approximate Improved Location
- Seismic Station - Approximate Location of Record
- H/V Spectral Ratio Measurement Location
- MASW and SASW Array

NOTES:
1. WGS 1984 COORDINATE SYSTEM
2. Image Source: ESRI, i-cubed, USDA FSA, USGS, AEX, GeoEye, Getmapping, Aerogrid, IGP

File Name: CI-DAN-I

Date: 4/7/2011

USGS science for a changing world

GEOVision geophysical services

RECOVERY.GOV

SITE MAP
CI•DAN

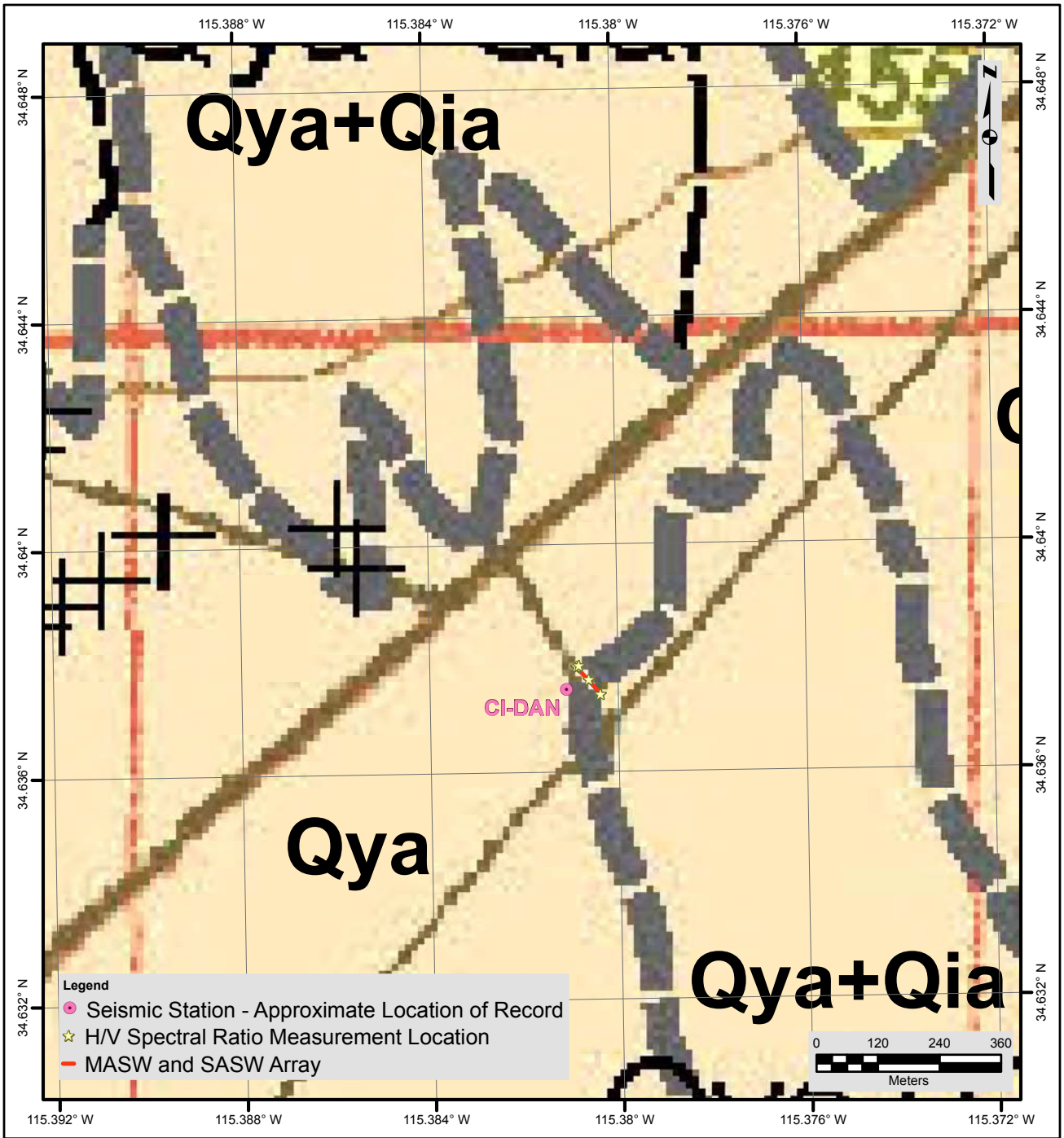

Description of Geologic Map Units

Qya = Quaternary (Holocene) young alluvial fan deposits
Qia = Quaternary (Pleistocene) intermediate alluvial fan deposits

NOTES:
1. WGS 1984 COORDINATE SYSTEM
2. Preliminary Surficial Geologic Map Database of the Amboy 30x60 Minute Quadrangle, California by David R Bedford, David M Miller, and Geoff A Phelps, 2006
3. See site map for details of geophysical survey

File Name: CI-DAN

Date: 4/1/2011

USGS science for a changing world

GEOVision geophysical services

RECOVERY.GOV

GEOLOGIC MAP
CI•DAN

Looking east at seismograph station CI.DAN (near corner of fence)

Looking northeast towards CI.DAN seismograph station (below sign on fence) and geophysical survey area (other side of fenced compound)

Looking southeast along MASW array DAN-1

Looking southeast along SASW array DAN-1

After several attempts to acquire HVSR data, plaster placed in shallow hole to couple HVSR sensors to loose gravelly soils

Location of Geophysical Testing Arrays:

Location	Latitude	Longitude
DAN-1, Southeast End of MASW Array	34.63736	-115.38043
DAN-1, Center of MASW and SASW Arrays	34.63761	-115.38068
DAN-1, Northwest End of MASW Array	34.63784	-115.38094
HVSR Sensor 507	34.63736	-115.38043
HVSR Sensor 453	34.63761	-115.38068
HVSR Sensor 450	34.63784	-115.38094

Notes: 1) WGS84 Coordinate System (decimal degrees)
2) Survey accuracy is estimated at 1 to 2 m

Results:

V_S Model

Depth to Top of Layer (m)	Layer Thickness (m)	S-Wave Velocity (m/s)	Inferred P-Wave Velocity (m/s)	Inferred Poisson's Ratio	Inferred Density (g/cm^3)
0	0.5	154	289	0.3	1.9
0.5	1.5	249	466	0.3	1.9
2	3	361	675	0.3	2.0
5	4	467	873	0.3	2.0
9	6	508	951	0.3	2.0
15	8	581	1086	0.3	2.0
23	12	629	1176	0.3	2.0
35	>10	886	1658	0.3	2.0

Observations/Discussion:

- Several attempts made to acquire HVSR data at this site due to potential limited microtremor energy in frequency range of interest, occasional heavy wind and difficulty coupling sensors in the loose gravelly soils. Best data obtained by placing plaster in a shallow hole to couple an aluminum sensor cradle or by digging deep holes.
- HVSR plots are similar at all measurement locations validating the 1-D velocity structure assumption.
- There is no distinct high amplitude HVSR peak at the site. There is, however, a possible weak HVSR peak at about 2.7 Hz, which could be indicative of relatively shallow bedrock (i.e. 60 to 90 m).
- Noise conditions at site were not sufficient to apply passive surface wave techniques.
- Surface wave dispersion data from SASW and MASW datasets are in good agreement at the site.
- Representative dispersion curves were generated for each surface wave data set using a moving average, polynomial curve fitting routine. These individual representative dispersion curves were combined and a representative dispersion curve generated for the combined data set for data modeling.
- Water table located at a depth of greater than 25 m based on seismic refraction survey design and absence of a water table refractor.
- Based on simple layer-based analysis of seismic refraction first arrival data, P-wave velocity in the upper 20 m ranges from about 500 to 850 m/s. Based on second arrivals and possible reflectors, there is inconclusive evidence of a geologic layer with P-wave velocity of about 1,100 m/s at a depth on the order of 20 to 25 m. Based on similar analysis cannot discount the possibility of either groundwater or bedrock at a depth between 35 and 50 m.
- A longer seismic refraction line would determine if either groundwater or bedrock is located within 60 m of the surface.
- Surface wave depth of investigation is about 45 m based on half of maximum wavelength criteria.
- V_{S30} is 477 m/s (Site Class C).
- Average S-wave velocity between 2 m (nominal sensor depth) and 32 m is 528 m/s.
- Average S-wave velocity of the upper 45 m (V_{S45}) is 548 m/s.

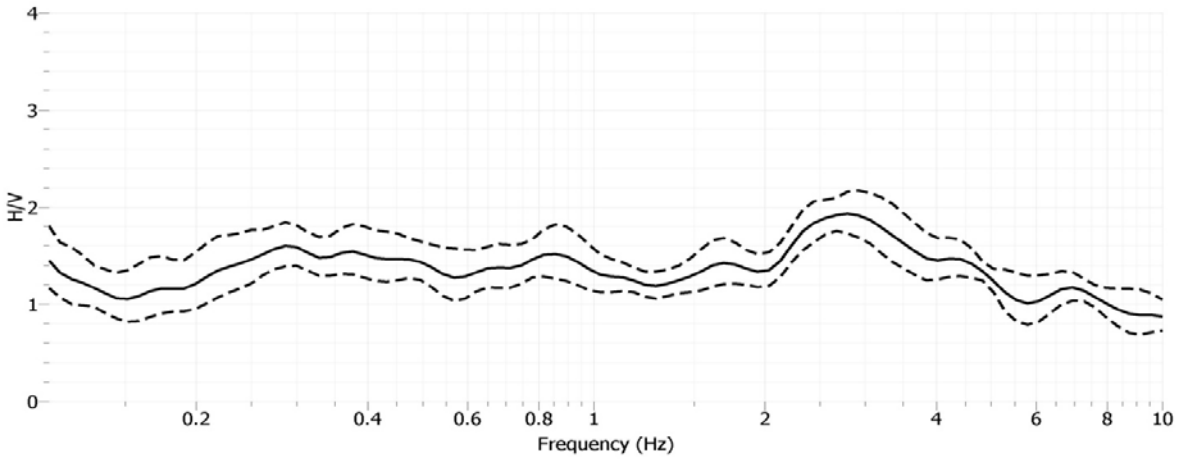

Site CI.DAN, H/V Spectral Ratio, Array DAN-1, Sensor 450

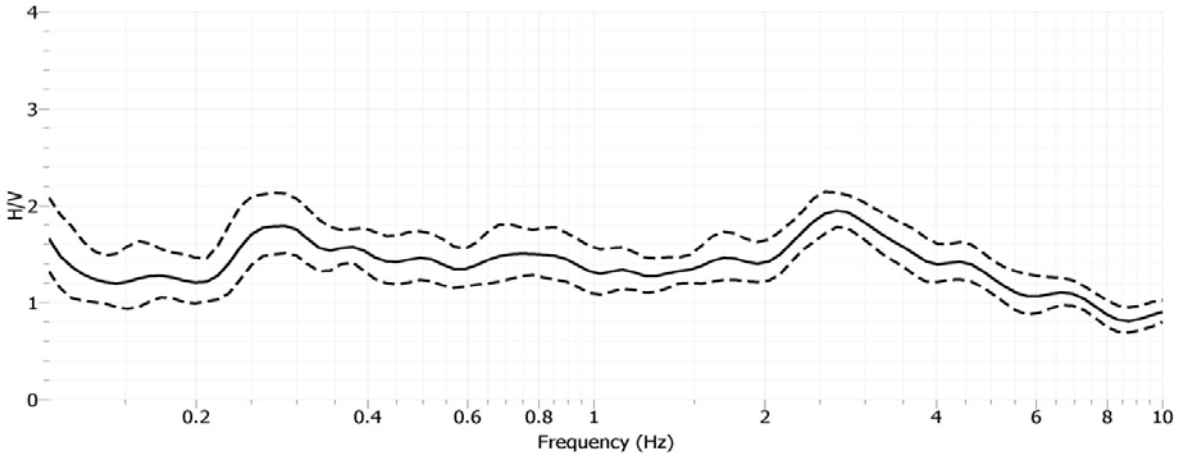

Site CI.DAN, H/V Spectral Ratio, Array DAN-1, Sensor 453

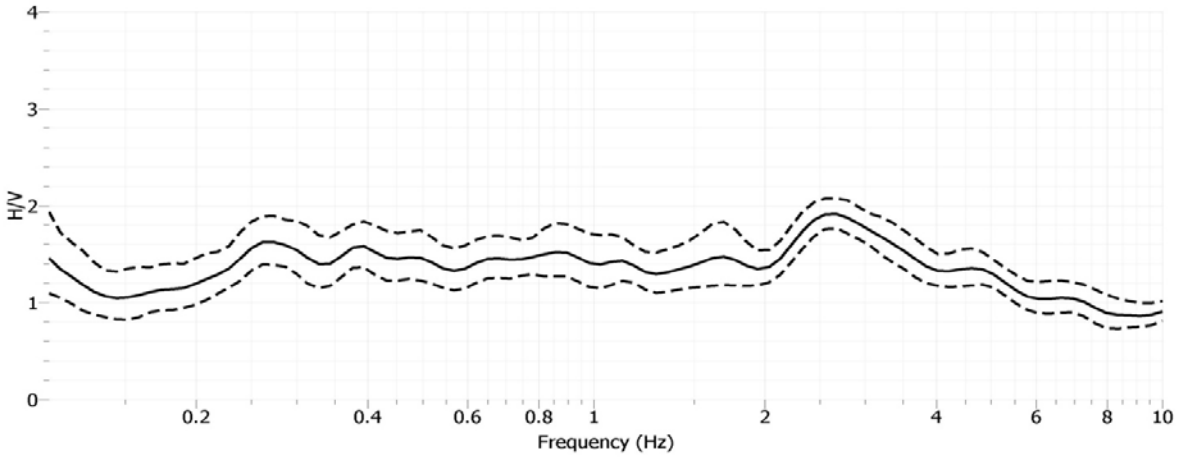

Site CI.DAN, H/V Spectral Ratio, Array DAN-1, Sensor 507

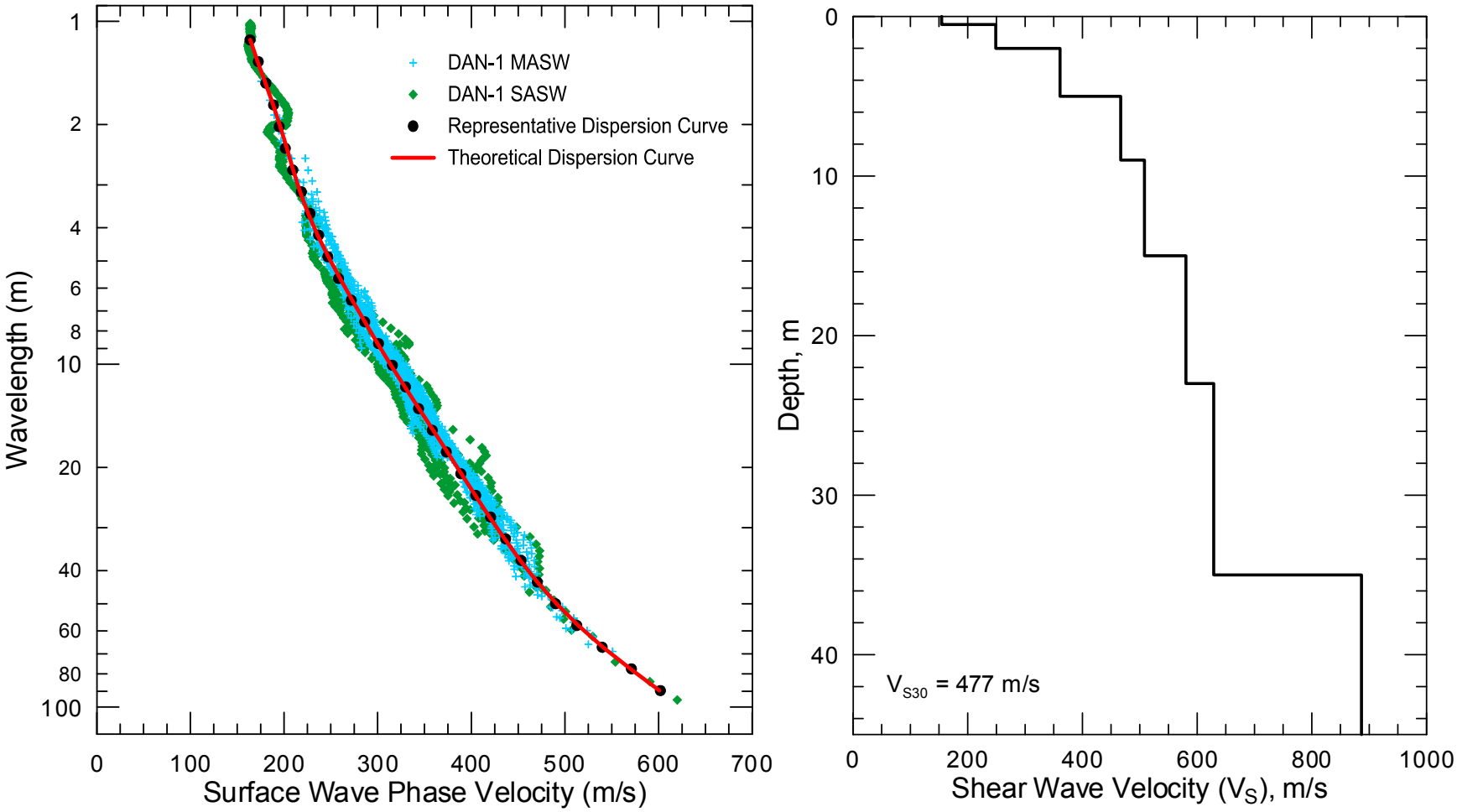

CI.DAN - Field, representative and inverted theoretical surface wave dispersion data (left) and associated V_S model (right)

Site CI.DNR

Location: Dunn Ranch, Anza, California

Latitude: 33.56667 **Longitude:** -116.63056

V_{S30} (measured): 361 m/s

V_{S30} (adjusted to more accurately reflect seismic station conditions): 411 m/s (average S-wave velocity between 4 and 34 m adjusting for 2 m nominal sensor depth and fact that weathered rock is slightly deeper beneath the seismic line than the seismic station). It is, therefore, recommended that a NEHRP Site Class C is used for this site rather than C/D as V_{S30} would indicate.

NEHRP Site Class: C/D (based on V_{S30}), C (based on adjusted V_{S30})

Geomatrix Code: IJC/IZC

Geologic Conditions/Observations: Seismic station located at the edge of an outcrop mapped as Paleozoic or Mesozoic Schist and between strands of the Casa Loma segment of the San Jacinto Fault Zone. Other outcrops in the site vicinity consist or Plio-Pleistocene Bautista Beds. Field observations indicate that the near surface rock is decomposed to very intensely weathered.

Site Conditions: Rural site with moderate traffic noise from SR-371 located about 500 m to the south. Relatively flat terrain along test area. Small hills located east and north of test area.

Geophysical Methods Utilized: HVSR, Seismic Refraction, MASW, ReMi™

Geophysical Testing Arrays:

1. Array DNR-1 (48 channel MASW and P-wave seismic refraction array utilizing 4.5 Hz vertical geophones spaced 1.5 m apart for a length of 70.5 m, forward and reverse shot locations with multiple source offsets and source types and multiple interior shot locations).
2. Passive surface wave data also acquired along MASW array DNR-1 during HVSR data acquisition.
3. Limited S-wave refraction data also acquired along array DNR-1 (24 channel array utilizing 28 Hz horizontal geophones spaced 3 m apart for a length of 69 m, several forward and reverse shot locations and a center shot).
4. Three HVSR measurement locations; two distributed along array DNR-1 and the other adjacent to the seismic station.

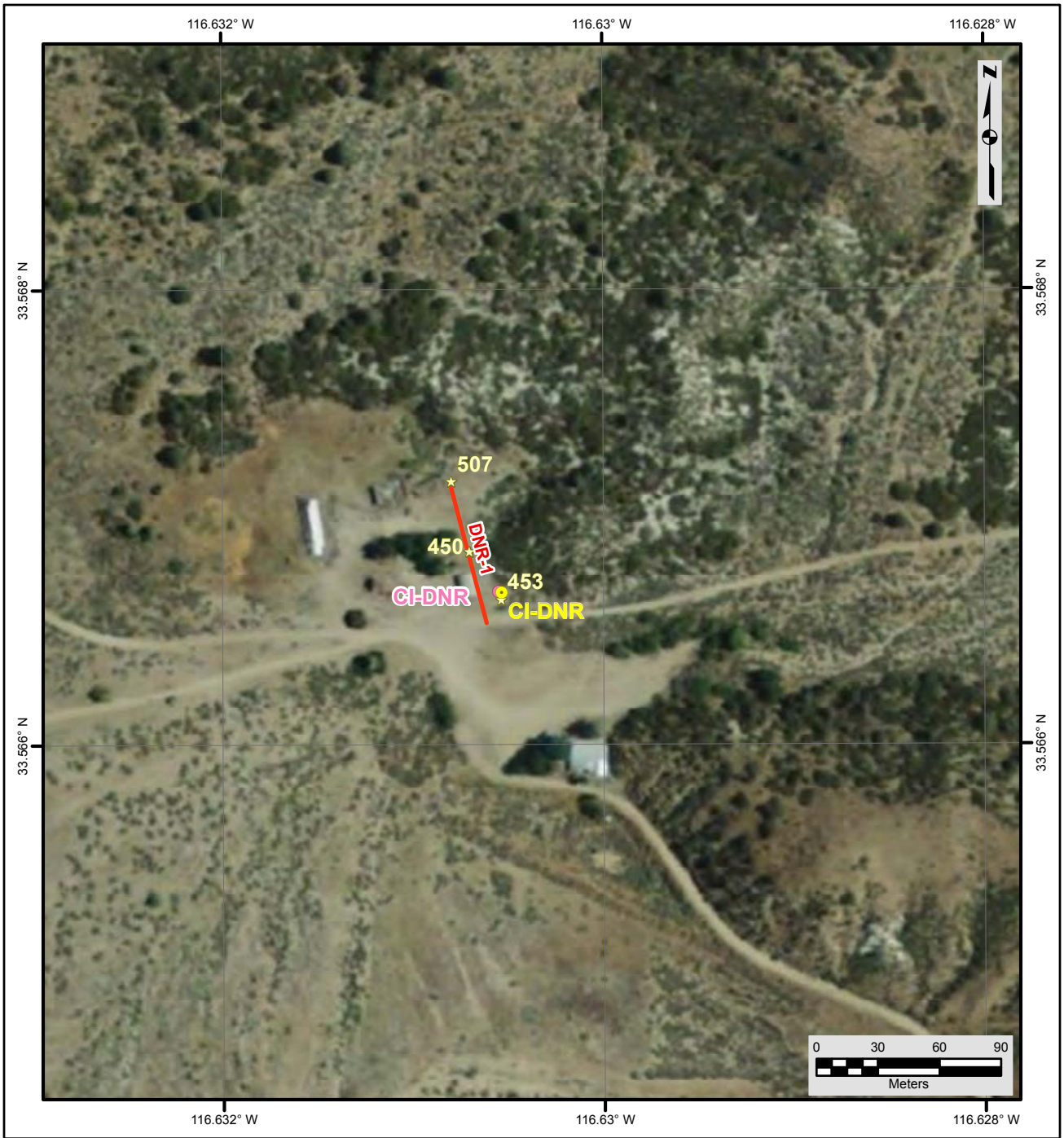

Legend

- Seismic Station - Approximate Surveyed Location
- Seismic Station - Approximate Location of Record
- H/V Spectral Ratio Measurement Location
- MASW and Seismic Refraction Array

NOTES:
1. WGS 1984 COORDINATE SYSTEM
2. Image Source: ESRI, i-cubed, USDA FSA, USGS, AEX, GeoEye, Getmapping, Aerogrid, IGP

File Name: CI-DNR-I

Date: 6/9/2011

USGS science for a changing world

GEOVision geophysical services

RECOVERY.GOV

SITE MAP
CI•DNR

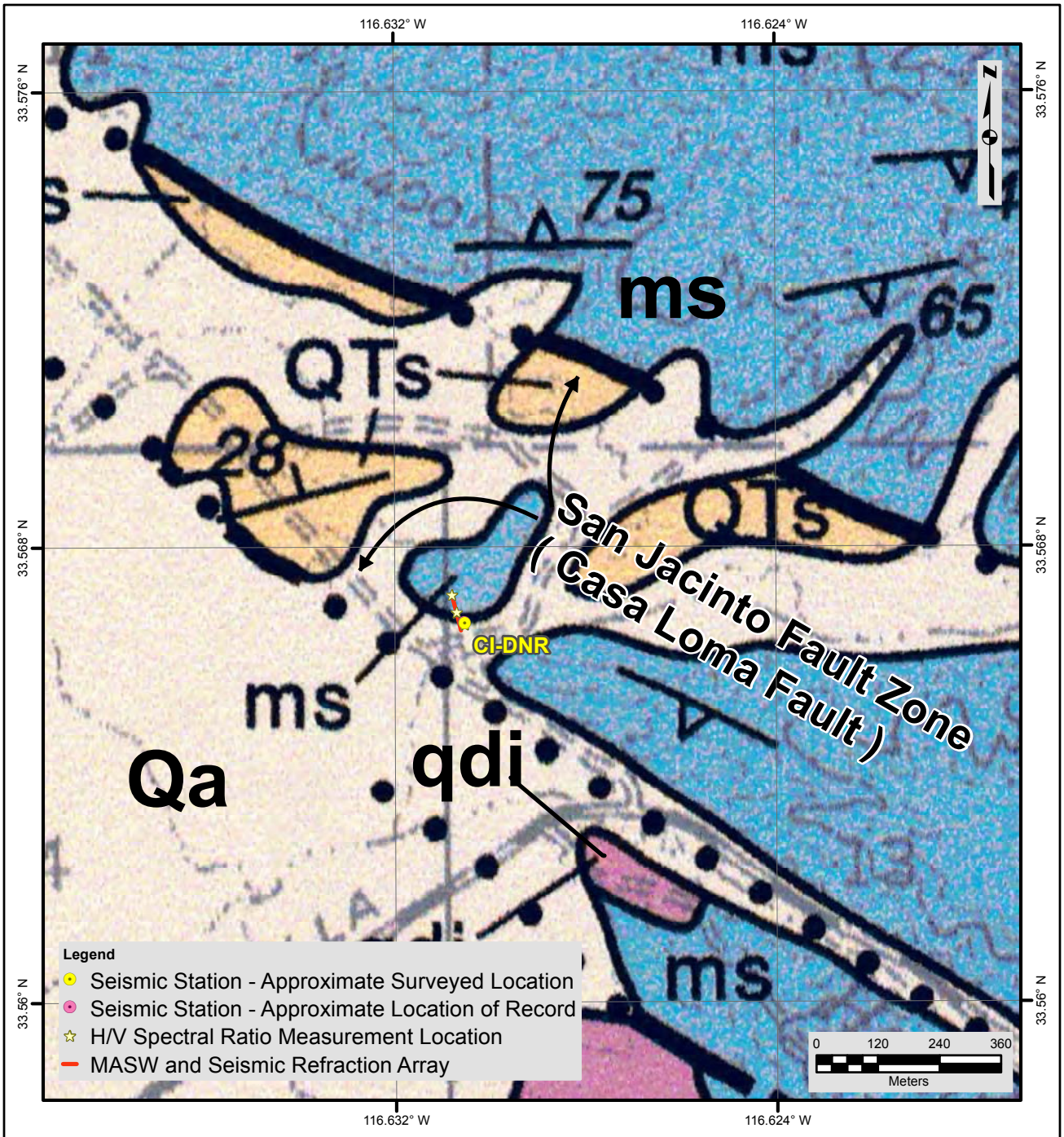

Description of Geologic Map Units

Qa = Quaternary (Holocene) alluvial sand and gravel of valley areas
QTs = Quaternary or Tertiary(Plio-Pleistocene) Bautista Beds; alluvial sandstone, arkosic, semi-lithified thin layers of claystone and pebble-cobble conglomerate of granitic detritus
qdi = Mesozoic (Cretaceous) quartz diorite to granodiorite, massive to slightly gneissoid with minor xenoliths
ms = Paleozoic or Mesozoic schist; fine grained, foliated, biotite, quartz and feldspar, ranges to fine grained gneiss

NOTES:
1. WGS 1984 COORDINATE SYSTEM
2. Geology Map of the Hemet & Idyllwild 15 Minute Quadrangles, Riverside County, California by Thomas W. Dibblee, Jr., 2008
3. See site map for details of geophysical survey

USGS science for a changing world

GEOVision geophysical services

RECOVERY.GOV

GEOLOGIC MAP
CI•DNR

File Name: CI-DNR

Date: 6/9/2011

Looking north along array DNR-1

Looking north towards HVSR sensor and CI.DNR seismic station

Looking north from center of array DNR-1

Nanometrics Trillium Compact seismic sensor used for HVSR measurements

Looking south at HVSR sensor 507 and array DNR-1

Location of Geophysical Testing Arrays:

Location	Latitude	Longitude
DNR-1, South End of Array	33.56653	-116.63062
DNR-1, Center of Array	33.56684	-116.63072
DNR-1, North End of Array	33.56715	-116.63082
HVSR Sensor 507	33.56715	-116.63081
HVSR Sensor 453	33.56664	-116.63055
HVSR Sensor 450	33.56685	-116.63071
CI.DNR Seismograph Station	33.56667	-116.63055

Notes: 1) WGS84 Coordinate System (decimal degrees)
2) Survey accuracy is estimated at 1 to 2 m

Results:

V_S Model

Depth to Top of Layer (m)	Layer Thickness (m)	S-Wave Velocity (m/s)	Inferred P-Wave Velocity (m/s)	Inferred Poisson's Ratio	Inferred Density (g/cm^3)
0	1	174	325	0.300	1.9
1	2	211	395	0.300	1.9
3	3	319	597	0.300	1.9
6	4	321	600	0.300	1.9
10	6	379	2300	0.486	2.0
16	8	443	2300	0.481	2.0
24	12	490	2300	0.476	2.0
36	>4	589	2300	0.465	2.0

Observations/Discussion:

- The site is located between strands of the Casa Loma segment of the San Jacinto Fault Zone.
- The HVSR curves are almost identical validating the 1-D velocity structure assumption.
- There is no clear HVSR peak at this site.
- Noise conditions at the site did not appear sufficient for application of passive surface wave techniques as the only significant noise source was moderate traffic on SR-371, located about 500 m south of array DNR-1 and somewhat perpendicular to the array. Passive surface wave data was, however, acquired on MASW array DNR-1 to check if a single road could be an effective source of passive surface wave energy.

- Both the ReMi™ and ESAC techniques used to extract surface wave dispersion data from the linear passive surface wave array.
- Interestingly, the surface wave dispersion data from active and passive surface wave data sets are in good agreement at this site although the dispersion data selected using the ReMi™ technique had to be constrained by the MASW and ESAC dispersion data.
- Representative dispersion curves were generated for each surface wave data set using a moving average, polynomial curve fitting routine. These individual representative dispersion curves were combined and a representative dispersion curve generated for the combined data set for data modeling.
- P-wave refraction data identified a 2,300 m/s refractor at a depth of about 10 m. Both layer based and tomographic inversion models were generated for the seismic refraction first arrival data. In the geologic environment of the site (adjacent outcrop of schist) it would be logical to assume that the high velocity refractor is associated with weathered rock; however, there is no evidence of high S-wave velocity in the surface wave dispersion data. Limited S-wave refraction data confirmed the absence of a high velocity rock layer and the 2,300 m/s P-wave velocity is likely associated with groundwater. It is possible that the Casa Loma Fault forms a groundwater barrier.
- The generalized reciprocal method was utilized to develop a three layer seismic refraction model with a 1 to 3 m thick upper layer of unsaturated sediments with V_P of about 350 m/s, an intermediate layer of unsaturated sediments with V_P varying from about 500 to 800 m/s and a lower layer of saturated sediments at a depth of approximately 9 to 12 m and V_P of about 2,300 m/s. It is possible that the saturated layer is perched on top of weathered rock. Depth of investigation of the P-wave seismic refraction survey is estimated at 15 to 20 m.
- Surface wave depth of investigation is about 40 m based on half of maximum wavelength criteria.
- Modeled V_S does not exceed 600 m/s in the upper 40 m, which was not expected for a site located at the edge of a weathered rock outcrop. The proximity of active faults to the site would explain the significant fracturing/weathering of the rock. The site should be inspected again to confirm that the seismic station is located on the schist rock unit rather than on Bautista Beds.
- V_{S30} is 361 m/s (NEHRP Site Class C/D).
- Average S-wave velocity between 2 m (nominal sensor depth) and 32 m is 391 m/s.
- Average S-wave velocity between 4 m (nominal sensor depth) and 34 m is 411 m/s.
- Considering that the seismic station is also about 11 m closer to the edge of the outcrop than the seismic line the site should be considered NEHRP Site Class C.
- Average S-wave velocity of the upper 40 m (V_{S40}) is 391 m/s.

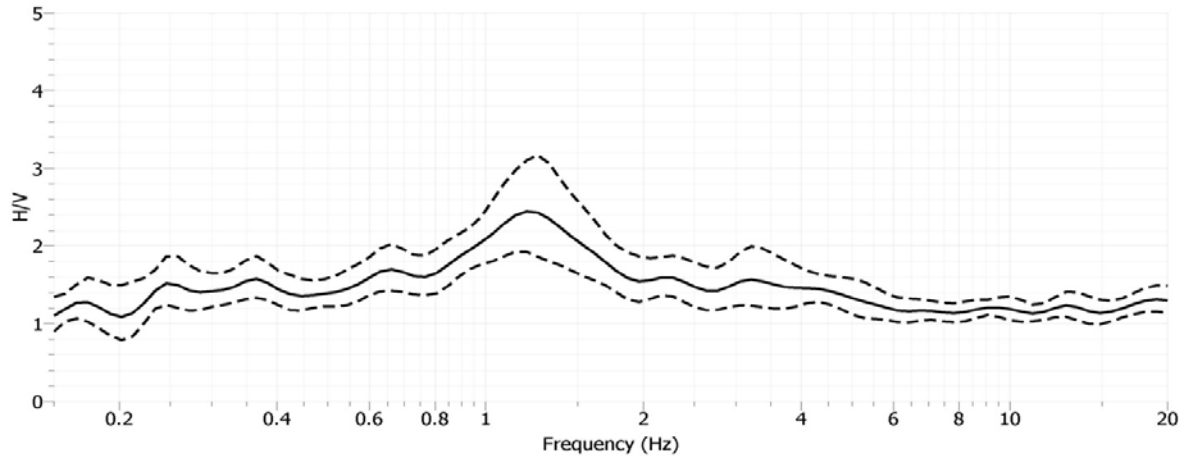

Site CI.DNR, H/V Spectral Ratio, Array DNR-1, Sensor 507

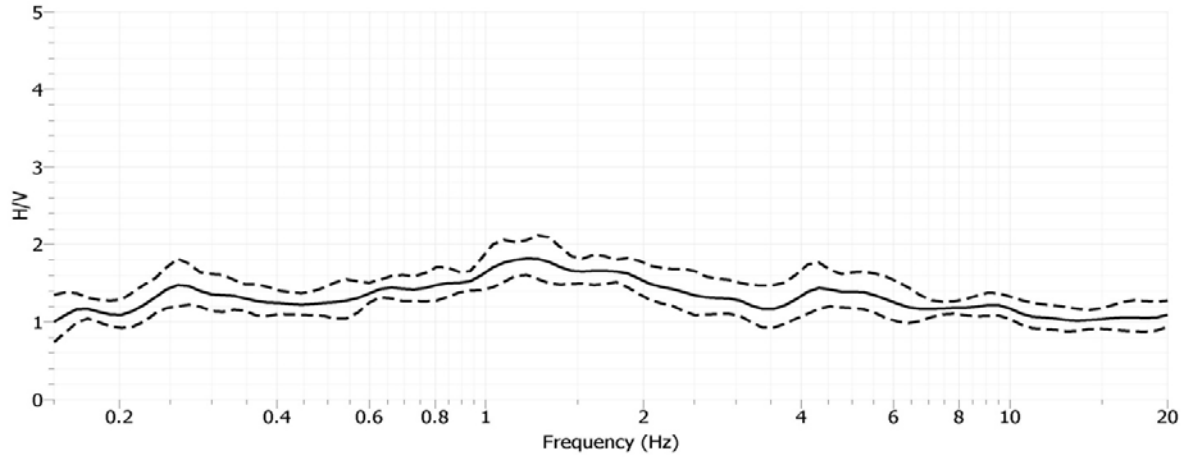

Site CI.DNR, H/V Spectral Ratio, Array DNR-1, Sensor 450

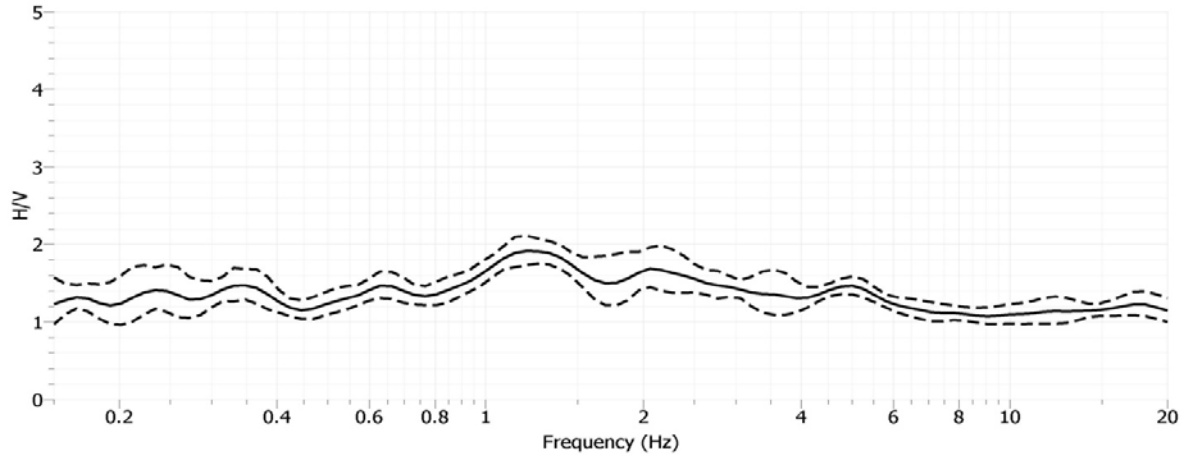

Site CI.DNR, H/V Spectral Ratio, near Seismic Station, Sensor 453

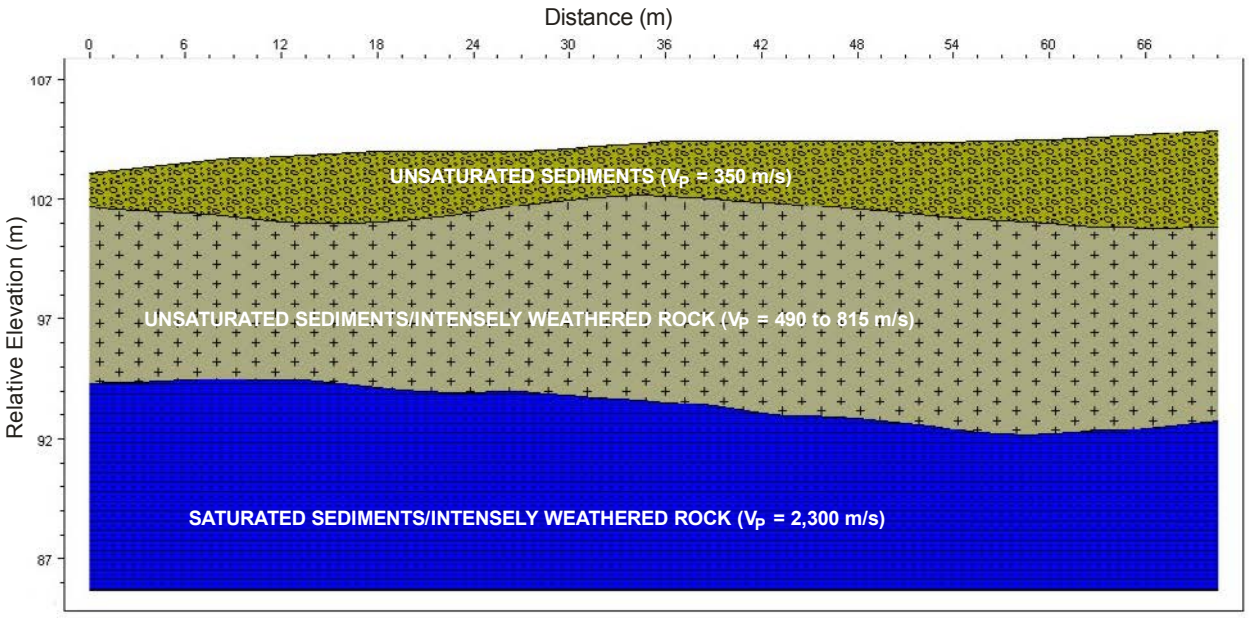

Array DNR-1 – Layer Based Seismic Refraction Model utilizing Generalized Reciprocal Method

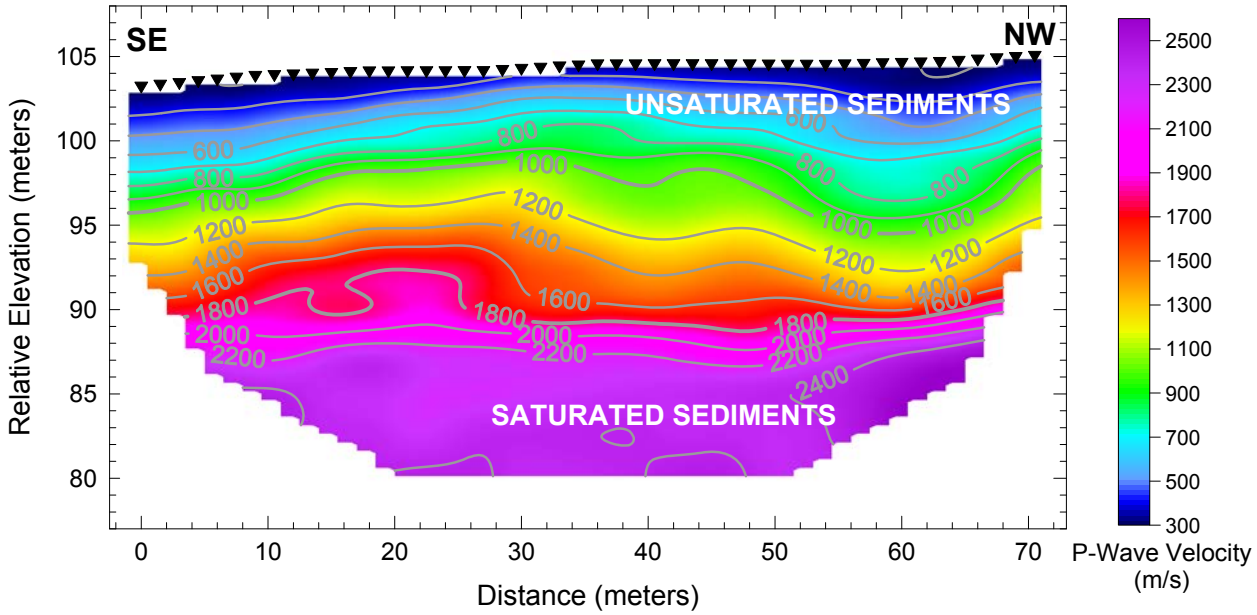

Array DNR-1 – Tomographic Seismic Refraction Model utilizing Smooth Velocity Gradient Starting Model

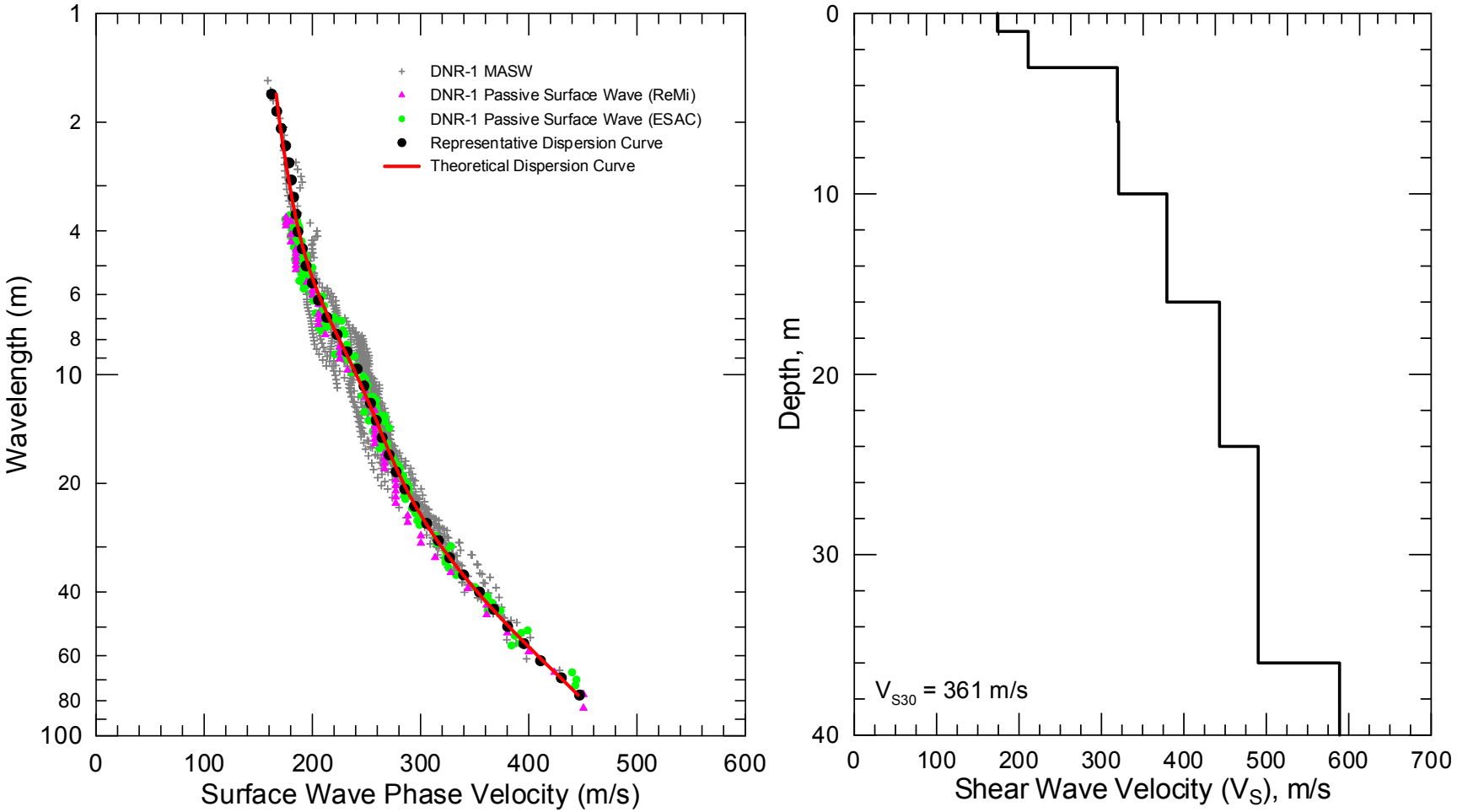

CI.DNR - Field, representative and inverted theoretical surface wave dispersion data (left) and associated V_S model (right)

Site CI.DPP

Location: Dos Picos County Park, 17953 Dos Picos Park Road, Ramona, California

Latitude: 32.99886 **Longitude:** -116.94188
(Station coordinates modified based on field GPS survey, WGS84 coordinate system)

V_{S30} (measured): 611 m/s (V_{S30} at the seismic station may be higher due to a possible thinner sediment layer overlying weathered bedrock).

V_{S30} (adjusted to more accurately reflect seismic station conditions): 830 m/s. Average S-wave velocity between 2 and 32 m (804 m/s), between 2.5 and 32.5 m (859 m/s) and between 1.5 and 31.5 m after replacing V_S of sediments between 1.5 and 2.5 m depth with that of weathered rock at 2.5 m depth (828 m/s) adjusting for 1.5 to 2 m nominal sensor depth and fact that weathered bedrock may be slightly shallower in the vicinity of the seismic station. The three adjusted V_{S30} values discussed above average 830 m/s.

NEHRP Site Class: C (based on adjusted V_{S30}), B (based on adjusted V_{S30}, which probably best reflects seismic station conditions).

Geomatrix Code: IGA/IGB

Geologic Conditions/Observations: Seismic station located on thin layer of soil or weathered rock overlying Mesozoic (Cretaceous) granitic rock.

Site Conditions: Rural site. Relatively planar topography in site vicinity. Seismic station located behind a small park facility building. Weathered granitic rock outcrops within 20 m of the seismic station and 45 to 55 m of the seismic line. The seismic sensors possibly sit on weathered rock.

Geophysical Methods Utilized: HVSR, Seismic Refraction (P- and S-wave), MASW (Rayleigh wave), MALW (Love wave)

Geophysical Testing Arrays:

1. Array DPP-1 (48 channel MASW and P-wave seismic refraction array utilizing 4.5 Hz vertical geophones spaced 1.5 m apart for a length of 70.5 m, forward and reverse shot locations with multiple source offsets and source types and multiple interior shot locations).
2. Array DPP-1 (24 channel S-wave seismic refraction array utilizing 28 Hz horizontal geophones spaced 3 m apart for a length of 69 m, forward and reverse shot locations with multiple source offsets and multiple interior shot locations). Common origin and orientation as P-wave refraction/MASW array of same name.

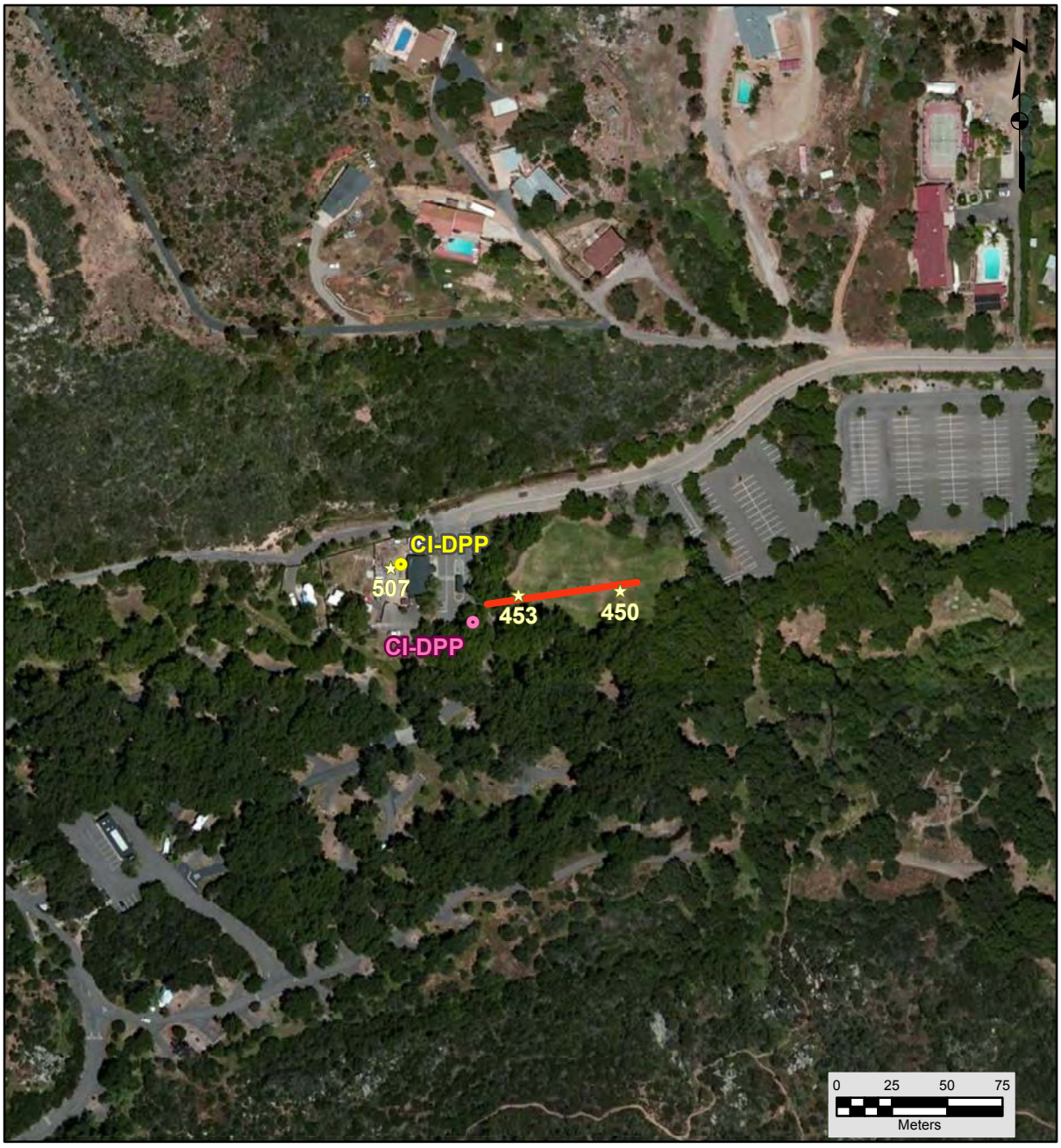

Legend

- Seismic Station - Approximate Surveyed Location
- Seismic Station - Approximate Location of Record
- H/V Spectral Ratio Measurement Location
- MASW and Seismic Refraction Array (P- and S-wave)

NOTES:
1. WGS 1984 COORDINATE SYSTEM
2. Image Source: (c) Microsoft Corporation and its data suppliers

File Name: CI-DPP-I

Date: 2/2/2012

USGS science for a changing world

GEOVision geophysical services

RECOVERY.GOV

SITE MAP
CI•DPP

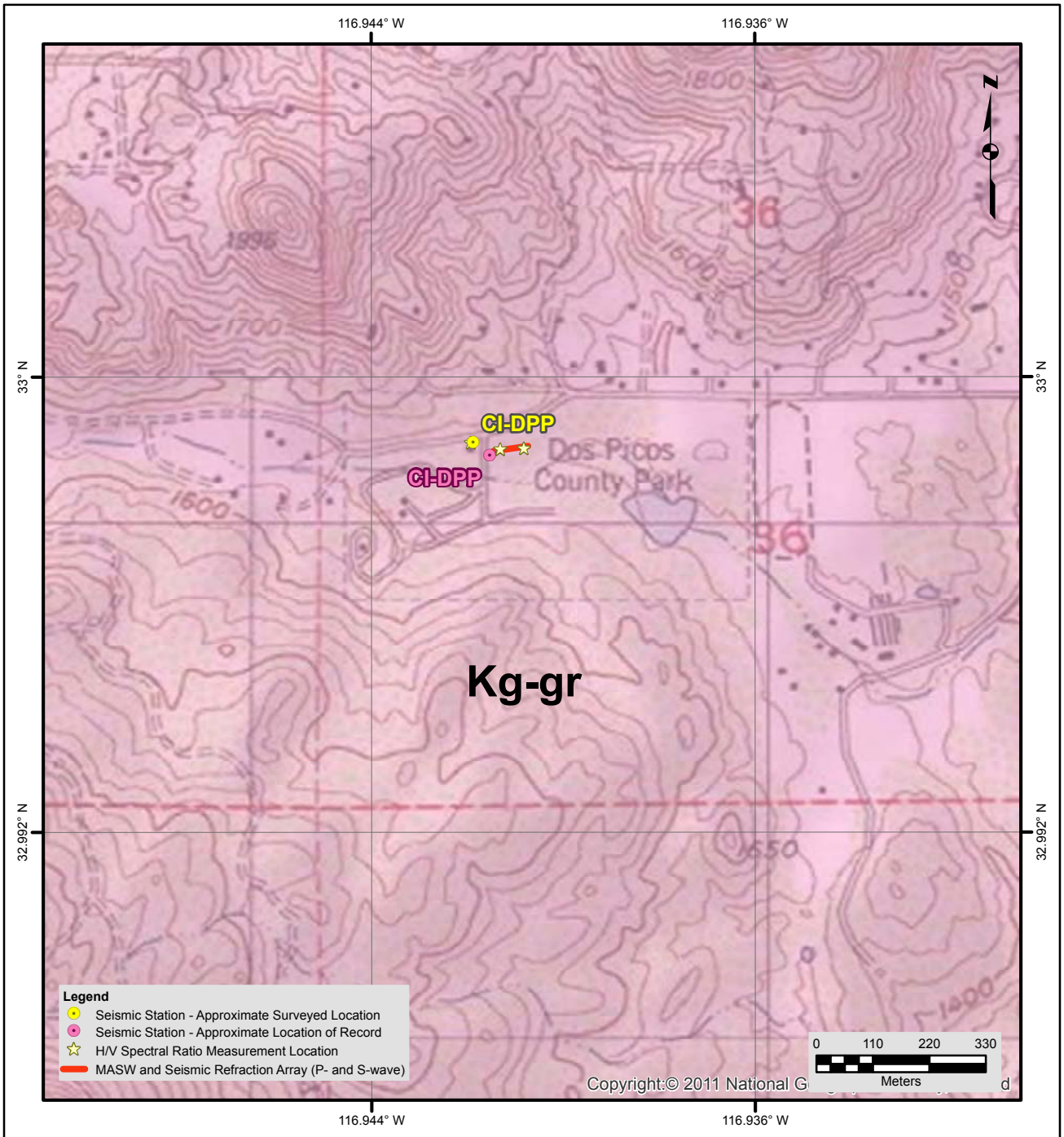

Description of Geologic Map Units

Kg-gr = Mesozoic (Cretaceous) granite, includes some granodiorite, mostly leucocratic, medium- to coarse-grained

NOTES:
1. WGS 1984 COORDINATE SYSTEM
2. Geology taken from:
Geology Map of the San Vincente Reservoir 7.5' Quadrangle, San Diego County, California by Siang S. Tan, 2002
and Geologic Map of California, Santa Ana Sheet Olaf P. Jenkins Edition, compilation by Thomas H. Rogers, 1965
3. See site map for details of geophysical survey

File Name: CI-DPP

Date: 10/18/2012

USGS science for a changing world

GEOVision geophysical services

RECOVERY.GOV

GEOLOGIC MAP
CI•DPP

CI.DPP seismic station and HVSR sensor 507

Looking east along array DPP-1 and
at HVSR sensor 453

Looking west towards end of array DPP-1 and
building behind which the seismic station is located

S-wave data acquisition on array DPP-1

Looking east along MALW array DPP-1

3. Array DPP-1 (48 channel MALW array utilizing 10 Hz horizontal geophones spaced 1.5 m apart for a length of 70.5 m, forward and reverse shot locations with multiple source offsets and a center shot locations). Common origin and orientation as P-wave refraction/MASW array of same name.
4. Three HVSR measurement locations: two distributed along array DPP-1 and the other adjacent to the seismic station.

Location of Geophysical Testing Arrays:

Location	Latitude	Longitude
DPP-1, West End of MASW/Refraction Array	32.99870	-116.94146
DPP-1, East End of MASW/Refraction Array	32.99878	-116.94074
HVSR Sensor 450	32.99875	-116.94082
HVSR Sensor 453	32.99873	-116.94131
HVSR Sensor 507	32.99884	-116.94193
CI.DPP Seismic Station	32.99886	-116.94188

Notes: 1) WGS84 Coordinate System (decimal degrees)
2) Survey accuracy is estimated at 1 to 2 m

Results:

V_S Model

Depth to Top of Layer (m)	Layer Thickness (m)	S-Wave Velocity (m/s)	Inferred P-Wave Velocity (m/s)	Assumed Poisson's Ratio	Assumed Density (g/cm^3)
0	0.4	89	166	0.3	1.6
0.4	2.1	182	340	0.3	1.7
2.5	3.5	485	907	0.3	2.0
6	5	547	1023	0.3	2.0
11	6	856	1602	0.3	2.1
17	>13	1340	2507	0.3	2.2

Notes: 1) Depth of investigation is about 30 m.
2) Poisson's ratio/P-wave velocity has no impact of Love wave modeling.
2) Bottom layer is a half space.

Observations/Discussion:

- The seismic station is located about 20 m from the nearest bedrock outcrop, whereas the seismic line is located 45 to 55 m from the outcrop. Bedrock is, therefore, expected to be slightly shallower in the vicinity of the seismic station. The site is mapped as granitic rock so there may only be a very thin residual soil layer overlying weathered rock.

Although there was not space adjacent to the seismic station to conduct testing, there may be space for a very short seismic line to confirm bedrock depth.

- There are no peaks in the HVSR data by which to assess lateral velocity variation. HVSR data quality at sensor 450 is not as good as that at sensors 453 and 507. Sensor 507 was placed on relatively hard fill near the seismic station, whereas sensors 453 and 450 were placed in soft organic soils.
- Noise conditions at the site were not sufficient for application of passive surface wave techniques.
- Rayleigh wave data quality did not appear to be very good in the field due to dominant higher modes associated with the shallow bedrock. Therefore, S-wave seismic refraction and MALW (Love wave) data were also acquired at this site.
- The P-wave first arrival data were picked to a greater degree of accuracy than the S-wave first arrival data because the S-wave is not typically the first energy on a seismic record, even when using a horizontal traction plank as an energy source. The air wave arrives before the direct soil arrival in the P-wave seismic records and an attempt was made to pick the direct arrival after the air wave, which is not always accurately conducted.
- The P- and S-wave seismic refraction data for array DPP-1 were modeled using a tomographic inversion routine with layer-based starting models. The seismic refraction models were extended to far offset shot locations to extend depth of investigation. It should be noted that a larger geophone spacing, rather than the utilization of far offset shot locations, is preferred for extending depth of investigation, when applying tomographic inversion routines. However, the seismic refraction data were acquired in conjunction with surface wave data, where a shorter array length is preferred.
- The P-wave seismic refraction survey design allowed P-wave velocity to be imaged to a maximum depth of about 20 to 25 m. The seismic refraction model indicates that P-wave velocity is about 200 m/s at the surface and increases to over 750 m/s at a nominal depth of about 2 m, 1,000 m/s at a depth of 3 to 5 m, 1,500 m/s at a depth of 5 to 10 m and over 3,000 m/s at a depth of 13 to 19 m. The maximum P-wave velocity in the central portion of the model, where depth of investigation is greatest is about 3,400 m/s.
- The S-wave seismic refraction survey design allowed S-wave velocity to be imaged to a maximum depth of about 20 to 25 m. The seismic refraction model indicates that S-wave velocity is about 125 to 150 m/s at the surface and increases to over 500 m/s at a nominal depth of 2.5 m, 800 m/s at a depth of 9 to 14 m, 1,000 m/s at a depth of 11 to 19 m and over 1,200 m/s at a depth of 19 to 22 m. The maximum S-wave velocity in the central portion of the model, where depth of investigation is greatest is about 1,350 m/s.
- MASW (Rayleigh wave) data quality is poor due to the high velocity shallow rock and, therefore, MASW data were not utilized for site characterization. MALW (Love wave) data was of significantly better quality with a dominant fundamental mode and were, therefore, used for site characterization.
- The minimum wavelength surface wave phase velocity data extracted from the 48-channel MALW array is about 9 m. Data reduction using seismic records from smaller hammer sources and a limited offset receiver array (i.e. less active geophones) allowed extraction of surface wave dispersion data to a minimum wavelength of about 1.5 m.
- There is nominally about 30 to 75 m/s scatter in MALW dispersion data likely due to the effects of lateral velocity variation.

- A representative dispersion curve was generated for the MALW data set using a moving average, polynomial curve fitting routine and used for modeling.
- Surface wave depth of investigation is assumed to be about 30 m. The maximum wavelength Love wave phase velocity used for modeling was about 90 m, which appears sufficient to image to 30 m depth.
- Several V_S models were generated from the Love wave phase velocity dispersion curve to demonstrate nonuniqueness. As expected V_{S30} is similar for all of the models, varying from 607 to 613 m/s.
- The S-wave refraction model indicates that weathered bedrock is located at an average depth of 2.5 m and one of the Love wave V_S models with 2.5 m depth to bedrock is assumed to be most representative of subsurface velocity structure.
- V_{S30} estimated from the central portion of the S-wave seismic refraction model is 659 m/s (Site Class C), about 7.5% higher than that estimated from the MALW V_S models.
- The S-wave refraction model has slightly higher V_S over the 3 to 6 m depth range and slightly lower V_S at depths greater than 20 m than the MALW V_S models. The S-wave refraction survey design may not permit accurate characterization of S-wave velocity structure at depths below 20 m. A longer seismic refraction line would better constrain the bedrock velocities at depth.
- Estimated V_S derived from the P-wave refraction model using an assumed Poisson's ratio of 0.3 is much higher than that in the S-wave refraction and MALW V_S models below a depth of about 13 m. A Poisson's ratio of 0.4 results in better agreement with the MALW V_S model and may indicate that the weathered and fractured granitic rock is saturated below a depth of 13 m. It is well documented that water filled fractures (cracks) in low porosity rocks will increase Poisson's ratio relative to unsaturated conditions, but it is not clear if an increase in Poisson's ratio to 0.4 is realistic for this type of media.
- V_{S30} from the presented MALW V_S model is 611 m/s (NEHRP Site Class C).
- Weathered bedrock is expected to be slightly shallower at the seismic station than beneath the seismic line. Assuming that the seismic sensor is about 1 to 2 m deep, there is a strong possibility that the seismic sensor sits on rock. Several approaches were, therefore, used to adjust V_{S30} for seismic station conditions including: calculating the average S-wave velocity between 2 and 32 m, 2.5 and 32.5 m and 1.5 and 31.5 m after replacing the V_S of the sediments above 2.5 m with that of the underlying weathered rock layer.
- Average S-wave velocity between 2 m and 32 m and 2.5 and 32.5 m is 804 and 859 m/s, respectively (NEHRP Site Class B).
- The average S-wave velocity between 1.5 and 31.5 m after replacing the V_S of the sediments between 1.5 and 2.5 m with that of the underlying weathered rock unit is 828 m/s.
- The average of the three adjusted V_{S30} values is 830 m/s (NEHRP Site Class B).
- Although it is not possible to conduct a 30 m deep surface wave sounding immediately adjacent to the seismic station, it may be possible to acquire seismic data along a very short array to determine the depth to weathered bedrock.

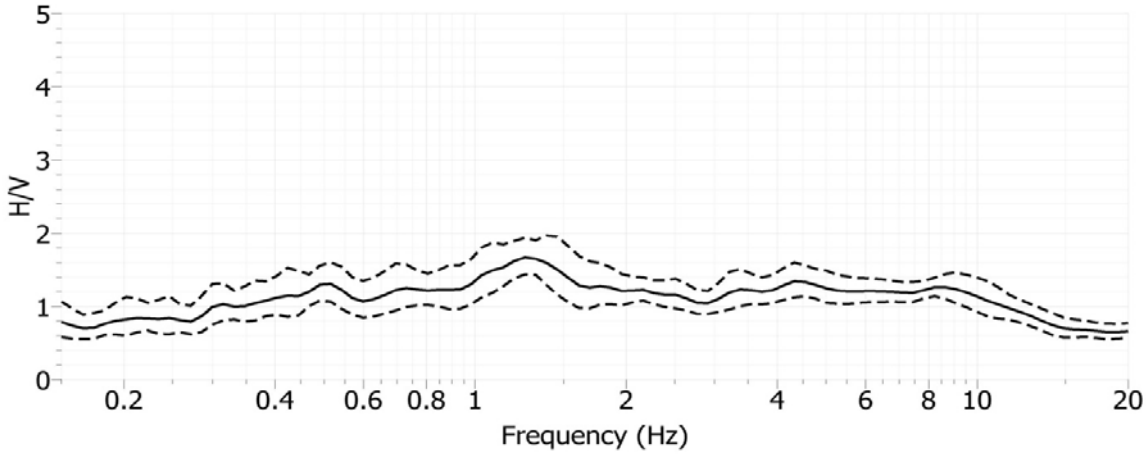

Site CI.DPP, H/V Spectral Ratio, Near Seismic Station, Sensor 507

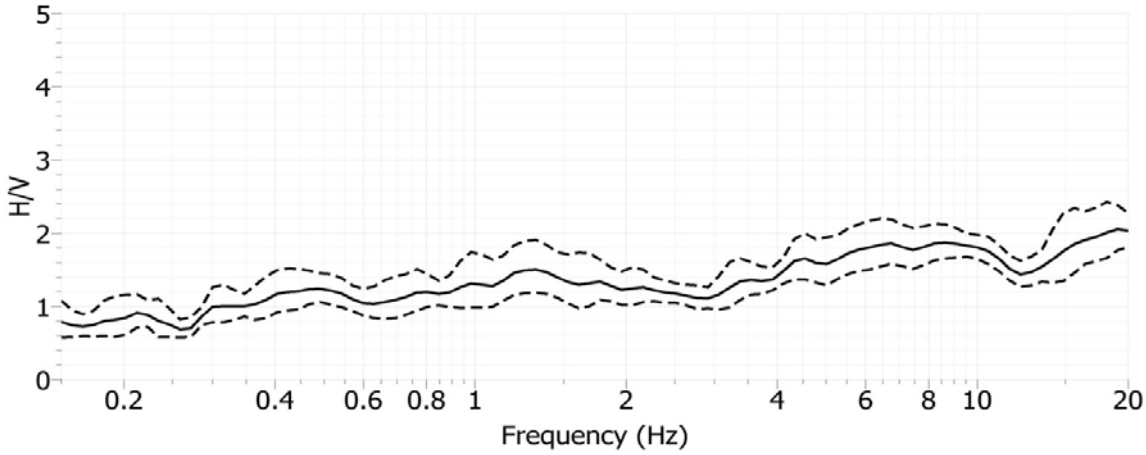

Site CI.DPP, H/V Spectral Ratio, Array DPP-1, Sensor 453

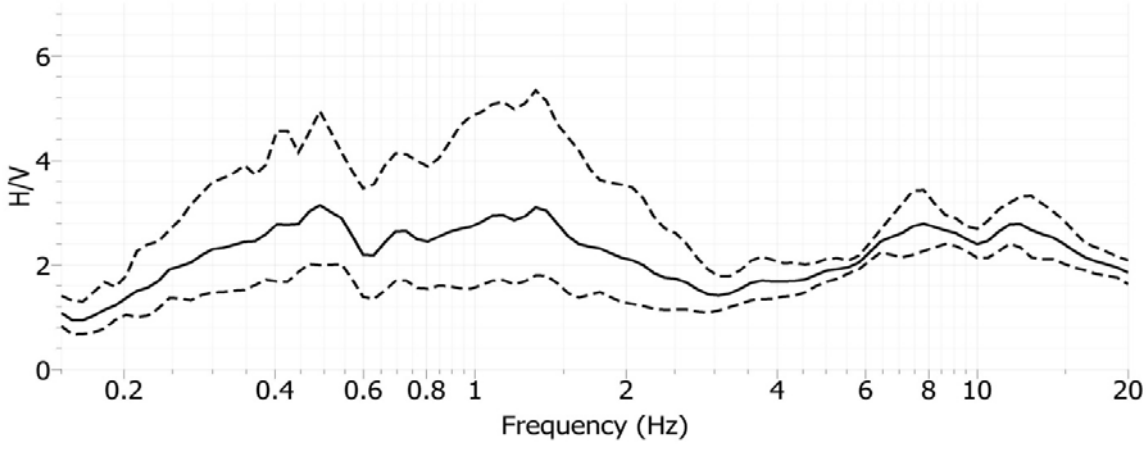

Site CI.DPP, H/V Spectral Ratio, Array DPP-1, Sensor 450

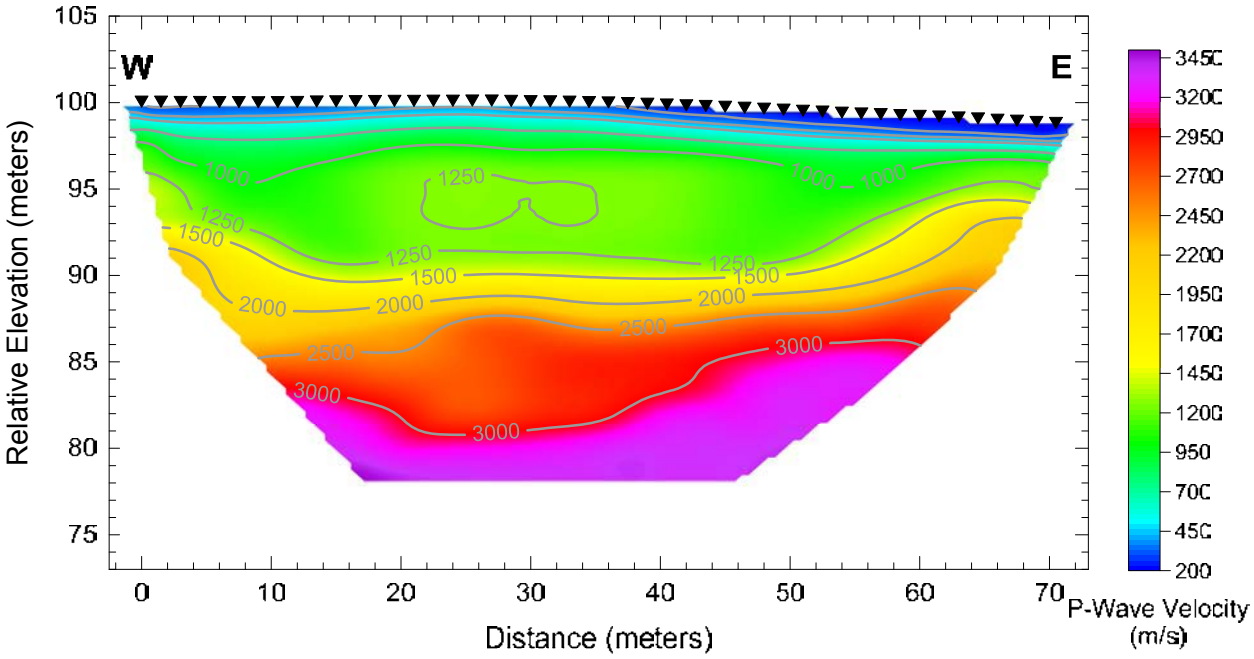

Array DPP-1 – P-wave Tomographic Seismic Refraction Model utilizing Layer Based Starting Model

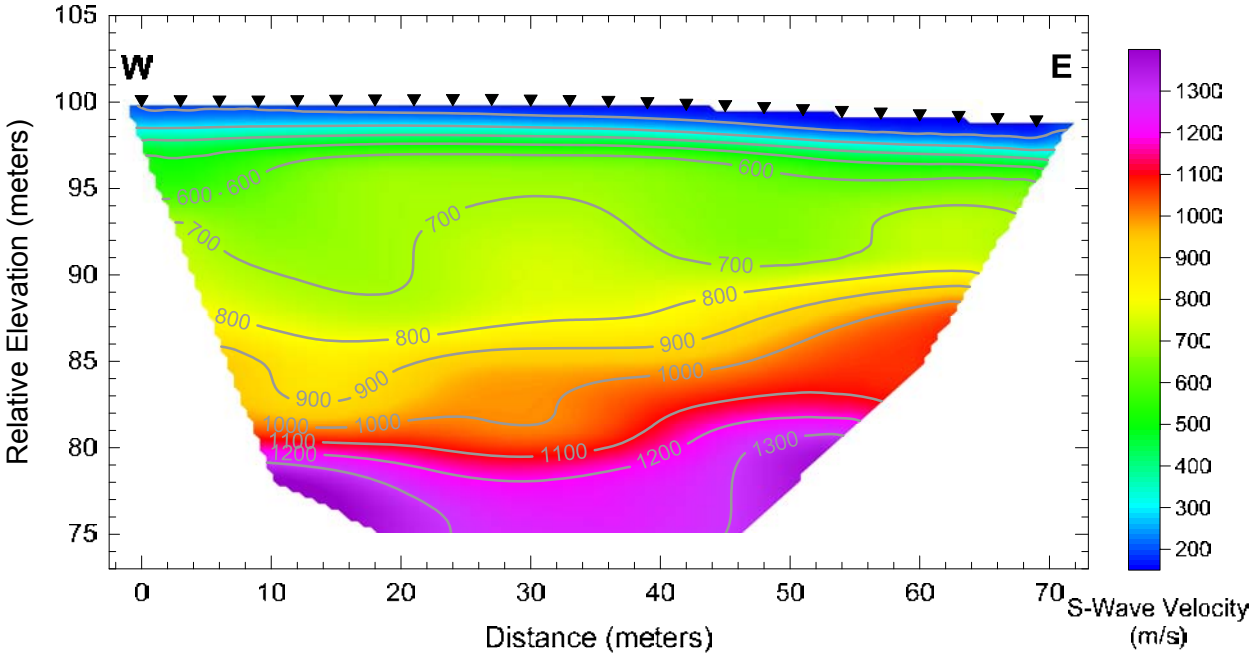

Array DPP-1 – S-wave Tomographic Seismic Refraction Model utilizing Layer Based Starting Model

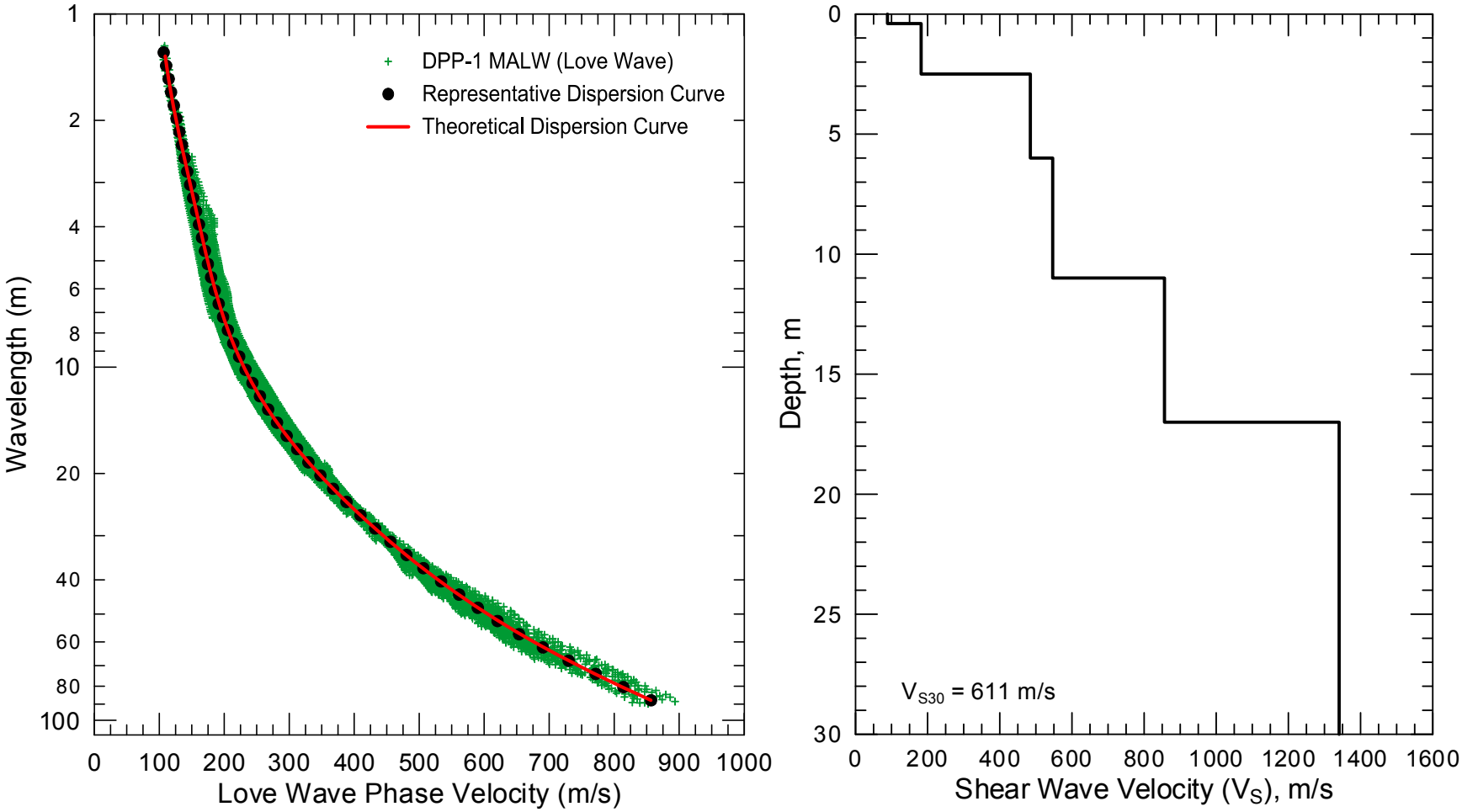

CI.DPP - Field, representative and inverted theoretical surface wave dispersion data (left) and associated V_S model (right)

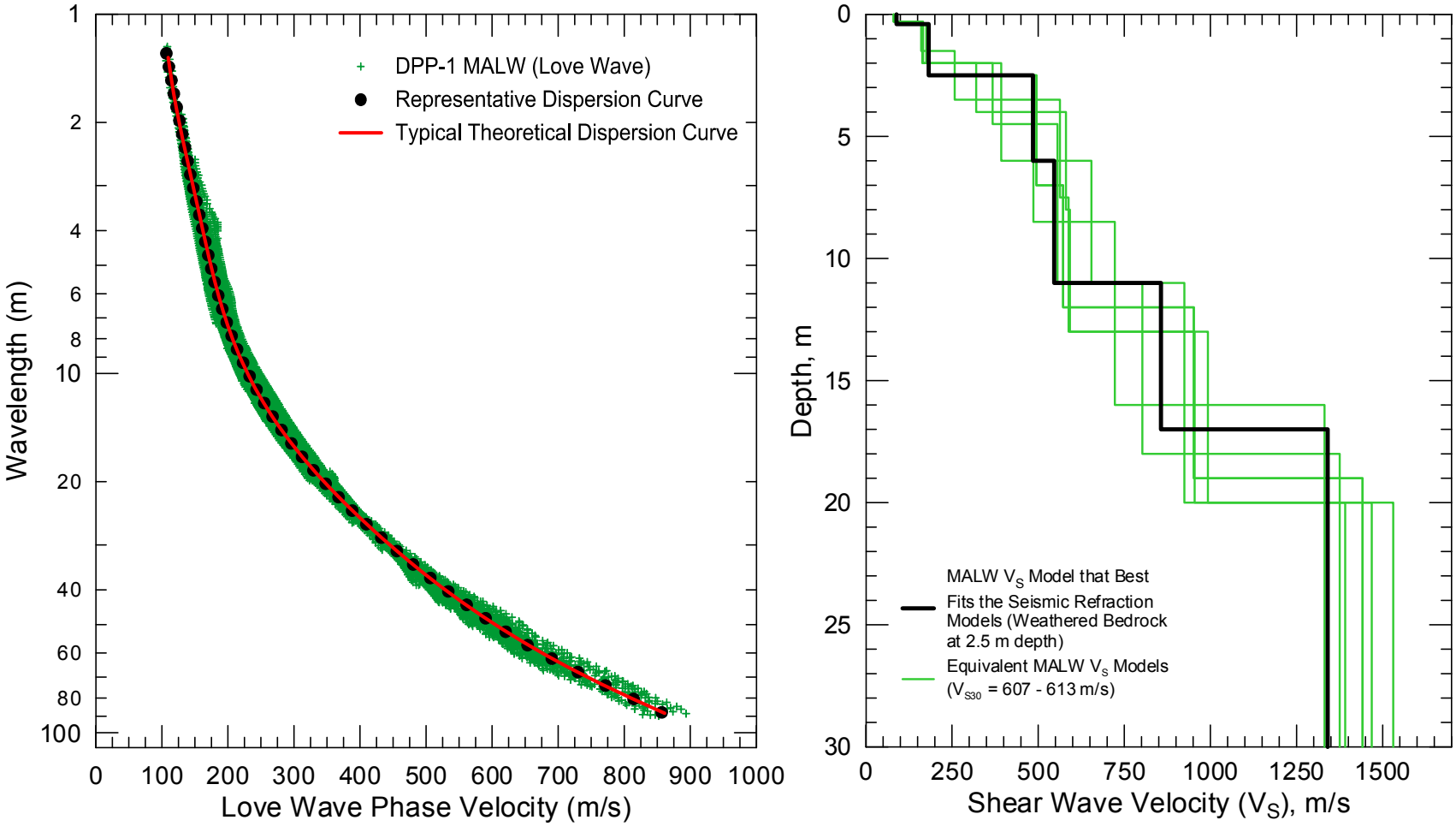

CI.DPP - Field, representative and inverted theoretical surface wave dispersion data (left) and associated equivalent V_S models (right)

Site CI.DRE

Location: University of California, Desert Research Extension Center, 1004 East Holton Road, El Centro, California

Latitude: 32.80535 **Longitude:** -115.44677

(Station coordinates modified based on field GPS survey, WGS84 coordinate system)

V_{S30} (measured): 196 m/s

V_{S30} (adjusted to more accurately reflect seismic station conditions): 216 m/s (average S-wave velocity between 2 and 32 m adjusting for nominal sensor depth)

NEHRP Site Class: D

Geomatrix Code: IHD

Geologic Conditions/Observations: Site located on geologic unit mapped as Quaternary (Holocene) lake deposits. Deep soil site.

Site Conditions: Rural site with sporadic traffic on nearby road. Relatively flat terrain in site vicinity.

Geophysical Methods Utilized: HVSR, MASW, SASW

Geophysical Testing Arrays:

1. Array DRE-1 (48 channel MASW array utilizing 4.5 Hz vertical geophones spaced 1.5 m apart for a length of 70.5 m, forward and reverse shot locations with multiple source offsets and source types and center shot location).
2. Array DRE-1 (SASW array with same midpoint and orientation as MASW array of same name utilizing 1 Hz vertical geophones and maximum receiver spacing of 30 m).
3. Three HVSR measurement locations distributed along array DRE-1.

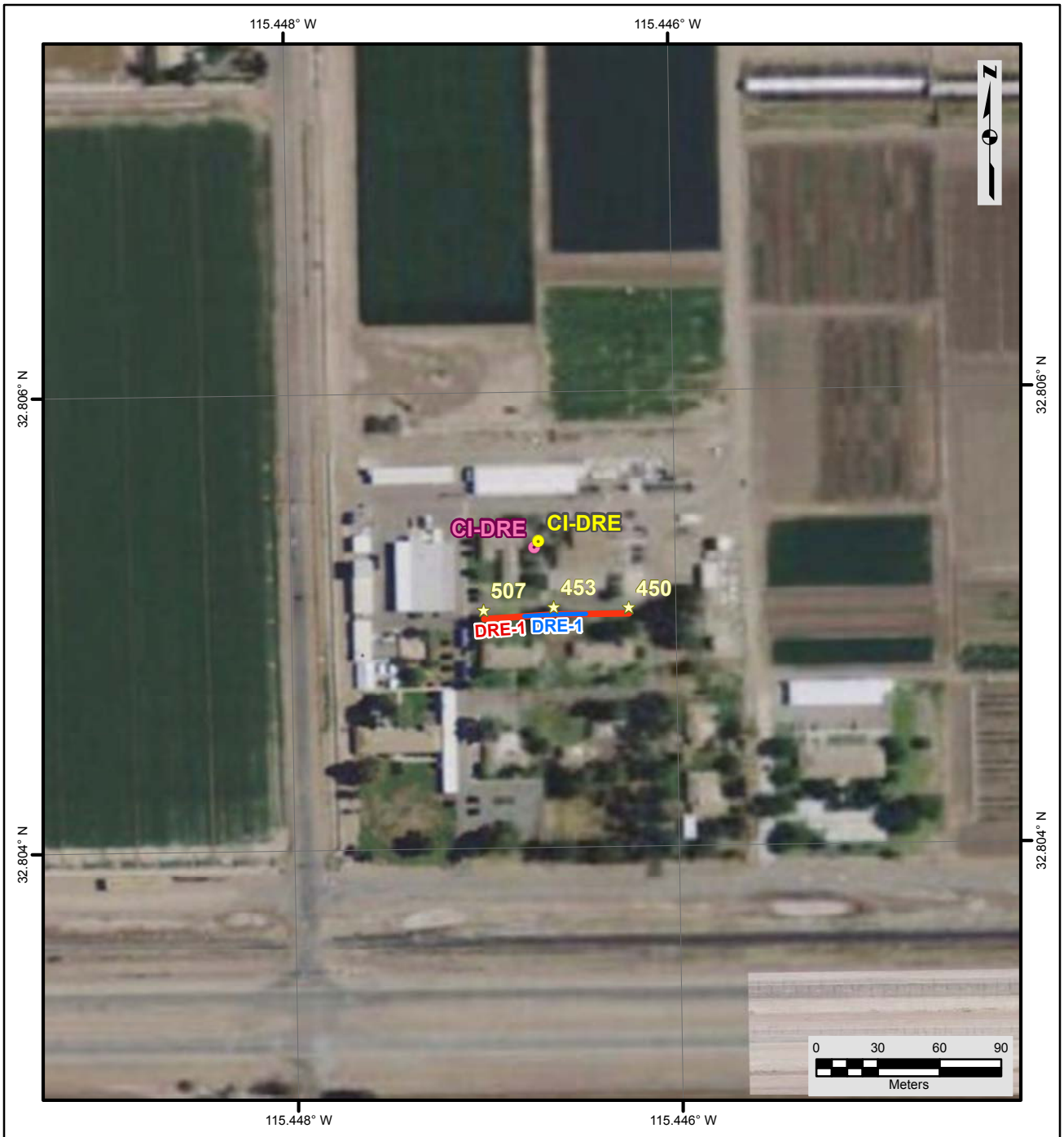

Legend

- Seismic Station - Approximate Surveyed Location
- Seismic Station - Approximate Location of Record
- H/V Spectral Ratio Location
- SASW Array
- MASW Array

NOTES:
1. WGS 1984 COORDINATE SYSTEM
2. Image Source: ESRI, i-cubed, USDA FSA, USGS, AEX, GeoEye, Getmapping, Aerogrid, IGP

File Name: CI-DRE-I

Date: 9/22/2011

USGS science for a changing world

GEOVision geophysical services

RECOVERY.GOV

SITE MAP
CI•DRE

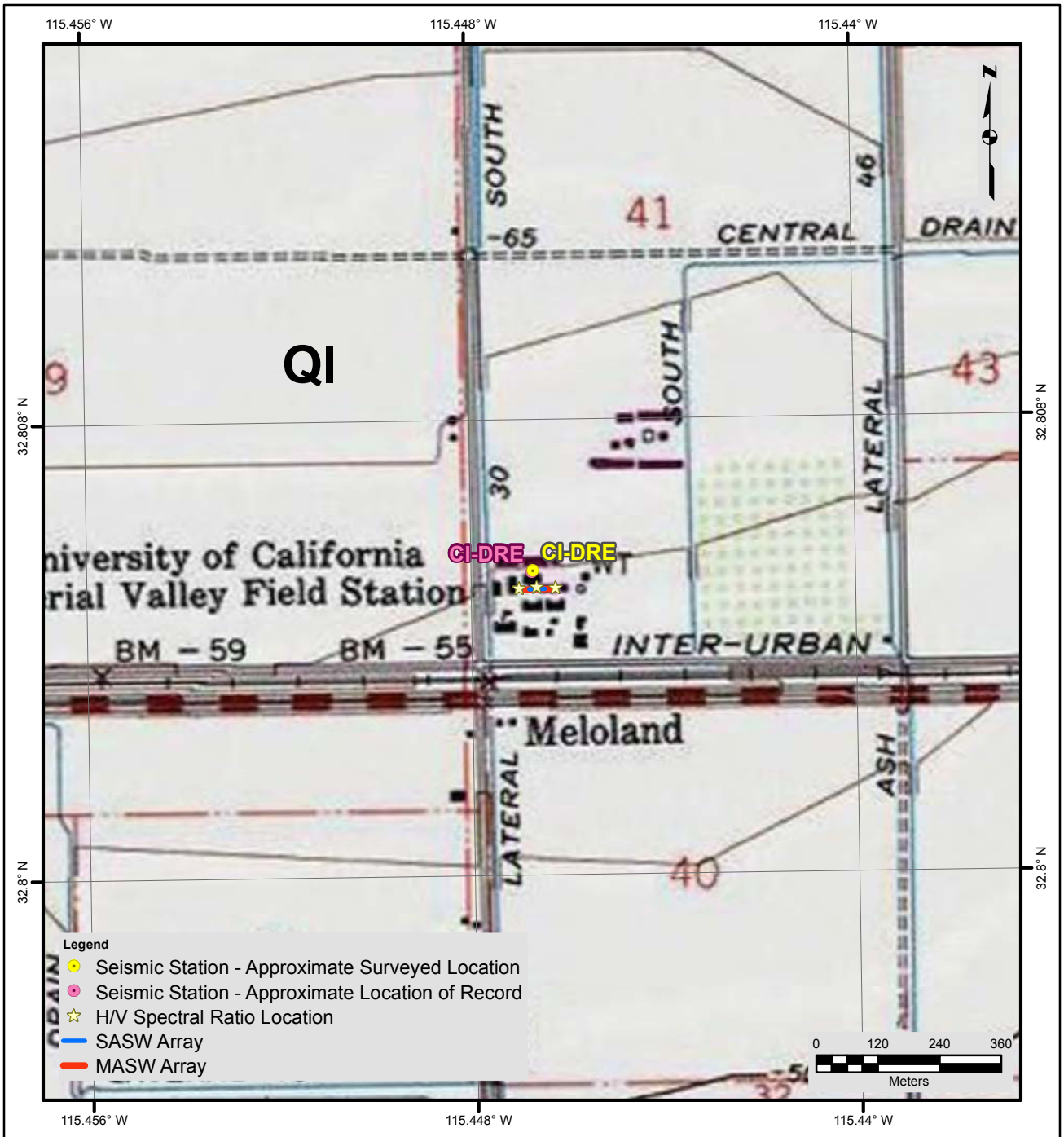

Description of Geologic Map Units

QI = Quaternary (Holocene) lake deposits

NOTES:
1. WGS 1984 COORDINATE SYSTEM
2. Geologic Units from Geologic Map of California, San Diego-El Centro Sheet, Olaf P Jenkins Edition;
Topographic imagery from ESRI ArcGIS Online and data partners including USGS and © 2007 National Geographic Society by Rudolph G. Strand, 1962
3. See site map for details of geophysical survey

File Name: CI-DRE

Date: 9/22/2011

USGS science for a changing world

GEOVision geophysical services

GEOLOGIC MAP
CI•DRE

Looking south towards seismic station CI.DRE and test area

Looking east along MASW array DRE-1

Looking northeast towards location of seismic station from west end of MASW array DRE-1 and HVSR sensor 507

Accelerated weight drop (AWD) being used as energy source on SASW array DRE-1

Looking east along SASW array DRE-1

Location of Geophysical Testing Arrays:

Location	Latitude	Longitude
DRE-1, West End of MASW Array	32.80501	-115.44706
DRE-1, Center of MASW and SASW Arrays	32.80502	-115.44669
DRE-1, East End of MASW Array	32.80502	-115.44630
HVSR Sensor 450	32.80505	-115.44630
HVSR Sensor 453	32.80506	-115.44669
HVSR Sensor 507	32.80505	-115.44706
CI.DRE Seismic Station	32.80535	-115.44677

Notes: 1) WGS84 Coordinate System (decimal degrees)
2) Survey accuracy is estimated at 1 to 2 m

Results:

V_S Model – MASW Array

Depth to Top of Layer (m)	Layer Thickness (m)	S-Wave Velocity (m/s)	Inferred P-Wave Velocity (m/s)	Assumed Poisson's Ratio	Assumed Density (g/cm^3)
0	1	77	144	0.300	1.8
1	2	126	237	0.300	1.8
3	2.5	170	318	0.300	1.8
5.5	5	258	482	0.300	1.9
10.5	4	181	1650	0.494	1.9
14.5	6	184	1650	0.494	1.9
20.5	6	243	1650	0.489	1.9
26.5	>3.5	313	1650	0.481	2.0

Notes: 1) Saturated sediments estimated at 10.5 m depth from seismic refraction first arrival data. The P-wave velocity of saturated sediments is about 1,650 m/s.
2) Depth of investigation is about 30 m.
3) Bottom layer is a half space.

Observations/Discussion:

- The HVSR curves are similar validating the 1-D velocity structure assumption.
- HVSR data quality is best at the location of sensor 450, particularly at low frequency. Sensor 453 has significant low frequency noise.
- There is a high amplitude HVSR peak at about 0.13 Hz, likely associated with the deep basement complex. The horizontal components of the HVSR data have a clear peak at about 0.14 Hz. Better characterization of such a low frequency HVSR peak would be possible if measurements were made at night for a longer duration and with particular

attention paid to sensor coupling. Measurements at different times would also determine if the HVSR peak is stable over time.

- The water table, with P-wave velocity of about 1,650 m/s was modeled at a depth of about 10.5 m based on interactive layer-based analysis of seismic refraction first arrival data. P-wave velocities of the unsaturated sediments range from about 275 to 300 m/s to a depth of 1 to 2 m, below which velocities are in the 350 to 425 m/s range to the water table.
- There is good reflectivity in the MASW seismic records with multiple reflectors in the approximate 40 to 125 m depth range.
- Noise conditions at the site were not sufficient to apply passive surface wave techniques.
- Dominant higher mode surface wave energy in the SASW data and some MASW seismic records indicate that a high velocity layer is present at shallow depth. It appeared that the fundamental mode was dominant on most MASW seismic records and, therefore, data analysis was limited to modeling of the MASW data.
- There is significant scatter in the MASW data at wavelengths greater than 50 m, corresponding to a frequency of about 4 Hz. The scatter is likely associated with limited energy from the accelerated weight drop energy source at frequencies below 4 to 5 Hz.
- The 60 m wavelength phase velocity data, the minimum required to develop a 30 m depth model, occurs at a frequency of about 3.5 Hz, 1 Hz lower than the natural frequency of the geophones utilized to acquire the data. It should be noted that the SASW data, acquired with 1 Hz geophones, had similar phase velocities at wavelengths in the 50 to 60 m range.
- A representative dispersion curve was generated for the MASW data set using a moving average, polynomial curve fitting routine for data modeling.
- A relative high velocity layer with thickness of 5 m is in the surface wave model at a depth of about 5.5 m. The thickness and velocity of this layer and the velocity of the underlying layer may not be well constrained, but are not expected to have a significant impact on V_{S30}.
- The S-wave velocity model was evaluated and the fundamental mode Rayleigh wave was confirmed to have the highest amplitude at all frequencies. The first higher mode, however, has only slightly less energy over the approximate 7 to 12 Hz range. Therefore, the possibility cannot be discounted that some modal superposition occurs with phase velocities slightly overestimated due to influence of the higher mode surface wave energy. If this were the case, forward modeling indicates that the S-wave velocity of the high velocity layer would be slightly overestimated and the velocity of the underlying two layers slightly underestimated. Interestingly, in this scenario V_{S30} remains almost unchanged.
- Surface wave depth of investigation is about 30 m based on half of maximum wavelength criteria.
- V_{S30} is 196 m/s (Site Class D).
- Average S-wave velocity between 2 m (nominal sensor depth) and 32 m is 216 m/s.

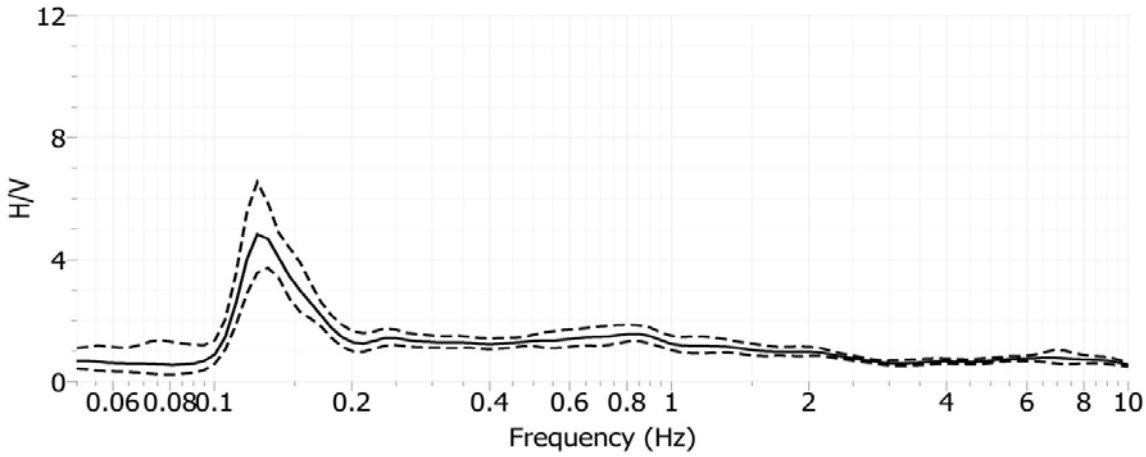

Site CI.DRE, H/V Spectral Ratio, Array DRE-1, Sensor 507

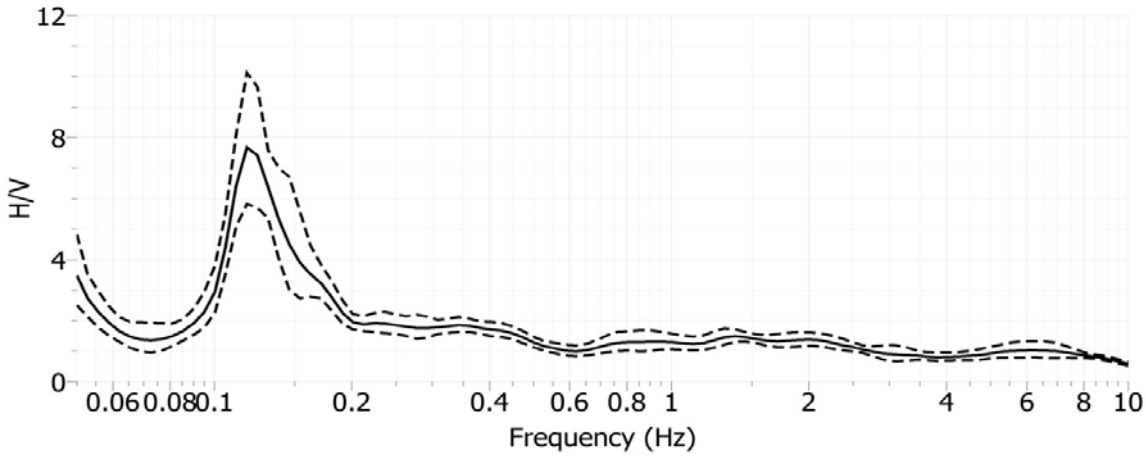

Site CI.DRE, H/V Spectral Ratio, Array DRE-1, Sensor 453

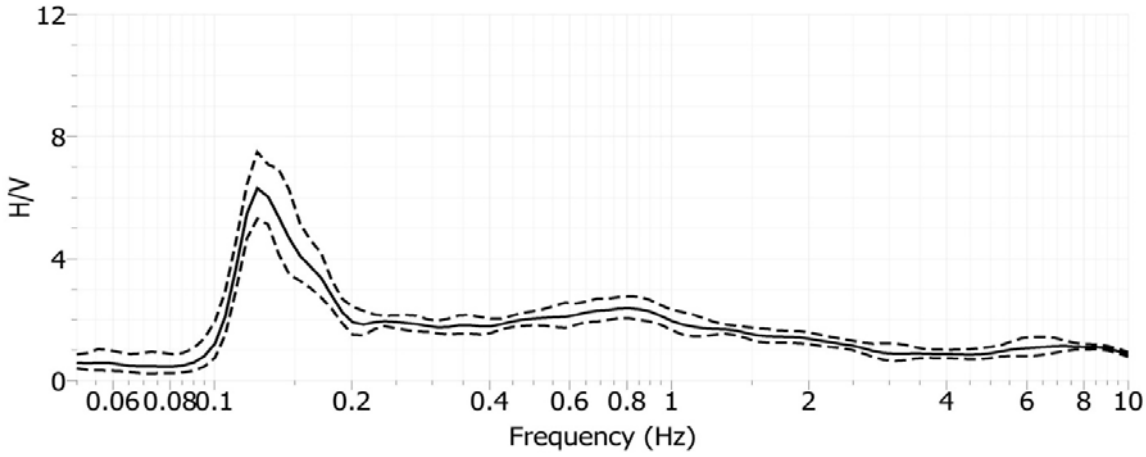

Site CI.DRE, H/V Spectral Ratio, Array DRE-1, Sensor 450

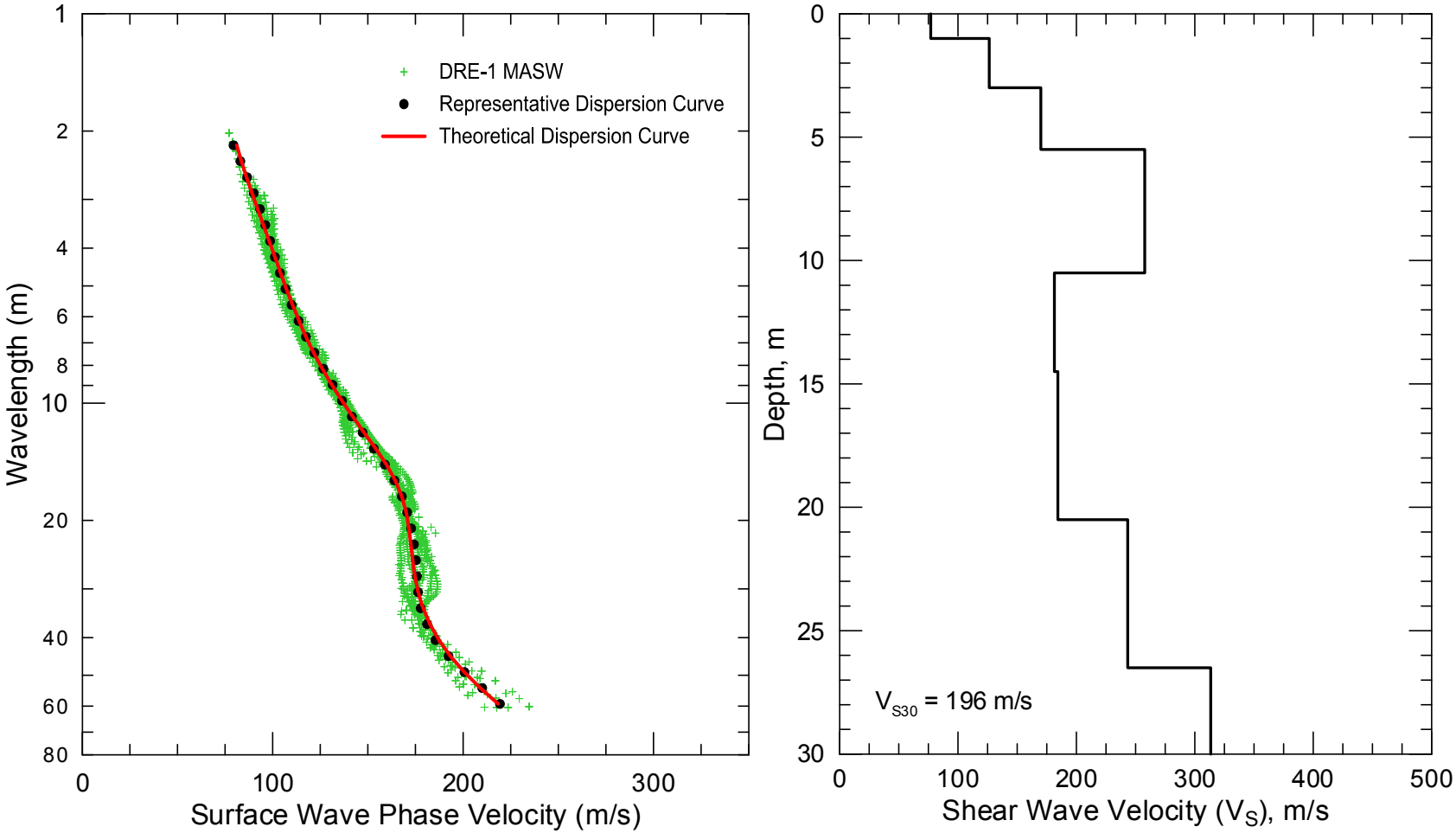

CI.DRE - Field, representative and inverted theoretical surface wave dispersion data (left) and associated V_S model (right)

Site CI.DSC

Location: California State University Desert Studies Center, Zzyzx Road, San Bernardino County, California

Latitude: 35.14255 **Longitude:** -116.10395
(Station coordinates provided by USGS, WGS84 coordinate system)

V_{S30} (measured): 1,329 m/s (based on S-wave seismic refraction model)

V_{S30} (adjusted to more accurately reflect seismic station conditions): 1,484 m/s (average S-wave velocity between 1 and 31 m to account for bedrock contact occurring at least 1 m shallower beneath the seismic station).

NEHRP Site Class: B or B/A (based on adjusted V_{S30})

Geomatrix Code: AHA/AZA

Geologic Conditions/Observations: Seismic station located on the concrete slab of a single story structure, on top of a unit mapped as Quaternary (Holocene) alluvium. Paleozoic (Carboniferous) limestone or dolomite outcrops immediately east of the seismic station and may be located at a depth of 1 m, or less, beneath the seismic station. Mesozoic granitic and metavolcanic rocks outcrop 300 to 500 m west of the site.

Site Conditions: Rural site. Seismic line located in a relatively flat area between bedrock outcrops. Seismic station located on the concrete slab of a research center building. Bedrock outcrops immediately east of the seismic station.

Geophysical Methods Utilized: HVSR, Seismic Refraction (P- and S-wave), MASW (Rayleigh wave), MALW (Love wave)

Geophysical Testing Arrays:

1. Array DSC-1 (48 channel MASW and P-wave seismic refraction array utilizing 4.5 Hz vertical geophones spaced 1.5 m apart for a length of 70.5 m, forward and reverse shot locations with multiple source offsets and source types (hammers only) and multiple interior shot locations).
2. Array DSC-1 (48 channel MALW and S-wave seismic refraction array utilizing 10 Hz horizontal geophones spaced 1.5 m apart for a length of 70.5 m, forward and reverse shot locations with multiple source offsets and multiple interior shot locations). Common origin and orientation as P-wave array of same name.
3. Three HVSR measurement locations: two distributed along array DSC-1 and the other adjacent to the seismic station.

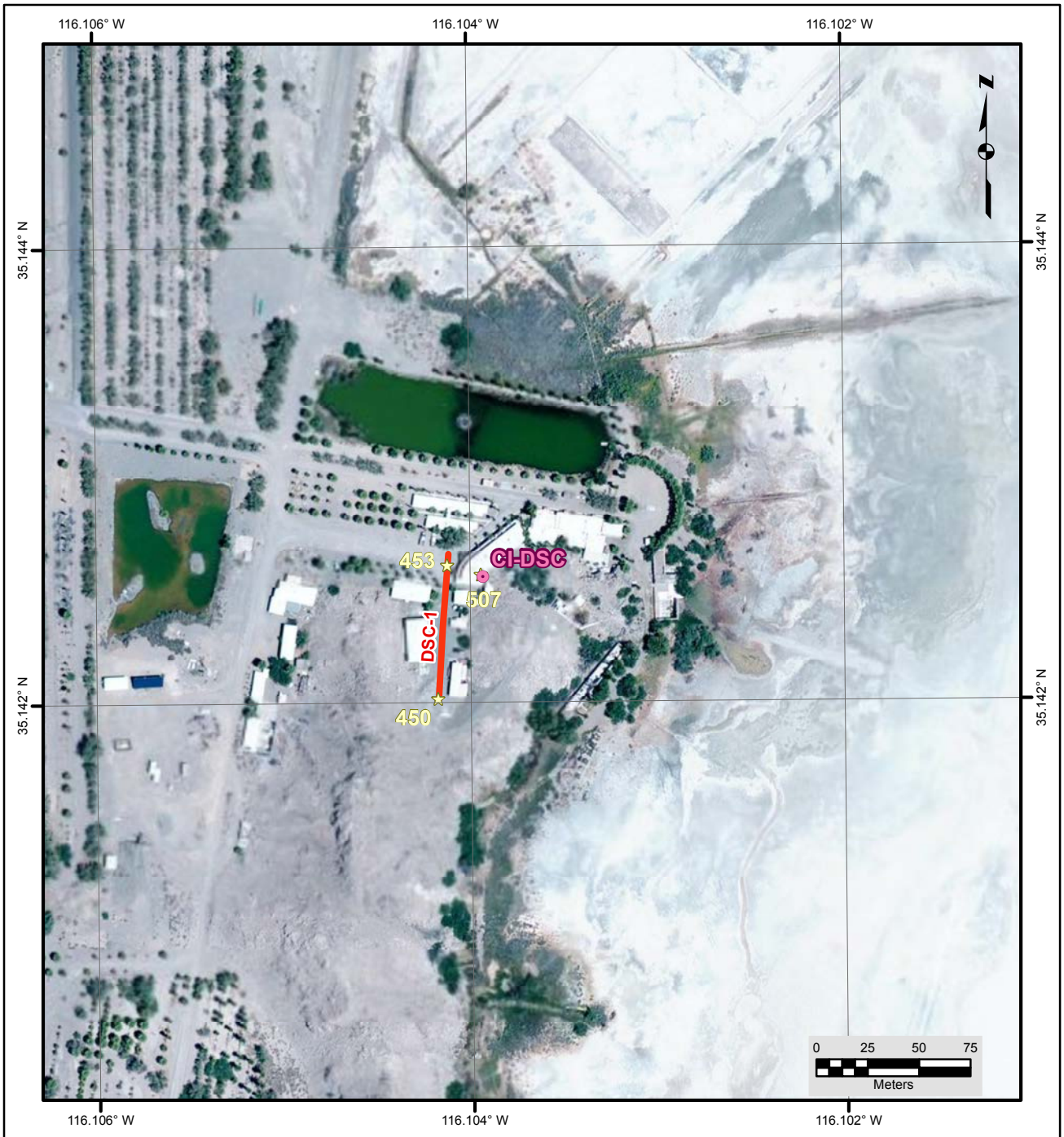

Legend

- Seismic Station - Approximate Location of Record
- H/V Spectral Ratio Measurement Location
- MASW and Seismic Refraction Array (P- and S-wave)

NOTES:
1. WGS 1984 COORDINATE SYSTEM
2. Image Source: (c) Microsoft Corporation and its data suppliers

File Name: CI-DSC-I

Date: 2/24/2012

USGS science for a changing world

GEOVision geophysical services

RECOVERY.GOV

SITE MAP
CI•DSC

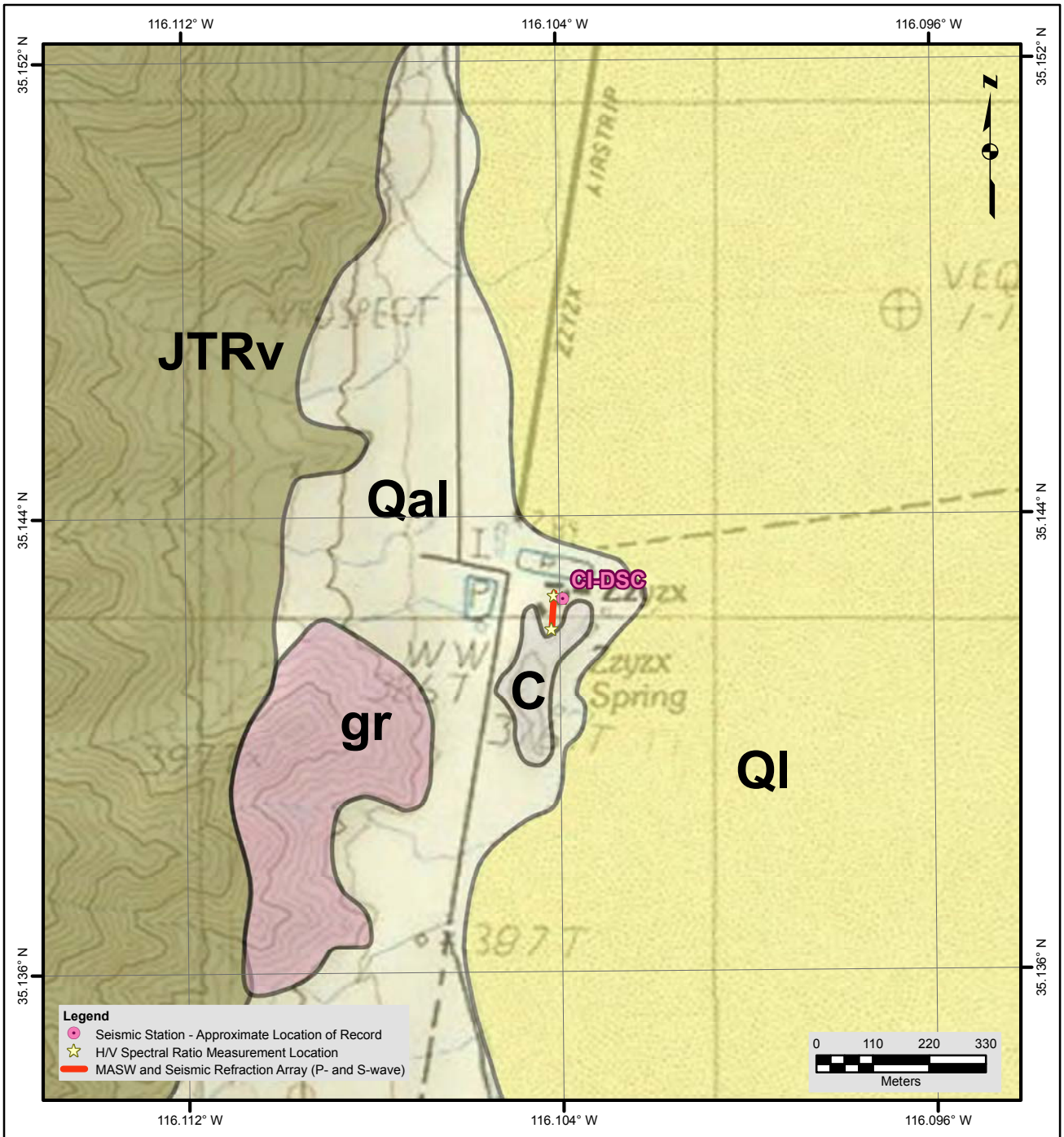

Description of Geologic Map Units

Qal = Quaternary (Holocene) alluvium
Ql = Quaternary (Holocene) lake deposits
gr = Mesozoic (Cretaceous) granitic rocks
JTRv = Mesozoic (Jurassic / Triassic) metavolcanic rocks
C = Paleozoic (Carboniferous) undivided marine deposits

NOTES:
1. WGS 1984 COORDINATE SYSTEM
2. Geology modified from:
Geologic Map of California Trona Sheet
by Charles W. Jennings, John L. Burnett
& Bennie W. Troxel, 1962
3. See site map for details of geophysical survey

File Name: CI-DSC
Date: 2/24/2012

USGS science for a changing world
GEOVision geophysical services

GEOLOGIC MAP
CI•DSC

RECOVERY.GOV

Looking south along array DSC-1 towards outcrop of Paleozoic carbonate rocks

Looking east towards building housing seismic station, the north end of array DSC-1 and HVSR sensor 453

Looking north towards HVSR sensor 450 and along array DSC-1

HVSR sensor 507 and CI.DSC seismic station

S-wave seismic refraction data acquisition on array DSC-1

Location of Geophysical Testing Arrays:

Location	Latitude	Longitude
DSC-1, South End of MASW/Refraction Array	35.14201	-116.10419
DSC-1, Center of MASW/Refraction Array	35.14233	-116.10417
DSC-1, North End of MASW/Refraction Array	35.14265	-116.10413
HVSR Sensor 450	35.14202	-116.10419
HVSR Sensor 453	35.14260	-116.10414
HVSR Sensor 507	35.14256	-116.10396

Notes: 1) WGS84 Coordinate System (decimal degrees)

2) Survey accuracy is estimated at 1 to 2 m.

3) Coordinates for HVSR sensor 507 are estimated.

Results:

Average V_P and Estimated V_S Model from Central Portion of P-wave Seismic Refraction Line

Depth to Top of Layer (m)	Layer Thickness (m)	P-Wave Velocity (m/s)	Estimated S-Wave Velocity (m/s)			
			Poisson's Ratio = 0.25	Poisson's Ratio = 0.30	Poisson's Ratio = 0.35	Poisson's Ratio = 0.40
0.00	0.33	597	345	319	287	244
0.33	0.66	686	396	367	330	280
0.99	0.66	776	448	415	373	317
1.65	0.66	799	461	427	384	326
2.31	0.66	1977	1142	1057	950	807
2.97	0.66	2328	1344	1245	1118	951
3.63	0.66	2602	1502	1391	1250	1062
4.29	1.39	3082	1779	1647	1480	1258
5.67	1.39	3809	2199	2036	1830	1555
7.06	1.39	3844	2219	2055	1846	1569
8.44	1.39	3990	2304	2133	1917	1629
9.83	1.39	4026	2325	2152	1934	1644
11.21	1.39	4039	2332	2159	1940	1649
12.60	Half Space	4138	2389	2212	1988	1689

Note: Not recommended to utilize estimated S-wave velocity from P-wave seismic refraction model because rock is saturated and Poisson's ratio is probably relatively highly variable.

Average V_S Model from Central Portion of S-wave Seismic Refraction Line

Depth to Top of Layer (m)	Layer Thickness (m)	S-Wave Velocity (m/s)
0.00	0.33	232
0.33	0.66	470
0.99	0.66	487
1.65	0.66	500
2.31	0.66	506
2.97	0.66	715
3.63	0.66	1060
4.29	1.39	1119
5.67	1.39	1267
7.06	1.39	1452
8.44	1.39	1522
9.83	1.39	1685
11.21	1.39	1767
12.60	1.39	1878
13.98	Half Space	2083

Observations/Discussion:

- The seismic station is located on the concrete slab of a small building at the base of an outcrop of carbonate rock, either limestone or dolomite. It could not be confirmed whether the building foundation sits on rock or a thin layer of alluvium or fill. Given the proximity of the seismic station to the outcrop, it is unlikely that there is more than 1 or 2 meters of fill or alluvium overlying rock.
- There are no distinct, high amplitude HVSR peaks on all three of the HVSR measurement locations. HVSR sensors 507 (near seismic station) and 450 (at south end of array DSC-1) have possible low amplitude HVSR peaks at a frequency of about 14 Hz.
- Field observations indicated that the MASW (Rayleigh wave) technique may not be effective at this site due to the thin layer of low velocity sediments overlying high velocity rock and/or lateral variability of the subsurface velocity structure. Therefore, both P- and S-wave seismic refraction data were collected and MALW (Love wave) data acquired.
- Geophysical testing was conducted as close as possible to the seismic station, in an area where there are likely subsurface utilities. P-wave seismic refraction data quality was good but S-wave seismic refraction data quality was significantly degraded by subsurface conditions and heavy winds during testing. It may be possible to obtain better quality data in lighter winds or at an alternate location. Consideration was given to testing on top of the limestone/dolomite outcrop adjacent to the seismic station; however, there is a

distinct possibility that the rock at the top of the outcrop is more weathered and, therefore, has lower seismic velocity than that at the base of the outcrop.

- Noise conditions at the site were not sufficient for application of passive surface wave techniques.
- Surface wave techniques were not expected to be effective at this site because of the very shallow high velocity bedrock. MALW (Love wave) data was of very poor quality and not utilized. An attempt was made to generate a coherent dispersion curve for the MASW (Rayleigh wave) data. A complete and coherent dispersion curve could not be developed, especially over the 15 to 30 m wavelength range. There was also significant scatter in long wavelength dispersion data due to possible thinning of the sediment layer to the south. Sufficient surface wave dispersion data was compiled to demonstrate that there is, on average, about 2 m of soil with S-wave velocity in the 225 to 275 m/s range overlying rock beneath the array. Additionally, the phase velocity of a 40 m wavelength Rayleigh wave (V_{R40}) was found to vary from about 1,100 to 1,250 m/s, averaging about 1,175 m/s. Assuming that V_{R40} is associated with the fundamental mode then V_{S30} is expected to be in the 1,130 to 1,306 m/s range and average 1,228 m/s, based on the relationship between V_{R40} and V_{S30} outlined in Brown, et al., 2000. V_{S30} would be lower if V_{R40} were associated with a higher mode or superimposed/mixed modes (modal superposition or mode mixing). The surface wave dispersion data also provides evidence that S-wave velocity exceeds 1,600 m/s at depth in the site vicinity.
- For reasons discussed above, site characterization was limited to the application of the P- and S-wave seismic refraction techniques.
- The P- and S-wave seismic refraction data for array DSC-1 were modeled using a tomographic inversion routine with layer-based starting models. The seismic refraction models were extended to far offset shot locations to extend depth of investigation. Due to space limitations the furthest offend shot locations were only 10 m from the nearest geophone. It should be noted that a larger geophone spacing, rather than the utilization of far offset shot locations, is preferred for extending depth of investigation when applying tomographic inversion routines. However, the seismic refraction data were acquired in conjunction with surface wave data acquisition, where a shorter array length is preferred, and there were space limitations at the site.
- The P-wave first arrival data were picked to a significantly greater degree of accuracy than the S-wave first arrival data. S-wave refraction data were very noisy due to heavy winds during testing and possibly subsurface conditions (e.g. utilities) and the possibility of significant error should be considered. Data acquisition at an alternate location in better environmental conditions may yield more reliable results.
- Review of P- and S-wave first arrival data indicates that P- and S-wave velocities exceed 3,500 and 1,600 m/s, respectively, at relatively shallow depth. Although MASW data was not of sufficient quality for modeling, Rayleigh wave phase velocity data also indicates that S-wave velocity likely exceeds 1,600 m/s at depth.
- The P-wave seismic refraction survey design allowed P-wave velocity to be imaged to a maximum depth of about 15 m. The seismic refraction model indicates that P-wave velocity is about 475 to 750 m/s at the surface and increases to about 1,500 m/s at a depth of 2 to 3 m, 3,000 m/s at a depth of 4 to 5 m and over 4,000 m/s at a depth of 5 to 12 m. The maximum P-wave velocity in the model is about 4,200 m/s, although seismic velocities this high are not well constrained with a relatively short (70.5 m) seismic line.

Such high P-wave velocities are indicative of slightly weathered rock and, therefore, we would expect velocity to increase very gradually with depth below 15 m.

- The S-wave seismic refraction survey design allowed S-wave velocity to be imaged to a maximum depth of about 15 m. The seismic refraction model indicates that S-wave velocity is about 250 to 400 m/s at the surface and increases to over 750 m/s at a depth of 2.5 to 6 m, 1,250 m/s at a depth of 4 to 10 m and over 1,750 m/s at a depth of 6 to 12 m. The maximum S-wave velocity in model is about 2,100 m/s. An S-wave velocity this high is indicative of slightly weathered rock and, therefore, we would expect velocity to only increase very gradually with depth below 15 m.
- There is some lateral velocity variation at the site, associated with both a variable thickness of the thin layer of alluvium overlying rock and variable weathering of rock.
- V_{S30} was estimated between 25.5 and 54 m along the S-wave refraction model, where depth of investigation was greatest, by projecting the velocity at 15 m depth to 30 m depth. Over this interval V_{S30} ranges from about 1,278 to 1,355 m/s, a 6% variation.
- An average V_S model was developed over the 25.5 to 54 m distance interval by averaging the slowness through each model cell and average V_{S30} was determined to be 1,329 m/s. Decreasing average V_S of the half space from 2,083 to 1,878 m/s, the average V_S of the cell above, only decreases V_{S30} by 4%.
- V_{P30} between 25.5 and 54 m in the P-wave seismic refraction model varies from about 2,746 to 3,105 m/s, a 12 % variation, and averages 2,865 m/s. Potential saturated alluvium at the northern end of the line may contribute to a larger variation in V_{P30} in the P-wave refraction model than V_{S30} in the S-wave refraction model. However, it should also be noted that the P-wave refraction model is better constrained due to more accurate first arrival data and the S-wave refraction model may be smoothed due to the increased error in first arrival data and higher RMS error in the model.
- Estimating V_{S30} from V_{P30} assuming constant Poisson's ratio is not recommended at this site because the bedrock and possibly the lowermost alluvium is saturated and, therefore, Poisson's ratio will be highly variable – lowest in the unsaturated sediments, highest in the saturated alluvium if present, and decreasing with depth in the saturated bedrock as fractures/joints become more sparse and thinner.
- Estimated V_{S30} assuming constant Poisson's ratio in the range of 0.25 to 0.4 results in V_{S30} in the 1,654 to 1,170 m/s range. This large variation in potential V_{S30} demonstrates the risks in attempting to estimate V_{S30} from P-wave velocity data, even with a realistic estimate of Poisson's ratio and this approach should only be used as a last resort. In fact, comparing the average V_S model from the S-wave seismic refraction model to estimated V_S models from the P-wave seismic refraction model (assuming that the S-wave refraction model is not too biased due to error) demonstrates that Poisson's ratio may be highly variable. A large increase in velocity occurs at slightly shallower depth in the P-wave refraction model, which indicates that the lowermost alluvium may be saturated. Poisson's ratio of the weathered and saturated rock above a depth of 10 m may be slightly higher than 0.4. Below 10 m, Poisson's ratio decreases with depth and may be between 0.3 and 0.35 below a depth of 15 m.
- For the purpose of site characterization, we recommend using the S-wave refraction model, even though potential error in the model is much higher than desirable. Consideration should be given to acquiring additional seismic refraction data in an area where data quality may be improved, such as the southwestern edge of the outcrop.

Seismic refraction data could be acquired on top of the outcrop; however, the weathering profile at higher elevation may be different than that in the immediate vicinity of the seismic station The average V_{S30} of 1,329 m/s is slightly higher than that estimated from V_{R40}, 1,130 to 1,306 m/s, averaging 1,228 m/s.

- In summary, V_{S30} is estimated to be 1,329 m/s (Site Class B), based on average velocity structure beneath the central portion of the S-wave seismic refraction line.
- Average S-wave velocity between 1 and 31 m to account for at least a 1 m decrease in the thickness of alluvium below the seismic station is 1,484 m/s (Site Class B/A).

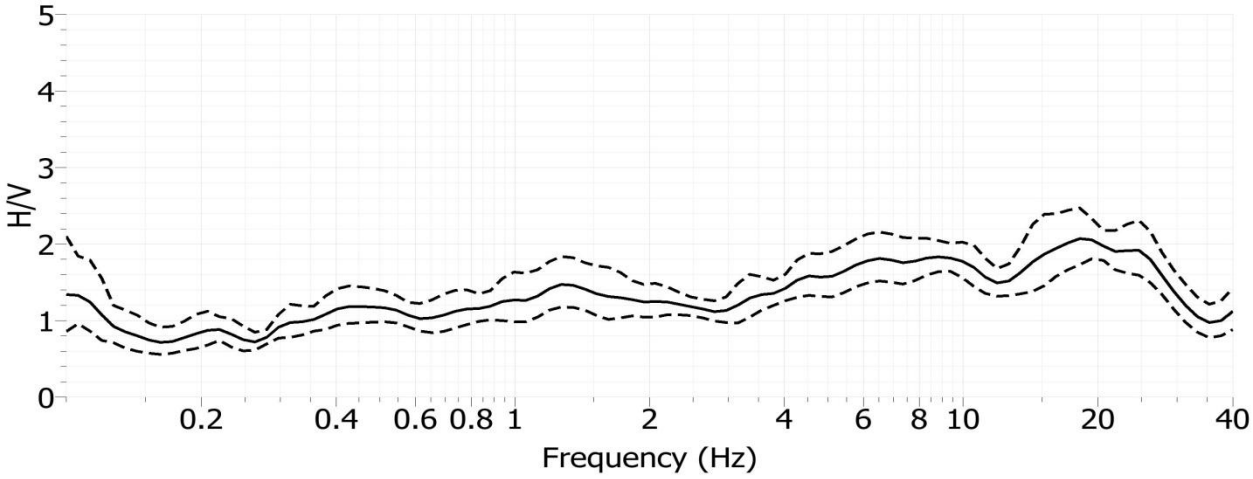

Site CI.DSC, H/V Spectral Ratio, Array DSC-1, Sensor 453

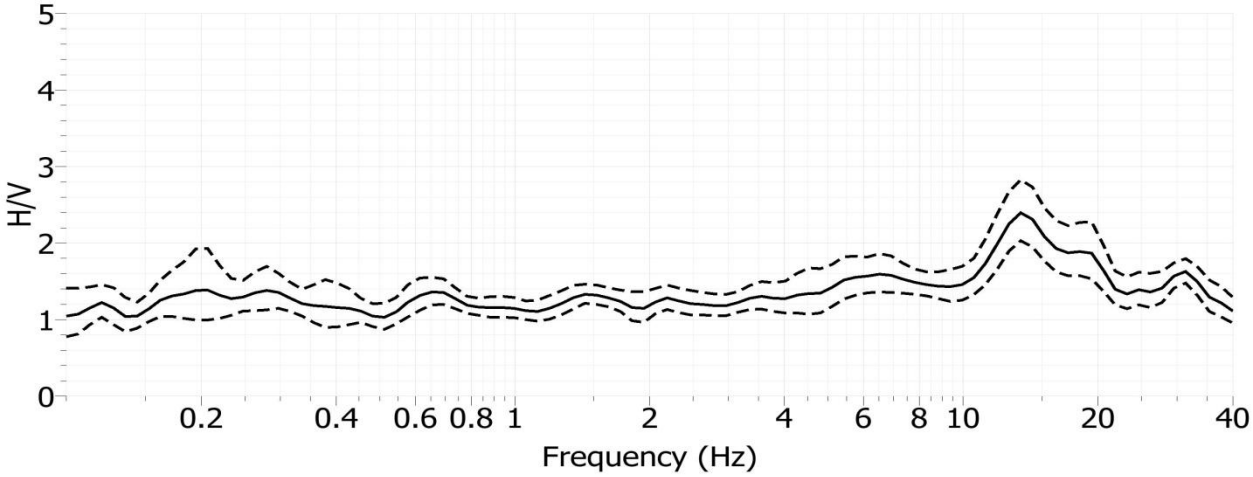

Site CI.DSC, H/V Spectral Ratio, Near Seismic Station, Sensor 507

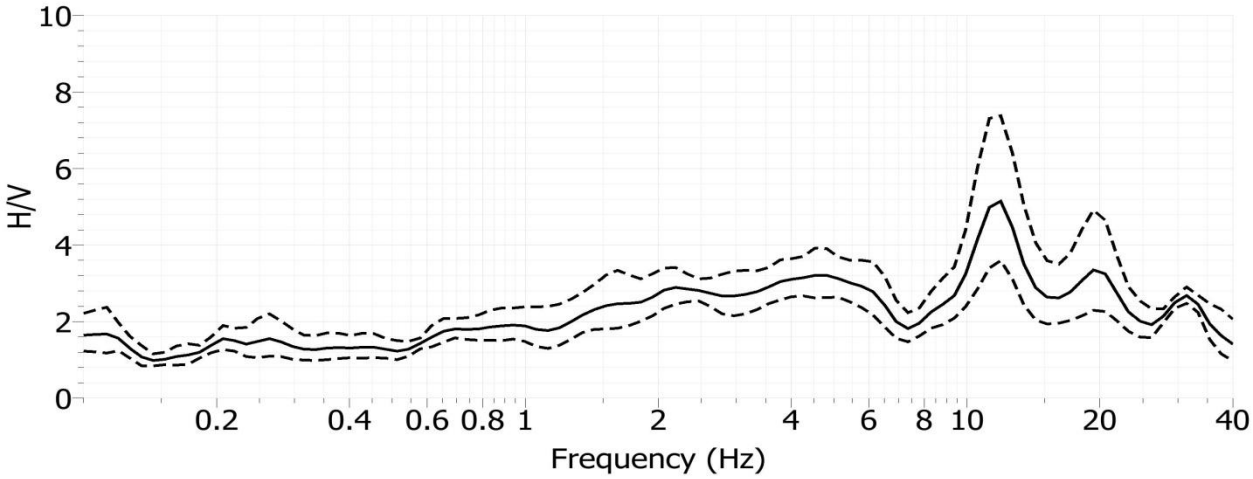

Site CI.DSC, H/V Spectral Ratio, Array DSC-1, Sensor 450

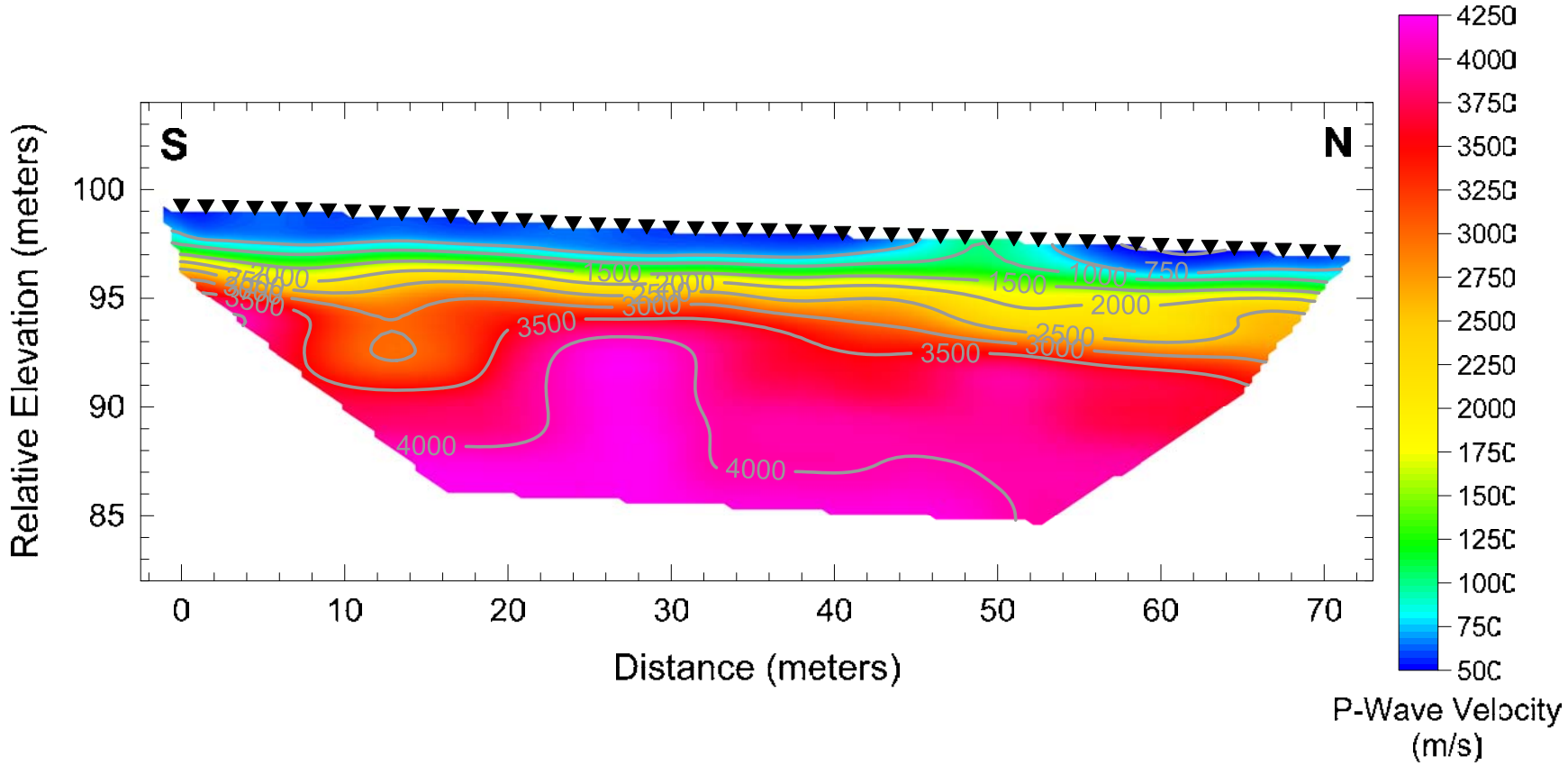

Array DSC-1 – P-wave Tomographic Seismic Refraction Model utilizing Layer Based Starting Model

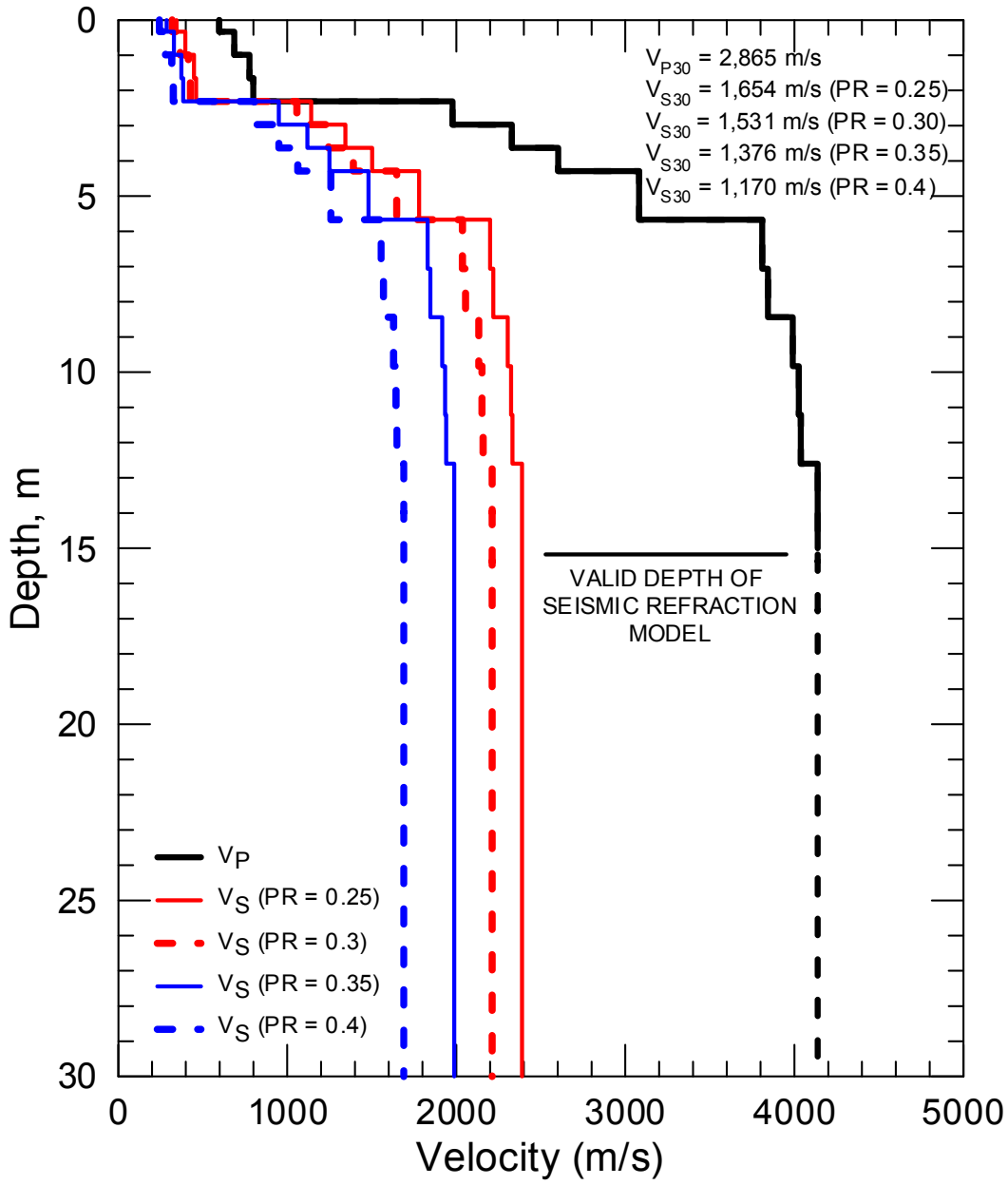

CI.DSC – Average P-wave velocity structure and estimated S-wave velocity structure between a distance of 25.5 and 54 m along the P-wave seismic refraction model for array DSC-1. Although the maximum seismic refraction depth of investigation is limited to about 15 m, P-wave velocity is very high at depth and is not expected to increase significantly between 15 and 30 m. A longer seismic line would be preferred to both more accurately model the high P-wave velocities and image to 30 m depth. P-wave velocity should not be used to estimate S-wave velocity at this site because bedrock and possibly the deeper zone of alluvium are saturated. A Poisson's ratio of 0.35 or greater may be plausible for saturated limestone or dolomite.

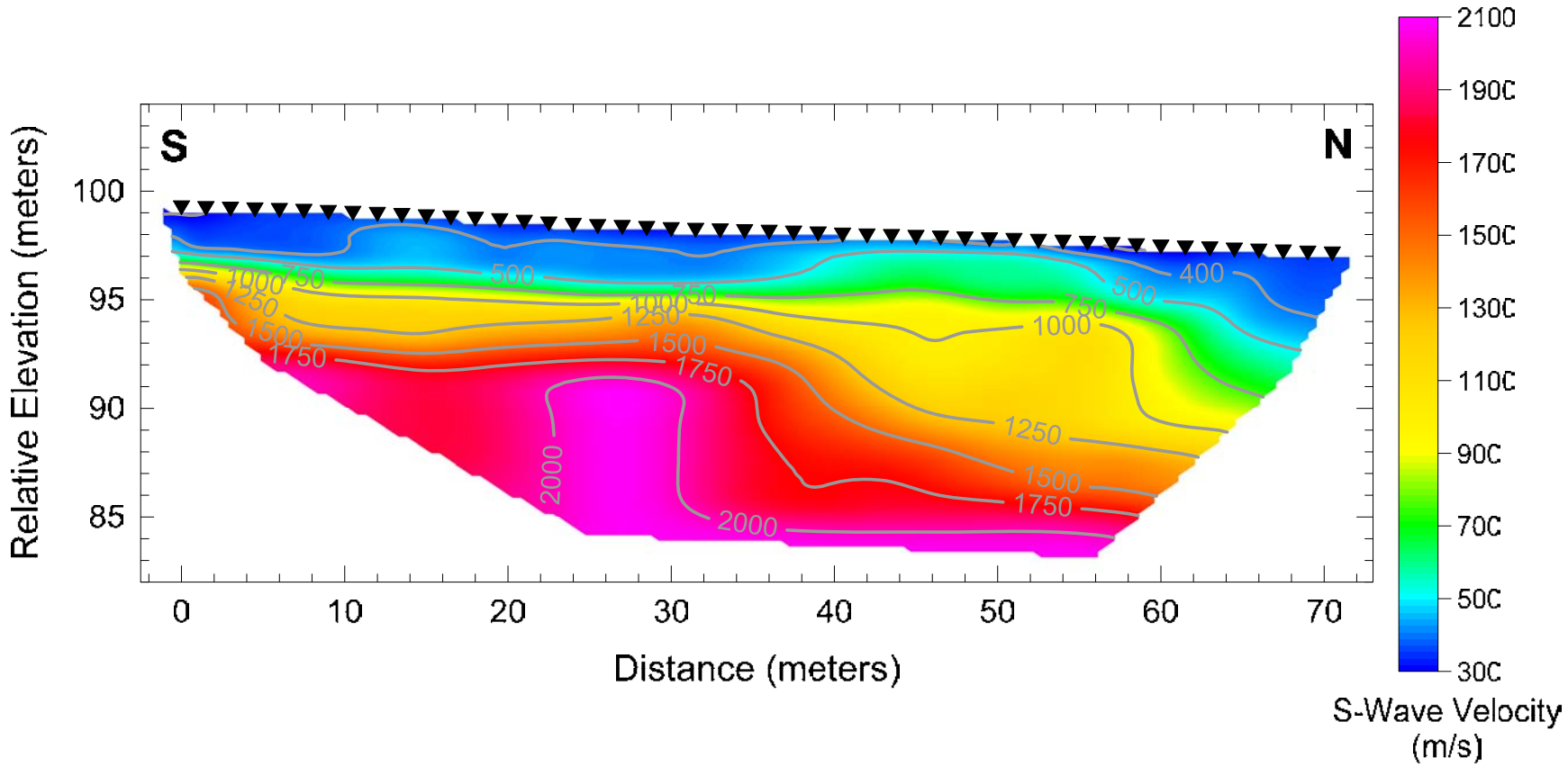

Array DSC-1 – S-wave Tomographic Seismic Refraction Model utilizing Layer Based Starting Model

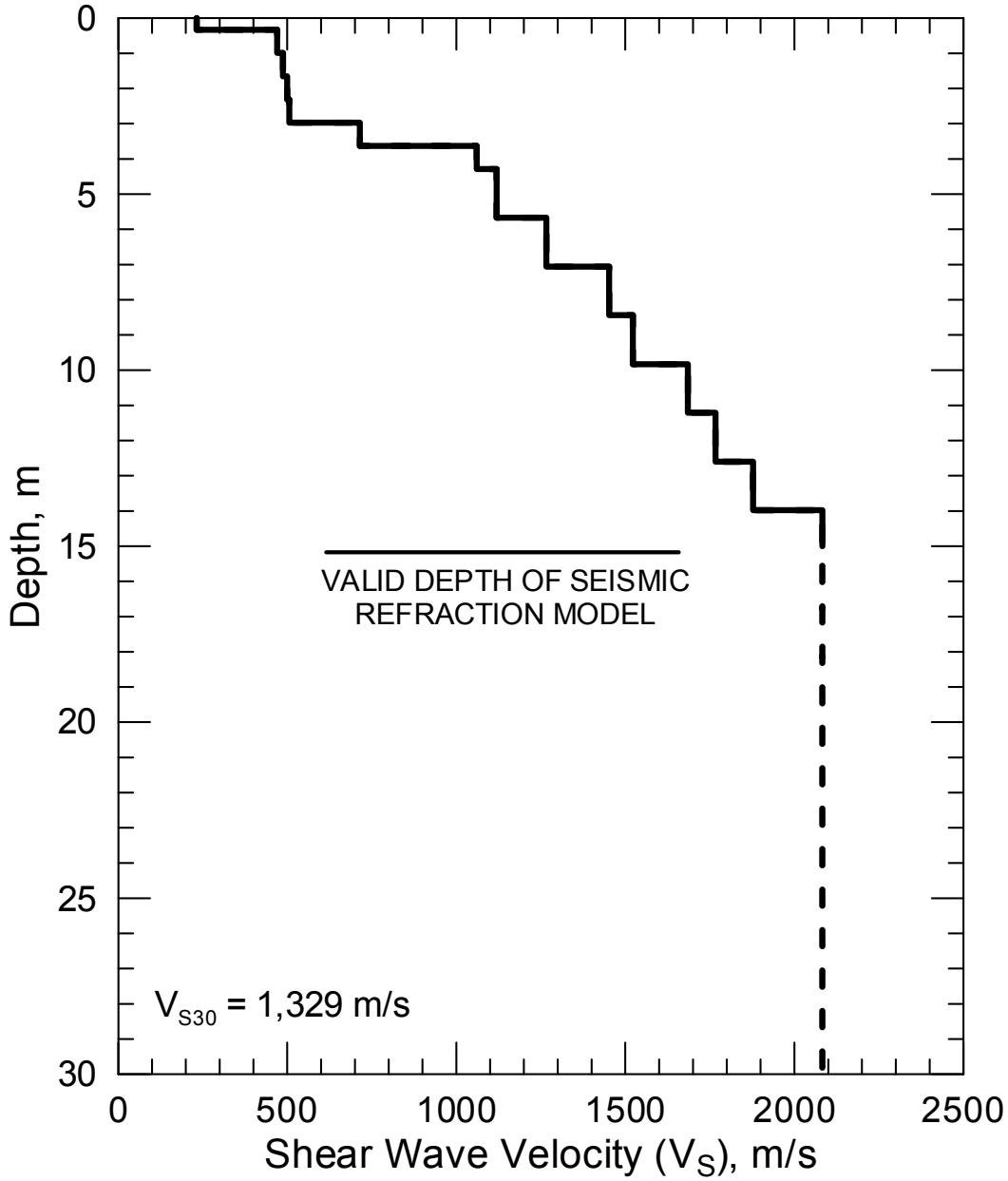

CI.DSC – Average S-wave velocity structure between a position of 25.5 and 54 m along the S-wave seismic refraction model for array DSC-1. Although the maximum seismic refraction depth of investigation is limited to about 15 m, S-wave velocity is very high at depth and is not expected to increase significantly between 15 and 30 m. A longer seismic line would be preferred to both more accurately model the high S-wave velocities and to image to 30 m depth.

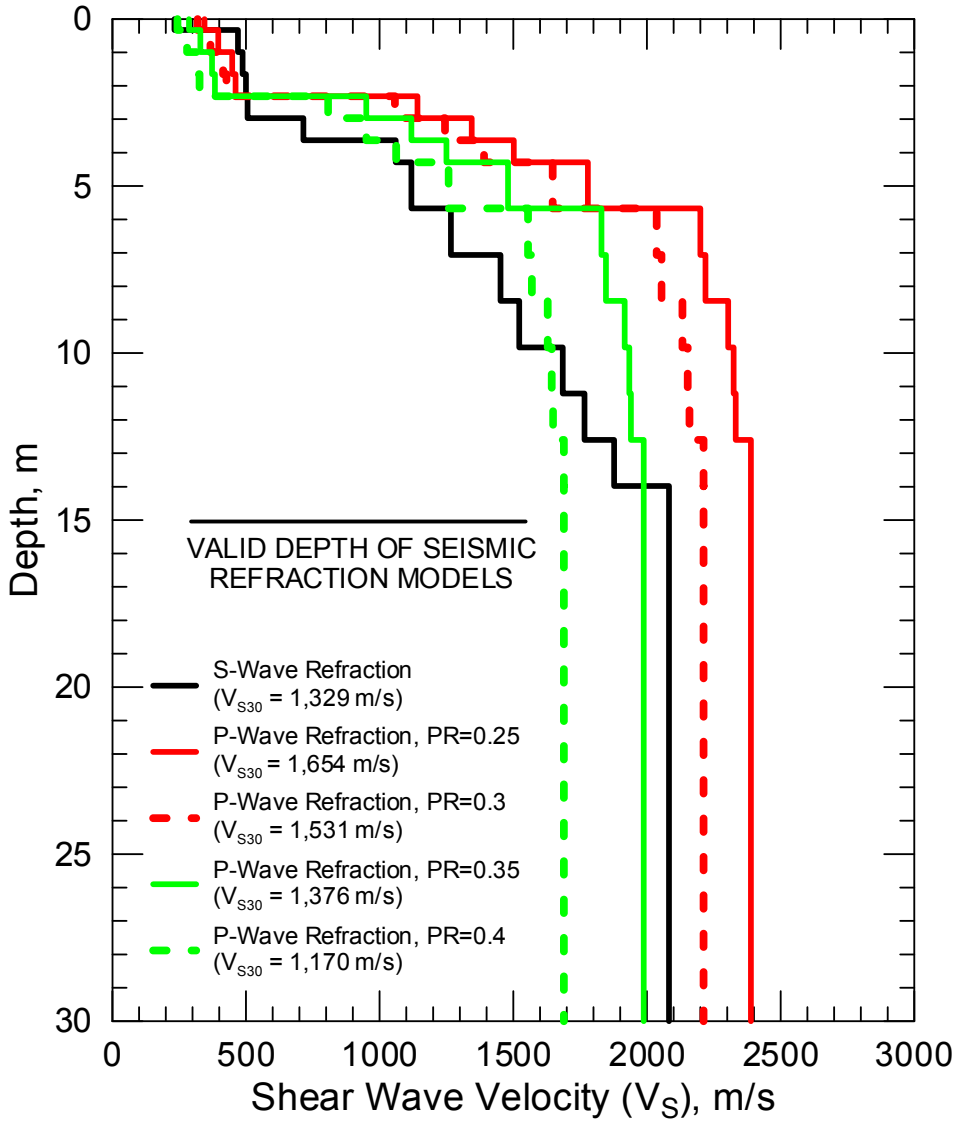

CI.DSC – Comparison of S-wave velocity models derived from the P- and S-wave seismic refraction data. High velocity bedrock is slightly deeper in the S-wave refraction model indicating that alluvium may be saturated immediately above bedrock. Based on data quality, P-wave velocity structure is more accurately defined at the site than S-wave velocity structure from the S-wave refraction survey. Possible model error aside, comparison of the S-wave velocity model and estimated S-wave velocity models from the P-wave seismic refraction survey indicates that Poisson's ratio of the uppermost weathered rock may be slightly higher than 0.4 and decreases with depth as rock becomes more competent, becoming slightly lower than 0.35 at a depth of about 15 m.

Site CI.DVT

Location: Desert View Tower, East of I-8, San Diego County, California

Previous Seismic Sensor Location

Latitude: 33.65915 **Longitude:** -116.10061

(Coordinates provided by USGS – WGS84 coordinate system)

Current Seismic Sensor Location

Latitude: 32.65877 **Longitude:** -116.09984

(Coordinates estimated using Google Earth after field inspection of seismic station – WGS84 coordinate system)

V_{S30} (measured): 625 m/s

V_{S30} (adjusted to more accurately reflect seismic station conditions): 625 m/s (no adjustment necessary, although replacing the S-wave velocity of the upper layer with that of the underlying layer to more accurately reflect conditions at the ends of the seismic array would increase V_{S30} to 679 m/s.)

NEHRP Site Class: C

Geomatrix Code: AGA/AGB

Geologic Conditions/Observations: Seismic station located on outcrop of weathered granitic rock (quartz diorite and granodiorite).

Site Conditions: Rural site located on a bedrock outcrop near the I-8 Freeway. Relatively flat terrain along test area, but hilly terrain in site vicinity.

Geophysical Methods Utilized: HVSR, Seismic Refraction, MASW, ReMi™

Geophysical Testing Arrays:

1. Array DVT-1 (48 channel MASW and P-wave seismic refraction array utilizing 4.5 Hz vertical geophones spaced 1.5 m apart for a length of 70.5 m, forward and reverse shot locations with multiple source offsets and source types and multiple interior shot locations).
2. Passive surface wave data also acquired along MASW array DVT-1 during HVSR data acquisition.
3. Three HVSR measurement locations distributed along array DVT-1.

Legend

- Seismic Station - Approximate Former Location
- Seismic Station - Approximate Current Location
- H/V Spectral Ratio Measurement Location
- MASW and Seismic Refraction

NOTES:
1. WGS 1984 COORDINATE SYSTEM
2. Image Source: ESRI, i-cubed, USDA FSA, USGS, AEX, GeoEye, Getmapping, Aerogrid, IGP

File Name: CI-DVT-I

Date: 6/15/2011

USGS science for a changing world

GEOVision geophysical services

RECOVERY.GOV

SITE MAP
CI•DVT

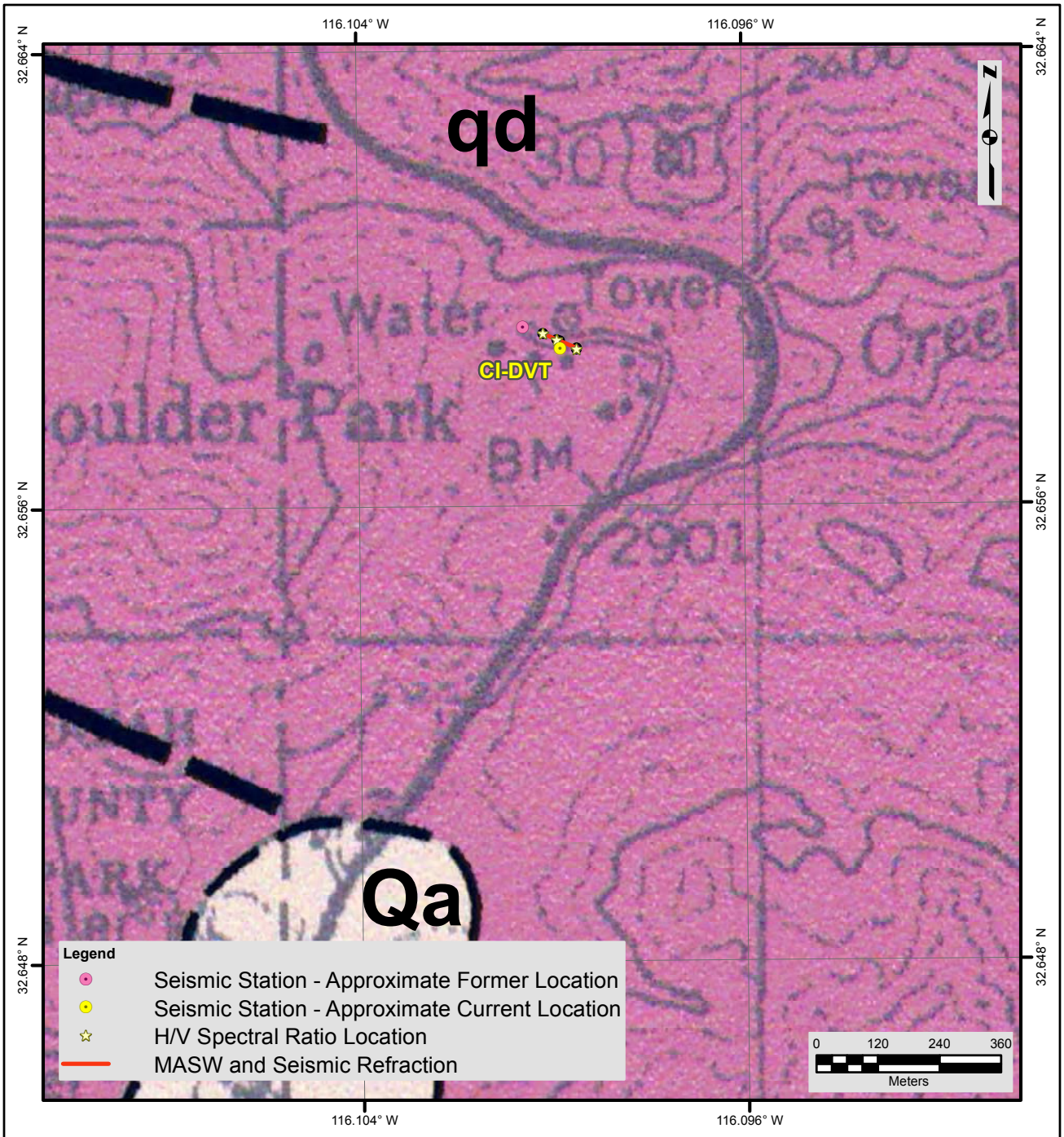

Description of Geologic Map Units

Qa = Quaternary (Holocene) alluvial clay and silt, grading to sandy gravel near mountains
qd =Mesozoic (Cretaceous) quartz diorite and granodiorite

NOTES:
1. WGS 1984 COORDINATE SYSTEM
2. Geologic Map of the Jacumba 15 Minute Quadrangle, San Diego and Imperial Counties, California By Thomas W. Dibblee, Jr., 2008
3. See site map for details of geophysical survey

File Name: CI-DVT

Date: 6/15/2011

USGS science for a changing world

GEOVision geophysical services

RECOVERY.GOV

GEOLOGIC MAP
CI•DVT

Looking south towards HVSR sensor 453 and house containing CI.DVT seismic station

Looking southwest towards array DVT-1 and structure housing CI.DVT seismic sensor

Looking northwest along MASW and seismic refraction array DVT-1

Looking northwest at HVSR station 507

Accelerated weight drop energy source utilized on MASW and seismic refraction array DVT-1

Location of Geophysical Testing Arrays:

Location	Latitude	Longitude
DVT-1, Northwest End of Array	32.65902	-116.10019
DVT-1, Center of Array	32.65890	-116.09984
DVT-1, Southeast End of Array	32.65877	-116.09949
HVSR Sensor 507	32.65875	-116.09949
HVSR Sensor 453	32.65892	-116.09990
HVSR Sensor 450	32.65903	-116.10019

Notes: 1) WGS84 Coordinate System (decimal degrees)
2) Survey accuracy is estimated at 1 to 2 m

Results:

V_S Model

Depth to Top of Layer (m)	Layer Thickness (m)	S-Wave Velocity (m/s)	Inferred P-Wave Velocity (m/s)	Inferred Poisson's Ratio	Inferred Density (g/cm^3)
0	2	233	436	0.3	1.9
2	3	417	780	0.3	2
5	4	546	1022	0.3	2
9	6	665	1245	0.3	2.1
15	9	813	1521	0.3	2.1
24	>6	1252	2342	0.3	2.2

Observations/Discussion:

- The HVSR curves are similar and there is no clear HVSR peak at this site. The absence of an HVSR peak is expected for a rock site. This site, however, has a significant weathering profile and the absence of an HVSR peak may indicate that velocity gradually increases with depth.
- Passive surface wave techniques were not expected to be effective at this site due to both geologic conditions and topographic variation between I-8, located 150 to 200 m from the site, and the test area. Passive surface wave data was, however, acquired on MASW array DVT-1 during HVSR data acquisition.
- Both the ReMi™ and ESAC techniques used to extract surface wave dispersion data from the linear passive surface wave array.
- Interestingly, the surface wave dispersion data from active and passive surface wave datasets are in good agreement at this site.

- Representative dispersion curves were generated for each surface wave data set using a moving average, polynomial curve fitting routine. These individual representative dispersion curves were combined and a representative dispersion curve generated for the combined data set for data modeling.
- P-wave refraction data is somewhat noisy due to heavy wind, traffic noise (on site and nearby freeway), geophone coupling (rock plate), and source limitations (limited access for weight drop). Additionally, there is evidence of out of plane refractors in some seismic refraction seismic records. The seismic refraction survey would have benefited from a longer profile, which was not feasible due to space and source limitations.
- Regardless of limitations, the P-wave refraction survey clearly shows that P-wave velocity generally increases with depth from about 900 m/s near the surface to over 2,000 m/s at a depth of 20 to 25 m. There is, however, a localized, thin zone of lower velocity weathered rock/residual soil in the central portion of the seismic array, which is the closest part of the array to the current seismic sensor location.
- Typical depth of investigation of a 70.5 m long P-wave seismic refraction line is estimated at 15 to 20 m. The model was extended to greater depth by utilizing off-end shots in tomographic inversion and the model clearly shows higher velocity bedrock at depth. However, P-wave velocities at depths greater than 20 m are not accurately resolved as forward and reverse first arrival coverage of the higher velocity bedrock unit was not obtained with the survey design.
- Clear evidence of lateral velocity variation in viewing surface wave energy on MASW seismic records.
- Generally, it was difficult to extract surface wave dispersion data at wavelengths less than about 10 m, likely the result of lateral velocity variation. Surface wave phase velocities were obtained at wavelengths as low as 4 m analyzing offset limited groups of geophones in the vicinity of the center of the array, which corresponds to the low velocity zone on the seismic refraction model and is also closest to the current location of the seismic station.
- Surface wave depth of investigation is about 30 m based on half of maximum wavelength criteria
- The surface wave model is generally consistent with P-wave velocity structure in the central portion of the seismic refraction model.
- V_{S30} is 625 m/s (NEHRP Site Class C).
- The surface wave dispersion data and seismic refraction model indicate that the near surface weathered rock/residual soil at the ends of the seismic line has higher seismic velocity than that in the central portion of the line. Replacing the S-wave velocity of the upper layer in the surface wave model with that of the underlying layer would increase V_{S30} to 679 m/s (NEHRP Site Class C).

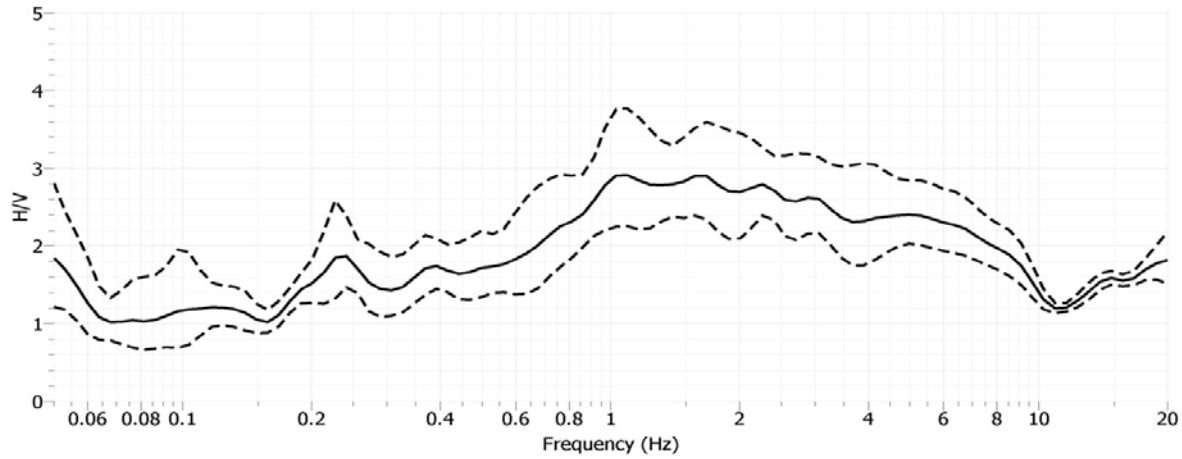

Site CI.DVT, H/V Spectral Ratio, Array DVT -1, Sensor 450

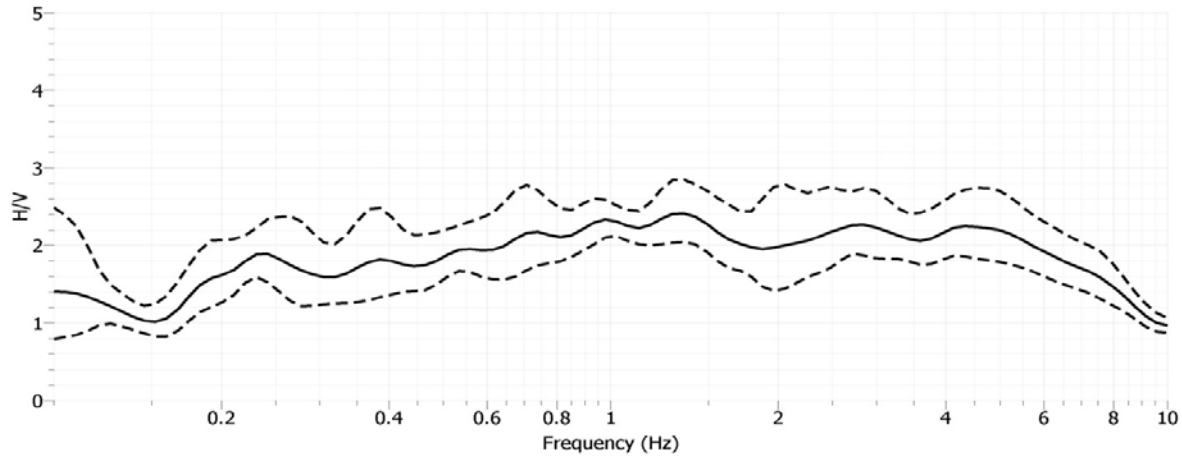

Site CI.DVT, H/V Spectral Ratio, Array DVT -1, Sensor 453

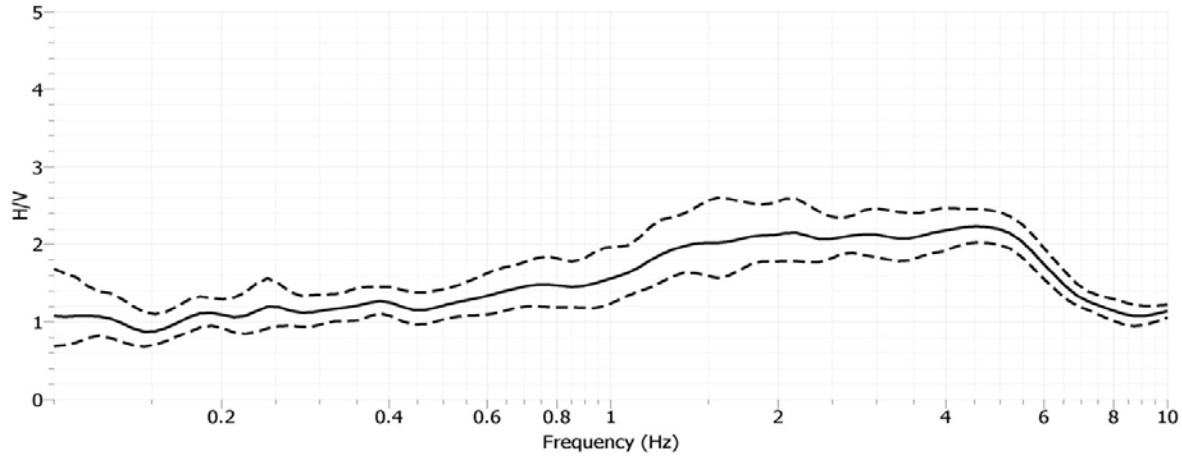

Site CI.DVT, H/V Spectral Ratio, Array DVT -1, Sensor 507

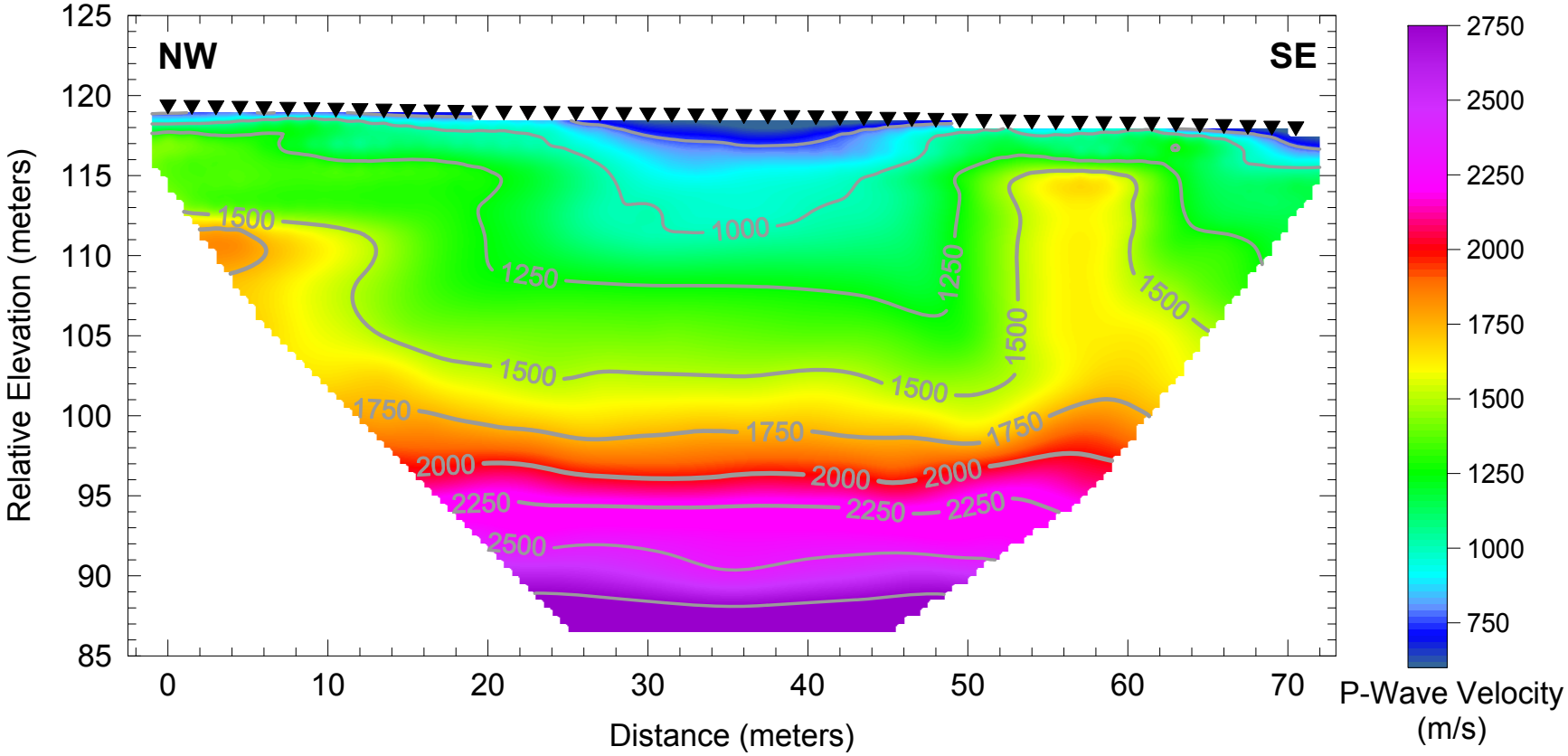

Array DVT-1 – Tomographic Seismic Refraction Model utilizing Smooth Velocity Gradient Starting Model

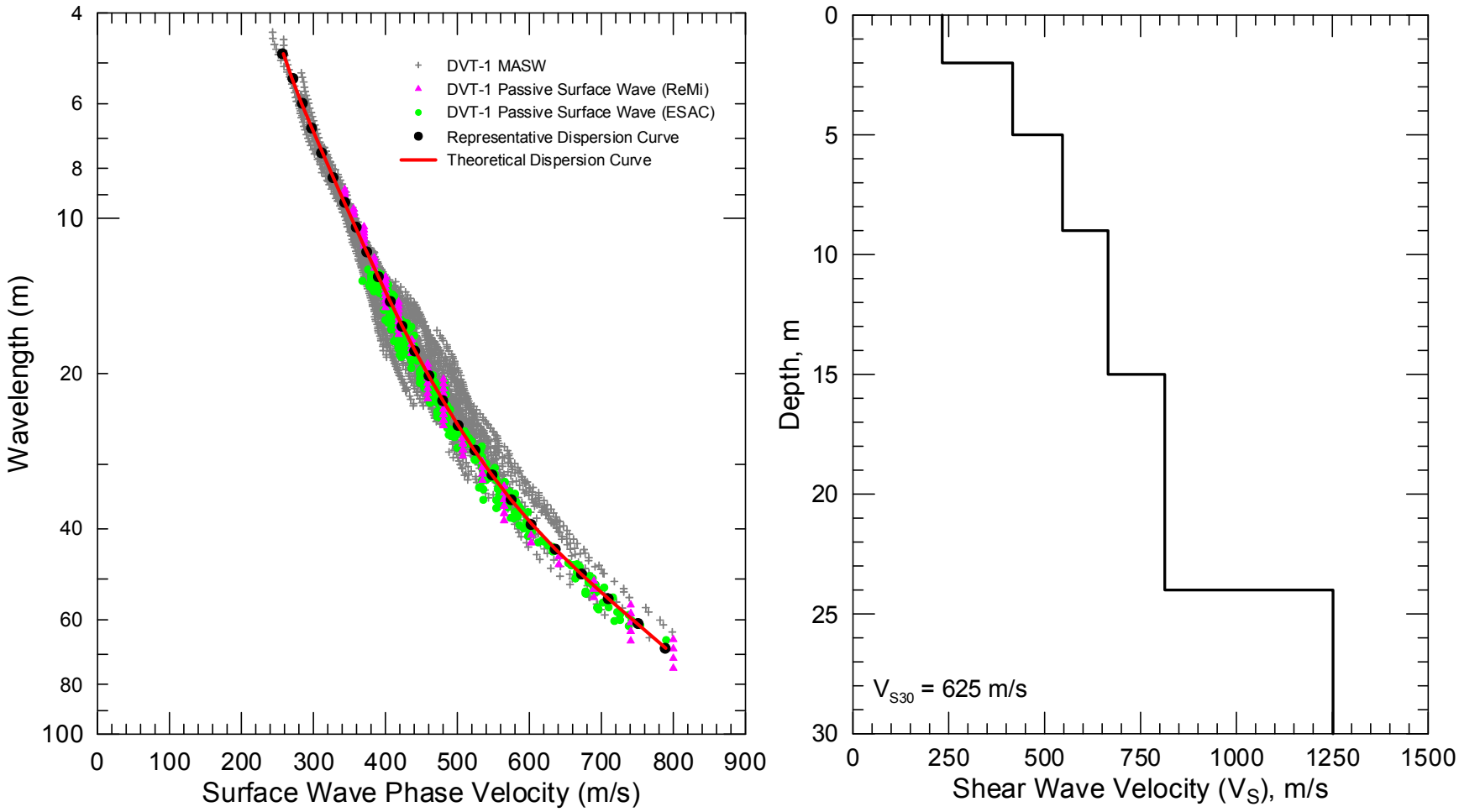

CI.DVT - Field, representative and inverted theoretical surface wave dispersion data (left) and associated V_S model (right)

Site CI.EDW2

Location: Edwards Air Force Base 2, Edwards, California

Latitude: 34.88110 **Longitude:** -117.99388
(Station coordinates provided by USGS, WGS84 coordinate system)

V_{S30} (measured): 1,242 m/s

V_{S30} (adjusted to more accurately reflect seismic station conditions): 1,445 m/s (average S-wave velocity between 1 and 31 m adjusting for 1 m assumed sensor depth).

NEHRP Site Class: B

Geomatrix Code: IGA

Geologic Conditions/Observations: Seismic station located on weathered Mesozoic (Cretaceous) quartz monzonite.

Site Conditions: Rural site. Relatively planar topography in site vicinity. Elevation gently decreases to the southeast in the test area. Some electric noise from nearby facilities.

Geophysical Methods Utilized: HVSR, Seismic Refraction (P- and S-wave), MASW (Rayleigh wave), MALW (Love wave)

Geophysical Testing Arrays:

1. Array EDW2-1 (48 channel MASW and P-wave seismic refraction array utilizing 4.5 Hz vertical geophones spaced 1.5 m apart for a length of 70.5 m, forward and reverse shot locations with multiple source offsets and source types and multiple interior shot locations).
2. Array EDW2-1 (48 channel MALW and S-wave seismic refraction array utilizing 10 Hz horizontal geophones spaced 1.5 m apart for a length of 70.5 m, forward and reverse shot locations with multiple source offsets and multiple interior shot locations). Coincident with P-wave array of same name.
3. Three HVSR measurement locations: two distributed along array EDW2-1 and the other adjacent to the seismic station.

Legend

- Seismic Station - Approximate Location of Record
- H/V Spectral Ratio Location
- MASW and Seismic Refraction Array (P- and S-wave)

NOTES:
1. WGS 1984 COORDINATE SYSTEM
2. Image Source: (c) Microsoft Corporation and its data suppliers

File Name: CI-EDW2-I

Date: 2/24/2012

USGS science for a changing world

GEOVision geophysical services

RECOVERY.GOV

SITE MAP
CI•EDW2

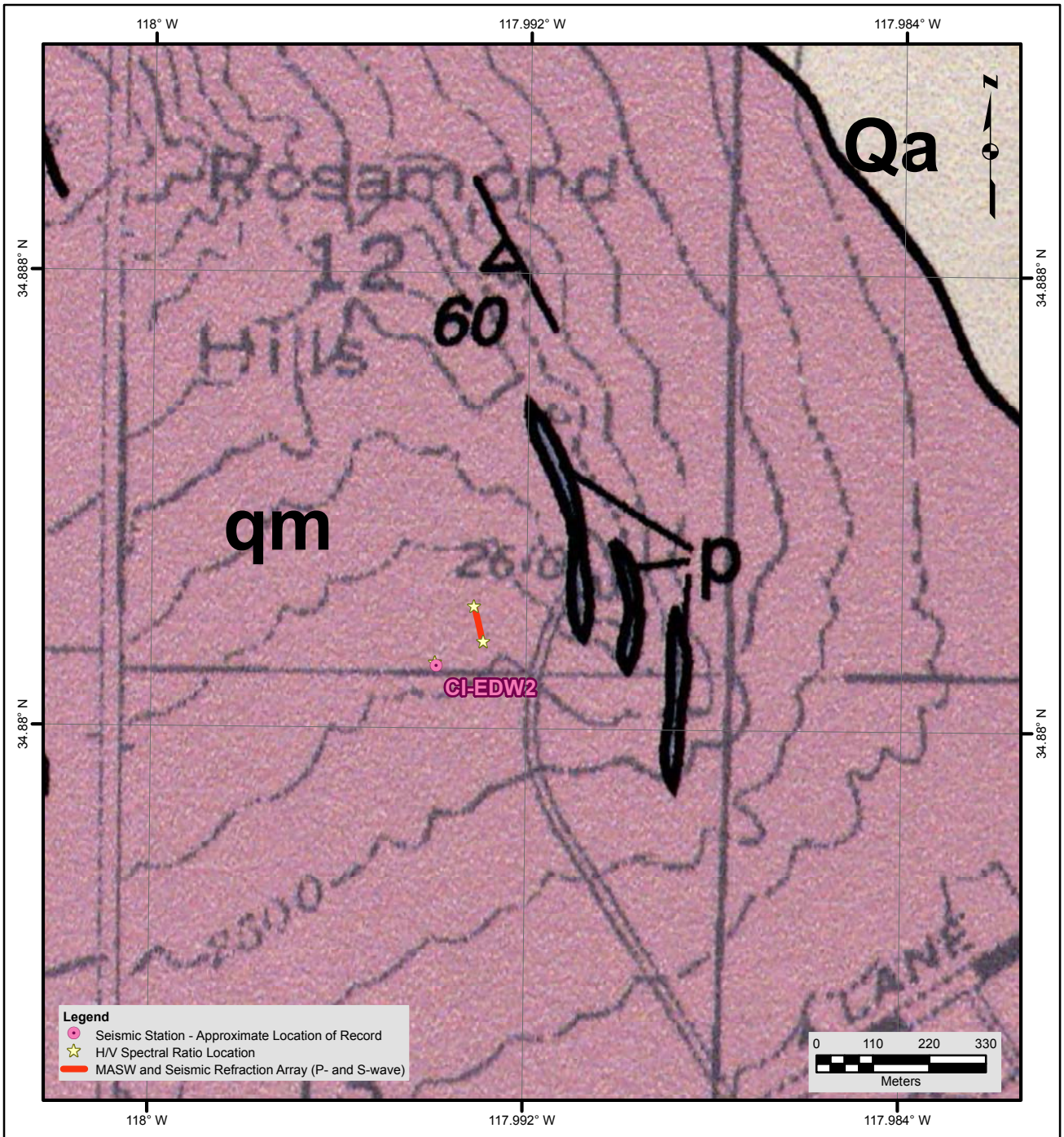

Description of Geologic Map Units

Qa = Quaternary (Holocene) alluvial silt, sand and gravel of valley areas and flood plains
p = Mesozoic (Jurassic to Cretaceous) pegmatite and aplite dikes swarms, intrusive into quartz monzonite
qm = Mesozoic (Jurassic to Cretaceous) quartz monzonite, massive, holocrystalline, medium- to course-grained

NOTES:
1. WGS 1984 COORDINATE SYSTEM
2. Geologic Map of the Rosamond & Rogers Lake 15 Minute Quadrangles, Kern and Los Angeles Counties, California by Thomas W. Dibblee, Jr., 2008
3. See site map for details of geophysical survey

File Name: CI-EDW2

Date: 2/24/2012

USGS science for a changing world

GEOVision geophysical services

GEOLOGIC MAP
CI•EDW2

RECOVERY.GOV

CI.EDW2 Seismic Station

HVSR sensor 453 near seismic station

Looking northwest along P-wave refraction/MASW array EDW2-1 towards HVSR sensor 450

Looking southeast along array EDW2-1

S-wave refraction and MASW data acquisition on array EDW2-1

Location of Geophysical Testing Arrays:

Location	Latitude	Longitude
EDW2-1, Northwest End of MASW/Refraction Array	34.88214	-117.99308
EDW2-1, Center of MASW/Refraction Array	34.88184	-117.99299
EDW2-1, Southeast End of MASW/Refraction Array	34.88153	-117.99290
HVSR Sensor 450	34.88152	-117.99288
HVSR Sensor 453	34.88116	-117.99391
HVSR Sensor 507	34.88215	-117.99309

Notes: 1) WGS84 Coordinate System (decimal degrees)
2) Survey accuracy is estimated at 2 to 3 m.

Results:

V_S Model from MALW (Love Wave) Sounding

Depth to Top of Layer (m)	Layer Thickness (m)	S-Wave Velocity (m/s)	Inferred P-Wave Velocity (m/s)	Assumed Poisson's Ratio	Assumed Density (g/cm^3)
0	0.75	216	404	0.3	1.8
0.75	3.25	618	1157	0.3	2.0
4	4	849	1589	0.3	2.1
8	>22	2054	3842	0.3	2.4

Notes: 1) Depth of investigation is about 25 to 30 m.
2) Bottom layer is a half space.

Average V_P and Estimated V_S Models from Central Portion of P-wave Seismic Refraction Line (Model Developed using Layered Starting Model)

Depth to Top of Layer (m)	Layer Thickness (m)	P-Wave Velocity (m/s)	Estimated S-Wave Velocity (m/s)			
			Poisson's Ratio = 0.25	Poisson's Ratio = 0.30	Poisson's Ratio = 0.3333	Poisson's Ratio = 0.35
0.00	0.51	543	314	290	272	261
0.51	1.02	928	536	496	464	446
1.53	1.02	1313	758	702	657	631
2.55	1.02	1413	816	755	706	679
3.57	1.02	1450	837	775	725	697
4.59	1.02	1476	852	789	738	709
5.61	1.02	1491	861	797	745	716
6.63	2.14	1501	866	802	750	721
8.77	2.14	2730	1576	1459	1365	1311
10.91	2.14	3824	2208	2044	1912	1837
13.05	2.14	4096	2365	2190	2048	1968
15.19	2.14	4219	2436	2255	2109	2027
17.33	2.14	4436	2561	2371	2218	2131
19.47	Half Space	4436	2561	2371	2218	2131

Observations/Discussion:

- There are no peaks in the HVSR data. HVSR data quality is best at sensor location 453 (near seismic station) and 507 (northwest end of array EDW2-1).
- Field observations indicated that the MASW (Rayleigh wave) technique may not be effective at this site and, therefore, both P- and S-wave seismic refraction surveys were conducted and MALW (Love wave) data acquired.
- P-wave seismic refraction first arrival data are of excellent quality. S-wave seismic refraction first arrival data quality were not considered good enough to use for site characterization purposes. However, review of S-wave first arrival data and comparison to P-wave first arrival data indicated that average Poisson's ratio is likely in the 0.3 to 0.333 range and that S-wave velocity exceeds 2,000 m/s at depth. It was possible to extract Love wave dispersion data from the dataset, although data were somewhat noisy.
- The P-wave seismic refraction data for array EDW2-1 were modeled using a tomographic inversion routine with a layer-based starting model. The seismic refraction model was extended to far offset shot locations to extend depth of investigation. It should be noted that a larger geophone spacing, rather than the utilization of far offset shot locations, is preferred for extending depth of investigation, when applying tomographic inversion routines. However, the seismic refraction data were acquired in conjunction with surface wave data, where a shorter array length is preferred.

- The P-wave seismic refraction survey design allowed P-wave velocity to be imaged to a maximum depth of about 21 m. The seismic refraction model indicates that P-wave velocity is nominally about 550 m/s at the surface and increases to 1,250 m/s at a depth of 1 to 4 m, 2,000 m/s at a depth of 7 to 10 m and over 4,000 m/s at a depth of 11 to 13 m. The maximum P-wave velocity in the models is about 4,500 m/s. A velocity this high would be more accurately determined with a longer line.
- There is some lateral velocity variation at the site, particularly a slight thickening of the lower velocity weathered zone to the southeast and slightly variable thickness of sediment/fill cover over weathered rock.
- V_{P30} was estimated between 21 and 52.5 m on the P-wave refraction model that used a layered starting model, by projecting the velocity at 20 m depth to 30 m depth. Over this interval, V_{P30} ranges from about 2,243 to 2,451 m/s, about a 14% variation over a 31 m long segment of the array. An average V_P model was developed over the 21 to 52.5 m distance interval by averaging the travel time through each model cell at a particular depth and average V_{P30} was determined to be 2,445 m/s.
- An average V_S model was estimated from the average V_P model using constant Poisson's ratio in the range of 0.25 to 0.35. Estimating V_{S30} from V_{P30} assuming constant Poisson's ratio in the range of 0.25 to 0.35 results in V_{S30} in the 1,412 to 1,223 m/s range. This large variation in potential V_{S30} demonstrates the risks in attempting to estimate V_{S30} from P-wave velocity data. Review of the S-wave refraction data indicated that Poisson's ratio likely averages 0.3 to 0.333. Additionally, shallow groundwater, which could slightly increase Poisson's ratio in the weathered rock, is not expected at this site.
- Noise conditions at the site were not sufficient for application of passive surface wave techniques.
- An attempt was made to reduce the MASW (Rayleigh wave) data and a Rayleigh wave phase velocity dispersion curve was developed. However, the dispersion curve could not be modeled at long wavelengths using the fundamental mode assumption and there was no clear jump to a higher mode. There is a distinct possibility of modal superposition occurring at long wavelengths/low frequencies. Occasionally, in this case modeling the dispersion curve using the average mode assumption can result in a more accurate velocity of the half space. The average mode assumption is not commonly made and we only apply it when modal superposition appears to occur at long wavelengths and the average mode assumption only significantly changes the V_S of the half space. There are several problems in attempting to model the dispersion curve with the average mode assumption including: sensitivity of relative higher mode amplitudes to Poisson's ratio, effect of lateral velocity variation, assumptions made in estimating the amplitude of surface wave mode are not necessarily valid (e.g. plane Rayleigh wave and not source-receiver geometry affects). At this site, the average mode assumption resulted in too much change to the velocity structure, relative to fundamental mode assumption, to be considered valid and, therefore, a reliable model could not be developed for the Rayleigh wave data.
- Even though a model was not developed for the Rayleigh wave dispersion curve, the phase velocity of a 40 m wavelength Rayleigh wave was determined to average about 1,175 m/s. Assuming that the fundamental mode prevails at 40 m wavelength, V_{S30} is estimated to be 1,228 using the $V_{S30} = 1.045V_{R40}$ relationship presented in Brown, et al,

2000. Forward modeling indicates that the fundamental mode V_{R40} may be overestimated by up to about 5% due to possible modal superposition.

- MALW (Love wave) data were expected to be dominated by the fundamental mode, given the velocity structure inherent in the seismic refraction model. Love wave data were, however, noisy and it was difficult to obtain Love wave dispersion data at wavelengths greater than 60 to 75 m.
- The minimum wavelength surface wave phase velocity data extracted from the 48-channel MALW array is about 14 m. Data reduction using seismic records from smaller hammer sources and a limited offset receiver array (i.e. less active geophones) allowed extraction of surface wave dispersion data to a minimum wavelength of about 4.5 m.
- There is nominally about 100 to 125 m/s scatter in MALW dispersion data likely due to the effects of lateral velocity variation.
- A representative dispersion curve was generated for the MALW data set using a moving average, polynomial curve fitting routine and used for modeling.
- Surface wave depth of investigation is assumed to be about 30 m. It does appear as though the MALW technique required longer wavelength Love wave phase velocity data to image to 30 m depth than the Rayleigh wave technique requires. The maximum wavelength Love wave phase velocity used for modeling was about 80 m, which may only be sufficient to image in the 25 to 30 m depth range. A 60 m wavelength is the minimum wavelength Rayleigh wave phase velocity required to image to 30 m depth.
- V_{S30} from the MALW V_S model is 1,242 m/s (Site Class B).
- Average S-wave velocity between 1 m and 31 m from the MALW V_S model, to account for assumed seismic sensor depth, is 1,445 m/s (Site Class B).
- V_{S30} estimated from the MALW V_S model compares favorably with that estimated from V_{R40} and that estimated from the P-wave seismic refraction model with assumed constant Poisson's ratio in the 0.3 to 0.333 range.
- The MALW and seismic refraction V_S models are in reasonable agreement, although the MALW model slightly underestimated the V_S of the half space relative to the seismic refraction model.
- For site characterization purposes, we recommend using the S-wave velocity structure derived from the MALW model, which is conservative (low) relative to that estimated from the S-wave refraction model.
- The velocity structure at this site makes it a good location to further investigate modal superposition in Rayleigh wave dispersion data and possible mechanisms for dealing with it. A longer P-wave seismic refraction line and another attempt at acquiring S-wave refraction data would be beneficial.

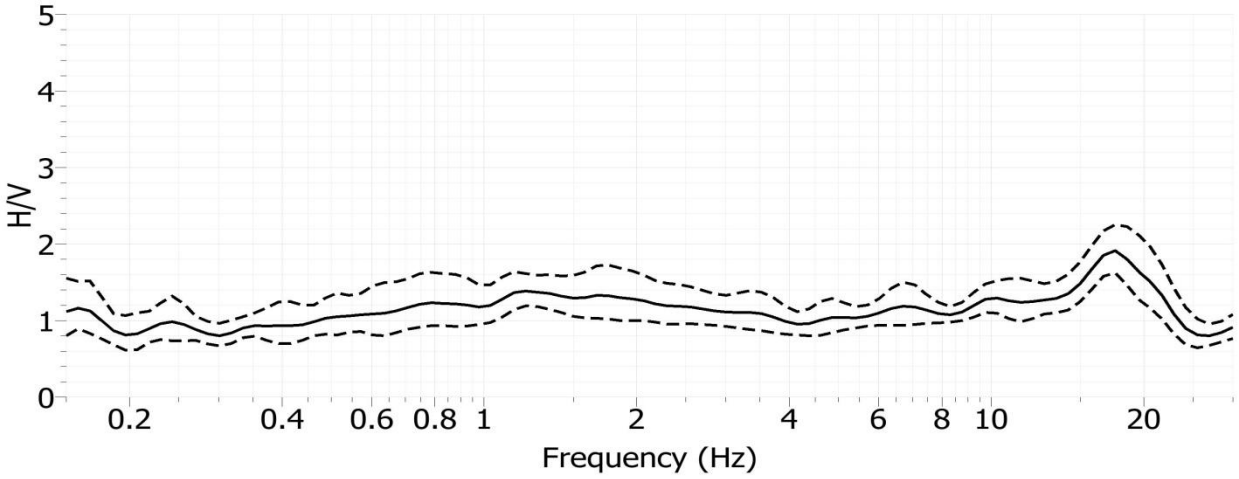

Site CI.EDW2, H/V Spectral Ratio, Array EDW2 -1, Sensor 507

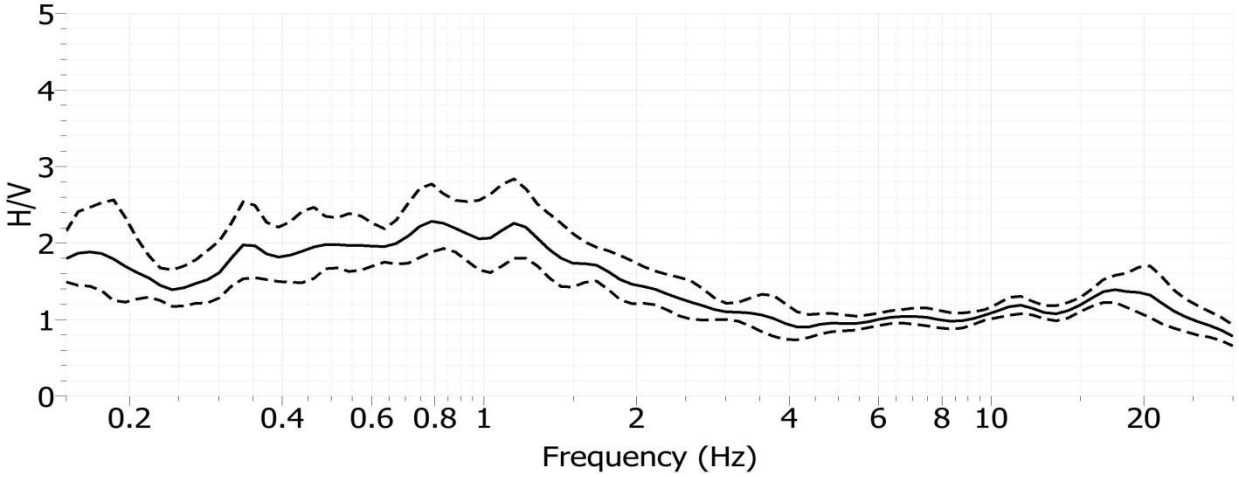

Site CI.EDW2, H/V Spectral Ratio, Array EDW2-1, Sensor 450

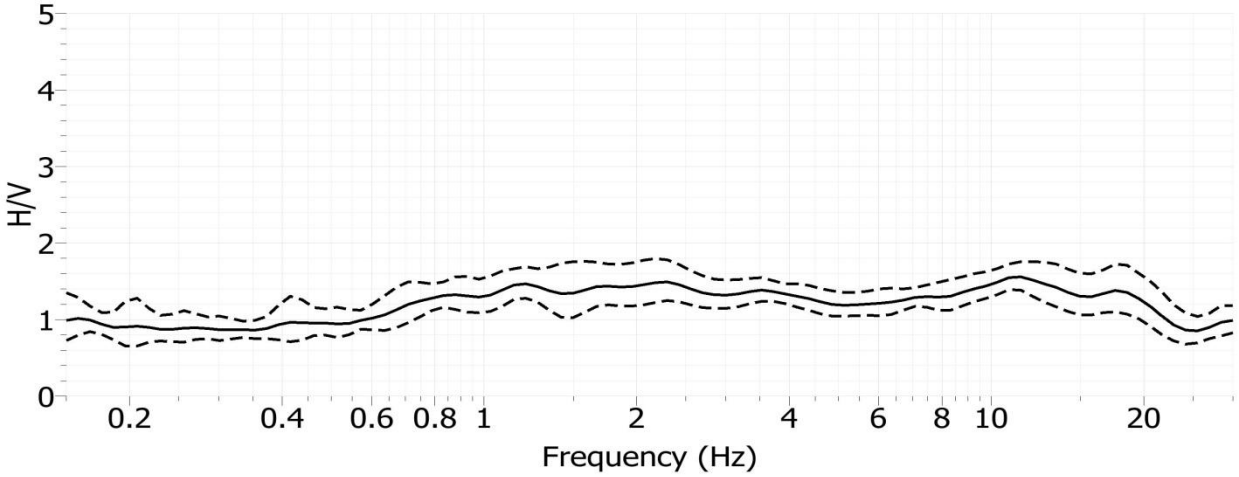

Site CI.EDW2, H/V Spectral Ratio, Near Seismic Station, Sensor 453

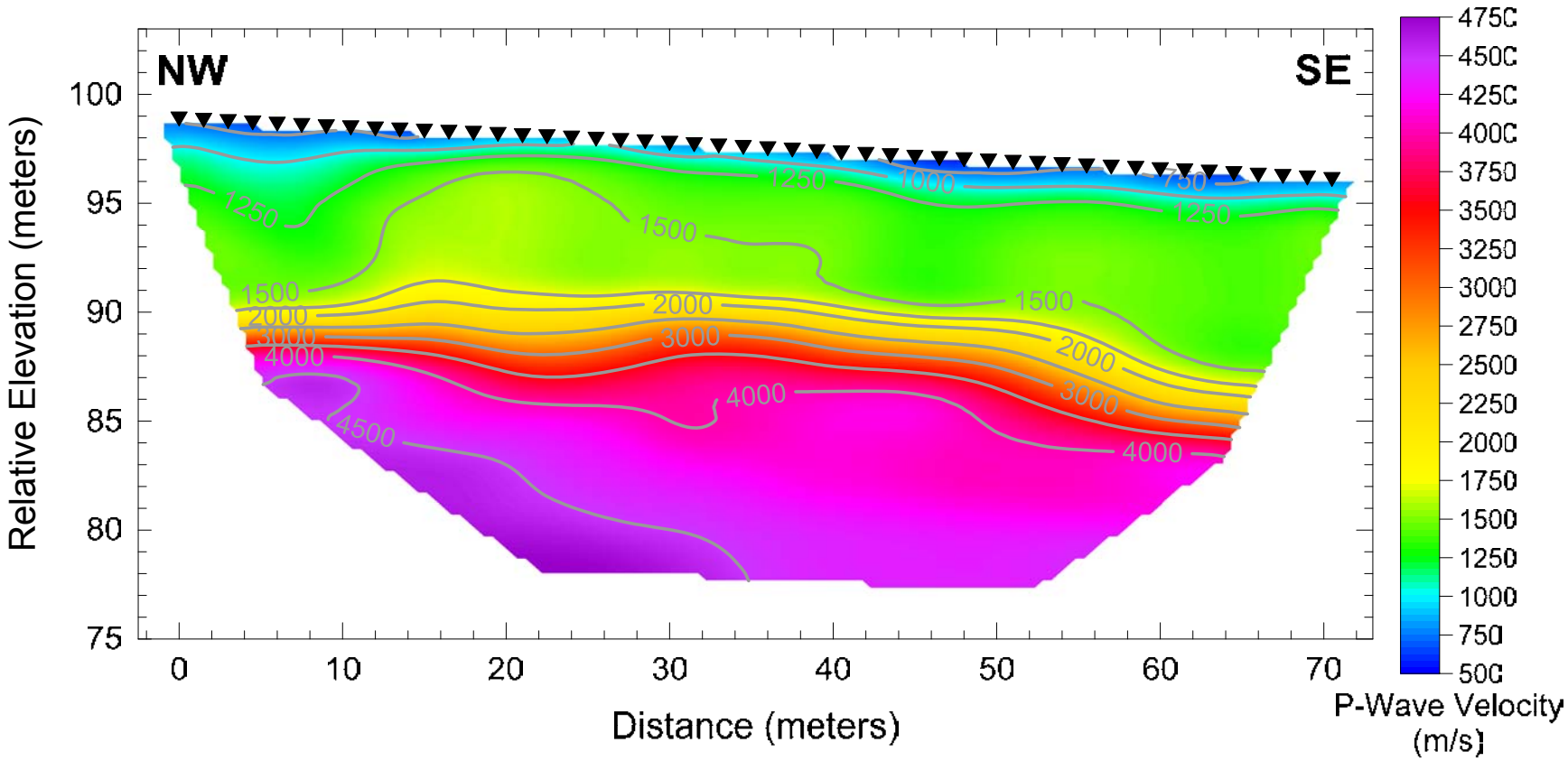

Array EDW2-1 – Tomographic seismic refraction model utilizing layer based starting model

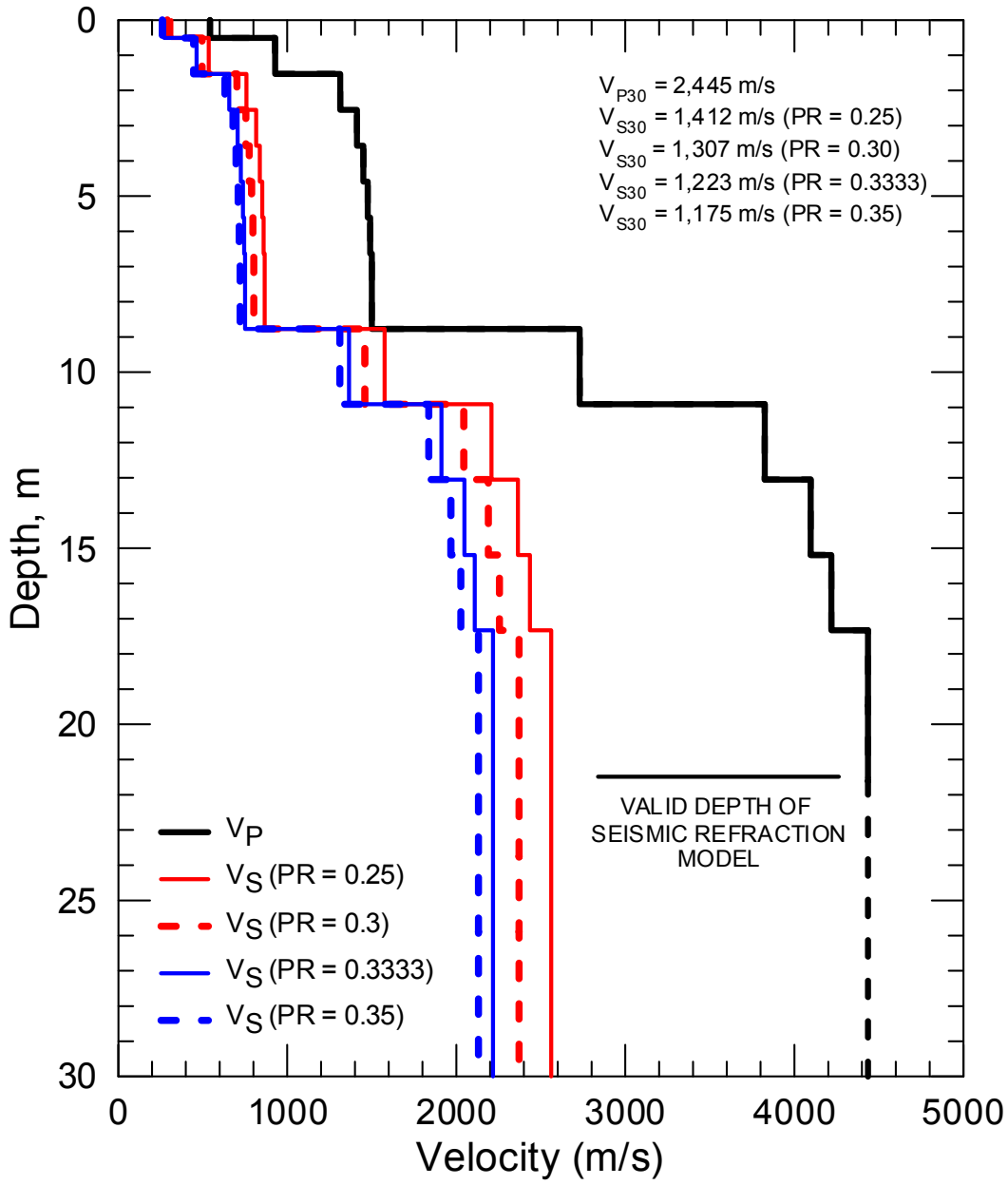

CI.EDW2 – Average P-wave velocity structure and estimated S-wave velocity structure between a position of 21 and 51.5 m on the P-wave seismic refraction model for array EDW2-1. Although the maximum seismic refraction depth of investigation is limited to about 21 m, P-wave velocity is very high at depth and is not expected to increase significantly between the valid depth of investigation and 30 m. A longer seismic line would be preferred to both more accurately model the high P-wave velocities and to image to 30 m depth.

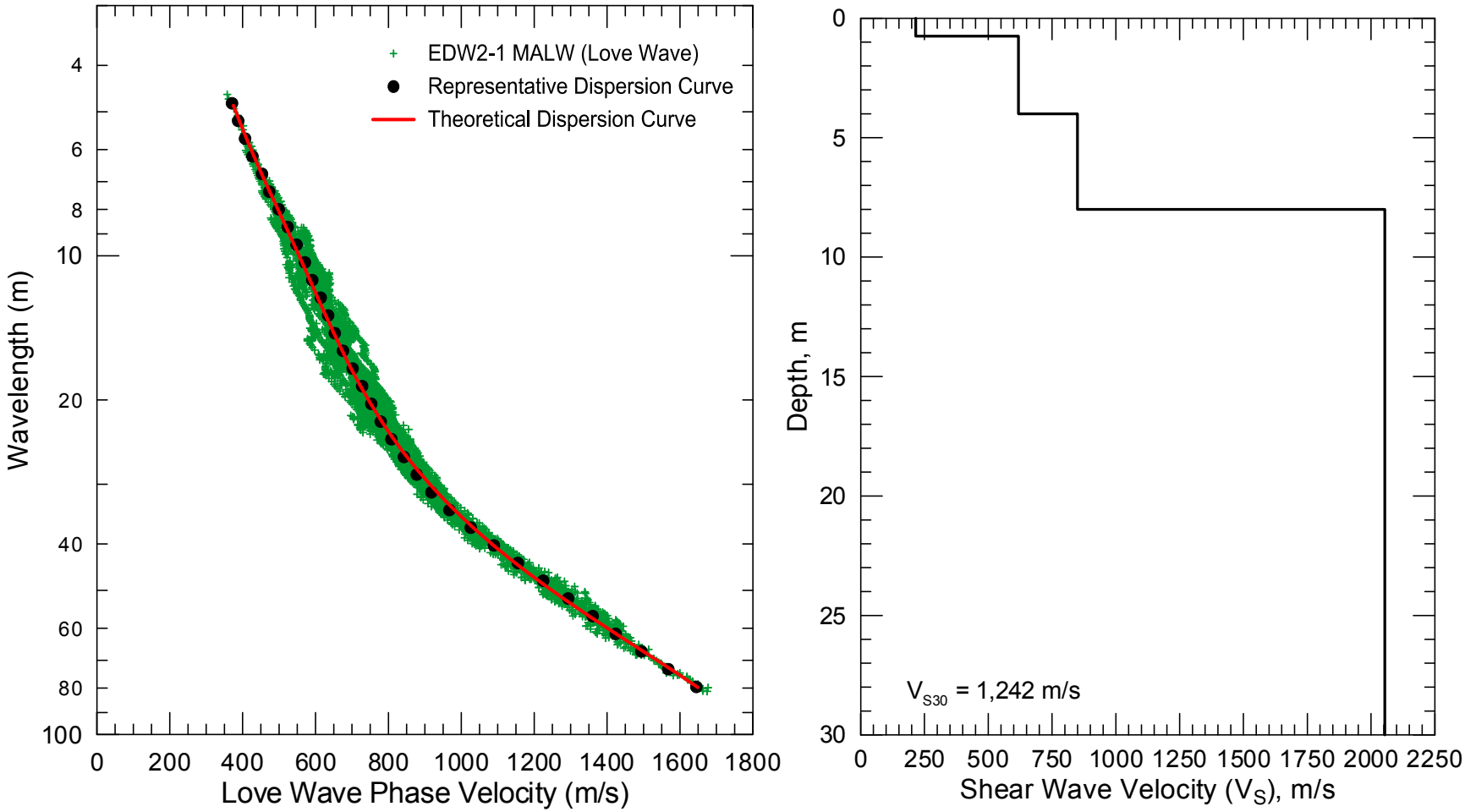

CI.EDW2 - Field, representative and inverted theoretical surface wave dispersion data (left) and associated V_S model (right)

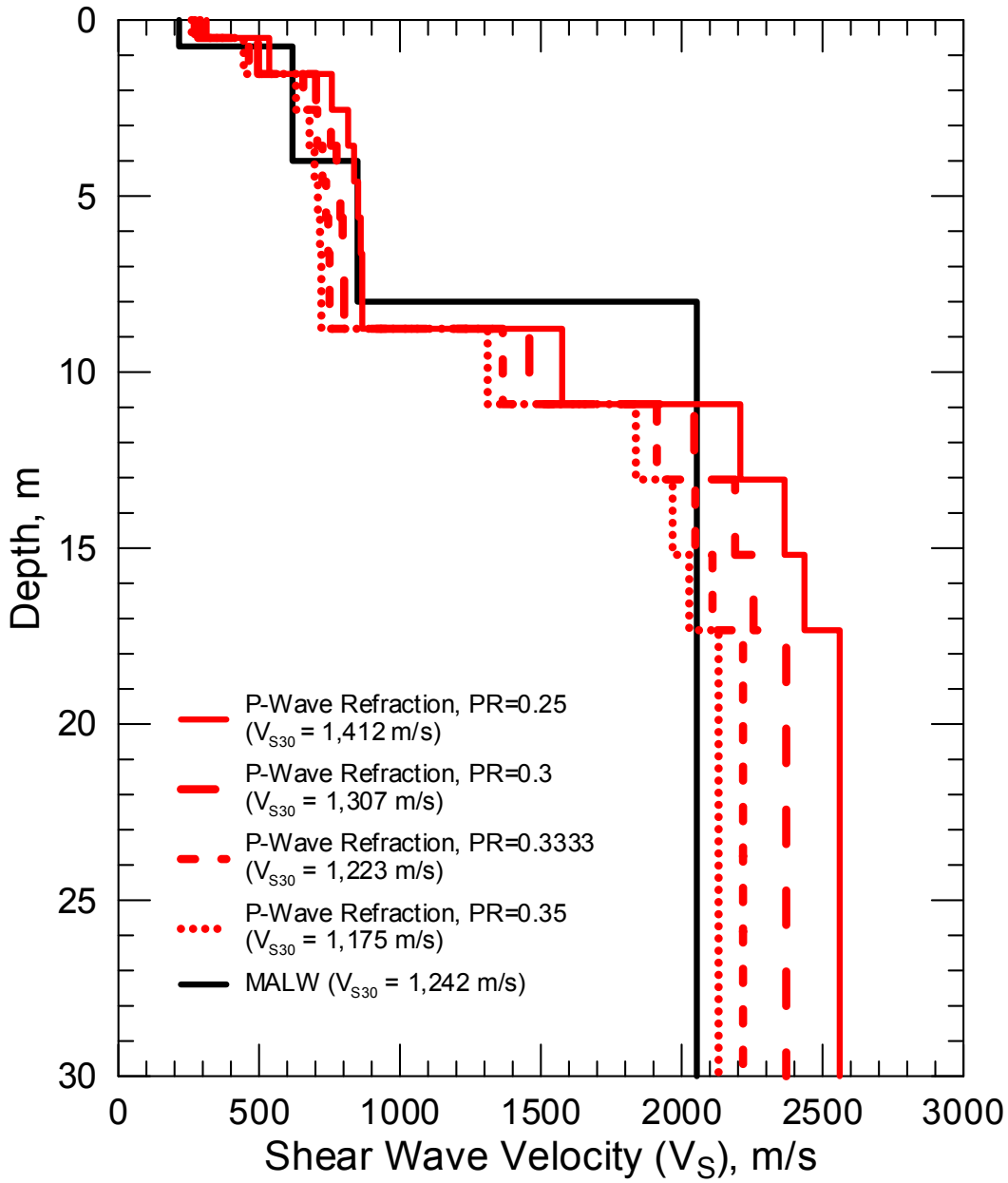

CI.EDW2 – Comparison of S-wave velocity models derived from the MALW (Love wave) and P-wave seismic refraction surveys

Site CI.EML

Location: El Monte County Park, San Diego County, California

Latitude: 32.89083 **Longitude:** -116.84566
(Station coordinates provided by USGS, WGS84 coordinate system)

V_{S30} (measured): 805 m/s

V_{S30} (adjusted to more accurately reflect seismic station conditions): 1,188 m/s (average S-wave velocity between 2 and 32 m adjusting for 2 m assumed sensor depth).

NEHRP Site Class: B

Geomatrix Code: IVA

Geologic Conditions/Observations: Seismic station located on thin layer of young Quaternary (Holocene) alluvium over Cretaceous metavolcanic rocks. It is possible that the seismic sensor is placed on rock.

Site Conditions: Rural site. Seismic station located at the toe of a slope of large hill of metavolcanic rock. Seismic testing conducted along the toe of slope with minimal elevation variation along the profile.

Geophysical Methods Utilized: HVSR, Seismic Refraction (P- and S-wave), MASW (Rayleigh wave), MALW (Love wave)

Geophysical Testing Arrays:

1. Array EML-1 (48 channel MASW and P-wave seismic refraction array utilizing 4.5 Hz vertical geophones spaced 1.5 m apart for a length of 70.5 m, forward and reverse shot locations with multiple source offsets and source types (hammers only) and multiple interior shot locations).
2. Array EML-1 (48 channel MALW and S-wave seismic refraction array utilizing 10 Hz horizontal geophones spaced 1.5 m apart for a length of 70.5 m, forward and reverse shot locations with multiple source offsets and source types (hammers only) and multiple interior shot locations). Coincident with P-wave array of same name.
3. Six HVSR measurement locations; three distributed along array EML-1, one adjacent to the seismic station, and two additional locations at varying distances from the bedrock outcrop.

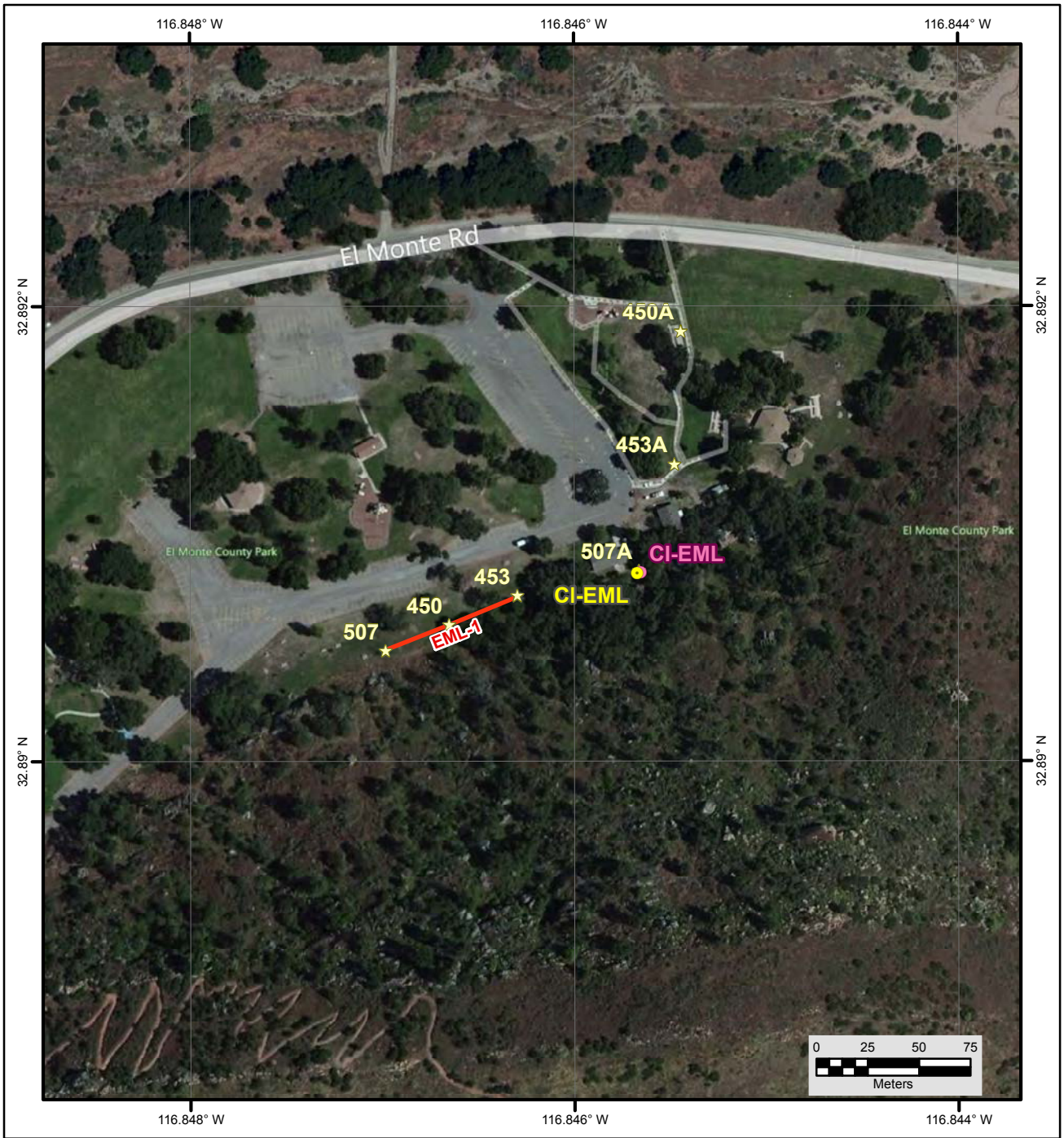

Legend

- Seismic Station - Approximate Surveyed Location
- Seismic Station - Approximate Location of Record
- H/V Spectral Ratio Location
- MASW and Seismic Refraction Array

NOTES:
1. WGS 1984 COORDINATE SYSTEM
2. Image Source: (c) Microsoft Corporation and its data suppliers

File Name: CI-EML-I

Date: 1/5/2012

USGS science for a changing world

GEOVision geophysical services

RECOVERY.GOV

SITE MAP
CI•EML

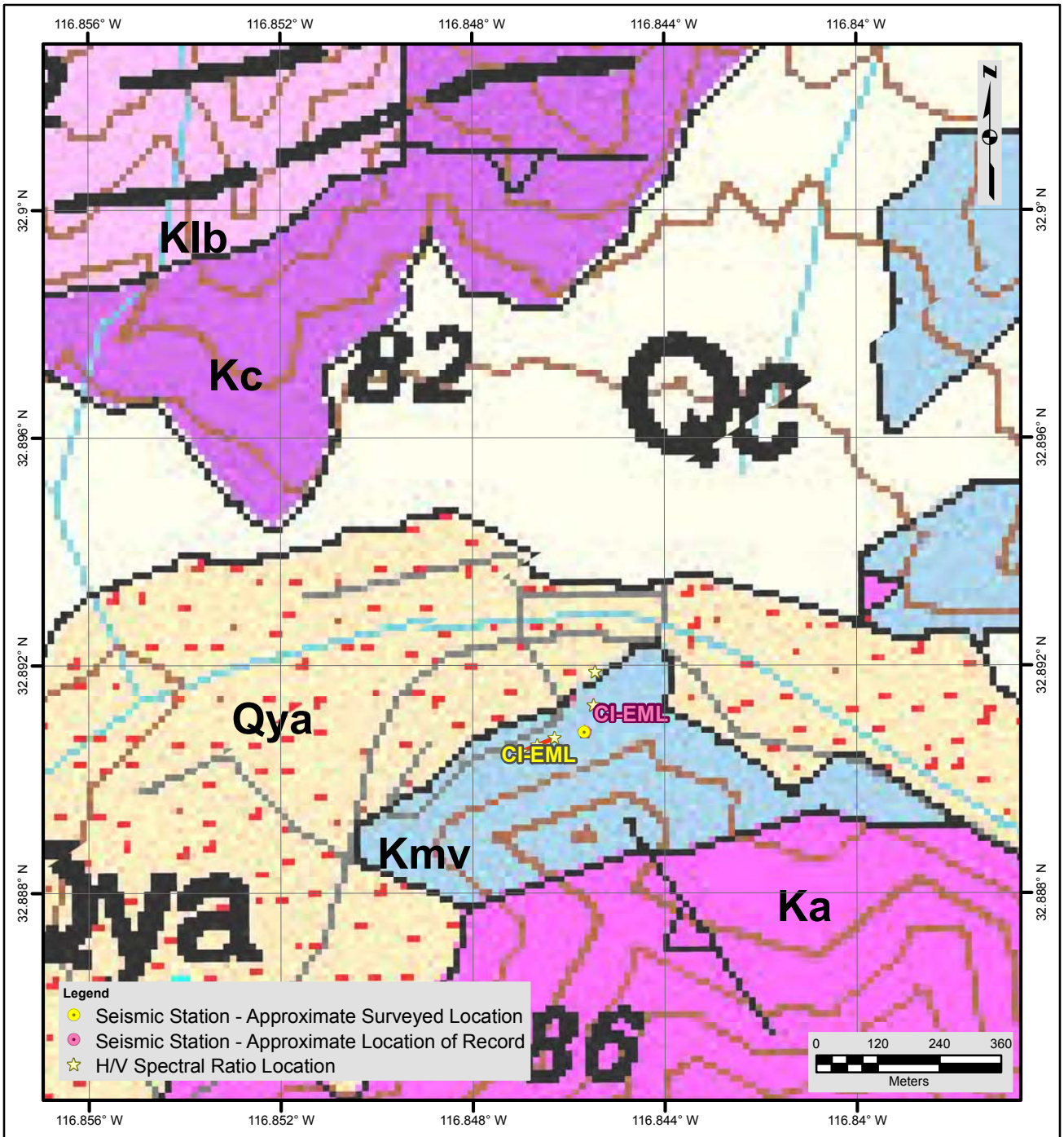

Description of Geologic Map Units

Qya = Quaternary (Holocene) young alluvium, sand silt and gravel in modern streambeds
Qc = Quaternary (Holocene and Pleistocene) colluvium, sand and gravel of slopewash, debris-flow and talus deposits
Klb = Mesozoic (Early Cretaceous) Tonalite of Las Bancas; hypersthene-biotite tonalite, quartz diorite, granodiorite, and lesser diorite, quartz monzodiorite and quartz norite, medium grained, weak foliation
Kc = Mesozoic (Early Cretaceous) Cuyamaca Gabbro; troctolite, anorthositic gabbro, gabbronorite, hornblend gabbro, minor hornblende diorite and leucodiorite, moderately to strongly foliated
Ka = Mesozoic (Early Cretaceous) Tonalite of Alpine; biotite-hornblende tonalite, lesser quartz diorite, and scarce granodioritic tonalite, medium to coarse-grained, moderately to strongly foliated, mafic inclusions
Kmv = Mesozoic (Early Cretaceous) metavolcanic rocks, amphibolite-facies metavolcanic tuff, tuff-breccia and flows of andesitic to basactic composition, somw meta quartzite, pelitic schist and metaconglomerate

NOTES:
1. WGS 1984 COORDINATE SYSTEM
2. Geologic Map of the El Cajon 30' x 60' Quadrangle, Southern California
by Victoria Todd, 2004
3. See site map for details of geophysical survey

USGS science for a changing world

GEOVision geophysical services

GEOLOGIC MAP
CI•EML

File Name: CI-EML

Date: 10/13/2011

Seismic Station CI.EML and HVSR sensor 507A

Looking northeast along P-wave refraction and MASW array EML-1

HVSR sensors 450, 453 and 507 near toe of slope of Cretaceous metavolcanic rock

Looking west along S-wave refraction and MALW array EML-1

Seismic data acquisition on P-wave array EML-1

Location of Geophysical Testing Arrays:

Location	Latitude	Longitude
EML-1, Southwest End of MASW/Refraction Array	32.89049	-116.84699
EML-1, Center of MASW/Refraction Array	32.89060	-116.84666
EML-1, Northest End of MASW/Refraction Array	32.89072	-116.84630
HVSR Sensor 450	32.89060	-116.84666
HVSR Sensor 453	32.89073	-116.84630
HVSR Sensor 507	32.89049	-116.84699
HVSR Sensor 450a	32.89189	-116.84545
HVSR Sensor 453a	32.89131	-116.84548
HVSR Sensor 507a	32.89084	-116.84567
CI.EML Seismic Station	32.89083	-116.84567

Notes: 1) WGS84 Coordinate System (decimal degrees)

2) Survey accuracy is estimated at 1 to 2 m.

Results:

Average V_S Model from Central Portion of S-wave Seismic Refraction Line

Depth to Top of Layer (m)	Layer Thickness (m)	S-Wave Velocity (m/s)
0.00	0.41	117
0.41	0.82	166
1.22	0.82	168
2.04	0.82	169
2.86	0.82	325
3.67	0.82	1065
4.49	0.82	1069
5.30	1.71	1080
7.02	1.71	1124
8.73	1.71	1250
10.44	1.71	1424
12.16	1.71	1589
13.87	1.71	1700
15.59	1.71	1937
17.30	1.71	1940
19.01	>11	1973

Observations/Discussion:

- The HVSR plots for measurement locations along array EML-1 (sensors 450, 507 and 453) and at the seismic station (sensor 507A) are very similar, validating the 1-D velocity structure assumption. Sensors 450, 507 and 507A all have a broad peak in the 8 to 15 Hz range, associated with the very shallow bedrock at the toe of slope. The HVSR peak at sensor location 450 is slightly lower frequency, in the 6 to 10 Hz range. The broad peak may reflect the three dimensional nature of the bedrock surface with bedrock depth deepening to the northwest. HVSR sensors 453A and 450A have distinct lower frequency peaks of 5.5 and 5.1 Hz, respectively, reflecting deeper bedrock at increasing distance from the outcrop. The HVSR data at sensors 453A and 450A demonstrates that site characterization can only be conducted along the toe of the slope of the rock outcrop.
- Noise conditions at the site were not sufficient for application of passive surface wave techniques.
- Surface wave techniques were not expected to be effective at this site because the bedrock surface may be dipping as much as 30 degrees to the northwest beneath the seismic profile. Site characterization was, therefore, limited to the application of the P- and S-wave seismic refraction techniques.
- The P- and S-wave seismic refraction data for array EML-1 were modeled using a tomographic inversion routine with layer-based starting models. The seismic refraction models were extended to far offset shot locations to extend depth of investigation. It should be noted that a larger geophone spacing, rather than the utilization of far offset shot locations, is preferred for extending depth of investigation, when applying tomographic inversion routines. However, the seismic refraction data were acquired in conjunction with surface wave data, where a shorter array length is preferred.
- The P-wave first arrival data were picked to a greater degree of accuracy than the S-wave first arrival data because the S-wave is not typically the first energy on a seismic record, even when using a horizontal traction plank as an energy source. The air wave arrives before the direct soil arrival in the P-wave seismic records and an attempt was made to pick the direct arrival after the air wave, which is not always easy.
- The P-wave seismic refraction survey design allowed P-wave velocity to be imaged to a maximum depth of about 19 m. The seismic refraction model indicates that P-wave velocity is about 250 to 300 m/s at the surface and increases to over 1,000 m/s at a depth of 2 to 5 m, 2,000 m/s at a depth of 4 to 8 m and over 3,000 m/s at a nominal depth of 8 to 16 m. The maximum P-wave velocity in the central portion of the model, where depth of investigation is greatest is about 3,500 m/s. A P-wave velocity this high is indicative of slightly weathered rock and, therefore, we would expect velocity to only increase very gradually with depth below 19 m.
- The S-wave seismic refraction survey design allowed S-wave velocity to be imaged to a maximum depth of about 19 m. The seismic refraction model indicates that S-wave velocity is about 125 to 150 m/s at the surface and increases to over 300 m/s 2 to 3 m, 1,000 m/s at a depth of 3 to 5 m, 1,250 m/s at a depth of 4 to 9 m and over 1,750 m/s at a depth of 13 to 18 m. The maximum S-wave velocity in the central portion of the model, where depth of investigation is greatest is about 2,000 m/s. An S-wave velocity this high is indicative of slightly weathered rock and, therefore, we would expect velocity to only increase very gradually with depth below 19 m.

- V_{S30} was estimated between 24 and 46.5 m on the S-wave refraction model, where depth of investigation is greatest, by projecting the velocity at 19 m depth to 30 m depth. Over this interval V_{S30} ranges from about 788 to 825 m/s, a 5% variation over a 22 m distance.
- An average V_S model was developed over the 24 to 46.5 m distance interval by averaging the slowness of each model cell and average V_{S30} was determined to be 805 m/s. Increasing V_S below 22 m from about 1,975 m/s to 2,250 m/s only increases V_{S30} to 816 m/s, a smaller change than that due to the lateral velocity variation along the line.
- V_{P30} between 24 and 46.5 m varies from about 1,353 to 1,435 m/s and averages 1,400 m/s. A Poisson's ratio of about 0.25 would yield the value of V_{S30} estimated from the S-wave seismic refraction survey, not unrealistic for relatively competent rock. Estimating V_{S30} from V_{P30} assuming constant Poisson's ratio in the range of 0.25 to 0.35 results in V_{S30} in the 808 to 673 m/s range. This large variation in potential V_{S30} demonstrates the risks in attempting to estimate V_{S30} from P-wave velocity data, even with a realistic estimate of Poisson's ratio and this approach should only be used as a last resort.
- In summary, V_{S30} is 805 m/s (Site Class B).
- Average S-wave velocity between 2 m (nominal sensor depth) and 32 m is 1,188 m/s (Site Class B).

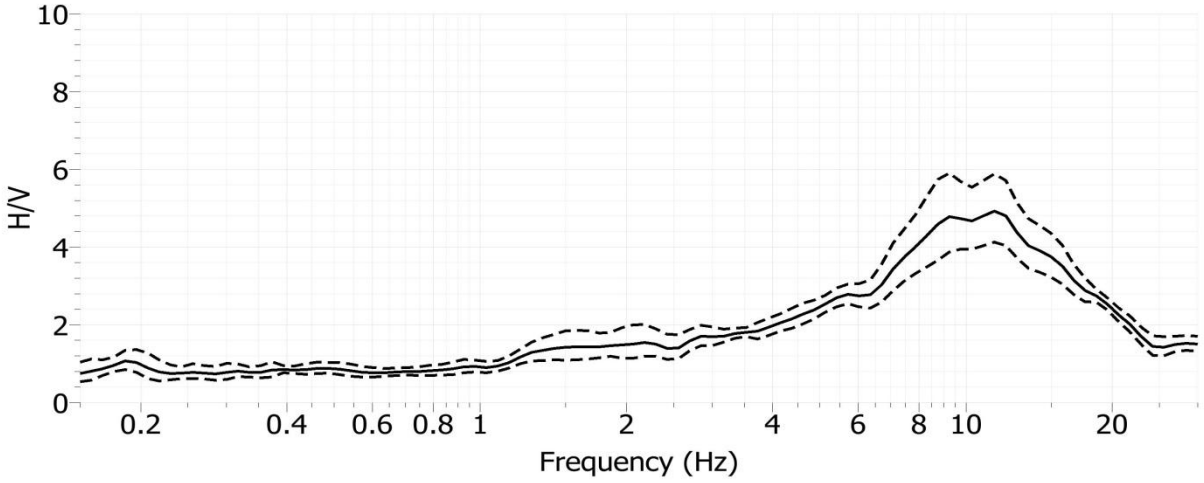

Site CI.EML, H/V Spectral Ratio, Array EML-1, Sensor 507

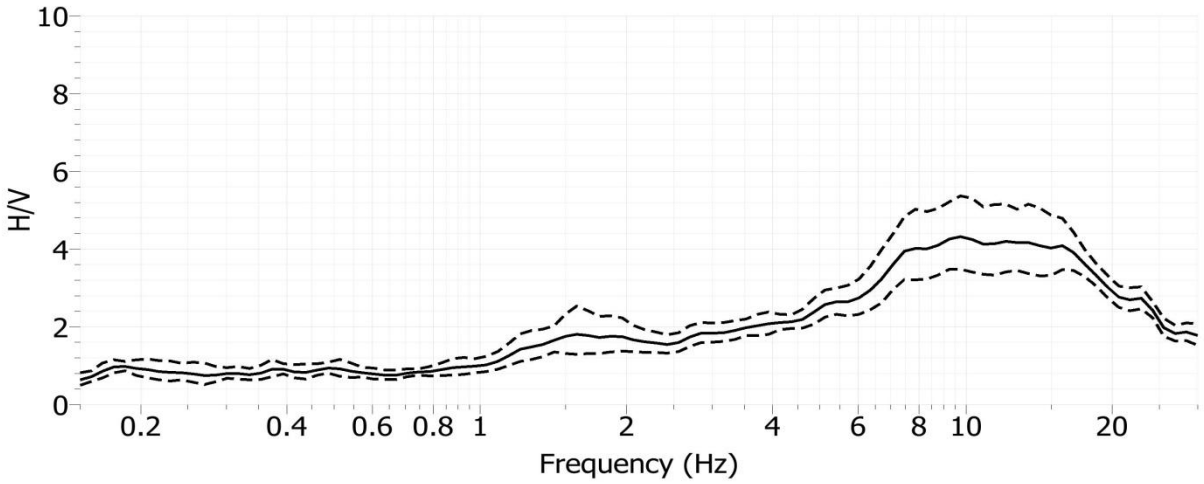

Site CI.EML, H/V Spectral Ratio, Array EML-1, Sensor 450

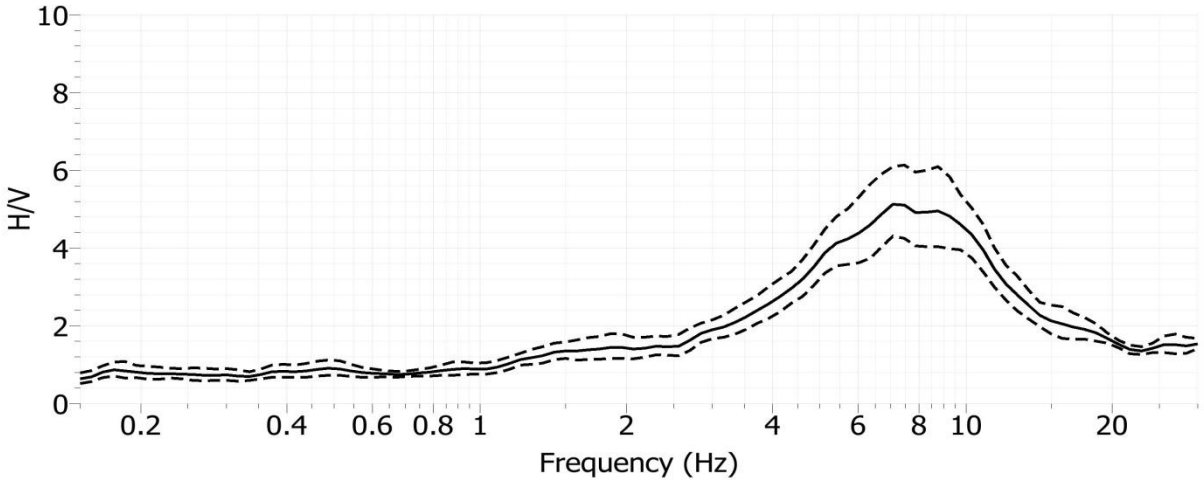

Site CI.EML, H/V Spectral Ratio, Array EML-1, Sensor 453

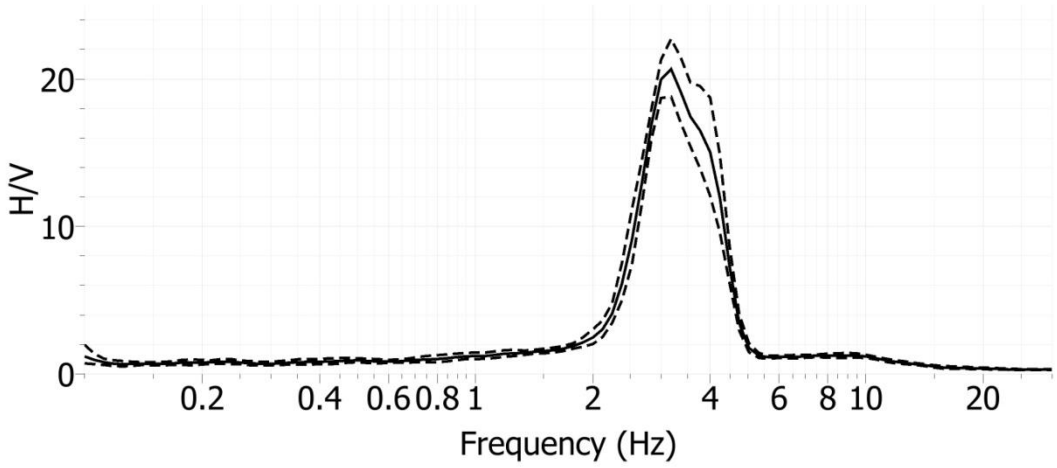

Site CI.EML, H/V Spectral Ratio, Sensor 450A

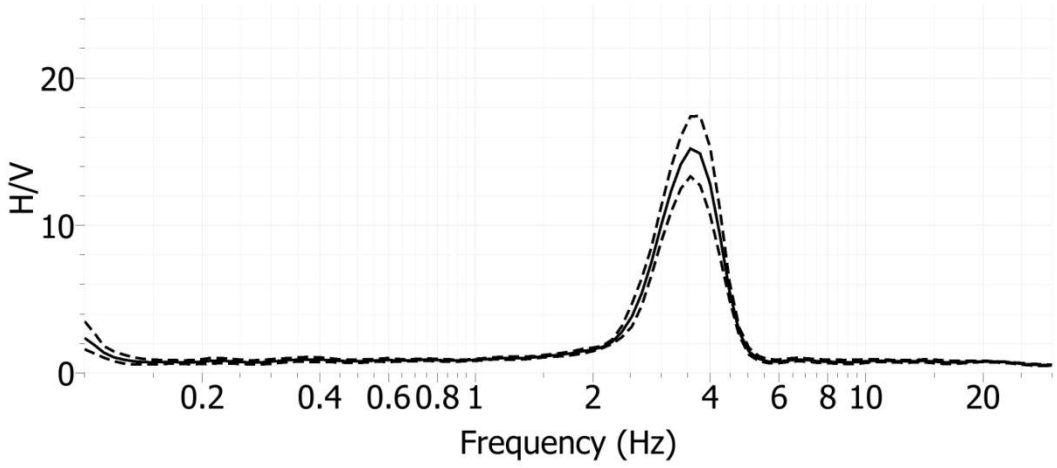

Site CI.EML, H/V Spectral Ratio, Sensor 453A

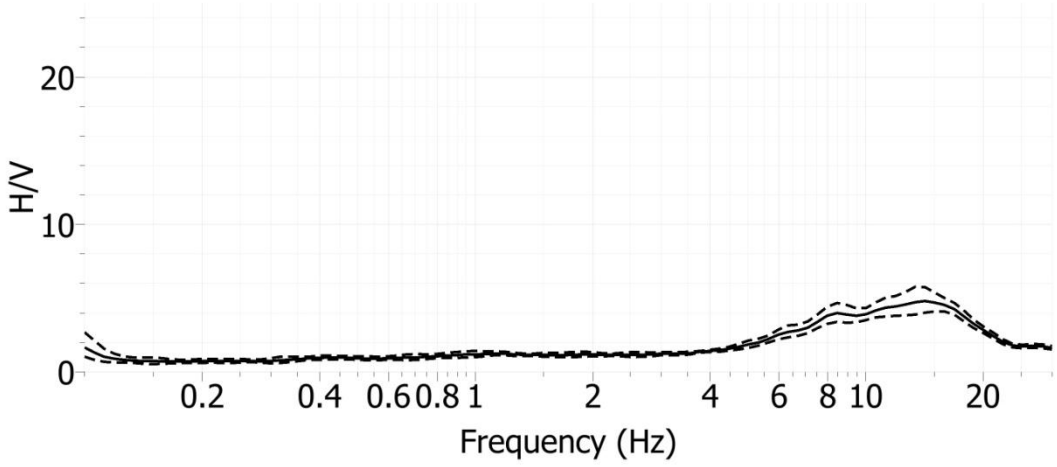

Site CI.EML, H/V Spectral Ratio, Near Seismic Station, Sensor 507A

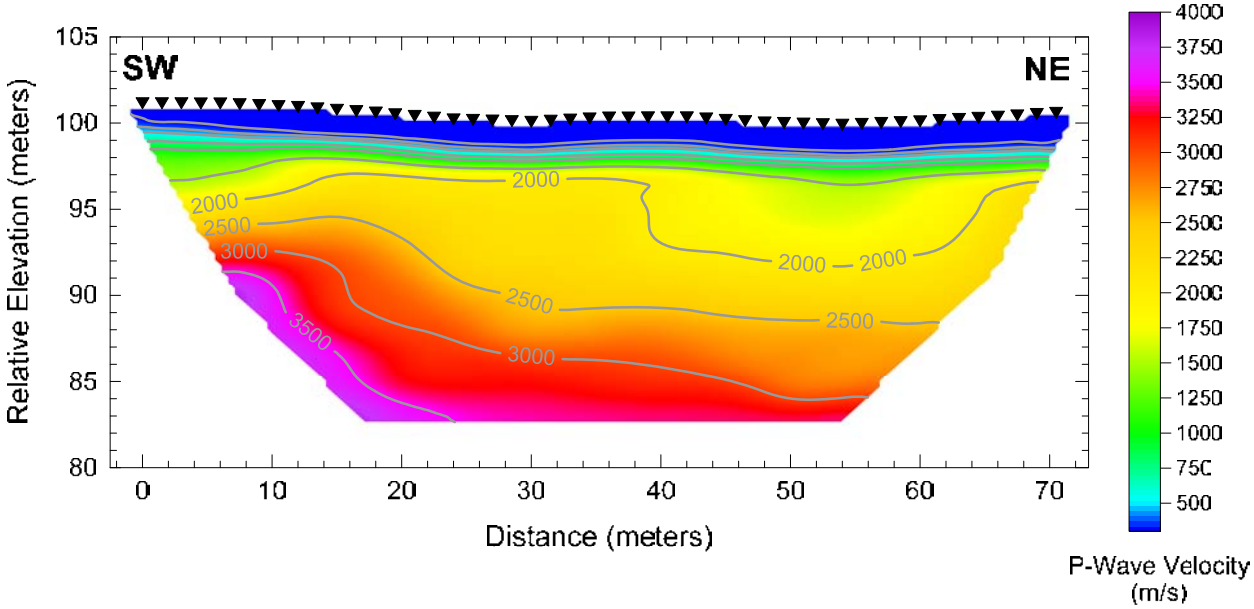

Array EML-1 – P-wave Tomographic Seismic Refraction Model utilizing Layer Based Starting Model

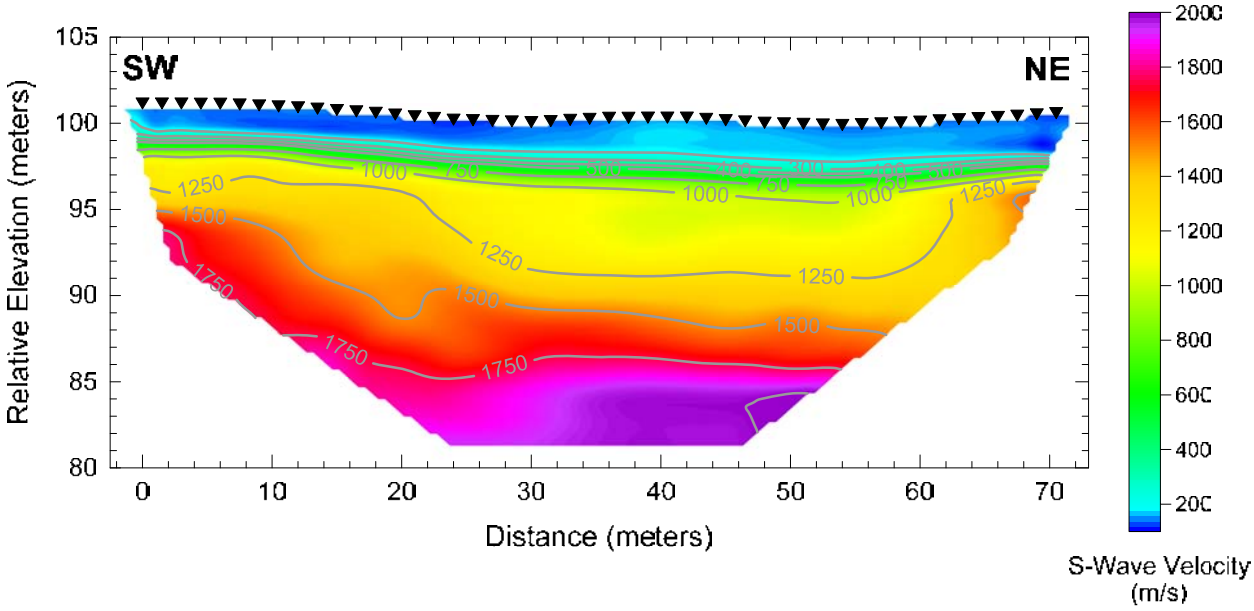

Array EML-1 – S-wave Tomographic Seismic Refraction Model utilizing Layer Based Starting Model

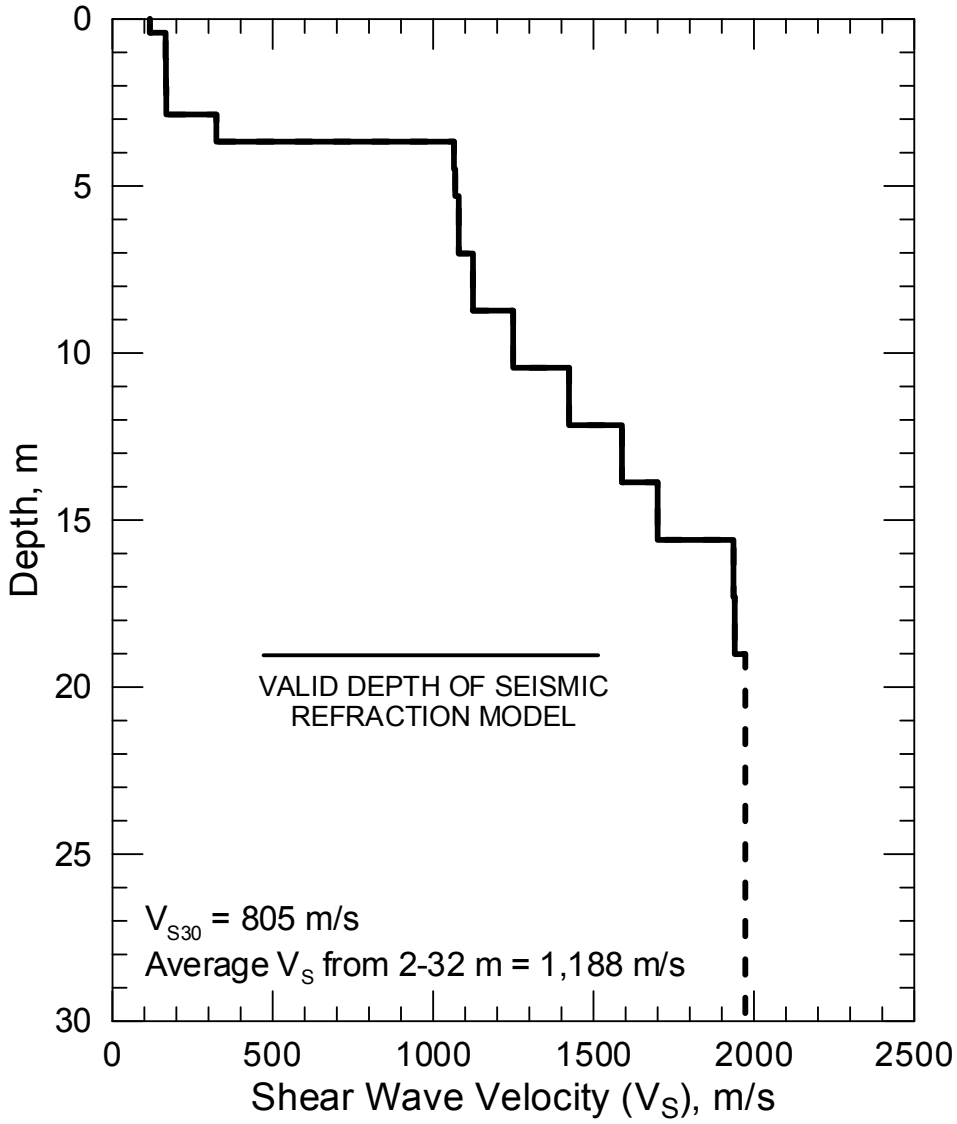

CI.EML – Average S-wave velocity structure between 24 and 46.5 m on S-wave seismic refraction array EML-1. Although seismic refraction depth of investigation limited to about 19 m, S-wave velocity is very high at 19 m depth and not expected to increase significantly between 19 and 30 m. Increasing S-wave velocity to 2,250 m/s below 22.5 m only increases V_{S30} to 816 m/s.

Site CI.ERR

Location: Kane Springs, San Felipe Wash, Elmore Desert Ranch, Borrego Springs, California

Latitude: 33.11645 **Longitude:** -115.82271

(Station coordinates modified based on field GPS survey, WGS84 coordinate system)

V_{S30} (measured): 238 m/s

V_{S30} (adjusted to more accurately reflect seismic station conditions): 253 m/s (average S-wave velocity between 2 and 32 m adjusting for nominal sensor depth)

NEHRP Site Class: D

Geomatrix Code: IHD

Geologic Conditions/Observations: Site located on geologic unit mapped as Quaternary (Holocene) thin claystone, gravel and sand deposits from former Lake Cahuilla. The Pliocene-Pleistocene Brawley Formation is mapped as outcropping about 100 m northwest of the seismic station, where it forms an anticline with moderately dipping beds. Deep soil site.

Site Conditions: Rural site. Relatively flat terrain in site vicinity.

Geophysical Methods Utilized: HVSR, MASW, SASW

Geophysical Testing Arrays:

1. Array ERR-1 (48 channel MASW array utilizing 4.5 Hz vertical geophones spaced 1.5 m apart for a length of 70.5 m, forward and reverse shot locations with multiple source offsets and source types and center shot location).
2. Array ERR-1 (SASW array with same midpoint and orientation as MASW array of same name utilizing 4.5 and 1 Hz vertical geophones and maximum receiver spacing of 32 m).
3. Three HVSR measurement locations; two distributed along array ERR-1 and one near the seismic station.

Legend

- Seismic Station - Approximate Surveyed Location
- Seismic Station - Approximate Location of Record
- H/V Spectral Ratio Location
- SASW Array
- MASW Array

NOTES:
1. WGS 1984 COORDINATE SYSTEM
2. Image Source: ESRI, i-cubed, USDA FSA, USGS, AEX, GeoEye, Getmapping, Aerogrid, IGP

File Name: CI-ERR-I

Date: 9/22/2011

USGS science for a changing world

GEOVision geophysical services

RECOVERY.GOV

SITE MAP
CI•ERR

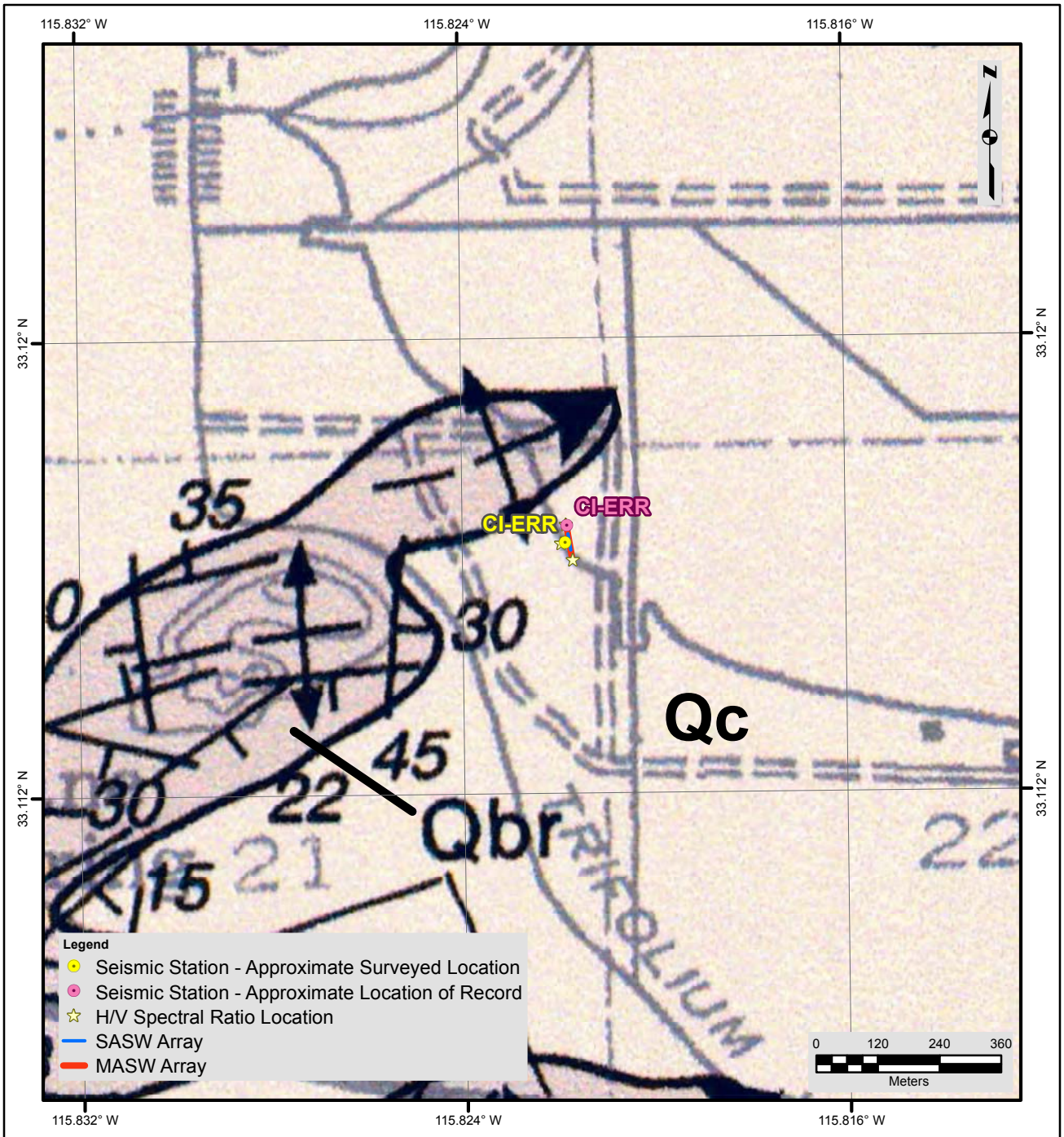

Description of Geologic Map Units

Qc = Quaternary (Holocene) Cahuilla Beds; thin series of claystones, sands and gravels deposited in former Lake Cahuilla, fossiliferous
Qbr = Quaternary (Pliocene - Pleistocene) Brawley Formation; claystone, thin sandstone strata with some pebbly beds locally

NOTES:
1. WGS 1984 COORDINATE SYSTEM
2. Geologic Map of the Kane Spring 15 Minute Quadrangle, Imperial County, California by Thomas W. Dibblee, Jr., 2008
3. See site map for details of geophysical survey

File Name: CI-ERR

Date: 9/15/2011

USGS science for a changing world

GEOVision geophysical services

RECOVERY.GOV

GEOLOGIC MAP
CI•ERR

Looking east from HVSR sensor 453 towards center of array ERR-1 and CI.ERR Seismic Station

Data acquisition with hammer source on MASW array ERR-1

Data acquisition with AWD on SASW array ERR-1

Looking south along array ERR-1 from HVSR sensor 507

Data acquisition with AWD on MASW array ERR-1

Location of Geophysical Testing Arrays:

Location	Latitude	Longitude
ERR-1, South end of MASW Array	33.11615	-115.82256
ERR-1, Center of MASW and SASW Arrays	33.11646	-115.82262
ERR-1, North end of MASW Array	33.11677	-115.82269
HVSR Sensor 450	33.11615	-115.82255
HVSR Sensor 453	33.11644	-115.82279
HVSR Sensor 507	33.11677	-115.82269
CI.ERR Seismic Station	33.11645	-115.82271

Notes: 1) WGS84 Coordinate System (decimal degrees)
2) Survey accuracy is estimated at 1 to 2 m

Results:

V_S Model – SASW Array

Depth to Top of Layer (m)	Layer Thickness (m)	S-Wave Velocity (m/s)	Inferred P-Wave Velocity (m/s)	Assumed Poisson's Ratio	Assumed Density (g/cm^3)
0	0.5	132	246	0.300	1.8
0.5	1.5	150	281	0.300	1.8
2	2	185	347	0.300	1.8
4	5	215	1650	0.491	1.9
9	6	223	1650	0.491	1.9
15	6	228	1650	0.490	1.9
21	>9	366	1650	0.474	2.0

Notes: 1) Saturated sediments estimated at 4 m depth from seismic refraction first arrival data. The P-wave velocity of saturated sediments is about 1,650 m/s.
2) Depth of investigation is about 30 m.
3) Bottom layer is a half space.

V_S Model – MASW Array

Depth to Top of Layer (m)	Layer Thickness (m)	S-Wave Velocity (m/s)	Inferred P-Wave Velocity (m/s)	Assumed Poisson's Ratio	Assumed Density (g/cm^3)
0	0.75	144	269	0.300	1.8
0.75	1.25	169	317	0.300	1.8
2	2	200	374	0.300	1.8
4	5	217	1650	0.491	1.9
9	7	226	1650	0.490	1.9
16	7	241	1650	0.489	1.9
23	>7	334	1650	0.479	2.0

Notes: 1) Saturated sediments estimated at 4 m depth from seismic refraction first arrival data. The P-wave velocity of saturated sediments is about 1,650 m/s.
2) Depth of investigation is about 30 m.
3) Bottom layer is a half space.

Observations/Discussion:

- The HVSR curves are very similar, validating the 1-D velocity structure assumption.
- HVSR sensor 450 appears to have the best data quality, particularly at low frequencies.
- Better quality data at frequencies below 0.2 Hz may be obtained if data were acquired for a longer duration with extra attention paid to sensor coupling.
- There is a relatively high amplitude HVSR peak at about 0.16 Hz and possibly another peak at a lower frequency of about 0.11 Hz, likely associated with the several kilometer deep basement complex. Low frequency noise, possibly related to sensor coupling or other environmental issues, impacts data at low frequencies making it difficult to accurately resolve the low frequency peak(s); which, although of scientific interest, are outside the scope of work.
- In addition to the low frequency HVSR peak, there also appears to be slightly elevated HVSR amplitude over the 0.3 to 0.9 Hz range.
- The water table was modeled at a depth on the order of 4 m based on interactive layer-based analysis of seismic refraction first arrival data. P-wave velocities of about 225 to 325 m/s and 1,650 m/s were modeled for unsaturated and saturated sediments, respectively. The seismic refraction data indicates that the water table surface has an apparent dip of about 2 degrees to the north.
- There is good reflectivity in the MASW seismic records with multiple reflectors in about the upper 25 to 150 m.
- Noise conditions at site were not sufficient to apply passive surface wave techniques.
- There is significant scatter in the SASW dispersion data, possibly due to the effects of shallow dipping geologic layers, influence of higher mode surface waves, or some other feature.
- There is sufficient difference in the surface wave dispersion data from the MASW and SASW soundings such that the data were modeled separately. The MASW data were

acquired along a 70.5 m receiver array, whereas, the SASW data were acquired with a maximum 32 m receiver spacing centered at the midpoint of the MASW array.

- For data modeling purposes, representative dispersion curves were generated for each surface wave data set using a moving average, polynomial curve fitting routine.
- The layer velocities in the S-wave velocity models derived from the SASW and MASW dispersion data generally agree to within 10% of velocity. The largest differences occur near the surface and in the depth and velocity of the lowest layer. Minor lateral velocity variation would explain the differences in near surface velocity structure as the near surface velocity structure is derived from different portions of the SASW and MASW arrays. Near surface velocities in the SASW model are representative of the velocity structure in the central several meters of the MASW array; whereas, near surface velocities in the MASW model are generally representative of one or both ends of the MASW array. The bottom layer in the SASW and MASW models could be associated with the Brawley Formation or another stiff layer. If this layer has shallow dip then the SASW and MASW models may differ slightly due to the different lengths of the receiver arrays.
- Surface wave depth of investigation is about 30 m based on half of maximum wavelength criteria.
- V_{S30} is 239 m/s for the SASW array and 237 m/s for the MASW array, averaging 238 m/s (Site Class D).
- Average S-wave velocity between 2 m (nominal sensor depth) and 32 m is 256 and 250 m/s for the SASW and MASW arrays, respectively and averages 253 m/s.

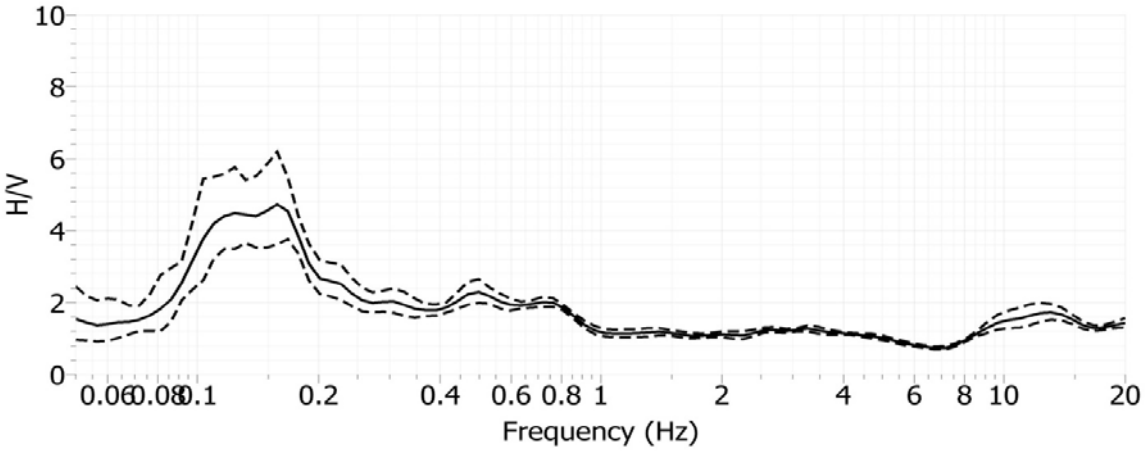

Site CI.ERR, H/V Spectral Ratio, Line ERR-1, Sensor 507

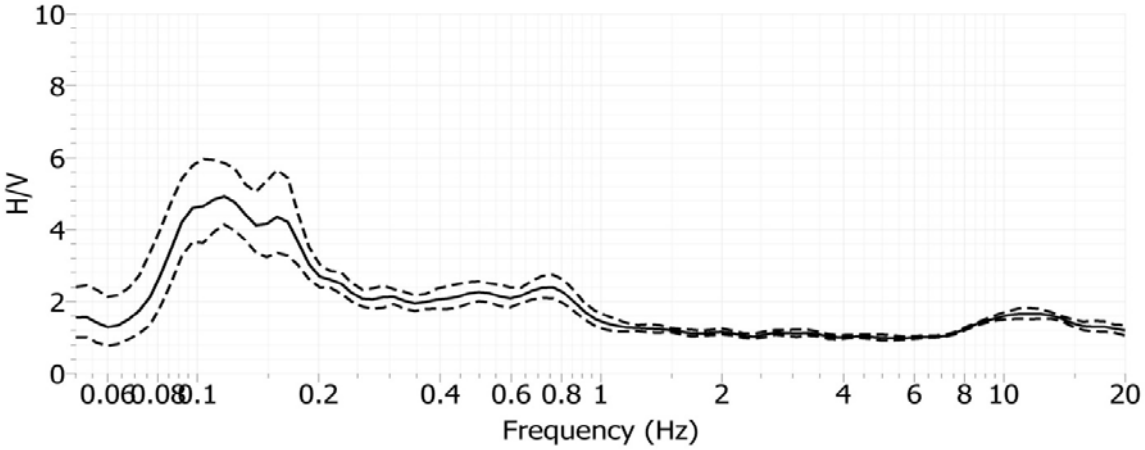

Site CI.ERR, H/V Spectral Ratio, Near Seismic Station, Sensor 453

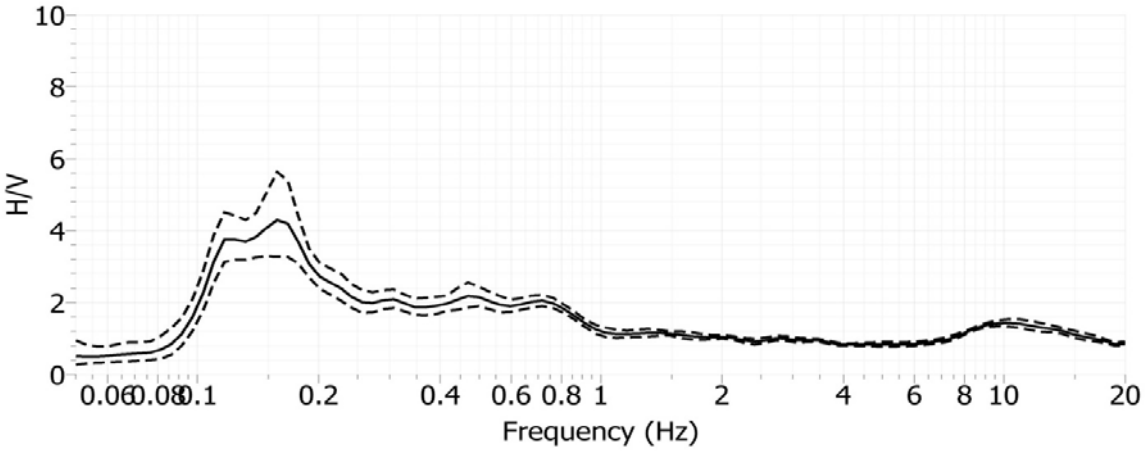

Site CI.ERR, H/V Spectral Ratio, Line ERR-1, Sensor 450

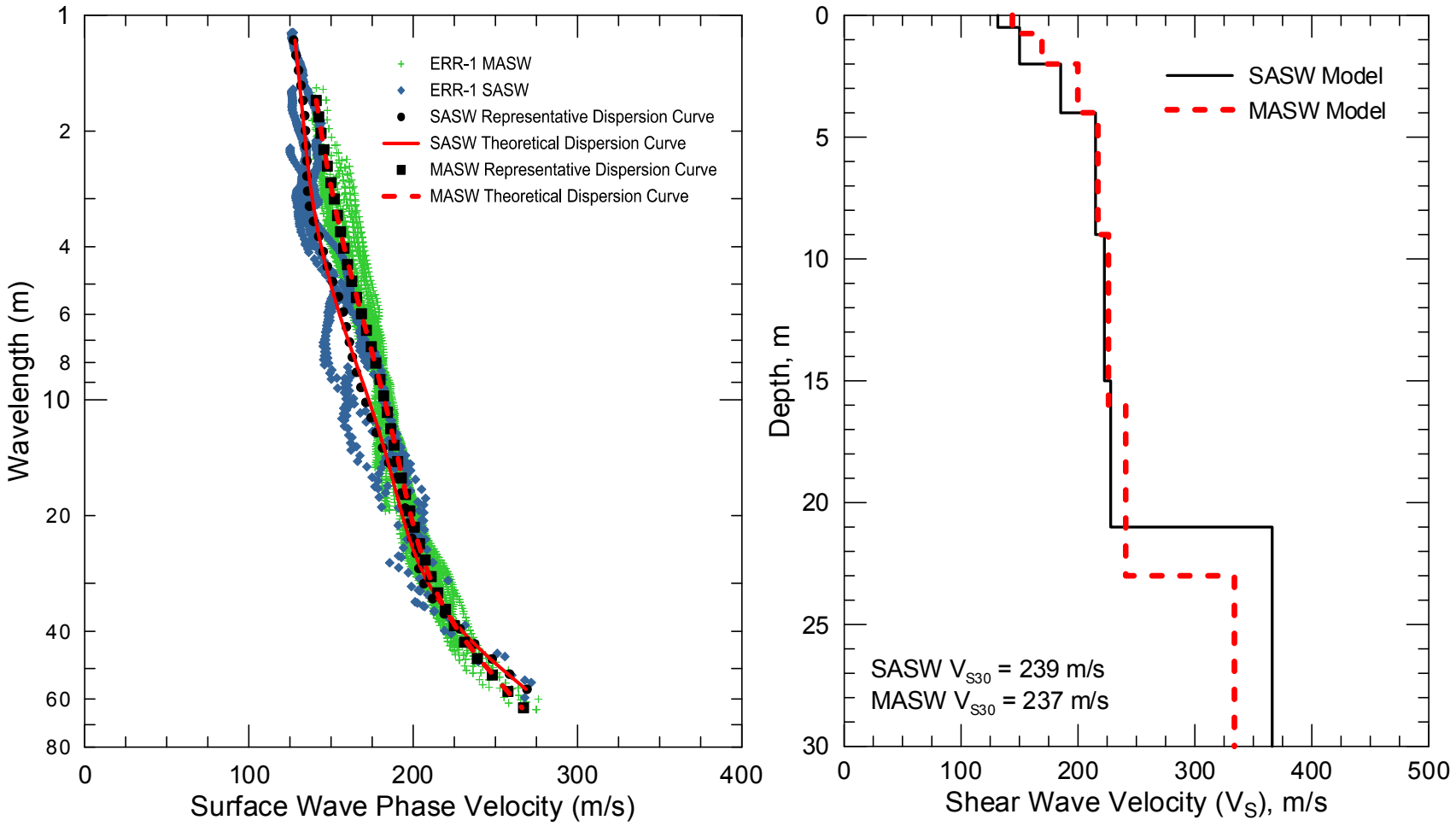

CI.ERR - Field, representative and inverted theoretical surface wave dispersion data (left) and associated V_S model (right)

Site CI.FHO

Location: Forest Home, Forest Falls, California

Latitude: 34.09355 **Longitude:** -116.93588
(Coordinates provided by USGS – WGS84 coordinate system)

V_{S30} (measured): 416 m/s

V_{S30} (adjusted to more accurately reflect seismic station conditions): 460 m/s (average S-wave velocity between 2 and 32 m adjusting for 2 m nominal sensor depth.)

NEHRP Site Class: C

Geomatrix Code: IQB/IQC

Geologic Conditions/Observations: Seismic station located on geologic unit mapped as Quaternary (Pleistocene) older terrace deposits. Outcrops of weathered gneiss are located both near the seismic station and test area. An outcrop of gneiss near the southwest end of the test area is decomposed. The inferred trace of the North Branch San Andreas Fault is located about 150 m south of the test area.

Site Conditions: Rural site. Sloping but relatively planar terrain along test area. Hilly terrain in site vicinity with steep mountain slopes about 250 m north and 600 m south of test area.

Geophysical Methods Utilized: HVSR, Seismic Refraction, MASW

Geophysical Testing Arrays:

1. Array FHO-1 (48 channel MASW array utilizing 4.5 Hz vertical geophones spaced 1.5 m apart for a length of 70.5 m, forward and reverse shot locations with multiple source offsets and source types and center shot location).
2. Array FHO-2 (48 channel MASW and seismic refraction array utilizing 4.5 Hz vertical geophones spaced 3 m apart for a length of 141 m, forward and reverse shot locations with multiple source offsets and source types and multiple interior shot locations).
3. Three HVSR measurement locations, two distributed along array FHO-1 and the other near the seismic station.

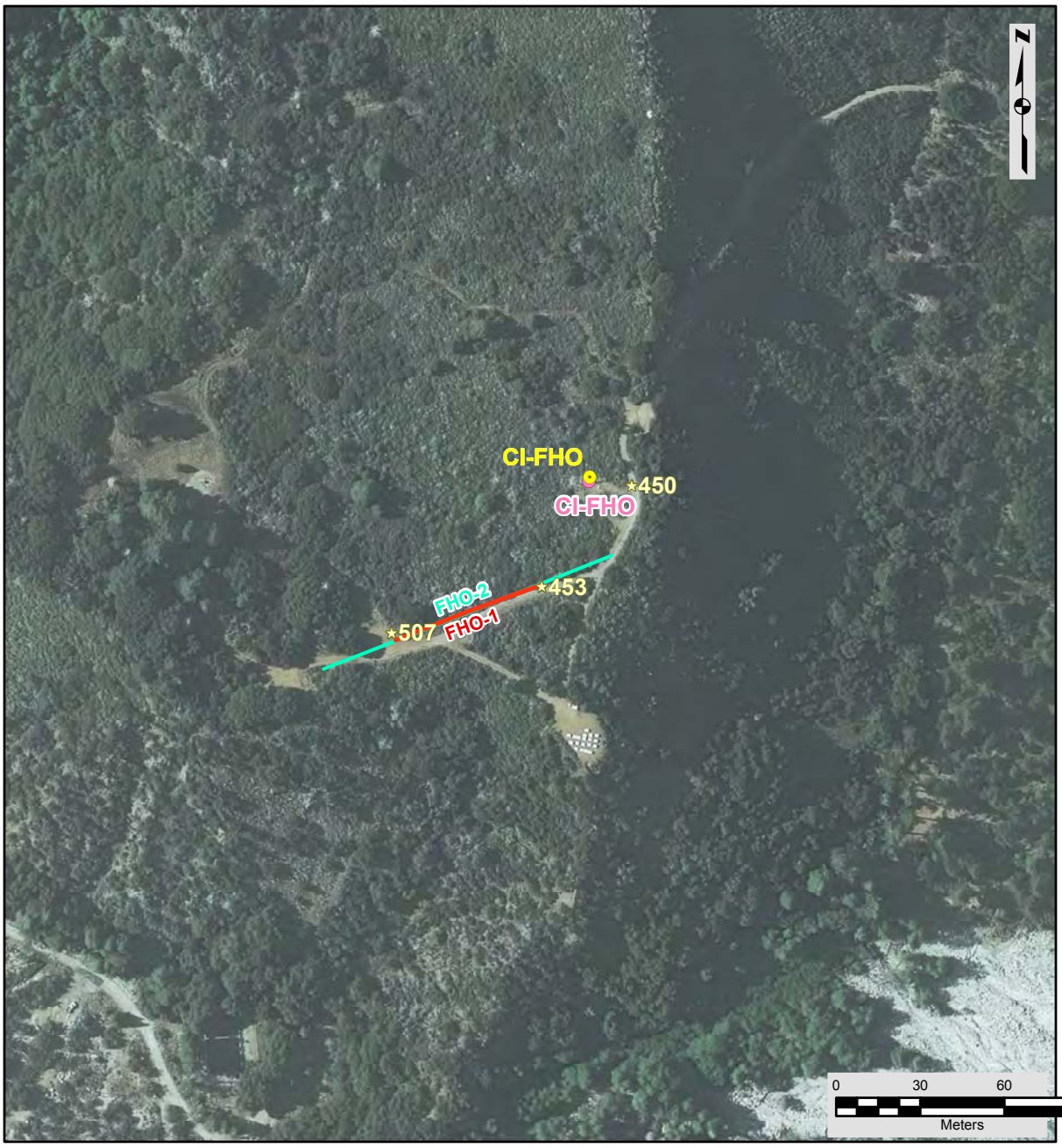

Legend

- Seismic Station - Approximate Surveyed Location
- Seismic Station - Approximate Location of Record
- H/V Spectral Ratio Measurement Location
- MASW and Seismic Refraction Array
- MASW Array

NOTES:
1. WGS 1984 COORDINATE SYSTEM
2. Image Source: ESRI, i-cubed, USDA FSA, USGS, AEX, GeoEye, Getmapping, Aerogrid, IGP

File Name: CI-FHO-I

Date: 5/12/2011

USGS science for a changing world

GEOVision geophysical services

RECOVERY.GOV

SITE MAP
CI•FHO

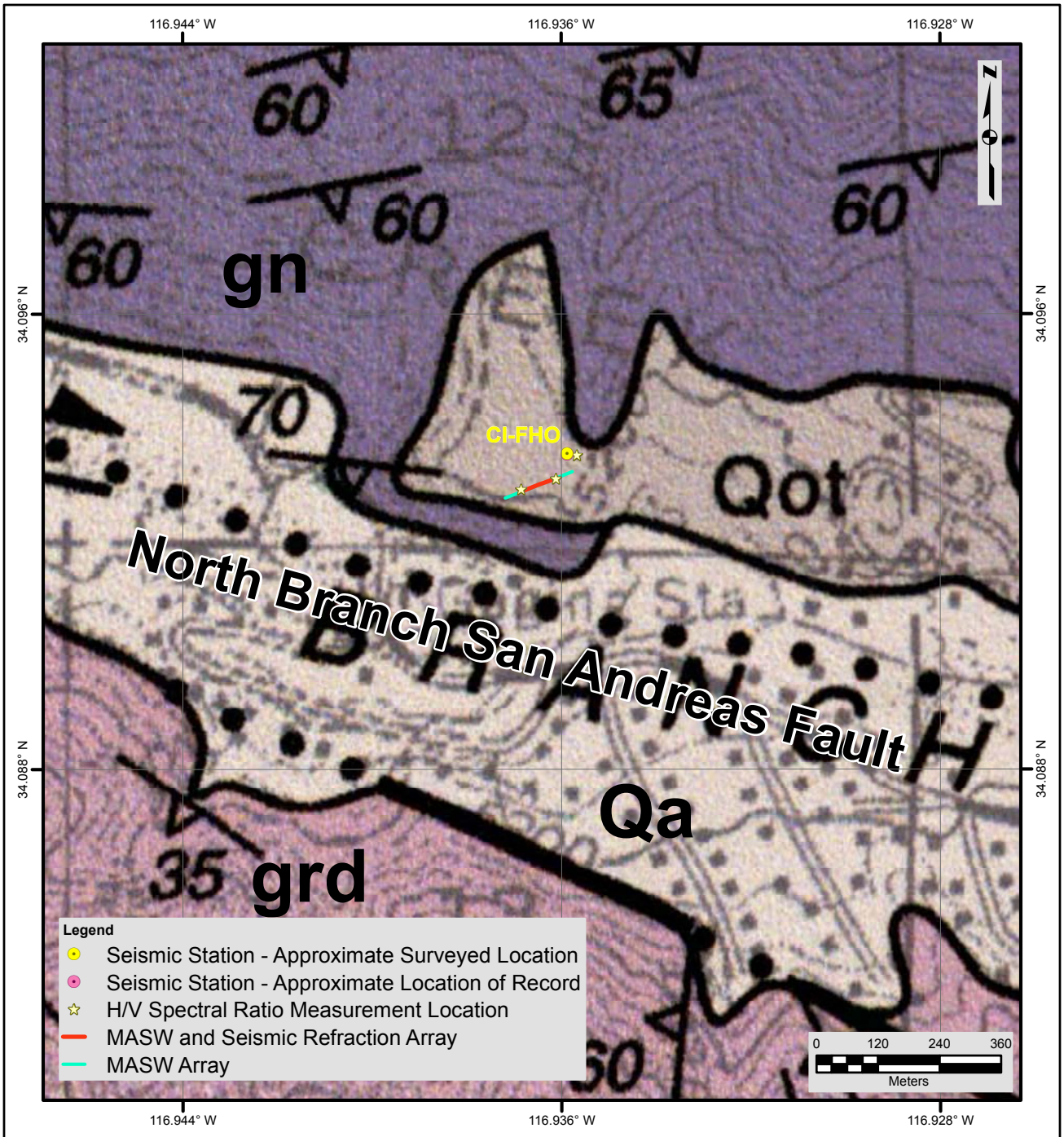

Description of Geologic Map Units

Qa = Quaternary (Holocene) alluvial silt, sand and gravel of floodplains and valleys
Qot = Quaternary (Pleistocene) older terrace gravels, unsorted boulders, cobble, course sand
gn = Gneiss, foliated
grd = Granodiorite to quartz diorite, intrusive into gneissic rocks

NOTES:
1. WGS 1984 COORDINATE SYSTEM
2. Geologic Map of the San Gorgonio Mountain & Morongo Valley 15 Minute Quadrangles, San Bernardino & Riverside Counties, California by Thomas W. Dibblee, Jr., 2008
3. See site map for details of geophysical survey

File Name: CI-FHO
Date: 6/15/2011

USGS science for a changing world
GEOVision geophysical services

GEOLOGIC MAP
CI•FHO

RECOVERY.GOV

Exposure of decomposed gneiss near the southwest end of array FHO-2

Seismic data acquisition system

Looking west towards seismic station CI.FHO and HVSR sensor 450

Looking northeast along seismic refraction and MASW array FHO-2

Looking southwest along MASW array FHO-1

Location of Geophysical Testing Arrays:

Location	Latitude	Longitude
FHO-1, Southwest End of Array	34.09289	-116.93683
FHO-1, Center of Array	34.09300	-116.93648
FHO-1, Northeast End of Array	34.09311	-116.93612
FHO-2, Southwest End of Array	34.09277	-116.93719
FHO-2, Center of Array	34.09300	-116.93648
FHO-2, Northeast End of Array	34.09323	-116.93577
HVSR Sensor 507	34.09292	-116.93685
HVSR Sensor 453	34.09310	-116.93612
HVSR Sensor 450	34.09352	-116.93567
CI.FHO Seismic Station	34.09353	-116.93588

Notes: 1) WGS84 Coordinate System (decimal degrees)
2) Survey accuracy is estimated at 1 to 2 m.

Results:

V_S Model

Depth to Top of Layer (m)	Layer Thickness (m)	S-Wave Velocity (m/s)	Inferred P-Wave Velocity (m/s)	Inferred Poisson's Ratio	Inferred Density (g/cm^3)
0	1	166	310	0.3	1.9
1	2	242	453	0.3	1.9
3	3	364	682	0.3	1.9
6	4	396	741	0.3	1.9
10	6	431	806	0.3	2.0
16	9	512	957	0.3	2.0
25	>5	622	1164	0.3	2.0

Observations/Discussion:

- The seismic station location is about 8 m higher in elevation than the test area.
- Mapped outcrops of gneiss are located near the seismic station and the southwestern end of array FHO-2. The outcrop of gneiss near the southwest end of array FHO-2 is decomposed.
- There is no conclusive HVSR peak at this site. There are two possible low amplitude peaks over the 3 to 5 Hz range. The HVSR plots are similar at frequencies below 2 Hz, but the relative amplitude and frequency of the peaks over the 3 to 5 Hz range differ. The absence of a clear HVSR peak may indicate that velocity gradually increases with depth. The topographic variation in the site vicinity and absence of local high frequency microtremor sources may also have an impact on the HVSR measurement results.
- Representative dispersion curves were generated for each surface wave data set using a moving average, polynomial curve fitting routine. These individual representative dispersion curves were combined and a representative dispersion curve generated for the combined data set for data modeling.
- Field review of off-end shot records on array FHO-1 indicated that a longer array would be beneficial for P-wave refraction data acquisition. To maximize depth of investigation, P-wave refraction data were, therefore, acquired along the 141 m array FHO-2.
- The P-wave refraction model shows P-wave velocity increasing with depth from about 400 m/s at the surface to over 1,200 m/s at a depth on the order of 25 m.
- Depth of investigation of the P-wave seismic refraction survey is estimated at 30 m.
- There is some scatter in the MASW surface wave dispersion data, likely the result of minor lateral velocity variation.
- Surface wave depth of investigation is about 30 m based on half of maximum wavelength criteria
- The inferred P-wave velocities in the surface wave model, assuming a Poisson's ratio of 0.3, are consistent with P-wave velocity structure in the seismic refraction model.
- V_{S30} is 416 m/s (Site Class C).
- Average S-wave velocity between 2 m (nominal sensor depth) and 32 m is 460 m/s.

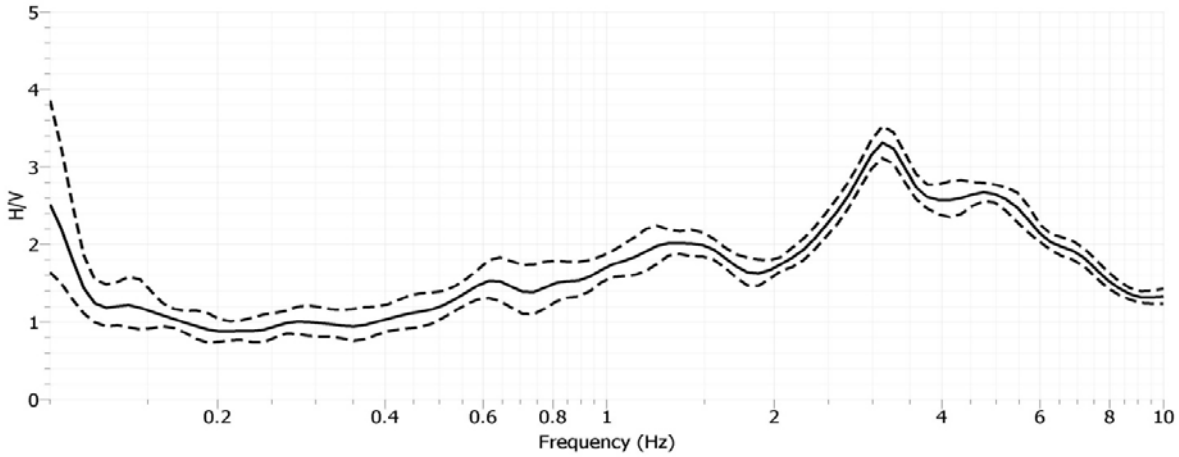

Site CI.FHO, H/V Spectral Ratio, Array FHO-1, Sensor 507

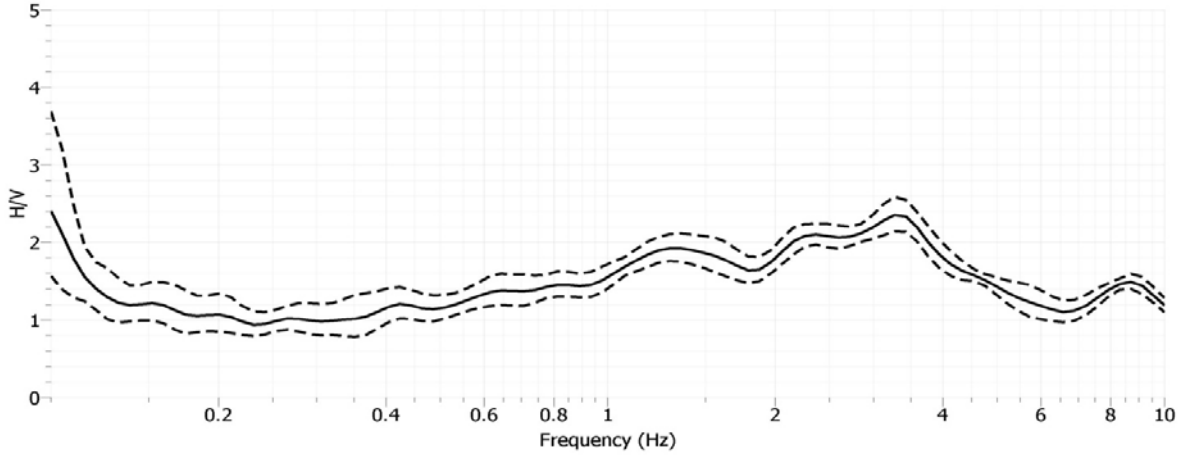

Site CI.FHO, H/V Spectral Ratio, Array FHO-1, Sensor 453

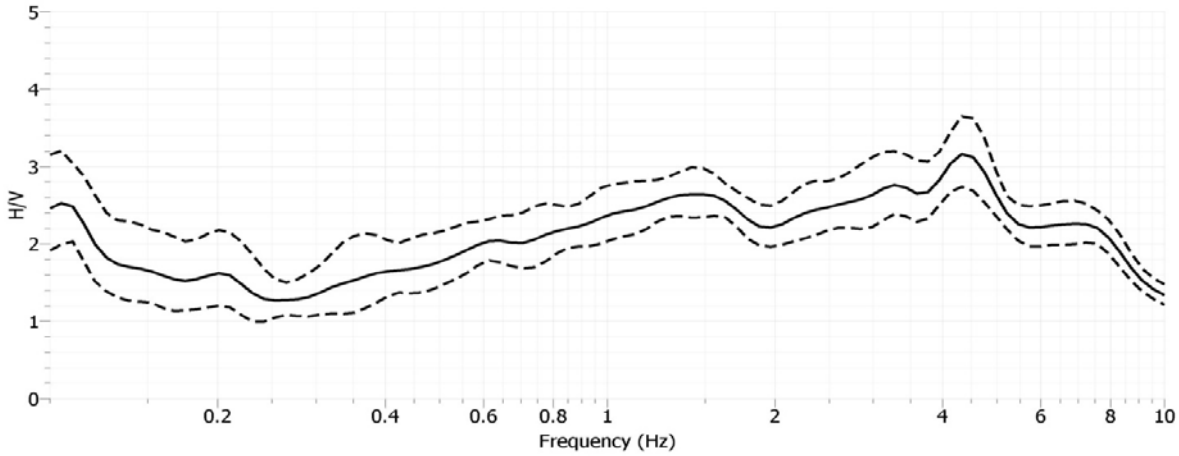

Site CI.FHO, H/V Spectral Ratio, Near Seismic Station, Sensor 450

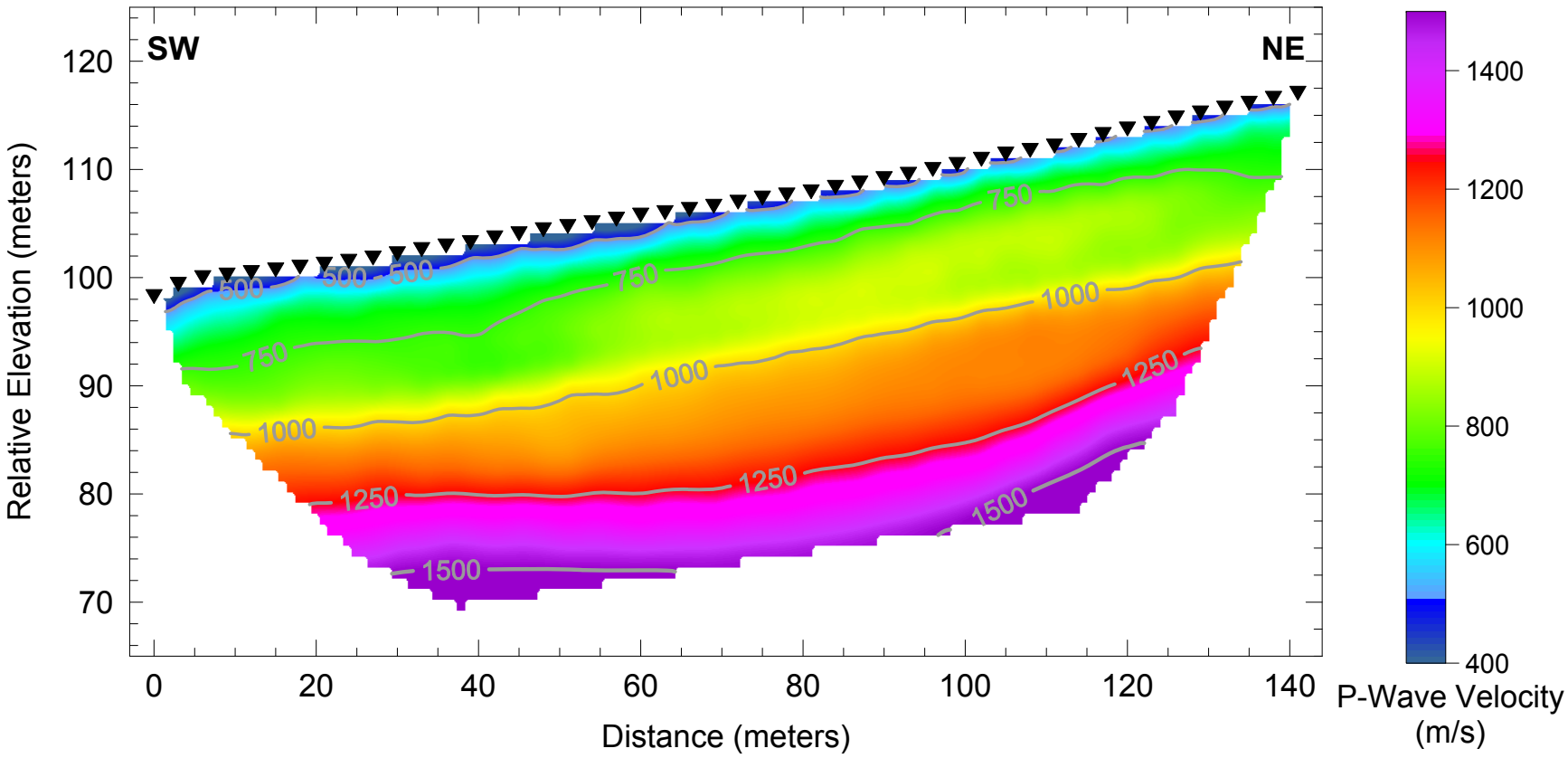

Array FHO-2 – Tomographic seismic refraction model developed using a smooth velocity gradient starting model

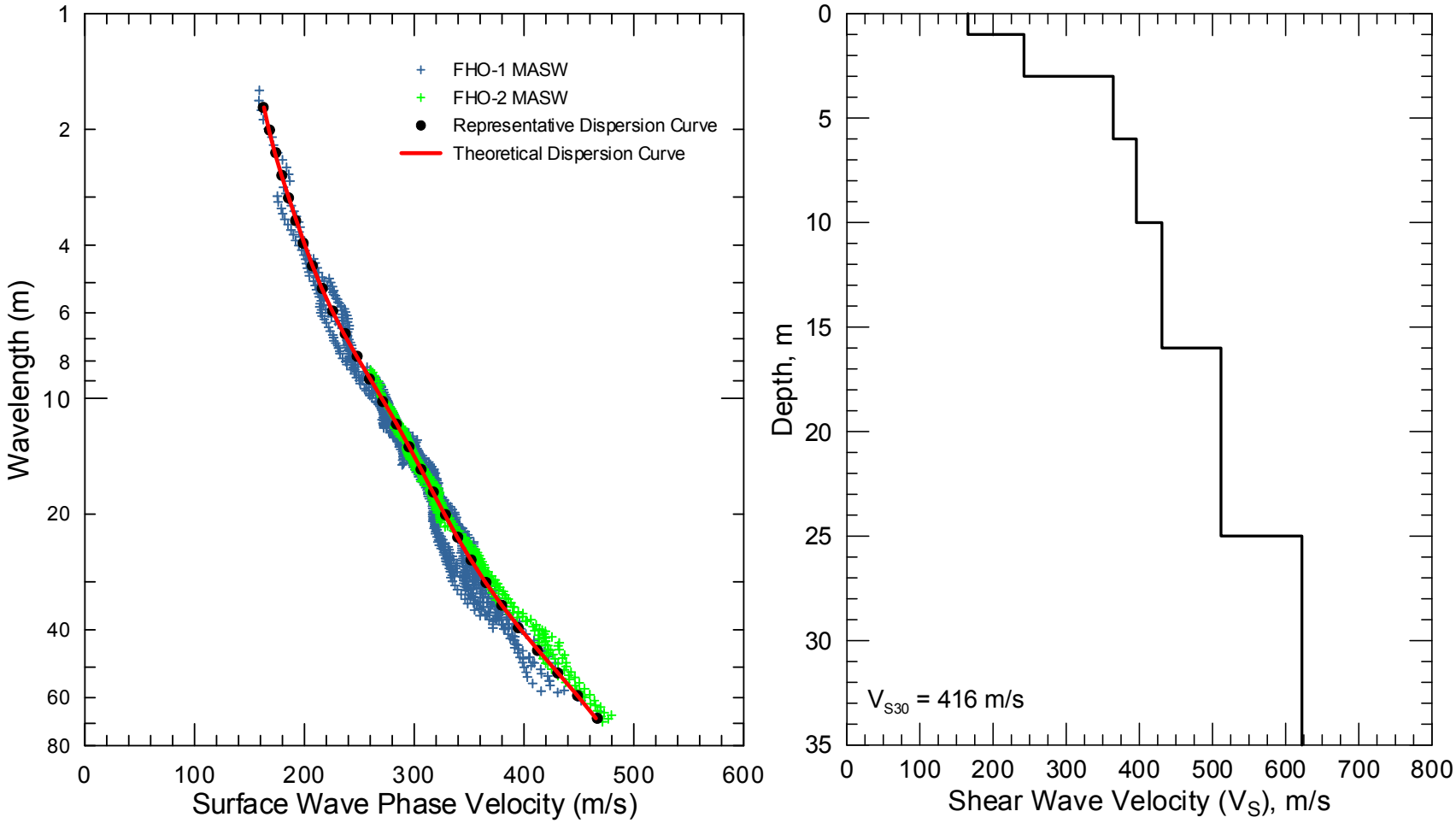

CI.FHO - Field, representative and inverted theoretical surface wave dispersion data (left) and associated V_S model (right)

Site CI.FIG

Location: Figueroa Mountain, Santa Barbara County, California

Latitude: 34.72832 **Longitude:** -119.98803
(Station coordinates provided by USGS, WGS84 coordinate system)

V_{S30} (measured): 489 m/s

V_{S30} (adjusted to more accurately reflect seismic station conditions): 602 (average S-wave velocity between 1.5 and 31.5 m adjusting for assumed seismic station depth) or 657 m/s (V_{S30} estimated by replacing V_S in upper 3.5 m with V_S of underlying unit to account for the seismic sensor likely being placed on weathered rock).

NEHRP Site Class: C

Geomatrix Code: IFB/IFA

Geologic Conditions/Observations: Seismic station located on Mesozoic (Jurassic and Cretaceous) Franciscan Assemblage (greenstone).

Site Conditions: Rural site. Site located on the side of a mountain with gentle decrease in elevation to the south. There was insufficient space to align seismic line parallel to slope. Therefore, the seismic line was oriented subparallel to slope with a 13 m elevation increase to the southwest along the 70.5 m long profile.

Geophysical Methods Utilized: HVSR, Seismic Refraction (P- and S-wave), MASW (Rayleigh wave), MALW (Love wave)

Geophysical Testing Arrays:

1. Array FIG-1 (48 channel MASW and P-wave seismic refraction array utilizing 4.5 Hz vertical geophones spaced 1.5 m apart for a length of 70.5 m, forward and reverse shot locations with multiple source offsets and source types and multiple interior shot locations).
2. Array FIG-1 (48 channel MALW and S-wave seismic refraction array utilizing 4.5 Hz horizontal geophones spaced 1.5 m apart for a length of 70.5 m, forward and reverse shot locations with multiple source offsets and multiple interior shot locations). Coincident with P-wave refraction/MASW array of same name.
3. Three HVSR measurement locations: two distributed along array FIG-1 and the other adjacent to the seismic station.

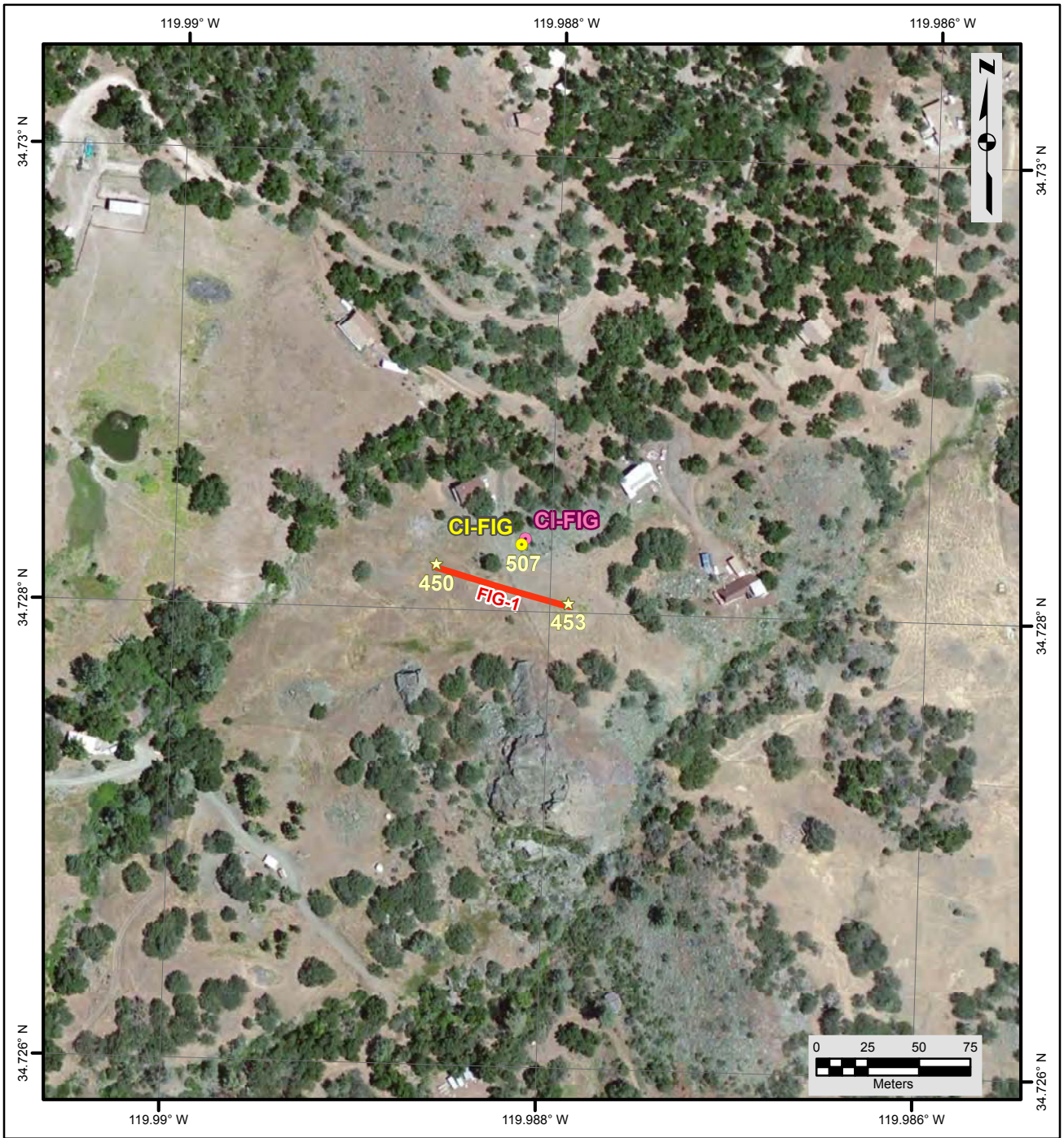

Legend

- Seismic Station - Approximate Surveyed Location
- Seismic Station - Approximate Location of Record
- H/V Spectral Ratio Location
- MASW and Seismic Refraction Line (S- and P-wave)

NOTES:
1. WGS 1984 COORDINATE SYSTEM
2. Image Source: ESRI, i-cubed, USDA FSA, USGS, AEX, GeoEye, Getmapping, Aerogrid, IGP

File Name: CI-FIG-I

Date: 2/7/2013

USGS science for a changing world

GEOVision geophysical services

RECOVERY.GOV

SITE MAP
CI•FIG

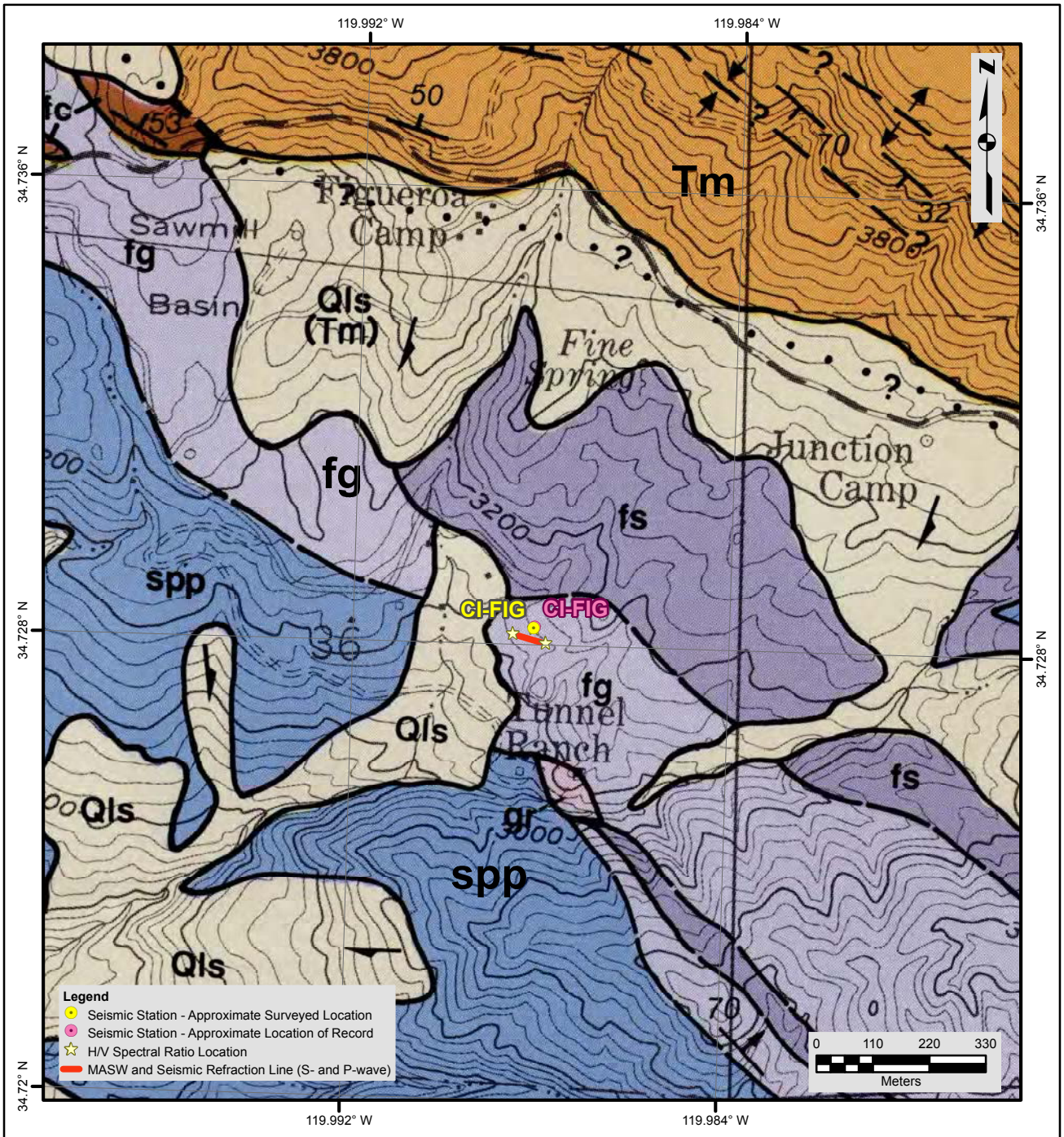

Description of Geologic Map Units

Qls = Quaternary (Holocene) landslide debris
Qls (Tm) = Quaternary (Holocene) Monterey Shale landslide debris
Tm = Tertiary (Miocene) Monterey Shale; marine biogenic upper shale unit, thin bedded, hard, platy siliceous
spp = Mesozoic (Jurassic & Cretaceous) partly serpentinized, peridotite ordanite, amorphous
fs = Mesozoic (Jurassic & Cretaceous) Franciscan Assemblage; graywacke and argilite, hard, coherent but severely fractured fine grained sandstone, massive
fg = Mesozoic (Jurassic & Cretaceous) Franciscan Assemblage; greenstone, massive, aphanitic, severely fractured
gr = Mesozoic (Jurassic & Cretaceous) Franciscan Assemblage; prehnite dioritic rock

NOTES:
1. WGS 1984 COORDINATE SYSTEM
2. Geologic Map of the Figueroa Mountain Quadrangle, Santa Barbara County, California by Thomas W. Dibblee, Jr., 1993
3. See site map for details of geophysical survey

USGS science for a changing world
GEOVision geophysical services

GEOLOGIC MAP
CI•FIG

File Name: CI-FIG
Date: 2/7/2013

Looking south towards seismic station CI.FIG and array FIG-1

Looking north at seismic station CI.FIG and HVSR sensor 507

Looking west along array FIG-1

Looking north towards seismic station from center of array FIG-1

Looking east along array FIG-1

Location of Geophysical Testing Arrays:

Location	Latitude	Longitude
FIG-1, Northwest End of MASW/Refraction Array	34.72818	-119.98851
FIG-1, Center of MASW/Refraction Array	34.72810	-119.98814
FIG-1, Southeast End of MASW/Refraction Array	34.72803	-119.98779
HVSR Sensor 450	34.72820	-119.98850
HVSR Sensor 453	34.72804	-119.98779
HVSR Sensor 507	34.72830	-119.98804
CI.FIG Seismic Station	34.72829	-119.98805

Notes: 1) WGS84 Coordinate System (decimal degrees)
2) Survey accuracy is estimated at 1 to 2 m.

Results:

V_S Model from MALW (Love Wave) Sounding

Depth to Top of Layer (m)	Layer Thickness (m)	S-Wave Velocity (m/s)	Inferred P-Wave Velocity (m/s)	Assumed Poisson's Ratio	Assumed Density (g/cm^3)
0	0.5	67	125	0.300	1.6
0.5	3	183	343	0.300	1.7
3.5	2.5	426	797	0.300	1.8
6	5	562	2312	0.469	2.0
11	7	714	2464	0.454	2.1
18	7	859	2609	0.439	2.1
25	>5	1053	2803	0.418	2.2

Notes: 1) Depth of investigation is about 30 m.
2) Weathered rock is assumed to be saturated below 6 m depth, based on P- and S-wave seismic refraction models. V_P of the saturated rock assumed to increase with depth from 2,300 to 2,800 m/s. The presence of saturated rock and assumed Poisson's ratio does not affect the V_S model.
3) Bottom layer is a half space.
4) Half space velocity is not well resolved.

Observations/Discussion:

- The center of array FIG-1 is only about 25 m from the seismic station; however, the seismic station appears to be closer to an outcrop of Franciscan greenstone, in which case there may be a thinner residual soil layer overlying rock at the seismic station. There were very limited locations to place a seismic line of sufficient length at the site due to both topography and multiple property owners.
- Outcrops of rock in the site vicinity give the impression of laterally variable velocity structure with the outcrops being less resistant to weathering and, therefore, most likely having higher seismic velocity. An additional seismic line from the seismic station to a rock outcrop south of array FIG-1 may be useful to characterize lateral velocity variation at the site.
- There are no distinct low frequency peaks in the HVSR data. There is, however, variable low amplitude HVSR peaks in the 8 to 15 Hz range which could be associated with a thin soil layer overlying weathered rock.
- Field observations indicated that the MASW (Rayleigh wave) technique was not effective at this site due to the thin layer of low velocity sediments overlying higher velocity rock and/or lateral variability of the subsurface velocity structure. Therefore, both P- and S-wave seismic refraction surveys were conducted and MALW (Love wave) data acquired.
- The P- and S-wave seismic refraction data for array FIG-1 were modeled using a tomographic inversion routine with a layer-based starting model. The seismic refraction models were extended to far offset shot locations to extend depth of investigation. It should be noted that a larger geophone spacing, rather than the utilization of far offset shot locations, is preferred for extending depth of investigation when applying tomographic inversion routines. However, the seismic refraction data were acquired in conjunction with surface wave data, where a shorter array length is preferred.
- As is often the case, the P-wave seismic refraction data set was of higher quality than the S-wave data set. The P-wave first arrival data were picked to a greater degree of accuracy than the S-wave first arrival data because the S-wave is not typically the first energy on a seismic record. The higher velocity bedrock first arrivals were relatively clear in the S-wave seismic records from offend shot locations. However, interpretation of the S-wave first arrival data from intermediate depth weathered rock on seismic records from interior shot locations was somewhat subjective. Therefore, the use of the S-wave seismic refraction data is not recommended for site characterization purposes. It may be possible to obtain higher quality S-wave seismic refraction data along an alternate array location at the site.
- The P-wave seismic refraction survey design allowed P-wave velocity to be imaged to a maximum depth of about 15 m. The seismic refraction model indicates that P-wave velocity is about 250 to 400 m/s at the surface and increases to 1,000 m/s at a depth of 2 to 4 m, 1,500 m/s at a depth of 3 to 7 m, 2,000 m/s at a depth of 4 to 9 m and over 2,500 m/s at a depth of 8 to 12 m.
- The S-wave seismic refraction survey design allowed S-wave velocity to be imaged to a maximum depth of about 15 to 20 m. The seismic refraction model indicates that S-wave velocity is about 80 to 150 m/s at the surface and increases to 300 m/s at a depth of 1.5 to 3 m, 600 m/s at a depth of 3 to 6 m and over 700 m/s at a depth of 5 to 15 m.

- Comparison of velocity structure in the P- and S-wave seismic refraction models indicate that the weathered rock is likely saturated below a depth on the order of 6 m. Below this depth S-wave velocities are on the order of 600 to 700 m/s while P-wave velocities are typically over 2,000 m/s.
- There is some lateral velocity variation at the site, likely associated with both a variable thickness of the residual soil layer and variable weathering of rock.
- Due to probable saturation at shallow depth, the P-wave seismic refraction model is not useful for assessing S-wave velocity structure at the site.
- Although not presented or recommended for site characterization, V_{S30} was estimated between 31.5 and 49.5 m on the S-wave refraction model, by projecting the velocity at 20 m depth to 30 m depth. Over this interval, V_{S30} ranges from about 515 to 535 m/s and averages 527 m/s. Because S-wave velocity is expected in gradually increase with depth below 20 m, this V_{S30} estimate would be expected to be conservative. It should be noted that the 31.5 to 49.5 m segment of the seismic line has higher velocity rock at shallower depth than other portions of the line and may, therefore, overestimate average V_{S30} beneath the array.
- Noise conditions at the site were not sufficient for application of passive surface wave techniques.
- MASW (Rayleigh wave) data were of poor quality due to the high velocity shallow rock and lateral velocity variation and were, therefore, not reduced. MALW (Love wave) data were of significantly better quality than the MASW data and were, therefore, reduced and modeled.
- The minimum wavelength surface wave phase velocity data extracted from the 48-channel MALW array is about 15 m. Data reduction using seismic records from smaller hammer sources and a limited offset receiver array (i.e. less active geophones) allowed extraction of surface wave dispersion data to a minimum wavelength of about 2 m. The smaller wavelength Love wave dispersion data was obtained from interior source locations. The offend shot locations did not generally provide usable small wavelength data.
- There is nominally about 40 to 60 m/s scatter in MALW dispersion data likely due to the effects of lateral velocity variation.
- A representative dispersion curve was generated for the MALW data set using a moving average, polynomial curve fitting routine and used for modeling.
- Surface wave depth of investigation is about 30 m. It appears as though the MALW technique requires longer wavelength Love wave phase velocity data to image to 30 m depth than the Rayleigh wave technique requires. The maximum wavelength Love wave phase velocity used for modeling was about 90 m, which is expected to be sufficient to image to 30 m depth. A 60 m wavelength is the minimum wavelength Rayleigh wave phase velocity required to image to 30 m depth. It should be noted that Love wave dispersion data at a 90 m wavelength occurred at a frequency of 8 Hz, and 10 Hz horizontal geophones were used for data acquisition at this site. Comparison of 4.5 and 10 Hz geophones at other sites indicates that this is probably not a significant issue.
- V_{S30} from the MALW V_S model is 489 m/s (Site Class C).
- Average S-wave velocity between 1.5 m and 31.5 m, to account for assumed seismic sensor depth, is 602 m/s (Site Class C). Alternatively, V_{S30} calculated after replacing the V_S of the low velocity soil in the upper 3.5 m with that of the underlying layer, to account

for probable shallower weathered rock beneath the seismic station and seismic station depth, is 657 m/s (Site Class C).

- V_{S30} estimated from the MALW data is about 8% less than that estimated from the S-wave seismic refraction data. However, V_{S30} is estimated from the higher velocity central portion of the seismic refraction model, which is probably not representative of average V_{S30} beneath the array. It is not recommended that the S-wave seismic refraction data be used for site characterization due to uncertainty in picking first arrival data associated with intermediate depth weathered rock from interior shot locations. Comparison of synthetic travel time data from the MALW V_S model to the S-wave seismic records from offend shot location requires a thinning of the upper two residual soil layers in the MALW V_S model to generally fit the offend seismic records, which is consistent with the seismic refraction model.
- Inspection of site geologic conditions and the seismic refraction and MALW models indicates that V_{S30} may have significant variability over small distances in the site vicinity.
- Significant lateral velocity variation appears to be the norm for a wide variety of sites with geologic units of Tertiary age or older. P- and/or S-wave seismic refraction techniques, especially along longer profiles, are the most efficient methods for quantifying lateral velocity variation in a wide variety of geologic conditions and offer a means of identifying areas which are relatively 1-D for surface wave testing. Although this approach was not implemented during this investigation, it should be considered for future investigations of older sediment and rock sites.
- Another common occurrence at rock sites is that V_{S30} adjusted for seismic station conditions can be 20% or more higher than measured V_{S30}. In such cases, it may be a prudent to conduct limited testing immediately adjacent to the seismic station, even if only very limited space is available, to more accurately make the adjustments to V_{S30}. This is an observation made during the investigation and has yet to be implemented or evaluated.
- An S-wave seismic refraction line, aligned approximately orthogonal to array FIG-1 and located between two outcrops of greenstone, may further characterize the lateral velocity variation at the site and S-wave velocity structure.

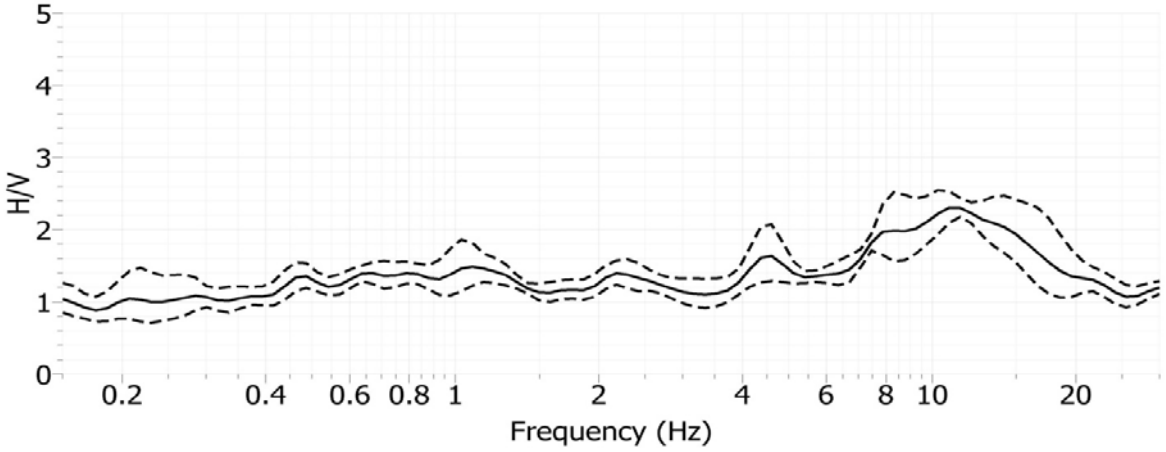

Site CI.FIG, H/V Spectral Ratio, Near Seismic Station, Sensor 507

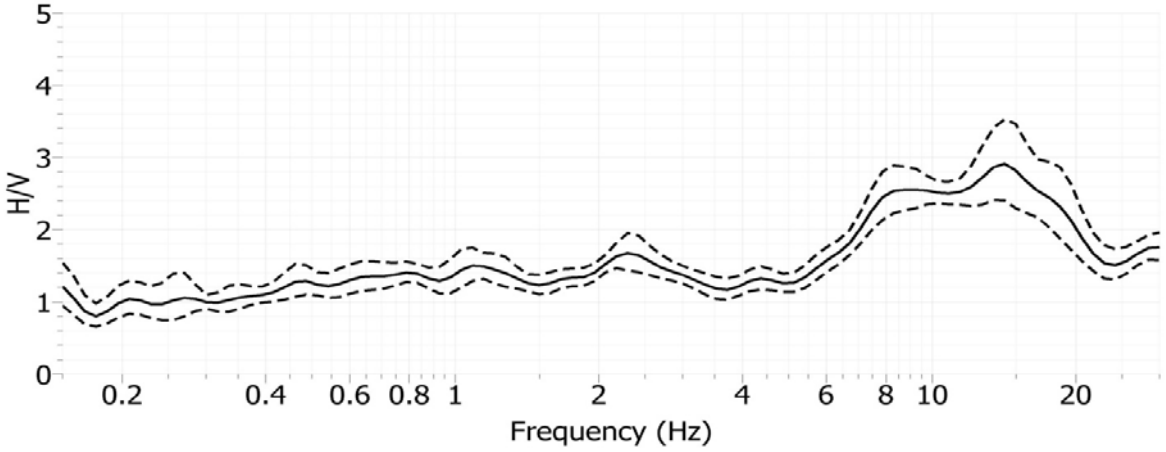

Site CI.FIG, H/V Spectral Ratio, Array FIG -1, Sensor 450

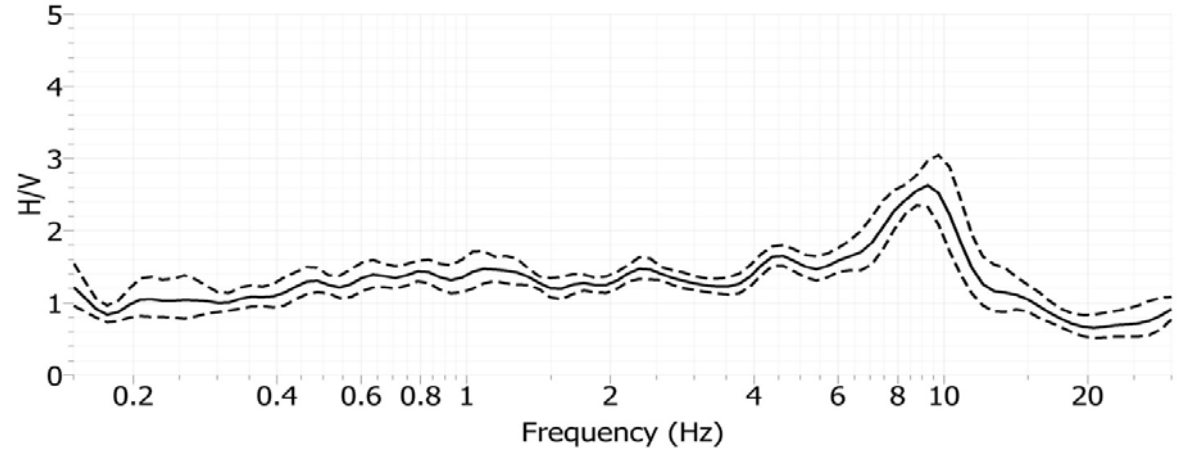

Site CI.FIG, H/V Spectral Ratio, Array FIG -1, Sensor 453

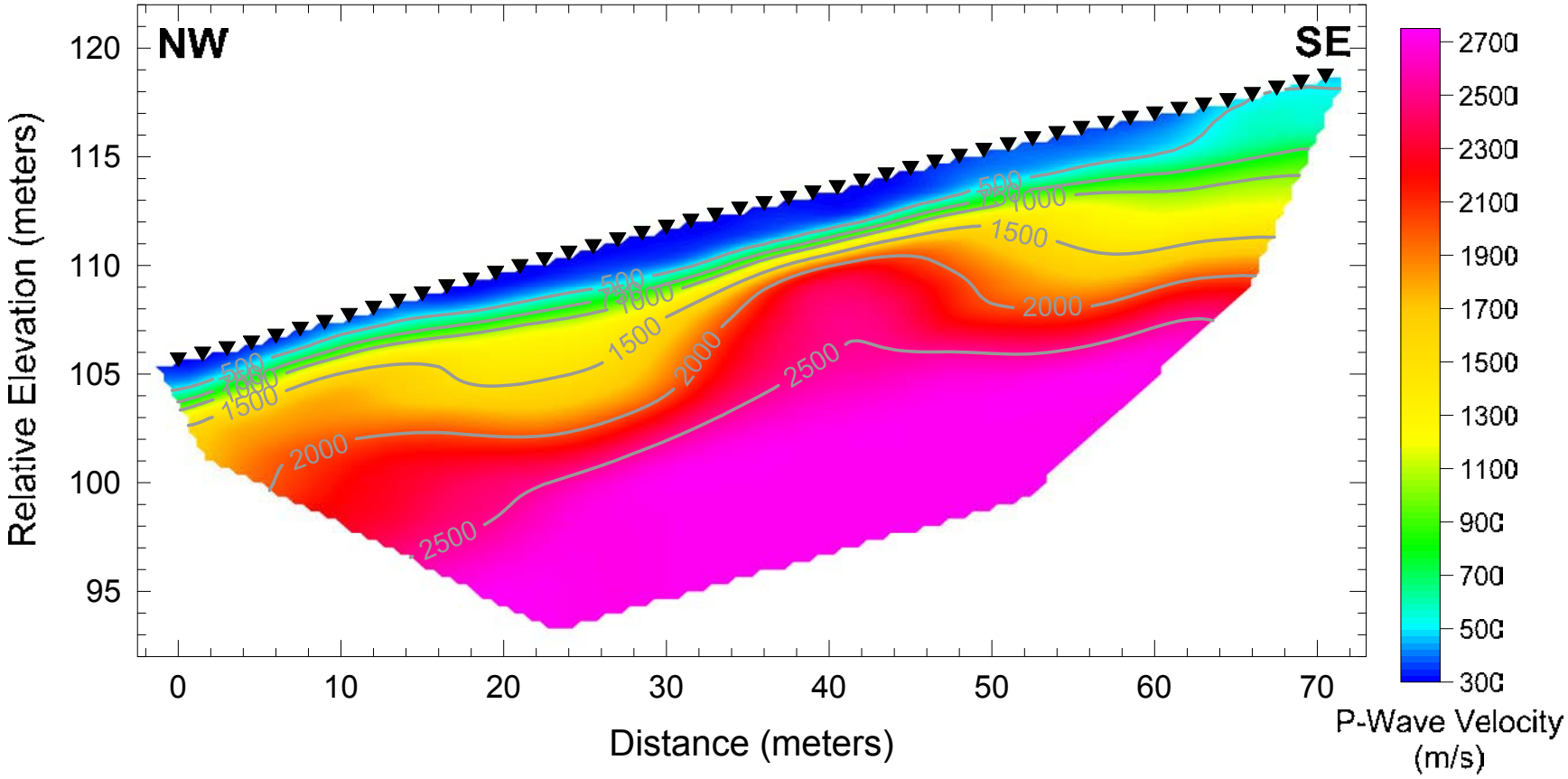

Array FIG-1 – P-wave Tomographic Seismic Refraction Model utilizing Layer Based Starting Model

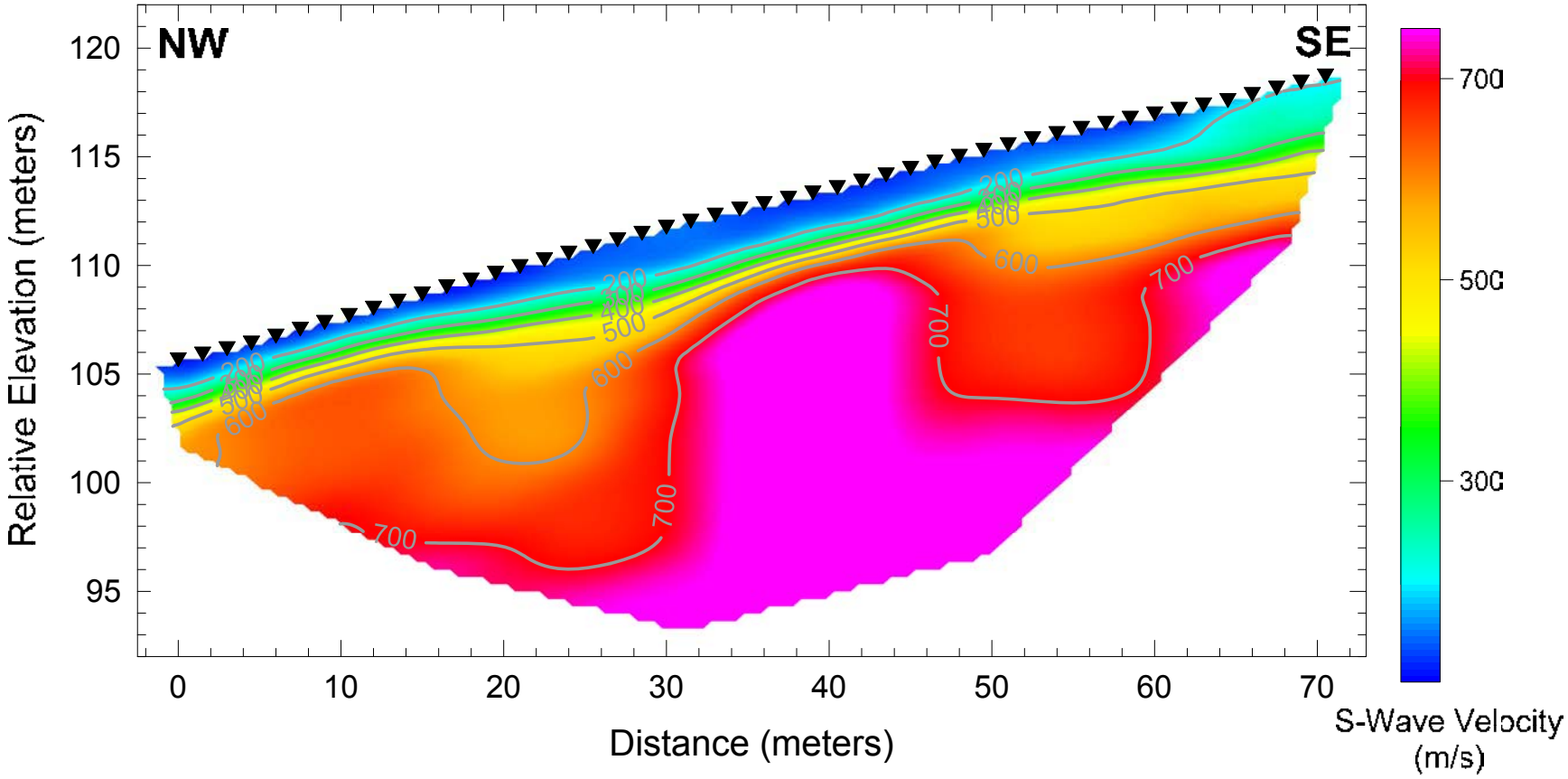

Array FIG-1 – S-wave Tomographic Seismic Refraction Model utilizing Layer Based Starting Model

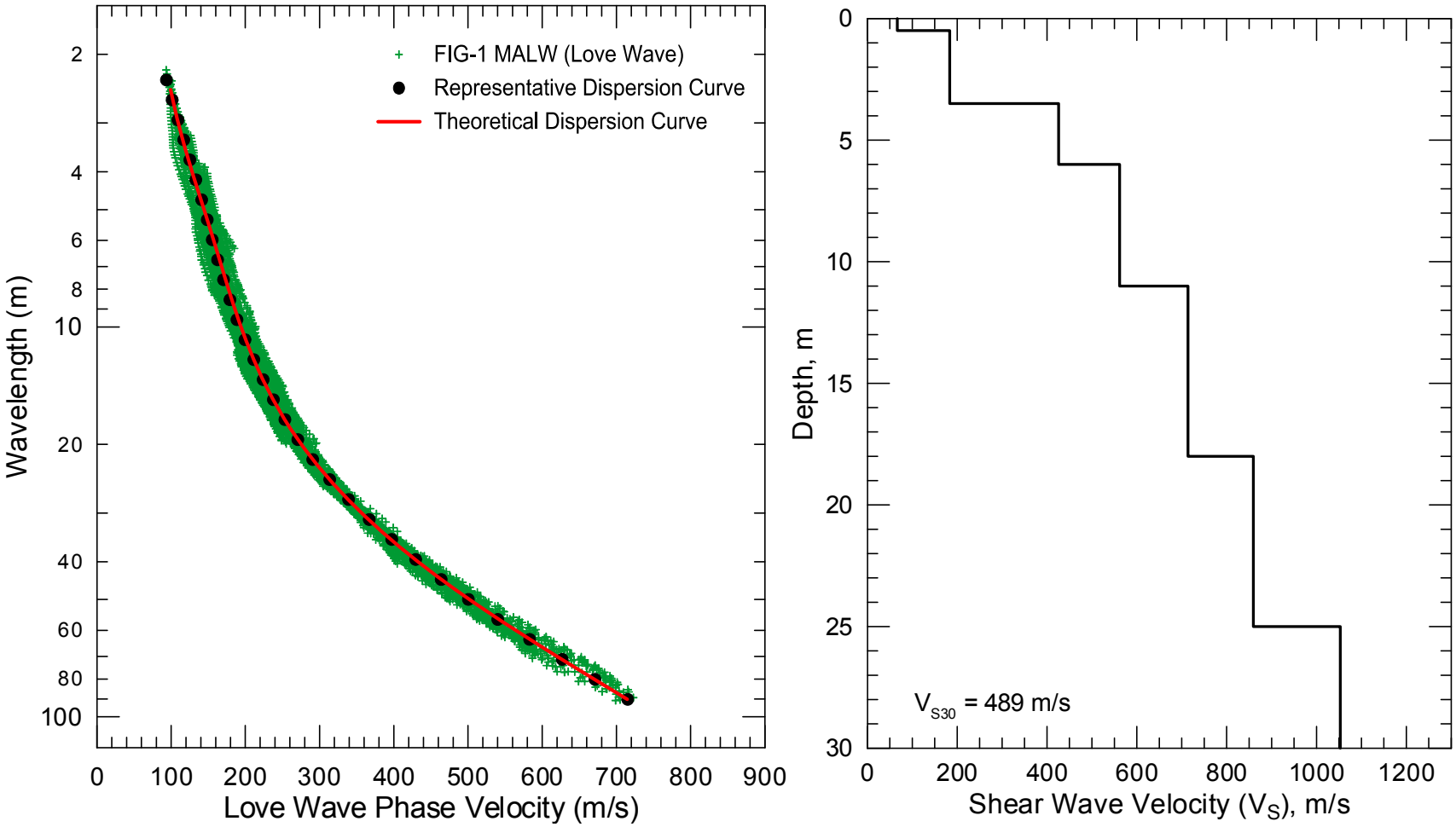

CI.FIG - Field, representative and inverted theoretical surface wave dispersion data (left) and associated V_S model (right)

Site CI.FUR

Location: Furnace Creek, California Highway 190, Death Valley, California

Latitude: 36.46717 **Longitude:** -116.86322

(Station coordinates modified based on field GPS survey, WGS84 coordinate system)

V_{S30} (measured): 433 m/s

V_{S30} (adjusted to more accurately reflect seismic station conditions): 456 m/s (average S-wave velocity between 2 and 32 m adjusting for nominal sensor depth)

NEHRP Site Class: C

Geomatrix Code: IQD/IPD

Geologic Conditions/Observations: Site located at mapped contact of Quaternary (Pleistocene) terrace deposits and geologic unit mapped as Tertiary (Pliocene) travertine. There are no visible outcrops of travertine adjacent to the site. The test area is in a similar geologic environment to the seismic station with scattered alluvial gravels overlying a white or light grey silt and/or clay. Terraces of Pleistocene alluvium appear to be located south and west of the test area and possible terraces of Pliocene silts and clays with a thin veneer of alluvium outcrop to north and east. Crystalline basement expected to be deep at this site.

Site Conditions: Rural site with no traffic. Relatively flat terrain in test area, but hilly/terraced terrain in immediate site vicinity.

Geophysical Methods Utilized: HVSR, Seismic Refraction, MASW, SASW

Geophysical Testing Arrays:

1. Array FUR-1 (48 channel MASW and seismic refraction array utilizing 4.5 Hz vertical geophones spaced 1.5 m apart for a length of 70.5 m, forward and reverse shot locations with multiple source offsets and source types and interior shot locations at a 12 geophone interval).
2. Array FUR-1 (SASW array with common midpoint and orientation as MASW array of same name utilizing 4.5 and 1 Hz vertical geophones and maximum receiver spacing of 32 m).
3. Three HVSR measurement locations distributed along array FUR-1.

Legend

- Seismic Station - Approximate Surveyed Location
- Seismic Station - Approximate Location of Record
- H/V Spectral Ratio Location
- SASW Array
- MASW and Refraction Array

NOTES:
1. WGS 1984 COORDINATE SYSTEM
2. Image Source: ESRI, i-cubed, USDA FSA, USGS, AEX, GeoEye, Getmapping, Aerogrid, IGP

File Name: CI-FUR-I

Date: 2/7/2013

USGS science for a changing world

GEOVision geophysical services

RECOVERY.GOV

SITE MAP
CI•FUR

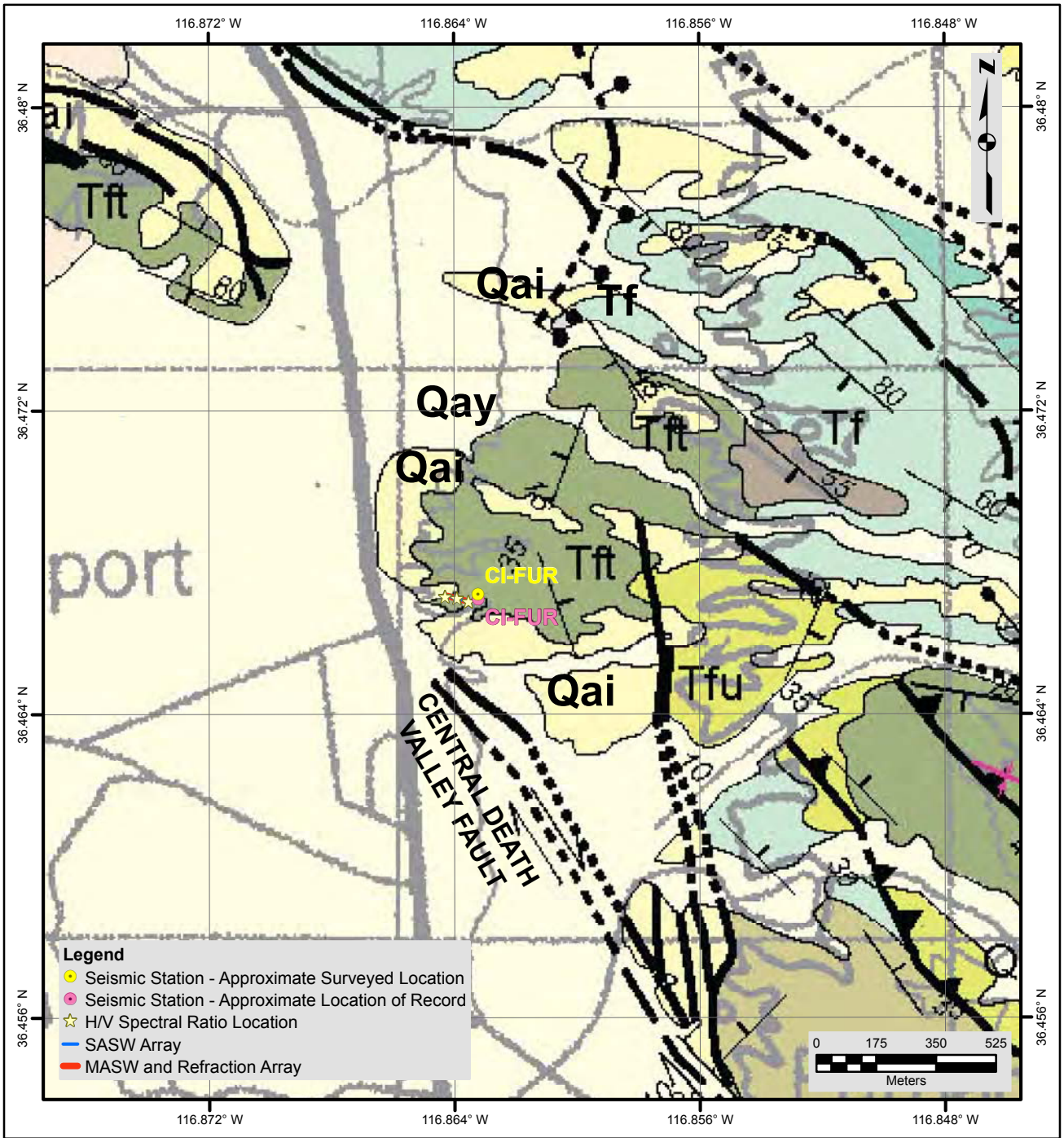

Description of Geologic Map Units

Qay = Quaternary (Holocene) alluvial deposits in recently active channels
Qai = Quaternary (Pleistocene) alluvial deposits in mid-level terraces
Tf = Tertiary (Pliocene) playa and playa margin rocks of Furnace Creek basin
Tft = Tertiary (Pliocene) travertine
Tfu = Tertiary (Pliocene) Upper claystone

NOTES:
1. WGS 1984 COORDINATE SYSTEM
2. Preliminary Geologic Map of the Southern Funeral Mountains and Adjacent Ground-Water Discharge Sites, Inyo County, California and Nye County, Nevada by Christopher J. Fridrich, Ren A. Thompson, Janet L. State, M.E. Berry, and Michael N. Machette, 2008
3. See site map for details of geophysical survey

File Name: CI-FUR

Date: 2/7/2013

USGS science for a changing world

GEOVision geophysical services

RECOVERY.GOV

GEOLOGIC MAP
CI•FUR

Looking northeast towards seismic station CI.FUR (behind building) and HVSR sensor 450

Looking east towards seismic station CI.FUR

Looking east towards center of SASW array FUR-1

Looking south at a Pleistocene alluvial terrace near the test line (note that alluvial layers do not have significant dip)

Looking southeast along MASW array FUR-1

Location of Geophysical Testing Arrays:

Location	Latitude	Longitude
FUR-1, Northwest End of MASW/Refraction Array	36.46713	-116.86430
FUR-1, Center of MASW and SASW Array	36.46705	-116.86392
FUR-1, Southeast End of MASW/Refraction Array	36.46697	-116.86354
HVSR Sensor 450	36.46696	-116.86354
HVSR Sensor 453	36.46706	-116.86391
HVSR Sensor 507	36.46710	-116.86430
CI.FUR Seismic Station	36.46717	-116.86322

Notes: 1) WGS84 Coordinate System (decimal degrees)
2) Survey accuracy is estimated at 1 to 2 m

Results:

V_S Model

Depth to Top of Layer (m)	Layer Thickness (m)	S-Wave Velocity (m/s)	Inferred P-Wave Velocity (m/s)	Inferred Poisson's Ratio	Inferred Density (g/cm^3)
0	1	278	520	0.300	1.9
1	5	326	610	0.300	1.9
6	3	561	1049	0.300	1.9
9	4	390	730	0.300	1.9
13	5	400	1550	0.464	2.0
18	7	477	1600	0.451	2.0
25	>5	655	1650	0.407	2.1

Observations/Discussion:

- Multiple mapped faults are located at distances between 300 and 600 m from the site.
- There are no clear peaks in HVSR plots by which to assess potential lateral velocity variation.
- Noise conditions at site were not sufficient to apply passive surface wave techniques.
- The generalized reciprocal method (GRM) was utilized to develop a three layer seismic refraction model for array FUR-1 with a 2 to 7 m thick upper layer of unsaturated sediments with V_P averaging about 590 m/s, an intermediate unsaturated sediment layer with V_P averaging about 1,050 and a lower layer of probable saturated sediments with V_P averaging about 1,575 m/s. This is likely a simplified model of subsurface velocity structure especially to the southeast of 48 m, where there is a lateral variation in subsurface velocities.
- A tomographic inversion of the first arrival data for array FUR-1 was also conducted using a three horizontal layer starting model based on interactive review of the travel time data and layer based modeling. There were not sufficient interior shots for a robust tomographic inversion of the first arrival data and the model reflects many of the characteristics of the starting model. The model, however, is very similar to the layer based model using the GRM even though the starting model for the tomographic inversion utilized horizontal layers.
- The seismic refraction models demonstrate that there is significant lateral velocity variation at the site, both in dip of subsurface horizons (GRM and tomographic models) and velocity (tomographic model). Such lateral velocity variation can complicate surface wave modeling.
- Surface wave dispersion data from the SASW and MASW data sets are in acceptable agreement at the site; however, it was not possible to extract SASW dispersion data at wavelengths greater than about 30 m due to the complexity of subsurface velocity structure. Therefore, only the MASW dispersion data were used for data analysis. The MASW seismic records show relatively complex wave propagation, including possible reflected surface waves, which could be indicative of lateral velocity variation, dipping layers, subsurface discontinuities, scatterers, etc.
- For reasons outlined above, MASW dispersion data were very difficult to reduce. Small wavelength (high frequency) surface wave dispersion data were extracted from seismic records at the southeast end of the array. High frequency surface wave dispersion data from the near-offset seismic records at the northwest end of the array and interior shots were not utilized for analysis as the effects of lateral velocity variation and potential complex subsurface velocity structure were clearly evident.
- For the purpose of data modeling, a representative dispersion curve was generated for selected MASW dispersion data using a moving average, polynomial curve fitting routine.
- Based on seismic refraction models the top of the saturated zone was constrained at a depth of 13 m for surface wave modeling.
- A high velocity layer (HVL) at a depth of about 6 m was required to model the surface wave dispersion data. This layer has an assumed P-wave velocity of 1,049 m/s, which is consistent with the seismic refraction models. The thickness and velocity of the HVL are not well constrained. The presence of a velocity inversion in the surface wave model

indicates that the seismic refraction models may slightly overestimate depth to the saturated zone.

- The possibility must be considered that subsurface velocity structure is very complex, especially if subsurface layers are dipping and/or the velocity inversion is not continuous.
- Surface wave data were modeled using the fundamental mode Rayleigh wave assumption. The resulting model was evaluated and found to not excite a dominant higher mode.
- The surface wave model is consistent with simplified P-wave refraction model considering unknown Poisson's ratio and lateral velocity variation.
- Surface wave depth of investigation is about 30 m based on half of maximum wavelength criteria.
- V_{S30} is 433 m/s (Site Class C).
- Average S-wave velocity between 2 m (nominal sensor depth) and 32 m is 456 m/s.
- Although velocity structure may be quite complex at the site with lateral velocity variation, potential dipping layers, probable high velocity layer beneath at least a portion of the seismic line, etc. the estimated V_{S30} is likely representative of average velocity structure and more accurate than the S-wave velocity model. V_{S30} at this site likely has higher error than is typical; however, the site is definitely Site Class C.

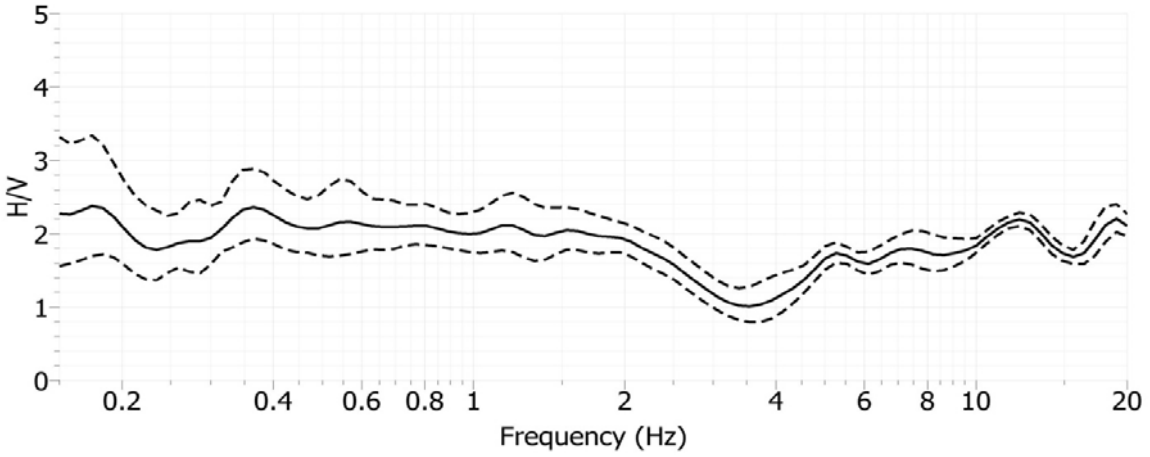

Site CI.FUR, H/V Spectral Ratio, Array FUR-1, Sensor 507

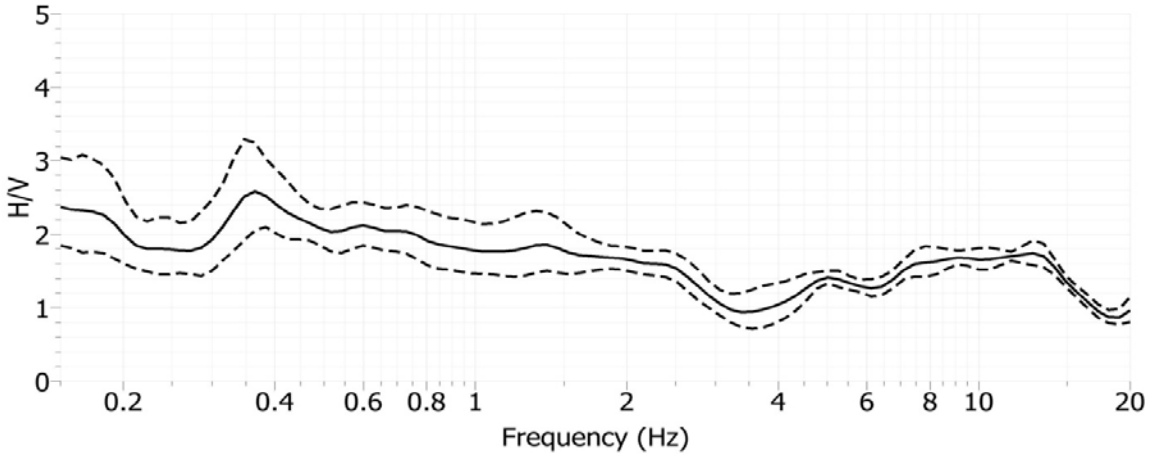

Site CI.FUR, H/V Spectral Ratio, Array FUR-1, Sensor 453

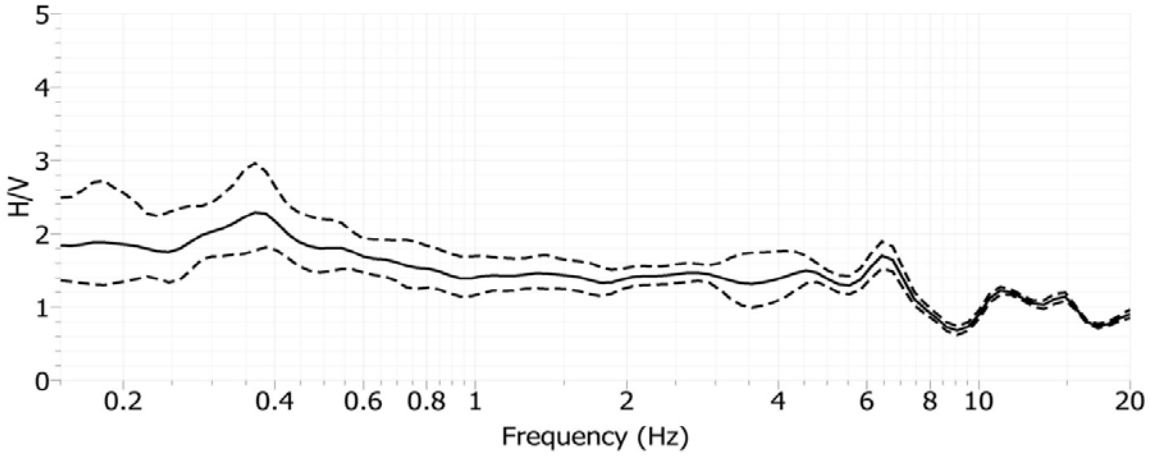

Site CI.FUR, H/V Spectral Ratio, Array FUR-1, Sensor 450

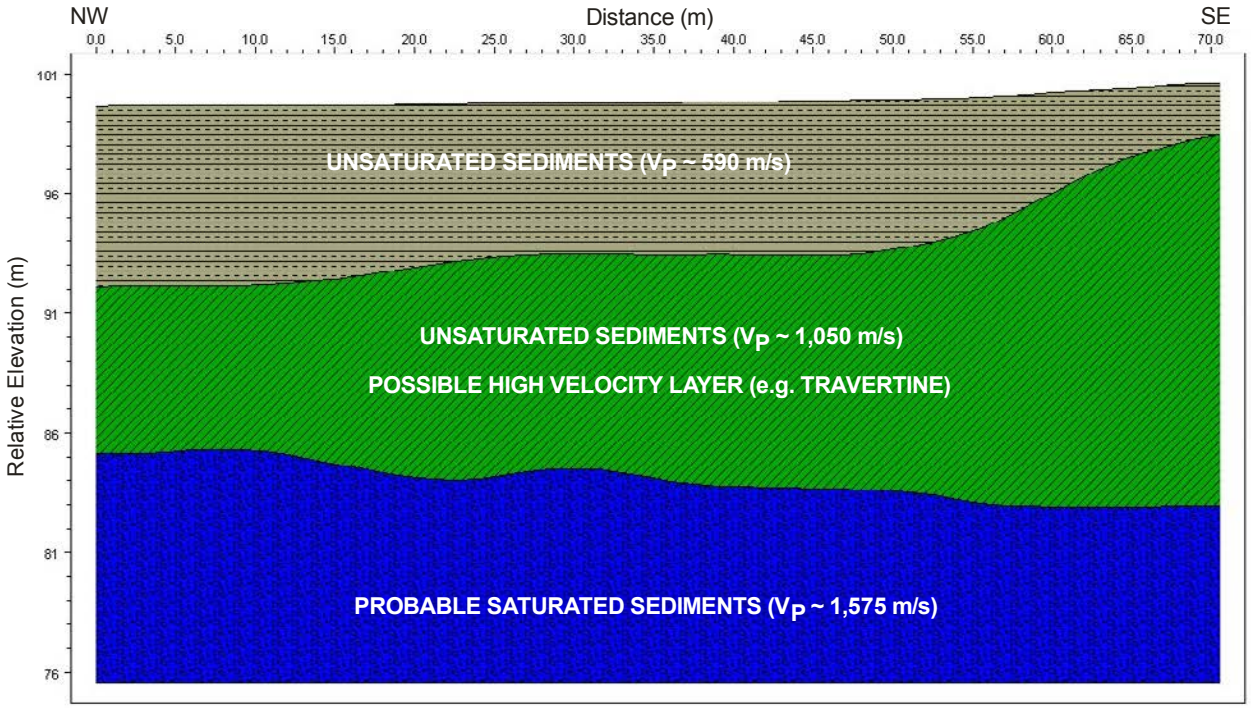

Array FUR-1 – Layer Based Seismic Refraction Model utilizing Generalized Reciprocal Method

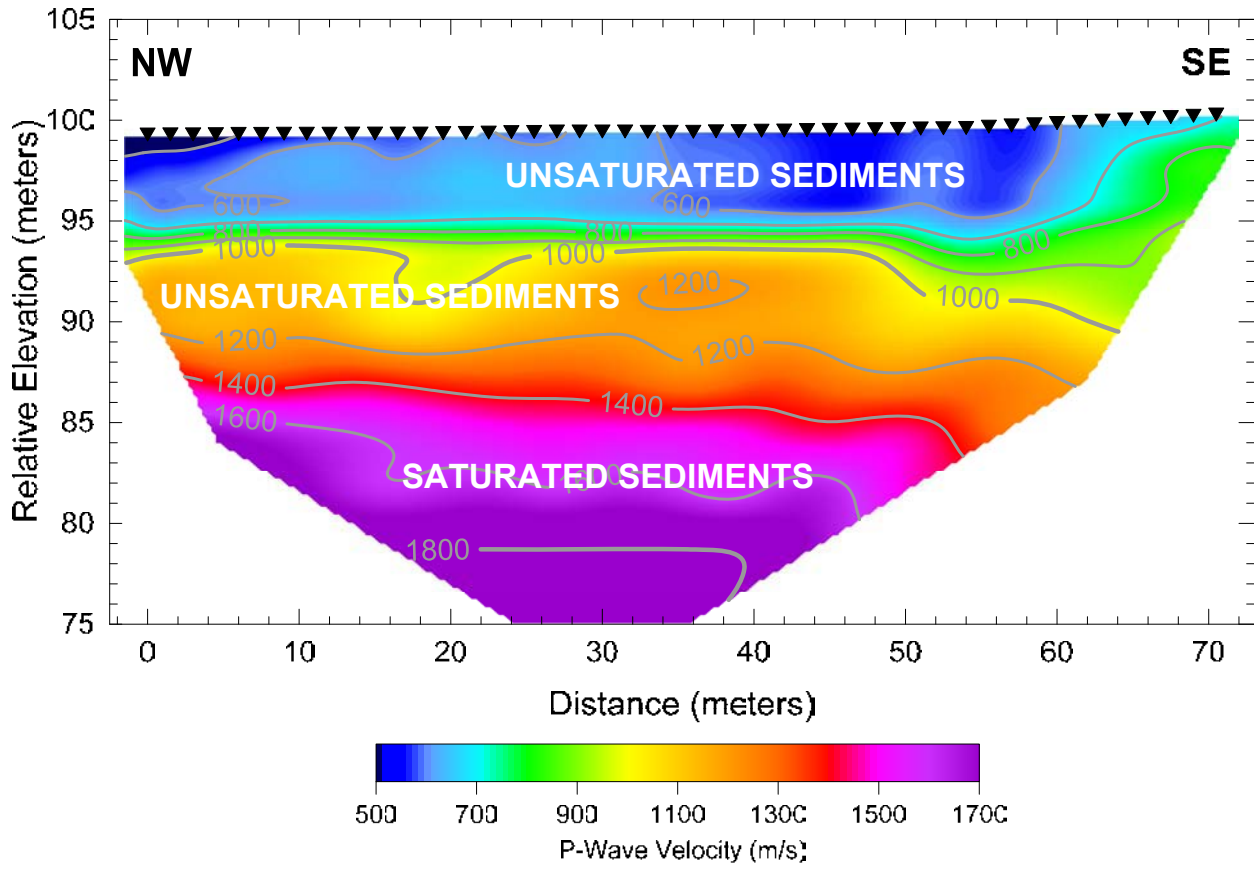

Array FUR-1 – Tomographic Seismic Refraction Model resulting from Layered Starting Model

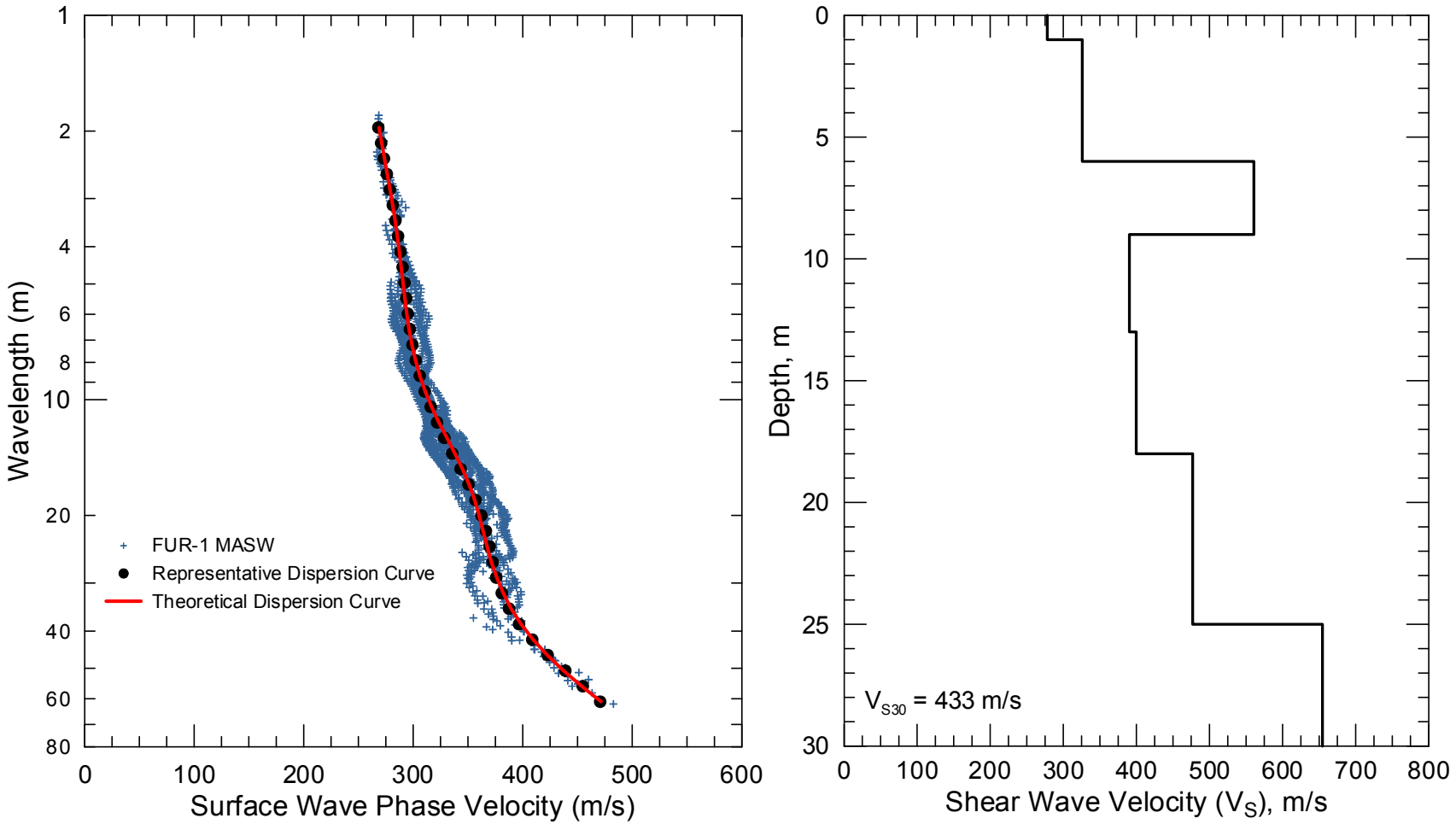

CI.FUR - Field, representative and inverted theoretical surface wave dispersion data (left) and associated V_S model (right) for MASW Array FUR-1.

Site CI.GATR

Location: Ground to Air Transmit and Receive Compound (GATR), Vandenberg Air Force Base, California

Latitude: 34.55266 **Longitude:** -120.50235
(Station coordinates provided by USGS, WGS84 coordinate system)

V_{S30} (measured): 338 m/s

V_{S30} (adjusted to more accurately reflect seismic station conditions): 345 m/s (average S-wave velocity between 0.5 and 30.5 m adjusting for expected 0.5 m sensor depth).

NEHRP Site Class: D/C

Geomatrix Code: IMB/IMD

Geologic Conditions/Observations: Seismic station located on Tertiary (Miocene) Monterey Shale (Upper Unit). Geologic bedding nominally dips about 25 degrees to the south-southeast in immediate site vicinity.

Site Conditions: Rural site. Undulating (hilly) topography in site vicinity. Seismic station and test area located on top of a small hill. Ground surface elevation decreases about 4 m to north along the 70.5 m long MASW and seismic refraction array.

Geophysical Methods Utilized: HVSR, Seismic Refraction, MASW

Geophysical Testing Arrays:

1. Array GATR-1 (48 channel MASW and P-wave seismic refraction array utilizing 4.5 Hz vertical geophones spaced 1.5 m apart for a length of 70.5 m, forward and reverse shot locations with multiple source offsets and source types and multiple interior shot locations).
2. Three HVSR measurement locations (Nanometrics Trillium Compact); two distributed along array GATR-1 and the other adjacent to the seismic station. HVSR measurements were also made with a Tromino ENGY near the seismic station.

Legend

- Seismic Station - Approximate Surveyed Location
- Seismic Station - Approximate Location of Record
- H/V Spectral Ratio Location
- MASW and Seismic Refraction Array

NOTES:
1. WGS 1984 COORDINATE SYSTEM
2. Image Source: ESRI, i-cubed, USDA FSA, USGS, AEX, GeoEye, Getmapping, Aerogrid, IGP

File Name: CI-GATR-I

Date: 10/13/2011

USGS science for a changing world

GEOVision geophysical services

RECOVERY.GOV

SITE MAP
CI•GATR

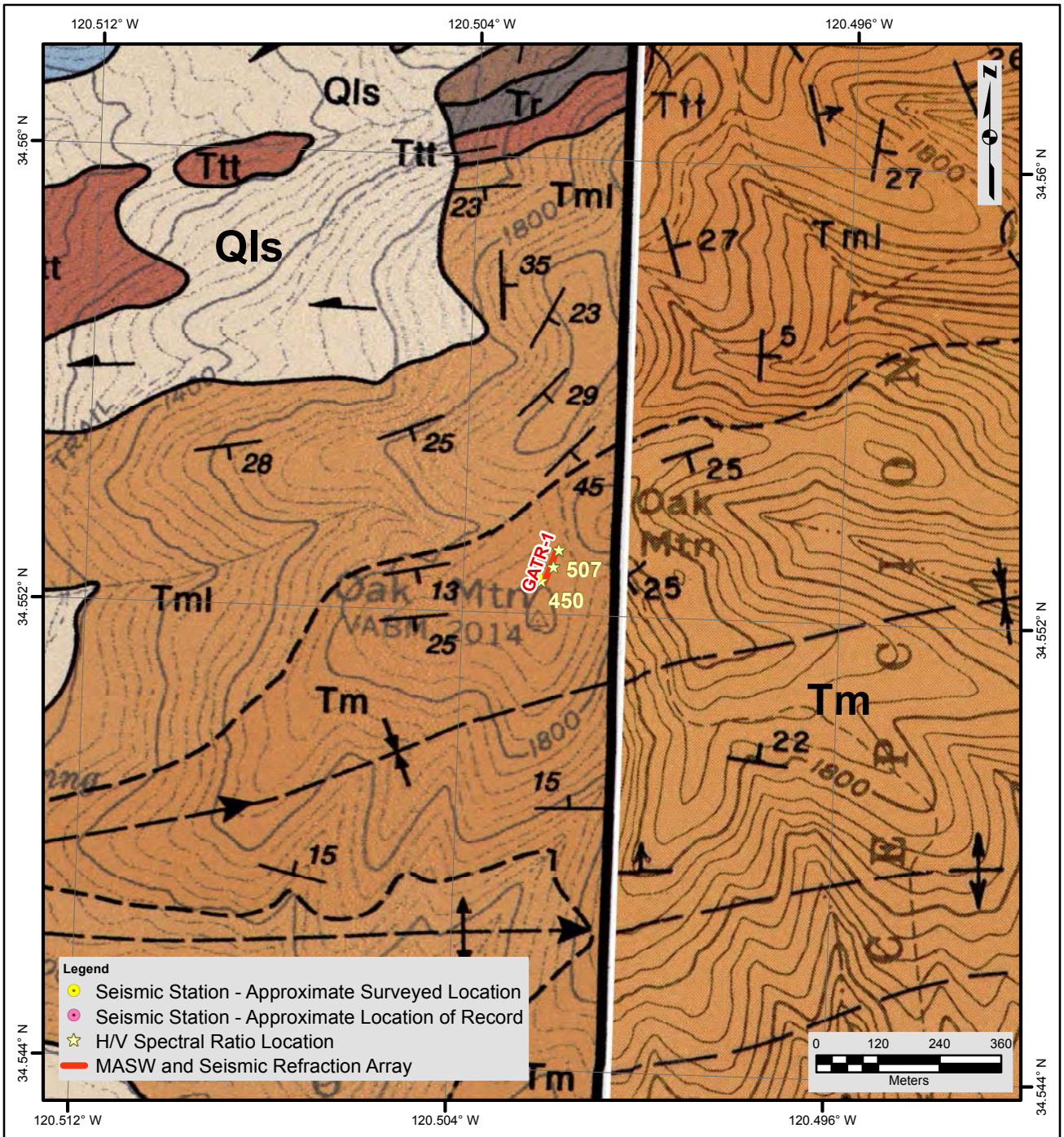

Description of Geologic Map Units

Qls = Quaternary (Holocene) landslide debris
Tm = Tertiary (Miocene) Monterey Shale, upper unit; thin bedded, hard, brittle siliceous shale, very cherty
Tml = Tertiary (Miocene) Monterey shale, lower unit; soft, punky, fissile to platy, semi-siliceous shale
Ttt = Tertiary (Miocene) Tranquillon Volcanic Formation; unbedded rhyolitic tuff-breccia

NOTES:
1. WGS 1984 COORDINATE SYSTEM
2. Geologic Map of the Lompoc Hills & Point Conception and Point Arguello & Tranquillon Mountain Quadrangles, Santa Barbara County, California By Thomas W. Dibblee, Jr., 1988
3. See site map for details of geophysical survey

File Name: CI-GATR

Date: 10/13/2011

USGS science for a changing world

GEOVision geophysical services

GEOLOGIC MAP
CI•GATR

RECOVERY.GOV

Looking west towards CI.GATR seismic station

Looking south at HVSR sensor 507

Looking north towards CI.GATR seismic station and array GATR-1

P-wave seismic refraction data acquisition

Looking northeast at HVSR sensors 450 and Tromino ENGR and array GATR-1

Location of Geophysical Testing Arrays:

Location	Latitude	Longitude
GATR-1, Southwest End of MASW/Refraction Array	34.55254	-120.50218
GATR-1, Center of MASW/Refraction Array	34.55284	-120.50206
GATR-1, Northeast End of MASW/Refraction Array	34.55314	-120.50194
HVSR Sensor 450	34.55258	-120.50224
HVSR Sensor 453	34.55284	-120.50200
HVSR Sensor 507	34.55313	-120.50189
HVSR Sensor Tromino ENGY	34.55259	-120.50226
CI.GATR Seismic Station	34.55265	-120.50234

Notes: 1) WGS84 Coordinate System (decimal degrees)
2) Survey accuracy is estimated at 1 to 2 m.

Results:

V_S Model 1

Depth to Top of Layer (m)	Layer Thickness (m)	S-Wave Velocity (m/s)	Inferred P-Wave Velocity (m/s)	Assumed Poisson's Ratio	Assumed Density (g/cm^3)
0	2	199	372	0.3	1.8
2	3	241	451	0.3	1.8
5	5	283	530	0.3	1.9
10	7	298	557	0.3	1.9
17	8	470	880	0.3	2.0
25	9	627	1173	0.3	2.1
34	>1	745	1395	0.3	2.1

Notes: 1) Depth of investigation is about 35 m.
2) Bottom layer is a half space.

V_S Model 2

Depth to Top of Layer (m)	Layer Thickness (m)	S-Wave Velocity (m/s)	Inferred P-Wave Velocity (m/s)	Assumed Poisson's Ratio	Assumed Density (g/cm^3)
0	2	199	371	0.3	1.8
2	3	242	453	0.3	1.8
5	5	277	518	0.3	1.9
10	11	322	603	0.3	1.9
21	>14	712	1331	0.3	2.1

Notes: 1) Depth of investigation is about 35 m.
2) Bottom layer is a half space.

Observations/Discussion:

- HVSR plots are very similar at every station, especially HVSR sensors 453 and 450, validating the 1-D velocity assumption.
- HVSR data were also recorded with a Tromino ENGY, which was located adjacent to the Nanometrics Trillium Compact sensor 450. Both HVSR sensors yielded similar results.
- There are no clear high frequency HVSR peaks, but there is elevated HVSR response between 0.7 and 6 Hz (i.e. broad peak or multiple low amplitude peaks), which may indicate that S-wave velocity increases with depth over a significant depth interval. It is unclear what effects dipping and folded geologic layers may have on HVSR response.
- The P-wave refraction data for array GATR-1 were modeled using a tomographic inversion routine with a smooth velocity gradient starting model. The seismic refraction model was extended to far offset shot locations to extend depth of investigation.
- Picking of seismic refraction first arrival data was complicated in some areas by a first arrival associated with the asphalt layer in the adjacent road.
- The seismic refraction survey design allowed P-wave velocity to be imaged to a maximum depth of about 20 m. The seismic refraction model shows that P-wave velocity is about 375 to 400 m/s at the surface, increasing to 500 m/s at a depth of 1 to 7 m and 800 m/s at a depth of 16 to 19 m.
- The seismic refraction survey indicates that there is some lateral velocity variation along the seismic line, with a slightly thicker sequence of lower velocity rock at the southern end of the line.
- The seismic refraction/MASW array was orientated almost perpendicular to strike of the geologic bedding, which dips on the order of 25 degrees in a southerly direction. An MASW array located adjacent to the seismic station and parallel to strike and of sufficient length to image to 30 m depth would have had significant topographic variation. Alternatively, it may have been possible to place a line approximately parallel to strike along E-W segment of a dirt road slightly further from the seismic station. The road is cut into a gently to steeply dipping slope, which is not ideal for surface wave testing. Ideally, a P-wave seismic refraction survey and MASW survey, if feasible, would be conducted parallel to strike in the future to demonstrate that velocity structure is somewhat independent of the attitude of the bedding in the site vicinity.
- Noise conditions at the site were not sufficient for application of passive surface wave techniques.
- The minimum wavelength surface wave phase velocity data extracted from the 48-channel MASW array was about 11 m. Reducing data from smaller hammer sources using a limited offset receiver array (i.e. less active geophones) allowed extraction of surface wave dispersion data to a minimum wavelength of about 3 m.
- Small wavelength/high frequency surface wave phase velocity data from small hammer shot locations at the north end of the array yielded slightly higher phase velocity data than shot locations at the south end of the array and was not used for data modeling. The lower phase velocity data from the south end of the array tied in better with surface wave data from far offset shots using larger energy sources and was considered more conservative. V_{S30} would not have significantly changed had the higher phase velocity, small wavelength phase velocity data been selected for modeling, as has been demonstrated at other sites.

- There is about 30 m/s scatter in the MASW dispersion data, particularly at wavelengths below 30 m, which is in part due to lateral velocity variation caused by differential weathering of near surface sedimentary rock.
- A representative dispersion curve was generated for the MASW data set using a moving average, polynomial curve fitting routine and used for modeling.
- Two V_S models were generated for the surface wave dispersion data: a model with gradual increase in velocity with depth after a large velocity increase at 17 m (Model 1) and a model with a minimal number of layers resulting is a large impedance contrast at 21 m depth (Model 2).
- Surface wave depth of investigation is about 35 m based on half of maximum wavelength criteria.
- The inferred P-wave velocities in surface wave model 1, based on an assumed Poisson's ratio of 0.3 and modeled S-wave velocity, are more consistent with the P-wave refraction models. Model 1 is therefore considered the more representative V_S model for the site.
- Both V_S models generate a synthetic HVSR peak at a frequency of about 4 Hz. Although there is elevated HVSR response at about 4 Hz in the field measurements, the elevated HVSR response extends to frequencies lower than 1 Hz, which may indicate that velocity increases with depth over a depth interval of 100 m, or more.
- The S-wave velocity model derived from the surface wave testing is believed to be representative of average subsurface velocity structure. However, geology at the site is complex with dipping bedding and the seismic line was oriented perpendicular to strike. It is difficult to predict the effect of dipping beds on surface wave dispersion data; however, the S-wave velocity model is consistent with observed P-wave velocities in seismic refraction data indicating that weathering may be a significant factor controlling shallow velocity structure.
- V_{S30} is 338 m/s for model 1 and 344 m/s for model 2 (Site Class D/C).
- Average S-wave velocity between 0.5 m (expected sensor depth) and 30.5 m is 345 and 351 m/s for models 1 and 2, respectively (Site Class D/C).

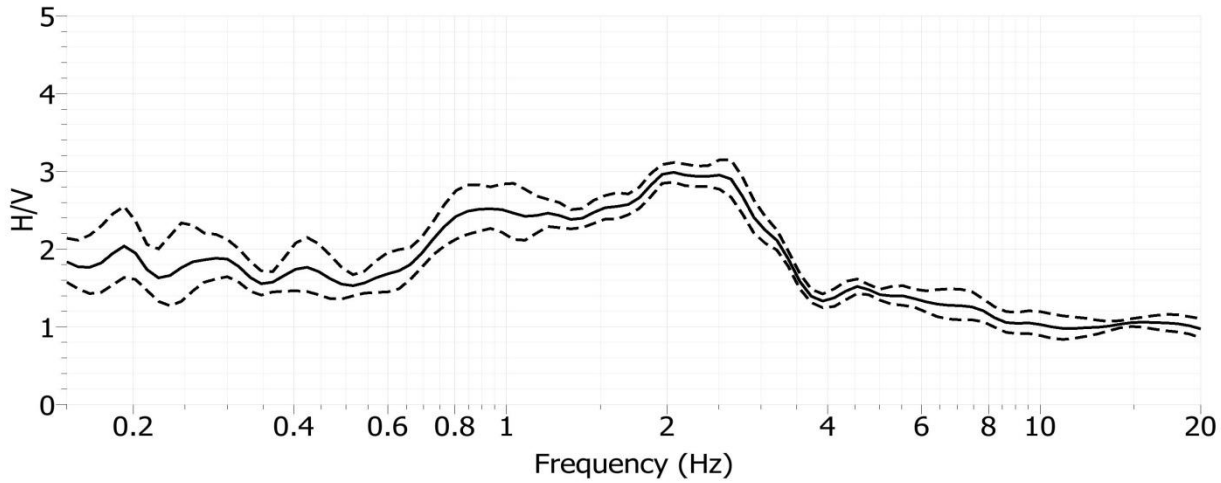

Site CI.GATR, H/V Spectral Ratio, Array GATR-1, Sensor 507

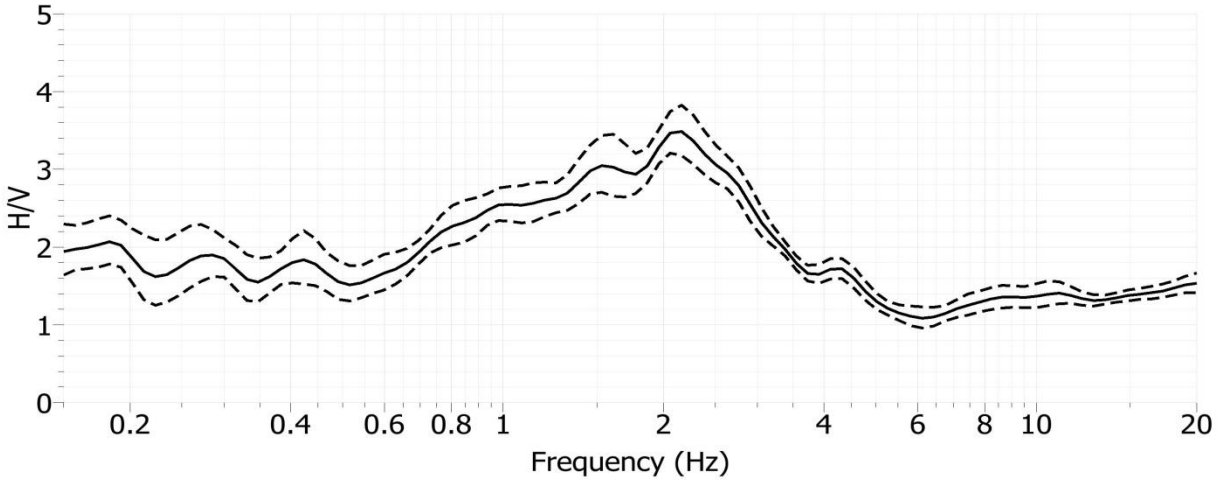

Site CI.GATR, H/V Spectral Ratio, Array GATR-1, Sensor 453

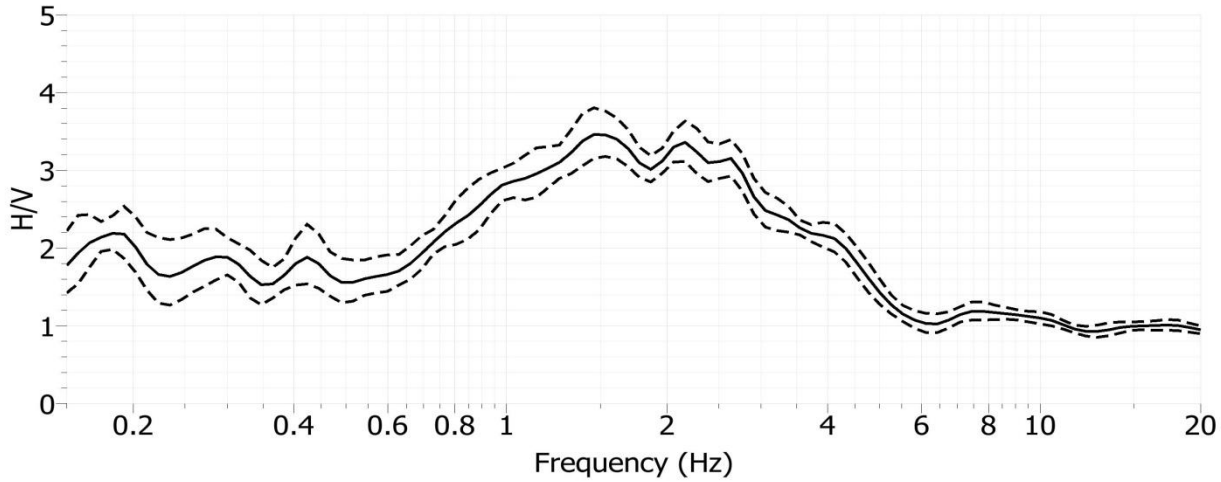

Site CI.GATR, H/V Spectral Ratio, Array GATR-1, Sensor 450

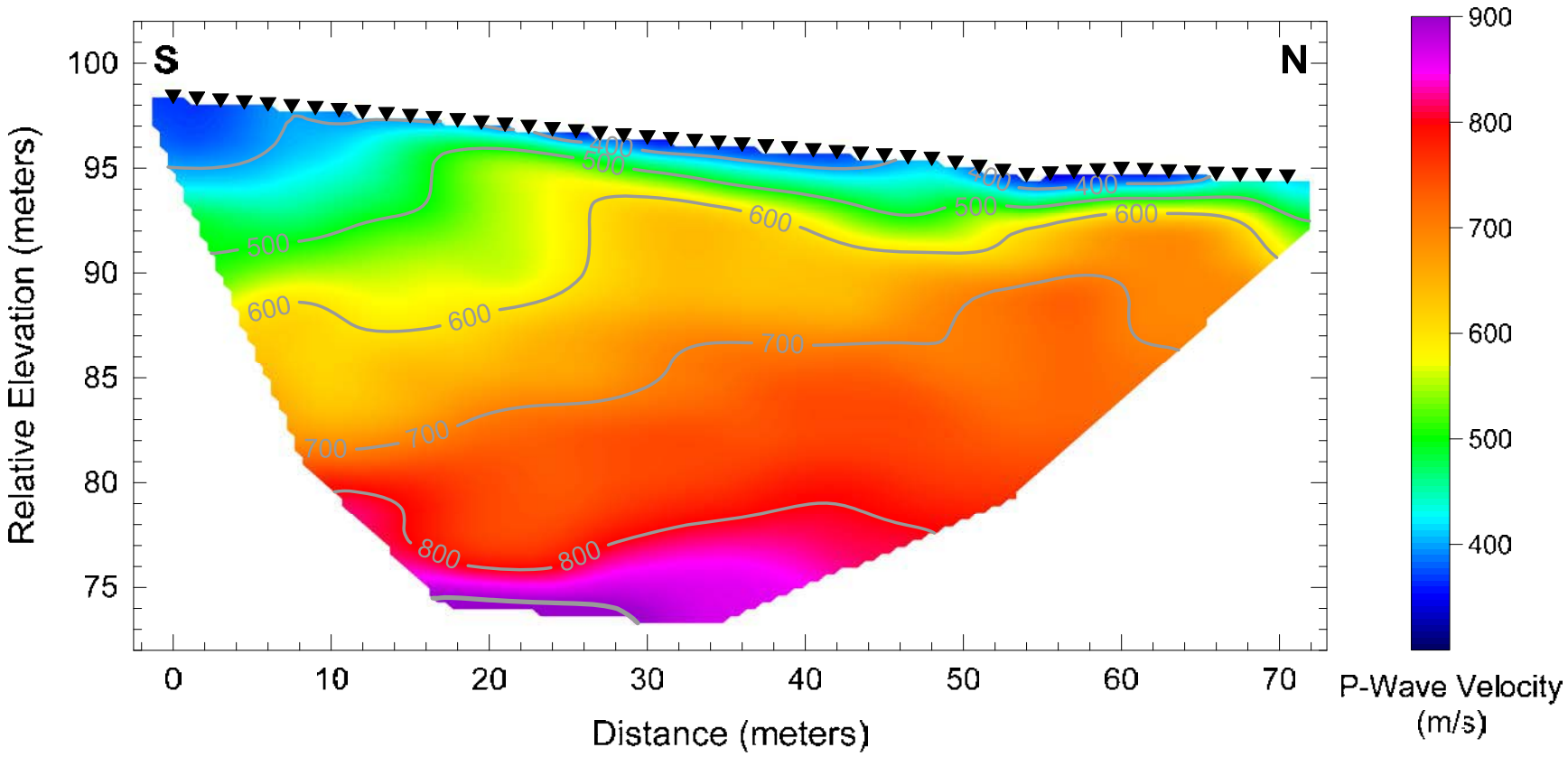

Array GATR-1 – Tomographic seismic refraction model utilizing smooth velocity gradient starting model

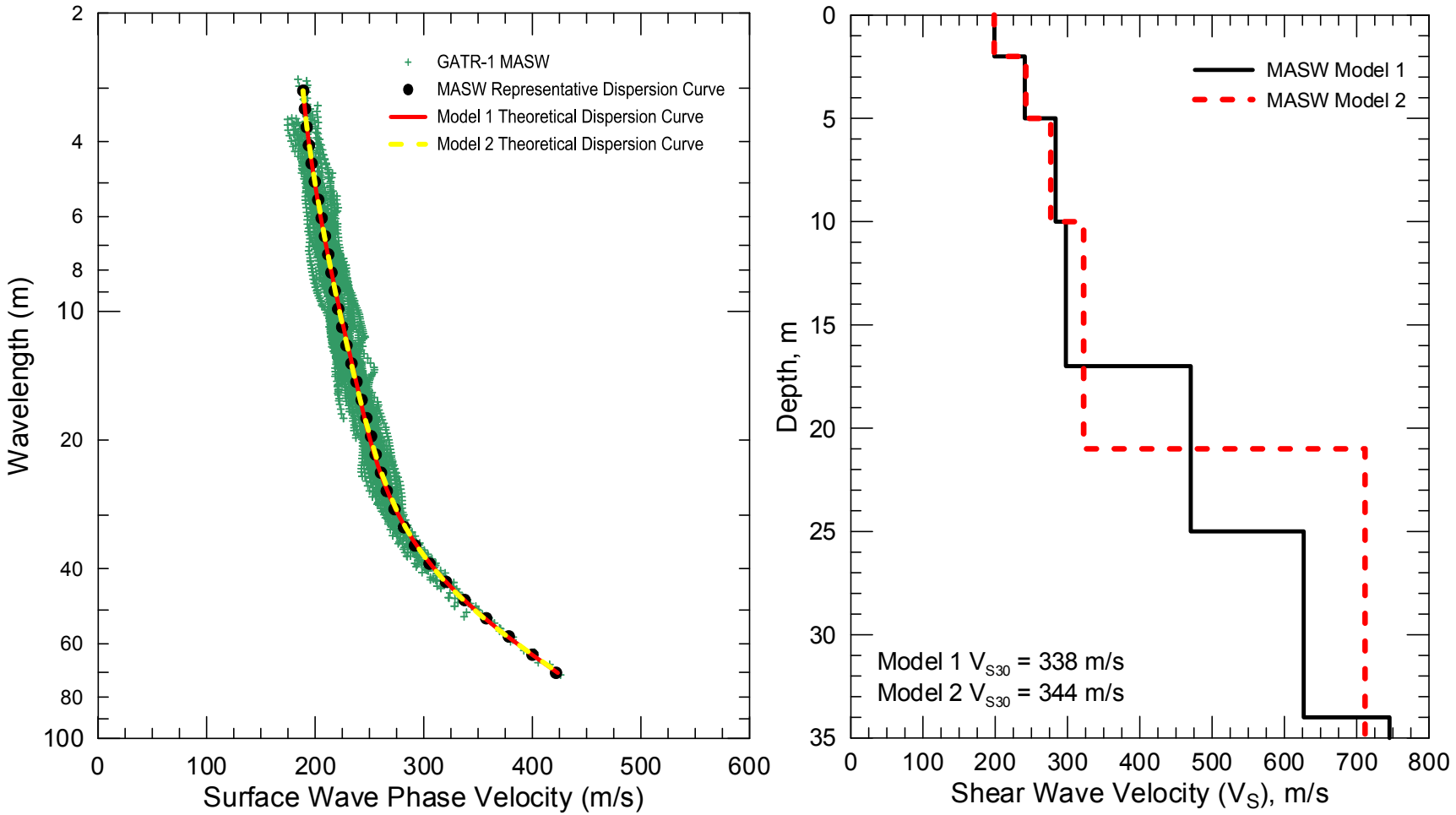

CI.GATR - Field, representative and inverted theoretical surface wave dispersion data (left) and associated V_S model (right)

Site CI.GLA

Location: Glamis, Black Mountain Road, Imperial County, California

Latitude: 33.05149 **Longitude:** -114.82706

(Coordinates provided by USGS – WGS84 coordinate system)

V_{S30} (measured): 743 m/s

V_{S30} (adjusted to more accurately reflect seismic station conditions): 816 - 852 m/s. The average V_S between 2 and 32 m, adjusting for the assumed 2 m sensor depth is 852 m/s. The average V_S between 1 and 31 m, adjusting for the shallowest feasible depth of the seismic sensor, is 816 m/s.

NEHRP Site Class: C/B

Geomatrix Code: IVA

Geologic Conditions/Observations: Seismic station located on outcrop of weathered Tertiary Basalt.

Site Conditions: Rural site located on a basalt outcrop at top of Black Mountain. Test array placed along mountain ridge with only about 3 m of elevation variation along the array. Moderate declines in ground surface elevation to west and east.

Geophysical Methods Utilized: HVSR, Seismic Refraction, MASW

Geophysical Testing Arrays:

1. Array GLA-1 (48 channel MASW and P-wave seismic refraction array utilizing 4.5 Hz vertical geophones spaced 1.5 m apart for a length of 70.5 m, forward and reverse shot locations with multiple source offsets and source types and multiple interior shot locations).
2. Three HVSR measurement locations distributed along array GLA-1.

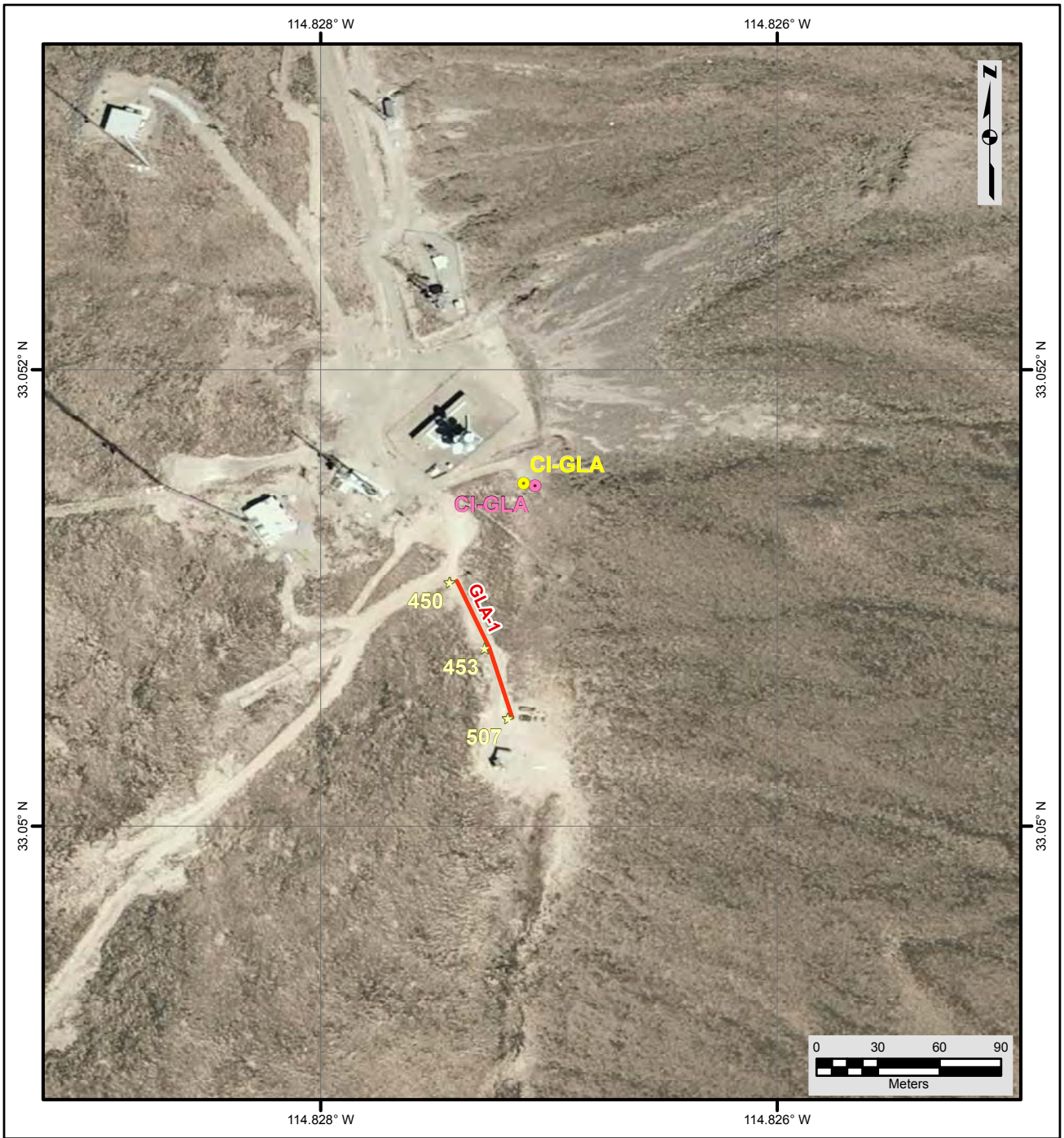

Legend

- H/V Spectral Ratio Measurement Location
- Seismic Station - Approximate Surveyed Location
- Seismic Station - Approximate Location of Record
- MASW and Seismic Refraction Array

NOTES:
1. WGS 1984 COORDINATE SYSTEM
2. Image Source: ESRI, i-cubed, USDA FSA, USGS, AEX, GeoEye, Getmapping, Aerogrid, IGP

File Name: CI-GLA-I

Date: 5/13/2011

USGS science for a changing world

GEOVision geophysical services

RECOVERY.GOV

SITE MAP
CI•GLA

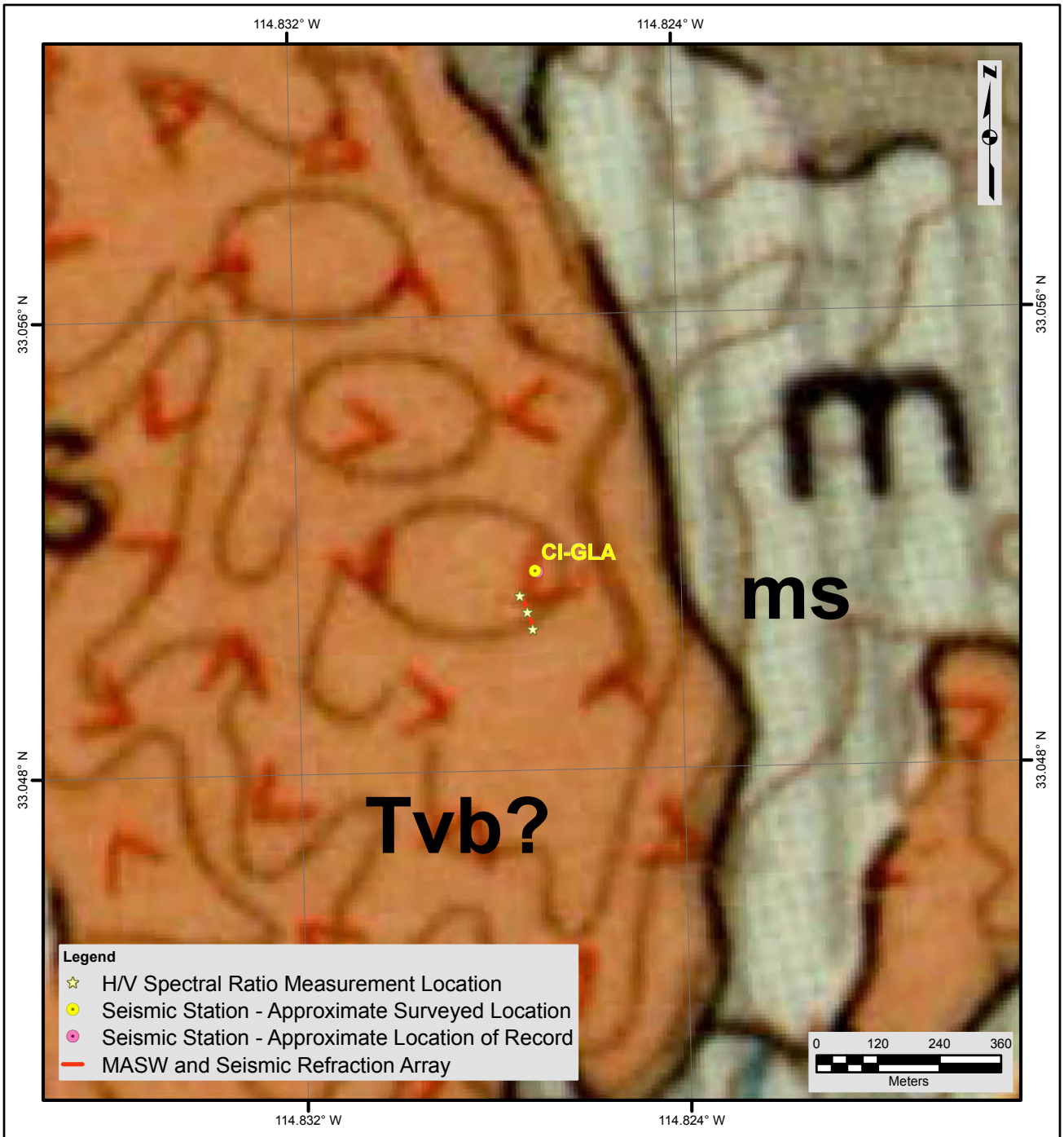

Description of Geologic Map Units

Tvb? = Tertiary volcanic, basalt
ms = Pre-Cretaceous metasedimentary rocks

NOTES:
1. WGS 1984 COORDINATE SYSTEM
2. Geologic Map of California Salton Sea Sheet, Olaf P. Jenkins Edition
Compilation by Charles W. Jennings, 1967
3. See site map for details of geophysical survey

File Name: CI-GLA

Date: 5/26/2011

USGS science for a changing world

GEOVision geophysical services

RECOVERY.GOV

GEOLOGIC MAP
CI•GLA

Looking south towards CI.GLA seismic station and array GLA-1

Looking northwest along MASW and seismic refraction array GLA-1

Data acquisition along a MASW and seismic refraction array GLA-1

Accelerated weight drop energy source used for off-end shot locations on array GLA-1

Near surface weathering of the basalt in the vicinity of seismic station CI.GLA

Location of Geophysical Testing Arrays:

Location	Latitude	Longitude
GLA-1, Southeast End of Array	33.05048	-114.82716
GLA-1, Center of Array	33.05078	-114.82728
GLA-1, Northwest End of Array	33.05108	-114.82740
HVSR Sensor 507	33.05047	-114.82718
HVSR Sensor 453	33.05078	-114.82726
HVSR Sensor 450	33.05107	-114.82744
CI.GLA Seismic Station	33.05150	-114.82711

Notes: 1) WGS84 Coordinate System (decimal degrees)
2) Survey accuracy is estimated at 1 to 2 m

Results:

V_S Model (assumed Poisson's ratio of 0.3)

Depth to Top of Layer (m)	Layer Thickness (m)	S-Wave Velocity (m/s)	Inferred P-Wave Velocity (m/s)	Inferred Poisson's Ratio	Inferred Density (g/cm^3)
0	1	221	414	0.3	1.9
1	2	405	758	0.3	2.0
3	3	634	1186	0.3	2.0
6	4	795	1488	0.3	2.1
10	6	891	1666	0.3	2.1
16	9	921	1724	0.3	2.1
25	>5	1079	2019	0.3	2.2

V_S Model (lower envelope of surface wave dispersion data and assumed Poisson's ratio of 0.3)

Depth to Top of Layer (m)	Layer Thickness (m)	S-Wave Velocity (m/s)	Inferred P-Wave Velocity (m/s)	Inferred Poisson's Ratio	Inferred Density (g/cm^3)
0	1	221	414	0.3	1.9
1	2	405	758	0.3	2.0
3	3	600	1123	0.3	2.0
6	4	700	1310	0.3	2.1
10	6	800	1497	0.3	2.1
16	9	925	1731	0.3	2.1
25	>5	1100	2058	0.3	2.2

V_S Model (upper envelope of surface wave dispersion data and assumed Poisson's ratio of 0.3)

Depth to Top of Layer (m)	Layer Thickness (m)	S-Wave Velocity (m/s)	Inferred P-Wave Velocity (m/s)	Inferred Poisson's Ratio	Inferred Density (g/cm^3)
0	1	221	414	0.3	1.9
1	2	405	758	0.3	2.0
3	3	650	1216	0.3	2.0
6	4	925	1731	0.3	2.1
10	6	950	1777	0.3	2.1
16	9	975	1824	0.3	2.1
25	>5	1050	1964	0.3	2.2

V_S Model (assumed Poisson's ratio of 0.3333)

Depth to Top of Layer (m)	Layer Thickness (m)	S-Wave Velocity (m/s)	Inferred P-Wave Velocity (m/s)	Inferred Poisson's Ratio	Inferred Density (g/cm^3)
0	1	219	437	0.3333	1.9
1	2	394	787	0.3333	2.0
3	3	608	1216	0.3333	2.0
6	4	769	1538	0.3333	2.1
10	6	870	1740	0.3333	2.1
16	9	907	1815	0.3333	2.1
25	>5	1066	2132	0.3333	2.2

Observations/Discussion:

- The HVSR curves are similar and there is low amplitude peak at 1.2 to 1.3 Hz associated with each sensor. Sensor 507 and, to a lesser degree, sensor 453 have high amplitude EM interference at about 5 minute intervals from a nearby microwave antenna. Sensor 507 also has a HVSR peak at about 5 Hz, which may be cultural rather than geologic. The best quality HVSR data is at sensor 450, which is furthest from the microwave antenna.
- Given the velocity structure at the site, a 1.25 Hz HVSR peak would be associated with a strong impedance contrast at a depth of over 200 m. It is unclear what the source of 1 Hz microtremor energy is at this remote site where the Colorado River is located 12 km to the east, Hwy 78 is located 12 km to the north and I-8 is located 32 km to the south.
- A representative dispersion curve was generated for the combined MASW data set using a moving average, polynomial curve fitting routine and used for data modeling.
- There was significant 120 Hz noise in the seismic data at the southernmost end of array GLA-1. The noise had the largest impact on the seismic refraction data at the southern 12 m of the array and was expected to have minimal impact on the surface wave data.

- The seismic refraction model shows P-wave velocity increasing with depth from about 400 m/s at the surface to over 1,750 m/s at a depth of 3 to 4 m.
- Depth of investigation of the P-wave seismic refraction survey is estimated at 10 to 15 m and there is no evidence that P-wave velocity significantly exceeds 2,000 m/s in the upper 15 m.
- Clear evidence of lateral velocity variation based on significant scatter in MASW surface wave dispersion data from multiple source locations.
- Generally, it was very difficult extracting surface wave dispersion data at wavelengths less than about 10 m, likely the result of lateral velocity variation and the high velocity near surface rock. Only two MASW seismic records from near the southern end of the line contributed surface wave dispersion data that was used for analysis over the 3 to 10 m wavelength range.
- Surface wave depth of investigation is about 30 m based on half of maximum wavelength criteria.
- Several V_S models were generated to 1) demonstrate the difference resulting from an assumed Poisson's ratio of 0.33 instead of the typically utilized 0.3 and 2) check model differences between lower and upper envelopes of surface wave dispersion data.
- The surface wave models slightly underestimate P-wave velocity structure observed in the seismic refraction model.
- The V_S model of the average representative dispersion curve with an assumed Poisson's ratio of 0.3 is used for site characterization purposes.
- V_{S30} is 743 m/s (Site Class C/B). Assumed Poisson's ratio of 0.3.
- An assumed Poisson's ratio of 0.3333 decreases V_{S30} to 727 m/s (2 % reduction).
- Modeling the lower and upper envelopes of the surface wave dispersion curve and assumed Poisson's ratio of 0.3 results in V_{S30} of 715 and 775 m/s (nominal 4 % change in V_{S30}).
- Average S-wave velocity between 2 m (assumed sensor depth) and 32 m is 852 m/s (Site Class B).
- Average S-wave velocity between 1 m (shallowest probable sensor depth) and 31 m is 816 m/s (Site Class B).
- The average S-wave velocity between 1 m (shallowest probable sensor depth) and 31 m is greater than 783 m/s (Site Class B) for all models presented. It is therefore justified to consider this site NERHP Site Class B or B/C.

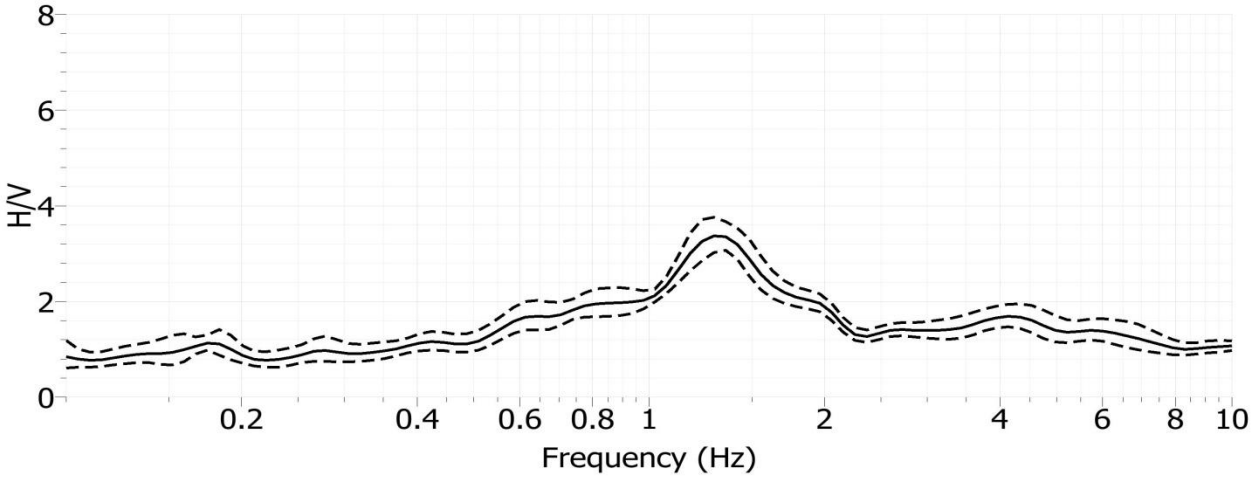

Site CI.GLA, H/V Spectral Ratio, Array GLA-1, Sensor 450

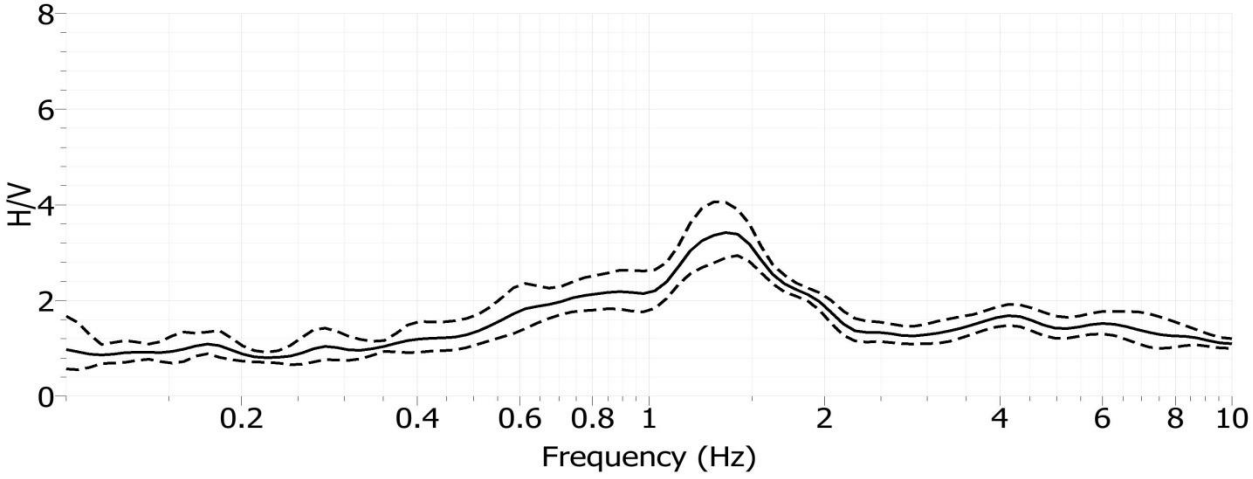

Site CI.GLA, H/V Spectral Ratio, Array GLA-1, Sensor 453

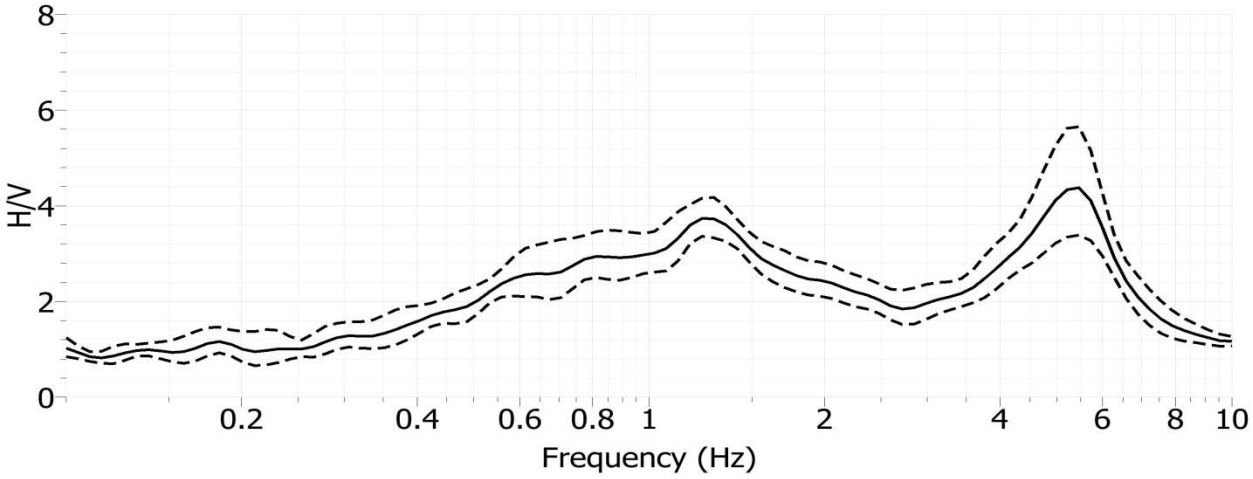

Site CI.GLA, H/V Spectral Ratio, Array GLA-1, Sensor 507

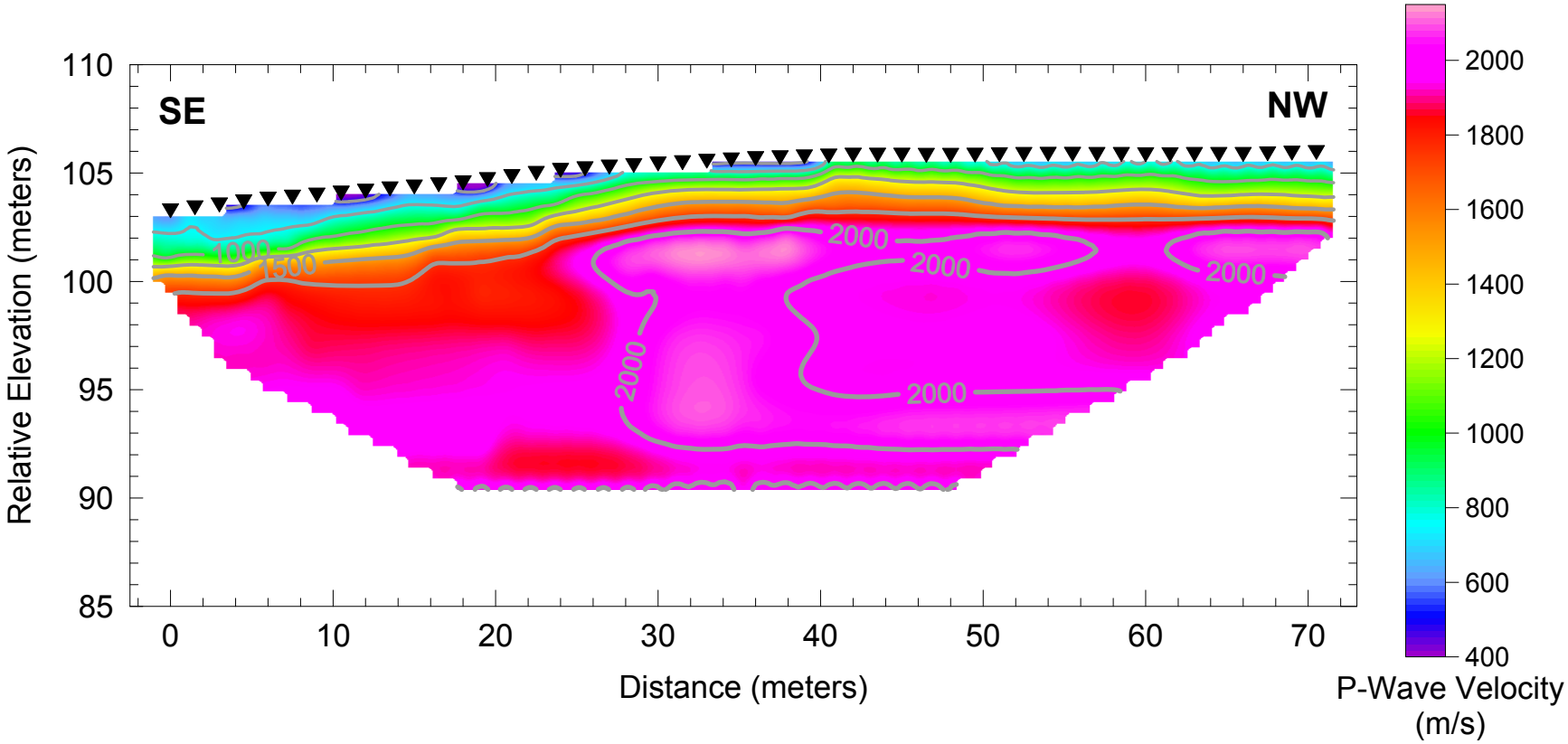

Array GLA-1 – Tomographic Seismic Refraction Model utilizing Smooth Velocity Gradient Starting Model

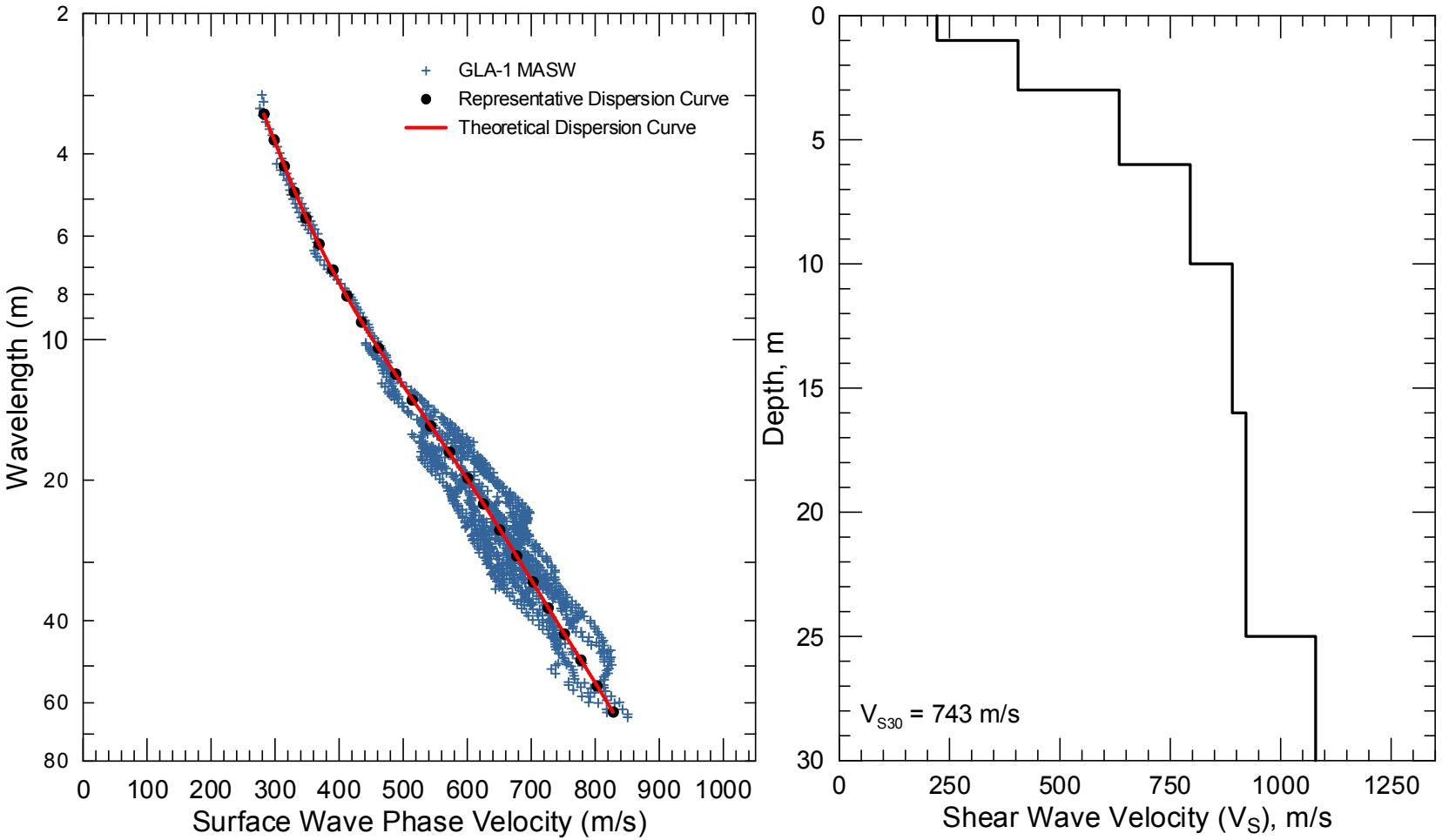

CI.GLA - Field, representative and inverted theoretical surface wave dispersion data (left) and associated V_S model with assumed Poisson's ratio of 0.3 (right)

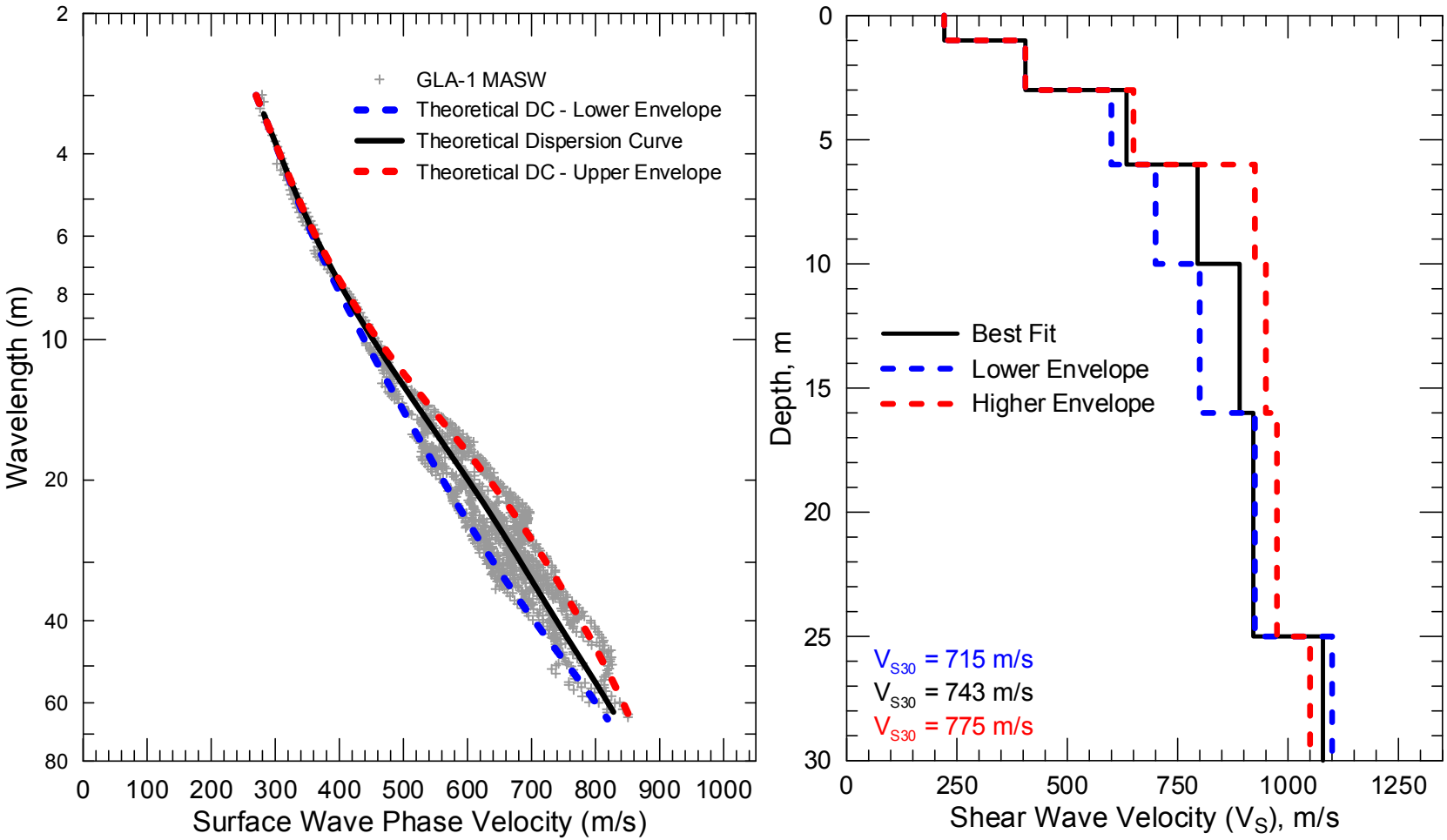

CI.GLA - Field, representative and inverted theoretical surface wave dispersion data (left) and associated V_S models fitting lower and upper envelope of surface wave dispersion data and with assumed Poisson's ratio of 0.3 (right)

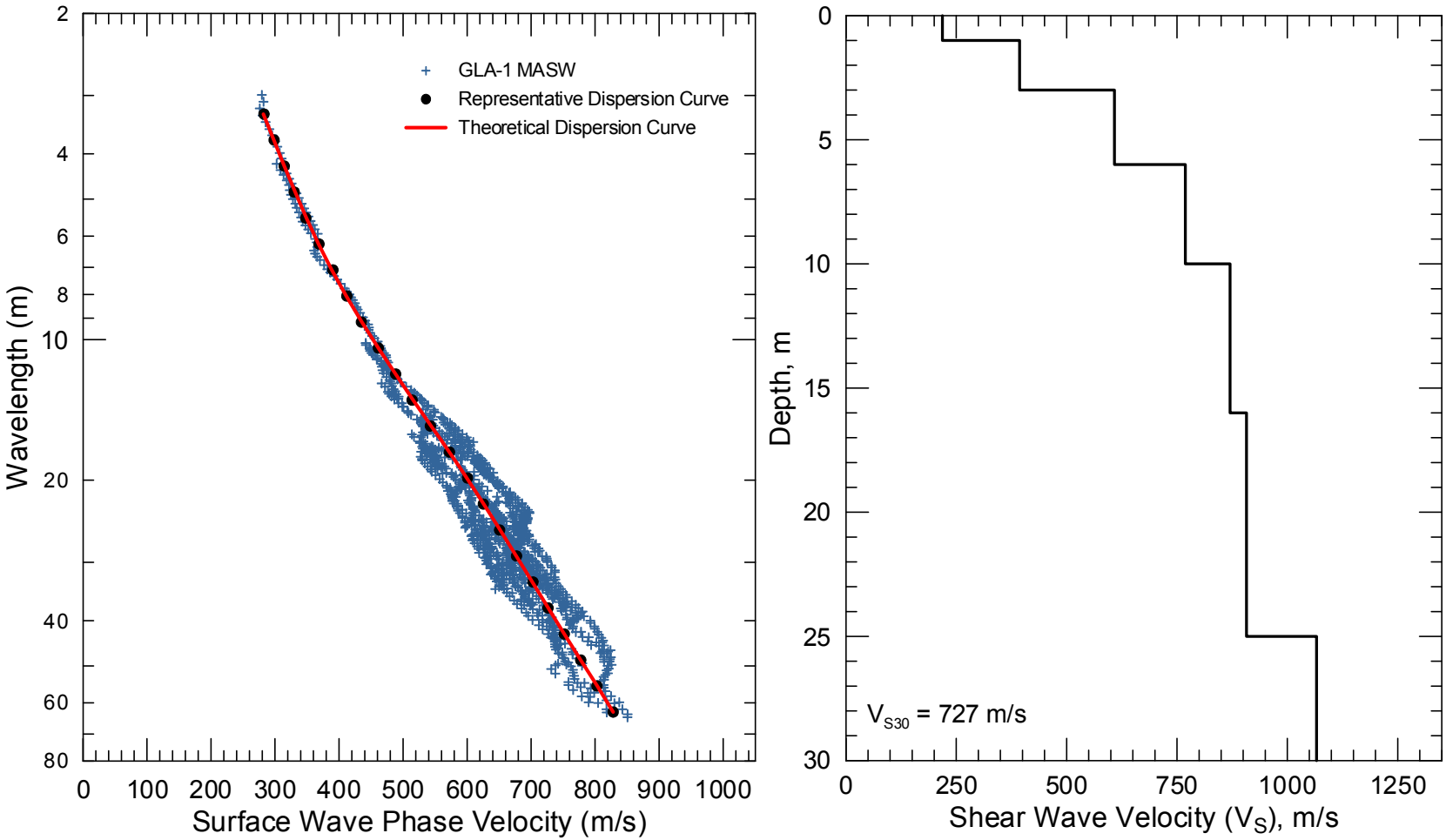

CI.GLA - Field, representative and inverted theoretical surface wave dispersion data (left) and associated V_S model with assumed Poisson's ratio of 0.33 (right)

Site CI.GMR

Location: Granite Mountains Research Center, Mojave National Preserve, California

Latitude: 34.78457 **Longitude:** -115.65994
(Station coordinates provided by USGS, WGS84 coordinate system)

V_{S30} (measured): 943 m/s (based on S-wave seismic refraction model where V_{S30} ranges from 850 to 1,058 m/s in the central portion of the seismic line).

V_{S30} (adjusted to more accurately reflect seismic station conditions): 1,270 (average S-wave velocity between 1.5 and 31.5 m adjusting for 1.5 m assumed sensor depth) or 1,412 m/s (V_{S30} estimated by replacing V_S in upper 3 m with V_S of underlying unit assuming that the seismic sensor is placed on rock).

NEHRP Site Class: B

Geomatrix Code: IHA/IGA

Geologic Conditions/Observations: Seismic station located on a thin layer of Quaternary (Holocene) alluvium overlying Mesozoic granitic rock. There are multiple rock outcrops in very close proximity to the seismic station. It is possible that the seismic sensors are placed on rock.

Site Conditions: Rural site. Steep, undulating topography in site vicinity; however, test area has relatively level topography.

Geophysical Methods Utilized: HVSR, Seismic Refraction (P- and S-wave), MASW (Rayleigh wave), MALW (Love wave)

Geophysical Testing Arrays:

1. Array GMR-1 (48 channel MASW and P-wave seismic refraction array utilizing 4.5 Hz vertical geophones spaced 1.5 m apart for a length of 70.5 m, forward and reverse shot locations with multiple source offsets and source types and multiple interior shot locations).
2. Array GMR-1 (48 channel MALW and S-wave seismic refraction array utilizing 10 Hz horizontal geophones spaced 1.5 m apart for a length of 70.5 m, forward and reverse shot locations with multiple source offsets and source types (hammers only) and multiple interior shot locations).
3. Three HVSR measurement locations distributed along array GMR-1.

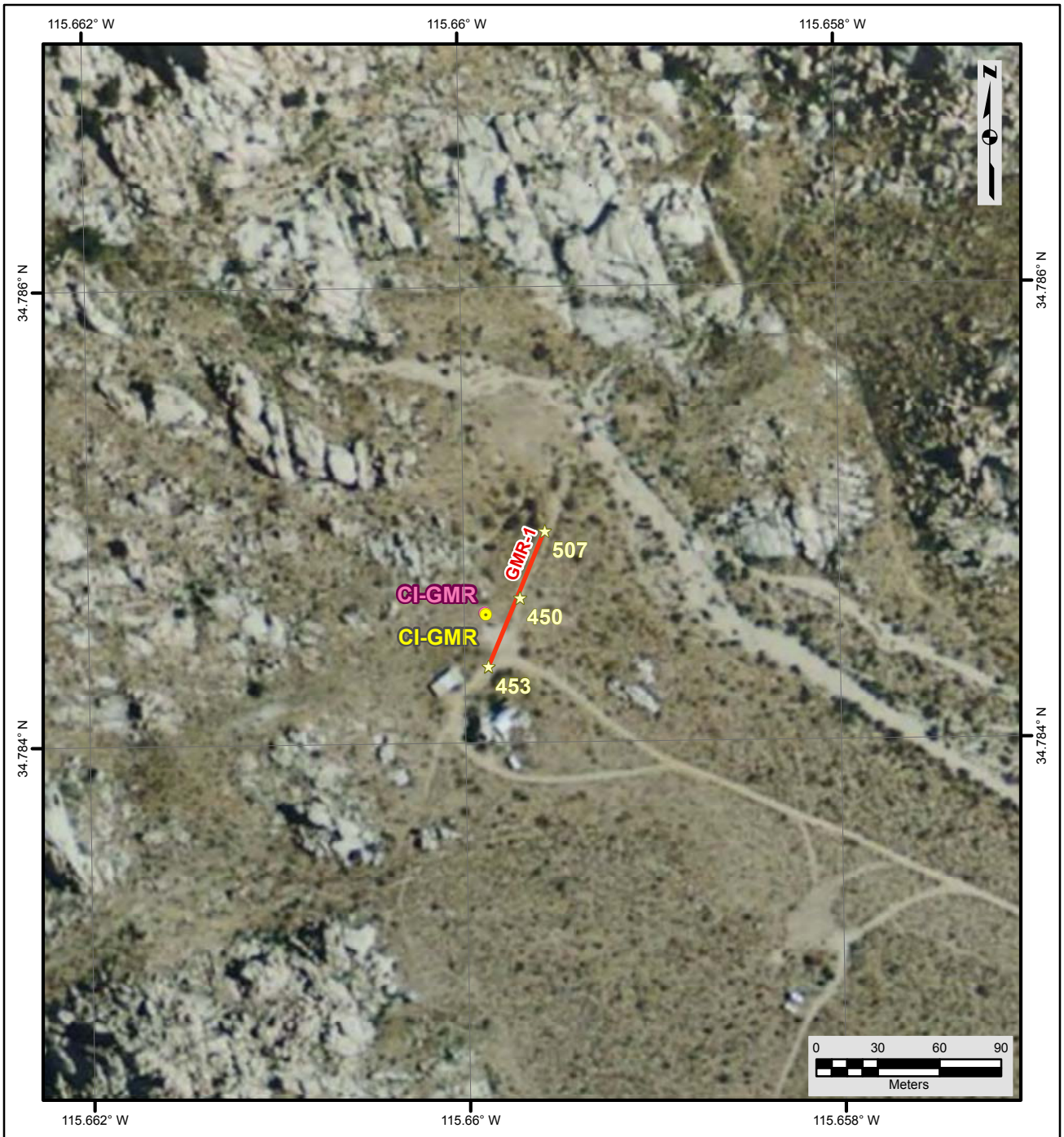

Legend

- Seismic Station - Approximate Surveyed Location
- Seismic Station - Approximate Location of Record
- H/V Spectral Ratio Location
- MASW and Seismic Refraction Array

NOTES:
1. WGS 1984 COORDINATE SYSTEM
2. Image Source: ESRI, i-cubed, USDA FSA, USGS, AEX, GeoEye, Getmapping, Aerogrid, IGP

File Name: CI-GMR-I

Date: 9/16/2011

USGS science for a changing world

GEOVision geophysical services

RECOVERY.GOV

SITE MAP
CI•GMR

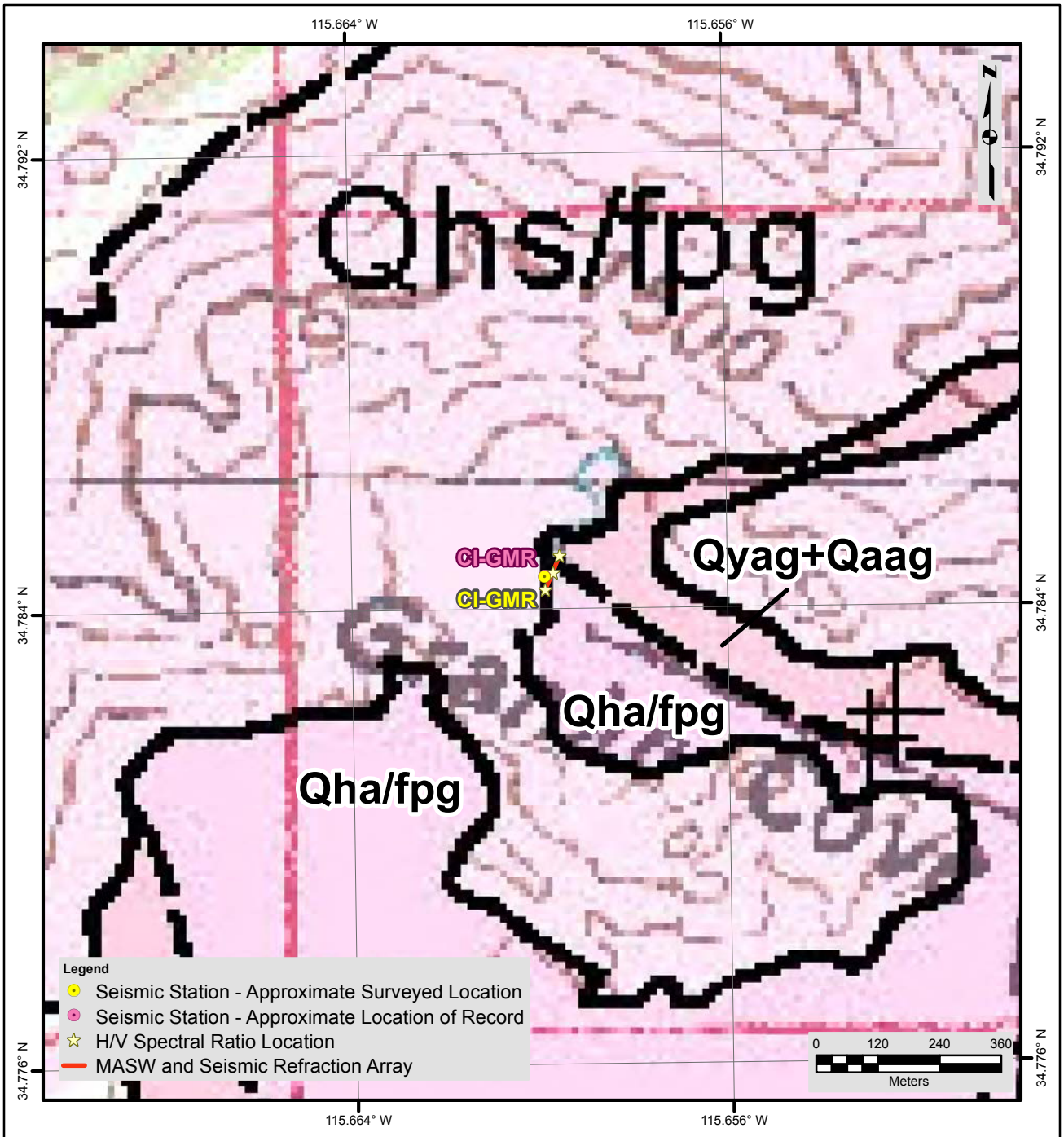

Description of Geologic Map Units

Qaag+Qyag = Quaternary (Holocene) Active granitic alluvial fan deposits, and Quaternary (Pleistocene to Holocene) Young granitic alluvial fan deposits
Qha = Quaternary (Pleistocene to Holocene) abundant hillslope deposits; colluvium, talus
Qhs = Quaternary (Pleistocene to Holocene) sparse hillslope deposits; colluvium, talus
fpg = Pre-Quarternary (mostly Cretaceous) Felsic plutonic rocks

NOTES:
1. WGS 1984 COORDINATE SYSTEM
2. Preliminary Surficial Geologic Map Database of the Amboy 30x60 Minute Quadrangle, California by David R Bedford, David M Miller, and Geoff A Phelps, 2006
3. See site map for details of geophysical survey

USGS science for a changing world

GEOVision geophysical services

RECOVERY.GOV

GEOLOGIC MAP
CI•GMR

File Name: CI-GMR

Date: 9/22/2011

CI.GMR Seismic Station

Data acquisition with hammer source on shear-wave array GMR-1

HVSR sensor 453 with seismic station in background

Looking northeast towards HVSR sensors 450 and 507

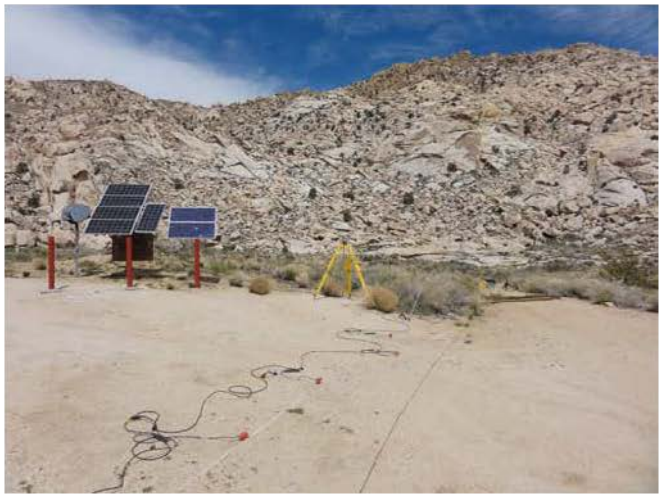

Looking northeast along P-wave array GMR-1

Location of Geophysical Testing Arrays:

Location	Latitude	Longitude
GMR-1, Southwest End of MASW/Refraction Array	34.78433	-115.65993
GMR-1, Center of MASW/Refraction Array	34.78463	-115.65977
GMR-1, Northeast End of MASW/Refraction Array	34.78493	-115.65962
HVSR Sensor 450	34.78463	-115.65975
HVSR Sensor 453	34.78433	-115.65992
HVSR Sensor 507	34.78493	-115.65961
CI.GMR Seismic Station	34.78456	-115.65993

Notes: 1) WGS84 Coordinate System (decimal degrees)

2) Survey accuracy is estimated at 1 to 2 m.

Results:

Average V_S Model from Central Portion of S-wave Seismic Refraction Line

Depth to Top of Layer (m)	Layer Thickness (m)	S-Wave Velocity (m/s)
0.00	0.43	154
0.43	0.87	175
1.30	0.87	183
2.17	0.87	184
3.03	0.87	457
3.90	0.87	1469
4.77	0.87	1619
5.63	1.82	1631
7.45	1.82	1747
9.28	1.82	1886
11.10	1.82	2191
12.92	1.82	2227
14.74	1.82	2228
16.56	1.82	2234
18.38	1.82	2235
20.20	1.82	2241
22.02	1.82	2242
23.84	Half Space	2247

Average V_P and Estimated V_S Models from Central Portion of P-wave Seismic Refraction Line

Depth to Top of Layer (m)	Layer Thickness (m)	P-Wave Velocity (m/s)	Estimated S-Wave Velocity (m/s)			
			Poisson's Ratio = 0.25	Poisson's Ratio = 0.30	Poisson's Ratio = 0.3333	Poisson's Ratio = 0.35
0.00	0.43	287	166	153	143	138
0.43	0.87	332	192	177	166	159
1.30	0.87	353	204	189	177	170
2.17	0.87	377	217	201	188	181
3.03	0.87	1083	625	579	542	520
3.90	0.87	2395	1382	1280	1197	1150
4.77	0.87	2415	1394	1291	1207	1160
5.63	1.82	2473	1428	1322	1237	1188
7.45	1.82	2650	1530	1417	1325	1273
9.28	1.82	3248	1875	1736	1624	1560
11.10	1.82	3466	2001	1852	1733	1665
12.92	1.82	4136	2388	2211	2068	1987
14.74	1.82	4179	2413	2234	2090	2008
16.56	1.82	4203	2427	2247	2102	2019
18.38	1.82	4258	2458	2276	2129	2045
20.20	1.82	4310	2488	2304	2155	2070
22.02	Half Space	4378	2527	2340	2189	2103

Observations/Discussion:

- The HVSR plots have different high frequency peaks between about 8.5 and 15 Hz. Assuming that the HVSR peaks are associated with shallow bedrock, they indicate that depth to shallow bedrock and/or the S-wave velocity of overlying rock may be slightly variable beneath the MASW/seismic refraction array.
- Noise conditions at the site were not sufficient for application of passive surface wave techniques.
- Rayleigh wave and Love wave techniques were not found to be effective at this site due to the thin layer of low velocity sediments overlying high velocity rock and/or lateral variability of the subsurface velocity structure. Site characterization was, therefore, limited to the application of the P- and S-wave seismic refraction techniques.
- The P- and S-wave seismic refraction data for array GMR-1 were modeled using a tomographic inversion routine with layer-based starting models. The seismic refraction models were extended to far offset shot locations to extend depth of investigation. It should be noted that a larger geophone spacing, rather than the utilization of far offset shot locations, is preferred for extending depth of investigation, when applying tomographic inversion routines. However, the seismic refraction data were acquired in conjunction with surface wave data, where a shorter array length is preferred.
- The P-wave first arrival data were picked to a greater degree of accuracy than the S-wave first arrival data because the S-wave is not typically the first energy on a seismic record, even when using a horizontal traction plank as an energy source. The air wave arrives before the direct soil arrival in the P-wave seismic records and an attempt was made to pick the direct arrival after the air wave, which is not always easy.
- The P-wave seismic refraction survey design allowed P-wave velocity to be imaged to a maximum depth of about 23 m. The seismic refraction model indicates that P-wave velocity is about 250 to 400 m/s at the surface and increases to over 2,000 m/s at a depth of 3 to 5 m and over 4,000 m/s at a nominal depth of 14 m. The maximum P-wave velocity in the central portion of the model, where depth of investigation is greatest, is about 4,400 m/s. A P-wave velocity this high is indicative of slightly weathered rock and, therefore, we would expect velocity to only increase very gradually with depth below 23 m.
- The S-wave seismic refraction survey design allowed S-wave velocity to be imaged to a maximum depth of about 24 m. The seismic refraction model indicates that S-wave velocity is about 125 to 200 m/s at the surface, increases to over 1,000 m/s at a depth of 3 to 5 m and to over 2,000 m/s at a depth of 11 to 12 m. The maximum S-wave velocity in the central portion of the model, where depth of investigation is greatest, is about 2,400 m/s. An S-wave velocity this high is indicative of slightly weathered rock and, therefore, we would expect velocity to only increase very gradually with depth below 24 m.
- V_{S30} was estimated between 19.5 and 46.5 m on the S-wave refraction model, where depth of investigation is greatest, by projecting the velocity at 24 m depth to 30 m depth. Over this interval, V_{S30} ranges from about 850 to 1,058 m/s, about a 25% variation over a 27 m distance.
- An average V_S model was developed over the 19.5 to 46.5 m distance interval by averaging the slowness of each model cell and average V_{S30} was determined to be 943 m/s.

- V_{P30} between 19.5 and 46.5 m varies from about 1,613 to 2,000 m/s and averages 1,776 m/s. A Poisson's ratio of about 0.3 would yield the value of V_{S30} estimated from the S-wave seismic refraction survey, not unrealistic for relatively competent rock. Estimating V_{S30} from V_{P30} assuming constant Poisson's ratio in the range of 0.25 to 0.35 results in V_{S30} in the 1,026 to 853 m/s range. This large variation in potential V_{S30} demonstrates the risks in attempting to estimate V_{S30} from P-wave velocity data, even with a realistic estimate of Poisson's ratio, and this approach should only be used as a last resort.
- The average V_S model estimated from the P-wave refraction model using an assumed Poisson's ratio of 0.3 is similar to the average V_S model from the S-wave refraction model with the exception of the 4 to 9 m depth range where V_S from the S-wave refraction survey is slightly higher.
- In summary, V_{S30}, as estimated from the S-wave seismic refraction survey, is 943 m/s (Site Class B).
- Average S-wave velocity between 1.5 m (assumed sensor depth) and 31.5 m is 1,270 m/s (Site Class B).
- It is possible that the seismic sensor is located on rock because both the HVSR data (higher frequency HVSR peak) and seismic refraction data indicate that bedrock is slightly shallower beneath the portion of the array closest to the seismic station. An adjusted V_{S30}, estimated by replacing the V_S of the upper 3 m with that of the underlying layer, is 1,412 m/s.
- V_{S30} is probably highly variable in the site vicinity and there are likely areas in close proximity to the seismic station without soil cover where V_{S30} exceeds 1,500 m/s.

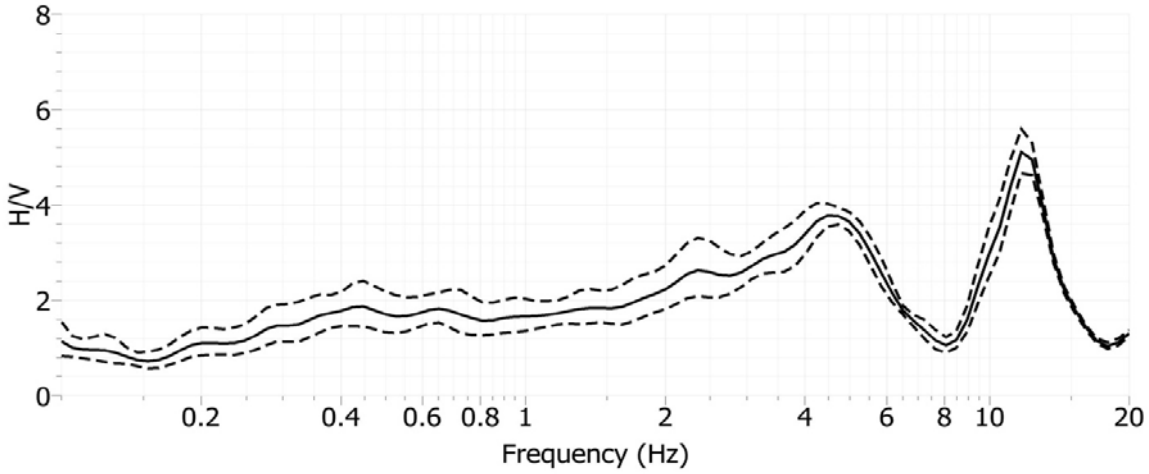

Site CI.GMR, H/V Spectral Ratio, Array GRM -1, Sensor 507

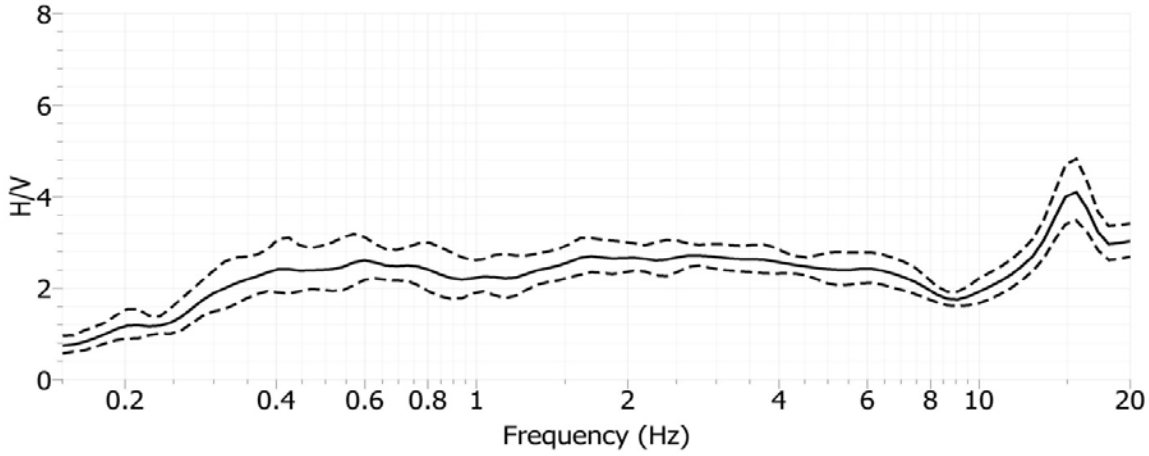

Site CI.GMR, H/V Spectral Ratio, Array GMR -1, Sensor 450

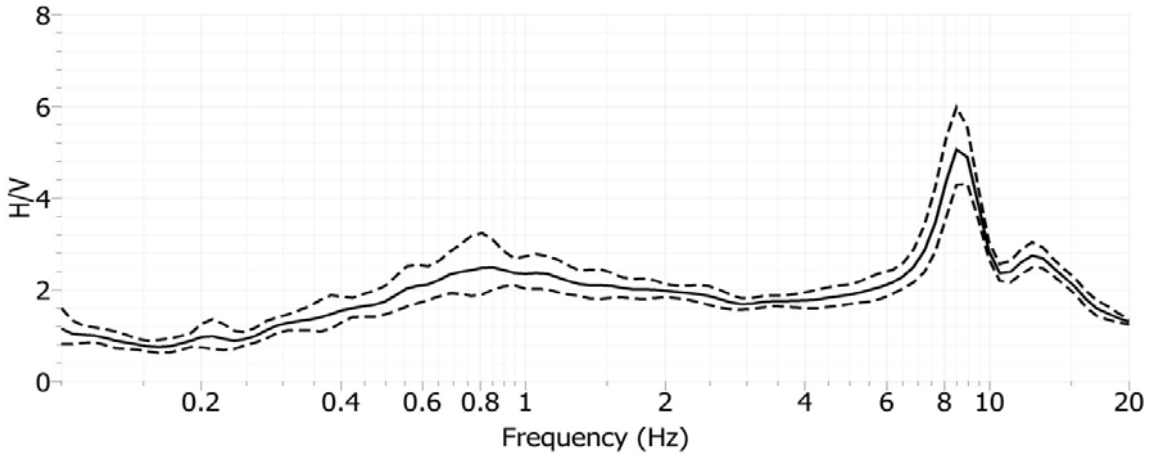

Site CI.GMR, H/V Spectral Ratio, Array GMR -1, Sensor 453

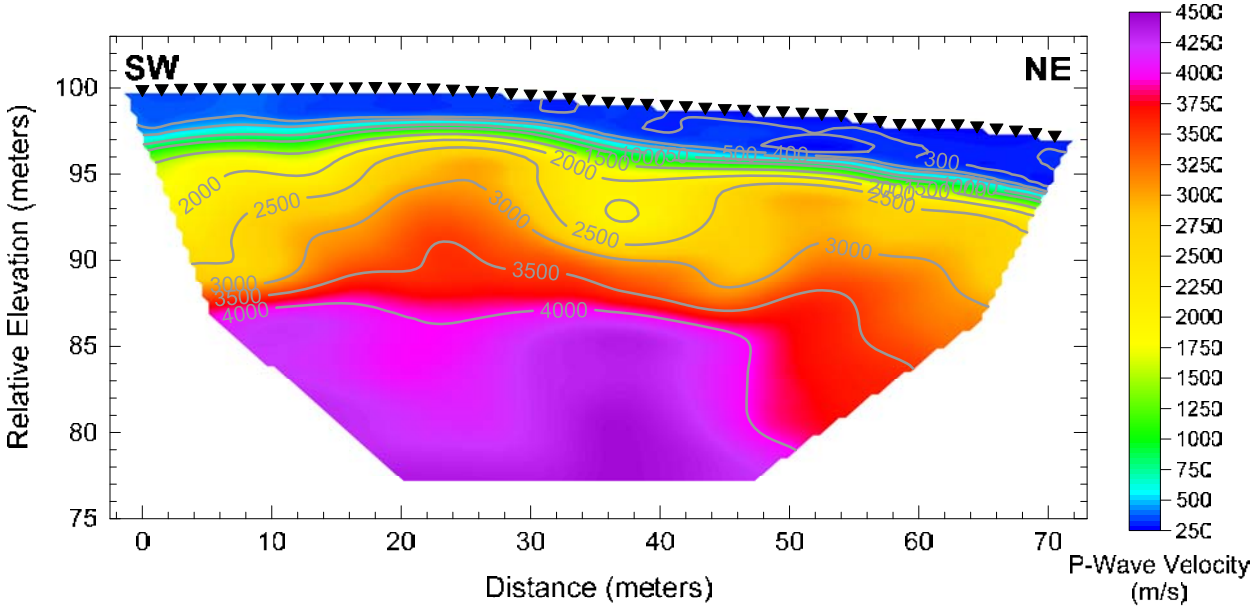

Array GMR-1 – P-wave Tomographic Seismic Refraction Model utilizing Layer Based Starting Model

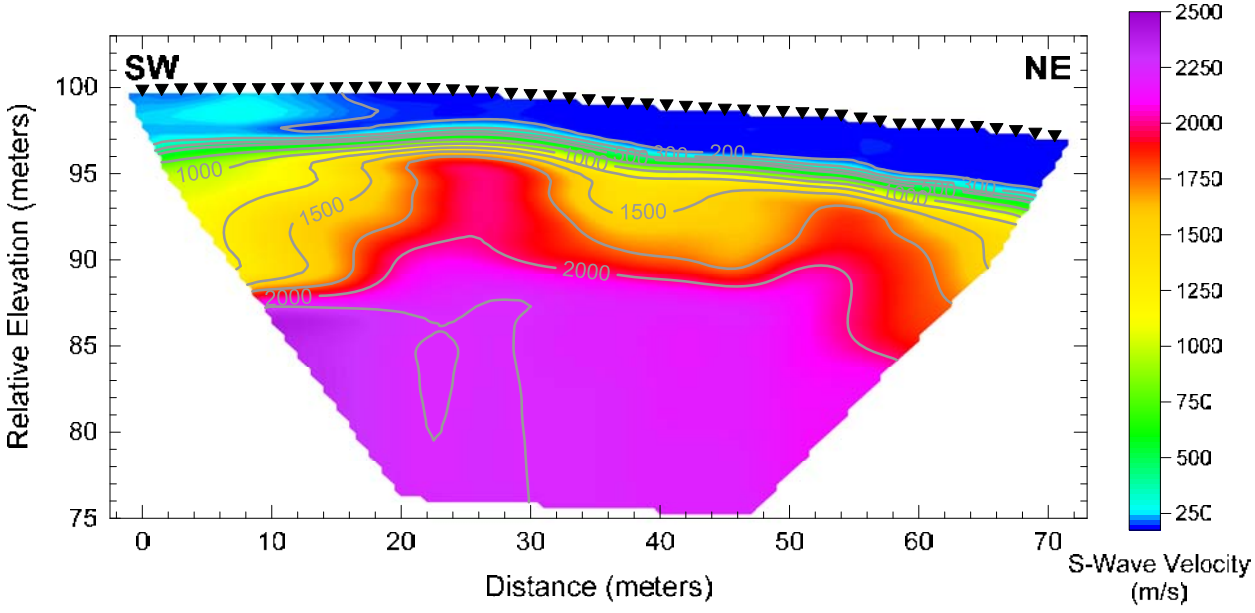

Array GMR-1 – S-wave Tomographic Seismic Refraction Model utilizing Layer Based Starting Model

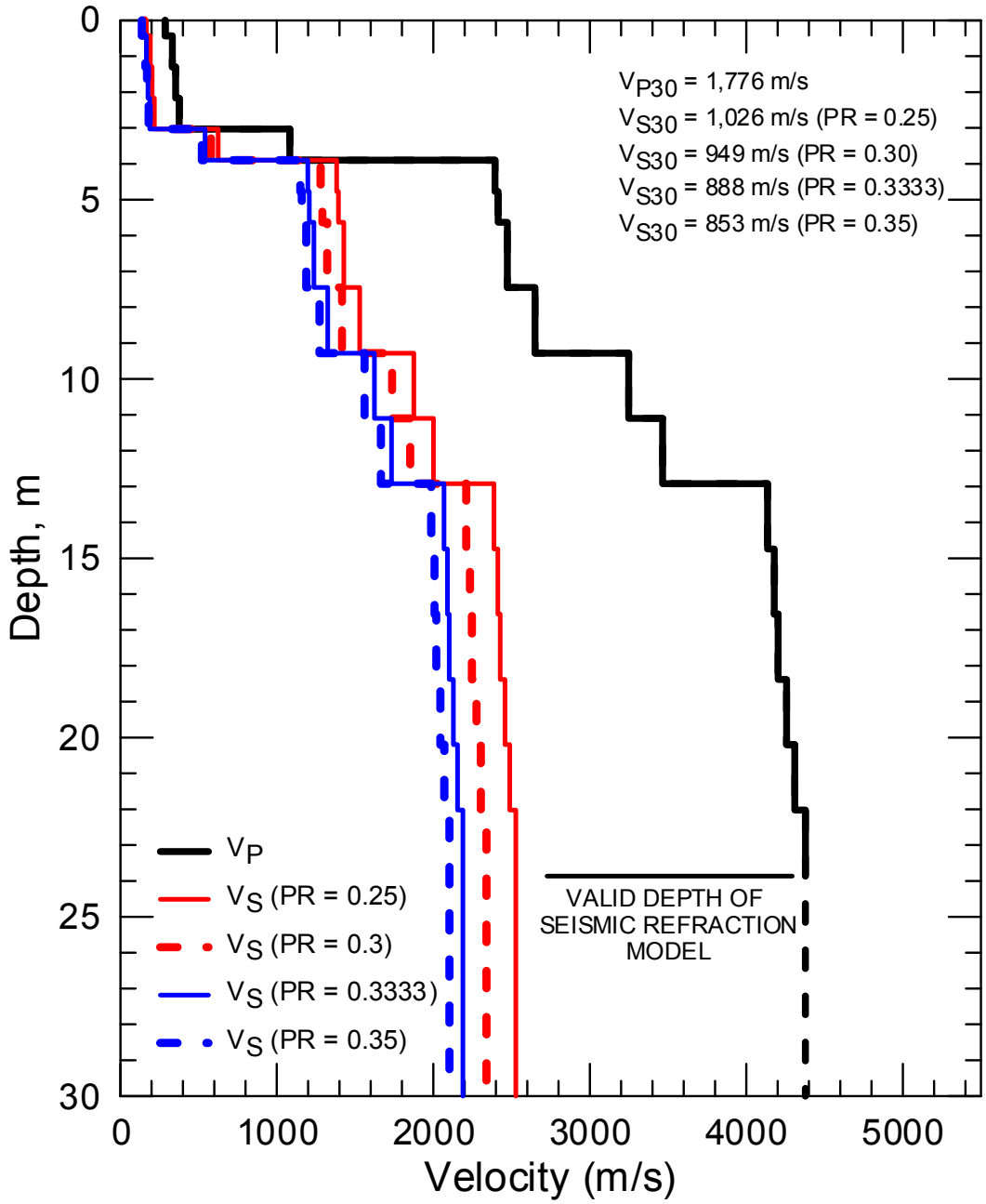

CI.GMR – Average P-wave velocity structure and estimated S-wave velocity structure between 19.5 and 46.5 m on P-wave seismic refraction array GMR-1. Although the maximum seismic refraction depth of investigation is limited to about 24 m, P-wave velocity is very high at the bottom of the model and is not expected to increase significantly between 24 and 30 m. A longer seismic line would be preferred to both more accurately model the high P-wave velocities and to image to 30 m depth.

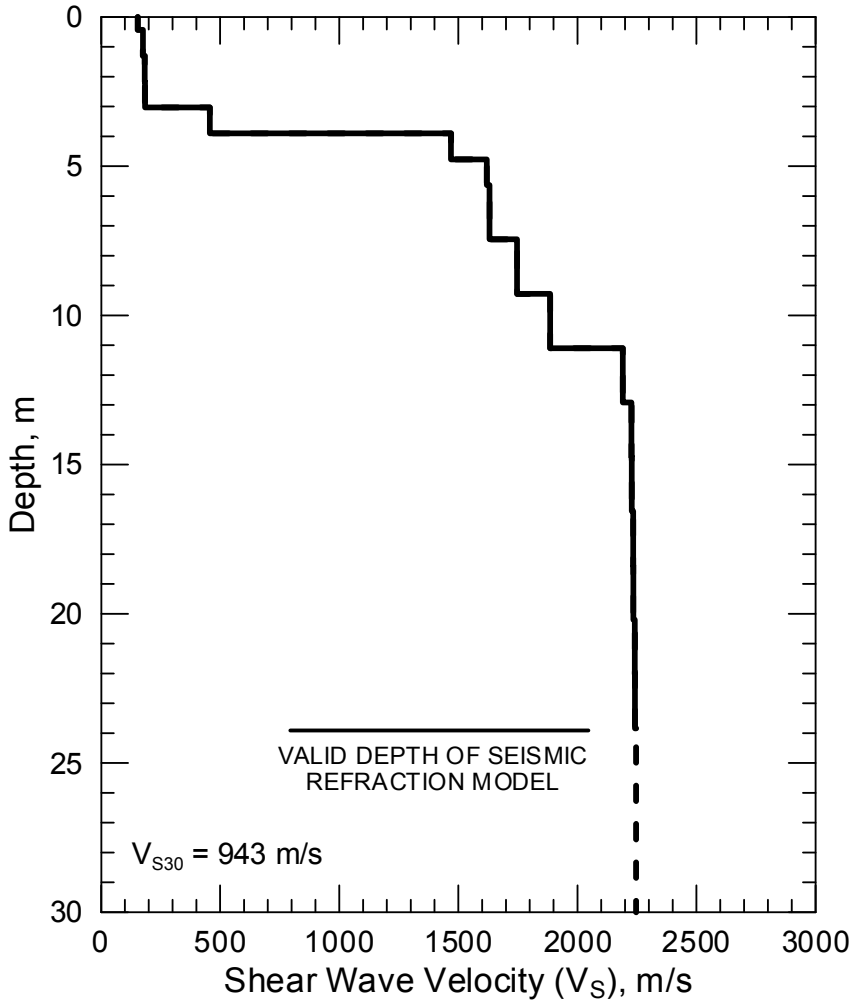

CI.GMR – Average S-wave velocity structure between 19.5 and 46.5 m on S-wave seismic refraction array GMR-1. Although seismic refraction depth of investigation limited to about 24 m, S-wave velocity is very high at the bottom of the model and not expected to increase significantly between the valid depth of exploration and 30 m.

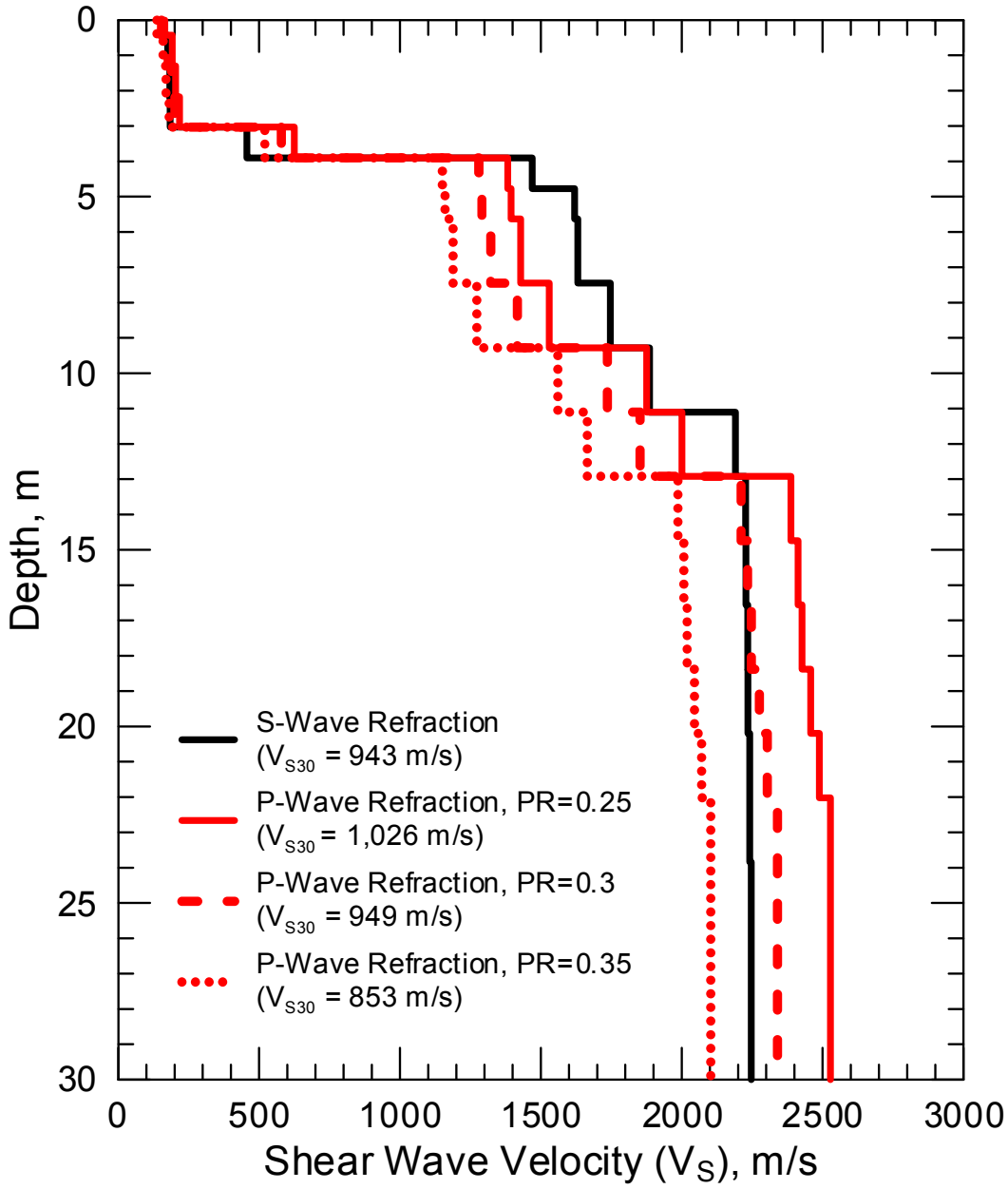

CI.GMR – Comparison of S-wave velocity models derived from the S-wave and P-wave seismic refraction surveys.

Site CI.GOR

Location: Green Oak Ranch, 1237 Green Oak Road, Vista, California

Seismic Sensor Location

Latitude: 33.15370 **Longitude:** -117.22921

(Coordinates provided by USGS – WGS84 coordinate system)

V_{S30} (measured): 559 m/s

V_{S30} (adjusted to more accurately reflect seismic station conditions): 623 m/s (average S-wave velocity between 2 and 32 m adjusting for 2 m nominal sensor depth.)

NEHRP Site Class: C

Geomatrix Code: IGA/IGB

Geologic Conditions/Observations: Seismic station located on outcrop of Cretaceous granitic rock (tonolite). Field inspection and geophysical data indicate that the near surface rock is decomposed to very intensely weathered. Some areas also contain a very thin layer of residual soil.

Site Conditions: Semi-urban site located on a weathered bedrock outcrop. Relatively flat terrain along test area but hilly terrain in site vicinity.

Geophysical Methods Utilized: HVSR, Seismic Refraction, MASW

Geophysical Testing Arrays:

1. Array GOR-1 (48 channel MASW and P-wave seismic refraction array utilizing 4.5 Hz vertical geophones spaced 1.5 m apart for a length of 70.5 m, forward and reverse shot locations with multiple source offsets and source types and multiple interior shot locations).
2. Three HVSR measurement locations distributed along array GOR-1.

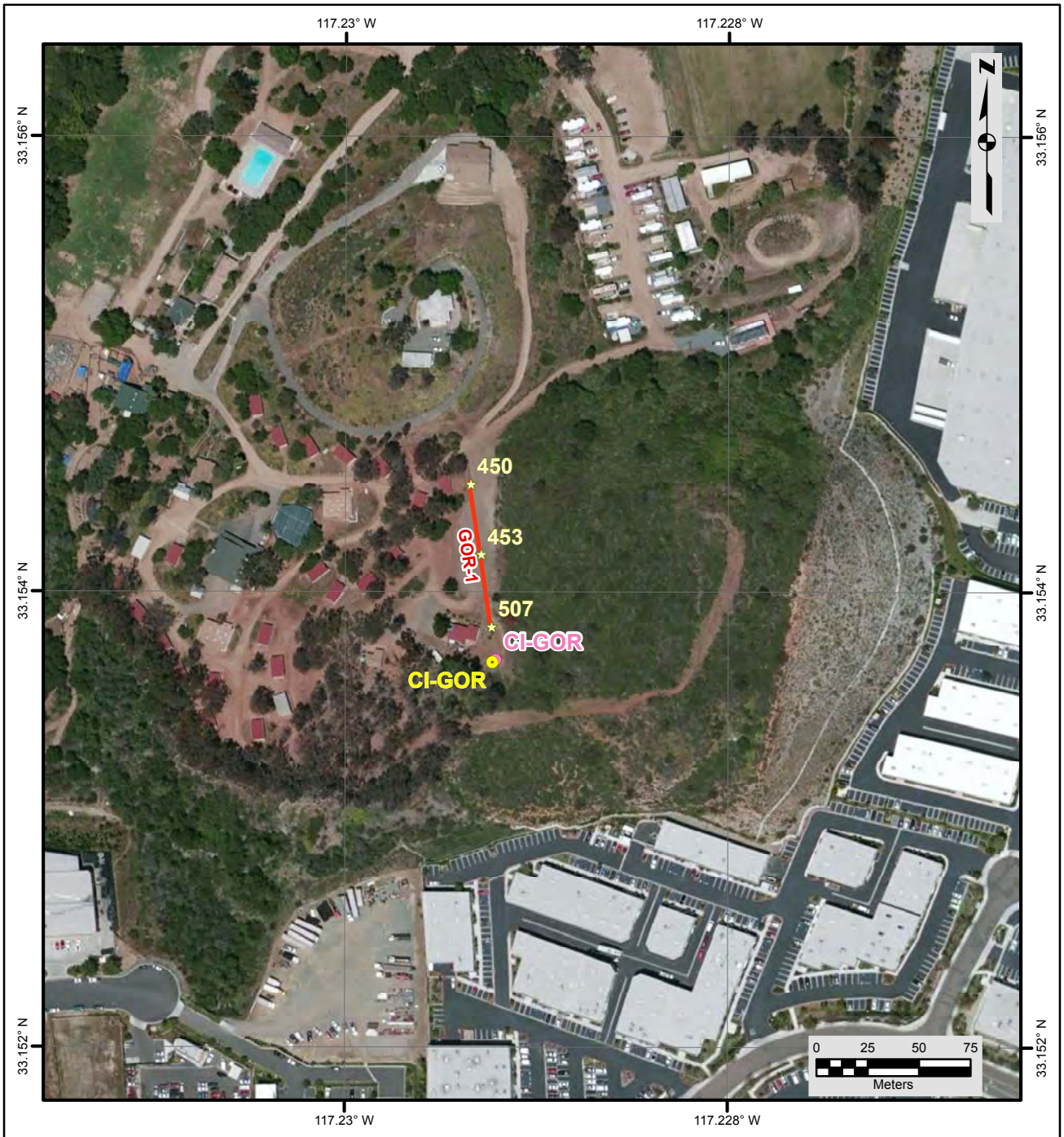

Legend

- Seismic Station - Approximate Surveyed Location
- Seismic Station - Approximate Location of Record
- H/V Spectral Ratio Location
- MASW and Seismic Reflection Array

NOTES:
1. WGS 1984 COORDINATE SYSTEM
2. Image Source: ESRI, i-cubed, USDA FSA, USGS, AEX, GeoEye, Getmapping, Aerogrid, IGP

File Name: CI-GOR-I

Date: 2/7/2013

USGS science for a changing world

GEOVision geophysical services

RECOVERY.GOV

SITE MAP
CI•GOR

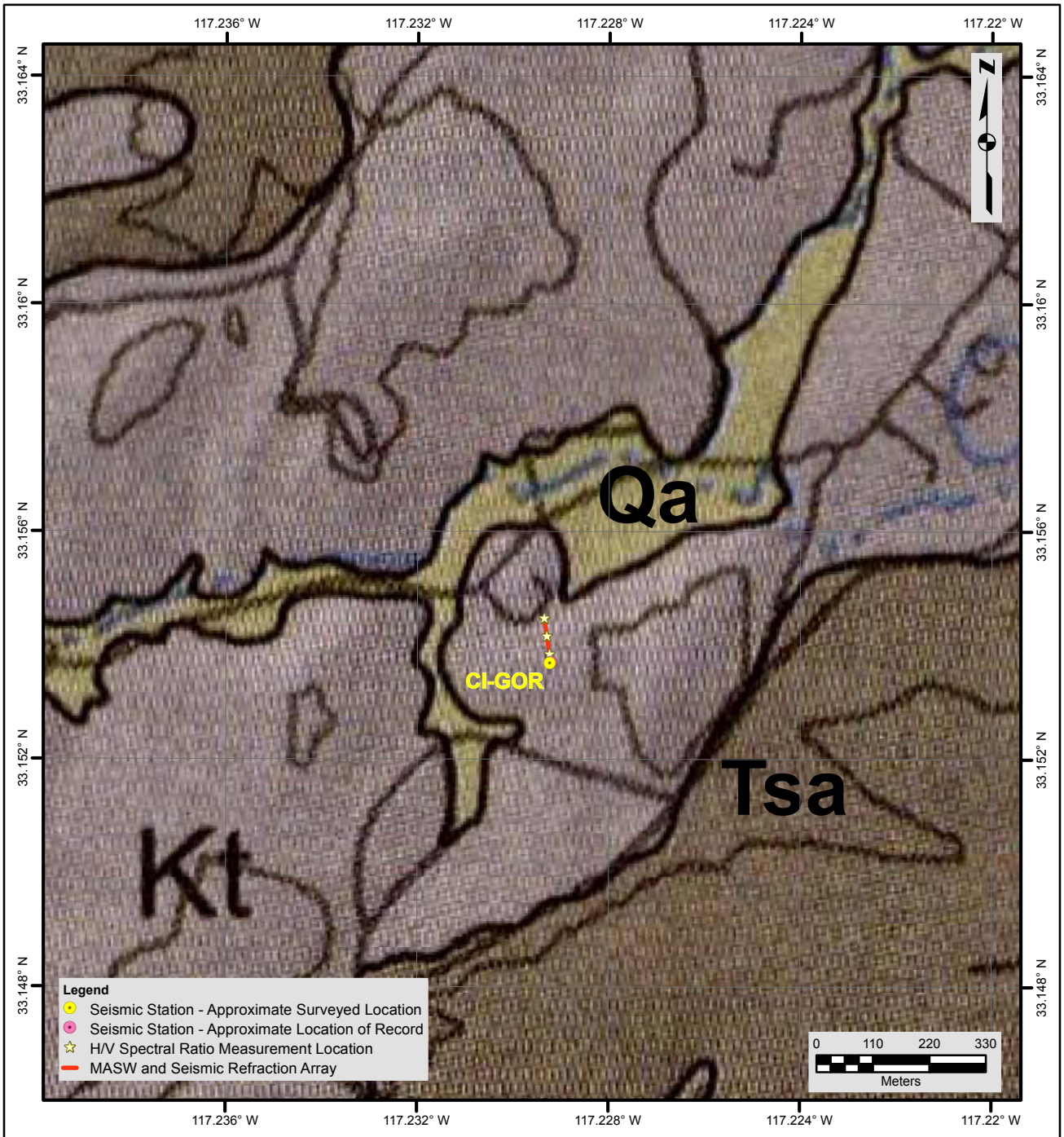

Description of Geologic Map Units

Qa = Quaternary (Holocene) alluvial flood-plain deposits
Tsa = Tertiary (Eocene) Santiago Formation
Kt = Mesozoic (Cretaceous) tonalite, undivided

NOTES:
1. WGS 1984 COORDINATE SYSTEM
2. Geologic Map of the Oceanside 30' x 60' Quadrangle, Southern California
by Michael P. Kennedy and Siang S. Tan, 2007
3. See site map for details of geophysical survey

File Name: CI-GOR

Date: 2/7/2013

USGS science for a changing world

GEOVision geophysical services

RECOVERY.GOV

GEOLOGIC MAP
CI•GOR

Looking north towards CI.GOR seismic station and along array GOR-1

Looking north towards HVSR sensor 507 and along array GOR-1

HVSR sensor 507 in shallow hole

Seismic data acquisition system and data acquisition using an accelerated weight drop energy source

20 lb sledge hammer source on MASW array GOR-1

Location of Geophysical Testing Arrays:

Location	Latitude	Longitude
GOR-1, South End of Array	33.15385	-117.22924
GOR-1, Center of Array	33.15417	-117.22929
GOR-1, North End of Array	33.15448	-117.22935
HVSR Sensor 507	33.15385	-117.22923
HVSR Sensor 453	33.15416	-117.22929
HVSR Sensor 450	33.15447	-117.22934
CI.GOR Seismic Station	33.15369	-117.22923

Notes: 1) WGS84 Coordinate System (decimal degrees)
2) Survey accuracy is estimated at 1 to 2 m

Results:

V_S Model 1 (Recommended for Purpose of Site Characterization)

Depth to Top of Layer (m)	Layer Thickness (m)	S-Wave Velocity (m/s)	Inferred P-Wave Velocity (m/s)	Inferred Poisson's Ratio	Inferred Density (g/cm^3)
0	1.5	253	473	0.3	1.9
1.5	2.5	380	711	0.3	2.0
4	6	468	875	0.3	2.0
10	10	514	961	0.3	2.0
20	>10	1129	2112	0.3	2.3

V_S Model 2

Depth to Top of Layer (m)	Layer Thickness (m)	S-Wave Velocity (m/s)	Inferred P-Wave Velocity (m/s)	Inferred Poisson's Ratio	Inferred Density (g/cm^3)
0	1.5	251	470	0.3	1.90
1.5	2.5	384	718	0.3	2.00
4	9	465	870	0.3	2.00
13	12	623	1165	0.3	2.00
25	>5	1398	2615	0.3	2.30

V_S Model 3

Depth to Top of Layer (m)	Layer Thickness (m)	S-Wave Velocity (m/s)	Inferred P-Wave Velocity (m/s)	Inferred Poisson's Ratio	Inferred Density (g/cm^3)
0	1.5	253	473	0.3	1.9
1.5	2.5	379	710	0.3	2.0
4	5	472	883	0.3	2.0
9	8	483	904	0.3	2.0
17	15	846	1583	0.3	2.1
32	>3	1458	2728	0.3	2.3

Observations/Discussion:

- HVSR plots are almost identical validating the 1-D velocity structure assumption.
- Clear HVSR peak in the 5.5 to 5.7 Hz range indicating a sharp impedance contrast at relatively shallow depth.
- Review of seismic refraction data indicates that P-wave velocity increases with depth with simplified velocity structure consisting of a 1 m thick layer of residual soil with P-wave velocity of about 500 m/s overlying a 2 to 5 m layer of decomposed rock with P-wave velocity of about 900 m/s underlain by intensely weathered rock with P-wave velocity of about 1,100 m/s. Off-end shots clearly indicate that P-wave velocity increases, possibly to over 2,000 m/s at a depth on the order of 20 to 25 m. A longer seismic line would be required to accurately characterize the high velocity layer; however, there is limited space at the site.
- A tomographic inversion of the seismic refraction first arrival data was conducted with the model extended to the off-end shot points in an attempt to approximately characterize velocity structure to the high velocity layer. The seismic refraction model is consistent with the simplified velocity structure discussed above and shows that the thickest sequence of lower velocity sediments/rock is limited to the ends of the profile.
- A representative dispersion curve was generated for the MASW data set using a moving average, polynomial curve fitting routine and used for modeling.
- Scatter in the MASW surface wave dispersion data is likely the result of near surface lateral velocity variation.
- Three V_S models with similar theoretical dispersion curves were generated for the surface wave dispersion data to illustrate the nonuniqueness of the surface wave inversion.
- The surface wave models are generally consistent with P-wave velocity structure in the seismic refraction model with the exception of the 1.5 to 10 m depth interval. P-wave velocity would need to increase to 900 to 1,100 m/s to satisfy the seismic refraction data. An increase in Poisson's ratio over this interval would improve the agreement between the seismic refraction and surface wave models; however, the difference is most likely due to the thicker sequence of lower velocity sediments/rock at the ends of the line (i.e. lateral velocity variation). High frequency surface wave dispersion data is definitely

biased towards the material properties at the ends of the lines as that is where most shot locations are positioned.

- V_S model 1 is most consistent with the 5.5 to 5.7 Hz HVSR peak based on the quarter wavelength approximation (depth to the impedance contrast is equal to the average V_S of the overlying sediments divided by 4 times the HVSR peak). Modeling of the HVSR data, however, indicates that all three V_S models yield approximately the same HVSR peak of 6.5 Hz, slightly higher than that measured in the field.
- Although the three V_S models are quite different at depths below 15 m, V_{S30} is very similar, ranging from 545 to 559 m/s (a 2.5% difference). Model 1 is used for the purpose of site characterization as it has intermediate depth to higher velocity rock.
- V_{S30} is 559 m/s (Site Class C).
- Average S-wave velocity between 2 m (nominal sensor depth) and 32 m is 623 m/s.

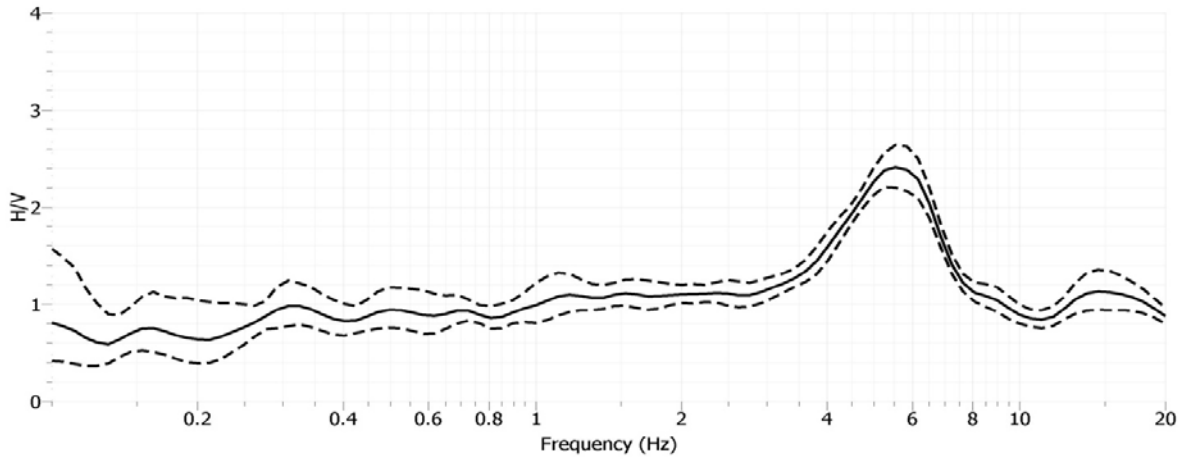

Site CI. GOR, H/V Spectral Ratio, Array GOR -1, Sensor 450

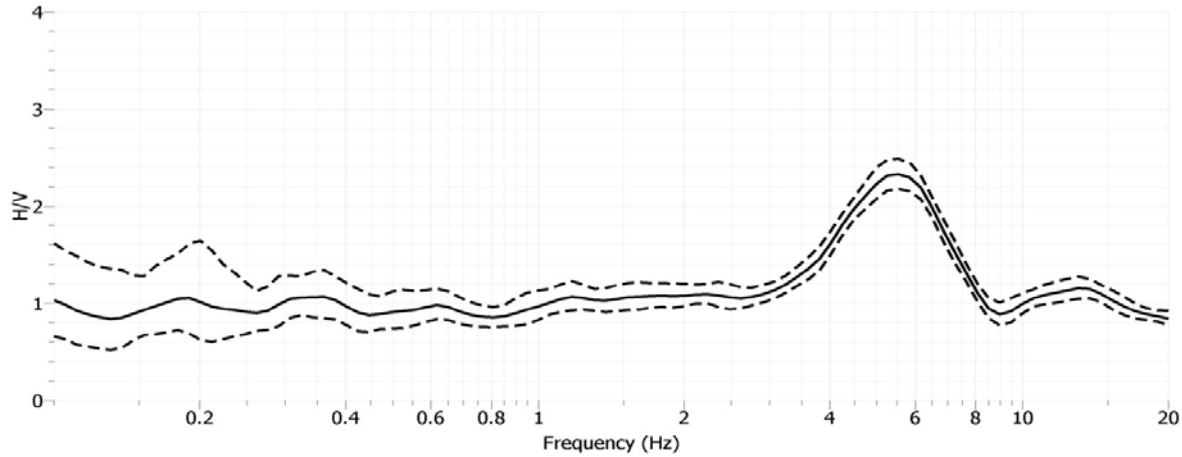

Site CI. GOR, H/V Spectral Ratio, Array GOR -1, Sensor 453

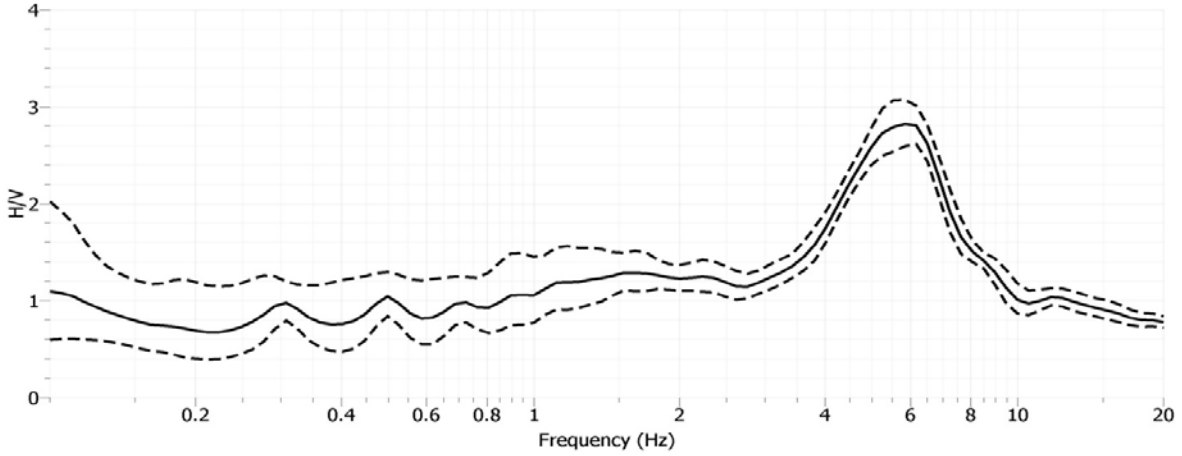

Site CI. GOR, H/V Spectral Ratio, Array GOR -1, Sensor 507

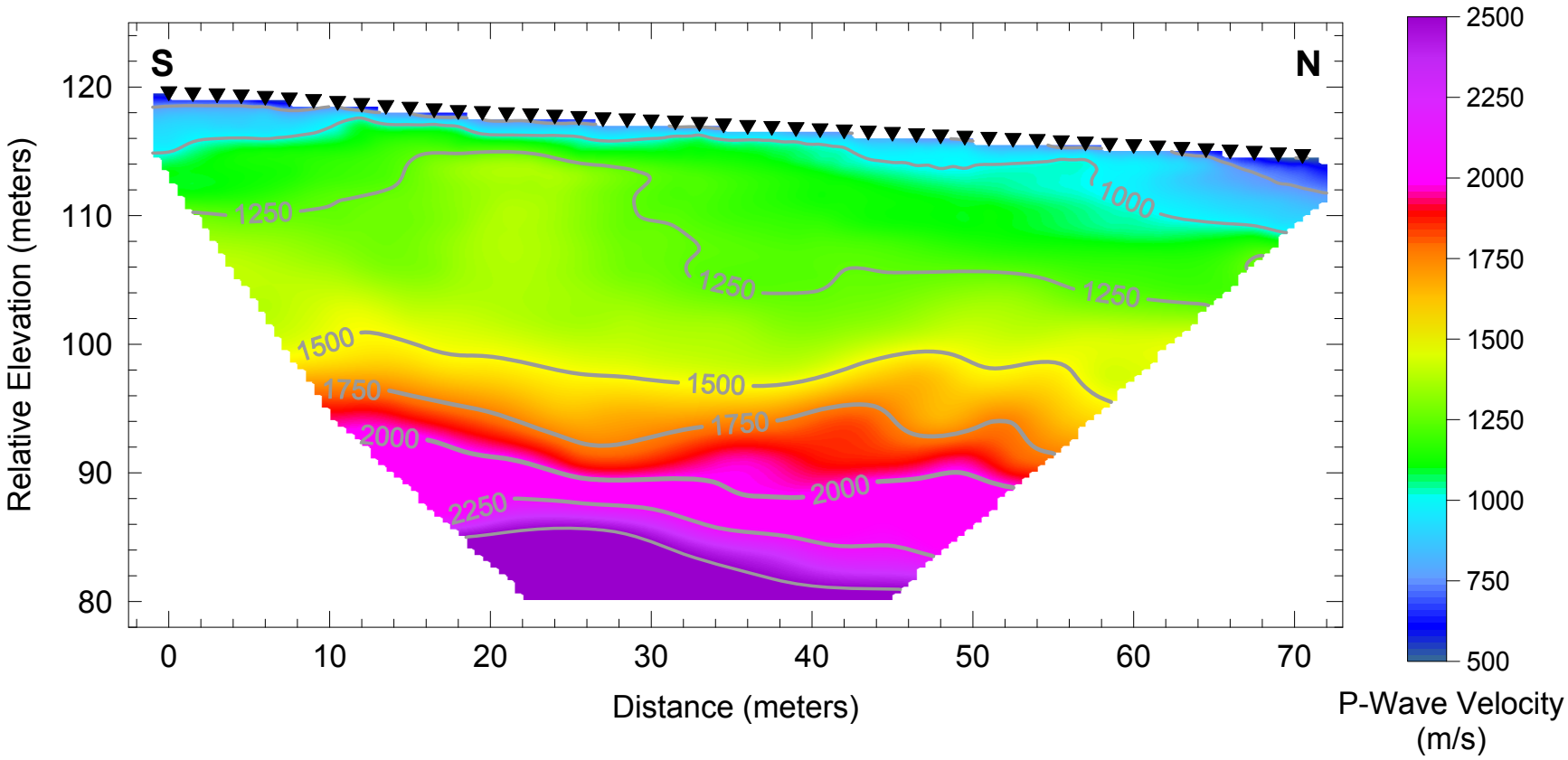

Array GOR-1 – Tomographic Seismic Refraction Model utilizing Smooth Velocity Gradient Starting Model

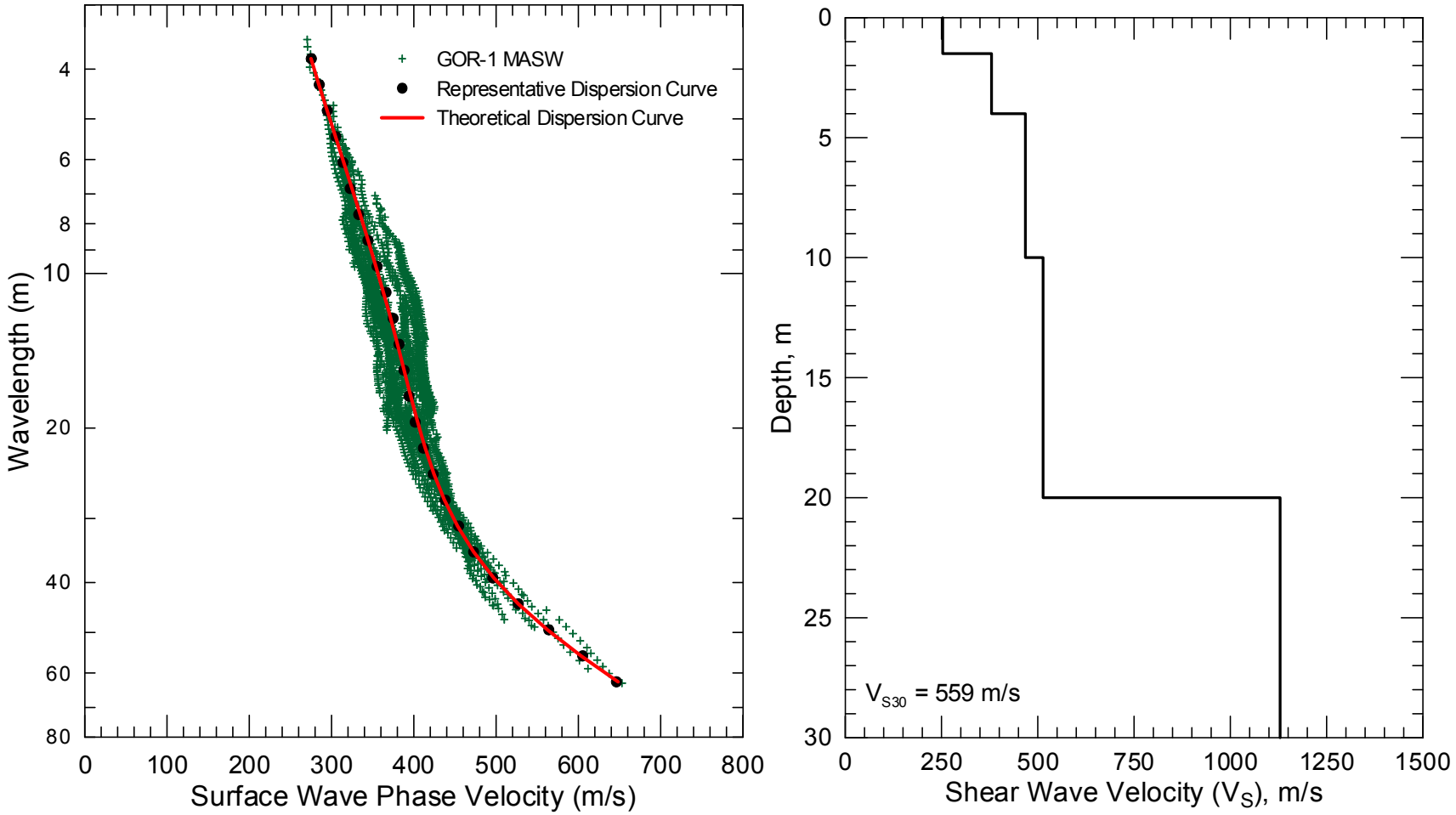

CI.GOR Model 1 - Field, representative and inverted theoretical surface wave dispersion data (left) and associated V_S model (right).

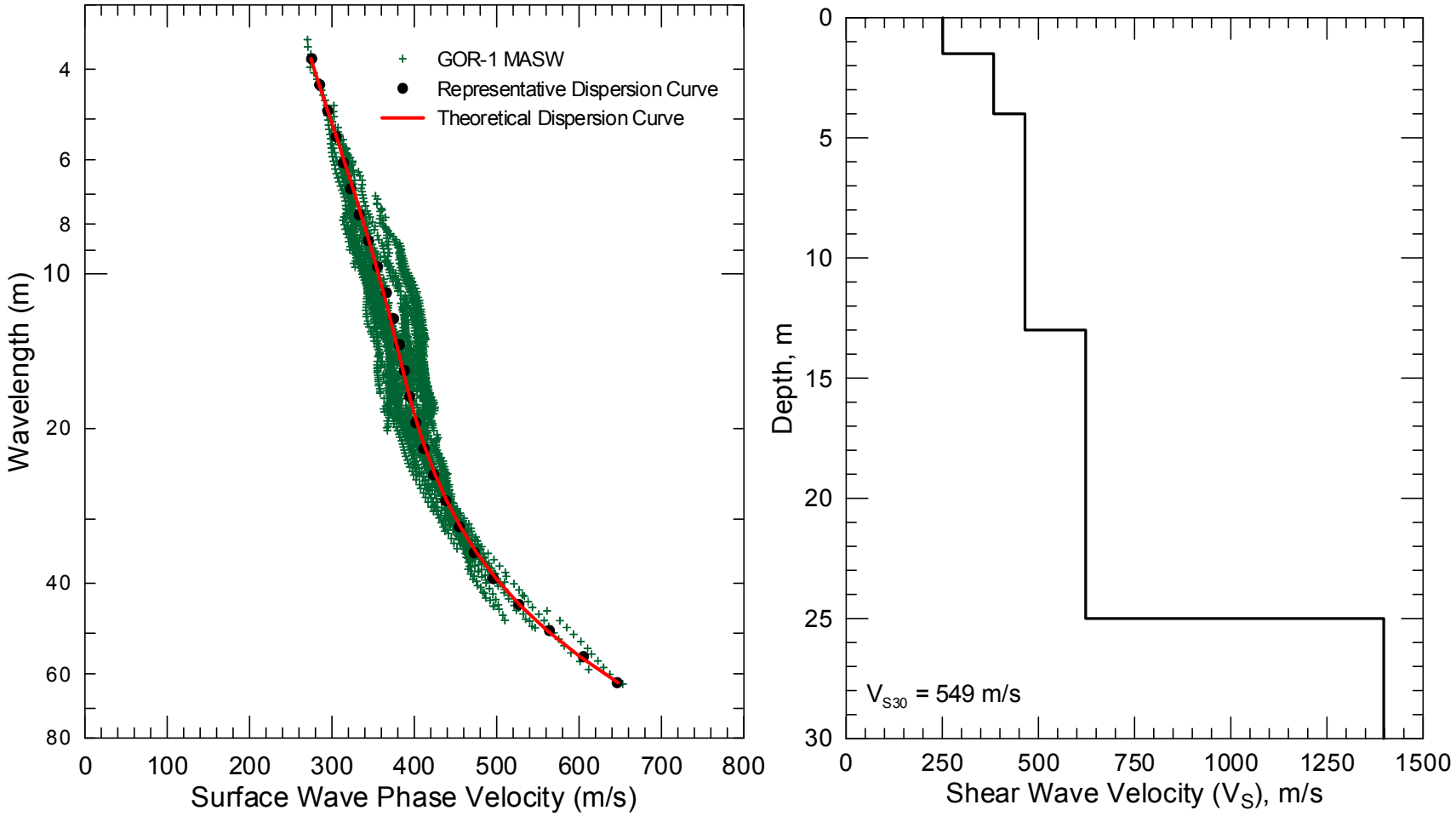

CI.GOR Model 2 - Field, representative and inverted theoretical surface wave dispersion data (left) and associated V_S model (right)

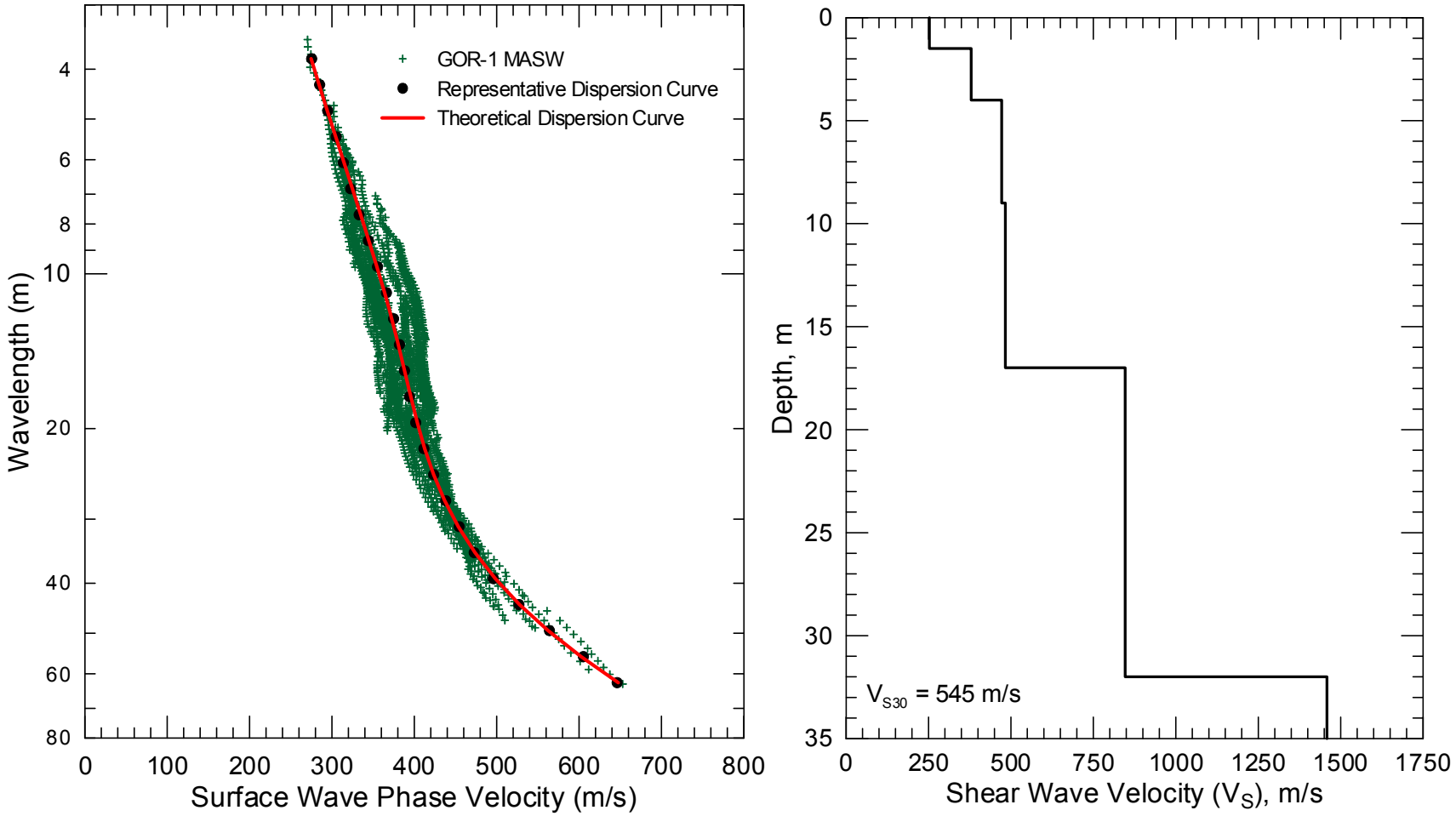

CI.GOR Model 3 - Field, representative and inverted theoretical surface wave dispersion data (left) and associated V_S model (right)

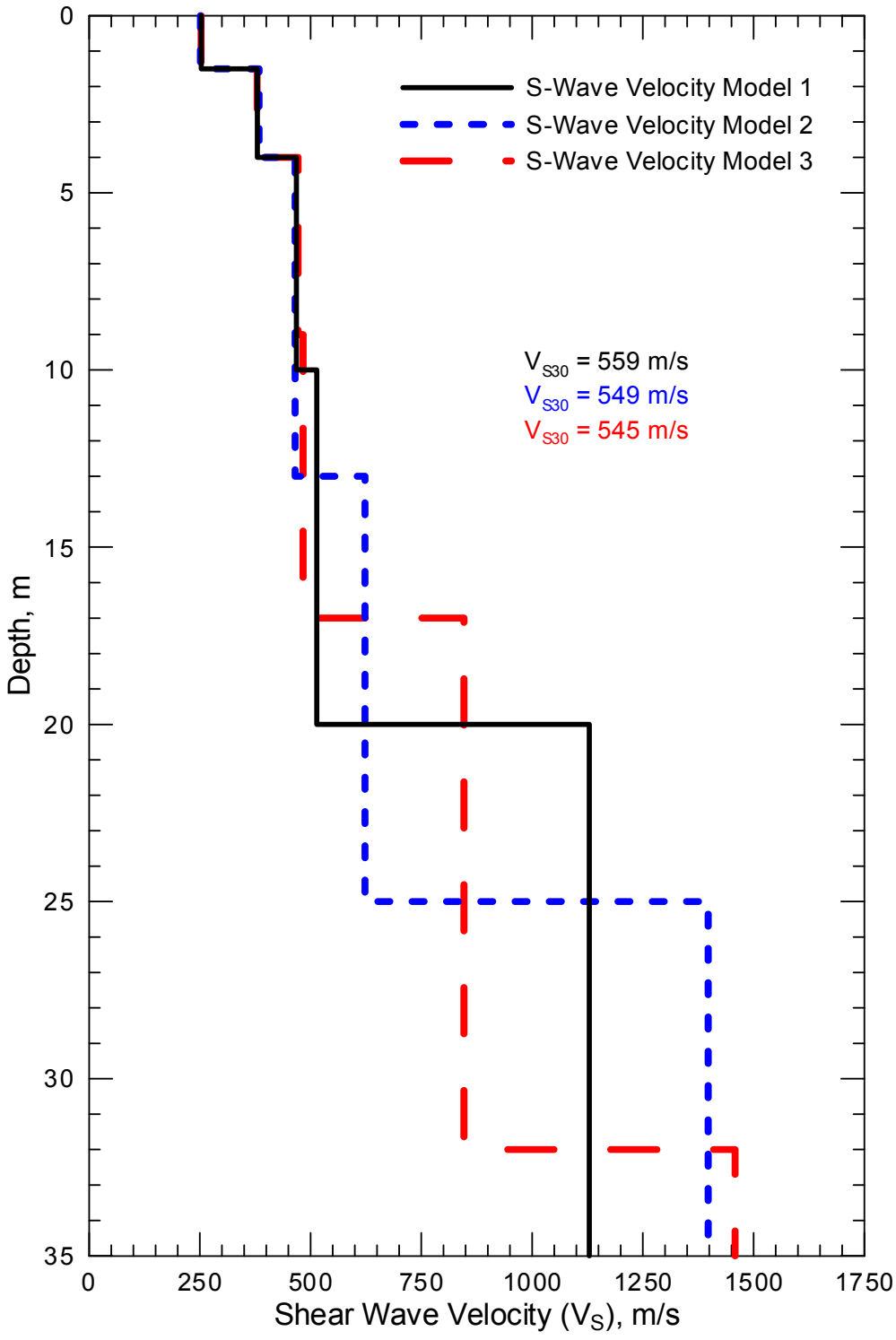

CI.GOR – Comparison of V_S models 1, 2 and 3.

Site CI.GRA

Location: Grapevine Ranger Station, Scotty's Castle Road, Death Valley, California

Latitude: 36.99606 **Longitude:** -117.36615

(Station coordinates modified based on field GPS survey, WGS84 coordinate system)

V_{S30} (measured): 386 m/s

V_{S30} (adjusted to more accurately reflect seismic station conditions): 407 m/s (average S-wave velocity between 2 and 32 m adjusting for nominal sensor depth)

NEHRP Site Class: C

Geomatrix Code: IHD

Geologic Conditions/Observations: Site located on geologic unit mapped as Holocene alluvium and 175 meters west of Tertiary sedimentary rock unit. The Furnace Creek fault is mapped in the vicinity of test area and, therefore, subsurface velocity structure could be highly variable. Crystalline basement expected to be deep at this site.

Site Conditions: Rural site with sporadic traffic on nearby road. Relatively flat terrain in test area with surface elevations gradually decreasing to south.

Geophysical Methods Utilized: HVSR, SASW, MASW, Seismic Refraction

Geophysical Testing Arrays:

1. Array GRA-1 (SASW array utilizing 1 Hz vertical geophones and maximum receiver spacing of 32 m). Array GRA-1 is as close to the seismic station as possible.
2. Array GRA-2 (48 channel MASW and seismic refraction array utilizing 4.5 Hz vertical geophones spaced 1.5 m apart for a length of 70.5 m, forward and reverse shot locations with multiple source offsets and source types and multiple interior shot locations). Array GRA-2 was not co-located with array GRA-1 due to inadequate space and could be located on the other side of a mapped fault.
3. Three HVSR measurement locations distributed along array GRA-1.

Legend

- Seismic Station - Approximate Surveyed Location
- Seismic Station - Approximate Location of Record
- H/V Spectral Ratio Location
- MASW and Refraction Array
- SASW Array

NOTES:
1. WGS 1984 COORDINATE SYSTEM
2. Image Source: ESRI, i-cubed, USDA FSA, USGS, AEX, GeoEye, Getmapping, Aerogrid, IGP

File Name: CI-GRA-I

Date: 2/7/2013

USGS science for a changing world

GEOVision geophysical services

RECOVERY.GOV

SITE MAP
CI•GRA

Description of Geologic Map Units

Qal = Quaternary (Holocene) alluvium
Tc = Tertiary nonmarine sediments (undivided)

NOTES:
1. WGS 1984 COORDINATE SYSTEM
2. Geologic Map of California (Olaf P. Jenkins edition), Death Valley Sheet
compiled by Charles W. Jennings, 1958
3. See site map for details of geophysical survey

File Name: CI-GRA

Date: 2/7/2013

USGS science for a changing world

GEOVision geophysical services

RECOVERY.GOV

GEOLOGIC MAP
CI•GRA

Looking northeast towards seismic station CI.GRA and test area

Looking northwest towards seismic station from HVSR sensor 507

Looking southeast along SASW array GRA-1

Looking southwest towards center of SASW array GRA-1 and seismic station

Looking south along MASW array GRA-2

Location of Geophysical Testing Arrays:

Location	Latitude	Longitude
GRA-1, Southeast End of SASW Receiver Array	36.99598	-117.36579
GRA-1, Center of SASW Array	36.99621	-117.36592
GRA-1, Northwest End of SASW Receiver Array	36.99644	-117.36605
GRA-2, Southeast End of MASW/Refraction Array	36.99671	-117.36601
GRA-2, Center of MASW/Refraction Array	36.99699	-117.36619
GRA-2, Northwest End of MASW/Refraction Array	36.99728	-117.36636
HVSR Sensor 450	36.99644	-117.36604
HVSR Sensor 453	36.99621	-117.36590
HVSR Sensor 507	36.99599	-117.36577
CI.GRA Seismic Station	36.99606	-117.36615

Notes: 1) WGS84 Coordinate System (decimal degrees)
2) Survey accuracy is estimated at 1 to 2 m

Results:

V_S Model – SASW Array GRA-1

Depth to Top of Layer (m)	Layer Thickness (m)	S-Wave Velocity (m/s)	Inferred P-Wave Velocity (m/s)	Inferred Poisson's Ratio	Inferred Density (g/cm^3)
0	1.5	254	475	0.300	1.9
1.5	2.5	316	591	0.300	1.9
4	6	292	545	0.300	1.9
10	2	429	803	0.300	1.9
12	14	441	2075	0.476	2.0
26	>4	577	2075	0.458	2.0

V_S Model – MASW Array GRA-2

Depth to Top of Layer (m)	Layer Thickness (m)	S-Wave Velocity (m/s)	Inferred P-Wave Velocity (m/s)	Inferred Poisson's Ratio	Inferred Density (g/cm^3)
0	0.75	202	377	0.300	1.9
0.75	4.25	349	652	0.300	1.9
5	7	442	827	0.300	1.9
12	13	291	2075	0.490	2.0
25	>5	603	2075	0.454	2.0

Note: Velocity model may not be reliable. More testing is required to determine if this array and/or array GRA-1 is located in or adjacent to a mapped fault zone.

Observations/Discussion:

- The Furnace Creek fault is mapped in close proximity to the site. The actual fault location is not visible on the surface.
- There are no clear peaks in HVSR plots by which to assess potential lateral velocity variation.
- Noise conditions at site were not sufficient to apply passive surface wave techniques.
- There were very few options for placement of surface wave arrays that allowed access with an accelerated weight drop energy source.
- Due to space limitations and faulting in the site vicinity, an SASW array and combined MASW/seismic refraction array were tested at different locations. The SASW array (GRA-1) is closest to the seismic station. MASW data were not acquired along array GRA-1 due to space limitations. A combined MASW and seismic refraction array (GRA-2) was placed along the edge of Scotty's Castle Road.
- The generalized reciprocal method was utilized to develop a two layer seismic refraction model for array GRA-2 with a 10.5 to 12.5 m thick upper layer of unsaturated sediments with V_P averaging about 550 m/s and a lower layer of saturated sediments with V_P averaging about 2,075 m/s.
- There is some reflectivity in the MASW seismic records with multiple reflectors in the approximate 35 to 100 m depth range. The reflectors may be dipping based on different positions on seismic records from forward and reverses shot locations. A shallow seismic reflection survey along a profile orthogonal to and crossing Scotty's Castle Road should be able to more accurately locate the fault mapped in the site vicinity.
- Surface wave dispersion data from SASW and MASW data sets are very different indicating that the arrays may be on different sides of the fault or that one or both of the arrays are in the mapped fault zone.
- The MASW seismic records appear to show relatively complex wave propagation. There appears to be poor signal quality in the portion of the seismic record containing the surface waves, possibly due to the presence of scatterers, subsurface discontinuities, lateral velocity variation, out of plane geologic structures, etc. Additionally, the spectral content of the seismic data is quite variable throughout the receiver array.
- Representative dispersion curves were generated for each surface wave data set using a moving average, polynomial curve fitting routine for purpose of data modeling.
- Based on the seismic refraction survey, the top of saturated sediments with V_P of about 2,075 m/s was constrained at a depth of 12 m during surface wave modeling.
- For reasons discussed above, the S-wave velocity model for SASW array GRA-1 is expected to be more reliable than that for MASW array GRA-2. The S-wave velocity model for array GRA-2 has a large velocity inversion at a depth of about 12 m. The model was generated assuming that the dispersion curve is associated with the fundamental mode Rayleigh wave. In this case, multi-mode modeling of the dispersion curve would only result in a minor improvement in the model because, although the first high mode is dominant over the 25 to 50 Hz frequency range (6 to 15 m wavelength range), phase velocities are only slightly greater than the fundamental mode. In fact, only minor changes to the model result in a dominant fundamental mode at all frequencies.

- Surface wave depth of investigation is about 30 m based on half of maximum wavelength criteria.
- Inferred P-wave velocities of the unsaturated zone in the surface wave model for SASW array GRA-1 are consistent with the P-wave refraction model for MASW array GRA-2, especially considering unknown Poisson's ratio. Inferred P-wave velocities of the unsaturated zone in the surface wave model for MASW array GRA-2 are not consistent with the associated P-wave refraction model, again indicating that the surface wave model for this array may not be reliable. It should, however, be noted that there may be significant differences in velocity structure on each side of the fault zone mapped near the seismic station. Velocity structure may also be highly variable in the immediate vicinity of the fault zone.
- V_{S30} is 386 m/s for array GRA-1 (Site Class C).
- Average S-wave velocity between 2 m (nominal sensor depth) and 32 m is 407 m/s for array GRA-1.
- V_{S30} is 354 m/s for array GRA-2 (Site Class D/C).
- Average S-wave velocity between 2 m (nominal sensor depth) and 32 m is 372 m/s for array GRA-2.
- The S-wave velocity model for array GRA-1 is believed to be more representative of velocity structure at the seismic station than that for array GRA-2 because the array is closer to the seismic station and array GRA-2 has complexities outlined above. It is, however, possible that both arrays are located in close proximity to a mapped fault zone where velocity structure may be highly variable. There is not space at the site for additional 30 m S-wave velocity soundings due to access restrictions for a vehicle; however, shallower MASW soundings could be conducted in the immediate vicinity of the seismic station for better understanding of near surface velocity variability. It may also be possible to map the fault location using the seismic reflection technique.
- Regardless of the geologic complexities in the vicinity of the seismic station, Site Class is expected to be D/C or C.

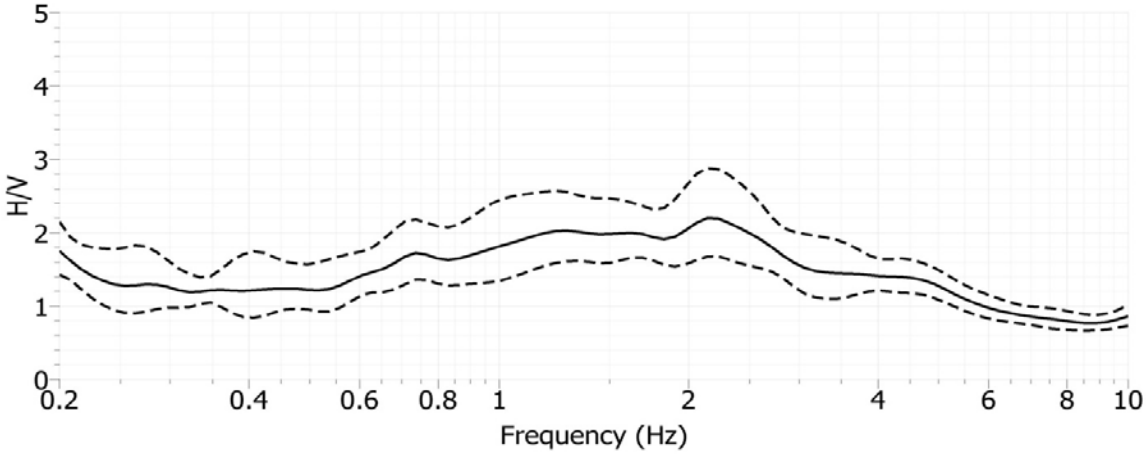

Site CI.GRA, H/V Spectral Ratio, Array GRA -1, Sensor 450

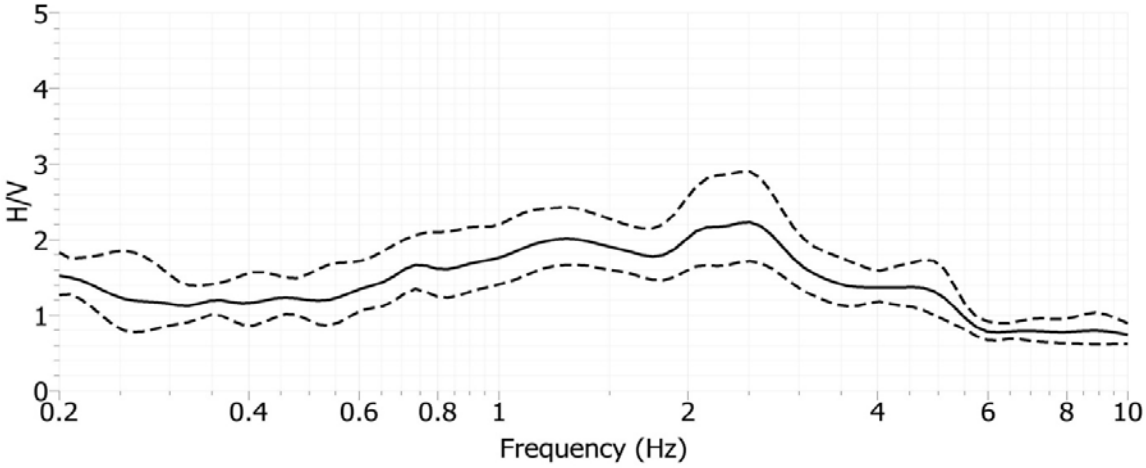

Site CI.GRA, H/V Spectral Ratio, Array GRA -1, Sensor 453

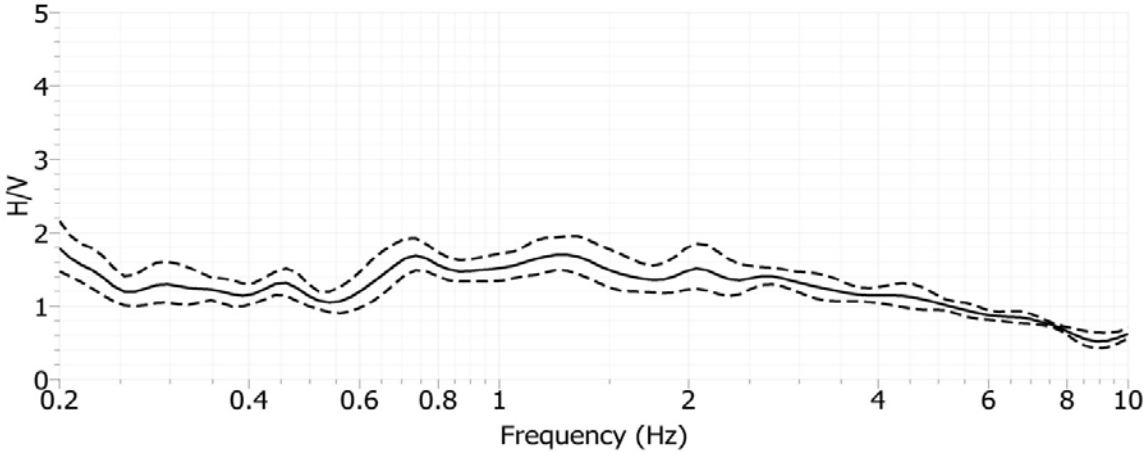

Site CI.GRA, H/V Spectral Ratio, Array GRA -1, Sensor 507

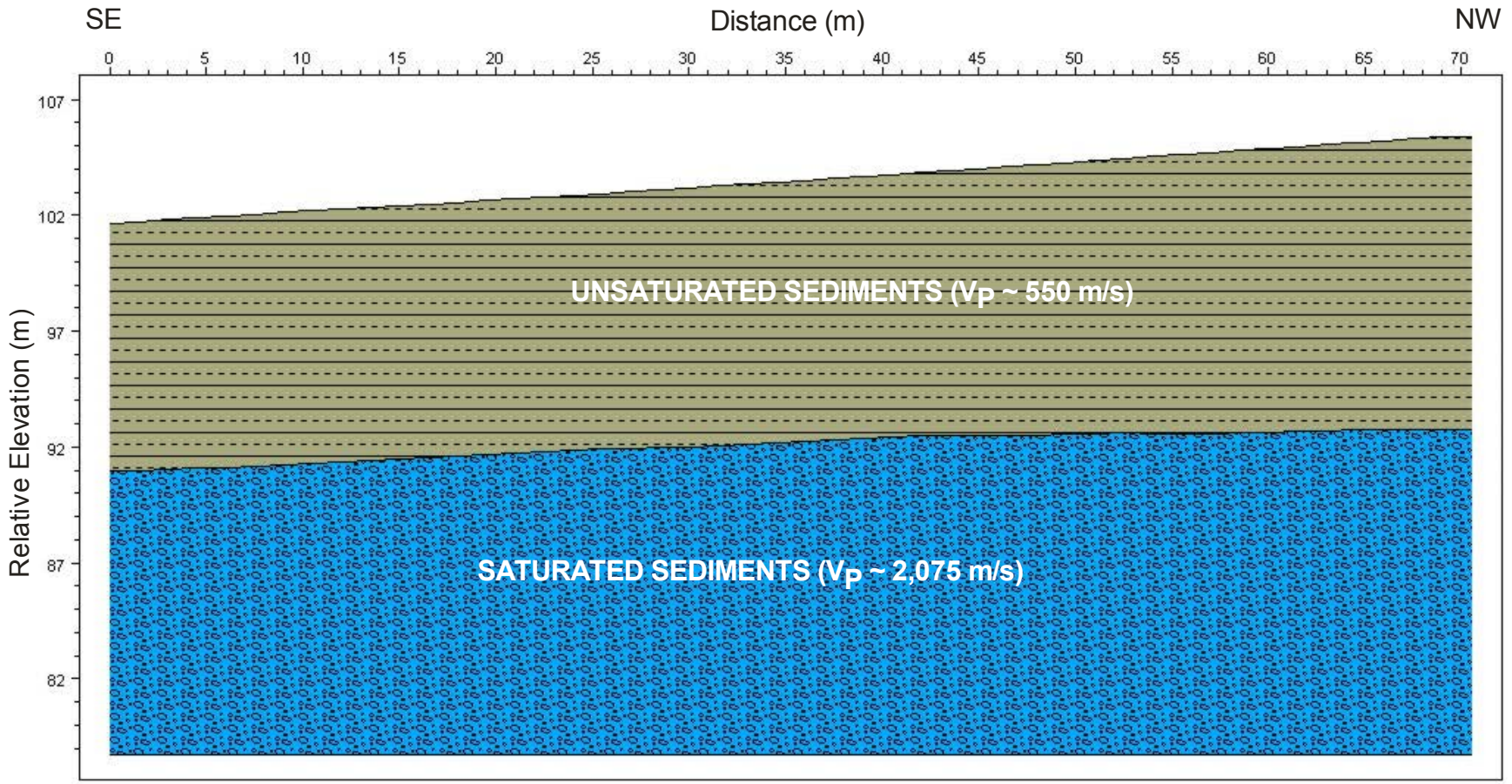

Array GRA-2 – Layer Based Seismic Refraction Model utilizing Generalized Reciprocal Method

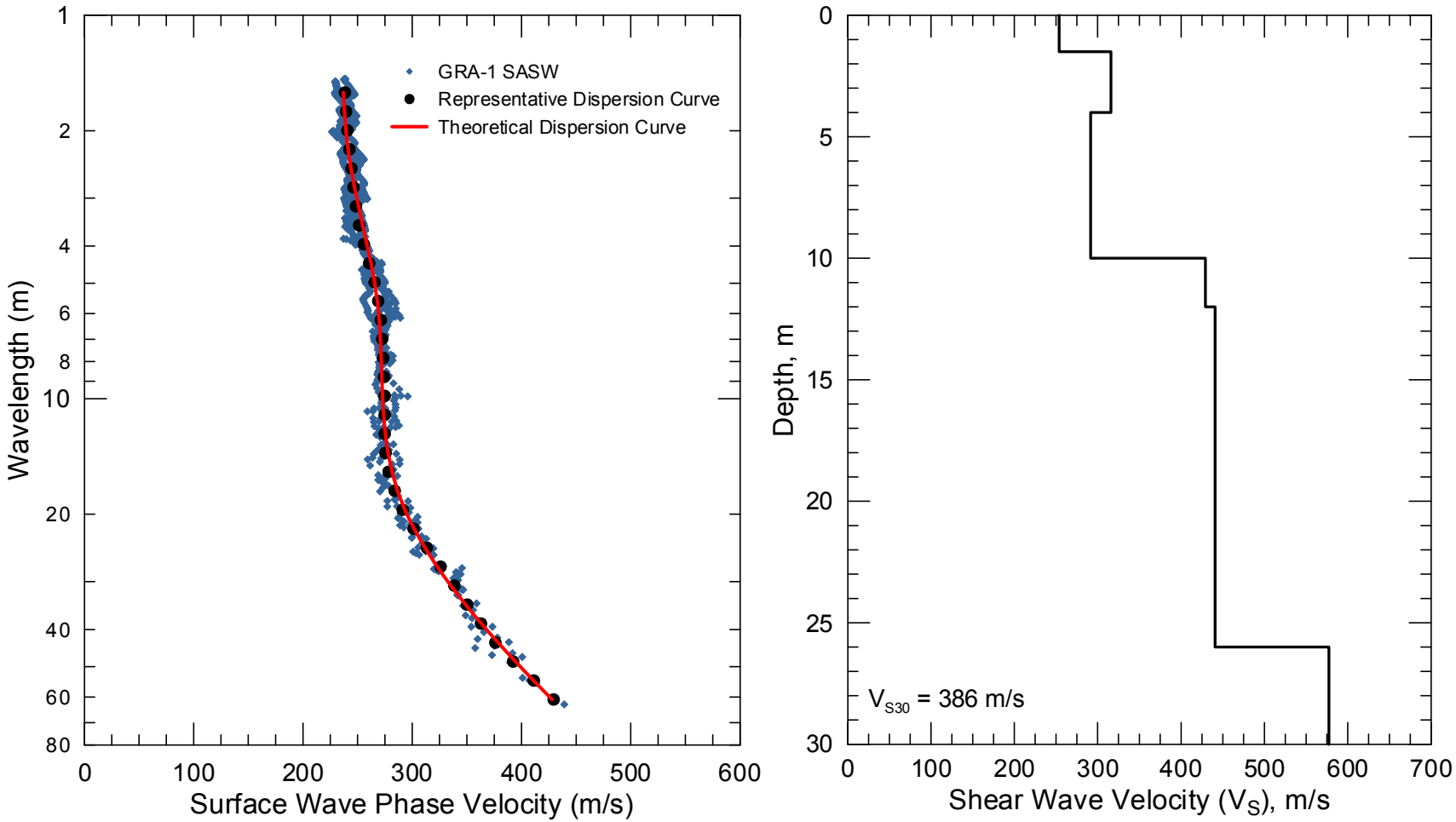

CI.GRA - Field, representative and inverted theoretical surface wave dispersion data (left) and associated V_S model (right) for SASW Array GRA-1

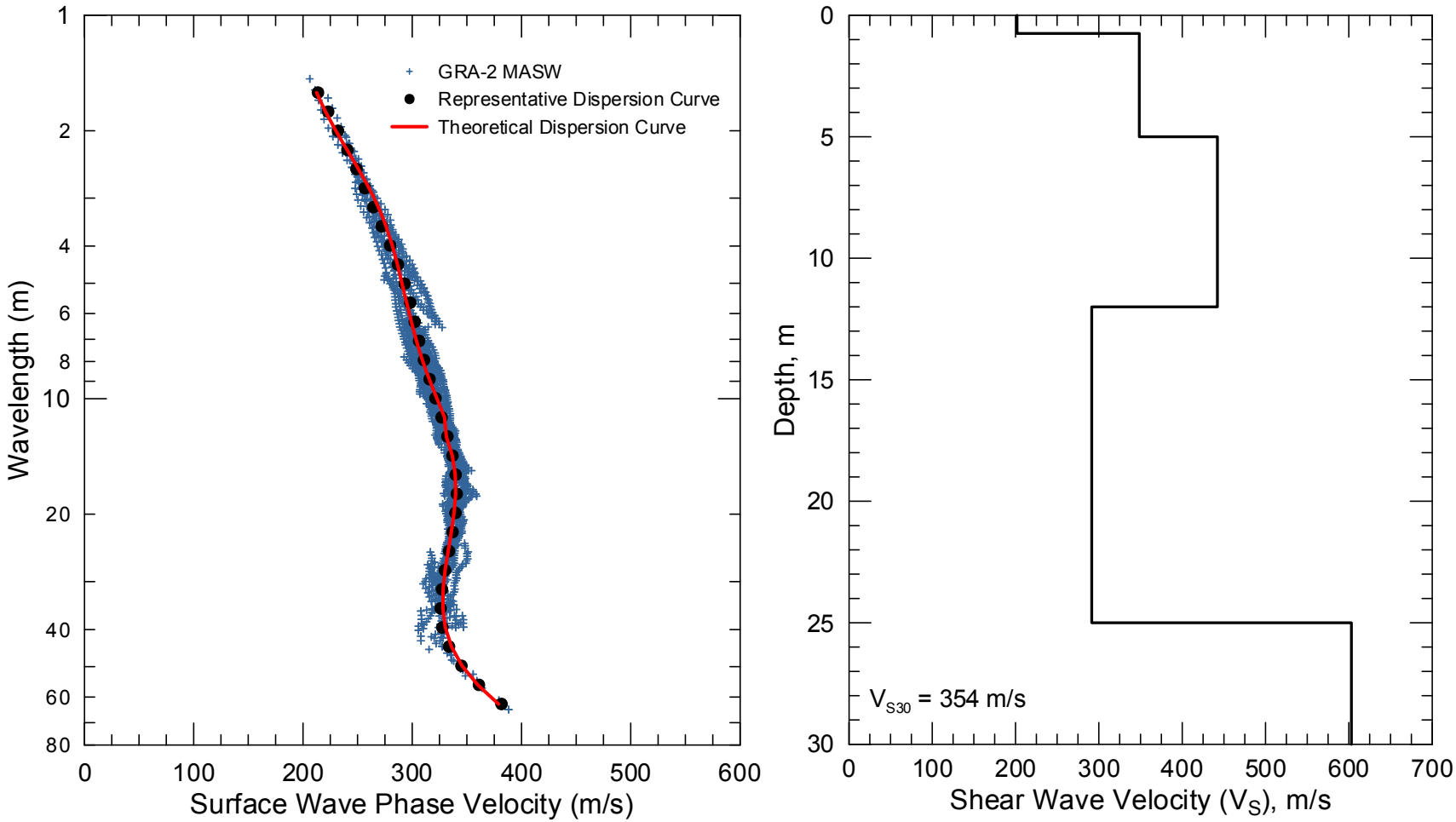

CI.GRA - Field, representative and inverted theoretical surface wave dispersion data (left) and associated V_S model (right) for MASW Array GRA-2. This sounding may be impacted by a fault zone and velocity model may not be representative of nominal site conditions.

Site CI.GSC

Location: Goldstone Deep Space Network Facility, Fort Irwin, San Bernardino County, California

Latitude: 35.30177 **Longitude:** -116.80574
(Station coordinates provided by USGS, WGS84 coordinate system)

V_{S30} (measured): 679 m/s

V_{S30} (adjusted to more accurately reflect seismic station conditions): 735 m/s (average S-wave velocity between 1 and 31 m adjusting for seismic sensor being located on a building pad likely placed on rock).

NEHRP Site Class: C

Geomatrix Code: AGA

Geologic Conditions/Observations: Geologic map indicates that seismic station is located on Quaternary (Pleistocene) volcanic basalt; however, field inspection indicates that the seismic station is located on Mesozoic granitic rocks.

Site Conditions: Rural site near large complex of buildings associated with the Goldstone Deep Space Network Facility. Seismic station located at the base of hill comprised of weathered granitic rocks. Seismic line located on relatively level surface with only about 1 m of elevation variation along line. There may be a thin layer of soil over weathered rock beneath the seismic line, whereas the seismic station is located inside a building that may sit on rock.

Geophysical Methods Utilized: HVSR, Seismic Refraction, MASW

Geophysical Testing Arrays:

1. Array GSC-1 (48 channel MASW and P-wave seismic refraction array utilizing 4.5 Hz vertical geophones spaced 1.5 m apart for a length of 70.5 m, forward and reverse shot locations with multiple source offsets and source types and multiple interior shot locations).
2. Three HVSR measurement locations: two on array GSC-1 and the other near the seismic station. HVSR measurements near the seismic station made with both a Nanometrics Trillium Compact and Tromino ENGY.

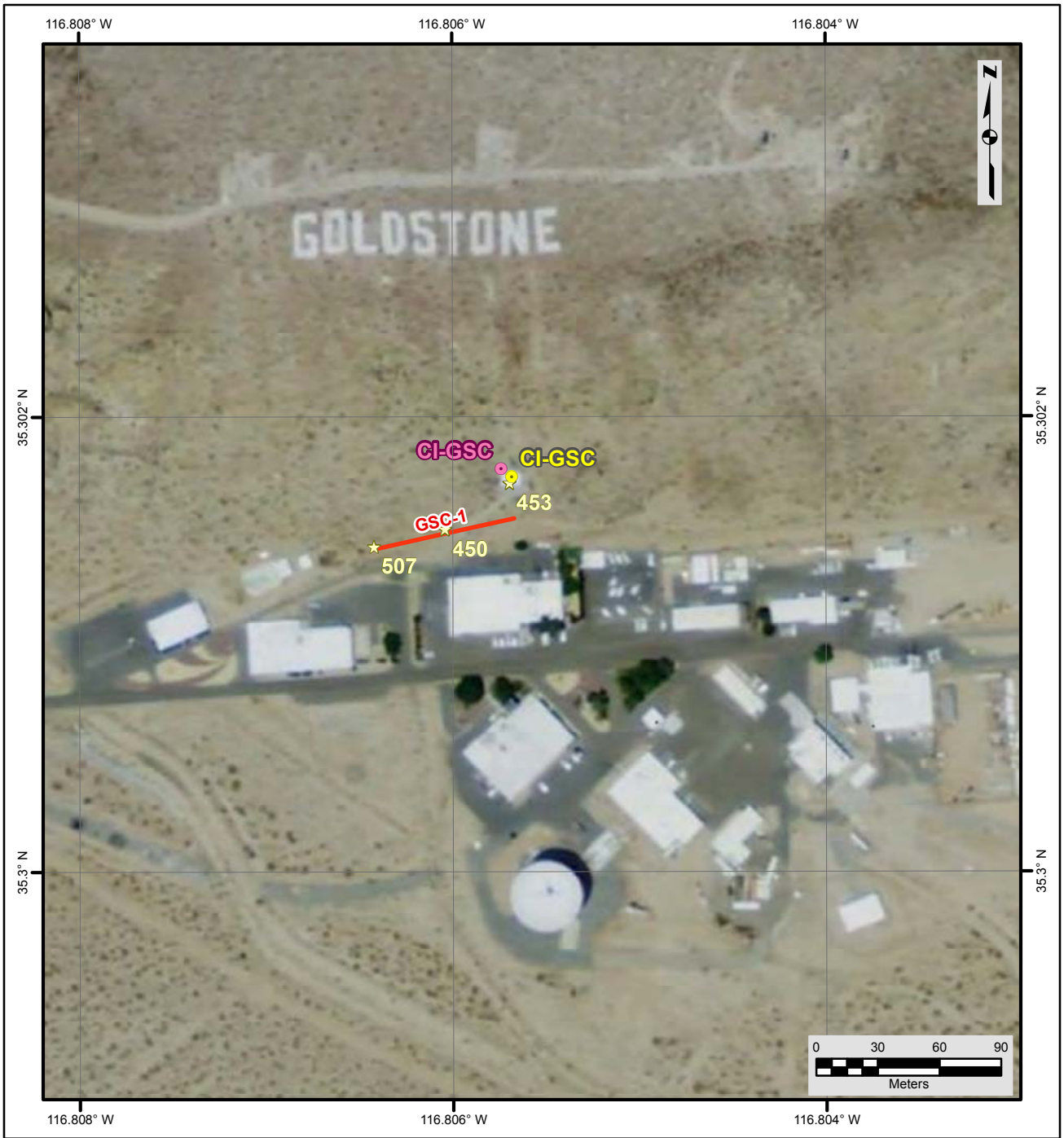

Legend

- Seismic Station - Approximate Surveyed Location
- Seismic Station - Approximate Location of Record
- H/V Spectral Ratio Location
- MASW and Seismic Refraction Array

NOTES:
1. WGS 1984 COORDINATE SYSTEM
2. Image Source: ESRI, i-cubed, USDA FSA, USGS, AEX, GeoEye, Getmapping, Aerogrid, IGP

File Name: CI-GSC-I

Date: 10/14/2011

USGS science for a changing world

GEOVision geophysical services

RECOVERY.GOV

SITE MAP
CI•GSC

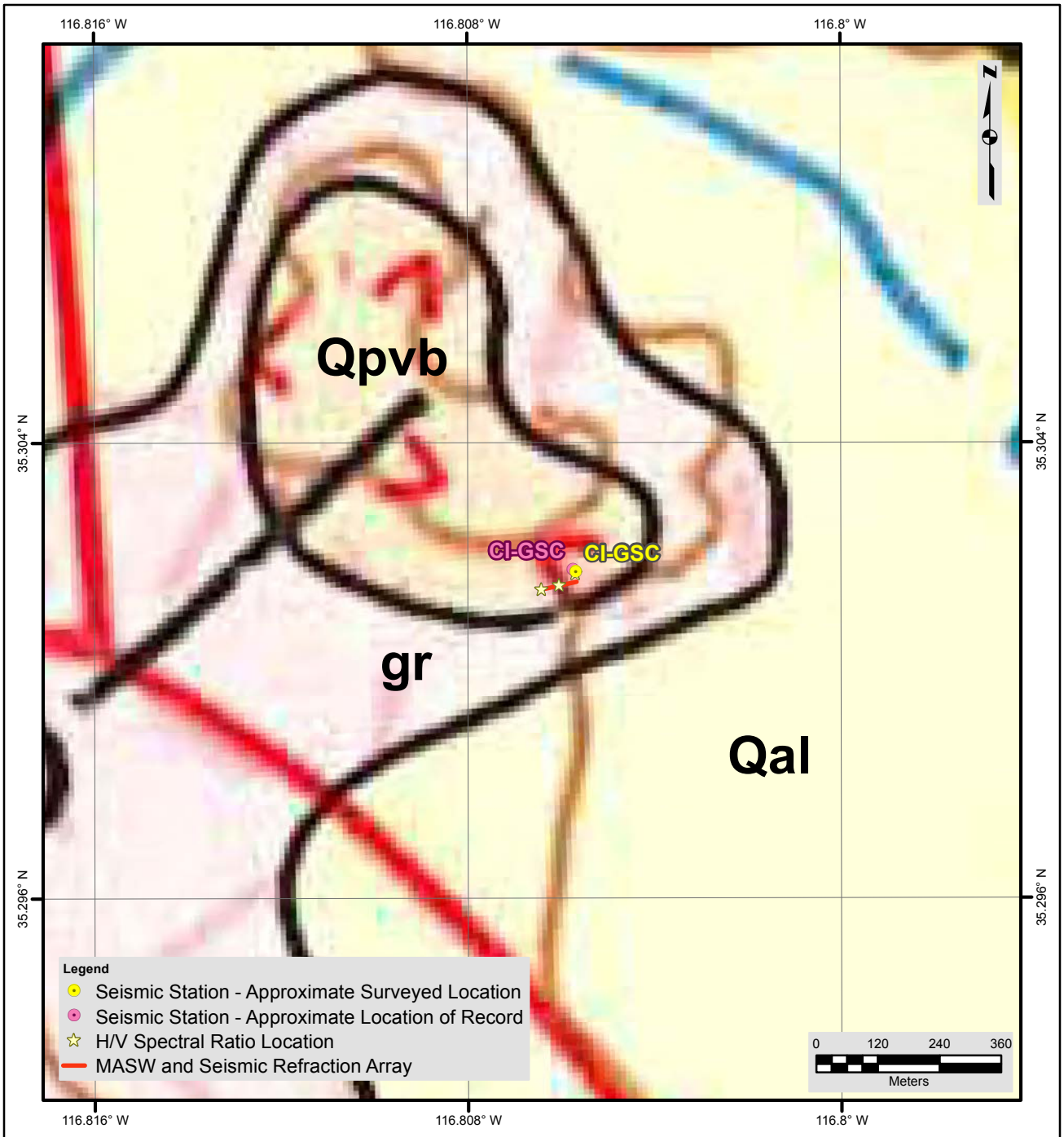

Description of Geologic Map Units

Qal = Quaternary (Holocene) alluvium
Qpvb = Quaternary (Pleistocene) volcanic basalt
gr = Mesozoic (Jurassic/Cretaceous) granitic rocks

NOTES:
1. WGS 1984 COORDINATE SYSTEM
2. Geologic Map of California, Trona Sheet
Olaf P. Jenkins Edition
compilation by Charles W. Jennings,
John L. Burnett, and Bennie W. Troxel, 1962
3. See site map for details of geophysical survey

File Name: CI-GSC

Date: 10/14/2011

USGS science for a changing world

GEOVision geophysical services

RECOVERY.GOV

GEOLOGIC MAP
CI•GSC

Looking at HVSR sensors 453 (Trillium Compact) and Tromino ENGR and the seismic station building

P-wave seismic refraction and MASW data acquisition along array GSC-1

Looking north towards Seismic Laboratory and eastern end of array GSC-1

Looking west along array GSC-1

Looking northeast towards Seismic Laboratory and center of array GSC-1

Location of Geophysical Testing Arrays:

Location	Latitude	Longitude
GSC-1, Southwest End of MASW/Seismic Refraction Array	35.30142	-116.80642
GSC-1, Center of MASW and Seismic Refraction Array	35.30149	-116.80604
GSC-1, Northeast End of MASW/Seismic Refraction Array	35.30155	-116.80567
HVSR Sensor 450	35.30150	-116.80604
HVSR Sensor 453	35.30171	-116.80570
HVSR Sensor 507	35.30143	-116.80642
HVSR Sensor Tromino	35.30170	-116.80570
CI.GSC Seismic Station Building	35.30174	-116.80568

Notes: 1) WGS84 Coordinate System (decimal degrees)
2) Survey accuracy is estimated at 1 to 2 m.

Results:

V_S Model

Depth to Top of Layer (m)	Layer Thickness (m)	S-Wave Velocity (m/s)	Inferred P-Wave Velocity (m/s)	Assumed Poisson's Ratio	Assumed Density (g/cm^3)
0	1	224	420	0.3	1.8
1	1.5	432	809	0.3	2.0
2.5	4.5	696	1302	0.3	2.1
7	7	732	1369	0.3	2.1
14	10	735	1375	0.3	2.1
24	>11	908	1699	0.3	2.1

Notes: 1) Depth of investigation is about 35 m.
2) Bottom layer is a half space.

Observations/Discussion:

- The seismic station is located in a building that may sit on either rock or a thin engineered pad over rock. The MASW/seismic refraction array is located adjacent to an outcrop of weathered granitic rocks where there is a thin layer of soil beneath the array.
- There are no significant HVSR peaks, as expected for a rock site.
- The P-wave refraction data collected along array GSC-1 were very noisy due to strong signal attenuation in the weathered rock and electrical noise from the adjacent facilities. Surface wave data quality is much better.
- A seismic refraction model is not presented due to poor data quality. Seismic refraction depth of investigation was only about 5 m and indicates that P-wave velocity is 350 to 600 m/s near the surface, increasing to over 1,500 m/s at a depth of 2 to 4 m.
- Noise conditions at the site were not sufficient for application of passive surface wave techniques.
- The minimum wavelength surface wave phase velocity data extracted from the 48-channel MASW array was about 14 m. Data reduction using seismic records from smaller hammer sources and a limited offset receiver array (i.e. less active geophones) allowed extraction of surface wave dispersion data to a minimum wavelength of about 4 m.
- There is about 75 m/s scatter in the MASW dispersion data over an intermediate wavelength range, likely the result of lateral velocity variation.
- A representative dispersion curve was generated for the MASW data set using a moving average, polynomial curve fitting routine and used for modeling.
- Surface wave depth of investigation is about 35 m based on half of maximum wavelength criteria.
- V_{S30} is 679 m/s (Site Class C).
- The scatter in the MASW data indicates that V_{S30} may vary by about 5% along the MASW array.
- Average S-wave velocity between 1 m (to account for the building housing the seismic station likely sitting on weathered rock with no low velocity soil layer) and 31 m is 735 m/s (Site Class C/B).

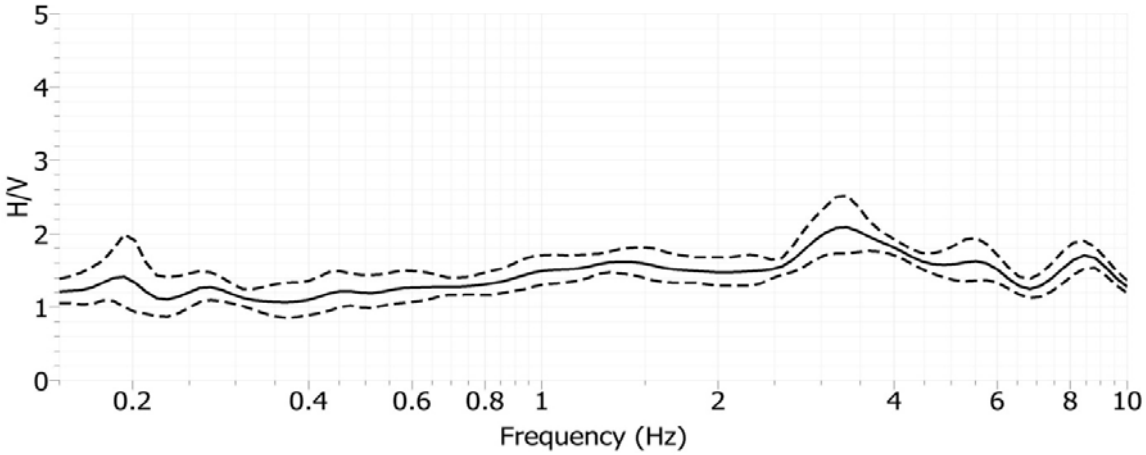

Site CI. GSC, H/V Spectral Ratio, Array GSC -1, Sensor 507

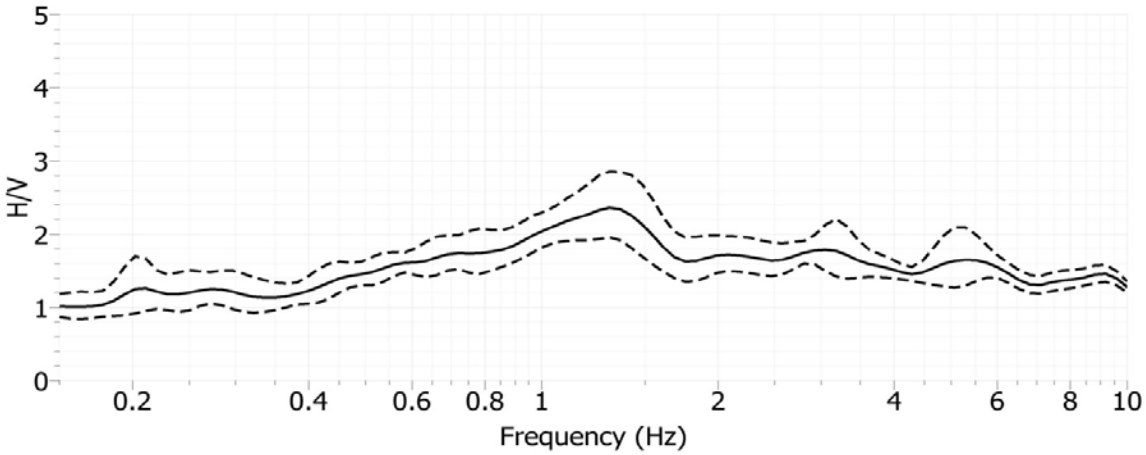

Site CI.GSC, H/V Spectral Ratio, Array GSC -1, Sensor 450

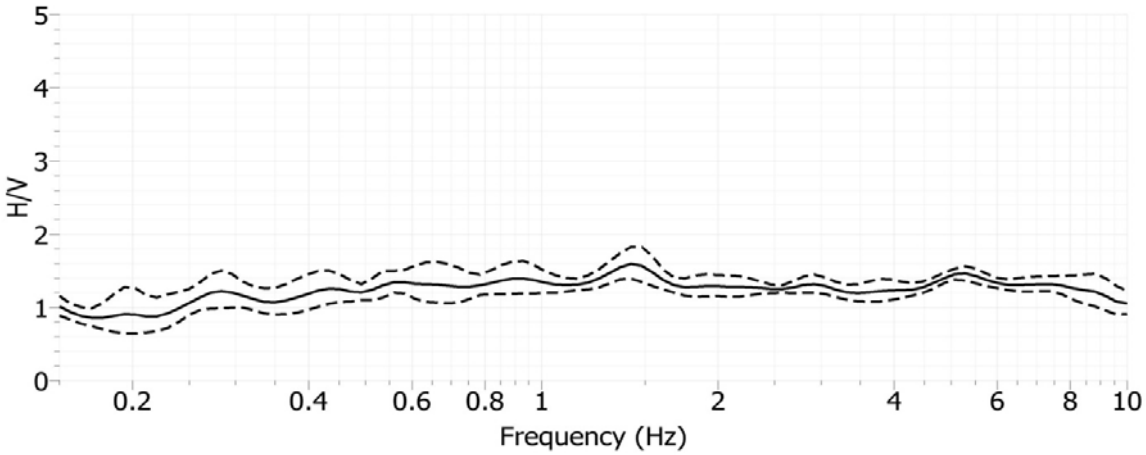

Site CI. GSC, H/V Spectral Ratio, Near Seismic Station, Sensor 453

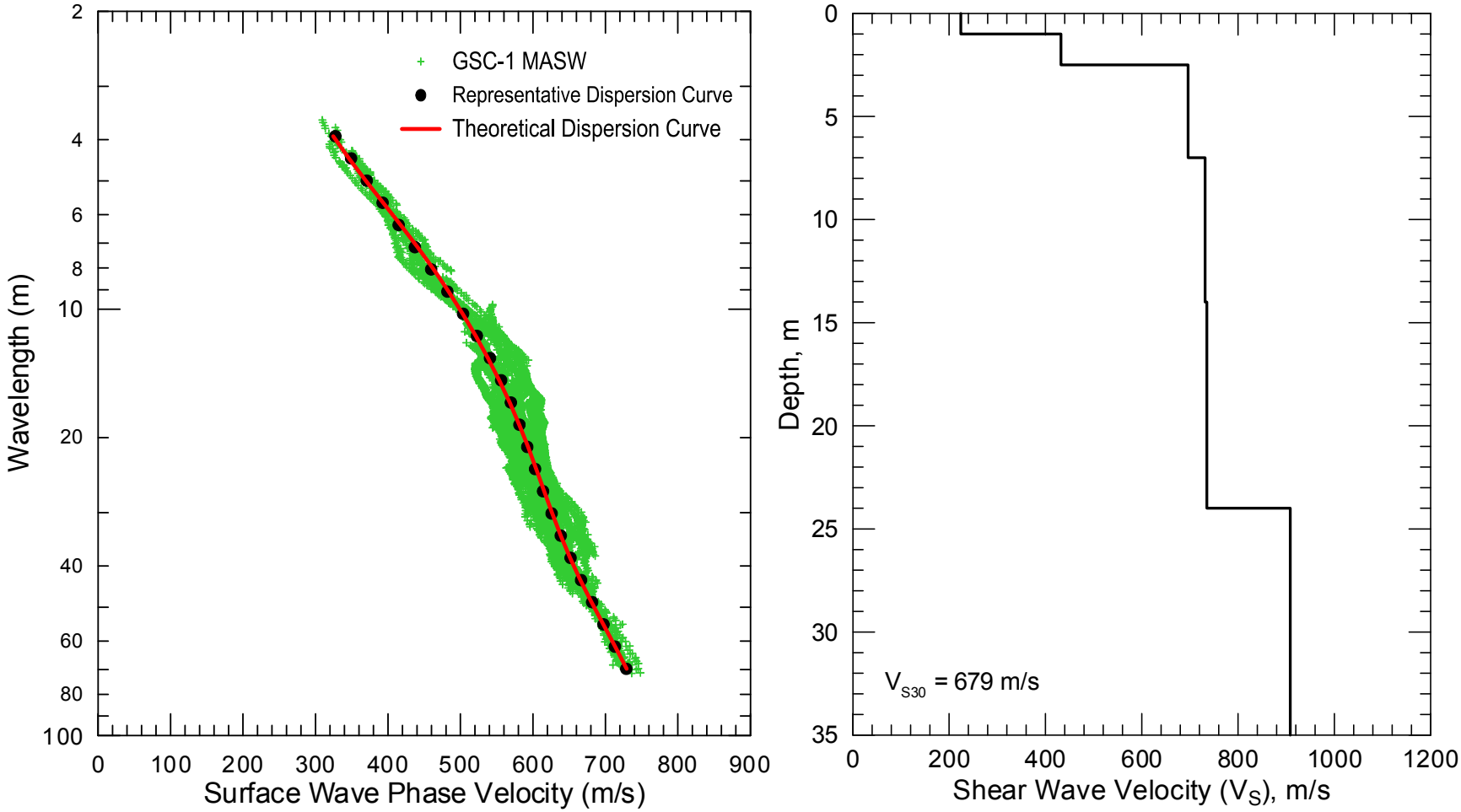

CI.GSC - Field, representative and inverted theoretical surface wave dispersion data (left) and associated V_S model (right)

Site CI.HEC

Location: Hector SBC/ATT Facility, North of Highway 40, San Bernardino County, California

Latitude: 34.82954 **Longitude:** -116.33637
(Station coordinates modified based on field GPS survey, WGS84 coordinate system)

V_{S30} (measured): 726 m/s
(Recommend using V_{S30} outlined below as the surface wave model includes a fill layer which is not present beneath the seismic station)

V_{S30} (adjusted to more accurately reflect seismic station conditions): 768 - 795 m/s (average S-wave velocity with velocity of upper layer replaced by that of underlying layer to average S-wave velocity between 1 and 31 m to reflect the fact that the seismic station is located on rock but the surface wave model includes a thin fill layer)

NEHRP Site Class: C/B

Geomatrix Code: IGA

Geologic Conditions/Observations: Seismic station located on weathered and fractured granitic rock (quartz monzonite to granite). Test area partially located on a leveled hilltop with a thin layer of fill over weathered rock. The seismic station is located on rock, in the center of the fill pad, near an outcrop.

Site Conditions: Rural site. Steep hilly terrain in site vicinity. Air conditioning units running in structures adjacent to test area. About 7 m of ground surface elevation variation along the 70.5 m long MASW and seismic refraction array HEC-2.

Geophysical Methods Utilized: HVSR, Seismic Refraction, MASW

Geophysical Testing Arrays:

1. Array HEC-1 (48 channel MASW and P-wave seismic refraction array utilizing 4.5 Hz vertical geophones spaced 1 m apart for a length of 47 m, forward and reverse shot locations with multiple source offsets and source types and center shot location).
2. Array HEC-2 (48 channel MASW and P-wave seismic refraction array utilizing 4.5 Hz vertical geophones spaced 1.5 m apart for a length of 70.5 m, forward and reverse shot locations with multiple source offsets and source types (hammers only) and center shot location).
3. Three HVSR measurement locations; two distributed along array HEC-2 and one near the seismic station.

Legend

- Seismic Station - Approximate Surveyed Location
- Seismic Station - Approximate Location of Record
- H/V Spectral Ratio Location
- MASW and Seismic Refraction Array

NOTES:
1. WGS 1984 COORDINATE SYSTEM
2. Image Source: ESRI, i-cubed, USDA FSA, USGS, AEX, GeoEye, Getmapping, Aerogrid, IGP

File Name: CI-HEC-I

Date: 9/16/2011

USGS science for a changing world

GEOVision geophysical services

RECOVERY.GOV

SITE MAP
CI•HEC

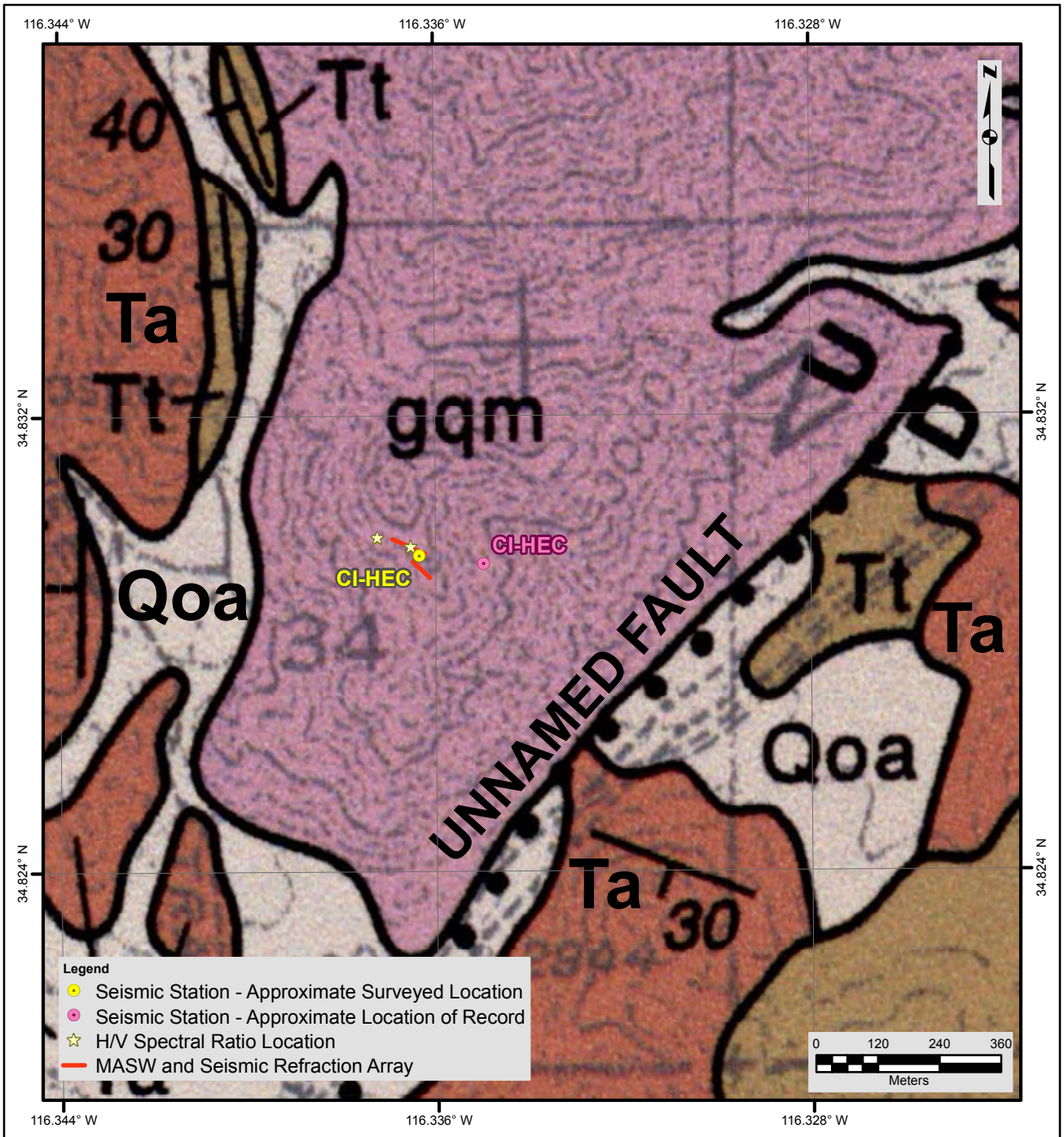

Description of Geologic Map Units

Qoa = Quaternary (Pleistocene) older alluvial cobble-pebble gravel and sand
Ta = Tertiary (Oligocene to Miocene) andesite, massive porphyritic, in places brecciated
Tt = Tertiary (Oligocene to Miocene) tuff breccia (mud flow and ash), massive to bedded, angular to subrounded, andesite fragments in tuff matrix
gqm = Mesozoic (Late Jurassic-Early Cretaceous) granite to quartz monzonite, hard, massive, medium to coarse-grained

NOTES:
1. WGS 1984 COORDINATE SYSTEM
2. Geologic Map of the Newberry & Cady Mountains 15 Minute Quadrangle, San Bernardino County, California by Thomas W. Dibblee, Jr., 2008
3. See site map for details of geophysical survey

File Name: CI-HEC
Date: 9/29/2011

USGS science for a changing world
GEOVision geophysical services

GEOLOGIC MAP
CI•HEC

RECOVERY.GOV

Enclosure housing seismic station
CI-HEC on fill pad

HVSR Sensor 450, near the center of
Array HEC-2

Looking southeast along Array HEC-1

HVSR Sensor 453

MASW and seismic refraction data acquisition at
southeast end of Array HEC-2, looking northwest

Location of Geophysical Testing Arrays:

Location	Latitude	Longitude
HEC-1, Northwest End of MASW/Refraction Array	34.82945	-116.33651
HEC-1, Center of MASW/Refraction Array	34.82929	-116.33631
HEC-1, Southeast End of MASW/Refraction Array	34.82916	-116.33615
HEC-2, Northwest End of MASW/Refraction Array	34.82984	-116.33694
HEC-2, Center of MASW/Refraction Array	34.82972	-116.33661
HEC-2, Southeast End of MASW/Refraction Array	34.82958	-116.33624
HVSR Sensor 453	34.82986	-116.33726
HVSR Sensor 450	34.82971	-116.33655
HVSR Sensor 507	34.82956	-116.33639
CI.HEC Seismic Station	34.82954	-116.33637

Notes: 1) WGS84 Coordinate System (decimal degrees)
2) Survey accuracy is estimated at 1 to 2 m.

Results:

V_S Model

Depth to Top of Layer (m)	Layer Thickness (m)	S-Wave Velocity (m/s)	Inferred P-Wave Velocity (m/s)	Assumed Poisson's Ratio	Assumed Density (g/cm^3)
0	1	225	422	0.3	1.8
1	1.5	451	843	0.3	1.9
2.5	9.5	812	1518	0.3	2.1
12	18	825	1543	0.3	2.1
30	>5	1155	2161	0.3	2.2

Notes: 1) Depth of investigation is about 35 m.
2) Bottom layer is a half space.

Observations/Discussion:

- The seismic station in located on a mountain top fill pad for communications antennas. Rock is exposed at the surface in the north central portion of the pad where the seismic station is located and the thickness of fill increases to the east and west.
- Array HEC-1 was located on the western side of the fill pad. A thick sequence of fill was found in this area, making the surface wave data not useful. Array HEC-2 is located partially on the western edge of the pad and north of the pad. There is a minimal thickness of fill beneath the array and, therefore, this array was utilized for site characterization. There are no other areas in which to attempt site characterization in close proximity to the seismic station.
- HVSR curves are similar at all sensor locations, with no peak, as expected for a rock site.
- There is some noise in the seismic refraction first arrival data due to noise from AC units on site and other electrical noise from antennas. Possible out of plane refractions from localized high velocity zones or dikes, scattering from heterogeneities and fractures in the rock, may also contribute to minor error in picking of seismic refraction first arrival data.
- Seismic refraction data were modeled using a tomographic inversion routine and a smooth velocity gradient starting model. The seismic refraction model indicates that P-wave velocity increases with depth from about 450 to 800 m/s at the surface, to 1,200 m/s at a depth of 1 to 5 m, 1,400 m/s at a depth of 2 to 9 m and 1,600 m/s at a depth of 4 to greater than 20 m.
- Seismic refraction depth of investigation is generally about 15 to 20 m.
- The seismic refraction model indicates that there is some lateral velocity variation beneath the line, particularly a thin layer of low velocity fill on the southeast end of the line.
- Lateral velocity variation and topography are expected to have some effect on MASW data collected at this site and there were no alternate areas to acquire data in reasonably close proximity to the seismic station. This is a very common problem with mountain top sites.
- Noise conditions at the site were not sufficient for application of passive surface wave techniques.
- The minimum wavelength surface wave phase velocity data extracted from the 48-channel MASW array was about 12 m. Reducing data from smaller hammer sources using a limited offset receiver array (i.e. less active geophones) generally allowed extraction of surface wave dispersion data to a minimum wavelength of about 6 m. Selected shot locations on the fill pad in the southern half of the array allowed extraction of surface wave dispersion data that tied into the full receiver array dispersion data to a minimum wavelength of about 2 m.
- There is significant scatter in the surface wave dispersion data due to lateral velocity variation caused by variable fill thickness, differential weathering, topography, etc. Selective use of over 70 reduced phase velocity data files was required to generate a coherent dispersion curve that tied into the phase velocity data reduced from the complete 48 channel receiver array. Even after this editing process, surface wave phase velocity data still deviates from the average by about 5 to 10 % of velocity over a wide wavelength range.

- A representative dispersion curve was generated for the MASW data set using a moving average, polynomial curve fitting routine and used for modeling.
- To prevent velocity inversions, which are probably not realistic for a weathered granitic rock environment, from occurring in the model, the number of layers in the model was reduced and layer thicknesses increased. Slightly smaller RMS errors would be obtained with more layers with less thickness, providing unrealistic velocity inversions are allowed in the model.
- Surface wave depth of investigation is about 35 m based on half of maximum wavelength criteria.
- The inferred P-wave velocities in the surface wave model, assuming a Poisson's ratio of 0.3, are generally consistent with P-wave velocity structure in the seismic refraction model, especially considering unknown Poisson's ratio. Inferred P-wave velocities between 2.5 and 20 m in the surface wave model are between about 1,500 and 1,550 m/s and generally correspond to the 1,400 to 1,600 m/s P-wave velocity zone in the seismic refraction model.
- V_{S30} is 726 m/s (Site Class C/B).
- V_{S30} is 768 m/s if the S-wave velocity of the upper layer is replaced by that of the underlying layer to account for the absence of a thin fill layer beneath the seismic station (Site Class B/C).
- Average S-wave velocity between 1 m and 31 m to compensate for the seismic station being located on rock but the surface wave model having a thin fill layer is 795 m/s (Site Class B/C).

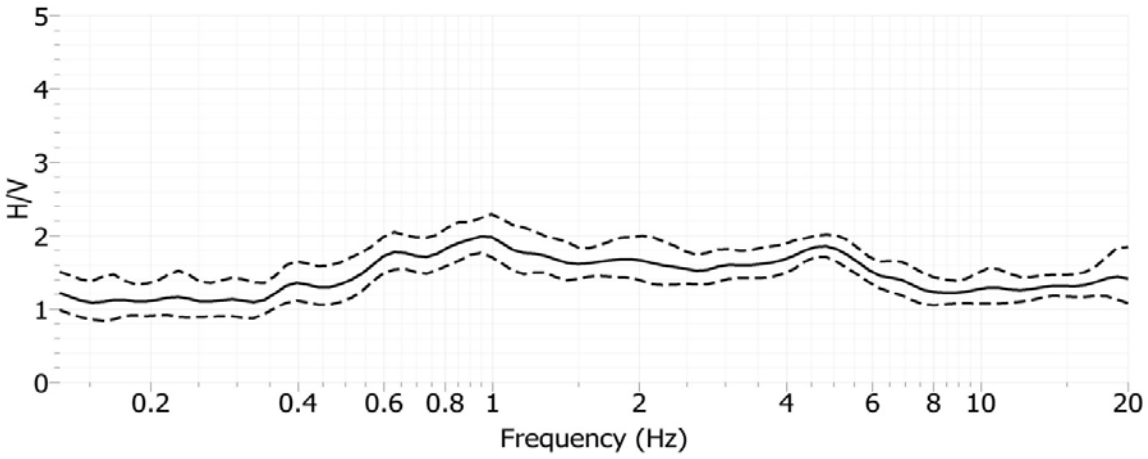

Site CI.HEC, H/V Spectral Ratio, Array HEC-2, Sensor 453

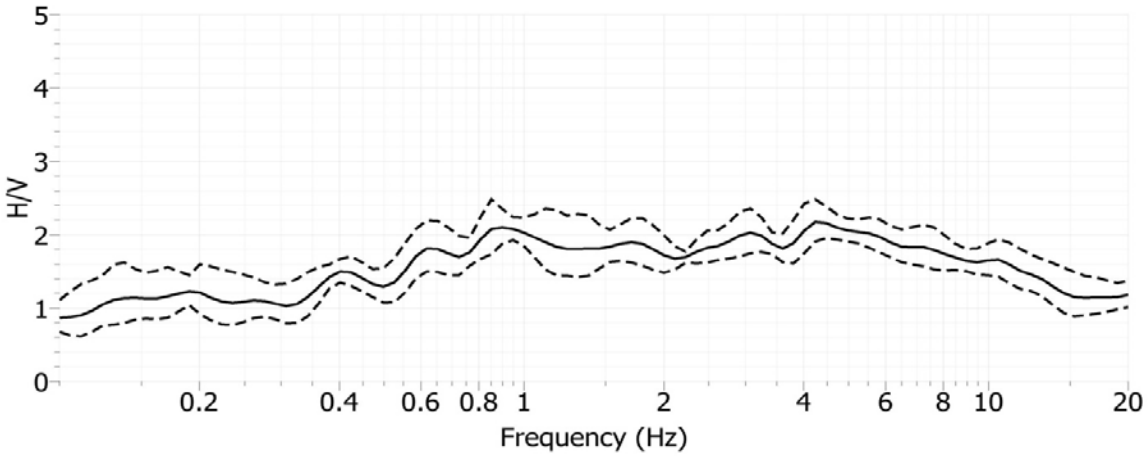

Site CI.HEC, H/V Spectral Ratio, Array HEC-2, Sensor 450

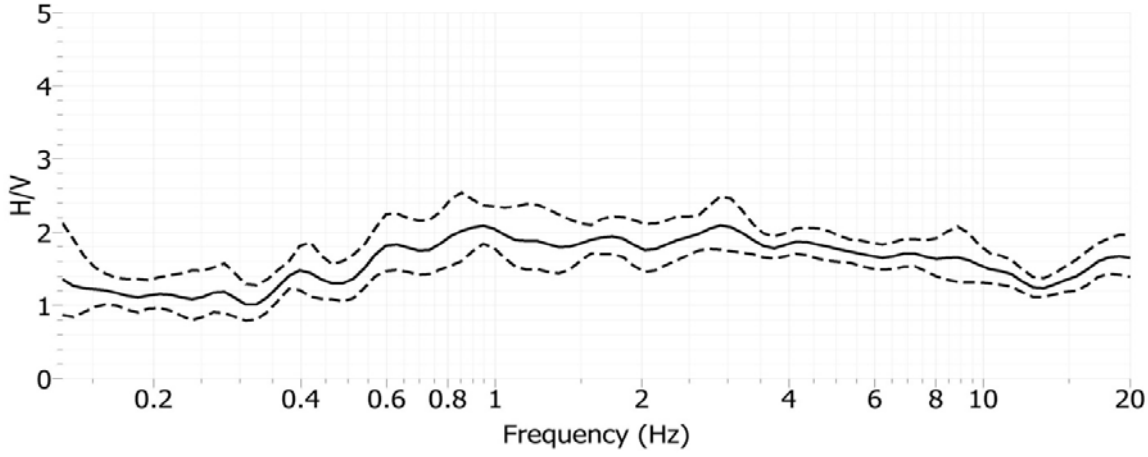

Site CI.HEC, H/V Spectral Ratio, Array HEC-2, Sensor 507

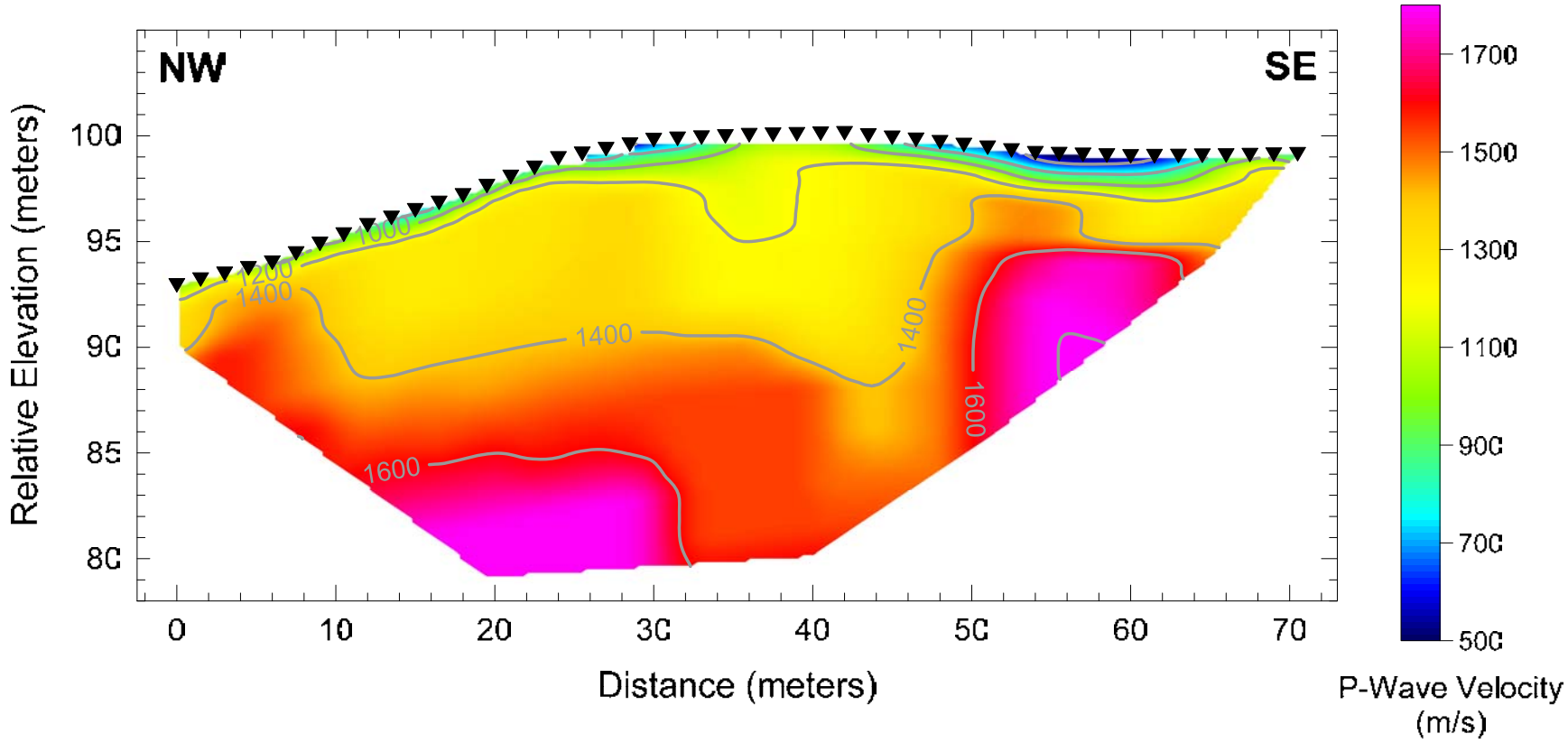

Array HEC-2 – Tomographic seismic refraction model utilizing smooth velocity gradient starting model

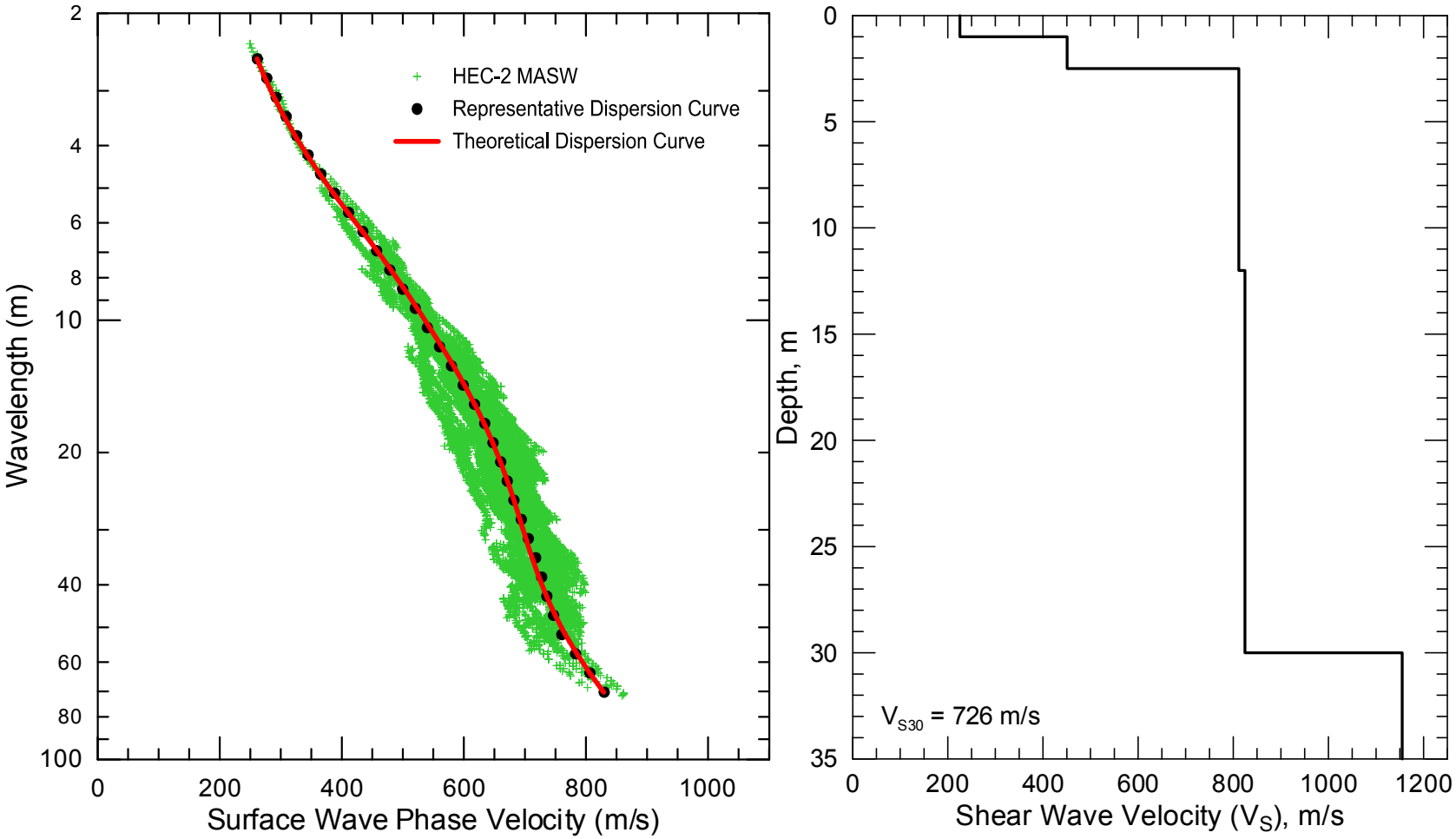

CI.HEC - Field, representative and inverted theoretical surface wave dispersion data (left) and associated V_S model (right)

Site CI.IDO

Location: Indio Hill, Dillon Road, Desert Hot Springs, California

Latitude: 33.79673 **Longitude:** -116.22153
(Station coordinates modified based on field GPS survey, WGS84 coordinate system)

V_{S30} (measured): 557 m/s

V_{S30} (adjusted to more accurately reflect seismic station conditions): 597 m/s (average S-wave velocity between 2 and 32 m adjusting for 2 m nominal sensor depth.)

NEHRP Site Class: C

Geomatrix Code: IQD

Geologic Conditions/Observations: Seismic station located on a Quaternary (Pleistocene) fanglomerate unit. Seismic station located near the apex of an anticline and geologic layers are expected to have shallow dip in the test area.

Site Conditions: Rural site. Steep, undulating topography in site vicinity. Seismic station located on top of a hill with steep decline to the east. Test area located along a dirt road cut into the side of a gently sloping hill.

Geophysical Methods Utilized: HVSR, Seismic Refraction, MASW

Geophysical Testing Arrays:

1. Array IDO-1 (48 channel MASW and P-wave seismic refraction array utilizing 4.5 Hz vertical geophones spaced 1.5 m apart for a length of 70.5 m, forward and reverse shot locations with multiple source offsets and source types and multiple interior shot locations).
2. Three HVSR measurement locations; two distributed along array IDO-1 and the other adjacent to the seismic station.

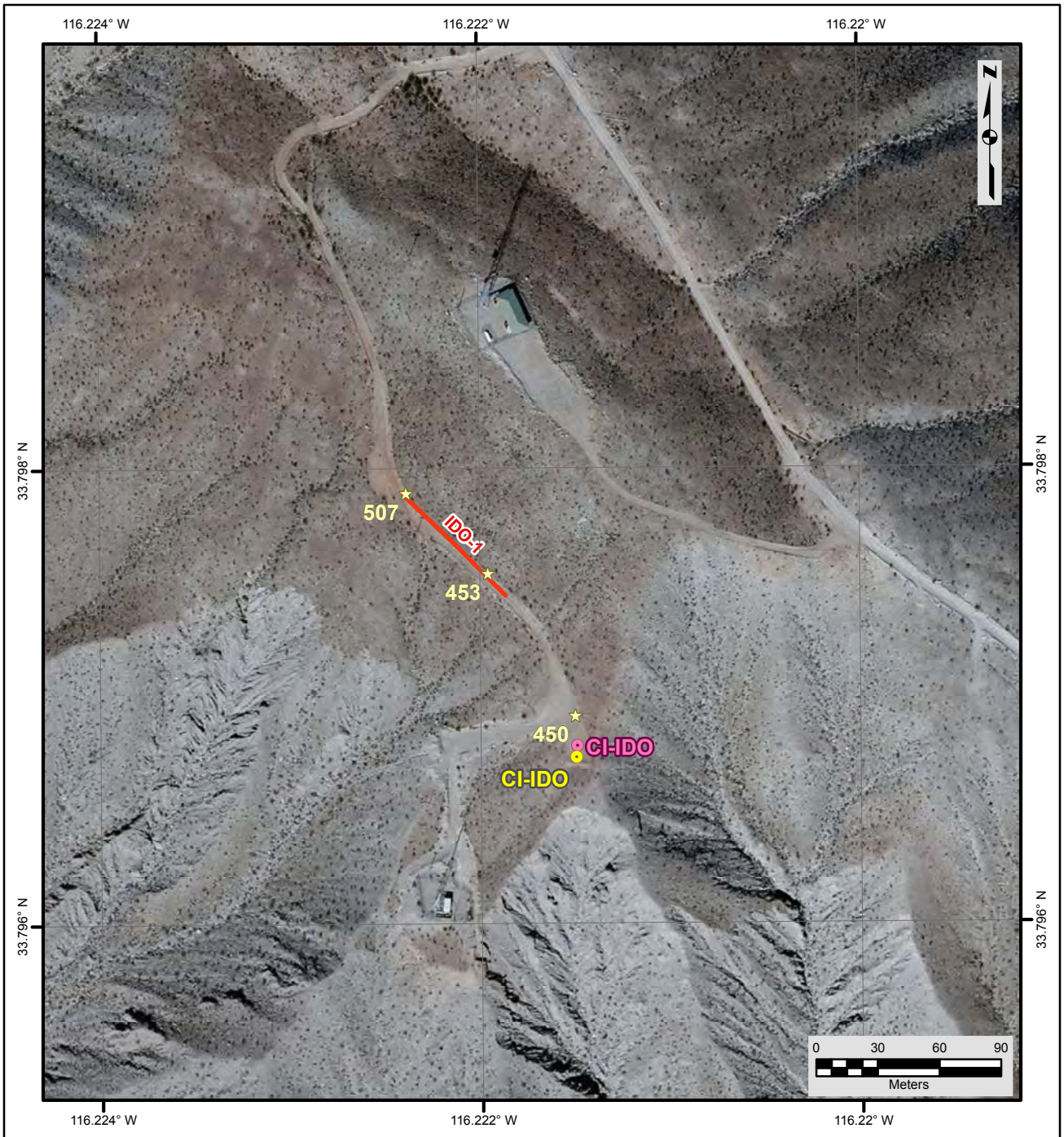

Legend

- Seismic Station - Approximate Surveyed Location
- Seismic Station - Approximate Location of Record
- H/V Spectral Ratio Location
- MASW and Seismic Refraction Array

NOTES:
1. WGS 1984 COORDINATE SYSTEM
2. Image Source: ESRI, i-cubed, USDA FSA, USGS, AEX, GeoEye, Getmapping, Aerogrid, IGP

File Name: CI-IDO-I

Date: 9/16/2011

USGS science for a changing world

GEOVision geophysical services

RECOVERY.GOV

SITE MAP
CI•IDO

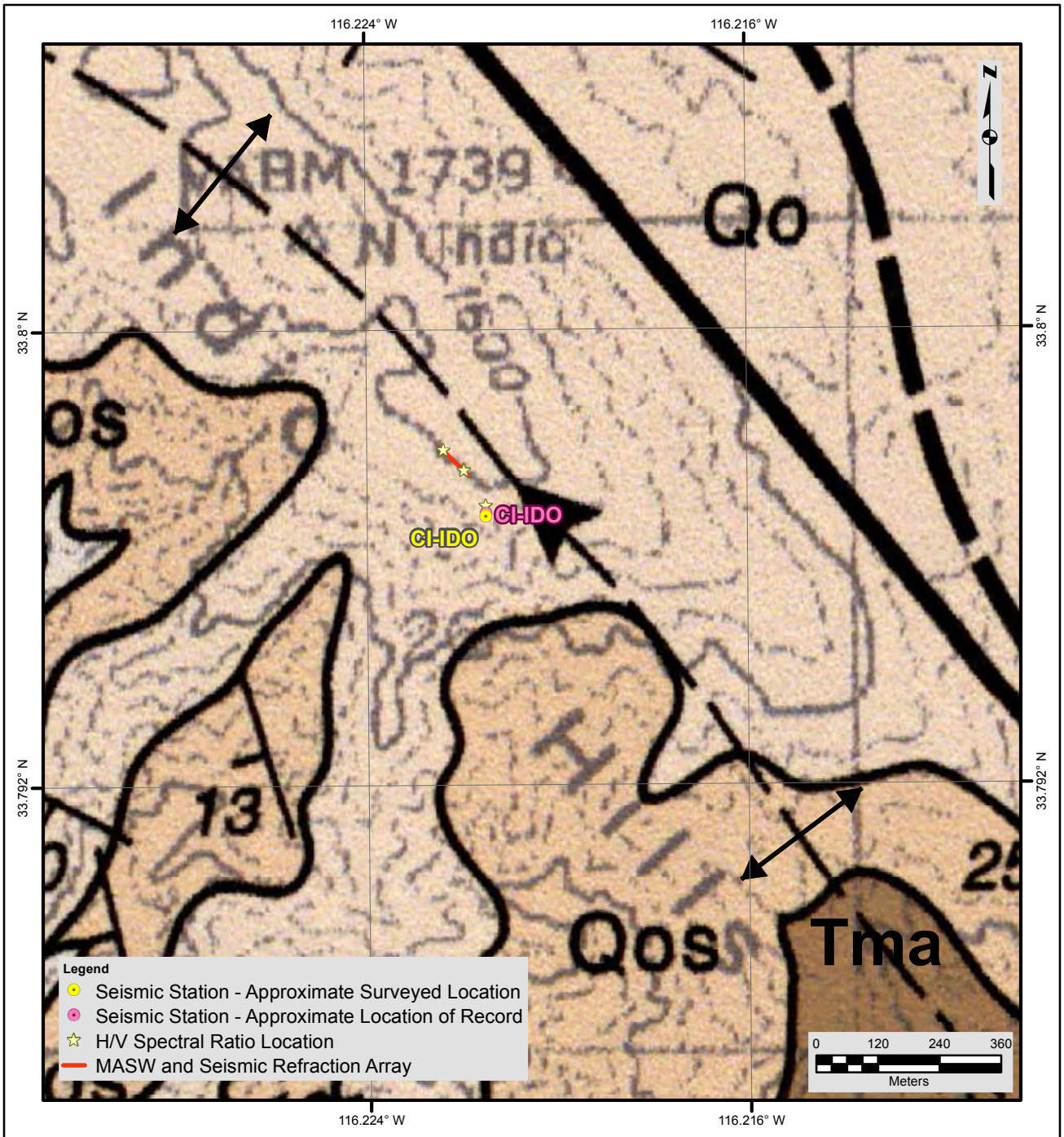

Description of Geologic Map Units

Qos = Quaternary (Pleistocene) older sand deposits, weakly indurated, dissected
Qo = Quaternary (Pleistocene) Ocotillo Formation; fanglomerate of sandstone, silts and tuff, some vertebrate fossil fragments
Tma = Tertiary (Miocene) Mecca Formation; clay, sandstone and conglomerate containing coarse angular to sub-rounded clasts of granitic and metamorphic debris, weakly to moderately lithified.

NOTES:
1. WGS 1984 COORDINATE SYSTEM
2. Geologic Map of the Thousand Palms & Lost Horse Mountains 15 Minute Quadrangles, Riverside County, California by Thomas W. Dibblee, Jr., 2008
3. See site map for details of geophysical survey

USGS science for a changing world

GEOVision geophysical services

RECOVERY.GOV

GEOLOGIC MAP
CI•IDO

File Name: CI-IDO

Date: 9/16/2011

Looking southeast towards seismic station and HVSR sensor 450 (Nanometrics Trillium)

HVSR sensor 507 placed in shallow hole

Looking southeast along MASW array IDO-1

Looking northwest along MASW array IDO-1 from HVSR sensor 453

MASW and seismic refraction data acquisition

Location of Geophysical Testing Arrays:

Location	Latitude	Longitude
IDO-1, Northwest End of Array	33.79789	-116.22243
IDO-1, Center of Array	33.79767	-116.22216
IDO-1, Southeast End of Array	33.79744	-116.22189
HVSR Sensor 450	33.79691	-116.22153
HVSR Sensor 453	33.79754	-116.22199
HVSR Sensor 507	33.79789	-116.22241
CI.IDO Seismic Station	33.79673	-116.22153

Notes: 1) WGS84 Coordinate System (decimal degrees)
2) Survey accuracy is estimated at 1 to 2 m

Results:

V_S Model

Depth to Top of Layer (m)	Layer Thickness (m)	S-Wave Velocity (m/s)	Inferred P-Wave Velocity (m/s)	Assumed Poisson's Ratio	Assumed Density (g/cm^3)
0	2	305	635	0.35	1.9
2	3	415	863	0.35	1.9
5	4	509	1059	0.35	2.0
9	7	618	1286	0.35	2.0
16	10	667	1388	0.35	2.0
26	>4	680	1416	0.35	2.0

Notes: 1) Depth of investigation is about 30 m.
2) Bottom layer is a half space.

Observations/Discussion:

- There are no clear peaks in the HVSR data.
- The seismic refraction model indicates that P-wave velocity increases with depth from 600 to 800 m/s near the surface to over 1,000 m/s at a depth of 1 to 2 m, over 1,300 m/s at a depth of 4 to 9 m and over 1,400 m/s at a depth of 6 to 11 m. With the exception of the southwest end of the line, the 1,300 and 1,400 m/s P-wave velocity contours are typically at depths of 7 to 9 and 8 to 11 m, respectively.
- The seismic refraction model indicates that there is some, but not significant, lateral velocity variation beneath the array.
- Noise conditions at the site were not sufficient for application of passive surface wave techniques.
- There is some scatter in MASW dispersion data, particularly at long wavelengths, likely due to lateral velocity variation associated with shallow dipping geologic layers. The placement of the MASW array on a road cut into a gentle slope and minor topographic variation along the array may also play a role in the scatter of the dispersion data.
- A representative dispersion curve was generated for the MASW data set using a moving average, polynomial curve fitting routine and used for modeling.
- An assumed Poisson's ratio of 0.35 was used for surface wave modeling as resulting P-wave velocities were in better agreement with the seismic refraction model.
- Inferred P-wave velocities in the surface wave model are slightly low (5 to 10%) relative to the P-wave refraction model, which is acceptable considering unknown Poisson's ratio.
- Surface wave depth of investigation is about 30 m based on half of maximum wavelength criteria.
- V_{S30} is 557 m/s (Site Class C).
- Average S-wave velocity between 2 m (nominal sensor depth) and 32 m is 597 m/s.

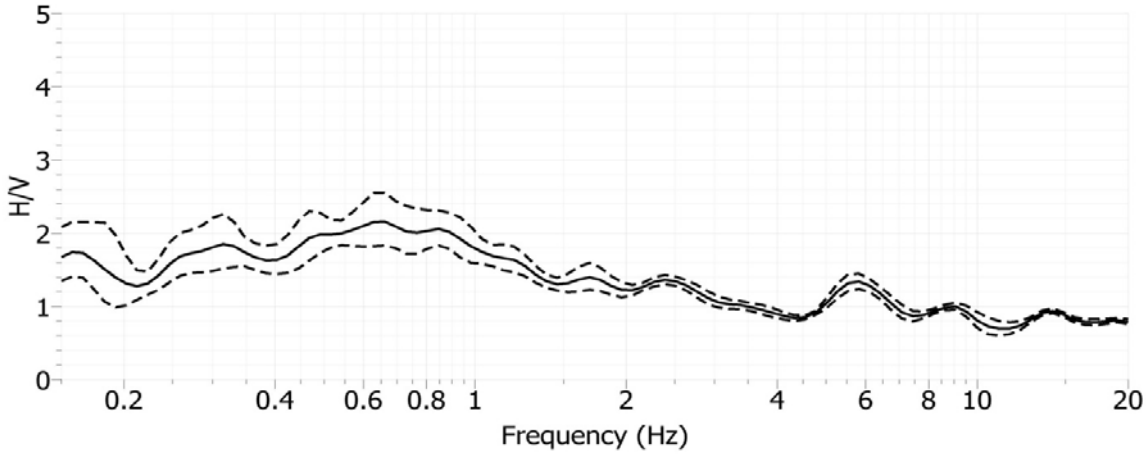

Site CI.IDO, H/V Spectral Ratio, Array IDO-1, Sensor 507

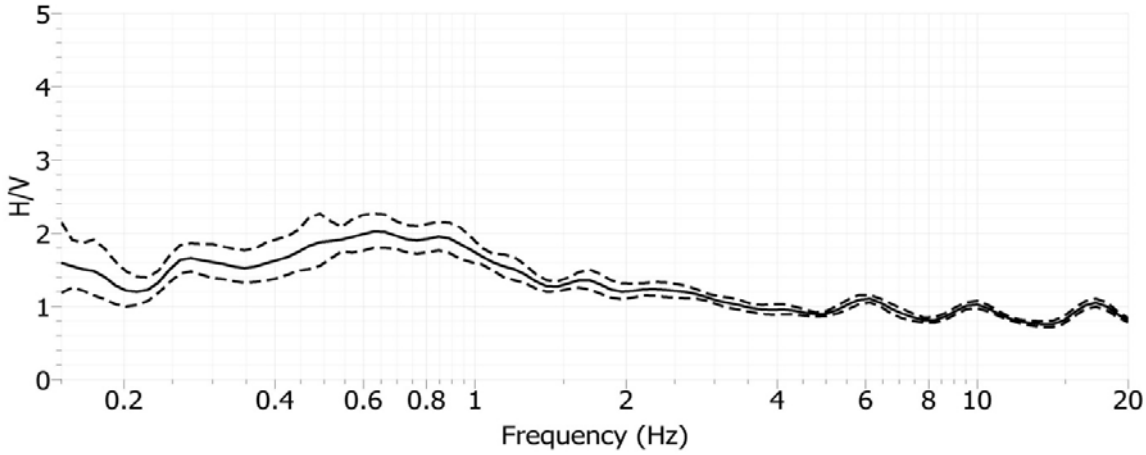

Site CI.IDO, H/V Spectral Ratio, Array IDO-1, Sensor 453

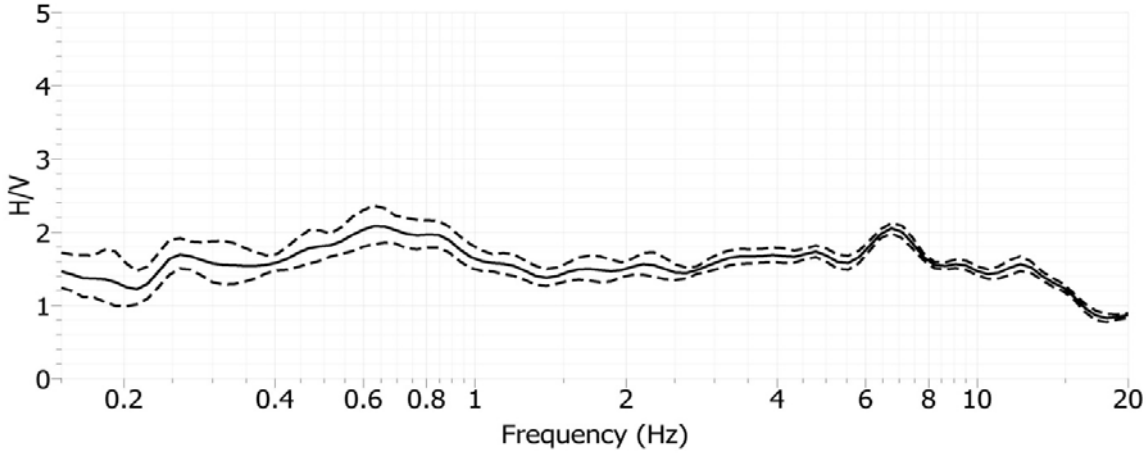

Site CI.IDO, H/V Spectral Ratio, Near Seismic Station, Sensor 450

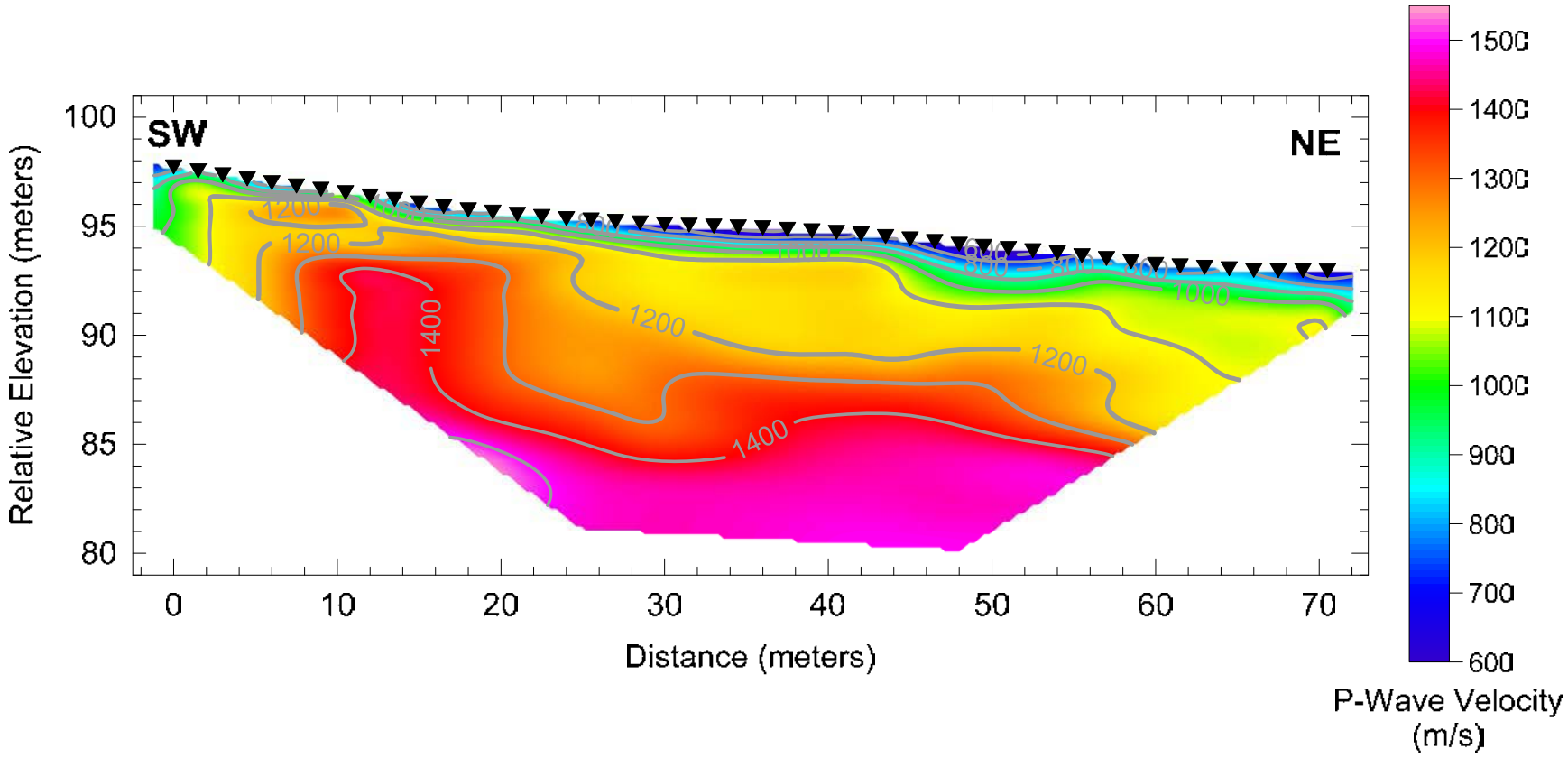

Array IDO-1 – Tomographic seismic refraction model utilizing smooth velocity gradient starting model

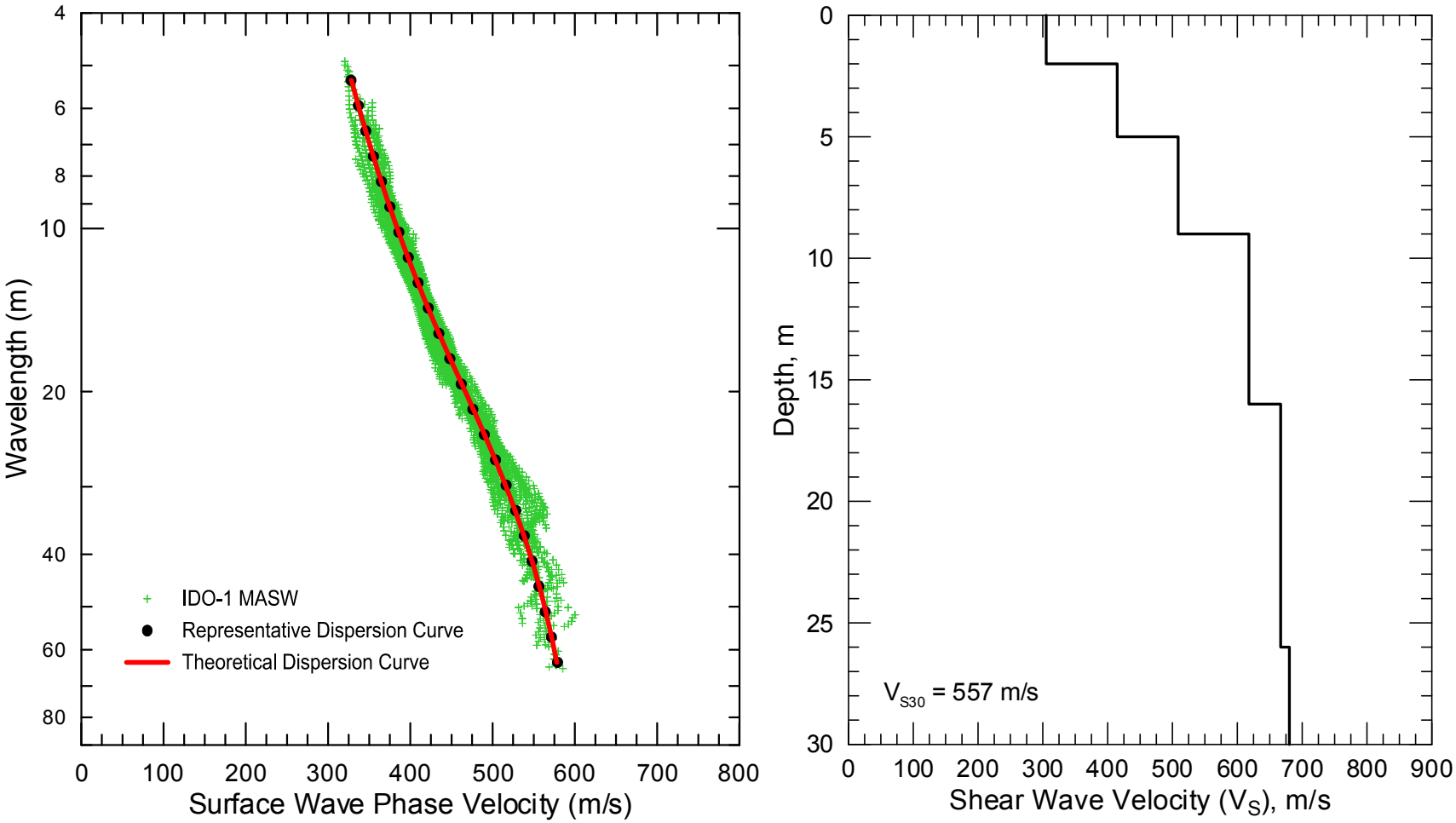

CI.IDO - Field, representative and inverted theoretical surface wave dispersion data (left) and associated V_S model (right)

Site CI.IKP

Location: In-Ko-Pah, San Diego County, California

Latitude: 32.65012 **Longitude:** -116.10948
(Station coordinates provided by USGS, WGS84 coordinate system)

V_{S30} (measured): 1,058 m/s

V_{S30} (adjusted to more accurately reflect seismic station conditions): 1,295 m/s (average S-wave velocity between 1.15 and 31.15 m adjusting for seismic sensor being placed on rock).

NEHRP Site Class: B

Geomatrix Code: IGA

Geologic Conditions/Observations: Seismic station located on Mesozoic granitic rocks (quartz diorite and granodiorite) of the Peninsular Ranges.

Site Conditions: Rural site. Seismic station located at the base of an outcrop of weathered granitic rocks. Rolling topography in site vicinity. Ground surface elevation decreases about 5 m to southeast along the 70.5 m seismic line.

Geophysical Methods Utilized: HVSR, Seismic Refraction, MASW

Geophysical Testing Arrays:

1. Array IKP-1 (48 channel MASW and P-wave seismic refraction array utilizing 4.5 Hz vertical geophones spaced 1.5 m apart for a length of 70.5 m, forward and reverse shot locations with multiple source offsets and source types (hammers only) and multiple interior shot locations).
2. Three HVSR measurement locations: one at each end of array IKP-1 and the other near the seismic station. HVSR measurements near the seismic station made with both a Nanometrics Trillium Compact and Tromino ENGY.

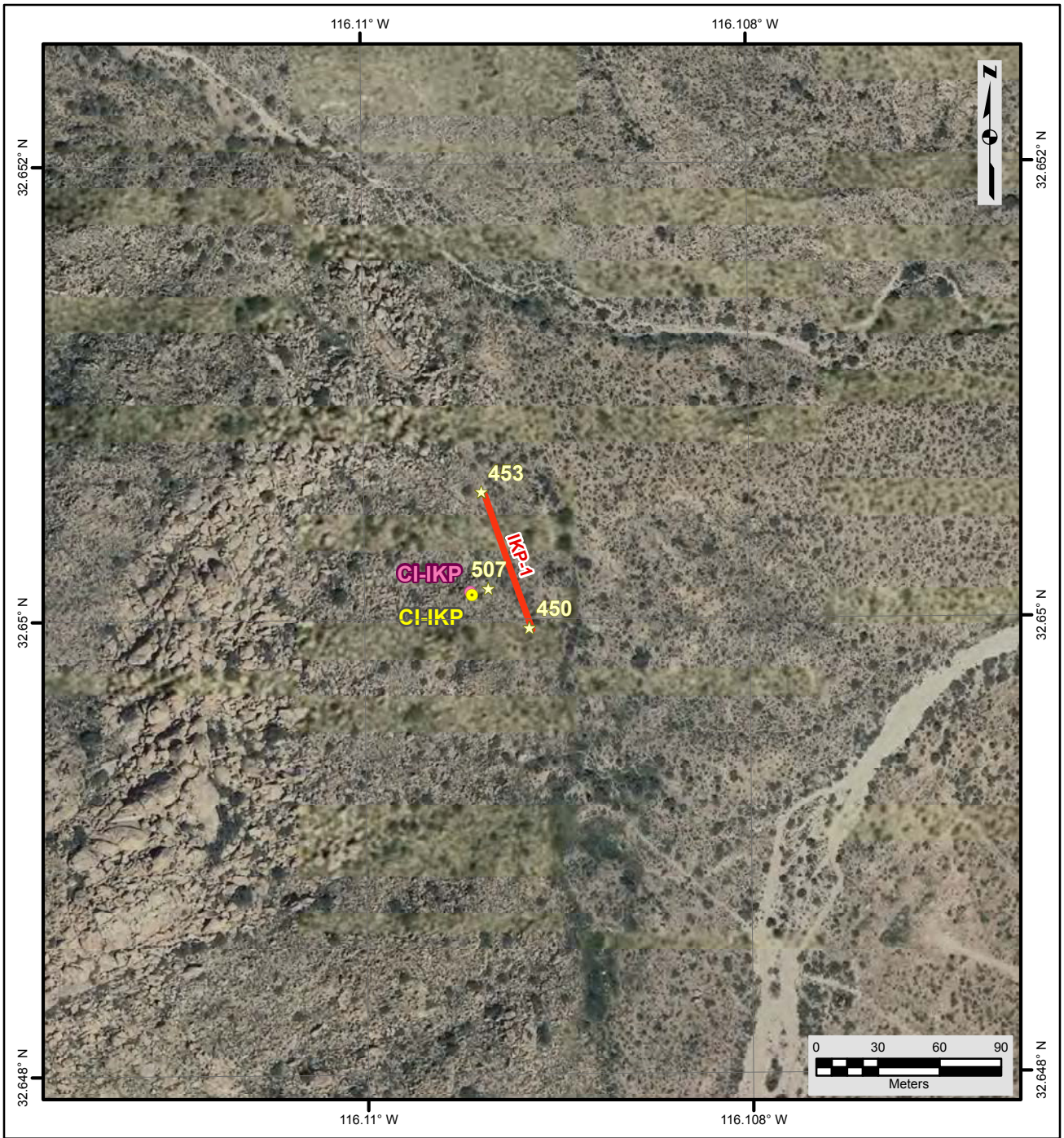

Legend

- Seismic Station - Approximate Surveyed Location
- Seismic Station - Approximate Location of Record
- H/V Spectral Ratio Location
- MASW and Seismic Refraction Array

NOTES:
1. WGS 1984 COORDINATE SYSTEM
2. Image Source: ESRI, i-cubed, USDA FSA, USGS, AEX, GeoEye, Getmapping, Aerogrid, IGP

File Name: CI-IKP-I

Date: 10/27/2011

USGS science for a changing world

GEOVision geophysical services

RECOVERY.GOV

SITE MAP
CI•IKP

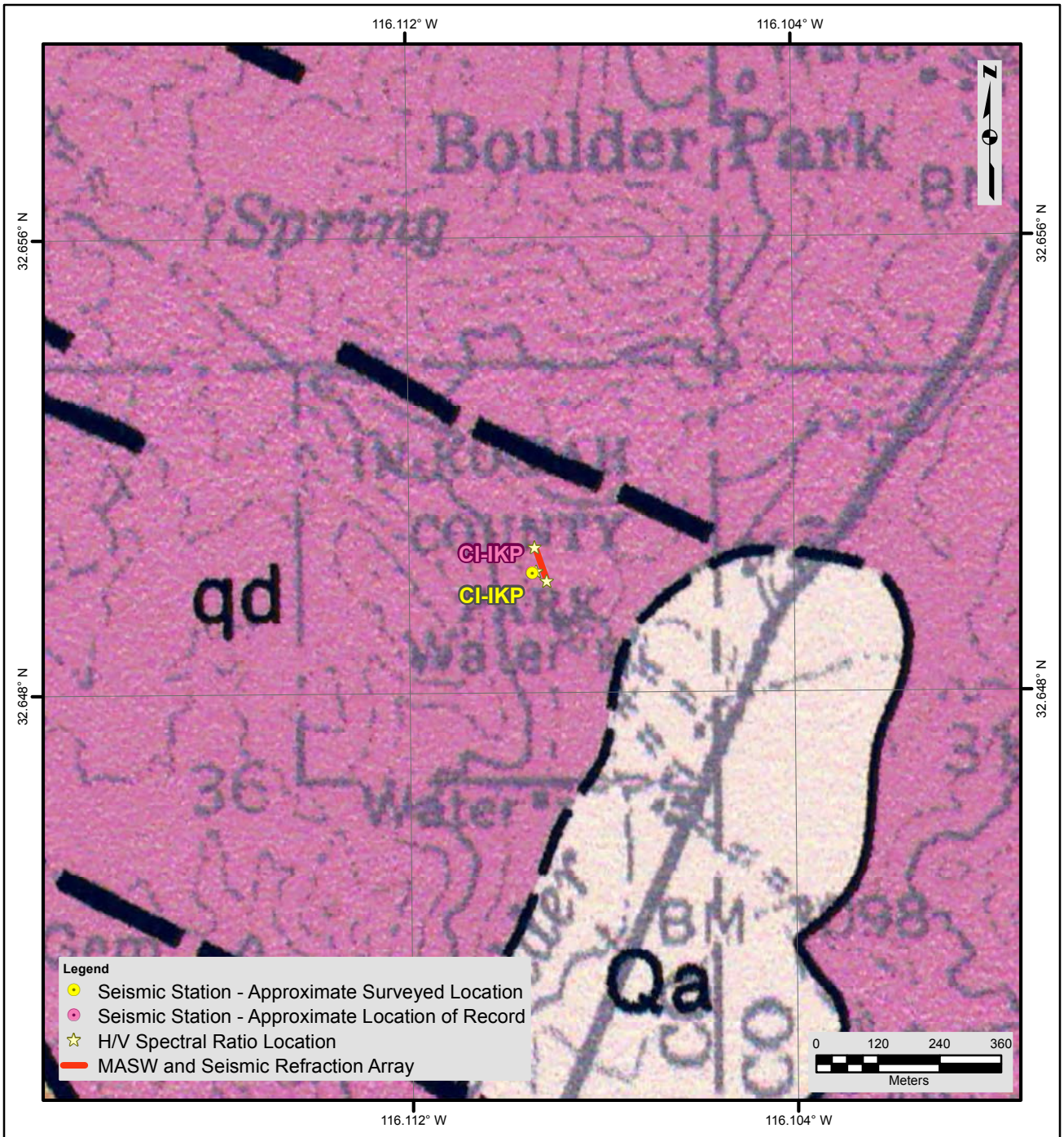

Description of Geologic Map Units

Qa = Quaternary (Holocene) alluvial clay and silt,
grading to sandy gravel near mountains
qd = Mesozoic or older (probably Cretaceous) quartz diorite and granodiorite

NOTES:
1. WGS 1984 COORDINATE SYSTEM
2. Geologic Map of the Jacumba 15 Minute Quadrangle, San Diego and Imperial Counties, California
By Thomas W. Dibblee, Jr., 2008
3. See site map for details of geophysical survey

File Name: CI-IKP

Date: 10/27/2011

USGS science for a changing world

GEOVision geophysical services

RECOVERY.GOV

GEOLOGIC MAP
CI•IKP

Looking east towards seismic station CI.IKP and array IKP-1

Seismic station CI.IKP

Looking west at HVSR sensor 507, Tromino ENGR and seismic station

Looking northwest along array IKP-1

Looking south towards center of array IKP-1 and seismic station

Location of Geophysical Testing Arrays:

Location	Latitude	Longitude
IKP-1, Southeast End of MASW/Refraction Array	32.64995	-116.10916
IKP-1, Center of MASW/Refraction Array	32.65025	-116.10928
IKP-1, Northwest End of MASW/Refraction Array	32.65055	-116.10940
HVSR Sensor 450	32.64996	-116.10917
HVSR Sensor 507	32.65013	-116.10939
HVSR Sensor 453	32.65056	-116.10942
HVSR Sensor Tromino ENGY	32.65013	-116.10939
CI.IKP Seismic Station	32.65011	-116.10947

Notes: 1) WGS84 Coordinate System (decimal degrees)
2) Survey accuracy is estimated at 1 to 2 m.

Results:

V_S Model

Depth to Top of Layer (m)	Layer Thickness (m)	S-Wave Velocity (m/s)	Inferred P-Wave Velocity (m/s)	Assumed Poisson's Ratio	Assumed Density (g/cm^3)
0	1.15	201	376	0.3	1.90
1.15	4.35	877	1641	0.3	2.15
5.5	6.5	1041	1947	0.3	2.20
12	8	1413	2643	0.3	2.30
20	9	1686	3154	0.3	2.40
29	>6	2246	4202	0.3	2.50

Notes: 1) Depth of investigation is about 35 m.
2) Bottom layer is a half space.

Observations/Discussion:

- Both the seismic station and MASW/seismic refraction array are located on weathered granitic rocks; although there is a thin layer of residual soil beneath portions of the MASW array.
- The HVSR curves are similar, validating the 1-D velocity structure assumption
- There are no significant HVSR peaks as expected for a rock site. There is, however, a very weak, but inconclusive, peak in the 7 to 8 Hz range that could be associated with the weathering profile in bedrock.
- The P-wave refraction data collected along array IKP-1 were modeled using a tomographic inversion routine with a smooth velocity gradient starting model. The seismic refraction model was extended to far offset shot locations to extend depth of investigation.
- The seismic refraction survey design allowed P-wave velocity to be imaged to a maximum depth of about 15 to 20 m. The seismic refraction model shows that P-wave velocity is about 450 to 500 m/s at the surface, increasing to 1,500 m/s at a depth of 1.5 to 4.5 m, 2,000 m/s at a depth of 3.5 to 7.5 m, 3,000 m/s at a nominal depth of 17 to 18 m and greater than 3,500 below a depth on the order of 21 m.
- The seismic refraction model indicates that there is some lateral velocity variation at this site as is typical at rock sites, which often have a variable thickness of residual soil and irregular weathering. The seismic model indicates that there is a slightly thicker sequence of residual soil and intensely weathered rock beneath the southern half of the line.
- Noise conditions at the site were not sufficient for application of passive surface wave techniques.
- MASW data modeling was conducted using only shot locations at the southeastern end of the line, which yielded the best quality surface wave dispersion due to the nature of the weathering profile in this portion of the line. Surface wave dispersion data from shot locations at the northwestern end of the line were in reasonable agreement between wavelengths of about 10 and 60 m, but had more noise (scatter) and did not yielded phase velocity data at wavelengths less than 10 m. The center shot location yield good quality phase velocity data when analysis was conducted using the southern 24 geophones with phase velocities slightly lower than those from the southern end shot at wavelengths below 10 m. This is consistent with the seismic refraction model, which shows a slightly thicker residual soil layer near the middle of the array. The center shot location did not yield usable phase velocity data at wavelengths below about 10 m when analysis was conducted using the northern 24 geophones.
- The high variability of surface wave phase velocity data at wavelengths below 10 m is a function of lateral velocity variation in the upper several meters, primarily caused by variable thickness of a thin residual soil layer and differential weathering of shallow rock. Normally in these conditions, a large ensemble of phase velocity data from multiple shot locations and selected receiver groups is compiled to generate an average, representative dispersion curve for modeling. At this site, the data quality from the southern shot locations was significantly better and, therefore, analysis limited to these data as discussed above.

- The minimum wavelength surface wave phase velocity data extracted from the 48-channel MASW array was about 16 m. Data reduction using seismic records from smaller hammer sources and a limited offset receiver array (i.e. less active geophones) allowed extraction of surface wave dispersion data to a minimum wavelength of about 2 m.
- A representative dispersion curve was generated for the MASW data set using a moving average, polynomial curve fitting routine and used for modeling.
- Surface wave depth of investigation is about 35 m based on half of maximum wavelength criteria.
- The inferred P-wave velocities in the surface wave model, assuming a Poisson's ratio of 0.3, are generally consistent with the average velocity structure in the seismic refraction model in the upper 20 m, the seismic refraction depth of investigation.
- V_{S30} is 1,058 m/s (Site Class B).
- Average S-wave velocity between 1.15 m (assumed sensor depth) and 31.15 m is 1,295 m/s. This compensates for the fact that the seismic sensor is placed on rock, whereas the surface wave model has a thin residual soil layer.

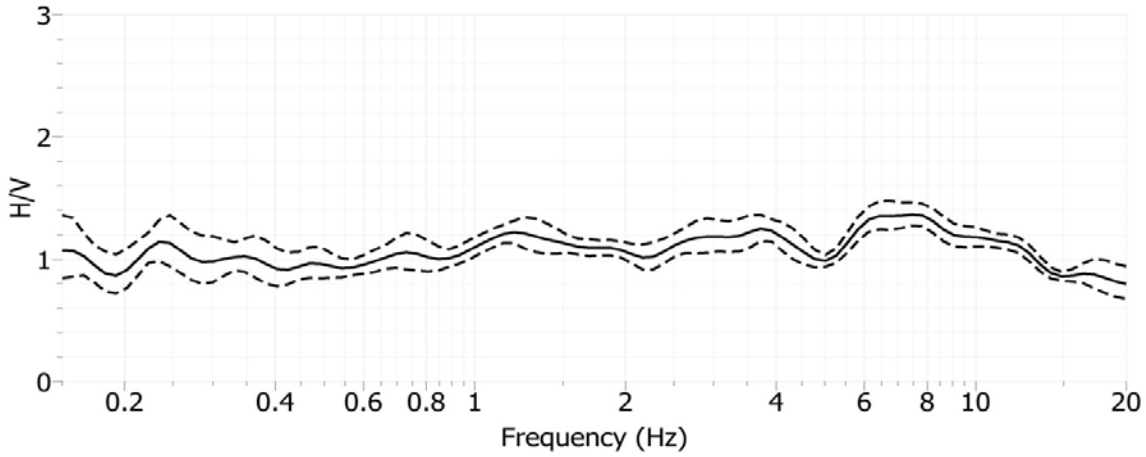

Site CI.IKP, H/V Spectral Ratio, Near Seismic Station, Sensor 453

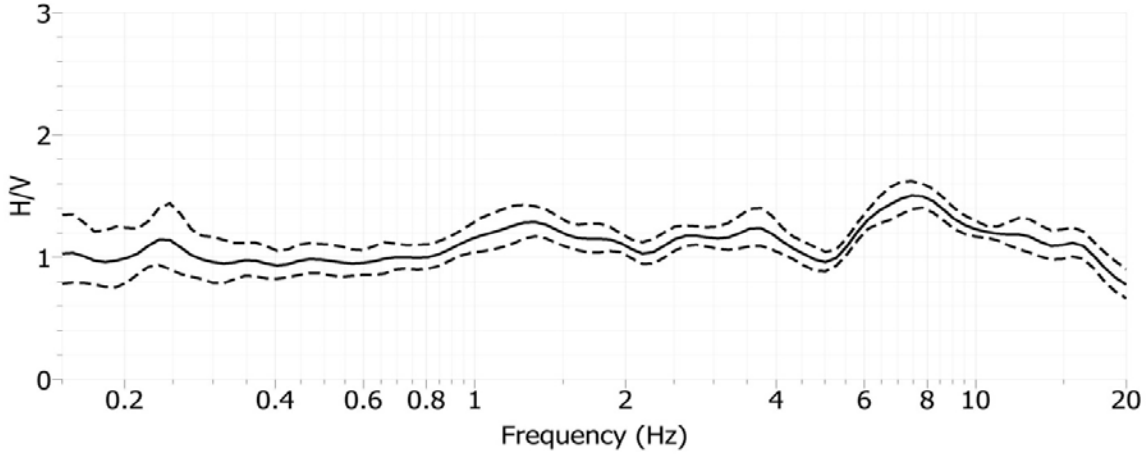

Site CI.IKP, H/V Spectral Ratio, Array IKP -1, Sensor 507

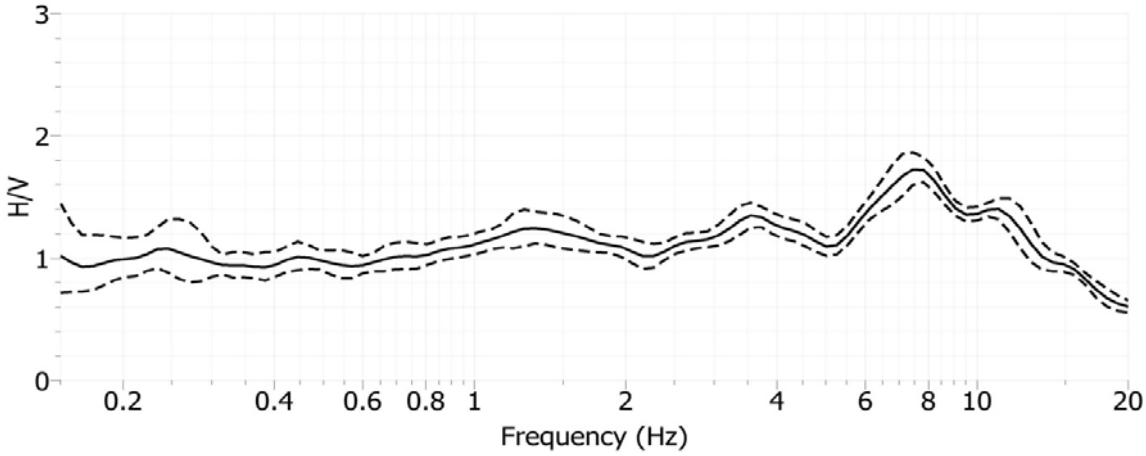

Site CI.IKP, H/V Spectral Ratio, Array IKP -1, Sensor 450

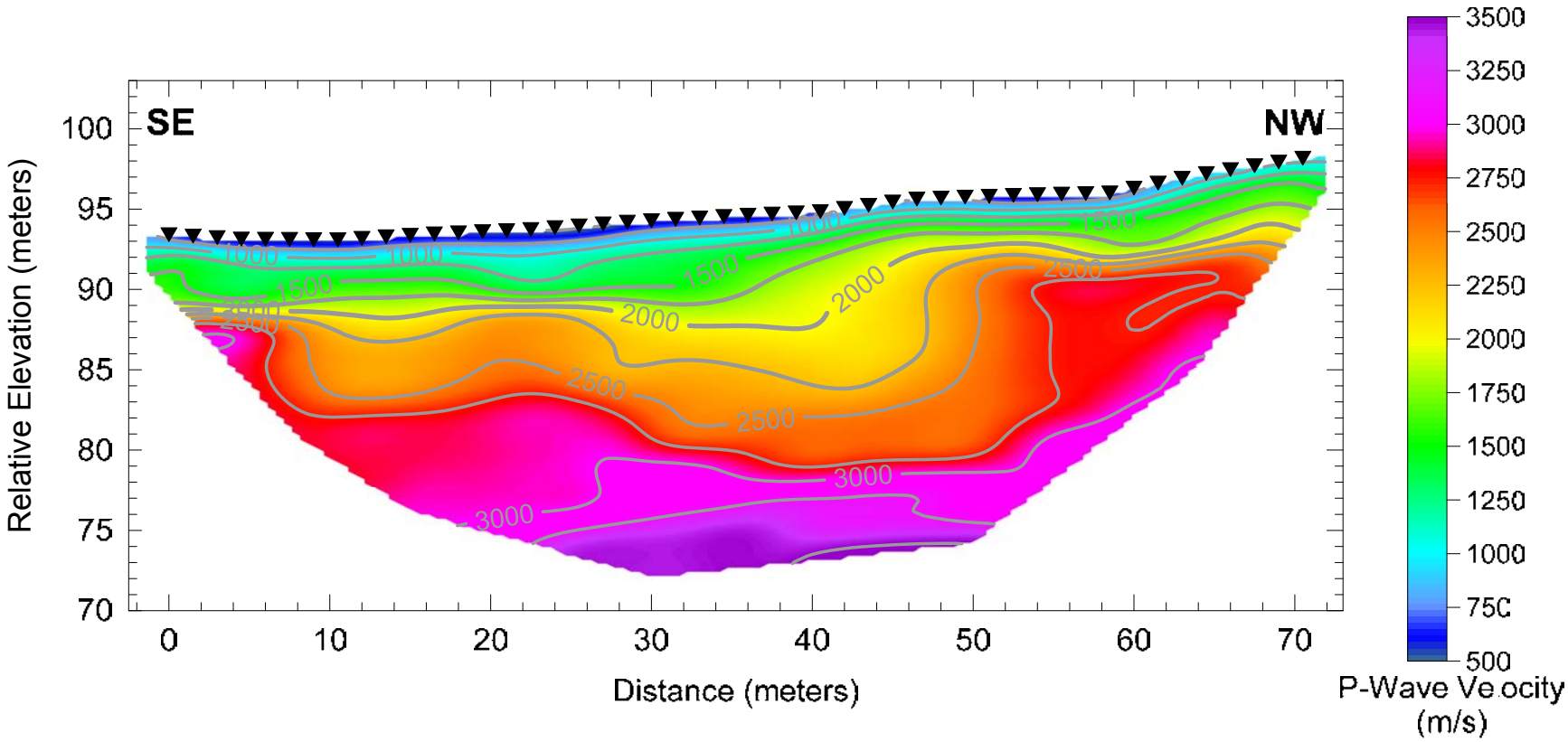

Array IKP-1 – Tomographic Seismic Refraction Model utilizing Smooth Velocity Gradient Starting Model

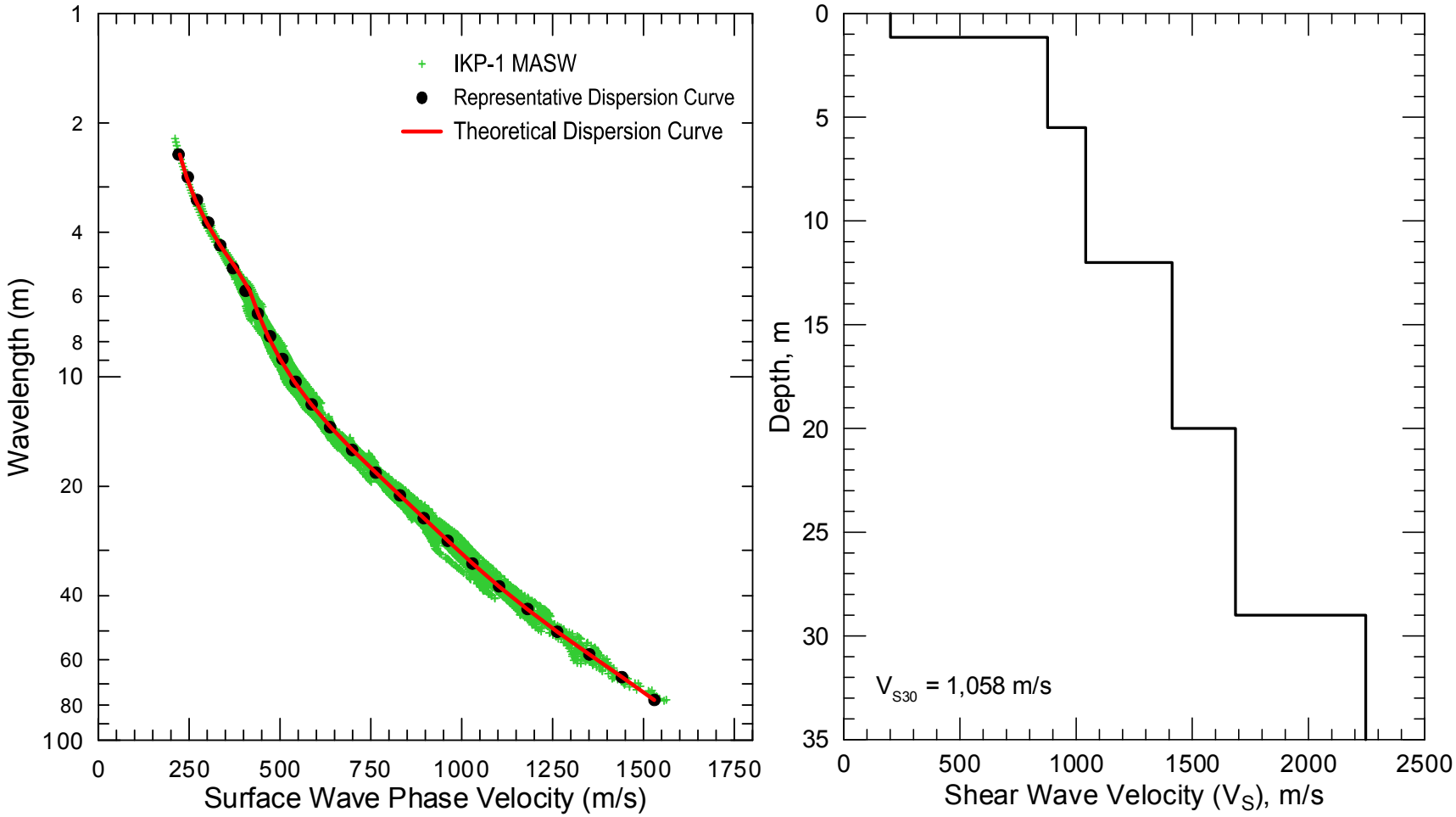

CI.IKP - Field, representative and inverted theoretical surface wave dispersion data (left) and associated V_S model (right)

Site CI.IRM

Location: Iron Mountain Pumping Station, San Bernardino County, California

Latitude: 34.15734 **Longitude:** -115.14513
(Station coordinates modified based on field GPS survey, WGS84 coordinate system)

V_{S30} (measured): 981 m/s

V_{S30} (adjusted to more accurately reflect seismic station conditions): 1,055 m/s (average S-wave velocity between 1 and 31 m adjusting for 1 m estimated sensor depth.)

NEHRP Site Class: B

Geomatrix Code: IGA

Geologic Conditions/Observations: Seismic station located on geologic unit mapped as Iron Granodiorite Gneiss. Field observations indicate that a thin layer of gravelly fill overlies weathered rock.

Site Conditions: Remote site located on mountain top graded flat to support communication site infrastructure. Steep topography in site vicinity.

Geophysical Methods Utilized: HVSR, Seismic Refraction, MASW

Geophysical Testing Arrays:

1. Array IRM-1 (48 channel MASW and P-wave seismic refraction array utilizing 4.5 Hz vertical geophones spaced 1.5 m apart for a length of 70.5 m, forward and reverse shot locations with multiple source offsets and source types and multiple interior shot locations).
2. Three HVSR measurement locations distributed along array IRM-1.

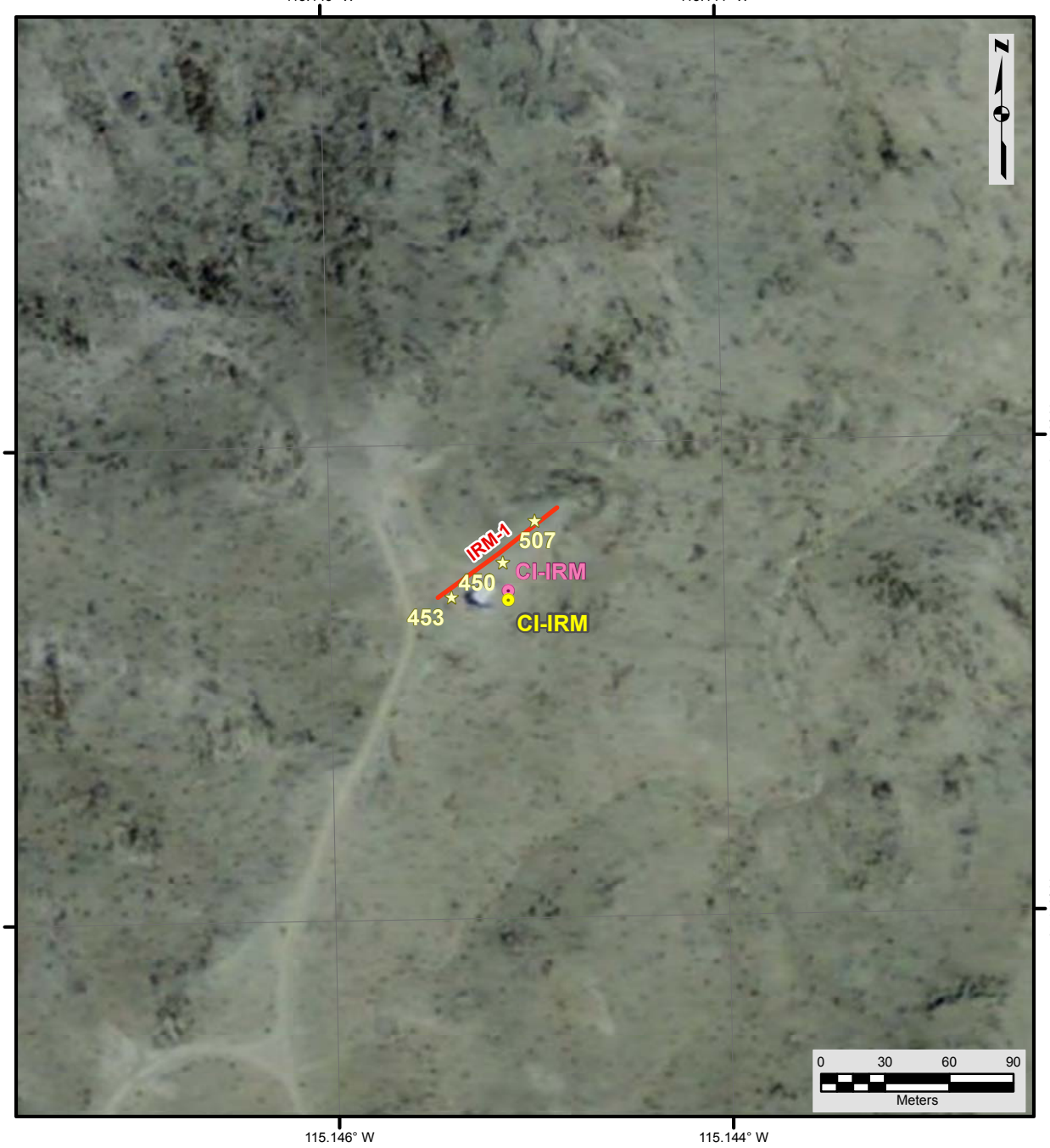

Legend

- Seismic Station - Approximate Surveyed Location
- Seismic Station - Approximate Location of Record
- H/V Spectral Ratio Location
- MASW and Seismic Refraction Array

NOTES:
1. WGS 1984 COORDINATE SYSTEM
2. Image Source: ESRI, i-cubed, USDA FSA, USGS, AEX, GeoEye, Getmapping, Aerogrid, IGP

File Name: CI-IRM-I

Date: 9/16/2011

USGS science for a changing world

GEOVision geophysical services

RECOVERY.GOV

SITE MAP
CI•IRM

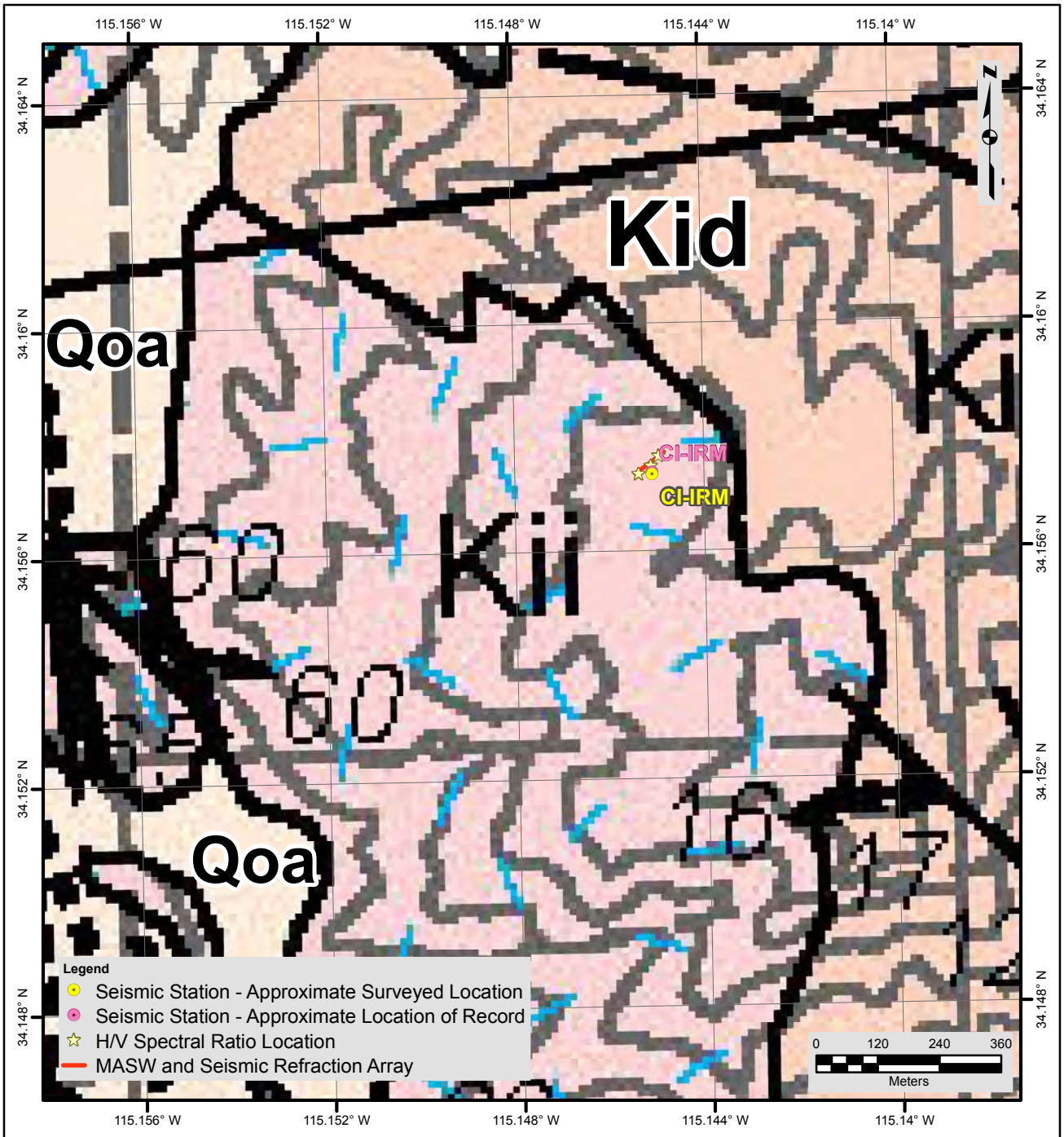

Description of Geologic Map Units

Qoa = Quaternary (Pleistocene) older alluvial angular sandy gravel
Kid = Mesozoic (Late Cretaceous) Danby Lake Granite Gneiss; medium-grained, leucocratic muscovite-biotite monzogranite gneiss
Kii = Mesozoic (Late Cretaceous) Iron Granodiorite Gneiss; Porphyritic, medium-grained biotite granodiorite gneiss

NOTES:
1. WGS 1984 COORDINATE SYSTEM
2. Geologic Map of the Sheep Hole Mountains 30' x 60' Quadrangle, San Bernardino and Riverside Counties, California by Keith A. Howard, 2002
3. See site map for details of geophysical survey

File Name: CI-IRM

Date: 9/16/2011

USGS science for a changing world

GEOVision geophysical services

RECOVERY.GOV

GEOLOGIC MAP
CI•IRM

CI.IRM seismic station

MASW/seismic refraction array IRM-1

Looking southwest along MASW array IRM-1, towards CI.IRM seismic station

Looking northeast along array IRM-1, towards HVSR sensor 450

Nanometrics Trillium Compact seismic sensor used for HVSR measurements

Location of Geophysical Testing Arrays:

Location	Latitude	Longitude
IRM-1, Southwest End of MASW/Refraction Array	34.15736	-115.14549
IRM-1, Center of MASW/Refraction Array	34.15754	-115.14518
IRM-1, Northeast End of MASW/Refraction Array	34.15773	-115.14488
HVSR Sensor 450	34.15750	-115.14516
HVSR Sensor 453	34.15736	-115.14542
HVSR Sensor 507	34.15767	-115.14499
CI.IRM Seismic Station	34.15734	-115.14513

Notes: 1) WGS84 Coordinate System (decimal degrees)
2) Survey accuracy is estimated at 1 to 2 m

Results:

V_S Model

Depth to Top of Layer (m)	Layer Thickness (m)	S-Wave Velocity (m/s)	Inferred P-Wave Velocity (m/s)	Assumed Poisson's Ratio	Assumed Density (g/cm^3)
0	1.5	350	655	0.3	2.0
1.5	2.5	697	1304	0.3	2.1
4	3	884	1654	0.3	2.2
7	4	1085	2030	0.3	2.3
11	6	1133	2119	0.3	2.4
17	8	1197	2239	0.3	2.4
25	>5	1373	2568	0.3	2.4

Observations/Discussion:

- The HVSR data quality is not very good due to difficultly coupling the sensors to the gravelly fill soils and heavy winds at time of survey. HVSR sensor 453 has the best quality data and, therefore, best represents site conditions.
- There is no clear HVSR peak at this site, as expected for a rock site.
- Based on tomographic analysis of seismic refraction first arrival data, P-wave velocity in the upper 15 m ranges from about 600 m/s near the surface to greater than 2,000 m/s at depths below 10 m.
- The seismic refraction model indicates that there is a thin layer of low velocity soil or fill overlying decomposed rock at this site. The sediment or fill thickness overlying rock

varies from about 0 to 2 m beneath the MASW and seismic refraction array. Depth of investigation of the P-wave seismic refraction survey is estimated at 10 to 15 m.

- Noise conditions at the site were not sufficient for application of passive surface wave techniques.
- There is significant scatter in the MASW dispersion data, about 5% of velocity, which is likely due to lateral velocity variation associated with differential weathering of near surface rock.
- A representative dispersion curve was generated for the MASW data set using a moving average, polynomial curve fitting routine and used for modeling.
- The surface wave model is generally consistent with the P-wave refraction model, especially considering unknown Poisson's ratio.
- Surface wave depth of investigation is about 30 m based on half of maximum wavelength criteria. Modeling of the upper and lower envelopes of the MASW dispersion data was not conducted but would result in about a 5% variation of V_{S30}.
- V_{S30} is 981 m/s (Site Class B).
- Average S-wave velocity between 1 m (nominal sensor depth) and 31 m is 1,055 m/s (Site Class B).

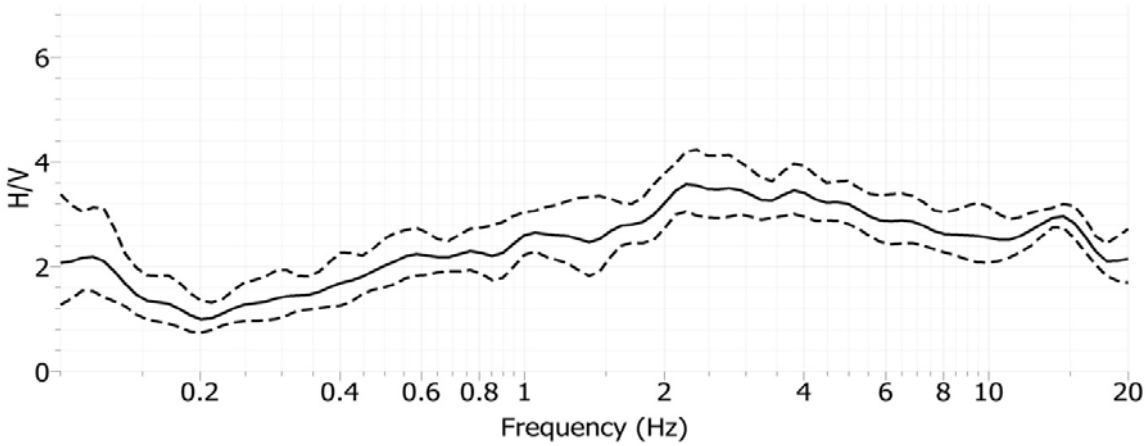

Site CI.IRM, H/V Spectral Ratio, Array IRM -1, Sensor 507

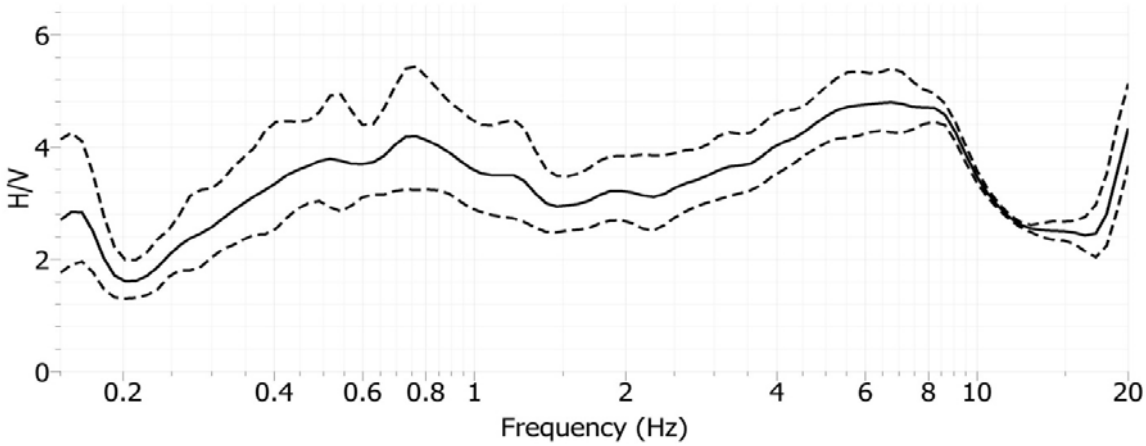

Site CI.IRM, H/V Spectral Ratio, Array IRM -1, Sensor 450

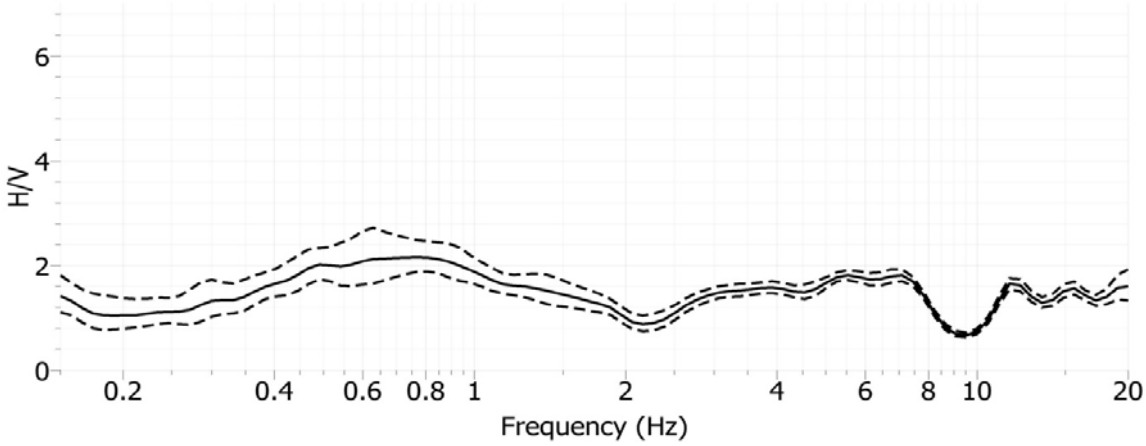

Site CI.IRM, H/V Spectral Ratio, Array IRM -1, Sensor 453

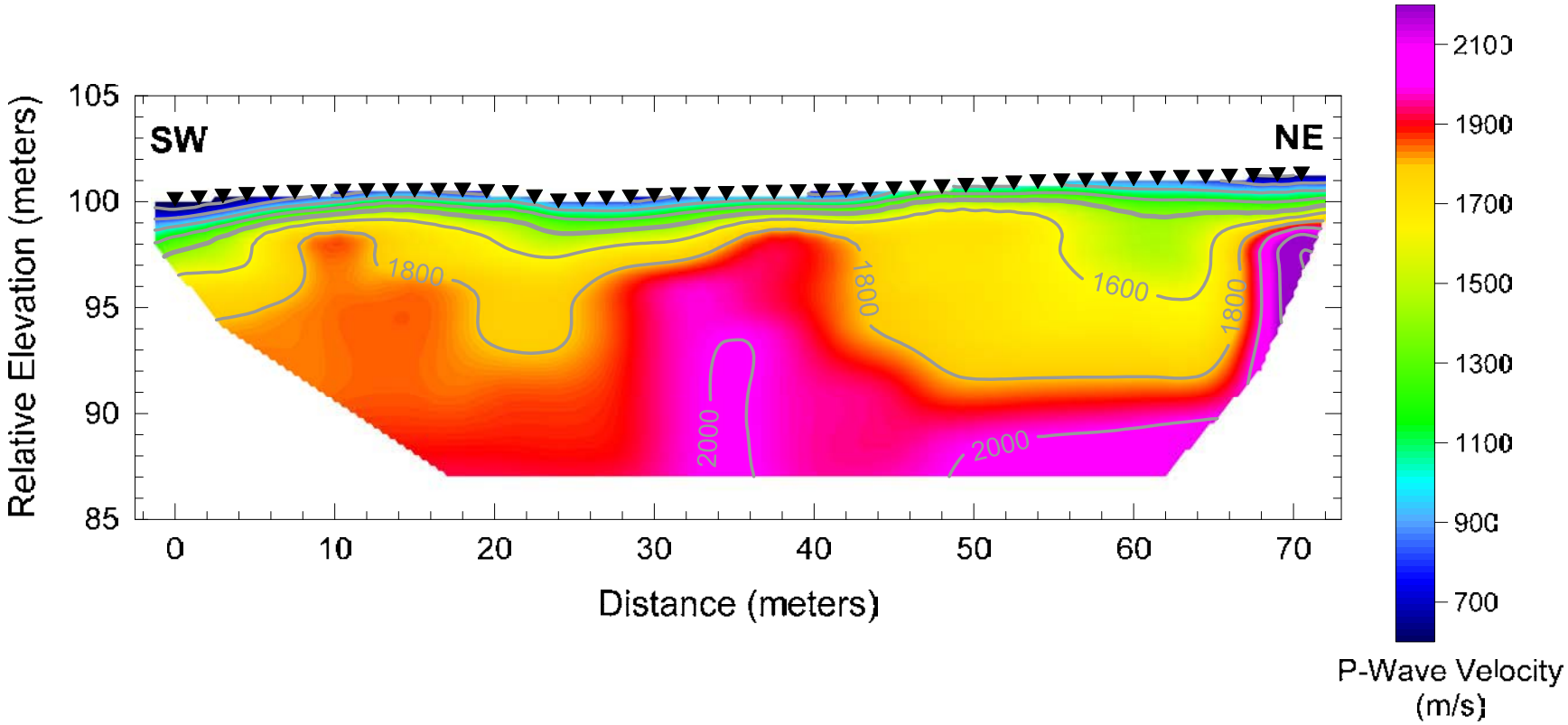

Array IRM-1 – Tomographic seismic refraction model utilizing smooth velocity gradient starting model

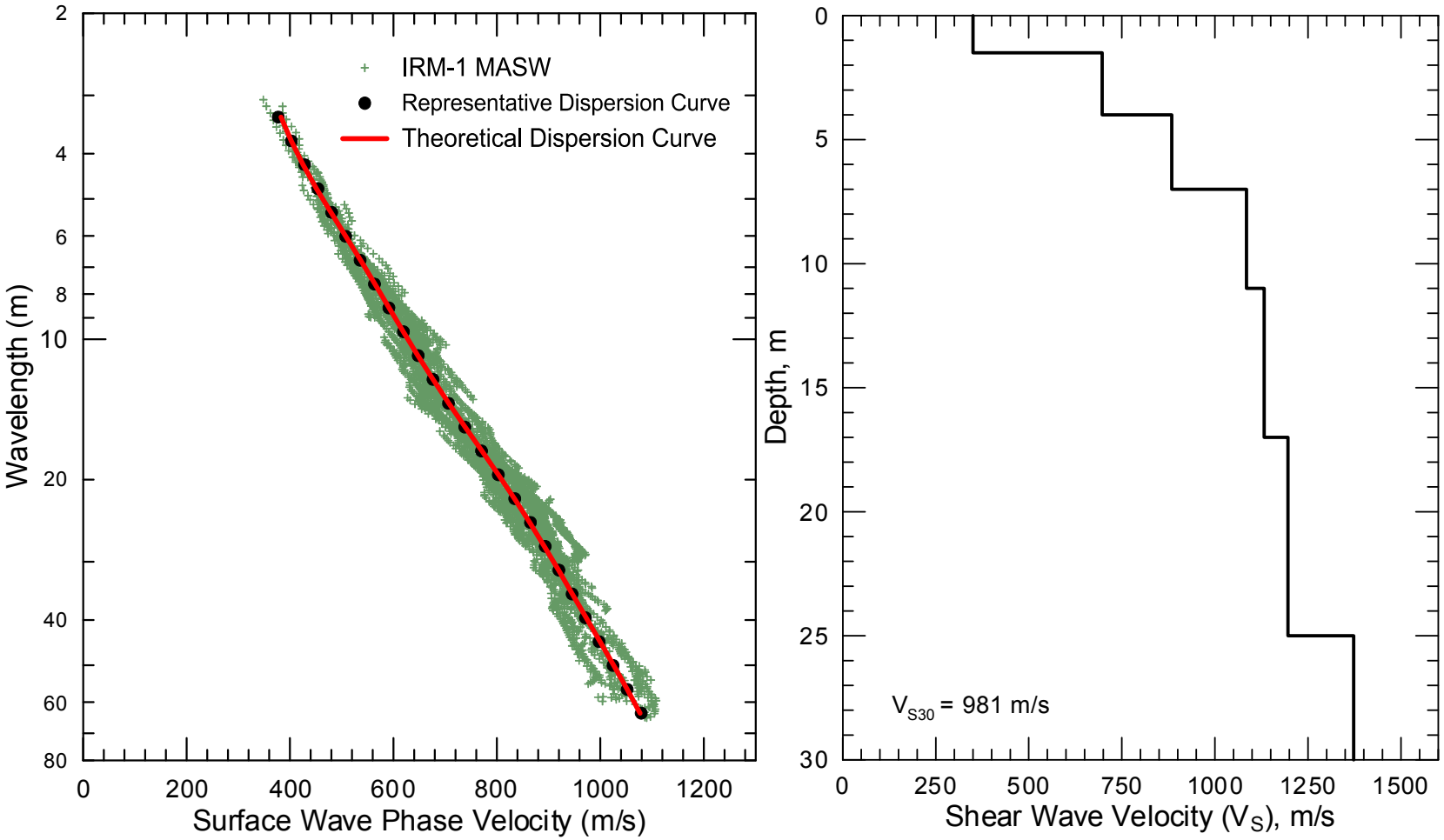

CI.IRM - Field, representative and inverted theoretical surface wave dispersion data (left) and associated V_S model (right)

Site CI.ISA

Location: Isabella, Lake Isabella, Kern County, California

Latitude: 35.66278 **Longitude:** -118.47403
(Station coordinates provided by USGS, WGS84 coordinate system)

V_{S30} (measured): 644 m/s

V_{S30} (adjusted to more accurately reflect seismic station conditions): 765/881 m/s (The seismic station is located about 28 m inside a tunnel with at least 10 m of overlying weathered rock. V_{S30} is 765 m/s assuming that the upper 4 m has V_S equal to that of the underlying layer and 881 m/s assuming that the average V_S between 5 and 35 m is representative of the seismic station).

NEHRP Site Class: C (based on V_{S30}), B/C (based on adjusted V_{S30})

Geomatrix Code: FGA

Geologic Conditions/Observations: Seismic station located on Cretaceous weathered granodiorite.

Site Conditions: Rural site. Seismic station located about 28.5 m from the entrance to a tunnel with 10 to 15 m of overlying weathered rock. Field inspection revealed that rock inside the tunnel is intensely weathered. Relatively steep topography in site vicinity. Test area located on relatively flat area cut into the side of a hill with a gradual topographic decline to the northeast.

Geophysical Methods Utilized: HVSR, Seismic Refraction, MASW

Geophysical Testing Arrays:

1. Array ISA-1 (48 channel MASW and P-wave seismic refraction array utilizing 4.5 Hz vertical geophones spaced 1.5 m apart for a length of 70.5 m, forward and reverse shot locations with multiple source offsets and source types and multiple interior shot locations).
2. Three HVSR measurement locations distributed along array ISA-1.

Legend

- Seismic Station - Approximate Location of Record
- H/V Spectral Ratio Location
- MASW and Seismic Refraction Array

NOTES:
1. WGS 1984 COORDINATE SYSTEM
2. Image Source: ESRI, i-cubed, USDA FSA, USGS, AEX, GeoEye, Getmapping, Aerogrid, IGP

File Name: CI-ISA-I

Date: 10/13/2011

USGS science for a changing world

GEOVision geophysical services

RECOVERY.GOV

SITE MAP
CI•ISA

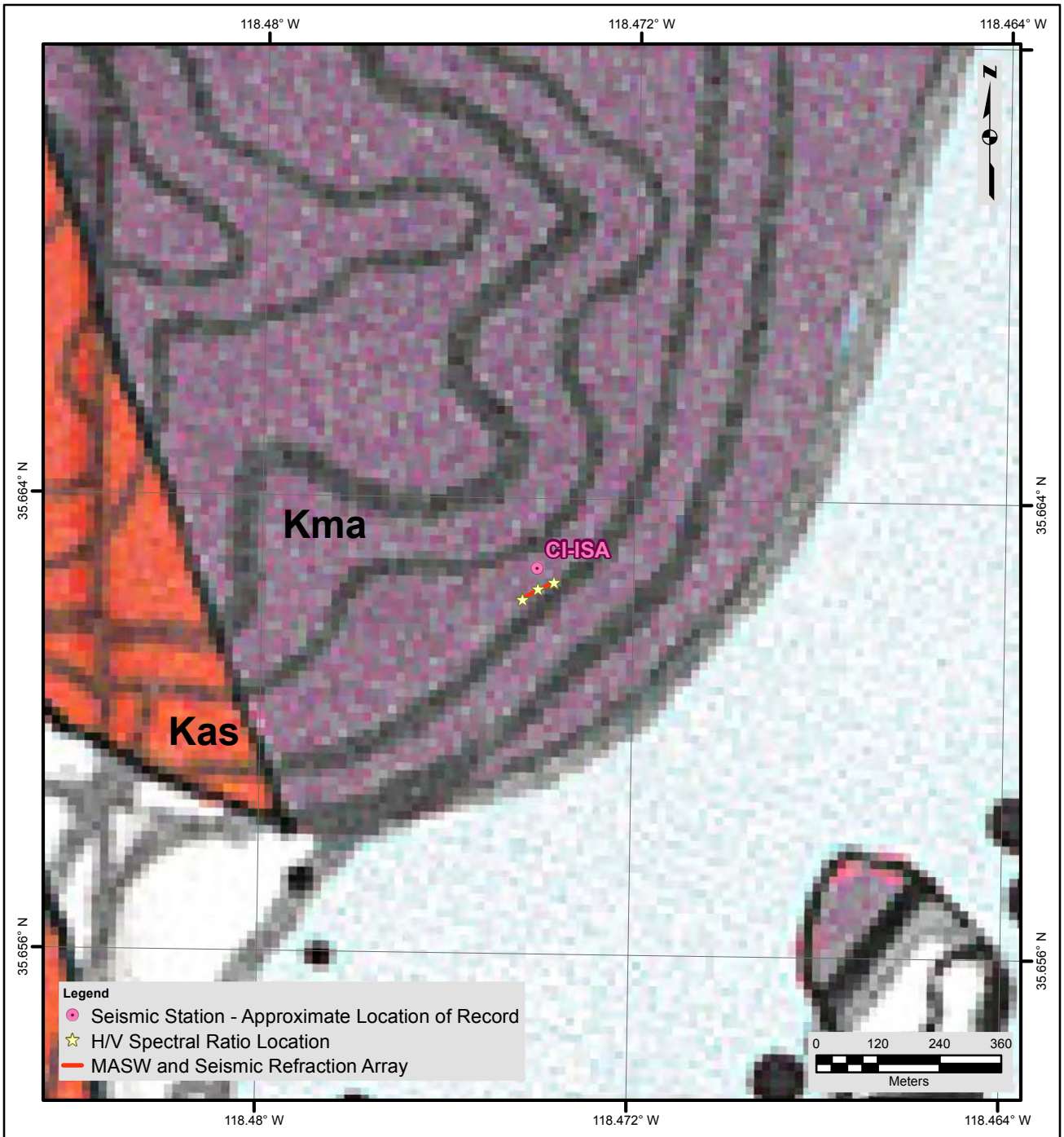

Description of Geologic Map Units

Kas = Late Cretaceous granodiorite of Alta Sierra, fine-grained
Kma = Late Cretaceous granodiorite of Mt Adelaide, course grained

NOTES:
1. WGS 1984 COORDINATE SYSTEM
2. Reconnaissance Geologic Map of Basement Rocks along the White Wolf-Breckenridge-Southern Kern Canyon Fault Zone, Southern Sierra Nevada, California by Donald C. Ross, 1980-1983
3. See site map for details of geophysical survey

File Name: CI-ISA

Date: 10/13/2011

USGS science for a changing world

GEOVision geophysical services

GEOLOGIC MAP
CI•ISA

RECOVERY.GOV

Looking northeast along array ISA-1 towards CI.ISA seismic station (about 28 m inside tunnel)

Looking northeast towards HVSR sensor 507 along array ISA-1

MASW/P-wave refraction data acquisition on array ISA-1

Looking southwest along array ISA-1 past HVSR sensor 453

Looking west across array ISA-1 at structure housing seismic station

Location of Geophysical Testing Arrays:

Location	Latitude	Longitude
ISA-1, Southwest End of MASW/Refraction Array	35.66223	-118.47436
ISA-1, Center of MASW/Refraction Array	35.66239	-118.47402
ISA-1, Northeast End of MASW/Refraction Array	35.66252	-118.47368
HVSR Sensor 450	35.66241	-118.47400
HVSR Sensor 453	35.66252	-118.47366
HVSR Sensor 507	35.66222	-118.47433

Notes: 1) WGS84 Coordinate System (decimal degrees)
2) Survey accuracy is estimated at 1 to 2 m.

Results:

V_S Model

Depth to Top of Layer (m)	Layer Thickness (m)	S-Wave Velocity (m/s)	Inferred P-Wave Velocity (m/s)	Assumed Poisson's Ratio	Assumed Density (g/cm^3)
0	1	186	347	0.3	1.70
1	1.5	268	502	0.3	1.80
2.5	2.5	482	901	0.3	1.90
5	4	569	1064	0.3	2.00
9	5	638	1193	0.3	2.10
14	6	874	1634	0.3	2.15
20	8	1107	2071	0.3	2.20
28	>7	1375	2573	0.3	2.25

Notes: 1) Depth of investigation is about 35 m.
2) Bottom layer is a half space.
3) Half space velocity not well resolved.

Observations/Discussion:

- The HVSR curves are generally similar, especially sensors 453 and 450, with two peaks in the 4.5 to 8 Hz range. Sensor 507 has an additional peak at about 12 Hz. The HVSR peaks are potentially associated with the weathering profile in the granitic rocks.
- It is unclear how topographic variation in the site vicinity may affect the HVSR measurements.
- The P-wave refraction data collected along array ISA-1 were modeled using a tomographic inversion routine with a smooth velocity gradient starting model.
- The seismic refraction survey design, including extension of the model to far offset source locations, allowed P-wave velocity to be imaged to a maximum depth of about 15 to 20 m. The seismic refraction model shows that P-wave velocity is about 300 to 450

m/s at the surface, increasing to 1,000 m/s at a depth of 1.5 to 5 m, 1,200 m/s at a depth of 6 to 11 m and greater than 1,600 m/s at a depth below 19 to 20 m.

- The seismic refraction model indicates that there is some lateral velocity variation at this site with a thicker weathered zone (lower velocity) at the northeast end of the line, but lower velocity at depth beneath the southwest end of the line. There were no reasonable alternate test locations at the site due to limited space and steep topography.
- Noise conditions at the site were not sufficient for application of passive surface wave techniques.
- Reduction of the MASW data was quite difficult due to lateral velocity variation, higher modes, scattering, etc.
- The minimum wavelength surface wave phase velocity data extracted from the 48-channel MASW array was about 11 m. Data reduction using seismic records from smaller hammer sources and a limited offset receiver array (i.e. less active geophones) allowed extraction of surface wave dispersion data to a minimum wavelength of about 2 m. Significant effort was also made reducing data from limited offset receiver arrays with interior seismic refraction sources to obtain surface wave dispersion data over intermediate wavelength ranges.
- Scatter in MASW dispersion data (about 40 to 75 m/s) is likely due, in part, to lateral velocity variation associated with differential weathering of near surface granitic rock.
- A representative dispersion curve was generated for the MASW data set using a moving average, polynomial curve fitting routine and used for modeling.
- Surface wave depth of investigation is about 35 m based on half of maximum wavelength criteria.
- The inferred P-wave velocities in the surface wave model, assuming a Poisson's ratio of 0.3, are generally consistent with the average velocity structure in the seismic refraction model in the upper 15 m.
- V_{S30} is 644 m/s (Site Class C).
- V_{S30} estimated from the surface wave sounding is likely lower than that at the seismic station, located 28.5 m inside a tunnel with about 10 to 15 m of overlying weathered rock. To obtain a better estimate of V_{S30} at the seismic station, the V_S of the upper 4m is replaced with that of the underlying layer and the average V_S is estimated between 5 and 35 m.
- V_{S30} is 765 m/s, if the V_S of the upper 4 m were replaced with that of the lower layer (Site Class B/C).
- Average S-wave velocity between 5 m and 35 m is 881 m/s. (Site Class B)
- A better approach to correlate the velocity structure at the seismic station to that measured would be to measure the near surface velocity (upper several meters) of the rock inside the tunnel using surface wave and/or seismic refraction techniques.

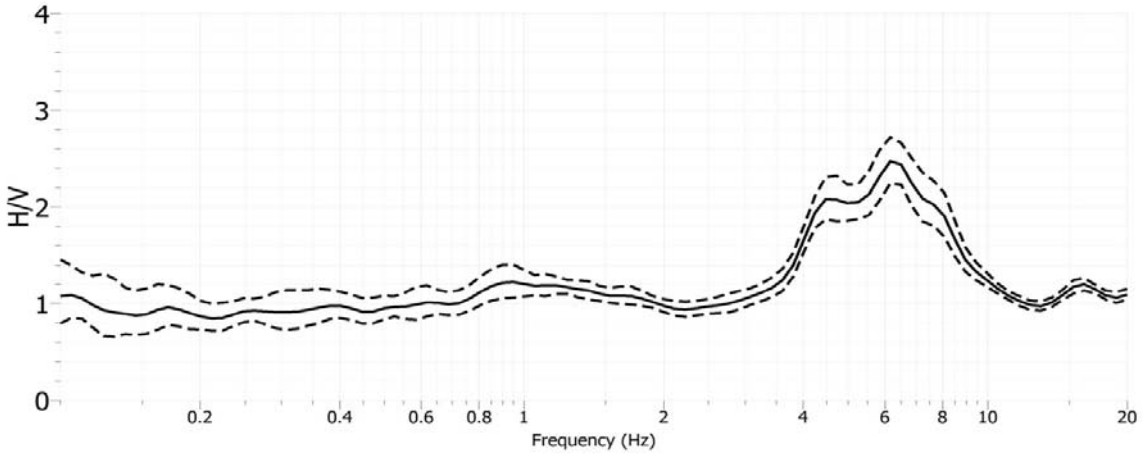

Site CI.ISA, H/V Spectral Ratio, Array ISA-1, Sensor 507

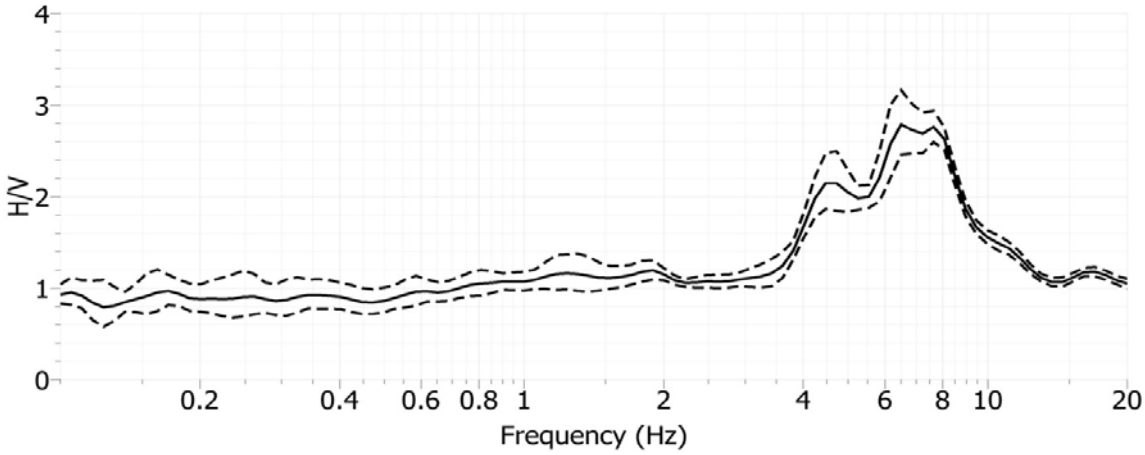

Site CI.ISA, H/V Spectral Ratio, Array ISA-1, Sensor 450

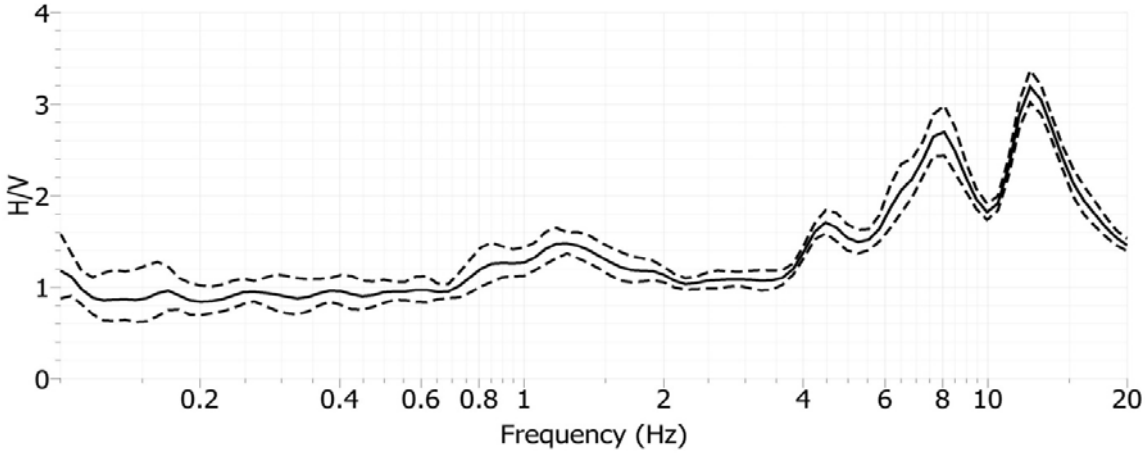

Site CI.ISA, H/V Spectral Ratio, Array ISA-1, Sensor 453

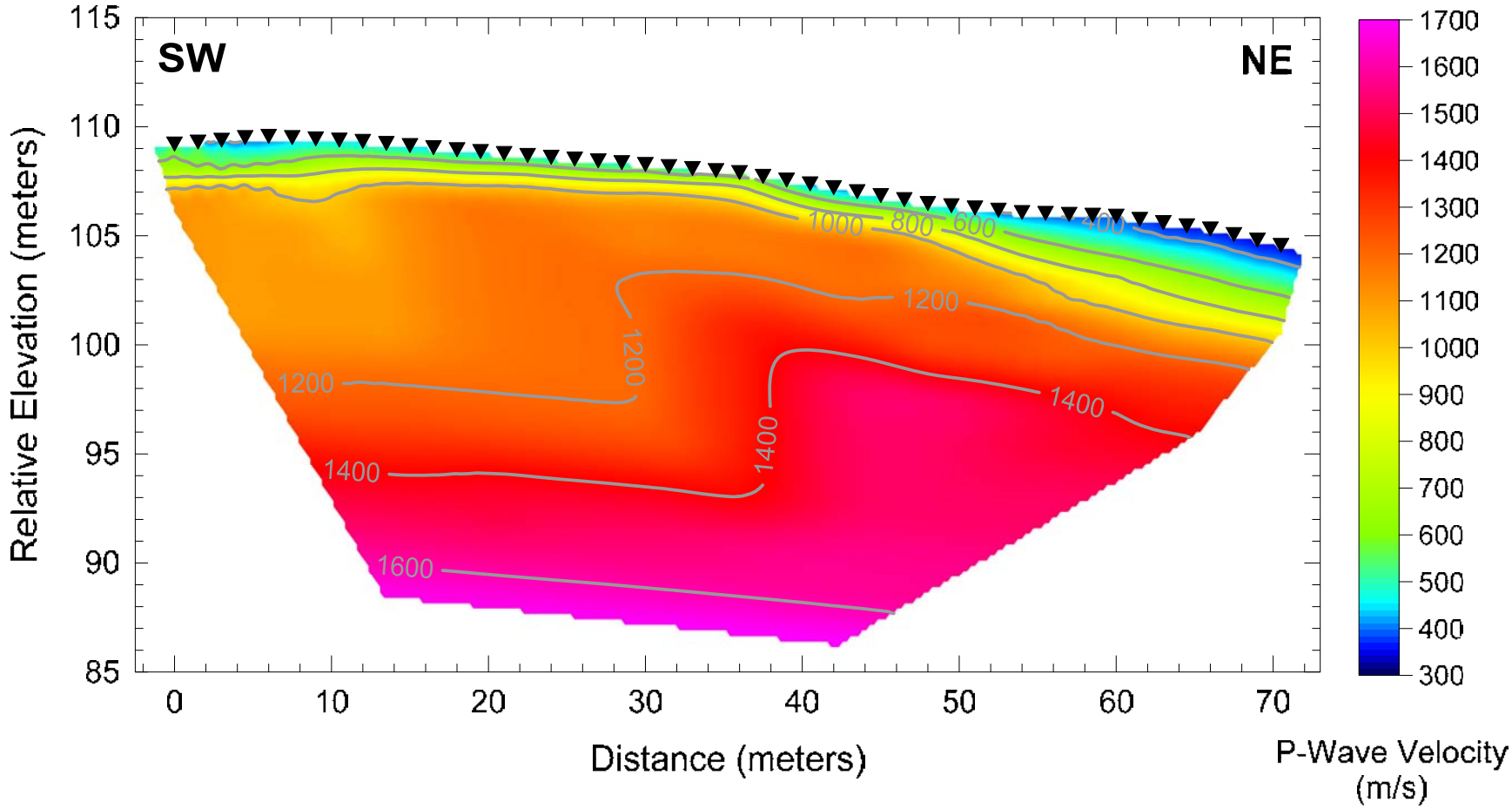

Array ISA-1 – Tomographic seismic refraction model utilizing smooth velocity gradient starting model

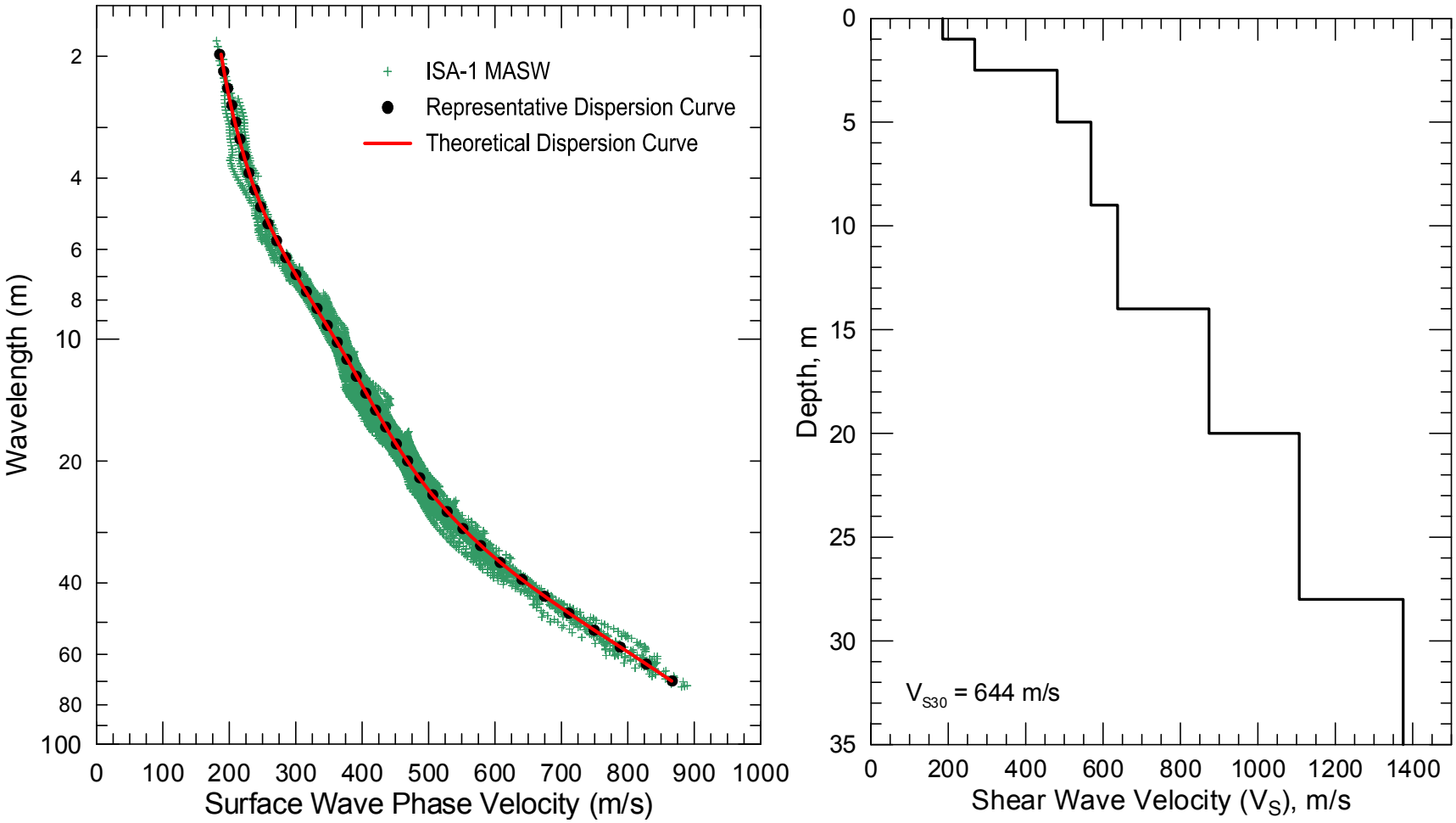

CI.ISA - Field, representative and inverted theoretical surface wave dispersion data (left) and associated V_S model (right)

Site CI.JEM

Location: Julian Eagle Mine, Julian, San Diego County, California

Latitude: 33.08098 **Longitude:** -116.59755
(Station coordinates provided by USGS, WGS84 coordinate system)

V_{S30} (measured): 501 m/s

V_{S30} (adjusted to more accurately reflect seismic station conditions): 559 m/s (average S-wave velocity between 1.5 and 31.5 m adjusting for seismic sensor location).

NEHRP Site Class: C

Geomatrix Code: IGB/INB

Geologic Conditions/Observations: Seismic station located on Jurassic granitic and metamorphic rocks (quartz diorite, schist and gneiss).

Site Conditions: Rural site. Seismic station located at the base of hill comprised of weathered bedrock. Hilly topography in site vicinity. Seismic line located along a dirt road consisting of a relatively planar surface with about a 2.5 m increase in ground surface elevation to the south along the 70.5 m long line.

Geophysical Methods Utilized: HVSR, Seismic Refraction, MASW

Geophysical Testing Arrays:

1. Array JEM-1 (48 channel MASW and P-wave seismic refraction array utilizing 4.5 Hz vertical geophones spaced 1.5 m apart for a length of 70.5 m, forward and reverse shot locations with multiple source offsets and source types and multiple interior shot locations).
2. Three HVSR measurement locations: one near each end of array JEM-1 and the other near the seismic station.

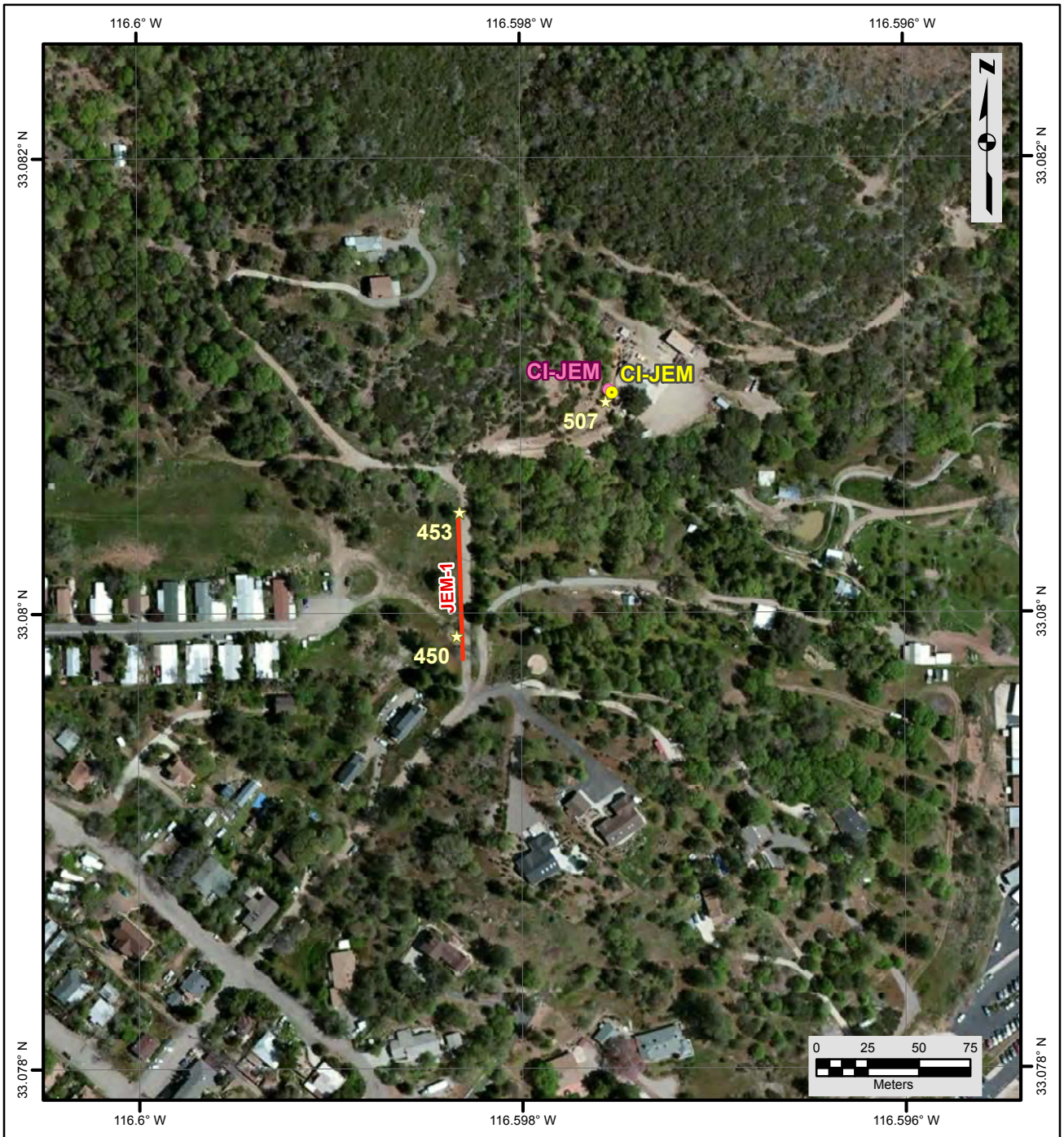

Legend

- Seismic Station - Approximate Surveyed Location
- Seismic Station - Approximate Location of Record
- H/V Spectral Ratio Location
- MASW and Seismic Refraction Array

NOTES:
1. WGS 1984 COORDINATE SYSTEM
2. Image Source: ESRI, i-cubed, USDA FSA, USGS, AEX, GeoEye, Getmapping, Aerogrid, IGP

File Name: CI-JEM-I

Date: 2/7/2013

USGS science for a changing world

GEOVision geophysical services

RECOVERY.GOV

SITE MAP
CI•JEM

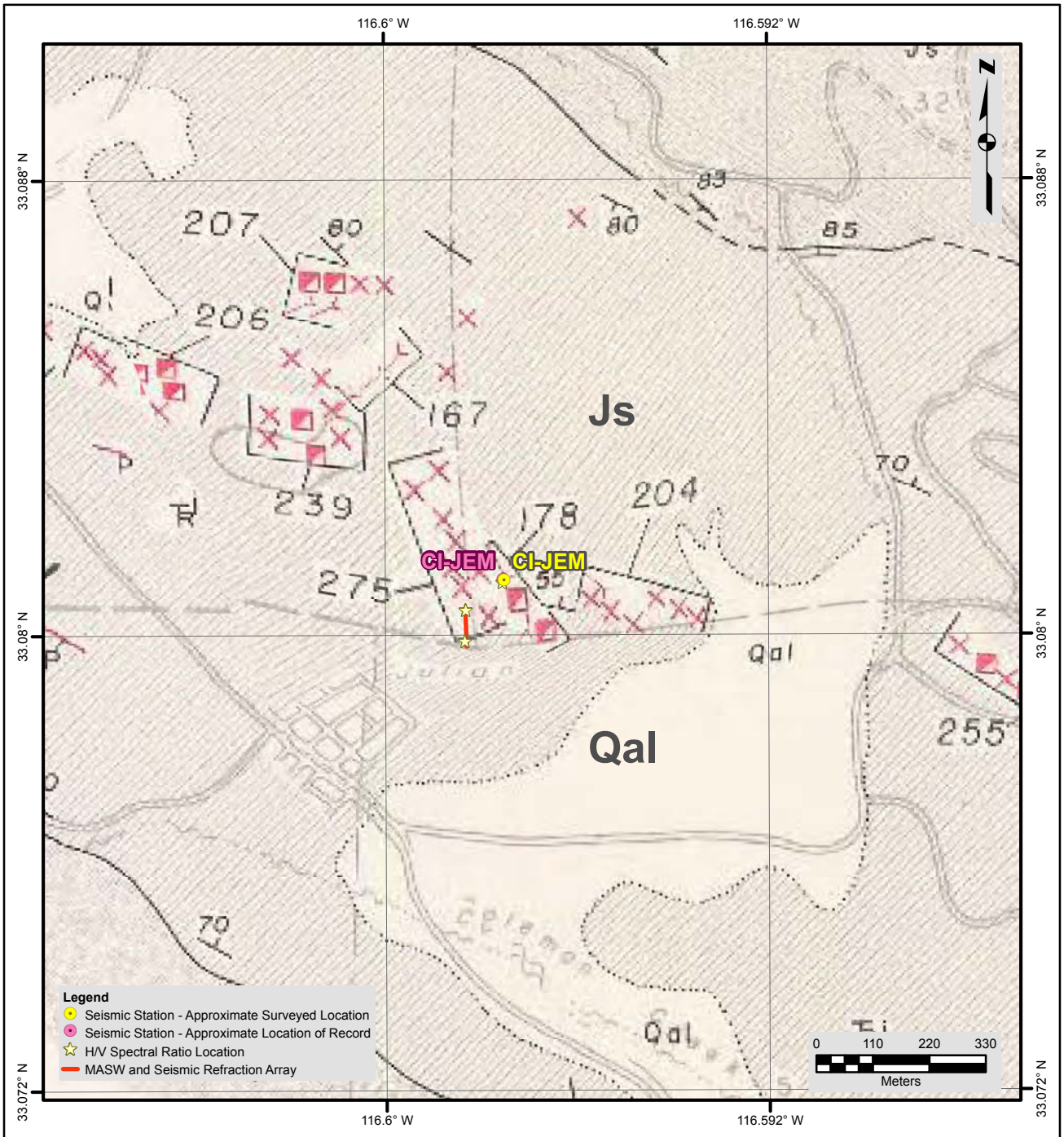

Description of Geologic Map Units

Qal = Quaternary (Holocene) alluvium
Js = Mesozoic (Jurassic) stonewall quartz diorite, schist and gneiss

NOTES:
1. WGS 1984 COORDINATE SYSTEM
2. Geology and Mineral Deposits of the Julian District, San Diego County, California by F. Harold Weber, Jr., 1956-1957
3. See site map for details of geophysical survey

File Name: CI-JEM

Date: 2/7/2013

USGS science for a changing world

GEOVision geophysical services

GEOLOGIC MAP
CI•JEM

Looking southwest at HVSR sensor 507 and seismic station CI.JEM

Looking at weathered rock in hill behind seismic station CI.JEM

Looking north along seismic refraction and MASW array JEM-1

HVSR sensor 453 in shallow hole

Looking south along array JEM-1

Location of Geophysical Testing Arrays:

Location	Latitude	Longitude
JEM-1, South End of MASW/Seismic Refraction Array	33.07979	-116.59831
JEM-1, Center of MASW/Seismic Refraction Array	33.08012	-116.59833
JEM-1, North End of MASW/Seismic Refraction Array	33.08044	-116.59835
HVSR Sensor 450	33.07990	-116.59835
HVSR Sensor 453	33.08044	-116.59833
HVSR Sensor 507	33.08093	-116.59757
CI.JEM Seismic Station	33.08097	-116.59753

Notes: 1) WGS84 Coordinate System (decimal degrees)
2) Survey accuracy is estimated at 1 to 2 m.

Results:

V_S Model 1

Depth to Top of Layer (m)	Layer Thickness (m)	S-Wave Velocity (m/s)	Inferred P-Wave Velocity (m/s)	Assumed Poisson's Ratio	Assumed Density (g/cm^3)
0	1.5	209	362	0.25	1.8
1.5	5.5	295	510	0.25	1.9
7	7	450	779	0.25	2.0
14	10	651	1127	0.25	2.1
24	>11	1742	3017	0.25	2.3

Notes: 1) Depth of investigation is about 35 m.
2) Bottom layer is a half space.
3) Velocity of half-space not well constrained.

V_S Model 2

Depth to Top of Layer (m)	Layer Thickness (m)	S-Wave Velocity (m/s)	Inferred P-Wave Velocity (m/s)	Assumed Poisson's Ratio	Assumed Density (g/cm^3)
0	1.5	210	363	0.25	1.8
1.5	5.5	293	508	0.25	1.9
7	6	470	815	0.25	2.0
13	6	492	853	0.25	2.0
19	>16	1437	2489	0.25	2.2

Notes: 1) Depth of investigation is about 35 m.
2) Bottom layer is a half space.
3) Velocity of half-space not well constrained.

V_S Model 3

Depth to Top of Layer (m)	Layer Thickness (m)	S-Wave Velocity (m/s)	Inferred P-Wave Velocity (m/s)	Assumed Poisson's Ratio	Assumed Density (g/cm^3)
0	1.5	210	363	0.25	1.8
1.5	5.5	293	508	0.25	1.9
7	10	469	812	0.25	2.0
17	12	938	1624	0.25	2.1
29	>6	1749	3029	0.25	2.3

Notes: 1) Depth of investigation is about 35 m.
2) Bottom layer is a half space.
3) Velocity of half-space not well constrained.

V_S Model 4 (Recommended Model)

Depth to Top of Layer (m)	Layer Thickness (m)	S-Wave Velocity (m/s)	Inferred P-Wave Velocity (m/s)	Assumed Poisson's Ratio	Assumed Density (g/cm^3)
0	1.5	210	364	0.25	1.80
1.5	5	291	504	0.25	1.90
6.5	5	426	738	0.25	2.00
11.5	5.5	508	879	0.25	2.00
17	6	759	1314	0.25	2.10
23	6	1177	2039	0.25	2.15
29	>6	1704	2952	0.25	2.25

Notes: 1) Depth of investigation is about 35 m.
2) Bottom layer is a half space.
3) Velocity of bottom two layers not well constrained.

Observations/Discussion:

- The seismic station is located at the base of a small hill comprised of weathered granitic and metamorphic rocks. The northern end of the MASW and seismic refraction array is located about 100 m southwest of the seismic station and is about 30 m south of the hill. The seismic line is also located on the same geologic unit and could not be placed closer to the seismic station due to space limitations.
- There are no significant HVSR peaks as expected for a rock site.
- Seismic refraction first arrivals are very weak and, in some areas, may occur from an out of plane refractor (e.g. dike, localized higher velocity zone). Alternatively, significant scattering from heterogeneities in the weathered rock may highly attenuate the refraction first arrival. Additionally, it is unclear if utility lines are located beneath the gravel road along which the seismic line was placed.

- The P-wave refraction data collected along array JEM-1 were modeled using a tomographic inversion routine with a smooth velocity gradient starting model. The seismic refraction model was extended to far offset shot locations to extend depth of investigation.
- The seismic refraction survey design allowed P-wave velocity to be imaged to a maximum depth of about 20 to 25 m. The seismic refraction model shows that P-wave velocity is about 450 to 500 m/s at the surface, increasing to 800 m/s at a depth of 2.5 to 7 m, 1,000 at a depth of 4 to 8 m, 1,500 m/s at a depth of 8 to 12 m, greater than 2,500 below a depth of 14 to 26 m, and likely exceeding 3,000 m/s in the upper 30 m.
- If seismic refraction data is indeed influenced by a high velocity out of plane refractor, then the seismic refraction model may overestimate P-wave velocity structure immediately beneath the profile.
- The seismic refraction model indicates that there is some lateral velocity variation at this site as is typical at weathered rock sites. The seismic model indicates that higher velocity, less weathered rock may occur at shallower depth beneath the northern portion of the line.
- Noise conditions at the site were not sufficient for application of passive surface wave techniques.
- The minimum wavelength surface wave phase velocity data extracted from the 48-channel MASW array was about 15 m. Data reduction using seismic records from smaller hammer sources and a limited offset receiver array (i.e. less active geophones), primarily from source locations in the southern portion of the line, allowed extraction of surface wave dispersion data to a minimum wavelength of about 2 m.
- There is nominally 50 to 60 m/s scatter in the MASW dispersion data, at least in part due to lateral velocity variation.
- A representative dispersion curve was generated for the MASW data set using a moving average, polynomial curve fitting routine and used for modeling.
- Surface wave depth of investigation is about 35 m based on half of maximum wavelength criteria.
- Four V_S models are presented demonstrating nonuniqueness in surface wave modeling. A Poisson's ratio of 0.25 was assumed for data modeling. These models attempt to illustrate the probable minimum, intermediate and maximum depths for the high velocity half space and a more gradual increase in velocity with depth. It should be noted that the velocity of the half space is not well resolved. There is only a 3.5 % variation in V_{S30} between the models. Model 4 exhibits the smoothest velocity variation (more layers) and represents the average velocity conditions and, therefore, is the better single model to represent site conditions.
- These models were all developed assuming that the phase velocity data represents the fundamental mode; however, testing indicates that the first higher mode may have equal or slightly greater relative amplitude than the fundamental mode over the 6 to 10 Hz range (wavelengths greater than about 50 m). Higher modes are not well defined in the wavefield transform images and there is no clear evidence of the first higher mode at predicted phase velocities over the 6 to 10 Hz frequency range. Even small changes to the velocity structure can significantly alter the amplitude of higher modes and the effects of lateral velocity variation, variable Poisson's ratio, density, etc. can be significant and difficult to predict. If modal superposition were to occur at low frequencies, then V_S

would be slightly overestimated at depth; however, the velocity at depth appears conservative relative to the P-wave seismic refraction model. The refraction model does, however, also have a certain degree of uncertainty.

- The effect of variable Poisson's ratio, in the 0.2 to 0.35 range, on the models is also demonstrated. Over this range, a 0.05 increase in Poisson's Ratio decreases V_{S30} by about 5%. The variation in V_{S30} associated with changes in Poisson's Ratio is much larger than expected (a 2% change may be more realistic although more testing is required) and may indicate that phase velocities at wavelengths greater than 50 m may result from superposition of the fundamental and first higher mode. This would also explain some of the significant variation in the velocity of the half space.
- The inferred P-wave velocities in the surface wave models are generally lower at intermediate depths than average velocity structure in the seismic refraction model in the upper 25 m. As discussed above, the possibility cannot be discounted that the seismic refraction model overestimates P-wave velocity structure at intermediate depths.
- Sites with sharp increases in velocity at depth (i.e. sediments over rock, abrupt reduction in weathering) present the most significant challenges with nonuniqueness and the largest variation in V_{S30} associated with nonuniqueness, which is still quite low. Often seismic refraction surveys, possibly HVSR (questionable) or alternate geophysical testing can help determine the most appropriate velocity model. At this site, seismic refraction may not be particularly useful as the first arrival may be associated with an out of plane refractor or thin high velocity layer, which results in underestimated depth to the high velocity unit. Further investigation needs to be made regarding the degree to which joint inversion of Rayleigh and Love wave phase velocity data can reduce nonuniqueness, if at all. Love wave data may be more useful at sites with similar velocity structure as this as Poisson's ratio has no effect on Love wave dispersion data and the fundamental mode is expected to be dominant at low frequencies/long wavelengths.
- V_{S30} is 498, 513, 495 and 496 m/s for Models 1 to 4, respectively, and averages 501 m/s (Site Class C).
- Average S-wave velocity between 1.5 m (compensating for assumed sensor depth and fact that seismic sensor is located adjacent to a hill of possibly less weathered rock) and 31.5 m is 557, 573, 552 and 553 m/s for Models 1 to 3, respectively, averaging 559 m/s.
- Further investigation is warranted at this site to 1) confirm that the weathering profile at the seismic station is similar to that at the seismic line, 2) assess the effect of potential modal superposition at low frequencies on the V_S models and 3) acquire Love wave MASW (MALW) data, which may be less affected by the higher modes at low frequencies.

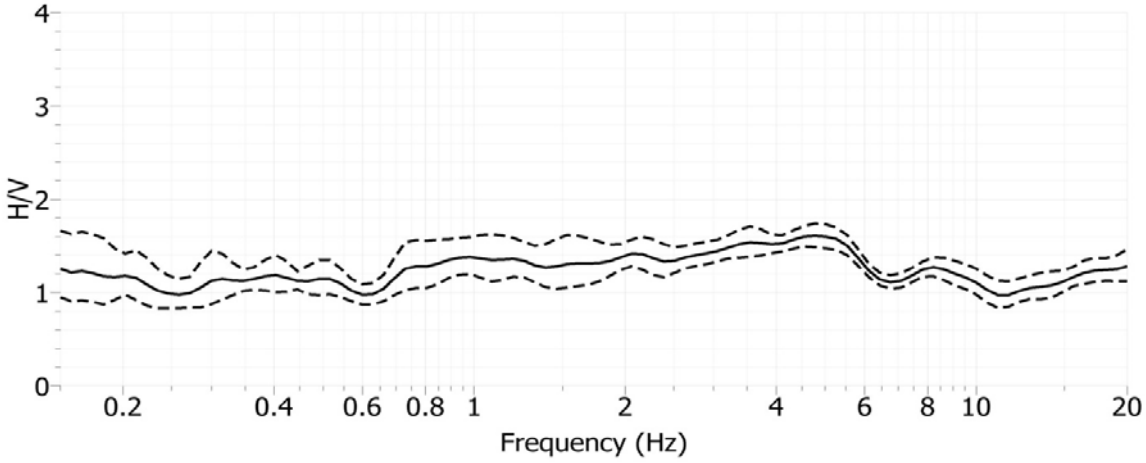

Site CI.JEM, H/V Spectral Ratio, Near Seismic Station, Sensor 507

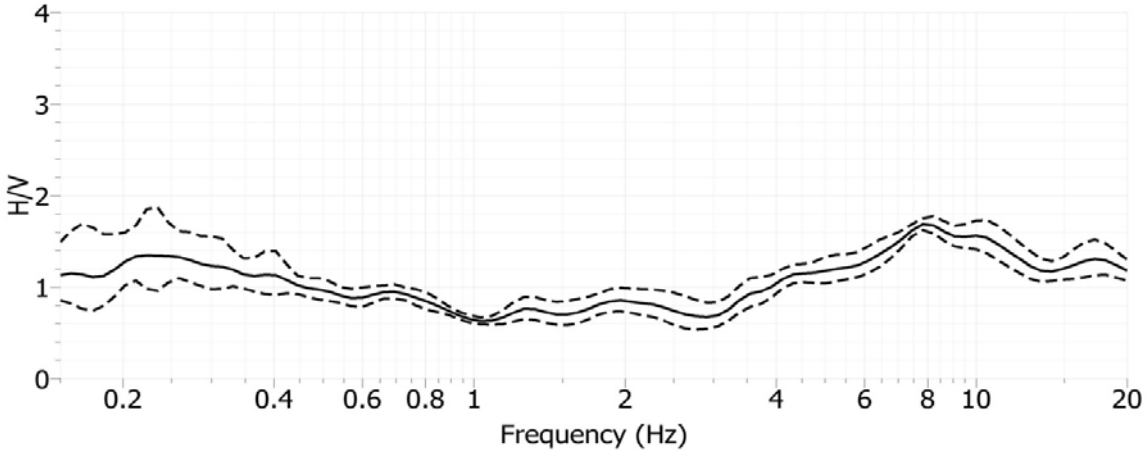

Site CI.JEM, H/V Spectral Ratio, Array JEM-1, Sensor 453

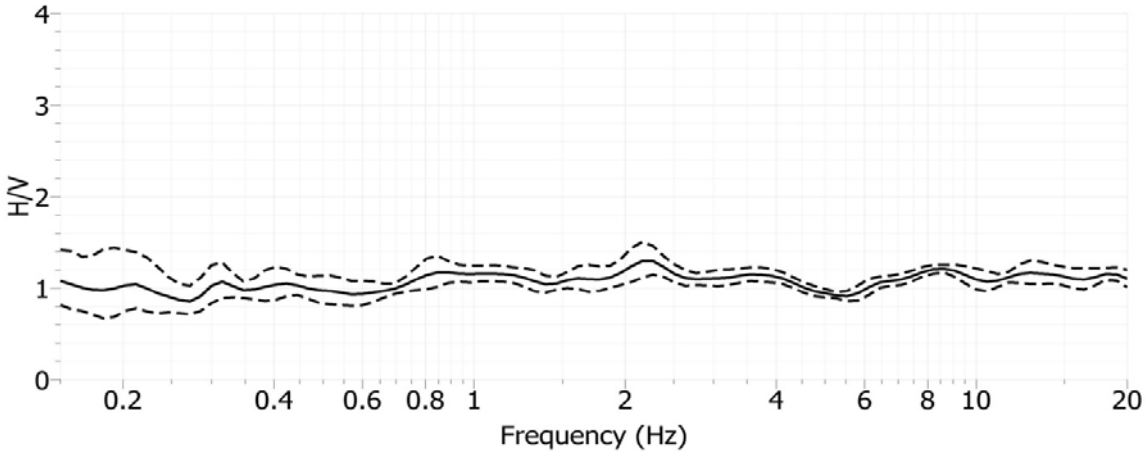

Site CI.JEM, H/V Spectral Ratio, Array JEM-1, Sensor 450

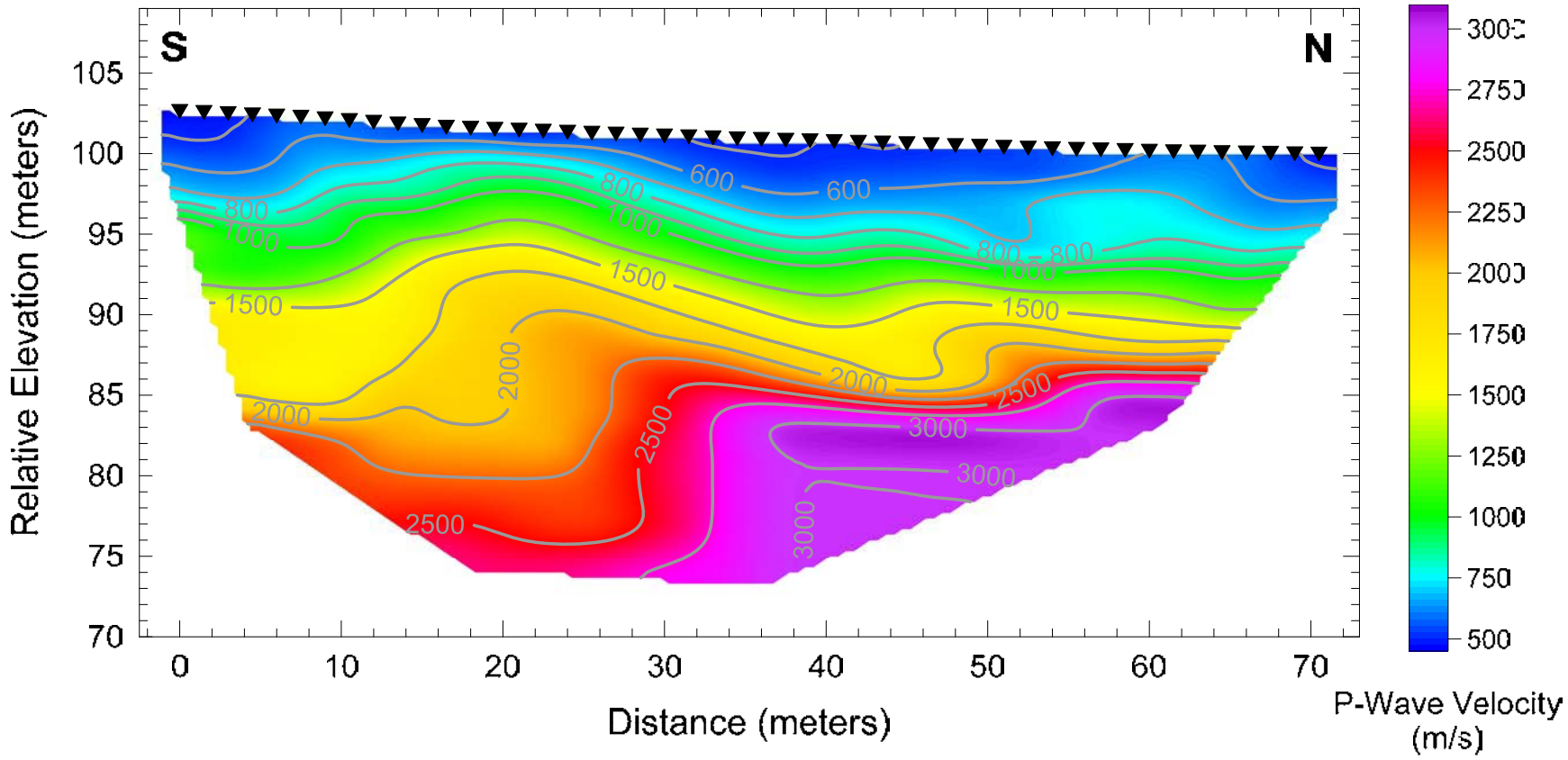

Array JEM-1 – Tomographic Seismic Refraction Model utilizing Smooth Velocity Gradient Starting Model

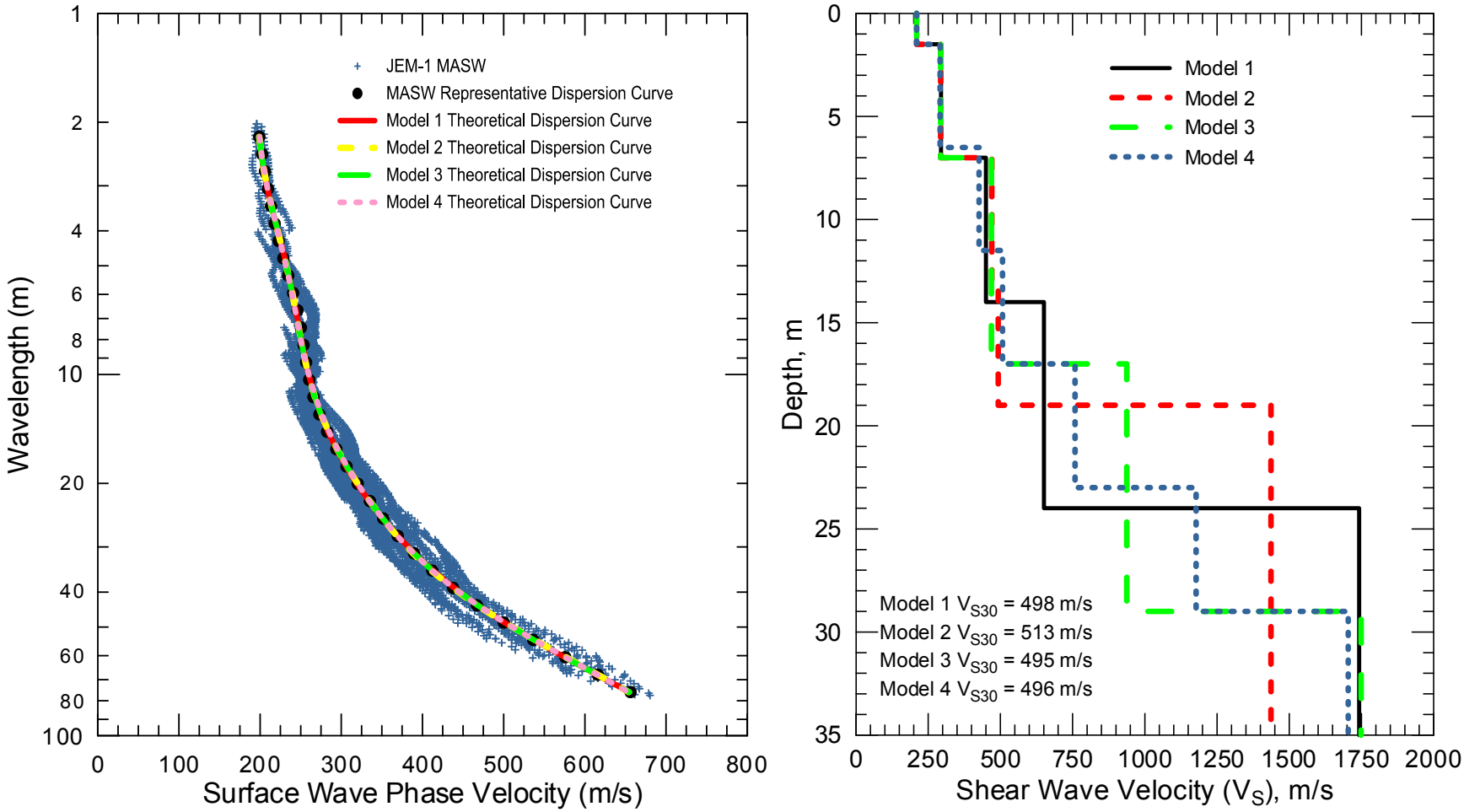

CI.JEM - Field, representative and inverted theoretical surface wave dispersion data (left) and equivalent V_S models (right) using a Poisson's ratio of 0.25.

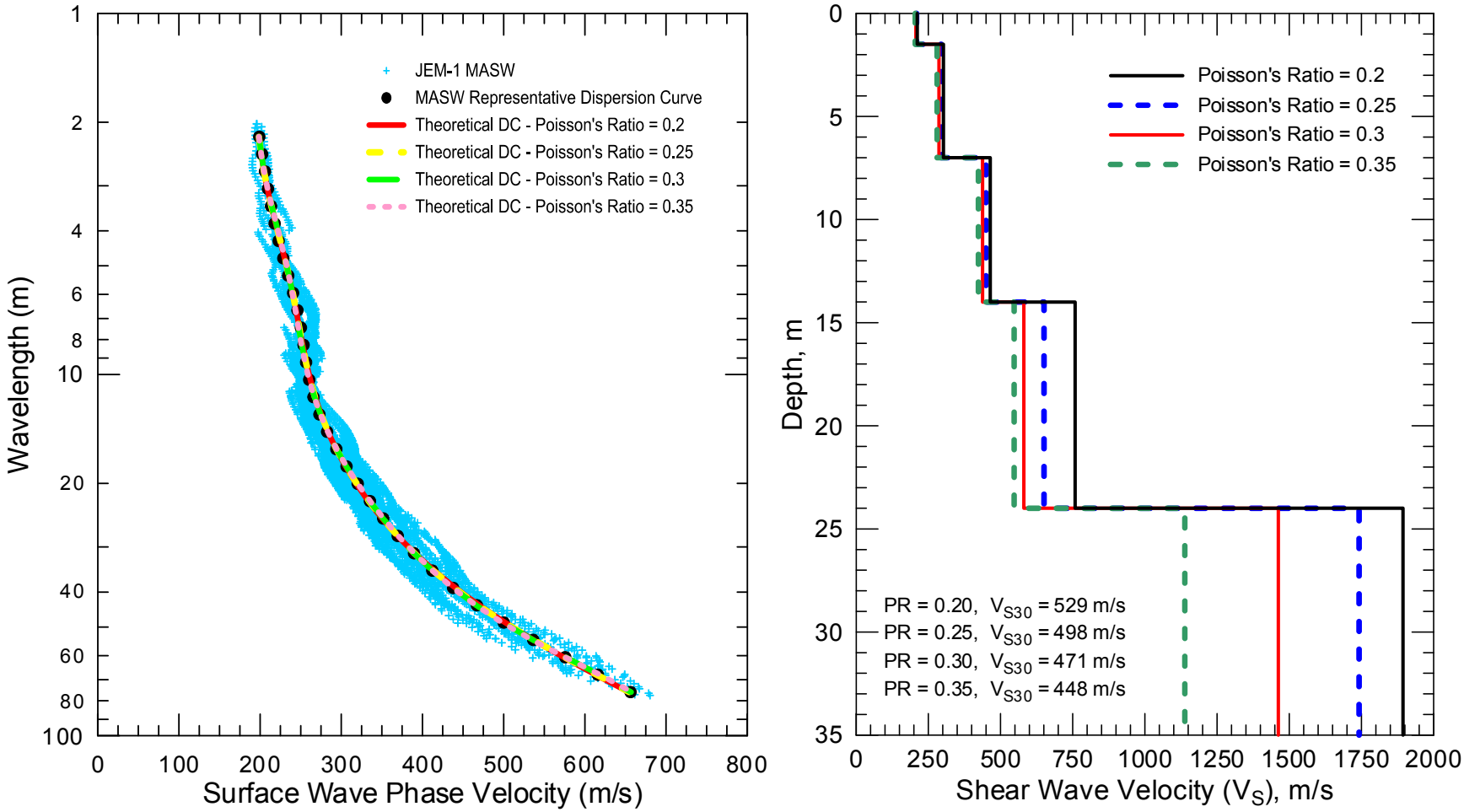

CI.JEM - Field, representative and inverted theoretical surface wave dispersion data (left) and V_S models utilizing different values of Poisson's Ratio (right). Note the significant variation in the V_S of the half-space, which is not well resolved. The variation of the half space velocity is more than expected from the variable Poisson's ratio and may result from the fact that phase velocities at wavelengths greater than 50 m may be associated with superposition of the fundamental and first higher modes; whereas, modeling is based on fundamental mode assumption.

Site CI.JRC2

Location: Joshua Ridge 2, China Lake Naval Weapons Center, Inyo County, California

Latitude: 35.98249 **Longitude:** -117.80885
(Station coordinates provided by USGS, WGS84 coordinate system)

V_{S30} (measured): 623 m/s

V_{S30} (adjusted to more accurately reflect seismic station conditions): 729 m/s (average S-wave velocity between 1.5 and 31.5 m adjusting for 1.5 m assumed sensor depth).

NEHRP Site Class: C

Geomatrix Code: IVB

Geologic Conditions/Observations: Quaternary (Pleistocene) volcanic tuff.

Site Conditions: Rural site located on ridge top with relatively steep terrain in site vicinity. Ground surface elevation gradually increases about 5 m to the southeast along array JRC2-1, Relatively flat terrain in the immediate vicinity of array JRC2-2.

Geophysical Methods Utilized: HVSR, Seismic Refraction, MASW, SASW

Geophysical Testing Arrays:

1. Array JRC2-1 (48 channel MASW and seismic refraction array utilizing 4.5 Hz vertical geophones spaced 1.5 m apart for a length of 70.5 m, forward and reverse shot locations with multiple source offsets and source types and multiple interior shot locations).
2. Array JRC2-2 (SASW array with data acquired using 4.5 and 1 Hz geophones, common center point geometry as possible, forward and reverse shot locations).
3. Three HVSR measurement locations distributed along JRC2-1.

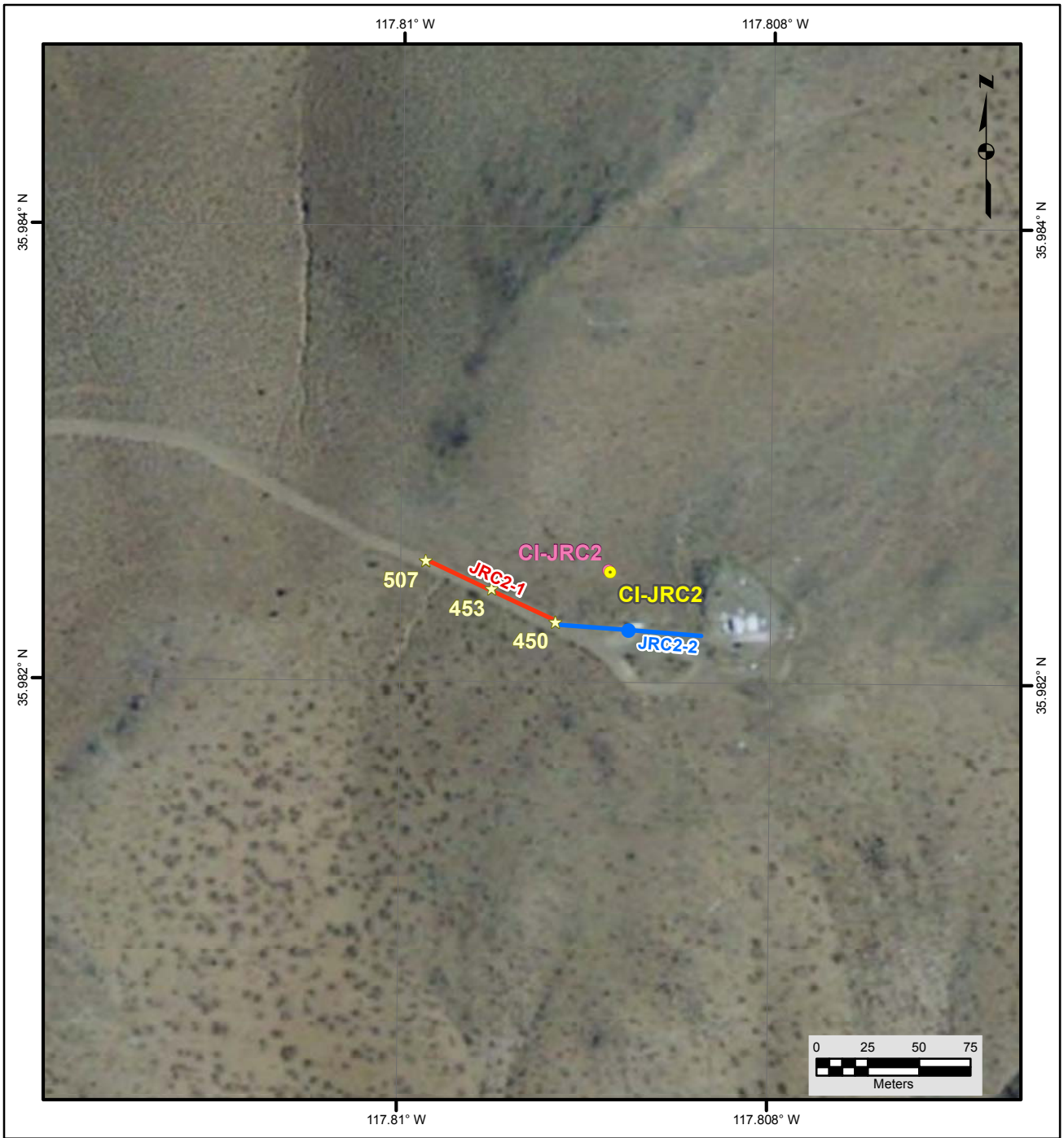

Legend

- Seismic Station - Approximate Surveyed Location
- Seismic Station - Approximate Location of Record
- H/V Spectral Ratio Location
- MASW and Refraction Array
- SASW Array
- Center of SASW Array

NOTES:
1. WGS 1984 COORDINATE SYSTEM
2. Image Source: ESRI, i-cubed, USDA FSA, USGS, AEX, GeoEye, Getmapping, Aerogrid, IGP

File Name: CI-JRC2-I

Date: 1/4/2012

USGS science for a changing world

GEOVision geophysical services

RECOVERY.GOV

SITE MAP
CI•JRC2

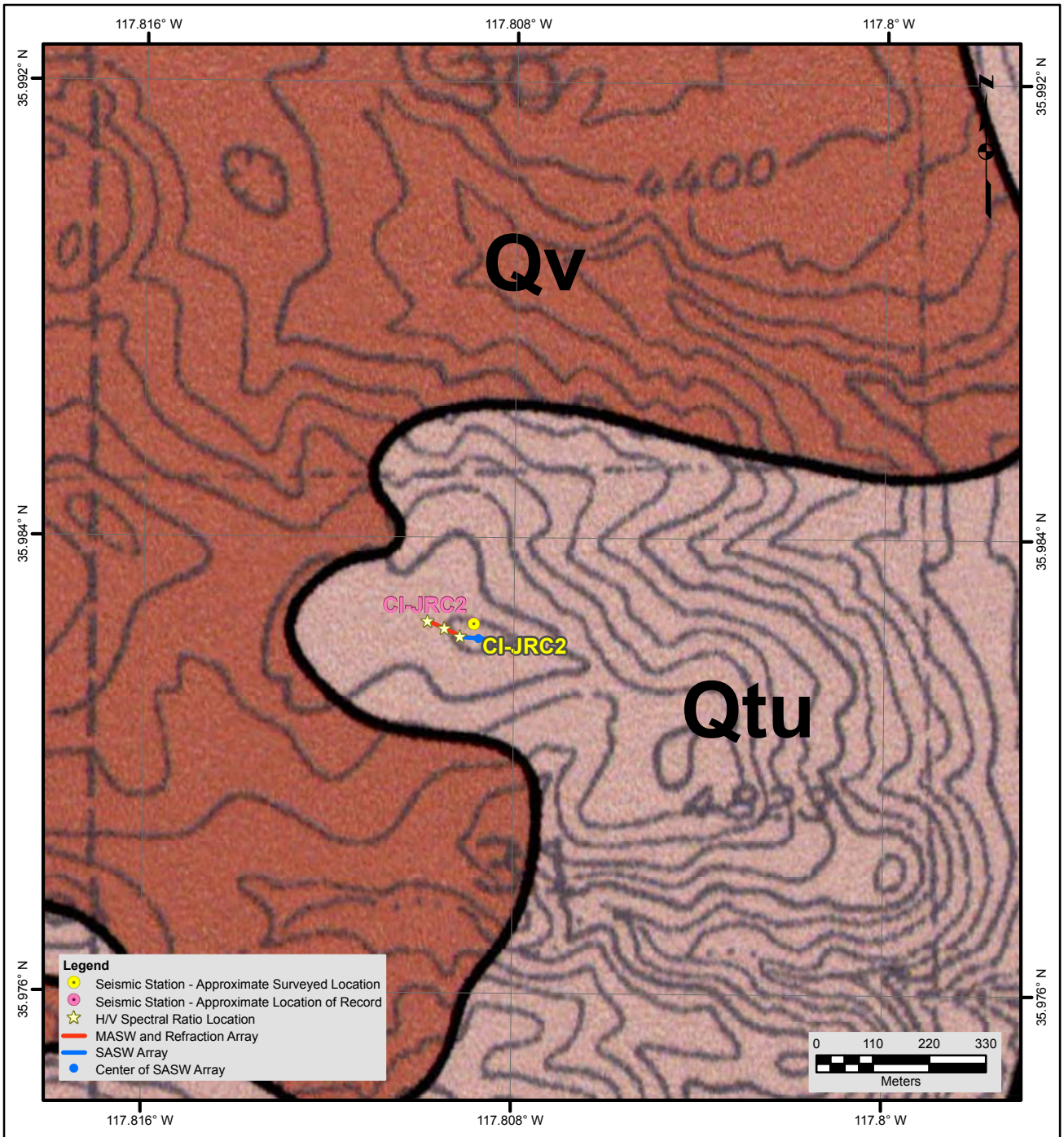

Description of Geologic Map Units

Qv = Quaternary volcanic rocks
Qtu = Quaternary tuff

NOTES:
1. WGS 1984 COORDINATE SYSTEM
2. Geologic Map of the Little Lake 15 Minute Quadrangle, Tulare, Kern & Inyo Counties, California by Thomas W. Dibblee, Jr., 2008
3. See site map for details of geophysical survey

File Name: CI-JRC2

Date: 1/4/2012

USGS science for a changing world

GEOVision geophysical services

RECOVERY.GOV

GEOLOGIC MAP
CI•JRC2

Seismic station CI.JRC2

HVSR measurements

Looking northwest along array JRC2-1

Nanometrics Trillium seismometer used for HVSR measurements

Location of Geophysical Testing Arrays:

Location	Latitude	Longitude
JRC2-1, Northwest End of MASW/Refraction Array	35.98253	-117.80983
JRC2-1, Center of MASW/Refraction Array	35.98240	-117.80948
JRC2-1, Southeast End of MASW/Refraction Array	35.98227	-117.80913
JRC2-2, Northwest End of SASW Array	35.98225	-117.80914
JRC2-2, Center of SASW Array	35.98223	-117.80874
JRC2-2, Southeast End of SASW Array	35.98221	-117.80835
HVSR Sensor 450	35.98226	-117.80914
HVSR Sensor 453	35.98241	-117.80948
HVSR Sensor 507	35.98253	-117.80984
CI.JRC2 Seismic Station	35.98248	-117.80884

Notes: 1) WGS84 Coordinate System (decimal degrees)
2) Survey accuracy is estimated at 1 to 2 m

Results:

V_S Model – SASW Array JRC2-2

Depth to Top of Layer (m)	Layer Thickness (m)	S-Wave Velocity (m/s)	Inferred P-Wave Velocity (m/s)	Inferred Poisson's Ratio	Inferred Density (g/cm^3)
0	1	158	295	0.3	1.7
1	1.5	235	439	0.3	1.8
2.5	3	443	829	0.3	2.0
5.5	17.5	802	1500	0.3	2.1
23	>7	1025	1918	0.3	2.2

Notes: 1) Depth of investigation is about 27 to 30 m.
2) Bottom layer is a half space.
3) Half space velocity not well resolved.

Observations/Discussion:

- HVSR plots are very similar validating the 1-D velocity assumption.
- There are no significant HVSR peaks at the site; although there is elevated HVSR response between about 1.5 and 12 Hz.
- The P-wave seismic refraction data for array JRC2-1 were modeled using a tomographic inversion routine with a layer-based starting model. The seismic refraction model was only extended to a 5 m offset shot location.
- The P-wave seismic refraction survey design allowed P-wave velocity to be imaged to a maximum depth of about 15 to 20 m. The seismic refraction model indicates that P-wave velocity is about 400 to 700 m/s at the surface and increases to 800 m/s at a depth of 8 to 14 m, 1,200 m/s at a depth of 13 to 16 m and over 1,600 m/s at a depth of about 16 to 20 m.
- The P-wave seismic refraction model indicates that there is significant near surface lateral velocity variation. Of particular concern was the apparent shallowing of higher velocity rock towards the southeast, indicating that subsurface velocities may be higher in the vicinity of the seismic station. Review of seismic records for array JRC2-1 also show a significant geologic structure that disrupts surface wave propagation in the southeastern portion of the line.
- Due to lateral velocity variation and associated uncertainty reducing the MASW data from array JRC2-1, an SASW sounding (array JRC2-2) was conducted on the pad southeast of array JRC2-1. There was not sufficient space in this area for an MASW array. Additionally, due to space limitations, the center of the 20 to 36 m SASW receiver spacings had to be moved for forward and reverse source locations.
- SASW data reduction from the 20 to 36 m receiver spacings was complicated by lateral velocity variation, in part associated with a thicker sequence of fill to the east. Because the forward and reverse source locations for these receiver spacings had a different midpoint, the resulting phase velocity data were different due to the lateral velocity variation. Therefore, only the SASW data from the 20 to 36 m receiver spacing collected with the receivers centered on the western portion of the pad, closest to the seismic station, were used for modeling.
- For the purpose of data modeling, a moving average, polynomial curve fitting routine was used to generate a representative dispersion curves for the SASW data.
- The S-wave velocity of the half space in the SASW model is not well resolved and will be overestimated if the SASW dispersion curve is not representative of the fundamental mode. Reduction of the S-wave velocity of the half space to that of the overlying layer only reduces V_{S30} by about 4%.
- Surface wave depth of investigation is about 27 to 30 m based on half of maximum wavelength criteria.
- V_{S30} for SASW array JRC2-2 is 623 m/s (Site Class C).
- Average S-wave velocity between 1.5 m (assumed sensor depth) and 31.5 m is 729 m/s.

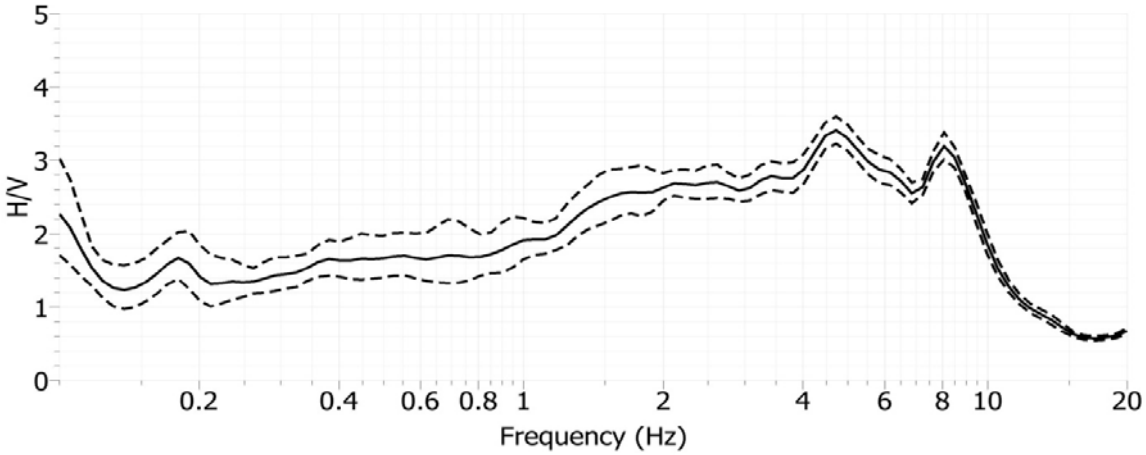

Site CI. JRC2, H/V Spectral Ratio, Array JRC2-1, Sensor 507

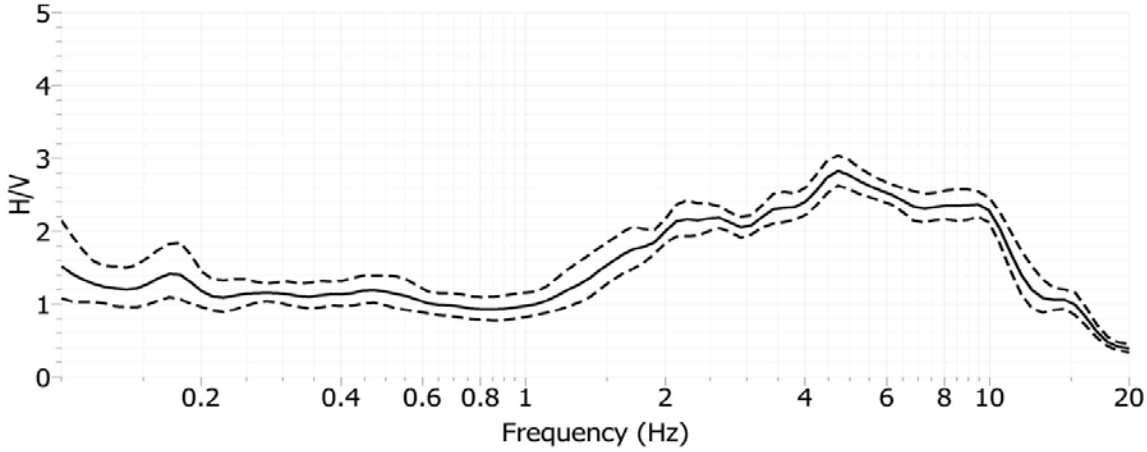

Site CI. JRC2, H/V Spectral Ratio, Array JRC2-1, Sensor 453

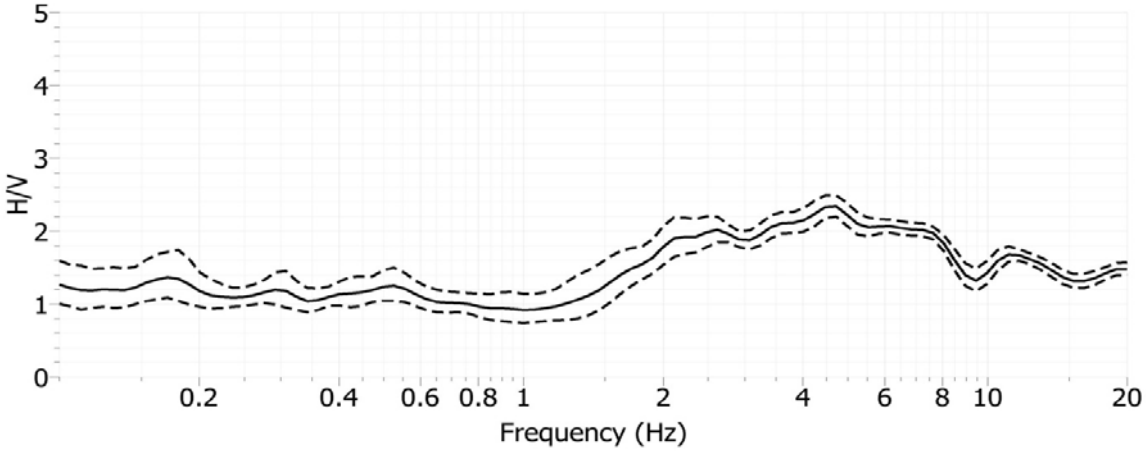

Site CI.JRC2, H/V Spectral Ratio, Array JRC2-1, Sensor 450

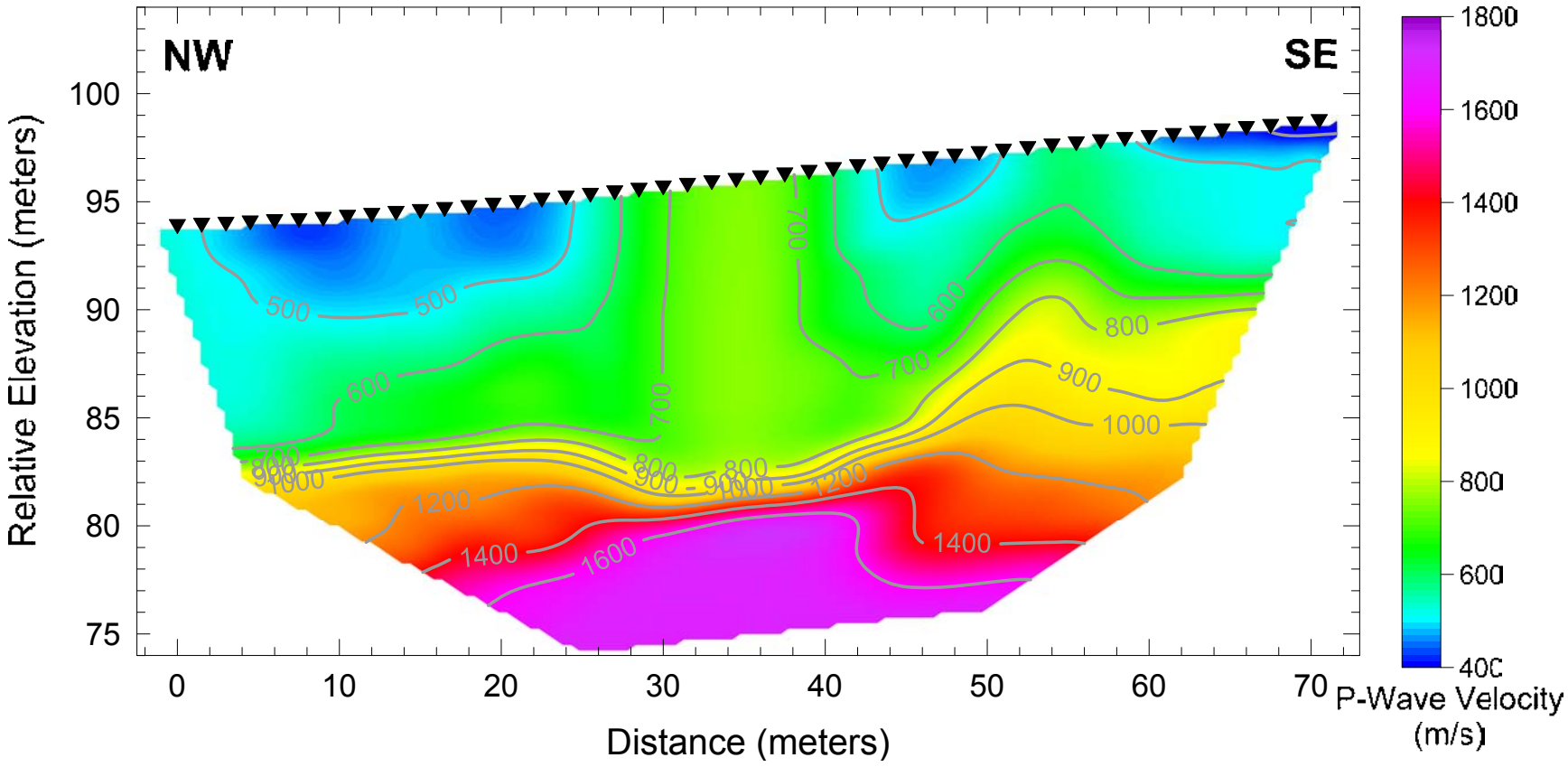

Array JRC2-1 – P-wave Tomographic Seismic Refraction Model utilizing Layer Based Starting Model

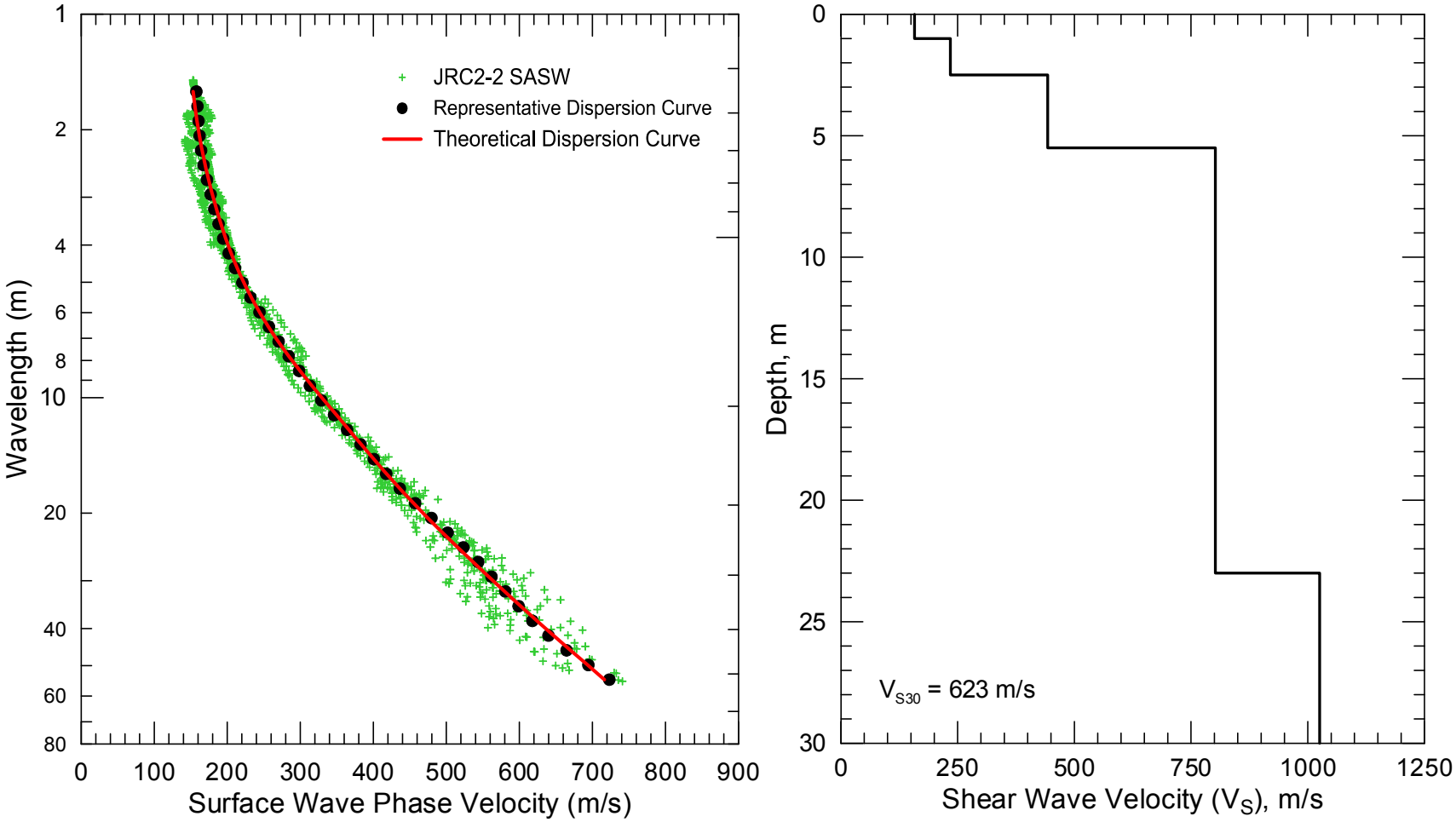

CI.JRC2 - Field, representative and inverted theoretical surface wave dispersion data (left) and associated V_S model (right)

Site CI.JVA

Location: Mojave Water Agency Facility, near intersection of Pony Road and Datura Terrace, Johnson Valley, California

Latitude: 34.36622 **Longitude:** -116.61266
(Could not survey station location because no access to gated compound. Station is very close to provided coordinates, WGS84 coordinate system.)

V_{S30} (measured): 383 m/s

V_{S30} (adjusted to more accurately reflect seismic station conditions): 417 m/s (average S-wave velocity between 2 and 32 m adjusting for assumed sensor depth).

NEHRP Site Class: C

Geomatrix Code: IHD

Geologic Conditions/Observations: Site located on geologic unit mapped as Quaternary (Holocene) young alluvial fan deposits. Small bedrock outcrop located about 500 m south to southeast of site. Bedrock depth is unclear at the site, but is greater than 45 m based on limited seismic refraction/reflection data and could be on the order of 100 m based on HVSR data.

Site Conditions: Rural site with sporadic traffic on nearby Highway 247 (Old Woman Springs Road) located about 400 m north of site. Relatively flat terrain in site vicinity with ground surface elevation gently decreasing to north.

Geophysical Methods Utilized: HVSR, MASW, SASW

Geophysical Testing Arrays:

1. Array JVA-1 (48 channel MASW array utilizing 4.5 Hz vertical geophones spaced 1.5 m apart for a length of 70.5 m, forward and reverse shot locations with multiple source offsets and source types and center shot location).
2. Array JVA-1 (SASW array with common midpoint and orientation as MASW array of same name utilizing 4.5 and 1 Hz vertical geophones and maximum receiver spacing of 32 m).
3. Three HVSR measurement locations distributed along array JVA-1.

Legend

- Seismic Station - Approximate Location of Record
- H/V Spectral Ratio Measurement Location
- MASW and SASW Array

NOTES:
1. WGS 1984 COORDINATE SYSTEM
2. Image Source: ESRI, i-cubed, USDA FSA, USGS, AEX, GeoEye, Getmapping, Aerogrid, IGP

File Name: CI-JVA-I

Date: 4/1/2011

USGS science for a changing world

GEOVision geophysical services

RECOVERY.GOV

SITE MAP
CI•JVA

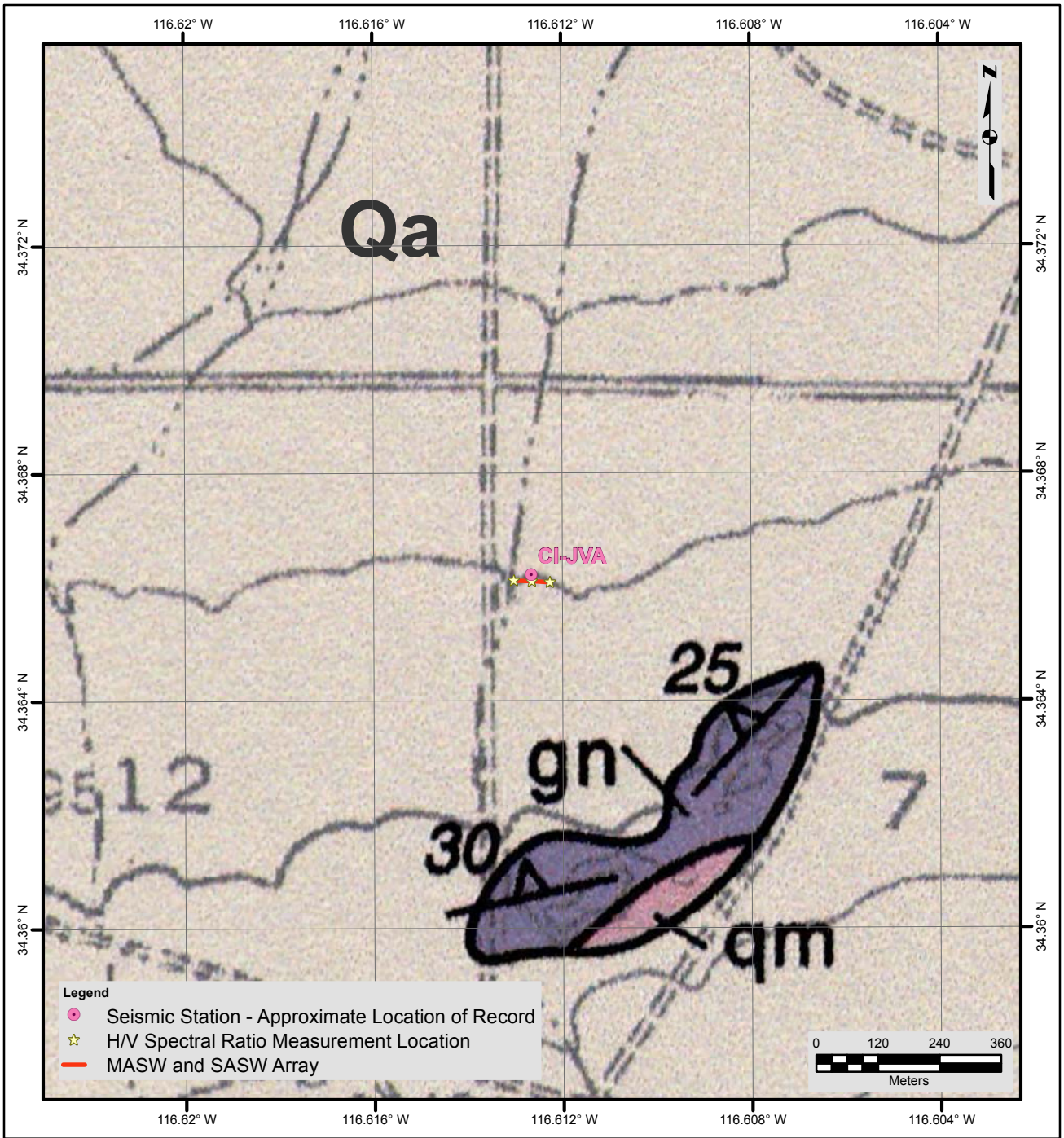

Description of Geologic Map Units

Qa = Quaternary (Holocene) alluvial silt, sand and gravel of valley areas and floodplains of canyons
qm = Mesozoic (Late Jurassic to early Cretaceous) quartz monzonite, massive, non-gneissoid, medium- to coarse-grained, porphyritic
gn = Precambrian gneiss, fine to coarse-grained

NOTES:
1. WGS 1984 COORDINATE SYSTEM
2. Geologic Map of the Old Woman Springs & Emerson Lake Quadrangles, San Bernardino County, California by Thomas W. Dibblee, Jr., 2008
3. See site map for details of geophysical survey

File Name: CI-JVA

Date: 7/21/2011

USGS science for a changing world

GEOVision geophysical services

RECOVERY.GOV

GEOLOGIC MAP
CI•JVA

Looking north at HVSR sensor 450 and seismograph station CI.JVA

Looking east along MASW array JVA-1

Looking north at SASW array JVA-1 and seismograph station CI.JVA

SASW data acquisition along array JVA-1

Large hole required to couple HVSR sensors in sandy soils

Location of Geophysical Testing Arrays:

Location	Latitude	Longitude
JVA-1, West End of MASW Array	34.36611	-116.61303
JVA-1, Center of MASW and SASW Arrays	34.36610	-116.61265
JVA-1, East End of MASW Array	34.36608	-116.61227
HVSR Sensor 507	34.36611	-116.61303
HVSR Sensor 453	34.36609	-116.61226
HVSR Sensor 450	34.36610	-116.61265

Notes: 1) WGS84 Coordinate System (decimal degrees)
2) Survey accuracy is estimated at 1 to 2 m.

Results:

V_S Model

Depth to Top of Layer (m)	Layer Thickness (m)	S-Wave Velocity (m/s)	Inferred P-Wave Velocity (m/s)	Assumed Poisson's Ratio	Assumed Density (g/cm^3)
0	1	159	297	0.3	1.70
1	2	230	430	0.3	1.75
3	3	324	606	0.3	1.80
6	4	422	790	0.3	1.85
10	5	432	809	0.3	1.85
15	8	441	825	0.3	1.90
23	9	470	879	0.3	1.90
32	>8	572	1069	0.3	2.00

Notes: 1) Depth of investigation is about 40 m.
2) Bottom layer is a half space.

Observations/Discussion:

- HVSR plots are similar at all measurement locations, validating the 1-D velocity structure assumption.
- HVSR peak at 1.5 to 1.6 Hz, which could be indicative of intermediate depth bedrock (e.g. 100 to 150 m).
- Noise conditions at site were not sufficient to apply passive surface wave techniques.
- Surface wave dispersion data from SASW and MASW datasets are in reasonable agreement at the site. However, SASW dispersion data are complicated by dominant higher modes and were not used for data modeling.

- Dominant higher mode in the 30 to 55 Hz range in MASW data but no conclusive high velocity layer in surface wave or seismic refraction data. It was, however, possible to pick the probable fundamental mode over this frequency range using limited offset receiver gathers. Both 1st and 2nd higher modes appear clear in wavefield transform image and were picked, but not used for modeling. MASW data were modeled using the fundamental mode assumption although multi-mode inversion may be worthwhile at this site.
- The maximum wavelength extracted from a specific receiver gather was generally set to the lesser of 81 m or 1.25 times the distance from the source to midpoint of receiver gather. This is slightly more aggressive than the Yoon and Rix (2009) near field criteria.
- The minimum wavelength surface wave phase velocity data extracted from the 48-channel MASW array is about 12 m. Data reduction using seismic records from smaller hammer sources and a limited offset receiver array (i.e. less active geophones) allowed extraction of surface wave dispersion data to a minimum wavelength of about 1.3 m.
- There is nominally about 50 m/s scatter in the MASW dispersion data likely due, in part, to lateral velocity variation.
- A representative dispersion curve was generated for the MASW data set using a moving average, polynomial curve fitting routine and used for modeling.
- Water table estimated at a depth of greater than 45 m based on possible water table reflector. Assuming the reflector is horizontal, the RMS P-wave velocity of sediments overlying reflector is about 700 to 750 m/s. The 1.5 Hz HVSR peak and velocity structure indicates that the reflector is too shallow to be associated with bedrock.
- Based on simple layer-based analysis of seismic refraction first arrival data, P-wave velocity in the upper 20 m ranges from about 280 m/s at the surface to 750 m/s at a depth of about 18 m. No clear evidence of P-wave velocity exceeding 900 m/s above water table, which is estimated at a depth on the order of 45 m. Inferred P-wave velocities in surface wave model are slightly higher than those outlined above, although a Poisson's ratio slightly lower than the inferred 0.3 could explain the difference.
- A longer seismic refraction line would determine if either groundwater or bedrock is located within 60 m of the surface, but is not pertinent for estimation of shallow S-wave velocity structure.
- Surface wave depth of investigation is about 40 m based on half of maximum wavelength criteria.
- V_{S30} is 383 m/s (NEHRP Site Class C).
- Average S-wave velocity between 2 m (assumed sensor depth) and 32 m is 417 m/s (NEHRP Site Class C).
- The average S-wave velocity of the upper 40 m (V_{S40}) is 414 m/s.
- Using the quarter wavelength approximation, the geologic contact associated with the 1.5 to 1.6 Hz HVSR peak is located at a minimum depth of about 65 m assuming that V_{S40} represents the average V_S of the geologic units overlying the contact. V_S is expected to gradually increase with depth below 40 m and, therefore, the geologic contact associated with the HVSR peak is more likely in the 80 to 100 m depth range.

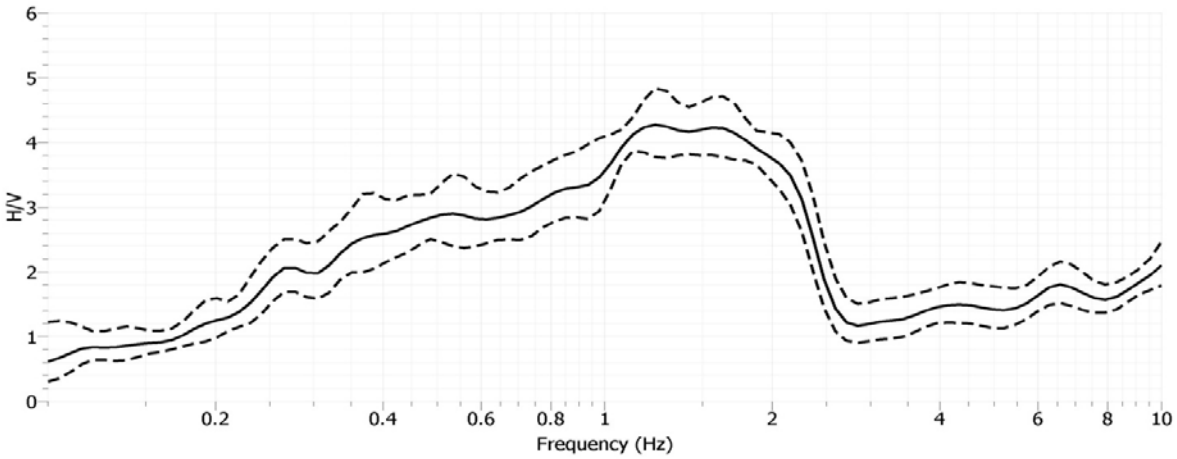

Site CI.JVA, H/V Spectral Ratio, Array JVA-1, Sensor 507

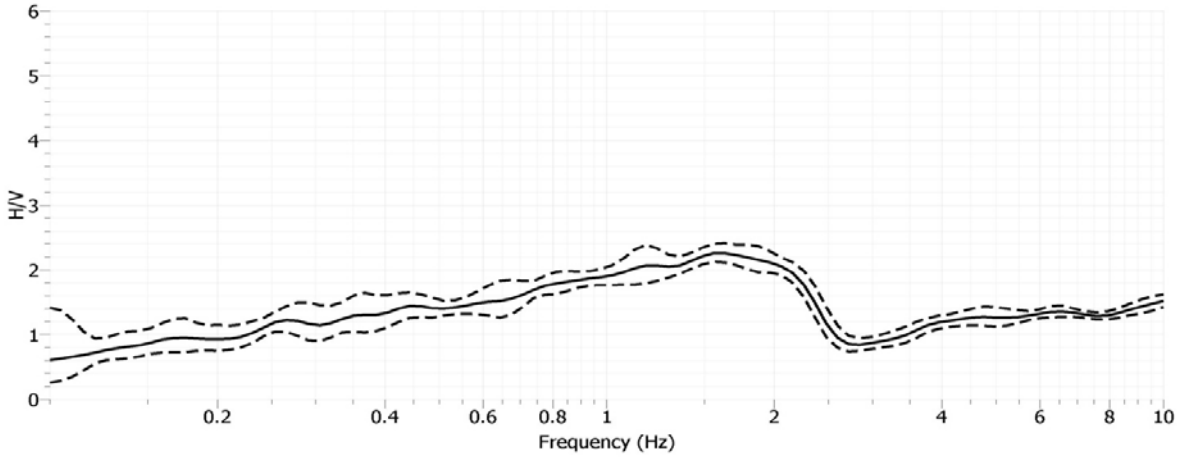

Site CI.JVA, H/V Spectral Ratio, Array JVA-1, Sensor 450

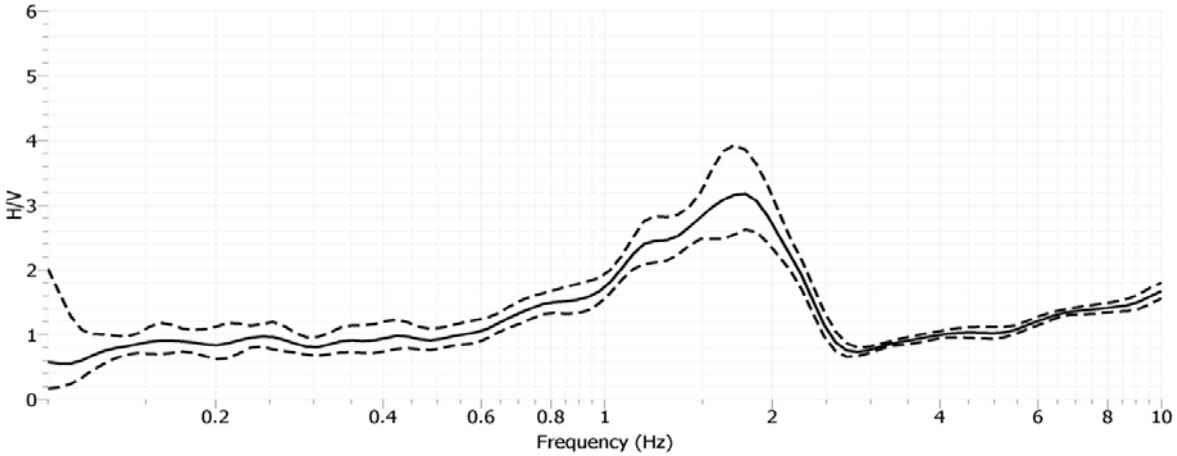

Site CI JVA, H/V Spectral Ratio, Array JVA-1, Sensor 453

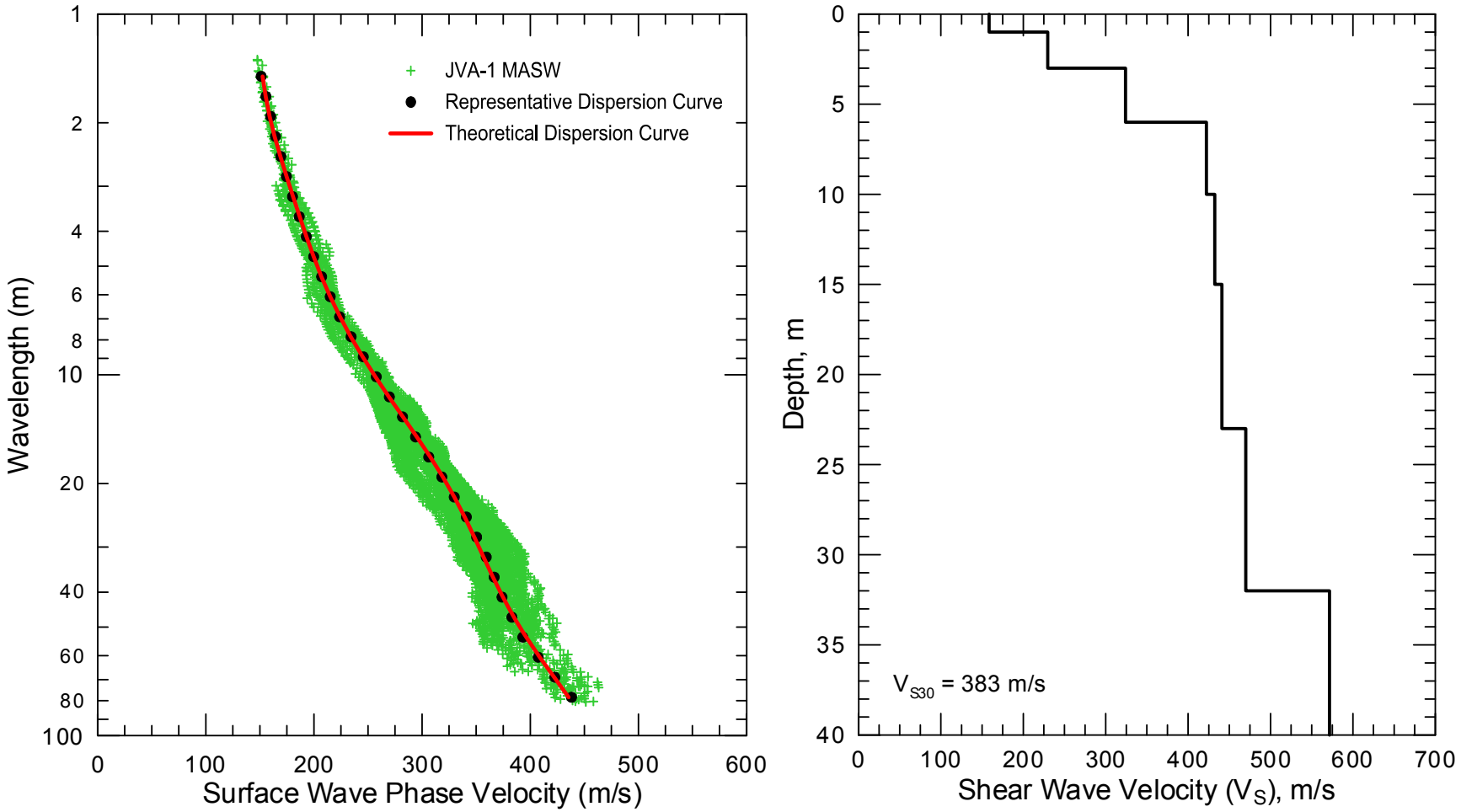

CI.JVA - Field, representative and inverted theoretical surface wave dispersion data (left) and associated V_S model (right)

Site CI.LAF

Location: La Fresa Substation, 17680 Yukon Ave, Torrance, California

Latitude: 33.86889 **Longitude:** -118.33143
(Station coordinates provided by USGS, WGS84 coordinate system)

V_{S30} (measured): 257 m/s

V_{S30} (adjusted to more accurately reflect seismic station conditions): 278 m/s (average S-wave velocity between 2 and 32 m adjusting for assumed 2 m sensor depth).

NEHRP Site Class: D

Geomatrix Code: IHD

Geologic Conditions/Observations: Site located in area mapped as Quaternary (Holocene) loamy alluvial deposits. Expected deep soil site.

Site Conditions: Urban site with significant traffic noise from nearby roads. Relatively flat terrain in site vicinity.

Geophysical Methods Utilized: HVSR, seismic refraction, MASW, array microtremor, ReMi™

Geophysical Testing Arrays:

1. Arrays LAF-1 (24 channel linear array utilizing 4.5 Hz vertical geophones spaced 4.5 m apart for an array length of 103.5 m) and LAF-2 (24 channel linear array utilizing 4.5 Hz vertical geophones spaced 5 m apart for an array length of 115 m) used to acquire passive surface wave data. Arrays combined to form an "L" shaped array.
2. Array LAF-3 (48 channel MASW and seismic refraction array utilizing 4.5 Hz vertical geophones spaced 1 m apart for a length of 47 m, forward and reverse shot locations with multiple source offsets and source types and three interior shot locations).
3. Three HVSR measurement locations distributed along arrays LAF-1 to LAF-3.

Legend

- Seismic Station - Approximate Surveyed Location
- Seismic Station - Approximate Location of Record
- H/V Spectral Ratio Location
- MASW and Seismic Refraction Array
- Passive Surface Wave Array

NOTES:
1. WGS 1984 COORDINATE SYSTEM
2. Image Source: ESRI, i-cubed, USDA FSA, USGS, AEX, GeoEye, Getmapping, Aerogrid, IGP

File Name: CI-LAF-I

Date: 2/7/2013

USGS science for a changing world

GEOVision geophysical services

RECOVERY.GOV

SITE MAP
CI•LAF

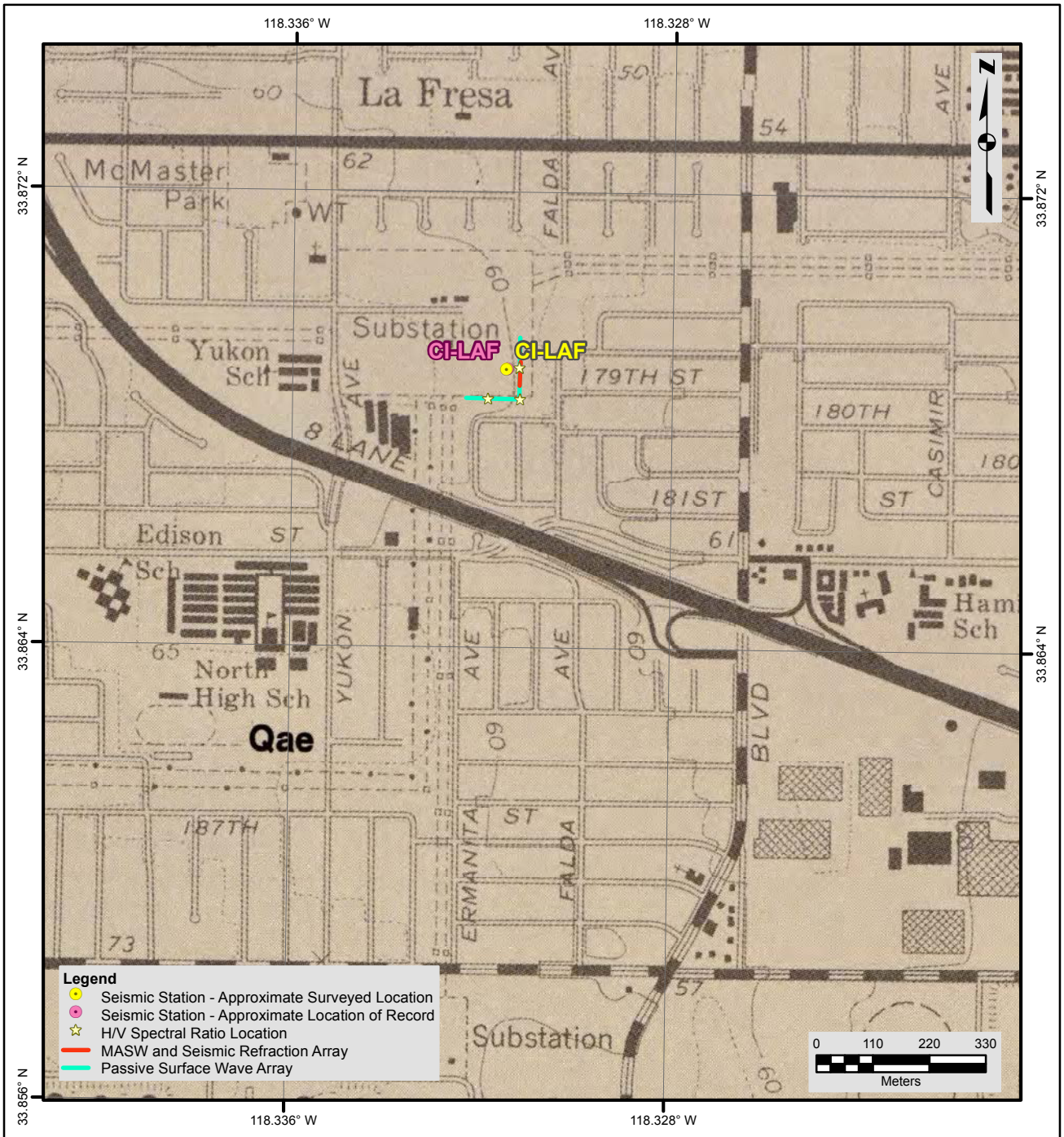

Description of Geologic Map Units

Qae = Quaternary (Holocene) alluvium, mostly loamy clay of valleys and flood plains, slightly elevated and locally dissected

NOTES:
1. WGS 1984 COORDINATE SYSTEM
2. Geologic Map of the Palos Verdes Peninsula and Vicinity, Redondo Beach, Torrance, and San Pedro Quadrangles, Los Angeles County, California by Thomas W. Dibblee, Jr., 1999
3. See site map for details of geophysical survey

File Name: CI-LAF

Date: 2/7/2013

USGS science for a changing world

GEOVision geophysical services

GEOLOGIC MAP
CI•LAF

RECOVERY.GOV

CI.LAF seismic station

Looking south along MASW array LAF-3 towards accelerated weight drop (AWD) energy source

HVSR sensor 453

Looking west along passive surface wave array LAF-1 towards HVSR sensor 450

Looking north along MASW array LAF-3

Location of Geophysical Testing Arrays:

Location	Latitude	Longitude
LAF-1, West End of Passive Array	33.86838	-118.33230
LAF-1, East End of Passive Array	33.86836	-118.33117
LAF-2, South End of Passive Array	33.86842	-118.33118
LAF-2, North End of Passive Array	33.86944	-118.33117
LAF-3, South End of MASW Array	33.86860	-118.33117
LAF-3, Center of MASW Array	33.86880	-118.33117
LAF-3, North End of MASW Array	33.86902	-118.33116
HVSR Sensor 450	33.86837	-118.33183
HVSR Sensor 453	33.86836	-118.33116
HVSR Sensor 507	33.86891	-118.33118
CI.LAF Seismic Station	33.86888	-118.33145

Notes: 1) WGS84 Coordinate System (decimal degrees)
2) Survey accuracy is estimated at 1 to 2 m

Results:

V_S Model

Depth to Top of Layer (m)	Layer Thickness (m)	S-Wave Velocity (m/s)	Inferred P-Wave Velocity (m/s)	Assumed Poisson's Ratio	Assumed Density (g/cm^3)
0	1	121	226	0.300	1.6
1	2	159	298	0.300	1.6
3	2	250	468	0.300	1.7
5	2	348	652	0.300	1.8
7	4	172	322	0.300	1.7
11	9	317	593	0.300	1.8
20	10	329	1750	0.482	1.9
30	12	345	1750	0.480	1.9
42	15	423	1750	0.469	2.0
57	20	500	1750	0.455	2.0
77	>13	596	1750	0.434	2.1

Notes: 1) Saturated zone, with assumed V_P of 1,750 m/s, constrained at a depth of about 20 m based on observation of possible seismic reflection from water table.
2) Depth of investigation is about 90 m.
2) Bottom layer is a half space.

Observations/Discussion:

- The HVSR curves are almost identical at frequencies below 10 Hz, validating the 1-D velocity structure assumption. There are, however, no significant high frequency HVSR peaks by which to characterize shallow velocity structure.
- High amplitude HVSR peak at 0.15 Hz, which is consistent for a very deep sedimentary basin.
- Noise conditions at site (multi-directional or omni-directional noise sources) appeared sufficient for successful application of passive surface wave techniques.
- ESAC technique used to extract surface wave dispersion data from passive "L" array data. Both the ReMi™ and ESAC techniques used to extract surface wave dispersion data from the linear arrays. Only the higher quality "L" array dispersion data and linear array LAF-2, oriented almost perpendicular to I-405, were used for analysis.
- A dominant higher mode(s) was identified over the 8 to 18 Hz frequency range in both the active and passive surface wave data. The fundamental mode could not be accurately identified in the MASW data over the 10 to 18 Hz frequency range; however, an attempt was made to pick the fundamental mode over this frequency range. Most of the higher mode surface wave energy in the MASW data was indentified while analyzing seismic records with source locations at the south end of the array. Picking of higher mode energy was much more complicated from seismic records with source locations at the north end of the array. The differences in higher modes between source locations at each end of the array may indicate that near surface velocity structure is not 1-D in nature. Dominant higher modes are also an issue at intermediate frequencies in the passive surface wave data and the fundamental mode could only be identified at frequencies below 8 Hz.
- A dominant higher mode at intermediate frequencies is often indicative of a high velocity layer.
- Fundamental mode surface wave dispersion data from active and passive surface wave data sets are in acceptable agreement although the two data sets only overlap over a very small wavelength range. Higher mode surface wave identified in the various data sets are, however, different due to inherent differences between the methods and/or lateral velocity variation.
- Representative dispersion curves were generated for each surface wave data set using a moving average, polynomial curve fitting routine. These individual representative dispersion curves were combined and a representative dispersion curve generated for the combined data set for modeling purposes.
- Water table located at a depth on the order of 20 m based on interactive fitting to a reflector assumed to be associated with the top of the saturated zone. P-wave velocity of the saturated zone is assumed to be 1,750 m/s.
- A V_S model was developed from the surface wave data set using the fundamental mode assumption, although the fundamental mode may not have been accurately indentified between a frequency of 10 and 18 Hz. A thin high velocity layer at a depth of about 5 m was required to fit the dispersion curve. The thickness and velocity of this layer and the underlying low velocity layer are not well resolved and there are likely significant equivalence issues with these layers; however, the average velocity structure over the depth interval associated with these layers probably adequately resolved. A layer-based

seismic refraction model for array LAF-3 confirms that there is a layer with V_P of about 785 m/s (V_S on the order of 400 m/s) at a depth as shallow as 5 m. The surface wave dispersion data and interactive fitting of a possible reflector at about 20 m depth both require that seismic velocity decrease below this layer.

- To date we have not been successful at implementing multi-mode modeling of the surface wave dispersion data collected at this site. First, the higher modes are different on the multiple surface wave data sets with the passive surface wave data generating a higher mode associated with either the 1st or 2nd higher modes and the MASW data generating a higher mode that may jump across multiple modes. Secondly, the fundamental mode should have dominant energy over the 8 to 18 Hz range for the V_S model developed and we have yet to define velocity structure that both fits the fundamental mode data and excites dominant higher modes at intermediate frequencies. The higher mode surface wave energy may be sensitive to minor 2-D variations in velocity structure. Additionally, changes to assumed Poisson's ratio and depth/thickness of the high velocity layer may have a significant impact on higher mode energy. Although, we have yet to successfully develop a multi-mode V_S model, an argument can be made that the fundamental mode V_S model is consistent with the observed higher modes and average velocity structure is likely reasonably well characterized.
- Surface wave depth of investigation is about 90 m based on half of maximum wavelength criteria and assuming that surface wave dispersion data at frequencies as low as 2.5 Hz are valid utilizing 4.5 Hz geophones (low frequency geophone phase response differences will cancel out if noise is omni-directional and/or the phase response differences are random in nature).
- V_{S30} is 257 m/s (NEHRP Site Class D).
- The average V_S between 2 and 32 m, to account for assumed seismic sensor depth, is 278 m/s (NEHRP Site Class D)
- Average S-wave velocity of the upper 90 m (V_{S90}) is 402 m/s.

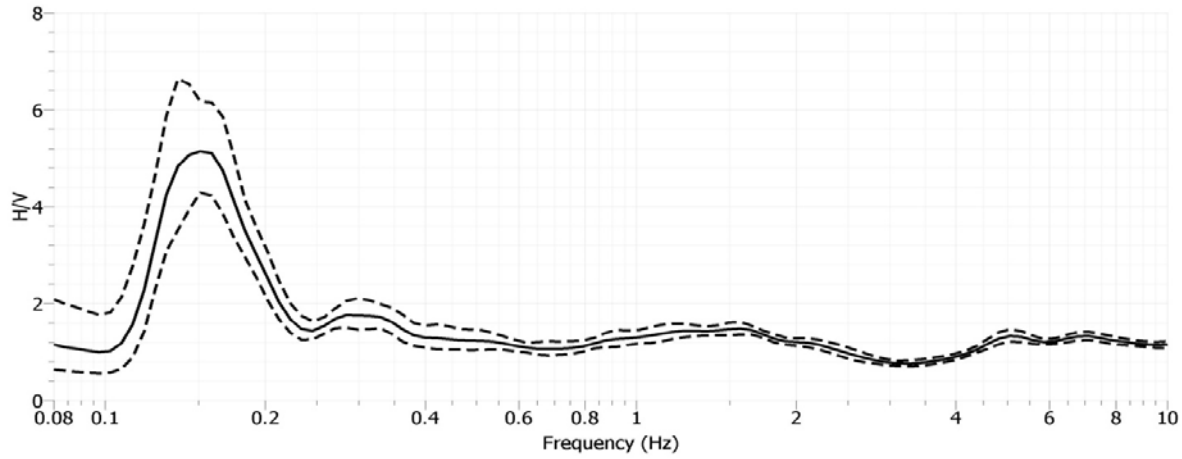

Site CI.LAF, H/V Spectral Ratio, Array LAF-1, Sensor 450

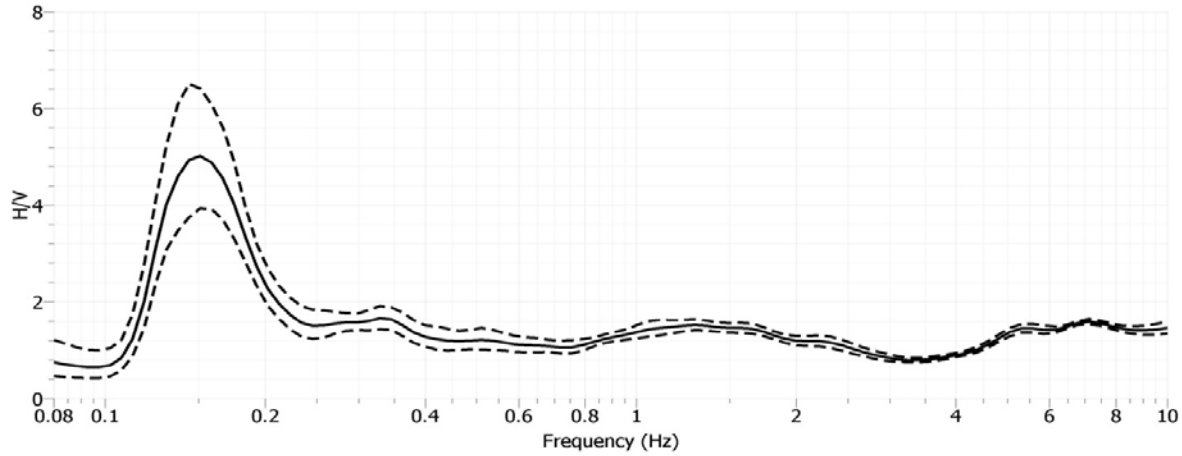

Site CI.LAF, H/V Spectral Ratio, Array LAF-1&2, Sensor 453

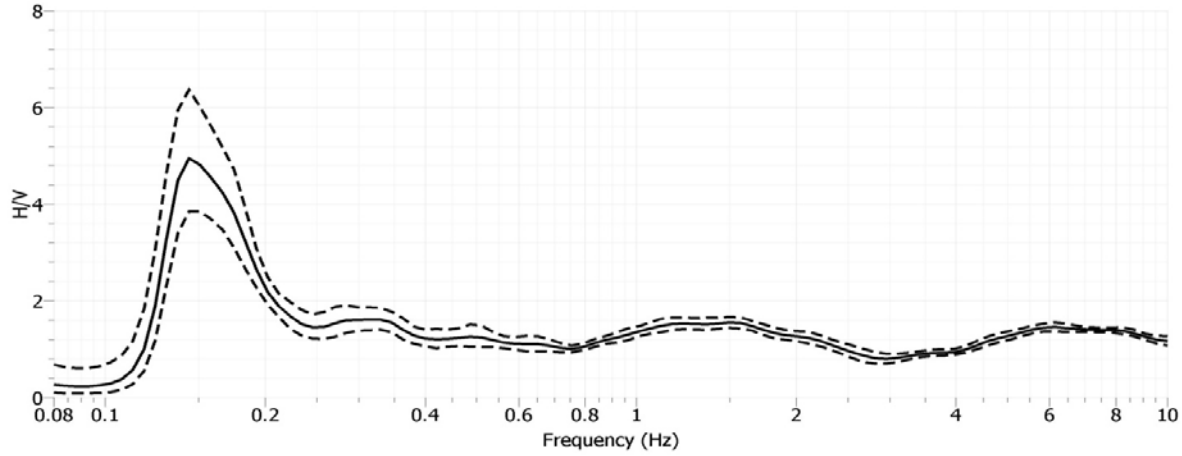

Site CI.LAF, H/V Spectral Ratio, Array LAF-2&3, Sensor 507

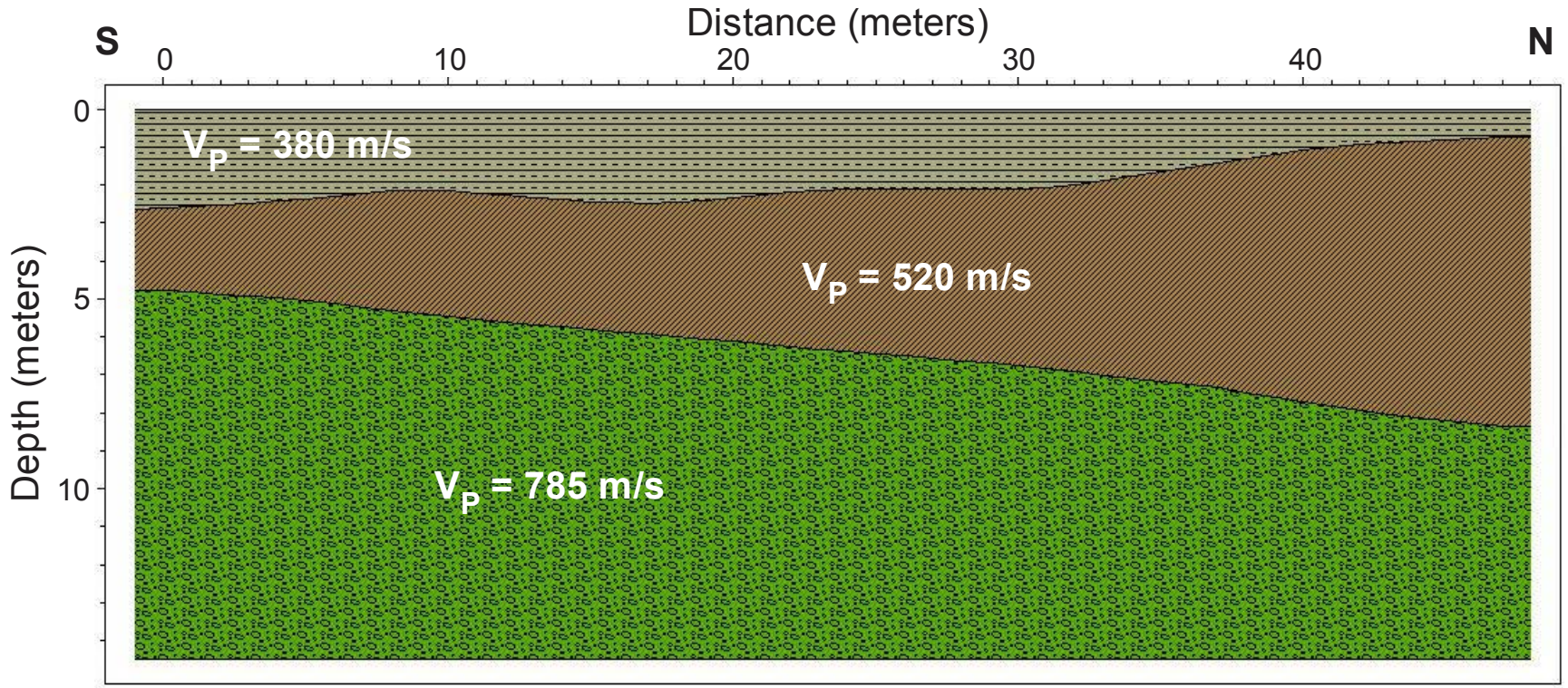

Array LAF-3 – Seismic refraction model developed using the generalized reciprocal method (GRM). The surface wave data indicates that the layer at a depth of 5 to 7 m with V_P = 785 m/s may be a high velocity layer with sufficient thickness to transmit a head wave over a distance of more than 50 m. The seismic refraction model indicates that the possible high velocity layer may be deepening to the north although velocity structure in the fill and near surface sediments may be more complex than depicted by the seismic refraction model.

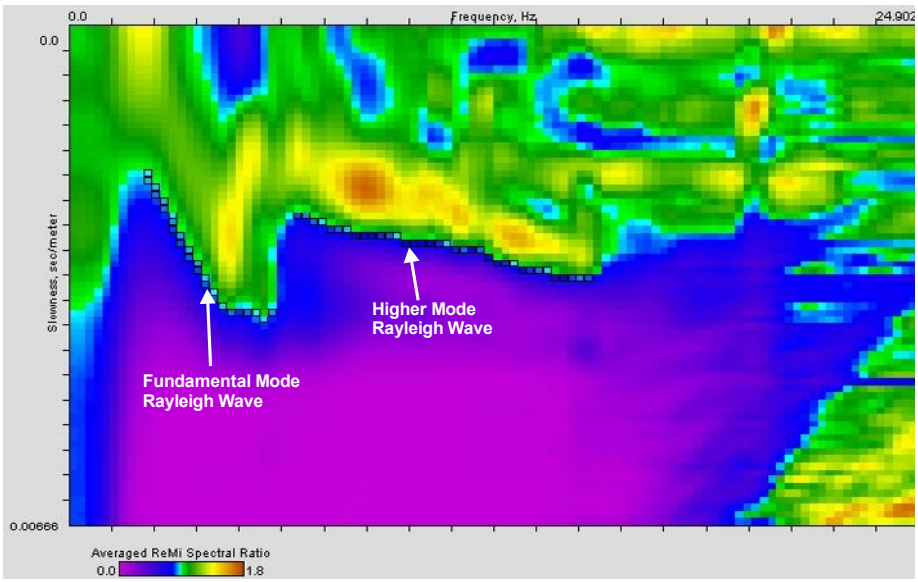

Analysis of passive surface wave data acquired along linear array LAF-2 using the ReMi™ technique. Note the dominant higher mode energy at frequencies greater than about 8 Hz.

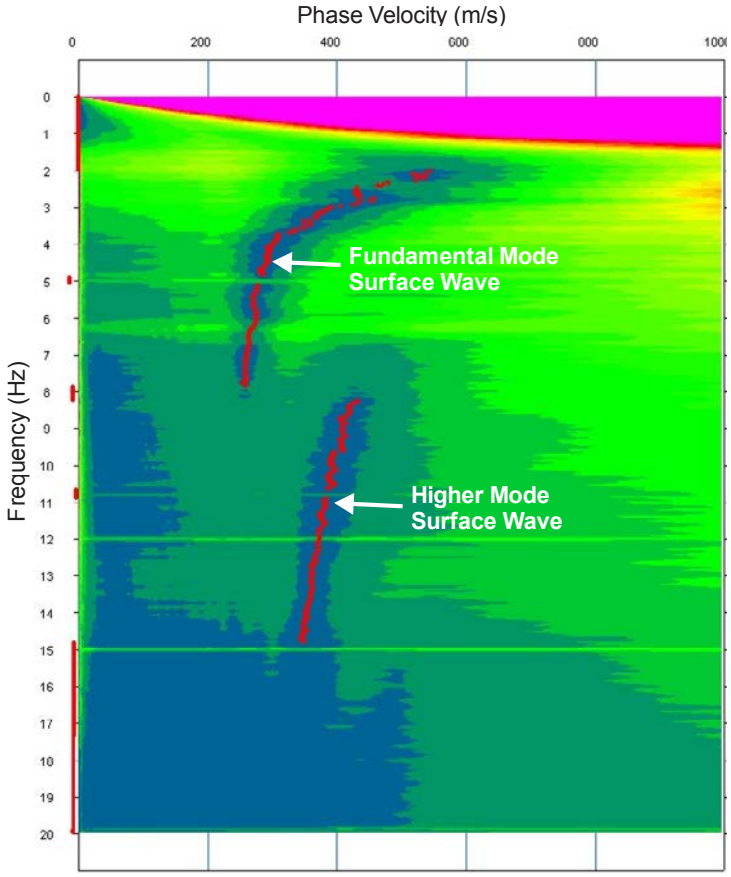

Analysis of passive surface wave data acquired along “L” array LAF-1/2 using the ESAC technique. Note the dominant higher mode energy at frequencies greater than about 8 Hz.

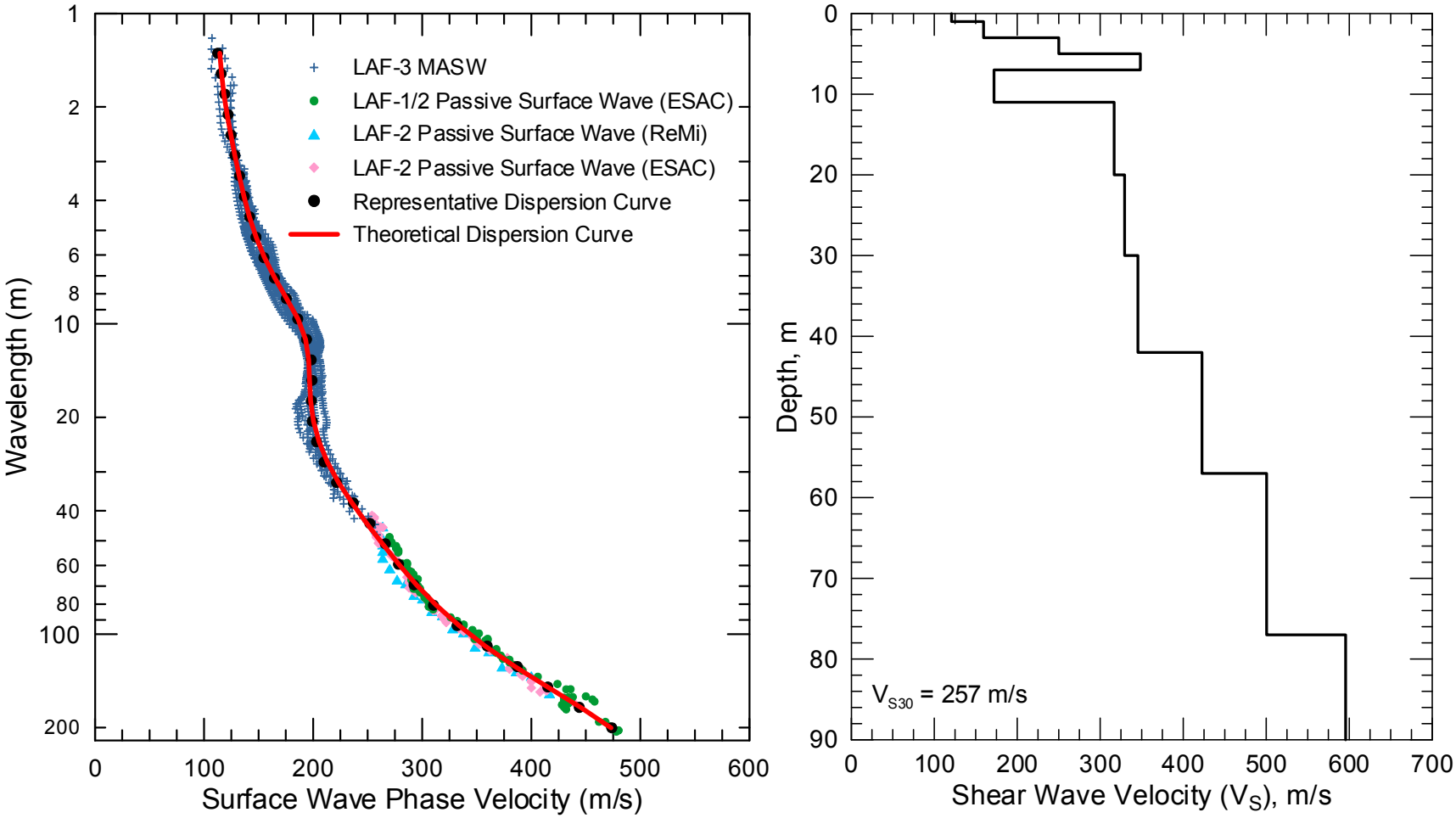

CI.LAF - Field, representative and inverted theoretical surface wave dispersion data (left) and associated V_S model (right)

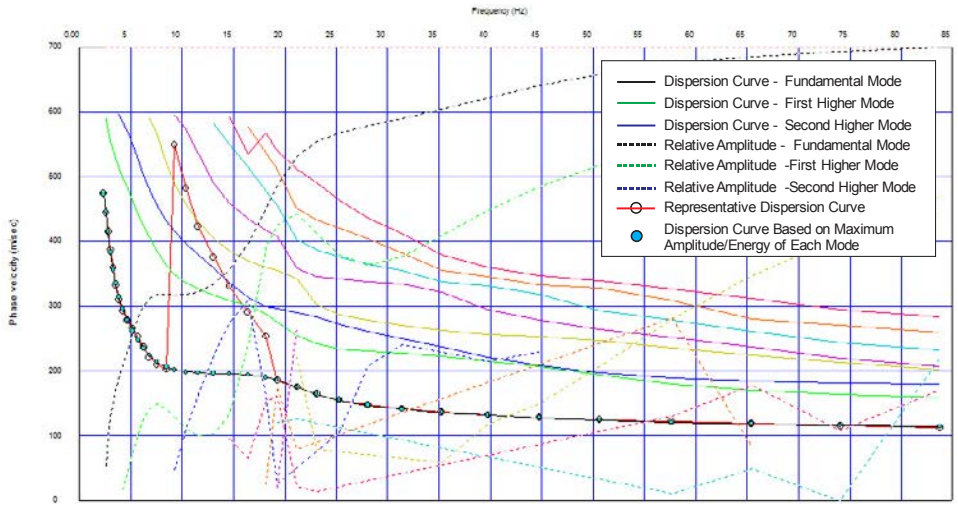

Calculated Rayleigh wave phase velocity modes for fundamental mode for V_S Model. The higher mode segment of the representative dispersion curve is from the MASW data (Array LAF-3). The higher mode(s) in the MASW data appear to jump from the 1st to 3rd higher modes. Both the first and second higher modes have significant energy over the 10 to 25 Hz range; however, for this V_S model the fundamental mode should be dominant at all frequencies (plane wave assumption and 1-D velocity structure). The higher modes are dominant over the 10 to 18 Hz frequency range in the field data and the fundamental mode could not be conclusively/accurately identified over this frequency range.

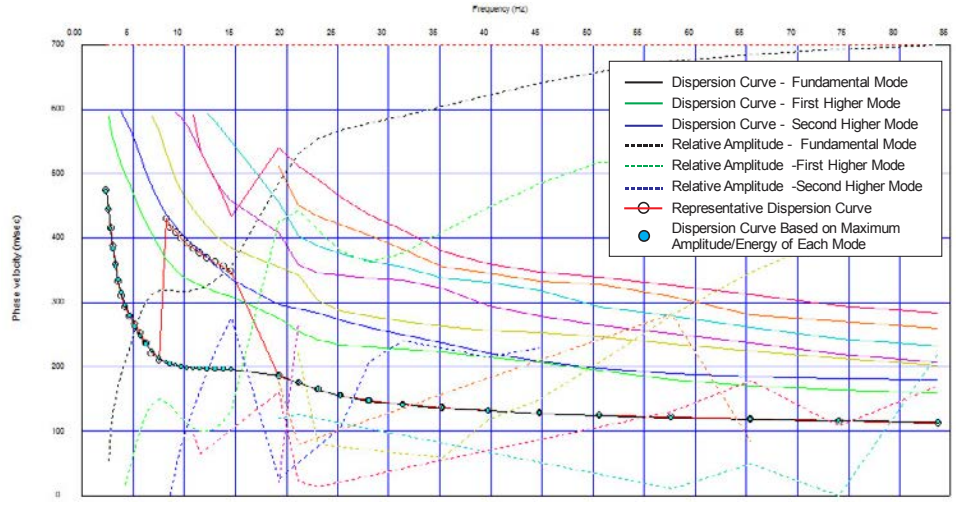

Calculated Rayleigh wave phase velocity modes for fundamental mode for V_S Model. The higher mode segment of the representative dispersion curve is from the passive "L" array data (Array LAF-1/2). The higher mode in the passive surface data appear to track the 2nd higher mode. Both the first and second higher modes have significant energy over the 10 to 25 Hz range; however, for this V_S model the fundamental mode should be dominant at all frequencies (plane wave assumption and 1-D velocity structure). The higher modes are dominant over the 8 to 15 Hz frequency range in the field data and the fundamental mode could not be identified over this frequency range.

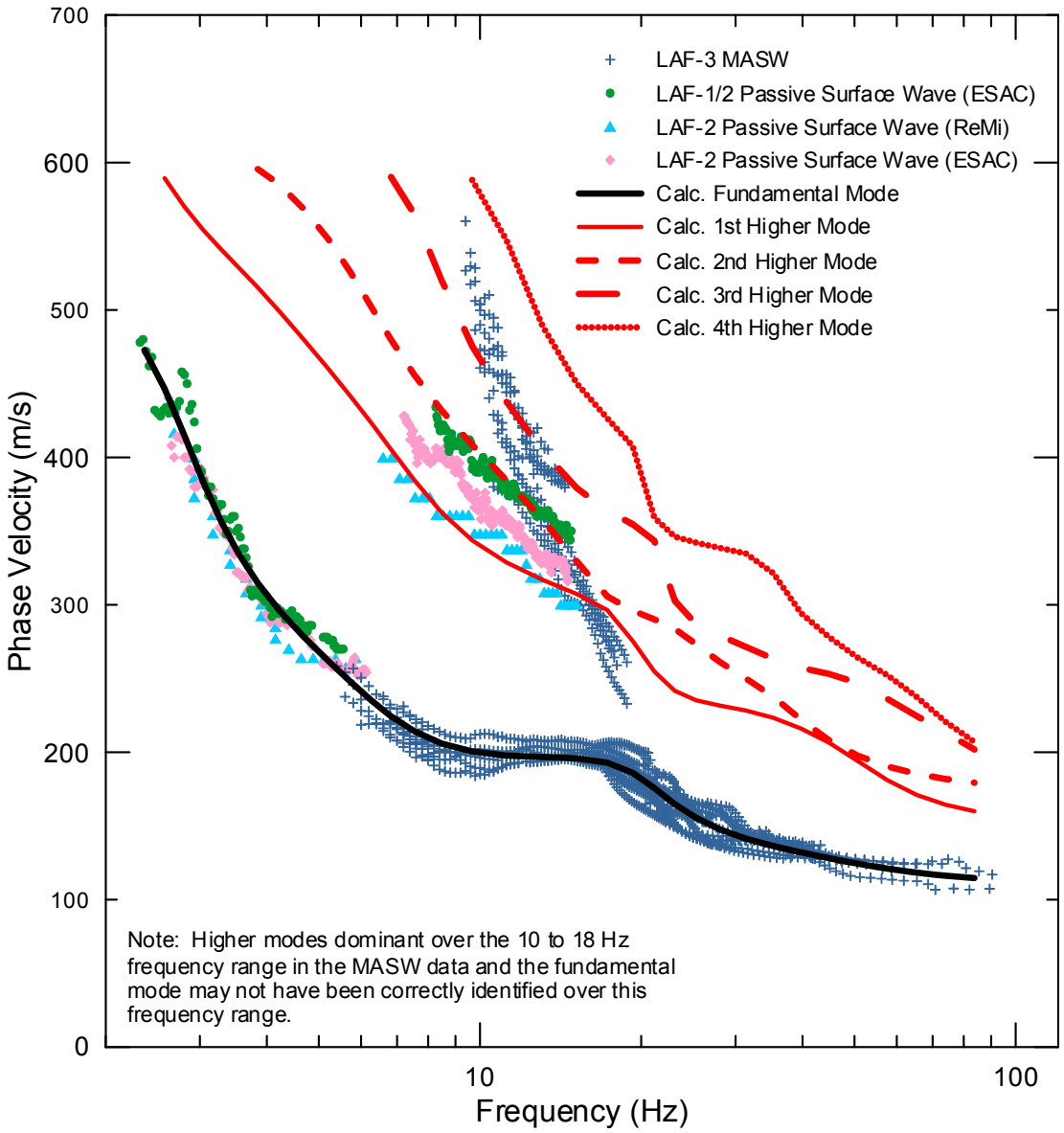

Fundamental mode and higher mode surface wave dispersion data extracted from the MASW and passive surface wave data sets. The higher mode surface wave data extracted from linear passive surface wave array LAF-2 using both the ESAC and ReMi techniques and from the passive "L" array LAF-1/2 using the ESAC technique track either the first and/or second higher modes. The higher mode surface wave data extracted from MASW array LAF-3 appears to jump from the first to third higher modes. The fundamental mode was not clear in the MASW data over the 10 to 18 Hz range (i.e. higher modes always had the most energy) and may have not been correctly interpreted over this frequency range. Multi-mode modeling has not been successfully implemented at this time because the higher modes are slightly different in the various surface wave data sets and we have yet to identify a velocity structure that would excite dominant first and second higher modes over the 8 to 18 Hz frequency range. Even a small degree of lateral velocity variation and variable thickness and/or depth of the high velocity layer would significantly complicate modeling.

Site CI.LCP

Location: Los Alamos County Park, 50 Drum Canyon Road, Los Alamos, California

Latitude: 34.73547 **Longitude:** -120.27984
(Station coordinates modified based on field observation of station location and identification of approximate station location on Google Earth – could not survey the seismic station due to tree cover, WGS84 coordinate system)

V_{S30} (measured): 259 m/s

V_{S30} (adjusted to more accurately reflect seismic station conditions): 267 m/s (average S-wave velocity between 1 and 31 m adjusting for 1 m assumed sensor depth).

NEHRP Site Class: D

Geomatrix Code: IHD

Geologic Conditions/Observations: Quaternary (Holocene) alluvium overlying Quaternary and Tertiary conglomerate and sandstone units. Quaternary/Tertiary Paso Robles Formation outcrops less than 15 meters to the west and about 75 meters to the east of the seismic station. Bedding within the Paso Robles Formation has near vertical dip.

Site Conditions: Semi-rural site with some noise sources from traffic in site vicinity (county park). Relatively planar terrain in test area with ground elevation gently decreasing to the north and hilly terrain to the east and the west.

Geophysical Methods Utilized: HVSR, seismic refraction, MASW, SASW

Geophysical Testing Arrays:

1. Array LCP-1 (48 channel MASW and seismic refraction array utilizing 4.5 Hz vertical geophones spaced 1.5 m apart for a length of 70.5 m, forward and reverse shot locations with multiple source offsets and source types and multiple interior shot locations).
2. Array LCP-2 (SASW array at a different location than MASW array LCP-1. SASW data acquired using 4.5 and 1 Hz geophones, common source and common center point geometry, forward and reverse shot locations).
3. Three HVSR measurement locations distributed along LCP-1.

Legend

- Seismic Station - Approximate Surveyed Location
- Seismic Station - Approximate Location of Record
- H/V Spectral Ratio Location
- MASW and Refraction Array
- SASW Array

NOTES:
1. WGS 1984 COORDINATE SYSTEM
2. Image Source: ESRI, i-cubed, USDA FSA, USGS, AEX, GeoEye, Getmapping, Aerogrid, IGP

File Name: CI-LCP-I

Date: 8/19/2011

USGS science for a changing world

GEOVision geophysical services

RECOVERY.GOV

SITE MAP
CI•LCP

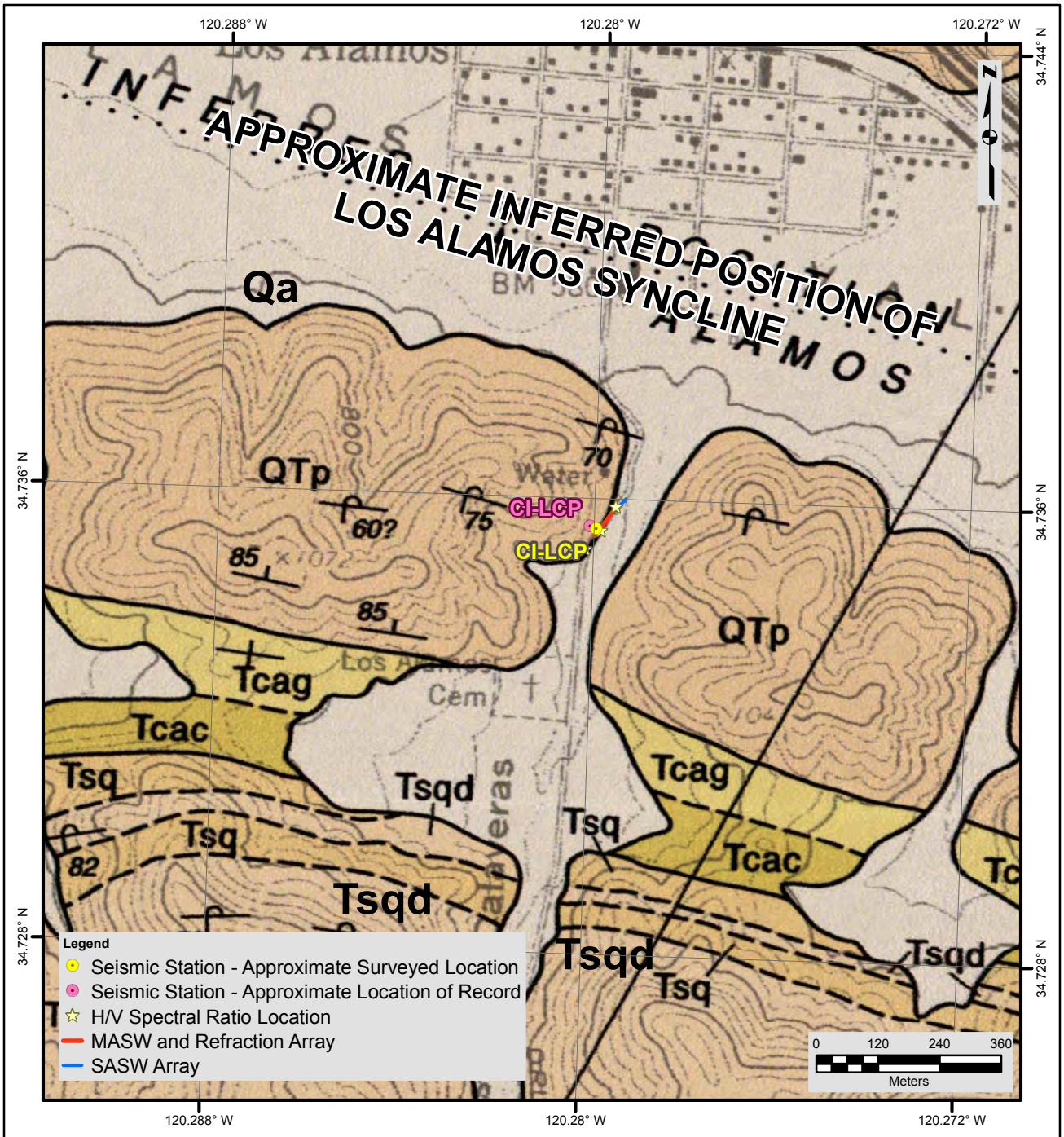

Description of Geologic Map Units

Qa = Quaternary (Holocene) valley, floodplain & stream channel alluvial deposits of gravel, sand & clay
Qtp = Quaternary (Pleistocene) Paso Robles Formation; conglomerate of gravel; siliceous shale pebbles
Tcag = Tertiary (Pliocene) Careaga Sandstone; Graciosa member, soft sandstone or sand
Tcac = Tertiary (Pliocene) Careaga Sandstone; Cebada member, soft fine-grained sandstone or sand
Tsq = Tertiary (Miocene) Sisquoc Formation; soft, slightly diatomaceous claystone
Tsqd = Tertiary (Miocene) Sisquoc Formation; Diatomaceous claystone or shale, semi-siliceous

NOTES:
1. WGS 1984 COORDINATE SYSTEM
2. Geologic Map of the Los Alamos Quadrangle, Santa Barbara County, California by Thomas W. Dibblee, Jr., 1993
3. See site map for details of geophysical survey

File Name: CI-LCP

Date: 8/19/2011

USGS science for a changing world

GEOVision geophysical services

RECOVERY.GOV

GEOLOGIC MAP
CI•LCP

Looking northeast towards HVSR sensor 453 and CI.LCP seismic station

Looking southwest along MASW array LCP-1

Looking southwest along MASW array LCP-1

Looking southwest along SASW array LCP-2 and towards location of seismic sensor CI.LCP

Looking south along SASW array LCP-2

Location of Geophysical Testing Arrays:

Location	Latitude	Longitude
LCP-1, South end of Array	34.73535	-120.27985
LCP-1, Center of Array	34.73560	-120.27964
LCP-1, North end of Array	34.73587	-120.27943
LCP-2, 0 meters, South end of Array	34.73547	-120.27980
LCP-2, 40 meters along Array	34.73573	-120.27952
LCP-2, 60 meters along Array	34.73587	-120.27938
LCP-2, 80 meters, North end of Array	34.73601	-120.27922
HVSR Sensor 450	34.73511	-120.28005
HVSR Sensor 453	34.73545	-120.27973
HVSR Sensor 507	34.73587	-120.27943
CI.LCP Seismic Station	34.73544	-120.27974

Notes: 1) WGS84 Coordinate System (decimal degrees)

2) Survey accuracy is estimated at 3 to 4 m, GPS signal blocked by trees in some areas

Results:

V_S Model – MASW Array LCP-1

Depth to Top of Layer (m)	Layer Thickness (m)	S-Wave Velocity (m/s)	Inferred P-Wave Velocity (m/s)	Inferred Poisson's Ratio	Inferred Density (g/cm^3)
0	1.5	160	320	0.333	1.8
1.5	2.5	175	350	0.333	1.8
4	3	195	389	0.333	1.8
7	5	246	491	0.333	1.8
12	12	259	519	0.333	1.9
24	>11	486	973	0.333	2.0

V_S Model – SASW Array LCP-2

Depth to Top of Layer (m)	Layer Thickness (m)	S-Wave Velocity (m/s)	Inferred P-Wave Velocity (m/s)	Inferred Poisson's Ratio	Inferred Density (g/cm^3)
0	1.5	181	363	0.333	1.8
1.5	2	174	348	0.333	1.8
3.5	4	214	428	0.333	1.8
7.5	5.5	230	460	0.333	1.8
13	11	273	546	0.333	1.9
24	>11	521	1042	0.333	2.0

Observations/Discussion:

- HVSR plots are very similar below a frequency of 8 Hz validating the 1-D velocity assumption.
- There are no significant HVSR peaks at the site.
- Noise conditions at site were not sufficient to apply passive surface wave techniques.
- Because the Paso Robles Formation outcrops less than 15 m from the seismic station, the seismic refraction and MASW array was placed as close to the seismic station as possible and orientated subparallel to the outcrop. The Paso Robles Formation may not be any deeper than 6 to 12 m beneath the seismic array but likely deepens to the east. Ideally, an additional seismic line would have been placed across the narrow valley in an attempt to map the depth to the Paso Robles Formation; however, a road and parking lot in the Los Alamos County Park make this impractical.
- Based on tomographic inversion of the array LCP-1 seismic refraction first arrival data utilizing a layer-based starting model, P-wave velocity in the upper 25 m is about 300 m/s near the surface, then gradually increases with depth to 500 m/s at a depth of about 7 to 10 m and then to 700 m/s at a depth of about 15 m. Below 15 m P-wave velocity relatively abruptly increases to about 1,100 m/s and then may increase again to over 1,400 m/s below a depth of 25 m.
- The interpretation of the seismic refraction model is complicated because the Paso Robles Formation, expected at a depth on the order of 6 to 12 m based on proximity to an outcrop, has near vertical dip. A diffuse boundary between the alluvium and top of the Paso Robles Formation may correspond to the 500 m/s velocity contour in the 7 to 10 m depth range. The 700 to 800 m/s velocity contours at about 15 m depth may correspond to less weathered Paso Robles Formation and the increase in P-wave velocity below a depth of 25 m may correspond to saturated sediments. A longer seismic refraction line may have helped characterize velocity structure and particularly to confirm the presence of the saturated zone.
- The MASW and SASW arrays were not co-located and there was a small difference in the surface wave dispersion data between the two data sets. Therefore, the two data sets were modeled separately.
- For the purpose of data modeling, a moving average, polynomial curve fitting routine was used to generate separate representative dispersion curves for the SASW and MASW data.
- Water table depth may be on the order of 30 m based on the seismic refraction model and, therefore, was not constrained in the surface wave models.
- S-wave velocities are lower than expected between a depth of about 14 and 24 m based on the P-wave seismic refraction model. Perhaps Poisson's ratio is higher than 0.33 in this interval or partial saturation of the sediments is increasing P-wave velocity, although P-wave velocity does not generally begin to rise due to pore water until over 98 % saturation.
- A significant increase is S-wave velocity to about 500 m/s is modeled at 24 m depth in both the MASW and SASW models, deeper than would be anticipated based on the P-wave seismic refraction data. It is unlikely that this is associated with a layer in the Paso Robles Formation due to the near vertical dip of the bedding. It is more likely that the overlying sediments are more weathered.

- Surface wave depth of investigation is about 35 m based on half of maximum wavelength criteria.
- V_{S30} for MASW array LCP-1 is 254 m/s and V_{S30} for SASW array LCP-2 is 263 m/s.
- V_{S30} averages 259 m/s (Site Class D).
- Average S-wave velocity between 1 m (assumed sensor depth) and 31 m is 264 m/s for MASW array LCP-1 and 271 m/s for SASW array LCP-2 and averages 267 m/s.

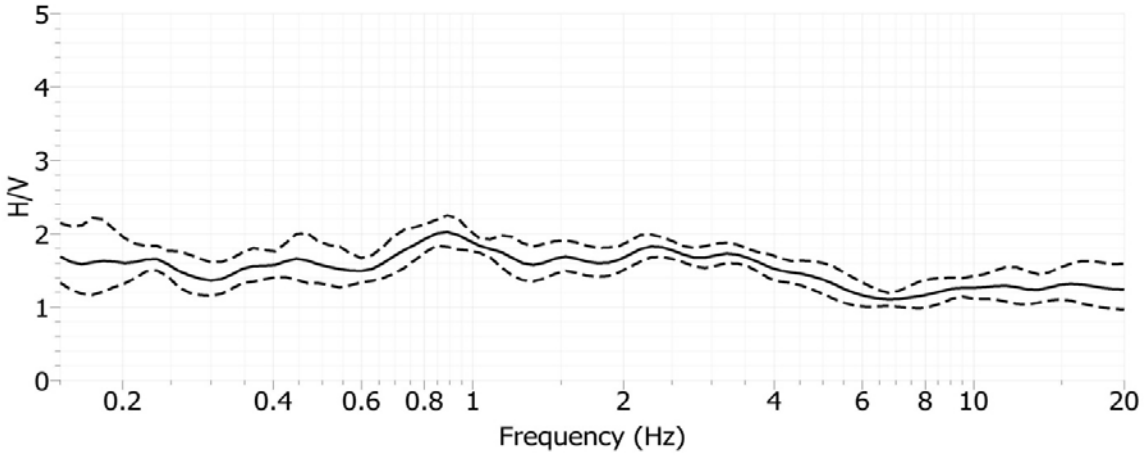

Site CI.LCP, H/V Spectral Ratio, Array LCP -1, Sensor 507

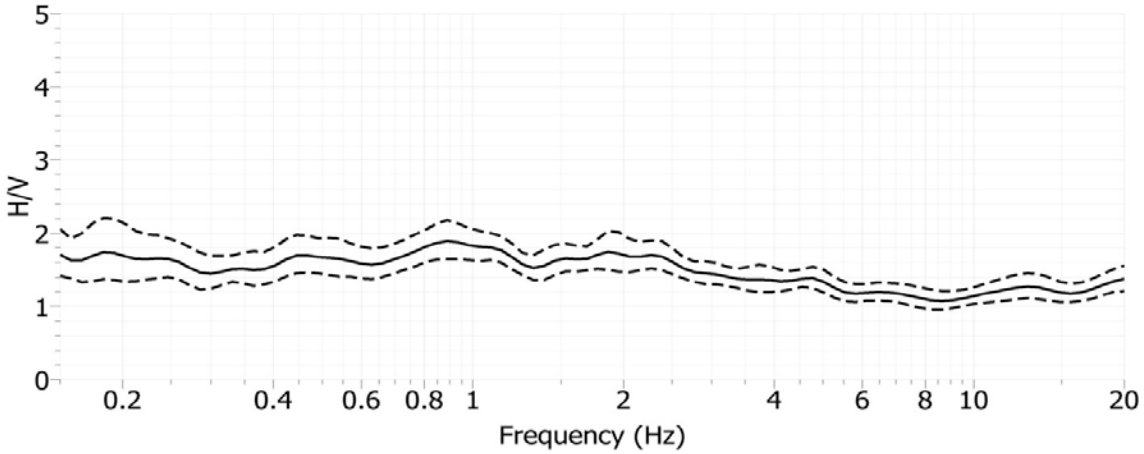

Site CI.LCP, H/V Spectral Ratio, Near Seismic Station, Sensor 453

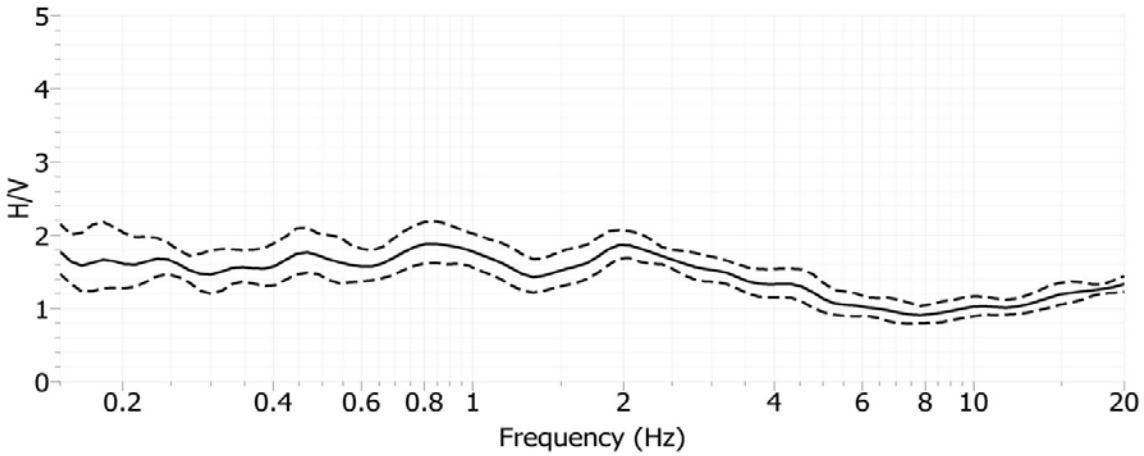

Site CI.LCP, H/V Spectral Ratio, Array LCP -1, Sensor 450

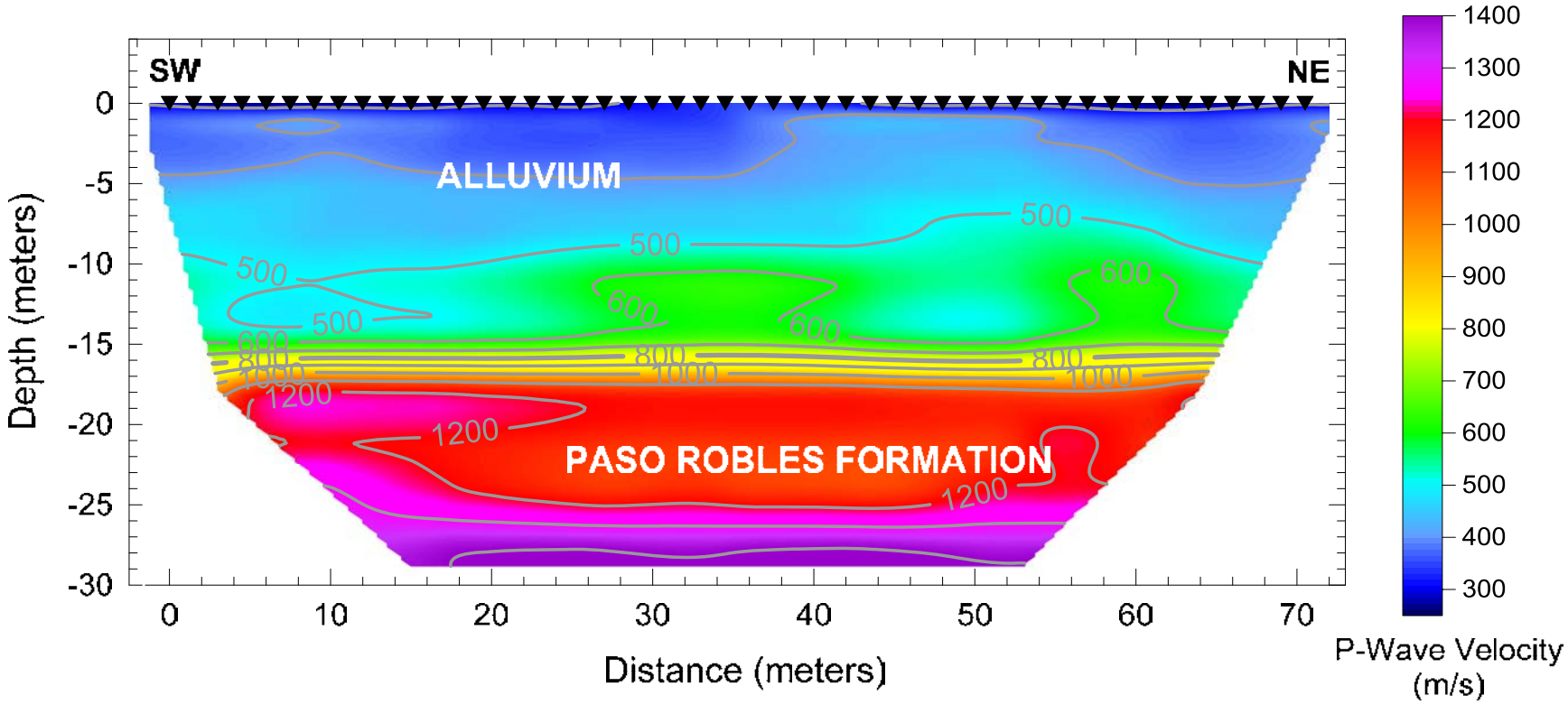

Array LCP-1 – Tomographic Seismic Refraction Model utilizing Layer Based Starting Model

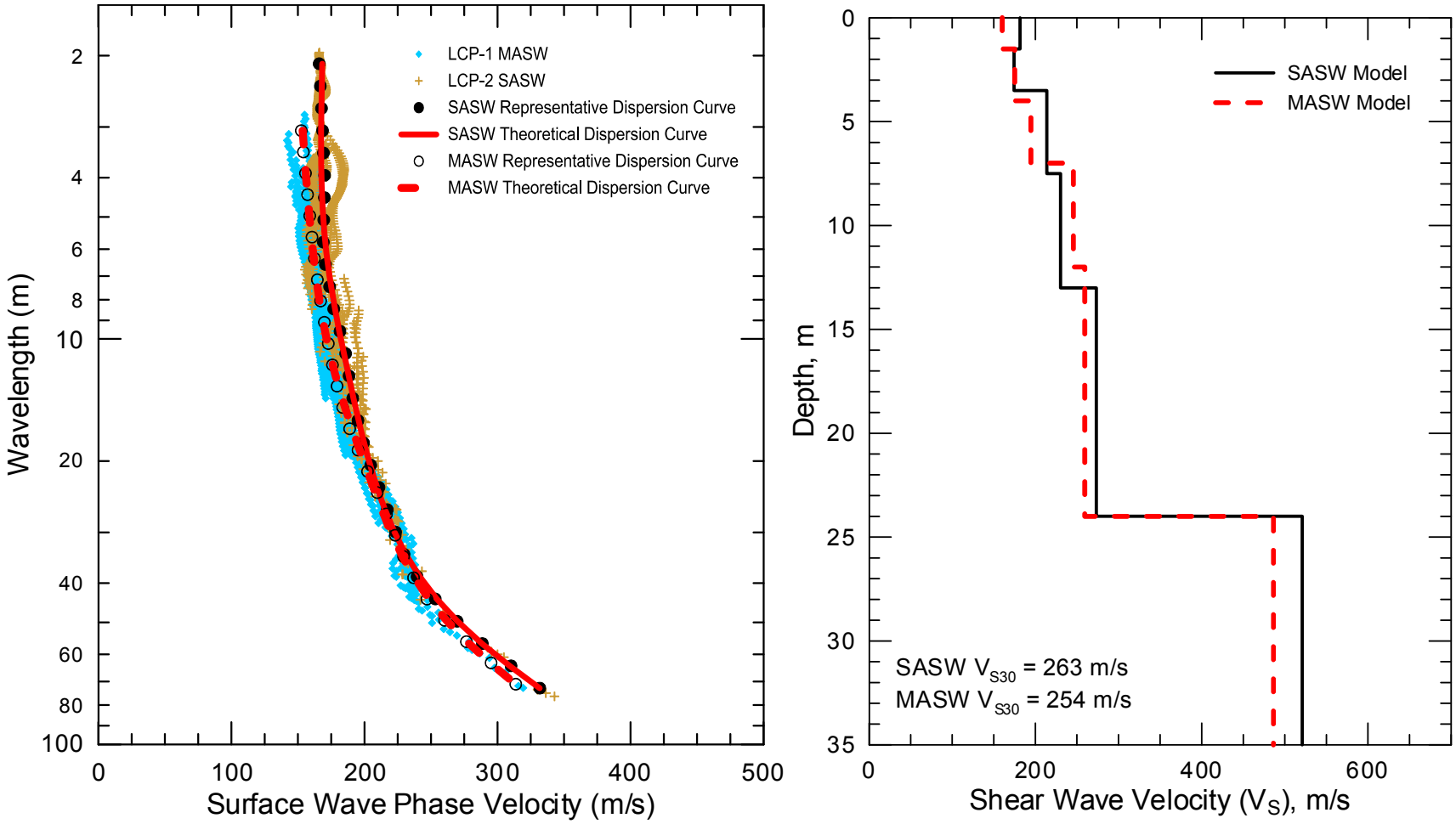

CI.LCP - Field, representative and inverted theoretical surface wave dispersion data (left) and associated V_S model (right)

Site CI.LDF

Location: AT&T Facility, near intersection of Lanfair Road and Cedar Canyon Road, Lanfair, California

Latitude: 35.13066 **Longitude:** -115.18416
(Station coordinates provided by USGS, WGS84 coordinate system)

V_{S30} (measured): 453 m/s

V_{S30} (adjusted to more accurately reflect seismic station conditions): 487 m/s (average S-wave velocity between 2 and 32 m adjusting for nominal sensor depth).

NEHRP Site Class: C

Geomatrix Code: IHD

Geologic Conditions/Observations: Site located on Quaternary (Holocene) alluvium. Nearest bedrock outcrop is about 2 km from site.

Site Conditions: Rural site. Relatively flat terrain in site vicinity with ground surface elevation gently decreasing to southeast.

Geophysical Methods Utilized: HVSR, MASW

Geophysical Testing Arrays:

1. Array LDF-1 (48 channel MASW array utilizing 4.5 Hz vertical geophones spaced 1.5 m apart for a length of 70.5 m, forward and reverse shot locations with multiple source offsets and source types and center shot location).
2. Array LDF-2 (48 channel MASW array utilizing 4.5 Hz vertical geophones spaced 3 m apart for a length of 141 m, forward and reverse shot locations with multiple source offsets and source types and multiple interior shot locations).
3. Three HVSR measurement locations distributed along array LDF-1.

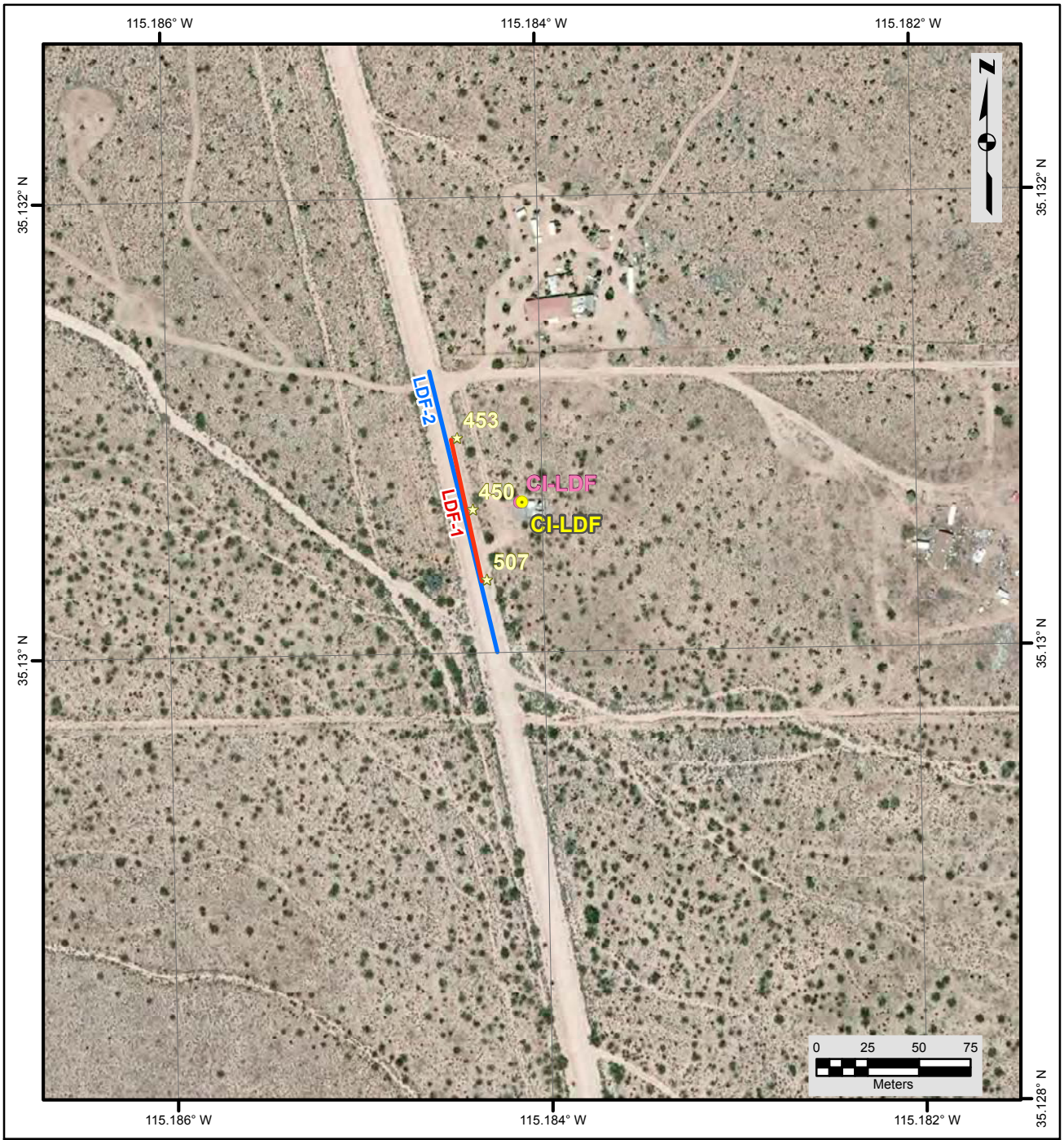

Legend

- Seismic Station - Approximate Surveyed Location
- Seismic Station - Approximate Location of Record
- H/V Spectral Ratio Measurement Location
- MASW Array
- MASW Array

NOTES:
1. WGS 1984 COORDINATE SYSTEM
2. Image Source: ESRI, i-cubed, USDA FSA, USGS, AEX, GeoEye, Getmapping, Aerogrid, IGP

File Name: CI-LDF-I-2

Date: 2/7/2013

USGS science for a changing world

GEOVision geophysical services

RECOVERY.GOV

SITE MAP
CI•LDF

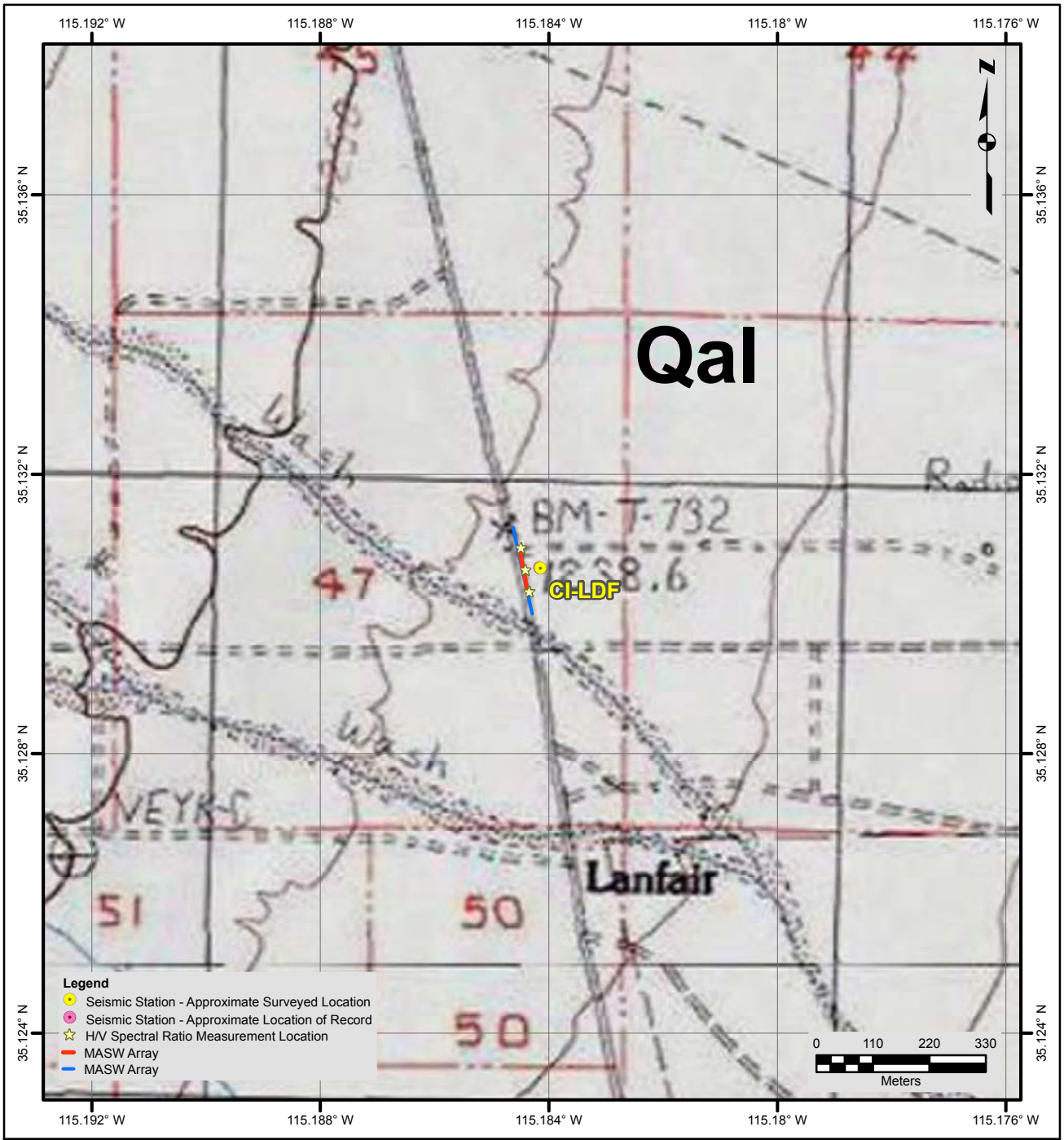

Description of Geologic Map Units

Qal = Quaternary (Holocene) alluvium

NOTES:
1. WGS 1984 COORDINATE SYSTEM
2. 2. Topo Image Sources: USGS, FAO, NPS, EPA, NRCAN, GeoBase, Esri, DeLorme, TANA, Intermap, AND, other suppliers, and the GIS community
3. Geologic Map Units from:
Geologic Map of California, Kingman Sheet
Olaf P. Jenkins Edition compiled by Charles W. Jennings, 1961
3. See site map for details of geophysical survey

File Name: CI-LDF-2

Date: 2/7/2013

USGS science for a changing world

GEOVision geophysical services

RECOVERY.GOV

GEOLOGIC MAP
CI•LDF

Seismograph station CI.LDF

Looking east towards array LDF-1 and seismograph station

HVSR sensor 453 in shallow hole and covered to protect from wind

Looking northwest along array LDF-1

MASW data acquisition along array LDF-2

Location of Geophysical Testing Arrays:

Location	Latitude	Longitude
LDF-1, Southeast End of MASW Array	35.13031	-115.18437
LDF-1, Center of MASW Array	35.13063	-115.18444
LDF-1, Northwest End of MASW Array	35.13094	-115.18452
LDF-2, Southeast End of MASW Array	35.13000	-115.18429
LDF-2, Center of MASW Array	35.13062	-115.18446
LDF-2, Northwest End of MASW Array	35.13124	-115.18463
HVSR Sensor 507	35.13032	-115.18434
HVSR Sensor 453	35.13094	-115.18449
HVSR Sensor 450	35.13063	-115.18441
CI.LDF Seismic Station	35.13066	-115.18415

Notes: 1) WGS84 Coordinate System (decimal degrees)
2) Survey accuracy is estimated at 1 to 2 m.

Results:

V_S Model 1

Depth to Top of Layer (m)	Layer Thickness (m)	S-Wave Velocity (m/s)	Inferred P-Wave Velocity (m/s)	Assumed Poisson's Ratio	Assumed Density (g/cm^3)
0	3	260	487	0.3	1.80
3	3	314	588	0.3	1.85
6	6	385	721	0.3	1.90
12	6	591	1106	0.3	2.00
18	8	610	1141	0.3	2.05
26	10	629	1177	0.3	2.05
36	15	660	1234	0.3	2.05
51	>4	679	1271	0.3	2.10

Notes: 1) Saturated zone located at a depth of greater than 60 m based on survey design and absence of water table refractor.
2) Depth of investigation is about 55 m.
3) Bottom layer is a half space.

V_S Model 2

Depth to Top of Layer (m)	Layer Thickness (m)	S-Wave Velocity (m/s)	Inferred P-Wave Velocity (m/s)	Assumed Poisson's Ratio	Assumed Density (g/cm^3)
0	3	260	486	0.3	1.80
3	3	321	600	0.3	1.85
6	6	372	696	0.3	1.90
12	6	666	1245	0.3	2.05
18	8	586	1096	0.3	2.00
26	10	632	1182	0.3	2.05
36	15	642	1202	0.3	2.05
51	>4	695	1301	0.3	2.10

Notes: 1) Saturated zone located at a depth of greater than 60 m based on survey design and absence of water table refractor.
2) Depth of investigation is about 55 m.
3) Bottom layer is a half space.

Observations/Discussion:

- HVSR plots are similar at all measurement locations, validating the 1-D velocity structure assumption.
- There is no distinct high amplitude HVSR peak at the site. There is, however, a possible weak and broad HVSR peak in the 0.45 to 0.5 Hz range.
- Field inspection of Rayleigh wave dispersion data from the 70.5 m long MASW array LDF-1 indicated that subsurface soils had relatively high S-wave velocity (V_S) making it possible for the available weight drop energy source to image to a depth greater than 30 m. Therefore, MASW data were also acquired along the 141 m long array LDF-2 in an attempt to extend depth of investigation.
- Based on simple layer-based analysis of seismic refraction first arrival data, P-wave velocity in the upper 30 m ranges from about 425 m/s at the surface to 650 to 675 m/s at a depth of 1 to 2 m, 750 to 775 m/s at a depth of 3 to 5 m and about 1,250 m/s at a depth of about 10 to 12 m. The 1,250 m/s refractor attenuates rapidly with distance from the source and eventually disappears, which indicates that there is a velocity inversion beneath a relatively thin layer. There is no evidence of P-wave velocity exceeding 1,500 m/s in the upper 50 to 60 m.
- Water table located at a depth of greater than 60 m based on survey design and absence of a water table refractor.
- There is a possible reflector in the seismic records that could be associated with the water table or other geologic structure at a depth on the order of 100 m.
- Noise conditions at site were not sufficient to apply passive surface wave techniques.

- Rayleigh wave dispersion data were reduced from both the 70.5 m long array LDF-1 and 141 m long array LDF-2.
- To minimize near field effects, the maximum wavelength Rayleigh wave data extracted from the data set was set equal to the lesser of 80 m for array LDF-1, 115 m for array LDF-2 or 1.2 times the distance between the source and midpoint of the active receiver array. A 115 m wavelength Rayleigh wave occurs at an average frequency of about 4.7 Hz.
- The minimum wavelength Rayleigh wave phase velocity data extracted from 48-channel MASW arrays LDF-1 and LDF-2 was 7 an 10 m, respectively. Reducing data from smaller hammer sources using a limited offset receiver array (i.e. less active geophones) allowed for extraction of surface wave dispersion data from arrays LDF-1 and LDF-2 to a minimum wavelength of about 2.5 and 3.5 m, respectively.
- There is nominally about 50 to 70 m/s of scatter in MASW dispersion data, which is in part due to lateral velocity variation.
- Interestingly, source offset and array length has a noticeable effect on Rayleigh wave phase velocity at wavelengths greater than about 30 m at this site.
- A moving average, polynomial curve fitting routine was used to generate a representative dispersion curve from an ensemble of MASW dispersion curves resulting from analysis of multiple, reversed source offsets and source types from both arrays LDF-1 and LDF-2.
- Surface wave depth of investigation is about 55 m based on the one half of maximum wavelength criteria.
- Two V_S models were developed from the Rayleigh wave dispersion curve, both to demonstrate nonuniqueness and to develop a model consistent with seismic refraction observations. V_S increases with depth in Model 1; whereas, a high velocity layer is permitted in Model 2 at a depth of 12 m to reflect observations made in seismic refraction first arrival data. The velocity and thickness of the high velocity layer are not well constrained and, as shown in Model 1, a velocity inversion at depth is not required to model the dispersion data. Both presented models should be considered valid, but not unique, representations of subsurface velocity structure. As is typical of the inversion of geophysical data, the models are not unique and multiple other models would fit the observations equally well. In the case of the inversion of surface wave dispersion data, it can be shown, however, that V_{S30} is much better constrained that the actual V_S models.
- The surface wave V_S models are consistent with the simplified P-wave refraction model considering uncertainty in Poisson's ratio.
- V_{S30} is 453 and 454 m/s for Models 1 and 2, respectively averaging 453 m/s (NEHRP Site Class C).
- Adjusted V_{S30}, the average S-wave velocity between 2 m (nominal sensor depth) and 32 m is 486 and 488 m/s for Models 1 and 2, respectively averaging 487 m/s.
- Scatter in the Rayleigh wave phase velocity data is such that V_{S30} may vary by as much as about 7% beneath the MASW arrays; assuming that the scatter is associated with lateral velocity variation rather than some other phenomenon.

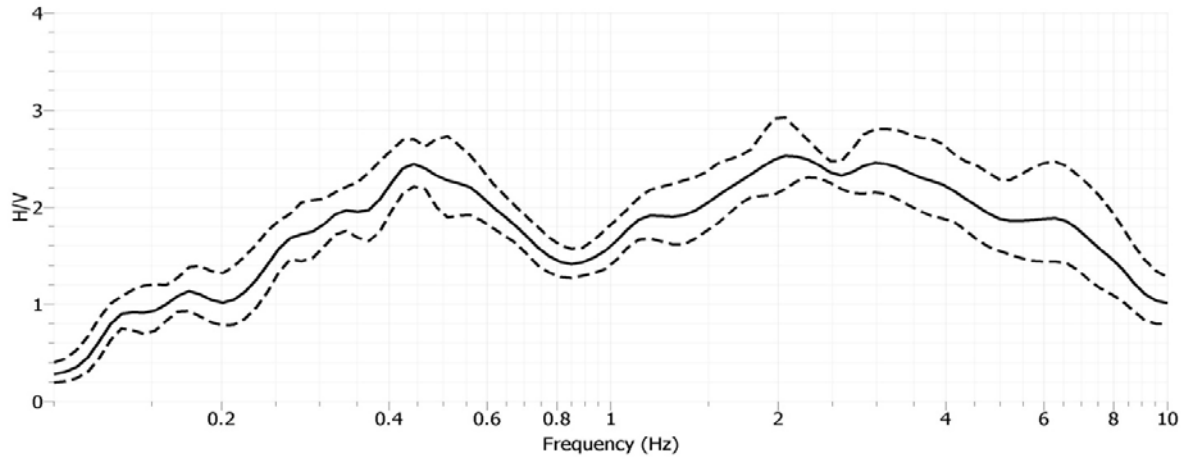

Site CI.LDF, H/V Spectral Ratio, Array LDF-1, Sensor 453

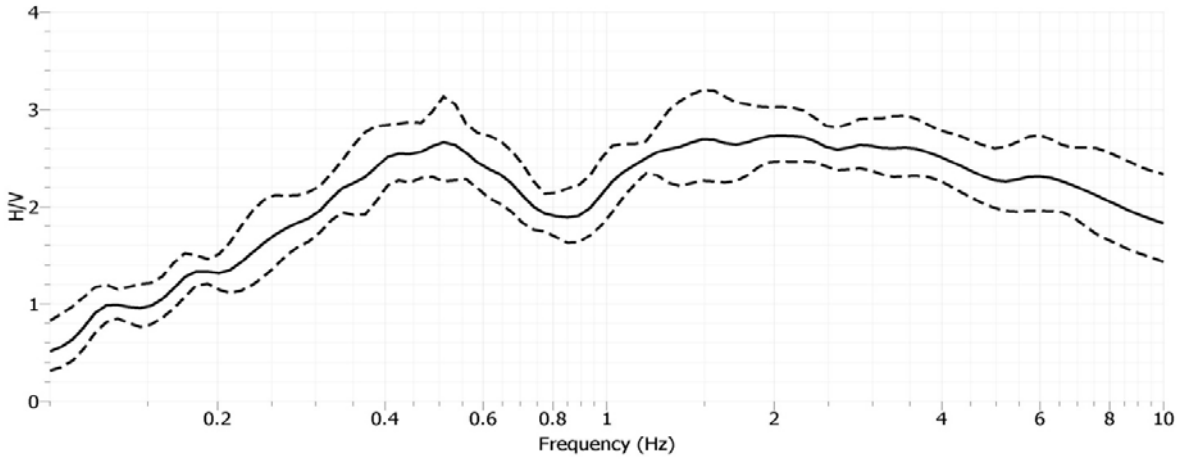

Site CI.LDF, H/V Spectral Ratio, Array LDF-1, Sensor 450

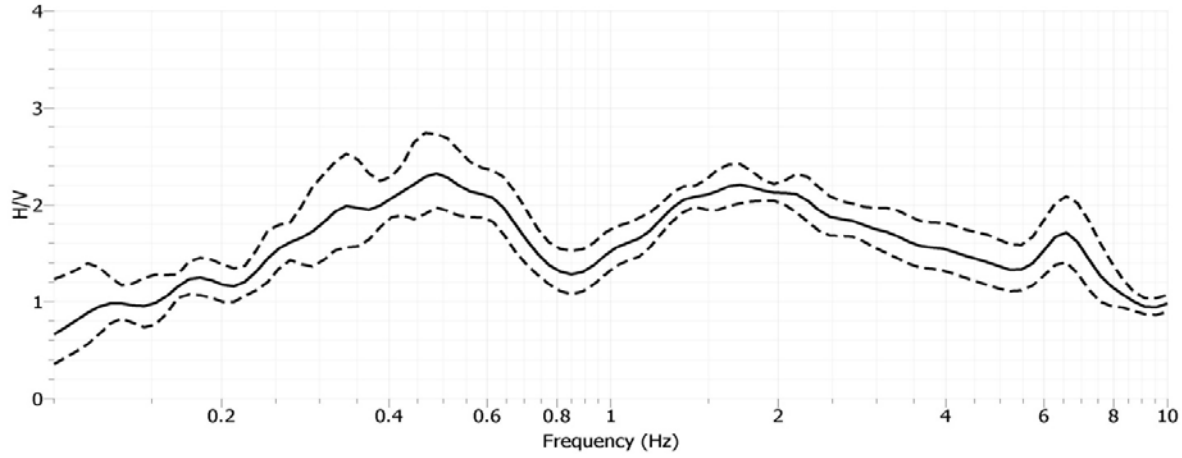

Site CI.LDF, H/V Spectral Ratio, Array LDF-1, Sensor 507

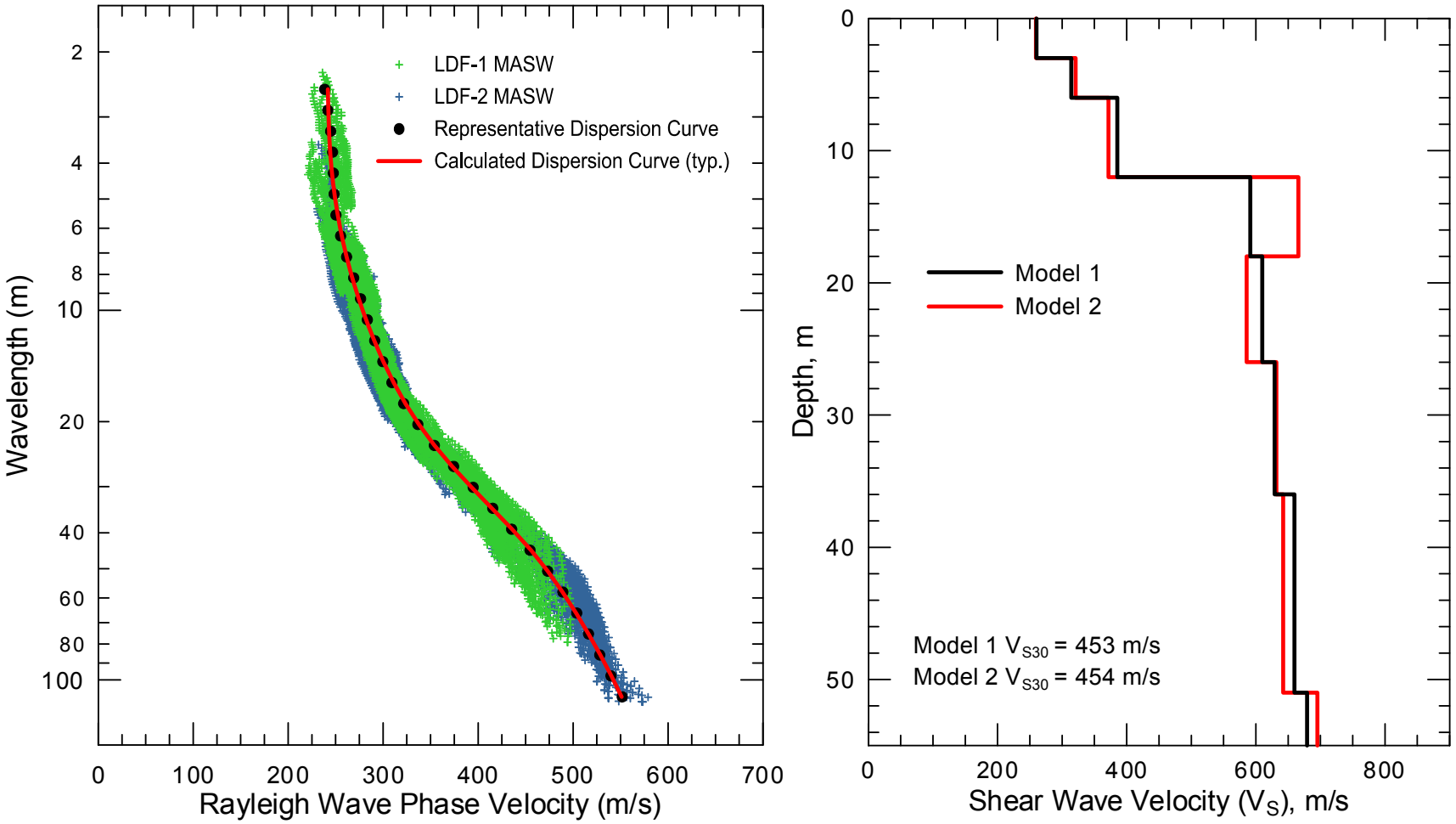

CI.LDF - Field, representative and inverted theoretical surface wave dispersion data (left) and associated V_S models (right)

Site CI.LDR

Location: Willow Springs Road, Mojave, California

Latitude: 34.99060 **Longitude:** -118.34156

(Coordinates provided by USGS – WGS84 coordinate system)

V_{S30} (measured): 378 m/s

V_{S30} (adjusted to more accurately reflect seismic station conditions): 415 m/s (average S-wave velocity between 2 and 32 m adjusting for 2 m nominal sensor depth.)

NEHRP Site Class: C

Geomatrix Code: IQD

Geologic Conditions/Observations: Seismic station located on geologic unit mapped as older Quaternary (Pleistocene) alluvial gravel and sand deposits. An outcrop of quartz monzonite is located about 0.7 km west of the seismic station.

Site Conditions: Rural site. No traffic noise on nearby roads. Relatively flat topography in test area. Ground surface elevations decrease gradually to southeast.

Geophysical Methods Utilized: HVSR, MASW

Geophysical Testing Arrays:

1. Array LDR-1 (48 channel MASW array utilizing 4.5 Hz vertical geophones spaced 1.5 m apart for a length of 70.5 m, forward and reverse shot locations with multiple source offsets and source types and center shot location).
2. Array LDR-2 (48 channel MASW array utilizing 4.5 Hz vertical geophones spaced 3 m apart for a length of 141 m, forward and reverse shot locations with multiple source offsets and source types and multiple interior shot locations). Array LDR-2 has the same midpoint and orientation as array LDR-1.
3. Three HVSR measurement locations; two distributed along array LDR-1 and the other near the seismic station.

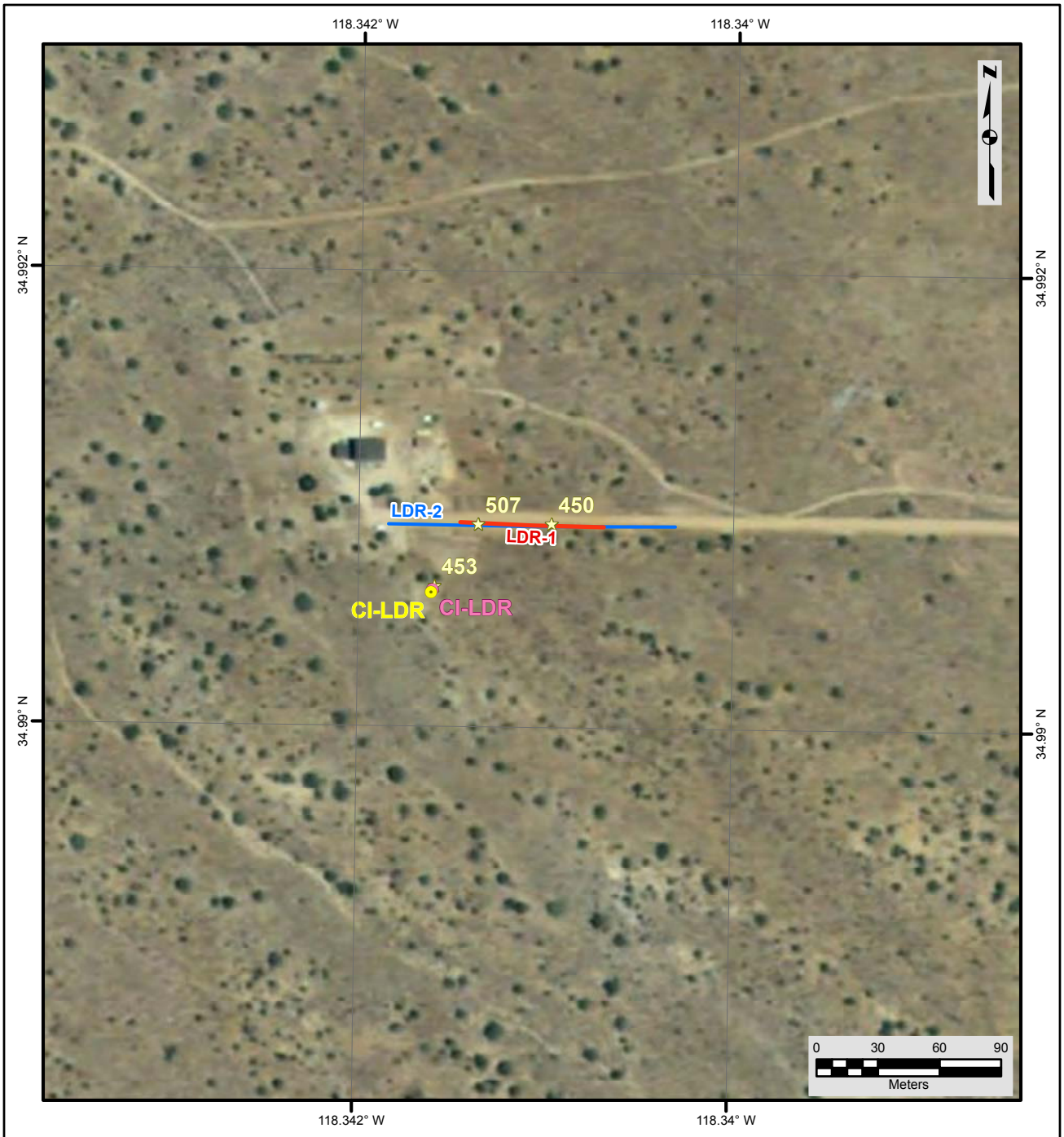

Legend

- Seismic Station - Approximate Surveyed Location
- Seismic Station - Approximate Location of Record
- H/V Spectral Ratio Location
- MASW Array
- MASW and Refraction Array

NOTES:
1. WGS 1984 COORDINATE SYSTEM
2. Image Source: ESRI, i-cubed, USDA FSA, USGS, AEX, GeoEye, Getmapping, Aerogrid, IGP

File Name: CI-LDR-I

Date: 6/29/2011

USGS science for a changing world

GEOVision geophysical services

RECOVERY.GOV

SITE MAP
CI•LDR

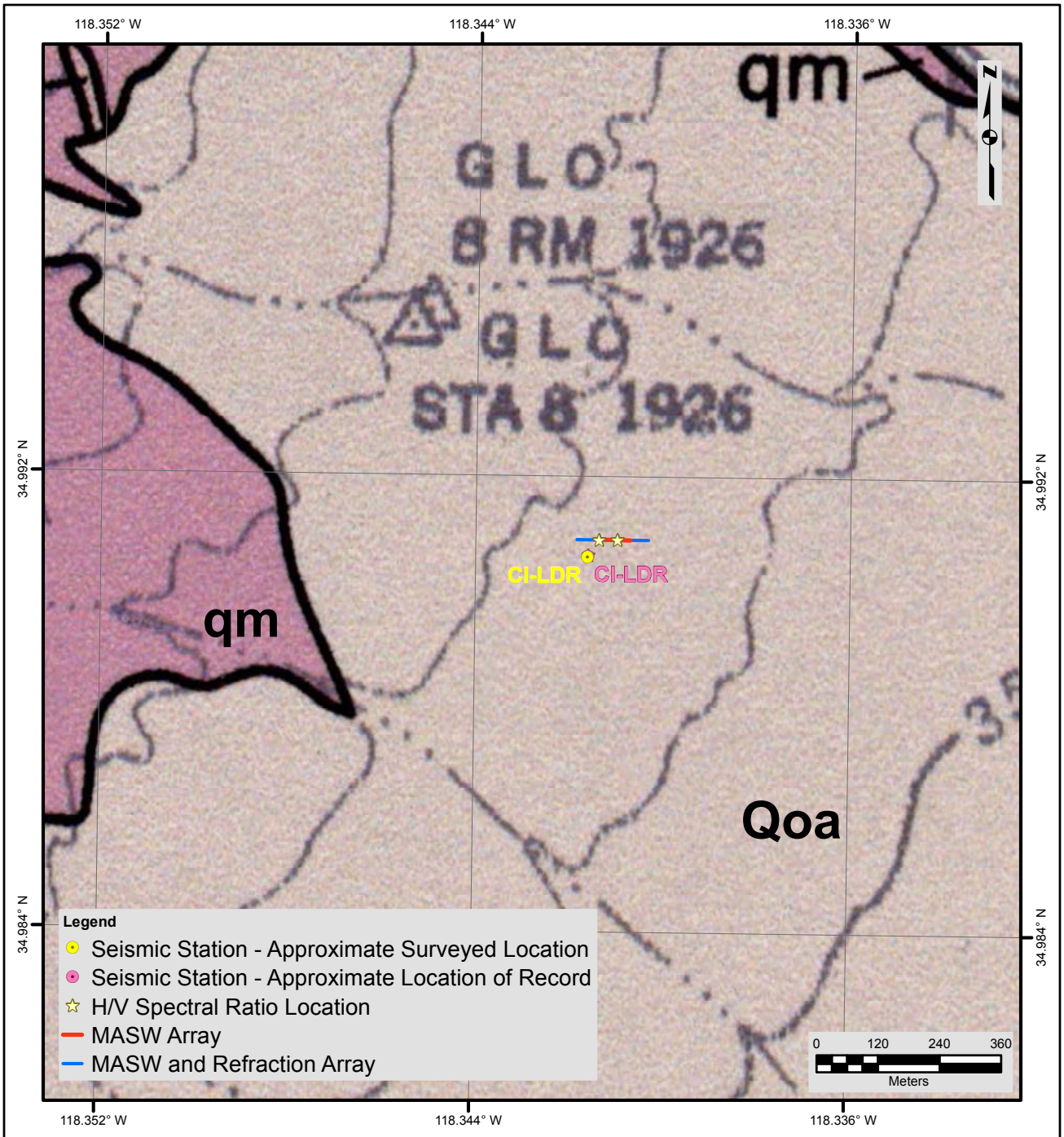

Description of Geologic Map Units

Qoa = Quaternary (Holocene) alluvial gravel and sand of unsorted detrutus, poorly bedded
qm = Mesozoic (Jurassic or Cretaceous) Quartz monzonite, medium- to coarse-grained, massive

NOTES:
1. WGS 1984 COORDINATE SYSTEM
2. Geologic Map of the Neenach & Willow Springs Quadrangles, Kern & Los Angeles Counties, California by Thomas W. Dibblee, Jr., 2008
3. See site map for details of geophysical survey

File Name: CI-LDR

Date: 6/29/2011

USGS science for a changing world

GEOVision geophysical services

GEOLOGIC MAP
CI•LDR

RECOVERY.GOV

Looking north towards CI.LDR seismic station

Looking south towards seismic station from HVSR sensor 507

Looking south towards seismic station from west end of MASW array LDR-1

Looking east along MASW array LDR-2

Looking west along MASW array LDR-2

Location of Geophysical Testing Arrays:

Location	Latitude	Longitude
LDR-1, West End of MASW Array	34.99090	-118.34142
LDR-1, Center of MASW Array	34.99089	-118.34103
LDR-1, East End of MASW Array	34.99088	-118.34065
LDR-2, West End of MASW/Refraction Array	34.99089	-118.34180
LDR-2, Center of MASW/Refraction Array	34.99088	-118.34103
LDR-2, East End of MASW/Refraction Array	34.99089	-118.34027
HVSR Sensor 453	34.99062	-118.34155
HVSR Sensor 507	34.99089	-118.34132
HVSR Sensor 450	34.99089	-118.34093
CI.LDR Seismic Station	34.99059	-118.34157

Notes: 1) WGS84 Coordinate System (decimal degrees)

2) Survey accuracy is estimated at 1 to 2 m

Results:

V_S Model

Depth to Top of Layer (m)	Layer Thickness (m)	S-Wave Velocity (m/s)	Inferred P-Wave Velocity (m/s)	Inferred Poisson's Ratio	Inferred Density (g/cm^3)
0	1.5	164	328	0.333	1.9
1.5	2.5	275	550	0.333	1.9
4	4	328	657	0.333	1.9
8	6	370	740	0.333	1.9
14	9	455	910	0.333	2.0
23	12	536	1072	0.333	2.0
35	>10	865	1730	0.333	2.1

Observations/Discussion:

- There is no conclusive dominant HVSR peak at this site, rather there may be multiple low amplitude peaks. The HVSR plots are similar at frequencies below 8 Hz with possible, but inconclusive, low amplitude HVSR peaks near 3.5, 1.6 and 1 Hz. There is a trough on all of the HVSR plots at between 2 and 3 Hz. Low amplitude HVSR peaks above 10 Hz are different on all of the plots, which would indicate that very shallow velocity structure is variable; however, the source of high frequency microtremor energy is not clear. The absence of local high frequency microtremor sources may also have an impact on the HVSR measurement results.

- Based on simple, interactive horizontal layer-based analysis of seismic refraction first arrival data, P-wave velocity in the upper 40 m ranges from about 400 m/s near the surface to as high as 1,800 m/s at a depth on the order of 35 m (about 0 to 4 m of sediments with velocity in the 400 to 500 m/s range, then sediments with a velocity of 675 to 775 m/s to a depth of 9 to 12 m, then sediments with a velocity of 900 to 1,000 m/s to a depth of 33 to 38 m, underlain by sediments with a velocity as high as 1,800 m/s.
- Review of the first arrival data indicated that there is some lateral velocity variation in the near surface sediments. As an example, the low velocity layer at the surface discussed above ranges in thickness from about 0 to 4 m.
- The layer with P-wave velocity of about 1,800 m/s would often be associated with saturated sediments; however, surface wave dispersion data indicates that there could be a large S-wave velocity impedance contrast in the depth range of this layer.
- Noise conditions at site were not sufficient to apply passive surface wave techniques.
- Surface wave dispersion data from arrays LDR-1 and LDR-2 are in good agreement.
- SASW analysis of selected MASW receiver pairs was conducted in an attempt to obtain higher frequency (smaller wavelength) surface wave dispersion data.
- There is some scatter in the MASW surface wave dispersion data, likely the result of minor lateral velocity variation.
- Surface wave phase velocities at small wavelengths (high frequencies) resulting from limited offset analysis of seismic data at the western end of the MASW arrays were higher than those from shot locations at the eastern end of the arrays due to lateral velocity variation discussed above. The lower phase velocity data from the eastern and center shot locations better fit the MASW data extracted from the complete seismic records and were used for analysis.
- Representative dispersion curves were generated for each surface wave data set using a moving average, polynomial curve fitting routine. These individual representative dispersion curves were combined and a representative dispersion curve generated for the combined data set for data modeling.
- Surface wave depth of investigation is about 45 m based on half of maximum wavelength criteria.
- The inferred P-wave velocities in the surface wave model, assuming a Poisson's ratio of 0.3333, are generally consistent with simplified P-wave velocity structure in the seismic refraction model.
- V_{S30} is 378 m/s (Site Class C).
- The upper 1.5 m thick low velocity layer is not present beneath the entire line based on seismic refraction data and limited offset range surface wave dispersion data at the west end of the arrays. If this layer were replaced with the velocity of the underlying layer then V_{S30} would be 396 m/s.
- Average S-wave velocity between 2 m (nominal sensor depth) and 32 m is 415 m/s.

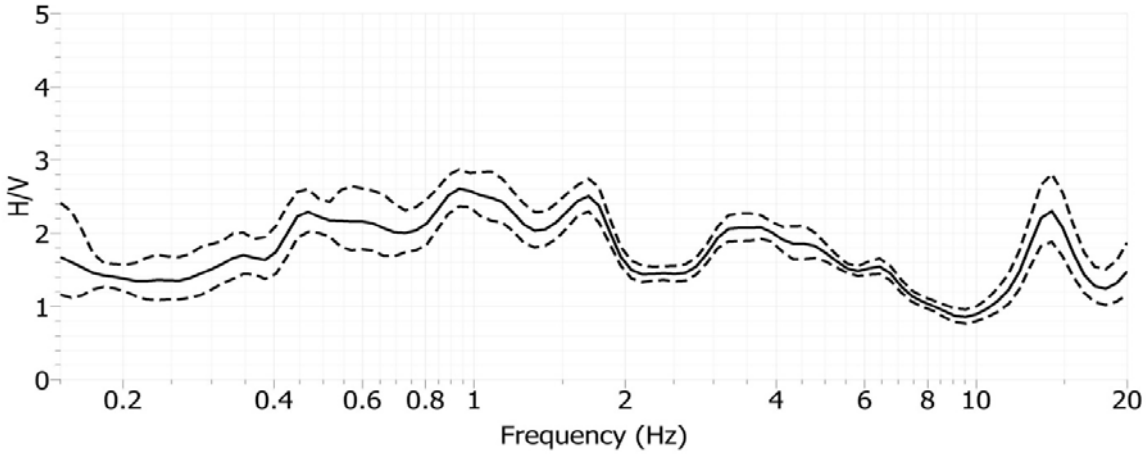

Site CI.LDR, H/V Spectral Ratio, Near Seismic Station, Sensor 453

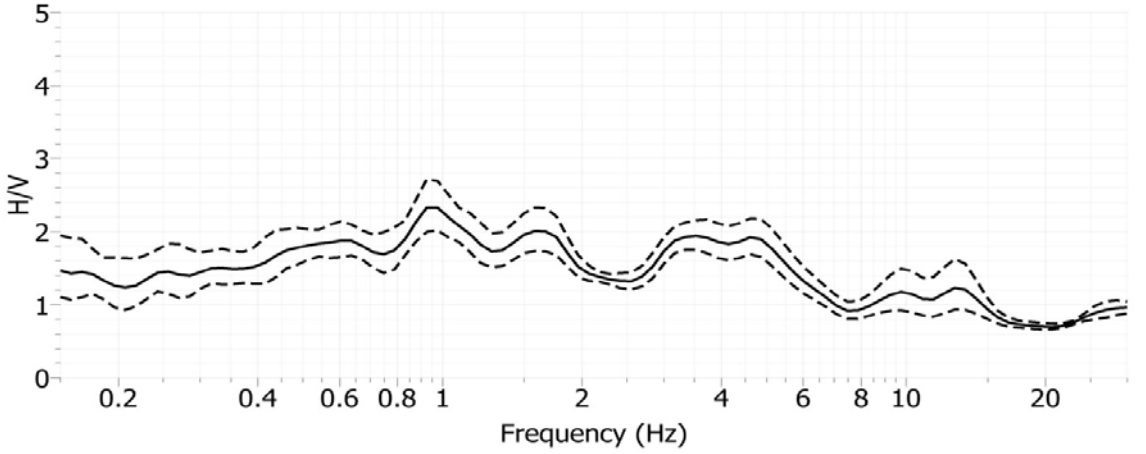

Site CI.LDR, H/V Spectral Ratio, Array LDR -1, Sensor 507

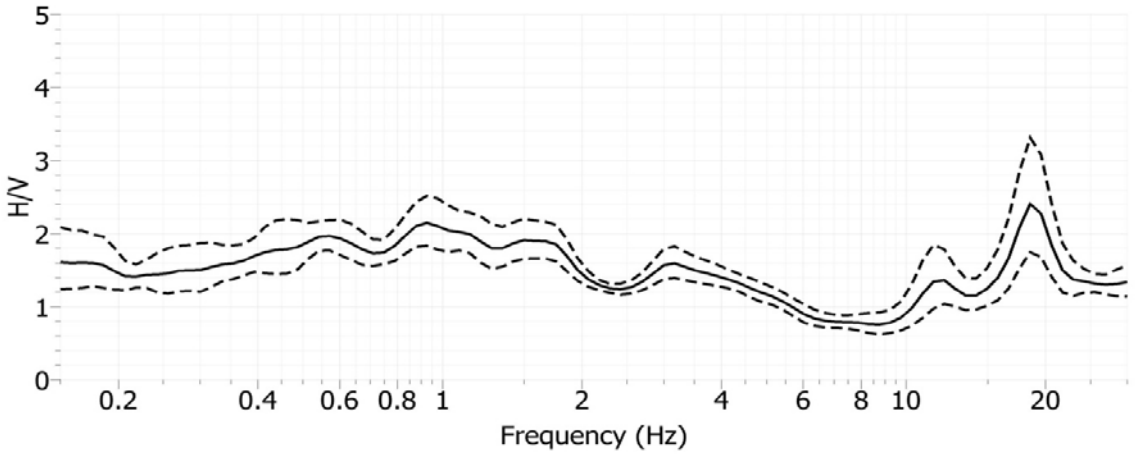

Site CI.LDR, H/V Spectral Ratio, Array LDR -1, Sensor 450

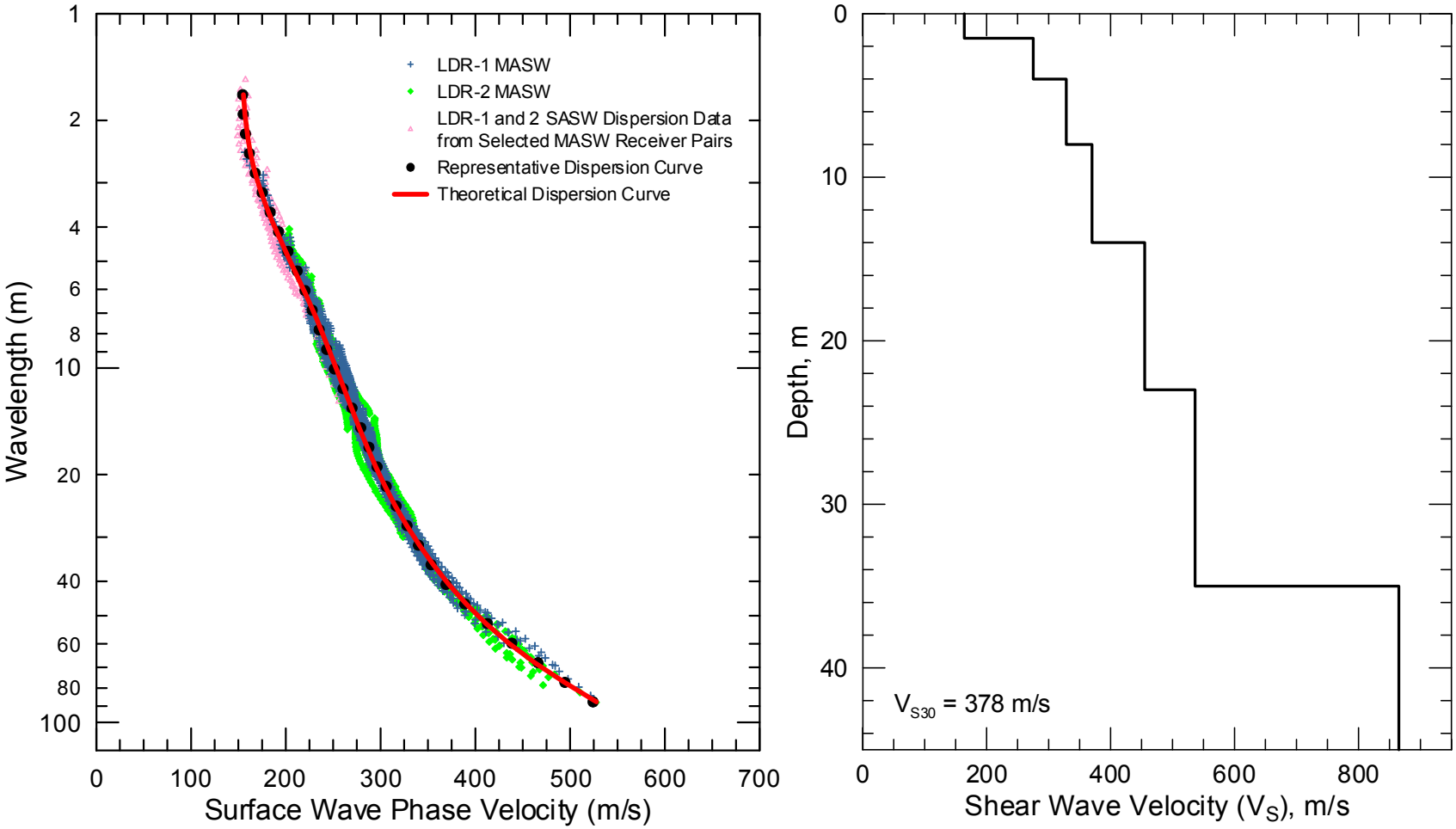

CI.LDR - Field, representative and inverted theoretical surface wave dispersion data (left) and associated V_S model (right)

Site CI.LEV

Location: AT&T Building, Leona Valley, California

Latitude: 34.61404 **Longitude:** -118.28929
(Station coordinates modified based on identification of approximate station location on Google Earth – could not survey the seismic station as located inside an inaccessible building, WGS84 coordinate system)

V_{S30} (measured): 505 m/s

V_{S30} (adjusted to more accurately reflect seismic station conditions): 505 m/s (no adjustment necessary).

NEHRP Site Class: C

Geomatrix Code: AHB

Geologic Conditions/Observations: Site located on unit mapped as Quaternary (Holocene) alluvium, in a narrow valley fault bound valley. The inferred location of the Nadeau fault is located about 200 m southwest of the site and an unnamed inferred fault is located about 100 m northeast of the site. The San Andreas fault is located about 450 m northeast of the site. A mapped outcrop of Mesozoic quartz diorite is located about 60 m northwest of the site, indicating that crystalline bedrock is located at very shallow depth in the site vicinity. Given the proximity to faulting, the bedrock is likely highly fractured.

Site Conditions: Suburban site with sparse traffic noise from nearby roads. Relatively flat terrain in immediate site vicinity. Weathered crystalline basement mapped as quartz diorite outcrops approximately 60 m northwest of the seismic station.

Geophysical Methods Utilized: HVSR, Seismic Refraction (P-wave and limited S-wave), MASW (Rayleigh wave), MALW (Love wave)

Geophysical Testing Arrays:

1. Array LEV-1 (48 channel MASW and P-wave seismic refraction array utilizing 4.5 Hz vertical geophones spaced 1.5 m apart for a length of 70.5 m, forward and reverse shot locations with multiple source offsets and source types and multiple interior shot locations).
2. Array LEV-1 (48 channel MALW and limited S-wave seismic refraction array utilizing 10 Hz horizontal geophones spaced 1.5 m apart for a length of 70.5 m, forward and reverse shot locations with multiple source offsets and a center shot location). Coincident with P-wave refraction and MASW array of same name.
3. Four HVSR measurement locations; two distributed along array LEV-1 and two adjacent to the AT&T building housing the seismic station.

Legend

- Seismic Station - Approximate Improved Location
- Seismic Station - Approximate Location of Record
- H/V Spectral Ratio Location
- MASW and Seismic Refraction Array (P- and S-wave)

NOTES:
1. WGS 1984 COORDINATE SYSTEM
2. Image Source: ESRI, i-cubed, USDA FSA, USGS, AEX, GeoEye, Getmapping, Aerogrid, IGP

File Name: CI-LEV-I

Date: 2/7/2013

USGS science for a changing world

GEOVision geophysical services

RECOVERY.GOV

SITE MAP
CI•LEV

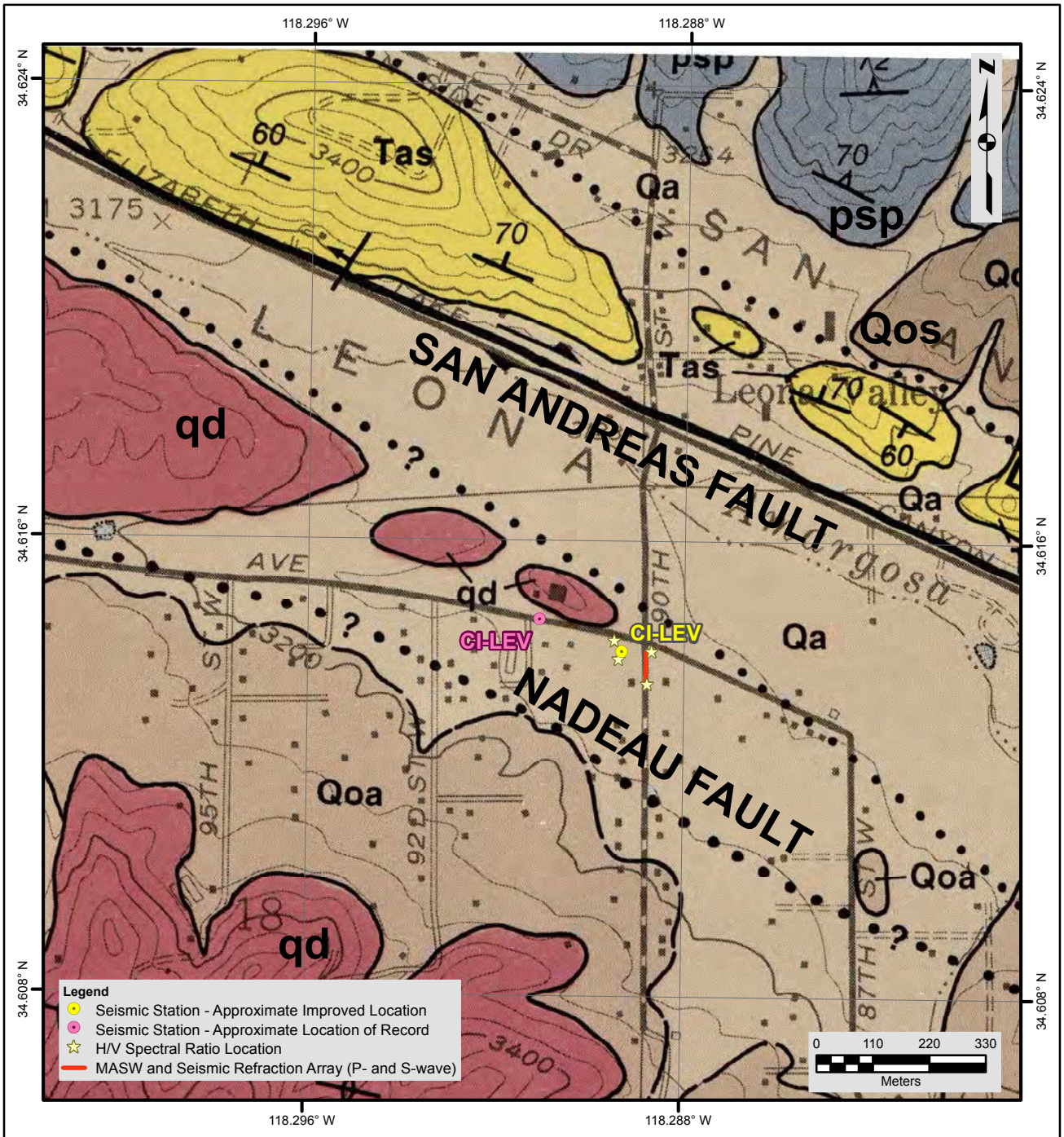

Description of Geologic Map Units

Qa = Quaternary (Holocene) alluvial gravel, sand and silt
Qoa = Quaternary (Pleistocene) allluvial gravel and sand of mostly granitic detritus
Qos = Quaternary (Pleistocene) alluvial gravel and sand of mostly schist detritus
Tas = Tertiary (Pliocene) Anaverde Formation; sandstone
qd = Mesozoic or older quartz diorite to granodiorite, biotite-rich, locally gneissoid
psp = Mesozoic or older Pelona Schist; schist of Portal Ridge, biotite-rich

NOTES:
1. WGS 1984 COORDINATE SYSTEM
2. Geologic Map of the Sleepy Valley and Ritter Ridge Quadrangles, Los Angeles County, California by Thomas W. Dibblee, Jr., 1997
3. See site map for details of geophysical survey

File Name: CI-LEV

Date: 2/7/2013

USGS science for a changing world

GEOVision geophysical services

RECOVERY.GOV

GEOLOGIC MAP
CI•LEV

Looking north towards building housing CI.LEV seismic station and HVSR sensor 453A

Looking west towards HVSR sensor 450, building housing seismic station and north end of array LEV-1

Data acquisition with hammer source on MASW and P-wave seismic refraction array LEV-1

Looking south along MASW and P-wave seismic refraction array LEV-1

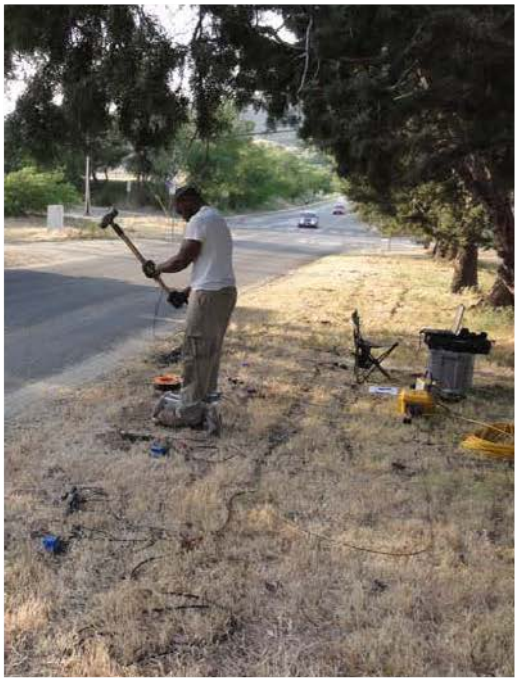

Data acquisition with aluminum plate source on MALW (Love wave) array LEV-1

Location of Geophysical Testing Arrays:

Location	Latitude	Longitude
LEV-1, South End of MASW/Refraction Array	34.61343	-118.28877
LEV-1, North End of MASW/Refraction Array	34.61405	-118.28877
HVSR Sensor 450	34.61406	-118.28865
HVSR Sensor 453	34.61349	-118.28874
HVSR Sensor 453A	34.61393	-118.28935
HVSR Sensor 507	34.61425	-118.28944

Notes: 1) WGS84 Coordinate System (decimal degrees)
2) Survey accuracy is estimated at 1 to 2 m.

Results:

V_S Model 1

Depth to Top of Layer (m)	Layer Thickness (m)	S-Wave Velocity (m/s)	Inferred P-Wave Velocity (m/s)	Inferred Poisson's Ratio	Inferred Density (g/cm^3)
0	1	161	301	0.3	1.7
1	2	199	371	0.3	1.7
3	6.75	320	599	0.3	1.8
9.75	>20	946	1770	0.3	2.1

Notes: 1) Depth of investigation is about 25 to 30 m.
2) Bottom layer is a half space.

V_S Model 2

Depth to Top of Layer (m)	Layer Thickness (m)	S-Wave Velocity (m/s)	Inferred P-Wave Velocity (m/s)	Inferred Poisson's Ratio	Inferred Density (g/cm^3)
0	1	154	288	0.3	1.7
1	2	219	409	0.3	1.7
3	5	276	517	0.3	1.8
8	>22	810	1515	0.3	2.1

Notes: 1) Depth of investigation is about 25 to 30 m.
2) Bottom layer is a half space.

V_S Model 3

Depth to Top of Layer (m)	Layer Thickness (m)	S-Wave Velocity (m/s)	Inferred P-Wave Velocity (m/s)	Inferred Poisson's Ratio	Inferred Density (g/cm^3)
0	1	158	295	0.3	1.7
1	2	206	386	0.3	1.7
3	6	303	568	0.3	1.8
9	>21	877	1642	0.3	2.1

Notes: 1) Depth of investigation is about 25 to 30 m.
2) Bottom layer is a half space.

V_S Model 4

Depth to Top of Layer (m)	Layer Thickness (m)	S-Wave Velocity (m/s)	Inferred P-Wave Velocity (m/s)	Inferred Poisson's Ratio	Inferred Density (g/cm^3)
0	1	162	303	0.3	1.7
1	2	196	367	0.3	1.7
3	7	325	609	0.3	1.8
10	>20	976	1826	0.3	2.1

Notes: 1) Depth of investigation is about 25 to 30 m.
2) Bottom layer is a half space.

Observations/Discussion:

- The HVSR plots at the four measurement locations are all different indicating small variations in bedrock depth and/or average S-wave velocity of overlying sediments and possibly a variable weathering profile within rock. The highest frequency HVSR peak is about 4 Hz at sensor 507, 9 Hz at sensor 453, 7 Hz at sensor 450 and 8 Hz at sensor 453A. Interestingly, the lowest frequency peak occurs at sensor location 507, which is closest to the mapped bedrock outcrop. Sensor 453A, located immediately south of the building housing the seismic sensor, has an HVSR response relatively similar to that at sensor 453, located on array LEV-1. There are also possible, but variable, lower frequency peaks that could be associated with the weathering profile in bedrock.
- Array LEV-1 was located immediately adjacent to a road and the presence of relatively high velocity road base limited the application of the seismic refraction technique to accurately image depth to bedrock. The P-wave and S-wave seismic refraction data were, however, reviewed to determine approximate seismic velocity of the near surface bedrock. Bedrock was found to have an approximate P-wave velocity of about 3,000 m/s and S-wave velocity of about 1,000 m/s. This V_P/V_S ratio equates to a Poisson's ratio of about 0.44, which, if correct, would indicate that the rock is both highly fractured and saturated. If not highly fractured, the presence of water would not significantly affect Poisson's ratio. It might be worthwhile to attempt to access private property in the site vicinity to avoid the effects of asphalt/road base on the seismic refraction data and more thoroughly characterize the seismic properties of the rock.
- Noise conditions at site were not sufficient to apply passive surface wave techniques.
- MASW (Rayleigh wave) data quality is poor due to the high velocity shallow rock, which causes dominant higher modes and were, therefore, not reduced. MALW (Love wave) data were of significantly better quality than the MASW data and were, therefore, reduced and modeled.
- It was difficult extracting Love wave dispersion data at wavelengths less than 9 m and, therefore, SASW analysis was conducted on selected MALW receiver pairs to supplement the small wavelength/high frequency Love wave phase velocity data.
- The minimum wavelength surface wave phase velocity data extracted from the 48-channel MALW array is about 17 m. Data reduction using seismic records from smaller hammer sources and a limited offset receiver array (i.e. less active geophones) allowed extraction of surface wave dispersion data to a minimum wavelength of about 4 m. SASW analysis of small receiver spacing MALW data allowed extraction of Love wave phase velocity data to a wavelength of about 2 m.
- MALW data were acquired using 10 Hz horizontal geophones. The maximum wavelength Love wave phase velocity utilized for modeling was about 77 m, equivalent to a frequency of 7.8 Hz, slightly below the natural frequency of the geophone. The use of 4.5 Hz horizontal geophones, which were not available until later in the project, would have been more appropriate. We are not seeing significant scatter in the low frequency/long wavelength phase velocities from forward and reverse data, indicating that any phase response differences in the geophones near the natural frequency appears to be cancelling out.
- There is nominally about 40 m/s scatter in MALW dispersion data likely due to the effects of lateral velocity variation.

- A stringent maximum wavelength criterion was utilized to minimize potential near field effects.
- A representative dispersion curve was generated for the MALW data set using a moving average, polynomial curve fitting routine and used for modeling.
- Surface wave depth of investigation is assumed to be about 30 m. It does appear as though the MALW technique required longer wavelength Love wave phase velocity data to image to 30 m depth than the Rayleigh wave technique requires. The maximum wavelength Love wave phase velocity used for modeling was about 77 m, which may still not be enough to image to 30 m depth. A 60 m wavelength is the minimum wavelength Rayleigh wave phase velocity required to image to 30 m depth.
- Four models were developed for the Love wave dispersion curve to demonstrate nonuniqueness. The V_S models have bedrock depth ranging from 8 to 10 m and a constant velocity for bedrock. RMS error increases significantly once bedrock gets out of this depth range.
- V_{S30} for the four MALW V_S models ranges from 493 to 514 m/s and averages 505 m/s (Site Class C).
- The V_S models with bedrock at 9.75 and 10 m depth (Models 1 and 4) have half space S-wave velocities of 946 and 976 m/s, which are closest to the approximate 1,000 m/s S-wave velocity observed in the limited analysis of S-wave seismic refraction data. A 25% increase in the S-wave velocity only increases V_{S30} by 7.5%. The variable bedrock depth in the site vicinity will have a large local effect on V_{S30}.
- Site characterization efforts at this site would benefit from an S-wave seismic refraction survey conducted in a soil covered area (would require access to private property) to better characterize the S-wave velocity structure of the weathered bedrock.

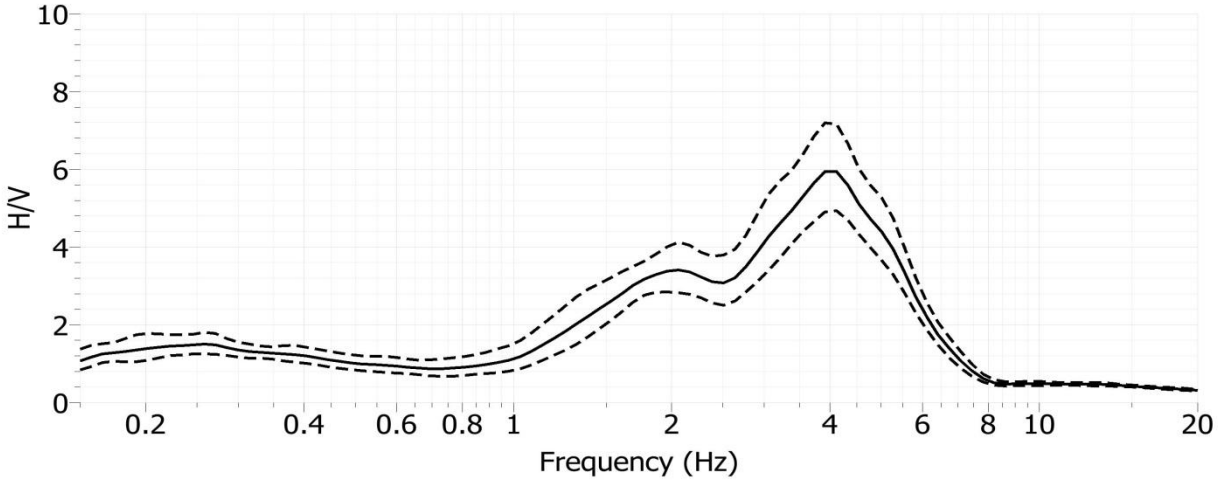

Site CI.LEV, H/V Spectral Ratio, Near AT&T building, Sensor 507

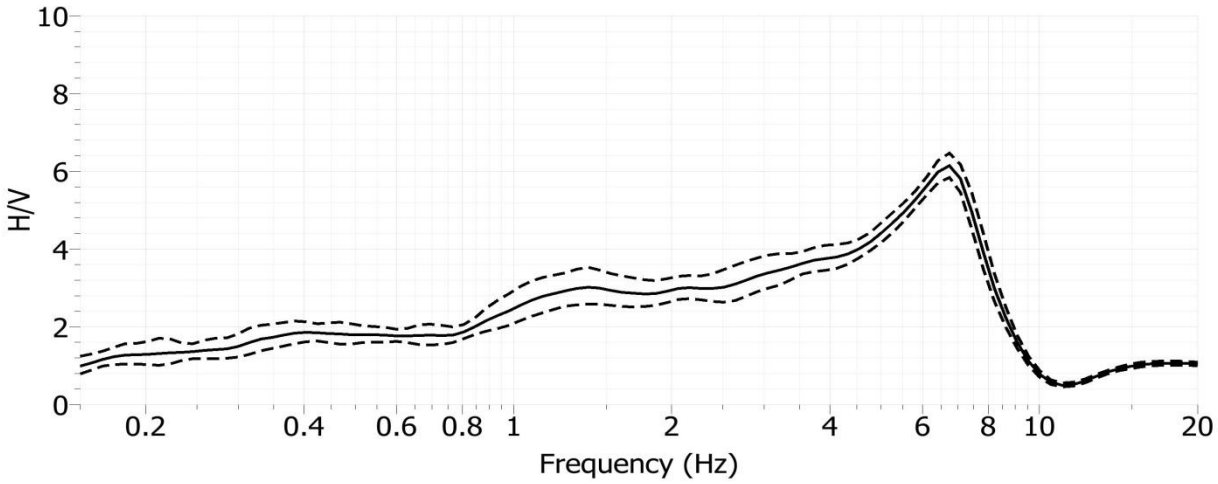

Site CI.LEV, H/V Spectral Ratio, Array LEV-1, Sensor 450

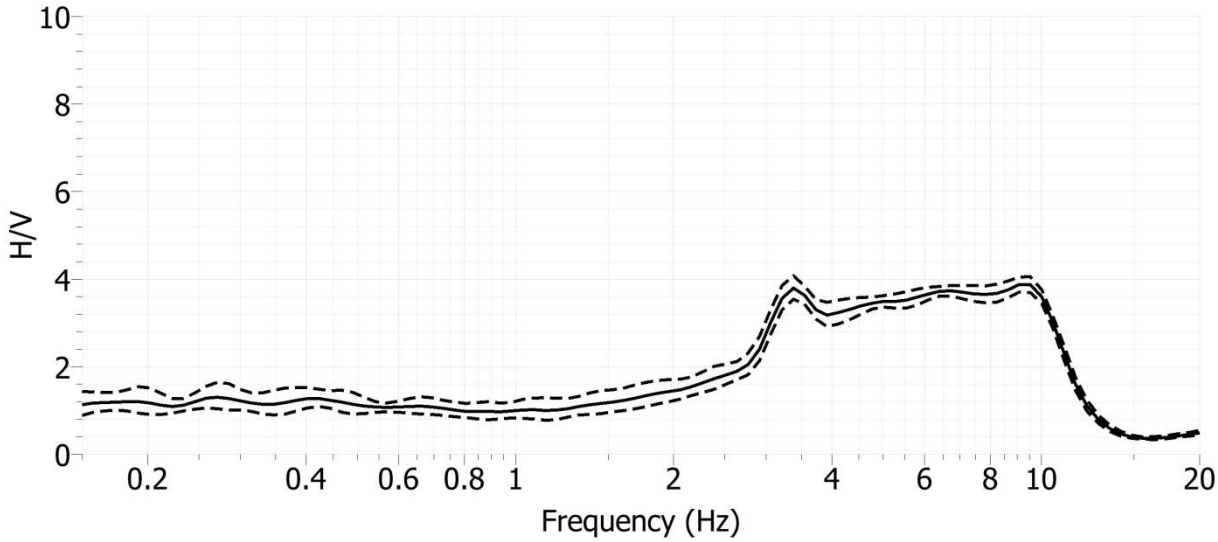

Site CI.LEV, H/V Spectral Ratio, Near AT&T building, Sensor 453A

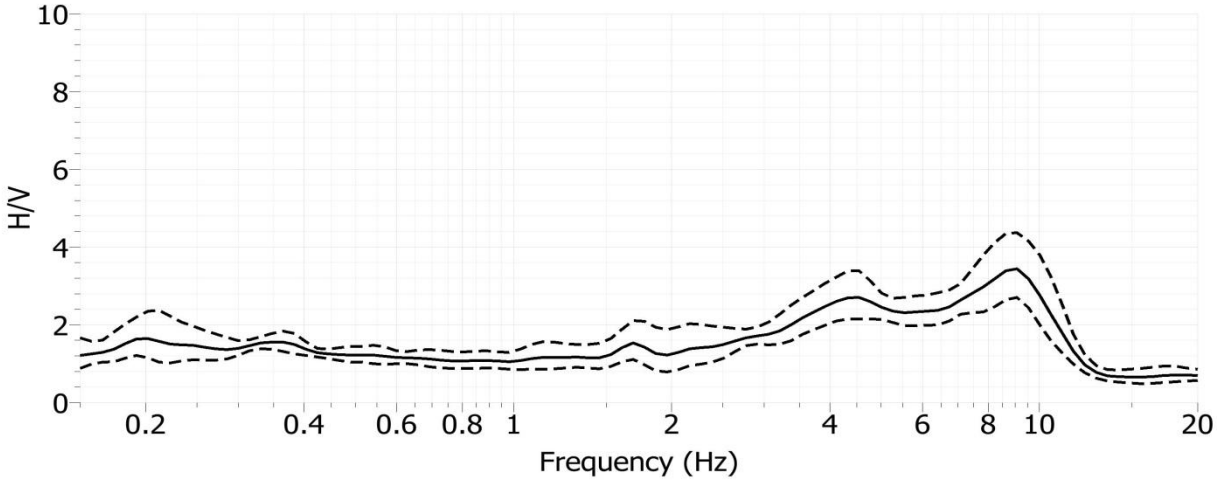

Site CI.LEV, H/V Spectral Ratio, Array LEV-1, Sensor 453

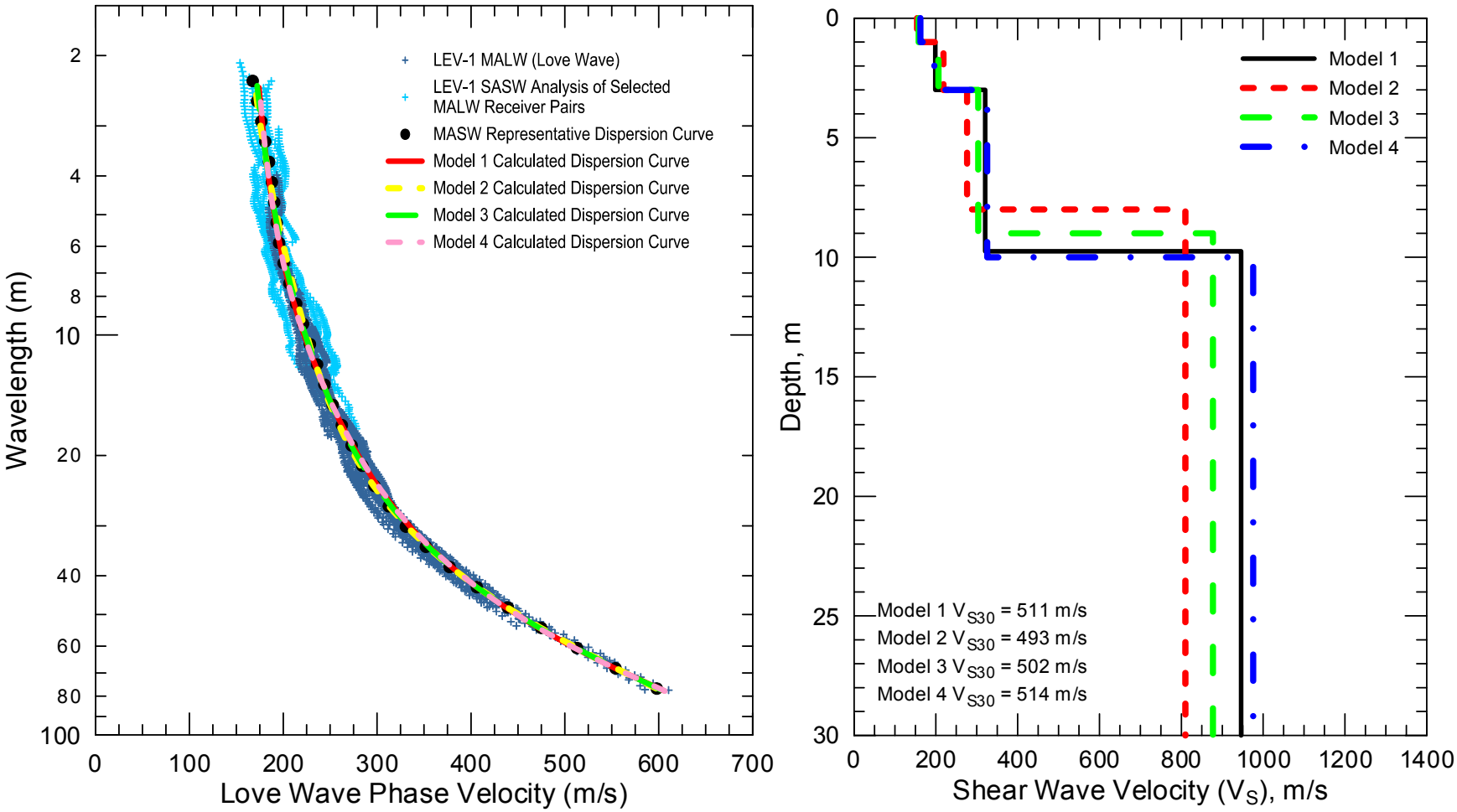

CI.LEV - Field, representative and inverted theoretical Love wave dispersion data (left) and associated V_S models (right)

Site CI.LJR

Location: Lone Juniper Ranch, 41415 Tejon Pass Road, Gorman, Los Angeles County, California

Latitude: 34.80762 **Longitude:** -118.86775
(Station coordinates provided by USGS, WGS84 coordinate system)

V_{S30} (measured): 303 m/s

V_{S30} (adjusted to more accurately reflect seismic station conditions): 325 m/s (average S-wave velocity between 2 and 32 m adjusting for assumed sensor depth).

NEHRP Site Class: D

Geomatrix Code: IGB/IGC

Geologic Conditions/Observations: Seismic station located on geologic unit mapped as Mesozoic (Cretaceous) quartz monzonite. Field inspection reveals that the surficial conditions consist of residual soil and that rock outcrops near the site are decomposed. The San Andreas Fault is located about 600 m south of the seismic station.

Site Conditions: Rural site located on mountain top. Test area located on top of ridge with ground surface elevation decreasing about 2 m to the northwest along the 70.5 m long MASW and seismic refraction array.

Geophysical Methods Utilized: HVSR, Seismic Refraction (P- and S-wave), MASW (Rayleigh Wave) and MALW (Love Wave)

Geophysical Testing Arrays:

1. Array LJR-1 (48 channel MASW and P-wave seismic refraction array utilizing 4.5 Hz vertical geophones spaced 1.5 m apart for a length of 70.5 m, forward and reverse shot locations with multiple source offsets and source types and multiple interior shot locations).
2. Array LJR-1 (48 channel MALW and S-wave seismic refraction array utilizing 10/4.5 Hz horizontal geophones spaced 1.5 m apart for a length of 70.5 m, forward and reverse shot locations with multiple source offsets and multiple interior shot locations). Coincident with P-wave array of same name.
3. Three HVSR measurement locations distributed along array LJR-1.

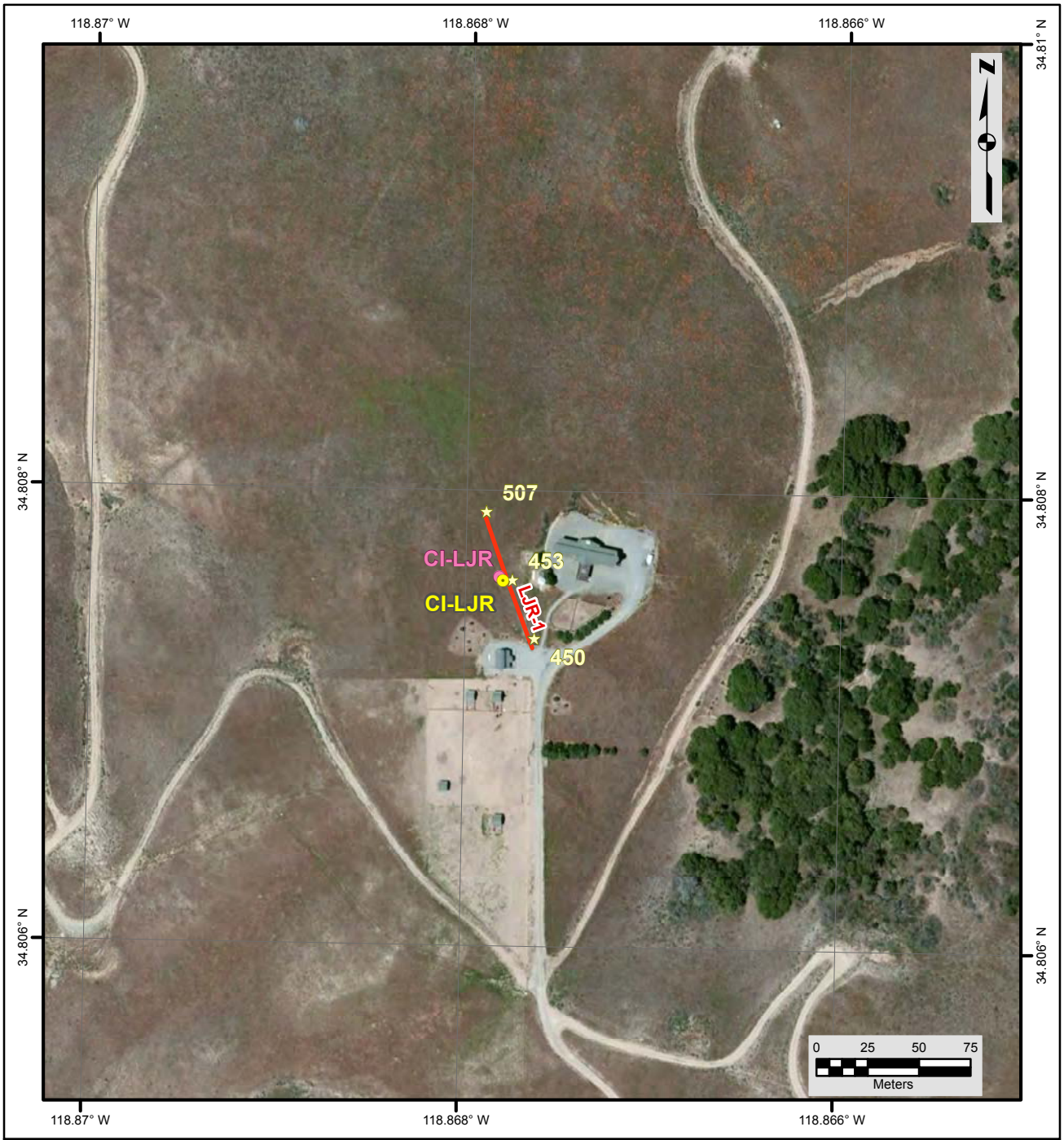

Legend

- Seismic Station - Approximate Surveyed Location
- Seismic Station - Approximate Location of Record
- H/V Spectral Ratio Location
- MASW and Seismic Refraction Array (P- and S-wave)

NOTES:
1. WGS 1984 COORDINATE SYSTEM
2. Image Source: ESRI, i-cubed, USDA FSA, USGS, AEX, GeoEye, Getmapping, Aerogrid, IGP

File Name: CI-LJR-I

Date: 2/7/2013

USGS science for a changing world

GEOVision geophysical services

RECOVERY.GOV

SITE MAP
CI•LJR

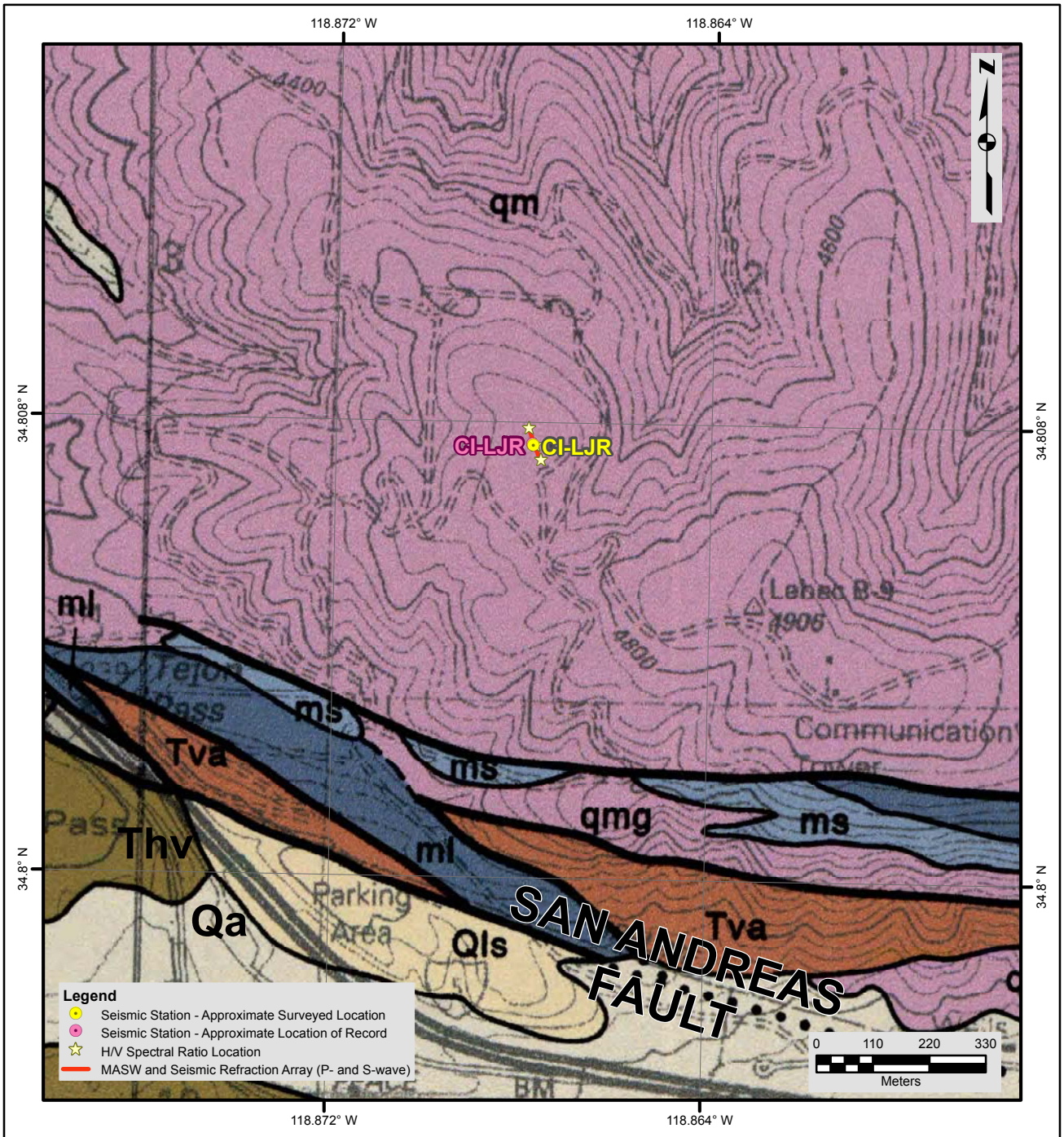

Description of Geologic Map Units

Qa = Quaternary (Holocene) alluvial gravel, sand and clay of valley areas
Qls = Quaternary (Pleistocene) landslide debris
Thv = Quaternary (Pliocene) Hungry Valley Formation; non-marine fluvial sediments, undivided, conglomerate to sandstone
Tva = Tertiary (Miocene) Neenach Volcanic Formation; andesitic flow-breccia, some biotite
qm/qmg = Mesozoic (Cretaceous) quartz monzonite/granite
ms = Mesozoic (Cretaceous) schist-phylite; biotite mica, quartz and feldspar, in part gneissic
ml = Mesozoic (Cretaceous) marble; limestone or dolomite

NOTES:
1. WGS 1984 COORDINATE SYSTEM
2. Geologic Map of the Frazier Mountain & Lebec Quadrangles, Los Angeles, Ventura & Kern Counties, California by Thomas W. Dibblee, Jr., 2006
3. See site map for details of geophysical survey

USGS science for a changing world
GEOVision geophysical services

GEOLOGIC MAP
CI•LJR

RECOVERY.GOV

File Name: CI-LJR
Date: 2/7/2013

Looking west at HVSR sensor 453 and CI.LJR seismic station

HVSR sensor placed in shallow hole

Looking southeast along array LJR-1 towards seismic station

Looking northwest along array LJR-1 towards seismic station

S-wave refraction and MALW data acquisition

Location of Geophysical Testing Arrays:

Location	Latitude	Longitude
LJR-1, Southeast End of MASW/Refraction Array	34.80731	-118.86757
LJR-1, Center of MASW/Refraction Array	34.80761	-118.86771
LJR-1, Northwest End of MASW/Refraction Array	34.80790	-118.86784
HVSR Sensor 450	34.80735	-118.86756
HVSR Sensor 453	34.80761	-118.86768
HVSR Sensor 507	34.80791	-118.86783
CI.LJR Seismic Station	34.80760	-118.86773

Notes: 1) WGS84 Coordinate System (decimal degrees)
2) Survey accuracy is estimated at 1 to 2 m.

Results:

V_S Model

Depth to Top of Layer (m)	Layer Thickness (m)	S-Wave Velocity (m/s)	Inferred P-Wave Velocity (m/s)	Assumed Poisson's Ratio	Assumed Density (g/cm^3)
0	1	164	306	0.3	1.7
1	2	205	384	0.3	1.7
3	3	223	417	0.3	1.7
6	4	243	455	0.3	1.7
10	6	308	576	0.3	1.8
16	8	389	727	0.3	1.8
24	>6	459	859	0.3	1.9

Notes: 1) Depth of investigation is about 30 m.
2) Bottom layer is a half space.

Observations/Discussion:

- HVSR plots at the three measurement stations are almost identical at frequencies below about 4 Hz, with slight differences at higher frequencies.
- There is a distinct HVSR peak at about 1.6 Hz. Given the velocity structure at the site, as discussed later, this peak could indicate a large impedance contrast associated with more competent bedrock at a depth on the order of 50 m, or more.
- The P-wave refraction data for array LJR-1 were modeled using a tomographic inversion routine with both smooth velocity gradient and layer-based starting models. The S-wave refraction data for array LJR-1 were modeled using a tomographic inversion routine with a smooth velocity gradient starting model. The seismic refraction models were extended to far offset shot locations to extend depth of investigation. A larger geophone spacing rather than the utilization of far offset shot locations is preferred for extending depth of investigation, when applying tomographic inversion routines.
- The P-wave first arrival data were picked to a greater degree of accuracy than the S-wave first arrival data because the S-wave is not typically the first energy on a seismic record, even when using a horizontal traction plank as an energy source. In the P-wave seismic data the air wave arrives before the direct soil arrival and an attempt was made to pick the direct arrival later in time than the air wave, which is not always easy.
- The P-wave seismic refraction survey design allowed P-wave velocity to be imaged to a maximum depth of about 30 m, although a longer profile is preferred to image to this depth. The seismic refraction models utilizing layer based and smooth velocity gradient starting models are quite similar with P-wave velocity of about 250 to 300 m/s at the surface, increasing to over 400 m/s at a depth of 1 to 5 m, 600 m/s at a depth of 7 to 10 m, 800 m/s at a depth of 15 to 21 m and over 1,000 m/s at a nominal depth of 25 to 30 m.
- The S-wave seismic refraction survey design allowed S-wave velocity structure to be imaged to a maximum depth of about 30 m. S-wave velocity is 150 to 200 m/s at the surface, increasing to over 300 m/s at a depth of 7 to 10 m, 400 m/s at a depth of 15 to 20 m and over 500 m/s at a nominal depth of 29 m.
- The P- and S-wave seismic refraction models indicate that there is some lateral velocity variation with a gradual thickening sequence of lower velocity, more intensely weathered or decomposed rock to the northwest.
- Noise conditions at the site were not sufficient for application of passive surface wave techniques.
- Review of Rayleigh wave (MASW) data indicated that higher modes were dominant over a wide frequency range. The source of dominant higher mode energy Rayleigh wave data is not clear. Therefore, S-wave refraction and Love wave (MALW) data were acquired at the site. Dominant higher modes are not a significant issue in Love wave (MALW) data. Therefore, modeling of Love wave, rather than Rayleigh wave, phase velocity data was conducted at this site. It should be noted, however, that the Love wave data were acquired using 4.5 Hz horizontal geophones and a hammer/traction plank energy source. To develop a V_S model to 30 m depth it was necessary to pick Love wave phase velocity data to a frequency of about 4.5 Hz, which is likely pushing the limits of the energy source. Consideration should be given to reacquiring the Love wave data with a lower frequency energy source, providing a cost effective energy source can be identified.

- The minimum wavelength Love wave phase velocity data extracted from the 48-channel MASW array was about 3.5 m. Reducing data from smaller hammer sources using a limited offset receiver array (i.e. less active geophones) allowed for extraction of surface wave dispersion data to a minimum wavelength of about 2.5 m, an insignificant gain.
- There is about 20 to 40 m/s of scatter in MALW dispersion data, which is in part due to lateral velocity variation caused by differential weathering of near surface rock/residual soil.
- A representative dispersion curve was generated for the MALW data set using a moving average, polynomial curve fitting routine and used for modeling.
- Surface wave depth of investigation is about 30 m based on one-half to one-third of maximum wavelength criteria and a maximum wavelength of about 82 m.
- V_{S30} derived from the Love wave V_S model is 303 m/s (Site Class D).
- The average S-wave velocity between 2 and 32 m depth is 325 m/s.
- The S-wave seismic refraction model yields a V_{S30} of about 317 to 332 m/s between a position of 24 and 45 m where depth of investigation is greatest. The average V_{S30} over this interval is about 323 m/s, 6 % higher than that estimated from the MALW sounding. It should be noted that the S-wave refraction survey was not optimally designed to image to 30 m depth and may have higher error than the surface wave sounding.

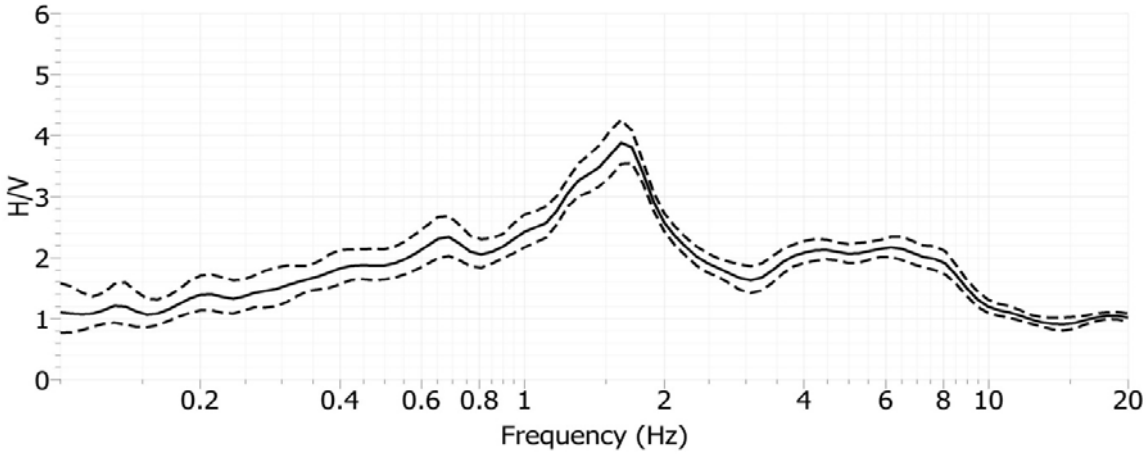

Site CI.LJR, H/V Spectral Ratio, Array LJR-1, Sensor 507

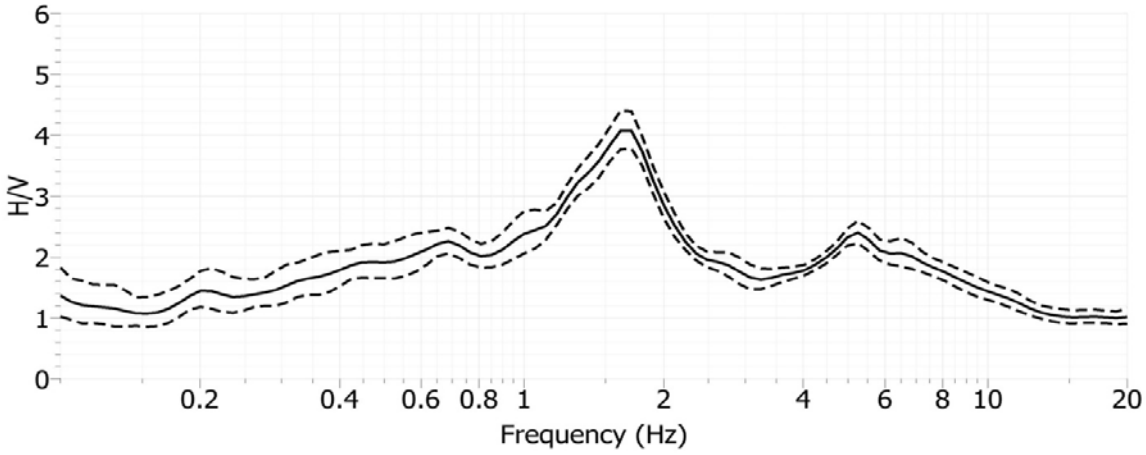

Site CI.LJR, H/V Spectral Ratio, Array LJR-1, Sensor 453

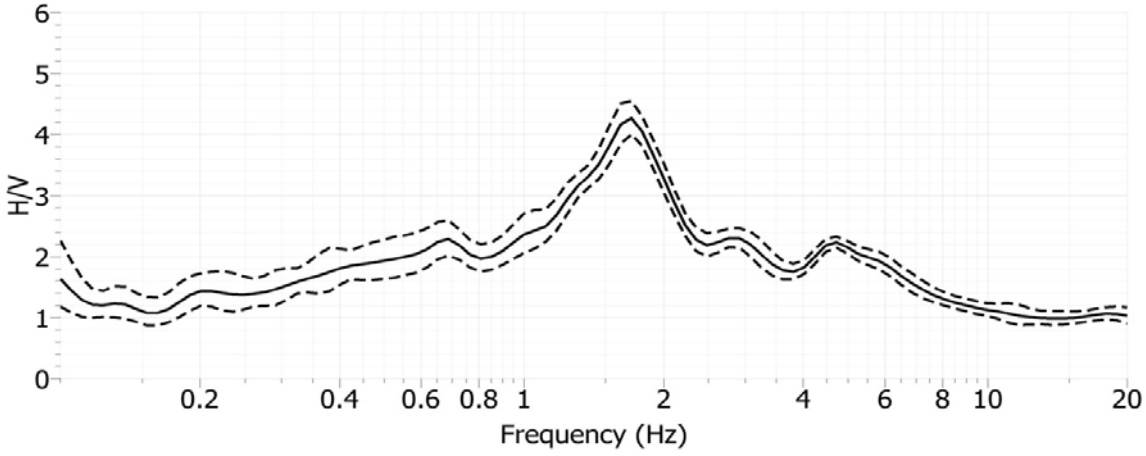

Site CI.LJR, H/V Spectral Ratio, Array LJR-1, Sensor 450

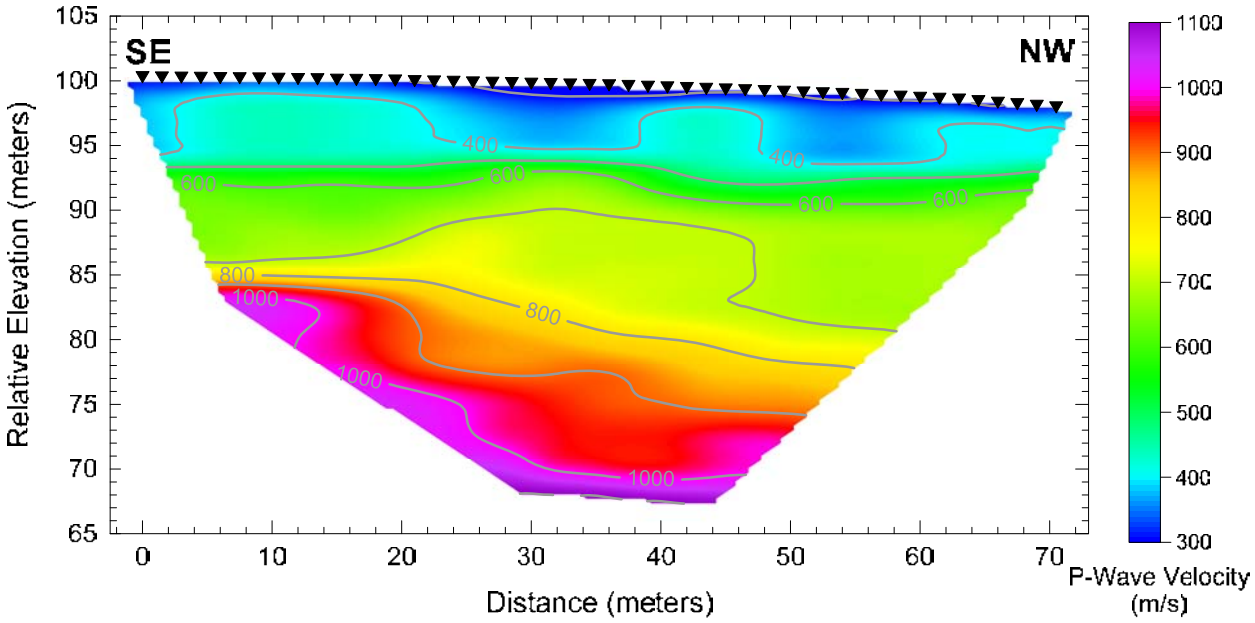

Array LJR-1 – P-wave tomographic seismic refraction model developed utilizing a layer based starting model

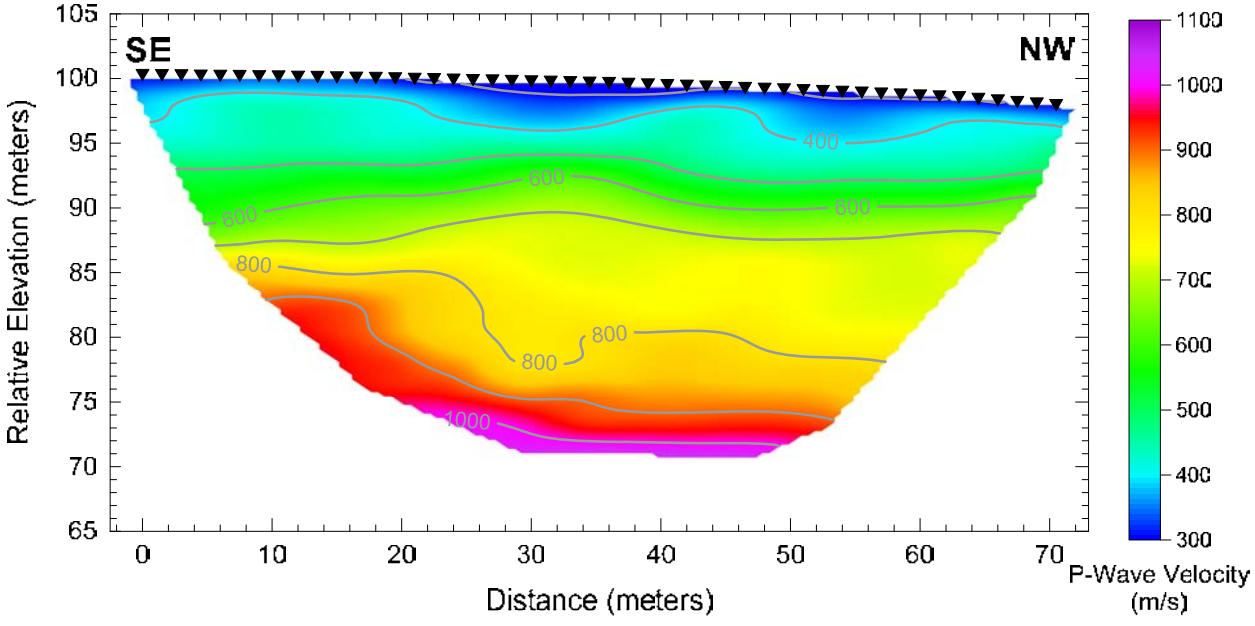

Array LJR-1 – P-wave tomographic seismic refraction model developed utilizing a smooth velocity gradient starting model

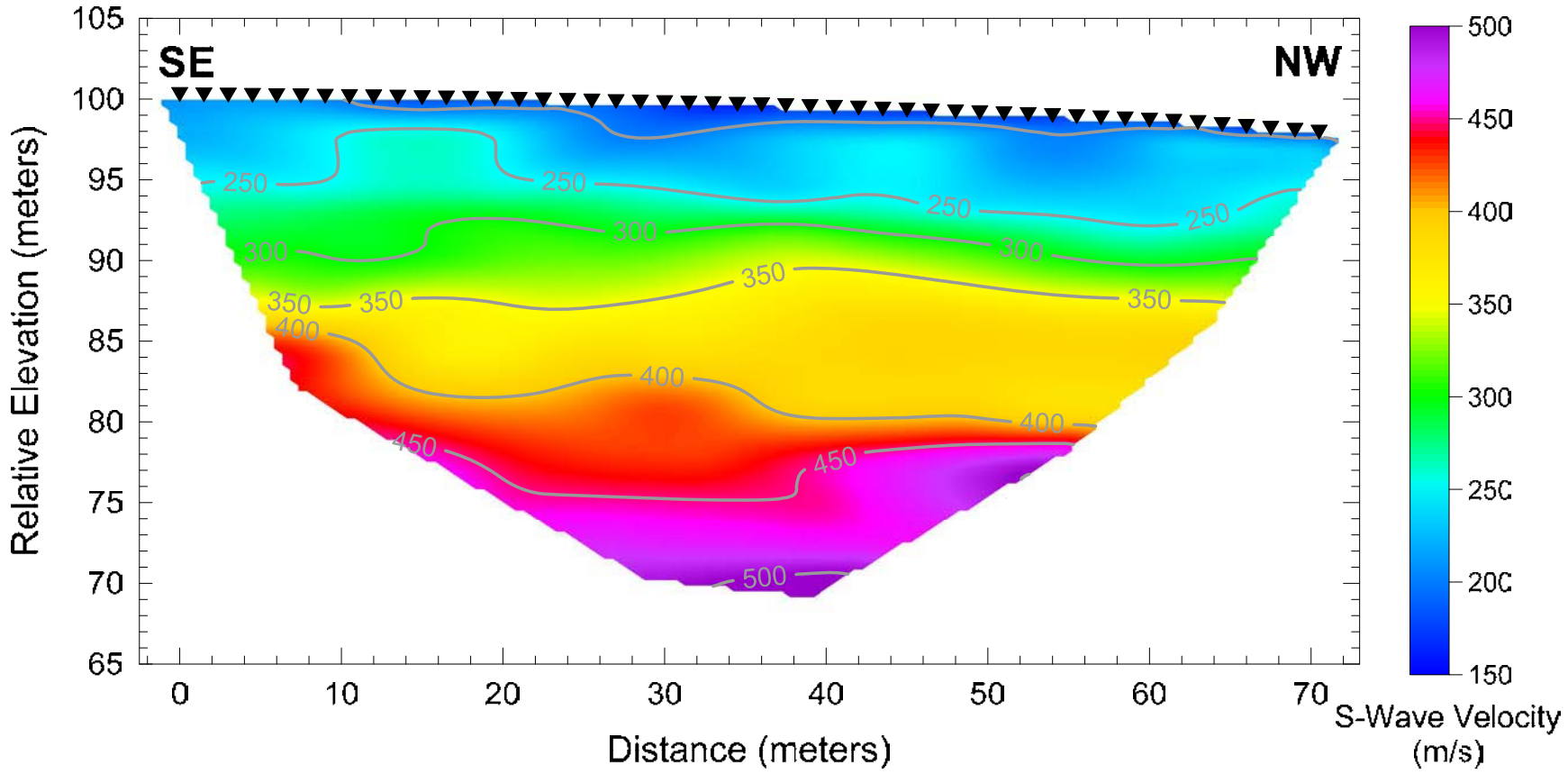

Array LJR-1 – S-wave tomographic seismic refraction model developed utilizing a smooth velocity gradient starting model

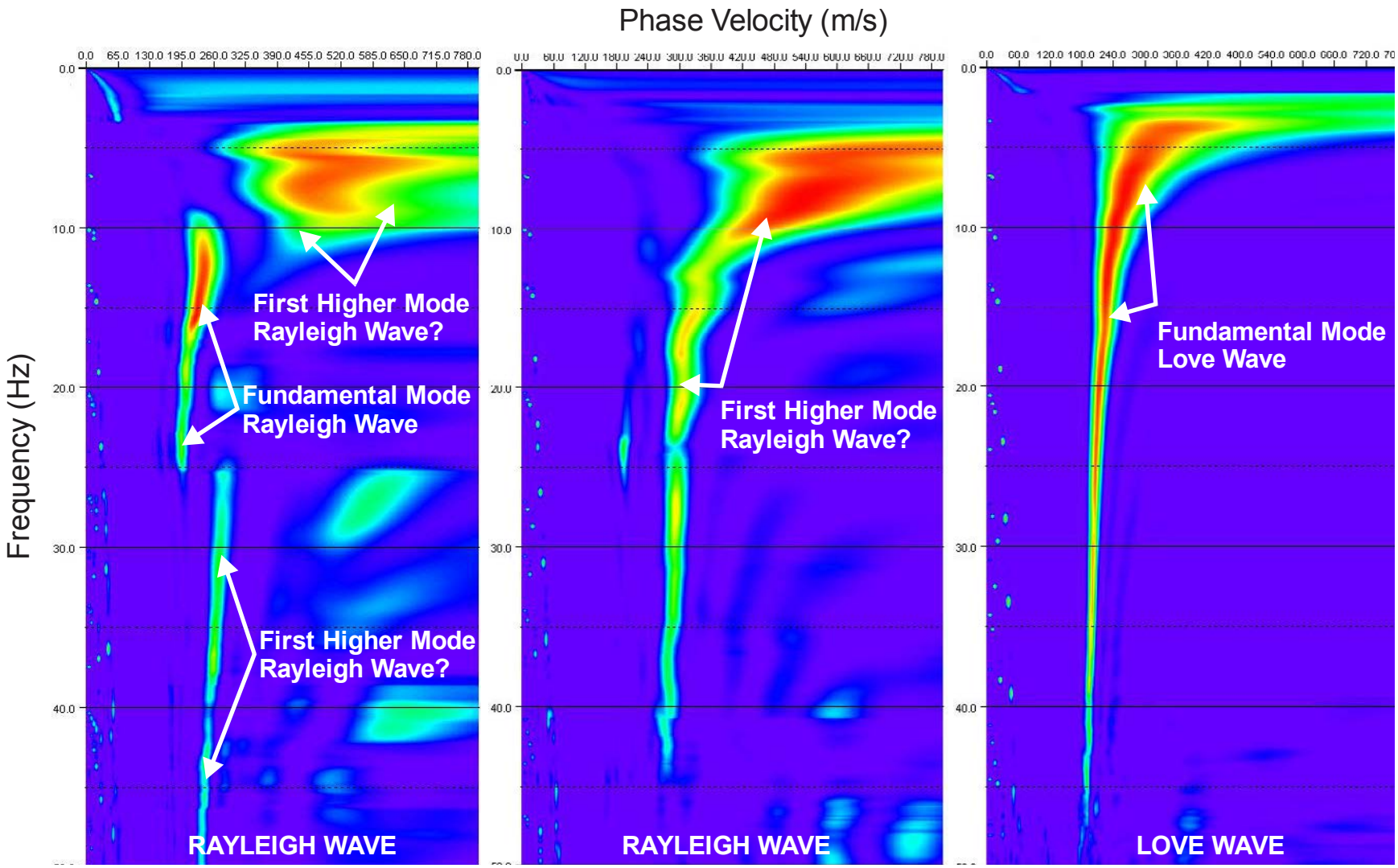

Array LJR-1 – Comparison of Rayleigh and Love wave overtone images demonstrating dominant higher mode energy in the Rayleigh wave data. Rayleigh wave overtone images from seismic records with source offsets of 1 m (left) and 30 m (center).

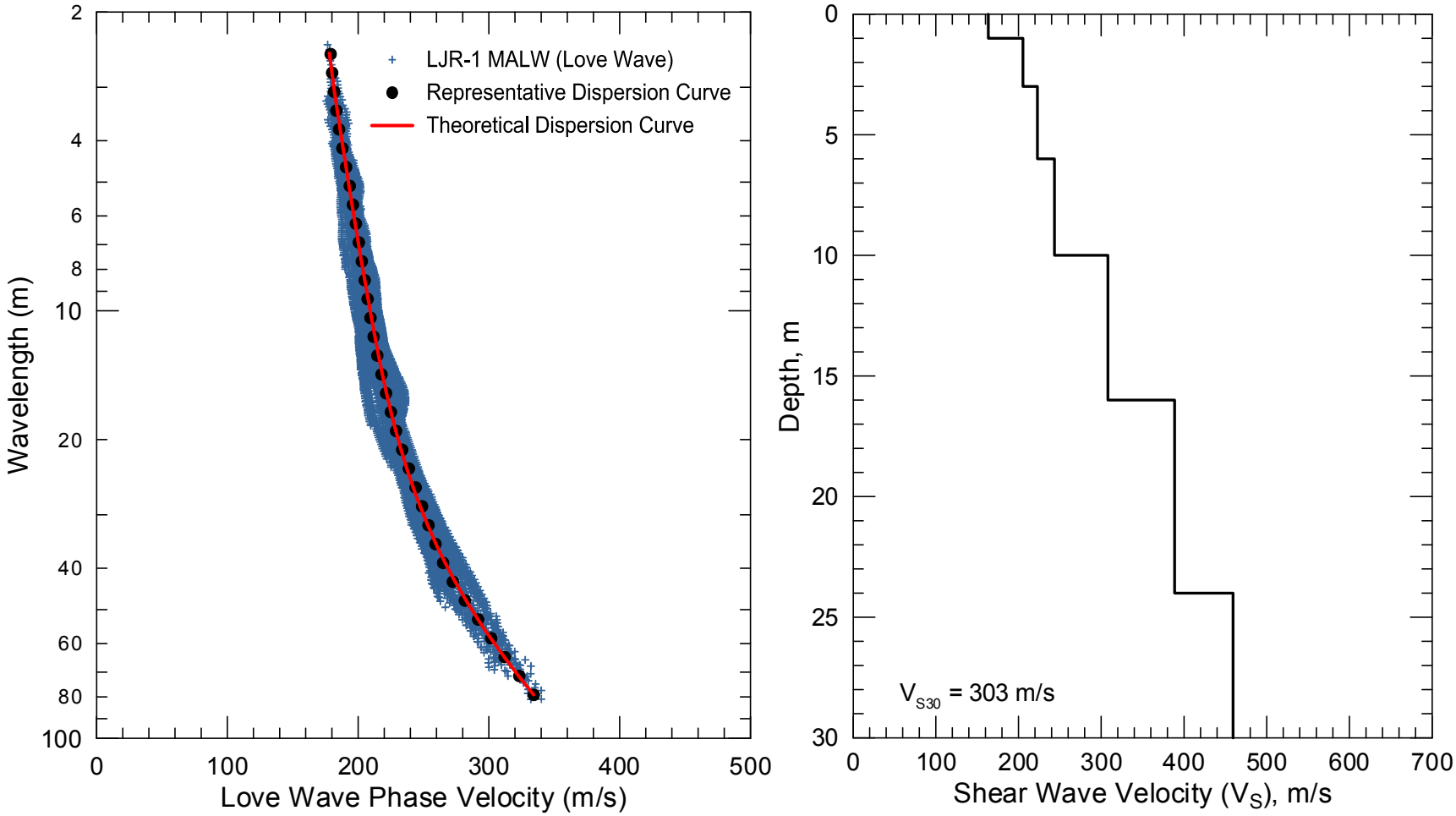

CI.LJR - Field, representative and inverted theoretical surface wave dispersion data (left) and associated V_S model (right)

Site CI.LPC

Location: Lone Pine Canyon, 5329 Lone Pine Canyon Road, San Bernardino County, California

Latitude: 34.31478 **Longitude:** -117.54642

(Coordinates provided by USGS – WGS84 coordinate system)

V_{S30} (measured): 506 m/s

V_{S30} (adjusted to more accurately reflect seismic station conditions): 542 m/s (average S-wave velocity between 1 and 31 m adjusting for assumed 1 m sensor depth).

NEHRP Site Class: C

Geomatrix Code: IHB/IHC

Geologic Conditions/Observations: Seismic station located on geologic unit mapped as Quaternary (Holocene) alluvial gravel and sand deposits. Seismic station is located in the San Andreas Fault Zone. Site located in 600 meter wide valley associated with fault zone, with Pelona Schist outcropping 150 meters to the southwest and gneiss outcropping 400 meters to the northeast.

Site Conditions: Rural site. Windy conditions during testing. Relatively gentle topography in test vicinity with gradual elevation decreasing to the southwest.

Geophysical Methods Utilized: HVSR, Seismic Refraction, MASW

Geophysical Testing Arrays:

1. Array LPC-1 (48 channel MASW and P-wave seismic refraction array utilizing 4.5 Hz vertical geophones spaced 1.5 m apart for a length of 70.5 m, forward and reverse shot locations with multiple source offsets and source types and center shot location).
2. Array LPC-2 (48 channel P-wave seismic refraction array utilizing 4.5 Hz vertical geophones spaced 3 m apart for a length of 141 m, forward and reverse shot locations with multiple source offsets and source types and multiple interior shot locations).
3. Three HVSR measurement locations; two distributed along array LPC-1 and the other near the seismic station.

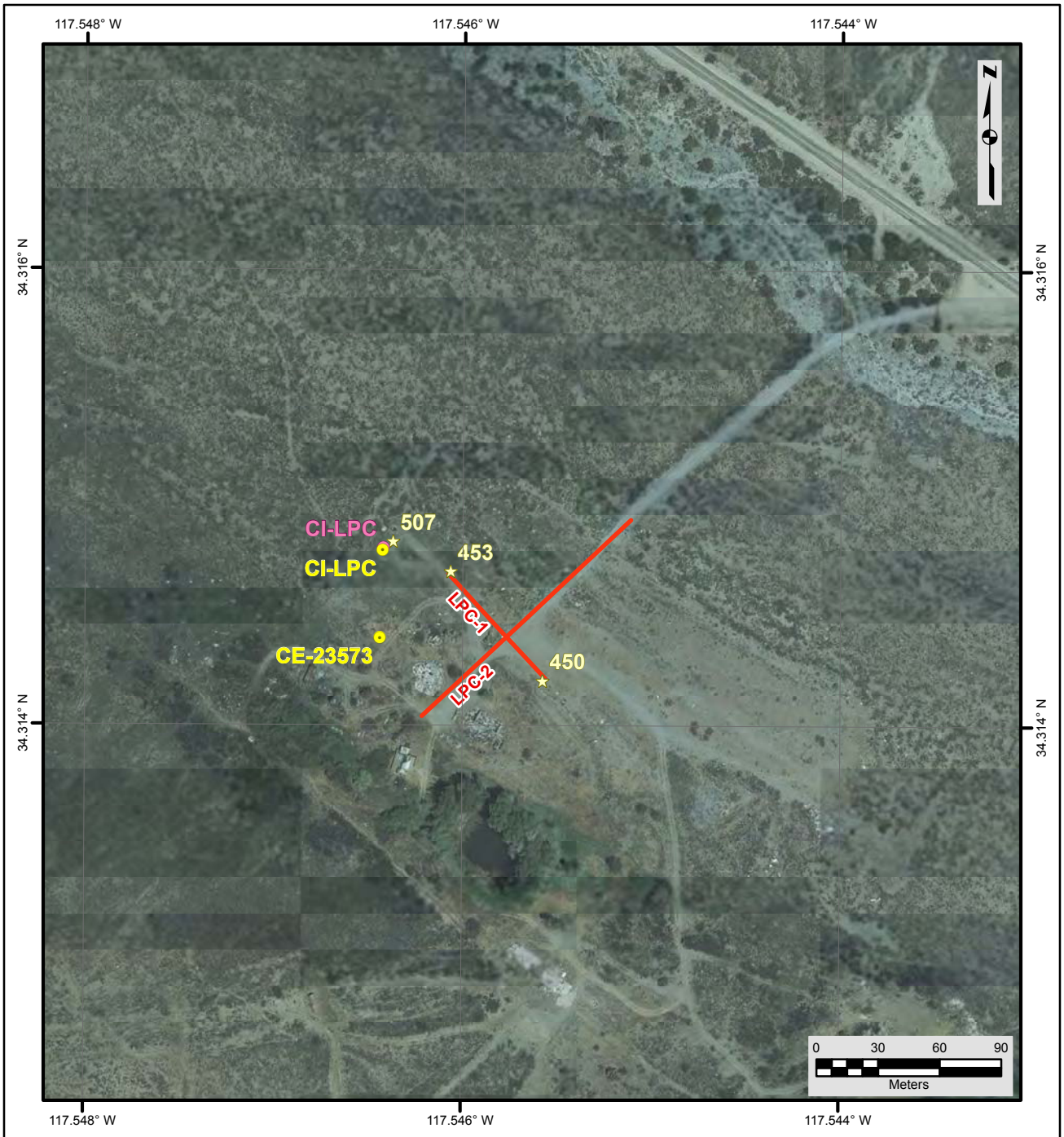

Legend

- Seismic Station - Approximate Surveyed Location
- Seismic Station - Approximate Location of Record
- H/V Spectral Ratio Location
- MASW and Seismic Refraction Array

NOTES:
1. WGS 1984 COORDINATE SYSTEM
2. Image Source: ESRI, i-cubed, USDA FSA, USGS, AEX, GeoEye, Getmapping, Aerogrid, IGP

File Name: CI-LPC-I

Date: 9/16/2011

USGS science for a changing world

GEOVision geophysical services

RECOVERY.GOV

SITE MAP
CI•LPC

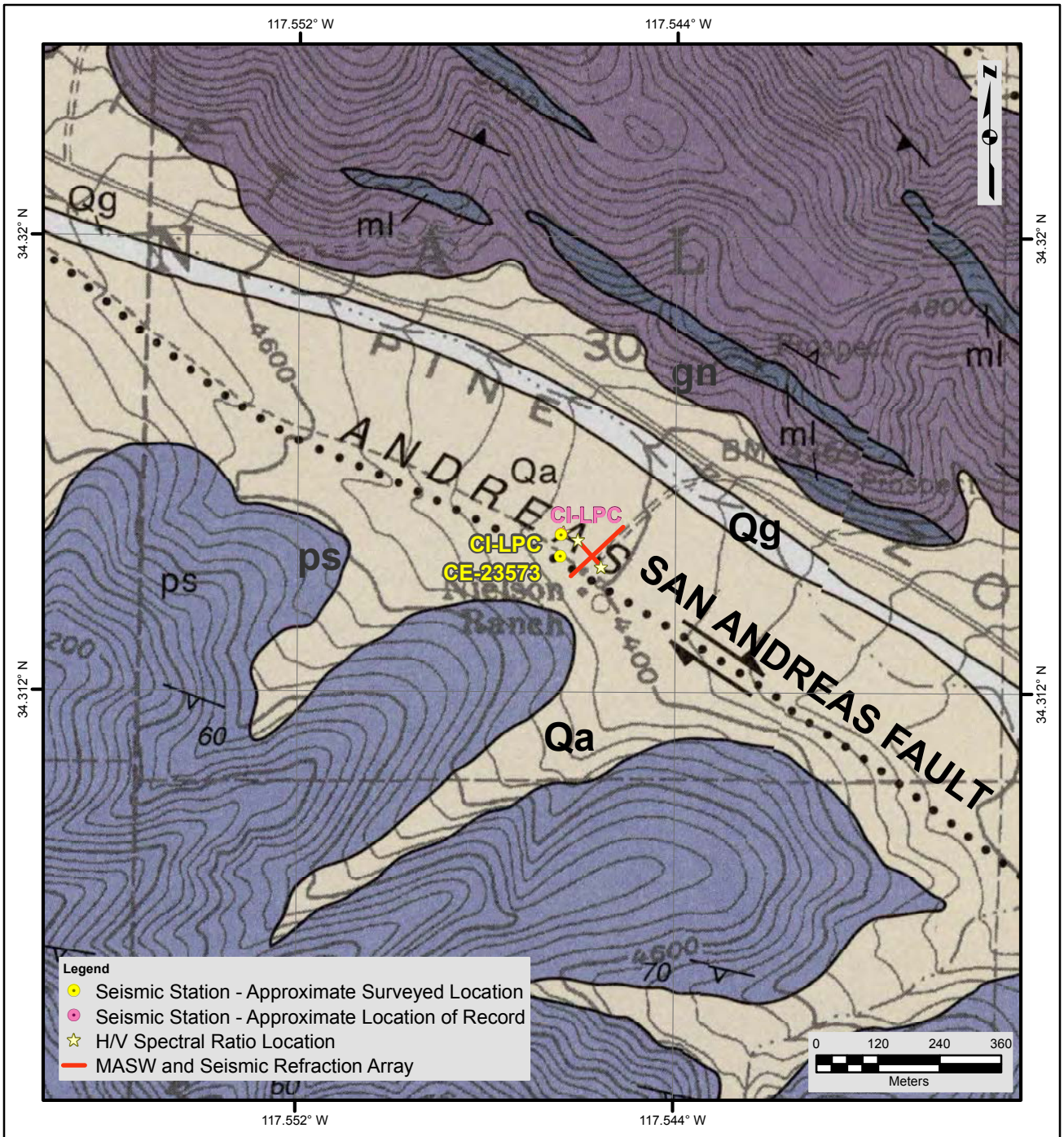

Description of Geologic Map Units

Qg = Quaternary (Holocene) alluvial gravel and sand of stream channels
Qa = Quaternary (Holocene) alluvial gravel and sand of valley areas
ps = Mesozoic (Cretaceous)Pelona Schist; calcaceous, foliated
gn = Precambrian (?) gneiss, hard, closely fractured
ml = Precambrian (?) marble, medium to coarse crystalline

NOTES:
1. WGS 1984 COORDINATE SYSTEM
2. Geologic Map of the Telegraph Peak and Phelan Quadrangles, San Bernardino County, California by Thomas W. Dibblee, Jr., 2003
3. See site map for details of geophysical survey

File Name: CI-LPC

Date: 9/16/2011

USGS science for a changing world

GEOVision geophysical services

RECOVERY.GOV

GEOLOGIC MAP
CI•LPC

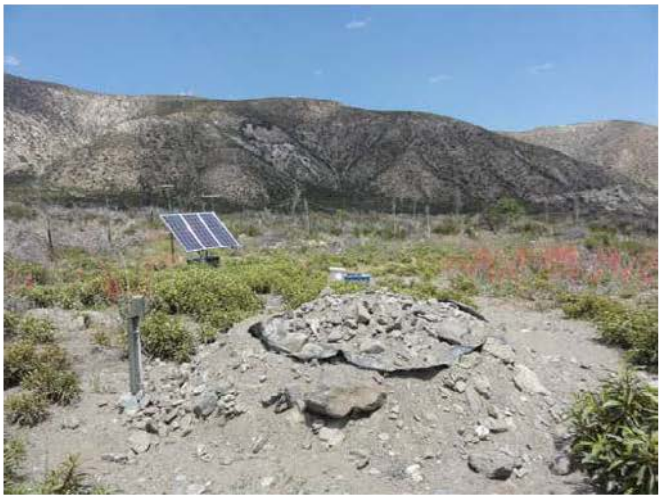

Looking northeast towards CI.LPC seismic station

Looking northwest along Array LPC-1

Plaster used to couple HVSR sensors to loose, gravelly surficial sediments

Looking northeast along Array LPC-2

Looking northwest towards seismic station from northwest end of Array LPC-1

Location of Geophysical Testing Arrays:

Location	Latitude	Longitude
LPC-1, Northwest End of MASW/Refraction Array	34.31467	-117.54608
LPC-1, Center of MASW/Refraction Array	34.31444	-117.54582
LPC-1, Southeast End of MASW/Refraction Array	34.31420	-117.54556
LPC-2, Southwest End of Seismic Refraction Array	34.31404	-117.54621
LPC-2, Center of Seismic Refraction Array	34.31447	-117.54567
LPC-2, Northeast End of Seismic Refraction Array	34.31490	-117.54511
HVSR Sensor 450	34.31420	-117.54557
HVSR Sensor 453	34.31468	-117.54606
HVSR Sensor 507	34.31481	-117.54637
CE.23573 Seismic Station	34.31438	-117.54644
CI.LPC Seismic Station	34.31477	-117.54642

Notes: 1) WGS84 Coordinate System (decimal degrees).
2) Survey accuracy is estimated at 1 to 2 m.

Results:

V_S Model

Depth to Top of Layer (m)	Layer Thickness (m)	S-Wave Velocity (m/s)	Inferred P-Wave Velocity (m/s)	Assumed Poisson's Ratio	Assumed Density (g/cm^3)
0	1	184	344	0.3	1.8
1	2	294	551	0.3	1.8
3	3	427	798	0.3	1.9
6	4	505	945	0.3	2.0
10	6	603	1127	0.3	2.1
16	9	616	1152	0.3	2.1
25	>5	664	1242	0.3	2.1

Notes: 1) Depth of investigation is about 30 m.
2) Bottom layer is a half space.

Observations/Discussion:

- Seismic station CI.LPC is located in the San Andreas Fault Zone. Seismic station CE.23573 is also located in close proximity to the test area.
- The HVSR curves are almost identical at frequencies below 10 Hz, validating the 1-D velocity approximation.
- There are no high amplitude peaks in the HVSR data.

- MASW array LPC-1 was aligned parallel to the San Andreas Fault Zone and as close as possible to the seismic station. Seismic refraction array LPC-2 was aligned perpendicular to the fault zone to demonstrate that there is not significant out of plane structures near array LPC-1 that could affect surface wave propagation. MASW analysis was not conducted on the array LPC-2 seismic data, but is possible.
- The P-wave refraction data for array LPC-1 were modeled using a tomographic inversion routine with both layer based and smooth velocity gradient starting models.
- The seismic refraction models for array LPC-1 indicate that P-wave velocity ranges from 400 to 500 m/s at the surface and increases to about 800 m/s at a depth of 2 to 4 m and exceeds 1,100 m/s below a depth of 5 to 9 m.
- The P-wave refraction data for array LPC-2 were modeled using a tomographic inversion routine with a layer based starting model generated using the time-term method. The model shows P-wave velocity increasing with depth from about 400 to 600 m/s at the surface to over 1, 000 m/s at a depth of 4 to 12 m, below which velocity varies from 1,000 to about 1, 250 m/s to about 40 m depth where velocity may increase to over 2,500 m/s. The velocity and geometry of the high velocity layer at the base of the model is not well constrained due to inadequate line length and source offset. This high velocity layer could be associated with either saturated sediments or weathered rock.
- The site conditions were not conducive to application of passive surface wave techniques.
- There is some scatter in the MASW surface wave dispersion data, possibly in part due to minor lateral velocity variation.
- The minimum wavelength surface wave phase velocity data extracted from the 48-channel MASW array was about 12 m. Data reduction using seismic records from smaller hammer sources and a limited offset receiver array (i.e. less active geophones) allowed extraction of surface wave dispersion data to a minimum wavelength of about 2 m.
- Surface wave phase velocity data at wavelengths smaller than about 5 m primarily extracted from a 3 lb hammer shot locations in the center and at the southeast end of the array with limited receiver offset. The similar shot location at the northwest end of the array yielded phase velocity data with slightly higher velocity and we opted to model the lower small wavelength phase velocities.
- A representative dispersion curve was generated for the MASW surface wave data set using a moving average, polynomial curve fitting routine and used for data modeling.
- Surface wave depth of investigation is about 30 m based on half of maximum wavelength criteria
- The inferred P-wave velocities in the surface wave model, assuming a Poisson's ratio of 0.3, are consistent with P-wave velocity structure in the seismic refraction models.
- S-wave velocity exceeds 400 m/s at a depth of 3 m and 600 m/s at a depth of 10 m. Velocities higher than 500 to 600 m/s are not expected to be associated with Holocene sediments and are likely associated with older sediments or, possibly, intensely fractured rock in the fault zone.
- V_{S30} is 506 m/s (Site Class C).
- Average S-wave velocity between 1 m (assumed sensor depth) and 31 m is 542 m/s.

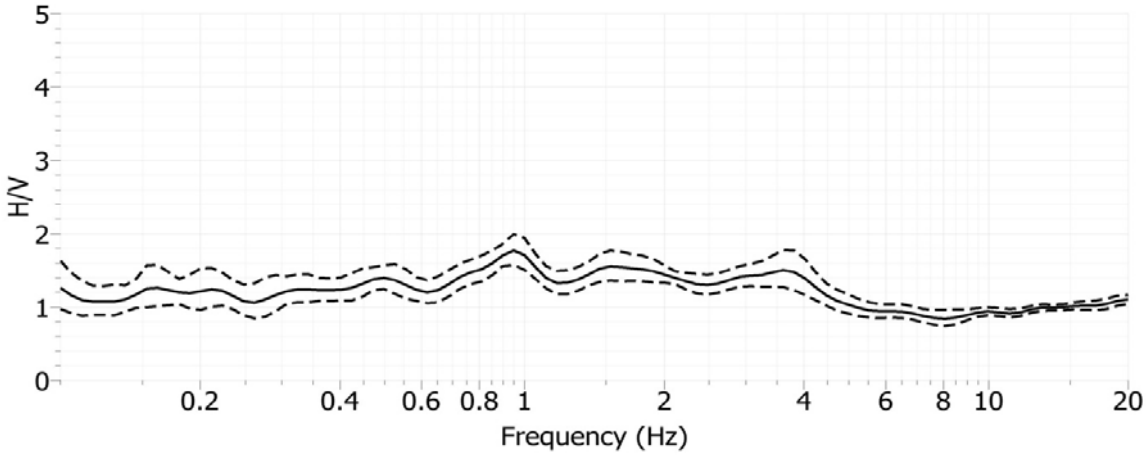

Site CI.LPC, H/V Spectral Ratio, Near Seismic Station, Sensor 507

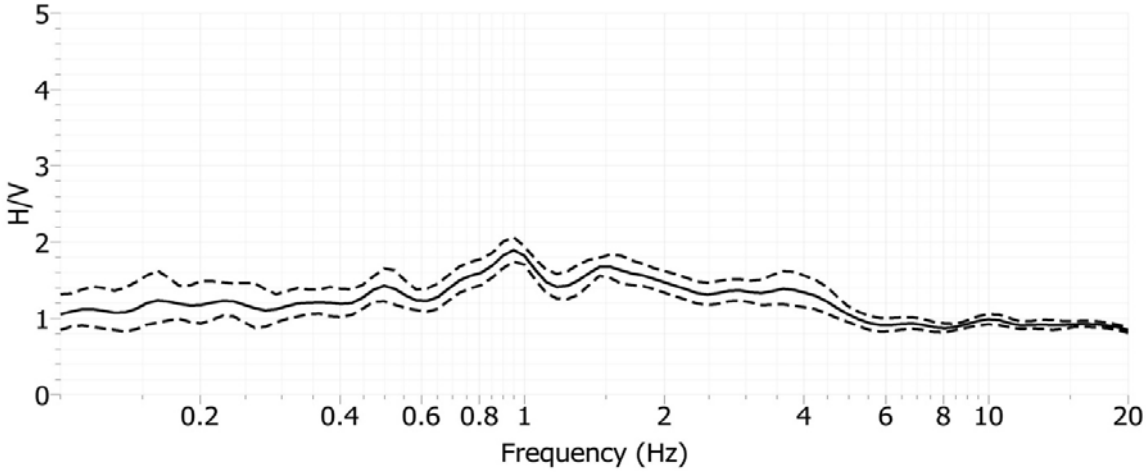

Site CI.LPC, H/V Spectral Ratio, Array LPC-1, Sensor 453

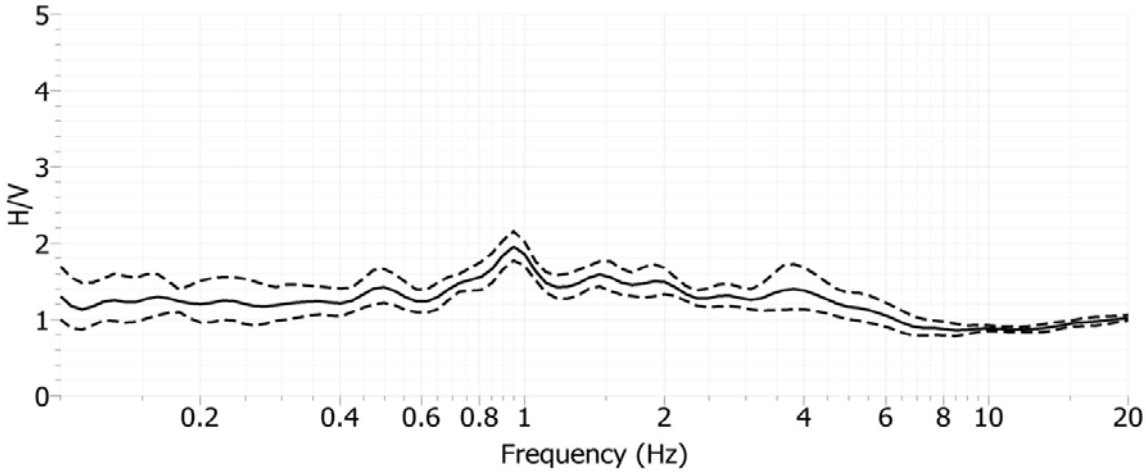

Site CI.LPC, H/V Spectral Ratio, Array LPC-1, Sensor 450

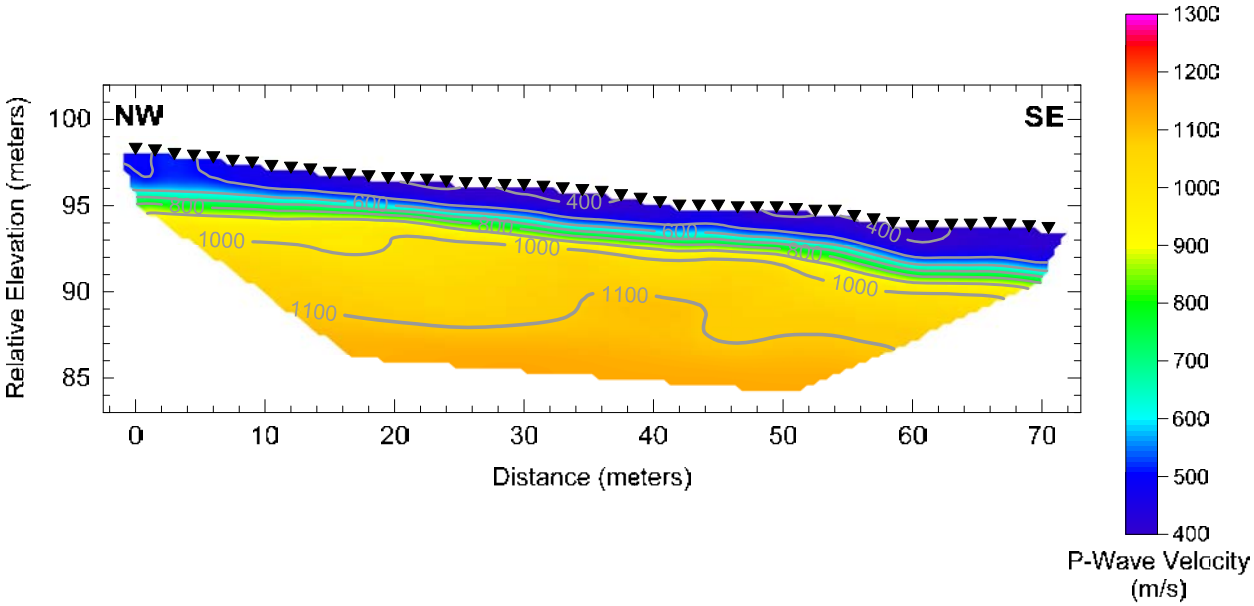

Array LPC-1 – Tomographic Seismic Refraction Model utilizing Layer Based Starting Model

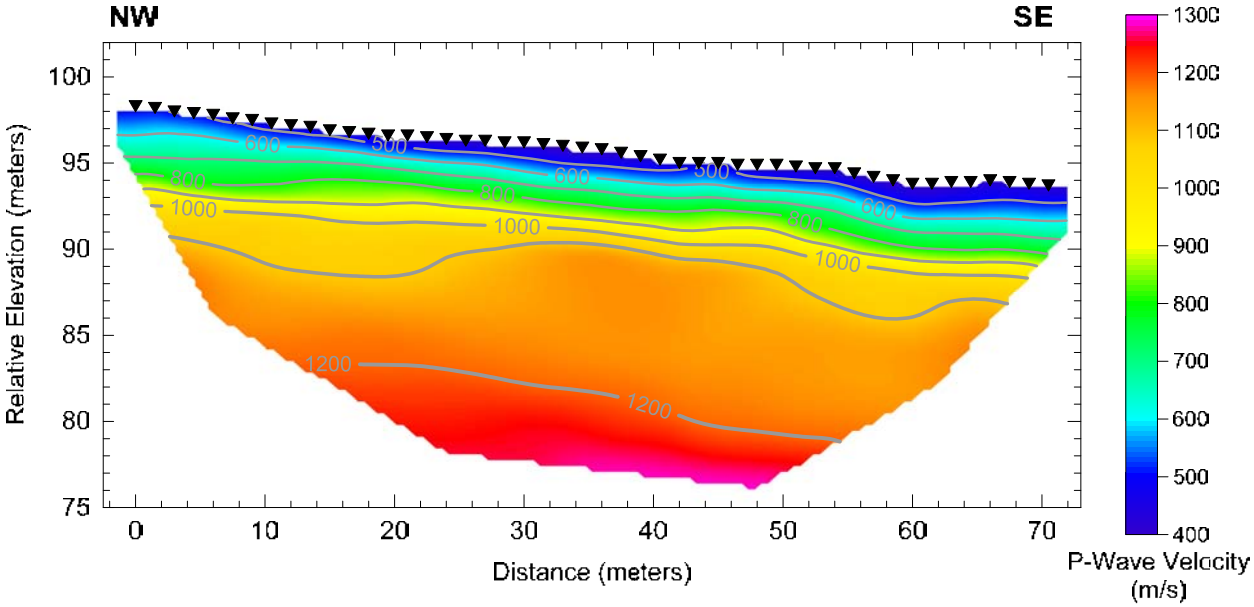

Array LPC-1 – Tomographic Seismic Refraction Model utilizing Smooth Velocity Gradient Starting Model

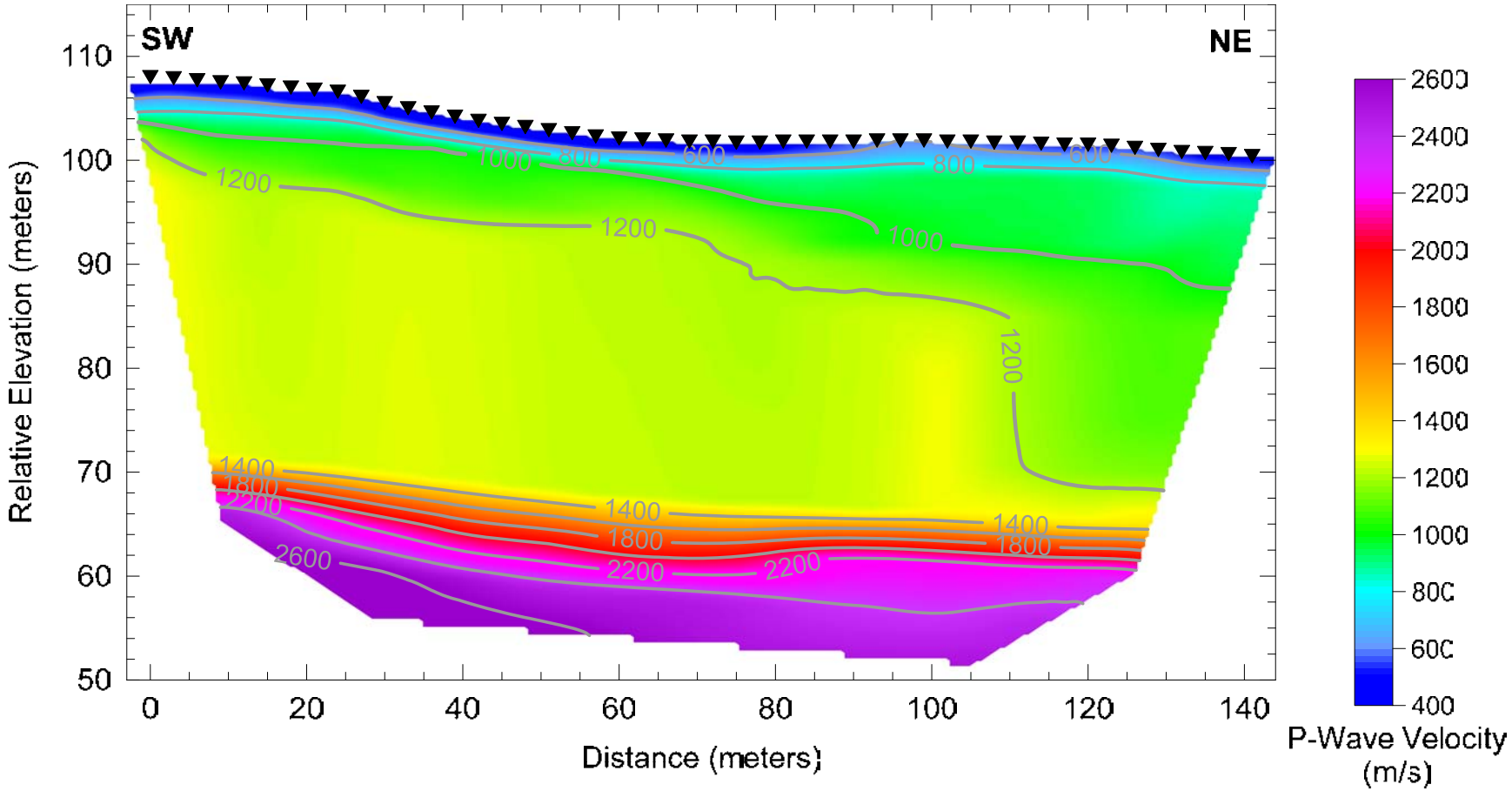

Note: High velocity layer at base of model exists, but is poorly constrained (both velocity and geometry) due to inadequate line length and shot offsets. This layer could be associated with either weathered rock or saturated sediments depending upon nature of geologic material beneath the seismic line.

Array LPC-2 – Tomographic Seismic Refraction Model utilizing Layer Based Starting Model

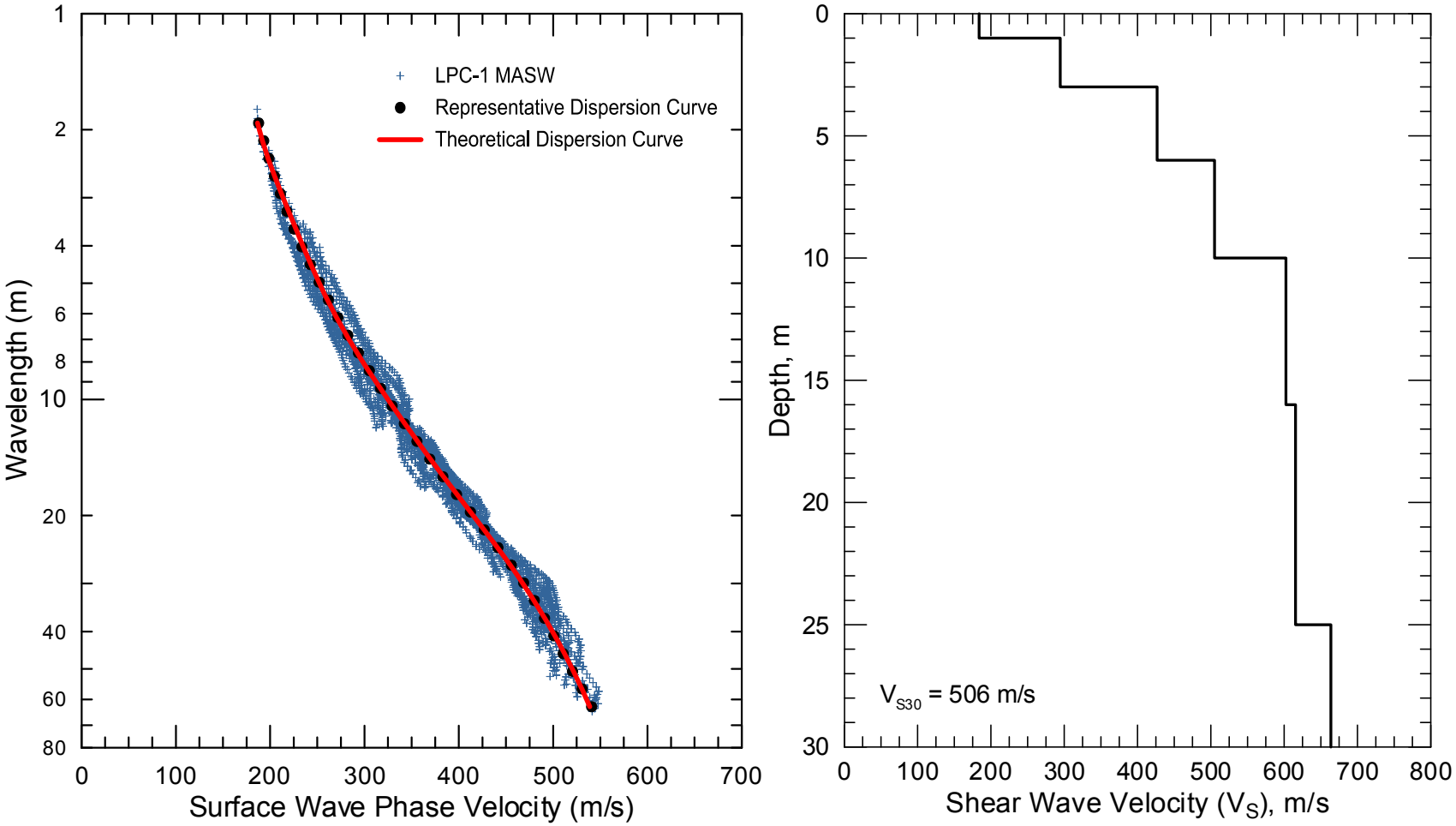

CI.LPC - Field, representative and inverted theoretical surface wave dispersion data (left) and associated V_S model (right)

Site CI.LRL

Location: Laurel Mountain, Ridgecrest, Kern County, California

Latitude: 35.47954 **Longitude:** -117.68212
(Station coordinates provided by USGS, WGS84 coordinate system)

V_{S30} (measured): 511 m/s

V_{S30} (adjusted to more accurately reflect seismic station conditions): 596 m/s (average S-wave velocity between 1 and 31 m adjusting for inferred 1 m sensor depth).

NEHRP Site Class: C

Geomatrix Code: IGA/IGB

Geologic Conditions/Observations: Seismic station located Mesozoic (Jurassic to Cretaceous) granodiorite.

Site Conditions: Rural site. Seismic station located on top of a mountain near communications antennas. Steep topography in site vicinity. Seismic line located on a gradual slope with an approximate 7 m elevation decrease to the northeast along the 70.5 m long line.

Geophysical Methods Utilized: HVSR, Seismic Refraction, MASW

Geophysical Testing Arrays:

1. Array LRL-1 (48 channel MASW and P-wave seismic refraction array utilizing 4.5 Hz vertical geophones spaced 1.5 m apart for a length of 70.5 m, forward and reverse shot locations with multiple source offsets and source types (hammers only) and multiple interior shot locations).
2. Three HVSR measurement locations: two distributed along array LRL-1 and one adjacent the seismic station.

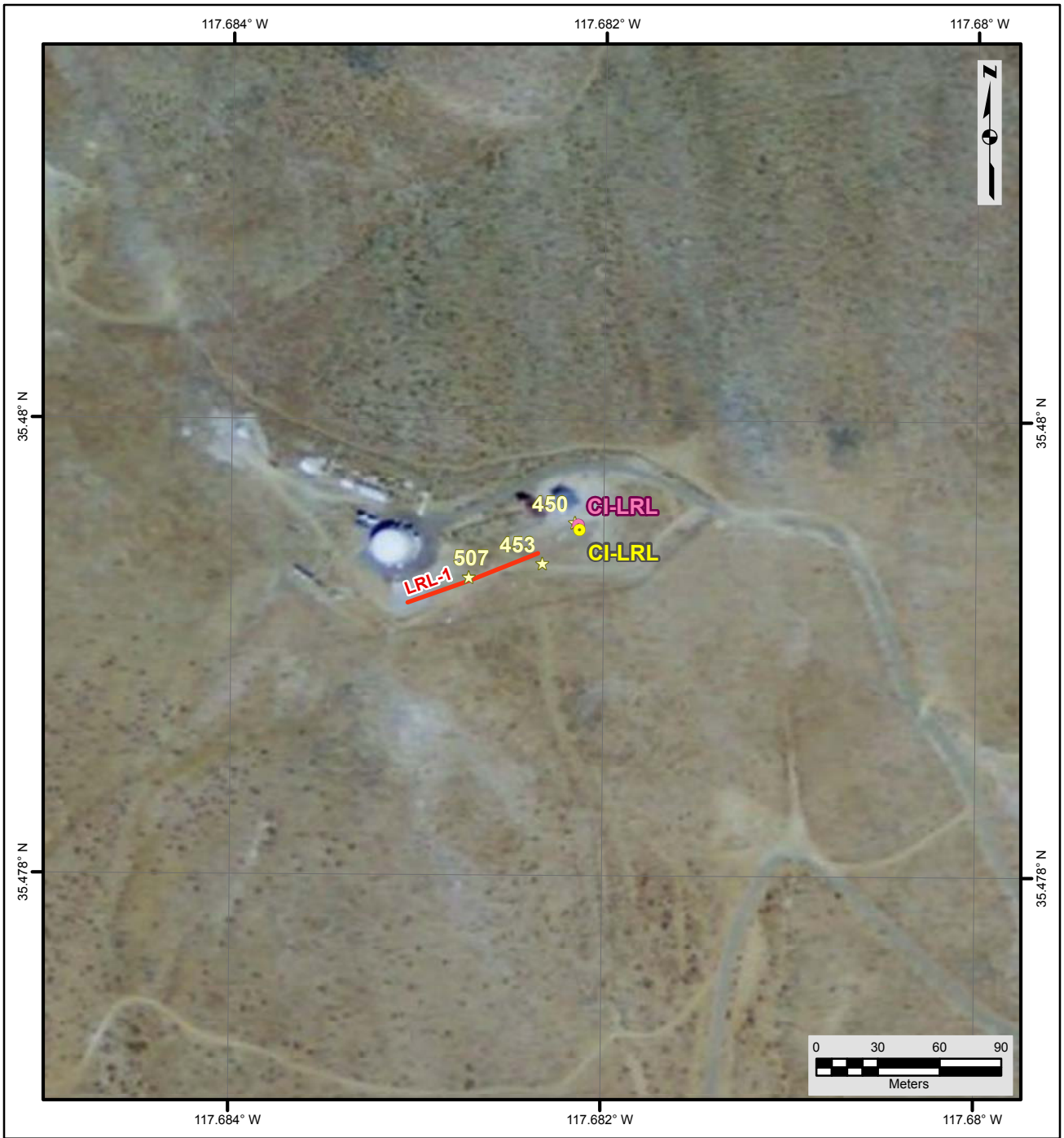

Legend

- Seismic Station - Approximate Surveyed Location
- Seismic Station - Approximate Location of Record
- H/V Spectral Ratio Location
- MASW and Seismic Refraction Array

NOTES:
1. WGS 1984 COORDINATE SYSTEM
2. Image Source: ESRI, i-cubed, USDA FSA, USGS, AEX, GeoEye, Getmapping, Aerogrid, IGP

File Name: CI-LRL-I

Date: 10/13/2011

USGS science for a changing world

GEOVision geophysical services

RECOVERY.GOV

SITE MAP
CI•LRL

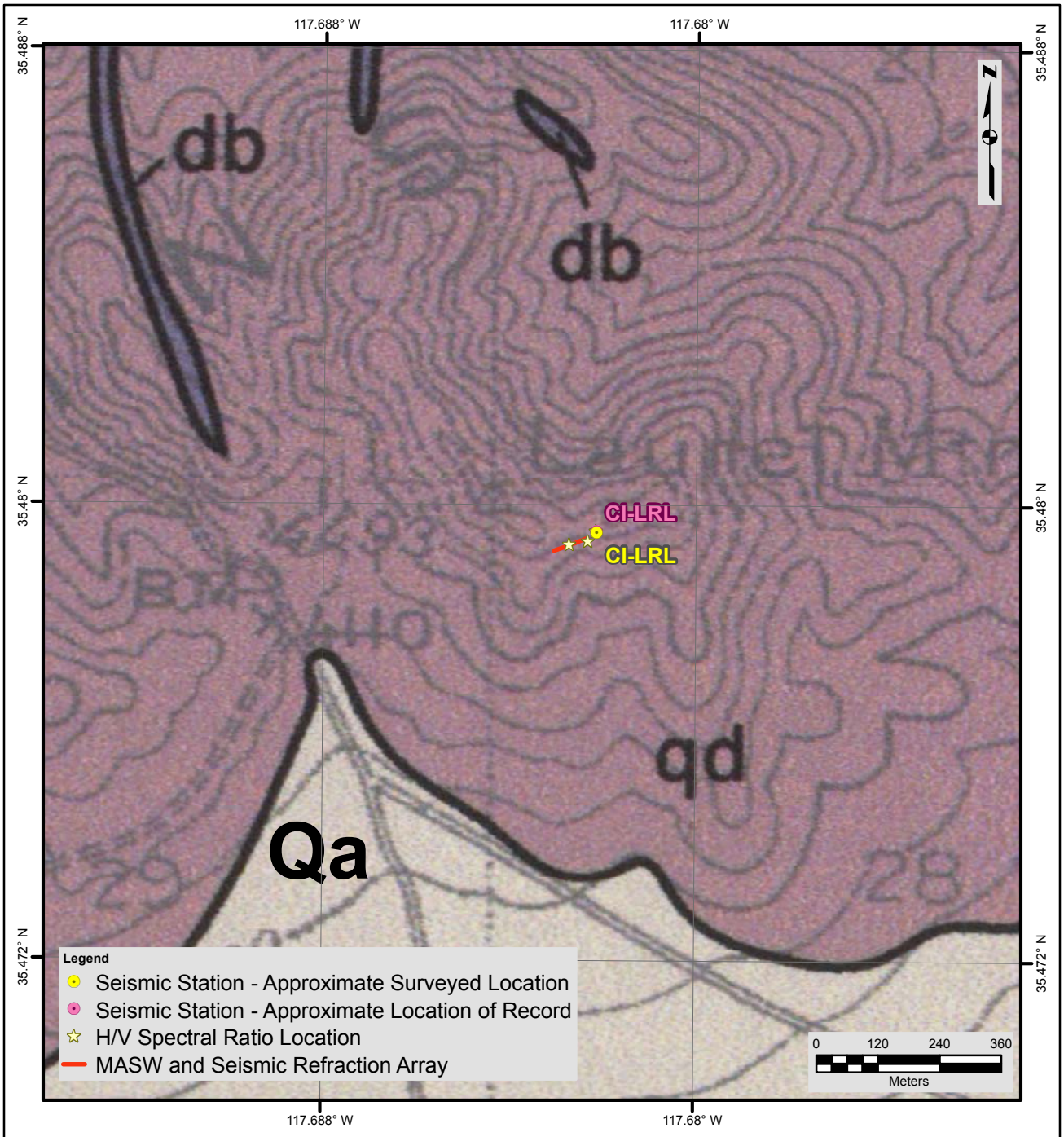

Description of Geologic Map Units

Qa = Quaternary (Holocene) alluvial gravel and sand
db = Tertiary (Pliocene) diabase dikes, fine grained, massive
qd = Mesozoic (Jurassic and Cretaceous) quartz diorite, massive to rarely gneissoid, medium-grained

NOTES:
1. WGS 1984 COORDINATE SYSTEM
2. Geologic Map of the Randsburg 15 Minute Quadrangle Kern & San Bernardino Counties, California by Thomas W. Dibblee Jr., 2008
3. See site map for details of geophysical survey

File Name: CI-LRL

Date: 10/13/2011

USGS science for a changing world

GEOVision geophysical services

RECOVERY.GOV

GEOLOGIC MAP
CI•LRL

CI.LRL seismic station

Looking downhill northeast along array LRL-1

Facing approximately east, looking down slope from top of outcrop at array LRL-1

HVSR sensor 453 on plaster

MASW data acquisition along array LRL-1

Location of Geophysical Testing Arrays:

Location	Latitude	Longitude
LRL-1, Southwest End of MASW/Refraction Array	35.47920	-117.68304
LRL-1, Center of MASW/Refraction Array	35.47929	-117.68270
LRL-1, Northeast End of MASW/Refraction Array	35.47941	-117.68234
HVSR Sensor 450	35.47955	-117.68214
HVSR Sensor 453	35.47937	-117.68231
HVSR Sensor 507	35.47931	-117.68271
CI.LRL Seismic Station	35.47952	-117.68211

Notes: 1) WGS84 Coordinate System (decimal degrees)
2) Survey accuracy is estimated at 1 to 2 m.

Results:

V_S Model

Depth to Top of Layer (m)	Layer Thickness (m)	S-Wave Velocity (m/s)	Inferred P-Wave Velocity (m/s)	Assumed Poisson's Ratio	Assumed Density (g/cm^3)
0	1	106	198	0.3	1.70
1	1.5	253	474	0.3	1.80
2.5	3	390	730	0.3	1.90
5.5	4	587	1099	0.3	2.00
9.5	6	647	1210	0.3	2.10
15.5	9	659	1233	0.3	2.10
24.5	>5.5	930	1740	0.3	2.15

Notes: 1) Depth of investigation is about 30 m.
2) Bottom layer is a half space.

Observations/Discussion:

- There are no distinct HVSR peaks. The HVSR plot for sensor 450, located adjacent to the seismic station, is slightly different that the HVSR plots for sensors 453 and 507, which are located along array LRL-1. Given that the site is located on a mountain top, the variation in HVSR response could have as much to do with topography as variation in velocity structure.
- The P-wave refraction data collected along array LRL-1 were modeled using a tomographic inversion routine with a smooth velocity gradient starting model. The

seismic refraction model was extended to far offset shot locations to extend depth of investigation.

- The seismic refraction survey design allowed P-wave velocity to be imaged to a maximum depth of about 15 m. The seismic refraction model shows that P-wave velocity is about 400 to 500 m/s at the surface, increasing to 1,000 m/s at a depth of 5 to 6 m and 1,400 m/s at a depth of 12 to greater than 16 m.
- The seismic refraction model indicates that there is some lateral velocity variation at this site. The model shows higher P-wave velocities at depth beneath the southwest end of the line than below the northeast end of the line. There were no reasonable alternate test locations at the site due to limited space and steep topography.
- Noise conditions at the site were not sufficient for application of passive surface wave techniques.
- MASW data reduction was somewhat complicated. Generally source locations at the southwest end of the array did not yield reliable Rayleigh wave phase velocity data at long wavelengths. Additionally, small wavelength phase velocity data associated with source locations at this end of the array were of a slightly higher velocity than that from source locations at the opposite end of the array and were not used for analysis. SASW analysis was conducted on seismic data from selected receiver pairs of source locations at the northeast end of the array to supplement the Rayleigh wave phase velocity data at small wavelengths/high frequencies.
- The minimum wavelength surface wave phase velocity data extracted from the 48-channel MASW array was about 16 m. Data reduction using seismic records from smaller hammer sources and a limited offset receiver array (i.e. less active geophones) allowed extraction of surface wave dispersion data to a minimum wavelength of about 4 m. SASW analysis of selected MASW receiver pairs associated with source locations at the northeast end of the array allowed extraction of surface wave dispersion data to a minimum wavelength of about 3 m
- There is about 50 to 60 m/s scatter in MASW dispersion data, which is likely due, in part, to lateral velocity variation associated with differential weathering of near surface bedrock.
- A representative dispersion curve was generated for the MASW data set using a moving average, polynomial curve fitting routine and used for modeling.
- Surface wave depth of investigation is about 30 m based on half of maximum wavelength criteria.
- The inferred P-wave velocities in the surface wave model, assuming a Poisson's ratio of 0.3, are generally consistent with the average velocity structure in the seismic refraction model in the upper 15 m, the seismic refraction depth of investigation.
- V_{S30} is 511 m/s (Site Class C).
- Average S-wave velocity between 1 m (assumed sensor depth) and 31 m is 596 m/s.

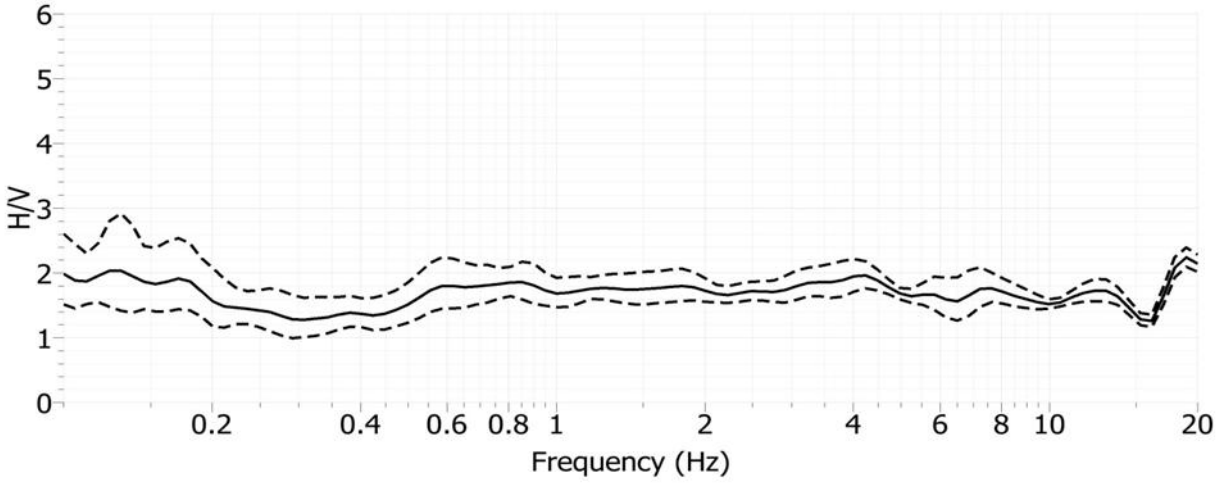

Site CI.LRL, H/V Spectral Ratio, Array LRL-1, Sensor 507

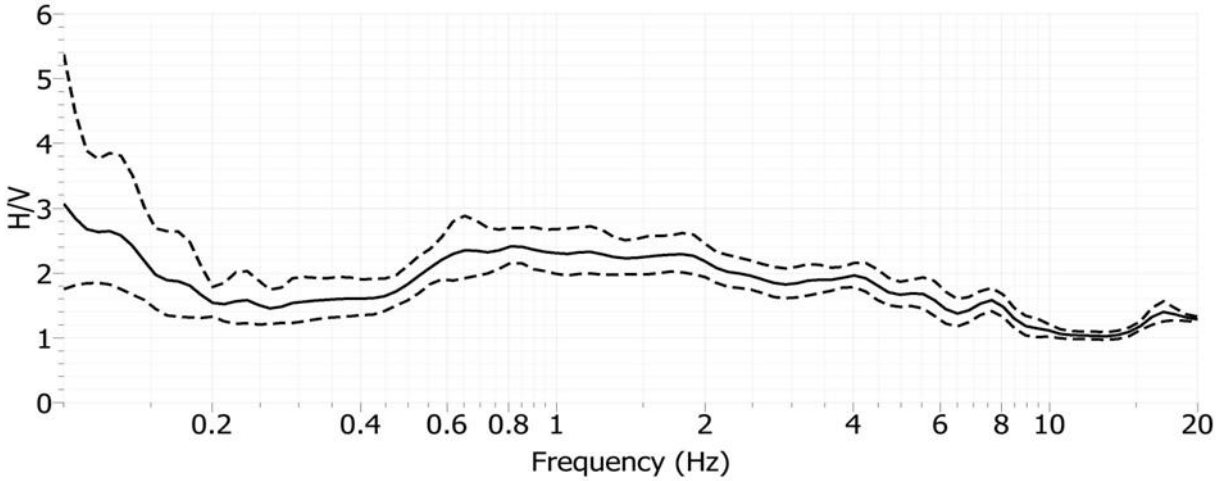

Site CI.LRL, H/V Spectral Ratio, Array LRL-1, Sensor 453

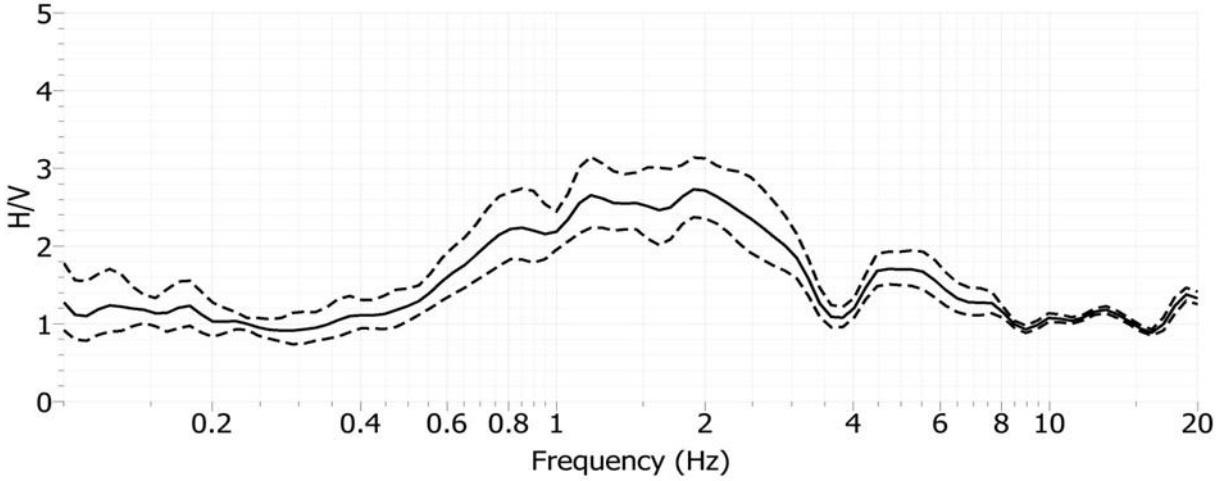

Site CI.LRL, H/V Spectral Ratio, Near Seismic Station, Sensor 450

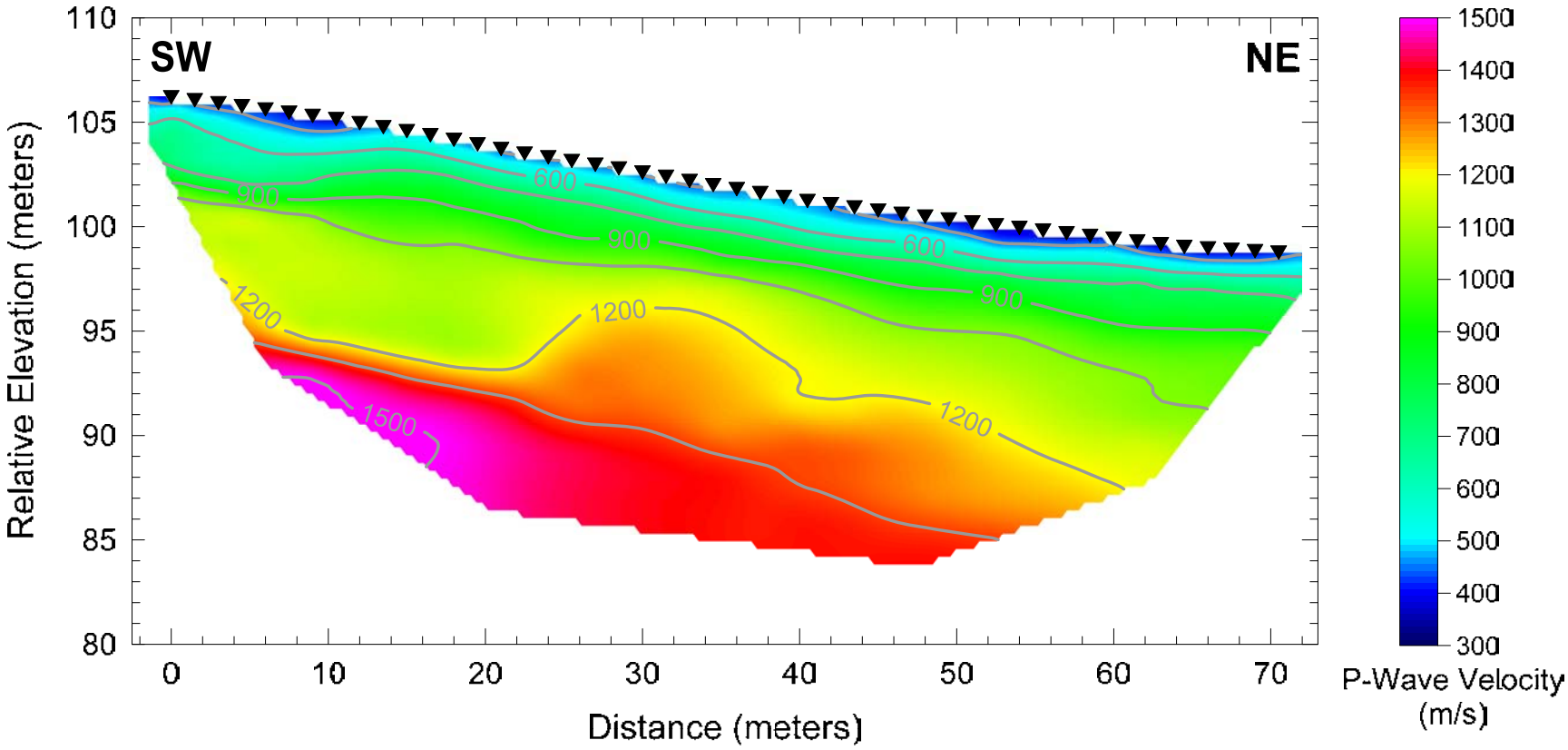

Array LRL-1 – Tomographic seismic refraction model utilizing smooth velocity gradient starting model

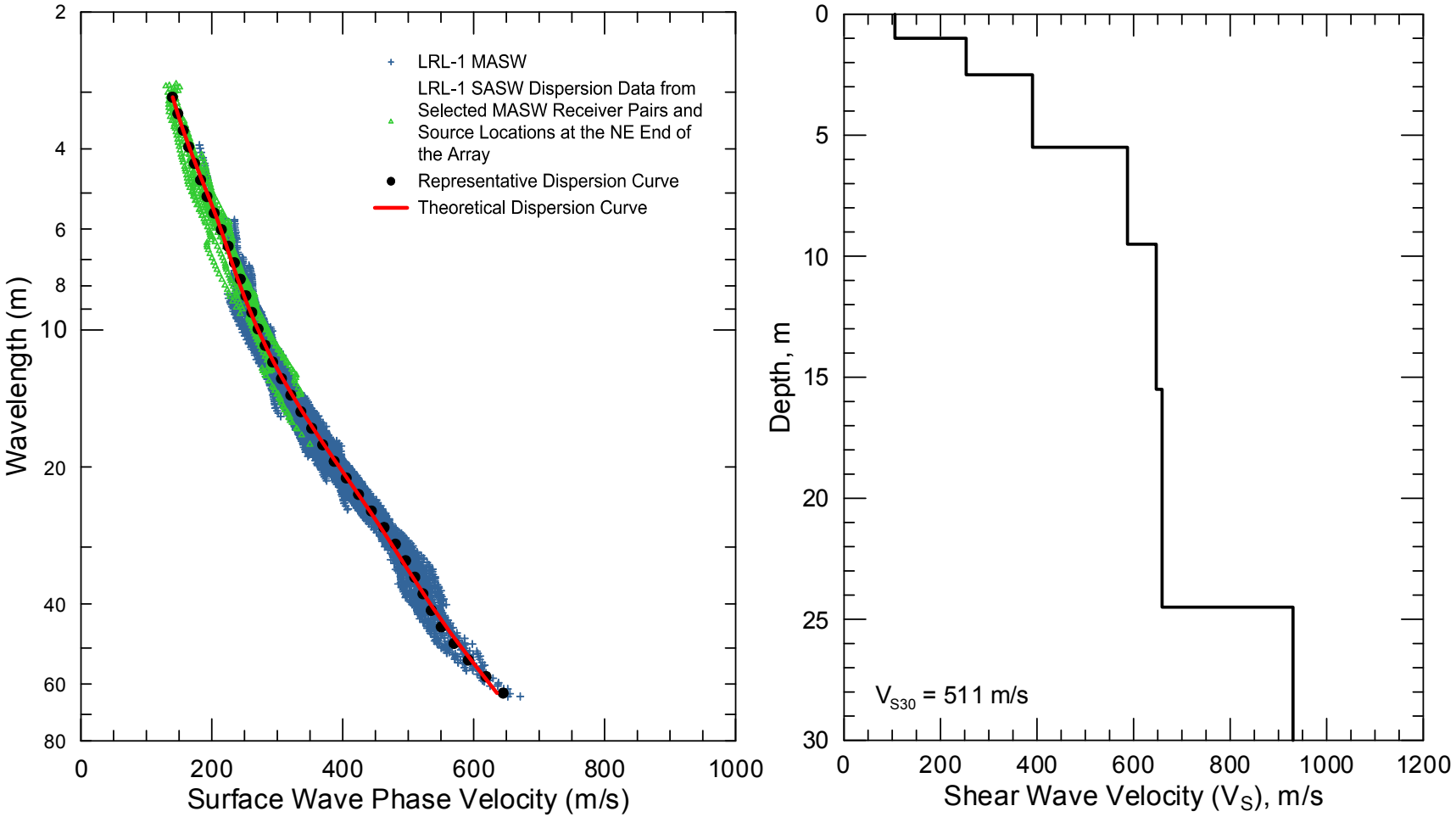

CI.LRL - Field, representative and inverted theoretical surface wave dispersion data (left) and associated V_S model (right)

Site CI.LUG

Location: Southern California Edison Lugo Substation, 6655 Escondido Drive, near Hesperia, California

Latitude: 34.36560 **Longitude:** -117.36683

(Station coordinates provided by USGS – WGS84 Coordinate System)

V_{S30} (measured): 365 m/s

V_{S30} (adjusted to more accurately reflect seismic station conditions): 381 m/s (average S-wave velocity between 2 and 32 m adjusting for nominal sensor depth)

NEHRP Site Class: C/D

Geomatrix Code: IQD

Geologic Conditions/Observations: Site located on geologic unit mapped as Pleistocene old alluvium (Shoemaker gravel). Crystalline basement expected to be deep at this site.

Site Conditions: Rural site with construction activities on the facility during testing. Relatively flat terrain in test area.

Geophysical Methods Utilized: HVSR, MASW, SASW

Geophysical Testing Arrays:

1. Array LUG-1 (48 channel MASW array utilizing 4.5 Hz vertical geophones spaced 1.5 m apart for a length of 70.5 m, forward and reverse shot locations with multiple source offsets and source types and center shot location).
2. Array LUG-1 (SASW array with common midpoint and orientation as MASW array of same name utilizing 4.5 and 1 Hz vertical geophones and maximum receiver spacing of 48 m).
3. Three HVSR measurement locations distributed along array LUG-1.

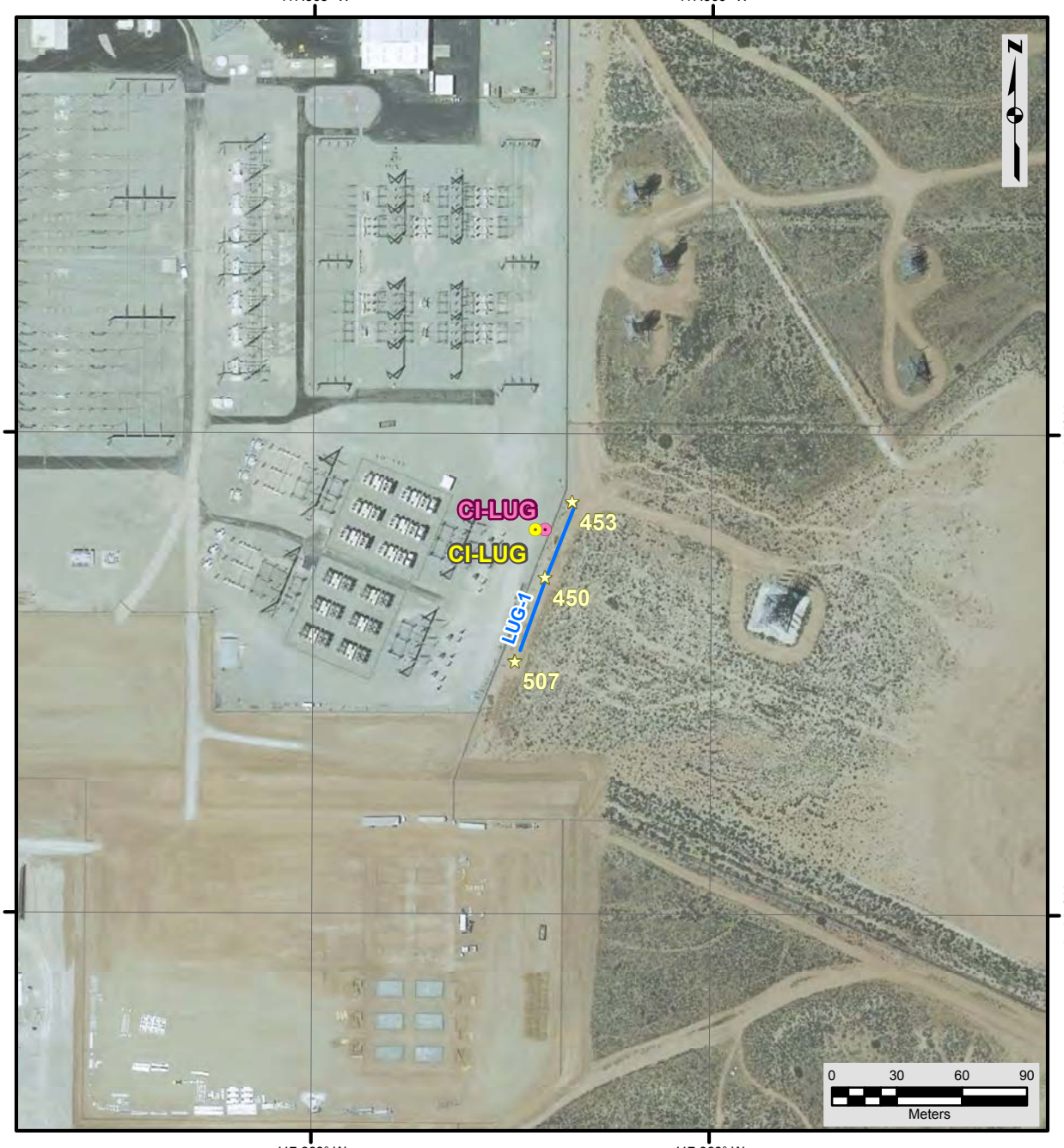

Legend

- Seismic Station - Approximate Surveyed Location
- Seismic Station - Approximate Location of Record
- H/V Spectral Ratio Location
- MASW and SASW Array

NOTES:
1. WGS 1984 COORDINATE SYSTEM
2. Image Source: ESRI, i-cubed, USDA FSA, USGS, AEX, GeoEye, Getmapping, Aerogrid, IGP

File Name: CI-LUG-I

Date: 10/20/2011

USGS science for a changing world

GEOVision geophysical services

RECOVERY.GOV

SITE MAP
CI•LUG

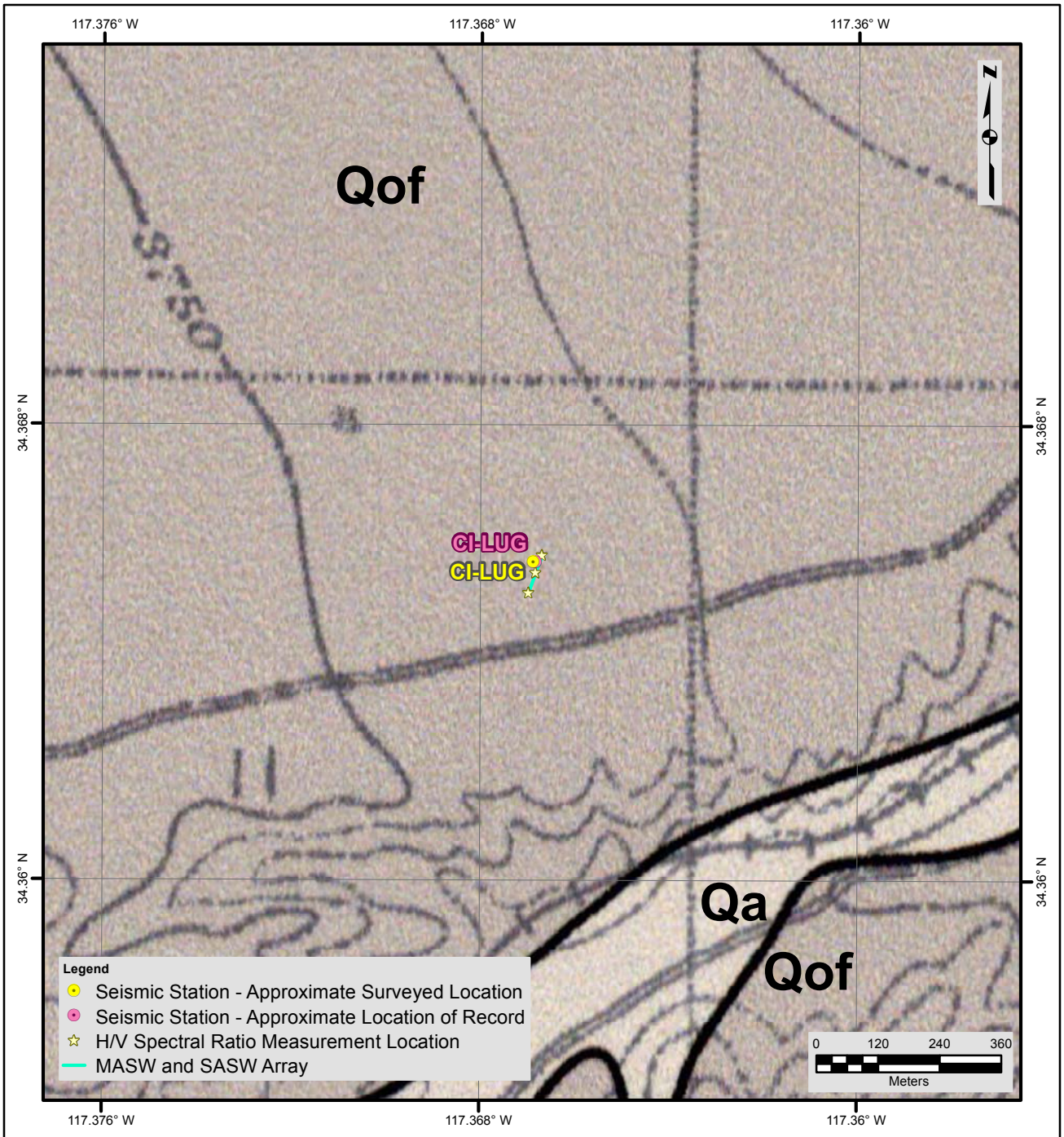

Description of Geologic Map Units

Qa =Quaternary (Holocene) alluvial sand and gravel
Qof = Quaternary (Pleistocene) Shoemaker Gravel; older alluvial fan gravel, detritus of gneissic and plutonic rocks

NOTES:
1. WGS 1984 COORDINATE SYSTEM
2. Geologic Map of the Hesperia 15 Minute Quadrangle, San Bernardino County, California by Thomas W. Dibblee, Jr., 2008
3. See site map for details of geophysical survey

File Name: CI-LUG

Date: 10/20/2011

USGS science for a changing world

GEOVision geophysical services

RECOVERY.GOV

GEOLOGIC MAP
CI•LUG

Looking north towards HVSR sensor 450 and CI.LUG seismic station

Looking north towards center of MASW array LUG-1 and seismic station

Looking north to northeast from center of MASW array LUG-1

CI.LUG seismic station

SASW array LUG-1

Location of Geophysical Testing Arrays:

Location	Latitude	Longitude
LUG-1, South End of MASW Array	34.36510	-117.36696
LUG-1, Center of MASW and SASW Arrays	34.36541	-117.36682
LUG-1, North End of MASW Array	34.36571	-117.36668
HVSR Sensor 507	34.36505	-117.36698
HVSR Sensor 453	34.36572	-117.36670
HVSR Sensor 450	34.36540	-117.36683
CI.LUG Seismic Station	34.36560	-117.36688

Notes: 1) WGS84 Coordinate System (decimal degrees)
2) Survey accuracy is estimated at 1 to 2 m

Results:

V_S Model from SASW Array LUG-1

Depth to Top of Layer (m)	Layer Thickness (m)	S-Wave Velocity (m/s)	Inferred P-Wave Velocity (m/s)	Inferred Poisson's Ratio	Inferred Density (g/cm^3)
0	1	247	462	0.3	1.9
1	2	257	481	0.3	1.9
3	3	277	518	0.3	1.9
6	4	305	570	0.3	1.9
10	6	398	745	0.3	1.9
16	9	419	784	0.3	1.9
25	>5	447	837	0.3	1.9

V_S Model from MASW Array LUG-1

Depth to Top of Layer (m)	Layer Thickness (m)	S-Wave Velocity (m/s)	Inferred P-Wave Velocity (m/s)	Inferred Poisson's Ratio	Inferred Density (g/cm^3)
0	1	245	459	0.3	1.9
1	1	283	529	0.3	1.9
2	8	330	617	0.3	1.9
10	14	388	725	0.3	1.9
24	>6	464	868	0.3	1.9

Observations/Discussion:

- HVSR plots are similar at all measurement locations validating the 1-D velocity structure assumption.
- There is a distinct HVSR peak at about 0.3 Hz, which is indicative of deep basement at the site.
- Noise conditions at the site were not sufficient to apply passive surface wave techniques.
- Surface wave dispersion data from SASW and MASW datasets are not in good agreement over the 3 to 20 m wavelength range, most likely as the result of lateral velocity variation. Limited MASW data extracted from the reverse end shot and forward direction center shot does agree with the SASW data over this wavelength range, but was not used for analysis. It appears that near surface sediments at the southern end of the line have higher S-wave velocity than those at the northern end of the line. SASW and MASW data were modeled separately to determine range of subsurface velocities.
- Representative dispersion curves were generated for each surface wave data set using a moving average, polynomial curve fitting routine.
- Water table located at a depth of greater than 30 m based on seismic refraction survey design, absence of a water table refractor. Possible reflector is observed at a depth of about 30 to 35 m but does not appear to be the water table based on first arrival data.
- Based on simple horizontal layer-based analysis of seismic refraction first arrival data, P-wave velocity in the upper 15 m ranges from about 550 m/s near the surface to 675 m/s at depths below 3 m. The RMS velocity of sediments overlying a potential reflector at a depth of 30 to 35 m is about 700 m/s indicating the P-wave velocity may be on the order of 775 m/s at depths below 15 m.
- Surface wave depth of investigation is about 30 m based on half of maximum wavelength criteria.
- Surface wave models are generally consistent with simplified P-wave refraction model considering unknown Poisson's ratio.
- With the exception of the 2 to 6 m depth interval, S-wave layer velocities from the SASW and MASW models are within 10 %.
- V_{S30} is 359 m/s for SASW array and 371 m/s for MASW array, averaging 365 m/s (Site Class C/D).
- Average S-wave velocity between 2 m (nominal sensor depth) and 32 m is 375 m/s for SASW array and 386 m/s for MASW array, averaging 381 m/s.

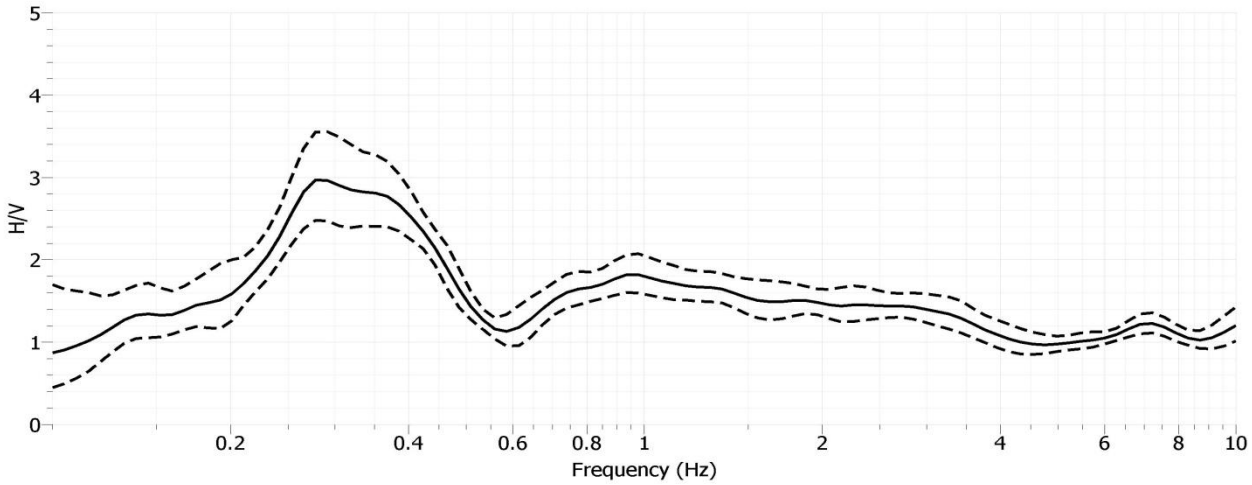

Site CI. LUG, H/V Spectral Ratio, Array LUG-1, Sensor 453

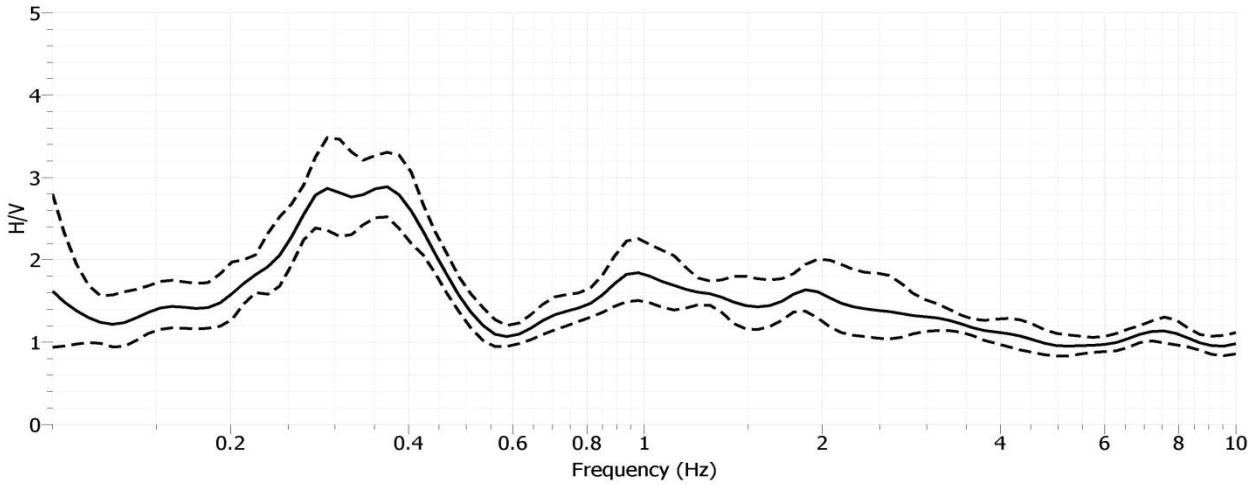

Site CI. LUG, H/V Spectral Ratio, Array LUG-1, Sensor 450

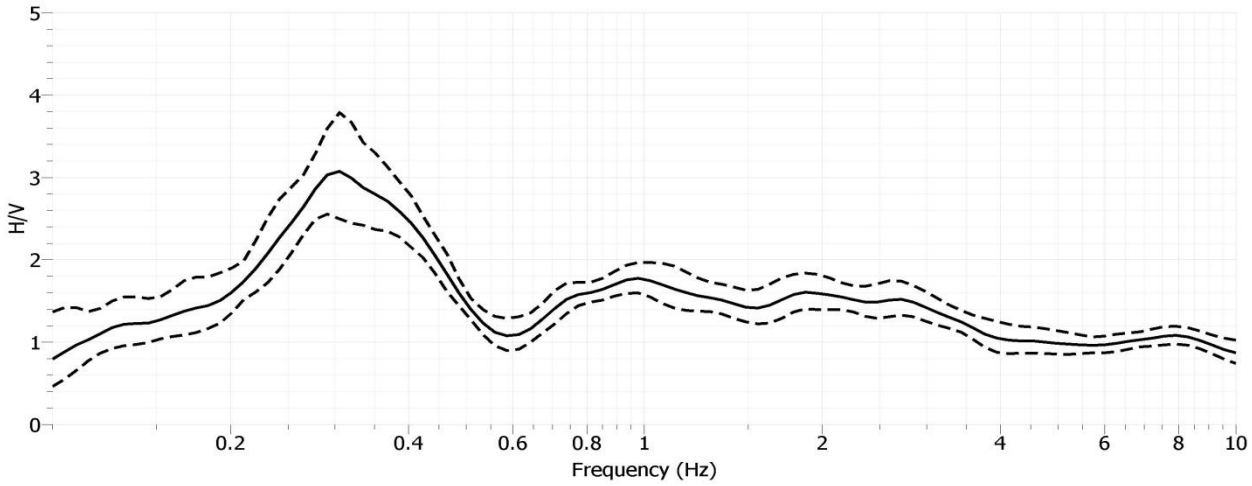

Site CI. LUG, H/V Spectral Ratio, Array LUG-1, Sensor 507

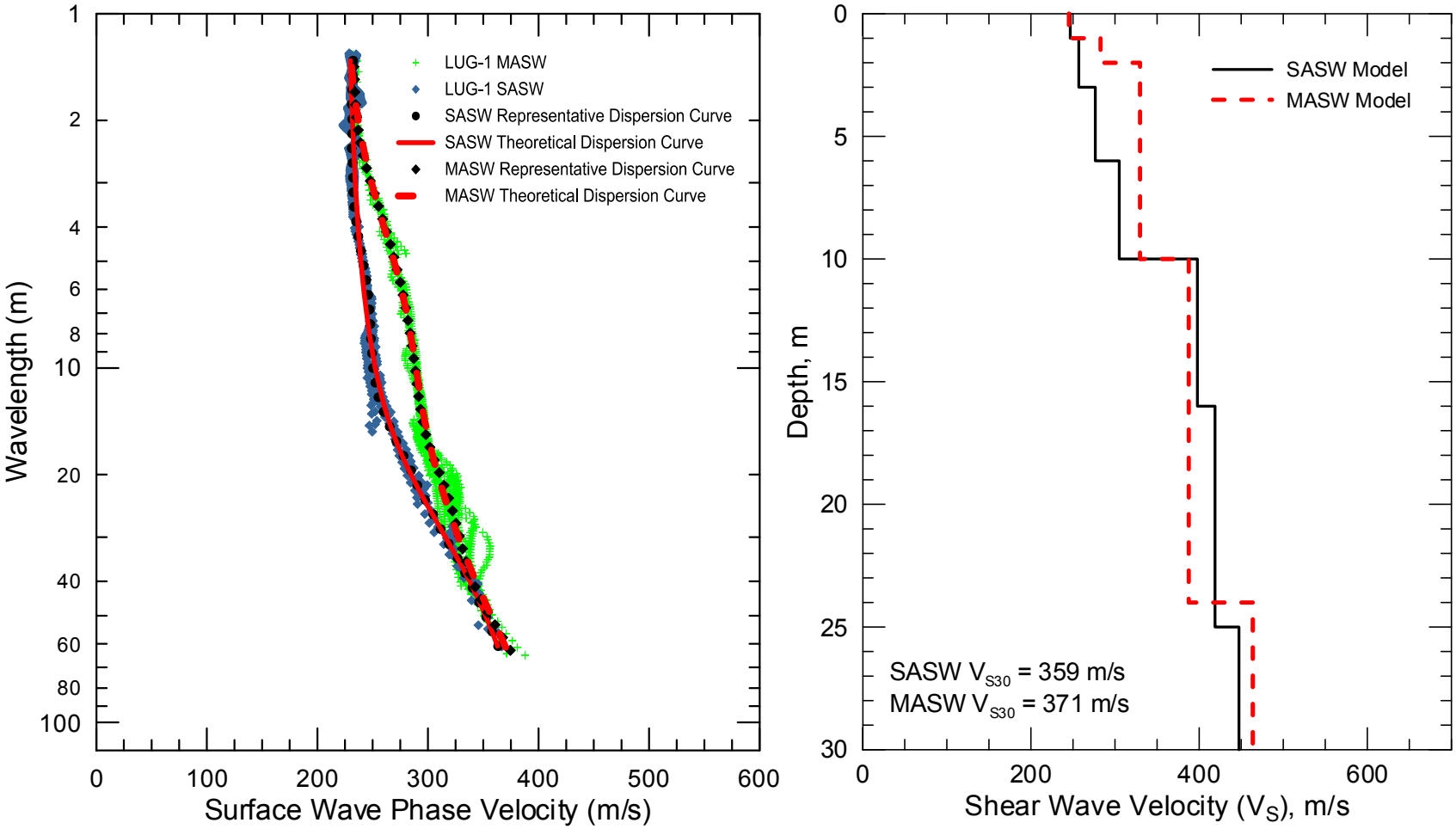

CI.LUG - Field, representative and inverted theoretical surface wave dispersion data (left) and associated V_S model (right)

Site CI.MCT

Location: Marine Corps Air Ground Combat Center, Twentynine Palms, San Bernardino County, California

Latitude: 34.22645 **Longitude:** -116.04073
(Station coordinates provided by USGS, WGS84 coordinate system)

V_{S30} (measured): 1,188 m/s (±20%, or more, in site vicinity based on lateral velocity variation beneath seismic refraction array. V_{S30} at seismic station may be lower than that presented based on seismic refraction model for array MCT-2).

V_{S30} (adjusted to more accurately reflect seismic station conditions): 1,188 m/s (no adjustment necessary).

NEHRP Site Class: B

Geomatrix Code: IGA

Geologic Conditions/Observations: Site located on geologic unit mapped as Mesozoic (Jurassic to Cretaceous) quartz monzonite. Field observations indicate that the near surface rock is intensely weathered and highly fractured.

Site Conditions: Rural site located on top of a small hill. Undulating (hilly) topography in site vicinity.

Geophysical Methods Utilized: HVSR, Seismic Refraction (P- and S-wave), MASW (Rayleigh wave), MALW (Love wave)

Geophysical Testing Arrays:

1. Array MCT-1 (48 channel MASW and P-wave seismic refraction array utilizing 4.5 Hz vertical geophones spaced 1 m apart for a length of 47 m, forward and reverse shot locations with multiple source offsets and source types (hammers only) and multiple interior shot locations).
2. Array MCT-1 (24 channel MALW and S-wave refraction array utilizing 10 Hz horizontal geophones spaced 2 m apart for a length of 46 m, several forward and reverse shot locations and multiple interior shot locations. Same origin and orientation as P-wave array of same name).
3. Array MCT-2 (48 channel P-wave seismic refraction array utilizing 4.5 Hz vertical geophones spaced 2.5 m apart for a length of 117.5 m, forward and reverse shot locations with multiple source offsets and multiple interior shot locations).
4. Array MCT-3 (48 channel MASW and P-wave seismic refraction array, utilizing 4.5 Hz vertical geophones spaced 1.5 m apart for a length of 70.5 m, forward and reverse

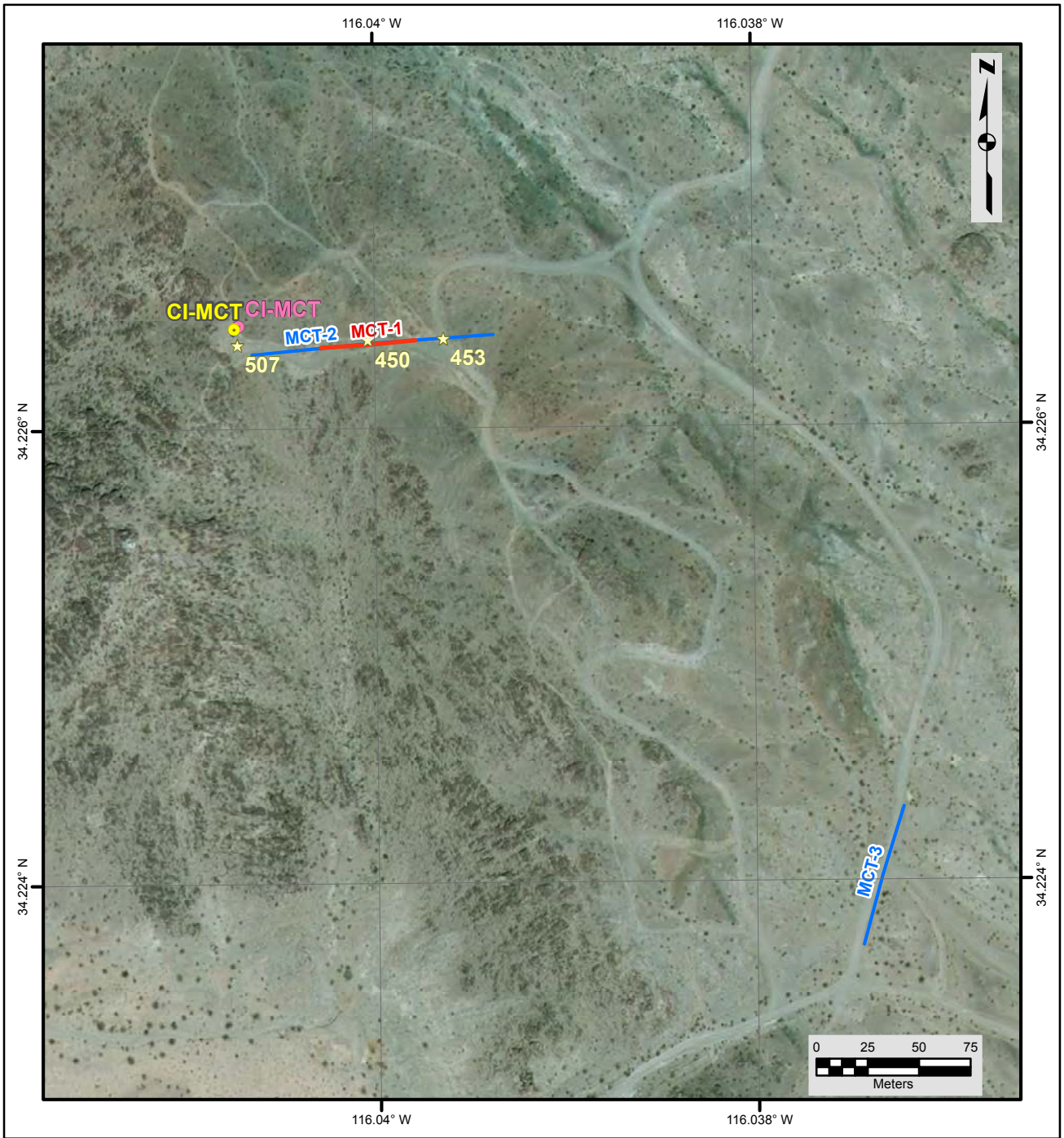

Legend

- Seismic Station - Approximate Surveyed Location
- Seismic Station - Approximate Location of Record
- H/V Spectral Ratio Location
- MASW and Seismic Refraction Array
- MASW and Seismic Refraction Array

NOTES:
1. WGS 1984 COORDINATE SYSTEM
2. Image Source: ESRI, i-cubed, USDA FSA, USGS, AEX, GeoEye, Getmapping, Aerogrid, IGP

File Name: CI-MCT-I

Date: 2/7/2013

USGS science for a changing world

GEOVision geophysical services

RECOVERY.GOV

SITE MAP
CI•MCT

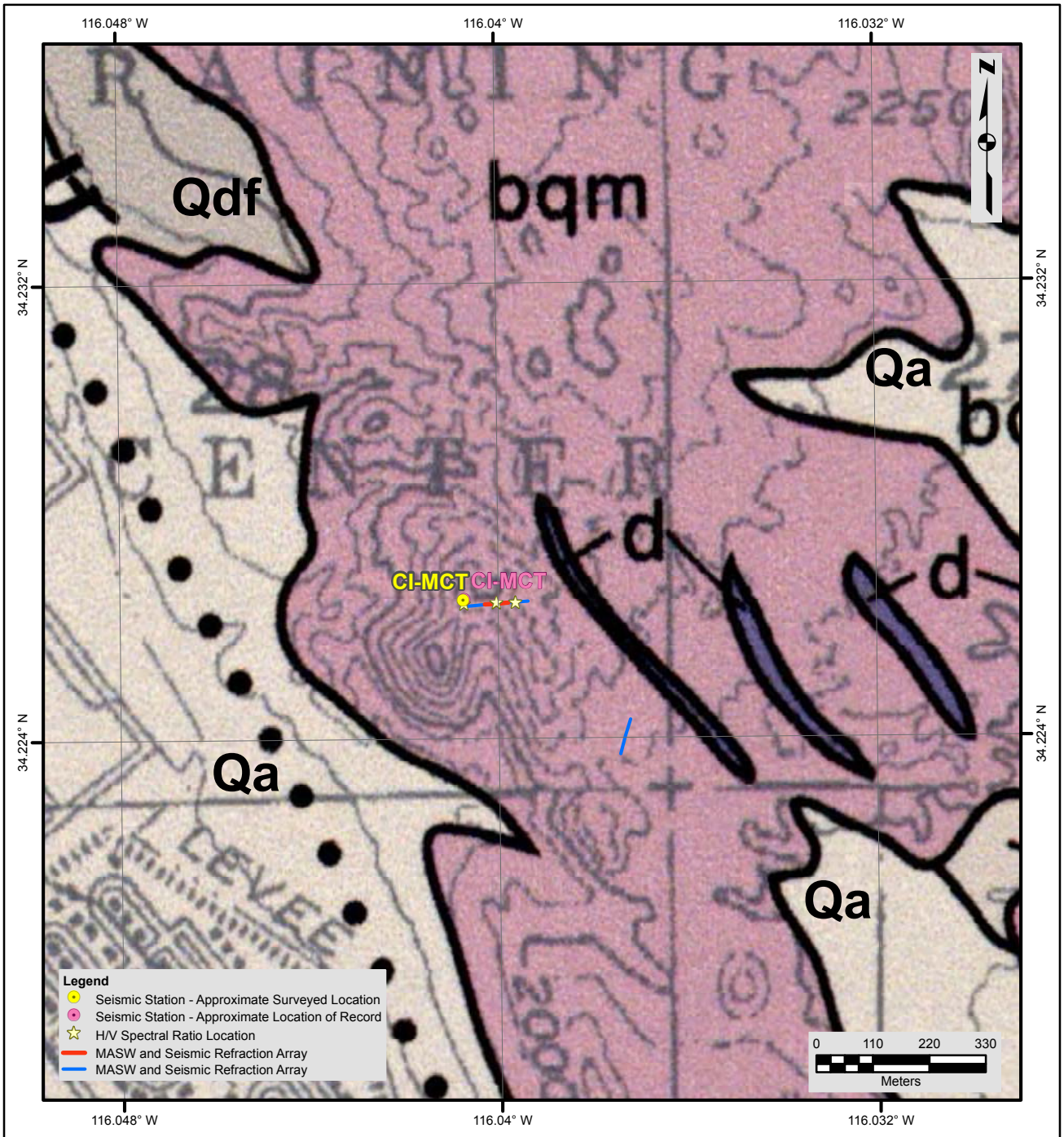

Description of Geologic Map Units

Qa = Quaternary (Holocene) alluvial sand and gravel
Qdf = Quaternary (Pleistocene ?) dissected alluvial fan gravel and sand
d = Mesozoic (Jurassic-Cretaceous) mafic dikes, dioritic or andesitic
bqm = Mesozoic (Jurassic-Cretaceous) biotite quartz monzonite

NOTES:
1. WGS 1984 COORDINATE SYSTEM
2. Geologic Map of the Joshua Tree & Twentynine Palms 15 Minute Quadrangles, Riverside & San Bernardino Counties, California by Thomas W. Dibblee, Jr., 2008
3. See site map for details of geophysical survey

File Name: CI-MCT

Date: 2/7/2013

USGS science for a changing world

GEOVision geophysical services

RECOVERY.GOV

GEOLOGIC MAP
CI•MCT

Looking north at CI.MCT seismic station and HVSR sensor 507

Looking east along array MCT-1

Looking northeast towards seismic station and array MCT-1

S-wave Refraction Data Acquisition Using Aluminum Plate

Looking west along array MCT-1

shot locations with multiple source offsets and source types (hammers only) and multiple interior shot locations).

5. Three HVSR measurement locations distributed along array MCT-1.

Location of Geophysical Testing Arrays:

Location	Latitude	Longitude
MCT-1, West End of MASW/Refraction Array	34.22636	-116.04030
MCT-1, Center of MASW/Refraction Array	34.22637	-116.04005
MCT-1, East End of MASW/Refraction Array	34.22639	-116.03980
MCT-2, West End of Seismic Refraction Array	34.22633	-116.04066
MCT-2, Center of Seismic Refraction Array	34.22638	-116.04002
MCT-2, East End of Seismic Refraction Array	34.22641	-116.03938
MCT-3, Southwest End of MASW/Refraction Array	34.22371	-116.03745
MCT-3, Center of MASW/Refraction Array	34.22402	-116.03735
MCT-3, Northeast End of MASW/Refraction Array	34.22432	-116.03723
HVSR Sensor 450	34.22639	-116.04004
HVSR Sensor 453	34.22639	-116.03965
HVSR Sensor 507	34.22637	-116.04074
CI.MCT Seismic Station	34.22644	-116.04075

Notes: 1) WGS84 Coordinate System (decimal degrees)

2) Survey accuracy is estimated at 1 to 2 m.

Results:

Average V_P Model and Estimated V_S Models from Central Portion of P-wave Seismic Refraction Array MCT-1

Depth to Top of Layer (m)	Layer Thickness (m)	P-Wave Velocity (m/s)	Estimated S-Wave Velocity (m/s)			
			Poisson's Ratio = 0.25	Poisson's Ratio = 0.3	Poisson's Ratio = 0.35	Poisson's Ratio = 0.4
0.00	0.45	419	242	224	201	171
0.45	0.89	542	313	289	260	221
1.34	0.89	1025	592	548	492	418
2.23	0.89	1248	720	667	599	509
3.12	0.89	1643	949	878	789	671
4.01	0.89	1847	1067	987	887	754
4.90	0.89	1881	1086	1005	904	768
5.79	1.87	1964	1134	1050	944	802
7.66	1.87	2175	1256	1163	1045	888
9.53	1.87	2424	1399	1296	1164	990
11.40	1.87	2493	1439	1333	1198	1018
13.26	1.87	2777	1604	1485	1334	1134
15.13	1.87	3030	1750	1620	1456	1237
17.00	1.87	3337	1927	1784	1603	1362
18.87	1.87	3507	2025	1875	1685	1432
20.74	1.87	3759	2170	2009	1806	1535
22.61	Half Space	4046	2336	2163	1943	1652

Average V_S Model from Central Portion of S-wave Seismic Refraction Array MCT-1

Depth to Top of Layer (m)	Layer Thickness (m)	S-Wave Velocity (m/s)
0.00	0.45	178
0.45	0.89	339
1.34	0.89	662
2.23	0.89	847
3.12	0.89	1149
4.01	0.89	1202
4.90	0.89	1265
5.79	1.87	1382
7.66	1.87	1435
9.53	1.87	1601
11.40	1.87	1636
13.27	1.87	1706
15.14	1.87	1858
17.01	1.87	1915

Average V_P Model and Estimated V_S Models from Central Portion of P-wave Seismic Refraction Array MCT-2

Depth to Top of Layer (m)	Layer Thickness (m)	P-Wave Velocity (m/s)	Estimated S-Wave Velocity (m/s)			
			Poisson's Ratio = 0.25	Poisson's Ratio = 0.3	Poisson's Ratio = 0.35	Poisson's Ratio = 0.4
0.00	0.54	491	283	262	236	200
0.54	1.08	956	552	511	459	390
1.62	1.08	1220	704	652	586	498
2.70	1.08	1504	868	804	722	614
3.78	1.08	1847	1066	987	887	754
4.86	1.08	1893	1093	1012	909	773
5.94	1.08	1966	1135	1051	944	803
7.02	2.27	2160	1247	1155	1038	882
9.29	2.27	2229	1287	1191	1071	910
11.55	2.27	2478	1431	1324	1190	1012
13.82	2.27	2813	1624	1504	1351	1148
16.09	2.27	3026	1747	1617	1454	1235
18.36	2.27	3268	1887	1747	1570	1334
20.62	2.27	3279	1893	1752	1575	1338
22.89	2.27	3346	1932	1788	1607	1366
25.16	2.27	3470	2004	1855	1667	1417
27.43	Half Space	3627	2094	1939	1742	1481

Site CI.MIK

Location: California Institute of Technology, Millikan, Pasadena, California

Latitude: 34.13688 **Longitude:** -118.12601

(Station coordinates provided by USGS – WGS84 coordinate system)

V_{S30} (measured): 333 m/s

V_{S30} (adjusted to more accurately reflect seismic station conditions): 376 m/s (average S-wave velocity between 4 and 34 m adjusting for assumed depth of the foundation of the Millikan Library)

NEHRP Site Class: D/C

Geomatrix Code: DQD/EQD/GQD

Geologic Conditions/Observations: Site located in area mapped as Quaternary (Pleistocene) old alluvial fan deposits. Deep soil site.

Site Conditions: Urban site with significant traffic noise from nearby roads. Relatively flat terrain in site vicinity with ground surface elevation gently decreasing to south.

Geophysical Methods Utilized: HVSR, MASW, array microtremor, ReMi™

Geophysical Testing Arrays:

1. Array MIK-1 (48 channel "110.25 degree L" shaped passive surface wave array utilizing 4.5 Hz vertical geophones spaced 3 m apart on the W-E leg along E. California Blvd. and 4 m apart on the SE-NW leg along Arden Rd., resulting in 72 and 92 m lengths of the linear segments
2. Array MIK-2 (48 channel MASW array, located along the SW-NW segment of array MIK-1, utilizing 4.5 Hz vertical geophones spaced 1 m apart for a length of 47 m, forward and reverse shot locations with multiple source offsets and source types and center shot location).
3. Array CRP-1 (48 channel "L" shaped passive surface wave array utilizing 4.5 Hz vertical geophones spaced 3 m apart on the W-E leg along E. California Blvd. and 5 m apart on the S-N leg along S. Wilson Ave., resulting in 72 and 115 m lengths of the linear segments. This array is approximately equidistant from the Millikan Library as array MIK-1 and 2.
4. Array CRP-2 (48 channel MASW array, located along the S-N segment of array CRP-1, utilizing 4.5 Hz vertical geophones spaced 1 m apart for a length of 47 m,

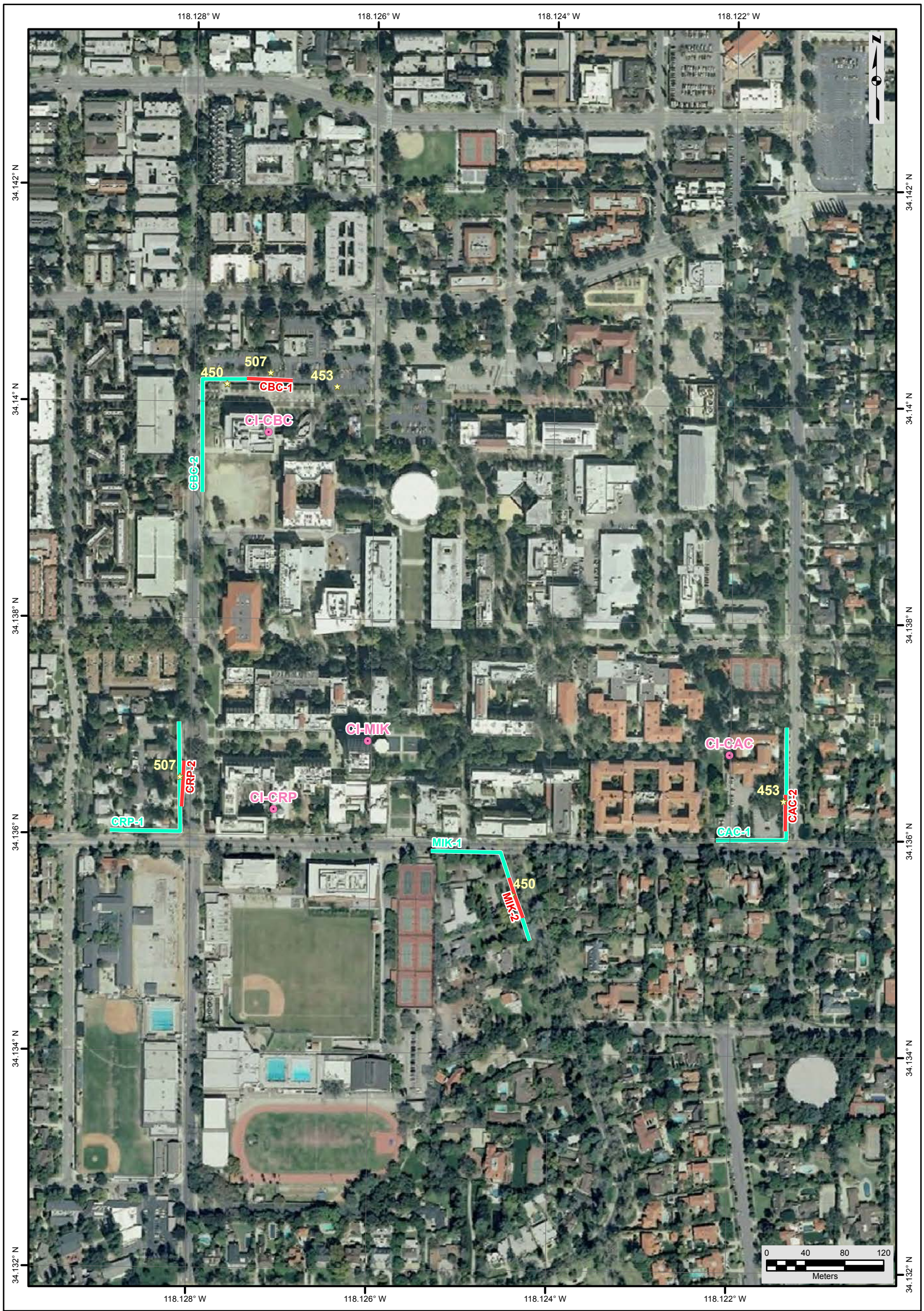

Legend

- Seismic Station - Approximate Location of Record
- H/V Spectral Ratio Measurement Location
- MASW Array
- Passive SASW Array

NOTES:
1. WGS 1984 COORDINATE SYSTEM
2. Image Source: ESRI, i-cubed, USDA FSA, USGS, AEX, GeoEye, Getmapping, Aerogrid, IGP

File Name: Caltech-I

Date: 5/16/2011

GEOVision geophysical services

SITE MAP
CI•CAC, CI•CBC, CI•CRP, CI•MIK

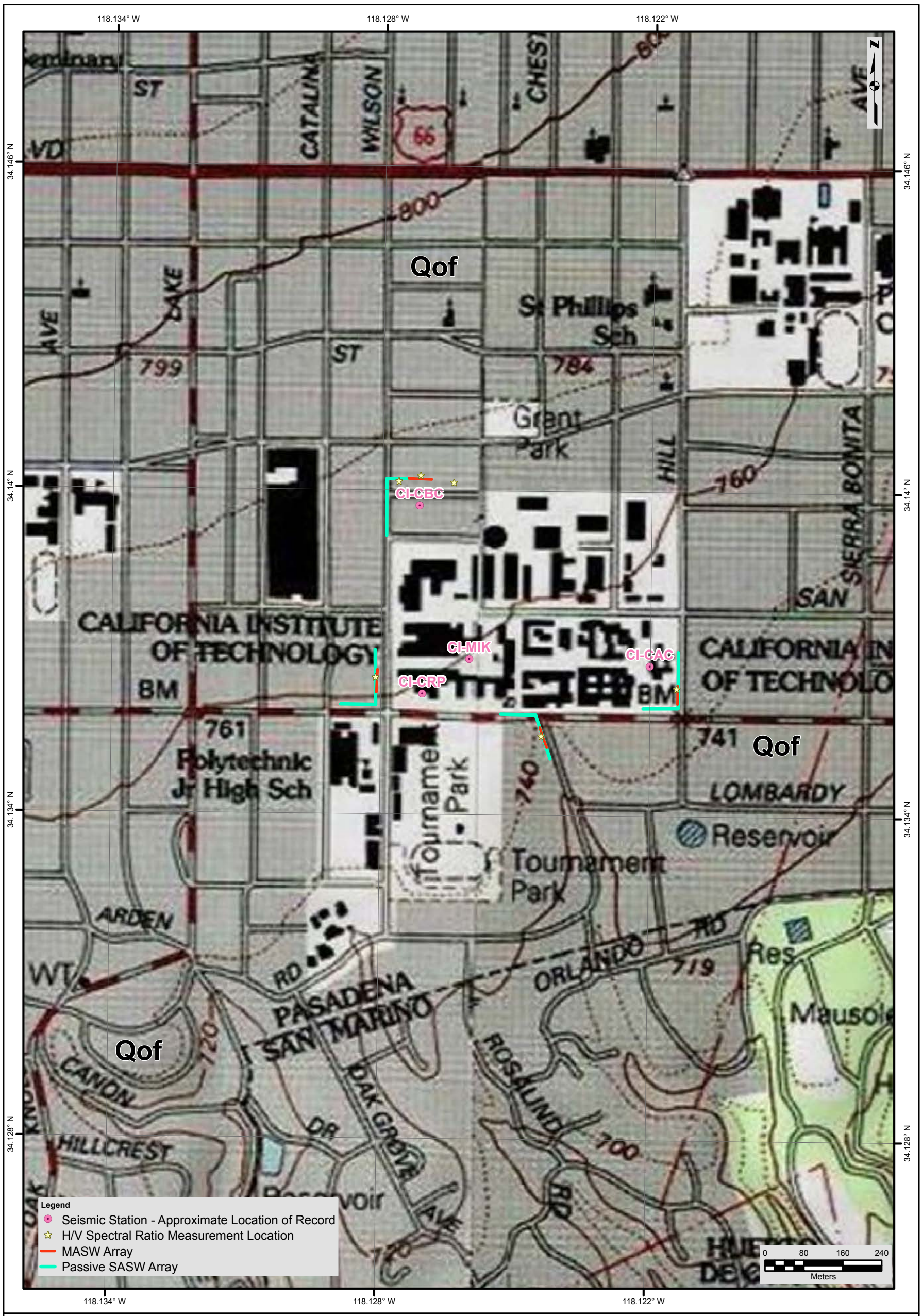

Description of Geologic Map Units

Qof = Quaternary (Holocene) alluvial fan gravel and sand

NOTES:
1. WGS 1984 COORDINATE SYSTEM
2. Topo Image Sources: USGS, FAO, NPS, EPA, NRCAN, GeoBase, Esri, DeLorme, TANA, Intermap and other suppliers and the GIS community
3. Geologic Map Units from:
Geologic Map of the Mt Wilson and Azusa Quadrangles, Los Angeles County, California by Thomas W. Dibblee, Jr., 1998 and
Geologic Map of the Pasadena Quadrangle, Los Angeles County, California by Thomas W. Dibblee, Jr., 1999
4. See site map for details of geophysical survey

File Name: Caltech

Date: 5/26/2011

GEOVision geophysical services

GEOLOGIC MAP
CI•CAC, CI•CBC, CI•CRP, CI•MIK

Looking northwest towards Millikan Library from the corner of passive surface wave array MIK-1

Looking northwest along MASW array MIK-2

Looking southeast along MASW array MIK-2

forward and reverse shot locations with multiple source offsets and source types and center shot location).

5. Three HVSR measurement locations, one on array MIK-1 and the others on nearby arrays CRP-1 and CAC-1.

Location of Geophysical Testing Arrays:

Location	Latitude	Longitude
MIK-1, West End of Array, Channel 1	34.13587	-118.12530
MIK-1, Corner of Array, Channel 25	34.13586	-118.12452
MIK-1, Southeast End of Array, Channel 48	34.13505	-118.12419
MIK-2, Southeast End of Array	34.13526	-118.12427
MIK-2, Center of Array	34.13544	-118.12435
MIK-2, Northwest End of Array	34.13563	-118.12443
CRP-1, West End of Array, Channel 1	34.13603	-118.12887
CRP-1, Corner of Array, Channel 25	34.13603	-118.12809
CRP-1, North End of Array, Channel 48	34.13704	-118.12811
CRP-2, South End of Array	34.13625	-118.12807
CRP-2, Center of Array	34.13643	-118.12806
CRP-2, North End of Array	34.13668	-118.12806
HVSR Sensor 507 (on array CRP-1)	34.13653	-118.12809
HVSR Sensor 453 (on array CAC-1)	34.13636	-118.12138
HVSR Sensor 450 (on array MIK-1)	34.13547	-118.12439

Notes: 1) WGS84 Coordinate System (decimal degrees)

2) Survey accuracy is estimated at 1 to 3 m

Results:

V_S Model – Arrays MIK-1 and MIK-2

Depth to Top of Layer (m)	Layer Thickness (m)	S-Wave Velocity (m/s)	Inferred P-Wave Velocity (m/s)	Inferred Poisson's Ratio	Inferred Density (g/cm^3)
0	1	158	295	0.300	1.9
1	2	232	435	0.300	1.9
3	3	279	521	0.300	1.9
6	4	304	569	0.300	1.9
10	6	360	673	0.300	1.9
16	10	373	698	0.300	1.9
26	14	416	778	0.300	1.9
40	18	476	1600	0.452	2.0
58	>2	537	1600	0.436	2.0

V_S Model – Arrays CRP-1 and CRP-2

Depth to Top of Layer (m)	Layer Thickness (m)	S-Wave Velocity (m/s)	Inferred P-Wave Velocity (m/s)	Inferred Poisson's Ratio	Inferred Density (g/cm^3)
0	1	139	260	0.300	1.9
1	2	211	395	0.300	1.9
3	3	304	569	0.300	1.9
6	4	324	607	0.300	1.9
10	6	352	658	0.300	1.9
16	9	411	770	0.300	1.9
25	15	478	894	0.300	1.9
40	20	535	1600	0.437	2.0
60	>15	599	1600	0.418	2.0

Observations/Discussion:

- Surface wave testing conducted on the perimeter of the Caltech campus due to basements on most buildings, dense utilities and possible tunnels connecting buildings on campus.
- Limited photographs taken during field testing as much of the field work was conducted at night. Passive surface wave measurements were typically made in the late afternoon to early evening when there was sufficient traffic noise. MASW data were generally acquired in the early evening when there was less traffic, but not too late so as to disturb residences. HVSR data were acquired between 11 pm and 2 am when there was minimal traffic noise.
- The HVSR curves are almost identical validating the 1-D velocity structure assumption with respect to deep geologic structure. There are no high frequency peaks by which to determine if shallow velocity structure is uniform.
- There is a clear HVSR peak in the 0.54 to 0.55 Hz range on all the HVSR plots, even though the test locations are about 300 m apart. An HVSR peak in the 0.55 Hz range is consistent with an expected basement depth on the order of 300 m in the site vicinity.
- Noise conditions at site (multi-directional or omni-directional noise sources) appeared sufficient for successful application of passive surface wave techniques with the closest noise source being the west to east trending E. California Blvd.
- Both arrays MIK-1/2 and CRP-1/2 are approximately equidistant from the Millikan Library.
- ESAC technique used to extract surface wave dispersion data from passive "L" array data. Both the ReMi™ and ESAC techniques used to extract surface wave dispersion data from the linear arrays.
- Only the "L" array passive surface wave data used for analysis of array MIK-1. As expected, the E-W linear array segment did not provide useful surface wave dispersion data as it was located along E. California Blvd (i.e. parallel to the oncoming traffic). The SE-NW linear yielded better agreement with the "L" array. Both the "L" array passive surface wave data and S-N linear array (both ESAC and ReMi™ analysis) yielded comparable surface wave dispersion curves and were used for data analysis.
- Surface wave dispersion data from active and passive surface wave data sets are in good agreement at this site. The surface wave dispersion data from the two techniques overlap over the 16 to 40 m and 8 to 43 m wavelength ranges on arrays CRP-1/2 and MIK-1/2, respectively. Slight differences in the surface wave dispersion data are attributed to near surface lateral velocity variation and the fact that the MASW data were acquired along a 47 m long array, whereas the passive surface wave data were acquired along a much larger array. Near surface lateral velocity variation is expected for this site due to all of the construction that has occurred over a long period of time.
- Representative dispersion curves were generated for each surface wave data set using a moving average, polynomial curve fitting routine. These individual representative dispersion curves were combined and a representative dispersion curve generated for the combined data set for data modeling.
- No evidence of a water table refractor in the MASW seismic records due to both high noise levels and short array length. There is a potential, but inconclusive, reflector at a depth on the order of 40 m that could be associated with the water table. Therefore, the

saturated zone, with inferred P-wave velocity of 1,600 m/s, was assumed to be located at a depth of 40 m for modeling purposes.

- Surface wave depth of investigation is about 55 m for arrays MIK-1 and 2 and 75 m for arrays CRP-1 and 2 based on half of maximum wavelength criteria and assuming that surface wave dispersion data at frequencies as low as 3 to 3.6 Hz are valid utilizing 4.5 Hz geophones (low frequency geophone phase response differences will cancel out if noise is omni-directional and/or the phase response differences are random in nature).
- Subsurface S-wave velocities are slightly higher in the vicinity of array CRP-1 than array MIK-1, particularly at depths greater than 16 m.
- V_{S30} is 326 and 340 m/s for arrays MIK-1/2 and CRP-1/2, respectively. Average V_{S30} between the two arrays is 333 m/s (Site Class D).
- Average S-wave velocity between 4 m (estimated depth of the foundation of the Millikan Library) and 34 m is 361 and 391 m/s for arrays MIK-1/2 and CRP-1/2, respectively and averages 376 m/s (Site Class C/D).
- Average S-wave velocity of the upper 55 m for array MIK-1/2 (V_{S55}) is 373 m/s. Average S-wave velocity of the upper 75 m for array CRP-1/2 (V_{S75}) is 437 m/s.

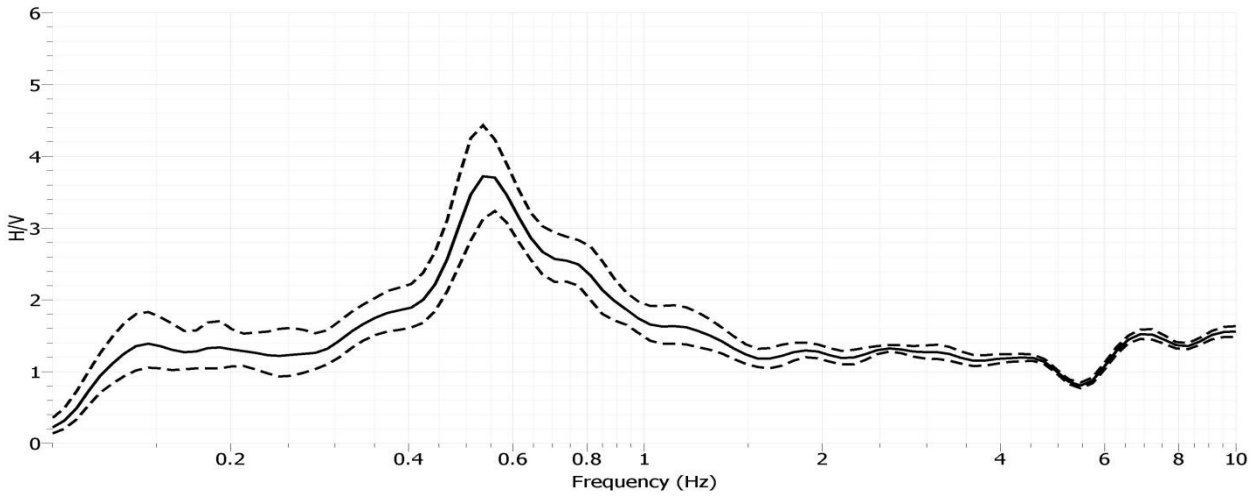

Site CI.CRP, H/V Spectral Ratio, Array CRP-1/2, Sensor 507

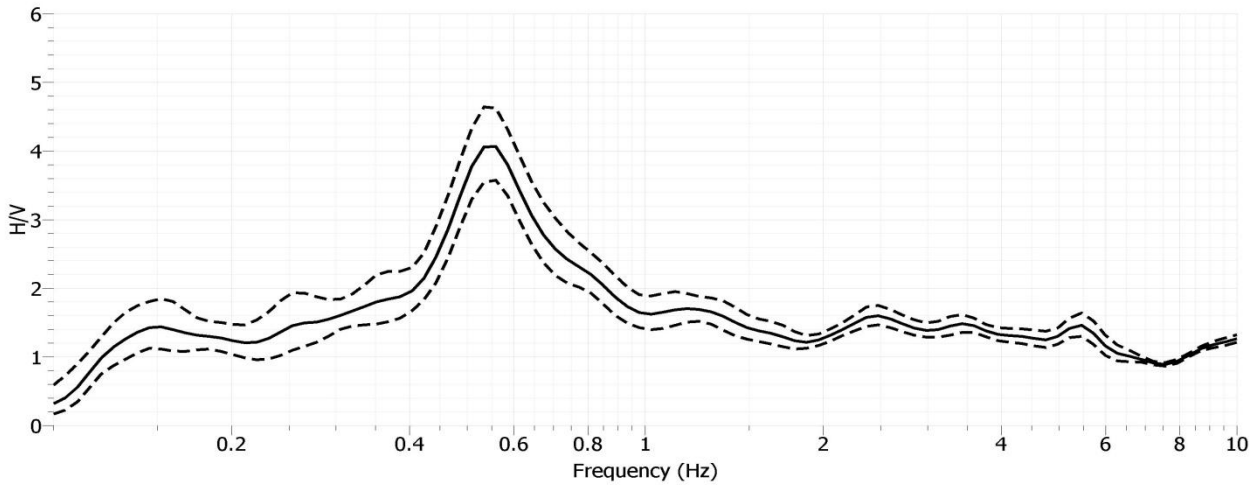

Site CI.MIK, H/V Spectral Ratio, Array MIK-1/2, Sensor 450

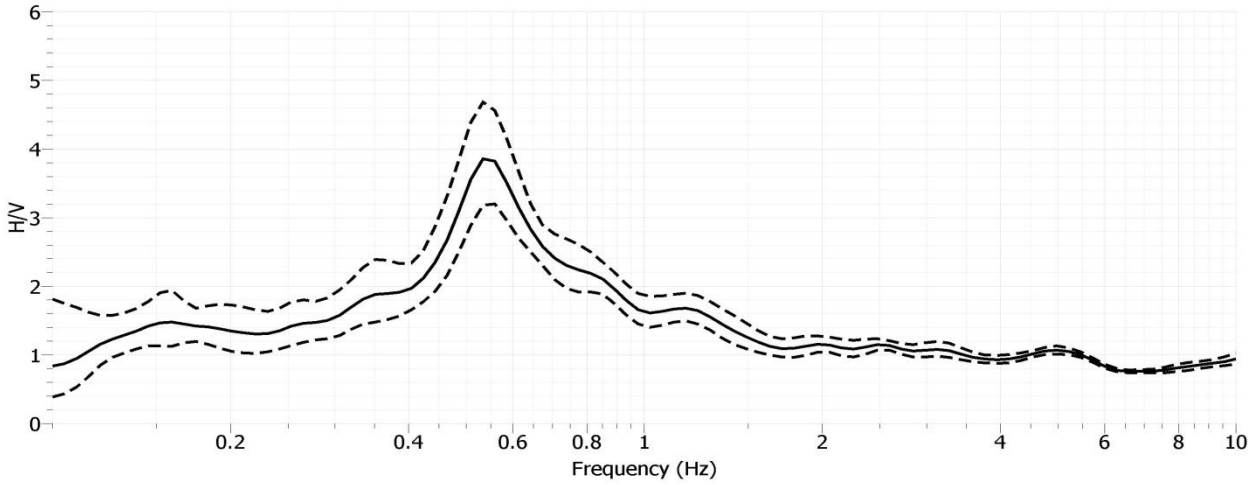

Site CI.CAC, H/V Spectral Ratio, Array CAC-1/2, Sensor 453

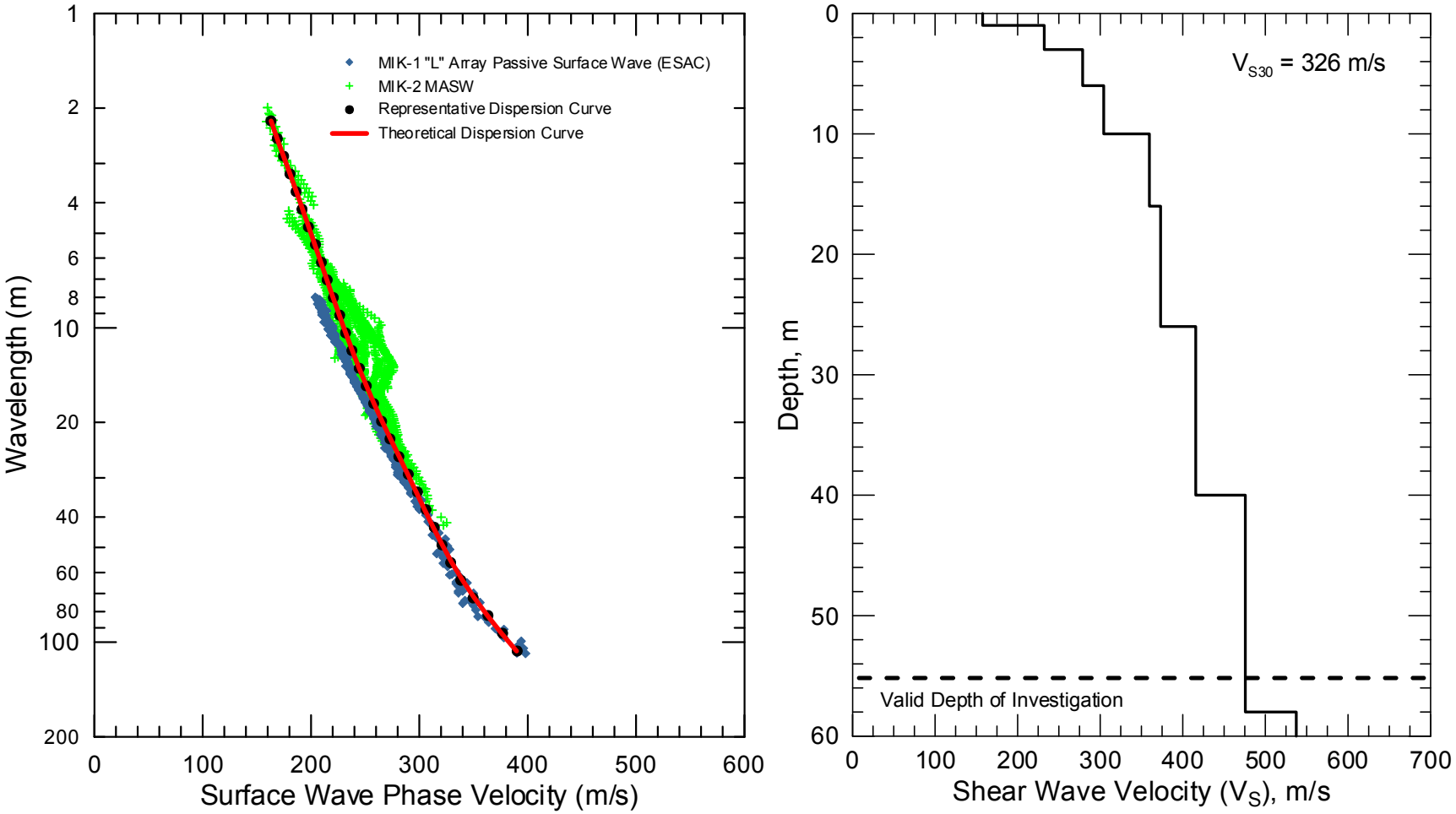

CI.MIK (Arrays MIK-1 and MIK-2) - Field, representative and inverted theoretical surface wave dispersion data (left) and associated V_S model (right)

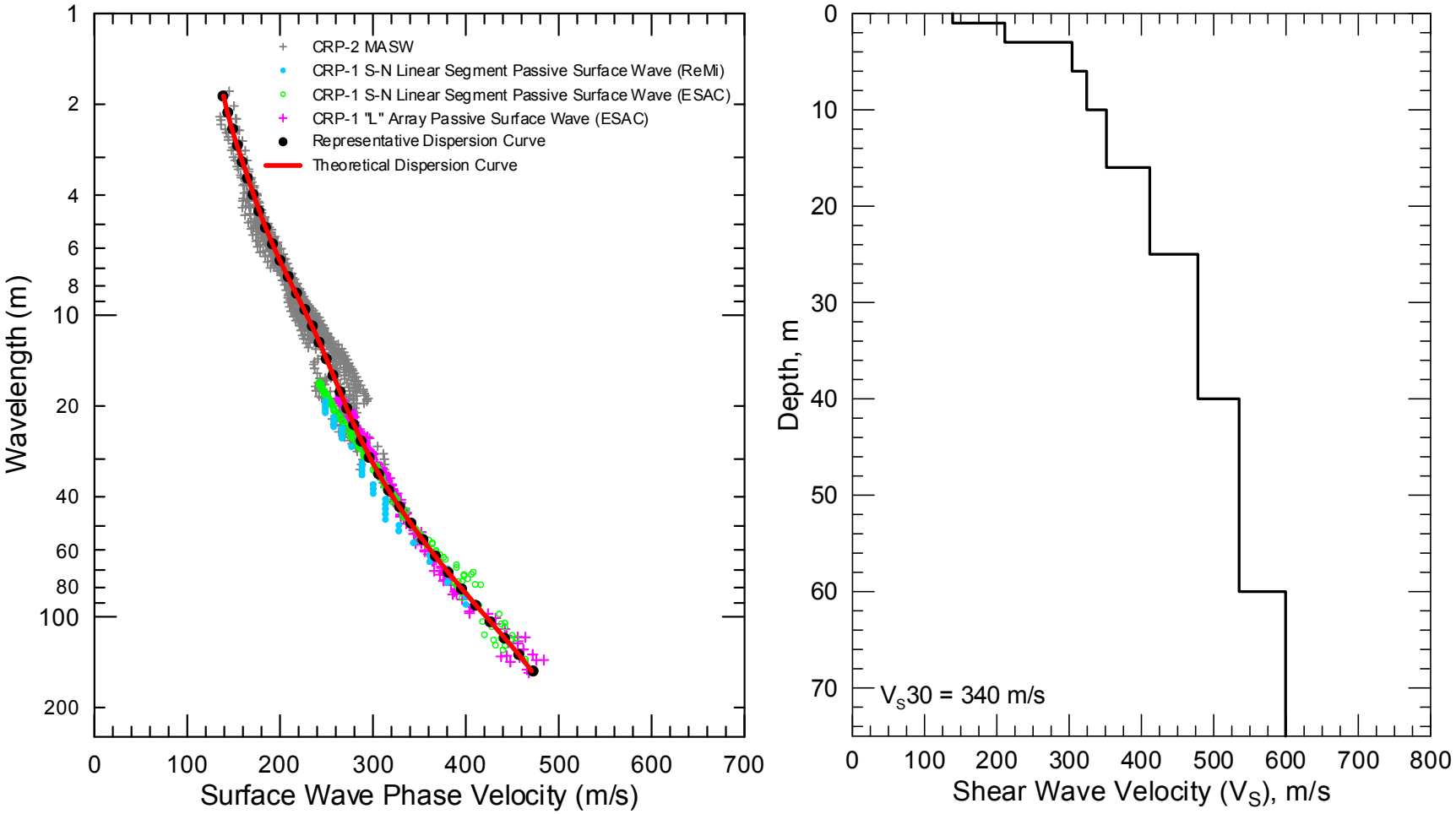

CI.MIK (Arrays CRP-1 and CRP-2) - Field, representative and inverted theoretical surface wave dispersion data (left) and associated V_S model (right)

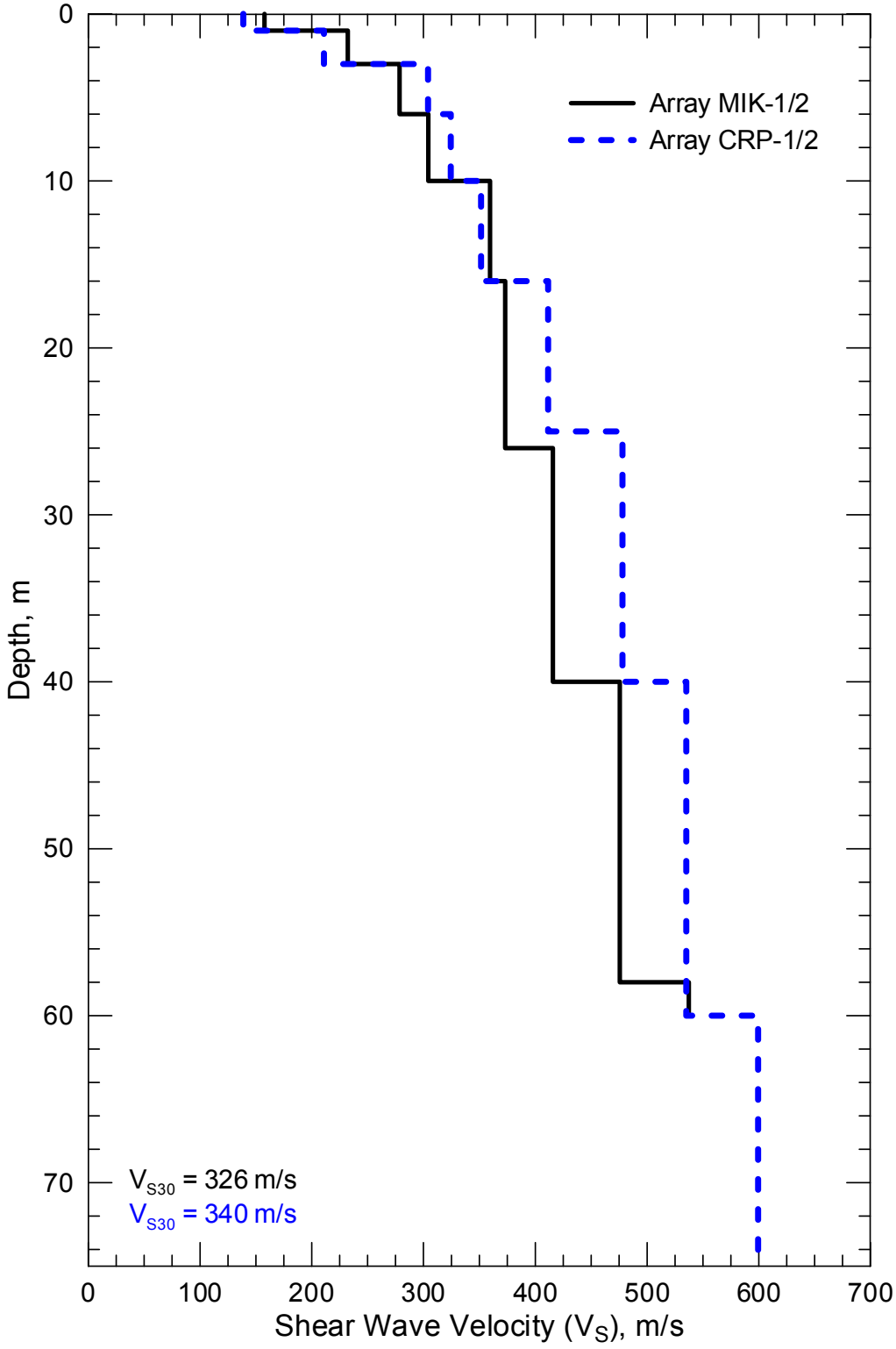

CI.MIK – Comparison of V_S models from arrays MIK-1 and 2 and CRP-1 and 2

Observations/Discussion:

- This site was visited on two occasions. During the first site visit on 12/17/10, P- and S-wave refraction data were acquired along the 46 to 47 m long array MCT-1. MASW and MALW data were also acquired along this array, but not expected to be effective because the array was located along a gravel road cut into the site of a small hill. HVSR data were also acquired at three locations along array MCT-1. As is often the case, P-wave refraction data were of much better quality than the S-wave refraction data. During the second site visit on 9/23/11, P-wave refraction data were acquired along the 117.5 m long array MCT-2 to extend depth of investigation. Array MCT-2 is coincidently located with array MCT-1. P-wave refraction and MASW data were also acquired along array MCT-3, located about 400 m southeast of the seismic station, to determine if MASW data could be successfully acquired in this geologic environment.
- There are no distinct HVSR peaks at this site. There is, however, elevated HVSR response over the 0.5 to 2 Hz range. Further review of the HVSR data revealed that a single horizontal component was primarily responsible for the elevated HVSR response, and it is, therefore, not clear if the broad weak HVSR peak has a geologic source. The amplitude of the elevated HVSR response is much higher at sensor location 450 and may result from poor sensor coupling in an area with a thicker zone of fill.
- As expected, the MASW and MALW data collected along array MCT-1 were not of sufficient quality to permit characterization of subsurface velocity structure in the vicinity of the seismic station. Site characterization was, therefore, limited to analysis of the P- and S-wave seismic refraction data collected along array MCT-1 and P-wave refraction data collected along the longer array MCT-2. Array MCT-3 is not used for site characterization as it is located 400 m from the seismic station and at a significantly lower elevation. MASW data are, however, of much better quality along this array.
- The P-wave seismic refraction data for array MCT-1 were modeled using a tomographic inversion routine with a smooth velocity gradient starting model. The model was extended to off-end shot locations to extend depth of investigation. A longer array is preferred to extend depth of investigation over utilization of far offset shot locations when applying tomographic inversion routines and, therefore, P-wave refraction array MCT-1 was later replaced with array MCT-2. A gradual increase in velocity with depth at the site and the utilization of the far offset source locations allowed a maximum depth of investigation of about 23 m, quite deep for a 47 m long array. The seismic refraction model indicates that P-wave velocity is about 350 to 600 m/s at the surface and increases to 2,000 m/s at a depth of 2 to 7 m, 3,000 m/s at a depth of 6 to 13 m and over 3,500 m/s at a depth of 15 m, or greater.
- The average P-wave velocity of the upper 30 m (V_{P30}) was estimated between 15 and 30 m on the array MCT-1 refraction model, where depth of investigation is greatest, by projecting the velocity at 23 m depth to 30 m depth. P-wave velocity likely continues to increase with depth below 23 m; however, the effect of this velocity increase on estimated V_{P30} may be balanced by the tendency of tomographic inversion routines to often overestimate velocity at the base of the model. V_{P30} ranges from about 1,905 to 2,461 m/s over the 15 to 30 m position interval, a 25% variation over only 15 m. An average V_P model was developed over the 15 to 30 m distance interval by horizontally averaging the travel time of each model cell and cell thickness and average V_{P30} was

determined to be 2,170 m/s. Assuming constant Poisson's ratios of 0.25, 0.3, 0.35 and 0.4 would result in an estimated V_{S30} of 1,253, 1,160, 1,042 and 886 m/s, respectively. Weathered bedrock is not expected to be saturated in the upper 30 m and, therefore, a realistic estimate of Poisson's ratio would be about 0.3.

- The S-wave refraction data for array MCT-1 were modeled using a tomographic inversion routine with a smooth velocity gradient starting model. The seismic refraction model was extended to limited far offset shot locations to extend depth of investigation. S-wave refraction data quality is not very good and at most the S-wave refraction data should be used to guide estimation of S-wave velocity structure from P-wave refraction data. There was typically not good polarity reversal on seismic records from shot locations at the opposite sides of the S-wave plank. The resulting S-wave refraction model is, therefore, not considered as accurate as the P-wave velocity model and should not be used alone for site characterization.
- The array MCT-1 S-wave seismic refraction survey design allowed S-wave velocity to be imaged to a maximum depth of about 18 m. The S-wave refraction model is much smoother than the P-wave refraction model due to the larger geophone spacing and larger error in the first arrival data. The seismic refraction model indicates that S-wave velocity is about 150 to 250 m/s at the surface and increases to 1,000 m/s at a depth of 2 to 3 m, 1,500 m/s at a depth of 4 to 11 m and over 2,000 m/s at a depth of 15 m, or greater. The S-wave refraction model generally overestimates V_S relative to V_S estimated from the P-wave refraction model using nominal values of Poisson's ratio and should not be used for site characterization.
- V_{S30} was estimated between 14 and 30 m on the S-wave refraction model, where depth of investigation is greatest, by projecting the velocity at 18 m depth to 30 m depth. Over this interval V_{S30} ranges from about 1,210 to 1,329 m/s, a 9% variation. An average V_S model was developed over the 14 to 30 m distance interval by horizontally averaging the travel time of each model cell and cell thickness and average V_{S30} was determined to be 1,271 m/s. Although the S-wave refraction model is not particularly reliable and appears to overestimate S-wave velocity over a large depth range, V_{S30} is only about 10% higher than that estimated over a similar position range from the P-wave refraction model and assumed constant Poisson's ratio of 0.3.
- The P-wave seismic refraction data for array MCT-2 were modeled using a tomographic inversion routine with a smooth velocity gradient starting model. The model was extended to limited off-end shot locations to extend depth of investigation. Depth of investigation for array MCT-2 is about 30 m. The seismic refraction model indicates that P-wave velocity is about 350 to 600 m/s at the surface and increases to 2,000 m/s at a depth of 2 to 15 m, 3,000 m/s at a depth of 11 to 25 m, 3,500 m/s at a depth of 15 to 28 m and over 4,000 m/s at a depth of 29 m, or greater. The P-wave velocity model has similar velocity structure in the region of overlap with array MCT-1. Lateral resolution is somewhat less due to the larger geophone spacing. As previously discussed, array MCT-1 appears to slightly overestimate P-wave velocity at the base of the model based on the more accurately resolved velocity structure at depth for array MCT-2.
- The average P-wave velocity of the upper 30 m (V_{P30}) was estimated between 25 and 85 m on the array MCT-2 refraction model, where depth of investigation is greatest. V_{P30} ranges from about 1,615 to 2,612 m/s over the 25 to 85 m position interval; a 44% variation over a 60 m distance interval. An average V_P model was developed over the 25

to 85 m distance interval by horizontally averaging the travel time of each model cell and cell thickness and average V_{P30} was determined to be 2,222 m/s. Assuming constant Poisson's ratios of 0.25, 0.3, 0.35 and 0.4 would result in an estimated V_{S30} of 1,283, 1,188, 1,067 and 907 m/s, respectively. Weathered bedrock is not expected to be saturated in the upper 30 m and, therefore, a realistic estimate of Poisson's ratio would be about 0.3.

- The P-wave seismic refraction data for array MCT-3 were modeled using a tomographic inversion routine with a smooth velocity gradient starting model. The model was extended to off-end shot locations to extend depth of investigation. Maximum depth of investigation was about 20 m. The seismic refraction model indicates that P-wave velocity is about 350 to 600 m/s at the surface and increases to 2,000 m/s at a depth of 2 to 8 m, 3,000 m/s at a depth of 6 to 17 m and over 4,000 m/s at a depth of 12 to 20 m. P-wave velocities at depth beneath array MCT-3 are typically higher than observed beneath arrays MCT-1 and MCT-2 with V_{P30} being about 10% higher. Therefore, this array cannot be used for site characterization.
- MASW data collected along array MCT-3 are not presented as this array is not considered representative of seismic station conditions.
- For the purpose of site characterization, we recommend using V_{S30} estimated from the average P-wave velocity model for array MCT-2 and a constant assumed Poisson's ratio of 0.3, which is equal to 1,188 m/s (NEHRP Site Class B). There is over 40% variation in V_{P30} beneath array MCT-2, and the seismic refraction model indicates that V_{S30} may be slightly lower at the seismic station than the average estimated for the array. Even with the uncertainty in the estimated V_{S30} at the seismic station due to use of P-wave refraction data and significant lateral velocity variation, the site is clearly NEHRP Site Class B.
- The minimum value of V_{P30} estimated from array MCT-2 and a Poisson's ratio of 0.35, considered high for weathered granitic rock, would still result in estimated V_{S30} above 760 m/s (Class C/B velocity boundary). The maximum value of V_{P30} estimated from array MCT-2 and a Poisson's ratio of 0.25, considered low for weathered granitic rock, would result in estimated V_{S30} at the 1,500 m/s Class B/A velocity boundary.

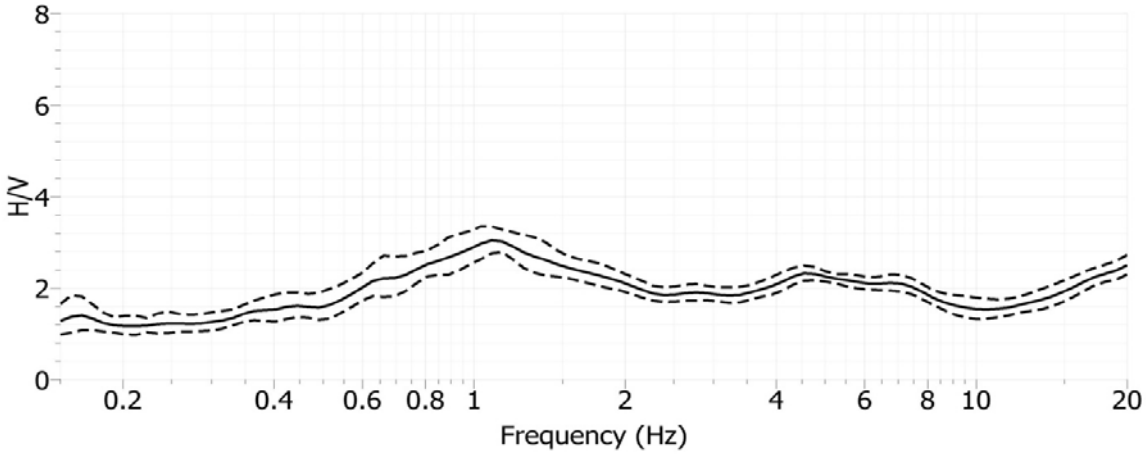

Site CI-MCT, H/V Spectral Ratio, Array MCT-1, Sensor 507

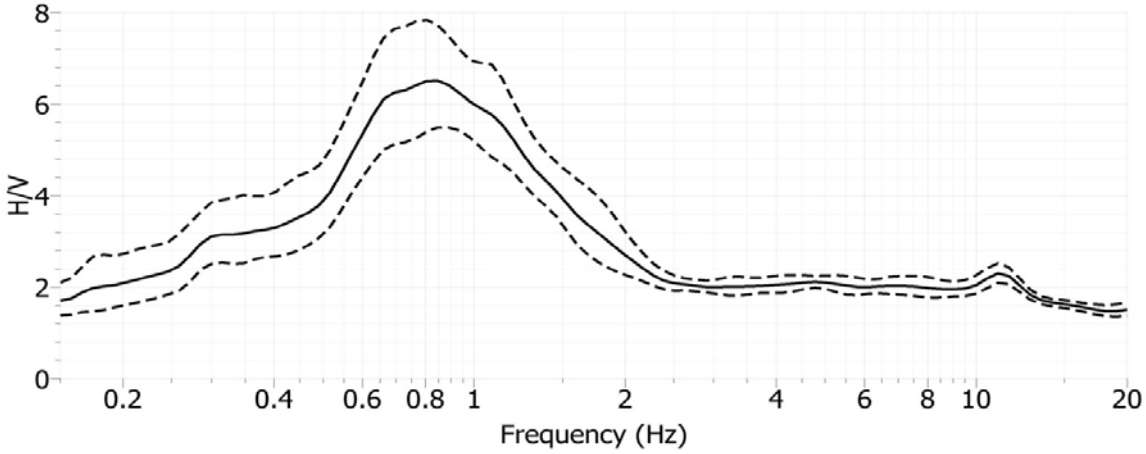

Site CI-MCT, H/V Spectral Ratio, Array MCT-1, Sensor 450

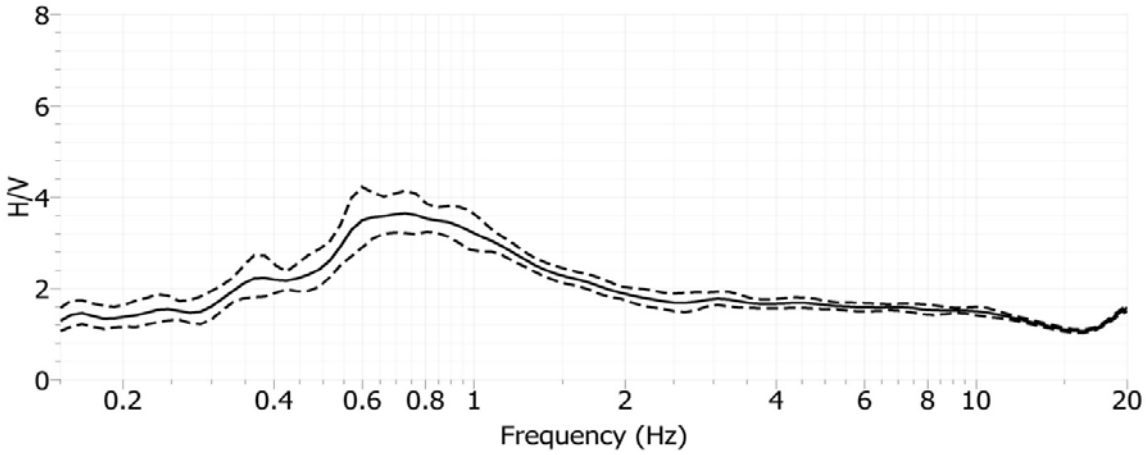

Site CI-MCT, H/V Spectral Ratio, Array MCT-1, Sensor 453

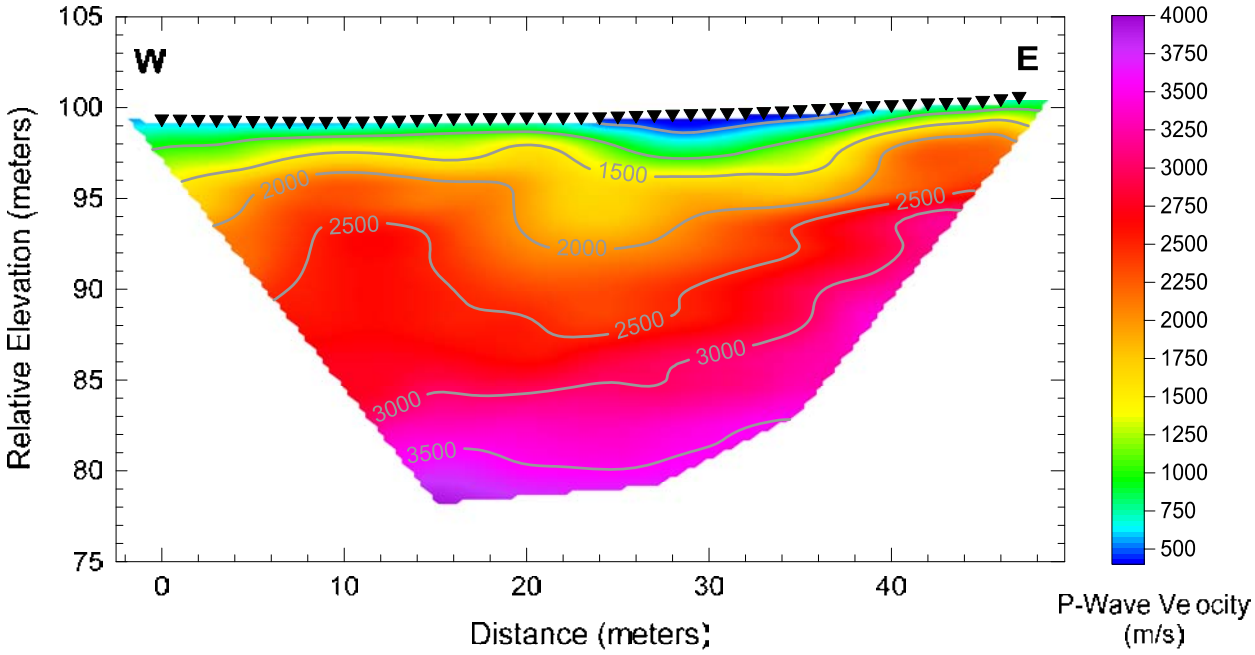

Array MCT-1 – P-wave Tomographic Seismic Refraction Model Developed using a Smooth Velocity Gradient Starting Model

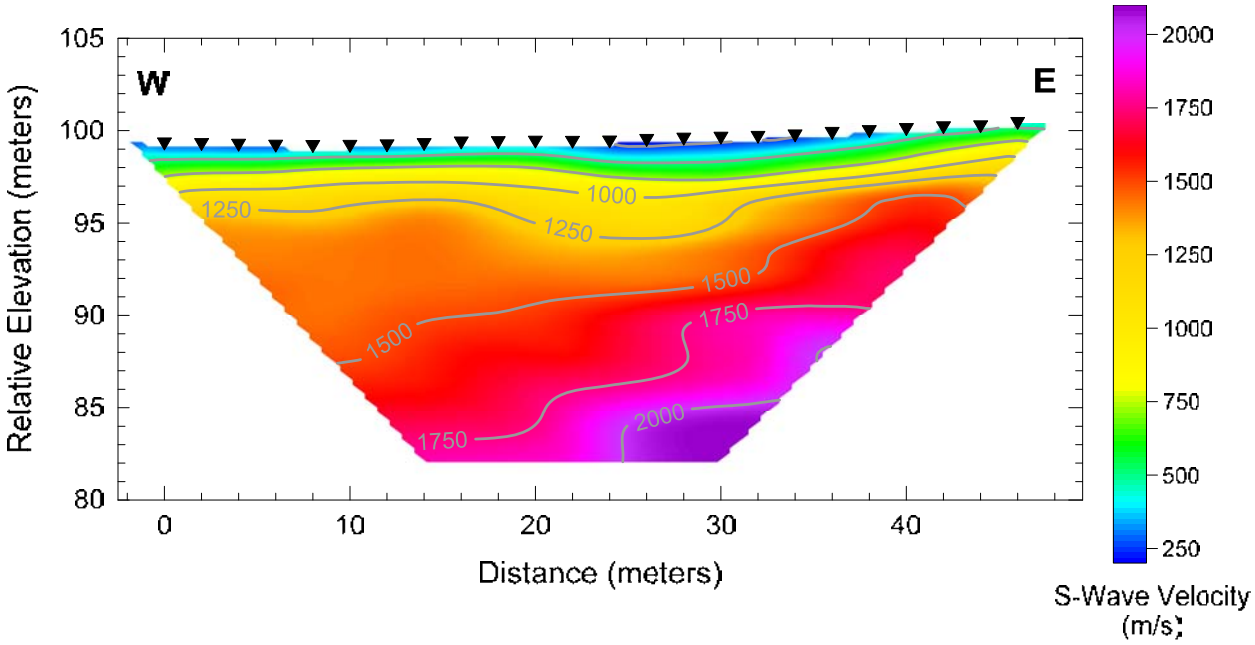

Array MCT-1 – S-wave Tomographic Seismic Refraction Model Developed using a Smooth Velocity Gradient Starting Model

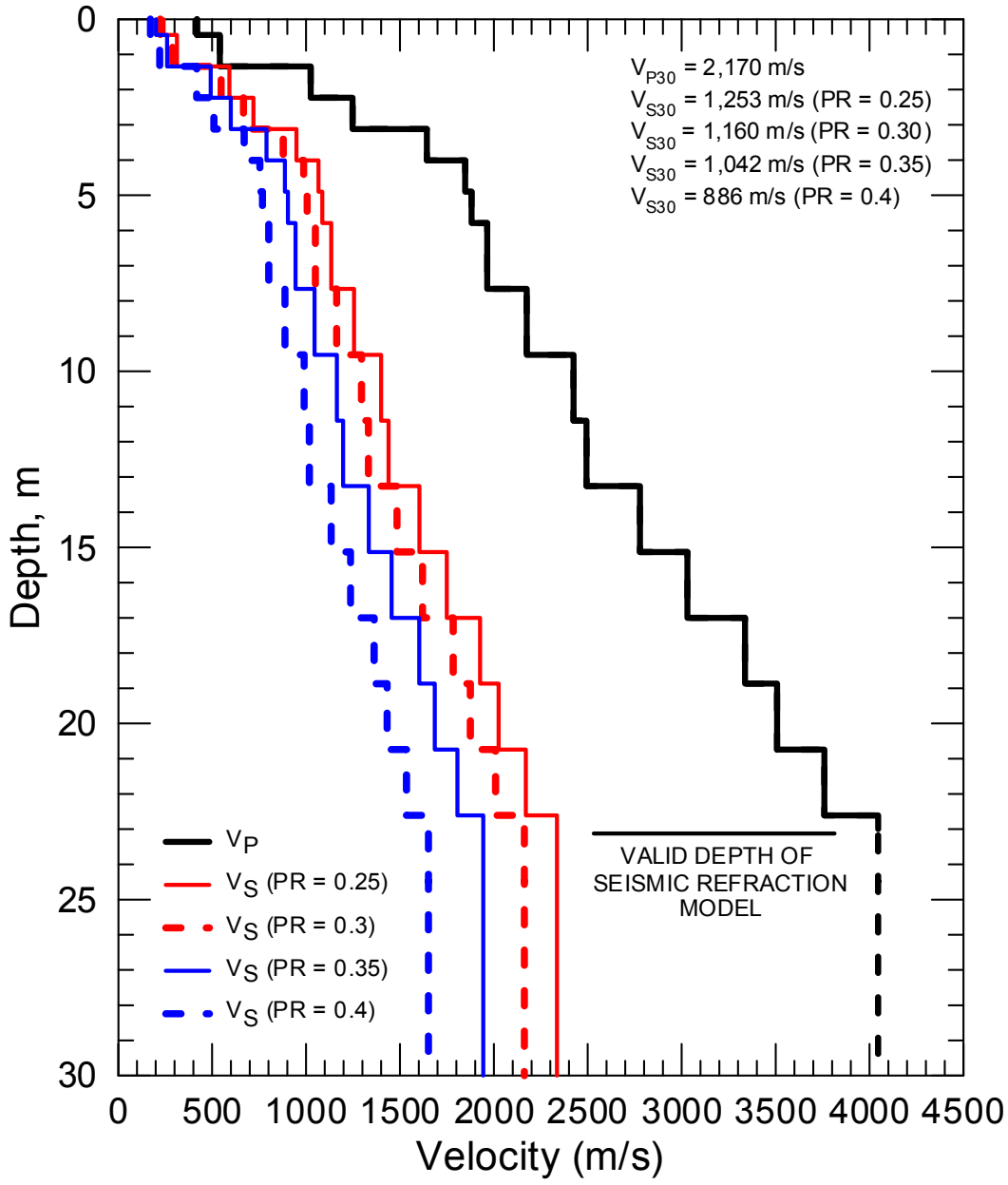

CI.MCT – Average P-wave velocity structure and estimated S-wave velocity structure between a position of 15 and 30 m on the P-wave seismic refraction model for array MCT-1 developed using a smooth velocity gradient starting model. The maximum seismic refraction depth of investigation is limited to about 23 m and P-wave velocity is assumed to be constant between 23 and 30 m.

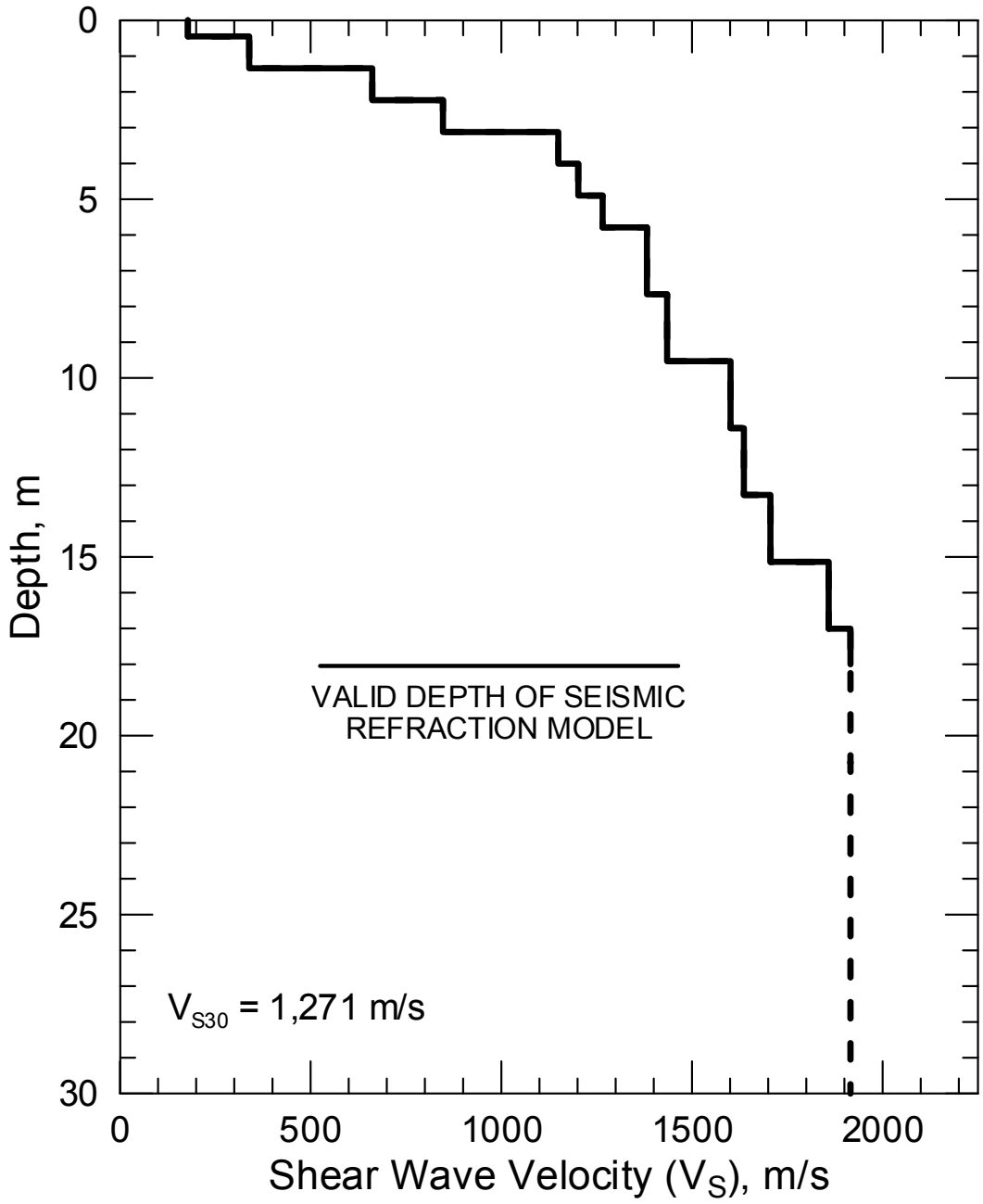

CI.MCT – Average S-wave velocity structure between 14 and 30 m on S-wave seismic refraction array MCT-1. Seismic refraction depth of investigation is limited to about 17 m and S-wave velocity is assumed to be constant below this depth.

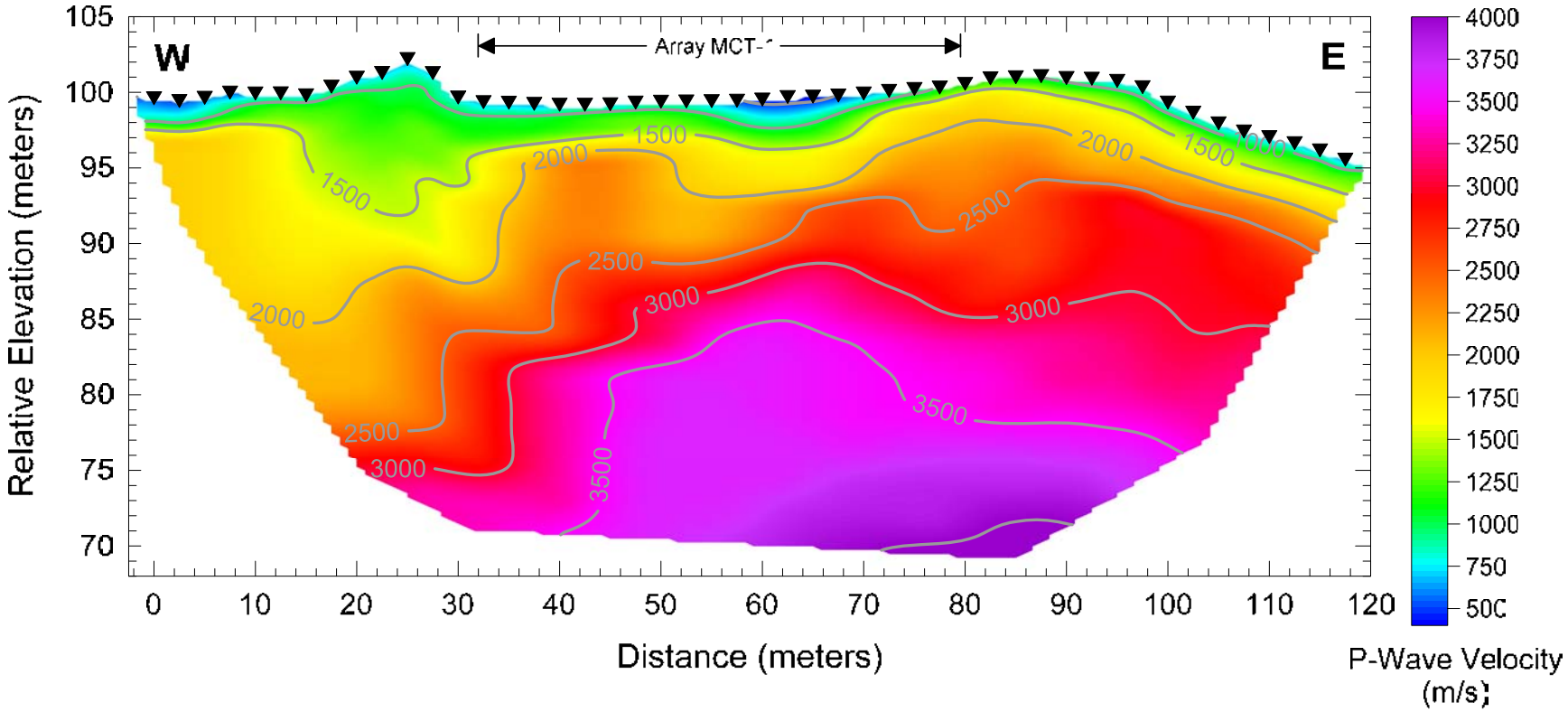

Array MCT-2 – P-wave Tomographic Seismic Refraction Model Developed using a Smooth Velocity Gradient Starting Model

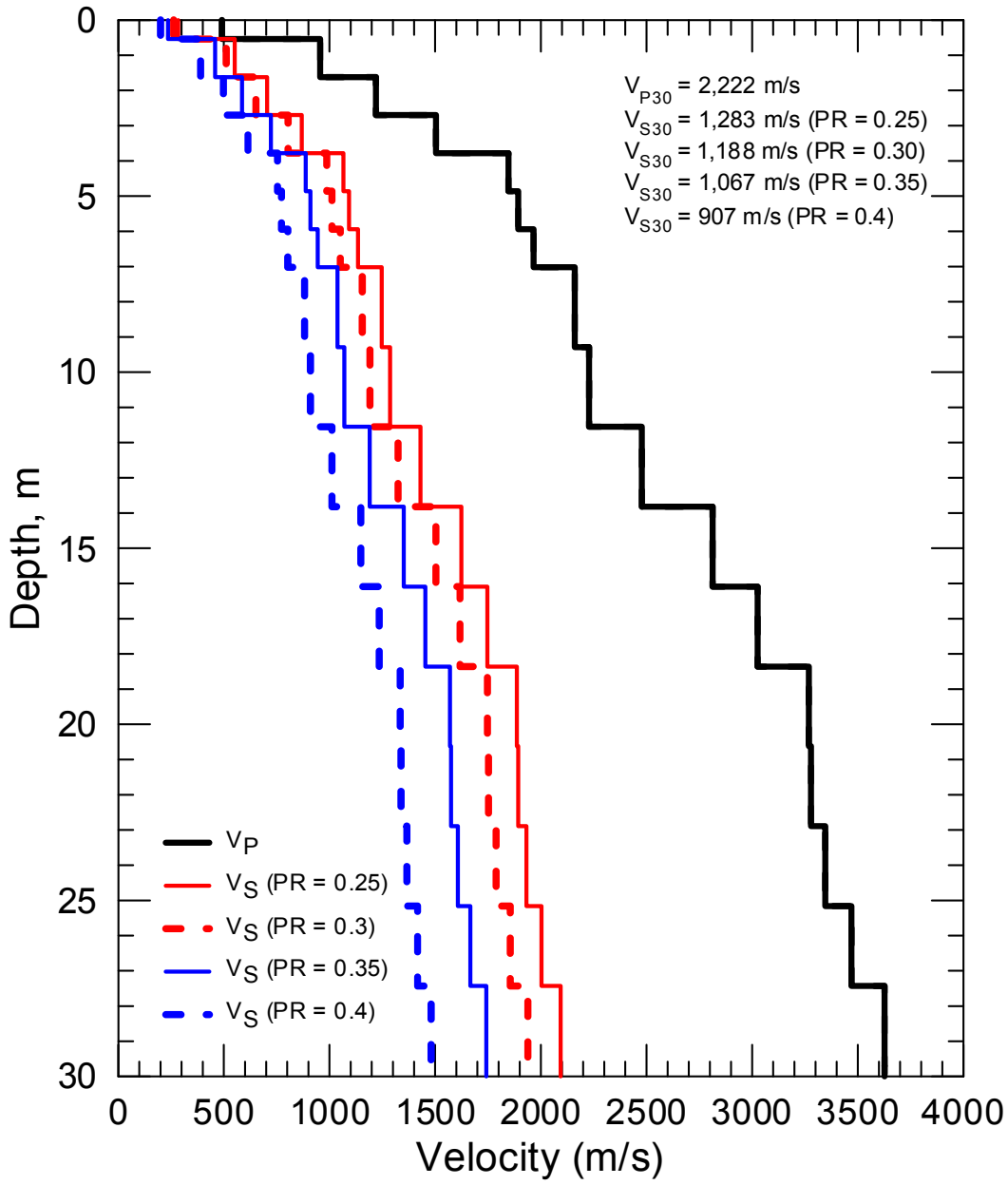

CI.MCT – Average P-wave velocity structure and estimated S-wave velocity structure between a position of 25 and 85 m on the P-wave seismic refraction model for array MCT-2 developed using a smooth velocity gradient starting model.

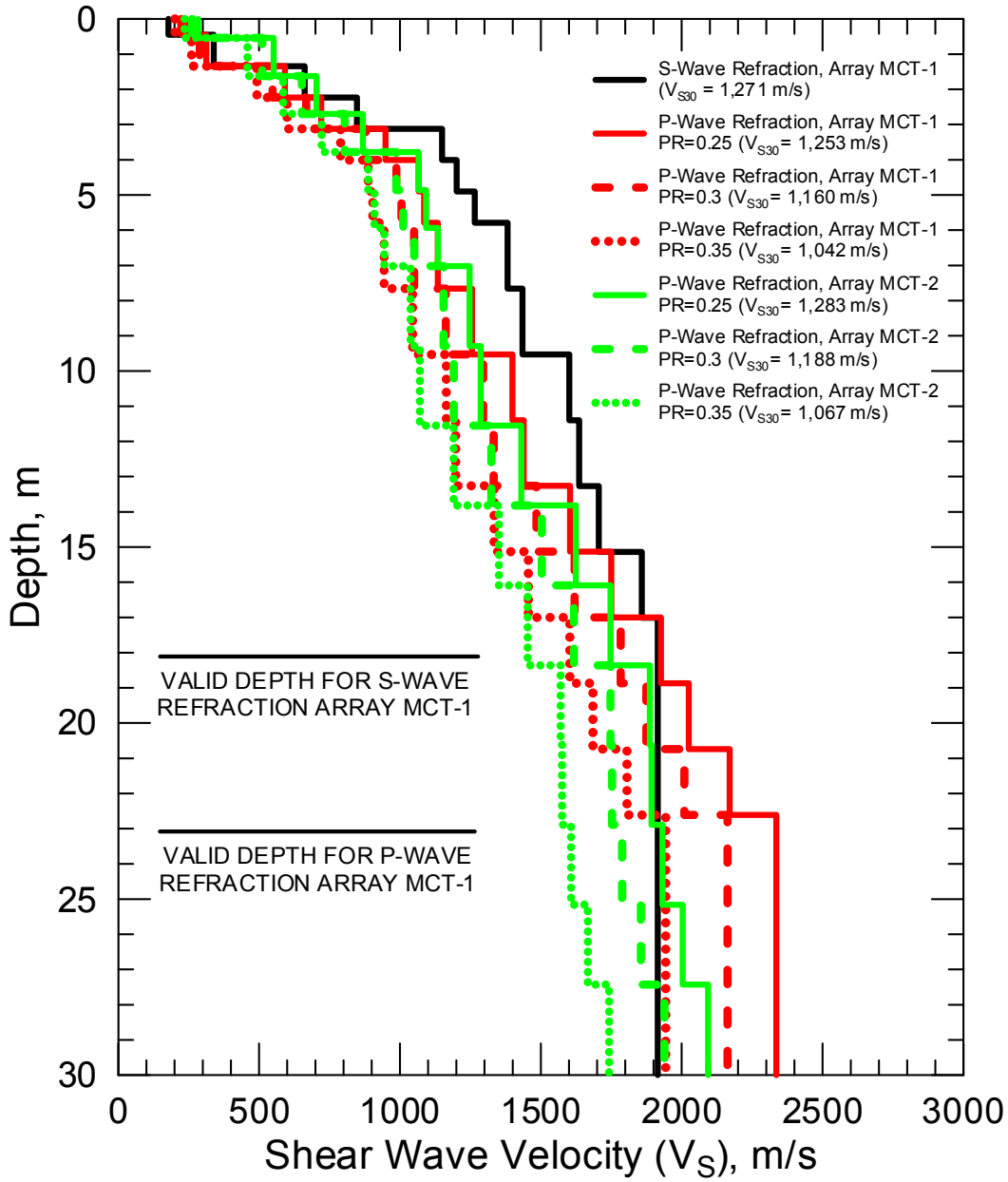

CI.MCT – Comparison of S-wave velocity models derived from the S-wave seismic refraction survey along array MCT-1 and P-wave seismic refraction surveys along arrays MCT-1 and MCT-2. The S-wave seismic refraction data were difficult to interpret and, therefore, the S-wave refraction model is not as reliable as the P-wave refraction models. The S-wave refraction model appears to overestimate V_S over the 3 to 15 m depth interval, relative to the P-wave refraction model. The average V_S models estimated from P-wave refraction arrays MCT-1 and MCT-2 are very similar, especially at depths below 20 m. The average V_S models from the longer P-wave refraction array MCT-2 are expected to be more reliable at depths below 20 m.

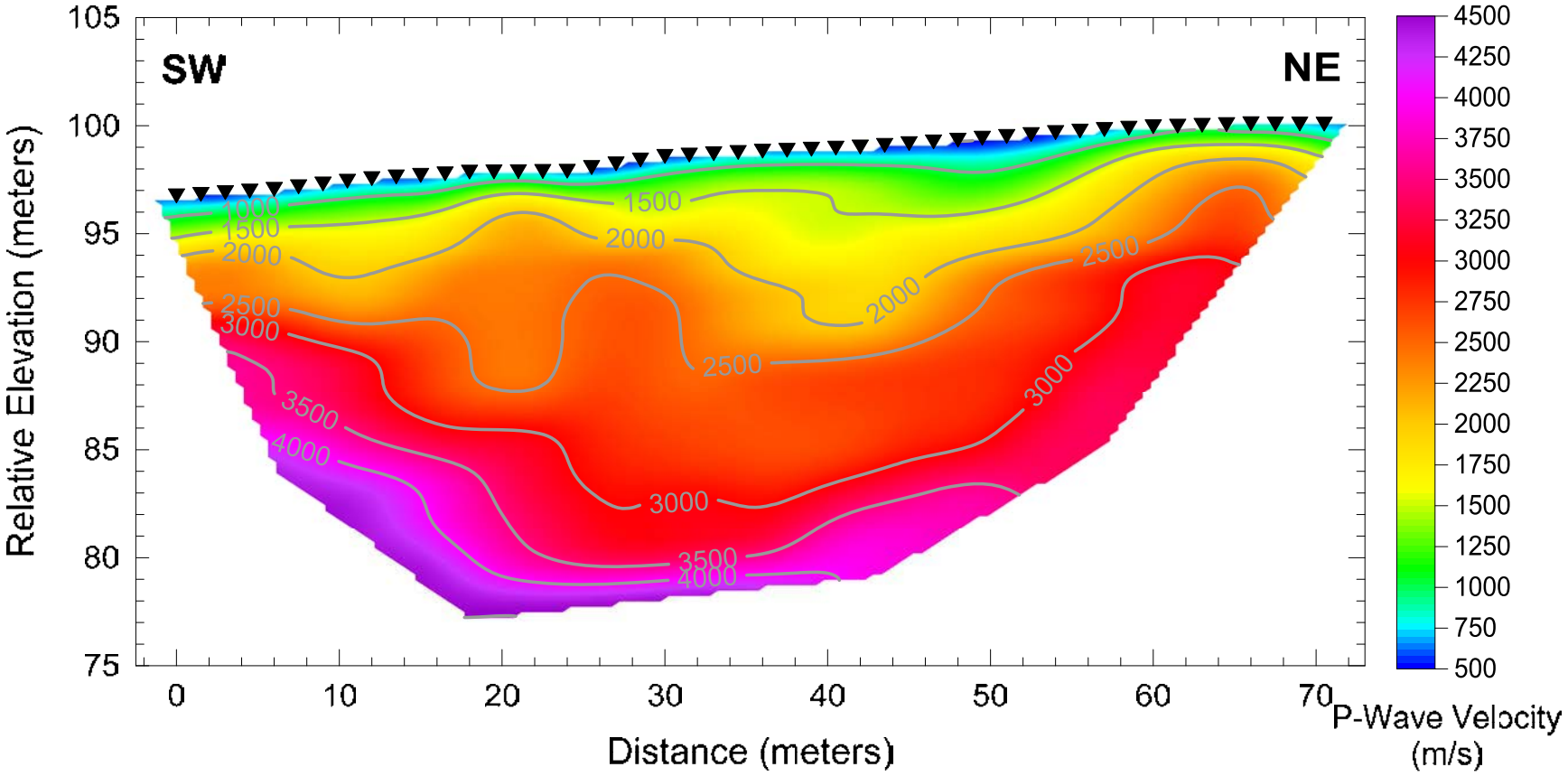

Array MCT-3 – P-wave Tomographic Seismic Refraction Model Developed using a Smooth Velocity Gradient Starting Model

Site CI.MLAC

Location: Mammoth Lakes Airport, Mono County, California

Latitude: 37.63019 **Longitude:** -118.83605
(Station coordinates provided by USGS, WGS84 coordinate system)

V_{S30} (measured): 308 m/s

V_{S30} (adjusted to more accurately reflect seismic station conditions): 322 m/s (average S-wave velocity between 2 and 32 m adjusting for 1 m assumed sensor depth).

NEHRP Site Class: D

Geomatrix Code: IQD

Geologic Conditions/Observations: Seismic station located on Quaternary (Pleistocene) old alluvium. Quaternary volcanic rocks outcrop about 150 m east of the site (rhyolite of Hot Creek) and 500 m northwest of the site (basalt). The site is located between mapped strands of the Hilton Creek Fault Zone.

Site Conditions: Rural site with only three significant noise sources in the site vicinity: SR-395 located about 600 m southeast of the site, the airport located about 550 m southeast of the site and a quarry located about 400 m northeast of the site. Relatively flat terrain in the immediate site vicinity.

Geophysical Methods Utilized: HVSR, MASW, SASW, Array Microtremor, ReMi™

Geophysical Testing Arrays:

1. Arrays MLAC-1 (24 channel linear array utilizing 4.5 Hz vertical geophones spaced 7.5 m apart for an array length of 172.5 m) and MLAC-2 (24 channel linear array utilizing 4.5 Hz vertical geophones spaced 3 m apart for an array length of 69 m) used to acquire passive surface wave data. Arrays combined to form a "T" shaped array. Limited seismic refraction data also acquired along array MLAC-1.
2. Array MLAC-3 (SASW array with midpoint at intersection of arrays MLAC-1 and MLAC-2 and same orientation as array MLAC-1. SASW data acquired using 1 Hz geophones, common center point geometry, forward and reverse shot locations and receiver spacings of 2 to 40 m).
3. Array MLAC-4 (48 channel MASW array utilizing 4.5 Hz vertical geophones spaced 1.5 m apart for a length of 70.5 m, forward and reverse shot locations with multiple source offsets and source types and center shot location). The center of array MLAC-4 is near that of array MLAC-3

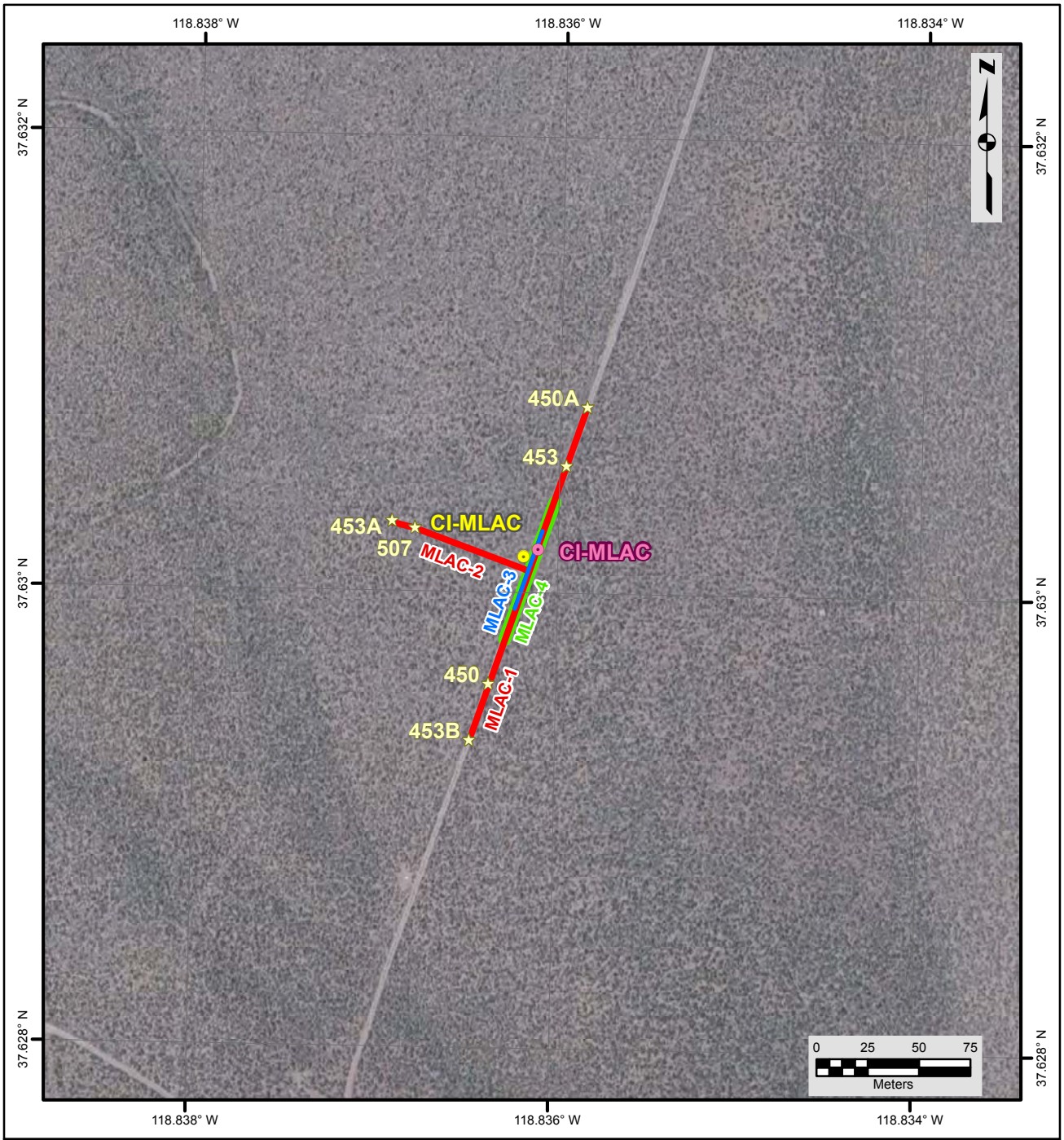

Legend

- Seismic Station - Approximate Surveyed Location
- Seismic Station - Approximate Location of Record
- H/V Spectral Ratio Location
- SASW Array
- Passive Surface Wave Array
- MASW Array

NOTES:
1. WGS 1984 COORDINATE SYSTEM
2. Image Source: ESRI, i-cubed, USDA FSA, USGS, AEX, GeoEye, Getmapping, Aerogrid, IGP

File Name: CI-MLAC-1

Date: 2/7/2013

USGS science for a changing world

GEOVision geophysical services

RECOVERY.GOV

SITE MAP
CI•MLAC

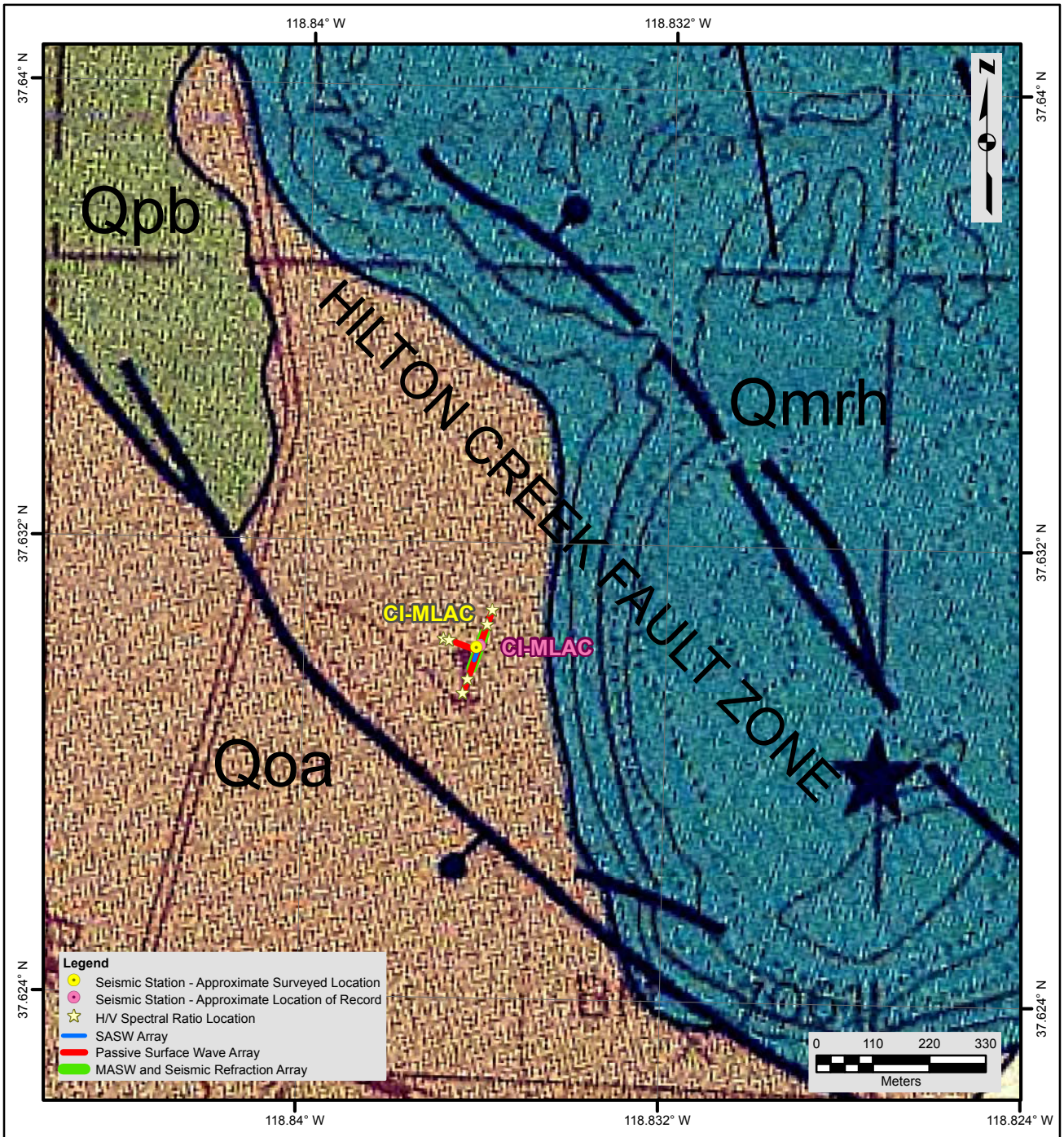

Description of Geologic Map Units

Qoa = Quaternary (Pleistocene) older alluvium, stream deposits undergoing erosion and dissection, glacial outwash and periglacial sediments
Qpb = Quaternary (Pleistocene) porphyritic basalt, coarsly porphyritic trachybasaltic lava and cinders
Qmrh = Quaternary (Pleistocene to Holocene) rhyolite of Hot creek, sparsely porphyritic high-silica rhyolite, texture variable from vitrophyre to felsite to pumice

NOTES:
1. WGS 1984 COORDINATE SYSTEM
2. Geologic Map of Long Valley Caldera, Mono-Inyo Craters Volcanic Chain, and Vicinity, Eastern California by Roy A. Bailey, 1989
3. See site map for details of geophysical survey

File Name: CI-MLAC

Date: 2/7/2013

USGS science for a changing world

GEOVision geophysical services

GEOLOGIC MAP
CI•MLAC

RECOVERY.GOV

Looking northeast at intersection of array MLAC-1 and MLAC-2 and CI.MLAC seismic station

Looking northeast towards seismic station and array MLAC-4

GPS data acquisition at HVSR sensor

SASW data acquisition on array MLAC-3

SASW data acquisition using accelerated weight drop energy source

4. Six HVSR measurement locations distributed along arrays MLAC-1 to MLAC-4. Three HVSR measurement locations occupied on 8/23/10, one on 10/29/11 and two on 11/11/11.

Location of Geophysical Testing Arrays:

Location	Latitude	Longitude
MLAC-1, Southwest End of Array, Geophone 1	37.62935	-118.83641
MLAC-1 and MLAC-2 Intersection	37.63010	-118.83610
MLAC-1, Northeast End of Array, Geophone 24	37.63082	-118.83579
MLAC-2, Southeast End of Array, Geophone 25	37.63010	-118.83613
MLAC-2, Northwest End of Array, Geophone 48	37.63030	-118.83686
MLAC-3, Center of SASW Array	37.63010	-118.83610
MLAC-4, Southwest End of Array	37.62979	-118.83622
MLAC-4, Center of Array	37.63010	-118.83609
MLAC-4, Northeast End of Array	37.63040	-118.83596
HVSR Sensor 450	37.62960	-118.83631
HVSR Sensor 453	37.63056	-118.83590
HVSR Sensor 507	37.63028	-118.83673
HVSR Sensor 453A	37.63031	-118.83686
HVSR Sensor 453B	37.62935	-118.83641
HVSR Sensor 450A	37.63082	-118.83579
CI.MLAC Seismic Station	37.63016	-118.83613

Notes: 1) WGS84 Coordinate System (decimal degrees)

2) Survey accuracy is estimated at 1 to 3 m.

Results:

V_S Model – SASW Array MLAC-3

Depth to Top of Layer (m)	Layer Thickness (m)	S-Wave Velocity (m/s)	Inferred P-Wave Velocity (m/s)	Assumed Poisson's Ratio	Assumed Density (g/cm^3)
0	2	207	386	0.300	1.7
2	3	255	477	0.300	1.7
5	4	317	594	0.300	1.8
9	4	348	651	0.300	1.8
13	7	325	1750	0.482	1.9
20	9	313	1750	0.483	1.9
29	>6	447	1750	0.465	2.0

Notes: 1) Saturated sediments estimated at 13 m depth from seismic refraction first arrival data. The P-wave velocity of saturated sediments is about 1,750 m/s.
2) Depth of investigation is about 35 m.
3) Bottom layer is a half space.

V_S Model – MASW Array MLAC-4

Depth to Top of Layer (m)	Layer Thickness (m)	S-Wave Velocity (m/s)	Inferred P-Wave Velocity (m/s)	Assumed Poisson's Ratio	Assumed Density (g/cm^3)
0	2	267	500	0.300	1.7
2	3	305	571	0.300	1.7
5	8	321	600	0.300	1.8
13	16	307	1750	0.484	1.9
29	>6	444	1750	0.466	2.0

Notes: 1) Saturated sediments estimated at 13 m depth from seismic refraction first arrival data. The P-wave velocity of saturated sediments is about 1,750 m/s.
2) Depth of investigation is about 35 m.
3) Bottom layer is a half space.

Observations/Discussion:

- The HVSR data acquired on 8/23/10 (sensor locations 450, 453 and 507) are similar validating the 1-D velocity structure assumption. There is an HVSR peak at about 0.8 Hz and a broad zone of elevated HVSR response between 0.2 and 0.5 Hz. The Nanometrics Trillium sensors were placed on a small ceramic plate and not covered. A ceramic plate was later learned to not be the best method of coupling the sensors to the ground and covering the sensors in the event of wind was later learned to be critical. There was only very light wind during data acquisition and all HVSR plots are very similar, therefore, the data is considered valid.
- The HVSR data acquired on 10/29/11 (sensor location 292A) and 11/11/11 (sensor locations 292B and 450A) are also similar, but slightly different that the data acquired the previous year. The sensors were coupled to the ground using a small aluminum tripod in a shallow hole and covered with a plastic bucket. The HVSR data still has the same general characteristics of the data acquired the previous year; however, the 0.8 Hz peak has much lower amplitude and the lower frequency peak is much higher amplitude and possibly slightly lower frequency. The broad, low frequency peak(s) occurs between 0.2 and 0.5 Hz with maxima at about 0.25 to 0.3 Hz.
- The water table, with P-wave velocity of about 1,750 m/s was modeled at a depth of about 13 m based on interactive layer-based analysis of seismic refraction first arrival data. P-wave velocities of the unsaturated sediments range from about 500 m/s at the surface to about 650 to 675 m/s at a depth of about 2.5 m.
- There is good reflectivity in the MASW seismic records with multiple reflectors in the approximate 45 to 150+ m depth range. There is a high amplitude reflector at a depth of greater than 150 m and would be the shallowest depth of volcanic rock beneath the line and could also be the source of the 0.8 Hz HVSR peak.
- Noise conditions at the site were not considered sufficient to apply passive surface wave techniques; however, passive surface wave data were acquired to evaluate the technique in less than ideal conditions. The only noise sources at the site consisted of SR-395 about 600 m southwest of the site, traffic into the airport located about 550 m southwest of the site and a quarry located about 400 m northwest of the site.
- The passive linear array data were not usable due to obvious directional noise bias. The "T" array passive surface wave data were processed using the SPAC technique. Data quality was acceptable, but phase velocities were slightly higher than the MASW and SASW data and, therefore, the passive surface wave data were not utilized.
- The SASW and MASW surface wave dispersion data are sufficiently different to require separate modeling.
- SASW dispersion data are interesting and we don't have an explanation for the signature of the dispersion data, which almost forms two separate dispersion curves. The signature of the dispersion data is very similar to that observed at CI.BOM and more work is needed to understand the type of velocity structure that causes such a response. Only the lower phase velocity portion of the SASW dispersion data were modeled and are expected to yield a conservative velocity model.
- The MASW dispersion data more closely tracks the higher phase velocity segment of the SASW dispersion curve.
- There is about 25 m/s scatter in the MASW dispersion data over the 15 to 40 m wavelength range.

- The minimum wavelength surface wave phase velocity data extracted from the 48-channel MASW array MLAC-4 was about 7 m. Reducing data from smaller hammer sources using a limited offset receiver array (i.e. less active geophones) allowed extraction of surface wave dispersion data to a minimum wavelength of about 2 m.
- A representative dispersion curve was generated for the MASW and SASW data sets using a moving average, polynomial curve fitting routine for data modeling.
- The only significant difference between the SASW and MASW models occurs in the upper 5 m and is likely associated with lateral velocity variation in near surface sediments. The SASW model represents near surface velocity structure near the center of the MASW array, whereas the MASW model represents near surface velocity structure near the ends of the MASW array.
- Surface wave depth of investigation is about 35 m based on half of maximum wavelength criteria.
- V_{S30} is 306 m/s for SASW array MLAC-3 and 310 m/s MASW array MLAC-4.
- The average V_{S30} between the SASW and MASW models is 308 m/s (Site Class D).
- V_{S30} is almost identical between the MASW and SASW models even though there is significant difference in Rayleigh wave phase velocity at wavelengths smaller than 20 m.
- Average S-wave velocity between 2 m (assumed sensor depth) and 32 m is 323 m/s for SASW array MLAC-3 and 320 m/s for MASW array MLAC-4.
- Average S-wave velocity between 2 m (assumed sensor depth) and 32 m for the SASW and MASW models is 322 m/s.

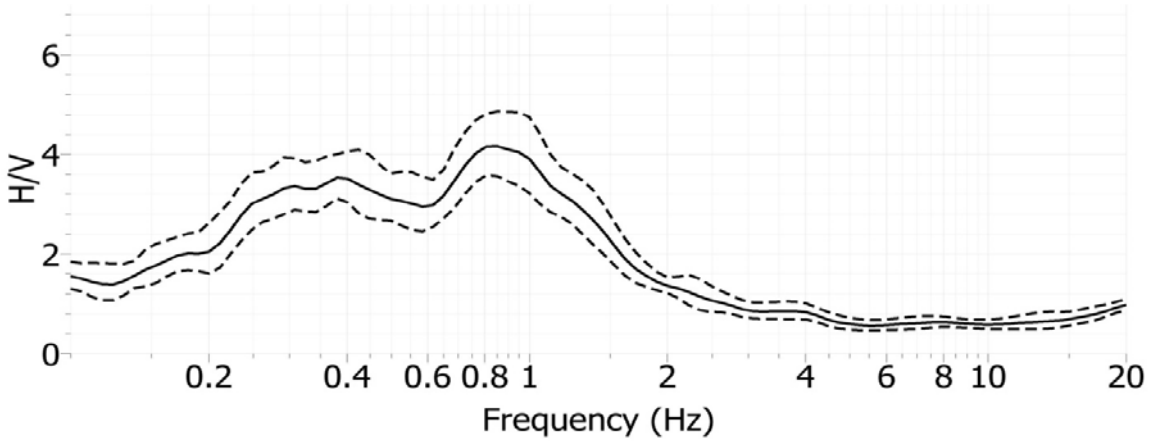

Site CI.MLAC, H/V Spectral Ratio, Array MLAC-1, Sensor 453

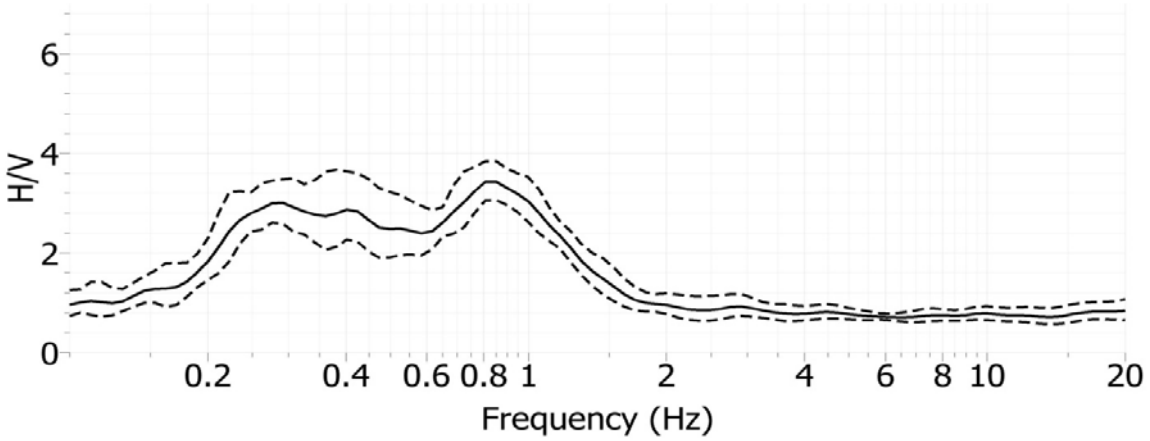

Site CI.MLAC, H/V Spectral Ratio, Array MLAC-2, Sensor 507

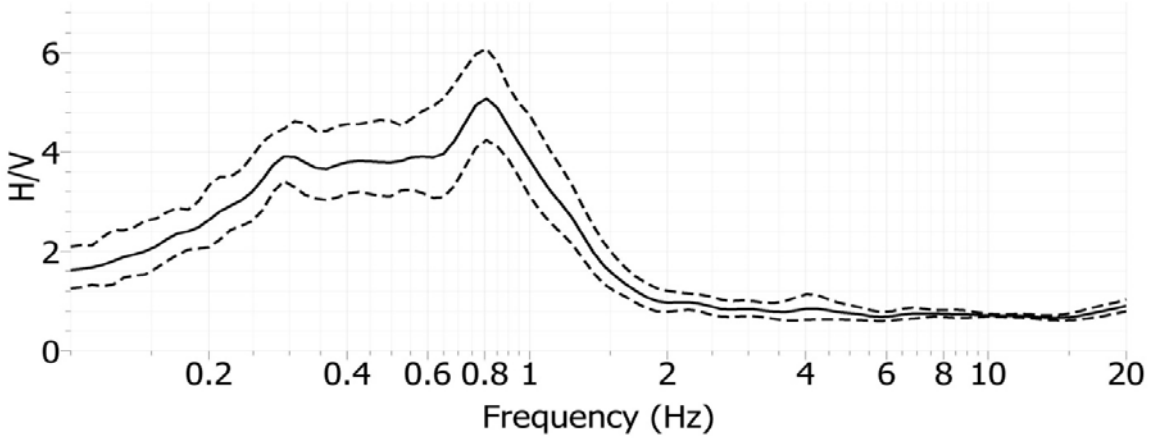

Site CI.MLAC, H/V Spectral Ratio, Array MLAC-1, Sensor 450

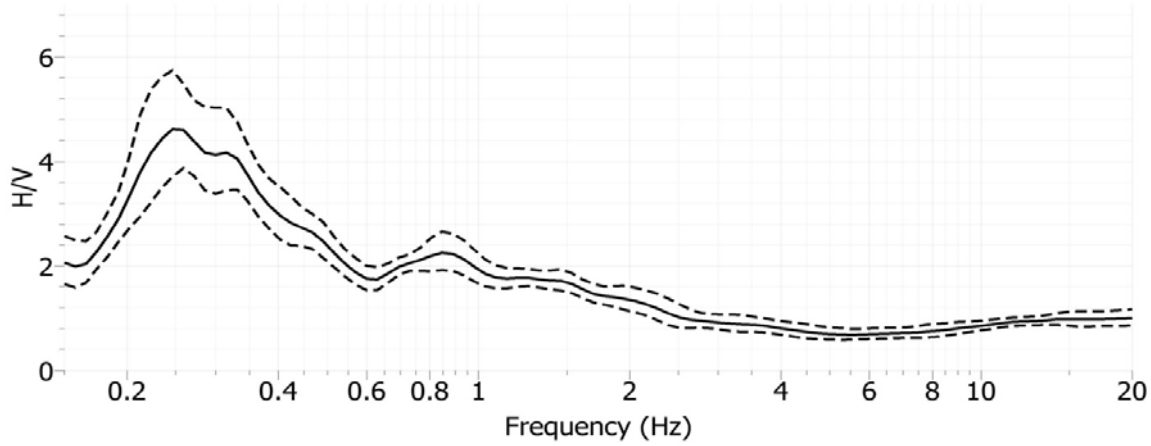

Site CI.MLAC, H/V Spectral Ratio, Array MLAC-1, Sensor 450A

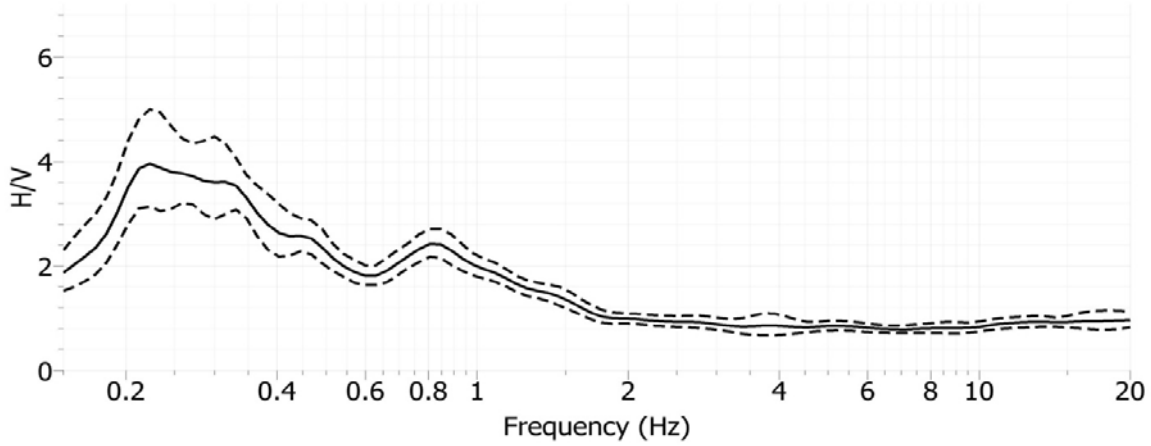

Site CI.MLAC, H/V Spectral Ratio, Array MLAC-2, Sensor 453A

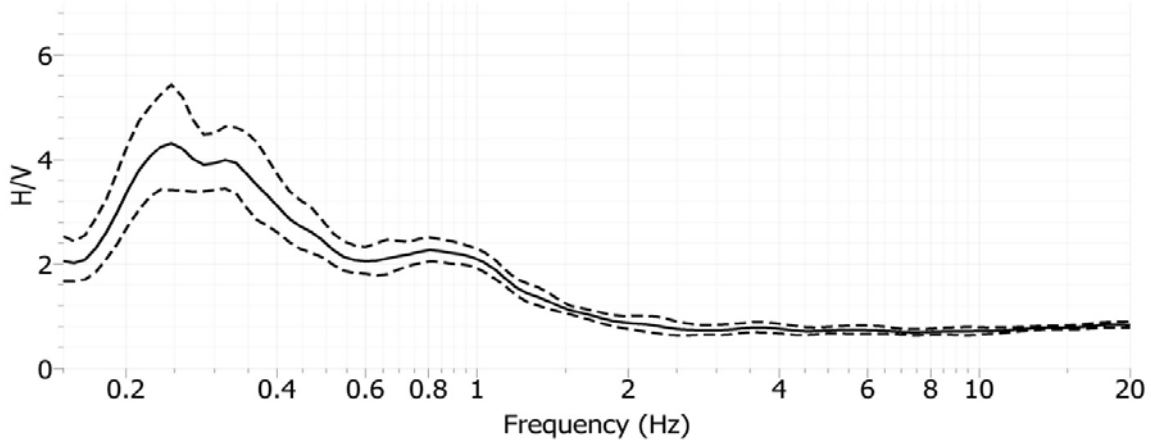

Site CI.MLAC, H/V Spectral Ratio, Array MLAC-1, Sensor 453B

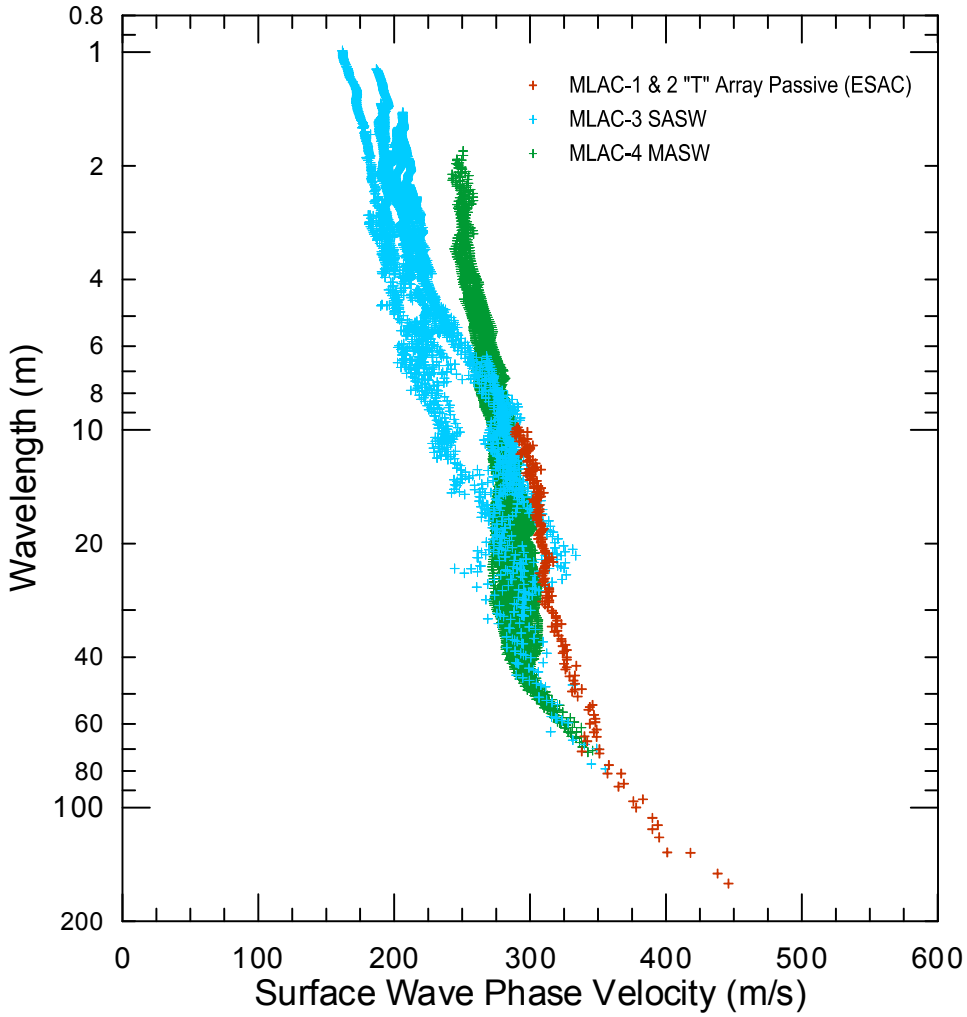

CI.MLAC – Rayleigh wave phase velocity data from the passive "T" shaped array (MLAC 1 and 2), SASW array (MLAC-3) and MASW array (MLAC-4). Noise conditions at the site were not considered suitable for effective use of passive surface wave data. Therefore, the passive surface wave dispersion curve was not used for analysis, although it is relatively consistent with the MASW and SASW data. The passive surface wave phase velocities are slightly higher than the MASW and SASW phase velocities over a wide frequency range, which may be the result of lateral velocity variation rather than ineffectiveness of the technique in this low noise environment. The SASW dispersion curve is quite complex and only the lower phase velocities were used for modeling in order to develop a V_S model to represent the lower near surface velocities. The MASW phase velocities are higher than the SASW phase velocities at wavelengths smaller than 6 m, track the higher SASW phase velocities between wavelengths of 6 and 30 m and are equal to the SASW phase velocities at wavelengths larger than 30 m. MASW data reduction using a center shot location, which sampled the same region as the SASW sounding, yielded Rayleigh wave phase velocities similar to those derived from the SASW array. This data is not presented and was not used for analysis, but indicates that the difference between the MASW and SASW dispersion data at small wavelengths is likely associated with lateral velocity variation.

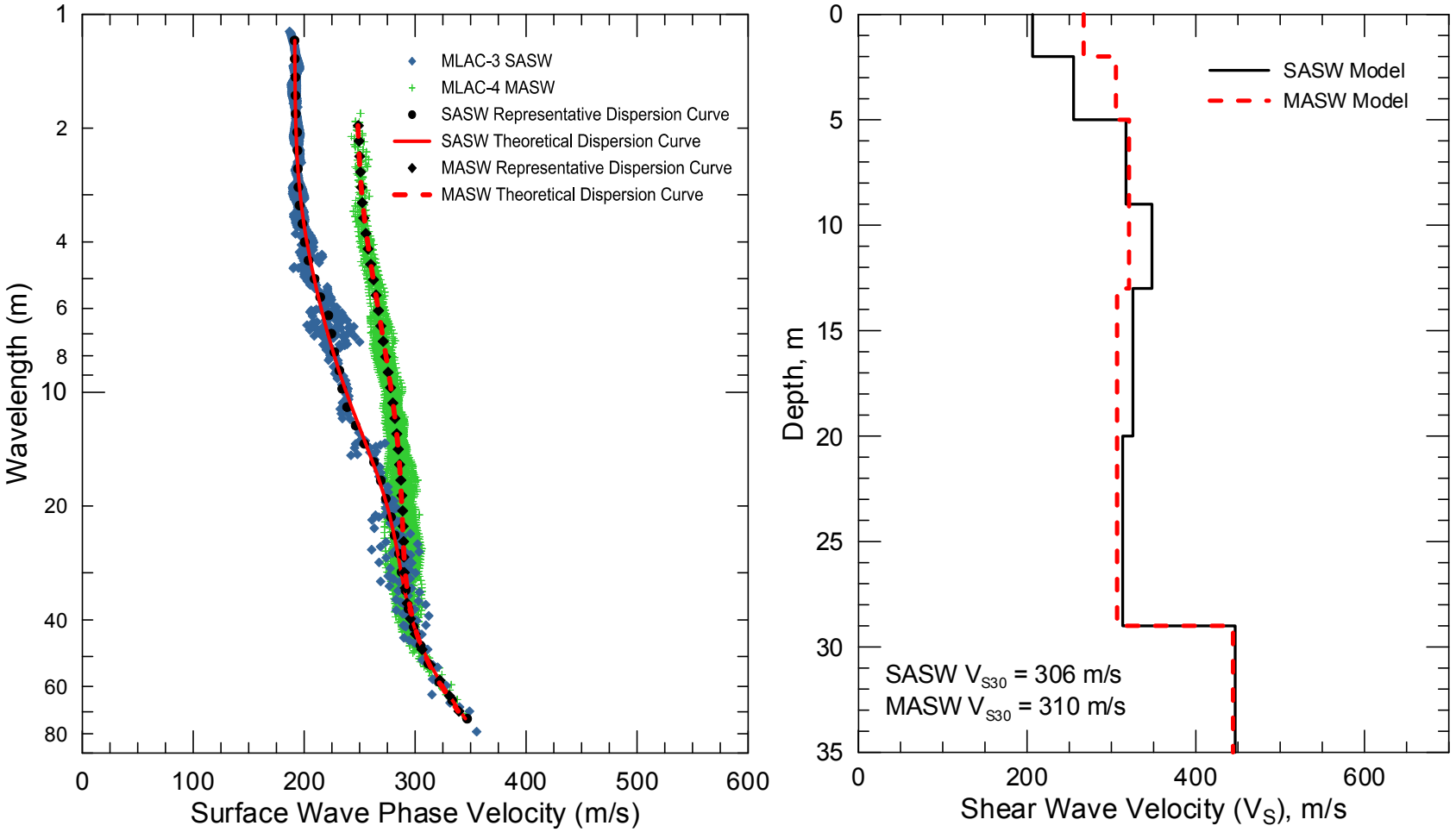

CI.MLAC - Field, representative and inverted theoretical surface wave dispersion data (left) and associated V_S models (right) for SASW array MLAC-3 and MASW array MLAC-4

Site CI.MPI

Location: Mount Pinos, Los Padres National Forest, California

Latitude: 34.81260 **Longitude:** -119.14523
(Station coordinates modified based on field GPS survey, WGS84 coordinate system)

V_{S30} (measured): 452 m/s

V_{S30} (adjusted to more accurately reflect seismic station conditions): 536 m/s (S-wave velocity of upper 3 layers replaced with that of underlying layer to account for seismic station being placed on weathered rock when there is a residual soil/decomposed rock layer at the surface beneath the MASW array).

NEHRP Site Class: C

Geomatrix Code: IGB

Geologic Conditions/Observations: Seismic station located on weathered Mesozoic granitic rocks.

Site Conditions: Rural site. Seismic station located on a mountain top near communications antennas and structures. Steep topography in site vicinity. Test area located on a relatively planar surface with about a 6 m elevation increase to the southeast along the 70.5 m long MASW and seismic refraction array.

Geophysical Methods Utilized: HVSR, Seismic Refraction, MASW

Geophysical Testing Arrays:

1. Array MPI-1 (48 channel MASW and P-wave seismic refraction array utilizing 4.5 Hz vertical geophones spaced 1.5 m apart for a length of 70.5 m, forward and reverse shot locations with multiple source offsets and source types (hammers only) and multiple interior shot locations).
2. Three HVSR measurement locations distributed along array MPI-1.

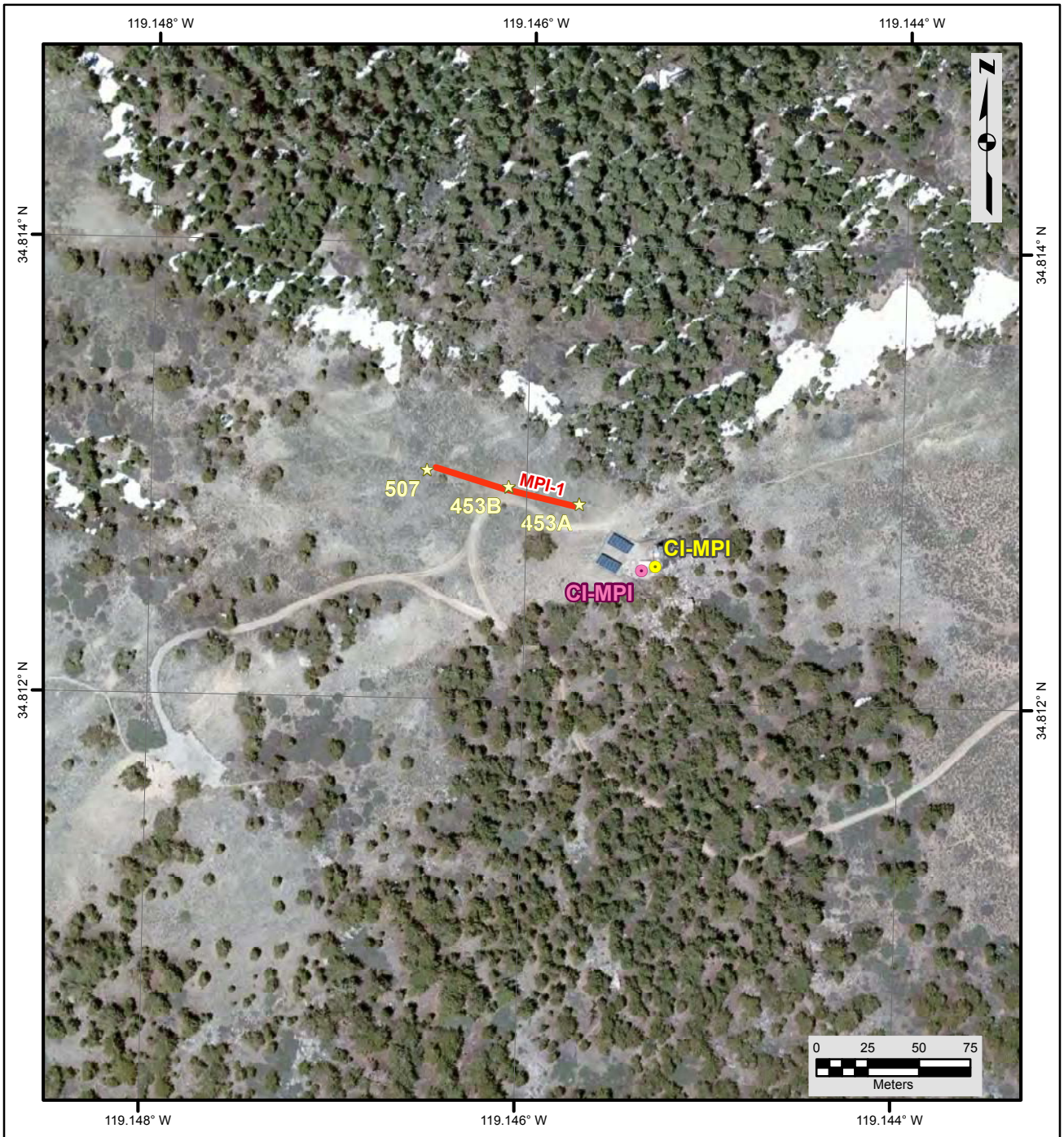

Legend

- Seismic Station - Approximate Surveyed Location
- Seismic Station - Approximate Location of Record
- H/V Spectral Ration Location
- MASW and Seismic Refraction Array

NOTES:
1. WGS 1984 COORDINATE SYSTEM
2. Image Source: ESRI, i-cubed, USDA FSA, USGS, AEX, GeoEye, Getmapping, Aerogrid, IGP

File Name: CI-MPI-I

Date: 2/7/2013

USGS science for a changing world

GEOVision geophysical services

RECOVERY.GOV

SITE MAP
CI•MPI

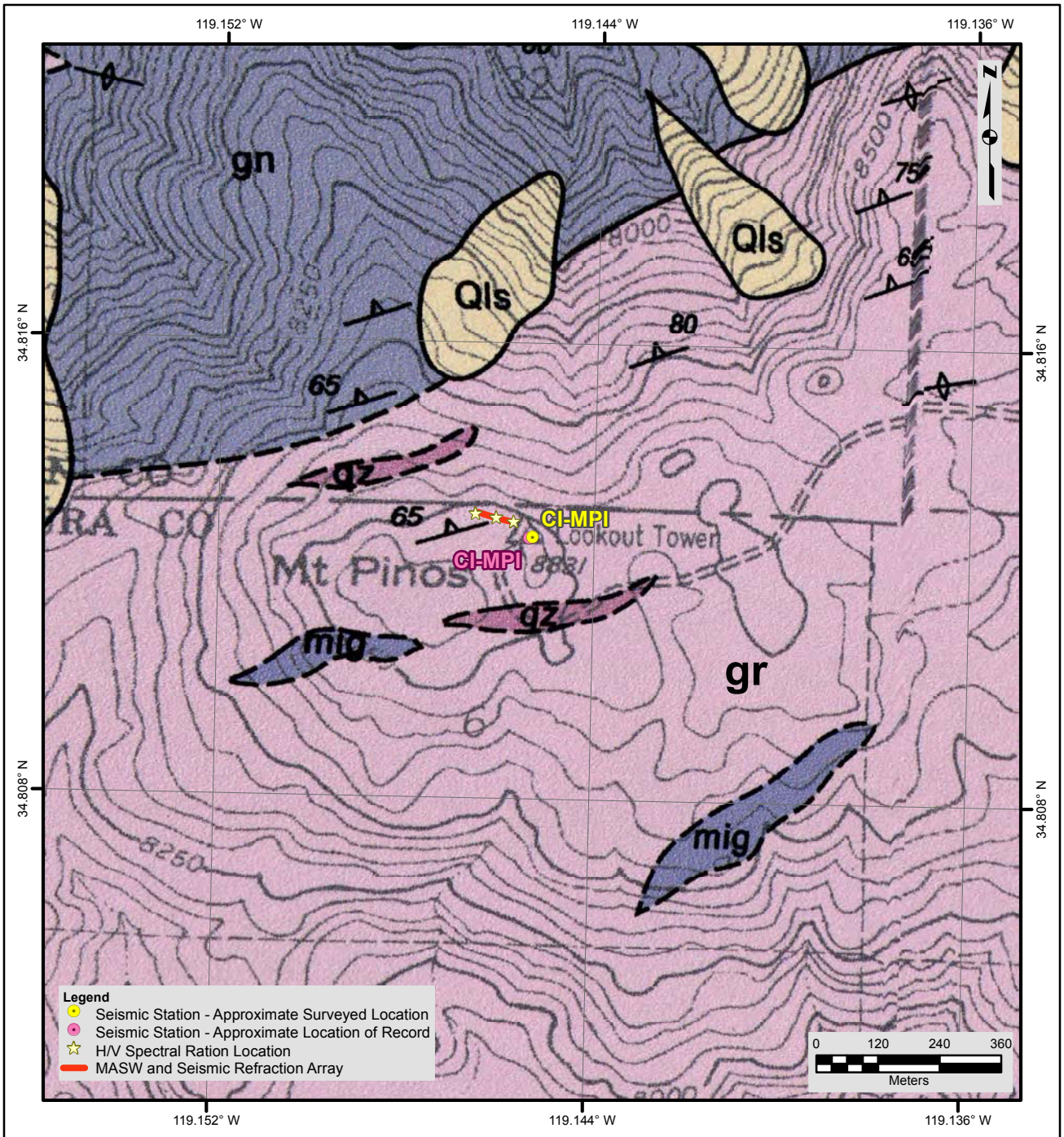

Description of Geologic Map Units

Qls = Quaternary (Pleistocene) landslide debris
gr = Mesozoic (Cretaceous) granite to quartz monzonite
qz = Mesozoic (Cretaceous) quartz monzonite; medium-grained
mig = Precambrian to Mesozoic migmatite, somewhat gneissoid
gn = Precambrian banded gneiss

NOTES:
1. WGS 1984 COORDINATE SYSTEM
2. Geologic Map of the Sawmill Mountain Quadrangle, Ventura & Kern Counties, California by Thomas W. Dibblee, Jr., 2006
3. See site map for details of geophysical survey

File Name: CI-MPI

Date: 11/10/2011

USGS science for a changing world

GEOVision geophysical services

GEOLOGIC MAP
CI•MPI

RECOVERY.GOV

CI.MPI seismic station

Looking southeast along array MPI-1 towards seismic station and at HVSR sensor 453

HVSR sensors placed in shallow holes

Looking northwest along array MPI-1

MASW and seismic refraction data acquisition

Location of Geophysical Testing Arrays:

Location	Latitude	Longitude
MPI-1, Northwest End of MASW/Seismic Refraction Array	34.81301	-119.14641
MPI-1, Center of MASW/Seismic Refraction Array	34.81293	-119.14604
MPI-1, Southeast End of MASW/Seismic Refraction Array	34.81286	-119.14566
HVSR Sensor 453B	34.81294	-119.14602
HVSR Sensor 453A	34.81287	-119.14564
HVSR Sensor 507	34.81300	-119.14645
HVSR Sensor Tromino ENGY	34.81294	-119.14600
CI.MPI Seismic Station	34.81260	-119.14523

Notes: 1) WGS84 Coordinate System (decimal degrees)
2) Survey accuracy is estimated at 1 to 2 m.

Results:

V_S Model 1 (Fundamental Mode Assumption)

Depth to Top of Layer (m)	Layer Thickness (m)	S-Wave Velocity (m/s)	Inferred P-Wave Velocity (m/s)	Assumed Poisson's Ratio	Assumed Density (g/cm^3)
0	1.5	192	359	0.3	1.7
1.5	2	240	449	0.3	1.8
3.5	2.5	287	536	0.3	1.8
6	4	404	755	0.3	1.9
10	5	459	859	0.3	2.0
15	6	813	1521	0.3	2.1
21	7	1147	2146	0.3	2.2
28	>2	1509	2823	0.3	2.3

Notes: 1) Depth of investigation is about 30 m.
2) Bottom layer is a half space.
3) V_S not well constrained below 21 m depth.

V_S Model 2 (Average Mode Assumption)

Depth to Top of Layer (m)	Layer Thickness (m)	S-Wave Velocity (m/s)	Inferred P-Wave Velocity (m/s)	Assumed Poisson's Ratio	Assumed Density (g/cm^3)
0	1.5	184	345	0.3	1.70
1.5	2	246	461	0.3	1.80
3.5	2.5	277	518	0.3	1.80
6	4	402	752	0.3	1.90
10	5	480	897	0.3	2.00
15	6	662	1238	0.3	2.10
21	7	756	1414	0.3	2.10
28	>2	843	1577	0.3	2.10

Notes: 1) Depth of investigation is about 30 m.
2) Bottom layer is a half space.
3) V_S not well constrained below 21 m depth.

Observations/Discussion:

- The HVSR curves are similar at frequencies below 3 Hz, but differ at higher frequencies, indicating that there may be some lateral velocity variation in near surface weathered rock.
- All HVSR curves have a low amplitude peak at about 2.2 Hz.
- The P-wave refraction data collected along array MPI-1 were modeled using a tomographic inversion routine with a smooth velocity gradient starting model. The seismic refraction model was not extended to far offset shot locations more than 10 m from the near geophone.
- The seismic refraction survey design allowed P-wave velocity to be imaged to a maximum depth of about 15 to 20 m. The seismic refraction model shows that P-wave velocity is about 350 to 450 m/s at the surface, increasing to 600 m/s at a depth of 1 to 4 m, 800 m/s at a depth of 1 to 7 m and 1,200 m/s at a depth of 8 to 17 m.
- Review of far offset seismic records, which were not used for modeling, provides no evidence of P-wave velocity exceeding 1,800 to 2,000 m/s in the upper 30 m. A longer seismic line with weight drop access would be required for confirmation.
- The seismic refraction model indicates that there is significant lateral velocity variation at this site with higher P-wave velocities at shallower depth at the west and east ends of the line.
- Noise conditions at the site were not sufficient for application of passive surface wave techniques.
- MASW data reduction was very difficult, most likely due to significant lateral velocity variation. In fact, it was not possible to reduce MASW data using the full 48 channel receiver spread, with 30 to 36 channels being the most used for analysis. There is

obvious lateral velocity variation on the seismic records, particularly beneath the easternmost 12 channels (geophones 36 to 48). This line should have been moved, although there are limited potential test locations in the site vicinity. Additionally, as this site required a military escort, there was a limited time window in which to acquire geophysical data.

- There is about 50 to 70 m/s scatter in MASW dispersion data, which is likely the result of lateral velocity variation.
- A representative dispersion curve was generated for the MASW data set using a moving average, polynomial curve fitting routine and used for modeling.
- Two V_S models were generated from the surface wave data. The first (Model 1) assumes that the dispersion curve consists of only the fundamental mode Rayleigh wave. Further modeling reveals that the resulting V_S model should excite a dominant first higher mode at low frequencies. There is likely insufficient resolution in the v-f transform (overtone image) to isolate the fundamental mode and first higher mode at low frequencies resulting in modal superposition. Given the relatively high velocities at the site, a significantly longer receiver array (several hundred meters) would be required to obtain sufficient resolution in v-f space to separately identify the fundamental and first higher modes. This type of space is generally not available at rock sites and longer arrays invariably introduce more lateral velocity variation. Because of possible modal superposition at low frequencies, an alternate V_S model (Model 2) was developed assuming the observed dispersion curve is more accurately represented by the average/effective mode (average of all modes based on relative amplitude of each mode for a far-field source and plane wave). We cannot state with certainty that the observed dispersion data consists of the average mode and it is not possible to quantify the effects of lateral velocity variation on the relative amplitude of the Rayleigh wave modes, but this may be a better option than incorrectly assuming that the dispersion data is the fundamental mode. In the event of modal superposition at low frequencies a V_S model based on the fundamental mode assumption will invariably overestimate velocity at depth.
- There is a 9% difference inV_{S30} between the fundamental and average mode V_S models. The two models are almost identical in the upper 15 m. The average mode V_S model has significantly lower V_S at depths greater than 15 m. We believe that the average mode model may more accurately reflect the S-wave velocity at depths below 15 m, although this cannot be stated with certainty. If the dispersion curve were modeled assuming that the dispersion curve jumps from the fundamental mode to first higher mode at low frequencies, then V_S at depth would be even lower.
- Surface wave depth of investigation is about 30 m based on half of maximum wavelength criteria.
- The inferred P-wave velocities in surface wave models, based on an assumed Poisson's ratio of 0.3 and modeled S-wave velocity, are generally consistent with the central portion of the P-wave refraction model in the upper 15 m. Model 2, based on the average/effective mode assumption, is in better agreement with the P-wave seismic refraction model at depths below 15 m.
- V_{S30} is 496 m/s for Model 1 (fundamental mode assumption) and 452 m/s Model 2 (average mode assumption), averaging 474 m/s (Site Class C).

- V_{S30} estimated after replacing the V_S of the upper three (3) layers with that of the underlying layer to account for the fact that the seismic station is placed on a localized small rock outcrop is 594 m/s for Model 1 and 536 m/s for Model 2, averaging 565 m/s.
- We recommend that the average/effective mode V_S model be used for the purpose of site characterization.
- Additional testing is warranted at this site. An alternate test location with less lateral velocity variation should be explored although there may not be feasible alternate test locations. Love wave MASW (MALW) techniques may not suffer from the potential modal superposition that seems to plague Rayleigh wave MASW in environments such as this. SASW testing may be feasible, given that there is an SASW modeling routine capable of addressing the influence of body waves and higher modes. Finally, a longer seismic refraction line may help confirm the most appropriate surface wave model.

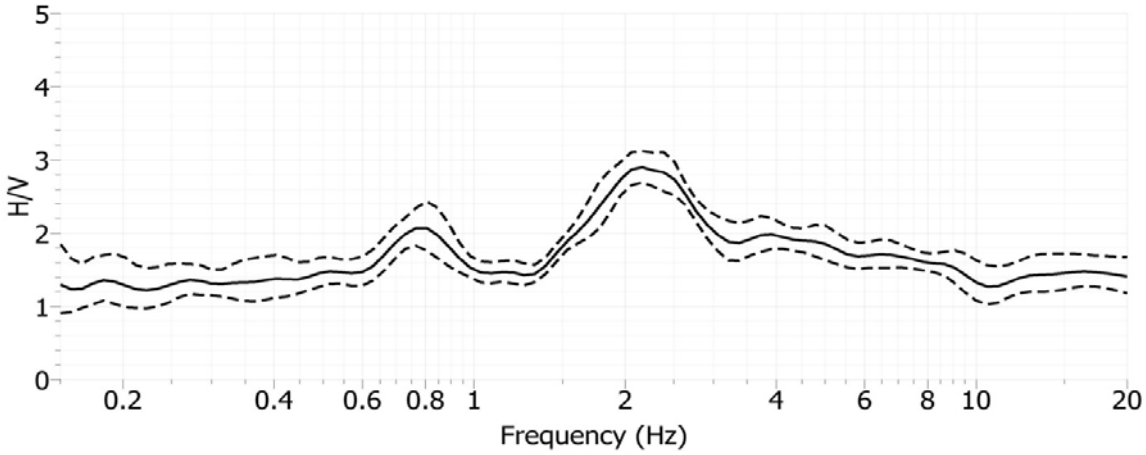

Site CI.MPI, H/V Spectral Ratio, Array MPI-1, Sensor 507

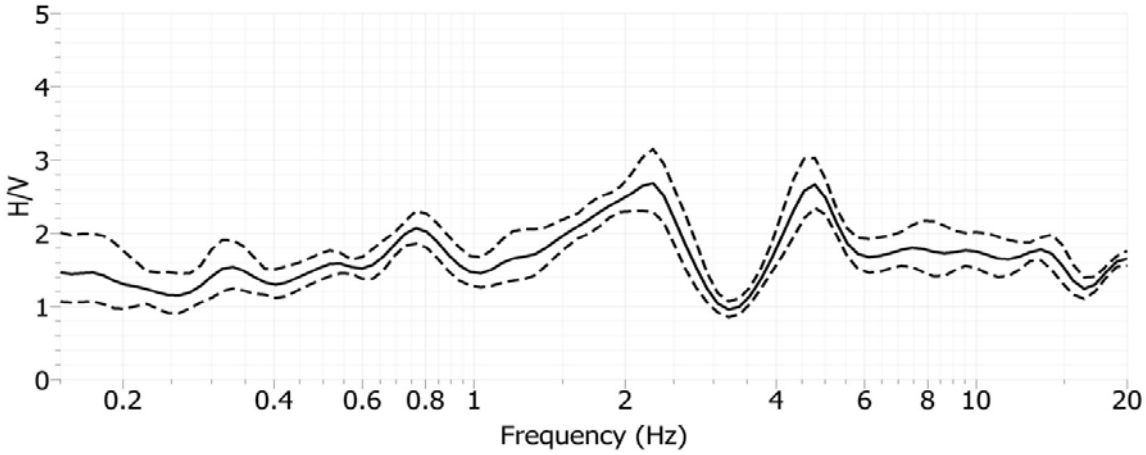

Site CI.MPI, H/V Spectral Ratio, Array MPI-1, Sensor 453B

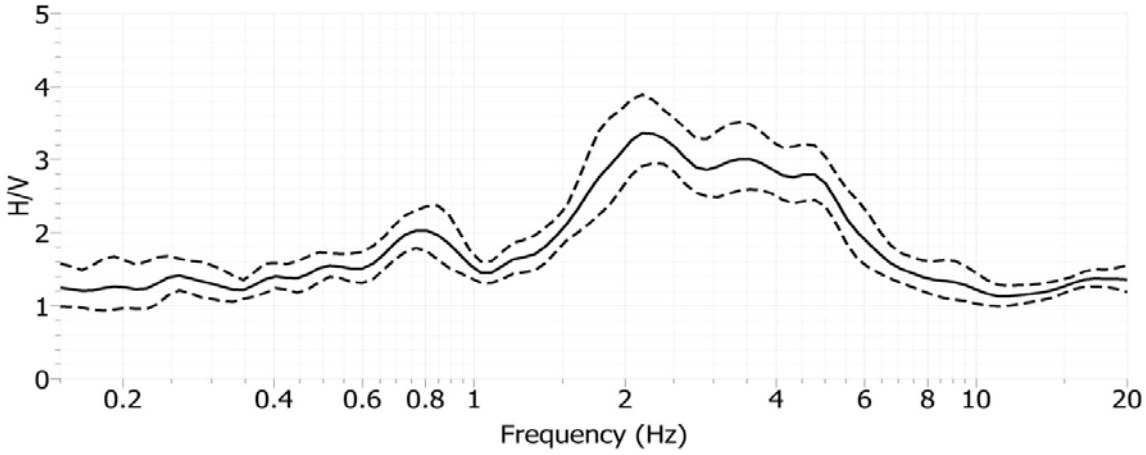

Site CI.MPI, H/V Spectral Ratio, Array MPI-1, Sensor 453A

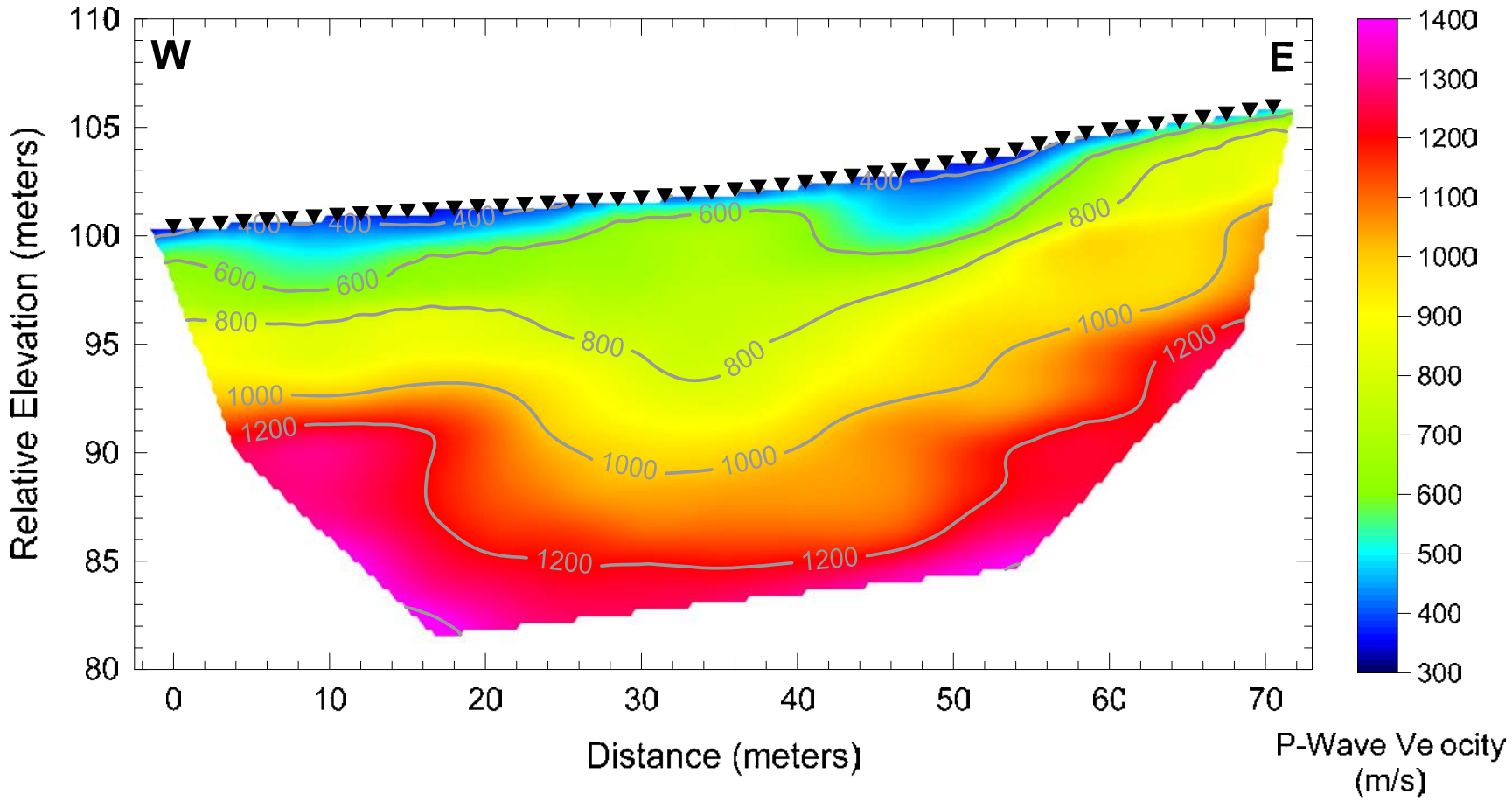

Array MPI-1 – Tomographic seismic refraction model utilizing smooth velocity gradient starting model

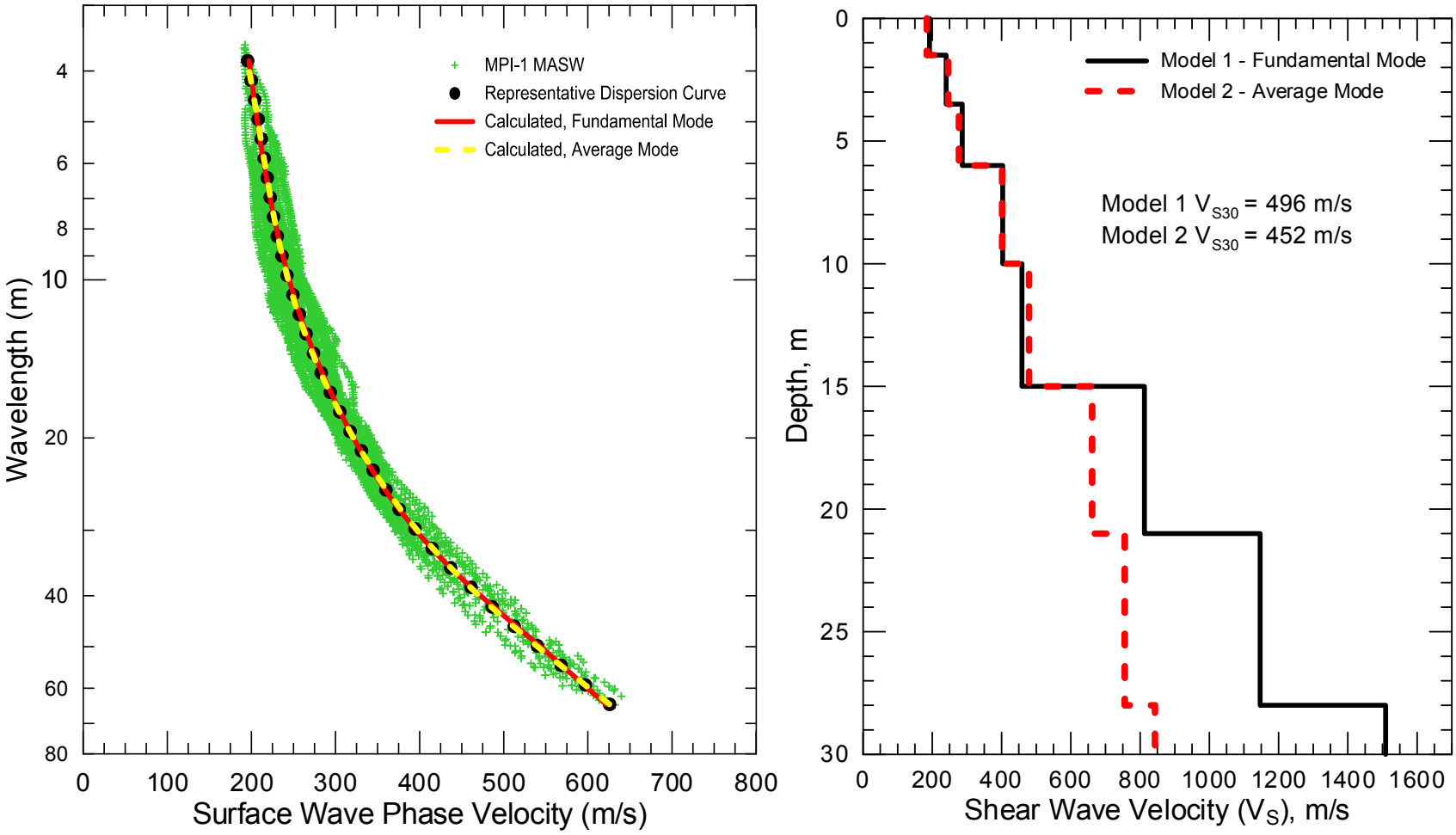

CI.MPI - Field, representative and inverted theoretical surface wave dispersion data (left) and associated V_S model (right)

Site CI.MPP

Location: McPherson Peak, Los Padres National Forest, California

Latitude: 34.88848 **Longitude:** -119.81362
(Station coordinates provided by USGS, WGS84 coordinate system)

V_{S30} (measured): 522 m/s

V_{S30} (adjusted to more accurately reflect seismic station conditions): 558 m/s (average S-wave velocity between 1 and 31 m adjusting for inferred 1 m sensor depth).

NEHRP Site Class: C

Geomatrix Code: IEB/ILB

Geologic Conditions/Observations: Seismic station located on Tertiary (Paleocene to Eocene) sandstone. The sandstone is dipping 20 to 30 degrees to the southwest in the site vicinity.

Site Conditions: Rural site. Seismic station located near telecommunications antennas on top of a mountain. Steep topography in site vicinity. Seismic testing conducted on top of mountain with only about 4 to 5 m of elevation relief along the 70.5 m long array.

Geophysical Methods Utilized: HVSR, Seismic Refraction, MASW

Geophysical Testing Arrays:

1. Array MPP-1 (48 channel MASW and P-wave seismic refraction array utilizing 4.5 Hz vertical geophones spaced 1.5 m apart for a length of 70.5 m, forward and reverse shot locations with multiple source offsets and source types (hammers only) and multiple interior shot locations).
2. Three HVSR measurement locations; two distributed along array MPP-1 and one adjacent to the seismic station.

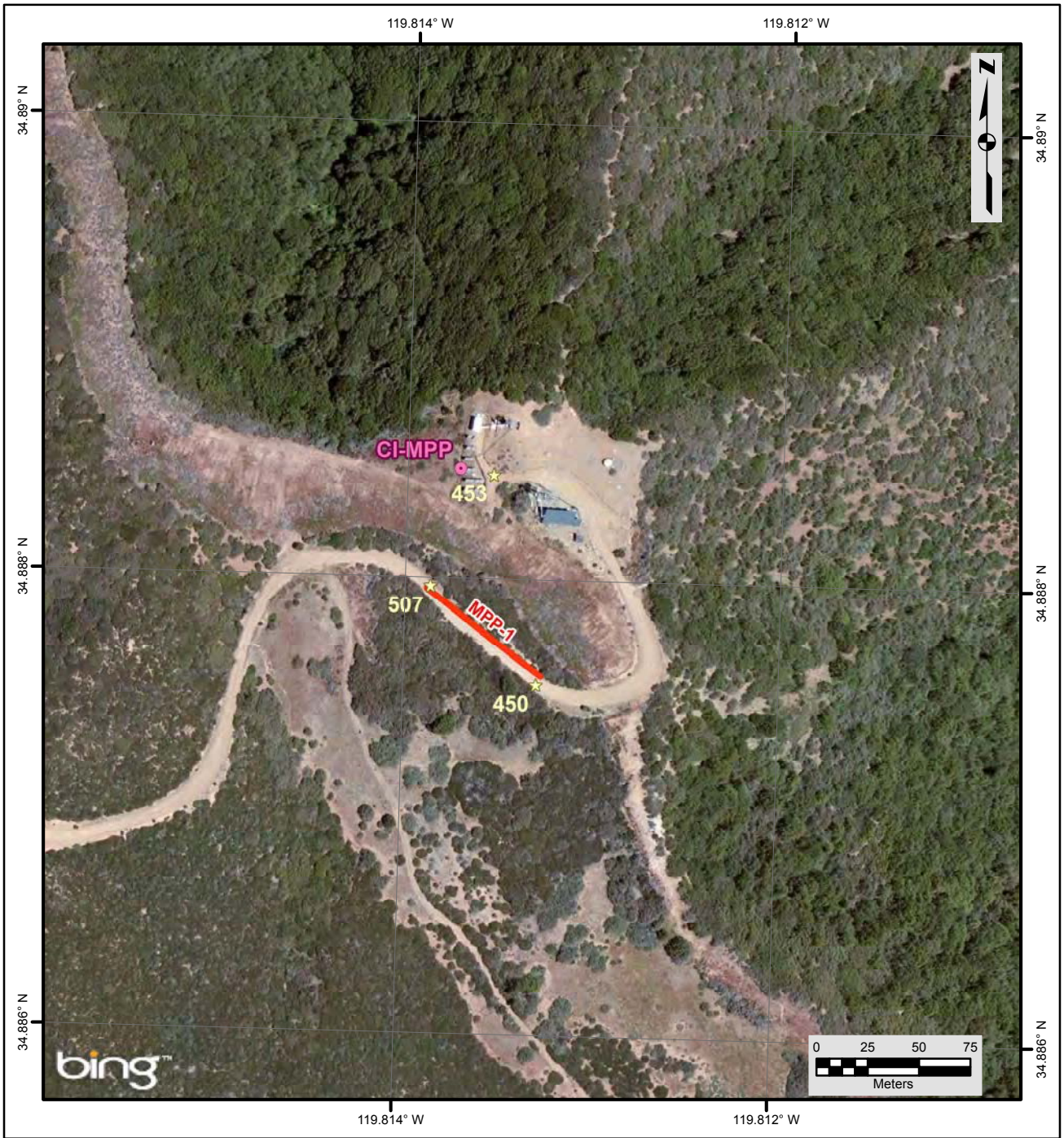

Legend

- Seismic Station - Approximate Location of Record
- H/V Spectral Ratio Location
- MASW and Seismic Refraction Array

NOTES:
1. WGS 1984 COORDINATE SYSTEM
2. Image Source: (c) Microsoft Corporation and its data suppliers

File Name: CI-MPP-I

Date: 2/7/2013

USGS science for a changing world

GEOVision geophysical services

RECOVERY.GOV

SITE MAP
CI•MPP

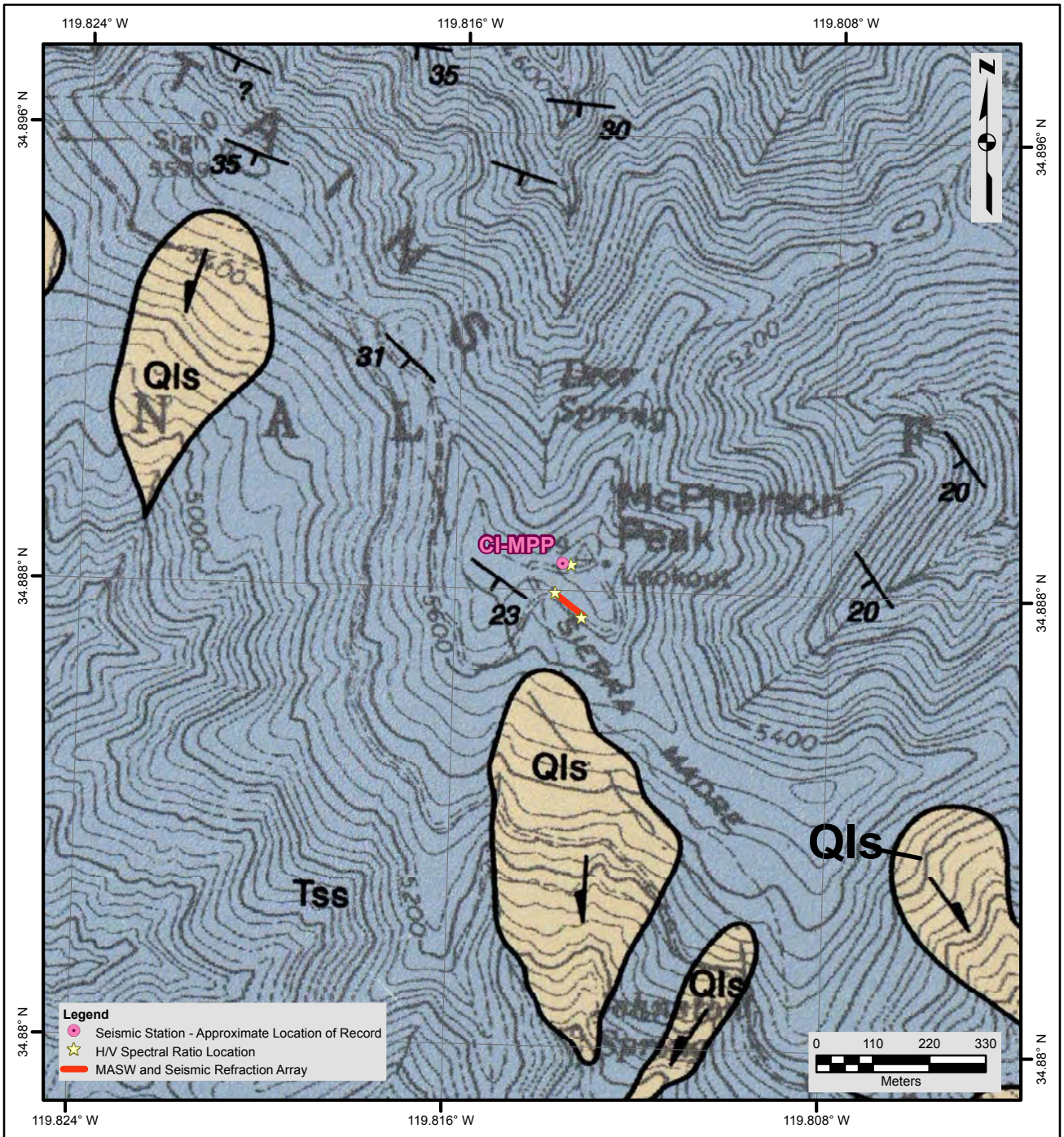

Description of Geologic Map Units

Qls = Quaternary (Pleistocene to Holocene) landslide debris
Tss = Tertiary (Paleocene to Eocene) sandstone, hard but fractured, arkosic, slightly micaceous, locally conglomeratic

NOTES:
1. WGS 1984 COORDINATE SYSTEM
2. Geologic Map of the Peak Mountain Quadrangle, San Luis Obispo and Santa Barbara Counties, California by Thomas W. Dibblee, Jr., 2005
3. See site map for details of geophysical survey

File Name: CI-MPP

Date: 2/7/2013

USGS science for a changing world

GEOVision geophysical services

GEOLOGIC MAP
CI•MPP

RECOVERY.GOV

CI.MPP seismic station and HVSR sensor 453 (Trillium) and Tromino ENGR

MASW and seismic refraction data acquisition at southeast end of array MPP-1

Looking southeast along array MPP-1 past HVSR sensor 507

GPS data acquisition at center of array MPP-1

MASW data acquisition at northwest end of array MPP-1using a 3-lb hammer

Location of Geophysical Testing Arrays:

Location	Latitude	Longitude
MPP-1, Southwest End of MASW/Refraction Array	34.88795	-119.81378
MPP-1, Center of MASW/Refraction Array	34.88776	-119.81348
MPP-1, Northeast End of MASW/Refraction Array	34.88757	-119.81317
HVSR Sensor 450	34.88754	-119.81319
HVSR Sensor 453	34.88846	-119.81344
HVSR Sensor 507	34.88796	-119.81376

Notes: 1) WGS84 Coordinate System (decimal degrees)
2) Survey accuracy is estimated at 1 to 2 m.

Results:

V_S Model

Depth to Top of Layer (m)	Layer Thickness (m)	S-Wave Velocity (m/s)	Inferred P-Wave Velocity (m/s)	Assumed Poisson's Ratio	Assumed Density (g/cm^3)
0	1	199	373	0.3	1.7
1	2	299	559	0.3	1.8
3	3	402	752	0.3	1.9
6	22	615	1150	0.3	2.0
28	>7	790	1478	0.3	2.1

Notes: 1) Depth of investigation is about 35 m.
2) Bottom layer is a half space.

V_S Model (lower envelope of surface wave dispersion data)

Depth to Top of Layer (m)	Layer Thickness (m)	S-Wave Velocity (m/s)	Inferred P-Wave Velocity (m/s)	Assumed Poisson's Ratio	Assumed Density (g/cm^3)
0	1	210	393	0.3	1.7
1	2	260	486	0.3	1.8
3	3	340	636	0.3	1.9
6	8	530	992	0.3	2.0
14	14	625	1169	0.3	2.0
28	>7	780	1459	0.3	2.1

Notes: 1) Depth of investigation is about 35 m.
2) Bottom layer is a half space.

V_S Model (upper envelope of surface wave dispersion data)

Depth to Top of Layer (m)	Layer Thickness (m)	S-Wave Velocity (m/s)	Inferred P-Wave Velocity (m/s)	Assumed Poisson's Ratio	Assumed Density (g/cm^3)
0	1	200	374	0.3	1.7
1	2	325	608	0.3	1.8
3	3	460	861	0.3	1.9
6	22	660	1235	0.3	2.0
28	>7	820	1534	0.3	2.1

Notes: 1) Depth of investigation is about 35 m.
2) Bottom layer is a half space.

Observations/Discussion:

- MASW and seismic refraction array MPP-1 was aligned approximately parallel to the mapped strike of geologic bedding in the site vicinity.
- The HVSR curves are almost identical, although there are no distinct high frequency peaks by which to assess shallow lateral velocity variation. Although there are no distinct HVSR peaks there is a potential, subtle low amplitude HVSR peak at about 1.4 Hz on all of the plots. The HVSR technique cannot be expected to be effective at this mountain top site with dipping geologic bedding.
- The P-wave refraction data collected along array MPP-1 were modeled using a tomographic inversion routine with a smooth velocity gradient starting model. The seismic refraction model was extended to far offset shot locations to extend depth of investigation.
- The seismic refraction survey design allowed P-wave velocity to be imaged to a maximum depth of about 20 m.
- The seismic refraction model shows that P-wave velocity is about 500 to 700 m/s at the surface, increasing to 1,000 m/s at a depth of 1 to 7 m, 1,400 m/s at a depth of 6 to 10 m and 1,600 m/s at a depth of 6 to 12 m.
- The seismic refraction model indicates that there is lateral velocity variation at this site, especially in the upper 7 m. The 1,000 m/s P-wave velocity contour is located at a depth of about 1 to 2 m beneath the northwestern half of the line, but is 4 to 7 m deep beneath the southeastern half of the line. There were no reasonable alternate test locations at the site with vehicle access due to limited space and steep topography. It may be possible to access alternate test locations on foot.
- Geologic environments such as this, with dipping geologic layers, are not always conducive to surface wave testing because velocity structure generally does not satisfy the homogeneous, horizontal layer assumption. However, surface wave methods can still be effective if shallow velocity structure is dominated by weathering rather than layering and there is not significant lateral velocity variation.

- Noise conditions at the site were not sufficient for application of passive surface wave techniques.
- MASW data reduction was very difficult due to lateral velocity variation and/or the dipping geologic layers. Over 125 dispersion curves were generated, utilizing all offend source locations at the southeast and northwest ends of the arrays (multiple source offsets and hammer sizes) and all interior seismic refraction shots and a variety of receiver gathers. About 70% of the reduced dispersion curves formed a coherent dispersion curve when combined, albeit with significant scatter, and the remaining dispersion curves were rejected. The accepted small wavelength dispersion curves primarily reflect the lower velocities at the southeast end of the array. Most of the rejected dispersion curves had maximum wavelengths less than 15 m and higher phase velocities reflective of near surface velocity structure at the northwest end of the array. These dispersion curves did not tie in well with longer wavelength dispersion curves from the complete 48 channel receiver array.
- The maximum wavelength Rayleigh wave phase velocity was generally set to 1.2 times the distance between the source and center of the active receiver array.
- To fill in the Rayleigh wave phase velocity data at small wavelengths, SASW analysis was conducted on the seismic data for selected receiver pairs in the southeastern portion of the array where near surface velocities are lowest.
- The minimum wavelength surface wave phase velocity data extracted from the 48-channel MASW array is about 15 and 27 m for source locations at the northwest and southeast ends of the array, respectively. Reducing data from smaller hammer sources using a limited offset receiver array (i.e. less active geophones) allowed for extraction of surface wave dispersion data to a minimum wavelength of about 3 m.
- There is significant scatter in MASW dispersion data (about 80 to 120 m/s), which is likely the result of lateral velocity variation caused by differential weathering of near surface rock and variable thickness of a residual soil layer. This scatter in the phase velocity data remains after removal of about 30 % of the reduced dispersion curve segments, primarily dispersion curves with maximum wavelengths less than 15 m resulting from analysis of limited offset receiver arrays from source locations in the northwestern portion of the array.
- A representative dispersion curve was generated for the MASW data set using a moving average, polynomial curve fitting routine and used for modeling.
- Because of the large scatter in the Rayleigh wave phase velocity data, the upper and lower envelopes of the dispersion curve were also modeled using a forward modeling routine.
- Surface wave depth of investigation is about 35m based on half of maximum wavelength criteria.
- The surface wave models slightly underestimate P-wave velocity structure observed in the seismic refraction model below a depth of about 10 m. Above 10 m, surface wave phase velocity data were selected for modeling that were most representative of the lower near surface velocities beneath the southeastern portion of the line. Poisson's ratio may be higher at depth than the assumed 0.3 using for data modeling.
- V_{S30} is 522 m/s (Site Class C).
- Average S-wave velocity between 1 m (assumed sensor depth) and 31 m is 558 m/s.

- V_{S30} of the models fitting the lower and upper envelopes of the dispersion curve is 489 and 561 m/s, respectively (Site Class C).
- The scatter in the Rayleigh wave phase velocity data indicates that V_{S30} could vary by more than 10 % beneath array MPP-1.
- Average S-wave velocity between 1 m (assumed sensor depth) and 31 m for the lower and upper envelope models is 555 and 604 m/s, respectively.
- Seismic velocity structure appears to be highly variable beneath array MPP-1, especially in the upper 7 m. The presented V_S models should, therefore, only be considered representative of generalized velocity structure beneath the array. Another test location should be considered at this site. Alternatively, a common midpoint SASW array centered at the northwestern and southeastern portions of the array may not suffer as much from the lateral velocity variation. Regardless of the accuracy of the layer velocities in the V_S model and possible large variability of V_{S30} in the site vicinity, the site can safely be classified as Site Class C.

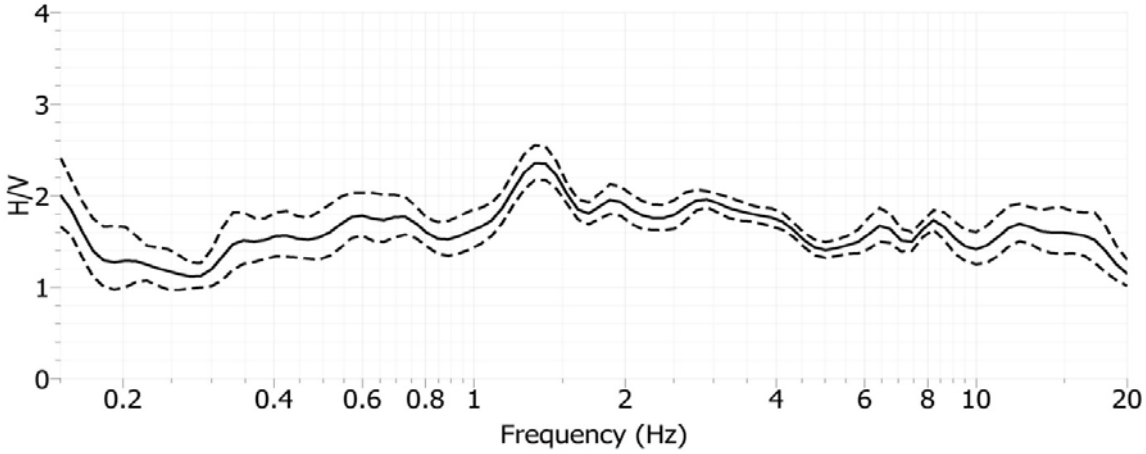

Site CI.MPP, H/V Spectral Ratio, Near Seismic Station, Sensor 453

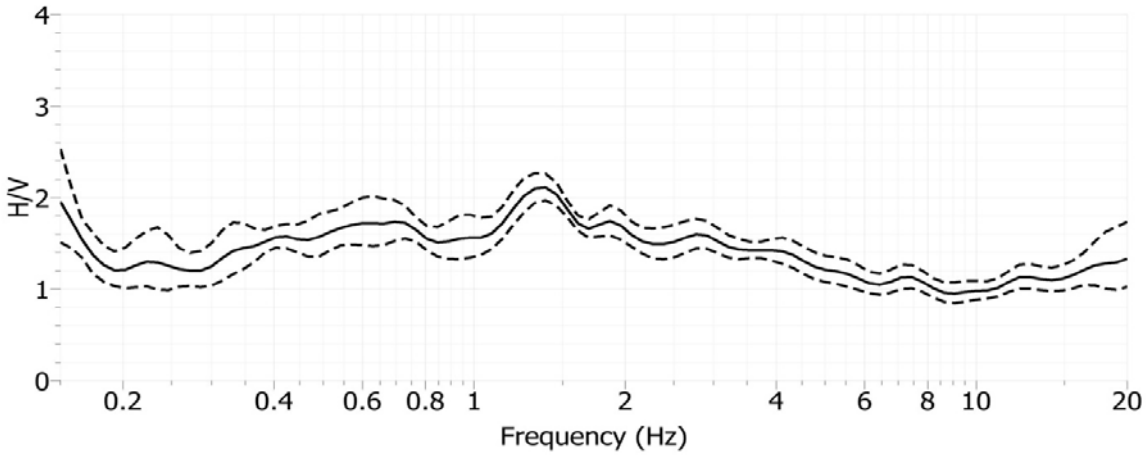

Site CI.MPP, H/V Spectral Ratio, Array MPP-1, Sensor 507

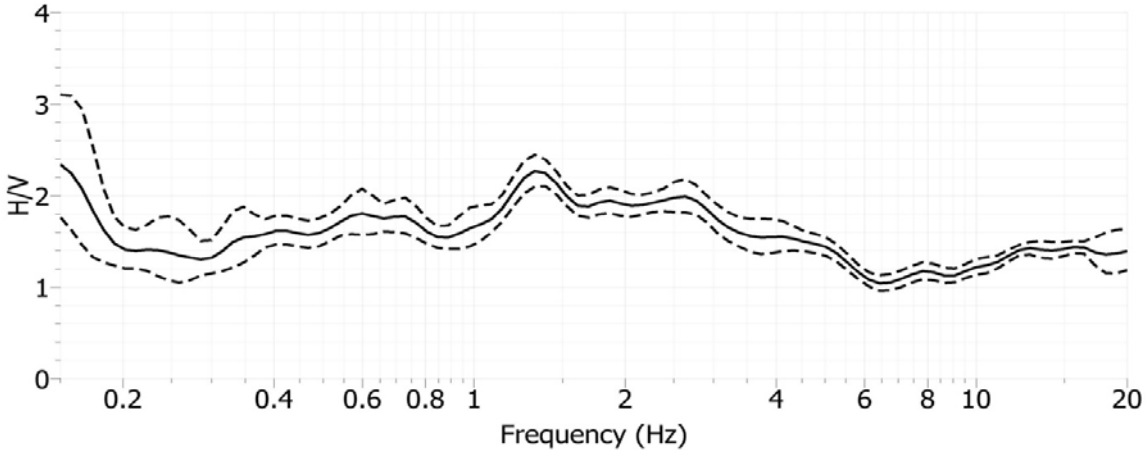

Site CI.MPP, H/V Spectral Ratio, Array MPP-1, Sensor 450

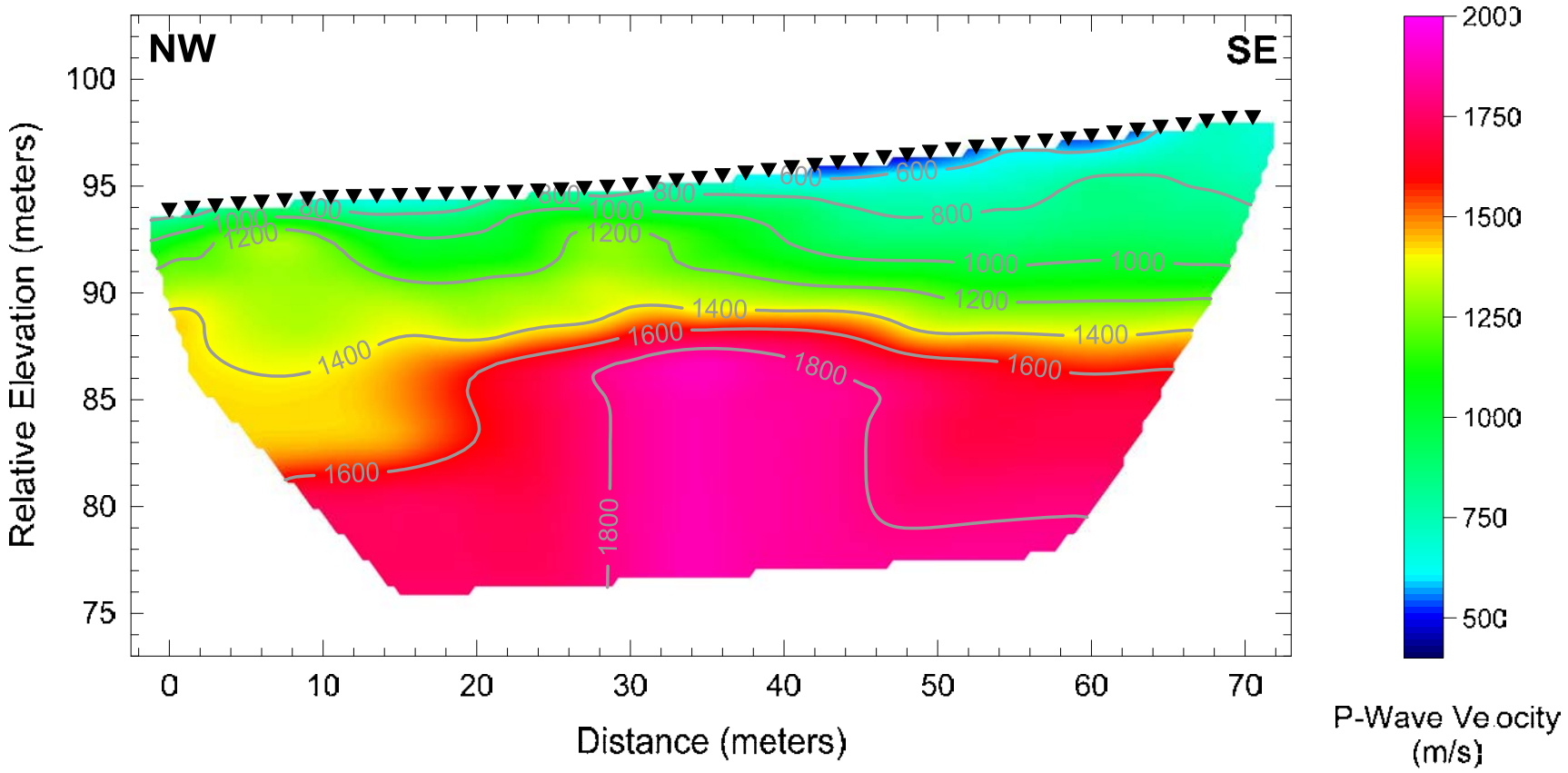

Array MPP-1 – Tomographic seismic refraction model utilizing smooth velocity gradient starting model

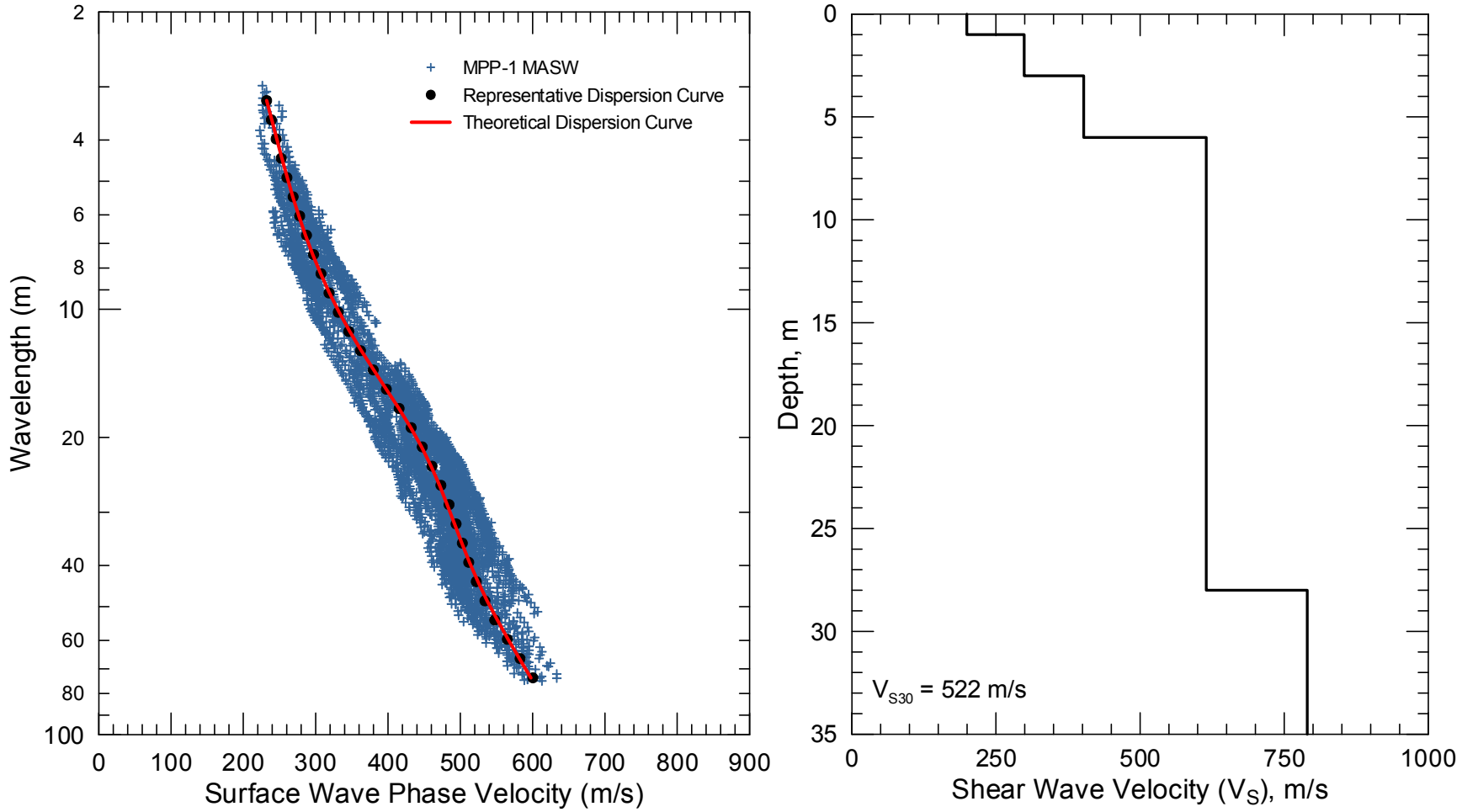

CI.MPP - Field, representative and inverted theoretical surface wave dispersion data (left) and associated V_S model. There is significant lateral velocity variation, as evident in the seismic refraction model and by the scatter in the Rayleigh wave phase velocity data, at this site and the model should be considered representative of average velocity structure.

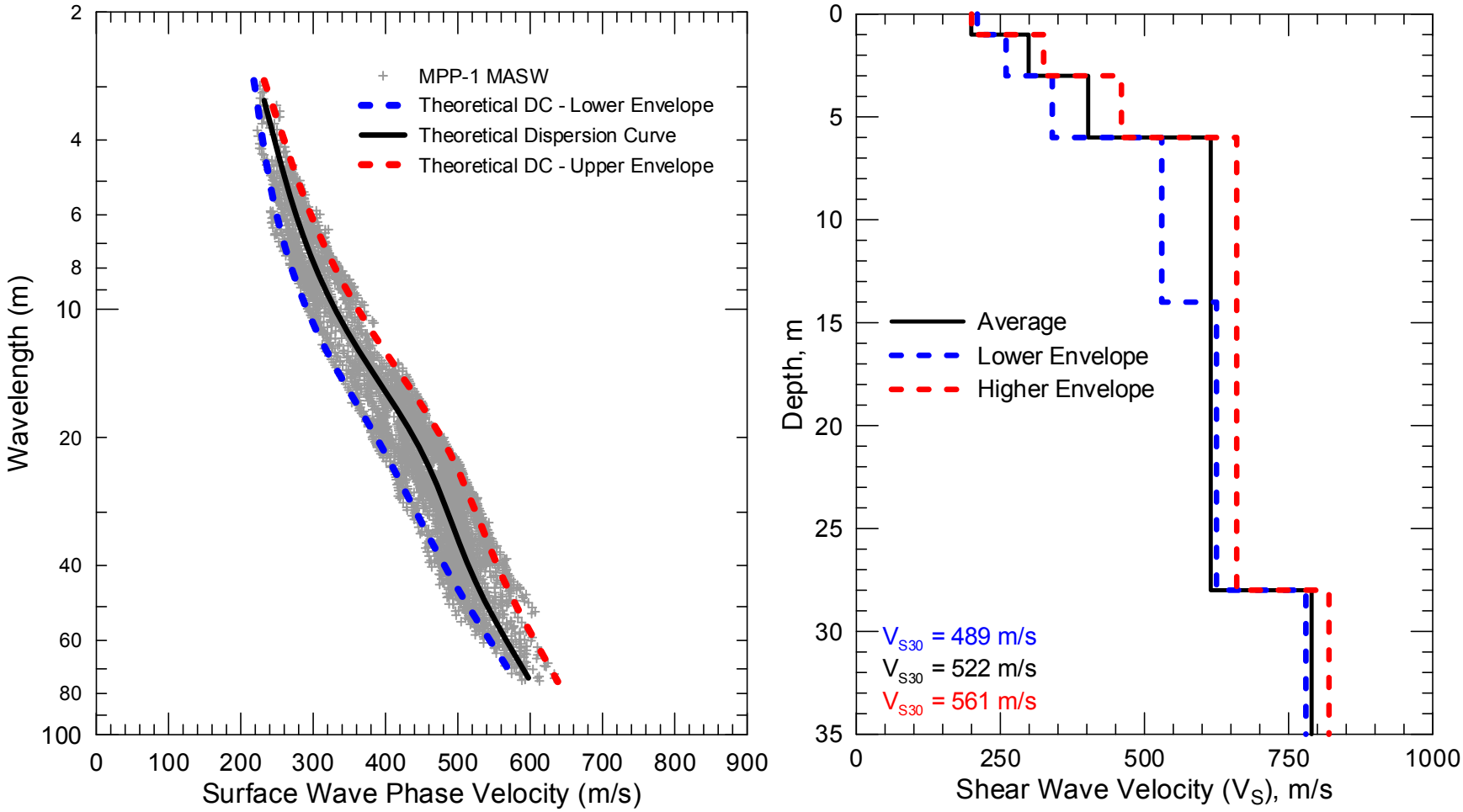

CI.MPP - Field, representative and inverted theoretical surface wave dispersion data (left) and associated V_S models fitting lower and upper envelope of surface wave dispersion data (right). There is more velocity variation in the upper several meters than depicted because selective use of small wavelength phase velocity was made to bias models towards the lower near surface velocities.

Site CI.MSC

Location: Mission Creek, San Bernardino County, California

Latitude: 34.03852 **Longitude:** -116.64795
(Station coordinates provided by USGS, WGS84 coordinate system)

V_{S30} (measured): 377 m/s

V_{S30} (adjusted to more accurately reflect seismic station conditions): 434 m/s (average S-wave velocity between 1.5 and 31.5 m adjusting for assumed sensor depth).

NEHRP Site Class: C

Geomatrix Code: INB

Geologic Conditions/Observations: Seismic station located on geologic unit mapped as Precambrian gneiss. Field inspection reveals that much of the near surface rock in the immediate site vicinity is decomposed to intensely weathered. The San Andreas Fault Zone is located about 1 km south of the site.

Site Conditions: Rural site located on a narrow bedrock ridge. Steep topography to the sides of the ridge.

Geophysical Methods Utilized: HVSR, Seismic Refraction (P- and limited S-wave), MASW (Rayleigh Wave) and limited MALW (Love Wave)

Geophysical Testing Arrays:

1. Array MSC-1 (48 channel MASW and P-wave seismic refraction array utilizing 4.5 Hz vertical geophones spaced 1.5 m apart for a length of 70.5 m, forward and reverse shot locations with multiple source offsets and source types (hammers only) and multiple interior shot locations).
2. Array MSC-2 (24 channel MASW and P-wave seismic refraction array utilizing 4.5 Hz vertical geophones spaced 6 m apart for a length of 138 m, forward and reverse shot locations with maximum 6 m source offset and source types (hammers only) and multiple interior shot locations).
3. Limited S-wave seismic refraction and MALW (Love wave) data acquired along array MSC-2 (10 Hz horizontal geophones, end shots, 6 m offend shots and a center shot).
4. Three HVSR measurement locations distributed along array MSC-1.

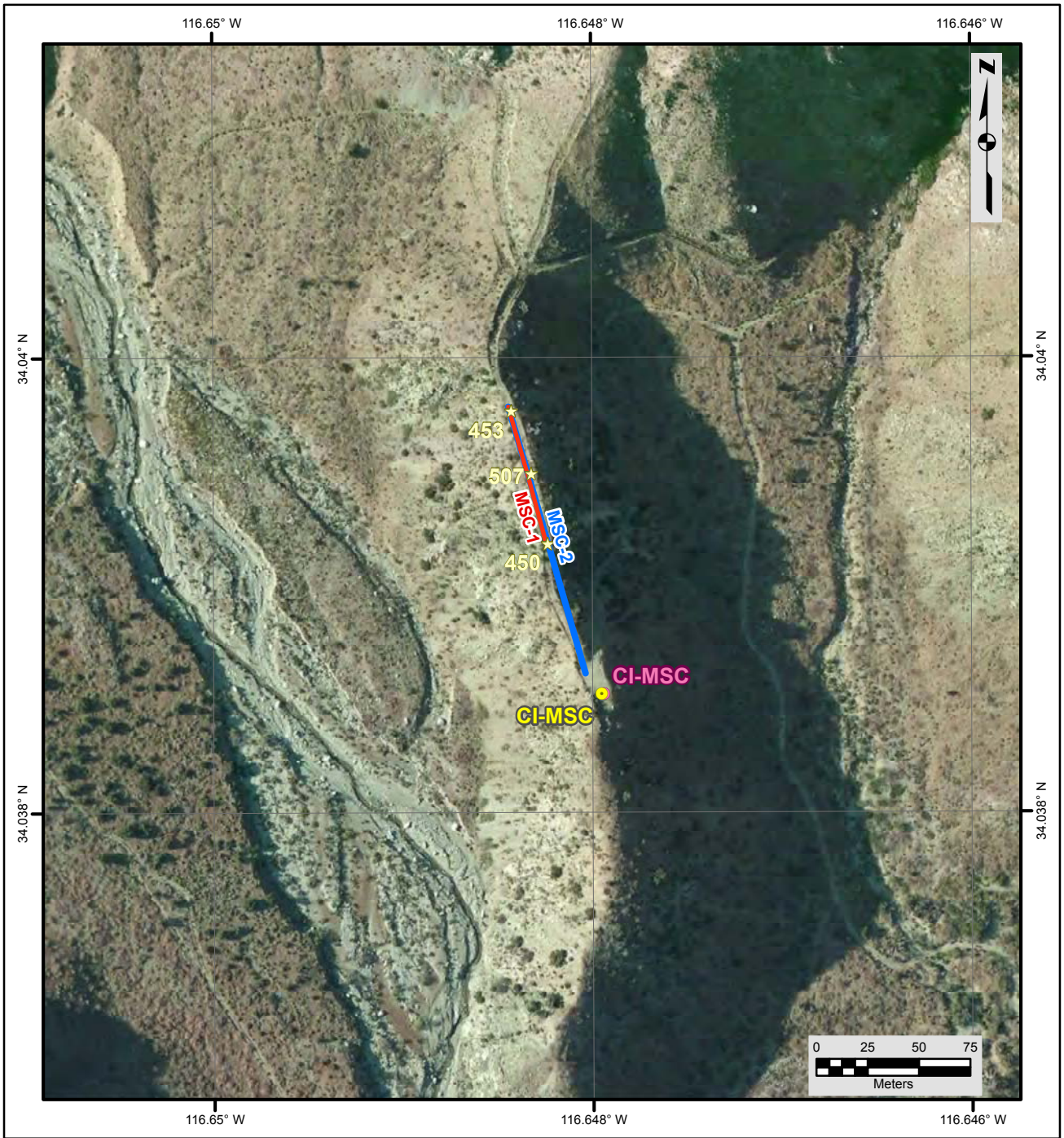

Legend

- Seismic Station - Approximate Surveyed Location
- Seismic Station - Approximate Location of Record
- H/V Spectral Ratio Location
- MASW and Seismic Refraction Array (P- and S-wave)
- Seismic Refraction Array

NOTES:
1. WGS 1984 COORDINATE SYSTEM
2. Image Source: ESRI, i-cubed, USDA FSA, USGS, AEX, GeoEye, Getmapping, Aerogrid, IGP

File Name: CI-MSC-I

Date: 2/7/2013

USGS science for a changing world

GEOVision geophysical services

RECOVERY.GOV

SITE MAP
CI•MSC

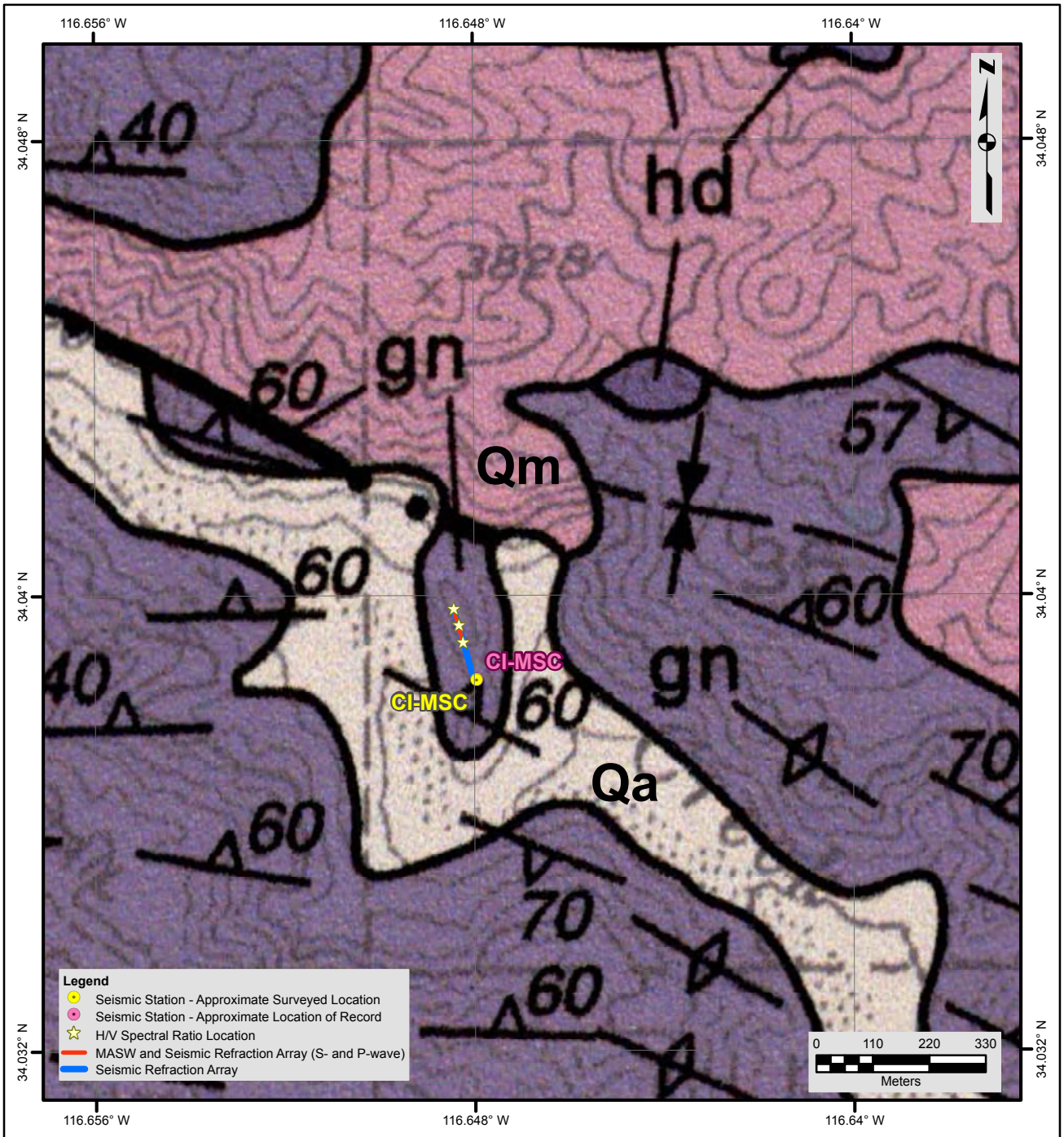

Description of Geologic Map Units

Qa = Quaternary (Holocene) alluvial silt, sand and gravel
qm = Mesozoic (Cretaceous) quartz monzonite
hd = Mesozoic (Cretaceous) hornblende diorite
gn = Precambrian gneiss

NOTES:
1. WGS 1984 COORDINATE SYSTEM
2. Geologic Map of the San Gorgonio Mountain & Morongo Valley 15 Minute Quadrangles, San Bernardino & Riverside Counties, California by Thomas W. Dibblee, Jr., 2008
3. See site map for details of geophysical survey

File Name: CI-MSC

Date: 2/7/2013

USGS science for a changing world

GEOVision geophysical services

GEOLOGIC MAP
CI•MSC

RECOVERY.GOV

CI.MSC seismic station

Seismic station located on intensely weathered rock

Arrays MSC-1 and MSC-2 located along narrow ridge of decomposed to intensely weathered rock

Looking northwest along array MSC-1

S-wave data acquisition along array MSC-2

Location of Geophysical Testing Arrays:

Location	Latitude	Longitude
MSC-1, Southeast End of MASW/Refraction Array	34.03918	-116.64825
MSC-1, Center of MASW/Refraction Array	34.03948	-116.64835
MSC-1, Northwest End of MASW/Refraction Array	34.03978	-116.64845
MSC-2, Southeast End of MASW/Refraction Array	34.03861	-116.64805
MSC-2, Center of MASW/Refraction Array	34.03919	-116.64825
MSC-2, Northwest End of MASW/Refraction Array	34.03978	-116.64845
HVSR Sensor 450	34.03918	-116.64825
HVSR Sensor 453	34.03976	-116.64844
HVSR Sensor 507	34.03949	-116.64833
CI.MSC Seismic Station	34.03852	-116.64796

Notes: 1) WGS84 Coordinate System (decimal degrees)
2) Survey accuracy is estimated at 1 to 2 m.

Results:

V_S Model

Depth to Top of Layer (m)	Layer Thickness (m)	S-Wave Velocity (m/s)	Inferred P-Wave Velocity (m/s)	Assumed Poisson's Ratio	Assumed Density (g/cm^3)
0	0.75	88	164	0.3	1.6
0.75	3.75	207	387	0.3	1.7
4.5	4	292	546	0.3	1.8
8.5	6.5	434	813	0.3	1.9
15	7	556	1041	0.3	2.0
22	7	674	1261	0.3	2.1
29	>1	849	1588	0.3	2.1

Notes: 1) Depth of investigation is about 30 m.
2) Bottom layer is a half space.
3) Half space V_S not well resolved.

Observations/Discussion:

- Although not identical, there are similarities in the HVSR plots at the three measurement stations, especially those for sensors 450 and 507. The effectiveness of the HVSR technique on a ridge top site, such as this, is questionable. There are no distinct, high amplitude HVSR peaks, although there is a possible low amplitude HVSR peak in the 3.5 to 5 Hz range at sensor locations 450 and 507.

- This site required USGS escort and only one day was set aside for field work, which limited the field effort at what turned out to be a complicated site. As was standard procedure for characterization of rock sites, MASW and P-wave seismic refraction data were acquired along a 70.5 m long array with 48 geophones spaced 1.5 m apart. After field review of the data, it became clear that the refraction array was not long enough to characterize a relatively high velocity refractor at depth and that dominant higher modes contaminated the surface wave data. In fact, most energy appears to be contained in the first higher mode at all source locations (both MASW and interior refraction shot locations) except for the source locations offset 1.5 to 10 m from the northwest end of the array. At the time of the field investigation, Love wave techniques were utilized for sites with a thin sediment layer overlying bedrock, but had not yet been considered for other problematic sites. Later, we would learn that Love wave techniques offered a means of characterizing a wide variety of sites where dominant higher modes plagued Rayleigh wave data. Fortunately, as it turns out, at the time of this investigation, all P- and S-refraction data were acquired with a minimum 1 s record length to at least permit review of surface wave data. After realizing that the MASW data acquired along array MSC-1 may not be sufficient for site characterization, at least using fundamental modeling techniques, a decision was made to acquire S-wave refraction data, S-wave seismic refraction data acquisition was attempted along a 138 m long array using twenty-four 10 Hz horizontal geophones spaced 6 m apart. Clear S-wave first arrivals could not be identified, possibly due to interference from P-waves reflecting from the sides of the ridge and/or other converted waves. Even though not effective, limited S-wave refraction data were acquired using source locations at both ends of the array, source locations offset 6 m from each end of the array (as much as space would allow) and a source location at the center of the array. With what little time was left in the day, P-wave seismic refraction data were acquired along the same array, to at least ensure that one data set capable of imaging to 30 m depth was obtained.
- The P-wave refraction data for arrays MSC-1 (70.5 m long) and MSC-2 (138 m long) were modeled using a tomographic inversion routine with a smooth velocity gradient starting model. Array MSC-1 is located between a position of 67.5 and 138 m on array MSC-2. As mentioned above the limited S-wave refraction data were not useable. The seismic refraction models were extended to far offset shot locations (maximum 30 m offset for array MSC-1 and 6 m offset for array MSC-2) to extend depth of investigation.
- The P-wave first arrival data were of excellent quality. The air wave arrives before the direct soil arrival on the P-wave refraction shot records; however, picking the later arrival to an acceptable degree of accuracy was possible.
- The P-wave seismic refraction survey design for array MSC-1 allowed P-wave velocity to be imaged to a maximum depth of about 30 m. P-wave velocity is about 200 to 300 m/s at the surface, increasing to 500 m/s at a depth of 2.5 to 4 m, 800 m/s at a depth of 9 to 14 m, 1,200 m/s at a depth of 18 to 25 m and over 1,600 m/s at a nominal depth of 28 m.
- The P-wave seismic refraction survey design for array MSC-2 allowed P-wave velocity to be imaged to a maximum depth of about 45 m. P-wave velocity is about 200 to 300 m/s at the surface, increasing to 500 m/s at a depth of 3 to 4 m, 800 m/s at a depth of 10 to 12 m, 1,200 m/s at a depth of 18 to 27 m, 1,600 m/s at a nominal depth of 26 to 39 m

and 2,000 m/s at a depth of 31 m, or more. The seismic line is located on a ridge top and groundwater is not expected in the upper 45 m.

- The P-wave velocity structure is consistent between arrays MSC-1 and MSC-2 with longer array MSC-2 imaging to greater depth and array MSC-1 (more channels and smaller geophone spacing) having much greater horizontal resolution.
- The average P-wave velocity of the upper 30 m (V_{P30}) was estimated between 12 and 132 m on the P-wave refraction model for array MSC-2. It should be noted that reversed first arrival coverage for the higher velocity zones at depth near the ends of the array. In fact, the critical distance of the high velocity refractor at a depth below 30 m, is 60 m, or more. V_{P30} ranges from about 653 to 795 m/s between a position of 12 to 132 m, a 20% variation.
- An average V_P model was developed over the 12 to 132 m distance interval by horizontally averaging the travel time of each model cell and cell thickness and average V_{P30} was determined to be 717 m/s. Assuming constant Poisson's ratios of 0.25, 0.3, 0.35 and 0.4 would result in an estimated V_{S30} of 417, 386, 347 and 295 m/s, respectively. Bedrock is not expected to be saturated in the upper 30 m, therefore, Poisson's ratio in the 0.25 to 0.35 range is probable.
- Similar analysis of the seismic refraction model for array MSC-1 yielded similar results, which are not presented because MALW was interpreted from the longer array MSC-2.
- The P-wave seismic refraction models indicate that there is some lateral velocity variation with a gradual thickening sequence of lower velocity, more intensely weathered or decomposed rock to the northwest.
- Noise conditions at the site were not sufficient for application of passive surface wave techniques.
- Review of Rayleigh wave (MASW) data indicated that higher modes were dominant over a wide frequency range. The source of dominant higher mode energy Rayleigh wave data is not clear, but we expect it may be associated with a thin layer of very low velocity, relative to underlying layer, residual soil or, possibly, and irregular damping profile. Dominant higher modes were not, however, a significant issue in Love wave (MALW) data and, fortunately, Love wave phase velocity data could be extracted from the limited S-wave refraction data set acquired along array MSC-2. Therefore, modeling of Love wave, rather than Rayleigh wave, phase velocity data was conducted at this site. It should be noted, however, that the Love wave data were acquired using 10 Hz horizontal geophones and a hammer/traction plank energy source. To develop a V_S model to 30 m depth it was necessary to pick Love wave phase velocity data to a frequency of about 5.5 Hz, which is below the natural frequency of the geophone and, possibly, pushing the limits of the energy source. Consideration should be given to reacquiring the Love wave data with 4.5 Hz geophones using a shorter 48-channel array, but does not appear necessary (see below). A lower frequency energy source would also be beneficial. It should also be noted that S-wave refraction data were acquired along array MSC-2, without particular attention made to surface wave propagation. A 1 second record length was common practice at the time of the field investigation to at least allow review of surface wave data from refraction data sets; however, given the length of the array and low subsurface seismic velocity, a longer record length would have been preferred. The 1 second record length was marginally sufficient to capture the complete surface wave package.

- It should also be noted that the seismic line is located along a narrow ridge. It is unclear what effect the geometry of the ridge may have on surface wave propagation. However, as noted below, the V_S model developed from limited MALW data is consistent with P-wave refraction models and, therefore, considered valid.
- Although Rayleigh wave data were not used for site characterization, it may be possible to pick and model the first higher mode or extract sufficient fundamental mode data from several seismic records for modeling.
- The minimum wavelength Love wave phase velocity data extracted from the MALW array was about 4 m. SASW analysis using selected receiver pairs and source offset equal to receiver spacing allowed extraction of Love wave phase velocity data to a minimum wavelength of about 2 m. These data were combined with the MALW dispersion data for analysis.
- There is about 40 m/s of scatter in MALW dispersion data, which is in part due to lateral velocity variation caused by differential weathering of near surface rock.
- A representative dispersion curve was generated for the MALW data set using a moving average, polynomial curve fitting routine and used for modeling.
- Surface wave depth of investigation is about 30 m based on a third of maximum wavelength. It appears that longer wavelength Love wave phase velocity data are needed to image to 30 m than for Rayleigh waves.
- V_{S30} derived from the Love wave V_S model is 377 m/s (NEHRP Site Class C).
- The average S-wave velocity between 1.5 and 31.5 m, to account for assumed sensor depth, is 434 m/s. (NEHRP Site Class C).
- V_{S30} derived from the Love wave V_S model is consistent with that derived from the estimated S-wave velocity model derived from the average P-wave refraction model and an assumed constant Poisson's ratio of slightly greater than 0.3.
- Ideally, Love wave data would be acquired along array MSC-1 using a 48 channel array of 4.5 Hz horizontal geophones and a lower frequency energy source, if a cost effective source could be identified. However, the V_S model developed using the limited MALW dispersion data acquired along array MSC-2 compares favorably with the P-wave seismic refraction models and, therefore, additional site characterization is not necessary. This is one of a number of sites that does not have shallow high velocity bedrock where Love wave techniques appeared to perform better than Rayleigh wave techniques, at least with regards to fundamental mode modeling. More research is needed to understand the exact mechanism exciting dominant higher modes in the Rayleigh wave data, but we suspect that the dominant higher modes arise from a thin, very low velocity residual soil layer at the surface resulting in a large impedance contrast at shallow depth or, possibly, an large change in damping/seismic Q, which could be plausible in weathered rock environments but unlikely in soil environments. Interestingly, all problems with dominant higher modes in the Rayleigh wave data, except for shallow rock sites and sediment sites with high velocity layers, have occurred at either weathered crystalline rock sites or Tertiary, or older, sedimentary rock sites with significant weathering. Very low velocity residual soil layers occur at all of these sites and damping properties are unknown.

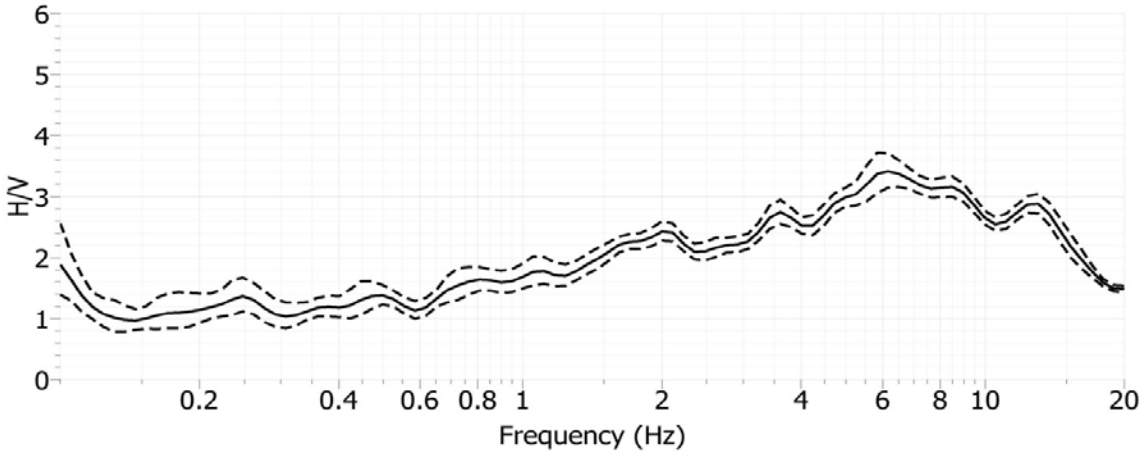

Site CI.MSC, H/V Spectral Ratio, Array MSC-1, Sensor 453

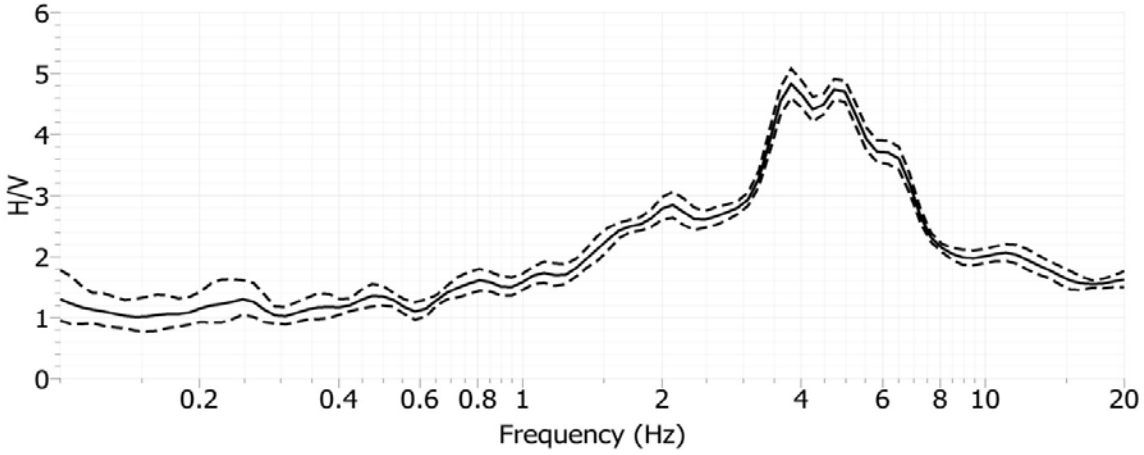

Site CI.MSC, H/V Spectral Ratio, Array MSC-1, Sensor 507

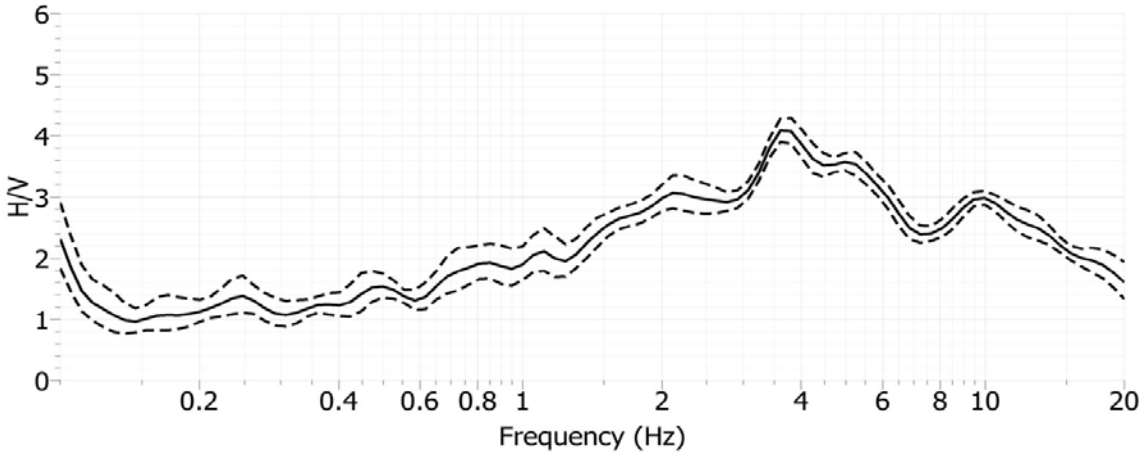

Site CI.MSC, H/V Spectral Ratio, Array MSC-1, Sensor 450

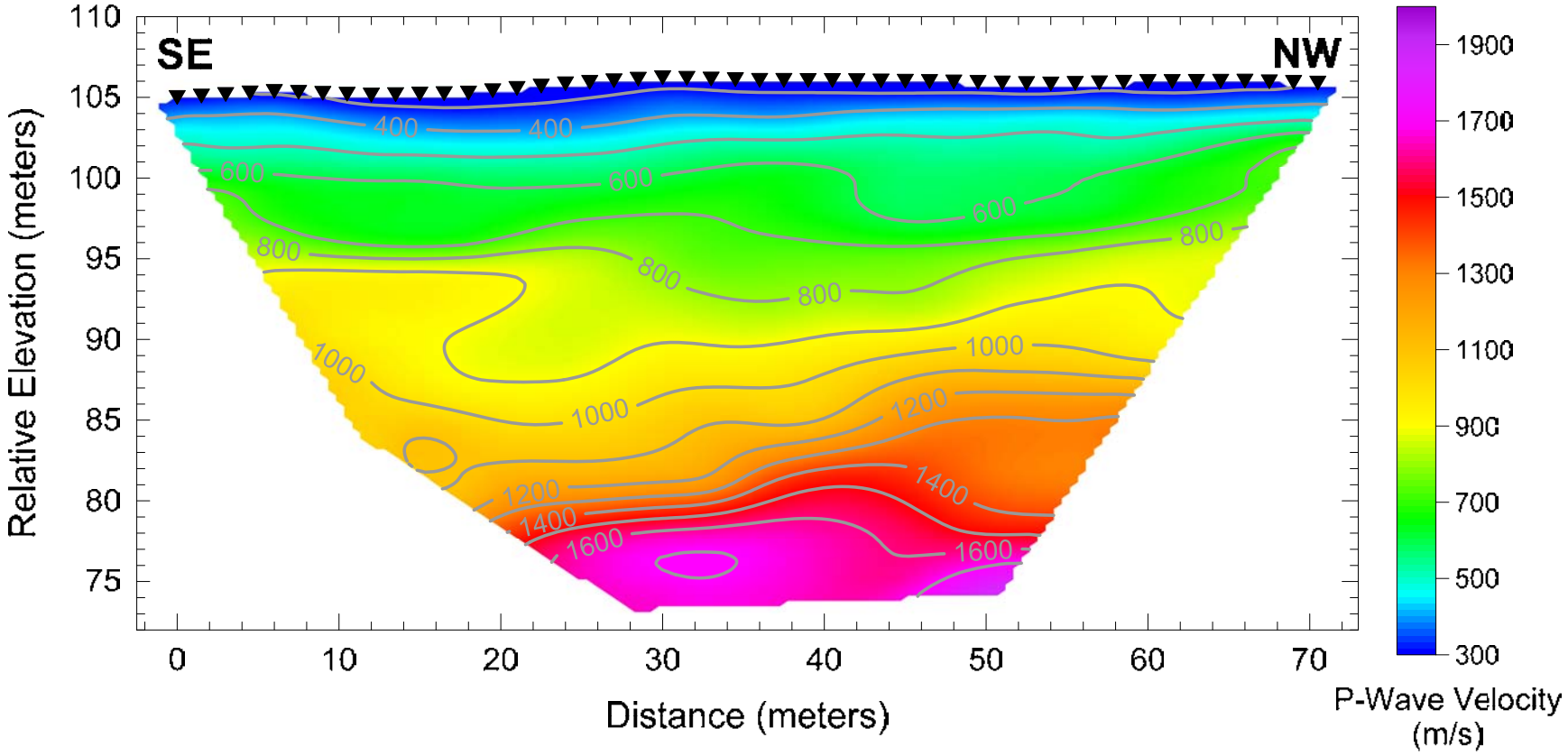

Array MSC-1 – P-wave Tomographic Seismic Refraction Model utilizing Smooth Velocity Gradient Starting Model

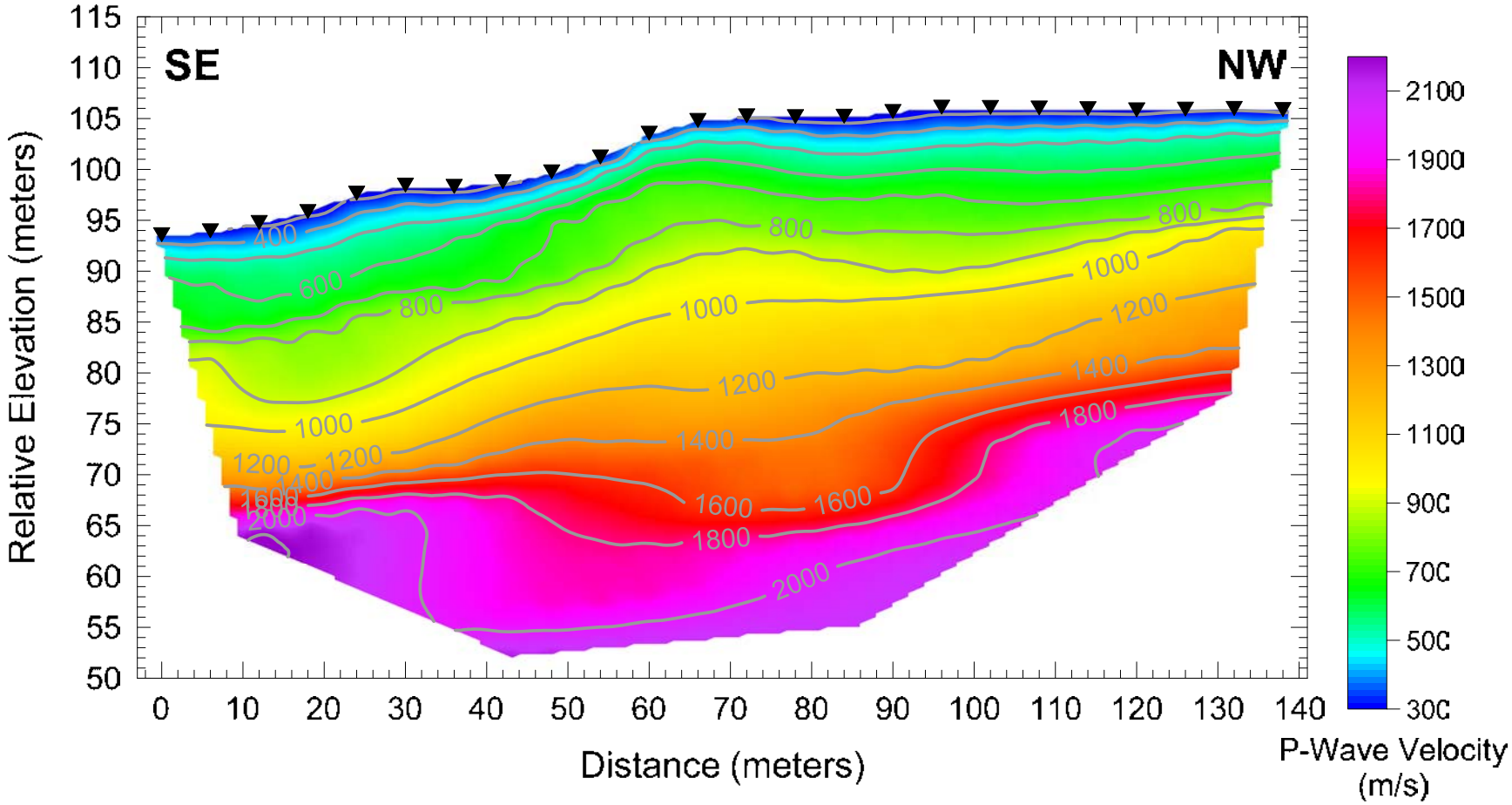

Array MSC-2 – P-wave Tomographic Seismic Refraction Model utilizing Smooth Velocity Gradient Starting Model. Array MSC-1 is located between a position of 67.5 and 138 m.

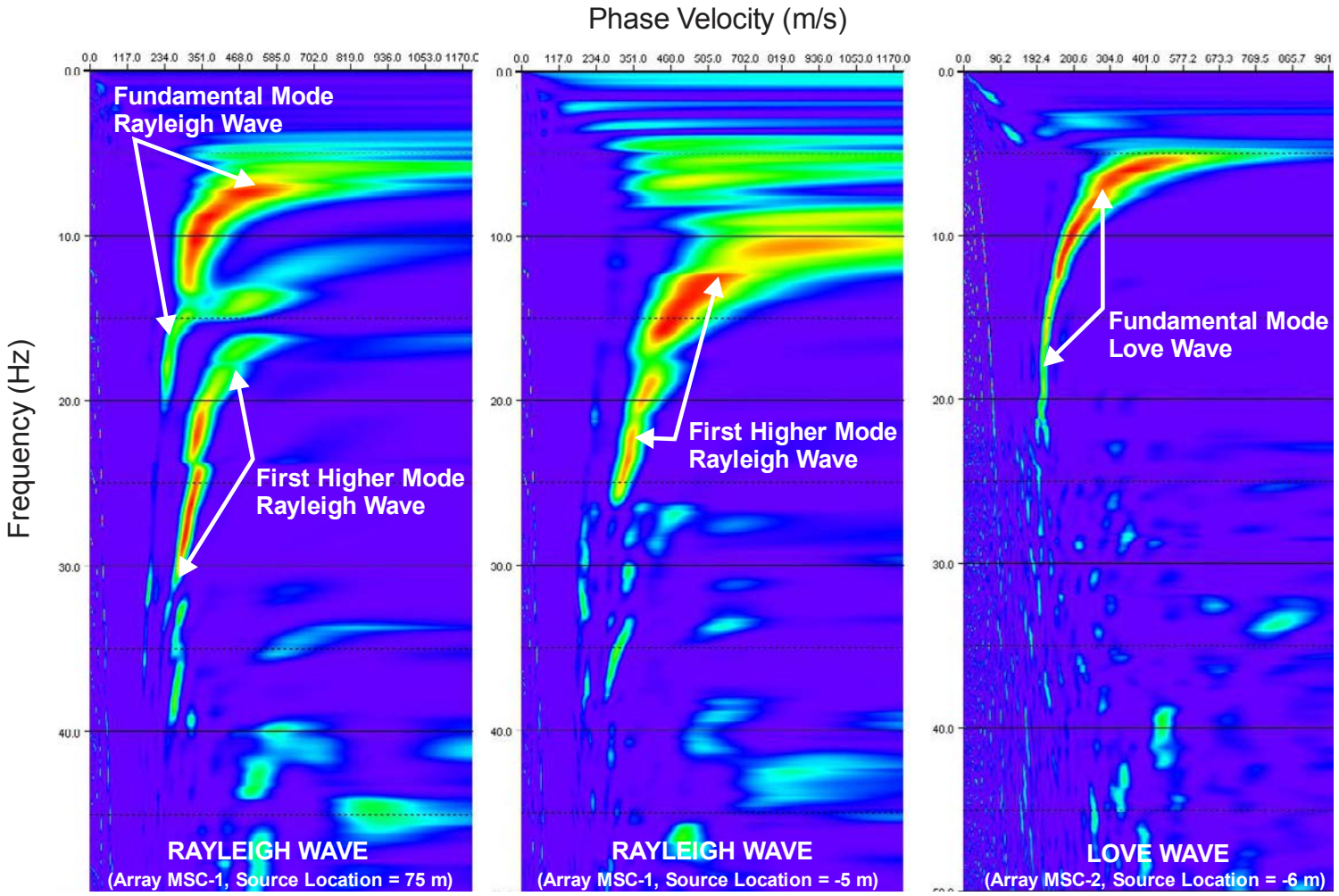

CI.MSC – Comparison of Rayleigh and Love wave overtone images demonstrating dominant higher mode energy in the Rayleigh wave data. Only several source locations with offsets of 1.5 to 10 m from the northwest end of the MASW (Rayleigh wave) arrays MSC-1 and MSC-2 yielded significant fundamental mode energy. Therefore, Love wave dispersion data from MALW array MSC-2 were used for site characterization. However, it may have been possible to extract sufficient fundamental mode Raleigh wave energy from arrays MSC-1 and MSC-2 or, alternatively, attempt modeling of the first higher mode.

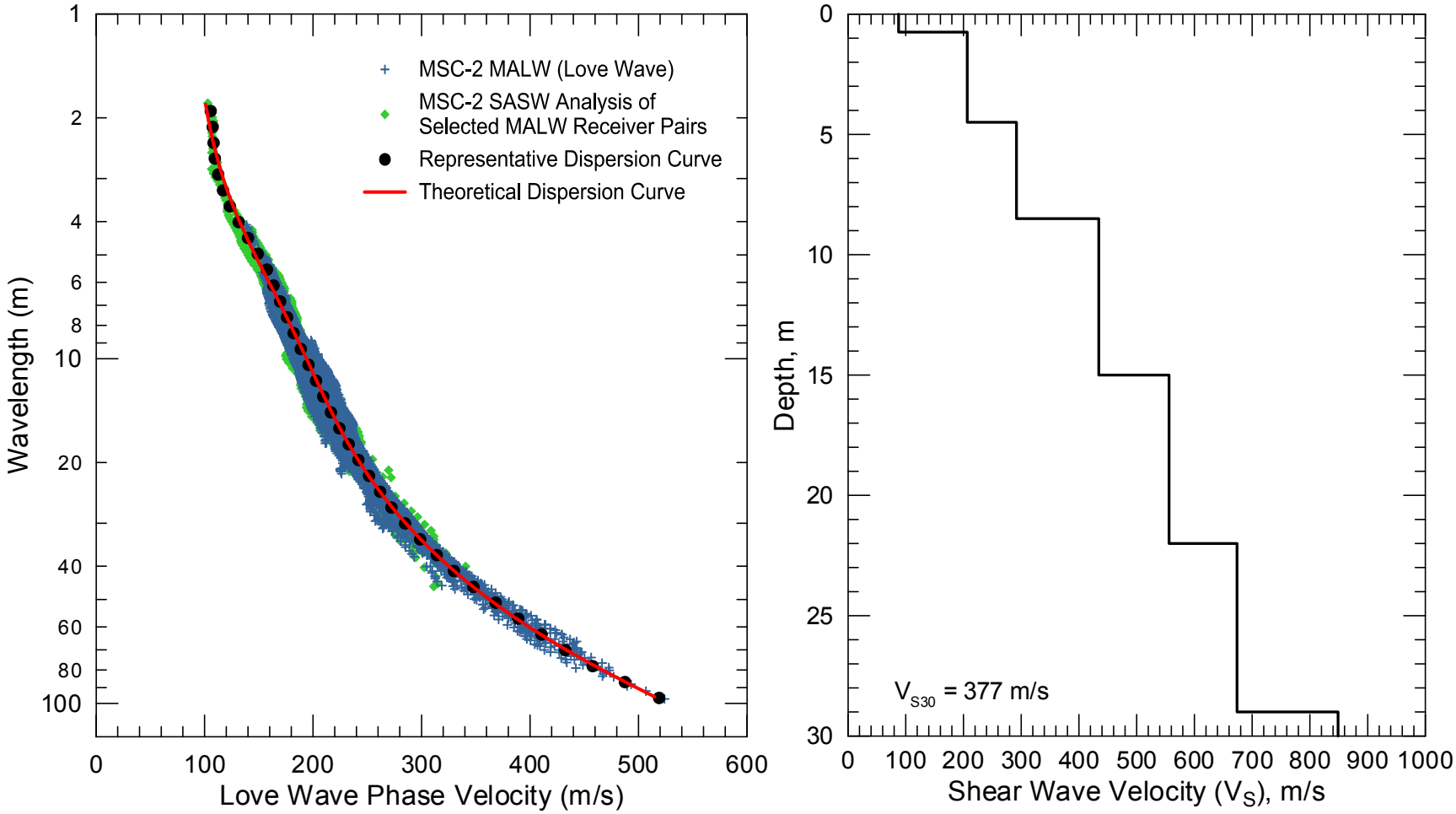

CI.MSC - Field, representative and inverted theoretical Love wave dispersion data (left) and associated V_S model (right)

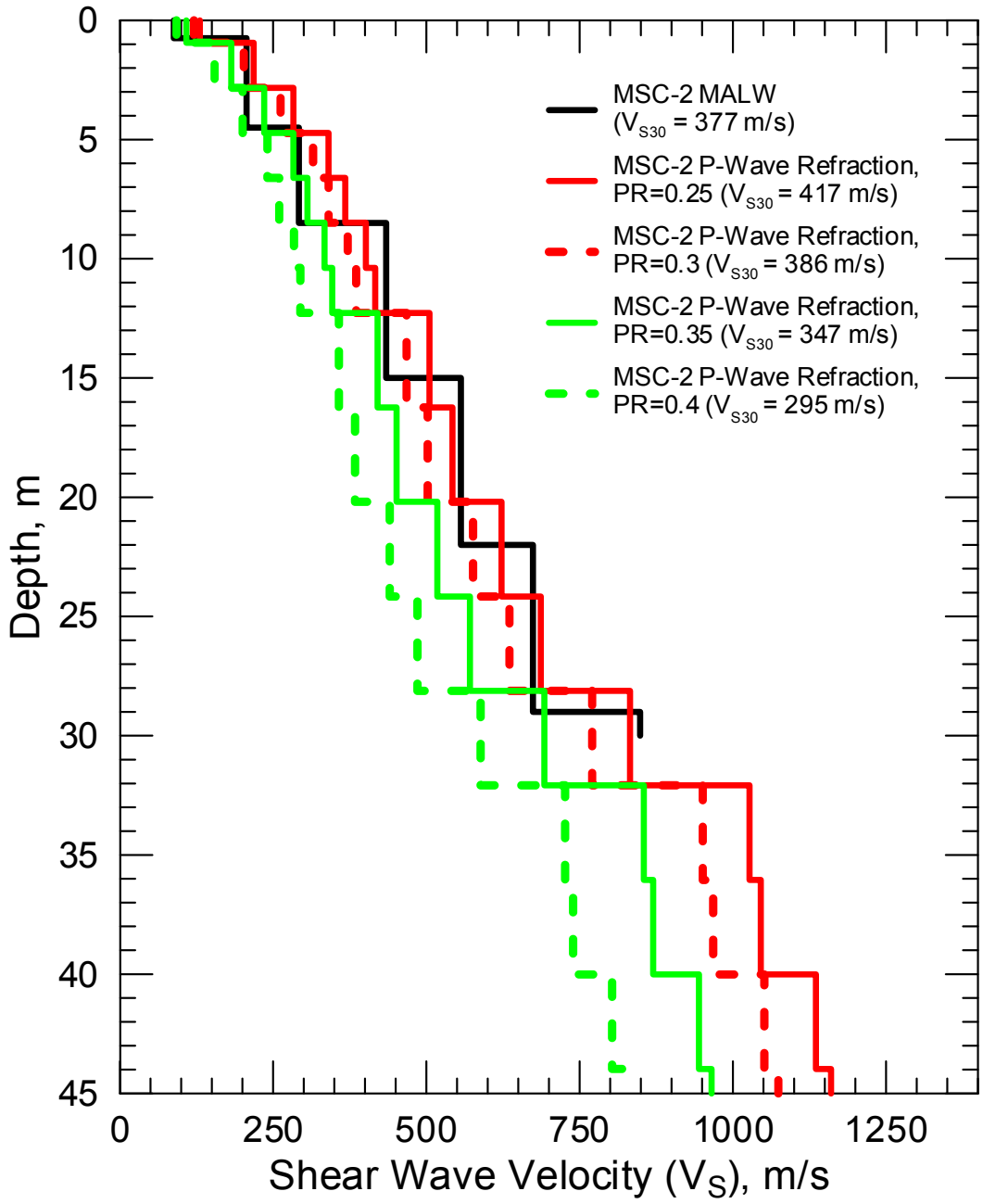

CI.MSC – Comparison of the S-wave velocity model derived from the MALW data and estimated V_S models derived from the P-wave refraction data assuming constant Poisson's ratio. V_{S30} calculated from the MALW V_S model compares favorably with that derived from the P-wave refraction model assuming a constant Poisson's ratio of 0.3, which is considered acceptable for decomposed and intensely weathered rock.

Site CI.MSJ

Location: Mount San Jacinto College, San Jacinto, California

Latitude: 33.80801 **Longitude:** -116.96789
(Station coordinates provided by USGS, WGS84 coordinate system)

V_{S30} (measured): 244 m/s

V_{S30} (adjusted to more accurately reflect seismic station conditions): 255 m/s (average S-wave velocity between 2 and 32 m adjusting for nominal sensor depth).

NEHRP Site Class: D

Geomatrix Code: IHD

Geologic Conditions/Observations: Site located in area mapped as Quaternary (Holocene) young alluvial deposits. Site located on a graben bound by the Claremont strand of the San Jacinto Fault about 1.25 km to east and the Casa Loma branch to the west. Basement is expected to be relatively deep at this site.

Site Conditions: Developed site with moderate traffic noise from nearby roads. Relatively flat terrain in site vicinity.

Geophysical Methods Utilized: HVSR, MASW, array microtremor, ReMi™

Geophysical Testing Arrays:

1. Arrays MSJ-1 (24 channel linear array utilizing 4.5 Hz vertical geophones spaced 5 m apart for an array length of 115 m) and MSJ-2 (24 channel linear array utilizing 4.5 Hz vertical geophones spaced 4 m apart for an array length of 92 m) used to acquire passive surface wave data. Arrays combined to form a "T" shaped array.
2. Arrays MSJ-1 and MSJ-2 were also used to acquire limited MASW and seismic refraction data (reversed off-end shot locations and center shot with accelerated weight drop energy source).
3. Array MSJ-3 (48 channel MASW array, aligned along array MSJ-2, utilizing 4.5 Hz vertical geophones spaced 1.5 m apart for a length of 70.5 m, forward and reverse shot locations with multiple source offsets and source types and center shot location).
4. Three HVSR measurement locations: one located near seismograph station and one each located on arrays MSJ-1 and MSJ-2.

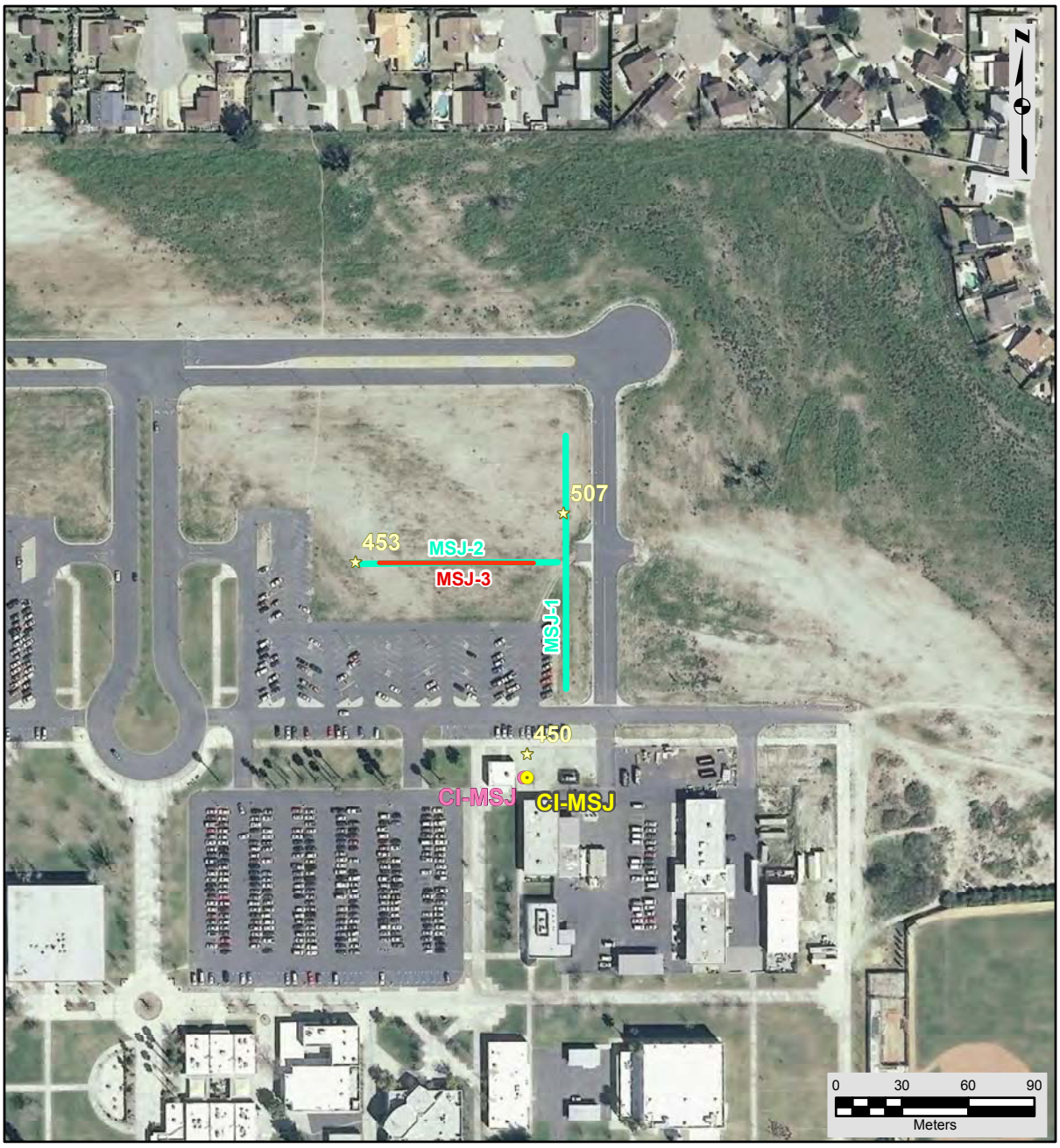

Legend

- Seismic Station - Approximate Surveyed Location
- Seismic Station - Approximate Location of Record
- H/V Spectral Ratio Measurement Location
- MASW Array
- Passive Surface Wave Array

NOTES:
1. WGS 1984 COORDINATE SYSTEM
2. Image Source: ESRI, i-cubed, USDA FSA, USGS, AEX, GeoEye, Getmapping, Aerogrid, IGP

File Name: CI-MSJ-I

Date: 4/1/2011

USGS science for a changing world

GEOVision geophysical services

RECOVERY.GOV

SITE MAP
CI•MSJ

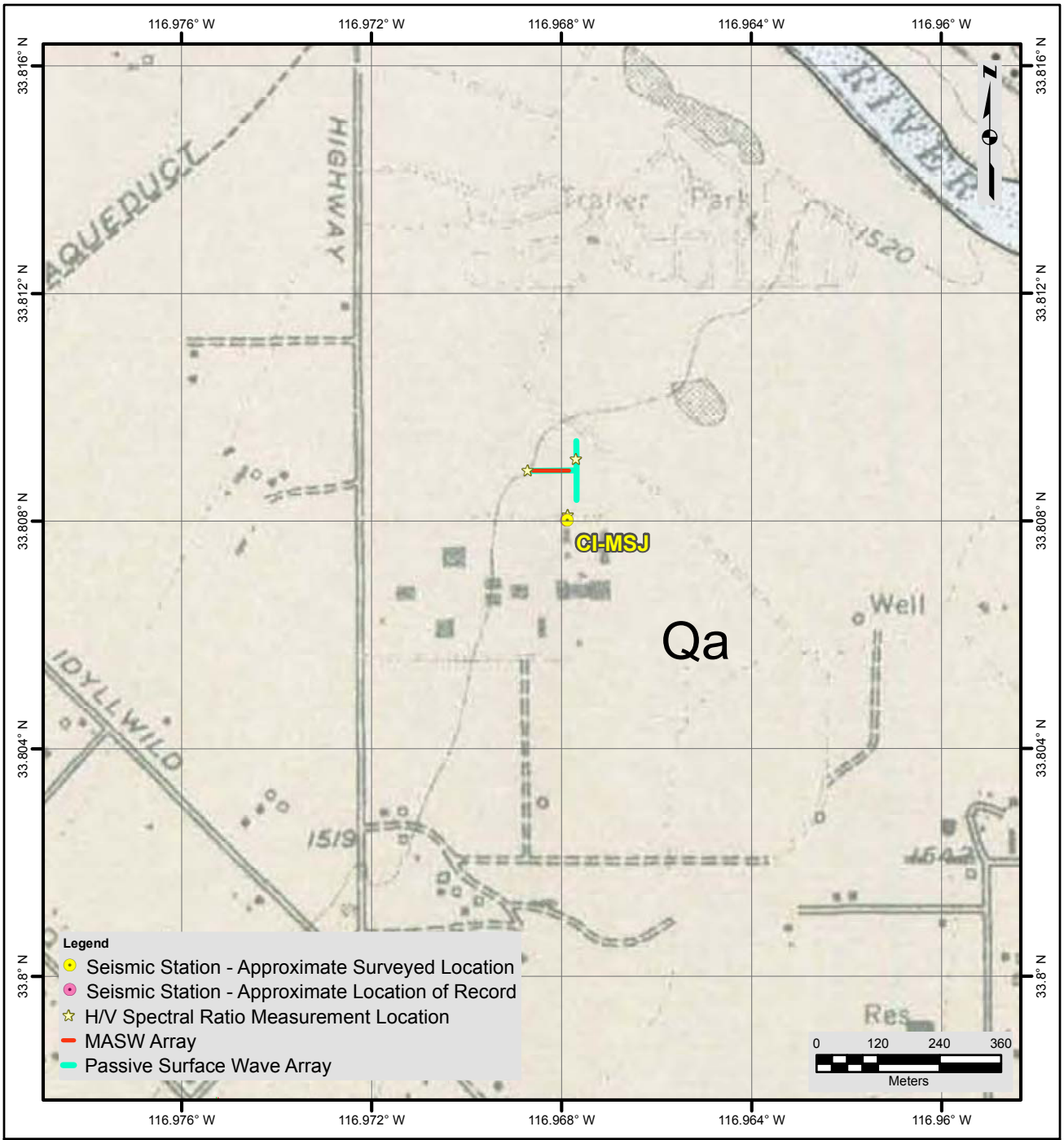

Description of Geologic Map Units

Qa = Quaternary (Holocene) alluvial sand and clay of valley areas, covered by grey soil, includes stream channel gravel and sand in mountain area

NOTES:
1. WGS 1984 COORDINATE SYSTEM
2. Geologic Map of the San Jacinto Quadrangle, Riverside County, California
By Thomas W. Dibblee, Jr., 2003
3. See site map for details of geophysical survey

File Name: CI-MSJ

Date: 4/15/2011

USGS science for a changing world

GEOVision geophysical services

RECOVERY.GOV

GEOLOGIC MAP
CI•MSJ

Looking south towards CI.MSJ seismograph station from the intersection of arrays MSJ-1 and MSJ-2

Looking north towards seismograph station CI.MSJ, HVSR sensor 450 and test area

Looking north along array MSJ-1 towards HVSR sensor 507

MASW data acquisition using accelerated weight drop source

Looking southeast towards seismograph station CI.MSJ from HVSR sensor 453

Location of Geophysical Testing Arrays:

Location	Latitude	Longitude
MSJ-1, South End of Array, Channel 1	33.80837	-116.96768
MSJ-1, North End of Array, Channel 24	33.80941	-116.96769
MSJ-2, East End of Array, Channel 25	33.80889	-116.96773
MSJ-2, West End of Array, Channel 48	33.80888	-116.96871
MSJ-3, West End of Array	33.80889	-116.96860
MSJ-3, Center of Array	33.80889	-116.96822
MSJ-3, East End of Array	33.80889	-116.96784
HVSR Sensor 507	33.80909	-116.96770
HVSR Sensor 453	33.80889	-116.96871
HVSR Sensor 450	33.80811	-116.96787
CI.MSJ Seismograph Station	33.80801	-116.96788

Notes: 1) WGS84 Coordinate System (decimal degrees)

2) Survey accuracy is estimated at 1 to 2 m.

Results:

V_S Model

Depth to Top of Layer (m)	Layer Thickness (m)	S-Wave Velocity (m/s)	Inferred P-Wave Velocity (m/s)	Inferred Poisson's Ratio	Inferred Density (g/cm^3)
0	1	170	317	0.300	1.9
1	2	177	331	0.300	1.9
3	2	213	398	0.300	1.9
5	3	228	427	0.300	1.9
8	5	230	1750	0.491	2.0
13	8	255	1750	0.489	2.0
21	11	301	1750	0.485	2.0
32	15	374	1750	0.476	2.0
47	20	439	1750	0.466	2.0
67	>8	482	1750	0.459	2.0

Observations/Discussion:

- The HVSR curves are almost identical, validating the 1-D velocity structure assumption.
- HVSR curves are complex with no clear dominant HVSR peak. The highest amplitude peak occurs at about 0.17 Hz, which would imply very deep basement in the site vicinity. There is also a broad low amplitude peak at about 0.8 Hz.
- Noise conditions at site appeared sufficient to attempt passive surface wave techniques although most noise sources were located west and south of the site. The relatively high traffic State Street and Ramona Expressway are located about 0.5 km west and 0.7 km south of the test area, respectively.
- ESAC technique used to extract surface wave dispersion data from passive "T" array data. Both the ReMi™ and ESAC techniques used to extract surface wave dispersion data from the linear arrays.
- Useful surface wave dispersion data not obtained from linear passive surface wave array MSJ-2, possibly because most noise emanated from the south, perpendicular to the array. Passive surface wave data acquired with array was, therefore, not used for data analysis. Surface wave dispersion data extracted from array MSJ-1 using the ESAC technique is in better agreement with the "T" array dispersion data than that extracted using the ReMi™ technique. Good quality MASW data was obtained from arrays MSJ-1 and MSJ-2.
- Surface wave dispersion data from active and passive surface wave ("T" array and linear array MSJ-1) datasets are in good agreement at this site.
- Scatter in the dispersion data, particularly at small wavelengths/high frequencies, likely results from near surface lateral velocity variation.
- Representative dispersion curves were generated for each surface wave data set using a moving average, polynomial curve fitting routine. These individual representative dispersion curves were combined and a representative dispersion curve generated for the combined data set for data modeling.
- Water table located at a depth of about 8 m based on interactive layer-based analysis of seismic refraction first arrival data. P-wave velocity of about 1,750 m/s modeled for upper portion of saturated zone.
- There are multiple reflectors in the upper 100 m that are clearly evident on the seismic records. The RMS velocity of the sediments overlying the reflectors introduces the possibility that the water table refractor may be associated with perched water rather than the regional aquifer. The water table, however, is assumed to be located at a depth of 8 m for modeling of the surface wave dispersion data.
- Surface wave depth of investigation is about 75 m based on half of maximum wavelength criteria and assuming that surface wave dispersion data at frequencies as low as 3 Hz are valid utilizing 4.5 Hz geophones (low frequency geophone phase response differences will cancel out if noise is truly omni-directional and/or the phase response differences are random in nature).
- V_{S30} is 244 m/s (Site Class D).
- Average S-wave velocity between 2 m (nominal sensor depth) and 32 m is 255 m/s.
- Average S-wave velocity of the upper 75 m (V_{S75}) is 324 m/s.

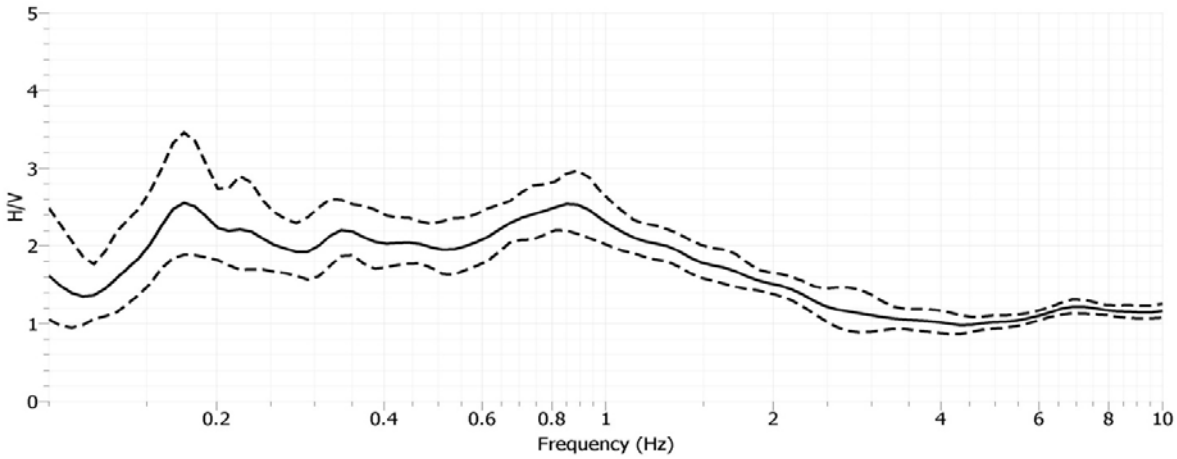

Site CI.MSJ, H/V Spectral Ratio, Array MSJ-1, Sensor 507

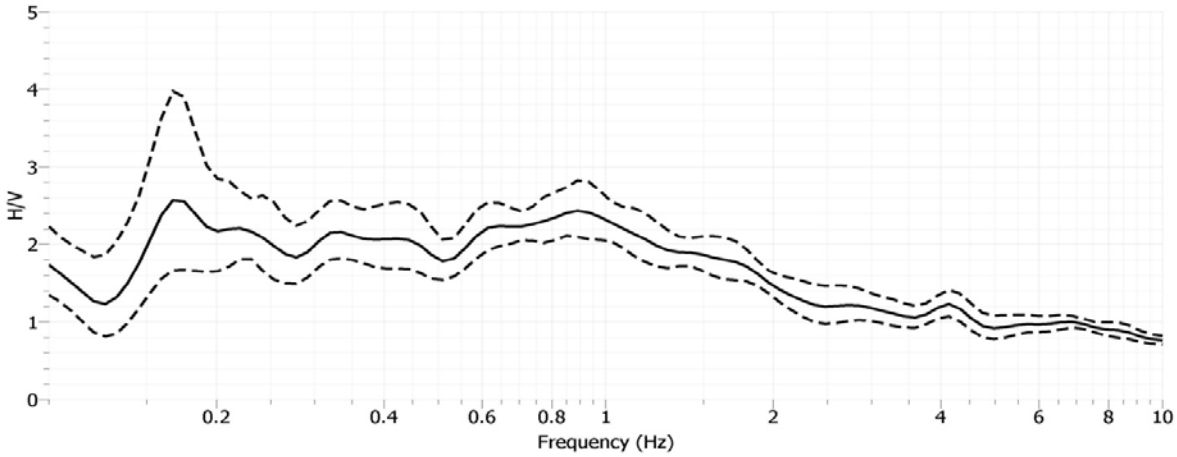

Site CI.MSJ, H/V Spectral Ratio, Array MSJ-2, Sensor 453

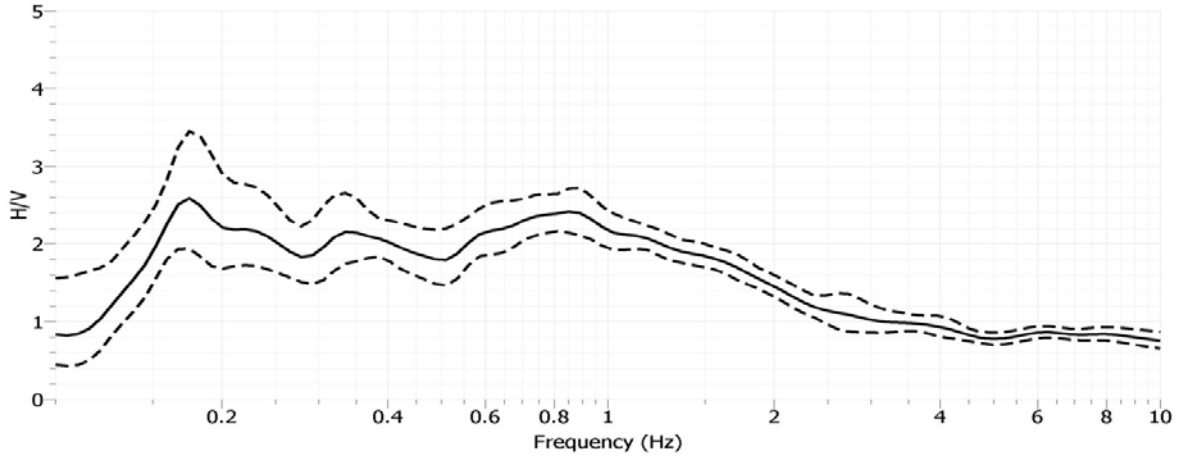

Site CI.MSJ, H/V Spectral Ratio, Near Seismic Station, Sensor 450

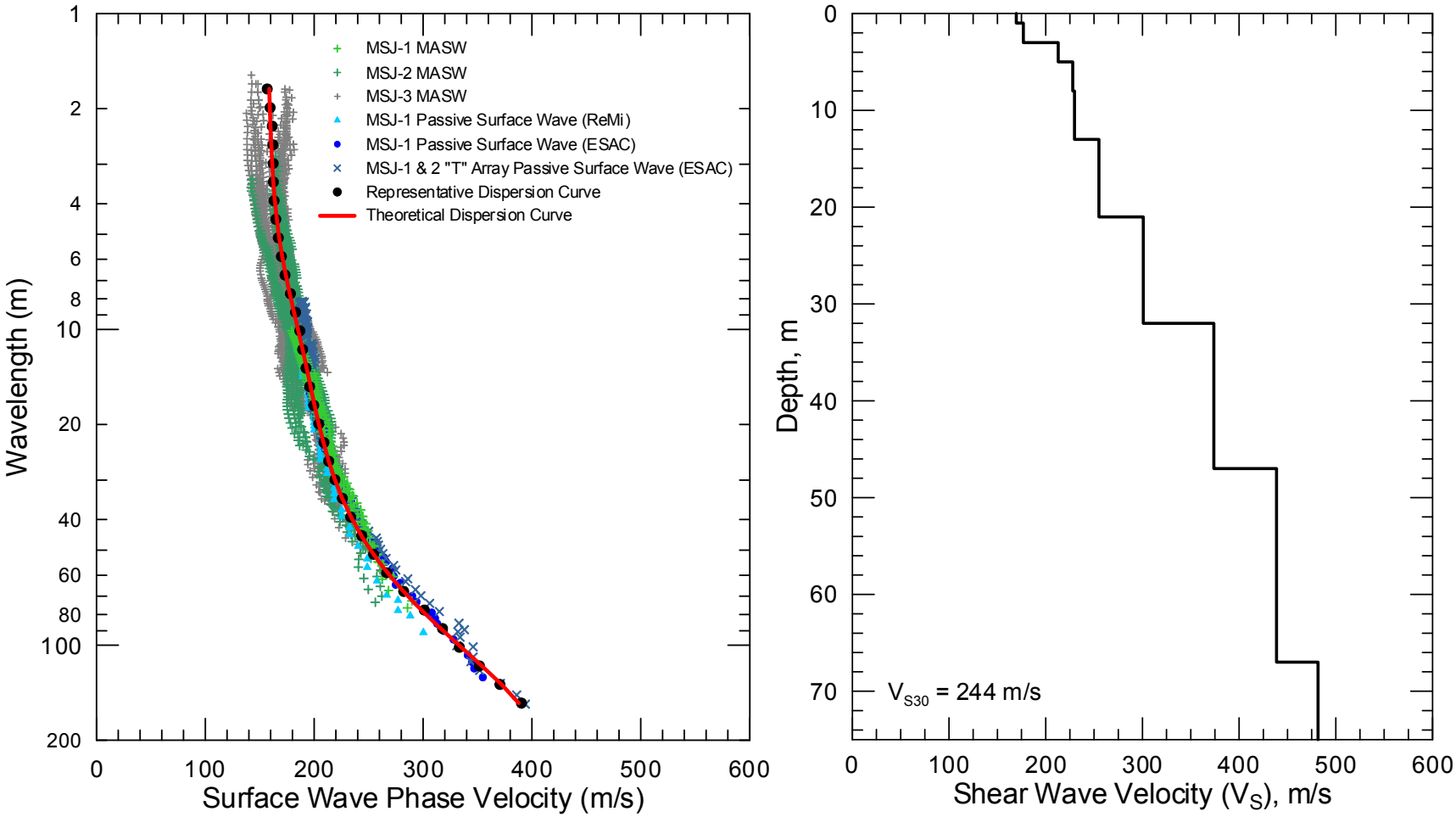

CI.MSJ - Field, representative and inverted theoretical surface wave dispersion data (left) and associated V_S model (right)

Site CI.MTP

Location: Mountain Pass, San Bernardino County, California

Latitude: 35.48434 **Longitude:** -115.55320
(Station coordinates provided by USGS, WGS84 coordinate system)

V_{S30} (measured): 956 m/s

V_{S30} (adjusted to more accurately reflect seismic station conditions): 1,079 m/s (average S-wave velocity between 1 and 31 m to account for seismic sensor not being placed on fill).

NEHRP Site Class: B

Geomatrix Code: IZA

Geologic Conditions/Observations: Seismic station located on geologic unit mapped as Precambrian metamorphic rocks. However, field inspection indicates that the seismic station is located on a Paleozoic limestone or dolomite overlying metamorphic rocks.

Site Conditions: Rural site located on a ridge top. Steep topography in site vicinity.

Geophysical Methods Utilized: HVSR, Seismic Refraction, MASW

Geophysical Testing Arrays:

1. Array MTP-1 (48 channel MASW and P-wave seismic refraction array utilizing 4.5 Hz vertical geophones spaced 1.5 m apart for a length of 70.5 m, forward and reverse shot locations with multiple source offsets and source types and multiple interior shot locations).
2. Array MTP-2 (48 channel MASW and P-wave seismic refraction array utilizing 4.5 Hz vertical geophones spaced 1.5 m apart for a length of 70.5 m, forward and reverse shot locations with multiple source offsets and source types and multiple interior shot locations).
3. Three HVSR measurement locations distributed along array MTP-1.

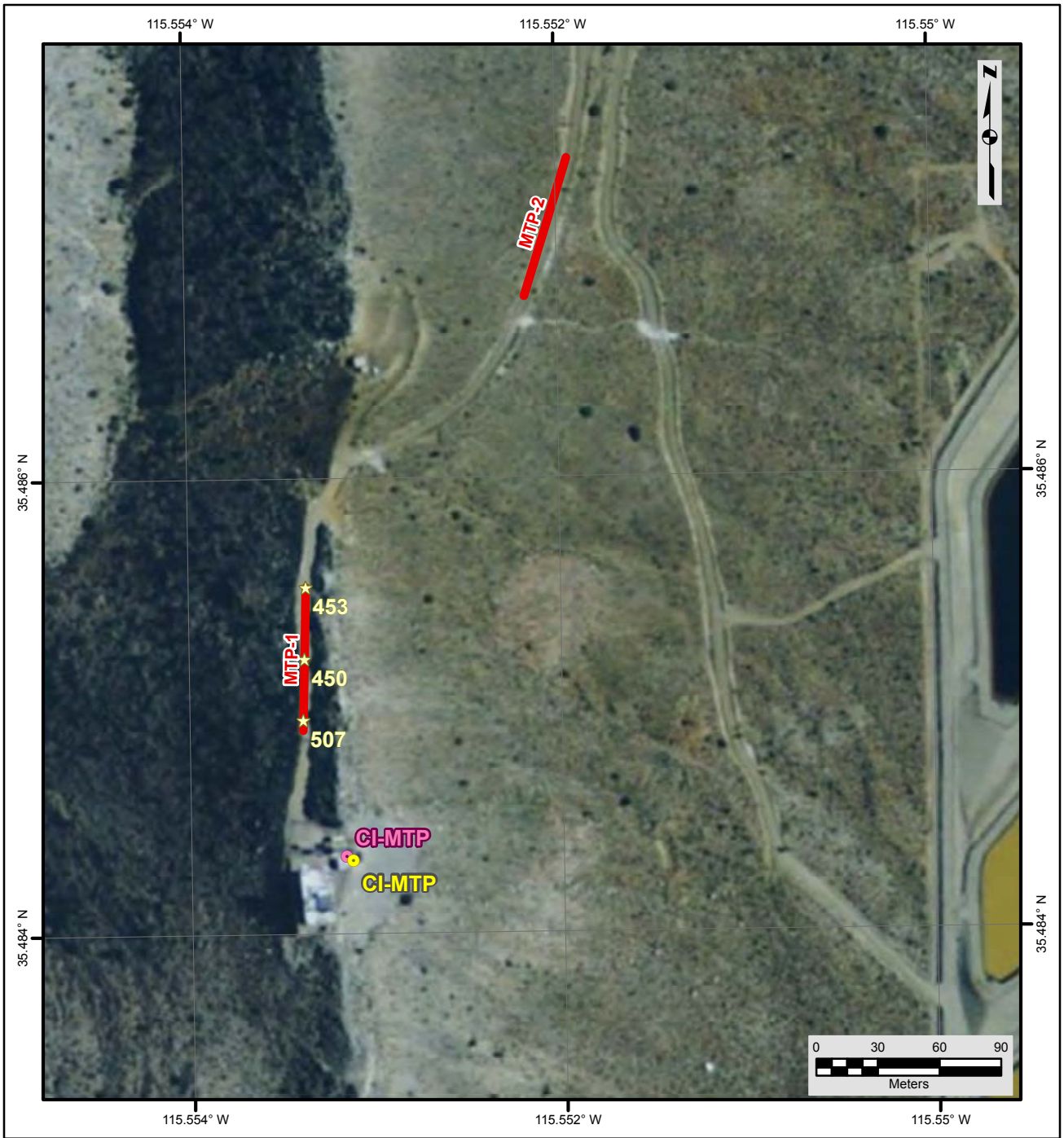

Legend

- ☆ H/V Spectral Ratio Location
- Seismic Station - Approximate Surveyed Location
- Seismic Station - Approximate Location of Record
- MASW and Seismic Refraction Array

NOTES:
1. WGS 1984 COORDINATE SYSTEM
2. Image Source: ESRI, i-cubed, USDA FSA, USGS, AEX, GeoEye, Getmapping, Aerogrid, IGP

File Name: CI-MTP-I

Date: 10/13/2011

USGS science for a changing world

GEOVision geophysical services

RECOVERY.GOV

SITE MAP
CI•MTP

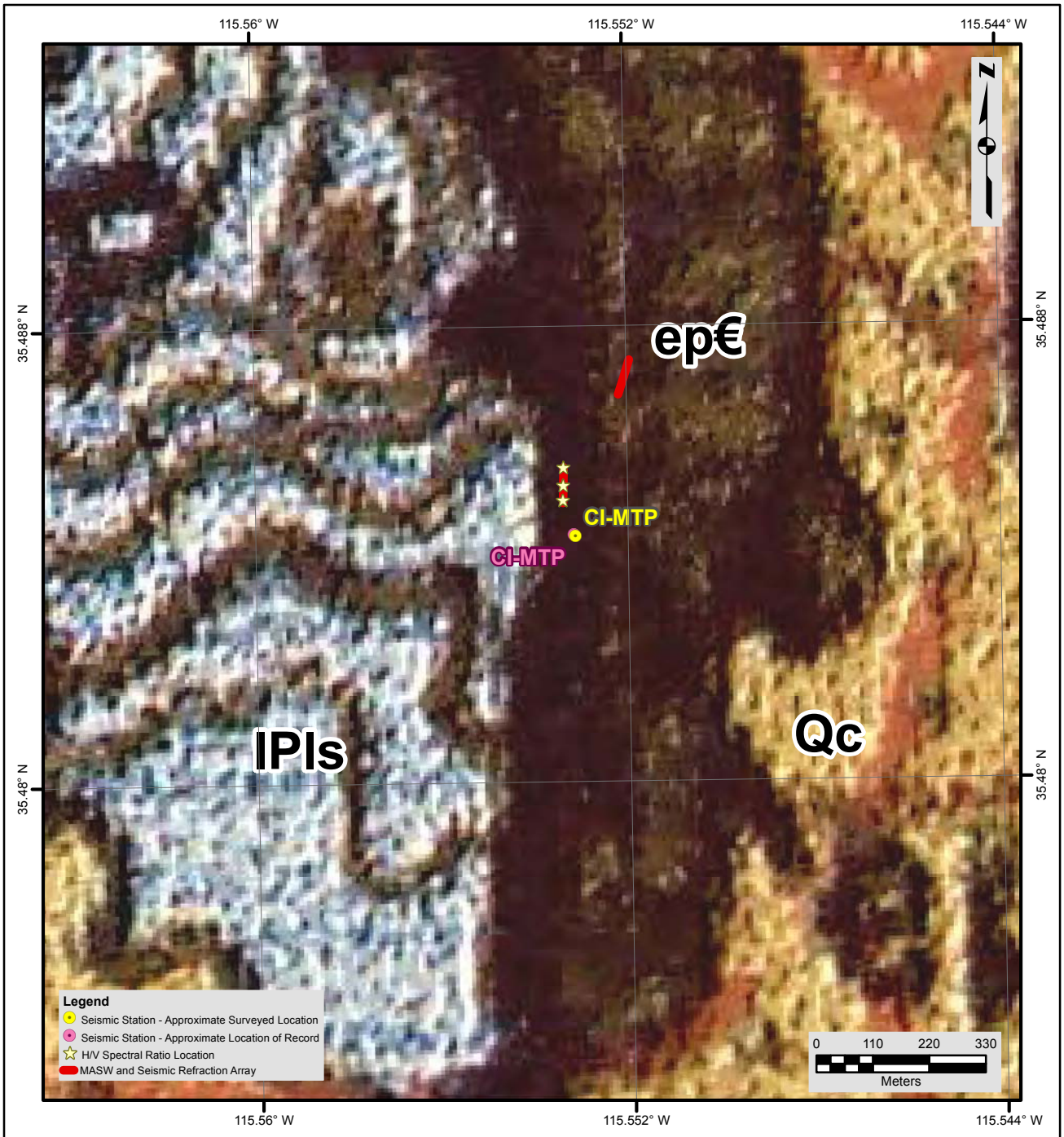

Description of Geologic Map Units

Qc = Quaternary (Pleistocene) nonmarine deposits
IPls = Paleozoic (Undivided) limestone or dolomite
ep€ = Earlier Precambrian metamorphic rocks

NOTES:
1. WGS 1984 COORDINATE SYSTEM
2. Geologic Map of California
Kingman Sheet Olaf P. Jenkins Edition
compiled by Charles W. Jennings, 1961
3. See site map for details of geophysical survey

File Name: CI-MTP

Date: 5/10/2012

USGS science for a changing world

GEOVision geophysical services

GEOLOGIC MAP
CI•MTP

RECOVERY.GOV

Looking south at CI.MTP seismic station

Looking south towards location of array MTP-1

Looking southwest towards seismic station (below power pole on left) at Precambrian limestone or dolomite overlying Precambrian metamorphic rocks

Looking southwest along array MTP-2

Looking south along array MTP-1

Location of Geophysical Testing Arrays:

Location	Latitude	Longitude
MTP-1, South End of MASW/Refraction Array	35.48489	-115.55343
MTP-1, Center of MASW/Refraction Array	35.48521	-115.55341
MTP-1, North End of MASW/Refraction Array	35.48552	-115.55340
MTP-2, Southwest End of MASW/Refraction Array	35.48679	-115.55221
MTP-2, Center of MASW/Refraction Array	35.48709	-115.55209
MTP-2, Northeast End of MASW/Refraction Array	35.48740	-115.55197
HVSR Sensor 450	35.48521	-115.55341
HVSR Sensor 453	35.48552	-115.55340
HVSR Sensor 507	35.48494	-115.55342
CI.MTP Seismic Station	35.48432	-115.55317

Notes: 1) WGS84 Coordinate System (decimal degrees)
2) Survey accuracy is estimated at 1 to 2 m.

Results:

Array MTP-1 V_S Model 1 (Average Dispersion Curve)

Depth to Top of Layer (m)	Layer Thickness (m)	S-Wave Velocity (m/s)	Inferred P-Wave Velocity (m/s)	Inferred Poisson's Ratio	Inferred Density (g/cm^3)
0	0.75	214	400	0.3	1.70
0.75	1.75	371	694	0.3	1.90
2.5	3.5	802	1501	0.3	2.10
6	19	1201	2246	0.3	2.20
25	>10	1685	3152	0.3	2.30

Notes: 1) Depth of investigation is about 35 m.
2) Bottom layer is a half space.

Array MTP-1 V_S Model 2 (Lower Envelope of Dispersion Curve)

Depth to Top of Layer (m)	Layer Thickness (m)	S-Wave Velocity (m/s)	Inferred P-Wave Velocity (m/s)	Inferred Poisson's Ratio	Inferred Density (g/cm^3)
0	0.75	190	356	0.3	1.70
0.75	1.75	340	636	0.3	1.90
2.5	3.5	735	1375	0.3	2.10
6	19	1125	2105	0.3	2.20
25	>10	1625	3040	0.3	2.30

Notes: 1) Depth of investigation is about 35 m.
2) Bottom layer is a half space.

Array MTP-1 V_S Model 3 (Upper Envelope of Dispersion Curve)

Depth to Top of Layer (m)	Layer Thickness (m)	S-Wave Velocity (m/s)	Inferred P-Wave Velocity (m/s)	Inferred Poisson's Ratio	Inferred Density (g/cm^3)
0	0.75	240	449	0.3	1.70
0.75	1.75	380	711	0.3	1.90
2.5	3.5	825	1543	0.3	2.10
6	19	1325	2479	0.3	2.20
25	>10	1750	3274	0.3	2.30

Notes: 1) Depth of investigation is about 35 m.
2) Bottom layer is a half space.

Observations/Discussion:

- Field inspection indicates that the seismic station sits on a limestone or dolomite layer overlying gneiss. The limestone unit appears to have a thickness of about 20 m, or more, beneath the seismic station and is tilted down to the west. P-wave seismic refraction and MASW data were acquired along two arrays at the site. Array MTP-1 is located on the limestone/dolomite unit and is in close proximity to the seismic station. Array MPT-2 was located on the gneiss to determine whether the gneiss, which underlies the limestone/dolomite, has lower seismic velocity than the limestone/dolomite.
- The P-wave refraction data were of poor quality, likely due to scattering in the highly fractured and heterogeneous rock, and were, therefore, not modeled. P-wave refraction data were better along array MTP-2, but possible out of plane refractors would have resulted in an unreliable model. The first arrival data were, however, reviewed and P-wave velocity appears to exceed 3,000 m/s at depth.
- HVSR data were collected at three stations distributed along array MTP-1. The HVSR plots are very similar at every station, which would appear to validate the 1-D velocity assumption. There are no distinct high amplitude HVSR peaks, but there is a weak peak at about 7 Hz.
- Noise and geologic conditions at the site were not sufficient for application of passive surface wave techniques.
- MASW data along array MTP-1 were of better quality than that collected along array MTP-2 and, therefore, array MTP-1, which is located on the same geologic unit as the seismic station, is used for site characterization. There may be significantly more lateral velocity variation along array MTP-2, complicating interpretation, and MASW data collected along array MTP-2 have not been modeled at this time. The primary purpose of array MTP-2 was to confirm that S-wave velocity of the gneiss unit is not lower than that of the overlying limestone/dolomite. Review of preliminary Rayleigh wave phase dispersion data for array MTP-2 indicates that the phase velocity at 40 m wavelength (V_{R40}) is about 10% higher than that for array MTP-1. This would indicate that V_{S30} beneath array MTP-2 is slightly higher than that beneath array MTP-1.
- The maximum wavelength Rayleigh wave phase velocity data extracted from the array MTP-1 data set was typically set equal to the lesser of 80 m or 1.25 times the distance from the source to midpoint of the active receiver array.
- The minimum wavelength surface wave phase velocity data extracted from the 48-channel MASW array was about 26 m. The inability to extract small wavelength dispersion data from long receiver arrays often appears to be associated with near surface lateral velocity variation. Reducing data from smaller hammer sources using a limited offset receiver array (i.e. less active geophones) allowed for extraction of Rayleigh wave dispersion data to a minimum wavelength of about 2 m.
- There is significant 75 to 200 m/s scatter in Rayleigh wave dispersion data for array MTP-1, likely the result of lateral velocity variation. The scatter is largest at long wavelengths.
- A representative dispersion curve was generated for the MASW data set using a moving average, polynomial curve fitting routine and used for modeling.
- Because of the significant lateral velocity variation beneath array MTP-1, three models were developed for the MASW data set to explore the variation in V_{S30}. Model 1 fits the

representative dispersion curve and is, therefore, considered the average V_S model for the array. Models 2 and 3 fit the lower and upper envelopes of the Rayleigh wave dispersion data, respectively.

- Surface wave depth of investigation is about 35 m based on one-third of the maximum wavelength criteria.
- V_{S30} is 956, 887 and 1,028 m/s for MASW V_S Models 1 (average), 2 (lower envelope) and 3 (upper envelope), respectively (NEHRP Site Class B).
- Average S-wave velocity between 1 and 31 m, to account for seismic sensor not being placed on loose fill, is 1,079, 1,008 and 1,156 m/s for MASW V_S Models 1 to 3, respectively (NEHRP Site Class B).
- For the purpose of site characterization, we recommend using MASW V_S Model 1, the V_S model developed from the average representative dispersion curve.
- In conclusion, V_{S30} at the seismic station is estimated to be about 956 m/s (NEHRP Site Class B) and adjusted V_{S30} is 1,079 m/s (NEHRP Site Class B).
- The V_S models for the lower and upper envelopes of the dispersion curve indicate that V_{S30} may vary by ±7% in the vicinity of array MTP-1.

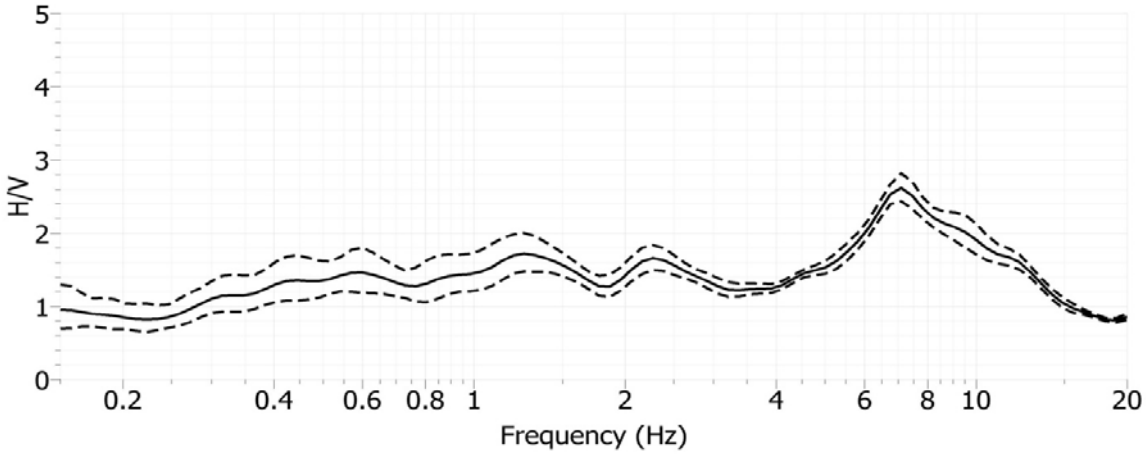

Site CI.MTP, H/V Spectral Ratio, Array MTP-1, Sensor 453

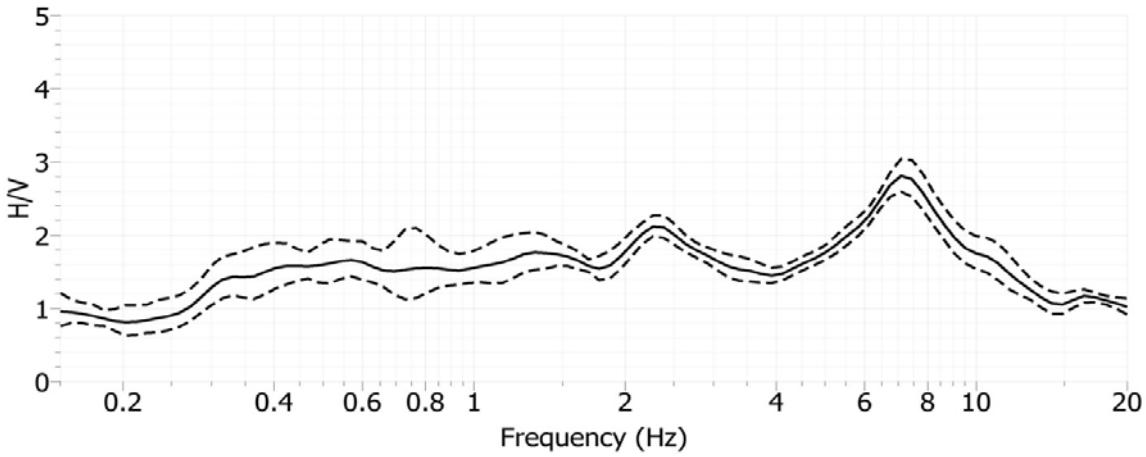

Site CI.MTP, H/V Spectral Ratio, Array MTP-1, Sensor 450

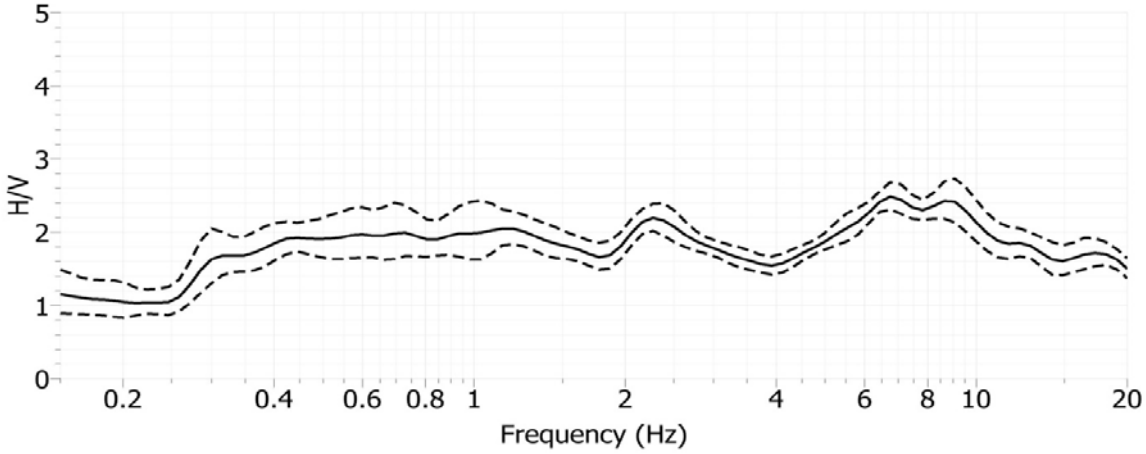

Site CI.MTP, H/V Spectral Ratio, Array MTP-1, Sensor 507

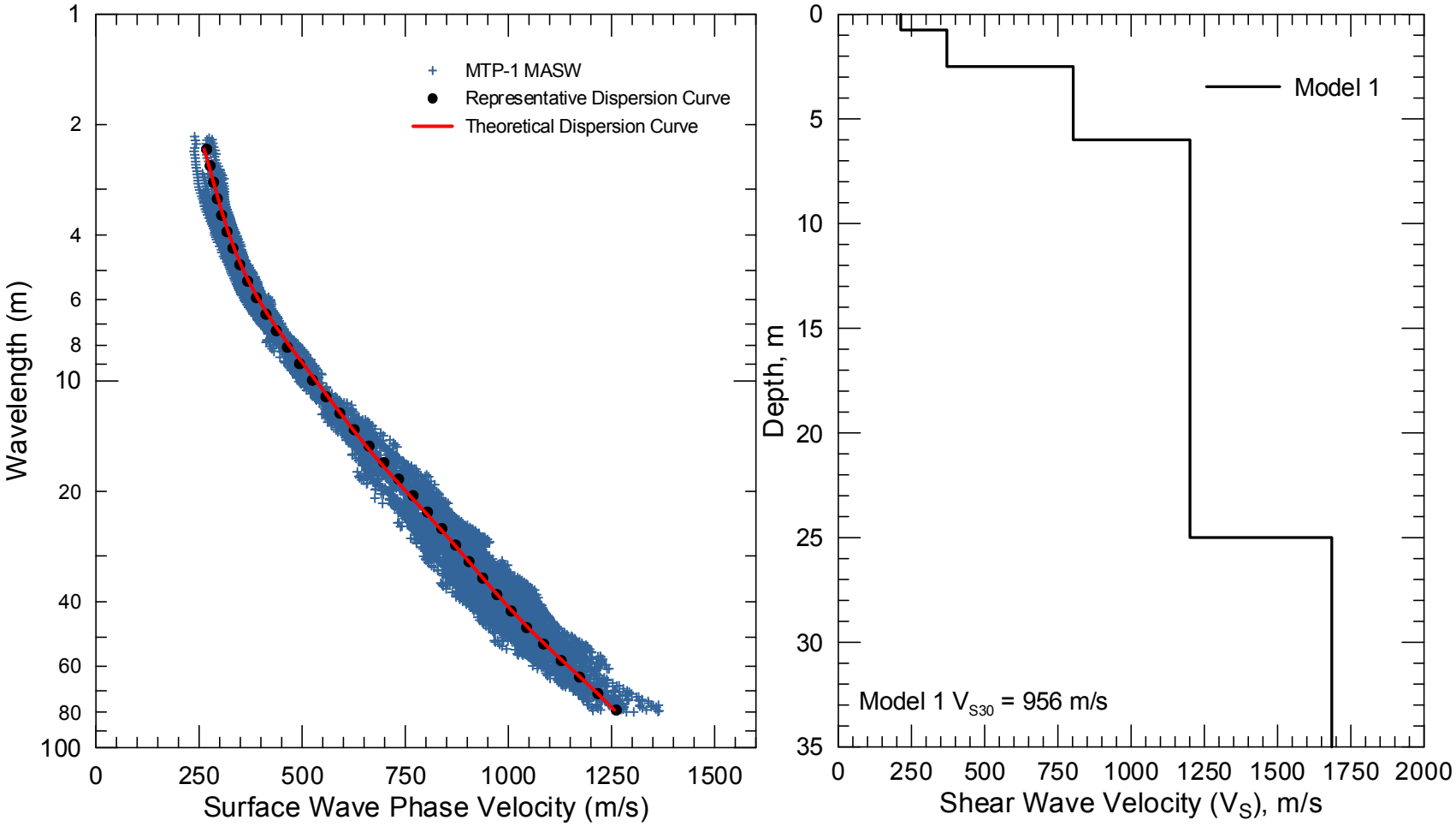

CI.MTP - Field, representative and inverted theoretical Rayleigh wave dispersion data (left) and associated V_S model (right)

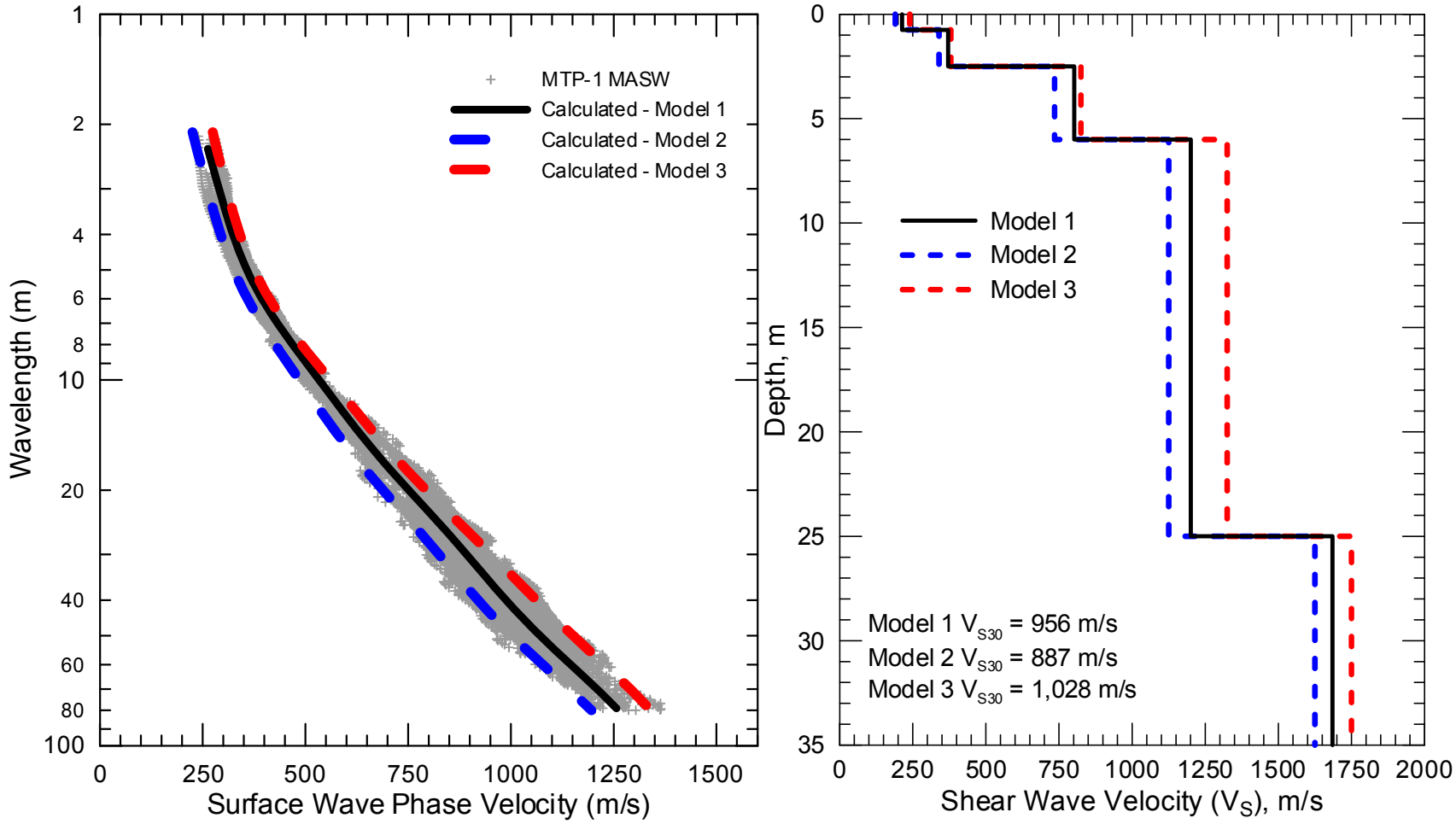

CI.MTP – Field and calculated Rayleigh wave dispersion data (left) and associated V_S models (right) fitting average (Model 1), lower envelope (Model 2) and upper envelope (Model 3) Rayleigh wave dispersion data.

Site CI.NBS

Location: Southern California Gas Facility, Gasco Road, South of National Trails Highway and I-40, Newberry Springs, California

Latitude: 34.78035 **Longitude:** -116.55798
(Station coordinates provided by USGS, WGS84 coordinate system)

V_{S30} (measured): 419 m/s

V_{S30} (adjusted to more accurately reflect seismic station conditions): 461 m/s (average S-wave velocity between 2 and 32 m adjusting for nominal sensor depth).

NEHRP Site Class: C

Geomatrix Code: IHD

Geologic Conditions/Observations: Site located on geologic unit mapped as Quaternary (Holocene) alluvium. Not clear how deep bedrock is in site vicinity but nearest outcrop is about 3.25 km to south.

Site Conditions: Rural site. I40 located about 3 km to north. Relatively flat terrain in site vicinity with ground surface elevation gently decreasing to southeast.

Geophysical Methods Utilized: HVSR, MASW, SASW

Geophysical Testing Arrays:

1. Array NBS-1 (48 channel MASW array utilizing 4.5 Hz vertical geophones spaced 1.5 m apart for a length of 70.5 m, forward and reverse shot locations with multiple source offsets and source types and center shot location).
2. Array NBS-1 (SASW array with common midpoint and orientation as MASW array of same name utilizing 4.5 and 1 Hz vertical geophones and maximum receiver spacing of 32 m).
3. Three HVSR measurement locations; two distributed along array NBS-1 and one located near seismograph station.

Legend

- Seismic Station - Approximate Location of Record
- H/V Spectral Ratio Measurement Location
- MASW and SASW Array

NOTES:
1. WGS 1984 COORDINATE SYSTEM
2. Image Source: ESRI, i-cubed, USDA FSA, USGS, AEX, GeoEye, Getmapping, Aerogrid, IGP

File Name: CI-NBS-I

Date: 4/1/2011

USGS science for a changing world

GEOVision geophysical services

RECOVERY.GOV

SITE MAP
CI•NBS

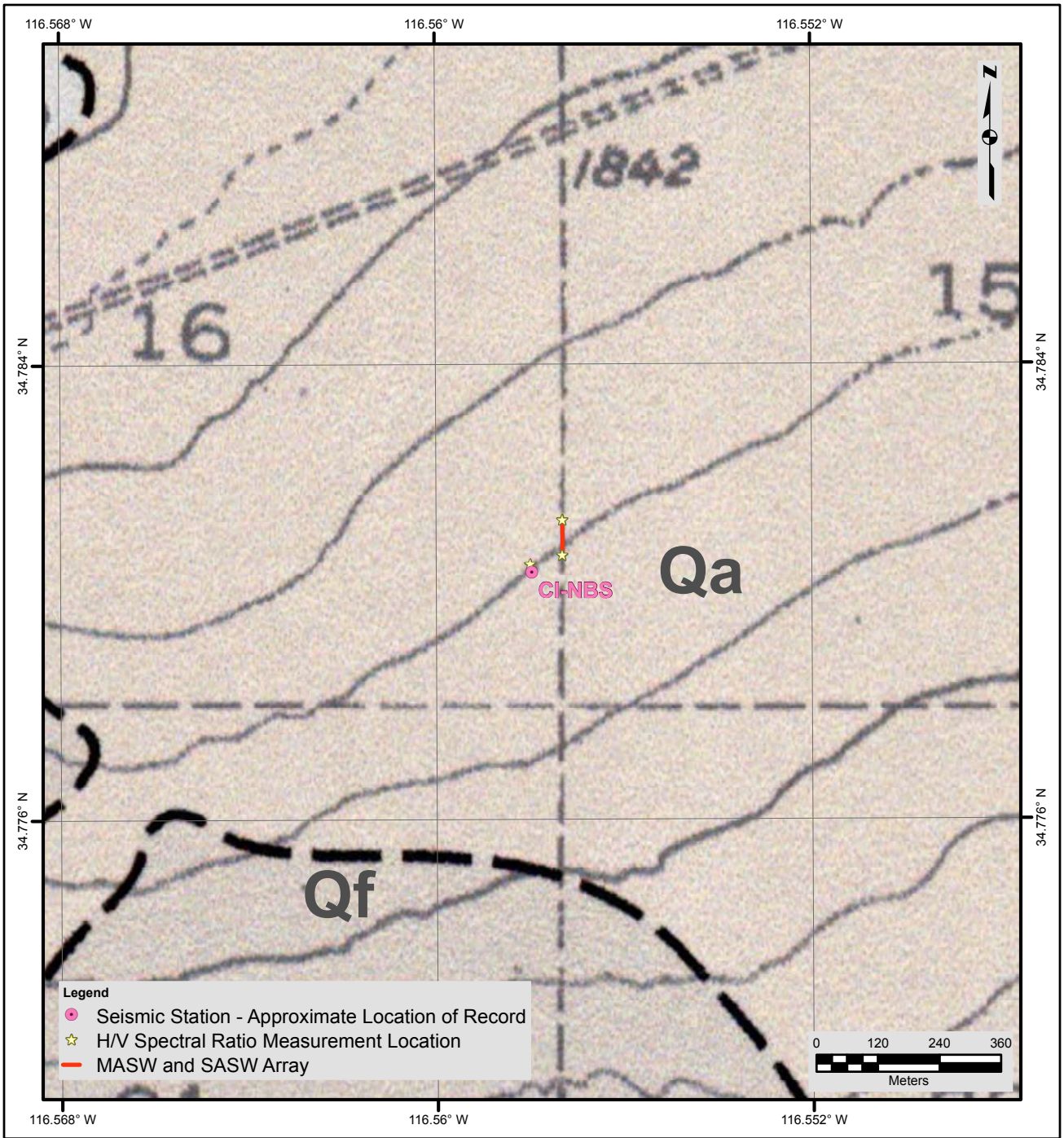

Description of Geologic Map Units

Qa = Quaternary (Holocene) alluvium, cobble-pebble gravel and sand near hills, grades to sand in valley areas
Qf = Quaternary (Holocene) alluvial fan gravel, coarse, unsorted

NOTES:
1. WGS 1984 COORDINATE SYSTEM
2. Geologic Map of the Newberry & Cady Mountains 15 Minute Quadrangle, San Bernardino County, California by Thomas W. Dibblee, Jr., 2008
3. See site map for details of geophysical survey

File Name: CI-NBS

Date: 4/15/2011

USGS science for a changing world

GEOVision geophysical services

GEOLOGIC MAP
CI•NBS

RECOVERY.GOV

Looking south at HVSR sensor 507 and seismograph station CI.NBS. Note coarse-grained soils near hole for HVSR sensor.

Looking southwest towards SASW array NBS-1 and seismograph station

Looking south towards HVSR sensor 450 and the facility housing the seismograph station

Data acquisition along SASW array NBS-1

Data acquisition along MASW array NBS-1

Location of Geophysical Testing Arrays:

Location	Latitude	Longitude
NBS-1, South End of MASW Array	34.78065	-116.55733
NBS-1, Center of MASW and SASW Arrays	34.78096	-116.55732
NBS-1, North End of MASW Array	34.78127	-116.55733
HVSR Sensor 507	34.78048	-116.55801
HVSR Sensor 453	34.78064	-116.55733
HVSR Sensor 450	34.78127	-116.55733

Notes: 1) WGS84 Coordinate System (decimal degrees)
2) Survey accuracy is estimated at 1 to 2 m.

Results:

V_S Model

Depth to Top of Layer (m)	Layer Thickness (m)	S-Wave Velocity (m/s)	Inferred P-Wave Velocity (m/s)	Inferred Poisson's Ratio	Inferred Density (g/cm^3)
0	0.5	166	311	0.3	1.9
0.5	1	196	367	0.3	1.9
1.5	2	276	516	0.3	1.9
3.5	3	351	656	0.3	1.9
6.5	4	424	794	0.3	2.0
10.5	6	475	888	0.3	2.0
16.5	9	509	952	0.3	2.0
25.5	>4.5	570	1067	0.3	2.0

Observations/Discussion:

- No access to gated compound housing seismograph station so the station location could not be surveyed. The provided seismic station coordinates do, however, appear to be accurate.
- Very difficult to couple HVSR sensors in gravelly soil.
- HVSR plots are generally similar at measurement locations; although the HVSR plot for sensor 507 (located near the seismic station) is slightly different from sensors 450 and 453 (located on array NBS-1) over the 3 to 10 Hz frequency range. Sensor 507 was placed in a deep hole in gravelly soils; whereas 450 and 453 were placed along a dirt road in sandy soil. It is possible that the slightly differing HVSR responses represent variable shallow velocity structure. Sensor 507 is also closer to a gas transfer station with running pumps/motors, which may contribute to the different HVSR response at high frequencies.
- There is no distinct high amplitude HVSR peak at the site. There is, however, a broad weak peak in the 0.8 to 0.9 Hz range.
- Noise conditions at site were not sufficient to apply passive surface wave techniques.
- Surface wave dispersion data from SASW and MASW datasets are in good agreement at the site.
- Representative dispersion curves were generated for each surface wave data set using a moving average, polynomial curve fitting routine. These individual representative dispersion curves were combined and a representative dispersion curve generated for the combined data set for data modeling.
- Water table located at a depth of greater than 30 m based on seismic refraction survey design and absence of a water table refractor.
- Based on simple layer-based analysis of seismic refraction first arrival data, P-wave velocity in the upper 20 m increases with depth from about 350 m/s at the surface to about 750 m/s at a depth of about 5 m and over 1,150 m/s at a depth of about 16 m.
- The surface wave model is consistent with P-wave refraction data, considering Poisson's ratio is unknown. The inferred P-wave velocities in the surface wave model would match the refraction data reasonably well if Poisson's ratio was increased to about 0.35. Increasing Poisson's ratio by 15% would result in about a 2% decrease in V_{S30}.
- Surface wave depth of investigation is about 30 m based on half of maximum wavelength criteria.
- V_{S30} is 419 m/s (Site Class C).
- Average S-wave velocity between 2 m (nominal sensor depth) and 32 m is 461 m/s.

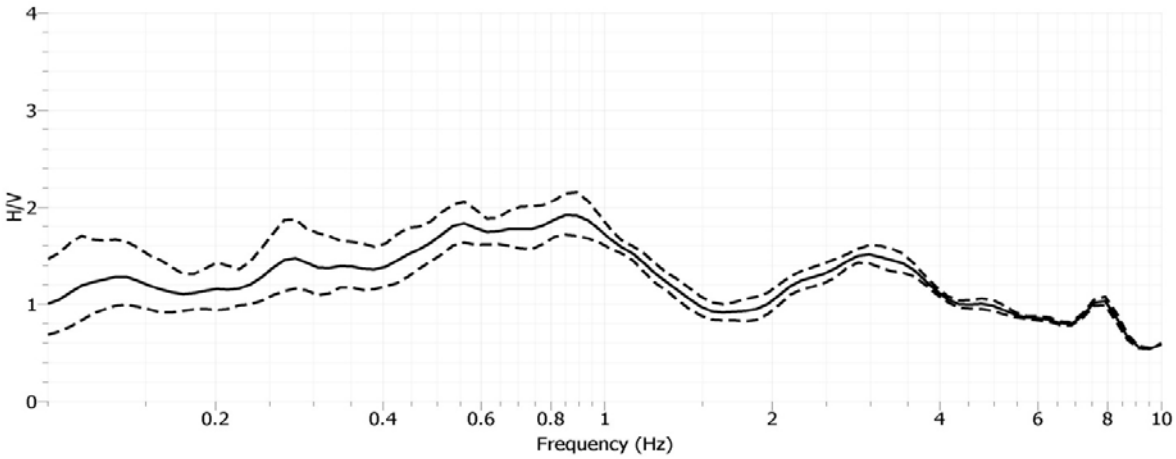

Site CI.NBS, H/V Spectral Ratio, Array NSB-1, Sensor 450

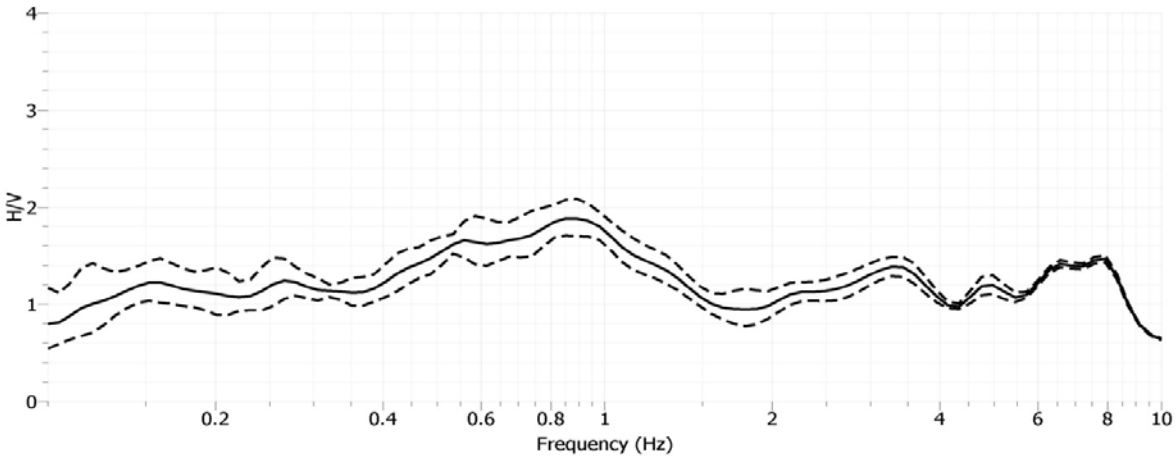

Site CI.NBS, H/V Spectral Ratio, Array NSB-1, Sensor 453

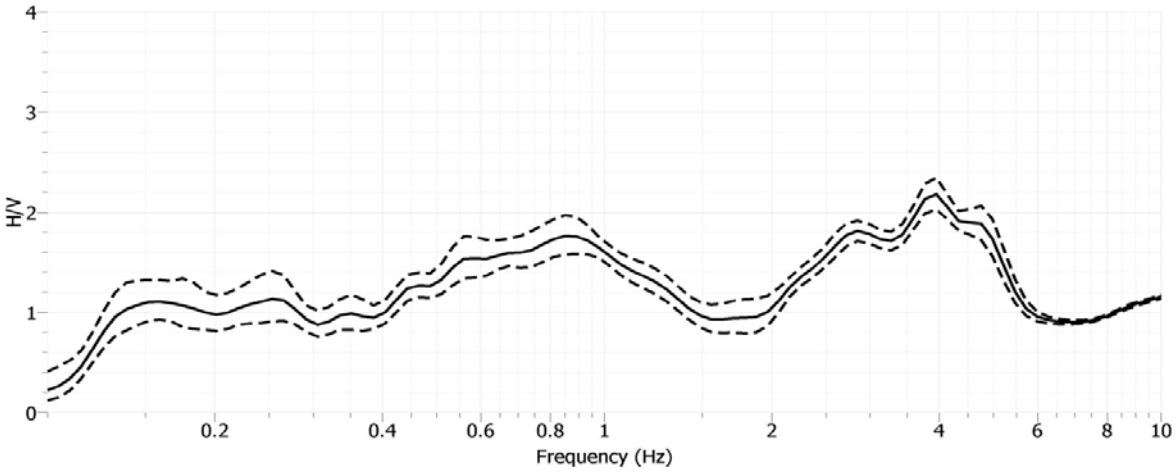

Site CI.NBS, H/V Spectral Ratio, Near Seismic Station, Sensor 507

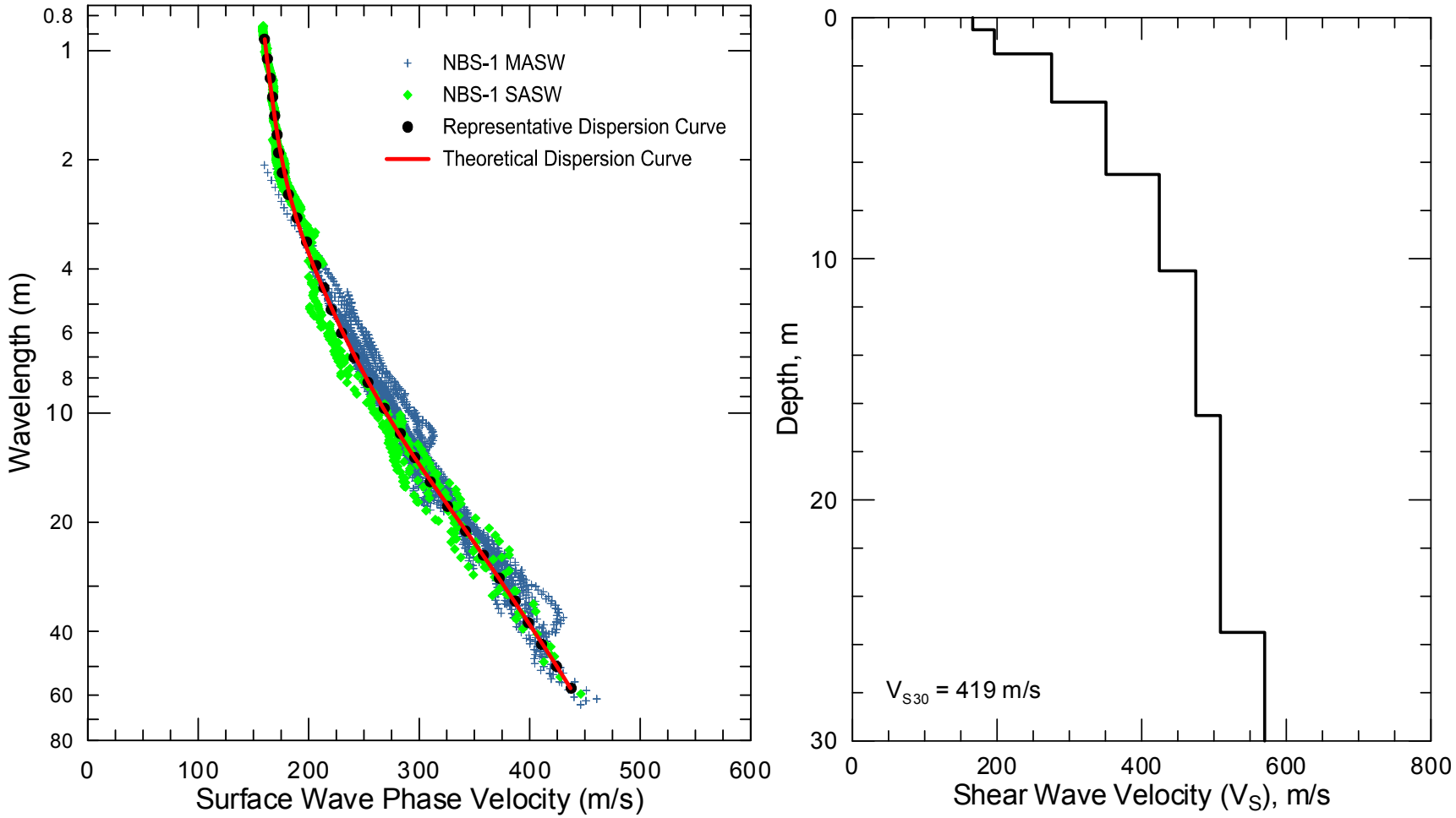

CI.NBS - Field, representative and inverted theoretical surface wave dispersion data (left) and associated V_S model (right)

Site CI.NEE2

Location: Needles Airport, Needles, California

Latitude: 34.76754 **Longitude:** -114.61883

(Station coordinates based on site GPS survey, WGS84 coordinate system)

V_{S30} (measured): 401 m/s

V_{S30} (adjusted to more accurately reflect seismic station conditions): 427 m/s (average S-wave velocity between 2 and 32 m adjusting for assumed sensor depth).

NEHRP Site Class: C

Geomatrix Code: IQD/IHD

Geologic Conditions/Observations: Site located on geologic unit mapped as Quaternary (Holocene to Pleistocene) alluvium.

Site Conditions: Rural site. Relatively flat terrain in test area. Surface elevation gradually declines to northeast.

Geophysical Methods Utilized: HVSR, MASW, SASW

Geophysical Testing Arrays:

1. Array NEE2-1 (48 channel MASW array utilizing 4.5 Hz vertical geophones spaced 1.5 m apart for a length of 70.5 m, forward and reverse shot locations with multiple source offsets and source types and center shot location).
2. Array NEE2-1 (SASW array with common midpoint and orientation as MASW array of same name utilizing 4.5 and 1 Hz vertical geophones and maximum receiver spacing of 40 m).
3. Array NEE2-2 (48 channel MASW array utilizing 4.5 Hz vertical geophones spaced 3 m apart for a length of 70.5 m, forward and reverse shot locations with multiple source offsets and center shot location).
4. Array NEE2-3 (SASW array located near southwest end of MASW array NEE2-1 utilizing 4.5 and 1 Hz vertical geophones and maximum receiver spacing of 32 m).
5. Array NEE2-4 (SASW array located near northeast end of MASW array NEE2-1 utilizing 4.5 and 1 Hz vertical geophones and maximum receiver spacing of 40 m).
6. Three HVSR measurement locations distributed along array NEE2-1.

Legend

- Seismic Station - Approximate Surveyed Location
- Seismic Station - Approximate Location of Record
- H/V Spectral Ratio Location
- SASW Array
- MASW and SASW Array
- MASW Array

NOTES:
1. WGS 1984 COORDINATE SYSTEM
2. Image Source: (c) Microsoft Corporation and its data suppliers

File Name: CI-NEE2-I

Date: 2/7/2013

USGS science for a changing world

GEOVision geophysical services

RECOVERY.GOV

SITE MAP
CI•NEE2

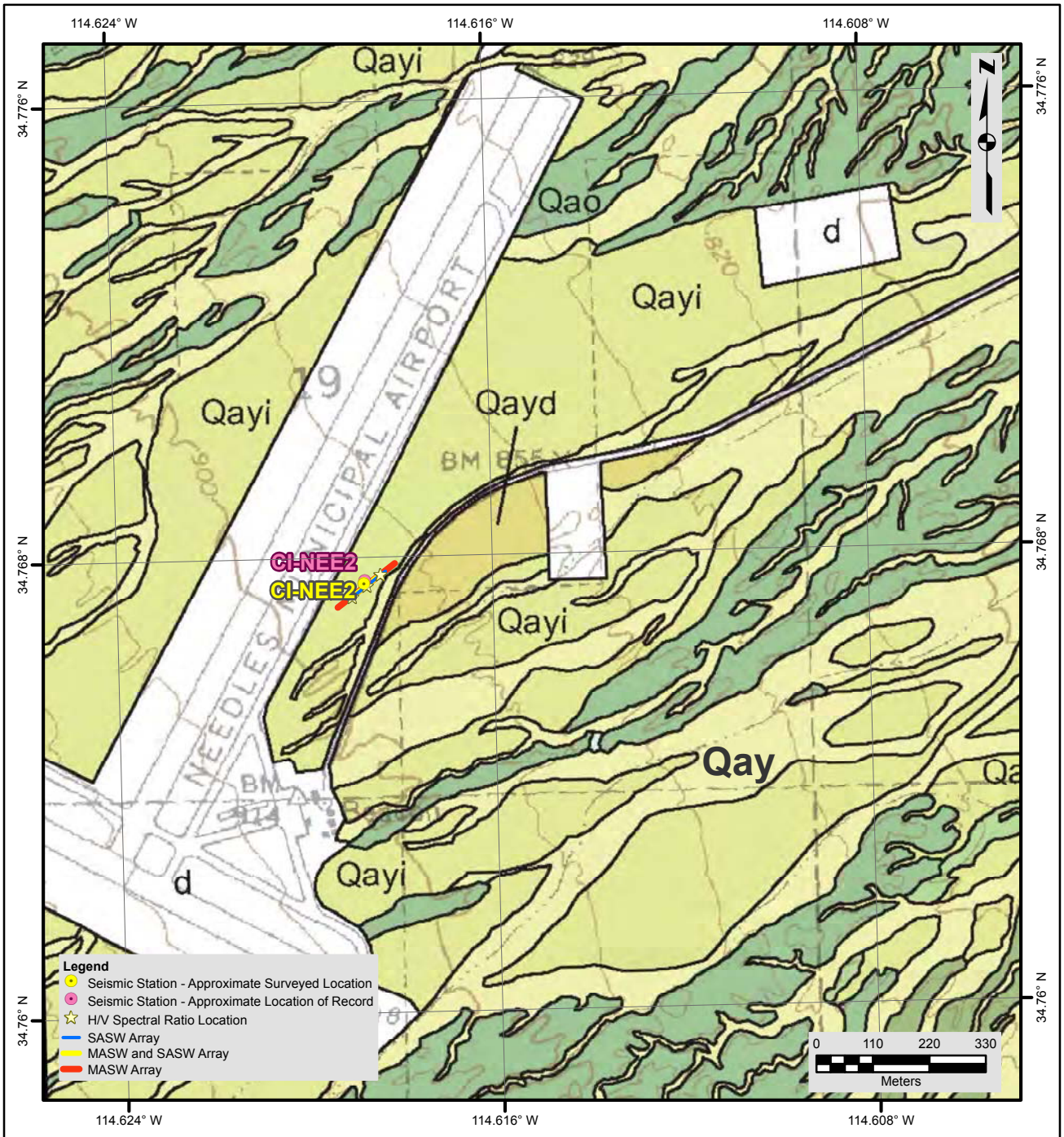

Description of Geologic Map Units

d = disturbed ground (historic)
Qay = Quaternary (Holocene) young piedmont gravels
Qayd = Quaternary (Holocene) Piedmont gravel deposits in diked, historically active washes
Qayi = Quaternary (Middle Holocene to Upper Pleistocene) youngest inactive piedmont gravels
Qao = Quaternary (Middle Pleistocene) older intermediate-age piedmont gravels

NOTES:
1. WGS 1984 COORDINATE SYSTEM
2. Geologic Map of the Needles 7.5' Quadrangle, California and Arizona (2009)
By Daniel V. Malmon, Keith A. howard, and Susan S. Priest
3. See site map for details of geophysical survey

File Name: CI-NEE2

Date: 2/7/2013

USGS science for a changing world

GEOVision geophysical services

GEOLOGIC MAP
CI•NEE2

RECOVERY.GOV

Looking northeast at seismic station CI.NEE2

Looking northeast towards seismic station and SASW array NEE2-3

Looking northeast along MASW array NEE2-1

Looking southwest along SASW array NEE2-1

Looking southwest at HVSR measurement locations along array NEE2-1

Location of Geophysical Testing Arrays:

Location	Latitude	Longitude
NEE2-1, Southwest End of MASW Array	34.76731	-114.61909
NEE2-1, Center of MASW and SASW Arrays	34.76750	-114.61878
NEE2-1, Northeast End of MASW Array	34.76769	-114.61848
NEE2-2, Southwest End of MASW Array	34.76713	-114.61940
NEE2-2, Northeast End of MASW Array	34.76788	-114.61817
NEE2-3, Southwest End of SASW Array	34.76726	-114.61916
NEE2-3, Center of SASW Array	34.76735	-114.61902
NEE2-3, Northeast End of SASW Array	34.76743	-114.61888
NEE2-4, Southwest End of SASW Array	34.76753	-114.61871
NEE2-4, Center of SASW Array	34.76764	-114.61854
NEE2-4, Northeast End of SASW Array	34.76775	-114.61837
HVSR Sensor 450	34.76731	-114.61909
HVSR Sensor 453	34.76750	-114.61877
HVSR Sensor 507	34.76769	-114.61848
CI.NEE2 Seismic Station	34.76754	-114.61883

Notes: 1) WGS84 Coordinate System (decimal degrees).
2) Survey accuracy is estimated at 1 to 2 m.

Results:

V_S Model – MASW Arrays NEE2-1 and NEE2-2

Depth to Top of Layer (m)	Layer Thickness (m)	S-Wave Velocity (m/s)	Inferred P-Wave Velocity (m/s)	Assumed Poisson's Ratio	Assumed Density (g/cm^3)
0	1	211	395	0.3	1.80
1	2	303	567	0.3	1.85
3	3	351	656	0.3	1.90
6	4	370	693	0.3	1.90
10	6	425	795	0.3	1.90
16	8	446	834	0.3	2.00
24	12	532	995	0.3	2.00
36	>4	633	1183	0.3	2.10

Notes: 1) Depth of investigation is about 40 m.
2) Bottom layer is a half space.

V_S Model – SASW Array NEE2-1 – Global 2-D Solution (plane Rayleigh wave - approximates fundamental mode)

Depth to Top of Layer (m)	Layer Thickness (m)	S-Wave Velocity (m/s)	Inferred P-Wave Velocity (m/s)	Assumed Poisson's Ratio	Assumed Density (g/cm^3)
0	1.25	199	373	0.3	1.80
1.25	1.75	299	559	0.3	1.85
3	3	337	630	0.3	1.90
6	4	351	656	0.3	1.90
10	6	432	808	0.3	1.90
16	8	450	843	0.3	2.00
24	12	517	966	0.3	2.00
36	>4	605	1131	0.3	2.10

Notes: 1) Depth of investigation is about 40 m.
2) Bottom layer is a half space.

V_S Model – SASW Array NEE2-1 – Global 3-D Solution (includes effects of body waves and higher modes – effective mode)

Depth to Top of Layer (m)	Layer Thickness (m)	S-Wave Velocity (m/s)	Inferred P-Wave Velocity (m/s)	Assumed Poisson's Ratio	Assumed Density (g/cm^3)
0	1.25	198	371	0.3	1.80
1.25	1.75	289	540	0.3	1.85
3	3	334	625	0.3	1.90
6	4	348	652	0.3	1.90
10	6	428	800	0.3	1.90
16	8	446	835	0.3	2.00
24	12	502	939	0.3	2.00
36	>4	588	1101	0.3	2.10

Notes: 1) Depth of investigation is about 40 m.
2) Bottom layer is a half space.

Observations/Discussion:

- After initial HVSR measurements were made and reviewed, HVSR sensor 453 was moved about 1 m and all measurements repeated for a short duration.
- HVSR plots are similar at all measurement locations below a frequency of about 10 Hz, validating the 1-D velocity structure assumption.
- There is a distinct HVSR peak in the 1.3 to 1.5 Hz range, which indicates that there is a significant increase in S-wave velocity, possibly associated with bedrock, at a depth on the order of 100 m. There is also a weak HVSR peak at about 5 Hz, which is likely due to a geologic structure at a depth of less than 30 m.
- Based on simple horizontal layer-based analysis of seismic refraction first arrival data, P-wave velocity in the upper 30 m ranges from about 475 to over 1,700 m/s (475 to 500 m/s at surface, 600 to 675 m/s at about 1.5 to 2.5 m, 700 to 800 m/s at about 5 to 8 m, 900 to 1,000 m/s at about 14 to 16 m and 1,500 to 1,700 m/s at about 30 to 35 m). The P-wave velocity of 1,500 to 1,700 m/s may be associated with saturated sediments.
- Noise conditions at site were not sufficient to apply passive surface wave techniques.
- Initial geophysical testing at this site consisted of MASW and SASW data acquisition along array NEE2-1. After reviewing the data it appeared that the surface wave dispersion curves at wavelengths near about 50 m were quite complex. Therefore, two additional SASW arrays (NEE2-3 and NEE2-4) were acquired near each end of MASW array NEE2-1 and MASW data were acquired along the longer array NEE2-2. Similar difficulties extracting surface wave dispersion data at wavelengths of about 50 m occurred on all of the SASW data sets. MASW dispersion data also had artifacts at similar wavelengths.
- Surface wave dispersion data from SASW and MASW data sets are in good agreement at the site, especially considering that the respective data sets are sampling different areas. The dispersion data for the two MASW arrays diverge at wavelengths greater than about 50 m and the dispersion curve for array NEE2-1 is complicated at wavelengths between 40 and 60 m. It was also very difficult to reduce SASW dispersion data associated with wavelengths near 50 m. There may be a geologic structure (e.g. velocity inversion) at a depth on the order of 25 to 30 m that complicates the MASW and SASW dispersion curves at long wavelengths, but is too thin to resolve. Separate models are generated for the combined MASW arrays and SASW array NEE2-1.
- It is possible that the velocity structure giving rise to the low amplitude HVSR peak at 5 Hz is in some way associated with the complex MASW and SASW dispersion curves at long wavelengths.
- The minimum wavelength surface wave phase velocity data extracted from the 48-channel 70.5 and 141 m long MASW arrays is about 7 and 8 m, respectively. Data reduction using seismic records from smaller hammer sources and/or a limited offset receiver array (i.e. less active geophones) allowed extraction of surface wave dispersion data to a minimum wavelength of about 1.5 and 5.5 m, respectively.
- There is nominally about 20 to 60 m/s scatter in MASW and SASW dispersion data likely due to the effects of lateral velocity variation.
- Representative dispersion curves were generated for each MASW data set using a moving average, polynomial curve fitting routine. These individual representative dispersion curves were combined and a representative dispersion curve generated for the

combined data set for data modeling. Similarly, for the purpose of modeling, a representative curve was generated for the dispersion data from SASW array NEE2-1.

- The potential saturated zone at about 30 to 35 m depth was not constrained for surface wave modeling as it will not significantly impact the resulting V_S models.
- Both MASW and SASW dispersion curves were modeled using the 2-D solution in the WinSASW software package, which uses the dynamic stiffness matrix for the forward solution. The 2-D solution assumes a plane Rayleigh wave and does not consider body waves and approximates the fundamental mode solution. The SASW dispersion data were also modeled using the 3-D global solution assuming that the receivers were located 2 and 4 wavelengths from the source. The 3-D global solution incorporates body waves and higher modes, modeling the effective dispersion curve. Individual SASW receiver pairs can be modeled separately with actual source-receiver geometry using the 3-D array solution, but was not conducted with this data set. The 3-D solution is most valuable when velocity structure is complex and dominant higher modes and/or modal superposition occurs. At this site, velocity appears to gradually increase with depth and there is very little difference between the 2-D and 3-D solutions.
- Surface wave depth of investigation is about 40 m based on half of maximum wavelength criteria.
- The surface wave models are relatively consistent with simplified P-wave refraction model, especially considering unknown Poisson's ratio.
- V_{S30} is 405 m/s for the combined MASW arrays NEE2-1 and NEE2-2 (Site Class C).
- Average S-wave velocity between 2 m (assumed sensor depth) and 32 m is 430 m/s for the combined MASW arrays.
- V_{S30} for SASW array NEE2-1 is 396 and 391 m/s for the 2-D and 3-D solutions, respectively (Site Class C).
- Average S-wave velocity between 2 m (assumed sensor depth) and 32 m for SASW array NEE2-1 is 424 and 418 m/s for the 2-D and 3-D solutions, respectively.
- Average V_{S30} for the MASW and SASW arrays (2-D solution) is 401 m/s (Site Class C).
- Average S-wave velocity between 2 m (assumed sensor depth) and 32 m is 427 m/s for the MASW and SASW arrays (2-D solution).
- This would be an excellent site to validate surface wave models versus a borehole velocity log, primarily because there could be complicated velocity structure (e.g. thin velocity inversion) at a depth on the order of 30 m that cannot be resolved with the surface wave data. Although velocity structure may be complicated at depth, V_{S30} is expected to be accurately resolved.

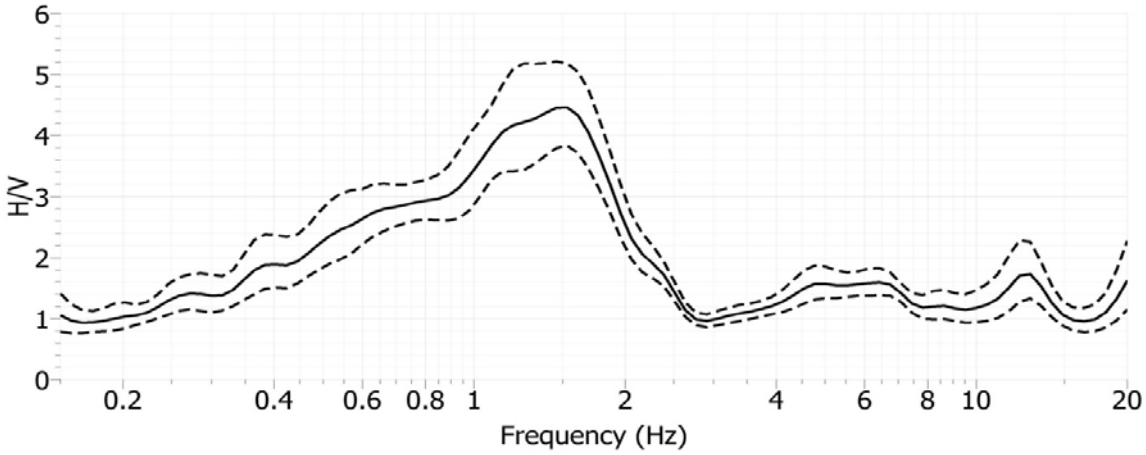

Site CI.NEE2, H/V Spectral Ratio, Array NEE2-1, Sensor 450

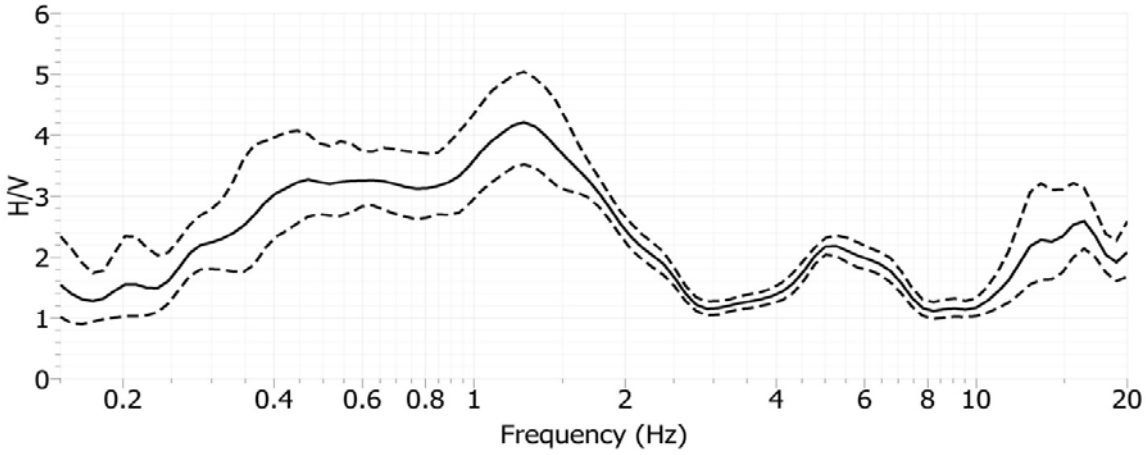

Site CI.NEE2, H/V Spectral Ratio, Array NEE2-1, Sensor 453

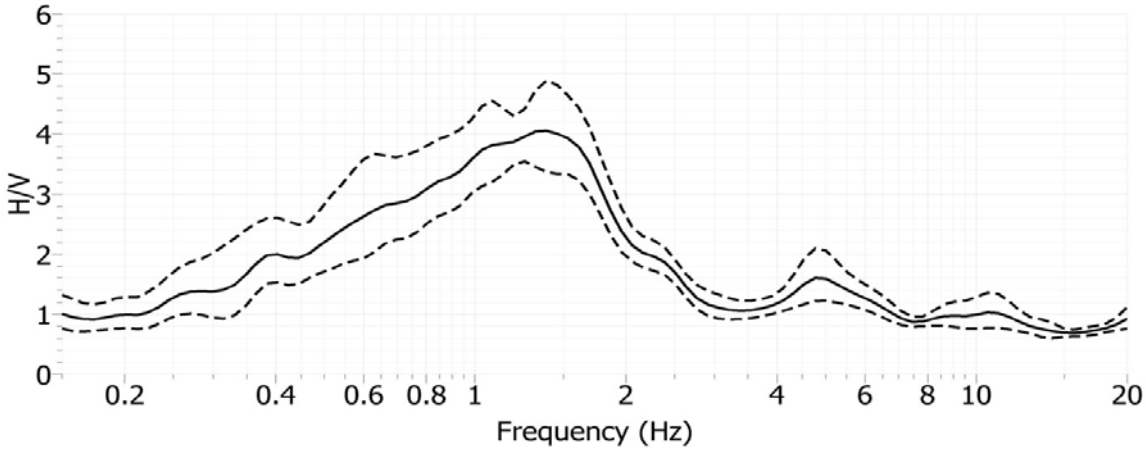

Site CI.NEE2, H/V Spectral Ratio, Array NEE2-1, Sensor 507

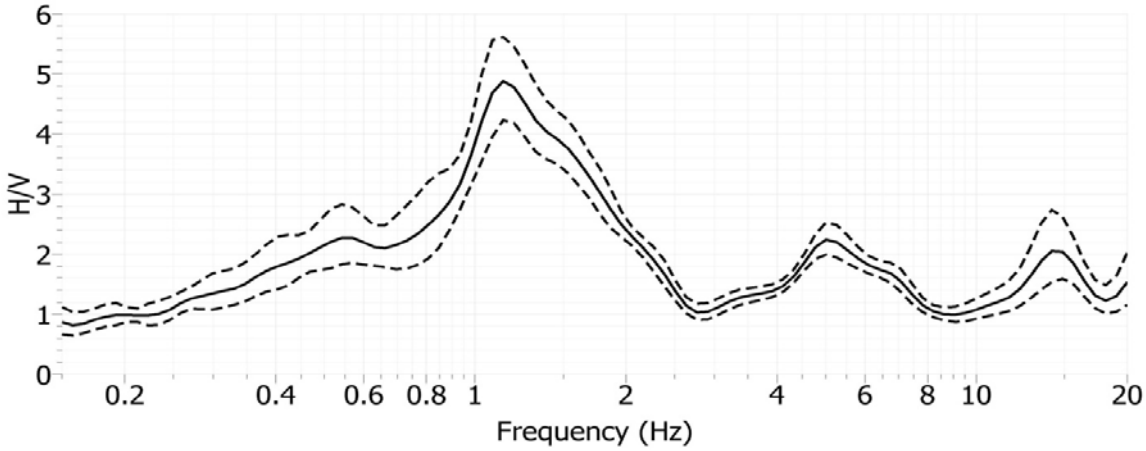

Site CI.NEE2, H/V Spectral Ratio, Array NEE2-1, Sensor 450 (repeat)

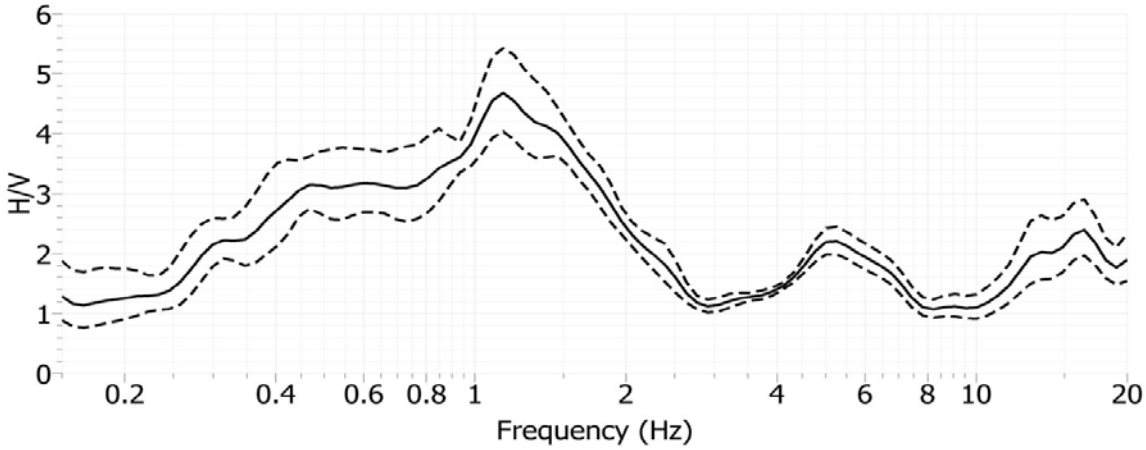

Site CI.NEE2, H/V Spectral Ratio, Array NEE2-1, Sensor 453 (repeat)

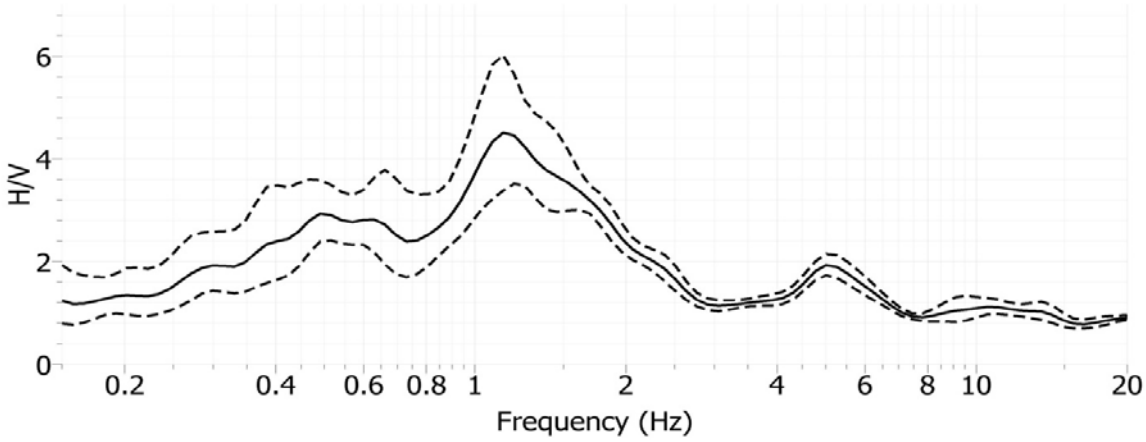

Site CI.NEE2, H/V Spectral Ratio, Array NEE2-1, Sensor 507 (repeat)

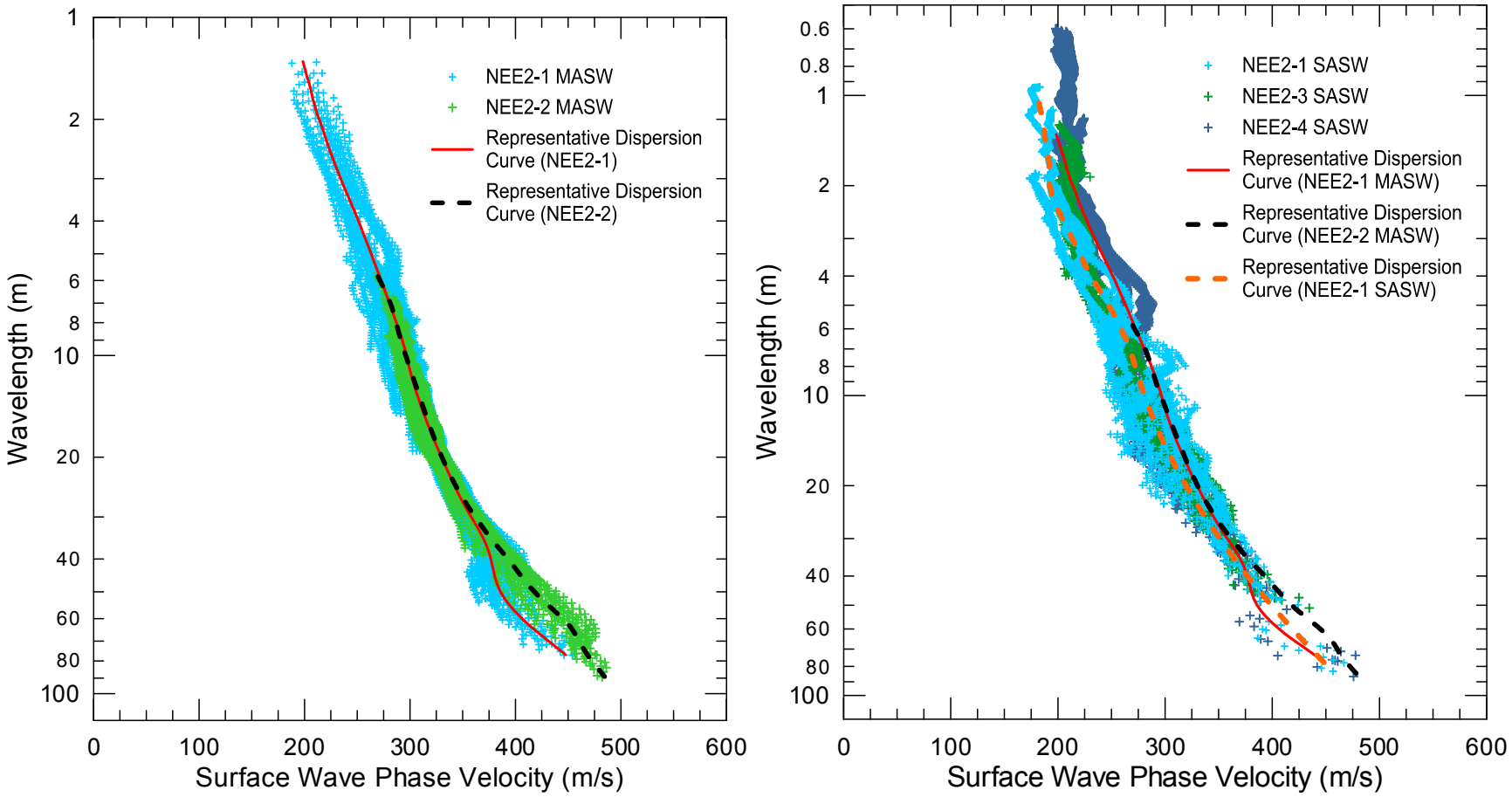

CI.NEE2 – Comparison of surface wave dispersion curves from MASW arrays NEE2-1 and NEE2-2 (left) and SASW dispersion data from arrays NEE2-1, NEE2-3 and NEE2-4 (right). The dispersion data for the two MASW arrays diverge at wavelengths greater than about 50 m. It was also very difficult to reduce SASW dispersion data associated with wavelengths near 50 m. There may be a geologic structure (e.g. velocity inversion) at a depth on the order of 25 to 30 m that complicates the MASW and SASW dispersion curves at long wavelengths, but is too thin to resolve. Separate models are generated for the combined MASW arrays and SASW array NEE2-1.

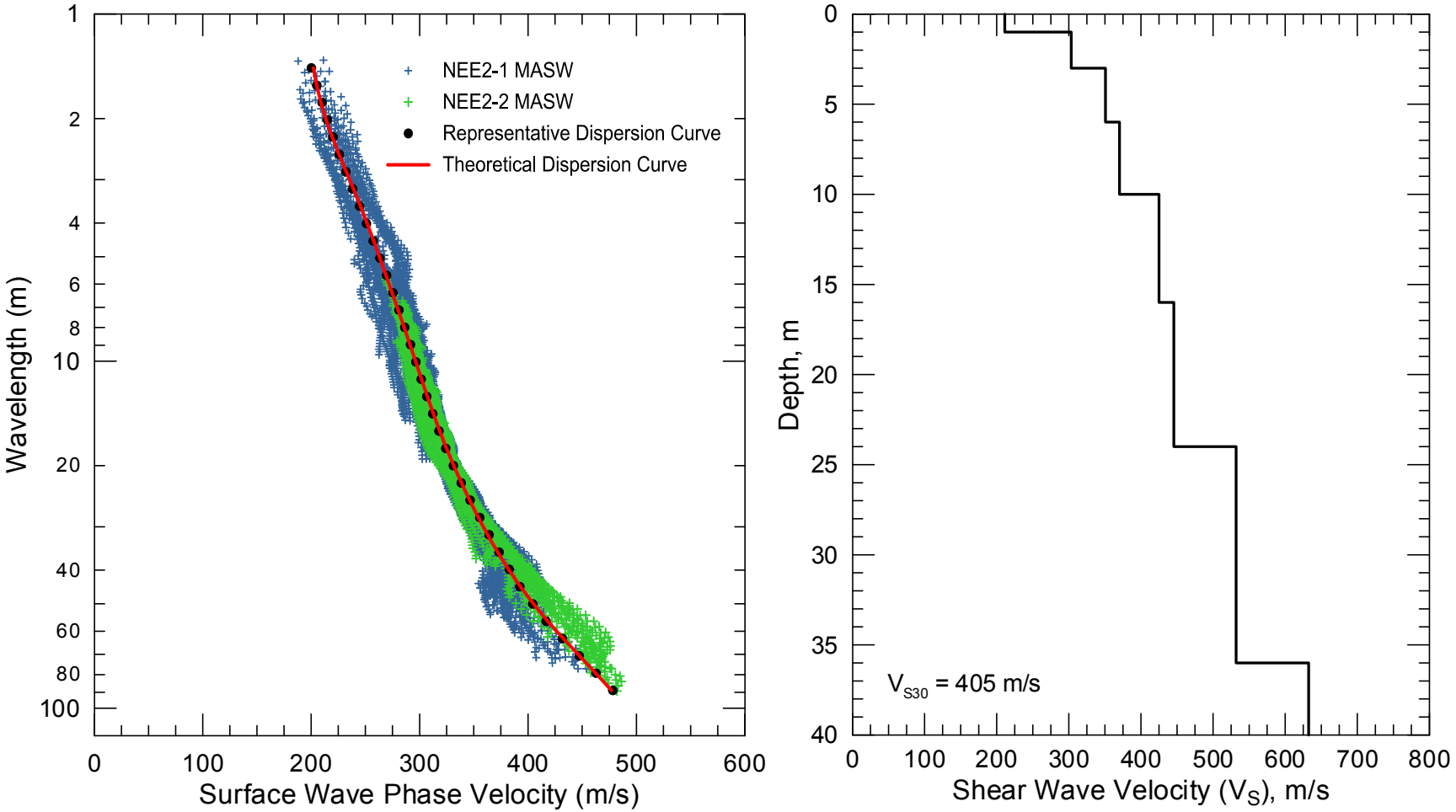

CI.NEE2 - Field, representative and inverted theoretical surface wave dispersion data (left) and associated V_S model (right) for combined MASW arrays NEE2-1 and NEE2-2

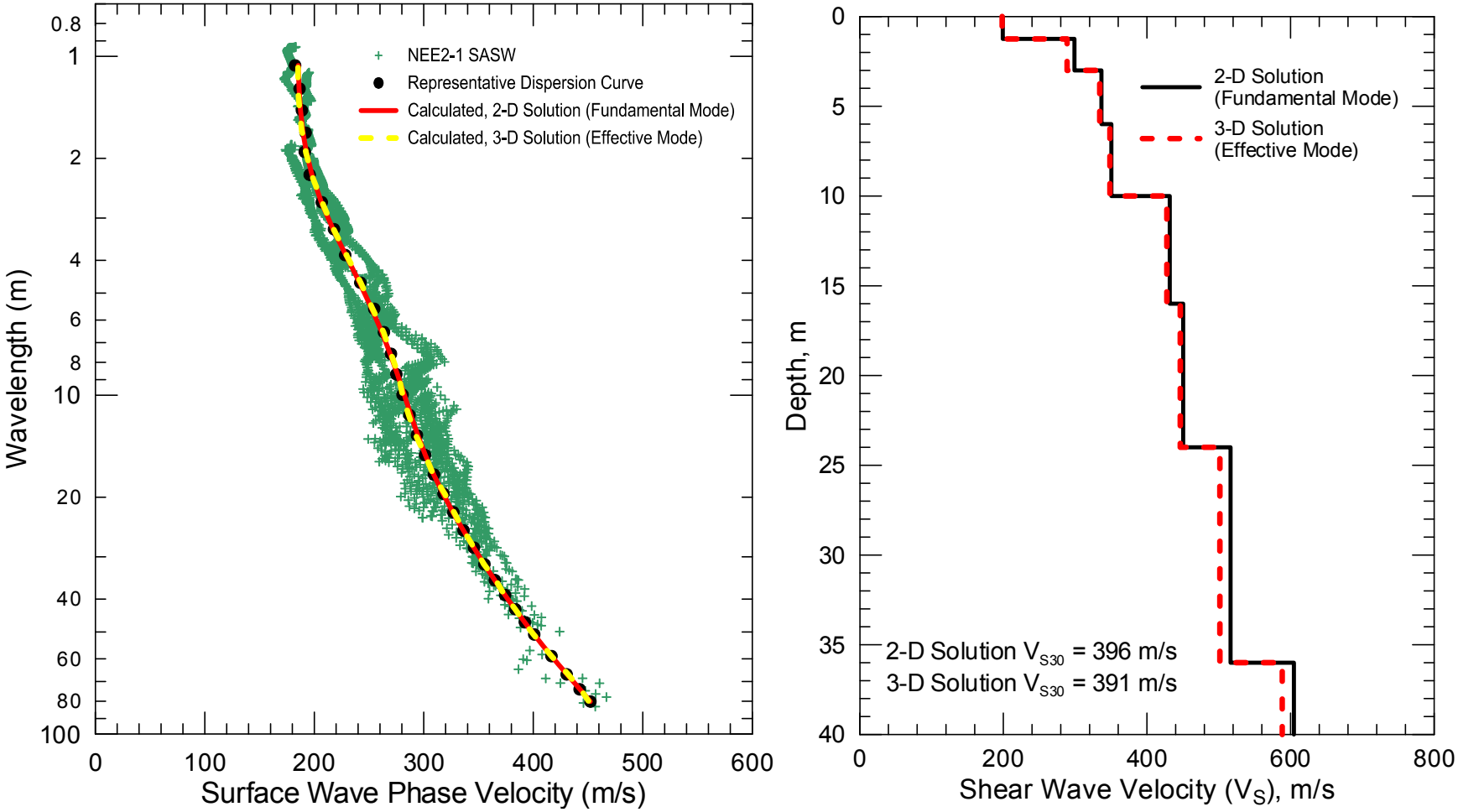

CI.NEE2 - Field, representative and inverted theoretical surface wave dispersion data (left) and associated V_S model (right) for SASW array NEE2-1

Site CI.NJQ

Location: Nojoqui Falls County Park, Alisal Road East, Goleta, California

Latitude: 34.53412 **Longitude:** -120.17737
(Station coordinates provided by USGS, WGS84 coordinate system)

V_{S30} (measured): 297 m/s

V_{S30} (adjusted to more accurately reflect seismic station conditions): 314 m/s (average S-wave velocity between 2 and 32 m adjusting for nominal sensor depth).

NEHRP Site Class: D

Geomatrix Code: IHD

Geologic Conditions/Observations: Quaternary (Holocene) alluvium overlying Tertiary and Cretaceous sandstone and shale units. Tertiary geologic units outcrop as close as 150 m to seismic station. The Santa Ynez fault is located about 300 m south of the site.

Site Conditions: Rural site with sporadic noise from traffic in site vicinity. Relatively flat terrain in test area with hills located about 200 m to south and north.

Geophysical Methods Utilized: HVSR, MASW, SASW

Geophysical Testing Arrays:

1. Array NJQ-1 (48 channel MASW array utilizing 4.5 Hz vertical geophones spaced 1.5 m apart for a length of 70.5 m, forward and reverse shot locations with multiple source offsets and source types and center shot location).
2. Array NJQ-1 (SASW array centered at the midpoint of and aligned along the MASW array with the same name. SASW data acquired using 4.5 and 1 Hz geophones, common center point and forward and reversed shot locations).
3. Three HVSR measurement locations; two distributed along NJQ-1 and one near the seismic station.

Legend

- Seismic Station - Approximate Surveyed Location
- Seismic Station - Approximate Location of Record
- H/V Spectral Ratio Location
- SASW Array
- MASW Array

NOTES:
1. WGS 1984 COORDINATE SYSTEM
2. Image Source: ESRI, i-cubed, USDA FSA, USGS, AEX, GeoEye, Getmapping, Aerogrid, IGP

File Name: CI-NJQ-I

Date: 8/19/2011

USGS science for a changing world

GEOVision geophysical services

RECOVERY.GOV

SITE MAP
CI•NJQ

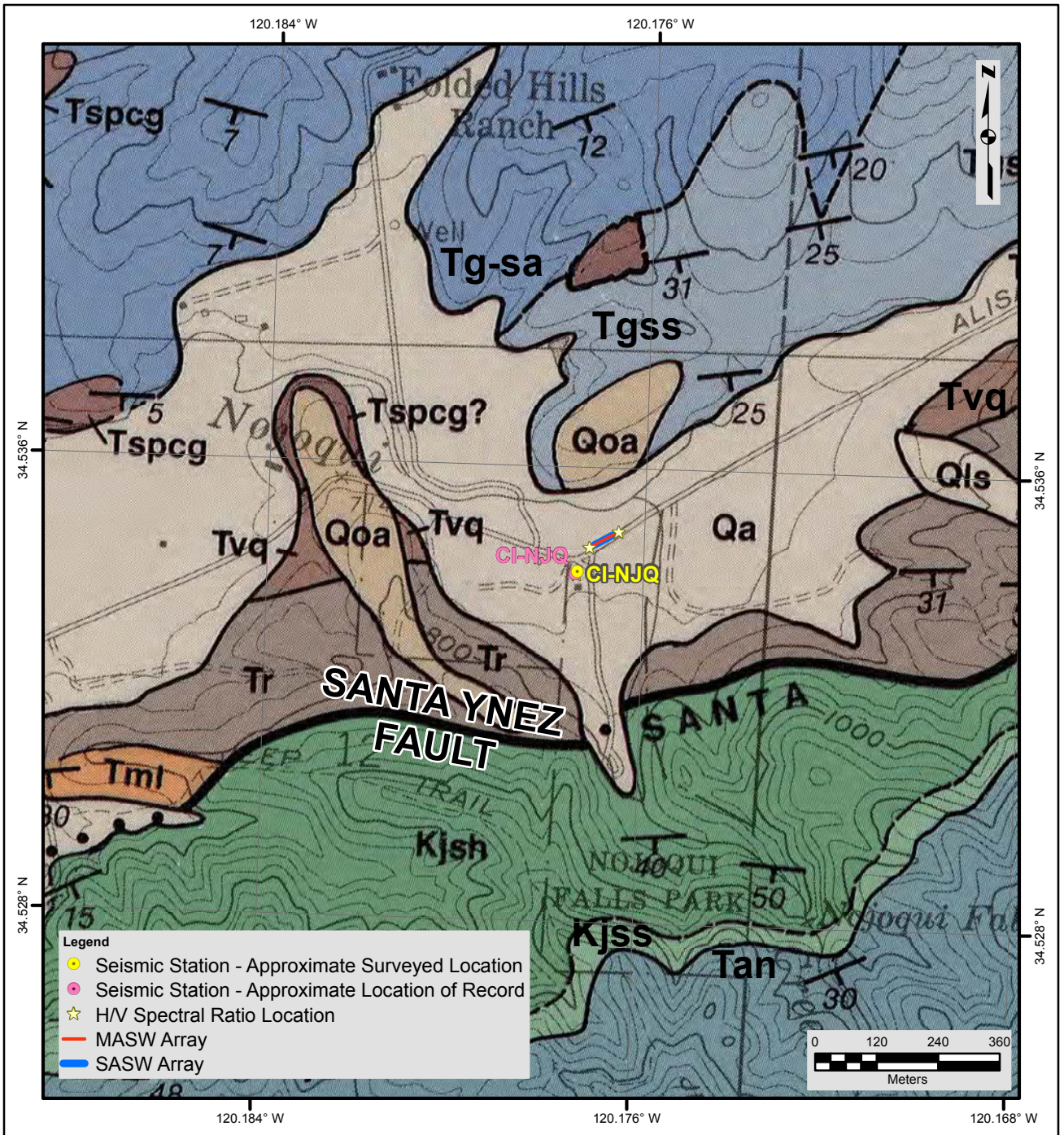

Description of Geologic Map Units

Qa = Quaternary (Holocene) valley and floodplain deposits of silt, sand and gravel
Qls = Quaternary (Holocene) landslide debris
Qoa = Quaternary (Pleistocene) undivided former terrace remnants
Tml = Tertiary (Miocene) Monterey Shale; lower unit, soft, punky, fissile to platy, semi-siliceous; Luisian-Relizian Stages
Tvq = Tertiary (Miocene) Vaqueros Sandstone and interbedded siltstone, calcareous lenses
Tspcg = Tertiary (Oligocene) Sespe Formation; conglomerate of mostly Franciscan and ultramatic detritus
Tgss = Tertiary (Oligocene) Gaviota Formation; hard, thick bedded arkosic sandstone
Tg-sa = Tertiary (Eocene to Oligocene) Gaviota-Sacate Formations; undifferentiated (clay shale and siltstone with arkosic sandstone, or conglomerate)
Tan = Tertiary (Eocene) Anita shale, micaceous clay shale
Kjss = Mesozoic (Upper Cretaceous) Jalama Formation; hard arkosic sandstone with thin shale partings
Kijsh =Mesozoic (Upper Cretaceous) Jalama Formation; hard but fractured micaceous shale, thin interbeds of sandstone, conglomerate and carbonates

NOTES:
1. WGS 1984 COORDINATE SYSTEM
2. Geologic Map of the Solvang and Gaviota Quadrangles, Santa Barbara County, California by Thomas W. Dibblee, Jr., 1988
3. See site map for details of geophysical survey

USGS science for a changing world
GEOVision geophysical services

GEOLOGIC MAP
CI•NJQ

File Name: CI-NJQ
Date: 8/19/2011

Looking east towards seismic station and HVSR sensor 507

Looking northeast along MASW array NJQ-1

Looking southwest along MASW array NJQ-1

Looking southwest along SASW array NJQ-1

Testing along SASW array NJQ-1

Location of Geophysical Testing Arrays:

Location	Latitude	Longitude
NJQ-1, Southwest end of MASW Array	34.53457	-120.17713
NJQ-1, Center of MASW and SASW Arrays	34.53473	-120.17679
NJQ-1, Northeast end of MASW Array	34.53489	-120.17646
HVSR Sensor 450	34.53488	-120.17647
HVSR Sensor 453	34.53459	-120.17707
HVSR Sensor 507	34.53411	-120.17734
CI.NJQ Seismic Station	34.53416	-120.17732

Notes: 1) WGS84 Coordinate System (decimal degrees)

2) Survey accuracy is estimated at 3 to 4 m, GPS signal blocked by trees in some areas

Results:

V_S Model – SASW Array NJQ-1

Depth to Top of Layer (m)	Layer Thickness (m)	S-Wave Velocity (m/s)	Inferred P-Wave Velocity (m/s)	Inferred Poisson's Ratio	Inferred Density (g/cm^3)
0	0.5	234	438	0.300	1.9
0.5	1	193	362	0.300	1.9
1.5	4.5	227	424	0.300	1.9
6	5	262	1600	0.486	2.0
11	7	306	1700	0.483	2.0
18	10	359	1800	0.479	2.0
28	>2	427	1800	0.470	2.0

V_S Model – MASW Array NJQ-1 – Model 1

Depth to Top of Layer (m)	Layer Thickness (m)	S-Wave Velocity (m/s)	Inferred P-Wave Velocity (m/s)	Inferred Poisson's Ratio	Inferred Density (g/cm^3)
0	1	225	421	0.300	1.9
1	2	211	395	0.300	1.9
3	3	227	425	0.300	1.9
6	5	290	1600	0.483	2.0
11	7	293	1700	0.485	2.0
18	10	362	1800	0.479	2.0
28	>2	462	1800	0.465	2.0

V_S Model – MASW Array NJQ-1 – Model 2

Depth to Top of Layer (m)	Layer Thickness (m)	S-Wave Velocity (m/s)	Inferred P-Wave Velocity (m/s)	Inferred Poisson's Ratio	Inferred Density (g/cm^3)
0	1	172	322	0.300	1.9
1	2	202	378	0.300	1.9
3	3	248	464	0.300	1.9
6	10	290	1600	0.483	2.0
16	12	349	1700	0.478	2.0
28	>2	466	1800	0.464	2.0

Observations/Discussion:

- The HVSR curves are very similar at frequencies below 20 Hz, although a trough in the 4 to 6 Hz range is slightly variable.
- There are no significant HVSR peaks at the site.
- Noise conditions at site were not sufficient to apply passive surface wave techniques.
- The water table is located at a depth on the order of about 6 m based on interactive layer-based analysis of seismic refraction first arrival data. P-wave velocities of about 350 and 1,800 m/s were modeled for unsaturated and saturated sediments, respectively.
- There is good reflectivity in the MASW seismic records with several possible reflectors in about the 30 to 125 m depth range. Subsurface geologic structure does not consist of horizontal layers due to reflector differences on forward and reverse shot records.
- Near surface lateral velocity variation was observed in the MASW data based on differing phase velocities at high frequencies (small wavelengths) from offset limited processing of small hammer source seismic records collected at each end of the array.
- Due to lateral velocity variation at the site, a moving average, polynomial curve fitting routine was used to generate separate representative dispersion curves for the SASW and MASW data. Two representative dispersion curves were generated for the MASW data, one with high frequency dispersion data from forward shot locations (Model 1) and the other with high frequency dispersion data from the reverse shot location and selected offset ranges from the center shot location (Model 2).
- Surface wave dispersion data from SASW data set and Model 1 MASW data set are in good agreement; however, each data set was modeled separately.
- Separate S-wave velocity versus depth models were developed for each representative dispersion curve.
- During surface wave modeling, the water table was constrained at a depth of 6m, based on seismic refraction data, and P-wave velocity of the saturated zone was assumed to increase with depth from 1,600 to 1,800 m/s.

- Due to lateral velocity variation observed in the MASW data as discussed above, three S-wave velocity models were generated, one for the SASW data and two for the MASW data. With the exception of the surface layer, the S-wave velocity of the layers in the three models vary by less than 10% and V_{S30} is almost identical.
- Surface wave depth of investigation is about 30 m based on half of maximum wavelength criteria.
- V_{S30} for SASW array NJQ-1 is 295 m/s and V_{S30} for MASW array NJQ-1 Models 1 and 2 is 299 and 297 m/s, respectively. The similarity of V_{S30} between the three models demonstrates the robustness of this parameter.
- V_{S30} averages 297 m/s (Site Class D).
- Average S-wave velocity between 2 m (nominal sensor depth) and 32 m is 310 m/s for SASW array NJQ-1, 314 m/s for MASW array NJQ-1 Model 1 and 318 m/s for MASW array NJQ-1 Model 2 and averages 314 m/s.

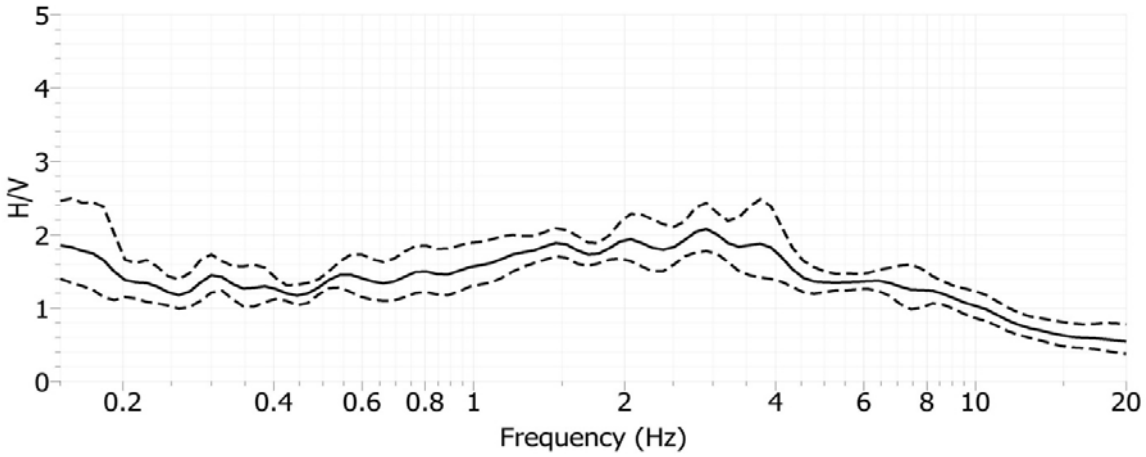

Site CI.NJQ, H/V Spectral Ratio, Array NJQ-1, Sensor 450

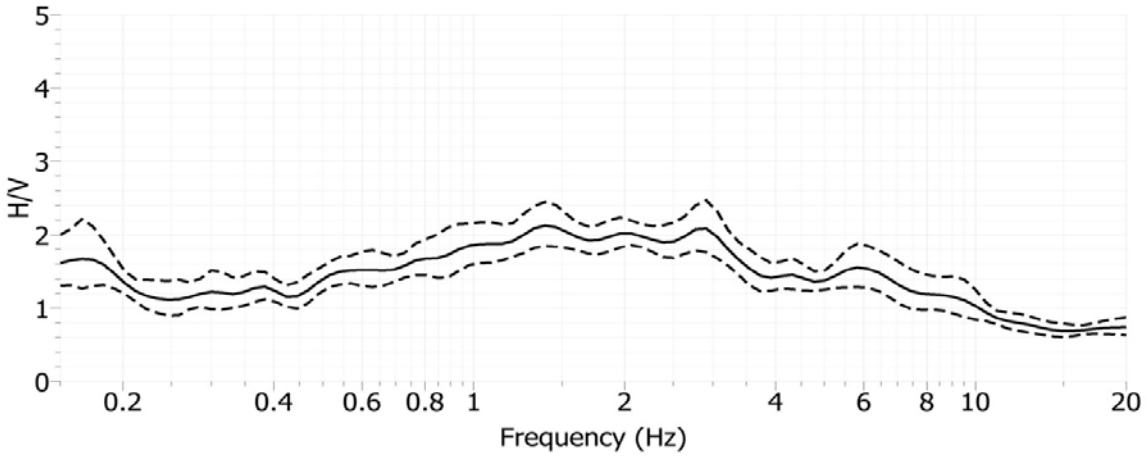

Site CI.NJQ, H/V Spectral Ratio, Array NJQ-1, Sensor 453

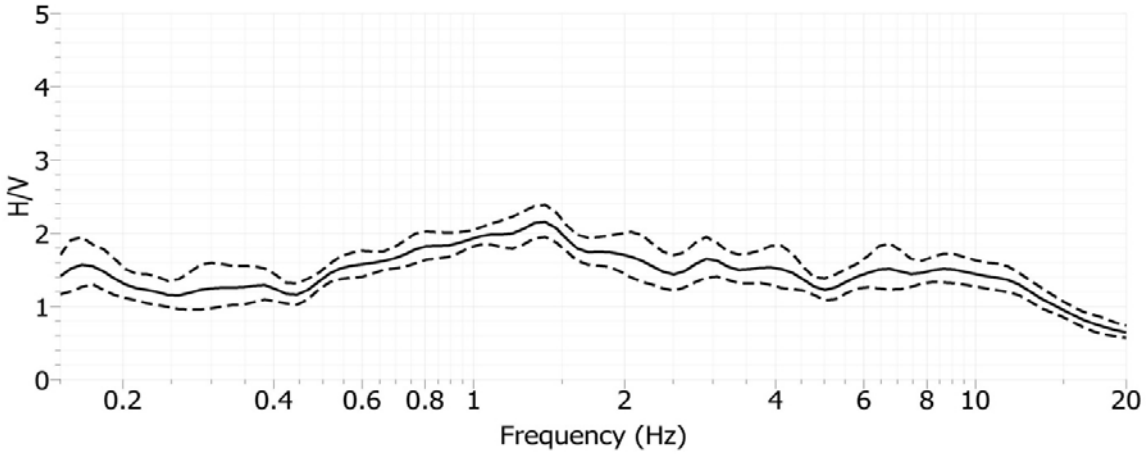

Site CI.NJQ, H/V Spectral Ratio, Near Seismic Station, Sensor 507

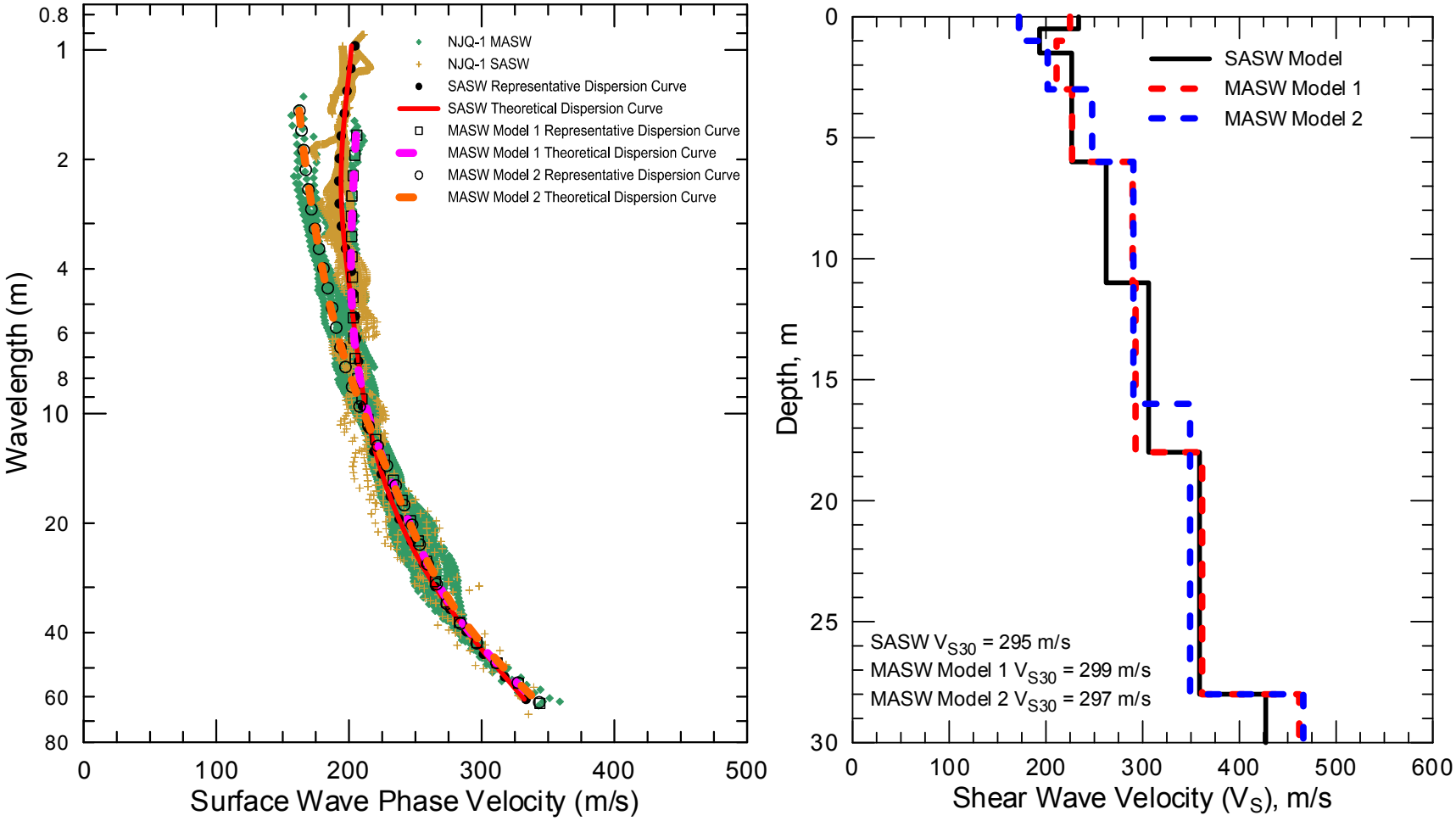

CI.NJQ - Field, representative and inverted theoretical surface wave dispersion data (left) and associated V_S model (right)

Site CI.NSS2

Location: North Shore Salton Sea 2, near Mecca, California

Latitude: 33.55553 **Longitude:** -115.94586

(Station coordinates provided by USGS, WGS84 coordinate system)

V_{S30} (measured): 352 m/s

V_{S30} (adjusted to more accurately reflect seismic station conditions): 377 m/s (average S-wave velocity between 2 and 32 m adjusting for nominal sensor depth).

NEHRP Site Class: D/C

Geomatrix Code: IHD

Geologic Conditions/Observations: Site located on geologic unit mapped as Quaternary (Holocene) alluvium. Tertiary Palm Spring Formation is mapped about 400 m northeast of site. Probable deep soil site.

Site Conditions: Rural site. Relatively flat terrain in site vicinity with ground surface elevation gently decreasing to southwest.

Geophysical Methods Utilized: HVSR, MASW, SASW

Geophysical Testing Arrays:

1. Array NSS2-1 (48 channel MASW array utilizing 4.5 Hz vertical geophones spaced 1.5 m apart for a length of 70.5 m, forward and reverse shot locations with multiple source offsets and source types and center shot location).
2. Array NSS2-1 (SASW array with common midpoint and orientation as MASW array of same name utilizing 4.5 and 1 Hz vertical geophones and maximum receiver spacing of 32 m).
3. Three HVSR measurement locations; two distributed along array NSS2-1 and one located near seismograph station.

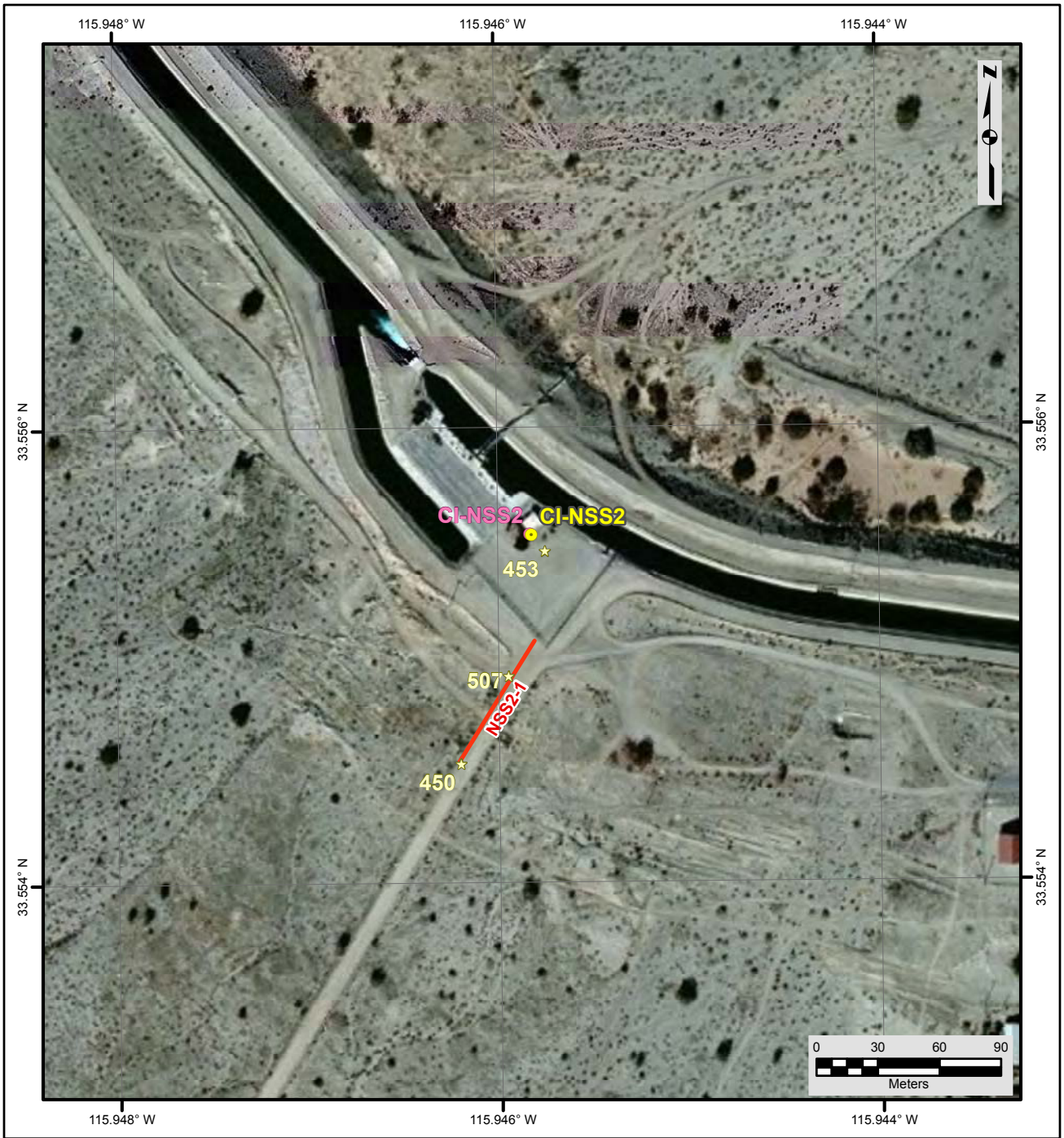

Legend

- Seismic Station - Approximate Surveyed Location
- Seismic Station - Approximate Location of Record
- H/V Spectral Ratio Measurement Location
- MASW Array

NOTES:
1. WGS 1984 COORDINATE SYSTEM
2. Image Source: ESRI, i-cubed, USDA FSA, USGS, AEX, GeoEye, Getmapping, Aerogrid, IGP

File Name: CI-NSS2-I

Date: 4/15/2011

USGS science for a changing world

GEOVision geophysical services

RECOVERY.GOV

SITE MAP
CI•NSS2

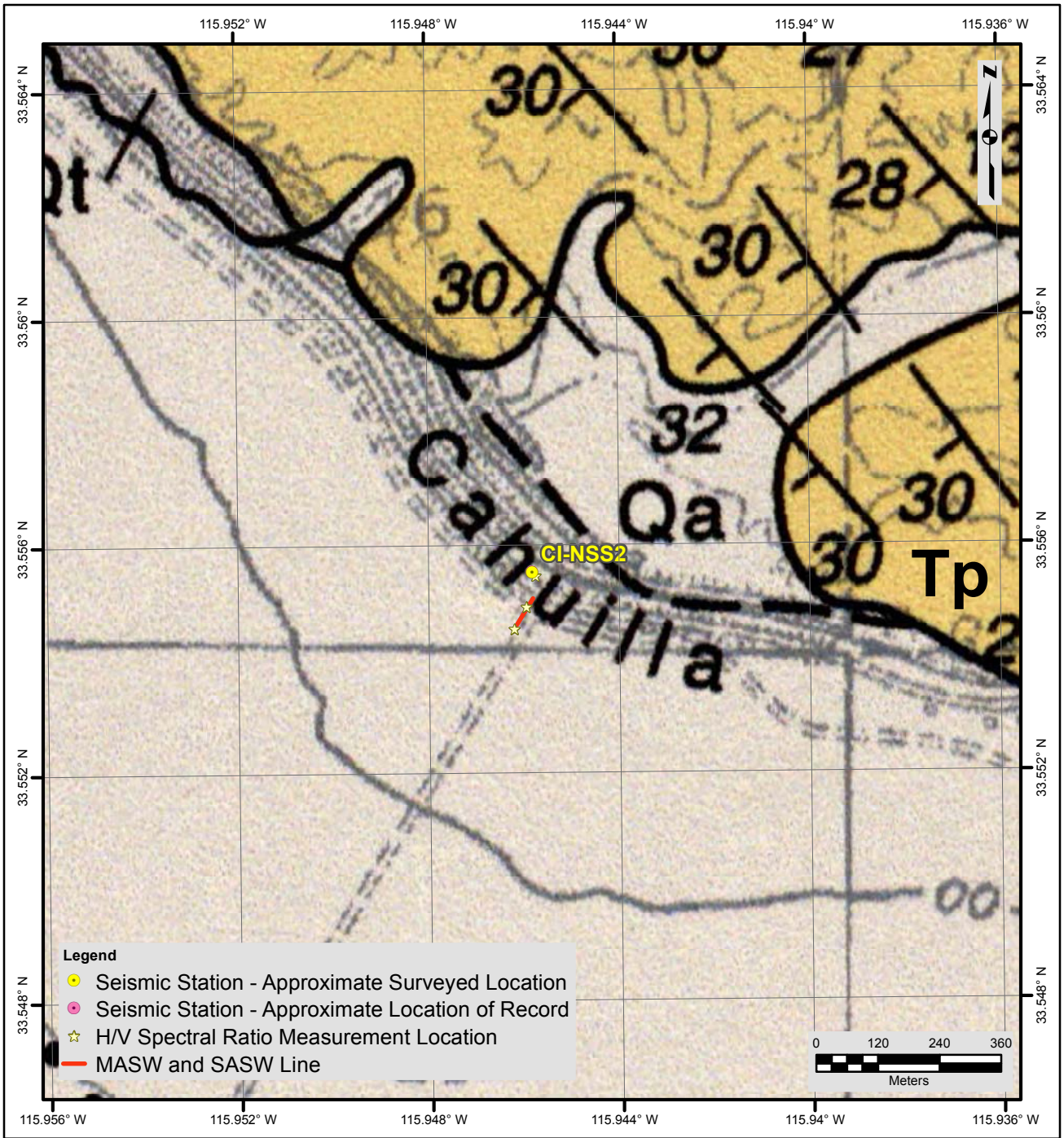

Description of Geologic Map Units

Qa = Quaternary (Holocene) alluvial sand, gravel, silt and clay of valley areas
Tp = Tertiary (Pliocene) Palm Spring Formation, laminated sandstones, arkosic, locally pebbly, interbedded red clays, weakly to moderately indurated

NOTES:
1. WGS 1984 COORDINATE SYSTEM
2. Geologic Map of the Cottonwood Spring & Canyon Spring 15 Minute Quadrangles, Riverside County, California by Thomas W. Dibblee, Jr., 2008
3. See site map for details of geophysical survey

File Name: CI-NSS2

Date: 7/21/2011

USGS science for a changing world

GEOVision geophysical services

RECOVERY.GOV

GEOLOGIC MAP
CI•NSS2

Looking northwest at HVSR sensor 453 and seismograph station CI.NSS2.

MASW data acquisition

Looking southwest along SASW array NSS2-1

Cluster test conducted at HVSR sensor 450 location to evaluate different approaches of coupling sensors in gravelly soils

Looking northeast along MASW array NSS2-1

Location of Geophysical Testing Arrays:

Location	Latitude	Longitude
NSS2-1, Southwest End of MASW Array	33.55453	-115.94624
NSS2-1, Center of MASW and SASW Arrays	33.55479	-115.94604
NSS2-1, Northeast End of MASW Array	33.55506	-115.94584
HVSR Sensor 507	33.55491	-115.94598
HVSR Sensor 453	33.55545	-115.94578
HVSR Sensor 450	33.55452	-115.94623
CI.NSS2 Seismograph Station	33.55553	-115.94585

Notes: 1) WGS84 Coordinate System (decimal degrees)

2) Survey accuracy is estimated at 1 to 2 m.

Results:

V_S Model – Combined SASW and MASW Data

Depth to Top of Layer (m)	Layer Thickness (m)	S-Wave Velocity (m/s)	Inferred P-Wave Velocity (m/s)	Inferred Poisson's Ratio	Inferred Density (g/cm^3)
0	0.5	177	331	0.3	1.9
0.5	1	200	373	0.3	1.9
1.5	1.5	240	449	0.3	1.9
3	2.5	273	511	0.3	1.9
5.5	4	331	619	0.3	1.9
9.5	6	358	669	0.3	1.9
15.5	9	409	765	0.3	2.0
24.5	>5.5	490	916	0.3	2.0

V_S Model –SASW Data

Depth to Top of Layer (m)	Layer Thickness (m)	S-Wave Velocity (m/s)	Inferred P-Wave Velocity (m/s)	Inferred Poisson's Ratio	Inferred Density (g/cm^3)
0	0.5	178	334	0.3	1.9
0.5	1	193	360	0.3	1.9
1.5	1.5	236	441	0.3	1.9
3	2.5	268	501	0.3	1.9
5.5	4	335	627	0.3	1.9
9.5	6	351	656	0.3	1.9
15.5	9	430	804	0.3	2.0
24.5	>5.5	532	994	0.3	2.0

V_S Model –MASW Data

Depth to Top of Layer (m)	Layer Thickness (m)	S-Wave Velocity (m/s)	Inferred P-Wave Velocity (m/s)	Inferred Poisson's Ratio	Inferred Density (g/cm^3)
0	0.5	191	357	0.3	1.9
0.5	1	208	389	0.3	1.9
1.5	1.5	251	470	0.3	1.9
3	2.5	276	517	0.3	1.9
5.5	4	334	626	0.3	1.9
9.5	6	358	670	0.3	1.9
15.5	9	376	703	0.3	2.0
24.5	>5.5	472	884	0.3	2.0

Observations/Discussion:

- Loose gravelly soils at site making HVSR sensor coupling difficult. Additionally, water flow in nearby Coachella Canal is a potential noise source.
- Significant noise in HVSR data at frequencies below 0.15 Hz.
- There is no distinct high amplitude HVSR peak at frequencies about 0.15 Hz.
- Improving the HVSR sensor coupling by utilizing a deeper hole and, if necessary, plaster to couple the sensor to the ground may result in better HVSR results, particularly at low frequencies.
- Noise conditions at site were not sufficient to apply passive surface wave techniques.
- Surface wave dispersion data from SASW and MASW datasets are in acceptable agreement at the site, although there is 15 to 20 m/s difference between the dispersion curves from each data set, particularly at small and large wavelengths. Differences in the two data sets may result from lateral velocity variation.
- Representative dispersion curves were generated for each surface wave data set using a moving average, polynomial curve fitting routine. For purposes of data modeling, these individual representative dispersion curves were combined, with higher weight given to the SASW dispersion data, and a representative dispersion curve generated for the combined data set.
- Because of the slight differences in dispersion data at long wavelengths separate V_S models were developed for each data set for comparison with the V_S model from the combined data set.
- Water table located at a depth of greater than 30 m based on seismic refraction survey design and absence of a water table refractor. The water table may be about 40 m deep based on possible water table reflector.
- Based on simple layer-based analysis of seismic refraction first arrival data, P-wave velocity in the upper 20 m increases with depth from about 350 m/s near the surface to about 800 m/s at a depth of about 17 m. Inferred P-wave velocities in the surface wave models are consistent with the simplified P-wave refraction velocities.

- Surface wave depth of investigation is about 30 m based on half of maximum wavelength criteria.
- V_{S30} is 352 m/s (Site Class D/C) for the combined data set.
- V_{S30} from the separate SASW and MASW models is 357 and 346 m/s, respectively, about a 1.5% difference from the combined data set.
- Average S-wave velocity between 2 and 32 m is 377 m/s for the combined data set.
- Average S-wave velocity between 2 and 32 m for the separate SASW and MASW models is 386 and 368 m/s, respectively.

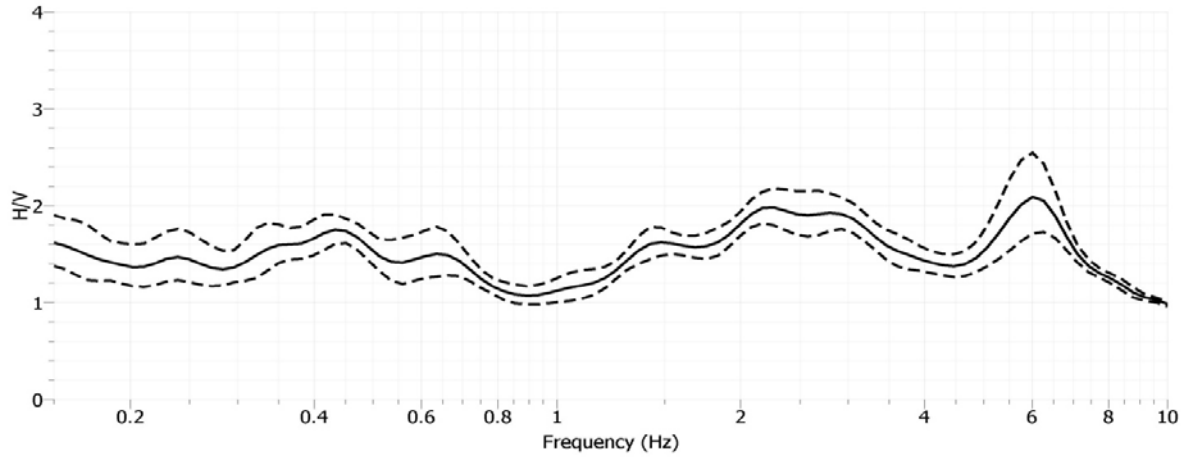

Site CI.NSS2, H/V Spectral Ratio, Near Seismic Station, Sensor 453

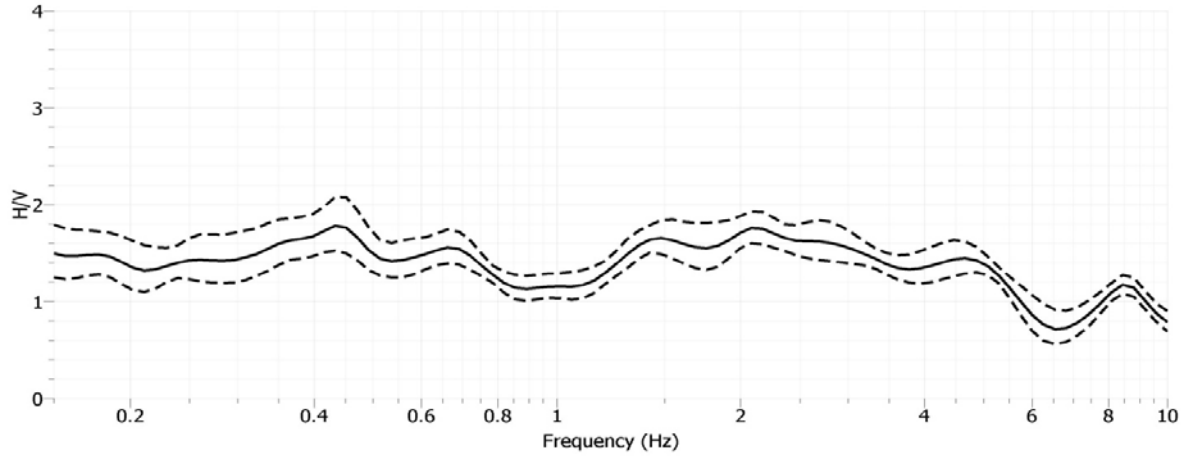

Site CI.NSS2, H/V Spectral Ratio, Array NSS2-1, Sensor 507

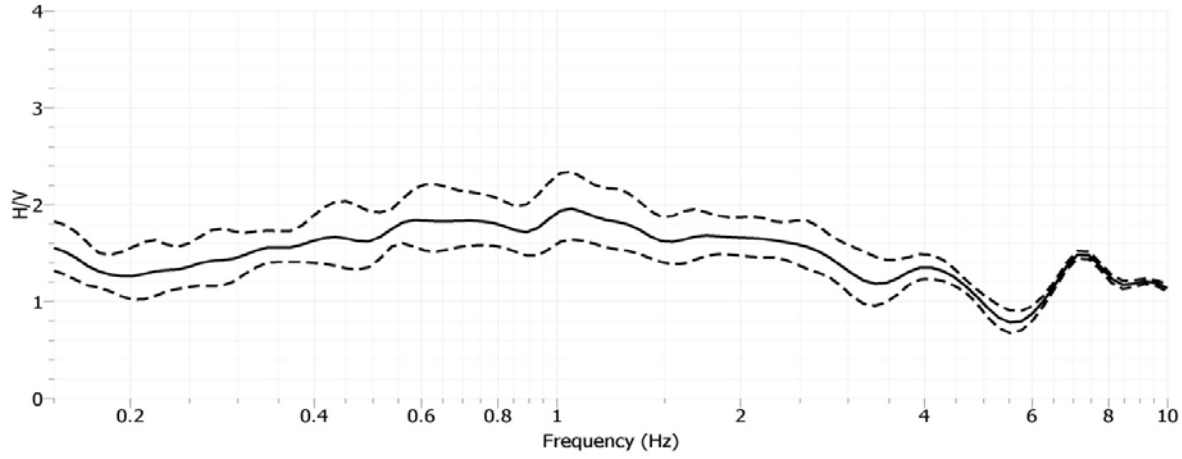

Site CI.NSS2, H/V Spectral Ratio, Array NSS2-1, Sensor 450

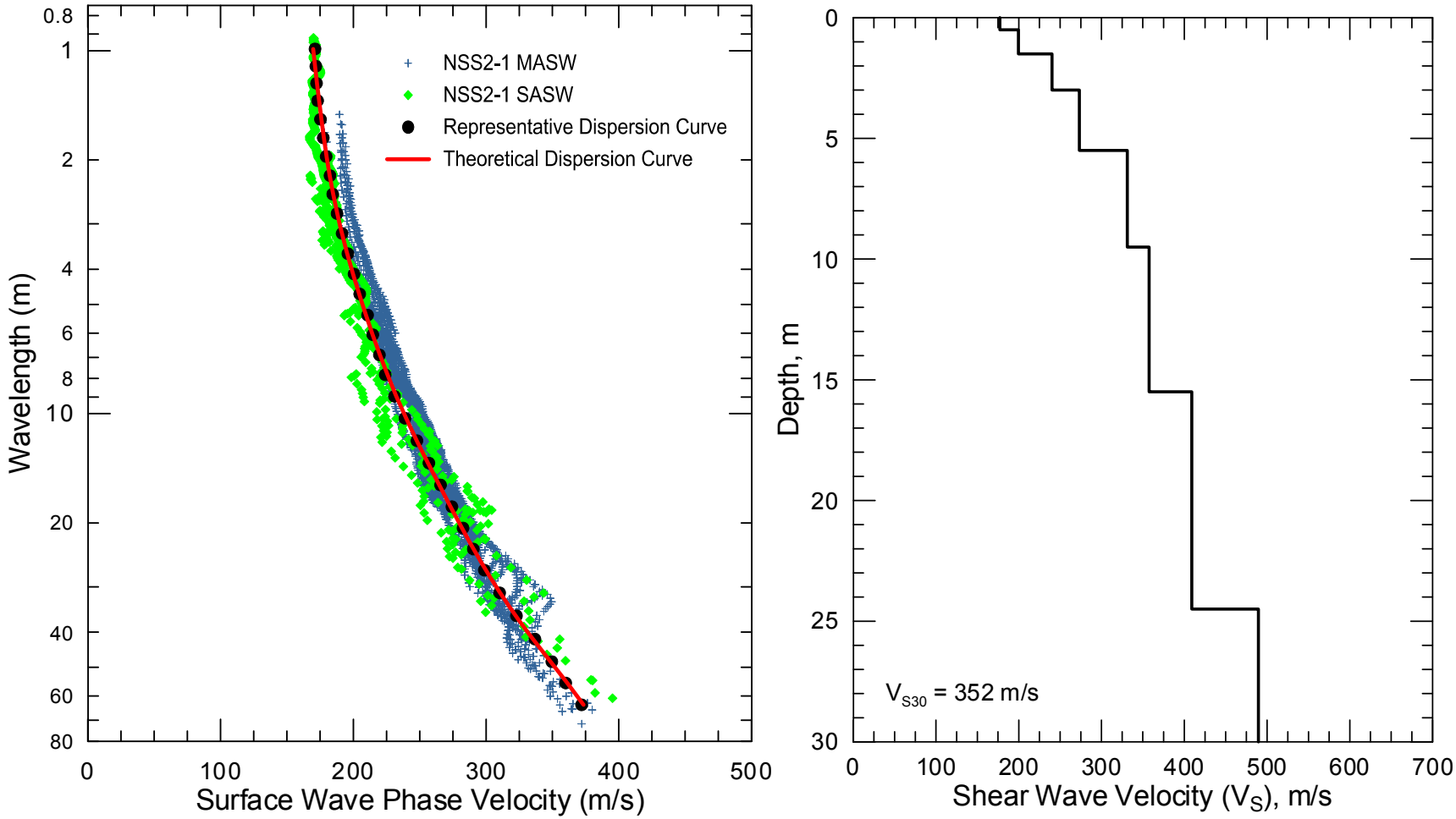

CI.NSS2 - Field, representative and inverted theoretical surface wave dispersion data (left) and associated V_S model (right)

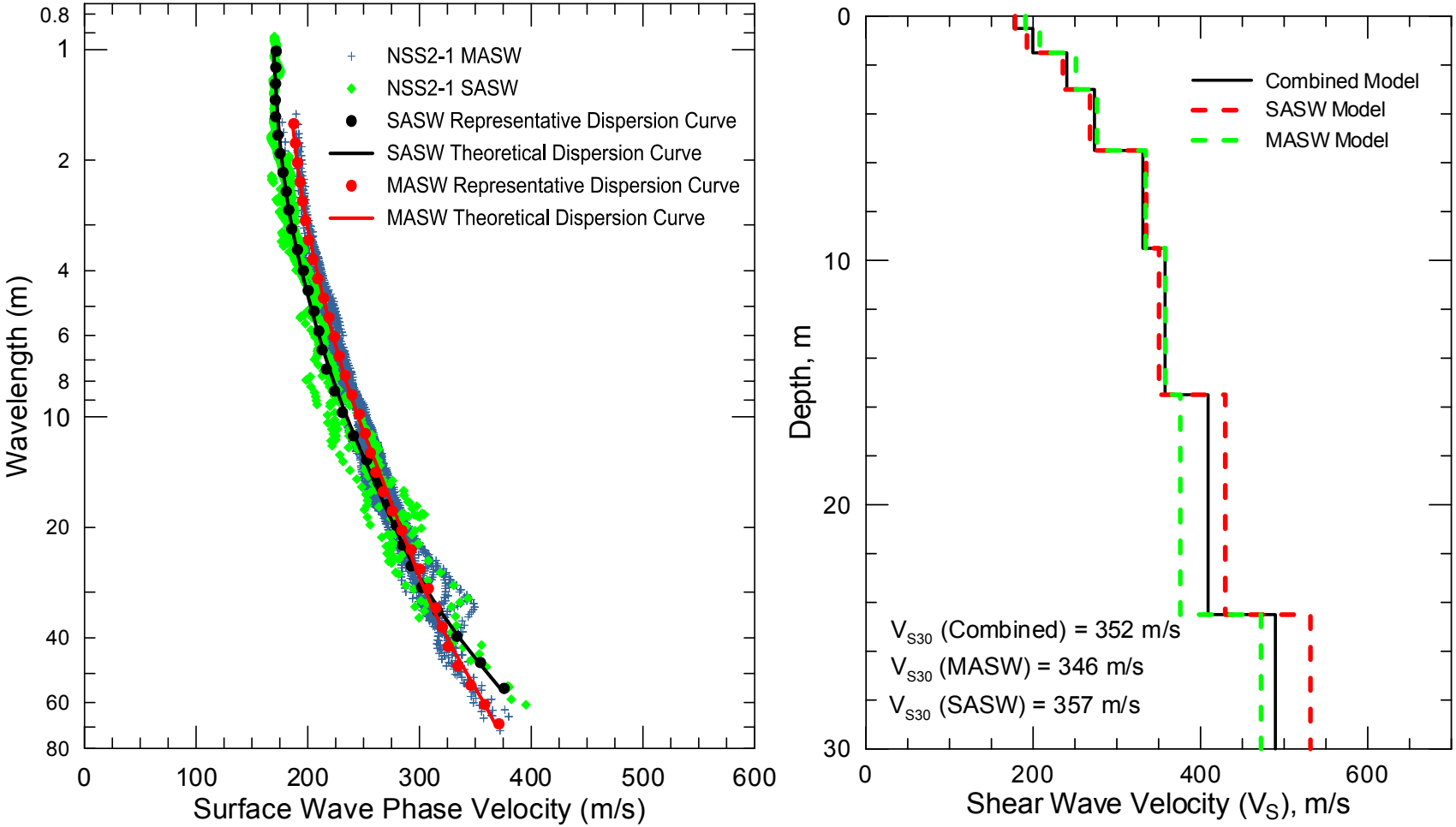

CI.NSS2 – Separate models for SASW and MASW dispersion data and comparison to the V_S model from the combined data

Site CI.OLP

Location: Otay Lakes Park, 2270 Wueste Road, Chula Vista, California

Latitude: 32.60778 **Longitude:** -116.93036
(Station coordinates modified based on field GPS survey, WGS84 coordinate system)

V_{S30} (measured): 489 m/s

V_{S30} (adjusted to more accurately reflect seismic station conditions): 548 m/s (average S-wave velocity between 1.5 and 31.5 m adjusting for 1.5 m assumed sensor depth).

NEHRP Site Class: C

Geomatrix Code: IVB

Geologic Conditions/Observations: Seismic station located on geologic unit mapped as the Jurassic and Cretaceous Santiago Peak Volcanics, mildly metamorphosed volcanic and volcaniclastic rocks. There is a thin layer of soil, possibly fill, over rock.

Site Conditions: Rural site. Rolling topography in site vicinity. Seismic line aligned parallel to a gradual slope with about a 4 m increase in surface elevation towards the east along the profile. Water treatment plant located to the west, sparse vehicle traffic during testing.

Geophysical Methods Utilized: HVSR, Seismic Refraction, MASW

Geophysical Testing Arrays:

1. Array OLP-1 (48 channel MASW and P-wave seismic refraction array utilizing 4.5 Hz vertical geophones spaced 1.5 m apart for a length of 70.5 m, forward and reverse shot locations with multiple source offsets and source types and center shot location).
2. Three HVSR measurement locations; two distributed along array OLP-1 and one near the seismic station.

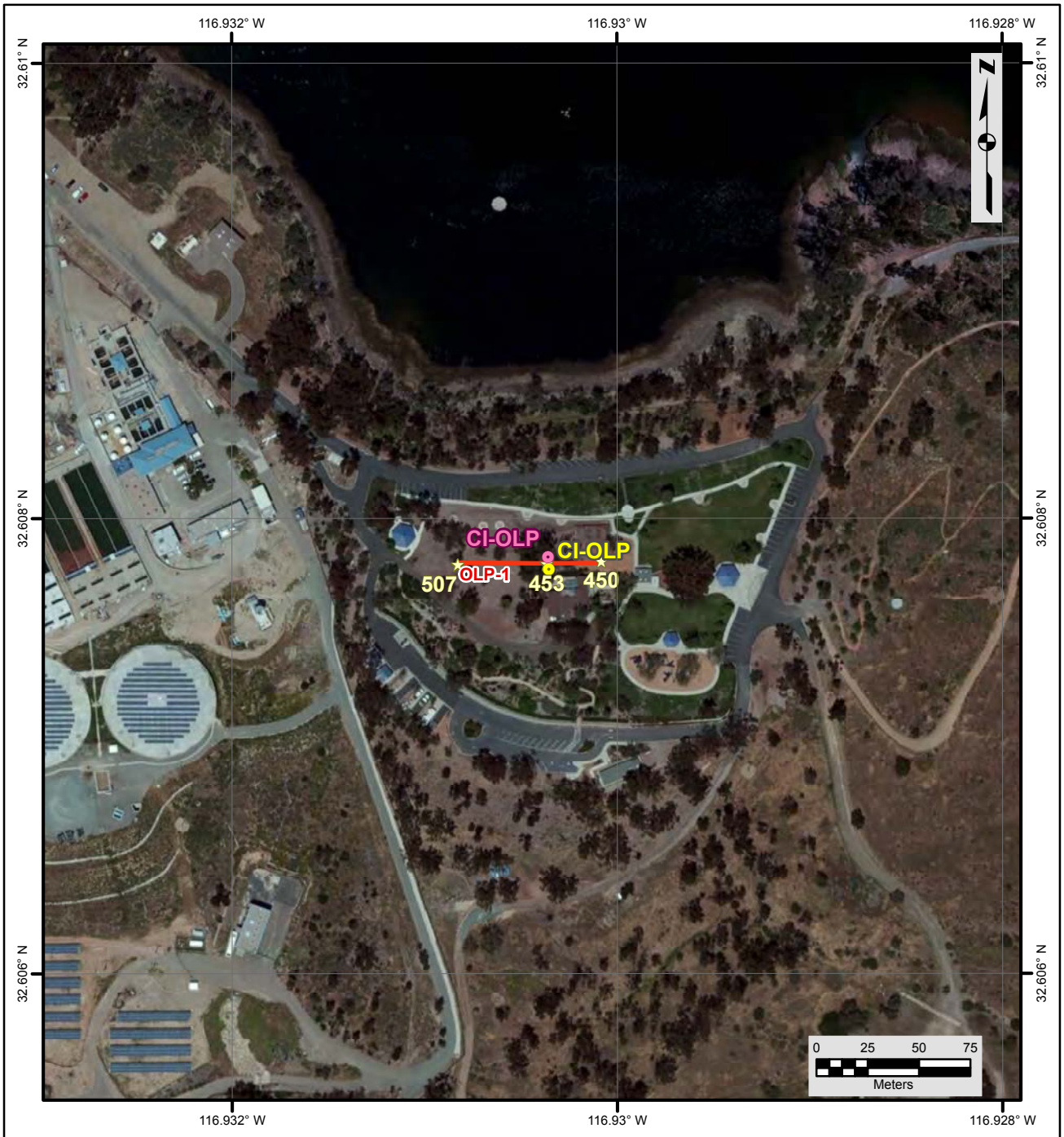

Legend

- Seismic Station - Approximate Surveyed Location
- Seismic Station - Approximate Location of Record
- H/V Spectral Ratio Location
- MASW and Seismic Refraction Array

NOTES:
1. WGS 1984 COORDINATE SYSTEM
2. Image Source: ESRI, i-cubed, USDA FSA, USGS, AEX, GeoEye, Getmapping, Aerogrid, IGP

File Name: CI-OLP-I

Date: 2/7/2013

USGS science for a changing world

GEOVision geophysical services

RECOVERY.GOV

SITE MAP
CI•OLP

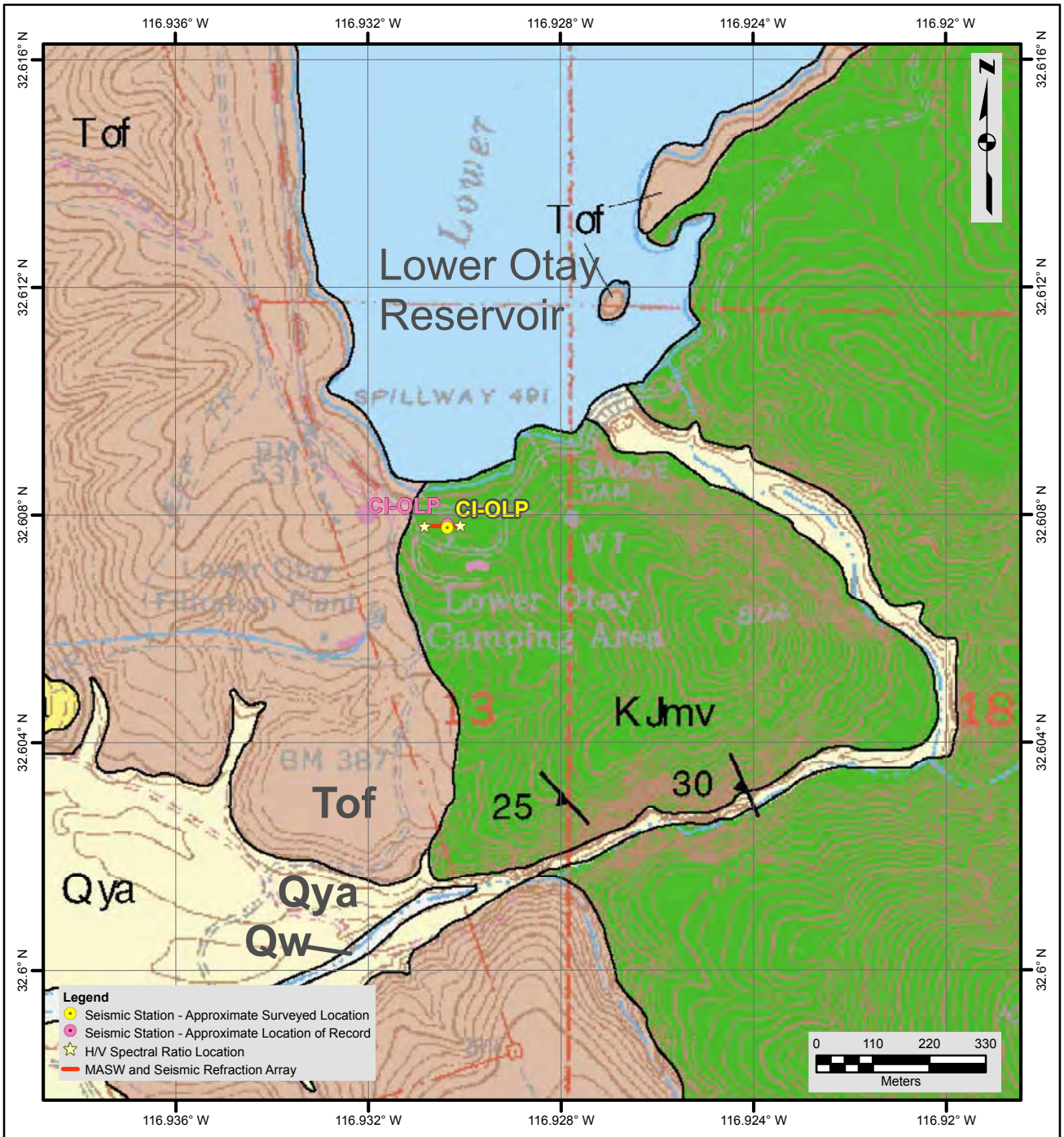

Description of Geologic Map Units

Qw = Quaternary (Holocene) active channel and wash deposits, sand, silt, gravel and clay
Qya = Quaternary (Holocene) young alluvial deposits, silt, clay, sand and gravel
Tof = Tertiary (Oligocene/Miocene) Otay formation; fanglomerate facies,
poorly cemented bouldery conglomerate and course-grained sandstone
KJmv = Mesozoic (Jurassic and Cretaceous) mildly metamorphosed volcanic,
volcaniclastic and sedimentary rocks

NOTES:
1. WGS 1984 COORDINATE SYSTEM
2. Geologic Map of the Otay Mesa 7.5' Quadrangle,
San Diego County, California
by Siang S. Tan and Michael P. Kennedy, 2002
3. See site map for details of geophysical survey

File Name: CI-OLP

Date: 2/7/2013

USGS science for a changing world

GEOVision geophysical services

GEOLOGIC MAP
CI•OLP

RECOVERY.GOV

CI.OLP seismic station

Looking east along array OLP-1 and at HVSR sensor 507

Looking south towards HVSR sensor 453 and the CI.OLP seismic station

Looking west along array OLP-1 towards seismic station

Looking east towards center of array OLP-1 and seismic station

Location of Geophysical Testing Arrays:

Location	Latitude	Longitude
OLP-1, West End of MASW/Refraction Array	32.60781	-116.93083
OLP-1, Center of MASW/Refraction Array	32.60780	-116.93044
OLP-1, East End of MASW/Refraction Array	32.60780	-116.93009
HVSR Sensor 450	32.60781	-116.93008
HVSR Sensor 453	32.60780	-116.93037
HVSR Sensor 507	32.60780	-116.93083
CI.OLP Seismic Station	32.60778	-116.93036

Notes: 1) WGS84 Coordinate System (decimal degrees)
2) Survey accuracy is estimated at 2 to 3 m.

Results:

V_S Model

Depth to Top of Layer (m)	Layer Thickness (m)	S-Wave Velocity (m/s)	Inferred P-Wave Velocity (m/s)	Assumed Poisson's Ratio	Assumed Density (g/cm^3)
0	1	152	284	0.300	1.70
1	1.5	223	417	0.300	1.70
2.5	2.5	346	647	0.300	1.80
5	4	497	930	0.300	2.00
9	10	606	2000	0.450	2.10
19	16	677	2200	0.448	2.10
35	>5	977	2400	0.401	2.15

Notes: 1) Saturated zone, with V_P of about 2,000 to 2,400 m/s, constrained at a depth of about 9 m based on seismic refraction survey.
2) Depth of investigation is about 40 m.
2) Bottom layer is a half space.

Observations/Discussion:

- HVSR plots are similar at every station, validating the 1-D velocity assumption. There appear to be two HVSR peaks at the site; the first between 3.4 and 3.6 Hz and the second between 4.5 and 4.7 Hz. The relative amplitude of the HVSR peaks is somewhat variable at the three measurement locations.
- The P-wave refraction data for array OLP-1 were modeled using a tomographic inversion routine with a layer based starting model. The seismic refraction model was extended to far offset shot locations to extend depth of investigation.
- The seismic refraction survey design allowed P-wave velocity to be imaged to a maximum depth of about 20 m. The seismic refraction model shows that P-wave velocity is about 250 to 400 m/s at the surface, increasing to 1,000 m/s at a depth of 3 to 6 m, 1,600 at a depth of 7 to 10 m and 2,200 m/s at a nominal depth of 16 m. P-wave velocity greater than 1,600 m/s are most likely associated with saturated volcanic rock. As the rock becomes more competent with depth, the effects of saturation on P-wave velocity are expected to decrease (i.e. Poisson's ratio will decrease).
- The seismic refraction model indicates that there is minor lateral velocity variation above the saturated zone at this site, with a slightly thicker sequence of low velocity soils at the eastern end of the line. The saturated zone masks potential lateral velocity variation at depths below 7 to 10 m.
- Noise conditions at the site were not sufficient for application of passive surface wave techniques.
- The minimum wavelength surface wave phase velocity data extracted from the 48-channel MASW array was about 28 m. Reducing data from smaller hammer sources using a limited offset receiver array (i.e. less active geophones) allowed for extraction of surface wave dispersion data to a minimum wavelength of about 2.5 m.
- There is about 50 to 100 m/s of scatter in MASW dispersion data, which is likely the result of lateral velocity variation caused by differential weathering of near surface rock and variable thickness of a thin soil layer. The lateral velocity variation is such that it was not possible to extract Rayleigh wave phase velocity data at wavelengths less than 28 m from the 48 channel MASW receiver array. Dominant higher modes were also an issue at smaller wavelengths/higher frequencies.
- A representative dispersion curve was generated for the MASW data set using a moving average, polynomial curve fitting routine and used for modeling.
- The saturated zone with P-wave velocity increasing with depth from 2,000 to 2,400 m/s was constrained at a depth of 9 m based on the seismic refraction survey.
- Surface wave depth of investigation is about 40 m based on half of maximum wavelength criteria.
- V_{S30} is 489 m/s (Site Class C).
- Average S-wave velocity between 1.5 m (assumed sensor depth) and 31.5 m is 548 m/s.

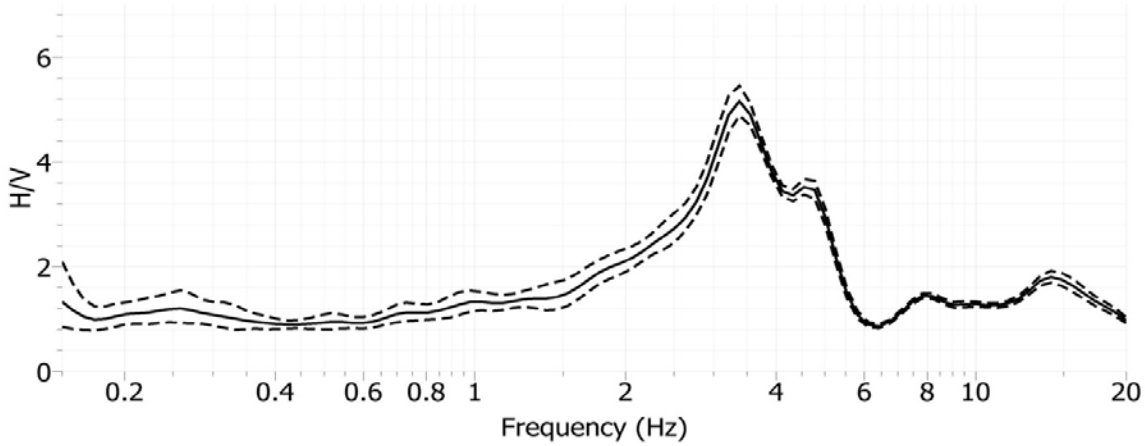

Site CI.OLP, H/V Spectral Ratio, Array OLP-1, Sensor 507

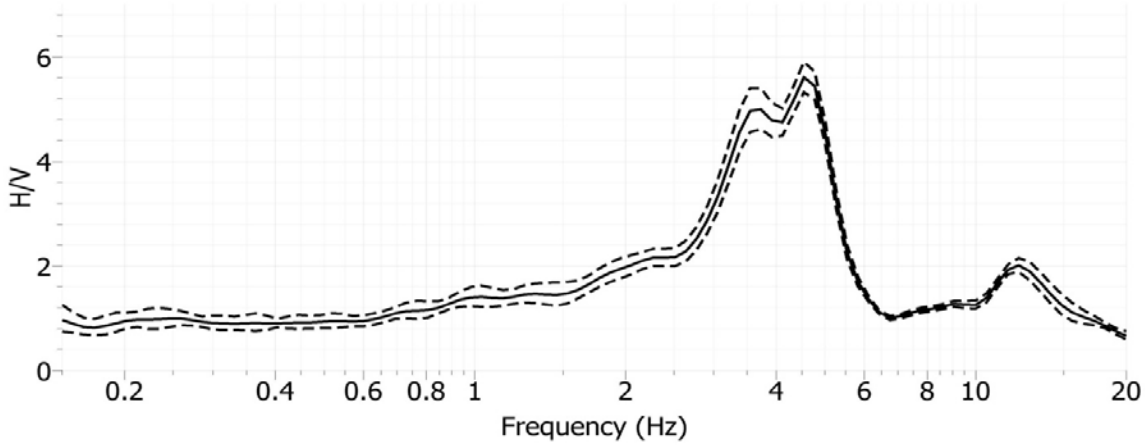

Site CI.OLP, H/V Spectral Ratio, Near Seismic Station, Sensor 453

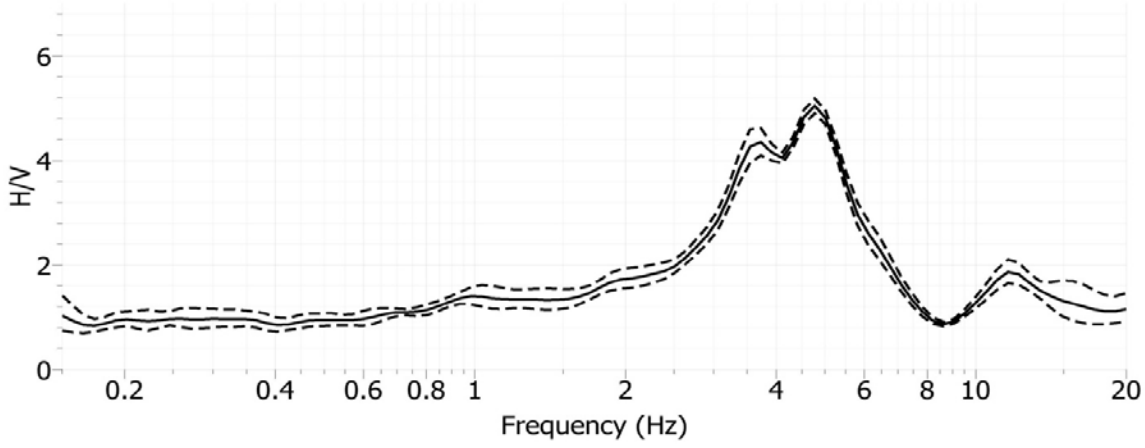

Site CI.OLP, H/V Spectral Ratio, Array OLP-1, Sensor 450

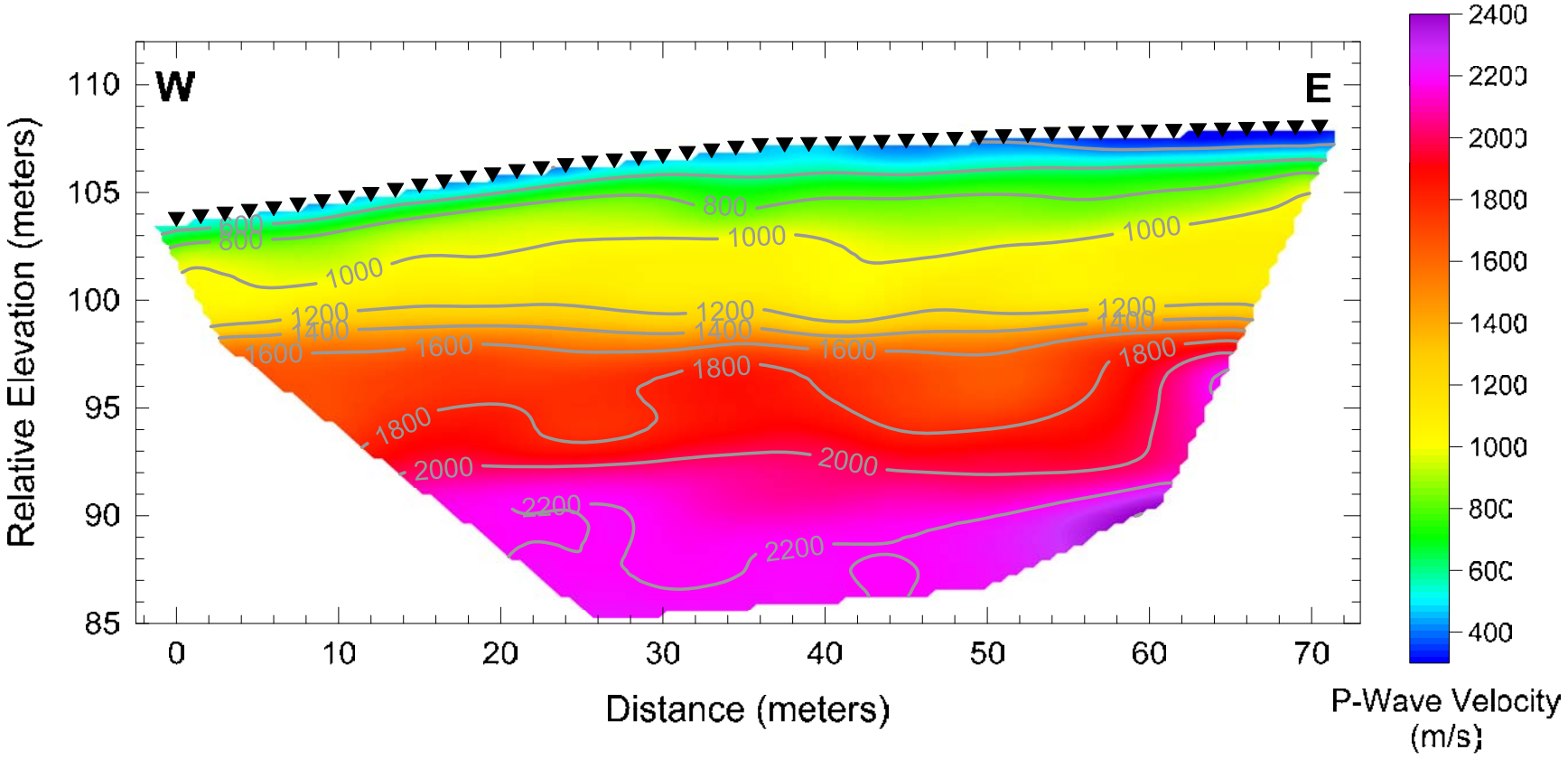

Array OLP-1 – Tomographic seismic refraction model utilizing layer based starting model

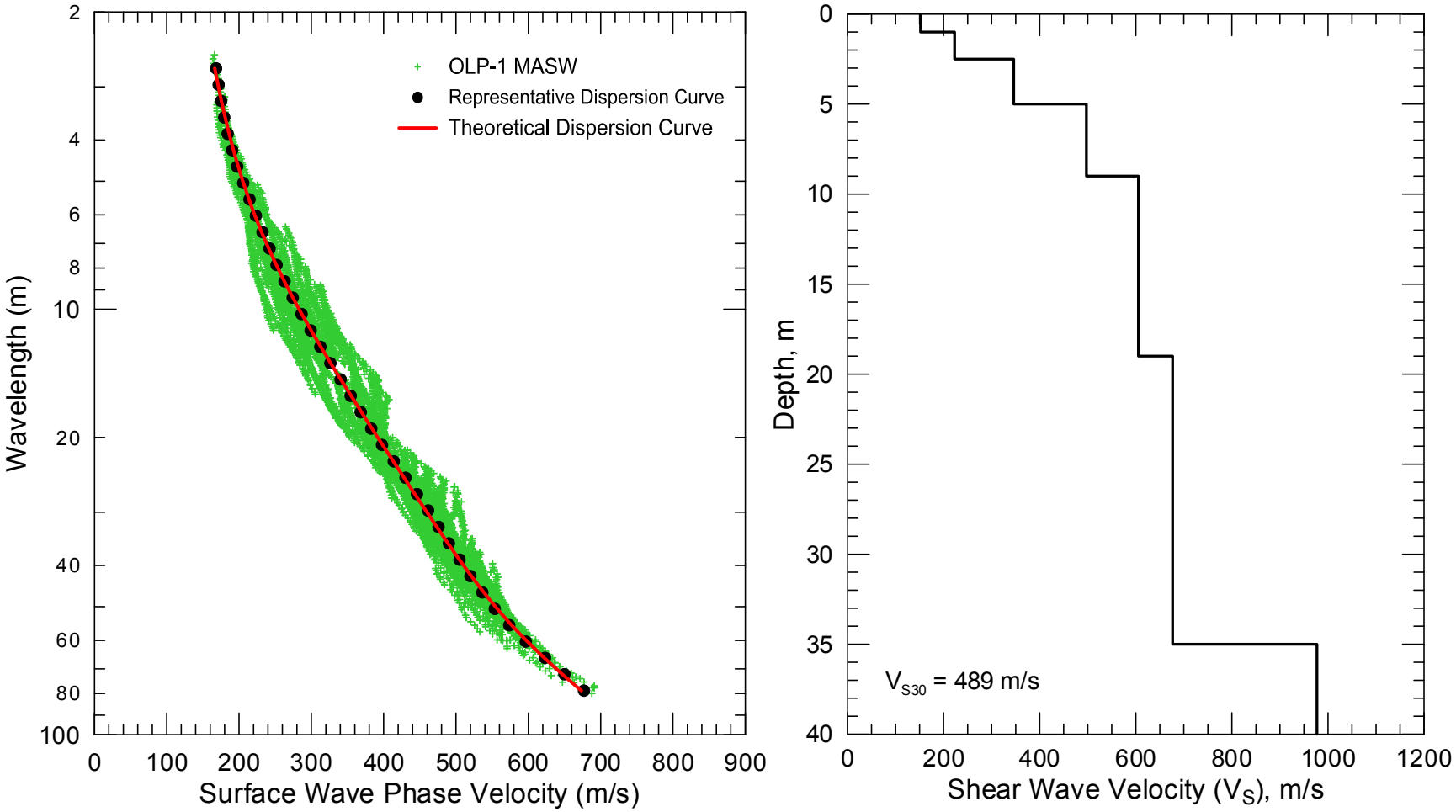

CI.OLP- Field, representative and inverted theoretical surface wave dispersion data (left) and associated V_S model (right)

Site CI.PASC

Location: Pasadena Art Center, College of Design, 1342 Carnarvon Drive, Pasadena, California

Latitude: 34.17141 **Longitude:** -118.18523
(Station coordinates provided by USGS, WGS84 coordinate system)

V_{S30} (measured): 714 m/s

V_{S30} (adjusted to more accurately reflect seismic station conditions): 988 m/s (average S-wave velocity between 4 and 34 m adjusting for assumed 4 m sensor depth).

NEHRP Site Class: C (based on V_{S30}), B (based on adjusted V_{S30})

Geomatrix Code: IGA

Geologic Conditions/Observations: Seismic station located on geologic unit mapped as Mesozoic (Cretaceous) quartz diorite.

Site Conditions: Suburban site located on gently rolling hills. Ground surface elevation decreases about 6.5 m to the southwest along the 70.5 m long MASW and seismic refraction array.

Geophysical Methods Utilized: HVSR, Seismic Refraction, MASW

Geophysical Testing Arrays:

1. Array PASC-1 (48 channel MASW and P-wave seismic refraction array utilizing 4.5 Hz vertical geophones spaced 1.5 m apart for a length of 70.5 m, forward and reverse shot locations with multiple source offsets and source types and multiple interior shot locations).
2. Three HVSR measurement locations: two distributed along array PASC-1 and one adjacent to the seismic station. HVSR measurements were also made with a Tromino ENGY near the seismic station.

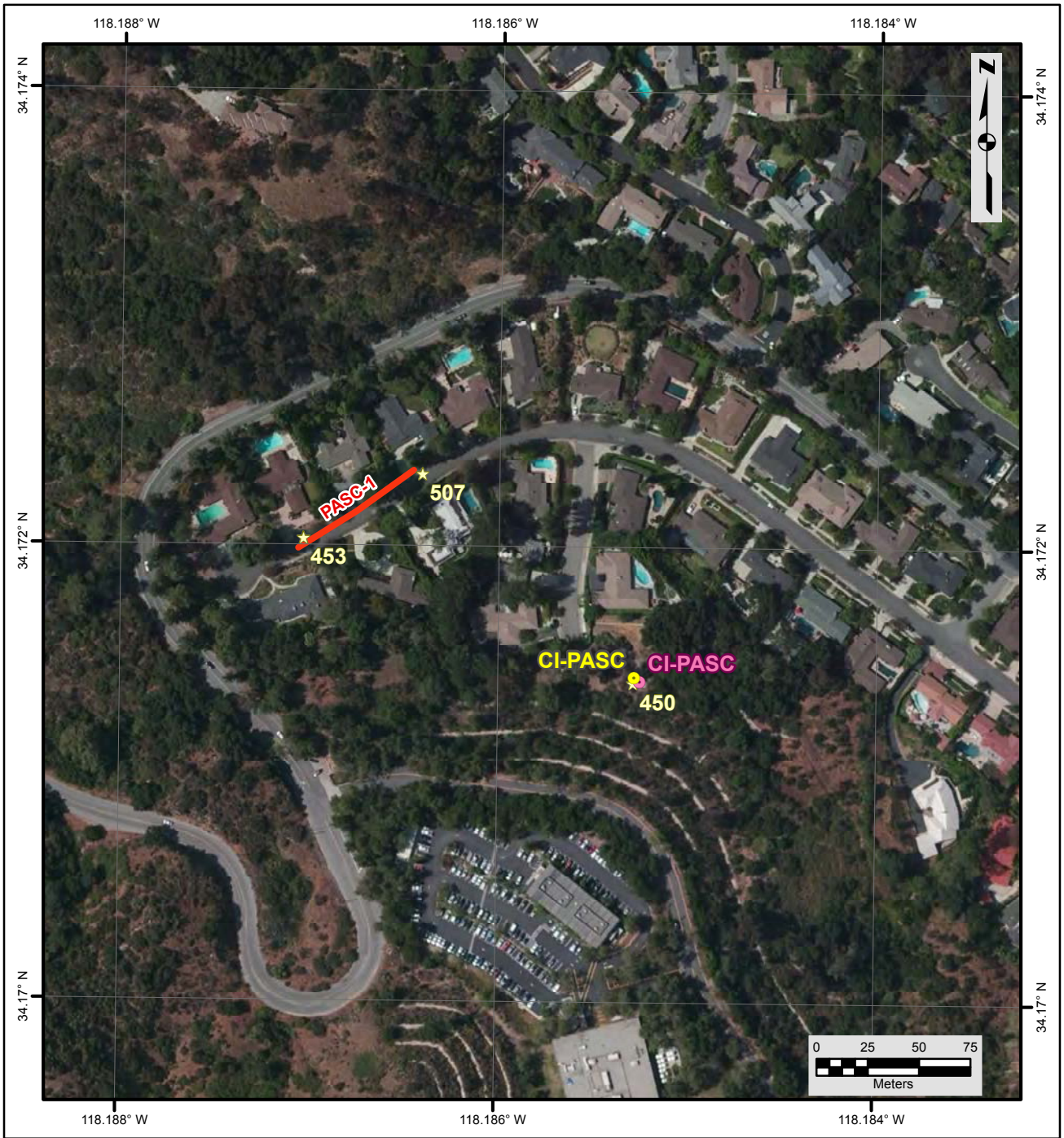

Legend

- Seismic Station - Approximate Surveyed Location
- Seismic Station - Approximate Location of Record
- H/V Spectral Ratio Location
- MASW and Seismic Refraction Array

NOTES:
1. WGS 1984 COORDINATE SYSTEM
2. Image Source: ESRI, i-cubed, USDA FSA, USGS, AEX, GeoEye, Getmapping, Aerogrid, IGP

File Name: CI-PASC-I

Date: 2/7/2013

USGS science for a changing world

GEOVision geophysical services

RECOVERY.GOV

SITE MAP
CI•PASC

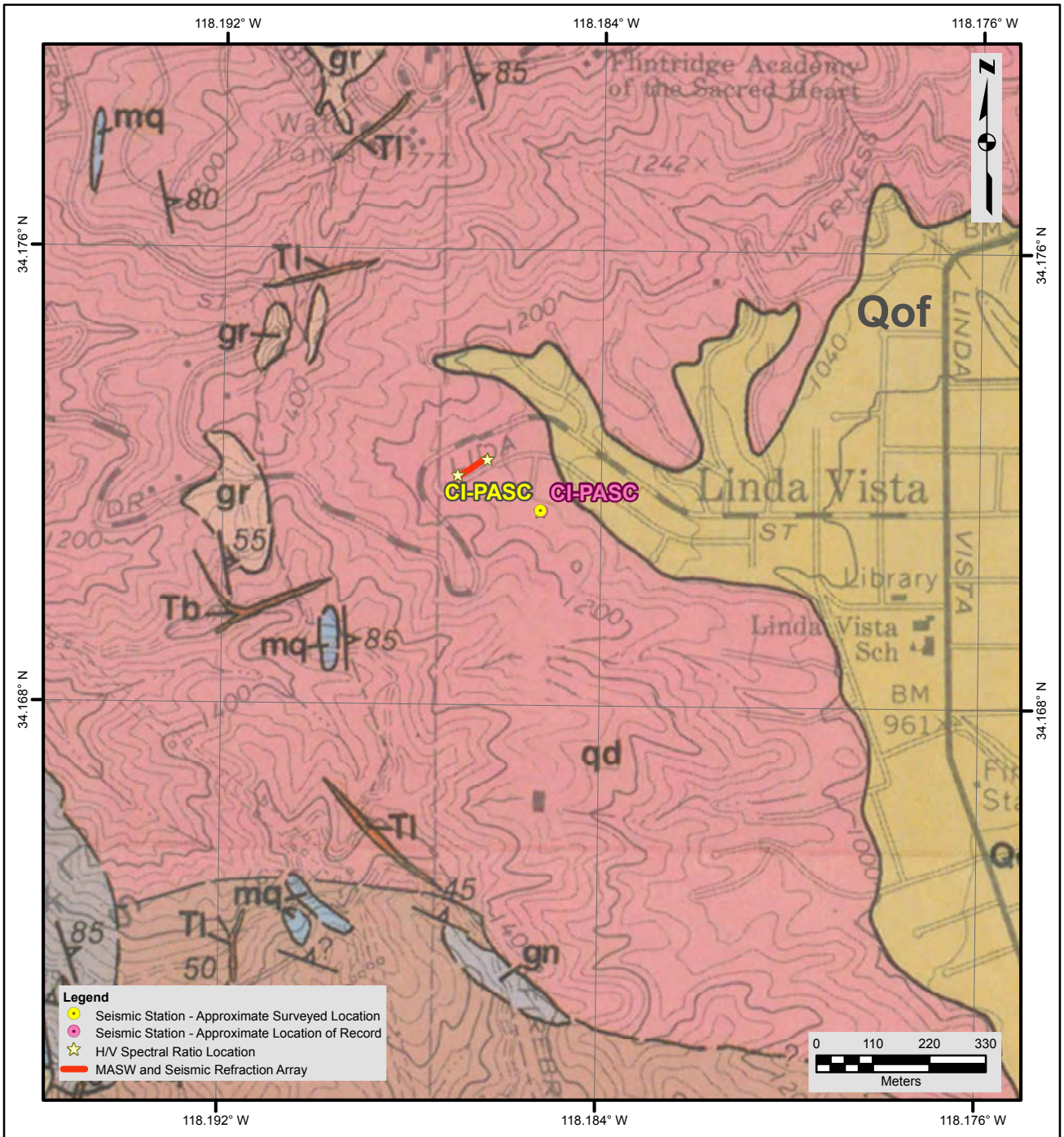

Description of Geologic Map Units

Qof = Quaternary (Pleistocene) alluvial fan gravel and sand derived from San Gabriel Mountains
Tb = Tertiary (Pre-Miocene) thin dikes of fine-grained basaltic, intrusive rocks
Tl = Tertiary (Pre-Miocene) thin dikes of latite porphyry
gr = Mesozoic (Cretaceous) medium- to fine-grained massive granitic rock mostly of quartz monzonite and granodiorite composition
qd = Mesozoic (Cretaceous) massive, non-gneissoid quartz diorite
mq =Precambrian or Paleozoic quartzite, quartz or quartzo-feldspathic rock, and schist
gn = Precambrian gneiss; in part contorted, migmatized with quartz diorite (qd) and complexly intruded or injected by leucogranitic rocks (gr)

NOTES:
1. WGS 1984 COORDINATE SYSTEM
2. Geologic Map of the Pasadena Quadrangle, Los Angeles County, California
By Thomas W. Dibblee, Jr., 1989
3. See site map for details of geophysical survey

File Name: CI-PASC
Date: 2/7/2013

USGS science for a changing world
GEOVision geophysical services

GEOLOGIC MAP
CI•PASC

Looking at seismic station and HVSR sensors 450 (Nanometrics Trillium Compact) and Micromed Tromino ENGR

Looking northeast along array PASC-1

Nanometrics Trillium Compact and Micromed Tromino ENGR seismic sensors

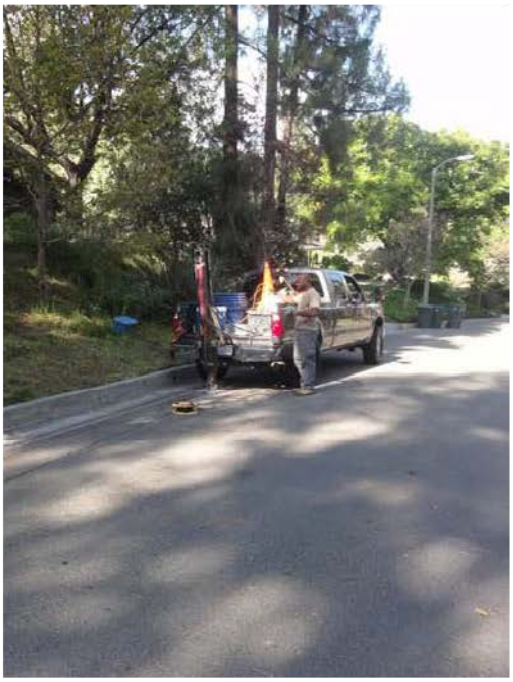

Accelerated weight drop energy source

Looking northeast along array PASC-1 and at HVSR sensor 453

Location of Geophysical Testing Arrays:

Location	Latitude	Longitude
PASC-1, Southwest End of MASW/Refraction Array	34.17198	-118.18704
PASC-1, Center of MASW/Refraction Array	34.17215	-118.18673
PASC-1, Northeast End of MASW/Refraction Array	34.17233	-118.18644
HVSR Sensor 450 (Nanometrics Trillium Compact)	34.17140	-118.18526
HVSR Sensor 453 (Nanometrics Trillium Compact)	34.17203	-118.18701
HVSR Sensor 507 (Nanometrics Trillium Compact)	34.17231	-118.18639
HVSR Sensor TRO-1 (Micromed Tromino ENGY)	34.17139	-118.18524
CI.PASC Seismic Station	34.17143	-118.18526

Notes: 1) WGS84 Coordinate System (decimal degrees)
2) Survey accuracy is estimated at 1 to 2 m.

Results:

V_S Model 1FM (Fundamental Mode Assumption)

Depth to Top of Layer (m)	Layer Thickness (m)	S-Wave Velocity (m/s)	Inferred P-Wave Velocity (m/s)	Assumed Poisson's Ratio	Assumed Density (g/cm^3)
0	1	214	400	0.300	1.80
1	2.5	316	591	0.300	1.85
3.5	6	397	742	0.300	1.90
9.5	7	1021	1910	0.300	2.20
16.5	>18.5	1812	3390	0.300	2.40

Notes: 1) Depth of investigation is about 35 m.
2) Bottom layer is a half space.
3) Half space velocity not well resolved.

V_S Model 1AM (Average Mode Assumption)

Depth to Top of Layer (m)	Layer Thickness (m)	S-Wave Velocity (m/s)	Inferred P-Wave Velocity (m/s)	Assumed Poisson's Ratio	Assumed Density (g/cm^3)
0	1	241	452	0.300	1.80
1	2.5	292	547	0.300	1.80
3.5	6	406	759	0.300	1.90
9.5	7	802	1501	0.300	2.10
16.5	13	897	1679	0.300	2.15
29.5	>5.5	1448	2708	0.300	2.20

Notes: 1) Depth of investigation is about 35 m.
2) Bottom layer is a half space.

Observations/Discussion:

- There was not sufficient space in close proximity to the seismic station to locate an MASW or seismic refraction array of sufficient length to image to 30 m depth. Therefore, array PASC-1 was located along a road about 150 m northwest of the seismic station. The location of array PASC-1 is at similar elevation to the seismic station.
- Review of photographs taken during installation of seismic station CI.PASC indicates that the seismic sensors may be as much as 4 m below ground surface and that the near surface rock is sufficiently weathered to allow excavation by an excavator.
- All HVSR plots are different at frequencies above 2 Hz, indicating that there may be lateral velocity variation along array PASC-1 and that the near surface velocity structure beneath array PASC-1 may be slightly different than that at the seismic station. The HVSR measurement locations near the seismic station may be located on top of or immediately adjacent to the former excavation for the seismic station, which may affect the HVSR response.
- HVSR data were also recorded with a Micromed Tromino ENGY, which was located adjacent to the Nanometrics Trillium Compact sensor 450. Both HVSR sensors yielded almost identical results.
- The P-wave seismic refraction data collected along array PASC-1 could not be modeled due to strong first arrival energy from the asphalt/concrete layer at the surface. This interference made it impossible to accurately constrain near surface P-wave velocity structure. Seismic records from off-end source locations were, however, reviewed to determine the approximate bedrock P-wave velocity range.
- Review of the seismic data indicates that weathered bedrock has a P-wave velocity in the 2,000 to 2,500 m/s range at a depth below 5 to 9 m, depending on near surface velocity structure, which could not be accurately determined. The P-wave velocity of the weathered bedrock appears to exceed 3,500 m/s at a depth below 15 to 20 m.
- Noise conditions at the site were not sufficient for successful application of passive surface wave techniques.
- It was difficult to extract Rayleigh wave phase velocity data over the 15 to 20 Hz frequency range (20 to 40 m wavelength range). The possibility that the fundamental mode jumps to the first higher mode over this frequency range cannot be discounted.
- The near field criteria typically applied during this investigation were significantly relaxed in order to obtain phase velocity data to as long a wavelength as feasible, in order to better constrain bedrock velocity. The maximum wavelength was set to 2.25 times the distance between the source and midpoint of the active receiver array for off-end source locations and receiver arrays consisting of 36 or more geophones, with the maximum wavelength not to exceed 140 m. The maximum wavelength for interior source locations and receiver arrays of less than 36 geophones was set to 1.4 times the source to midpoint of receiver array distance. It is highly probable that long wavelength Rayleigh wave phase velocity data suffer from near field effects, which typically result in underestimated phase velocity. Additionally, some of the scatter in the dispersion data at long wavelengths may be the result of near field effects, rather than lateral velocity variation.
- The minimum wavelength surface wave phase velocity data extracted from the 48-channel MASW array was about 4 m, although it was not generally possible to extract dispersion data over the 20 to 30 m wavelength range using the 48 channel receiver array.

Reducing data from smaller hammer sources using a limited offset receiver array (i.e. less active geophones) allowed for extraction of surface wave dispersion data to a minimum wavelength of about 2 m. MASW analysis of a limited group of receivers and SASW analysis of selected receiver pairs from the 3 lb hammer shot located at -1.5 m allowed for extraction of phase velocity data to a wavelength of about 1.3 m.

- There is about 150 m/s of scatter in MASW dispersion data. At short wavelengths the scatter is likely the result of lateral velocity variation. At long wavelengths the scatter is likely the result of both near field effects and lateral velocity variation.
- A representative dispersion curve was generated for the MASW data set using a moving average, polynomial curve fitting routine and used for modeling.
- Modeling of the dispersion curve assuming fundamental mode (V_S Model 1FM) did not result in a particularly good fit between the observed and calculated dispersion curve. Multi-mode analysis of the V_S model resulting from the fundamental mode assumption indicates that the fundamental mode should jump to the first higher mode at a frequency between 15 and 20 Hz, which, coincidently, is the frequency range where it was difficult to extract dispersion data from the MASW seismic records. Multi-mode analysis also indicates that the cut-off frequency for the first higher mode (frequency below which the first higher mode does not exist) may occur at about 10 Hz with the dispersion curve dropping back to the fundamental mode at lower frequencies. The actual cut-off frequency is affected by velocity structure much deeper than the depth of investigation and can, therefore, not be accurately estimated. In fact, not being able to accurately constrain deep velocity structure can complicate multi-mode, average/effective mode and SASW 3-D array and global inversions at sites with velocity structure such as this.
- To account for the possible mode jump or modal superposition at low frequencies, the dispersion curve was also modeled using the average/effective mode assumption; which, in this case, effectively models a jump from fundamental mode to first higher mode between 15 and 20 Hz (V_S Model 1AM). It should be noted that the algorithm used to estimate the higher modes and relative amplitude of the higher modes assumes a plane wave (i.e. infinite source location) and does not include body wave effects. A true multi-mode inversion for this data set, with the portion of the dispersion curve below 15 Hz and above 20 Hz assigned to the first higher mode and fundamental mode, respectively, would result in a similar V_S model, with possibly slightly lower Vs at depth.
- Surface wave depth of investigation is about 35 m based on half of maximum wavelength criteria.
- V_{S30} is 714 and 588 m/s for Models 1FM and 1AM, respectively (NEHRP Site Class C).
- Although, there is evidence pointing to the average/effective mode V_S model being more valid than the fundamental mode V_S model, the inferred P-wave velocity, based on an assumed Poisson's ratio of 0.3, below a depth of 9.5 m in the average mode model is not consistent with inspection of seismic refraction first arrival data. A Poisson's ratio of 0.4, or more, would be required for the average mode model to be consistent with seismic refraction data observations. Even if the weathered crystalline rock were saturated at depths below 9.5 m, which is improbable, it would appear unlikely for Poisson's ratio to exceed 0.4. Therefore, the fundamental mode V_S model, which has inferred P-wave velocities consistent with seismic refraction data, is assumed to be representative of subsurface velocity structure at this time.

- Average S-wave velocity between 4 m, assumed sensor depth, and 34 m is 988 and 752 m/s for Models 1FM and 1AM, respectively. Adjusted V_{S30} for the fundamental mode V_S model indicates that the site can be classified as NEHRP Site Class B. Adjusted V_{S30} for the average mode V_S model indicates that the site can be classified as NEHRP Site Class C/B.
- The fundamental mode V_S model is most consistent with bedrock P-wave velocities observed in the seismic refraction shot records and, therefore, should be used for the purpose of site characterization. Further research is required to identify possible reasons for the dispersion curve, at sites such as this, representing the fundamental mode when the velocity structure implies that the first higher mode should be dominant at low frequencies. One item to be investigated is the influence of lateral velocity variation on both higher mode amplitude and the accuracy of V_S models derived from surface wave dispersion data.
- Although there is not sufficient space adjacent to the seismic station for a 30 m surface wave or seismic refraction sounding, some seismic testing should be conducted in closer proximity to the seismic station to confirm that near surface velocity structure, which has the largest effect on V_{S30}, is similar to that beneath array PASC-1 and, if not, allow a more accurate adjustment to be made to V_{S30}.
- Lateral velocity variation has been the largest single factor complicating characterization of rock sites during this investigation. Future investigations should consider some testing as close as possible to the seismic station to correlate near surface velocity structure at the seismic station to that beneath a test array placed in an area with sufficient space to image to 30 m depth.

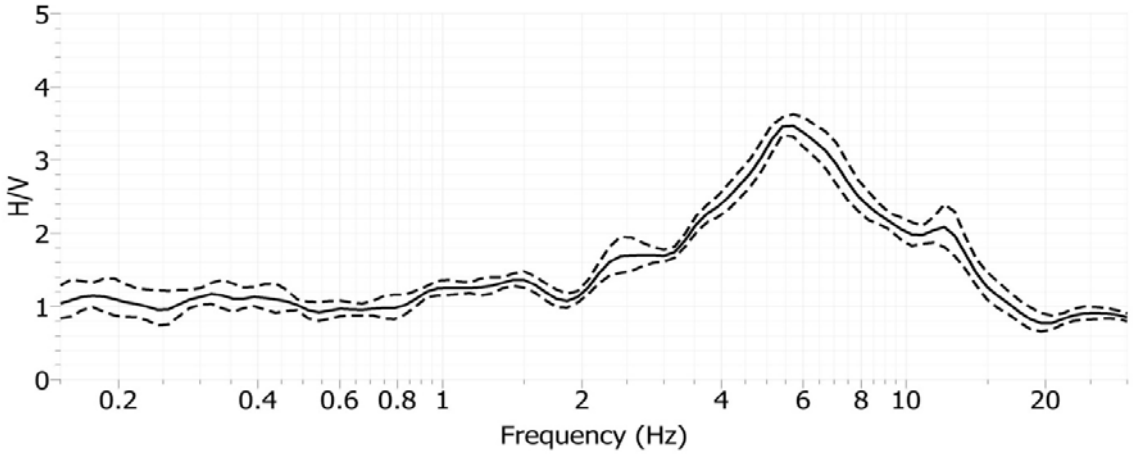

Site CI.PASC, H/V Spectral Ratio, Array PASC-1, Sensor 507

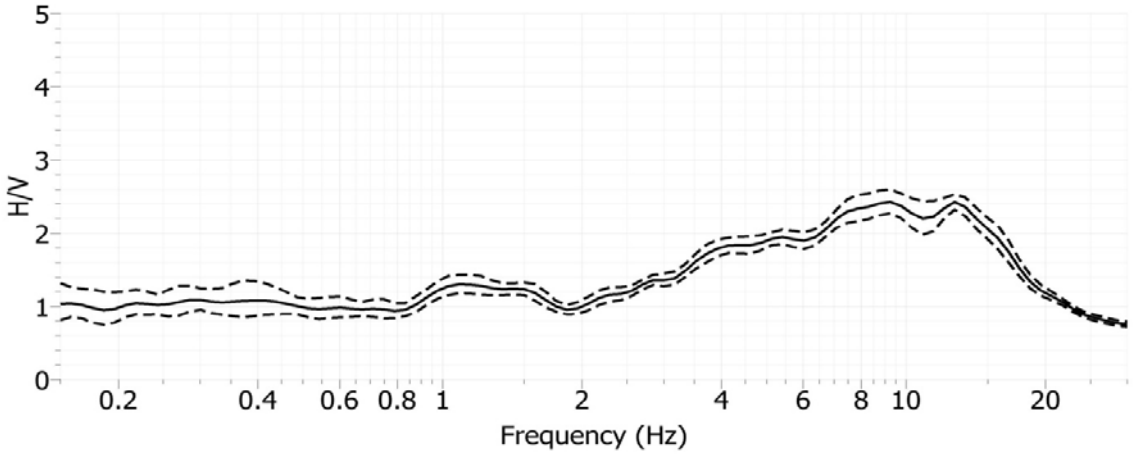

Site CI.PASC, H/V Spectral Ratio, Array PASC-1, Sensor 453

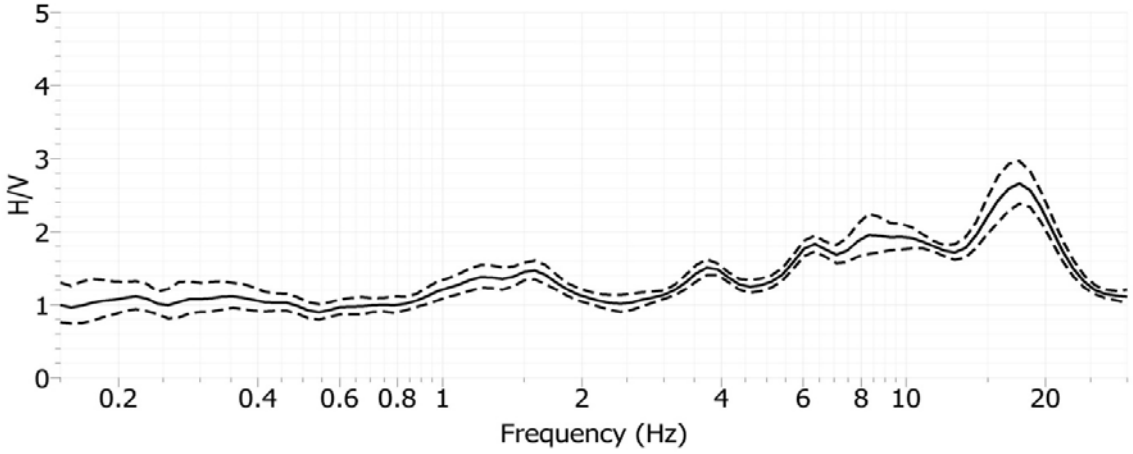

Site CI.PASC, H/V Spectral Ratio, Near Seismic Station, Sensor 450

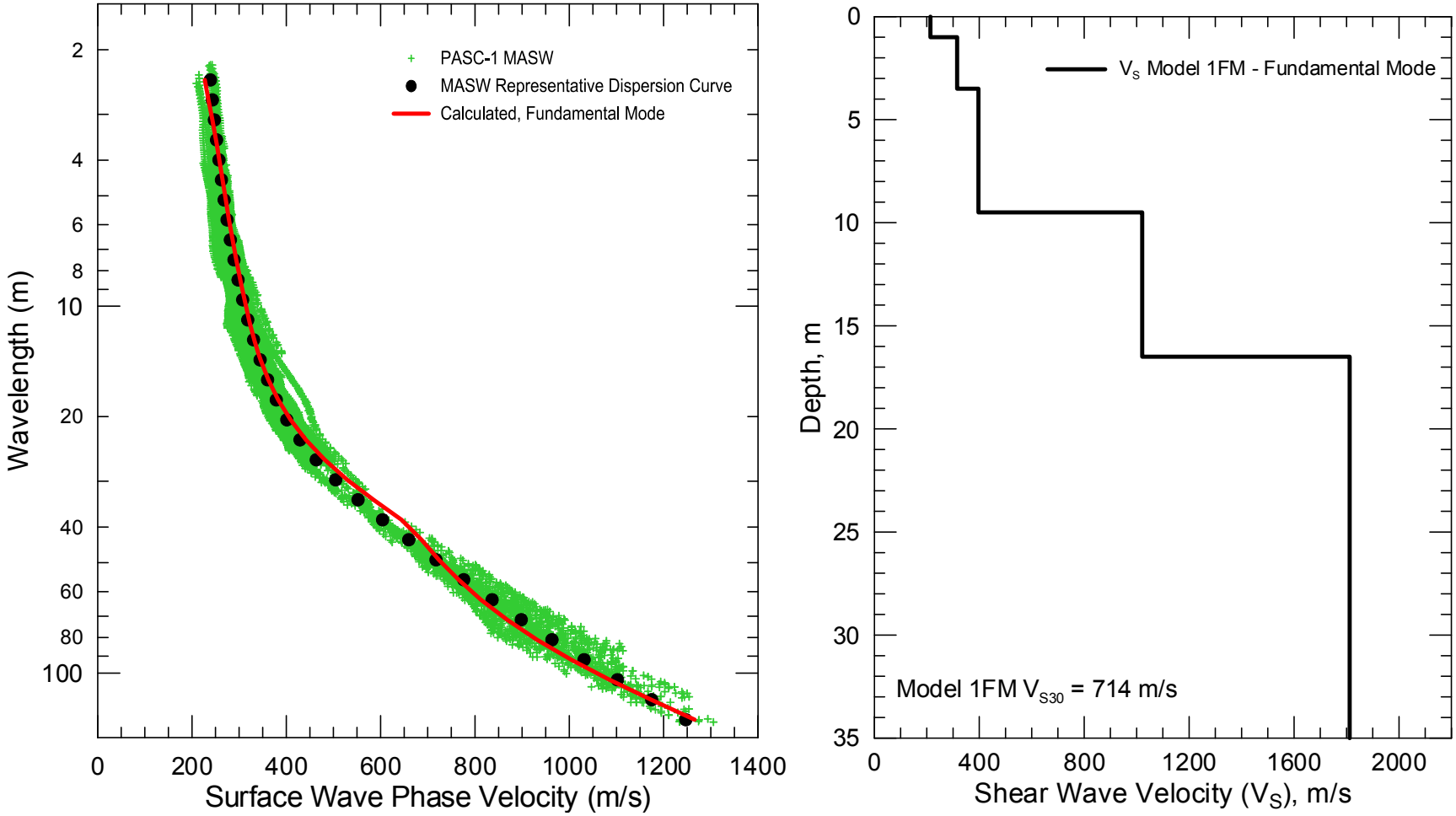

CI.PASC - Field, representative and inverted theoretical surface wave dispersion data (left) and associated V_S model (right) for fundamental mode assumption.

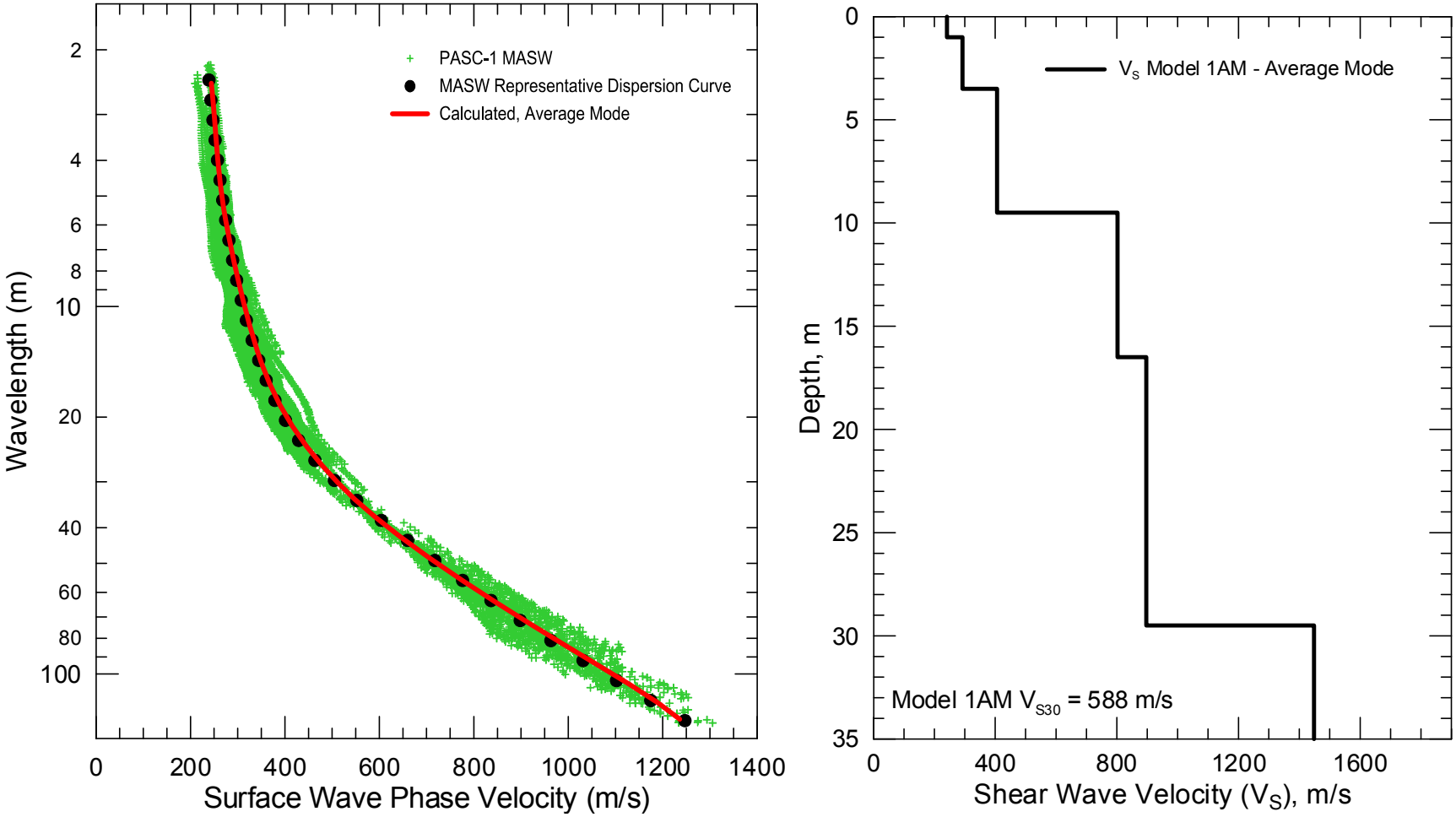

CI.PASC - Field, representative and inverted theoretical surface wave dispersion data (left) and associated V_S model (right) for average mode assumption.

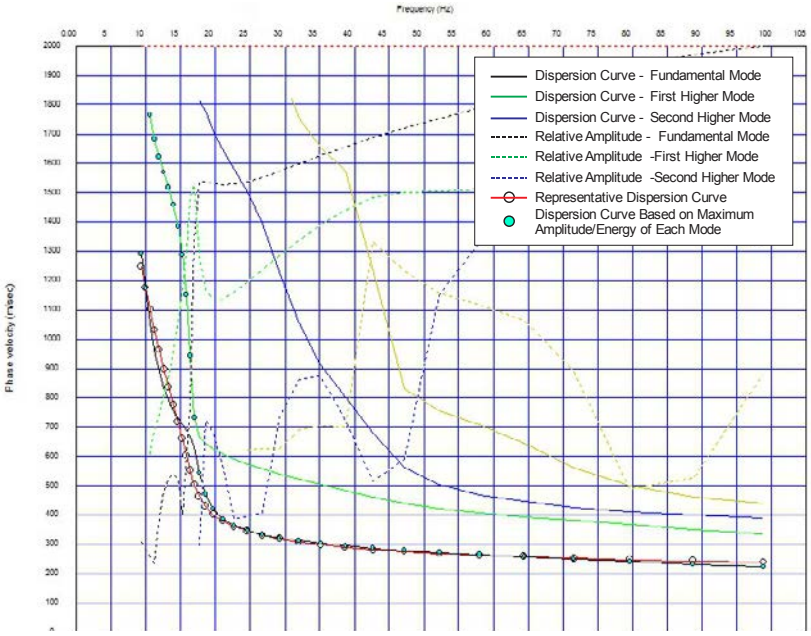

Calculated Rayleigh wave modes for fundamental mode for V_S Model 1FM demonstrating that this model should excite a dominant higher mode at frequencies below 17 Hz. However, a dominant fundamental mode at the lowest frequencies is also possible. It should be noted, however, that the analytical routine used to estimate the amplitudes of the higher modes does not include the source location or body wave effects and makes a plane wave assumption. It was difficult fitting a fundamental mode dispersion curve to the representative dispersion curve.

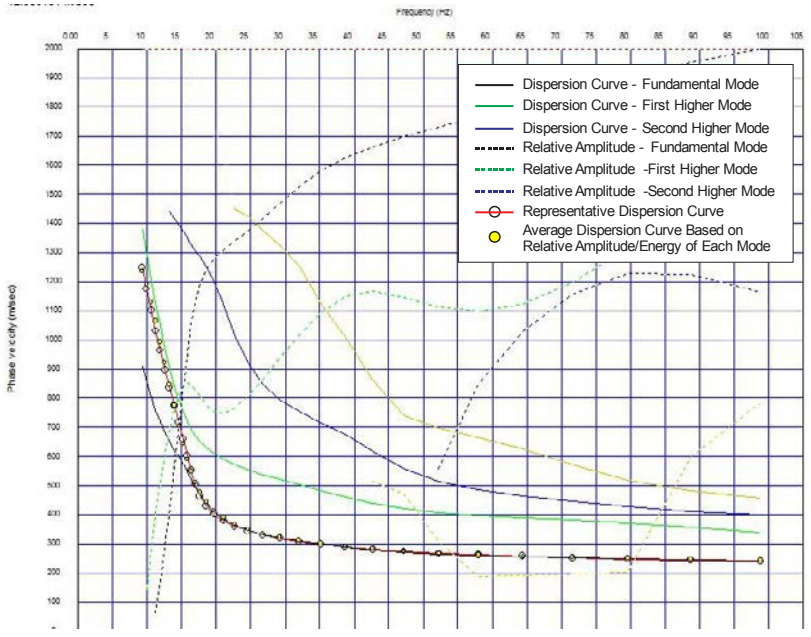

Calculated Rayleigh wave phase velocity modes for V_S Model 1AM developed using the average mode assumption in an attempt to account for possible modal superposition (mode mixing) at low frequencies. The V_S model is very similar to what would have been derived with a multi-mode inversion assuming fundamental mode at frequencies higher than 17 Hz and first higher mode at frequencies less than 15 Hz.

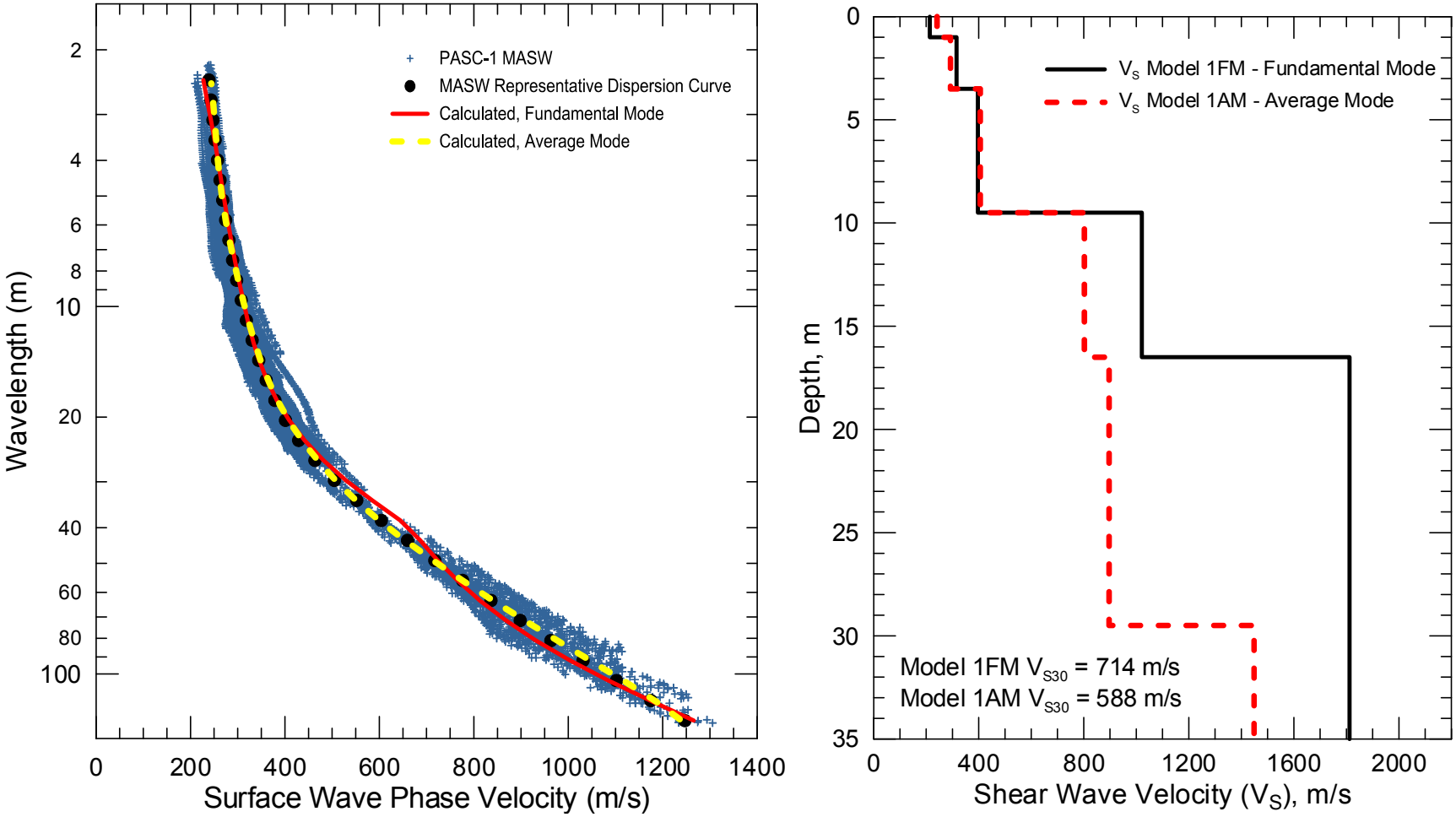

CI.PASC - Field, representative and inverted theoretical surface wave dispersion data (left) and associated V_S models (right) for fundamental and average mode assumption.

Site CI.PDM

Location: Parker Dam, California

Latitude: 34.30330 **Longitude:** -114.14218
(Station coordinates modified based on site GPS survey and are in WGS84 coordinate system)

V_{S30} (measured): 1,312 m/s (depending on the shallow bedrock weathering profile, V_{S30} at the seismic station may be higher due to absence of a thin sediment layer).

V_{S30} (adjusted to more accurately reflect seismic station conditions): 1,560 m/s (average S-wave velocity between 1 and 31 m adjusting for 1 m assumed sensor depth).

NEHRP Site Class: B/A

Geomatrix Code: INA

Geologic Conditions/Observations: Seismic station located on Precambrian igneous and metamorphic rocks.

Site Conditions: Rural site. Steep, undulating topography in site vicinity. Seismic station located on top of a small hill. Test area located along a small drainage with gentle topographic decline to northeast.

Geophysical Methods Utilized: HVSR, P-wave Seismic Refraction, MASW

Geophysical Testing Arrays:

1. Array PDM-1 (48 channel MASW and P-wave seismic refraction array utilizing 4.5 Hz vertical geophones spaced 1.5 m apart for a length of 70.5 m, forward and reverse shot locations with multiple source offsets and source types (hammers only) and multiple interior shot locations).
2. Three HVSR measurement locations; two distributed along array PDM-1 and the other adjacent to the seismic station.

Legend

- Seismic Station - Approximate Surveyed Location
- Seismic Station - Approximate Location of Record
- H/V Spectral Ratio Measurement Location
- MASW and Seismic Reflection Array

NOTES:
1. WGS 1984 COORDINATE SYSTEM
2. Image Source: ESRI, i-cubed, USDA FSA, USGS, AEX, GeoEye, Getmapping, Aerogrid, IGP

File Name: CI-PDM-I

Date: 5/13/2011

USGS science for a changing world

GEOVision geophysical services

RECOVERY.GOV

SITE MAP
CI•PDM

Description of Geologic Map Units

Qal = Quaternary (Holocene) Alluvium
pCc = Precambrian igneous and metamorphic rock complex

NOTES:
1. WGS 1984 COORDINATE SYSTEM
2. Geologic Map of California
Needles Sheet
by Charles C. Bishop, 1963
3. See site map for details of geophysical survey

File Name: CI-PDM

Date: 5/26/2011

USGS science for a changing world

GEOVision geophysical services

RECOVERY.GOV

GEOLOGIC MAP
CI•PDM

Looking northwest towards HVSR sensor 453 and CI.PDM seismic station

Looking northeast from northern end of array PDM-1 towards location of seismic sensor CI.PDM

Rock exposed in drainage along which array PDM-1 was placed

Looking southwest along MASW array PDM-1

Looking northeast along MASW array PDM-1

Location of Geophysical Testing Arrays:

Location	Latitude	Longitude
PDM-1, Southwest End of Array	34.30269	-114.14411
PDM-1, Center of Array	34.30292	-114.14385
PDM-1, Northeast End of Array	34.30315	-114.14358
HVSR Sensor 507	34.30272	-114.14404
HVSR Sensor 453	34.30329	-114.14214
HVSR Sensor 450	34.30319	-114.14347
CI.PDM Seismic Station	34.30330	-114.14218

Notes: 1) WGS84 Coordinate System (decimal degrees)

2) Survey accuracy is estimated at 1 to 2 m.

Results:

V_S Model

Depth to Top of Layer (m)	Layer Thickness (m)	S-Wave Velocity (m/s)	Inferred P-Wave Velocity (m/s)	Assumed Poisson's Ratio	Assumed Density (g/cm^3)
0	0.8	203	380	0.3	1.80
0.8	10.2	1234	2308	0.3	2.20
11	18	1769	3309	0.3	2.35
29	>1	2093	3916	0.3	2.50

Observations/Discussion:

- The HVSR curves are very similar validating the 1-D velocity structure assumption. There HVSR amplitudes are, however, slightly higher at sensor 453 located near the seismic station.
- There is a possible, but inconclusive, weak HVSR peak in the 0.8 to 0.9 Hz range. It is unclear what the significance of this peak is given that the site is a hard rock site.
- The P-wave refraction data for array PDM-1 were modeled using a tomographic inversion routine with a layer based starting model. The seismic refraction model was extended to far offset shot locations to extend depth of investigation.
- P-wave refraction data indicates that the P-wave velocity of bedrock generally exceeds 3,000 m/s at a depth of about 5 m. Field observations and the seismic refraction model indicate that the sediment thickness overlying rock varies from about 0 to 2 m beneath the MASW and seismic refraction array.
- Noise conditions at the site were not sufficient for application of passive surface wave techniques.
- A representative dispersion curve was generated for the MASW data set using a moving average, polynomial curve fitting routine and used for modeling.
- It was difficult extracting surface wave dispersion data at small wavelengths due to the high velocity shallow rock.
- The minimum wavelength surface wave phase velocity data extracted from the 48-channel MASW array was about 30 m. Reducing data from smaller hammer sources using a limited offset receiver array (i.e. less active geophones) allowed for extraction of surface wave dispersion data to a minimum wavelength of about 3.5 m.
- Scatter in MASW dispersion data is likely due to lateral velocity variation associated with both a very thin sediment layer of variable thickness (0 to 2 m) and differential weathering of near surface rock.
- Surface wave depth of investigation is about 30 m based on half of maximum wavelength criteria.
- The V_S model is generally consistent with the P-wave seismic refraction model. However, the seismic refraction model indicates that V_S may be slightly higher than that modeled over the 5 to 11 m depth range.
- V_{S30} is 1,312 m/s (NEHRP Site Class B).
- V_{S30} would be higher if not for the thin sediment layer overlying rock on portions of the MASW array. Soil is not present at the seismic station; however, there may be a thicker sequence of weathered rock at the seismic station than beneath the MASW array.
- Average S-wave velocity between 1 m (assumed sensor depth) and 31 m is 1,560 m/s (NEHRP Site Class A).
- V_{S30} at the location of the seismic station will depend on the local shallow weathering profile in rock. Although there is not enough space at the seismic station to conduct a surface wave sounding to a depth of 30 m, there is enough space to investigate the weathering profile in the upper 10 m using surface wave and seismic refraction techniques. This was not conducted during the current investigation, but is recommended during a future investigation.

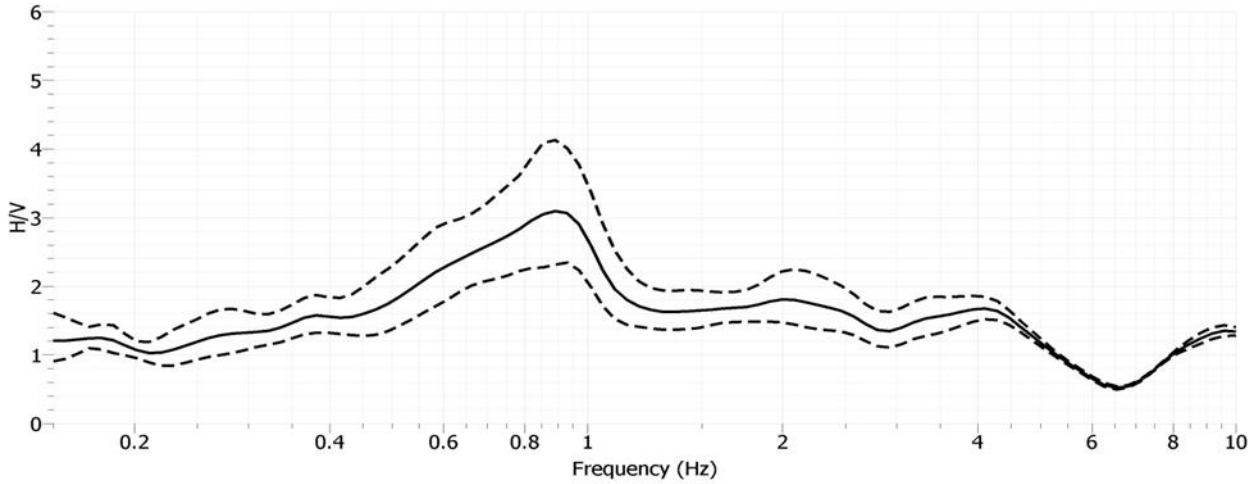

Site CI.PDM, H/V Spectral Ratio, Array PDM-1, Sensor 507

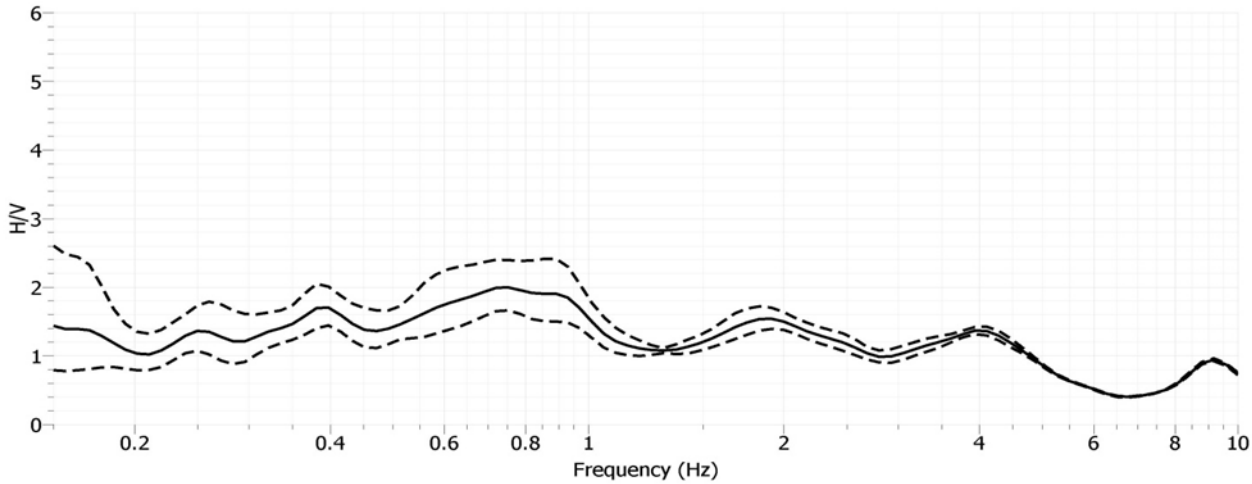

Site CI.PDM, H/V Spectral Ratio, Array PDM-1, Sensor 450

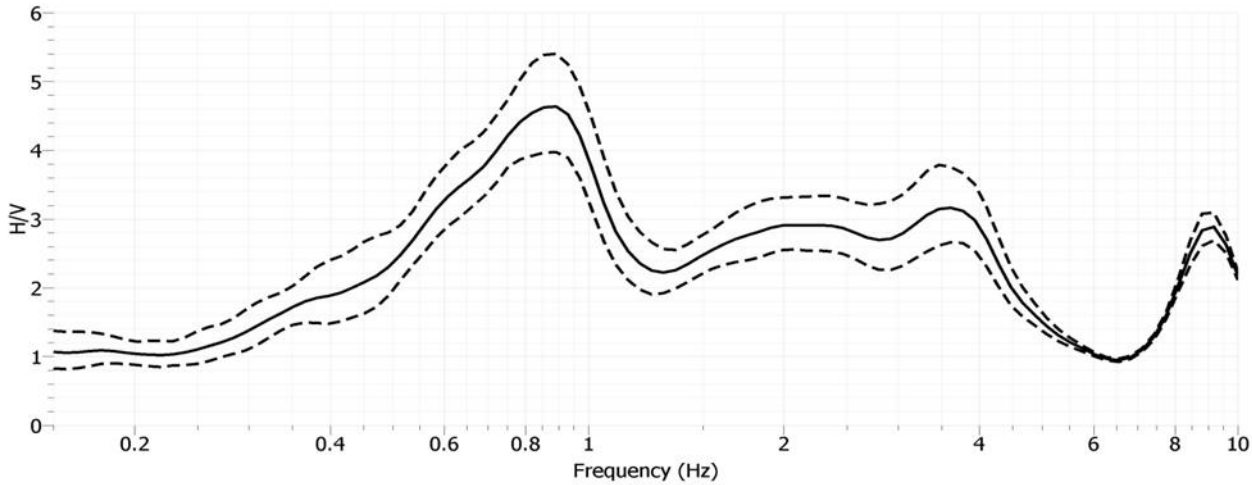

Site CI.PDM, H/V Spectral Ratio, near Seismic Station, Sensor 453

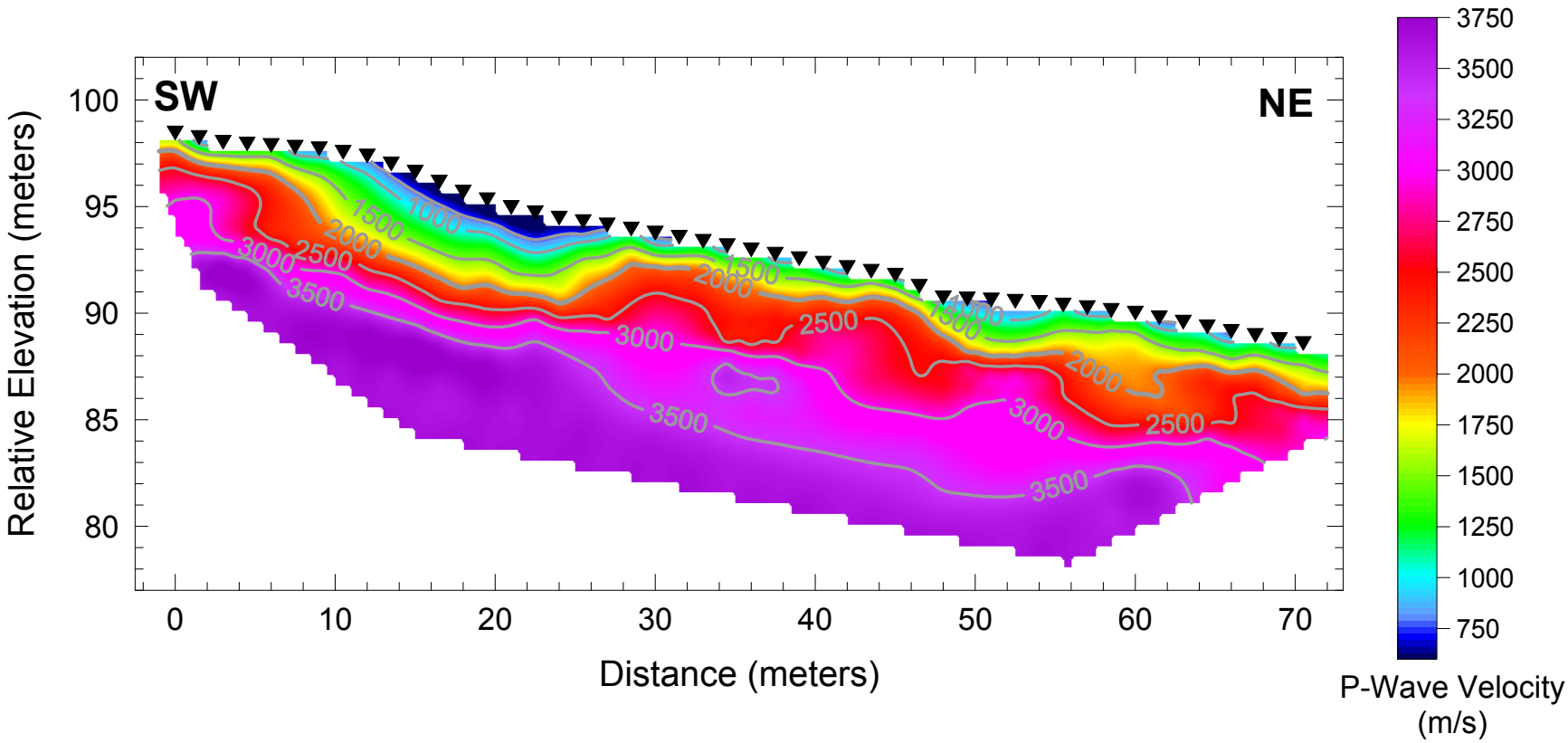

Array PDM-1 – Tomographic seismic refraction model utilizing smooth velocity gradient starting model

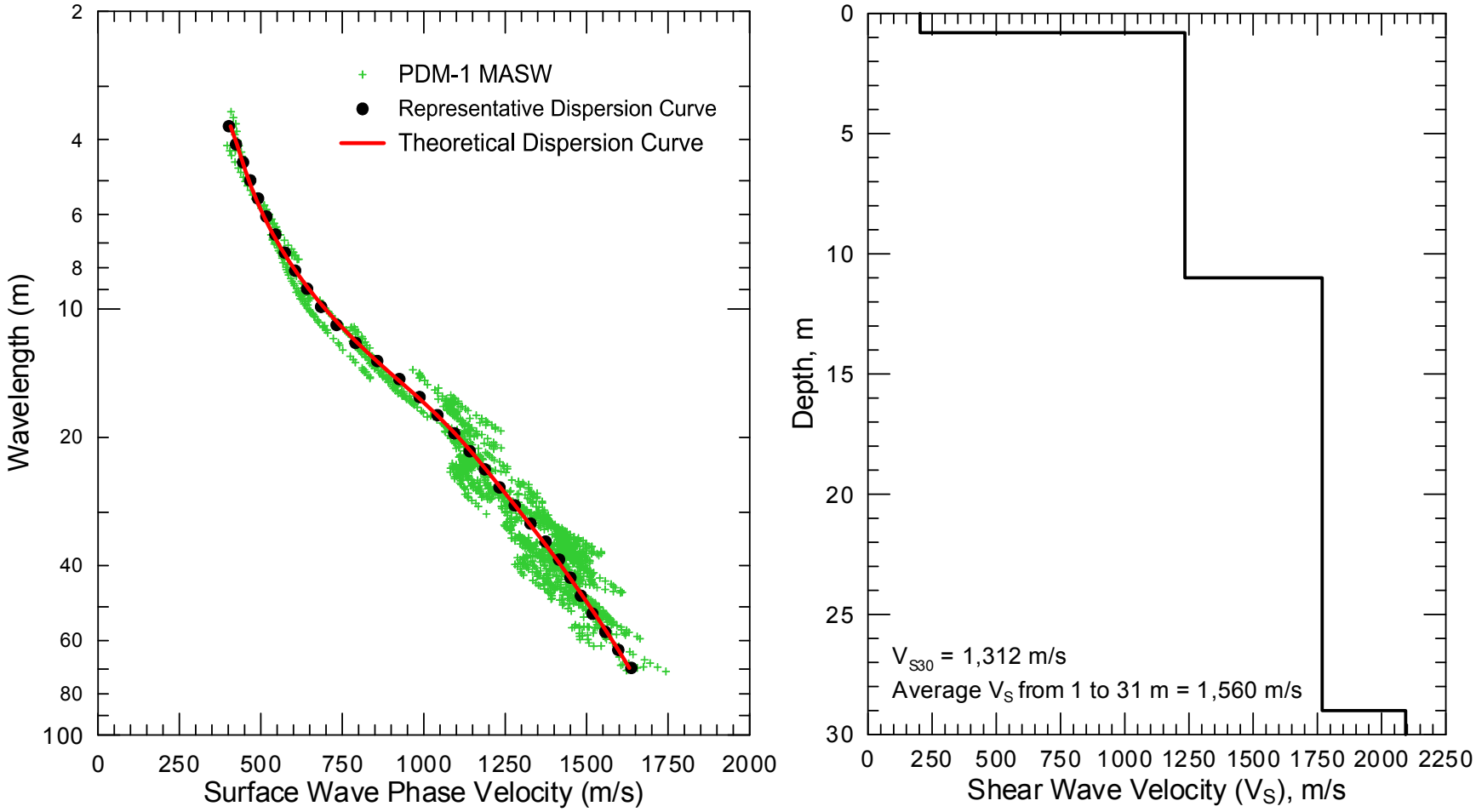

CI.PDM - Field, representative and inverted theoretical surface wave dispersion data (left) and associated V_S model (right)

Site CI.PHL

Location: Park Hill, San Luis Obispo County, California

Latitude: 35.40773 **Longitude:** -120.54556
(Station coordinates provided by USGS, WGS84 coordinate system)

V_{S30} (measured): 384 m/s

V_{S30} (adjusted to more accurately reflect seismic station conditions): 428 m/s (average S-wave velocity between 1.5 and 31.5 m adjusting for assumed 1.5 m sensor depth).

NEHRP Site Class: C

Geomatrix Code: IHB

Geologic Conditions/Observations: Seismic station located on geologic unit mapped as Quaternary (Holocene) stream channel gravel and sand. Mesozoic (Cretaceous) granitic rocks (granodiorite and quartz monzonite) are expected to be located at relatively shallow depth.

Site Conditions: Rural site located in a narrow valley with hilly/mountainous topography to the north and south.

Geophysical Methods Utilized: HVSR, Seismic Refraction (P- and S-wave), MASW (Rayleigh Wave), MALW (Love Wave)

Geophysical Testing Arrays:

1. Array PHL-1 (48 channel MASW and P-wave seismic refraction array utilizing 4.5 Hz vertical geophones spaced 1.5 m apart for a length of 70.5 m, forward and reverse shot locations with multiple source offsets and source types and multiple interior shot locations).
2. Array PHL-1 (48 channel MALW and S-wave seismic refraction array utilizing 4.5 Hz horizontal geophones spaced 1.5 m apart for a length of 70.5 m, forward and reverse shot locations with multiple source offsets and source types and multiple interior shot locations). Same location as P-wave seismic refraction and MASW array of same name.
3. Three HVSR measurement locations: two distributed along array PHL-1 and one adjacent to the seismic station. HVSR data were acquired using a Nanometrics Trillium Compact seismometer. An additional HVSR measurement was made adjacent to the seismic station using a Micromed Tromino ENGY.

Legend

- Seismic Station - Approximate Surveyed Location
- Seismic Station - Approximate Location of Record
- H/V Spectral Ratio Location
- MASW and Seismic Refraction Array

NOTES:
1. WGS 1984 COORDINATE SYSTEM
2. Image Source: (c) Microsoft Corporation and its data suppliers

File Name: CI-PHL-I

Date: 2/7/2013

USGS science for a changing world

GEOVision geophysical services

RECOVERY.GOV

SITE MAP
CI•PHL

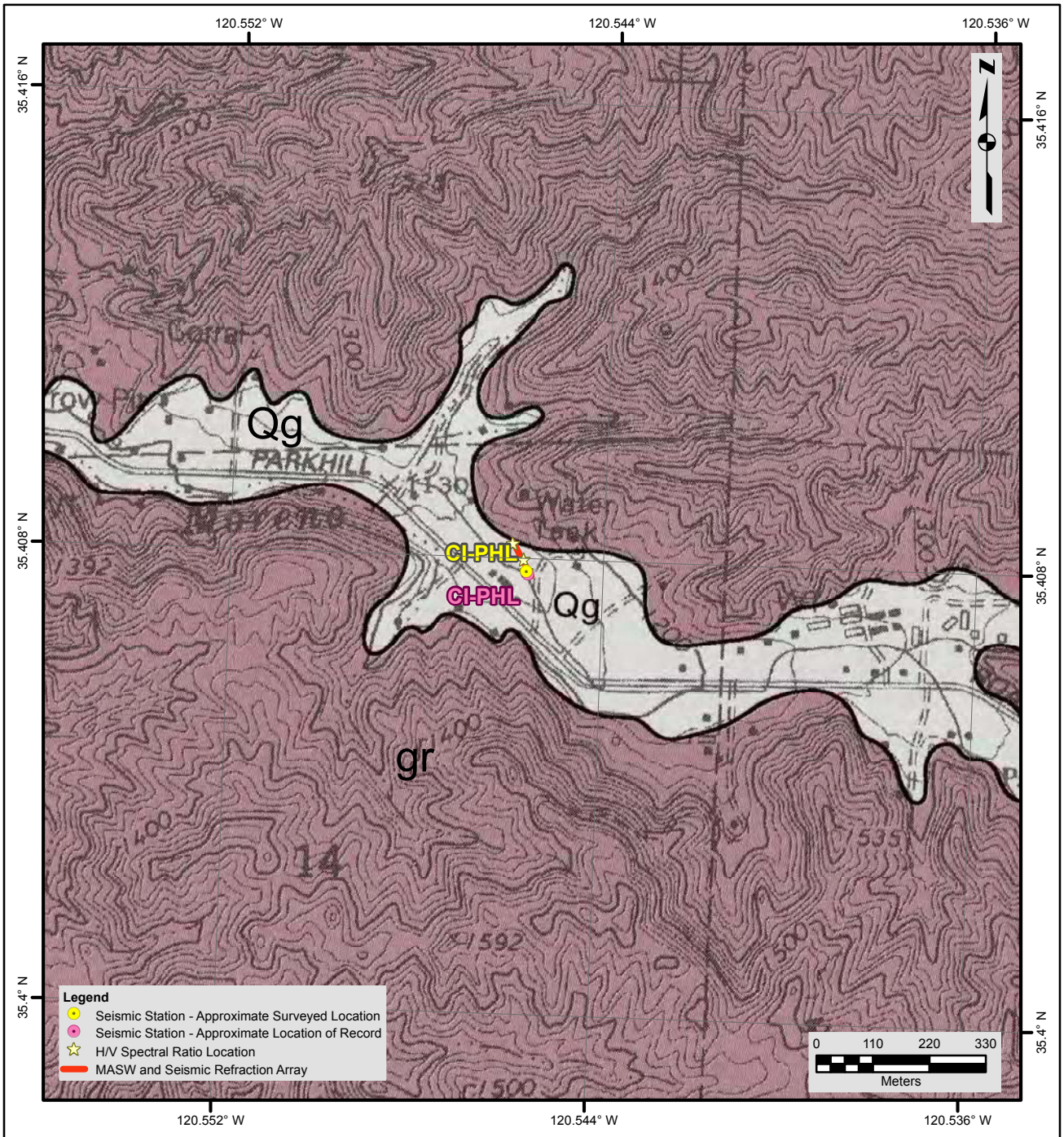

Description of Geologic Map Units

Qg = Quaternary (Holocene) Stream channel gravel and sand
gr = Mesozoic (Cretaceous) granitic rocks, granodiorite to quartz monzonite, medium-grained holocrystalline, massive

NOTES:
1. WGS 1984 COORDINATE SYSTEM
2. Geologic Map of the Santa Margarita Quadrangle, San Luis Obispo County, California by Thomas W. Dibblee, Jr., 2004
3. See site map for details of geophysical survey

File Name: CI-PHL

Date: 2/7/2013

USGS science for a changing world

GEOVision geophysical services

RECOVERY.GOV

GEOLOGIC MAP
CI•PHL

CI.PHL seismic station

Looking southeast at HVSR sensor 453B

Looking northwest along P-wave seismic refraction and MASW array PHL-1

S-wave seismic refraction data acquisition along array PHL-1

Looking southeast towards center of array PHL-1

Location of Geophysical Testing Arrays:

Location	Latitude	Longitude
PHL-1, Southeast End of MASW/Refraction Array	35.40770	-120.54549
PHL-1, Center of MASW/Refraction Array	35.40797	-120.54569
PHL-1, Northwest End of MASW/Refraction Array	35.40828	-120.54590
HVSR Sensor 453A	35.40798	-120.54566
HVSR Sensor 453B	35.40825	-120.54590
HVSR Sensor 507	35.40778	-120.54559
HVSR Sensor Tromino ENGY (TRO-1)	35.40780	-120.54559
CI.PHL Seismic Station	35.40777	-120.54560

Notes: 1) WGS84 Coordinate System (decimal degrees)
2) Survey accuracy is estimated at 1 to 2 m.

Results:

MASW V_S Model 1 (Average Dispersion Curve)

Depth to Top of Layer (m)	Layer Thickness (m)	S-Wave Velocity (m/s)	Inferred P-Wave Velocity (m/s)	Inferred Poisson's Ratio	Inferred Density (g/cm^3)
0	1.5	154	287	0.3	1.70
1.5	2.5	207	387	0.3	1.75
4	9	275	515	0.3	1.80
13	11	729	1363	0.3	2.10
24	>6	1418	2653	0.3	2.20

Notes: 1) Depth of investigation is about 30 m.
2) Bottom layer is a half space.
3) Bedrock velocity not well constrained.

MASW V_S Model 2 (Lower Envelope of Dispersion Curve)

Depth to Top of Layer (m)	Layer Thickness (m)	S-Wave Velocity (m/s)	Inferred P-Wave Velocity (m/s)	Inferred Poisson's Ratio	Inferred Density (g/cm^3)
0	1.5	140	262	0.3	1.70
1.5	2.5	190	356	0.3	1.75
4	10	260	486	0.3	1.80
14	11	900	1684	0.3	2.10
25	>5	1500	2806	0.3	2.20

Notes: 1) Depth of investigation is about 30 m.
2) Bottom layer is a half space.
3) Bedrock velocity not well constrained.

MASW V_S Model 3 (Upper Envelope of Dispersion Curve at Small Wavelengths and Lower Envelope at Long Wavelengths)

Depth to Top of Layer (m)	Layer Thickness (m)	S-Wave Velocity (m/s)	Inferred P-Wave Velocity (m/s)	Inferred Poisson's Ratio	Inferred Density (g/cm^3)
0	1.5	167	312	0.3	1.70
1.5	2.5	210	393	0.3	1.75
4	11	280	524	0.3	1.80
15	11	729	1364	0.3	2.10
26	>4	1418	2653	0.3	2.20

Notes: 1) Depth of investigation is about 30 m.
2) Bottom layer is a half space.
3) Bedrock velocity not well constrained.

MASW V_S Model 4 (Upper Envelope of Dispersion Curve)

Depth to Top of Layer (m)	Layer Thickness (m)	S-Wave Velocity (m/s)	Inferred P-Wave Velocity (m/s)	Inferred Poisson's Ratio	Inferred Density (g/cm^3)
0	1.5	167	312	0.3	1.70
1.5	2.5	210	393	0.3	1.75
4	8	280	524	0.3	1.80
12	11	729	1364	0.3	2.10
23	>7	1418	2653	0.3	2.20

Notes: 1) Depth of investigation is about 30 m.
2) Bottom layer is a half space.
3) Bedrock velocity not well constrained.

MASW V_S Model 5 (Lower Envelope of Dispersion Curve at Small Wavelengths and Upper Envelope at Long Wavelengths)

Depth to Top of Layer (m)	Layer Thickness (m)	S-Wave Velocity (m/s)	Inferred P-Wave Velocity (m/s)	Inferred Poisson's Ratio	Inferred Density (g/cm^3)
0	1.5	140	262	0.3	1.70
1.5	2.5	190	356	0.3	1.75
4	6	260	486	0.3	1.80
10	11	729	1364	0.3	2.10
21	>9	1418	2653	0.3	2.20

Notes: 1) Depth of investigation is about 30 m.
2) Bottom layer is a half space.
3) Bedrock velocity not well constrained.

Average V_P Model and Estimated V_S Models from Central Portion of P-wave Seismic Refraction Array PHL-1

Depth to Top of Layer (m)	Layer Thickness (m)	P-Wave Velocity (m/s)	Estimated S-Wave Velocity (m/s)			
			Poisson's Ratio = 0.25	Poisson's Ratio = 0.3	Poisson's Ratio = 0.35	Poisson's Ratio = 0.4
0.00	0.50	298	172	159	143	122
0.50	1.01	307	177	164	147	125
1.51	1.01	354	204	189	170	144
2.52	1.01	391	226	209	188	159
3.53	1.01	393	227	210	189	160
4.54	1.01	395	228	211	190	161
5.55	1.01	395	228	211	190	161
6.56	2.12	397	229	212	191	162
8.68	2.12	517	299	276	248	211
10.80	2.12	1474	851	788	708	602
12.92	2.12	1534	886	820	737	626
15.04	2.12	1622	936	867	779	662
17.16	2.12	1843	1064	985	886	753
19.27	2.12	2017	1164	1078	969	823
21.39	2.12	2659	1535	1421	1277	1085
23.51	2.12	2941	1698	1572	1413	1201
25.63	2.12	3367	1944	1800	1617	1375
27.75	Half Space	3516	2030	1879	1689	1435

Average V_S Model from Central Portion of S-wave Seismic Refraction Array PHL-1

Depth to Top of Layer (m)	Layer Thickness (m)	S-Wave Velocity (m/s)
0.00	0.51	107
0.51	1.01	218
1.52	1.01	229
2.53	1.01	252
3.54	1.01	254
4.55	1.01	257
5.56	1.01	258
6.58	2.12	261
8.70	2.12	352
10.83	2.12	500
12.95	2.12	669
15.08	2.12	727
17.20	2.12	730
19.32	2.12	739
21.45	2.12	785
23.57	2.12	921
25.70	Half Space	1314

Observations/Discussion:

- The seismic station is located in a narrow (~200 m wide) valley between mountains comprised of Cretaceous granitic rocks. The presence of a parking lot and property boundaries in the vicinity of the seismic station severely limited the choice of possible orientations for geophysical testing arrays. Ideally array PHL-1 would have been oriented parallel to the axis of the valley in order to maintain relatively uniform bedrock depth; however, this was not possible. The bedrock outcrop is not as close to the northwestern end of array PHL-1 as the geologic map indicates. The orientation of array PHL-1 is such that depth to bedrock is expected to gradually decrease to the northwest. The seismic station is located near the southeastern end of array PHL-1, where bedrock is expected to be deepest.
- This site was visited on two occasions. HVSR, P-wave seismic refraction and MASW data were acquired along array PHL-1 during the initial site visit. Preliminary review of the data indicated that MASW data interpretation may be difficult and, therefore, S-wave seismic refraction and MALW data were acquired at the site at a later date.
- HVSR data collected at the three measurement locations have high frequency HVSR peaks in the 3.5 to 6 Hz range, as expected for a site with relatively shallow bedrock. Data from HVSR sensor 507 (Nanometrics Trillium Compact), located next to the

seismic station near the southeastern end of array PHL-1, where bedrock is expected to be deepest, has a relatively narrow HVSR peak at about 3.7 Hz. HVSR measurements were also made adjacent to Trillium sensor 507, with a Tromino ENGY and yielded similar results. This data is not presented as it is considered redundant. HVSR data from sensors 453A and 453B have much broader peaks between 3.5 and 6 Hz. These broad peaks likely result from the three dimensional nature of the bedrock surface in the site vicinity.

- The P- and S-wave seismic refraction data for array PHL-1 were modeled using a tomographic inversion routine with layer based (two layer) starting models. The seismic refraction models were extended to far offset shot locations to extend depth of investigation. Ideally, the seismic refraction data would have been acquired along a longer array; however, the seismic refraction data was acquired in conjunction with MASW/MALW data, which benefits from a shorter array.
- The P-wave first arrival data were picked to greater degree of accuracy than the S-wave first arrival data because there were often strong P-wave arrivals before the S-wave arrivals and possible converted waves as first arrivals on several seismic records. Generally, S-wave refraction models should be checked against P-wave refraction models, unless there is a shallow saturated zone, to confirm that the S-wave refraction model is realistic and that converted waves have not been interpreted as S-waves. At this site, the P-wave seismic refraction model is expected to be more accurate.
- The P-wave seismic refraction survey design allowed P-wave velocity to be imaged to a maximum depth of about 28 m, although a longer profile would have imaged velocity structure below a depth of 20 to 25 m with more accuracy. The seismic refraction model indicates that P-wave velocity is about 275 to 350 m/s at the surface and increases to over 1,000 m/s at a depth of 7 to 12 m, 1,500 m/s at a depth of 9 to 17 m, 2,000 m/s at a depth of 14 to 20 m and over 3,000 m/s at a depth of 20 to 25 m. The maximum P-wave velocity in the model is about 3,500 m/s. The top of bedrock probably tracks the 1,000 to 1,250 m/s contours at a depth of about 7 to 15 m, with bedrock depth decreasing to the northwest. The S-wave seismic refraction model, discussed below, confirms that P-wave velocities in the 1,250 to 2,000 m/s range are associated with weathered bedrock rather than saturated sediments. The increase in weathered bedrock velocity to over 2,000 m/s may be associated with either a decrease in weathering or, possibly, saturation of the rock.
- The S-wave seismic refraction survey design allowed S-wave velocity to be imaged to a maximum depth of about 26 m, although a longer profile would have imaged velocity structure below a depth of 20 to 25 m with more accuracy. The seismic refraction model indicates that S-wave velocity is about 150 to 200 m/s at the surface and increases to over 300 m/s at a depth of 2 to 9 m, 500 m/s at a depth of 7 to 13 m and over 1,000 m/s at a depth of 13 to 25 m. The maximum S-wave velocity in the model is about 1,400 m/s. The top of the bedrock surface probably tracks the 500 to 600 m/s contours at a depth of 7 to 15 m. Bedrock depth decreases to the northwest, which is consistent with the P-wave refraction model. The high V_P to V_S ratio at depths below about 20 m introduces the possibility that bedrock is saturated below this depth, although this cannot be stated conclusively due to potential model errors at depth.
- The average P-wave velocity of the upper 30 m (V_{P30}) was estimated between 24 and 48 m along the P-wave refraction model, where depth of investigation is greatest. To

estimate V_{P30}, the P-wave velocity at a depth of 28 m, nominal depth of investigation, was projected to 30 m depth. V_{P30} ranges from about 769 to 914 m/s over the 24 to 48 m position interval, an 18% variation, and is expected to decrease and increase to the southeast and northwest, respectively. An average V_P model was developed over the 24 to 48 m distance interval by horizontally averaging the travel time of each model cell and cell thickness and average V_{P30} was determined to be 819 m/s. Assuming constant Poisson's ratios of 0.25, 0.3, 0.35 and 0.4 would result in an estimated V_{S30} of 473, 438, 393 and 334 m/s, respectively. The average V_S between 1.5 and 31.5 m, to account for assumed 1.5 m sensor depth, is 539, 499, 448, and 381 m/s for constant Poisson's ratios of 0.25, 0.3, 0.35 and 0.4, respectively. The seismic station is located towards the southeastern end of the array where bedrock is deeper, and V_{S30} and adjusted V_{S30} are expected to be about 10% lower than the average values.

- V_{S30} was estimated between 15 and 48 m along the S-wave refraction model, where depth of investigation is greatest, by projecting the velocity at 26 m depth to 30 m depth. Over this interval V_{S30} ranges from about 412 to 506 m/s, a 22% variation over a 33 m distance. An average V_S model was developed over the 15 to 48 m distance interval by horizontally averaging the travel time of each model cell and cell thickness and average V_{S30} was determined to be 440 m/s. The average V_S between 1.5 and 31.5 m, to account for assumed 1.5 m sensor depth, is 499 m/s. The seismic station is located towards the southeastern end of the array where bedrock is deeper and V_{S30} and adjusted V_{S30} are expected to be about 10% lower than the average values.
- Noise conditions at the site were not sufficient for application of passive surface wave techniques.
- Both MASW and MALW data were acquired along array PHL-1. It was difficult to extract long wavelength Rayleigh/Love wave dispersion data from the data sets, possibly due to the shallow dipping bedrock unit. It was not generally possible to extract long wavelength Rayleigh wave phase velocity data from far offset shot locations. Long wavelength phase velocity data was only obtained from source locations offset 1.5 and 5 m from the near geophone at each end of the array, which required the near field criteria to be relaxed to obtain the necessary 60+ m wavelength required to image to 30 m depth. There is significant scatter in both small wavelength dispersion data due to near surface lateral velocity variation and long wavelength dispersion data due to the slightly dipping bedrock surface. Only the MASW dataset was selected for modeling; however, the Love wave dispersion data appears consistent with the Rayleigh wave dispersion data. A relatively abrupt increase in S-wave velocity at shallow depth is typically expected to excite a dominant 1st higher mode in Rayleigh wave data at low frequencies, but the fundamental mode should remain dominant in Love wave dispersion data. Because the dispersion curves from the two data sets appear to be relatively consistent it would appear that the fundamental mode Rayleigh wave is dominant at low frequencies/long wavelengths. More investigation into the effects of lateral velocity variation on higher mode Rayleigh waves may shed light on to why the fundamental mode occasionally remains dominant at sites where the 1-D V_S model indicates that the first higher mode should have the most energy at low frequencies.
- The minimum wavelength surface wave phase velocity data extracted from the MASW array was about 1.5 m.

- The maximum wavelength extracted from the MASW data was generally set equal to the 1.5 times the distance from the source to midpoint of the receiver array. The maximum wavelength Rayleigh wave phase velocity data extracted from the MASW data was about 70 m.
- There is typically about 30 to 75 m/s of scatter in the MASW dispersion data, which is likely the result of lateral velocity variation.
- A representative dispersion curve was generated for the MASW data set using a moving average, polynomial curve fitting routine and used for modeling.
- MASW data was modeled using the fundamental mode assumption and bedrock V_S is not well constrained in the surface wave models.
- Because of the variable bedrock depth beneath the array, five models were developed for the MASW data set to explore the variation in V_{S30}. As shown above for the seismic refraction models, there is expected to be more than 20% variation in V_{S30}, primarily due to the slight (~5 degree) dip of the bedrock surface. The seismic station is located towards the southeastern end of the line, where bedrock is deepest and, therefore, V_{S30} should be lower than average values determined for the array. Model 1 fits the representative dispersion curve and is, therefore, considered the average V_S model for the array. The modeled bedrock depth of 13 m for Model 1 is slightly deeper than the average bedrock depth in the seismic refraction models. Model 2 fits the lower envelope of the dispersion data and has a modeled bedrock depth of 14 m, near the maximum bedrock depth observed in the refraction models. Model 3 fits the upper and lower envelope of the dispersion data at small and long wavelengths, respectively and has bedrock modeled at a depth of 15 m, the maximum depth interpreted in the seismic refraction models. Model 4 fits the upper envelope of the dispersion data and has bedrock modeled at a depth of 12 m, significantly deeper than the minimum depth to bedrock interpreted from the seismic refraction data. Model 5 fits the lower and upper envelope of the dispersion data at small and long wavelengths, respectively and has bedrock modeled at a depth of 10 m, slightly deeper than the minimum depth interpreted from the seismic refraction data. Models 2 and 3, with the deepest modeled depth to bedrock, are likely most representative of velocity structure near the seismic station.
- Surface wave depth of investigation is about 30 m based on half of maximum wavelength criteria.
- V_{S30} is 406, 385, 384, 432 and 439 m/s for MASW V_S Models 1 to 5, respectively (NEHRP Site Class C). The lowest V_{S30} of 384 m/s (MASW V_S Model 3) is considered most representative of seismic station conditions.
- Average S-wave velocity between 1.5 m (assumed sensor depth) and 31.5 m is 460, 440, 428, 487 and 511 m/s for MASW V_S Models 1 to 5, respectively (NEHRP Site Class C). The lowest adjusted V_{S30} of 428 m/s (MASW V_S Model 3) is considered most representative of seismic station conditions.
- The S-wave refraction V_S model is generally consistent with the MASW V_S models, but has higher V_S in to 1 to 4 m depth range. The V_S model estimates from the P-wave refraction model using constant Poisson's ratios of 0.3 and 0.35 have slightly lower V_S between depths of 4 and 9 m and generally higher V_S at depths below 18 m than the MASW and S-wave refraction V_S models. The higher V_S at depth estimated from the P-wave refraction model may indicate that weathered rock is saturated at depth with Poisson's ratio slightly higher than 0.35. Some of the differences in the V_S models may

be related to nonuniqueness and with additional data modeling it may be possible to develop more similar models. Although there are subtle differences in the V_S models developed using the three geophysical methods, estimates of V_{S30} from each data set are within about 10%. The average V_S models developed from the seismic refraction models are best compared with MASW V_S Model 1. MASW V_S Model 1 has a V_{S30} of 406 m/s compared to 440 m/s for the average V_S model from the S-wave seismic refraction survey and 438 and 393 m/s for the average P-wave refraction model with assumed constant Poisson's ratios of 0.3 and 0.35, respectively.

- For the purpose of site characterization, we recommend using MASW V_S Model 3. This model has the largest depth to bedrock and lowest value of V_{S30} and adjusted V_{S30} and is considered appropriate as the seismic station is located adjacent to the portion of the MASW array with deepest bedrock.
- In summary, V_{S30} is about 384 m/s (NEHRP Site Class C) and adjusted V_{S30} is 428 m/s (NEHRP Site Class C). NEHRP Site Class will likely drop to Class D a relatively small distance (<30 m) south of the seismic station as bedrock gets deeper.

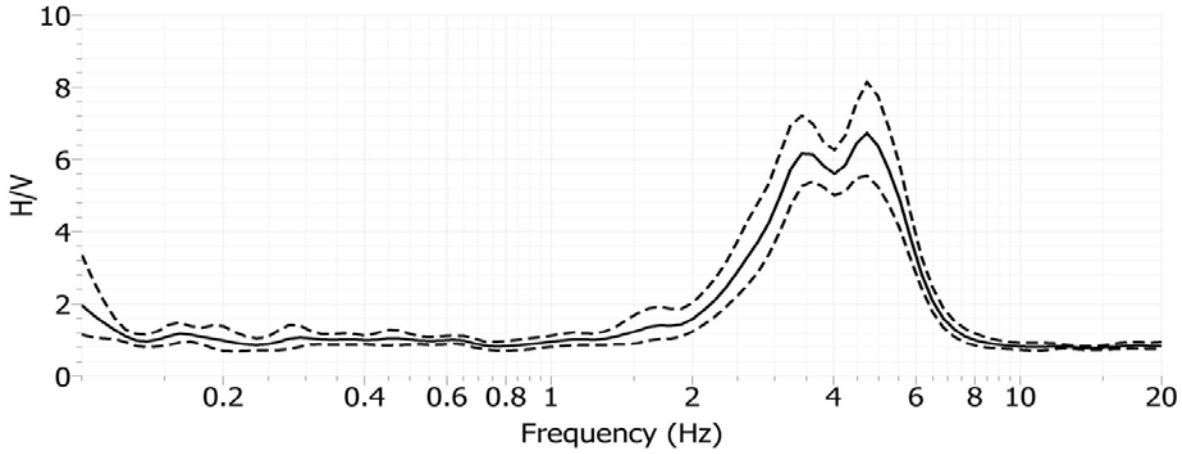

Site CI.PHL, H/V Spectral Ratio, Array PHL-1, Sensor 453B

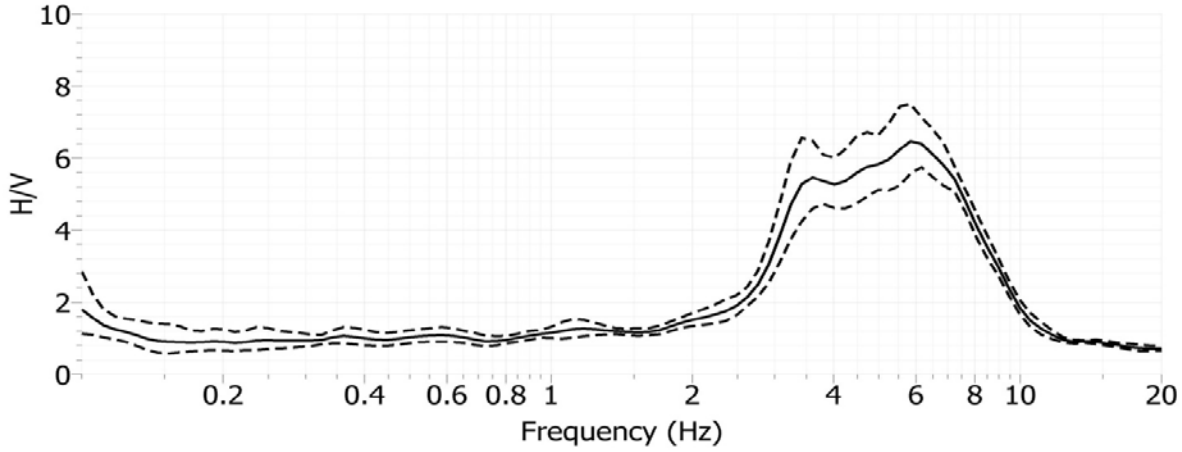

Site CI.PHL, H/V Spectral Ratio, Array PHL-1, Sensor 453A

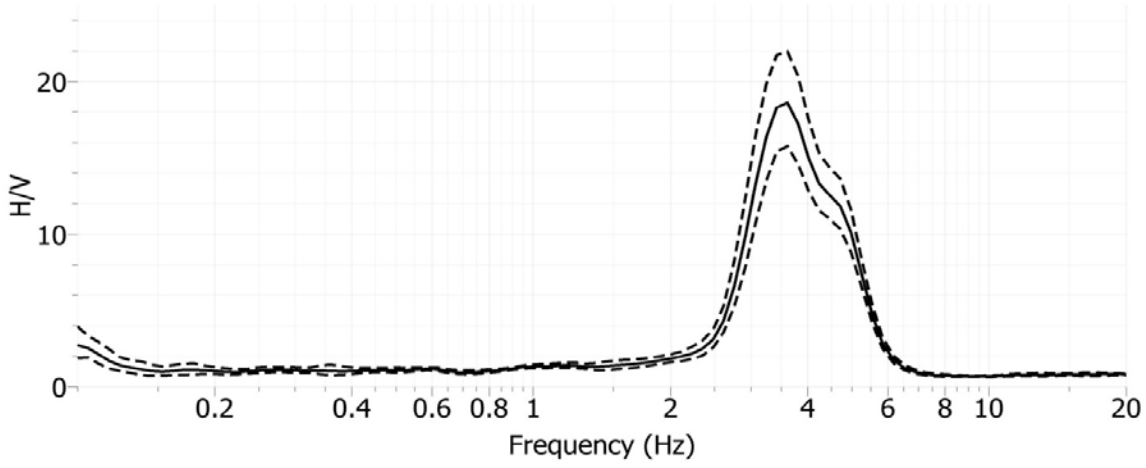

Site CI.PHL, H/V Spectral Ratio, Array PHL-1, Sensor 507

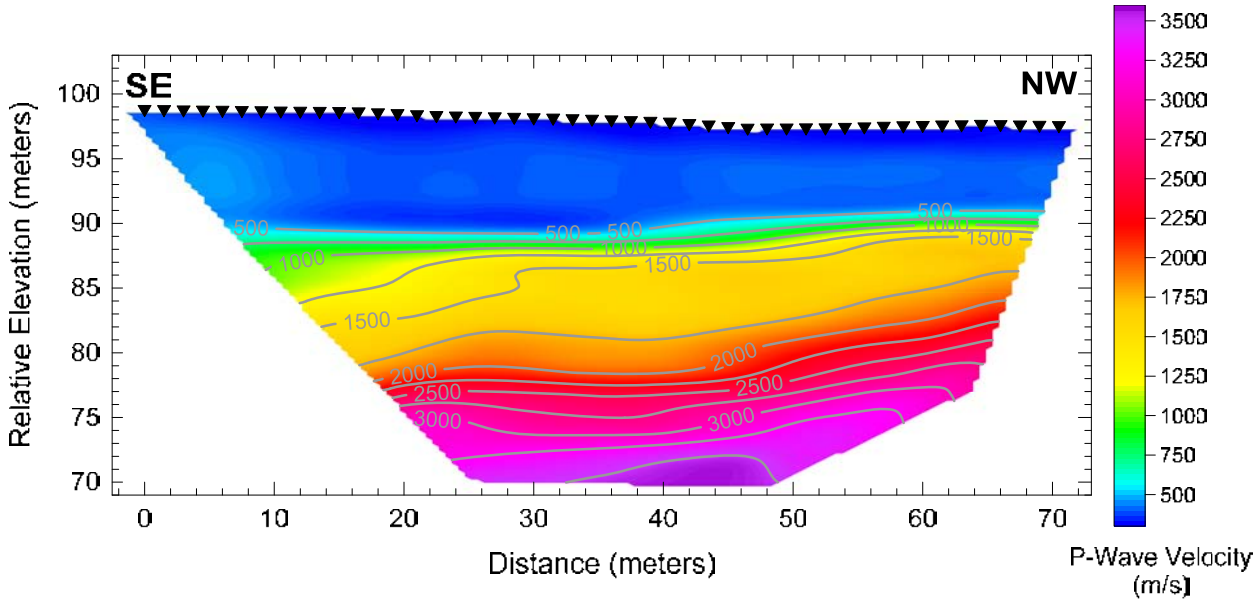

Array PHL-1 – P-wave Tomographic Seismic Refraction Model Developed using a Layer Based Starting Model

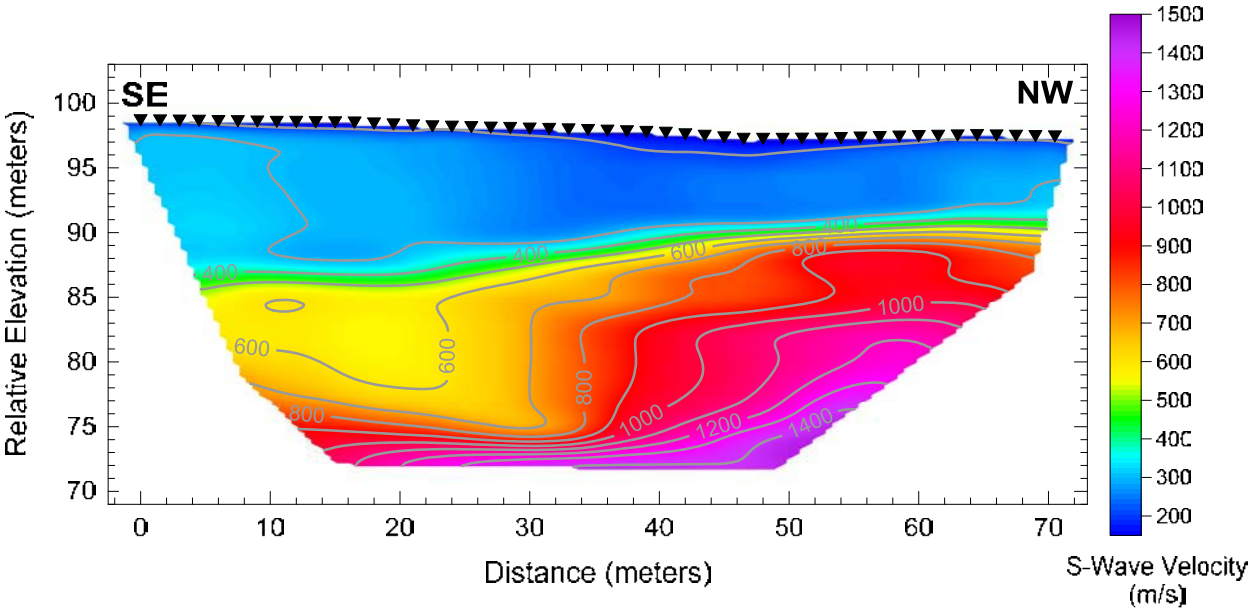

Array PHL-1 – S-wave Tomographic Seismic Refraction Model Developed using a Layer Based Starting Model

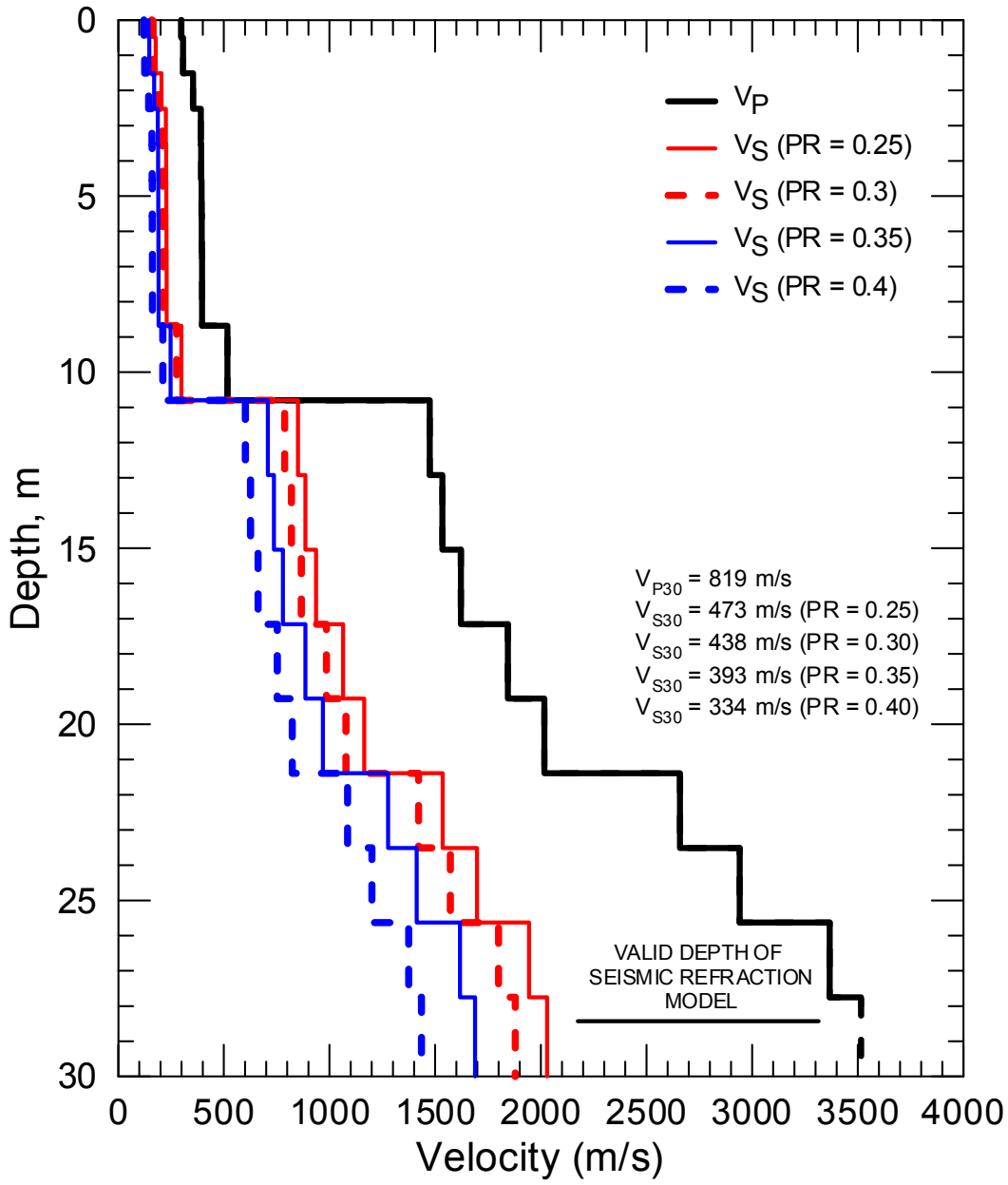

CI.PHL – Average P-wave velocity structure and estimated S-wave velocity structure between a distance of 24 and 48 m along the P-wave seismic refraction model for array PHL-1.

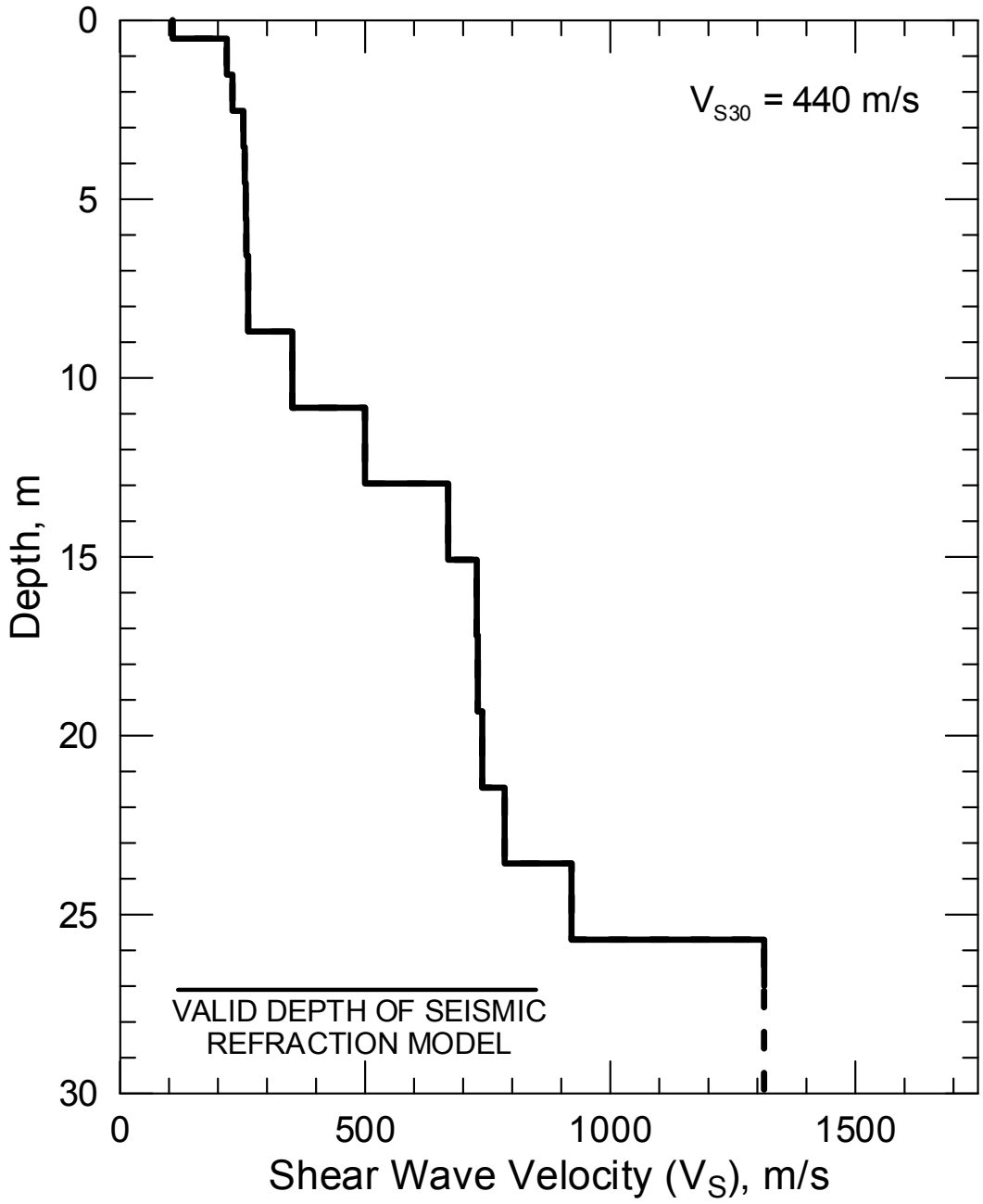

CI.PHL – Average S-wave velocity structure between 15 and 48 m on S-wave seismic refraction array PHL-1. Seismic refraction depth of investigation is limited to about 24 m and S-wave velocity is assumed to be constant below this depth.

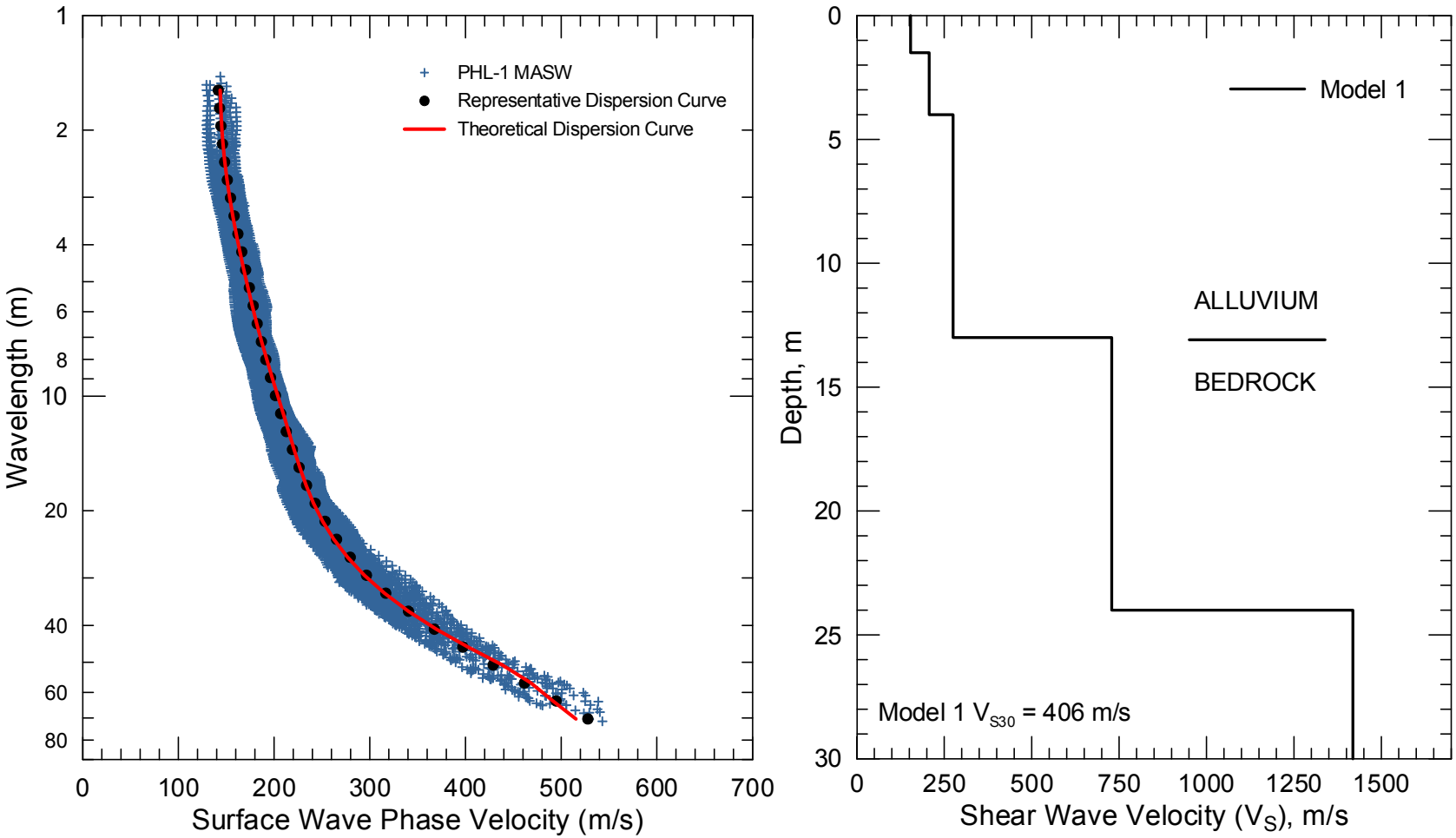

CI.PHL - Field, representative and inverted theoretical surface wave dispersion data (left) and associated V_S model (right)

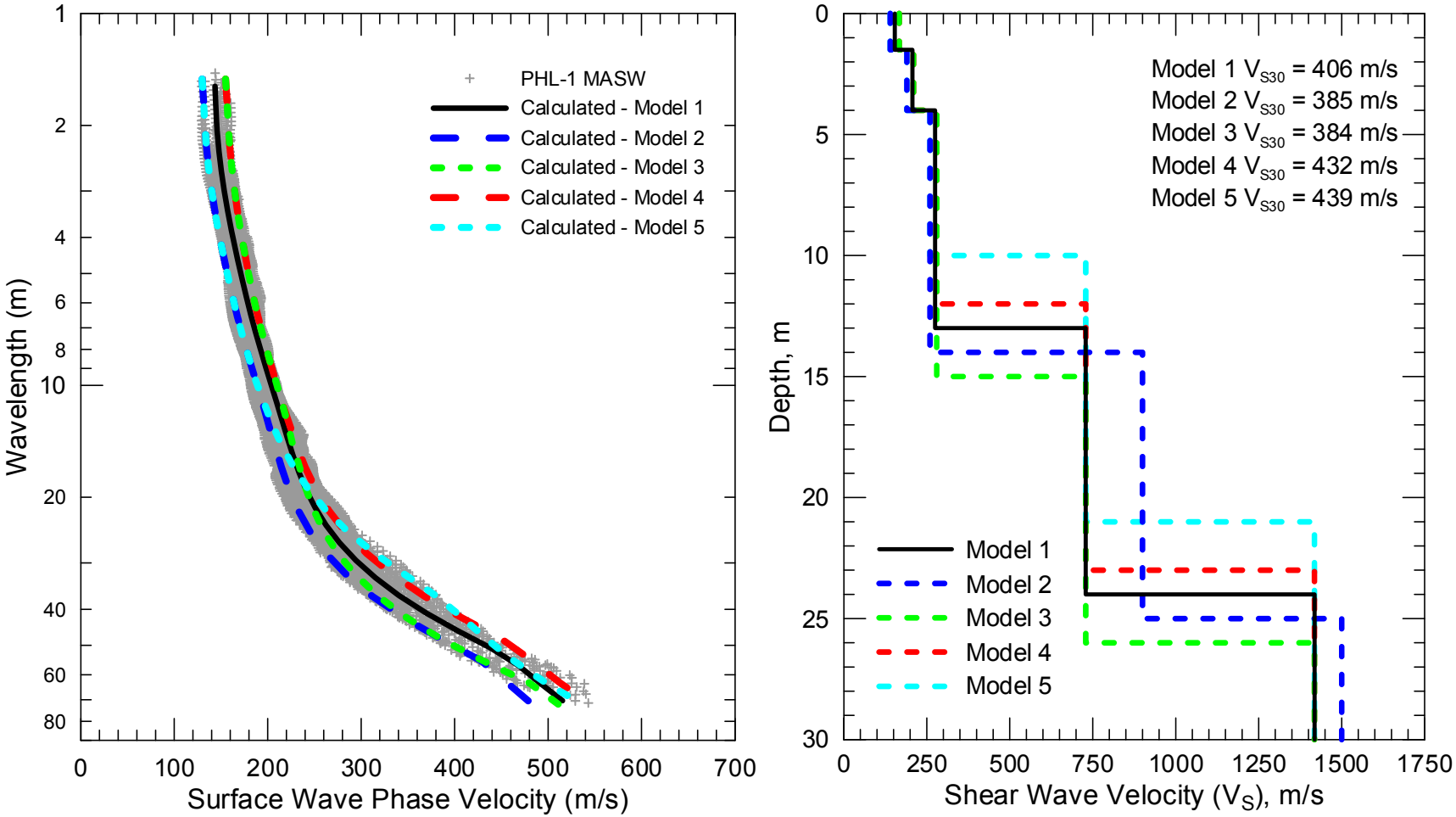

CI.PHL – Field and calculated surface wave dispersion data (left) and associated V_S models (right) fitting average (Model 1), lower envelope (Model 2), upper envelope at small wavelengths and lower envelope at large wavelengths (Model 3), upper envelope (Model 4) and lower envelope at small wavelengths and upper envelope at large wavelengths (Model 5) surface wave dispersion data

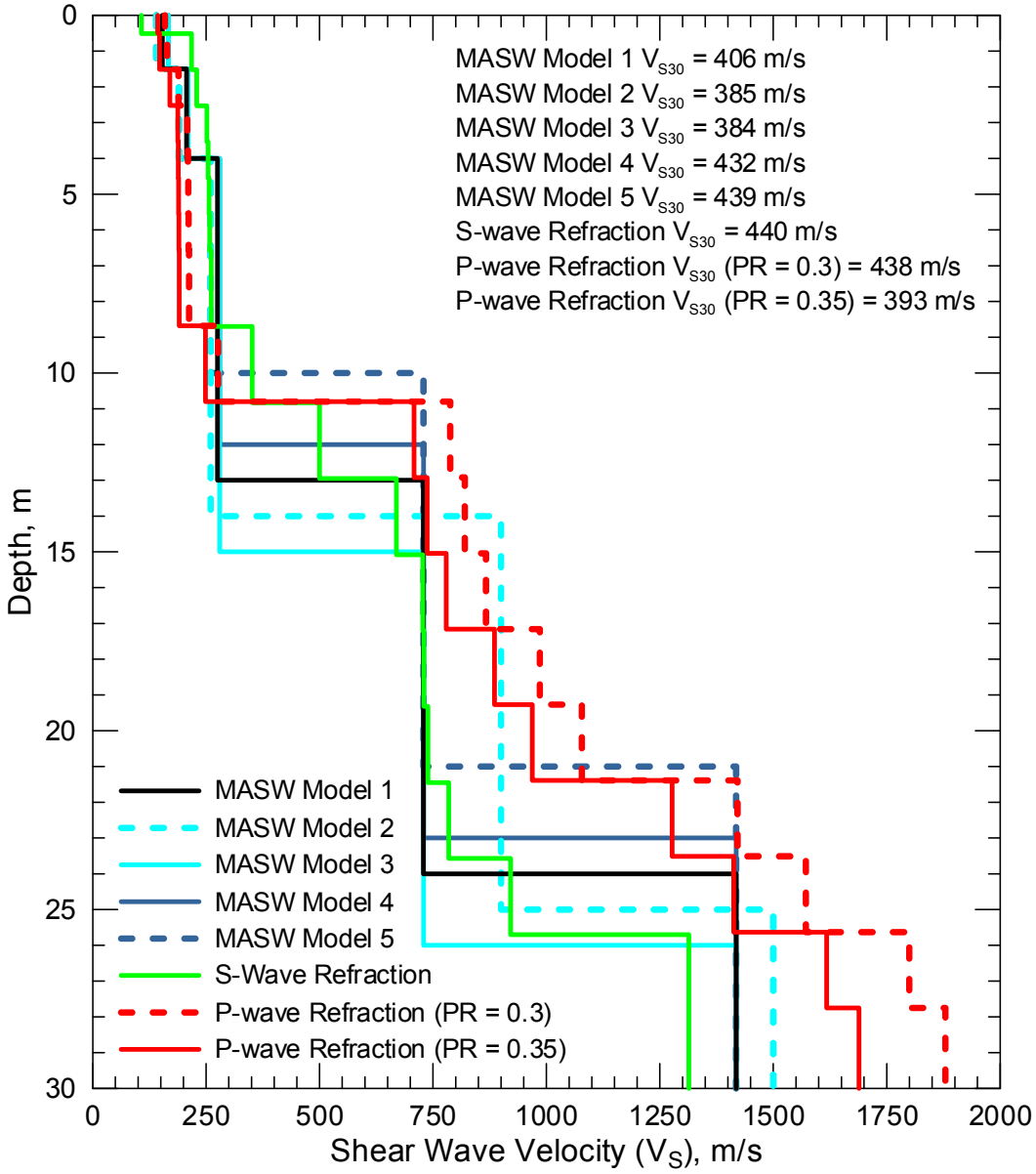

CI.PHL – Comparison of V_S models derived from MASW and P- and S-wave seismic refraction data. The S-wave refraction V_S model is generally consistent with the MASW V_S models, but has higher V_S in to 1 to 4 m depth range. The V_S model estimates from the P-wave refraction model using a constant Poisson's ratio of 0.3 and 0.35 has slightly lower V_S between depths of 4 and 9 m and generally higher V_S at depths below 18 m than the MASW and S-wave refraction V_S models. The higher V_S at depth estimated from the P-wave refraction model may indicate that weathered rock is saturated at depth, with a Poisson's ratio slightly higher than 0.35. Some of the differences in the V_S models may be related to nonuniqueness and with additional data modeling it may be possible to develop more similar. Although there are subtle differences in the V_S models developed using the three geophysical methods, estimates of V_{S30} from each data set are within about 10%.

Site CI.PLC

Location: Palm Springs City Hall, Palm Springs, California

Latitude: 33.82436 **Longitude:** -116.51195
(Station coordinates provided by USGS, WGS84 coordinate system)

V_{S30} (measured): 346 m/s

V_{S30} (adjusted to more accurately reflect seismic station conditions): 371 m/s (average S-wave velocity between 2 and 32 m adjusting for nominal sensor depth).

NEHRP Site Class: D/C

Geomatrix Code: IHD

Geologic Conditions/Observations: Site located in area mapped as Quaternary (Holocene) alluvium. Deep soil site.

Site Conditions: Urban site with significant traffic noise from nearby roads. Relatively flat terrain in site vicinity.

Geophysical Methods Utilized: HVSR, MASW, array microtremor, ReMi™

Geophysical Testing Arrays:

1. Arrays PLC-1 and PLC-2 (24 channel linear arrays utilizing 4.5 Hz vertical geophones spaced 4 m apart for an array length of 92 m) used to acquire passive surface wave data. Arrays combined to form an "L" shaped array.
2. Arrays PLC-1 and PLC-2 were also used to acquire limited MASW and seismic refraction data (reversed off-end shots with accelerated weight drop energy source).
3. Array PLC-3 (48 channel MASW array utilizing 4.5 Hz vertical geophones spaced 1 m apart for a length of 47 m, forward and reverse shot locations with multiple source offsets and source types and center shot location).
4. Three HVSR measurement locations: one located on each of arrays PLC-1 and PLC-2 and the other near the seismic station.

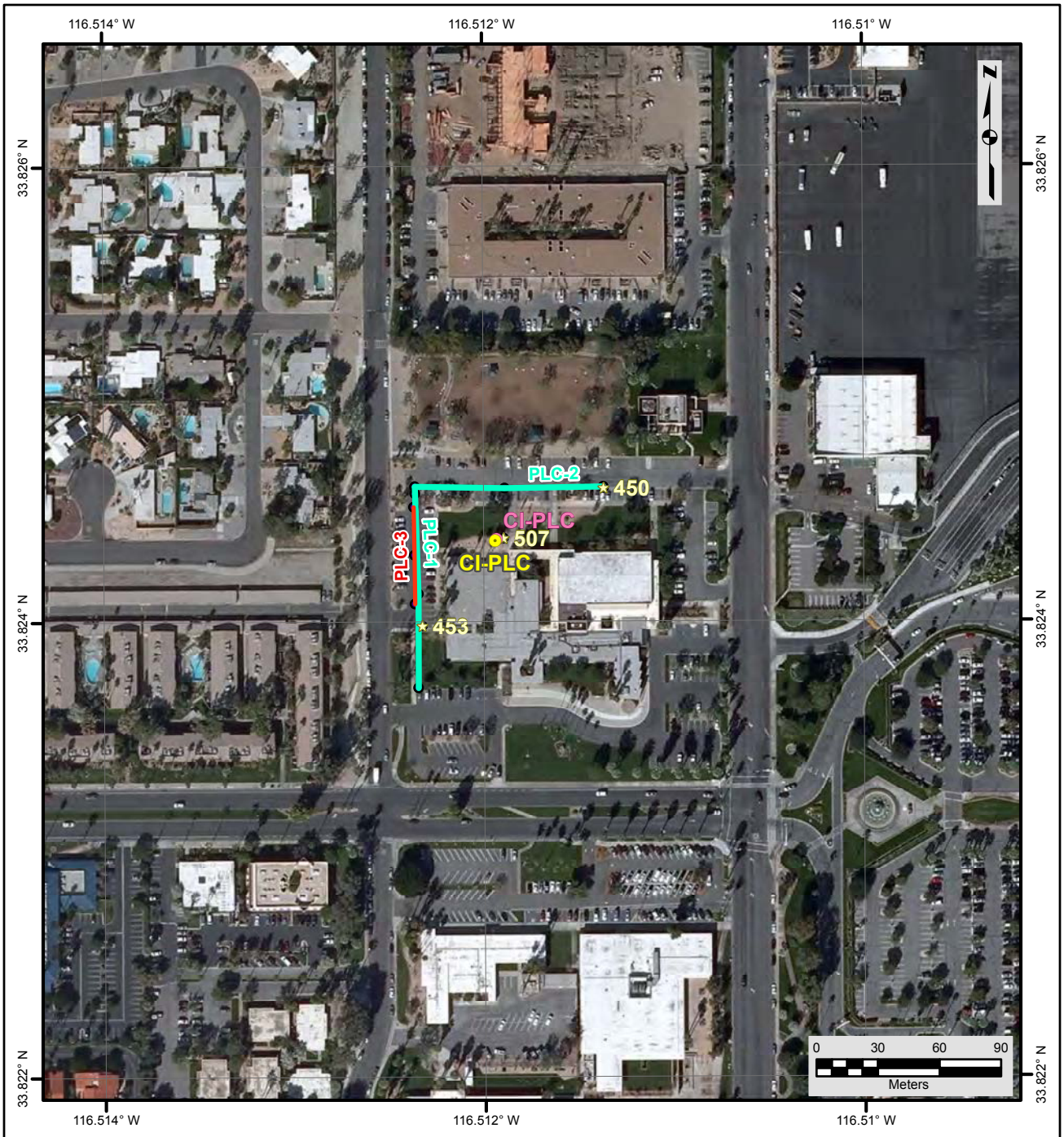

Legend

- Seismic Station - Approximate Surveyed Location
- Seismic Station - Approximate Location of Record
- H/V Spectral Ratio Measurement Location
- MASW Array
- Passive Surface Wave Array

NOTES:
1. WGS 1984 COORDINATE SYSTEM
2. Image Source: ESRI, i-cubed, USDA FSA, USGS, AEX, GeoEye, Getmapping, Aerogrid, IGP

File Name: CI-PLC-I

Date: 4/7/2011

USGS science for a changing world

GEOVision geophysical services

RECOVERY.GOV

SITE MAP
CI•PLC

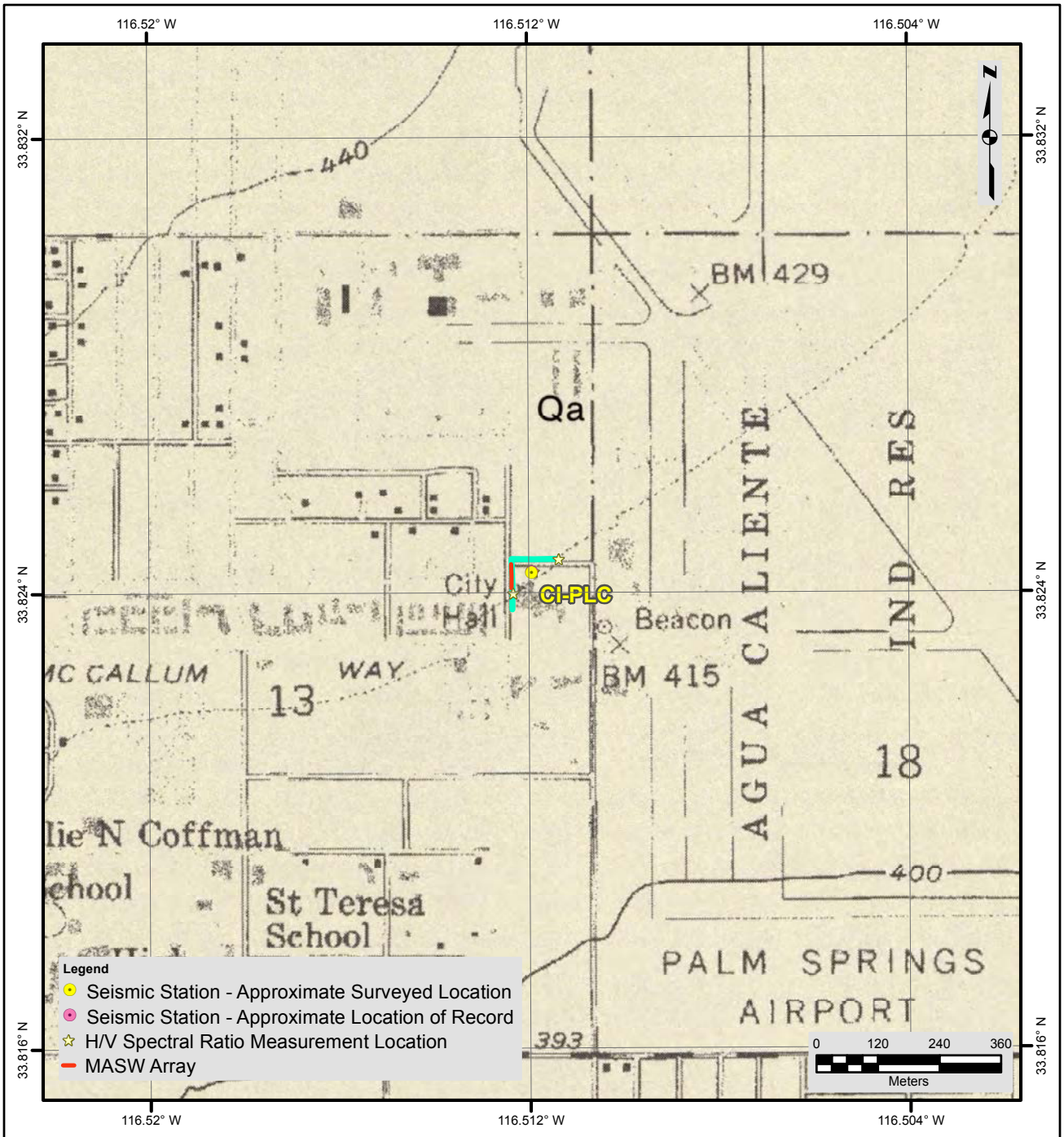

Description of Geologic Map Units

Qa = Quaternary (Holocene) alluvial sand and gravel of valley areas

NOTES:
1. WGS 1984 COORDINATE SYSTEM
2. Geologic Map of the Palm Springs Quadrangle Riverside County, California by Thomas W. Dibblee, Jr., 2004
3. See site map for details of geophysical survey

File Name: CI-PLC

Date: 4/1/2011

USGS science for a changing world

GEOVision geophysical services

RECOVERY.GOV

GEOLOGIC MAP
CI•PLC

CI.PLC Seismograph Station

Looking north along passive surface wave array PLC-1

Looking east towards CI.PLC seismograph station and HVSR sensor 507

Looking north along MASW array PLC-3

Looking south towards seismograph station from center of passive surface wave array PLC-2

Location of Geophysical Testing Arrays:

Location	Latitude	Longitude
PLC-1, South End of Array, Channel 1	33.82371	-116.51236
PLC-1, North End of Array, Channel 24	33.82456	-116.51238
PLC-2, West End of Array, Channel 25	33.82459	-116.51238
PLC-2, East End of Array, Channel 48	33.82459	-116.51139
PLC-3, South End of Array	33.82408	-116.51238
PLC-3, Center of Array	33.82429	-116.51238
PLC-3, North End of Array	33.82450	-116.51239
HVSR Sensor 507	33.82437	-116.51191
HVSR Sensor 453	33.82398	-116.51234
HVSR Sensor 450	33.82459	-116.51139
CI.PLC Seismograph Station	33.82436	-116.51196

Notes: 1) WGS84 Coordinate System (decimal degrees)

2) Survey accuracy is estimated at 1 to 2 m.

Results:

V_S Model

Depth to Top of Layer (m)	Layer Thickness (m)	S-Wave Velocity (m/s)	Inferred P-Wave Velocity (m/s)	Inferred Poisson's Ratio	Inferred Density (g/cm^3)
0	1	192	360	0.3	1.9
1	2	213	399	0.3	1.9
3	3	301	562	0.3	1.9
6	4	323	604	0.3	1.9
10	5	341	637	0.3	1.9
15	7	386	722	0.3	1.9
22	12	475	888	0.3	2.0
34	>26	498	932	0.3	2.0

Observations/Discussion:

- The HVSR curves are almost identical, validating the 1-D velocity structure assumption.
- Clear HVSR peak at about 0.42 Hz indicating that bedrock is moderately deep at the site.
- Noise conditions at site (multi-directional or omni-directional noise sources) appeared sufficient for successful application of passive surface wave techniques.
- ESAC technique used to extract surface wave dispersion data from passive "L" array data. Both the ReMi™ and ESAC techniques used to extract surface wave dispersion data from the linear arrays.
- Surface wave dispersion data from active and passive surface wave datasets are in good agreement at this site; however, only the more reliable "L" array data used for modeling.
- Passive linear array dispersion data resulting from ReMi™ analysis significantly diverges from that resulting from ESAC analysis at wavelengths greater than the array length.
- Representative dispersion curves were generated for each utilized surface wave data set (MASW arrays PLC-1 and PLC-3 and passive surface wave data from the combined arrays PLC-1 and PLC-2 forming an "L" array) using a moving average, polynomial curve fitting routine. These individual representative dispersion curves were combined and a representative dispersion curve generated for the combined data set for data modeling.
- Water table located at a depth of greater than 30 m based on interactive layer-based on absence of a water table refractor in seismic records. Additionally there is no clear reflector that could be associated with the water table.
- Based on simple layer-based analysis of seismic refraction first arrival data, P-wave velocity in the upper 25 m ranges from about 375 m/s at the surface to 600 m/s at a depth of about 4 m to about 1,000 m/s at a depth of 20 m. Note that the presence of intermediate velocity hidden layers (layers of insufficient thickness to give rise to a first arrival) would increase the depth of all of the above contacts.
- Inferred P-wave velocities from surface wave model are consistent with simple P-wave seismic refraction model, especially when considering that Poisson's ratio is unknown.
- Surface wave depth of investigation is greater than 60 m based on half of maximum wavelength criteria and assuming that surface wave dispersion data at frequencies as low as 3 Hz are valid utilizing 4.5 Hz geophones (low frequency geophone phase response differences will cancel out if noise is truly omni-directional and/or the phase response differences are random in nature).
- V_{S30} is 346 m/s (Site Class D).
- Average S-wave velocity between 2 m (assumed seismic sensor depth) and 32 m is 371 m/s (Site Class C).
- Average S-wave velocity of the upper 60 m (V_{S60}) is 408 m/s.

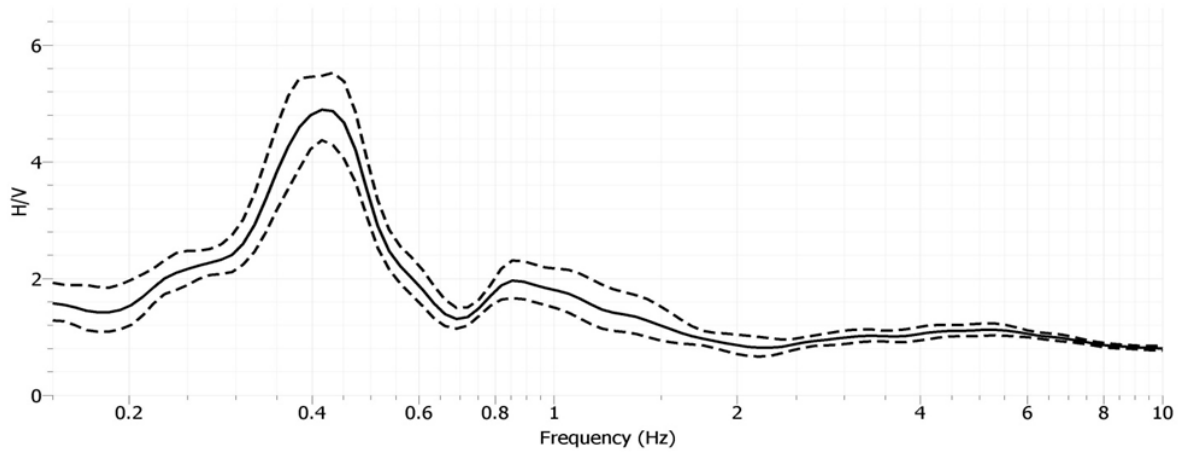

Site CI.PLC, H/V Spectral Ratio, Array PLC-1, Sensor 453

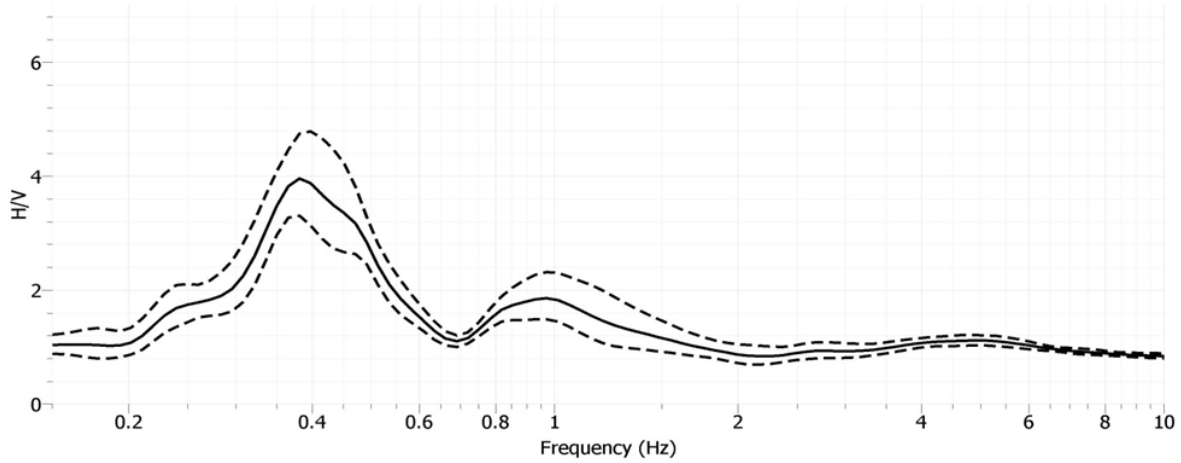

Site CI.PLC, H/V Spectral Ratio, Near Seismic Station, Sensor 507

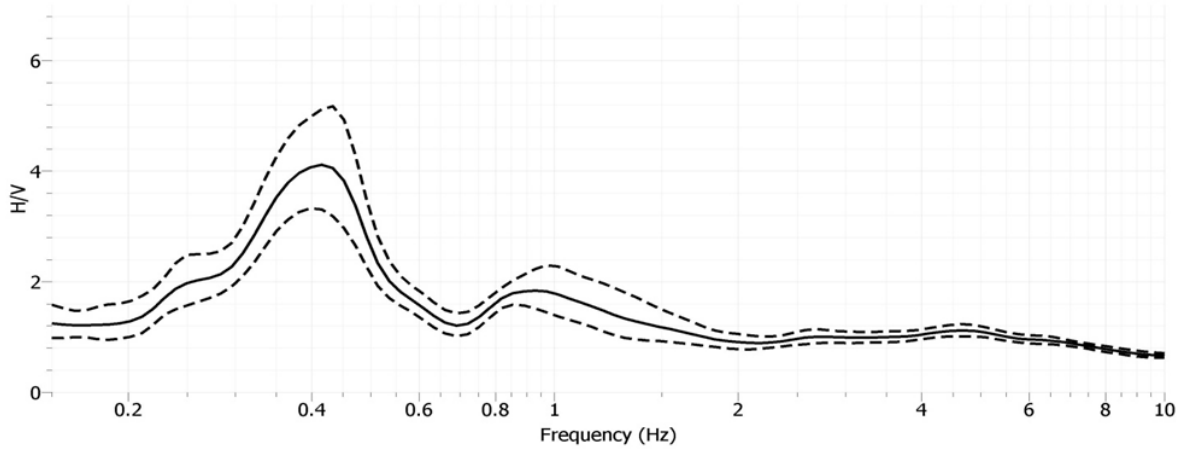

Site CI.PLC, H/V Spectral Ratio, Array PLC-1, Sensor 450

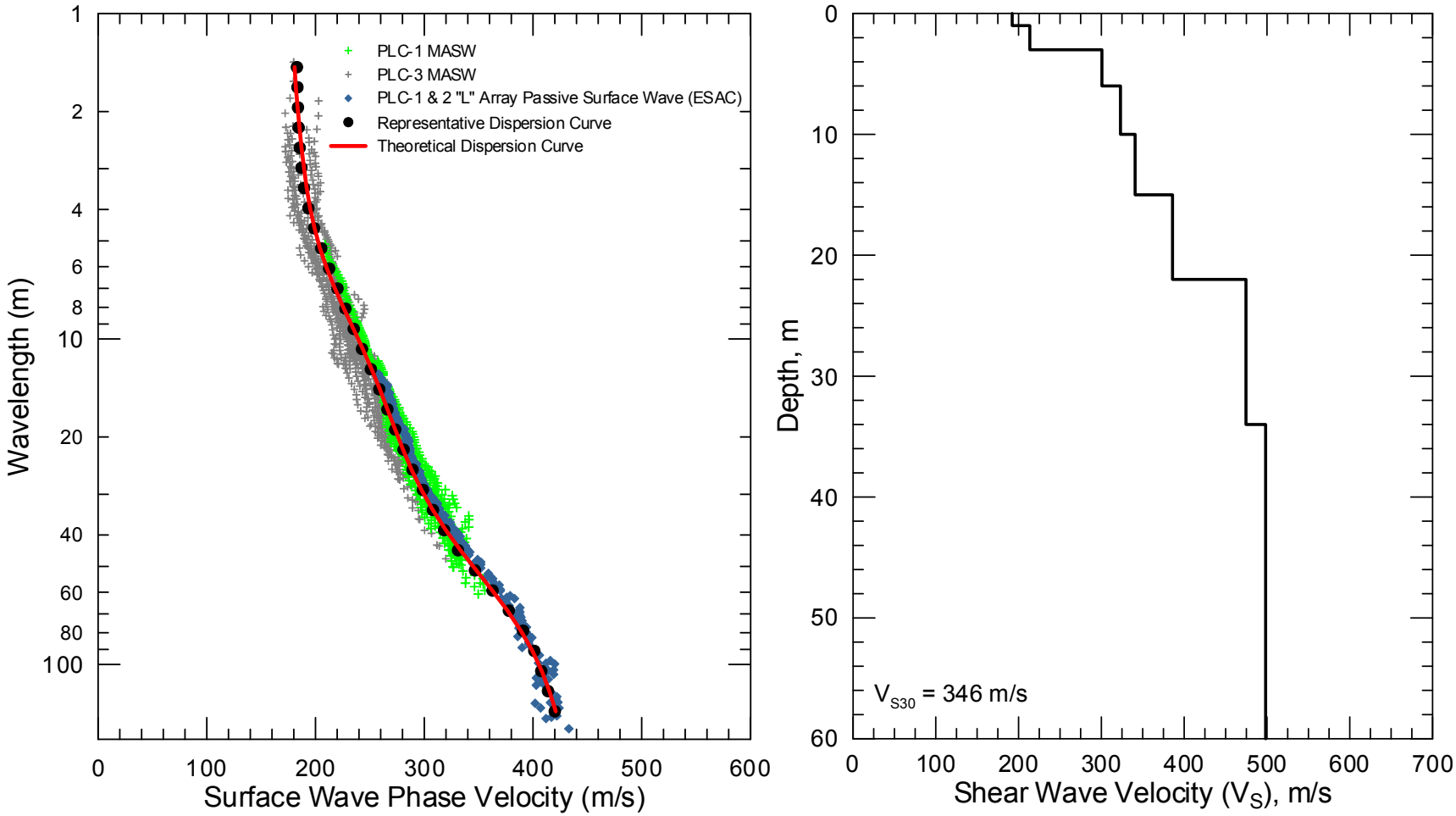

CI.PLC - Field, representative and inverted theoretical surface wave dispersion data (left) and associated V_S model (right)

Site CI.PLM

Location: Palomar Observatory, Palomar, San Diego County, California

Latitude: 33.35361 **Longitude:** -116.86265
(Station coordinates provided by USGS, WGS84 coordinate system)

V_{S30} (measured): 465 m/s

V_{S30} (adjusted to more accurately reflect seismic station conditions): 540 m/s (average S-wave velocity between 2.5 and 32.5 m to account for seismic sensor being located about 2.5 m below grade).

NEHRP Site Class: C

Geomatrix Code: AGB

Geologic Conditions/Observations: Seismic station located on geologic unit mapped as Mesozoic granitic rocks.

Site Conditions: Rural site located on a mountain. Undulating to steep topography in the site vicinity.

Geophysical Methods Utilized: HVSR, Seismic Refraction, MASW

Geophysical Testing Arrays:

1. Array PLM-1 (48 channel MASW and P-wave seismic refraction array utilizing 4.5 Hz vertical geophones spaced 1.5 m apart for a length of 70.5 m, forward and reverse shot locations with multiple source offsets and source types and multiple interior shot locations).
2. Array PLM-2 (48 channel MASW and P-wave seismic refraction array utilizing 4.5 Hz vertical geophones spaced 1.5 m apart for a length of 70.5 m, forward and reverse shot locations with multiple source offsets and source types and multiple interior shot locations).
3. Four HVSR measurement locations: three distributed along array PLM-1 and one adjacent to the seismic station and array PLM-2.

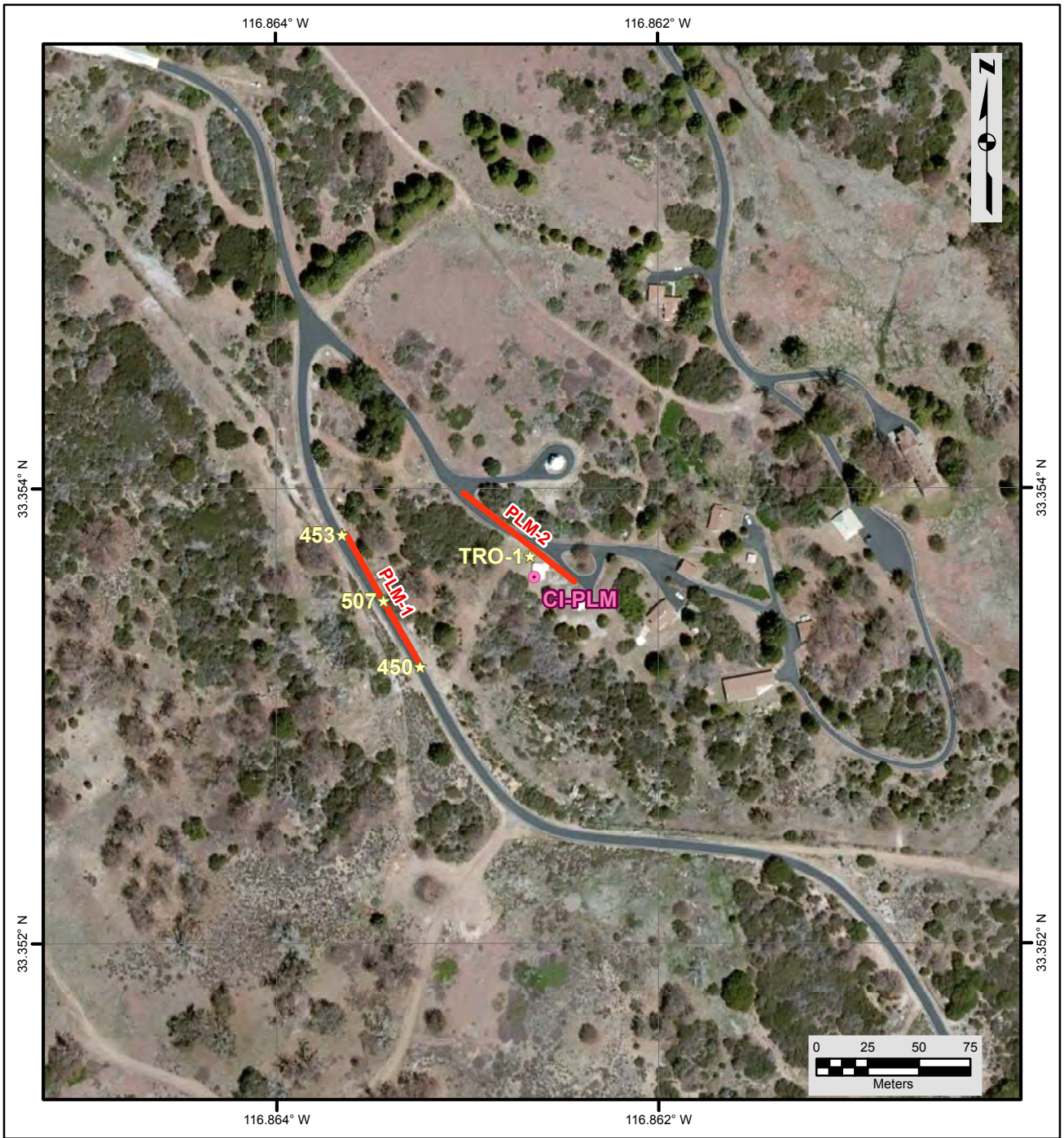

Legend

- Seismic Station - Approximate Location of Record
- H/V Spectral Ratio Location
- MASW and Seismic Refraction Array

NOTES:
1. WGS 1984 COORDINATE SYSTEM
2. Image Source: ESRI, i-cubed, USDA FSA, USGS, AEX, GeoEye, Getmapping, Aerogrid, IGP

File Name: CI-PLM-I

Date: 2/7/2013

USGS science for a changing world

GEOVision geophysical services

RECOVERY.GOV

SITE MAP
CI•PLM

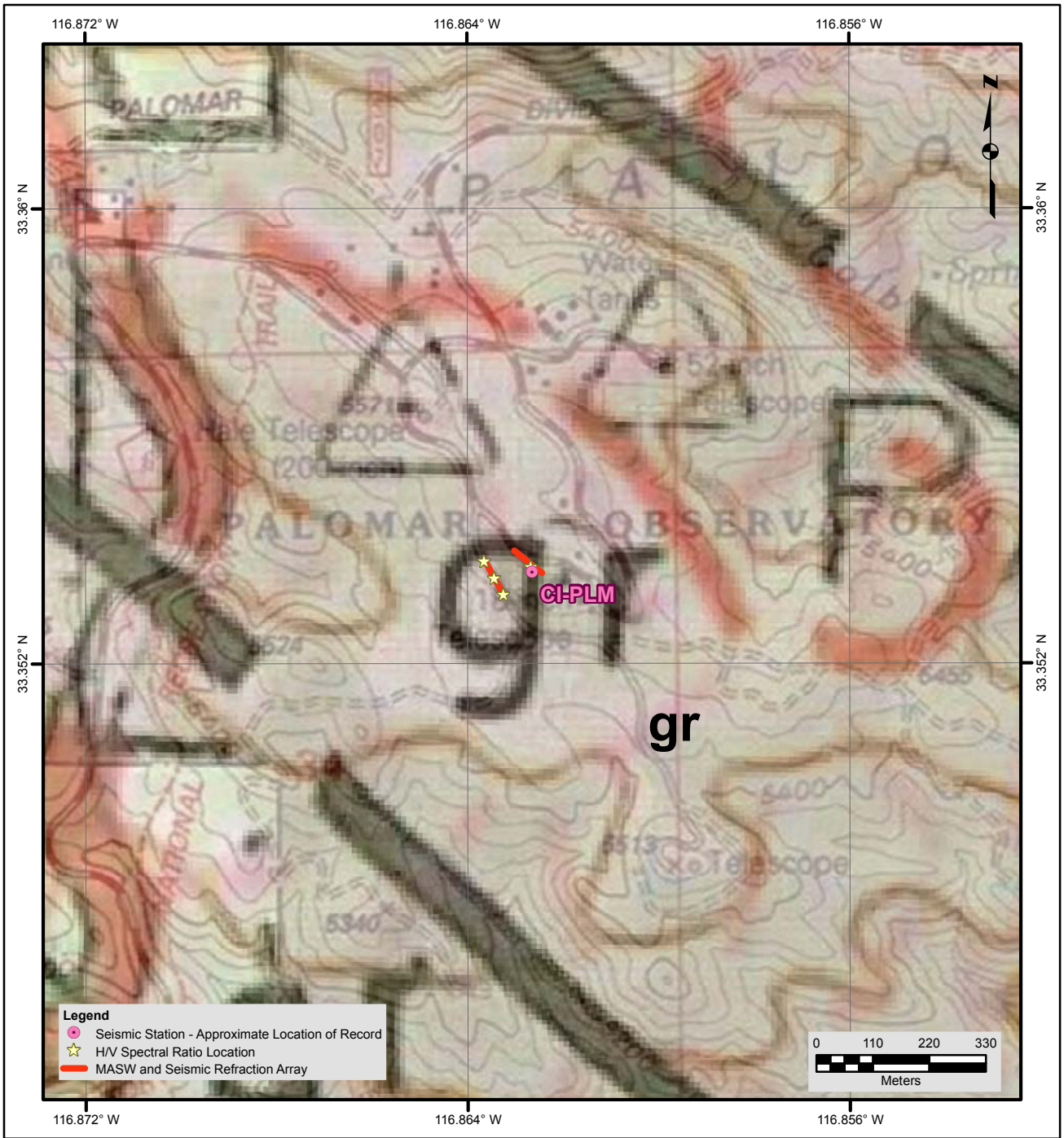

Description of Geologic Map Units

gr = Mesozoic (Jurassic to Cretaceous) granitic rocks

NOTES:
1. WGS 1984 COORDINATE SYSTEM
2. Geologic Map of California Santa Ana Sheet, Olaf P Jenkins Edition
Compiled by Thomas H. Rogers, 1965
3. See site map for details of geophysical survey

File Name: CI-PLM

Date: 5/10/2012

USGS science for a changing world

GEOVision geophysical services

RECOVERY.GOV

GEOLOGIC MAP
CI•PLM

Looking at structure housing the seismic station CI.PLM

Looking northeast towards center of array PLM-1, HVSR sensor 507 and structure housing seismic station

Looking southeast along array PLM-1

Granitic rocks are very intensely weathered in site vicinity

Looking northwest along array PLM-2 towards structure housing the seismic station

Location of Geophysical Testing Arrays:

Location	Latitude	Longitude
PLM-1, Southeast End of MASW/Refraction Array	33.35322	-116.86324
PLM-1, Center of MASW/Refraction Array	33.35349	-116.86343
PLM-1, Northwest End of MASW/Refraction Array	33.35380	-116.86363
PLM-2, Northwest End of MASW/Refraction Array	33.35398	-116.86302
PLM-2, Center of MASW/Refraction Array	33.35380	-116.86272
PLM-2, Southeast End of MASW/Refraction Array	33.35359	-116.86244
HVSR Sensor 450 (Nanometrics Trillium Compact)	33.35322	-116.86325
HVSR Sensor 453 (Nanometrics Trillium Compact)	33.35380	-116.86366
HVSR Sensor 507 (Nanometrics Trillium Compact)	33.35351	-116.86344
HVSR Sensor TRO-1 (Micromed Tromino ENGY)	33.35370	-116.86267

Notes: 1) WGS84 Coordinate System (decimal degrees)
2) Survey accuracy is estimated at 2 to 3 m.

Results:

V_S Model (MASW Array PLM-2)

Depth to Top of Layer (m)	Layer Thickness (m)	S-Wave Velocity (m/s)	Inferred P-Wave Velocity (m/s)	Assumed Poisson's Ratio	Assumed Density (g/cm^3)
0	1	182	341	0.3	1.60
1	2	251	469	0.3	1.70
3	3	297	555	0.3	1.75
6	5	419	783	0.3	1.90
11	6	485	907	0.3	2.00
17	8	688	1287	0.3	2.10
25	>5	1000	1871	0.3	2.20

Notes: 1) Depth of investigation is about 30 m.
2) Bottom layer is a half space.

Observations/Discussion:

- This site was visited on two occasions. During the first site visit on 2/22/11, MASW, P-wave seismic refraction and HVSR data were acquired along array PLM-1. Preliminary data reduction indicated that MASW data were difficult to work with; therefore, the site was revisited on 9/7/11 with MASW and P-wave seismic refraction data being acquired along array PLM-2. An additional HVSR measurement was also made adjacent to the structure housing the seismic station. MASW data collected along array PLM-2 were slightly easier to work with than that acquired along array PLM-1.
- There are no distinct peaks in any of the HVSR data collected at this site. The HVSR plots at the three measurement locations on array PLM-1 are very similar, with the exception of HVSR sensor 453 having slightly higher amplitude response or weak peaks between 1.5 and 6 Hz.
- Arrays PLM-1 and PLM-2 were located adjacent to or on asphalt roads. First arrival data at small offsets from the source were contaminated by the high velocity arrival from the asphalt and subgrade, particularly for seismic refraction data collected along array PLM-2. First arrival data near the source were easier to pick on seismic records from array PLM-1; however, near surface velocity structure could still not be accurately resolved. Later arrivals from weathered bedrock were not affected by the asphalt and, therefore, bedrock P-wave velocity can be relatively accurately resolved. Only a P-wave velocity model for array PLM-1 is presented as we do not believe that near surface velocity structure is accurately enough resolved in the seismic refraction model for array PLM-2.
- The P-wave refraction data for array PLM-1 were modeled using a tomographic inversion routine with a smooth velocity gradient starting model. The seismic refraction model was extended to far offset shot locations to extend depth of investigation.
- The seismic refraction survey design for array PLM-1 allowed P-wave velocity to be imaged to a maximum depth of about 23 m. The seismic refraction model shows that P-wave velocity is about 300 to 400 m/s at the surface, increasing to 500 m/s at a depth of 1 to 4 m, 1,000 m/s at a depth of 6 to 11 m, 2,000 m/s at a depth of 16 to 20 m and greater than 2,500 m/s at a depth of 19 to 21 m. The maximum P-wave velocity in the model is about 3,000 m/s.
- The average P-wave velocity of the upper 30 m (V_{P30}) was estimated between 27 and 60 m on the array PLM-1 refraction model, where depth of investigation is greatest, by projecting the velocity at 23 m depth to 30 m depth. V_{P30} ranges from about 994 to 1,169 m/s over the 27 to 60 m position interval, a 16% variation. An average V_P model was developed over the 27 to 60 m distance interval by horizontally averaging the travel time of each model cell and cell thickness and average V_{P30} was determined to be 1,081 m/s. Assuming constant Poisson's ratios of 0.25, 0.3, 0.35 and 0.4 would result in an estimated V_{S30} of 624, 578, 519 and 414 m/s, respectively. The possibility cannot be discounted that weathered bedrock is saturated below a depth of 20 m. A Poisson's ratio on the order of 0.3 and 0.4, or less, is reasonable for unsaturated and saturated weathered rock, respectively. Even though Poisson's ratio is not precisely known, the P-wave refraction model for array PLM-1 clearly indicates that the site is NEHRP Site Class C.
- Noise conditions at the site were not sufficient for application of passive surface wave techniques.
- MASW data reduction was complicated by significant scattering of surface wave energy from heterogeneities in the weathered rock and lateral velocity variation. MASW data

from both arrays were difficult to reduce. It was, however, easier to compile a coherent, probable fundamental mode dispersion curve from the MASW data collected along array PLM-2. Therefore, only the MASW dispersion data collected along array PLM-2, which is located closer to the seismic station, were modeled for the purpose of site characterization.

- The maximum wavelength Rayleigh wave extracted from the MASW data collected along array PLM-2 was generally set to the lesser of 70 m or 1.3 times the distance between the source and midpoint of the receiver array.
- The minimum wavelength surface wave phase velocity data extracted from the 48-channel MASW array PLM-2 was about 35 m. It was only possible to extract dispersion data from the 48-channel receiver array using source locations at the southeast end of the array. It was very difficult to extract dispersion data from source locations at the northwest end of the array. Reducing data from smaller hammer sources using a limited offset receiver array (i.e. less active geophones) allowed for extraction of surface wave dispersion data to a minimum wavelength of about 2 m.
- Due to lateral velocity variation, selective use of dispersion curves extracted from the data set was necessary to develop a coherent dispersion curve. This dispersion curve appears to be biased towards lower near surface seismic velocities.
- A representative dispersion curve was generated for the MASW data set using a moving average, polynomial curve fitting routine and used for modeling.
- Surface wave depth of investigation is about 30 m based on half of maximum wavelength criteria.
- Surface wave data was modeled using the fundamental mode assumption. Subsequent review of the V_S model indicated that superposition of the fundamental and first higher modes could occur at the longest wavelengths, in which case the half space velocity would be slightly overestimated with little effect on V_{S30}. Effective mode modeling was not applied to this dataset because a significant change in the V_S model was not expected.
- Review of the refraction data for array PLM-2 and surface wave data for array PLM-1 indicates that P-wave velocity structure beneath array PLM-2 is either similar to or slightly higher than that beneath array PLM-1. The inferred P-wave velocities in the V_S model for MASW array PLM-2, based on an assumed Poisson's ratio of 0.3 and modeled S-wave velocity, are generally lower than P-wave velocity in the array PLM-1 P-wave refraction model, particularly at depths below 10 m. Of course, Poisson's ratio of the weathered granitic rocks is not known. The depth of the saturated zone and its affect on Poisson's ratio is also not known.
- V_{S30} is 465 m/s (NEHRP Site Class C).
- The seismic station is located about 2.5 m below ground surface. The average S-wave velocity between 2.5 and 32.5 m, to account for approximate seismic sensor depth, is 540 m/s (NEHRP Site Class C).
- The S-wave velocity model derived from the surface wave testing is believed to be representative of the lower bound of subsurface seismic velocities in the immediate site vicinity. Given the significant near surface lateral velocity variation and scatter in the surface wave dispersion data, V_{S30} is probably more accurately constrained than the actual V_S model. The scatter in the surface wave dispersion is such that the presented V_{S30} may vary by 10% in the immediate site vicinity, not enough to change NEHRP Site

Class. The V_S model developed from the MASW data may be biased towards the lower S-wave velocities beneath the array.

- Both the seismic refraction and surface wave models clearly indicate that the site is NEHRP Site Class C. The average velocity structure in the P-wave refraction model seems to indicate that average V_{S30} may be higher than that determined from the MASW sounding, although Poisson's ratio is not accurately known. V_{S30} estimated from the MASW data for array PLM-2 appears to be most consistent with lower V_{P30} estimates from the refraction model for array PLM-1.
- Arrays PLM-1 and PLM-2 are located as close as possible to the seismic station. It may be possible to identify a location where better quality seismic refraction and MASW data can be acquired at greater distance from the seismic station, in which case uncertainty associated with lateral velocity variation becomes problematic. The possibility cannot be discounted that Love wave techniques may perform better at this site, although scattering associated with heterogeneities in the rock would also be problematic for the MALW technique.

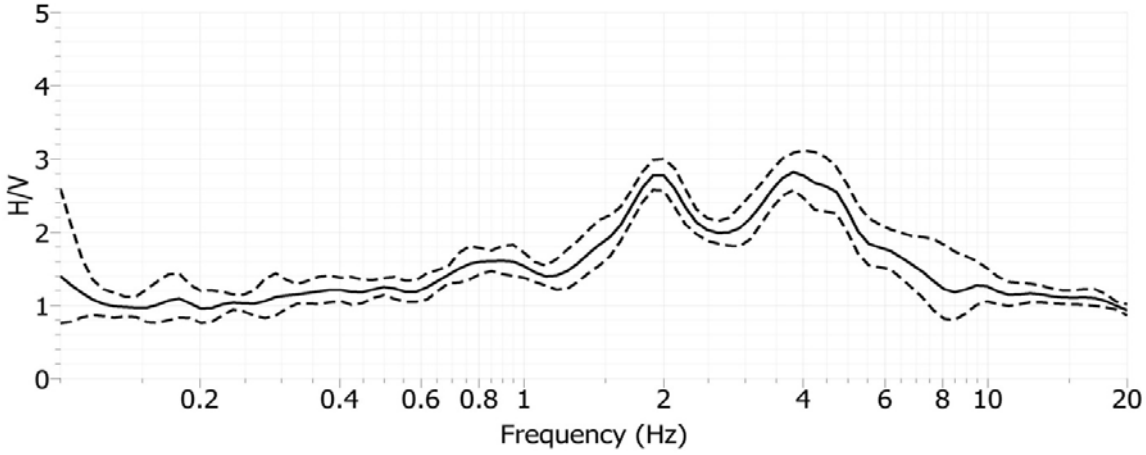

Site CI.PLM, H/V Spectral Ratio, Array PLM-1, Sensor 453

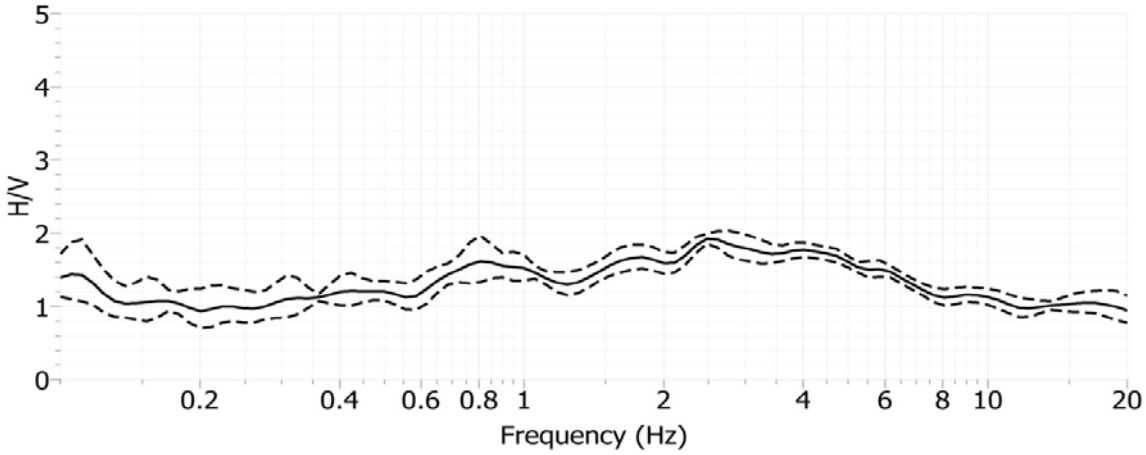

Site CI.PLM, H/V Spectral Ratio, Array PLM-1, Sensor 507

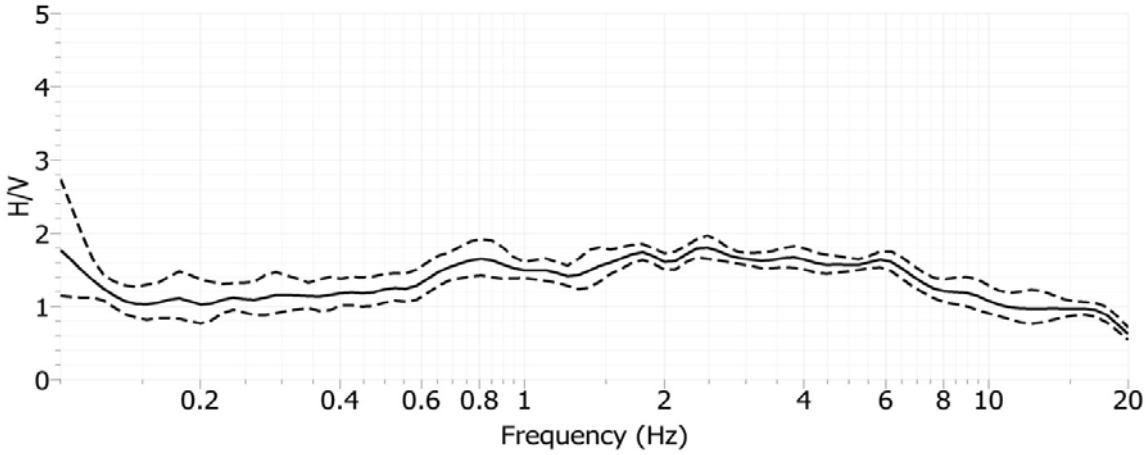

Site CI.PLM, H/V Spectral Ratio, Array PLM-1, Sensor 450

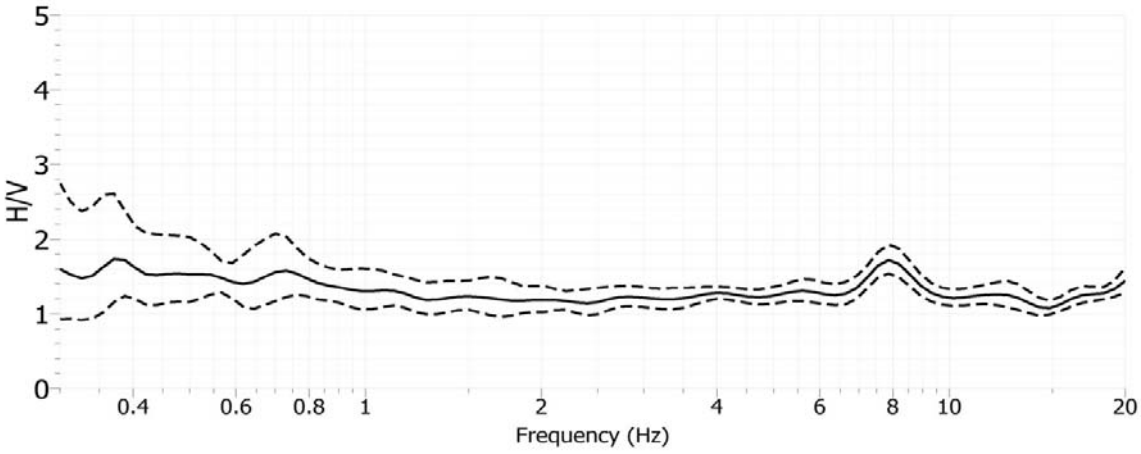

Site CI.PLM, H/V Spectral Ratio, Near Seismic Station, Sensor TRO-1

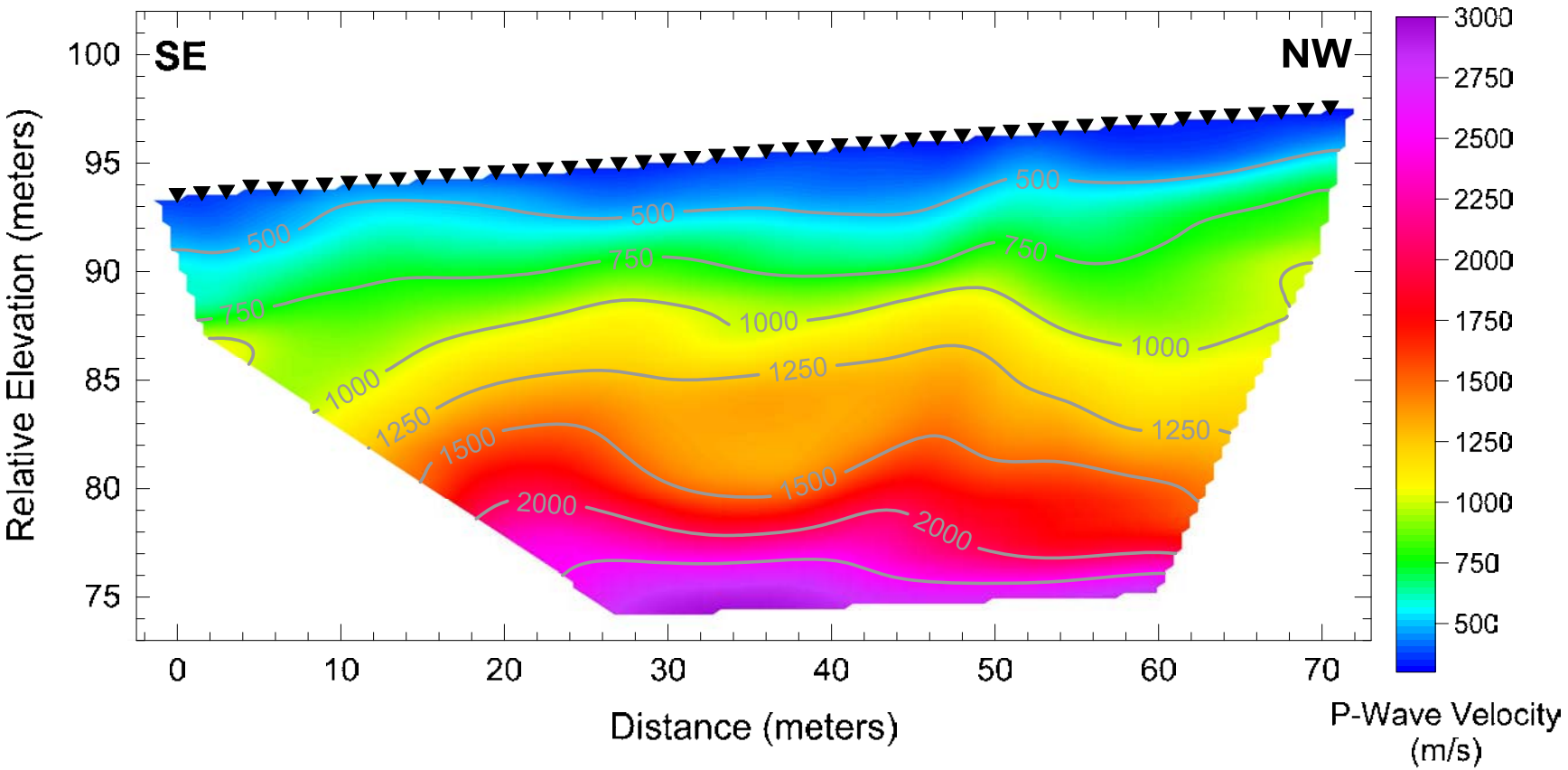

Array PLM-1 – Tomographic seismic refraction model developed using a smooth velocity gradient starting model

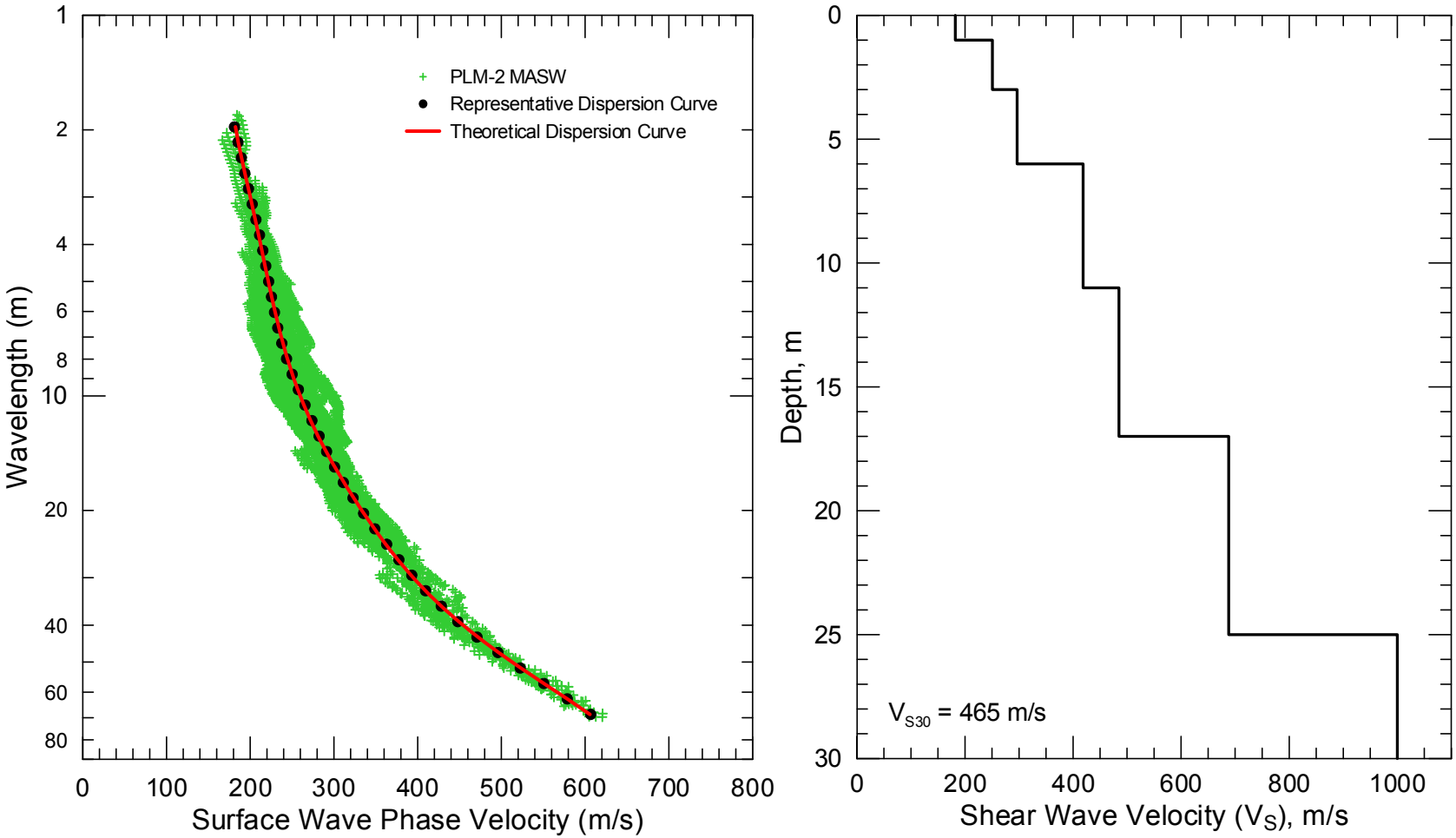

CI.PLM - Field, representative and inverted theoretical surface wave dispersion data (left) and associated V_S model (right) for MASW array PLM-2

Site CI.PLS

Location: Pleasants Peak Radio Facility, Riverside County, California

Latitude: 33.79530 **Longitude:** -117.60906
(Station coordinates provided by USGS, WGS84 coordinate system)

V_{S30} (measured): 699 m/s

V_{S30} (adjusted to more accurately reflect seismic station conditions): 699 m/s (no adjustment necessary).

NEHRP Site Class: C

Geomatrix Code: AJA

Geologic Conditions/Observations: Seismic station located on geologic unit mapped as Mesozoic (Jurassic) Bedford Canyon Formation, which consists of metasedimentary rock. Geologic maps indicate that bedding dips about 30 to 55 degrees to the east-northeast in the immediate site vicinity.

Site Conditions: Remote site located on mountain top graded flat to support communication site infrastructure. Steep, mountainous topography in site vicinity.

Geophysical Methods Utilized: HVSR, Seismic Refraction, MASW

Geophysical Testing Arrays:

1. Array PLS-1 (24 channel MASW and P-wave seismic refraction array utilizing 4.5 Hz vertical geophones spaced 2 m apart for a length of 46 m, forward and reverse shot locations with multiple source offsets and source types and multiple interior shot locations).
2. Array PLS-2 (48 channel MASW and P-wave seismic refraction array utilizing 4.5 Hz vertical geophones spaced 1.5 m apart for a length of 70.5 m, forward and reverse shot locations with multiple source offsets and source types and multiple interior shot locations).
3. Array PLS-3 (48 channel MASW and P-wave seismic refraction array utilizing 4.5 Hz vertical geophones spaced 1.5 m apart for a length of 70.5 m, forward and reverse shot locations with multiple source offsets and source types and multiple interior shot locations).
4. Three HVSR measurement locations: one each near the center of arrays PLS-1, PLS-2 and PLS-3.

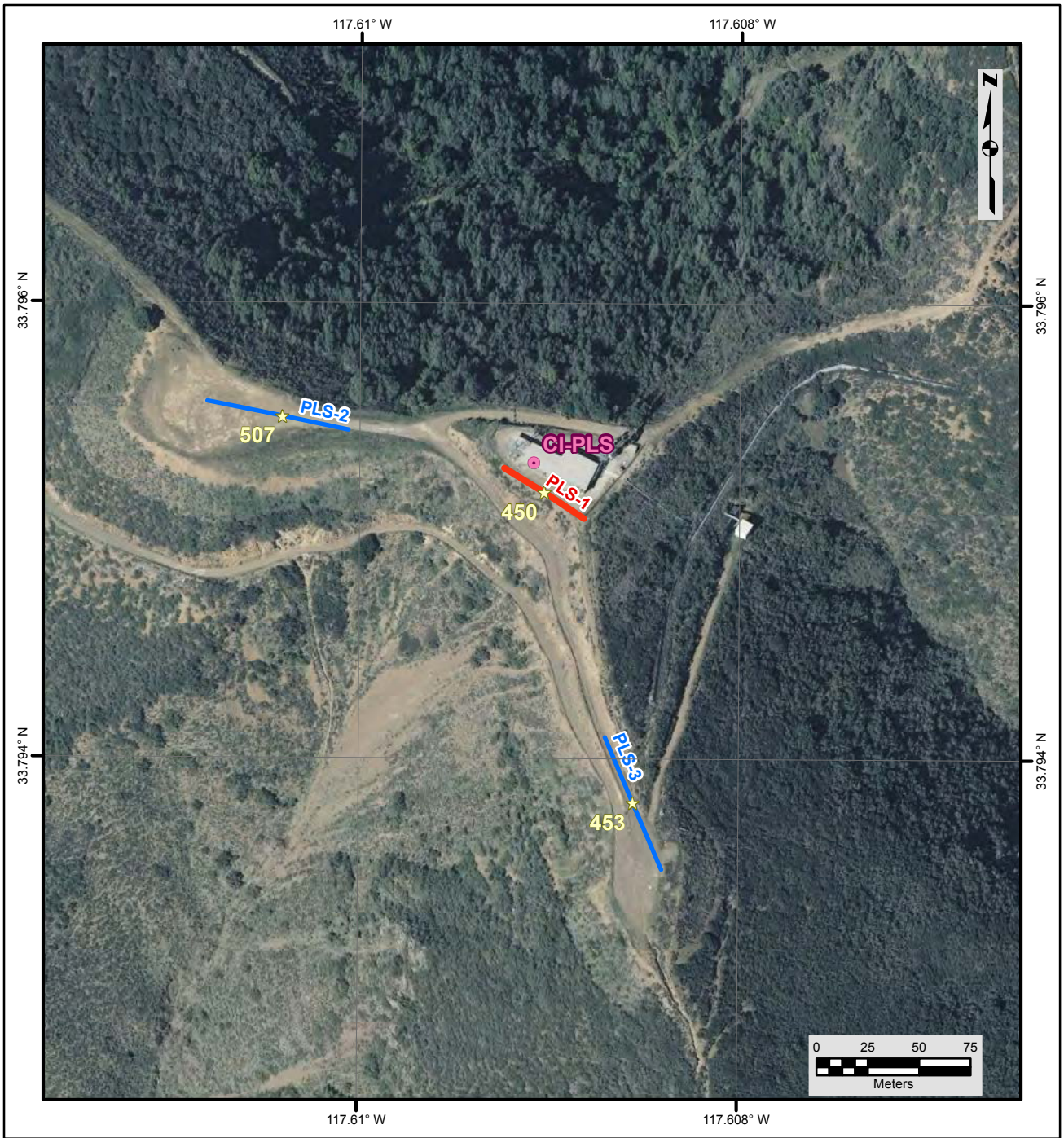

Legend

- Seismic Station - Approximate Location of Record
- H/V Spectral Ratio Location
- MASW and Seismic Refraction Array
- MASW and Seismic Refraction Array (NO SASW)

NOTES:
1. WGS 1984 COORDINATE SYSTEM
2. Image Source: ESRI, i-cubed, USDA FSA, USGS, AEX, GeoEye, Getmapping, Aerogrid, IGP

File Name: CI-PLS-I

Date: 5/10/2012

USGS science for a changing world

GEOVision geophysical services

RECOVERY.GOV

SITE MAP
CI•PLS

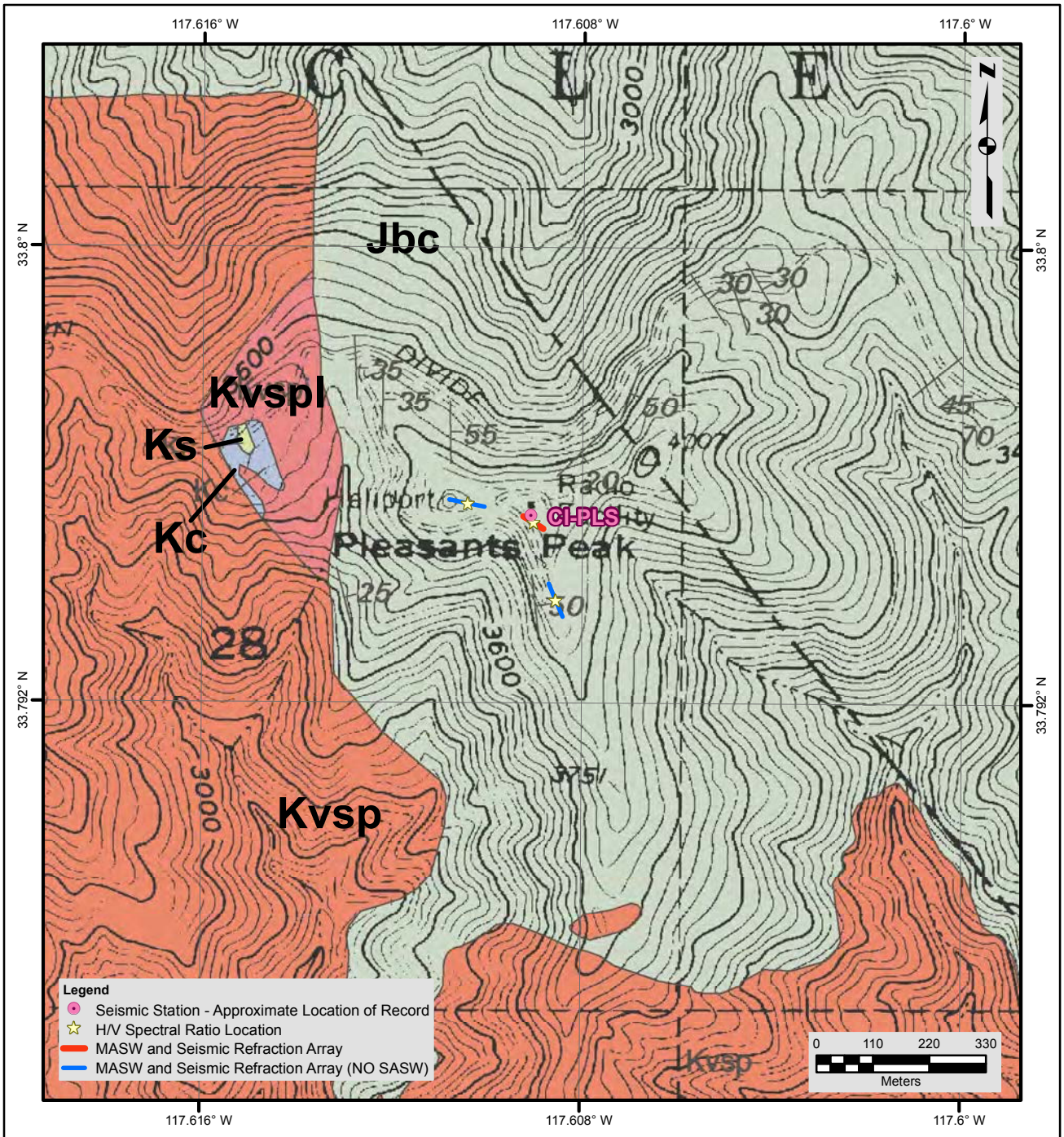

Description of Geologic Map Units

Ks = Mesozoic (Cretaceous) Serpentinite, highly deformed, slickensided
Kc = Mesozoic (Cretaceous) Carbonate-silicate rock
Kvsp = Mesozoic (Cretaceous) Santiago Peak Volcanics; basaltic andesite, andesite, dacite, rhyloite, volcaniclastic breccia, welded tuff, and epiclastic rocks
Kvspi = Mesozoic (Cretaceous) intrusive rocks associated with Santiago Peak Volcanics; porphyritic plagioclase, clinopyroxene, and altered orthopyroxene
Jbc = Mesozoic (Jurassic) Bedford Canyon Formation; slightly metamorphosed interlayered argillite, slate, graywacke and quartzite

NOTES:
1. WGS 1984 COORDINATE SYSTEM
2. Geologic Map of the Corona South 7.5' Quadrangle, Riverside and Orange Counties, California (Version 1.0) By C.H. Gray, Jr., Douglas M. Morton, and F.H. Weber, Jr.
3. See site map for details of geophysical survey

USGS science for a changing world

GEOVision geophysical services

RECOVERY.GOV

GEOLOGIC MAP
CI•PLS

File Name: CI-PLS

Date: 5/10/2012

CI.PLS seismic station

Looking north from array PLS-1 towards corner of building housing the seismic station

Looking northwest along array PLS-1 and at building housing the seismic station

Looking southeast along array PLS-2 and at building housing the seismic station (at the top of the hill)

Looking northwest along array PLS-3 and at building housing the seismic station (at the top of the hill)

Location of Geophysical Testing Arrays:

Location	Latitude	Longitude
PLS-1, Southeast End of MASW/Refraction Array	33.79505	-117.60880
PLS-1, Center of MASW/Refraction Array	33.79517	-117.60901
PLS-1, Northwest End of MASW/Refraction Array	33.79527	-117.60922
PLS-2, Northwest End of MASW/Refraction Array	33.79557	-117.61078
PLS-2, Center of MASW/Refraction Array	33.79550	-117.61041
PLS-2, Southeast End of MASW/Refraction Array	33.79544	-117.61004
PLS-3, Southeast End of MASW/Refraction Array	33.79351	-117.60838
PLS-3, Center of MASW/Refraction Array	33.79381	-117.60853
PLS-3, Northwest End of MASW/Refraction Array	33.79410	-117.60868
HVSR Sensor 450	33.79517	-117.60901
HVSR Sensor 507	33.79550	-117.61039
HVSR Sensor 453	33.79381	-117.60853

Notes: 1) WGS84 Coordinate System (decimal degrees)
2) Survey accuracy is estimated at 1 to 2 m.

Results:

V_S Model

Depth to Top of Layer (m)	Layer Thickness (m)	S-Wave Velocity (m/s)	Inferred P-Wave Velocity (m/s)	Assumed Poisson's Ratio	Assumed Density (g/cm^3)
0	1	301	564	0.3	1.90
1	2	504	943	0.3	2.00
3	3	617	1155	0.3	2.05
6	4	703	1314	0.3	2.10
10	8	791	1480	0.3	2.10
18	>12	802	1501	0.3	2.10

Notes: 1) Depth of investigation is about 30 m.
2) Bottom layer is a half space.

Observations/Discussion:

- P-wave seismic refraction and MASW data were acquired along three arrays at this site to characterize lateral velocity variation in the Bedford Canyon Formation. Array PLS-1 is located closest to the seismic station and is used for site characterization
- The HVSR plots are very similar at every station, although there are no distinct HVSR peaks. There is very subtle elevated HVSR response between about 0.7 and 6 Hz on the HVSR plots.
- The P-wave refraction data for arrays PLS-1, PLS-2 and PLS-3 were modeled using a tomographic inversion routine with a smooth velocity gradient starting model. The seismic refraction models were extended to far offset shot locations to extend depth of investigation.
- The seismic refraction survey design allowed P-wave velocity to be imaged to a maximum depth of about 11, 15 and 12 m for arrays PLS-1, PLS-2 and PLS-3 respectively. The seismic refraction models indicate that there is significant near surface lateral velocity variation beneath all of the arrays. The relative low velocity sediments in the upper several meters at the southeastern end of each array may be associated with fill. The P-wave velocity of the metasedimentary rock typically exceeds 1,300 to 1,400 m/s at a depth of about 10 m beneath all of the arrays. The maximum P-wave velocity modeled in the upper 15 m is about 1,650 m/s.
- The seismic refraction/MASW arrays were orientated at various angles to the strike of the geologic bedding, which dips on the order of 30 to 55 degrees in an easterly direction. For surface wave methods to be effective in such environments, the seismic velocity of the geologic bedding must be relatively uniform with near surface velocity variation primarily being a function of weathering.
- Noise conditions at the site were not sufficient for application of passive surface wave techniques.
- Lateral velocity variation at this site is such that development of coherent surface wave dispersion curves was challenging. Array PLS-1 yielded the best quality surface wave dispersion data and, based on its proximity to the seismic station, was used for site characterization. Analysis of the surface wave data for arrays PLS-2 and PLS-3 is significantly complicated by lateral velocity variation and has not been completed at this time.
- The near field criteria typically applied during this investigation was significantly relaxed to allow surface wave dispersion data to be extracted from array PLS-1 to a wavelength of 60 m. Long wavelength Rayleigh wave phase velocity data were only extracted from source locations offset from the southeast end of the array.
- The minimum wavelength surface wave phase velocity data extracted from the 48-channel MASW array PLS-1 was about 13 m. Reducing data from smaller hammer sources using a limited offset receiver array (i.e. less active geophones) allowed for extraction of surface wave dispersion data to a minimum wavelength of about 2 m.
- There is nominally about 75 to 100 m/s of scatter in MASW dispersion data, which is likely due to lateral velocity variation caused by differential weathering of near surface rock.
- A representative dispersion curve was generated for the MASW data set using a moving average, polynomial curve fitting routine and used for modeling.

- Surface wave depth of investigation is about 30 m based on half of maximum wavelength criteria.
- The inferred P-wave velocities in the surface wave model, based on an assumed Poisson's ratio of 0.3 and modeled S-wave velocity, are generally consistent with the P-wave refraction model for array PLS-1 in the upper 10 m, especially considering unknown Poisson's ratio.
- The S-wave velocity model derived from the surface wave testing is believed to be representative of average subsurface velocity structure. However, geology at the site is complex, with dipping bedding, and the seismic line was oriented perpendicular to strike. It is difficult to predict the effect of dipping beds on surface wave dispersion data.
- V_{S30} is 699 m/s (Site Class C).
- Lateral velocity variation is such that V_{S30} likely varies by 5 to 10% in the immediate vicinity of the seismic station.

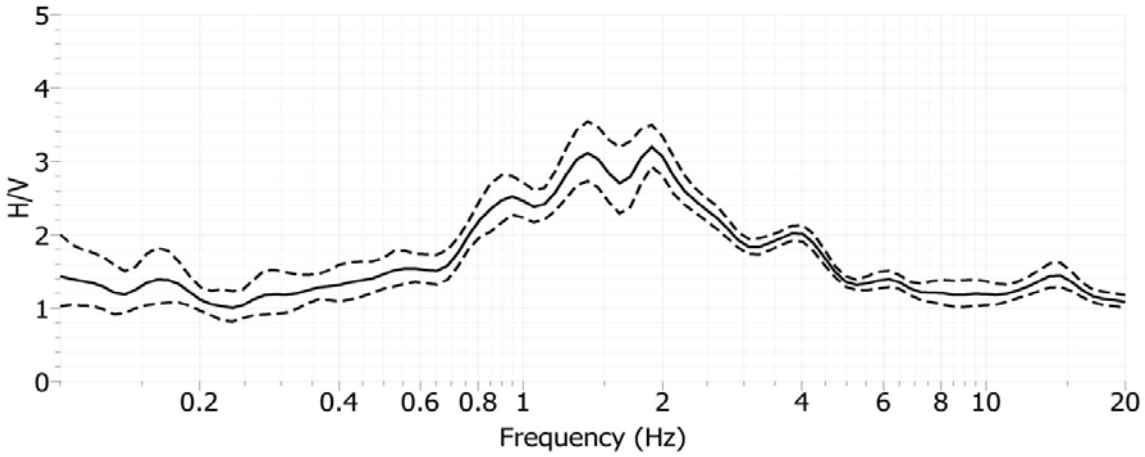

Site CI.PLS, H/V Spectral Ratio, Array PLS-2, Sensor 507

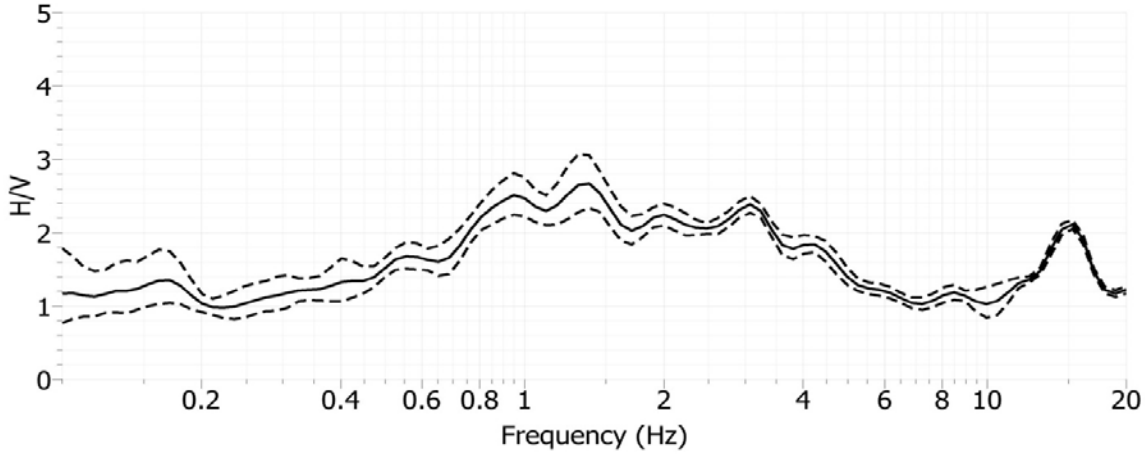

Site CI.PLS, H/V Spectral Ratio, Array PLS-1, Sensor 450

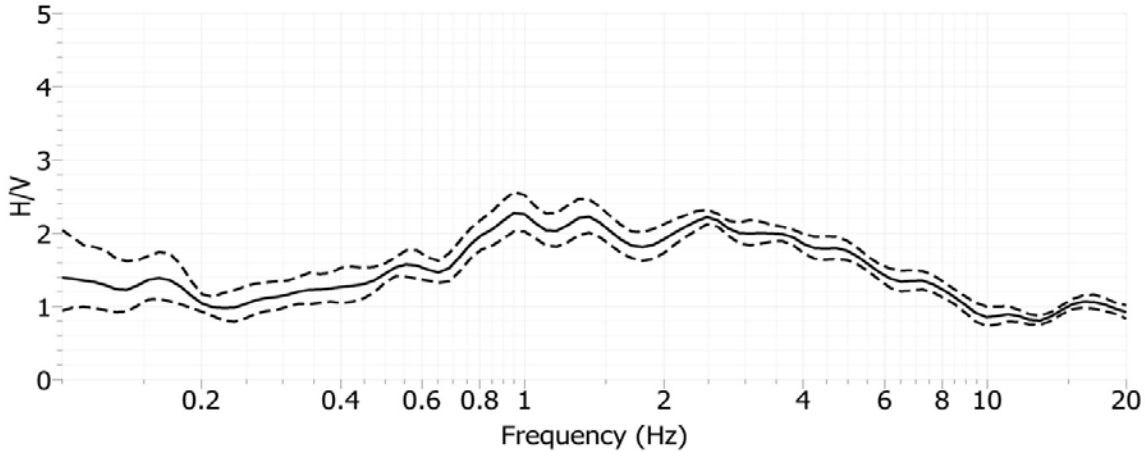

Site CI.PLS, H/V Spectral Ratio, Array PLS-3, Sensor 453

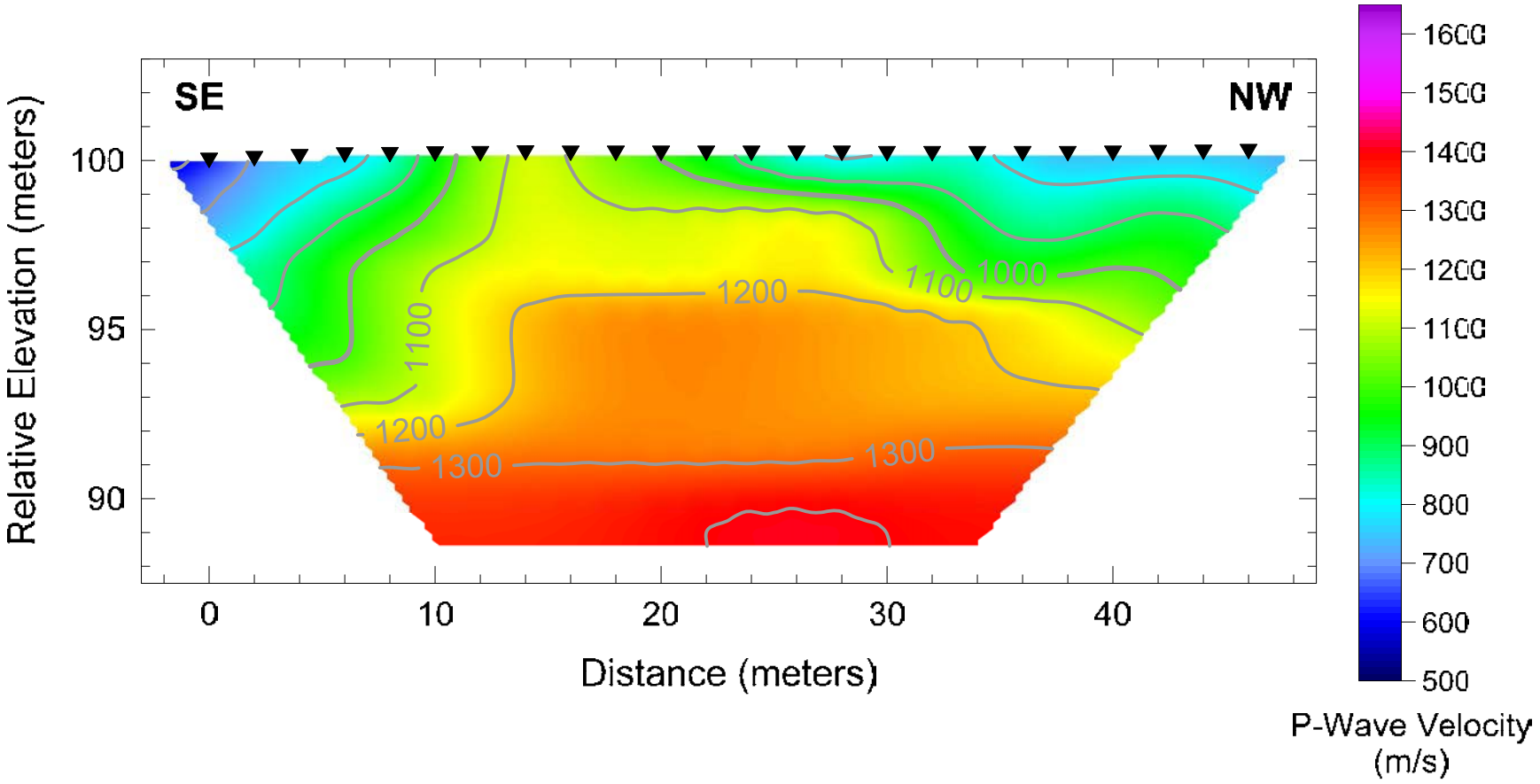

Array PLS-1 – P-wave tomographic seismic refraction model developed using a smooth velocity gradient starting model

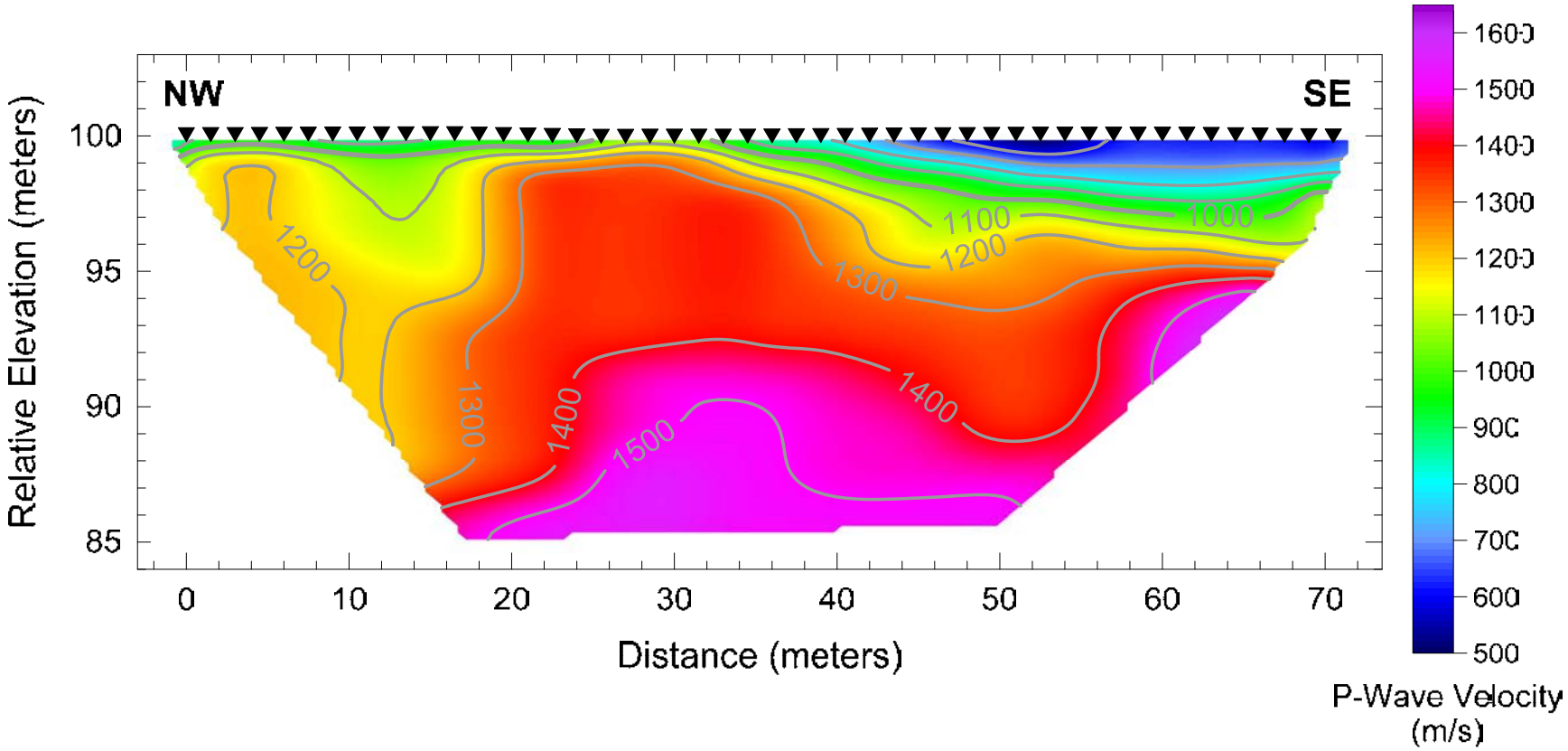

Array PLS-2 – P-wave tomographic seismic refraction model developed using a smooth velocity gradient starting model

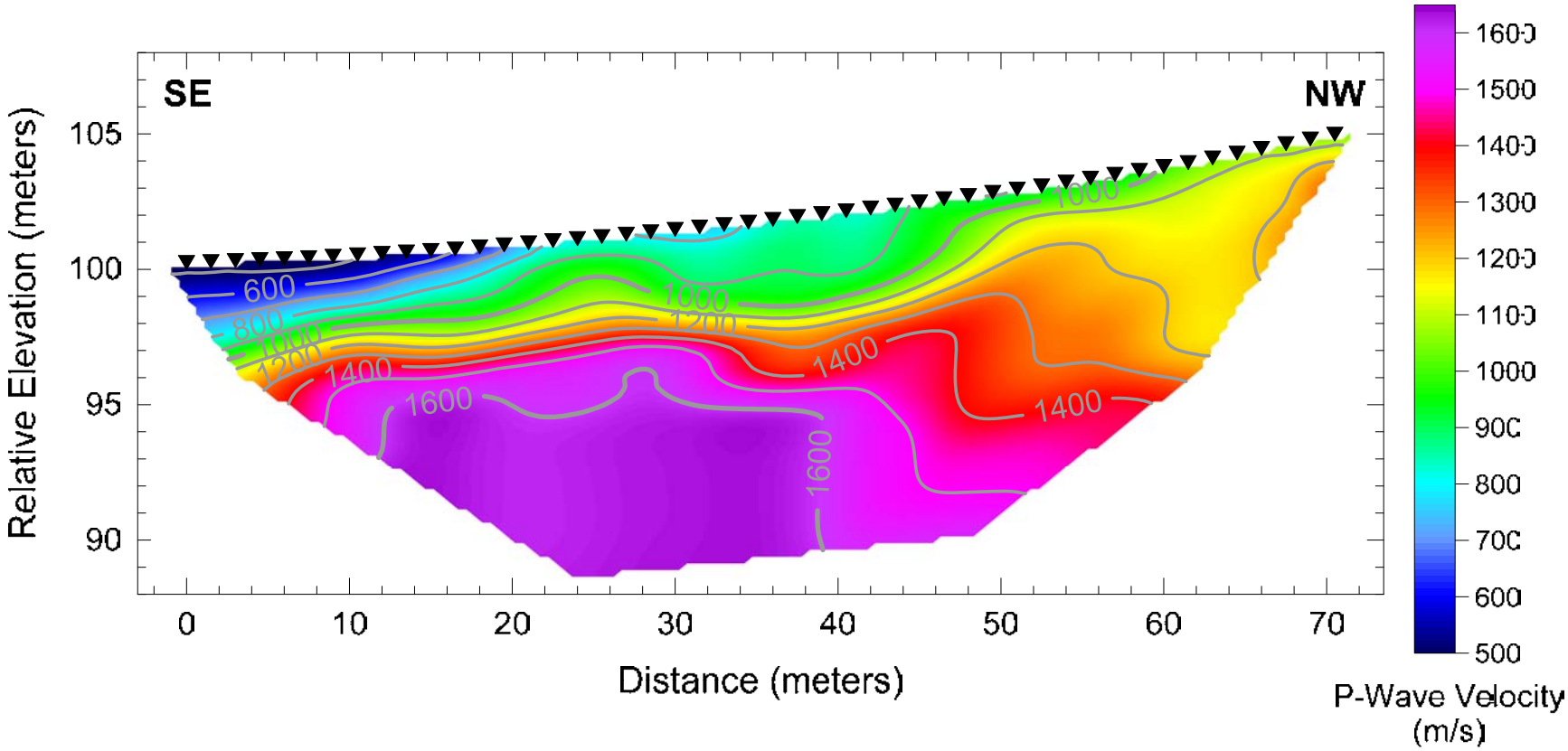

Array PLS-3 – P-wave tomographic seismic refraction model developed using a smooth velocity gradient starting model

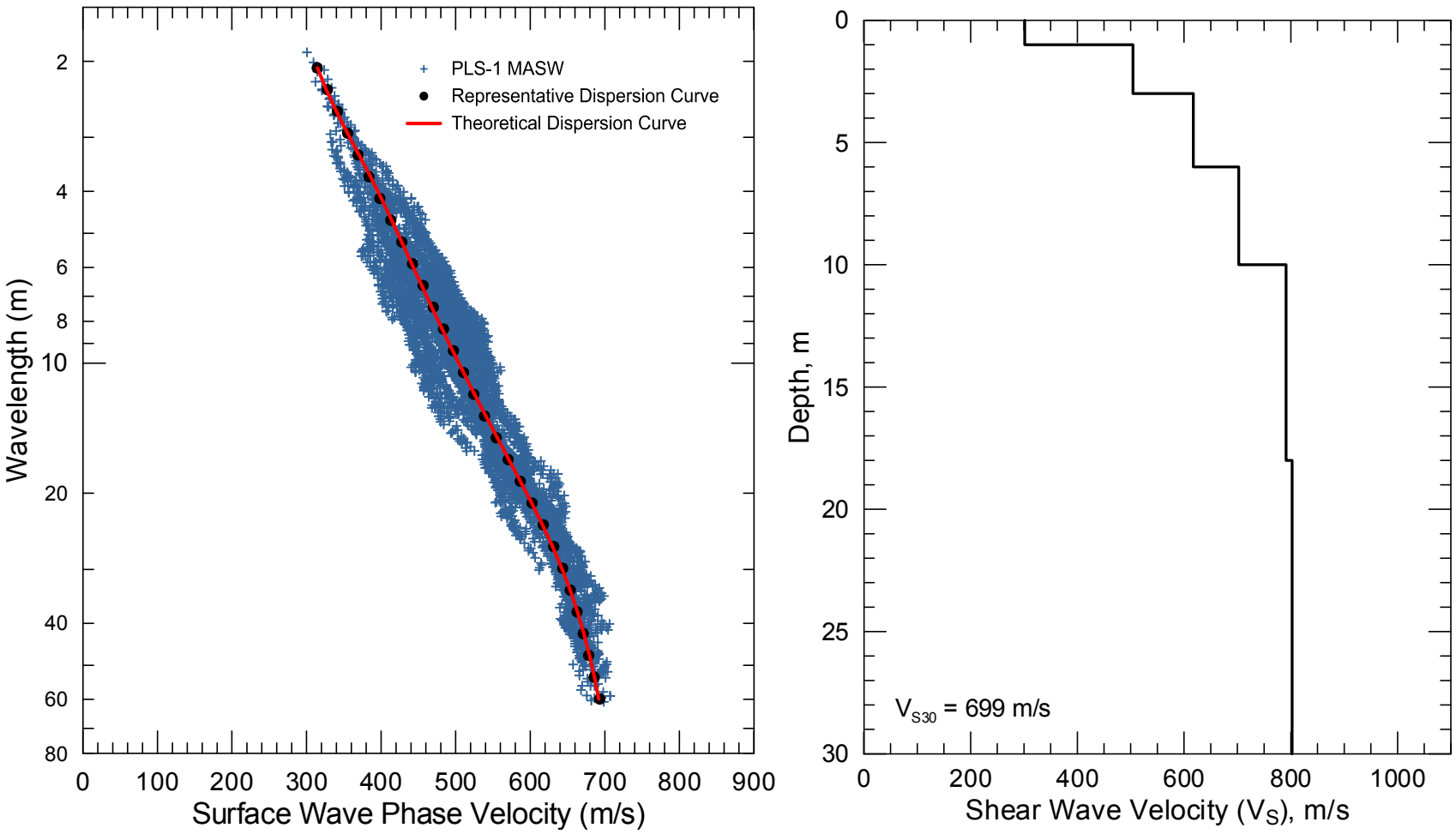

CI.PLS - Field, representative and inverted theoretical surface wave dispersion data (left) and associated V_S model (right) for array PLS-1

Site CI.PMD

Location: Palm Desert, Riverside County, California

Latitude: 33.64785 **Longitude:** -116.37769
(Station coordinates provided by USGS, WGS84 coordinate system)

V_{S30} (measured): 786 m/s (±10% based on lateral velocity variation and model uncertainty)

V_{S30} (adjusted to more accurately reflect seismic station conditions): 978 m/s (average S-wave velocity between 1.5 and 31.5 m adjusting for assumed sensor depth and sensor being located on weathered rock).

NEHRP Site Class: B

Geomatrix Code: IGA

Geologic Conditions/Observations: Seismic station located at the toe of slope of an outcrop of Mesozoic (Cretaceous) quartz diorite.

Site Conditions: Rural site. Seismic station located at the edge of a very narrow (225 m wide) valley at the toe of slope of a mountain. Steep topography in the site vicinity. MASW/seismic refraction array located along toe of slope of a mountain with a gradual 8 m decrease in ground surface elevation to the northeast along the 70.5 m array.

Geophysical Methods Utilized: HVSR, Seismic Refraction, MASW

Geophysical Testing Arrays:

1. Array PMD-1 (48 channel MASW and seismic refraction array utilizing 4.5 Hz vertical geophones spaced 1.5 m apart for a length of 70.5 m, forward and reverse shot locations with multiple source offsets and source types (hammers only) and multiple interior shot locations).
2. Three HVSR measurement locations: one at each end of array PMD-1 and the other adjacent to the seismic station.

Legend

- Seismic Station - Approximate Surveyed Location
- Seismic Station - Approximate Location of Record
- H/V Spectral Ratio Location
- MASW and Seismic Refraction Array

NOTES:
1. WGS 1984 COORDINATE SYSTEM
2. Image Source: ESRI, i-cubed, USDA FSA, USGS, AEX, GeoEye, Getmapping, Aerogrid, IGP

File Name: CI-PMD-I

Date: 3/21/2012

USGS science for a changing world

GEOVision geophysical services

RECOVERY.GOV

SITE MAP
CI•PMD

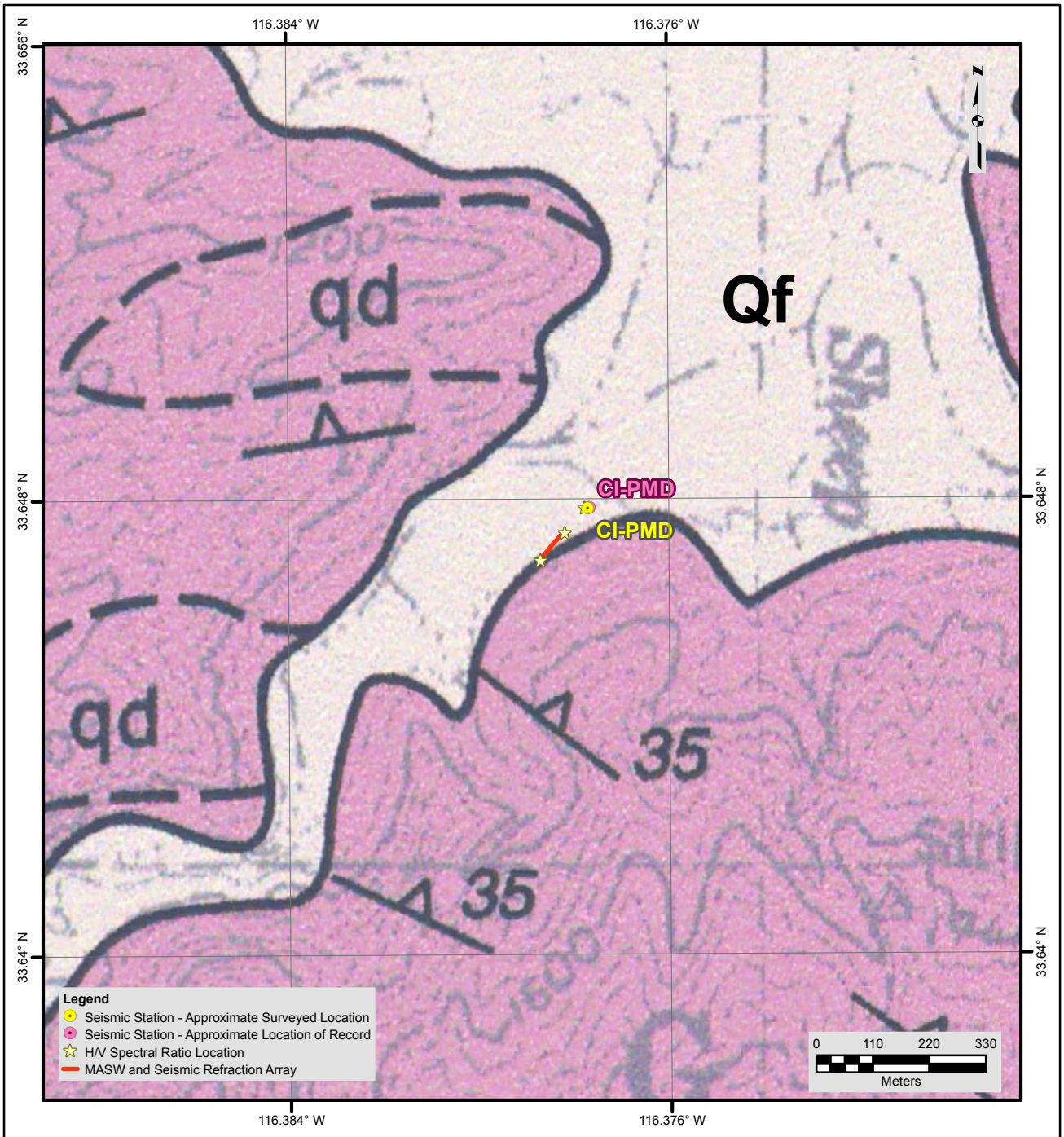

Description of Geologic Map Units

Qf =Quaternary (Holocene) alluvial fan gravel
qd = Mesozoic (Cretaceous) quartz diorite, massive to gneissoid

NOTES:
1. WGS 1984 COORDINATE SYSTEM
2. Geologic Map of the Palm Desert & Coachella 15 Minute Quadrangles, Riverside County, California By Thomas W. Dibblee, Jr., 2008
3. See site map for details of geophysical survey

File Name: CI-PMD

Date: 3/21/2012

USGS science for a changing world

GEOVision geophysical services

RECOVERY.GOV

GEOLOGIC MAP
CI•PMD

Looking south at seismic station CI.PMD

Looking northeast from center of array PMD-1

Looking at HVSR sensor 453 and seismic station

Acquisition of high frequency MASW data with 3 lb hammer

Looking southwest along array PMD-1 and at HVSR sensor 450

Location of Geophysical Testing Arrays:

Location	Latitude	Longitude
PMD-1, Southwest End of MASW/Refraction Array	33.64695	-116.37871
PMD-1, Center of MASW/Refraction Array	33.64719	-116.37848
PMD-1, Northeast End of MASW/Refraction Array	33.64741	-116.37824
HVSR Sensor 450	33.64741	-116.37821
HVSR Sensor 453	33.64785	-116.37779
HVSR Sensor 507	33.64693	-116.37872
CI.PMD Seismic Station	33.64784	-116.37772

Notes: 1) WGS84 Coordinate System (decimal degrees)
2) Survey accuracy is estimated at 1 to 3 m.

Results:

Average V_P and Estimated V_S Models from Central Portion of P-wave Seismic Refraction Array PMD-1

Depth to Top of Layer (m)	Layer Thickness (m)	P-Wave Velocity (m/s)	Estimated S-Wave Velocity (m/s)			
			Poisson's Ratio = 0.25	Poisson's Ratio = 0.30	Poisson's Ratio = 0.35	Poisson's Ratio = 0.40
0.00	0.56	357	206	191	171	146
0.56	1.13	515	297	275	247	210
1.69	1.13	822	474	439	395	335
2.81	1.13	1014	585	542	487	414
3.94	1.13	1234	713	660	593	504
5.07	1.13	1315	759	703	632	537
6.19	1.13	1362	787	728	654	556
7.32	2.36	1481	855	792	712	605
9.68	2.36	1581	913	845	760	646
12.05	2.36	1763	1018	942	847	720
14.41	2.36	2079	1200	1111	999	849
16.77	2.36	2402	1387	1284	1154	981
19.14	2.36	2811	1623	1502	1350	1148
21.50	Half Space	2811	1623	1503	1351	1148

Notes: 1) V_{S30} = 899, 833, 748 and 636 m/s for constant Poisson's ratio = 0.25, 0.3, 0.35 and 0.4, respectively.
2) Average V_S from 1.5 to 31.5 m is 1057, 978, 879 and 747 m/s for constant Poisson's ratio = 0.25, 0.3, 0.35 and 0.4, respectively.

V_S Model from MASW Data with Fundamental Mode Assumption

Depth to Top of Layer (m)	Layer Thickness (m)	S-Wave Velocity (m/s)	Inferred P-Wave Velocity (m/s)	Assumed Poisson's Ratio	Assumed Density (g/cm^3)
0	1	156	291	0.3	1.70
1	1.5	277	519	0.3	1.80
2.5	2.5	490	917	0.3	2.00
5	4	596	1116	0.3	2.10
9	5	975	1824	0.3	2.15
14	7	1436	2686	0.3	2.30
21	>9	1993	3729	0.3	2.40

Notes: 1) Depth of investigation is about 30 m.
2) Bottom layer is a half space.
3) Half space velocity not well resolved and most likely overestimated.
4) V_{S30} = 786 m/s.

V_S Model from MASW Data with Average Mode Assumption (possibly not valid)

Depth to Top of Layer (m)	Layer Thickness (m)	S-Wave Velocity (m/s)	Inferred P-Wave Velocity (m/s)	Assumed Poisson's Ratio	Assumed Density (g/cm^3)
0	1	169	316	0.3	1.70
1	1.5	279	521	0.3	1.80
2.5	2.5	411	769	0.3	1.90
5	4	521	975	0.3	2.00
9	5	890	1666	0.3	2.15
14	7	951	1779	0.3	2.15
21	>9	1350	2526	0.3	2.30

Notes: 1) Depth of investigation is about 30 m.
2) Bottom layer is a half space.
3) Half space velocity not well resolved.
4) V_{S30} = 671 m/s.

V_S Model from MASW Data using 3-D Global Inversion in WinSASW Software Package (not valid)

Depth to Top of Layer (m)	Layer Thickness (m)	S-Wave Velocity (m/s)	Inferred P-Wave Velocity (m/s)	Assumed Poisson's Ratio	Assumed Density (g/cm^3)
0	1	163	305	0.3	1.70
1	1.5	276	517	0.3	1.80
2.5	2.5	363	679	0.3	1.90
5	4	530	991	0.3	2.00
9	5	810	1515	0.3	2.15
14	7	952	1782	0.3	2.15
21	>9	1357	2538	0.3	2.30

Notes: 1) Depth of investigation is about 30 m.
2) Bottom layer is a half space.
3) Half space velocity not well resolved.
4) V_{S30} = 650 m/s.

Observations/Discussion:

- The HVSR curves are very similar at frequencies below 8 Hz. There is a possible weak HVSR peak at about 5 Hz, which is best defined on the HVSR plot for sensor 507.
- The seismic station is located at the base of an outcrop of granitic rock. In this situation, the only feasible location for geophysical testing is an array aligned along the toe of slope. Surface waves are difficult to apply in this situation unless the bedrock surface only has shallow slope orthogonal to the array. In these types of environments, we have had the most success applying the S-wave seismic refraction technique. However, S-wave seismic refraction data were not acquired at this site as the technique was not in common use on the project at the time of the field investigation. Upon more careful review of aerial photo coverage, a better location for testing may have been in a small drainage about 100 m southeast of the seismic station.
- P-wave seismic refraction data quality was excellent. The P-wave seismic refraction data for array PMD-1 were modeled using a tomographic inversion routine with a smooth velocity gradient starting model. The model was extended to far offset source locations to extend depth of investigation. A longer array, rather than the utilization of far offset shot locations, is preferred for extending depth of investigation, when applying tomographic inversion routines. However, the seismic refraction data were acquired in conjunction with surface wave data, where a shorter array length is preferred.
- The P-wave seismic refraction survey design allowed P-wave velocity to be imaged to a maximum depth of about 24 m. The seismic refraction model indicates that P-wave velocity is about 400 to 500 m/s at the surface and increases to 1,000 m/s at a depth of 2

to 6 m, 1,500 m/s at a depth of 7 to 11 m, 2,000 m/s at a depth of 13 to 15 m and over 3,000 m/s at a depth greater than 19 m.

- The seismic refraction survey indicates that there is some lateral velocity variation beneath the array associated with variable thickness of the sediments overlying bedrock and differential weathering within bedrock.
- The average P-wave velocity of the upper 30 m (V_{P30}) was estimated between 21 and 49.5 m on the P-wave refraction model, where depth of investigation is greatest, by projecting the velocity at 21.5 m depth to 30 m depth. The average V_P at 21.5 m is very high and only expected to gradually increase with depth. Additionally, even a significant increase in the velocity below 21.5 m will only have a small effect of V_{P30}. V_{P30} ranges from about 1,459 to 1,646 m/s between a position of 21 to 49.5 m, a 12% variation.
- An average V_P model was developed over the 21 to 49.5 m distance interval by horizontally averaging the travel time of each model cell or slowness, if cells have uniform thickness, and cell thickness and average V_{P30} was determined to be 1,558 m/s. Assuming a constant Poisson's ratio of 0.25, 0.3, 0.35 and 0.4 would result in an estimated V_{S30} of 899, 833, 748 and 636 m/s, respectively. Bedrock is not expected to be saturated in the upper 30 m and, therefore, Poisson's ratio in the 0.25 to 0.35 range is probable. Average S-wave velocity between 1.5 and 31.5 m, to account for assumed sensor depth and the fact that the sensor appears to be placed on rock, is 1057, 978, 879 and 747 m/s for constant Poisson's ratio of 0.25, 0.3, 0.35 and 0.4, respectively.
- Noise conditions at the site were not sufficient for application of passive surface wave techniques.
- MASW (Rayleigh wave) data were difficult to reduce due to lateral velocity variation, a possible dipping bedrock surface beneath the seismic line and probable variable thickness of the sediment layer beneath the array. Dominant higher modes also appeared to be problematic as might be expected for a thin sediment layer overlying high velocity weathered rock. For many of the source locations it was difficult to extract surface wave dispersion data using the complete 48 channel receiver array. The near field wavelength restriction applied on this investigation had to be relaxed somewhat to obtain Rayleigh wave phase velocity data to a wavelength of 60 m. To minimize near field effects, the maximum wavelength was set to between 1.2 and 1.4 times the distance between the source and center of the active receiver array for this data set. A factor of 1 to 1.2 has been more commonly applied during this investigation.
- The minimum wavelength Rayleigh wave phase velocity data extracted from the data set is about 3 m.
- There is nominally about 100 to 120 m/s scatter in MASW dispersion data, likely due to the effects of lateral velocity variation.
- A representative dispersion curve was generated for the MASW data set using a moving average, polynomial curve fitting routine and used for modeling.
- The velocity structure at this site is such that higher modes may dominate over a wide frequency range. The fundamental mode appears to be recovered at high frequencies using limited offset receiver gathers and small offset source locations. The fundamental mode may also be recovered at low frequencies; however, data modeling introduced the possibility that the fundamental mode may jump to the first higher mode at frequencies below 40 Hz. Alternatively, the fundamental and first higher modes may become superimposed at low frequencies. Currently there are limited mechanisms to deal with

possible modal superposition in MASW data. The SASW technique has an available 3-D array based inversion to attempt to deal with this issue. In the future, direct comparison of dispersion curves generated using the MASW and SASW techniques will be made at sites similar to this to better understand the problem and explore possible solutions.

- V_{R40} is in the 730 to 830 m/s range which would result in an estimated V_{S30} of 763 to 867 m/s, based on the Brown, et al., 2000 relationship, assuming that the dispersion curve at 40 m wavelength is the fundamental mode. V_{S30} would be lower if the dispersion curve were associated with the first higher mode or if modal superposition occurs at low frequencies. V_{S30} from the average seismic refraction V_P model using a Poisson's ratio of 0.3 to represent typical unsaturated conditions is 833 m/s, which is consistent with the values above.
- The MASW data were modeled using both the fundamental mode assumption (2-D solution in the WinSASW software package, which is approximately equivalent to fundamental mode) and average/effective mode assumption (observed dispersion curve consists of the average of all modes based on relative amplitude of each mode estimated for a plane Rayleigh wave). The average/effective mode assumption is an attempt to deal with modal superposition that may occur at low frequencies due to lack of resolution partially associated with finite receiver array length. However, the analytical method used to estimate the relative energy of each mode does not consider source-receiver geometry and assumes a far-field source and plane Rayleigh wave and no body wave effects, making it much for suitable to modeling of passive surface wave data. It is well documented that source-receiver geometry affects the energy in higher modes and, therefore, the average mode assumption may not always be accurate. However, modeling of average mode may result in a more accurate model than incorrectly assuming that the dispersion curve is fundamental mode, especially if only the lowest frequency portion of the dispersion curve is affected by modal superposition. Finally, in another attempt to deal with possible modal superposition or dominant higher modes, the MASW dispersion data was modeled using the 3-D global inversion option in the WinSASW software package. This modeling routine is designed to model SASW data acquired with a pair of receivers and is not generally be applicable to MASW data. Interestingly, the average mode and 3-D global inversion models are very similar at this site.
- Surface wave depth of investigation is about 30 m based on the one half to one third of maximum wavelength criteria.
- V_{S30} is 786 m/s for the V_S model developed using the fundamental mode assumption (NEHRP Site Class B).
- Average S-wave velocity between 1.5 and 31.5 m, to account for assumed sensor depth and the fact that the sensor appears to be placed on rock, is 978 m/s for the fundamental mode surface wave model.
- Decreasing the velocity of the half space to that of the overlying layer in the fundamental mode model decreases V_{S30} to 752 m/s and the average V_S between 1.5 and 31.5 m to 917 m/s.
- V_{S30} is 671 and 650 m/s for the average mode and 3-D global inversion surface wave models, respectively (NEHRP Site Class C).
- Average S-wave velocity between 1.5 and 31.5 m is 787 and 763 m/s for the average mode and 3-D global inversion surface wave models, respectively.

- The estimates of V_{S30} and the average V_S between 1.5 and 31.5 m from the average mode and 3-D global inversion V_S models are not supported by the seismic refraction model. An average Poisson's ratio of slightly less than 0.4 would be required for these models to be relatively consistent with the average refraction model, which is not realistic for unsaturated weathered crystalline rock.
- There are inconsistencies between the various V_S models developed from the surface wave and P-wave refraction data. Conditions are not ideal for acquisition of surface wave data and MASW data reduction was quite difficult. Lateral velocity variation may contribute to the difference in the seismic refraction and surface wave models. We only present the average velocity structure from the P-wave refraction model and not the portions of the model with highest and lowest estimated V_{P30}. Additionally, we only present a single V_S model to represent the surface wave data rather than an ensemble of models to reflect nonuniqueness. There may be other models that are in better agreement with the seismic refraction models and fit within the error bars defined by the scatter in the dispersion data.
- For site characterization purposes, we recommend using the S-wave velocity structure derived from the MASW model developed using the fundamental mode assumption. Although we expect the velocity of the half space to be overestimated in this model, the model yields a V_{S30} estimate consistent with the P-wave refraction model with an assumed constant Poisson's ratio in the 0.3 to 0.35 range, which is realistic for weathered rock.
- There is uncertainty in the V_S models at this site, related to uncertainty in which Rayleigh wave modes are dominant, and acquisition of S-wave seismic refraction and MALW (Love wave) data is recommended to better constrain subsurface velocity structure. Alternatively, SASW data acquisition could be considered to evaluate if 3-D array based SASW inversion generates a more reliable V_S model in this type of environment. However, this site is not particularly suited for surface wave methods as the bedrock surface dips orthogonally to an array orientated along the toe of slope. Testing in a small drainage channel, located between two bedrock ridges about 100 m south of the seismic station may yield better results. Regardless of the uncertainly, with data modeling at this site, all presented models indicate that once V_{S30} is adjusted for seismic station conditions that site falls into NEHRP Site Class B.

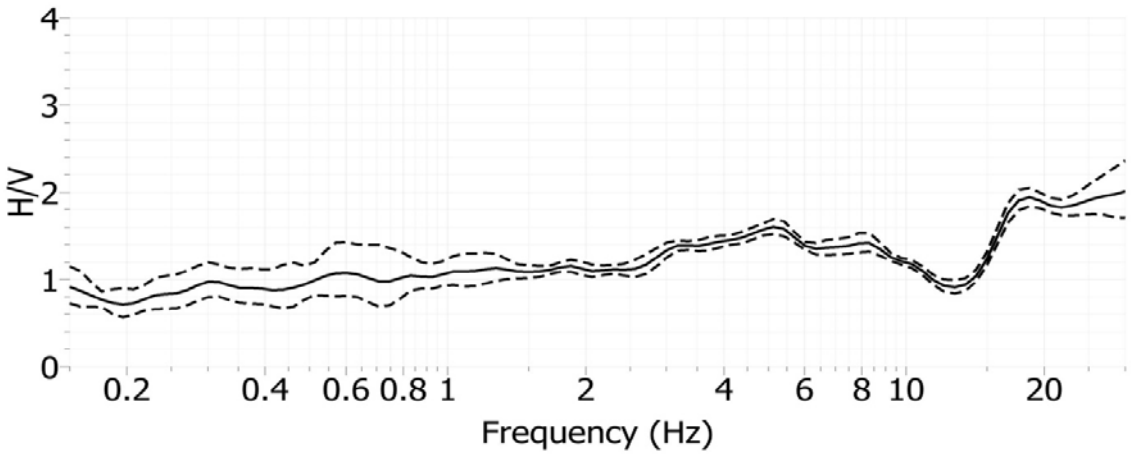

Site CI.PMD, H/V Spectral Ratio, Near Seismic Station, Sensor 453

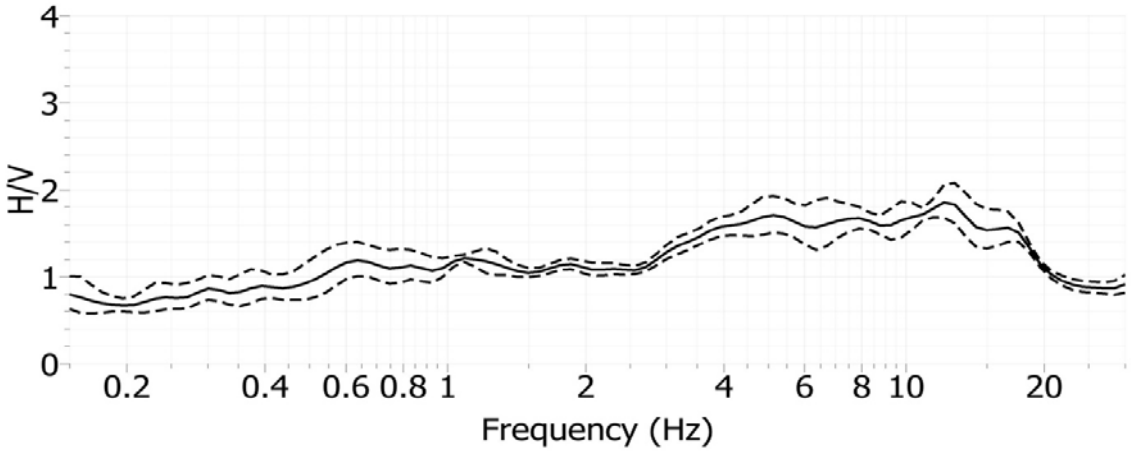

Site CI.PMD, H/V Spectral Ratio, Array PMD-1, Sensor 450

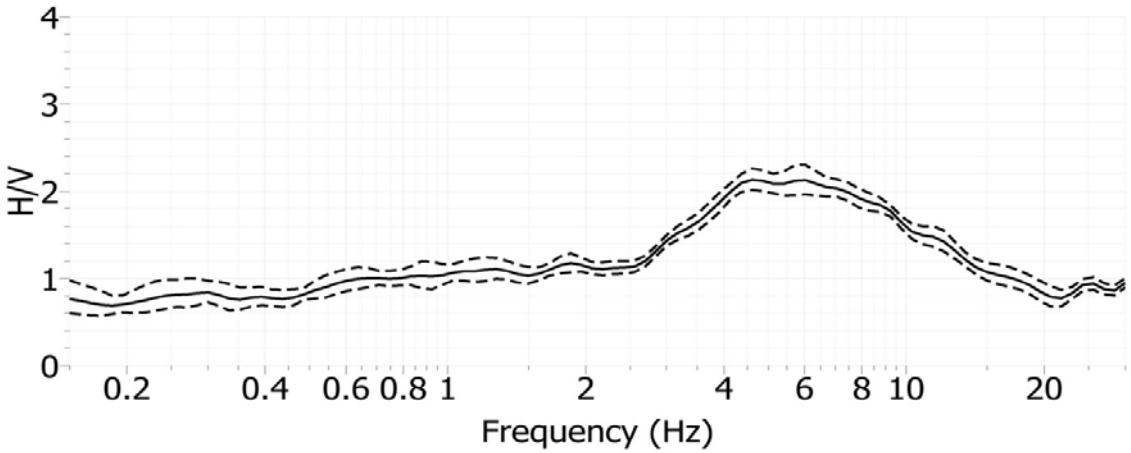

Site CI.PMD, H/V Spectral Ratio, Array PMD-1, Sensor 507

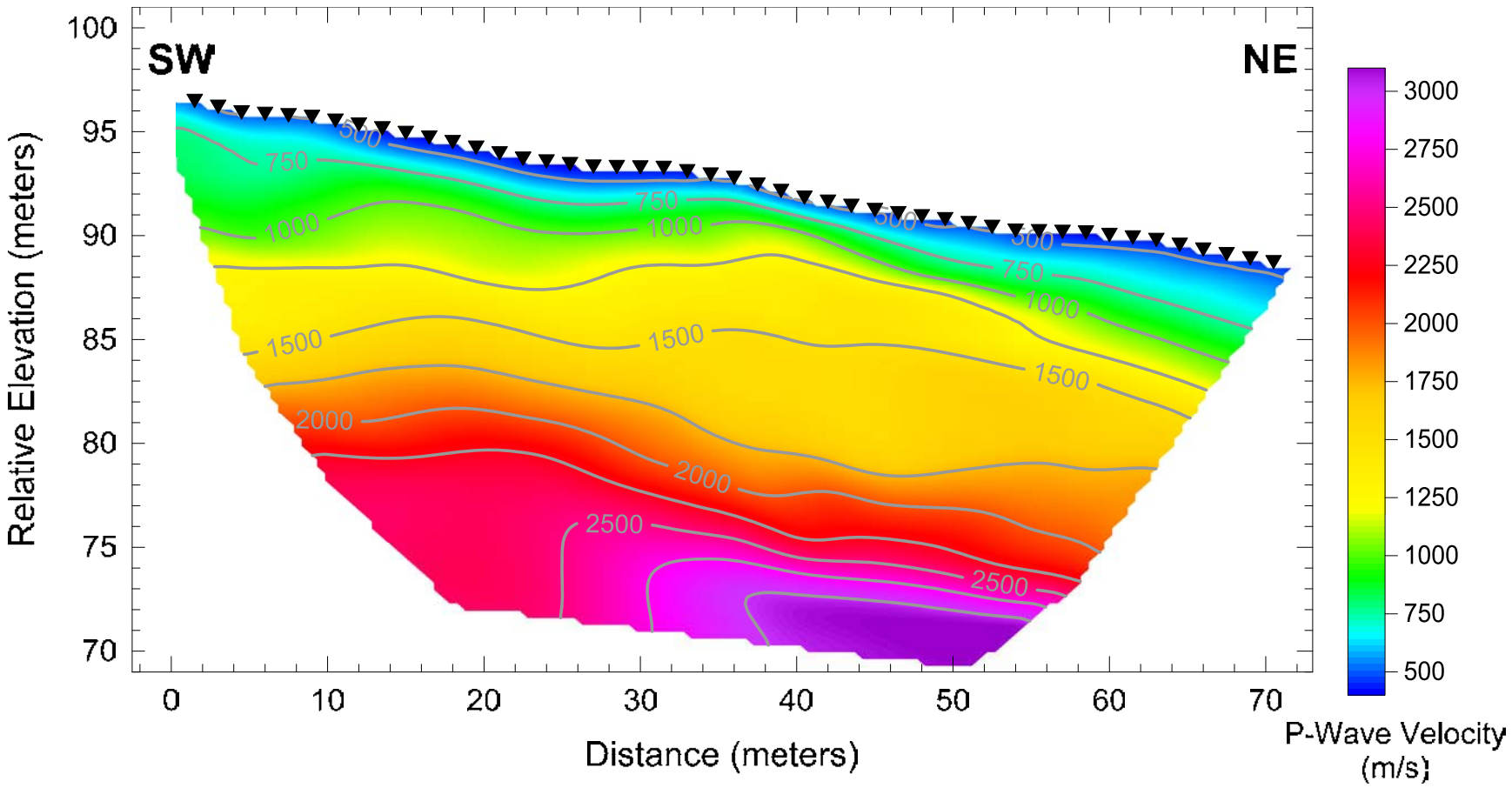

Array PMD-1 – Tomographic Seismic Refraction Model developed utilizing Smooth Velocity Gradient Starting Model

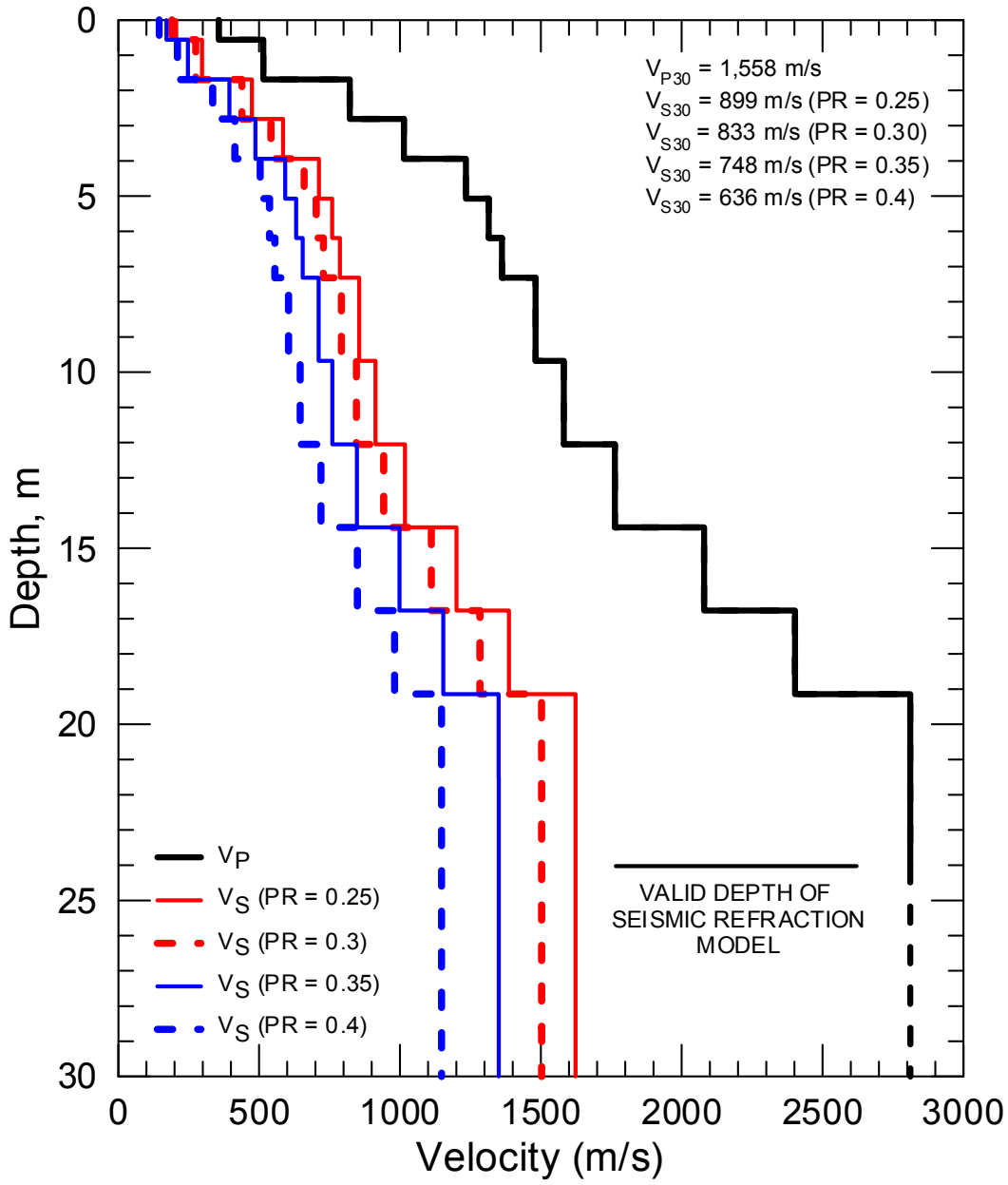

CI.PMD – Average P-wave velocity structure and estimated S-wave velocity structure between a position of 21 and 49.5 m on the P-wave seismic refraction model for array PMD-1.

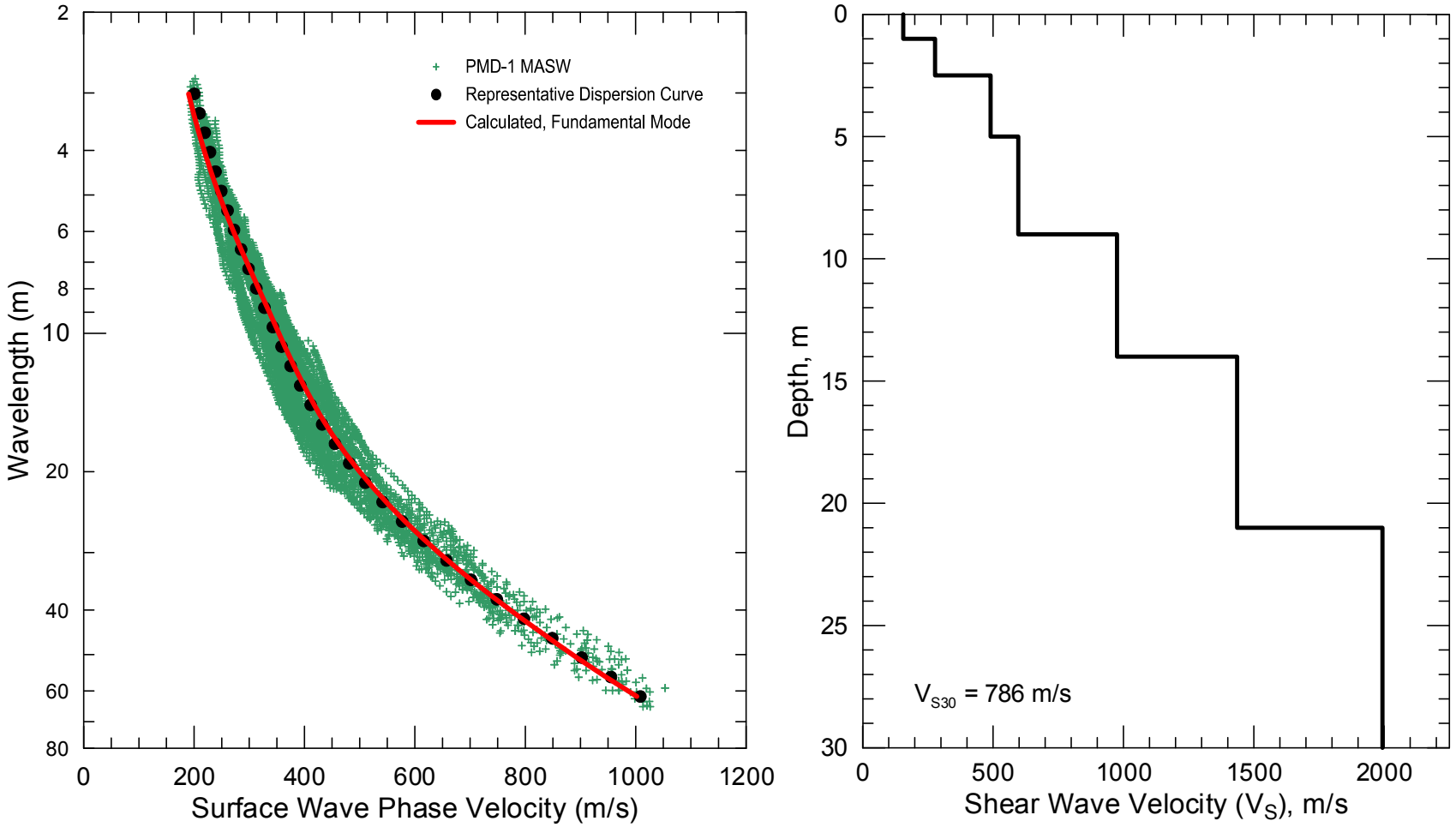

CI.PMD - Field, representative and inverted theoretical surface wave dispersion data (left) and associated V_S model (right) for fundamental mode assumption

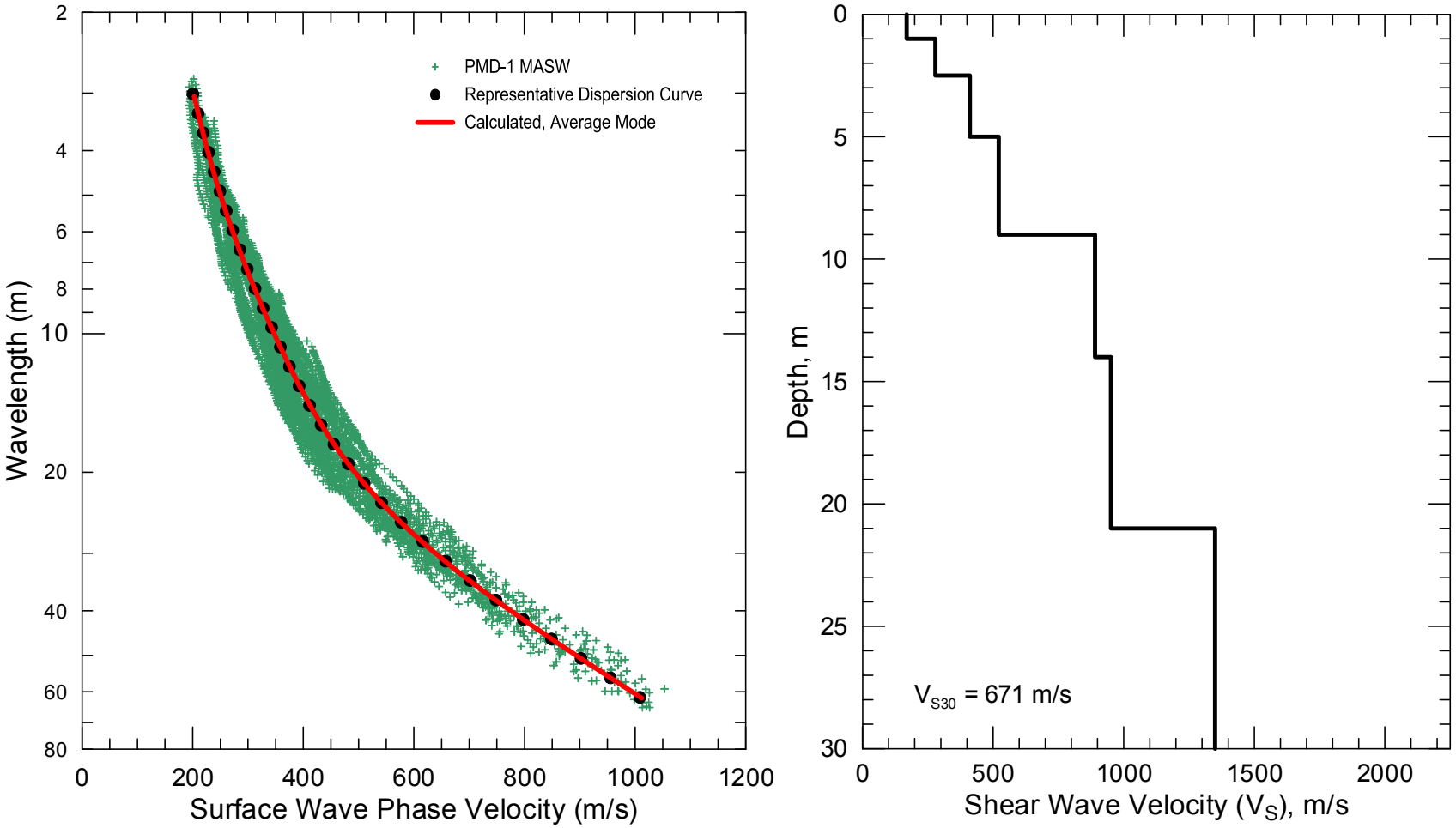

CI.PMD - Field, representative and inverted theoretical surface wave dispersion data (left) and associated V_S model (right) for average mode assumption

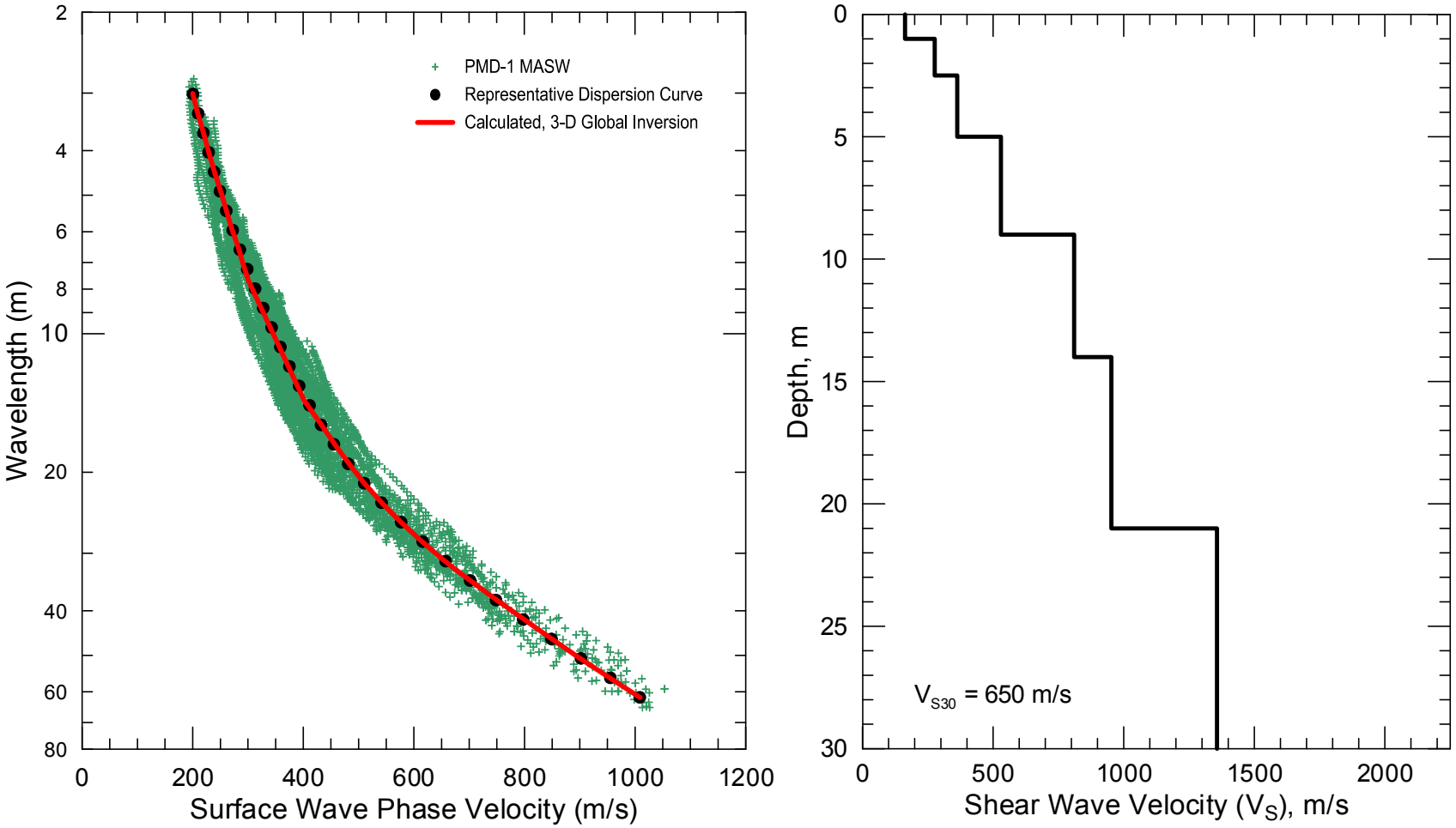

CI.PMD - Field, representative and inverted theoretical surface wave dispersion data (left) and associated V_S model (right) utilizing 3-D global inversion routine in WinSASW software package (use of this modeling approach is not defensible)

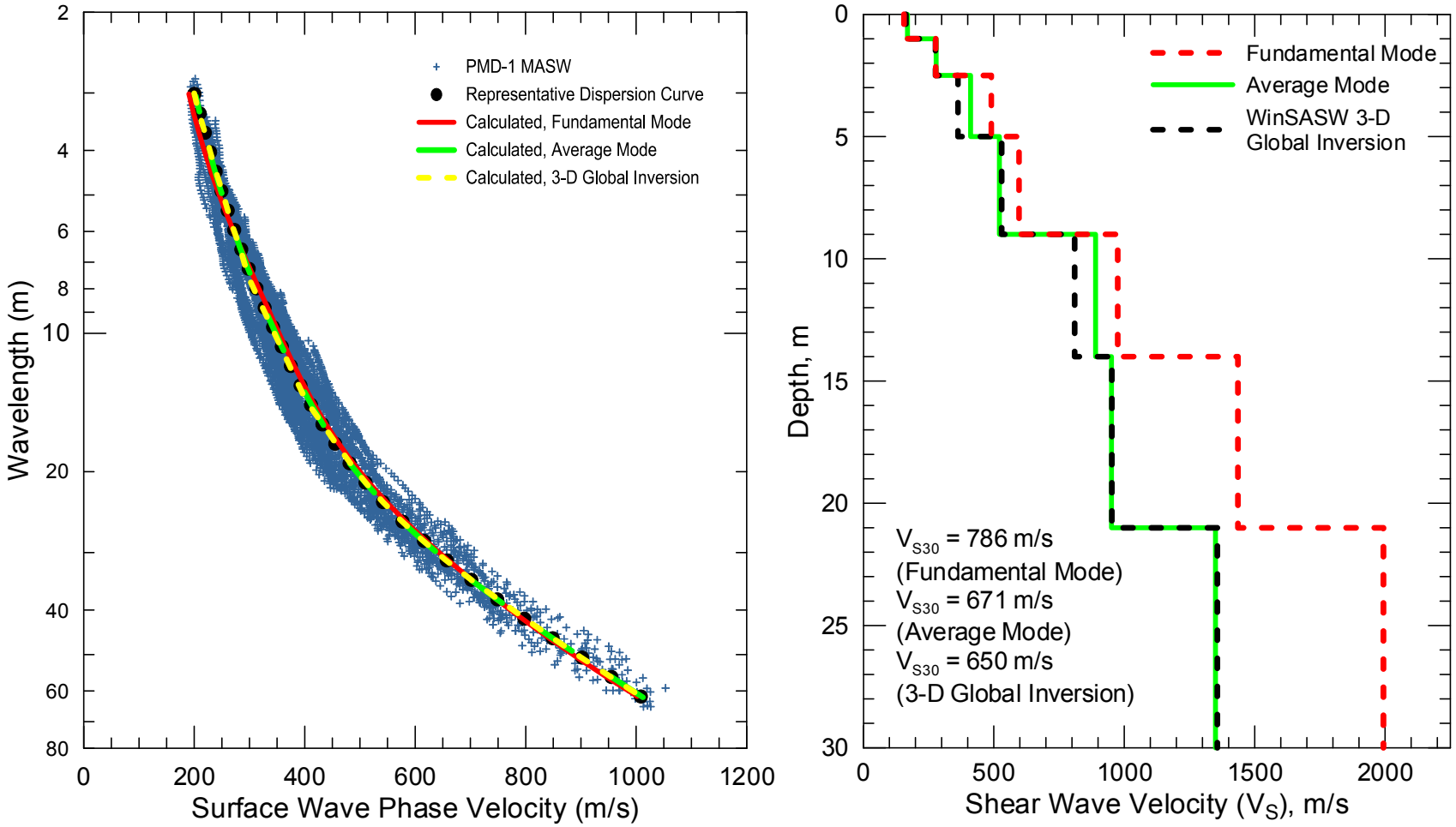

CI.PMD - Field, representative and inverted theoretical surface wave dispersion data (left) and associated V_S models (right) for fundamental and average mode assumption and 3-D global inversion

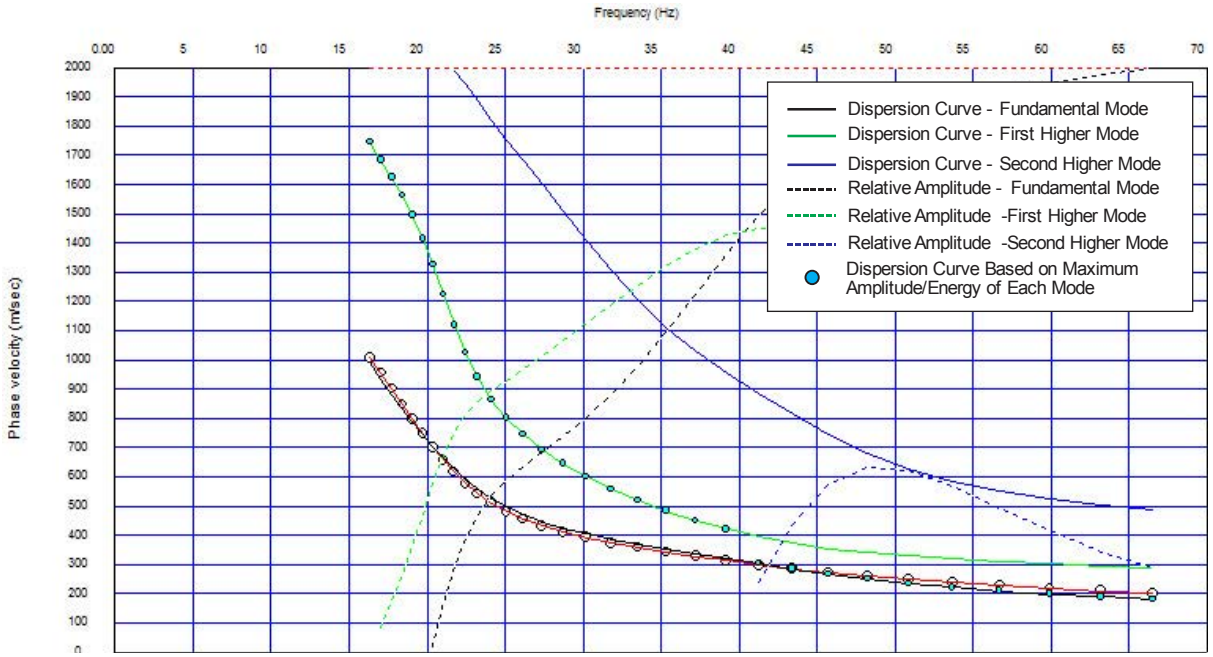

Calculated Rayleigh wave phase velocity modes for fundamental mode V_S model demonstrating that this mode should excite a dominant higher mode at frequencies below 40 Hz. It should be noted, however, that the analytical routine used to estimate the amplitudes of the higher modes does not include the source location and makes a plane wave assumption.

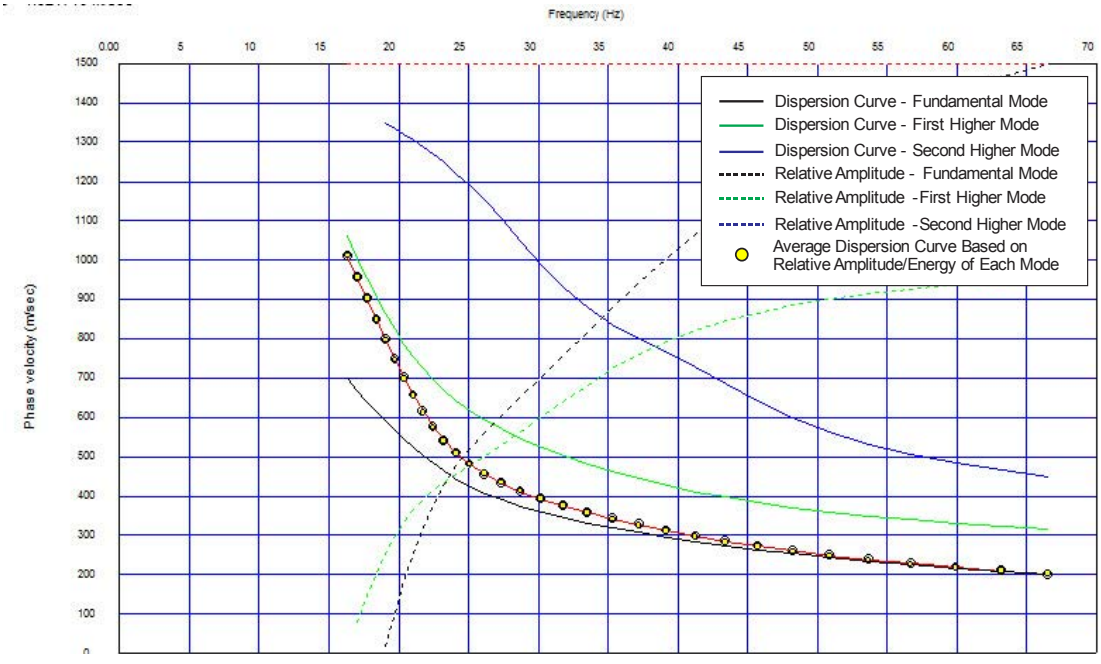

Calculated Rayleigh wave phase velocity modes for V_S model developed using the average mode assumption in an attempt to account for possible modal superposition (mode mixing) at low frequencies.

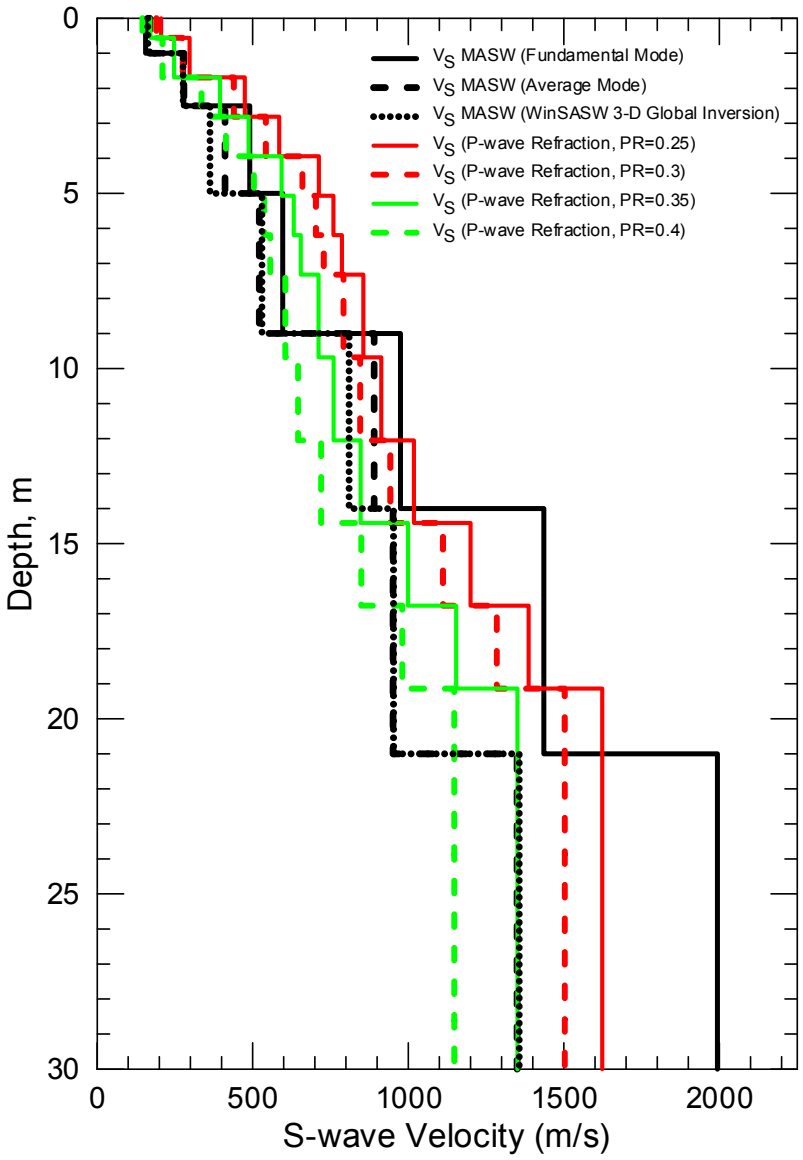

CI.PMD – Comparison of S-wave velocity models derived from the MASW and P-wave seismic refraction surveys. The S-wave model generated from the Rayleigh wave phase velocity dispersion data using the fundamental mode assumption agrees best with the seismic refraction models (a Poisson's ratio of 0.3 is realistic for weathered rock), although V_S appears significantly overestimated at depth due to possible modal superposition or mode jumping. We typically apply the average mode assumption when only the half space velocity is modified, to account for modal superposition at low frequencies. In this case, V_S of all layers below 3 m depth are lowered and the average mode model cannot be considered valid. The analytical routine used for the WinSASW 3-D global inversion is not designed for MASW data and is not considered valid; although, interestingly, the average mode and 3-D global inversions result in similar Vs models at this site. The average mode and 3-D global inversion models would be feasible at depth if the weathered rock were saturated, which is unknown but not expected. An S-wave seismic refraction and/or MALW (Love wave) survey may yield better results at this site.

Site CI.RCT

Location: SCE Rector Substation, near Visalia, California

Latitude: 36.30523 **Longitude:** -119.24384
(Station coordinates provided by USGS with station location confirmed in field, WGS84 coordinate system)

V_{S30} (measured): 282 m/s

V_{S30} (adjusted to more accurately reflect seismic station conditions): 301 m/s (average S-wave velocity between 2 and 32 m adjusting for nominal 2 m seismic sensor depth).

NEHRP Site Class: D

Geomatrix Code: IHD

Geologic Conditions/Observations: Quaternary (Holocene) alluvial fan deposits, deep soil site.

Site Conditions: Rural site with significant, albeit directionally biased, noise sources from agricultural activity to northwest, road construction to southeast and lightly traveled road to east. Relatively flat terrain in site vicinity.

Geophysical Methods Utilized: HVSR, MASW, SASW, array microtremor, ReMi™

Geophysical Testing Arrays:

1. Arrays RCT-1 (24 channel array utilizing 4.5 Hz vertical geophones spaced 6 m apart for a length of 138 m) and RCT-2 (24 channel array utilizing 4.5 Hz vertical geophones spaced 3 m apart for a length of 69 m) used to acquire passive surface wave data. The arrays were combined to form a "T" array and separated to form linear arrays.
2. Arrays RCT-1 and RCT-2 were also used to acquire limited MASW and seismic refraction data (off-end shots with accelerated weight drop energy source).
3. Array RCT-3 (48 channel MASW array utilizing 4.5 Hz vertical geophones spaced 1 m apart for a length of 47 m and a common midpoint SASW array utilizing 1 Hz geophones with maximum receiver spacing of 36 m). Array RCT-3 was aligned along array RCT-1 and centered at the intersection of arrays RCT-1 and RCT-2.
4. Three HVSR measurement locations distributed along arrays RCT-1 and RCT-2.

Legend

- Seismic Station - Approximate Location of Record
- H/V Spectral Ratio Measurement Location
- MASW and SASW Array
- Passive Surface Wave Array

NOTES:
1. WGS 1984 COORDINATE SYSTEM
2. Image Source: ESRI, i-cubed, USDA FSA, USGS, AEX, GeoEye, Getmapping, Aerogrid, IGP

File Name: CI-RCT-I

Date: 6/18/2012

USGS science for a changing world

GEOVision geophysical services

SITE MAP
CI•RCT

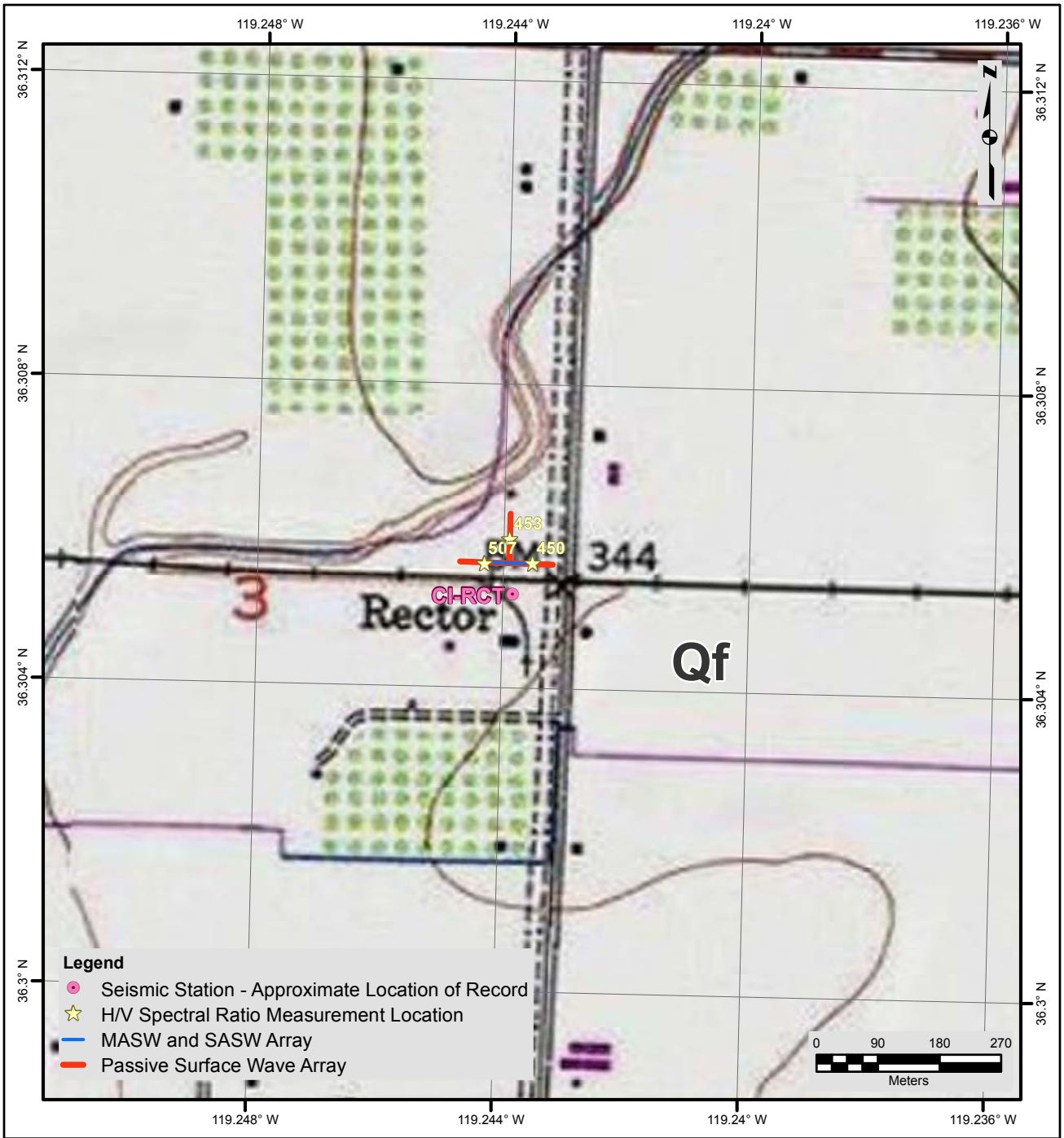

Description of Geologic Map Units

Qf = Quaternary (Holocene) alluvial fan deposits of the Great Valley

NOTES:
1. WGS 1984 COORDINATE SYSTEM
2. Topo Image Sources: USGS, FAO, NPS, EPA, NRCAN, GeoBase, Esri, DeLorme, TANA, Intermap, AND, other suppliers, and the GIS community
3. Geologic Map Units from:
Geologic Map of California (Olaf P. Jenkins edition),
Fresno Sheet
compiled by Robert A Matthews and John L. Burnett, 1965
4. See site map for details of geophysical survey

File Name: CI-RCT

Date: 4/7/2011

USGS science for a changing world

GEOVision geophysical services

RECOVERY.GOV

GEOLOGIC MAP
CI•RCT

CI.RCT seismograph station

Looking south towards intersection of RCT-1 and RCT-2 and seismograph station

Looking southeast towards seismograph station from HVSR sensor 507

RCT-3 SASW array

RCT-3 MASW array

Location of Geophysical Testing Arrays:

Location	Latitude	Longitude
RCT-1, West End of Array	36.30565	-119.24470
RCT-1, East End of Array	36.30564	-119.24320
RCT-2, South End of Array	36.30567	-119.24390
RCT-2, North End of Array	36.30629	-119.24390
RCT-3, Center of Array	36.30565	-119.24390
HVSR Sensor 507	36.30564	-119.24431
HVSR Sensor 453	36.30596	-119.24391
HVSR Sensor 450	36.30564	-119.24352

Notes: 1) WGS84 Coordinate System (decimal degrees)
2) RCT-3 aligned along RCT-1
3) Survey accuracy is estimated at 1 to 2 m

Results:

V_S Model

Depth to Top of Layer (m)	Layer Thickness (m)	S-Wave Velocity (m/s)	Inferred P-Wave Velocity (m/s)	Assumed Poisson's Ratio	Assumed Density (g/cm^3)
0	2	175	327	0.300	1.7
2	5	209	391	0.300	1.8
7	5	242	452	0.300	1.8
12	5	299	559	0.300	1.8
17	10	378	2000	0.481	1.9
27	13	428	2000	0.476	1.9
40	>10	512	2000	0.465	2.0

Observations/Discussion:

- HVSR curves are generally similar at all stations, validating the 1-D velocity assumption. There are, however, subtle differences between the HVSR curves. The high amplitude HVSR response at low frequencies for sensor 507 appears to be associated with a sensor coupling/deployment issue and should not be considered valid.
- Broad HVSR peak or multiple peaks in the 0.35 to 0.55 Hz range. Low frequency peaks, such as these, are consistent with a deep soil site.
- Distinct low amplitude, secondary HVSR peaks at about 0.9 and 3.5 Hz at all measurement locations.
- The noise conditions at this site are not ideal for application of passive surface wave techniques due to limited and possibly directionally biased noise sources near site. There are, however, more significant noise sources (i.e. high traffic roads and developed areas) at distances of 1.5 km, or more, from site. Even with these limitations, the passive surface wave data is in good agreement with the active surface wave data and slightly extends depth of investigation.
- ESAC technique used to extract surface wave dispersion data from passive "T" array data. Both the ReMi™ and ESAC techniques used to extract surface wave dispersion data from the passive linear arrays.
- Surface wave dispersion data from all active and passive surface wave datasets are in very good agreement at this site.
- SASW data provides surface wave dispersion data at slightly smaller wavelengths (higher frequencies) than the MASW data.
- MASW data were acquired along the long, linear passive surface wave arrays to obtain long wavelength surface wave data without concern of near field effects in the frequency range of interest.
- For the purpose of data modeling, a representative dispersion curve was generated for the combined surface wave data set using a moving average, polynomial curve fitting routine.
- Water table depth constrained at about 17 m based on a simple, 2-layer interactive analysis of seismic refraction data from MASW shot records (375 m/s V_P for unsaturated sediments and 2,000 m/s V_P for saturated sediments).
- Surface wave depth of investigation is about 50 m, based on half maximum wavelength criteria.
- V_{S30} is 282 m/s (Site Class D).
- Average S-wave velocity between 2 m (nominal sensor depth) and 32 m is 301 m/s.
- Average S-wave velocity of the upper 50 m (V_{S50}) is 335 m/s.

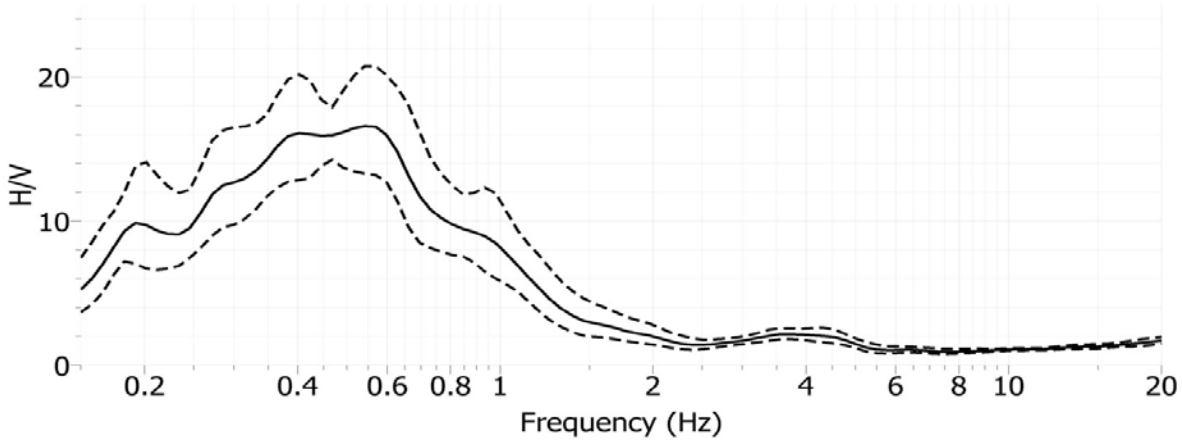

Site CI.RCT, H/V Spectral Ratio, Array RCT-1, Sensor 507 (Not Reliable at Low Frequency)

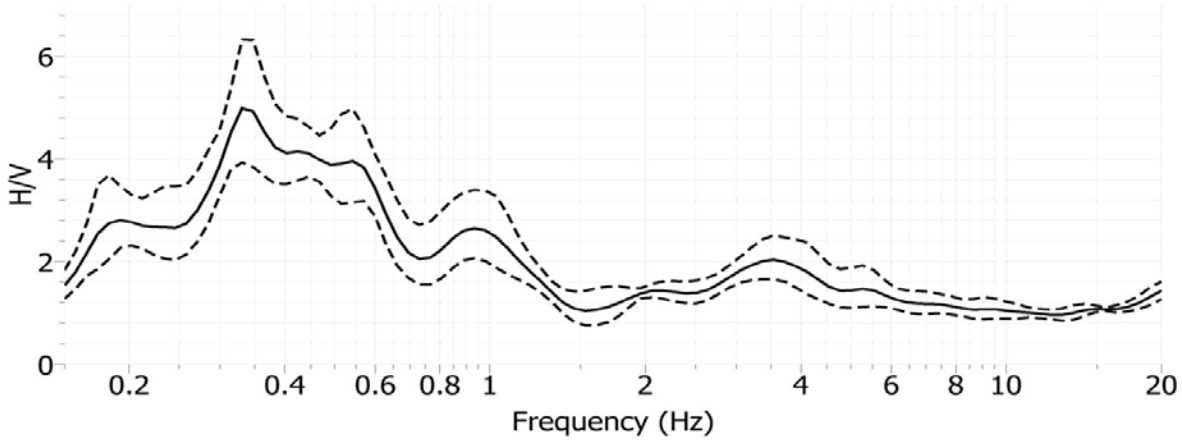

Site CI.RCT, H/V Spectral Ratio, Array RCT-2, Sensor 453

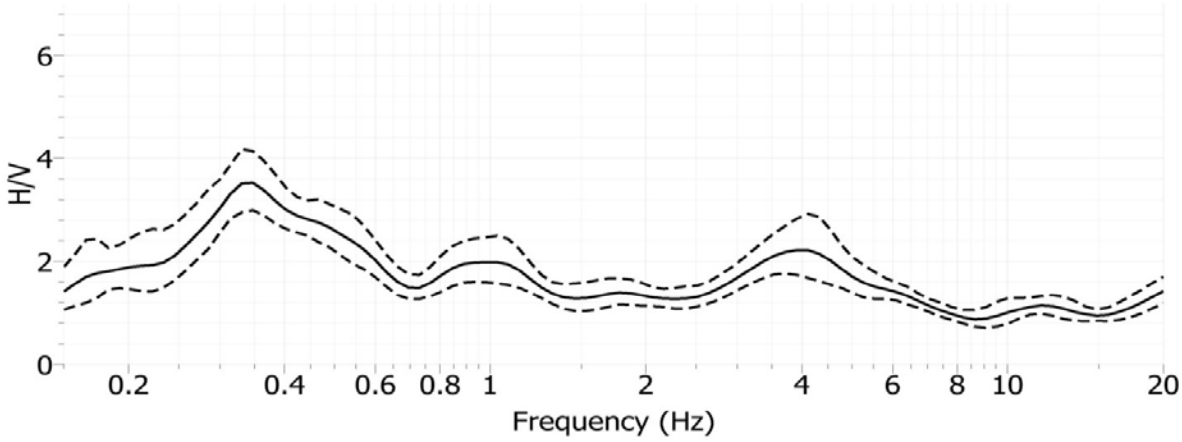

Site CI.RCT, H/V Spectral Ratio, Array RCT-1, Sensor 450

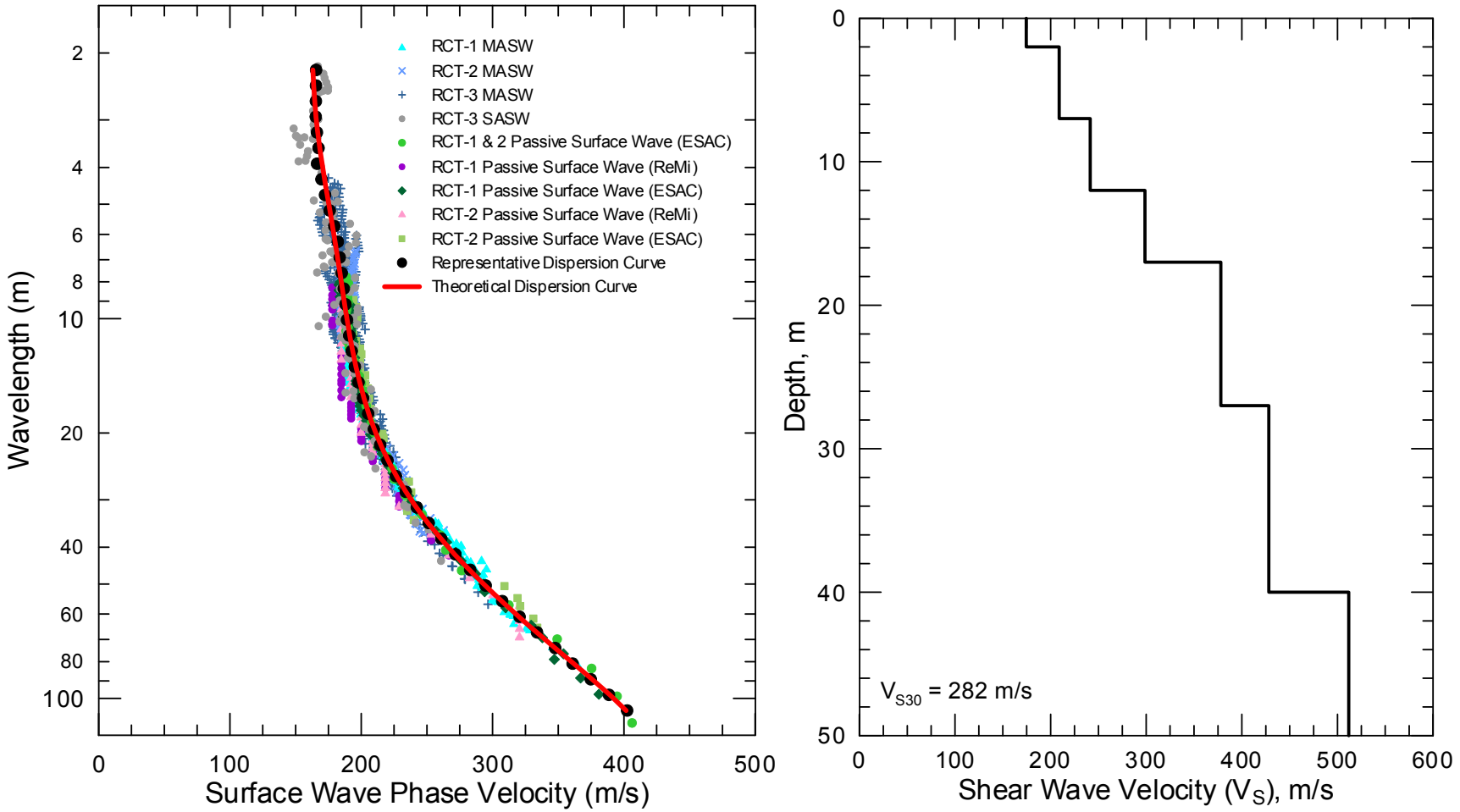

CI.RCT - Field, representative and inverted theoretical surface wave dispersion data (left) and associated V_S model (right)

Site CI.RRX

Location: Southern California Edison Barstow Service Center, 30553 E. Rimrock Road, Barstow, California

Latitude: 34.87499 **Longitude:** -116.99683

(Station coordinates modified based on field GPS survey)

V_{S30} (measured): 372 m/s

V_{S30} (adjusted to more accurately reflect seismic station conditions): 396 m/s (average S-wave velocity between 2 and 32 m adjusting for nominal sensor depth)

NEHRP Site Class: C

Geomatrix Code: IQD/IHD

Geologic Conditions/Observations: Site located on geologic unit mapped as Holocene alluvium, but within 100 m of mapped Pleistocene old alluvium. Seismic sensors located on a pad cut about 2 m below natural ground surface and it is possible that the seismic sensor sits on Pleistocene rather than Holocene sediments. Crystalline basement expected to be deep at this site.

Site Conditions: Rural site with sporadic traffic on nearby streets. Relatively flat terrain in test area. Surface topography gradually declines to north.

Geophysical Methods Utilized: HVSR, MASW, SASW

Geophysical Testing Arrays:

1. Array RRX-1 (48 channel MASW array utilizing 4.5 Hz vertical geophones spaced 1.5 m apart for a length of 70.5 m, forward and reverse shot locations with multiple source offsets and source types and center shot location).
2. Array RRX-1 (SASW array with common midpoint and orientation as MASW array of same name utilizing 4.5 and 1 Hz vertical geophones and maximum receiver spacing of 48 m).
3. Three HVSR measurement locations distributed along array RRX-1.

Legend

- Seismic Station - Approximate Location of Record
- Seismic Station - Approximate Surveyed Location
- H/V Spectral Ratio Measurement Location
- MASW and SASW Array

NOTES:
1. WGS 1984 COORDINATE SYSTEM
2. Image Source: ESRI, i-cubed, USDA FSA, USGS, AEX, GeoEye, Getmapping, Aerogrid, IGP

File Name: CI-RRX-I

Date: 5/12/2011

USGS science for a changing world

GEOVision geophysical services

RECOVERY.GOV

SITE MAP
CI•RRX

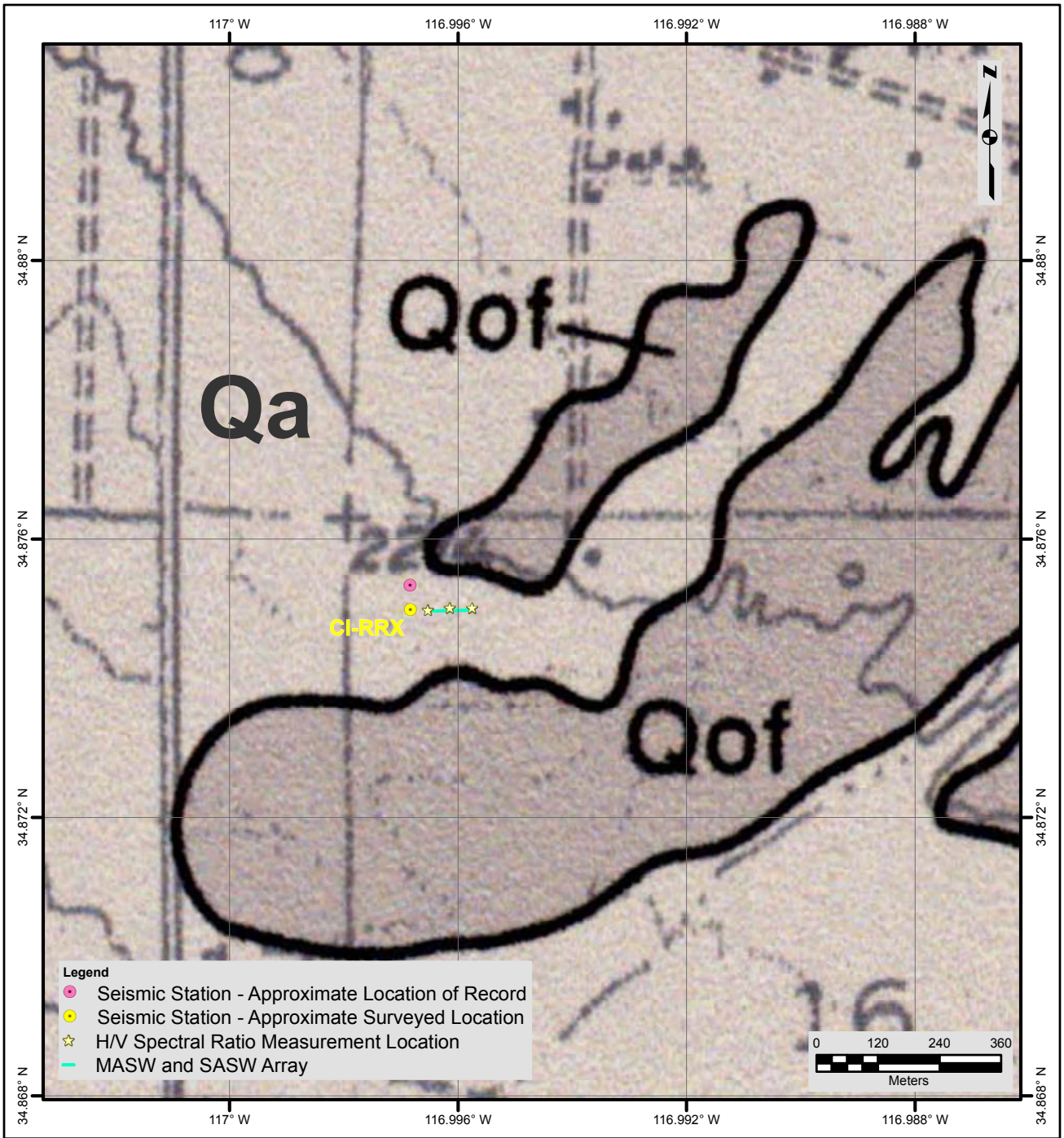

Description of Geologic Map Units

Qa = Quaternary (Holocene) alluvial sand of valley areas
Qof = Quaternary (Pleistocene) older alluvium, fanglomerate and gravel boulders, cobbles and pebbles in weakly to moderately consolidated sandy matrix

NOTES:
1. WGS 1984 COORDINATE SYSTEM
2. Geologic Map of the Barstow & Daggett 15 Minute Quadrangles, San Bernardino County, California by Thomas W. Dibblee, Jr., 2008
3. See site map for details of geophysical survey

File Name: CI-RRX

Date: 5/26/2011

USGS science for a changing world

GEOVision geophysical services

RECOVERY.GOV

GEOLOGIC MAP
CI•RRX

Looking west towards HVSR sensor 507 and CI.RRX seismic station

CI.RRX seismic station

SASW array RRX-1

Looking east along MASW array RRX-1

Nanometrics Trillium Compact seismic sensor used for HVSR measurements

Location of Geophysical Testing Arrays:

Location	Latitude	Longitude
RRX-1, West End of MASW Array	34.87497	-116.99653
RRX-1, Center of MASW and SASW Arrays	34.87497	-116.99614
RRX-1, East End of MASW Array	34.87498	-116.99575
HVSR Sensor 507	34.87498	-116.99653
HVSR Sensor 453	34.87501	-116.99614
HVSR Sensor 450	34.87500	-116.99575
CI.RRX Seismic Station	34.87499	-116.99683

Notes: 1) WGS84 Coordinate System (decimal degrees)

2) Survey accuracy is estimated at 1 to 2 m

Results:

V_S Model

Depth to Top of Layer (m)	Layer Thickness (m)	S-Wave Velocity (m/s)	Inferred P-Wave Velocity (m/s)	Inferred Poisson's Ratio	Inferred Density (g/cm^3)
0	1	189	354	0.3	1.9
1	2	266	497	0.3	1.9
3	3	307	575	0.3	1.9
6	3	326	610	0.3	1.9
9	6	410	767	0.3	1.9
15	9	416	778	0.3	1.9
24	>6	477	893	0.3	1.9

Observations/Discussion:

- HVSR plots are similar at all measurement locations validating the 1-D velocity structure assumption.
- There is low amplitude HVSR peak at about 0.85 Hz, which would be indicative of a large impedance contrast at a depth on the order of 150 to 200 m, depending upon S-wave velocity structure. Based on the signature of the HVSR curves at lower frequencies, this HVSR peak may be associated with a sediment layer rather than the basement complex.
- Noise conditions at site were not sufficient to apply passive surface wave techniques.
- Surface wave dispersion data from SASW and MASW data sets are in good agreement at the site, although both data sets were not easy to reduce. The MASW seismic records show relatively complex wave propagation, which could be indicative of lateral velocity variation, dipping layers, subsurface discontinuities, scatterers, etc.
- Representative dispersion curves were generated for each surface wave data set using a moving average, polynomial curve fitting routine. These individual representative dispersion curves were combined and a representative dispersion curve generated for the combined data set for data modeling.
- Water table located at a depth of greater than 30 m based on seismic refraction survey design, absence of a water table refractor and no clear reflectors.
- Based on simple horizontal layer-based analysis of seismic refraction first arrival data, P-wave velocity in the upper 20 m ranges from about 500 to 1,000 m/s (about 10 m of sediments with velocity in the 500 to 625 m/s range overlying sediments with velocity in the 850 to 1,000 m/s range).
- Surface wave depth of investigation is about 30 m based on half of maximum wavelength criteria.
- Surface wave model is consistent with simplified P-wave refraction model considering unknown Poisson's ratio.
- V_{S30} is 372 m/s (Site Class C).
- Average S-wave velocity between 2 m (nominal sensor depth) and 32 m is 396 m/s.

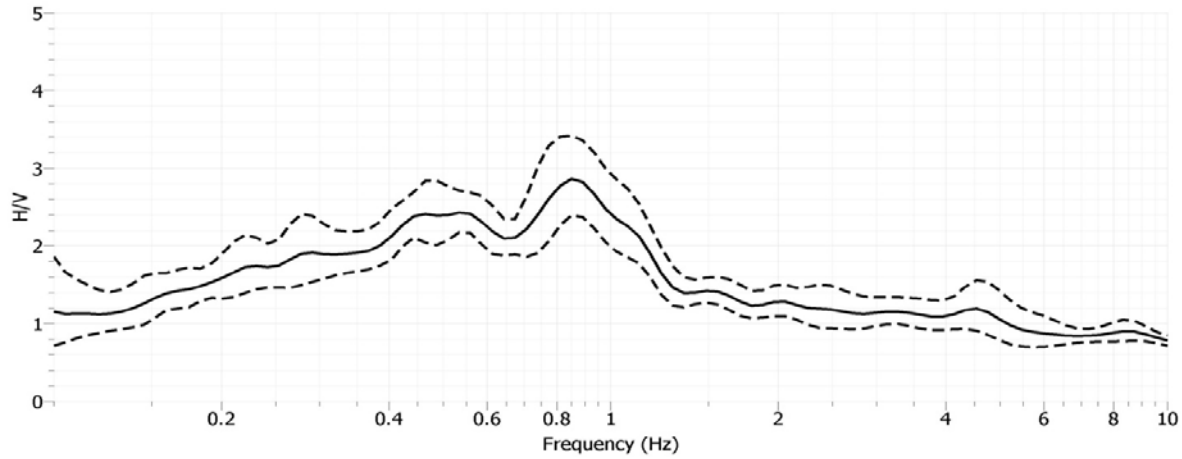

Site CI.RRX, H/V Spectral Ratio, Array RRX -1, Sensor 507

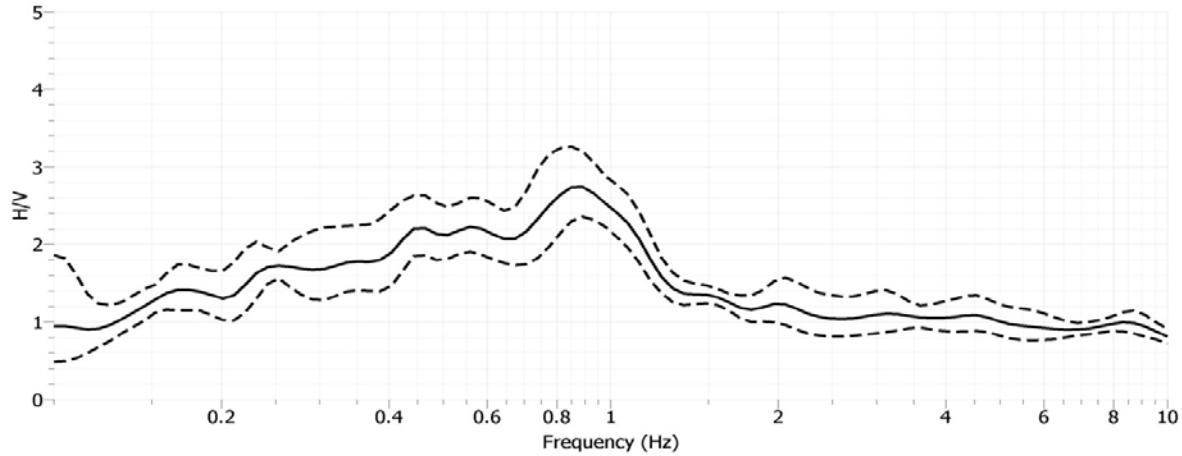

Site CI.RRX, H/V Spectral Ratio, Array RRX -1, Sensor 453

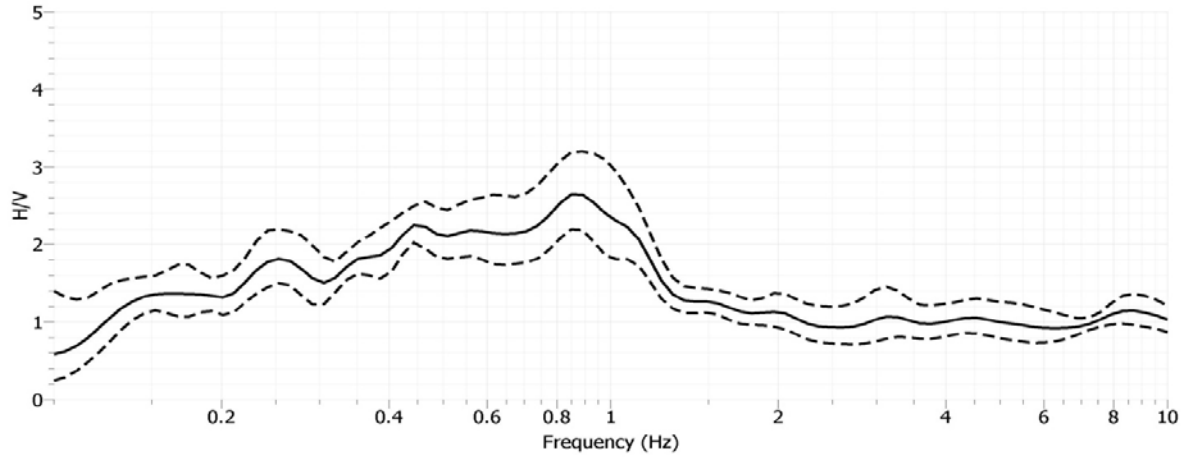

Site CI.RRX, H/V Spectral Ratio, Array RRX -1, Sensor 450

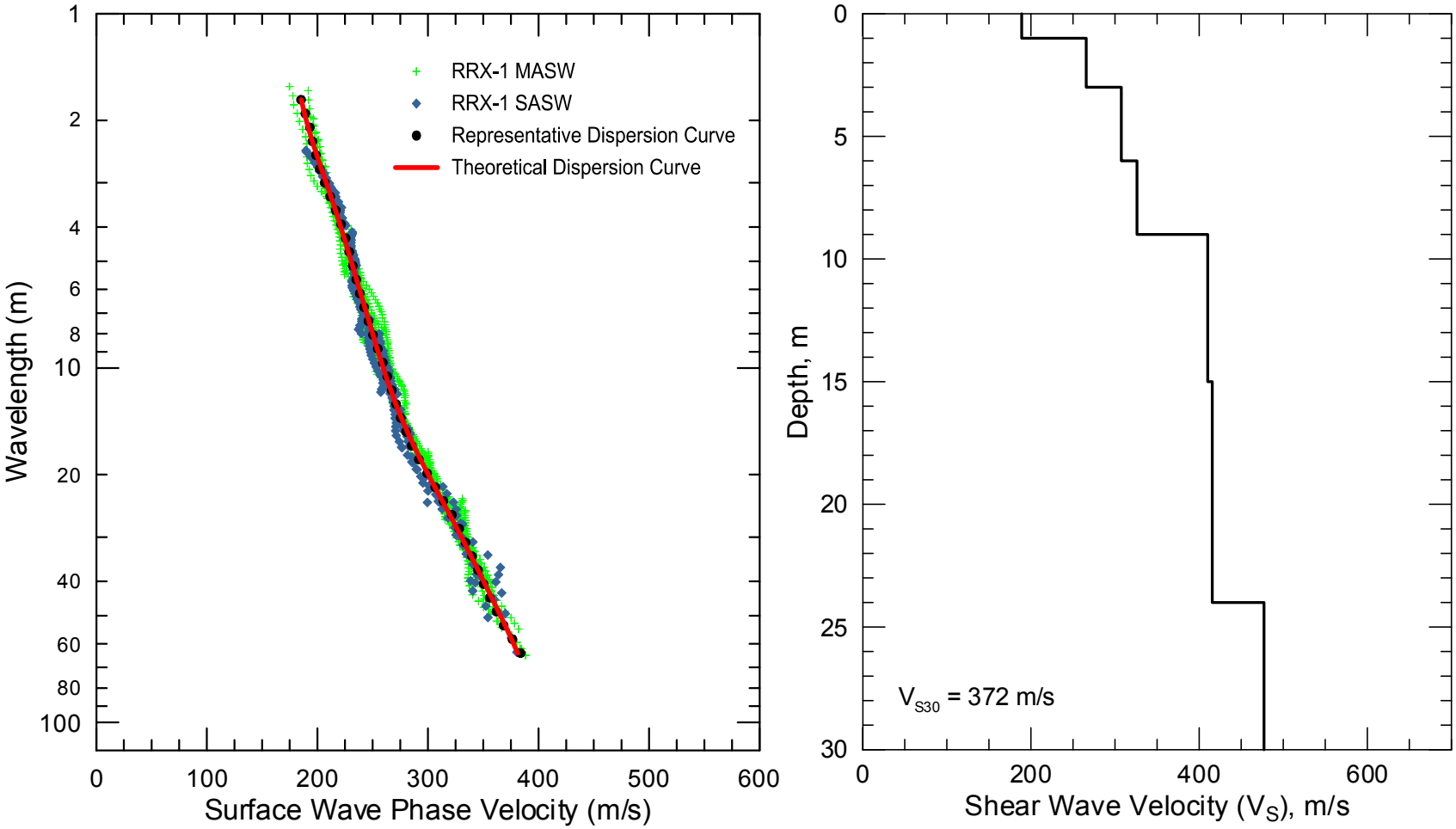

CI.RRX - Field, representative and inverted theoretical surface wave dispersion data (left) and associated V_S model (right)

Site CI.RSB and CI.RSS

Location: Tomas Rivera Library, University of California, Riverside, California

CI.RSB Latitude: 33.97327 **CI.RSB Longitude:** -117.32755
(Station coordinates modified based on site GPS survey and further adjustment was made using site photographs and ESRI Imagery because of tree cover, WGS84 coordinate system).

CI.RSS Latitude: 33.97327 **CI.RSS Longitude:** -117.32755
(Station coordinates modified based on site GPS survey and further adjustment was made using site photographs and ESRI Imagery because of tree cover, WGS84 coordinate system). We have been unable to confirm if CI.RSS remains in the surface enclosure for CI.RSB or has been moved to the storeroom housing the seismic recording equipment or alternate location).

V_{S30} (measured): 360 m/s

V_{S30} (adjusted to more accurately reflect seismic station conditions): 360 m/s (no adjustment necessary for the surface sensor CI.RSS); 663 m/s (average V_S between 31.9 and 61.9 m to account for CI.RSB upper borehole sensor depth). CI.RSB lower sensor located in granitic bedrock at 99.1 m depth.

NEHRP Site Class: C/D

Geomatrix Code: FHC (CI.RSB), LHC/BHC (CI.RSS)

Geologic Conditions/Observations: Site located in area mapped as Quaternary (Holocene) alluvial sand and gravelly sand deposits. Competent granitic rock located at a depth of about 88 to 90 m based on borehole PS suspension log.

Site Conditions: Urban site with significant pedestrian and vehicular noise from university campus. Relatively flat terrain in site vicinity.

Geophysical Methods Utilized: HVSR, MASW, array microtremor, ReMi™

Geophysical Testing Arrays:

1. Array RSB-1 (48 channel MASW array utilizing 4.5 Hz vertical geophones spaced 1 m apart for a length of 47 m, forward and reverse shot locations with multiple source offsets and hammer source types and center shot location).
2. Array RSB-2 (24 channel, linear passive surface wave array utilizing 4.5 Hz vertical geophones spaced 4 m apart for an array length of 92 m).
3. Array RSB-3 (24 channel, linear passive surface wave array utilizing 4.5 Hz vertical geophones spaced 6 m apart for an array length of 138 m).

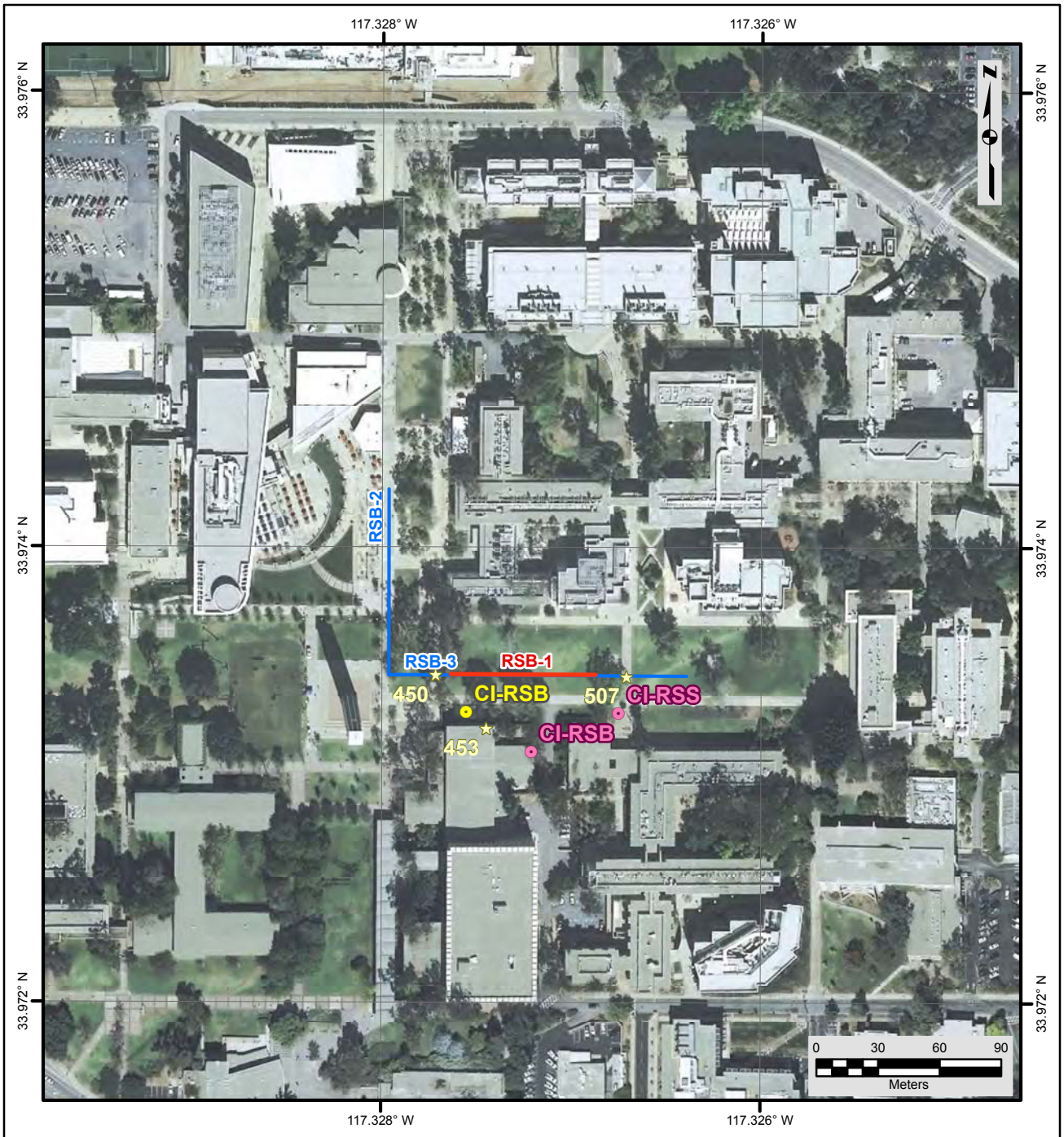

Legend

- Seismic Station - Approximate Improved Location
- Seismic Station - Approximate Location of Record
- H/V Spectral Ratio Location
- MASW Array
- Passive Surface Wave Array

NOTES:
1. WGS 1984 COORDINATE SYSTEM
2. Image Source: ESRI, i-cubed, USDA FSA, USGS, AEX, GeoEye, Getmapping, Aerogrid, IGP

File Name: CI-RSB-I

Date: 10/14/2011

USGS science for a changing world

GEOVision geophysical services

RECOVERY.GOV

SITE MAP
CI•RSB

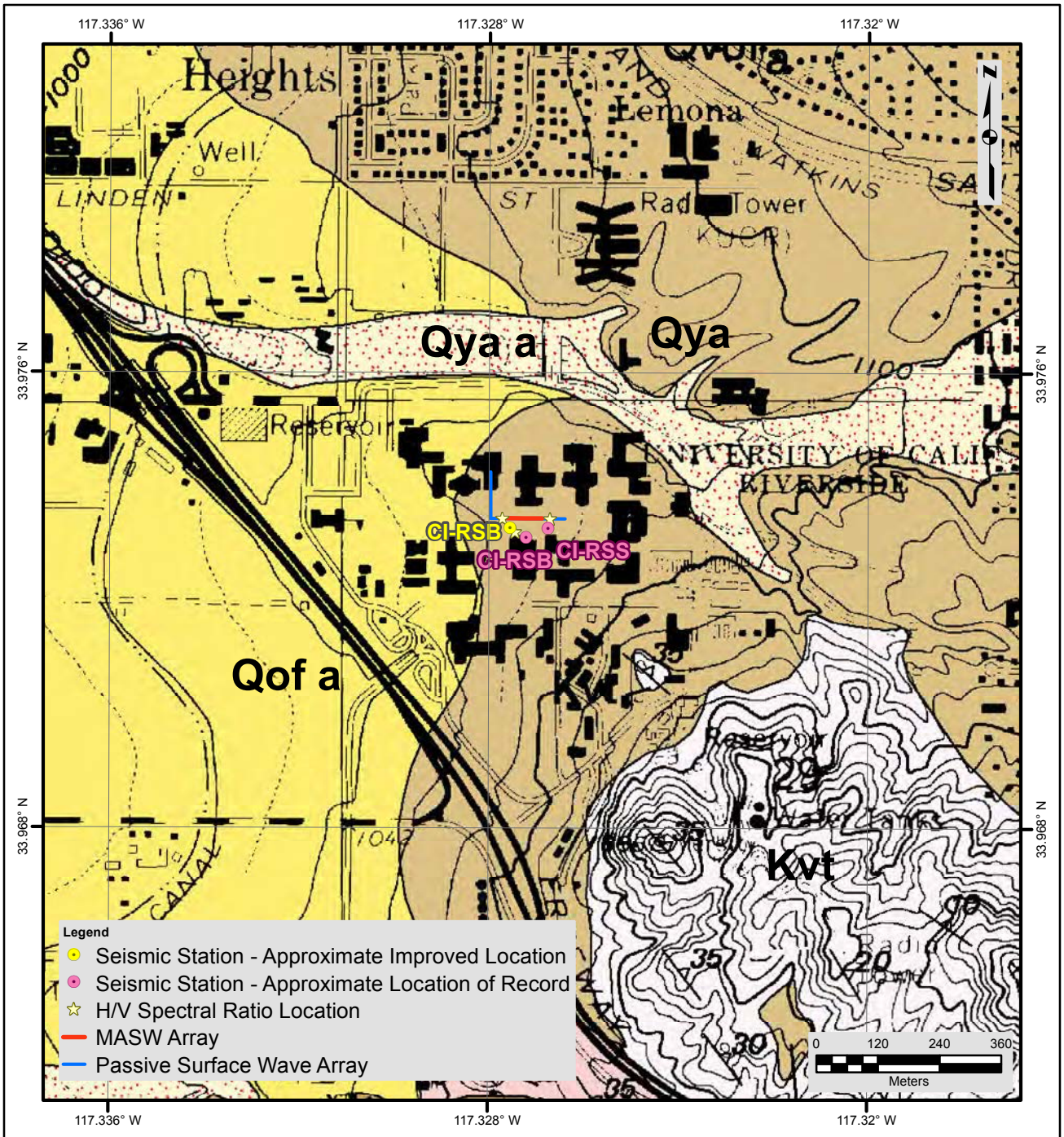

Description of Geologic Map Units

Qya, Qya a = Quaternary (Holocene) young axial channel deposits; medium to fine grained sand, a-arenaceous
Qof a = Quaternary (Pleistocene) old alluvial fan deposits; indurated, sandy, capped with pedogenic soils
Kvt = Mesozoic (Cretaceous) Val Verde tonalite, biotite-horneblende tonalite

NOTES:
1. WGS 1984 COORDINATE SYSTEM
2. Geologic Map of the Riverside East 7.5' Quadrangle, Riverside County, California, Version 1.0 by Douglas M. Morton and Brett Cox, 1988, 1996-7
3. See site map for details of geophysical survey

File Name: CI-RSB

Date: 10/14/2011

USGS science for a changing world

GEOVision geophysical services

GEOLOGIC MAP
CI•RSB

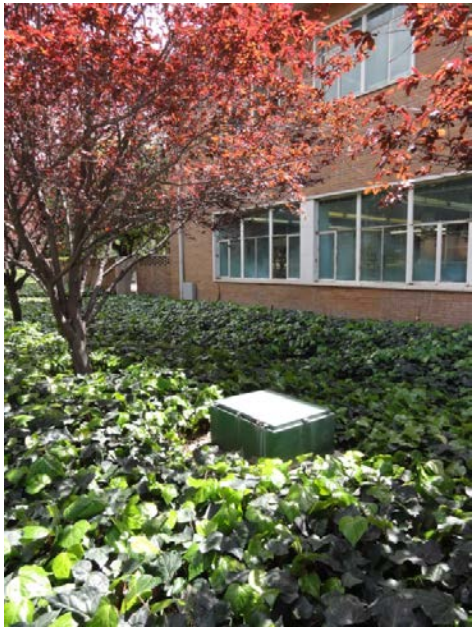

Seismic Station CI.RSB outside Tomas Rivera Library, UC Riverside

HVSR Sensor 453 outside room housing seismic recording equipment

Looking north along passive surface wave array RSB-2

Looking east along passive surface wave array RSB-3

Looking southeast towards HVSR sensor 450 and Tomas Rivera Library

Looking west along MASW array RSB-1

Looking south from western end of MASW array RSB-1

4. Arrays RSB-2 and RSB-3 combined to form an “L” shaped passive surface wave array.
5. Three HVSR measurement locations; two located along array RSB-3 and the other on the first floor of the Tomas Rivera Library next to the room housing the recording instrumentation. The seismic sensors are located in a borehole outside the library (CI.RSB).

Location of Geophysical Testing Arrays:

Location	Latitude	Longitude
RSB-1, West End of MASW Array	33.97344	-117.32762
RSB-1, Center of MASW Array	33.97344	-117.32724
RSB-1, East End of MASW Array	33.97344	-117.32686
RSB-2, North End of Array	33.97425	-117.32795
RSB-2, South End of Array	33.97344	-117.32795
RSB-3, West End of Array	33.97344	-117.32788
RSB-3, East End of Array	33.97343	-117.32638
HVSR Sensor 453	33.97320	-117.32744
HVSR Sensor 450	33.97344	-117.32771
HVSR Sensor 507	33.97343	-117.32670
CI.RSS Seismic Station	33.97327	-117.32755
CI.RSB Seismic Station	33.97327	-117.32755

Notes: 1) WGS84 Coordinate System (decimal degrees).
2) Survey accuracy is estimated at 3 to 4 m.
3) HVSR sensor 453 not surveyed as located inside building. Approximate location determined based on ESRI Imagery and field observations.
4) Surveyed seismic station not accurate due to tree cover and moved based on field observations.
5) At one time CI.RSS was located in surface enclosure for CI.RSB, but may have been moved to Tomas Rivera Library.

Results:

V_S Model 1

Depth to Top of Layer (m)	Layer Thickness (m)	S-Wave Velocity (m/s)	Inferred P-Wave Velocity (m/s)	Assumed Poisson's Ratio	Assumed Density (g/cm^3)
0	3	202	377	0.3	1.8
3	3	272	508	0.3	1.8
6	5	351	657	0.3	1.9
11	7	357	669	0.3	1.9
18	10	490	916	0.3	2.0
28	14	553	1035	0.3	2.0
42	20	723	1352	0.3	2.1
62	>13	885	1656	0.3	2.1

Notes: 1) Depth of investigation is about 75 m.
2) Bottom layer is a half space.

V_S Model 2

Depth to Top of Layer (m)	Layer Thickness (m)	S-Wave Velocity (m/s)	Inferred P-Wave Velocity (m/s)	Assumed Poisson's Ratio	Assumed Density (g/cm^3)
0	3	201	377	0.3	1.8
3	3	274	512	0.3	1.8
6	5	352	658	0.3	1.9
11	8	359	671	0.3	1.9
19	10	527	986	0.3	2.0
29	14	612	1146	0.3	2.0
43	22	710	1329	0.3	2.1
65	>10	885	1656	0.3	2.1

Notes: 1) Depth of investigation is about 75 m.
2) Bottom layer is a half space.

Observations/Discussion:

- At the time of installation, CI.RSB seismic station was comprised of two Kinemetrics Hyposensors located at depths of 99.1 (granitic bedrock) and 31.9 (alluvium) meters in a borehole outside the UC Riverside Tomas Rivera Library and a Kinemetrics Episensor located on the surface immediately adjacent to the borehole. The recording equipment for the accelerometers is located in a small storeroom in the library. CI.RSS is thought to be the surface sensor associated with CI.RSB and we have not yet confirmed if the sensor remains in place or moved to the storeroom housing the seismic recording equipment or alternate location.
- Oyo PS suspension logging was conducted in the CI.RSB borehole in 1998, prior to borehole sensor installation.
- HVSR sensor 453 was located in the Tomas Rivera library next to a storeroom where the CI.RSB recording equipment is located. At this location the library does not have a basement level although it does appear have a basement further to the south. HVSR sensors 450 and 507 were located along passive surface wave array RSB-3. HVSR measurements were made at these locations both on a concrete sidewalk and in the adjacent grass covered area. During data acquisition, there was heavy pedestrian and vehicular traffic near the HVSR sensors located outside the building.
- HVSR data quality was best at sensor 453, located in the Tomas Rivera library. The sensor 450 and 507 locations on the concrete sidewalks had some low frequency noise, which was mitigated during processing. Permission was not obtained to dig holes in the grass and, therefore, sensor coupling in the grass was not ideal and this data is not presented.
- All HVSR plots show a well defined peak at 2.2 to 2.4 Hz, with data quality best for the sensor located in the building. This peak is consistent with the large impedance contrast associated with bedrock located at a depth of about 88 to 90 m.
- Noise conditions at site (multi-directional or omni-directional noise sources) appeared sufficient for successful application of passive surface wave techniques. It should be noted, however, that many buildings in the site vicinity have basements, which may several affect passive surface wave propagation in the area. The numerous utility corridors present on university campus may also degrade high frequency surface wave data, if located in the immediate vicinity of the arrays.
- ESAC technique used to extract surface wave dispersion data from passive "L" array data. Both the ReMi™ and ESAC techniques used to extract surface wave dispersion data from the linear array. Linear passive surface wave array RSB-2 did not provide useful surface wave data. Surface wave data from passive linear array RSB-3, extracted using the ESAC technique, are in better agreement with the "L" array data, although phase velocities are slightly lower at long wavelengths. Surface wave data from passive linear array RSB-3, extracted using the ReMi™ technique, are in good agreement with MASW data at wavelengths in the 12 to 60 m range, but appear to underestimate phase velocity at greater wavelengths, relative to ESAC analysis of the same array and the "L" array. Passive surface data is adequate for data modeling, but data quality definitely appears to be degraded by basements in buildings surrounding the site.
- MASW data acquisition was limited to hammer sources and, given the noise levels at the site, surface wave phase velocities are likely only valid to a wavelength of about 40 m, corresponding to a frequency of about 8 Hz. MASW surface wave dispersion data were,

however, extracted to a maximum wavelength of about 60 m, corresponding to a frequency of about 6.5 Hz, generally beyond the reliable capability of a 20 lb sledge hammer. Data at these longer wavelengths are, however, in acceptable agreement with the passive surface wave data.

- Surface wave dispersion data from active and passive surface wave datasets are in good agreement at this site, although there is limited overlap between the multiple data sets. The minimum wavelength extracted from the passive "L" array is about 45 m. The minimum wavelength extracted from ESAC analysis of the array RSB-3 passive surface wave data is 12 m, although no dispersion data were picked over the 34 to 45 m wavelength range. The minimum wavelength extracted from ReMi™ analysis of the array RSB-3 passive surface wave data is also 12 m and the dispersion data is in acceptable agreement with the MASW data, but was not used for modeling.
- Representative dispersion curves were generated for each surface wave data set using a moving average, polynomial curve fitting routine. These individual representative dispersion curves were combined and a representative dispersion curve generated for the combined data set for data modeling. Two representative dispersion curves were developed for modeling. The first (Model 1) combined MASW data and the passive surface wave data from array RSB-3 and the "L" array (combined arrays RSB-2 and RSB-3). The second (Model 2) combined only the MASW data and "L" array passive surface wave data.
- Water table located at a depth of 71 m, based on PS suspension log in the CI.RSB borehole (increase in P-wave velocity to over 2,000 m/s with no associated increase in S-wave velocity).
- Surface wave depth of investigation is about 75 m based on one half of maximum wavelength criteria.
- The velocity and depth of the half space in the surface wave models is not well resolved. In fact, this layer is not necessary if the high velocity bedrock were to be fixed in the models at 88 m depth.
- V_{S30} is 358 m/s for Model 1 and 362 m/s for Model 2, averaging 360 m/s (NEHRP Site Class D/C).
- Seismic station CI.RSS is located on ground surface and, therefore, V_{S30} is representative of seismic station conditions. Seismic station CI.RSB, however, has borehole sensors at depths of about 31.9 and 99.1 m. The average V_S between 31.9 and 61.9 m to reflect velocity structure beneath the uppermost borehole sensor (adjusted V_{S30}) is 655 m/s for Model 1 and 671 m/s for Model 2, averaging 663 m/s.
- Average S-wave velocity of the upper 75 m (V_{S75}) is 507 and 512 m/s for Models 1 and 2, respectively and averages 510 m/s.
- An Oyo PS suspension log was previously acquired in the CI.RSB borehole, located near the test area. V_{S30} developed from the PS log higher resolution receiver to receiver analysis is 395 m/s (NEHRP Site Class C), about 10% higher than the surface wave sounding. V_{S30} developed from the PS log lower resolution source to receiver analysis is 391 m/s (NEHRP Site Class C), about 9% higher than the surface wave sounding. The difference between the surface wave and PS log velocities may be the result of lateral velocity variation, with the surface wave V_S models reflecting average velocity structure in the area beneath the measurement arrays and the PS log reflecting velocity structure immediately adjacent to the borehole. Alternatively, the difference between surface wave

and PS suspension log velocities may be a function of body wave dispersion associated with damping/seismic quality factor (Q). The dominant frequency of S-wave data in a PS suspension log is typically in the 200 to 1000 Hz range, whereas, surface wave measurements are generally made over the 50 Hz (shallow velocity structure) to 1 Hz (deep velocity structure) frequency range.

- S-wave velocity Model 2, developed using only the MASW and "L" array passive surface wave data, is most similar to the PS suspension log.
- The average V_S between 31.9 and 61.9 m to reflect velocity structure beneath the uppermost borehole sensor (adjusted V_{S30}) from the PS log receiver to receiver analysis is 760 m/s, about 13% higher than the V_S models from the surface wave data. Adjusted V_{S30} from the PS log source to receiver analysis is 705 m/s, about 6% higher than the V_S models from the surface wave data. V_S beneath the lowermost borehole seismic sensor, located at a depth of 99.1 m, is greater than 2,500 m/s based on the Oyo PS suspension log.
- V_{S75} developed from the PS log higher resolution receiver to receiver analysis is 555 m/s, about 9% higher than surface wave sounding. V_{S75} developed from the PS log lower resolution source to receiver analysis is 539 m/s, about 6% higher than surface wave sounding.
- The average S-wave velocity of the 88 m thick sedimentary section overlying bedrock is 593 m/s from the PS log receiver to receiver analysis and 575 m/s from the source to receiver analysis.
- The V_S models developed from the surface wave dispersion data are used for the purpose of site characterization, although the Oyo PS suspension log probably more accurately represents velocity structure in the seismic station CI.RSB borehole.

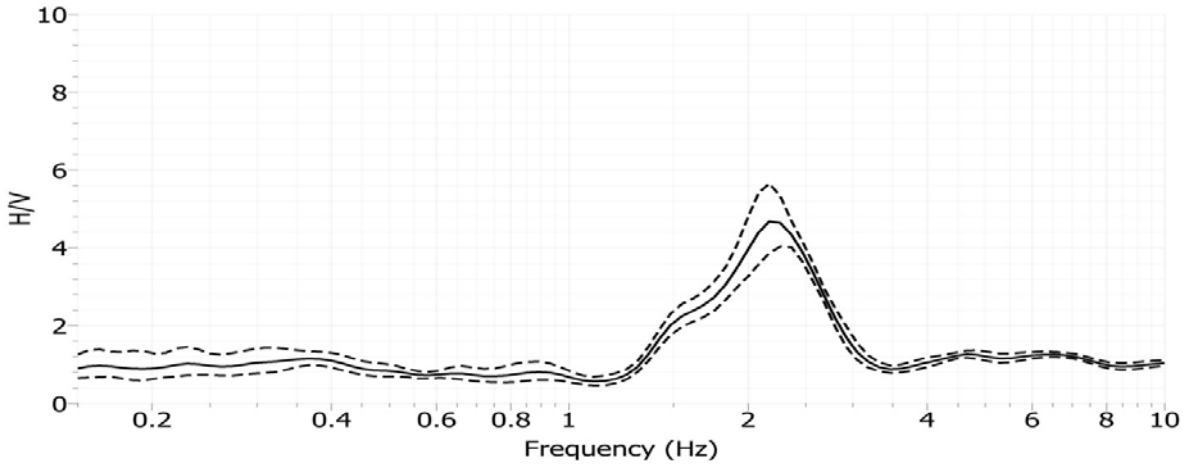

Site CI.RSB, H/V Spectral Ratio, Array RSB-1, Sensor 450

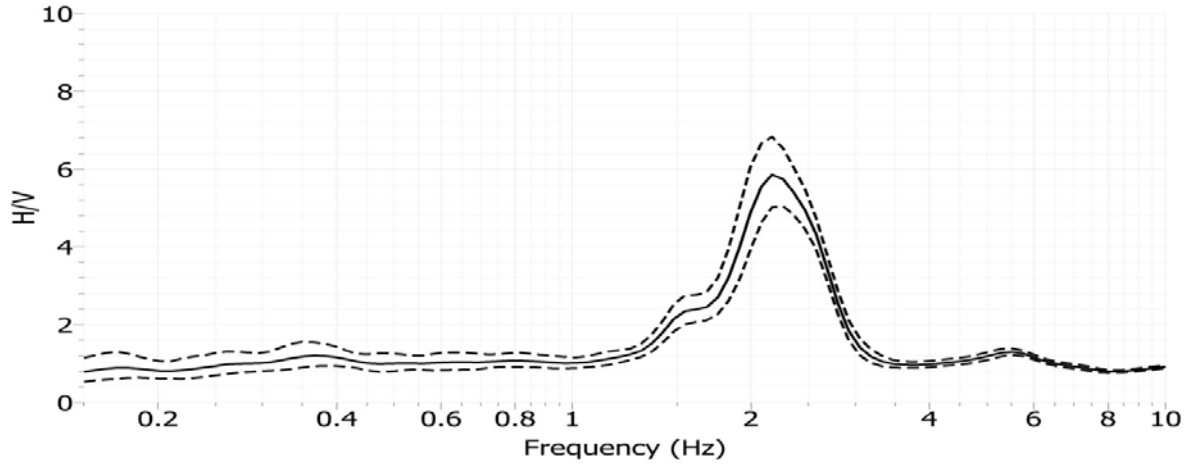

Site CI.RSB, H/V Spectral Ratio, Inside Tomas Rivera Library, Sensor 453

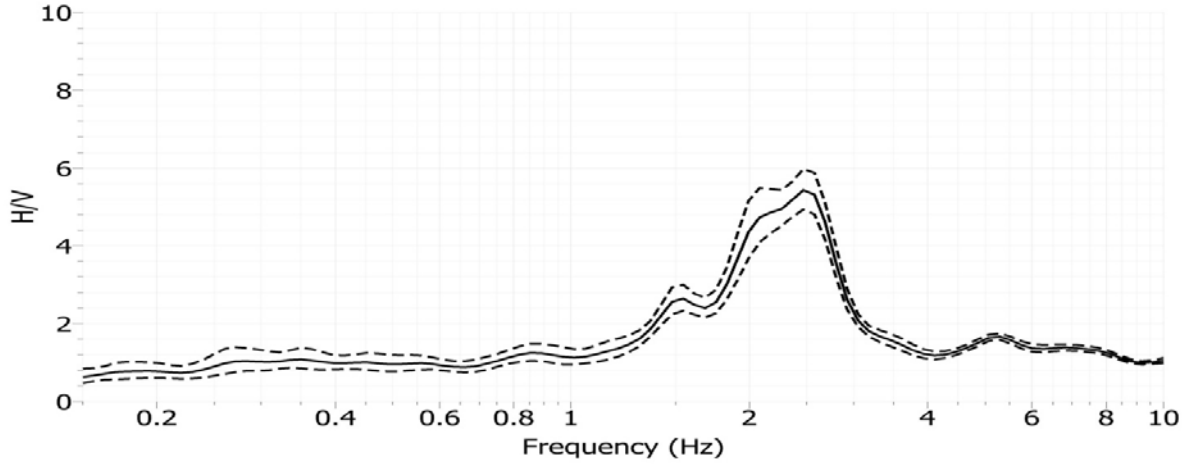

Site CI.RSB, H/V Spectral Ratio, Array RSB-1, Sensor 507

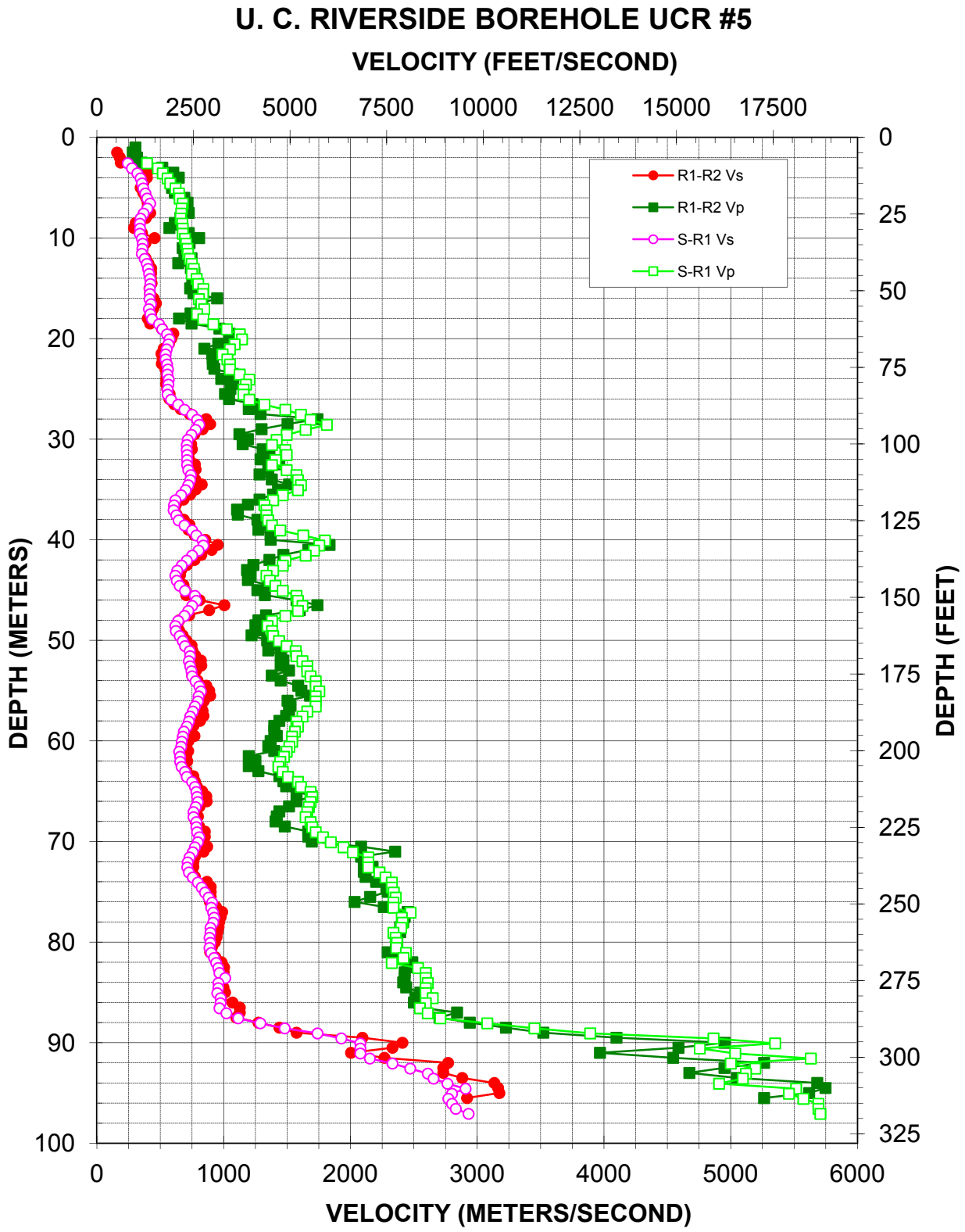

CI.RSB- Oyo PS suspension log conducted as part UC/CLC Campus Earthquake Program. Source to receiver (S-R1) and receiver to receiver (R1-R2) analysis.

CI.RSB - Oyo PS suspension log conducted as part of the UC/CLC Campus Earthquake Program. Receiver to Receiver (R1-R2) analysis.

DEPTH (m)	Vs (m/s)	Vp (m/s)	DEPTH (m)	Vs (m/s)	Vp (m/s)	DEPTH (m)	Vs (m/s)	Vp (m/s)
1.5	159	282	19.5	602	1047	37.5	629	1111
2.0	180	316	20.0	587	1042	38.0	685	1266
2.5	188	352	20.5	568	957	38.5	730	1299
3.0	322	515	21.0	526	847	39.0	722	1274
3.5	397	602	21.5	509	909	39.5	769	1370
4.0	394	645	22.0	518	913	40.0	855	1370
4.5	366	617	22.5	512	913	40.5	952	1835
5.0	345	592	23.0	539	926	41.0	905	1667
5.5	365	613	23.5	548	1070	41.5	823	1471
6.0	388	690	24.0	546	980	42.0	769	1361
6.5	400	714	24.5	545	1075	42.5	709	1235
7.0	398	694	25.0	554	1053	43.0	664	1183
7.5	420	725	25.5	573	1010	43.5	656	1212
8.0	386	658	26.0	571	1042	44.0	645	1190
8.5	306	613	26.5	608	1227	44.5	683	1351
9.0	292	571	27.0	660	1198	45.0	694	1266
9.5	355	725	27.5	733	1290	45.5	704	1325
10.0	455	806	28.0	862	1739	46.0	810	1575
10.5	383	730	28.5	893	1504	46.5	1005	1739
11.0	361	676	29.0	833	1299	47.0	885	1600
11.5	357	690	29.5	769	1124	47.5	727	1333
12.0	383	746	30.0	730	1190	48.0	649	1274
12.5	405	641	30.5	743	1149	48.5	633	1250
13.0	427	741	31.0	749	1307	49.0	647	1282
13.5	427	769	31.5	722	1361	49.5	676	1220
14.0	426	752	32.0	727	1290	50.0	704	1342
14.5	431	763	32.5	772	1439	50.5	746	1418
15.0	414	735	33.0	778	1351	51.0	752	1351
15.5	418	760	33.5	746	1282	51.5	775	1449
16.0	446	948	34.0	775	1379	52.0	820	1471
16.5	465	820	34.5	826	1515	52.5	823	1449
17.0	444	833	35.0	778	1429	53.0	781	1515
17.5	427	738	35.5	735	1389	53.5	752	1379
18.0	401	647	36.0	683	1282	54.0	794	1449
18.5	419	746	36.5	623	1190	54.5	862	1587
19.0	512	966	37.0	612	1105	55.0	885	1613

CI.RSB - Oyo PS suspension log conducted as part of the UC/CLC Campus Earthquake Program. Receiver to receiver (R1-R2) analysis (cont.)

DEPTH (m)	Vs (m/s)	Vp (m/s)	DEPTH (m)	Vs (m/s)	Vp (m/s)	DEPTH (m)	Vs (m/s)	Vp (m/s)
55.5	893	1681	73.5	772	2119	91.5	2268	4545
56.0	844	1504	74.0	868	2203	92.0	2770	5263
56.5	823	1527	74.5	897	2283	92.5	2732	4950
57.0	833	1515	75.0	897	2294	93.0	2732	4673
57.5	840	1493	75.5	897	2155	93.5	2882	5050
58.0	813	1439	76.0	891	2033	94.0	3135	5682
58.5	760	1399	76.5	939	2262	94.5	3165	5747
59.0	741	1399	77.0	988	2451	95.0	3175	5618
59.5	769	1418	77.5	976	2427	95.5	2920	5263
60.0	722	1370	78.0	964	2415			
60.5	704	1351	78.5	959	2392			
61.0	719	1399	79.0	950	2392			
61.5	702	1198	79.5	943	2370			
62.0	712	1250	80.0	930	2358			
62.5	687	1198	80.5	907	2370			
63.0	707	1274	81.0	893	2294			
63.5	760	1439	81.5	935	2347			
64.0	772	1471	82.0	983	2488			
64.5	787	1493	82.5	1003	2451			
65.0	830	1575	83.0	1000	2427			
65.5	862	1695	83.5	990	2427			
66.0	866	1575	84.0	985	2415			
66.5	810	1515	84.5	998	2439			
67.0	784	1439	85.0	1010	2551			
67.5	797	1418	85.5	980	2513			
68.0	778	1408	86.0	1070	2500			
68.5	806	1481	86.5	1127	2551			
69.0	851	1667	87.0	1127	2841			
69.5	851	1667	87.5	1099	2703			
70.0	844	1695	88.0	1274	2941			
70.5	870	2083	88.5	1439	3226			
71.0	840	2353	89.0	1575	3521			
71.5	772	2083	89.5	2094	4098			
72.0	760	2105	90.0	2410	4950			
72.5	760	2174	90.5	2331	4587			
73.0	749	2105	91.0	2004	3968			

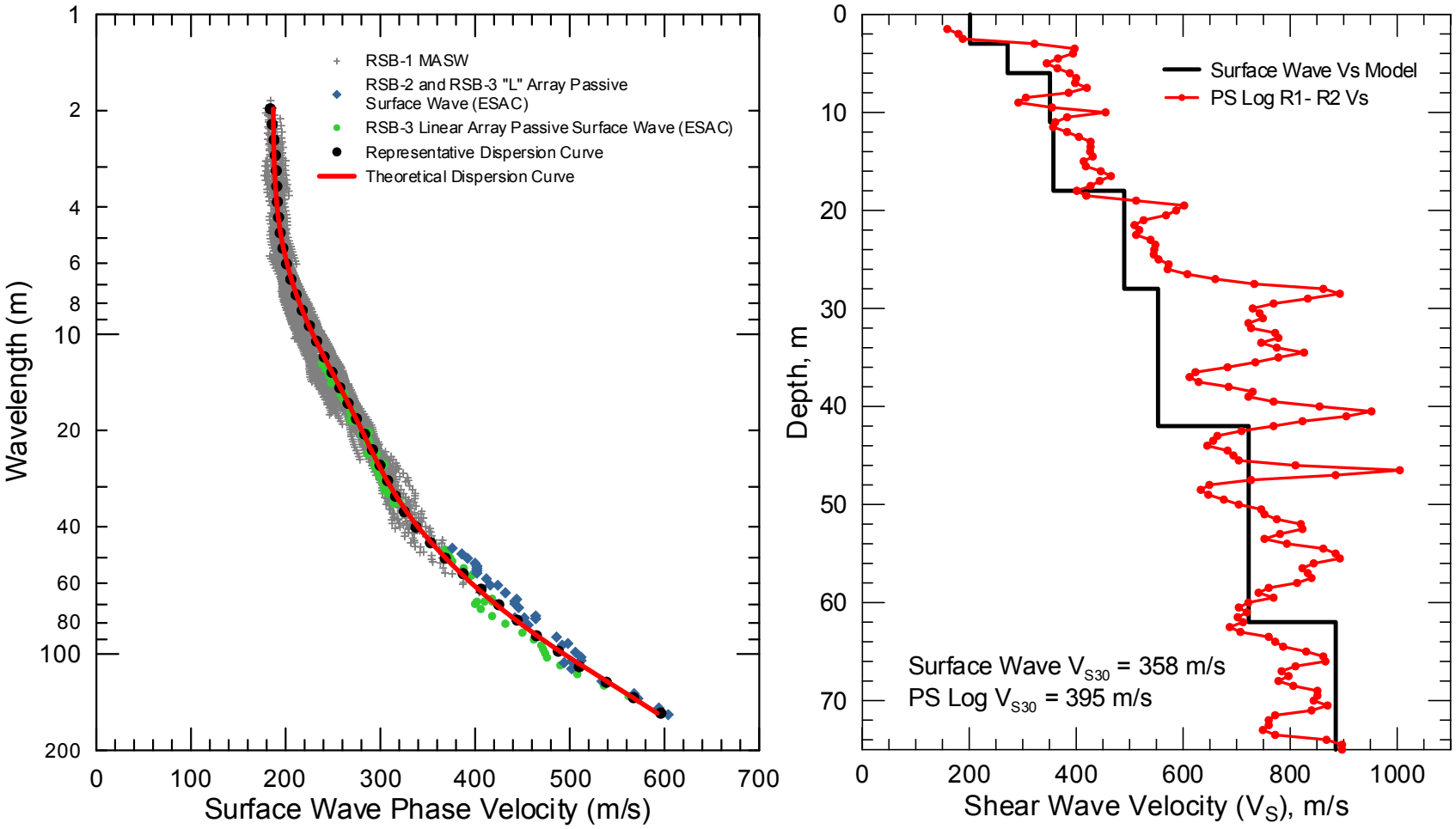

CI.RSB and CI.RSS - Field, representative and inverted theoretical surface wave dispersion data (left) and associated V_S model (right) – Model 1

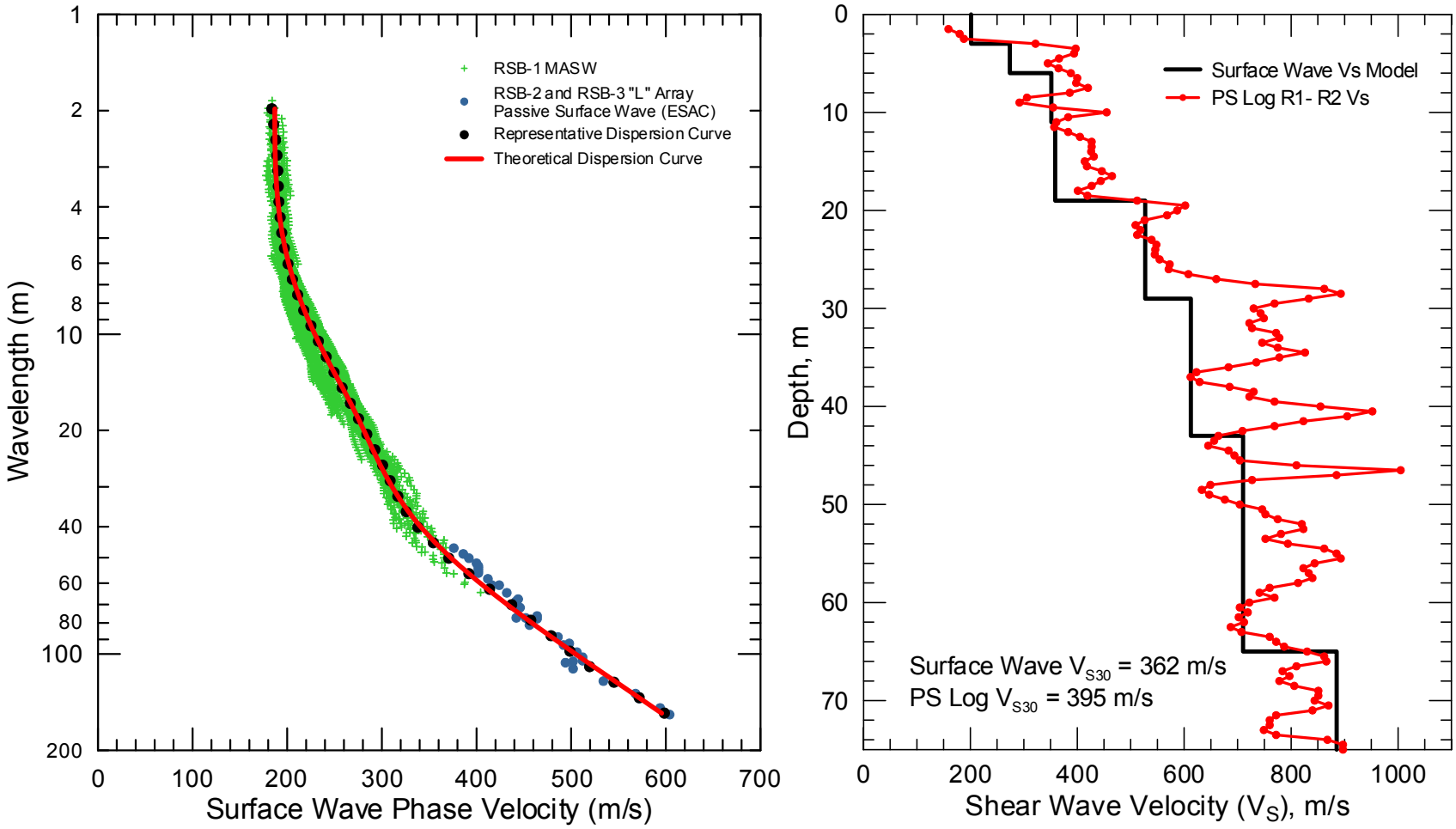

CI.RSB and CI.RSS - Field, representative and inverted theoretical surface wave dispersion data (left) and associated V_S model (right) – Model 2

Site CI.RXH

Location: Rock Hill, Salton Sea National Wildlife Refuge, Imperial County, California

Latitude: 33.18313 **Longitude:** -115.62257
(Station coordinates provided by USGS, WGS84 coordinate system)

V_{S30} (measured): 309 m/s

V_{S30} (adjusted to more accurately reflect seismic station conditions): 324 m/s (average S-wave velocity between 1 and 31 m adjusting for inferred depth of seismic sensor).

NEHRP Site Class: D

Geomatrix Code: IVD

Geologic Conditions/Observations: Seismic station located on a small hill mapped as Quaternary (Holocene) volcanic rhyolite.

Site Conditions: Rural site. Seismic station located on a small hill (Rock Hill) comprised of very intensly weathered rhyolite. In the vicinity of the seismic station, the rhyolite appears to have weathered to boulders, cobbles and soil, although at the northwest end of Rock Hill the rhyolite is significantly less weathered. With the exception of Rock Hill, the terrain is flat in the site vicinity.

Geophysical Methods Utilized: HVSR, Seismic Refraction, MASW

Geophysical Testing Arrays:

1. Array RXH-1 (48 channel MASW and P-wave seismic refraction array utilizing 4.5 Hz vertical geophones spaced 1.5 m apart for a length of 70.5 m, forward and reverse shot locations with multiple source offsets and source types and multiple interior shot locations).
2. Array RXH-2 (48 channel P-wave seismic refraction array utilizing 4.5 Hz vertical geophones spaced 1.5 m apart for a length of 70.5 m, forward, reverse and multiple interior shot locations).
3. Three HVSR measurement locations distributed along array RXH-1.

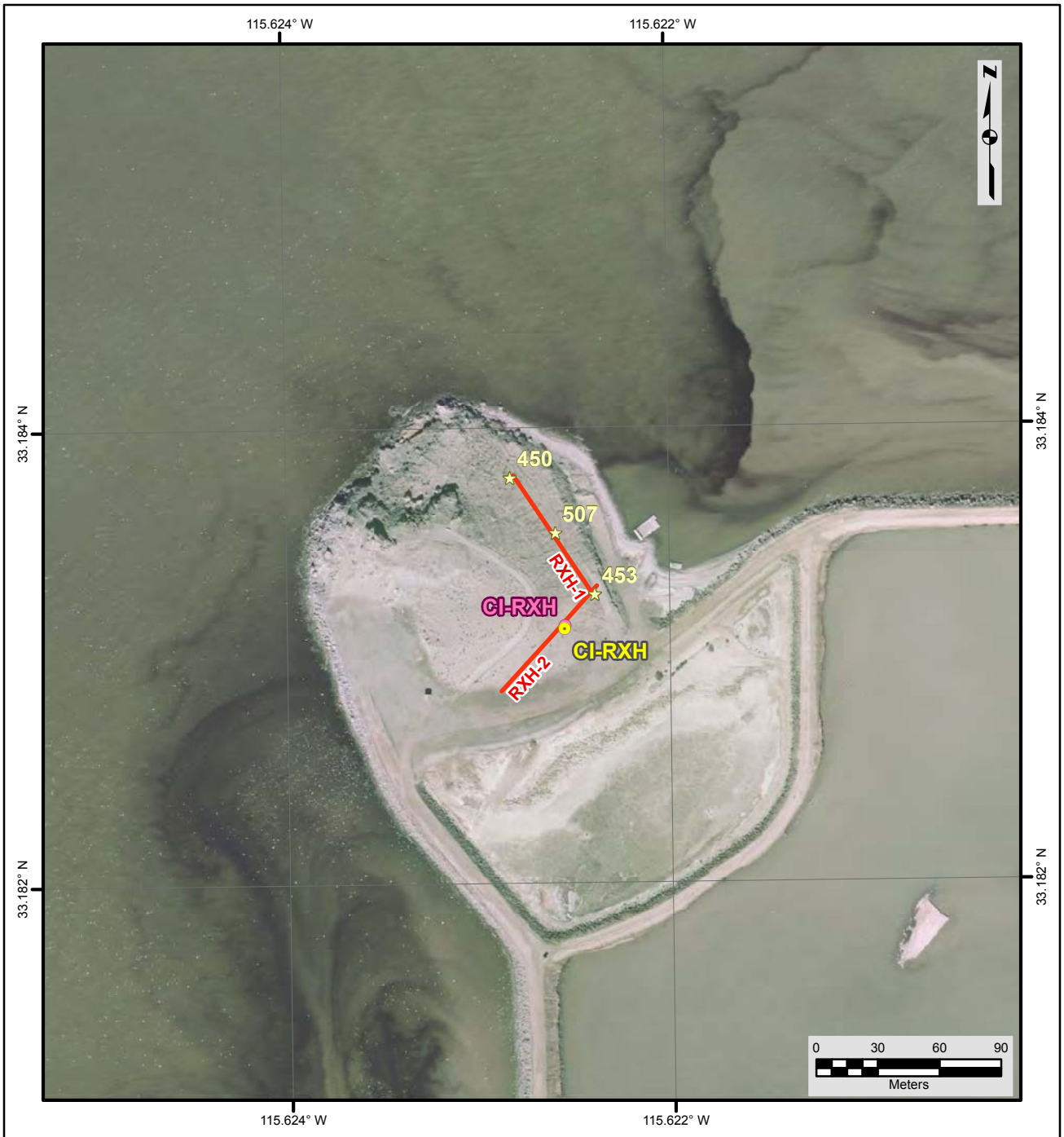

Legend

- Seismic Station - Approximate Surveyed Location
- Seismic Station - Approximate Location of Record
- H/V Spectral Ratio Location
- MASW and Seismic Refraction Array

NOTES:
1. WGS 1984 COORDINATE SYSTEM
2. Image Source: ESRI, i-cubed, USDA FSA, USGS, AEX, GeoEye, Getmapping, Aerogrid, IGP

File Name: CI-RXH-I

Date: 10/27/2011

USGS science for a changing world

GEOVision geophysical services

RECOVERY.GOV

SITE MAP
CI•RXH

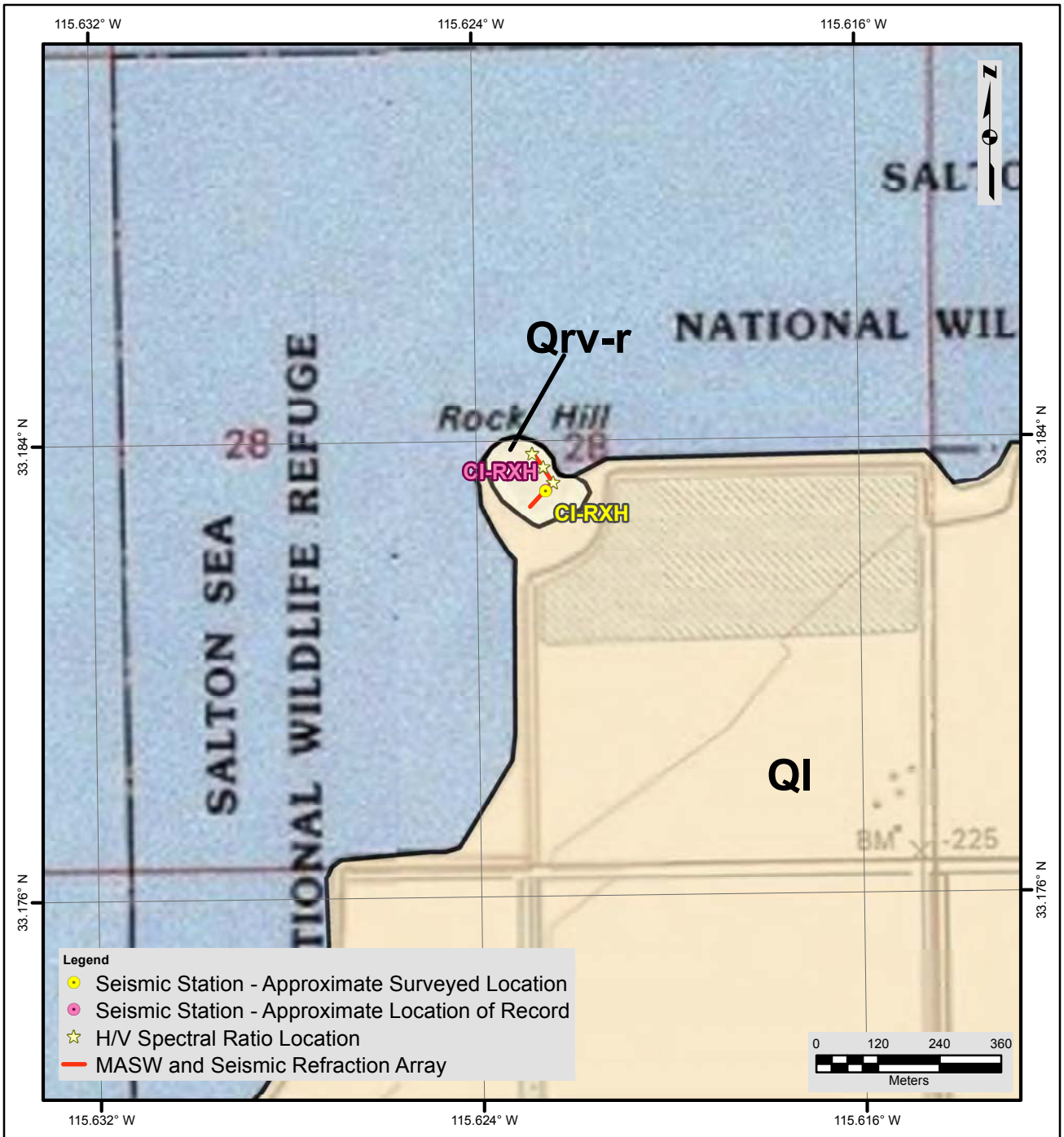

Description of Geologic Map Units

QI = Quaternary (Pleistocene to Holocene) lake deposits
Qrv-r = Quaternary (Holocene) recent volcanic, rhyolite

NOTES:
1. WGS 1984 COORDINATE SYSTEM
2. Topo Image Sources: USGS, FAO, NPS, EPA, NRCAN, GeoBase, Esri, DeLorme, TANA, Intermap, AND, other suppliers, and the GIS community
3. Geologic Map Units from:
Geologic Map of California, Salton Sea Sheet,
Olaf P Jenkins Edition
by Charles W. Jennings, 1967
3. See site map for details of geophysical survey

File Name: CI-RXH
Date: 10/27/2011

USGS science for a changing world
GEOVision geophysical services

GEOLOGIC MAP
CI•RXH

RECOVERY.GOV

Looking northeast towards seismic station CI.RXH and location of array RXH-1

Looking southeast along array RXH-1 and at HVSR sensor 450

Seismic refraction array RXH-2 placed adjacent to seismic station to demonstrate that near surface velocity structure is similar to array RXH-1

Looking northwest towards the center of array RXH-1

Holocene volcanic rhyolite has weathered to cobbles, boulders and soil in the vicinity of array RXH-1. There is less weathered rock at the northwest end of Rock Hill

Location of Geophysical Testing Arrays:

Location	Latitude	Longitude
RXH-1, Southeast End of MASW/Seismic Refraction Array	33.18326	-115.62242
RXH-1, Center of MASW/Seismic Refraction Array	33.18353	-115.62263
RXH-1, Northwest End of MASW/Seismic Refraction Array	33.18379	-115.62283
RXH-2, Southwest End of Seismic Refraction Array	33.18284	-115.62291
RXH-2, Center of Seismic Refraction Array	33.18307	-115.62265
RXH-2, Northeast End of Seismic Refraction Array	33.18330	-115.62240
HVSR Sensor 450	33.18378	-115.62285
HVSR Sensor 453	33.18327	-115.62241
HVSR Sensor 507	33.18354	-115.62262
CI.RXH Seismic Station	33.18312	-115.62257

Notes: 1) WGS84 Coordinate System (decimal degrees)
2) Survey accuracy is estimated at 1 to 2 m.

Results:

V_S Model

Depth to Top of Layer (m)	Layer Thickness (m)	S-Wave Velocity (m/s)	Inferred P-Wave Velocity (m/s)	Assumed Poisson's Ratio	Assumed Density (g/cm^3)
0	1	153	287	0.300	1.8
1	2.5	182	340	0.300	1.8
3.5	2.5	193	362	0.300	1.8
6	2.5	254	475	0.300	1.8
8.5	4	345	1600	0.476	2.0
12.5	6	372	1600	0.471	2.0
18.5	8	420	1600	0.463	2.0
26.5	>3.5	482	1600	0.450	2.0

Notes: 1) Saturated zone, with V_P of about 1,600 m/s, constrained at a depth of 8.5 m based on seismic refraction survey.
2) Depth of investigation is about 30 m.
2) Bottom layer is a half space.

Observations/Discussion:

- Both the seismic station and MASW/seismic refraction arrays are located on very intensely weathered volcanic rocks. After observing low seismic velocities beneath array RXH-1, seismic refraction data were acquired along array RXH-2, located adjacent to the seismic station, to demonstrate that velocity structure was similar in the immediate vicinity of the seismic station.

- The HVSR curves are similar, validating the 1-D velocity structure assumption
- There is a high amplitude HVSR peak in the 4 to 4.5 Hz range and a broad zone of elevated HVSR response (multiple low amplitude peaks) over the 0.2 to 0.5 Hz range.
- The P-wave refraction data collected along arrays RHX-1 and RHX-2 were modeled using a tomographic inversion routine with layer based starting model.
- There is a clear water table refractor in the seismic records, but it has very low amplitude.
- The seismic refraction survey design allowed P-wave velocity to be imaged to a maximum depth of about 15 m. The seismic refraction models for arrays RXH-1 and RXH-2 show that P-wave velocity is about 325 to 425 m/s in the upper 8 to 9 m and then rapidly increases to over 1,500 m/s in what is interpreted as saturated sediments/very intensely weathered rock. P-wave velocity of the saturated zone is slightly higher beneath array RXH-2.
- Near surface P-wave velocity structure beneath array RXH-2 is similar to that beneath array RXH-1, indicating that MASW array RXH-1 is adequately located to characterize the seismic station.
- Noise conditions at the site were not sufficient for application of passive surface wave techniques.
- There is about 40 m/s scatter in the Rayleigh wave phase velocity data over a wide wavelength/frequency range. This is relatively high for a site with such low velocities, but expected due to lateral velocity variation associated with differential weathering of the rhyolite. It was particularly difficult reducing MASW dispersion data at wavelengths greater than 45 m, thereby more scatter than normal is observed at large wavelengths. The scatter in the MASW dispersion data are not expected to significantly impact V_{S30}, although the scatter does imply that V_{S30} could vary by 5 to 10% beneath the array.
- The minimum wavelength surface wave phase velocity data extracted from the 48-channel MASW array was about 6 m. Data reduction using seismic records from smaller hammer sources and a limited offset receiver array (i.e. less active geophones) allowed extraction of surface wave dispersion data to a minimum wavelength of about 1.5 m.
- A representative dispersion curve was generated for the MASW data set using a moving average, polynomial curve fitting routine and used for modeling.
- Surface wave depth of investigation is about 30 m based on half of maximum wavelength criteria.
- The inferred P-wave velocities in the surface wave model above the saturated zone are generally consistent with the average velocity structure in the seismic refraction model.
- The HVSR peak in the 4 to 4.5 Hz range may be associated with the increase in V_S below a depth of 8.5 m.
- V_{S30} is 309 m/s (Site Class D).
- Average S-wave velocity between 1 m (inferred sensor depth) and 31 m is 324 m/s.

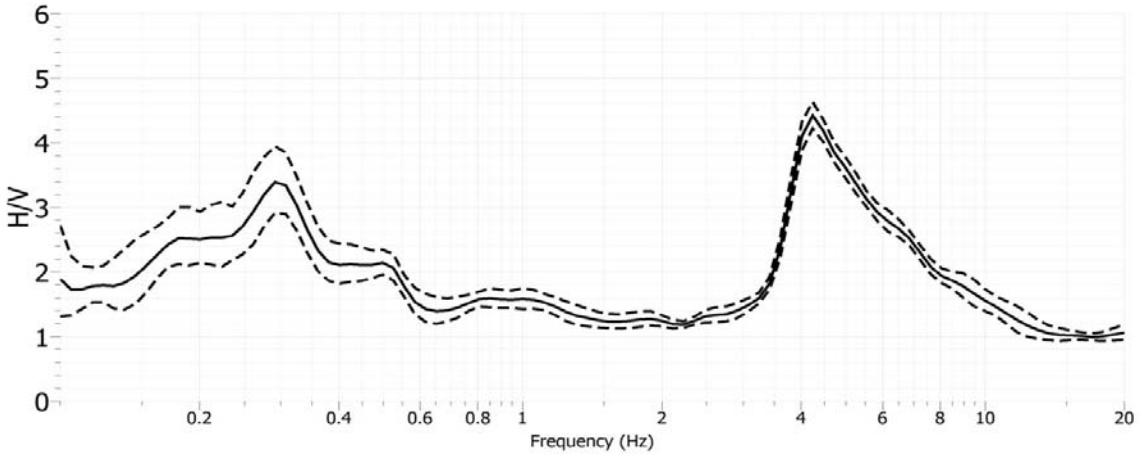

Site CI.RXH, H/V Spectral Ratio, Array RXH-1, Sensor 450

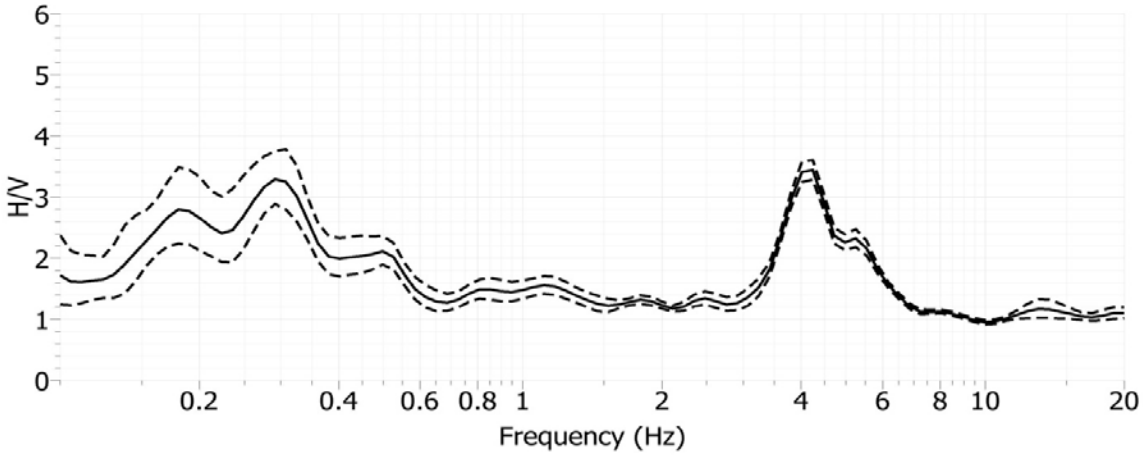

Site CI.RXH, H/V Spectral Ratio, Array RXH-1, Sensor 507

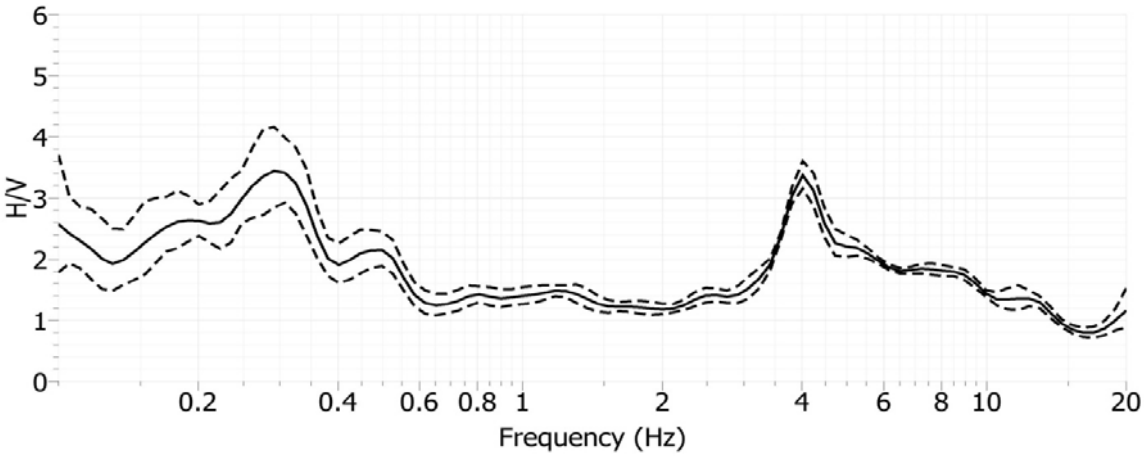

Site CI.RXH, H/V Spectral Ratio, Array RXH-1, Sensor 453

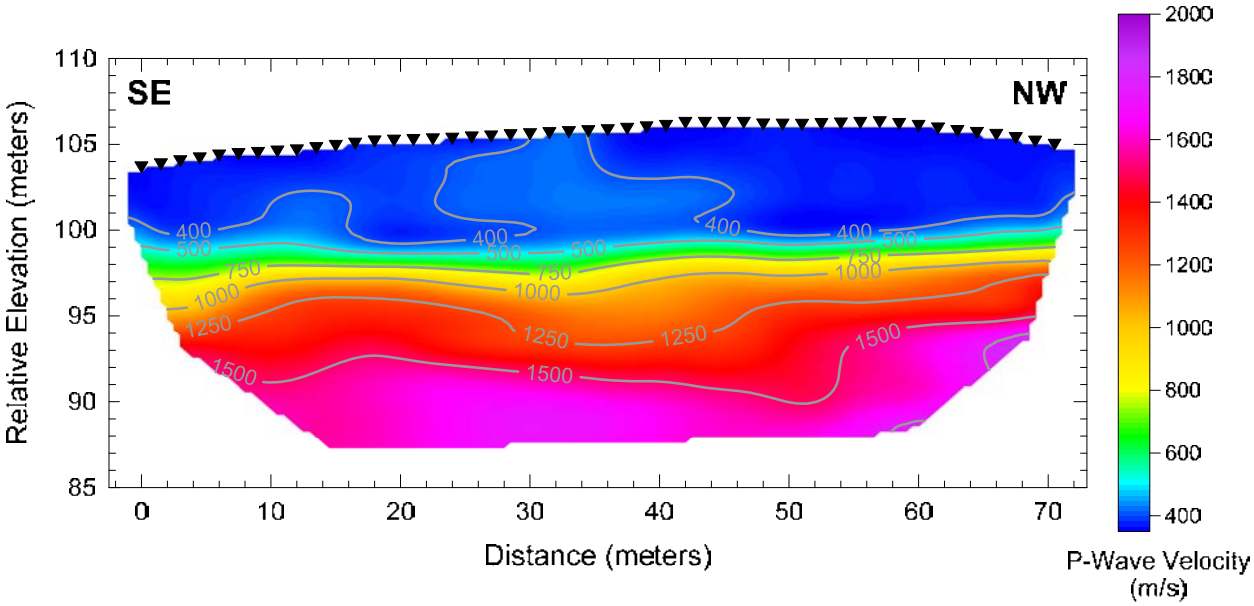

Array RXH-1 – Tomographic Seismic Refraction Model utilizing Layer Based Starting Model

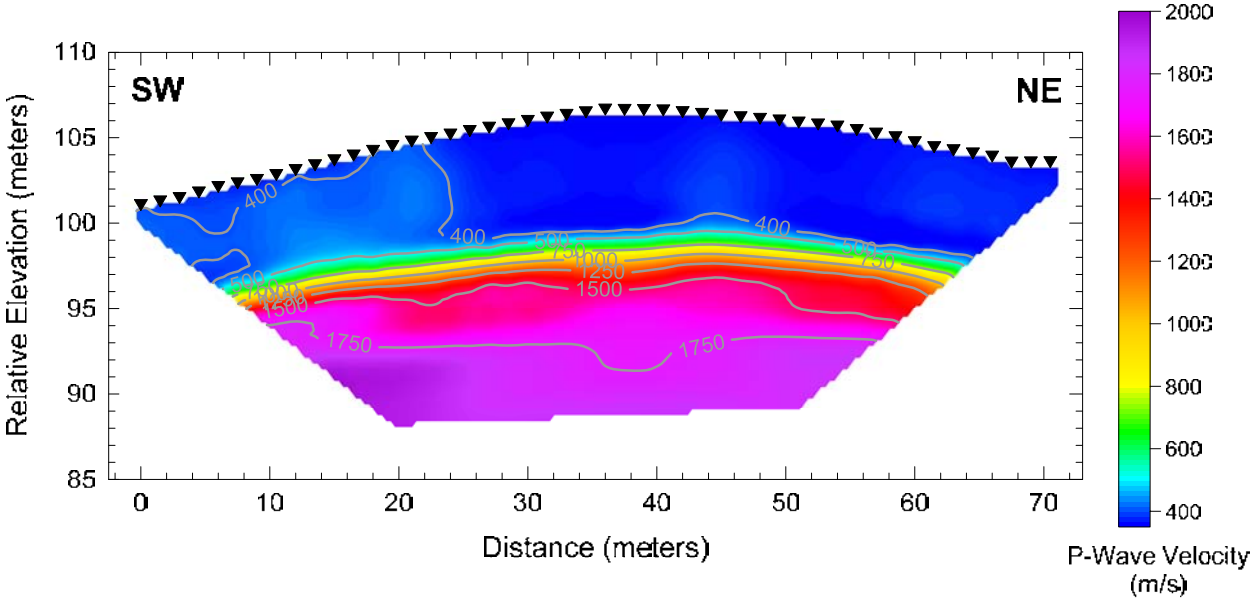

Array RXH-2 – Tomographic Seismic Refraction Model utilizing Layer Based Starting Model

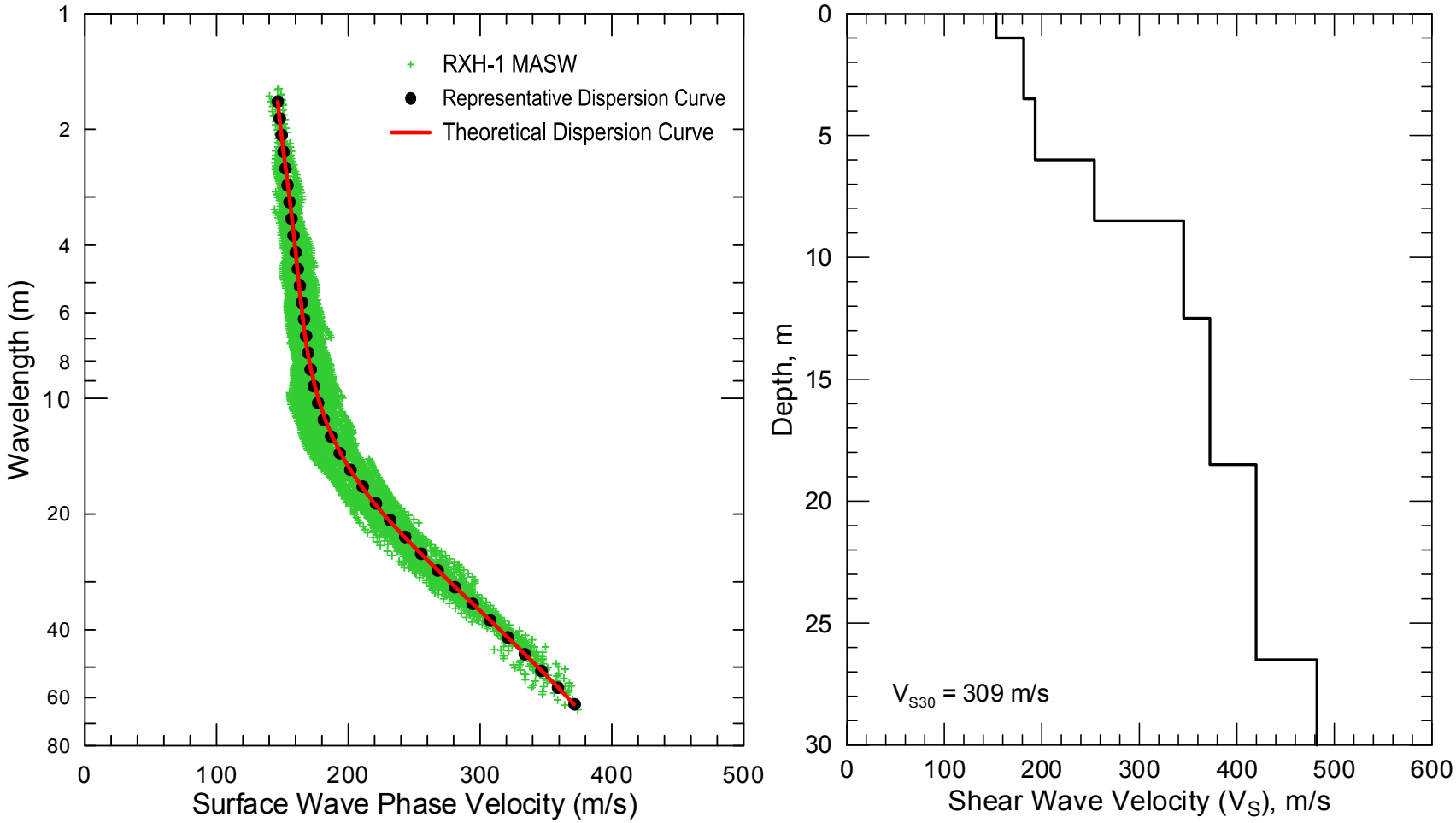

CI.RXH - Field, representative and inverted theoretical surface wave dispersion data (left) and associated V_S model (right)

Site CI.SAL

Location: Salton City, Imperial County, California

Latitude: 33.28010 **Longitude:** -115.98585
(Station coordinates provided by USGS, WGS84 coordinate system)

V_{S30} (measured): 253 m/s

V_{S30} (adjusted to more accurately reflect seismic station conditions): 264 m/s (average S-wave velocity between 1 and 31 m adjusting for assumed seismic sensor depth and the fact that the sensor is located on compacted fill).

NEHRP Site Class: D

Geomatrix Code: IQD

Geologic Conditions/Observations: Quaternary (Pleistocene) old alluvium. Quaternary Cahuilla beds or, possibly, Tertiary Palm Springs Formation may outcrop about 50 m west of survey area. Probable deep soil site.

Site Conditions: Rural site. Relatively flat topography in site vicinity with gradual decrease in ground surface elevation to east.

Geophysical Methods Utilized: HVSR, MASW

Geophysical Testing Arrays:

1. Array SAL-1 (48 channel MASW array utilizing 4.5 Hz vertical geophones spaced 1.5 m apart for a length of 70.5 m, forward and reverse shot locations with multiple source offsets and source types and center shot location).
2. Three HVSR measurement locations distributed along SAL-1.

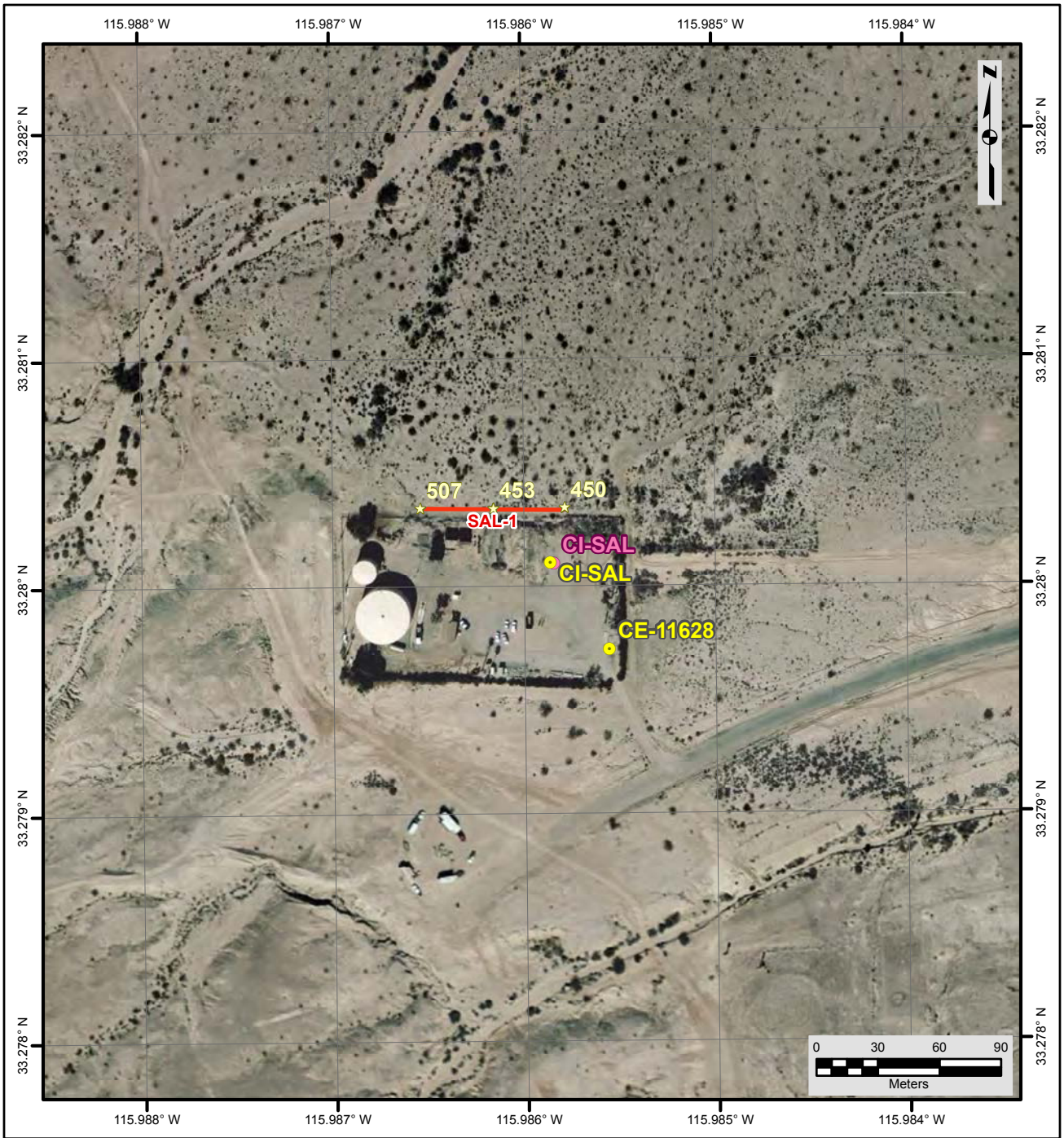

Legend

- Seismic Station - Approximate Surveyed Location
- Seismic Station - Approximate Location of Record
- H/V Spectral Ratio Measurement Location
- MASW Array

NOTES:
1. WGS 1984 COORDINATE SYSTEM
2. Image Source: ESRI, i-cubed, USDA FSA, USGS, AEX, GeoEye, Getmapping, Aerogrid, IGP

File Name: CI-SAL-I

Date: 4/1/2011

USGS science for a changing world

GEOVision geophysical services

RECOVERY.GOV

SITE MAP
CI•SAL

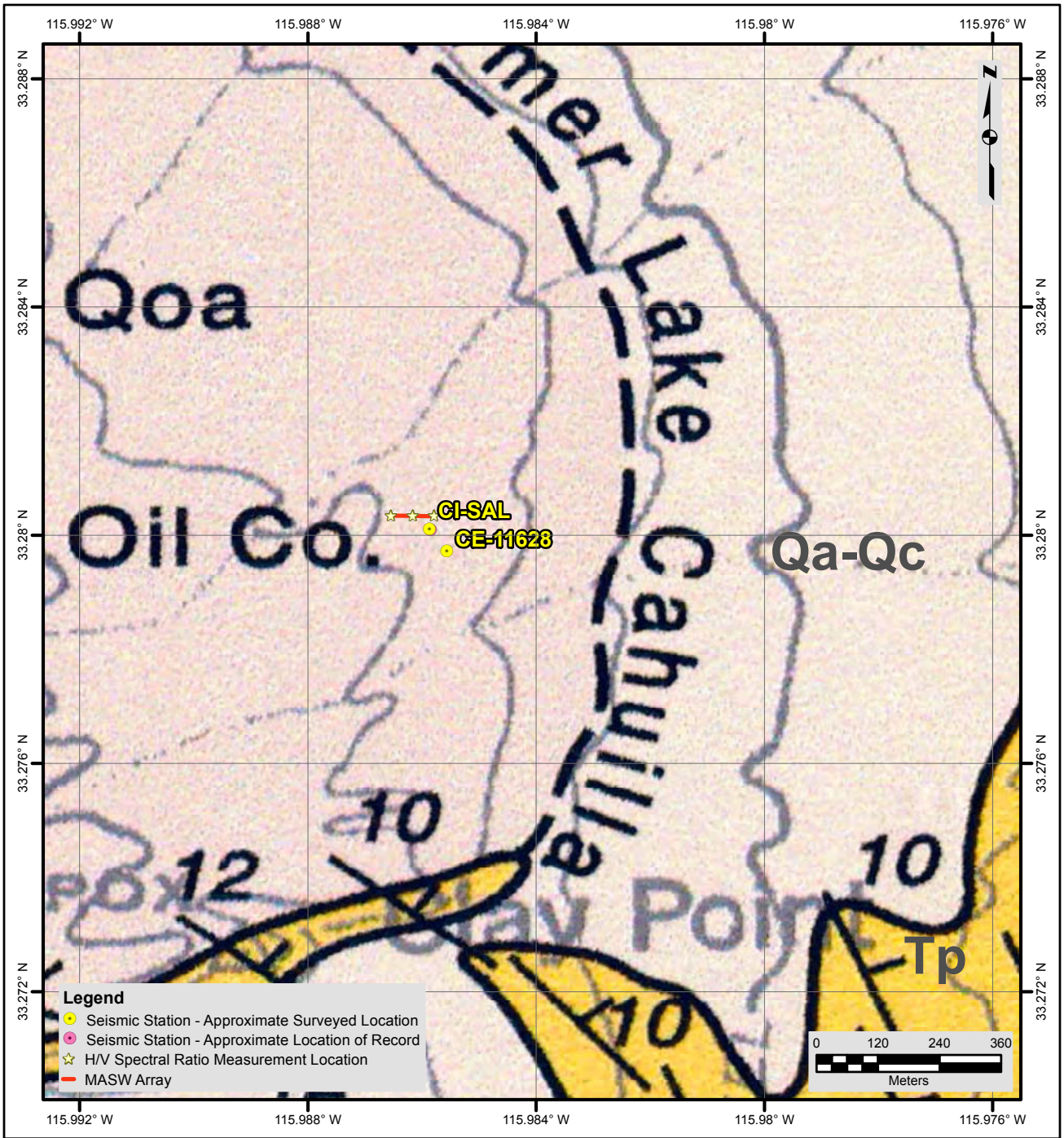

Description of Geologic Map Units

Qa = Quaternary (Holocene) alluvial sand, gravel, silt and clay of valley areas
Qc = Quaternary (Holocene) Cahuilla beds; thin series of claystones, sands, and gravels, fossiliferous
Qoa = Quaternary (Pleistocene) older dissected alluvial gravel
Tp = Tertiary (Pliocene) Palm Spring Formation; laminated sandstones, arkosic, with interbedded red clays, includes fossil hardwoods

NOTES:
1. WGS 1984 COORDINATE SYSTEM
2. Geologic Map of the Durmid 15 Minute Quadrangle, Riverside and Imperial Counties, California by Thomas W. Dibblee, Jr., 2006
4. See site map for details of geophysical survey

File Name: CI-SAL

Date: 4/1/2011

USGS science for a changing world

GEOVision geophysical services

RECOVERY.GOV

GEOLOGIC MAP
CI•SAL

Looking south from array SAL-1
towards CI.SAL seismic station

Looking southeast towards seismic station from
HVSR sensor 507

Looking east at HVSR sensors along array SAL-1

Looking west along MASW array SAL-1

Location of Geophysical Testing Arrays:

Location	Latitude	Longitude
SAL-1, West End of Array	33.28034	-115.98654
SAL-1, Center of Array	33.28034	-115.98616
SAL-1, East End of Array	33.28033	-115.98579
HVSR Sensor 507	33.28034	-115.98655
HVSR Sensor 453	33.28034	-115.98616
HVSR Sensor 450	33.28035	-115.98579
CI.SAL Seismic Station	33.28010	-115.98587
CE.11628 Seismic Station	33.27972	-115.98556

Notes: 1) WGS84 Coordinate System (decimal degrees)
2) Typical survey accuracy is estimated at 1 to 2 m.

Results:

V_S Model

Depth to Top of Layer (m)	Layer Thickness (m)	S-Wave Velocity (m/s)	Inferred P-Wave Velocity (m/s)	Assumed Poisson's Ratio	Assumed Density (g/cm^3)
0	1	133	249	0.300	1.7
1	2	182	340	0.300	1.8
3	2	202	378	0.300	1.8
5	4	234	437	0.300	1.8
9	6	249	1575	0.487	1.9
15	8	273	1575	0.485	1.9
23	10	358	1575	0.473	1.9
33	>2	447	1575	0.456	2.0

Notes: 1) Saturated zone, with V_P of about 1,575 m/s, constrained at a depth of about 9 m based on seismic refraction analysis.
2) Depth of investigation is about 35 m.
3) Bottom layer is a half space.

Observations/Discussion:

- HVSR curves very similar at all stations validating the 1-D velocity assumption.
- HVSR peak in the 0.21 to 0.22 Hz range, which is consistent with a deep soil site.
- Possible secondary HVSR peak(s) in the 0.45 to 0.7 Hz range.
- Noise conditions at site were not sufficient to apply passive surface wave techniques.
- The minimum wavelength Rayleigh wave phase velocity data extracted from the 48-channel MASW array was about 4 m. Reducing data from smaller hammer sources using a limited offset receiver array (i.e. less active geophones) allowed for extraction of surface wave dispersion data to a minimum wavelength of about 2 m.
- The maximum wavelength extracted from the MASW data was generally set equal to about the distance from the source to midpoint of the receiver array. The maximum wavelength Rayleigh wave phase velocity data extracted from the MASW data was about 70 m.
- There is nominally about 25 m/s of scatter in the MASW dispersion data, which is likely the result of minor lateral velocity variation.
- A representative dispersion curve was generated for the MASW data set using a moving average, polynomial curve fitting routine and used for modeling.
- Water table depth constrained at about 8 to 9 m based on a simple, 3-layer interactive analysis of seismic refraction data from MASW shot records (300 m/s V_P to depth of 1.5 m overlying 500 m/s V_P for unsaturated sediments, underlain by 1,575 m/s V_P for saturated sediments).
- Surface wave depth of investigation is about35 m, based on half of maximum wavelength criteria.
- Seismic station located on fill pad up to about 2 m higher in elevation than array SAL-1.
- V_{S30} is 253 m/s (NEHRP Site Class D).
- Average S-wave velocity between 1 and 31 m to account for assumed seismic sensor depth and the fact that the sensor is located on compacted fill is 264 m/s (NEHRP Site Class D).

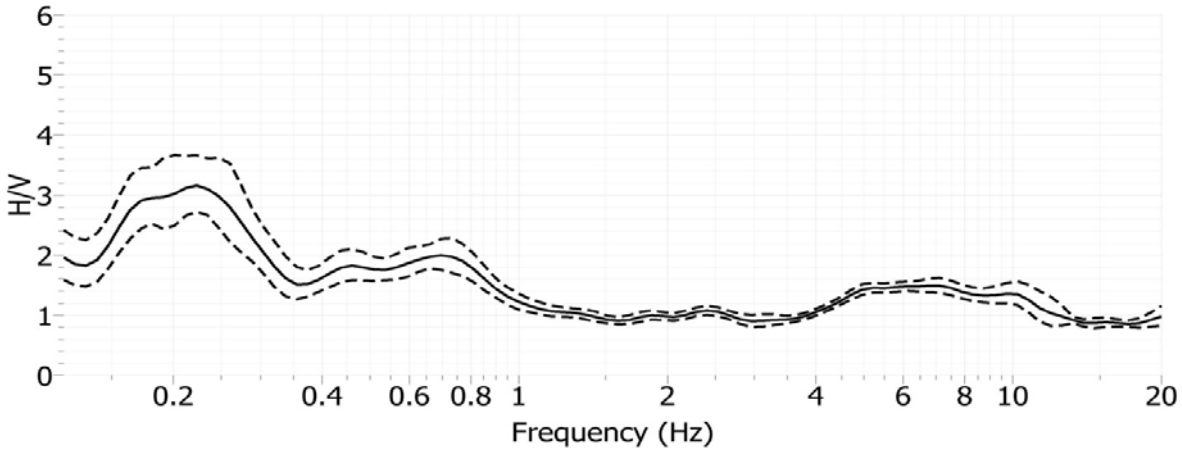

Site CI.SAL, H/V Spectral Ratio, Array SAL-1, Sensor 507

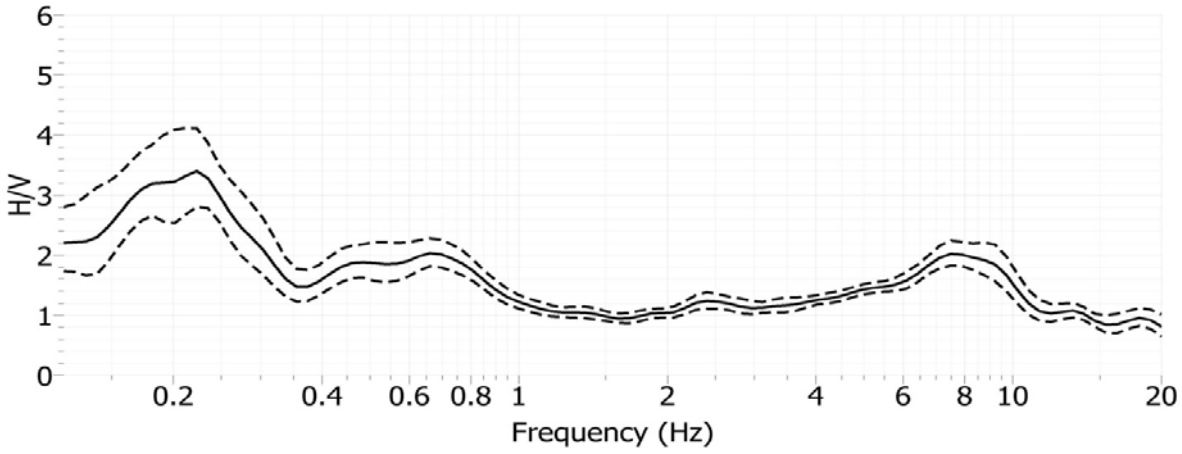

Site CI.SAL, H/V Spectral Ratio, Array SAL-1, Sensor 453

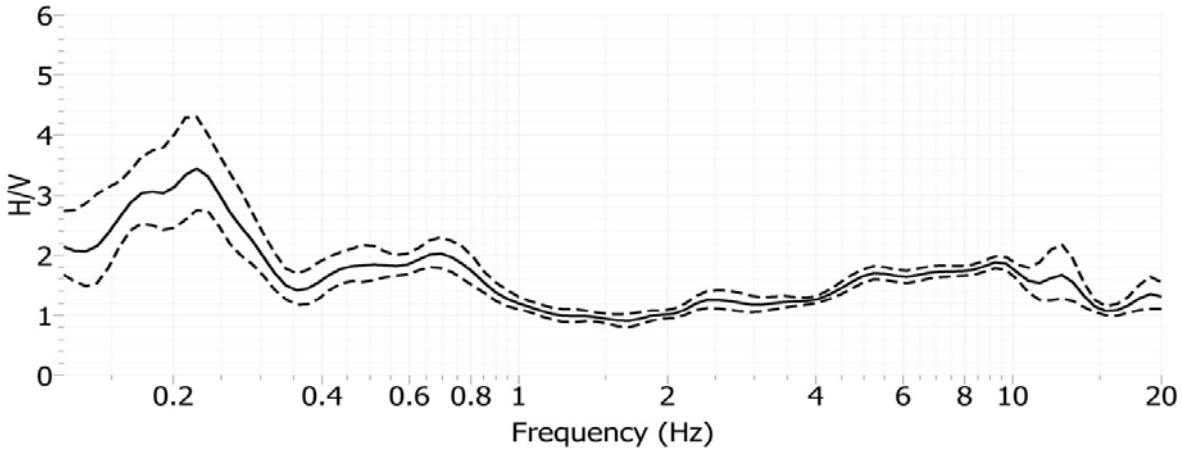

Site CI.SAL, H/V Spectral Ratio, Array SAL-1, Sensor 450

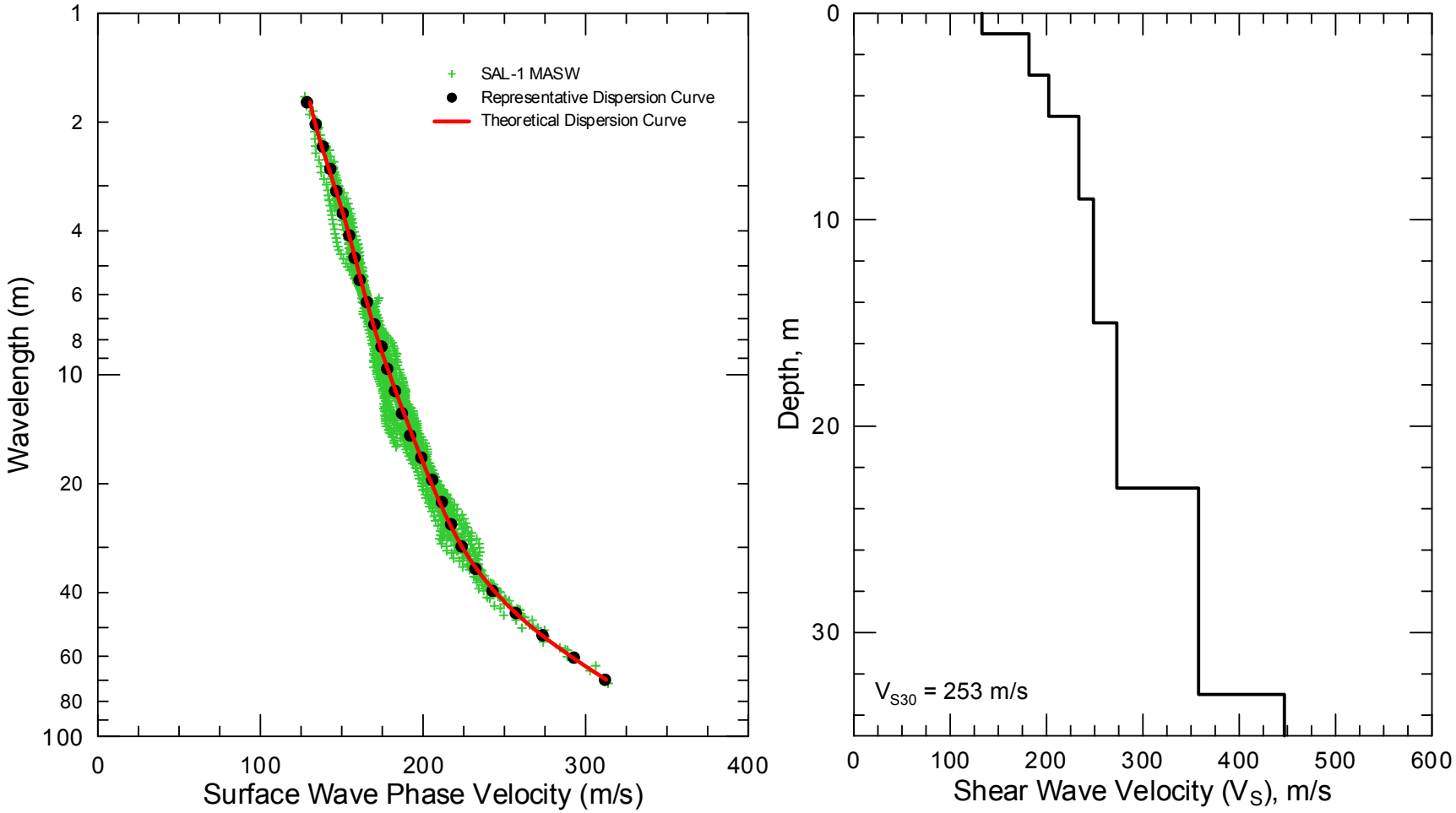

CI.SAL - Field, representative and inverted theoretical surface wave dispersion data (left) and associated V_S model (right)

Site CI.SAN

Location: AT&T, 3220 S. Bristol St., Santa Ana, California

Latitude: 33.70442 **Longitude:** -117.88669

(Station coordinates modified based on field observation of station location and identification of approximate station location on Google Earth – could not survey the seismic station as located inside a building, WGS84 coordinate system)

V_{S30} (measured): 222 m/s

V_{S30} (adjusted to more accurately reflect seismic station conditions): 222 m/s (no adjustment necessary)

NEHRP Site Class: D

Geomatrix Code: BHD or GHD (sensor on first floor of structure and there may be subsurface levels in structure, but could not be visually confirmed)

Geologic Conditions/Observations: Site located in area mapped as Quaternary (Holocene) alluvium. Deep soil site.

Site Conditions: Urban site with significant traffic noise from nearby roads and railroad. Relatively flat terrain in site vicinity.

Geophysical Methods Utilized: HVSR, MASW, array microtremor, ReMi™

Geophysical Testing Arrays:

1. Arrays SAN-1 (24 channel linear array utilizing 4.5 Hz vertical geophones spaced 4 m apart for an array length of 92 m) and SAN-2 (24 channel linear array utilizing 4.5 Hz vertical geophones spaced 5 m apart for an array length of 115 m) used to acquire passive surface wave data. Arrays combined to form an "L" shaped array.
2. Array SAN-3 (48 channel MASW array utilizing 4.5 Hz vertical geophones spaced 1 m apart for a length of 47 m, forward and reverse shot locations with multiple source offsets and source types (hammers only) and center shot location).
3. Three HVSR measurement locations distributed along array SAN-3 and one additional measurement location inside building next to seismic station.

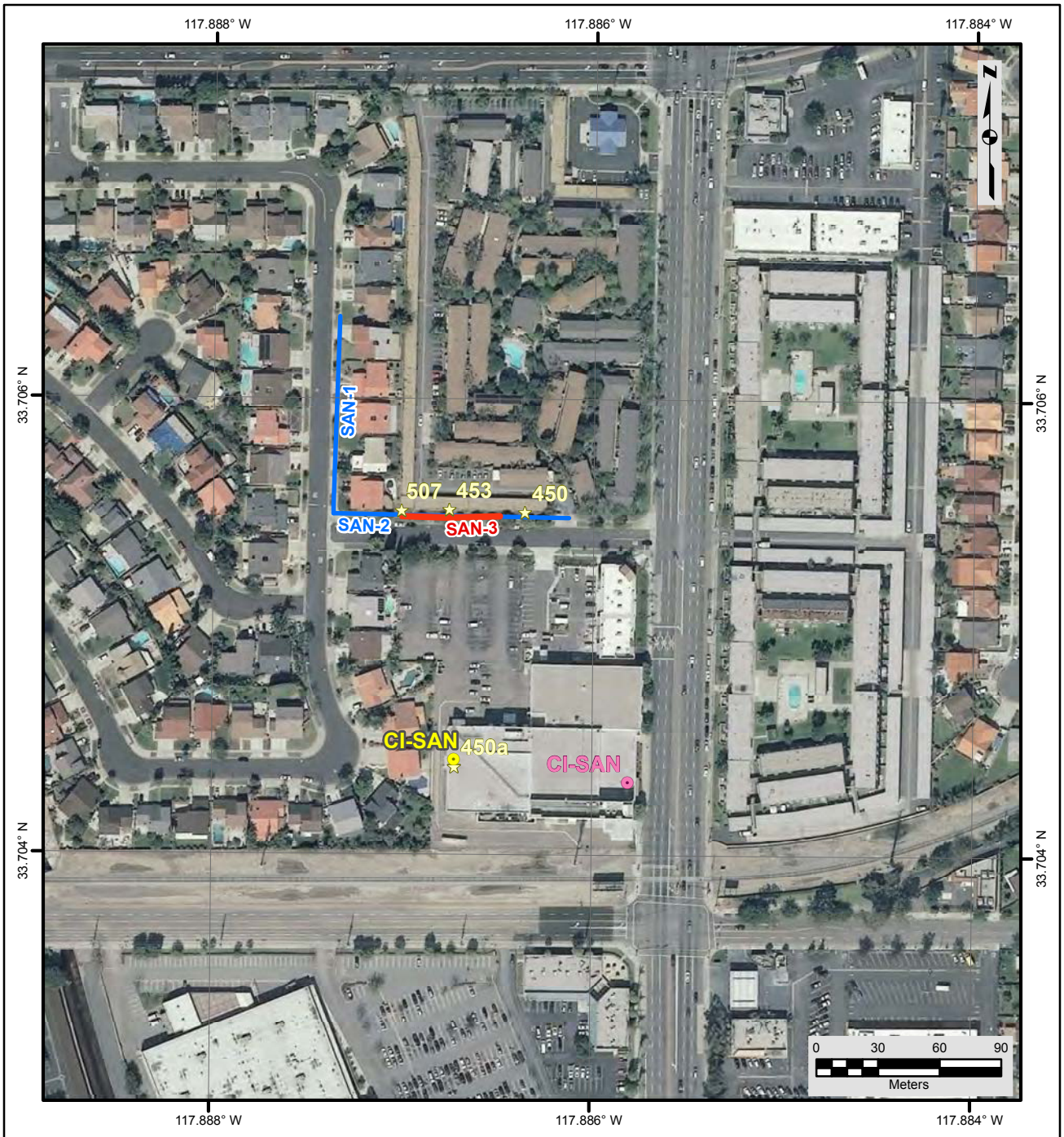

Legend

- Seismic Station - Approximate Surveyed Location
- Seismic Station - Approximate Location of Record
- H/V Spectral Ratio Location
- MASW Array
- Passive Array

NOTES:
1. WGS 1984 COORDINATE SYSTEM
2. Image Source: ESRI, i-cubed, USDA FSA, USGS, AEX, GeoEye, Getmapping, Aerogrid, IGP

File Name: CI-SAN-I

Date: 7/15/2011

USGS science for a changing world

GEOVision geophysical services

RECOVERY.GOV

SITE MAP
CI•SAN

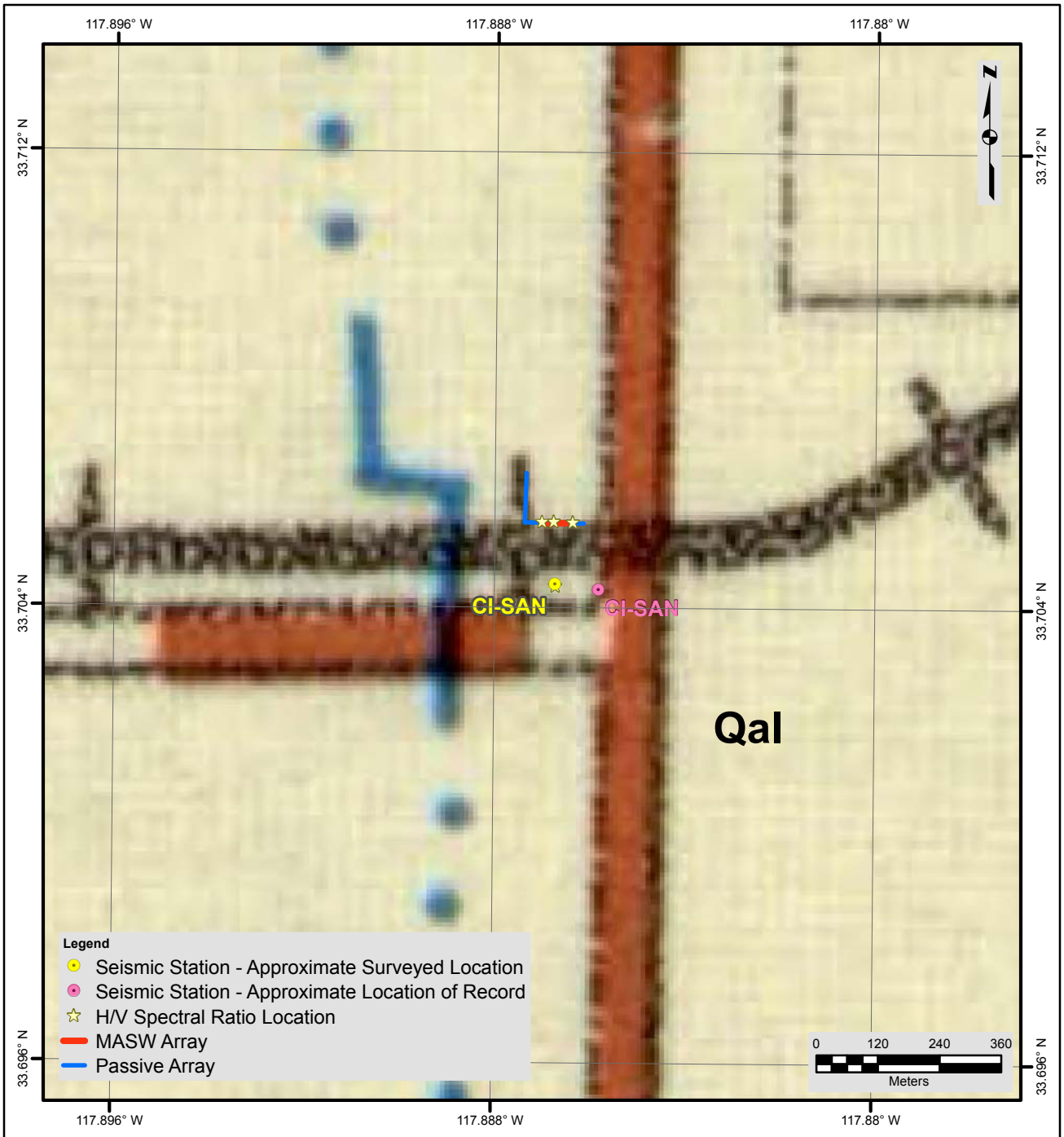

Description of Geologic Map Units

Qal = Quaternary (Holocene) alluvium

NOTES:
1. WGS 1984 COORDINATE SYSTEM
2. Geologic Map of California, Santa Ana Sheet
Olaf P. Jenkins Edition
Compilation by Thomas H. Rogers, 1965
3. See site map for details of geophysical survey

File Name: CI-SAN

Date: 7/15/2011

USGS science for a changing world

GEOVision geophysical services

RECOVERY.GOV

GEOLOGIC MAP
CI•SAN

CI.SAN Seismic Station

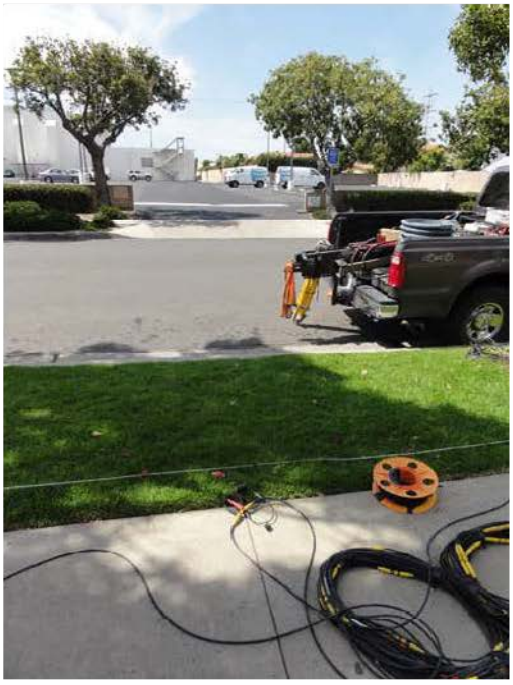

Looking south towards seismic station CI.SAN from passive surface wave array SAN-2

HVSR Sensor 450A adjacent to seismic station

Looking east along MASW array SAN-3

Looking north along passive surface wave array SAN-1

Location of Geophysical Testing Arrays:

Location	Latitude	Longitude
SAN-1, North End of Passive SW Array	33.70636	-117.88731
SAN-1, South End of Passive SW Array	33.70553	-117.88734
SAN-2, West End of Passive SW Array	33.70549	-117.88734
SAN-2, East End of Passive SW Array	33.70548	-117.88610
SAN-3, East End of MASW Array	33.70548	-117.88698
SAN-3, Center of MASW Array	33.70548	-117.88673
SAN-3, West End of MASW Array	33.70549	-117.88646
HVSR Sensor 450	33.70550	-117.88633
HVSR Sensor 450a	33.70442	-117.88669
HVSR Sensor 453	33.70551	-117.88673
HVSR Sensor 507	33.70551	-117.88698
CI.SAN Seismic Station	33.70442	-117.88669

Notes: 1) WGS84 Coordinate System (decimal degrees)
2) Survey accuracy is estimated at 1 to 2 m
3) CI.SAN Seismic Station and HVSR Sensor 450a were not surveyed with a GPS, but estimated using Google Earth and field observations.

Results:

V_S Model

Depth to Top of Layer (m)	Layer Thickness (m)	S-Wave Velocity (m/s)	Inferred P-Wave Velocity (m/s)	Inferred Poisson's Ratio	Inferred Density (g/cm^3)
0	1	99	185	0.300	1.9
1	1.5	133	248	0.300	1.9
2.5	2.5	138	258	0.300	1.9
5	4	171	1600	0.494	2.0
9	6	245	1600	0.488	2.0
15	9	301	1600	0.482	2.0
24	12	340	1600	0.476	2.0
36	15	407	1600	0.465	2.0
51	>19	477	1600	0.451	2.1

Observations/Discussion:

- The building housing seismic station CI-SAN may have subsurface levels, which could not be substantiated. The seismic sensor is on the first floor of the structure.
- The HVSR curves are almost identical at frequencies below 10 Hz, validating the 1-D velocity structure assumption. There are, however, no significant high frequency HVSR peaks by which to characterize shallow velocity structure.
- The HVSR measurements made inside the building housing the seismic sensors are almost identical to those made outside of the building.
- High amplitude HVSR peak at 0.16 Hz, which is consistent for a very deep sedimentary basin.
- Noise conditions at site (multi-directional or omni-directional noise sources) appeared sufficient for successful application of passive surface wave techniques.
- ESAC technique used to extract surface wave dispersion data from passive "L" array data. Both the ReMi™ and ESAC techniques used to extract surface wave dispersion data from the linear arrays. Only the higher quality "L" array dispersion data used for analysis. The linear arrays yielded similar dispersion curves that deviate no more than 25 m/s from the "L" array dispersion curve.
- Surface wave dispersion data from active and passive surface wave data sets are in excellent agreement at this site.
- Representative dispersion curves were generated for each surface wave data set using a moving average, polynomial curve fitting routine. These individual representative dispersion curves were combined and a representative dispersion curve generated for the combined data set for data modeling.
- The water table was modeled at a depth on the order of 5 m based on interactive layer-based analysis of seismic refraction first arrival data, which was very noisy due to heavy vehicle traffic in site vicinity. P-wave velocities of about 350 and 1,600 m/s were modeled for unsaturated and saturated sediments, respectively.
- Surface wave depth of investigation is about 70 m based on half of maximum wavelength criteria and assuming that surface wave dispersion data at frequencies as low as 2.8 Hz are valid utilizing 4.5 Hz geophones (low frequency geophone phase response differences will cancel out if noise is omni-directional and/or the phase response differences are random in nature).
- V_{S30} is 222 m/s (Site Class D).
- Average S-wave velocity of the upper 70 m (V_{S70}) is 369 m/s.

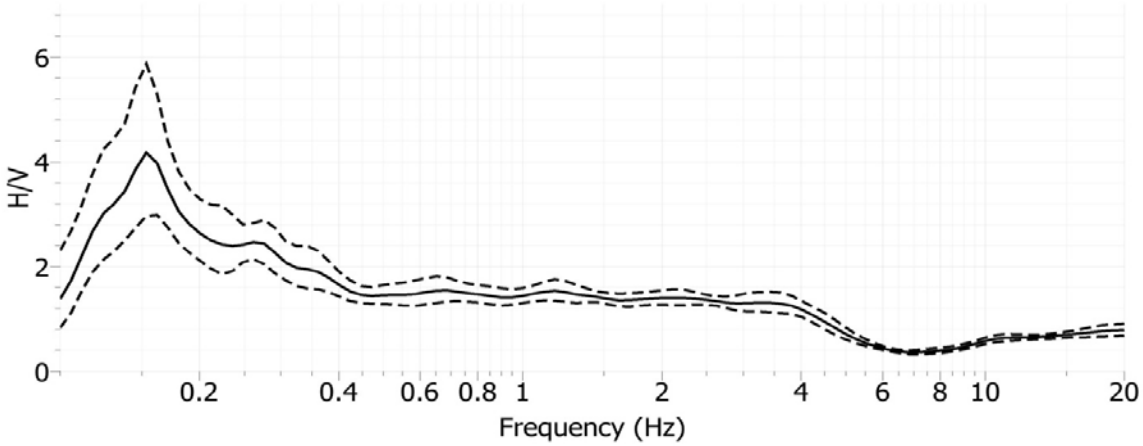

Site CI.SAN, H/V Spectral Ratio, Array SAN-3, Sensor 507

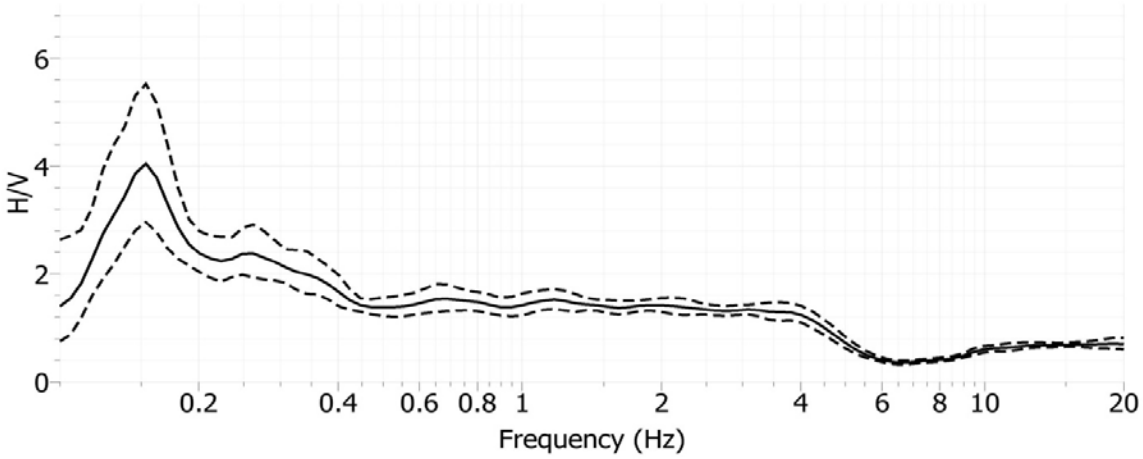

Site CI. SAN, H/V Spectral Ratio, Array SAN-3, Sensor 453

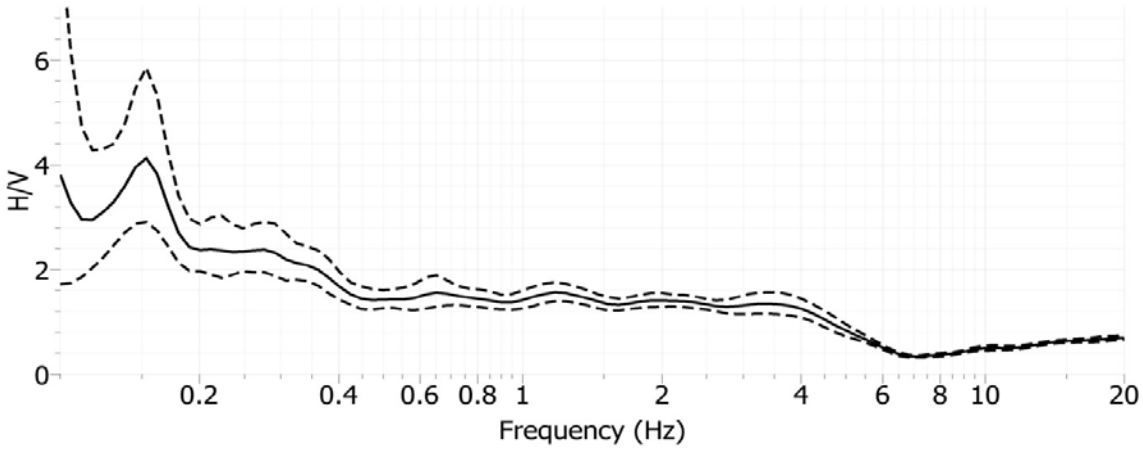

Site CI. SAN, H/V Spectral Ratio, Array SAN-2, Sensor 450

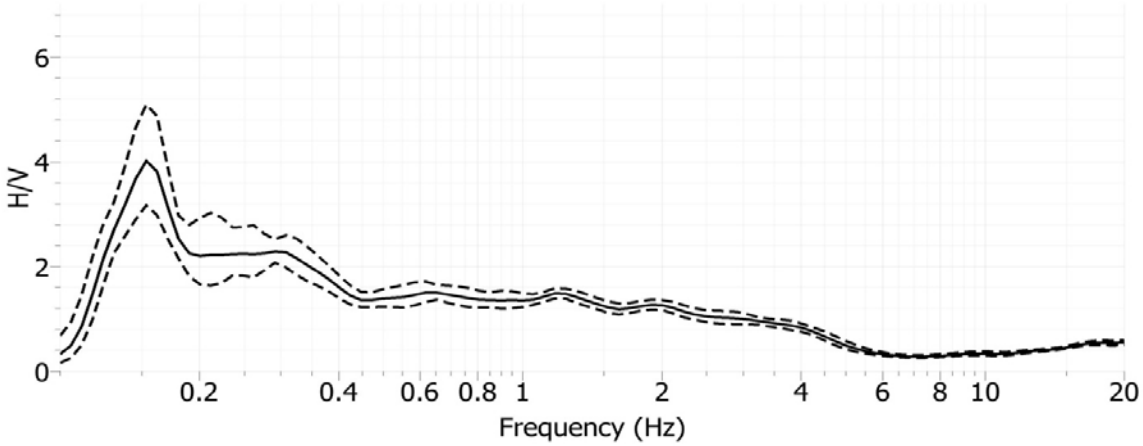

Site CI.SAN, H/V Spectral Ratio, Adjacent to Seismic Station, Sensor 450A

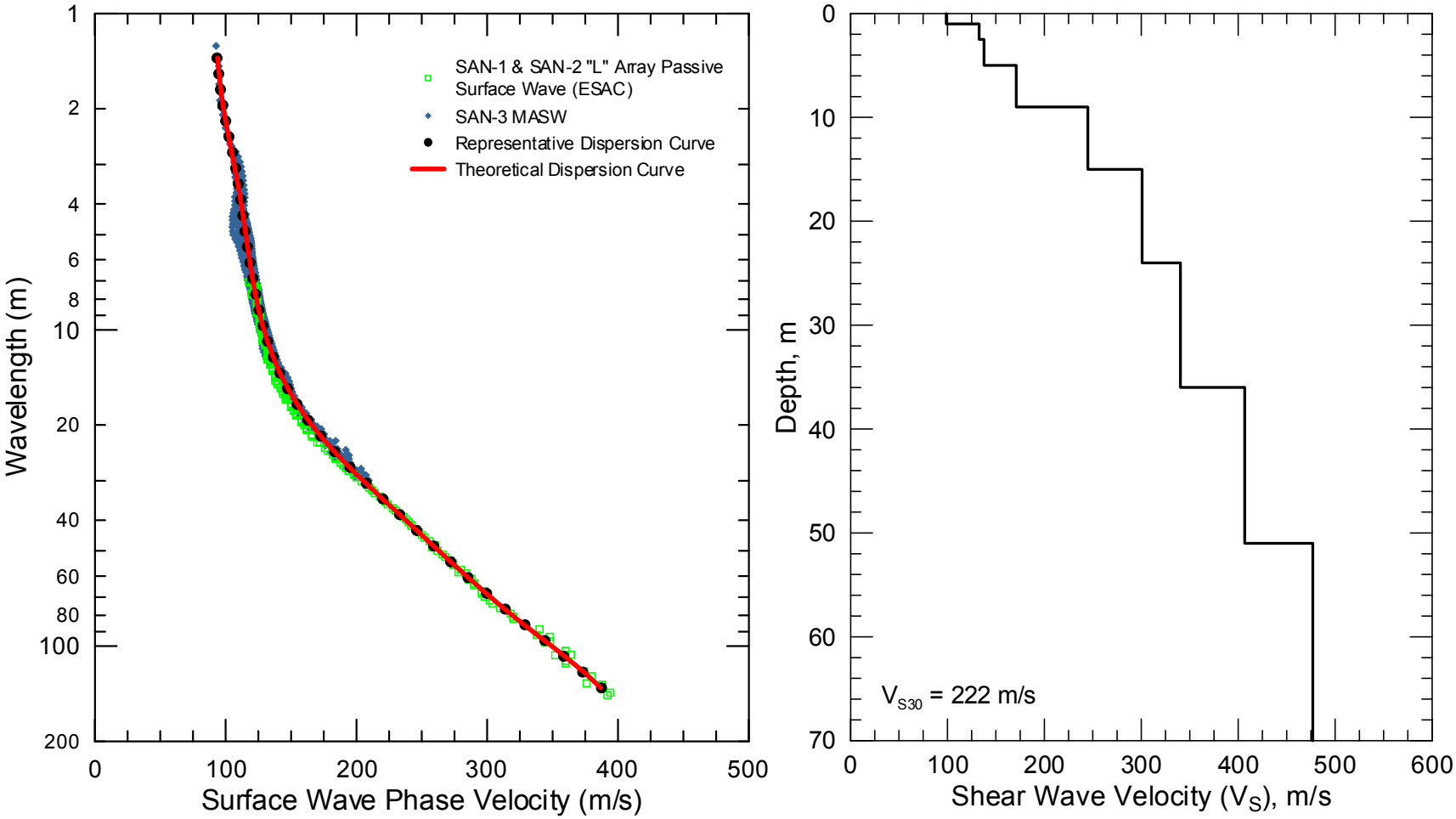

CI.SAN - Field, representative and inverted theoretical surface wave dispersion data (left) and associated V_S model (right)

Site CI.SBB2

Location: Saddle Butte State Park, Los Angeles County, California

Latitude: 34.68844 **Longitude:** -117.82420
(Station coordinates from site GPS survey, WGS84 coordinate system)

V_{S30} (measured): 1,131 m/s

V_{S30} (adjusted to more accurately reflect seismic station conditions): 1,319 m/s (average S-wave velocity between 1 and 31 m adjusting for assumed 1 m sensor depth).

NEHRP Site Class: B

Geomatrix Code: IGA

Geologic Conditions/Observations: Seismic station located on geologic unit mapped as Mesozoic (Late Jurassic to Cretaceous) quartz monzonite.

Site Conditions: Rural site located on a small bedrock outcrop. There is about 2 m of elevation variation along the 70.5 m long MASW and seismic refraction array.

Geophysical Methods Utilized: HVSR, Seismic Refraction, MASW

Geophysical Testing Arrays:

1. Array SBB2-1 (48 channel MASW and P-wave seismic refraction array utilizing 4.5 Hz vertical geophones spaced 1.5 m apart for a length of 70.5 m, forward and reverse shot locations with multiple source offsets and source types and multiple interior shot locations).
2. Three HVSR measurement locations: two distributed along array SBB2-1 and one adjacent to the seismic station.

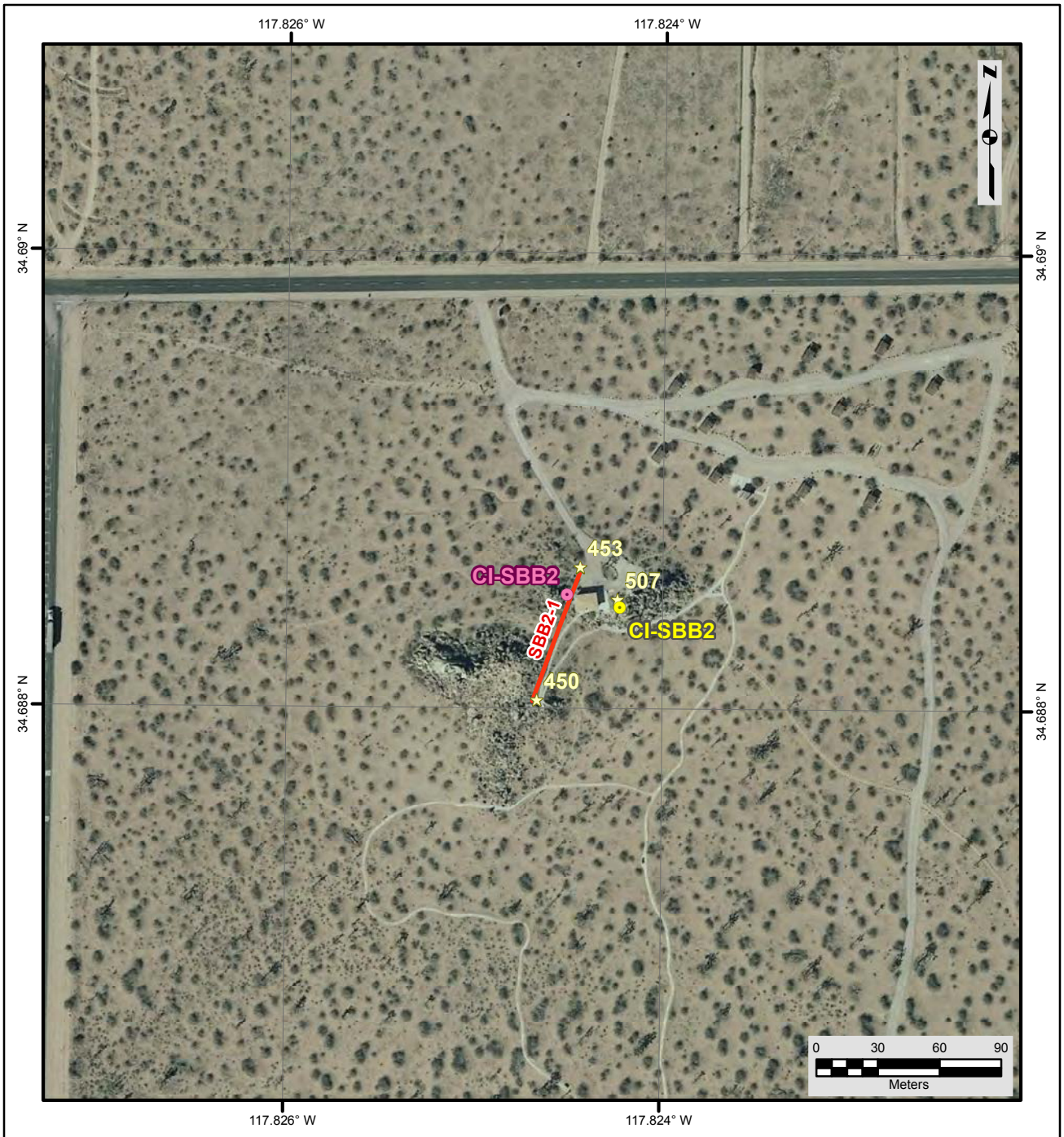

Legend

- Seismic Station - Approximate Surveyed Location
- Seismic Station - Approximate Location of Record
- H/V Spectral Ratio Location
- MASW and Seismic Refraction Array

NOTES:
1. WGS 1984 COORDINATE SYSTEM
2. Image Source: ESRI, i-cubed, USDA FSA, USGS, AEX, GeoEye, Getmapping, Aerogrid, IGP

File Name: CI-SBB2-I

Date: 10/13/2011

USGS science for a changing world

GEOVision geophysical services

RECOVERY.GOV

SITE MAP
CI•SBB2

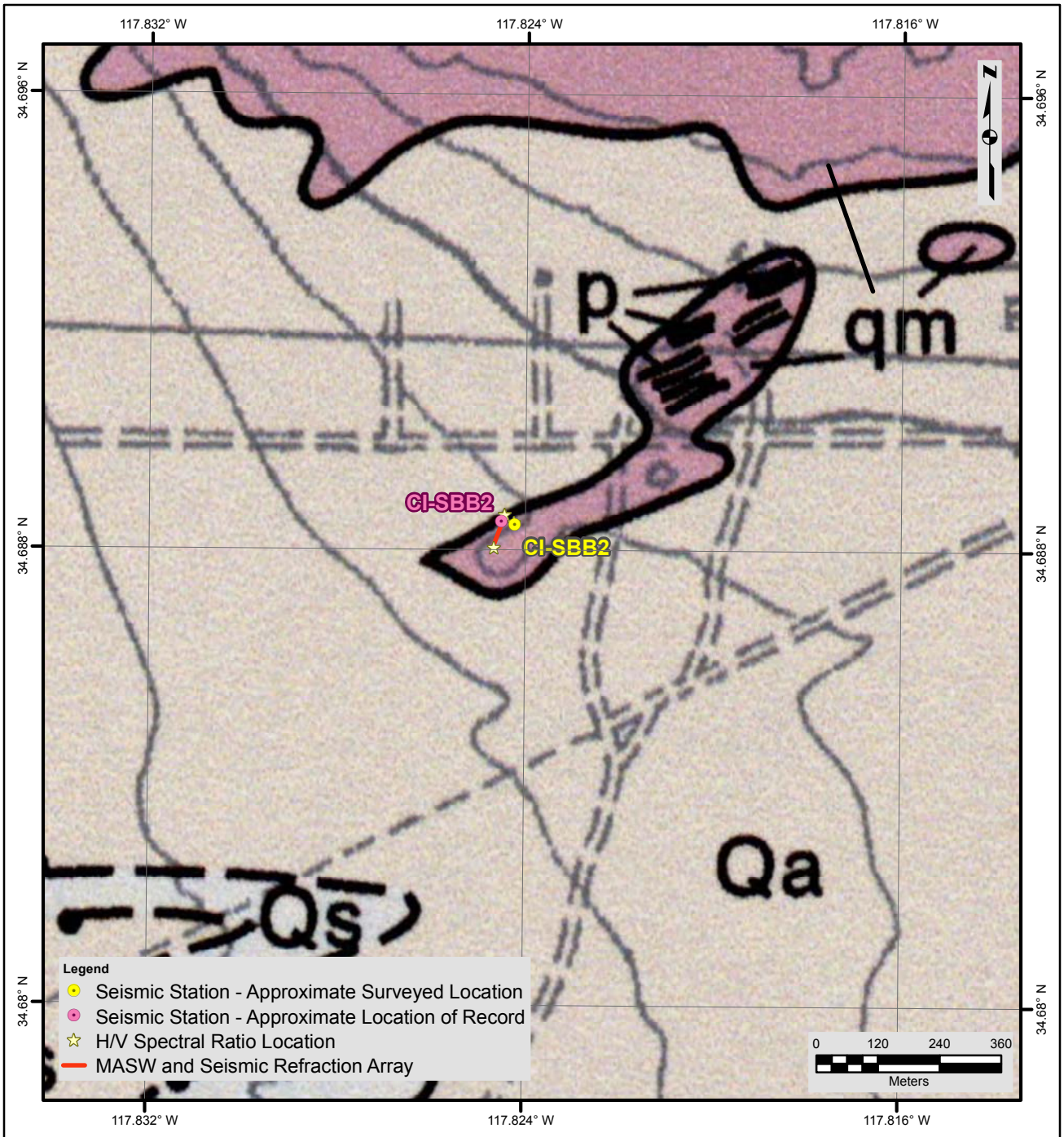

Description of Geologic Map Units

Qa = Quaternary (Holocene) alluvial gravel, sand and silt
Qs = Quaternary (Holocene) loose, windblown sand of dunes and dune ridges
p = Mesozoic or Tertiary pegmatite dikes with some gradations to aplite, coarsely crystalline
qm = Mesozoic (Late Jurassic to Cretaceous) quartz monzonite,
massive to rarely gneissoid, medium-grained

NOTES:
1. WGS 1984 COORDINATE SYSTEM
2. Geologic Map of the Lancaster & Alpine Butte 15 Minute Quadrangles, Los Angeles County, California by Thomas W. Dibblee, Jr., 2008
3. See site map for details of geophysical survey

File Name: CI-SBB2
Date: 10/13/2011

USGS science for a changing world
GEOVision geophysical services

GEOLOGIC MAP
CI•SBB2

RECOVERY.GOV

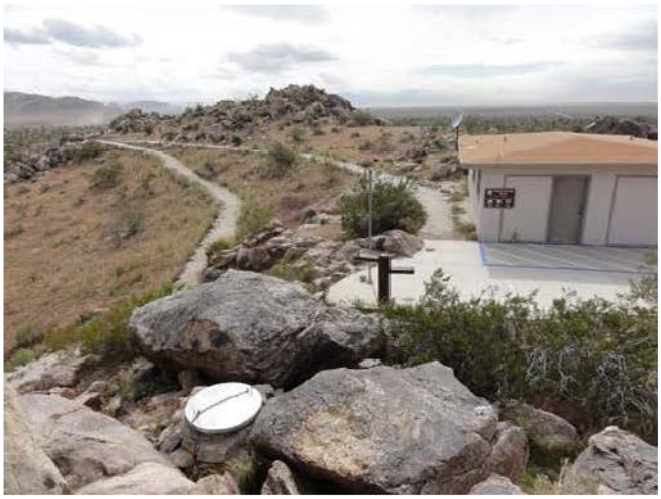

Looking south at CI.SBB2 seismic station

Looking south at HVSR sensor 507 (seismic station behind bolder in background)

Looking southwest towards test area

Looking southwest along array SBB2-1

Looking northeast along array SBB2-1

Location of Geophysical Testing Arrays:

Location	Latitude	Longitude
SBB2-1, Southwest End of MASW/Refraction Array	34.68803	-117.82466
SBB2-1, Center of MASW/Refraction Array	34.68833	-117.82453
SBB2-1, Northeast End of MASW/Refraction Array	34.68862	-117.82440
HVSR Sensor 450	34.68803	-117.82464
HVSR Sensor 453	34.68862	-117.82441
HVSR Sensor 507	34.68848	-117.82421
CI.SBB2 Seismic Station	34.68844	-117.82420

Notes: 1) WGS84 Coordinate System (decimal degrees)
2) Survey accuracy is estimated at 1 to 2 m.

Results:

V_S Model (MASW Array)

Depth to Top of Layer (m)	Layer Thickness (m)	S-Wave Velocity (m/s)	Inferred P-Wave Velocity (m/s)	Assumed Poisson's Ratio	Assumed Density (g/cm^3)
0	1	240	449	0.3	1.80
1	2	410	767	0.3	2.00
3	3	1015	1900	0.3	2.15
6	4	1144	2141	0.3	2.20
10	5	1399	2617	0.3	2.30
15	6	1845	3452	0.3	2.40
21	8	2102	3932	0.3	2.50
29	>6	2552	4774	0.3	2.60

Notes: 1) Depth of investigation is about 35 m.
2) Bottom layer is a half space.
3) Half space velocity not well constrained.

Average V_P and Estimated V_S Models from Central Portion of P-wave Seismic Refraction Line

Depth to Top of Layer (m)	Layer Thickness (m)	P-Wave Velocity (m/s)	Estimated S-Wave Velocity (m/s)				
			Poisson's Ratio = 0.25	Poisson's Ratio = 0.3	Poisson's Ratio = 0.333	Poisson's Ratio = 0.35	Poisson's Ratio = 0.4
0.00	0.43	454	262	242	227	218	185
0.43	0.86	863	498	461	431	414	352
1.29	0.86	1226	708	655	613	589	500
2.15	0.86	1504	868	804	752	722	614
3.00	0.86	1881	1086	1006	941	904	768
3.86	0.86	2001	1155	1070	1001	961	817
4.72	0.86	2127	1228	1137	1064	1022	868
5.58	1.80	2408	1390	1287	1204	1157	983
7.38	1.80	2605	1504	1392	1303	1251	1063
9.18	1.80	2831	1634	1513	1415	1360	1156
10.98	1.80	3205	1851	1713	1603	1540	1309
12.79	1.80	3335	1925	1782	1667	1602	1361
14.59	1.80	3456	1995	1847	1728	1660	1411
16.39	1.80	3553	2051	1899	1777	1707	1451
18.19	1.80	3706	2140	1981	1853	1780	1513
19.99	Half Space	3805	2197	2034	1903	1828	1553

Observations/Discussion:

- There are no distinct HVSR peaks at the site as expected for a rock site.
- The P-wave seismic refraction data for array SBB2-1 were modeled using a tomographic inversion routine with a smooth velocity gradient starting model. The P-wave seismic refraction model was extended to far offset shot locations to extend depth of investigation. It should be noted that a larger geophone spacing, rather than the utilization of far offset shot locations, is preferred for extending depth of investigation, when applying tomographic inversion routines. However, the seismic refraction data were acquired in conjunction with surface wave data, where a shorter array length is preferred.
- The P-wave seismic refraction survey design allowed P-wave velocity to be imaged to a maximum depth of about 22 m. The seismic refraction model indicates that P-wave velocity is about 250 to 700 m/s at the surface and increases to over 1,500 m/s at a depth of 1 to 4 m, 2,500 m/s at a depth of 2.5 to 10 m and over 3,500 m/s at a depth of 10 to 16 m. The maximum P-wave velocity in the central portion of the model, where depth of investigation is greatest, is close to 4,000 m/s.

- The seismic refraction survey indicates that there is significant lateral velocity variation at the site, as is often the norm for rock sites.
- The average P-wave velocity of the upper 30 m (V_{P30}) was estimated between 19.5 and 54 m on the P-wave refraction model, where depth of investigation is greatest. To estimate $V_{P30,}$ the P-wave velocity at a depth of 22 m, nominal depth of investigation, was projected to 30 m depth. V_{P30} ranges from about 2,153 to 2,878 m/s over the 19.5 to 54 m position interval, a 28% variation over a distance of 34.5 m.
- An average V_P model was developed over the 19.5 to 54 m distance interval by horizontally averaging the travel time of each model cell and the cell thickness and average V_{P30} was determined to be 2,537 m/s. Assuming constant Poisson's ratios of 0.25, 0.3, 0.3333, 0.35 and 0.4 would result in an estimated V_{S30} of 1,465, 1,356, 1,269, 1,219 and 1,036 m/s, respectively. Saturation is not expected in the upper 30 m and, therefore, Poisson's ratio of the weathered rock is not expected to be higher than 0.333.
- Noise conditions at the site were not sufficient for application of passive surface wave techniques.
- The lateral velocity variation at the site was such that MASW data reduction was quite difficult. Coherent dispersion data were only obtained at wavelengths greater than about 40 m using long (i.e. 36 to 48 geophone) receiver arrays. Small wavelength (high frequency) dispersion data were extracted from limited offset receiver arrays from end shot and interior source locations. It was particularly difficult extracting intermediate wavelength (15 to 35 m) dispersion data and the near field criteria typically applied during this investigation had to be significantly relaxed to fill in the intermediate wavelength range. The maximum wavelength dispersion data extracted from the data set was 80 m. About 85% of the picked dispersion curves were used for analysis. The lowest Rayleigh wave phase velocities at small wavelengths originated from interior source locations near thicker zones of low velocity near surface rock and were not used for analysis. The lateral velocity variation at this site is severe enough to where V_S models developed from surface wave techniques may not be representative of average velocity structure beneath the array.
- The minimum wavelength surface wave phase velocity data extracted from the 48-channel MASW array is about 38 m. Data reduction using seismic records from smaller hammer sources and a limited offset receiver array (i.e. less active geophones) allowed extraction of surface wave dispersion data to a minimum wavelength of about 4 m.
- There is nominally about 125 to 175 m/s scatter in MASW dispersion data selected for modeling, likely due to the effects of lateral velocity variation.
- A representative dispersion curve was generated for the MASW data set using a moving average, polynomial curve fitting routine and used for modeling.
- The Rayleigh wave dispersion curve was modeled using the fundamental mode assumption.
- Although a minimum Rayleigh wave wavelength of only 4 m was obtained from the MASW data, a 1 m thick low velocity layer was permitted in the V_S model based on observations in the seismic refraction data.
- Surface wave depth of investigation is about 35 m based on the one half of maximum wavelength criteria.

- There is acceptable agreement between the average V_S models calculated from the P-wave seismic refraction model assuming constant values of Poisson's ratio and the V_S model resulting from inversion of the Rayleigh wave phase velocity data.
- Subsequent analysis of the V_S model derived from the surface wave data based on the fundamental mode assumption indicates that the first higher mode is expected to be dominant over a wide frequency range and that average/effective mode modeling should be considered. However, the fundamental mode V_S model is in reasonable agreement with the P-wave refraction data and it is possible that lateral velocity variation is such that the Rayleigh wave dispersion curve derived from the MASW data more closely reflects the fundamental mode. Effective mode or multi-mode modeling was, therefore, not attempted on this dataset. More research is needed into the effects of lateral velocity variation on both the amplitude of higher mode surface waves and the validity of surface wave V_S models.
- V_{S30} from the MASW V_S model is 1,131 m/s (NEHRP Site Class B).
- Average S-wave velocity between a depth of 1 and 31 m, to account for assumed seismic sensor depth, is 1,319 m/s (NEHRP Site Class B).
- V_{S30} from the average P-wave seismic refraction model and assumed constant Poisson's ratio of 0.3 and 0.3333 is 1,356 and 1,269 m/s (Site Class B), respectively, 20 and 12% higher than that measured using the MASW technique. The lowest V_{P30} in the central portion of the P-wave seismic refraction model (position of 36 m) is 2,153 m/s, resulting in estimated V_{S30} of 1,151 and 1,077 m/s for an assumed constant Poisson's ratio of 0.3 and 0.3333, respectively. The lower bound of V_{S30} estimated from the P-wave refraction model is more consistent with the MASW V_S model.
- Average S-wave velocity between a depth of 0.5 (approximate base of lowest velocity sediment layer) and 30.5 m from the average P-wave velocity model is 1,585, 1,468, 1,373, 1,319 and 1,121 m/s for assumed constant Poisson's ratios of 0.25, 0.3, 0.3333, 0.35 and 0.4, respectively.
- For site characterization purposes, the use of the MASW V_S model is recommended. This model may reflect the lower bound of V_{S30} in the site vicinity. Alternatively, the seismic refraction model may reflect the upper bound of V_{P30} and estimated V_{S30}, if out of plane refractors occur as first arrivals beneath segments of the seismic line. It is always a possibility in weathered rock environments that the smallest P- or S-wave travel time between source and receiver is not through material directly beneath the array. The seismic refraction model indicates that there is more than 28% variation of V_{P30}, and therefore V_{S30}, over distances as small as 34 m. It is difficult to precisely predict the effects of lateral velocity variation of the surface wave dispersion data and resulting V_S model and estimated V_{S30} is probably more accurate than the actual V_S models.
- The site is characterized as having V_{S30} in the mid to upper velocity range of NEHRP Site Class B. Based on lateral velocity variation observed in the seismic refraction data there are possibly localized areas on the bedrock outcrop where adjusted V_{S30} is NEHRP Site Class A.

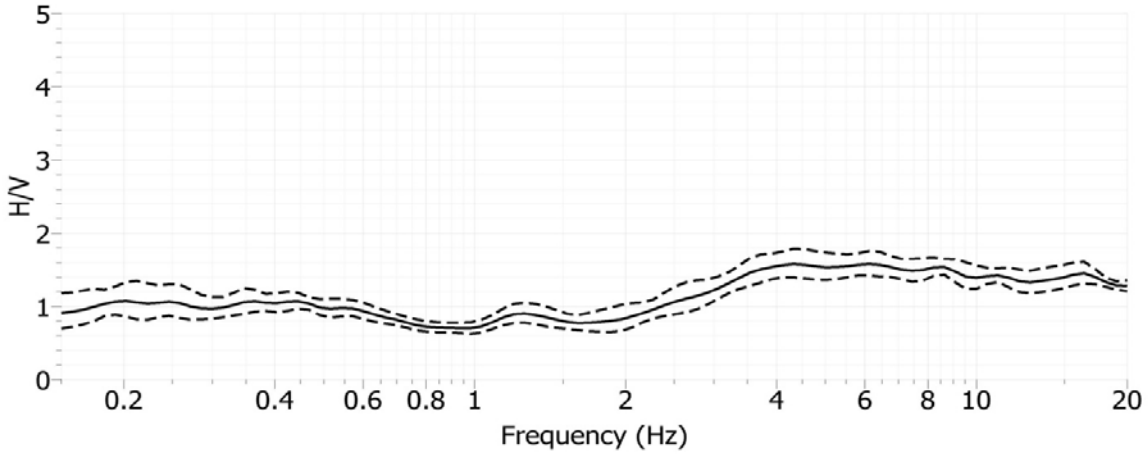

Site CI.SBB2, H/V Spectral Ratio, Array SBB2-1, Sensor 453

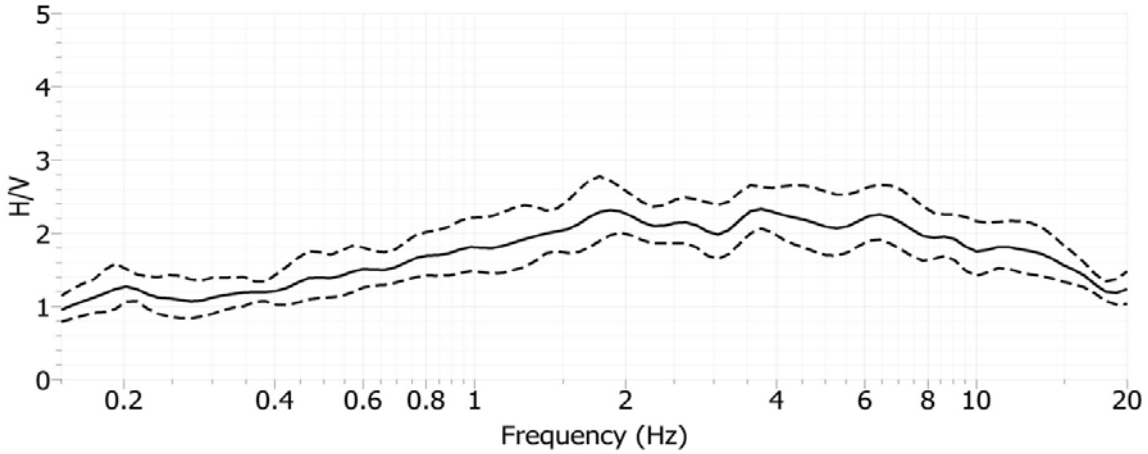

Site CI.SBB2, H/V Spectral Ratio, Near Seismic Station, Sensor 507

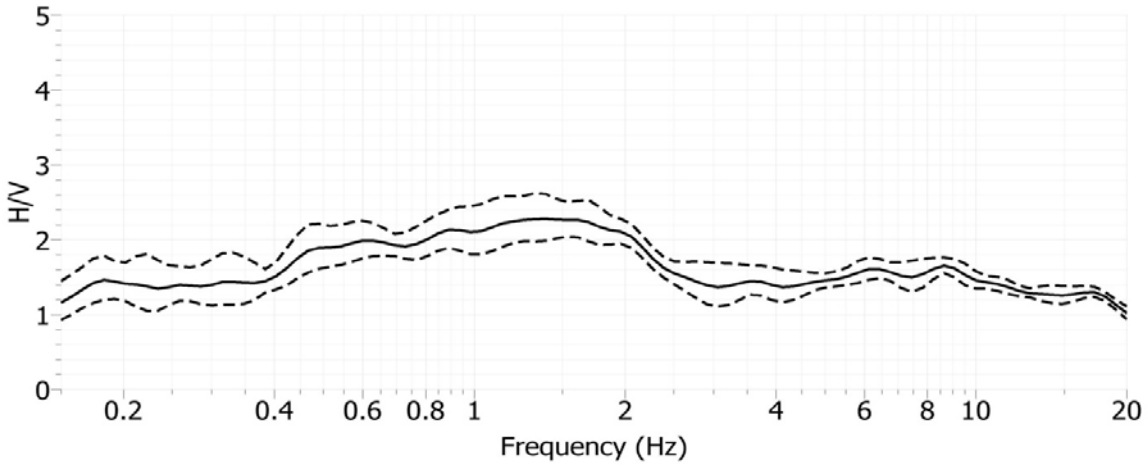

Site CI.SBB2, H/V Spectral Ratio, Array SBB2-1, Sensor 450

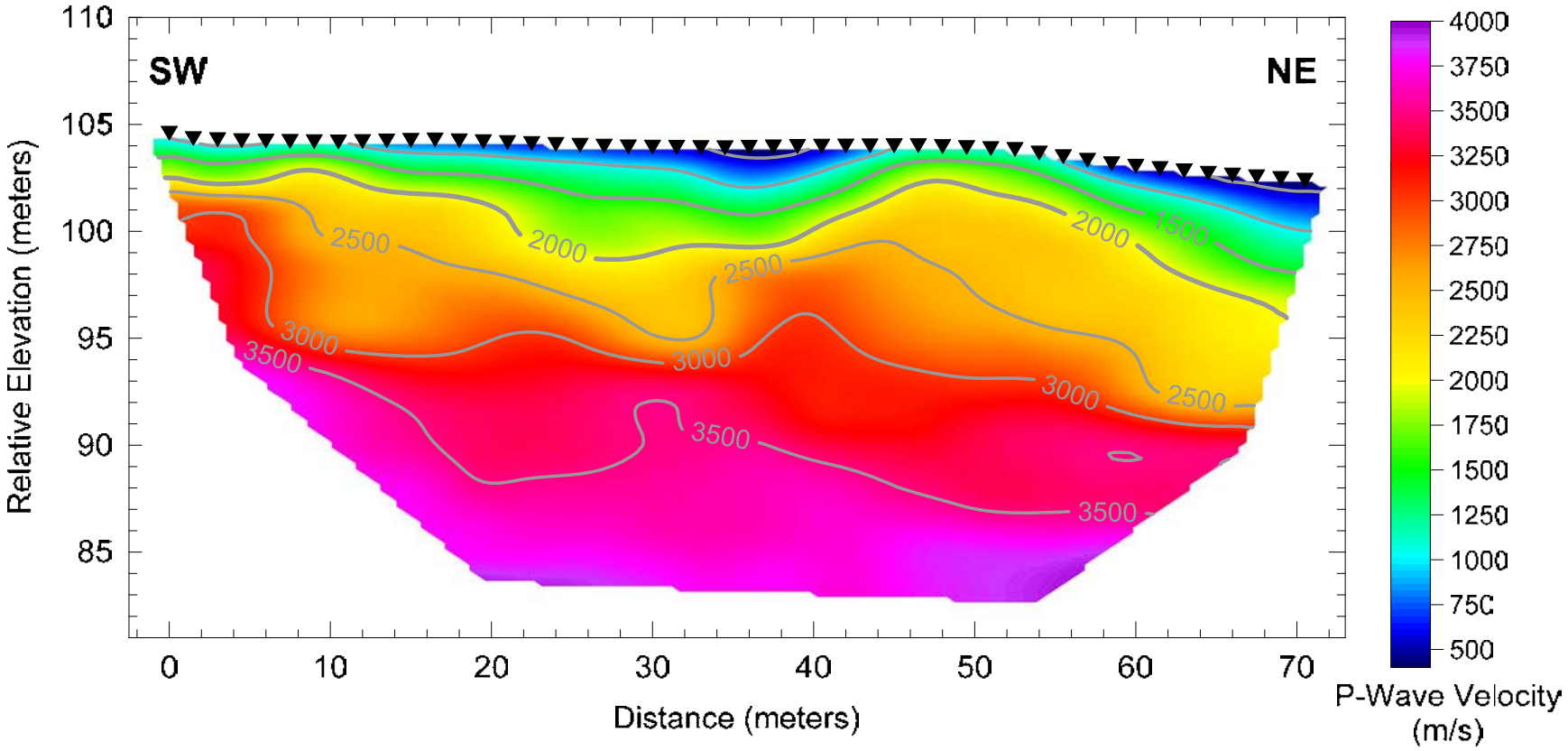

Array SBB2-1 – P-wave tomographic seismic refraction model developed utilizing a smooth velocity gradient starting model

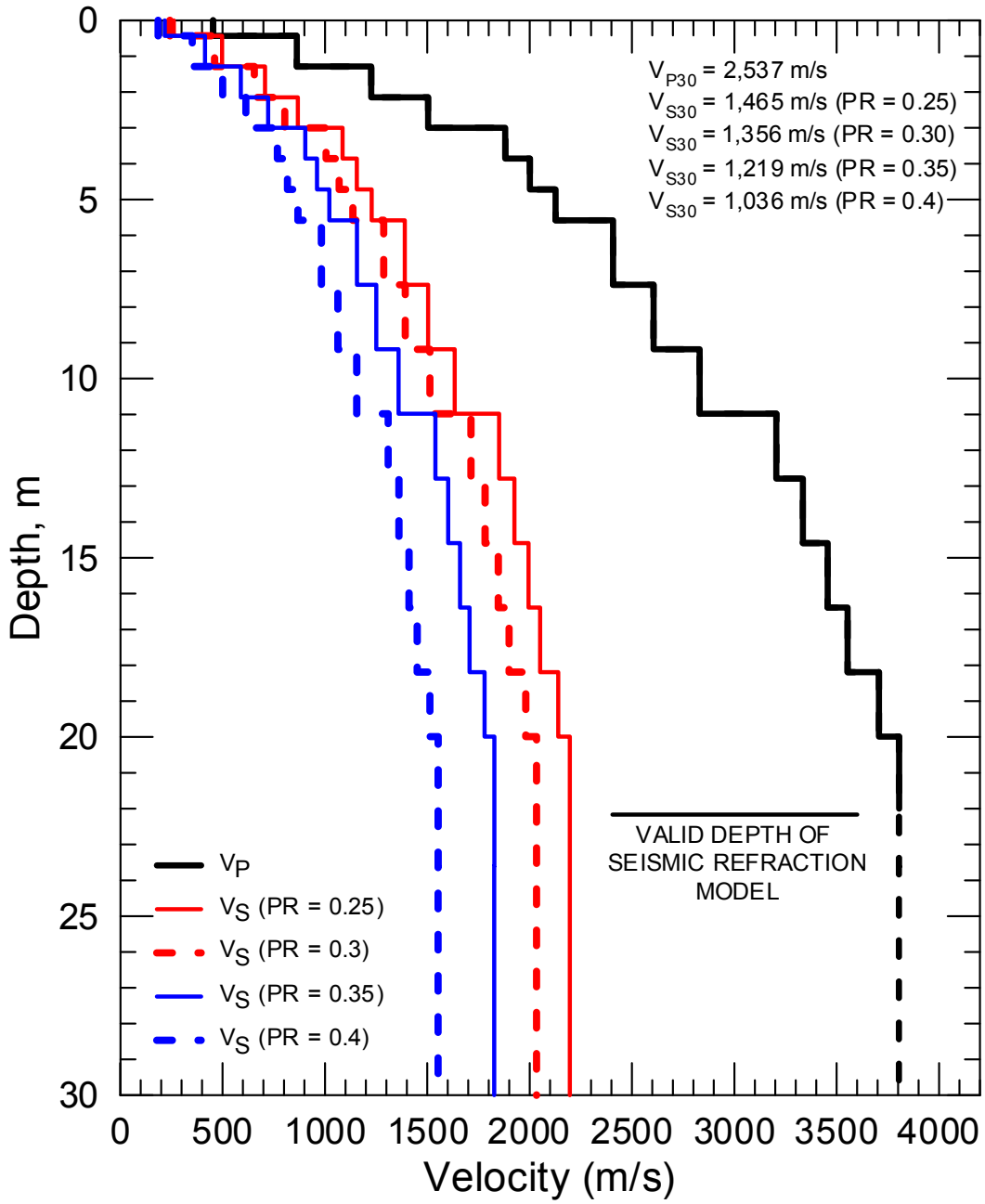

CI.SBB2 – Average P-wave velocity structure and estimated S-wave velocity structure between a distance of 19.5 and 54 m along the P-wave seismic refraction model for array SBB2-1. Maximum seismic refraction depth of investigation is limited to about 22 m and P-wave velocity is assumed to be constant between 22 and 30 m. P-wave velocity is very high at a depth of 22 m and not expected to increase significantly between 22 and 30 m.

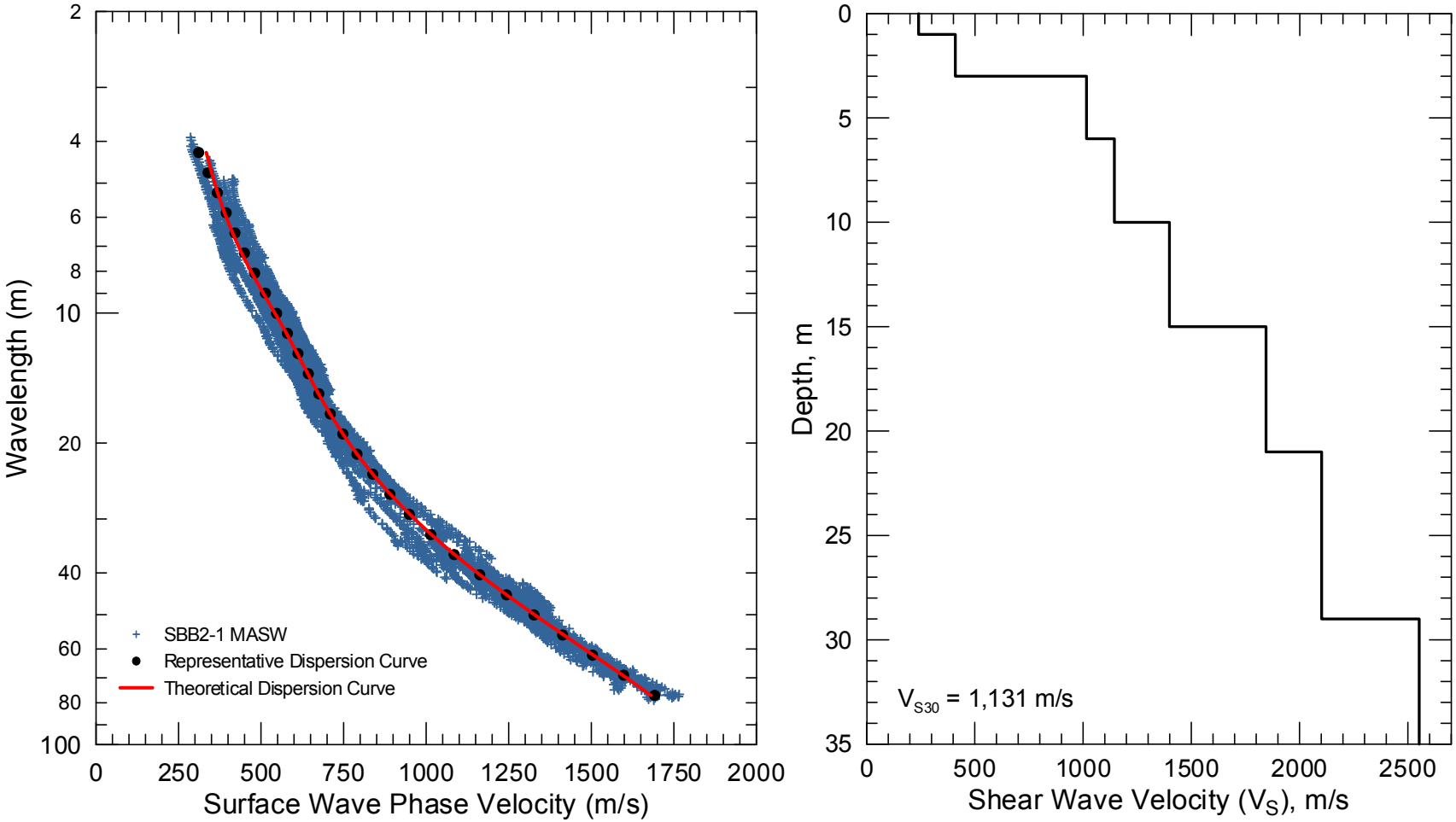

CI.SBB2 - Field, representative and inverted theoretical surface wave dispersion data (left) and associated V_S model (right)

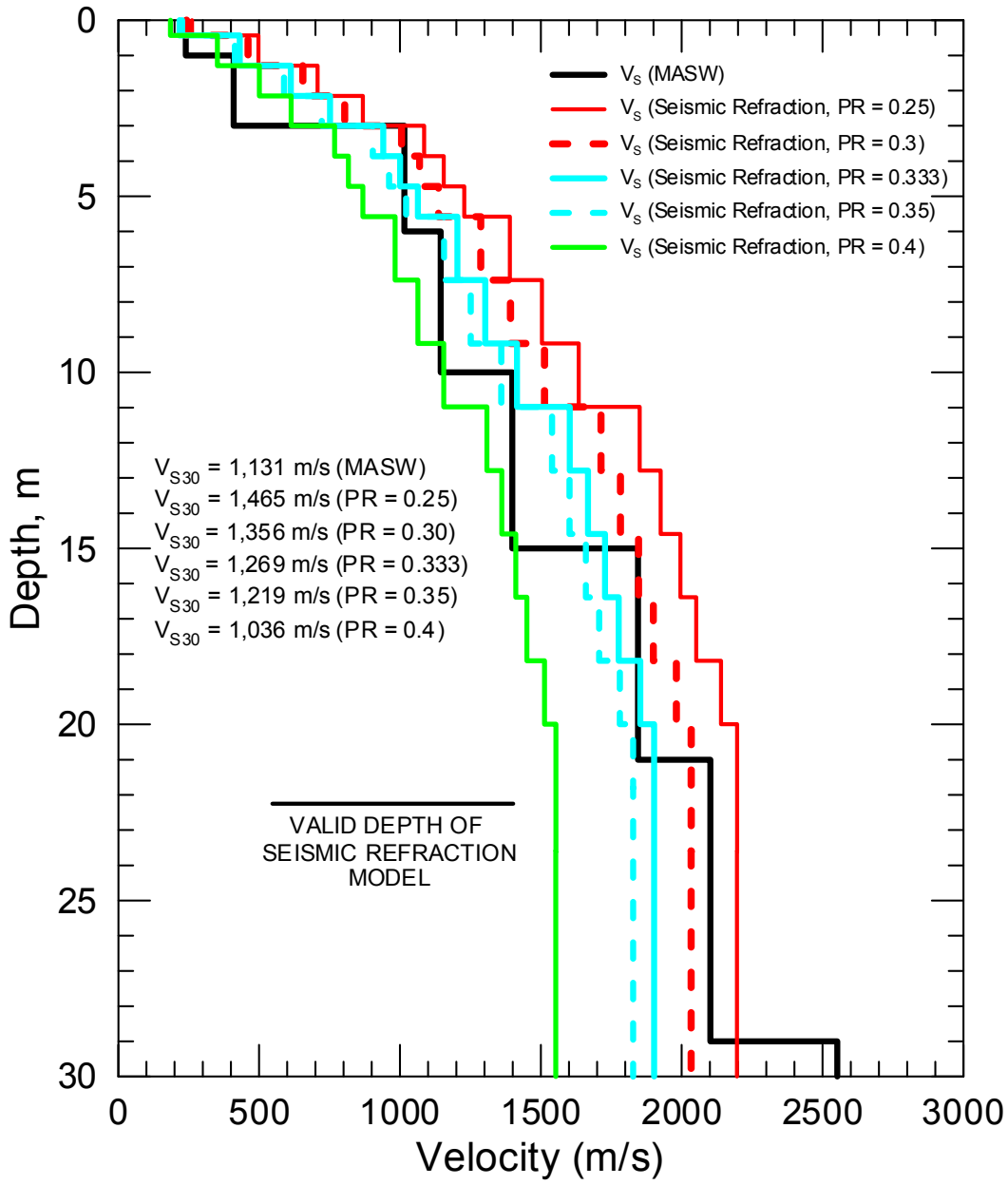

CI.SBB2 – Comparison of S-wave velocity models derived from the array SBB2-1 MASW and average P-wave velocity model using constant Poisson's ratio in the 0.25 to 0.4 range. The MASW V_S model underestimates V_{S30} relative to the P-wave refraction model with a Poisson's ratio in the 0.3 to 0.33 range. V_{P30} estimated from the average V_P model varies by ±15% in the central portion of the seismic line and it is possible that the MASW V_S model is biased towards the lower velocities. Alternatively, if out of plane refractors give rise to seismic refraction first arrivals then the seismic refraction model would be biased towards the higher velocities in the immediate vicinity of the array.

Site CI.SBC

Location: Santa Barbara Museum, Santa Barbara, California

Latitude: 34.44076 **Longitude:** -119.71492
(Station coordinates provided by USGS, WGS84 coordinate system)

V_{S30} (measured): 485 m/s

V_{S30} (adjusted to more accurately reflect seismic station conditions): 507 m/s (average S-wave velocity between 3 and 33 m adjusting for sensor being located in a basement).

NEHRP Site Class: C

Geomatrix Code: CHD

Geologic Conditions/Observations: Site located in area mapped as Quaternary (Holocene) alluvium, near deposits of older Pleistocene alluvium and younger Holocene stream channel deposits. The inferred location of the Mission Ridge Fault is located about 300 m northwest of the site.

Site Conditions: Urban site with significant traffic noise from nearby roads. Gentle topographic decline to south/southwest in site vicinity. Seismic station located at basement level inside museum building.

Geophysical Methods Utilized: HVSR, MASW, array microtremor, ReMi™

Geophysical Testing Arrays:

1. Arrays SBC-1 (24 channel linear array utilizing 4.5 Hz vertical geophones spaced 3 m apart for an array length of 69 m) and SBC-2 (24 channel linear array utilizing 4.5 Hz vertical geophones spaced 4 m apart for an array length of 92 m) used to acquire passive surface wave data. Arrays combined to form an "L" shaped array.
2. Array SBC-3 (48 channel array utilizing 4.5 Hz vertical geophones spaced 1 m apart for a length of 47 m, forward and reverse shot locations with multiple source offsets and source types (hammers only) and center shot location).
3. Three HVSR measurement locations distributed along arrays SBC-2 and SBC-3.

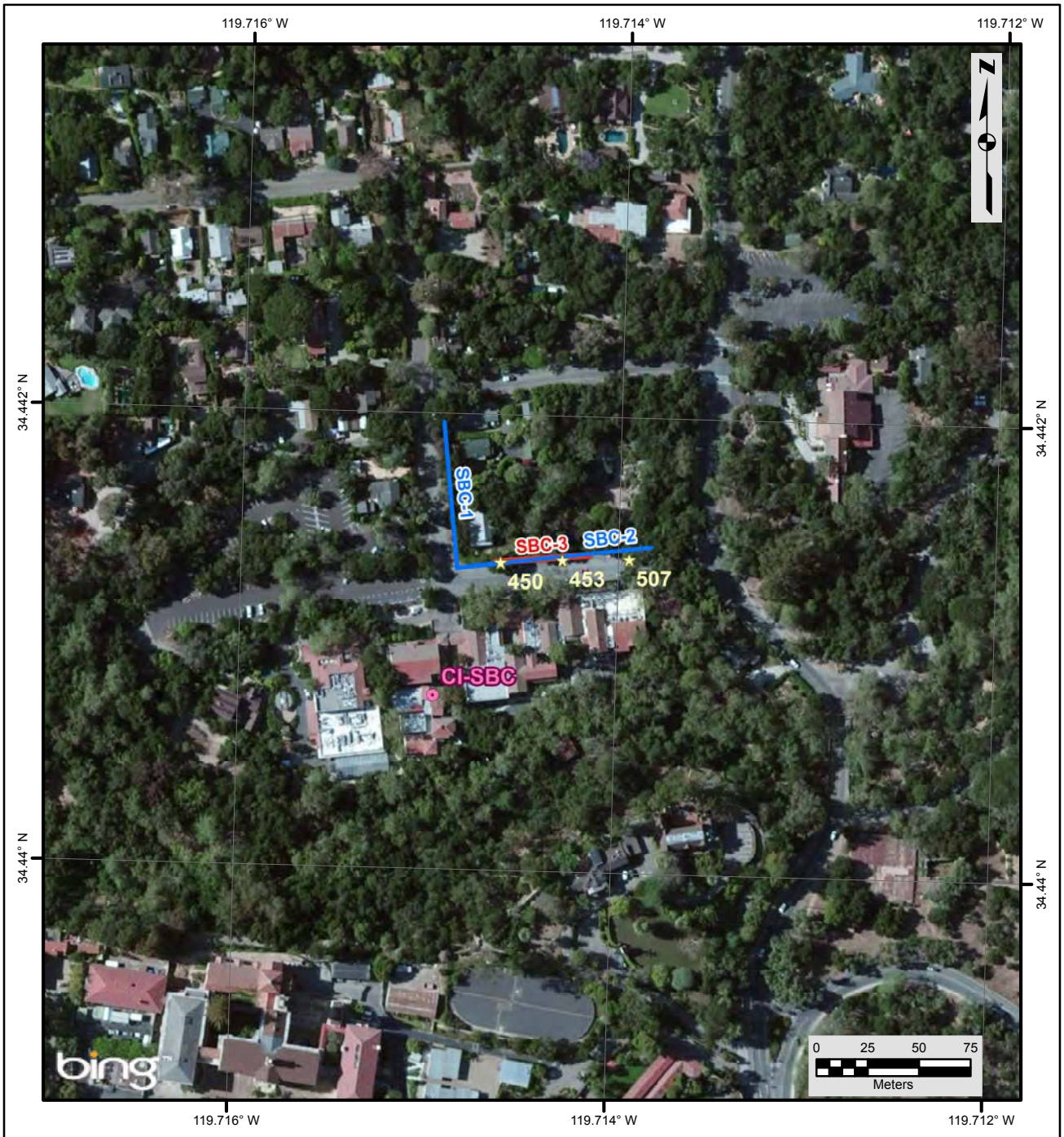

Legend

- Seismic Station - Approximate Location of Record
- H/V Spectral Ratio Location
- Passive Surface Wave Array
- MASW Array

NOTES:
1. WGS 1984 COORDINATE SYSTEM
2. Image Source: (c) Microsoft Corporation and its data suppliers

File Name: CI-SBC-I

Date: 2/7/2013

USGS science for a changing world

GEOVision geophysical services

RECOVERY.GOV

SITE MAP
CI•SBC

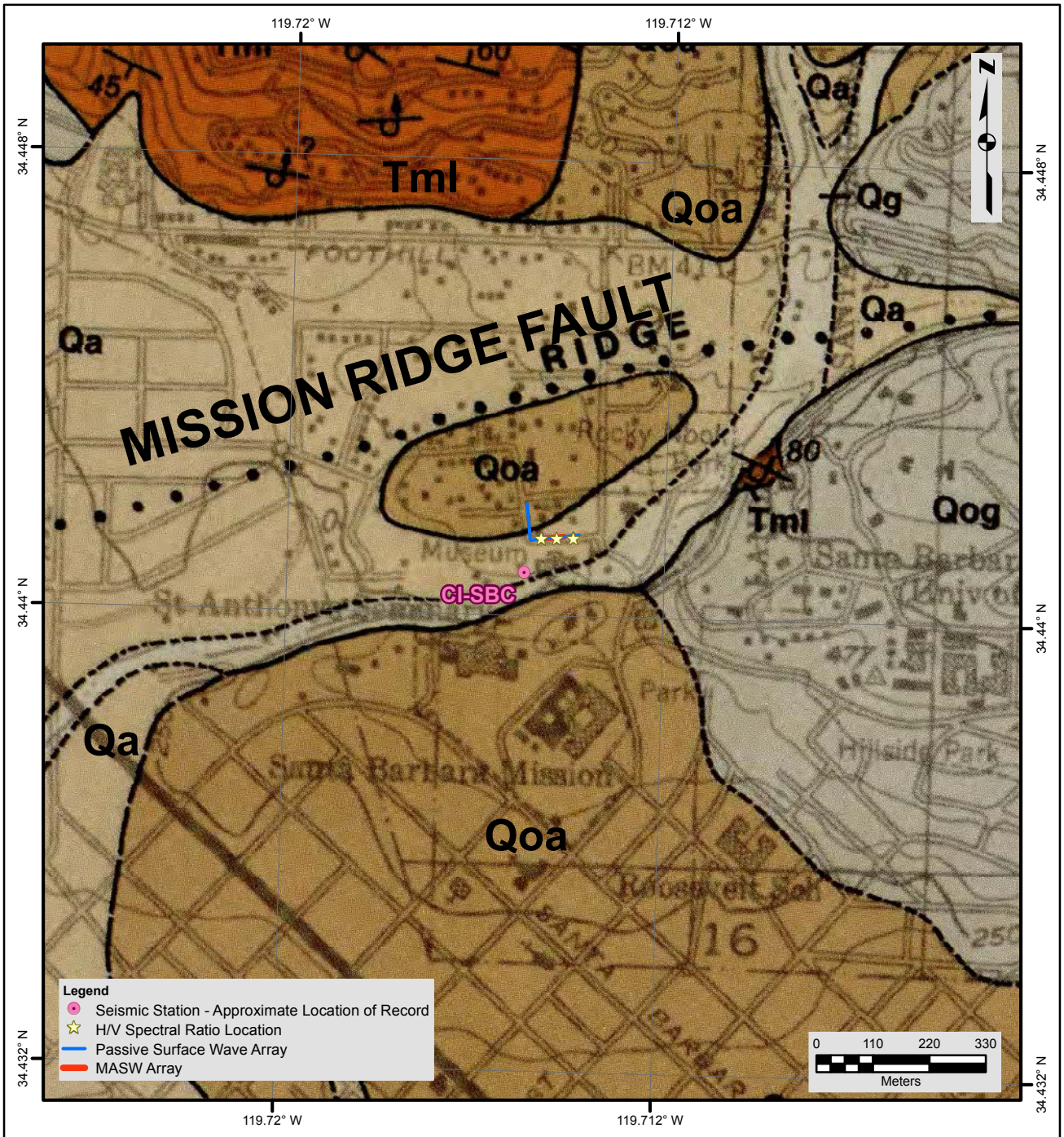

Description of Geologic Map Units

Qg = Quaternary (Holocene) stream channel deposits, mostly gravel and sand
Qa = Quaternary (Holocene) alluvium, unconsolidated floodplain deposits of silt, sand and gravel
Qoa = Quaternary (Pleistocene) former alluvial deposits of silt, sand and gravel
Qog = Quaternary (Pleistocene) cobble-boulder fan gravel and fanglomerate deposits
Tml = Tertiary (Miocene) Monterey Formation; lower shale unit, soft, marine clay shale with interbeds of hard siliceous shale and thin limestone strata

NOTES:
1. WGS 1984 COORDINATE SYSTEM
2. Geologic Map of the Santa Barbara Quadrangle, Santa Barbara County, California by Thomas W. Dibblee, Jr., 1986
3. See site map for details of geophysical survey

File Name: CI-SBC
Date: 2/7/2013

USGS science for a changing world
GEOVision geophysical services

GEOLOGIC MAP
CI•SBC

RECOVERY.GOV

CI.SBC seismic station

Looking south along passive surface wave array SBC-1

Looking west along MASW array SBC-3

Looking west along passive array SBC-2 and at HVSR sensors 450 (Trillium Compact) and Tromino ENGR

Looking east along passive surface wave array SBC-2

Location of Geophysical Testing Arrays:

Location	Latitude	Longitude
SBC-1, North End of Passive Array	34.44195	-119.71489
SBC-1, South End of Passive Array	34.44132	-119.71481
SBC-2, West End of Passive Array	34.44133	-119.71478
SBC-2, East End of Passive Array	34.44143	-119.71379
SBC-3, West End of MASW Array	34.44135	-119.71460
SBC-3, Center of MASW Array	34.44137	-119.71436
SBC-3, East End of MASW Array	34.44139	-119.71411
HVSR Sensor 450	34.44135	-119.71458
HVSR Sensor 453	34.44137	-119.71425
HVSR Sensor 507	34.44138	-119.71390

Notes: 1) WGS84 Coordinate System (decimal degrees)
2) Survey accuracy is estimated at 3 to 4 m.

Results:

V_S Model

Depth to Top of Layer (m)	Layer Thickness (m)	S-Wave Velocity (m/s)	Inferred P-Wave Velocity (m/s)	Assumed Poisson's Ratio	Assumed Density (g/cm^3)
0	1	319	596	0.300	1.9
1	1.5	415	777	0.300	1.9
2.5	2.5	438	819	0.300	1.9
5	8	471	1900	0.467	2.0
13	10	494	1900	0.464	2.0
23	12	574	1900	0.450	2.0
35	>10	666	1900	0.430	2.1

Notes: 1) Saturated sediments with V_P = 1,900 m/s estimated at a depth of about 5 m based on seismic refraction data.
2) Depth of investigation is about 45 m.
3) Bottom layer is a half space.

Observations/Discussion:

- Geophysical testing was conducted on the streets near the Santa Barbara Museum. The parking lot next to the museum had heavy traffic at the time of the field investigation (early evening). MASW testing in the parking lot would have been preferred, although it may be difficult to find a time when the parking lot is not in use. Testing at night is not possible due to nearby residences, although HVSR data collection at night would have been preferred.
- Three geologic units are mapped in the site vicinity: Holocene stream channel deposits, Holocene alluvium and Pleistocene old alluvium. The seismic station is mapped as being located on Holocene alluvium. The MASW array and one passive array (one leg of the "L" array) are located on mapped Holocene alluvium. The other passive array is primarily located on mapped Pleistocene alluvium. These geologic units could not be differentiated in the field due to development.
- Transient noise from nearby vehicle traffic complicated HVSR data reduction.
- The HVSR curves are almost identical although there are, however, no significant high frequency HVSR peaks to characterize variability of shallow velocity structure.
- There is no distinct high amplitude HVSR peak at the site. There is a possible, but inconclusive, low amplitude peak in the 0.2 Hz range, which would be indicative of very deep bedrock.
- Seismic refraction first arrival data on the MASW seismic records were reviewed and there is a possibility that saturated sediments with P-wave velocity of about 1,900 m/s may be present at a depth on the order of 5 m. Depth is very approximate because a high velocity wave propagating through the asphalt limited our ability to accurately determine the average velocity of the unsaturated sediments. The possibility cannot be discounted that the possible saturated layer is just a thin perched water zone.
- Noise conditions at site (multi-directional or omni-directional noise sources) appeared sufficient for successful application of passive surface wave techniques.
- The ESAC technique was used to extract surface wave dispersion data from passive "L" array data. Both the ReMi™ and ESAC techniques were used to extract surface wave dispersion data from the linear arrays. Surface wave dispersion data from passive arrays SBC-1, SBC-2 and the combined L-array are different, due to apparent lateral velocity variation. The passive surface wave data acquired along linear array SBC-2 and processed using the ESAC and ReMi™ techniques are in good agreement with the MASW data (ReMi™ data is in best agreement). Passive array SBC-1 has lower phase velocities and the combined array SBC-1/2 has intermediate phase velocities.
- Due to apparent lateral velocity variation at the site the MASW data from array SBC-3 were only combined with the passive surface wave data collected along array SBC-2 and processed with the ReMi™ technique. This combined surface wave data set was used for site characterization. Both of these arrays are located on Holocene alluvium, the same geologic unit the seismic station is mapped as being on.
- The average Rayleigh wave phase velocity at a wavelength of 40 m (V_{R40}) was reviewed to assess the relative variation in V_{S30} in the immediate site vicinity. Brown, et al, 2000 published an empirical relationship between V_{R40} and V_{S30}, which is $V_{S30} = 1.045V_{R40}$ and can be used for a first order estimate of V_{S30}. V_{R40} is about 455 m/s for MASW array SBC-3, 465 m/s for the adjacent passive linear array SBC-2 processed using the ReMi™

software, 485 m/s for array SBC-2 processed using the ESAC technique, 400 m/s for passive linear array SBC-1 processed using both the ESAC and ReMi™ techniques, and 430 m/s for the combined passive arrays SBC-1 and 2 ("L" array). This site was characterized using the dispersion curves from MASW array SBC-3 and the linear passive array SBC-2 processed using ReMi™, which have an average V_{R40} of about 460 m/s. These arrays are located on the same geologic unit as the seismic station and, therefore, modeling results are considered representative of seismic station conditions. However, it should be considered that V_{S30} may be on the order of 10 to 15% lower in the immediate site vicinity, based on the lower estimated V_{R40} associated with array SBC-1.

- The minimum wavelength Rayleigh wave extracted from the linear passive array SBC-2 was about 9 m. The maximum wavelength was fixed to the length of the array, which was 92 m. The minimum wavelength Rayleigh wave extracted from the MASW data was about 2 m.
- There is about 50 m/s scatter in the MASW dispersion data, likely the result of lateral velocity variation.
- Representative dispersion curves were generated for each surface wave data set using a moving average, polynomial curve fitting routine. These individual representative dispersion curves were combined and a representative dispersion curve generated for the combined data set for data modeling.
- The saturated zone with estimated P-wave velocity of 1,900 m/s was fixed at a depth of 5 m during surface wave data modeling, based on review of seismic refraction first arrivals on the MASW seismic records.
- Surface wave depth of investigation is about 45 m based on half of maximum wavelength criteria.
- V_{S30} is 485 m/s (NEHRP Site Class C).
- Average S-wave velocity between a depth of 3 and 33 m, to account for the seismic station being located in a basement, is 507 m/s (NEHRP Site Class C).
- Average S-wave velocity of the upper 45 m (V_{S45}) is 526 m/s.

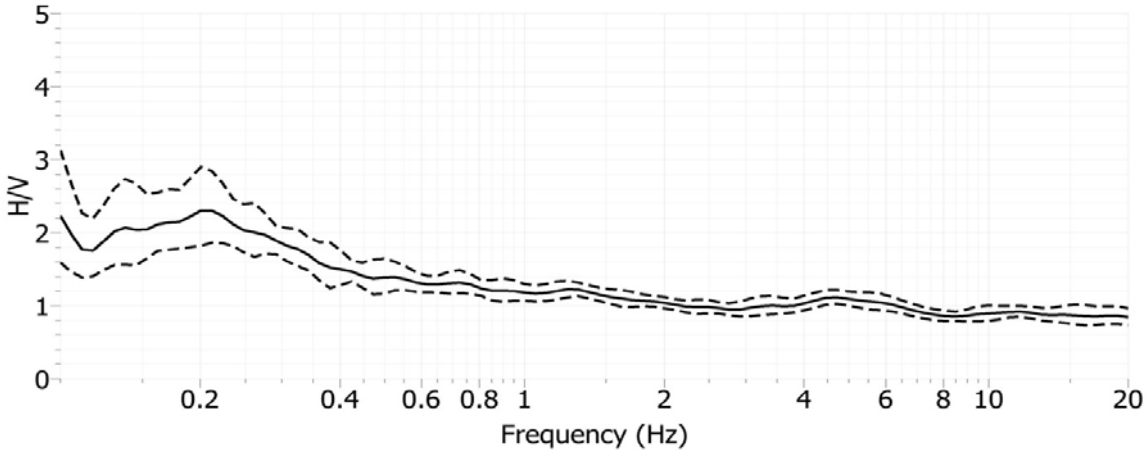

Site CI.SBC, H/V Spectral Ratio, Arrays SBC-2/3, Sensor 450

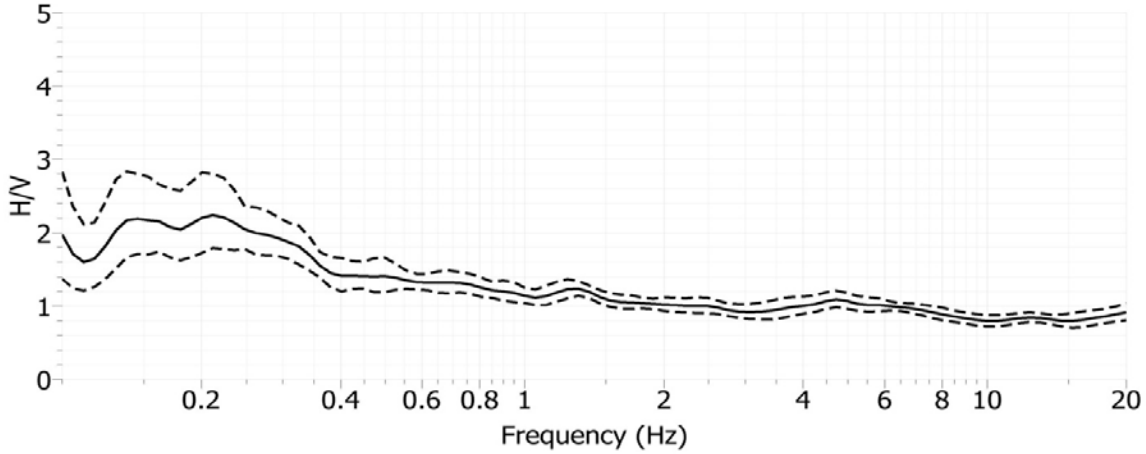

Site CI.SBC, H/V Spectral Ratio, Arrays SBC-2/3, Sensor 453

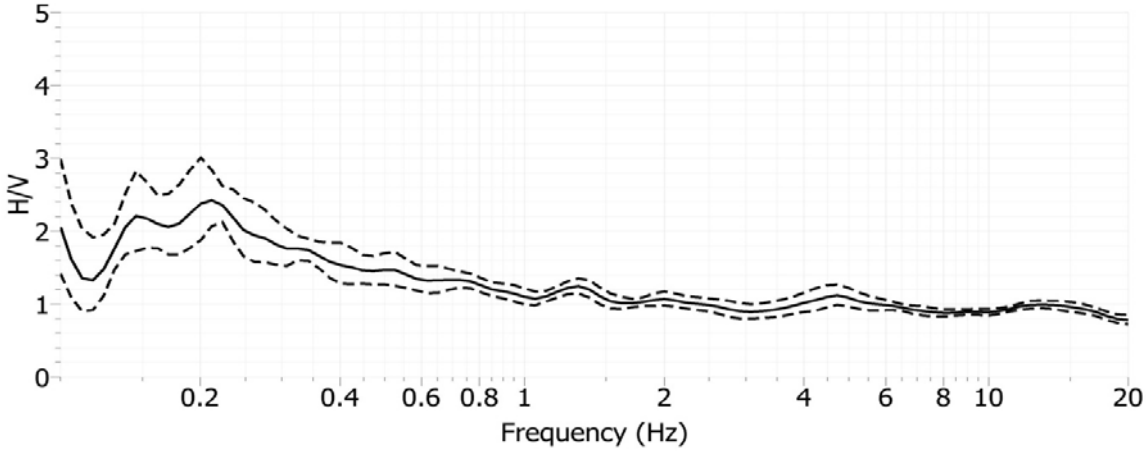

Site CI.SBC, H/V Spectral Ratio, Array SBC-2, Sensor 507

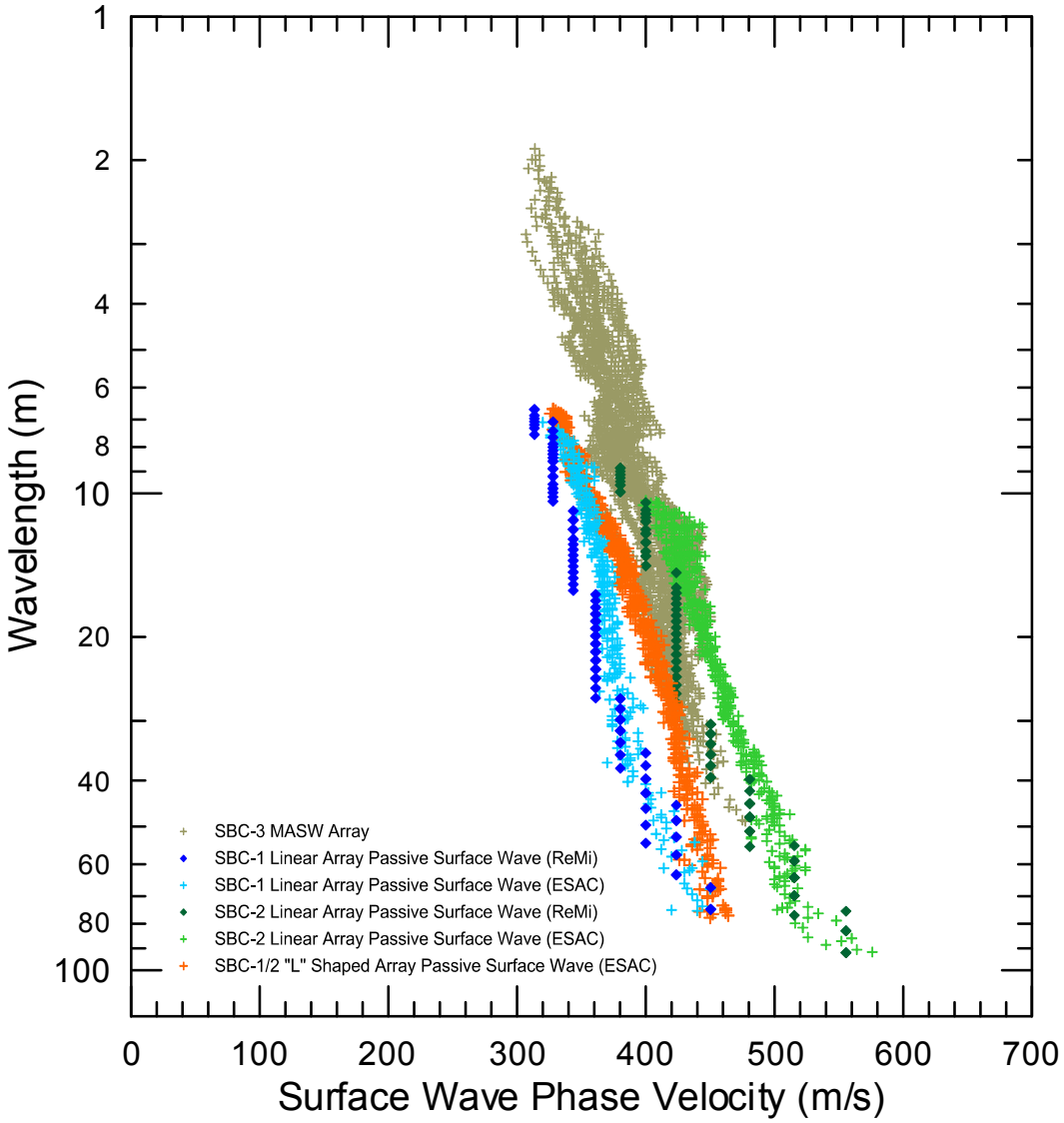

CI.SBC – Observed active and passive Rayleigh wave phase velocity data. The passive surface wave arrays consist of two linear segments (arrays SBC-1 and SBC-2), which were combined to form an "L" shaped array. Passive surface wave data were reduced from both of the linear arrays and the "L" array. The MASW array, SBC-3, was centered along linear passive surface wave array SBC-2. The linear and "L" shaped passive surface wave arrays all yield slightly different dispersion curves due to probable lateral velocity variation. As expected the "L" array yields intermediate phase velocities to the two linear arrays. The dispersion data extracted from linear passive array SBC-1 utilizing both the ESAC and ReMi™ techniques are in good agreement. There is a slight difference in the dispersion data extracted from linear passive array SBC-2 utilizing both the ESAC and ReMi™ techniques. Although this difference is not significant (maximum difference of about 20 m/s, which less than the scatter in the MASW dispersion data), the ReMi™ data are in better agreement with the MASW data and were used for modeling. Arrays SBC-1 and the combined array SBC-1/2 were not used for modeling. Modeling of array SBC-1 would likely result in an estimated V_{S30} about 10 to 15% lower than that from the combined arrays SBC-2 and SBC-3.

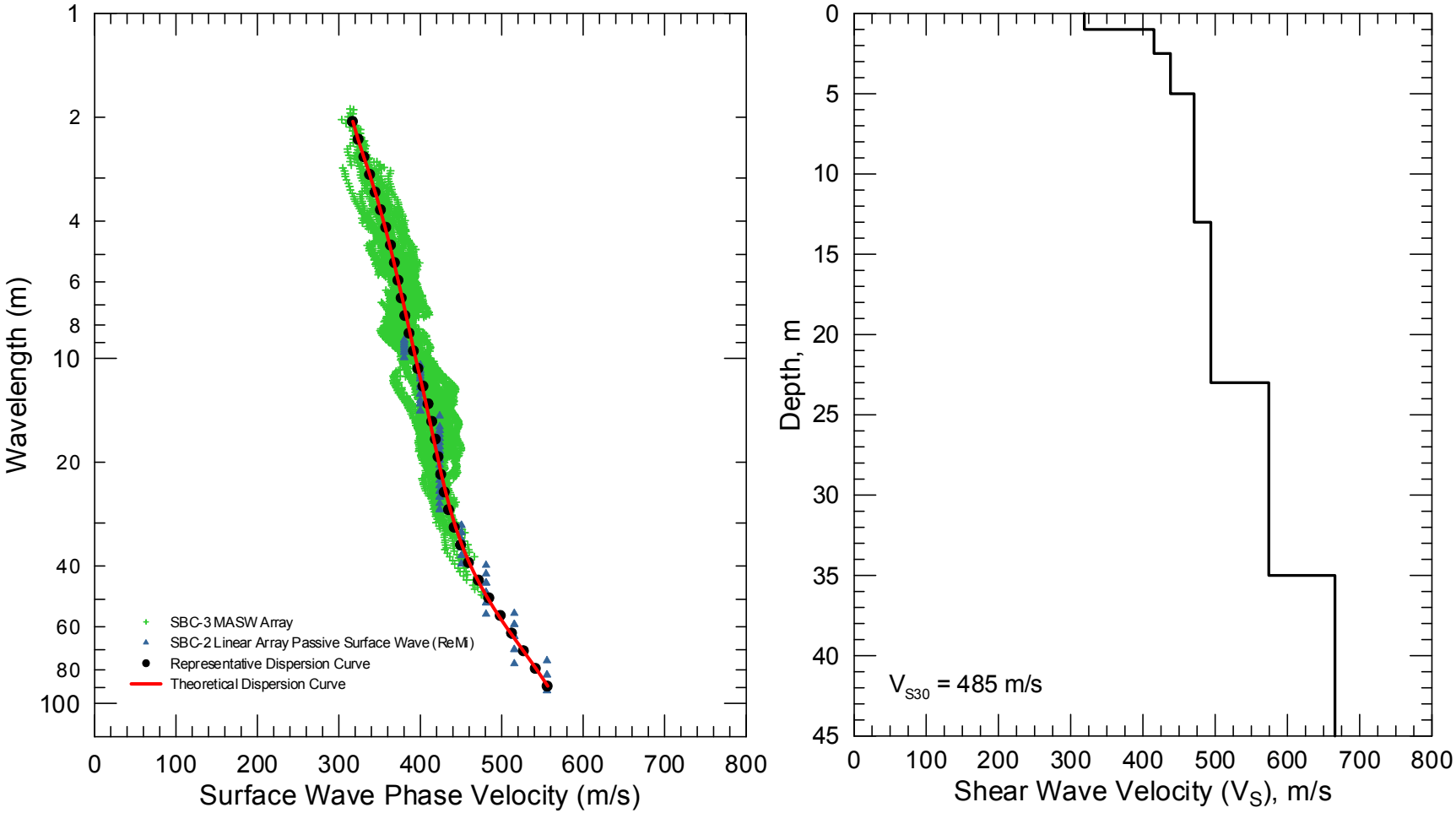

CI.SBC - Field, representative and inverted theoretical surface wave dispersion data (left) and associated V_S model (right)

Site CI.SBI

Location: Santa Barbara Island, Channel Islands, California

Latitude: 33.48046 **Longitude:** -119.02986
(Station coordinates provided by USGS, WGS84 coordinate system)

V_{S30} (measured): 854 m/s (±20% variation in site vicinity)

V_{S30} (adjusted to more accurately reflect seismic station conditions): 1,043 m/s (average S-wave velocity between 1 and 31 m adjusting for inferred 1 m sensor depth and because seismic sensors are likely placed on rock).

NEHRP Site Class: B

Geomatrix Code: KQA/KVA

Geologic Conditions/Observations: Site geologic conditions consist of a thin layer of Quaternary (Pleistocene to Holocene) old alluvium overlying Tertiary (Miocene) volcanic rocks. The seismic sensors are likely placed directly on volcanic rock.

Site Conditions: Rural site. Gentle topographic decline to the east in site vicinity. Steep cliffs at edge of ocean located about 150 m east of seismic station.

Geophysical Methods Utilized: HVSR, Seismic Refraction, MASW

Geophysical Testing Arrays:

1. Array SBI-1 (48 channel MASW and P-wave seismic refraction array utilizing 4.5 Hz vertical geophones spaced 1.5 m apart for a length of 70.5 m, forward and reverse shot locations with multiple source offsets and hammer source types and multiple interior shot locations).
2. Three HVSR measurement locations: two distributed along array SBI-1 and one adjacent to the seismic station.

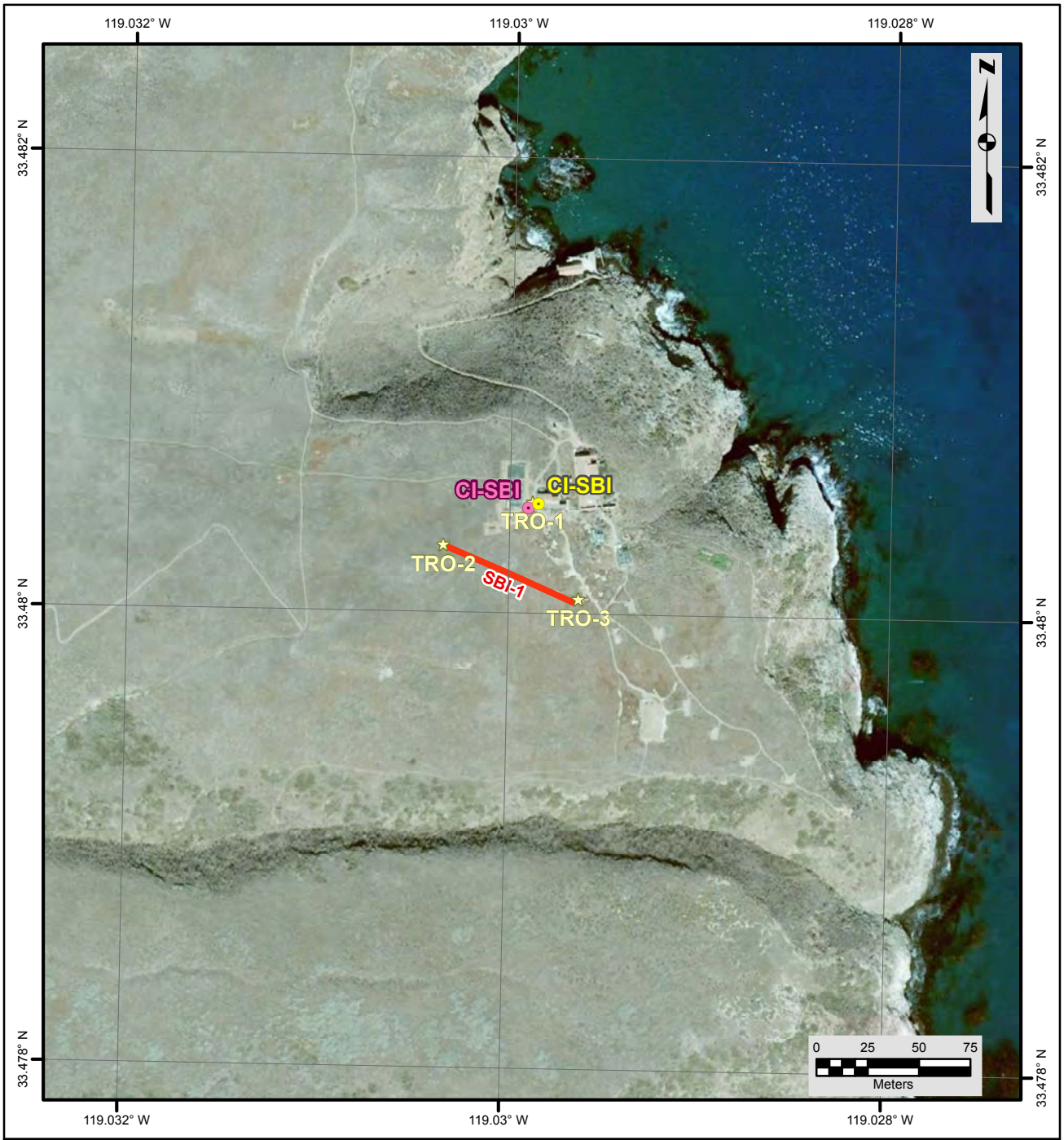

Legend

- Seismic Station - Approximate Surveyed Location
- Seismic Station - Approximate Location of Record
- H/V Spectral Ratio Location
- MASW and Seismic Refraction Array

NOTES:
1. WGS 1984 COORDINATE SYSTEM
2. Image Source: ESRI, i-cubed, USDA FSA, USGS, AEX, GeoEye, Getmapping, Aerogrid, IGP

File Name: CI-SBI-I

Date: 2/7/2013

USGS science for a changing world

GEOVision geophysical services

RECOVERY.GOV

SITE MAP
CI•SBI

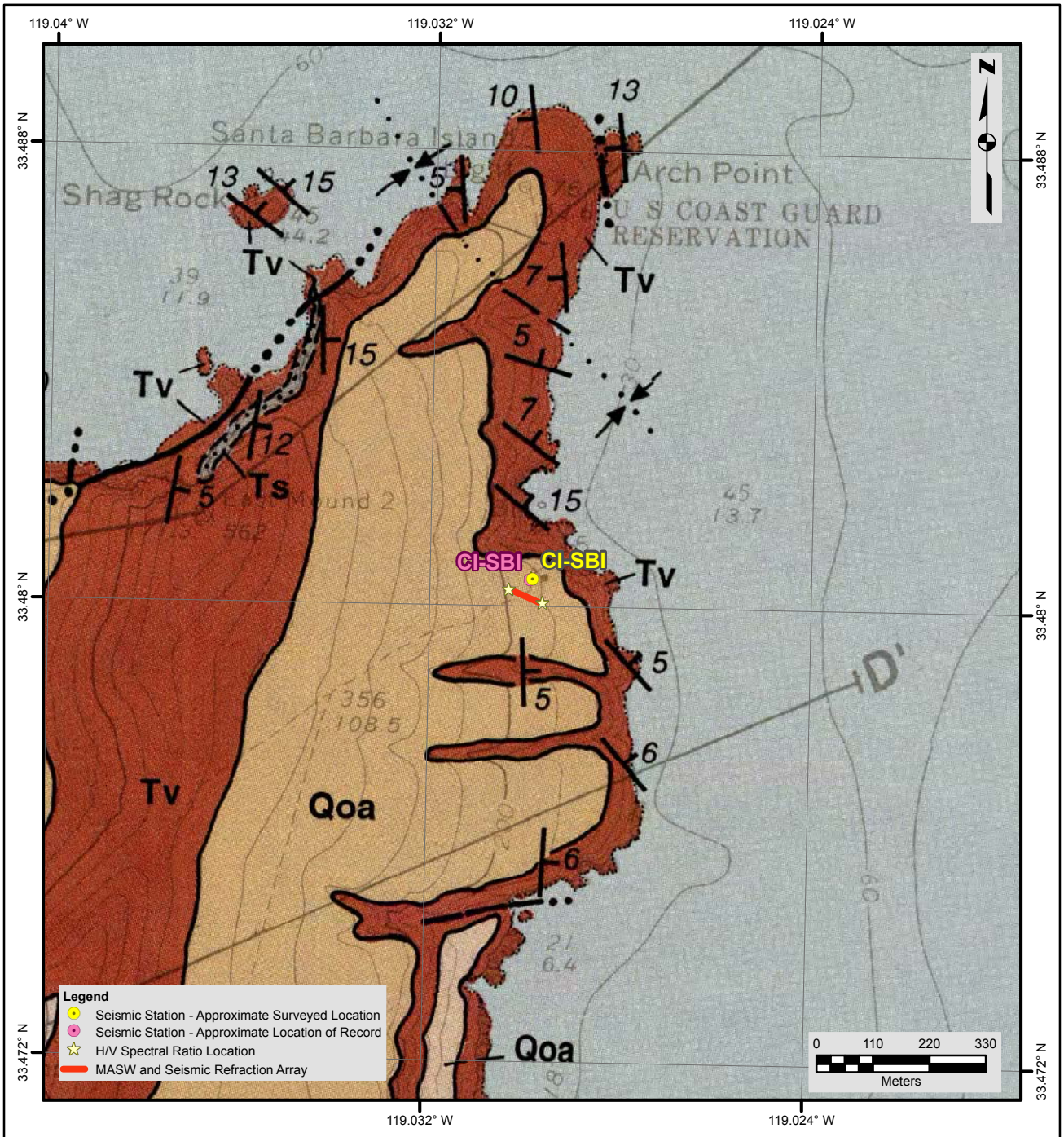

Description of Geologic Map Units

Qoa = Quaternary (Pleistocene to Holocene) old alluvium on wave-cut terraces, clay soil with thin basal conglomerate and breccia of pebbles of volcanic rocks in calcereous matrix
Tv = Tertiary (Miocene) basaltic-andesitic rock flows and flow breccias, some pillow structure, lenses
Ts = Tertiary (Miocene) sedimentary volcanic rocks - tuffaceous siltstone, claystone and shale

NOTES:
1. WGS 1984 COORDINATE SYSTEM
2. Geologic Map of Anacapa and Santa Barbara Islands, Channel Islands National Park, Ventura and Santa Barbara Counties, California by Thomas W. Dibblee, Jr., 2001
3. See site map for details of geophysical survey

File Name: CI-SBI

Date: 2/7/2013

USGS science for a changing world

GEOVision geophysical services

GEOLOGIC MAP
CI•SBI

RECOVERY.GOV

Looking north at CI.SBI seismic station (beneath solar panel)

Looking northeast at CI.SBI seismic station

Looking at HVSR sensor location TRO-1 next to seismic station

Looking southeast along array SBI-1 and at HVSR sensor TRO-2

Looking north towards location of seismic station from center of array SBI-1

Location of Geophysical Testing Arrays:

Location	Latitude	Longitude
SBI-1, Northwest End of MASW/Refraction Array	33.48029	-119.03030
SBI-1, Center of MASW/Refraction Array	33.48017	-119.02996
SBI-1, Southeast End of MASW/Refraction Array	33.48005	-119.02961
HVSR Sensor Tromino ENGY (TRO-1)	33.48049	-119.02984
HVSR Sensor Tromino ENGY (TRO-2)	33.48029	-119.03030
HVSR Sensor Tromino ENGY (TRO-3)	33.48006	-119.02959
CI.SBI Seismic Station	33.48048	-119.02981

Notes: 1) WGS84 Coordinate System (decimal degrees)
2) Survey accuracy is estimated at 1 to 2 m.

Results:

V_S Model 1FM (Lower Bound)

Depth to Top of Layer (m)	Layer Thickness (m)	S-Wave Velocity (m/s)	Inferred P-Wave Velocity (m/s)	Assumed Poisson's Ratio	Assumed Density (g/cm^3)
0	0.5	76	142	0.3	1.7
0.5	0.75	338	633	0.3	1.9
1.25	2.75	538	1007	0.3	2.0
4	6	759	1419	0.3	2.1
10	9	1057	1978	0.3	2.2
19	>11	2223	4159	0.3	2.4

Notes: 1) Data modeled assuming dispersion curve is the fundamental mode.
2) Depth of investigation is about 30 m.
3) Bottom layer is a half space.
4) Velocity of half-space not well constrained.

V_S Model 1AM (Lower Bound)

Depth to Top of Layer (m)	Layer Thickness (m)	S-Wave Velocity (m/s)	Inferred P-Wave Velocity (m/s)	Assumed Poisson's Ratio	Assumed Density (g/cm^3)
0	0.5	76	142	0.3	1.7
0.5	0.75	338	632	0.3	1.9
1.25	2.75	538	1007	0.3	2.0
4	6	759	1420	0.3	2.1
10	9	1045	1955	0.3	2.2
19	>11	1750	3274	0.3	2.4

Notes: 1) Fundamental mode V_S model adjusted assuming dispersion curve is the average mode (based on relative amplitude of the fundamental and higher surface wave modes) below 25 Hz.
2) Depth of investigation is about 30 m.
3) Bottom layer is a half space.
4) Velocity of half space not well constrained.

V_S Model 2FM (Upper Bound)

Depth to Top of Layer (m)	Layer Thickness (m)	S-Wave Velocity (m/s)	Inferred P-Wave Velocity (m/s)	Assumed Poisson's Ratio	Assumed Density (g/cm^3)
0	0.5	106	199	0.3	1.70
0.5	1	394	737	0.3	1.80
1.5	2	558	1044	0.3	2.00
3.5	2.5	731	1367	0.3	2.10
6	6	842	1574	0.3	2.10
12	8	1296	2425	0.3	2.20
20	>10	2101	3930	0.3	2.40

Notes: 1) Data modeled assuming dispersion curve is the fundamental mode.
2) Depth of investigation is about 30 m.
3) Bottom layer is a half space.
4) Velocity of half-space not well constrained.

V_S Model 2AM (Upper Bound)

Depth to Top of Layer (m)	Layer Thickness (m)	S-Wave Velocity (m/s)	Inferred P-Wave Velocity (m/s)	Assumed Poisson's Ratio	Assumed Density (g/cm^3)
0	0.5	106	198	0.3	1.7
0.5	1	394	737	0.3	1.8
1.5	2	558	1044	0.3	2.0
3.5	2.5	731	1368	0.3	2.1
6	6	841	1573	0.3	2.1
12	8	1275	2385	0.3	2.2
20	>10	1665	3115	0.3	2.4

Notes: 1) Fundamental mode V_S model adjusted assuming dispersion curve is the average mode (based on relative amplitude of the fundamental and higher surface wave modes) below 25 Hz.
2) Depth of investigation is about 30 m.
3) Bottom layer is a half space.
4) Velocity of half space not well constrained.

Average V_P Model and Estimated Constant Poisson's Ratio V_S Models from Seismic Refraction Model resulting from Tomographic Inversion with Layered Starting Model

Depth to Top of Layer (m)	Layer Thickness (m)	P-Wave Velocity (m/s)	Estimated S-Wave Velocity (m/s)			
			Poisson's Ratio = 0.25	Poisson's Ratio = 0.30	Poisson's Ratio = 0.3333	Poisson's Ratio = 0.35
0.00	0.42	217	125	116	108	104
0.42	0.84	378	218	202	189	182
1.25	0.84	614	354	328	307	295
2.09	0.84	1305	754	698	653	627
2.92	0.84	1455	840	778	728	699
3.76	0.84	1738	1003	929	869	835
4.59	0.84	1890	1091	1010	945	908
5.43	1.75	2029	1171	1085	1014	975
7.18	1.75	2045	1181	1093	1023	983
8.94	1.75	2177	1257	1164	1089	1046
10.69	1.75	2265	1308	1211	1133	1088
12.44	1.75	2270	1311	1214	1135	1091
14.20	1.75	2281	1317	1219	1141	1096
15.95	1.75	2293	1324	1226	1146	1102
17.70	1.75	2336	1349	1249	1168	1122
19.46	1.75	2447	1413	1308	1224	1176
21.21	1.75	2715	1568	1451	1358	1304
22.97	Half Space	2967	1713	1586	1483	1425

Average V_P Model and Estimated Constant Poisson's Ratio V_S Models from Seismic Refraction Model resulting from Tomographic Inversion with Smooth Velocity Gradient Starting Model

Depth to Top of Layer (m)	Layer Thickness (m)	P-Wave Velocity (m/s)	Estimated S-Wave Velocity (m/s)			
			Poisson's Ratio = 0.25	Poisson's Ratio = 0.30	Poisson's Ratio = 0.3333	Poisson's Ratio = 0.35
0.00	0.62	213	123	114	107	102
0.62	1.24	540	312	289	270	259
1.86	1.24	1110	641	593	555	533
3.10	1.24	1556	898	831	778	747
4.34	1.24	1848	1067	988	924	888
5.58	1.24	2031	1173	1086	1016	976
6.82	1.24	2069	1195	1106	1035	994
8.06	2.60	2137	1234	1142	1069	1027
10.66	2.60	2253	1301	1204	1126	1082
13.26	2.60	2261	1305	1208	1130	1086
15.86	2.60	2318	1339	1239	1159	1114
18.46	2.60	2389	1379	1277	1195	1148
21.07	2.60	2742	1583	1466	1371	1317
23.67	2.60	2957	1707	1581	1478	1420
26.27	Half Space	3076	1776	1644	1538	1478

Observations/Discussion:

- Geologic conditions at this site consist of a thin layer of alluvium overlying volcanic rock. The seismic station is likely placed directly on rock, although this needs to be confirmed.
- Due to limited time on site, MASW and P-wave seismic refraction data could only be acquired along a single array with no opportunity to move the array or acquire S-wave refraction and MALW data. Additional data acquisition may be needed at this site, in which case arrangements would have to be made to stay overnight.
- HVSR peaks at the three measurement locations are variable indicating that there is lateral velocity variation at this site; both beneath the seismic array and differing at the seismic station. The HVSR measurement made near the seismic station (TRO-1) has no peak or a very high frequency peak at about 55 to 66 Hz, which could have a cultural source. The absence of an HVSR peak indicates that the seismic station may sit on rock. The HVSR peak at sensor location TRO-2, located at the northwest end of array SBI-1, is at a significantly higher frequency than that at sensor location TRO-3, located at the southeast end of array SBI-1, indicating that the zone of sediments and/or weathered rock is thicker at the southeast end of the array.
- Under normal conditions, differing HVSR response would require an alternate test location; however, there was insufficient time during the initial mobilization to this difficult to access site. Additionally, if significant lateral velocity variation exists at the site, then some testing would also be required in very close proximity to the seismic station to facilitate correlation of velocity structure from the geophysical array to that at the seismic station.
- The P-wave seismic refraction data collected along array SBI-1 were modeled using a tomographic inversion routine with both a smooth velocity gradient and layer based starting model. The models were extended to far offset shot locations to extend depth of investigation. A longer array would have been preferred to image velocity structure to 30 m depth; however, data acquisition was limited to the use of a sledge hammer energy source.
- The seismic refraction survey design allowed P-wave velocity structure to be imaged to a maximum depth of 24 to 27 m; although a longer seismic line would have permitted velocity structure to be more accurately characterized at depths below 20 m. The seismic refraction models show that P-wave velocity is about 200 to 350 m/s at the surface, increasing to 1,000 m/s at a depth of 0.5 to 4 m, 2,000 m/s at a nominal depth of 3 to 19 m and 3,000 m/s at depth of 22 m, or more. It is unlikely that the volcanic rock is saturated in the upper 30 m at this site and, therefore, it is practical to estimate V_S from V_P using realistic values of Poisson's ratio.
- The seismic refraction models indicate that there is significant lateral velocity variation at this site, most significantly a slight thickening of a low velocity sediment layer and a thickening of the weathered rock to the southeast. Between a position of 22.5 and 49.5 m on the seismic line there is a 45% variation in the average P-wave velocity of the upper 30 m (V_{P30}), relative to the average V_{P30} over this interval. The lateral velocity variation observed in the seismic refraction model is consistent with HVSR observations. This significant near surface lateral velocity variation is the source of the significant scatter in surface wave dispersion data at small to intermediate wavelengths, as discussed below.

- V_{P30} was estimated between 22.5 and 49.5 m on the P-wave refraction model, resulting from tomographic inversion with a layered starting model, by projecting the velocity at 24 m depth to 30 m depth. Over this interval, V_{P30} ranges from about 1,345 to 2,112 m/s, about a 45% variation over a 27 m long segment of the array. An average V_P model was developed over the 27 to 49.5 m distance interval by averaging the travel time through each model cell at a particular depth and average V_{P30} was determined to be 1,693 m/s.
- An average V_S model was estimated from the average V_P model using constant Poisson's ratio in the range of 0.25 to 0.35. Estimating V_{S30} from V_{P30} assuming constant Poisson's ratio in the range of 0.25 to 0.35 results in V_{S30} in the 977 to 813 m/s range.
- Estimating V_{S30} from the highest estimated V_{P30} in the central portion of array SBI-1 (2,112 m/s at a position of 22.5 m), assuming constant Poisson's ratio in the 0.25 to 0.35 range, results in V_{S30} in the 1,219 to 1,015 m/s range. Estimating V_{S30} from the lowest estimated V_{P30} in the central portion of array SBI-1 (1,348 at a position of 49.5 m) assuming constant Poisson's ratio in the 0.25 to 0.35 range results in V_{S30} in the 778 to 647 m/s range. It should be noted that adjusting V_{S30} for seismic station conditions by estimated the average S-wave velocity between 1 and 31 m results in a minimum estimated V_{S30} of 788 m/s (position of 49.5 m with constant Poisson's ratio of 0.35) and a maximum estimated V_{S30} of 1,304 m/s (position of 22.5 m with constant Poisson's ratio of 0.30 as Poisson's ratio of 0.25 considered too low). Therefore, irrespective of lateral velocity variation, the site can safely be characterized as NEHRP Site Class B based on P-wave seismic refraction data.
- The seismic refraction model resulting from tomographic inversion using a smooth velocity gradient starting model yields very similar results and, therefore, is not discussed in detail.
- Noise conditions at the site were not sufficient for application of passive surface wave techniques.
- MASW data reduction was difficult due to significant lateral velocity variation, which resulted in significant scatter in Rayleigh wave phase velocity data at small to intermediate wavelengths and minor divergence of dispersion curves at long wavelengths. Two separate dispersion curves representative of the lower and upper bounds of the composite dispersion data were extracted. The dispersion curve representative of the lower bound of the Rayleigh wave phase velocity data was constructed by combining dispersion curves from limited offset receiver gathers from source locations at the southeast end of the array, selected interior source locations and large offset receiver gathers from source locations at the northwest end of the array. The dispersion curve representative of the upper bound of the Rayleigh wave phase velocity data was constructed by combining dispersion curves from limited offset receiver gathers from source locations at the northwest end of the array, selected interior source locations and large offset receiver gathers from source locations at the southeast end of the array.
- The minimum wavelength Rayleigh wave phase velocity data extracted from the 48-channel MASW array was 16 m. Reducing data from smaller hammer sources using a limited offset receiver array (i.e. less active geophones) allowed for extraction of surface wave dispersion data to a minimum wavelength of about 1.5 to 3 m.
- A maximum 70 m wavelength Rayleigh wave was extracted from the MASW data by slightly relaxing the near field criteria typically applied during this investigation.

- There is significant scatter of about 75 to 150 m/s in the two separate Rayleigh wave dispersion curves selected for modeling, likely the result of lateral velocity variation.
- Representative dispersion curves were generated for the two MASW data sets (lower and upper bounds of the composite dispersion curve) using a moving average, polynomial curve fitting routine and used for modeling.
- V_{R40} is 918 and 983 m/s for the lower and upper bound dispersion curves, receptively, which would result in an estimated V_{S30} of 960 and 1,027 m/s, based on the Brown, et al., 2000 relationship, assuming that the dispersion curve at 40 m wavelength consists of the fundamental mode. V_{S30} would be lower if the dispersion curve were associated with the first higher mode or if modal superposition occurs at low frequencies. Additionally, V_{S30} may vary by 5% or more based on the scatter in the Raleigh wave phase velocity data. V_{S30} from the average seismic refraction V_P model using a Poisson's ratio of 0.3 to represent typical unsaturated conditions is 905 m/s (6 to 12 % lower than that estimated from V_{R40}), but varies from 720 to 1,129 m/s beneath the central portion of the array.
- The velocity structure at this site consisting of a thin low velocity layer over much higher velocity weathered rock is such that higher modes may dominate over a wide frequency range. Ideally, the surface wave data would have been acquired along an array located on volcanic rock; however, in the immediate site vicinity rock is only exposed in drainages and in nearby cliffs. Due to the potential for dominant higher modes and/or modal superposition, the surface wave data were modeled using several strategies with the seismic refraction model used to confirm the better model. These strategies consisted of the fundamental mode assumption (2-D solution in the WinSASW software package, which is approximately equivalent to fundamental mode); average/effective mode assumption (observed dispersion curve consists of the average of all modes based on relative amplitude of each mode estimated assuming a far-field, plane Rayleigh wave and no body wave affects); adjustment of fundamental mode V_S model to fit average/effective mode at frequencies below 25 Hz and the 3-D global inversion option in the WinSASW software package. Both the average/effective mode assumption and 3-D global inversion are attempts to deal with possible modal superposition and/or dominant higher modes where there are not clear jumps to the higher mode. The analytical method used to estimate average/effective mode based on the relative energy of each mode assumes a far-field, plane Rayleigh wave and does not consider source-receiver geometry or body wave affects. It is well documented that source-receiver geometry affects the amplitudes of higher mode surface waves and, therefore, the average mode assumption may not always be accurate. However, modeling of the average mode will often result in more accurate V_S models than incorrectly assuming that the dispersion curve represents the fundamental mode, especially when only the lowest frequency portion or the dispersion curve is affected by modal superposition. The WinSASW 3-D global inversion is designed for SASW analysis and is not generally considered applicable to MASW data analysis. None of the techniques addressed above can account for the effects of lateral velocity variation on the dispersion curves or for the effect of lateral velocity variation on the amplitude of higher modes.
- The fundamental mode V_S models significantly overestimate V_S of the half space relative to the P-wave seismic refraction models. Multi-mode analysis of these models indicates a complex relationship between the fundamental and first higher modes. Assuming a 1-D velocity structure (not a valid assumption at this site), the fundamental mode V_S model

for the upper bound dispersion curve is expected to have a dominant first higher mode at high and low frequencies and dominant fundamental mode at intermediate frequencies. The fundamental mode V_S model for the lower bound dispersion curve yields similar results except that the fundamental mode should be dominant at the highest frequencies. It should be noted that the modal energy is very sensitive to model parameters and even small changes to layer thickness or velocity can have significant effect on the relative amplitude of the surface wave modes. For this reason, we prefer to only use the average/effective mode assumption when only the V_S of the half space is affected (i.e. the average mode only deviates from the fundamental mode at low frequencies).

- Because the estimated average/effective mode dispersion curve deviated from the fundamental mode at all but the highest frequencies, a modeling strategy was employed where the velocity of the half space and overlying layer were adjusted until the calculated dispersion curve fit the average mode at frequencies lower than 25 Hz.
- Multi-mode analysis of the V_S model developed for the upper bound dispersion curve using the average mode assumption indicates that the observed dispersion curve falls between the fundamental and first higher modes over almost the entire frequency range. One would expect that resolution in v-f space is sufficient such that modal superposition would not occur at higher frequencies and, therefore, this model is expected to underestimate V_S at shallow to intermediate depths. Similar analysis of the V_S model resulting from 3-D global inversion reveals that the observed dispersion curve generally tracks 1st higher mode over a wide frequency range. The possibility that the 1st higher mode is dominant over a wide frequency range cannot be completely discounted.
- Multi-mode analysis of the V_S model developed for the lower bound dispersion curve using both the average/effective mode assumption and 3-D global inversion indicates that the observed dispersion curves track the fundamental mode at high frequencies (> 60 Hz), gradually move towards the first higher mode between 55 and 45 Hz and closely track the first higher mode at lower frequencies. If the observed dispersion curve is actually the fundamental mode at all but the lowest frequencies, then these models will underestimate V_S at shallow to intermediate depth.
- Comparison of the V_S models developed from the lower and upper bound dispersion curves, using the four strategies discussed above, indicates that the V_S models developed using the fundamental mode assumption, with the half space velocity adjusted to fit the average mode at frequencies less that 25 Hz, best fits the estimated V_S models from the seismic refraction data. Although shown graphically, V_S models resulting from the average mode assumption and 3-D global inversion are not presented in tabular form as these modeling approaches are not really defensible and do not agree with the seismic refraction models at shallow depth.
- Surface wave depth of investigation is about 30 m based on the one half to one third of maximum wavelength criteria.
- V_{S30} is 850 and 928 m/s for the fundamental mode surface wave models of the lower and upper bound dispersion curves, respectively, averaging 889 m/s (NEHRP Site Class B). This is about 12% less than that estimated from V_{R40}. A similar observation has been made at other sites with a very thin low velocity layer overlying significantly higher velocity sediments or rock.
- Average S-wave velocity between 1 and 31 m, to account for assumed sensor depth and sensor likely being placed on rock, is 1,084 and 1,119 m/s for the fundamental mode

surface wave models of the lower and upper bound dispersion curves, respectively, averaging 1,102 m/s (NEHRP Site Class B).

- V_{S30} is 817 and 891 m/s for the fundamental mode surface wave models with average mode adjustment below 25 Hz of the lower and upper bound dispersion curves, respectively, averaging 854 m/s (NEHRP Site Class B).
- Average S-wave velocity between 1 and 31 m, to account for assumed sensor depth and sensor likely being placed on rock, is 1,026 and 1,060 m/s for the fundamental mode surface wave models with average mode adjustment below 25 Hz of the lower and upper bound dispersion curves, respectively, averaging 1,043 m/s (NEHRP Site Class B).
- For the purpose of site characterization, we recommend using the V_S models developed using the fundamental mode V_S model adjusted to average/effective mode at frequencies less than 25 Hz as this model has a more realistic half space velocity relative to the fundamental mode model. These models generally fall within 10% of the V_S models (low, average and high) estimated from the central portion of the P-wave refraction model using an assumed constant Poisson's ratio of 0.3. Slightly increasing Poisson's ratio of the uppermost 10 m of weathered rock and slightly decreasing Poisson's ratio below a depth of 20 m would result in better agreement between the models. The average V_{S30} estimated from the surface wave sounding, 854 m/s, compares favorably with that estimated from the average V_P model using an assumed constant Poisson's ratio of 0.3, 905 m/s, especially considering that there is at least a 45% variation in V_{S30} beneath the seismic line.
- There is uncertainty in the V_S models at this site, related to both uncertainty in which Rayleigh wave modes are dominant and extreme lateral velocity variation. However, we can state with confidence that adjusted V_{S30} at the seismic station will fall into NEHRP Site Class B, regardless of lateral velocity variation.
- Additional geophysical investigation would reduce the uncertainty in the V_S models at this site. A short seismic line or SASW sounding immediately adjacent to the seismic station would facilitate correlation of seismic station velocity structure to that beneath the longer arrays needed to image to 30 m depth. Multiple seismic lines would better quantify the degree of lateral velocity variation in the immediate site vicinity. Finally, the S-wave seismic refraction and MALW (Love wave) techniques may yield less subjective and, therefore, more reliable V_S models at this site, assuming that good quality data can be obtained. This type of site (thin low velocity layer over higher velocity sediments/rock) is very challenging for MASW and SASW analysis and would provide a good proving ground to evaluate advanced analytical techniques for modeling higher modes and modal superposition.

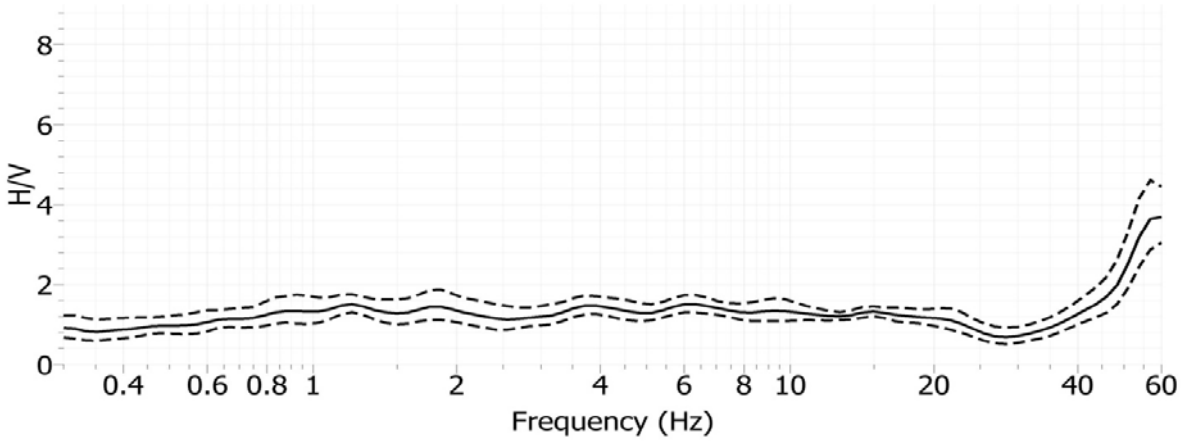

Site CI.SBI, H/V Spectral Ratio, Near Seismic Station, Sensor TRO-1

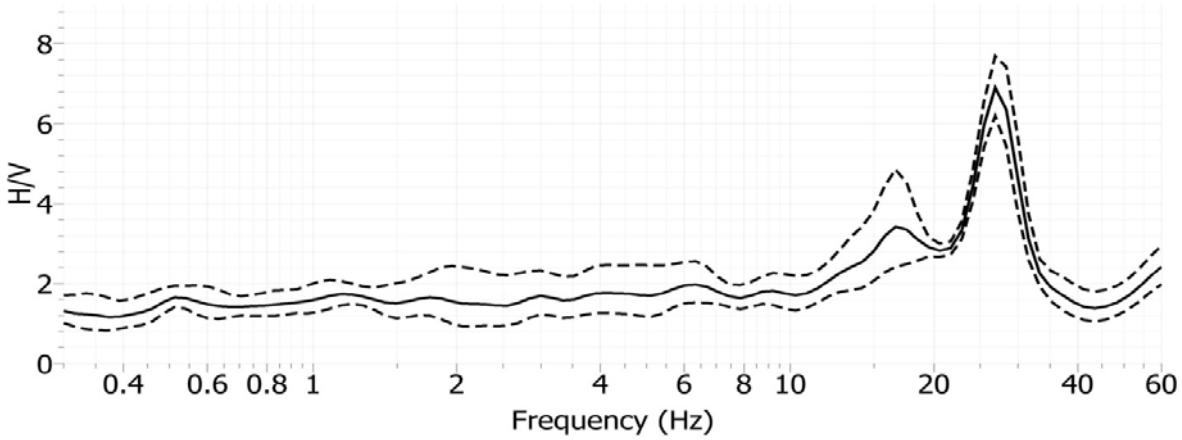

Site CI.SBI, H/V Spectral Ratio, Array SBI-1, Sensor TRO-2

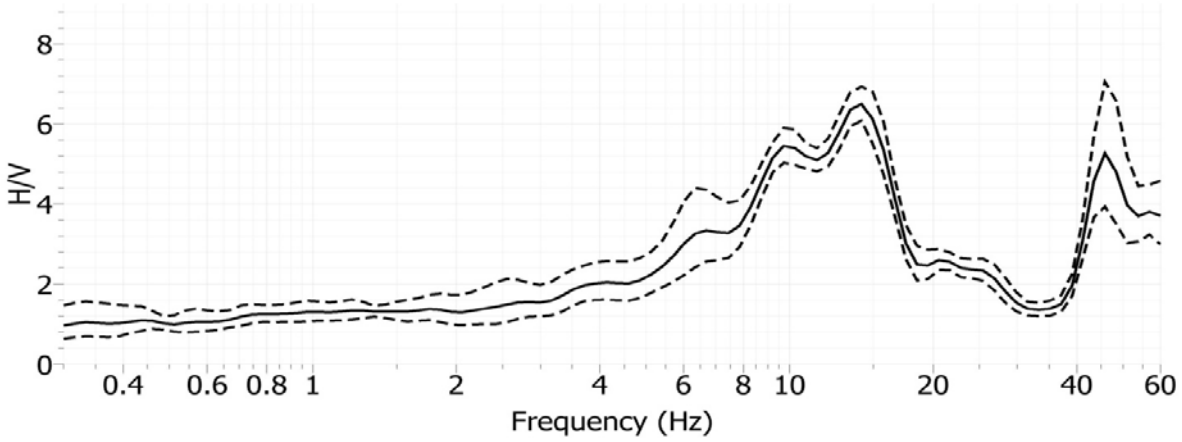

Site CI.SBI, H/V Spectral Ratio, Array SBI-1, Sensor TRO-3

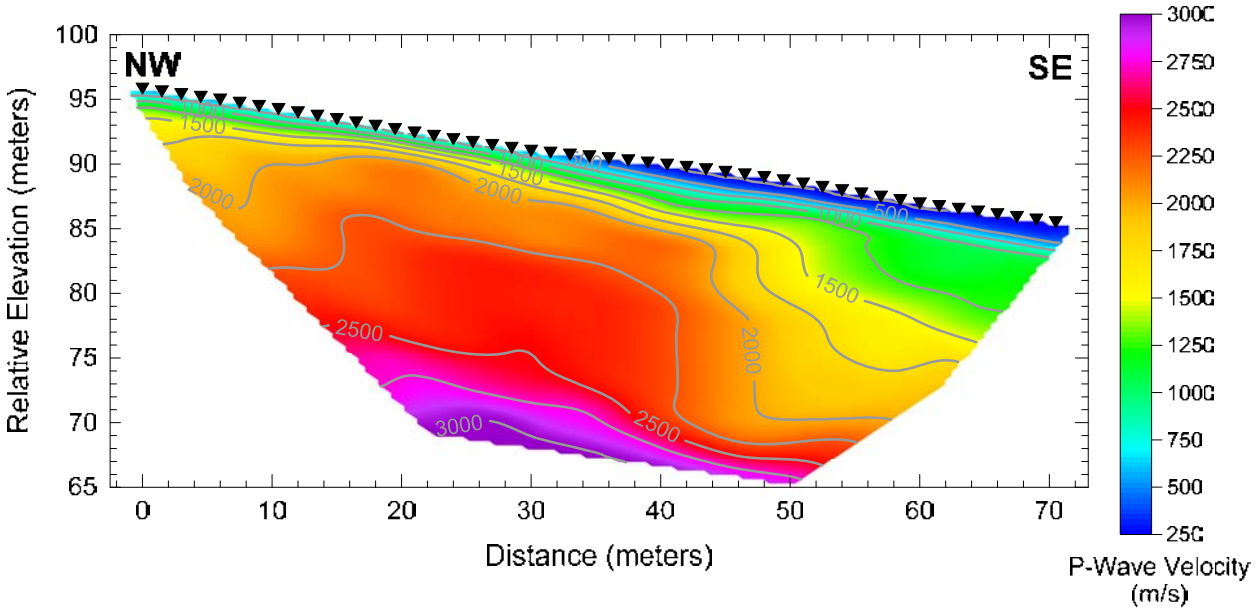

Array SBI-1 – P-wave Tomographic Seismic Refraction Model utilizing Layer Based Starting Model

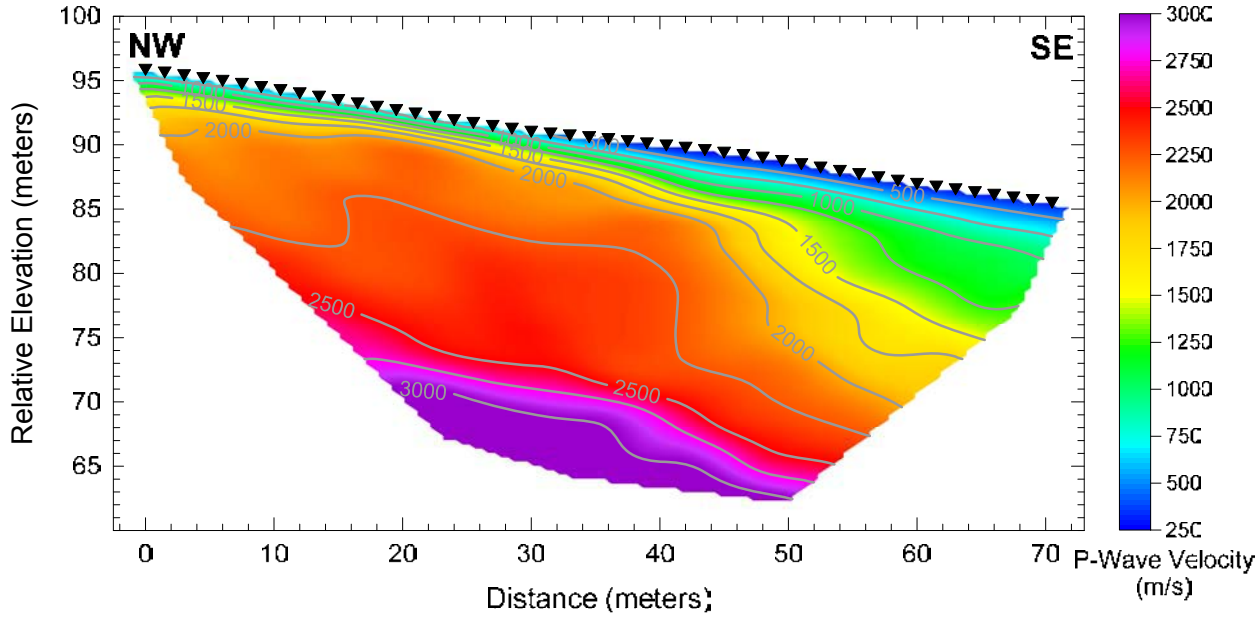

Array SBI-1 – P-wave Tomographic Seismic Refraction Model utilizing Smooth Velocity Gradient Starting Model

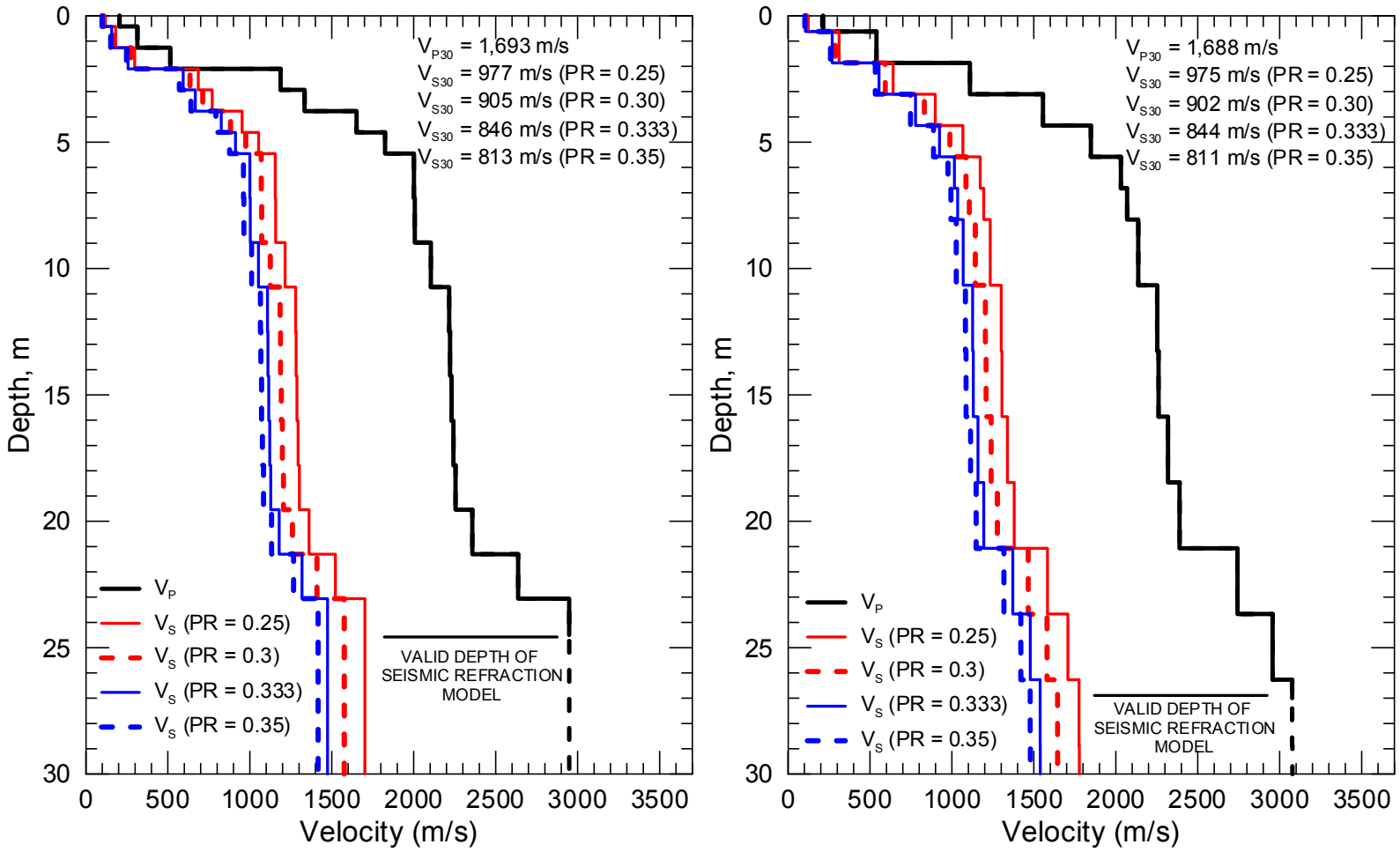

CI.SBI – Average P-wave velocity structure and estimated S-wave velocity structure between a position of 22.5 and 49.5 m on the P-wave seismic refraction models for array SBI-1 that utilized both layered (left) and smooth velocity gradient (right) starting models. Although the maximum seismic refraction depth of investigation is limited to about 24 to 27 m, P-wave velocity is very high at the bottom of the model and is not expected to increase significantly between the valid depth of investigation and 30 m.

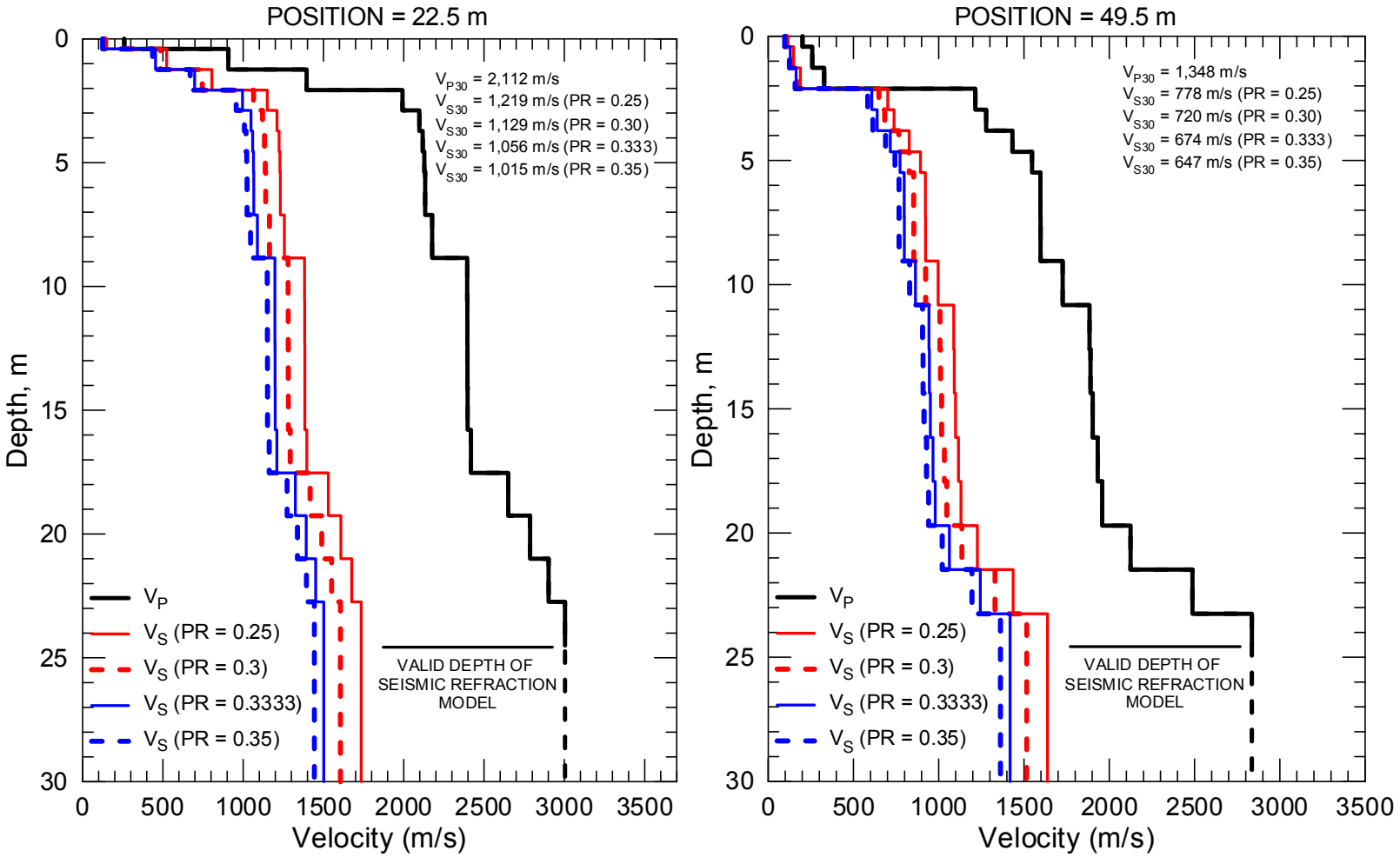

CI.SBI –P-wave velocity structure and estimated S-wave velocity structure at a position of 22.5 (maximum V_{P30}) and 49.5 m (minimum V_{P30}) on the P-wave seismic refraction model for array SBI-1 that utilized a layered starting model. The P-wave refraction model developed using a smooth velocity gradient starting model is very similar to that developed using a layered starting model with almost identical V_{P30} and is, therefore, not presented.

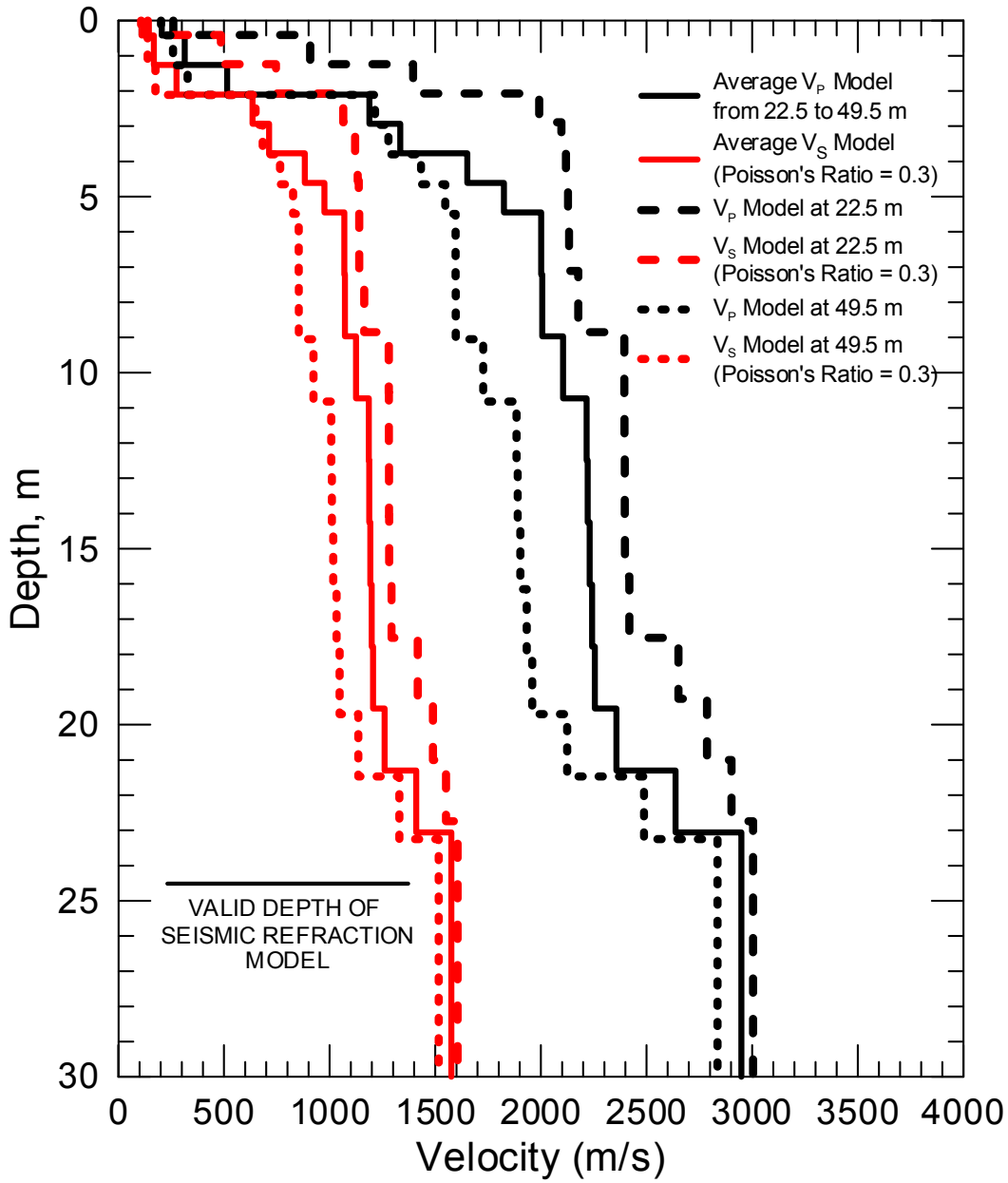

CI.SBI - Comparison of P-wave and estimated S-wave velocity structure between the average P-wave velocity model and models with minimum and maximum V_{P30}. There is about 45% variation in V_{P30} between a position of 22.5 and 49.5 m on array SBI-1, which will significantly impact any attempt to model surface wave dispersion data. Although not confirmed, the weathered rock is not expected to be saturated in the upper 30 m and it may, therefore, be possible to estimate V_{S30} to an acceptable degree of accuracy using nominal ranges of Poisson's ratio for weathered rock.

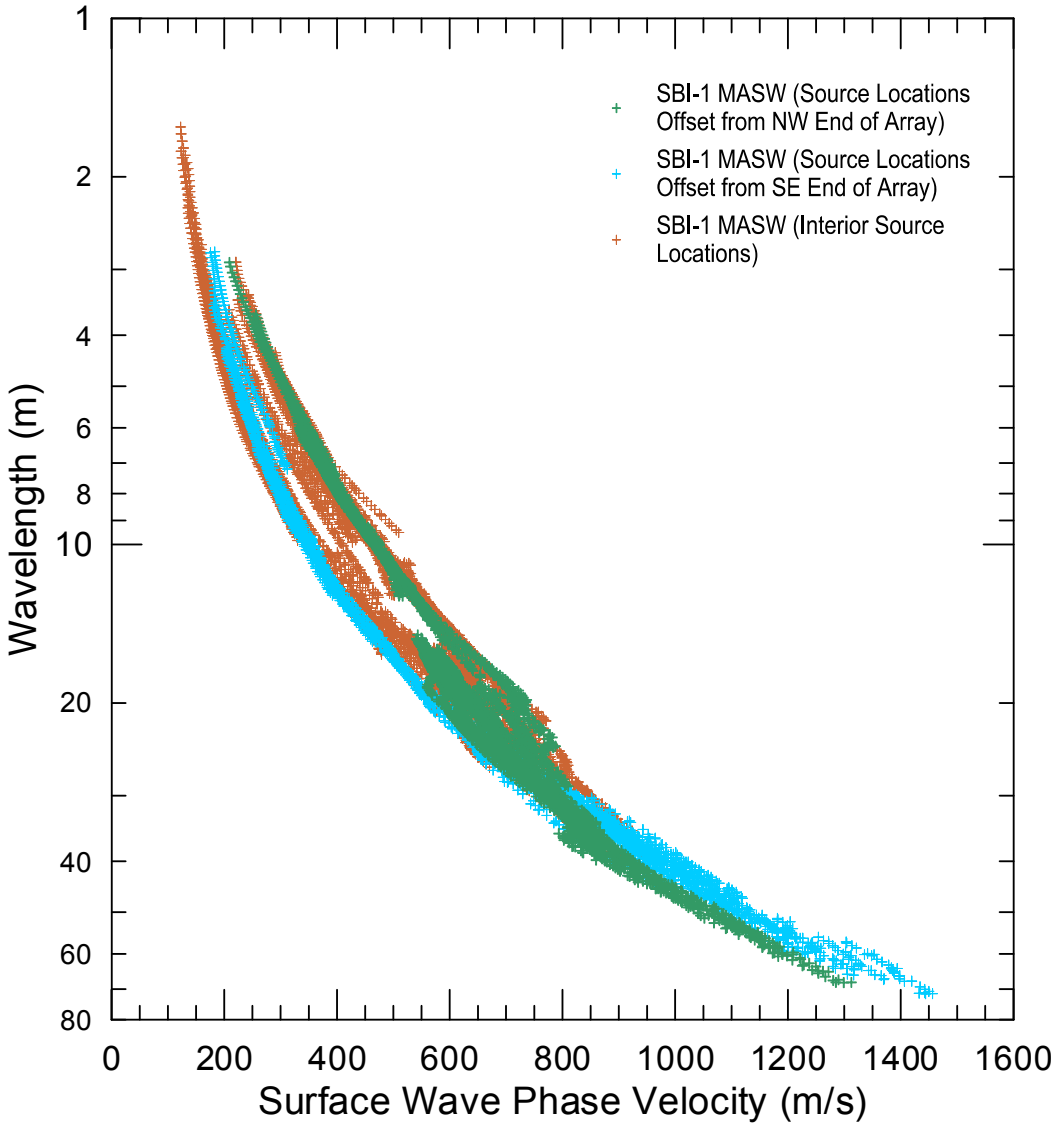

CI.SBI – Rayleigh wave phase velocity data from source locations offset from the northwest and southeast ends of the array and from interior source locations (i.e. seismic refraction sources) clearly showing the effects of near surface lateral velocity variation. There are two distinct dispersion curves at small to intermediate wavelengths due to a significant thickening to the southeast of the uppermost weathered zone. There is also a slight divergence of the dispersion curves at long wavelengths from northwest and southeast source locations. The Rayleigh wave phase velocity at a 40 m wavelength (V_{R40}) is similar indicating the V_{S30} estimates made from the surface wave models may be representative of the average velocity structure beneath the line. Although the surface wave models may accurately estimate average V_{S30} beneath the array, it is unclear whether the S-wave velocity structure in the models will accurately represent the highly variable subsurface velocity structure evident in the seismic refraction models. This surface wave dispersion data were modeled by developing two dispersion curves that define the upper and lower bounds of the Rayleigh wave phase velocity data.

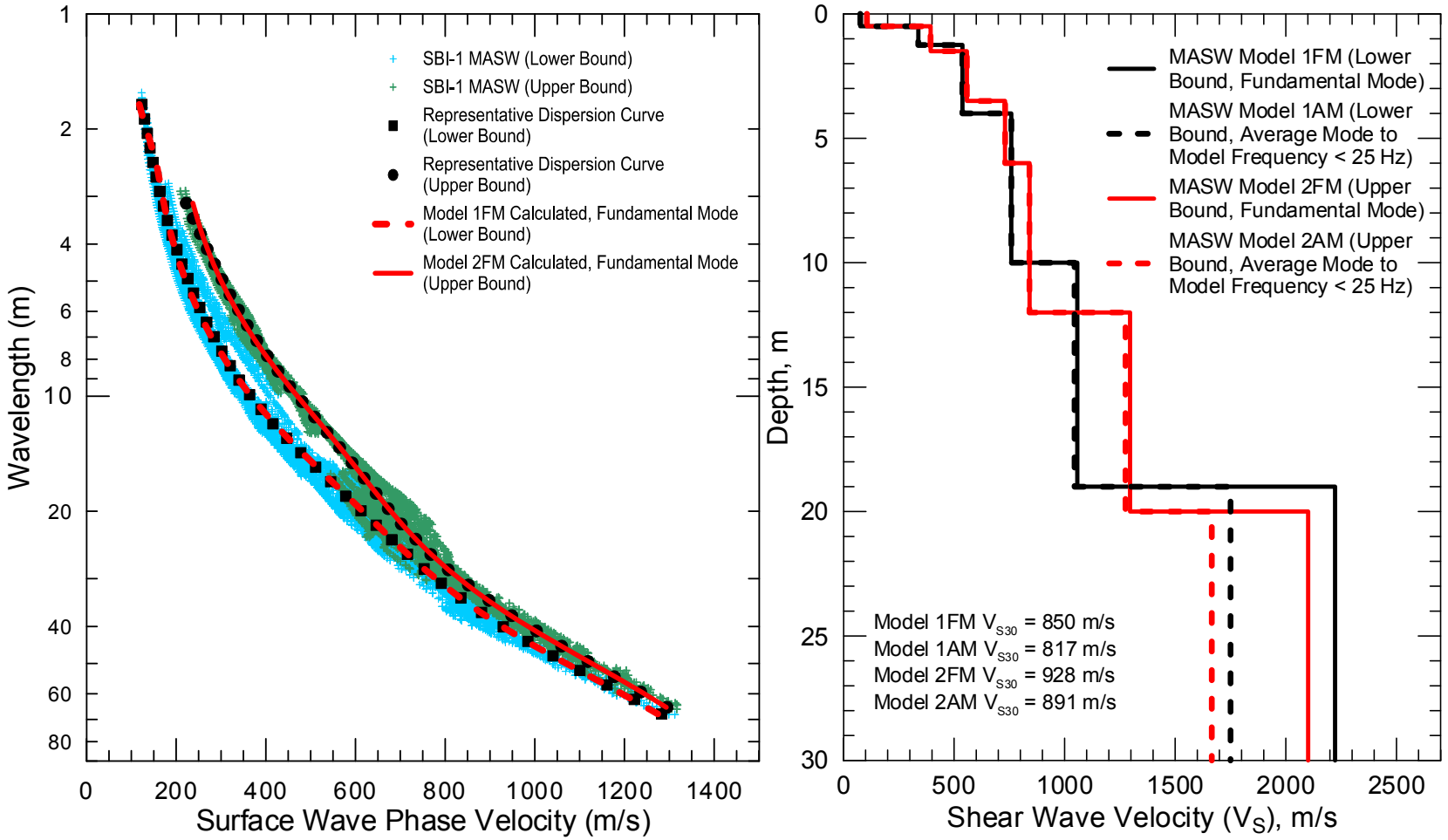

CI.SBI - Field, representative and inverted theoretical surface wave dispersion data (left) and associated V_S models (right) based on fundamental mode assumption and with model adjusted to fit average mode at frequencies less than 25 Hz. Fitting the average mode to account for possible modal superposition between the fundamental mode and first higher mode appears to yield a more realistic estimate of the half space velocity. However, the half space velocity should be considered to be poorly constrained. Due to near surface lateral velocity variation, primarily due to a slight thickening of low velocity alluvium and weathered volcanic rock to the southeast, two representative dispersion curves that approximately correlate to the upper and lower bounds were modeled.

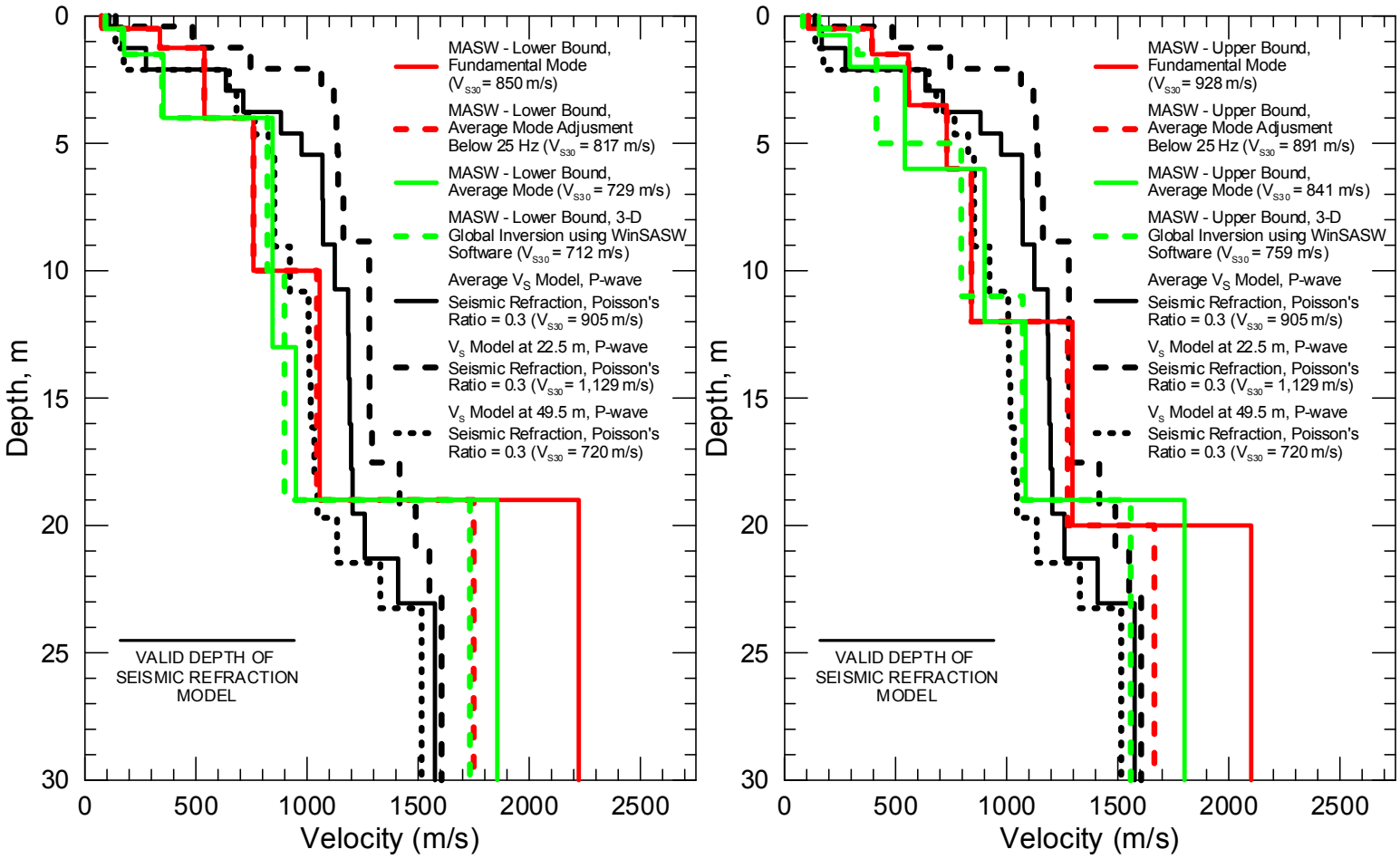

CI.SBI – Comparison of S-wave velocity models derived from the MASW lower (left) and upper (right) bound dispersion curves (fundamental mode, average mode adjustment below 25 Hz, average mode and 3-D global inversion in WinSASW software) and P-wave seismic refraction survey (estimated from average V_P model, maximum V_P model at 22.5 m and minimum V_P model at 49.5 m using assumed constant Poisson's ratio of 0.3). The seismic refraction models presented for comparison result from tomographic inversion with a layered starting model. The most appropriate MASW V_S model is that based on the fundamental mode assumption with average mode adjustments below 25 Hz, which result in a more realistic velocity of the half space. The MASW V_S models developed using the average mode assumption and 3-D global inversion are presented for discussion and should not be utilized.

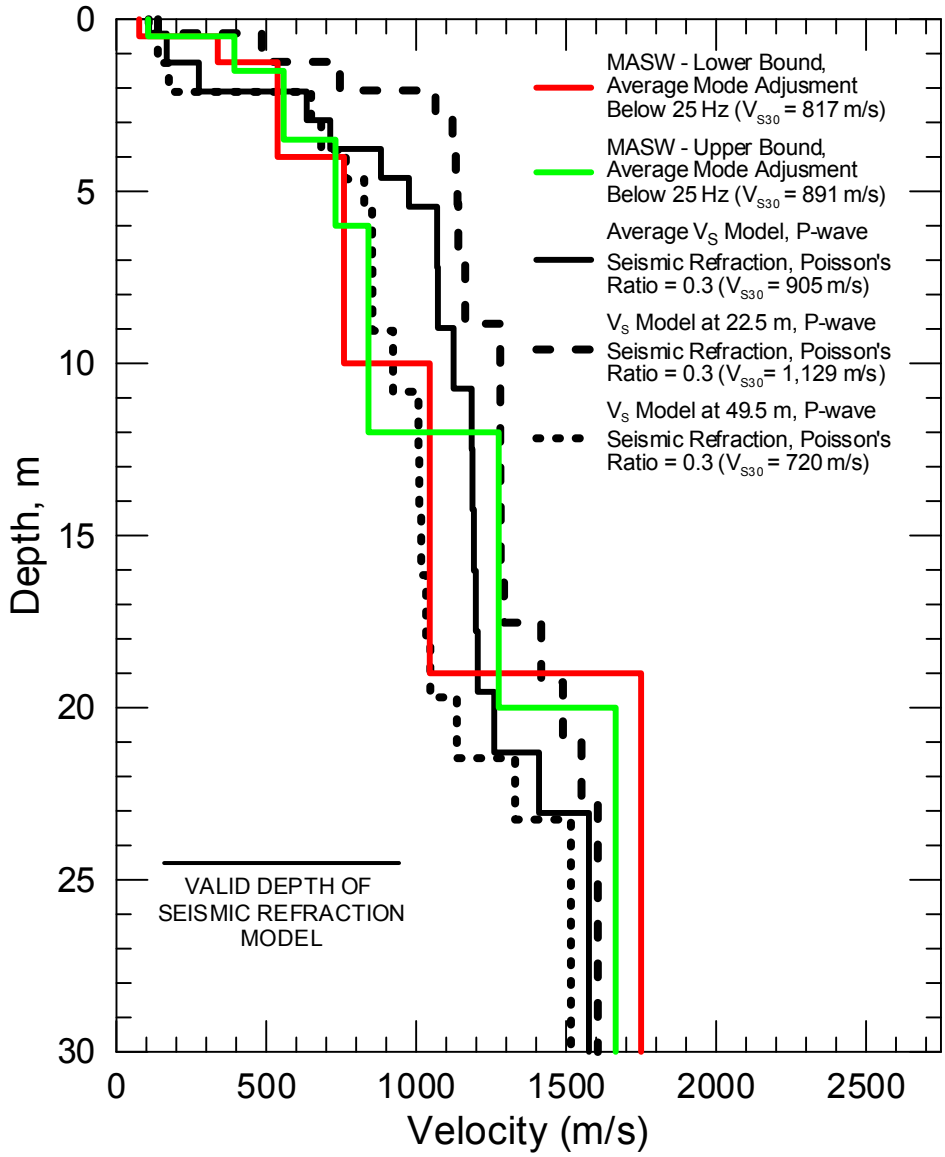

CI.SBI – Comparison of S-wave velocity models derived from the MASW lower and upper bound dispersion curves (based on the fundamental mode assumption with average mode adjustments below 25 Hz) and P-wave seismic refraction survey (estimated from average V_P model, maximum V_P model at 22.5 m and minimum V_P model at 49.5 m using assumed constant Poisson's ratio of 0.3). The seismic refraction models presented for comparison result from tomographic inversion with a layered starting model. Several modeling strategies were utilized to model the MASW data and the presented MASW V_S models are believed to be the most representative of subsurface velocity structure. However, given the significant lateral velocity variation beneath the seismic line, S-wave velocity structure inferred from the P-wave seismic refraction model could be considered more accurate. The volcanic rocks underlying the site are not expected to be saturated and either an assumed constant Poisson's ratio of 0.3 or a decrease in Poisson's ratio with depth from 0.35 or 0.33 at the surface to 0.25 at depth may adequately convert V_P to V_S.

Site CI.SBPX

Location: Strawberry Peak, Twin Peaks, California

Latitude: 34.23246 **Longitude:**-117.23490
(Station coordinates modified based on field GPS survey, WGS84 coordinate system)

V_{S30} (measured): 393 m/s

V_{S30} (adjusted to more accurately reflect seismic station conditions): 441 m/s (average S-wave velocity between 1 and 31 m adjusting for inferred 1 m sensor depth).

NEHRP Site Class: C

Geomatrix Code: IGB

Geologic Conditions/Observations: Seismic station located on weathered Mesozoic (Cretaceous) granitic rocks.

Site Conditions: Rural site. Seismic station located on a mountain top near radio communications antennas. Test area located on an undulating surface with about 8 m of elevation variation along the 70.5 m seismic line. Steep topography in site vicinity.

Geophysical Methods Utilized: HVSR, Seismic Refraction, MASW

Geophysical Testing Arrays:

1. Array SBPX-1 (48 channel MASW and P-wave seismic refraction array utilizing 4.5 Hz vertical geophones spaced 1.5 m apart for a length of 70.5 m, forward and reverse shot locations with multiple source offsets and source types and multiple interior shot locations).
2. Three HVSR measurement locations: two distributed along array SBPX-1 and one near the seismic station.

Legend

- Seismic Station - Approximate Surveyed Location
- Seismic Station - Approximate Location of Record
- H/V Spectral Ratio Location
- MASW and Seismic Refraction Array

NOTES:
1. WGS 1984 COORDINATE SYSTEM
2. Image Source: ESRI, i-cubed, USDA FSA, USGS, AEX, GeoEye, Getmapping, Aerogrid, IGP

File Name: CI-SBPX-I

Date: 2/7/2013

USGS science for a changing world

GEOVision geophysical services

RECOVERY.GOV

SITE MAP
CI•SBPX

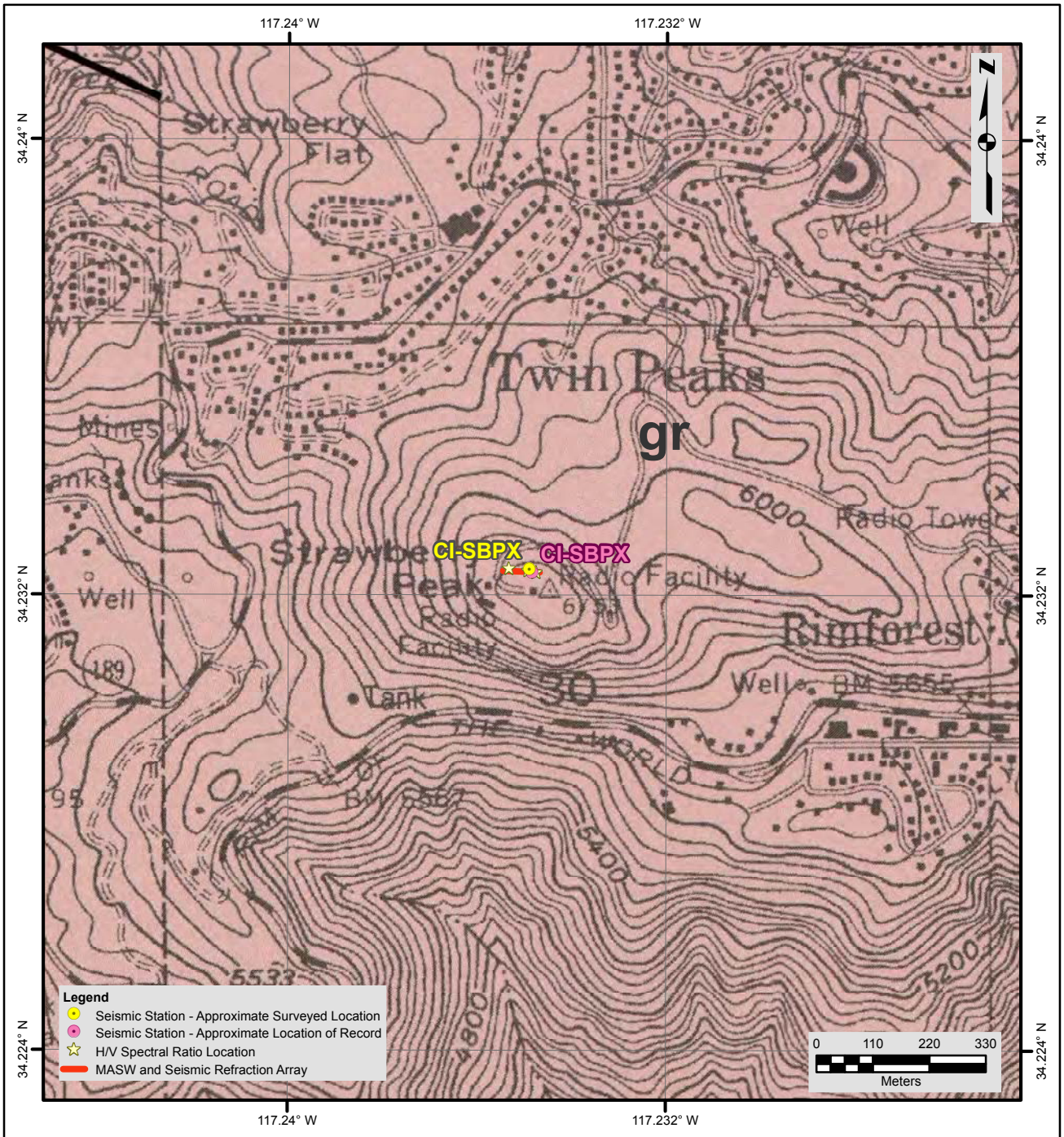

Description of Geologic Map Units

gr = Mesozoic (Cretaceous) Leucocratic granitic rocks, mostly quartz monzonite or monzogranite, massive, intrusive

NOTES:
1. WGS 1984 COORDINATE SYSTEM
2. Geologic Map of the Harrison Mountain / North ½ of Redlands Quadrangles, Riverside & San Bernardino Counties, California by Thomas W. Dibblee, Jr., 2004
3. See site map for details of geophysical survey

File Name: CI-SBPX

Date: 2/7/2013

USGS science for a changing world

GEOVision geophysical services

GEOLOGIC MAP
CI•SBPX

RECOVERY.GOV

Looking west towards HVSR sensor 450 and CI.SBPX seismic station

Looking east past HVSR sensor 453

Looking west past HVSR sensor 507 towards seismic station

Looking south at seismic station and HVSR sensor 450

MASW and P-wave refraction data acquisition

Location of Geophysical Testing Arrays:

Location	Latitude	Longitude
SBPX-1, West End of MASW/Refraction Array	34.23242	-117.23545
SBPX-1, East End of MASW/Refraction Array	34.23240	-117.23468
HVSR Sensor 450	34.23243	-117.23492
HVSR Sensor 453	34.23246	-117.23533
HVSR Sensor 507	34.23240	-117.23476
CI.SBPX Seismic Station	34.23246	-117.23490

Notes: 1) WGS84 Coordinate System (decimal degrees)
2) Survey accuracy is estimated at 1 to 2 m.

Results:

V_S Model 1FM

Depth to Top of Layer (m)	Layer Thickness (m)	S-Wave Velocity (m/s)	Inferred P-Wave Velocity (m/s)	Assumed Poisson's Ratio	Assumed Density (g/cm^3)
0	1	106	199	0.3	1.7
1	1.75	194	363	0.3	1.7
2.75	2.75	309	578	0.3	1.8
5.5	4	336	629	0.3	1.8
9.5	5.5	411	768	0.3	1.9
15	8	645	1206	0.3	2.1
23	>7	1052	1967	0.3	2.2

Notes: 1) Data modeled assuming dispersion curve is the fundamental mode.
2) Depth of investigation is about 30 m.
3) Bottom layer is a half space.
4) Velocity of half-space not well constrained.

V_S Model 1AM

Depth to Top of Layer (m)	Layer Thickness (m)	S-Wave Velocity (m/s)	Inferred P-Wave Velocity (m/s)	Assumed Poisson's Ratio	Assumed Density (g/cm^3)
0	1	105	197	0.3	1.7
1	1.75	198	370	0.3	1.7
2.75	2.75	267	500	0.3	1.8
5.5	4	327	612	0.3	1.8
9.5	5.5	432	808	0.3	1.9
15	8	567	1061	0.3	2.0
23	>7	818	1529	0.3	2.1

Notes: 1) Data modeled assuming dispersion curve is the average mode (based on relative amplitude of the fundamental and higher surface wave modes).
2) Depth of investigation is about 30 m.
3) Bottom layer is a half space.
4) Velocity of half space not well constrained.

Observations/Discussion:

- Geologic conditions at the site, based on field observations, consist of a thin layer of sediments over weathered granitic rock.
- HVSR plots have many similarities, but are not identical. There are no distinct high amplitude HVSR peaks, but multiple, possible low amplitude peaks.
- The P-wave refraction data for array SBPX-1 were modeled using a tomographic inversion routine with a smooth velocity gradient starting model. The seismic refraction data were modeled without extending the model to far offset shot locations.
- The seismic refraction survey design allowed P-wave velocity to be imaged to a maximum depth of about 15 m. The seismic refraction model shows that P-wave velocity is about 350 to 400 m/s at the surface, increasing to 600 m/s at a nominal depth of 3 to 5 m, 800 m/s at a depth of 6 to 12 m and 1,000 m/s at a nominal depth of 15 to 18 m.
- There is some lateral velocity variation indicated in the seismic data probably caused by a variable weathering profile along the array. The seismic model shows that less weathered (higher velocity) rock is located at shallower depth at the west end of array SBPX-1.
- Noise conditions at the site were not sufficient for application of passive surface wave techniques.
- The minimum wavelength surface wave phase velocity data extracted from the 48-channel MASW array is about 10.5 m. Data reduction using seismic records from smaller hammer sources and a limited offset receiver array (i.e. less active geophones) allowed extraction of surface wave dispersion data to a minimum wavelength of about 2 m.
- There is nominally about 50 m/s scatter in MASW dispersion data likely due to lateral velocity variation associated with both variable thickness of the sediment layer and differential weathering of near surface granitic bedrock.

- A representative dispersion curve was generated for the MASW data set using a moving average, polynomial curve fitting routine and used for modeling.
- Several V_S models were generated from the surface wave data. Models 1FM, 2FM and 3FM were developed assuming the dispersion curve consists of only the fundamental mode Rayleigh wave and assumed Poisson's ratios of 0.3, 0.25 and 0.35, respectively. Further modeling reveals that these V_S models should excite a dominant first higher mode at low frequencies. Due to relatively high velocities, it is expected that there is insufficient resolution in the v-f transform (overtone image) to isolate the fundamental mode and first higher mode at low frequencies, resulting in modal superposition. Given the high velocities at the site, a significantly longer receiver array (several hundred meters) would be required to obtain sufficient resolution in v-f space to separately identify the fundamental and first higher modes. This type of space is generally not available at rock sites and longer arrays invariably introduce more lateral velocity variation. Because of possible modal superposition, alternate V_S models (Models 1AM, 2AM and 3AM) were developed assuming the observed dispersion curve consists of the average/effective mode (average of all modes based on relative amplitude in each mode for a far-field, plane Rayleigh wave). We cannot state with certainty that the observed dispersion data consists of the average/effective mode, but this may be a better option than incorrectly assuming that the dispersion data is the fundamental mode. The most significant unknown is the effect of lateral velocity variation on the amplitude of the Rayleigh wave modes and resulting estimates of effective mode.
- Interestingly, V_{S30} is quite similar between the fundamental and average mode models, with average mode models yielding V_{S30} about 5 to 6 % lower than the fundamental mode models.
- A 0.05 increase in Poisson's ratio decreases V_{S30} by 5 to 6 % for both the fundamental mode and average mode models, and vice versa. For the purpose of site characterization, a Poisson's ratio of 0.3 is assumed.
- Love wave MASW was not applied at this site because data quality appeared to be acceptable in the field. Love wave MASW may be better suited to characterizing sites with the observed or similar velocity structure because the fundamental mode should be dominant at low frequencies and Poisson's ratio is not an issue.
- Surface wave depth of investigation is about 30 m based on half of maximum wavelength criteria.
- The inferred P-wave velocities in the surface wave models are generally consistent with the seismic refraction model. The surface wave models based on the average mode assumption appears to be in better agreement with the P-wave refraction model at depths below about 10 m.
- V_{S30} is 419 m/s for Model 1FM (fundamental mode, Poisson's ratio of 0.3) and 393 m/s for Model 1AM (average mode, Poisson's ratio of 0.3) - Site Class C.
- Average S-wave velocity between 1 m (inferred sensor depth) and 31 m is 475 and 441 m/s, for Models 1FM and 1AM, respectively.
- The seismic refraction data was reviewed and does not support the high velocity of the half space in the fundamental mode V_S model (Model 1FM); therefore, the average/effective mode V_S model (Model 1AM) is recommended for the purpose of site characterization.

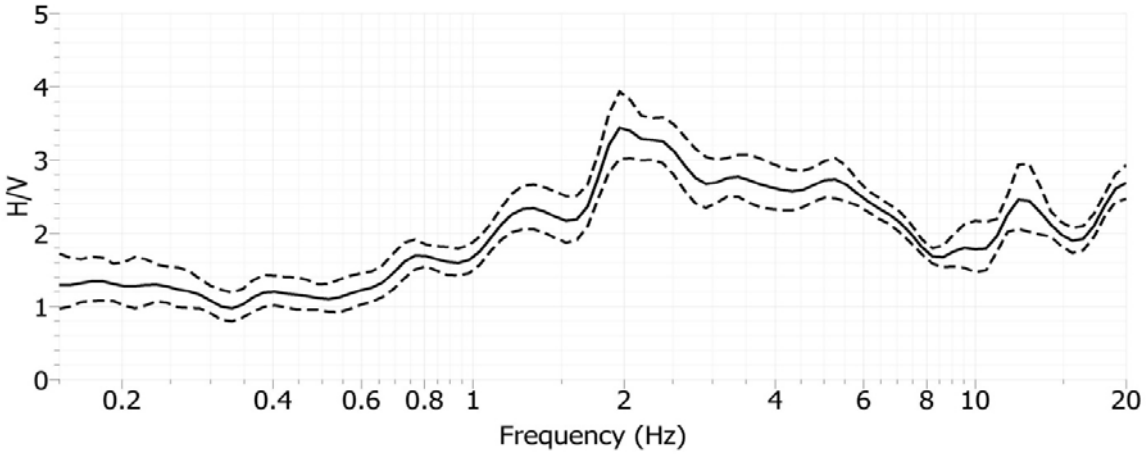

Site CI.SBPX, H/V Spectral Ratio, Array SBPX-1, Sensor 453

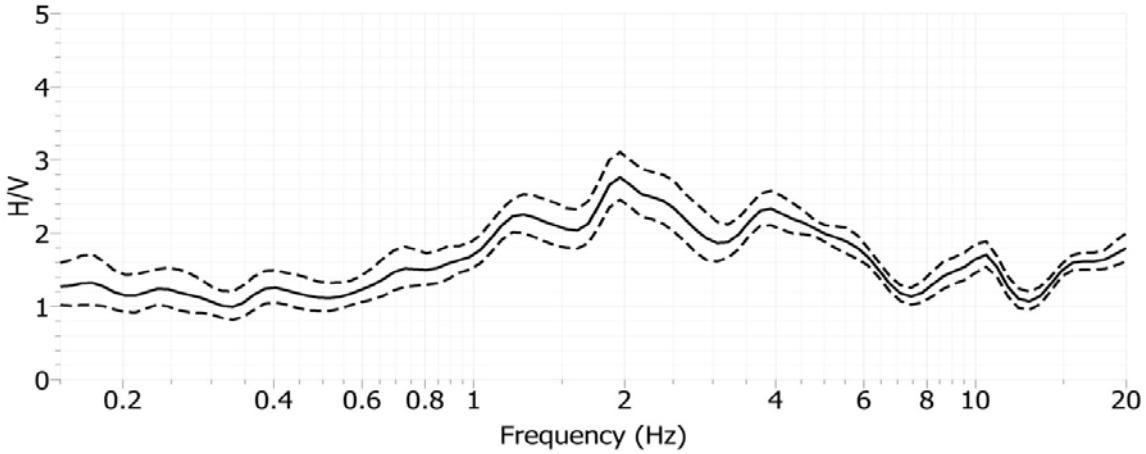

Site CI.SBPX, H/V Spectral Ratio, Near Seismic Station, Sensor 450

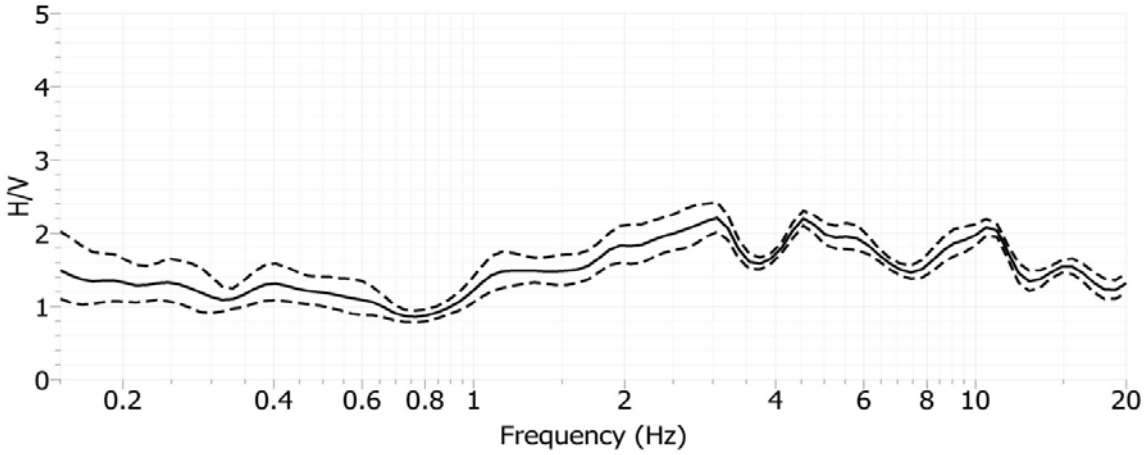

Site CI.SBPX, H/V Spectral Ratio, Array SBPX-1, Sensor 507

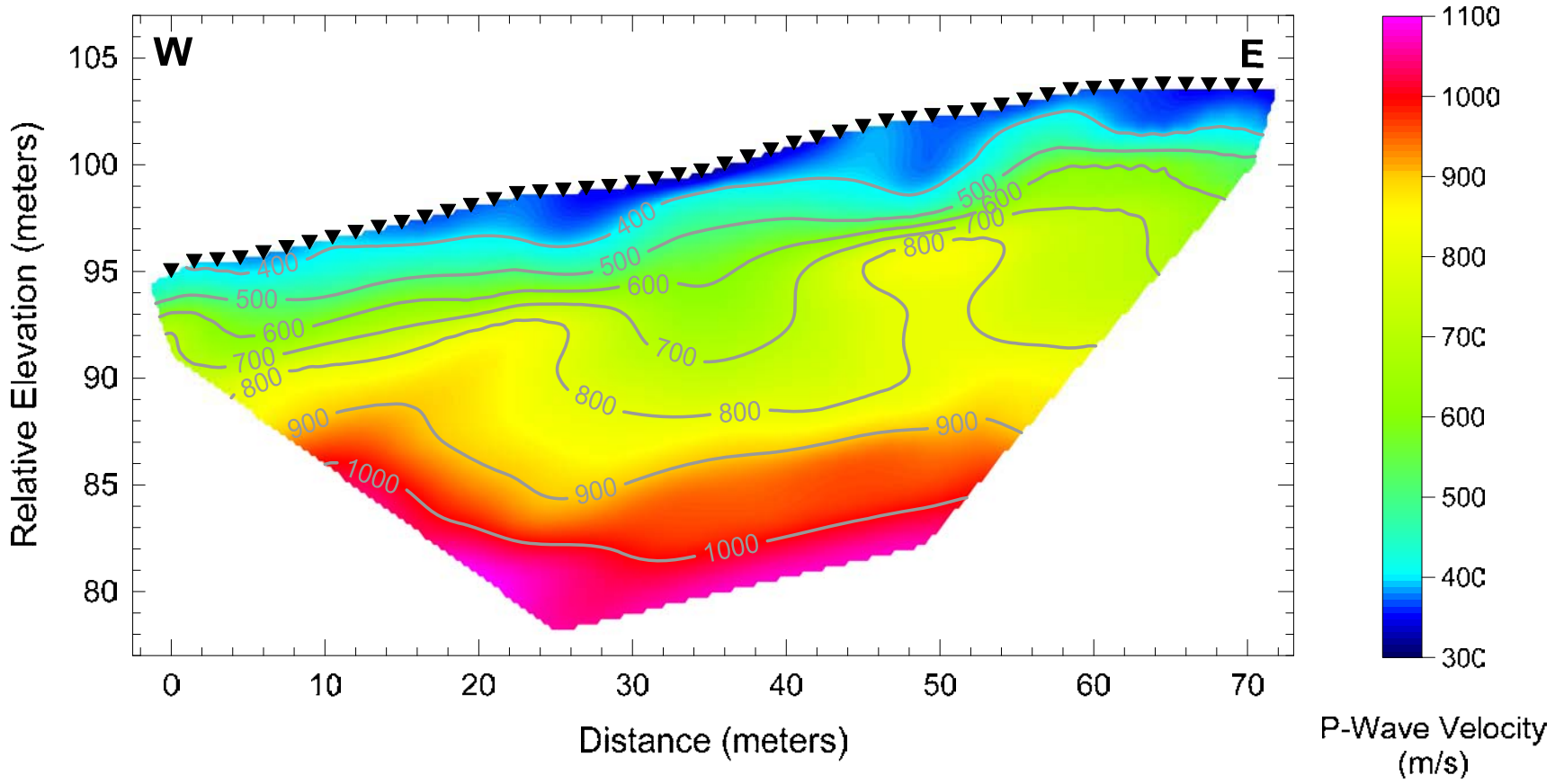

Array SBPX-1 – Tomographic seismic refraction model utilizing smooth velocity gradient starting model

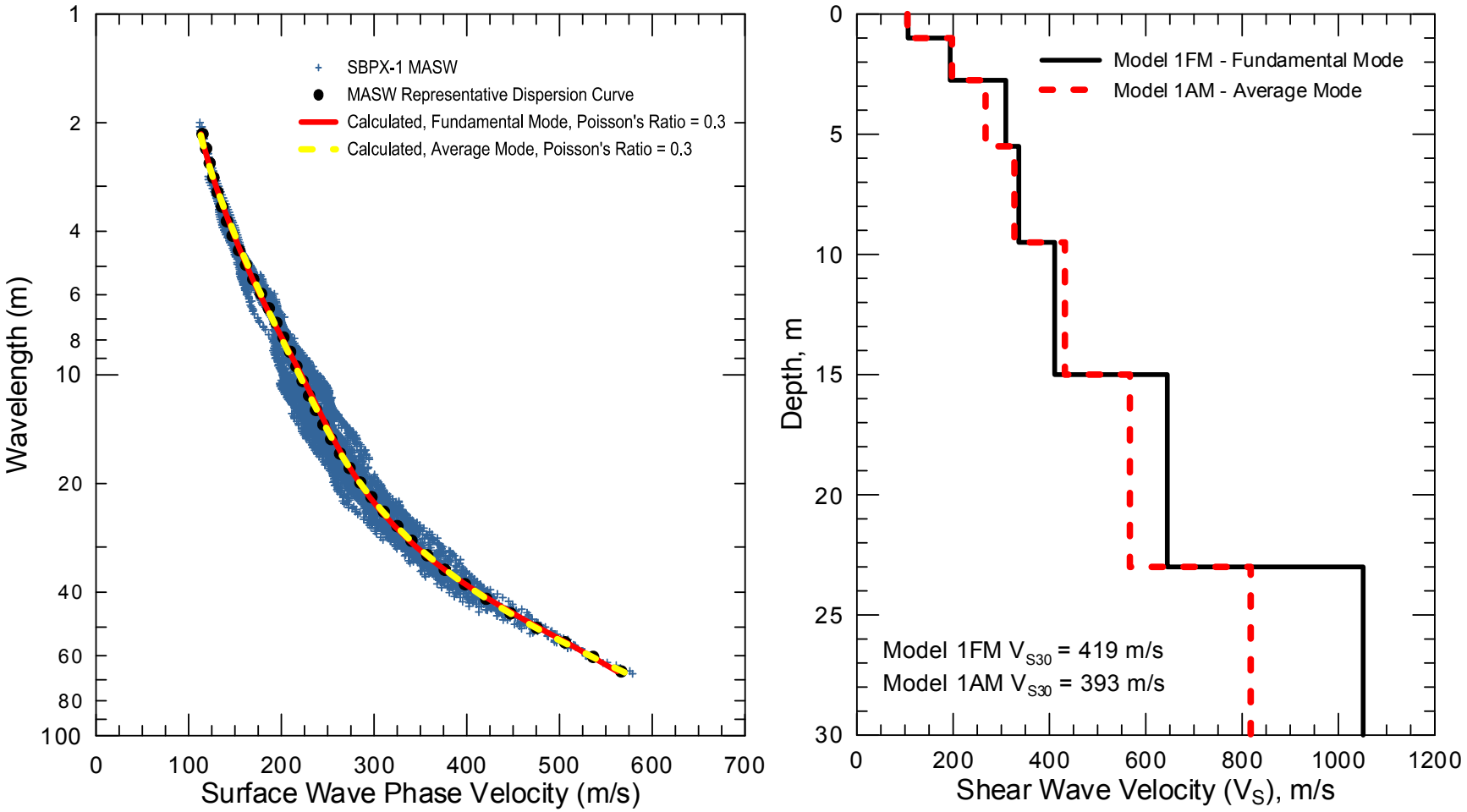

CI.SBPX - Field, representative and inverted theoretical surface wave dispersion data (left) and V_S models assuming both fundamental mode and average mode (right).

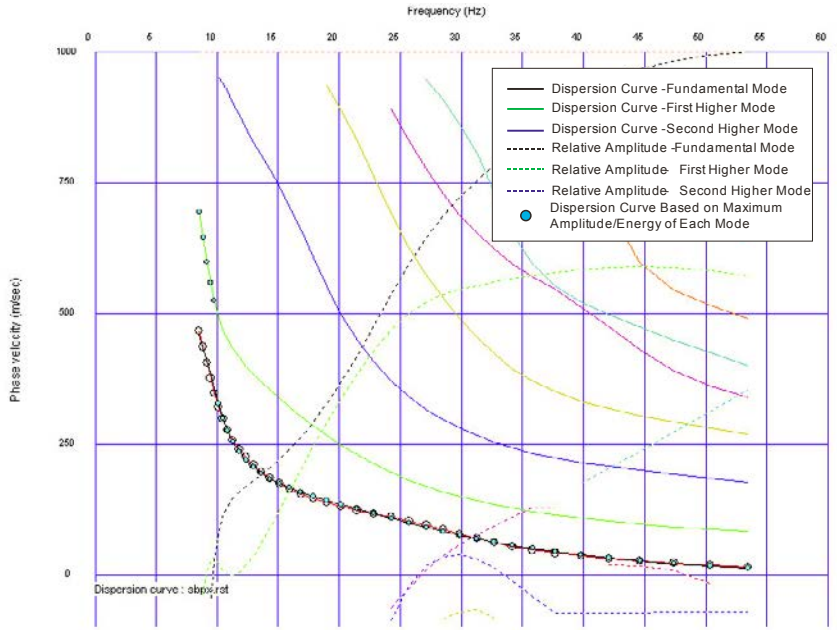

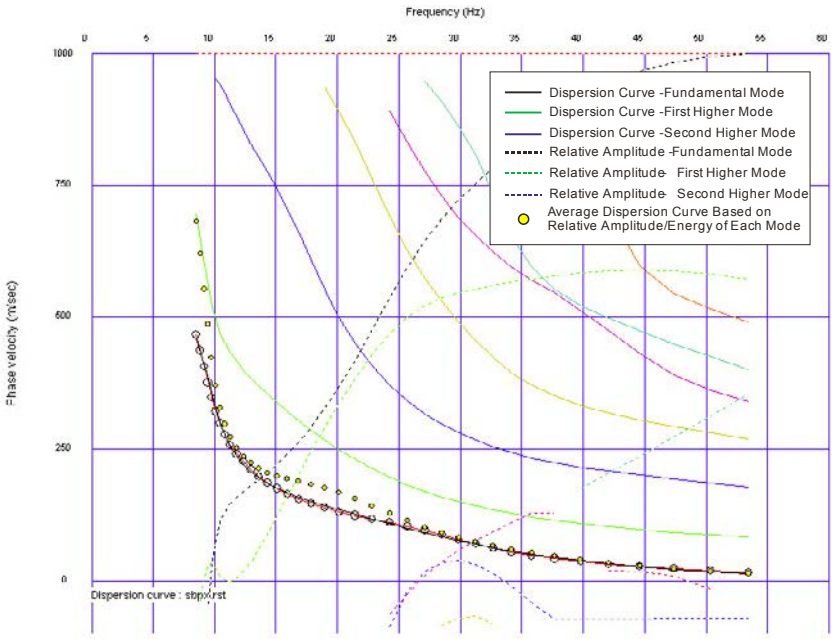

CI.SBPX – Calculated Rayleigh wave phase velocity modes with maximum amplitude (left) and the effective (average) mode (right) for the V_S model developed for the fundamental mode assumption and a Poisson's ratio of 0.3. Because there is no clear jump between the fundamental and first higher modes at low frequencies (i.e. the modes are superimposed), effective (average) mode modeling is expected to be more feasible than multi-mode modeling. Modeling of the effective (average) mode is not in common practice. It is probable that the fundamental mode is correctly identified at intermediate to high frequencies (e.g. over the 15 to 25 Hz range where modal superposition is implied in the upper right figure) with the average mode approximately representing modal superposition at low frequencies. In cases of possible modal superposition, effective (average) mode modeling may be the best solution at this time and result in more accurate velocities at depth.

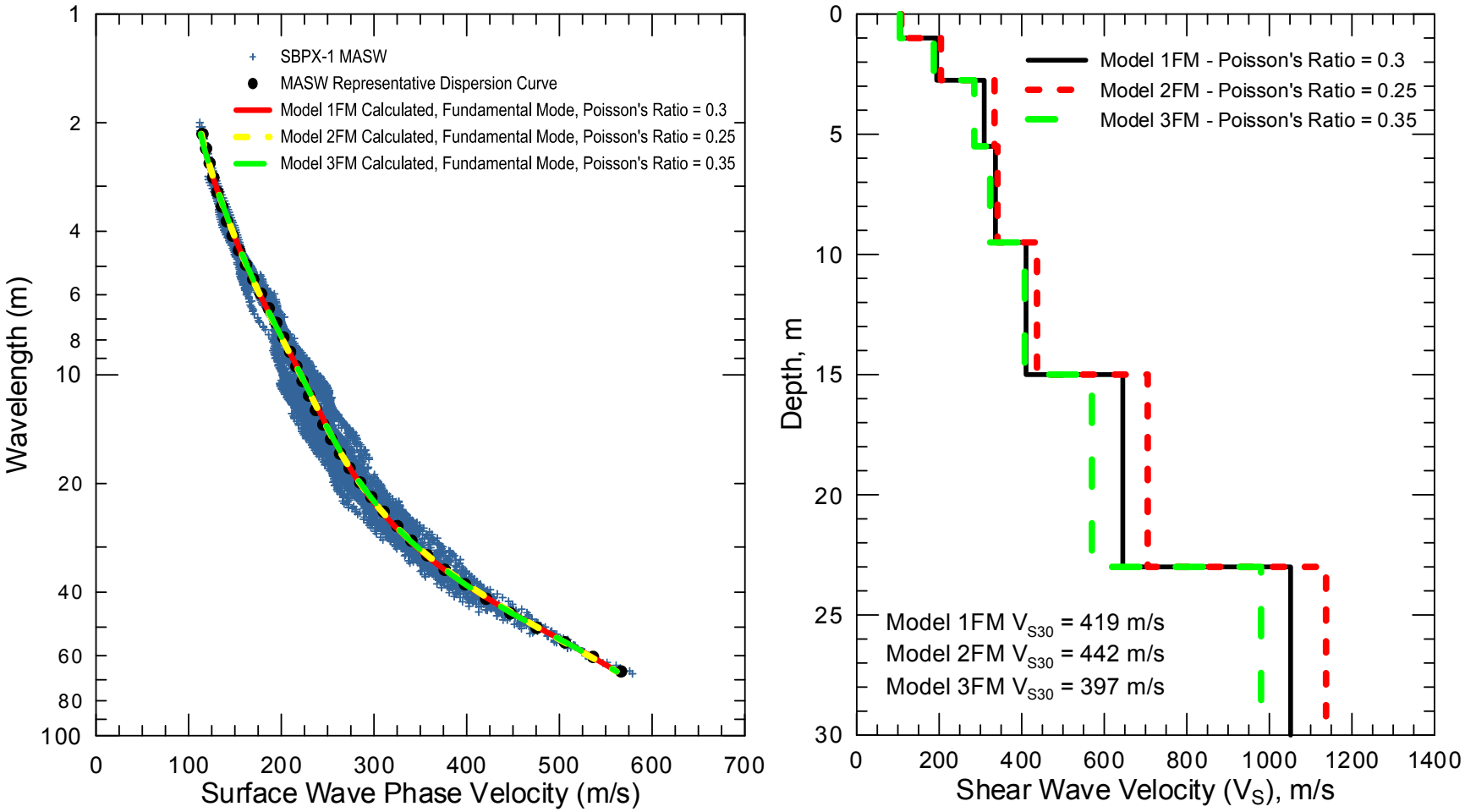

CI.SBPX - Field, representative and inverted theoretical surface wave dispersion data (left) and V_S models based on different values of Poisson's ratio and fundamental mode assumption (right).

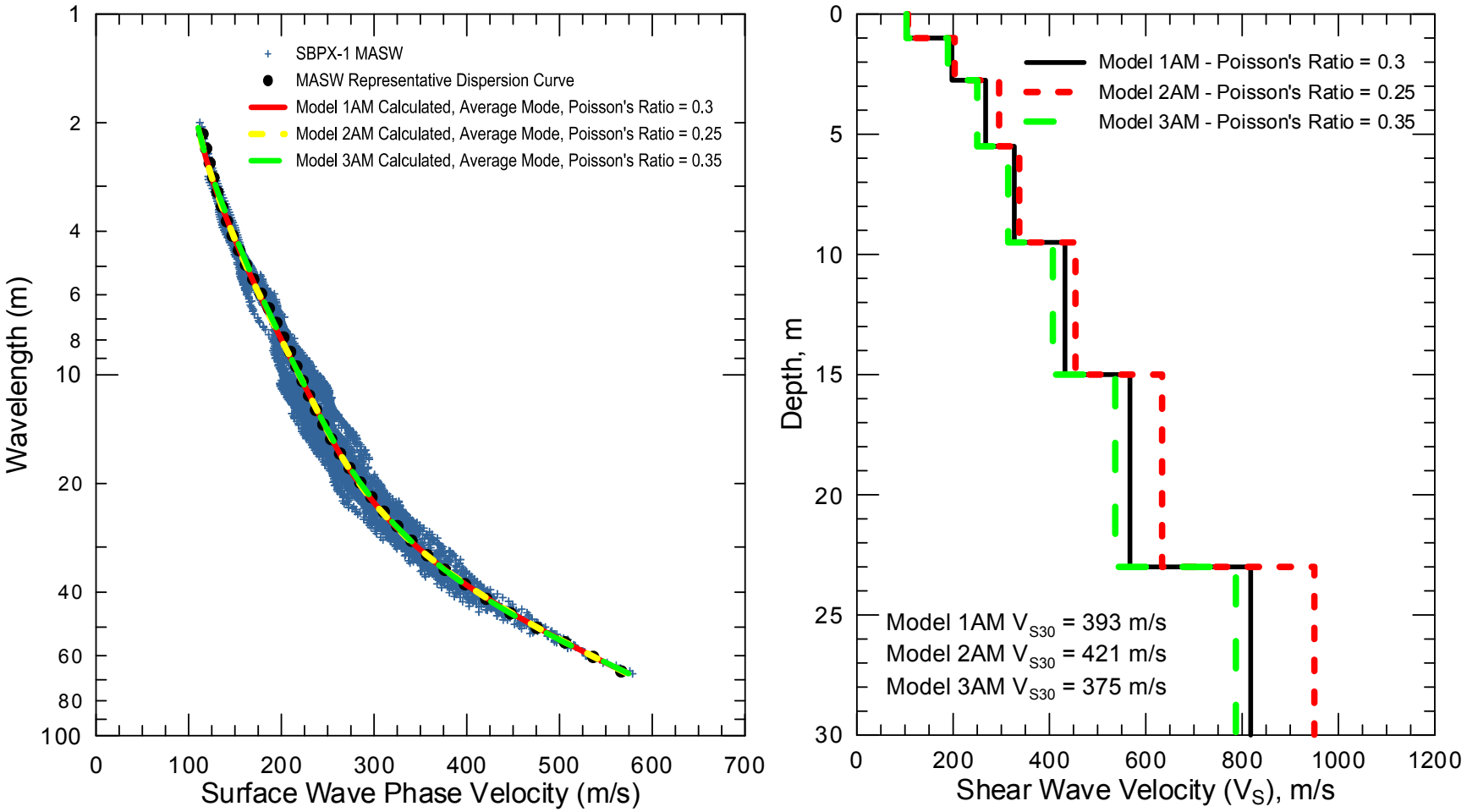

CI.SBPX - Field, representative and inverted theoretical surface wave dispersion data (left) and V_S models utilizing different values of Poisson's ratio and average mode assumption (right).

Site CI.SCI2

Location: San Clemente Island, Los Angeles County. California

Latitude: 32.97990 **Longitude:** -118.54697
(Station coordinates provided by USGS, WGS84 coordinate system)

V_{S30} (measured): 442 m/s

V_{S30} (adjusted to more accurately reflect seismic station conditions): 442 m/s (no adjustment necessary).

NEHRP Site Class: C

Geomatrix Code: AQB/AVB

Geologic Conditions/Observations: Seismic station located on geologic unit mapped as Quaternary (Pleistocene) sand deposits. Tertiary (Miocene) rhyolite outcrops near the site and may be located at shallow depth.

Site Conditions: Rural site located on an island with undulating hilly topography. The test location was alongside a gravel road.

Geophysical Methods Utilized: HVSR, Seismic Refraction (P- and S-wave), MASW (Rayleigh wave), MALW (Love wave)

Geophysical Testing Arrays:

1. Array SCI2-1 (48 channel MASW and P-wave seismic refraction array utilizing 4.5 Hz vertical geophones spaced 1.5 m apart for a length of 70.5 m, forward and reverse shot locations with multiple source offsets and source types and multiple interior shot locations).
2. Array SCI2-1 (48 channel MALW and S-wave seismic refraction array utilizing 4.5 Hz horizontal geophones spaced 1.5 m apart for a length of 70.5 m, coincident with MASW and P-wave seismic refraction array of same name).
3. Three HVSR measurement locations: two distributed along array SCI2-1 and one adjacent to the seismic station.

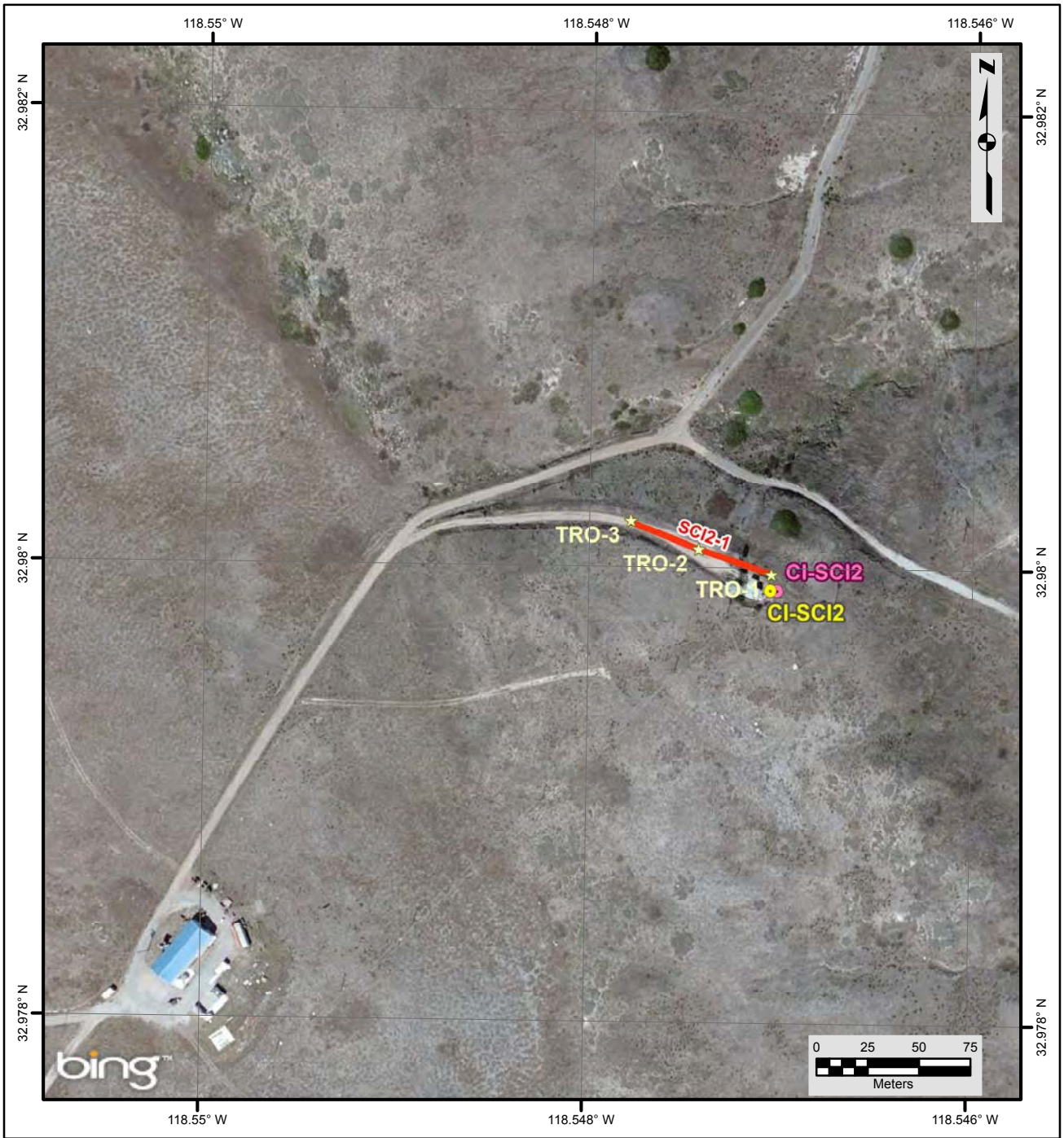

Legend

- Seismic Station - Approximate Surveyed Location
- Seismic Station - Approximate Location of Record
- H/V Spectral Ratio Location
- MASW and Seismic Refraction Array

NOTES:
1. WGS 1984 COORDINATE SYSTEM
2. Image Source: (c) Microsoft Corporation and its suppliers

File Name: CI-SCI2-I

Date: 2/7/2013

USGS science for a changing world

GEOVision geophysical services

RECOVERY.GOV

SITE MAP
CI•SCI2

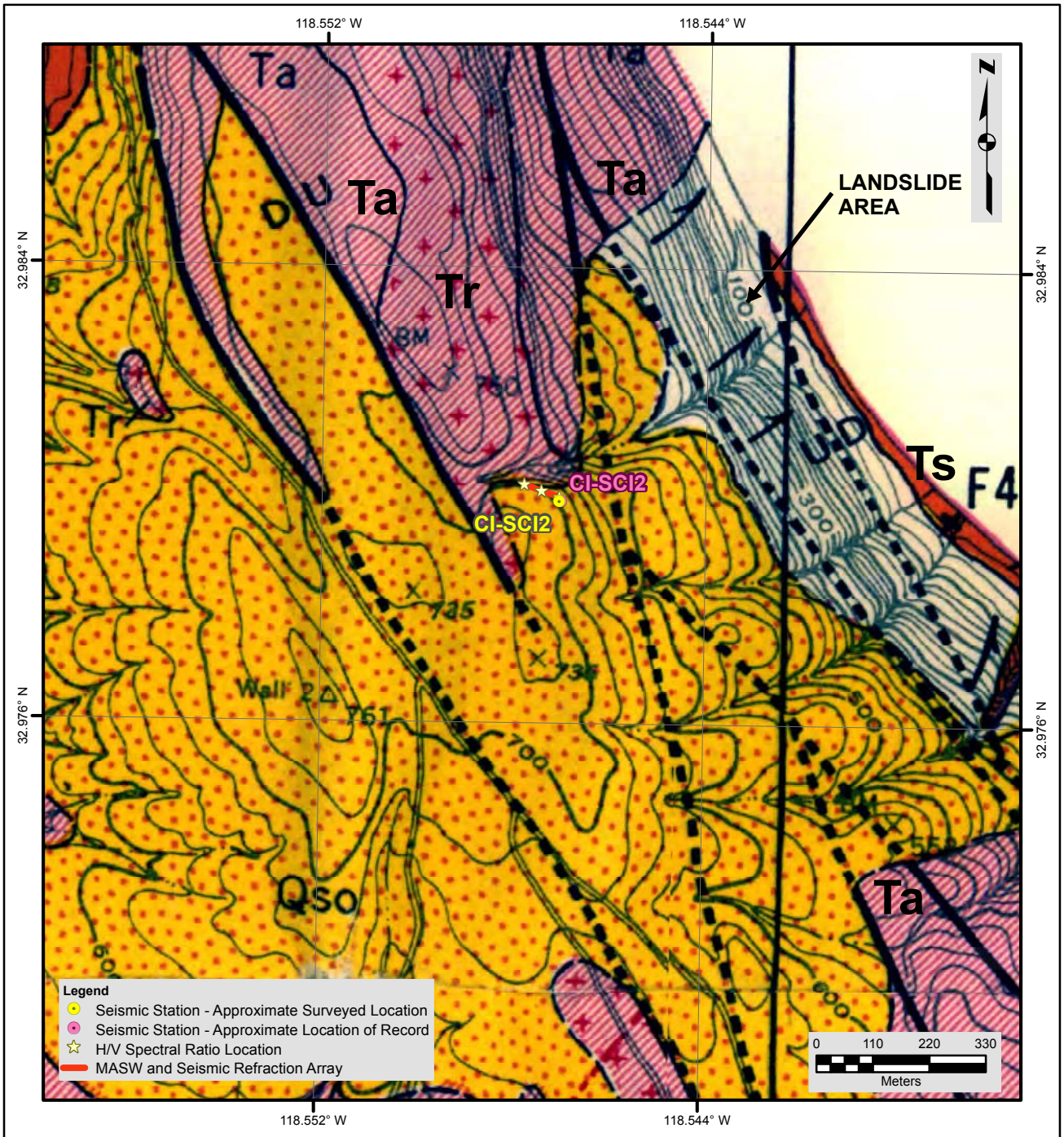

Description of Geologic Map Units

Qso = Quaternary (Pleistocene?) older sand deposits; sand, silt and clay, mostly weathered, locally cemented
Ts = Tertiary (Miocene) marine sedimentary rocks; thin-bedded siltstone shale diatomite and limestone, basal sandstone composed of volcanic detritus
Tr = Tertiary (Miocene) ryholite; massive to prominently flow-banded porphyritic rock, minor tuff
Ta = Tertiary (Miocene) andesite; volcanic flows and pyroclastic rocks, highly fractured and vesicular

NOTES:
1. WGS 1984 COORDINATE SYSTEM
2. Geologic Map and Sections of San Clemente Island, California, by F.H. Olmstead with U.S. Dept. of the Navy, 1958
3. See site map for details of geophysical survey

File Name: CI-SCI2

Date: 2/7/2013

USGS science for a changing world

GEOVision geophysical services

GEOLOGIC MAP
CI•SCI2

CI.SCI2 seismic station

CI.SCI2 seismic station

Looking southeast along array SCI2-1 towards building housing seismic station and at HVSR station TRO-3

Looking northwest towards center of array SCI2-1 and HVSR station TRO-2

P-wave seismic refraction acquisition along array SCI2-1

Location of Geophysical Testing Arrays:

Location	Latitude	Longitude
SCI2-1, Northwest End of MASW/Refraction Array	32.98019	-118.54774
SCI2-1, Center of MASW/Refraction Array	32.98008	-118.54738
SCI2-1, Southeast End of Refraction/MASW Array	32.97998	-118.54702
HVSR Sensor Tromino ENGY (TRO-1)	32.97997	-118.54700
HVSR Sensor Tromino ENGY (TRO-2)	32.98008	-118.54738
HVSR Sensor Tromino ENGY (TRO-3)	32.98020	-118.54773
CI.SCI2 Seismic Station	32.97990	-118.54701

Notes: 1) WGS84 Coordinate System (decimal degrees)
2) Survey accuracy is estimated at 1 to 2 m

Results:

V_S Model

Depth to Top of Layer (m)	Layer Thickness (m)	S-Wave Velocity (m/s)	Inferred P-Wave Velocity (m/s)	Assumed Poisson's Ratio	Assumed Density (g/cm^3)
0	1.5	210	394	0.3	1.70
1.5	2.5	273	510	0.3	1.80
4	4	336	628	0.3	1.90
8	5	358	670	0.3	1.90
13	7	539	1009	0.3	2.00
20	8	753	1409	0.3	2.10
28	>2	979	1831	0.3	2.15

Notes: 1) Depth of investigation is about 30 m.
2) Bottom layer is a half space.
3) Half space velocity not well resolved.

Observations/Discussion:

- Seismic testing was conducted along a gravel road near the seismic station as this was the only location in both close proximity and similar elevation to the seismic station. Both P- and S-wave seismic refraction, MASW and MALW data were acquired along a single array. S-wave seismic refraction and MALW data were of poor quality and not used for site characterization.
- HVSR plots are different at every station indicating that there is likely lateral velocity variation at this site. All HVSR plots do, however, have elevated HVSR response at a frequency between 1.5 and 8 Hz. There are no distinct HVSR peaks that occur at every measurement location.

- The P-wave refraction data for array SCI2-1 were modeled using a tomographic inversion routine with a smooth velocity gradient starting model. The seismic refraction model was extended to far offset shot locations to extend depth of investigation.
- The seismic refraction survey design allowed P-wave velocity to be imaged to a maximum depth of about 18 m. The seismic refraction model shows that P-wave velocity is about 300 to 450 m/s at the surface, increasing to 600 m/s at a depth of 1 to 5 m, 800 m/s at a depth of 5 to 8 m, 1,000 m/s at a depth of 8 to 11 m and greater than 1,100 m/s at a depth of 9 to 18 m. The maximum P-wave velocity in the upper 18 m is about 1,200 m/s. P-wave velocities greater than 600 to 700 m/s are likely associated with weathered ryholite, which outcrops in the site vicinity.
- The seismic refraction model indicates that there is significant near surface lateral velocity variation at this site.
- Noise conditions at the site were not sufficient for application of passive surface wave techniques.
- MASW data reduction was complicated by the near surface lateral velocity variation, which resulted in significant scatter, about 40 to 60 m/s, in the surface wave dispersion data.
- The minimum wavelength surface wave phase velocity data extracted from the 48-channel MASW array was about 20 m. Reducing data from smaller hammer sources using a limited offset receiver array (i.e. less active geophones) allowed for extraction of surface wave dispersion data to a minimum wavelength of about 3.5 m.
- A representative dispersion curve was generated for the MASW data set using a moving average, polynomial curve fitting routine and used for modeling.
- Surface wave depth of investigation is about 30 m based on half of maximum wavelength criteria.
- The inferred P-wave velocities in the surface wave model, based on an assumed Poisson's ratio of 0.3 and modeled S-wave velocity, are consistent with the P-wave refraction model at shallow depths but appear to overestimate the depth at which P-wave velocity exceeds 1,000 m/s. The seismic refraction survey did not image to great enough depth to validate the relatively high S-wave velocities at depths below 20 m in the surface wave model.
- V_{S30} is 442 m/s (NEHRP Site Class C).
- The S-wave velocity model derived from the surface wave testing is believed to be representative of average subsurface velocity structure. However, given the significant near surface lateral velocity variation and scatter in the surface wave dispersion data, V_{S30} is probably more accurately constrained than the actual V_S model. The scatter in the surface wave dispersion is such that the presented V_{S30} may vary by 5 to 10% in the immediate site vicinity, not enough to change NEHRP Site Class.

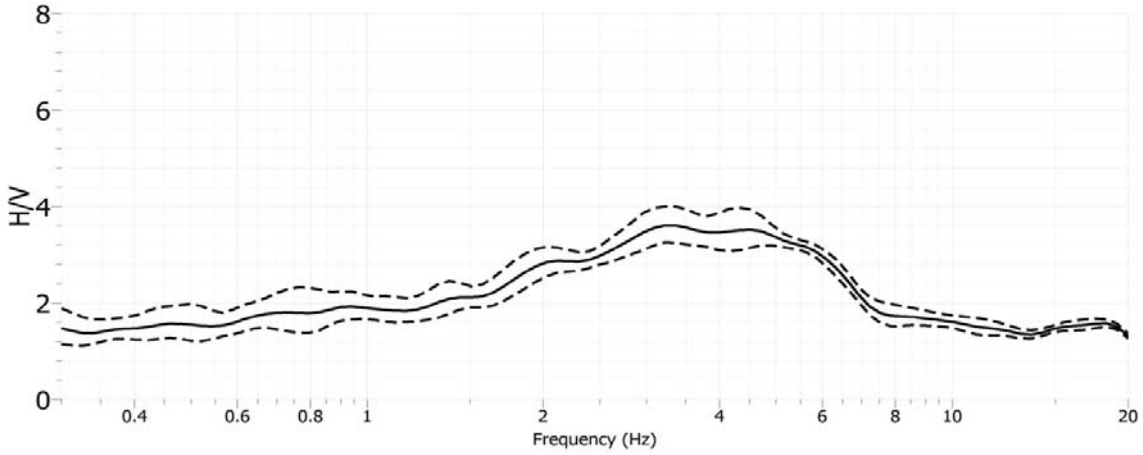

Site CI.SCI2, H/V Spectral Ratio, Array SCI2-1, Sensor TRO-3

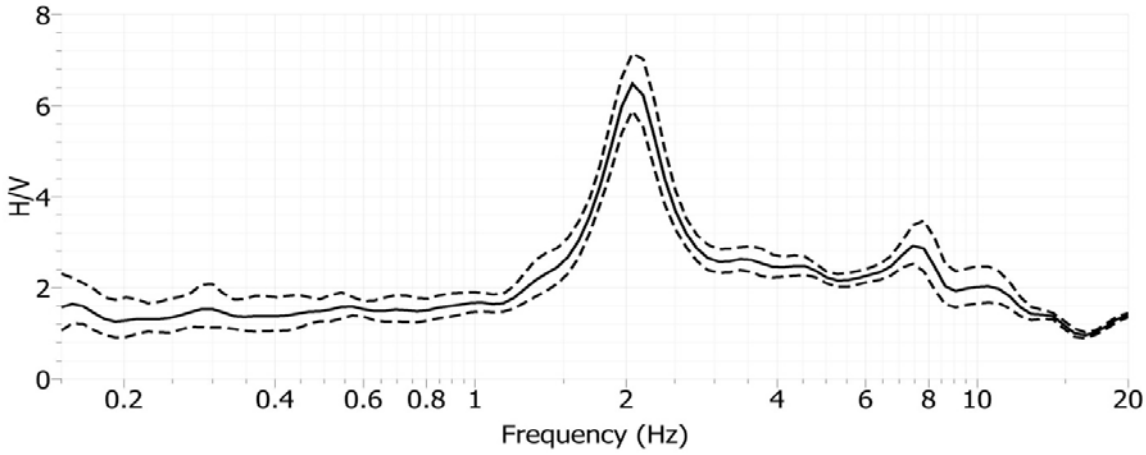

Site CI.SCI2, H/V Spectral Ratio, Array SCI2-1, Sensor TRO-2

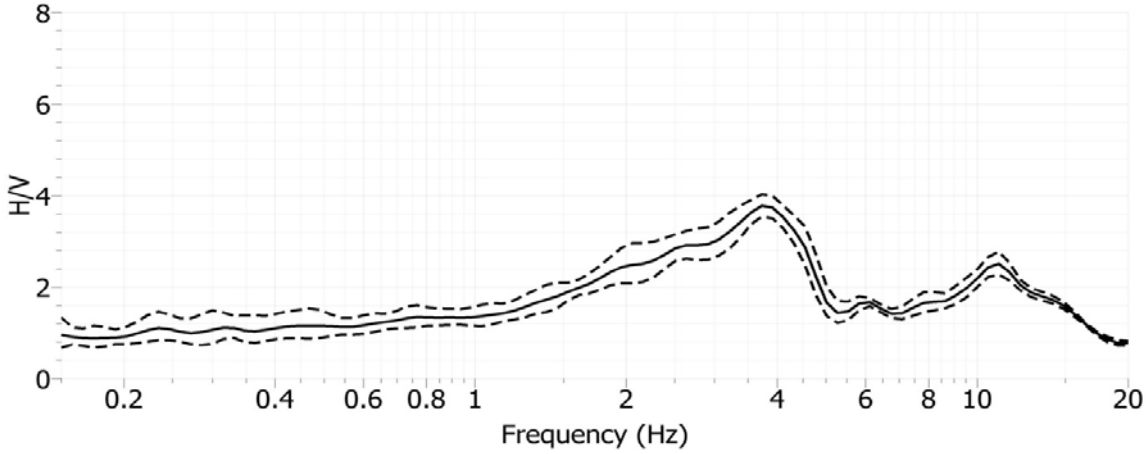

Site CI.SCI2, H/V Spectral Ratio, Array SCI2-1, Sensor TRO-1

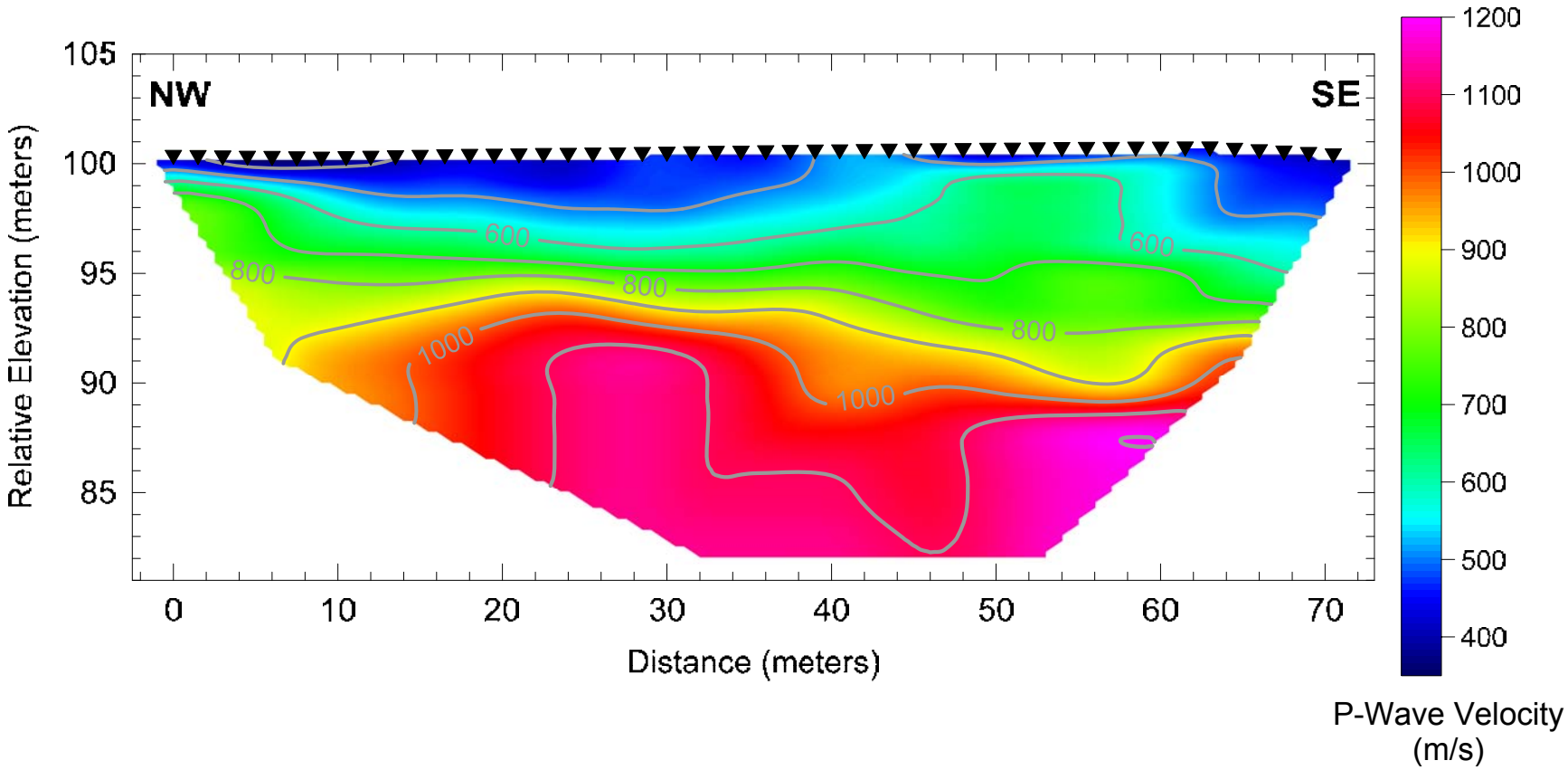

Array SCI2-1 – Tomographic seismic refraction model developed using a smooth velocity gradient starting model

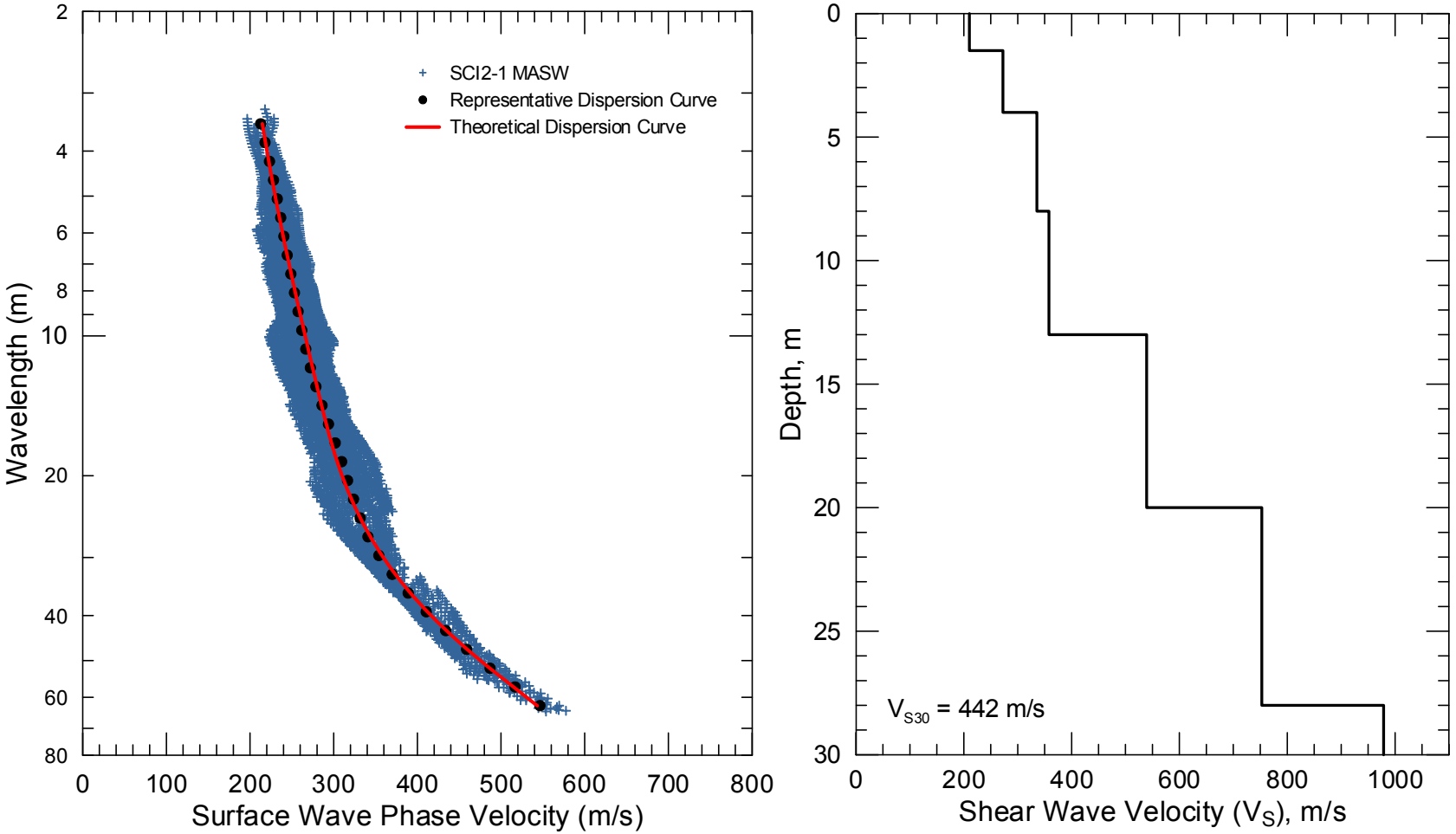

CI.SCI2 - Field, representative and inverted theoretical surface wave dispersion data (left) and associated V_S model (right)

Site CI.SCZ2

Location: Santa Cruz Island 2, Santa Barbara County, California

Latitude: 33.99549 **Longitude:** -119.63514

(Station coordinates modified based on field GPS survey, WGS84 coordinate system)

V_{S30} (measured): 313 m/s

V_{S30} (adjusted to more accurately reflect seismic station conditions): 325 m/s (average S-wave velocity between 1 and 31 m adjusting for inferred sensor depth).

NEHRP Site Class: D

Geomatrix Code: IMD

Geologic Conditions/Observations: Site located on geologic unit mapped as Tertiary (Miocene) Monterey Formation; a thin bedded marine siliceous shale that is closely fractured and crumbly. The attitude of the bedding is highly variable in the site vicinity with nominal mapped dips of 20 to 30 degrees to the northeast, southeast, south and north. The seismic station is located in close proximity to a mapped syncline.

Site Conditions: Rural site. Hilly topography in site vicinity. There is about a 4 m increase in elevation to the southeast along the 70.5 m long seismic line.

Geophysical Methods Utilized: HVSR, MASW

Geophysical Testing Arrays:

1. Array SCZ2-1 (48 channel MASW array utilizing 4.5 Hz vertical geophones spaced 1.5 m apart for a length of 70.5 m, forward and reverse shot locations with multiple source offsets and source types and multiple interior shots).
2. Three HVSR measurement locations: two distributed along array SCZ2-1 and the other near the seismic station.

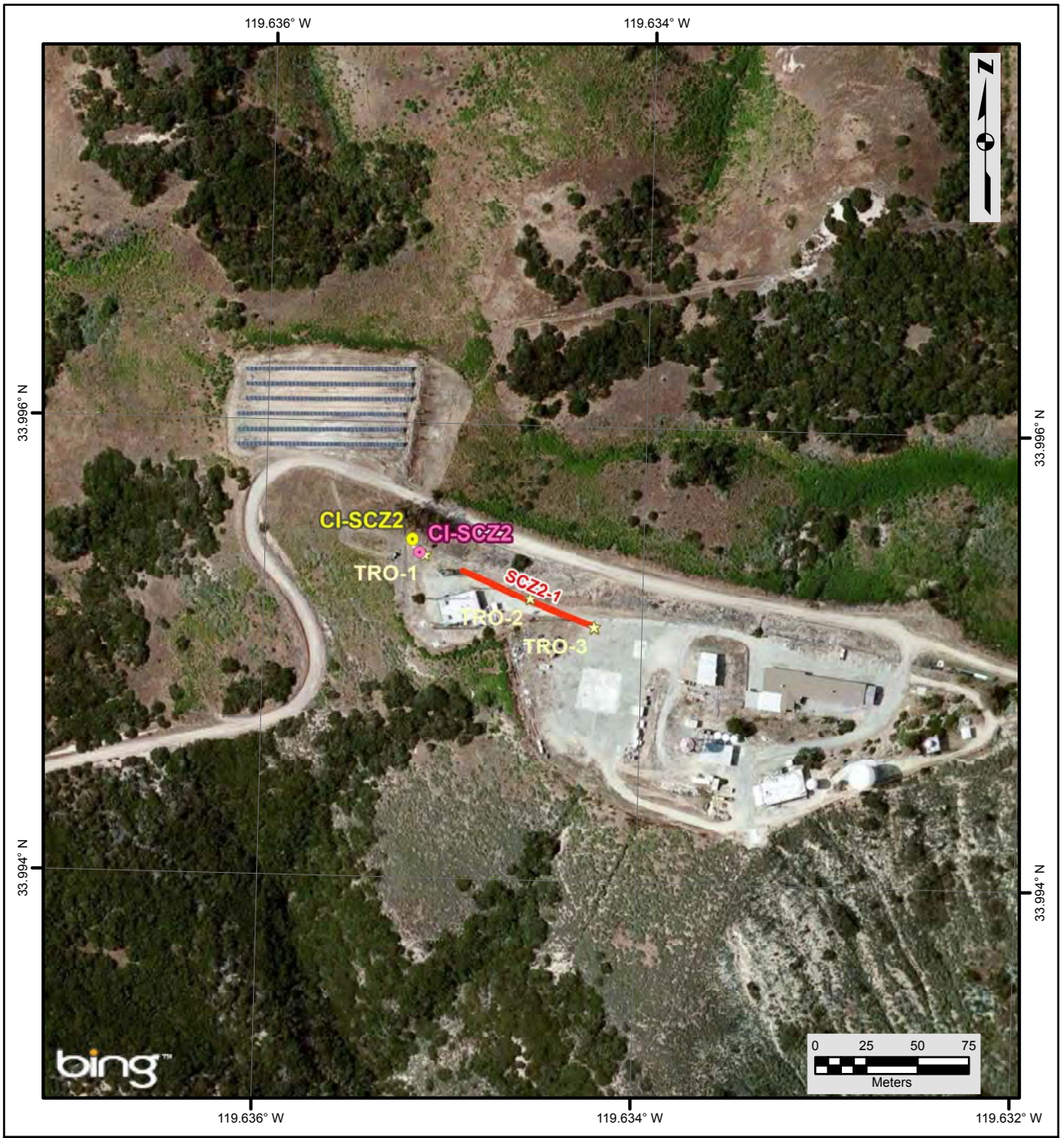

Legend

- Seismic Station - Approximate Surveyed Location
- Seismic Station - Approximate Location of Record
- H/V Spectral Ratio Location
- MASW and Seismic Refraction Array

NOTES:
1. WGS 1984 COORDINATE SYSTEM
2. Image Source: (c) Microsoft Corporation and its suppliers

File Name: CI-SCZ2-I

Date: 2/7/2013

USGS science for a changing world

GEOVision geophysical services

RECOVERY.GOV

SITE MAP
CI•SCZ2

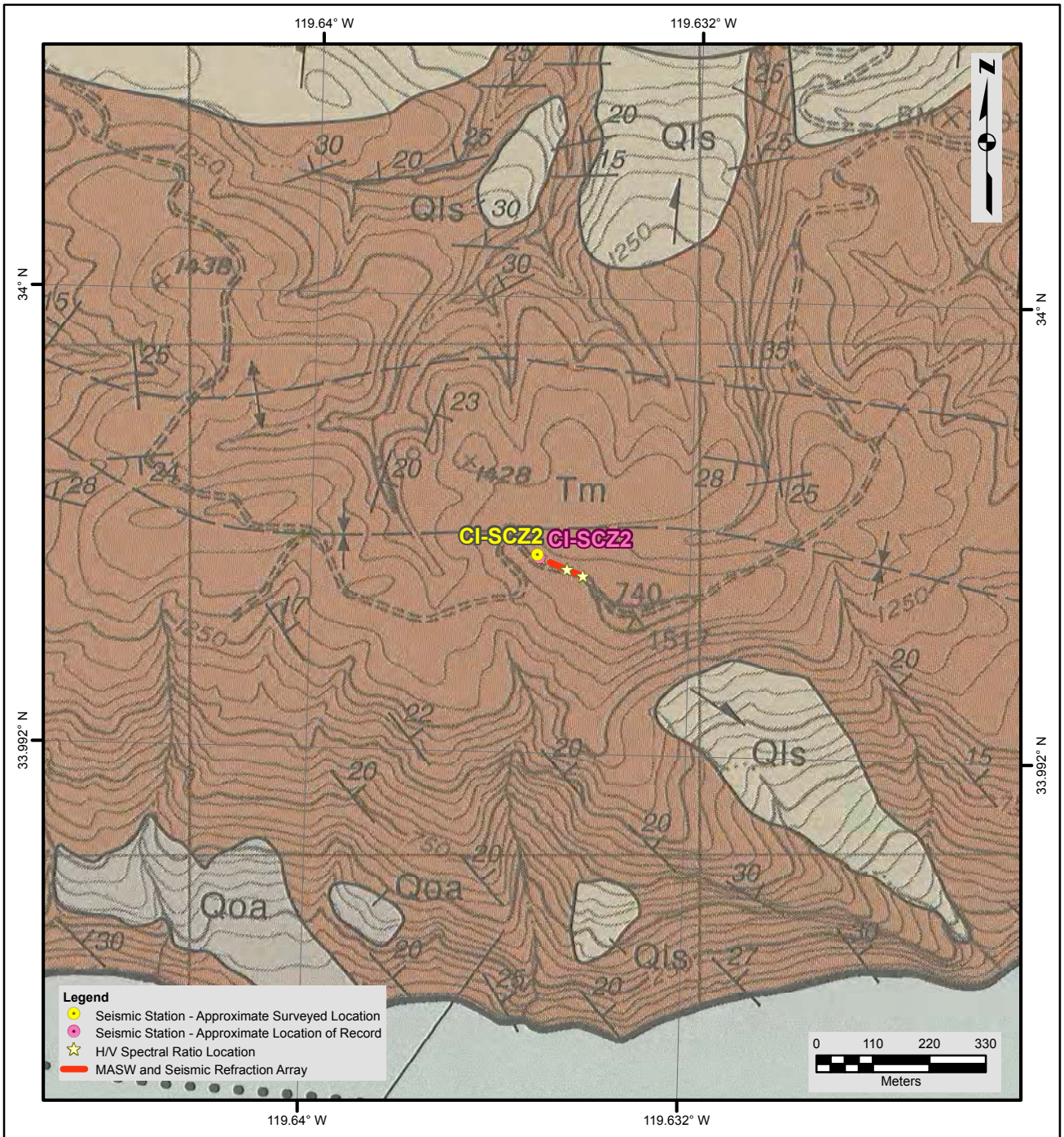

Description of Geologic Map Units

Qls = Quaternary (Holocene) landslide debris, mostly Monterey Shale (Tm)
Qoa = Quaternary (Pleistocene) terrace sediments, older alluvium derived from local bedrock, gray, slightly indurated
Tm = Tertiary (Miocene) Monterey Formation; thin bedded siliceous shale, marine, crumbly, closely fractured

NOTES:
1. WGS 1984 COORDINATE SYSTEM
2. Geologic Map of Eastern Santa Cruz Island, Santa Barbara, California by Thomas W. Dibblee, Jr., 2001
3. See site map for details of geophysical survey

File Name: CI-SCZ2
Date: 2/7/2013

USGS science for a changing world
GEOVision geophysical services

GEOLOGIC MAP
CI•SCZ2

Looking southeast at CI.SCZ2 seismic station

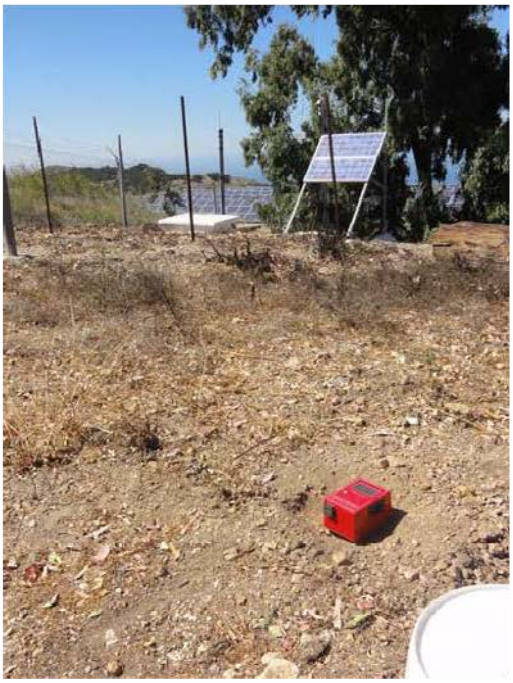

HVSR station TRO-1 (Tromino ENGR) located near seismic station

Looking southeast towards array SCZ2-1 from seismic station

Looking northwest from center of array CI.SCZ2 and at HVSR station TRO-2

Looking southeast along array SCZ2-1

Location of Geophysical Testing Arrays:

Location	Latitude	Longitude
SCZ2-1, Northwest End of MASW/Refraction Array	33.99535	-119.63487
SCZ2-1, Center of MASW/Refraction Array	33.99523	-119.63451
SCZ2-1, Southeast End of MASW/Refraction Array	33.99512	-119.63417
HVSR Sensor Tromino ENGY (TRO-1)	33.99542	-119.63507
HVSR Sensor Tromino ENGY (TRO-2)	33.99524	-119.63451
HVSR Sensor Tromino ENGY (TRO-3)	33.99512	-119.63417
CI.SCZ2 Seismic Station	33.99549	-119.63514

Notes: 1) WGS84 Coordinate System (decimal degrees)
2) Survey accuracy is estimated at 1 to 2 m.

Results:

V_S Model 1

Depth to Top of Layer (m)	Layer Thickness (m)	S-Wave Velocity (m/s)	Inferred P-Wave Velocity (m/s)	Assumed Poisson's Ratio	Assumed Density (g/cm^3)
0	1	182	340	0.3	1.70
1	2	214	400	0.3	1.70
3	3	233	435	0.3	1.70
6	5	251	470	0.3	1.75
11	7	301	564	0.3	1.80
18	8	461	862	0.3	1.90
26	>4	528	988	0.3	1.90

Notes: 1) Depth of investigation is about 30 m.
2) Bottom layer is a half space.

V_S Model 2

Depth to Top of Layer (m)	Layer Thickness (m)	S-Wave Velocity (m/s)	Inferred P-Wave Velocity (m/s)	Assumed Poisson's Ratio	Assumed Density (g/cm^3)
0	1	182	341	0.3	1.70
1	2	212	397	0.3	1.70
3	3	237	443	0.3	1.70
6	4	248	464	0.3	1.75
10	5	265	495	0.3	1.80
15	7	414	775	0.3	1.90
22	>8	506	947	0.3	1.90

Notes: 1) Depth of investigation is about 30 m.
2) Bottom layer is a half space.

V_S Model 3

Depth to Top of Layer (m)	Layer Thickness (m)	S-Wave Velocity (m/s)	Inferred P-Wave Velocity (m/s)	Assumed Poisson's Ratio	Assumed Density (g/cm^3)
0	1	181	340	0.3	1.70
1	2	214	400	0.3	1.70
3	3	233	435	0.3	1.70
6	6	250	468	0.3	1.75
12	9	344	643	0.3	1.80
21	8	468	875	0.3	1.90
29	>1	560	1047	0.3	1.90

Notes: 1) Depth of investigation is about 30 m.
2) Bottom layer is a half space.

Observations/Discussion:

- HVSR plots are generally similar at all measurement locations, although there are no clear distinct HVSR peaks, validating the 1-D velocity structure assumption. There is an elevated HVSR response in the 0.5 to 2.5 Hz range with possible weak peaks at about 0.8 and 1.5 Hz.
- P-wave seismic refraction data were acquired at this site, but was considered too noisy to model. Structures in the site vicinity generated significant noise. The P-wave refraction data were, however, reviewed and sediments in the upper 10 m, or more, have very low P-wave velocity. There is evidence of a higher velocity refractor at a depth on the order of 15 to 25 m. There is no evidence of shallow groundwater at the site.
- Noise conditions at the site were not sufficient to apply passive surface wave techniques.
- Only hammer energy sources were utilized at the site due to the remote location and transportation limitations. A 30 m depth of investigation is generally the maximum depth of investigation for a 20 lb sledge hammer at a very stiff soil site with low noise. At this site, a Rayleigh wave with 40 m wavelength occurs at a frequency of about 7.5 Hz, which can reliably be obtained with a 20 lb hammer. However, a 70 m wavelength Rayleigh wave occurs at a frequency of about 5.5 Hz, which is pushing the envelope for a 20 lb sledge hammer. Scatter in the surface wave dispersion data is no worse at long wavelengths (low frequencies) than at shorter wavelengths (high frequencies) so the phase velocity data are probably reliable to a wavelength of about 60 m.
- The minimum wavelength surface wave phase velocity data extracted from the 48-channel MASW array is about 12 m. Data reduction using seismic records from smaller hammer sources and a limited offset receiver array (i.e. less active geophones) allowed extraction of surface wave dispersion data to a minimum wavelength of about 1.5 m.
- There is nominally about 30 to 40 m/s scatter in the MASW dispersion data likely due to lateral velocity variation.
- A representative dispersion curve was generated for the MASW data set using a moving average, polynomial curve fitting routine and used for modeling.
- Three V_S models (Models 1 to 3) were generated to demonstrate the nonuniqueness in the inversion of surface wave phase velocity data. As expected, V_{S30} is almost identical between the three models. Model 1 has intermediate depth to the impedance contrast and should be utilized if a single model is used to represent subsurface velocity structure.
- Surface wave depth of investigation is about 30 m based on half of maximum wavelength criteria.
- V_{S30} is 313, 315 and 310 m/s for Models 1 to 3, respectively and averages 313 m/s (Site Class D).
- Average S-wave velocity between 1 m (inferred sensor depth) and 31 m is 325, 327 and 322 m/s for Models 1 to 3, respectively and averages 325 m/s (Site Class D).

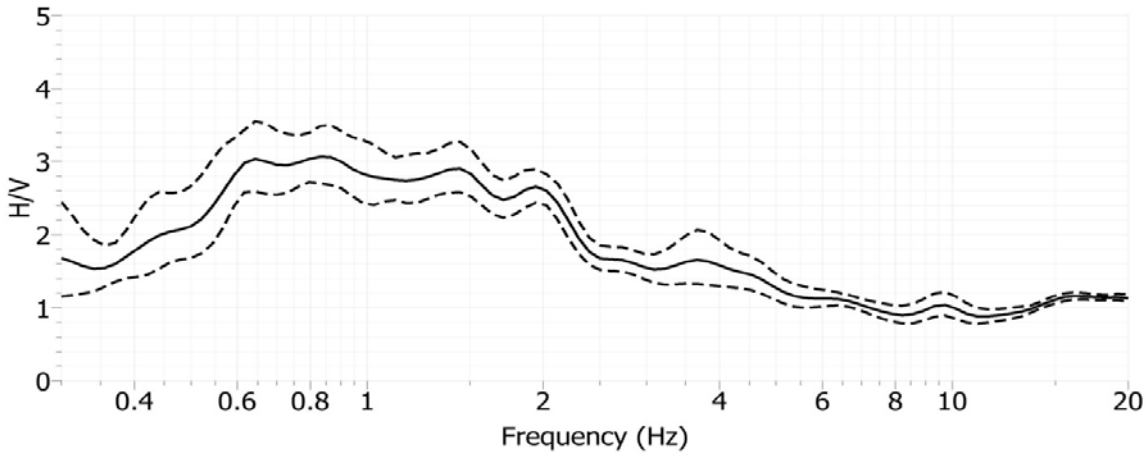

Site CI.SCZ2, H/V Spectral Ratio, Near Seismic Station, TRO-1

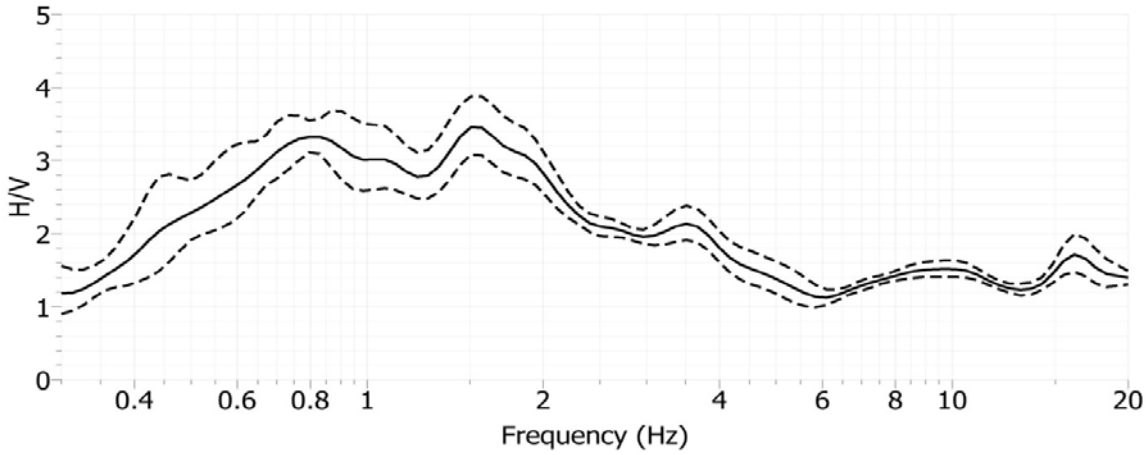

Site CI.SCZ2, H/V Spectral Ratio, Array SCZ2-1, TRO-2

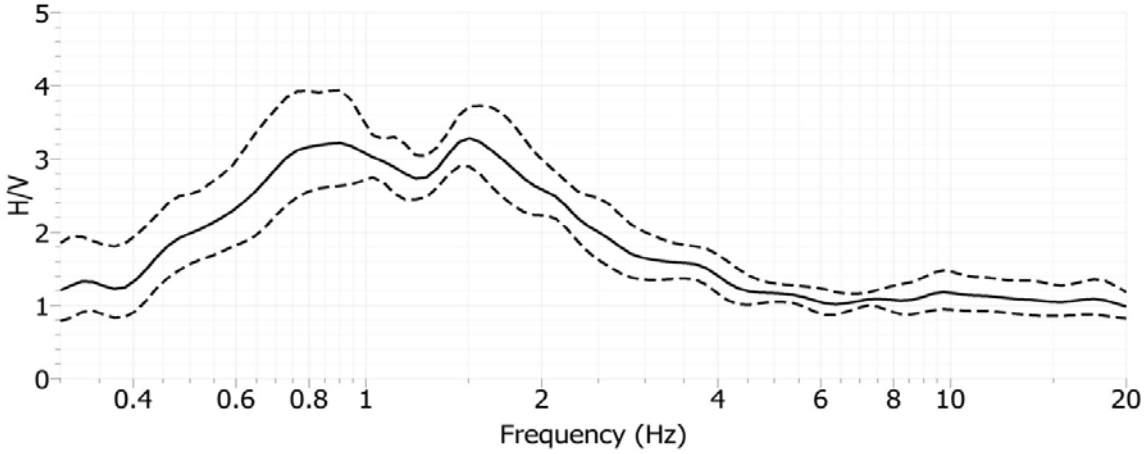

Site CI.SCZ2, H/V Spectral Ratio, Array SCZ2-1, TRO-3

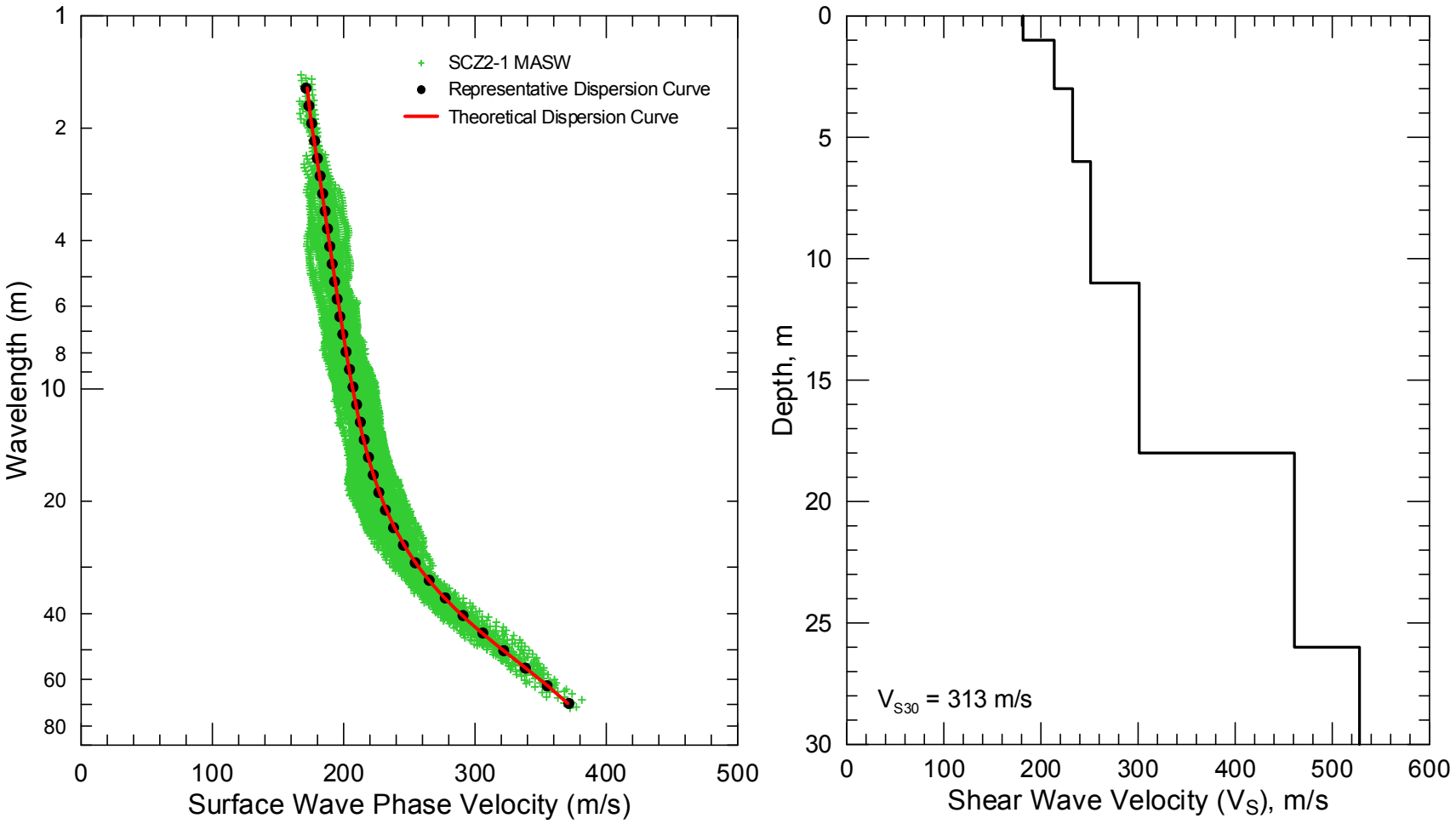

CI.SCZ2 - Field, representative and inverted theoretical surface wave dispersion data (left) and associated V_S model (right)

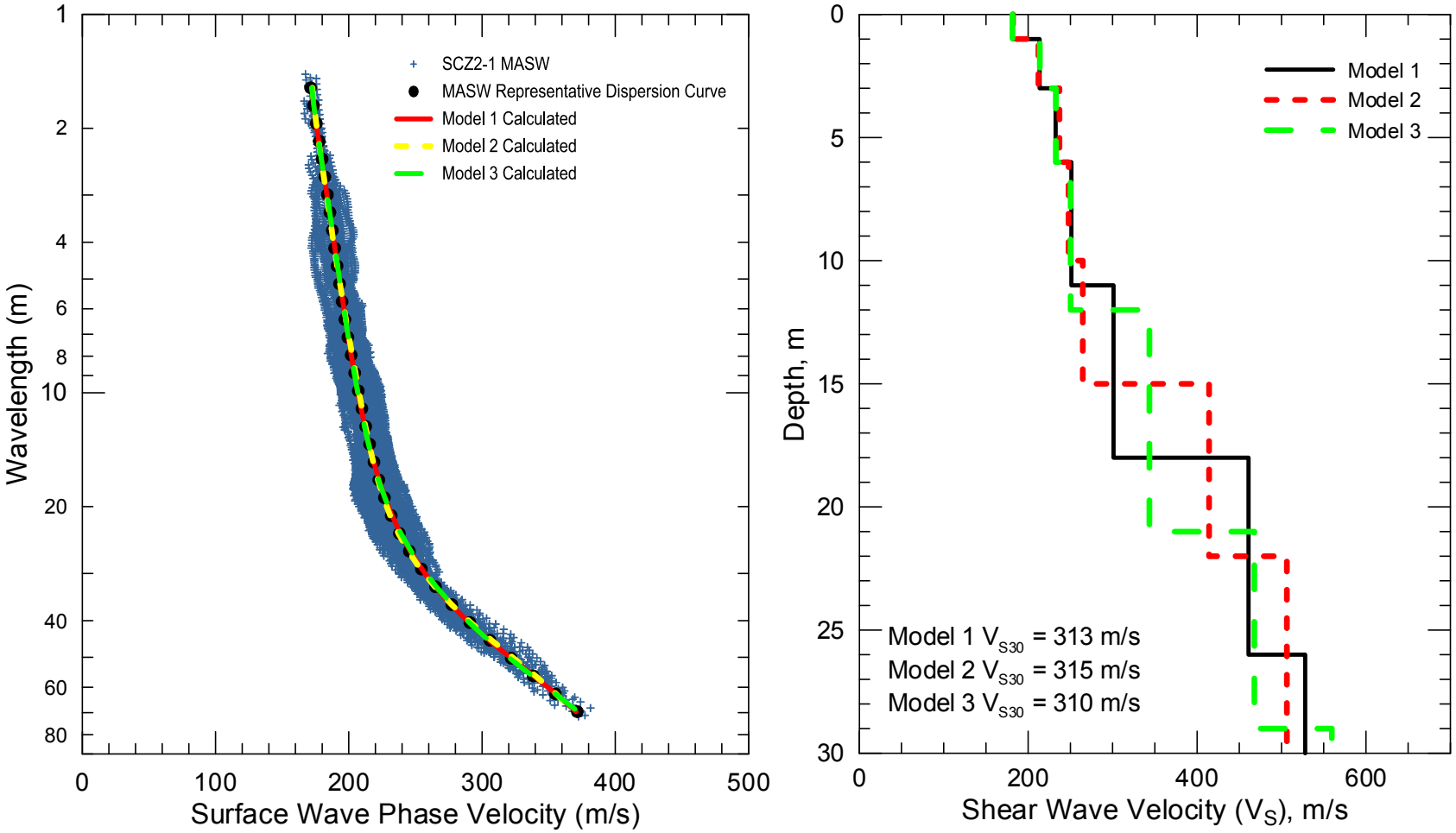

CI.SCZ2 - Field, representative and inverted theoretical surface wave dispersion data (left) and associated V_S models (right) demonstrating nonuniqueness.

Site CI.SDG

Location: San Diego Gas & Electric Mission Control Center, San Diego, California

Latitude: 32.78400 **Longitude:** -117.13805
(Station coordinates provided by USGS, WGS84 coordinate system)

V_{S30} (measured): 439 m/s

V_{S30} (adjusted to more accurately reflect seismic station conditions): 439 m/s (no adjustment necessary).

NEHRP Site Class: C

Geomatrix Code: IQD

Geologic Conditions/Observations: Seismic station located on Quaternary (Pleistocene) old alluvial flood plain deposits. Both Tertiary (Middle Eocene) Mission Valley Formation (sandstone) and Stadium Conglomerate located in close proximity to seismic station.

Site Conditions: Developed site. Hilly topography in site vicinity. Topography declines gently to the northwest in the test area (about 3.5 m over the 70.5 m MASW array). There was limited space for testing at the site.

Geophysical Methods Utilized: HVSR, Seismic Refraction, MASW

Geophysical Testing Arrays:

1. Array SDG-1 (48 channel MASW and P-wave seismic refraction array utilizing 4.5 Hz vertical geophones spaced 1.5 m apart for a length of 70.5 m, forward and reverse shot locations with multiple source offsets and source types and multiple interior shot locations).
2. Three HVSR measurement locations distributed along array SDG-1.

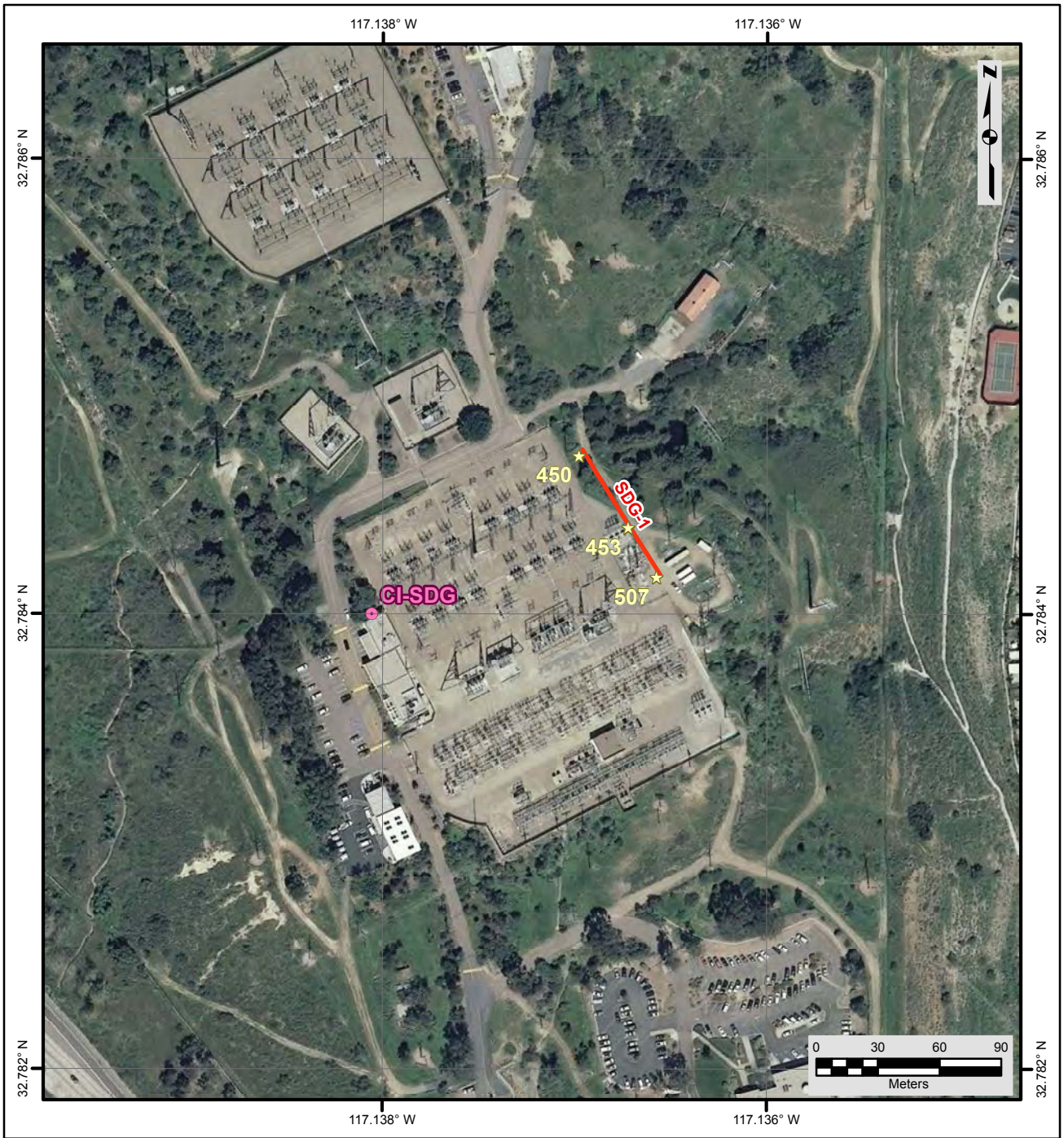

Legend

- Seismic Station - Approximate Location of Record
- H/V Spectral Ratio Location
- MASW and Seismic Refraction Array

NOTES:
1. WGS 1984 COORDINATE SYSTEM
2. Image Source: ESRI, i-cubed, USDA FSA, USGS, AEX, GeoEye, Getmapping, Aerogrid, IGP

File Name: CI-SDG-I

Date: 10/13/2011

USGS science for a changing world

GEOVision geophysical services

RECOVERY.GOV

SITE MAP
CI•SDG

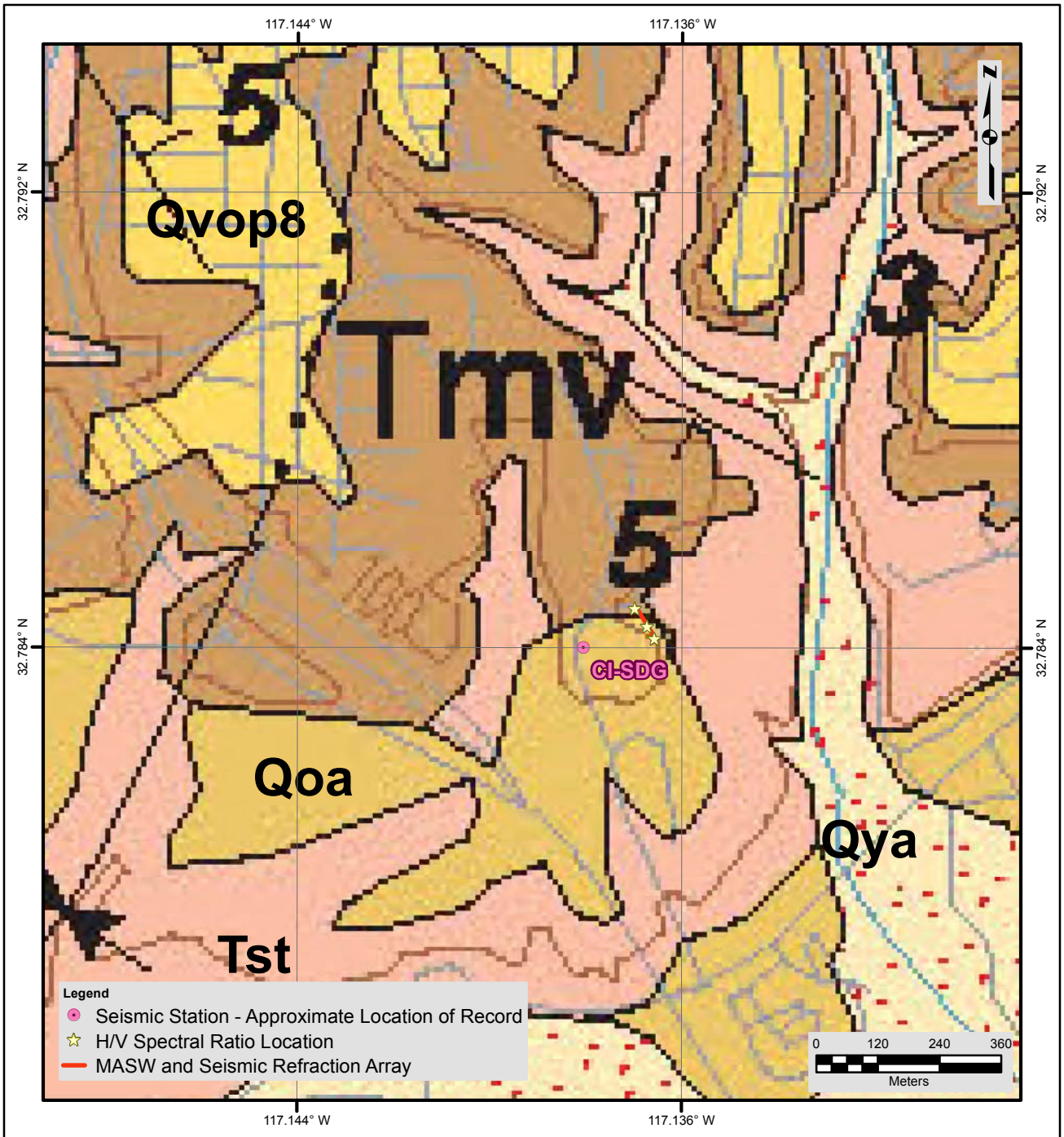

Description of Geologic Map Units

Qya = Quaternary (Holocene) young alluvial flood-plain deposits, poorly consolidated and sorted
Qoa = Quaternary (Pleistocene) older alluvial flood-plain deposits, poorly sorted
Qvop8 = Quaternary (Middle to Early Pleistocene) very old paralic deposits, siltstone to conglomerate
Tmv = Tertiary (Middle Eocene) Mission Valley Formation; sandstone, soft, minor cobble conglomerate
Tst = Tertiary (Middle Eocene) Stadium Conglomerate, cobble conglomerate, massive, coarse sandstone matrix

NOTES:
1. WGS 1984 COORDINATE SYSTEM
2. Geologic Map of the San Diego 30' x 60' Quadrangle, Southern California
by Michael P. Kennedy and Siang S. Tan, 2008
3. See site map for details of geophysical survey

File Name: CI-SDG

Date: 10/13/2011

USGS science for a changing world

GEOVision geophysical services

RECOVERY.GOV

GEOLOGIC MAP
CI•SDG

Looking northeast at CI.SDG seismic station.
Array SDG-1 on other site of substation

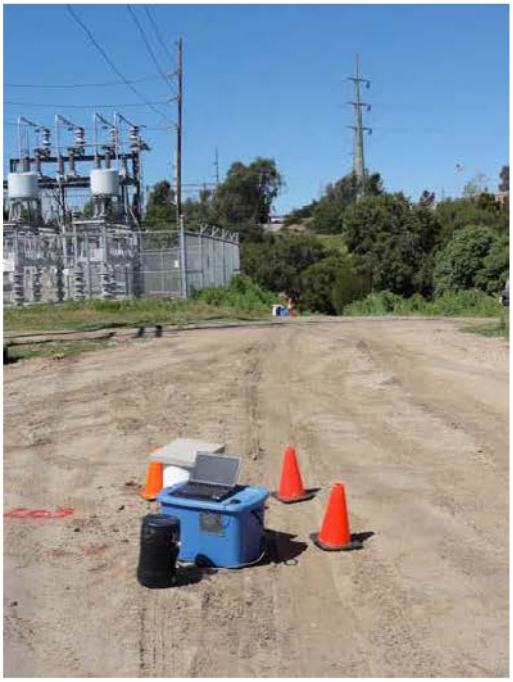

Looking northwest along array SDG-1
and at HVSR sensor 507

Looking northwest along array SDG-1

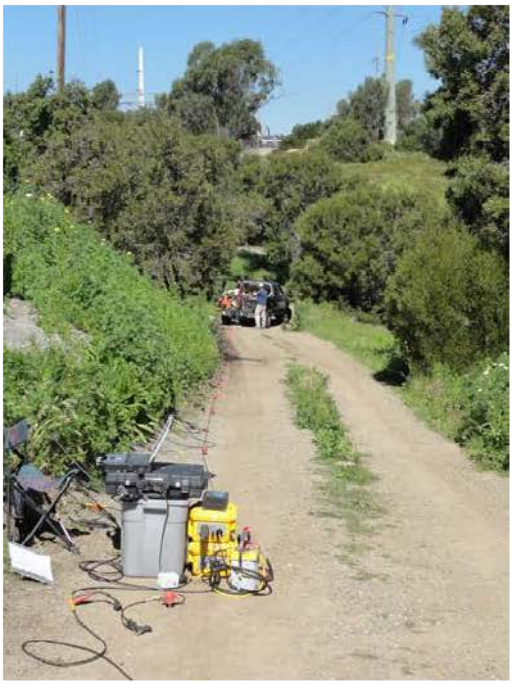

MASW data acquisition using
accelerated weight drop energy source

MASW data acquisition with 20 lb hammer source

Location of Geophysical Testing Arrays:

Location	Latitude	Longitude
SDG-1, Southeast End of MASW/Refraction Array	32.78417	-117.13655
SDG-1, Center of MASW/Refraction Array	32.78444	-117.13675
SDG-1, Northwest End of MASW/Refraction Array	32.78472	-117.13696
HVSR Sensor 450	32.78470	-117.13697
HVSR Sensor 453	32.78438	-117.13672
HVSR Sensor 507	32.78416	-117.13657

Notes: 1) WGS84 Coordinate System (decimal degrees)
2) Survey accuracy is estimated at 1 to 3 m.

Results:

V_S Model 1FM (Southeast Source Locations)

Depth to Top of Layer (m)	Layer Thickness (m)	S-Wave Velocity (m/s)	Inferred P-Wave Velocity (m/s)	Assumed Poisson's Ratio	Assumed Density (g/cm^3)
0	0.9	236	442	0.3	1.7
0.9	2.6	451	844	0.3	1.9
3.5	2.5	311	581	0.3	1.8
6	3.5	258	482	0.3	1.8
9.5	4	391	731	0.3	1.9
13.5	5	544	1018	0.3	2.0
18.5	6	623	1166	0.3	2.1
24.5	>5.5	724	1354	0.3	2.1

Notes: 1) Data modeled assuming dispersion curve is the fundamental mode.
2) Depth of investigation is about 30 m.
3) Bottom layer is a half space.

V_S Model 1AM (Southeast Source Locations)

Depth to Top of Layer (m)	Layer Thickness (m)	S-Wave Velocity (m/s)	Inferred P-Wave Velocity (m/s)	Assumed Poisson's Ratio	Assumed Density (g/cm^3)
0	0.75	226	422	0.3	1.7
0.75	2.75	396	740	0.3	1.9
3.5	2.5	309	578	0.3	1.8
6	3.5	281	526	0.3	1.8
9.5	4	360	674	0.3	1.9
13.5	5	536	1002	0.3	2.0
18.5	6	618	1157	0.3	2.1
24.5	>5.5	711	1330	0.3	2.1

Notes: 1) Data modeled assuming dispersion curve is the average mode (based on relative amplitude of the fundamental and higher surface wave modes).
2) Depth of investigation is about 30 m.
3) Bottom layer is a half space.

V_S Model 2 (Northwest Source Locations)

Depth to Top of Layer (m)	Layer Thickness (m)	S-Wave Velocity (m/s)	Inferred P-Wave Velocity (m/s)	Assumed Poisson's Ratio	Assumed Density (g/cm^3)
0	1	180	337	0.3	1.7
1	2	281	527	0.3	1.8
3	3	250	468	0.3	1.8
6	4	369	690	0.3	1.9
10	5	396	741	0.3	1.9
15	6	464	867	0.3	2.0
21	7	572	1070	0.3	2.1
28	>2	694	1298	0.3	2.1

Notes: 1) Data modeled assuming dispersion curve is the fundamental mode.
2) Depth of investigation is about 30 m.
3) Bottom layer is a half space.

Observations/Discussion:

- Geophysical testing was conducted as close to the seismic station as feasible, while still attempting to remain on the same geologic unit. The seismic station is mapped as being located on older Quaternary alluvium, although Tertiary sandstone (Mission Valley Formation) and conglomerate (Stadium Conglomerate) are mapped nearby. The MASW array SDG-1 crosses the mapped contact of the older alluvium and Mission Valley Formation and is very close to the mapped contact of the Stadium Conglomerate. Mapped geologic contacts could not be quickly verified in the field due to soil cover.
- HVSR data quality is excellent and the three HVSR curves are almost identical, which would appear to validate the 1-D velocity model assumption. There is a strong HVSR peak at about 0.9 Hz and weak peak at about 5 Hz. There is a very subtle difference in the HVSR plots for sensor 450, located on the mapped Mission Valley Formation, and sensors 453 and 507, located on mapped older alluvium, between 6 and 8 Hz.
- No attempt was made to reduce the seismic refraction data due to strong 180 Hz noise, associated with the substation and, more importantly, the possible presence of a high velocity layer beneath a portion of the seismic line identified in MASW data.
- Noise conditions at the site were not sufficient for application of passive surface wave techniques.
- The minimum wavelength surface wave phase velocity data extracted from the 48-channel MASW array is about 16 m for source locations off the southeast end of the array and 18 m for source locations off the northwest end of the array. Data reduction using seismic records from smaller hammer sources and a limited offset receiver array (i.e. less active geophones) allowed extraction of surface wave dispersion data to a minimum wavelength of about 1 to 2 m.
- There is significant scatter in MASW dispersion data due to lateral velocity variation. Rayleigh wave velocity data at wavelengths less than 16 to 18 m were only generated using limited offset receiver gathers and clearly show two surface wave dispersion curves that can be used to characterize the site. One dispersion curve is constructed from source locations at the southeast end of the array and the other from source locations at the northwest end of the array, both supplemented by interior shot location dispersion data.
- A total of about 140 separate dispersion curves were reduced from the MASW data acquired at this site. About 60 files were used in each of the separate dispersion curves utilized for modeling.
- A representative dispersion curve was generated for each MASW data set using a moving average, polynomial curve fitting routine and used for modeling.
- Several V_S models were generated from the surface wave data. Models 1FM and 2 were developed for the southeast source location and northwest source location dispersion curves, respectively, assuming fundamental mode only (WinSASW 2D solution) and Poisson's ratio of 0.3. It should be noted that in cases of high velocity surface or near surface layers the 2D solution in the WinSASW software package effectively models fundamental mode at long wavelengths, but can approximately account for modal superposition that occurs at small wavelengths/high frequencies. The calculated dispersion curve associated with Model 1FM, derived using the 2D solution in the WinSASW software package, generally fits the representative dispersion curve with the exception of a modeling artifact at a wavelength of about 5 m. Subsequent modeling

revealed that this V_S model should excite dominant higher modes at intermediate to high frequencies. Therefore, an alternate V_S model (Model 1AM) was developed assuming the observed dispersion curve consists of the average/effective mode (average of all modes based on relative amplitude of each mode for a far-field, plane Rayleigh wave). Interestingly, the multi-mode response for Model 1FM shows that the representative dispersion curve closely tracks the fundamental mode at frequencies lower than 45 Hz and higher than 120 Hz and the first and second higher modes between 45 and 120 Hz. This model, therefore, may actually be a relatively accurate representation of subsurface velocity structure, the effects of lateral velocity variation aside. In fact, the fundamental and average mode V_S models exhibit very similar velocity structure and V_{S30}, illustrating the effectiveness of the 2D solution in the WinSASW software package at modeling this type of velocity structure. The fundamental mode assumption is valid for Model 2 and with this V_S model the 2D solution in the WinSASW software package and the fundamental mode are equivalent.

- Surface wave depth of investigation is about 30 m based on half of maximum wavelength criteria.
- V_{S30} is 442 m/s for Model 1FM (fundamental mode) and 437 m/s for Model 1AM (average mode). The average V_{S30} between the two models is 439 m/s (NEHRP Site Class C). The velocity structure in the two models is quite similar. A multi-mode inversion is expected to also yield a similar V_S model.
- V_{S30} is 394 m/s for Model 2 (NEHRP Site Class C), 9% lower than that for Models 1FM and 1AM.
- Even though there is significant near surface lateral velocity variation at this site, which is not clear in HVSR data, V_{S30} appears to be relatively well constrained.
- Models 1FM and 1AM are considered most representative of the velocity structure in the immediate vicinity of the seismic station as the southeast end of the MASW array is located on the same mapped geologic unit as the seismic station.

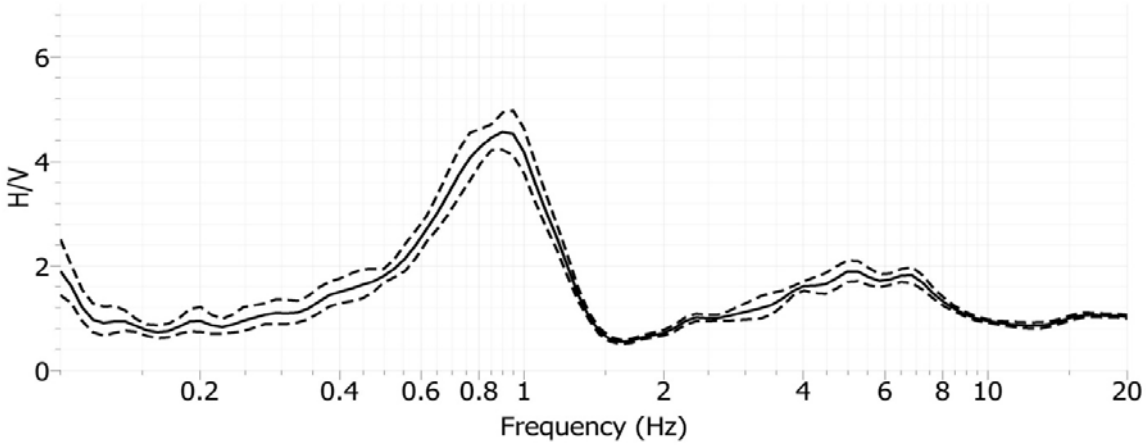

Site CI.SDG, H/V Spectral Ratio, Array SDG-1, Sensor 450

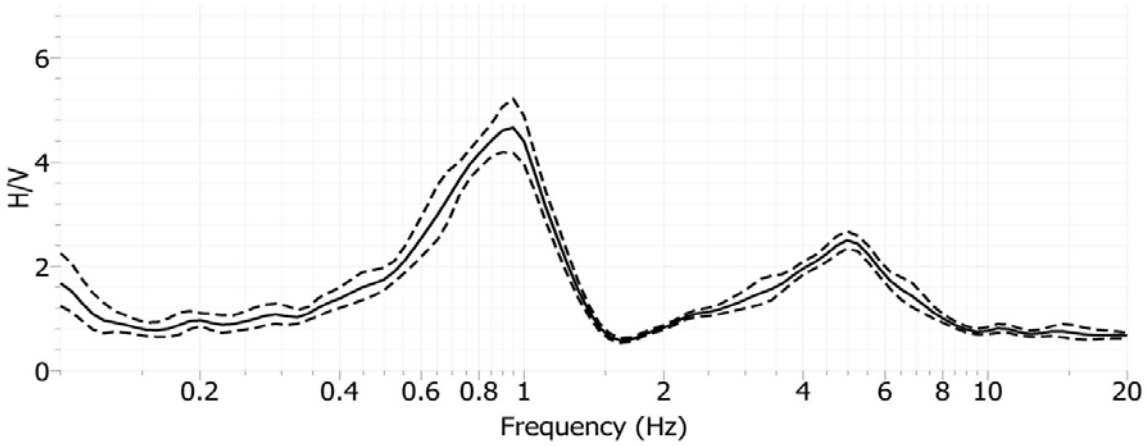

Site CI.SDG, H/V Spectral Ratio, Array SDG-1, Sensor 453

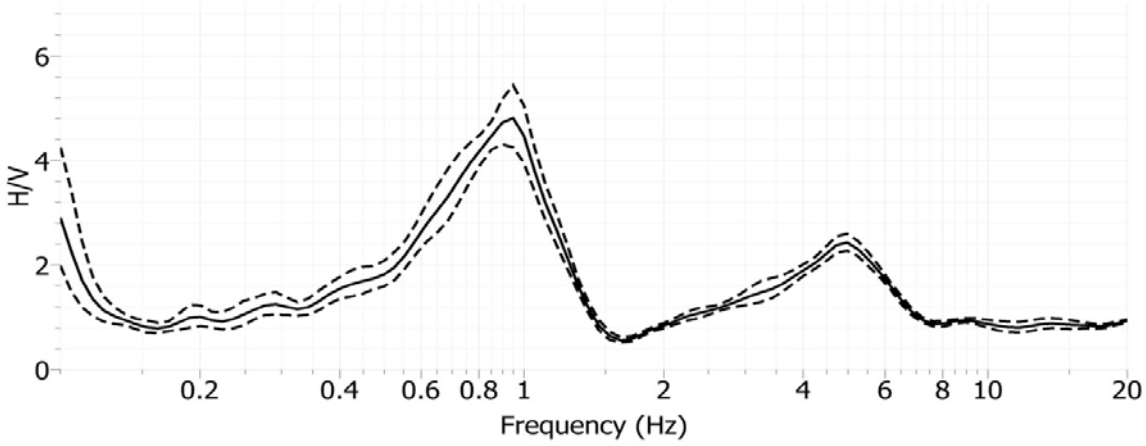

Site CI.SDG, H/V Spectral Ratio, Array SDG-1, Sensor 507

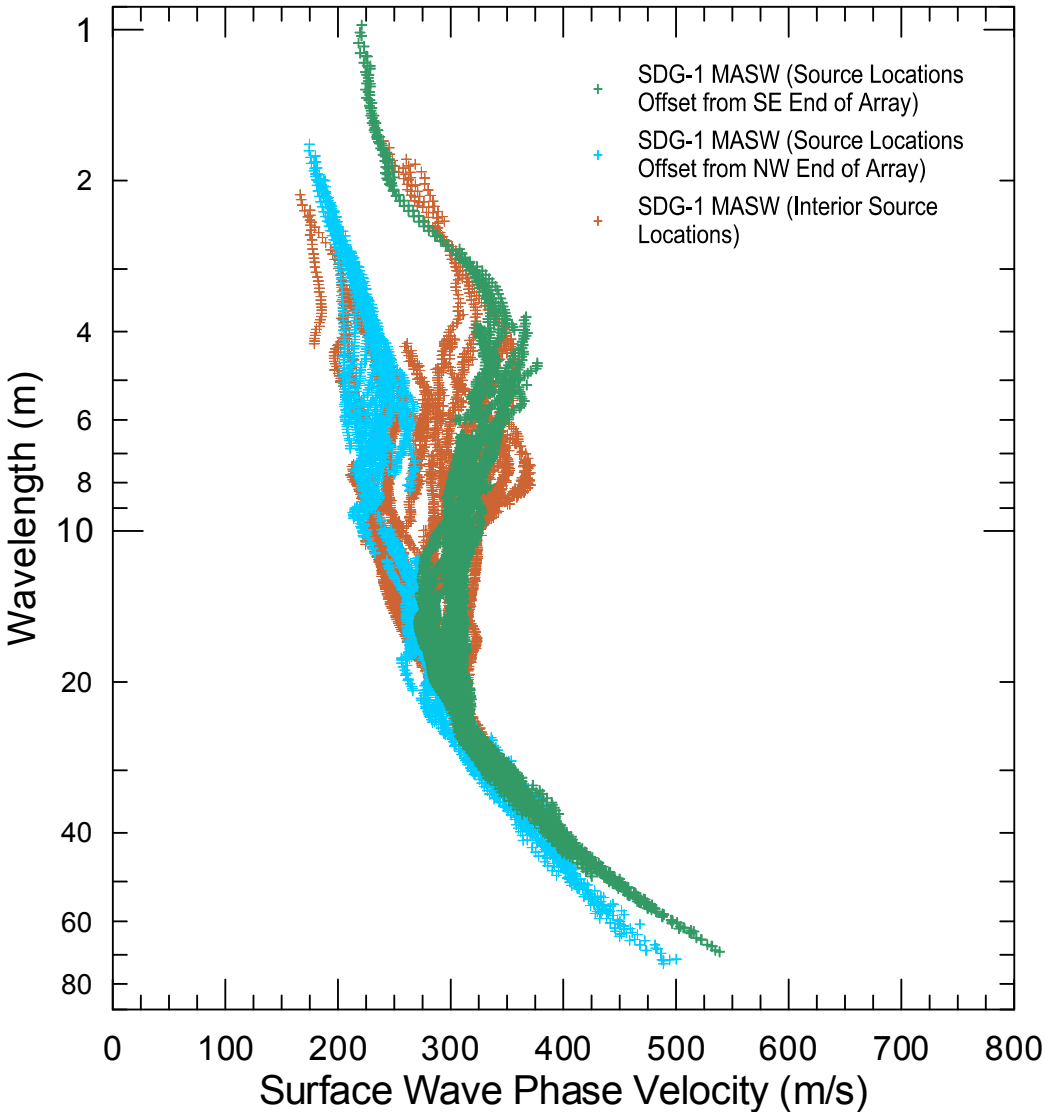

CI.SDG – Rayleigh wave phase velocity data from source locations offset from the southeast and northwest ends of the array and from interior source locations (i.e. seismic refraction sources) clearly showing the effects of near surface lateral velocity variation. It is possible that the MASW array crosses a geologic contact, although this could not be confirmed in the field. The only other feasible test location at this site would have required testing inside the electric transmission yard, which was not permitted due to safety concerns. Rayleigh wave phase velocity data at wavelengths less than 16 m were only generated from limited offset receiver gathers. It appears that the site can be characterized by two dispersion curves; one consisting of source locations at the southeast end of the array and the other consisting of source locations at the northwest end of the array, both supplemented by interior shot location dispersion data. A total of about 140 separate dispersion curves were reduced from the MASW data acquired at this site. About 60 files were used in each of the separate dispersion curves utilized for modeling.

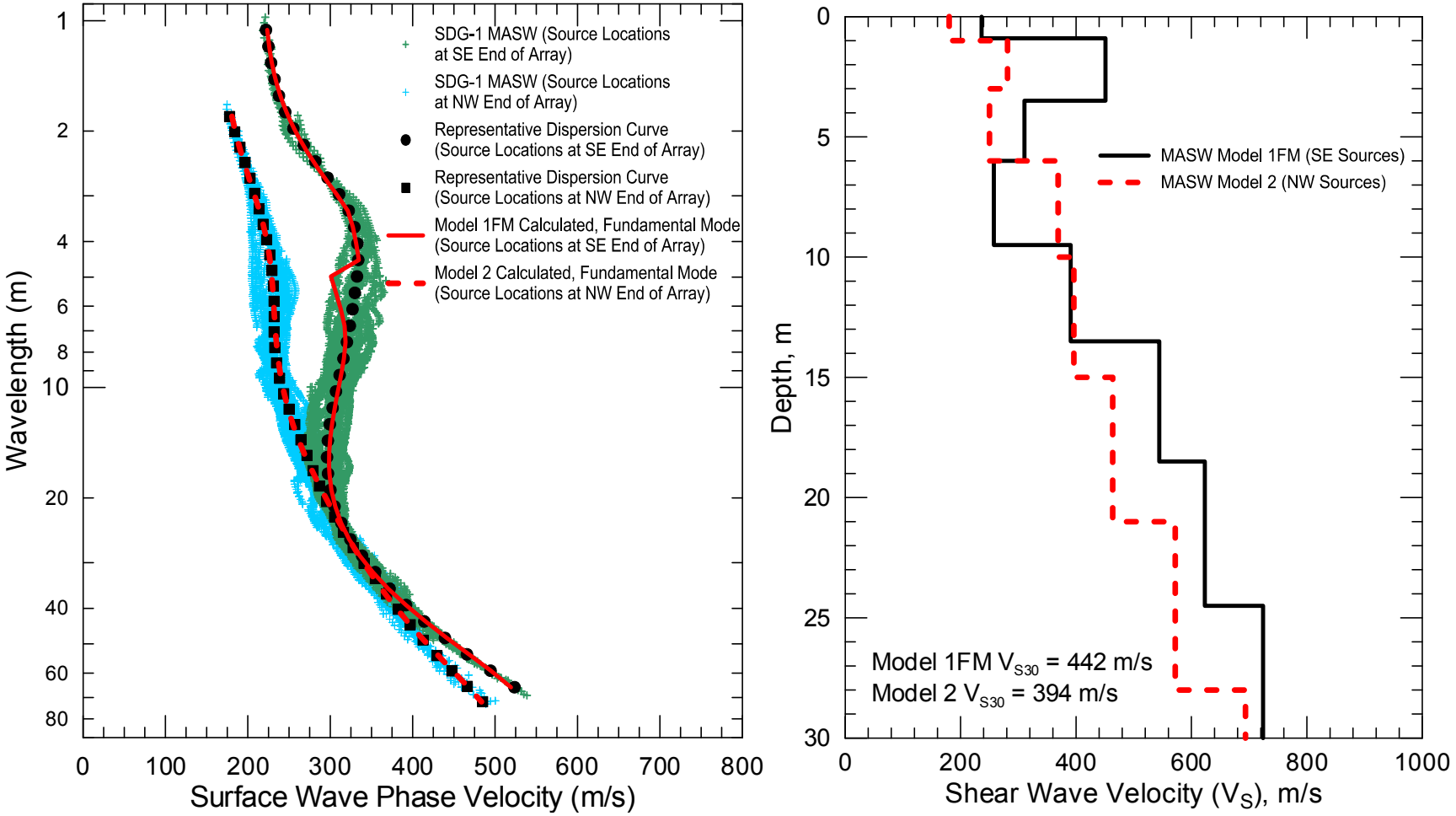

CI.SDG - Field, representative and inverted theoretical surface wave dispersion data (left) and associated V_S models (right) based on fundamental mode assumption. Due to significant near surface lateral velocity variation two representative dispersion curves were modeled. The Rayleigh wave dispersion curve developed from sources at the southeast end of the array has probable dominant higher modes at small wavelengths and could not be effectively modeled using the fundamental mode assumption.

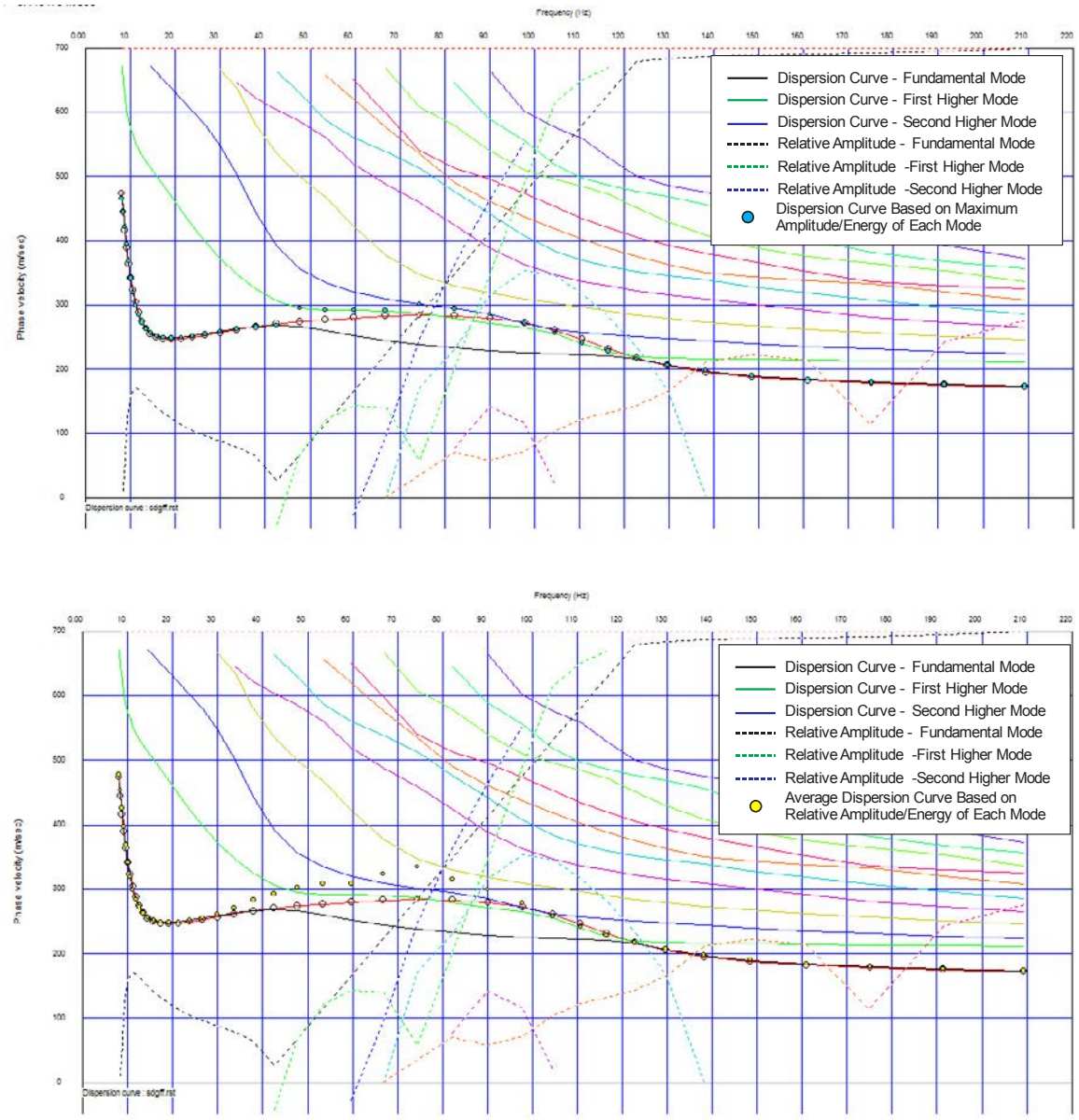

Calculated Rayleigh wave phase velocity modes for Model 1FM with the mode having maximum amplitude identified (top) and the average mode (average response based on relative amplitude of all modes) identified (bottom). Interestingly, Model 1FM maybe representative of subsurface velocity structure as the dispersion curve segment between 50 and 120 Hz very closely fits the first higher mode with the remaining segments of the dispersion curve fitting the fundamental mode. It may be possible to model this data using a multi-mode algorithm with the 50 to 120 Hz segment of the dispersion curve assigned to the first higher mode and the remaining portion of the dispersion curve assigned to the fundamental mode. However, much of the dispersion curve at frequencies above was generated from small receiver groups and modal superposition is likely. Therefore, the dispersion curve was modeled assuming that the dispersion curve was representative of the average mode.

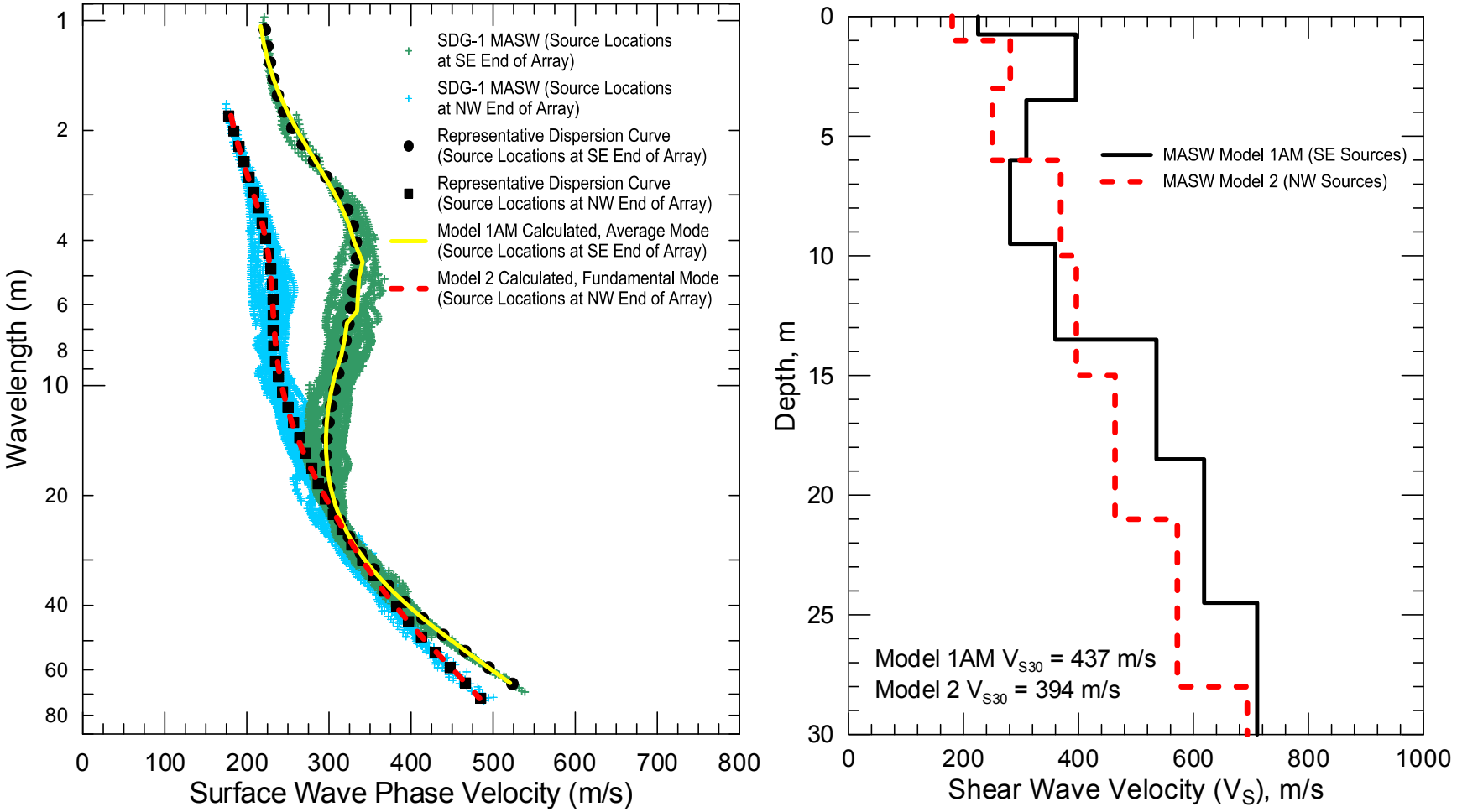

CI.SDG - Field, representative and inverted theoretical surface wave dispersion data (left) and associated V_S models (right). Model 1AM is based on the average mode assumption, which is more appropriate than the fundamental mode assumption with this data set. It may also be possible to generate a multi-mode model for this dispersion curve although small wavelength dispersion data was reduced from small groups of receivers and modal superposition is a distinct possibility.

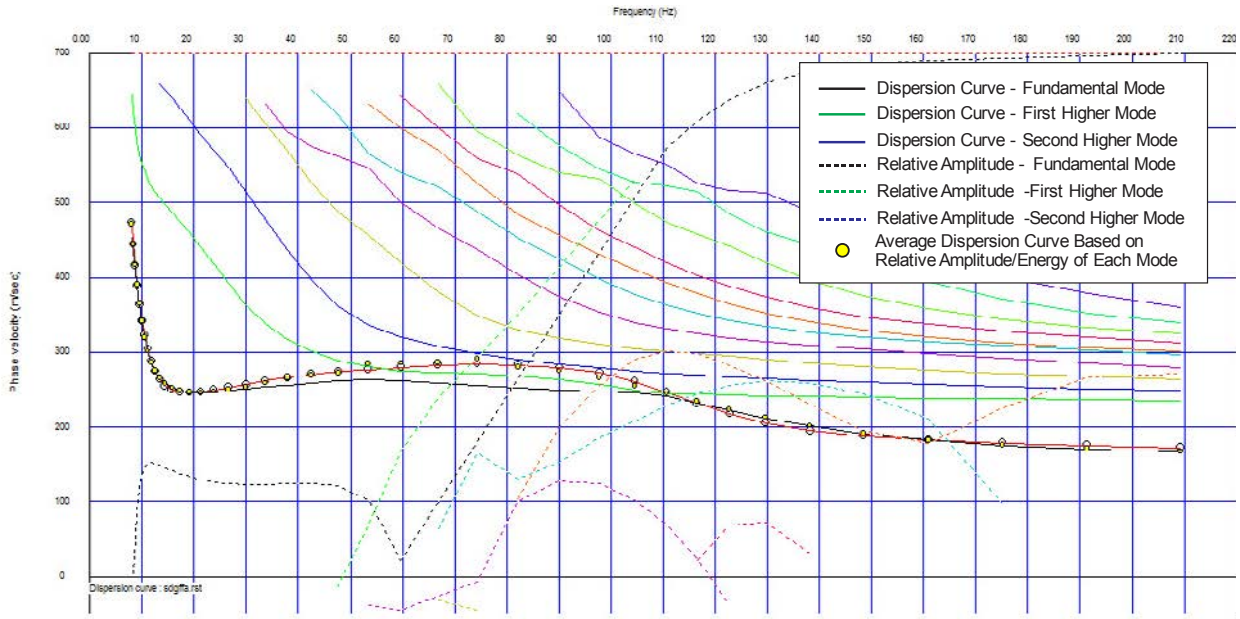

Calculated Rayleigh wave phase velocity modes for Models 1AM based on the average mode assumption.

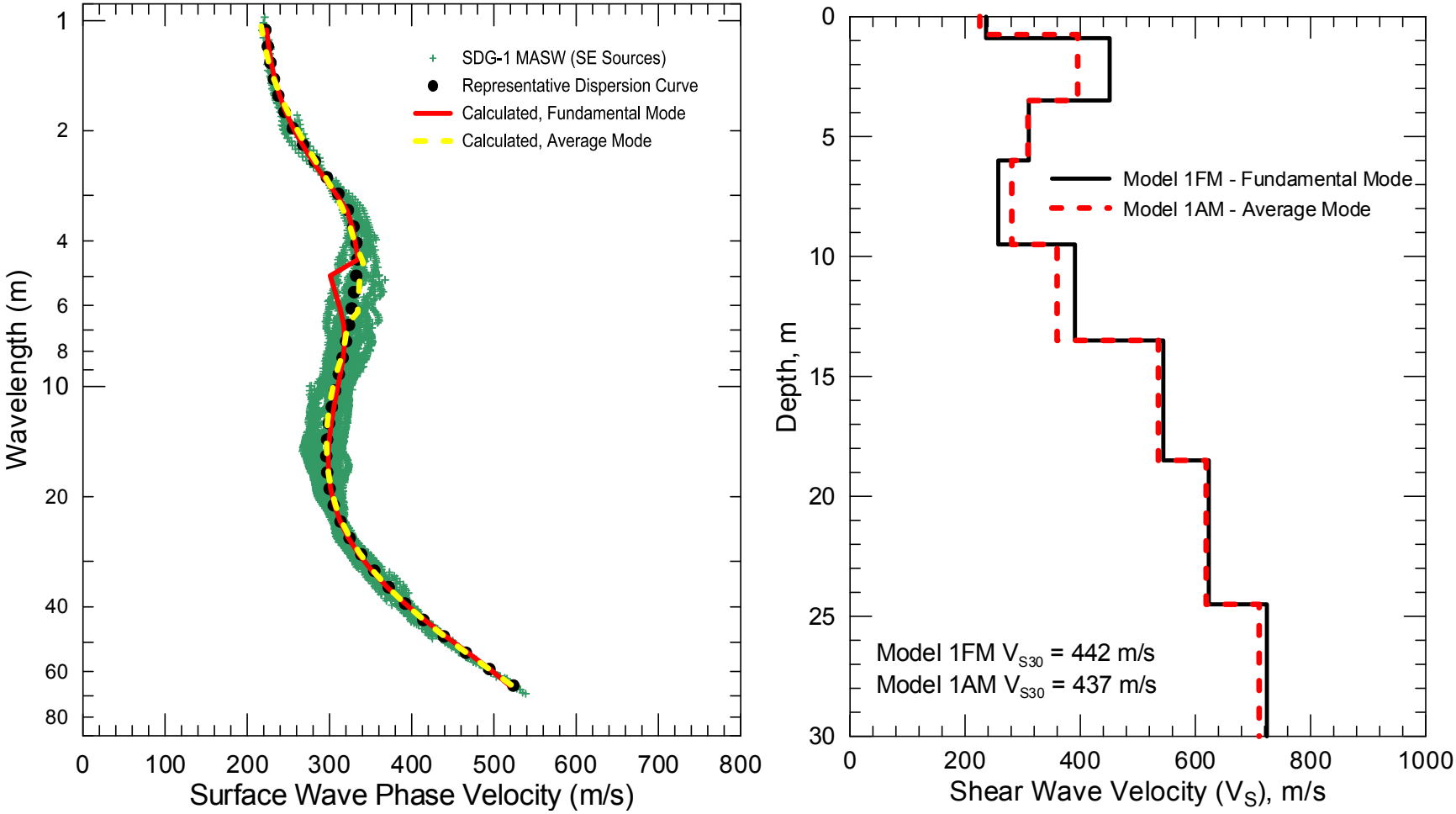

CI.SDG - Field, representative and inverted theoretical surface wave dispersion data (left) and associated V_S models (right) based on both fundamental and average mode assumptions and for source locations at the southeast end of the array.

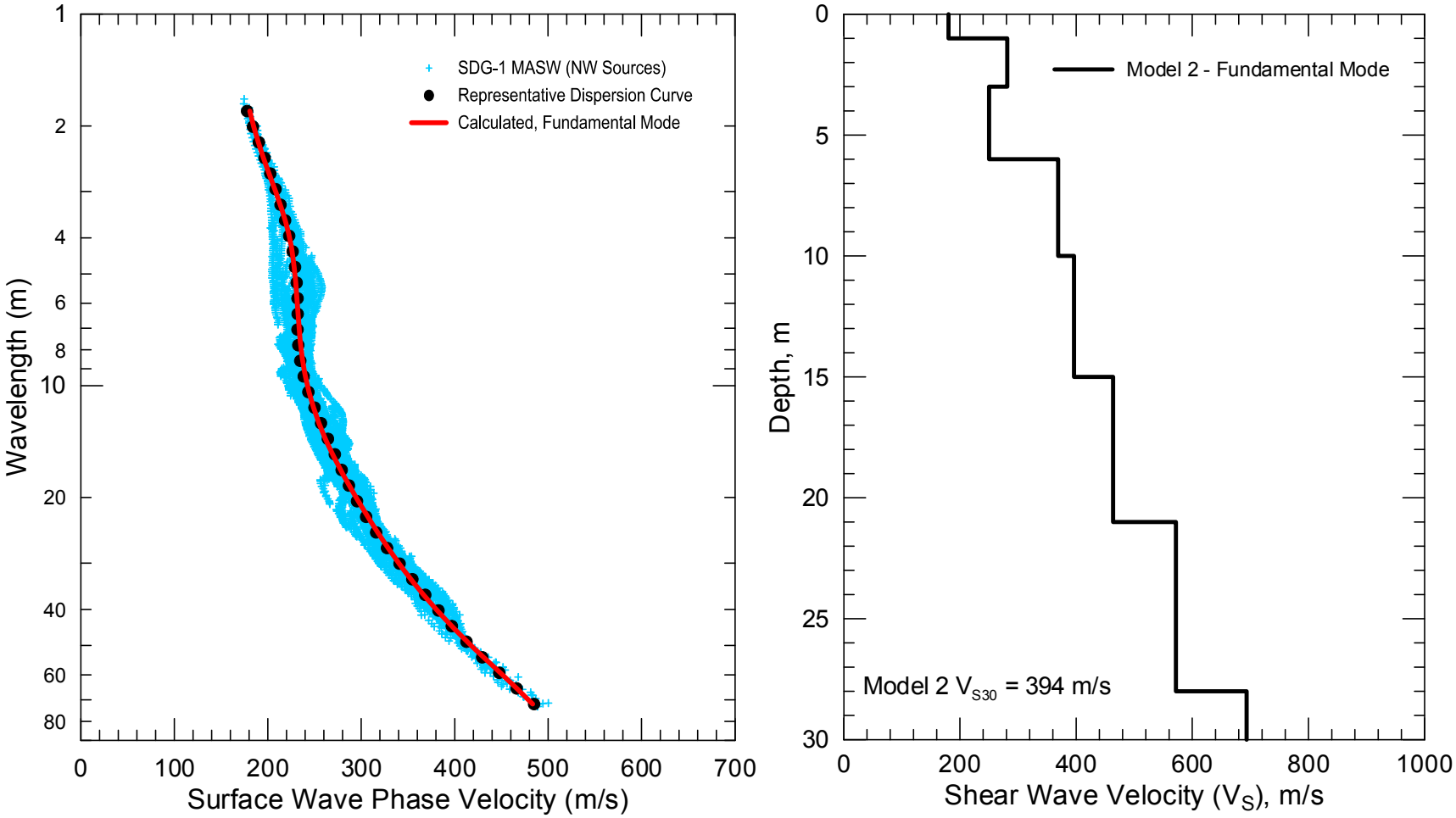

CI.SDG - Field, representative and inverted theoretical surface wave dispersion data (left) and associated V_S model (right) based on fundamental mode assumption for source locations at the northwest end of the array.

Site CI.SDR

Location: San Diego County Road Department, 11970 Singer Lane, Spring Valley, California

Latitude: 32.73561 **Longitude:** -116.94241
(Station coordinates provided by USGS, WGS84 coordinate system)

V_{S30} (measured): 827 m/s (±10% based on expected lateral velocity variation)

V_{S30} (adjusted to more accurately reflect seismic station conditions): 861 m/s (V_{S30} calculated after replacing velocity of upper 0.5 m thick layer in S-wave refraction V_S model with velocity of underlying layer to account for seismic station likely resting on weathered rock).

NEHRP Site Class: B/C

Geomatrix Code: KGA/IGA

Geologic Conditions/Observations: Seismic station located on geologic unit mapped as Mesozoic (Cretaceous) tonalite, granodiorite and quartz diorite.

Site Conditions: Suburban site located at the base of a large hill comprised of granitic rock. Relatively level terrain along the geophysical test arrays.

Geophysical Methods Utilized: HVSR, Seismic Refraction (P- and S-wave), MASW, MALW

Geophysical Testing Arrays:

1. Array SDR-1 (48 channel MASW and P-wave seismic refraction array utilizing 4.5 Hz vertical geophones spaced 1.5 m apart for a length of 70.5 m, forward and reverse shot locations with multiple source offsets and source types and multiple interior shot locations).
2. Array SDR-1 (48 channel MALW and S-wave refraction array, coincident with P-wave refraction/MASW array of same name, utilizing 10 Hz horizontal geophones spaced 1.5 m apart for a length of 70.5 m, forward and reverse shot locations with multiple source offsets and multiple interior shot locations).
3. Array SDR-2 (48 channel MASW and P-wave seismic refraction array utilizing 4.5 Hz vertical geophones spaced 1.5 m apart for a length of 70.5 m, forward and reverse shot locations with multiple source offsets and source types and multiple interior shot locations).
4. Three HVSR measurement locations distributed along array SDR-1.

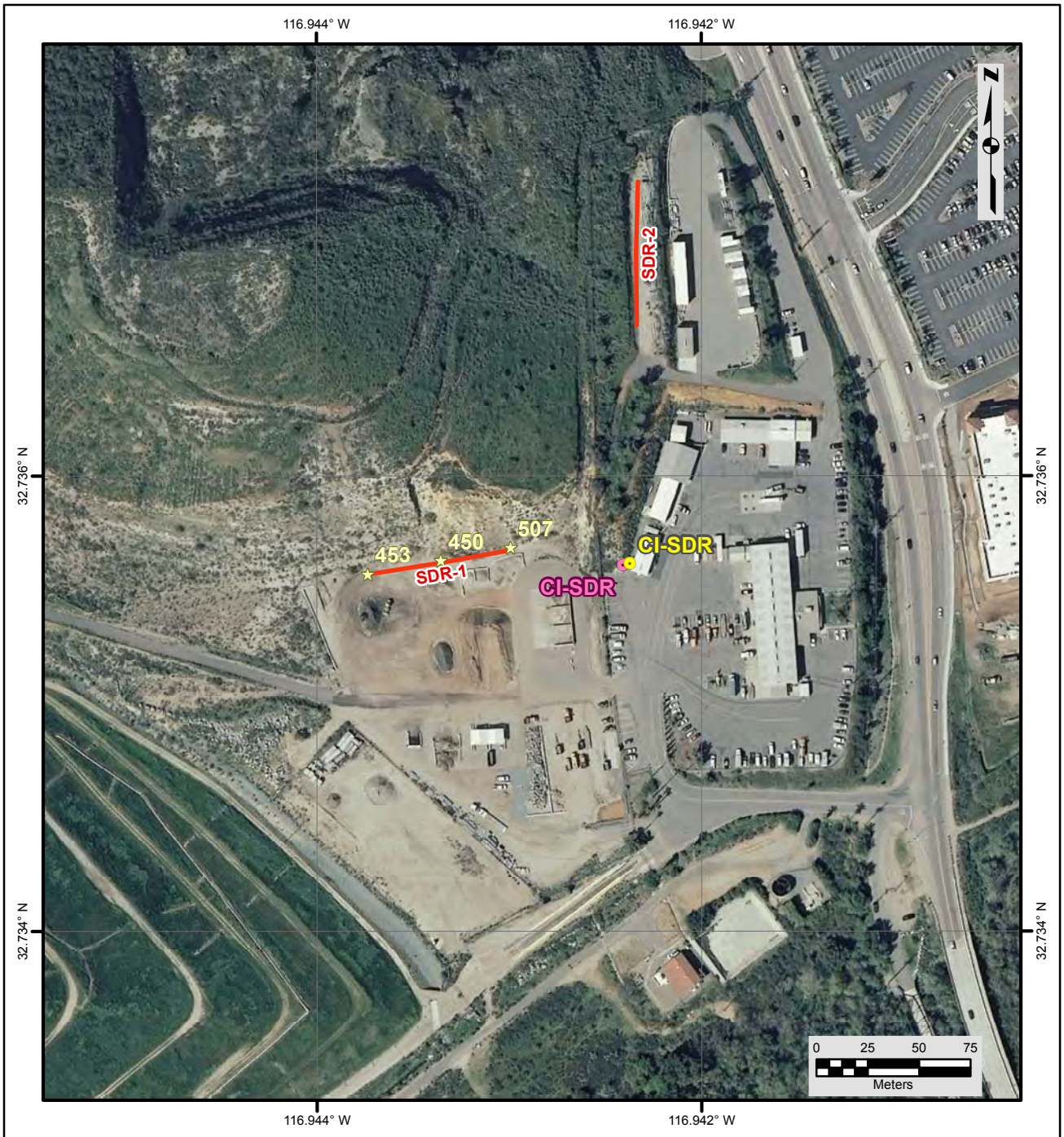

Legend

- Seismic Station - Approximate Surveyed Location
- Seismic Station - Approximate Location of Record
- H/V Spectral Ratio Location
- MASW and Seismic Refraction Array

NOTES:
1. WGS 1984 COORDINATE SYSTEM
2. Image Source: ESRI, i-cubed, USDA FSA, USGS, AEX, GeoEye, Getmapping, Aerogrid, IGP

File Name: CI-SDR-I

Date: 4/12/2012

USGS science for a changing world

GEOVision geophysical services

RECOVERY.GOV

SITE MAP
CI•SDR

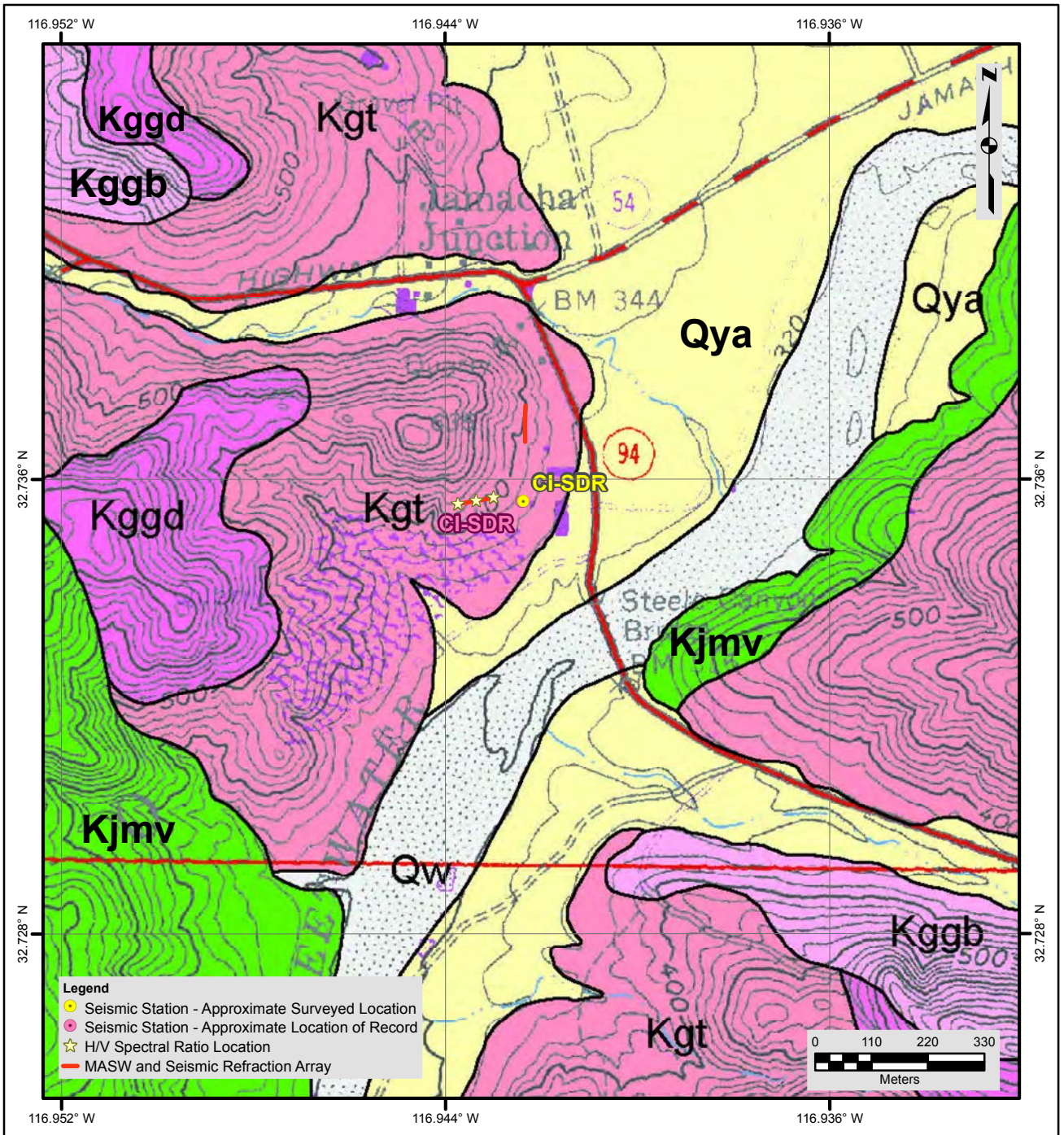

Description of Geologic Map Units

Qw = Quaternary (Holocene) active channel and wash deposits, sand, silt, gravel and clay
Qya = Quaternary (Holocene) alluvial deposits, silt, clay, sand and gravel
Kgt = Mesozoic (Cretaceous) tonalite, some granodiorite and quartz diorite
Kggd = Mesozoic (Cretaceous) granodiorite, some tonalite and monzogranite
Kggb = Mesozoic (Cretaceous) gabbro, some peridotite, norite, quartz gabbro
Kjmv = Mesozoic (Jurassic or Cretaceous) mildly metamorphosed volcanic, volcaniclastic and sedmentary rocks; basalt to rhyolite, mostly andesite and dacite

NOTES:
1. WGS 1984 COORDINATE SYSTEM
2. Geologic Map of the Jamul Mountains 7.5' Quadrangle, San Diego County, California by Siang S. Tan, 2002
3. See site map for details of geophysical survey

File Name: CI-SDR

Date: 3/29/2012

USGS science for a changing world

GEOVision geophysical services

RECOVERY.GOV

GEOLOGIC MAP
CI•SDR

Looking east along array SDR-1 and at HVSR sensor 453

CI.SDR seismic station

Looking east along array SDR-1 towards the location of the seismic station on other side of hill

Looking south along array SDR-2

S-wave refraction data acquisition along array SDR-1

Location of Geophysical Testing Arrays:

Location	Latitude	Longitude
SDR-1, West End of MASW/Refraction Array	32.73557	-116.94374
SDR-1, Center of MASW/Refraction Array	32.73562	-116.94336
SDR-1, East End of MASW/Refraction Array	32.73567	-116.94299
SDR-2, North End of MASW/Refraction Array	32.73729	-116.94233
SDR-2, Center of MASW/Refraction Array	32.73698	-116.94234
SDR-2, South End of MASW/Refraction Array	32.73666	-116.94234
HVSR Sensor 450	32.73563	-116.94336
HVSR Sensor 453	32.73557	-116.94374
HVSR Sensor 507	32.73569	-116.94299
CI.SDR Seismic Station	32.73562	-116.94238

Notes: 1) WGS84 Coordinate System (decimal degrees)

2) Survey accuracy is estimated at 1 to 2 m.

Results:

Average V_P Model and Estimated V_S Models from Central Portion of P-wave Seismic Refraction Array SDR-1

Depth to Top of Layer (m)	Layer Thickness (m)	P-Wave Velocity (m/s)	Estimated S-Wave Velocity (m/s)			
			Poisson's Ratio = 0.25	Poisson's Ratio = 0.3	Poisson's Ratio = 0.35	Poisson's Ratio = 0.4
0.00	0.61	399	231	213	192	163
0.61	1.22	657	379	351	316	268
1.83	1.22	872	503	466	419	356
3.06	1.22	955	552	511	459	390
4.28	1.22	1001	578	535	481	409
5.50	1.22	1032	596	552	496	421
6.72	1.22	1103	637	590	530	450
7.95	2.57	1414	816	756	679	577
10.51	2.57	1848	1067	988	888	755
13.08	2.57	2075	1198	1109	997	847
15.65	2.57	2848	1644	1522	1368	1163
18.22	2.57	2949	1703	1577	1417	1204
20.78	2.57	3166	1828	1692	1521	1292
23.35	Half Space	3800	2194	2031	1825	1551

Average V_P Model and Estimated V_S Model using Variable Poisson's Ratio from Central Portion of P-wave Seismic Refraction Array SDR-1

Depth to Top of Layer (m)	Layer Thickness (m)	P-Wave Velocity (m/s)	Estimated S-wave Velocity (m/s)	Inferred Poisson's Ratio
0.00	0.61	399	213	0.300
0.61	1.22	657	351	0.300
1.83	1.22	872	466	0.300
3.06	1.22	955	511	0.300
4.28	1.22	1001	535	0.300
5.50	1.22	1032	552	0.300
6.72	1.22	1103	590	0.300
7.95	2.57	1414	756	0.300
10.51	2.57	1848	988	0.300
13.08	2.57	2075	1109	0.300
15.65	2.57	2848	1163	0.400
18.22	2.57	2949	1204	0.400
20.78	2.57	3166	1292	0.400
23.35	Half Space	3800	1551	0.400

Average V_S Model from Central Portion of S-wave Seismic Refraction Array SDR-1

Depth to Top of Layer (m)	Layer Thickness (m)	S-Wave Velocity (m/s)
0.00	0.47	163
0.47	0.95	325
1.42	0.95	484
2.37	0.95	550
3.31	0.95	556
4.26	0.95	570
5.20	0.95	593
6.15	1.99	698
8.14	1.99	778
10.12	1.99	875
12.11	1.99	917
14.10	1.99	1023
16.09	1.99	1078
18.07	1.99	1249
20.06	1.99	1330
22.05	1.99	1407
24.03	1.99	1540.46
26.02	Half Space	1641.88

Average V_P Model and Estimated V_S Models from Central Portion of P-wave Seismic Refraction Array SDR-2

Depth to Top of Layer (m)	Layer Thickness (m)	P-Wave Velocity (m/s)	Estimated S-Wave Velocity (m/s)			
			Poisson's Ratio = 0.25	Poisson's Ratio = 0.3	Poisson's Ratio = 0.35	Poisson's Ratio = 0.4
0.00	0.51	485	280	259	233	198
0.51	1.02	904	522	483	434	369
1.54	1.02	1202	694	643	577	491
2.56	1.02	1321	763	706	635	539
3.58	1.02	1395	806	746	670	570
4.61	1.02	1401	809	749	673	572
5.63	1.02	1422	821	760	683	580
6.66	2.15	1439	831	769	691	587
8.81	2.15	1486	858	794	714	607
10.96	2.15	1638	945	875	787	669
13.11	2.15	1701	982	909	817	694
15.26	2.15	1857	1072	992	892	758
17.41	2.15	1943	1122	1038	933	793
19.56	2.15	2088	1206	1116	1003	853
21.71	Half Space	2109	1217	1127	1013	861

Observations/Discussion:

- Seismic station CI.SDR is located at the toe of a hill comprised of weathered granitic rock. The seismic sensor is located in a vault 1 to 2 m deep and likely rests on rock. Geologic maps indicate that much of the San Diego County Road Department facility adjacent to the hill has been cut into weathered rock. It was, therefore, possible to conduct geophysical testing in areas where weathered granitic rocks were at the surface or immediately beneath the surface.
- This site was visited on two occasions to attempt site characterization. During the first site visit on 3/09/11, P- and S-wave seismic refraction, MASW and MALW data were acquired along array SDR-1, located in a relatively flat area at the base of the hill that had been cut into weathered rock. Ground surface elevation along array SDR-1 is similar to that at the seismic station. Preliminary data reduction revealed that lateral velocity variation beneath array SDR-1 is such that a reliable Rayleigh or Love wave dispersion curve could not be extracted from the data set. Additionally, comparison of preliminary P- and S-wave seismic refraction models indicated that bedrock may be saturated at intermediate depth. Therefore, P-wave seismic refraction and MASW data were acquired along array SDR-2 on 3/21/12. This was the only other plausible test location, where

data could be acquired during business hours. Array SDR-2 was located at about a 10 m higher elevation than array SDR-1 and the seismic station.

- HVSR data is similar at the three measurement locations; however, there are no distinct high amplitude HVSR peaks. There is a slightly elevated HVSR response between about 4 and 15 Hz at all of the measurement locations.
- Surface wave data acquired along arrays SDR-1 and SDR-2 were not considered useable due to lateral velocity variation beneath the arrays. It may be possible that areas that have more 1-D weathering profiles are present in the site vicinity; however, the only other possible test areas are located in the facility parking lot where access would have to be arranged after business hours. With multiple SASW tests, in the parking lot, it may be possible to identify an area where acceptable quality surface wave dispersion data can be obtained. The SASW technique requires a shorter receiver array than the MASW technique to reliably image to 30 m depth and, therefore, may have more success at sites with significant lateral velocity variation. Alternatively, shorter MASW arrays with the dispersion data reduced using the cylindrical beamformer of Zywicki, 1999 to minimize near field effects may have success at sites with significant lateral velocity variation. Regarding lateral velocity variation, more research is needed on the effects of the amount of lateral velocity variation and type of lateral velocity variation (e.g. shallow dip, undulating geologic contact) on V_S models and V_{S30} estimates developed using surface wave techniques.
- Although it was not possible to generate a reliable dispersion curve to model the surface wave data, the MASW data were screened to estimate the 40 m wavelength Rayleigh wave phase velocity (V_{R40}). V_{R40} was found to vary by more than 10% and average about 650 m/s and 600 m/s on arrays SDR-1 and SDR-2, respectively, which would result in an estimated V_{S30} of 679 and 627 m/s, based on the Brown, et al., 2000 relationship. As will be seen below, these V_{S30} estimates are significantly lower than those estimated from the seismic refraction testing and additional testing is likely going to be required to characterize this site. It should be noted that, due to lateral velocity variation, V_{R40} could only be estimated from limited offset receiver gathers at selected source locations and may not be reliable or reflective of average velocity structure beneath the arrays.
- The P- and S-wave seismic refraction data for array SDR-1 were modeled using a tomographic inversion routine with a smooth velocity gradient starting model. The models were extended to off-end shot locations to extend depth of investigation. The depth of investigation for the P- and S-wave refraction models is about 24 and 27 m, respectively. Interpretation of S-wave first arrival was difficult on some seismic records due to strong P-wave energy, poor polarity reversal from source locations on opposite sides of the plank and possible converted waves and/or out of plane refractors in some areas. The P-wave velocity model is, therefore, likely more accurate than the S-wave model. The P- and S-wave seismic refraction models show the same general velocity structure in the upper 15 m with the S-wave velocity model being somewhat smoother due to noisier first arrival data. P-wave velocity below depth of about 16 m is high relative to S-wave velocity, indicating that the weathered rock may be saturated below this depth.
- The P-wave seismic refraction model for array SDR-1 indicates that P-wave velocity is about 300 to 600 m/s at the surface and increases to over 1,000 m/s at a depth of 1 to 7 m, 1,500 m/s at a depth of 7 to 14 m, 2,500 m/s at a depth of about 13 to 19 m and over

3,500 m/s at a depth of 18 to 22 m. The average P-wave velocity of the upper 30 m (V_{P30}) was estimated between 19.5 and 42 m on the array SDR-1 V_P model, where depth of investigation is greatest, by projecting the velocity at a depth of 24 m to 30 m depth. V_P is very high at a depth of 24 m and probably does not increase significantly between 24 and 30 m. V_{P30} ranges from about 1,531 to 1,765 m/s over this interval; a 14% variation over a distance of 22.5 m. Variation in V_{P30} beneath the entire array is likely somewhat higher than 14 %. An average V_P model was developed over the 19.5 to 42 m distance interval by horizontally averaging the travel time of each model cell and cell thickness and average V_{P30} was determined to be 1,634 m/s. Assuming constant Poisson's ratios of 0.25, 0.3, 0.35 and 0.4 would result in an estimated V_{S30} of 943, 873, 785 and 667 m/s, respectively. The seismic station most likely rests on rock, and V_{S30} is adjusted for seismic station conditions by replacing the P-wave velocity of the upper 0.6 m thick layer with that of the underlying layer. The adjusted V_{P30} is 1,689 m/s. Assuming constant Poisson's ratios of 0.25, 0.3, 0.35 and 0.4 would result in estimated adjusted V_{S30} of 975, 903, 811 and 690 m/s, respectively.

- The S-wave seismic refraction model for array SDR-1 indicates that S-wave velocity is about 150 to 250 m/s at the surface and increases to over 600 m/s at a depth of 3 to 6 m, 1,000 m/s at a depth of 7 to 16 m and over 1,600 m/s at a depth of 18 to 25 m. V_{S30} was estimated between 19.5 and 42 m on the S-wave refraction model, where depth of investigation is greatest, by projecting the velocity at 27 m depth to 30 m depth. Over this interval V_{S30} ranges from about 810 to 860 m/s, a 6% variation. There is less apparent lateral velocity variation than the P-wave model along the same array, probably the result of a smoother velocity model resulting from higher error in the first arrival data. An average V_S model was developed over the 19.5 to 42 m distance interval by horizontally averaging the travel time of each model cell and cell thickness and average V_{S30} was determined to be 827 m/s. The seismic station most likely rests on rock, and V_{S30} is adjusted for seismic station conditions by replacing the S-wave velocity of the upper 0.6 m thick layer with that of the underlying layer and the adjusted V_{S30} is 861 m/s.
- Comparison of P- and S-wave refraction models from array SDR-1 indicates that a higher Poisson's ratio is required below a depth of 16 m for estimated V_S from the P-wave refraction model to concur with that from the S-wave refraction model. This may indicate that the weathered rock is saturated below a depth of about 16 m. Therefore, an estimated S-wave velocity model was developed from the average V_P model using variable Poisson's ratio of 0.3 and 0.4 above and below a depth of 15.7 m, respectively. V_{S30} and adjusted V_{S30} from this model are 814 and 839 m/s, respectively, which are in good agreement with the estimates made from the S-wave refraction model. Therefore, even though the S-wave refraction model is not as accurate as the P-wave refraction model due to much higher uncertainty in first arrival data, V_{S30} appears to be consistent between the two models.
- The P-wave seismic refraction data for array SDR-2 were modeled using a tomographic inversion routine with a smooth velocity gradient starting model. The model was extended to off-end shot locations to extend depth of investigation. The depth of investigation for the P-wave refraction model is about 23 m. The P-wave seismic refraction model for array SDR-2 indicates that P-wave velocity is about 350 to 600 m/s at the surface and increases to over 1,000 m/s at a depth of 1 to 2 m, 1,500 m/s at a depth of 2 to 15 m and over 2,000 m/s at a depth of about 6 to 20. There is a zone of shallow

high velocity weathered rock at the northern end of the line with P-wave velocity of 2,500 m/s, or more. P-wave velocity structure beneath array SDR-2, which is about 10 m higher in elevation than array SDR-1 and the seismic station, is significantly different than that for array SDR-1, which is both closer to and at a similar elevation to the seismic station. Therefore, array SDR-2 should not be used to characterize seismic station velocity structure.

- The average P-wave velocity of the upper 30 m (V_{P30}) was estimated between 25.5 and 48 m on the array SDR-2 V_P model, where depth of investigation is greatest, by projecting the velocity at a depth of 23 m to 30 m depth. V_P may increase gradually with depth below 23 m, but this will not significantly affect estimates of V_{P30}. V_{P30} ranges from about 1,544 to 1,772 m/s over this interval; a 14% variation over a distance of 22.5 m. Based on the velocity model, V_{P30} appears to be increasing to the north and decreasing to the south of the 25.5 to 48 m interval and there is likely more than 25% variation in V_{P30} beneath the entire array. An average V_P model was developed over the 25.5 to 48 m distance interval by horizontally averaging the travel time of each model cell and cell thickness and average V_{P30} was determined to be 1,600 m/s. Assuming constant Poisson's ratios of 0.25, 0.3, 0.35 and 0.4 would result in an estimated V_{S30} of 924, 855, 769 and 653 m/s, respectively. The seismic station most likely rests on rock, and V_{S30} is adjusted for seismic station conditions by replacing the P-wave velocity of the upper 0.5 m thick layer with that of the underlying layer. The adjusted V_{P30} is 1,643 m/s. Assuming constant Poisson's ratios of 0.25, 0.3, 0.35 and 0.4 would result in estimated adjusted V_{S30} of 949, 878, 789 and 671 m/s, respectively.
- Although MASW data could not be modeled at this site, review of the data indicates that V_{S30} may be over 15% lower than that determined from the P- and S-wave seismic refraction surveys. There are likely areas beneath the seismic refraction arrays where V_{S30} is 10% lower than the presented average V_{S30} beneath the central portion of the arrays and it may be the V_{R40} estimates made from the surface wave data are skewed to the lower velocities at the site. More investigation is needed into the effects of lateral velocity variation on surface wave dispersion data and whether reliable V_{S30} estimates can be made from surface wave dispersion data when lateral velocity variation is too great. Due to the significant lateral velocity variation at this site, the possibility cannot be discounted that some first arrival data in the seismic refraction data sets arise from out of plane refractors, in which case the seismic refraction models would overestimate the seismic velocities immediately beneath the arrays.
- At this time, we recommend that the average velocity structure from the S-wave refraction model be used for the purpose of site characterization. It should be recognized that there is likely more than 10% variation in V_{S30} in the immediate vicinity of the seismic station due to lateral velocity variation. There are likely areas in close proximity to the seismic station where V_{S30} falls into both the NEHRP Site Class C and B categories.
- In conclusion, V_{S30} and adjusted V_{S30} averages about 827 and 861 m/s (NEHRP Site Class B/C to B), respectively, beneath the central portion of the S-wave refraction model for array SDR-1. This is consistent with V_{S30} estimates made from the P-wave refraction model along the same array, but appears to be significantly higher than that would have been obtained had it been possible to extract a coherent surface wave dispersion curve from the MASW data.

- Due to uncertainty in the V_{S30} estimate for this site, additional attempts to acquire surface wave data are warranted. Surface wave testing will only be effective at this site if a location can be identified where there is less lateral velocity variation than observed beneath arrays SDR-1 and SDR-2. SASW testing may achieve the greatest success because a 30 m V_S model can be obtained using a much shorter receiver array, relative to MASW testing. The only other possible test locations are in the parking lot adjacent to the seismic station and multiple tests may be required to identify a location where surface wave testing is successful.

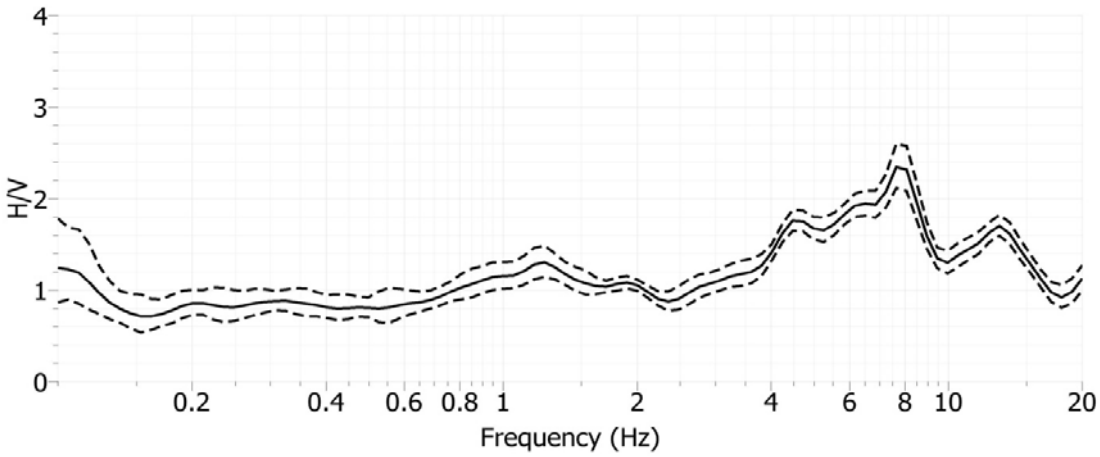

Site CI.SDR, H/V Spectral Ratio, Array SDR-1, Sensor 453

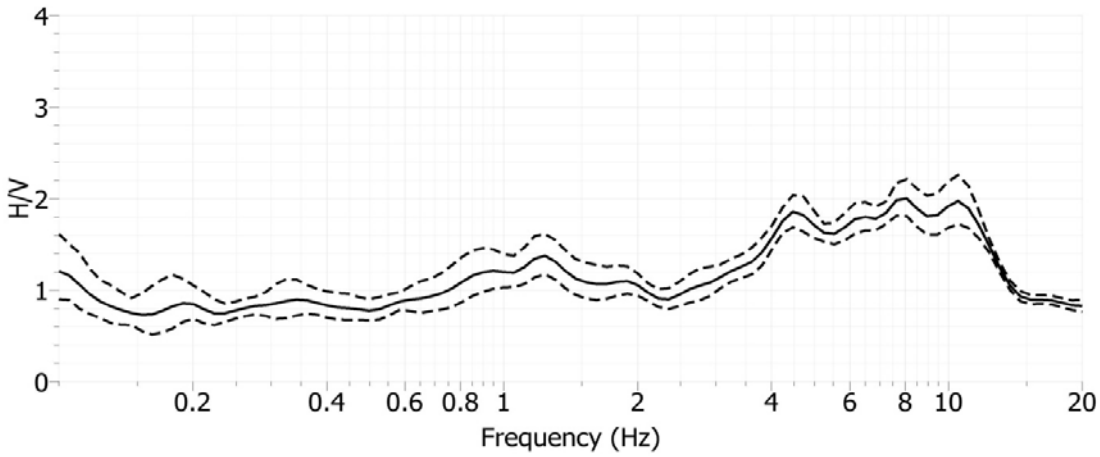

Site CI.SDR, H/V Spectral Ratio, Array SDR-1, Sensor 450

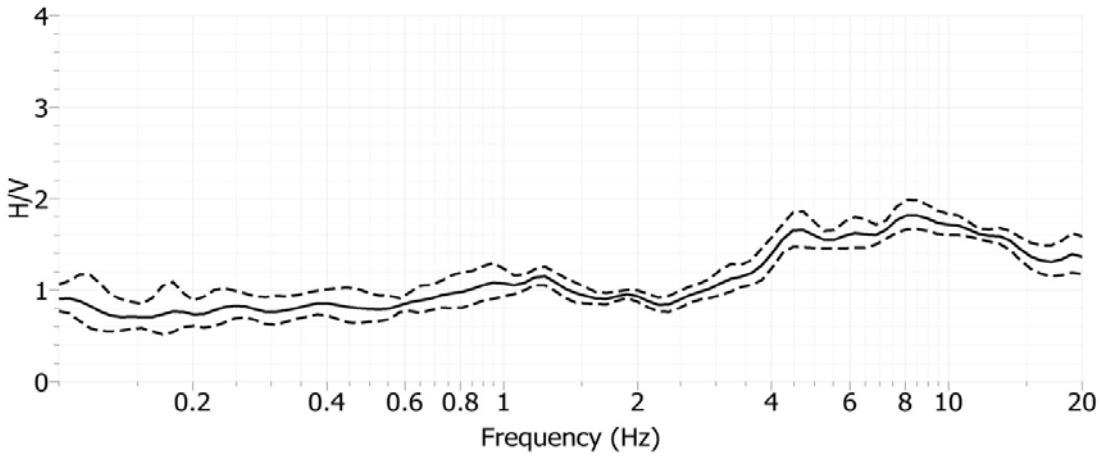

Site CI.SDR, H/V Spectral Ratio, Array SDR-1, Sensor 507

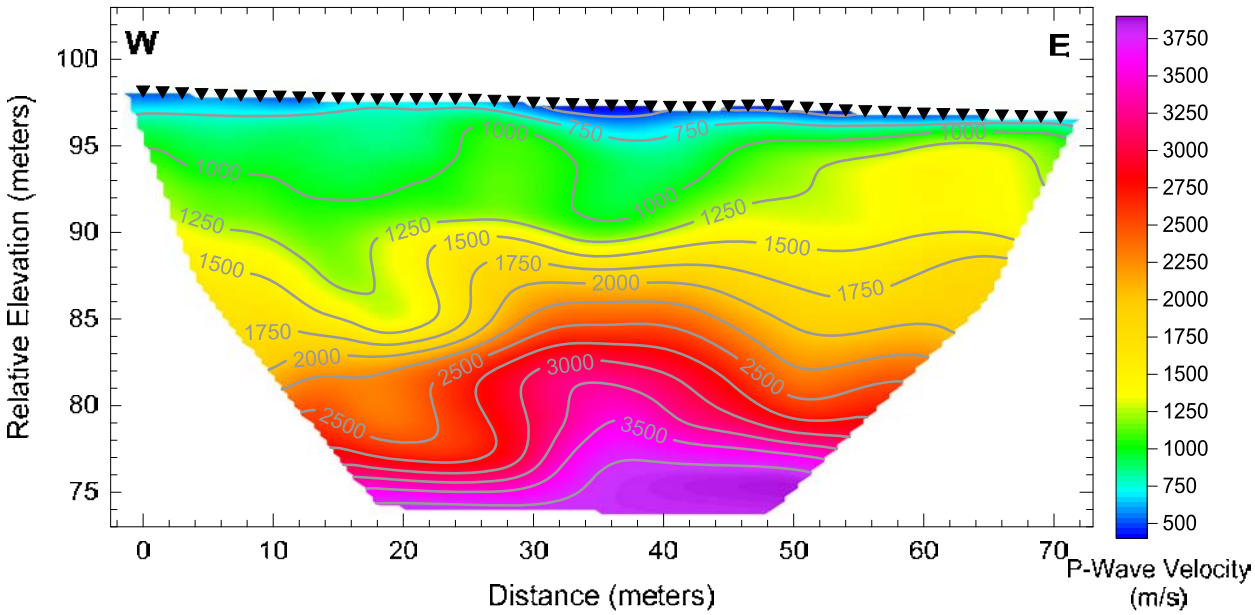

Array SDR-1 – P-wave Tomographic Seismic Refraction Model Developed using a Smooth Velocity Gradient Starting Model

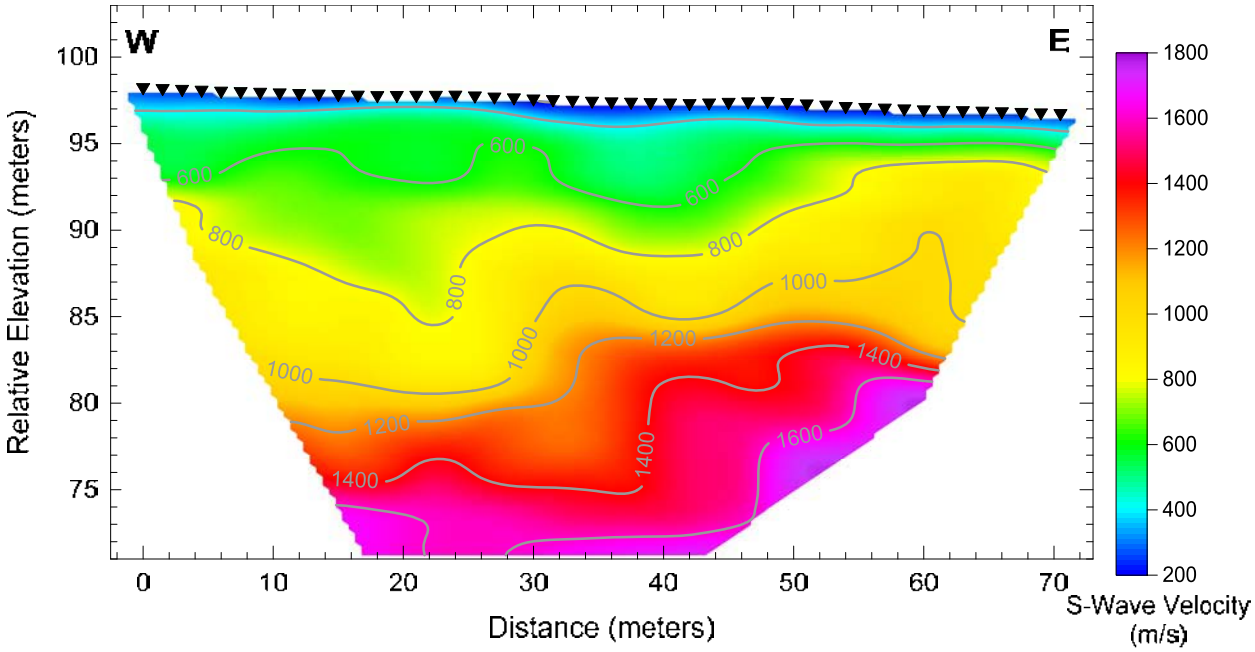

Array SDR-1 – S-wave Tomographic Seismic Refraction Model Developed using a Smooth Velocity Gradient Starting Model

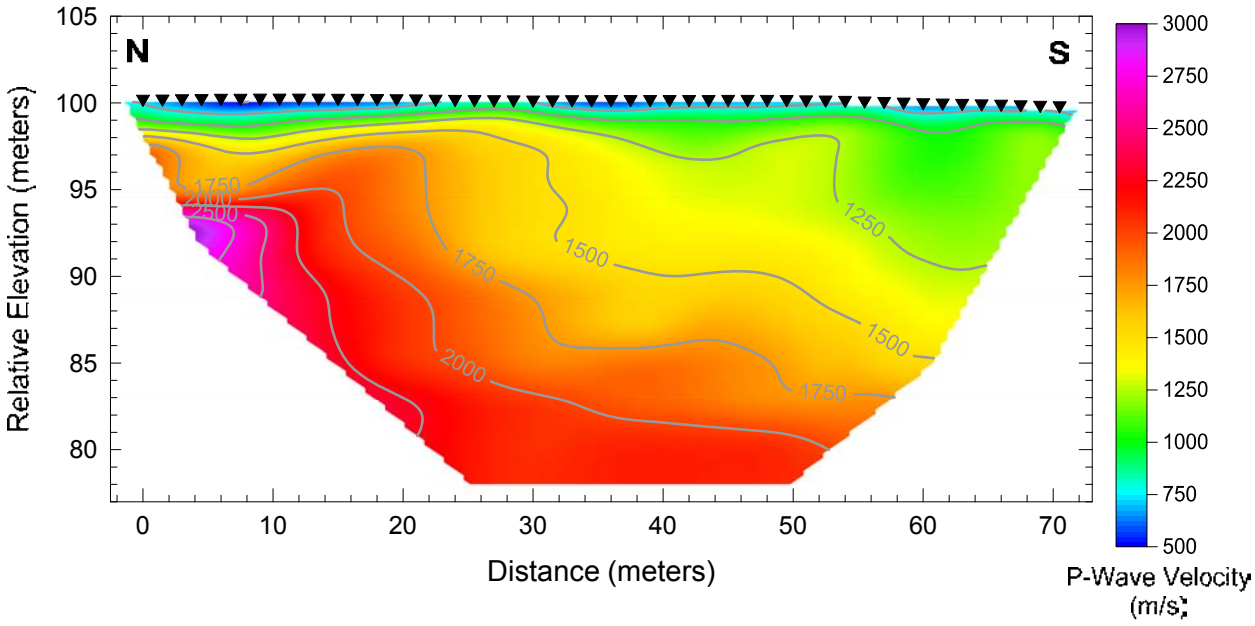

Array SDR-2 – P-wave Tomographic Seismic Refraction Model Developed using a Smooth Velocity Gradient Starting Model

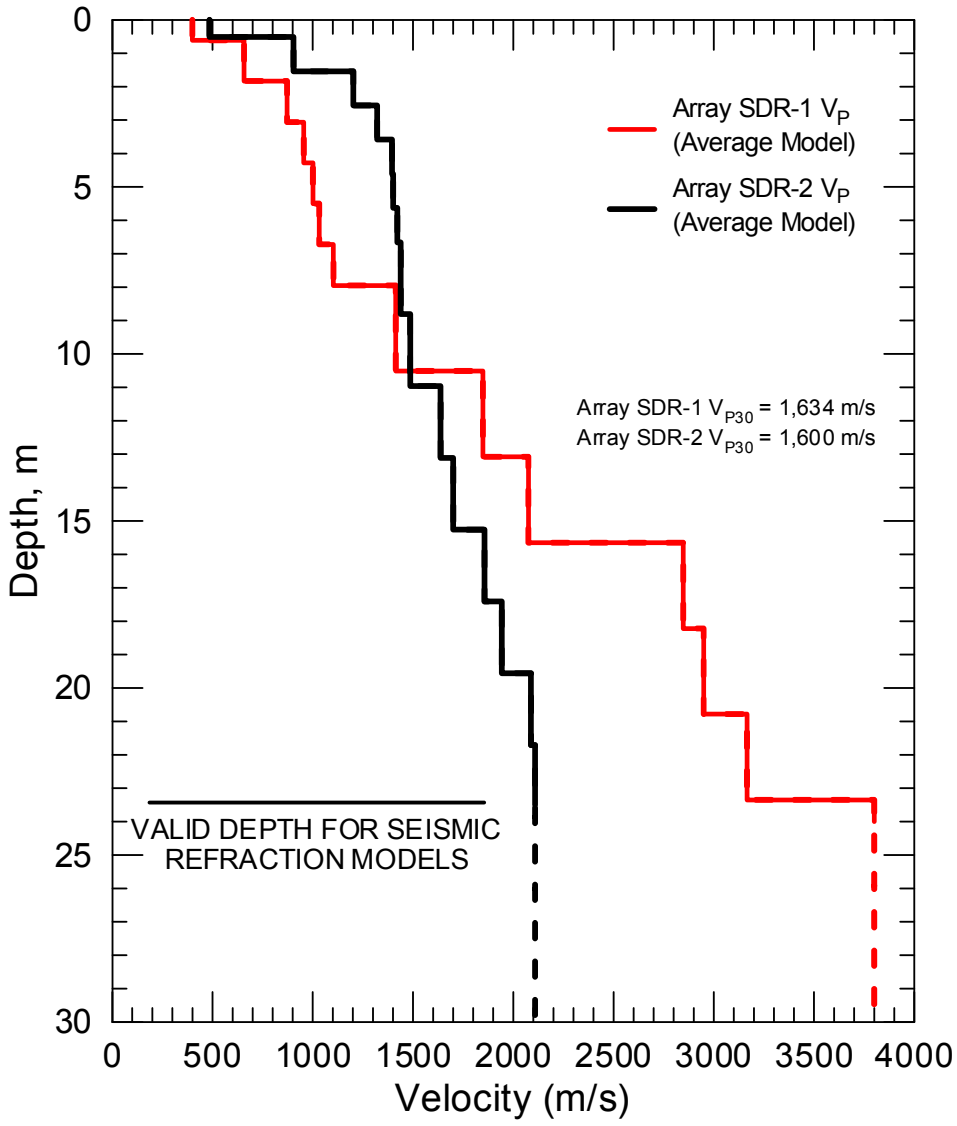

CI.SDR – Average V_P models between 19.5 and 42 m on array SDR-1 and between 25.5and 48 m on array SDR-2. Array SDR-2 is located at an approximate 10 m higher elevation than array SDR-1. Depth of investigation was limited to about 22 to 24 m and the models were extrapolated to 30 m depth. The differing velocity structure indicates that the bedrock weathering profiles are very different beneath the two arrays. The high P-wave velocities below a depth of 16 m on array SDR-1 could be associated with saturated weathered rock, based on the S-wave refraction model for the array. There is about a 14% variation in V_{P30} along the central 22.5 m segment of each array and variation in V_{P30} is likely much greater than 14% beneath the entire arrays.

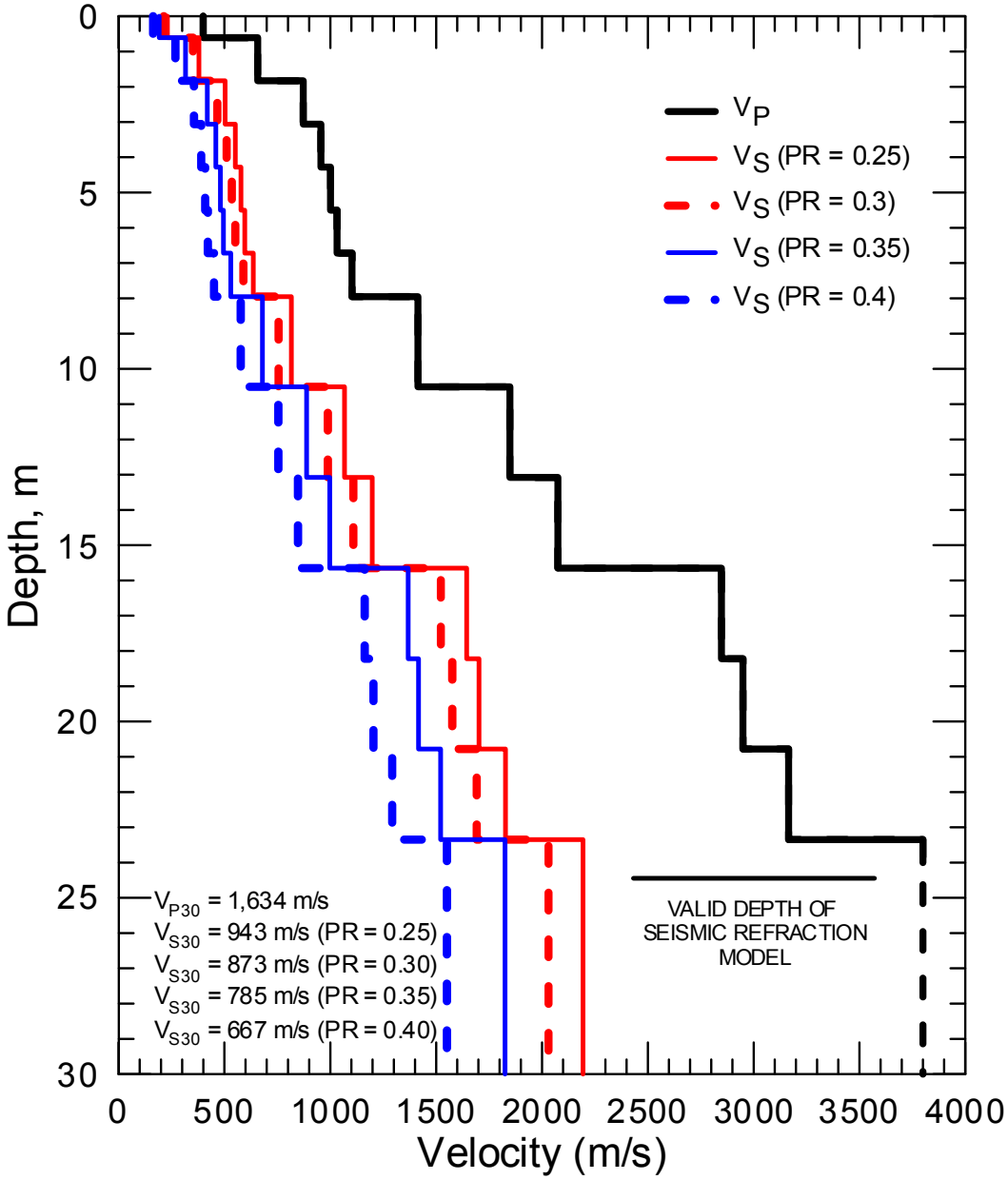

CI.SDR – Average P-wave velocity structure and estimated S-wave velocity structure between a position of 19.5 and 42 m on the P-wave seismic refraction model for array SDR-1. The maximum seismic refraction depth of investigation is limited to about 24 m; however, P-wave velocity is not expected to significantly increase with depth between 24 and 30 m.

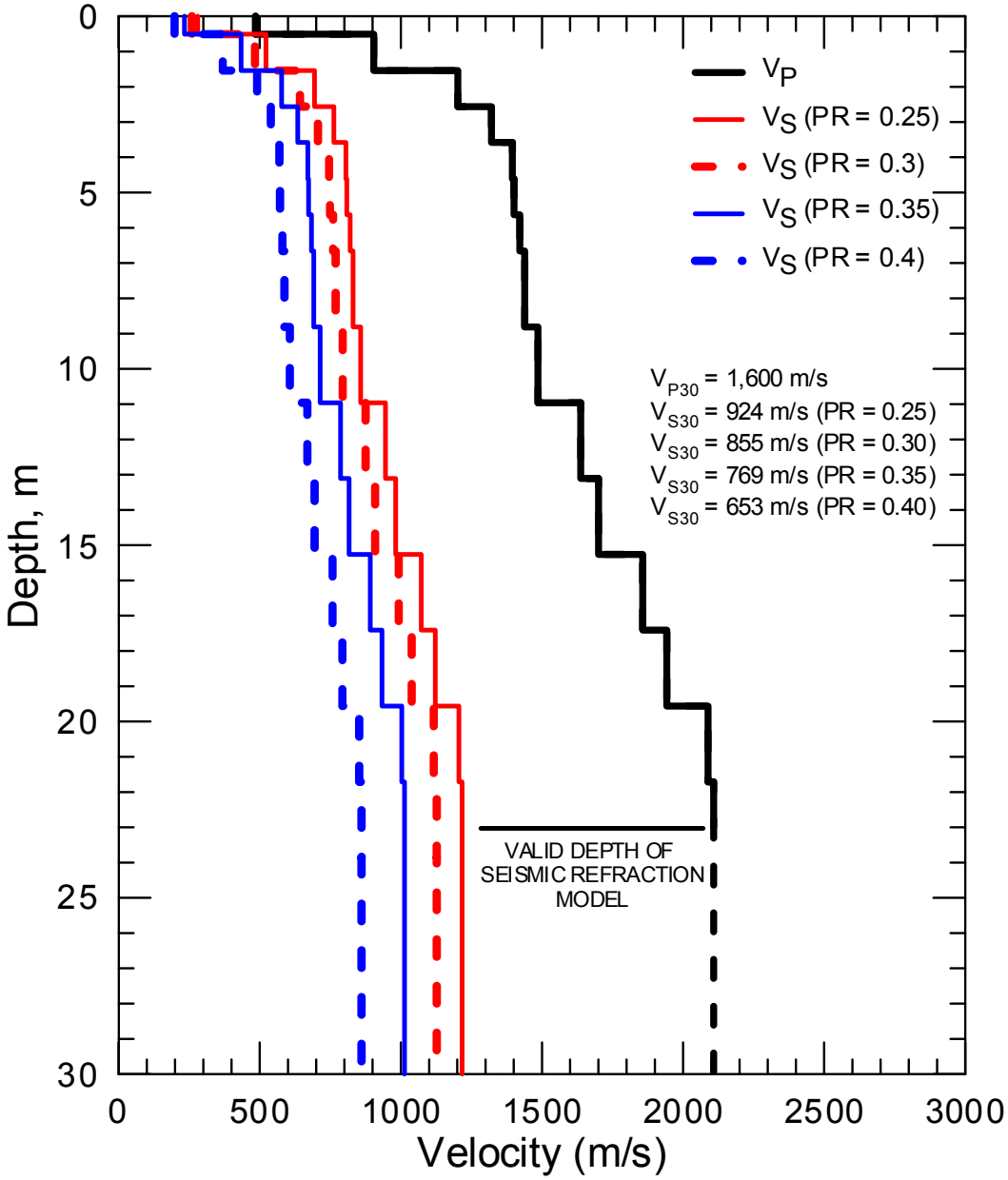

CI.SDR – Average P-wave velocity structure and estimated S-wave velocity structure between a position of 25.5 and 48 m on the P-wave seismic refraction model for array SDR-2. Array SDR-2 should not be used for site characterization because the array is at different elevation than the seismic station and the velocity structure is much different than that for array SDR-1, which is located closer to the seismic station.

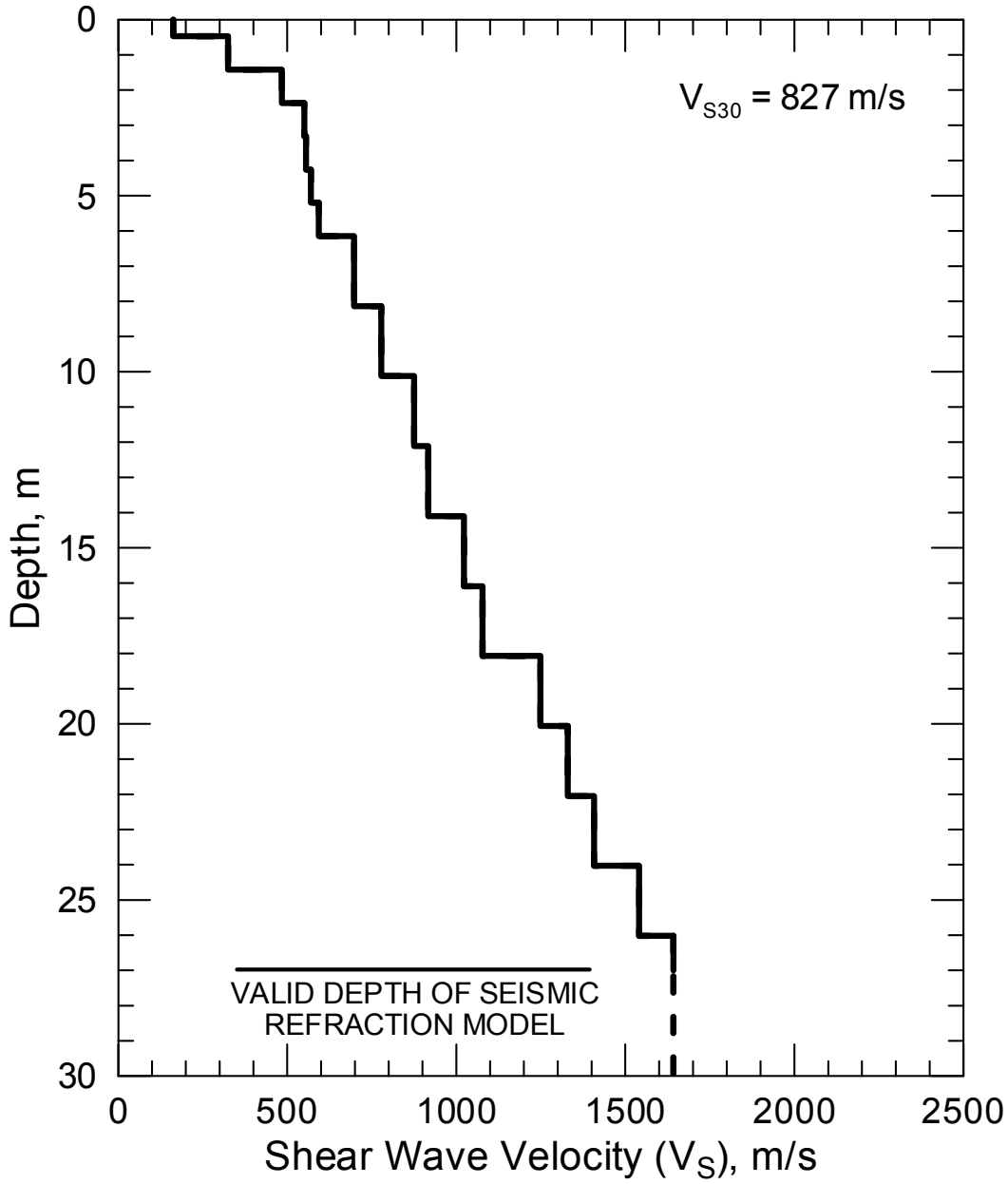

CI.SDR – Average S-wave velocity structure between a position of 19.5 and 42 m on the S-wave seismic refraction model for array SDR-1. S-wave first arrival data was difficult to accurately interpret on some seismic records due to strong P-wave arrivals and possible converted waves and/or out of plane refractors. As is often the case, P-wave seismic refraction data could be more accurately analyzed.

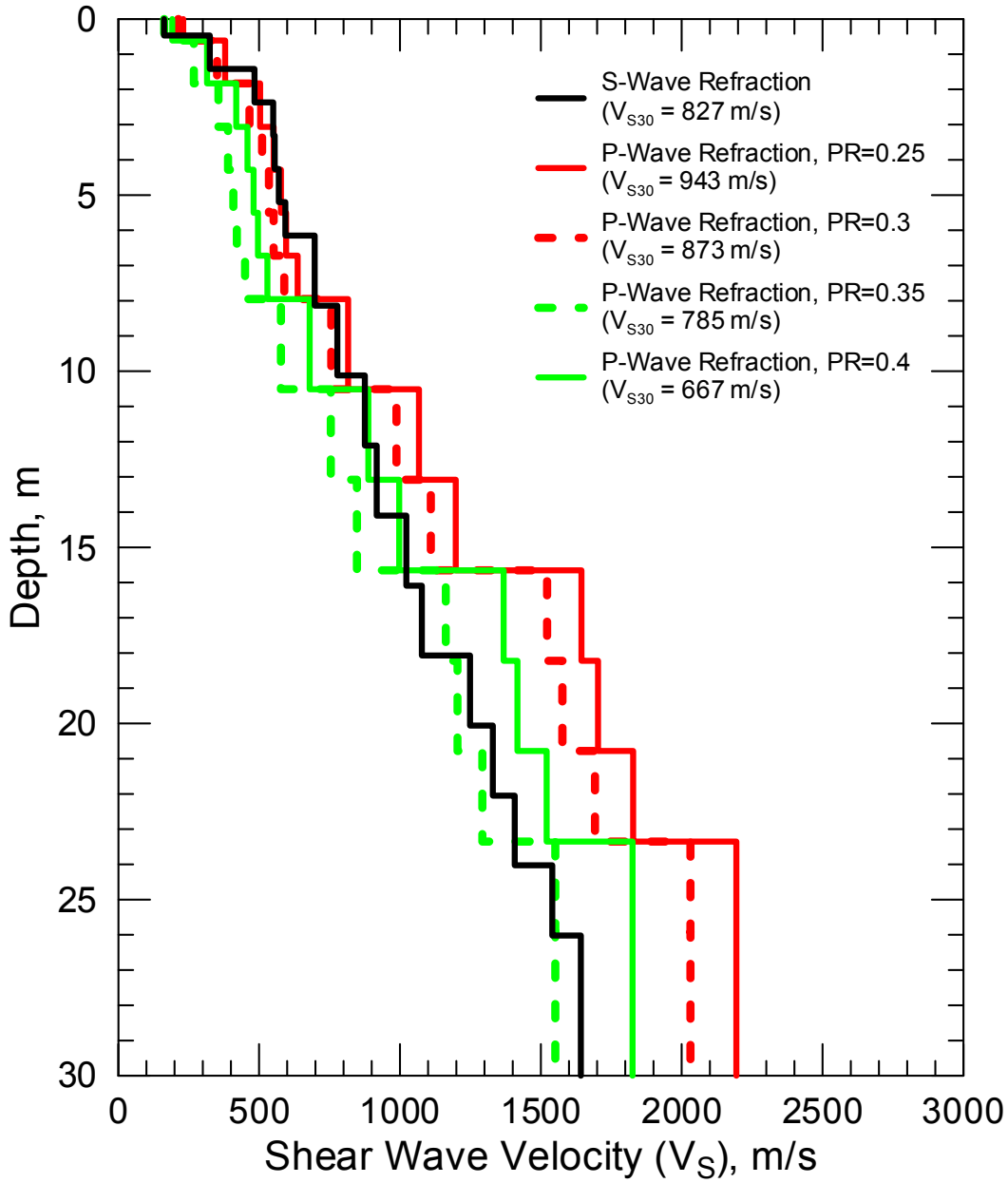

CI.SDR – Comparison of S-wave velocity models derived from the P- and S-wave seismic refraction survey along array SDR-1. S-wave wave velocity is estimated from the average P-wave velocity model between 19.5 and 42 m on array SDR-1, assuming constant Poisson's ratio of 0.25, 0.3, 0.35 and 0.4. The V_S model from the S-wave seismic refraction survey indicates that weathered rock may be saturated below a depth of about 13 to 16 m, based on the relatively high Poisson's ratio required for the estimated V_S from the P-wave refraction model to equal that from the S-wave refraction model.

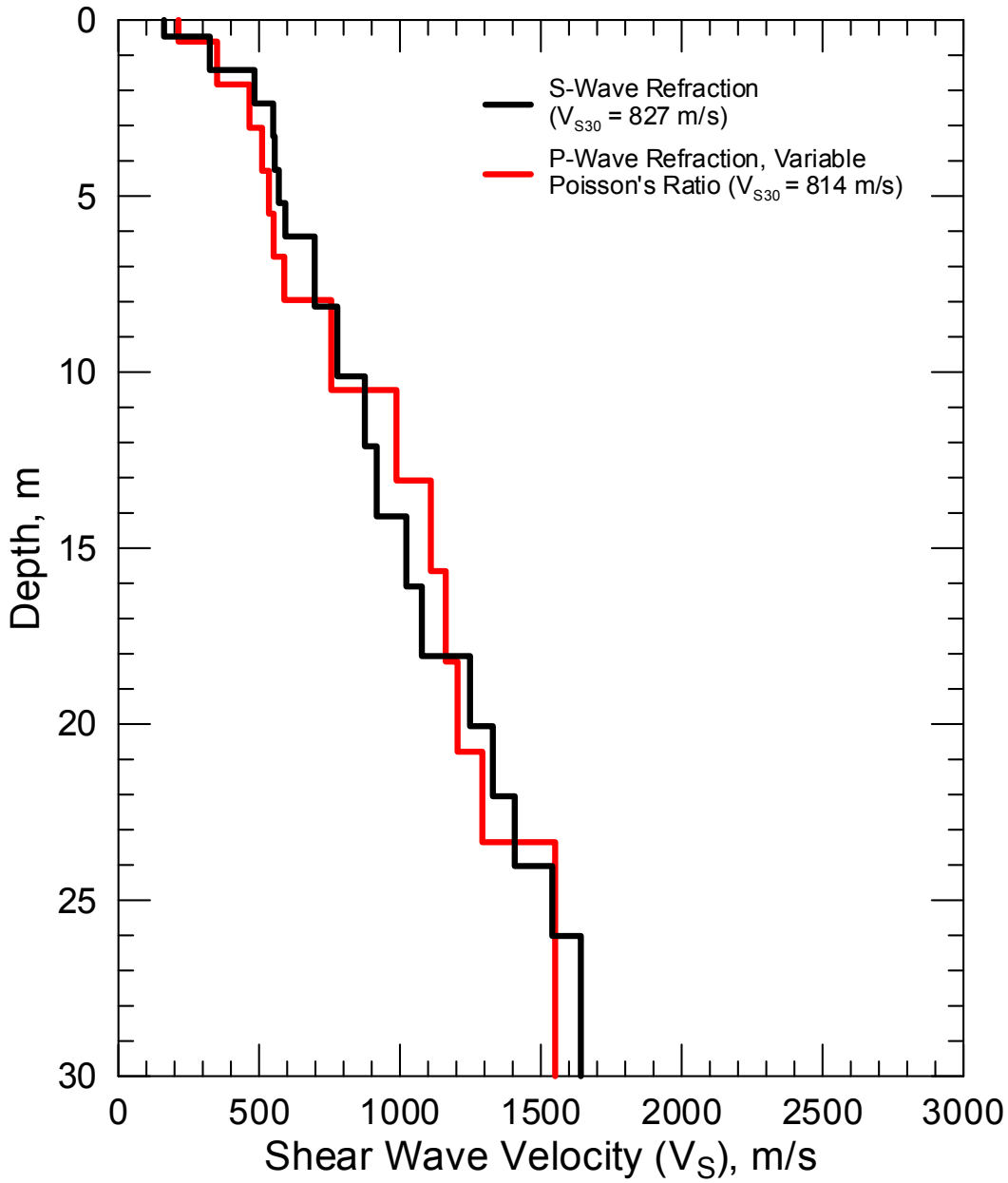

CI.SDR – Comparison of S-wave velocity models derived from the P- and S-wave seismic refraction survey along array SDR-1. S-wave wave velocity is estimated from the average P-wave velocity model between 19.5 and 42 m on array SDR-1, assuming a variable Poisson's ratio of 0.3 and 0.4 above and below a depth of 15.7 m, respectively.

Site CI.SHO

Location: Shoshone, Furnace Creek Wash Road, Shoshone, California

Latitude: 35.89964 **Longitude:** -116.27518
(Station coordinates modified based on field GPS survey, WGS84 coordinate system)

V_{S30} (measured): 356 m/s

V_{S30} (adjusted to more accurately reflect seismic station conditions): 377 m/s (average S-wave velocity between 1 and 31 m adjusting for expected sensor depth)

NEHRP Site Class: D/C

Geomatrix Code: IQD

Geologic Conditions/Observations: Site located in area mapped as an old alluvial fan surface with interfingered units of Quaternary (Holocene) alluvium and older Quaternary (Pleistocene) alluvium. Seismic station located on geologic unit mapped as Pleistocene alluvium. Crystalline basement expected to be relatively deep at this site.

Site Conditions: Rural site with no traffic noise. Relatively flat terrain in test area. Incised channel immediately south of test area. Hilly terrain in site vicinity due to large channels incised into old alluvial fans.

Geophysical Methods Utilized: HVSR, MASW, SASW

Geophysical Testing Arrays:

1. Array SHO-1 (48 channel MASW array utilizing 4.5 Hz vertical geophones spaced 1.5 m apart for a length of 70.5 m, forward and reverse shot locations with multiple source offsets and source types and center shot location).
2. Array SHO-1 (SASW array with common midpoint and orientation as MASW array of same name utilizing 4.5 and 1 Hz vertical geophones and maximum receiver spacing of 40 m).
3. Three HVSR measurement locations distributed evenly along array SHO-1.

Legend

- Seismic Station - Approximate Surveyed Location
- Seismic Station - Approximate Location of Record
- H/V Spectral Ratio Location
- SASW Array
- MASW Array

NOTES:
1. WGS 1984 COORDINATE SYSTEM
2. Image Source: ESRI, i-cubed, USDA FSA, USGS, AEX, GeoEye, Getmapping, Aerogrid, IGP

File Name: CI-SHO-I

Date: 7/18/2011

USGS science for a changing world

GEOVision geophysical services

RECOVERY.GOV

SITE MAP
CI•SHO

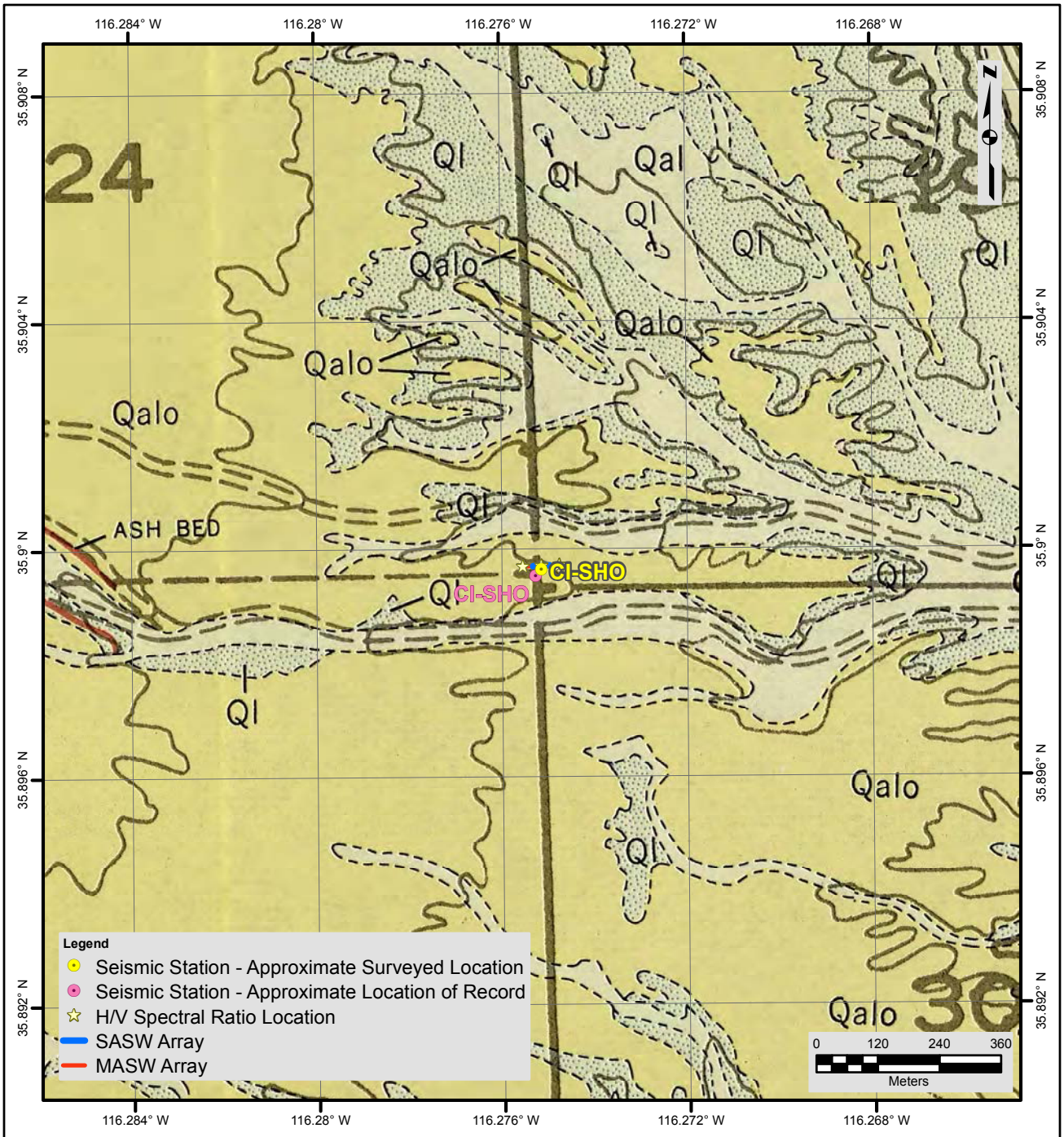

Description of Geologic Map Units

Qal = Quaternary (Holocene) alluvium
Qalo = Quaternary (Pleistocene) older alluvium
Ql = Quaternary (Pleistocene) lacustrine deposits

NOTES:
1. WGS 1984 COORDINATE SYSTEM
2. Geologic Map of the N.E. ¼ Shoshone 15-Minute Quadrangle, Inyo County, California by Charles W. Chesterman, 1973
3. See site map for details of geophysical survey

File Name: CI-SHO

Date: 7/7/2011

USGS science for a changing world

GEOVision geophysical services

GEOLOGIC MAP
CI•SHO

RECOVERY.GOV

Looking southeast towards CI.SHO seismic station and center of MASW array SHO-1

Looking north towards CI.SHO seismic station and HVSR sensor 507

Looking east along MASW array SHO-1

Looking at exposure of possible high velocity cemented sediments or caliche overlying lower velocity sediments in a drainage south of test area

Looking east along SASW array SHO-1

Location of Geophysical Testing Arrays:

Location	Latitude	Longitude
SHO-1, West End of MASW Array	35.89969	-116.27557
SHO-1, Center of MASW and SASW Arrays	35.89970	-116.27518
SHO-1, East End of MASW Array	35.89972	-116.27479
HVSR Sensor 450	35.89973	-116.27479
HVSR Sensor 453	35.89972	-116.27518
HVSR Sensor 507	35.89970	-116.27558
CI.SHO Seismic Station	35.89964	-116.27518

Notes: 1) WGS84 Coordinate System (decimal degrees)
2) Survey accuracy is estimated at 1 to 2 m

Results:

V_S Model from SASW Array SHO-1

Depth to Top of Layer (m)	Layer Thickness (m)	S-Wave Velocity (m/s)	Inferred P-Wave Velocity (m/s)	Inferred Poisson's Ratio	Inferred Density (g/cm^3)
0	0.75	112	210	0.300	1.8
0.75	1.75	243	455	0.300	1.9
2.5	2.5	394	738	0.300	1.9
5	15	355	663	0.300	1.9
20	10	461	1800	0.465	2.0
30	>5	579	1800	0.442	2.0

V_S Model from MASW Array SHO-1

Depth to Top of Layer (m)	Layer Thickness (m)	S-Wave Velocity (m/s)	Inferred P-Wave Velocity (m/s)	Inferred Poisson's Ratio	Inferred Density (g/cm^3)
0	1	183	343	0.300	1.8
1	1	266	497	0.300	1.9
2	3	394	738	0.300	1.9
5	6	330	617	0.300	1.9
11	9	351	657	0.300	1.9
20	10	422	1800	0.471	2.0
30	>5	533	1800	0.452	2.0

Observations/Discussion:

- HVSR measurements were made on different days. Data for sensors 453 and 507 were acquired in the early evening of one day and data for sensor 450 was acquired the next morning to replace a poor quality measurement.
- HVSR data are similar at every station, validating the 1-D velocity assumption.
- There is a probable low amplitude HVSR peak at about 0.6 to 0.65 Hz which if associated with bedrock, would be indicative of moderately deep basement at the site (250 to 350 m range). There is also a possible, but inconclusive, very weak secondary peak in the 1.2 to 1.4 Hz range.
- Noise conditions at the site were not sufficient to apply passive surface wave techniques.
- Seismic records clearly indicate the presence of a shallow, thin high velocity layer based on attenuation of a high velocity first arrival with distance. Simplified analysis of the seismic refraction data indicates that there is 1 to 2 m of low velocity sediments with P-wave velocity of 350 to 450 m/s overlying the high velocity layer with velocity of about 725 to 825 m/s. Depending on the velocity of the underlying sediments, a water table refractor is present at a depth on the order of 17 to 23 m.
- As mentioned above, it is not possible to accurately define water table depth from refraction data alone due to shallow high velocity layer and unknown velocity structure below. A 20 m water table depth was used for surface wave data modeling.
- The presence of a high velocity layer (HVL) complicates interpretation of the SASW and MASW data due to the potential presence of dominant higher modes over some frequency ranges. Furthermore the HVL may be at variable depth and may have slight dip and variable velocity. Different SASW and MASW dispersion curves were selected for modeling, neither of which appear to have significant problems with dominant higher modes. These dispersion curves have significant differences at wavelengths less than 12 m due to a combination of the above factors and variable velocity of the surficial sediments.
- Only forward end shots were used for low wavelength MASW dispersion data. MASW dispersion data from center shots yielded surface wave dispersion data more similar to the lower phase velocities in the SASW dispersion data. Reverse shots did not yield small wavelength/high frequency surface wave dispersion data.
- It is possible to extract surface wave dispersion data from both the MASW and SASW data that are more similar at small wavelengths, but using the MASW center shots and larger source to near receiver offset SASW data. However, such a data set suffers from dominant higher modes at small wavelengths/high frequencies and does not allow exploration of the variability of the subsurface velocity structure.
- Representative dispersion curves were generated for each surface wave data set using a moving average, polynomial curve fitting routine.
- Surface wave depth of investigation is about 35 m based on half of maximum wavelength criteria.
- At shallow depths, inferred P-wave velocities in the surface wave models are generally consistent with simplified P-wave refraction model considering unknown Poisson's ratio, except P-wave refraction data indicates that the high velocity layer is shallower than in the surface wave models. P-wave refraction data does not accurately constrain the thickness of the HVL or velocity structure below.

- With the exception of the upper 1 m, S-wave layer velocities from the SASW and MASW models are within 10 %.
- V_{S30} is 356 m/s for SASW array and 356 m/s for MASW array, averaging 356 m/s (Site Class D/C).
- Average S-wave velocity between 1 m (expected sensor depth) and 31 m is 383 m/s for SASW array and 371 m/s for MASW array, averaging 377 m/s.

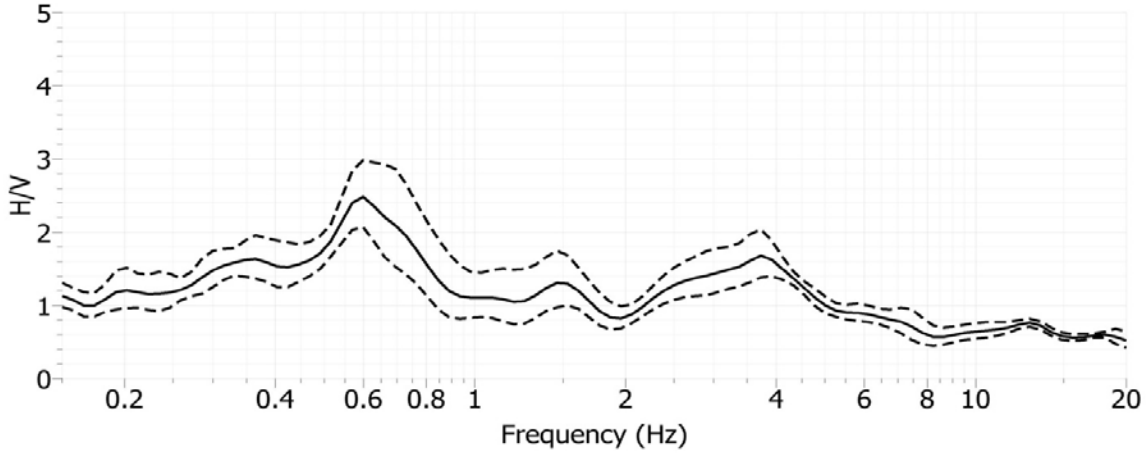

Site CI.SHO, H/V Spectral Ratio, Array SHO-1, Sensor 507

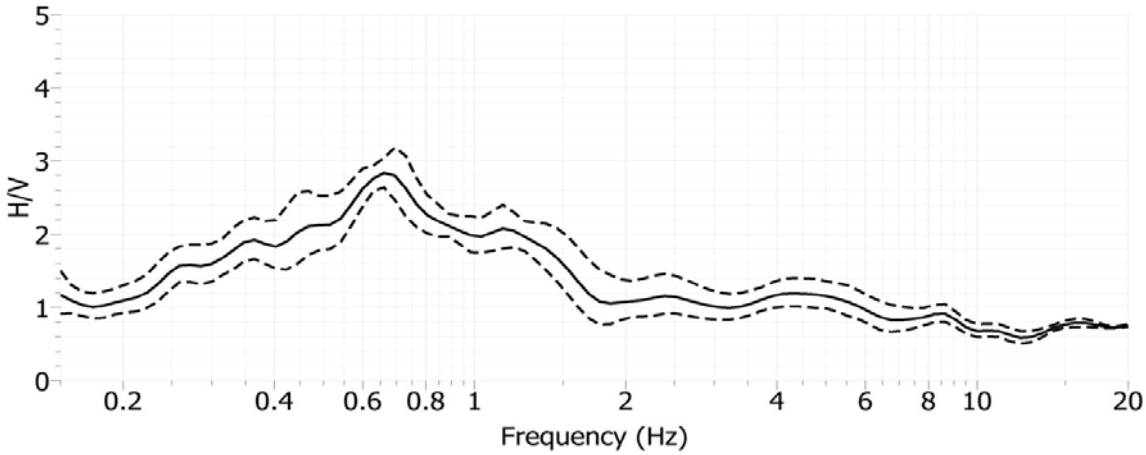

Site CI.SHO, H/V Spectral Ratio, Array SHO-1, Sensor 453

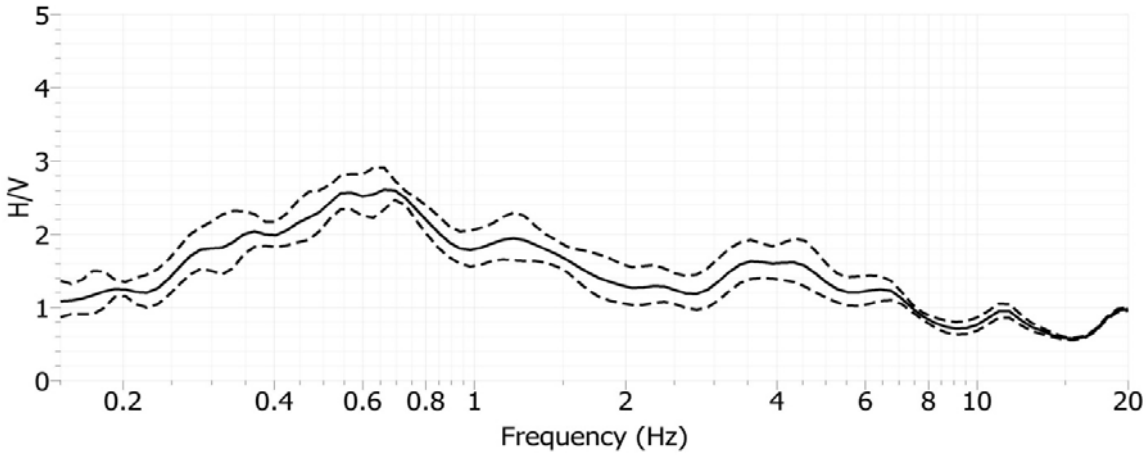

Site CI.SHO, H/V Spectral Ratio, Array SHO-1, Sensor 450

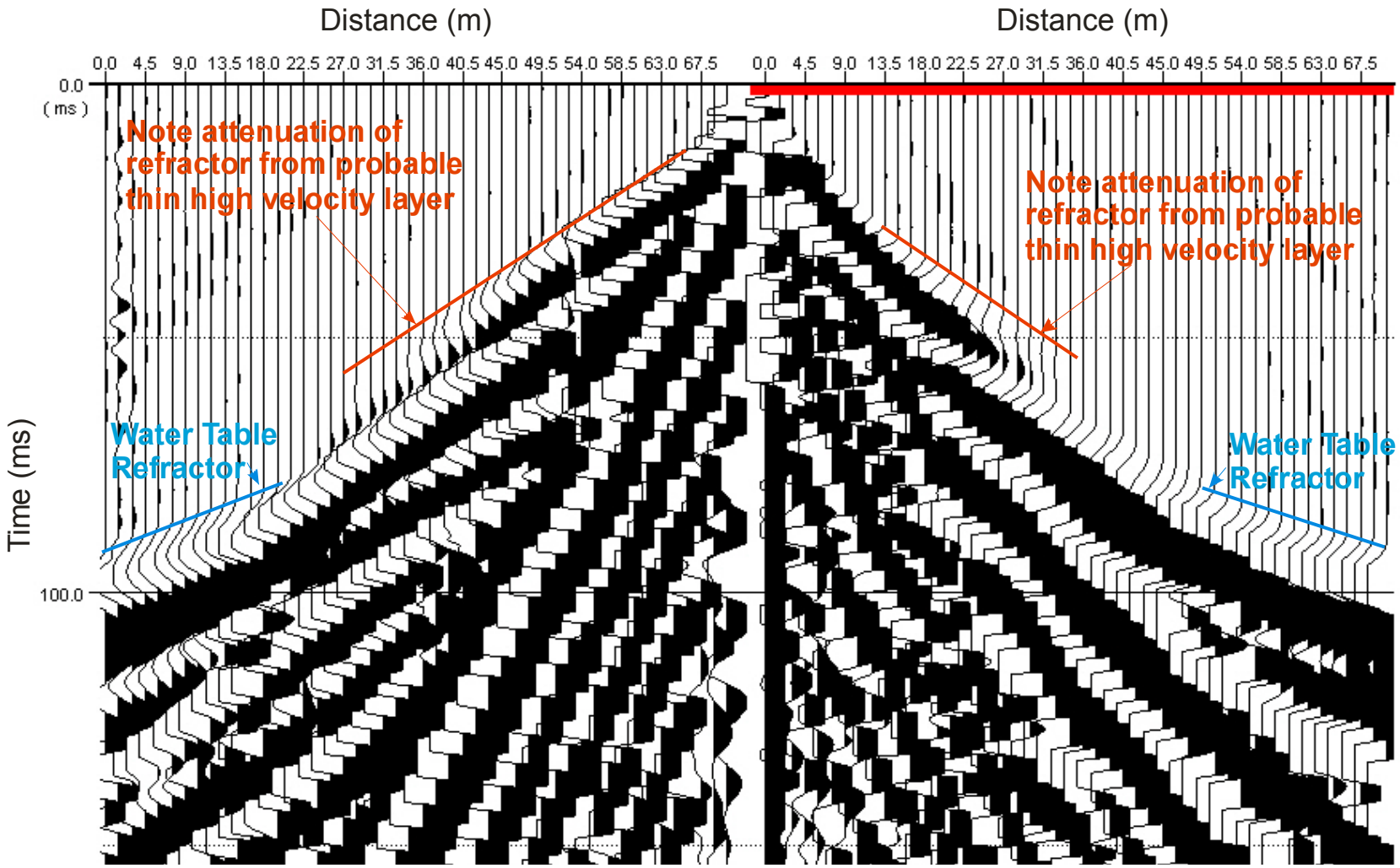

CI.SHO – Forward and reverse MASW seismic records showing the attenuation of the head wave propagating along a thin high velocity layer

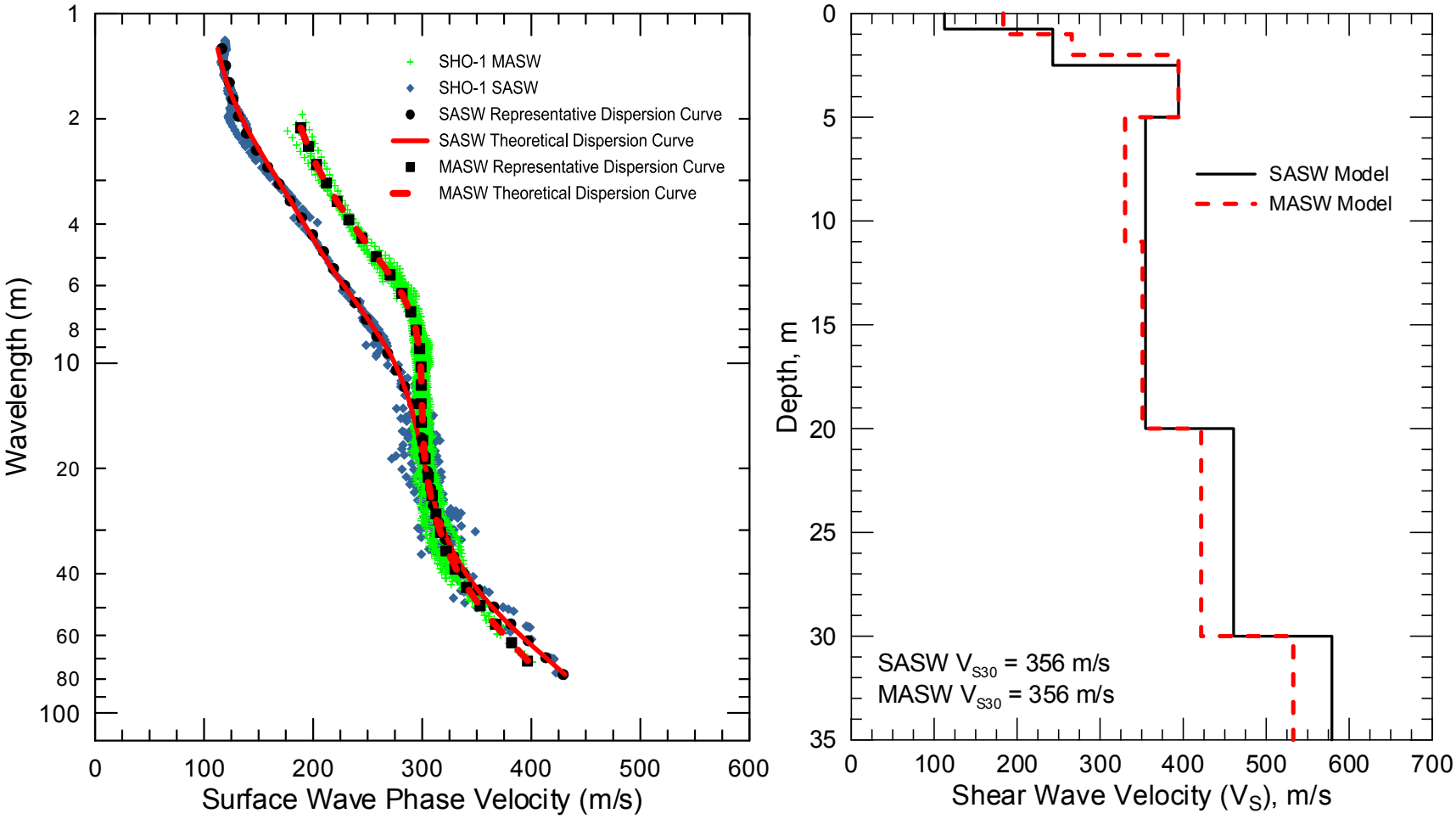

CI.SHO - Field, representative and inverted theoretical surface wave dispersion data (left) and associated V_S model (right)

Site CI.SIO

Location: AT&T, 10609 Telegraph Road, Saticoy, California

Latitude: 34.29224 **Longitude:** -119.16694

(Station coordinates modified based on field observation of station location and identification of approximate station location on Google Earth and/or ESRI Imagery– could not survey the seismic station as located inside a building, WGS84 coordinate system)

V_{S30} (measured): 249 m/s

V_{S30} (adjusted to more accurately reflect seismic station conditions): 249 m/s (no adjustment necessary)

NEHRP Site Class: D

Geomatrix Code: AHD

Geologic Conditions/Observations: Site located in area mapped as Quaternary (Holocene) alluvium.

Site Conditions: Suburban site with significant traffic noise from nearby roads. Relatively flat terrain in site vicinity. Gradual decrease in surface elevation to southeast.

Geophysical Methods Utilized: HVSR, MASW, array microtremor, ReMi™

Geophysical Testing Arrays:

1. Arrays SIO-1 (24 channel linear array utilizing 4.5 Hz vertical geophones spaced 3 m apart for an array length of 69 m) and SIO-2 (24 channel linear array utilizing 4.5 Hz vertical geophones spaced 5 m apart for an array length of 115 m) used to acquire passive surface wave data. Arrays combined to form an "L" shaped array.
2. Array SIO-3 (48 channel MASW array utilizing 4.5 Hz vertical geophones spaced 1 m apart for a length of 47 m, forward and reverse shot locations with multiple source offsets and source types (hammers only) and center shot location).
3. Three HVSR measurement locations, two distributed along arrays SIO-1 and SIO-3 and one next to the building housing the seismic sensor.

Legend

- Seismic Station - Approximate Surveyed Location
- Seismic Station - Approximate Location of Record
- H/V Spectral Ratio Location
- MASW Array
- Passive Surface Wave Array

NOTES:
1. WGS 1984 COORDINATE SYSTEM
2. Image Source: ESRI, i-cubed, USDA FSA, USGS, AEX, GeoEye, Getmapping, Aerogrid, IGP

File Name: CI-SIO-I

Date: 2/7/2013

USGS science for a changing world

GEOVision geophysical services

RECOVERY.GOV

SITE MAP
CI•SIO

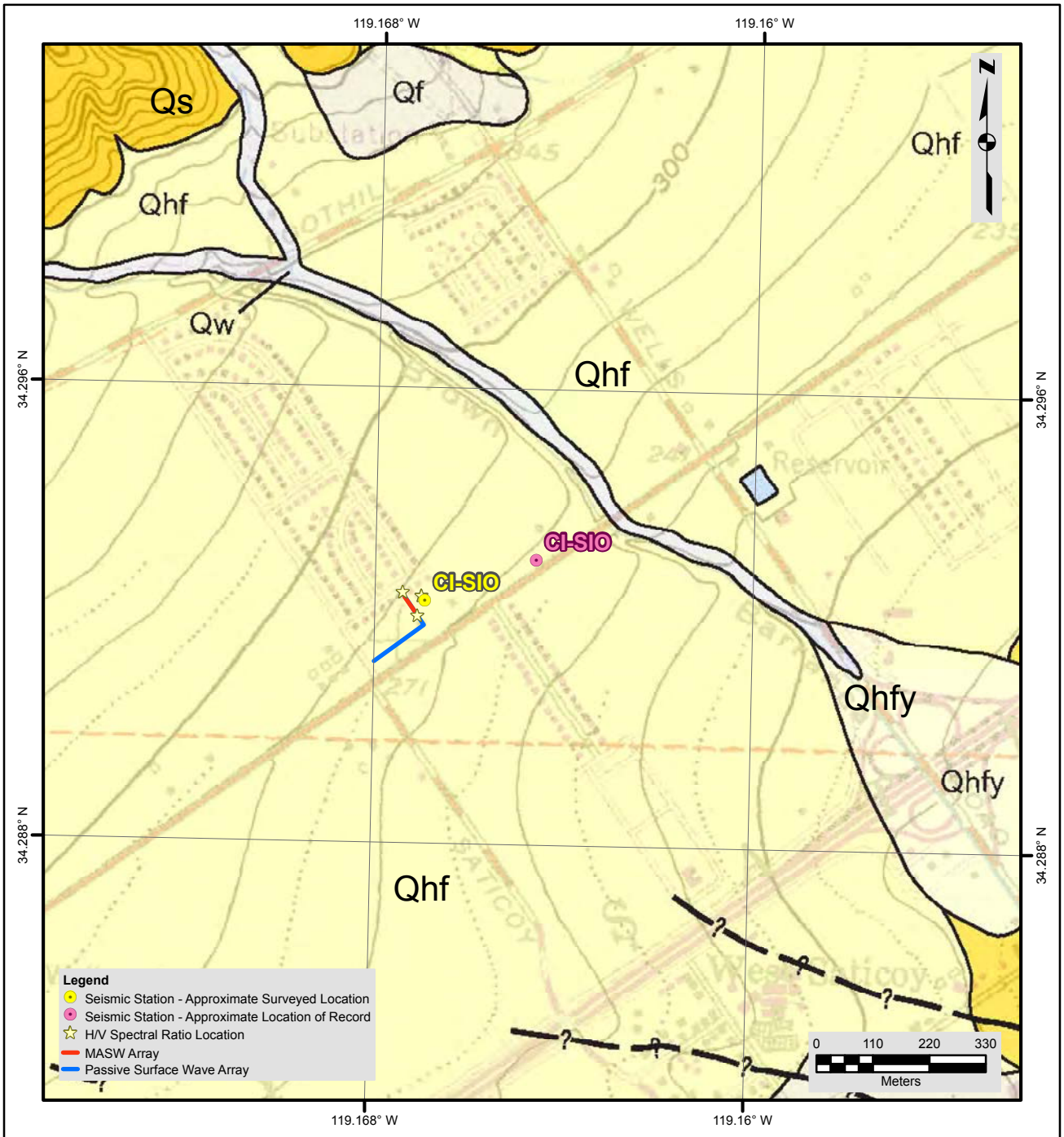

Description of Geologic Map Units

Qw = Quaternary (Holocene) wash deposits, unconsolidated silt, sand and gravel
Qhfy = Quaternary (Holocene) alluvial fan deposits, gravel, sand, silt and clay
Qhf = Quaternary (Late Holocene) alluvial fan deposits, sandy clay with gravel
Qf = Quaternary (Late Pleistocene to Holocene) alluvial fan deposits, sand gravel, silt and clay
Qs = Quaternary (Pleistocene) Saugus Formation; weakly consolidated alluvial deposits of sandstone and siliceous shale, gravel and cobbles in sandy matrix

NOTES:
1. WGS 1984 COORDINATE SYSTEM
2. Geologic Map of the Saticoy 7.5' Quadrangle, Ventura County, California, Version 1.0 by Siang S. Tan, Kevin B. Clahan and Anne M. Rosinski, 2004
3. See site map for details of geophysical survey

File Name: CI-SIO

Date: 2/7/2013

USGS science for a changing world

GEOVision geophysical services

GEOLOGIC MAP
CI•SIO

RECOVERY.GOV

CI.SIO Seismic Station

HVSR Data Acquisition Outside Building Housing Seismic Sensor

MASW Data Acquisition on Array SIO-3

Looking Northwest along Array SIO-1

Looking Southwest along Array SIO-2

Location of Geophysical Testing Arrays:

Location	Latitude	Longitude
SIO-1, Northwest end of "L" Array	34.29235	-119.16739
SIO-1, Corner of "L" Array	34.29183	-119.16695
SIO-2, Southwest end of "L" Array	34.29117	-119.16799
SIO-3, Southeast end of MASW Array	34.29197	-119.16707
SIO-3, Center of MASW Array	34.29217	-119.16723
SIO-3, Northwest end of MASW Array	34.29232	-119.16737
HVSR Sensor 450	34.29235	-119.16701
HVSR Sensor 453	34.29240	-119.16741
HVSR Sensor 507	34.29199	-119.16709
CI.SIO Seismic Station	34.29224	-119.16694

Notes: 1) WGS84 Coordinate System (decimal degrees)

2) Survey accuracy is estimated at 2 to 3 m

3) CI.SIO Seismic Station was not surveyed with GPS because it is located inside a building. The location of the seismic station was estimated using Google Earth/ESRI Imagery and field observations.

Results:

V_S Model

Depth to Top of Layer (m)	Layer Thickness (m)	S-Wave Velocity (m/s)	Inferred P-Wave Velocity (m/s)	Assumed Poisson's Ratio	Assumed Density (g/cm^3)
0	1.5	122	229	0.300	1.8
1.5	2	189	353	0.300	1.8
3.5	4.5	261	488	0.300	1.9
8	8	265	496	0.300	1.9
16	10	266	1600	0.486	2.0
26	12	318	1650	0.481	2.0
38	15	389	1650	0.471	2.0
53	15	482	1700	0.456	2.1
68	>12	584	1700	0.433	2.1

Notes: 1) Saturated sediments estimated at 16 m depth from seismic refraction first arrival and possible reflection.

2) P-wave velocity assumed to increase with depth in saturated zone from 1,600 to 1,700 m/s. Too much noise in seismic refraction data to accurately estimate velocity.

3) Depth of investigation is about 80 m.

4) Bottom layer is a half space.

Observations/Discussion:

- The HVSR curves are almost identical at frequencies below 10 Hz, validating the 1-D velocity structure assumption.
- Low amplitude HVSR peak at about 1.3 Hz. There is no low frequency HVSR peak associated with basement complex, although HVSR data is noisy at frequencies below 0.2 Hz. Night time measurements may improve data quality at low frequencies.
- Noise conditions at site (multi-directional or omni-directional noise sources) appeared sufficient for successful application of passive surface wave techniques.
- ESAC technique used to extract surface wave dispersion data from passive "L" array data. Both the ReMi™ and ESAC techniques used to extract surface wave dispersion data from the linear arrays. Only the higher quality "L" array dispersion data used for analysis. The linear arrays yielded dispersion curves that differ from the "L" array dispersion curve by no more than 30 m/s. However, array SIO-1 is not long enough (69 m) to be effective and is located next to a building with potential utilities, lateral velocity variation, etc. Array SIO-2 is located along Telegraph Road, so there is potential for a strong in-line directional noise bias. A passive array located in the residential community about 100 m northwest of the seismic station may be more appropriate.
- Surface wave dispersion data from active and passive surface wave data sets are in good agreement at this site. The MASW array is located adjacent to a building in order to be located along a segment of the passive array. There is some near surface lateral velocity variation due to the building fill pad and possible utilities in the vicinity of the MASW array; however, surface wave dispersion data in reasonable agreement with passive data was obtained by focusing on data from the northern portion of the array, which is further from the building.
- Representative dispersion curves were generated for each surface wave data set using a moving average, polynomial curve fitting routine. These individual representative dispersion curves were combined and a representative dispersion curve generated for the combined data set for data modeling.
- The water table was modeled at a depth on the order of 16 m based on interactive layer-based analysis of seismic refraction first arrival data and potential water table reflection, which was very noisy due to heavy vehicle traffic in site vicinity. P-wave velocities of saturated sediments assumed to increase gradually with depth from 1,600 to 1,650 m/s, respectively.
- Surface wave depth of investigation is about 80 m based on half of maximum wavelength criteria and assuming that surface wave dispersion data at frequencies as low as 2.5 Hz are valid utilizing 4.5 Hz geophones (low frequency geophone phase response differences will cancel out if noise is omni-directional and/or the phase response differences are random in nature).
- The S-wave velocity model, developed from the active and passive surface wave data, generates a synthetic HVSR peak of about 1.6 Hz, assuming an equal distribution of Rayleigh and Love waves and no higher modes, which is reasonably close to the observed 1.3 Hz peak.
- V_{S30} is 249 m/s (Site Class D).
- Average S-wave velocity of the upper 80 m (V_{S80}) is 339 m/s.

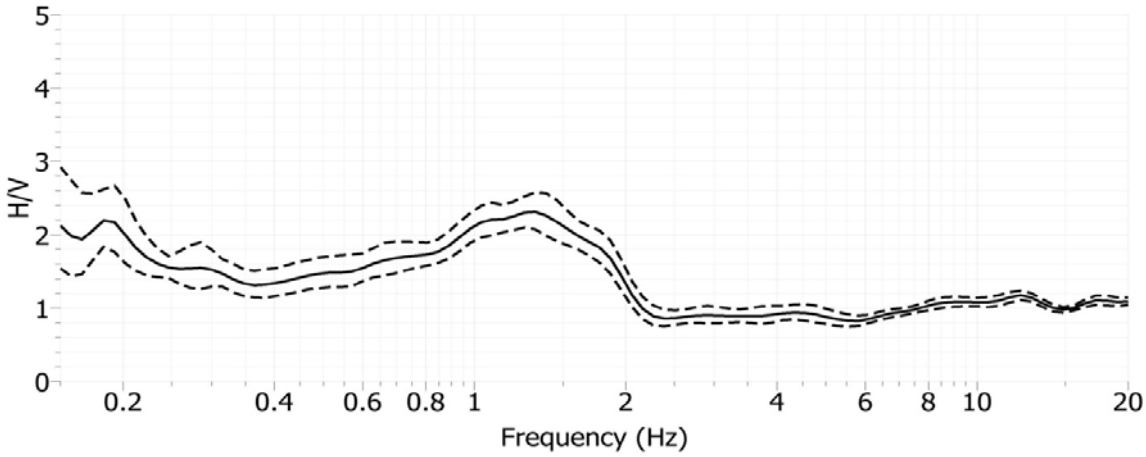

Site CI.SIO, H/V Spectral Ratio, Array SIO-3, Sensor 453

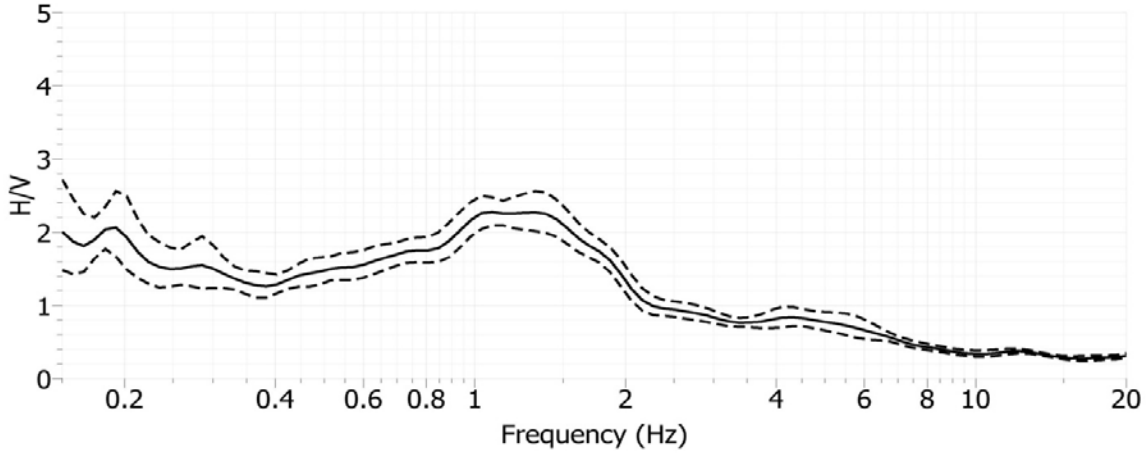

Site CI.SIO, H/V Spectral Ratio, Near Seismic Station, Sensor 450

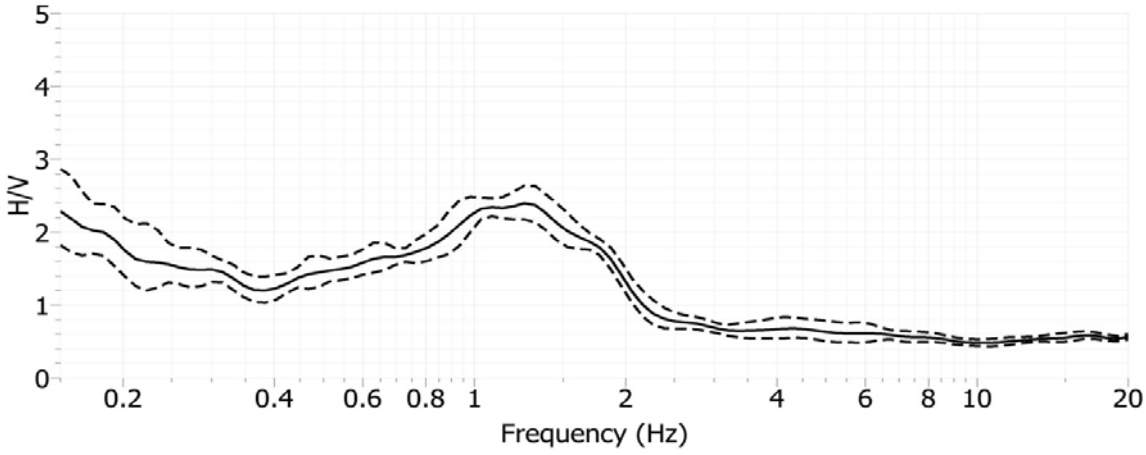

Site CI.SIO, H/V Spectral Ratio, Array SIO-1, Sensor 507

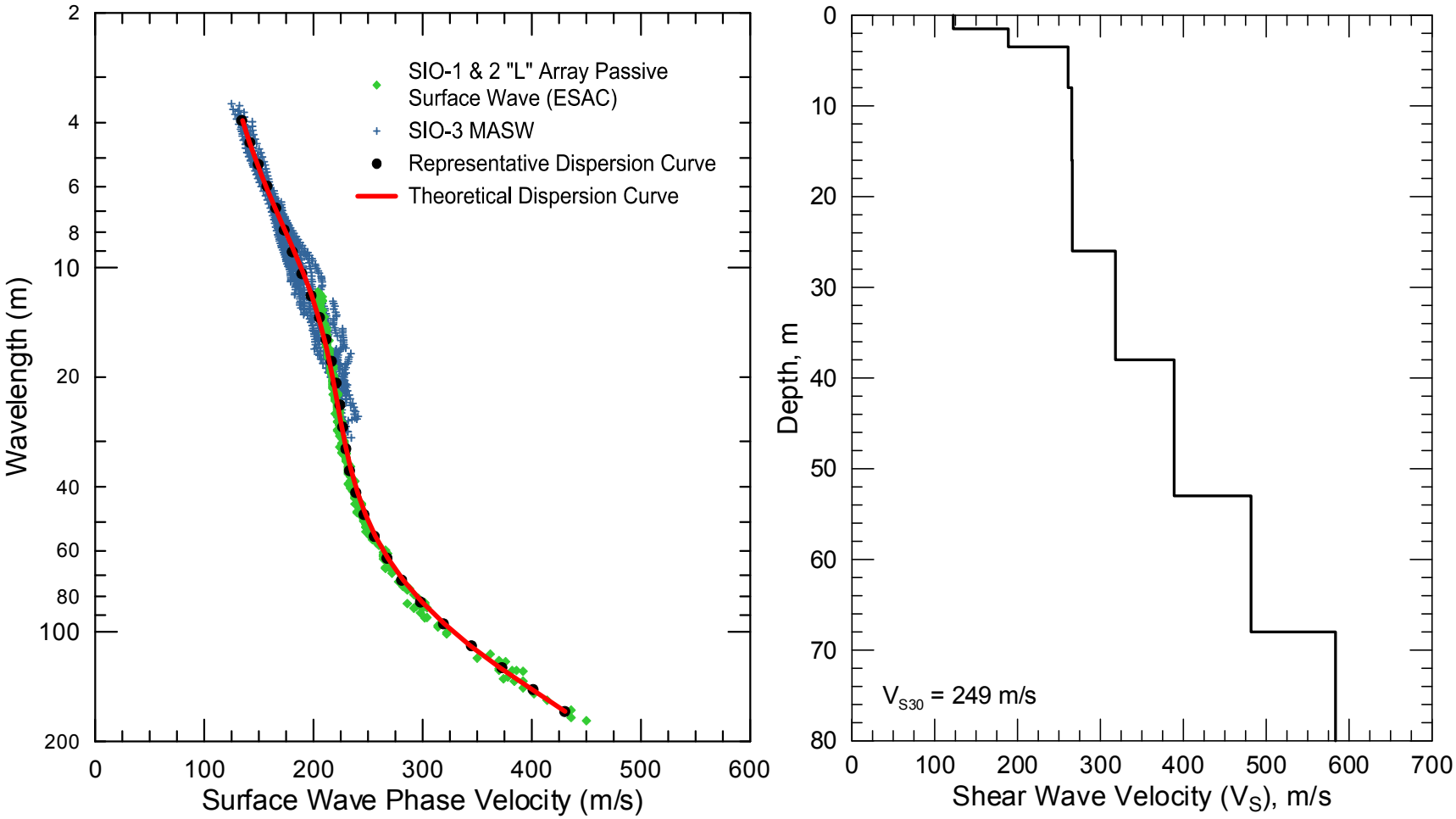

CI.SIO - Field, representative and inverted theoretical surface wave dispersion data (left) and associated V_S model (right)

Site CI.SLA

Location: Slate Mountain, Inyo County, California

Latitude: 35.89095 **Longitude:** -117.28332
(Station coordinates provided by USGS, WGS84 coordinate system)

V_{S30} (measured): 482 m/s

V_{S30} (adjusted to more accurately reflect seismic station conditions): 521 m/s (average S-wave velocity between 1.5 and 31.5 m adjusting for inferred 1.5 m sensor depth).

NEHRP Site Class: C

Geomatrix Code: IVA

Geologic Conditions/Observations: Seismic station located on Tertiary (Pliocene or Miocene) andesitic to basaltic flows. Mapped outcrop of undifferentiated plutonic and metamorphic rocks within 200 m of site.

Site Conditions: Rural site. Seismic station located on top of a mountain peak. Relatively steep topography in site vicinity. Test area located on a hilltop with a relatively flat surface.

Geophysical Methods Utilized: HVSR, Seismic Refraction, MASW

Geophysical Testing Arrays:

1. Array SLA-1 (48 channel MASW and P-wave seismic refraction array utilizing 4.5 Hz vertical geophones spaced 1.5 m apart for a length of 70.5 m, forward and reverse shot locations with multiple source offsets and source types and multiple interior shot locations).
2. Three HVSR measurement locations distributed along array SLA-1.

Legend

- Seismic Station - Approximate Surveyed Location
- Seismic Station - Approximate Location of Record
- H/V Spectral Ratio Location
- MASW and Seismic Refraction Array

NOTES:
1. WGS 1984 COORDINATE SYSTEM
2. Image Source: ESRI, i-cubed, USDA FSA, USGS, AEX, GeoEye, Getmapping, Aerogrid, IGP

File Name: CI-SLA-I

Date: 2/7/2013

USGS science for a changing world

GEOVision geophysical services

RECOVERY.GOV

SITE MAP
CI•SLA

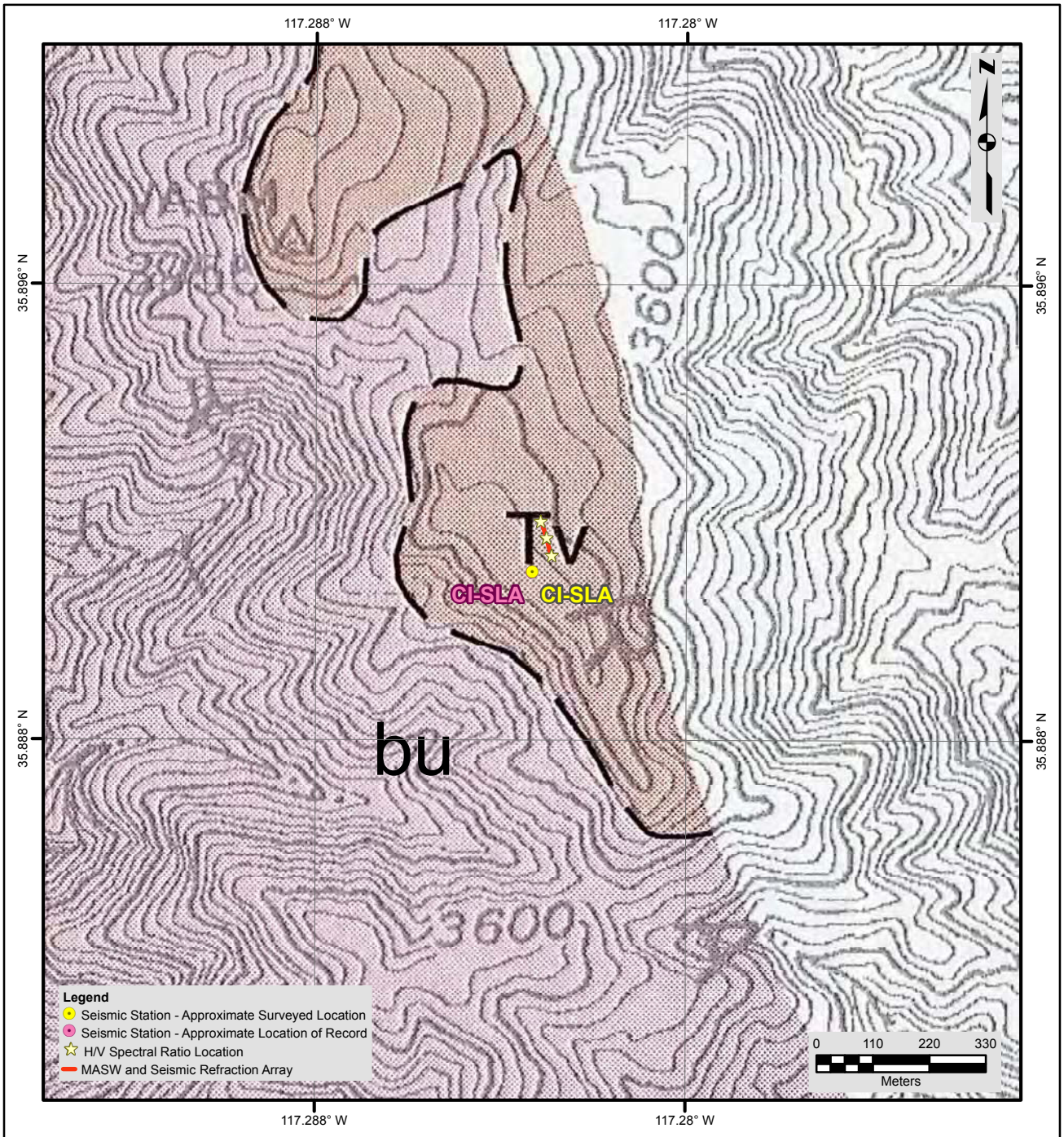

Description of Geologic Map Units

Tv = Tertiary (Pliocene or Miocene) volcanic rock; andesitic and basaltic flows, some tuffs and breccias
bu = Pre-Tertiary bedrock; undifferentiated, mostly plutonic and metamorphic rocks

NOTES:
1. WGS 1984 COORDINATE SYSTEM
2. Geologic Map of the Searles Valley, Inyo and San Bernardino Counties, California by George I. Smith, 2009
3. See site map for details of geophysical survey

File Name: CI-SLA

Date: 2/7/2013

USGS science for a changing world

GEOVision geophysical services

GEOLOGIC MAP
CI•SLA

RECOVERY.GOV

CI.SLA seismic station (beneath GPS unit in center of photo)

Looking south along array SLA-1 and at HVSR sensor 450

Looking south past HVSR sensor 507 along array SLA-1

MASW and seismic refraction data acquisition on array SLA-1

P-wave refraction data acquisition using accelerated weight drop energy source

Location of Geophysical Testing Arrays:

Location	Latitude	Longitude
SLA-1, Southeast End of MASW/ Seismic Refraction Array	35.89124	-117.28291
SLA-1, Center of MASW/Seismic Refraction Array	35.89155	-117.28302
SLA-1, Northwest End of MASW/Seismic Refraction Array	35.89184	-117.28312
HVSR Sensor 450	35.89155	-117.28300
HVSR Sensor 453	35.89124	-117.28290
HVSR Sensor 507/453B	35.89185	-117.28313
CI.SLA Seismic Station	35.89095	-117.28331

Notes: 1) WGS84 Coordinate System (decimal degrees)
2) Survey accuracy is estimated at 1 to 2 m.

Results:

V_S Model

Depth to Top of Layer (m)	Layer Thickness (m)	S-Wave Velocity (m/s)	Inferred P-Wave Velocity (m/s)	Assumed Poisson's Ratio	Assumed Density (g/cm^3)
0	2	232	433	0.3	1.7
2	2.5	288	539	0.3	1.8
4.5	3.5	380	711	0.3	1.9
8	4	489	915	0.3	2.0
12	6	563	1053	0.3	2.0
18	8	663	1240	0.3	2.1
26	>9	823	1540	0.3	2.1

Notes: 1) Depth of investigation is about 35 m.
2) Bottom layer is a half space.

Observations/Discussion:

- The HVSR curves are generally similar with a low amplitude peak in the 1.25 to 2.5 Hz range. HVSR measurements were made on two occasions. The original data collected with sensor 507 had significant low frequency noise. HVSR data acquisition was repeated at this location (sensor 453B) about 3 months later with the 1.25 to 2.5 Hz HVSR peak being repeatable.
- The HVSR peak in the 1.25 to 2.5 Hz range could be associated with the contact between weathered Tertiary volcanic rocks and underlying plutonic and metamorphic rocks.
- The P-wave refraction data collected along array SLA-1 were not of high enough quality to generate a seismic refraction model. The geologic conditions at the testing did not allow for accurate picking of first arrival times due to probable out of plane refractors from localized high velocity zones. The seismic refraction data were, however, reviewed for general velocity structure. Lateral velocity variation is evident in the seismic records, both in the seismic refraction first arrival data and surface waves.
- The seismic refraction data show that the P-wave velocity is about 500 to 700 m/s at the surface, increasing to about 1,000 m/s at depth of less than 15 m.
- Noise conditions at the site were not sufficient for application of passive surface wave techniques.
- The minimum wavelength surface wave phase velocity data extracted from the 48-channel MASW array was about 13 m. Data reduction using seismic records from smaller hammer sources and a limited offset receiver array (i.e. less active geophones) allowed extraction of surface wave dispersion data to a minimum wavelength of about 4.5 m. Scatter in MASW dispersion data is likely due, in part, to lateral velocity variation associated with both a very thin sediment/fill layer of variable thickness and differential weathering of near surface volcanic rock.
- There is significant scatter (60 to 100 m/s) in the surface wave dispersion data, likely due to lateral velocity variation. Lateral velocity variation is clear on the seismic records in both the P-wave and surface wave waveforms.
- Small wavelength (high frequency) Rayleigh wave phase velocities are higher at the north end of the array and only the more conservative (slower) high frequency phase velocity data from shot locations near the center and southern end of the array were used for analysis.
- A representative dispersion curve was generated for the MASW data set using a moving average, polynomial curve fitting routine and used for modeling.
- Surface wave depth of investigation is about 35 m based on half of maximum wavelength criteria.
- V_{S30} is 482 m/s (Site Class C).
- Average S-wave velocity between 1.5 m (assumed sensor depth) and 31.5 m is 521 m/s.
- Although there is significant lateral velocity variation at the site, we believe that the V_S model derived from the surface wave dispersion data is representative of average site conditions. The scatter in the surface wave dispersion data indicates that V_{S30} may vary by 10% beneath the array.

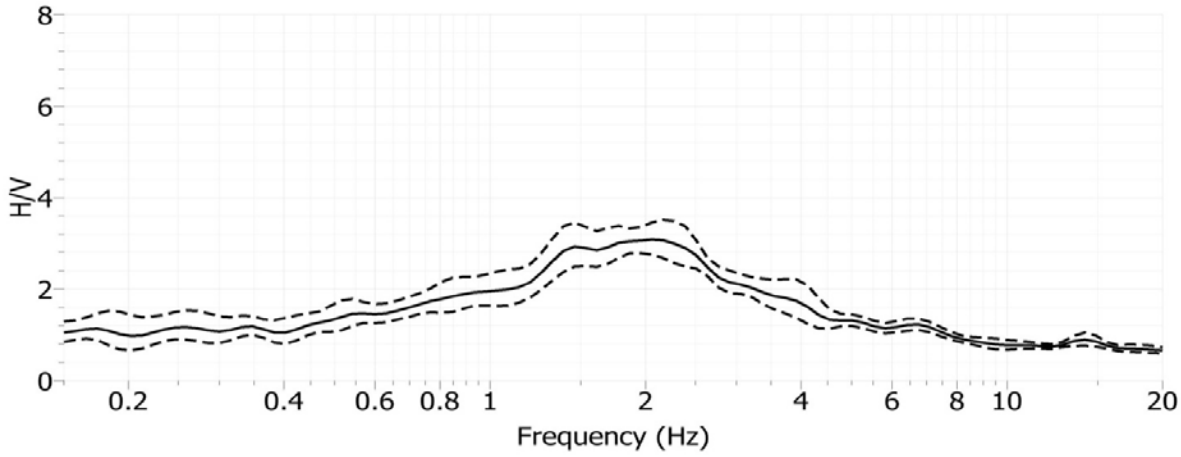

Site CI.SLA, H/V Spectral Ratio, Array SLA-1, Sensor 453B

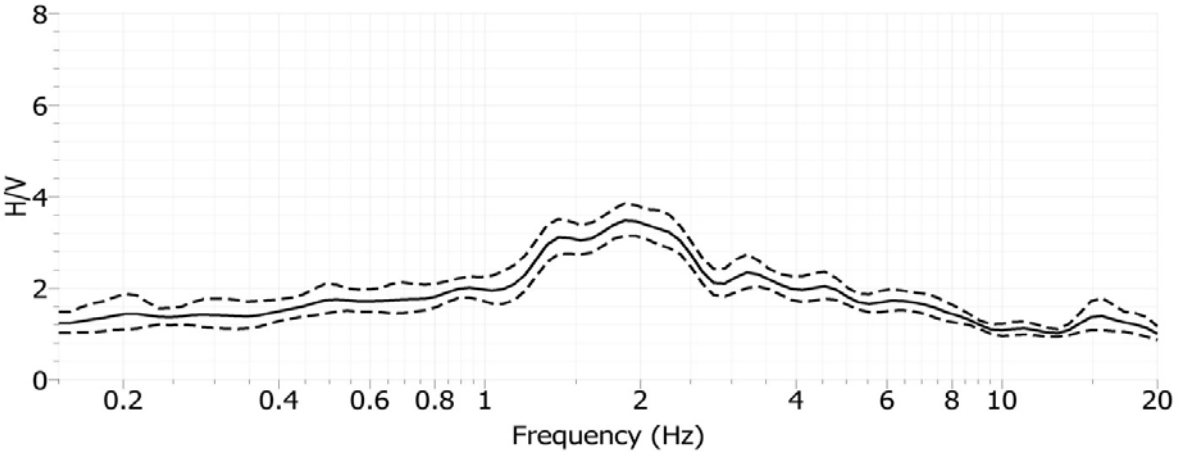

Site CI.SLA, H/V Spectral Ratio, Array SLA-1, Sensor 450

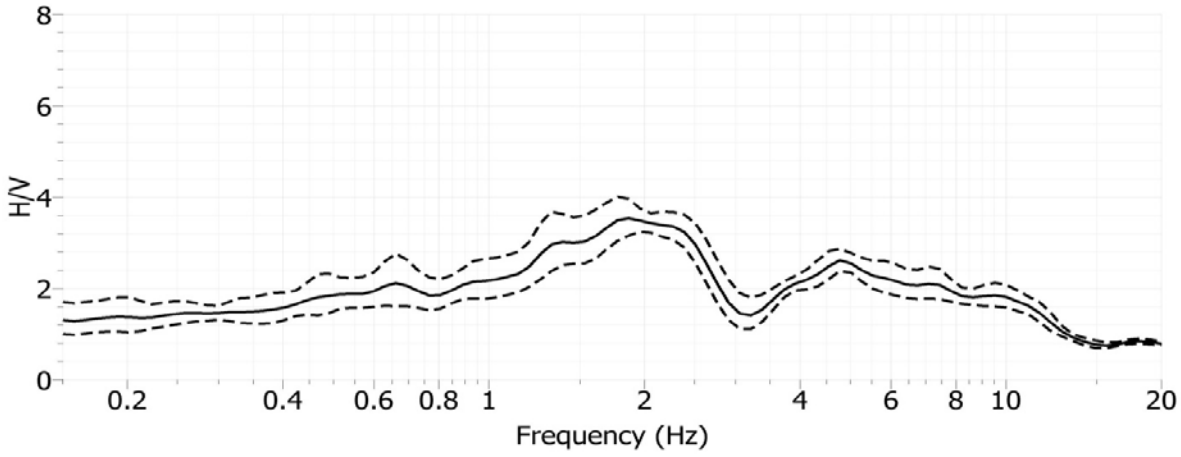

Site CI.SLA, H/V Spectral Ratio, Array SLA-1, Sensor 453

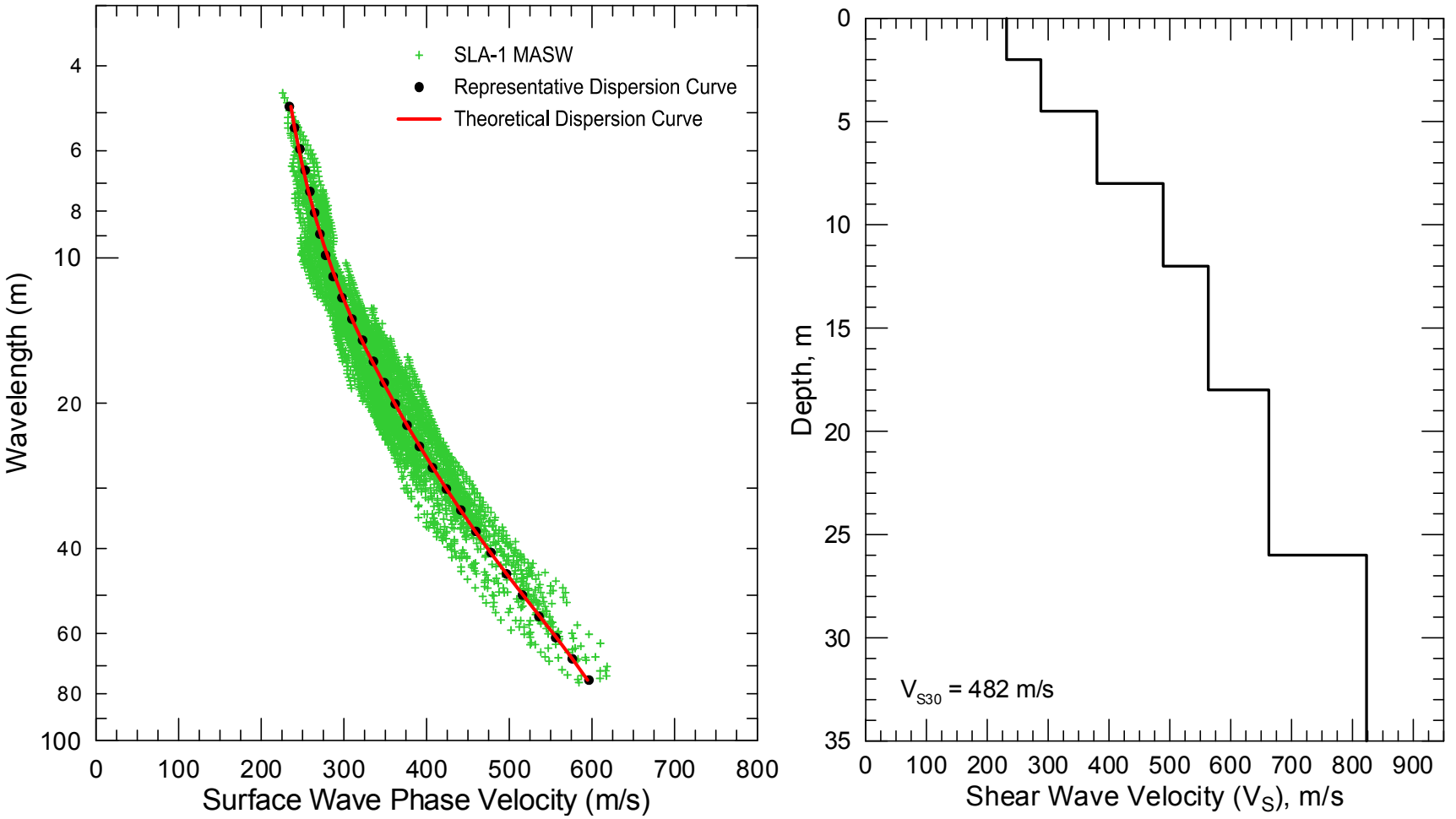

CI.SLA - Field, representative and inverted theoretical surface wave dispersion data (left) and associated V_S model (right)

Site CI.SLB

Location: IID Communication Facility, Salton Beach, North Shore of Salton Sea, Riverside County, California

Latitude: 33.48519 **Longitude:** -115.86643
(Station coordinates provided by USGS, WGS84 coordinate system)

V_{S30} (measured): 336 m/s

V_{S30} (adjusted to more accurately reflect seismic station conditions): 377 m/s (average S-wave velocity between 2 and 32 m adjusting for 2 m assumed sensor depth).

NEHRP Site Class: D/C

Geomatrix Code: IHD

Geologic Conditions/Observations: Seismic station located at mapped contact of geologic units mapped as Quaternary (Holocene) alluvial sand and gravel deposits and Cahuilla beds and Holocene Cahuilla gravel bar deposits. Field observations unable to confirm this geologic contact, but geophysical arrays are placed on same geologic material as seismic station. San Andreas Fault located about 1.5 km southwest of site. Tertiary Palm Springs Formation outcrops less than 1 km southwest and northeast of site. Expected deep soil site.

Site Conditions: Rural site. Tall radio antennae located near seismic station and test area. Flat terrain in site vicinity.

Geophysical Methods Utilized: HVSR, MASW, SASW

Geophysical Testing Arrays:

1. Array SLB-1 (48 channel MASW array utilizing 4.5 Hz vertical geophones spaced 1.5 m apart for a length of 70.5 m, forward and reverse shot locations with multiple source offsets and source types and center shot location).
2. Array SLB-1 (SASW array with same midpoint and orientation as MASW array SLB-1. SASW data acquired using 1 Hz geophones, common source and common center point geometry, forward and reverse shot locations).
3. Three HVSR measurement locations distributed along SLB-1.

Legend

- Seismic Station - Approximate Surveyed Location
- Seismic Station - Approximate Location of Record
- H/V Spectral Ratio Location
- SASW Array
- MASW Array

NOTES:
1. WGS 1984 COORDINATE SYSTEM
2. Image Source: ESRI, i-cubed, USDA FSA, USGS, AEX, GeoEye, Getmapping, Aerogrid, IGP

File Name: CI-SLB-I

Date: 9/22/2011

USGS science for a changing world

GEOVision geophysical services

RECOVERY.GOV

SITE MAP
CI•SLB

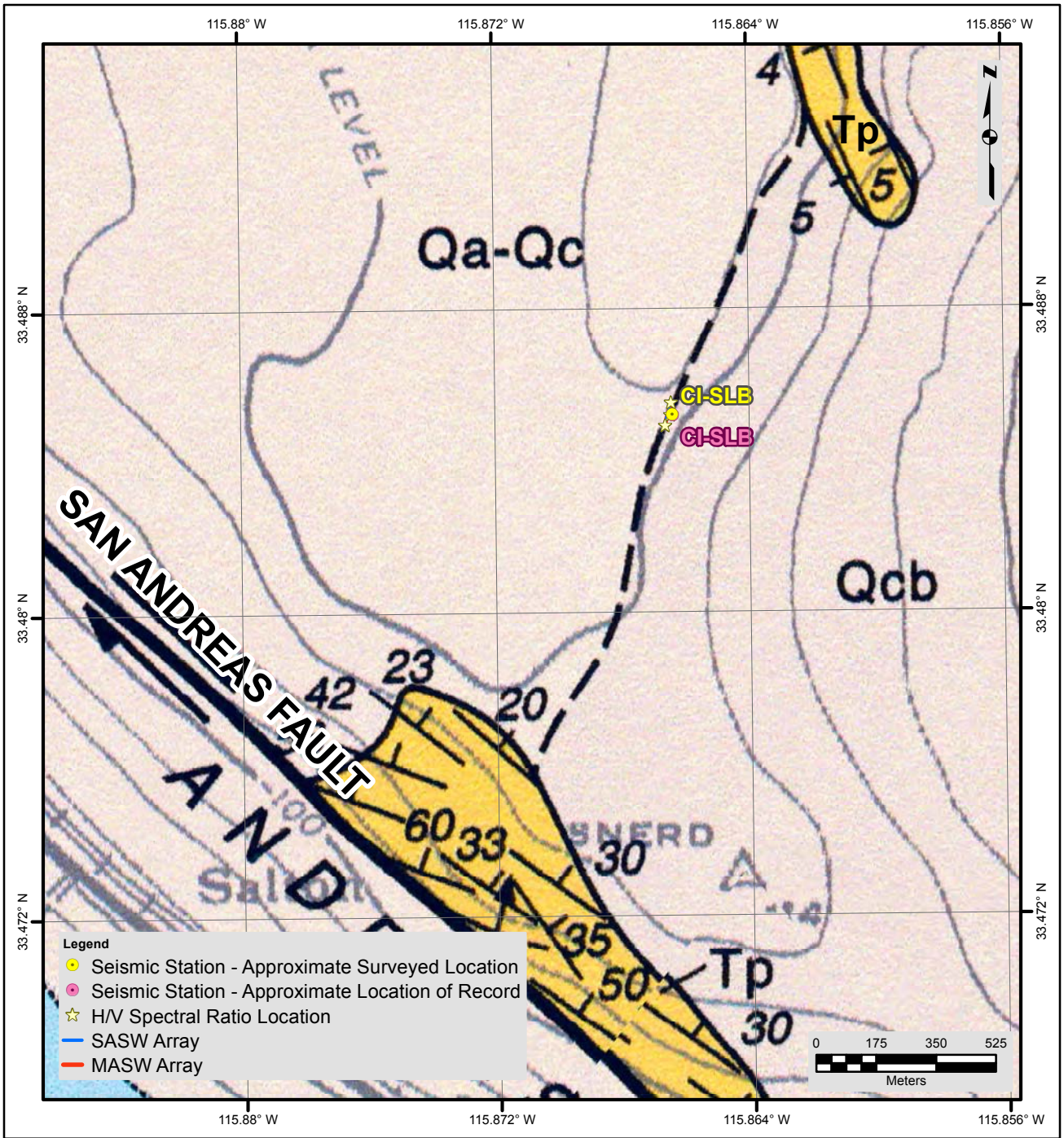

Description of Geologic Map Units

Qa-Qc = Quaternary (Holocene) alluvial sand, gravel, silt and clay of valley areas - Cahuilla beds, thin series of tan-gray claystones, sands, and gravels, fossiliferous
Qcb = Quaternary (Holocene) Cahuilla Gravel Bar; gravel and sand deposited as a bar on east side of former Lake Cahuilla
Tp = Tertiary (Pliocene) Palm Spring Formation; pink-gray laminated sandstones, arkosic, with interbedded red clays

NOTES:
1. WGS 1984 COORDINATE SYSTEM
2. Geologic Map of the Durmid 15 Minute Quadrangle, Riverside and Imperial Counties, California by Thomas W. Dibblee, Jr., 2006
3. See site map for details of geophysical survey

USGS science for a changing world

GEOVision geophysical services

RECOVERY.GOV

GEOLOGIC MAP
CI•SLB

File Name: CI-SLB

Date: 9/22/2011

Looking east towards CI.SLB seismic station and center of MASW array SLB-1

Looking northeast along MASW array SLB-1

SASW data acquisition with hammer source on SLB-1

Looking southwest towards data acquisition with AWD along MASW array SLB-1

Looking towards seismic station CI.SLB during MASW data acquisition with hammer source

Location of Geophysical Testing Arrays:

Location	Latitude	Longitude
SLB-1, Southwest End of MASW Array	33.48492	-115.86669
SLB-1, Center of MASW and SASW Arrays	33.48522	-115.86658
SLB-1, Northeast End of MASW Array	33.48553	-115.86647
HVSR Sensor 450	33.48520	-115.86650
HVSR Sensor 453	33.48553	-115.86648
HVSR Sensor 507	33.48492	-115.86667
CI.SLB Seismic Station	33.48520	-115.86645

Notes: 1) WGS84 Coordinate System (decimal degrees)
2) Survey accuracy is estimated at 1 to 2 m

Results:

V_S Model – Combined MASW and SASW Surface Wave Dispersion Data

Depth to Top of Layer (m)	Layer Thickness (m)	S-Wave Velocity (m/s)	Inferred P-Wave Velocity (m/s)	Assumed Poisson's Ratio	Assumed Density (g/cm^3)
0	0.5	98	183	0.300	1.7
0.5	1	184	344	0.300	1.8
1.5	1.5	226	422	0.300	1.8
3	3	311	582	0.300	1.9
6	5	319	596	0.300	2.0
11	7	379	710	0.300	2.0
18	12	426	796	0.300	2.0
30	>2	624	2000	0.446	2.1

Notes: 1) Saturated sediments estimated at 30 m depth from seismic refraction first arrival data. P-wave velocity of saturated sediments assumed to be 2,000 m/s.
2) Depth of investigation is about 32 m.
3) Bottom layer is a half space.
4) Velocity of half space not well constrained due to depth, relative to depth of investigation.

V_S Model – MASW Array SLB-1

Depth to Top of Layer (m)	Layer Thickness (m)	S-Wave Velocity (m/s)	Inferred P-Wave Velocity (m/s)	Assumed Poisson's Ratio	Assumed Density (g/cm^3)
0	1	144	270	0.300	1.8
1	2	219	410	0.300	1.8
3	3	304	569	0.300	1.9
6	5	349	653	0.300	2.0
11	7	370	692	0.300	2.0
18	12	408	763	0.300	2.0
30	>2	665	2000	0.438	2.1

Notes: 1) Saturated sediments estimated at 30 m depth from seismic refraction first arrival data. P-wave velocity of saturated sediments assumed to be 2,000 m/s.
2) Depth of investigation is about 32 m.
3) Bottom layer is a half space.
4) Velocity of half space not well constrained due to depth, relative to depth of investigation.

V_S Model – SASW Array SLB-1

Depth to Top of Layer (m)	Layer Thickness (m)	S-Wave Velocity (m/s)	Inferred P-Wave Velocity (m/s)	Assumed Poisson's Ratio	Assumed Density (g/cm^3)
0	0.5	99	185	0.300	1.7
0.5	1	166	311	0.300	1.8
1.5	1.5	222	415	0.300	1.8
3	3	312	584	0.300	1.9
6	5	314	587	0.300	2.0
11	7	363	679	0.300	2.0
18	12	463	866	0.300	2.0
30	>2	646	2000	0.442	2.1

Notes: 1) Saturated sediments estimated at 30 m depth from seismic refraction first arrival data. P-wave velocity of saturated sediments assumed to be 2,000 m/s.
2) Depth of investigation is about 32 m.
3) Bottom layer is a half space.
4) Velocity of half space not well constrained due to depth, relative to depth of investigation.

Observations/Discussion:

- HVSR plots are very similar validating the 1-D velocity assumption.
- There is a broad, weak HVSR peak in the 3 Hz range, which could potentially be associated with the top of the Tertiary Palm Springs Formation at relatively shallow depth (i.e. upper 40 m). There is no low frequency peak associated with the basement complex, which is expected to be very deep at this site.
- Noise conditions at the site were not sufficient to apply passive surface wave techniques.
- Dominant higher mode surface wave energy over the 20 to 35 Hz range in forward direction MASW shot records; however, dominant higher mode surface waves were not an issue for reverse direction shot records. Dominant higher mode surface wave energy also appeared to complicate reduction of SASW data.
- Surface wave dispersion data from SASW and MASW datasets are in acceptable agreement, but there are sufficient differences to justify modeling both the combined data set and the individual data sets to determine range of subsurface velocities.
- For the purpose of data modeling, a moving average, polynomial curve fitting routine was used to generate separate representative dispersion curves for the SASW and MASW data. Additionally, these representative dispersion curves were combined to form a composite representative dispersion curve for modeling.
- Based on simple, horizontal layer-based analysis of seismic refraction first arrival data, P-wave velocity in the upper 30 m ranges from about 350 m/s near the surface to 500 to 550 m/s at a depth of 2 to 3 m and 675 to 775 m/s at a depth of about 6 to 7 m. A high velocity refractor likely associated with the water table is identified at a depth of 27 to 30 m. There was not sufficient source offset to accurately constrain the P-wave velocity of the saturated zone, but velocity appears to exceed 2,000 m/s.
- Water table depth constrained at a depth of 30 m and with P-wave velocity of 2,000 m/s for surface wave modeling.
- P-wave velocities in surface wave model, based on an assumed Poisson's ratio of 0.3, are consistent with P-wave velocities in seismic refraction first arrival data.
- A significant increase in S-wave velocity to over 600 m/s is modeled at 30 m depth in both the MASW and SASW models. The S-wave velocity of this layer is not well resolved due to the layers depth relative to depth of investigation. A significant increase in S-wave velocity in this depth range is, however, supported by the weak HVSR peak at approximately 3 Hz.
- The S-wave velocity models developed from the SASW and MASW data generate a synthetic HVSR peak at about 3.2 Hz, relatively close to the observed 3 Hz peak.
- S-wave velocities in the three surface wave models agree to within about 10% of velocity.
- Surface wave depth of investigation is about 32 m based on half of maximum wavelength criteria.
- V_{S30} for the MASW array is 339 m/s and V_{S30} for the SASW array is also 339 m/s.
- V_{S30} for the combined MASW and SASW data set is 336 m/s (Site Class D).
- Average S-wave velocity between 2 m (assumed sensor depth) and 32 m is 375 m/s for the MASW array and 383 m/s for the SASW array.
- Average S-wave velocity between 2 m (assumed sensor depth) and 32 m for the combined MASW and SASW data set is 377 m/s (Site Class C).

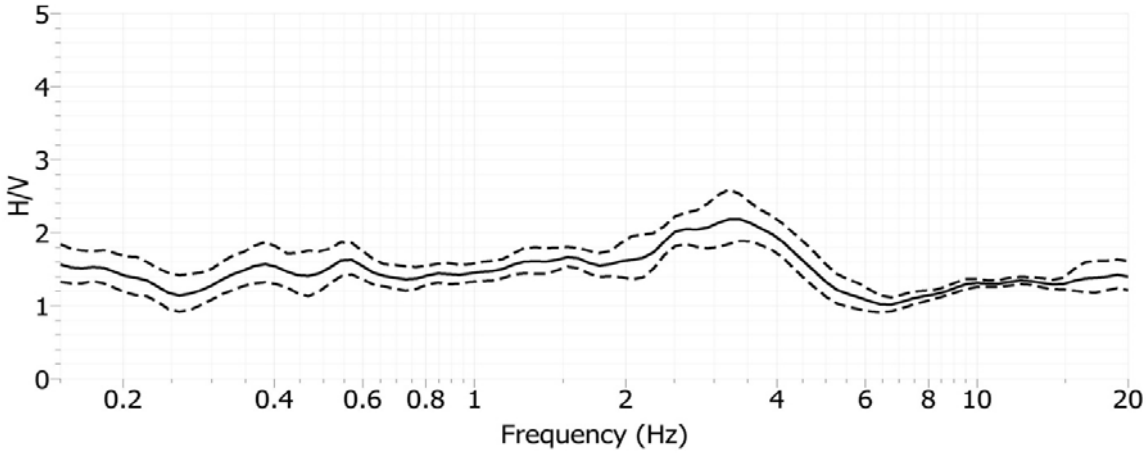

Site CI.SLB, H/V Spectral Ratio, Array SLB-1, Sensor 453

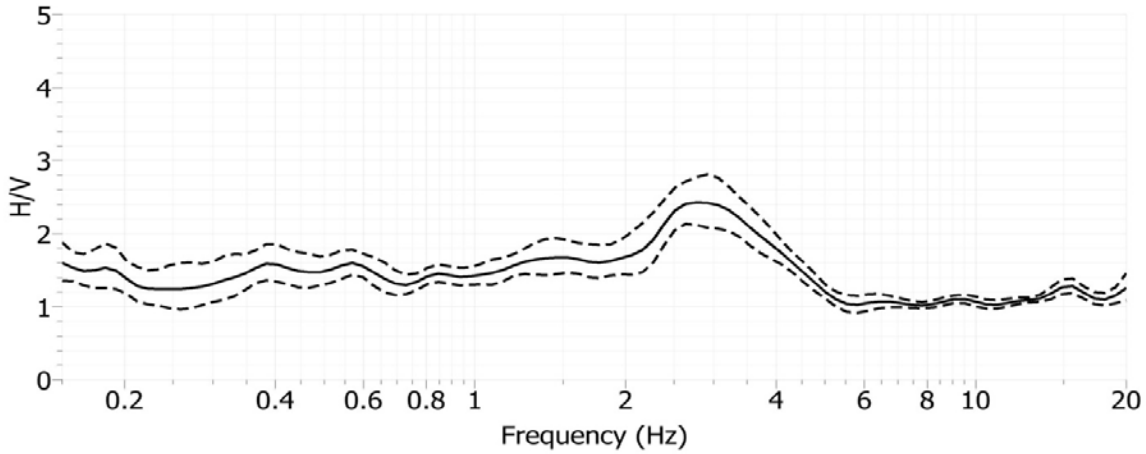

Site CI.SLB, H/V Spectral Ratio, Array SLB-1, Sensor 450

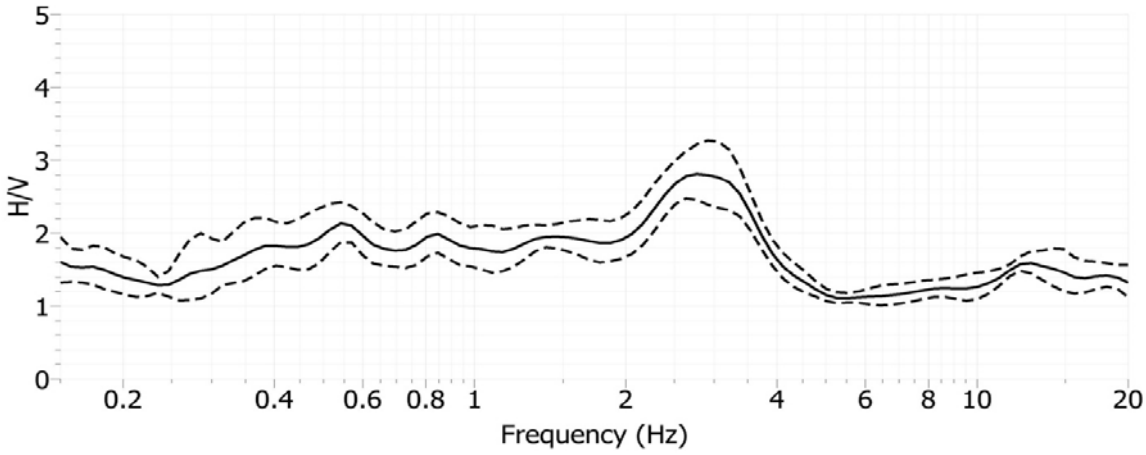

Site CI.SLB, H/V Spectral Ratio, Array SLB-1, Sensor 507

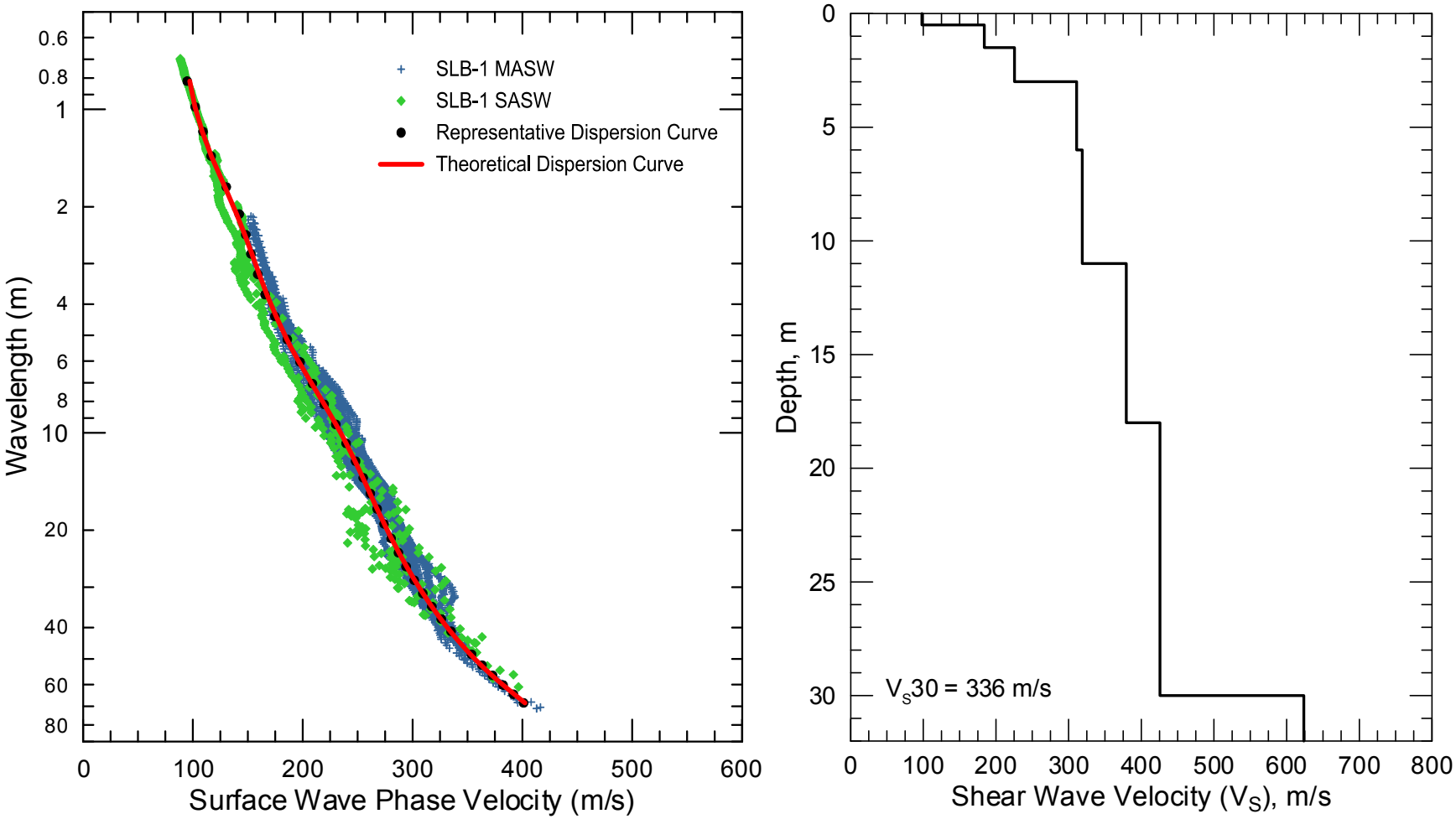

CI.SLB - Field, representative and inverted theoretical surface wave dispersion data (left) and associated V_S model (right), combined MASW and SASW data

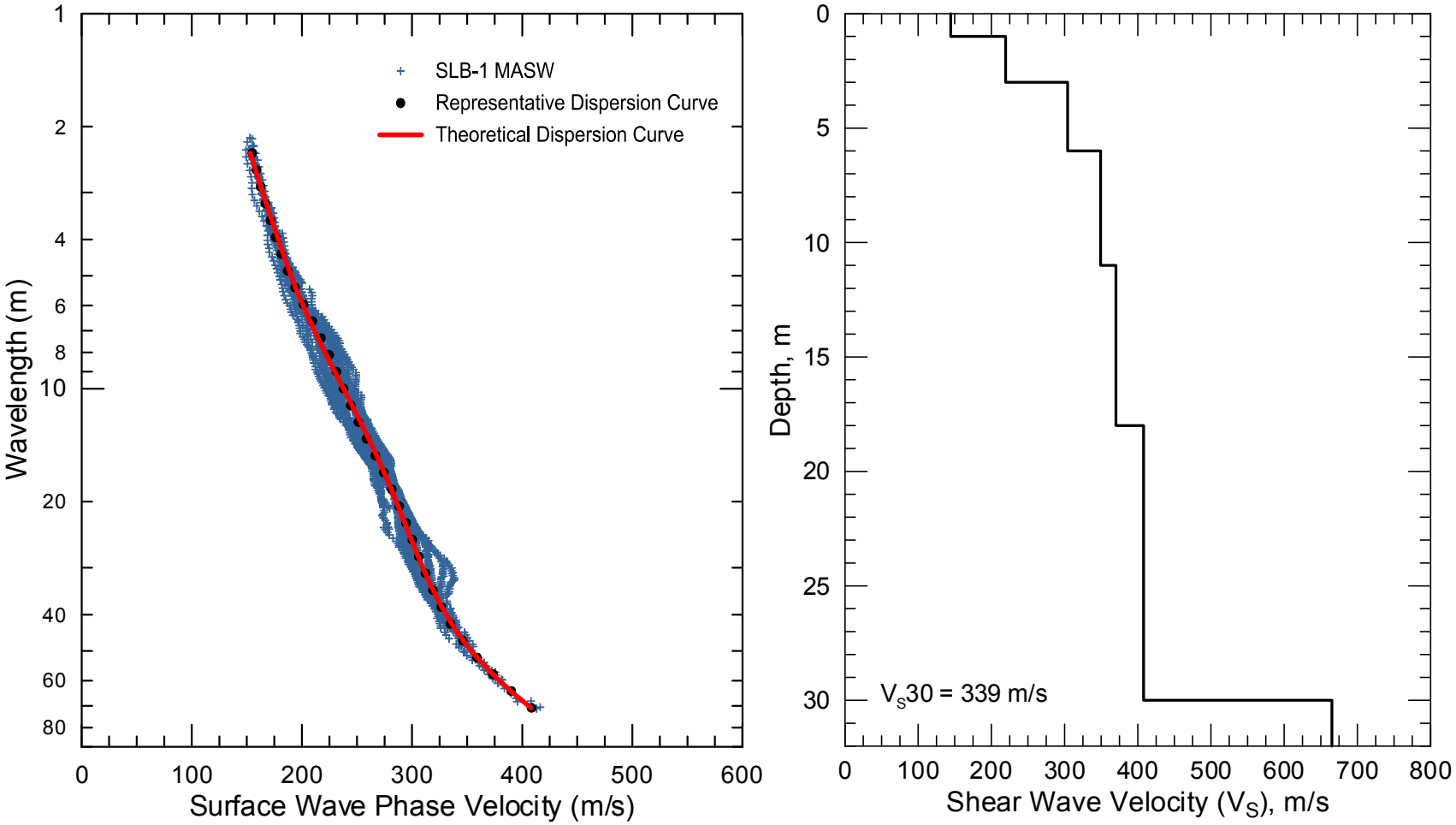

CI.SLB - Field, representative and inverted theoretical surface wave dispersion data (left) and associated V_S model (right), MASW array SLB-1

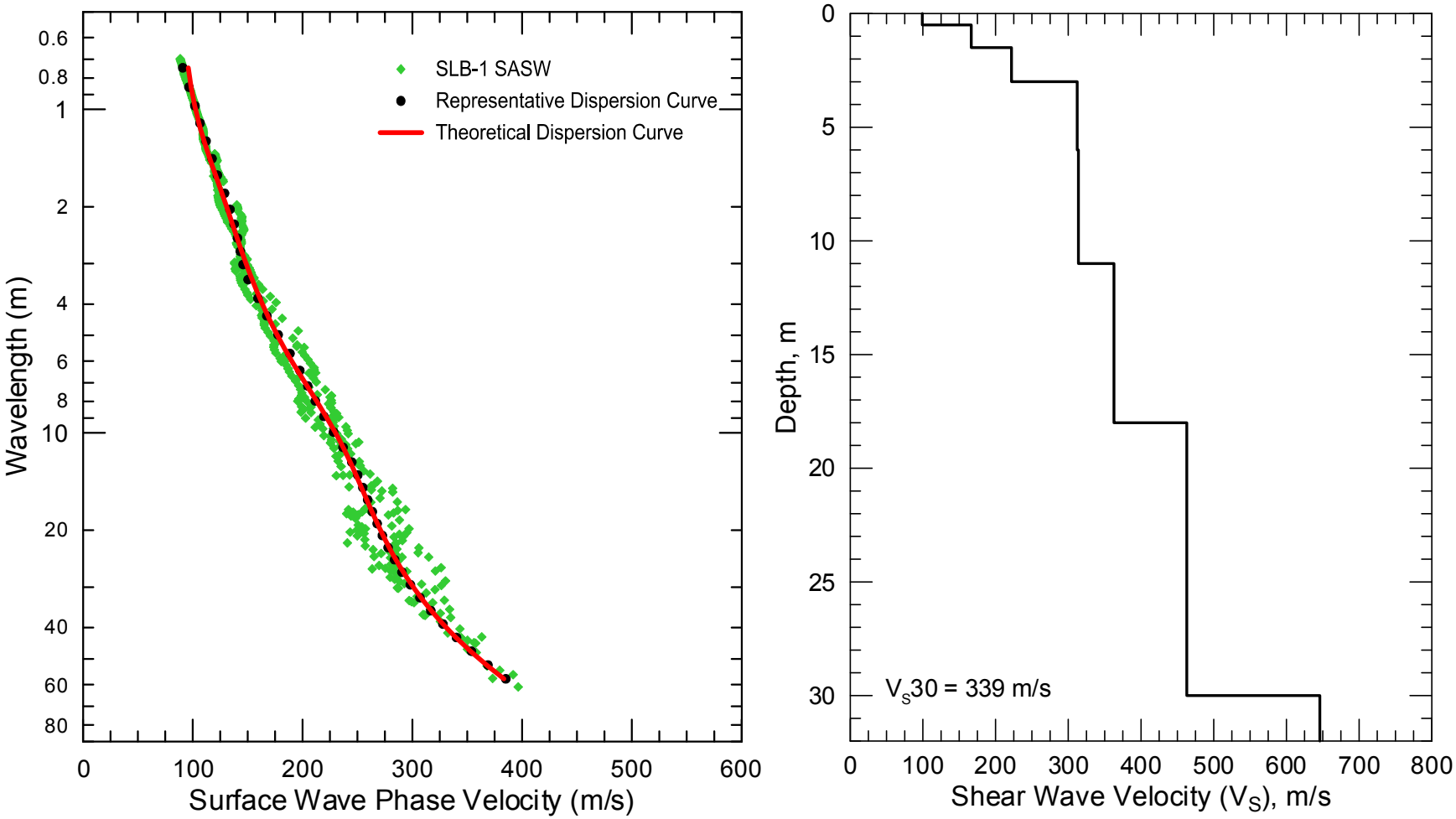

CI.SLB - Field, representative and inverted theoretical surface wave dispersion data (left) and associated V_S model (right), SASW array SLB-1

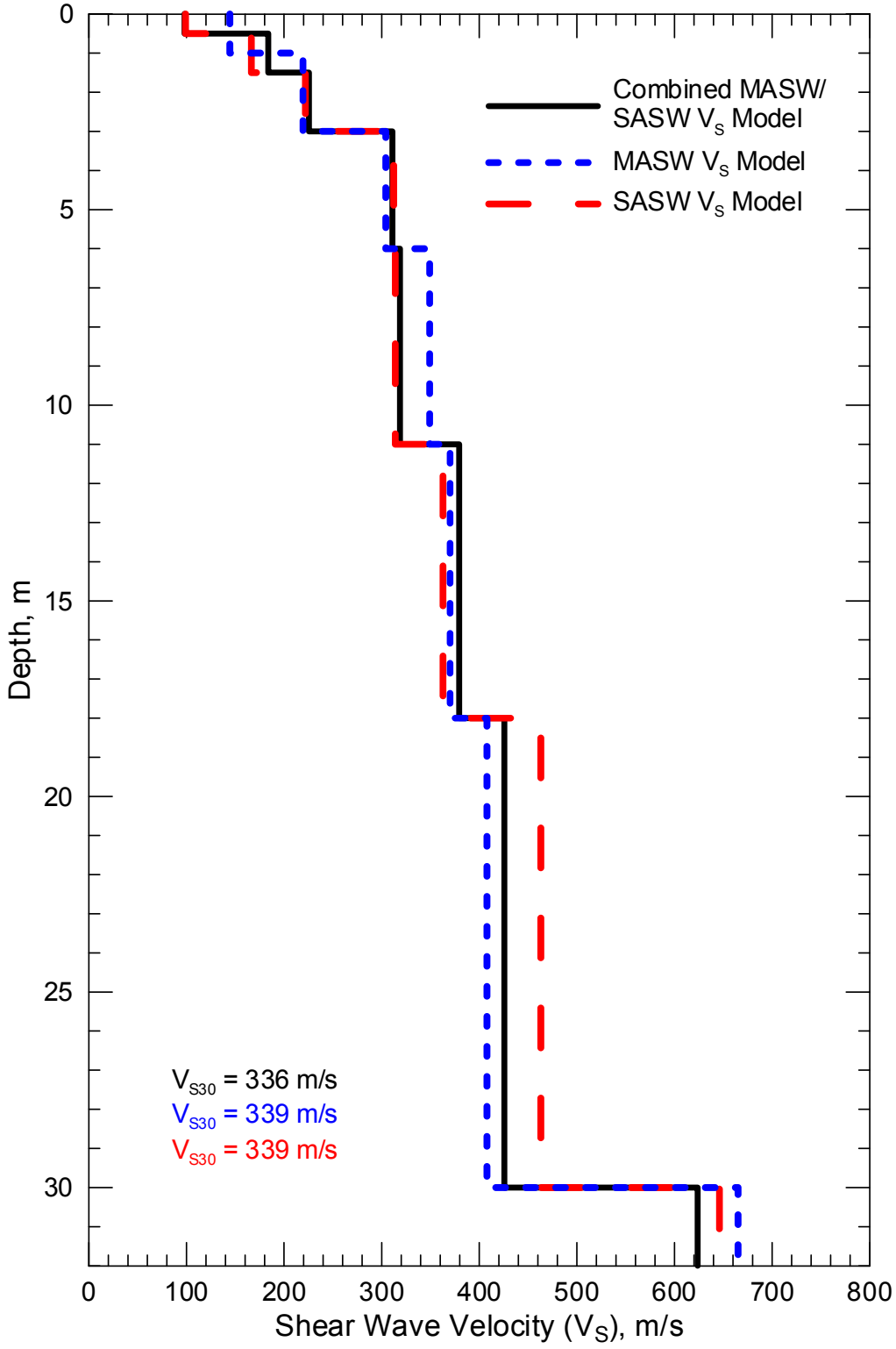

CI.SLB – Comparison of MASW, SASW and combined MASW/SASW V_S models

Site CI.SLR

Location: Skyland Ranch, 19750 Highway 243, Riverside County, California

Latitude: 33.83359 **Longitude:** -116.79737
(Station coordinates provided by USGS, WGS84 coordinate system)

V_{S30} (measured): 503 m/s

V_{S30} (adjusted to more accurately reflect seismic station conditions): 617 m/s (average S-wave velocity between 2 and 32 m adjusting for assumed depth of sensor).

NEHRP Site Class: C

Geomatrix Code: IGB

Geologic Conditions/Observations: Seismic station located on geologic unit mapped as Mesozoic (Cretaceous) intrusive granitic rocks consisting of tonalite, quartz diorite and granodiorite. There is a residual soil or organic soil layer at the surface and bedrock outcrops appear very intensely weathered.

Site Conditions: Rural site located in area of gently rolling terrain. There is steep mountainous terrain in close proximity to site.

Geophysical Methods Utilized: HVSR, P- and S-wave Seismic Refraction, MASW (Rayleigh wave, MALW (Love wave)

Geophysical Testing Arrays:

1. Array SLR-1 (48 channel MASW, MALW and P- and S-wave seismic refraction array utilizing 4.5 Hz vertical or horizontal geophones spaced 1.5 m apart for a length of 70.5 m, forward and reverse shot locations with multiple source offsets and source types and multiple interior shot locations).
2. Three HVSR measurement locations distributed along array SLR-1.

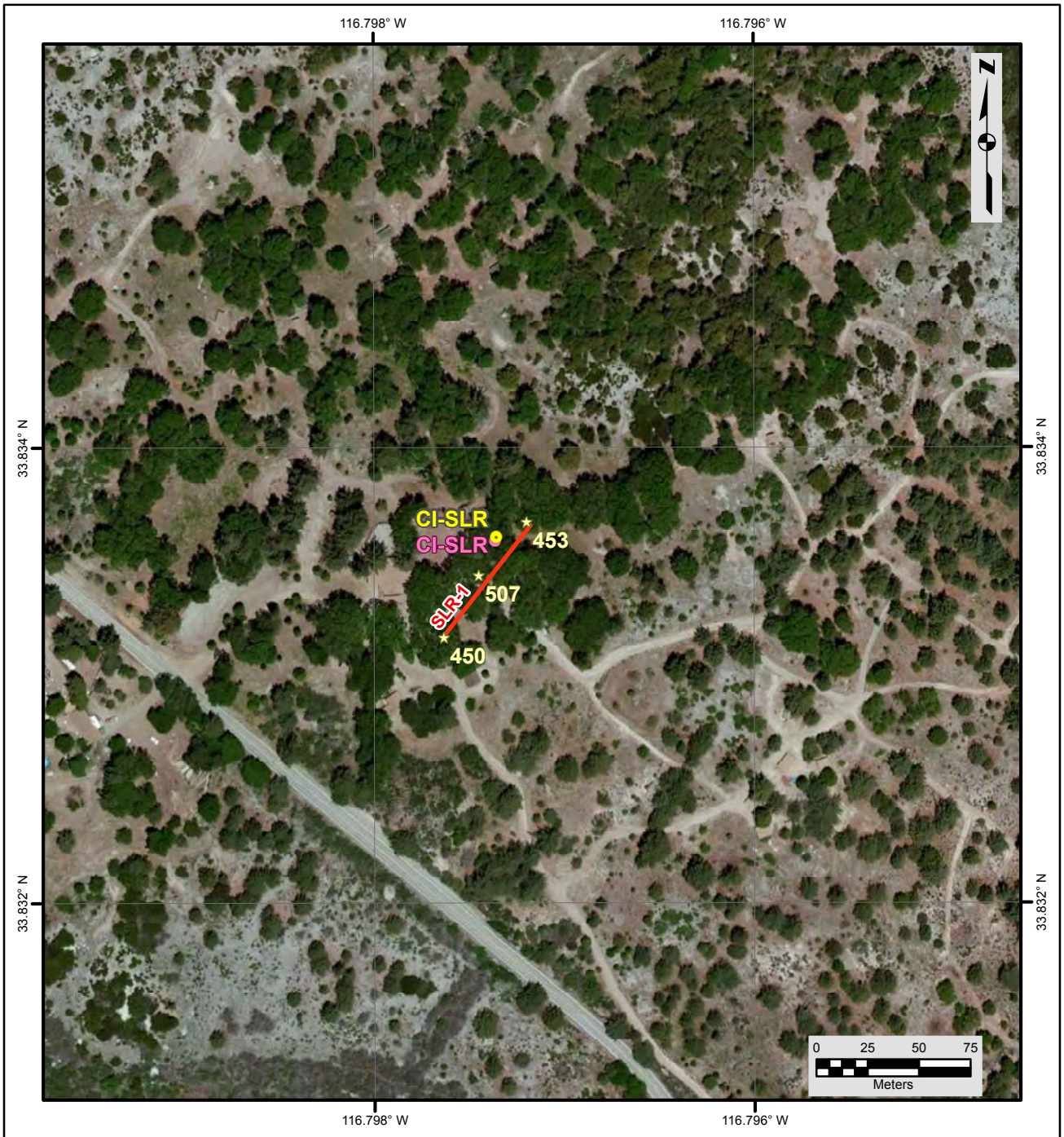

Legend

- Seismic Station - Approximate Surveyed Location
- Seismic Station - Approximate Location of Record
- H/V Spectral Ratio Location
- MASW and Seismic Refraction Line

NOTES:
1. WGS 1984 COORDINATE SYSTEM
2. Image Source: ESRI, i-cubed, USDA FSA, USGS, AEX, GeoEye, Getmapping, Aerogrid, IGP

File Name: CI-SLR-I

Date: 2/7/2013

USGS science for a changing world

GEOVision geophysical services

RECOVERY.GOV

SITE MAP
CI•SLR

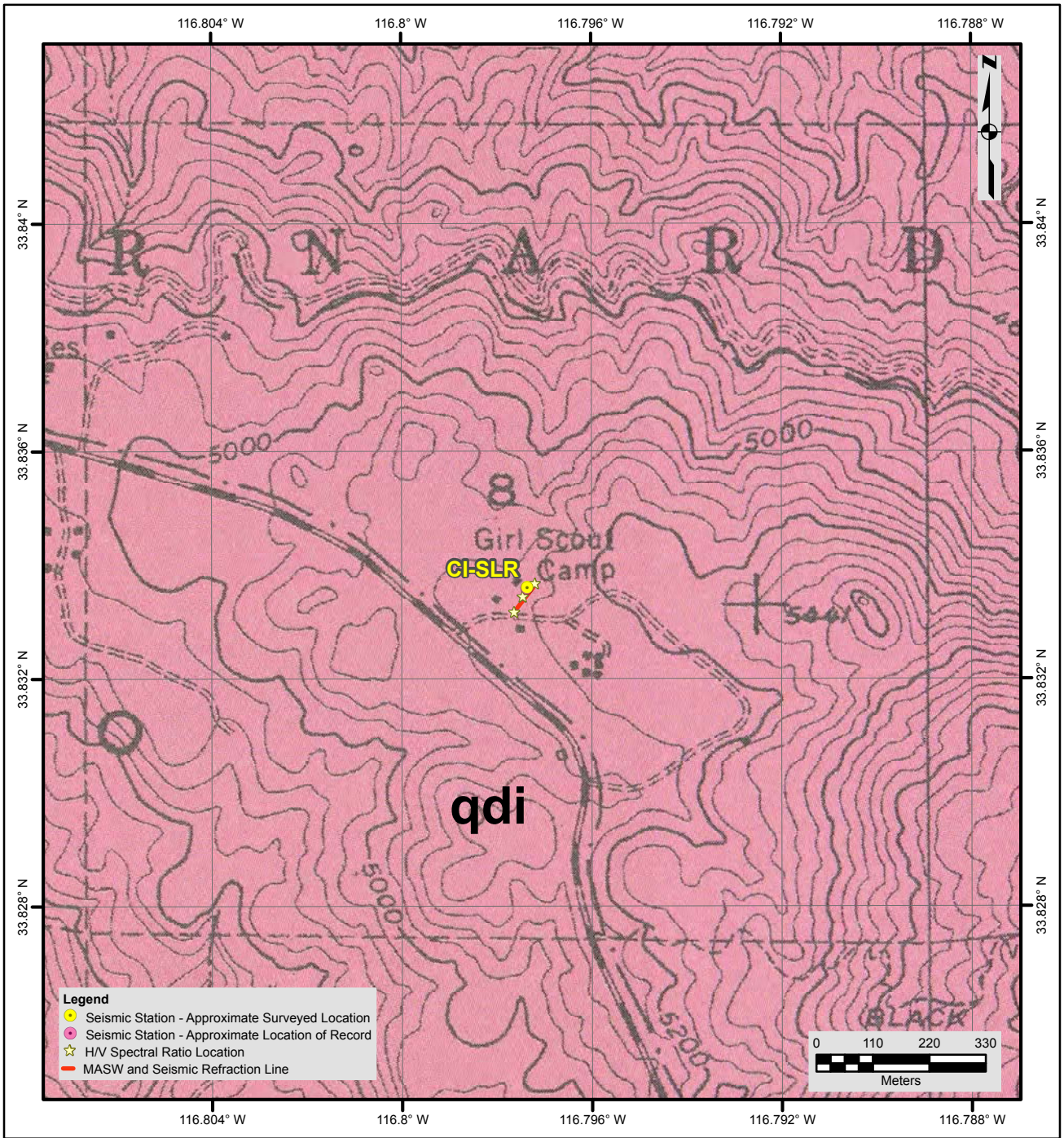

Description of Geologic Map Units

qdi = Mesozoic (Cretaceous) quartz diorite (tonalite), ranges to granodiorite

NOTES:
1. WGS 1984 COORDINATE SYSTEM
2. Geologic Map of the Lake Fulmore Quadrangle, Riverside County, California by Thomas W. Dibblee, Jr., 2004
3. See site map for details of geophysical survey

File Name: CI-SLR

Date: 2/7/2013

USGS science for a changing world

GEOVision geophysical services

RECOVERY.GOV

GEOLOGIC MAP
CI•SLR

Looking north at HVSR sensor 453 and CI.SLR seismic station from near center of array SLR-1

Looking northeast along array SLR-1 and at HVSR sensor 450

Looking north at center of array SLR-1, seismic station and HVSR sensor 507

S-wave seismic refraction and Love wave MASW data acquisition

P-wave seismic refraction and Rayleigh wave MASW data acquisition

Location of Geophysical Testing Arrays:

Location	Latitude	Longitude
SLR-1, Southwest End of MASW/ Seismic Refraction Array	33.83317	-116.79764
SLR-1, Center of MASW/Seismic Refraction Array	33.83343	-116.79744
SLR-1, Northeast End of MASW/Seismic Refraction Array	33.83366	-116.79718
HVSR Sensor 450	33.83317	-116.79764
HVSR Sensor 453	33.83367	-116.79720
HVSR Sensor 507	33.83344	-116.79746
CI.SLR Seismic Station	33.83361	-116.79736

Notes: 1) WGS84 Coordinate System (decimal degrees)
2) Survey accuracy is estimated at 1 to 2 m.

Results:

V_S Model (MASW - Rayleigh wave)

Depth to Top of Layer (m)	Layer Thickness (m)	S-Wave Velocity (m/s)	Inferred P-Wave Velocity (m/s)	Assumed Poisson's Ratio	Assumed Density (g/cm^3)
0	0.75	118	176	0.1	1.70
0.75	1.75	177	265	0.1	1.80
2.5	2	231	347	0.1	1.90
4.5	2.5	267	400	0.1	1.90
7	4	584	876	0.1	2.10
11	7	690	1036	0.1	2.10
18	9	931	1397	0.1	2.10
27	>8	1063	1594	0.1	2.15

Notes: 1) Depth of investigation is about 35 m.
2) Bottom layer is a half space.
3) Half space velocity not well resolved.

V_S Model (MALW - Love Wave)

Depth to Top of Layer (m)	Layer Thickness (m)	S-Wave Velocity (m/s)	Assumed Density (g/cm^3)
0	0.75	130	1.70
0.75	1.75	184	1.80
2.5	2	346	1.90
4.5	2.5	468	1.90
7	4	632	2.10
11	7	700	2.10
18	9	860	2.10
27	>3	1034	2.15

Notes: 1) Depth of investigation is about 30 m.
2) Bottom layer is a half space.
3) Half space velocity not well resolved.

Average V_P and Estimated V_S Models from Central Portion of P-wave Seismic Refraction Line (Smooth Velocity Gradient Starting Model)

Depth to Top of Layer (m)	Layer Thickness (m)	P-Wave Velocity (m/s)	Estimated S-Wave Velocity (m/s)				
			Poisson's Ratio = 0.10	Poisson's Ratio = 0.15	Poisson's Ratio = 0.20	Poisson's Ratio = 0.25	Poisson's Ratio = 0.30
0.00	0.59	179	119	115	110	103	96
0.59	1.17	257	171	165	158	148	137
1.76	1.17	395	263	253	242	228	211
2.93	1.17	543	362	349	333	314	290
4.11	1.17	675	450	433	413	390	361
5.28	1.17	796	531	511	487	460	425
6.46	1.17	823	549	528	504	475	440
7.63	2.47	890	593	571	545	514	476
10.10	2.47	919	613	590	563	531	491
12.56	2.47	958	638	615	586	553	512
15.03	2.47	1007	671	646	617	582	538
17.49	2.47	1072	715	688	657	619	573
19.96	2.47	1115	743	715	683	644	596
22.42	2.47	1195	797	767	732	690	639
24.89	2.47	1254	836	804	768	724	670
27.35	2.47	1323	882	849	810	764	707
29.82	Half Space	1393	928	894	853	804	744

Average V_S Model from Central Portion of S-wave Refraction Line (Smooth Velocity Gradient Starting Model)

Depth to Top of Layer (m)	Layer Thickness (m)	S-Wave Velocity (m/s)
0.00	0.59	118
0.59	1.17	177
1.76	1.17	275
2.93	1.17	373
4.11	1.17	459
5.28	1.17	542
6.46	1.17	553
7.63	2.47	586
10.10	2.47	624
12.56	2.47	652
15.03	2.47	696
17.49	2.47	770
19.96	2.47	793
22.42	2.47	843
24.89	2.47	869
27.35	2.47	930
29.82	Half Space	947

Observations/Discussion:

- HVSR plots for sensors 453 and 507 are similar with slightly elevated HVSR response over the 0.5 to 6 Hz range, but with no distinct peaks. The HVSR plot for station 450 differs from the other stations and has no significant peaks. Coupling may have been an issue for sensors 453 and 507, which were placed in very loose organic soils. HVSR measurements should be repeated at this site, although the relevance of HVSR measurements at this mountainous site is not clear.
- The P-wave first arrival data were picked to a greater degree of accuracy than the S-wave first arrival data as the P-wave data were generally of better quality. A smaller energy source was used for S-wave data acquisition and S-wave seismic records appear to have weak P-wave arrivals before the S-wave arrivals complicating analysis. There is also some uncertainty in picking the first arrival associated with the uppermost low velocity soil layer in both the P- and S-wave refraction data. In the P-wave seismic data, the air wave arrives before the direct soil arrival; however, it was possible to reasonably accurately pick the later soil arrival.
- The P- and S-wave refraction data for array SLR-1 were modeled using a tomographic inversion routine with both smooth velocity gradient and layer-based starting models.

The seismic refraction models were extended to far offset shot locations to extend depth of investigation. A larger geophone spacing is preferred for extending depth of investigation when applying tomographic inversion routines.

- The P-wave seismic refraction survey design allowed P-wave velocity to be imaged to a maximum depth of about 17 m with a layer based starting model and 25 m with a smooth velocity gradient starting model. The two seismic refraction models are quite similar in the upper 15 m with P-wave velocity of about 200 m/s near the surface, increasing to over 800 m/s at a depth of 3 to 7 m and over 1,000 m/s at a depth of 5 to 16 m. The primary difference between the models is that the layer based starting model results in a thicker sequence of low velocity sediments at the surface, with 1.5 to 2 m of sediments with P-wave velocity of less than 300 m/s. The seismic refraction model that utilized a smooth velocity starting model provides some evidence that P-wave velocity may increase to about 1,200 m/s at a nominal depth of 20 m and 1,400 m/s at a nominal depth of 28 m.
- The average P-wave velocity of the upper 30 m (V_{P30}) was estimated between 21 and 51 m on the P-wave refraction model, where depth of investigation was greatest. V_{P30} ranges from about 732 to 852 m/s over the 21 to 51 m interval, a 16% variation.
- An average V_P model was developed over the 21 to 51 m distance interval by horizontally averaging the travel time of each model cell and cell thickness and average V_{P30} was determined to be 777 m/s. Assuming constant Poisson's ratios of 0.1, 0.15, 0.2, 0.25 and 0.3 would result in an estimated V_{S30} of 518, 498, 476, 448 and 415 m/s, respectively.
- The S-wave seismic refraction survey design allowed S-wave velocity structure to be imaged to a maximum depth of about 18 m with a layer based starting model and 25 m with a smooth velocity gradient starting model. The two seismic refraction models are quite similar in the upper 15 m with S-wave velocity of less than 150 m/s at the surface, increasing to over 600 m/s at a depth of 4 to 11 m and over 800 m/s at a depth of 16 to 21 m. The S-wave seismic refraction model that utilized a smooth velocity starting model provides some evidence that S-wave velocity may increase to over 900 m/s at a nominal depth of about 27 m.
- The average S-wave velocity of the upper 30 m (V_{S30}) was estimated between 21 and 51 m on the S-wave refraction model, where depth of investigation is greatest. Over this interval, V_{S30} ranges from about 507 to 600 m/s, a 17% variation. An average V_S model was developed over the 21 to 51 m distance interval by horizontally averaging the travel time of each model cell and cell thickness and average V_{S30} was determined to be 533 m/s.
- The P- and S-wave seismic refraction models indicate that there is near surface lateral velocity variation at the site, with higher velocity, less weathered rock at shallow depth beneath the southwestern portion of the line.
- Inspection of the seismic refraction models indicates that V_P/V_S is nominally about 1.5, indicating a Poisson's ratio of about 0.1. This is an unusually low Poisson's ratio and should be further investigated for confirmation. The possibility cannot be discounted that out of plane refractors and/or converted waves skew the S-wave refraction model to higher incorrect velocities.
- Noise conditions at the site were not sufficient for application of passive surface wave techniques.

- Both Rayleigh wave and Love wave MASW data were acquired at the site, although the two data sets were acquired at different times, about 7 months apart.
- The minimum wavelength Rayleigh wave phase velocity data extracted from the 48-channel MASW array was about 12 m. Reducing data from smaller hammer sources using a limited offset receiver array (i.e. less active geophones) allowed for extraction of surface wave dispersion data to a minimum wavelength of about 1 m. The minimum wavelength Love wave phase velocity data extracted from the 48-channel MALW array was about 8 m. Reducing data using a limited offset receiver array (i.e. less active geophones) allowed for extraction of surface wave dispersion data to a minimum wavelength of about 1.5 m.
- A maximum 70 and 90 m wavelength was extracted from the MASW (Rayleigh wave) and MALW (Love wave) data, respectively.
- There is typically about 30 to 50 m/s of scatter in both the Rayleigh and Love wave dispersion data, likely the result of velocity variation caused by differential weathering of near surface rock and variable thickness of a thin residual soil layer. There is larger scatter (> 75 m/s) in the Love wave dispersion data at wavelengths greater than 70 m due to geologic conditions, limited low frequency source energy and possible near field effects.
- A representative dispersion curve was generated for the Rayleigh and Love wave data sets using a moving average, polynomial curve fitting routine and used for modeling. Rayleigh and Love wave dispersion data were modeled using the fundamental mode assumption.
- Surface wave depth of investigation is about 35 m for the Rayleigh wave models and 30 m for the Love wave model. We expect that Love wave phase velocity wavelengths of about 90 m are required to develop a V_S model to a depth of 30 m compared to a 60 m wavelength for Rayleigh wave phase velocity data.
- It should be noted that inversion of Rayleigh and Love wave dispersion data result in models of S_V- and S_H-velocity, respectively. Small differences in S_V and S_H-velocity can occur in anisotropic media.
- Rayleigh wave phase velocity dispersion data could only be modeled with the fundamental mode assumption using values of Poisson's ratio of less than about 0.25. A Poisson's ratio of 0.1 yielded a V_S model with the lowest RMS error. Use of a Poisson's ratio of greater than 0.25 yielded unrealistic V_S models, relative to the refraction models, that further evaluation indicated could generate a dominant first higher mode at low frequencies. Additionally, as Poisson's ratio increases, V_{S30} decreases quite significantly. Under the more typical 0.25 to 0.35 range of Poisson's ratio for unsaturated sediments and rock, Poisson's ratio is generally assumed to have a minimal affect on V_{S30}. As demonstrated herein, use of the correct value of Poisson's ratio becomes more critical when outside the typical range.
- We assume that the V_S model developed from the Rayleigh wave dispersion data, using a Poisson's ratio of 0.1, is most representative of site conditions as this model is in better agreement with other V_S models developed at the site.
- Several equivalent V_S models were developed for the Love wave dispersion data to demonstrate the insensitivity of V_{S30} to nonuniqueness. Because Love waves are only composed of S_H waves, variations in Poisson's ratio do not affect the V_S model. The

smoothest (most layers) V_S model developed from the Love wave dispersion data, which also has the lowest RMS error, is assumed to be most representative of site conditions.

- The V_S models developed from the Rayleigh and Love wave methods are significantly different over the 2.5 to 7 m depth range, but similar at other depths. Over this depth range V_S in the Love wave model is 50 to 75% greater than that in the Rayleigh wave model, much more than can be likely explained by anisotropy.
- V_{S30} is 470 m/s for the Rayleigh wave model (Poisson's ratio = 0.1) and 535 m/s for the Love wave model (Site Class C). The 13% difference in V_{S30} is primarily associated with the difference in velocity structure in the two models between depths of 2.5 and 7 m.
- It should be noted that modeling of the Rayleigh wave dispersion curve with a Poisson's ratio of 0.3 and fundamental mode assumption would result in an estimated V_{S30} of 390 m/s, significantly lower than above, but still NEHRP Site Class C.
- The average V_{S30} of the Rayleigh wave and Love wave V_S models is 503 m/s (NEHRP Site Class C).
- Average S-wave velocity between 2 m (assumed sensor depth) and 32 m (adjusted V_{S30}) is 575 m/s for the Rayleigh wave model and 660 m/s for the Love wave model. The 14% difference in adjusted V_{S30} is primarily associated with the difference velocity structure between depths of 2.5 and 7 m.
- Average S-wave velocity of the Rayleigh wave and Love wave V_S models between 2 and 32 m depth is 617 m/s.
- The S-wave seismic refraction and MALW V_S models are generally similar and have almost the same $V_{S30,}$ although the MALW V_S model has slightly higher V_S at depths greater than 18 m. The V_S estimated from the P-wave refraction model with an unusually low Poisson's ratio of 0.1 is also similar to the S-wave refraction and MALW V_S models. The MASW V_S model has much lower V_S over the 2.5 to 7 m depth range, likely more than can be associated with anisotropy, but is relatively consistent with the MALW V_S model at greater depths.
- It would be worthwhile to conduct additional testing at this site to study the mechanisms resulting in different Rayleigh and Love wave V_S models over the 2.5 to 7 m depth range and determine if Poisson's ratio is as low as 0.1. The only mechanisms that could cause the seismic refraction models to overestimate velocity over the 2.5 to 7 m depth interval would be a shallow high velocity layer, out of plane refractor or possible converted waves in the S-wave refraction data. A shallow high velocity layer would not be expected in a crystalline rock weathering profile and there is no evidence of such a layer in the surface wave dispersion data. At this time, we have no explanation, other than anisotropy, as to the difference in V_S over the 2.5 to 7 m depth interval between the Rayleigh and Love wave V_S models.
- For the purpose of site characterization at this time, we recommend averaging the presented V_S models and V_{S30} developed from the Rayleigh and Love wave dispersion data.

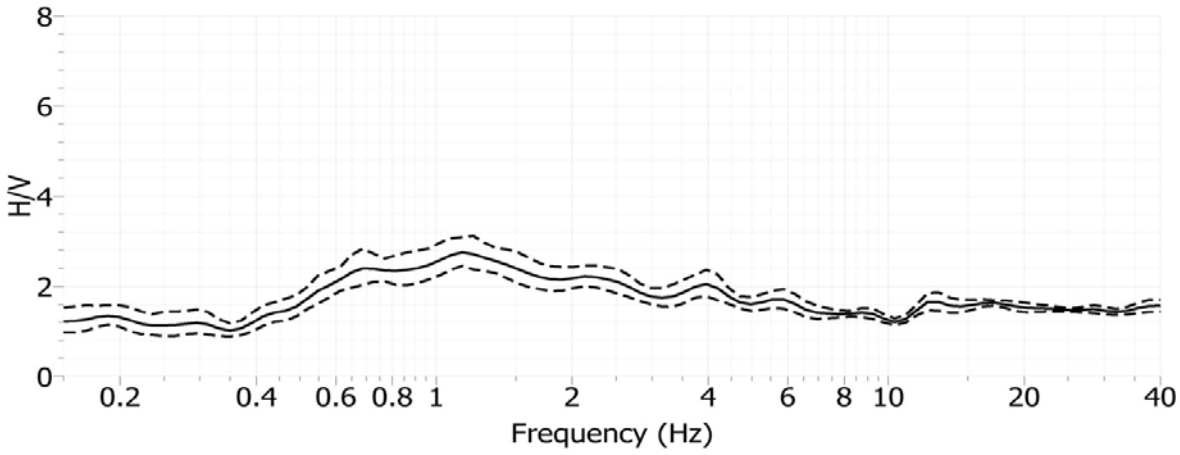

Site CI.SLR, H/V Spectral Ratio, Array SLR-1, Sensor 453

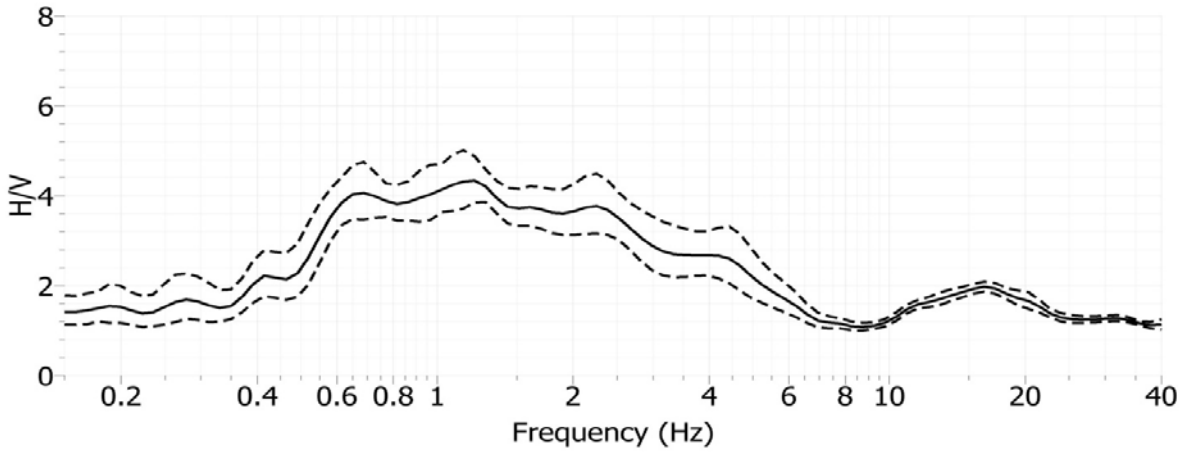

Site CI.SLR, H/V Spectral Ratio, Array SLR-1, Sensor 507

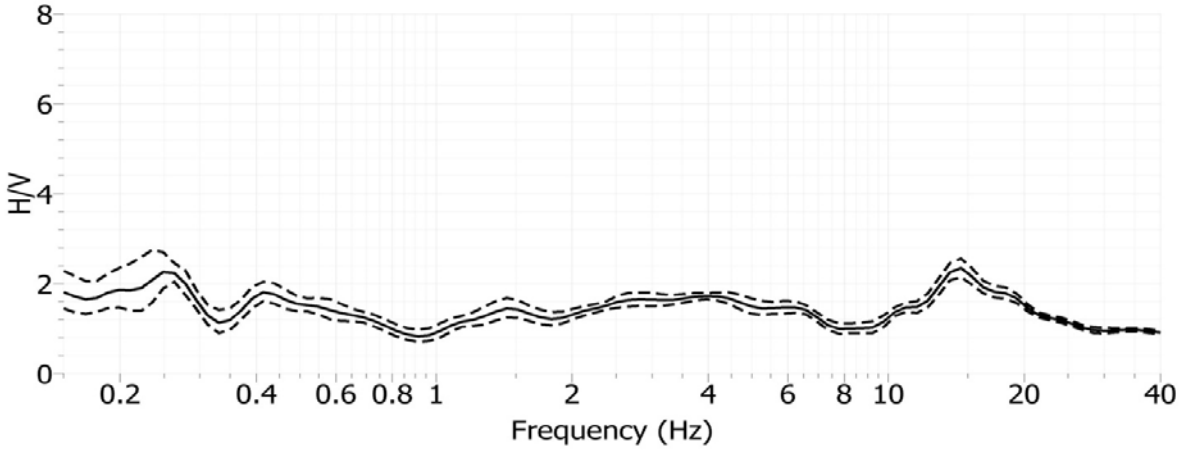

Site CI.SLR, H/V Spectral Ratio, Array SLR-1, Sensor 450

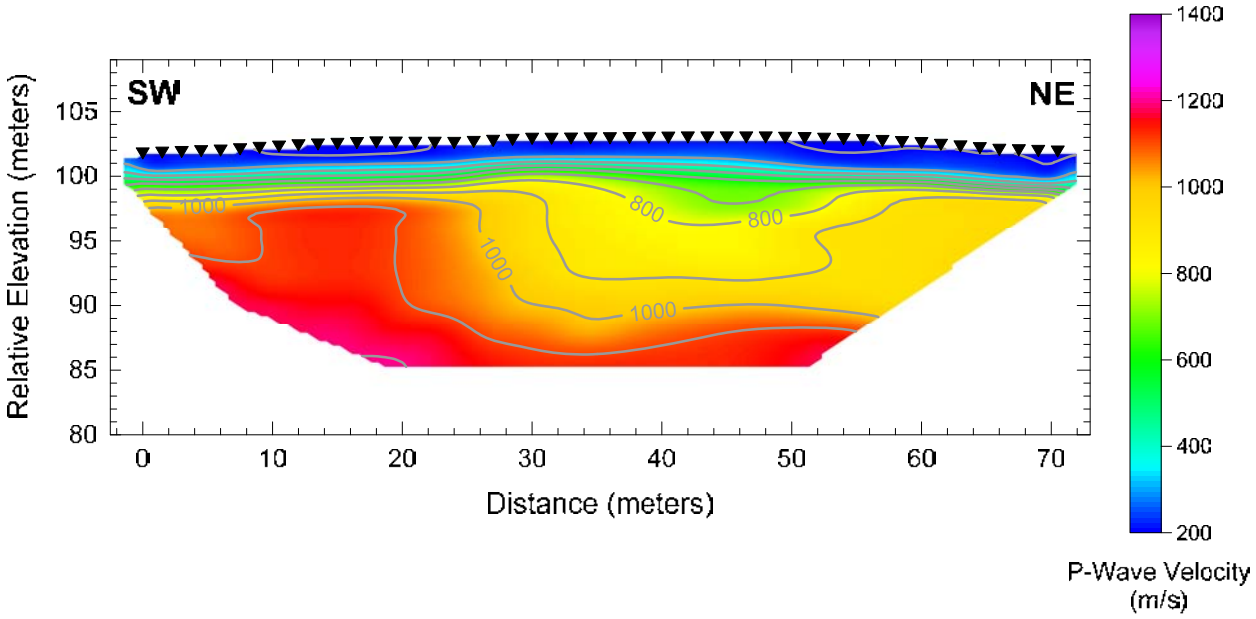

Array SLR-1 – P-wave tomographic seismic refraction model developed utilizing a layer based starting model

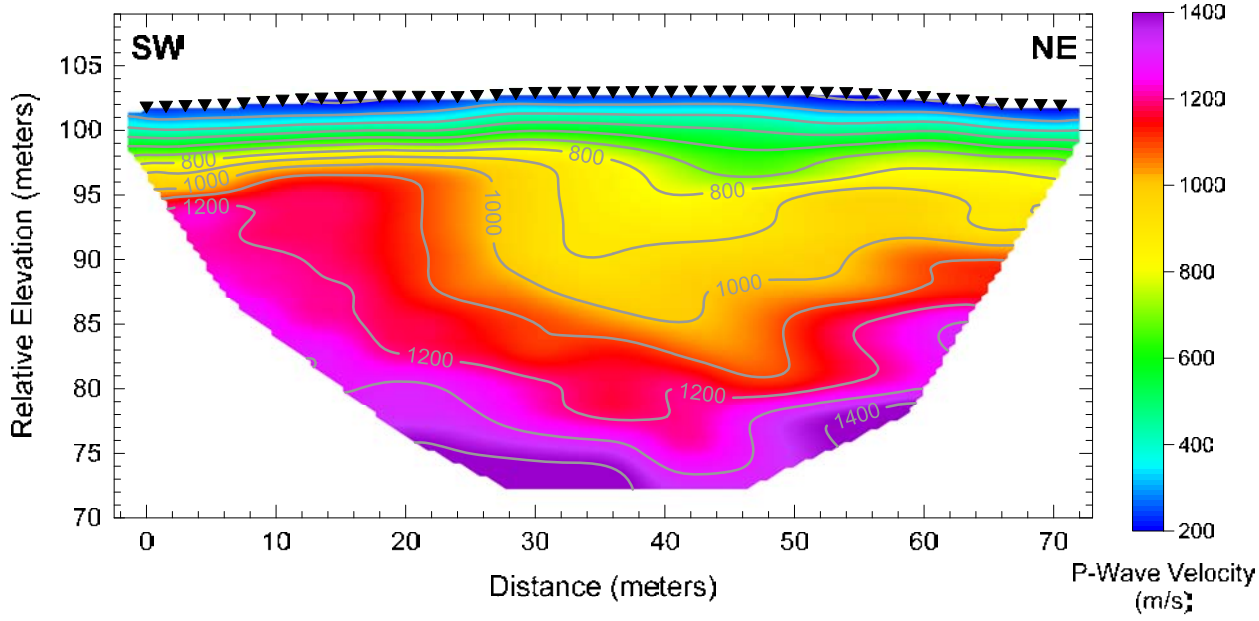

Array SLR-1 – P-wave tomographic seismic refraction model developed utilizing a smooth velocity gradient starting model

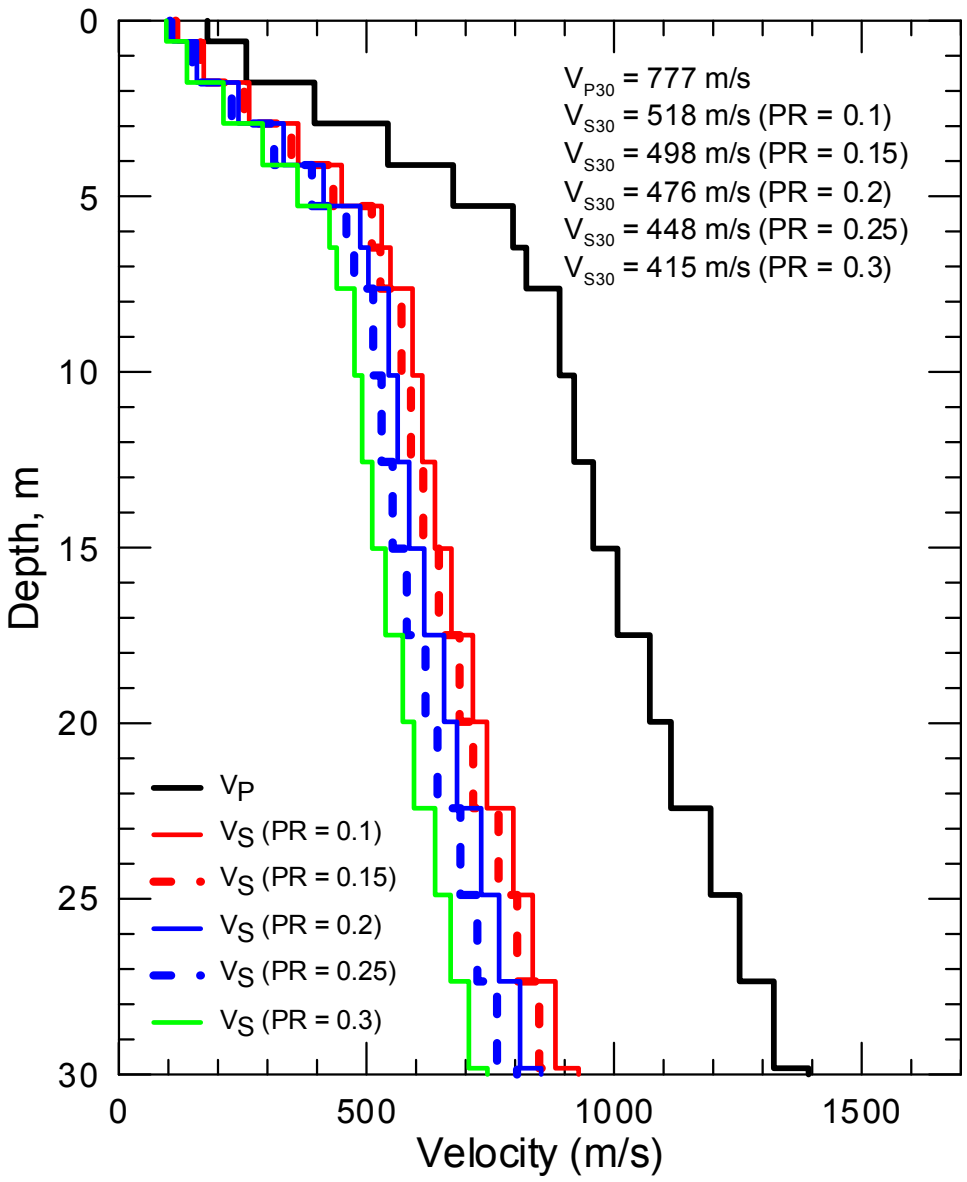

CI.SLR – Average P-wave velocity structure and estimated S-wave velocity structure between a position of 21 and 51 m on the array SLR-1 P-wave seismic refraction model developed using a smooth velocity gradient starting model.

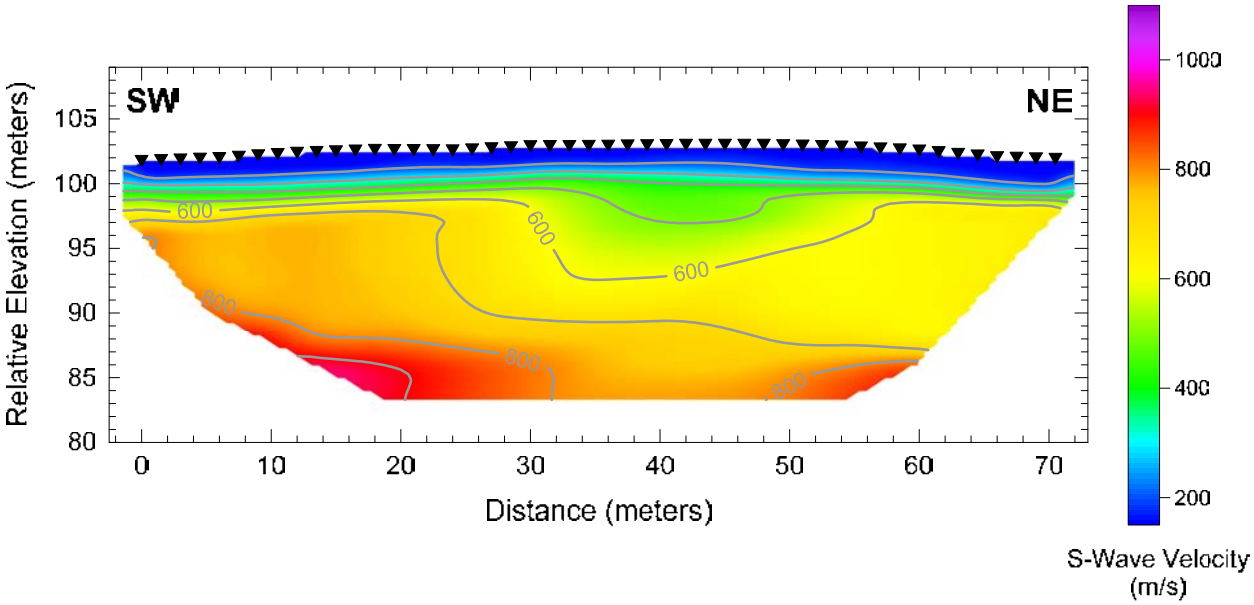

Array SLR-1 – S-wave tomographic seismic refraction model developed utilizing a layer based starting model

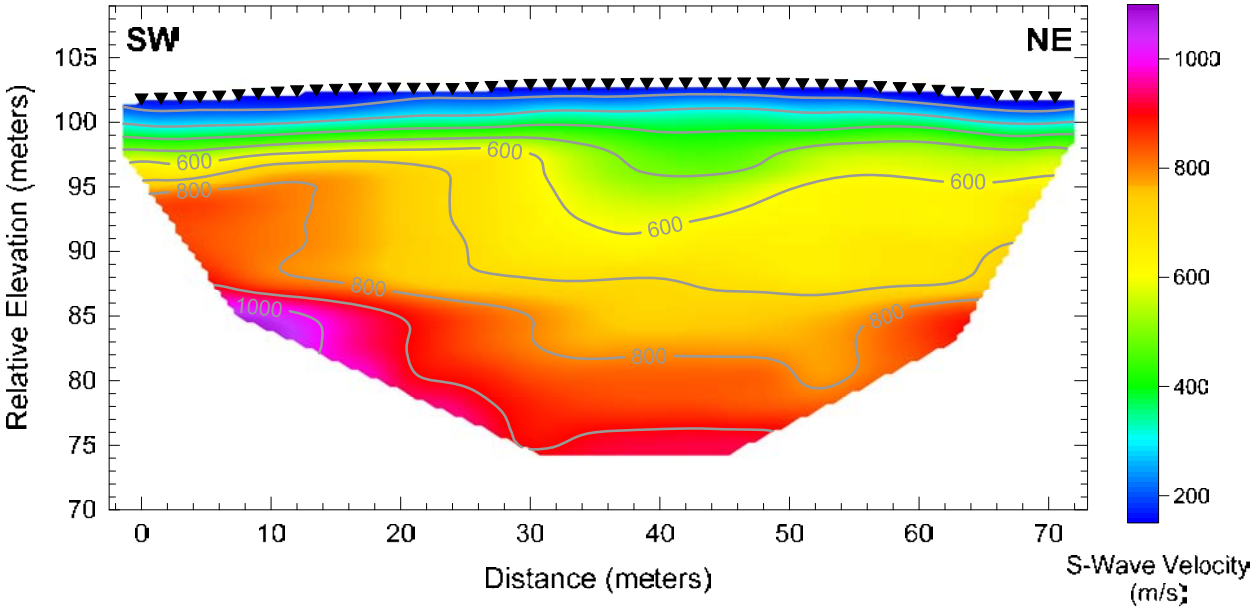

Array SLR-1 – S-wave tomographic seismic refraction model developed utilizing a smooth velocity gradient starting model

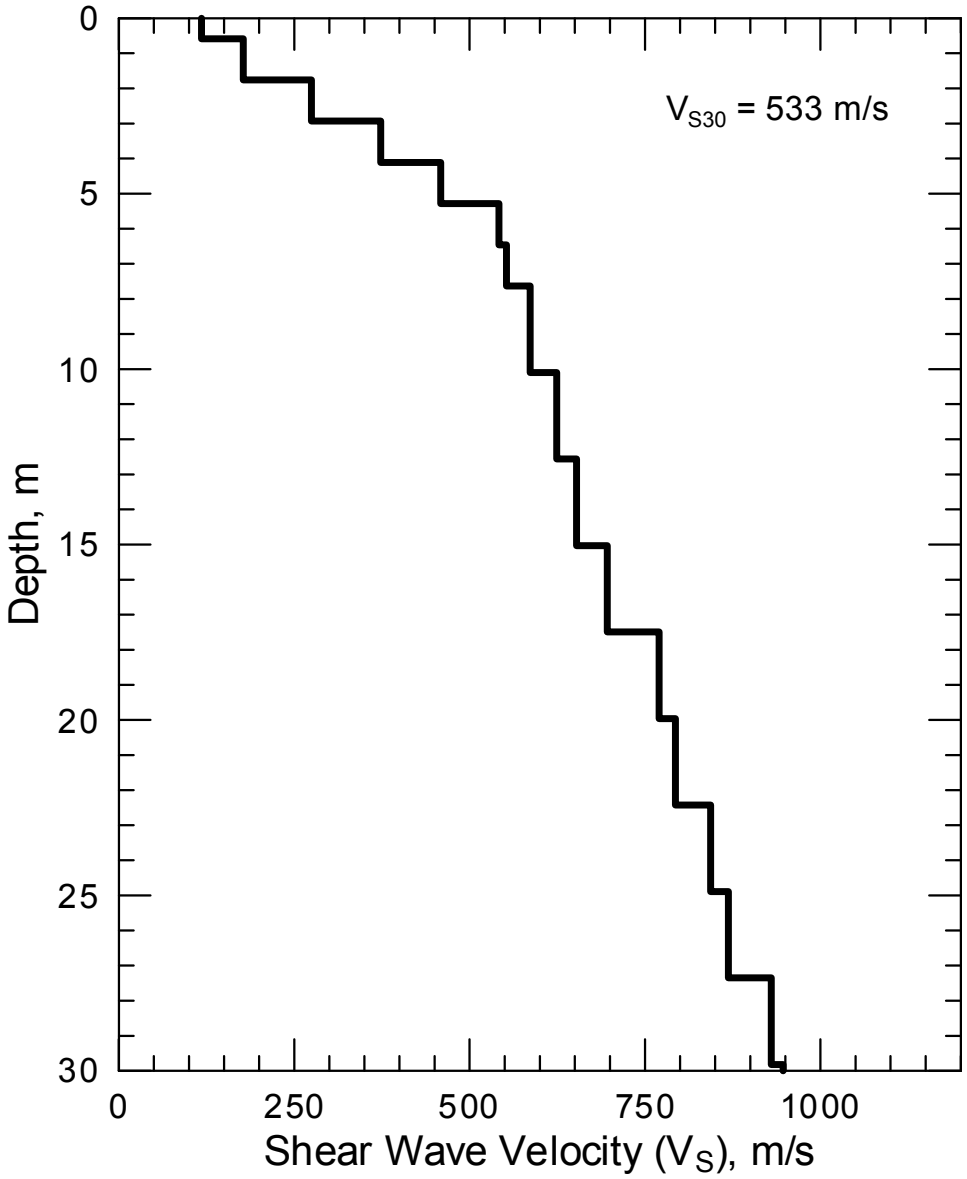

CI.SLR – Average S-wave velocity structure between a position of 21 and 51 m on the array SLR-1 S-wave seismic refraction model developed using a smooth velocity gradient starting model.

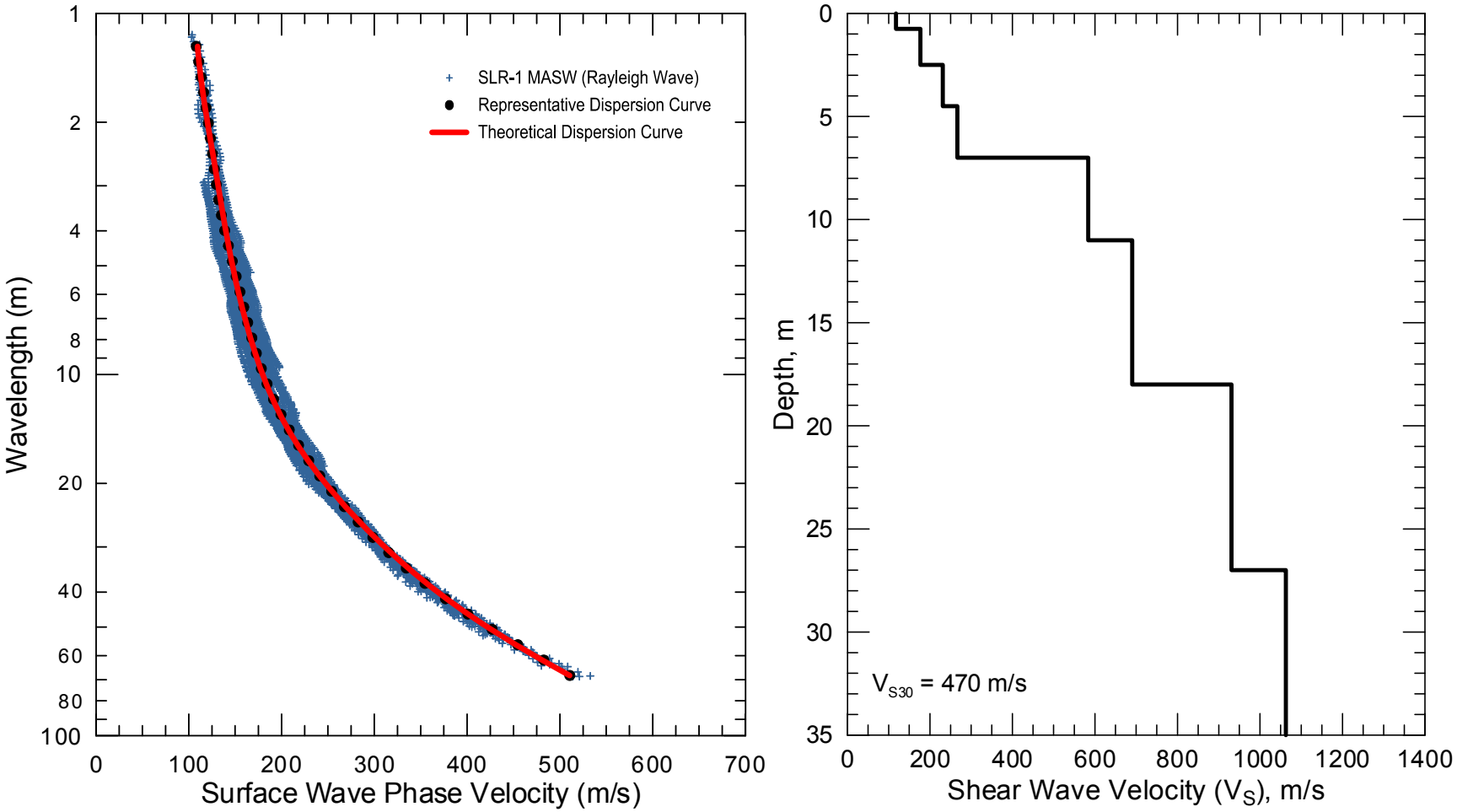

CI.SLR - Field, representative and inverted theoretical surface wave dispersion data (left) and associated V_S model (right) for Rayleigh wave data. Modeling was conducted using a Poisson's ratio of 0.1, which is unrealistically low, but supported by P- and S-wave seismic refraction data.

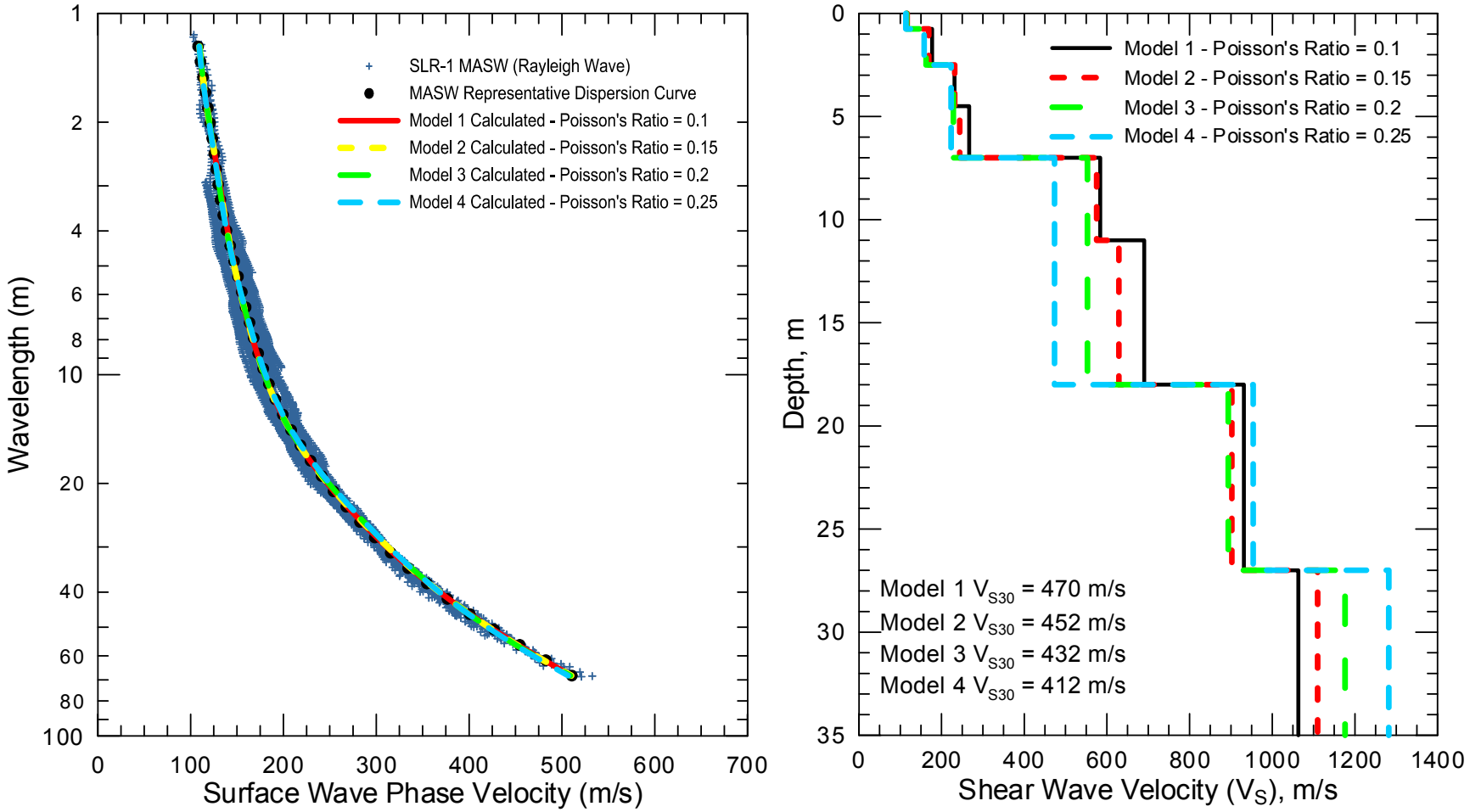

CI.SLR - Field, representative and inverted theoretical surface wave dispersion data (left) and V_S models utilizing different values of Poisson's ratio (right) for Rayleigh wave data. Higher values of Poisson's ratio resulted in unrealistic S-wave velocity models relative to the seismic refraction models and are also expected to excite a dominant first higher mode at low frequencies.

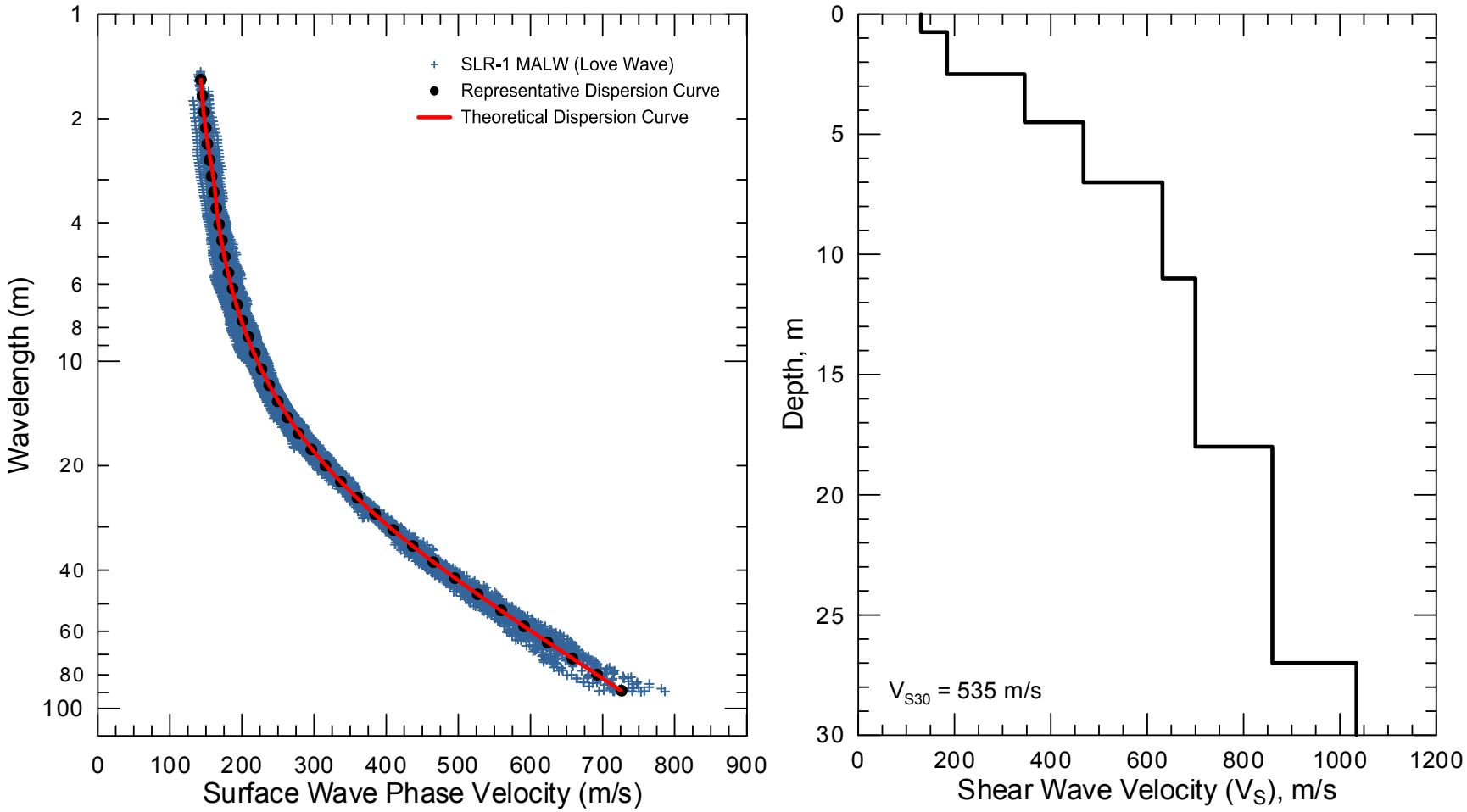

CI.SLR - Field, representative and inverted theoretical surface wave dispersion data (left) and associated V_S model (right) for Love wave data

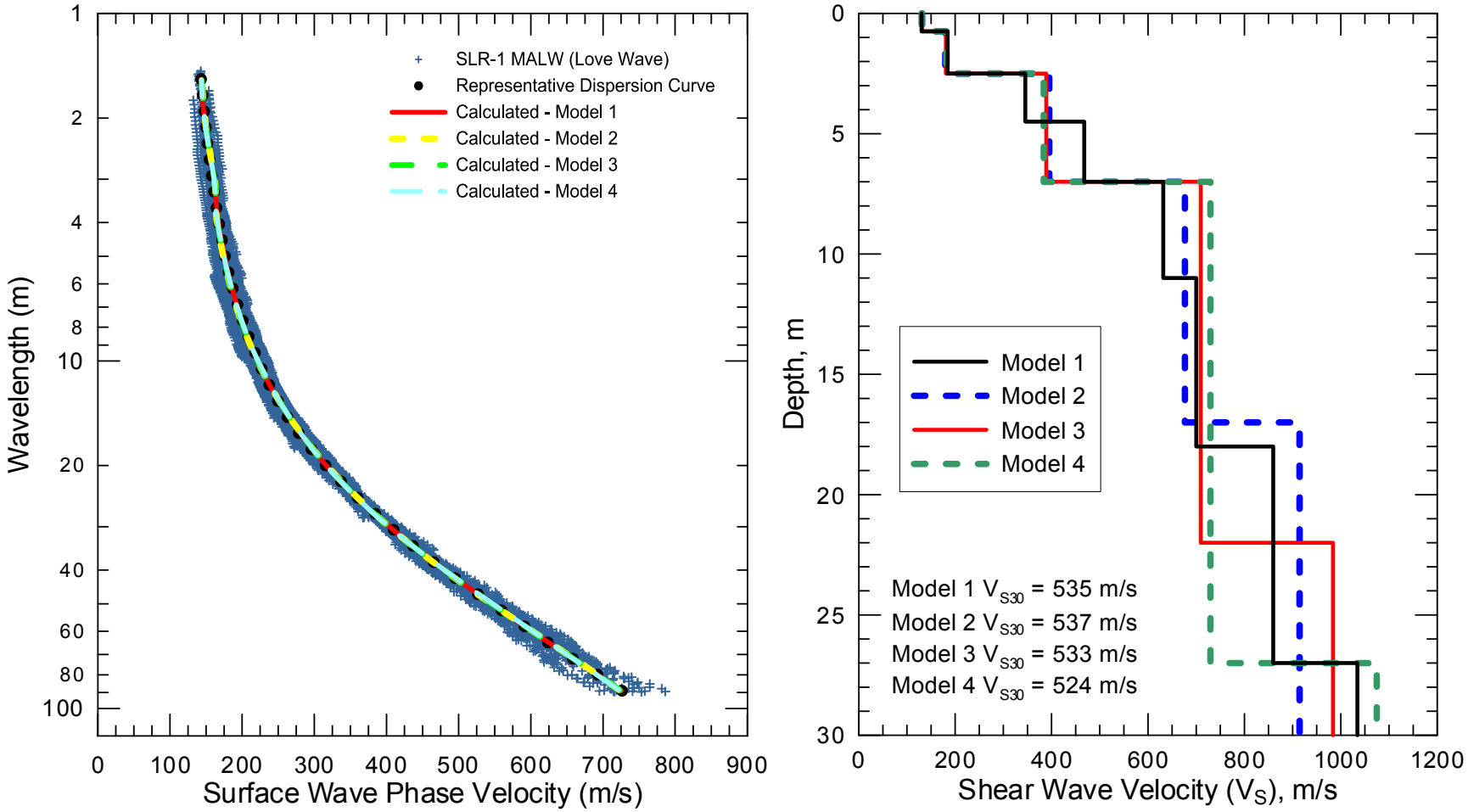

CI.SLR - Field, representative and inverted theoretical surface wave dispersion data (left) and equivalent V_S models (right) for Love wave data

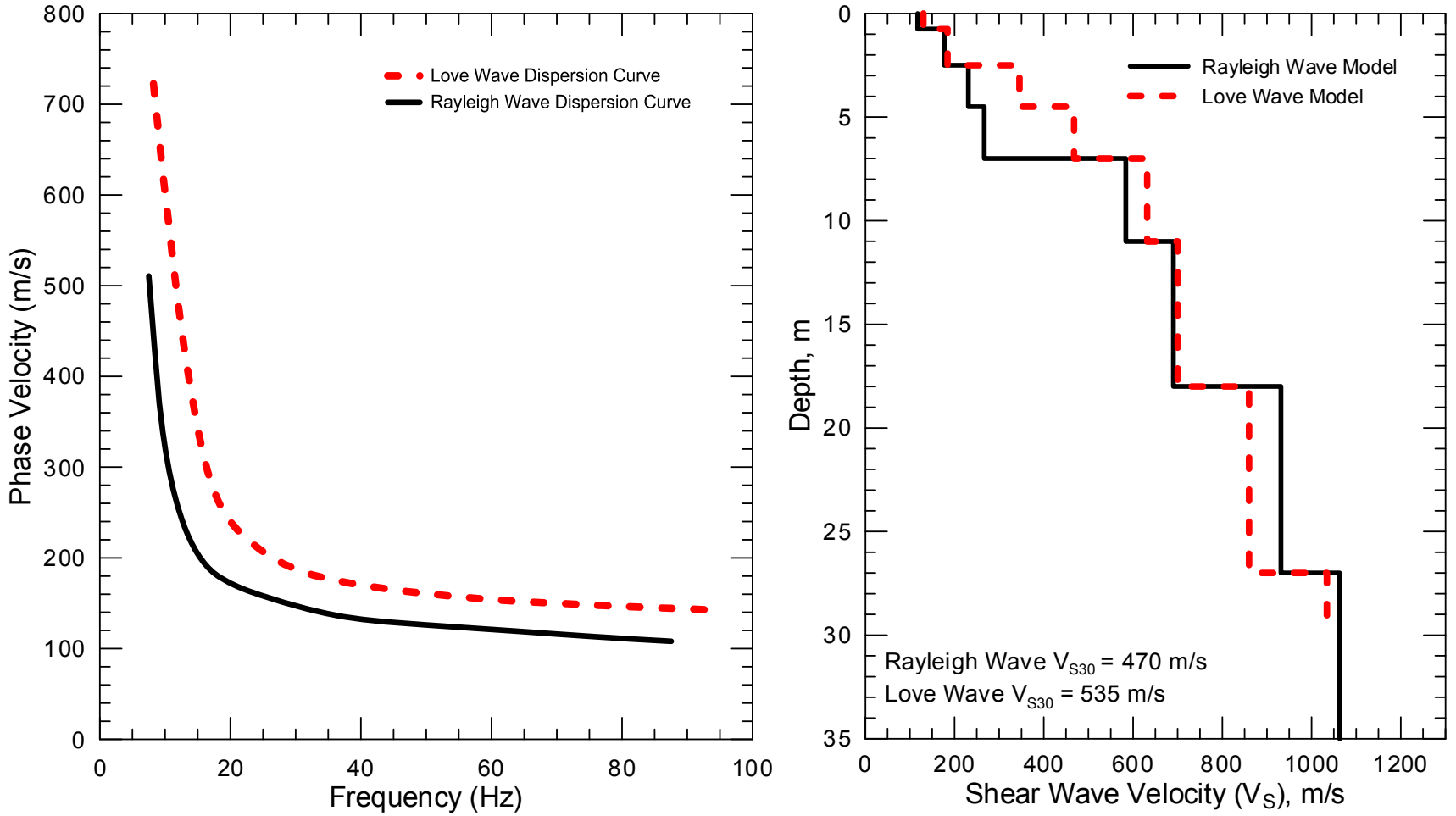

CI.SLR – Rayleigh and Love wave phase velocity dispersion curves (left) and associated V_S models (right). The V_S model from the Love wave data has significantly higher V_S over the 2.5 to 7 m depth range, much higher than can be explained by anisotropy. This site may also have unusually low Poisson's ratio and additional study is warranted.

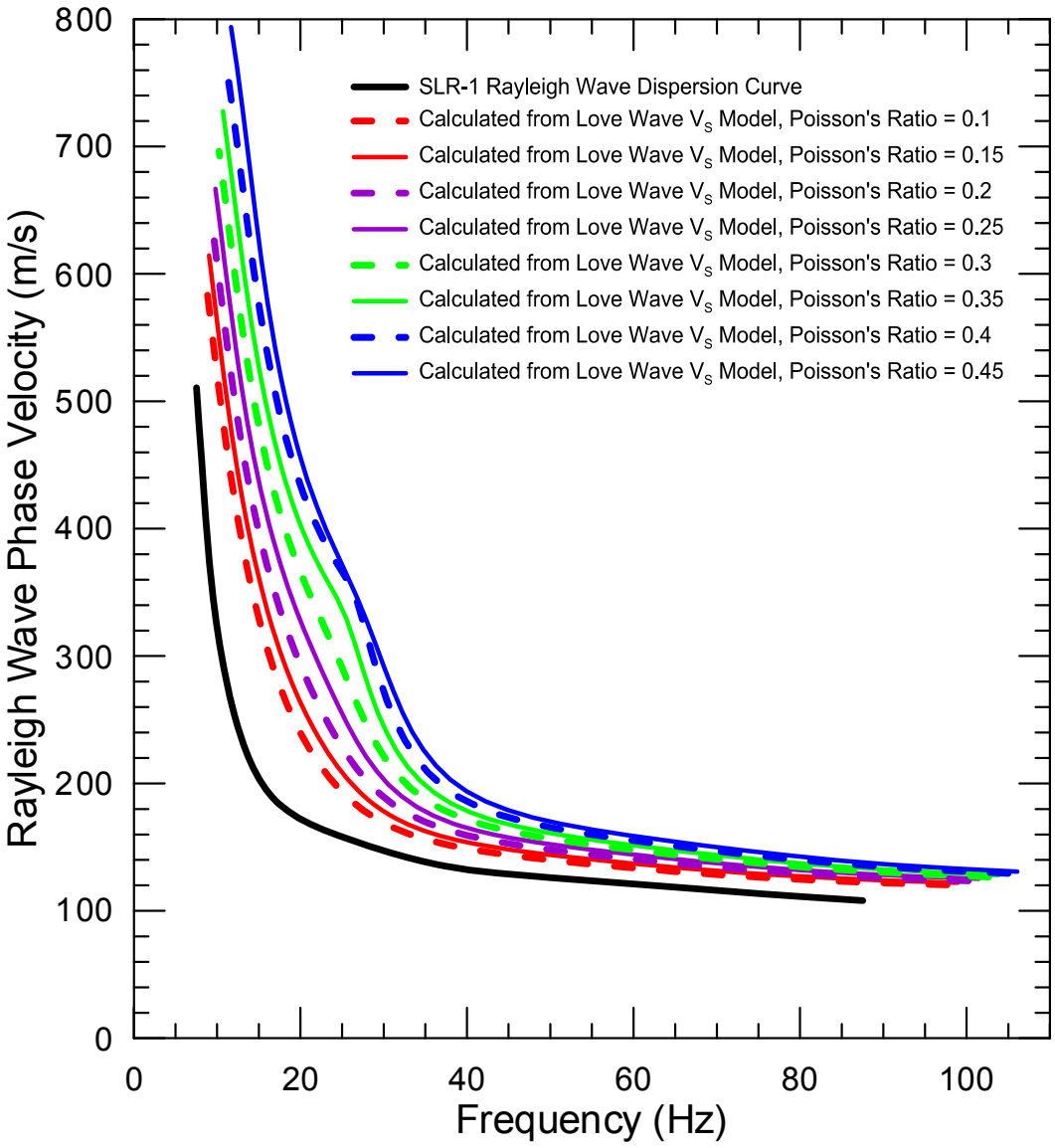

Comparison of Rayleigh wave dispersion curve to calculated fundamental mode Rayleigh wave dispersion curves using the Love wave V_S model and varying Poisson's ratio. A Poisson's ratio of 0.4, or greater, is not realistic for the higher velocity weathered crystalline rock, even if saturated.

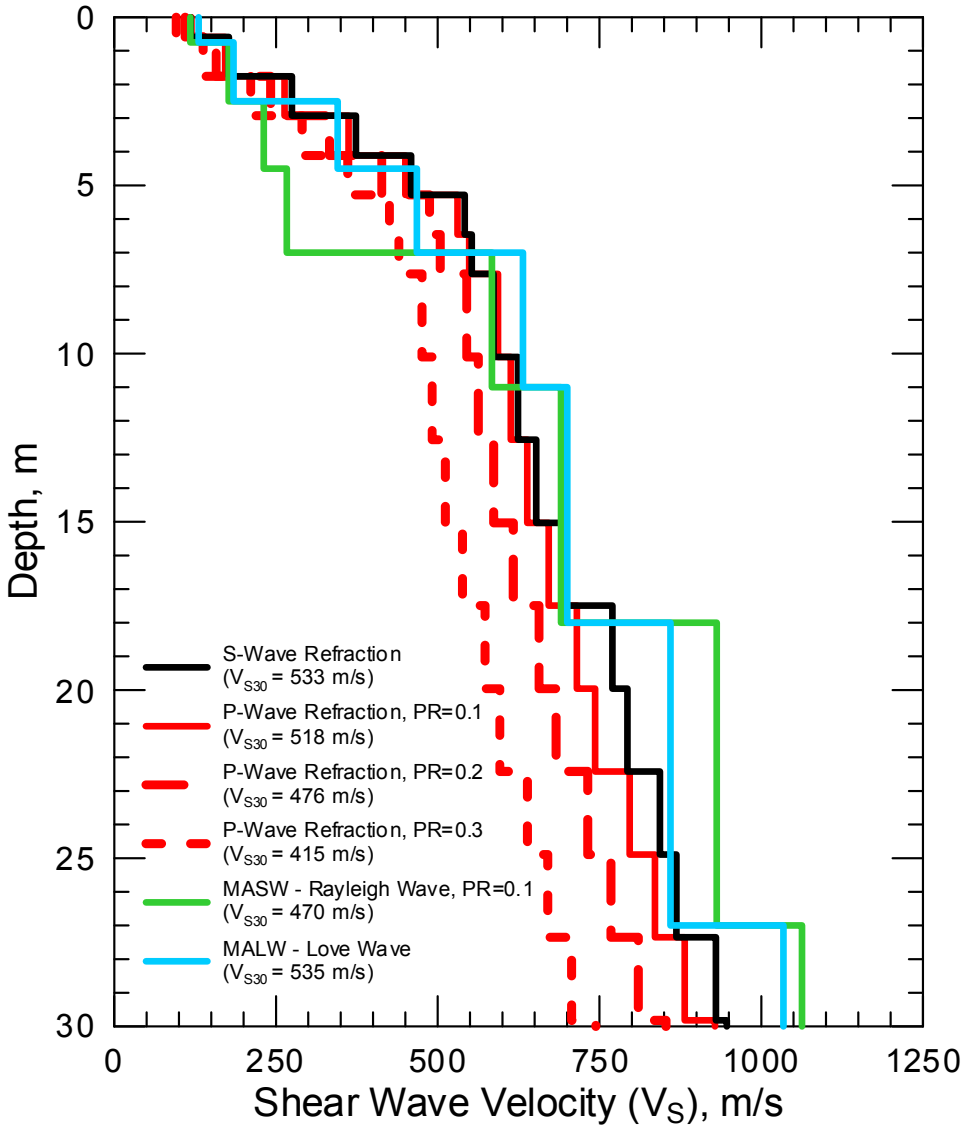

CI.SLR – Comparison of S-wave velocity models derived from the MASW (Rayleigh wave), MALW (Love wave) and the P- and S-wave seismic refraction surveys. The P- and S-wave seismic refraction models and MALW V_S model generally agree for an unusually low Poisson's ratio of 0.1, although the MALW V_S model has slightly higher V_S at depths greater than 18 m. The MASW V_S model has much lower V_S over the 2.5 to 7 m depth range, more that can easily be explained by anisotropy, but is relatively consistent with the MALW V_S model at greater depths.

Site CI.SMM

Location: Soda Lake Road, Simmler, California

Latitude: 35.31402 **Longitude:** -119.99579

(Station coordinates modified based on field GPS survey, WGS84 Coordinate System)

V_{S30} (measured): 225 m/s

V_{S30} (adjusted to more accurately reflect seismic station conditions): 235 m/s (average S-wave velocity between 2 and 32 m adjusting for nominal sensor depth)

NEHRP Site Class: D

Geomatrix Code: IHD

Geologic Conditions/Observations: Site located on geologic unit mapped as Quaternary (Holocene) alluvial clay, sand and gravel. Relative depth to crystalline basement is not clear at this site, but likely deeper than 100 to 150 m based on HVSR data and seismic reflection events in MASW seismic records.

Site Conditions: Rural site with sporadic traffic on nearby road. Relatively flat terrain in test area.

Geophysical Methods Utilized: HVSR, MASW, SASW

Geophysical Testing Arrays:

1. Array SMM-1 (48 channel MASW array utilizing 4.5 Hz vertical geophones spaced 1.5 m apart for a length of 70.5 m, forward and reverse shot locations with multiple source offsets and source types and center shot location).
2. Array SMM-1 (SASW array with common midpoint and orientation as MASW array of same name utilizing 4.5 and 1 Hz vertical geophones and maximum receiver spacing of 32 m).
3. Three HVSR measurement locations; two distributed along array SMM-1 and one near the seismic station.

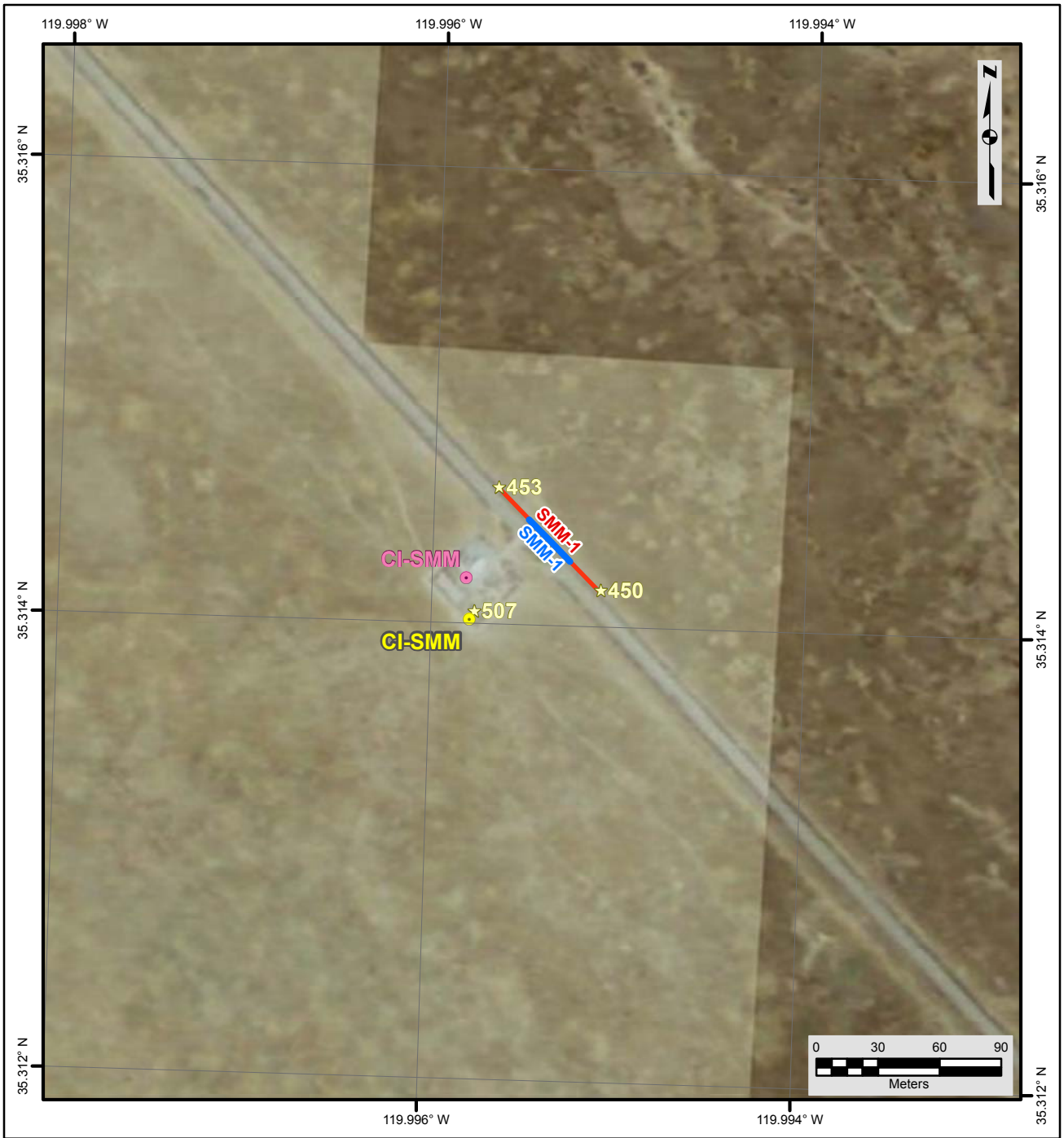

Legend

- Seismic Station - Approximate Surveyed Location
- Seismic Station - Approximate Location of Record
- H/V Spectral Ratio Location
- SASW Array
- MASW Array

NOTES:
1. WGS 1984 COORDINATE SYSTEM
2. Image Source: ESRI, i-cubed, USDA FSA, USGS, AEX, GeoEye, Getmapping, Aerogrid, IGP

File Name: CI-SMM-I

Date: 7/15/2011

USGS science for a changing world

GEOVision geophysical services

RECOVERY.GOV

SITE MAP
CI•SMM

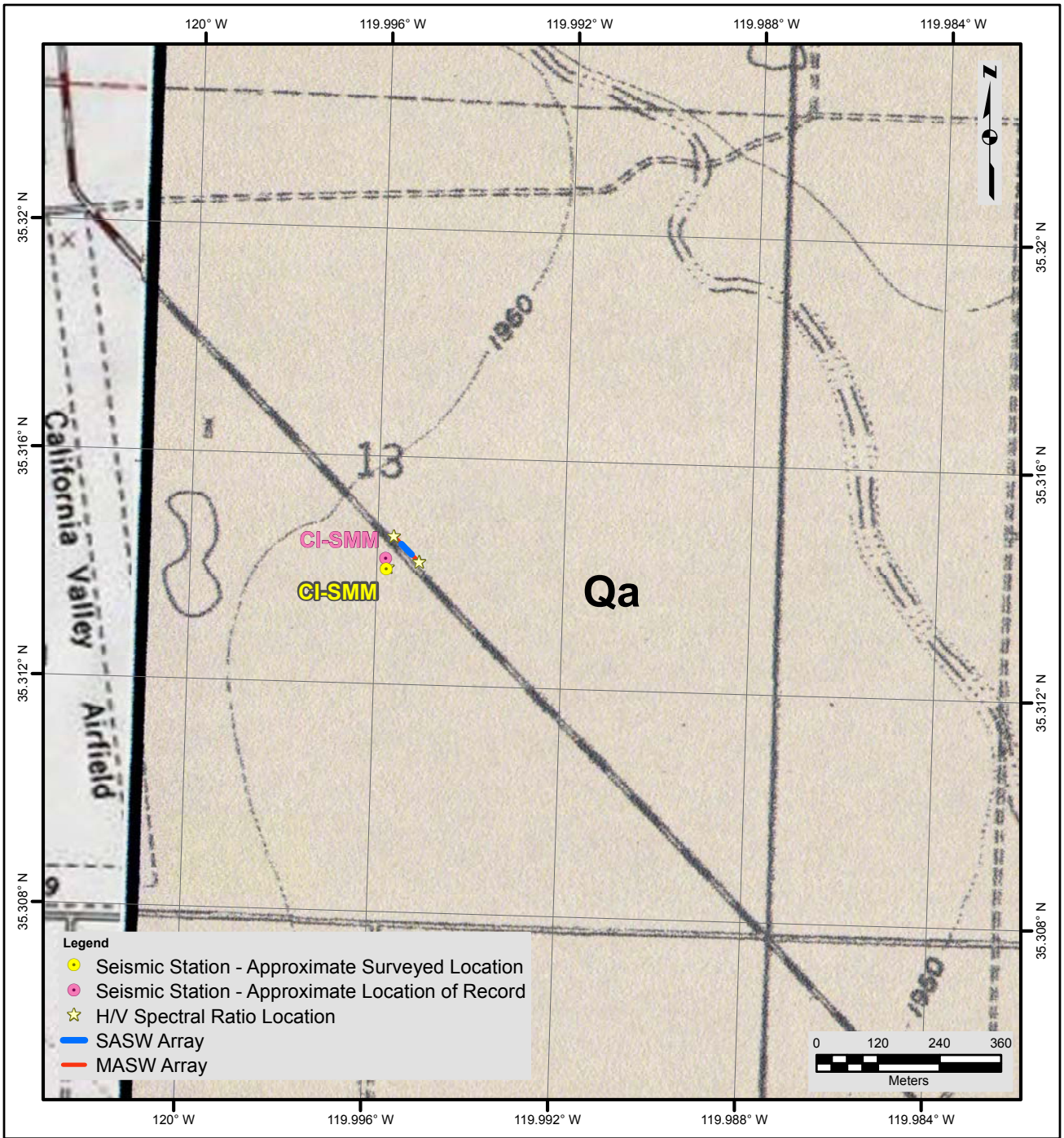

Description of Geologic Map Units

Qa = Quaternary (Holocene) alluvial clay, sand and gravel of valley areas

NOTES:
1. WGS 1984 COORDINATE SYSTEM
2. Geologic Map of the Simmler Quadrangle, San Luis Obispo & Kern Counties, California by Thomas W. Dibblee, Jr., 2005
3. See site map for details of geophysical survey

File Name: CI-SMM

Date: 7/7/2011

USGS science for a changing world

GEOVision geophysical services

GEOLOGIC MAP
CI•SMM

RECOVERY.GOV

Looking southwest towards seismic station CI.SMM from array SMM-1

Looking southeast along MASW array SMM-1

Looking northwest towards HVSR sensor 453

Looking southeast towards seismic station from SASW array SMM-1

Looking northwest along SASW array SMM-1

Location of Geophysical Testing Arrays:

Location	Latitude	Longitude
SMM-1, Northwest End of MASW Array	35.31460	-119.99565
SMM-1, Center of MASW and SASW Arrays	35.31437	-119.99537
SMM-1, Southeast End of MASW Array	35.31415	-119.99510
HVSR Sensor 450	35.31416	-119.99509
HVSR Sensor 453	35.31460	-119.99565
HVSR Sensor 507	35.31405	-119.99576
CI.SMM Seismic Station	35.31402	-119.99579

Notes: 1) WGS84 Coordinate System (decimal degrees)
2) Survey accuracy is estimated at 1 to 2 m

Results:

V_S Model

Depth to Top of Layer (m)	Layer Thickness (m)	S-Wave Velocity (m/s)	Inferred P-Wave Velocity (m/s)	Inferred Poisson's Ratio	Inferred Density (g/cm^3)
0	1	128	240	0.300	1.9
1	4	223	417	0.300	1.9
5	8	235	1650	0.490	2.0
13	12	211	1650	0.492	2.0
25	>5	297	1650	0.483	2.0

Observations/Discussion:

- The HVSR curves are similar at frequencies below 10 Hz, validating the 1-D velocity structure assumption.
- There is a broad, low amplitude HVSR peak with maximum response at about 0.9 to 0.95 Hz. This peak may be indicative of a large impedance contrast at a depth on the order of 75 to 150 m, depending upon S-wave velocity structure. Based on the signature of the HVSR curves at lower frequencies, this HVSR peak may be associated with a sediment layer rather than the basement complex.
- Noise conditions at site were not sufficient to apply passive surface wave techniques.
- Surface wave dispersion data from SASW and MASW data sets are in good agreement at the site. It was not possible to extract surface wave phase velocity data at wavelengths less than 2.5 m, likely due to near surface lateral velocity variation associated with animal burrows, nearby subsurface utilities, a possible thin high velocity layer at about 1 m depth, etc.

- Representative dispersion curves were generated for each surface wave data set using a moving average, polynomial curve fitting routine. These individual representative dispersion curves were combined and a representative dispersion curve generated for the combined data set for data modeling.
- The water table was modeled at a depth on the order of 5 m based on interactive layer-based analysis of seismic refraction first arrival data. P-wave velocities of about 350 to 650 m/s and 1,600 m/s were modeled for unsaturated and saturated sediments, respectively. The seismic refraction data indicates that there may be a very, thin high velocity layer at a depth of 1 m.
- There is excellent reflectivity in the MASW seismic records with multiple reflectors in the approximate 30 to 150 m depth range. The deep reflectors indicate that the 0.9 to 0.95 Hz HVSR peak may not be associated with crystalline basement.
- Surface wave depth of investigation is about 30 m based on half of maximum wavelength criteria.
- V_{S30} is 225 m/s (Site Class D).
- Average S-wave velocity between 2 m (nominal sensor depth) and 32 m is 235 m/s.

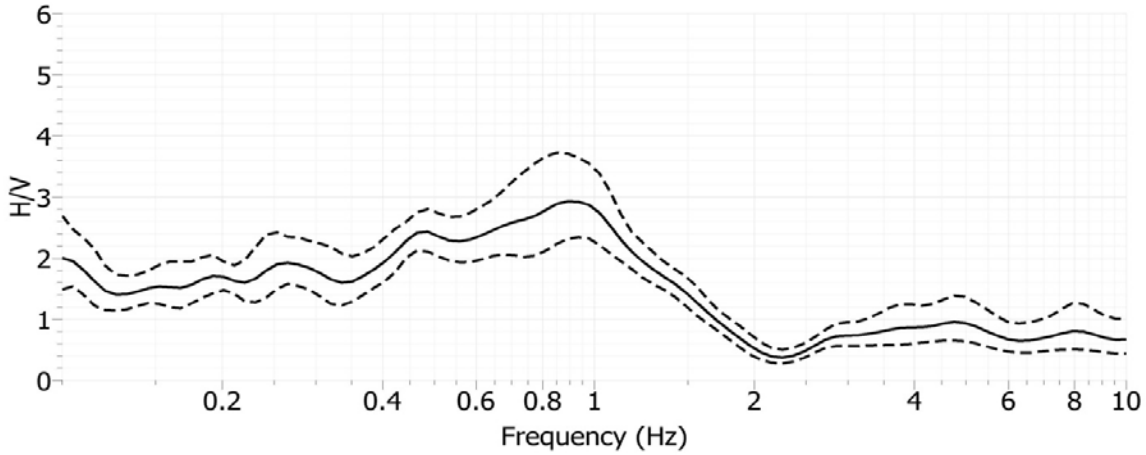

Site CI.SMM, H/V Spectral Ratio, Array SMM-1, Sensor 453

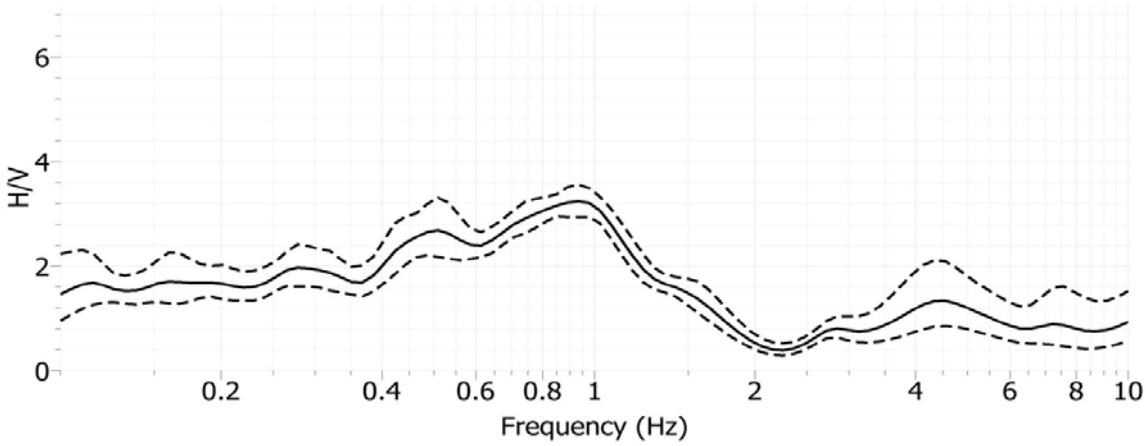

Site CI. SMM, H/V Spectral Ratio, Array SMM-1, Sensor 450

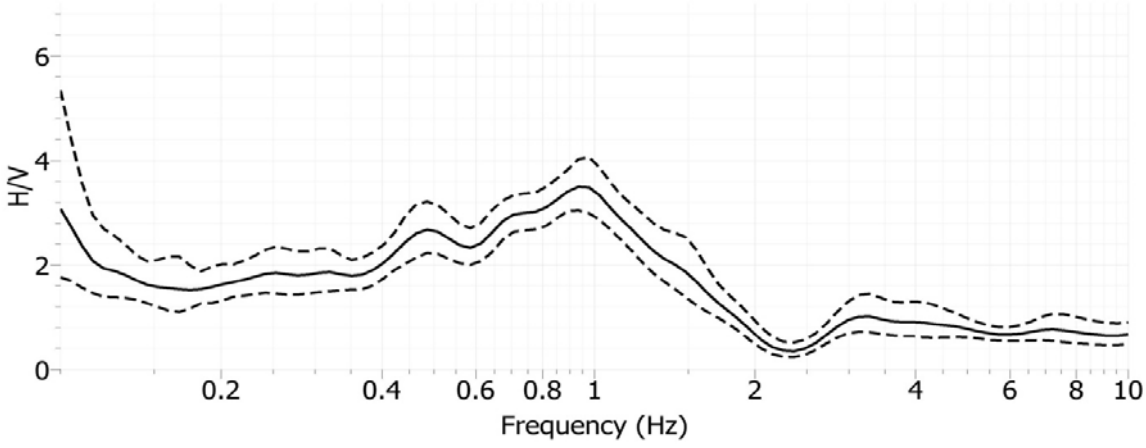

Site CI. SMM, H/V Spectral Ratio, Adjacent to Seismic Station, Sensor 507

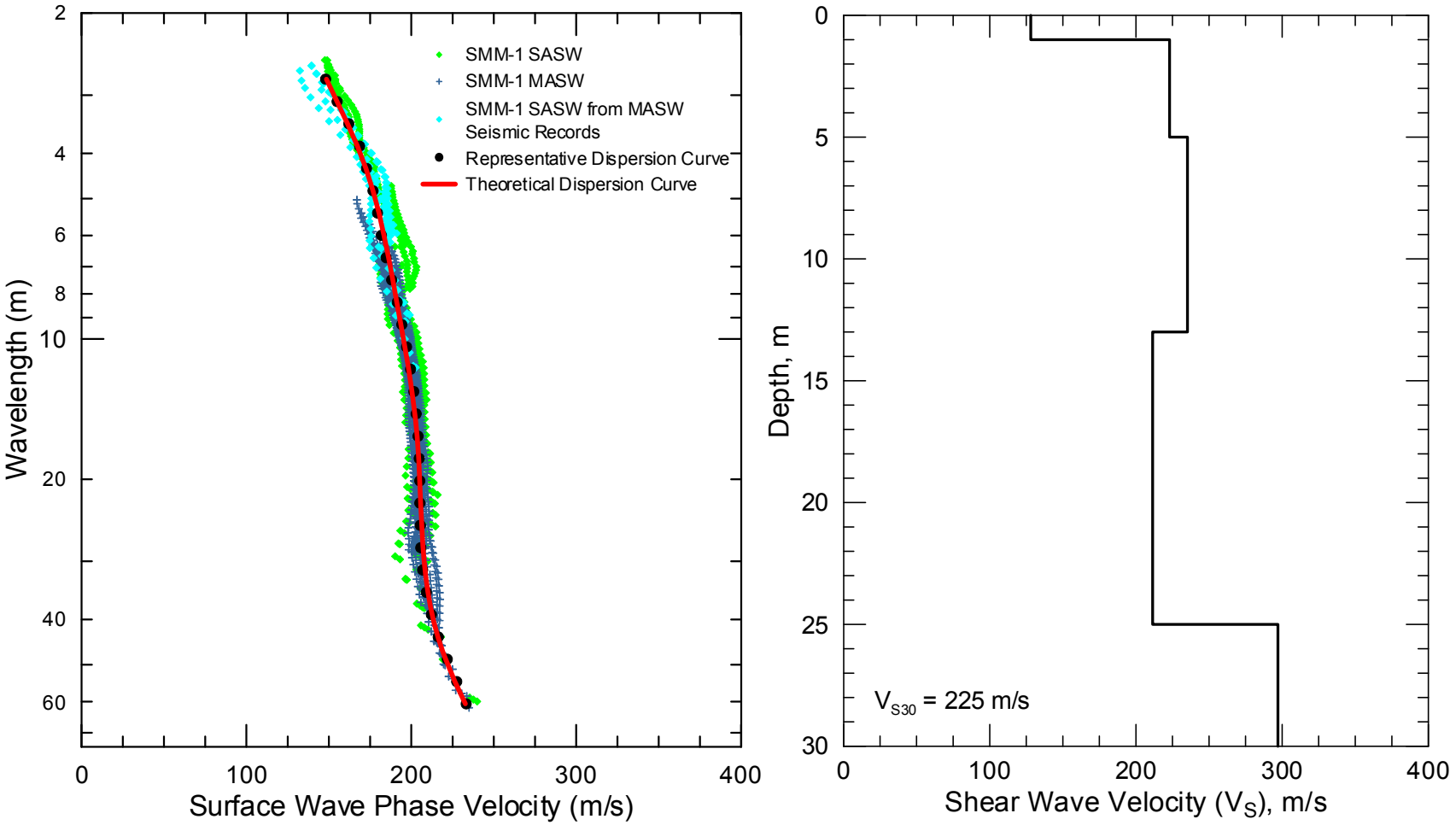

CI.SMM - Field, representative and inverted theoretical surface wave dispersion data (left) and associated V_S model (right)

Site CI.SMR

Location: Santa Margarita Ranch, Santa Margarita, California

Latitude: 35.37688 **Longitude:** -120.61236
(Station coordinates modified based on field GPS survey, WGS84 coordinate system)

V_{S30} (measured): 847 m/s

V_{S30} (adjusted to more accurately reflect seismic station conditions): 1,054 m/s (average S-wave velocity between 1.5 and 31.5 m adjusting for assumed sensor depth).

NEHRP Site Class: B

Geomatrix Code: IKA

Geologic Conditions/Observations: Seismic station located on the Mesozoic (Cretaceous) Atascadero Formation, a marine sandstone. The Rinconada Fault Zone is located about 270 m east of the seismic station. Mapped bedding attitudes on geologic maps indicate that the sandstone generally dips about 25 to 40 degrees to the southwest in the site vicinity.

Site Conditions: Rural site. Rolling, hilly terrain in site vicinity. There is about 2 m of elevation variation along the 70.5 m long seismic refraction and MASW array.

Geophysical Methods Utilized: HVSR, Seismic Refraction, MASW

Geophysical Testing Arrays:

1. Array SMR-1 (48 channel MASW and P-wave seismic refraction array utilizing 4.5 Hz vertical geophones spaced 1.5 m apart for a length of 70.5 m, forward and reverse shot locations with multiple source offsets and source types and multiple interior shot locations).
2. Three HVSR measurement locations: two distributed along array SMR-1 and one near the seismic station.

Legend

- Seismic Station - Approximate Surveyed Location
- Seismic Station - Approximate Location of Record
- H/V Spectral Ratio Location
- MASW and Seismic Refraction Array

NOTES:
1. WGS 1984 COORDINATE SYSTEM
2. Image Source: (c) 2011 Microsoft Corporation and its data suppliers

File Name: CI-SMR-I

Date: 2/7/2013

USGS science for a changing world

GEOVision geophysical services

RECOVERY.GOV

SITE MAP
CI•SMR

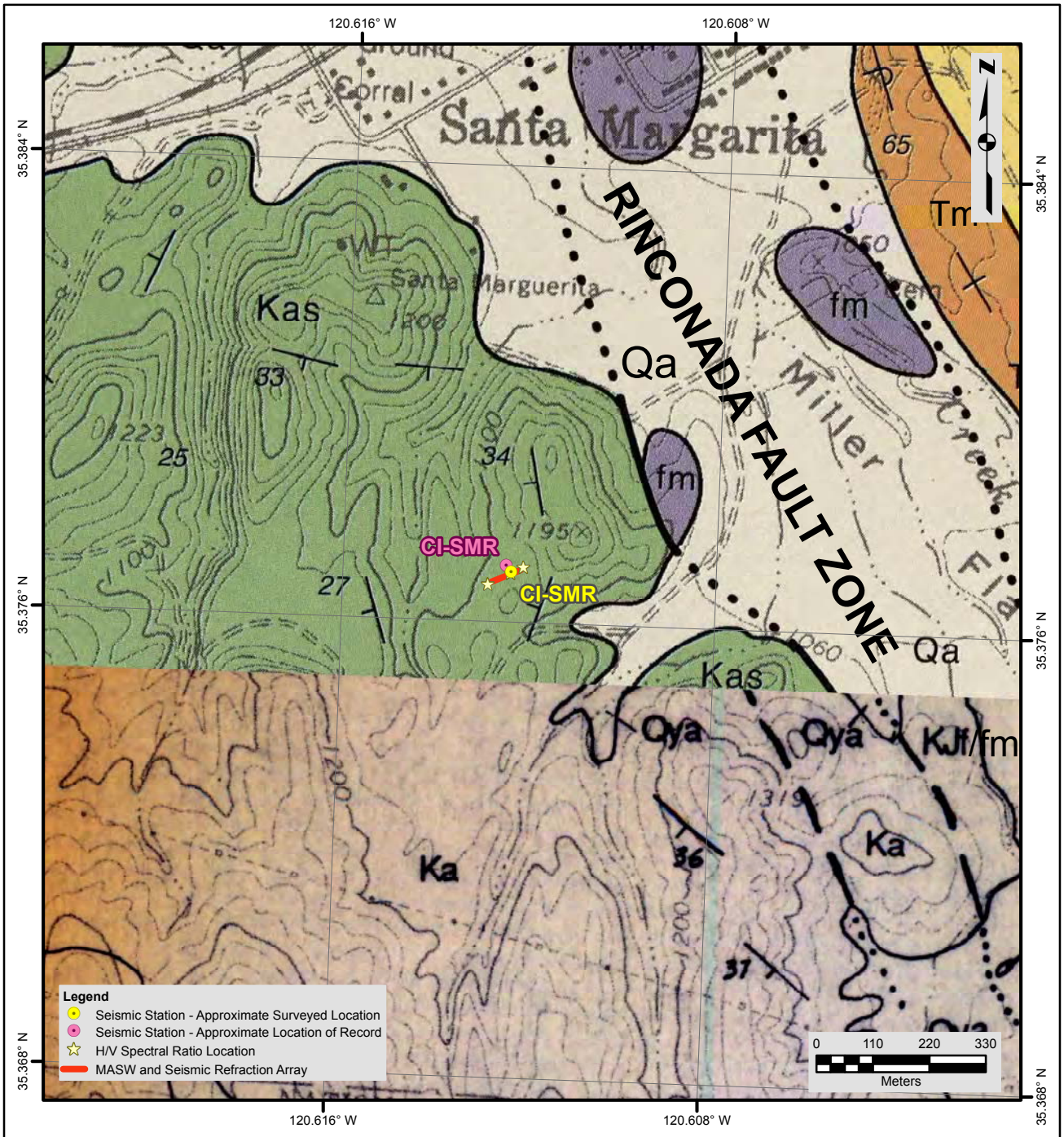

Description of Geologic Map Units

Qa/Qya = Quaternary (Holocene) alluvium/sand, gravel & silt
Tm = Tertiary (Miocene) Monterey shale; upper part, silaceous shale, thin bedded, platy, porcellaneous, locally cherty
Kas/Ka = Mesozoic (Cretaceous) Atascadero Formation; marine, clastic, lithified, hard, arkosic sandstone, minor micaceous clay shale/siltstone, mudstone
KJf/fm = Mesozoic (Jurassic and Cretaceous) Franciscan Assemblage; melange of claystone, graywacke-sandstone, chert, and blueschist, pervasively sheared, slightly metamorphosed

NOTES:
1. WGS 1984 COORDINATE SYSTEM
2. Geologic Map of the Santa Margarita and Lopez Mountain Quadrangles, San Luis Obispo County, California by Thomas W. Dibblee, Jr., 2004 and Hugh McLean, 1990
3. See site map for details of geophysical survey

File Name: CI-SMR

Date: 2/7/2013

USGS science for a changing world

GEOVision geophysical services

GEOLOGIC MAP
CI•SMR

RECOVERY.GOV

CI.SMR seismic station

Accelerated weight drop energy source on MASW array SMR-1

20 lb sledge hammer energy source on MASW and seismic refraction array SMR-1

Looking at HVSR sensor 450, seismic station and MASW array SMR-1

Looking northeast along array SMR-1 towards seismic station

Location of Geophysical Testing Arrays:

Location	Latitude	Longitude
SMR-1, Southwest End of MASW Array	35.37666	-120.61286
SMR-1, Center of MASW Array	35.37679	-120.61251
SMR-1, Northeast End of MASW Array	35.37692	-120.61215
HVSR Sensor 507	35.37697	-120.61210
HVSR Sensor 450	35.37686	-120.61237
HVSR Sensor 453	35.37665	-120.61285
CI.SMR Seismic Station	35.37688	-120.61236

Notes: 1) WGS84 Coordinate System (decimal degrees)

2) Survey accuracy is estimated at 2 to 3 m.

Results:

Average V_P Model and Estimated Constant Poisson's Ratio V_S Models from Seismic Refraction Model resulting from Tomographic Inversion with Layered Starting Model

Depth to Top of Layer (m)	Layer Thickness (m)	P-Wave Velocity (m/s)	Estimated S-Wave Velocity (m/s)				
			Poisson's Ratio = 0.25	Poisson's Ratio = 0.30	Poisson's Ratio = 0.35	Poisson's Ratio = 0.4	Poisson's Ratio = 0.45
0.00	0.44	405	234	217	195	165	122
0.44	0.88	461	266	246	221	188	139
1.32	0.88	1153	666	616	554	471	348
2.20	0.88	1470	849	786	706	600	443
3.08	0.88	1565	904	837	752	639	472
3.96	0.88	1583	914	846	760	646	477
4.84	0.88	1617	934	865	777	660	488
5.72	1.85	1642	948	878	789	670	495
7.57	1.85	2416	1395	1291	1161	986	728
9.42	1.85	2807	1620	1500	1348	1146	846
11.26	1.85	2971	1715	1588	1427	1213	896
13.11	1.85	3297	1904	1763	1584	1346	994
14.96	1.85	3300	1905	1764	1585	1347	995
16.81	1.85	3328	1922	1779	1599	1359	1003
18.66	1.85	3363	1942	1798	1616	1373	1014
20.50	Half Space	3513	2028	1878	1688	1434	1059

Note: Estimated V_{S30} = 641 to 1,227 m/s, for constant Poisson's ratio 0.45 to 0.25, demonstrating that P-wave refraction models cannot be used to infer S-wave velocity , especially if the saturated zone is present in the model at unknown depth.

Average V_P Model from Seismic Refraction Model Resulting from Tomographic Inversion with Layered Starting Model and Estimated V_S Model using Conservative Values of Poisson's Ratio for Unsaturated and Assumed Saturated Sediments/Rock

Depth to Top of Layer (m)	Layer Thickness (m)	P-Wave Velocity (m/s)	Estimated S-wave Velocity (m/s)	Assumed Poisson's Ratio
0.00	0.44	405	195	0.350
0.44	0.88	461	221	0.350
1.32	0.88	1153	554	0.350
2.20	0.88	1470	706	0.350
3.08	0.88	1565	752	0.350
3.96	0.88	1583	760	0.350
4.84	0.88	1617	777	0.350
5.72	1.85	1642	789	0.350
7.57	1.85	2416	873	0.425
9.42	1.85	2807	1014	0.425
11.26	1.85	2971	1073	0.425
13.11	1.85	3297	1191	0.425
14.96	1.85	3300	1192	0.425
16.81	1.85	3328	1202	0.425
18.66	1.85	3363	1215	0.425
20.50	Half Space	3513	1269	0.425

Notes: 1) Saturated zone assumed at 7.5 m depth.
2) Estimated V_{S30} = 878 m/s.

V_S Model from MASW Data with Fundamental Mode Assumption

Depth to Top of Layer (m)	Layer Thickness (m)	S-Wave Velocity (m/s)	Inferred P-Wave Velocity (m/s)	Assumed Poisson's Ratio	Assumed Density (g/cm^3)
0	0.5	101	188	0.300	1.7
0.5	2	335	626	0.300	1.8
2.5	2.5	447	836	0.300	2.0
5	2.5	738	1381	0.300	2.1
7.5	>22.5	1454	3000	0.346	2.3

Notes: 1) Saturated zone with V_P of 3,000 m/s inferred at depth of about 7.5 m from seismic refraction model.
2) Depth of investigation is about 30 m.
3) Bottom layer is a half space.
4) V_{S30} = 847 m/s.

V_S Model from MASW Data with Average/Effective Mode Assumption

Depth to Top of Layer (m)	Layer Thickness (m)	S-Wave Velocity (m/s)	Inferred P-Wave Velocity (m/s)	Assumed Poisson's Ratio	Assumed Density (g/cm^3)
0	1	189	354	0.300	1.70
1	2	298	558	0.300	1.80
3	3	536	1003	0.300	2.00
6	3	747	2000	0.419	2.10
9	6	872	2750	0.444	2.10
15	12	1079	3000	0.426	2.15
27	>3	1302	3000	0.384	2.20

Notes: 1) Saturated zone with V_P of 2,000 to 3,000 m/s inferred at depth of about 6 to 9 m from seismic refraction model.
2) Depth of investigation is about 30 m.
3) Model extended below bottom layer.
4) V_{S30} = 716 m/s.

V_S Model from MASW Data using 3-D Global Inversion in WinSASW Software Package (not valid)

Depth to Top of Layer (m)	Layer Thickness (m)	S-Wave Velocity (m/s)	Inferred P-Wave Velocity (m/s)	Assumed Poisson's Ratio	Assumed Density (g/cm^3)
0	1	180	337	0.3	1.7
1	2	295	552	0.3	1.8
3	2.5	483	903	0.3	2.0
5.5	3.5	778	2000	0.411	2.1
9	20	836	3000	0.458	2.1
29	>1	1150	3000	0.414	2.2

Notes: 1) Saturated zone with V_P of 2,000 to 3,000 m/s inferred at depth of about 5.5 to 9 m from seismic refraction model.
2) Depth of investigation is about 30 m.
3) Bottom layer is a half space.
4) V_{S30} = 641 m/s.

Observations/Discussion:

- There is no distinct HVSR peak that occurs consistently at all of the HVSR measurement locations.
- The MASW and seismic refraction array appears to almost be orthogonal to or at a high angle to mapped strike of geologic bedding in the site vicinity. Bedding attitudes were not, however, confirmed in the field due to a thin residual soil layer overlying rock.
- MASW data appeared of sufficient quality as to not require S-wave seismic refraction and MALW data for site characterization. As it will become apparent below, S-wave refraction and MALW data would have been highly useful at this site.
- The P-wave refraction data for array SMR-1 were modeled using a tomographic inversion routine with both layer-based and smooth velocity gradient starting models. The seismic refraction models were extended to far offset shot locations to extend the depth of investigation. A larger geophone spacing is preferred for extending the depth of investigation, when applying tomographic inversion routines.
- The P-wave seismic refraction survey design allowed P-wave velocity to be imaged to a maximum depth of 20 m or more. The seismic refraction models show that P-wave velocity is about 375 to 500 m/s at the surface and increases to 1,250 m/s at a depth of 1 to 3 m, 2,000 m/s at a depth of 6 to 8 m and 3,000 m/s at a depth of 8 to 12 m. The maximum P-wave velocity in the models is about 3,500 m/s. It is unclear if P-wave velocity is affected by a potential saturated zone; however, the possibility should be considered that P-wave velocities over 2,500 m/s are associated with saturated sandstone.
- The possibility of saturated rock, makes the P-wave velocity models not useful for estimating S-wave velocity structure to validate the surface wave models. Under normal conditions the surface wave models will confirm the presence of saturated sediments/rock; however, possible dominant higher modes in the Rayleigh wave phase velocity data result in significant uncertainty. S-wave seismic refraction and/or MALW data would be required to determine if high P-wave velocities are associated with saturated rock.
- V_{P30} was estimated between 27 and 49.5 m on the P-wave refraction model, that used a layered starting model, by projecting the velocity at 21 m depth to 30 m depth. Over this interval, V_{P30} ranges from about 2,037 to 2,246 m/s, about a 10% variation over a 22 m long segment of the array. An average V_P model was developed over the 27 to 49.5 m distance interval by averaging the travel time through each model cell at a particular depth and average V_{P30} was determined to be 2,125 m/s.
- An average V_S model was estimated from the average V_P model using constant Poisson's ratio in the range of 0.25 to 0.45. Estimating V_{S30} from V_{P30} assuming constant Poisson's ratio in the range of 0.25 to 0.45 results in V_{S30} in the 1,227 to 641 m/s range. This large variation in potential V_{S30} demonstrates the risks in attempting to estimate V_{S30} from P-wave velocity data, especially when sediments or rock may be saturated, resulting in higher Poisson's ratios.
- An average V_S model was also estimated from the average V_P model by assuming a conservative Poisson's ratio of 0.35 and 0.425 for unsaturated and saturated sediments/rock, respectively. The saturated zone was assumed to be present at a depth of 7.5 m, based on an abrupt increase in P-wave velocity from 1,640 to 2,420 m/s. V_{S30} is 878 m/s for this model.

- Noise conditions at the site were not sufficient for application of passive surface wave techniques.
- MASW data reduction was difficult, with a dominant higher mode often being present at high frequencies The fundamental mode appeared to be dominant at lower frequencies; however, because the subsurface velocity structure consists of a thin soil layer over much harder rock, the possibility of modal superposition or a dominant first higher mode at low frequencies cannot be discounted. The use of smaller hammer energy sources and limited offset receiver arrays appeared to permit extraction of the fundamental mode at high frequencies.
- The minimum wavelength Rayleigh wave phase velocity data extracted from the 48-channel MASW array was 35 m, primarily the result of a dominant higher mode at smaller wavelengths (higher frequencies). Reducing data from smaller hammer sources using a limited offset receiver array (i.e. less active geophones) allowed for extraction of surface wave dispersion data to a minimum wavelength of about 2 m.
- A maximum 80 m wavelength Rayleigh wave was extracted from the MASW data by slightly relaxing the near field criteria typically applied during this investigation. The maximum wavelength Rayleigh wave was set equal to 1.2 times the source to midpoint of receiver array distance.
- There is significant scatter of about 80 to 120 m/s in Rayleigh wave dispersion data, likely the result of lateral velocity variation. Generally, long wavelength phase velocity data from source locations offset from the northeast end of the array were not utilized as phase velocities were about 10% lower than those from the opposite direction and did not tie into the coherent dispersion curve at smaller wavelengths.
- A representative dispersion curve was generated for the edited MASW data set using a moving average, polynomial curve fitting routine and used for modeling.
- The velocity structure at this site is such that higher modes may dominate over a wide frequency range. Generally two or three modes were evident in the v-f transforms. The fundamental mode appears to be recovered at high frequencies using limited offset receiver gathers and small offset source locations. The fundamental mode may also be recovered at low frequencies; however, data modeling introduced the possibility that the fundamental mode may jump to the first higher mode at low frequencies. It is, therefore, unclear if the higher mode observed in many v-f transform images (overtone images) is the first or second higher mode.
- V_{R40} is 895 m/s which would result in an estimated V_{S30} of 935 m/s, based on the Brown, et al., 2000 relationship, assuming that the dispersion curve at 40 m wavelength is the fundamental mode. V_{S30} would be lower if the dispersion curve were associated with the first higher mode or if modal superposition occurs at low frequencies. Additionally, V_{S30} may be as much as 10% lower based on lower V_{R40} on source locations offset from the northeast end of the array. V_{S30} from the average seismic refraction V_P model using a Poisson's ratio of 0.325 to represent typical unsaturated conditions is 1,082 m/s. This is significantly higher than that estimated from the surface wave dispersion curve and would tend to indicate that saturation affects P-wave velocity.
- The MASW data were modeled using both the fundamental mode assumption (2-D solution in the WinSASW software package, which is approximately equivalent to fundamental mode) and average/effective mode assumption (observed dispersion curve consists of the average of all modes based on relative amplitude of each mode estimated

for a far-field, plane Rayleigh wave). The average mode assumption is an attempt to deal with modal superposition that may occur at low frequencies due to lack of resolution partially associated with finite receiver array length. However, the analytical method used to estimate the relative amplitude of each mode assumes a plane Rayleigh wave and does not consider source-receiver geometry. It is well documented that source-receiver geometry affects the energy in higher modes and, therefore, this particular average/effective mode assumption may not always be accurate. However, modeling of average mode may lead to more correct results than incorrectly assuming that the dispersion curve is fundamental mode, especially if only the lowest frequency portion or the dispersion curve is affected by modal superposition. Finally, in another attempt to deal with possible modal superposition or dominant higher modes the MASW dispersion data was modeled using the 3-D global inversion option in the WinSASW software package. This modeling routine is designed to model SASW data acquired with a pair of receivers and may not generally be applicable to MASW data.

- The resulting fundamental mode and 3-D global inversion V_S models were evaluated to determine if dominant higher modes are expected. Multi-mode analysis of the fundamental mode V_S model indicated that the first higher mode should be dominant at frequencies below about 40 Hz and there is a possibility that the first higher mode terminates at a frequency between 20 and 25 Hz, in which case the fundamental mode will be dominant at lower frequencies. If the first higher mode does not exist below a low frequency bound then the fundamental mode assumption may be the only approach to model the data. Alternatively, multi-mode modeling routines could be considered. Multi-mode analysis of the 3-D global inversion V_S model indicated that the modeling routine was effectively modeling intermediate to low frequency portions of the dispersion curve as the first higher mode. If the first higher mode were not dominant at low to intermediate frequencies, this model would significantly underestimate S-wave velocity at depth. Likewise the average mode model would also underestimate S-wave velocity at depth if the lowest frequency portion of the dispersion curve were indeed the fundamental mode.
- Surface wave depth of investigation is about 30 m based on the one half to one third of maximum wavelength criteria.
- V_{S30} is 847 m/s for the fundamental mode surface wave model (NEHRP Site Class B).
- Average S-wave velocity between 1.5 m (assumed sensor depth) and 31.5 m is 1,054 m/s for the fundamental mode surface wave model.
- V_{S30} 716 and 641 m/s for the average mode and 3-D global inversion surface wave models, respectively (NEHRP Site Class C).
- Average S-wave velocity between 1.5 m (assumed sensor depth) and 31.5 m is 831 and 735 m/s for the average mode and 3-D global inversion surface wave models, respectively.
- Comparison of S-wave velocity models derived from the MASW and P-wave seismic refraction surveys indicate that S-wave velocities inferred from the P-wave seismic refraction model are generally higher than those from the surface wave sounding over the 1.5 to 5.5 m depth range. S-wave models generated from the Rayleigh wave phase velocity dispersion data using the fundamental mode and average mode assumptions and the 3-D global inversion in the WinSASW software package are generally consistent in the upper 7 to 9 m and significantly different below. The WinSASW 3-D global

inversion is definitely not valid based on inferred S-wave velocities from the P-wave refraction model. This is not unexpected, as this analytical routine is not designed for MASW data. Both the fundamental mode and average mode models are feasible depending on the Poisson's ratio of the saturated sandstone unit.

- The best estimate of V_S structure from the average P-wave velocity model, assuming Poisson's ratio of 0.35 and 0.425 for unsaturated and saturated sediments/rock, respectively yields an estimated V_{S30} of 878 m/s. This is similar to the V_{S30} estimate from the fundamental mode surface wave model, although there are distinct differences between the models.
- For site characterization purposes, we recommend using the S-wave velocity structure derived from the MASW model developed using the fundamental mode assumption. However, the possibility should be considered that V_{S30} is 10%, or more, lower than that presented. The MASW model developed using the average mode assumption appears to be conservative and although resulting V_{S30} is indicative of NEHRP Site Class C/B, adjusted V_{S30} is indicative of NEHRP Site Class B. Therefore, we can state with confidence that the velocity structure at the seismic station can be classified as NEHRP Site Class B.
- There is uncertainty in the V_S models at this site, related to uncertainty in which Rayleigh wave modes are dominant, and acquisition of S-wave seismic refraction and MALW (Love wave) data is recommended to better constrain subsurface velocity structure.

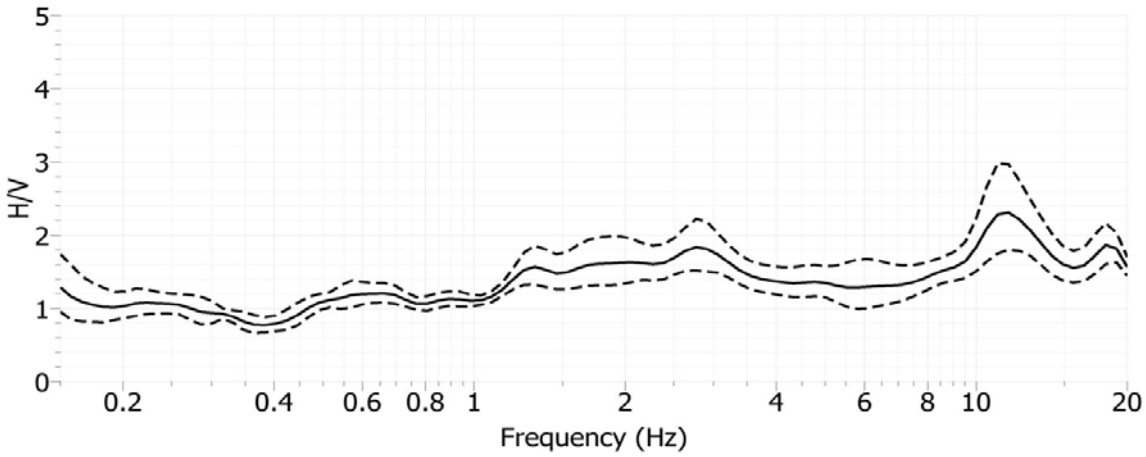

Site CI.SMR, H/V Spectral Ratio, Array SMR-1, Sensor 453

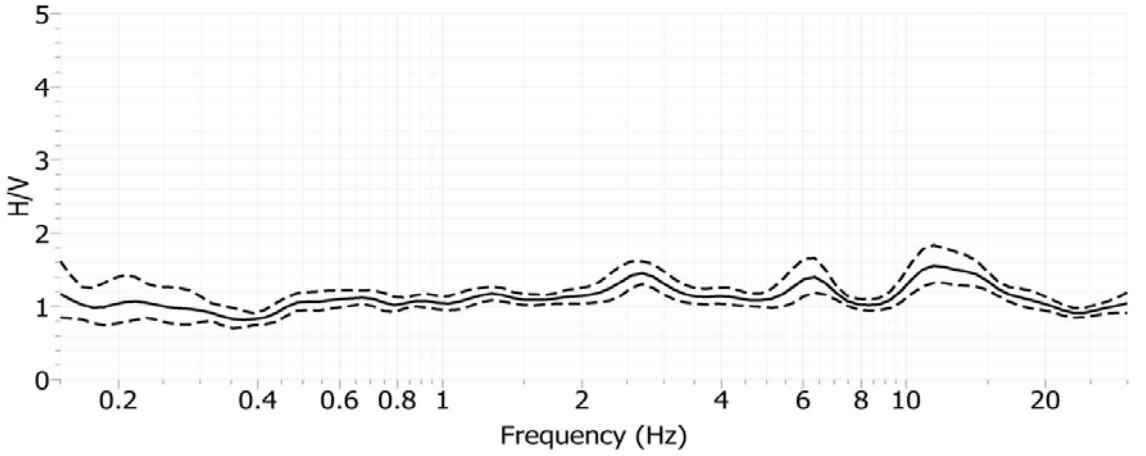

Site CI.SMR, H/V Spectral Ratio, Near Seismic Station, Sensor 450

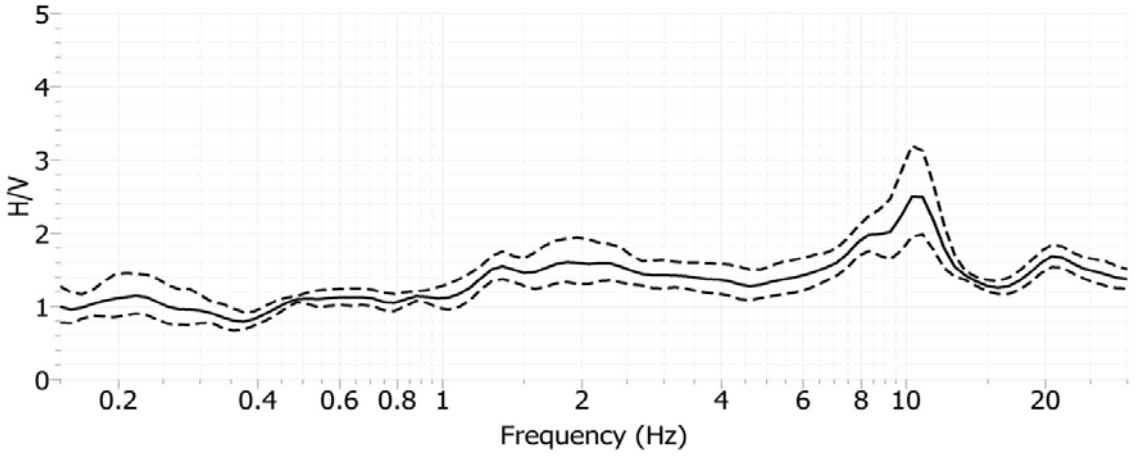

Site CI.SMR, H/V Spectral Ratio, Array SMR-1, Sensor 507

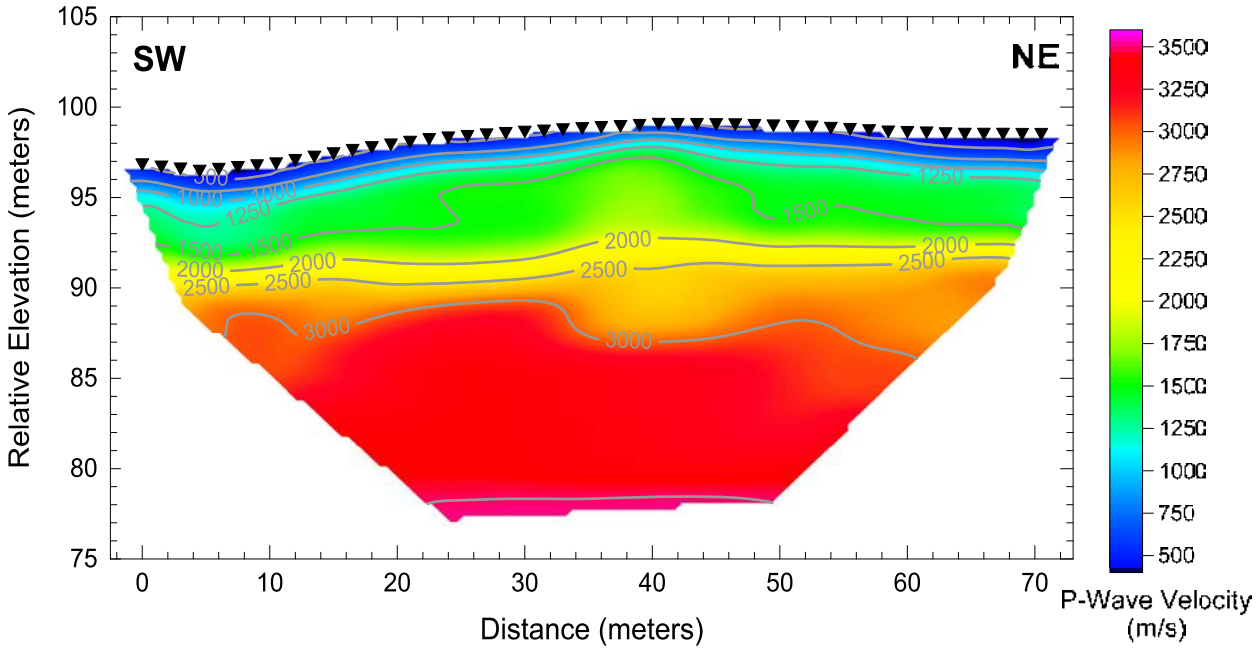

Array SMR-1 – P-wave tomographic seismic refraction model developed utilizing a layer based starting model

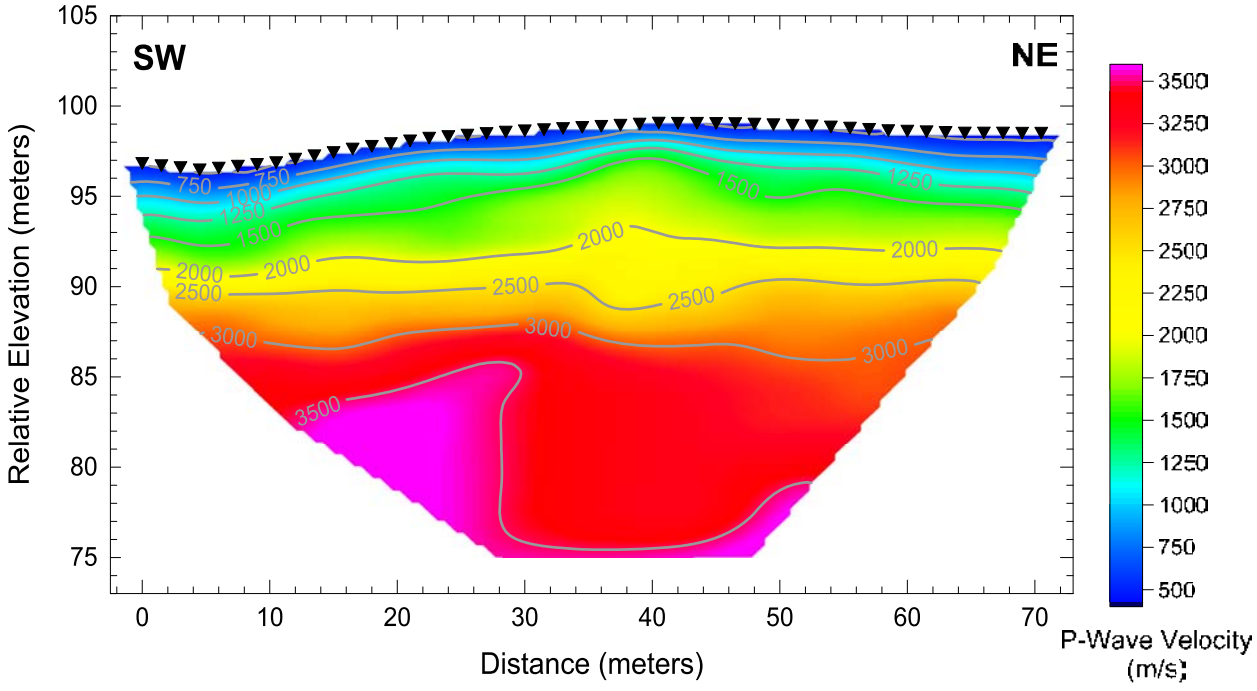

Array SMR-1 – P-wave tomographic seismic refraction model developed utilizing a smooth velocity gradient starting model

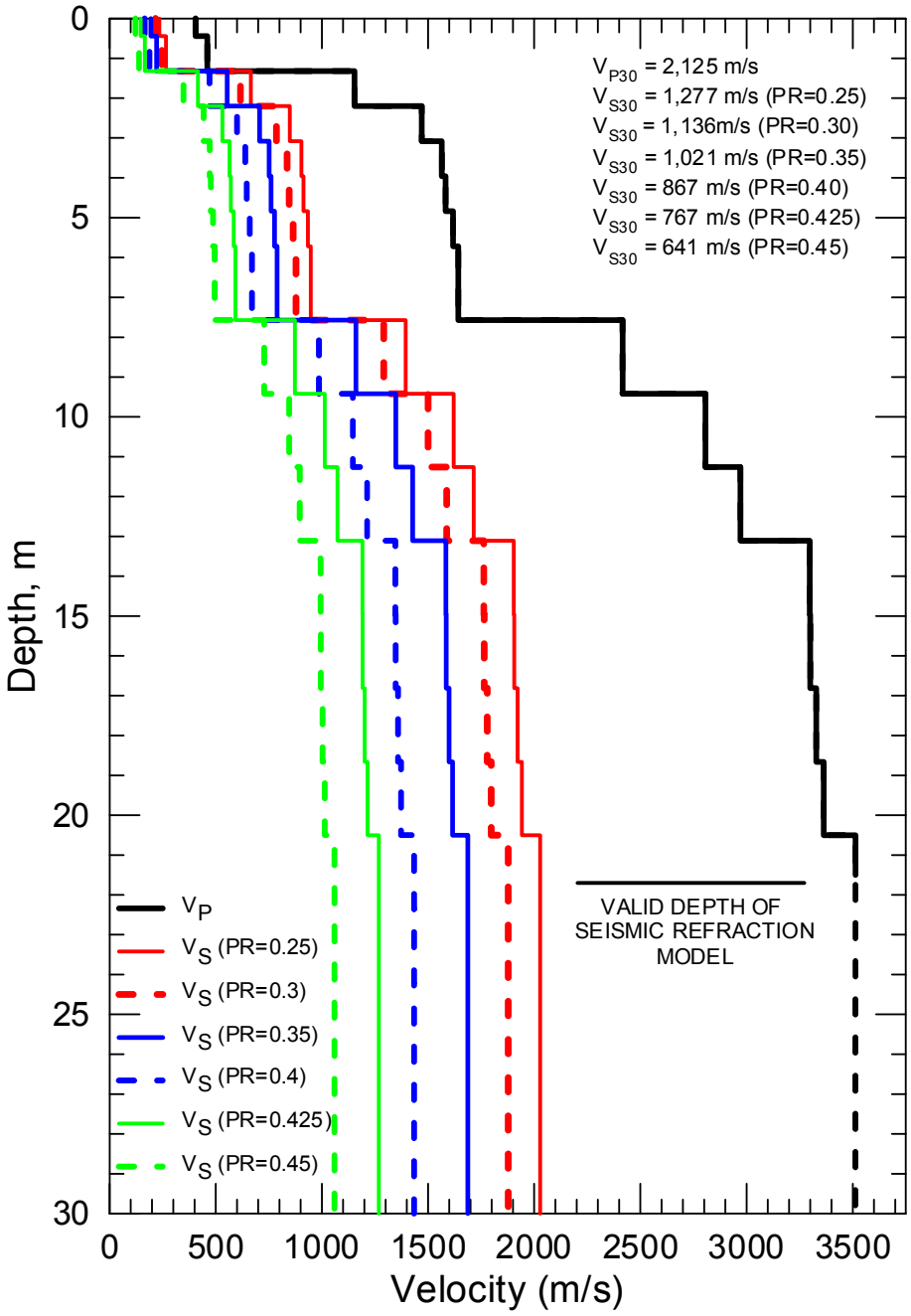

CI.SMR – Average P-wave velocity structure and estimated S-wave velocity structure between a position of 27 and 49.5 m on the P-wave seismic refraction model for array SMR-1 that utilized a layered starting model. Although the maximum seismic refraction depth of investigation is limited to about 21 m, P-wave velocity is very high at depth and is not expected to increase significantly between the valid depth of investigation and 30 m. A longer seismic line would be preferred to both more accurately model the high P-wave velocities and to image to 30 m depth. The possibility of the sandstone being saturated at some depth beneath the site severely limits the use of P-wave velocity to estimate S-wave velocity assuming a constant Poisson's ratio.

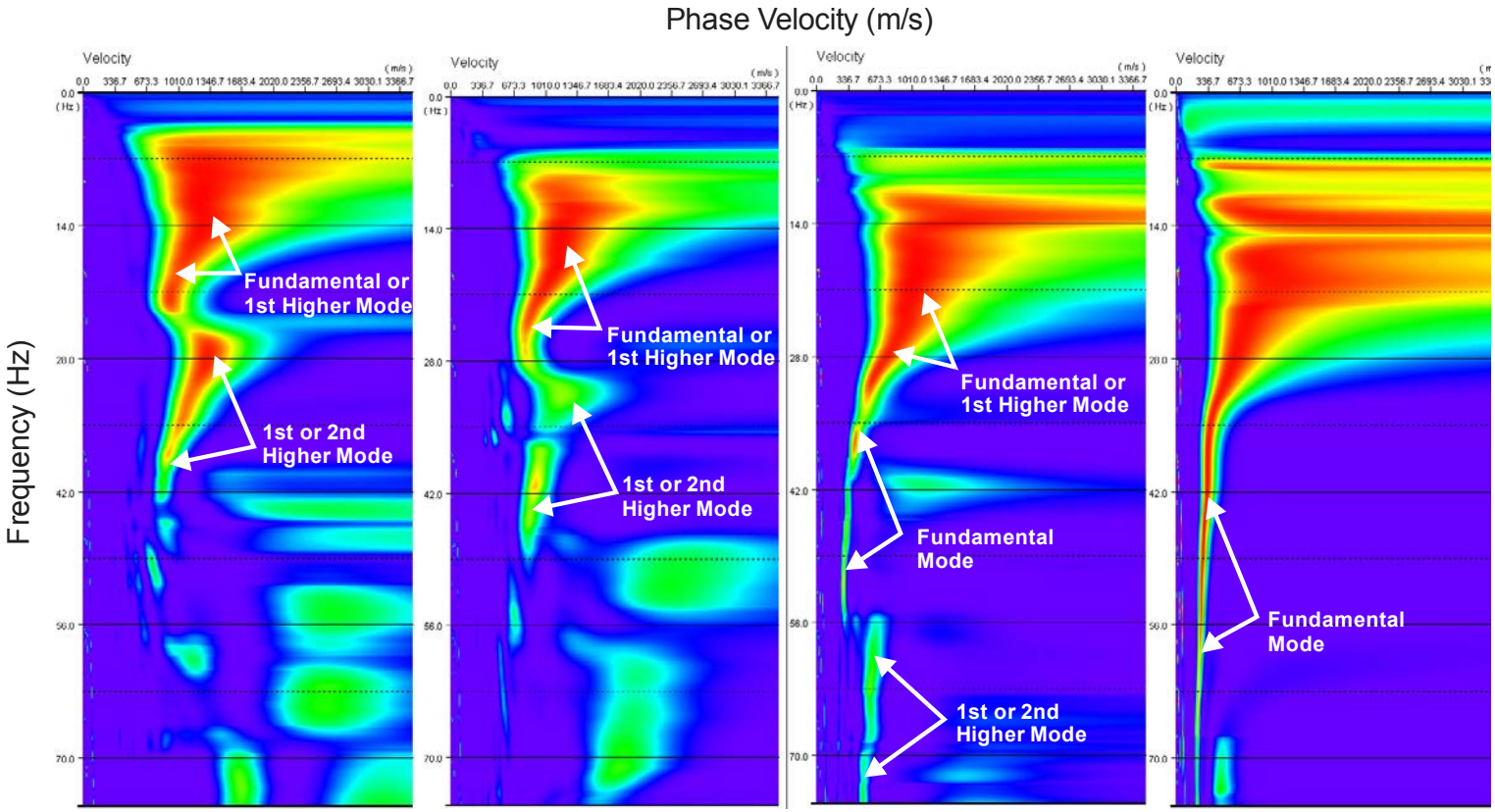

Array SMR-1 – Comparison of Rayleigh wave dispersion curves for various source types, source offsets and receiver arrays. This site consists of a thin low velocity layer over much higher velocity rock and it is, therefore, not clear if the fundamental mode is dominant at low frequencies, which is typically the case. This figure clearly illustrates the effect of source-receiver geometry on the relative amplitude of higher modes demonstrating the need for analytical routines that include source-receiver geometry. Generally, only source independent (i.e. plane wave) analytical routines have been applied during this investigation. One exception is the 3-D global or array based inversion routines available in the WinSASW software package. Similar analytical methods are needed for MASW analysis. Review of the P-wave seismic refraction models supports either a dominant fundamental mode or modal superposition at low frequencies.

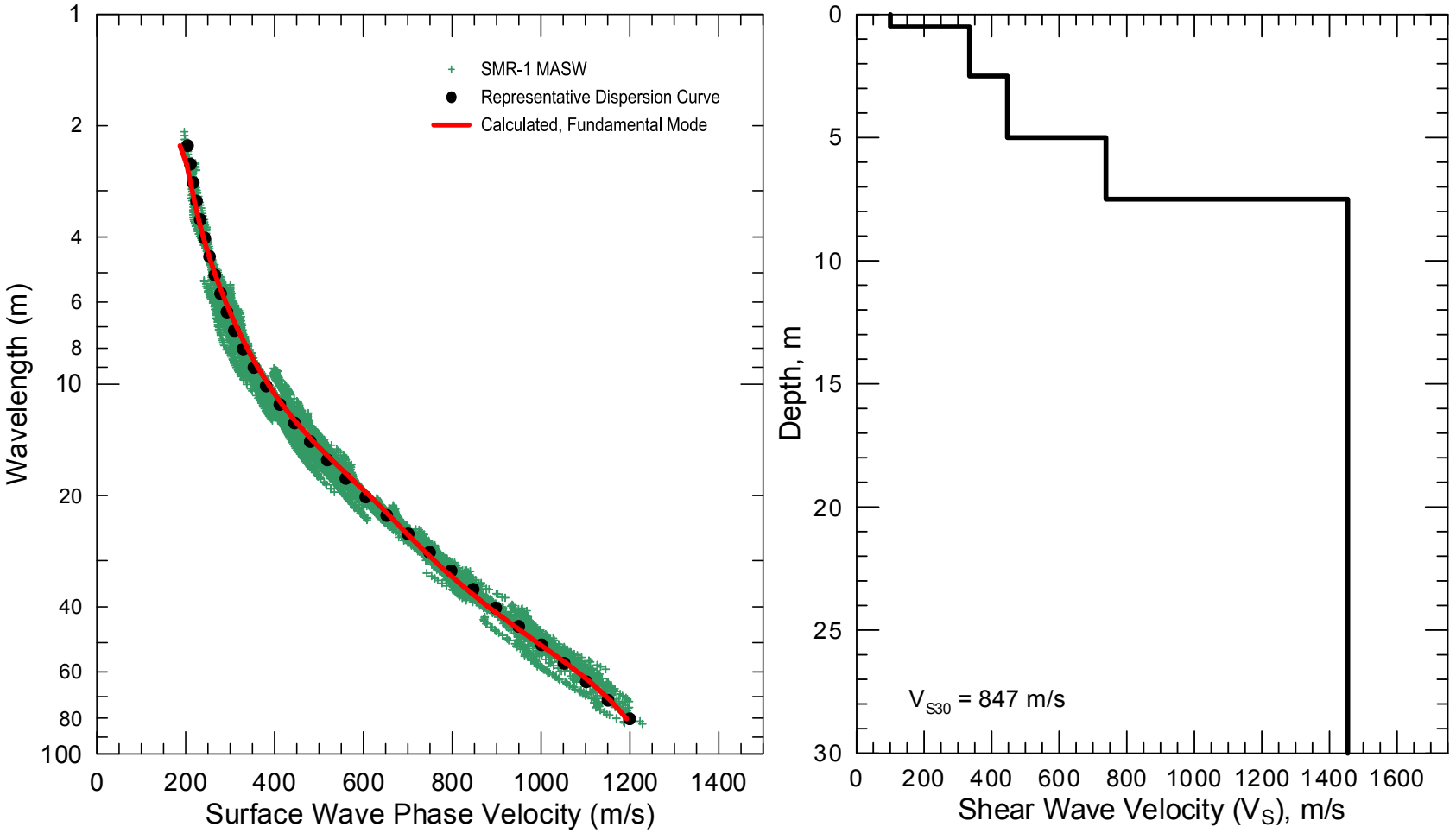

CI.SMR - Field, representative and inverted theoretical surface wave dispersion data (left) and associated V_S model (right) for fundamental mode assumption

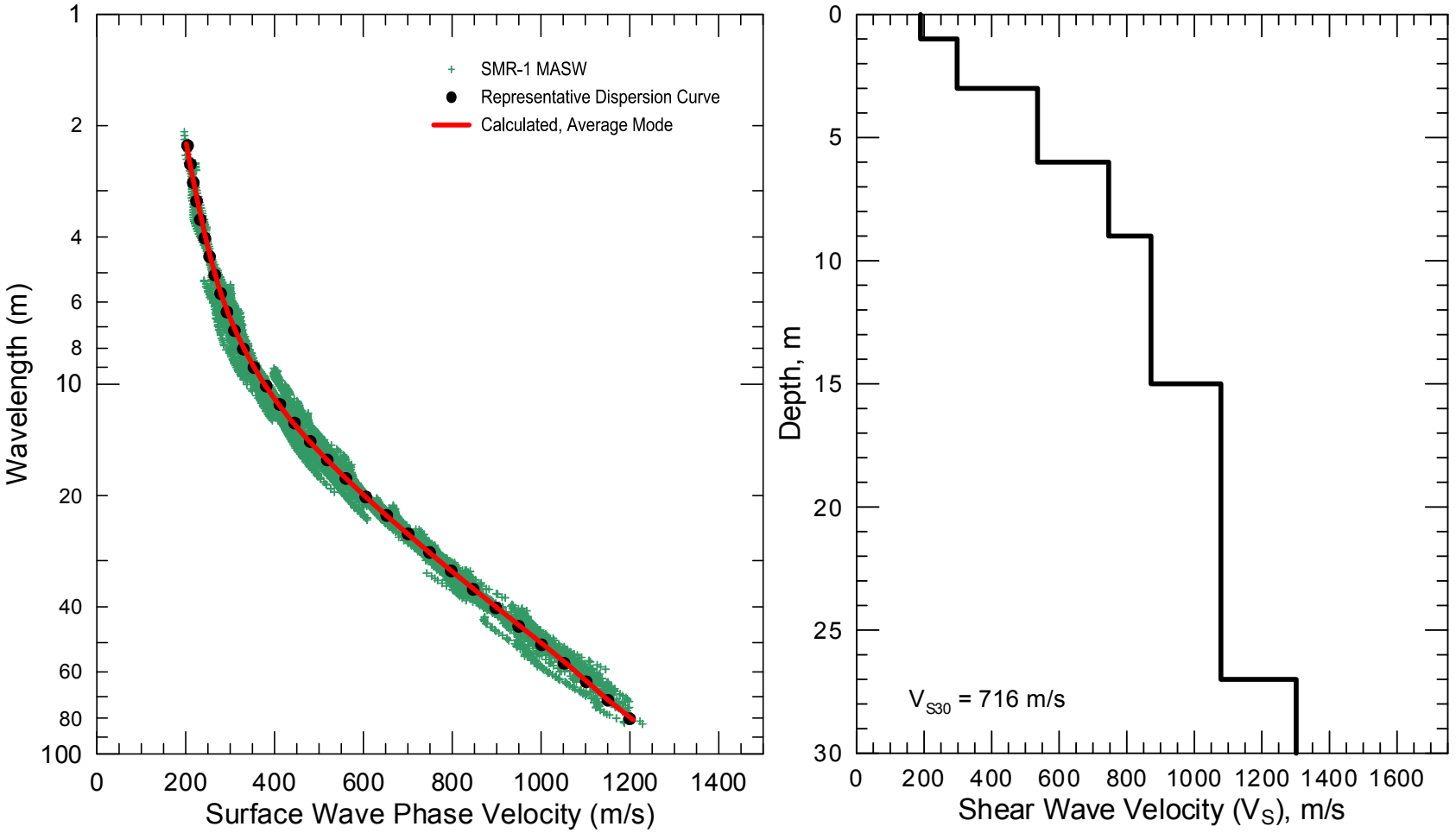

CI.SMR - Field, representative and inverted theoretical surface wave dispersion data (left) and associated V_S model (right) for average mode assumption

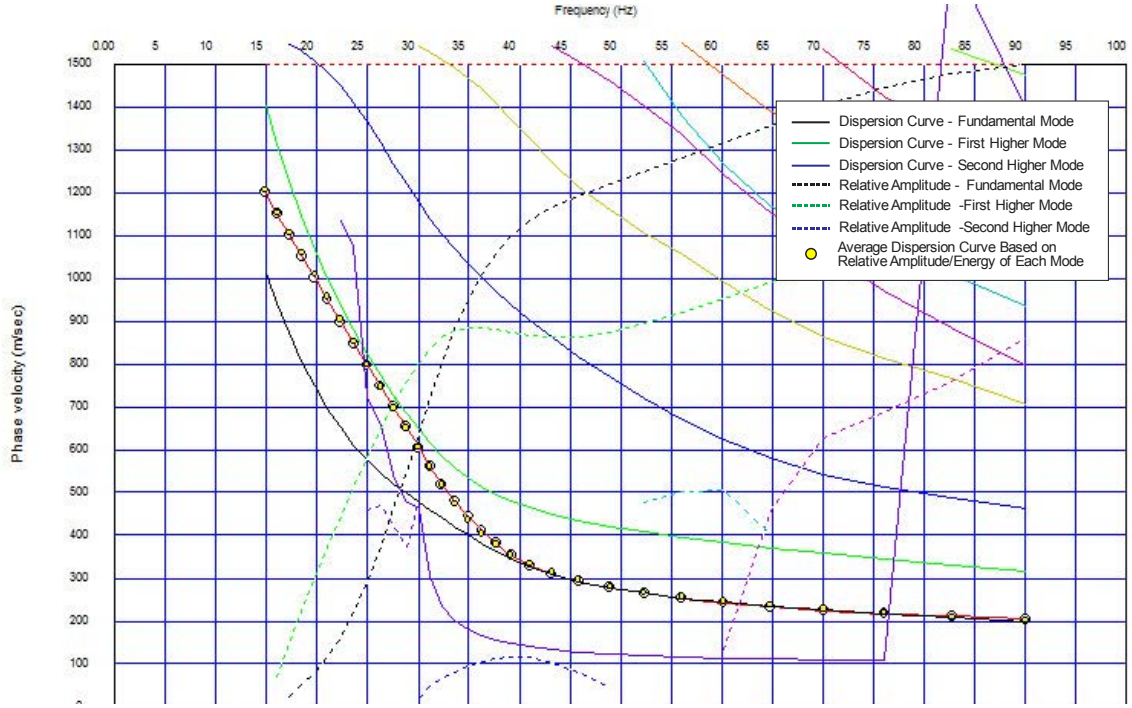

Calculated Rayleigh wave phase velocity modes for the V_S model developed using the average mode assumption in an attempt to account for possible modal superposition (mode mixing) at low frequencies. The average mode for most closely tracks the first higher mode at frequencies below 30 Hz. The modeled V_S will be underestimated at depth if the representative dispersion curve actually reflects the fundamental mode and slightly overestimated at depth if the representative dispersion curve actually reflects the first higher mode. If correct, this model indicates that the higher mode energy observed in the v-f transform of MASW seismic records is associated with the second higher mode. However, the second higher mode does not seem to have high amplitude relative to the fundamental and first higher modes.

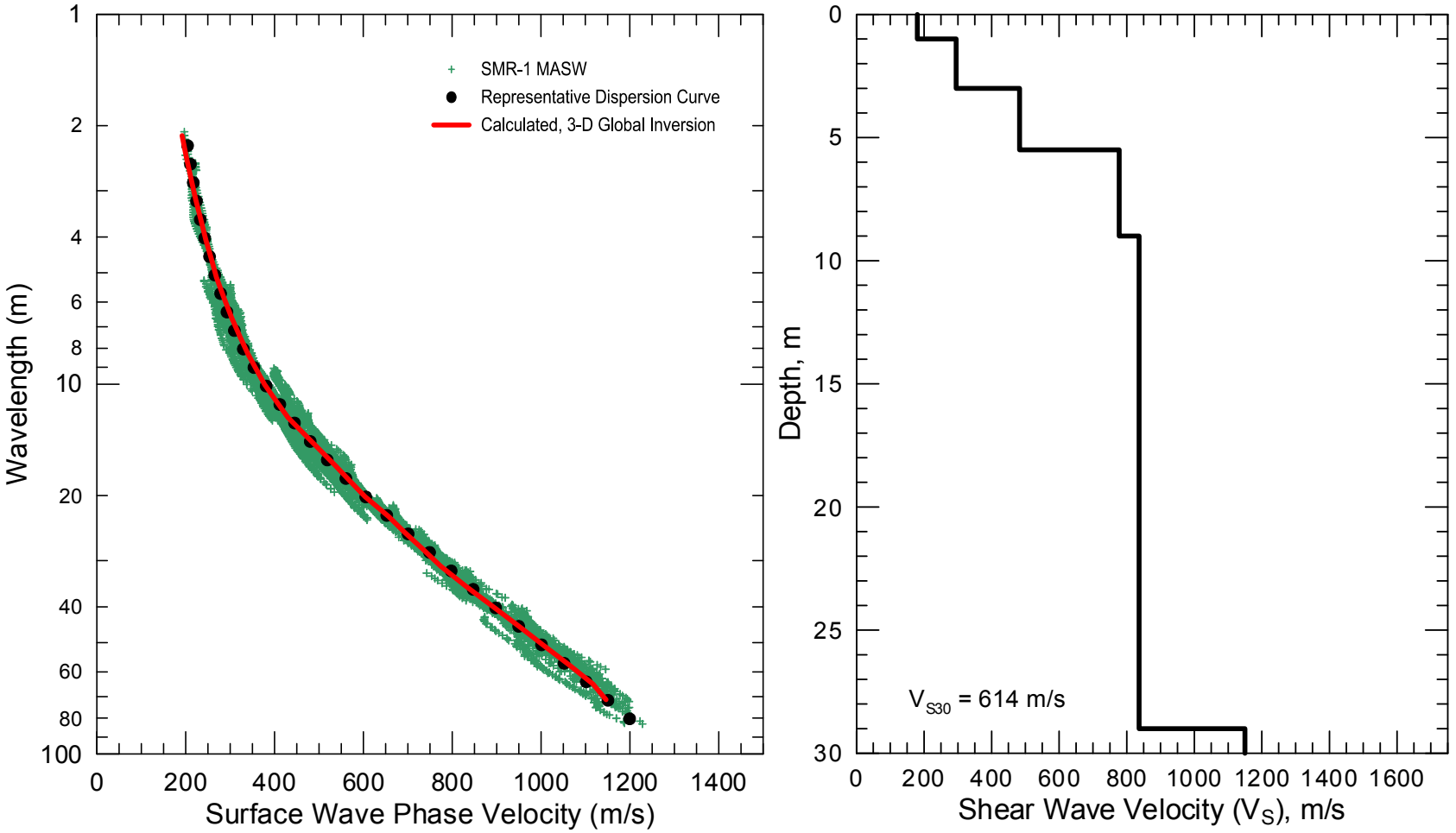

CI.SMR - Field, representative and inverted theoretical surface wave dispersion data (left) and associated V_S model (right) utilizing 3-D global inversion routine in WinSASW software package (it is unlikely that this model is valid)

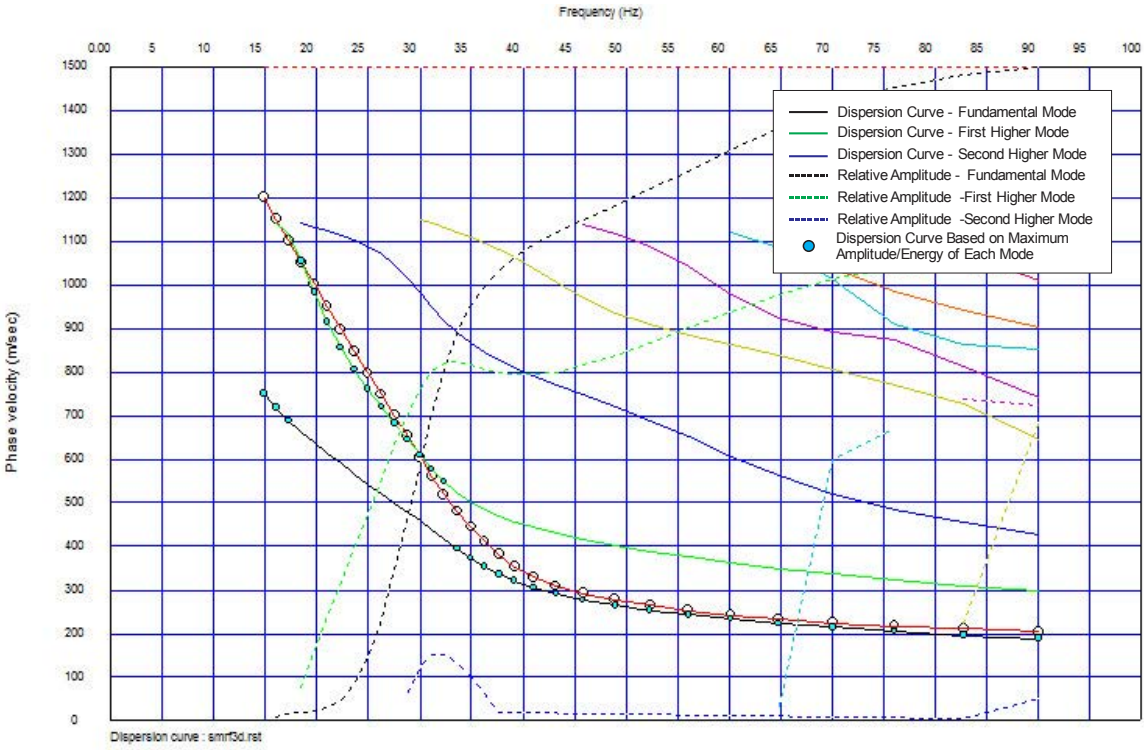

Calculated Rayleigh wave phase velocity modes for the V_S model developed using the 3-D global inversion in the WinSASW software package (Model 2), which is generally not considered applicable to MASW surface wave dispersion data. Generally, the 3-D global inversion appears to be fitting the fundamental mode at high frequencies and the first higher mode at lower frequencies. This would mean that the higher mode energy observed in the v-f transform of MASW seismic records is associated with the second higher mode. However, the second higher mode does not seem to have high amplitude relative to the fundamental and first higher modes.

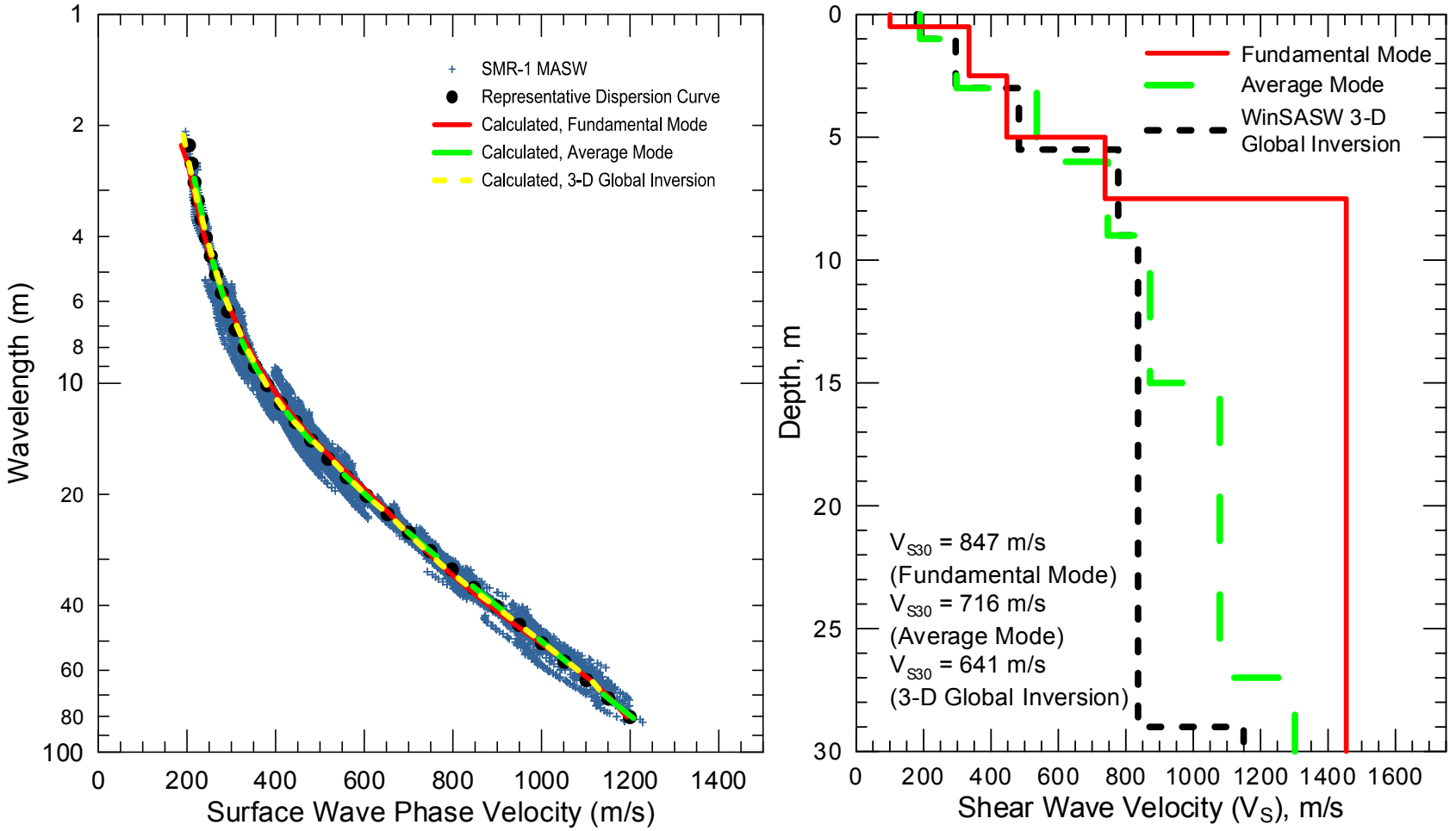

CI.SMR - Field, representative and inverted theoretical surface wave dispersion data (left) and associated V_S models (right) for fundamental and average mode assumption and 3-D global inversion

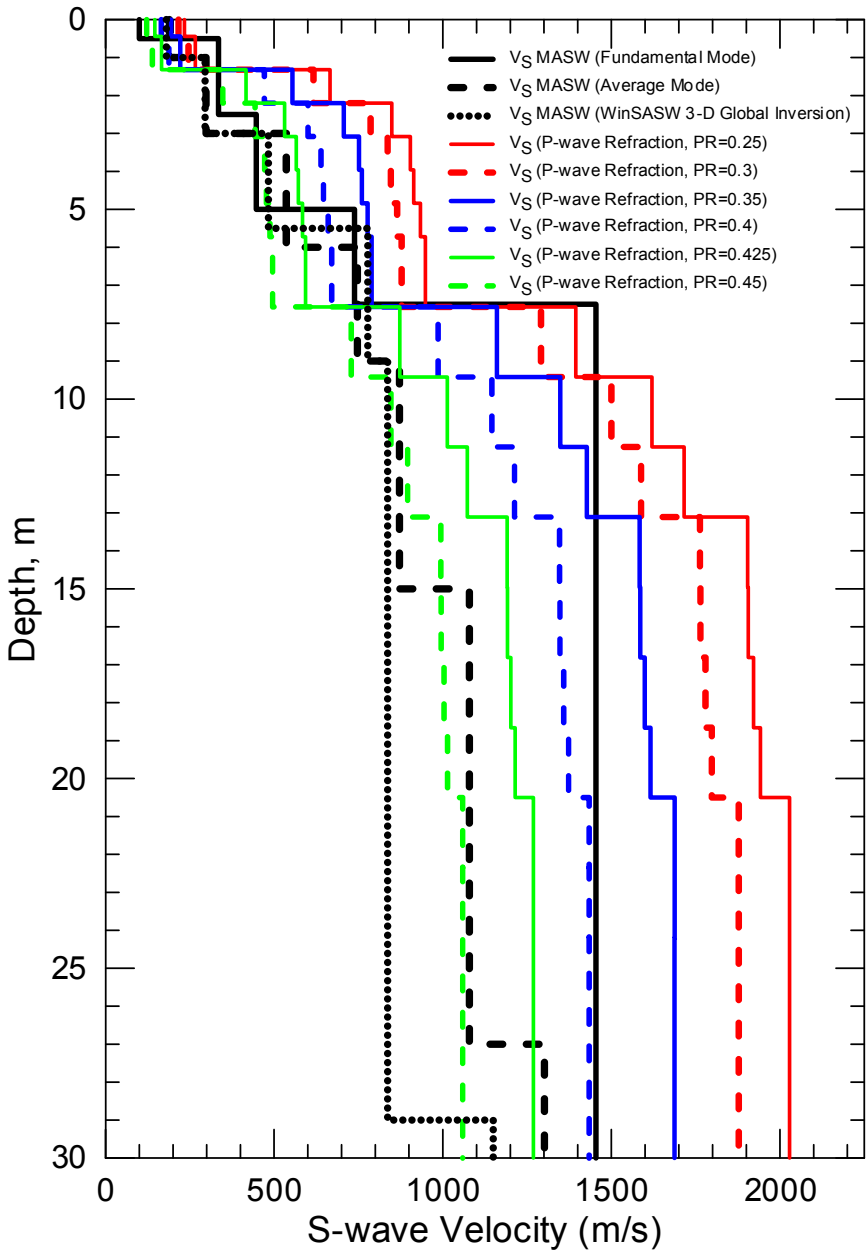

CI.SMR – Comparison of S-wave velocity models derived from the MASW and P-wave seismic refraction surveys. S-wave velocities inferred from the P-wave seismic refraction model are generally higher than those from the surface wave sounding over the 1.5 to 5.5 m depth range. S-wave models generated from the Rayleigh wave phase velocity dispersion data using the fundamental mode and average mode assumptions and the 3-D global inversion in the WinSASW software package are generally consistent in the upper 7 to 9 m and significantly different below. The WinSASW 3-D global inversion is definitely not valid based on inferred S-wave velocities from the P-wave refraction model. This is not unexpected, as this analytical routine is not designed for MASW data. Both the fundamental mode and average mode models are feasible depending on the Poisson's ratio of the saturated sandstone unit. An S-wave seismic refraction and/or MALW (Love wave) survey may yield better results at this site.

Site CI.SMV

Location: AT&T, East Los Angeles Avenue and Sycamore Drive, Simi Valley, California

Latitude: 34.27091 **Longitude:** -118.74407

(Station coordinates provided by USGS, WGS84 coordinate system)

V_{S30} (measured): 260 m/s

V_{S30} (adjusted to more accurately reflect seismic station conditions): 278 m/s (average S-wave velocity between 3 and 33 m adjusting for sensor possibly being located in basement).

NEHRP Site Class: D

Geomatrix Code: AHD

Geologic Conditions/Observations: Site located in area mapped as Quaternary (Holocene) alluvium.

Site Conditions: Urban site with significant traffic noise from nearby roads. Relatively flat terrain in site vicinity. Gradual decrease in surface elevation to southwest.

Geophysical Methods Utilized: HVSR, MASW, array microtremor, ReMi™

Geophysical Testing Arrays:

1. Arrays SMV-1 (24 channel linear array utilizing 4.5 Hz vertical geophones spaced 4 m apart for an array length of 92 m) and SMV-2 (24 channel linear array utilizing 4.5 Hz vertical geophones spaced 3 m apart for an array length of 69 m) used to acquire passive surface wave data. Arrays combined to form an "L" shaped array.
2. Array SMV-3 (48 channel MASW array utilizing 4.5 Hz vertical geophones spaced 1 m apart for a length of 47 m, forward and reverse shot locations with multiple source offsets and source types (hammers only) and center shot location).
3. Three HVSR measurement locations; two distributed along array SMV-3 and one at the corner of arrays SMV-1 and SMV-2.

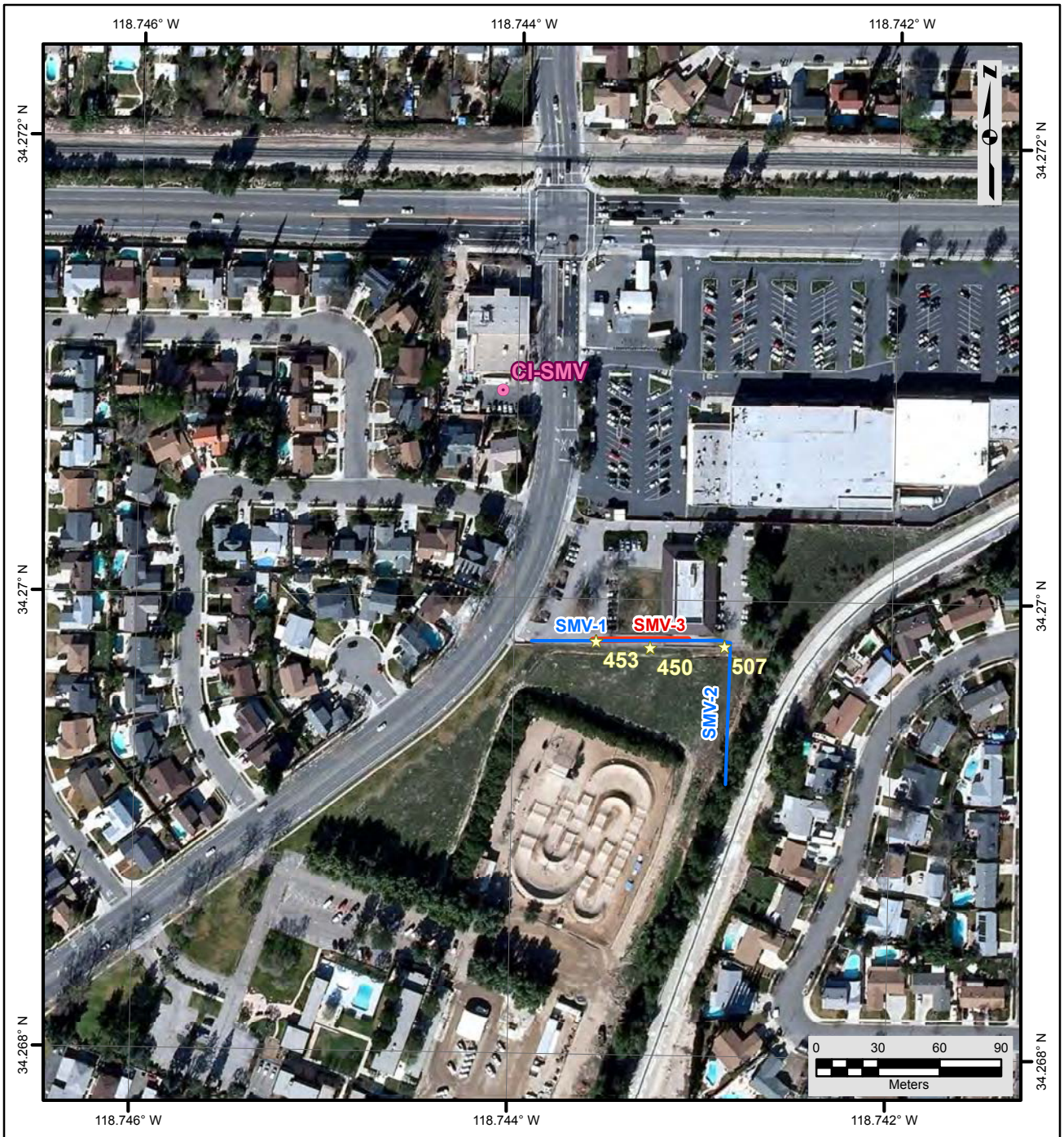

Legend

- Seismic Station - Approximate Location of Record
- H/V Spectral Ratio Location
- Passive Surface Wave Array
- MASW Array

NOTES:
1. WGS 1984 COORDINATE SYSTEM
2. Image Source: ESRI, i-cubed, USDA FSA, USGS, AEX, GeoEye, Getmapping, Aerogrid, IGP

File Name: CI-SMV-I

Date: 9/22/2011

USGS science for a changing world

GEOVision geophysical services

RECOVERY.GOV

SITE MAP
CI•SMV

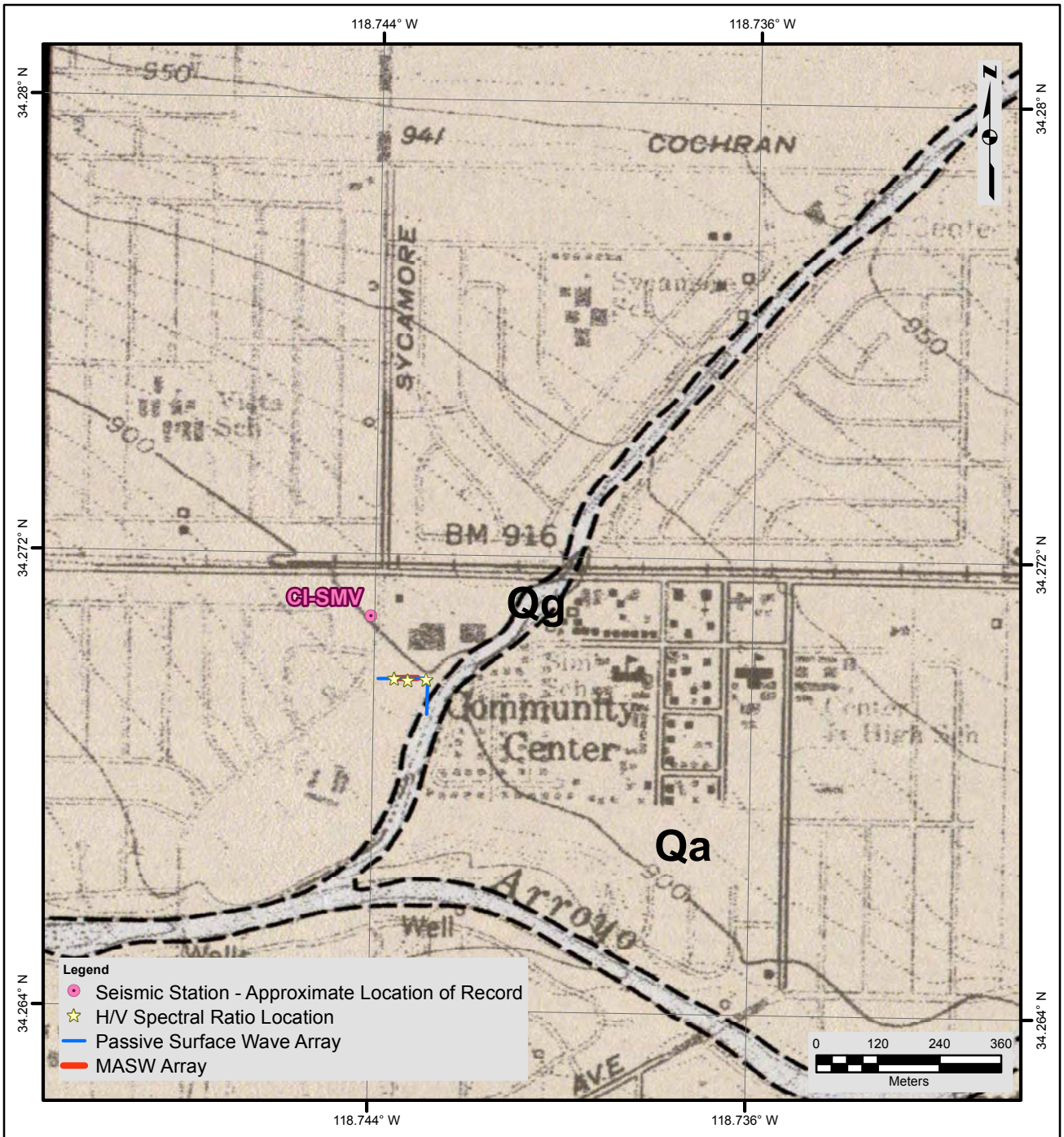

Description of Geologic Map Units

Qg = Quaternary (Holocene) gravel and sand of major stream channels
Qa = Quaternary (Holocene) alluvial gravel, sand and clay of valley and floodplain areas

NOTES:
1. WGS 1984 COORDINATE SYSTEM
2. Geologic Map of the Santa Susana Quadrangle, Ventura and Los Angeles Counties, California by Thomas W. Dibblee, Jr., 1992
3. See site map for details of geophysical survey

File Name: CI-SMV

Date: 9/22/2011

USGS science for a changing world

GEOVision geophysical services

GEOLOGIC MAP
CI•SMV

RECOVERY.GOV

HVSR sensor 450 in shallow hole

Station GPS receiver outside building housing CI.SMV seismic station

Northeast corner of passive surface wave arrays SMV-1 and SMV-2

Looking northwest from HVSR sensors 453 (Nanometrics Trillium) and Tromino ENGR towards building housing seismic station

Looking west along array SMV-1 and the location of array SMV-3

Location of Geophysical Testing Arrays:

Location	Latitude	Longitude
SMV-1, West End of Array	34.26981	-118.74390
SMV-1, East End of Array	34.26983	-118.74290
SMV-2, North End of Array	34.26982	-118.74285
SMV-2, South End of Array	34.26920	-118.74286
SMV-3, West End of Array	34.26982	-118.74357
SMV-3, Center of Array	34.26983	-118.74332
SMV-3, East End of Array	34.26983	-118.74307
HVSR Sensor 450	34.26979	-118.74327
HVSR Sensor 453	34.26982	-118.74356
HVSR Sensor 507	34.26980	-118.74288

Notes: 1) WGS84 Coordinate System (decimal degrees)
2) Survey accuracy is estimated at 1 to 2 m

Results:

V_S Model

Depth to Top of Layer (m)	Layer Thickness (m)	S-Wave Velocity (m/s)	Inferred P-Wave Velocity (m/s)	Assumed Poisson's Ratio	Assumed Density (g/cm^3)
0	1	144	270	0.3	1.8
1	2	203	381	0.3	1.8
3	3	208	389	0.3	1.8
6	4	229	429	0.3	1.8
10	6	266	498	0.3	1.9
16	9	309	578	0.3	1.9
25	12	329	615	0.3	2.0
37	15	483	903	0.3	2.1
52	20	596	1115	0.3	2.1
72	>8	725	1356	0.3	2.1

Notes: 1) Depth of investigation is about 80 m.
2) Bottom layer is a half space.

Observations/Discussion:

- Surface wave testing conducted 150 m from seismic station because there was not sufficient space closer to the station.
- The HVSR curves are almost identical, validating the 1-D velocity structure assumption. There are, however, no significant high frequency HVSR peaks by which to characterize shallow velocity structure.
- Possible very low amplitude and broad HVSR peak(s) between about 1 and 2 Hz. There is no low frequency HVSR peak associated with basement complex.
- Noise conditions at site (multi-directional or omni-directional noise sources) appeared sufficient for successful application of passive surface wave techniques.
- ESAC technique used to extract surface wave dispersion data from passive "L" array data. Both the ReMi™ and ESAC techniques used to extract surface wave dispersion data from the linear arrays. Only the higher quality "L" array dispersion data used for analysis.
- Excellent MASW data quality with no significant complications due to lateral velocity variation.
- The largest source used for MASW data acquisition consisted of a 20 lb sledge hammer and, therefore, surface wave dispersion data at frequencies lower than 7 Hz were not extracted from the MASW data.
- Surface wave dispersion data from active and passive surface wave data sets are in excellent agreement over the 6.5 to 33 m overlapping wavelength range.
- Representative dispersion curves were generated for each surface wave data set using a moving average, polynomial curve fitting routine. These individual representative dispersion curves were combined and a representative dispersion curve generated for the combined data set for data modeling.
- Review of seismic refraction first arrival data indicates that near surface P-wave velocity is in the 300 to 400 m/s range. Significant noise, due to traffic, in the seismic refraction data; however, there is no evidence of saturated sediments in the upper 15 m.
- Surface wave depth of investigation is about 80 m based on half of maximum wavelength criteria and assuming that surface wave dispersion data at frequencies as low as 2.7 Hz are valid utilizing 4.5 Hz geophones (low frequency geophone phase response differences will cancel out if noise is omni-directional and/or the phase response differences are random in nature).
- V_{S30} is 260 m/s (Site Class D).
- Average S-wave velocity between 3 m (assumed sensor depth if located in basement and 33 m is 278 m/s.
- Average S-wave velocity of the upper 80 m (V_{S80}) is 377 m/s.

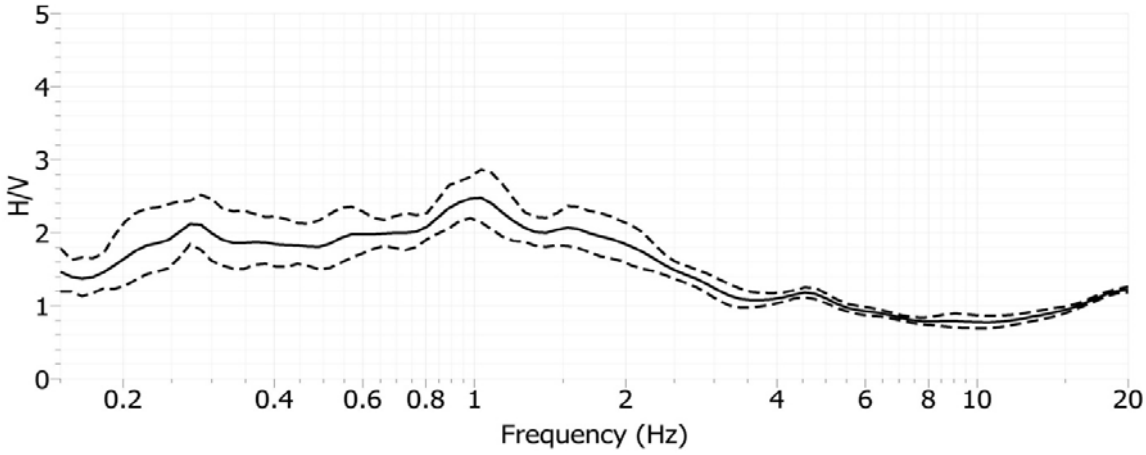

Site CI.SMV, H/V Spectral Ratio, Array SMV-1, Sensor 453

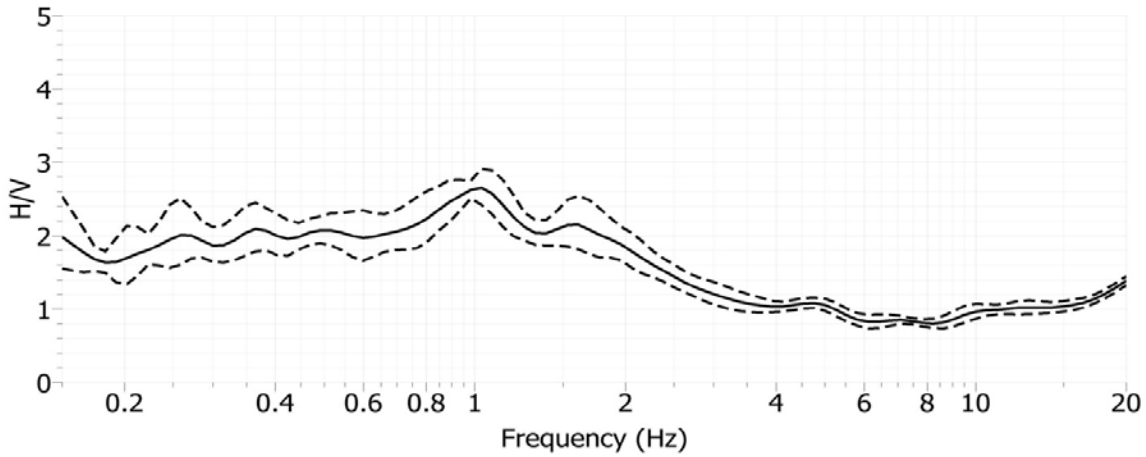

Site C.SMV, H/V Spectral Ratio, Array SMV-1, Sensor 450

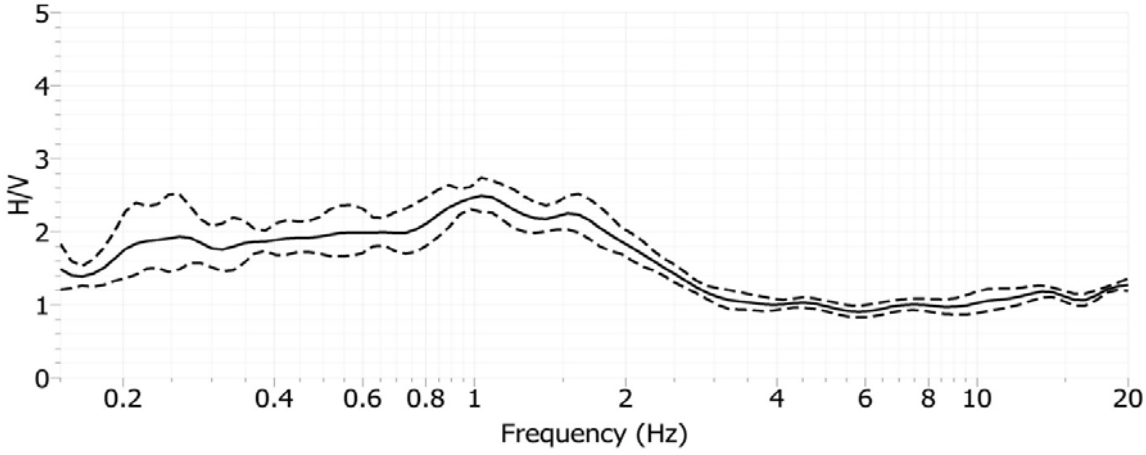

Site CI.SMV, H/V Spectral Ratio, Array SMV-1, Sensor 507

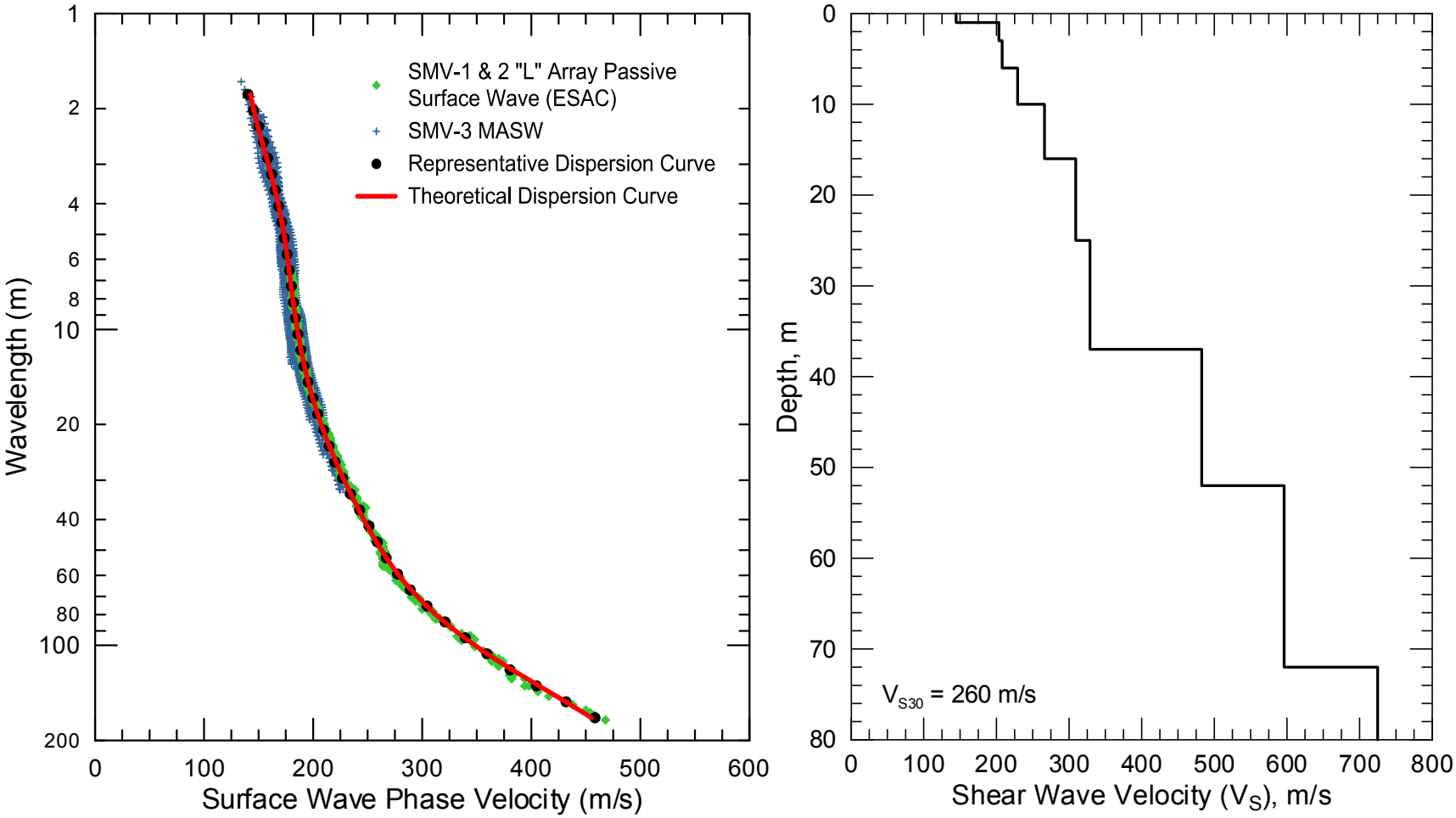

CI.SMV - Field, representative and inverted theoretical surface wave dispersion data (left) and associated V_S model (right)

Site CI.SMW

Location: Santa Maria Wineman, 415 Wineman Road, Hwy. 166, Nipomo, California

Latitude: 35.01108 **Longitude:** -120.40997

(Station coordinates provided by USGS, WGS84 coordinate system)

V_{S30} (measured): 676 m/s

V_{S30} (adjusted to more accurately reflect seismic station conditions): 742 m/s (average S-wave velocity between 1.5 and 31.5 m adjusting for assumed sensor depth and for fact that the seismic sensor is placed on weathered rock) or 734 m/s (average S-wave velocity of upper 30 m calculated after replacing S-wave velocity of 1.5 m thick sediment layer with that of underlying layer).

NEHRP Site Class: C

Geomatrix Code: IVA

Geologic Conditions/Observations: Seismic station located on the Tertiary (Miocene) Obispo Formation, which consists of volcanic rocks, primarily basalt. The geologic contact between the Obispo Formation and Tertiary (Miocene) Monterey Formation is mapped about 30 m northeast of the seismic station. Field inspection revealed no evidence of Monterey Formation near the site and that the Obispo Formation consists of a welded tuff in the site vicinity.

Site Conditions: Rural site. Rolling topography in site vicinity. Seismic station located on top of a small hill. Rock is very fractured in test area and covered by thin layer of soil.

Geophysical Methods Utilized: HVSR, Seismic Refraction, MASW

Geophysical Testing Arrays:

1. Array SMW-1 (48 channel MASW and P-wave seismic refraction array utilizing 4.5 Hz vertical geophones spaced 1.5 m apart for a length of 70.5 m, forward and reverse shot locations with multiple source offsets and source types and multiple interior shot locations).
2. Three HVSR measurement locations: two distributed along array SMW-1 and the other adjacent to the seismic station.

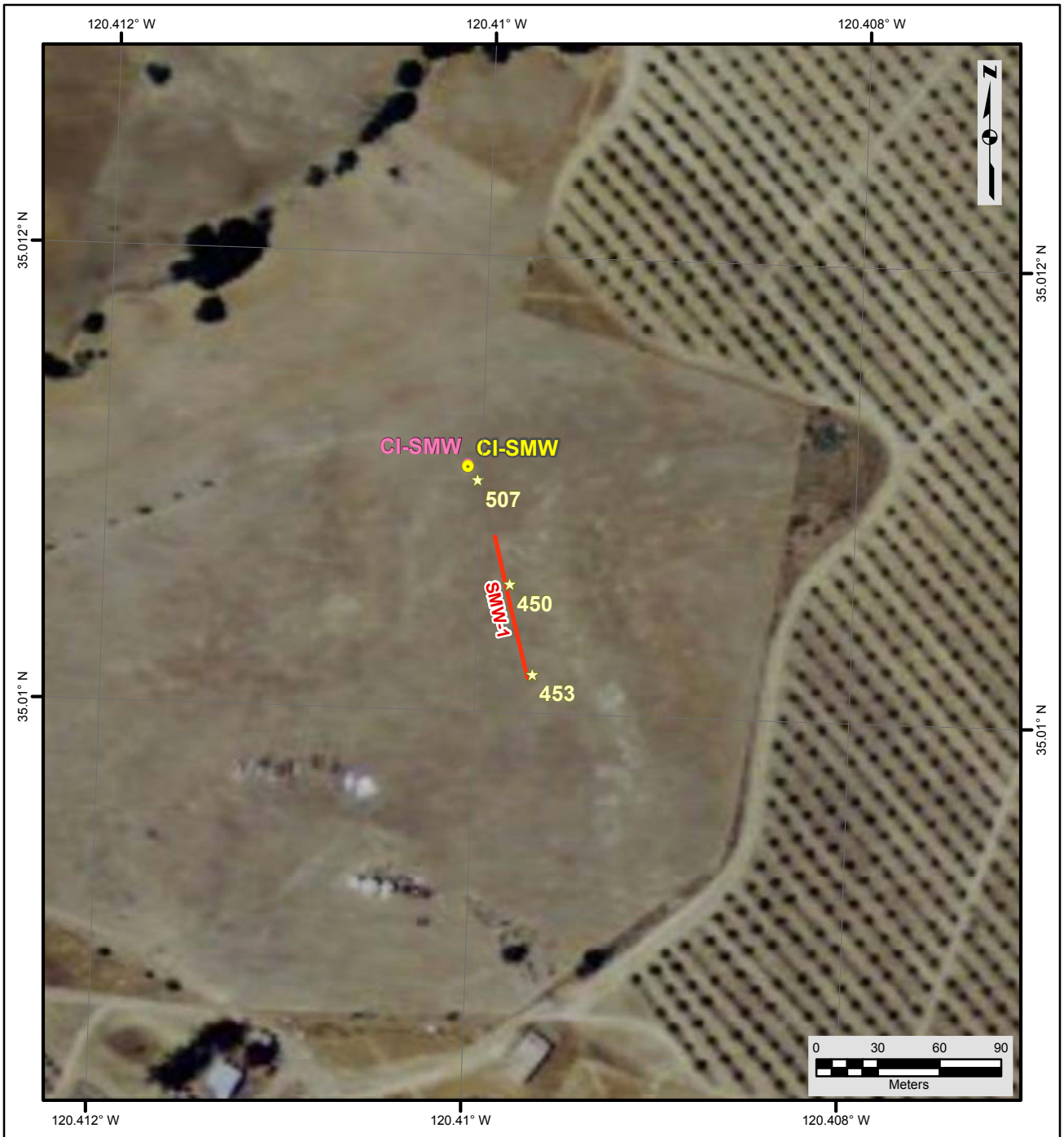

Legend

- Seismic Station - Approximate Surveyed Location
- Seismic Station - Approximate Location of Record
- H/V Spectral Ratio Location
- MASW and Seismic Refraction Array

NOTES:
1. WGS 1984 COORDINATE SYSTEM
2. Image Source: ESRI, i-cubed, USDA FSA, USGS, AEX, GeoEye, Getmapping, Aerogrid, IGP

File Name: CI-SMW-I

Date: 9/16/2011

USGS science for a changing world

GEOVision geophysical services

RECOVERY.GOV

SITE MAP
CI•SMW

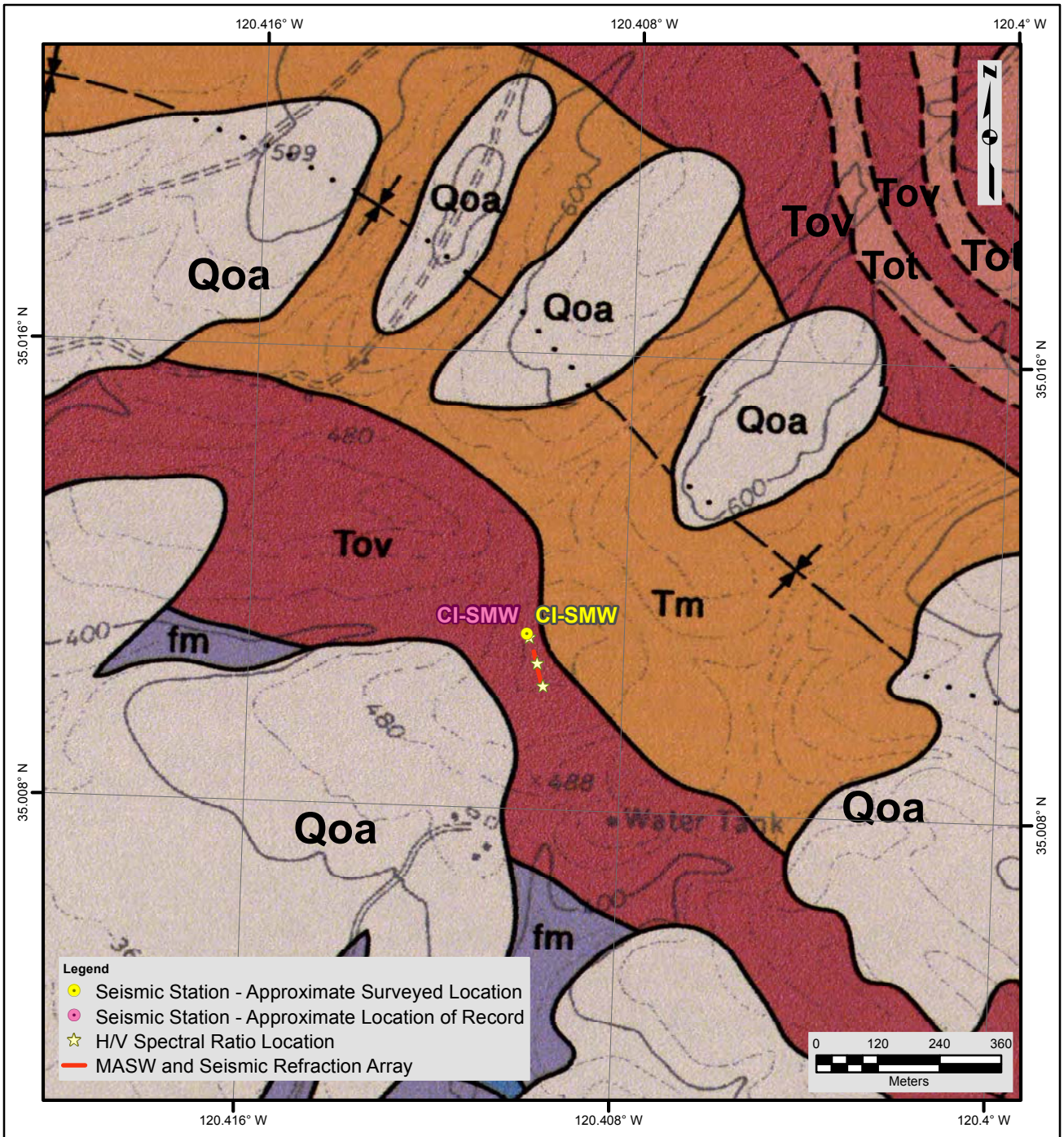

Description of Geologic Map Units

Qoa = Quaternary (Pleistocene) alluvial deposits of mostly volcanic detritus
Tm = Tertiary (Miocene) Monterey Formation; siliceous shale, thin-bedded
Tov = Tertiary (Miocene) Obispo Formation; volcanic rocks, mostly basalt, fine-grained, massive to vaguely bedded
Tot = Tertiary (Miocene) Obispo Formation; tuff breccia, medium to coarse grained, massive to vaguely bedded
fm = Mesozoic (Jurassic to Cretaceous) melange of fragments of graywacke, greenstone, and chert in sheared dark gougy claystone matrix

NOTES:
1. WGS 1984 COORDINATE SYSTEM
2. Geologic Map of the Nipomo Quadrangle, San Luis Obispo County, California by Thomas W. Dibblee, Jr., 2006
3. See site map for details of geophysical survey

USGS science for a changing world
GEOVision geophysical services

GEOLOGIC MAP
CI•SMW

RECOVERY.GOV

File Name: CI-SMW
Date: 9/16/2011

CI.SMW seismic station

Data acquisition with sledge hammer energy source on array SMW-1

Looking northwest towards HVSR sensor 507 and seismic station

Data acquisition with accelerated weight drop energy source on array SMW-1

Looking north along array SMW-1

Location of Geophysical Testing Arrays:

Location	Latitude	Longitude
SMW-1, South end of Array	35.01016	-120.40962
SMW-1, Center of Array	35.01046	-120.40972
SMW-1, North end of Array	35.01077	-120.40981
HVSR Sensor 450	35.01056	-120.40972
HVSR Sensor 453	35.01017	-120.40959
HVSR Sensor 507	35.01101	-120.40991
CI-SMW Seismic Station	35.01107	-120.40997

Notes: 1) WGS84 Coordinate System (decimal degrees)
2) Survey accuracy is estimated at 1 to 2 m.

Results:

V_S Model

Depth to Top of Layer (m)	Layer Thickness (m)	S-Wave Velocity (m/s)	Inferred P-Wave Velocity (m/s)	Assumed Poisson's Ratio	Assumed Density (g/cm^3)
0	1.5	247	462	0.3	1.80
1.5	2.5	588	1099	0.3	2.00
4	27.5	764	1429	0.3	2.10
31.5	>3.5	935	1749	0.3	2.15

Notes: 1) Depth of investigation is about 35 m.
2) Bottom layer is a half space.

Observations/Discussion:

- The HVSR curves are very similar validating the 1-D velocity structure assumption.
- There is a broad zone of elevated HVSR response between 1.5 and 6 Hz on all of the measurement locations. Additionally, there is a slightly variable, high frequency HVSR peak or multiple peaks in the 9 to 14 Hz range.
- P-wave seismic refraction data were acquired at this site, but data quality appeared poor because first arrival data may have consisted of out of plane refractors in some areas. P-wave refraction models are, therefore, not presented. The P-wave refraction data were, however, reviewed and the maximum P-wave velocity in the upper 15 m was determined to be about 1,500 m/s, or more.
- Noise conditions at the site were not sufficient for application of passive surface wave techniques.
- There is nominally about 70 m/s scatter in MASW dispersion data, which is likely due to lateral velocity variation associated with both a very thin sediment layer of variable thickness (0 to 2 m) and differential weathering of near surface rock.
- Selected use of MASW dispersion data was made so that the small wavelength/high frequency portion of the dispersion curve was representative of portions of the array with the thickest sequence of low velocity sediments near the surface. Over 75% of the reduced dispersion curve segments were used to construct the representative dispersion curve.
- The maximum wavelength phase velocity data extracted from a receiver array was set to 1.1 to 1.2 times the distance from the source to center of the receiver array in order to minimize near field effects.
- The minimum wavelength surface wave phase velocity data extracted from the 48-channel MASW array is about 15 m. Data reduction using seismic records from smaller hammer sources and a limited offset receiver array (i.e. less active geophones) allowed extraction of surface wave dispersion data to a minimum wavelength of about 3.5 m.
- A representative dispersion curve was generated for the MASW data set using a moving average, polynomial curve fitting routine and used for modeling.
- The Rayleigh wave dispersion curve was modeled using the fundamental mode assumption.
- The surface wave V_S model was kept simple (i.e. minimal number of layers) because of probable lateral velocity variation. Utilization of finer layering would have resulted in a minor velocity inversion at depth.
- Surface wave depth of investigation is about 35 m based on half of maximum wavelength criteria.
- V_{S30} is 676 m/s (Site Class C).
- Average S-wave velocity between 1.5 m (nominal sensor depth) and 31.5 m is 745 m/s (Site Class C/B).
- V_{S30} calculated after replacing S-wave velocity of 1.5 m thick sediment layer with that of underlying layer is 734 m/s (Site Class C/B).

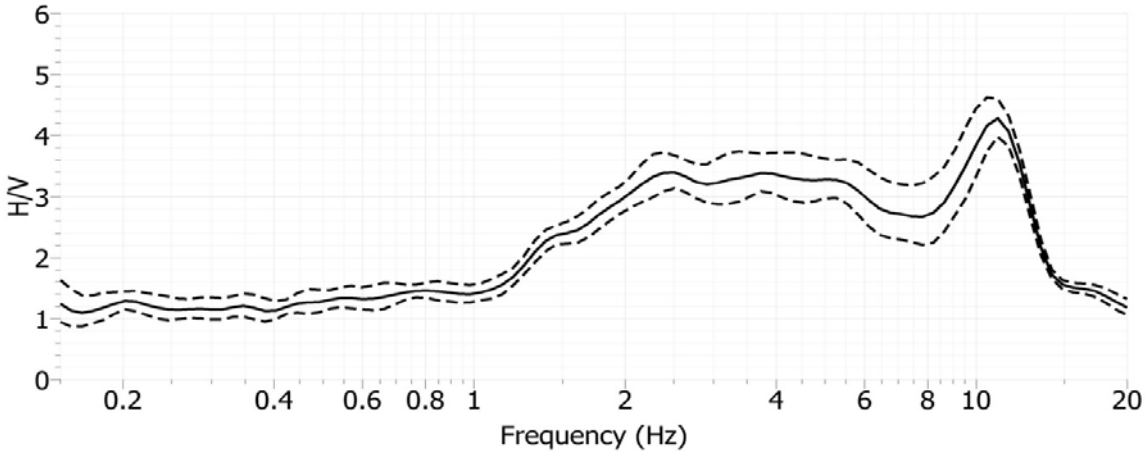

Site CI.SMW, H/V Spectral Ratio, Near Seismic Station, Sensor 507

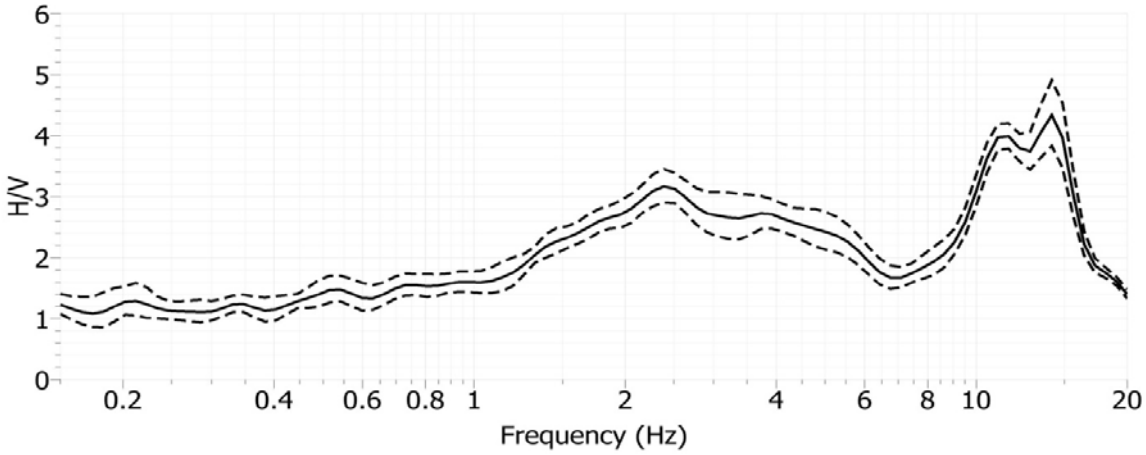

Site CI.SMW, H/V Spectral Ratio, Array SMW-1, Sensor 450

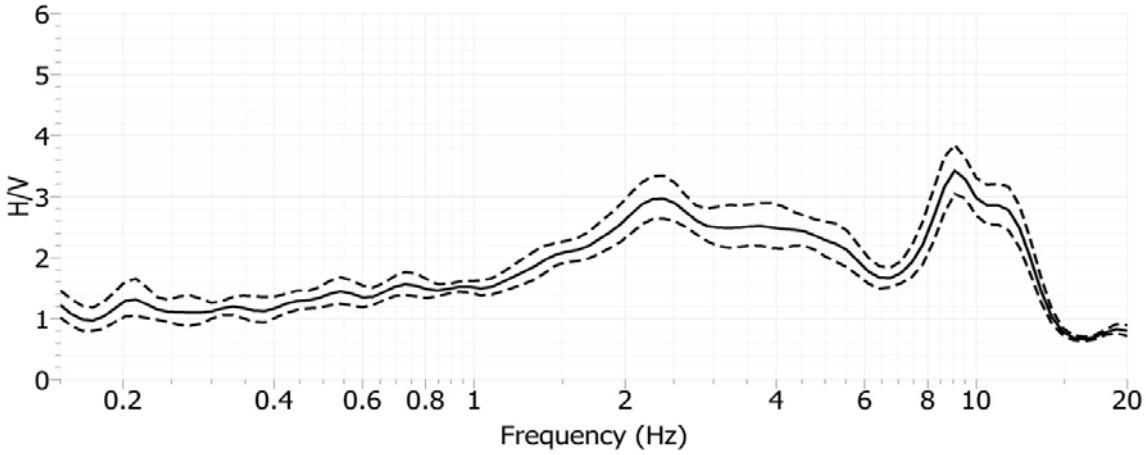

Site CI.SMW, H/V Spectral Ratio, Array SMW-1, Sensor 453

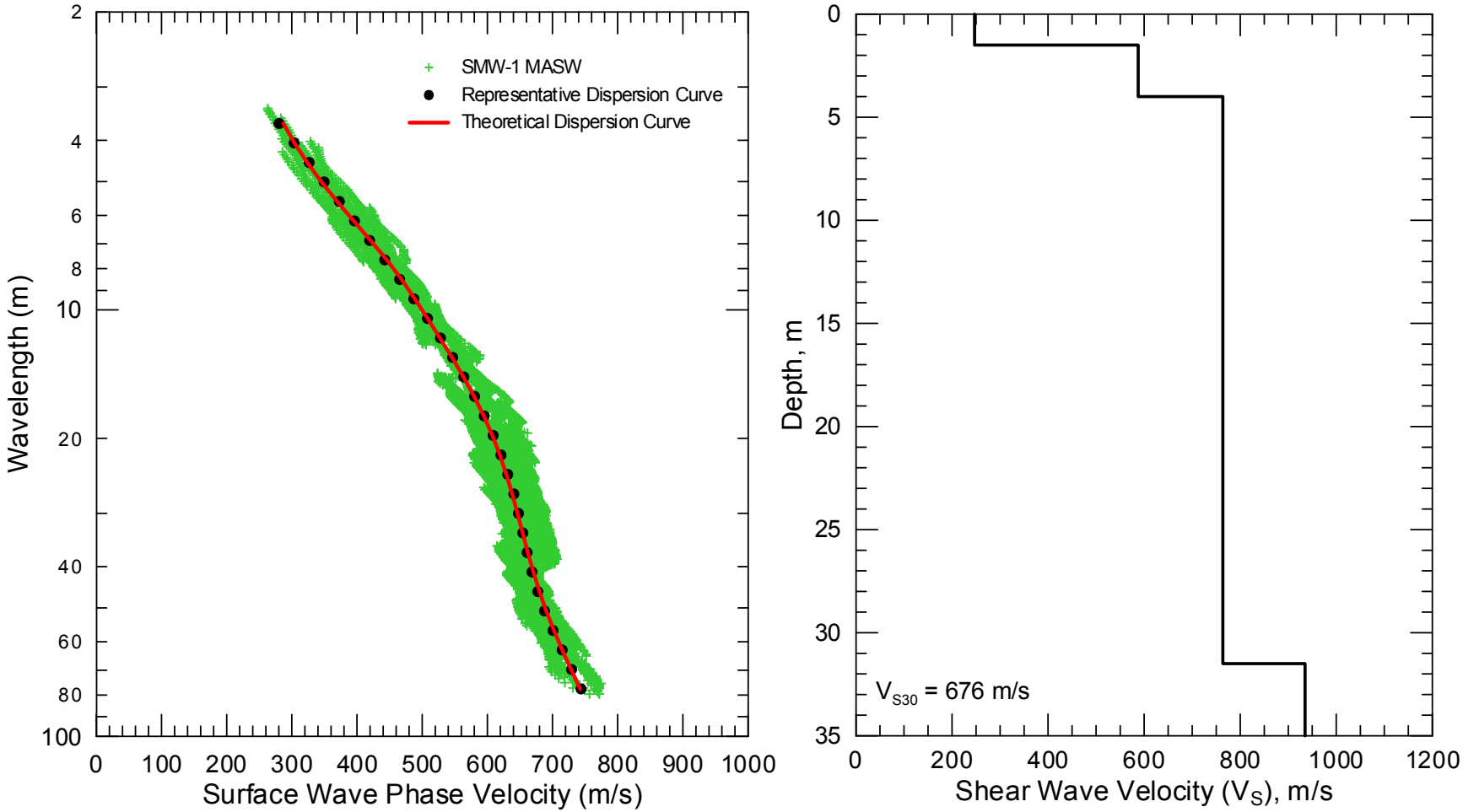

CI.SMW - Field, representative and inverted theoretical surface wave dispersion data (left) and associated V_S model (right)

Site CI.SNCC

Location: San Nicolas Island, Ventura County, California

Latitude: 33.24786 **Longitude:** -119.52437
(Station coordinates modified based on field GPS survey, WGS84 coordinate system)

V_{S30} (measured): 541 m/s

V_{S30} (adjusted to more accurately reflect seismic station conditions): 668 m/s (average S-wave velocity between 3 and 33 m adjusting for estimated 3 m sensor depth).

NEHRP Site Class: C

Geomatrix Code: FQB

Geologic Conditions/Observations: Surficial geologic unit at site mapped as Quaternary (Holocene) unconsolidated, wind-transported sand and lime-cemented sand. Quaternary (Upper Pleistocene) marine terrace deposits consisting of silt, sand, gravel and rubble are also mapped in the vicinity. Tertiary sandstone and siltstone units outcrop within 300 m of the site. Field observations indicate that a layer of sandy loose soil overlies more compacted soil at the surface. The seismic sensor is located in a bunker, approximately 3 m below ground surface and is most likely on Pleistocene marine terrace deposits or Tertiary sandstone/siltstone.

Site Conditions: Remote site located on a hill at the high point of the island. Ground surface elevation does not change along the 70.5 m long MASW and seismic refraction array.

Geophysical Methods Utilized: HVSR, Seismic Refraction, MASW

Geophysical Testing Arrays:

1. Array SNCC-1 (48 channel MASW and P-wave seismic refraction array utilizing 4.5 Hz vertical geophones spaced 1.5 m apart for a length of 70.5 m, forward and reverse shot locations with multiple source offsets and hammer source types and multiple interior shot locations).
2. Three HVSR measurement locations distributed along array SNCC-1.

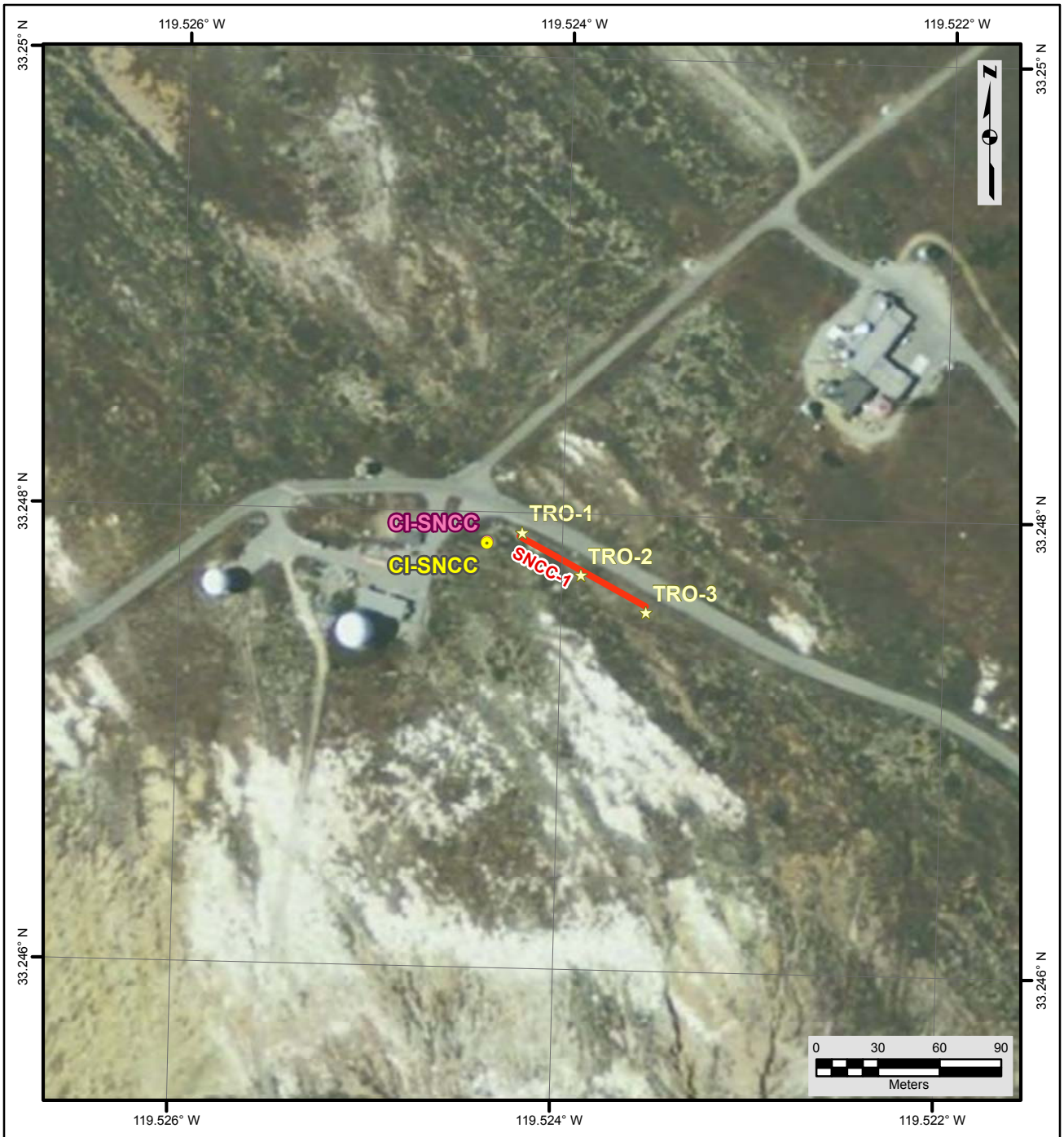

Legend

- Seismic Station - Approximate Surveyed Location
- Seismic Station - Approximate Location of Record
- H/V Spectral Ratio Location
- MASW and Seismic Refraction Array

NOTES:
1. WGS 1984 COORDINATE SYSTEM
2. Image Source: ESRI, i-cubed, USDA FSA, USGS, AEX, GeoEye, Getmapping, Aerogrid, IGP

File Name: CI-SNCC-I

Date: 11/14/2011

USGS science for a changing world

GEOVision geophysical services

RECOVERY.GOV

SITE MAP
CI•SNCC

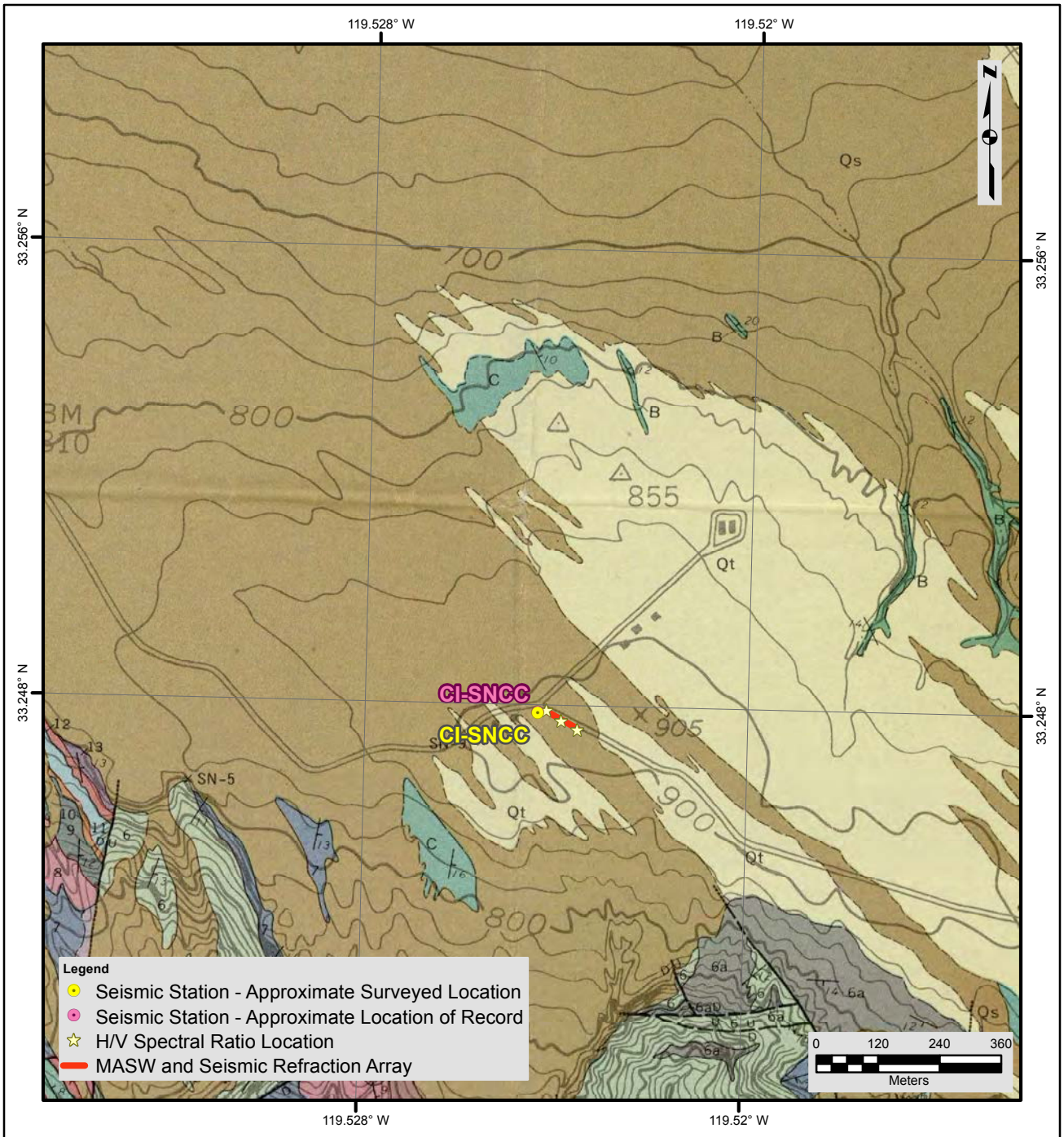

Description of Geologic Map Units

Qs = Quaternary (Holocene) wind-transported sand, unconsolidated, sand and lime-cemented sand
Qt = Quaternary (Upper Pleistocene) marine terrace deposits, silt, sand, gravel and rubble
7 = Tertiary (Middle to Upper Eocene) thick-bedded sandstone, few thin siltstone interbeds
6 & 6a = Tertiary (Middle to Upper Eocene) interbedded thin bedded siltstone and sandstone, few thin sandstone interbeds
B = Tertiary (Middle to Upper Eocene) siltstone, undifferentiated, unknown stratigraphic position between 5 and 17
C = Tertiary (Middle to Upper Eocene) sandstone, undifferentiated, unknown stratigraphic position between 6 and 18

NOTES:
1. WGS 1984 COORDINATE SYSTEM
2. Geologic Map and Sections of San Nicolas Island, California by J.G. Vedder, R.L. Harbour, R.M. Norris, R.L. Burnside, N.C. Privrasky, and D.H. Milton, 1955-1956
3. See site map for details of geophysical survey

USGS science for a changing world
GEOVision geophysical services

GEOLOGIC MAP
CI•SNCC

File Name: CI-SNCC
Date: 11/17/2011

Looking northwest towards bunker housing CI.SNCC seismic station

Looking northwest along array SNCC-1

CI.SNCC seismic station in a military bunker

P-wave seismic refraction data acquisition

MASW data acquisition along array SNCC-1

Location of Geophysical Testing Arrays:

Location	Latitude	Longitude
SNCC-1, Northwest End of Array	33.24790	-119.52420
SNCC-1, Center of Array	33.24775	-119.52387
SNCC-1, Southeast End of Array	33.24760	-119.52353
HVSR Sensor Tromino 1 (TRO-1)	33.24791	-119.52419
HVSR Sensor Tromino 2 (TRO-2)	33.24773	-119.52388
HVSR Sensor Tromino 3 (TRO-3)	33.24757	-119.52353
CI.SNCC Seismic Station	33.24786	-119.52437

Notes: 1) WGS84 Coordinate System (decimal degrees).
2) Survey accuracy is estimated at 1 to 2 m.

Results:

Depth to Top of Layer (m)	Layer Thickness (m)	S-Wave Velocity (m/s)	Inferred P-Wave Velocity (m/s)	Assumed Poisson's Ratio	Assumed Density (g/cm^3)
0	1	169	316	0.3	1.7
1	2	258	482	0.3	1.8
3	3	372	695	0.3	1.9
6	4	450	842	0.3	2.0
10	5	718	1343	0.3	2.1
15	7	809	1514	0.3	2.1
22	9	866	1620	0.3	2.1
31	>4	1022	1911	0.3	2.1

Notes: 1) Depth of investigation is about 35 m.
2) Bottom layer is a half space.

Observations/Discussion:

- The HVSR plots are similar at all sensor locations, with data quality appearing best at sensor locations TRO-1 and TRO-2. There is a weak HVSR peak in the 6 to 8 Hz range, possibly associated with shallow sedimentary rock.
- Two models were generated for the seismic refraction data using tomographic inversion; one using a layer based starting model and the other using a smooth velocity gradient starting model. The seismic refraction models were extended to far offset shot locations. Extending the model to far offset shot locations allowed depth of investigation to be increased to validate the surface wave model at depth. Both seismic refraction models have similar RMS errors.
- Both seismic refraction models show similar P-wave velocity structure. The seismic refraction models indicate that P-wave velocity is about 400 to 600 m/s at the surface, increasing to 1,000 m/s at a depth of 5 to 9 m. The velocity model developed using a

layer based starting model, increases to 1,200 to 1,400 m/s at a nominal depth of 11 to 16 m and greater than 1,600 m/s at a depth below 12 to 18 m. The velocity model developed using a smooth velocity gradient starting model shows a gradual increase in P-wave velocity to 1,200 to 1,400 m/s at a nominal depth of 10 to 15m and greater than 1,600 m/s at a depth below 15 to 20m.

- Extending the models to far offset shot locations allowed the model to be extended to a greater depth (about 20 m), revealing layers with P-wave velocity on the order of 1,600 to 1,800 m/s at nominal depths of 12 m to 20 m. It should be noted that a longer receiver array would be required to accurately image velocity structure at these depths; however, the far offset shot locations do support P-wave velocity continuing to increase with depth below 15 m.
- The seismic refraction model indicates that there is some lateral velocity variation at this site, with higher P-wave velocities at shallower depth near the southeast end of the line.
- Noise conditions at the site were not sufficient for application of passive surface wave techniques.
- There is about 30 to 80 m/s scatter in the MASW dispersion data, which is partially due to lateral velocity variation.
- The minimum wavelength surface wave phase velocity data extracted from the 48-channel MASW array was about 5 m. Data reduction using seismic records from smaller hammer sources and a limited offset receiver array (i.e. less active geophones) allowed extraction of surface wave dispersion data to a minimum wavelength of about 2 m.
- A representative dispersion curve was generated for the MASW data set using a moving average, polynomial curve fitting routine and used for modeling.
- The Rayleigh wave dispersion data was modeled using the fundamental mode assumption.
- The surface wave model is generally consistent with the P-wave refraction model, especially considering unknown Poisson's ratio, and also demonstrates that the P-wave velocities higher than 1,500 m/s in the seismic refraction model are associated with sedimentary rock rather than saturated sediments.
- Surface wave depth of investigation is about 35 m based on half of maximum wavelength criteria.
- Subsequent analysis of the V_S model resulting from inversion of the Rayleigh wave phase velocity data using the fundamental mode assumption indicated that the first higher mode could be dominant at low frequencies/long wavelengths. It is, therefore, possible that superposition (mode mixing) of the fundamental and first high modes occurs at low frequencies. The V_S model is, however, consistent with the P-wave seismic refraction model at depth and, therefore, effective mode routines were not applied to this data set. It is possible that lateral velocity is such that the fundamental mode remains dominant at long wavelengths. More research is needed into the effects of minor lateral velocity variation on both V_S models derived from surface wave dispersion data and the relative amplitude of higher mode surface waves.
- V_{S30} is 541 m/s (NEHRP Site Class C).
- Average S-wave velocity between 3 m (estimated sensor depth) and 33 m is 668 m/s (NEHRP Site Class C).
- The 80 m/s scatter in the Rayleigh wave phase velocity data at a 40 m wavelength, indicates about 40 m/s variation in that V_{S30} may vary by as much as 7.5 percent.

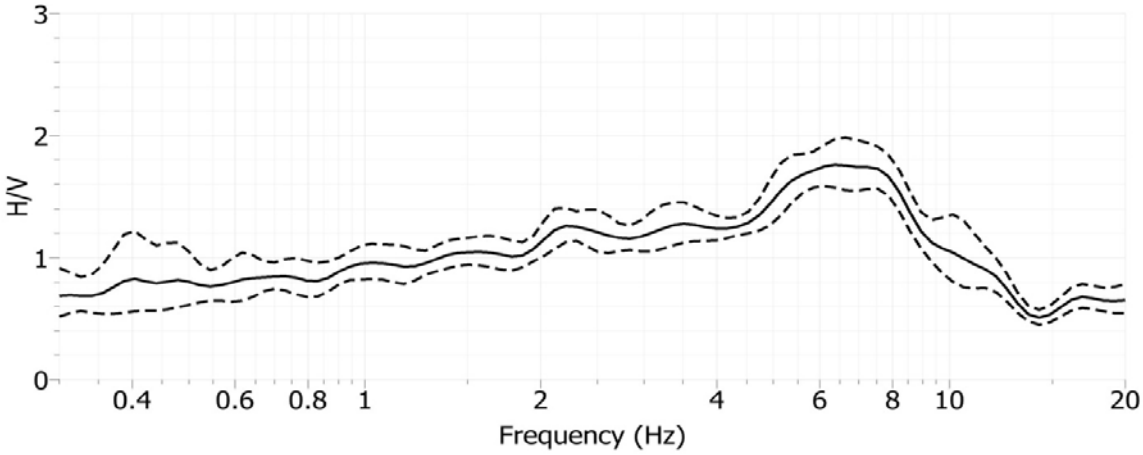

Site CI.SNCC, H/V Spectral Ratio, Array SNCC-1, Sensor TRO-1

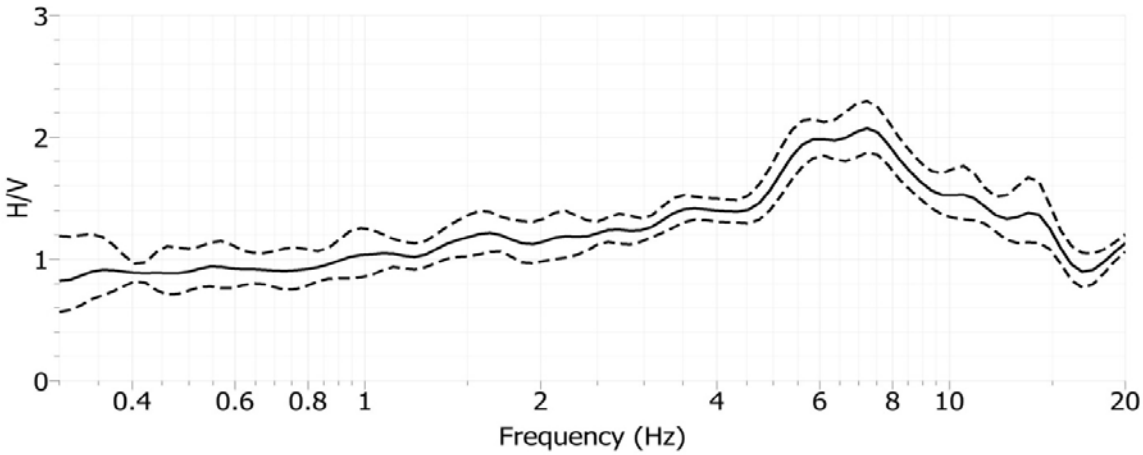

Site CI.SNCC, H/V Spectral Ratio, Array SNCC-1, Sensor TRO-2

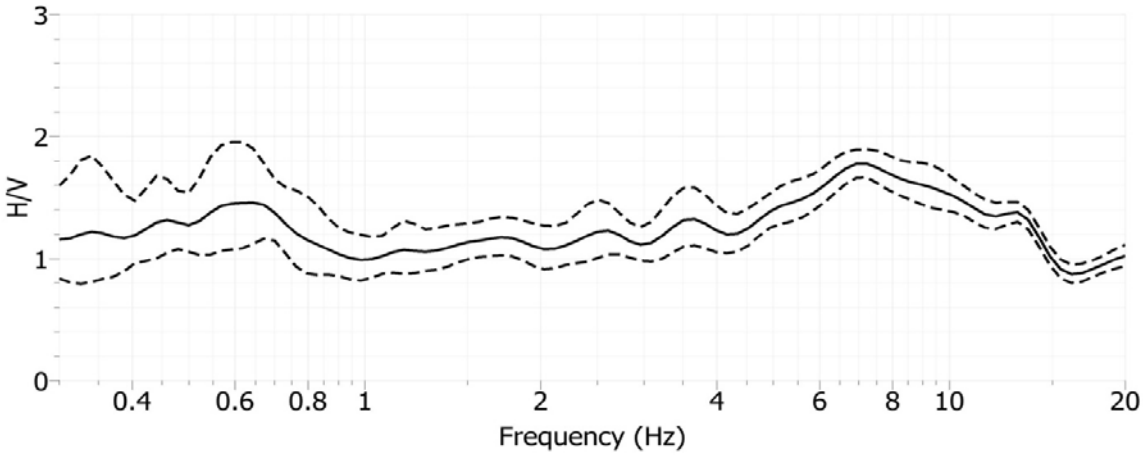

Site CI.SNCC, H/V Spectral Ratio, Array SNCC-1, Sensor TRO-3

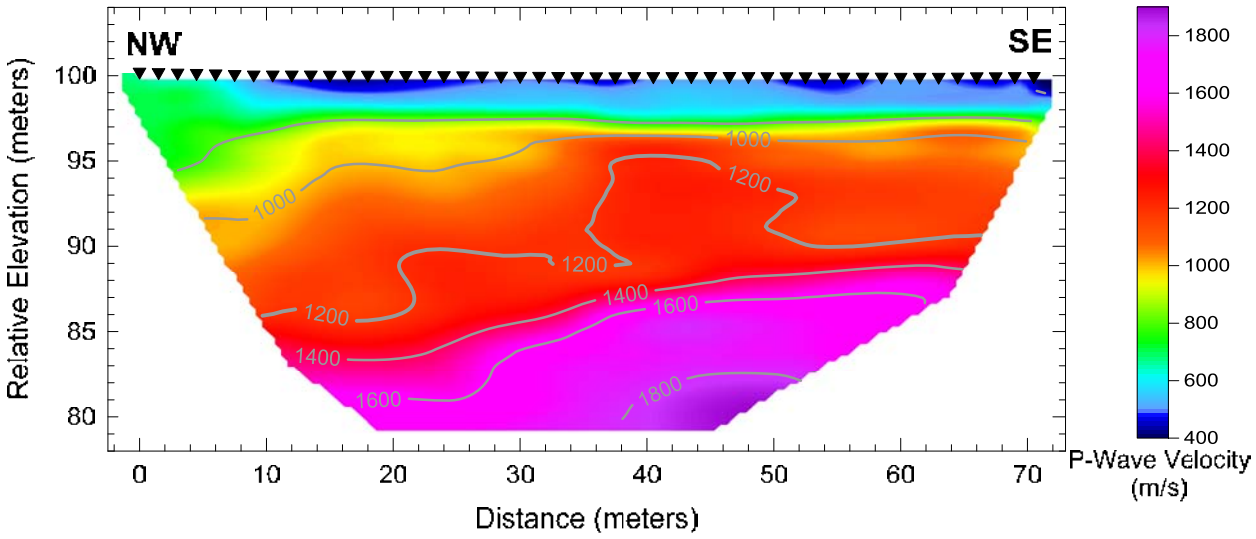

Array SNCC-1 – Tomographic Seismic Refraction Model utilizing Layer Based Starting Model

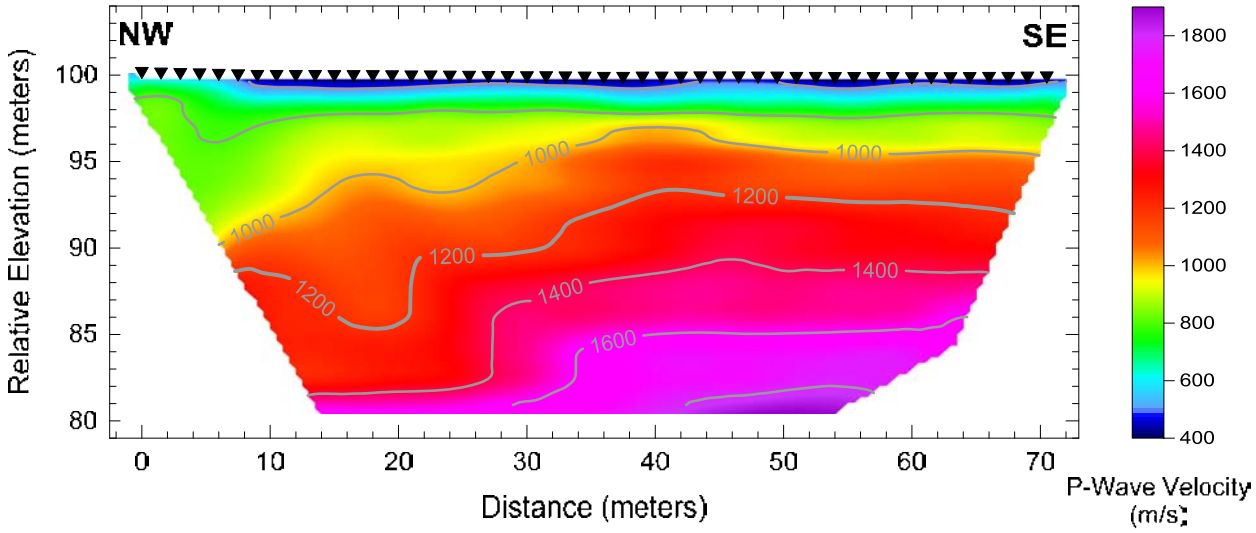

Array SNCC-1 – Tomographic Seismic Refraction Model utilizing Smooth Velocity Gradient Starting Model

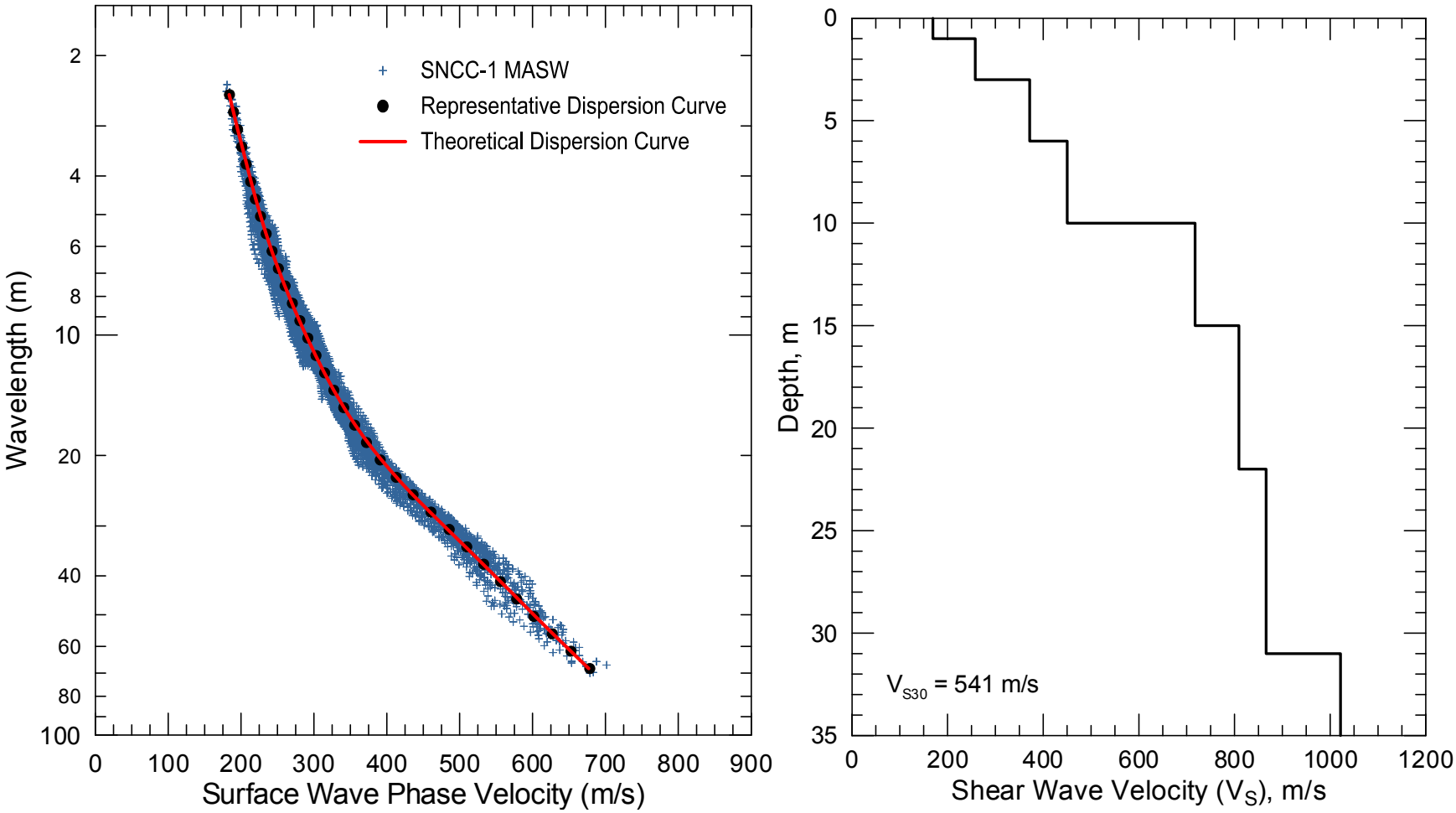

CI.SNCC - Field, representative and inverted theoretical surface wave dispersion data (left) and associated V_S model (right)

Site CI.SNO

Location: Snow Peak, San Bernardino National Forest, San Bernardino County, California

Latitude: 34.03515 **Longitude:** -116.80778
(Station coordinates provided by USGS, WGS84 coordinate system

V_{S30} (measured): 503 m/s (weathering at the site is such that V_{S30} could easily be 20% higher at the seismic station).

V_{S30} (adjusted to more accurately reflect seismic station conditions): 553 m/s (average S-wave velocity between 1.5 and 31.5 m adjusting for 1.5 m assumed sensor depth).

NEHRP Site Class: C

Geomatrix Code: INB

Geologic Conditions/Observations: Seismic station located on Precambrian gneiss. San Andreas Fault Zone located about 1 km north of the seismic station.

Site Conditions: Rural site. Steep, undulating topography in site vicinity. Seismic station located on mountain ridge. Test area located near the top of a mountain with steady topographic decline to the east.

Geophysical Methods Utilized: HVSR, Seismic Refraction, MASW

Geophysical Testing Arrays:

1. Array SNO-1 (48 channel MASW and P-wave seismic refraction array utilizing 4.5 Hz vertical geophones spaced 1.5 m apart for a length of 70.5 m, forward and reverse shot locations with multiple source offsets and source types and multiple interior shot locations).
2. Three HVSR measurement locations: two distributed along array SNO-1 and one adjacent to the seismic station.

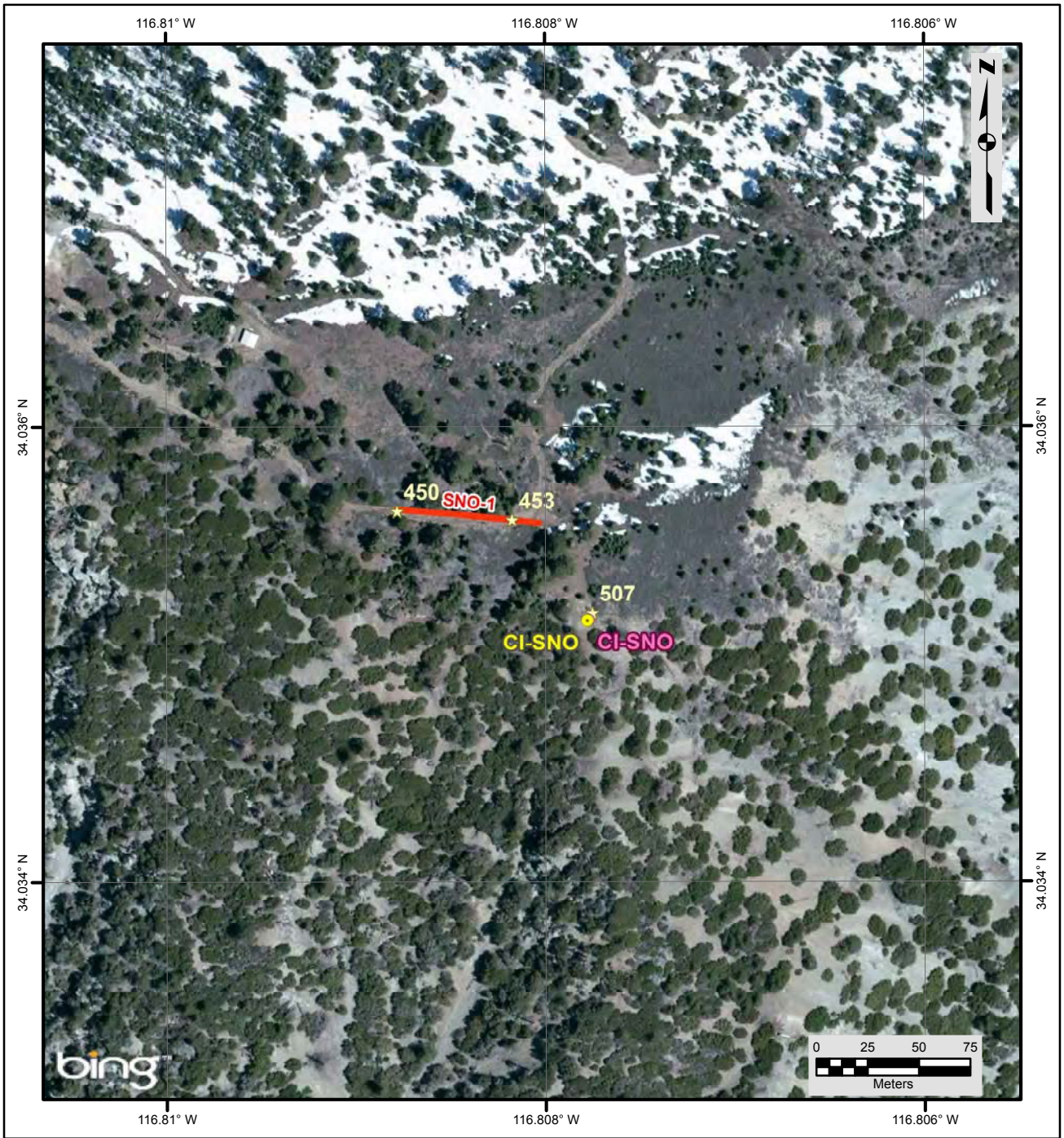

Legend

- Seismic Station - Approximate Surveyed Location
- Seismic Station - Approximate Location of Record
- H/V Spectral Ratio Location
- MASW and Seismic Refraction Array

NOTES:
1. WGS 1984 COORDINATE SYSTEM
2. Image Source: (c) Microsoft Corporation and its data suppliers

File Name: CI-SNO-I

Date: 2/7/2013

USGS science for a changing world

GEOVision geophysical services

RECOVERY.GOV

SITE MAP
CI•SNO

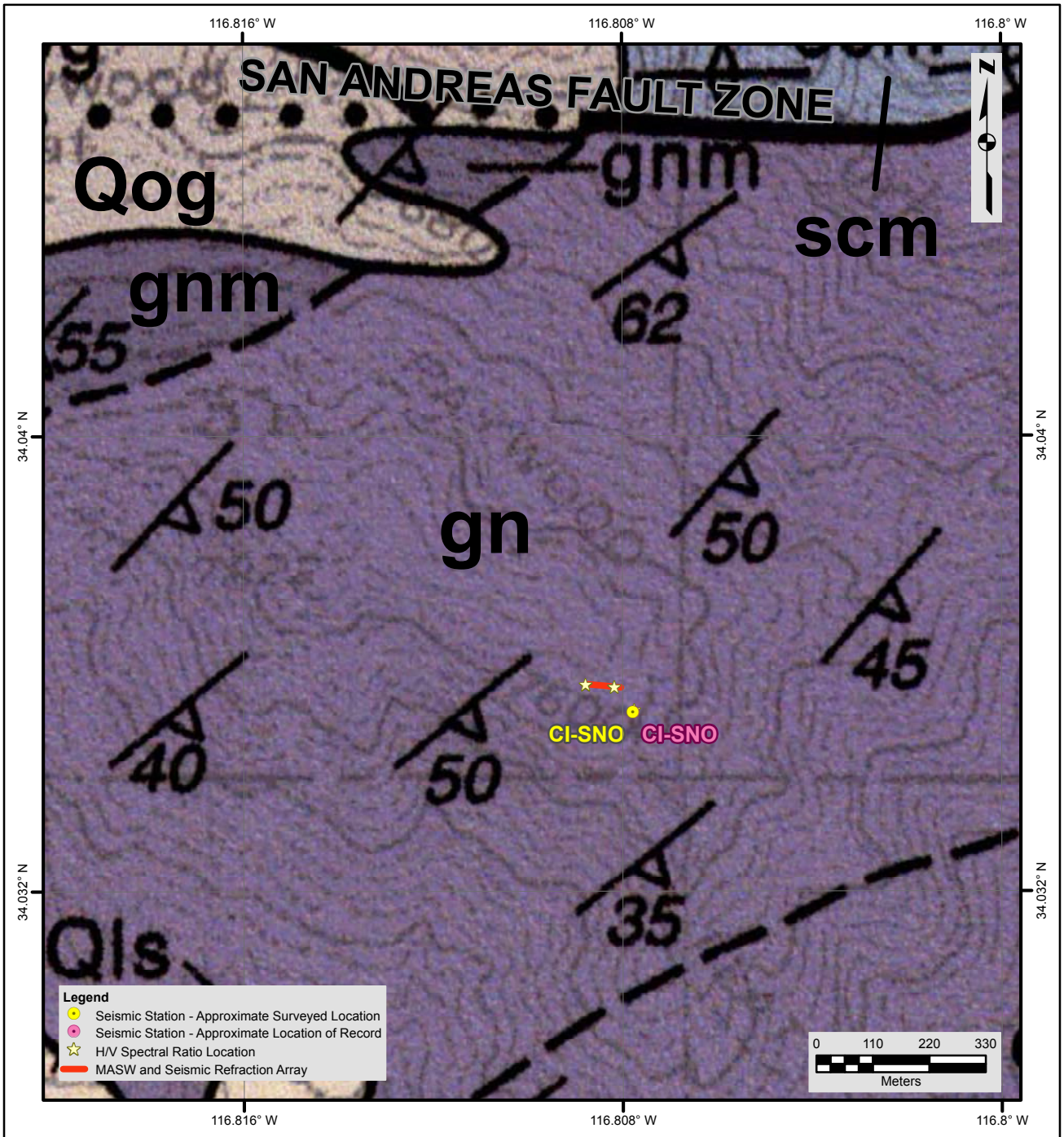

Description of Geologic Map Units

Qls = Quaternary (Pleistocene to Holocene) landslide rubble, rock debris
Qog = Quaternary (Pleistocene) gravel or fanglomerate, massive to crudely bedded, unsorted boulders, cobbles, and pebbles in coarse, gritty arkosic sand matrix
gn = Precambrian gneiss, laminated gneiss to gneissoid quartz diorite
gnm = Precambrian mylonitic or cataclastic gneiss
scm = Precambrian mylonitic schist, hard

NOTES:
1. WGS 1984 COORDINATE SYSTEM
2. Geologic Map of the San Gorgonio Mountain & Morongo Valley 15 Minute Quadrangles, San Bernardino & Riverside Counties, California by Thomas W. Dibblee, Jr., 2008
3. See site map for details of geophysical survey

USGS science for a changing world
GEOVision geophysical services

GEOLOGIC MAP
CI•SNO

RECOVERY.GOV

File Name: CI-SNO
Date: 2/7/2013

HVSR measurements next to seismic station

Seismic station CI.SNO

Looking west along array SNO-1 and at HVSR sensor 453

Looking east along array SNO-1

Seismic refraction and MASW data acquisition on array SNO-1

Location of Geophysical Testing Arrays:

Location	Latitude	Longitude
SNO-1, Northwest End of MASW/Refraction Array	34.03563	-116.80879
SNO-1, Center of MASW/Refraction Array	34.03561	-116.80842
SNO-1, Southeast End of MASW/Refraction Array	34.03558	-116.80804
HVSR Sensor 450	34.03563	-116.80879
HVSR Sensor 453	34.03559	-116.80818
HVSR Sensor 507	34.03518	-116.80776
CI.SNO Seismic Station	34.03515	-116.80779

Notes: 1) WGS84 Coordinate System (decimal degrees)
2) Survey accuracy is estimated at 1 to 2 m.

Results:

V_S Model (MASW Sounding)

Depth to Top of Layer (m)	Layer Thickness (m)	S-Wave Velocity (m/s)	Inferred P-Wave Velocity (m/s)	Assumed Poisson's Ratio	Assumed Density (g/cm^3)
0	1	184	344	0.3	1.7
1	2	250	468	0.3	1.8
3	3	326	609	0.3	1.9
6	5	511	955	0.3	2.0
11	7	661	1236	0.3	2.1
18	10	720	1346	0.3	2.1
28	>7	740	1384	0.3	2.1

Notes: 1) Depth of investigation is about 35 m.
2) Bottom layer is a half space.
3) Surface wave model may be biased towards a lower half space velocity..

Average V_P and Estimated V_S Models from Central Portion of P-wave Seismic Refraction Line

Depth to Top of Layer (m)	Layer Thickness (m)	P-Wave Velocity (m/s)	Estimated S-Wave Velocity (m/s)			
			Poisson's Ratio = 0.25	Poisson's Ratio = 0.30	Poisson's Ratio = 0.3333	Poisson's Ratio = 0.35
0.00	0.50	513	296	274	256	246
0.50	1.00	561	324	300	281	270
1.50	1.00	682	394	365	341	328
2.50	1.00	722	417	386	361	347
3.50	1.00	900	519	481	450	432
4.50	1.00	943	544	504	471	453
5.50	1.00	983	567	525	491	472
6.50	2.10	1094	631	585	547	525
8.60	2.10	1186	685	634	593	570
10.70	2.10	1367	789	731	683	657
12.80	2.10	1413	816	756	707	679
14.90	2.10	1544	892	825	772	742
17.00	2.10	1620	935	866	810	778
19.10	2.10	1744	1007	932	872	838
21.20	Half Space	1789	1033	957	895	860

V_P and Estimated V_S Models from a Position of 24 m on the P-wave Seismic Refraction Line where Lowest Velocities occur in the Central Portion of the Line

Depth to Top of Layer (m)	Layer Thickness (m)	P-Wave Velocity (m/s)	Estimated S-Wave Velocity (m/s)			
			Poisson's Ratio = 0.25	Poisson's Ratio = 0.30	Poisson's Ratio = 0.3333	Poisson's Ratio = 0.35
0.00	0.50	473	273	253	237	227
0.50	1.00	511	295	273	256	246
1.50	1.00	603	348	322	301	290
2.50	1.00	681	393	364	341	327
3.50	1.00	771	445	412	385	370
4.50	1.00	844	487	451	422	406
5.50	1.00	921	532	492	460	442
6.50	2.10	1017	587	544	509	489
8.60	2.10	1204	695	644	602	579
10.69	2.10	1324	764	708	662	636
12.79	2.10	1406	812	751	703	675
14.89	2.10	1443	833	772	722	693
16.99	2.10	1555	898	831	778	747
19.09	2.10	1557	899	832	779	748
21.19	Half Space	1593	920	851	796	765

Observations/Discussion:

- There are no distinct, high amplitude HVSR peaks at the site. There is a possible, but inconclusive, weak HVSR peak at about 1.5 Hz, which could be associated with the base of the uppermost weathered zone.
- The P-wave seismic refraction data for array SNO-1 were modeled using a tomographic inversion routine with a layered starting model. The P-wave seismic refraction model was extended to far offset shot locations to extend depth of investigation. It should be noted that a larger geophone spacing, rather than the utilization of far offset shot locations, is preferred for extending depth of investigation, when applying tomographic inversion routines. However, the seismic refraction data were acquired in conjunction with surface wave data, where a shorter array length is preferred.
- The P-wave seismic refraction survey design allowed P-wave velocity to be imaged to a maximum depth of about 23 m. The seismic refraction model indicates that P-wave velocity is about 400 to 600 m/s at the surface and increases to over 1,000 m/s at a depth of 2 to 6 m, 1,200 m/s at a depth of 2.5 to 8.5 m, 1,400 m/s at a depth of 8 to 13 m and over 1,800 m/s at a depth of 16 m, or more. The maximum P-wave velocity in the central portion of the model, where depth of investigation is greatest, is slightly greater than 2,000 m/s.
- The seismic refraction survey indicates that there is significant lateral velocity variation at the site with the lower velocity weathered zone thickening to the west.
- The average P-wave velocity of the upper 30 m (V_{P30}) was estimated between 18 and 48 m on the P-wave refraction model, where depth of investigation is greatest. To estimate V_{P30} the P-wave velocity at a depth of 23 m, nominal depth of investigation, was projected to 30 m depth. V_{P30} ranges from about 1,142 to 1,383 m/s over the 18 to 45 m position interval, a 20% variation. The lowest estimated V_{P30} over this distance interval occurs at a position of 24 m on the profile.
- An average V_P model was developed over the 18 to 45 m distance interval by horizontally averaging the travel time of each model cell and cell thickness and average V_{P30} was determined to be 1,235 m/s. Assuming constant Poisson's ratios of 0.25, 0.3, 0.3333 and 0.35 would result in an estimated V_{S30} of 713, 660, 618 and 593 m/s, respectively. If the highly weathered rock is saturated, Poisson's ratio could plausibly be higher than 0.35.
- The lowest value of V_{P30} over the 18 to 45 m distance interval is 1,142 m/s and occurs at a position of 24 m. Assuming constant Poisson's ratios of 0.25, 0.3, 0.3333 and 0.35 would result in an estimated V_{S30} of 659, 610, 571 and 549 m/s, respectively.
- The highest value of V_{P30} over the 18 to 45 m distance interval is 1,383 m/s and occurs at a position of 42 m. Assuming constant Poisson's ratios of 0.25, 0.3, 0.3333 and 0.35 would result in an estimated V_{S30} of 798, 739, 692 and 664 m/s, respectively. It should be noted that the eastern end of the line with higher velocities is closest to the seismic station.
- Noise conditions at the site were not sufficient for application of passive surface wave techniques.
- MASW (Rayleigh wave) data were not easy to reduce, especially at wavelengths greater than 40 m, due to lateral velocity variation. It was necessary to be quite selective in

Rayleigh wave dispersion data used to construct the dispersion curve for modeling. Long wavelength Rayleigh wave dispersion consists of data from source locations at the eastern end of the line where wave propagation is towards the lower velocity western end of the line. Rayleigh wave phase velocity data at long wavelengths from western source locations were not significantly different, just difficult to reduce and tie into the final dispersion curve. Shot locations from the lower velocity western end and center of the array were the primary source of small wavelength/high frequency phase velocity data. Therefore, it would appear logical to assume that the resulting V_S model will be biased towards the lower velocities beneath the array.

- The minimum wavelength surface wave phase velocity data extracted from the 48-channel MASW array is about 15 m. Data reduction using seismic records from smaller hammer sources and a limited offset receiver array (i.e. less active geophones) allowed extraction of surface wave dispersion data to a minimum wavelength of about 1.5 m.
- There is nominally about 50 to 70 m/s scatter in MASW dispersion data selected for modeling, likely due to the effects of lateral velocity variation.
- A representative dispersion curve was generated for the MASW data set using a moving average, polynomial curve fitting routine and used for modeling.
- Surface wave depth of investigation is about 35 m based on half of maximum wavelength criteria.
- V_{S30} from the MASW V_S model is 503 m/s (NEHRP Site Class C).
- Average S-wave velocity between a depth of 1.5 and 31.5 m, to account for assumed seismic sensor depth, is 553 m/s (NEHRP Site Class C).
- V_{S30} from the average P-wave seismic refraction model and assumed constant Poisson's ratio of 0.3333 is 618 m/s (Site Class C), over 20% higher than that measured using the MASW technique. The lowest V_{S30} from the central portion of the P-wave seismic refraction model and assumed constant Poisson's ratio of 0.3333 is 571 m/s, about 13% higher than that measured using the MASW technique. The estimated V_S model from a position of 24 m along the array with assumed constant Poisson's ratio of 0.35 is closest to the MASW V_S model. If the highly weathered rock is saturated at shallow depth, then the average Poisson's ratio could plausibly be higher than 0.33, which would result in lower estimated V_{S30}. An S-wave refraction survey would be better able to characterize subsurface S-wave velocity structure, assuming converted waves are not an issue.
- For site characterization purposes, the use of the MASW V_S model is recommended. This model likely reflects the lower bound of V_{S30} in the site vicinity. It is plausible that V_{S30} is higher at the seismic station, based on increasing velocities to the east in the seismic refraction model, but not enough to move the site to Site Class B. The MASW array was located as close as possible to the seismic station while avoiding undulating topography and remaining on a road. It may be possible to acquire P- and S-wave refraction data closer to the seismic station assuming vegetation is not too dense. There is too much topographic variation closer to the seismic station to acquire surface wave data, although even a shallow surface wave sounding closer to the seismic station would help adjust the model from array SNO-1 to seismic station conditions.

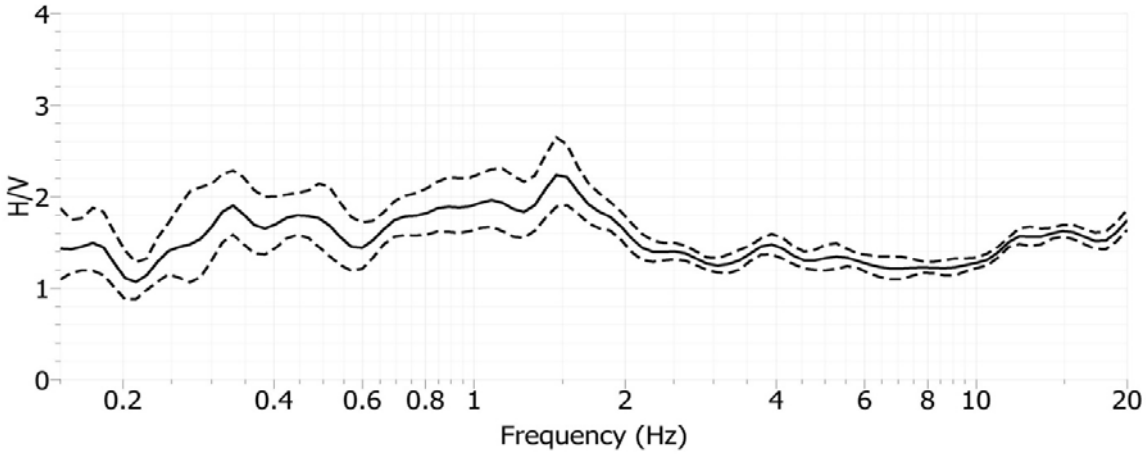

Site CI.SNO, H/V Spectral Ratio, Array SNO-1, Sensor 450

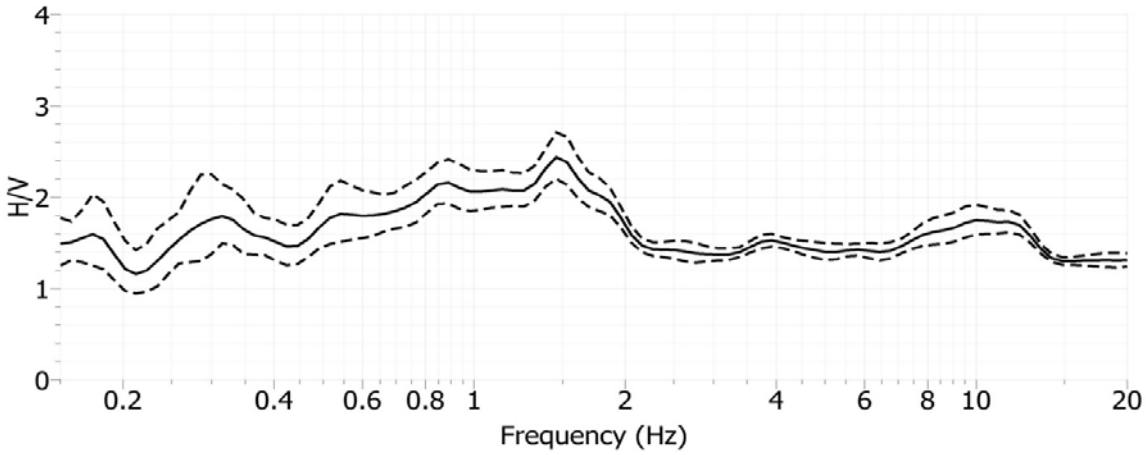

Site CI.SNO, H/V Spectral Ratio, Array SNO-1, Sensor 453

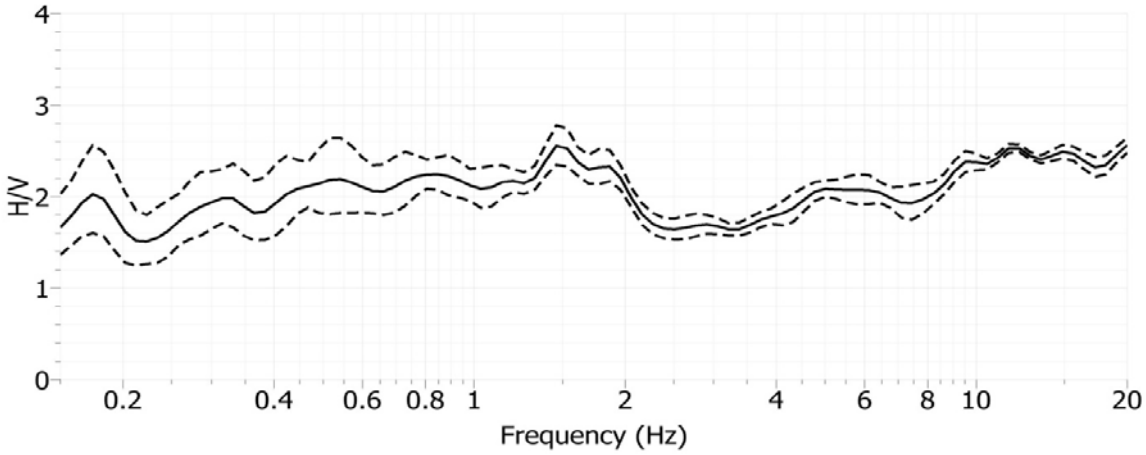

Site CI.SNO, H/V Spectral Ratio, Near Seismic Station, Sensor 507

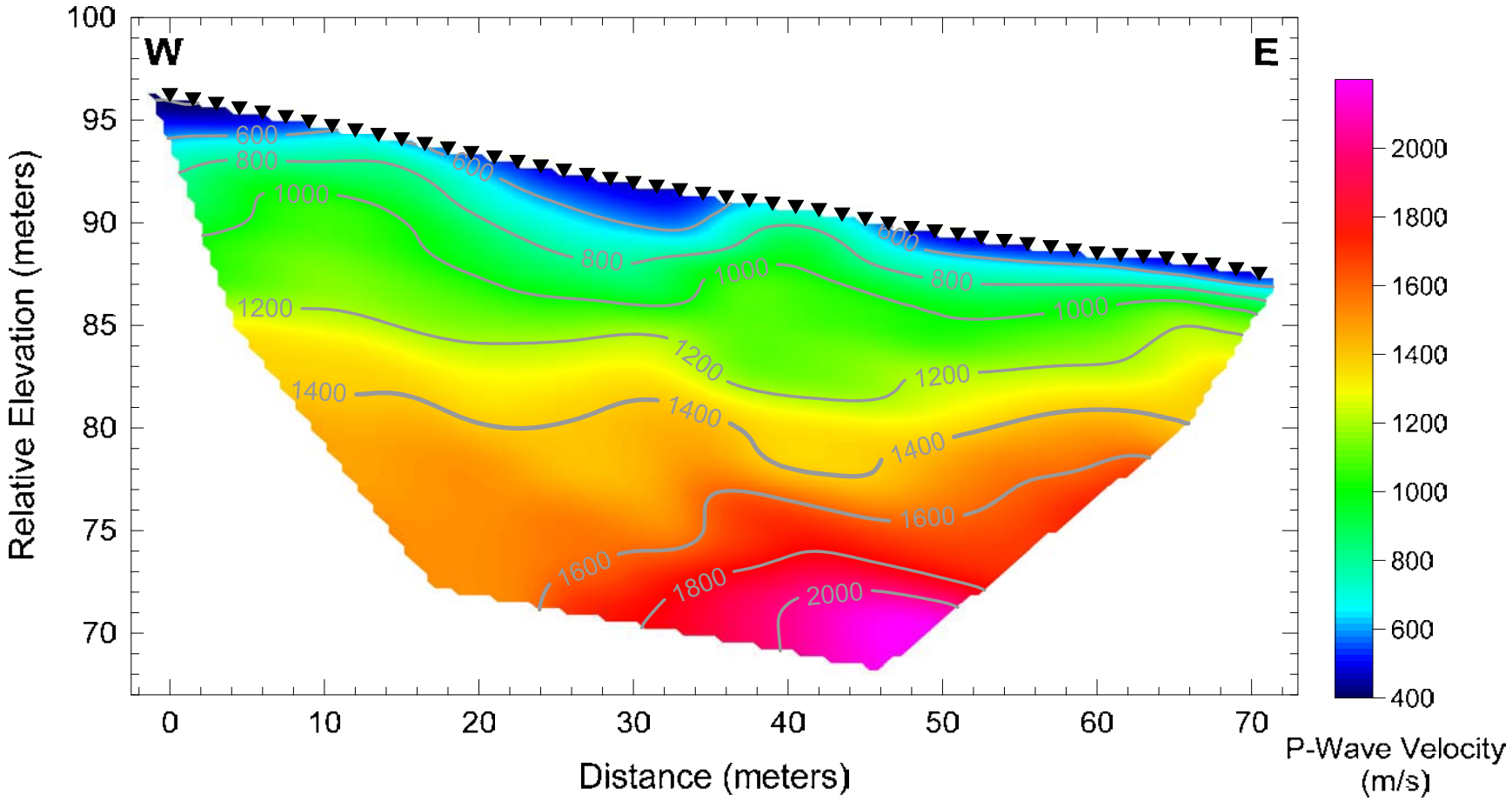

Array SNO-1 – Tomographic seismic refraction model utilizing smooth velocity gradient starting model

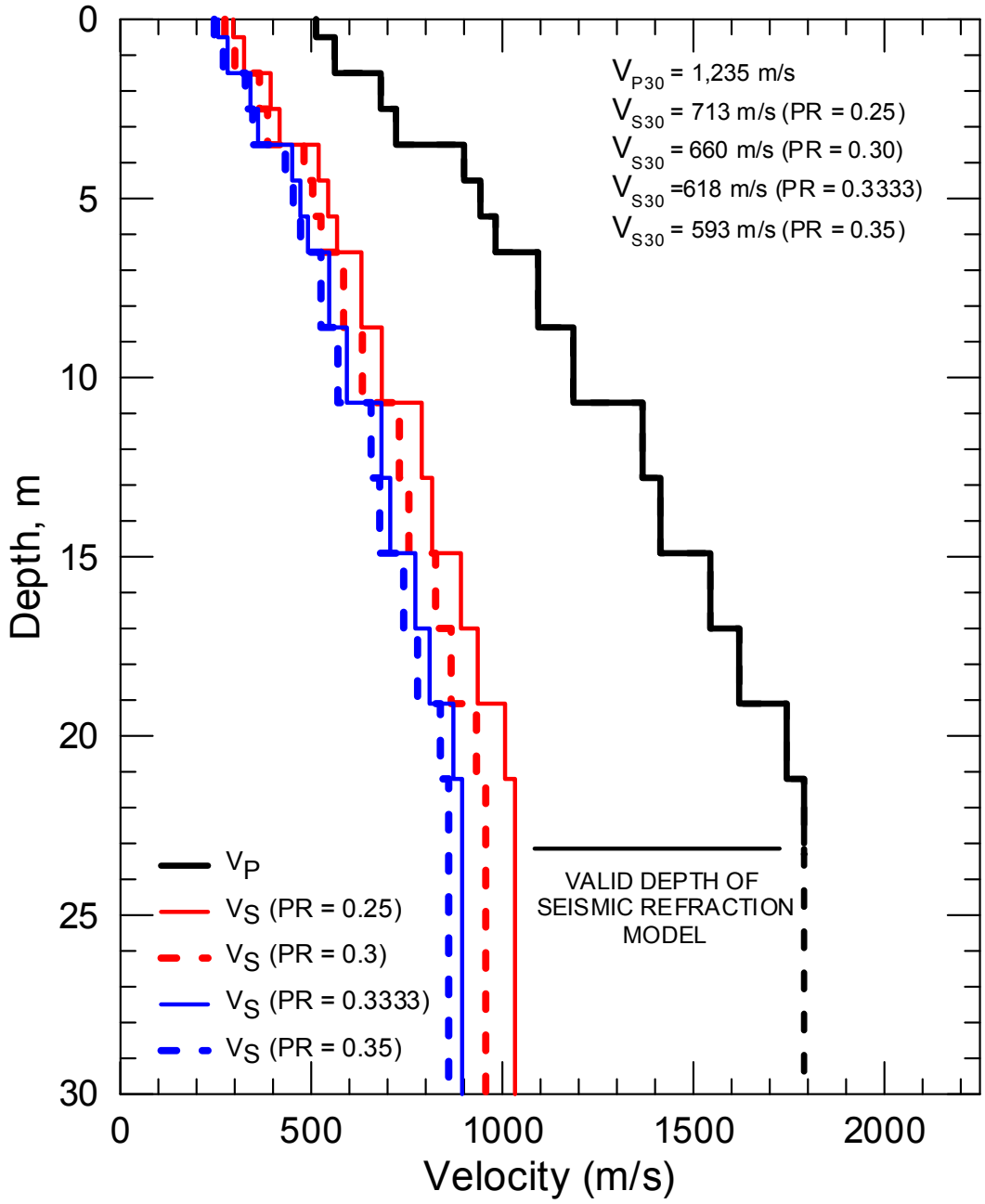

CI.SNO – Average P-wave velocity structure and estimated S-wave velocity structure between 18 and 45 m on P-wave seismic refraction array SNO-1. P-wave velocity is not well constrained below a depth of 23 m and computations are made assuming that velocity is constant below this depth. A longer seismic line would be preferred to more accurately image P-wave velocity structure to a 30 m depth.

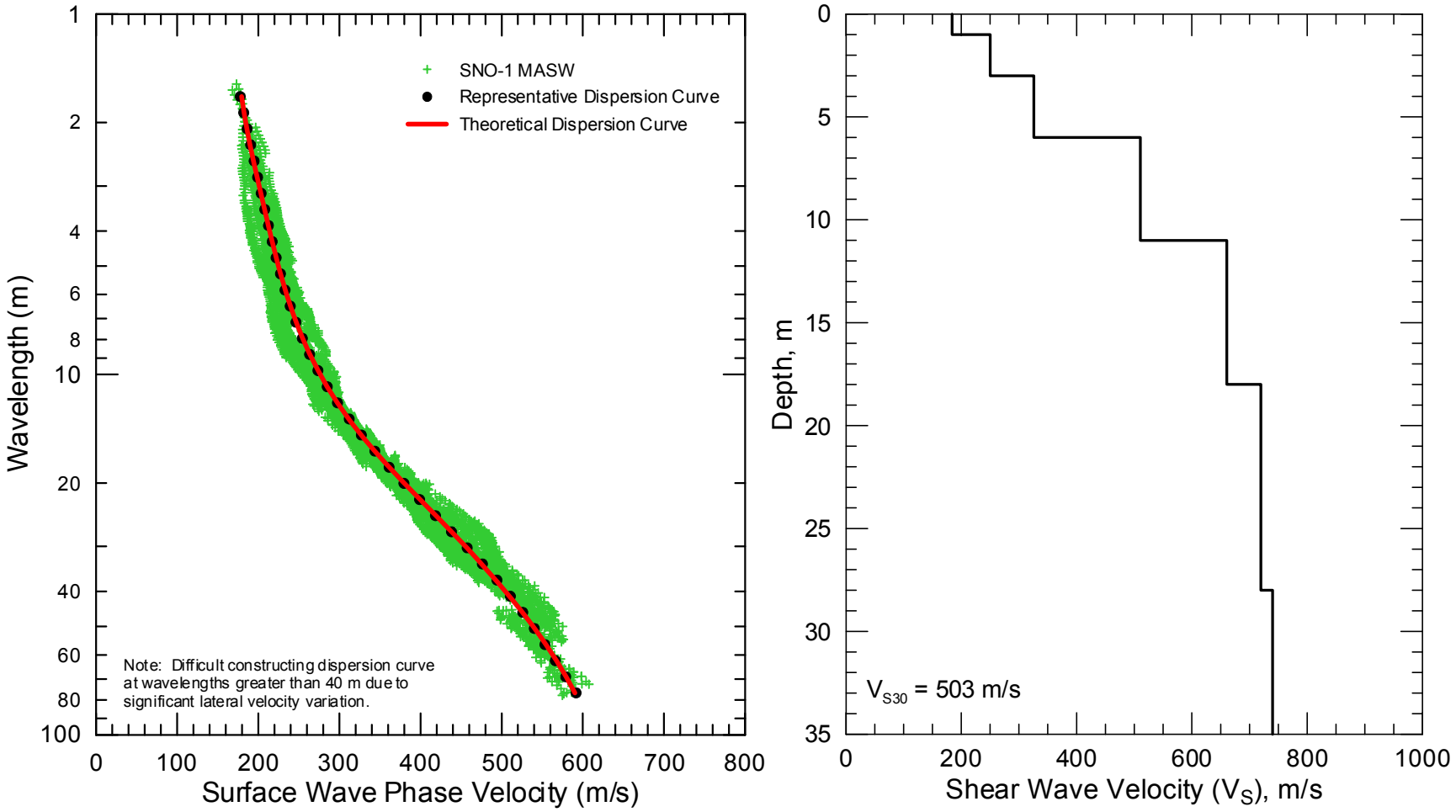

CI.SNO - Field, representative and inverted theoretical surface wave dispersion data (left) and associated V_S model (right)

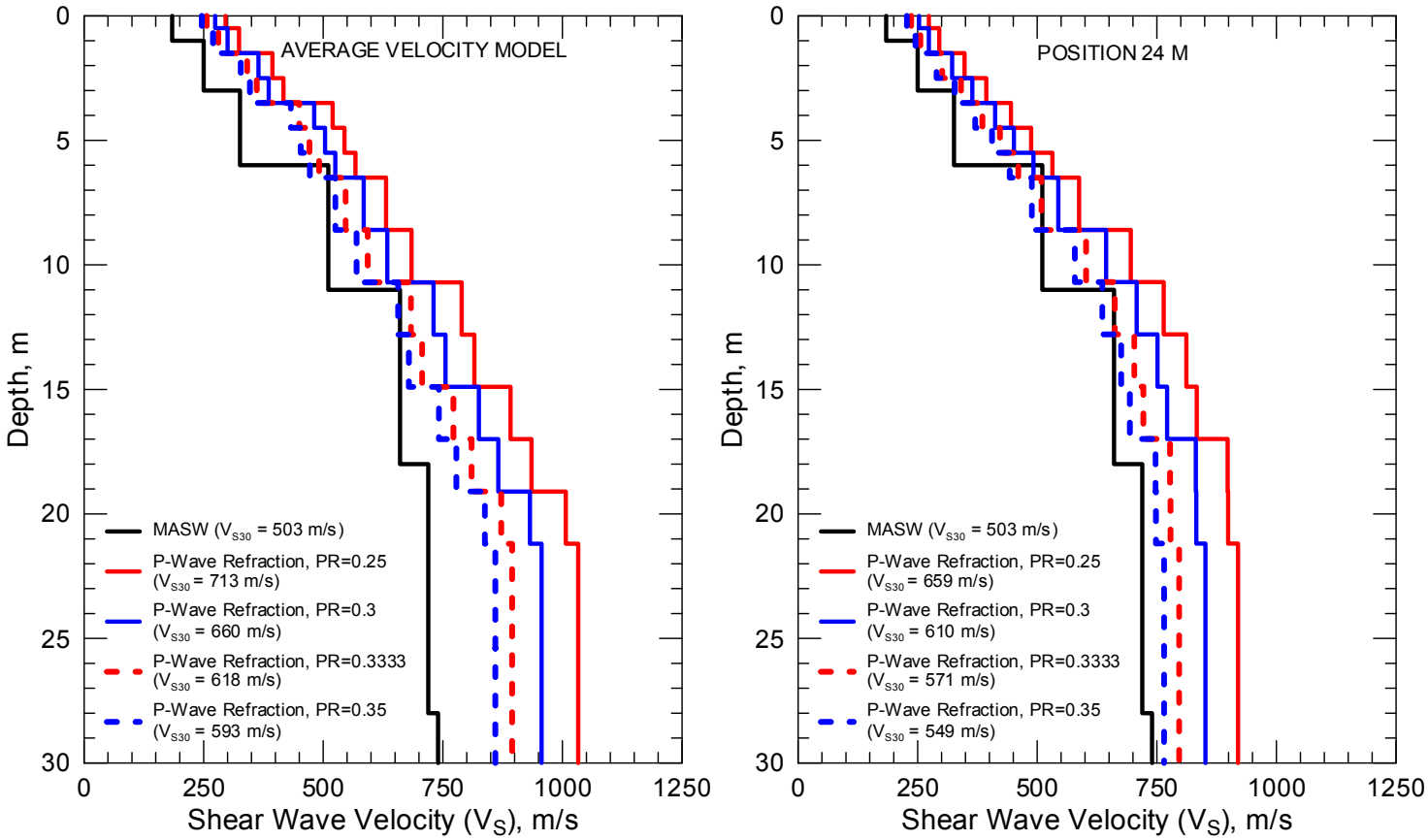

CI.SNO – Summary of S-wave velocity models derived from the MASW (Rayleigh wave) and P-wave seismic refraction surveys. S-wave velocity was estimated from the P-wave seismic refraction model assuming constant Poisson's ratio in the 0.2 to 0.35 range. Estimated S-wave velocity from the average P-wave velocity structure over the 18 to 45 m distance interval on array SNO-1 and the P-wave velocity structure with the lowest V_{P30} over this interval (distance of 24 m along the profile) are presented on the left and right, respectively. The P-wave seismic refraction model appears to be overestimating S-wave velocity structure relative to the surface wave model, unless the weathered rock is saturated at shallow depth and Poisson's ratio exceeds 0.35. There is, however, an approximate 20% variation in V_{P30} over the 18 to 45 m interval. Construction of the surface wave dispersion curve for modeling was very difficult due to lateral velocity variation and the MASW dispersion data selected for modeling may skew the V_S model to the lower velocities beneath the array.

Site CI.SPG2

Location: Springville 2, Scicon County School, Springville, California

Latitude: 36.20057 **Longitude:** -118.76624
(Station coordinates provided by USGS, WGS84 coordinate system)

V_{S30} (measured): 910 m/s

V_{S30} (adjusted to more accurately reflect seismic station conditions): 987 m/s (average S-wave velocity between 1 and 31 m adjusting for inferred 1 m sensor depth).

NEHRP Site Class: B

Geomatrix Code: IGA

Geologic Conditions/Observations: Seismic station located on Mesozoic weathered granitic rocks.

Site Conditions: Rural site. Mountainous topography is site vicinity. Test area located along a relatively planar ridge surface with topography declining gently to the northeast. There was limited space for testing at the site.

Geophysical Methods Utilized: HVSR, Seismic Refraction, MASW

Geophysical Testing Arrays:

1. Array SPG2-1 (48 channel MASW and P-wave seismic refraction array utilizing 4.5 Hz vertical geophones spaced 1 m apart for a length of 47 m, forward and reverse shot locations with multiple source offsets and source types and multiple interior shot locations).
2. Three HVSR measurement locations: two distributed along array SPG2-1 and one adjacent to the seismic station.

Legend

- Seismic Station - Approximate Surveyed Location
- Seismic Station - Approximate Location of Record
- H/V Spectral Ratio Location
- MASW and Seismic Refraction Array

NOTES:
1. WGS 1984 COORDINATE SYSTEM
2. Image Source: ESRI, i-cubed, USDA FSA, USGS, AEX, GeoEye, Getmapping, Aerogrid, IGP

File Name: CI-SPG2-I

Date: 10/13/2011

USGS science for a changing world

GEOVision geophysical services

RECOVERY.GOV

SITE MAP
CI•SPG2

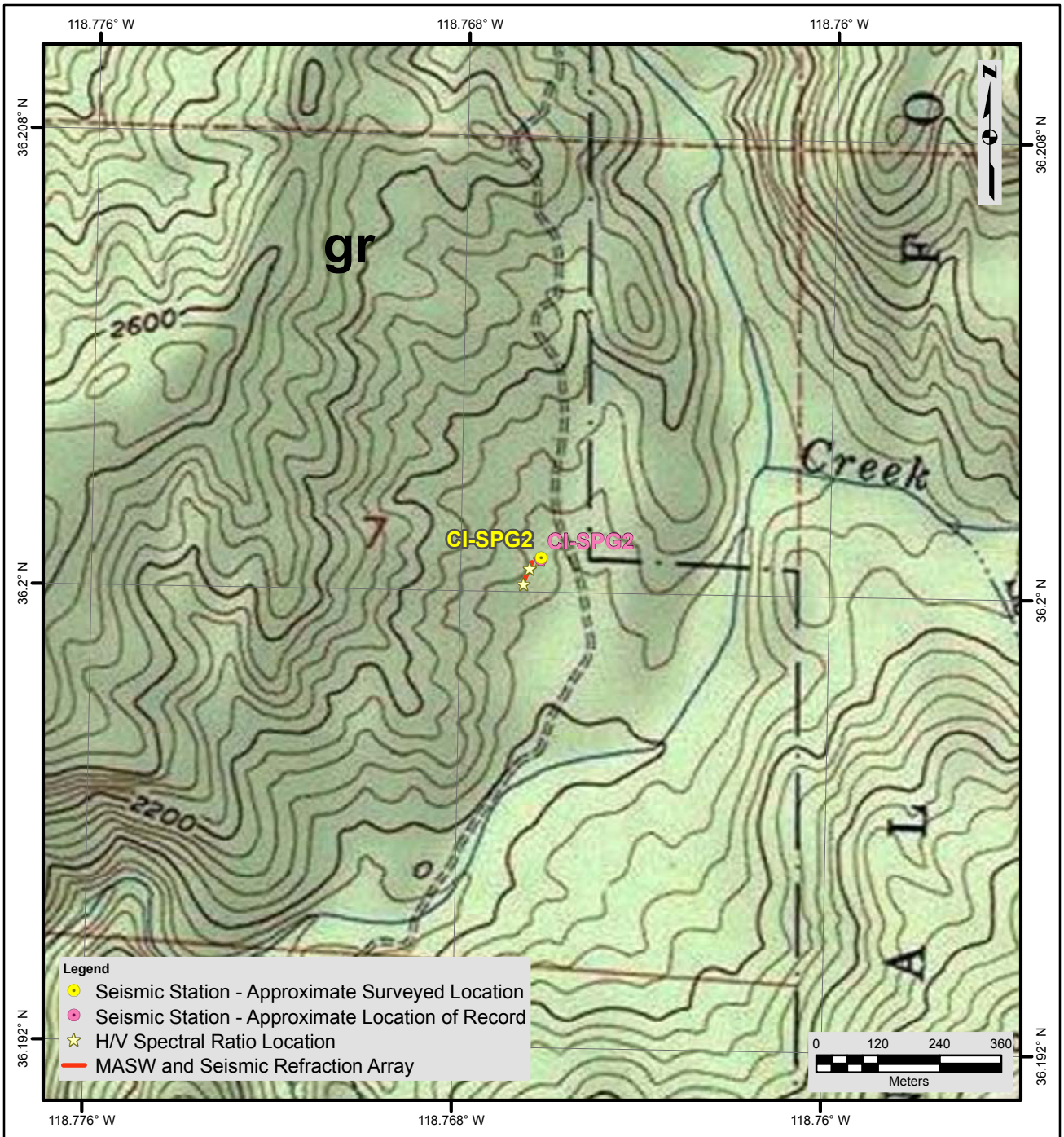

Description of Geologic Map Units

gr = Mesozoic granitic rocks

NOTES:
1. WGS 1984 COORDINATE SYSTEM
2. Geologic Map of California (Olaf P. Jenkins edition), Fresno Sheet, compiled by Robert A Matthews and John L. Burnett, 1965
3. See site map for details of geophysical survey

File Name: CI-SPG2

Date: 10/13/2011

USGS science for a changing world

GEOVision geophysical services

RECOVERY.GOV

GEOLOGIC MAP
CI•SPG2

Looking north at HVSR sensor 453 and CI.SPG2 seismic station

Looking southwest along array SPG2-1 past HVSR sensor 507

Looking southeast towards seismic station and array SPG2-1

Looking northeast along array SPG2-1 and at HVSR sensor 450

Looking northeast towards seismic station and northeast end of array SPG2-1

Location of Geophysical Testing Arrays:

Location	Latitude	Longitude
SPG2-1, Southwest End of MASW/Refraction Array	36.20012	-118.76663
SPG2-1, Center of MASW/Refraction Array	36.20033	-118.76653
SPG2-1, Northeast End of MASW/Refraction Array	36.20052	-118.76644
HVSR Sensor 450	36.20013	-118.76661
HVSR Sensor 453	36.20057	-118.76625
HVSR Sensor 507	36.20040	-118.76648
CI.SPG2 Seismic Station	36.20060	-118.76623

Notes: 1) WGS84 Coordinate System (decimal degrees).
2) Survey accuracy is estimated at 1 to 2 m.

Results:

V_S Model 1FM (Southwest Source Locations)

Depth to Top of Layer (m)	Layer Thickness (m)	S-Wave Velocity (m/s)	Inferred P-Wave Velocity (m/s)	Assumed Poisson's Ratio	Assumed Density (g/cm^3)
0	1	235	439	0.3	1.8
1	1.5	347	649	0.3	1.9
2.5	2.5	506	947	0.3	2.0
5	7	912	1706	0.3	2.1
12	7	1097	2052	0.3	2.1
19	7	2045	3826	0.3	2.4
26	>4	2593	4850	0.3	2.5

Notes: 1) Data modeled assuming dispersion curve is the fundamental mode.
2) Depth of investigation is about 30 m.
3) Bottom layer is a half space.
4) Velocity of half-space not well constrained.

V_S Model 1AM (Southwest Source Locations)

Depth to Top of Layer (m)	Layer Thickness (m)	S-Wave Velocity (m/s)	Inferred P-Wave Velocity (m/s)	Assumed Poisson's Ratio	Assumed Density (g/cm^3)
0	1	235	439	0.3	1.80
1	1.5	342	640	0.3	1.90
2.5	2.5	515	963	0.3	2.00
5	6	732	1369	0.3	2.10
11	7	989	1851	0.3	2.15
18	7	1690	3163	0.3	2.40
25	>5	1715	3208	0.3	2.40

Notes: 1) Data modeled assuming dispersion curve is the average mode (based on relative amplitude of the fundamental and higher surface wave modes).
2) Depth of investigation is about 30 m.
3) Bottom layer is a half space.
4) Velocity of half space not well constrained.

V_S Model 2FM (Northeast Source Locations)

Depth to Top of Layer (m)	Layer Thickness (m)	S-Wave Velocity (m/s)	Inferred P-Wave Velocity (m/s)	Assumed Poisson's Ratio	Assumed Density (g/cm^3)
0	1	317	594	0.3	1.80
1	2	453	848	0.3	1.90
3	4	693	1297	0.3	2.10
7	6	845	1582	0.3	2.10
13	7	1065	1993	0.3	2.15
20	8	1972	3689	0.3	2.40
28	>2	2235	4182	0.3	2.50

Notes: 1) Data modeled assuming dispersion curve is the fundamental mode.
2) Depth of investigation is about 30 m.
3) Bottom layer is a half space.
4) Velocity of half-space not well constrained.

V_S Model 2AM (Northeast Source Locations)

Depth to Top of Layer (m)	Layer Thickness (m)	S-Wave Velocity (m/s)	Inferred P-Wave Velocity (m/s)	Assumed Poisson's Ratio	Assumed Density (g/cm^3)
0	1	316	592	0.3	1.8
1	1.5	444	830	0.3	1.9
2.5	2.5	589	1102	0.3	2.0
5	6	763	1427	0.3	2.1
11	7	980	1834	0.3	2.1
18	7	1648	3084	0.3	2.4
25	>5	1700	3180	0.3	2.4

Notes: 1) Data modeled assuming dispersion curve is the average mode
(based on relative amplitude of the fundamental and higher surface wave modes).
2) Depth of investigation is about 30 m.
3) Bottom layer is a half space.
4) Velocity of half space not well constrained.

Observations/Discussion:

- The best quality HVSR data was collected at sensor 450 and to a lesser degree sensor 453. Sensor 507 yielded high amplitude noise over the 0.6 to 3 Hz range, likely due to sensor coupling, and is not presented. There are no significant HVSR peaks at the location of sensor 450. Consideration should be given to repeating HVSR data at this site, if the site is visited again in the future, although HVSR data is not expected to be particularly useful at this rock site in a rural environment.
- The P-wave seismic refraction data collected along array SPG2-1 were modeled using a tomographic inversion routine with both a smooth velocity gradient and layer based starting model. The layer based starting model was extended to far offset shot locations to extend depth of investigation. The smooth velocity gradient starting model was not extended to far offset shot locations.
- The seismic refraction survey design allowed P-wave velocity structure to be reliably imaged to a maximum depth of 10 to 15 m. The seismic refraction models show that P-wave velocity is about 400 to 1,000 m/s at the surface, increasing to 1,500 m/s at a depth of 1 to 4 m and to 2,000 m/s at a nominal depth of 6 to 12 m. Although not well constrained, both models show P-wave velocity exceeding 3,000 m/s at a depth below 13 to 18 m.
- The seismic refraction models indicate that there is some lateral velocity variation at this site, most significantly a slight thickening of a low velocity sediment/decomposed rock layer to the southwest. We believe that this small near surface lateral velocity variation is the source of the significant scatter in surface wave dispersion data at small wavelengths, as discussed below.

- Noise conditions at the site were not sufficient for application of passive surface wave techniques.
- The minimum wavelength surface wave phase velocity data extracted from the 48-channel MASW array is about 10 m for source locations off the northeast end of the array and 22 m for source locations off the southwest end of the array. Data reduction using seismic records from smaller hammer sources and a limited offset receiver array (i.e. less active geophones) allowed extraction of surface wave dispersion data to a minimum wavelength of about 2.5 m.
- There is significant scatter of up to 200 m/s in MASW dispersion data at small wavelengths due to a slight thickening to the southwest of a low velocity sediment/decomposed rock layer, as supported by the seismic refraction models. Therefore, the MASW data were modeled by developing two dispersion curves: one from interior and southwest source locations defining the lower envelope and the other from interior and northeast source locations defining the upper envelop of the Rayleigh wave phase velocity data.
- A representative dispersion curve was generated for each MASW data set using a moving average, polynomial curve fitting routine and used for modeling.
- Several V_S models were generated from the surface wave data. Models 1FM and 2FM were developed for the southwest source location and northeast source location dispersion curves, respectively, assuming fundamental mode only and Poisson's ratio of 0.3. Further modeling revealed that these V_S models may excite a dominant first higher mode at low frequencies. There is expected to be insufficient resolution in the v-f transform (overtone image) to isolate the fundamental mode and first higher mode at low frequencies resulting, which would result in modal superposition (mode mixing). Therefore, alternate V_S models (Models 1AM and 2AM) were developed assuming the observed dispersion curve consists of the average/effective mode (average of all modes based on relative amplitude of each mode for a far-field, plane Rayleigh wave). The algorithm used to estimate average mode does not consider source offset (i.e. infinite source location assumed) of body wave effects. We cannot state with certainty that the observed dispersion data consists of the average mode, but this may be a better option than incorrectly assuming that the dispersion data is the fundamental mode.
- There is a significant difference in the relative amplitude of the first higher mode between Models 1FM and 2FM. This may indicate that average mode computations may not be reliable at this site due to the unpredictable effects of the lateral velocity variation. Alternatively, an argument could be made that the representative dispersion curve used to develop model 2FM is the first higher mode associated with Model 1FM rather than fundamental mode. The seismic refraction model does, however, support the presence of near surface lateral velocity variation observed between the models.
- Another problem in working with the average/effective mode is that there may be sufficient resolution at high frequencies to correctly identify the fundamental mode. At these frequencies the average mode phase velocity may be slightly higher than the fundamental mode phase velocity, in which case modeling based on the average mode may slightly underestimate the associated V_S. This potential problem is most clear for Model 1AM, where the fundamental mode and average mode deviate over a wide frequency range. On Model 2AM, however, the fundamental mode and average mode only differ significantly at low frequencies.

- Interestingly, V_{S30} is quite similar for Models 1FM, 2FM and 2AM. Model 1AM has about a 10% lower V_{S30} for reasons discussed above. It is also interesting to note that Models 1FM and 2FM have quite different V_S over a wide depth range, whereas Models 1AM and 2AM are almost identical at depths below 5 m.
- Surface wave depth of investigation is about 30 m based on half of maximum wavelength criteria.
- The inferred P-wave velocities in the surface wave models are generally lower than those in the seismic refraction models. The surface wave models based on the average mode assumption appear to have more realistic P-wave velocities at depths below 18 m, however, a longer refraction line would be required to accurately constrain P-wave velocities at these depths.
- V_{S30} is 922 m/s for Model 1FM (fundamental mode) and 837 m/s for Model 1AM (average mode). The average V_{S30} between the two models is 879 m/s (NEHRP Site Class B). The significant difference in velocity structure between these two models is related to the significant difference between the fundamental mode and average mode dispersion curves.
- Average S-wave velocity between 1 m (inferred sensor depth) and 31 m is 1,046 and 933 m/s, for Models 1FM and 1AM, respectively, averaging 990 m/s.
- V_{S30} is 939 m/s for Model 2FM (fundamental mode) and 910 m/s for Model 2AM (average mode). The average V_{S30} between the two models is 924 m/s (NEHRP Site Class B). The V_S models are relatively similar, once different layer thicknesses are accounted for, except for lower V_S of the deepest two layers in the average mode model.
- Average S-wave velocity between 1 m (inferred sensor depth) and 31 m is 1,026 and 987 m/s, for Models 2FM and 2AM, respectively, averaging 1,006 m/s.
- Models 2FM and 2AM are considered most representative of the velocity structure in the immediate vicinity of the seismic station as the northeast end of the MASW array is closest to the seismic station. For the purpose of site characterization, we recommend using the V_S model developed using the average/effective mode assumption (Model 2AM) as V_S below a depth of 18 m is more consistent with the P-wave refraction model. Regardless of the V_S model used for site characterization, the site falls into the NEHRP Site Class B velocity range.
- This site would benefit from additional investigation. A longer P-wave seismic refraction line would better constrain P-wave velocity at depth. A common center point SASW sounding would not suffer as much from the significant lateral velocity variation. An MALW (Love wave) array would not be as severely impacted from probable dominant higher mode issues, but lateral velocity variation would still be an issue. MASW data acquisition and processing schemes designed to minimize the effects of lateral velocity variation need to be further investigated.

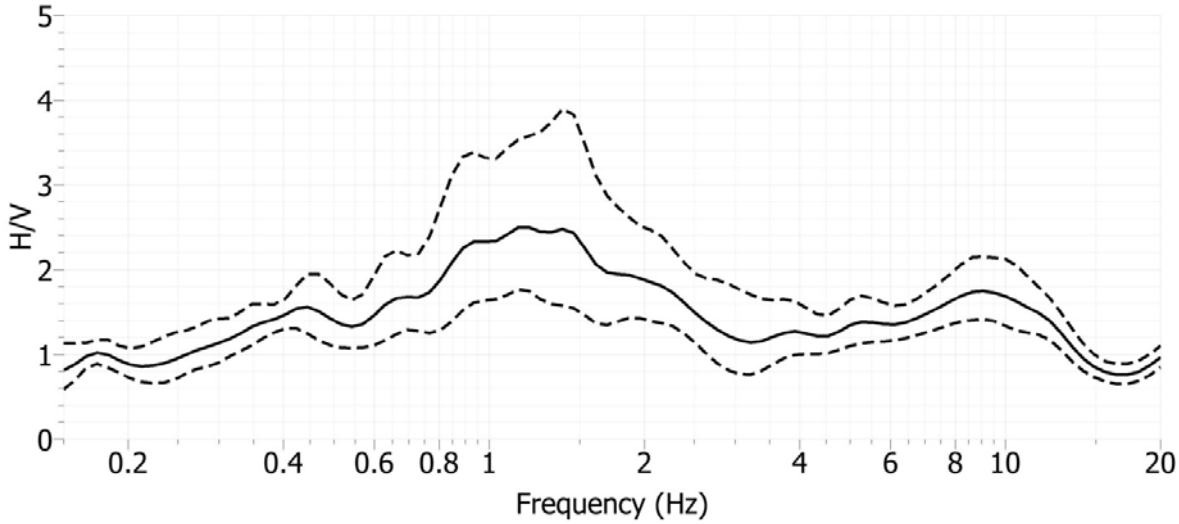

Site CI.SPG2, H/V Spectral Ratio, Near Seismic Station, Sensor 453

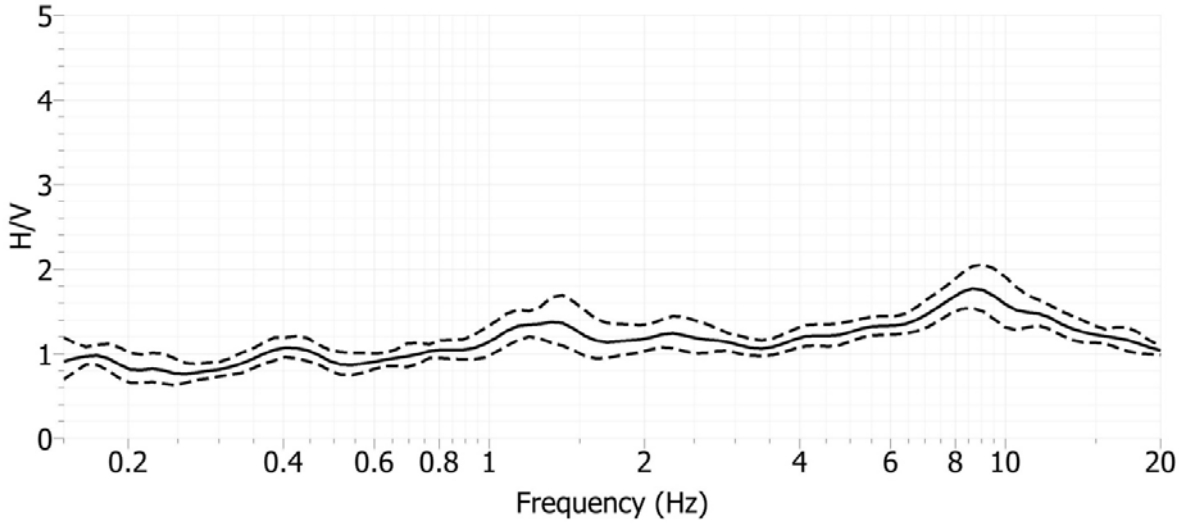

Site CI.SPG2, H/V Spectral Ratio, Array SPG2-1, Sensor 450

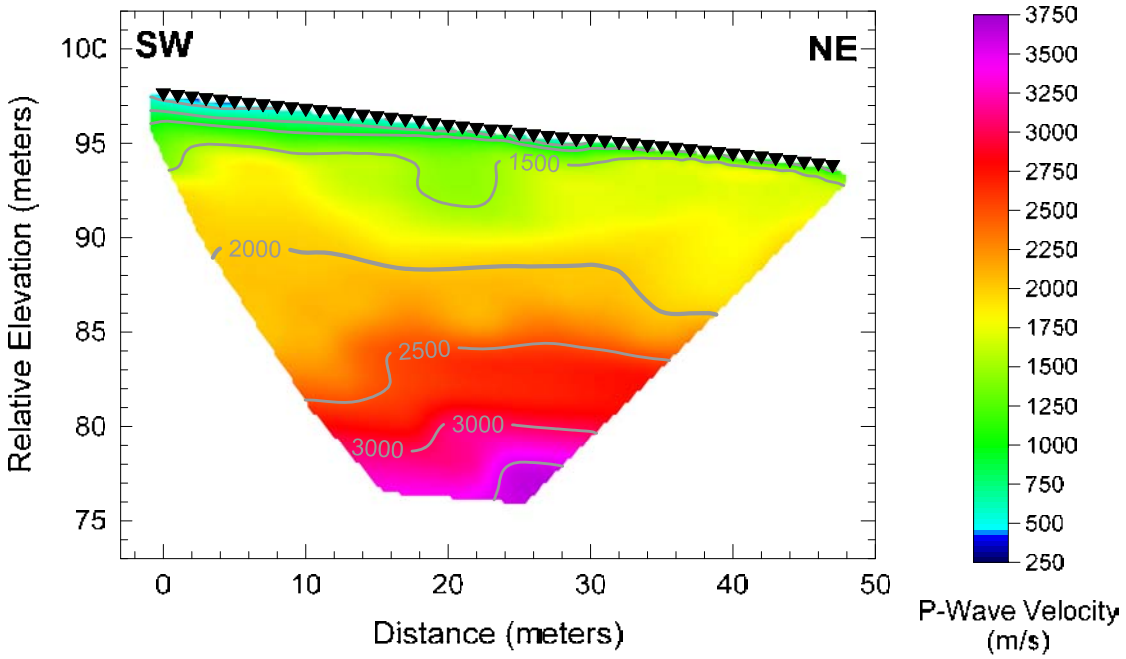

Array SPG2-1 – Tomographic Seismic Refraction Model utilizing Smooth Velocity Gradient Starting Model

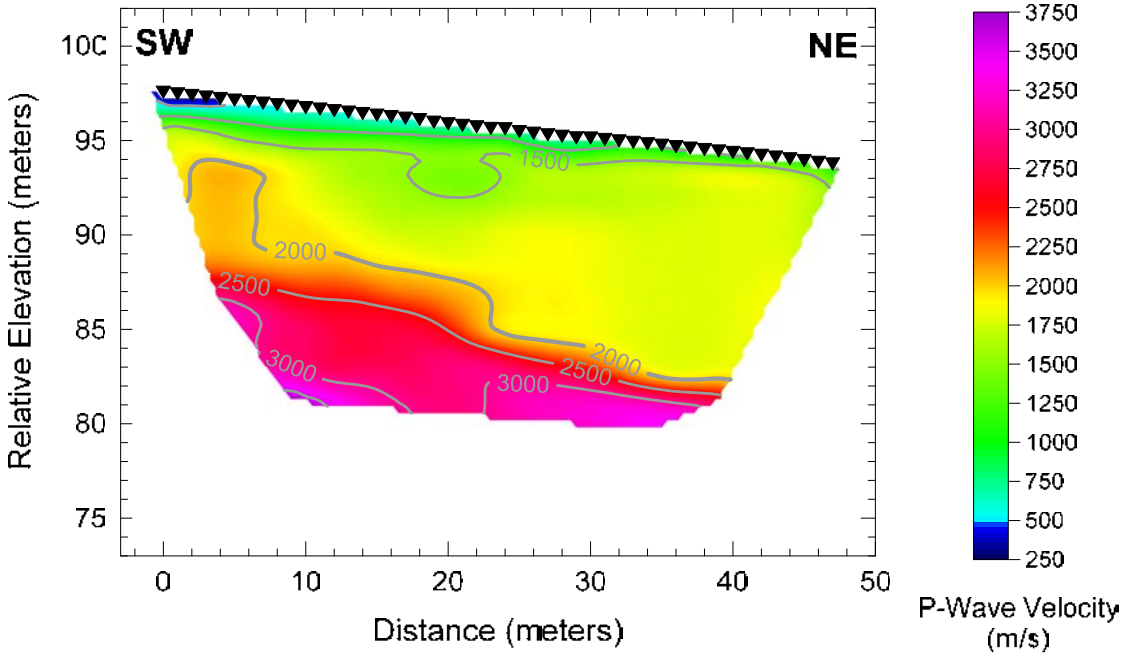

Array SPG2-1 – Tomographic Seismic Refraction Model utilizing Layer Based Starting Model

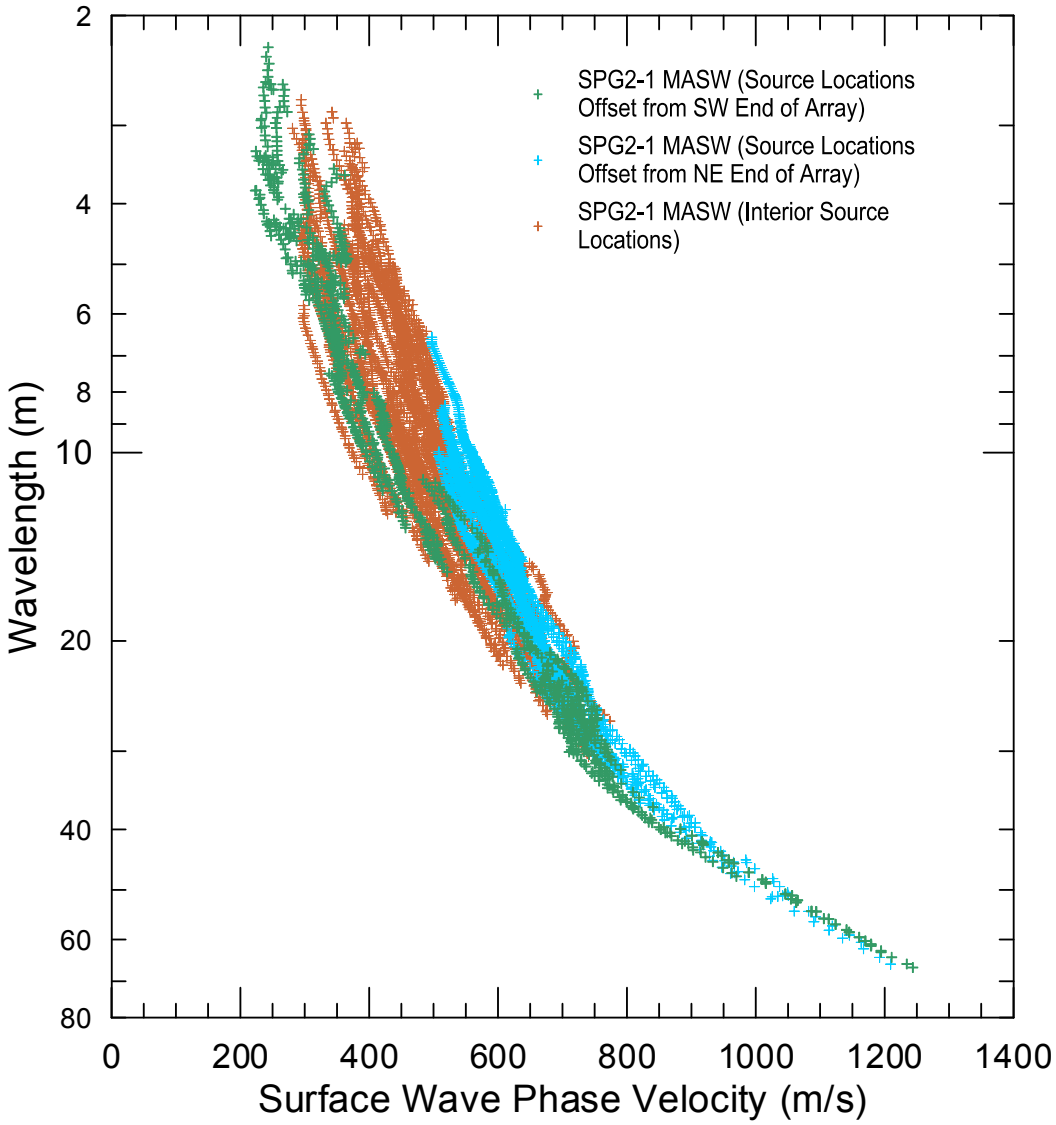

CI.SPG2 – Rayleigh wave phase velocity data from source locations offset from the southwest and northeast ends of the array and from interior source locations (i.e. seismic refraction sources) clearly showing the effects of near surface lateral velocity variation. There is significant scatter (about 200 m/s) at small wavelengths due to a slight thickening to the southwest of a low velocity sediment/decomposed rock layer as shown in seismic refraction models. This data were modeled by developing two dispersion curves: one from interior and southwest source locations defining the lower envelope and the other from interior and northeast source locations defining the upper envelop of the dispersion data. Although the seismic refraction model supports the observed lateral velocity variation at small wavelengths in the Rayleigh wave dispersion data, the possibility cannot be completely discounted that the higher phase velocities at small wavelengths are associated with higher mode Rayleigh waves.

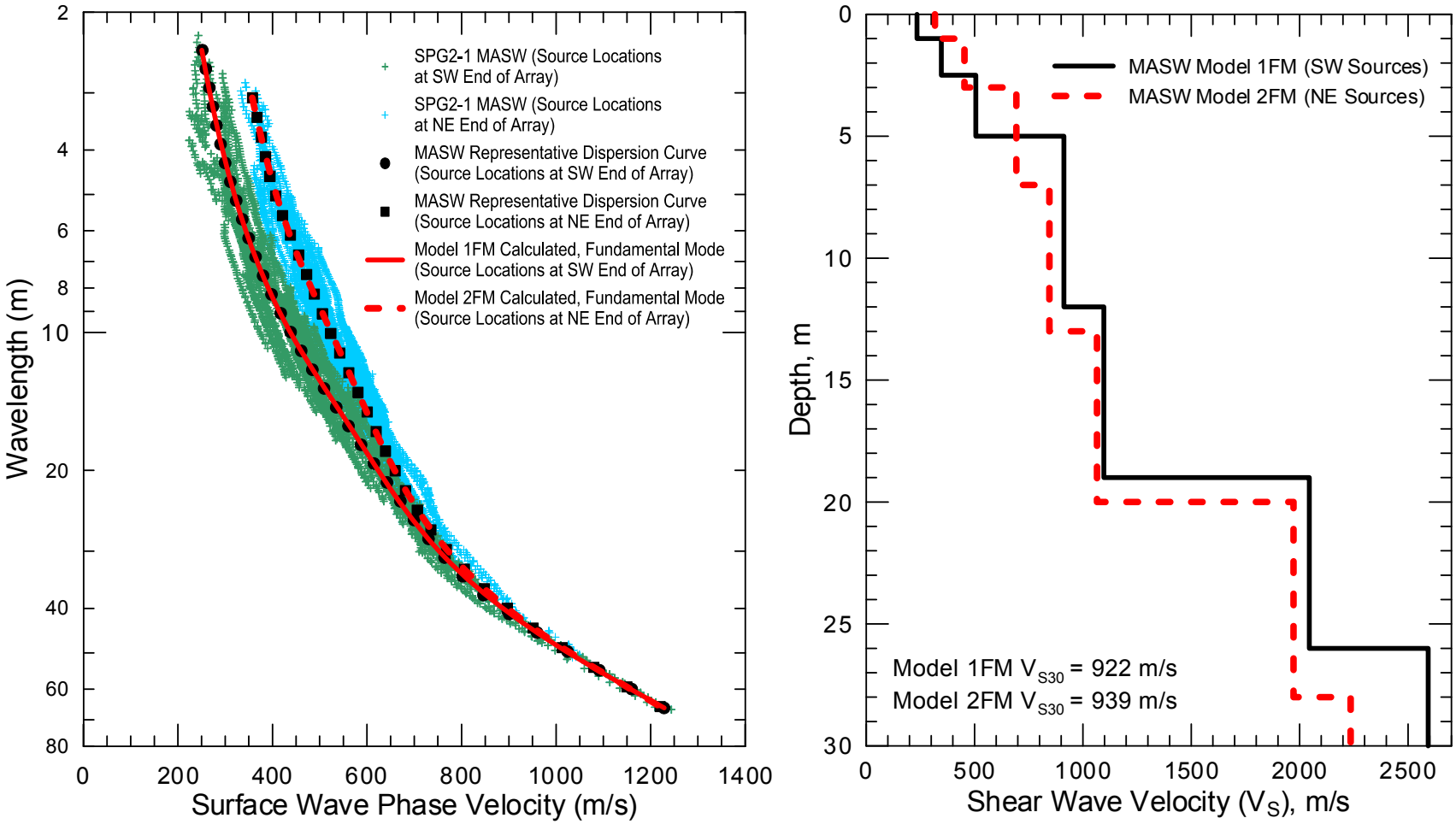

CI.SPG2 - Field, representative and inverted theoretical surface wave dispersion data (left) and associated V_S models (right) based on fundamental mode assumption. Due to near surface lateral velocity variation, primarily due to a slight thickening of low velocity soil and decomposed rock to the southwest, two representative dispersion curves were modeled.

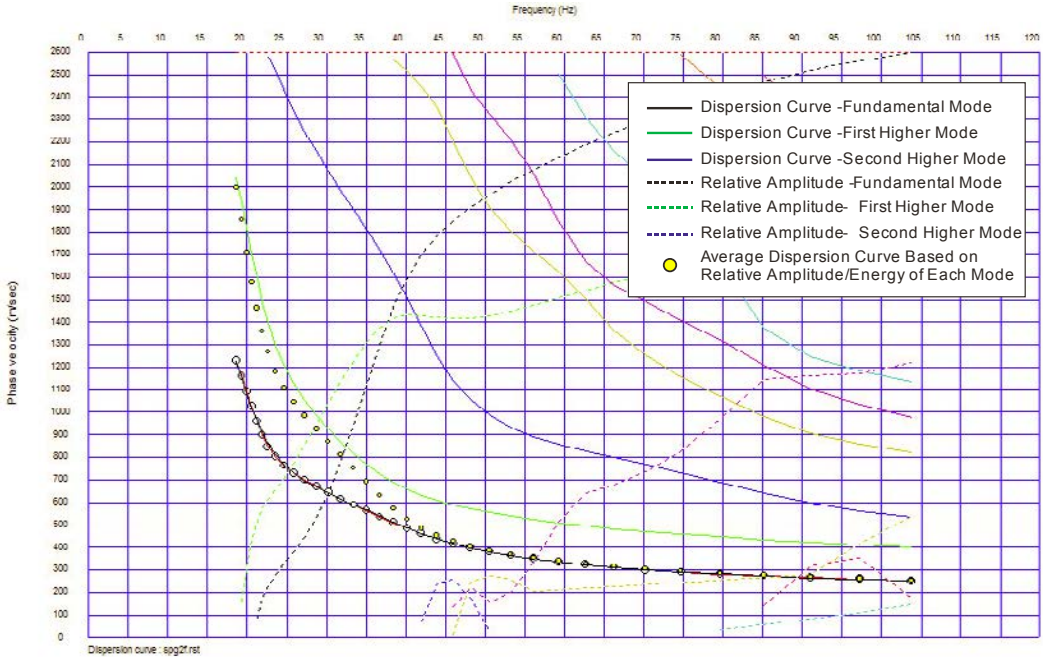

Model 1FM (SW Sources) – Calculated Rayleigh Wave Modes

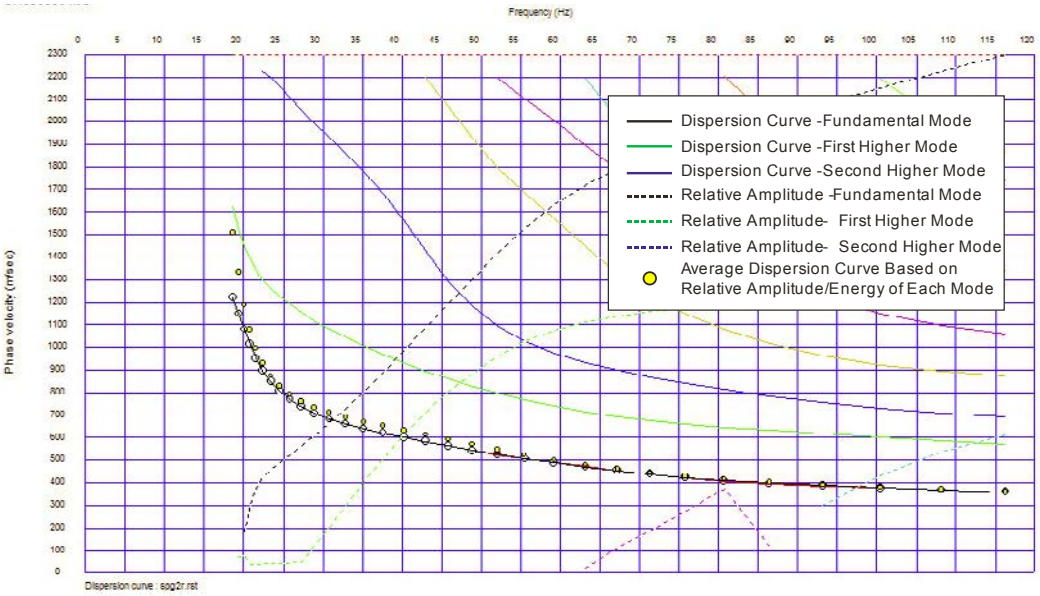

Model 2FM (NE Sources) – Calculated Rayleigh Wave Modes

Calculated Rayleigh wave phase velocity modes for Models 1FM and 2FM. Model 1FM is expected to have significant problems with a dominant first higher mode, whereas Model 2FM has less of a problem. Due to possible modal superposition at low frequencies and because the velocity of the deeper layers in the fundamental mode V_S models are unrealistically high, alternate V_S models were developed by assuming that the average/effective mode is representative of the observed dispersion curve. However, it is not possible to account for the effects of lateral velocity variation on the relative amplitude of the Rayleigh wave modes.

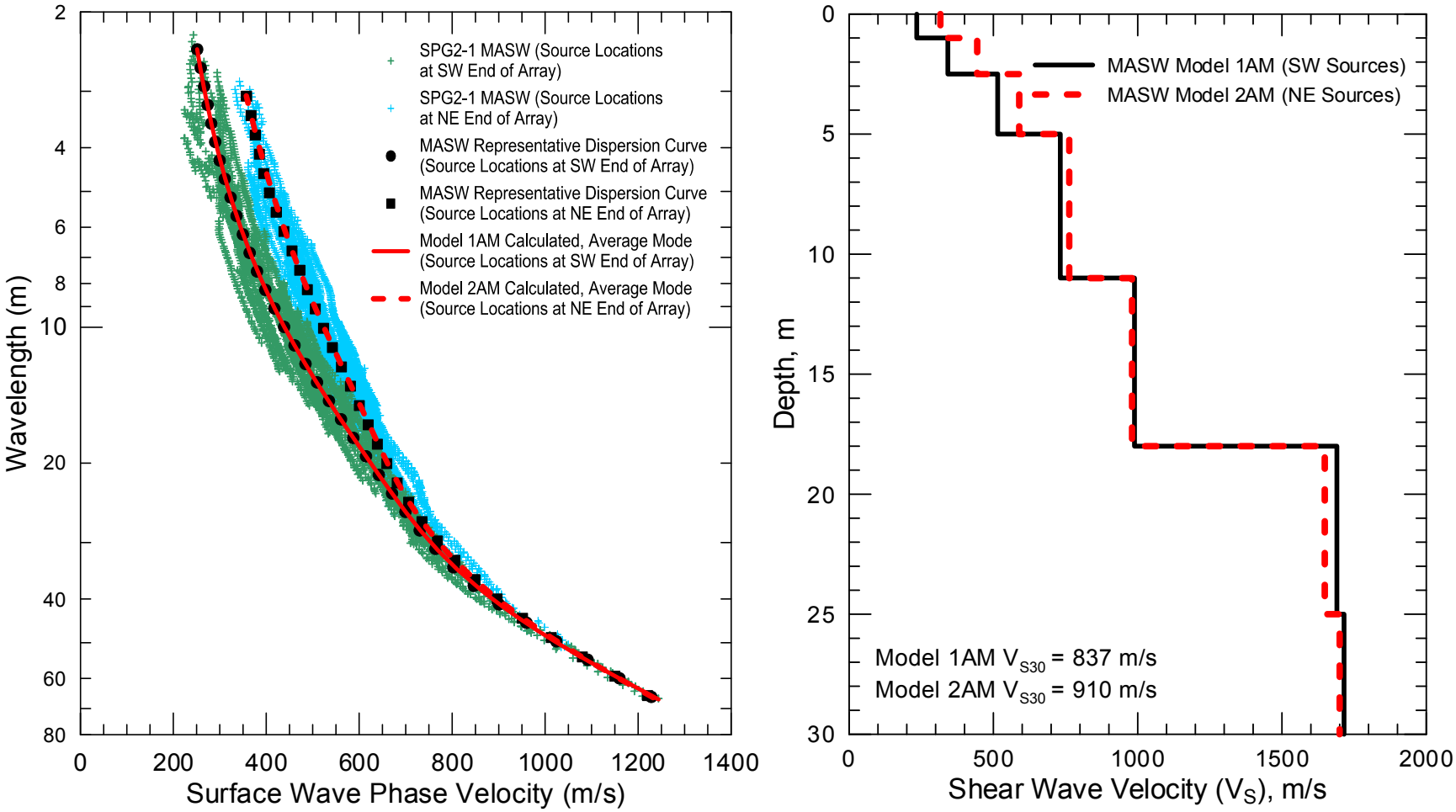

CI.SPG2 - Field, representative and inverted theoretical surface wave dispersion data (left) and associated V_S models (right) based on average mode assumption. Due to near surface lateral velocity variation, primarily due to a slight thickening of low velocity soil and decomposed rock to the southwest, two representative dispersion curves were modeled.

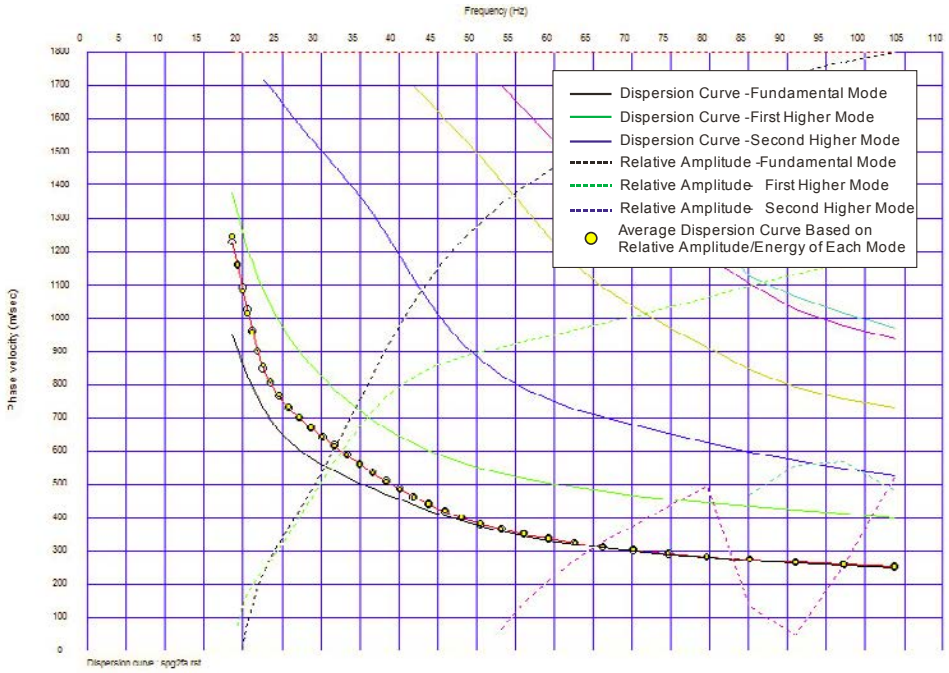

Model 1AM (SW Sources) – Calculated Rayleigh Wave Modes

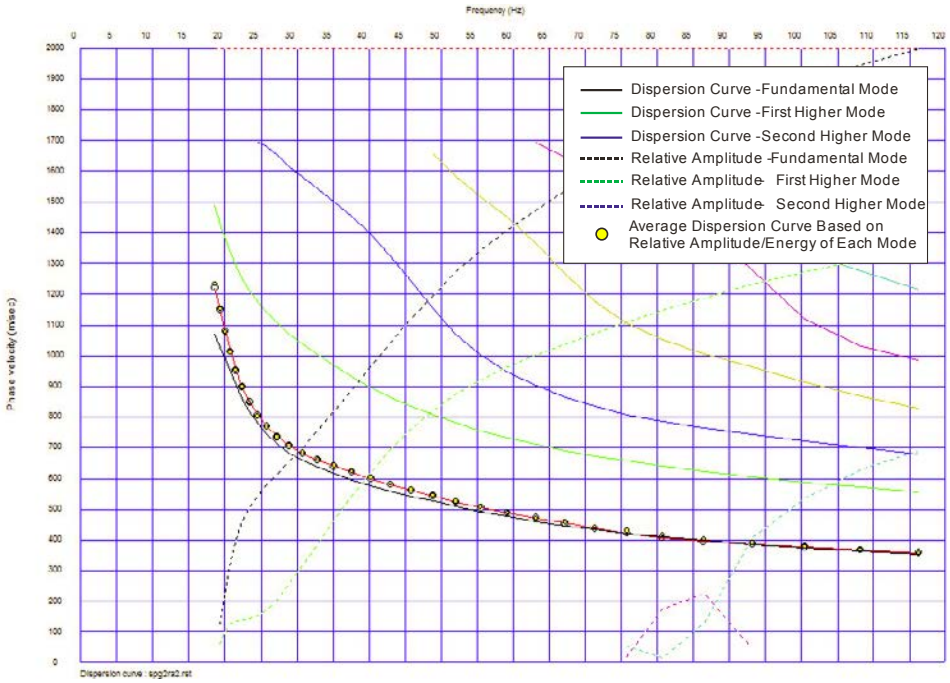

Model 2AM (NE Sources) – Calculated Rayleigh Wave Modes

Calculated Rayleigh wave phase velocity modes for V_S Models 1AM and 2AM, which were developed using the average mode assumption. The average mode for Model 1AM is significantly different from the fundamental mode over a wide frequency range. The modeled V_S will be underestimated over a wide depth interval if the representative dispersion curve actually reflects the fundamental mode at all but the lowest frequencies. The average mode for Model 2AM only diverges significantly from the fundamental mode at low frequencies.

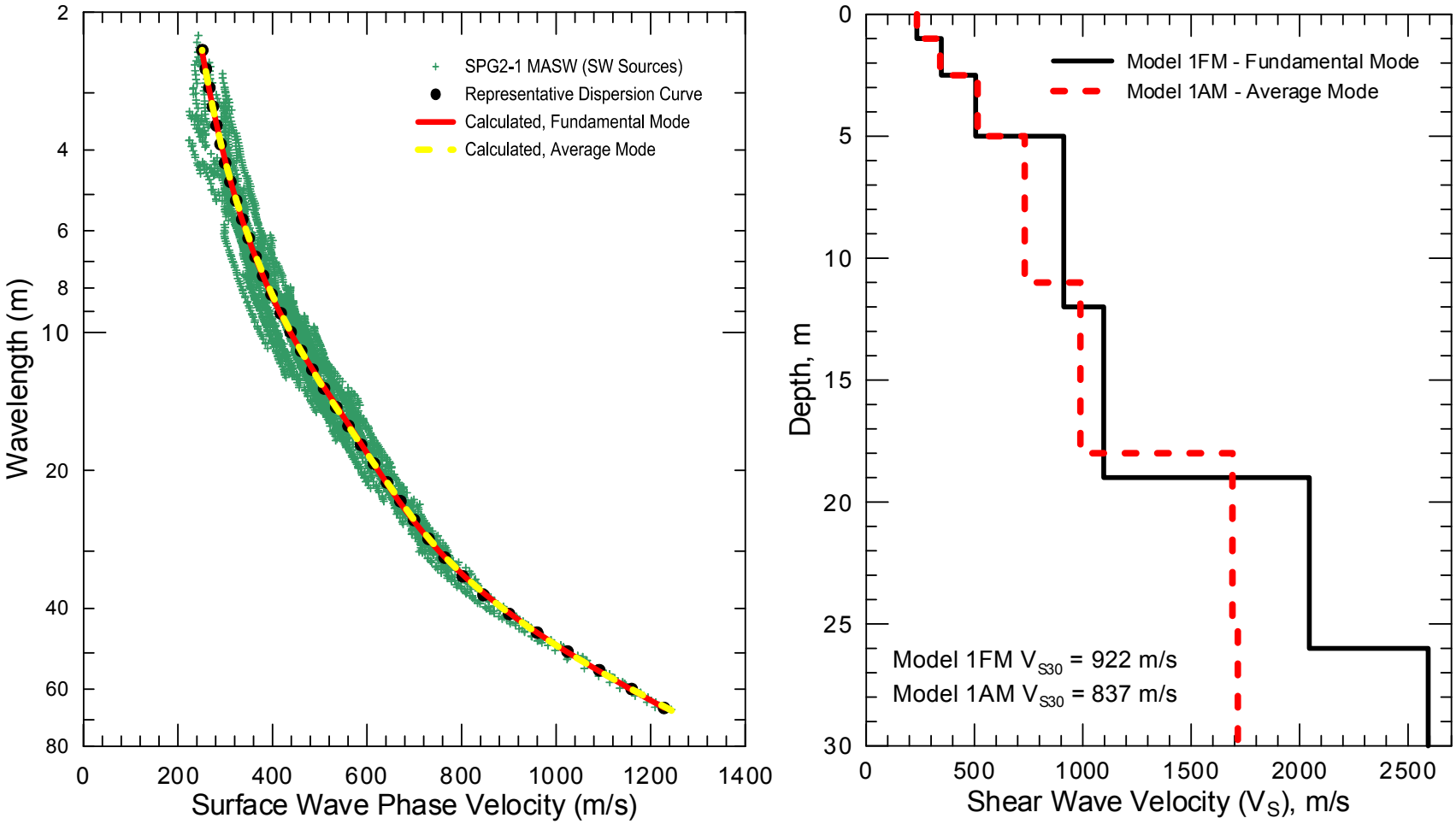

CI.SPG2 - Field, representative and inverted theoretical surface wave dispersion data (left) and associated V_S models (right) based on both fundamental and average mode assumptions and for source locations at the southwest end of the array.

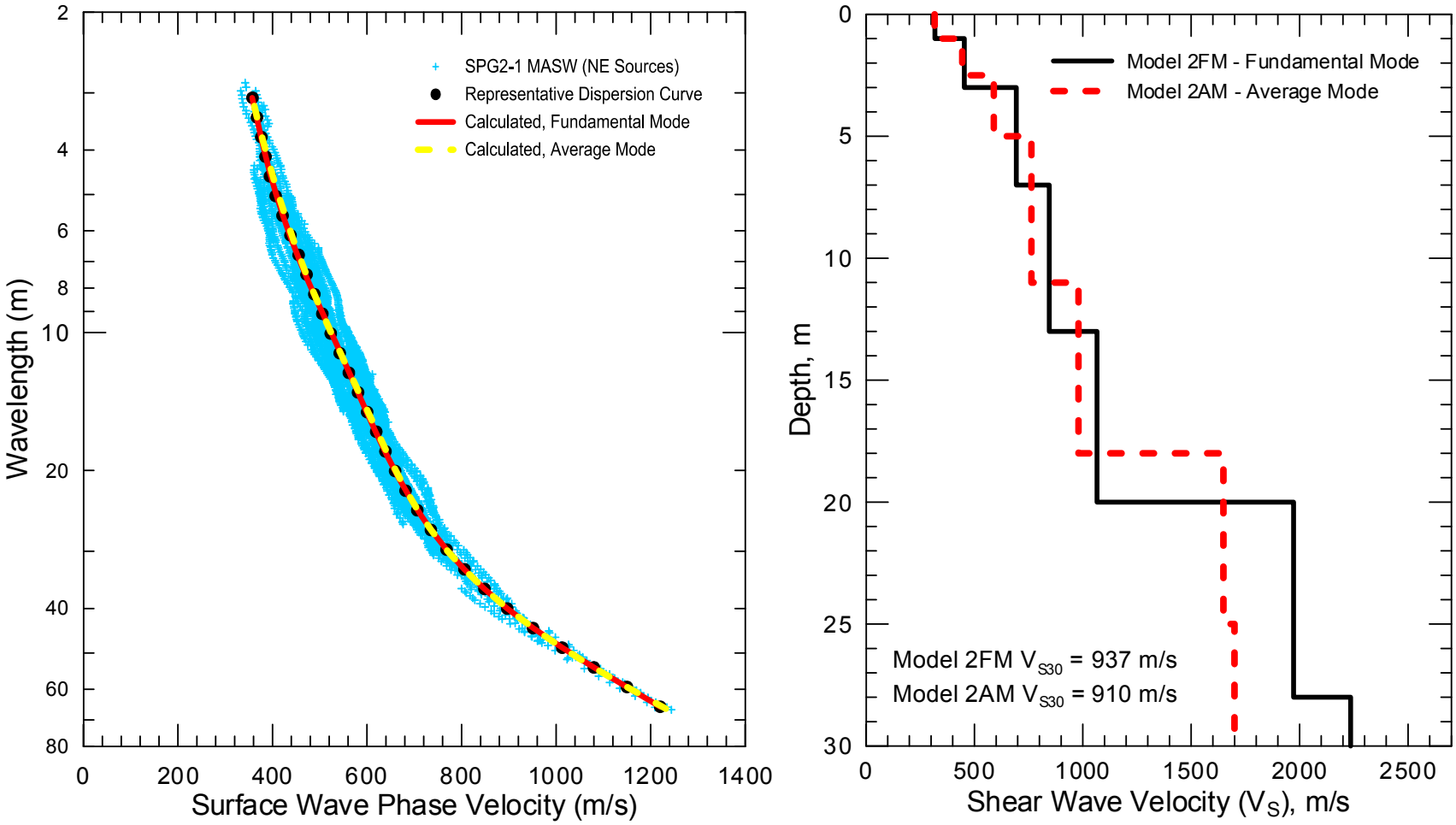

CI.SPG2 - Field, representative and inverted theoretical surface wave dispersion data (left) and associated V_S models (right) based on both fundamental and average mode assumptions and for source locations at the northeast end of the array.

Site CI.SWS

Location: Sam W. Stewart, El Centro Naval Bombing Range, Superstition Hills, Imperial County, California

Latitude: 32.94503 **Longitude:** -115.79990
(Station coordinates modified based on field GPS survey, WGS84 coordinate system)

V_{S30} (measured): 525 m/s (±10% lateral velocity variation)

V_{S30} (adjusted to more accurately reflect seismic station conditions): 587 m/s (average S-wave velocity between 1.5 and 31.5 m adjusting for assumed sensor depth).

NEHRP Site Class: C

Geomatrix Code: IGA/IGB

Geologic Conditions/Observations: Seismic station located on weathered Mesozoic (Jurassic to Late Triassic) granodiorite of the Southern California batholith.

Site Conditions: Rural site. Hilly topography in site vicinity. Seismic station located on Mesozoic granitic bedrock covered by eolian dune sands. Test area located on a relatively planar surface gently sloping to the northeast.

Geophysical Methods Utilized: HVSR, Seismic Refraction, MASW

Geophysical Testing Arrays:

1. Array SWS-1 (48 channel MASW and P-wave seismic refraction array utilizing 4.5 Hz vertical geophones spaced 1.5 m apart for a length of 70.5 m, forward and reverse shot locations with multiple source offsets and source types and multiple interior shot locations).
2. Three HVSR measurement locations distributed along array SWS-1.

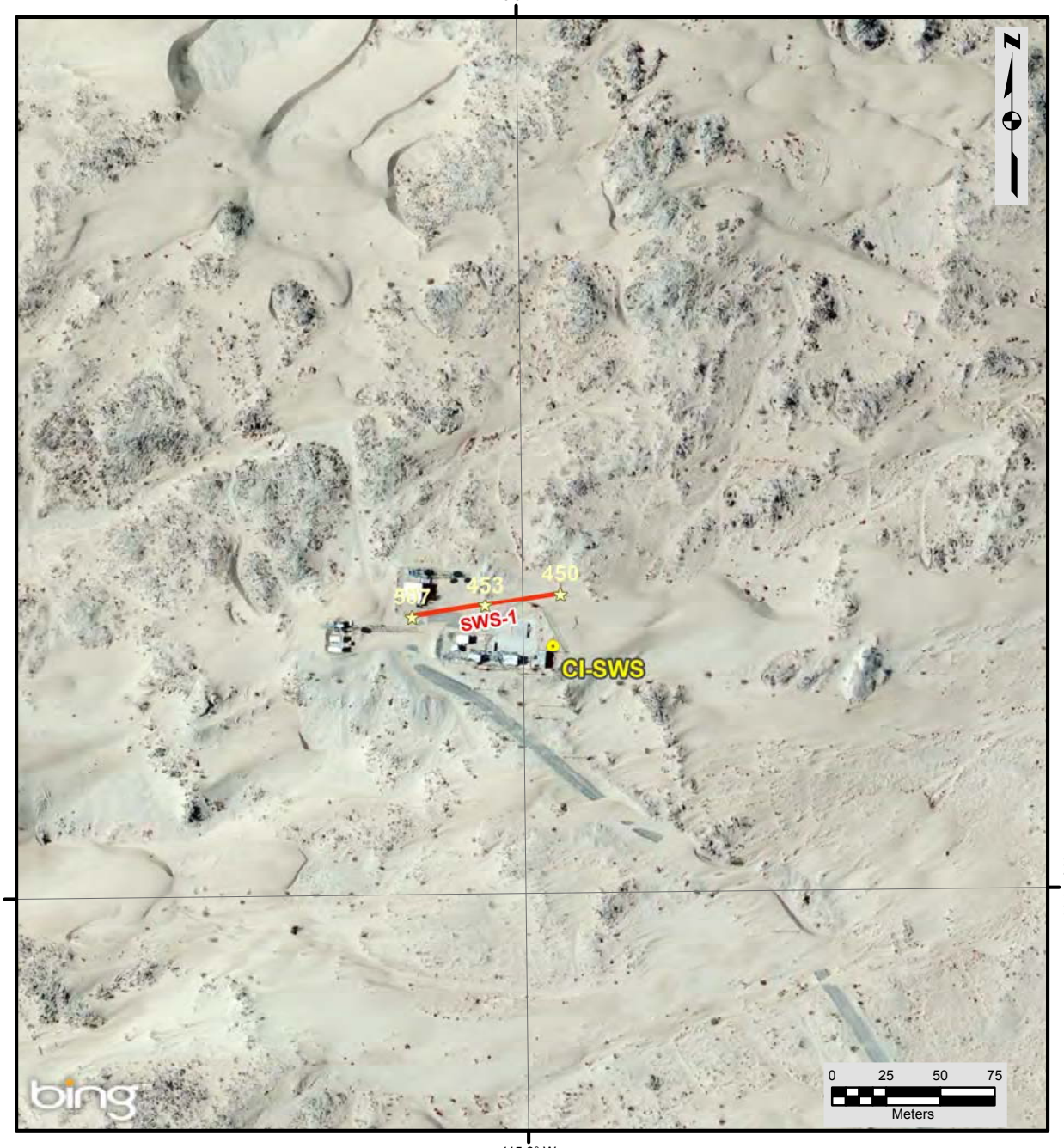

Legend

- Seismic Station - Approximate Surveyed Location
- Seismic Station - Approximate Location of Record
- H/V Spectral Ratio Location
- MASW and Seismic Refraction Array

NOTES:
1. WGS 1984 COORDINATE SYSTEM
2. Image Source: (c) Microsoft Corporation and its data suppliers

File Name: CI-SWS-I

Date: 2/7/2013

USGS science for a changing world

GEOVision geophysical services

RECOVERY.GOV

SITE MAP
CI•SWS

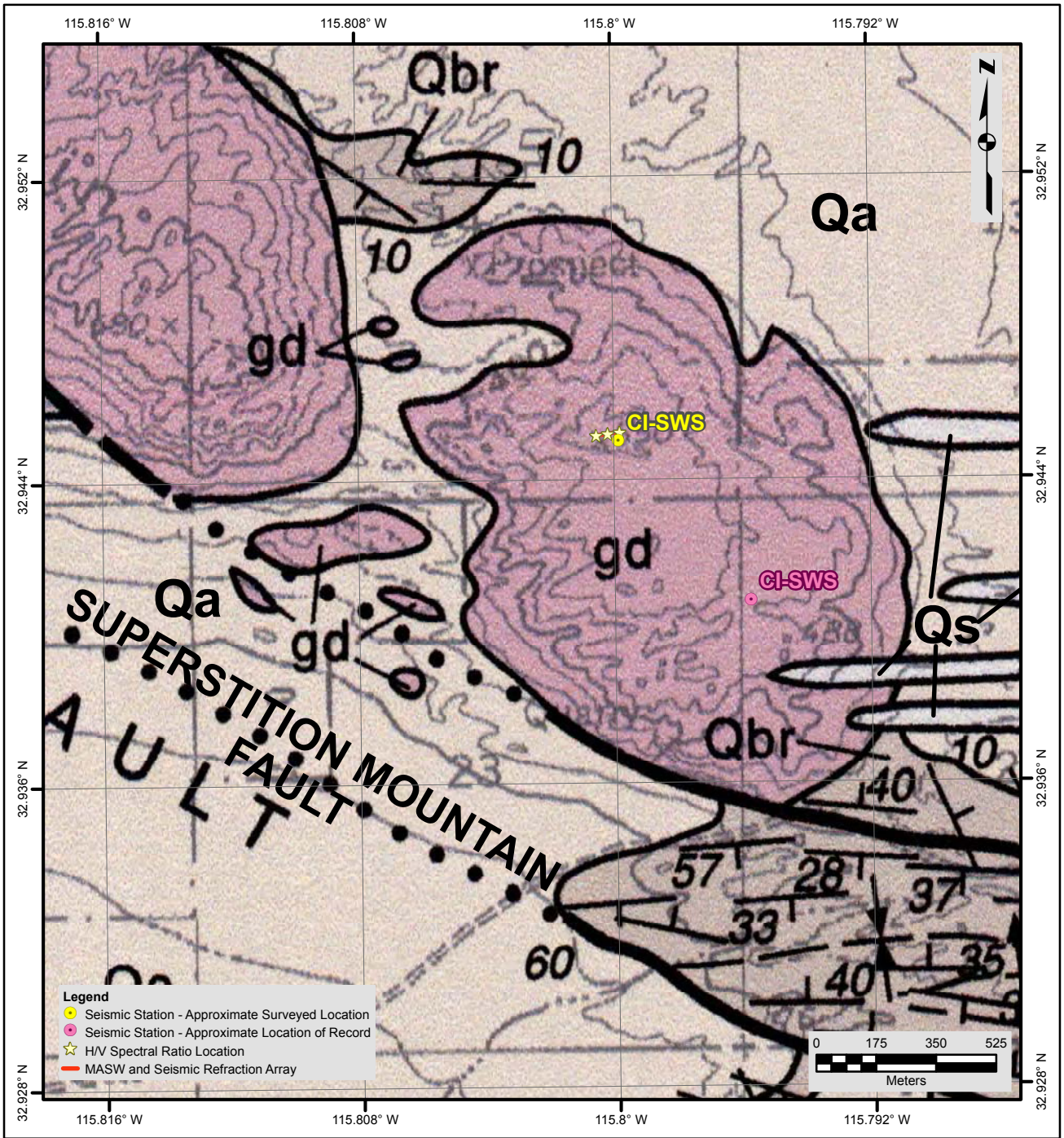

Description of Geologic Map Units

Qa = Quaternary (Holocene) alluvial sand, gravel, silt and clay of valleys areas
Qs = Quaternary (Holocene) windblown dune sand, thin veneers to broad dunes at least 20 feet thick
Qbr = Quaternary (Late Pliocene to Pleistocene) Brawley Formation; lacustrine facies of Ocotillo Conglomerate; claystone, thin sandstone strata with some pebbly beds locally
gd = Mesozoic (Jurassic to Late Triasic) granodiorite

NOTES:
1. WGS 1984 COORDINATE SYSTEM
2. Geologic Map of Plaster city & Brawley 15 Minute Quadrangles, Imperial County, California by Thomas W. Dibblee, Jr., 2008
3. See site map for details of geophysical survey

USGS science for a changing world

GEOVision geophysical services

RECOVERY.GOV

GEOLOGIC MAP
CI•SWS

File Name: CI-SWS

Date: 2/7/2013

CI.SWS seismic station to left of structure

CI.SWS seismic station

Looking southeast towards center of array SWS-1, HVSR sensor 453 and seismic station

P-wave refraction data acquisition along array SWS-1

Looking southwest along array SWS-1

Location of Geophysical Testing Arrays:

Location	Latitude	Longitude
SWS-1, Southwest End of MASW/Refraction Array	32.94516	-115.80059
SWS-1, Center of MASW/Refraction Array	32.94520	-115.80023
SWS-1, Northeast End of MASW/Refraction Array	32.94525	-115.79986
HVSR Sensor 450	32.94524	-115.79986
HVSR Sensor 453	32.94520	-115.80023
HVSR Sensor 507	32.94515	-115.80059
CI.SWS Seismic Station	32.94503	-115.79990

Notes: 1) WGS84 Coordinate System (decimal degrees)
2) Survey accuracy is estimated at 1 to 2 m.

Results:

V_S Model for Southwestern Half of MASW Array

Depth to Top of Layer (m)	Layer Thickness (m)	S-Wave Velocity (m/s)	Inferred P-Wave Velocity (m/s)	Inferred Poisson's Ratio	Inferred Density (g/cm^3)
0	1	208	389	0.3	1.8
1	2	317	594	0.3	1.9
3	5	474	887	0.3	1.9
8	14	588	1101	0.3	2.0
22	>8	932	1743	0.3	2.2

Notes: 1) Depth of investigation is about 30 m.
2) Bottom layer is a half space.
3) V_S of half space is not well constrained.

V_S Model for Northeastern Half of MASW Array

Depth to Top of Layer (m)	Layer Thickness (m)	S-Wave Velocity (m/s)	Inferred P-Wave Velocity (m/s)	Inferred Poisson's Ratio	Inferred Density (g/cm^3)
0	0.5	121	226	0.3	1.7
0.5	1.5	202	378	0.3	1.8
2	3.5	303	567	0.3	1.8
5.5	6	515	964	0.3	1.9
11.5	9	552	1032	0.3	2.0
20.5	>9.5	985	1842	0.3	2.1

Notes: 1) Depth of investigation is about 30 m.
2) Bottom layer is a half space.
3) V_S of half space is not well constrained.

Average V_P and Estimated V_S Models from Central Portion of P-wave Seismic Refraction Line

Depth to Top of Layer (m)	Layer Thickness (m)	P-Wave Velocity (m/s)	Estimated S-Wave Velocity (m/s)			
			Poisson's Ratio = 0.25	Poisson's Ratio = 0.30	Poisson's Ratio = 0.3333	Poisson's Ratio = 0.35
0.00	0.42	445	257	238	223	214
0.42	0.84	490	283	262	245	235
1.26	0.84	555	320	297	277	266
2.11	0.84	738	426	394	369	354
2.95	0.84	750	433	401	375	360
3.79	0.84	767	443	410	383	368
4.64	0.84	779	450	416	389	374
5.48	1.77	857	495	458	429	412
7.25	1.77	910	525	486	455	437
9.02	1.77	938	542	502	469	451
10.79	1.77	985	569	526	492	473
12.56	1.77	1010	583	540	505	485
14.33	1.77	1055	609	564	528	507
16.10	1.77	1090	629	583	545	524
17.87	1.77	1132	654	605	566	544
19.64	1.77	1156	668	618	578	555
21.41	1.77	1250	722	668	625	600
23.18	Half Space	1265	730	676	633	608

V_P and Estimated V_S Models from a Position of 45 m on the P-wave Seismic Refraction Line where Lowest Velocities occur in the Central Portion of the Line – Most Representative of the Northeastern Half of the Seismic Line

Depth to Top of Layer (m)	Layer Thickness (m)	P-Wave Velocity (m/s)	Estimated S-Wave Velocity (m/s)			
			Poisson's Ratio = 0.25	Poisson's Ratio = 0.30	Poisson's Ratio = 0.3333	Poisson's Ratio = 0.35
0.00	0.42	390	225	208	195	187
0.42	0.84	390	225	209	195	187
1.26	0.84	415	240	222	207	199
2.11	0.84	477	275	255	238	229
2.95	0.84	488	282	261	244	235
3.79	0.84	517	299	277	259	249
4.64	0.84	554	320	296	277	266
5.48	1.77	723	418	387	362	347
7.25	1.77	855	493	457	427	411
9.02	1.77	913	527	488	456	439
10.79	1.77	969	559	518	484	465
12.56	1.77	987	570	528	493	474
14.33	1.77	1017	587	544	509	489
16.10	1.77	1034	597	553	517	497
17.87	1.77	1060	612	567	530	509
19.64	1.77	1144	660	611	572	549
21.41	1.77	1238	715	662	619	595
23.18	Half Space	1343	775	718	671	645

V_P and Estimated V_S Models from a Position of 34.5 m on the P-wave Seismic Refraction Line where Highest Velocities occur in the Central Portion of the Line

Depth to Top of Layer (m)	Layer Thickness (m)	P-Wave Velocity (m/s)	Estimated S-Wave Velocity (m/s)			
			Poisson's Ratio = 0.25	Poisson's Ratio = 0.30	Poisson's Ratio = 0.3333	Poisson's Ratio = 0.35
0.00	0.42	458	264	245	229	220
0.42	0.84	551	318	295	276	265
1.26	0.84	698	403	373	349	335
2.11	0.84	899	519	481	450	432
2.95	0.84	942	544	503	471	452
3.79	0.84	975	563	521	488	469
4.64	0.84	976	564	522	488	469
5.48	1.77	977	564	522	489	470
7.25	1.77	978	565	523	489	470
9.02	1.77	988	570	528	494	475
10.79	1.77	995	575	532	498	478
12.57	1.77	1009	582	539	504	485
14.34	1.77	1073	620	574	537	516
16.11	1.77	1105	638	591	553	531
17.88	1.77	1191	688	637	596	572
19.65	1.77	1198	691	640	599	575
21.42	1.77	1230	710	657	615	591
23.19	Half Space	1242	717	664	621	597

V_P and Estimated V_S Models from a Position of 25.5 m on the P-wave Seismic Refraction Line – Most Representative of the Southwestern Half of the Seismic Line

Depth to Top of Layer (m)	Layer Thickness (m)	P-Wave Velocity (m/s)	Estimated S-Wave Velocity (m/s)			
			Poisson's Ratio = 0.25	Poisson's Ratio = 0.30	Poisson's Ratio = 0.3333	Poisson's Ratio = 0.35
0.00	0.42	498	287	266	249	239
0.42	0.84	565	326	302	282	271
1.26	0.84	582	336	311	291	280
2.11	0.84	762	440	407	381	366
2.95	0.84	763	440	408	381	366
3.79	0.84	764	441	408	382	367
4.63	0.84	765	442	409	382	367
5.48	1.77	767	443	410	384	369
7.24	1.77	813	470	435	407	391
9.01	1.77	867	501	463	433	416
10.78	1.77	971	561	519	485	466
12.55	1.77	972	561	520	486	467
14.32	1.77	1023	591	547	512	492
16.09	1.77	1099	635	588	550	528
17.86	1.77	1103	637	590	552	530
19.63	1.77	1103	637	590	552	530
21.40	1.77	1266	731	677	633	608
23.17	Half Space	1267	732	677	634	609

Observations/Discussion:

- The HVSR curves are similar, especially those for sensors 453 and 507, which would appear to validate the 1-D velocity structure assumption.
- There are no distinct, high amplitude HVSR peaks. There is, however, a possible, but inconclusive, weak HVSR peak in the 2 to 3 Hz. This HVSR peak could be associated with a velocity increase from highly weathered to relatively competent rock.
- The P-wave seismic refraction data for array SWS-1 were modeled using a tomographic inversion routine with a smooth velocity gradient starting model. The P-wave seismic refraction model was extended to far offset shot locations to extend depth of investigation. It should be noted that a larger geophone spacing, rather than the utilization of far offset shot locations, is preferred for extending depth of investigation, when applying tomographic inversion routines. However, the seismic refraction data were acquired in conjunction with surface wave data, where a shorter array length is preferred.

- The P-wave seismic refraction survey design allowed P-wave velocity to be imaged to a maximum depth of about 20 to 24 m. The seismic refraction model indicates that P-wave velocity is about 350 to 600 m/s at the surface and increases to 700 m/s at a depth of 2 to 8 m, 900 m/s at a depth of 3 to 15 m, 1,000 m/s at a depth of 12 to 17 m and over 1,200 m/s at a nominal depth of 20 m. The maximum P-wave velocity in the central portion of the model, where depth of investigation is greatest, is about 1,275 m/s.
- The seismic refraction survey indicates that there is significant lateral velocity variation at the site with lower near surface velocities beneath the northeastern half of the line and an elevated zone of higher velocity weathered rock beneath the central portion of the seismic line.
- The average P-wave velocity of the upper 30 m (V_{P30}) was estimated between 25.5 and 45 m on the P-wave refraction model, where depth of investigation is greatest. To estimate V_{P30} the P-wave velocity at a depth of 23 m, nominal depth of investigation, was projected to 30 m depth. V_{P30} ranges from about 853 to 1,023 m/s between a position of 25.5 to 45 m, an 18% variation. The lowest and highest estimated V_{P30} over this distance interval occurs at a position of 45 and 34.5 m, respectively. V_{P30} is expected to be lower than the maximum beneath much of the southwest half of the seismic line and may be slightly lower than the minimum northeast of a position of 45 m.
- An average V_P model was developed over the 25.5 to 45 m distance interval by horizontally averaging the travel time of each model cell and cell thickness and average V_{P30} was determined to be 959 m/s. Assuming constant Poisson's ratios of 0.25, 0.3, 0.3333 and 0.35 would result in an estimated V_{S30} of 554, 513, 479 and 461 m/s, respectively. Bedrock is not expected to be saturated in the upper 30 m, therefore, Poisson's ratio in the 0.25 to 0.35 range is probable. Estimated V_{P30} and V_{S30} are expected to be slightly conservative (low) because velocity likely continues to increase with depth below a depth of 23 m, the maximum depth of investigation. However, a 50% increase of the half-space velocity from 1,265 to 1,898 m/s only increases V_{P30} by 6%.
- The lowest value of V_{P30} over the 25.5 to 45 m distance interval, 853 m/s, occurs at a position of 45 m and may continue to decrease to the northeast. Assuming constant Poisson's ratios of 0.25, 0.3, 0.3333 and 0.35 would result in an estimated V_{S30} of 472, 456, 426 and 410 m/s, respectively. The velocity structure at a position of 45 m is likely most representative of the northeastern half of the seismic line.
- The highest value of V_{P30} over the 25.5 to 45 m distance interval, 1,024 m/s, occurs at a position of 34.5 m. Assuming constant Poisson's ratios of 0.25, 0.3, 0.3333 and 0.35 would result in an estimated V_{S30} of 591, 547, 512 and 492 m/s, respectively.
- At a position of 25.5 m, considered most representative of the southwestern half of the seismic line, V_{P30} is 946 m/s. Assuming constant Poisson's ratios of 0.25, 0.3, 0.3333 and 0.35 would result in an estimated V_{S30} of 546, 506, 473 and 455 m/s, respectively.
- Noise conditions at the site were not sufficient for application of passive surface wave techniques.
- MASW (Rayleigh wave) data were difficult to reduce due to the differing near-surface velocity structure beneath each half of the line and a narrow elevated zone of higher velocity rock beneath the central portion of the line. Surface wave dispersion data could only be extracted from the seismic records by considering each half of the MASW array separately. SASW analysis of selected MASW receiver pairs from off-end source locations was also conducted to better constrain the dispersion curves. Extraction of long

wavelength surface wave dispersion data required use of geophones near the center of the array, both for MASW and SASW analysis, where wave propagation has been impacted by the elevated zone of higher velocities. This shallow higher velocity zone is expected to have some unknown effect on the resulting V_S models, likely at depths below about 20 m. Ideally, an alternate location would have been identified for site characterization, although significant 2-D velocity variation may be the norm in the immediate site vicinity.

- Dispersion curves from MASW analysis and SASW analysis of selected MASW receiver pairs were combined into a single dispersion curve for analysis.
- There is nominally about 50 to 80 m/s scatter in MASW/SASW dispersion data selected for modeling, likely due to the effects of lateral velocity variation.
- Representative dispersion curves were generated for the MASW data sets using a moving average, polynomial curve fitting routine and used for modeling.
- Separate V_S models were generated for the southwest and northeast portions of the MASW arrays.
- Surface wave depth of investigation is about 30 m based on half of maximum wavelength criteria.
- There is a strong possibility that the velocity of the half space in the MASW V_S models is overestimated due to the effects of the shallow, high velocity zone in the central portion of the seismic line and/or possible modal superposition at low frequencies. The seismic refraction models likely underestimate velocity below a depth of 20 to 24 m due to limited depth of investigation. Most likely V_S below a depth of 20 m falls somewhere between that estimated in the MASW models and that estimated from the seismic refraction models with an assumed Poisson's ratio of 0.3.
- The V_P and estimated V_S structure at various positions along the seismic refraction profile (average, 25.5 m, 34.5 m and 45 m) are very similar below a depth of about 10 m, but significantly different at shallower depths.
- For the purpose of discussion, the MASW V_S model from the southwestern half of the array is compared to the P-wave seismic refraction model at a position of 25.5 m. V_{S30} for the southwest half of the MASW array is 555 m/s while estimated V_{S30} at a position of 25.5 m on the seismic refraction model (assumed Poisson's ratio = 0.3) is 513 m/s. Decreasing V_S of the half space in the MASW model and increasing V_S below 23 m in the seismic refraction model would yield similar estimates of V_{S30}.
- For the purpose of discussion, the MASW V_S model from the northeastern half of the array is compared to the P-wave seismic refraction model at a position of 45 m. V_{S30} for the northeast half of the MASW array is 494 m/s while estimated V_{S30} at a position of 45 m on the seismic refraction model (assumed Poisson's ratio = 0.3) is 456 m/s. Decreasing V_S of the half space in the MASW model and increasing V_S below 23 m in the seismic refraction model would yield similar estimates of V_{S30}.
- V_{S30} from the MASW V_S models for the southwest and northeast portions of the MASW arrays is 555 and 494 m/s, respectively, and averages 525 m/s (NEHRP Site Class C).
- Average S-wave velocity between a depth of 1.5 and 31.5 m, to account for assumed seismic sensor depth, is 609 and 565 m/s for the southwest and northeast portions of the MASW array, respectively, and averages 587 m/s (NEHRP Site Class C).
- V_{S30} estimated from the average P-wave seismic refraction velocity model for the central portion of the seismic line with assumed constant Poisson's ratio of 0.3 is 513 m/s

(NEHRP Site Class C). Average V_{S30} beneath the entire seismic line is expected to be lower than that mentioned above.

- Average S-wave velocity between a depth of 1.5 and 31.5 m from the average P-wave seismic refraction velocity model with assumed constant Poisson's ratio of 0.3 is 551 m/s (NEHRP Site Class C).
- V_{S30} estimated from the P-wave seismic refraction velocity model (assumed constant Poisson's ratio of 0.3) at positions of 25.5 and 45 m is 506 and 456 m/s, respectively and averages 481 m/s (NEHRP Site Class C).
- Average S-wave velocity between a depth of 1.5 and 31.5 m from the P-wave seismic refraction velocity model at positions of 25.5 and 45 m (assumed constant Poisson's ratio of 0.3) is 536 and 497 m/s, respectively, and averages 516 m/s (NEHRP Site Class C).
- For the purpose of site characterization, we recommend using the mean V_{S30} and adjusted V_{S30} from the two MASW V_S models, which are 525 and 587 m/s, respectively. These parameters vary by at least 10% in the immediate vicinity of the seismic line.
- Although data analysis at this site was complicated and the P-wave seismic refraction and MASW models may underestimate and overestimate velocity structure, respectively, at depths below about 20 m the site is clearly in the intermediate range of NEHRP Site Class C and the presented estimate of V_{S30} definitely falls within the variable range in the immediate site vicinity
- A longer P-wave seismic refraction line would permit velocity structure to be imaged to 30 m depth; however, there is limited space at this site. S-wave refraction would be difficult to implement because a portable energy source will not couple well to the weathered rock and truck access for hold down weight on a traction plank is not possible at all locations. Using P-wave seismic refraction to identify areas with minimal lateral velocity variation and then conducting common midpoint SASW tests in these locations may provide more reliable results. SASW testing only requires a maximum receiver spacing of 30 m to image to 30 m depth; whereas, the MASW technique requires an array at least twice that length, at least when utilizing wavefield transforms based on an assumed planar wavefront.

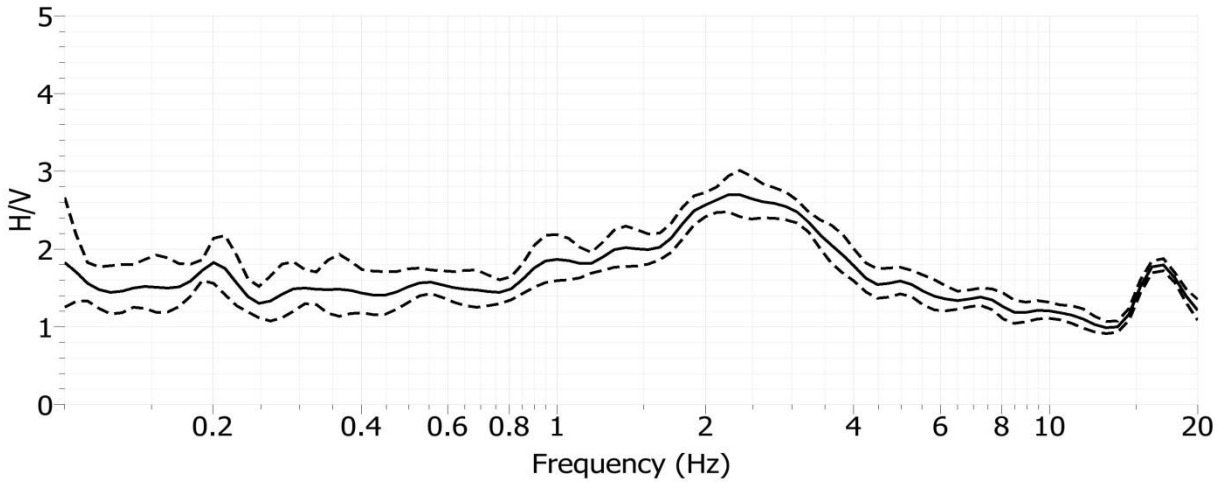

Site CI.SWS, H/V Spectral Ratio, Array SW-1, Sensor 507

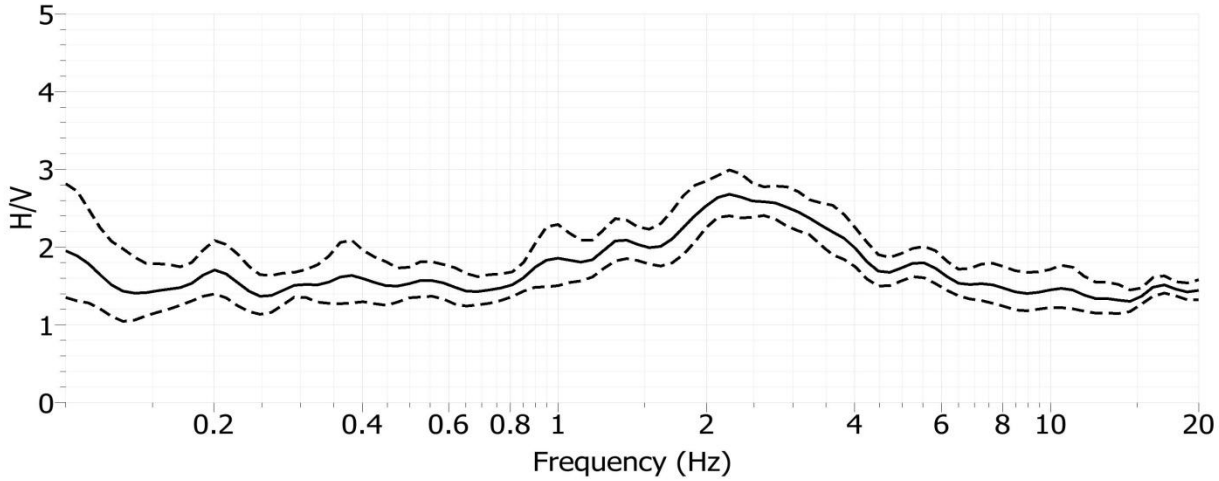

Site CI.SWS, H/V Spectral Ratio, Array SWS-1, Sensor 453

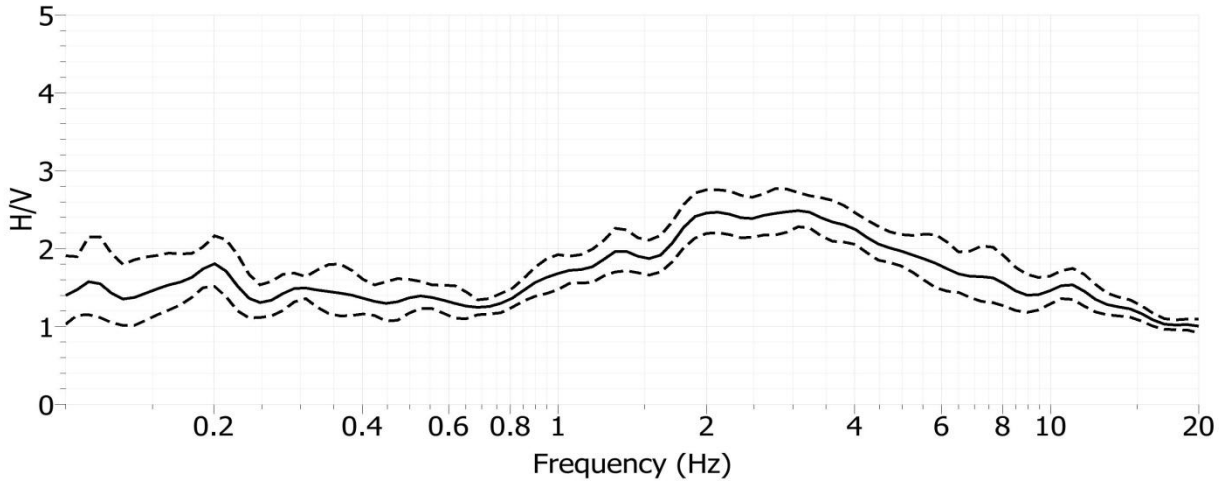

Site CI.SWS, H/V Spectral Ratio, Array SWS-1, Sensor 450

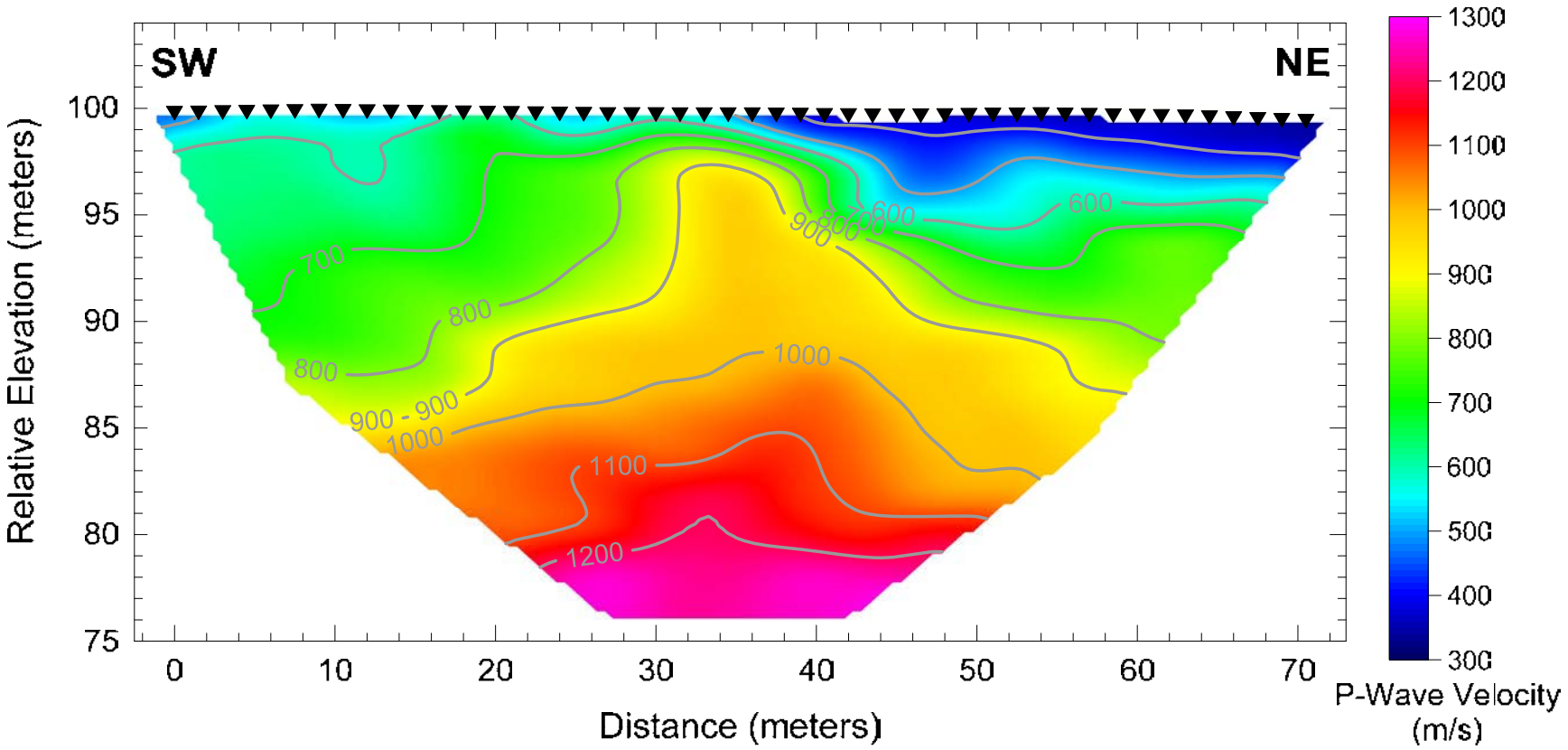

Array SWS-1 – Tomographic seismic refraction model utilizing smooth velocity gradient starting model

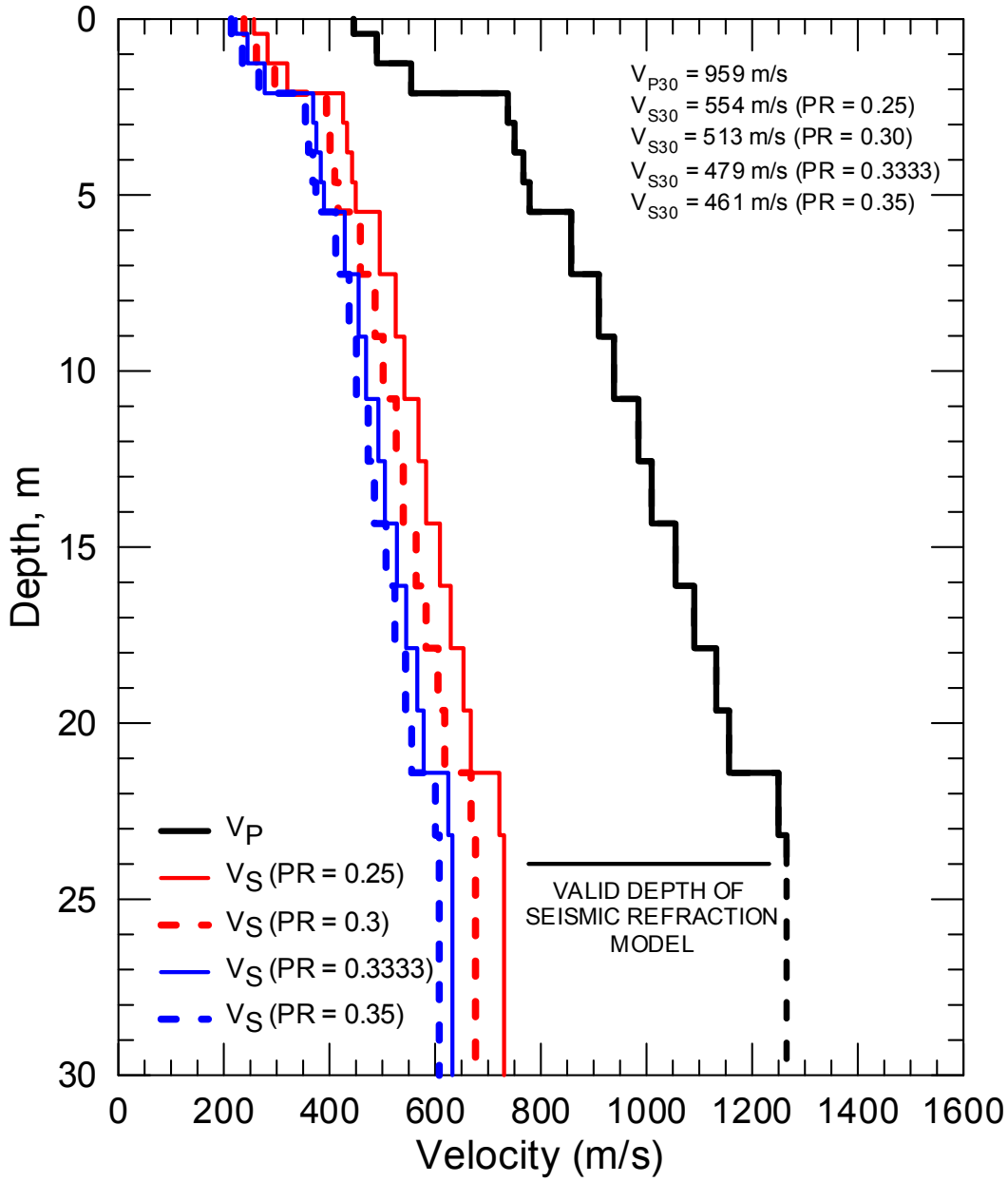

CI.SWS – Average P-wave velocity structure and estimated S-wave velocity structure between 25.5 and 45 m on P-wave seismic refraction array SWS-1. P-wave velocity is not well constrained below a depth of 23 m and computations are made assuming that velocity is constant below this depth. A 50% increase in velocity of the half space only increases V_{P30} by 6%. A longer seismic line would be preferred to more accurately image P-wave velocity structure to a 30 m depth.

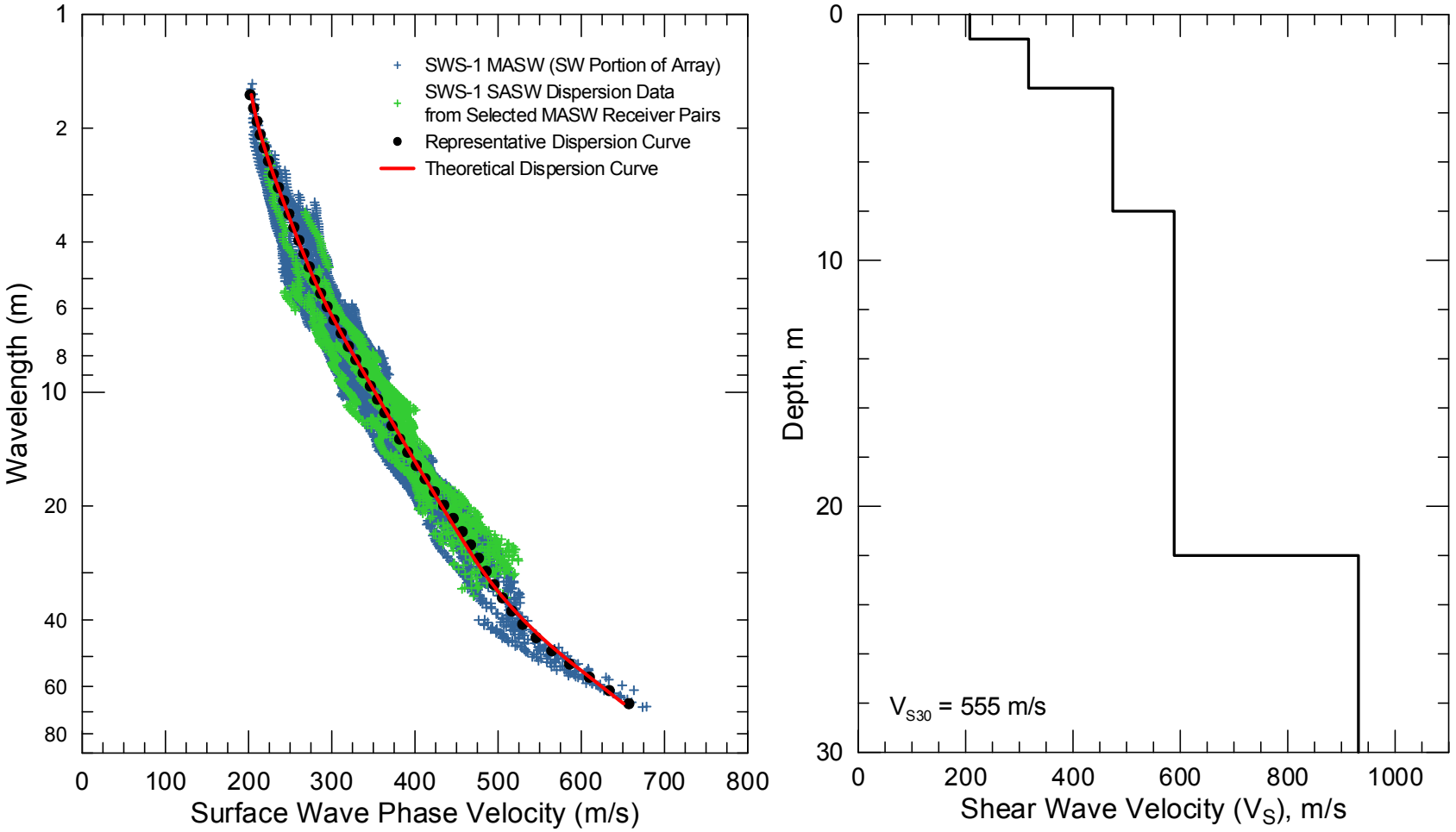

CI.SWS - Field, representative and inverted theoretical surface wave dispersion data (left) and associated V_S model (right) for the southwestern half of array SWS-1

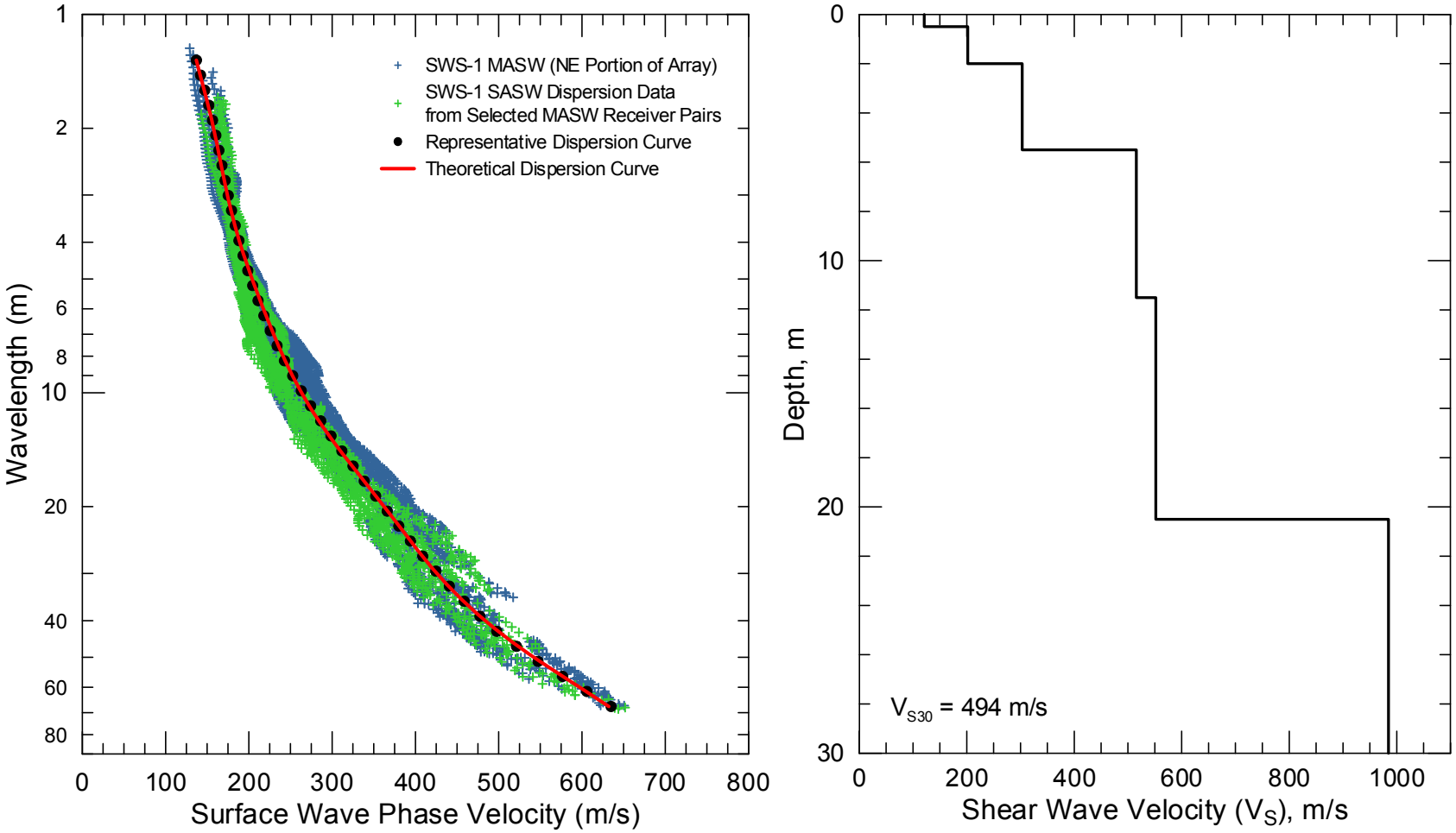

CI.SWS - Field, representative and inverted theoretical surface wave dispersion data (left) and associated V_S model (right) for the northeastern half of array SWS-1

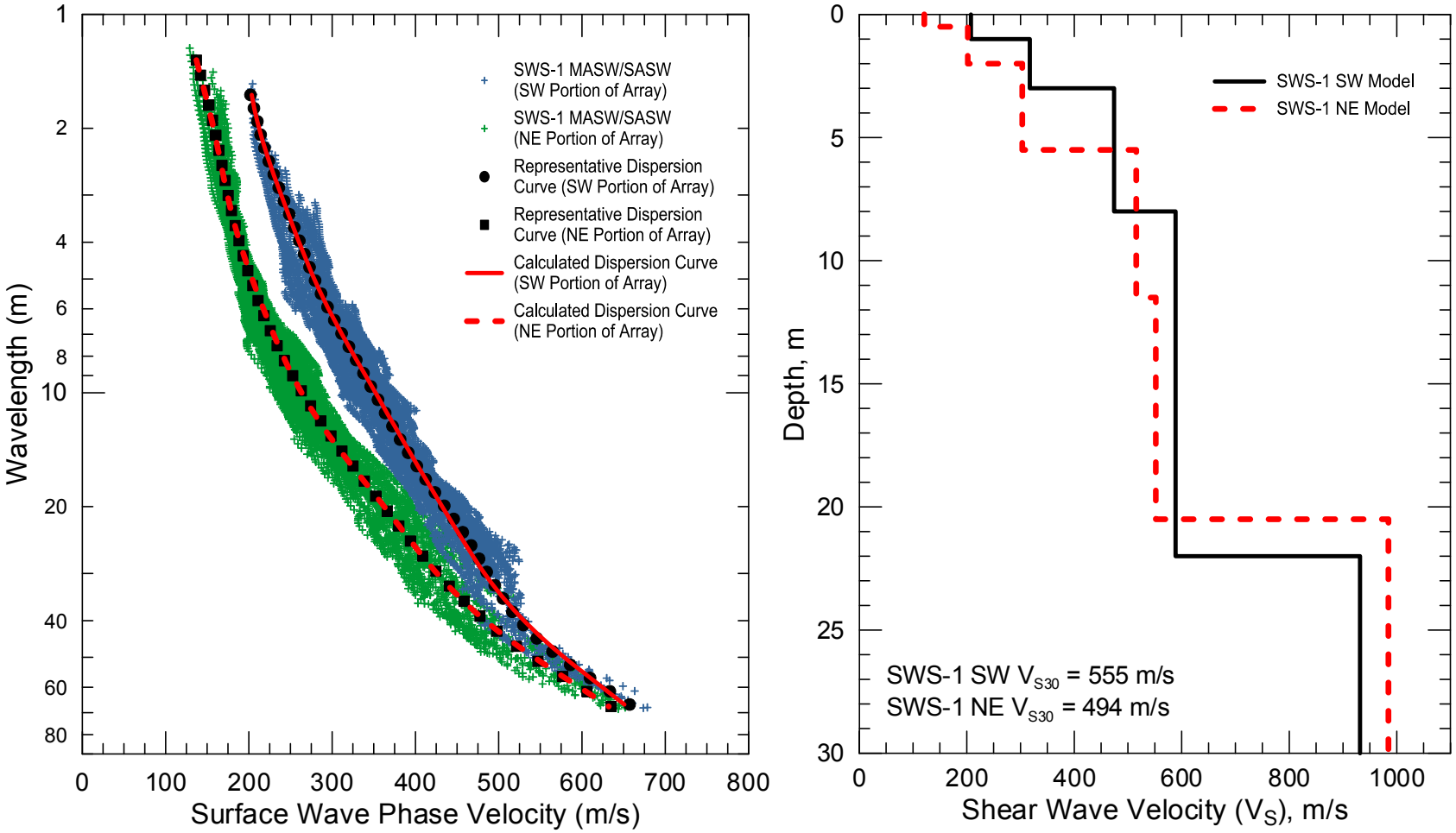

CI.SWS - Field, representative and inverted theoretical surface wave dispersion data (left) and associated V_S models (right)

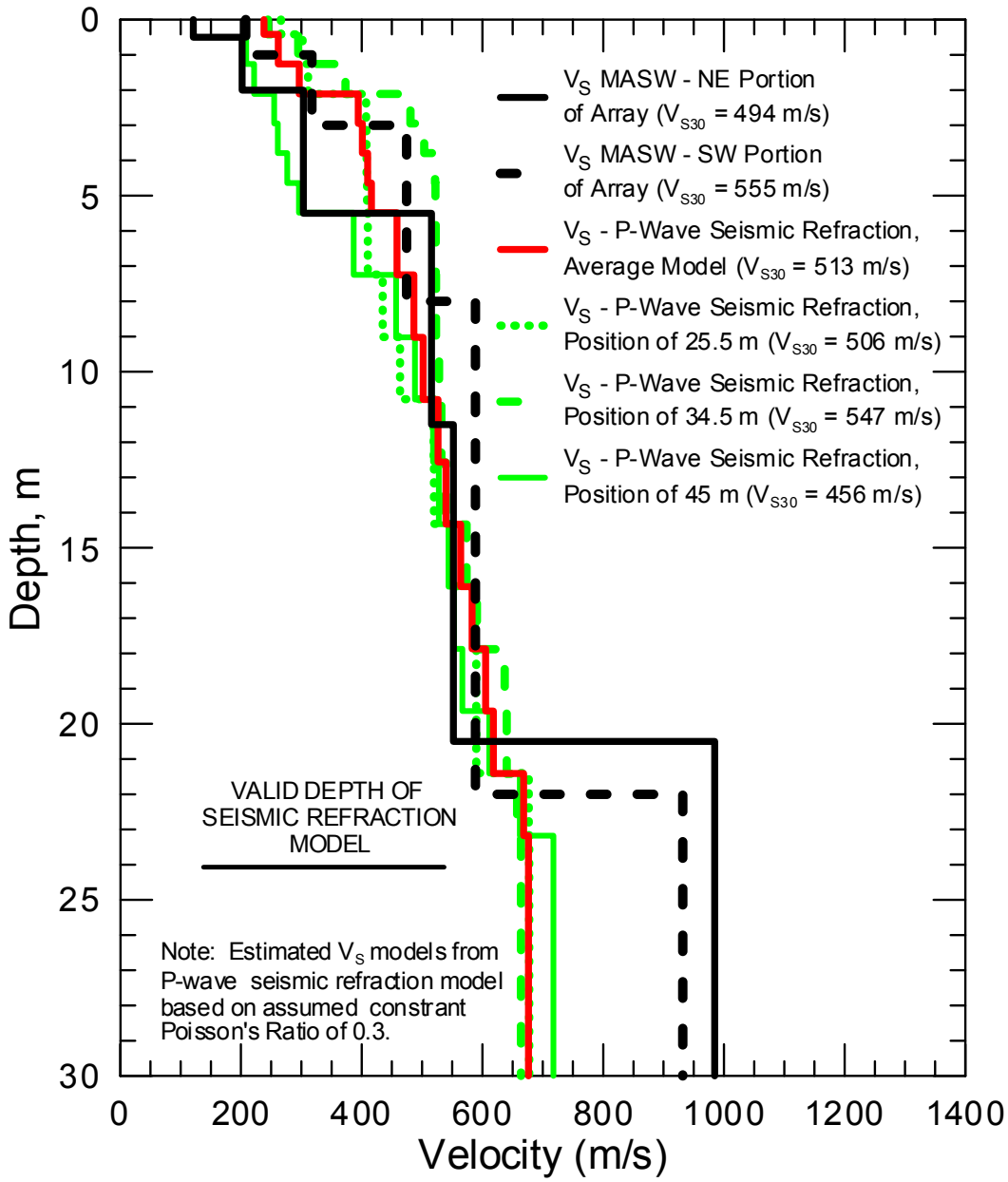

CI.SWS – Summary of S-wave velocity models derived from the MASW (Rayleigh wave) and P-wave seismic refraction surveys. S-wave velocity was estimated from the P-wave seismic refraction models (average over 25.5 to 45 m distance, 25.5 m, maximum V_{P30} at 34.5 m, and minimum V_{P30} at 45 m) assuming a constant Poisson's ratio of 0.3. There is significant lateral velocity variation in the upper 10 m, based on the seismic refraction models, which complicated MASW interpretation. S-wave velocity, estimated from the P-wave seismic refraction models, is probably underestimated below a depth of 23 m due to limited depth of investigation. The S-wave velocity below a depth of 21 m on the MASW models may be overestimated due to the influence of lateral velocity variation and/or modal superposition. Below a depth of 20 m, S-wave velocity is likely between that depicted by the seismic refraction and MASW models.

Site CI.SYP

Location: Santa Ynez Peak, Los Padres National Forest, California

Latitude: 34.52775 **Longitude:** -119.97834
(Station coordinates provided by USGS, WGS84 coordinate system)

V_{S30} (measured): 440 m/s

V_{S30} (adjusted to more accurately reflect seismic station conditions): 470 m/s (average S-wave velocity between 1.5 and 31.5 m adjusting for inferred 1.5 m sensor depth).

NEHRP Site Class: C

Geomatrix Code: IEB

Geologic Conditions/Observations: Seismic station located on Tertiary (Eocene) sedimentary sandstone with shale, dipping about 30 to 40 degrees to the south in the site vicinity.

Site Conditions: Rural site. Seismic station located on top of a mountain peak. Steep topography in site vicinity. Test area located on a hilltop with a steady topographic decline to the southwest.

Geophysical Methods Utilized: HVSR, Seismic Refraction, MASW

Geophysical Testing Arrays:

1. Array SYP-1 (48 channel MASW and P-wave seismic refraction array utilizing 4.5 Hz vertical geophones spaced 1.5 m apart for a length of 70.5 m, forward and reverse shot locations with multiple source offsets and source types (hammers only) and multiple interior shot locations).
2. Four HVSR measurement locations distributed along or near array SYP-1.

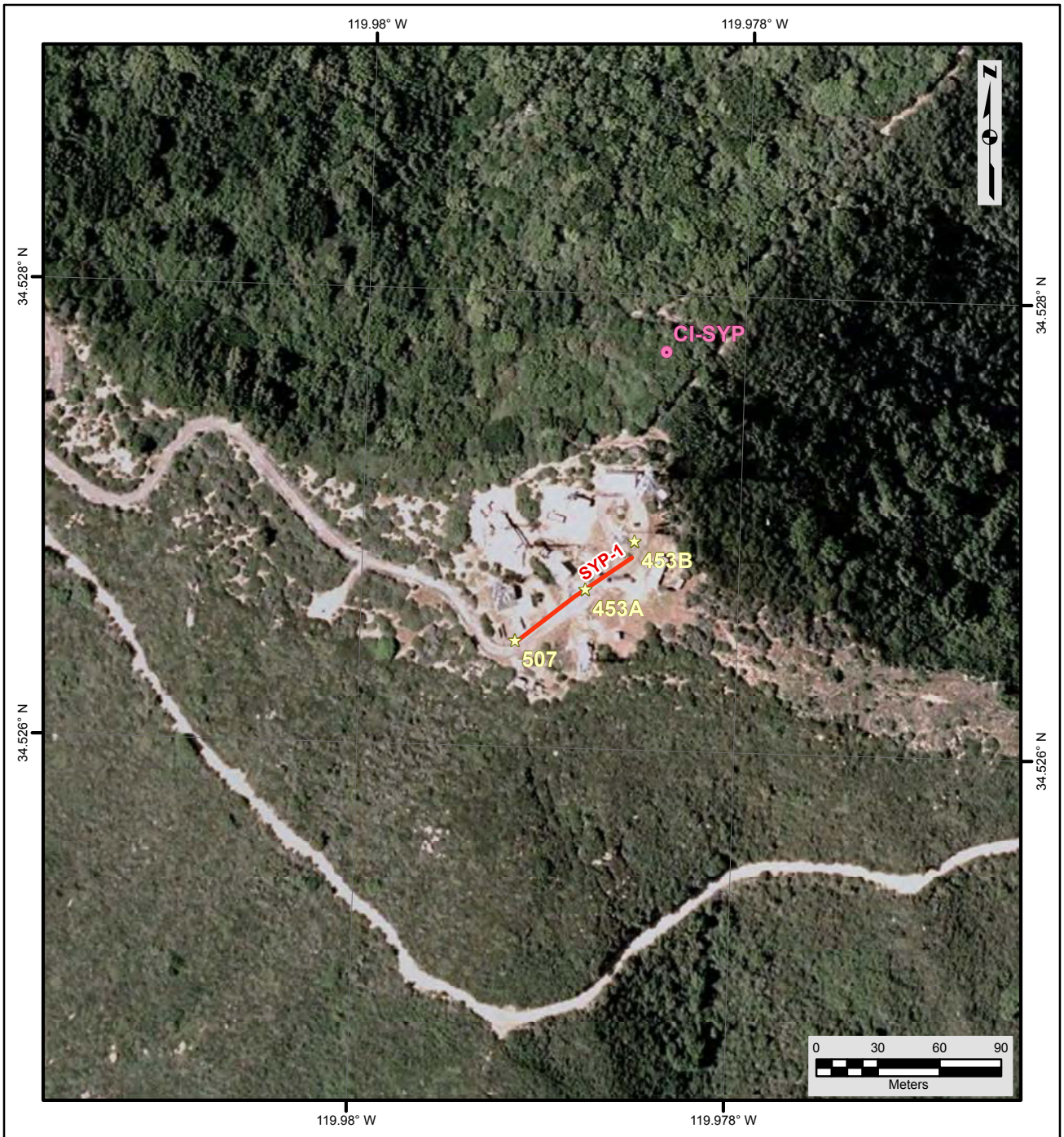

Legend

- Seismic Station - Approximate Location of Record
- H/V Spectral Ratio Location
- MASW and Seismic Refraction Array

NOTES:
1. WGS 1984 COORDINATE SYSTEM
2. Image Source: ESRI, i-cubed, USDA FSA, USGS, AEX, GeoEye, Getmapping, Aerogrid, IGP

File Name: CI-SYP-I

Date: 10/6/2011

USGS science for a changing world

GEOVision geophysical services

RECOVERY.GOV

SITE MAP
CI•SYP

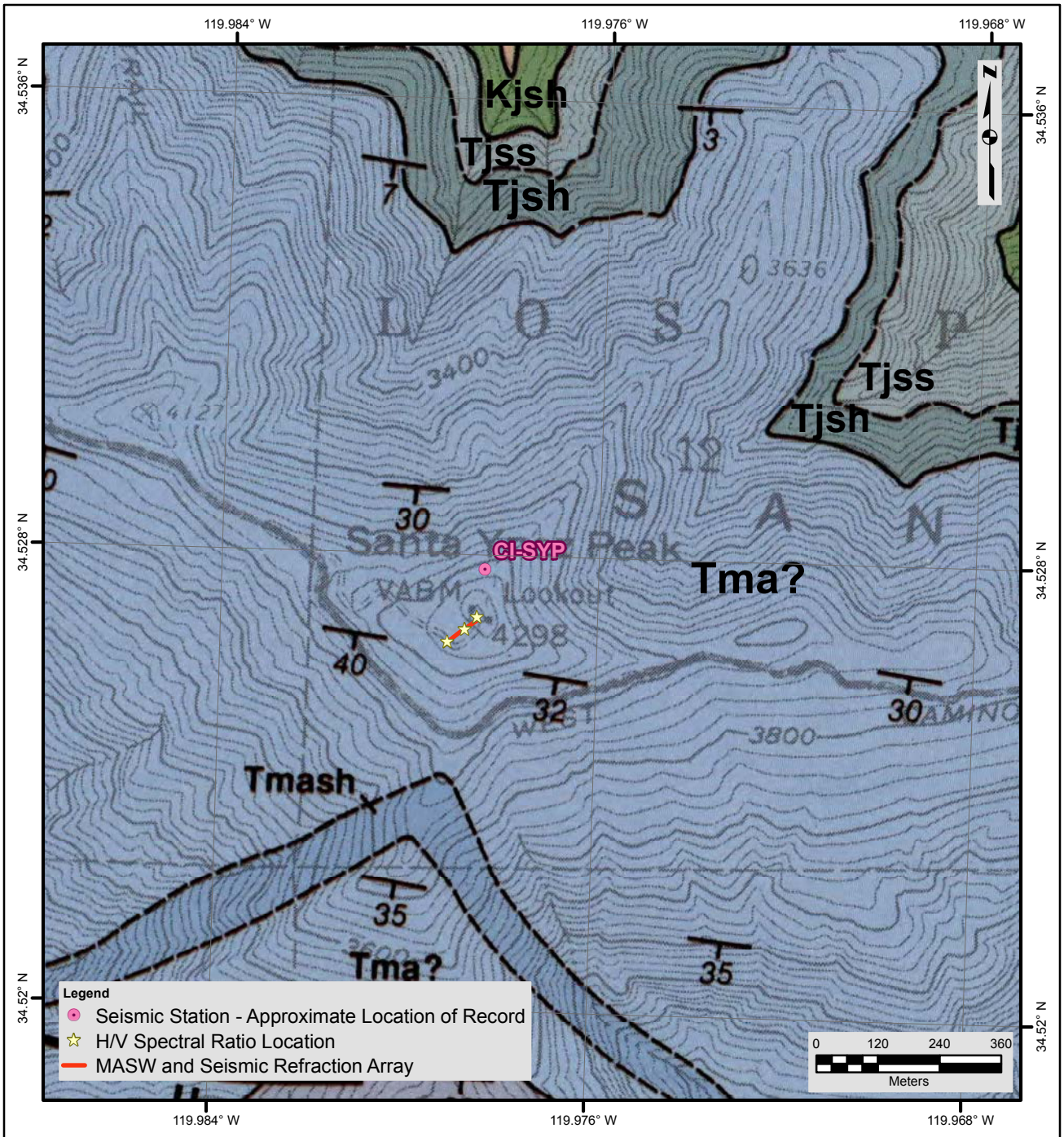

Description of Geologic Map Units

Tma = Tertiary (Eocene) Matilija (?) Sandstone; hard, thick bedded, arkosic sandstone, thin to thick with micaceous shale
Tmash = Tertiary (Eocene) Matilija (?) Sandstone; micaceous shale with minor sandstone interbeds
Tjsh = Tertiary (Eocene) Jucal or Anita Formation; micaceous shale with thin interbeds of hard, arkosic sandstone
Tjss = Tertiary (Eocene) Jucal or Anita Formation; hard, arkosic sandstone with minor interbeds of micaceous shale

NOTES:
1. WGS 1984 COORDINATE SYSTEM
2. Geologic Map of the Lake Cachuma Quadrangle, Santa Barbara County, California by Thomas W. Dibblee, Jr., 1987
3. See site map for details of geophysical survey

File Name: CI-SYP
Date: 10/6/2011

USGS science for a changing world
GEOVision geophysical services

GEOLOGIC MAP
CI•SYP

Looking northeast along array SYP-1 and at HVSR Sensor 453

Looking southwest along array SYP-1

HVSR sensor placed in shallow hole

P-wave seismic refraction data acquisition

MASW and seismic refraction data acquisition along array SYP-1

Location of Geophysical Testing Arrays:

Location	Latitude	Longitude
SYP-1, Southwest End of MASW/Refraction Array	34.52646	-119.97910
SYP-1, Center of MASW/Refraction Array	34.52666	-119.97879
SYP-1, Northeast End of MASW/Refraction Array	34.52684	-119.97849
HVSR Sensor 453A	34.52670	-119.97873
HVSR Sensor 453B	34.52692	-119.97848
HVSR Sensor 507	34.52647	-119.97910

Notes: 1) WGS84 Coordinate System (decimal degrees)
2) Survey accuracy is estimated at 1 to 2 m

Results:

V_S Model

Depth to Top of Layer (m)	Layer Thickness (m)	S-Wave Velocity (m/s)	Inferred P-Wave Velocity (m/s)	Assumed Poisson's Ratio	Assumed Density (g/cm^3)
0	1	216	405	0.3	1.8
1	2	266	497	0.3	1.8
3	3	284	532	0.3	1.8
6	4	403	755	0.3	1.9
10	5	473	884	0.3	2.0
15	6	526	984	0.3	2.0
21	>9	666	1246	0.3	2.1

Notes: 1) Depth of investigation is about 30 m.
2) Bottom layer is a half space.

Observations/Discussion:

- Seismic station location could not be verified in the field due to heavy vegetation.
- The HVSR curves are generally similar although there are subtle differences at frequencies greater than 5 Hz and also in the 2.5 Hz range. All HVSR curves do, however, have a clear peak at about 1.2 Hz and trough at about 3.3 Hz.
- The 1.2 Hz HVSR peak is associated with a velocity structure at greater depth than imaged by the surface wave sounding.
- The P-wave refraction data collected along array SYP-1 were modeled using a tomographic inversion routine with a smooth velocity gradient starting model. The seismic refraction model was extended to far offset shot locations to extend depth of investigation.
- The seismic refraction survey design allowed P-wave velocity to be imaged to a maximum depth of about 15 to 20 m. The seismic refraction model shows that P-wave

velocity is about 350 to 450 m/s at the surface, increasing to 500 m/s at a depth of 1 to 4 m, 700 m/s at a depth of 4 to 8 m and 900 m/s at a depth of 5 to 19 m.

- The seismic refraction model indicates that there is lateral velocity variation at this site with higher P-wave velocities at shallower depth at the southwest end of the line. There were no reasonable alternate test locations at the site due to limited space and steep topography.
- The sandstone unit at the site dips about 30 to 40 degrees to the south. It was not possible to orient seismic lines parallel and/or perpendicular to strike. Geologic environments are not always conducive to surface wave testing because velocity structure generally does not satisfy the homogeneous, horizontal layer assumption. However, surface wave methods can still be effective if shallow velocity structure is dominated by weathering rather than layering and there is not significant lateral velocity variation.
- Noise conditions at the site were not sufficient for application of passive surface wave techniques.
- Due to limited space maximum source offset was 15 m, rather than the typical 30 m. Therefore, the maximum wavelength extracted from surface wave data had to be increased to 1.3 times the distance from the source to the center of the active receiver array. To minimize near field effects we have typically been using a maximum wavelength of 1 to 1.1 times the distance from the source to the center of the active receiver array. The larger factor used for this array does not appear to be degrading the quality of the surface wave dispersion data.
- The minimum wavelength surface wave phase velocity data extracted from the 48-channel MASW array was about 24 m, although data with wavelengths this small were only extracted from seismic records associated with two of the offend source locations. Generally, extraction of surface wave data from the 48-channel MASW array was difficult due to apparent lateral velocity variation and/or dominant higher modes. Data reduction using seismic records from smaller hammer sources and a limited offset receiver array (i.e. less active geophones) allowed extraction of surface wave dispersion data to a minimum wavelength of about 2.5 m. Significant effort was also made reducing data from limited offset receiver arrays with larger hammer sources to obtain surface wave dispersion data over intermediate wavelength ranges.
- Scatter in MASW dispersion data is likely due, in part, to lateral velocity variation associated with both a very thin sediment/fill layer of variable thickness and differential weathering of near surface sedimentary rock.
- A representative dispersion curve was generated for the MASW data set using a moving average, polynomial curve fitting routine and used for modeling.
- Surface wave depth of investigation is about 30 m based on half of maximum wavelength criteria.
- The inferred P-wave velocities in the surface wave model, assuming a Poisson's ratio of 0.3, are generally consistent with the average velocity structure in the seismic refraction model in the upper 15 m, the seismic refraction depth of investigation.
- V_{S30} is 440 m/s (Site Class C).
- Average S-wave velocity between 1.5 m (assumed sensor depth) and 31.5 m is 470 m/s.

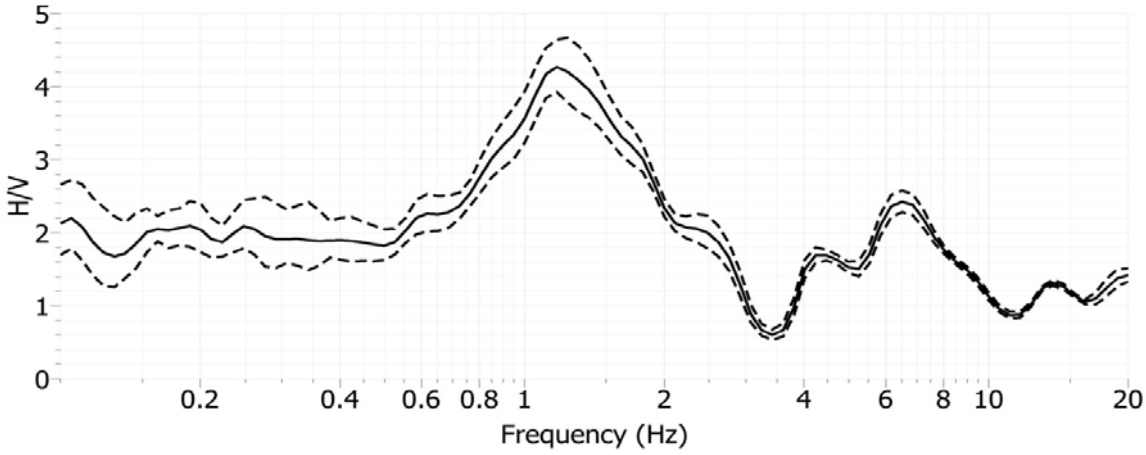

Site CI.SYP, H/V Spectral Ratio, Array SYP-1, Sensor 453b

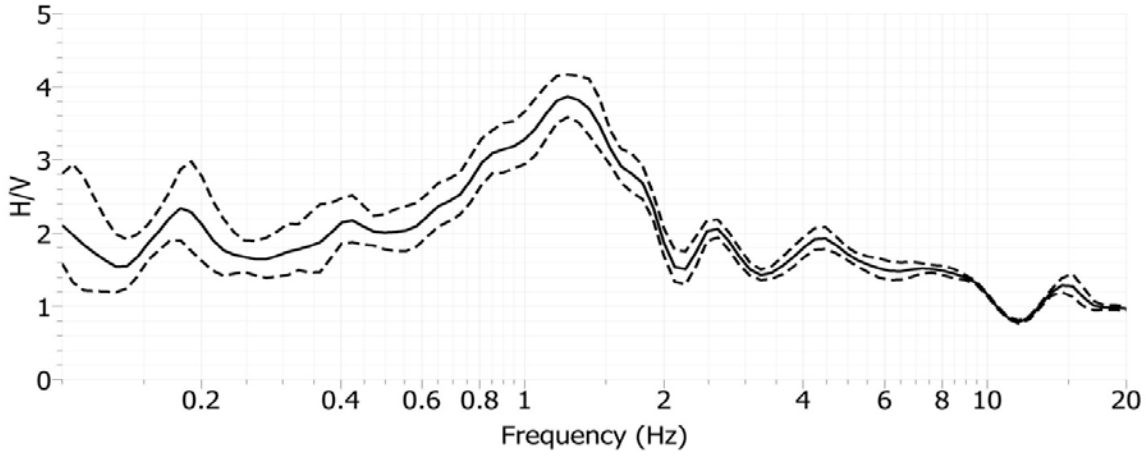

Site CI.SYP, H/V Spectral Ratio, Array SYP-1, Sensor 453a

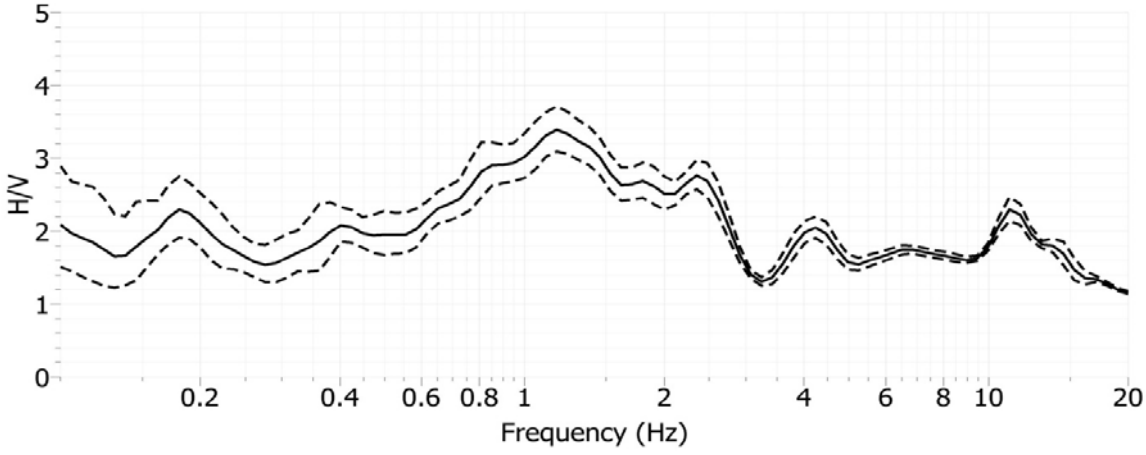

Site CI.SYP, H/V Spectral Ratio, Array SYP-1, Sensor 507

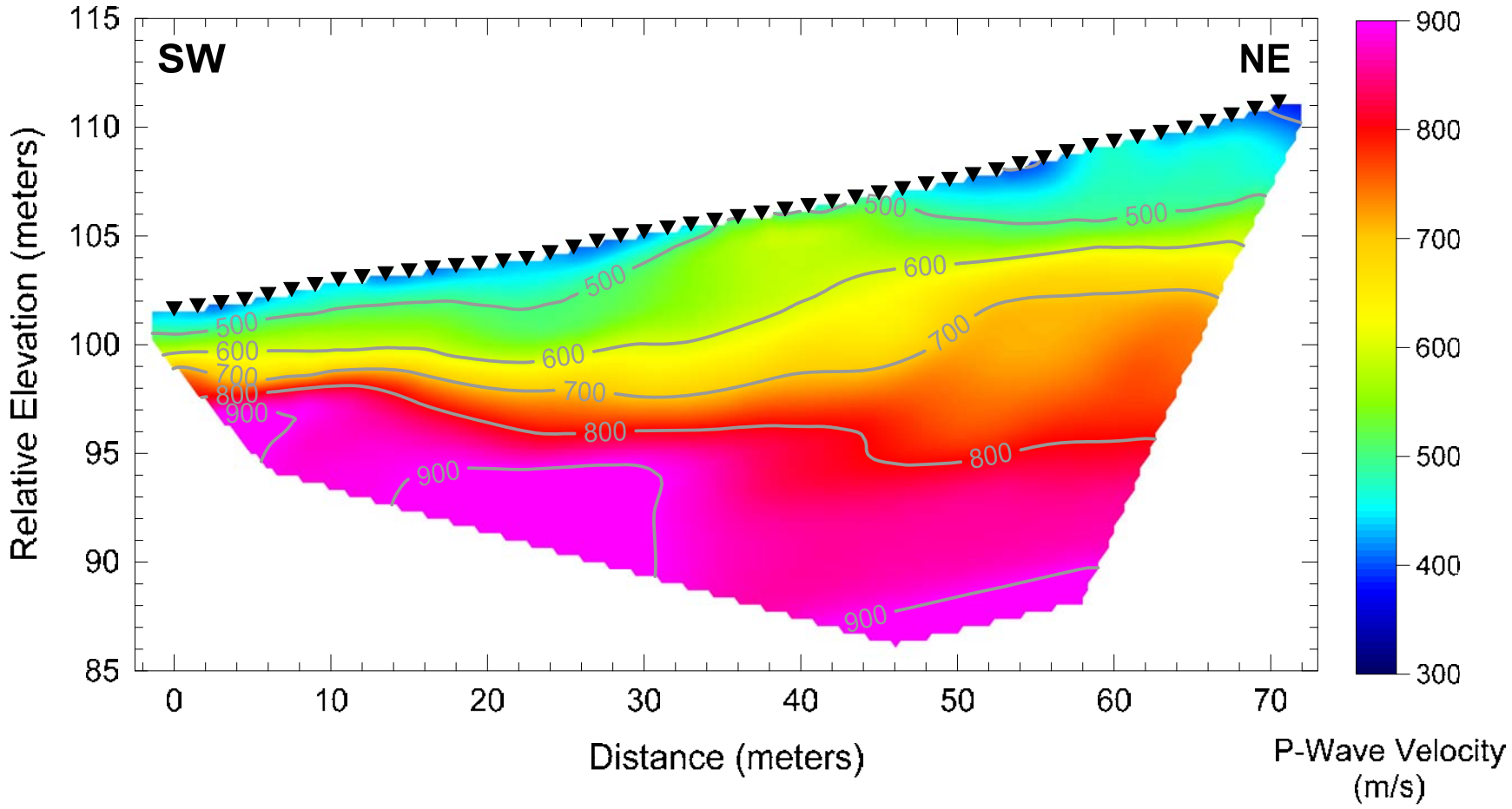

Array SYP-1 – Tomographic seismic refraction model utilizing smooth velocity gradient starting model

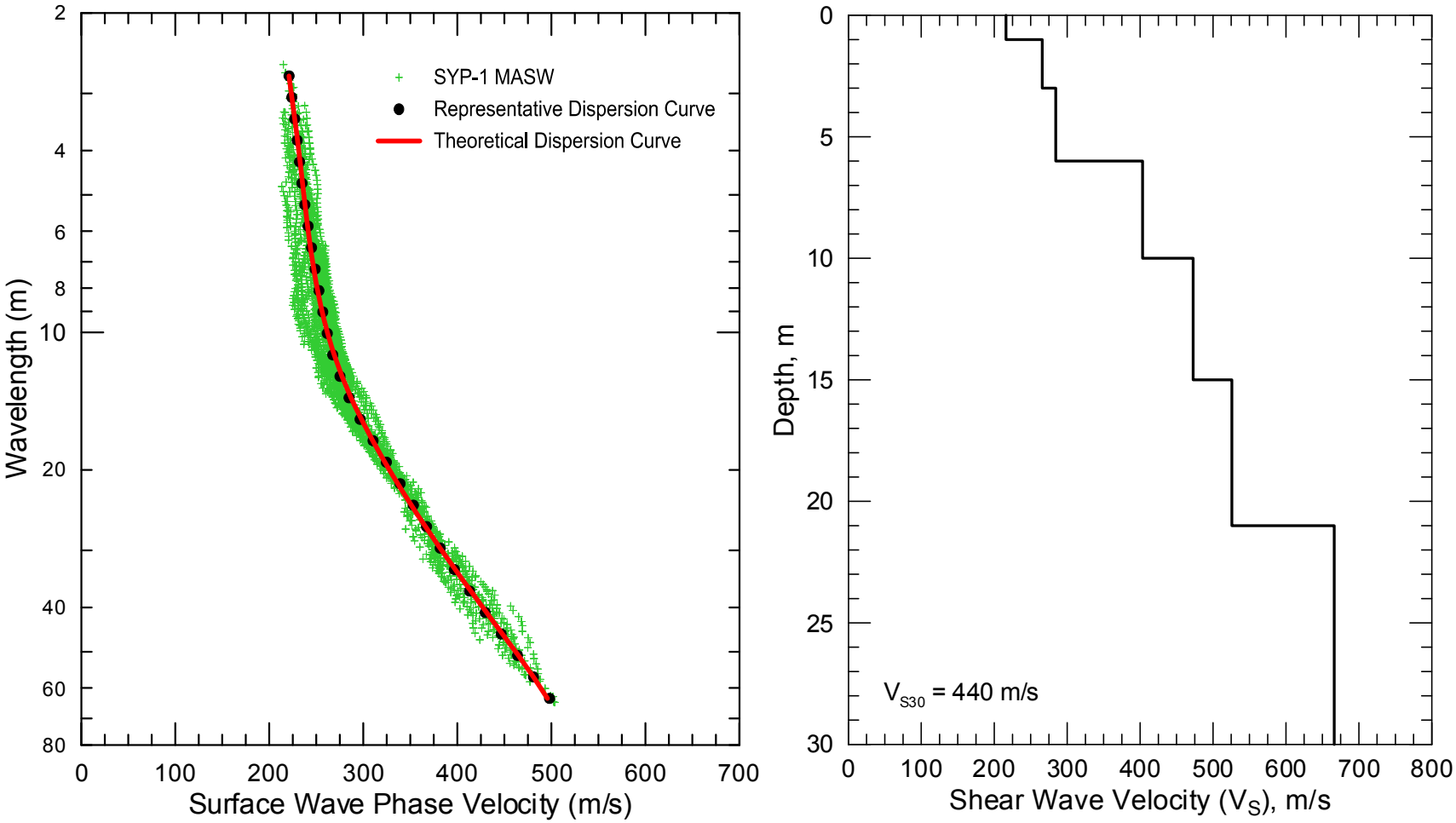

CI.SYP - Field, representative and inverted theoretical surface wave dispersion data (left) and associated V_S model (right)

Site CI.TA2

Location: JPL Table Mountain Facility, Wrightwood, California

Former Location Latitude: 34.38203 **Former Location Longitude:** -117.67822
(Station coordinates provided by USGS, WGS84 coordinate system)

V_{S30} (measured): 565 m/s

V_{S30} (adjusted to more accurately reflect seismic station conditions): 565 m/s (no adjustment necessary).

NEHRP Site Class: C

Geomatrix Code: ANB

Geologic Conditions/Observations: Seismic station located on geologic unit mapped as Precambrian gneiss. Mapped outcrop of Precambrian limestone dolomite marble in site vicinity. Outcrops of weathered gneiss are located north of the seismic station and south of the test area.

Site Conditions: Rural site located on a mountain top. Steep terrain in site vicinity. Ground surface elevation does not change significantly along the MASW and seismic refraction arrays.

Geophysical Methods Utilized: HVSR, Seismic Refraction, MASW

Geophysical Testing Arrays:

1. Array TA2-1 (48 channel MASW array utilizing 4.5 Hz vertical geophones spaced 1.5 m apart for a length of 70.5 m, forward and reverse shot locations with multiple source offsets and source types and multiple interior shot locations).
2. Array TA2-2 (48 channel MASW and P-wave seismic refraction array utilizing 4.5 Hz vertical geophones spaced 2.5 m apart for a length of 117.5 m, forward and reverse shot locations with multiple source offsets and source types and multiple interior shot locations).
3. Three HVSR measurement locations, two distributed along array TA2-1 and the other adjacent to the current seismic station.

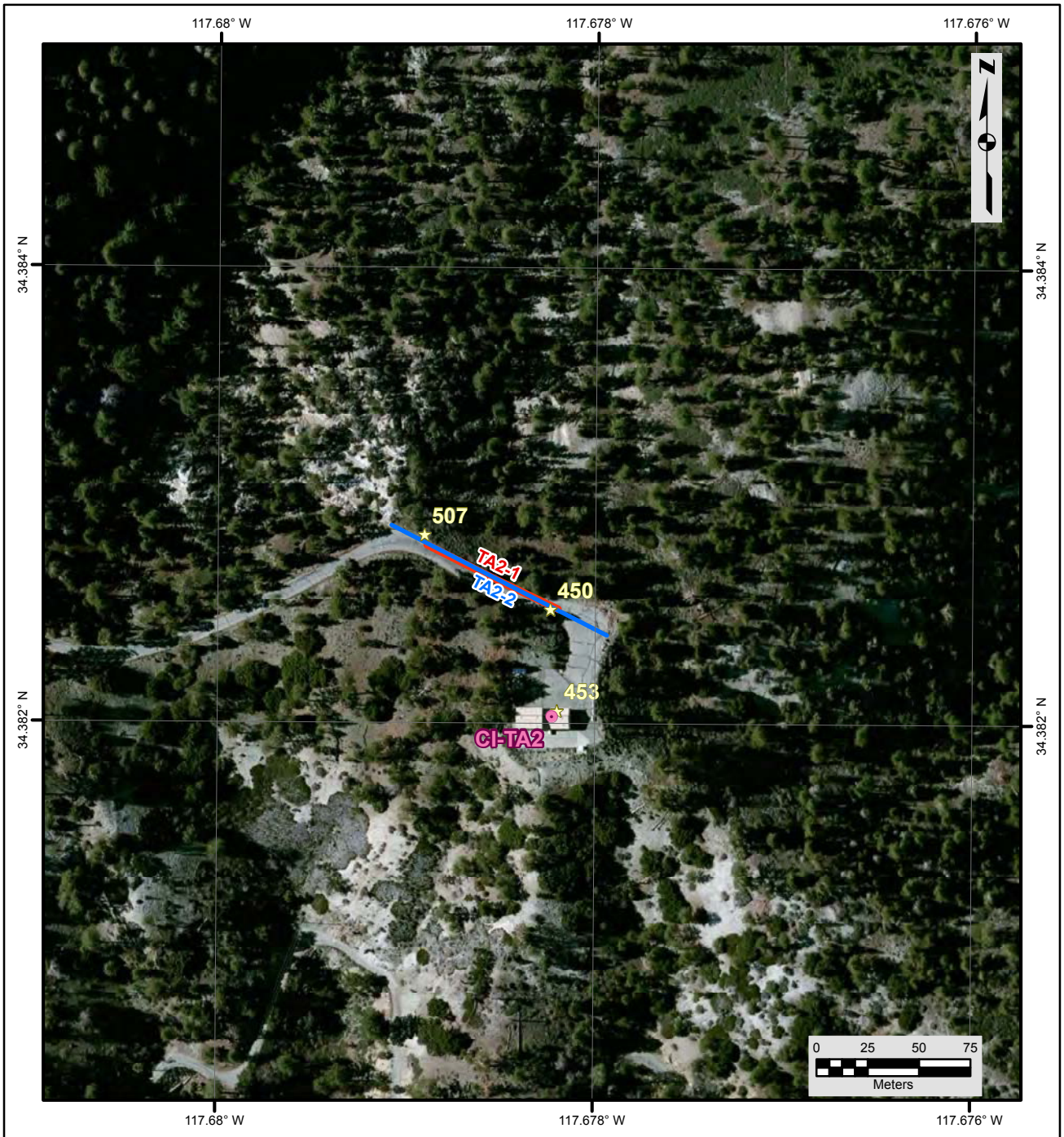

Legend

- Seismic Station - Approximate Location of Record
- H/V Spectral Ratio Location
- MASW and Seismic Refraction Array
- MASW and Seismic Refraction Array

NOTES:
1. WGS 1984 COORDINATE SYSTEM
2. Image Source: ESRI, i-cubed, USDA FSA, USGS, AEX, GeoEye, Getmapping, Aerogrid, IGP

File Name: CI-TA2-I

Date: 2/7/2013

USGS science for a changing world

GEOVision geophysical services

RECOVERY.GOV

SITE MAP
CI•TA2

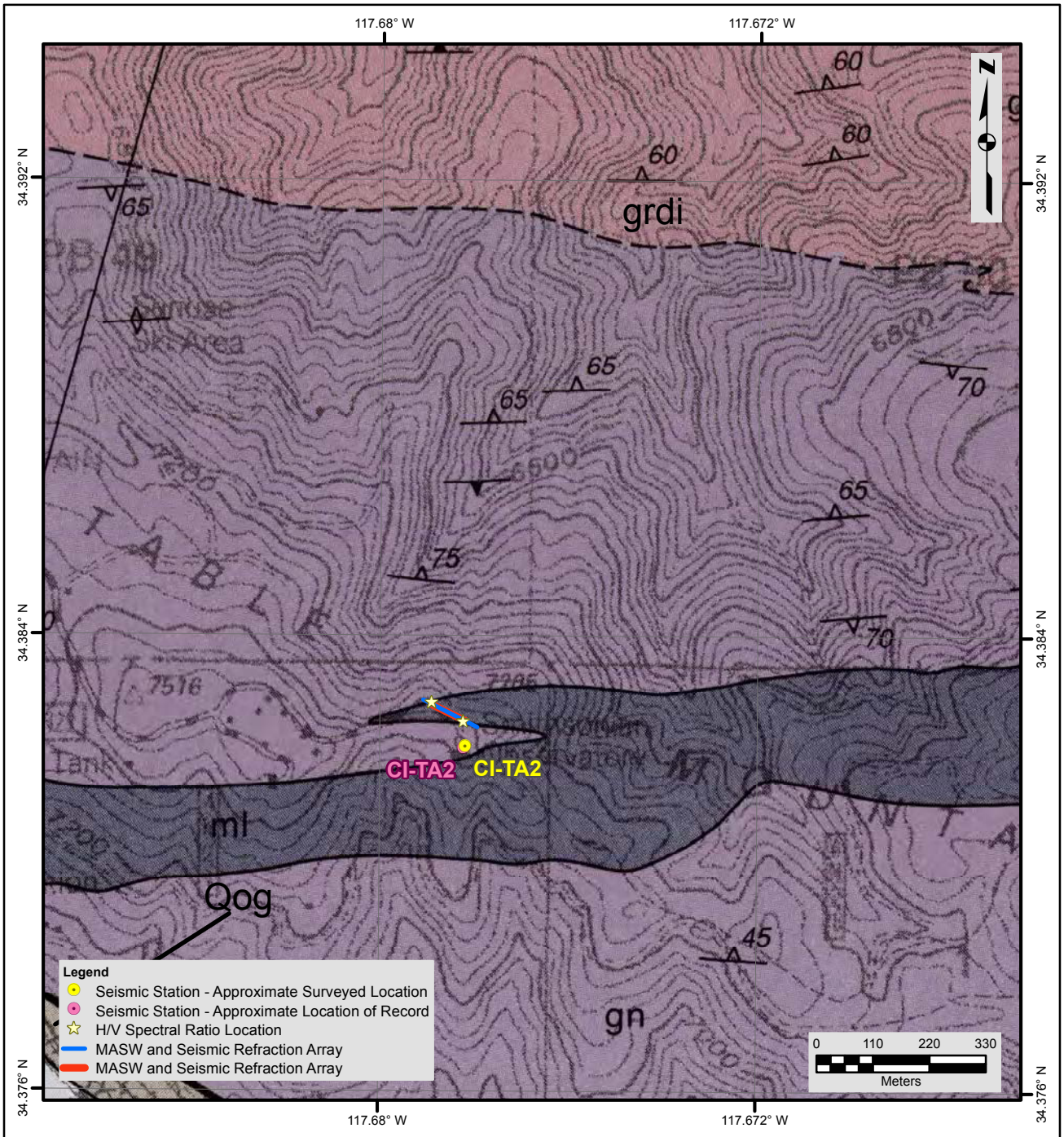

Description of Geologic Map Units

Qog = Quaternary (Pleistocene) alluvial fan gravel of granitic, gneissic and minor schist detritus
grdi = Mesozoic granodiorite, medium-grained, includes some gneiss
ml = Precambrian limestone dolomite marble
gn = Precambrian gneiss, hard, closely fractured and brittle

NOTES:
1. WGS 1984 COORDINATE SYSTEM
2. Geologic Map of the Mescal Creek Quadrangle, Los Angeles and San Bernardino Counties, California by Thomas W. Dibblee, Jr., 2002
3. See site map for details of geophysical survey

File Name: CI-TA2

Date: 2/7/2013

USGS science for a changing world

GEOVision geophysical services

GEOLOGIC MAP
CI•TA2

RECOVERY.GOV

Looking southwest toward building housing CI.TA2 seismic station and array TA2-2

Looking at CI.TA2 seismic station and adjacent HVSR measurement locations

Looking southeast at HVSR sensor 507 and array TA2-1

MASW data acquisition using accelerated weight drop along seismic array TA2-1

Looking southeast along seismic array TA2-2 on asphalt and geophones with rock plates

Location of Geophysical Testing Arrays:

Location	Latitude	Longitude
TA2-1, Northwest End of MASW/Refraction Arrays	34.38282	-117.67898
TA2-1, Center of MASW/Refraction Array	34.38264	-117.67854
TA2-1, Southeast End of MASW/Refraction Array	34.38250	-117.67819
TA2-2, Northwest End of Refraction Array	34.38287	-117.67908
TA2-2, Southeast End of Refraction Array	34.38239	-117.67793
HVSR Sensor 450	34.38250	-117.67823
HVSR Sensor 507	34.38283	-117.67890
HVSR Sensor 453	34.38205	-117.67819
CI.TA2 Seismic Station	34.38206	-117.67819

Notes: 1) WGS84 Coordinate System (decimal degrees)

2) Survey accuracy is estimated at 1 to 2 m.

3) Seismic station and HVSR sensor 453 located in building and location is estimated.

Results:

V_S Model 1 (Fundamental Mode Assumption)

Depth to Top of Layer (m)	Layer Thickness (m)	S-Wave Velocity (m/s)	Inferred P-Wave Velocity (m/s)	Assumed Poisson's Ratio	Assumed Density (g/cm^3)
0	1	208	389	0.3	1.7
1	1.5	250	467	0.3	1.8
2.5	2.5	345	646	0.3	1.9
5	4	498	932	0.3	2.0
9	5	678	1268	0.3	2.1
14	6	770	1441	0.3	2.1
20	8	1167	2184	0.3	2.2
28	>7	1488	2784	0.3	2.3

Notes: 1) Depth of investigation is about 35 m.

2) Bottom layer is a half space.

V_S Model 2 (Average Mode Assumption)

Depth to Top of Layer (m)	Layer Thickness (m)	S-Wave Velocity (m/s)	Inferred P-Wave Velocity (m/s)	Assumed Poisson's Ratio	Assumed Density (g/cm^3)
0	1	206	385	0.3	1.70
1	1.5	250	467	0.3	1.80
2.5	2.5	341	639	0.3	1.90
5	4	488	912	0.3	2.00
9	5	597	1117	0.3	2.10
14	6	724	1355	0.3	2.10
20	8	956	1788	0.3	2.15
28	>7	1176	2201	0.3	2.20

Notes: 1) Depth of investigation is about 35 m.
2) Bottom layer is a half space.

Observations/Discussion:

- There are subtle differences between the HVSR plots, although the plots have similar general characteristics.
- There are no clear high amplitude HVSR peaks, but there is a low amplitude peak in the 2 to 4.5 Hz range and centered at about 3 Hz.
- Field review of off-end shot records on array TA2-1 indicated that a longer array would be beneficial for P-wave refraction data acquisition. To maximize depth of investigation, P-wave refraction data were, therefore, acquired along the 117.5 m array TA2-2.
- The P-wave refraction data for array TA2-2 were modeled using a tomographic inversion routine with a smooth velocity gradient starting model.
- The seismic refraction survey design allowed P-wave velocity to be imaged to a maximum depth of about 25 to 30 m. The seismic refraction model indicates P-wave velocity is about 400 to 500 m/s at the surface, increasing to 600 m/s at a depth of about 2 to 5 m, 1,000 m/s at a depth of about 5 to 12 m, 1,400 m/s at a depth of about 11 to 20 m and is over 1,800 m/s below a depth of about 24 to 28 m.
- Noise conditions at the site were not sufficient for application of passive surface wave techniques.
- The minimum wavelength surface wave phase velocity data extracted from the 48-channel MASW arrays TA2-1 and TA2-2 was about 8 and 15 m, respectively. Reducing data from smaller hammer sources using a limited offset receiver array (i.e. less active geophones) allowed extraction of surface wave dispersion data to a minimum wavelength of about 1.5 and 3 m, respectively.
- There is about 30 to 60 m/s scatter in the MASW dispersion data, which is in part due to lateral velocity variation.

- Representative dispersion curves were generated for each surface wave data set using a moving average, polynomial curve fitting routine. These individual representative dispersion curves were combined and a representative dispersion curve generated for the combined data set for data modeling.
- Two V_S models were generated from the surface wave data. The first (Model 1) assumes that the dispersion curve is representative of the fundamental mode Rayleigh wave. Further modeling reveals that this V_S model should excite a dominant first higher mode at low frequencies. There is likely insufficient resolution in the v-f transform (overtone image) to isolate the fundamental mode and first higher mode at low frequencies resulting in modal superposition (mode mixing). Given the relatively high velocities at the site, a significantly longer receiver array (several hundred meters) would be required to obtain sufficient resolution in v-f space to separately identify the fundamental and first higher modes. This type of space is generally not available at rock sites and longer arrays invariably introduce more lateral velocity variation. Because of possible modal superposition at low frequencies, an alternate V_S model (Model 2) was developed assuming the observed dispersion curve consists of the average/effective mode (average of all modes based on relative amplitude in each mode for a far-field, plane Rayleigh wave with no body wave effects). We cannot state with certainty that the observed dispersion data consists of the average mode, but this may be a better option than incorrectly assuming that the dispersion data is the fundamental mode. In the event of modal superposition at low frequencies a V_S model based on the fundamental mode assumption will invariably overestimate velocity at depth.
- There is a 7% difference inV_{S30} between the fundamental and average mode models. The two models are almost identical in the upper 9 m. The average mode model has slightly lower V_S between depths of 9 and 20 m and much lower V_S at depths greater than 20 m.
- Surface wave depth of investigation is about 35 m based on half of maximum wavelength criteria.
- The inferred P-wave velocities in both surface wave models, based on an assumed Poisson's ratio of 0.3 and modeled S-wave velocity, are generally consistent with the P-wave refraction model in the upper 10 m. Model 2, based on the average mode assumption, is in better agreement with the P-wave seismic refraction model at depths below 10 m.
- V_{S30} is 607 m/s for Model 1 (fundamental mode assumption) and 565 m/s Model 2 (average mode assumption), averaging 586 m/s (NEHRP Class C).
- For the purpose of site characterization, we recommend use of the average/effective mode V_S model (Model 2), which is in better agreement with the P-wave seismic refraction model.
- This site may be more effectively characterized using the S-wave refraction and MALW (Love wave) techniques because the velocity structure at this site is expected to yield a dominant fundamental mode Love wave at all frequencies.

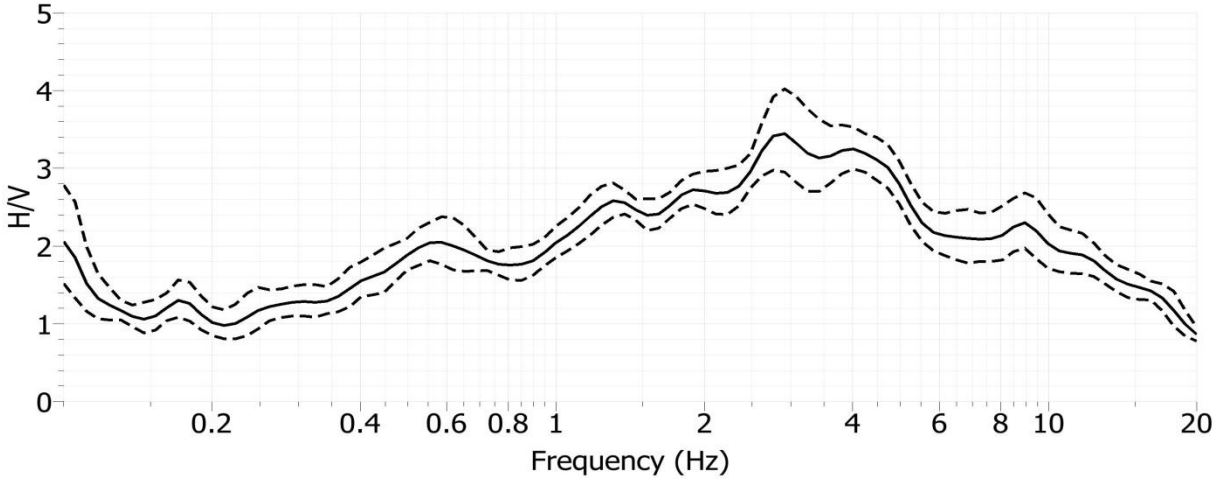

Site CI.TA2, H/V Spectral Ratio, Array TA2-1, Sensor 507

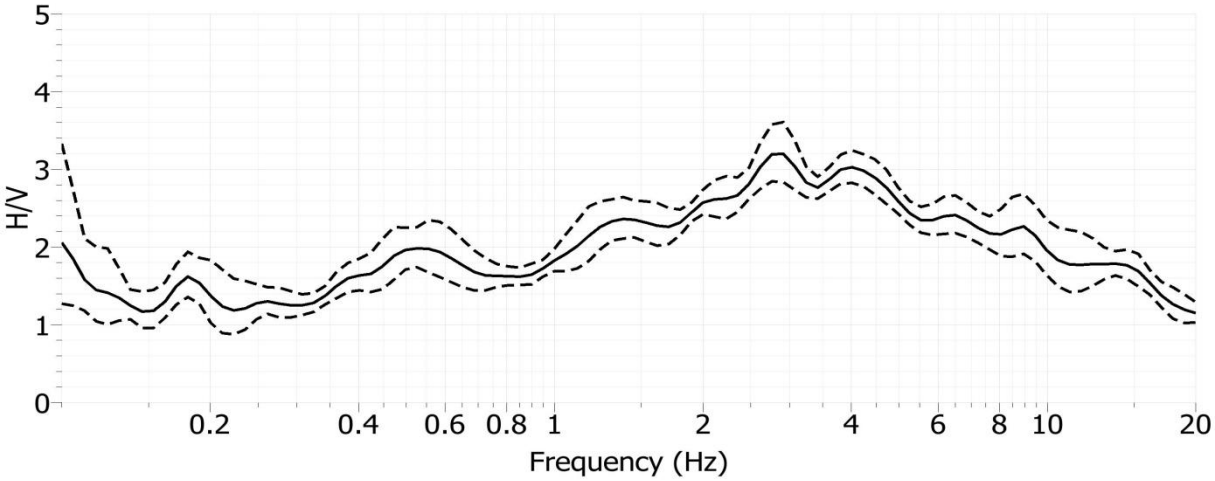

Site CI.TA2, H/V Spectral Ratio, Array TA2-1, Sensor 450

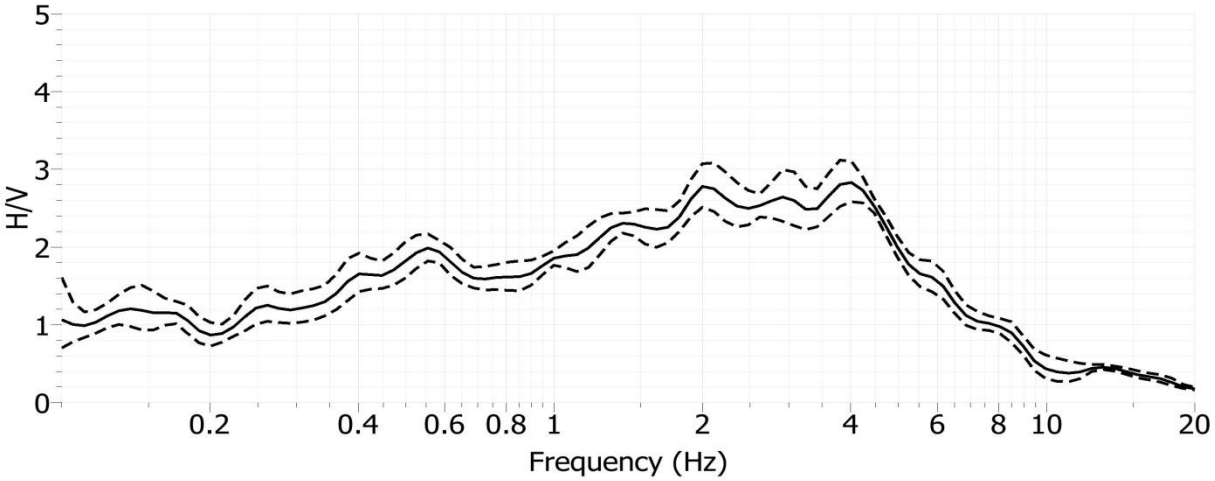

Site CI.TA2, H/V Spectral Ratio, Near Seismic Station, Sensor 453

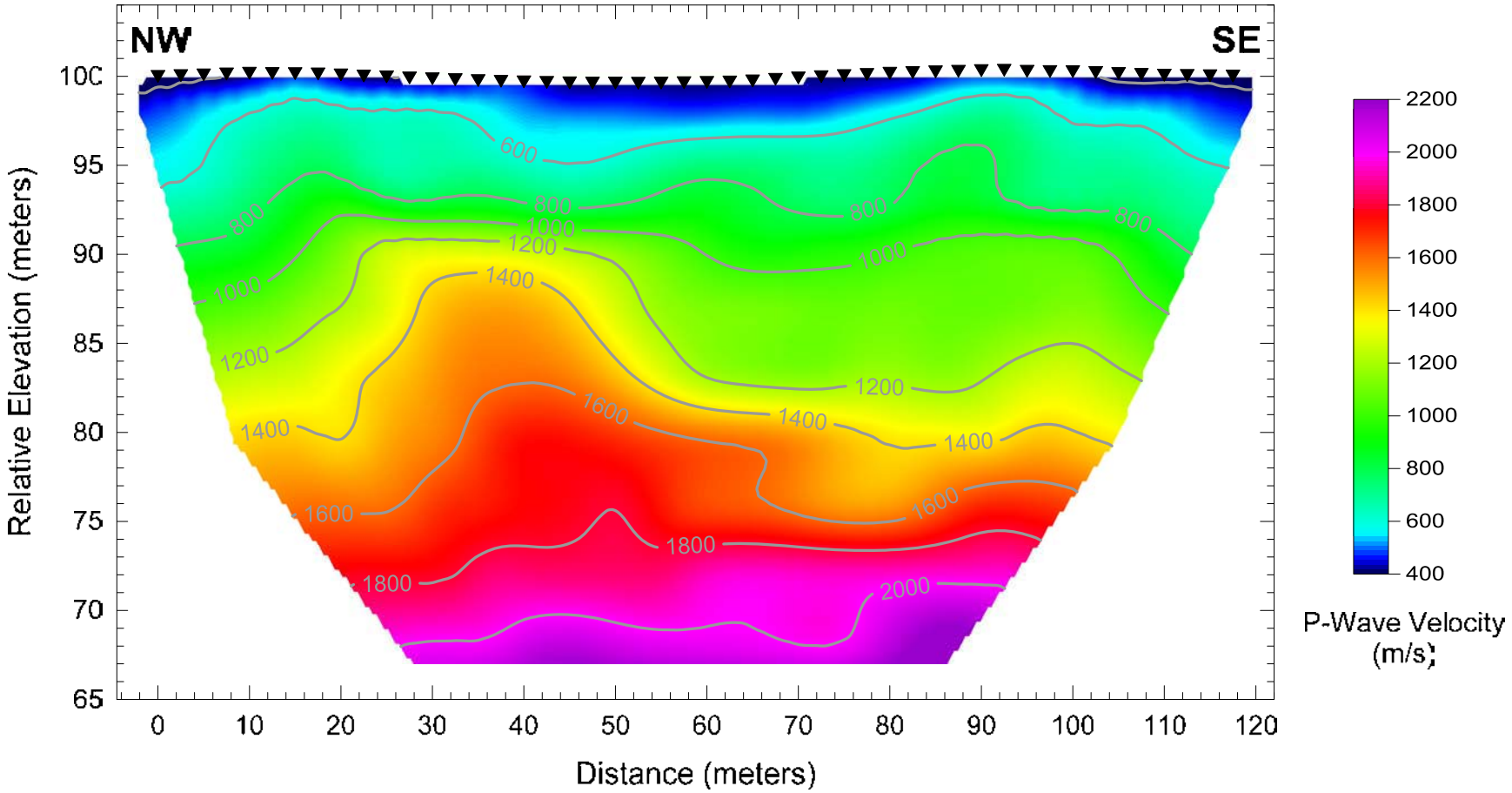

Array TA2-2 – Tomographic seismic refraction model developed utilizing a smooth velocity gradient starting model

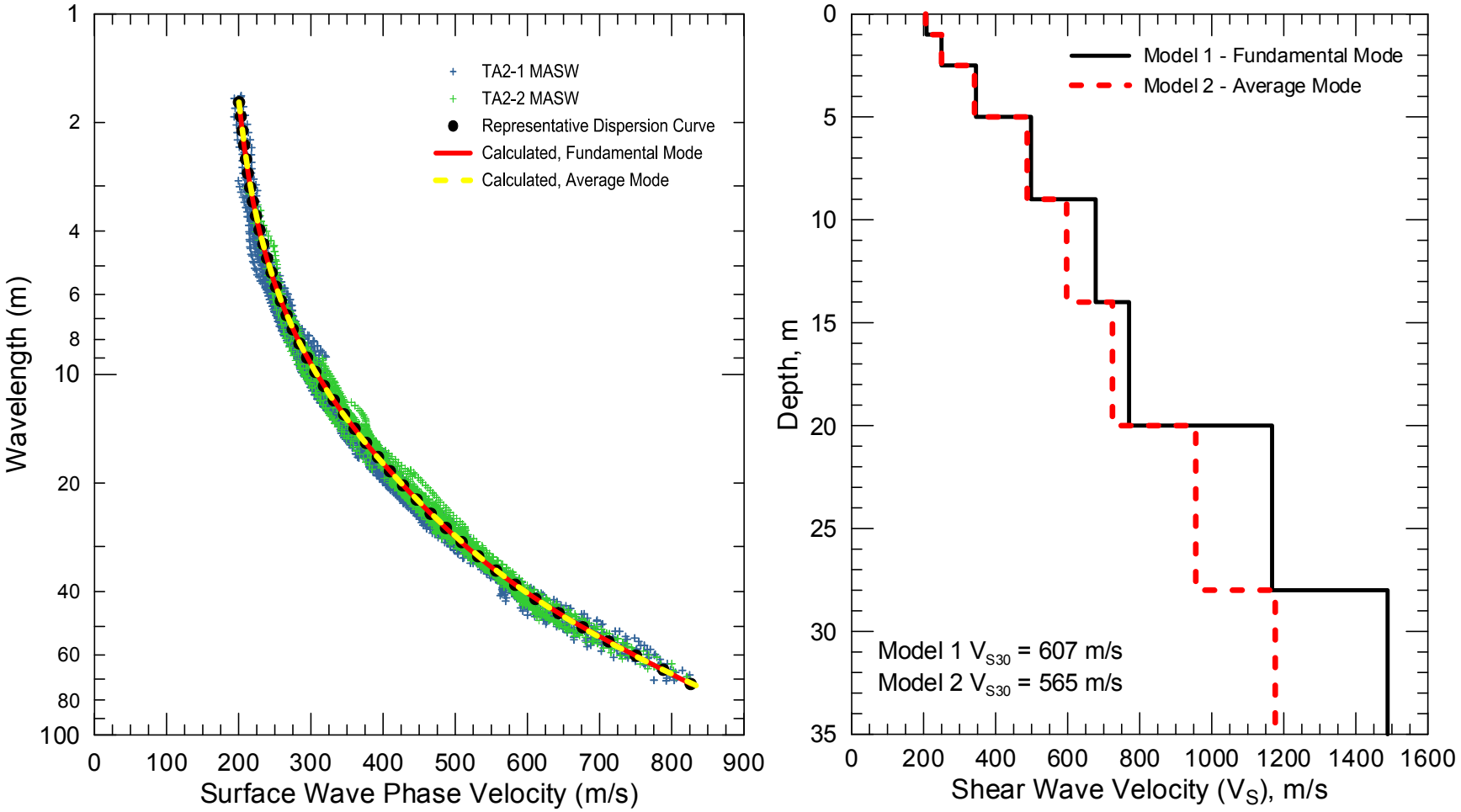

CI.TA2 - Field, representative and inverted theoretical surface wave dispersion data (left) and associated V_S model (right)

Site CI.TEH

Location: Cattani Ranch, Kern County, California

Latitude: 35.29130 **Longitude:** -118.42079
(Station coordinates provided by USGS, WGS84 coordinate system)

V_{S30} (measured): 895 m/s (±15% due to lateral velocity variation and error)

V_{S30} (adjusted to more accurately reflect seismic station conditions): 1,076 m/s (average S-wave velocity between 2 and 32 m adjusting for assumed 2 m sensor depth, ±15% due to lateral velocity variation and error).

NEHRP Site Class: B

Geomatrix Code: IGA

Geologic Conditions/Observations: Seismic station located on geologic unit mapped as Mesozoic (Cretaceous to Jurassic) granitic rocks. Field observations indicate that the surficial granitic rock is highly decomposed.

Site Conditions: Rural site located in the mountains near a dry river channel. Undulating, hilly topography in site vicinity. Ground surface elevation decreases about 3 m along the 70.5 m long MASW and seismic refraction array.

Geophysical Methods Utilized: HVSR, Seismic Refraction (P- and S-wave), MASW

Geophysical Testing Arrays:

1. Array TEH-1 (48 channel MASW and P-wave seismic refraction array utilizing 4.5 Hz vertical geophones spaced 1.5 m apart for a length of 70.5 m, forward and reverse shot locations with multiple source offsets and source types and multiple interior shot locations).
2. Array TEH-1 (24 channel S-wave seismic refraction array utilizing 10 Hz horizontal geophones spaced 4 m apart for a length of 69 m, forward and reverse shot locations with multiple source offsets and multiple interior shot locations). Same origin and orientation as P-wave refraction and MASW array of same name.
3. Three HVSR measurement locations distributed along array TEH-1.

Legend

- Seismic Station - Approximate Surveyed Location
- Seismic Station - Approximate Location of Record
- H/V Spectral Ratio Location
- MASW and Seismic Refraction Array

NOTES:
1. WGS 1984 COORDINATE SYSTEM
2. Image Source: ESRI, i-cubed, USDA FSA, USGS, AEX, GeoEye, Getmapping, Aerogrid, IGP

File Name: CI-TEH-I

Date: 10/13/2011

USGS science for a changing world

GEOVision geophysical services

RECOVERY.GOV

SITE MAP
CI•TEH

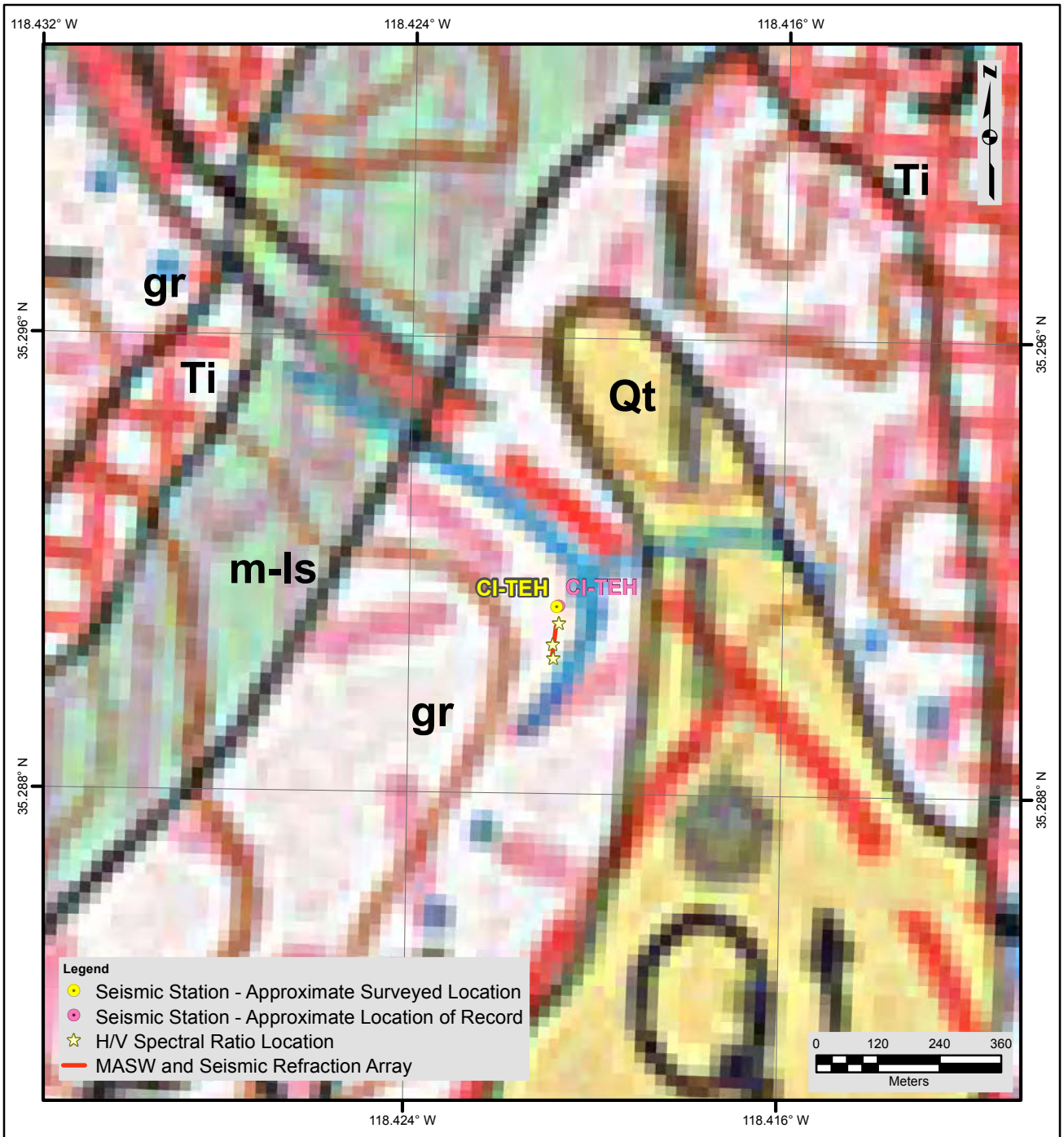

Description of Geologic Map Units

Qt = Quaternary (Pleistocene) nonmarine terrace deposits
Ti-r - Tertiary (Undivided) intrusive rhyolite
gr = Mesozoic (Cretaceous to Jurassic) granitic rocks
m-ls = Pre-Cretaceous (Undivided) metamorphic rocks, limestone or dolomite

NOTES:
1. WGS 1984 COORDINATE SYSTEM
2. Geologic Map of California (Olaf P. Jenkins Edition), Bakersfield Sheet
compilation by Arthur R. Smith, 1964
3. See site map for details of geophysical survey

File Name: CI-TEH

Date: 10/13/2011

USGS science for a changing world

GEOVision geophysical services

GEOLOGIC MAP
CI•TEH

RECOVERY.GOV

Looking south towards CI.TEH seismic station (left of drum) and location of array TEH-1 (behind building)

Looking north along S-wave seismic refraction array TEH-1

Looking north along MASW array TEH-1

S-wave seismic refraction data acquisition

Looking south along MASW array TEH-1

Location of Geophysical Testing Arrays:

Location	Latitude	Longitude
TEH-1, South End of MASW/Refraction Array	35.29032	-118.42094
TEH-1, Center of MASW/Refraction Array	35.29063	-118.42089
TEH-1, North End of MASW/Refraction Array	35.29094	-118.42085
HVSR Sensor 450	35.29038	-118.42090
HVSR Sensor 453	35.29100	-118.42079
HVSR Sensor 507	35.29063	-118.42091
CI.TEH Seismic Station	35.29129	-118.42084

Notes: 1) WGS84 Coordinate System (decimal degrees)
2) Survey accuracy is estimated at 2 to 3 m.

Results:

V_S Model 1FM (Fundamental Mode)

Depth to Top of Layer (m)	Layer Thickness (m)	S-Wave Velocity (m/s)	Inferred P-Wave Velocity (m/s)	Assumed Poisson's Ratio	Assumed Density (g/cm^3)
0	1	211	394	0.30	1.80
1	2	350	655	0.30	1.90
3	6	499	933	0.30	2.00
9	6	1027	1922	0.30	2.20
15	8	1802	3371	0.30	2.40
23	>7	2326	4351	0.30	2.50

Notes: 1) Depth of investigation is about 30 m.
2) Bottom layer is a half space.
3) Half space velocity not well resolved.

V_S Model 1AM (Average Mode)

Depth to Top of Layer (m)	Layer Thickness (m)	S-Wave Velocity (m/s)	Inferred P-Wave Velocity (m/s)	Assumed Poisson's Ratio	Assumed Density (g/cm^3)
0	1	231	431	0.30	1.80
1	2	337	631	0.30	1.90
3	6	487	912	0.30	2.00
9	8	1046	1958	0.30	2.20
17	11	1102	2063	0.30	2.20
28	>2	1269	2373	0.30	2.25

Notes: 1) Depth of investigation is about 30 m.
2) Bottom layer is a half space.
3) Half space velocity not well resolved.

Average V_P Model and Estimated V_S Models from Central Portion of P-wave Seismic Refraction Array TEH-1

Depth to Top of Layer (m)	Layer Thickness (m)	P-Wave Velocity (m/s)	Estimated S-Wave Velocity (m/s)				
			Poisson's Ratio = 0.25	Poisson's Ratio = 0.3	Poisson's Ratio = 0.3333	Poisson's Ratio = 0.35	Poisson's Ratio = 0.4
0.00	0.42	426	246	228	213	205	174
0.42	0.85	658	380	352	329	316	269
1.27	0.85	894	516	478	447	429	365
2.12	0.85	928	536	496	464	446	379
2.96	0.85	1100	635	588	550	529	449
3.81	0.85	1159	669	619	579	557	473
4.65	0.85	1218	703	651	609	585	497
5.50	1.78	1409	814	753	705	677	575
7.28	1.78	1743	1006	932	871	837	712
9.05	1.78	2126	1227	1136	1063	1021	868
10.83	1.78	2419	1397	1293	1209	1162	988
12.61	1.78	2709	1564	1448	1355	1302	1106
14.38	1.78	2984	1723	1595	1492	1433	1218
16.16	1.78	3204	1850	1713	1602	1539	1308
17.94	1.78	3751	2166	2005	1875	1802	1531
19.72	1.78	3770	2177	2015	1885	1811	1539
21.49	Half Space	3838	2216	2052	1919	1844	1567

Average V_S Model from Central Portion of S-wave Seismic Refraction Array TEH-1

Depth to Top of Layer (m)	Layer Thickness (m)	S-Wave Velocity (m/s)
0.00	0.47	208
0.47	0.93	344
1.40	0.93	536
2.34	0.93	559
3.27	0.93	776
4.20	0.93	828
5.14	0.93	893
6.07	1.96	988
8.04	1.96	1095
10.00	1.96	1194
11.96	1.96	1305
13.92	1.96	1324
15.89	1.96	1397
17.85	1.96	1453
19.81	1.96	1551
21.77	1.96	1645
23.73	Half Space	1725

Observations/Discussion:

- The seismic station is located in a small cellar and sensor depth is assumed to be 2 m.
- MASW and seismic refraction array TEH-1 was conducted in a location at similar elevation as the seismic station and thought to have the best chance of being representative of seismic station conditions. During acquisition of MASW data along this array, it became clear that MASW data quality was not very good and, therefore, S-wave seismic refraction data were also acquired along the array. Geophysical testing was conducted at this site before the potential benefits of MALW (Love wave) data acquisition was realized. It may be possible to find a location in the site vicinity more conducive to MASW data acquisition, but given the significant degree of lateral velocity variation often observed at rock sites additional effort would be required to correlate the velocity structure at the test location to the seismic station.
- HVSR data collected at sensor locations 453 and 507 are very noisy and should be repeated. These data were collected early in the project field investigation when strategies for deployment of the Nanometrics Trillium compact seismometer for HVSR measurements were still being developed. HVSR data at sensor location 450 appears to be of much better quality. There is no strong HVSR peak at sensor location 450.
- The P- and S-wave seismic refraction data for array TEH-1 were modeled using a tomographic inversion routine with smooth velocity gradient starting models. The seismic refraction models were extended to limited far offset shot locations to extend depth of investigation.
- The P-wave first arrival data were picked to greater degree of accuracy than the S-wave first arrival data because there were often strong P-wave arrivals before the S-wave arrivals and possible converted waves as first arrivals on several S-wave refraction seismic records. Generally, S-wave refraction models should be checked against P-wave refraction models, unless there is a shallow saturated zone, to confirm that the S-wave refraction model is realistic and that converted waves have not been interpreted as S-waves.
- The P-wave seismic refraction survey design allowed P-wave velocity to be imaged to a maximum depth of about 22 m. The seismic refraction model indicates that P-wave velocity is about 475 to 600 m/s at the surface and increases to over 1,000 m/s at a depth of 1 to 3 m, 2,000 m/s at a depth of 7 to 14 m, 3,000 m/s at a depth of 12 to 17 m and over 3,500 m/s at a depth of 16 to 20 m. The maximum P-wave velocity in the model is about 4,000 m/s.
- The S-wave seismic refraction survey design allowed S-wave velocity to be imaged to a maximum depth of about 24 m. The seismic refraction model indicates that S-wave velocity is about 225 to 300 m/s at the surface and increases to over 600 m/s at a depth of 1.5 to 3.5 m, 1,000 m/s at a depth of 6 to 12 m, 1,400 m/s at a depth of 11 to 22 m and over 1,800 m/s at a depth of 19 to greater than 25 m.
- The S-wave refraction model has less detail than the P-wave refraction model due to both the larger geophone spacing and larger error in the first arrival data. Both models generally show a thickening of the intermediate velocity weathered zone to the north and a slightly thicker zone of lower velocity decomposed rock near the surface between a position of about 25 and 45 m.

- The average P-wave velocity of the upper 30 m (V_{P30}) was estimated between 19.5 and 49.5 m on the P-wave refraction model, where depth of investigation is greatest. To estimate V_{P30} the P-wave velocity at a depth of 22 m, nominal depth of investigation, was projected to 30 m depth. V_{P30} ranges from about 1,899 to 2,146 m/s over the 19.5 to 49.5 m position interval, a 13% variation. An average V_P model was developed over the 19.5 to 49.5 m distance interval by horizontally averaging the travel time of each model cell and cell thickness and average V_{P30} was determined to be 1,980 m/s. Assuming constant Poisson's ratios of 0.25, 0.3, 0.3333, 0.35 and 0.4 would result in an estimated V_{S30} of 1,143, 1,058, 990, 951 and 808 m/s, respectively. The average V_S between 2 and 32 m to account for assumed sensor depth is 1,378, 1,275, 1,193, 1,146 and 974 m/s for constant Poisson's ratio of 0.25, 0.3, 0.3333, 0.35 and 0.4, respectively.
- V_{S30} was estimated between 19.5 and 49.5 m on the S-wave refraction model, where depth of investigation is greatest, by projecting the velocity at 24 m depth to 30 m depth. Over this interval V_{S30} ranges from about 979 to 1,107 m/s, a 12% variation over a 30 m distance. An average V_S model was developed over the 19.5 to 49.5 m distance interval by horizontally averaging the travel time of each model cell and cell thickness and average V_{S30} was determined to be 1,034 m/s. The average V_S between 2 and 32 m to account for assumed sensor depth is 1,245 m/s.
- The lowest value of V_{S30} over the 19.5 to 49.5 m distance interval on the S-wave refraction model occurs at a position of 49.5 m and is 979 m/s. V_{S30} likely continues to decrease to the north of 49.5 m. The highest value of V_{S30} over this interval is 1,107 m/s and occurs at a position of 19.5 m. V_{S30} may continue to gradually increase south of 19.5 m. The average V_S between 2 and 32 m at the locations of lowest and highest V_{S30} are 1,109 and 1,364 m/s, respectively.
- Noise conditions at the site were not sufficient for application of passive surface wave techniques.
- MASW data were very difficult to reduce, probably due to lateral velocity variation. Very little surface wave dispersion data could be reduced from the complete 48 channel receiver array. The near field criteria generally applied during this investigation had to be relaxed to obtain Rayleigh wave phase velocity data to a wavelength of 60 m. Over 75% of the picked dispersion curves were combined for analysis. Small wavelength phase velocity data generally reflects the lower near surface velocities beneath the array.
- The minimum wavelength surface wave phase velocity data extracted from the MASW array was about 3 m.
- There is typically about 120 m/s of scatter in the final MASW dispersion data, which is in part due to lateral velocity variation caused by differential weathering of near surface rock.
- A representative dispersion curve was generated for the MASW data set using a moving average, polynomial curve fitting routine and used for modeling.
- Multi-mode analysis of the V_S model resulting from the fundamental mode assumption (Vs Model 1FM) indicates that the fundamental mode should jump to the first higher mode at a frequency below 21 Hz. To account for the possible mode jump or modal superposition at low frequencies, the dispersion curve was also modeled using the average/effective mode assumption, which in this case simulated superposition of the fundamental and first higher modes at frequencies below 25 Hz (V_S Model 1AM). It should be noted that the algorithm used to estimate the higher modes and relative

amplitude of the higher modes assumes a far-field, plane Rayleigh wave (i.e. infinite source location) and does not include body wave effects.

- Surface wave depth of investigation is about 30 m based on half of maximum wavelength criteria.
- V_{S30} is 838 m/s for V_S Model 1FM (NEHRP Site Class B) and 718 m/s for V_S Model 1AM (NEHRP Site Class C).
- Average S-wave velocity between 2 m, assumed sensor depth, and 32 m is 1,033 and 832 m/s for V_S Models 1FM and 1AM, respectively (NEHRP Site Class B).
- The V_S models developed using the three geophysical methods are not consistent. V_S from the average S-wave seismic refraction model is higher than estimated V_S from the average P-wave refraction model over the 3 to 8 m depth range, possibly due to error in the model. V_S from the average S-wave seismic refraction model relative to the average P-wave refraction model could indicate that weathered rock is saturated below a depth of 15 m. The V_S model developed from the MASW data using the fundamental mode assumption is most consistent with the seismic refraction models, but significantly underestimates V_{S30} relative to the seismic refraction models. The surface wave V_S models generally underestimate V_S in the upper 15 m relative to the average seismic refraction models. There is some bias towards lower phase velocities in the small wavelength surface wave dispersion data, but not enough to account for the significant difference between the refraction and surface wave V_S models. Further research is required to identify possible reasons for the dispersion curve, at sites such as this, representing the fundamental mode when the velocity structure indicates that the first higher mode should be dominant at low frequencies. MASW data reduction was difficult and lateral velocity variation may be such that the V_S models developed from the MASW data are not valid. Alternatively, out-of-plane refractors, if occurring, would result in the seismic refraction models overestimating velocity structure beneath the array. High velocity layers would also result in refraction models overestimating subsurface velocities; however, velocity inversions are not typically observed in bedrock weathering profiles unless there is a significant change in rock composition.
- Lateral velocity variation has been the largest single factor complicating characterization of rock sites during this investigation and further research on the effects of lateral velocity variation on V_S models developed using surface wave methods, assuming a coherent dispersion curve can be constructed, is needed.
- For the purpose of site characterization, we average V_{S30} and adjusted V_{S30} (V_S between 2 and 32 m) between the average S-wave seismic refraction model, estimated V_S model from the average P-wave refraction model and assumed Poisson's ratio of 0.3333, and the MASW fundamental mode and average mode models.
- In summary, average V_{S30} between the surface wave and refraction V_S models is 895 m/s (NEHRP Site Class B) and adjusted V_{S30} is 1,076 m/s (NEHRP Site Class B). It should be assumed that there is 15% variation in the V_{S30} estimate due to lateral velocity variation and error.
- Regardless of the uncertainty in V_{S30} at this site, the site is definitely NEHRP Site Class B.
- This site warrants further investigation to better understand the differences between the surface wave and seismic refraction V_S models.

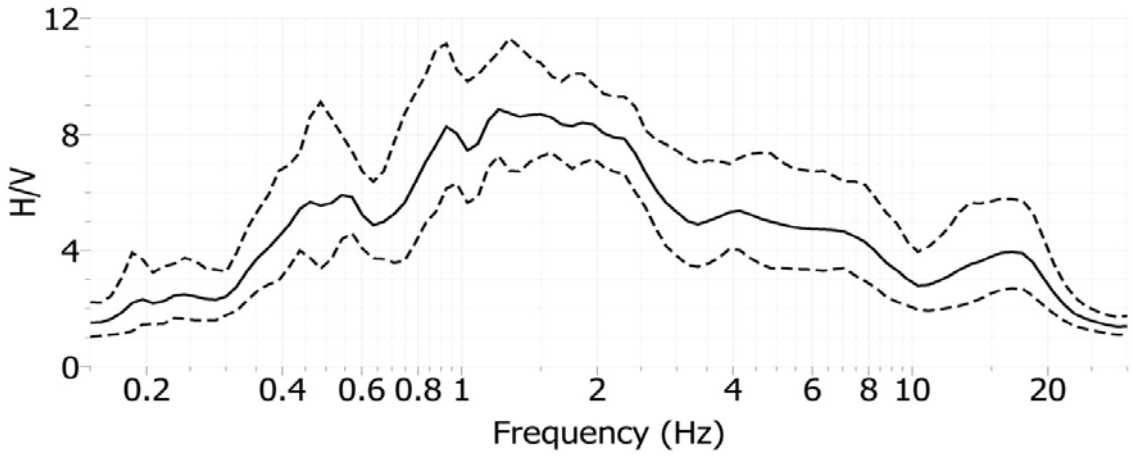

Site CI.TEH, H/V Spectral Ratio, Array TEH-1, Sensor 453

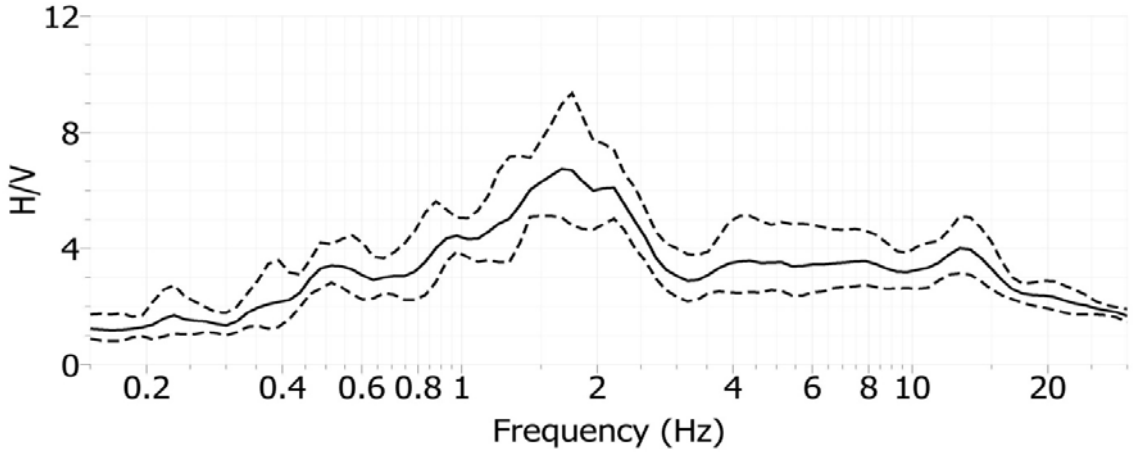

Site CI.TEH, H/V Spectral Ratio, Array TEH-1, Sensor 507

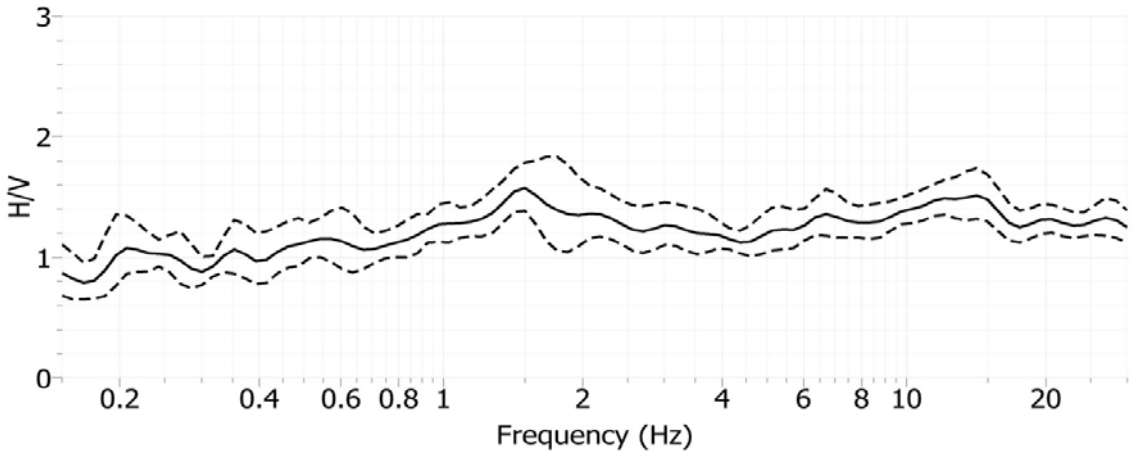

Site CI.TEH, H/V Spectral Ratio, Array TEH-1, Sensor 450

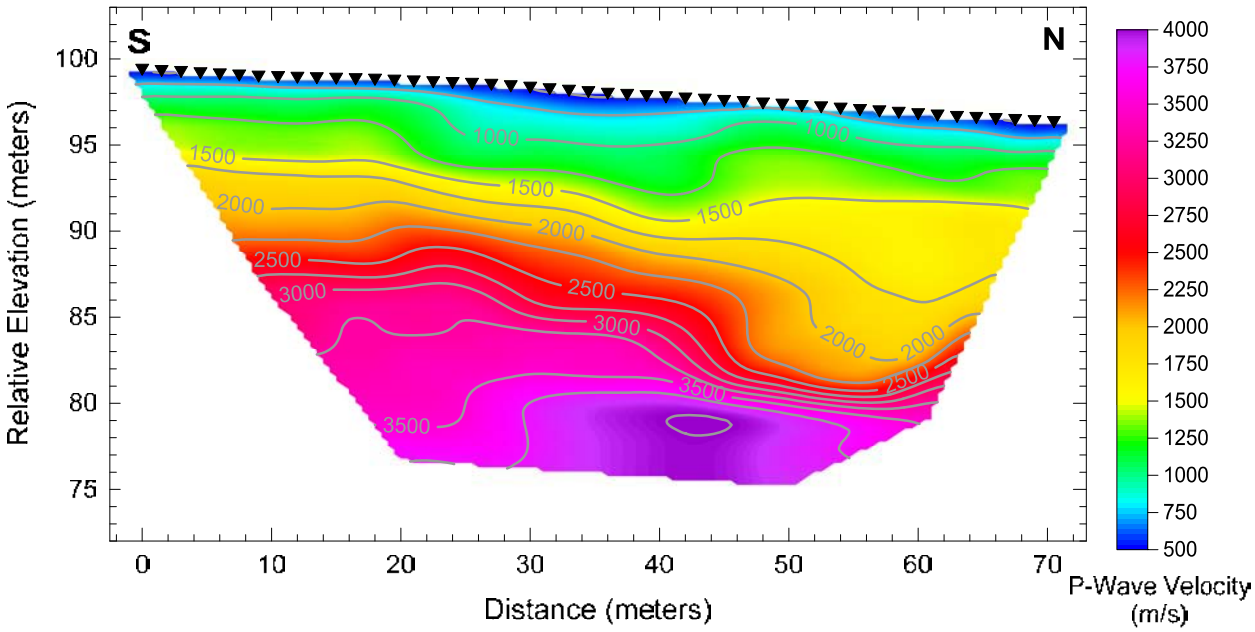

Array TEH-1 – P-wave Tomographic Seismic Refraction Model utilizing Smooth Velocity Gradient Starting Model

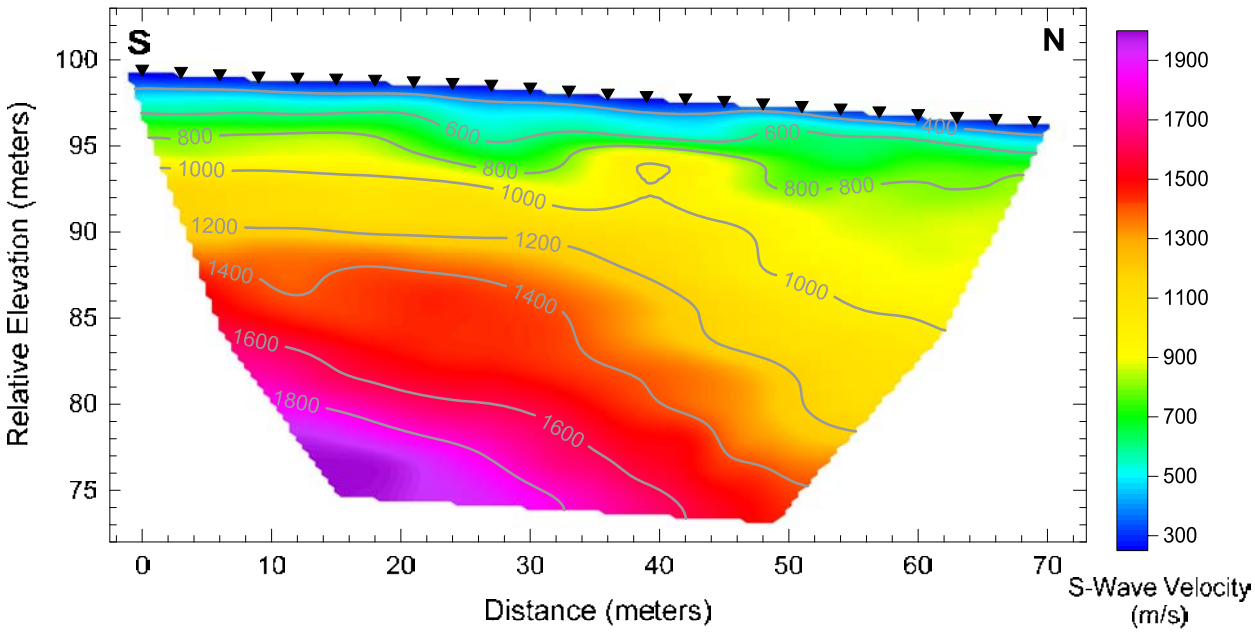

Array TEH-1 – S-wave Tomographic Seismic Refraction Model utilizing Smooth Velocity Gradient Starting Model

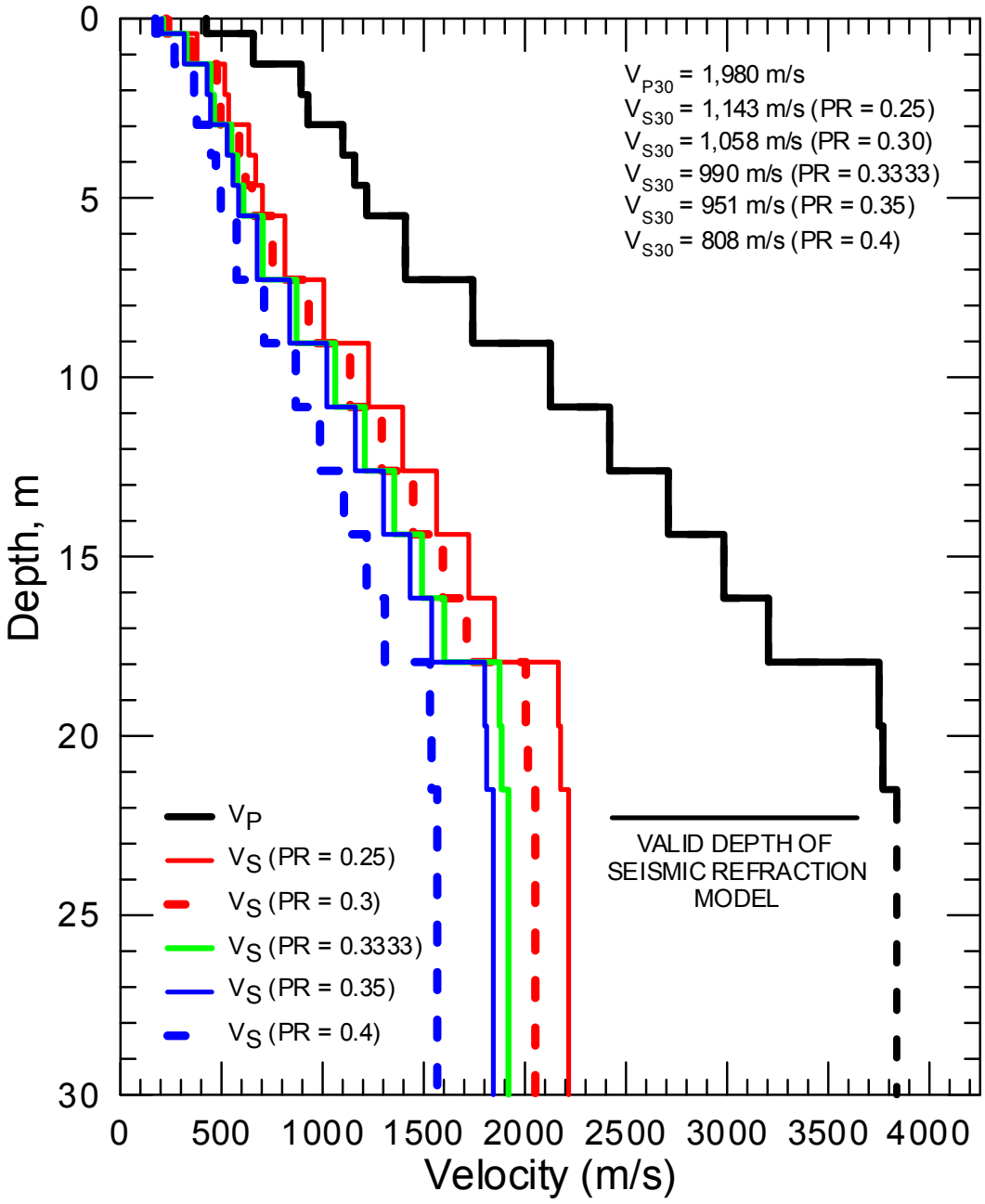

CI.TEH – Average P-wave velocity structure and estimated S-wave velocity structure between a distance of 19.5 and 49.5 m along the P-wave seismic refraction model for array TEH-1. Seismic refraction depth of investigation is limited to about 22 m. P-wave velocity is very high at a depth of 22 m and is not expected to increase significantly between a 22 and 30 m.

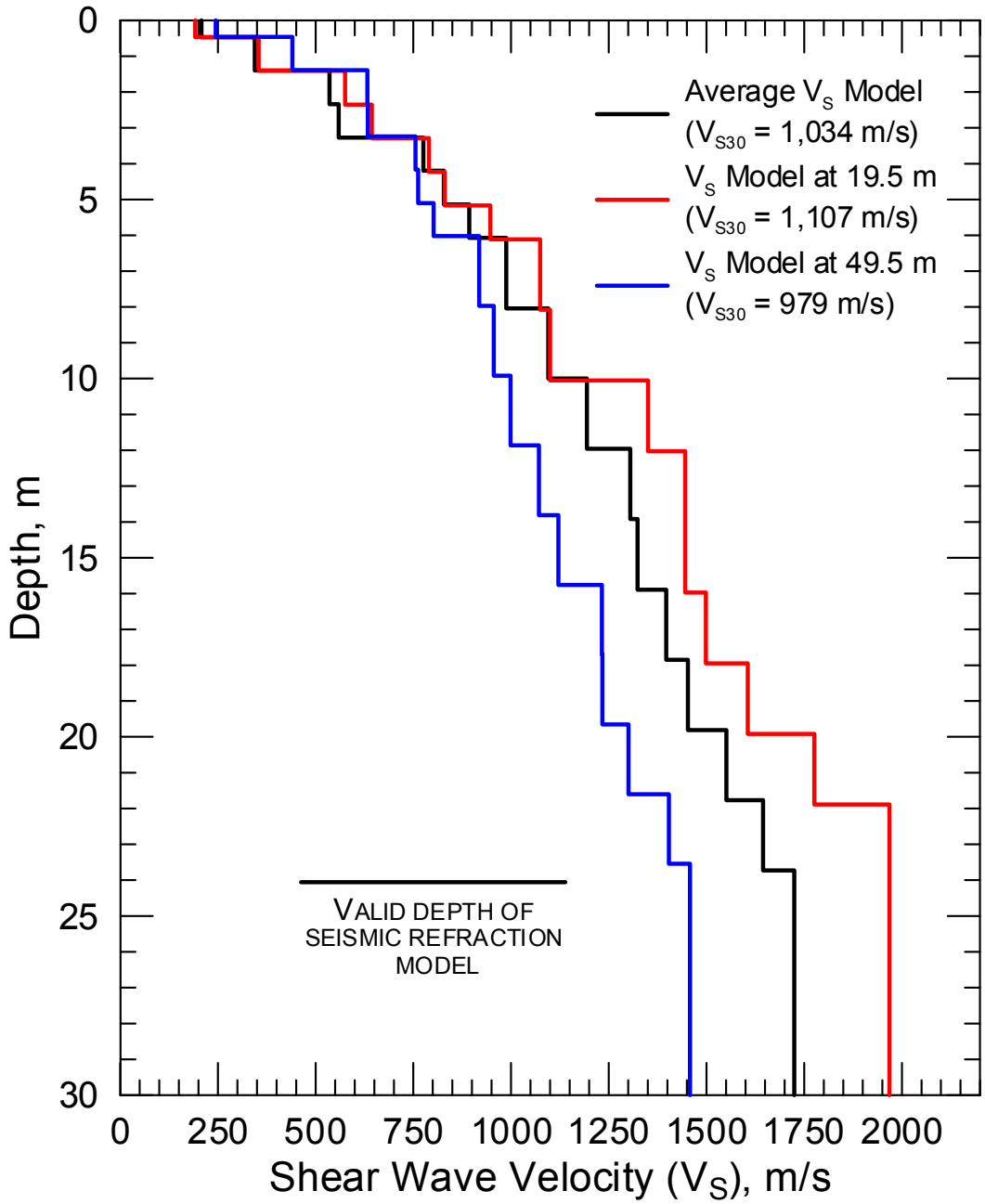

CI.TEH – Average S-wave velocity structure between 19.5 and 49.5 m beneath S-wave seismic refraction array TEH-1 and S-wave velocity structure at a position of 19.5 m (maximum V_{S30}), and 49.5 m (minimum V_{S30}). Seismic refraction depth of investigation is limited to about 24 m and S-wave velocity is assumed to be constant below this depth.

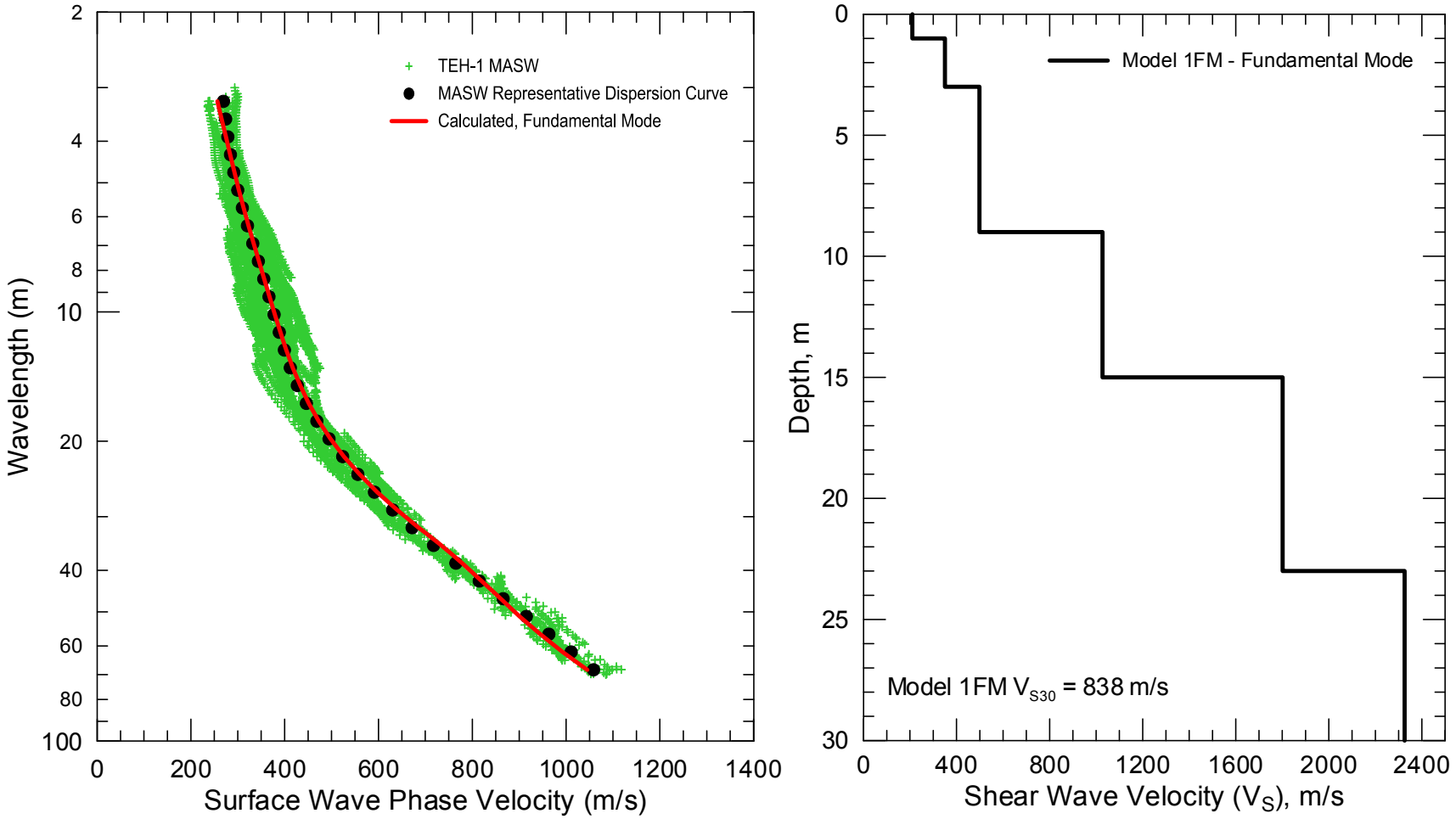

CI.TEH - Field, representative and inverted theoretical surface wave dispersion data (left) and associated V_S model (right) for fundamental mode assumption.

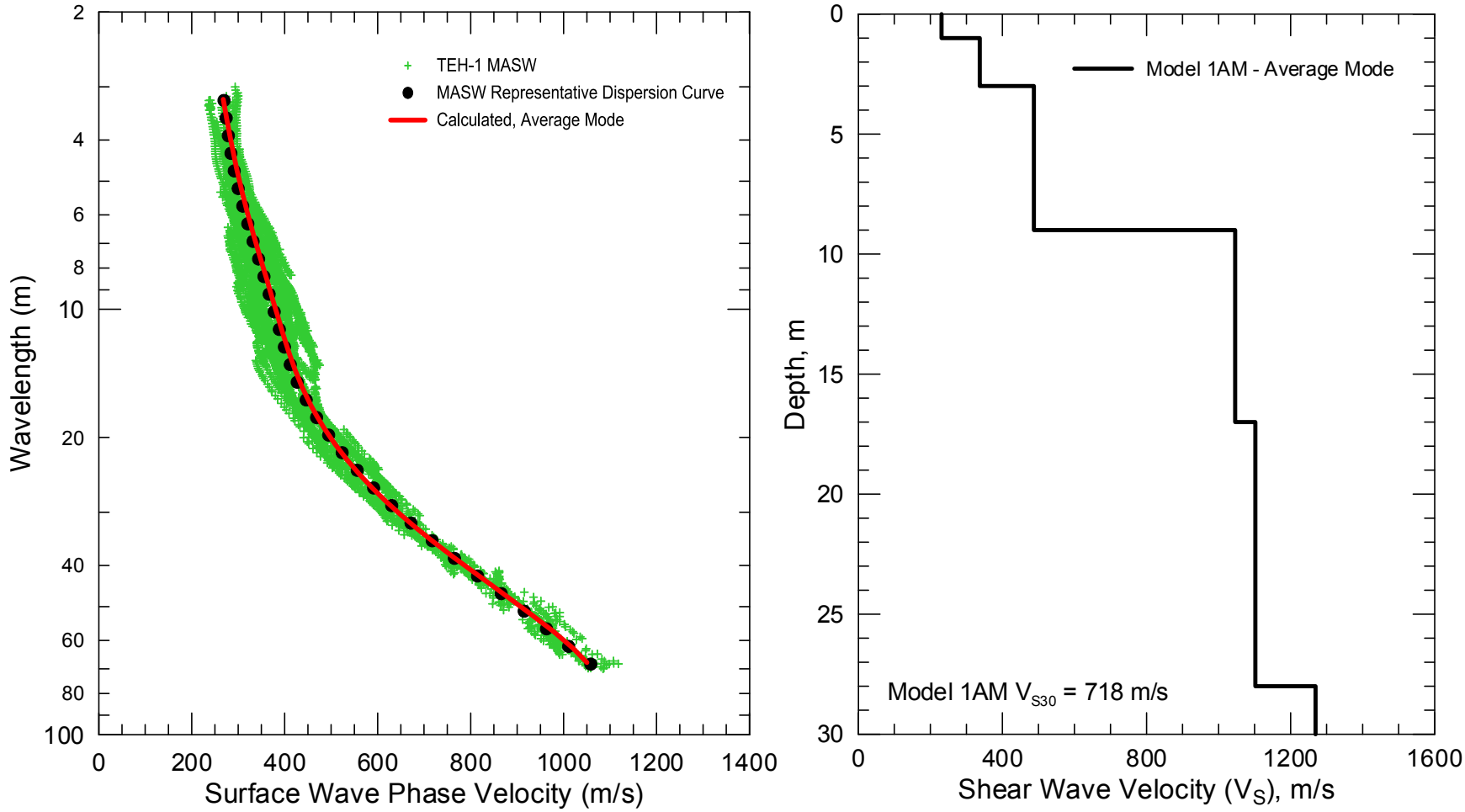

CI.TEH - Field, representative and inverted theoretical surface wave dispersion data (left) and associated V_S model (right) for average mode assumption.

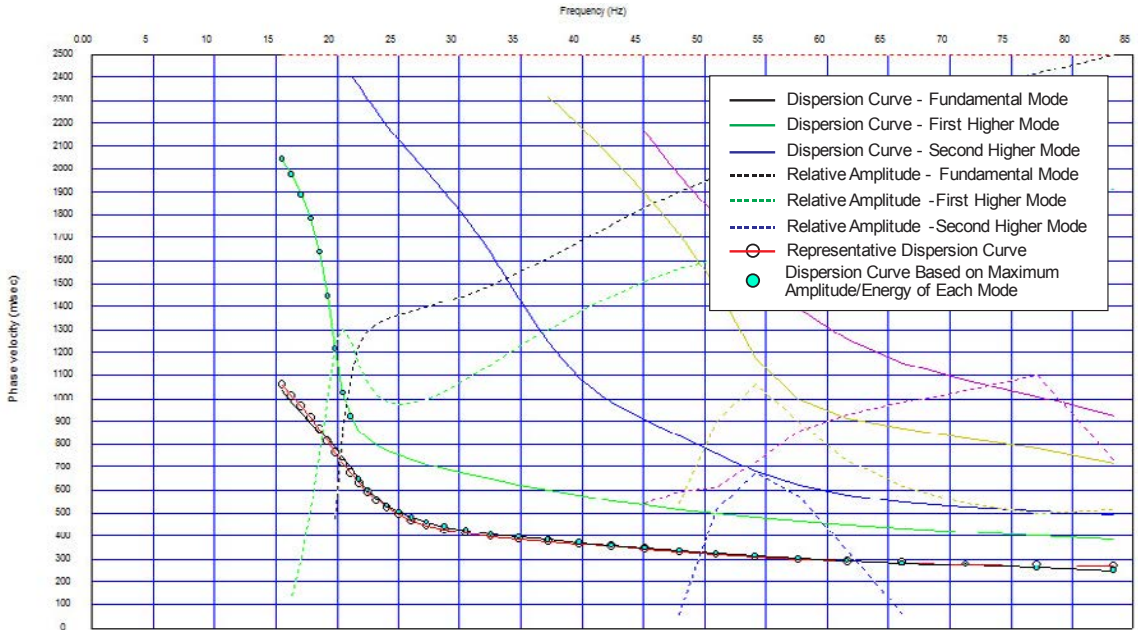

Calculated Rayleigh wave modes for fundamental mode V_S model 1FM demonstrating that the model should excite a dominant higher mode at frequencies below 21 Hz. It should be noted, however, that the analytical routine used to estimate the amplitudes of the higher modes makes a plane wave assumption (i.e. infinite source location) and does not include the effects of body waves.

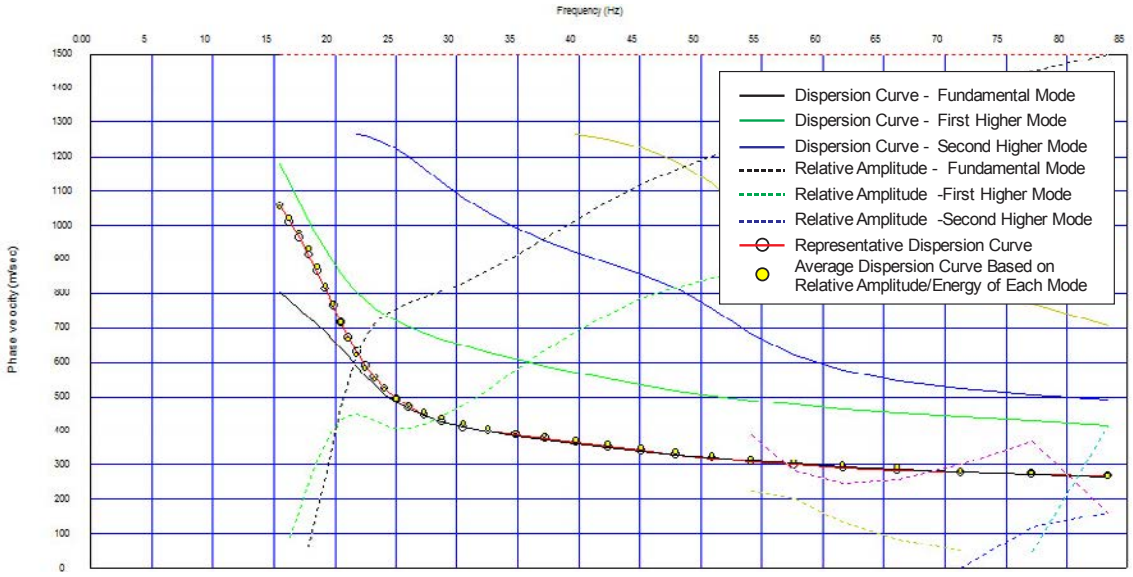

Calculated Rayleigh wave phase velocity modes for V_S model 1AM developed using the average mode assumption in an attempt to account for possible modal superposition (mode mixing) at low frequencies.

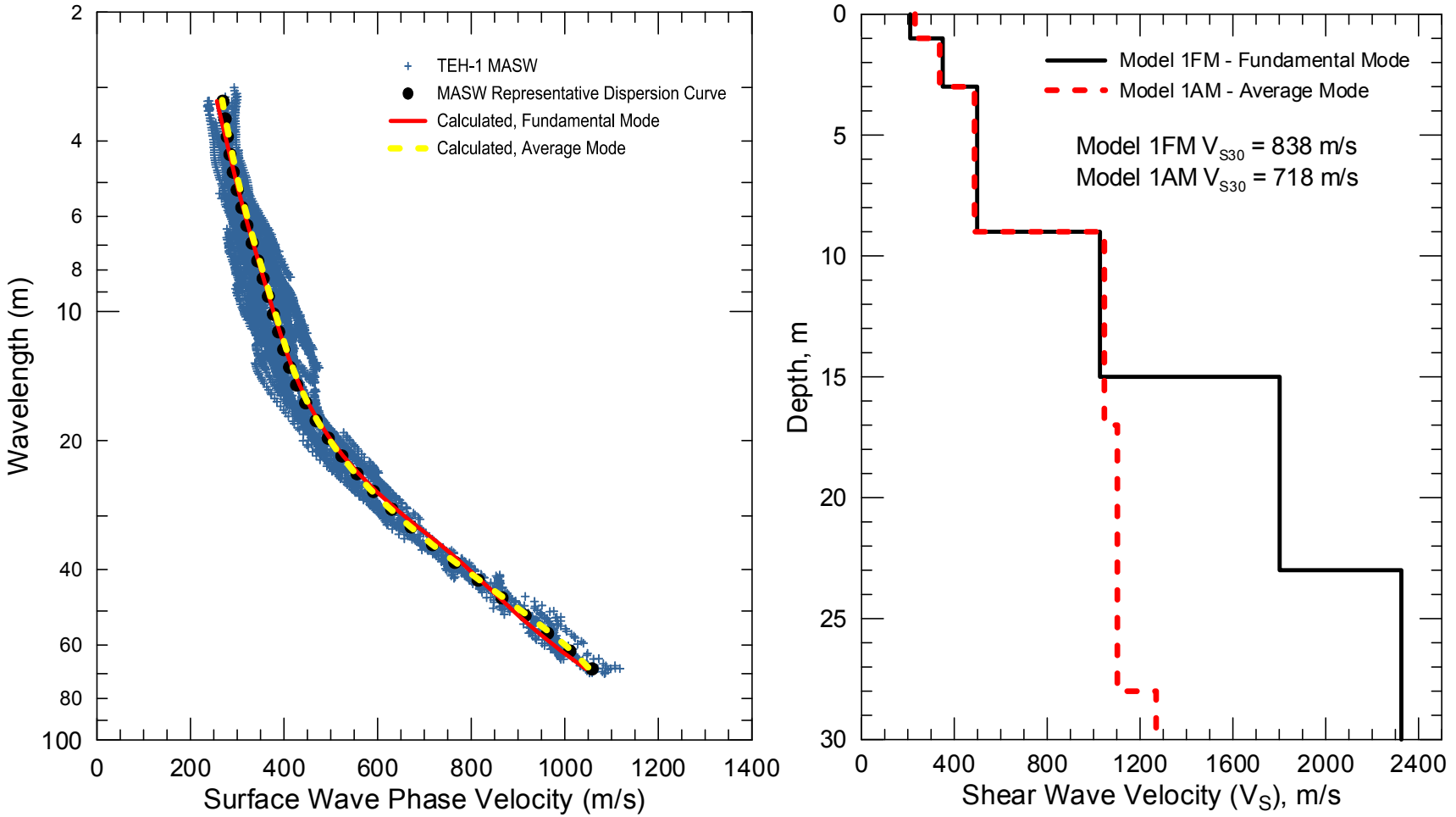

CI.TEH - Field, representative and inverted theoretical surface wave dispersion data (left) and associated V_S models (right) for fundamental and average mode assumption.

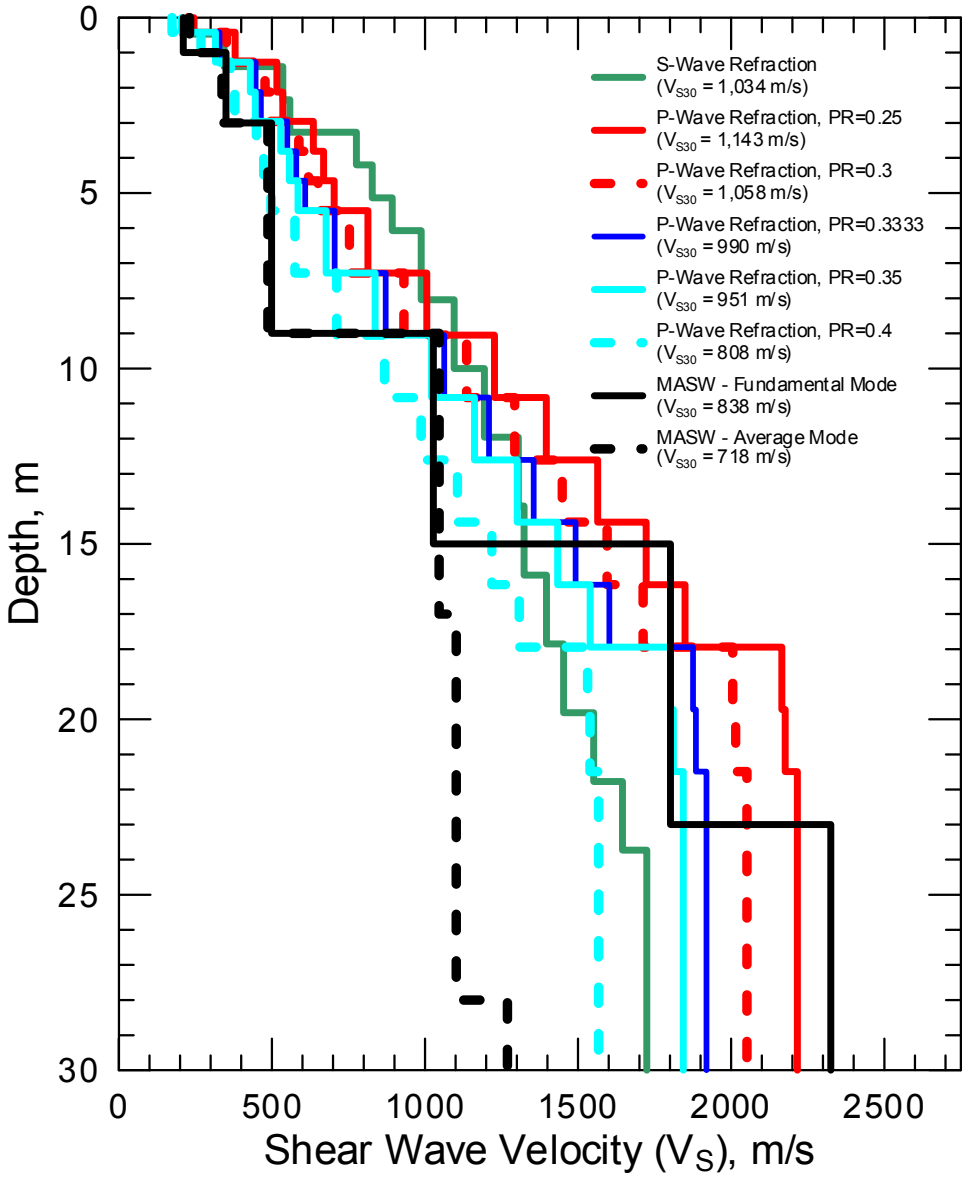

CI.TEH – Comparison of V_S models derived from MASW and P- and S-wave seismic refraction data. The V_S models developed using the three geophysical methods are not consistent. V_S from the average S-wave seismic refraction model is higher than that estimated from the average P-wave refraction model over the 3 to 8 m depth range, possibly due to error in the model. V_S from the average S-wave seismic refraction model relative to the average P-wave refraction model may indicate that weathered rock is saturated below a depth of 15 m. The V_S model developed from the MASW data using the fundamental mode assumption is most consistent with the seismic refraction models, but significantly underestimates V_{S30} relative to the seismic refraction models, primarily due to lower near surface velocities. MASW data reduction was difficult and lateral velocity variation may be such that the V_S models developed from the MASW data are not valid. Alternatively, out-of-plane refractors, if occurring, would result in the seismic refraction models overestimating velocities beneath the array.

Site CI.TFT

Location: Southern California Gas Company, 27680 Gas Company Road, Taft, California

Latitude: 35.14580 **Longitude:** -119.41941

(Station coordinates modified based on field observation of station location and identification of approximate station location on Google Earth – could not survey the seismic station as located inside a building, WGS84 coordinate system)

V_{S30} (measured): 332 m/s

V_{S30} (adjusted to more accurately reflect seismic station conditions): 367 m/s (average S-wave velocity between 2.6 and 32.6 m adjusting for approximate elevation difference between basement and ground surface. It should be noted that there is also a surface sensor located about 0.5 m below ground surface.)

NEHRP Site Class: D

Geomatrix Code: AHD/KHD (two sensor packages)

Geologic Conditions/Observations: Site located on geologic unit mapped as Quaternary (Holocene) alluvial gravel and sand. Pleistocene Tulare Formation (pebble gravel, sand and clay) outcrops about 200 m to the east of the test area. Crystalline basement expected to be deep at this site.

Site Conditions: Rural site with sporadic traffic on nearby road. Relatively flat terrain in test area with slight elevation decrease to the south.

Geophysical Methods Utilized: HVSR, MASW, SASW

Geophysical Testing Arrays:

1. Array TFT-1 (48 channel MASW array utilizing 4.5 Hz vertical geophones spaced 1.5 m apart for a length of 70.5 m, forward and reverse shot locations with multiple source offsets and source types and center shot location).
2. Array TFT-1 (SASW array with common midpoint and orientation as MASW array of same name utilizing 4.5 and 1 Hz vertical geophones and maximum receiver spacing of 32 m).
3. Three HVSR measurement locations distributed along array TFT-1.

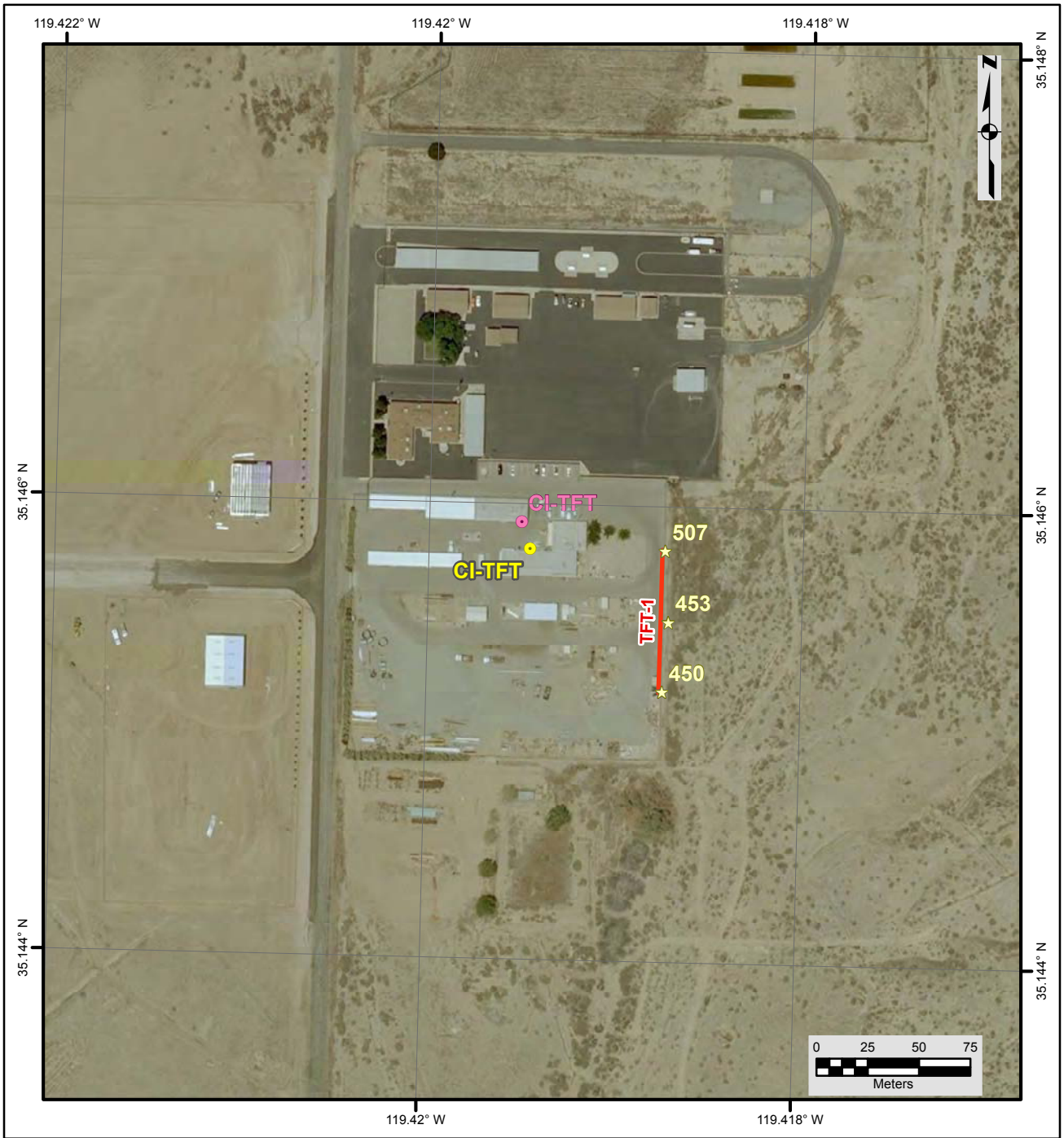

Legend

- Seismic Station - Approximate Improved Location
- Seismic Station - Approximate Location of Record
- H/V Spectral Ratio Location
- MASW and SASW Array

NOTES:
1. WGS 1984 COORDINATE SYSTEM
2. Image Source: ESRI, i-cubed, USDA FSA, USGS, AEX, GeoEye, Getmapping, Aerogrid, IGP

File Name: CI-TFT-I

Date: 10/18/2012

USGS science for a changing world

GEOVision geophysical services

RECOVERY.GOV

SITE MAP
CI•TFT

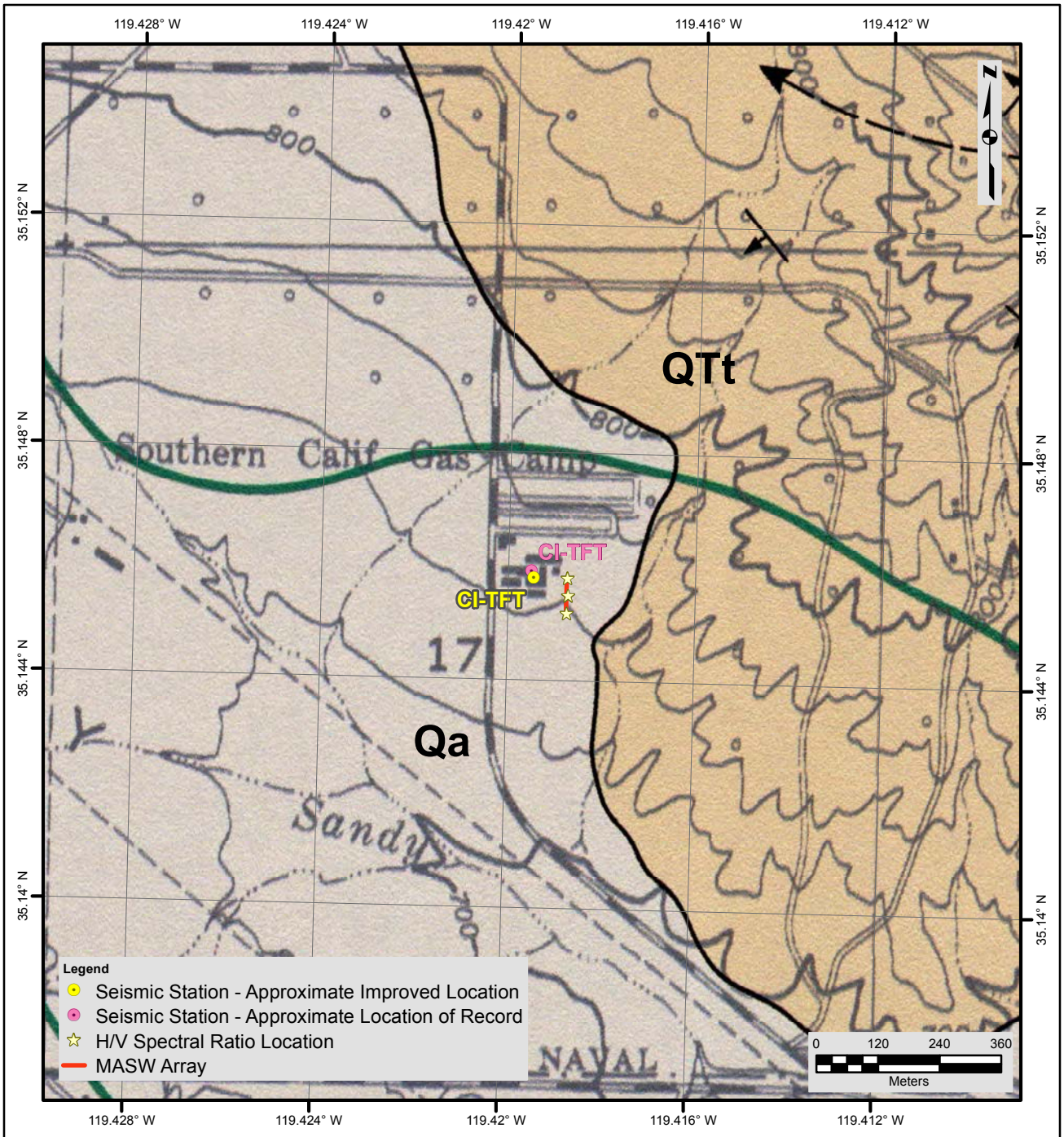

Description of Geologic Map Units

Qa = Quaternary (Holocene) alluvial gravel and sand of valley areas
QTt = Quaternary (Pleistocene) Tulare Formation; pebble gravel, sand and clay, mostly of Monterey siliceous shale debris

NOTES:
1. WGS 1984 COORDINATE SYSTEM
2. Geologic Map of the Taft and Mouth of Kern Quadrangles, Kern County, California by Thomas W. Dibblee, Jr., 2005
3. See site map for details of geophysical survey

File Name: CI-TFT

Date: 7/15/2011

USGS science for a changing world

GEOVision geophysical services

GEOLOGIC MAP
CI•TFT

RECOVERY.GOV

Seismic station CI.TFT in basement level of structure

Looking north towards structure housing seismic station CI.TFT and a surface sensor in PVC casing outside the building

Looking northwest towards seismic station, center of MASW array TFT-1 and HVSR sensor 453

Looking south along SASW array TFT-1

Looking south along MASW array TFT-1

Location of Geophysical Testing Arrays

Location	Latitude	Longitude
TFT-1, South end of MASW Array	35.14518	-119.41871
TFT-1, Center of MASW and SASW Arrays	35.14550	-119.41871
TFT-1, North end of MASW Array	35.14581	-119.41870
HVSR Sensor 450	35.14519	-119.41869
HVSR Sensor 453	35.14549	-119.41866
HVSR Sensor 507	35.14581	-119.41869

Notes: 1) WGS84 Coordinate System (decimal degrees)
2) Survey accuracy is estimated at 1 to 2 m

Results:

V_S Model

Depth to Top of Layer (m)	Layer Thickness (m)	S-Wave Velocity (m/s)	Inferred P-Wave Velocity (m/s)	Inferred Poisson's Ratio	Inferred Density (g/cm^3)
0	1	147	275	0.3	1.9
1	2	213	399	0.3	1.9
3	3	283	529	0.3	1.9
6	4	333	623	0.3	1.9
10	6	363	678	0.3	2.0
16	9	379	709	0.3	2.0
25	>5	445	833	0.3	2.0

Observations/Discussion:

- HVSR plots are similar at all measurement locations at frequencies below 10 Hz validating the 1-D velocity structure assumption.
- HVSR data quality not as good at sensor location 507 as at sensor locations 450 and 453. It may be possible to acquire better quality data if measurements are made at night.
- There is a low amplitude HVSR peak (or double peaks) in the 0.13 to 0.18 Hz range, confirming that the basement complex is very deep at the site.
- Noise conditions at site were not sufficient to apply passive surface wave techniques.
- Surface wave dispersion data from SASW and MASW data sets are in good agreement at the site.
- Representative dispersion curves were generated for each surface wave data set using a moving average, polynomial curve fitting routine. These individual representative dispersion curves were combined and a representative dispersion curve generated for the combined data set for purpose of data modeling.
- Water table located at a depth of greater than 30 m based on seismic refraction survey design, absence of a water table refractor and no clear reflectors.
- Based on simple horizontal layer-based analysis of seismic refraction first arrival data, P-wave velocity in the upper 20 m ranges from about 300 to 750 m/s (300 to 350 m/s to a depth of 1 to 2 m, 500 to 550 m/s to a depth of about 5 m, 600 to 625 m/s to a depth of about 15 to 16 m, then 750 m/s).
- Surface wave depth of investigation is about 30 m based on half of maximum wavelength criteria.
- The inferred P-wave velocities in the surface wave model are consistent with simplified P-wave refraction model, especially considering that Poisson's ratio is unknown.
- V_{S30} is 332 m/s (Site Class D).
- Average S-wave velocity between 2.6 m (basement sensor depth below ground surface) and 32.6 m is 367 m/s (Site Class D/C). There is also a surface sensor at this site.

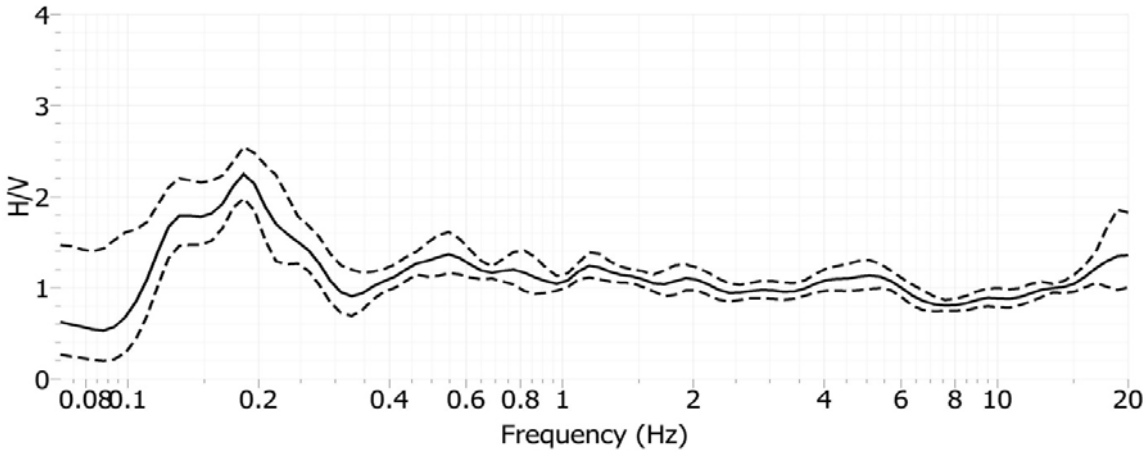

Site CI. TFT, H/V Spectral Ratio, Array TFT-1, Sensor 507

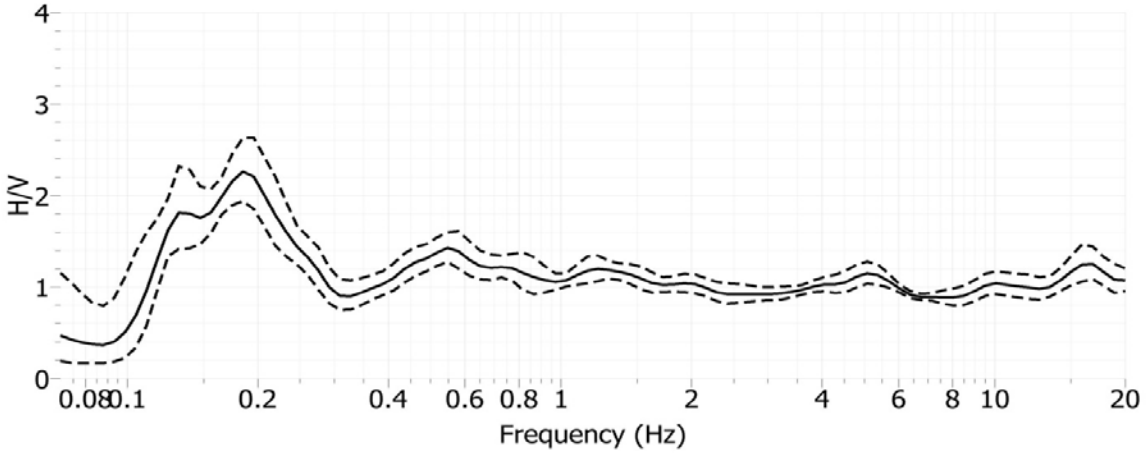

Site CI. TFT, H/V Spectral Ratio, Array TFT-1, Sensor 453

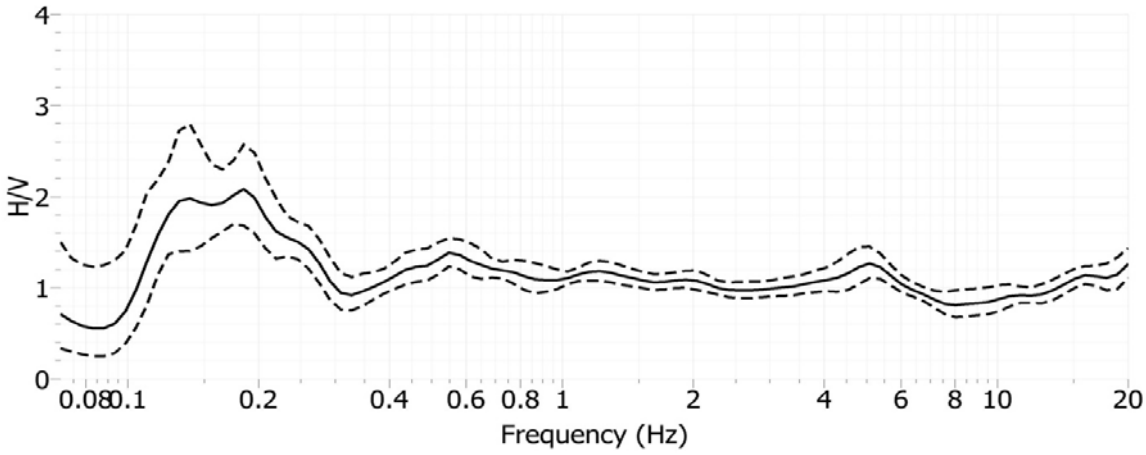

Site CI.TFT, H/V Spectral Ratio, Array TFT-1, Sensor 450

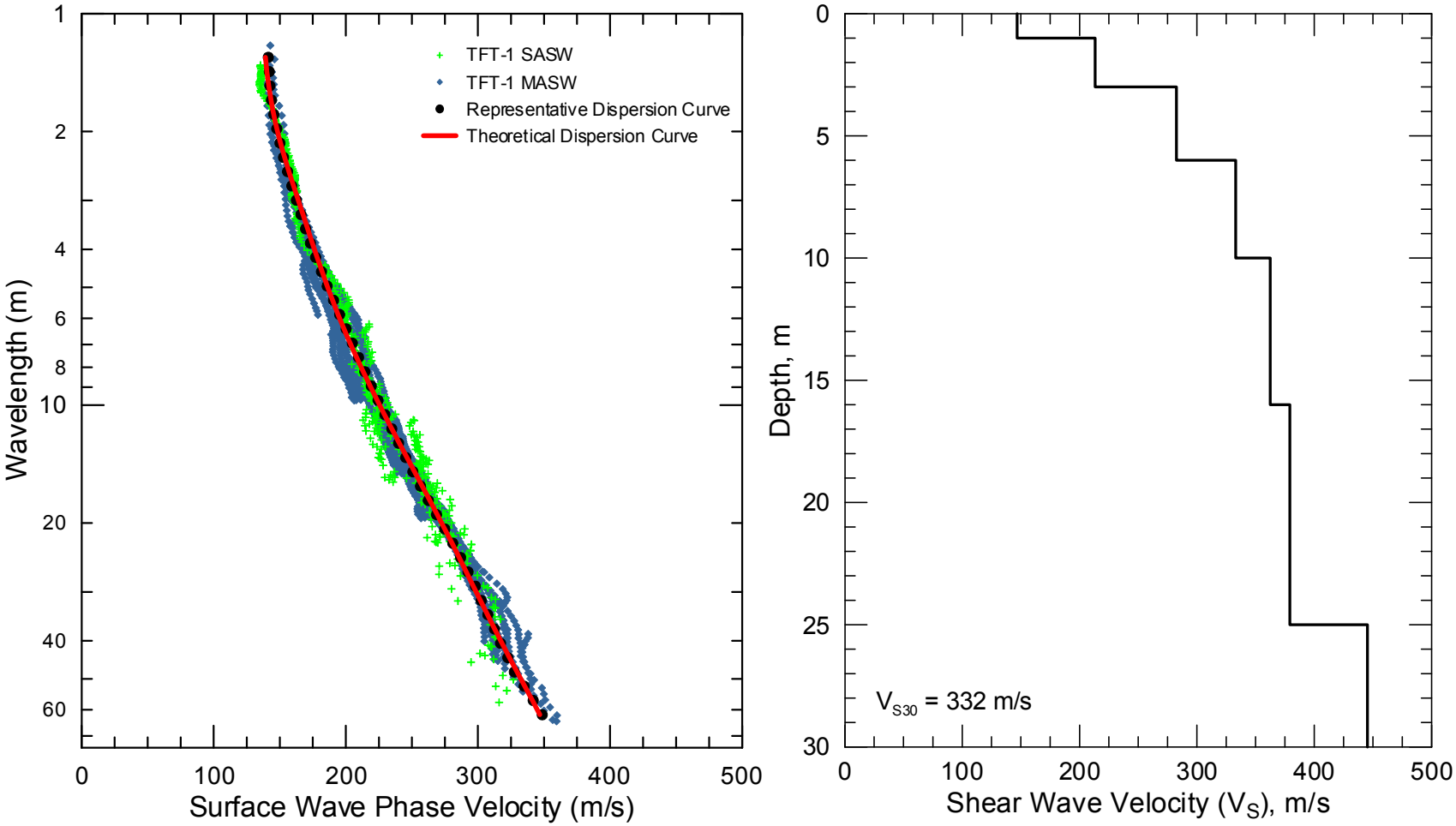

CI.TFT - Field, representative and inverted theoretical surface wave dispersion data (left) and associated V_S model (right)

Site CI.THM

Location: Thermal Canyon, Thermal, Riverside County, California

Latitude: 33.65066 **Longitude:** -116.07734
(Station coordinates provided by USGS, WGS84 coordinate system)

V_{S30} (measured): 452 m/s

V_{S30} (adjusted to more accurately reflect seismic station conditions): 480 m/s (average S-wave velocity between 2 and 32 m adjusting for 2 m nominal sensor depth).

NEHRP Site Class: C

Geomatrix Code: IQD

Geologic Conditions/Observations: Quaternary (Pleistocene) Ocotillo Formation. Seismic station located near axis of a syncline with bedding nominally dipping on the order of 30 degrees. San Andreas Fault Zone located about 350 meters southwest of the seismic station.

Site Conditions: Rural site. Test area located on relatively planar surface with elevation increasing gently to the east and surrounded by hilly terrain.

Geophysical Methods Utilized: HVSR, MASW

Geophysical Testing Arrays:

1. Array THM-1 (48 channel MASW array utilizing 4.5 Hz vertical geophones spaced 1.5 m apart for a length of 70.5 m, forward and reverse shot locations with multiple source offsets and hammer source types and several interior shot locations).
2. Three HVSR measurement locations distributed along array THM-1.

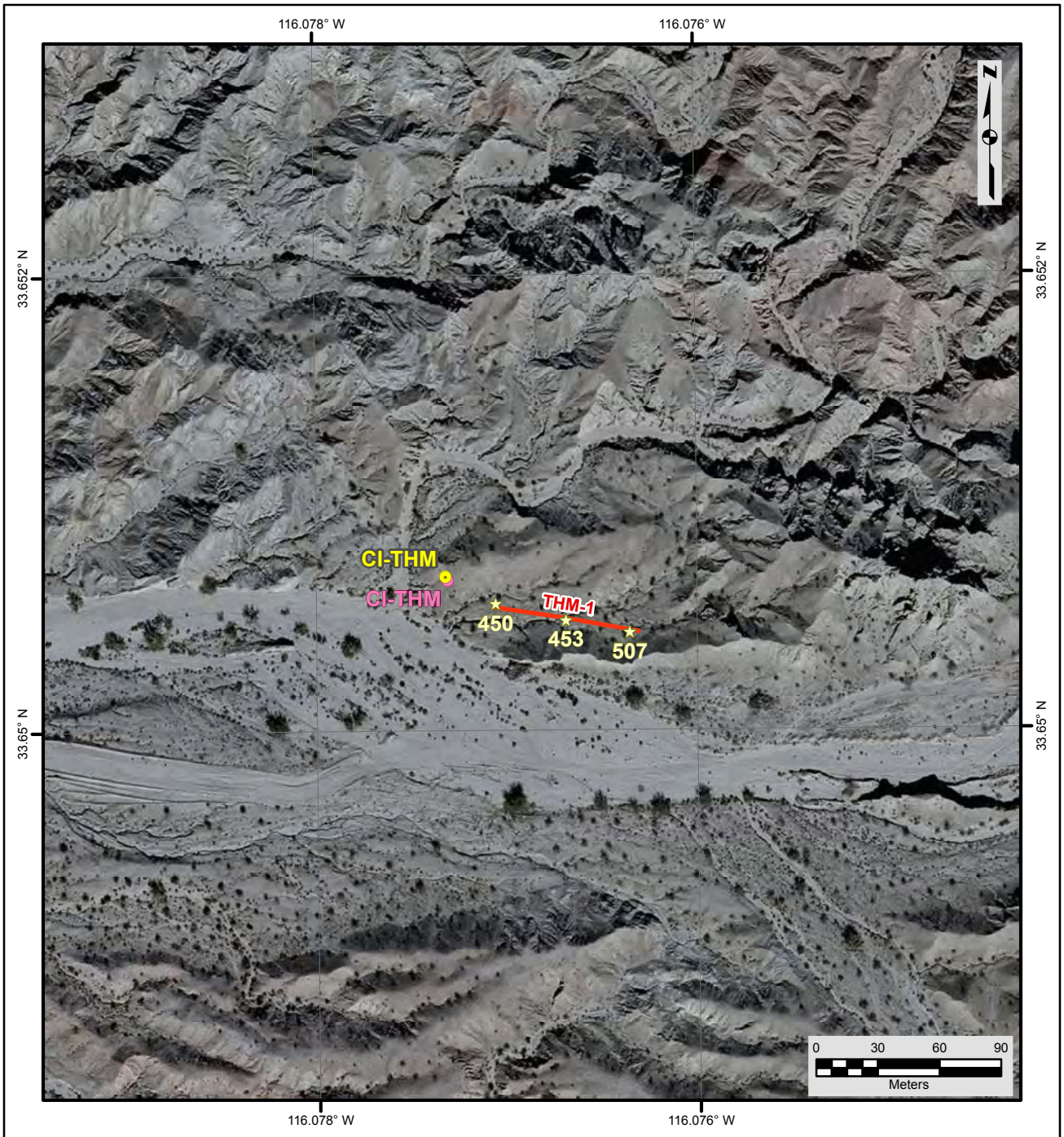

Legend

- Seismic Station - Approximate Surveyed Location
- Seismic Station - Approximate Location of Record
- H/V Spectral Ratio Location
- MASW Array

NOTES:
1. WGS 1984 COORDINATE SYSTEM
2. Image Source: ESRI, i-cubed, USDA FSA, USGS, AEX, GeoEye, Getmapping, Aerogrid, IGP

File Name: CI-THM-I

Date: 8/11/2011

USGS science for a changing world

GEOVision geophysical services

RECOVERY.GOV

SITE MAP
CI•THM

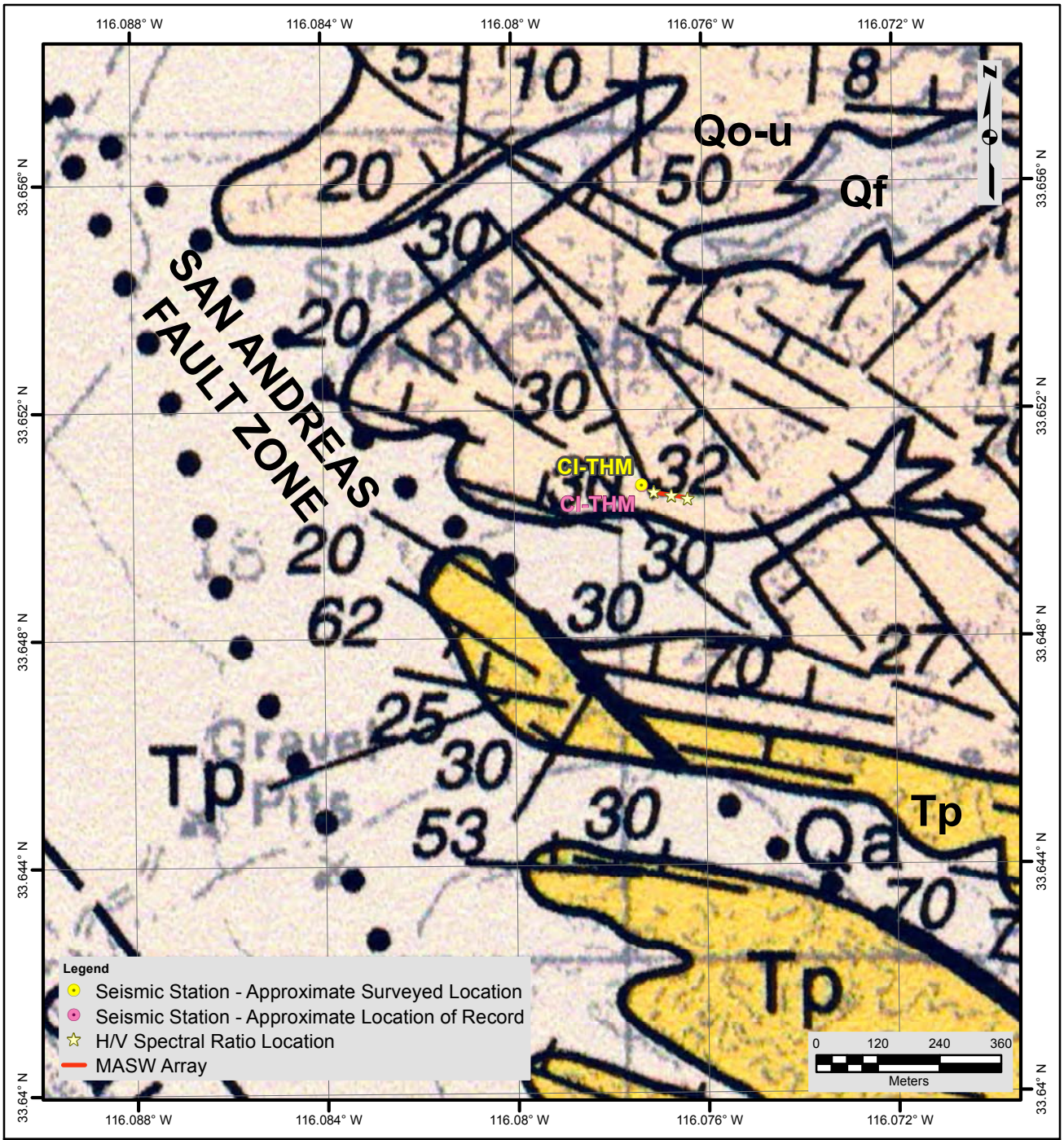

Description of Geologic Map Units

Qa = Quaternary (Holocene) alluvial sand and clay of valleys areas
Qf = Quaternary (Holocene) alluvial fan gravel
Qo-u = Tertiary (Pliocene) Ocotillo formation; upper unit, boulder-conglomerate
Tp = Tertiary (Pliocene) Palm Spring formation; sandstone, arkosic

NOTES:
1. WGS 1984 COORDINATE SYSTEM
2. Geologic Map of the Palm Desert & Coachella 15 Minute Quadrangles, Riverside County, California By Thomas W. Dibblee, Jr., 2008
3. See site map for details of geophysical survey

File Name: CI-THM

Date: 8/12/2011

USGS science for a changing world

GEOVision geophysical services

RECOVERY.GOV

GEOLOGIC MAP
CI•THM

Looking west at HVSR sensor 507 and MASW array THM-1

Looking east at seismic station CI.THM

MASW data acquisition

Looking east along array THM-1

Looking northwest towards HVSR sensor 450 and the seismic station

Location of Geophysical Testing Arrays:

Location	Latitude	Longitude
THM-1, West End of MASW Array	33.65054	-116.07709
THM-1, Center of MASW Array	33.65049	-116.07672
THM-1, East End of MASW Array	33.65043	-116.07634
HVSR Sensor 450	33.65056	-116.07709
HVSR Sensor 453	33.65048	-116.07672
HVSR Sensor 507	33.65043	-116.07638
CI.THM Seismic Station	33.65068	-116.07735

Notes: 1) WGS84 Coordinate System (decimal degrees).
2) Survey accuracy is estimated at 1 to 2 m.

Results:

V_S Model

Depth to Top of Layer (m)	Layer Thickness (m)	S-Wave Velocity (m/s)	Inferred P-Wave Velocity (m/s)	Assumed Poisson's Ratio	Assumed Density (g/cm^3)
0	1.5	243	454	0.300	1.8
1.5	2	406	760	0.300	1.9
3.5	5.5	517	967	0.300	1.9
9	7	409	766	0.300	1.9
16	7	450	842	0.300	1.9
23	>7	582	2000	0.454	2.0

Notes: 1) Saturated sediments estimated at 23 m depth from seismic refraction first arrival data. The P-wave velocity of saturated sediments is not well constrained due to limited offset, but appears to be greater than 2,000 m/s.
2) Depth of investigation is about 30 m.
3) Bottom layer is a half space.

Observations/Discussion:

- HVSR plots are very similar at every station, validating the 1-D velocity assumption.
- There are no clear high frequency HVSR peaks, but there is elevated HVSR response between 0.2 and 2 Hz at each station.
- Both the vertical and horizontal HVSR components have a spectral peak at about 0.14 Hz. There is no HVSR peak in this range although there could be one at lower frequency. Documenting an HVSR peak at such low frequency would require longer duration recording and a very stable sensor platform and would more easily be investigated by recording several hours of noise with the long period seismometer installed at station CI.THM.
- Based on interactive, horizontal layer-based analysis of seismic refraction first arrival data, P-wave velocity structure in the upper 25 m consists of a 1.5 to 2.5 m layer with P-wave velocity in the 450 to 550 m/s range, underlain by sediments with a P-wave velocity typically in the 800 to 875 m/s range to a depth of about 20 to 25 m, below which sediments may be saturated. P-wave velocity of the potential saturated zone cannot be accurately resolved due to insufficient array length, but appears to be over 2,000 m/s.
- Noise conditions at the site were not sufficient to apply passive surface wave techniques.
- The minimum wavelength surface wave phase velocity data extracted from the 48-channel MASW array was about 25 m with a possible dominant higher mode at smaller wavelengths (higher frequencies). Reducing data from smaller hammer sources using a limited offset receiver array (i.e. less active geophones) allowed extraction of surface wave dispersion data to a minimum wavelength of about 3.5 m. It should be noted that there is the possibility of modal superposition (modes combining) when the phase velocity resolution decreases as the number of geophones decreases.
- There is some scatter in the MASW dispersion data, which may be partially associated with lateral velocity variation.
- The nature of the MASW dispersion curve suggests that a velocity inversion may be present at the site. Seismic refraction data are inconclusive in regards to the presence of a high velocity later although does indicate that there is a certain degree of lateral velocity variation.
- A representative dispersion curve was generated for the combined MASW data set using a moving average, polynomial curve fitting routine and used for modeling.
- Water table depth constrained to about 23 m based on seismic refraction analysis discussed above (2,000 m/s V_P for saturated sediments).
- Surface wave depth of investigation is about 30 m based on half of maximum wavelength criteria.
- The inferred P-wave velocities in surface wave model, based on an assumed Poisson's ratio of 0.3 and modeled S-wave velocity, are consistent with simplified P-wave refraction model, especially considering the unknown Poisson's ratio.
- The S-wave velocity model derived from the surface wave testing is believed to be representative of average subsurface velocity structure. However, geology at the site is complex with folded bedding due to proximity of the site to the San Andreas Fault Zone. Due to limited feasible test locations at the site, the MASW array is neither parallel to nor orthogonal to the predominant strike of the bedding and the array is located near the axis

of a mapped syncline. Mapped dips of bedding are typically in the 30 degree range, although effective dip will be much less beneath the seismic array due to orientation of the array relative to strike of bedding. It is difficult to predict the effect of dipping beds on surface wave dispersion data; however, the S-wave velocity model is consistent with observed P-wave velocities in seismic refraction data and seismic refraction data does not indicate that there is significant lateral velocity variation at shallow depth.

- V_{S30} is 452 m/s (Site Class C).
- Average S-wave velocity between 2 m (nominal sensor depth) and 32 m is 480 m/s.

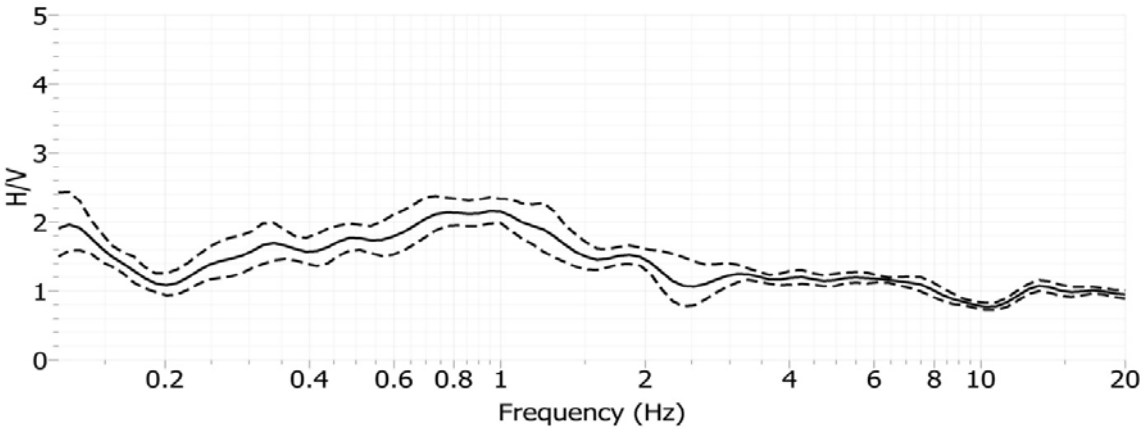

Site CI.THM, H/V Spectral Ratio, Array THM-1, Sensor 450

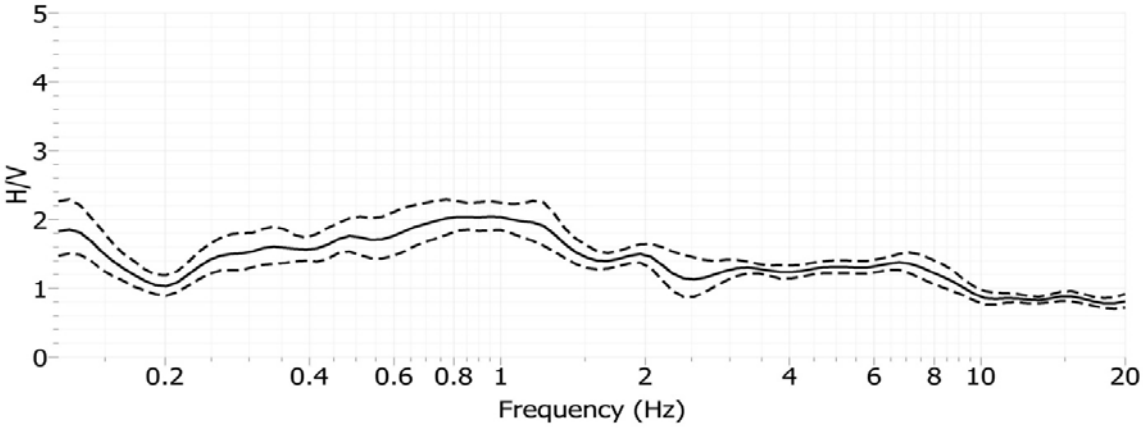

Site CI.THM, H/V Spectral Ratio, Array THM-1, Sensor 453

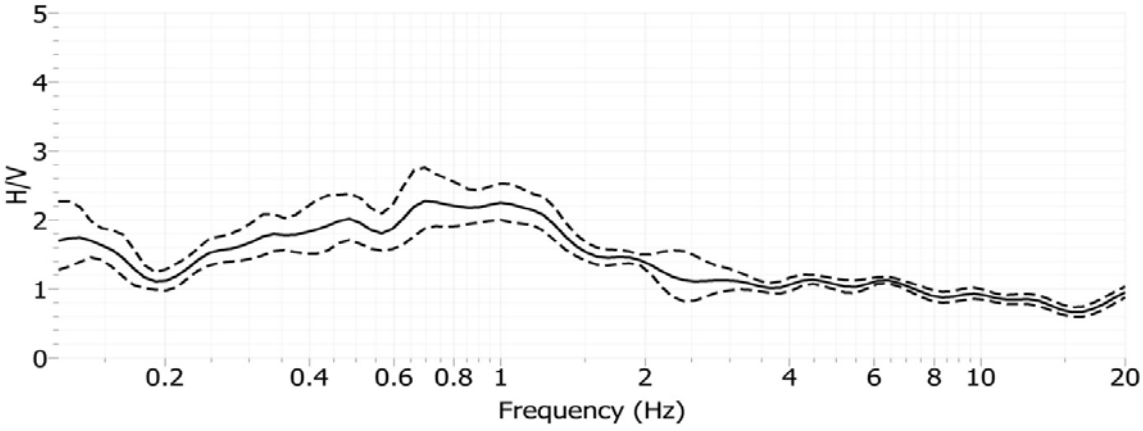

Site CI.THM, H/V Spectral Ratio, Array THM-1, Sensor 507

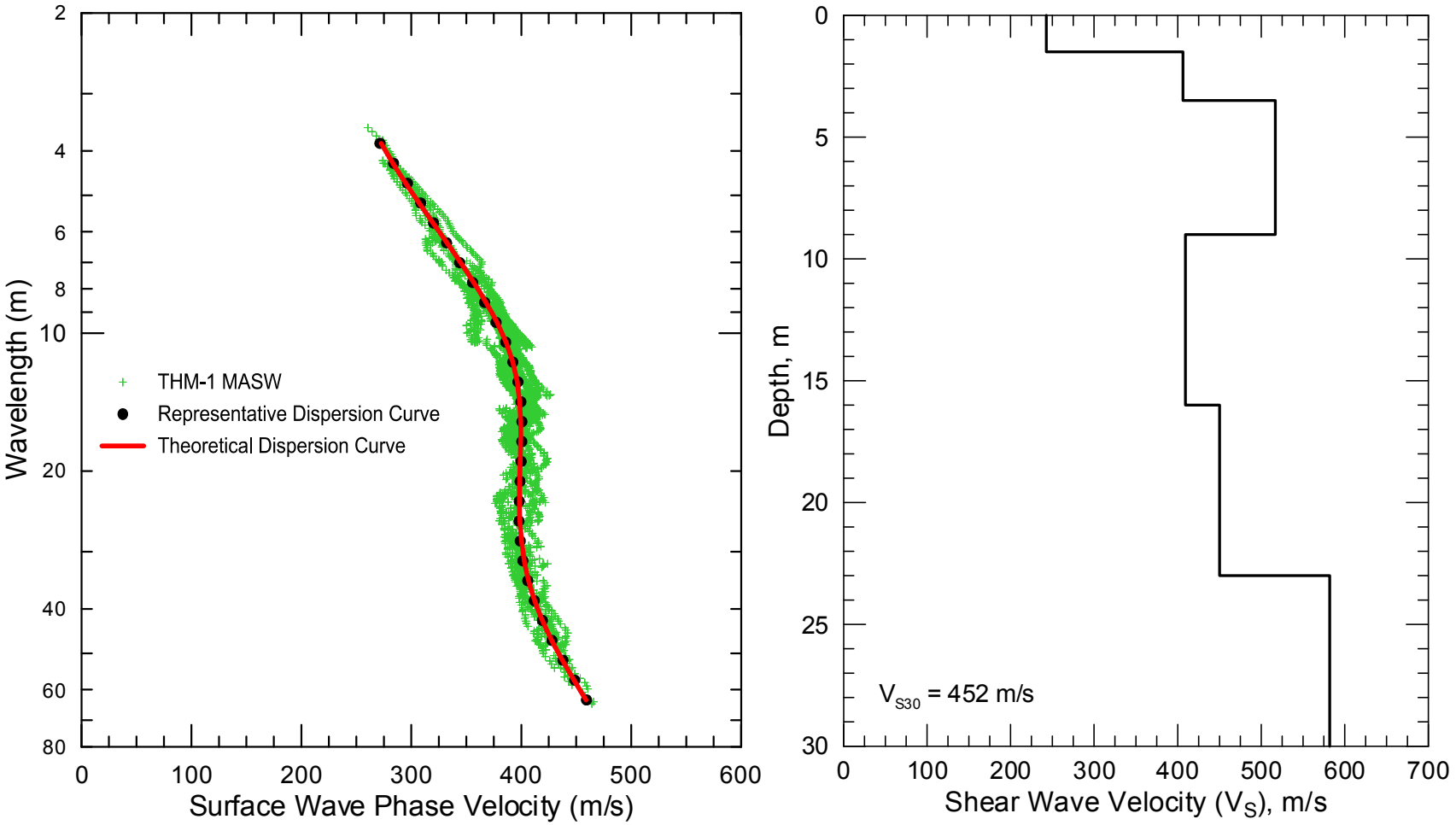

CI.THM - Field, representative and inverted theoretical surface wave dispersion data (left) and associated V_S model (right)

Site CI.TIN

Location: Tinemaha Reservoir, Inyo County, California

Latitude: 37.05422 **Longitude:** -118.23009
(Station coordinates provided by USGS, WGS84 coordinate system)

V_{S30} (measured): 396 m/s

V_{S30} (adjusted to more accurately reflect seismic station conditions): 396 m/s (no adjustment necessary).

NEHRP Site Class: C

Geomatrix Code: AVD/APD

Geologic Conditions/Observations: Seismic station located on geologic unit mapped as Tertiary (Pliocene) basalt flow. The basalt unit appears to be very thin and overlies a Tertiary (Pliocene) diatomite interbedded with lacustrine silt, sand and conglomerate. The Tertiary sediments are mapped as dipping about 30 to 45 degrees to the southwest in the site vicinity.

Site Conditions: Rural site. Test area located at toe of an outcrop of Tertiary volcanic and sedimentary rocks on relatively planar older alluvial surface. Noise from vehicle traffic on nearby SR-395.

Geophysical Methods Utilized: HVSR, Seismic Refraction, MASW

Geophysical Testing Arrays:

1. Array TIN-1 (48 channel MASW and P-wave seismic refraction array utilizing 4.5 Hz vertical geophones spaced 2 m apart for a length of 94 m, forward and reverse shot locations with multiple source offsets and source types and center shot location). Passive surface wave data also acquired along this linear array.
2. Array TIN-2 (48 channel MASW and P-wave seismic refraction array with same orientation and center location as TIN-1 utilizing 4.5 Hz vertical geophones spaced 1 m apart for a length of 47 m, forward and reverse shot locations with multiple source offsets and source types and center shot location).
3. Array TIN-3 (48 channel MASW and P-wave seismic refraction array utilizing 4.5 Hz vertical geophones spaced 1.5 m apart for a length of 70.5 m, forward and reverse shot locations with multiple source offsets and source types (hammers only) and center shot location).
4. Four HVSR measurement locations; three distributed along array TIN-1/TIN-2 and one along array TIN-3.

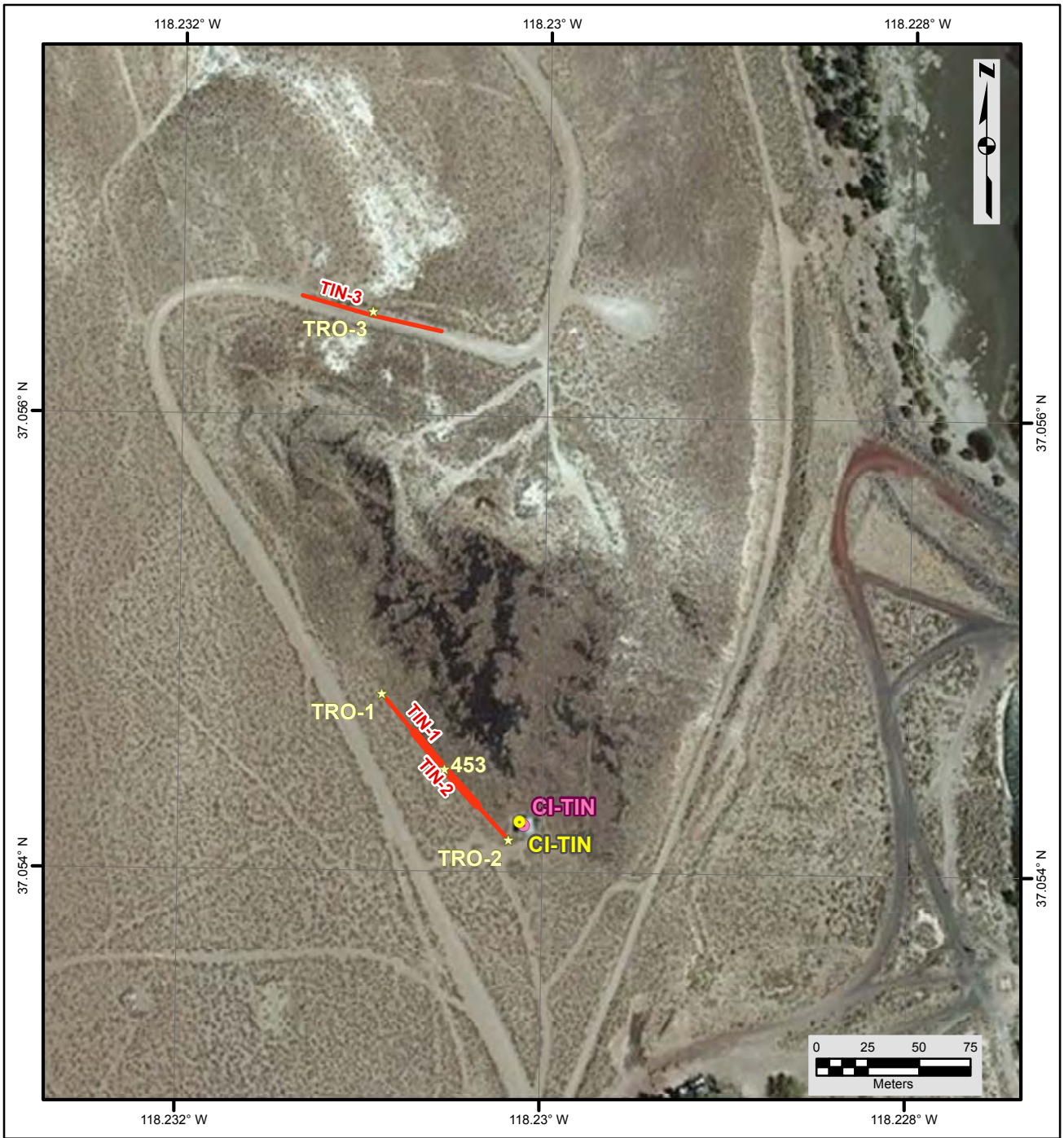

Legend

- Seismic Station - Approximate Surveyed Location
- Seismic Station - Approximate Location of Record
- H/V Spectral Ratio Location
- MASW, SASW and Seismic Refraction Array

NOTES:
1. WGS 1984 COORDINATE SYSTEM
2. Image Source: ESRI, i-cubed, USDA FSA, USGS, AEX, GeoEye, Getmapping, Aerogrid, IGP

File Name: CI-TIN-1

Date: 3/29/2012

USGS science for a changing world

GEOVision geophysical services

RECOVERY.GOV

SITE MAP
CI•TIN

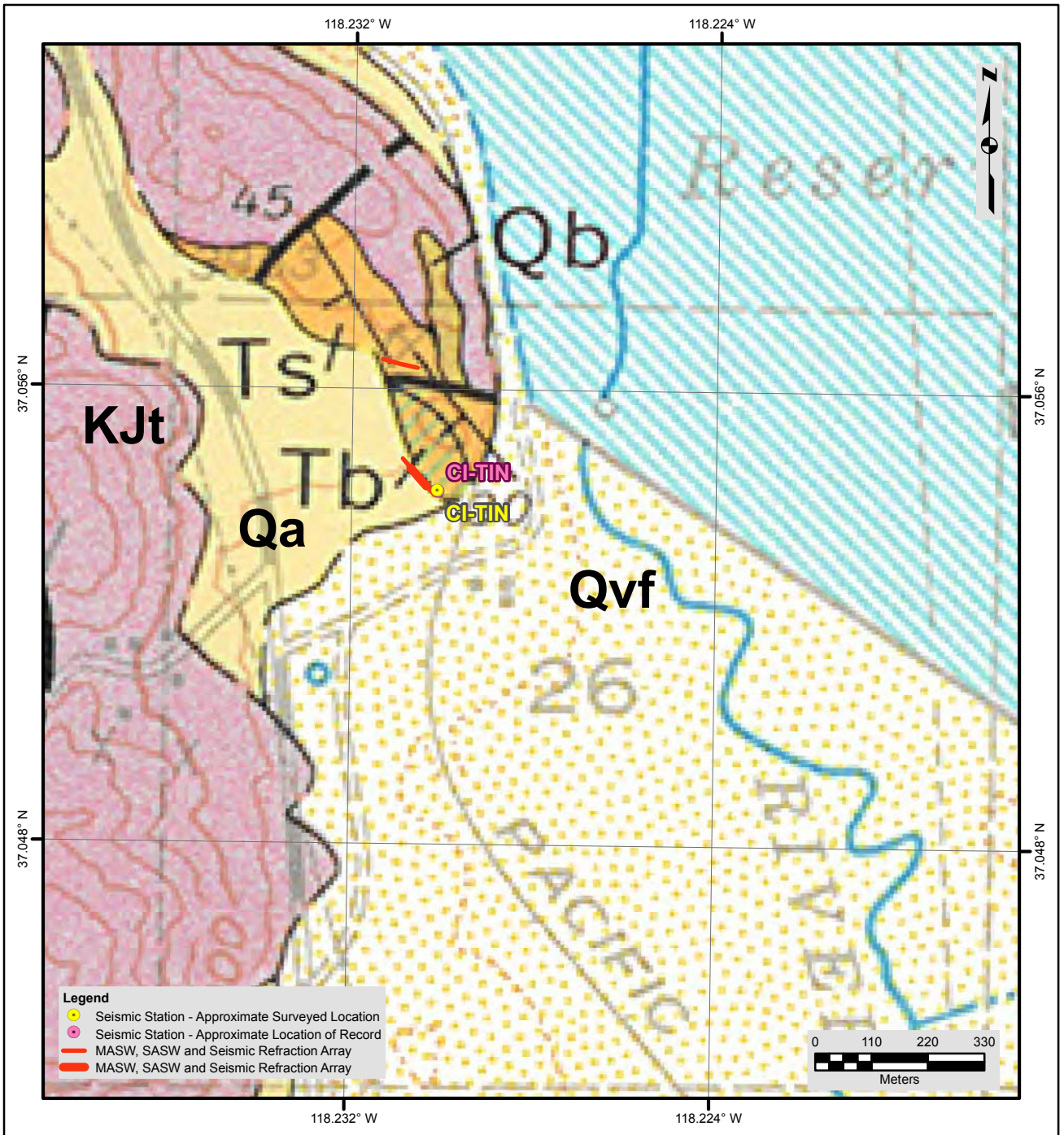

Description of Geologic Map Units

Qvf = Quaternary sand, silt, and clay in Owens Valley
Qa = Quaternary alluvial fans and stream gravel and sand in intermontane basins
Qb = Quaternary black olivine basalt
Tb = Tertiary (Pliocene) olivine basalt
Ts = Tertiary (Pliocene) diatomite, interbedded in lacustrine silt and sand and pebble conglomerate
KJt = Jurassic or Cretaceous Tinemaha granodiorite; medium-grained, epidotized

NOTES:
1. WGS 1984 COORDINATE SYSTEM
2. Geologic Map of the Waucoba Mountain Quadrangle, Inyo County, California by C. A. Nelson, 1966
3. See site map for details of geophysical survey

File Name: CI-TIN2
Date: 3/29/2012

USGS science for a changing world
GEOVision geophysical services

GEOLOGIC MAP
CI•TIN

RECOVERY.GOV

Looking north at building housing CI.TIN seismic station

Looking southeast along array TIN-1

Looking west at east side of basalt outcrop showing sedimentary rocks underlying the thin basalt layer

Looking northwest along array TIN-2

Looking northwest along array TIN-3

Location of Geophysical Testing Arrays:

Location	Latitude	Longitude
TIN-1, Southeast End of MASW/Refraction Array	37.05414	-118.23015
TIN-1, Center of MASW/Refraction Array	37.05445	-118.23051
TIN-1, Northwest End of MASW/Refraction Array	37.05478	-118.23086
TIN-2, Northwest End of MASW/Refraction Array	37.05428	-118.23032
TIN-2, Center of MASW/Refraction Array	37.05445	-118.23051
TIN-2, Southeast End of MASW/Refraction Array	37.05461	-118.23067
TIN-3, Northwest End of MASW/Refraction Array	37.05652	-118.23132
TIN-3, Center of MASW/Refraction Array	37.05644	-118.23094
TIN-3, Southeast End of MASW/Refraction Array	37.05637	-118.23055
HVSR Sensor Tromino ENGY (TRO-1)	37.05478	-118.23086
HVSR Sensor Tromino ENGY (TRO-2)	37.05414	-118.23015
HVSR Sensor Tromino ENGY (TRO-3)	37.05646	-118.23093
HVSR Sensor 453 (Nanometrics Trillium Compact)	37.05445	-118.23051
CI.TIN Seismic Sensor	37.05421	-118.23007

Notes: 1) WGS84 Coordinate System (decimal degrees)
2) Survey accuracy is estimated at 1 to 2 m
3) Seismic station location is average coordinates of four corners of building housing sensor.

Results:

MASW V_S Model 1 (Average Dispersion Curve)

Depth to Top of Layer (m)	Layer Thickness (m)	S-Wave Velocity (m/s)	Inferred P-Wave Velocity (m/s)	Inferred Poisson's Ratio	Inferred Density (g/cm^3)
0	1	221	413	0.3	1.7
1	2	267	499	0.3	1.8
3	10	456	853	0.3	1.9
13	11	393	736	0.3	1.9
24	>11	644	1204	0.3	2.0

Notes: 1) Depth of investigation is about 35 m.
2) Bottom layer is a half space.

MASW V_S Model 2 (Lower Envelope of Dispersion Curve)

Depth to Top of Layer (m)	Layer Thickness (m)	S-Wave Velocity (m/s)	Inferred P-Wave Velocity (m/s)	Inferred Poisson's Ratio	Inferred Density (g/cm^3)
0	1	190	356	0.3	1.7
1	2	250	468	0.3	1.8
3	10	425	795	0.3	1.9
13	13	395	739	0.3	1.9
26	>9	660	1235	0.3	2.0

Notes: 1) Depth of investigation is about 35 m.
2) Bottom layer is a half space.

MASW V_S Model 3 (Upper Envelope of Dispersion Curve at Small Wavelengths and Lower Envelope at Long Wavelengths)

Depth to Top of Layer (m)	Layer Thickness (m)	S-Wave Velocity (m/s)	Inferred P-Wave Velocity (m/s)	Inferred Poisson's Ratio	Inferred Density (g/cm^3)
0	1	230	430	0.3	1.7
1	2	290	543	0.3	1.8
3	10	420	786	0.3	1.9
13	13.5	395	739	0.3	1.9
26.5	>8.5	660	1235	0.3	2.0

Notes: 1) Depth of investigation is about 35 m.
2) Bottom layer is a half space.

MASW V_S Model 4 (Upper Envelope of Dispersion Curve)

Depth to Top of Layer (m)	Layer Thickness (m)	S-Wave Velocity (m/s)	Inferred P-Wave Velocity (m/s)	Inferred Poisson's Ratio	Inferred Density (g/cm^3)
0	1	230	430	0.3	1.7
1	2	280	524	0.3	1.8
3	10	490	917	0.3	1.9
13	12	410	767	0.3	1.9
25	>10	690	1291	0.3	2.0

Notes: 1) Depth of investigation is about 35 m.
2) Bottom layer is a half space.

MASW V_S Model 5 (Lower Envelope of Dispersion Curve at Small Wavelengths and Upper Envelope at Long Wavelengths)

Depth to Top of Layer (m)	Layer Thickness (m)	S-Wave Velocity (m/s)	Inferred P-Wave Velocity (m/s)	Inferred Poisson's Ratio	Inferred Density (g/cm^3)
0	1	190	356	0.3	1.7
1	2.25	250	468	0.3	1.8
3.25	9.75	520	973	0.3	1.9
13	12	410	767	0.3	1.9
25	>10	690	1291	0.3	2.0

Notes: 1) Depth of investigation is about 35 m.
2) Bottom layer is a half space.

Observations/Discussion:

- This site was visited on two occasions. During the first site visit on 8/18/10 seismic refraction data and MASW data were acquired along the 94 m long array TIN-1, located at the toe of slope of the basalt outcrop. Passive surface wave data were also acquired along this array to test the effectiveness of linear arrays with limited noise sources, the primary noise source being vehicular traffic on the nearby SR-395. HVSR data were also acquired during this site visit; however, procedures for acquiring good quality HVSR data with Nanometrics Trillium Compact seismometers were still under development and the HVSR data was not of acceptable quality. Preliminary review of the seismic refraction and MASW data indicated that data quality was not sufficient to accurately characterize subsurface velocity structure, possibly due to the steeply dipping Tertiary basalt and sedimentary rock unit beneath the array. Therefore, additional field investigation was conducted at the site on 10/24/11 with MASW data acquired along a shorter MASW array (TIN-2) with common center and orientation as array TIN-1. Three HVSR measurements were also made along arrays TIN-1/TIN-2 using Nanometrics Trillium Compact and Micromed Tromino ENGY seismometers. Because of the difficulty acquiring surface wave data at the toe of the basalt outcrop, seismic refraction and MASW data were also acquired along an array located on the Tertiary sediments underlying the thin basalt unit. There is a mapped fault located between this array and the basalt outcrop; however, field inspection and the geologic map indicates that the same Tertiary sediments are located on both sides of the fault.
- HVSR plots at the three sensor locations on array TIN-1 are generally similar with no high amplitude HVSR peaks. Two of the measurements were made using a Tromino ENGY and the other with a Nanometrics Trillium Compact. HVSR response is relatively similar between the two sensor types at frequencies about 1 Hz; however, the Trillium has better response at lower frequencies, as expected. An HVSR measurement was also made on array TIN-3 using the Tromino ENGY. HVSR response on this array is different from that on array TIN-1; however, there are no high frequency peaks by which to more thoroughly evaluate the data.

- Seismic refraction data acquired along arrays TIN-1 and TIN-3 was not analyzed due to poor data quality associated with noise from the nearby SR-395 and geologic conditions (weak refraction, out of plane refractors, etc.) MASW data collected along arrays TIN-1 and TIN-2 were also not of sufficient quality to characterize the site, probably because the weathered basalt layer and underlying sediments are dipping beneath the array. Interestingly, the passive surface wave data acquired, as a test, along array TIN-1 appears to be of better quality. The linear array, passive surface wave data were evaluated using the ReMi™ and SPAC/ESPAC techniques, both yielding similar surface wave dispersion curves. Unfortunately, the passive surface wave data did not yield phase velocity data at wavelengths below 15 to 20 m and could not be used along to develop a V_S model for array TIN-1. Additionally, given the limited noise sources and three dimensional nature of the geologic structure beneath array TIN-1, the passive surface wave data should only be used with caution.
- Array TIN-3 yielded much better quality MASW data; albeit with significant lateral velocity variation. The passive surface wave data acquired along array TIN-1 is in good agreement with the MASW data from array TIN-1 and generally tracks the lower envelope of the MASW dispersion data.
- The minimum wavelength Rayleigh wave phase velocity data extracted from the 48-channel MASW array was about 11 m. Reducing data from smaller hammer sources using a limited offset receiver array (i.e. less active geophones) allowed for extraction of surface wave dispersion data to a minimum wavelength of about 2.5 m.
- The maximum wavelength extracted from the MASW data was generally set equal to 1.25 times the distance from the source to midpoint of the receiver array. The maximum wavelength Rayleigh wave phase velocity data extracted from the MASW data was about 80 m.
- There is nominally about 70 m/s of scatter in the MASW dispersion data, which is likely the result of lateral velocity variation.
- A representative dispersion curve was generated for the MASW data set using a moving average, polynomial curve fitting routine and used for modeling.
- Because of the variable depth beneath the array, five models were developed for the MASW data set to explore the variation in V_{S30}. Model 1 fits the representative dispersion curve and is, therefore, considered the average V_S model for the array. Model 2 fits the lower envelope of the dispersion data and based on the passive surface wave data collected along array TIN-1 is expected to be most representative of seismic station conditions. Model 3 fits the upper and lower envelope of the dispersion data at small and long wavelengths, respectively. Model 4 fits the upper envelope of the dispersion data. Model 5 fits the lower and upper envelope of the dispersion data at small and long wavelengths.
- Surface wave depth of investigation is about 35 m based on half of maximum wavelength criteria.
- V_{S30} is 421, 396, 403, 439 and 431 m/s for MASW V_S Models 1 to 5, respectively (NEHRP Site Class C). The lowest V_{S30} of 396 m/s (MASW V_S Model 3) is considered most representative of seismic station conditions.
- Although there is significant scatter in the MASW dispersion data, there is only about 10% variation between the minimum and maximum V_{S30} estimates.

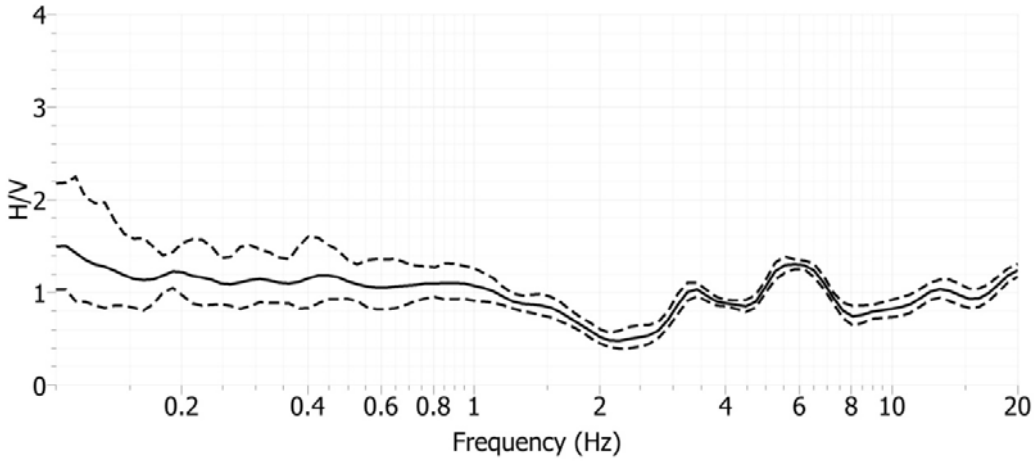

Site CI.TIN, H/V Spectral Ratio, Array TIN-3, Sensor TRO-3

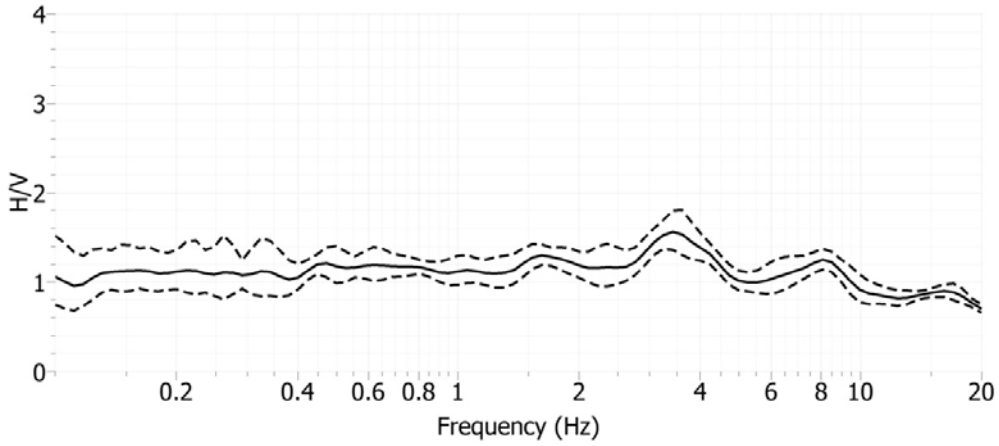

Site CI.TIN, H/V Spectral Ratio, Array TIN-1, Sensor TRO-1

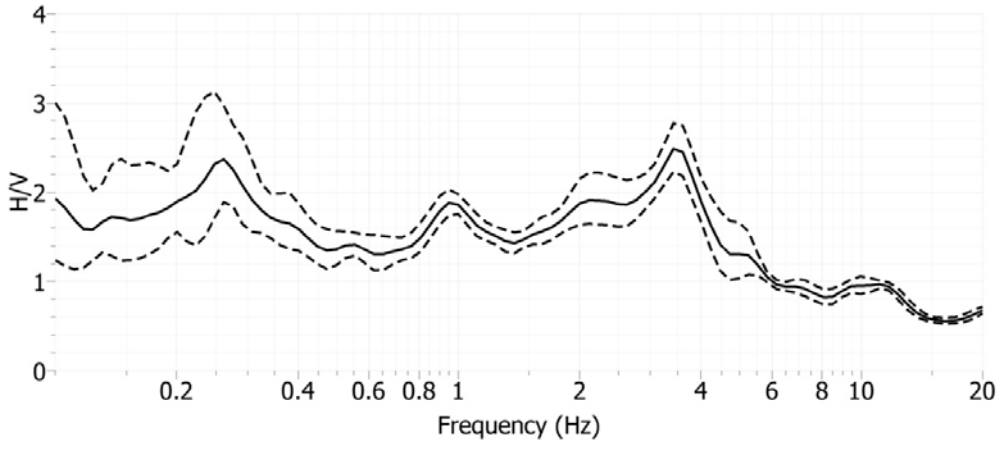

Site CI.TIN, H/V Spectral Ratio, Array TIN-1, Sensor 453

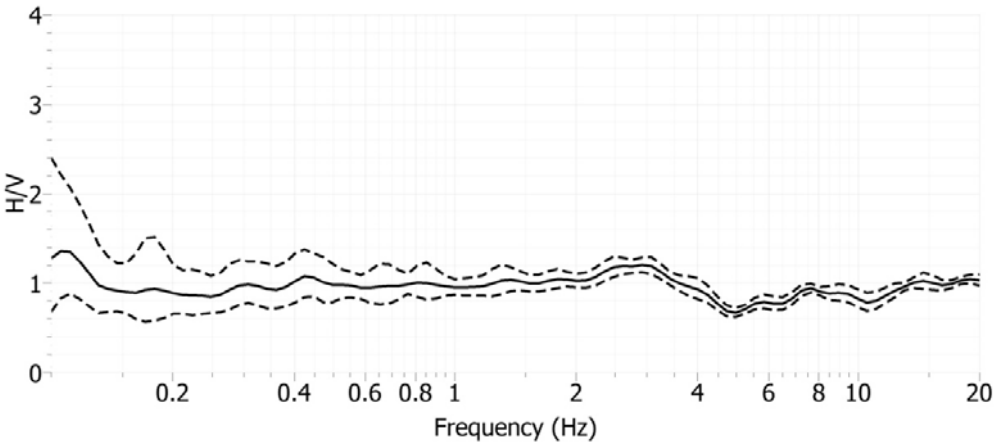

Site CI.TIN, H/V Spectral Ratio, Array TIN-1, Sensor TRO-2

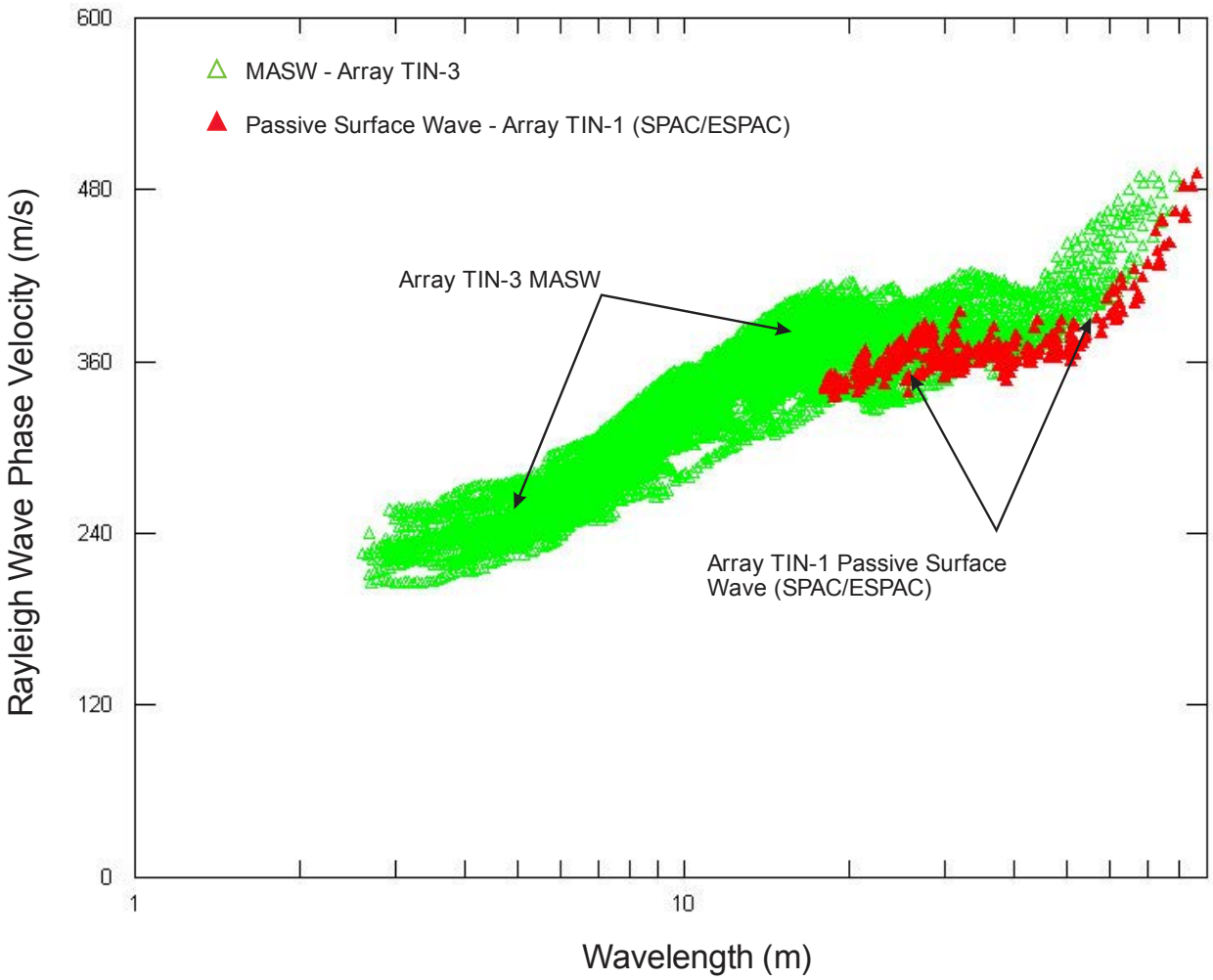

CI.TIN – Comparison of surface wave dispersion data from analysis of MASW data collected along array TIN-3 and analysis of passive surface wave data collected along array TIN-1 and reduced using the SPAC/ESPAC technique. Both dispersion curves are similar with the passive surface wave dispersion data closely tracking the lower envelope of the MASW data. The geologic and noise conditions at the site are not ideal for application of passive surface wave techniques; however, the passive surface wave data indicates that the MASW data collected along MASW array TIN-3 is closely representative of seismic station conditions.

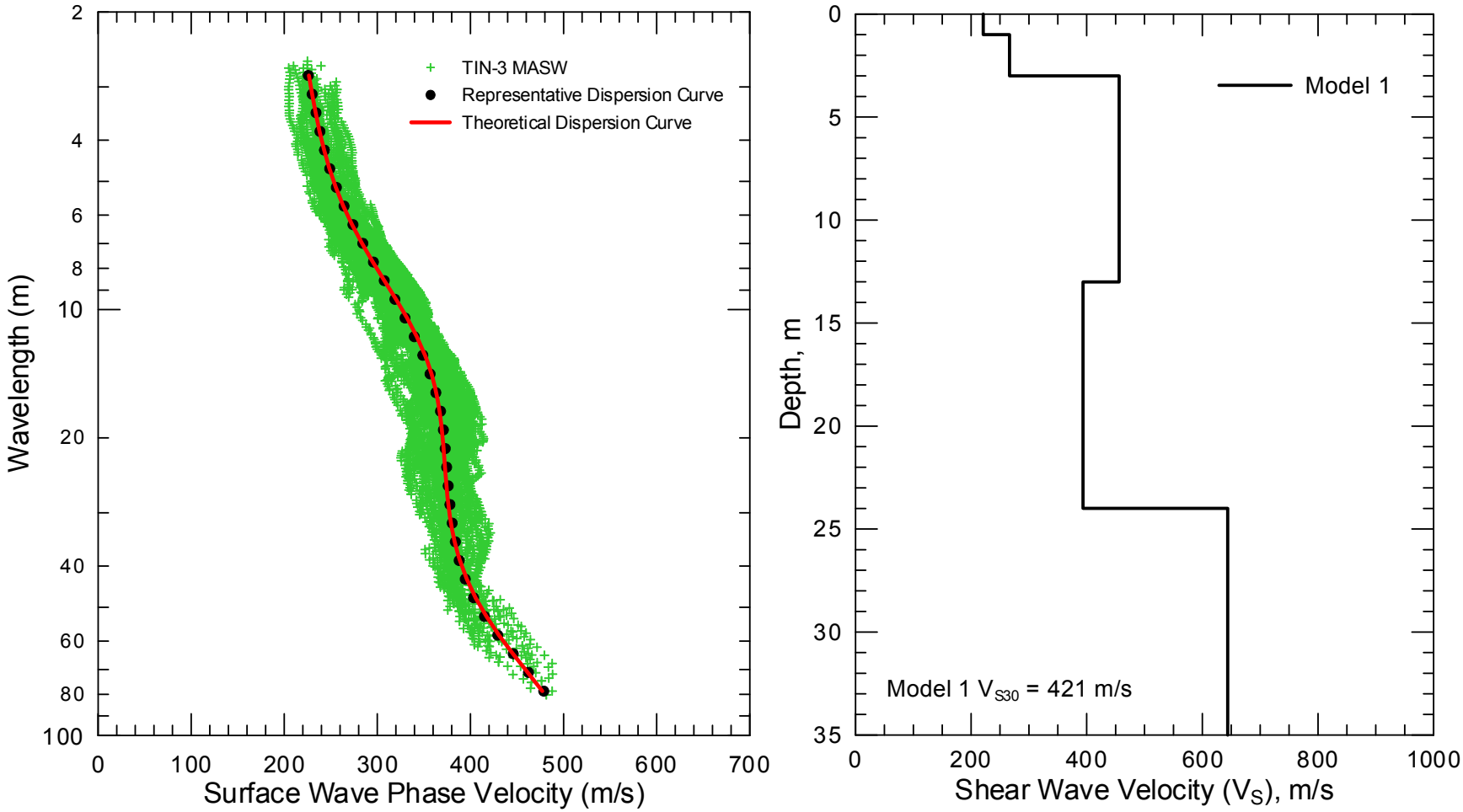

CI.TIN - Field, representative and inverted theoretical surface wave dispersion data (left) and associated V_S model (right)

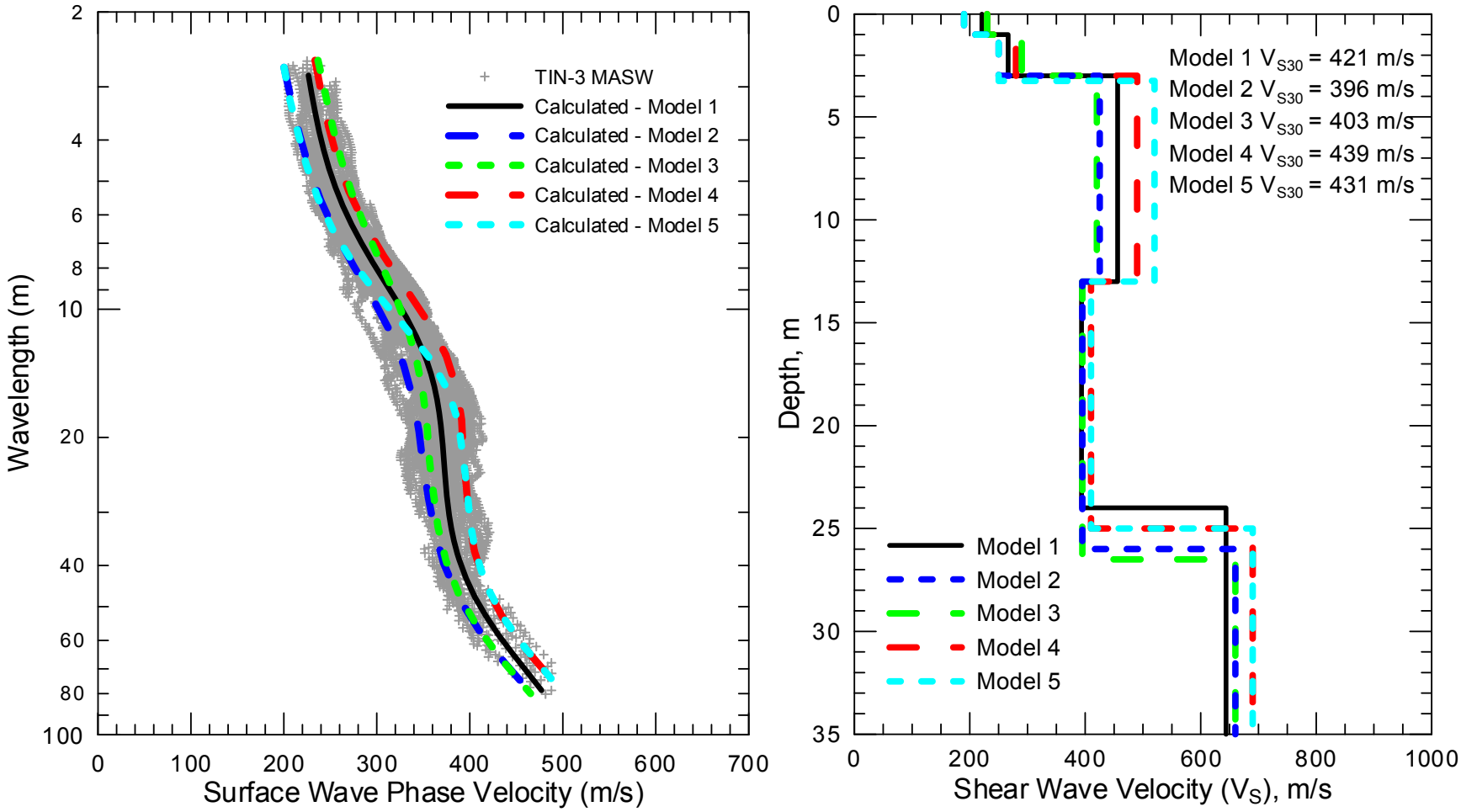

CI.TIN – Field and calculated surface wave dispersion data (left) and associated V_S models (right) fitting average (Model 1), lower envelope (Model 2), upper envelope at small wavelengths and lower envelope at large wavelengths (Model 3), upper envelope (Model 4) and lower envelope at small wavelengths and upper envelope at large wavelengths (Model 5) surface wave dispersion data

Site CI.TOR

Location: Toro Canyon, Riverside County, California

Latitude: 33.57526 **Longitude:** -116.22584
(Station coordinates provided by USGS, WGS84 coordinate system)

V_{S30} (measured): ~1,330 m/s (maximum estimate), ~1,100 ± 15% (realistic estimate - see discussion)

V_{S30} (adjusted to more accurately reflect seismic station conditions): 1,100 m/s (no adjustment necessary). The seismic station is about 8 m higher in elevation than the seismic line and the average depth of bedrock beneath the seismic line is about 4 to 5 m. Because bedrock beneath the testing array is about 12 m lower in elevation than that at the seismic station and not exposed, the possibility cannot be discounted that exposed bedrock is significantly more weathered than that beneath the test area.

NEHRP Site Class: B

Geomatrix Code: IGA

Geologic Conditions/Observations: Seismic station located on outcrop of Mesozoic (Cretaceous) quartz diorite. Based on field observations the possibility cannot be discounted that the seismic station sits on talus deposits rather than rock. Local topography, however, indicates that the seismic station is likely located on a small rock outcrop.

Site Conditions: Rural site. Seismic station located on the slope of a hill. Steep topography in site vicinity. Seismic testing conducted near and subparallel to the toe of slope.

Geophysical Methods Utilized: HVSR, Seismic Refraction (P- and S-wave), MASW (Rayleigh wave)

Geophysical Testing Arrays:

1. Array TOR-1 (48 channel MASW and P-wave seismic refraction array utilizing 4.5 Hz vertical geophones spaced 1.5 m apart for a length of 70.5 m, forward and reverse shot locations with multiple source offsets and source types and multiple interior shot locations).
2. Array TOR-1 (24 channel S-wave seismic refraction array utilizing 28 Hz horizontal geophones spaced 3 m apart for a length of 69 m, forward and reverse shot locations with limited source offsets and three interior shot locations). Common origin and orientation as P-wave array of same name.
3. Three HVSR measurement locations: one at each end of array TOR-1 and the other near the seismic station.

Legend

- Seismic Station - Approximate Surveyed Location
- Seismic Station - Approximate Location of Record
- H/V Spectral Ratio Location
- MASW and Seismic Refraction Array

NOTES:
1. WGS 1984 COORDINATE SYSTEM
2. Image Source: ESRI, i-cubed, USDA FSA, USGS, AEX, GeoEye, Getmapping, Aerogrid, IGP

File Name: CI-TOR-I

Date: 10/13/2011

USGS science for a changing world

GEOVision geophysical services

RECOVERY.GOV

SITE MAP
CI•TOR

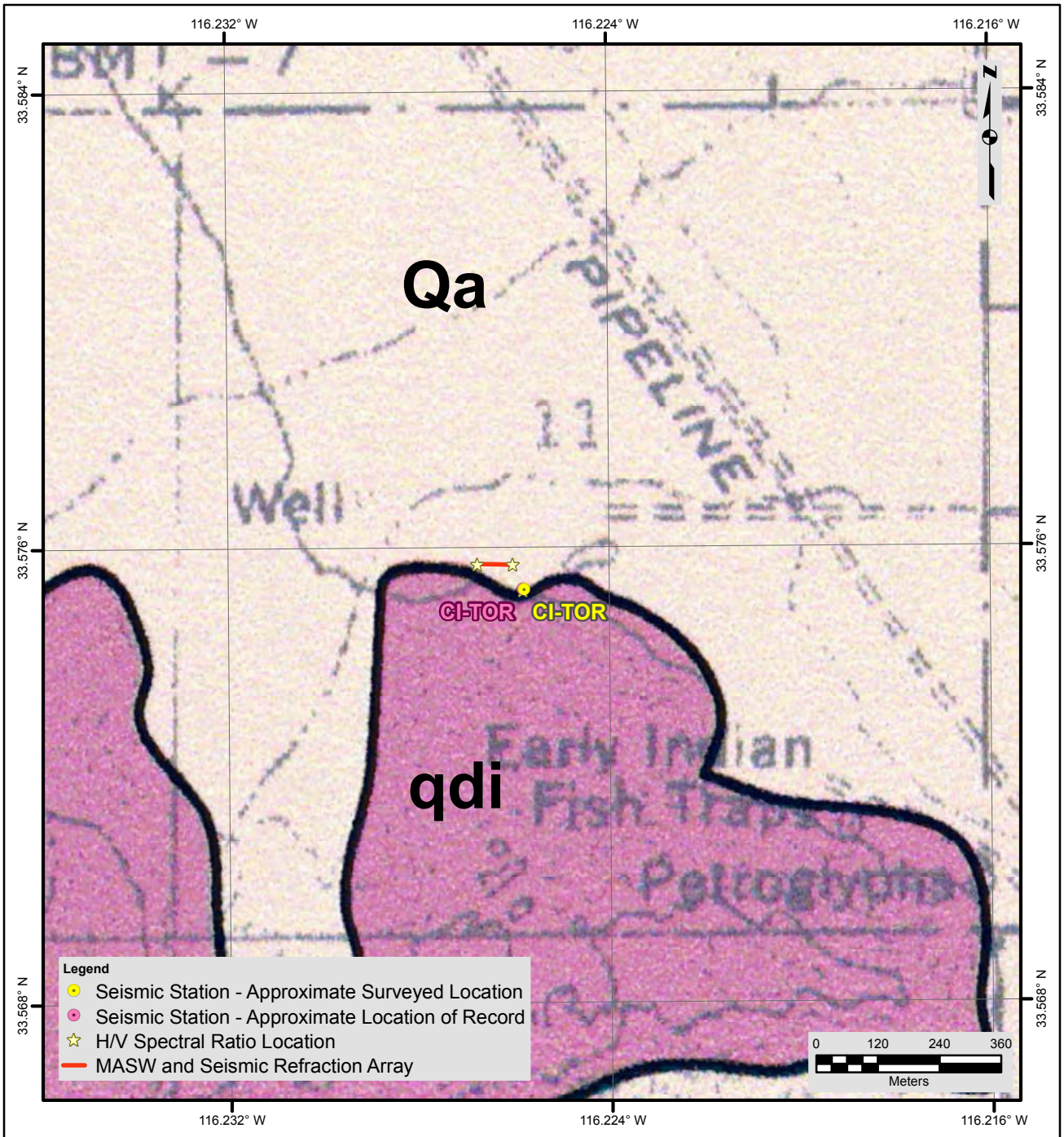

Description of Geologic Map Units

Qa = Quaternary (Holocene) alluvial sand and clay valleys areas
qdi = Mesozoic (Cretaceous) quartz diorite, massive to gneissoid

NOTES:
1. WGS 1984 COORDINATE SYSTEM
2. Geologic Map of the Palm Desert & Coachella 15 Minute Quadrangles, Riverside County, California By Thomas W. Dibblee, Jr., 2008
3. See site map for details of geophysical survey

File Name: CI-TOR

Date: 10/13/2011

USGS science for a changing world

GEOVision geophysical services

RECOVERY.GOV

GEOLOGIC MAP
CI•TOR

Looking north at CI.TOR seismic station and HVSR sensor 507

Looking east towards seismic station and at large boulders forming talus slope

Looking east along array TOR-1. Seismic station located on hill in upper right corner of photograph

Looking northwest towards center of array TOR-1 from near seismic station

Looking south towards seismic station on hill and east end of array TOR-1

Location of Geophysical Testing Array:

Location	Latitude	Longitude
TOR-1, West End of MASW/Refraction Array	33.57571	-116.22679
TOR-1, Center of MASW/Refraction Array	33.57570	-116.22641
TOR-1, East End of MASW/Refraction Array	33.57569	-116.22605
HVSR Sensor 450	33.57570	-116.22679
HVSR Sensor 453	33.57570	-116.22605
HVSR Sensor 507	33.57524	-116.22584
CI.TOR Seismic Station	33.57526	-116.22581

Notes: 1) WGS84 Coordinate System (decimal degrees)

2) Survey accuracy is estimated at 1 to 2 m.

Results:

Average V_P and Estimated V_S Models from Central Portion of P-wave Seismic Refraction Array TOR-1

Depth to Top of Layer (m)	Layer Thickness (m)	P-Wave Velocity (m/s)	Estimated S-Wave Velocity (m/s)			
			Poisson's Ratio = 0.20	Poisson's Ratio = 0.25	Poisson's Ratio = 0.30	Poisson's Ratio = 0.35
0.00	0.42	335	205	193	179	161
0.42	0.84	344	210	198	184	165
1.26	0.84	357	219	206	191	171
2.11	0.84	360	220	208	192	173
2.95	0.84	361	221	208	193	173
3.79	0.84	517	317	299	277	249
4.63	0.84	1794	1099	1036	959	862
5.47	1.77	1803	1104	1041	964	866
7.24	1.77	1861	1140	1075	995	894
9.01	1.77	2078	1273	1200	1111	998
10.78	1.77	2120	1298	1224	1133	1018
12.55	1.77	2272	1391	1312	1215	1092
14.32	1.77	2289	1402	1322	1224	1100
16.08	1.77	2347	1437	1355	1254	1127
17.85	1.77	2462	1508	1422	1316	1183
19.62	Half Space	2520	1543	1455	1347	1210

Observations/Discussion:

- Seismic station CI.TOR is located on the side of a hill consisting of granitic rock and talus deposits. The only feasible test location was at the base of the hill with an array orientated subparallel to the toe of slope. It was not feasible to test on bedrock due to the abundance of cobbles and boulders that form a talus slope.
- The HVSR plots for the three measurement locations are quite variable. Sensor 450, located at the west end of array TOR-1, has an HVSR peak at 18.5 Hz while sensor 453, located at the east of the end of the array, has a peak at about 10.5 Hz. High frequency HVSR peaks, such as these, are expected to be associated with the shallow bedrock beneath the array. Based on HVSR data it appears that bedrock deepens slightly to the east beneath the array or that the sediments in the vicinity of sensor 453 have lower V_S than in the vicinity of sensor 450. It should be noted that the bedrock surface is likely dipping orthogonal to array TOR-1, which will have some affect on the HVSR peaks. HVSR sensor 507, located on a talus slope adjacent to the seismic station, does not have an HVSR peak at a frequency of less than 40 Hz. However, HVSR data were later plotted to 100 Hz, the Nyquist frequency with a 200 Hz sample rate, and a peak is observed at a frequency of 72 Hz. High frequency HVSR peaks can often have cultural noise sources and the data were further reviewed to confirm that there are spectral peaks in both horizontal components, but not in the vertical component, providing some evidence that the peak may have a geologic source. The source of high frequency noise in the site vicinity is not clear and more literature review is necessary to determine if a geologic source for such a high frequency HVSR peak is reasonable. If the HVSR peak at sensor location 507 is associated with bedrock, then bedrock is very shallow, providing evidence that the seismic station is located on rock. It should also be noted that sensor locations 450 and 453 also have high frequency peaks at about 79 and 94 Hz, respectively, of unknown source.
- Noise conditions at the site were not sufficient for application of passive surface wave techniques.
- Surface wave techniques were not expected to be effective at this site because the bedrock surface is dipping to the north beneath the seismic profile. Site characterization was, therefore, limited to the application of the P- and S-wave seismic refraction techniques. Surface wave data were, however, reviewed. Rayleigh wave data were ineffective due to a significant increase in seismic velocity at shallow depth and the dipping bedrock. Although S-wave refraction data were acquired using 28 Hz horizontal geophones, it was still possible to review Love wave data, which was also ineffective.
- The P-wave seismic refraction data for array TOR-1 were modeled using a tomographic inversion routine with layer-based starting model. The seismic refraction model was extended to far offset shot locations to extend depth of investigation. It should be noted that a larger geophone spacing, rather than the utilization of far offset shot locations, is preferred for extending depth of investigation, when applying tomographic inversion routines. However, the seismic refraction data were acquired in conjunction with surface wave data, where a shorter array length is preferred. Only limited S-wave seismic refraction data were acquired, and the data were modeling using the layer-based generalized reciprocal method (GRM). The P-wave seismic refraction data were also modeled in this manner for correlation.

- The P-wave first arrival data were picked to a greater degree of accuracy than the S-wave first arrival data because the S-wave is not typically the first energy on a seismic record, even when using a horizontal traction plank as an energy source. Therefore, the P-wave refraction models likely provide a more accurate estimate of bedrock depth because near source first arrivals were much clearer in the P-wave refraction data. There was not good polarity reversal in the S-wave seismic records resulting from shots on opposite sides of the source. Therefore, S-wave first arrival data were picked after applying an S-wave stack (subtracting opposite polarity records to enhance S-wave and reduce amplitude of earlier arriving P-wave energy).
- The P-wave seismic refraction survey design allowed P-wave velocity to be imaged to a maximum depth of about 21 m. The seismic refraction model indicates that P-wave velocity is about 250 to 300 m/s at the surface and increases to over 1,500 m/s at a depth of 4 to 5 m, 2,000 m/s at a depth of 5 to 12 m and over 2,500 m/s at a depth of 16 m, or more.
- The S-wave seismic refraction data were modeled using the GRM to estimate approximate S-wave velocity of the bedrock unit, which was found to be about 1,350 m/s. The P-wave seismic refraction model indicates that there is some weathering in the uppermost bedrock and, therefore, this velocity should only be considered approximate. A GRM model was also developed for the P-wave refraction data. This model shows bedrock, with average P-wave velocity of about 2,230 m/s, deepening to the east from about 4 m at the west end of the line to 5.5 m at the east end of the line. Bedrock gradually deepening to the east is consistent with the HVSR observations. The tomographic inversion of the P-wave seismic refraction data using a layered starting model shows some weathering in the uppermost bedrock, which is not adequately represented by the simple GRM models. The bedrock V_P/V_S ratio is 1.65, resulting in a Poisson's ratio of about 0.21, which seems very low for weathered granitic rock.
- The average P-wave velocity of the upper 30 m (V_{P30}) was estimated between 22.5 and 54 m on the P-wave refraction model, where depth of investigation is greatest, by projecting the velocity at 20 m depth to 30 m depth. V_P below 20 m depth is only expected to gradually increase with depth. Additionally, even a significant increase in the velocity below 21.5 m will only have a small effect of V_{P30}. V_{P30} ranges from about 1,233 to 1,336 m/s between a position of 22.5 to 54 m, the variation primarily due to variable bedrock depth.
- An average V_P model was developed over the 22.5 to 54 m distance interval by horizontally averaging the travel time of each model cell and cell thickness and average V_{P30} was determined to be 1,271 m/s. Assuming a constant Poisson's ratio of 0.2, 0.25, 0.3 and 0.35 would result in an estimated V_{S30} of 778, 734, 680 and 611 m/s, respectively. V_{S30} is also adjusted to bedrock conditions by replacing V_P of the sediments above 4.6 m with the velocity of the underlying bedrock unit. Adjusted V_{S30} is 1330, 1254, 1161 and 1044 m/s for constant Poisson's ratio of 0.2, 0.25, 0.3 and 0.35, respectively. A more conservative adjustment to V_{S30} would assume that P-wave velocity of the upper 4.6 m is lower than that modeled at a depth of 4.6 m, to account for the seismic station being located at higher elevation and most likely on more intensely weathered rock. V_{S30} adjusted to bedrock conditions by replacing V_P of the sediments above 4.6 m with an assumed V_P of 1,000 m/s is 1158, 1094, 1011 and 909 m/s for constant Poisson's ratio of 0.2, 0.25, 0.3 and 0.35, respectively.

- Although, the S-wave seismic refraction data indicates that Poisson's ratio may be 0.21, we believe that, without additional evidence, a Poisson's ratio of 0.25 to 0.3 is more appropriate to estimate S-wave velocity from the P-wave refraction models. There is an approximate 12 m elevation difference between the seismic station and bedrock beneath array TOR-1. Bedrock in the upper 12 m beneath the seismic station is almost certainly more weathered than beneath array TOR-1. As evident in photographs, it would be very difficult to acquire seismic refraction data on the talus slope near the seismic station. It may, however, be possible to conduct a very short seismic line in the vicinity of the seismic station to determine seismic velocity in the upper several meters. Any seismic data acquired near the seismic station would allow more accurate adjustment of estimated V_{S30} from array TOR-1 to conditions at the seismic station.
- Maximum V_{S30} at the site is expected to be 1,330 m/s (NEHRP Site Class B), which is the value derived for bedrock in the P-wave seismic refraction model using an assumed Poisson's ratio of 0.2, in order to be consistent with the S-wave refraction model. We expect this estimated V_{S30} to be significantly overestimated because 1) bedrock encountered beneath array TOR-1 is about 12 m lower in elevation than the seismic station, 2) bedrock in the upper 12 m beneath the seismic station is likely significantly more weathered resulting in lower velocities than observed beneath array TOR-1 and 3) although we cannot discount a Poisson's ratio of 0.2, a Poisson's ratio of 0.3 is likely more realistic for the uppermost weathered rock at the seismic station. At this time we recommend using an estimated V_{S30} of 1,100 ±15% (NEHRP Site Class B) to represent site conditions at the seismic station, which is approximately equal to that estimated from the P-wave seismic refraction model using an assumed constant Poisson's ratio of 0.25 and replacing the 4.6 m of sediments with weathered rock having assumed P-wave velocity of 1,000 m/s.
- Additional field effort is needed to more accurately constrain V_{S30} at this seismic station. A longer P- and S-wave seismic refraction profile to map velocity structure to greater depth would be beneficial. More importantly, some attempt should be made to characterize velocity structure in the upper several meters at the seismic station. It would be very difficult to acquire P-wave seismic refraction data and impossible to acquire S-wave seismic refraction data on the talus slope, but maybe a better test location than the toe of slope can be identified. It may be possible to hike equipment to a ridge on the mountain, although this would be much higher elevation than the seismic station and the weathering profile in the rock may be much different.
- In retrospect, it may not have been a good idea to attempt to characterize this site without a borehole. However, even given the difficult conditions and significant uncertainty in estimated V_{S30}, the site is clearly NEHRP Site Class B.

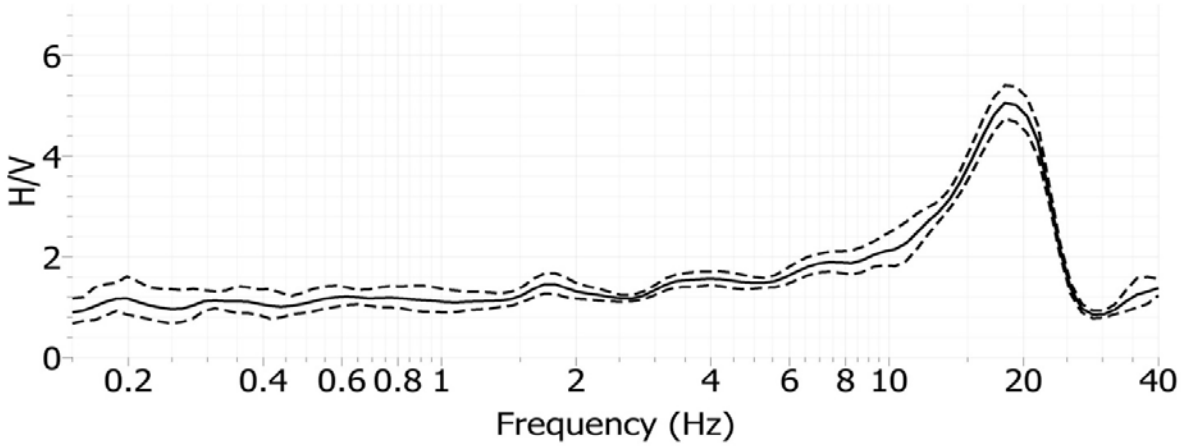

Site CI.TOR, H/V Spectral Ratio, Array TOR-1, Sensor 450

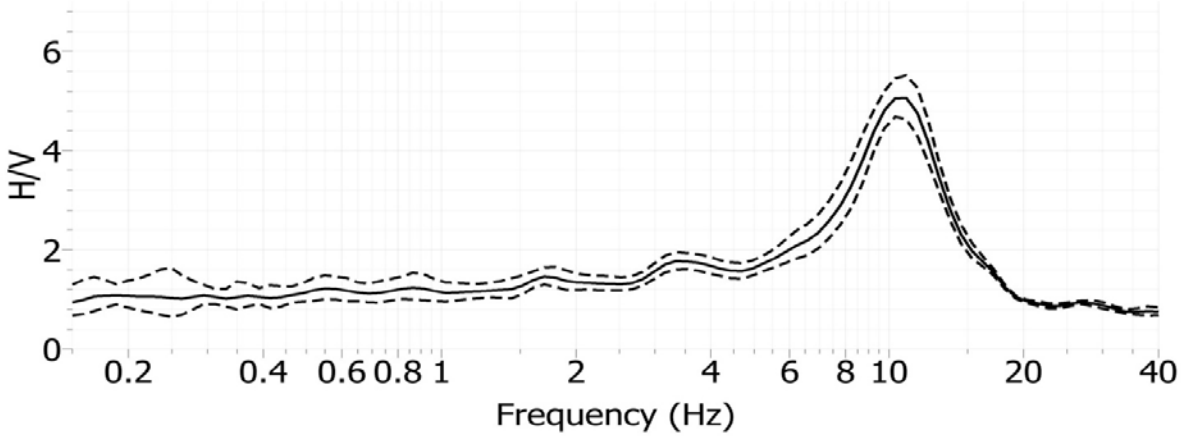

Site CI.TOR, H/V Spectral Ratio, Array TOR-1, Sensor 453

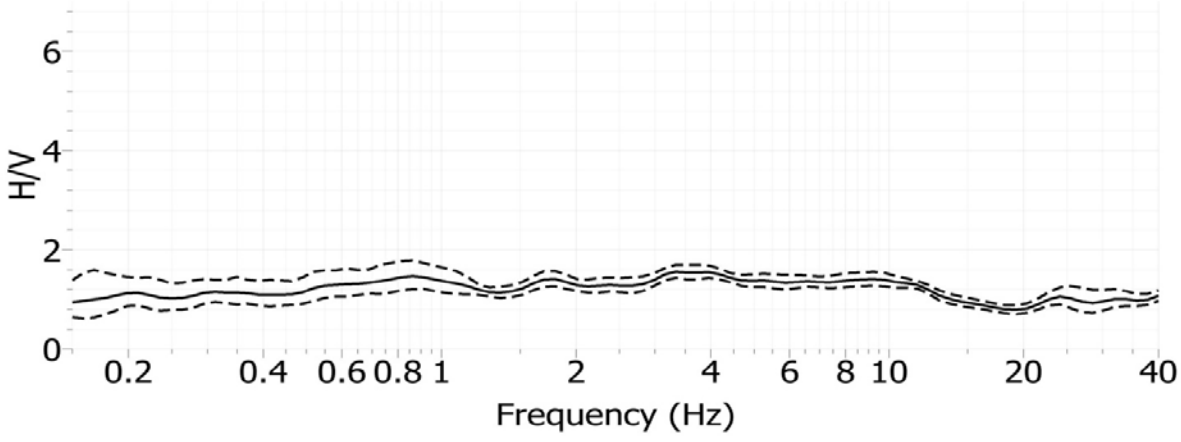

Site CI.TOR, H/V Spectral Ratio, Array TOR-1, Sensor 507

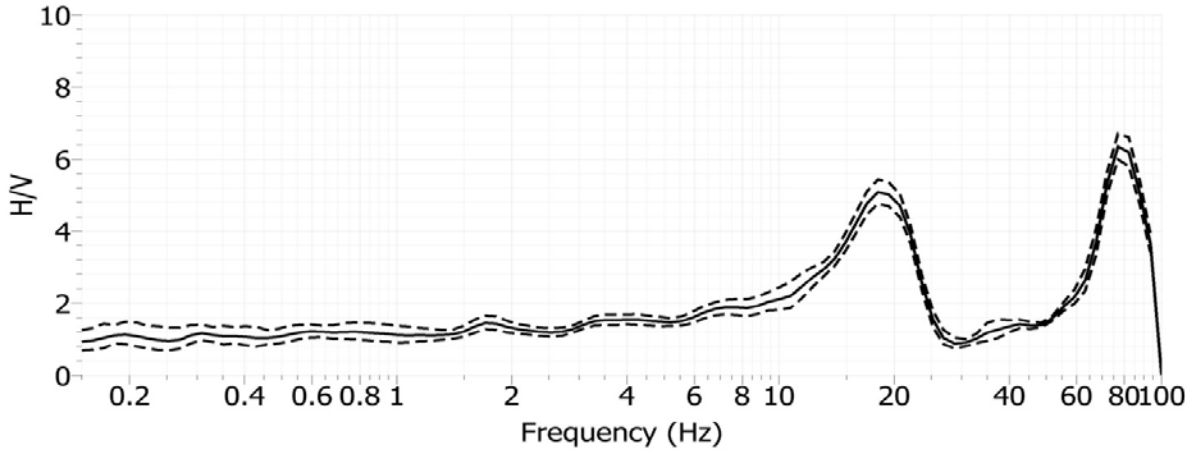

Site CI.TOR, H/V Spectral Ratio, Array TOR-1, Sensor 450

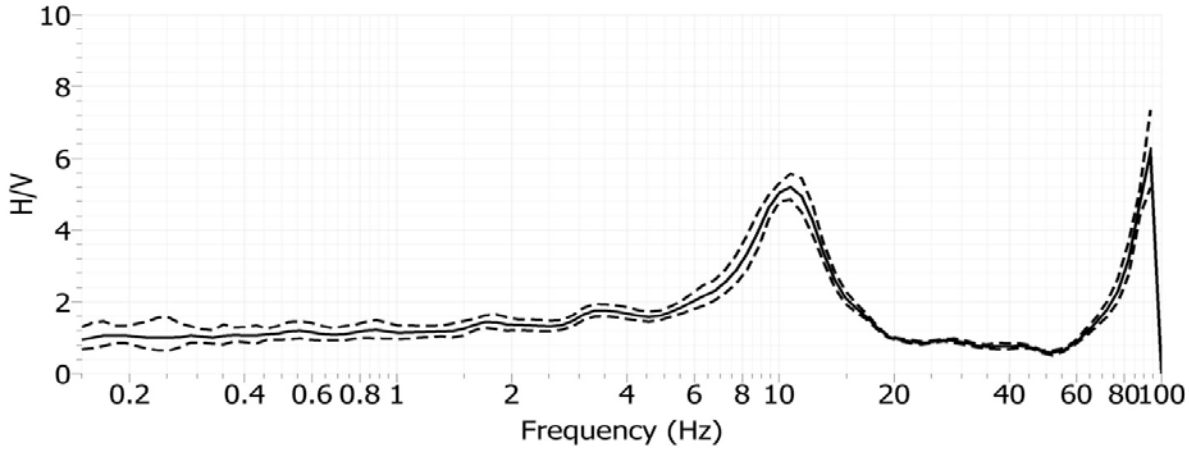

Site CI.TOR, H/V Spectral Ratio, Array TOR-1, Sensor 453

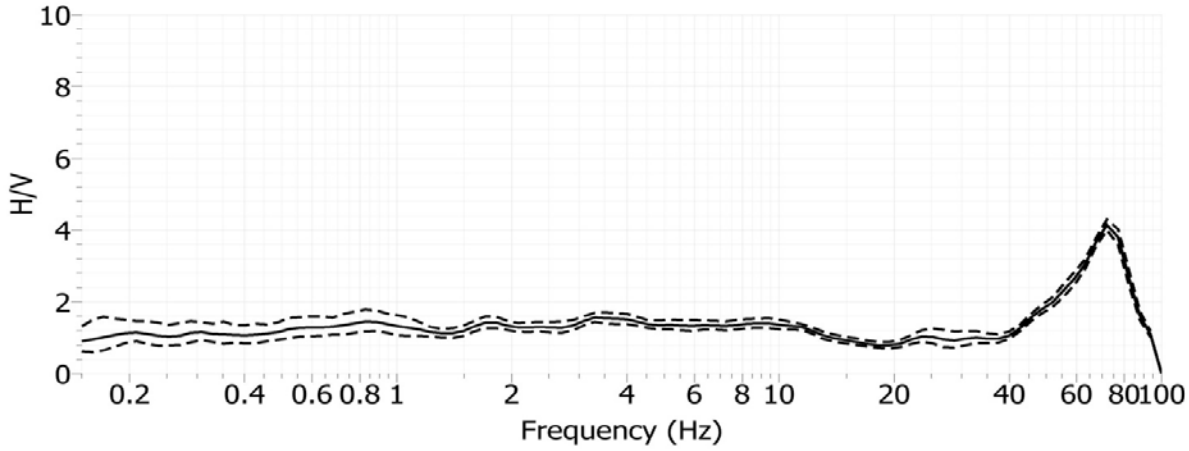

Site CI.TOR, H/V Spectral Ratio, Array TOR-1, Sensor 507

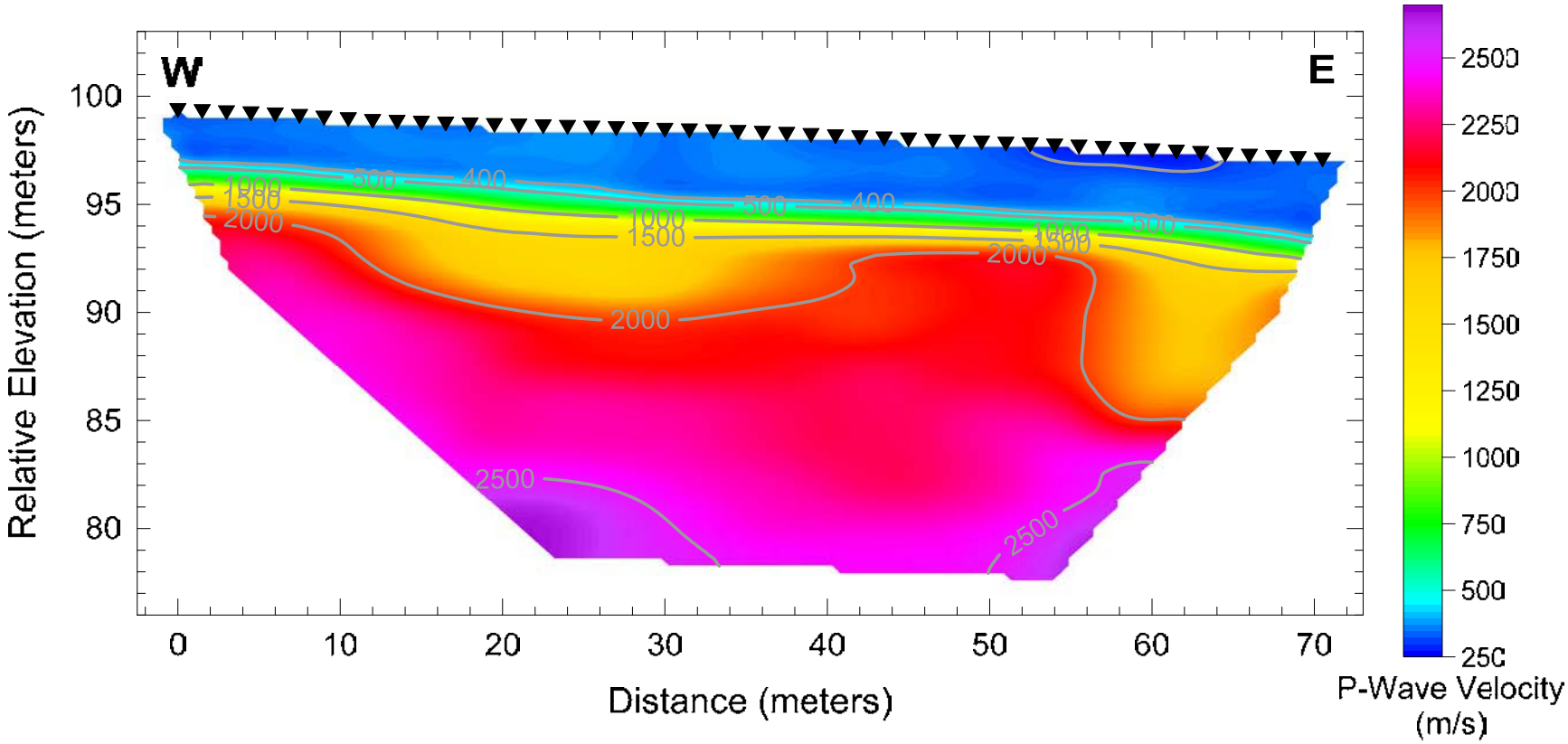

Array TOR-1 – P-wave tomographic seismic refraction model developed utilizing a layered starting model

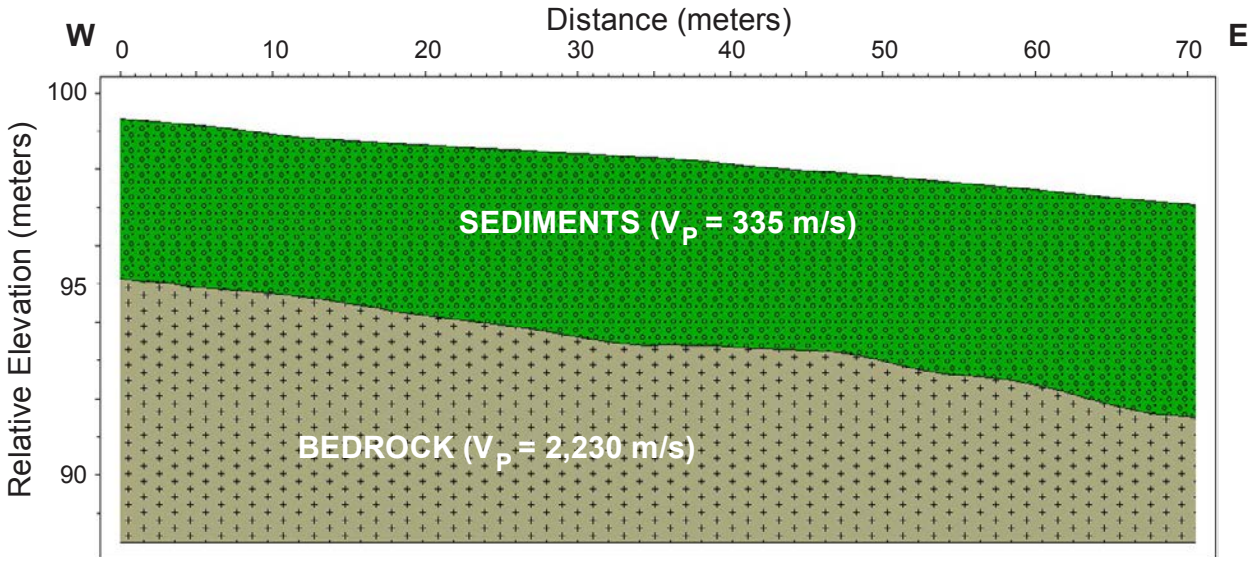

Array TOR-1 – P-wave Seismic Refraction Model Developed using Generalized Reciprocal Method

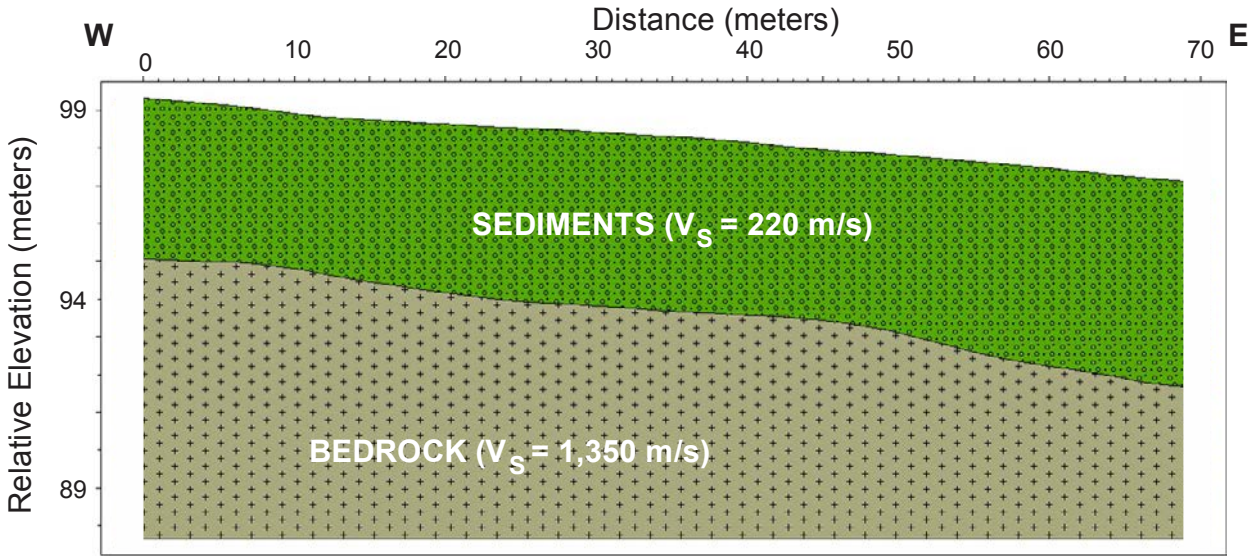

Array TOR-1 – S-wave Seismic Refraction Model Developed using Generalized Reciprocal Method

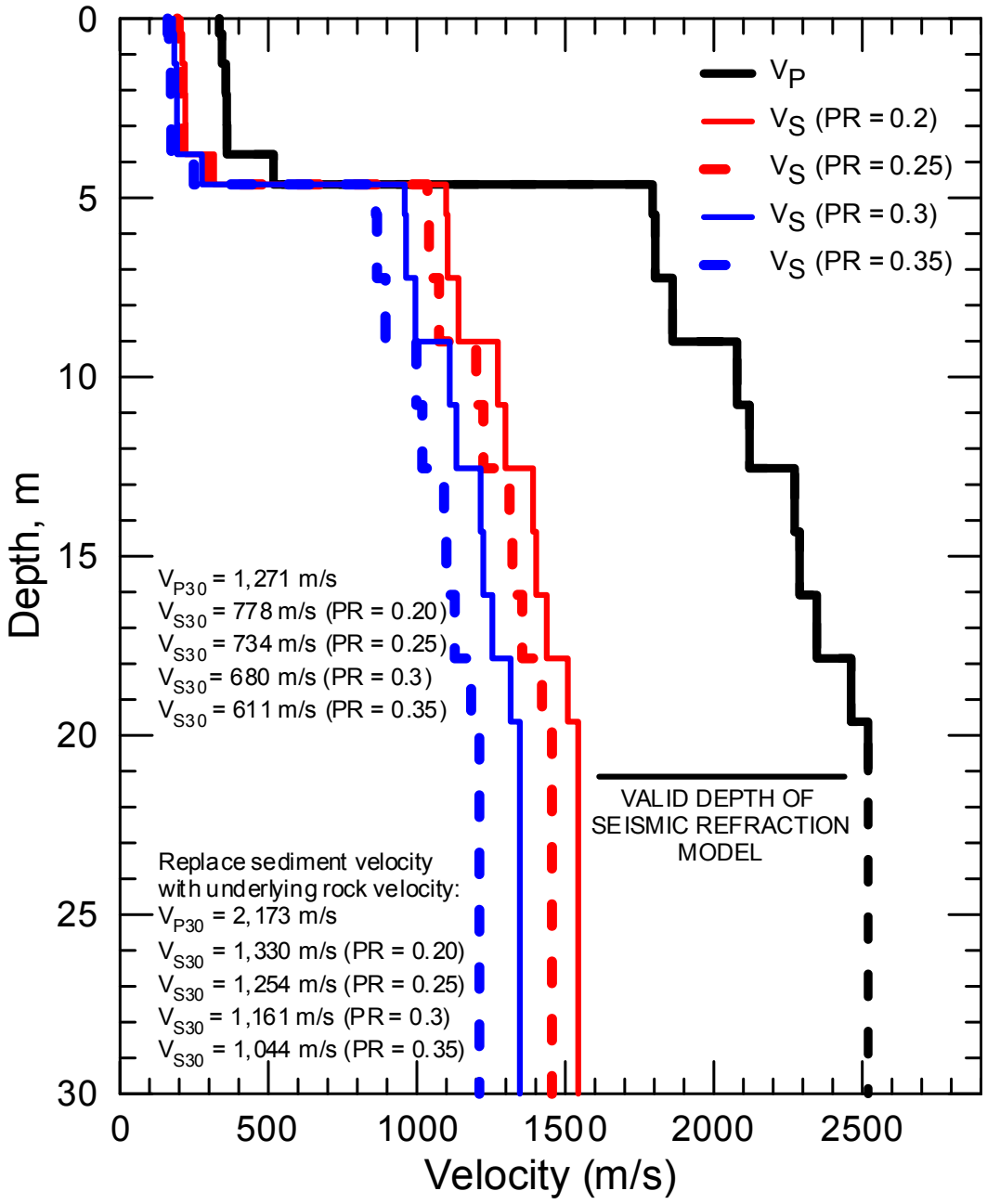

CI.TOR – Average P-wave velocity structure and estimated S-wave velocity structure between a position of 22.5 and 54 m on the P-wave seismic refraction model for array TOR-1 developed using a layered starting model. Although the maximum seismic refraction depth of investigation is limited to about 21 m, P-wave velocity is only expected to gradually increase with depth between 21 and 30 m.

Site CI.TUQ

Location: Turquoise Mountain, San Bernardino County, California

Latitude: 35.43584 **Longitude:** -115.92389
(Station coordinates provided by USGS, WGS84 coordinate system)

V_{S30} (measured): 819 m/s

V_{S30} (adjusted to more accurately reflect seismic station conditions): 853 m/s (average S-wave velocity between 1 and 31 m adjusting for 1 m assumed sensor depth).

NEHRP Site Class: B

Geomatrix Code: IGA

Geologic Conditions/Observations: Seismic station located on geologic unit mapped as Mesozoic granitic rocks. Field observations indicate that weathering is highly variable.

Site Conditions: Rural site located near the top of a mountain. Very steep mountainous terrain in site vicinity. Seismic station located next to large antenna and small portable structure.

Geophysical Methods Utilized: HVSR, Seismic Refraction, MASW

Geophysical Testing Arrays:

1. Array TUQ-1 (48 channel MASW and P-wave seismic refraction array utilizing 4.5 Hz vertical geophones spaced 1.5 m apart for a length of 70.5 m, forward and reverse shot locations with multiple source offsets and source types (hammers only) and multiple interior shot locations).
2. Array TUQ-2 (48 channel MASW and P-wave seismic refraction array utilizing 4.5 Hz vertical geophones spaced 1.5 m apart for a length of 70.5 m, forward and reverse shot locations with multiple source offsets and source types (hammers only) and multiple interior shot locations).
3. Three HVSR measurement locations distributed along array TUQ-1.

Legend

- Seismic Station - Approximate Surveyed Location
- Seismic Station - Approximate Location of Record
- H/V Spectral Ratio Location
- MASW and Seismic Refraction Array

NOTES:
1. WGS 1984 COORDINATE SYSTEM
2. Image Source: ESRI, i-cubed, USDA FSA, USGS, AEX, GeoEye, Getmapping, Aerogrid, IGP

File Name: CI-TUQ-I

Date: 2/7/2013

USGS science for a changing world

GEOVision geophysical services

RECOVERY.GOV

SITE MAP
CI•TUQ

Description of Geologic Map Units

gr = Mesozoic granitic rocks
epЄ = Earlier precambrian metamorphic rocks

NOTES:
1. WGS 1984 COORDINATE SYSTEM
2. Geologic Map of California
Kingman Sheet Olaf P. Jenkins Edition
compiled by Charles W. Jennings, 1961
3. See site map for details of geophysical survey

File Name: CI-TUQ

Date: 2/7/2013

USGS science for a changing world

GEOVision geophysical services

GEOLOGIC MAP
CI•TUQ

RECOVERY.GOV

CI.TUQ seismic station

Looking north at HVSR sensor 450 towards seismic station location

Looking northwest along array TUQ-1

Looking east along array TUQ-1

Looking east along array TUQ-2 towards seismic station on top of hill in background

Location of Geophysical Testing Arrays:

Location	Latitude	Longitude
TUQ-1, West End of MASW/Refraction Array	35.43536	-115.92364
TUQ-1, Center of MASW/Refraction Array	35.43540	-115.92325
TUQ-1, East End of MASW/Refraction Array	35.43543	-115.92287
TUQ-2, West End of MASW/Refraction Array	35.43650	-115.92791
TUQ-2, Center of MASW/Refraction Array	35.43647	-115.92753
TUQ-2, East End of MASW/Refraction Array	35.43644	-115.92715
HVSR Sensor 450	35.43538	-115.92364
HVSR Sensor 453	35.43540	-115.92326
HVSR Sensor 507	35.43544	-115.92287
CI.TUQ Seismic Station	35.43582	-115.92388

Notes: 1) WGS84 Coordinate System (decimal degrees)
2) Survey accuracy is estimated at 1 to 2 m.

Results:

V_S Model – Array TUQ-2

Depth to Top of Layer (m)	Layer Thickness (m)	S-Wave Velocity (m/s)	Inferred P-Wave Velocity (m/s)	Assumed Poisson's Ratio	Assumed Density (g/cm^3)
0	1.5	427	799	0.3	2.00
1.5	2	662	1239	0.3	2.10
3.5	2.5	707	1323	0.3	2.10
6	4	842	1576	0.3	2.15
10	7	878	1642	0.3	2.15
17	10	889	1663	0.3	2.15
27	>8	1152	2156	0.3	2.20

Notes: 1) Near surface velocity structure representative of west end of array.
2) Depth of investigation is about 35 m.
3) Bottom layer is a half space.
4) Velocity of half-space not well constrained.

Observations/Discussion:

- There is no clear HVSR peak at this site, as expected for a rock site.
- HVSR data quality is not as good at sensor location 453 and elevated HVSR response is likely related to field conditions, such as sensor coupling or poor sensor cable deployment (e.g. cable touching side of bucket covering sensor), rather than subsurface geologic conditions.
- Array TUQ-1 is located along a paved road cut into the side of the mountain and is the closest possible test location to the seismic station. Surface wave dispersion data at long wavelengths were not expected to be reliable at this site due to steep topography to the sides of the array. Surface wave data were, however, partially reduced for correlation with data collected at a more distant alternate test location. The average phase velocity of a 40 m Rayleigh wave (V_{R40}) is about 810 m/s for array TUQ-1. Surface wave dispersion data at wavelengths greater than 40 m definitely appear to be affected by the steep topography adjacent to the array. P-wave refraction data were also not considered reliable enough to model due to interference from the asphalt arrival, weak first arrival data and possible out of plane refractors. However, the reciprocal time (travel time from end shot to far receiver) was documented for comparison with that at an alternate test location.
- Array TUQ-2 was located about 350 m northwest of the seismic station on an adjacent ridge top. Seismic refraction data collected along this array were also not considered reliable enough to model; however, the reciprocal time was found to be within 4% of that from array TUQ-1, indicating that average shallow velocity structure is similar at the two sites. V_{R40} ranges from about 730 to 830 m/s, the scatter likely being associated with lateral velocity variation, and averages about 780 m/s, about 4% lower than that observed in limited dispersion data extracted from array TUQ-1. Therefore, array TUQ-2 is considered acceptable for the purpose of characterizing V_{S30} at the seismic station. The resulting velocity model may differ somewhat, but near surface velocity structure is expected to be highly variable in the site vicinity due to observed variable weathering of near surface rock.
- As discussed previously, seismic refraction data were not modeled as first arrival data could not be picked to an acceptable degree of accuracy to generate reliable velocity models. First arrivals were generally weak, possibly due to scattering in the highly fractured and weathered bedrock. Wind noise was also an issue during data acquisition along array TUQ-2. A high velocity arrival from the asphalt also was problematic in much of the seismic refraction data acquired along array TUQ-1. Reciprocal times could be relatively accurately identified and were similar between arrays TUQ-1 and TUQ-2, indicating that average near surface velocity structure is similar between the two arrays.
- Noise conditions at the site were not sufficient for application of passive surface wave techniques.
- As mentioned above, long wavelength surface wave dispersion data from array TUQ-1 were not expected to be reliable due to steep topography to the sides of the array. Limited data reduction was, however, conducted to estimate V_{R40} and correlate with dispersion data from array TUQ-2.
- There is significant near surface lateral velocity variation beneath array TUQ-2, which is evident in both seismic records and in reduced surface wave dispersion data. It appears as though the eastern half of the array has significantly higher near surface S-wave

velocity, but that Rayleigh wave phase velocities are similar at wavelengths greater than about 20 m. This is demonstrated by comparing dispersion data generated from receiver gathers comprised of geophones from each half of the array. Additionally, SASW type analysis was conducted using time history data from two receivers spaced 30 m apart from the 30 m offset source location at each end of the array. Again dispersion curves were similar at wavelengths greater than 20 m. Because each half of the MASW array yields similar long wavelength dispersion curves, it also appears possible to use MASW dispersion data from all receiver gathers (e.g. all 48 geophones). The small wavelength (high frequency) surface wave dispersion data extracted from array TUQ-1 is similar to the lower velocity surface wave dispersion data extracted from array TUQ-2. Therefore, for modeling, dispersion data originating from receiver gathers in the eastern half of the array (i.e. the dispersion data with higher phase velocity at small wavelengths) were not utilized.

- A total of over 150 dispersion curves were generated, utilizing all offend source locations at the west and east ends of the arrays (multiple source offsets and hammer sizes) and all interior seismic refraction shots and a variety of receiver gathers. The maximum wavelength did not exceed 1.2 times the distance from the source to midpoint of the receiver array, 20% over the maximum wavelength criteria established by Yoon and Rix (2009). As discussed above, all dispersion curves originating from receiver gathers limited to the eastern half of the array were rejected. Additional surface wave dispersion data that did not form a coherent dispersion curve were also rejected, resulting in only about 60% of the reduced dispersion curves used for analysis. The accepted small wavelength dispersion curves primarily reflect the lower velocities at the west end of the array.
- There is significant scatter in the final, selectively edited MASW dispersion data (about 100 to 120 m/s), which is likely the result of lateral velocity variation.
- The minimum wavelength surface wave phase velocity data extracted from the 48-channel MASW array was about 10 m. Data reduction using seismic records from smaller hammer sources and a limited offset receiver array (i.e. less active geophones), primarily from source locations in the southern portion of the line, allowed extraction of surface wave dispersion data to a minimum wavelength of about 4 m.
- A representative dispersion curve was generated for the extensively edited MASW data set using a moving average, polynomial curve fitting routine and used for modeling.
- Surface wave depth of investigation is about 35 m based on half of maximum wavelength criteria.
- V_{S30} is 819 m/s (Site Class B).
- Average S-wave velocity between 1 m (assumed sensor depth) and 31 m is 853 m/s.
- Modeling of the upper and lower envelopes of the MASW dispersion curves was not conducted, but would result in about a 5 to 7.5% variation of V_{S30}.
- Although there is significant lateral velocity variation in the site vicinity due to differential weathering in near surface bedrock, we believe that V_{S30} has been reasonably accurately characterized. The presented V_S model is biased towards the lower near surface S-wave velocity beneath the western half of array TUQ-2. Array TUQ-1 appears to have similar near surface velocity structure, although as noted near surface velocities are expected to be highly variable at the site.

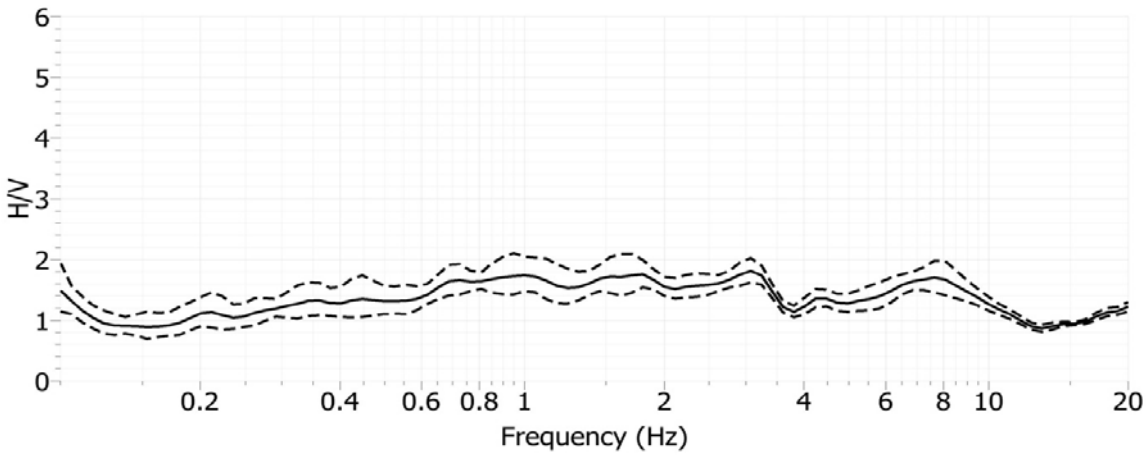

Site CI.TUQ, H/V Spectral Ratio, Array TUQ-1, Sensor 450

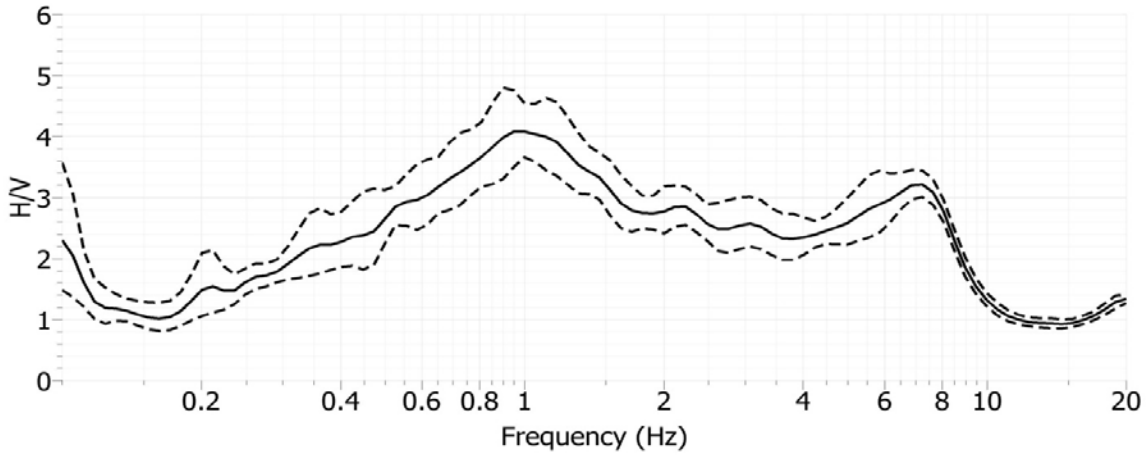

Site CI.TUQ, H/V Spectral Ratio, Array TUQ-1, Sensor 453

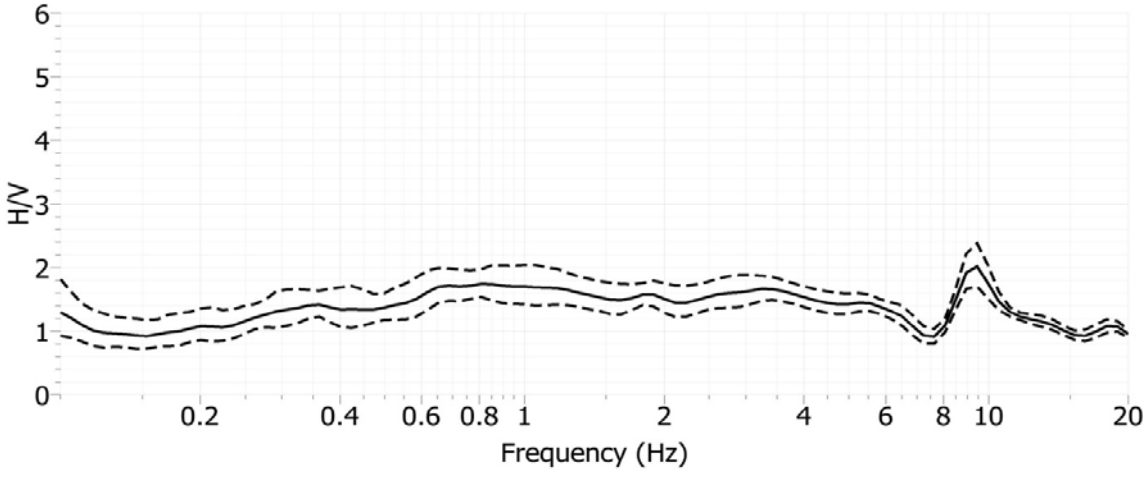

Site CI.TUQ, H/V Spectral Ratio, Array TUQ-1, Sensor 507

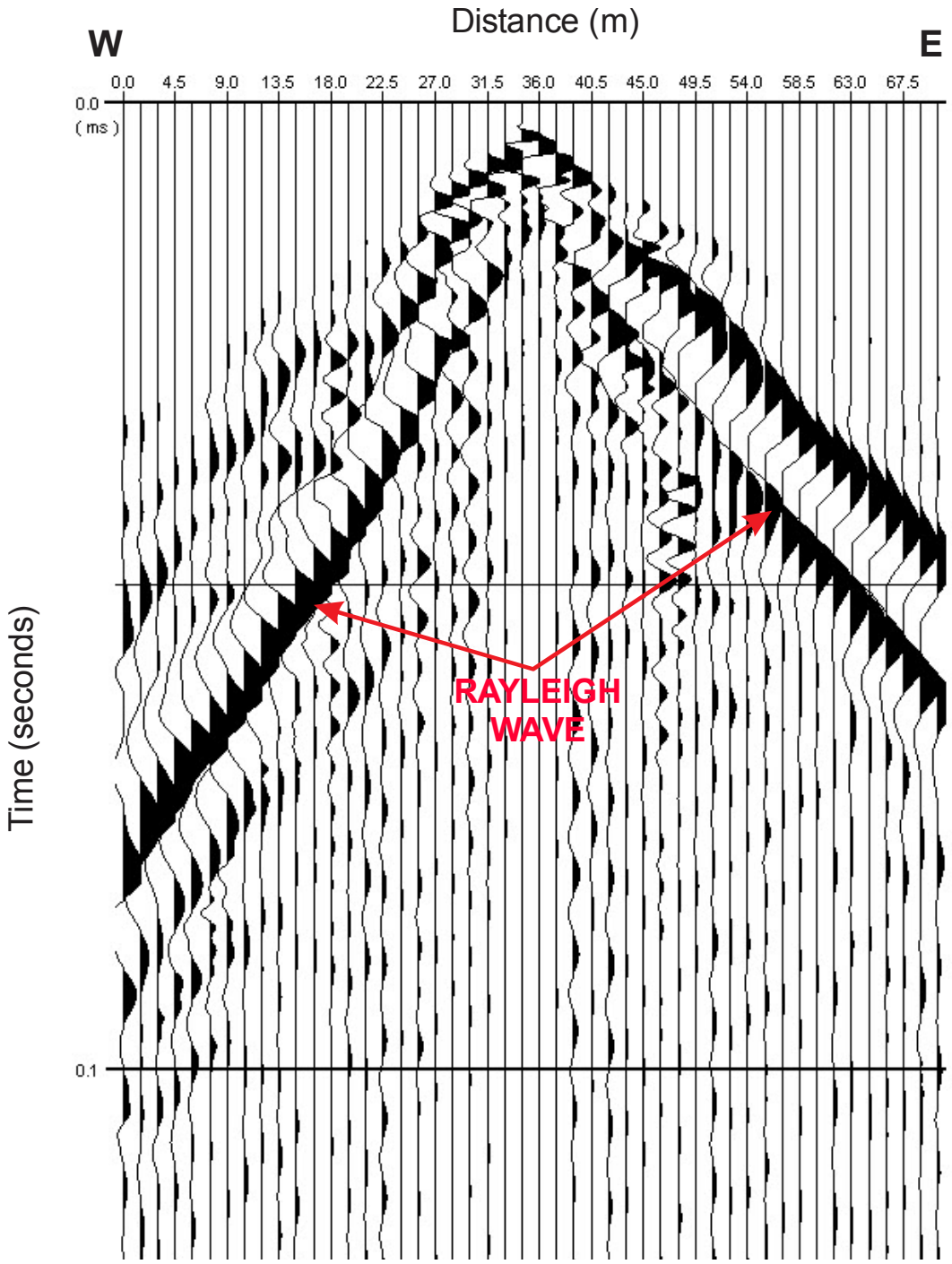

CI.TUQ – Seismic record from center shot location of array TUQ-2 illustrating the effects of near surface lateral velocity variation. There is a distinct difference in the velocity of surface wave energy propagating in the forward (east) and reverse (west) directions on the seismic record.

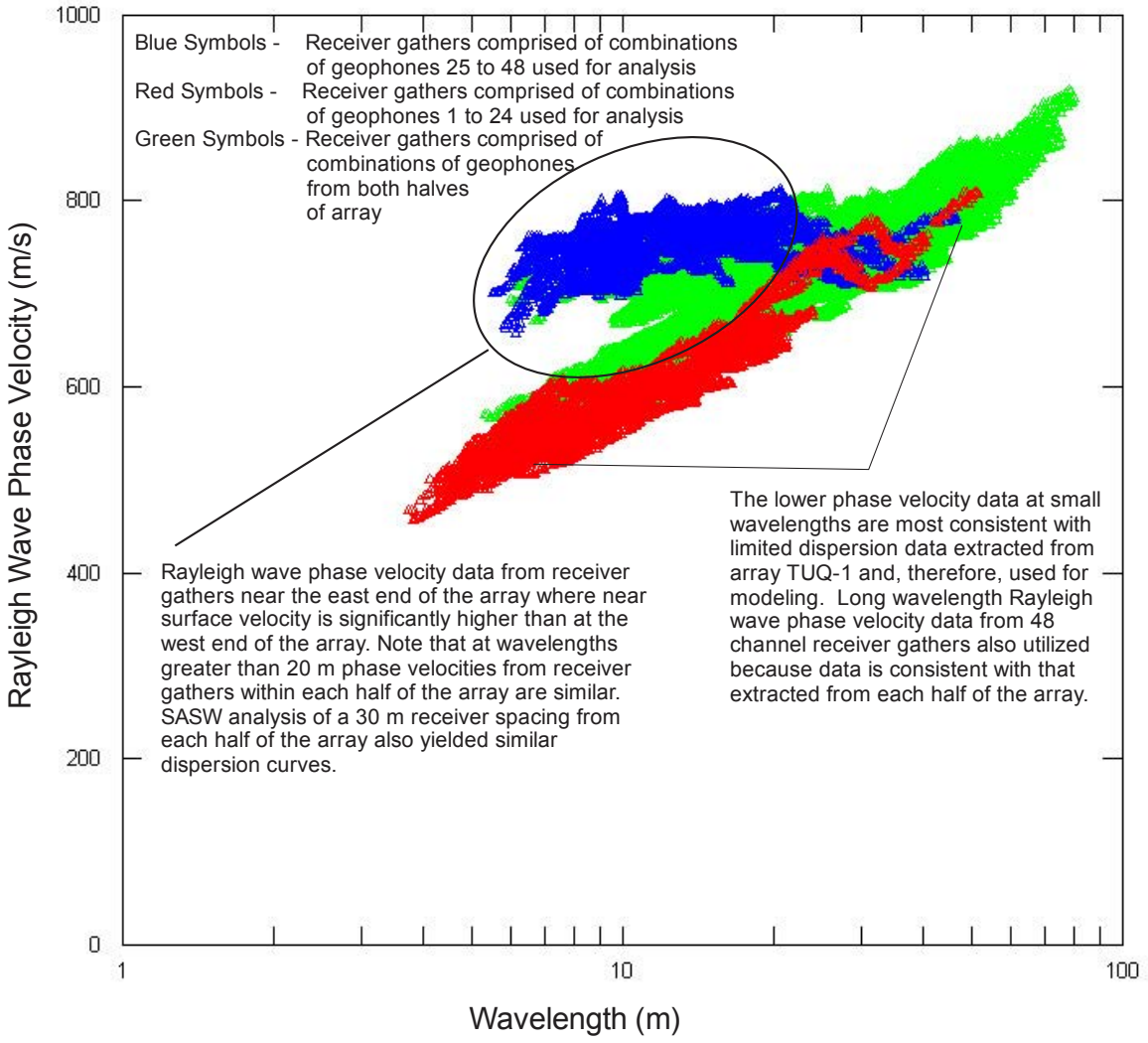

CI.TUQ – MASW dispersion data (right) from array TUQ-2 illustrating the effects of near surface lateral velocity variation. Rayleigh wave phase velocities from receiver gathers limited to the eastern half of the array are higher at small wavelengths than those limited to the western half of the array. The dispersion curves merge at long wavelengths (greater than 20 m), therefore no significant impact on V_{S30} is expected. In this case, the lower phase velocity data were selected for modeling because of better agreement with limited surface wave dispersion data extracted from array TUQ-1, located closer to the seismic station. Long wavelength dispersion data resulting from larger receiver gathers (e.g. all 48 channels) were included for modeling because the phase velocities are consistent with those from receiver gathers limited to the western and eastern portions of the array. Lateral velocity variation of varying degree is a common problem at weathered rock sites. Ideally, an alternate test location would have been identified; however, there are limited viable test locations at this site.

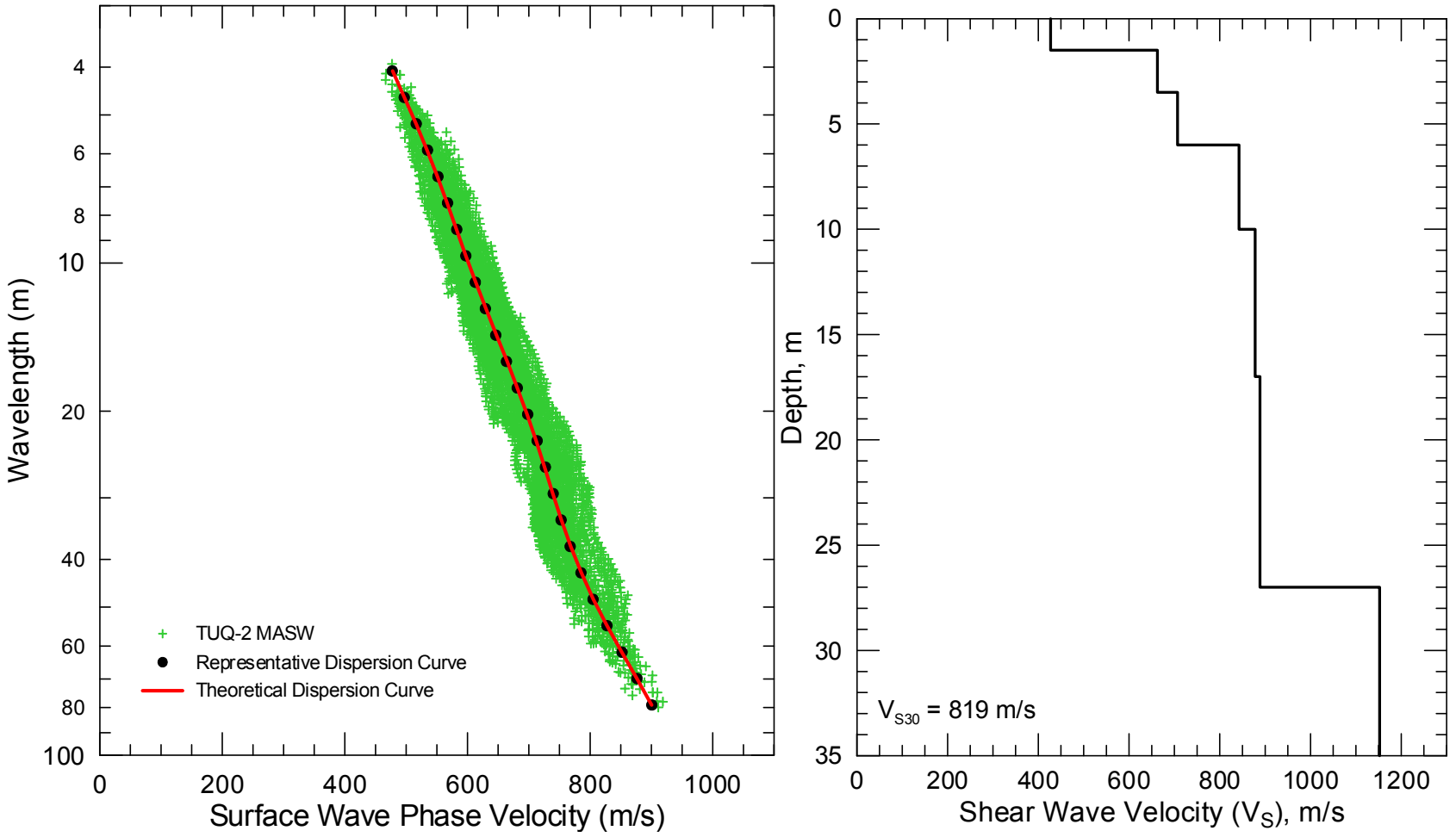

CI.TUQ - Field, representative and inverted theoretical surface wave dispersion data (left) and associated V_S model (right)

Site CI.USB

Location: UC Santa Barbara, Isla Vista, California

Latitude: 34.41357 **Longitude:** -119.84368
(Station coordinates modified based on field GPS survey, WGS84 coordinate system)

V_{S30} (measured): 300 m/s

V_{S30} (adjusted to more accurately reflect seismic station conditions): 300 m/s (no adjustment necessary for surface sensor).

NEHRP Site Class: D

Geomatrix Code: IQD/FQD

Geologic Conditions/Observations: Site located in area mapped as Quaternary (Pleistocene) older alluvial terraces overlying older sedimentary rocks. The Miocene Sisquoc Formation, which consists of a highly overconsolidated, high plasticity silt is located about 5 m deep at the site based on a borehole drilled for installation of the borehole accelerometers. The Sisquoc Formation dips about 35 to 40 degrees in a southerly direction in the site vicinity based on geologic maps.

Site Conditions: Campus site with significant noise from pedestrians and light vehicle traffic. Flat terrain in site vicinity.

Geophysical Methods Utilized: HVSR, MASW, array microtremor, ReMi™

Geophysical Testing Arrays:

1. Arrays USB-1 (24 channel linear array utilizing 4.5 Hz vertical geophones spaced 4 m apart for an array length of 92 m) and USB-2 (24 channel linear array utilizing 4.5 Hz vertical geophones spaced 5 m apart for an array length of 115 m) used to acquire passive surface wave data. Arrays combined to form an "L" shaped array.
2. Array USB-3 (24 channel MASW array utilizing 4.5 Hz vertical geophones spaced 1 m apart for a length of 23 m, forward and reverse shot locations with multiple source offsets and source types (hammers only) and center shot location).
3. Array USB-4 (24 channel MASW array utilizing 4.5 Hz vertical geophones spaced 3 m apart for a length of 69 m, limited forward and reverse shot locations with multiple source offsets and source types).
4. Three HVSR measurement locations; two distributed along array USB-2 and the other next to the seismic station.

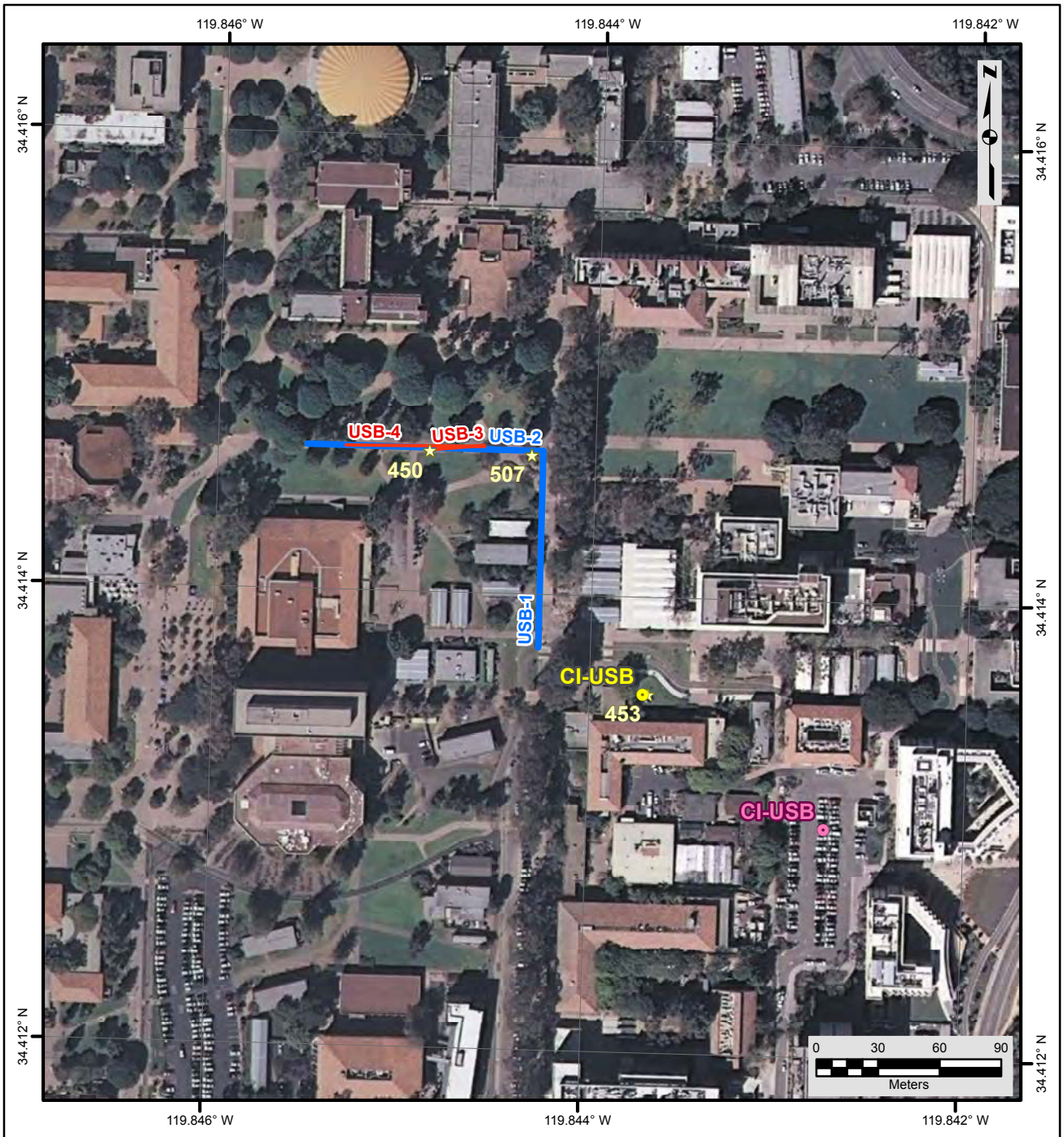

Legend

- Seismic Station - Approximate Surveyed Location
- Seismic Station - Approximate Location of Record
- H/V Spectral Ratio Location
- MASW Array
- Passive Surface Wave Array

NOTES:
1. WGS 1984 COORDINATE SYSTEM
2. Image Source: ESRI, i-cubed, USDA FSA, USGS, AEX, GeoEye, Getmapping, Aerogrid, IGP

File Name: CI-USB-I

Date: 10/13/2011

USGS science for a changing world

GEOVision geophysical services

RECOVERY.GOV

SITE MAP
CI•USB

Description of Geologic Map Units

Qs = Quaternary (Holocene) beach sand deposits
Qa = Quaternary (Holocene) alluvium; floodplain deposits of silt, sand and gravel
Qoa = Quaternary (Pleistocene) former alluvial deposits of silt, sand and gravel
Qsb = Tertiary & Quaternary (Pliocene & Pleistocene) Santa Barbara Formation; massive to bedded fossiliferous sand and silt
Tsq = Tertiary (Miocene) Sisquoc Shale; silty diatomaceous clay shale, breccia of shale detritus
Tm = Tertiary (Miocene) Monterey Formation; thin bedded, hard, platy to brittle siliceous shale

NOTES:
1. WGS 1984 COORDINATE SYSTEM
2. Geologic Map of the Goleta Quadrangle, Santa Barbara County, California by Thomas W. Dibblee, Jr., 1987
3. See site map for details of geophysical survey

USGS science for a changing world
GEOVision geophysical services

GEOLOGIC MAP
CI•USB

RECOVERY.GOV

File Name: CI-USB
Date: 10/6/2011

Looking east along array USB-2 at HVSR sensor 450

Looking at HVSR sensor 453 and seismic station CI.USB

Looking south along array USB-1

Looking east along array USB-3

Looking west along array USB-2

Location of Geophysical Testing Arrays:

Location	Latitude	Longitude
USB-1, South end of Array	34.41377	-119.84424
USB-1, North end of Array	34.41459	-119.84424
USB-2, West end of Array	34.41463	-119.84549
USB-2, East end of Array	34.41463	-119.84424
USB-3, West end of MASW Array	34.41462	-119.84480
USB-3, East end of MASW Array	34.41465	-119.84455
USB-4, West end of MASW Array	34.41463	-119.84528
USB-4, East end of MASW Array	34.41464	-119.84455
HVSR Sensor 450	34.41462	-119.84484
HVSR Sensor 453	34.41357	-119.84365
HVSR Sensor 507	34.41461	-119.84430
CI.USB Seismic Station	34.41357	-119.84368

Notes: 1) WGS84 Coordinate System (decimal degrees).
2) Survey accuracy is estimated at 1 to 2 m.

Results:

V_S Model

Depth to Top of Layer (m)	Layer Thickness (m)	S-Wave Velocity (m/s)	Inferred P-Wave Velocity (m/s)	Assumed Poisson's Ratio	Assumed Density (g/cm^3)
0	1	104	195	0.300	1.7
1	1.5	156	292	0.300	1.8
2.5	2.5	228	426	0.300	1.9
5	4	317	1500	0.477	2.0
9	6	358	1500	0.470	2.0
15	8	366	1550	0.471	2.0
23	10	378	1550	0.468	2.0
33	12	403	1600	0.466	2.0
45	>15	445	1600	0.458	2.0

Notes: 1) Saturated sediments estimated at 5 m depth from seismic refraction first arrival data. The P-wave velocity of saturated sediments is about 1,500 to 1,600 m/s.
2) Depth of investigation is about 60 m.
3) Bottom layer is a half space.

Observations/Discussion:

- Seismic station CI.USB consists of four 3-component accelerometers, two at the surface and the other two at 74 m depth in contiguous boreholes. At the time of installation, the two surface sensors consisted of Wilcoxon and Kinemetrics FBA accelerometers and the borehole sensors consisted of borehole equivalents of the surface sensors.
- Oyo PS suspension logging was conducted in the CI.USB borehole in 1997, prior to borehole sensor installation.
- HVSR sensor 507 was located near the corner of passive surface wave arrays USB-1 and USB-2. HVSR sensor 450 was located near arrays USB-2, USB-3 and USB-4 and HVSR sensor 453 was located adjacent to the seismic station. The HVSR sensors consisted on Nanometrics Trillium 120 second seismometers. HVSR data were also collected with a Tromino ENGY sensor adjacent to sensor 453.
- The HVSR curves are almost identical at frequencies below 4 Hz, but differ at higher frequencies, which may be related to the steeply dipping geologic units at the site. There are no significant HVSR peaks at this site. There appears to be low frequency noise in the HVSR data below 0.3 Hz although the possibility cannot be discounted that there is an HVSR peak on the order of 0.15 Hz. Data quality at low frequency would be improved by recording data for a longer period at night with better sensor coupling. The Tromino ENGY data are not presented, but is almost identical to Trillium sensor 453 at frequencies above 0.3 Hz, the low frequency limit of the Tromino.
- Noise conditions at site (multi-directional or omni-directional noise sources) appeared sufficient for successful application of passive surface wave techniques. It should be noted, however, that many buildings in the site vicinity have basements, which may severly affect passive surface wave propagation in the area. The numerous utility corridors present on university campus may also degrade high frequency surface wave data, if located in the immediate vicinity of the arrays.
- ESAC technique used to extract surface wave dispersion data from passive "L" array data. Both the ReMi™ and ESAC techniques used to extract surface wave dispersion data from the linear arrays. Only the higher quality "L" array dispersion data and the linear array data from array USB-2 (both ESAC and ReMi™) were used for analysis. Linear array USB-1 did not yield useful surface wave dispersion data.
- Passive surface wave phase velocity data were very noisy over the 8 to 11 Hz range, possibly due to noise from on site facilities. Additionally, it was not possible to extract MASW dispersion data at frequencies lower than 11 Hz, although the focus of the MASW survey was acquisition of high frequency surface wave data to supplement the passive surface wave data.
- Surface wave dispersion data from active and passive surface wave data sets overlap in the 7 to 30 m wavelength range are in very good agreement.
- Representative dispersion curves were generated for each surface wave data set using a moving average, polynomial curve fitting routine. These individual representative dispersion curves were combined and a representative dispersion curve generated for the combined data set for data modeling.
- The water table was modeled at a depth on the order of 5 m based on interactive layer-based analysis of seismic refraction first arrival data. P-wave velocities of about 250 to

400 m/s and 1,500 to 1,600 m/s were modeled for unsaturated and saturated sediments, respectively.

- Surface wave depth of investigation is about 60 m based on half of maximum wavelength criteria and assuming that surface wave dispersion data at frequencies as low as 3.4 Hz are valid utilizing 4.5 Hz geophones (low frequency geophone phase response differences will cancel out if noise is omni-directional and/or the phase response differences are random in nature).
- V_{S30} from the surface wave model is 300 m/s (Site Class D).
- An Oyo PS suspension log was previously acquired in CI.USB borehole located about 120 m from the center of the test area. V_{S30} developed from the PS log receiver to receiver analysis, utilizing the S-wave velocity structure from the surface wave model in the upper 6 m where there was no borehole velocity data, is 313 m/s, about 4% higher than the surface wave sounding. Due to the dipping geologic units at the site the borehole velocity log and surface wave sounding do not sample the same material, which may in part explain the small difference between the measurements. Alternatively, the difference between surface wave and PS Suspension log velocities may be a function of body wave dispersion associated with damping/seismic quality factor (Q). The dominant frequency of S-wave data in a PS Suspension log is typically over 200 Hz, whereas, surface wave measurements are generally made over the 50 Hz (shallow) to 1 Hz (deep) frequency range.
- Average S-wave velocity of the upper 60 m (V_{S60}) is 350 and 367 m/s from the surface wave model and PS suspension log, respectively, about a 5% difference.
- The average S-wave velocity to the accelerometers at 74 m depth (V_{S74}) using the PS suspension log supplemented by the surface wave model in the upper 6 m is 380 m/s.

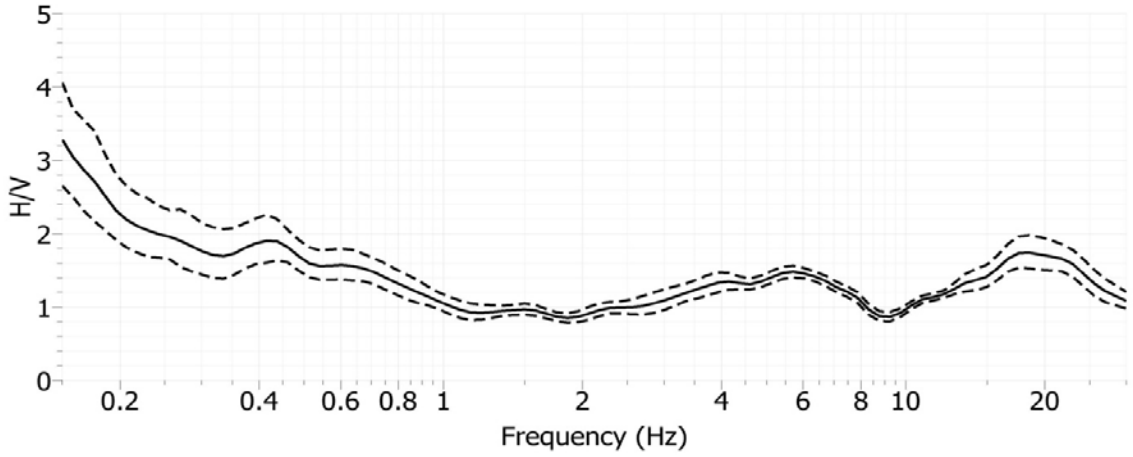

Site CI.USB, H/V Spectral Ratio, Array USB-2, Sensor 450

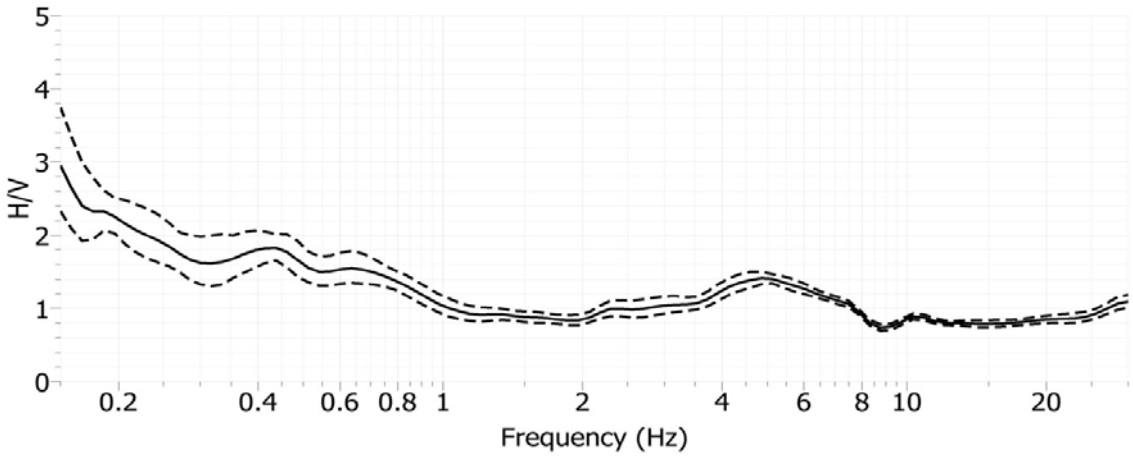

Site CI.USB, H/V Spectral Ratio, Array USB-2, Sensor 507

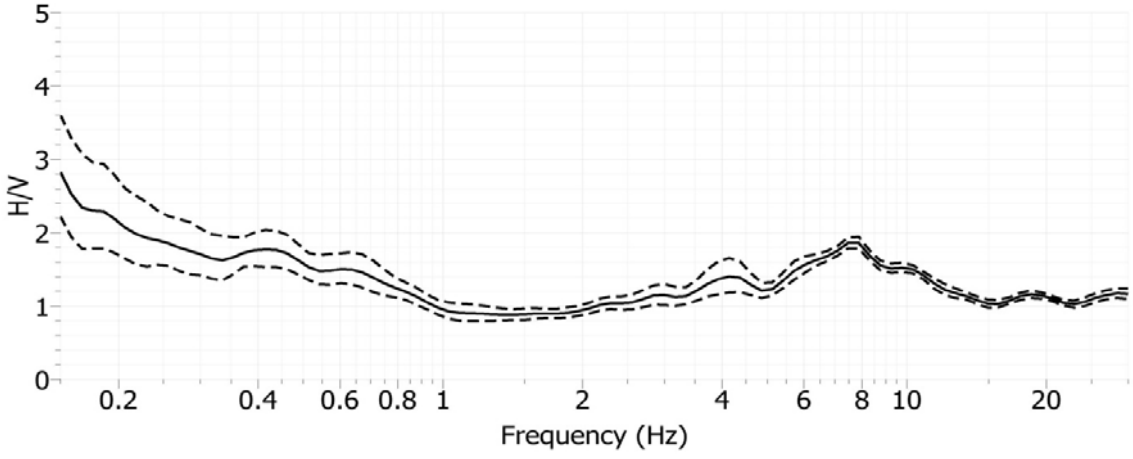

Site CI.USB, H/V Spectral Ratio, Near Seismic Station, Sensor 453

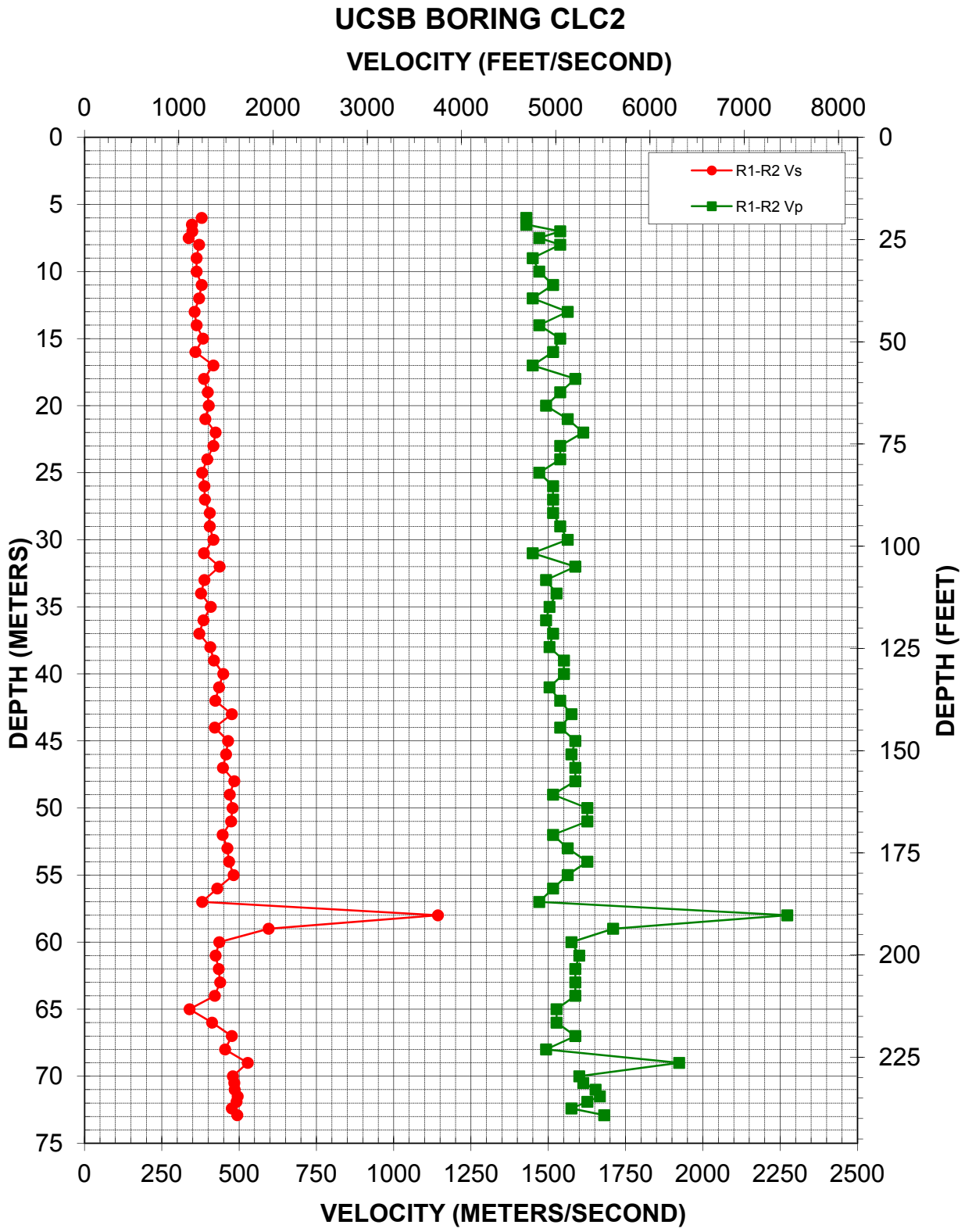

CI.USB- Oyo PS suspension log conducted as part UC/CLC Campus Earthquake Program. Receiver to receiver (R1-R2) analysis.

CI.USB - Oyo PS suspension log conducted as part of the UC/CLC Campus Earthquake Program. Receiver to Receiver (R1-R2) Analysis.

DEPTH (M)	Vs (M/SEC)	Vp (M/SEC)	DEPTH (M)	Vs (M/SEC)	Vp (M/SEC)
6.0	379	1429	41.0	435	1504
6.5	347	1429	42.0	423	1538
7.0	348	1538	43.0	476	1575
7.5	337	1471	44.0	421	1538
8.0	370	1538	45.0	464	1587
9.0	362	1449	46.0	458	1575
10.0	362	1471	47.0	447	1587
11.0	379	1515	48.0	484	1587
12.0	370	1449	49.0	469	1515
13.0	356	1563	50.0	478	1626
14.0	362	1471	51.0	474	1626
15.0	383	1538	52.0	446	1515
16.0	358	1515	53.0	462	1563
17.0	417	1449	54.0	467	1626
18.0	386	1587	55.0	482	1562
19.0	398	1538	56.0	429	1515
20.0	402	1493	57.0	380	1471
21.0	391	1563	58.0	1143	2273
22.0	424	1613	59.0	595	1709
23.0	417	1538	60.0	436	1575
24.0	397	1538	61.0	424	1600
25.0	380	1471	62.0	434	1587
26.0	388	1515	63.0	439	1587
27.0	389	1515	64.0	421	1587
28.0	405	1515	65.0	340	1527
29.0	405	1538	66.0	412	1527
30.0	417	1563	67.0	476	1587
31.0	386	1449	68.0	455	1493
32.0	437	1587	69.0	528	1923
33.0	388	1493	70.0	480	1600
34.0	377	1527	70.5	484	1613
35.0	408	1504	71.0	485	1653
36.0	385	1493	71.5	495	1667
37.0	371	1515	71.9	491	1626
38.0	407	1504	72.4	476	1575
39.0	418	1550	72.9	494	1681
40.0	448	1550			

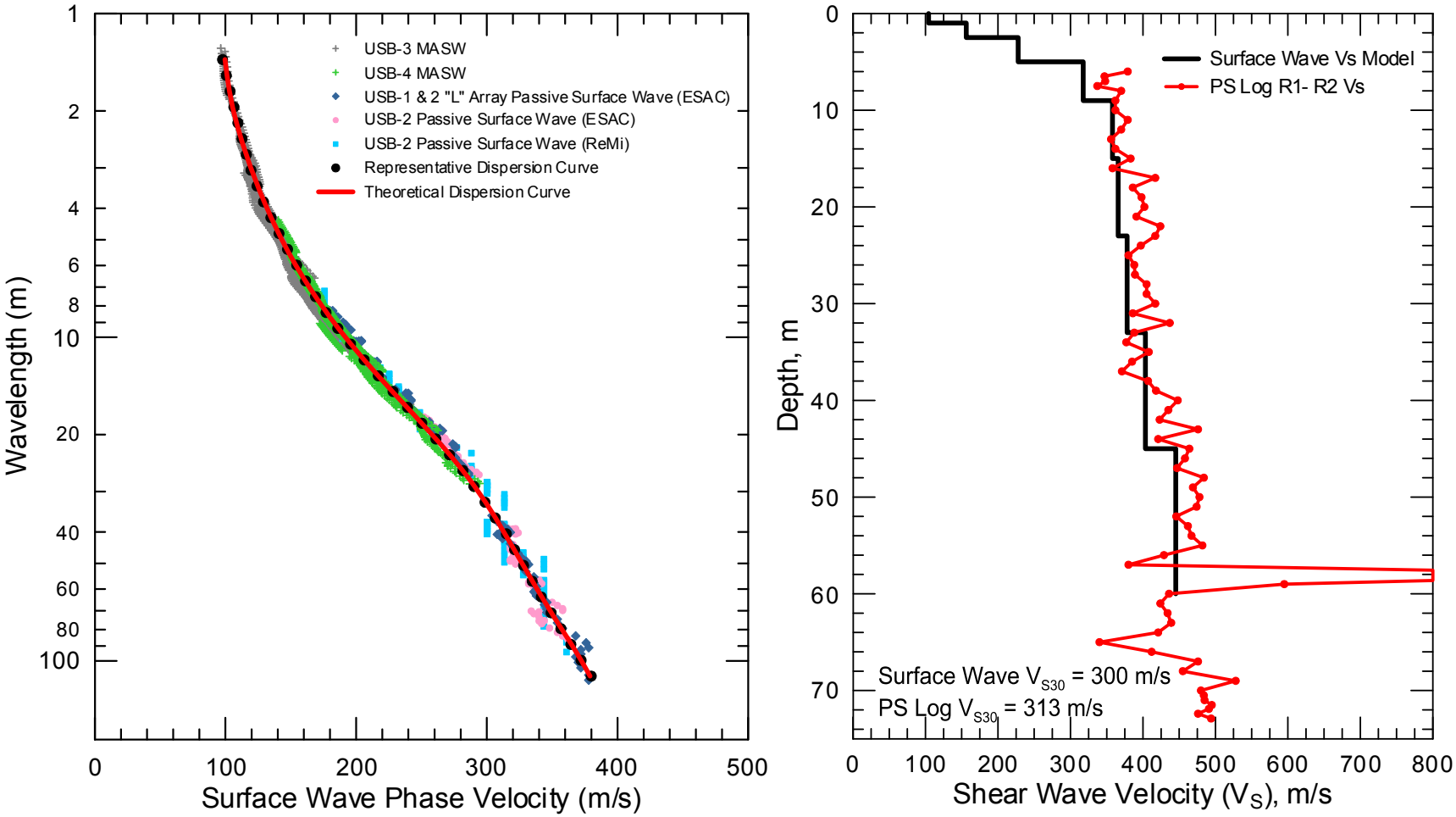

CI.USB - Field, representative and inverted theoretical surface wave dispersion data (left) and associated V_S model (right)

Site CI.VCS

Location: Southern California Edison, Vincent Substation, North Los Angeles Forest Highway, Palmdale, California

Latitude : 34.48372 **Longitude:** -118.11781
(Station coordinates modified based on field GPS survey, WGS84 coordinate system)

V_{S30} (measured): 405 m/s

V_{S30} (adjusted to more accurately reflect seismic station conditions): 433 m/s (no adjustment necessary)

NEHRP Site Class: C

Geomatrix Code: IQC

Geologic Conditions/Observations: Seismic station located on area mapped as Quaternary (Pleistocene) older elevated alluvial remnants. Crystalline bedrock outcrops approximately 450 meters south of the seismic station.

Site Conditions: Rural site with noise from nearby electric generating facilities and some vehicles. Antelope Valley Freeway located about 1.2 km northwest of site. Relatively flat terrain in site vicinity with surface elevation gently decreasing to the west.

Geophysical Methods Utilized: HVSR, MASW, array microtremor, ReMi™

Geophysical Testing Arrays:

1. Arrays VCS-1 (24 channel linear array utilizing 4.5 Hz vertical geophones spaced 5 m apart for an array length of 115 m) and VCS-2 (24 channel linear array utilizing 4.5 Hz vertical geophones spaced 4 m apart for an array length of 92 m) used to acquire passive surface wave data. Arrays combined to form an "L" shaped array.
2. Array VCS-3 (48 channel MASW array utilizing 4.5 Hz vertical geophones spaced 1.5 m apart for a length of 70.5 m, forward and reverse shot locations with multiple source offsets and source types and center shot location).
3. Three HVSR measurement locations distributed along array VCS-1 and VCS-2. Both Nanometrics Trillium and Tromino ENGY sensors used to make HVSR measurements.

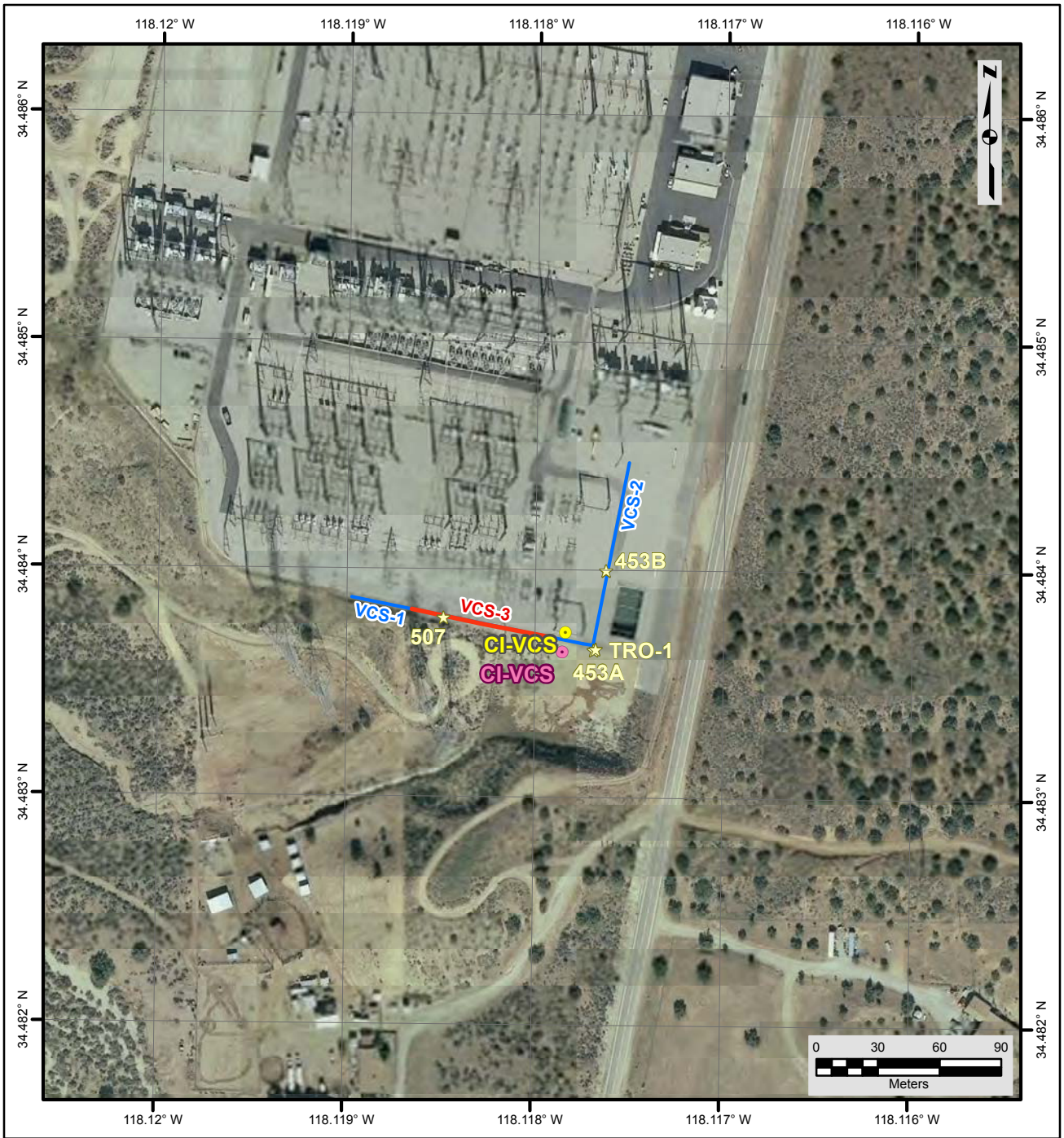

Legend

- Seismic Station - Approximate Surveyed Location
- Seismic Station - Approximate Location of Record
- H/V Spectral Ratio Location
- MASW Array
- Passive Surface Wave Array

NOTES:
1. WGS 1984 COORDINATE SYSTEM
2. Image Source: ESRI, i-cubed, USDA FSA, USGS, AEX, GeoEye, Getmapping, Aerogrid, IGP

File Name: CI-VCS-I

Date: 9/22/2011

USGS science for a changing world

GEOVision geophysical services

RECOVERY.GOV

SITE MAP
CI•VCS

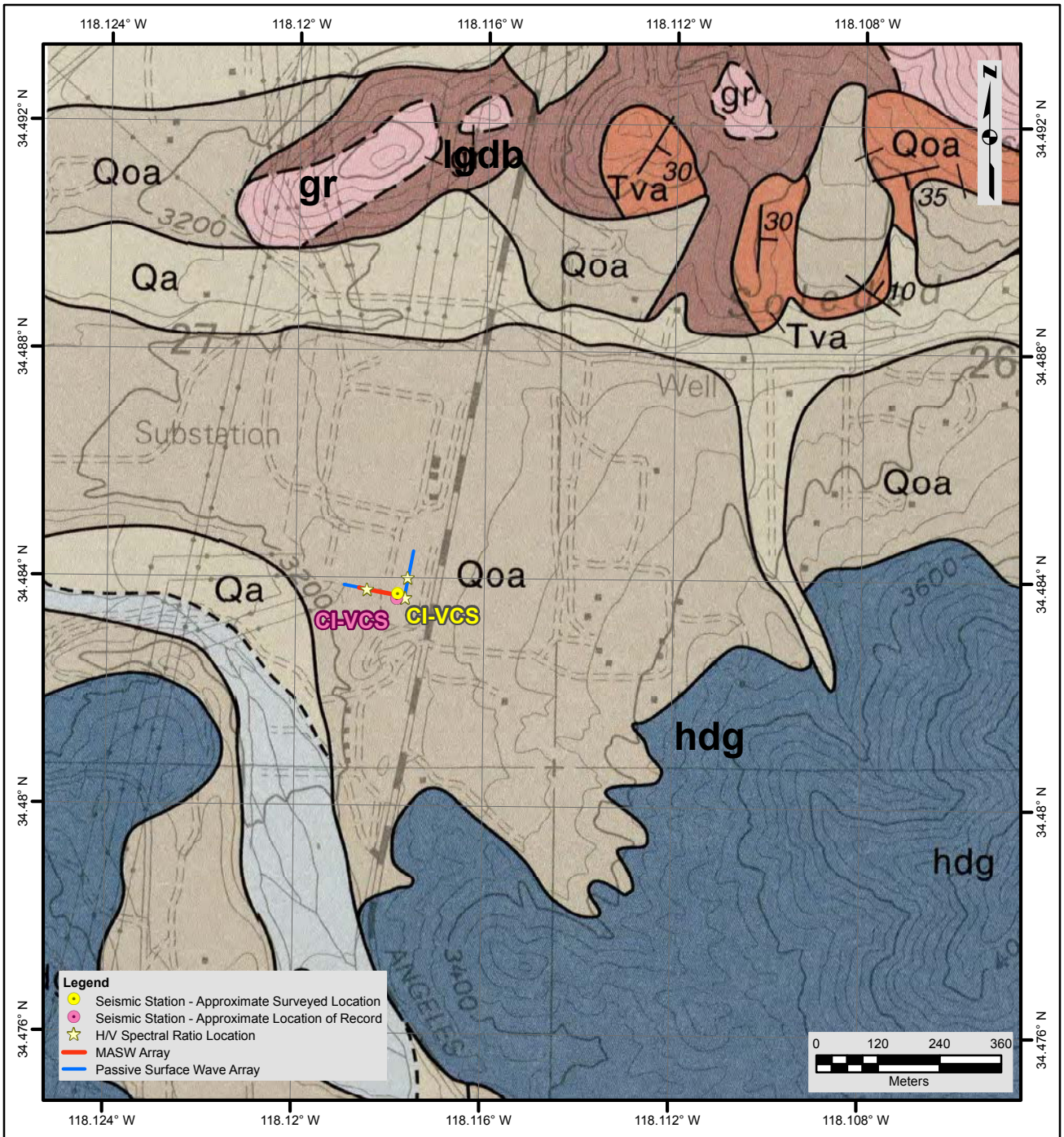

Description of Geologic Map Units

Qg = Quaternary (Holocene) gravel and sand of stream channels
Qa = Quaternary (Holocene) allluvial gravel, sand and silt/clay of valleys and canyon flood plains
Qoa = Quaternary (Pleistocene) older elevated remnants of alluvial gravel and sand
Tva = Tertiary (Oligocene) andesitic volcanic rocks, hard, resistant
gr = Mesozoic (Late Cretaceous or older) granitic rocks, hard, coherent, severely fractured, massive
lgdb = Mesozoic (Early Triassic) Lowe Granodiorite, massive to vaguely gneissoid, fractured
hdg = Mesozoic (or older) hornblende diorite gabbro; engulfed by Lowe Granodiorite, hard, fractured

NOTES:
1. WGS 1984 COORDINATE SYSTEM
2. Geologic Map of the Pacifico Mountain and Palmdale (South ½) Quadrangles, Los Angeles County, California by Thomas W. Dibblee, Jr., 2001
3. See site map for details of geophysical survey

File Name: CI-VCS

Date: 9/16/2011

USGS science for a changing world

GEOVision geophysical services

GEOLOGIC MAP
CI•VCS

RECOVERY.GOV

Looking south towards CI.VCS seismic station

Looking south along VCS-2 from HVSR sensor 450

Looking west along array VCS-1 towards HVSR sensor 507

Looking north towards corner of passive arrays VCS-1 and VCS-2 and HVSR sensor 453

Data acquisition with hammer source on MASW array VCS-3

Location of Geophysical Testing Arrays:

Location	Latitude	Longitude
VCS-1, West End of Array	34.48387	-118.11895
VCS-1, East End of Array	34.48368	-118.11772
VCS-2, South End of Array	34.48367	-118.11767
VCS-2, North End of Array	34.48447	-118.11749
VCS-3, West End of Array	34.48382	-118.11863
VCS-3, Center of Array	34.48376	-118.11825
VCS-3, East End of Array	34.48370	-118.11788
HVSR Sensor 453B (Trillium)	34.48400	-118.11760
HVSR Sensor 453A (Trillium)	34.48365	-118.11766
HVSR Sensor 507 (Trillium)	34.48379	-118.11846
Tromino ENGY Sensor (adjacent to Sensor 453A)	34.48365	-118.11765
CI.VCS Seismic Station	34.48372	-118.11781

Notes: 1) WGS84 Coordinate System (decimal degrees)
2) Survey accuracy is estimated at 1 to 2 m

Results:

V_S Model

Depth to Top of Layer (m)	Layer Thickness (m)	S-Wave Velocity (m/s)	Inferred P-Wave Velocity (m/s)	Assumed Poisson's Ratio	Assumed Density (g/cm^3)
0	1.5	193	360	0.3	1.8
1.5	4.5	365	682	0.3	1.9
6	8	403	754	0.3	2.0
14	18	469	877	0.3	2.0
32	>18	1188	2222	0.3	2.3

Notes: 1) Lowest layer is half space
2) Model valid to a depth of about 50 m
3) Velocity of bottom layer not well constrained

Observations/Discussion:

- There is significant 60 Hz noise in the HVSR and MASW seismic records. The HVSR data collected with the Tromino ENGY may be less affected by the 60 Hz noise as the system does not have cables. The 60 Hz noise should have a limited impact on HVSR and MASW data, but significantly impacts analysis of seismic refraction first arrival data.
- There is a low amplitude HVSR peak in the 2.5 to 4 Hz range, which could indicate relatively shallow bedrock at the site (i.e. 25 to 40 m depending on velocity structure) although the nearest outcrop of crystalline bedrock is about 450 m to the south. Alternatively, the weak HVSR peak could be associated with a significant increase in P- and S-wave velocity not associated with crystalline basement (e.g. volcanic or sedimentary rock or a high velocity gravel layer.)
- The HVSR peak is clearest at sensor 289 and occurs at about 3 Hz, although there could be double peaks at 2.5 and 3.2 Hz. The HVSR peak is weaker at sensor 292A and occurs between 3.2 and 3.5 Hz. Interestingly, the peak is clearer in the data collected with the Tromino ENGY, which was located adjacent to sensor 292A, and also slightly offset to 3.7 Hz. This may be the result of better coupling of the Tromino sensor and higher noise in the Trillium data due to cabling. Trillium sensor 289 HVSR data is more similar to the Tromino sensor data, but has a slightly lower frequency peak. The low amplitude HVSR peak is located at about 3.4 to 3.5 Hz at sensor 292B. The variable HVSR peaks likely result from variable depth of the geologic structure associated with the impedance contrast and lateral variability of sediment velocity structure.
- Noise conditions at site (multi-directional or omni-directional noise sources) did not seem sufficient for successful application of passive surface wave techniques (some vehicle traffic on adjacent Angeles Forest Highway, limited traffic on other nearby roads and the high traffic Antelope Valley Freeway located about 1.2 km from the site). Passive surface wave data were collected at this site in attempt to extend MASW depth of investigation.
- Based on simple horizontal layer-based analysis of seismic refraction first arrival data, P-wave velocity in the upper 10 m ranges from about 400 to 600 m/s near the surface to about 600 to 700 m/s between a depth of 1 and 10 m, or more. Data quality was significantly degraded by strong 60 Hz noise from the adjacent substation and it was not possible to accurately evaluate P-wave velocity structure below a depth of 10 to 15 m. There is, however, some evidence of a high velocity layer, such as bedrock or the saturated zone below a depth of about 25 m.
- ESAC technique used to extract surface wave dispersion data from passive "L" array data. The overall quality of the passive "L" array surface wave dispersion data is not very good, but is in reasonable agreement with the MASW dispersion data. Attempts were made to extract surface wave dispersion data from the linear arrays using both the ReMi™ and ESAC techniques with the ESAC data not being usable and the ReMi™ data of poor quality. Only the higher quality "L" array dispersion data and ReMi™ dispersion data from array VCS-1 were used for modeling.
- It was not possible to extract surface wave dispersion data at wavelengths below about 3.5 m due to lateral velocity variation, a dominant higher mode at high frequencies, and maybe due to possible utilities near the array. MASW analysis of seismic data acquired using small hammers and a limited offset range (e.g. small groups of receivers near the

source) and SASW analysis of selected MASW receiver pairs was able to obtain some surface wave dispersion data at smaller wavelengths, but it did not blend well with other data and was not utilized. Lateral velocity variation becomes quite apparent when MASW analysis is conducted using limited offset range data from shot points at opposite ends and the center of the receiver array.

- Surface wave dispersion data from active and passive surface wave data sets are in acceptable agreement over the overlapping frequency/wavelength range.
- Representative dispersion curves were generated for each surface wave data set using a moving average, polynomial curve fitting routine. These individual representative dispersion curves were combined and a representative dispersion curve generated for the combined data set for data modeling.
- There is a large increase in velocity at about 32 m depth in the surface wave model, which is associated with either crystalline basement or a large increase in velocity associated with a sedimentary or volcanic rock unit. The S-wave velocity of this layer is not well constrained in the model, but does not significantly affect V_{S30}. Although seismic refraction first arrival data is strongly degraded by 60 Hz noise, there is some evidence of the high velocity layer that could be associated with bedrock or groundwater at a depth of greater than 25 m.
- The surface wave model generates a synthetic HVSR peak at about 3.7 Hz although the velocity of the lower layer had to be decreased to about 975 m/s to match the HVSR amplitude. The software package utilized to develop the synthetic HVSR plots (Grilla developed by Micromed s.p.a.) is based on simulation of both Rayleigh and Love waves (50% Rayleigh wave and 50% Love wave assumption) propagating in multiple, horizontal, planar layers and is limited to the fundamental mode only.
- Surface wave depth of investigation is about 50 m based on half of maximum wavelength criteria.
- V_{S30} is 405 m/s (Site Class C).
- Average S-wave velocity between 2 m (nominal sensor depth) and 32 m is 433 m/s.

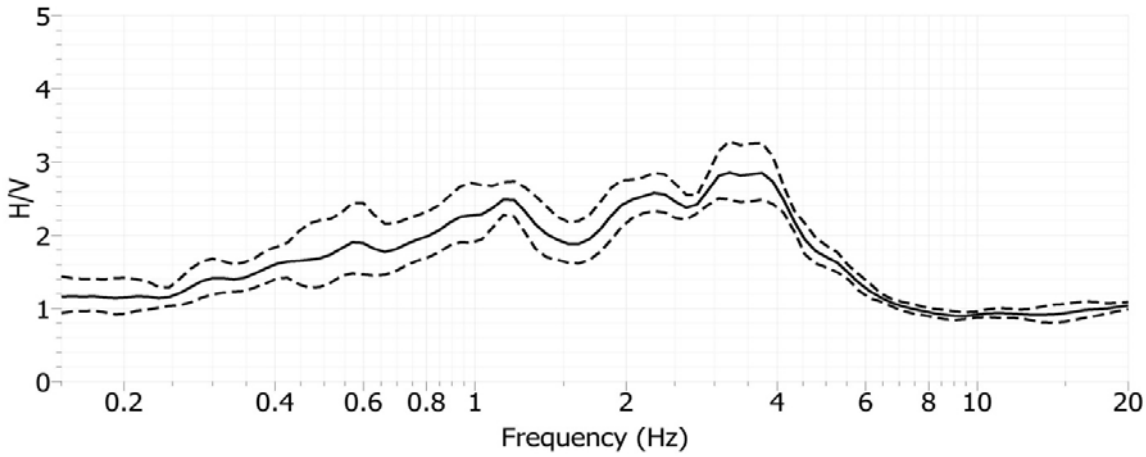

Site CI.VCS, H/V Spectral Ratio, Array VCS-1, Sensor 453B

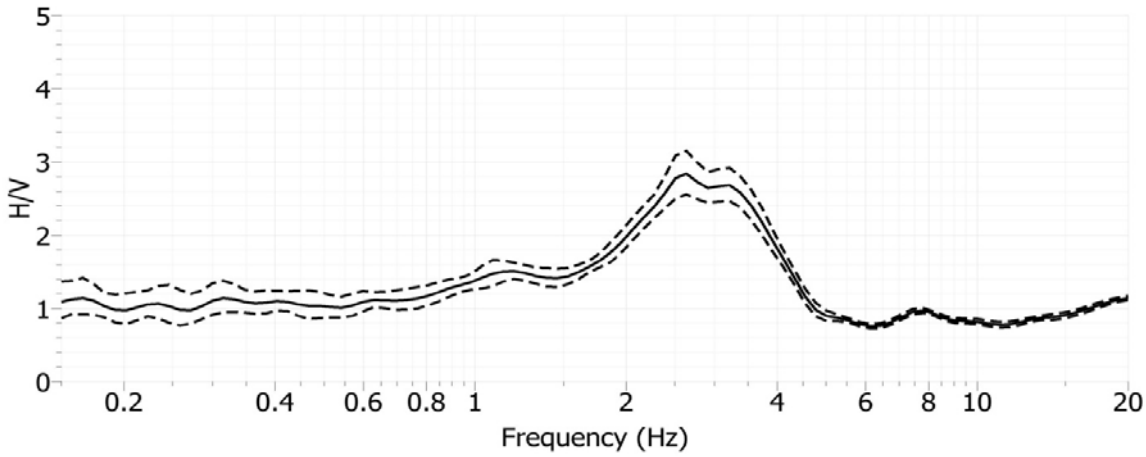

Site CI.VCS, H/V Spectral Ratio, Array VCS-2, Sensor 507

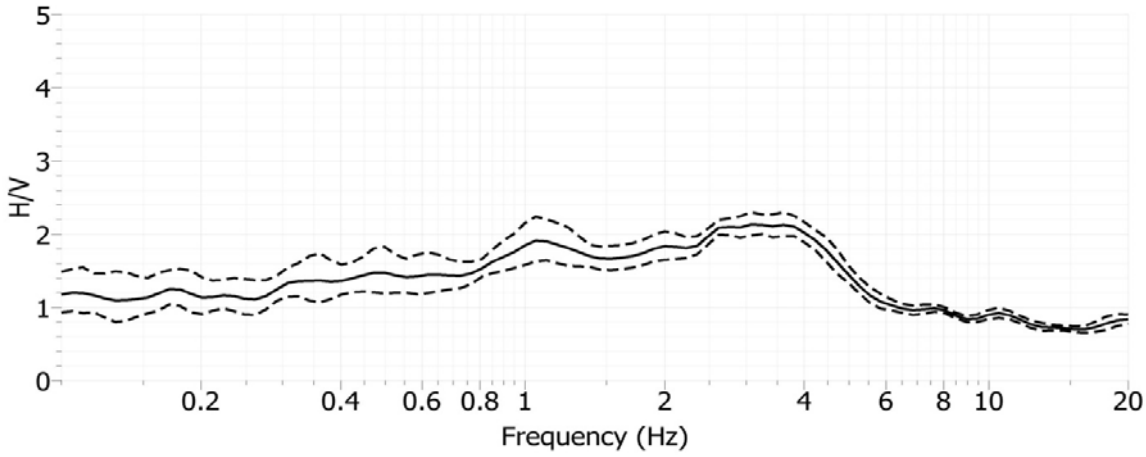

Site CI.VCS, H/V Spectral Ratio, Array VCS -1 and 2, Sensor 453A

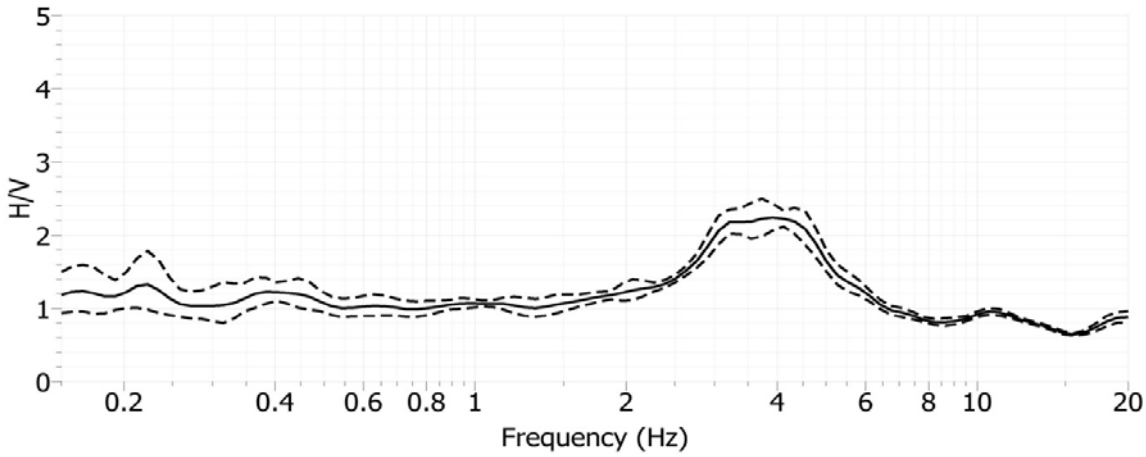

Site CI.VCS, H/V Spectral Ratio, Array VCS -1, Tromino ENGR, located adjacent to Trillium Sensor 453A

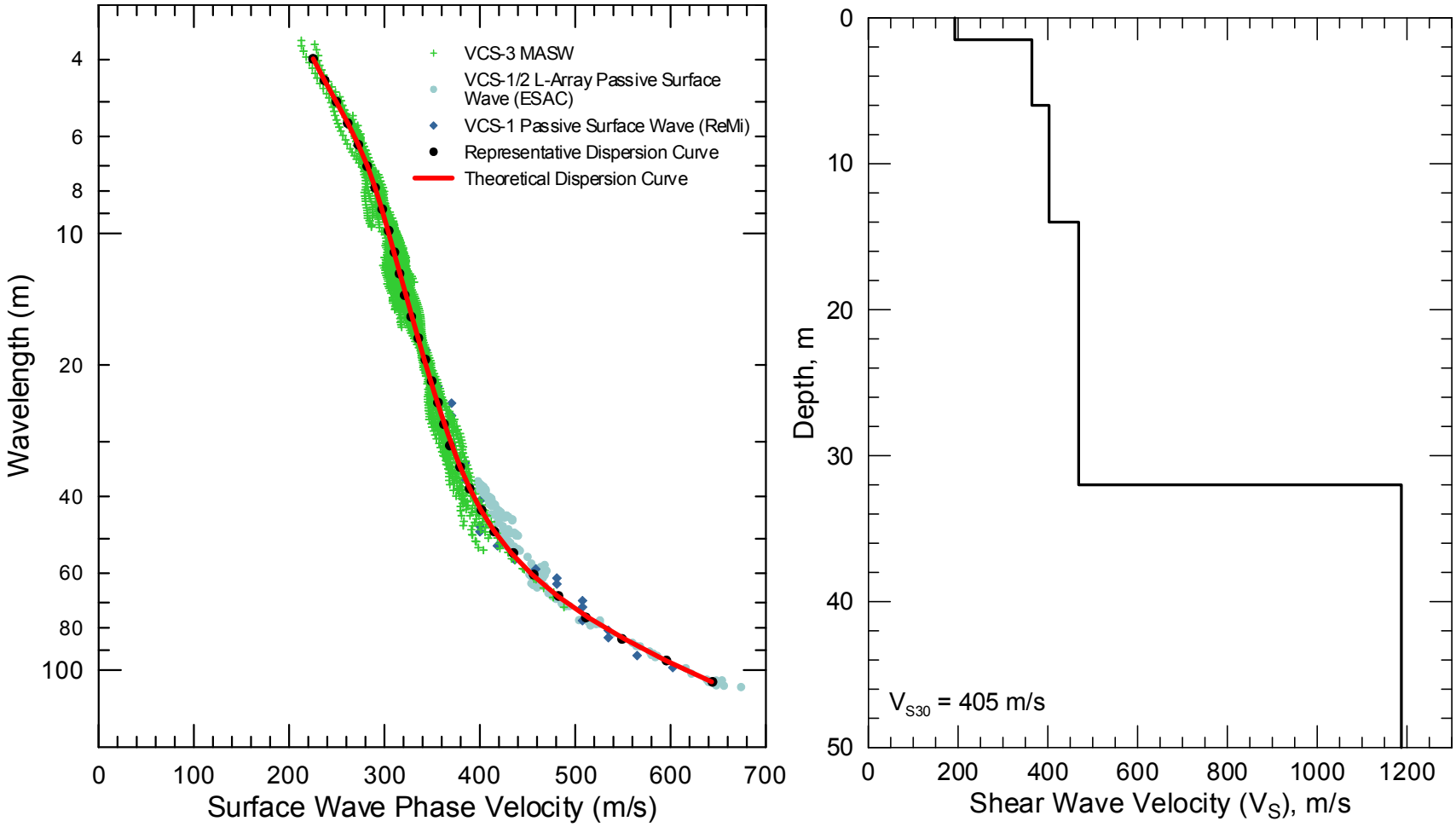

CI.VCS - Field, representative and inverted theoretical surface wave dispersion data (left) and associated V_S model (right)

Site CI.VES

Location: Vestal Substation, Tulare County, California

Latitude: 35.84088 **Longitude:** -119.08489
(Station coordinates modified based on field GPS survey, WGS84 coordinate system)

V_{S30} (measured): 393 m/s

V_{S30} (adjusted to more accurately reflect seismic station conditions): 456 m/s (average S-wave velocity between 2 and 32 m adjusting for 2 m assumed sensor depth).

NEHRP Site Class: C

Geomatrix Code: IQD

Geologic Conditions/Observations: Seismic station located on unit mapped as Quaternary (Pleistocene) older alluvial terrace deposits. Arrays VES-1 and VES-3 are located on the same mapped geologic unit as at the seismic station. Array VES-2 is located on a mapped Tertiary to Quaternary sandstone and conglomerate unit near the contact with the Quaternary older alluvial and terrace deposits. The geologic contact is not clearly visible at the site.

Site Conditions: Rural site with some noise from sporadic vehicle traffic on nearby roads. Relatively flat terrain in test area.

Geophysical Methods Utilized: HVSR, MASW, SASW

Geophysical Testing Arrays:

1. Array VES-1 (48 channel MASW array utilizing 4.5 Hz vertical geophones spaced 1.5 m apart for a length of 70.5 m, forward and reverse shot locations with multiple source offsets and source types and a center shot location).
2. Array VES-1 (SASW array with common midpoint and orientation as MASW array VES-1. SASW data acquired using 1 Hz geophones, common center point geometry, receiver spacings between 2 and 32 m, forward and reverse shot locations).
3. Array VES-2 (48 channel MASW array utilizing 4.5 Hz vertical geophones spaced 1 m apart for a length of 47 m, forward and reverse shot locations with multiple source offsets and source types and center shot location).
4. Array VES-3 (48 channel MASW array utilizing 4.5 Hz vertical geophones spaced 1 m apart for a length of 47 m, forward and reverse shot locations with multiple source offsets and source types and center shot location).
5. Three HVSR measurement locations distributed along VES-1.

Legend

- Seismic Station - Approximate Surveyed Location
- Seismic Station - Approximate Location of Record
- H/V Spectral Ratio Location
- SASW Array
- MASW Array

NOTES:
1. WGS 1984 COORDINATE SYSTEM
2. Image Source: ESRI, i-cubed, USDA FSA, USGS, AEX, GeoEye, Getmapping, Aerogrid, IGP

File Name: CI-VES-I

Date: 8/20/2011

USGS science for a changing world

GEOVision geophysical services

RECOVERY.GOV

SITE MAP
CI•VES

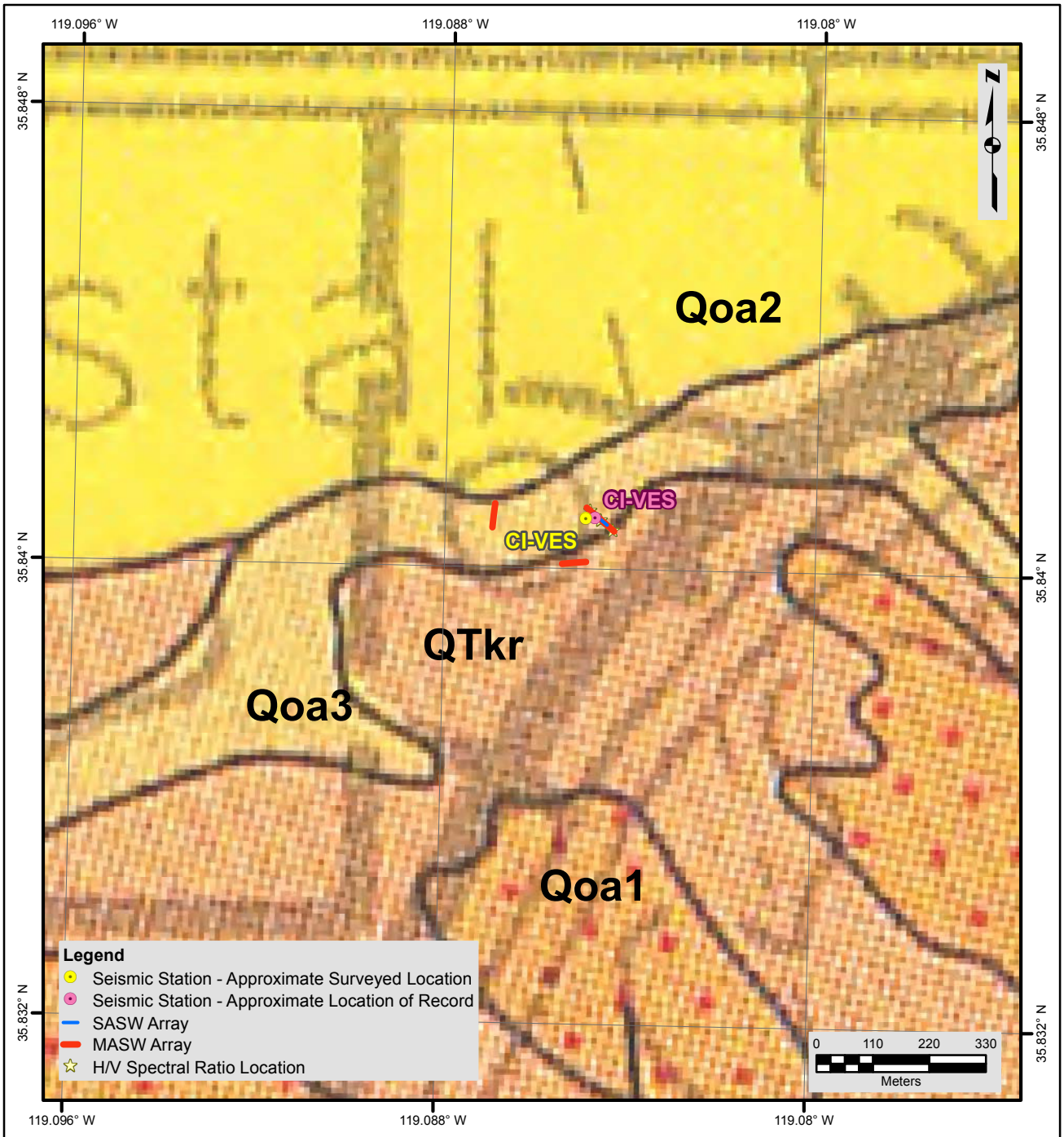

Description of Geologic Map Units

Qoa3 = Quaternary (Pleistocene) older Alluvium, underlying low to medium-high terraces along modern streams and in undissected old alluvial fans
Qoa2 = Quaternary (Pleistocene) older Alluvium, underlying higher terraces and in extensive older alluvial fans
Qoa1 = Quaternary (Pleistocene) older Alluvium, underlying dissected remnants of oldest alluvial fans
QTkr = Tertiary to Quaternary (Upper Miocene, Pliocene and Pleistocene) Kern River Formation – Nonmarine, coarse-grained pebbly arkosic sandstone and conglomerate, containing thin interbeds of drab-colored siltstone and mudstone

NOTES:
1. WGS 1984 COORDINATE SYSTEM
2. Geologic Map of the Southeastern Margin of the San Juaquin Valley, California by J. Alan Bartow, 1984
3. See site map for details of geophysical survey

File Name: CI-VES

Date: 4/12/2012

USGS science for a changing world

GEOVision geophysical services

GEOLOGIC MAP
CI•VES

RECOVERY.GOV

Looking southwest at MASW array VES-1, HVSR sensor 450 and CI.VES seismic station

Looking southeast along SASW array VES-1

Looking southeast along MASW array VES-1 and at seismic station

Looking west along MASW array VES-2

Looking east at MASW array VES-3

Location of Geophysical Testing Arrays:

Location	Latitude	Longitude
VES-1, Northwest End of MASW Array	35.84107	-119.08488
VES-1, Center of MASW and SASW Arrays	35.84087	-119.08457
VES-1, Southeast End of MASW Array	35.84067	-119.08428
VES-2, West End of MASW Array	35.84008	-119.08539
VES-2, Center of MASW Array	35.84010	-119.08513
VES-2, East End of MASW Array	35.84012	-119.08487
VES-3, South End of MASW Array	35.84069	-119.08690
VES-3, Center of MASW Array	35.84090	-119.08688
VES-3, North End of MASW Array	35.84111	-119.08685
HVSR Sensor 450	35.84103	-119.08480
HVSR Sensor 453	35.84086	-119.08457
HVSR Sensor 507	35.84069	-119.08430
CI.VES Seismic Station	35.84088	-119.08489

Notes: 1) WGS84 Coordinate System (decimal degrees)
2) Survey accuracy is estimated at 1 to 2 m.

Results:

V_S Model – MASW Array VES-1

Depth to Top of Layer (m)	Layer Thickness (m)	S-Wave Velocity (m/s)	Inferred P-Wave Velocity (m/s)	Assumed Poisson's Ratio	Assumed Density (g/cm^3)
0	1	115	216	0.300	1.6
1	2	182	341	0.300	1.7
3	3	283	530	0.300	1.8
6	3	455	851	0.300	1.9
9	18	527	987	0.300	2.0
27	>8	553	1034	0.300	2.0

Notes: 1) Depth of investigation is about 35 m.
2) Bottom layer is a half space.

Observations/Discussion:

- During acquisition of SASW and MASW data along array VES-1, possible dominant higher mode Rayleigh waves were observed over a wide frequency range. Therefore, MASW data were acquired along two other arrays (VES-2 and VES-3) to confirm that this was not a localized issue. Array VES-2 was located at about the same elevation as array VES-1 and reduction of MASW data obtained almost identical fundamental mode and higher mode Rayleigh wave data as array VES-1. Array VES-3 was located at a ground surface elevation 2 to 3 m lower than arrays VES-1 and VES-2. A hard pan layer was observed at the surface and it is, therefore, possible that a very thin high velocity layer at a depth of 2 to 3 m is the geologic feature complicating interpretation of the surface wave data collected along array VES-1. A steep velocity gradient at relatively shallow depth could also excite dominant higher modes at intermediate wavelengths. Array VES-3 also has significant issues with a dominant higher mode, but the higher mode differs from that observed on arrays VES-1 and VES-2. Only surface wave data collected along array VES-1 were modeled.
- HVSR plots are very similar below a frequency of 10 Hz with a high amplitude HVSR peak at 0.23 Hz, which is consistent for a deep sedimentary basin. There is a possible weak HVSR peak at variable frequencies in the 14 to 20 Hz range. If this HVSR peak were to have a geologic source, it could be associated with a structure at a depth of several meters.
- Noise conditions at site were not sufficient to apply passive surface wave techniques.
- Reduction of the SASW and MASW data acquired along array VES-1 was complicated by dominant higher mode Rayleigh wave energy. The fundamental mode is clearly identifiable in the MASW data at low frequencies (long wavelengths) and possibly clear at high frequencies (small wavelengths), but difficult to recover at intermediate frequencies/wavelengths. We believe that we were able to recover the fundamental mode at intermediate frequencies using limited offset receiver arrays from some shot locations. For similar reasons, SASW data reduction was also difficult and SASW data reduction focused on identifying only the fundamental mode. The probable fundamental mode dispersion curves interpreted from both SASW and MASW data are almost identical and, therefore, only the MASW dispersion curve was modeled.
- MASW data collected along arrays VES-2 and VES-3 were not modeled because the arrays were conducted to verify that the geologic complexities beneath array VES-1 were not localized. The fundamental mode and higher mode dispersion data for array VES-2 is almost identical to array VES-1. VES-3 also has issues with dominant higher modes with the fundamental mode dispersion data being almost identical to the other arrays, but the higher mode(s) being different. This array was located at an elevation about 2 to 3 m lower than that at arrays VES-1 and VES-2 and had a hard pan layer at the surface, which could be one of the geologic features complicating data interpretation.
- The near field criteria generally applied during this investigation was relaxed somewhat to obtain more dispersion data at intermediate wavelengths. The maximum wavelength was set equal to the smaller of 75 m or 1.3 times the distance between the source and midpoint of the receiver array.
- The minimum wavelength surface wave phase velocity data extracted from the 48-channel MASW array is about 17 m. Data reduction using seismic records from smaller

hammer sources and a limited offset receiver array (i.e. less active geophones) allowed extraction of surface wave dispersion data to a minimum wavelength of about 2 m.

- There is nominally about 50 m/s scatter in the MASW dispersion data likely due to lateral velocity variation.
- A representative dispersion curve was generated for the MASW data set using a moving average, polynomial curve fitting routine and used for modeling.
- Unsuccessful attempts were made at multi-mode modeling in order to identify the location and velocity of the possible shallow high velocity layer or other feature exciting dominant higher modes. It may be a very time consuming process to try and model a possible high velocity layer if it is thin relative to depth, there are multiple thin high velocity layers, or if the potential high velocity layer(s) are laterally variable.
- Although only the fundamental mode dispersion curve was modeled, resulting in no high velocity layers in the final V_S model, the general velocity structure is likely relatively accurate and V_{S30} is accurate.
- Subsequent modeling indicated that the fundamental mode V_S model should excite a dominant first higher mode at intermediate frequencies. Of course, the addition of a thin high velocity layer to the model would significantly affect the relative amplitude of the higher mode Rayleigh waves. It is likely that the combination of a possible, thin high velocity layer and a steep velocity gradient give rise to the observed dominant higher mode(s) at intermediate frequencies.
- Although arrays VES-2 and VES-3 were not modeled, the fundamental mode dispersion curves are almost identical to array VES-1 and, therefore, the velocity structure is similar.
- Surface wave depth of investigation is about 35 m based on half of maximum wavelength criteria.
- Although P-wave seismic refraction data were not acquired at this site, the MASW seismic records were reviewed to determine shallow P-wave velocity structure. Near surface P-wave velocities are typically higher than those in the MASW V_S model indicating that either Poisson's ratio is higher than the assumed value of 0.3 or there is a shallow high velocity layer that has not been resolved by the surface wave model.
- V_{S30} is 393 m/s (NEHRP Site Class C).
- The average V_S between 2 and 32 m, to account for assumed 2 m sensor depth, is 456 m/s (NEHRP Site Class C).
- It is possible that successful implementation of multi-mode modeling would refine the V_S model, but would probably not significantly change V_{S30}.

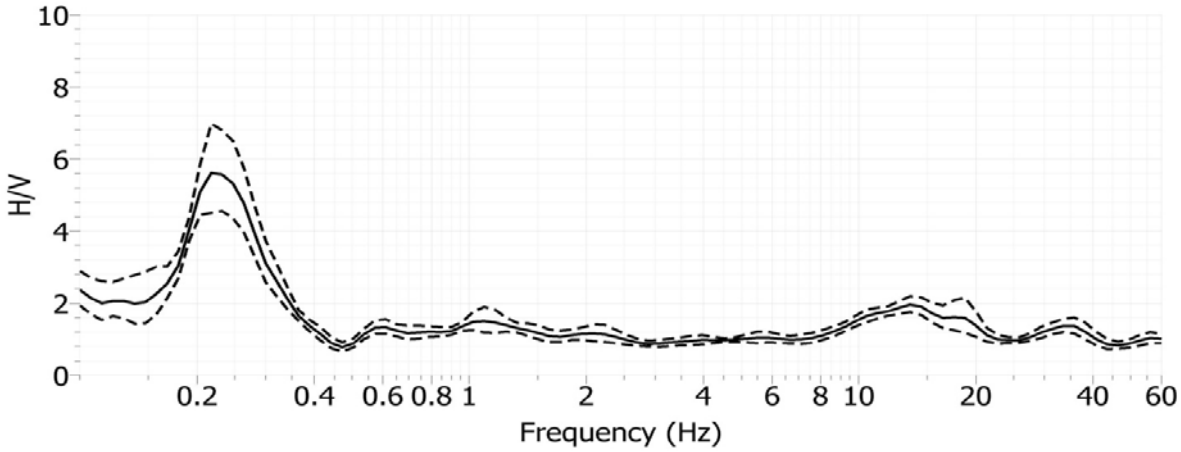

Site CI.VES, H/V Spectral Ratio, Array VE -1, Sensor 450

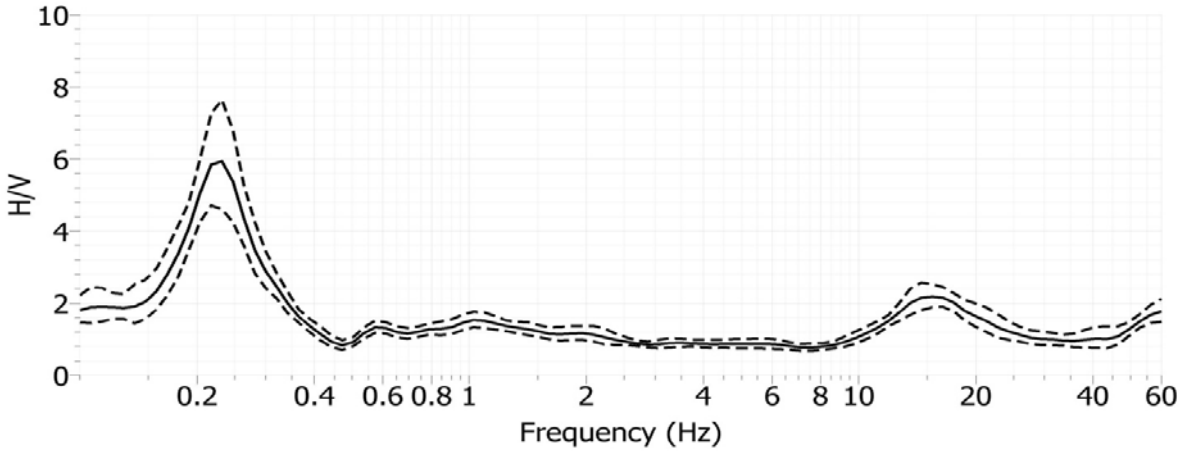

Site CI.VES, H/V Spectral Ratio, Array VES-1, Sensor 453

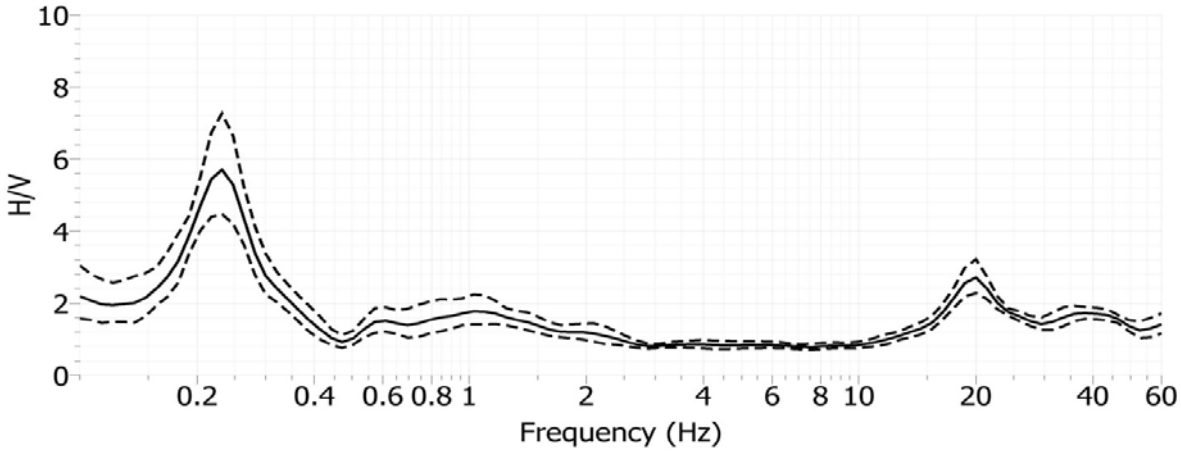

Site CI.VES, H/V Spectral Ratio, Array VES-1, Sensor 507

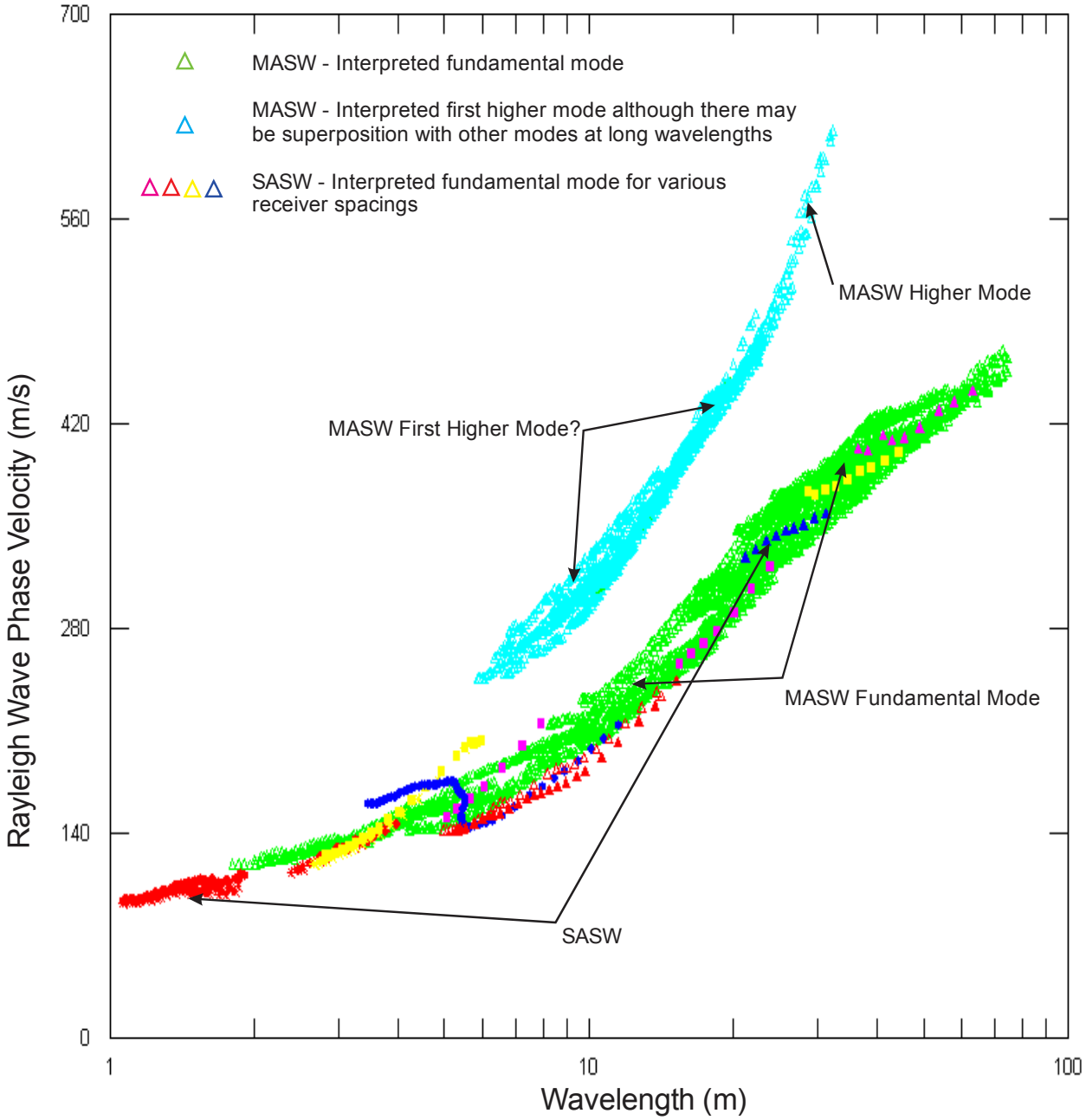

CI.VES – Reduced MASW and SASW data acquired along array VES-1. It was difficult to reduce MASW and SASW data due to a dominant higher mode at small wavelengths (high frequencies), possibly associated with a shallow, thin high velocity layer. SASW data were reduced with focus on extracting the fundamental mode, but there are still higher mode artifacts in the 4 to 10 m wavelength range. It was very difficult to extract the fundamental mode at intermediate frequencies from the MASW data. The fundamental mode Rayleigh wave phase velocity data interpreted from the MASW and SASW data are in very good agreement and only the MASW data were inverted to develop a V_S model. To date, we have not been successful at developing a V_S model that fits both the fundamental mode and higher mode(s).

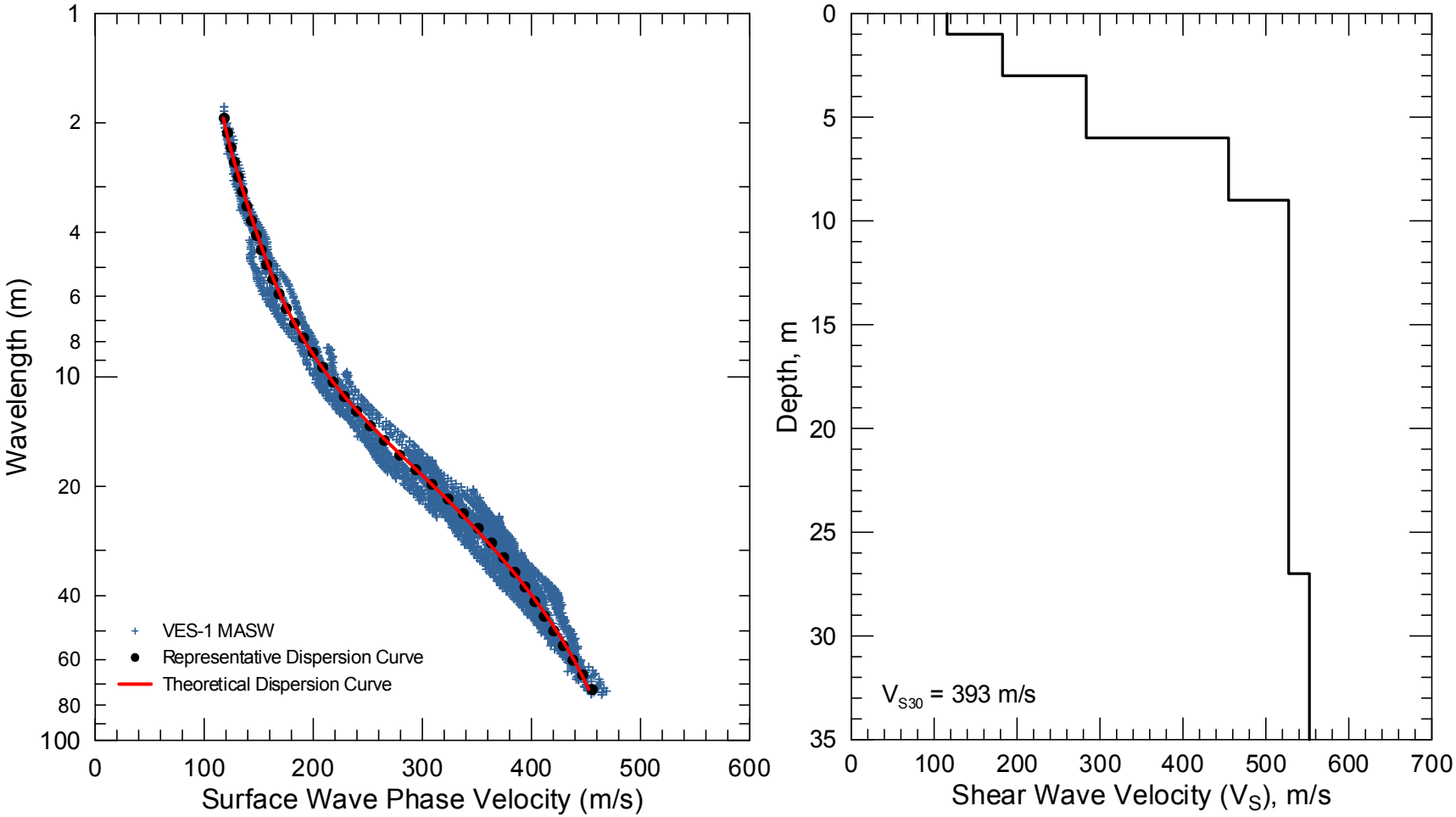

CI.VES - Field, representative and inverted theoretical surface wave dispersion data (left) and associated V_S model (right)

Site CI.VOG

Location: Valley Oaks Golf Course, Visalia, California

Latitude: 36.32097 **Longitude:** -119.38224
(Station coordinates modified based on field GPS survey, WGS84 coordinate system)

V_{S30} (measured): 341 m/s

V_{S30} (adjusted to more accurately reflect seismic station conditions): 358 m/s (average S-wave velocity between 1 and 31 m adjusting for 1 m assumed sensor depth).

NEHRP Site Class: D/C

Geomatrix Code: IHD

Geologic Conditions/Observations: Site located in area mapped as Quaternary (Holocene) alluvium, although there may be some artificial fill overlying alluvium. Expected deep soil site.

Site Conditions: Rural-Suburban site with significant noise from nearby golf course and maintenance yard. Relatively flat terrain in site vicinity.

Geophysical Methods Utilized: HVSR, MASW, array microtremor, ReMi™

Geophysical Testing Arrays:

1. Arrays VOG-1 (24 channel linear array utilizing 4.5 Hz and 1 Hz vertical geophones spaced 4 m apart for an array length of 92 m) and VOG-2 (24 channel linear array utilizing 4.5 Hz and 1 Hz vertical geophones spaced 3 m apart for an array length of 69 m) used to acquire passive surface wave data. Arrays combined to form an "L" shaped array.
2. Passive surface wave data also acquired along arrays VOG-1 and 2 using a 9 channel "L" array with 1-Hz geophones.
3. Array VOG-3 (48 channel MASW array utilizing 4.5 Hz vertical geophones spaced 1.5 m apart for a length of 70.5 m, forward and reverse shot locations with multiple source offsets and source types [hammers only at request of golf course staff] and center shot location).
4. Three HVSR measurement locations; two distributed along array VOG-3, one adjacent the seismic station.

Legend

- Seismic Station - Approximate Surveyed Location
- Seismic Station - Approximate Location of Record
- H/V Spectral Ratio Location
- MASW Array
- Passive Surface Wave Array

NOTES:
1. WGS 1984 COORDINATE SYSTEM
2. Image Source: ESRI, i-cubed, USDA FSA, USGS, AEX, GeoEye, Getmapping, Aerogrid, IGP

File Name: CI-VOG-I

Date: 9/16/2011

USGS science for a changing world

GEOVision geophysical services

RECOVERY.GOV

SITE MAP
CI•VOG

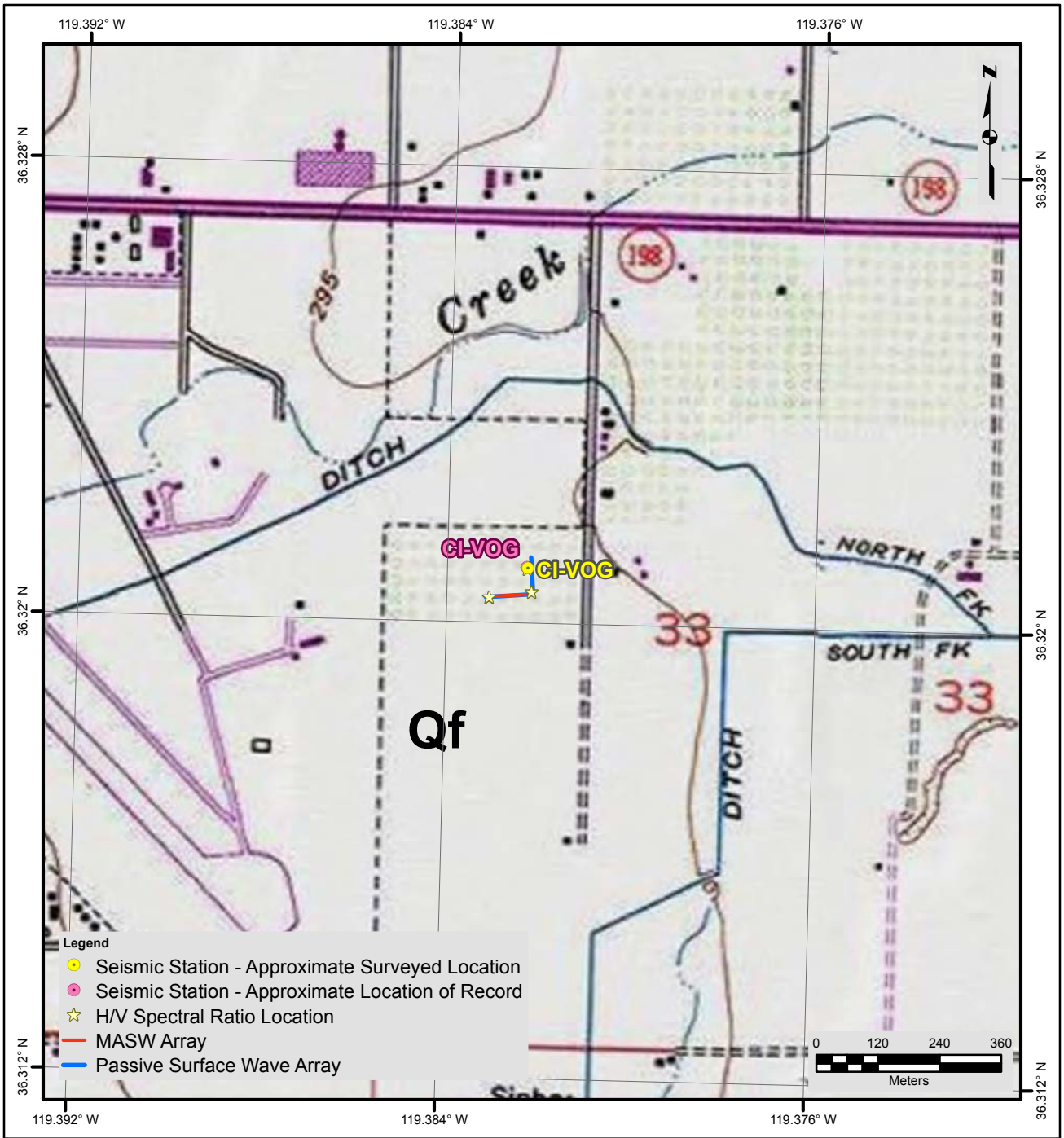

Description of Geologic Map Units

Qf = Quaternary (Holocene) alluvial fan deposits of the Great Valley

NOTES:
1. WGS 1984 COORDINATE SYSTEM
2. Geologic units from Geologic Map of California (Olaf P. Jenkins edition), Fresno Sheet compiled by Robert A Matthews and John L. Burnett, 1965; Topographic imagery from ESRI ArcGIS Online and data partners including USGS and © 2007 National Geographic Society
3. See site map for details of geophysical survey

File Name: CI-VOG

Date: 9/22/2011

USGS science for a changing world

GEOVision geophysical services

RECOVERY.GOV

GEOLOGIC MAP
CI•VOG

HVSR measurements near CI.VOG seismic station

Looking south along passive surface wave array VOG-2

Looking west along passive surface wave array VOG-1

MASW data acquisition along array VOG-3

Looking east long MASW array VOG-3

Location of Geophysical Testing Arrays:

Location	Latitude	Longitude
VOG-1, West End of Array	36.32044	-119.38314
VOG-1, East End of Array	36.32051	-119.38212
VOG-2, South End of Array	36.32053	-119.38212
VOG-2, North End of Array	36.32116	-119.38218
VOG-3, West End of MASW Array	36.32045	-119.38307
VOG-3, Center of MASW Array	36.32047	-119.38268
VOG-3, East End of MASW Array	36.32050	-119.38229
HVSR Sensor 450	36.32095	-119.38225
HVSR Sensor 453	36.32055	-119.38215
HVSR Sensor 507	36.32044	-119.38307
CI.VOG Seismic Station	36.32097	-119.38224

Notes: 1) WGS84 Coordinate System (decimal degrees)
2) Survey accuracy is estimated at 1 to 2 m

Results:

V_S Model

Depth to Top of Layer (m)	Layer Thickness (m)	S-Wave Velocity (m/s)	Inferred P-Wave Velocity (m/s)	Assumed Poisson's Ratio	Assumed Density (g/cm^3)
0	0.75	163	305	0.3	1.8
0.75	1.75	245	458	0.3	1.8
2.5	5.5	283	529	0.3	1.9
8	14	310	579	0.3	1.9
22	>13	692	1295	0.3	2.1

Notes: 1) Depth of investigation is about 35 m.
2) Bottom layer is a half space.

Observations/Discussion:

- The HVSR curves are almost identical with multiple peaks over a wide frequency range, validating the 1-D velocity structure assumption.
- There is a high amplitude HVSR peak at about 0.18 Hz, which is consistent for a very deep sedimentary basin. This HVSR peak is not well resolved due to low frequency noise. Acquisition of HVSR data for a longer duration at night, with particular attention paid to sensor coupling, would improve the low frequency HVSR data.
- There are low amplitude, broad, secondary HVSR peaks at about 0.9 and 3.9 Hz. The HVSR peak at 3.9 Hz is likely associated with a geologic structure within the depth of investigation of the surface wave testing.
- Seismic data acquisition was limited to the use of hammer sources at the request of maintenance personnel at the golf course. This was expected to limit depth of investigation of the MASW sounding and also result in higher noise levels in the seismic refraction first arrivals.
- Based on simple horizontal layer-based analysis of seismic refraction first arrival data, P-wave velocity in the upper 20 m ranges from about 400 to over 1,000 m/s (about 2 to 3 m of sediments with velocity in the 400 to 450 m/s range overlying sediments with velocity in the 500 to 600 m/s range, which are underlain by a high velocity layer at a depth of 18 to 25 m with velocity in the 1,000 to 1,500 m/s range). The depth and velocity of the deeper layer are not well constrained due to high noise levels at the site, limited offset and possible complicated velocity structure (thin high velocity layers, etc.).
- Noise conditions at site (multi-directional or omni-directional noise sources) appeared sufficient for successful application of passive surface wave techniques. The northwest trending Hwy 99 is located about 1.2 km west of the site, Sierra Blvd. about 500 m north of the site and the city of Visalia located east of the site. There was also some activity on the golf course.
- ESAC technique used to extract surface wave dispersion data from 48-channel passive "L" array data. Both the ReMi™ and ESAC techniques used to extract surface wave dispersion data from the linear arrays. The 9-channel "L" array data was not useful at this site. Almost all of the 24-channel linear array and 48-channel "L" array passive surface wave data were used for modeling.
- The passive surface wave data did not provide useful surface wave dispersion data below a frequency of 4.5 Hz and did not significantly extend depth of investigation beyond what is normally achieved with the MASW or SASW technique. However, the passive surface wave data was needed at this site as MASW data acquisition was limited to a 20 lb sledge hammer as the largest energy source, which is not adequate to image to a depth of 30 m.
- Although not usable, passive surface wave data at low frequencies may imply that there is an S-wave velocity inversion below the depth modeled.
- Surface wave phase velocity data were not extracted at frequencies below 7.5 Hz from the MASW data acquired with a 20 lb sledge hammer.
- There was significant variation in Rayleigh wave phase velocity data that were extracted from MASW seismic records with a limited receiver offset range at wavelengths below 5 m. This is most likely the result of near surface lateral velocity variation and selective use of small wavelength MASW phase velocity data was required to form a coherent dispersion curve.

- SASW analysis was conducted on selected MASW receiver pairs with small spacing in an attempt to obtain surface wave dispersion data at small wavelengths/higher frequencies.
- Surface wave dispersion data from active and passive surface wave data sets are in good agreement at this site.
- Representative dispersion curves were generated for each surface wave data set using a moving average, polynomial curve fitting routine. These individual representative dispersion curves were combined and a representative dispersion curve generated for the combined data set for data modeling.
- Surface wave model is consistent with simplified P-wave refraction model considering unknown Poisson's ratio.
- The S-wave velocity of the bottom layer is not well constrained.
- Based on observations of low frequency passive surface wave data, that could not be utilized, and multiple HVSR peaks, it should be assumed that there is a velocity inversion at some depth below the high velocity layer at the base of the S-wave velocity model.
- A synthetic HVSR peak of about 3.5 Hz would be associated with the S-wave velocity model, reasonably close to the observed 3.9 Hz peak. The HVSR data would better match the S-wave velocity model if the high velocity layer at the bottom of the model was a couple meters shallower.
- Surface wave depth of investigation is about 35 m based on half of maximum wavelength criteria.
- V_{S30} is 341 m/s (Site Class D).
- Average S-wave velocity between 1 m (assumed sensor depth) and 31 m is 358 m/s (Site Class D/C).

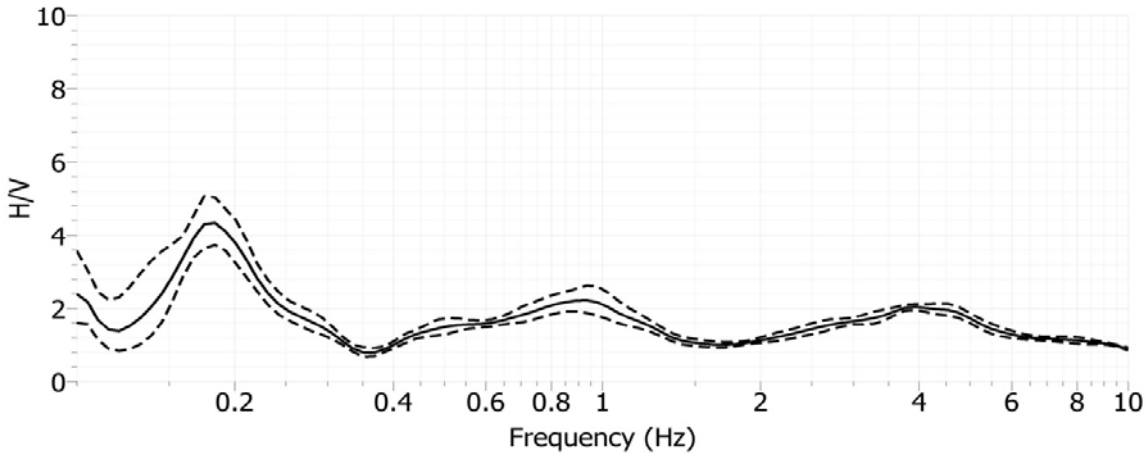

Site CI.VOG, H/V Spectral Ratio, Near Seismic Station, Sensor 450

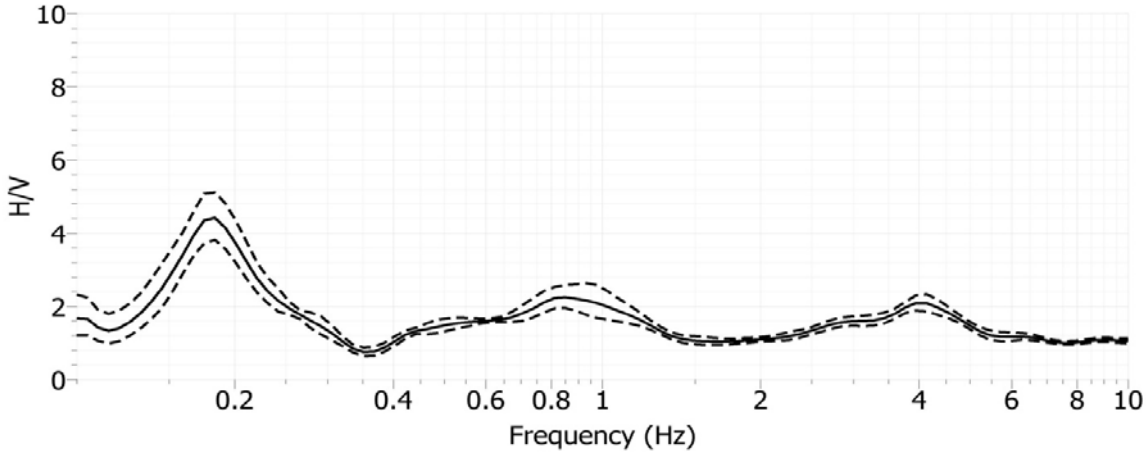

Site CI. VOG, H/V Spectral Ratio, Array VOG -1, Sensor 507

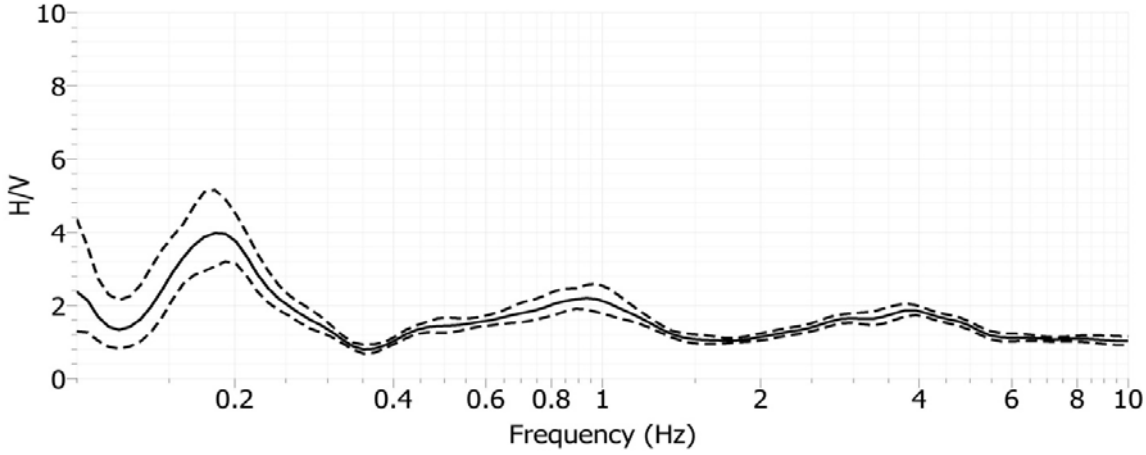

Site CI. VOG, H/V Spectral Ratio, Array VOG -1, Sensor 453

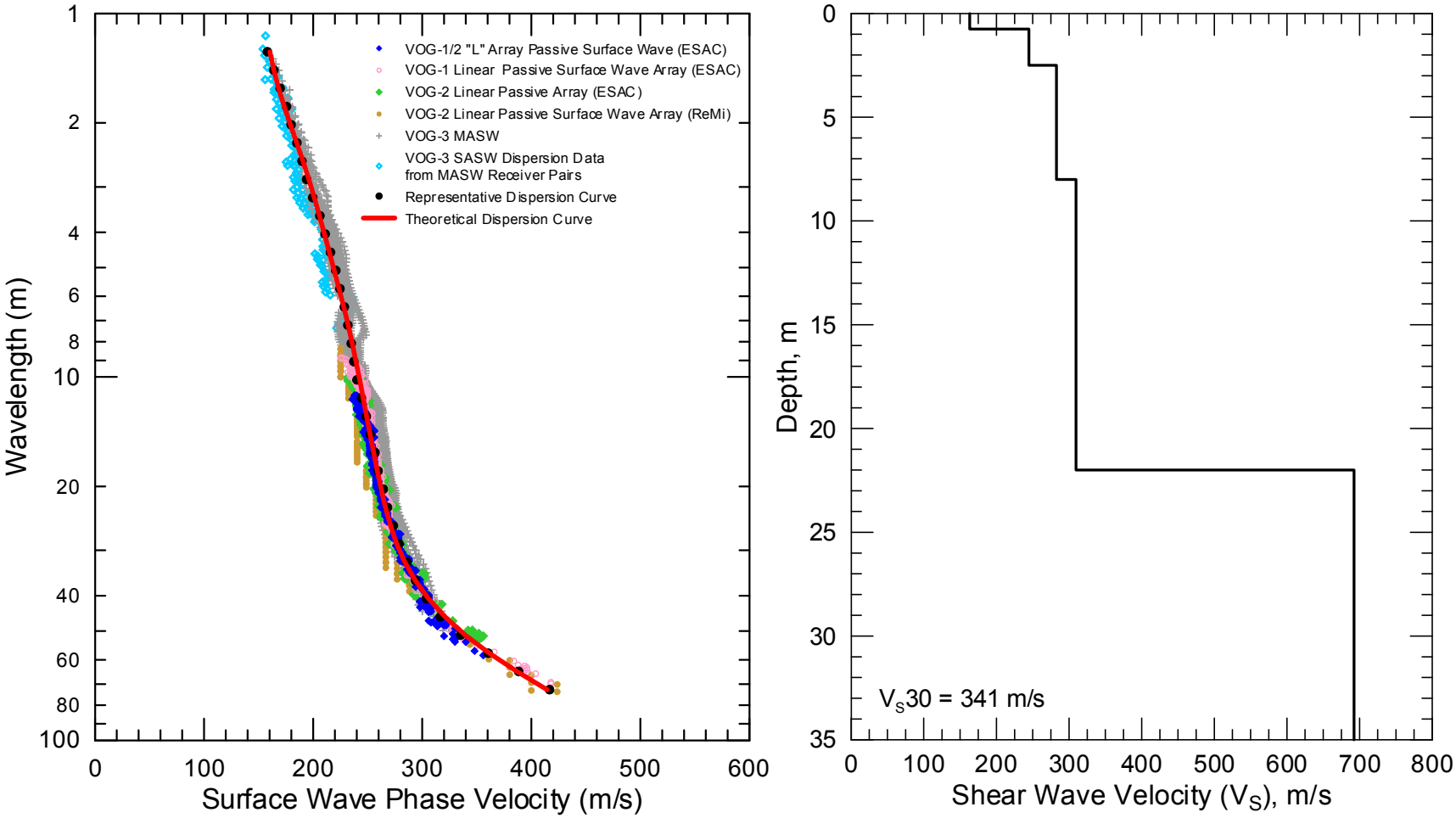

CI.VOG - Field, representative and inverted theoretical surface wave dispersion data (left) and associated V_S model (right)

Site CI.WBS

Location: Bird Spring Pass, Kern County, California

Latitude: 35.53664 **Longitude:** -118.14035
(Station coordinates provided by USGS, WGS84 coordinate system)

V_{S30} (measured): 402 m/s

V_{S30} (adjusted to more accurately reflect seismic station conditions): 426 m/s (average S-wave velocity between 1 and 31 m adjusting for inferred 1 m sensor depth).

NEHRP Site Class: C

Geomatrix Code: IGA

Geologic Conditions/Observations: Seismic station located on weathered Mesozoic granitic rocks.

Site Conditions: Rural site. Seismic station located on flat mountain top near communications antennas. Test area located on a relatively planar surface along a ridge with relatively steep topography to the sides.

Geophysical Methods Utilized: HVSR, Seismic Refraction, MASW

Geophysical Testing Arrays:

1. Array WBS-1 (48 channel MASW and P-wave seismic refraction array utilizing 4.5 Hz vertical geophones spaced 1.5 m apart for a length of 70.5 m, forward and reverse shot locations with multiple source offsets and source types and multiple interior shot locations).
2. Three HVSR measurement locations distributed along array WBS-1.

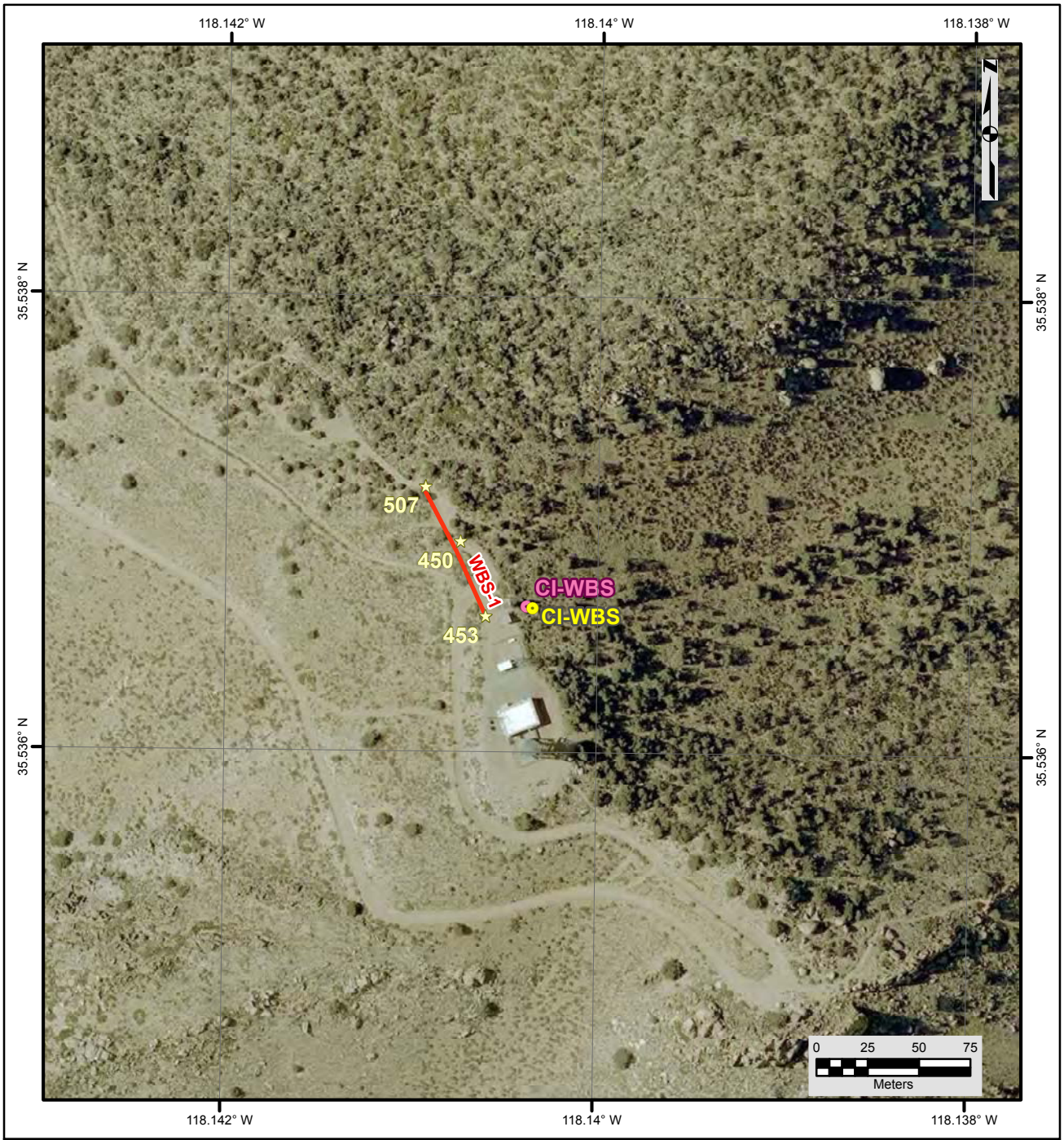

Legend

- Seismic Station - Approximate Surveyed Location
- Seismic Station - Approximate Location of Record
- H/V Spectral Ratio Location
- MASW and Seismic Refraction Array

NOTES:
1. WGS 1984 COORDINATE SYSTEM
2. Image Source: ESRI, i-cubed, USDA FSA, USGS, AEX, GeoEye, Getmapping, Aerogrid, IGP

File Name: CI-WBS-I

Date: 11/15/2012

USGS science for a changing world

GEOVision geophysical services

RECOVERY.GOV

SITE MAP
CI•WBS

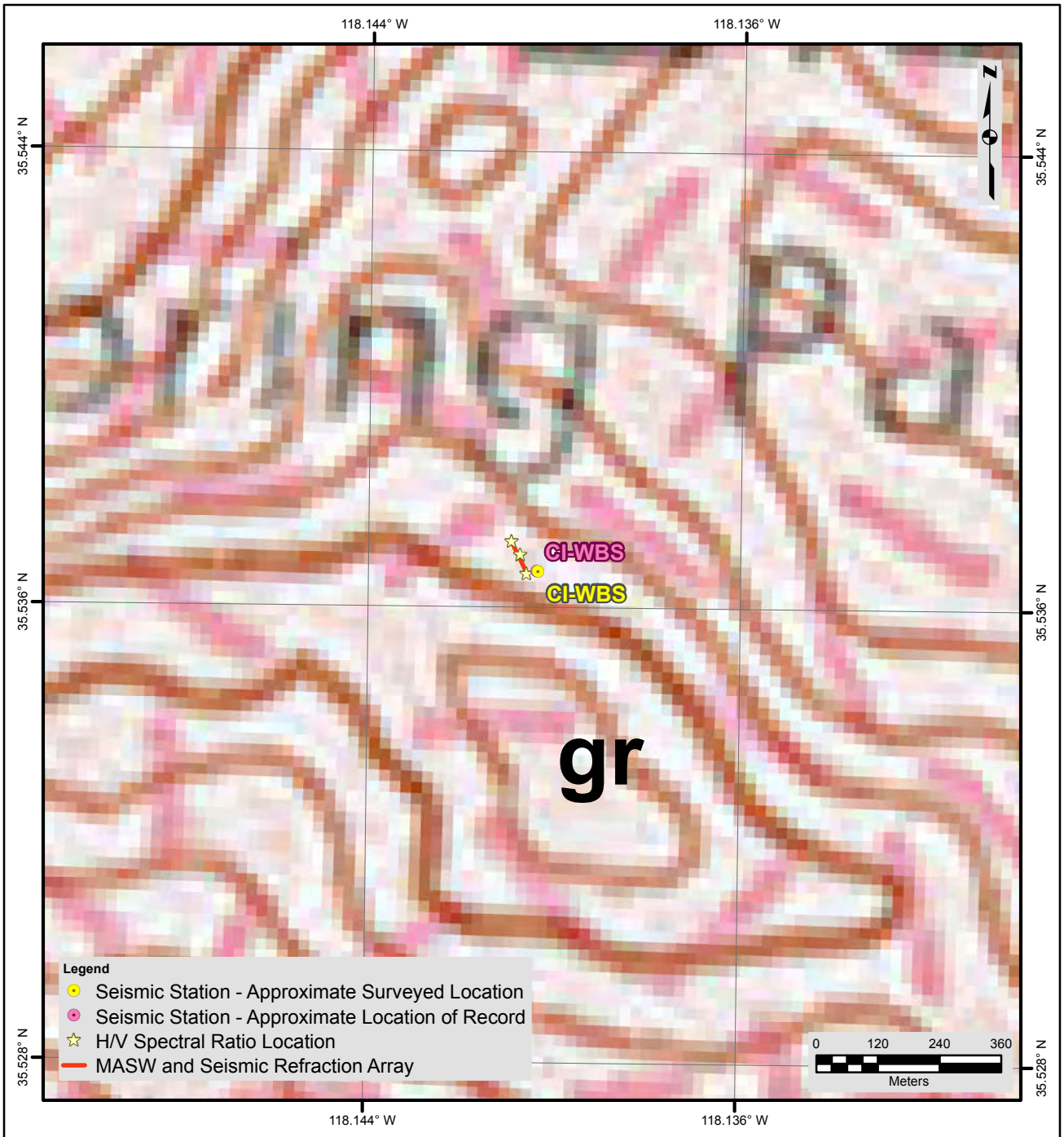

Description of Geologic Map Units

gr = Mesozoic (Cretaceous) granitic rocks

NOTES:
1. WGS 1984 COORDINATE SYSTEM
2. Geologic Map of California (Olaf P. Jenkins Edition), Bakersfield Sheet
compilation by Arthur R. Smith, 1964
3. See site map for details of geophysical survey

File Name: CI-WBS

Date: 10/14/2011

USGS science for a changing world

GEOVision geophysical services

RECOVERY.GOV

GEOLOGIC MAP
CI•WBS

Looking towards CI.WBS seismic station and test area

CI.WBS seismic station

Looking southeast towards center of array WBS-1 and HVSR sensor 450

Looking northwest along array WBS-1 and at HVSR sensor 453

Looking northwest along array WBS-1

Location of Geophysical Testing Arrays:

Location	Latitude	Longitude
WBS-1, Southeast End of MASW/Refraction Array	35.53660	-118.14057
WBS-1, Center of MASW/Refraction Array	35.53688	-118.14073
WBS-1, Northwest End of MASW/Refraction Array	35.53716	-118.14091
HVSR Sensor 450	35.53692	-118.14071
HVSR Sensor 453	35.53660	-118.14057
HVSR Sensor 507	35.53716	-118.14090
CI.WBS Seismic Station	35.53663	-118.14032

Notes: 1) WGS84 Coordinate System (decimal degrees)
2) Survey accuracy is estimated at 1 to 2 m.

Results:

V_S Model

Depth to Top of Layer (m)	Layer Thickness (m)	S-Wave Velocity (m/s)	Inferred P-Wave Velocity (m/s)	Assumed Poisson's Ratio	Assumed Density (g/cm^3)
0	1	178	332	0.3	1.7
1	2.5	315	590	0.3	1.8
3.5	4.5	366	685	0.3	1.9
8	7	385	720	0.3	1.9
15	7	418	782	0.3	2.0
22	7	562	1051	0.3	2.0
29	>6	726	1358	0.3	2.1

Notes: 1) Depth of investigation is about 35 m.
2) Bottom layer is a half space.

Observations/Discussion:

- Geologic conditions at the site, based on field observations, consist of a thin layer of sediments over weathered granitic rock. The seismic station is located on a mountain top and the seismic line was placed in an area where then ridge has the greatest width. There are no possible alternate test locations at this site. Seismic station likely placed directly on weathered granitic rock.
- HVSR sensors 450 and 507 have the best quality data. HVSR sensor 453 appears to have noise over a wide frequency range centered at 1 Hz, possibly associated with poor sensor coupling. HVSR data for sensors 450 and 507 are similar with no significant peaks. The utilization of HVSR data on a mountain peak site such as this is unclear.
- The P-wave refraction data for array WBS-1 were modeled using a tomographic inversion routine with a smooth velocity gradient starting model. The seismic refraction

data were modeled by extending the model to far offset shot locations. Extending the model to far offset shot locations allowed depth of investigation to be increased to validate the surface wave model at depth. A longer receiver array is preferred for extending depth of investigation, but at the expense of the efficiency in combining seismic refraction and MASW data acquisition along the shorter array.

- The seismic refraction survey design allowed P-wave velocity to be imaged to a maximum depth of over 20 m. The seismic refraction model shows that P-wave velocity is about 350 to 500 m/s at the surface, increasing to 600 m/s at a depth of 1 to 4 m, 800 m/s at a depth of 2 to 12 m and 1,000 m/s at a depth of 13 to 20 m. Utilization of far offset shot locations allowed the model to be extended to greater depth, revealing the possible presence of bedrock with P-wave velocity on the order of 1,200 m/s at nominal depths of 20 m to 27 m. It should be noted that a longer receiver array would be required to accurately image velocity structure at these depths; however, the far offset shot locations do support P-wave velocity continuing to increase with depth below 15 m.
- There is some lateral velocity variation indicated in the seismic data probably caused by a variable weathering profile along the array. The seismic model shows that less weathered (higher velocity) rock is located at shallower depth at the northwest end of array WBS-1 until about 5 m depth. However, at depths greater than 10 m, velocity structure is relatively uniform although less weathered (higher velocity) bedrock is found at slightly shallower depths on the southeast end of the array.
- Noise conditions at the site were not sufficient for application of passive surface wave techniques.
- MASW data reduction was quite difficult and source locations offset from the southeast end (forward direction) of the array generally did not provide good quality long wavelength phase velocity data. Therefore, most long wavelength Rayleigh wave phase velocity data originates from source locations offset from the northwest end of the array (reverse direction).
- There is nominally about 50 to 60 m/s scatter in MASW dispersion data, likely due to lateral velocity variation associated with both variable thickness of the sediment layer and differential weathering of near surface granitic bedrock.
- The minimum wavelength surface wave phase velocity data extracted from the 48-channel MASW array was about 7 m. Data reduction using seismic records from smaller hammer sources and a limited offset receiver array (i.e. less active geophones) allowed extraction of surface wave dispersion data to a minimum wavelength of about 2.5 m.
- A representative dispersion curve was generated for the MASW data set using a moving average, polynomial curve fitting routine and used for modeling.
- Surface wave depth of investigation is about 35 m based on half of maximum wavelength criteria.
- The inferred P-wave velocities in the surface wave model, assuming a Poisson's ratio of 0.3, are generally consistent with the seismic refraction model, although the seismic refraction model has slightly higher velocity at depths below 15 m.
- V_{S30} is 402 m/s (Site Class C).
- Average S-wave velocity between 1 m (inferred sensor depth) and 31 m is 426 m/s.

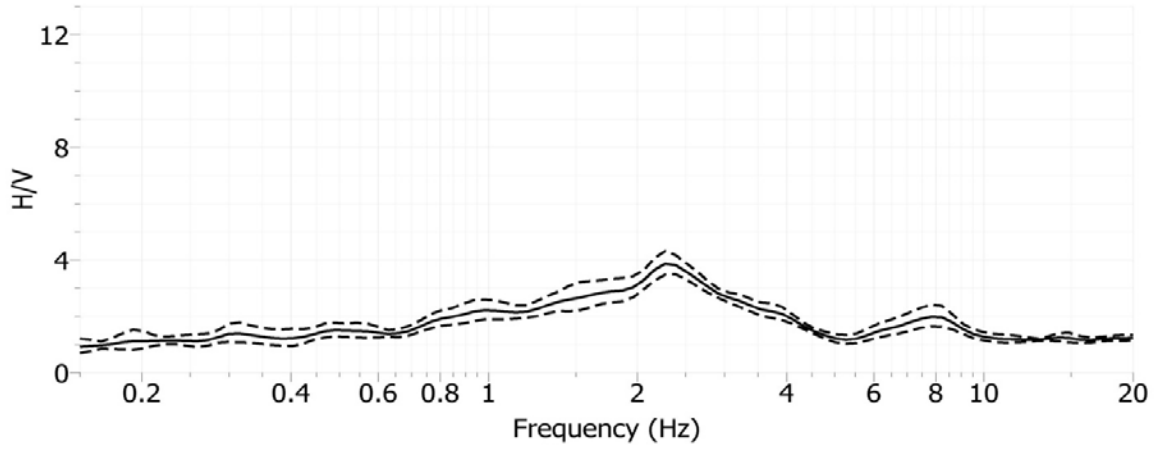

Site CI.WBS, H/V Spectral Ratio, Array WBS-1, Sensor 507

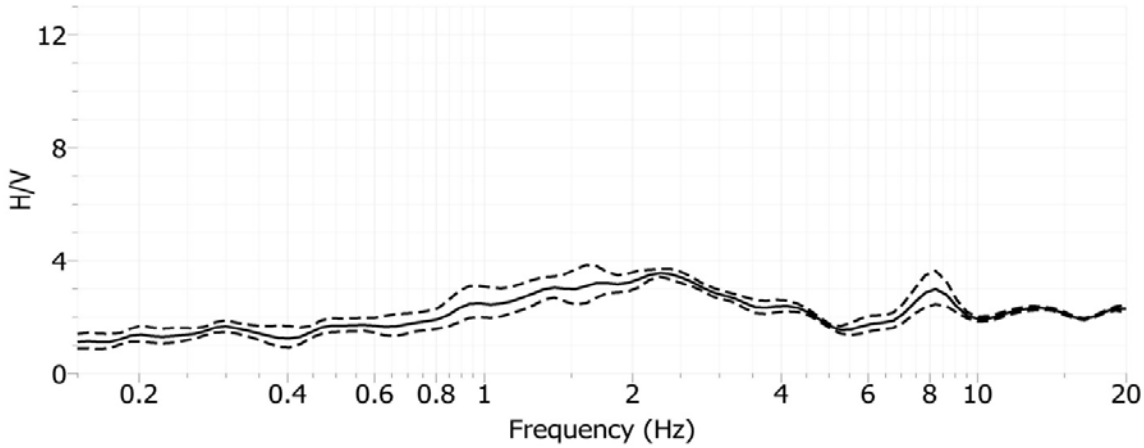

Site CI.WBS, H/V Spectral Ratio, Array WBS-1, Sensor 450

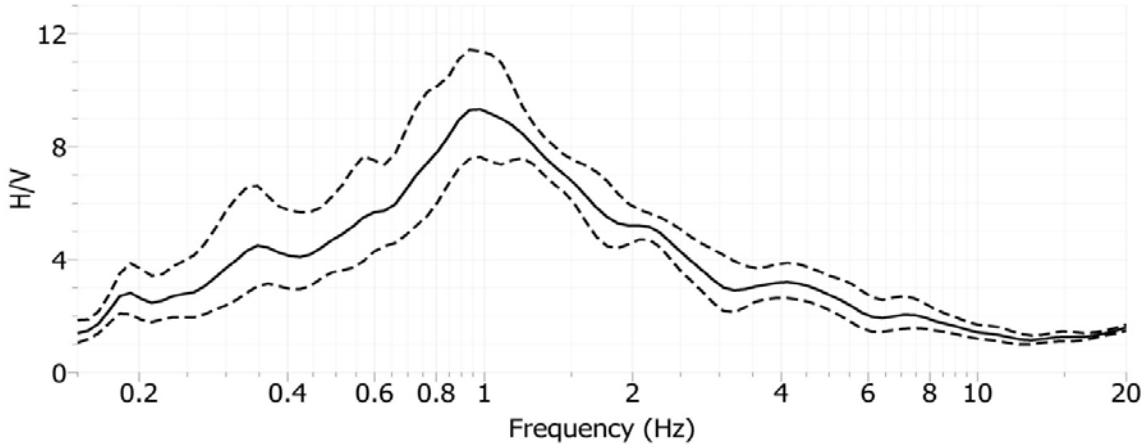

Site CI.WBS, H/V Spectral Ratio, Array WBS-1, Sensor 453 (Poor Quality)

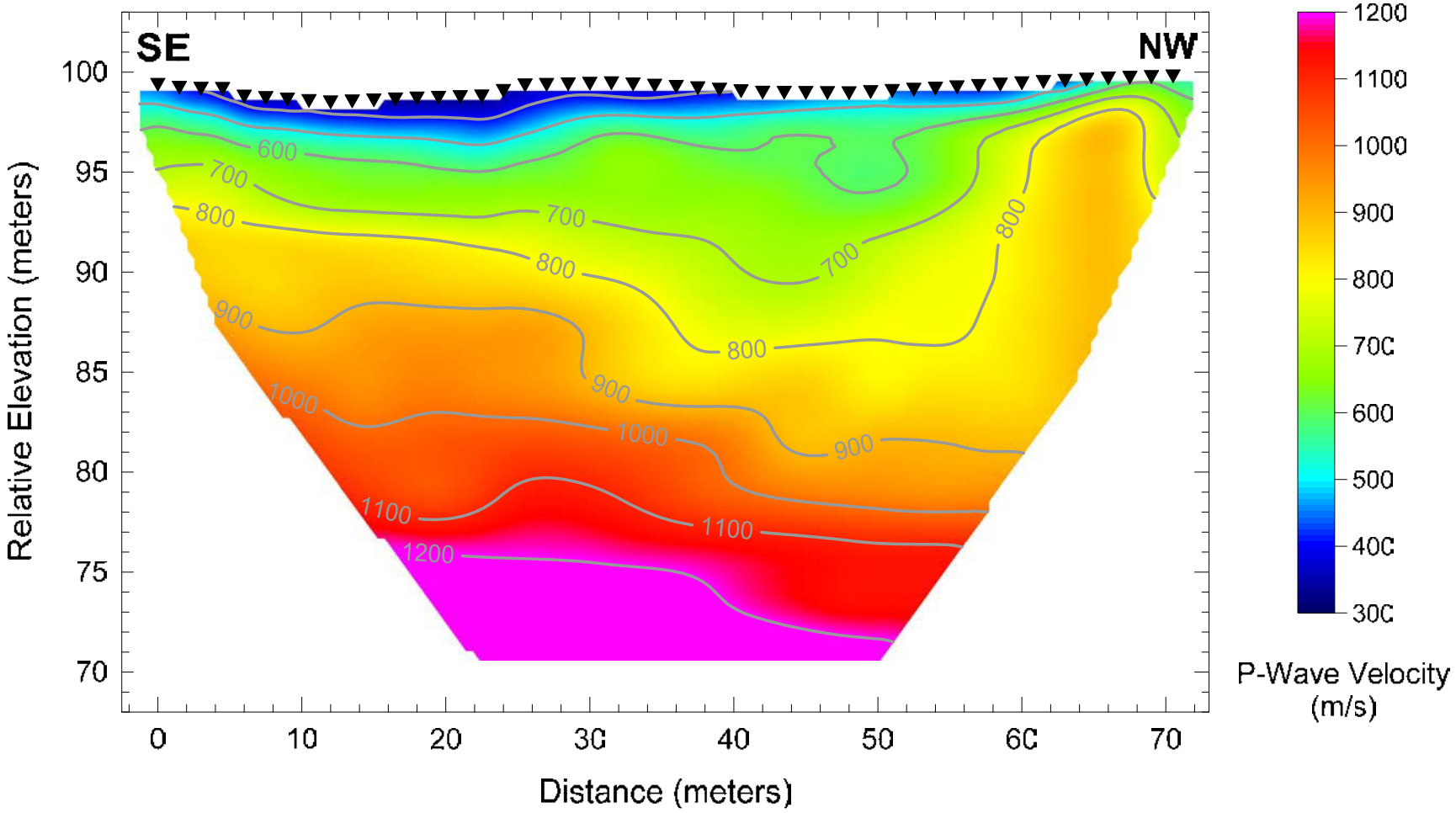

Array WBS-1 – Tomographic seismic refraction model utilizing smooth velocity gradient starting model

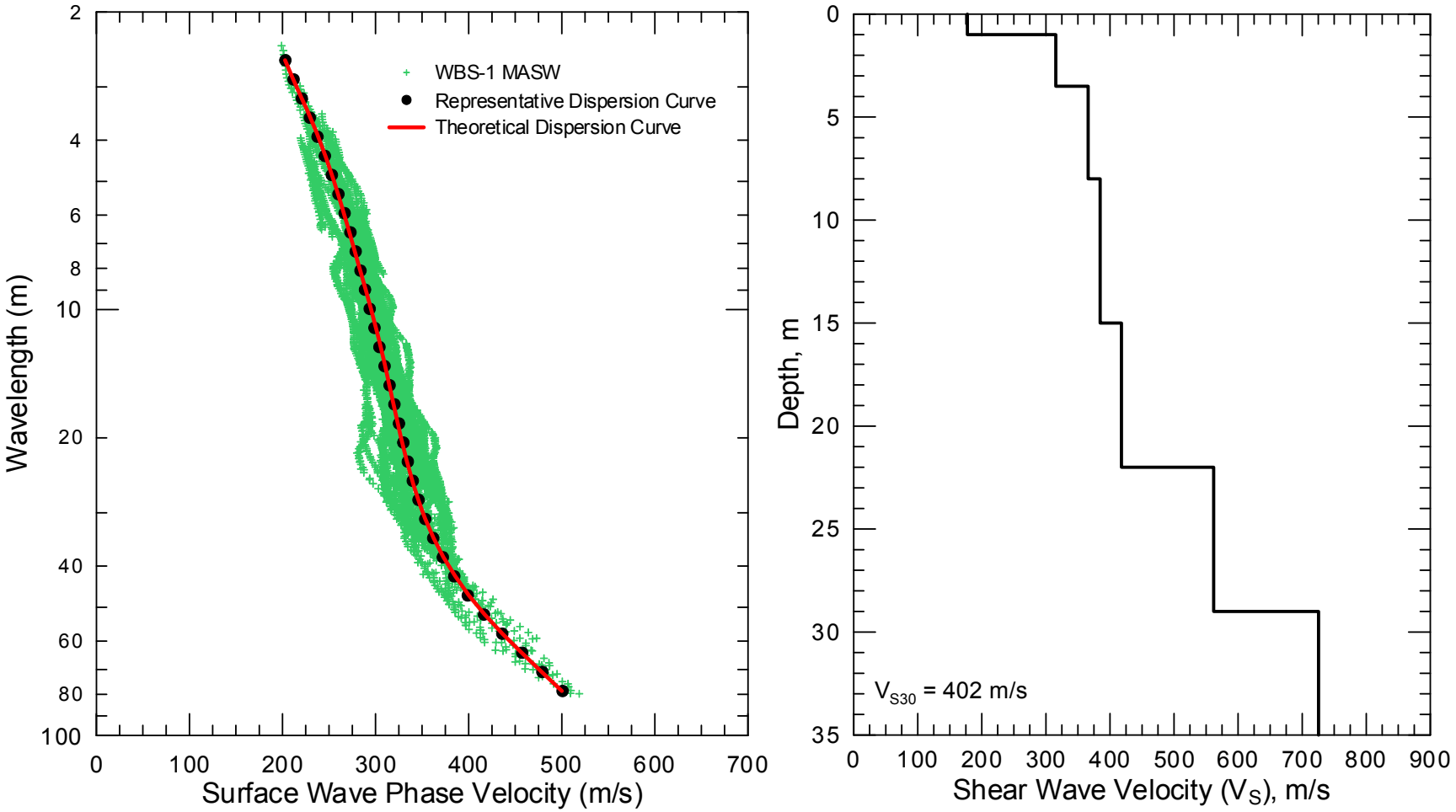

CI.WBS - Field, representative and inverted theoretical surface wave dispersion data (left) and associated V_S model (right)

Site CI.WES

Location: Westside Elementary School, El Centro, California

Latitude: 32.75905 **Longitude:** -115.73152

(Station coordinates modified based on field survey of station location)

V_{S30} (measured): 242 m/s

V_{S30} (adjusted to more accurately reflect seismic station conditions): 269 m/s (average S-wave velocity between 2 and 32 m adjusting for nominal sensor depth).

NEHRP Site Class: D

Geomatrix Code: IHD

Geologic Conditions/Observations: Site located on geologic units mapped as Quaternary (Holocene) alluvium and lake deposits of the former Lake Cahuilla. Deep soil site.

Site Conditions: Rural site. Relatively flat terrain in site vicinity with ground surface elevation gently decreasing to southwest.

Geophysical Methods Utilized: HVSR, MASW, SASW

Geophysical Testing Arrays:

1. Array WES-1 (48 channel MASW array utilizing 4.5 Hz vertical geophones spaced 1.5 m apart for a length of 70.5 m, forward and reverse shot locations with multiple source offsets and source types and center shot location).
2. Array WES-1 (SASW array with common midpoint and orientation as MASW array of same name utilizing 4.5 and 1 Hz vertical geophones and maximum receiver spacing of 32 m).
3. Array WES-2 (48 channel MASW array utilizing 4.5 Hz vertical geophones spaced 2.5 m apart for a length of 117.5 m, same midpoint as array WES-1, forward and reverse shot locations with multiple source offsets and source types and center shot location).
4. Three HVSR measurement locations; two distributed along array WES-1 and one located near seismograph station.

Legend

- Seismic Station - Approximate Location of Record
- Seismic Station - Approximate Surveyed Location
- H/V Spectral Ratio Measurement Location
- MASW and SASW Array
- MASW Array

NOTES:
1. WGS 1984 COORDINATE SYSTEM
2. Image Source: ESRI, i-cubed, USDA FSA, USGS, AEX, GeoEye, Getmapping, Aerogrid, IGP

File Name: CI-WES-I

Date: 4/27/2011

USGS science for a changing world

GEOVision geophysical services

RECOVERY.GOV

SITE MAP
CI•WES

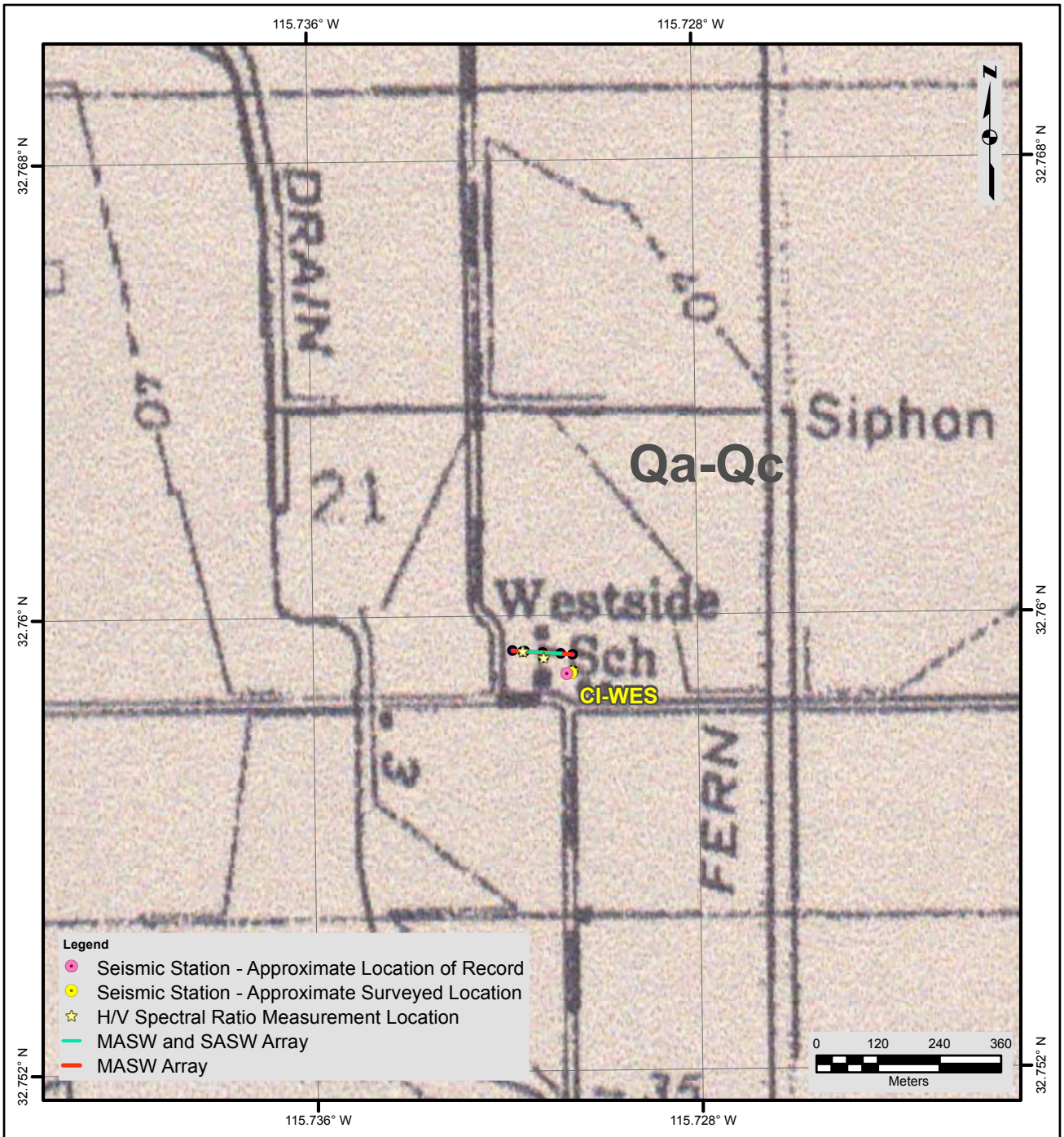

Description of Geologic Map Units

Qa = Quaternary (Holocene) alluvial sand, gravel, silt and clay of valleys area
Qc = Quaternary (Holocene) Cahuilla Beds, claystones, sands, and gravel deposits in former Lake Cahuilla, fossiliferous

NOTES:
1. WGS 1984 COORDINATE SYSTEM
2. Geologic Map of Plaster City & Brawley 15 Minute Quadrangles, Imperial County, California byThomas W. Dibblee, Jr., 2008
3. See site map for details of geophysical survey

File Name: CI-WES

Date: 4/27/2011

USGS science for a changing world

GEOVision geophysical services

GEOLOGIC MAP
CI•WES

RECOVERY.GOV

Looking west at HVSR sensor 450 and seismograph station CI.WES

Looking towards seismograph station from center of MASW arrav WES-1

Looking east along SASW array WES-1

MASW data acquisition

SASW data acquisition

Location of Geophysical Testing Arrays:

Location	Latitude	Longitude
WES-1, West End of MASW Array	32.75943	-115.73248
WES-1, Center of MASW and SASW Arrays	32.75941	-115.73211
WES-1, East End of MASW Array	32.75939	-115.73173
WES-2, West End of MASW Array	32.75945	-115.73273
WES-2, East End of MASW Array	32.75937	-115.73148
HVSR Sensor 507	32.75943	-115.73252
HVSR Sensor 453	32.75932	-115.73209
HVSR Sensor 450	32.75909	-115.73148
CI.WES Seismograph Station	32.75905	-115.73152

Notes: 1) WGS84 Coordinate System (decimal degrees)

2) Survey accuracy is estimated at 1 to 2 m

Results:

V_S Model

Depth to Top of Layer (m)	Layer Thickness (m)	S-Wave Velocity (m/s)	Inferred P-Wave Velocity (m/s)	Inferred Poisson's Ratio	Inferred Density (g/cm^3)
0	0.5	125	234	0.300	1.90
0.5	1	112	210	0.300	1.90
1.5	2	120	225	0.300	1.90
3.5	2	181	1700	0.494	2.00
5.5	4	204	1700	0.493	2.00
9.5	6	254	1700	0.489	2.00
15.5	8	313	1700	0.482	2.00
23.5	>6.5	443	1700	0.464	2.00

Observations/Discussion:

- HVSR plots are similar at all measurement locations validating the 1-D velocity structure assumption.
- Narrow HVSR peak at frequency of about 0.16 to 0.17 Hz confirming that the site is a deep soil site.
- Noise conditions at site were not sufficient to apply passive surface wave techniques.
- SASW data reduction was relatively straight forward. MASW data reduction was much more difficult due to possible dominant higher modes at low frequencies. Aggressive muting of higher mode surface waves on MASW seismic records was necessary. Muting of higher mode surface wave energy should be conducted with caution as even small changes in the mute window can have significant impacts on the dispersion curve. The presence of dominant higher modes in wavefield transforms of MASW data may indicate complex velocity structure (e.g. velocity inversion) at depth, possibly below the 30 m depth of investigation.
- The SASW and MASW experimental dispersion data utilized for analysis are in excellent agreement. Possible higher modes in MASW data, which were not considered for analysis, should be investigated further, but would require a larger energy source and lower frequency geophones.
- Representative dispersion curves were generated for each surface wave data set using a moving average, polynomial curve fitting routine. For purposes of data modeling, these individual representative dispersion curves were combined and a representative dispersion curve generated for the combined data set.
- Water table depth constrained at about 3.5 m based on a simple, 2-layer interactive analysis of seismic refraction data from MASW seismic records (300 m/s V_P for unsaturated sediments, 1,700 m/s V_P for saturated sediments).
- Multiple reflectors evident in MASW seismic records at depths on the order of 20 to 150 m. Slight difference in reflector NMO velocity between forward and reverse shot locations indicates that the reflectors may have shallow dip.
- Surface wave depth of investigation is about 30 m based on half of maximum wavelength criteria.
- The subsurface velocity structure may be more complicated than presented, possibly at a depth of greater than 30 m; however, V_S30 is expected to be reliable due to strong influence of near surface velocity structure.
- V_{S30} is 242 m/s (Site Class D) for the combined surface wave data set.
- Average S-wave velocity between 2 and 32 m is 269 m/s.

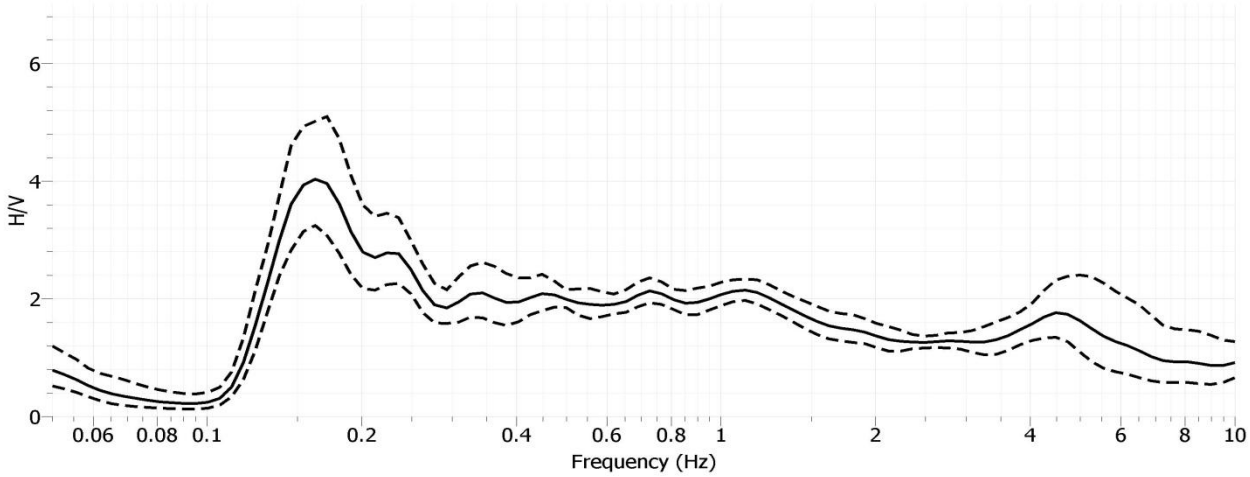

Site CI.WES, H/V Spectral Ratio, Array WES -1, Sensor 507

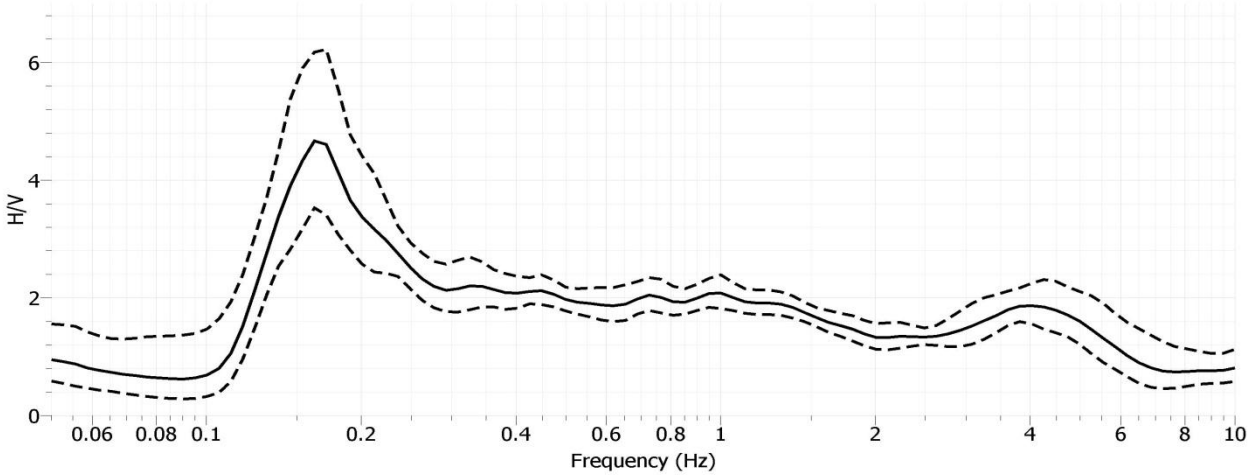

Site CI.WES, H/V Spectral Ratio, Array WES -1, Sensor 453

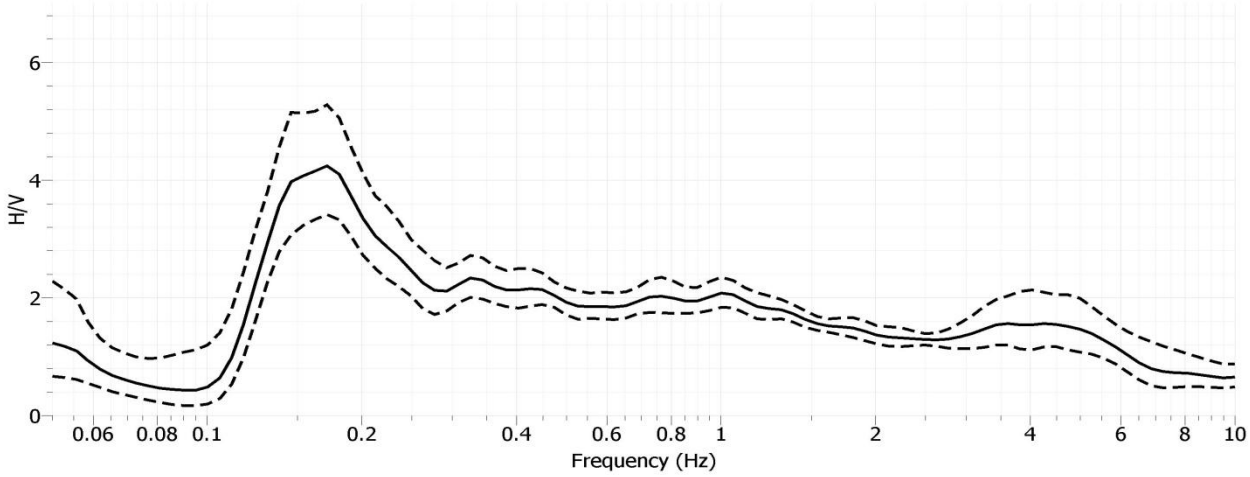

Site CI.WES, H/V Spectral Ratio, near Seismic Station, Sensor 450

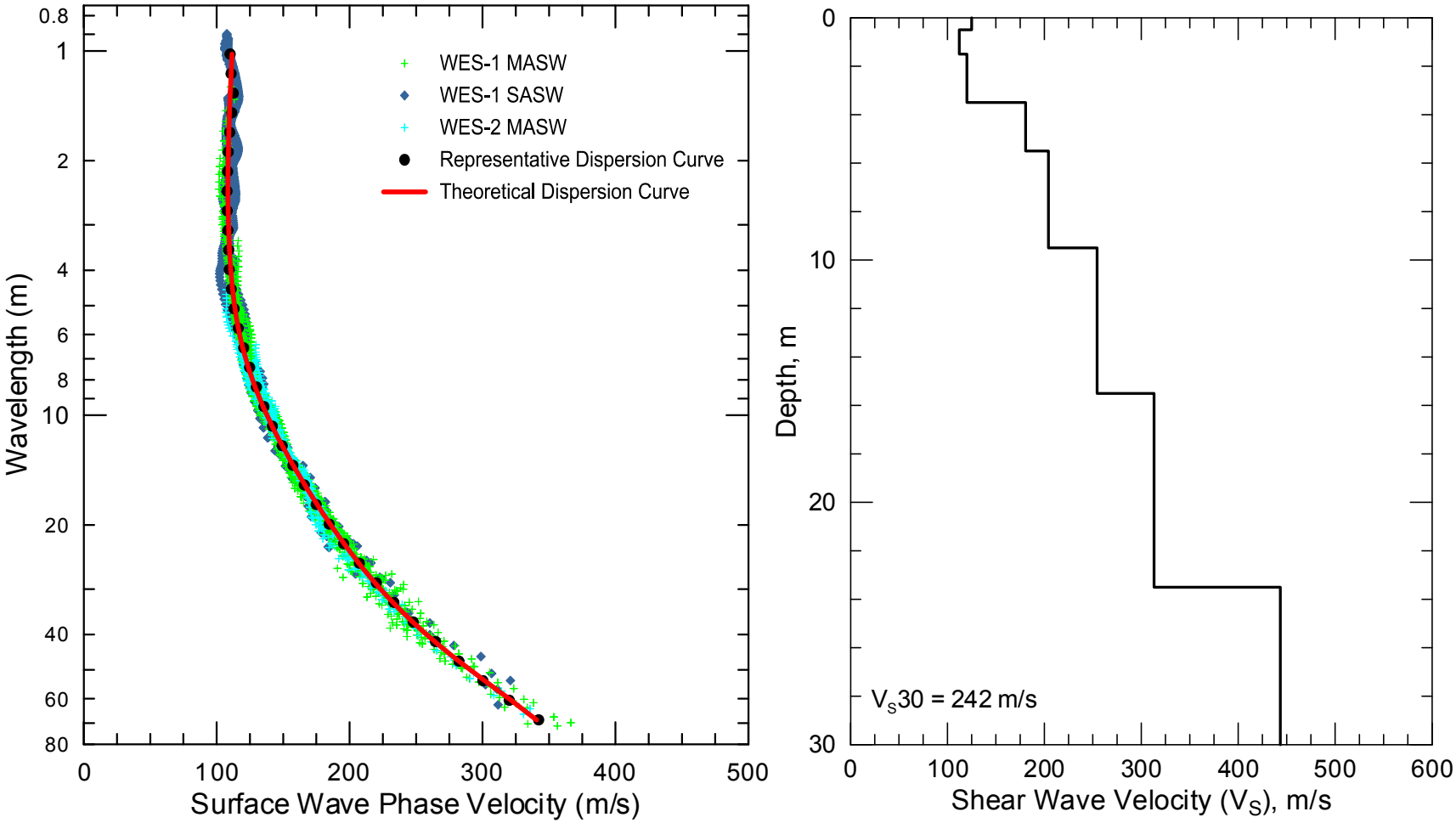

CI.WES - Field, representative and inverted theoretical surface wave dispersion data (left) and associated V_S model (right)

Site CI.WGR

Location: Wheeler Gorge Ranger Station, Ventura County, California

Latitude: 34.51085 **Longitude:** -119.27407
(Station coordinates provided by USGS, WGS84 coordinate system)

V_{S30} (measured): 660 m/s (616 to 743 m/s beneath central portion of S-wave seismic refraction array)

V_{S30} (adjusted to more accurately reflect seismic station conditions): 757 m/s (average S-wave velocity between 1 and 31 m adjusting for 1 m assumed sensor depth). Adjusted V_{S30} is 707 to 829 m/s beneath central portion of S-wave seismic refraction array.

NEHRP Site Class: C (based on V_{S30}), C/B (based on adjusted V_{S30})

Geomatrix Code: IKA

Geologic Conditions/Observations: Seismic station located on an outcrop of Upper Cretaceous clay shale with arkosic sandstone. Mapped location of the Santa Ynez fault is located immediately adjacent to the seismic station. The seismic station is located on the south side of the mapped fault. North of the fault, bedrock consists of Tertiary Coldwater Sandstone Formation.

Site Conditions: Rural site. Seismic station located at the base of large hill of shale and sandstone. Seismic testing conducted along the toe of slope with minimal elevation variation along the profile.

Geophysical Methods Utilized: HVSR, Seismic Refraction (P- and S-wave), MASW (Rayleigh wave), MALW (Love wave)

Geophysical Testing Arrays:

1. Array WGR-1 (48 channel MASW and P-wave seismic refraction array utilizing 4.5 Hz vertical geophones spaced 1.5 m apart for a length of 70.5 m, forward and reverse shot locations with multiple source offsets and source types (hammers only) and multiple interior shot locations).
2. Array WGR-1 (48 channel MASW and S-wave seismic refraction array utilizing 4.5 Hz horizontal geophones spaced 1.5 m apart for a length of 70.5 m, forward and reverse shot locations with multiple source offsets and multiple interior shot locations). Coincident with P-wave array of same name.
3. Three HVSR measurement locations: one near each end of array WGR-1 and the other adjacent to the seismic station.

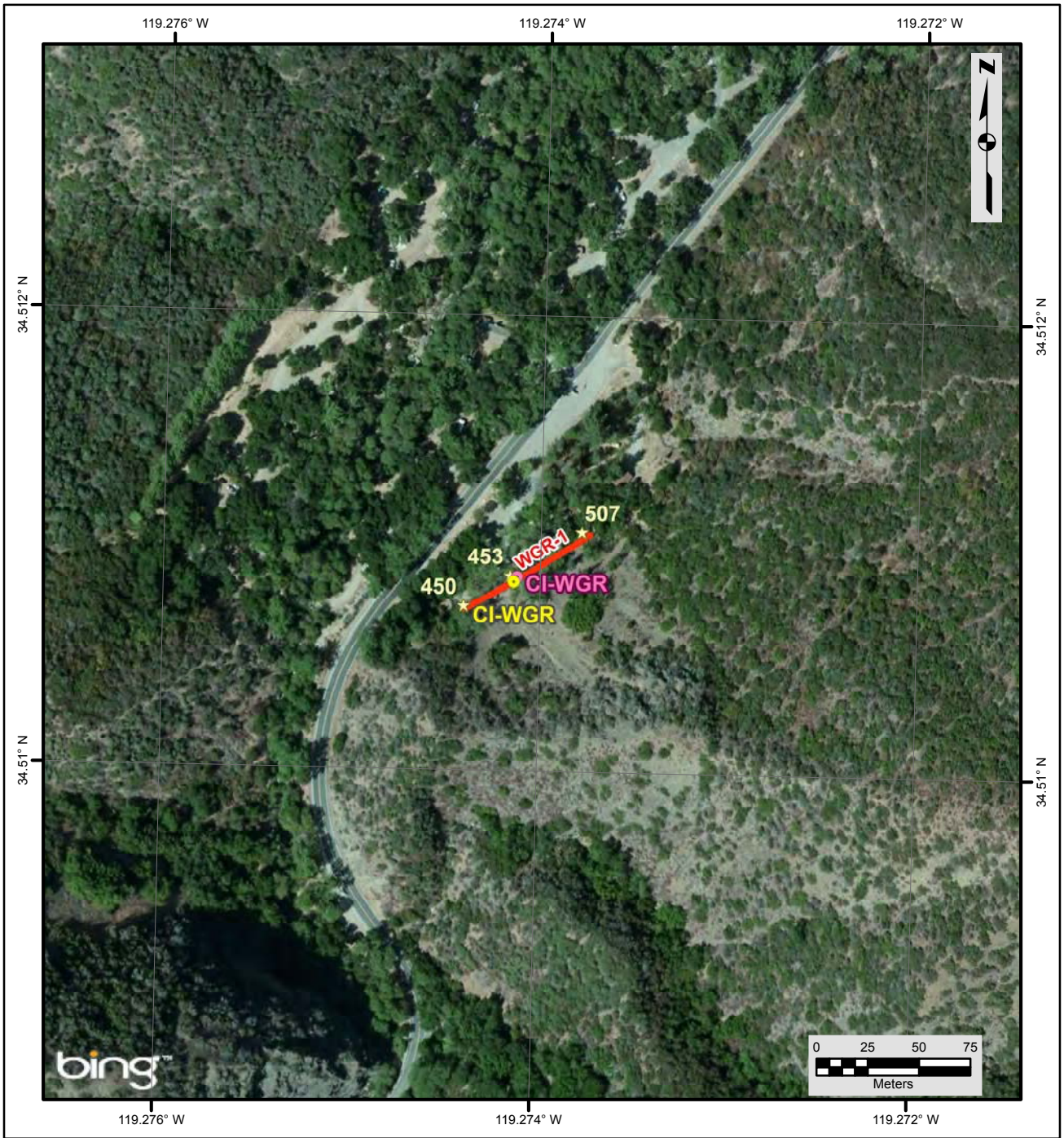

Legend

- Seismic Station - Approximate Surveyed Location
- Seismic Station - Approximate Location of Record
- H/V Spectral Ratio Location
- MASW and Seismic Refraction Array

NOTES:
1. WGS 1984 COORDINATE SYSTEM
2. Image Source: (c) Microsoft Corporation and its data suppliers

File Name: CI-WGR-I

Date: 2/7/2013

USGS science for a changing world

GEOVision geophysical services

RECOVERY.GOV

SITE MAP
CI•WGR

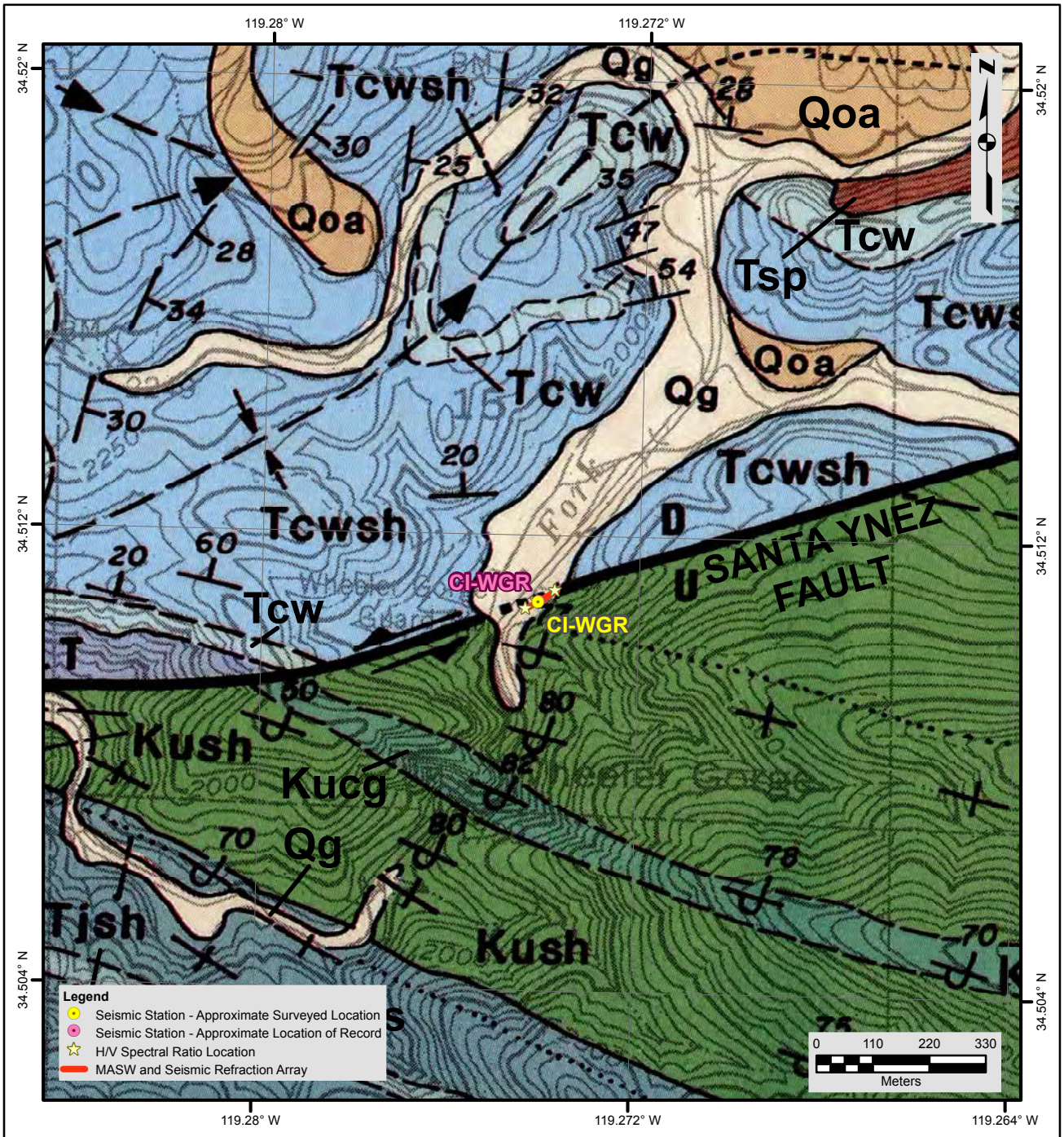

Description of Geologic Map Units

Qg = Quaternary (Holocene) stream channel deposits
Qoa = Quaternary (Pleistocene) older alluvial deposits
Tsp = Tertiary (Oligocene) Sespe Formation; sandstone with interbedded claystone
Tcw = Tertiary (Eocene to Oligocene) Coldwater Sandstone Formation; hard, bedded, arkosic sandstone with siltstone and shale
Tcwsh = Tertiary (Eocene to Oligocene) Coldwater Sandstone Formation; sandy siltstone and shale with arkosic sandstone
Tjsh = Tertiary (Eocene) Juncal Formation; micaceous shale with hard, arkosic sandstone
Tjss = Tertiary (Eocene) Juncal Formation; hard arkosic sandstone with micaceous shale
Kush = Upper Cretaceous micaceous clay shale with arkosic sandstone
Kucg = Upper Cretaceous cobble conglomerate in hard, arkosic sandstone matrix

NOTES:
1. WGS 1984 COORDINATE SYSTEM
2. Geologic Map of the Wheeler Springs Quadrangle, Ventura County, California by Thomas W. Dibblee, Jr., 1985
3. See site map for details of geophysical survey

USGS science for a changing world

GEOVision geophysical services

GEOLOGIC MAP
CI•WGR

File Name: CI-WGR
Date: 2/7/2013

Looking northeast along array WGR-1 at HVSR sensor 453 and CI.WGR seismic station

Looking northeast along array WGR-1

Looking southwest along array WGR-1 at HVSR sensor 453 and CI.WGR seismic station

S-wave data acquisition on array WGR-1

Looking south at outcropping shale and sandstone unit adjacent to seismic station

Location of Geophysical Testing Arrays:

Location	Latitude	Longitude
WGR-1, Southwest End of MASW/Refraction Array	34.51071	-119.27434
WGR-1, Center of MASW/Refraction Array	34.51086	-119.27402
WGR-1, Northeast End of MASW/Refraction Array	34.51104	-119.27369
HVSR Sensor 450	34.51072	-119.27435
HVSR Sensor 453	34.51086	-119.27411
HVSR Sensor 507	34.51105	-119.27373
CI.WGR Seismic Station	34.51083	-119.27409

Notes: 1) WGS84 Coordinate System (decimal degrees)

2) Survey accuracy is estimated at 3 to 4 m.

3) Location of HVSR sensor 507 estimated due to tree cover.

Results:

Average V_S Model from Central Portion of S-wave Seismic Refraction Line

Depth to Top of Layer (m)	Layer Thickness (m)	S-Wave Velocity (m/s)
0.00	0.40	101
0.40	0.80	204
1.20	0.80	350
2.00	0.80	407
2.80	0.80	460
3.60	0.80	522
4.40	0.80	560
5.20	1.68	655
6.88	1.68	704
8.56	1.68	754
10.25	1.68	831
11.93	1.68	864
13.61	1.68	884
15.29	1.68	920
16.97	Half Space	948

V_S Model from a Position of 27 m, Near the Seismic Station, on the S-wave Seismic Refraction Line

Depth to Top of Layer (m)	Layer Thickness (m)	S-Wave Velocity (m/s)
0.00	0.40	127
0.40	0.81	233
1.21	0.81	366
2.02	0.81	432
2.83	0.81	519
3.64	0.81	577
4.45	0.81	632
5.26	1.70	767
6.96	1.70	768
8.66	1.70	850
10.36	1.70	950
12.06	1.70	962
13.76	1.70	962
15.46	1.70	962
17.16	Half Space	990

Average V_P Model and Estimated V_S Models from Central Portion of P-wave Seismic Refraction Line

Depth to Top of Layer (m)	Layer Thickness (m)	P-Wave Velocity (m/s)	Estimated S-Wave Velocity (m/s)			
			Poisson's Ratio = 0.25	Poisson's Ratio = 0.30	Poisson's Ratio = 0.35	Poisson's Ratio = 0.40
0.00	0.40	208	120	111	100	85
0.40	0.80	420	242	224	202	171
1.20	0.80	683	394	365	328	279
2.00	0.80	1001	578	535	481	409
2.80	0.80	1201	693	642	577	490
3.61	0.80	1375	794	735	661	561
4.41	0.80	1532	884	819	736	625
5.21	1.68	1601	925	856	769	654
6.89	1.68	1661	959	888	798	678
8.57	1.68	1863	1076	996	895	761
10.26	1.68	1884	1088	1007	905	769
11.94	1.68	1976	1141	1056	949	807
13.62	1.68	2077	1199	1110	998	848
15.31	Half Space	2443	1410	1306	1173	997

Observations/Discussion:

- There are no distinct high amplitude HVSR peaks at the three measurement stations. HVSR sensors 450, located at the southwest end of array WGR-1, and 453, located adjacent to the seismic station, appear to have a low amplitude peak near a frequency of 20 Hz.
- The seismic station is located at the base of an outcrop of Cretaceous shale and sandstone and most likely sits on rock. The seismic testing array was located along the toe of slope and the bedrock surface is likely dipping steeply orthogonal to the array.
- The P- and S-wave seismic refraction data for array WGR-1 were modeled using a tomographic inversion routine with smooth velocity gradient starting models. The seismic refraction models were extended to limited far offset shot locations to extend depth of investigation. There was not sufficient space at the site for a longer seismic refraction profile.
- The P-wave first arrival data were picked to a greater degree of accuracy than the S-wave first arrival data because the S-wave is not typically the first energy on a seismic record, even when using a horizontal traction plank as an energy source. The air wave arrives before the direct soil arrival in the P-wave seismic records and an attempt was made to pick the direct arrival after the air wave, which is not always easy.
- The P-wave seismic refraction survey design allowed P-wave velocity to be imaged to a maximum depth of about 17 m. The seismic refraction model indicates that P-wave velocity is about 250 to 400 m/s at the surface and increases to over 1,000 m/s at a depth of 1 to 3 m, 1,500 m/s at a depth of 2 to 10 m, 2,000 m/s at a depth of 3 to 14 m and over 2,500 m/s at a depth of 4 to greater than 15 m.
- The S-wave seismic refraction survey design allowed S-wave velocity to be imaged to a maximum depth of about 19 m. The seismic refraction model indicates that S-wave velocity is about 100 to 200 m/s at the surface and increases to over 500 m/s at a depth of 1 to 5 m, 700 m/s at a depth of 5 to 12 m and over 900 m/s at a depth of 6 to 16 m.
- There is definite lateral velocity variation beneath array WGR-1 with both the P- and S-wave seismic refraction surveys revealing higher velocity sedimentary rock beneath the southwest half of the array. The northeast half of the array is closer to the mapped location of the Santa Ynez Fault where bedrock is expected to be more fractured.
- V_{S30} was estimated between 24 and 52.5 m on the S-wave refraction model, where depth of investigation is greatest, by projecting the velocity at 19 m depth to 30 m depth. Over this interval V_{S30} ranges from about 616 to 743 m/s, a 19% variation over a 28 m distance. Although the depth of investigation is limited to about 19 m, tomographic inversion routines often overestimate velocity at the base of the model, which may compensate for an expected slight increase in velocity with depth below 19 m. It should also be noted that geologic bedding is overturned and very steeply dipping south of the fault and there could be significant lateral velocity variation in the site vicinity.
- An average V_S model was developed over the 24 to 52.5 m distance interval by horizontally averaging the travel time of each model cell and cell thickness and average V_{S30} was determined to be 660 m/s. The average V_S between 1 and 31 m to account for assumed sensor depth is 757 m/s.
- The lowest value of V_{S30} over the 24 to 52.5 m distance interval is 616 m/s, occurs at a position of 52.5 m. The highest value of V_{S30} over this interval is 743 and occurs at a

position of 24 m. The seismic station is located near a position of 27 m where V_{S30} is 723 m/s. The average V_S between 1 and 31 m at the locations of lowest and highest V_{S30} and near the seismic station are 707, 829 and 816 m/s, respectively.

- V_{P30} between 24 and 52.5 m varies from about 1,368 to 2,007 m/s and averages 1,569 m/s. A constant Poisson's ratio of slightly lower than 0.4 would yield the value of V_{S30} estimated from the S-wave seismic refraction survey, indicating that the sedimentary rock is likely saturated at relatively shallow depth.
- Noise conditions at the site were not sufficient for application of passive surface wave techniques.
- Surface wave techniques were not expected to be effective at this site because the bedrock surface may be dipping as much as 30 degrees to the northwest beneath the seismic profile. Site characterization was, therefore, limited to the application of the P- and S-wave seismic refraction techniques. Rayleigh wave data were inspected and either a dominant higher mode or artifact associated with dipping bedrock occurred over a wide frequency range. Love wave data were also inspected and there was evidence of significant lateral velocity variation beneath the array resulting is large scatter in the dispersion data. The Love wave dispersion data seems to indicate that V_{S30} may be in the 525 to 625 m/s range, significantly lower than that measured by the S-wave seismic refraction survey. It is difficult to predict the effects of bedrock deepening orthogonally to the seismic line, but there is a strong possibility that it could result in underestimated V_{S30} from surface wave testing, assuming that a dispersion curve can be constructed. Therefore, the Love wave data are not considered valid.
- For the purpose of site characterization, we recommend using the average S-wave velocity structure between 24 and 52.5 m on the S-wave seismic refraction line. This estimated V_{S30} is slightly conservative and V_{S30} may be 10% higher beneath the seismic station. It should be noted that V_{S30} will decrease rapidly to the northwest from the seismic station as the sediment cover gets thicker. As an example, at a distance of 2 m northwest from the seismic station there could be an additional 1 m of sediment cover, which could decrease V_{S30} by over 10%.
- In summary, V_{S30} is 660 m/s (NEHRP Site Class C).
- Average S-wave velocity between 1 m (nominal sensor depth) and 31 m is 757 m/s (NEHRP Site Class C/B).

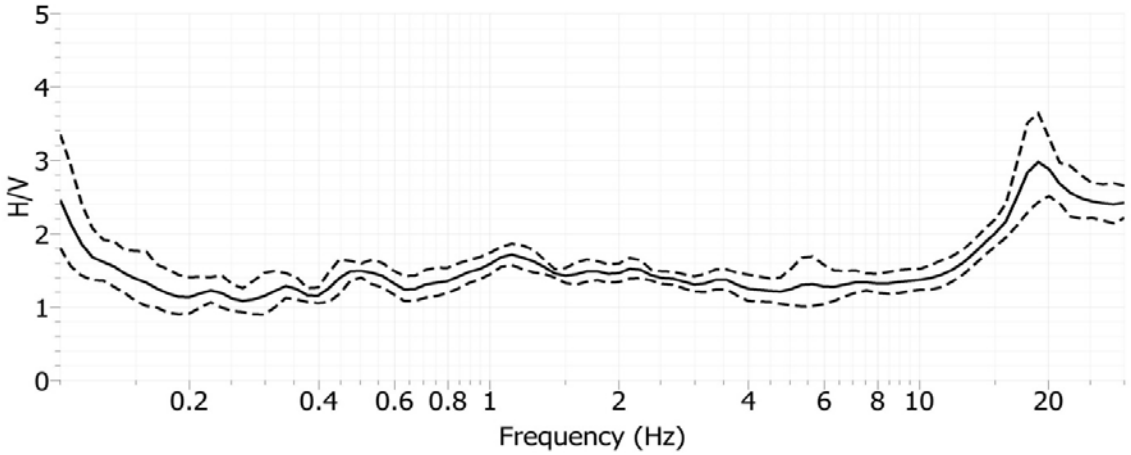

Site CI.WGR, H/V Spectral Ratio, Array WGR-1, Sensor 450

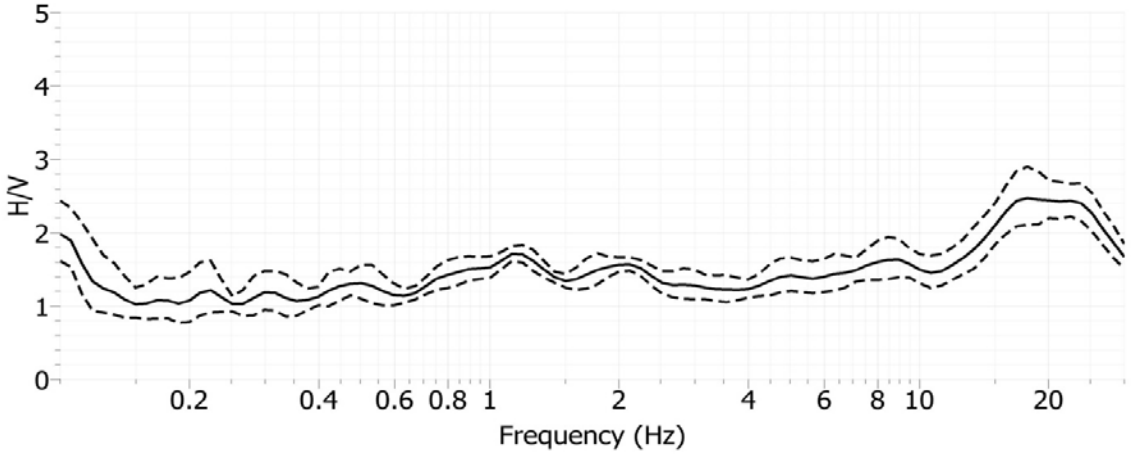

Site CI.WGR, H/V Spectral Ratio, Near Seismic Station, Sensor 453

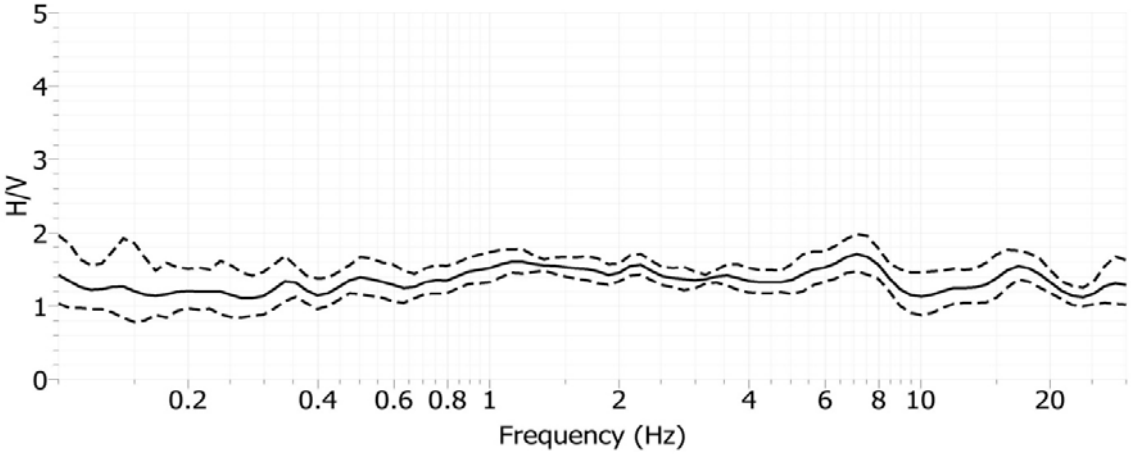

Site CI.WGR, H/V Spectral Ratio, Array WGR-1, Sensor 507

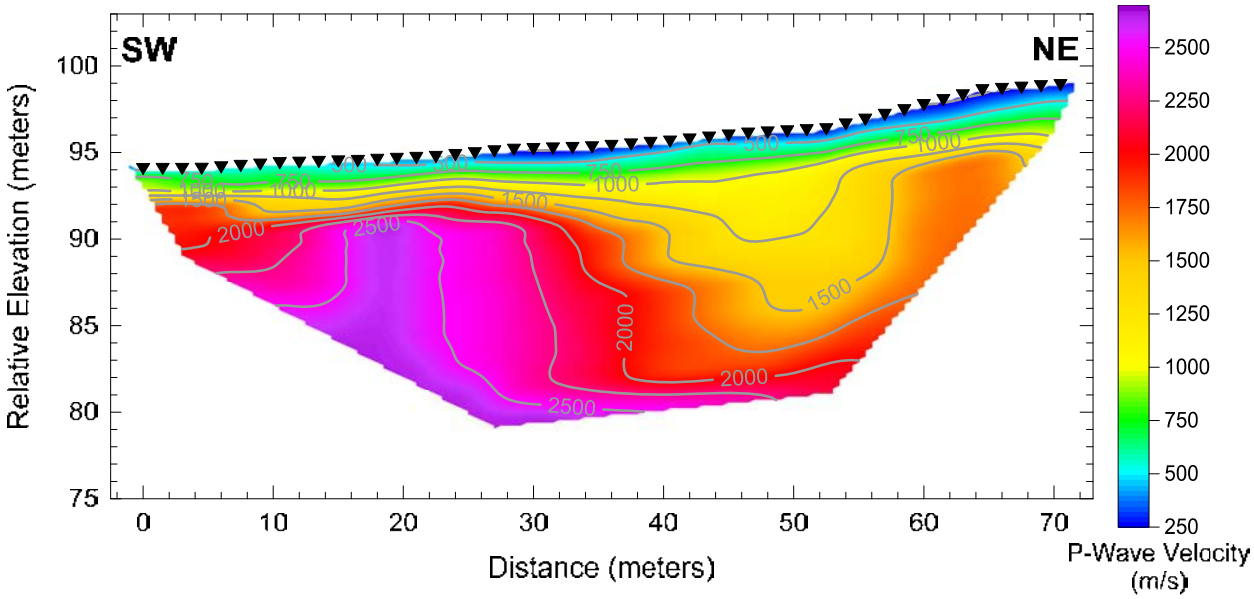

Array WGR-1 – P-wave Tomographic Seismic Refraction Model Developed using a Smooth Velocity Gradient Starting Model

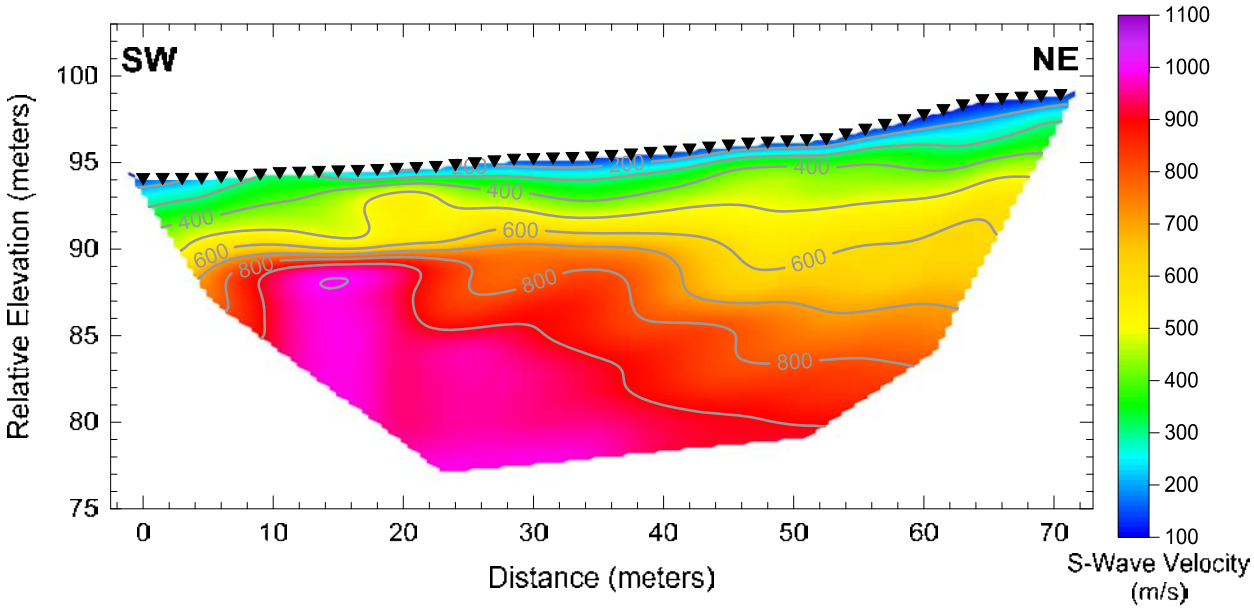

Array WGR-1 – S-wave Tomographic Seismic Refraction Model Developed using a Smooth Velocity Gradient Starting Model

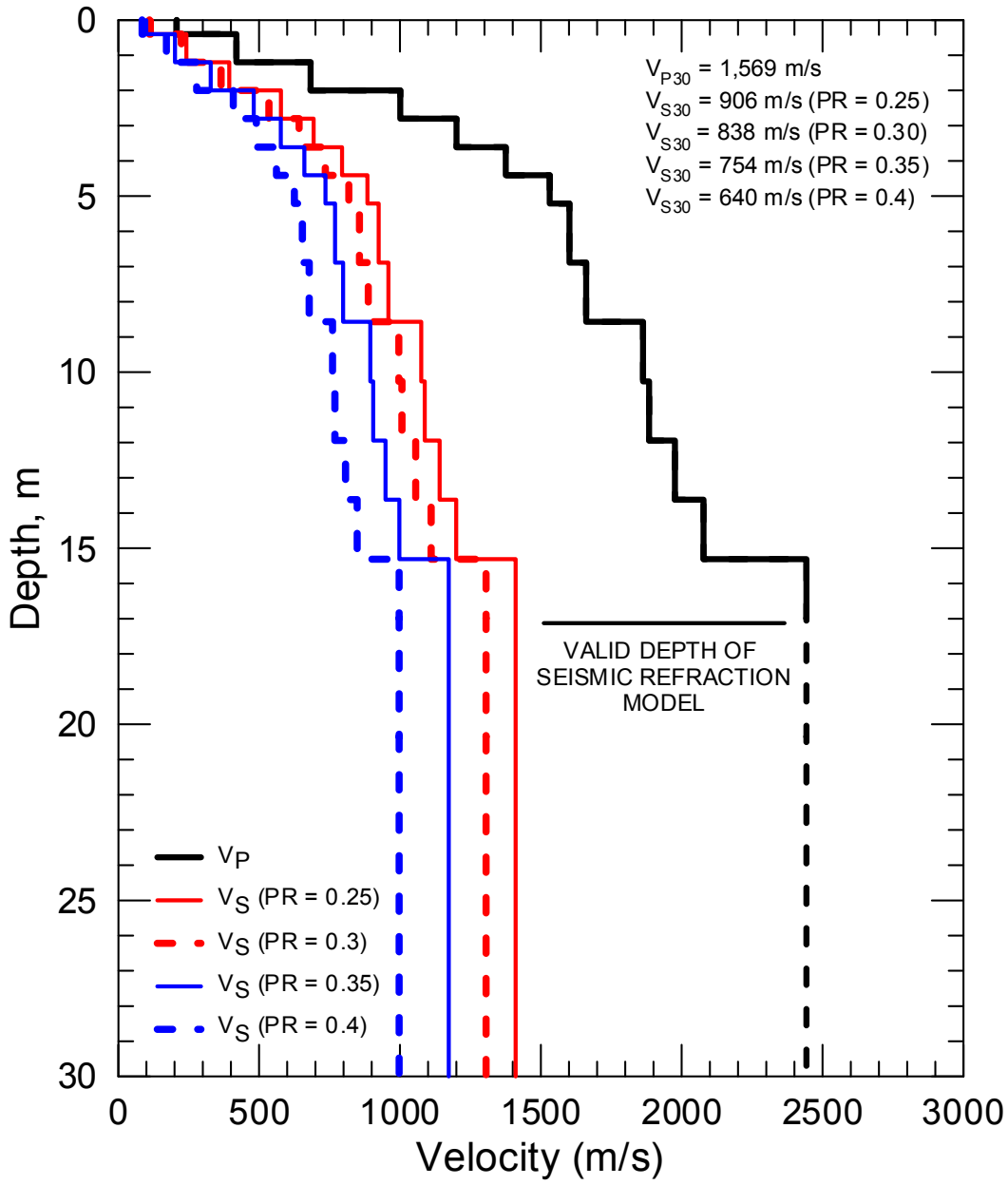

CI.WGR – Average P-wave velocity structure and estimated S-wave velocity structure between a distance of 24 and 52.5 m along the P-wave seismic refraction model for array WGR-1. Maximum seismic refraction depth of investigation is limited to about 17 m and P-wave velocity is assumed to be constant between 17 and 30 m. Space was not available for a longer seismic line to image to 30 m depth. P-wave velocity should not be used to estimate S-wave velocity at this site because the sedimentary rock may be saturated at unknown depth.

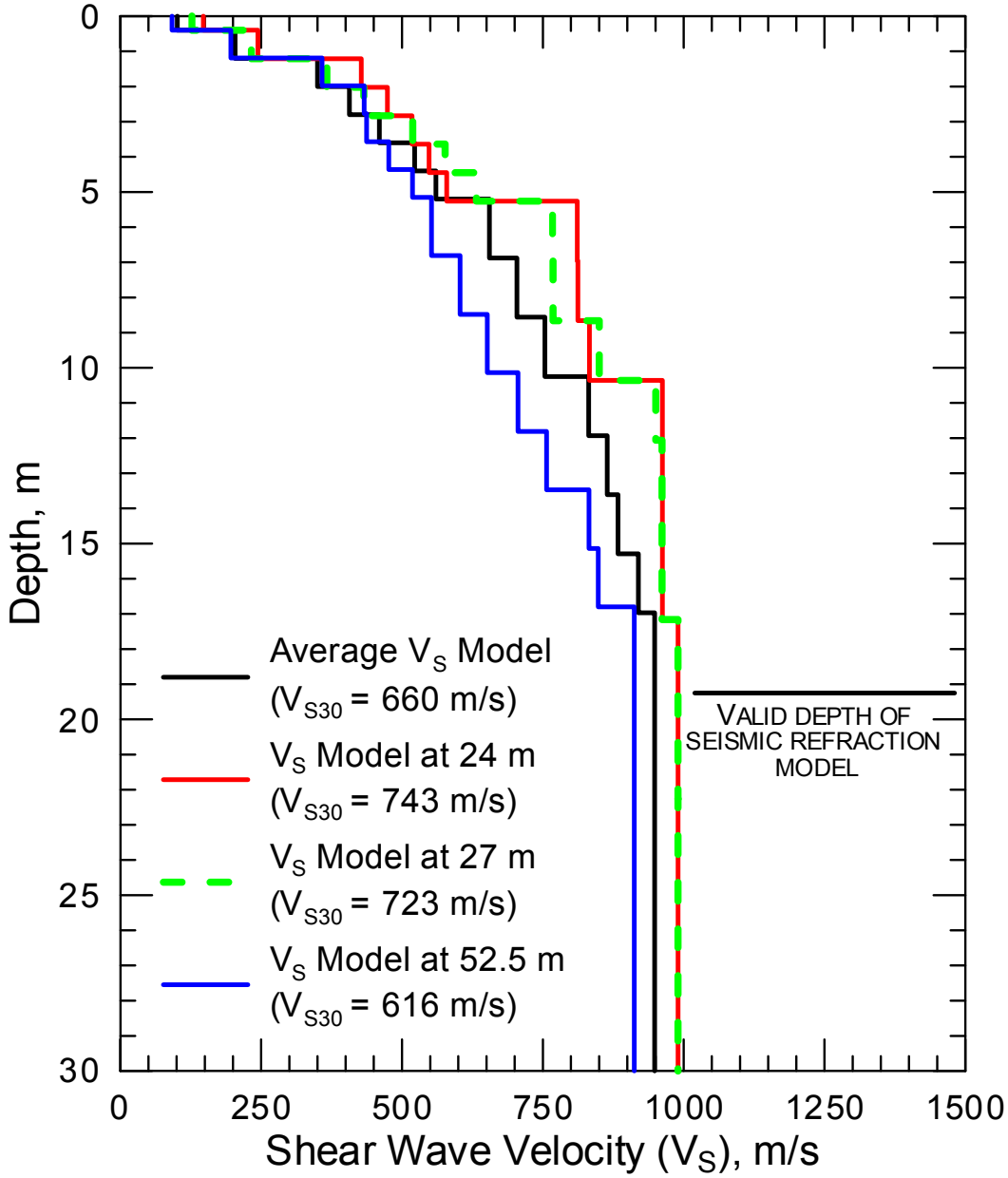

CI.WGR – Average S-wave velocity structure between 24 and 52.5 m beneath S-wave seismic refraction array WGR-1 and S-wave velocity structure at a position of 24 m (maximum V_{S30}), 27 m (near seismic station) and 52.5 m (minimum V_{S30}). Seismic refraction depth of investigation is limited to about 17 m and S-wave velocity is assumed to be constant below this depth. Interpolating constant velocity from 17 to 30 m is likely balanced by the tendency of tomographic routines to overestimate velocity at the base of the model. There is not sufficient space at the site for a longer seismic line and surface wave techniques are not applicable due to the steeply dipping bedrock surface.

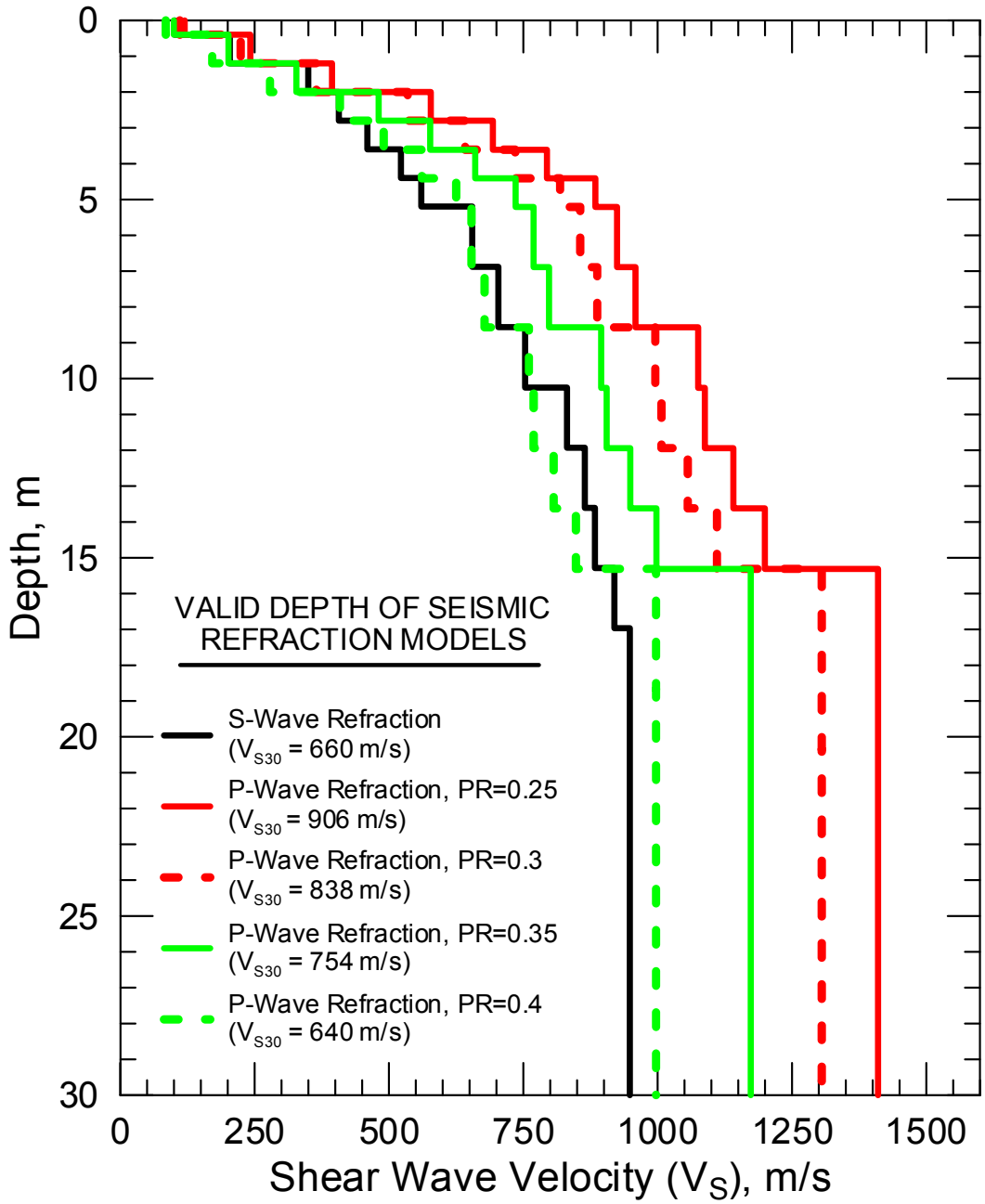

CI.WGR – Comparison of average S-wave velocity models derived from the P- and S-wave seismic refraction data. Below a depth of about 2 m, the average V_S model from the S-wave seismic refraction model closely tracks the average V_S model estimated from the P-wave refraction model assuming a constant Poisson's ratio of 0.4. This indicates that the sedimentary rock may be saturated at shallow depth.

Site CI.WNS

Location: Wonderland Avenue School, 8510 Wonderland Avenue, Los Angeles, California

Latitude: 34.11395 **Longitude:** -118.37967
(Station coordinates modified based on field observation of station location and identification of approximate station location on Google Earth – could not survey the seismic station as located inside a building, WGS84 coordinate system)

V_{S30} (measured): 1,043 m/s (based on previously acquired Oyo PS suspension log)

V_{S30} (adjusted to more accurately reflect seismic station conditions): 1,043 m/s (no adjustment necessary)

NEHRP Site Class: B

Geomatrix Code: BGA

Geologic Conditions/Observations: Seismic station located on geologic unit mapped as Mesozoic (Cretaceous) quartz diorite.

Site Conditions: Urban site located at an elementary school with undulating hilly topography in the site vicinity. There are very limited space and locations for geophysical testing due to development. The test locations were on asphalt or concrete.

Geophysical Methods Utilized: HVSR, Seismic Refraction, MASW

Geophysical Testing Arrays:

1. Array WNS-1 (48 channel MASW and P-wave seismic refraction array utilizing 4.5 Hz vertical geophones spaced 1.5 m apart for a length of 70.5 m, forward and reverse shot locations with limited source offsets and source types and multiple interior shot locations).
2. Array WNS-2 (48 channel MASW array utilizing 4.5 Hz vertical geophones spaced 1 m apart for a length of 47 m, forward and reverse shot locations with limited source offsets and source types and center shot location).
3. Array WNS-3 (48 channel P-wave seismic refraction array utilizing 4.5 Hz vertical geophones spaced 1.5 m apart for a length of 70.5 m, forward and reverse shot locations with limited source offsets and source types and multiple interior shot locations occupying the same center and orientation as WNS-2).
4. Three HVSR measurement locations: two distributed along array WNS-2 and one near the seismic station.

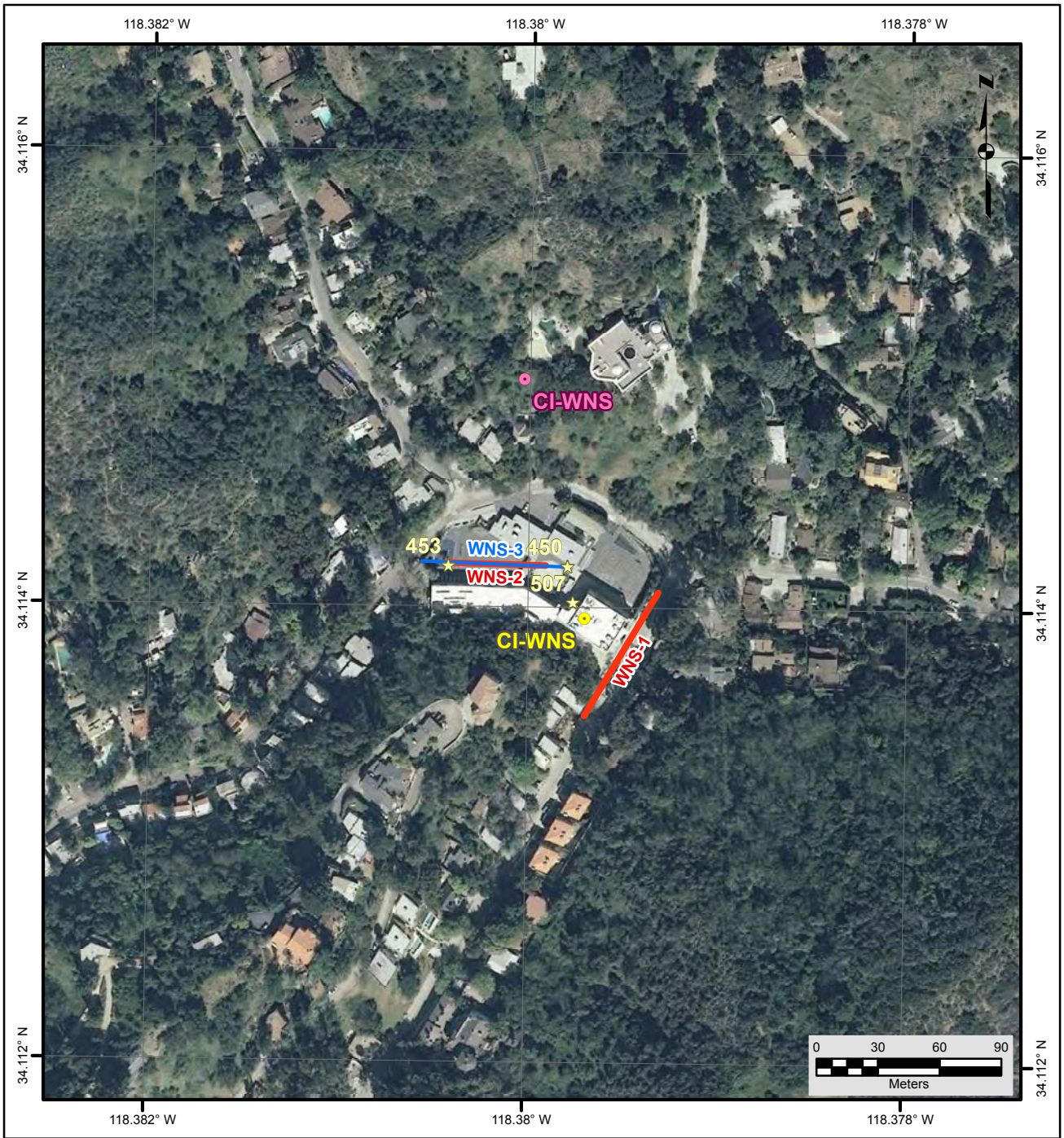

Legend

- Seismic Station - Approximate Surveyed Location
- Seismic Station - Approximate Location of Record
- H/V Spectral Ratio Location
- MASW and Seismic Refraction Array
- MASW and Seismic Refraction Array

NOTES:
1. WGS 1984 COORDINATE SYSTEM
2. Image Source: ESRI, i-cubed, USDA FSA, USGS, AEX, GeoEye, Getmapping, Aerogrid, IGP

File Name: CI-WNS-I

Date: 4/27/2012

USGS science for a changing world

GEOVision geophysical services

RECOVERY.GOV

SITE MAP
CI•WNS

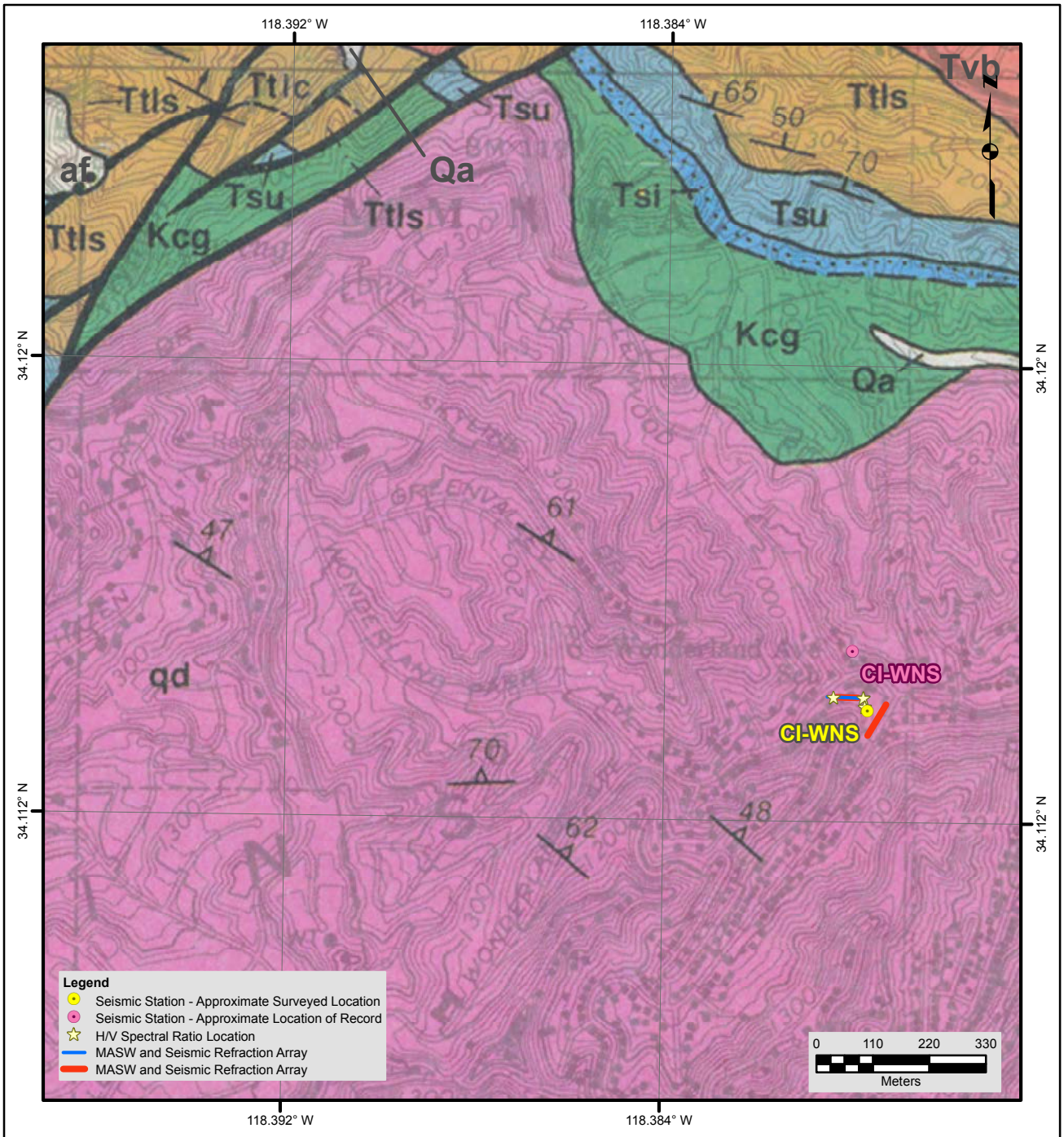

Description of Geologic Map Units

af = Quaternary (Holocene) artificial cut and fill
Qa = Quaternary (Holocene) alluvial gravel, sand, and silt-clay, includes gravel and sand of stream channels
Tvb = Tertiary (Miocene) basaltic volcanic rocks, fine grained, massive, rarely vesicular, incoherent where weathered
Ttls = Tertiary (Miocene) Lower Topanga Formation; semi-friable to hard arkosic sandstone, includes micaceous shale
Tsu = Tertiary (Paleocene) Santa Susana Formation; fine grained sandstone and vaguely bedded micaceous silty claystone
Tsi = Tertiary (Paleocene) Santa Susana Formation; Simi Conglomerate Member; vaguely bedded cobble conglomerate in sandstone matrix, few thin layers of sandstone and claystone
Kcg = Cretaceous (Upper) crudely bedded cobble conglomerate in hard sandstone matrix, includes interbedded sandstone
qd = Cretaceous quartz diorite, medium grained granitic rock, much fractured and deeply weathered, incoherent where weathered

NOTES:
1. WGS 1984 COORDINATE SYSTEM
2. Geologic Map of the Beverly Hills and Van Nuys (South ½) Quadrangles, Los Angeles County, California by Thomas W. Dibblee, Jr., 1991
3. See site map for details of geophysical survey

USGS science for a changing world
GEOVision geophysical services

GEOLOGIC MAP
CI•WNS

File Name: CI-WNS
Date: 4/27/2012

CI.WNS seismic station (in cabinet)

Looking southwest along array WNS-1

Looking northeast along array WNS-1

Looking west along array WNS-3

Looking east along array WNS-2

Location of Geophysical Testing Arrays:

Location	Latitude	Longitude
WNS-1, Southwest End of MASW/Refraction Array	34.11352	-118.37966
WNS-1, Northeast End of MASW/Refraction Array	34.11407	-118.37928
WNS-2, West End of MASW/Refraction Array	34.11419	-118.38041
WNS-2, Center of MASW/Refraction Array	34.11419	-118.38015
WNS-2, East End of MASW/Refraction Array	34.11418	-118.37988
WNS-3, West End of MASW/Refraction Array	34.11418	-118.38051
WNS-3, Center of MASW/Refraction Array	34.11419	-118.38015
WNS-3, East End of MASW/Refraction Array	34.11418	-118.37976
HVSR Sensor 453	34.11418	-118.38039
HVSR Sensor 450	34.11418	-118.37976
HVSR Sensor 507	34.11402	-118.37973
CI.WNS Seismic Station	34.11395	-118.37967

Notes: 1) WGS84 Coordinate System (decimal degrees)

2) Survey accuracy is estimated at 1 to 2 m.

3) Seismic station location based on site observations. Could not be surveyed as in building.

Observations/Discussion:

- Two unsuccessful attempts were made to characterize this site. There are limited locations where MASW and seismic refraction data could be acquired due to development in the site vicinity. Seismic refraction methods were not effective at this site as all possible survey areas have asphalt and/or concrete cover and there was significant traffic noise. The MASW technique was not effective due to lateral velocity variation and the presence of a thin sediment/fill layer overlying relatively high velocity rock. However, an Oyo PS suspension log was previously acquired at this site as part of the "Resolution of Site Response Issues from the Northridge Earthquake (ROSRINE)" Project and is used for the purpose of site characterization.
- The HVSR plots are different at high frequencies at the three HVSR measurement locations, possibly indicating that there is lateral velocity variation at the site. The HVSR plot at sensor location 450 has a broad peak between 3 and 13 Hz with a maxima at about 7 Hz. The HVSR plot at sensor location 507 does not exhibit a distinct peak, but has elevated HVSR response over the 6 to 15 Hz range. The HVSR plot at sensor location 453 has a distinct peak at about 12 Hz.
- The PS suspension log previously acquired on site did not accurately characterize velocity structure in the upper 2 m. MASW data were reviewed and near surface sediment/fill S-wave velocity was found to be about 225 m/s.
- The PS suspension log indicates that there are several meters of low velocity sediments/fill/decomposed rock at the site below which V_S gradually increases with depth reaching 1,600 to 1,800 m/s at a depth of about 10 m and over 2,000 m/s at a depth of 20 m.
- PS suspension velocity logs are presented for the receiver to receiver (R1-R2) analysis and also the source to receiver (S-R1) analysis, which is typically just used to validate the more accurate and better resolution R1-R2 analysis.
- V_{S30} was estimated from the PS suspension log R1-R2 analysis using a V_S of 225 m/s for the upper 2.25 m, based on MASW data, and is 1,043 m/s (NEHRP Site Class B). We recommend using this estimate of V_{S30} for site characterization.
- The S-R1 velocity log starts at a depth of 4.5 m and V_{S30} was estimated using a V_S of 225 m/s for the upper 2.25 m and V_S from the R1-R2 analysis for depths of 2.5 and 3 m. Estimated V_{S30} for the PS suspension log S-R1 analysis is 1,000 m/s (NEHRP Site Class B), which is consistent with that from the R1-R2 analysis.

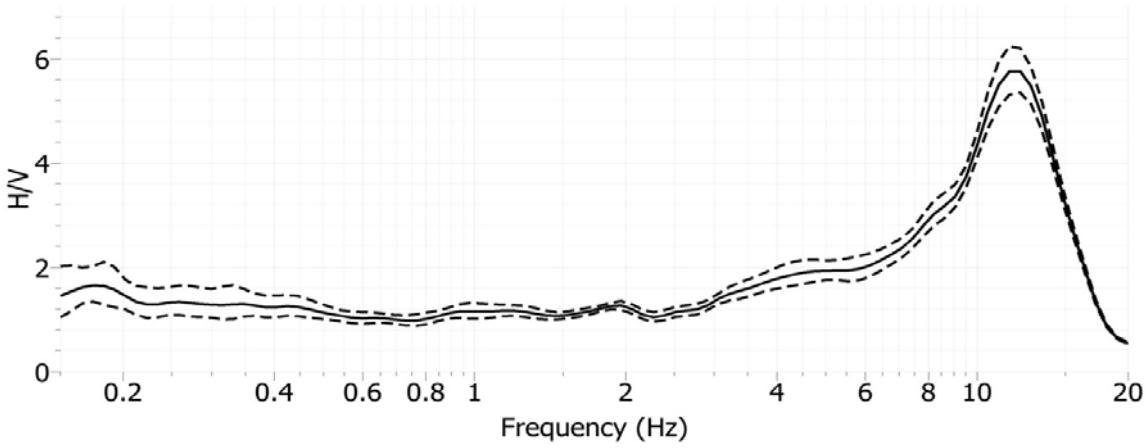

Site CI.WNS, H/V Spectral Ratio, Array WNS-1, Sensor 453

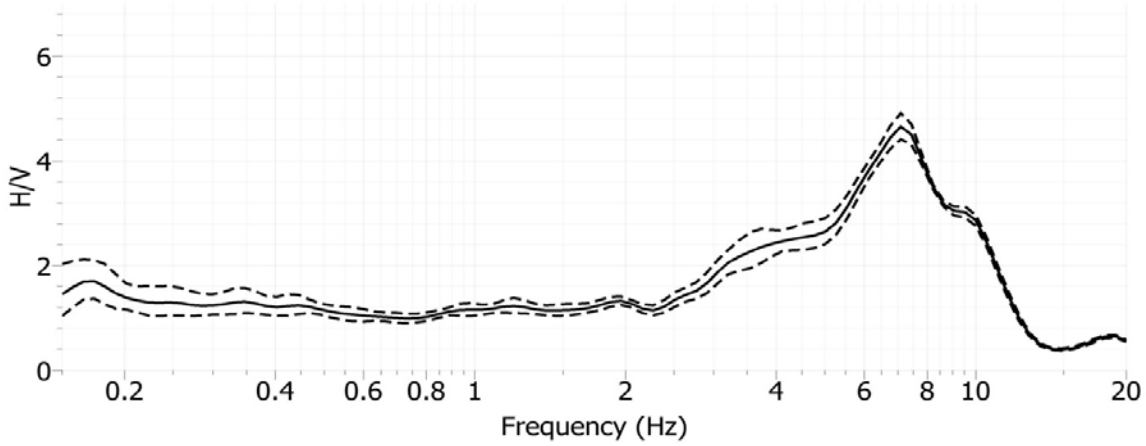

Site CI.WNS, H/V Spectral Ratio, Array WNS-1, Sensor 450

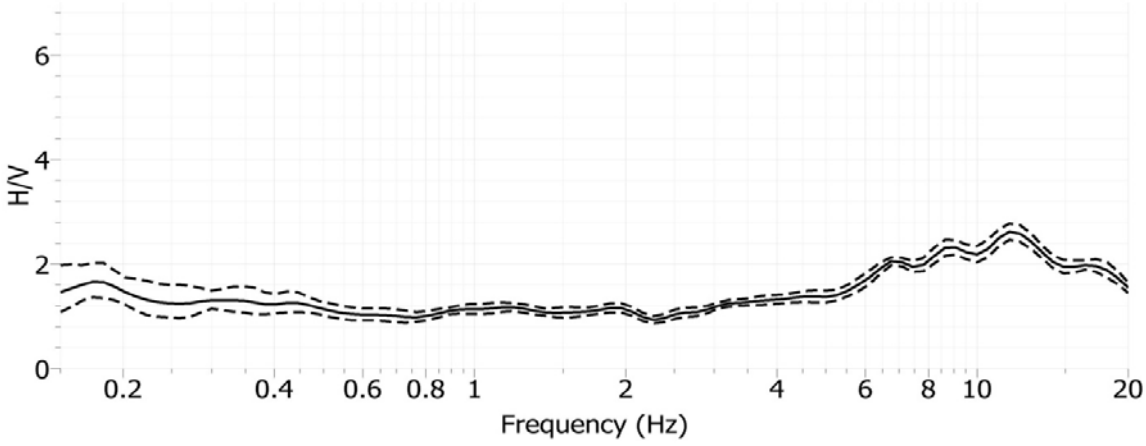

Site CI.WNS, H/V Spectral Ratio, Near Seismic Station, Sensor 507

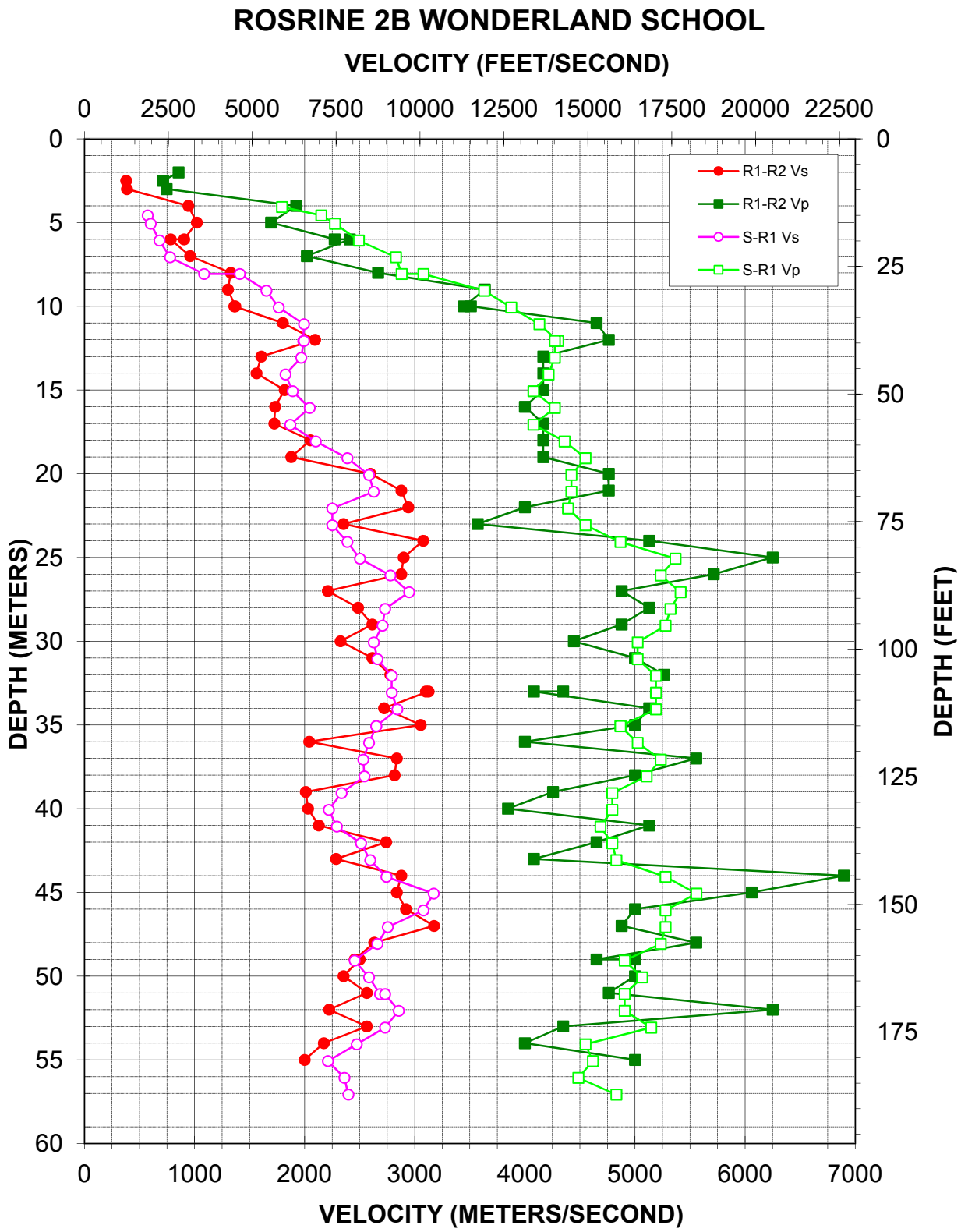

CI.WNS- Oyo PS suspension log conducted as part of the "Resolution of Site Response Issues from the Northridge Earthquake (ROSRINE)" Project. P- and S-wave velocity from receiver to receiver (R1-R2) and source to receiver (S-R1) analysis.

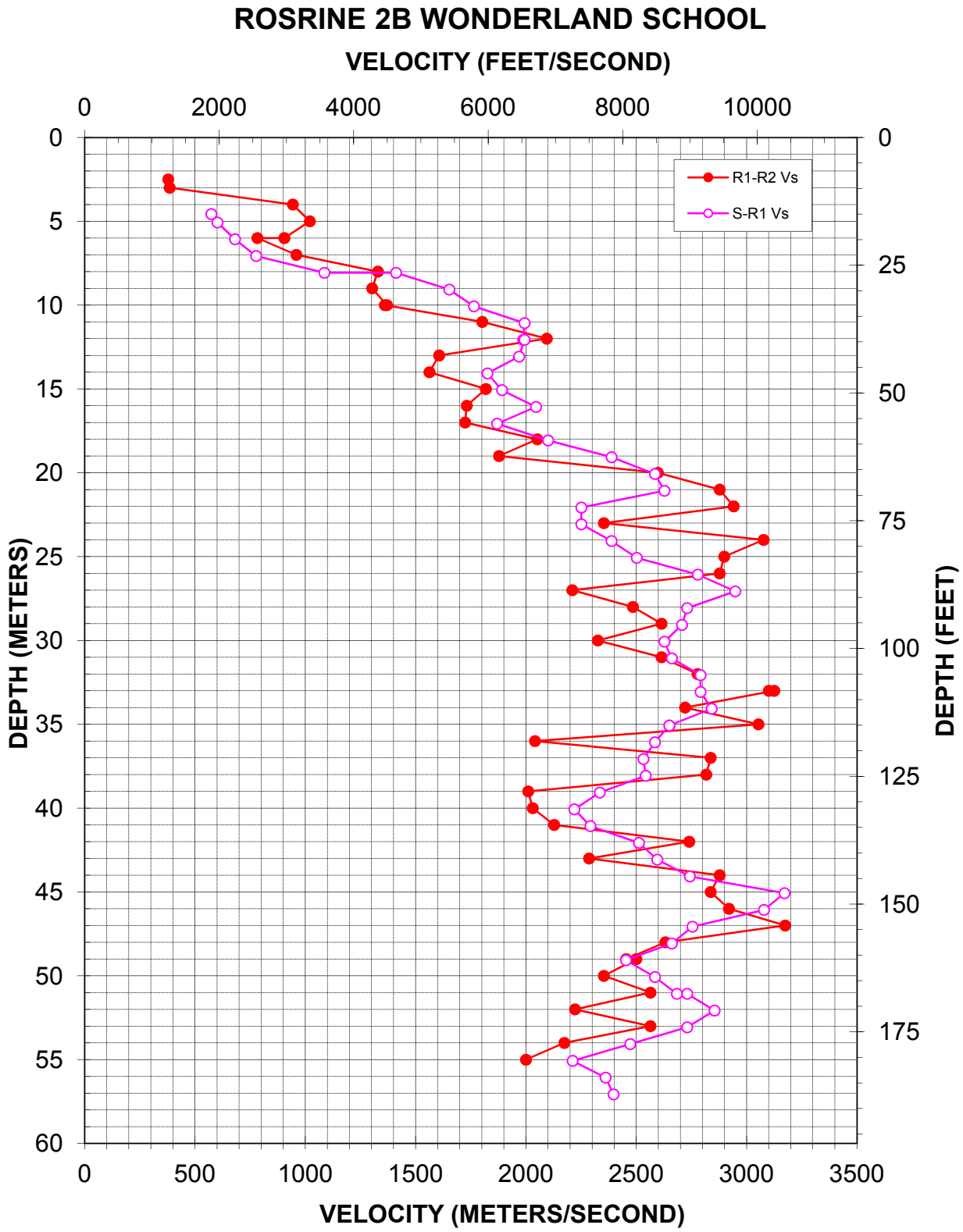

CI.WNS- Oyo PS suspension log conducted as part of the ROSRINE Project. S-wave velocity from receiver to receiver (R1-R2) and source to receiver (S-R1) analysis.

CI.WNS - Oyo PS suspension log conducted as part of the ROSRINE Project. Receiver to receiver (R1-R2) analysis.

Depth (m)	V_S (m/s)	V_P (m/s)	Depth (m)	V_S (m/s)	V_P (m/s)
2.5	379	714	30	2326	4444
3	385	746	31	2614	5000
4	943	1923	32	2778	5263
5	1020	1695	33	3101	4348
6	844	2341	33	3125	4082
7	959	2020	34	2721	5128
8	1329	2667	35	3053	5000
9	1303	3636	36	2041	4000
10	1365	3479	37	2837	5556
11	1802	4651	38	2817	5000
12	2094	4762	39	2010	4255
13	1606	4167	40	2030	3846
14	1563	4167	41	2128	5128
15	1818	4167	42	2740	4651
16	1732	4000	43	2286	4082
17	1724	4167	44	2878	6897
18	2051	4167	45	2837	6061
19	1878	4167	46	2920	5000
20	2597	4762	47	3175	4878
21	2878	4762	48	2632	5556
22	2941	4000	49	2454	4651
23	2353	3571	49	2500	5000
24	3077	5128	50	2353	5000
25	2899	6250	51	2564	4762
26	2878	5714	52	2222	6250
27	2210	4878	53	2564	4348
28	2484	5128	54	2174	4000
29	2614	4878	55	2000	5000

CI.WNS - Oyo PS suspension log conducted as part of the ROSRINE Project. Source to receiver (S1-R2) analysis.

Depth (m)	V_S (m/sec)	V_P (m/sec)	Depth (m)	V_S (m/sec)	V_P (m/sec)
4.57	574	2151	32.07	2791	5190
5.07	602	2275	33.07	2791	5190
6.07	681	2492	34.07	2842	5190
7.07	777	2829	35.07	2650	4868
8.07	1249	2980	35.07	2650	4868
9.07	1653	3630	36.07	2584	5024
10.07	1764	3877	37.07	2532	5233
11.07	1994	4132	38.07	2543	5106
12.07	1990	4287	39.07	2335	4794
13.07	1969	4272	40.07	2219	4794
14.07	1826	4215	41.07	2292	4687
15.07	1892	4078	42.07	2512	4794
16.07	2046	4272	43.07	2595	4831
17.07	1869	4078	44.07	2742	5277
18.07	2100	4361	45.07	3172	5558
19.07	2388	4551	46.07	3078	5277
20.07	2584	4423	47.07	2754	5277
21.07	2628	4423	48.07	2661	5233
22.07	2251	4392	49.07	2453	4906
23.07	2251	4551	50.07	2584	5065
24.07	2388	4868	51.07	2684	4906
25.07	2502	5368	51.07	2730	4906
26.07	2779	5233	52.07	2855	4906
27.07	2948	5414	53.07	2730	5148
28.07	2730	5322	54.07	2472	4551
29.07	2707	5277	55.07	2211	4618
30.07	2628	5024	56.07	2361	4486
31.07	2661	5024	57.07	2397	4831

Site CI.WWC

Location: West Wide Canyon, Riverside County, California

Latitude: 33.94068 **Longitude:** -116.40876
(Station coordinates provided by USGS, WGS84 coordinate system

V_{S30} (measured): 587 m/s

V_{S30} (adjusted to more accurately reflect seismic station conditions): 727 m/s (average S-wave velocity between 1.5 and 31.5 m adjusting for assumed 1.5 m sensor depth).

NEHRP Site Class: C

Geomatrix Code: INB

Geologic Conditions/Observations: Seismic station located on Pre-Mesozoic San Gorgonio Complex, which consists of migmatitic gneiss.

Site Conditions: Rural site. Steep, undulating topography in site vicinity. Seismic station located on weathered bedrock ridge. Geophysical testing conducted along the top of the ridge with about 2 m of elevation variation along the 70.5 m long array.

Geophysical Methods Utilized: HVSR, Seismic Refraction, MASW

Geophysical Testing Arrays:

1. Array WWC-1 (48 channel MASW and P-wave seismic refraction array utilizing 4.5 Hz vertical geophones spaced 1.5 m apart for a length of 70.5 m, forward and reverse shot locations with multiple source offsets and source types and multiple interior shot locations).
2. Three HVSR measurement locations distributed along array WWC-1.

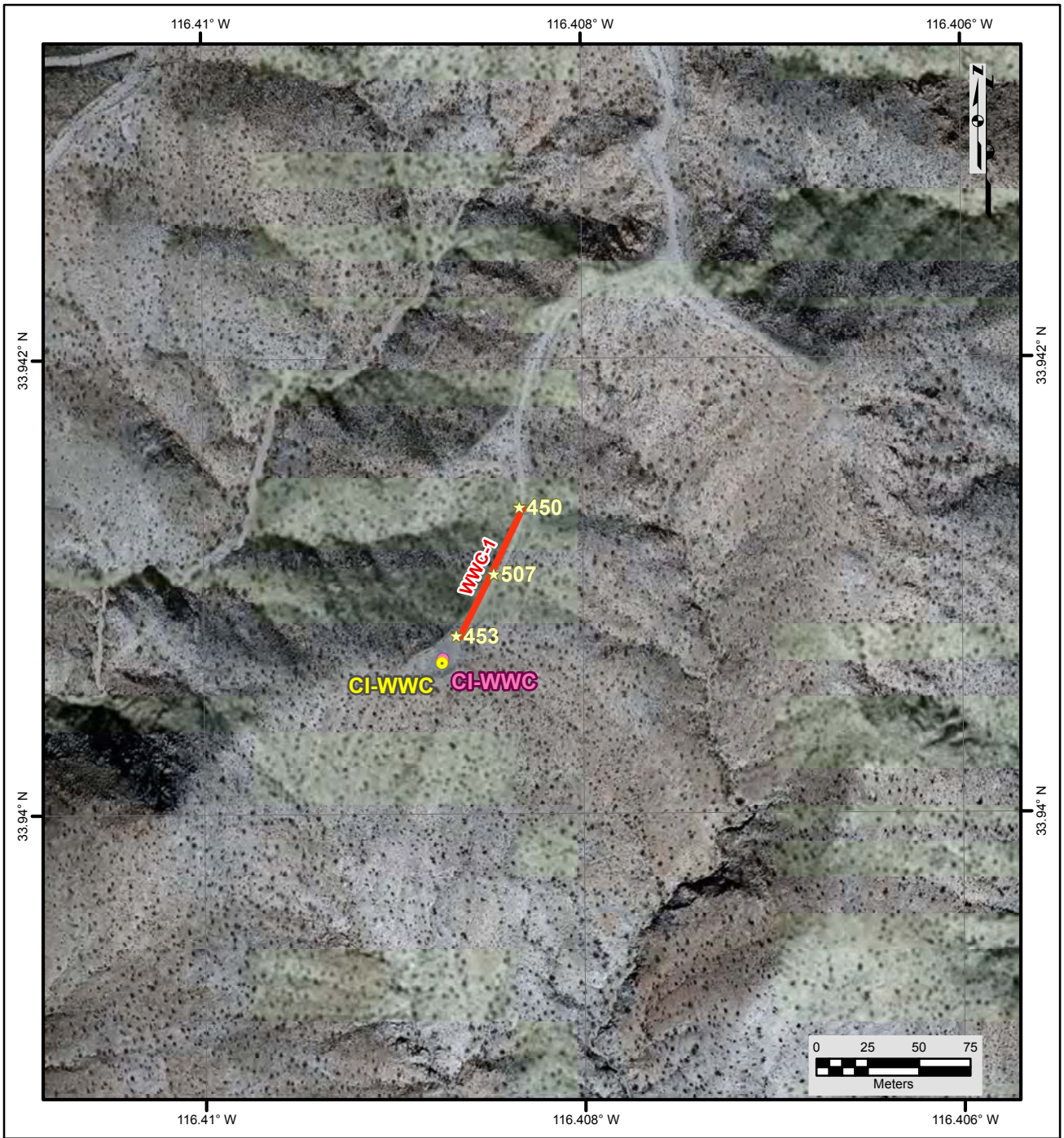

Legend

- Seismic Station - Approximate Surveyed Location
- Seismic Station - Approximate Location of Record
- H/V Spectral Ratio Location
- MASW and Seismic Refraction Array

NOTES:
1. WGS 1984 COORDINATE SYSTEM
2. Image Source: ESRI, i-cubed, USDA FSA, USGS, AEX, GeoEye, Getmapping, Aerogrid, IGP

File Name: CI-WWC-I

Date: 3/21/2012

USGS science for a changing world

GEOVision geophysical services

RECOVERY.GOV

SITE MAP
CI•WWC

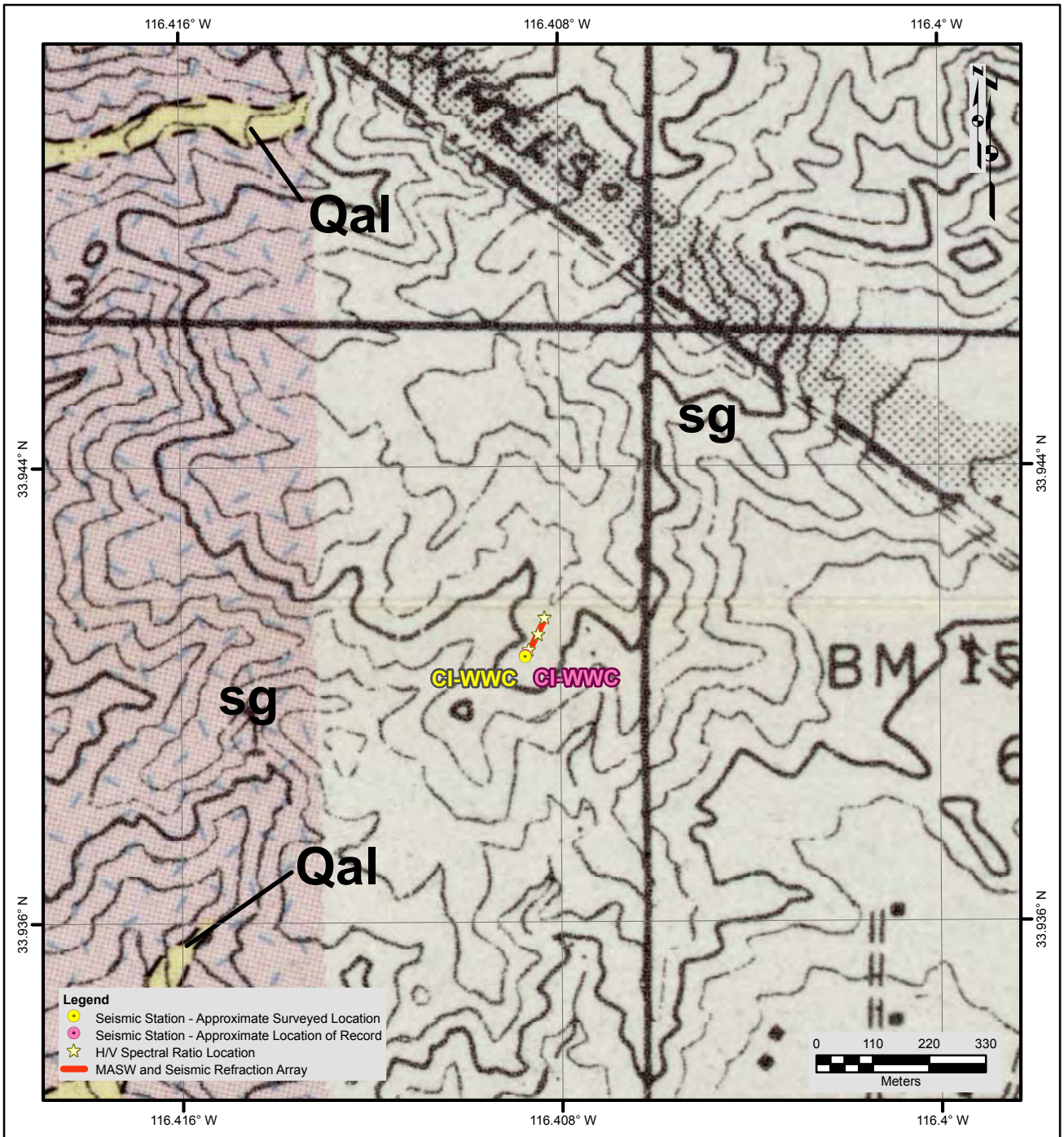

Description of Geologic Map Units

Qal = Quaternary (Holocene) alluvium
sg = Pre-Mesozoic San Gorgonio Complex (Chuckwalla Complex); mainly contorted migmatitic gneisses

NOTES:
1. WGS 1984 COORDINATE SYSTEM
2. Geologic Map and Sections of the Desert Hot Springs Area Riverside County, California by Richard J. Proctor, 1968
3. See site map for details of geophysical survey

File Name: CI-WWC

Date: 3/21/2012

USGS science for a changing world

GEOVision geophysical services

RECOVERY.GOV

GEOLOGIC MAP
CI•WWC

CI.WWC seismic station

Looking northeast along array WWC-1

Looking southwest at seismic station from southwest end of array WWC-1

Looking southwest along array WWC-1

MASW and seismic refraction data acquisition using accelerated weight drop energy source

Location of Geophysical Testing Arrays:

Location	Latitude	Longitude
WWC-1, Southwest End of MASW/Refraction Array	33.94077	-116.40867
WWC-1, Center of MASW/Refraction Array	33.94106	-116.40850
WWC-1, Northeast End of MASW/Refraction Array	33.94134	-116.40834
HVSR Sensor 450	33.94135	-116.40835
HVSR Sensor 453	33.94078	-116.40869
HVSR Sensor 507	33.94105	-116.40849
CI.WWC Seismic Station	33.94066	-116.40877

Notes: 1) WGS84 Coordinate System (decimal degrees)
2) Survey accuracy is estimated at 1 to 2 m.

Results:

V_S Model (MASW Sounding)

Depth to Top of Layer (m)	Layer Thickness (m)	S-Wave Velocity (m/s)	Inferred P-Wave Velocity (m/s)	Inferred Poisson's Ratio	Inferred Density (g/cm^3)
0	1	104	195	0.3	1.70
1	1.5	343	642	0.3	1.90
2.5	2.5	538	1006	0.3	2.00
5	4	562	1051	0.3	2.00
9	7	664	1242	0.3	2.10
16	9	828	1550	0.3	2.15
25	>5	1256	2349	0.3	2.25

Notes: 1) Depth of investigation is about 30 m.
2) Bottom layer is a half space.
3) Half space velocity not well constrained.

Average V_P and Estimated V_S Models from Central Portion of P-wave Seismic Refraction Line

Depth to Top of Layer (m)	Layer Thickness (m)	P-Wave Velocity (m/s)	Estimated S-Wave Velocity (m/s)			
			Poisson's Ratio = 0.25	Poisson's Ratio = 0.3	Poisson's Ratio = 0.3333	Poisson's Ratio = 0.35
0.00	0.60	296	171	158	148	142
0.60	1.21	541	312	289	270	260
1.81	1.21	791	456	423	395	380
3.02	1.21	921	532	492	461	443
4.22	1.21	956	552	511	478	459
5.43	1.21	1070	618	572	535	514
6.64	1.21	1079	623	577	540	518
7.85	2.53	1108	640	592	554	532
10.38	2.53	1213	701	649	607	583
12.91	2.53	1414	816	756	707	679
15.45	2.53	1801	1040	963	901	865
17.98	2.53	1834	1059	980	917	881
20.52	2.53	2090	1206	1117	1045	1004
23.05	2.53	2450	1414	1309	1225	1177
25.59	Half Space	3103	1791	1659	1552	1491

Note: Half space velocity may be overestimated and seismic refraction data can be adequately modeled with a half space P-wave velocity of about 2,500 m/s.

Observations/Discussion:

- There are no distinct, high amplitude HVSR peaks at the site. Heavy winds are very common at the site and HVSR data were acquired in moderate winds with the sensors covered. Data quality at sensor 453 may be degraded by conditions during testing and/or poor sensor coupling.
- The P-wave seismic refraction data for array WWC-1 were modeled using a tomographic inversion routine with a smooth velocity gradient starting model. The P-wave seismic refraction model was extended to far offset shot locations to extend depth of investigation. It should be noted that a larger geophone spacing, rather than the utilization of far offset shot locations, is preferred for extending depth of investigation, when applying tomographic inversion routines. However, the seismic refraction data were acquired in conjunction with surface wave data, where a shorter array length is preferred.
- The P-wave seismic refraction survey design allowed P-wave velocity to be imaged to a maximum depth of about 26 m, although 23 m may be more realistic. The seismic refraction model indicates that P-wave velocity is about 350 to 500 m/s at the surface and increases to over 1,000 m/s at a depth of 2.5 to 9 m, 1,500 m/s at a depth of 6 to 14 m, 2,000 m/s at a depth of 15 to 21 m and over 3,000 m/s at a nominal depth of 25 m. The

maximum P-wave velocity in the central portion of the model, where depth of investigation is greatest, is slightly greater than 3,100 m/s. P-wave velocities over 2,500 m/s, below a depth of about 23 m, are not well constrained and it was possible to model the data with a maximum allowable P-wave velocity of 2,500 m/s with inconsequential increase in RMS error. Care should always be taken interpreting seismic velocities near the base of models developed using tomographic inversion.

- The seismic refraction survey indicates that there is lateral velocity variation at the site, as is the norm for rock sites. There is a very thin, nominal 0.5 to 1 m thick, residual soil layer overlying weathered rock. This layer may have its greatest thickness and lowest velocity towards the northeast end of the array. The southwest end of the array, which is closest to the seismic station, has a thicker sequence of weathered rock with P-wave velocity less than 1,250 m/s.
- The average P-wave velocity of the upper 30 m (V_{P30}) was estimated between 21 and 46.5 m on the P-wave refraction model, where depth of investigation is greatest. To estimate V_{P30} the P-wave velocity at a depth of 26 m, nominal depth of investigation, was projected to 30 m depth. V_{P30} ranges from about 1,231 to 1,362 m/s over the 21 to 46.5 m position interval, a 10% variation. The lowest and highest estimated V_{P30} over this distance interval occur at a position of 21 and 46.5 m on the profile, respectively. Southwest of 21 m, V_{P30} is likely similar to that at 21 m, the minimum value. Northeast of 46.5 m, V_{P30} is likely higher than that at 46.5 m, the maximum value.
- An average V_P model was developed over the 21 to 46.5 m distance interval by horizontally averaging the travel time of each model cell, or slowness if cell thickness relatively uniform, and cell thickness and average V_{P30} were determined to be 1,291 m/s. Assuming constant Poisson's ratios of 0.25, 0.3, 0.3333 and 0.35 would result in an estimated V_{S30} of 745, 690, 645 and 620 m/s, respectively. Saturation is not expected in the upper 30 m and, therefore, Poisson's ratio of the weathered rock is not expected to be higher than 0.35.
- Noise conditions at the site were not sufficient for application of passive surface wave techniques.
- The minimum wavelength surface wave phase velocity data extracted from the 48-channel MASW array is about 17 m. Data reduction using seismic records from smaller hammer sources and a limited offset receiver array (i.e. less active geophones) allowed extraction of surface wave dispersion data to a minimum wavelength of about 5 m. It was very difficult to extract fundamental mode Rayleigh wave phase velocity data at wavelengths less than 8 m (frequency greater than 30 Hz), possibly because the velocity in the upper two to three meters is highly variable beneath the array. Higher modes were dominant at high frequencies for some seismic records. Slightly higher frequency Raleigh wave dispersion data were extracted from seismic records associated with source locations at the northeastern end of the array.
- There is nominally about 75 to 125 m/s scatter in MASW dispersion data selected for modeling, likely due to the effects of lateral velocity variation.
- The Rayleigh wave phase velocity at 40 m wavelength (V_{R40}) is in the 560 to 660 m/s range which would result in an estimated V_{S30} of 585 to 690 m/s, based on the Brown, et al., 2000 relationship, assuming that the dispersion curve at 40 m wavelength is the fundamental mode.

- A representative dispersion curve was generated for the MASW data set using a moving average, polynomial curve fitting routine and used for modeling.
- Although a minimum Rayleigh wave wavelength of only 5 m was obtained from the MASW data, a 1 m thick low velocity layer was permitted in the V_S model based on observations in the seismic refraction data.
- Surface wave depth of investigation is about 30 to 35 m based on the one half of maximum wavelength criteria.
- There is good agreement between the average V_S models calculated from the P-wave seismic refraction model assuming constant values of Poisson's ratio and the V_S model resulting from inversion of the Rayleigh wave phase velocity data, especially in the upper 16 to 20 m. Below a depth of 20 m, the MASW V_S model underestimates S-wave velocity relative to the seismic refraction model. The seismic refraction model may overestimate velocity below 24 m, but this does not completely account for the difference in the two models. Saturation of the rock would possibly increase Poisson's ratio of significantly fractured weathered rock, thereby lowering estimated S-wave velocity. Saturation of the rock is not expected in the upper 30 m as there is no flow in the adjacent canyons, but cannot be completely discounted.
- V_{S30} from the MASW V_S model is 587 m/s (NEHRP Site Class C).
- V_{S30} estimated from the MASW sounding is at the lower bound of that estimated based on V_{R40}, possibly because of the allowance of a thin low velocity layer in the model to be consistent with the seismic refraction model and to fit small wavelength dispersion data extracted for seismic records associated with several source locations at the northeast end of the array.
- Average S-wave velocity between a depth of 1.5 and 31.5 m, to account for assumed seismic sensor depth, is 727 m/s (NEHRP Site Class C).
- V_{S30} from the average P-wave seismic refraction model and assumed constant Poisson's ratio of 0.3333 is 645 m/s (Site Class C), 10% higher than that measured using the MASW technique. V_{S30} from the average P-wave seismic refraction model and assumed constant Poisson's ratio of 0.35 is 620 m/s (Site Class C), 6% higher than that measured using the MASW technique. The lowest V_{S30} in the central portion of the P-wave seismic refraction model (position of 21 m) is 591 m/s for an assumed constant Poisson's ratio of 0.35, similar to that measured with the MASW technique.
- Average S-wave velocity between a depth of 1.5 and 31.5 m from the average P-wave velocity model is 823, 762, 713 and 685 m/s for assumed constant Poisson's ratios of 0.25, 0.3, 0.3333 and 0.35, respectively.
- For site characterization purposes, the use of the MASW V_S model is recommended. This model likely reflects the lower bound of V_{S30} in the site vicinity, which is considered appropriate as the seismic station is located at the southwestern end of the seismic line where velocities are lowest. The seismic refraction model indicates that there is more than 10% variation of V_{S30} over distances as small as 25 m.

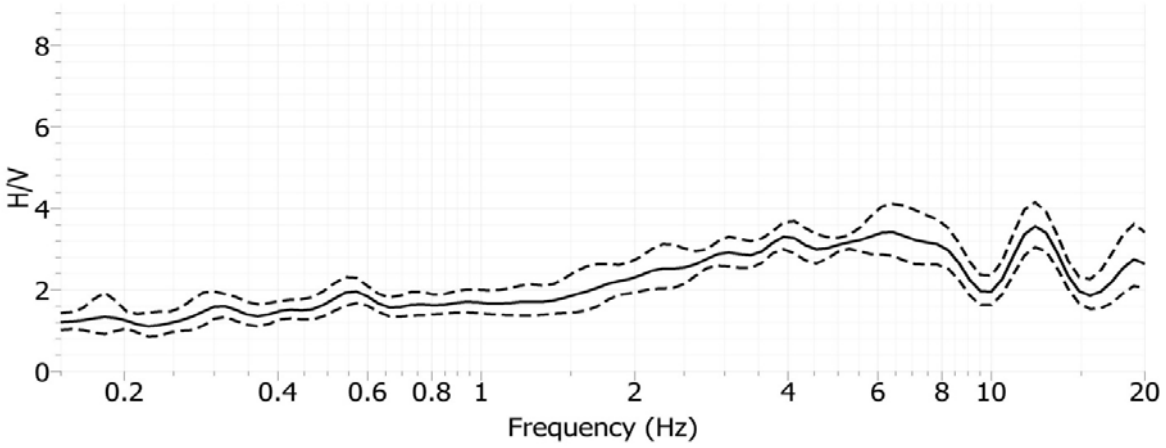

Site CI.WWC, H/V Spectral Ratio, Array WWC-1, Sensor 450

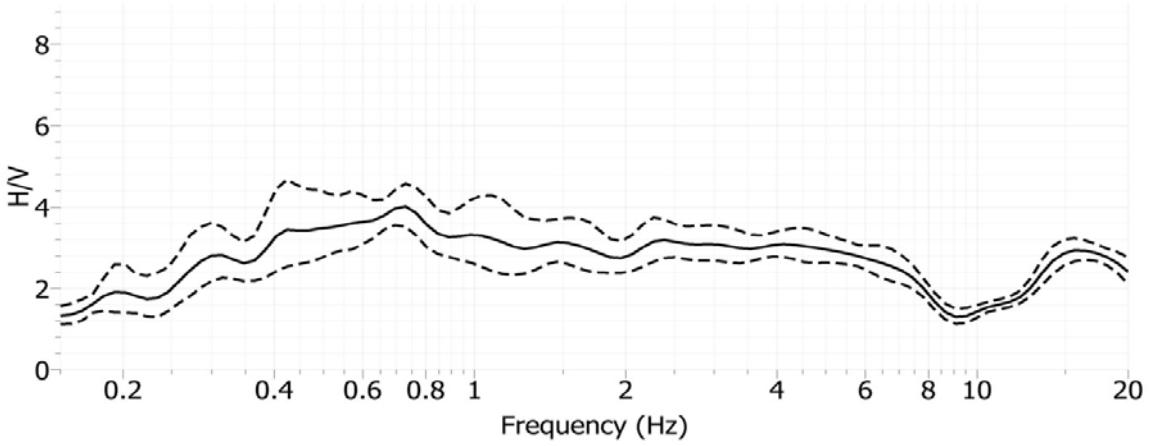

Site CI.WWC, H/V Spectral Ratio, Array WWC-1, Sensor 507

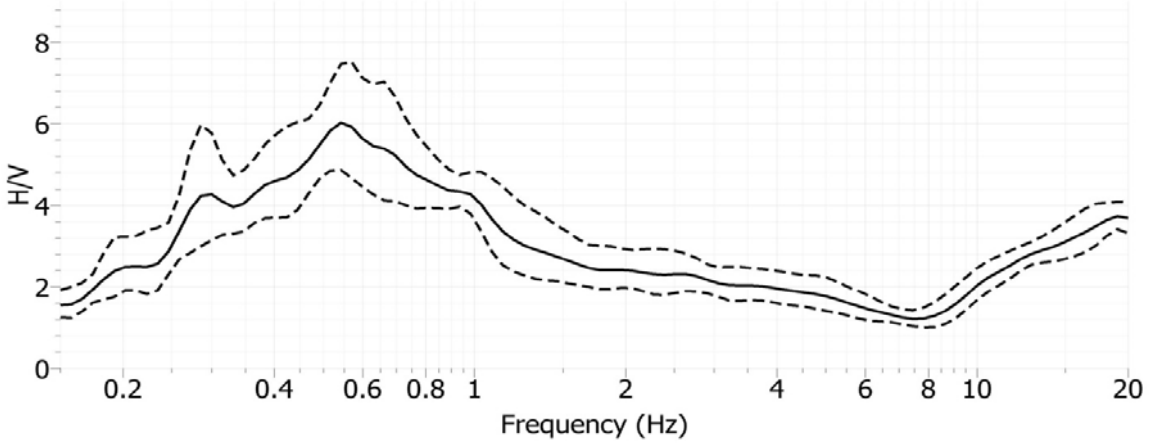

Site CI.WWC, H/V Spectral Ratio, Array WWC-1, Sensor 453

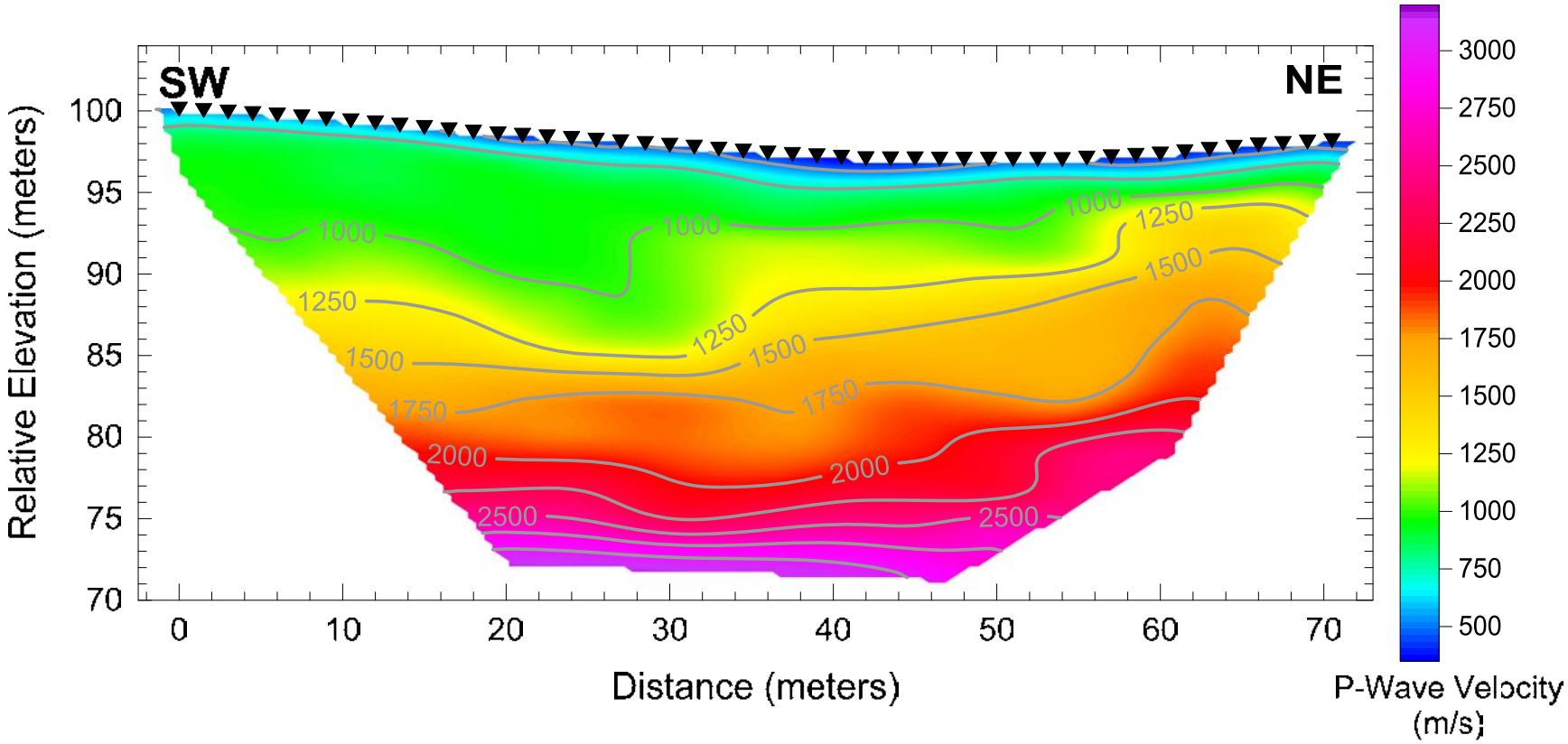

Array WWC-1 – P-wave tomographic seismic refraction model developed utilizing a smooth velocity gradient starting model

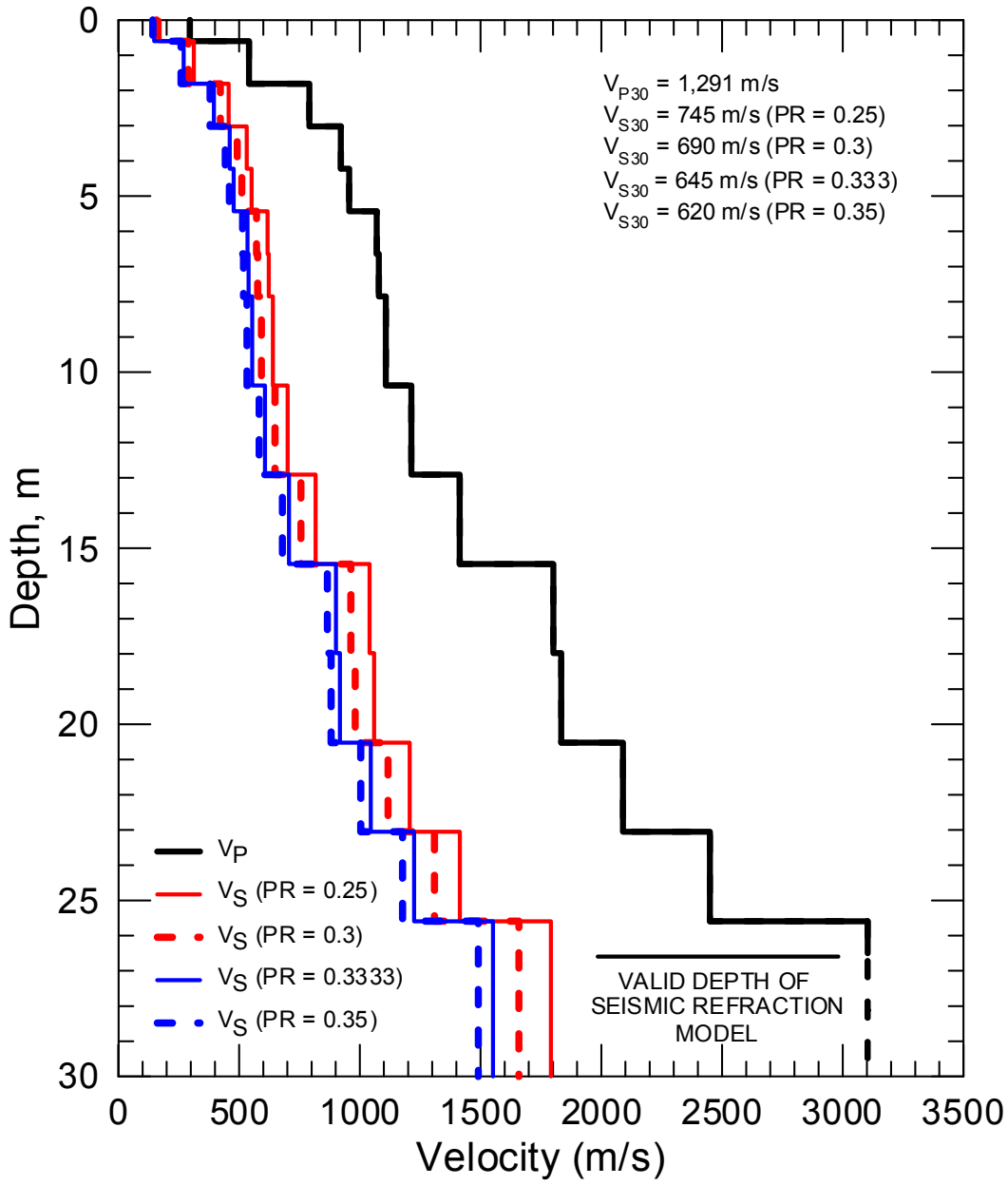

CI.WWC – Average P-wave velocity structure and estimated S-wave velocity structure between a position of 21 and 46.5 m on the P-wave seismic refraction model for array WWC-1. The bottom layer in the seismic refraction model is not well constrained and not required to model the first arrival data.

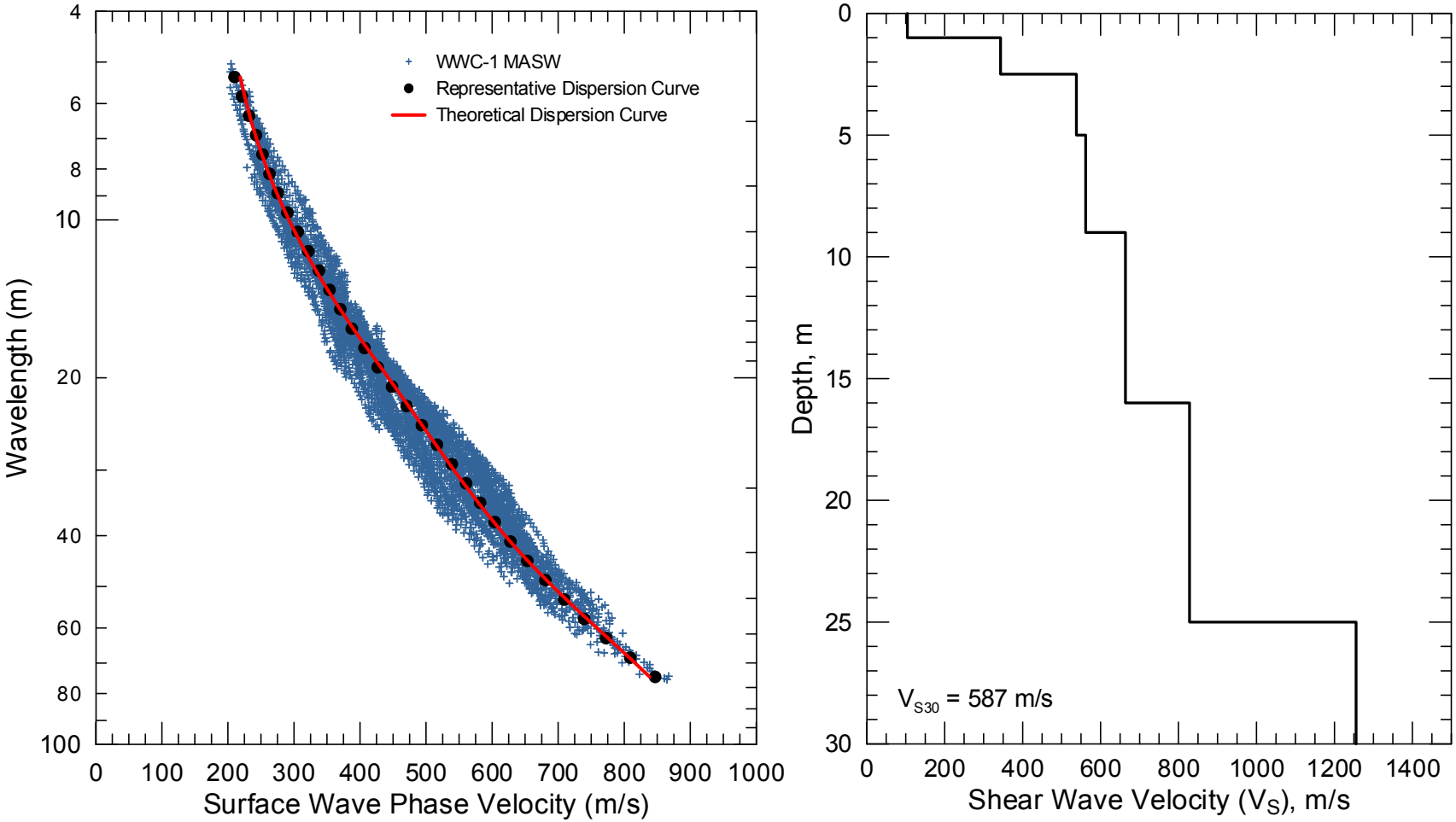

CI.WWC - Field, representative and inverted theoretical surface wave dispersion data (left) and associated V_S model (right)

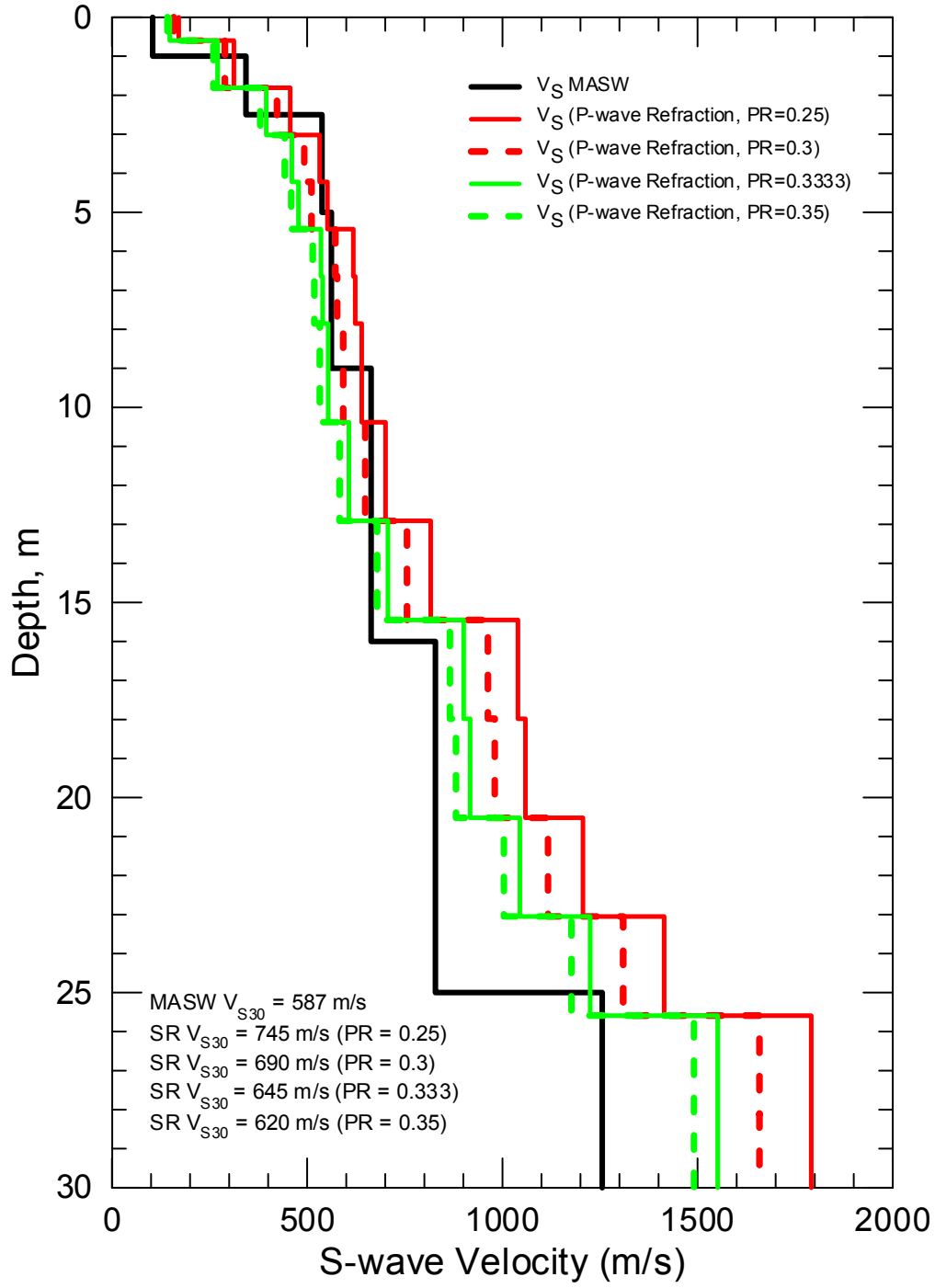

CI.WWC – Comparison of S-wave velocity models derived from the MASW and P-wave seismic refraction surveys. The V_S model from the MASW array is in good agreement with estimated V_S models from the P-wave refraction model at depths above 16 m, but slightly underestimates V_S, relative to the seismic refraction model, at greater depths. The seismic refraction line is not long enough to accurately constrain the velocity of the layer below 25 m and the data can be effectively modeled without this layer, which would improve agreement with the MASW model. If weathered rock were saturated at a depth below 20 m, Poisson's ratio would be higher resulting in lower V_S; however, saturation at such a depth is not expected at this site.

Site NC.BBGB

Location: Big Mountain, San Benito County, California

Latitude: 36.57849 **Longitude:** -121.03956
(Station coordinates provided by USGS, WGS84 coordinate system)

V_{S30} (measured): 285 m/s

V_{S30} (adjusted to more accurately reflect seismic station conditions): 312 m/s (average S-wave velocity between 1 and 31 m adjusting for assumed 1 m sensor depth and/or the sensor not being placed on loose top soil).

NEHRP Site Class: D

Geomatrix Code: IED

Geologic Conditions/Observations: Seismic station located on geologic unit mapped as Tertiary (Eocene) Kreyenhagen Shale. Geologic bedding is mapped as dipping about 60 degrees to the south-southwest in the immediate site vicinity.

Site Conditions: Rural site located on gently rolling hills. Test area located along a gently sloping hill with ground surface elevation increasing about 7 m to the north along the 70.5 m long MASW array BBGB-1 and 14 m to the north along the 141 m long seismic refraction and surface wave array BBGB-2.

Geophysical Methods Utilized: HVSR, Seismic Refraction (P- and S-wave), MASW (Rayleigh Wave) and MALW (Love Wave)

Geophysical Testing Arrays:

1. Array BBGB-1 (48 channel MASW and P-wave seismic refraction array utilizing 4.5 Hz vertical geophones spaced 1.5 m apart for a length of 70.5 m, forward and reverse shot locations with multiple source offsets and source types and multiple interior shot locations).
2. Array BBGB-2 (48 channel P-wave seismic refraction array utilizing 4.5 Hz vertical geophones spaced 3 m apart for a length of 141 m, forward and reverse shot locations with multiple source offsets and source types and multiple interior shot locations).
3. Array BBGB-2 (48 channel MALW and S-wave seismic refraction array utilizing 4.5 Hz horizontal geophones spaced 3 m apart for a length of 141 m, forward and reverse shot locations with multiple source offsets and multiple interior shot locations). Coincident with P-wave array of same name.
4. Three HVSR measurement locations: two distributed along array BBGB-1 and the other adjacent to the seismic station.

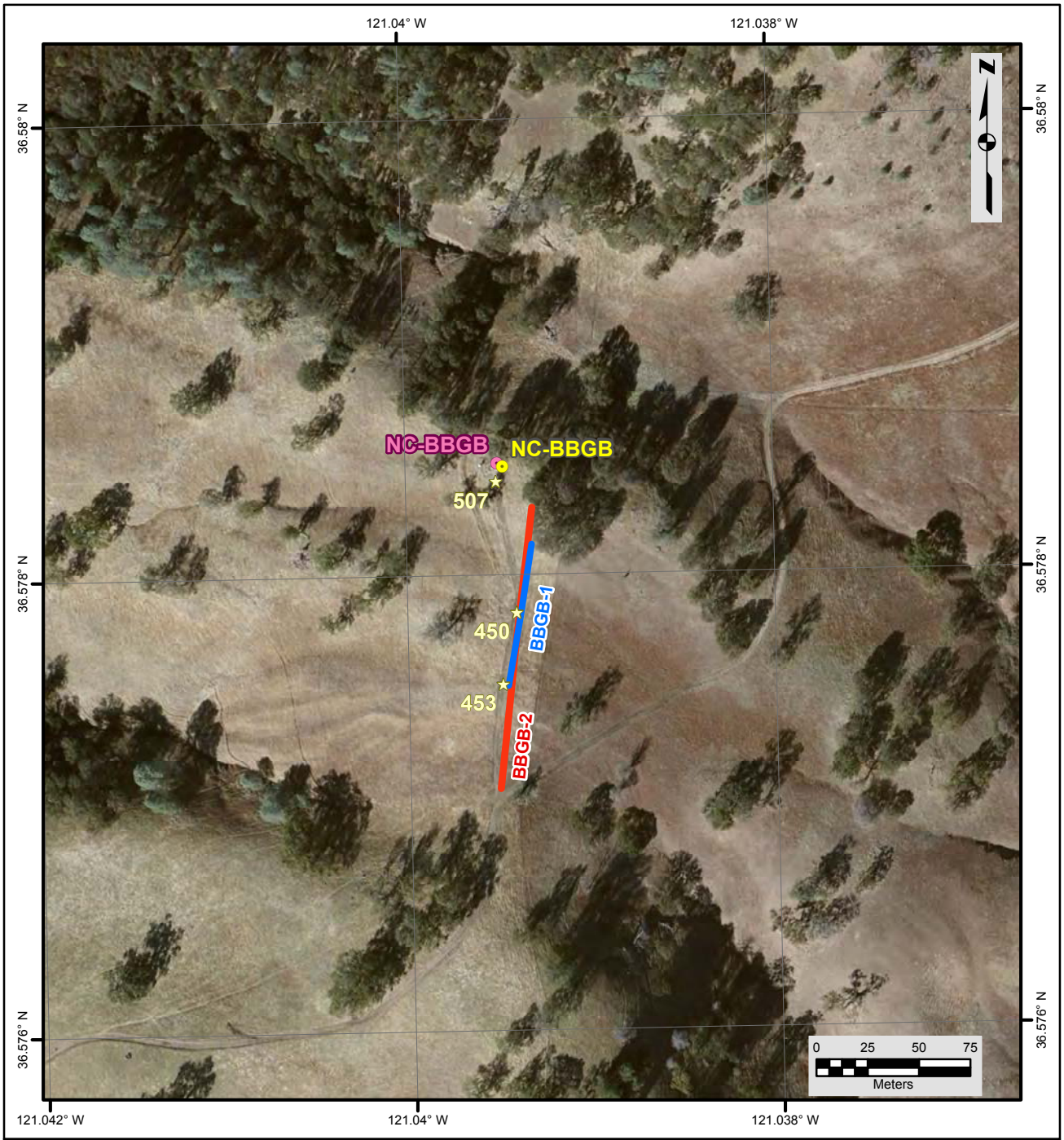

Legend

- Seismic Station - Approximate Surveyed Location
- Seismic Station - Approximate Location of Record
- H/V Spectral Ratio Location
- MASW and Seismic Refraction Array
- MASW and Seismic Refraction Array

NOTES:
1. WGS 1984 COORDINATE SYSTEM
2. Image Source: ESRI, i-cubed, USDA FSA, USGS, AEX, GeoEye, Getmapping, Aerogrid, IGP

File Name: NC-BBGB-I

Date: 2/7/2013

USGS science for a changing world

GEOVision geophysical services

RECOVERY.GOV

SITE MAP
NC•BBGB

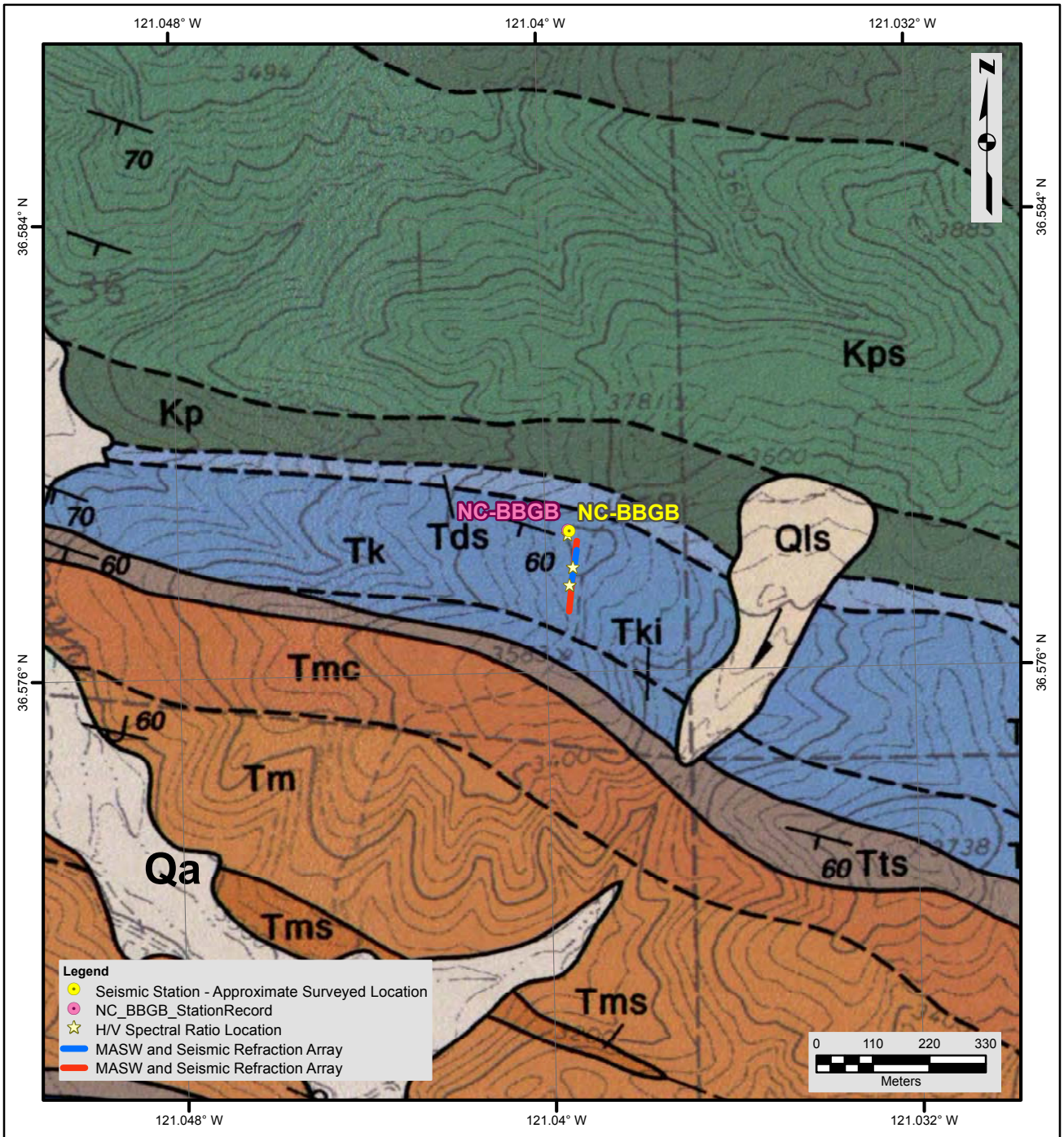

Description of Geologic Map Units

Qa = Quaternary (Holocene) alluvial gravel & sand of major stream channels
Qls = Quaternary (Pleistocene/Holocene) landslide rubble
Tms = Tertiary (Miocene) sandstone, fine to medium grained, arkosic
Tm = Tertiary (Miocene) Monterey shale; semi-siliceous, thin bedded, platy to silty with hackly fracture
Tmc = Tertiary (Miocene) Monterey (?) clay shale; soft, argillaceous, locally bentonitic
Tts = Tertiary (Miocene) Temblor sandstone; fine to medium grained, arkosic
Tki = Tertiary (Eocene) Kreyenhagen Shale; clay shale & semi-siliceous shale, micaceous, interbedded siliceous shale, thin bedded, soft, diatomaceous

Tk = Tertiary (Eocene) Kreyenhagen Shale; clay shale or claystone, micaceous, argillaceous
Tds = Tertiary (Eocene) Domengine Sandstone; sandstone and interbedded silty clay shale
Kp = Mesozoic (Upper Cretaceous) Panoche Formation; clay shale or claystone, bedded, micaceous, argillaceous
Kps = Mesozoic (Cretaceous) Panoche Formation; sandstone, hard, fine to medium grained, arkosic

NOTES:
1. WGS 1984 COORDINATE SYSTEM
2. Geologic Map of the San Benito Quadrangle San Benito County, California by Thomas W. Dibblee, Jr., 2007
3. See site map for details of geophysical survey

File Name: NC-BBGB

Date: 2/7/2013

USGS science for a changing world

GEOVision geophysical services

GEOLOGIC MAP
NC•BBGB

RECOVERY.GOV

Looking at NC.BBGB Seismic Station

P-wave seismic refraction and MASW data acquisition on array BBGB-1

S-wave seismic refraction and MALW data acquisition on array BBGB-2

Looking north along array BBGB-1 towards seismic station and at HVSR sensor 450

Looking south along MASW and P-wave refraction array BBGB-2

Location of Geophysical Testing Arrays:

Location	Latitude	Longitude
BBGB-1, South End of MASW/Refraction Array	36.57751	-121.03952
BBGB-1, Center of MASW/Refraction Array	36.57782	-121.03945
BBGB-1, North End of MASW/Refraction Array	36.57813	-121.03938
BBGB-2, South End of MASW/MALW/Refraction Array	36.57706	-121.03957
BBGB-2, Center of MASW/MALW/Refraction Array	36.57769	-121.03948
BBGB-2, North End of MASW/MALW/Refraction Array	36.57829	-121.03937
HVSR Sensor 450	36.57783	-121.03947
HVSR Sensor 453	36.57752	-121.03955
HVSR Sensor 507	36.57841	-121.03957
NC.BBGB Seismic Station	36.57847	-121.03953

Notes: 1) WGS84 Coordinate System (decimal degrees)
2) Survey accuracy is estimated at 1 to 2 m.

Results:

V_S Model 1 (Source Locations near South End of Array)

Depth to Top of Layer (m)	Layer Thickness (m)	S-Wave Velocity (m/s)	Inferred P-Wave Velocity (m/s)	Assumed Poisson's Ratio	Assumed Density (g/cm^3)
0	0.8	78	146	0.300	1.6
0.8	2.2	177	331	0.300	1.7
3	3	212	397	0.300	1.7
6	4	292	546	0.300	1.8
10	5	341	637	0.300	1.8
15	5	358	670	0.300	1.8
20	6	380	1750	0.475	1.9
26	>4	437	1750	0.467	1.9

Notes: 1) Saturated zone with V_P of about 1,750 m/s constrained at 20 m depth based on seismic refraction model, although no effect on Love wave model.
2) Depth of investigation is about 30 m.
3) Bottom layer is a half space.

V_S Model 2 (Source Locations near North End of Array)

Depth to Top of Layer (m)	Layer Thickness (m)	S-Wave Velocity (m/s)	Inferred P-Wave Velocity (m/s)	Assumed Poisson's Ratio	Assumed Density (g/cm^3)
0	1.5	87	163	0.300	1.6
1.5	2	183	342	0.300	1.7
3.5	2.5	248	465	0.300	1.7
6	4	283	529	0.300	1.8
10	5	324	606	0.300	1.8
15	5	353	660	0.300	1.8
20	6	391	1750	0.474	1.9
26	>4	438	1750	0.467	1.9

Notes: 1) Saturated zone with V_P of about 1,750 m/s constrained at 20 m depth based on seismic refraction model, although no effect on Love wave model.
2) Depth of investigation is about 30 m.
3) Bottom layer is a half space.

Observations/Discussion:

- The HVSR plots at the three measurement locations are generally similar, especially sensor location 507 near the seismic station and 453 near the southern end of array BBGB-1. There are, however, no distinct high amplitude HVSR peaks at the site.
- The seismic arrays were located almost orthogonal to strike of the geologic bedding. Attempting to acquire data parallel to strike would have introduced too much topographic variation along the arrays.
- During the first site visit, MASW and P-wave seismic refraction data were acquired along the 70.5 m long array BBGB-1. After preliminary data review, it was determined that additional geophysical data were required to characterize the site because higher modes dominated the Rayleigh wave dispersion data at high frequencies. Therefore, P-wave seismic refraction, MALW and S-wave seismic refraction data were acquired along a 141 m long array during a second site visit.
- P-wave seismic refraction first arrival data collected along array BBGB-2 are of excellent quality, although it was necessary to pick around the air wave at small receiver offsets. S-wave seismic refraction first arrival data quality was not considered good enough to use for site characterization purposes. However, review of S-wave first arrival data and comparison to P-wave first arrival data indicated that a high velocity refractor in the P-wave seismic refraction data is likely associated with the saturated zone. Additionally, there is no evidence of S-wave velocity exceeding 400 m/s until a depth of greater than about 25 m. It was possible to extract Love wave dispersion data from the dataset.
- The P-wave seismic refraction data for array BBGB-2 were modeled using a tomographic inversion routine with a layer-based starting model. The seismic refraction model was extended to far offset shot locations to extend depth of investigation.

- The P-wave seismic refraction survey design allowed P-wave velocity to be imaged to a maximum depth of about 30 m. The seismic refraction model indicates that P-wave velocity is about 225 to 300 m/s at the surface and increases to 600 m/s at a depth of 2 to 5 m, 800 m/s at a depth of 5 to 12 m and abruptly increases from 1,200 to over 1,600 m/s at a depth of about 14 to 24 m. The maximum P-wave velocity in the models is about 1,950 m/s. Review of the S-wave refraction data and surface wave data yields no evidence of high S-wave velocities associated with the P-wave velocities of greater than 1,400 m/s. Therefore, we conclude that this high velocity unit is associated with saturated sediments.
- Noise conditions at the site were not sufficient for application of passive surface wave techniques.
- Review of Rayleigh wave (MASW) data indicated that higher modes were dominant at higher frequencies with the smallest wavelength Rayleigh wave phase velocity data extracted from limited offset receiver arrays equal to about 8 m. The source of dominant higher mode energy Rayleigh wave data is not clear. Dominant higher modes were not, however, a significant issue in Love wave (MALW) data. Therefore, modeling of Love wave, rather than Rayleigh wave, phase velocity data was conducted at this site. It should be noted, however, that the Love wave data were acquired using 4.5 Hz horizontal geophones and a hammer/traction plank energy source. To develop a V_S model to 30 m depth it was necessary to pick Love wave phase velocity data to a frequency of about 4 Hz (90 m wavelength), which may be pushing the limits of the energy source.
- Even though a model was not developed for the Rayleigh wave dispersion curve, the phase velocity of a 40 m wavelength Rayleigh wave (V_{R40}) was determined to average about 290 m/s, which would result in an estimated V_{S30} of 303 m/s using the relationship presented in Brown, et al, 2000 ($V_{S30} = 1.045V_{R40}$).
- Compilation of a Love wave dispersion curve was complicated by near surface lateral velocity variation. There was clear divergence of the phase velocities at small wavelengths (high frequencies) generated from source locations at the south and north ends of the array. Therefore, the MALW data were modeled by developing two dispersion curves: one from interior and south off end source locations and the other from north off-end and interior source locations.
- The minimum wavelength Love wave phase velocity data extracted from the 48-channel MALW array was about 14 m. Reducing data from smaller hammer sources using a limited offset receiver array (i.e. less active geophones) allowed for extraction of surface wave dispersion data to a minimum wavelength of about 3.5 m.
- There is nominally about 30 m/s of scatter in MALW dispersion data, which is in part due to lateral velocity variation.
- A representative dispersion curve was generated for the MALW data set using a moving average, polynomial curve fitting routine and used for modeling.
- Although not necessary for modeling of Love wave dispersion data, the saturated zone with P-wave velocity of 1,750 m/s was anchored at a depth of 20 m during data modeling. An assumed Poisson's ratio of 0.3 was used for unsaturated sediments. Unlike Rayleigh wave data, Poisson's ratio has no impact on Love wave modeling. In reviewing the P-wave seismic refraction model, it appears that Poisson's ratio may be significantly higher than 0.3 in parts of the unsaturated zone.

- The V_S model developed for the Love wave dispersion curves developed from source locations at the south (Model 1) and north (Model 2) ends of array BBGB-2 are relatively similar with only a 2% difference in V_{S30}.
- Surface wave depth of investigation is about 30 m based on one third of maximum wavelength criteria.
- The S-wave velocity models derived from the surface wave testing are believed to be representative of average subsurface velocity structure. However, geology at the site is complex with steeply dipping bedding. The seismic line was oriented almost perpendicular to strike and surface topography did not allow acquisition of data parallel to strike. The S-wave velocities are very low at this site, indicating that the near surface Tertiary shale has weathered to soil, in which case the dip of the bedding will not significantly impact results.
- V_{S30} is 288 m/s for Model 1 and 282 m/s for Model 2, averaging 285 m/s (Site Class D).
- V_{S30} estimated from the MALW V_S model compares favorably with that estimated from V_{R40}, about 303 m/s.
- Average S-wave velocity between 1 m (compensating for assumed sensor depth and/or sensor not being placed on loose soil) and 31 m is 316 and 308 m/s for Models 1 and 2, respectively, averaging 312 m/s.

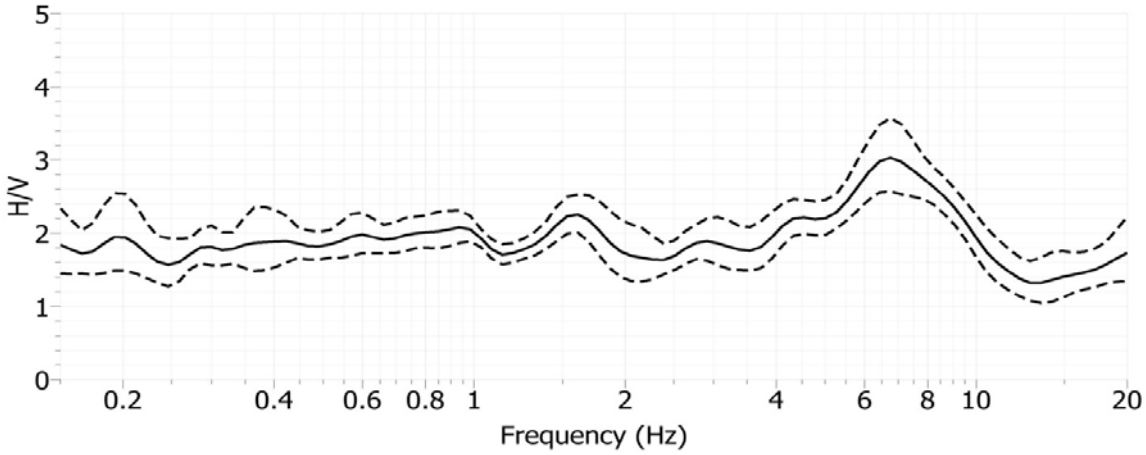

Site NC.BBGB, H/V Spectral Ratio, Near Seismic Station, Sensor 507

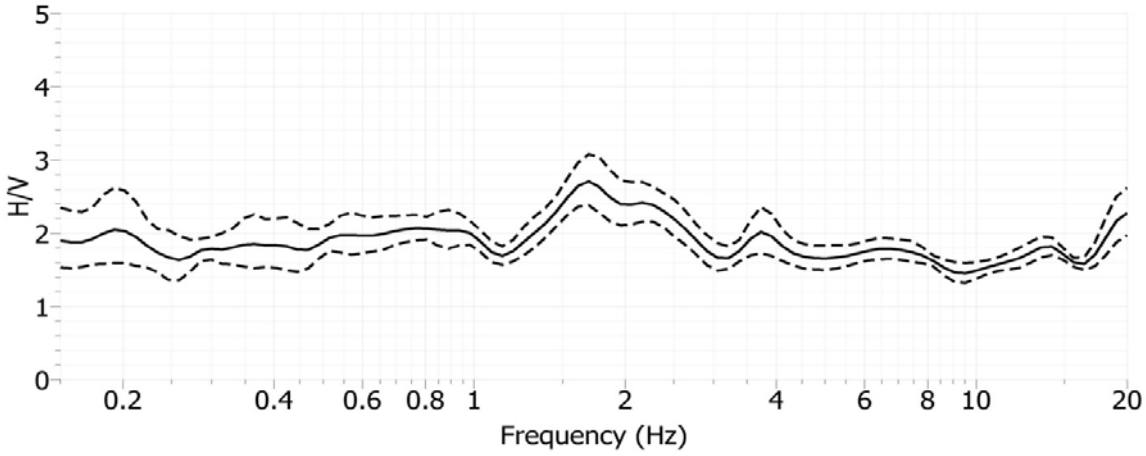

Site NC.BBGB, H/V Spectral Ratio, Array BBGB-1, Sensor 450

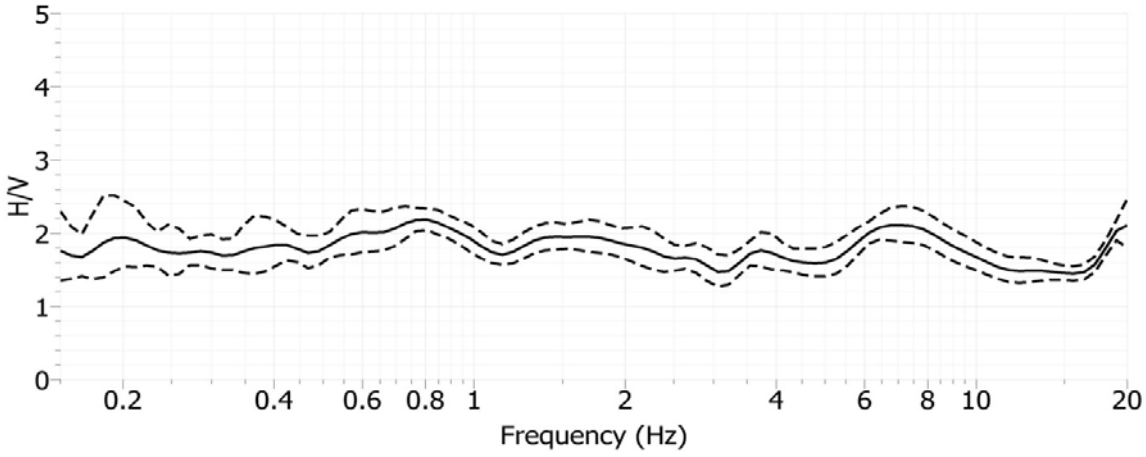

Site NC.BBGB, H/V Spectral Ratio, Array BBGB-1, Sensor 453

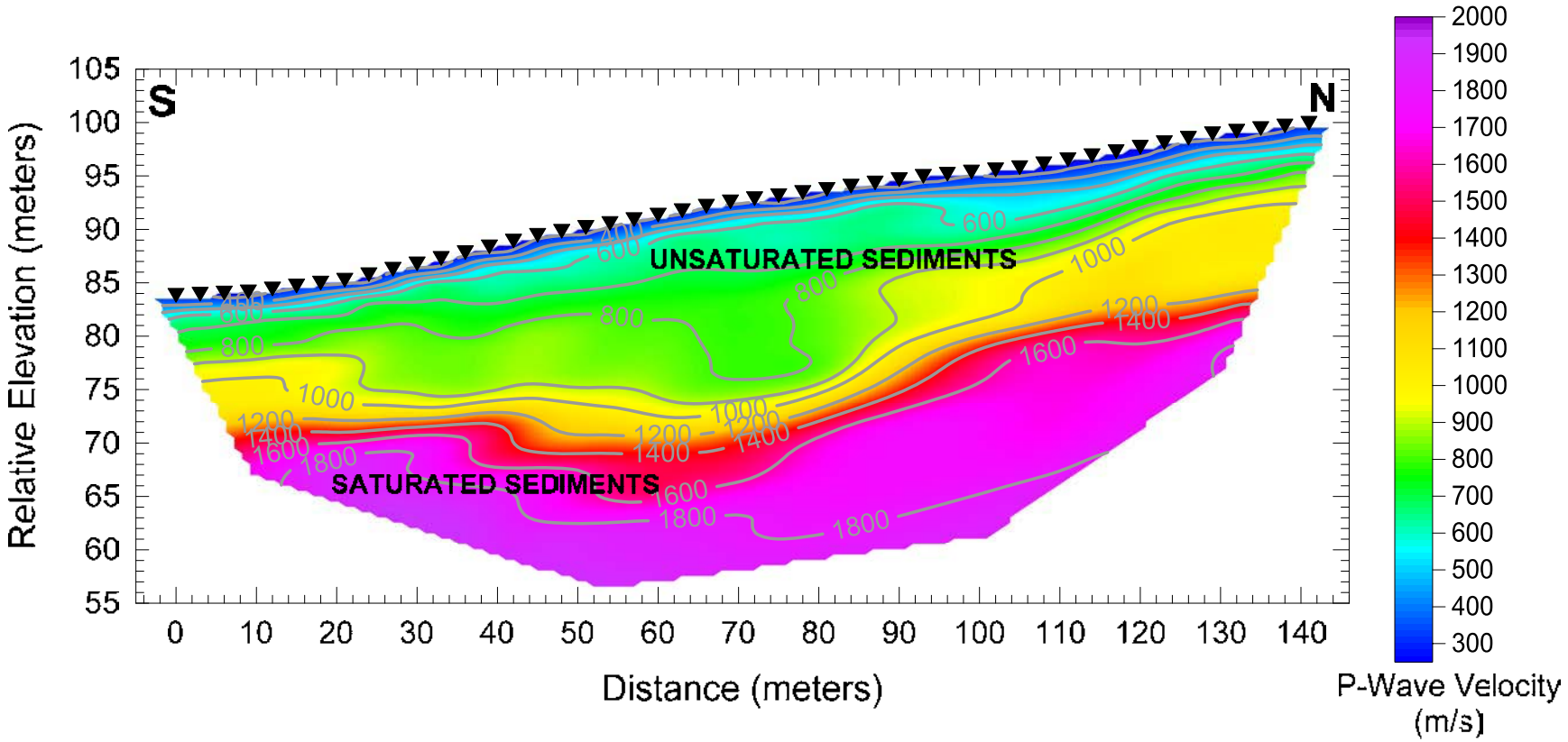

Array BBGB-2 – P-wave Tomographic Seismic Refraction Model utilizing Layer Based Starting Model

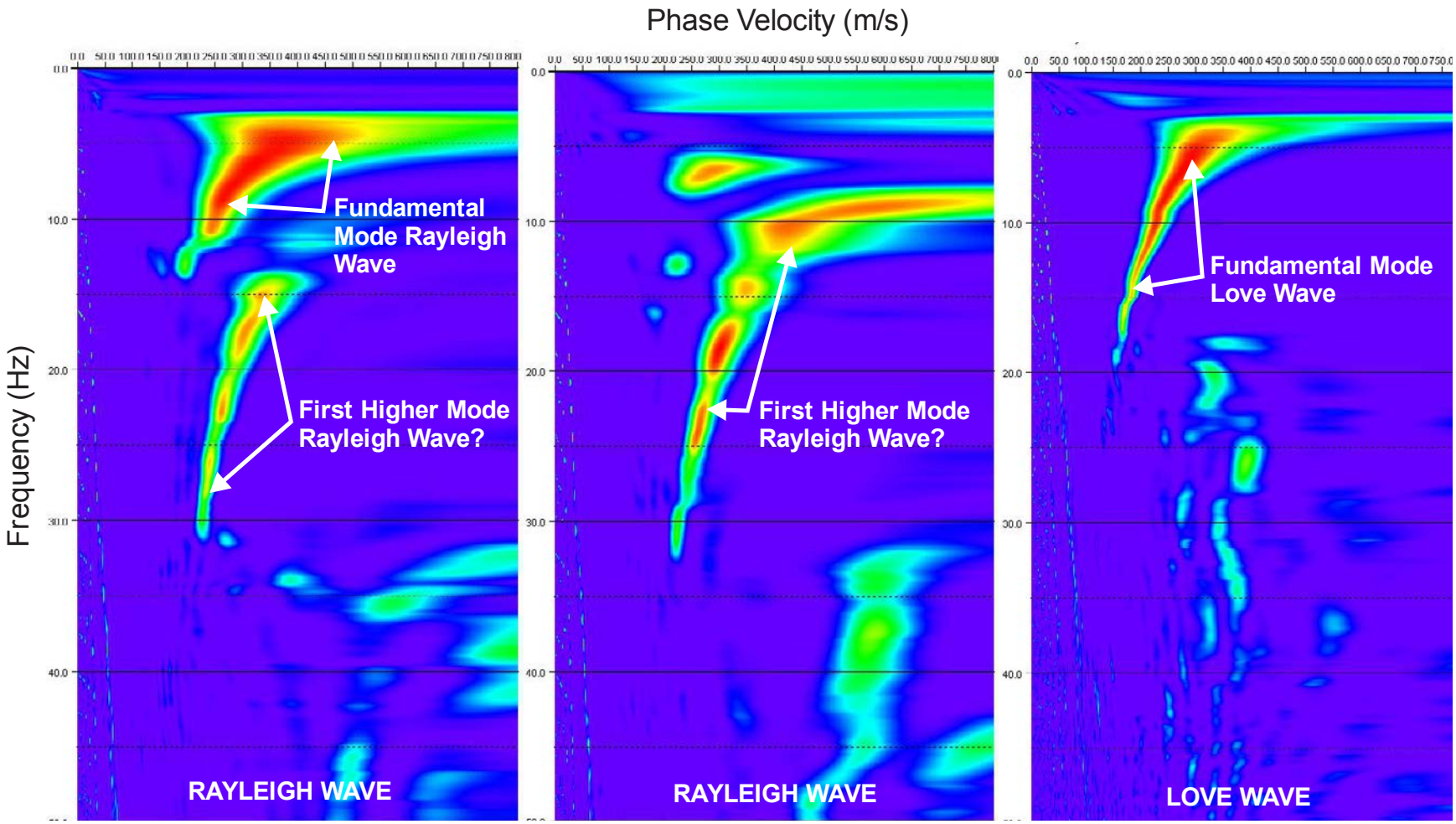

NC.BBGB – Comparison of Rayleigh and Love wave overtone images demonstrating dominant higher mode energy in the Rayleigh wave data. Example Rayleigh wave overtone images from seismic records with source locations at southern end (left) and northern end of array (center).

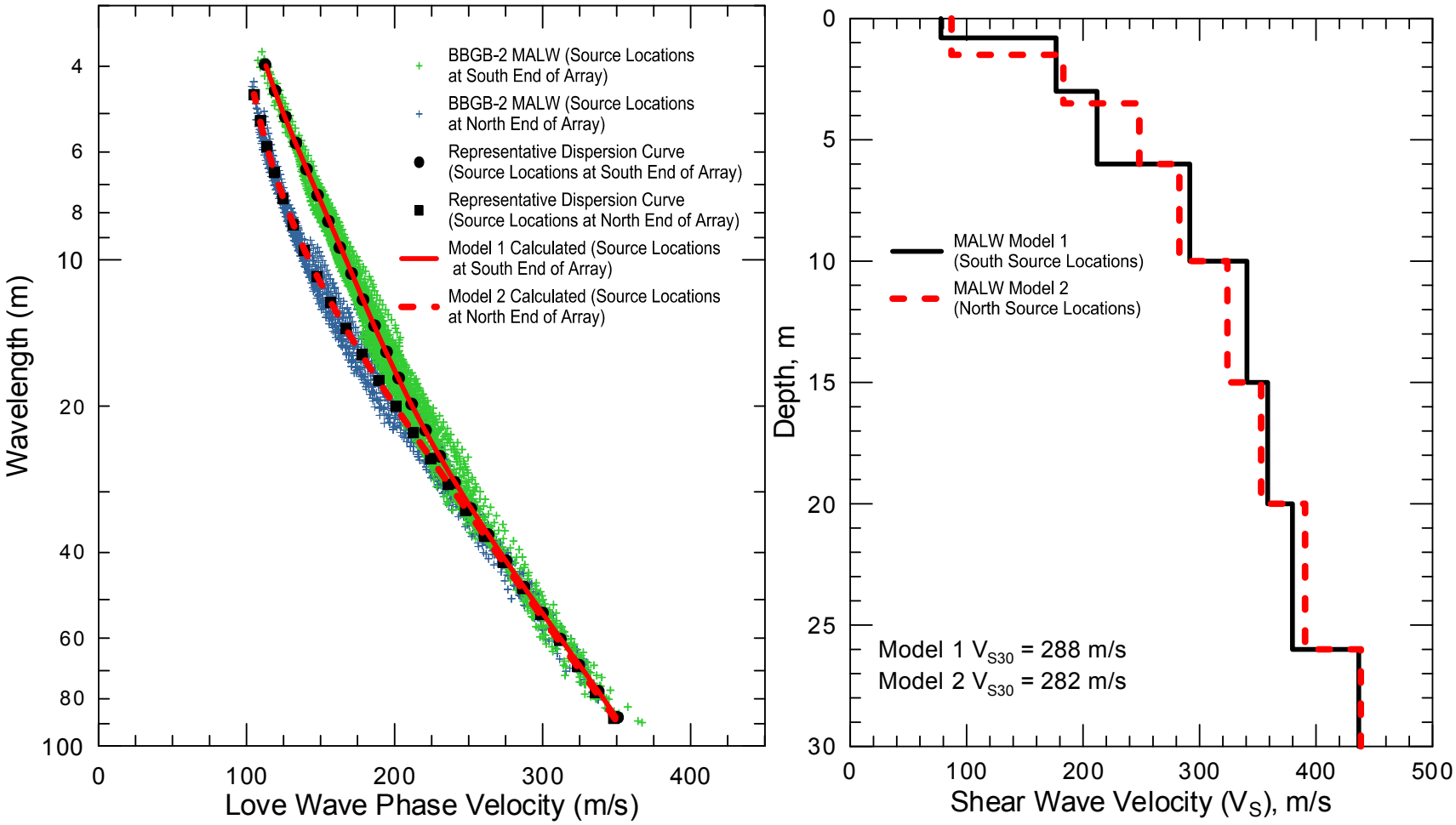

NC.BBGB - Field, representative and inverted theoretical Love wave dispersion data (left) and associated V_S models (right)

Site NC.BJOB

Location: Mount Johnson, San Benito County, California

Latitude: 36.61087 **Longitude:** -121.31467
(Station coordinates modified based on field GPS survey and may be for NC.BJOB2, coordinates provided for NC.BJOB have a typographical error, WGS84 coordinate system)

V_{S30} (measured): 486 m/s

V_{S30} (adjusted to more accurately reflect seismic station conditions): 528 m/s (average S-wave velocity between 1 and 31 m adjusting for assumed sensor depth and fact that sensor is unlikely placed on residual soil).

NEHRP Site Class: C

Geomatrix Code: IGB

Geologic Conditions/Observations: Seismic station located on Mesozoic (Cretaceous) quartz diorite bedrock.

Site Conditions: Rural site. Seismic station located on top of a small mountain peak. Hilly, undulating topography in site vicinity. Test area located on a hilltop with an approximate 8 m topographic decline to the southeast along the 70.5 m long seismic line.

Geophysical Methods Utilized: HVSR, Seismic Refraction, MASW

Geophysical Testing Arrays:

1. Array BJOB-1 (48 channel MASW and P-wave seismic refraction array utilizing 4.5 Hz vertical geophones spaced 1.5 m apart for a length of 70.5 m, forward and reverse shot locations with multiple source offsets and source types (hammers only) and multiple interior shot locations).
2. Three HVSR measurement locations: two distributed along array BJOB-1 and one adjacent the seismic station.

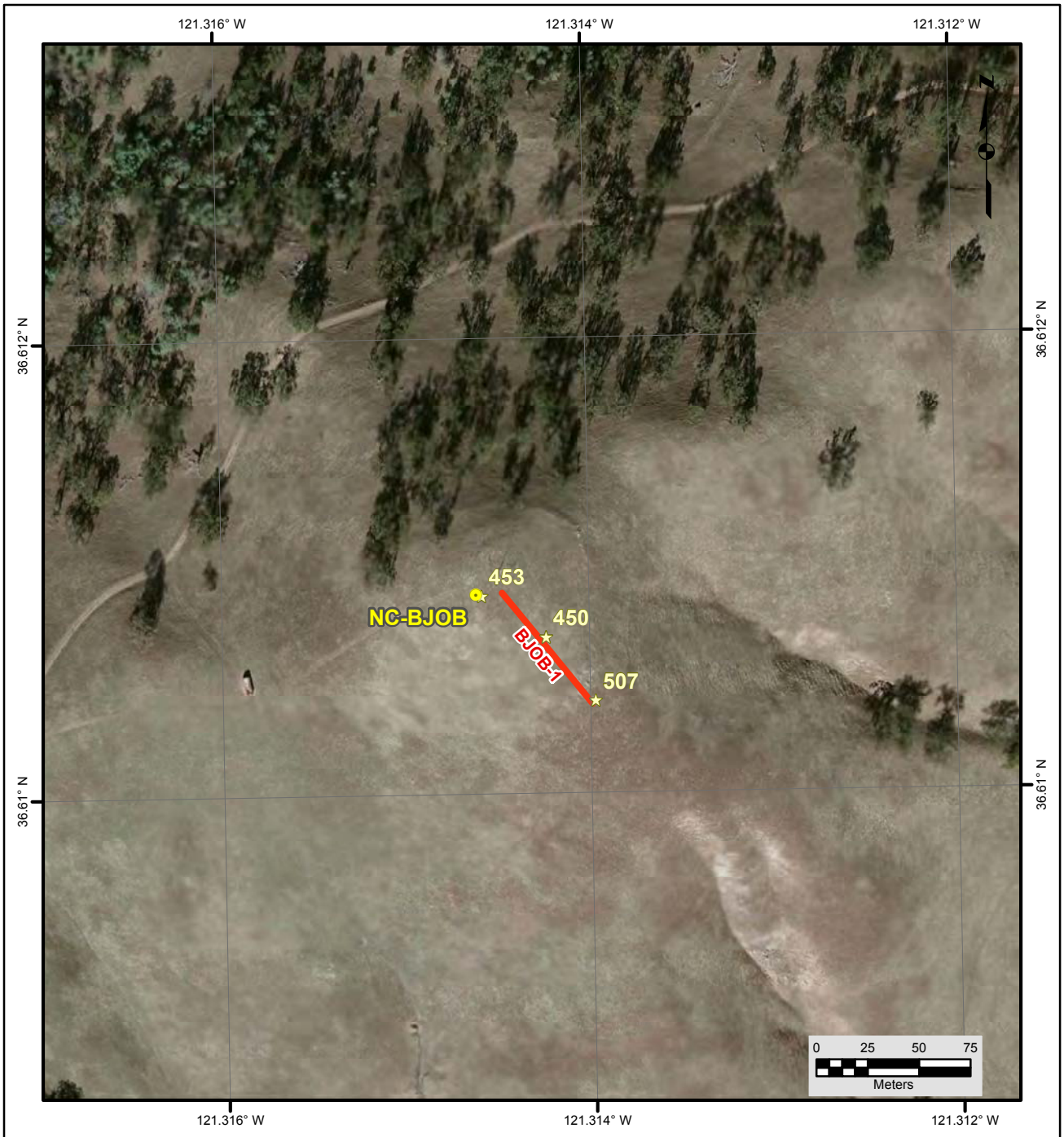

Legend

- Seismic Station - Approximate Surveyed Location
- H/V Spectral Ratio Location
- MASW and Seismic Refraction Array

NOTES:
1. WGS 1984 COORDINATE SYSTEM
2. Image Source: (c) Microsoft Corporation and its data suppliers

File Name: NC-BJOB-I

Date: 1/26/2012

USGS science for a changing world

GEOVision geophysical services

RECOVERY.GOV

SITE MAP
NC•BJOB

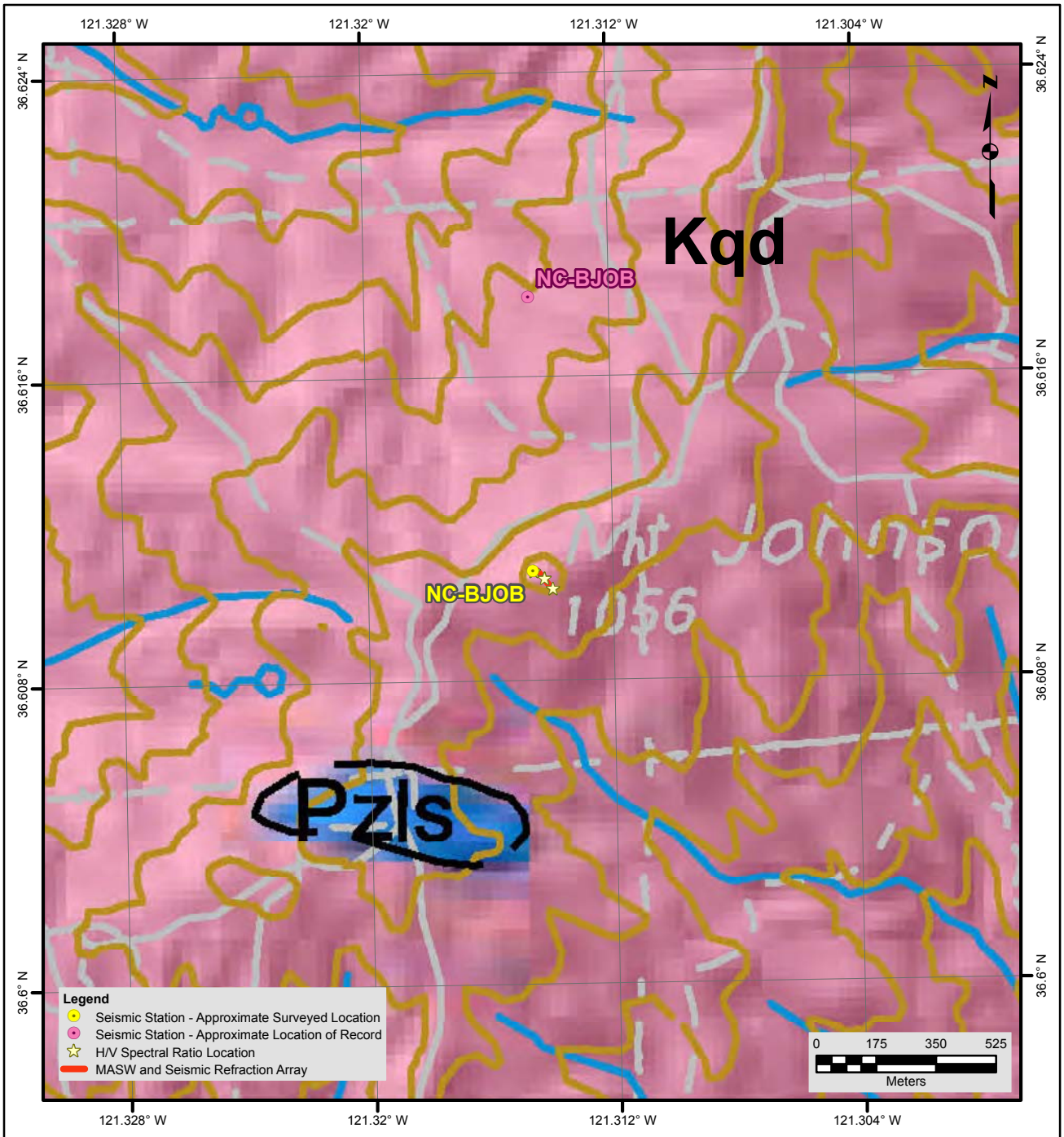

Description of Geologic Map Units

Kqd = Mesozoic (Cretaceous) quartz diorite
Pzls = Paleozoic ? carbonate rocks including Gabilan Limestone

NOTES:
1. WGS 1984 COORDINATE SYSTEM
2. Geologic Map of the Monterey 30'x60' Quadrangle and Adjacent Areas, California, compiled by David L. Wagner, H. Gary Greene, George J. Saucedo and Cynthia L. Pridmore, 2002
3. See site map for details of geophysical survey

File Name: NC-BJOB

Date: 2/2/2012

USGS science for a changing world

GEOVision geophysical services

GEOLOGIC MAP
NC•BJOB

RECOVERY.GOV

HVSR measurements adjacent to NC.BJOB or NC-BJOB2 seismic station

NC.BJOB2 seismic station

Looking towards the location of NC.BJOB (upper right corner) from NC.BJOB2 (lower left corner)

Looking southeast along array BJOB-1

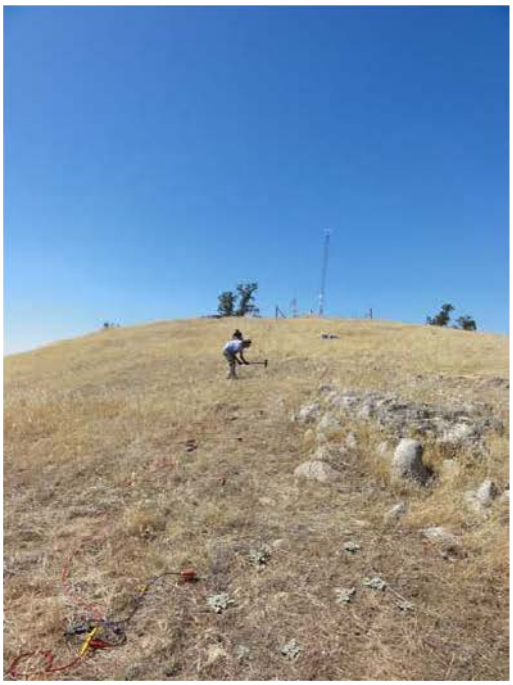

Looking northwest along array BJOB-1

Location of Geophysical Testing Arrays:

Location	Latitude	Longitude
BJOB-1, Northwest End of MASW/Refraction Array	36.61088	-121.31453
BJOB-1, Center of MASW/Refraction Array	36.61064	-121.31429
BJOB-1, Southeast End of MASW/Refraction Array	36.61039	-121.31404
HVSR Sensor 450	36.61069	-121.31429
HVSR Sensor 453	36.61087	-121.31464
HVSR Sensor 507	36.61041	-121.31403
NC.BJOB Seismic Station	36.61087	-121.31467

Notes: 1) WGS84 Coordinate System (decimal degrees)
2) Survey accuracy is estimated at 1 to 2 m.

Results:

V_S Model

Depth to Top of Layer (m)	Layer Thickness (m)	S-Wave Velocity (m/s)	Inferred P-Wave Velocity (m/s)	Assumed Poisson's Ratio	Assumed Density (g/cm^3)
0	1	166	311	0.3	1.7
1	2	308	576	0.3	1.8
3	5.5	465	869	0.3	1.9
8.5	15.5	502	940	0.3	2.0
24	>11	918	1717	0.3	2.1

Notes: 1) Depth of investigation is about 35 m.
2) Bottom layer is a half space
3) Half space velocity not well resolved.

Observations/Discussion:

- The HVSR curves at the three measurement locations are generally similar.
- There is a distinct, low amplitude HVSR peak in the 4.5 to 5.5 Hz range, which could be associated with the base of the uppermost weathered zone in the granitic rocks.
- The P-wave refraction data collected along array BJOB-1 were modeled using a tomographic inversion routine with a smooth velocity gradient starting model. The seismic refraction model was extended to far offset shot locations to extend depth of investigation.
- The seismic refraction survey design allowed P-wave velocity to be imaged to a maximum depth of about 20 m. The seismic refraction model shows that P-wave velocity is about 400 to 600 m/s at the surface, increasing to 900 m/s at a depth of 1 to 10

m and 1,200 m/s at a depth of 9 to 19 m. The maximum P-wave velocity in the model is about 1,400 m/s, located at a depth of about 20 m beneath the southeastern portion of the line.

- Site geologic conditions consist of a thin residual soil layer over weathered quartz diorite. The low P-wave velocities indicate that the granitic rocks are intensely weathered. The high velocity unit at the base of the model is not well resolved due to limited depth of investigation. A longer seismic refraction line would better resolve the relatively abrupt increase in velocity at the base of the model. The 4.5 to 5.5 Hz HVSR peak is likely associated with the base of the uppermost weathered zone.
- The seismic refraction model indicates that there is some lateral velocity variation at this site with higher P-wave velocities at shallower depth at the northwest end of the line. The weathering profile in rock appears somewhat irregular as probably the norm in weathered granitic rocks. There were no reasonable alternate test locations in close proximity to the seismic station due to limited space and steep topography.
- Noise conditions at the site were not sufficient for application of passive surface wave techniques.
- To minimize near field effects a maximum Rayleigh wave wavelength of 1.15 times the distance from the source to the center of the active receiver array was applied during MASW data reduction.
- The minimum wavelength surface wave phase velocity data extracted from the 48-channel MASW array was about 10 m. Seismic records with source locations at the northwest end of the array generally yielded the best quality surface wave data at long wavelengths. Data reduction using seismic records from smaller hammer sources and a limited offset receiver array (i.e. less active geophones) allowed extraction of surface wave dispersion data to a minimum wavelength of about 2 m.
- There is about 30 to 70 m/s scatter in MASW dispersion data, which is likely due, in part, to lateral velocity variation associated with both a very thin residual soil layer of variable thickness and differential weathering of near surface granitic rock.
- A representative dispersion curve was generated for the MASW data set using a moving average, polynomial curve fitting routine and used for modeling.
- Surface wave depth of investigation is about 35 m based on half of maximum wavelength criteria.
- The inferred P-wave velocities in the surface wave model, assuming a Poisson's ratio of 0.3, are most consistent with the average velocity structure at the southeast end of the seismic refraction model. The surface wave model shows a large increase in velocity at about 24 m. This is consistent with the 4.5 to 5.5 Hz HVSR peak and supported by the seismic refraction model, although a longer seismic refraction line would be required to accurately characterize velocity structure to this depth.
- V_{S30} is 486 m/s (Site Class C).
- Average S-wave velocity between 1 m and 31 m, to account for seismic sensor depth and the fact the seismic sensor is likely coupled to weathered rock rather than residual soil, is 528 m/s.

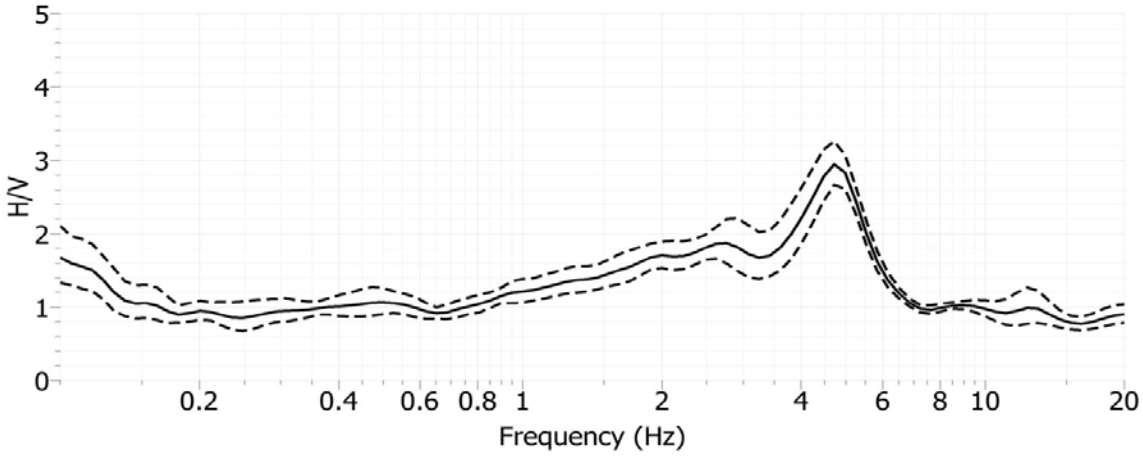

Site NC.BJOB, H/V Spectral Ratio, Near Seismic Station, Sensor 453

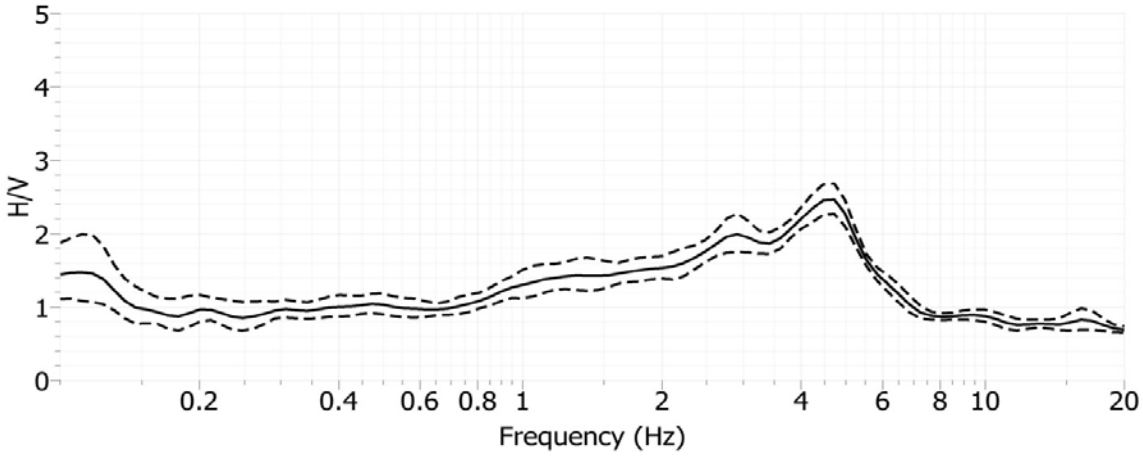

Site NC.BJOB, H/V Spectral Ratio, Array BJOB-1, Sensor 450

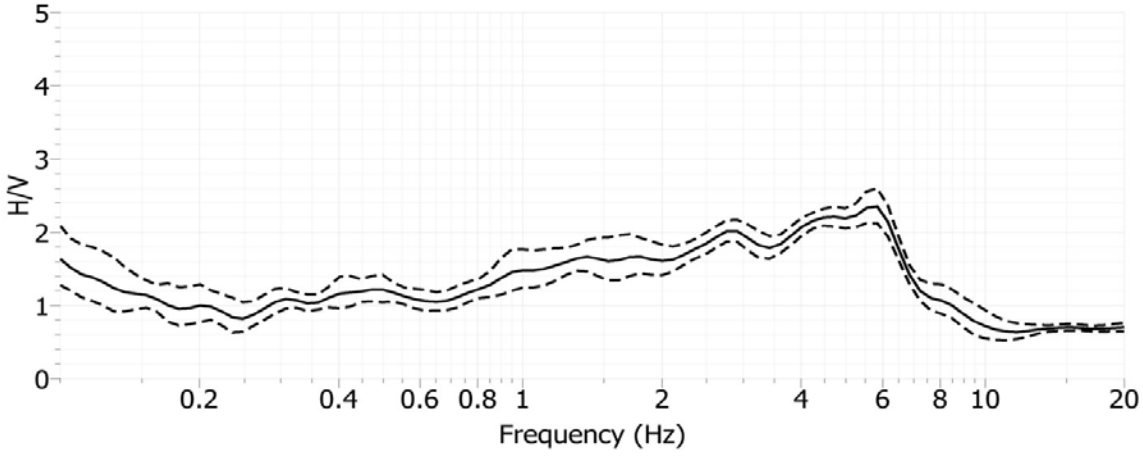

Site NC.BJOB, H/V Spectral Ratio, Array BJOB-1, Sensor 507

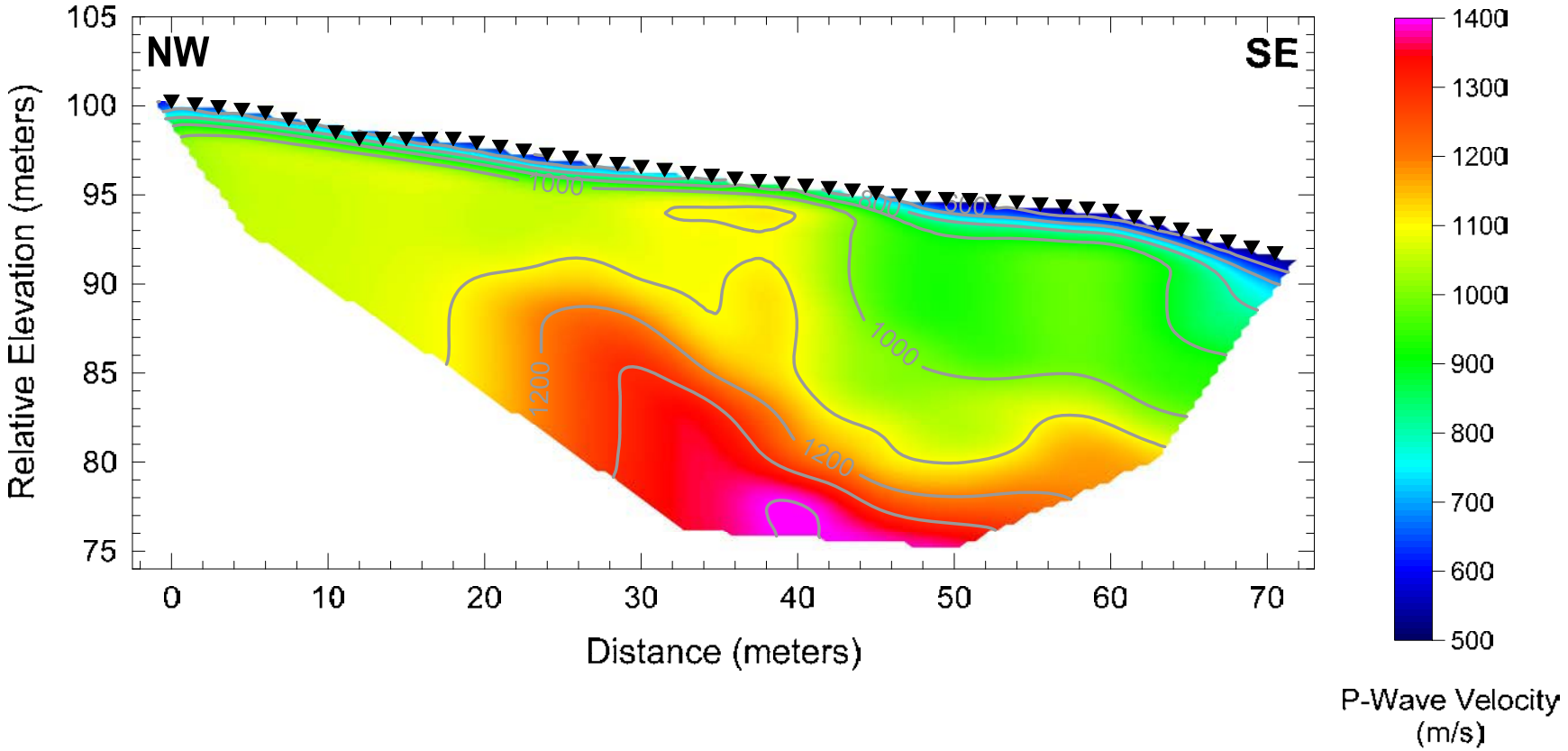

Array BJOB-1 – Tomographic seismic refraction model utilizing smooth velocity gradient starting model

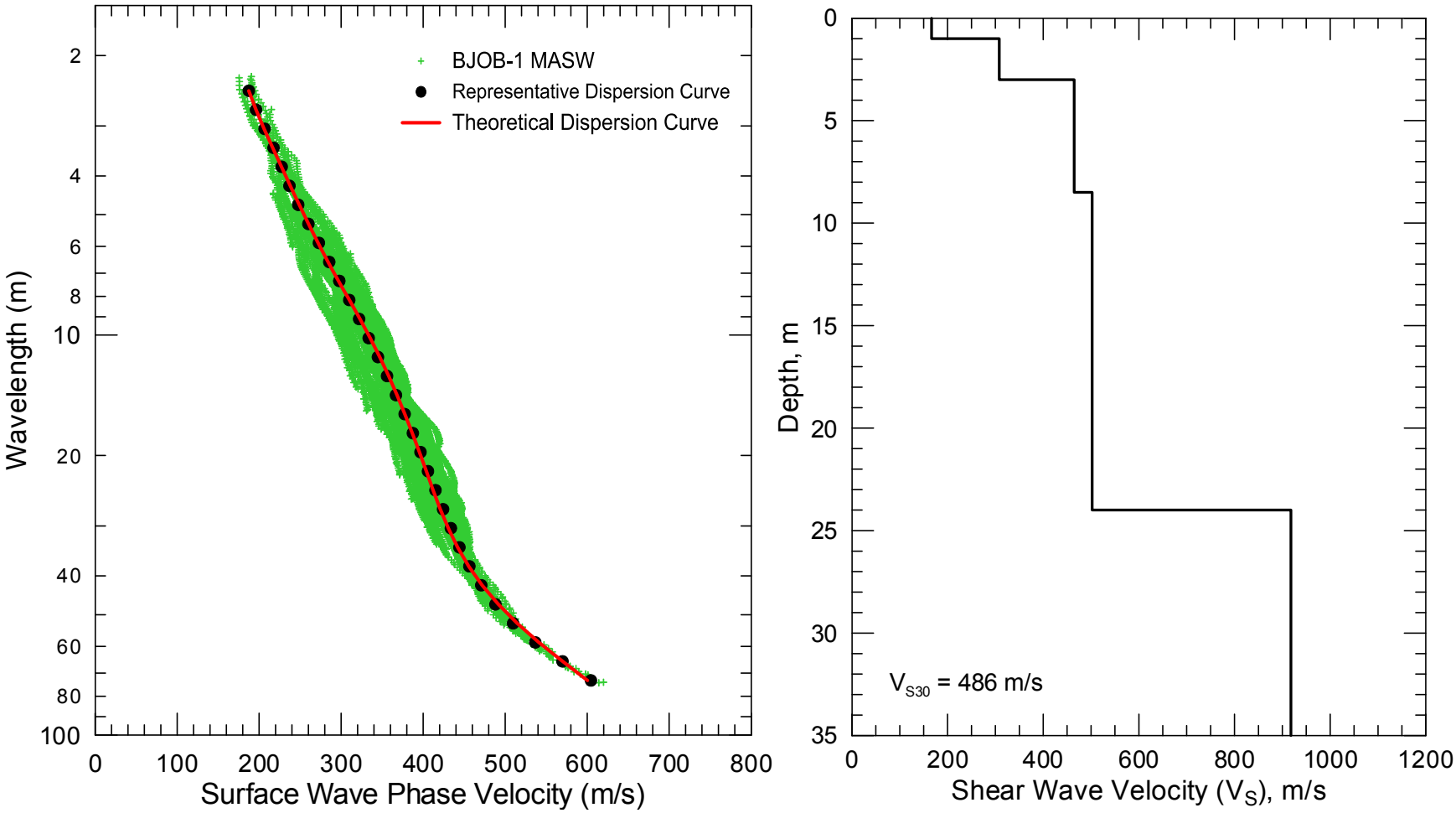

NC.BJOB- Field, representative and inverted theoretical surface wave dispersion data (left) and associated V_S model (right)

Site NC.CADB

Location: Anderson Reservoir, Morgan Hill, Santa Clara County, California

Latitude: 37.16346 **Longitude:** -121.62645
(Station coordinates provided by USGS, WGS84 coordinate system)

V_{S30} (measured): 600 m/s

V_{S30} (adjusted to more accurately reflect seismic station conditions): 600 m/s (no adjustment necessary).

NEHRP Site Class: C

Geomatrix Code: IFA

Geologic Conditions/Observations: Seismic station located on geologic unit mapped as Mesozoic (Jurassic-Cretaceous) Franciscan Assemblage, greenstone unit. The Coyote Fault is located about 0.4 km southwest of the site.

Site Conditions: Rural site. Undulating, hilly topography in site vicinity and around the reservoir. Seismic station located on top of a small hill. Test site located along edge of parking lot at bottom of hill to the west of the seismic station. The seismic station is located at about a 20 m higher elevation than the test area.

Geophysical Methods Utilized: HVSR, Seismic Refraction (P-wave), MASW (Rayleigh wave), MALW (Love wave)

Geophysical Testing Arrays:

1. Array CADB-1 (48 channel MASW and P-wave seismic refraction array, utilizing 4.5 Hz vertical geophones spaced 1.5 m apart for a length of 70.5 m, forward and reverse shot locations with multiple source offsets and source types and multiple interior shot locations).
2. Array CADB-1 (48 channel MALW array utilizing 10 Hz horizontal geophones spaced 1.5 m apart for a length of 70.5 m, several forward and reverse shot locations and a center shot).
3. Array CADB-2 (48 channel MASW and P-wave seismic refraction array utilizing 4.5 Hz vertical geophones spaced 2.5 m apart for a length of 117.5 m, forward and reverse shot locations with multiple source offsets and source types and multiple interior shot locations). Array CADB-2 is coincident with array CADB-1 with the southeast end of the array located 30 m southeast from the end of array CADB-1.
4. Three HVSR measurement locations: two distributed along array CADB-1 and the other near the seismic station.

Legend

- Seismic Station - Approximate Surveyed Location
- Seismic Station - Approximate Location of Record
- H/V Spectral Ratio Location
- Seismic Refraction Array
- MASW and Seismic Refraction Array (S- and P-wave)

NOTES:
1. WGS 1984 COORDINATE SYSTEM
2. Image Source: ESRI, i-cubed, USDA FSA, USGS, AEX, GeoEye, Getmapping, Aerogrid, IGP

File Name: NC-CADB-I

Date: 3/29/2012

USGS science for a changing world

GEOVision geophysical services

RECOVERY.GOV

SITE MAP
NC•CADB

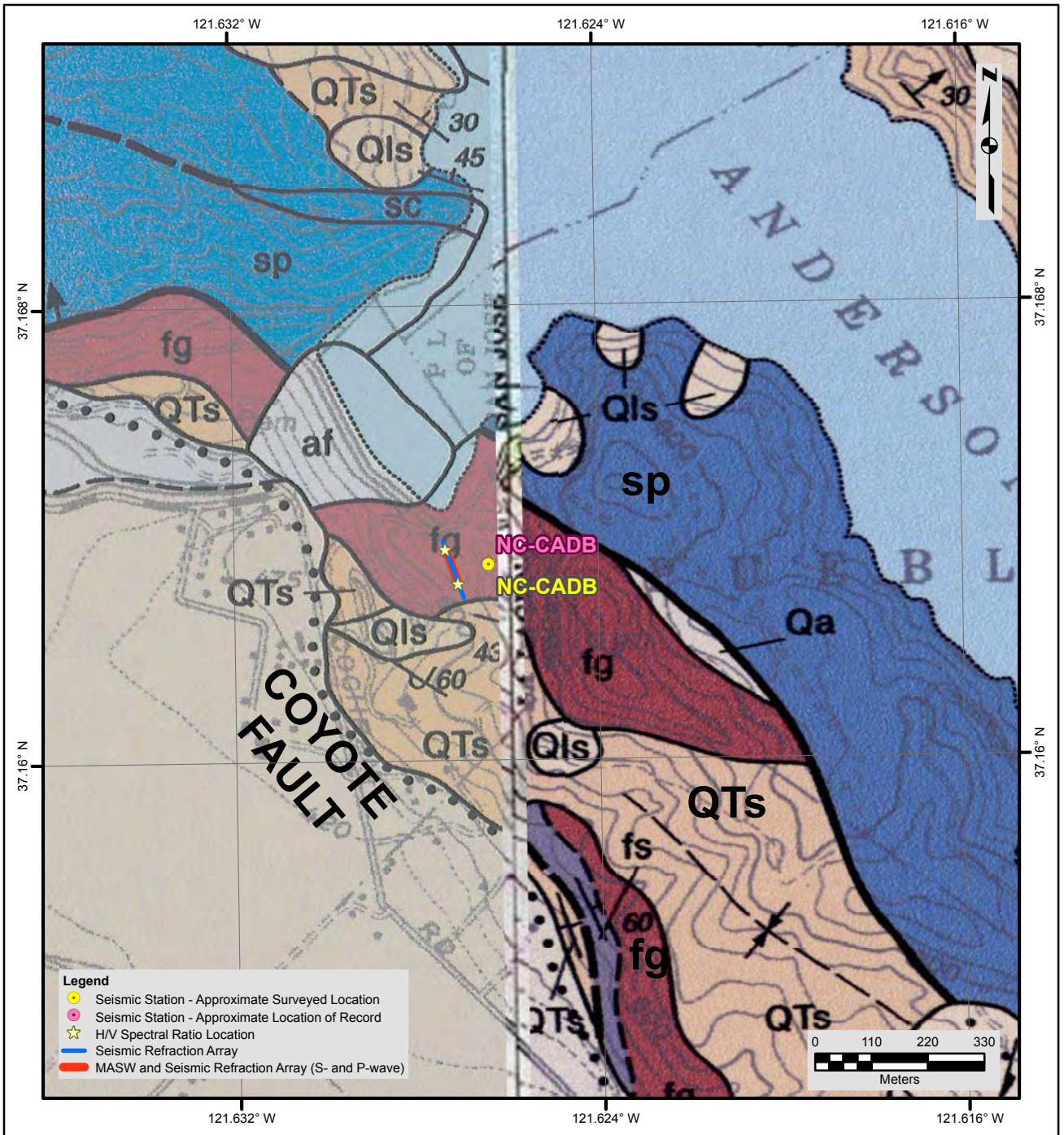

Description of Geologic Map Units

af = Quaternary (Holocene) artificial fill for Anderson Dam
Qg = Quaternary (Holocene) sand and gravel of Coyote Creek channel
Qa = Quaternary (Holocene) alluvial gravel, sand and clay of valleys
Qls = Quaternary (Holocene) landslide deposits, rubble derived from rocks upslope
QTs = Quaternary (Pleistocene/Pliocene) Santa Clara Formation; gravel/conglomerate, mostly pebbles, of volcanic rocks, silceous shale, moderately lithified, well bedded, interbeds of sandstone and claystone, tufff and basalt
sp = Mesozoic (Jurassic and Cretaceous) serpentinite, massive, fractured, slickensided
sc = Mesozoic (Jurassic and Cretaceous) serpentinite altered to ferruginous silica-carbonate rock
fg = Mesozoic (Jurassic and Cretaceous) Franciscan Assemblage; greenstone, massive, amorphous

NOTES:
1. WGS 1984 COORDINATE SYSTEM
2. Geologic Map of the Morgan Hill and Mount Sizer Quadrangles, Santa Clara County, California by Thomas W. Dibblee, Jr., 2005
3. See site map for details of geophysical survey

USGS science for a changing world
GEOVision geophysical services

GEOLOGIC MAP
NC•CADB

File Name: NC-CADB
Date: 4/5/2012

NC.CADB seismic station

Looking at HVSR sensor 507 and seismic station

S-wave refraction and MALW data acquisition along array CADB-1

Looking southeast along MASW array CADB-1 and at HVSR sensor 450. Seismic station located on hill to left in photograph

Looking northwest along P-wave seismic refraction array CADB-2

Location of Geophysical Testing Arrays:

Location	Latitude	Longitude
CADB-1, Southeast End of MASW/Refraction Array	37.16312	-121.62710
CADB-1, Center of MASW/Refraction Array	37.16342	-121.62724
CADB-1, Northwest End of MASW/Refraction Array	37.16371	-121.62737
CADB-2, Southeast End of Refraction array	37.16286	-121.62699
CADB-2, Center of Refraction array	37.16336	-121.62721
CADB-2, Northwest End of Refraction Array	37.16385	-121.62743
HVSR Sensor 450	37.16371	-121.62739
HVSR Sensor 453	37.16311	-121.62711
HVSR Sensor 507	37.16349	-121.62642
NC.CADB Seismic Station	37.16345	-121.62643

Notes: 1) WGS84 Coordinate System (decimal degrees)
2) Survey accuracy is estimated at 1 to 2 m.

Results:

V_S Model (MALW Array CADB-1)

Depth to Top of Layer (m)	Layer Thickness (m)	S-Wave Velocity (m/s)	Assumed Density (g/cm^3)
0	1	249	1.80
1	3	339	1.90
4	4	617	2.00
8	7	642	2.10
15	9	716	2.10
24	>6	837	2.15

Notes: 1) Depth of investigation is about 25 to 30 m.
2) Bottom layer is a half space.

Observations/Discussion:

- The seismic station is located on top of a small hill comprised of the Franciscan Assemblage greenstone unit. There was insufficient space on top of the hill to conduct a surface wave sounding to image to 30 m depth due to both topography and vegetation. Therefore, geophysical testing was conducted in a parking lot at the base of the hill on the order of 20 m lower in elevation and on the same mapped geologic unit. In retrospect, it would be prudent to conduct additional seismic testing (e.g. seismic refraction, SASW or MASW array) in the available space at the top of the hill to confirm that velocity structure is similar to that at the base of the hill.
- HVSR sensor locations 450 and 453 were located at the base of a hill along array CADB-1, whereas sensor location 507 was located on top of the hill next to the seismic station. HVSR response is similar at all sensor locations below a frequency of 3 Hz. HVSR sensors 450 and 453 have similar response at higher frequencies with a weak HVSR peak in the 4 to 5 Hz range. HVSR sensor 507 has a higher amplitude and higher frequency peak at about 8 Hz. This peak may mask the 4 to 5 Hz peak observed at sensor locations 450 and 453. The impedance contrast associated with the 8 Hz peak is expected to occur at very shallow depth. Assuming near surface weathered rock has a V_S of 320 m/s, then the abrupt increase in velocity associated with the 8 Hz peak would occur at a depth of about 10 m, based on the quarter wavelength approximation.
- The P-wave first arrival data from array CADB-2 were degraded by a high velocity first arrival from the asphalt and subgrade layer. This made it difficult to accurately constrain the P-wave velocity of the near surface sediments, but had no impact on determining the seismic velocity of deeper layers. Seismic refraction data from the shorter array CADB-1 were not modeled as the array is coincident with the longer array CADB-2. A complete S-wave seismic refraction data set was not acquired along array CADB-1, rather S-wave data acquisition along this array was limited to acquisition of MALW data. However, review of the S-wave seismic records indicated that S-wave velocity does not exceed 800 m/s in the upper 15 m.
- The P-wave refraction data for array CADB-2 were modeled using a tomographic inversion routine with a layer based starting model. The survey design for array CADB-2 allowed P-wave velocity to be imaged to a maximum depth of about 21 m. P-wave velocity is about 350 to 550 m/s at the surface and rapidly increases from 1,000 to 1,600 m/s at a depth on the order of 5 to 7 m. Although P-wave velocity is over 1,600 m/s, this geologic unit may not be saturated based on review of S-wave first arrival data and surface wave data. At a depth of about 10 to 16 m, P-wave velocity increases to over 2,200 m/s. This geologic unit is likely saturated based on S-wave first arrival data and surface wave data. The maximum P-wave velocity in the refraction model for array CADB-1 is about 2,800 m/s.
- Noise conditions at the site were not sufficient for application of passive surface wave techniques.
- It was not possible to construct a reliable and coherent dispersion curve from the MASW (Rayleigh wave) data, collected on arrays CADB-1 and CADB-2, over the wavelength range necessary to characterize S-wave velocity structure to a depth of 30 m. Lateral velocity variation and dominant higher modes contribute to the difficulty analyzing the MASW data. In fact, no reliable, long wavelength Rayleigh wave dispersion data could

be extracted from source locations offset from the northwest end of the array using the complete 48 channel receiver array. Although not modeled, the MASW data were screened to determine the approximate range for the Rayleigh wave phase velocity at a wavelength of 40 m (V_{R40}). V_{R40} was typically found to vary from about 550 to 650 m/s, averaging 600 m/s. The Brown, et al. (2000) relationship between V_{R40} and V_{S30} would, therefore, indicate that V_{S30} could average about 627 m/s, assuming that the 40 m wavelength Rayleigh wave phase velocity data are associated with the fundamental mode.

- The Love wave (MALW) data also suffered from lateral velocity variation and was difficult to reduce, but dominant higher modes were not an issue. Therefore, the MALW data collected along array CADB-1 were used for site characterization.
- Because 10 Hz horizontal geophones were used to acquire the MALW data at this site, Love wave phase velocity data to a minimum frequency of only 9 Hz (approximate 75 m wavelength) were extracted from the data set. There was also more scatter and/or error in the dispersion data at lower frequencies.
- There is significant scatter (60 to 100 m/s after selective use of data files) in the Love wave dispersion data, especially at intermediate wavelength ranges. The scatter in the dispersion data is most likely associated with lateral velocity variation.
- The minimum wavelength surface wave phase velocity data extracted from the 48-channel MALW array is about 8 m. Data reduction using limited maximum offset receiver arrays (i.e. less active geophones) allowed extraction of surface wave dispersion data to a minimum wavelength of about 4 m.
- A representative dispersion curve was generated for the MALW data set using a moving average, polynomial curve fitting routine and used for modeling.
- Surface wave depth of investigation is about 25 m based on a third of maximum wavelength. The V_S model is, however, sensitive to the layer at 24 m depth; therefore, it can be assumed that a 30 m depth of investigation was achieved with this data set.
- V_{S30} derived from the Love wave V_S model is 600 m/s (NEHRP Site Class C).
- V_{S30} derived from the Love wave V_S model is consistent with that estimated from the Rayleigh wave phase velocity data based on V_{R40}.
- The seismic station is located on a hill about 20 m higher in elevation than the location or arrays CADB-1 and CADB-2. The seismic station and geophysical testing arrays were, however, located on the same mapped geologic unit. Although it would not be possible to image S-wave velocity structure to 30 m depth adjacent to the seismic station due to lack of space and topography, limited testing should be conducted closer to the seismic station to confirm that the velocity structure at the base of the hill is similar to that at the top of the hill. The different high frequency HVSR response at the top and base of the hill supports the need for limited additional testing. Seismic refraction surveys can be conducted in rugged topography and it may be possible to acquire P- and/or S-wave refraction data along a long profile in the vicinity of the seismic station, although this may require limited brush removal.
- V_{S30} at the site is in the intermediate to high NEHRP Site Class C velocity range and it is unlikely that velocity structure at the seismic station is sufficiently different to where the Site Class would drop to D or increase to B.

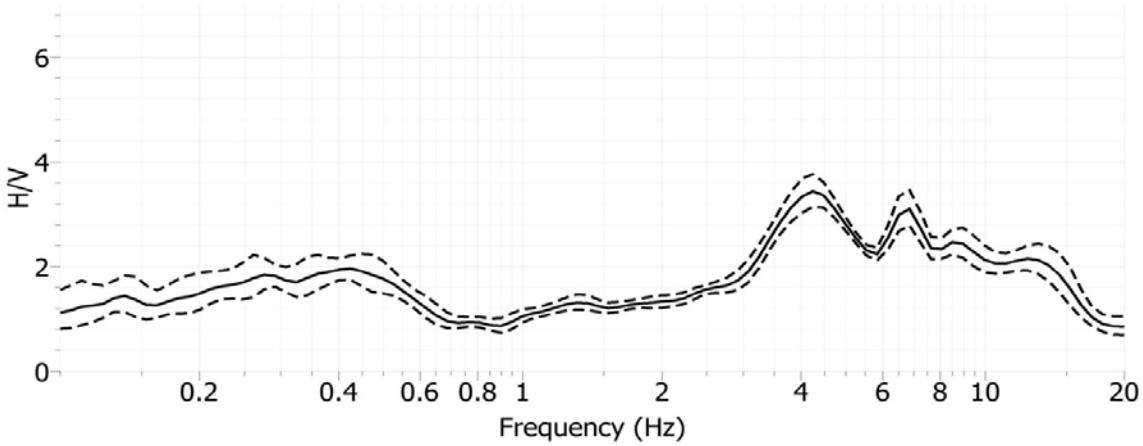

Site NC.CADB, H/V Spectral Ratio, Array CADB-1, Sensor 450

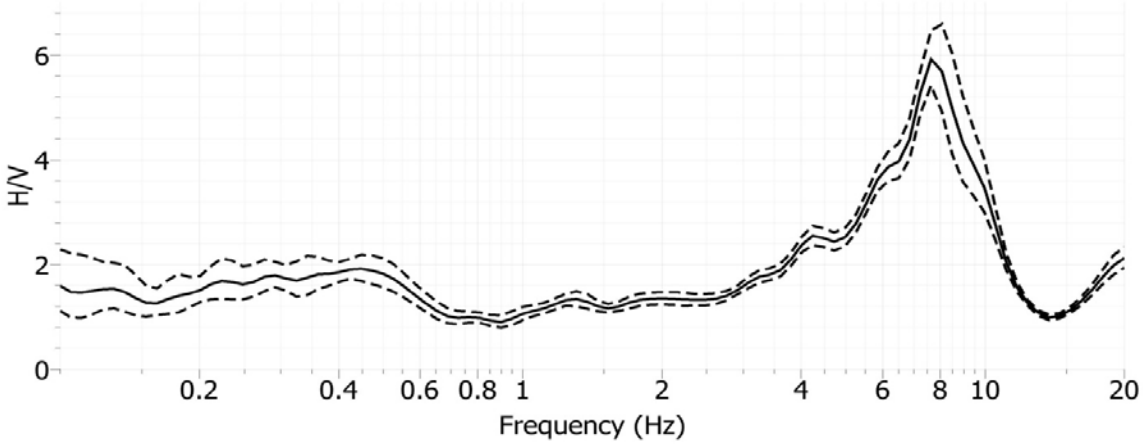

Site NC.CADB, H/V Spectral Ratio, Array CADB-1, Sensor 507

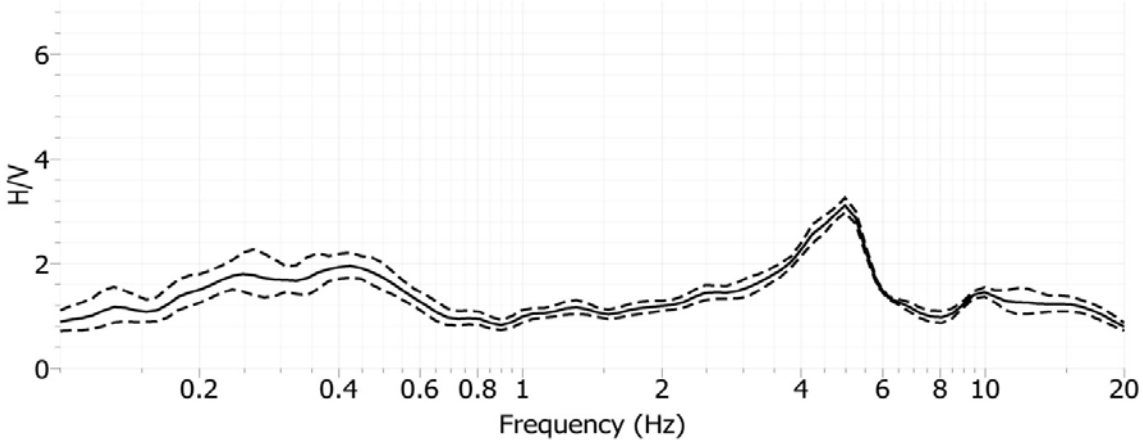

Site NC.CADB, H/V Spectral Ratio, Array CADB-1, Sensor 453

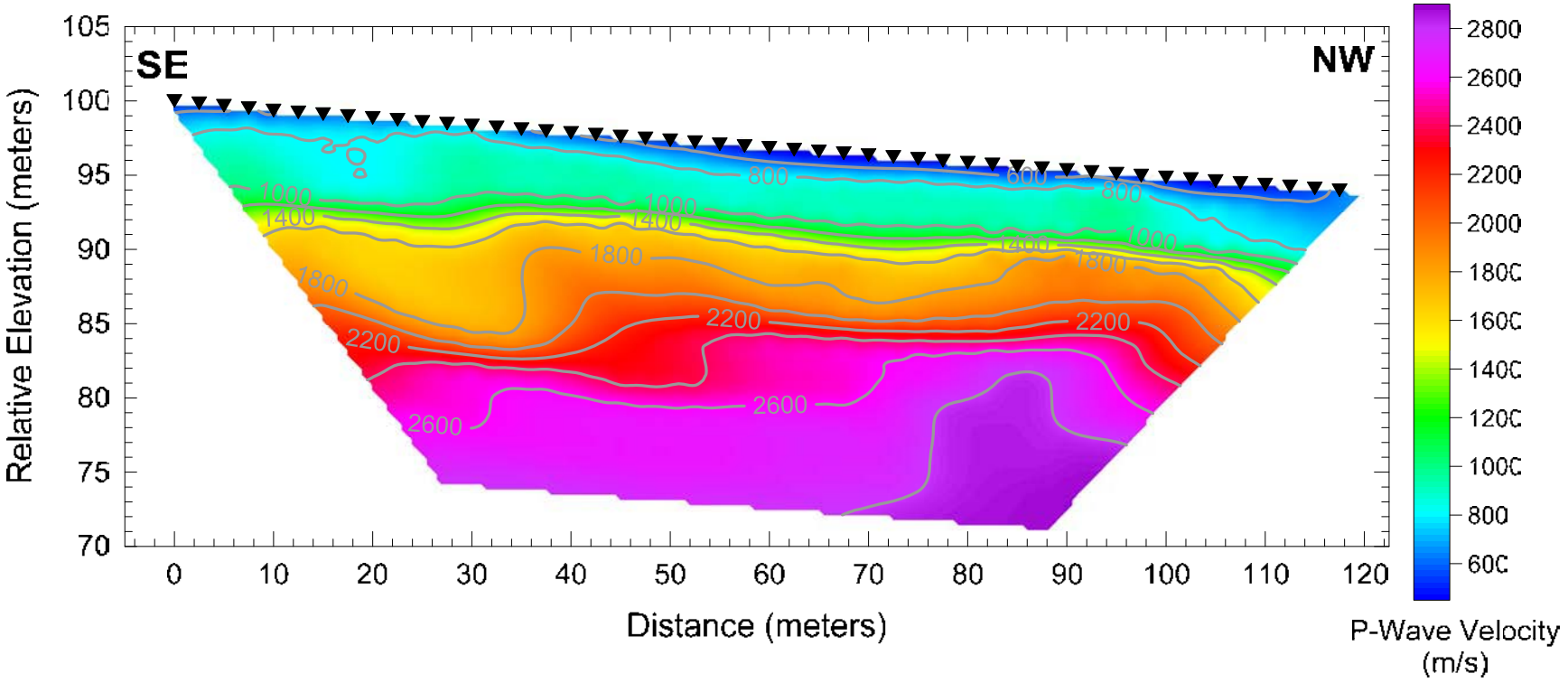

Array CADB-2 – Tomographic seismic refraction model developed using a layer-based starting model

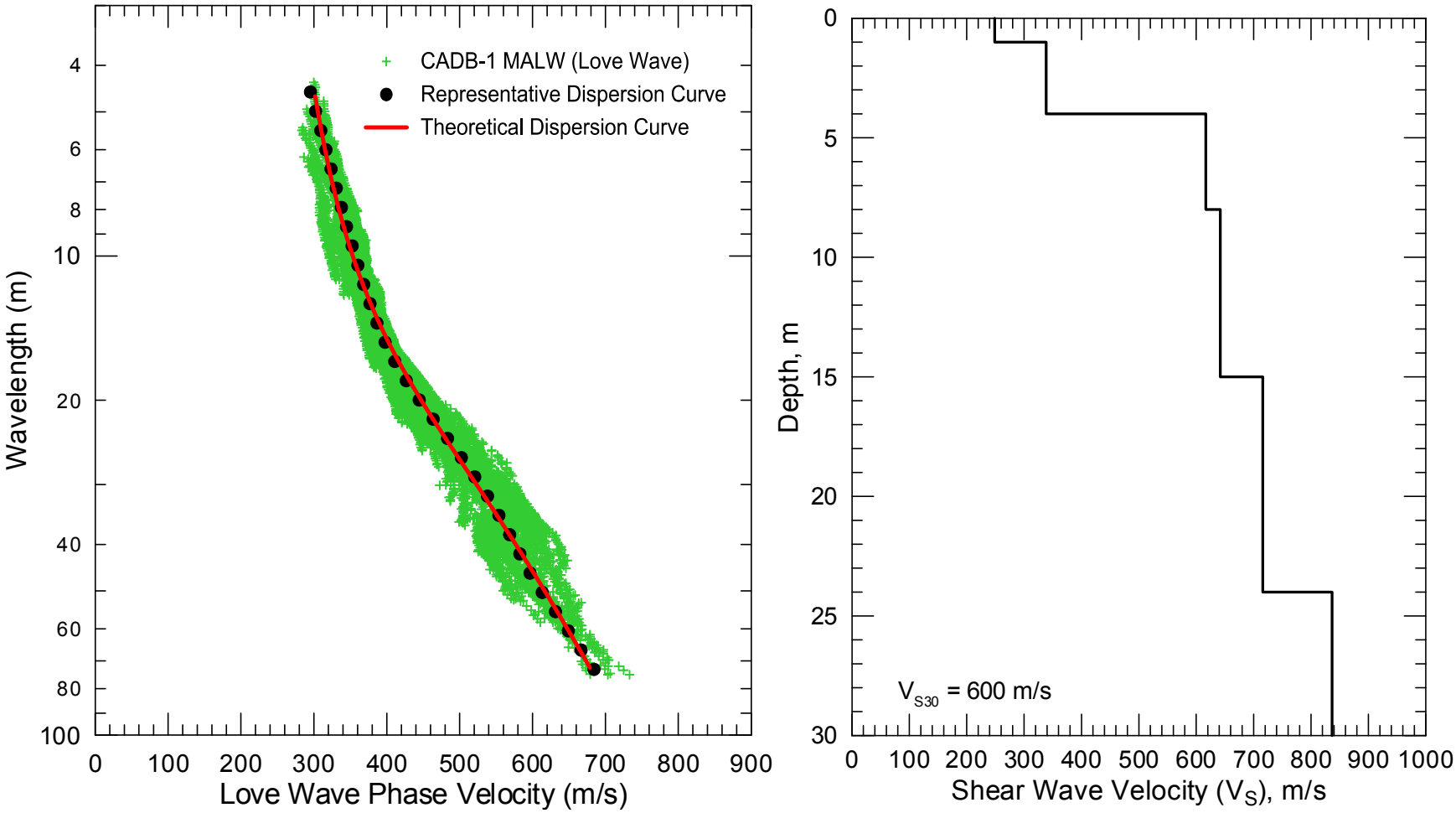

NC.CADB - Field, representative and inverted theoretical Love wave dispersion data (left) and associated V_S model (right)

Site NC.CAL

Location: Calaveras Reservoir, Santa Clara County, California

Latitude: 37.45035 **Longitude:** -121.80037
(Station coordinates provided by USGS, WGS84 coordinate system)

V_{S30} (measured): 519 m/s

V_{S30} (adjusted to more accurately reflect seismic station conditions): 557 m/s (average S-wave velocity between 1 and 31 m adjusting for assumed 1 m sensor depth).

NEHRP Site Class: C

Geomatrix Code: IHB/IFB

Geologic Conditions/Observations: Seismic station located on geologic unit mapped as Quaternary (Holocene) landslide rubble, which overlies Mesozoic (Jurassic and Cretaceous) Franciscan Assemblage, greywacke sandstone. Field observations indicate that a layer of soil overlies weathered shale. The Calaveras Fault is located about 1 km southwest of the site and an inferred, unnamed fault is located about 450 m southwest of the site.

Site Conditions: Rural site. Undulating topography in site vicinity near the reservoir. Test area located near the seismic station with approximately 5 m of topographic decline to the west along the 70.5 m long seismic line.

Geophysical Methods Utilized: HVSR, Seismic Refraction, MASW

Geophysical Testing Arrays:

1. Array CAL-1 (48 channel MASW and P-wave seismic refraction array, utilizing 4.5 Hz vertical geophones spaced 1.5 m apart for a length of 70.5 m, forward and reverse shot locations with multiple source offsets and source types (hammers only) and multiple interior shot locations).
2. Three HVSR measurement locations: two distributed along array CAL-1 and the other near the seismic station.

Legend

- Seismic Station - Approximate Surveyed Location
- Seismic Station - Approximate Location of Record
- H/V Spectral Ratio Location
- MASW and Seismic Refraction Array

NOTES:
1. WGS 1984 COORDINATE SYSTEM
2. Image Source: ESRI, i-cubed, USDA FSA, USGS, AEX, GeoEye, Getmapping, Aerogrid, IGP

File Name: NC-CAL-I

Date: 11/3/2011

USGS science for a changing world

GEOVision geophysical services

RECOVERY.GOV

SITE MAP
NC•CAL

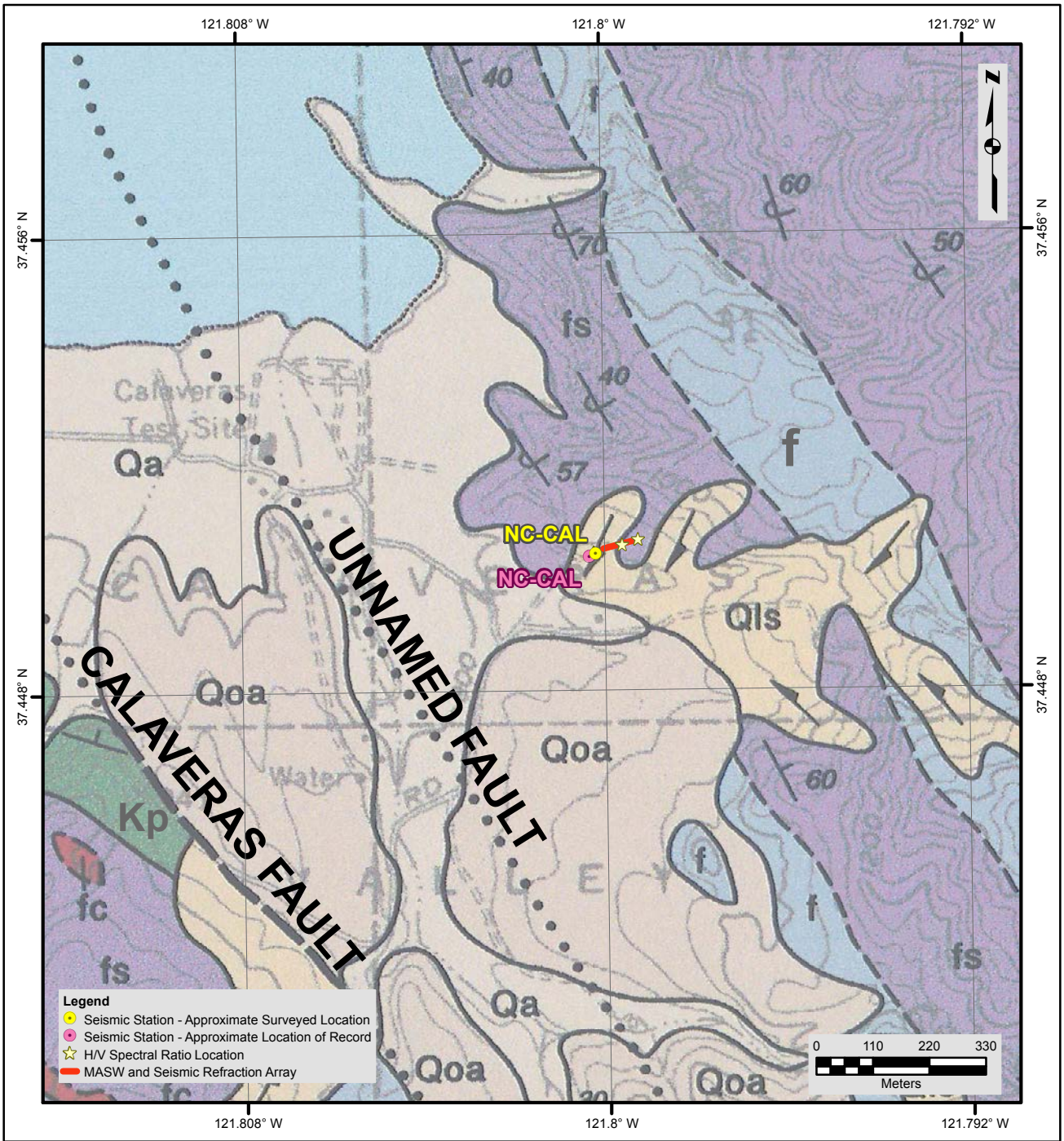

Description of Geologic Map Units

Qa = Quaternary (Holocene) alluvial gravel, sand and clay and alluvial fan deposits
Qls = Quaternary (Pleistocene to Holocene) rubble derived from rocks upslope
Qoa = Quaternary (Pleistocene) older alluvium
Kp = Late Cretaceous Panoche Formation; clay shale or mudstone, micaceous
fc = Late Jurassic and Cretaceous Franciscan Assemblage; chert, thin bedded, contorted, in part jasperized
f = Late Jurassic and Cretaceous Franciscan Assemblage; clay shale, micaceous, sheared
fs = Late Jurassic and Cretaceous Franciscan Assemblage; graywacke sandstone fine to medium grained, massive to bedded, hard

NOTES:
1. WGS 1984 COORDINATE SYSTEM
2. Geologic Map of the Calaveras Reservoir Quadrangle, Alameda and Santa Clara Counties, California by Thomas W. Dibblee, Jr., 2005
3. See site map for details of geophysical survey

USGS science for a changing world

GEOVision geophysical services

GEOLOGIC MAP
NC•CAL

File Name: NC-CAL
Date: 4/27/2012

NC.CAL seismic station

NC.CAL seismic station

Looking west towards center of array CAL-1 and HVSR sensor 450

Looking east along array CAL-1

Looking west along array CAL-1 and at HVSR sensor 507

Location of Geophysical Testing Arrays:

Location	Latitude	Longitude
CAL-1, Southwest End of MASW/Refraction Array	37.45048	-121.80005
CAL-1, Center of MASW/Refraction Array	37.45055	-121.79966
CAL-1, Northeast End of MASW/Refraction Array	37.45063	-121.79928
HVSR Sensor 450	37.45055	-121.79964
HVSR Sensor 453	37.45042	-121.80026
HVSR Sensor 507	37.45064	-121.79929
NC.CAL Seismic Station	37.45040	-121.80023

Notes: 1) WGS84 Coordinate System (decimal degrees)
2) Survey accuracy is estimated at 1 to 2 m.

Results:

V_S Model

Depth to Top of Layer (m)	Layer Thickness (m)	S-Wave Velocity (m/s)	Inferred P-Wave Velocity (m/s)	Assumed Poisson's Ratio	Assumed Density (g/cm^3)
0	1.5	205	383	0.300	1.70
1.5	2.5	331	619	0.300	1.80
4	4	413	772	0.300	1.90
8	5	609	2500	0.468	2.10
13	7	634	2500	0.466	2.10
20	10	712	2750	0.464	2.15
30	>10	1091	3000	0.424	2.20

Notes: 1) Saturated sedimentary rock with V_P of about 2,500 to 3,000 m/s located at an approximate depth of 8 m based on seismic refraction survey.
2) Depth of investigation is about 40 m.
3) Bottom layer is a half space.

Observations/Discussion:

- Array CAL-1, as plotted on the geologic map, is located on both Quaternary landslide deposits and Franciscan greywacke sandstone. Field inspection indicates that the array is located on a thin sediment layer, possibly landslide deposits, overlying Franciscan Assemblage sedimentary rocks. Weathered Franciscan shale rather than sandstone is exposed in a drainage near the site. Franciscan rocks are very steeply dipping and possibly overturned in the site vicinity. Array CAL-1 is located almost perpendicular to strike of the geologic bedding. An array orientated parallel to strike would have had too much topographic variation.
- HVSR plots are very similar at every station at frequencies below 6 Hz, but differ at higher frequencies. There are no clear high amplitude HVSR peaks, although there are possible weak peaks at frequencies higher than 7 Hz.
- The P-wave refraction data for array CAL-1 were modeled using a tomographic inversion routine with a layer based starting model. The seismic refraction model was extended to far offset shot locations to extend depth of investigation.
- The seismic refraction survey design allowed P-wave velocity to be imaged to a maximum depth of about 19 m. The seismic refraction model shows that P-wave velocity is about 400 to 650 m/s at the surface, increasing to 1,000 m/s at a depth of 2 to 4 m, 1,600 m/s at a depth of 6 to 9 m, 2,400 m/s at a depth of 8 to 13 m, and over 2,800 m/s at a depth of 12 to 17 m. P-wave velocity over 1,600 m/s is probably associated with saturated Franciscan sedimentary rock.
- With the exception of a thin low velocity surficial layer of variable thickness, the seismic refraction model does not reveal significant lateral velocity variation. However, the shallow saturated zone may mask laterally variable S-wave velocity.
- Noise conditions at the site were not sufficient for application of passive surface wave techniques.
- MASW data were difficult to reduce because of dominant higher modes over a wide frequency range. We believe, however, that the fundamental mode has been successfully extracted from the MASW seismic records. The fundamental mode could not be recovered from 48 channel receiver arrays and near offset shot locations. Low frequency (long wavelength) fundamental mode Rayleigh wave phase velocity data were only recovered from source locations offset 30 m from each end of the array. This is interesting because higher modes often become more problematic as source offset increases. The fundamental mode was recovered at high frequencies using limited offset receiver arrays. As has been observed at other similar sites, the MALW (Love wave) technique may perform better than the MASW technique at this site. However, MALW data were not acquired at this site because the difficulties with data analysis were not recognized in the field.
- Due to the difficulty extracting surface wave dispersion data from the full 48 channel receiver array, the near field criteria typically applied during this investigation was relaxed somewhat. The maximum wavelength was set equal to the lesser of 90 m or 1.3 times the distance from the source to midpoint of the receiver array. The maximum wavelength had to be reduced on several files where modal superposition appeared to occur at long wavelengths.

- The minimum wavelength surface wave phase velocity data extracted from the 48-channel MASW array was about 30 m, although dispersion data were only recovered from a 48 channel array with source locations offset 30 m from each end of the array and 20 m from one end of the array. Reducing data from smaller hammer sources using a limited offset receiver array (i.e. less active geophones) allowed for extraction of surface wave dispersion data to a minimum wavelength of about 2.5 m.
- There is about 50 to 80 m/s of scatter in MASW dispersion data, which is in part due to lateral velocity variation caused by differential weathering of near surface sedimentary rock and variable thickness of a thin low velocity sediment layer.
- A representative dispersion curve was generated for the MASW data set using a moving average, polynomial curve fitting routine and used for modeling.
- Surface wave depth of investigation is about 40 m based on half of maximum wavelength criteria.
- The saturated zone with V_P between 2,500 and 3,000 m/s was constrained at an approximate depth of 8 m based on the seismic refraction model.
- Near surface S-wave velocities in the V_S model from the surface wave dispersion data are somewhat lower than might be expected from the seismic refraction model. Possible explanations include a Poisson's ratio of greater than 0.3 for the shallow sediments or a shallow high velocity layer. A shallow high velocity layer could excite dominant higher modes, but the presence of such a layer at this site is inconclusive.
- The S-wave velocity model derived from the surface wave testing is believed to be representative of average subsurface velocity structure. However, geology at the site is complex, with dipping bedding and the seismic line was oriented perpendicular to strike. It is difficult to predict the effect of dipping beds on surface wave dispersion data. If the sedimentary rock units have relatively uniform velocity structure and changes in V_S are dominated by weathering, then the dipping bedding may not have a significant effect on the surface wave data. The source of the dominant higher mode(s) in the MASW data is not known. It is possible that a MALW (Love wave) sounding may perform better at this site.
- V_{S30} is 510 m/s (NEHRP Site Class C).
- Average S-wave velocity between 1 m (assumed sensor depth) and 31 m is 557 m/s (NEHRP Site Class C).
- Regardless of the complexities in data analysis, the site is clearly NEHRP Site Class C.

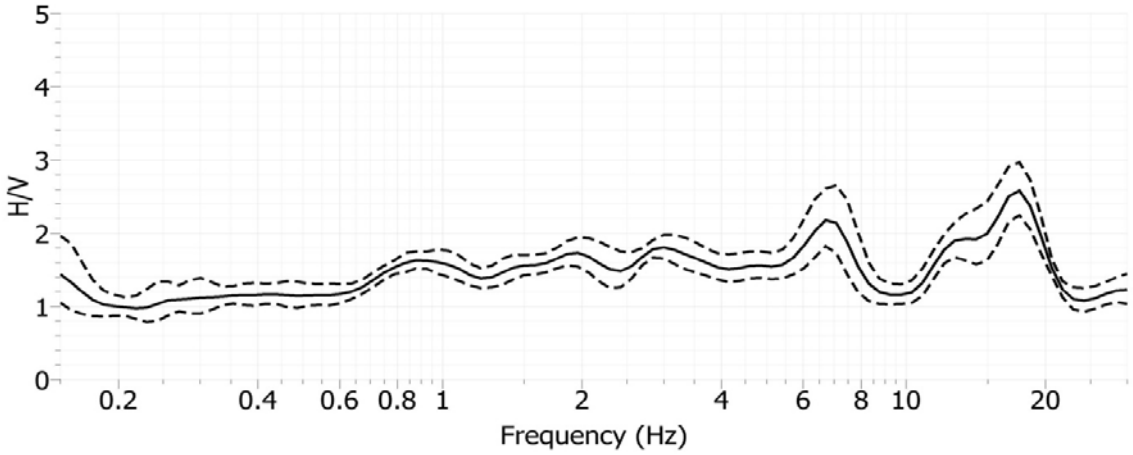

Site NC.CAL, H/V Spectral Ratio, Near Seismic Station, Sensor 453

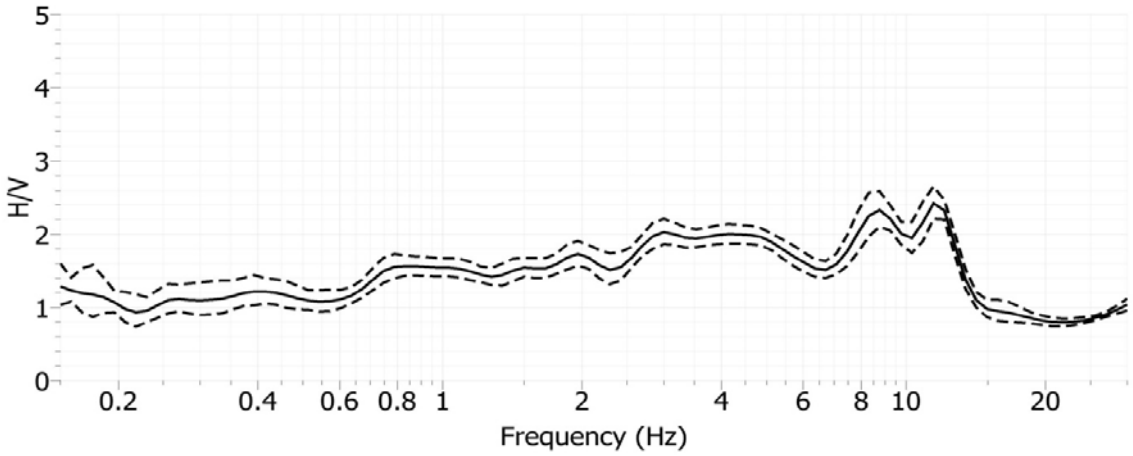

Site NC.CAL, H/V Spectral Ratio, Array CAL-1, Sensor 450

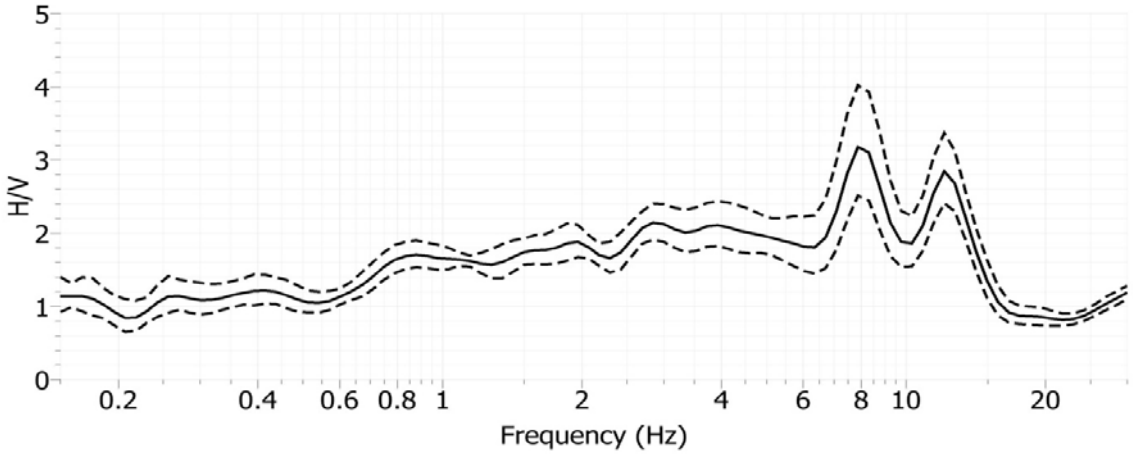

Site NC.CAL, H/V Spectral Ratio, Array CAL-1, Sensor 507

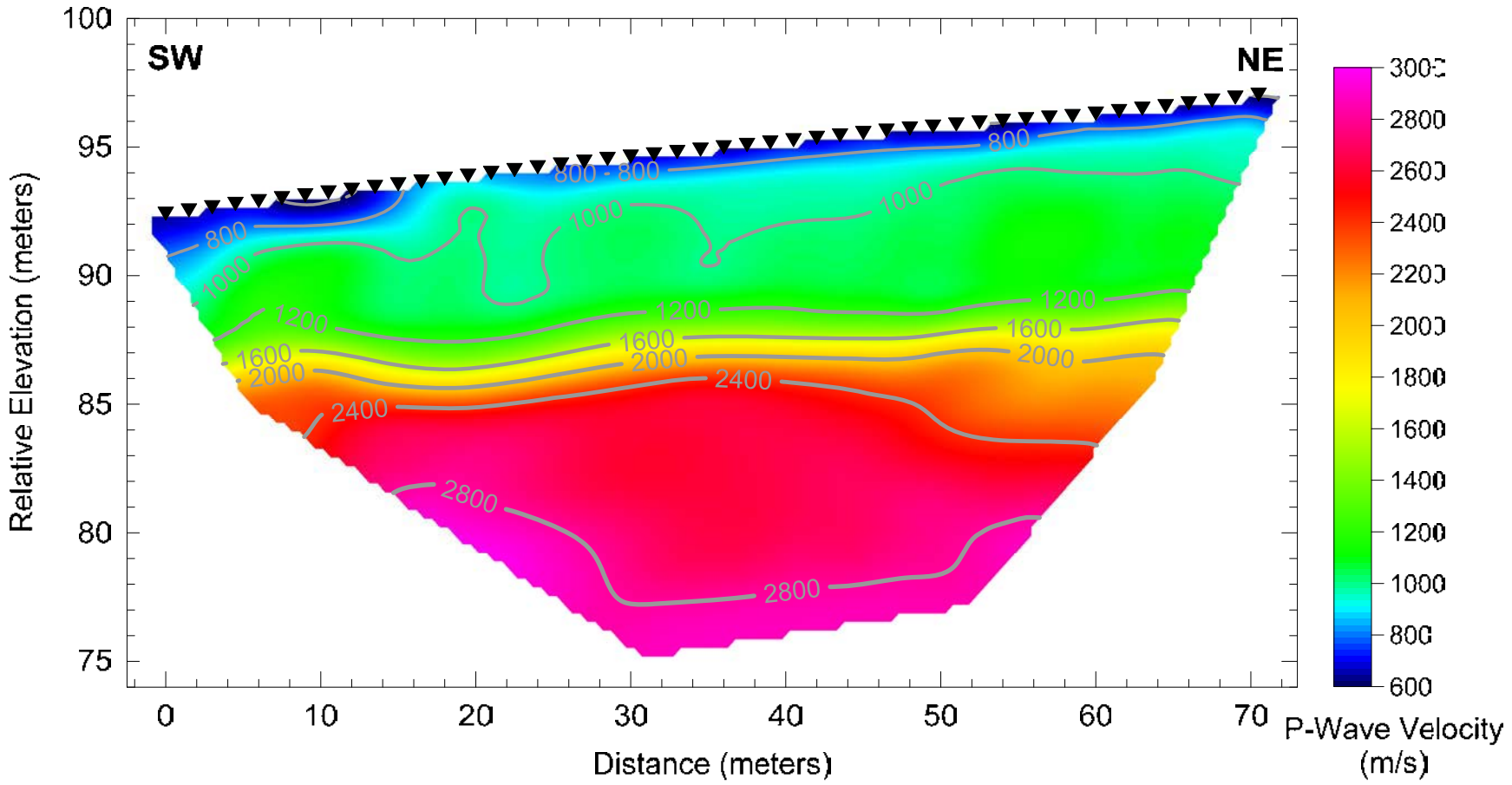

Array CAL-1 – Tomographic seismic refraction model developed using a layer-based starting model

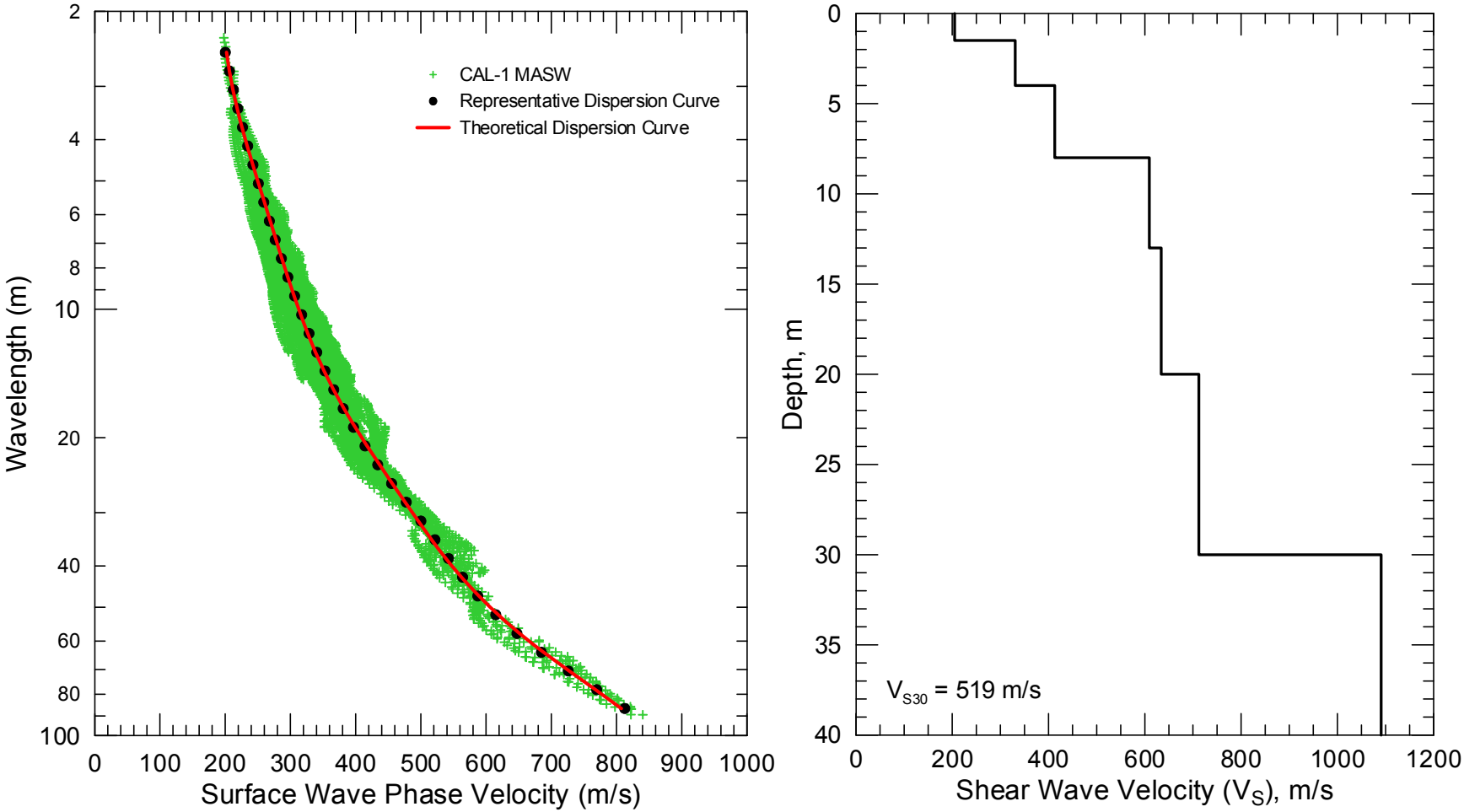

NC.CAL - Field, representative and inverted theoretical surface wave dispersion data (left) and associated V_S model (right)

Site NC.CCOB

Location: Coe Ranch, Santa Clara County, California

Latitude: 37.25898 **Longitude:** -121.67311
(Station coordinates provided by USGS, WGS84 coordinate system)

V_{S30} (measured): 400 m/s

V_{S30} (adjusted to more accurately reflect seismic station conditions): 414 m/s (average S-wave velocity between 1 and 31 m adjusting for assumed sensor depth).

NEHRP Site Class: C

Geomatrix Code: IKD

Geologic Conditions/Observations: Seismic station located on geologic unit mapped as Mesozoic (Cretaceous) Panoche Formation, a clay shale or mudstone. The mapped location of the Calaveras Fault is about 250 m west of the seismic station. The geologic maps indicate that bedding in the immediate site vicinity has a steep dip (50 to 60 degrees) to the northeast.

Site Conditions: Rural site located on gently rolling hills.

Geophysical Methods Utilized: HVSR, P- and S-wave Seismic Refraction, MASW (Rayleigh wave) and MALW (Love wave)

Geophysical Testing Arrays:

1. Array CCOB-1 (48 channel MASW and P-wave seismic refraction array utilizing 4.5 Hz vertical geophones spaced 1.5 m apart for a length of 70.5 m, forward and reverse shot locations with multiple source offsets and source types and multiple interior shot locations).
2. Array CCOB-2 (48 channel MASW, MALW and P- and S-wave seismic refraction array utilizing 4.5 Hz vertical or horizontal geophones spaced 1.5 m apart for a length of 70.5 m, forward and reverse shot locations with multiple source offsets and source types and multiple interior shot locations).
3. Three HVSR measurement locations: two distributed along array CCOB-1 and one near the seismic station.

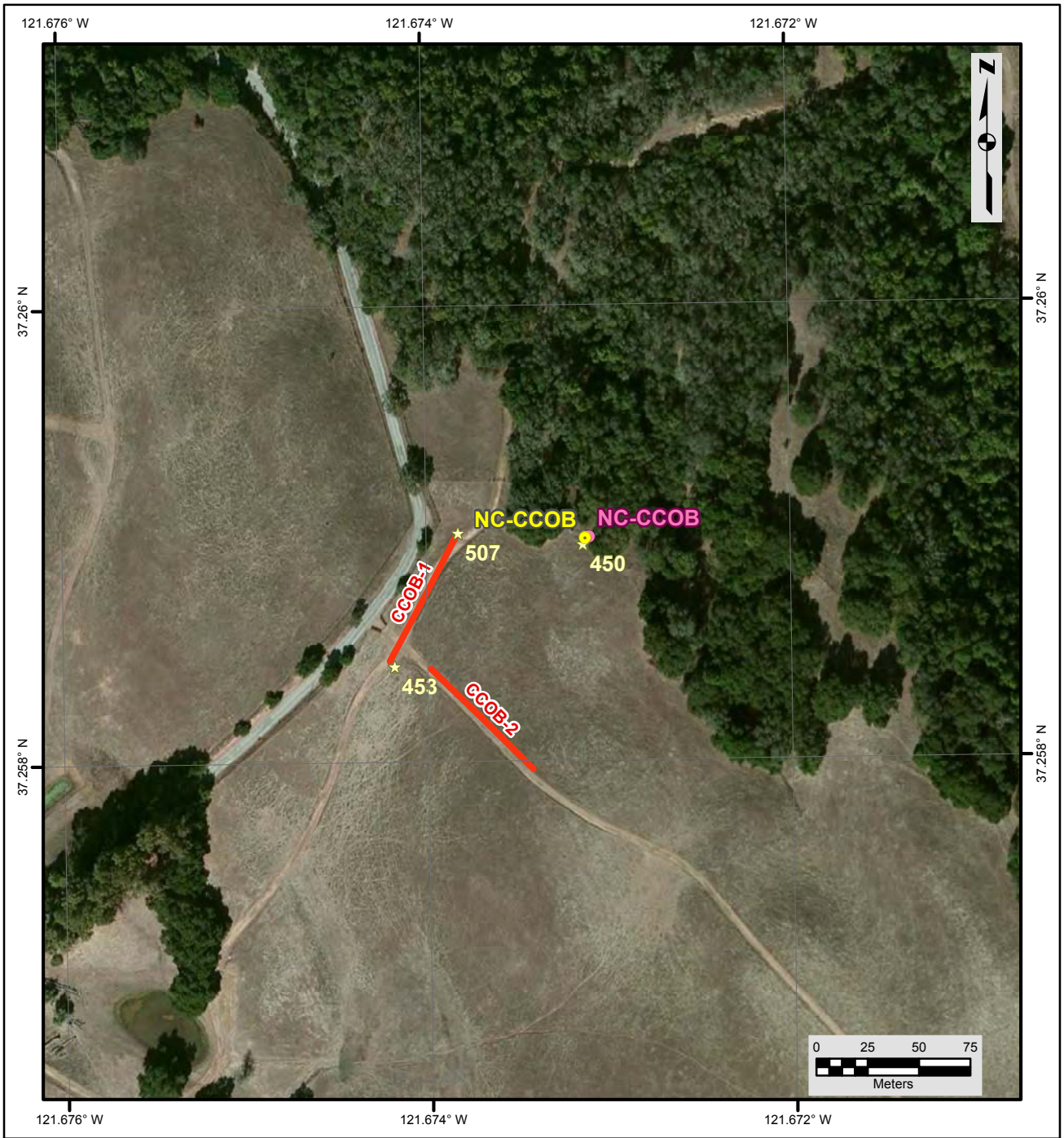

Legend

- Seismic Station - Approximate Surveyed Location
- Seismic Station - Approximate Location of Record
- H/V Spectral Ratio Location
- MASW and Seismic Refraction Array

NOTES:
1. WGS 1984 COORDINATE SYSTEM
2. Image Source: ESRI, i-cubed, USDA FSA, USGS, AEX, GeoEye, Getmapping, Aerogrid, IGP

File Name: NC-CCOB-I

Date: 2/7/2013

USGS science for a changing world

GEOVision geophysical services

RECOVERY.GOV

SITE MAP
NC•CCOB

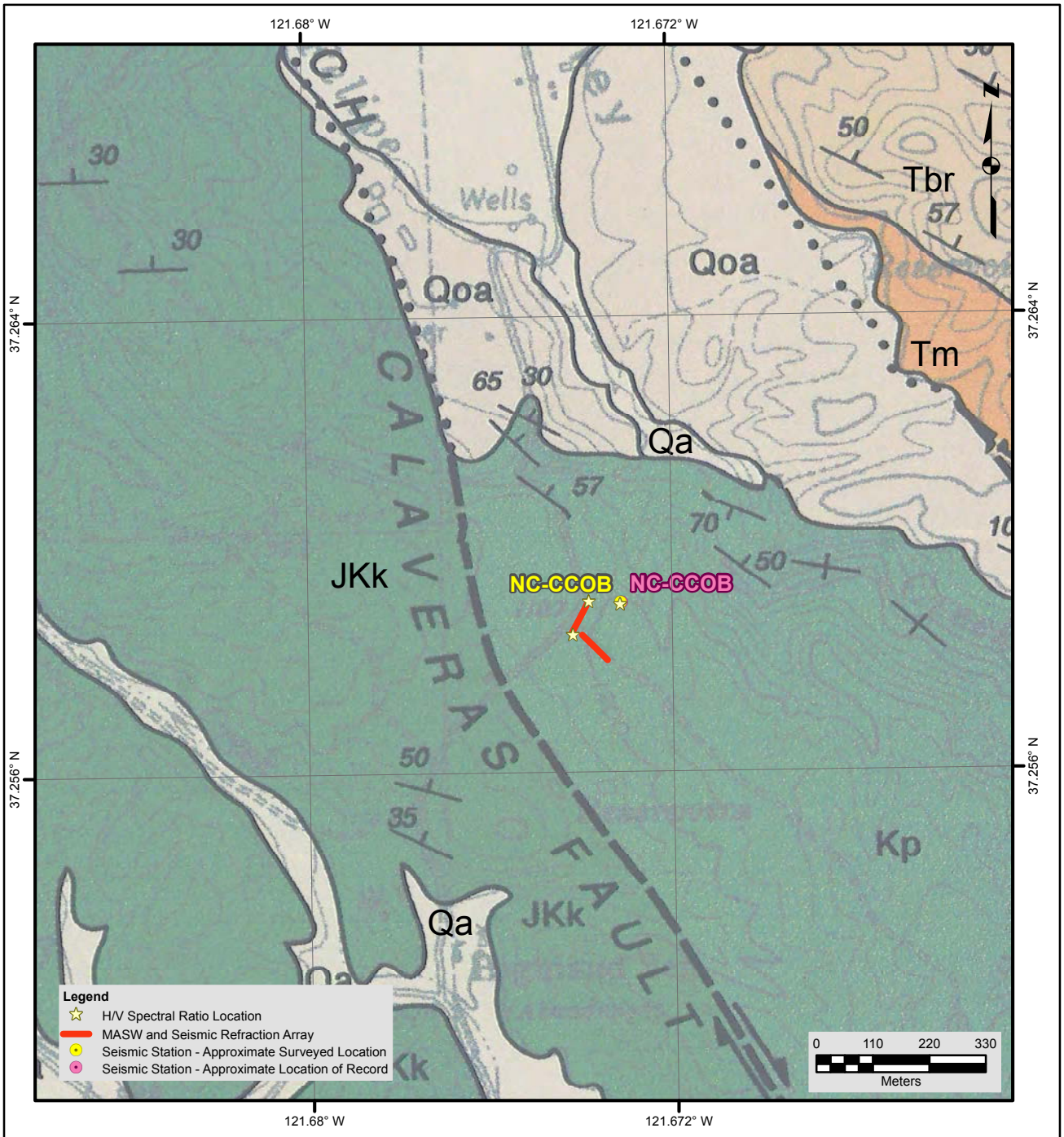

Description of Geologic Map Units

Qa = Quaternary (Holocene) alluvial gravel, sand and clay
Qoa = Quaternary (Pleistocene) alluvial fan deposits, dissected
Tbr = Tertiary (Miocene) Briones Formation; sandstone, lithified, arkosic, locally fossiliferous
Tm = Tertiary (Miocene) Monterey Formation; lithified siliceous shale, platy, locally cherty
Kp = Mesozoic (Cretaceous) Panoche Formation; clay shale or mudstone, micaceous, indurated
JKk = Mesozoic (Jurassic and Cretaceous) Knoxville Formation; clay shale or mudstone, micaceous, lithified

NOTES:
1. WGS 1984 COORDINATE SYSTEM
2. Geologic Map of the Lick Observatory Quadrangle, Santa Clara County, California by Thomas W. Dibblee, Jr., 2005
3. See site map for details of geophysical survey

USGS science for a changing world
GEOVision geophysical services

GEOLOGIC MAP
NC•CCOB

File Name: NC-CCOB
Date: 2/7/2013

Seismic station NC.CCOB

Looking at HVSR sensors 450 (Trillium Compact) and Tromino ENGR and seismic station

Looking northeast along array CCOB-1

Looking southwest along array CCOB-1

Looking northwest along array CCOB-2

Location of Geophysical Testing Arrays:

Location	Latitude	Longitude
CCOB-1, Southwest End of MASW/Refraction Array	37.25844	-121.67421
CCOB-1, Center of MASW/Refraction Array	37.25872	-121.67402
CCOB-1, Northeast End of MASW/Refraction array	37.25899	-121.67384
CCOB-2, Northwest End of MASW/Refraction Array	37.25841	-121.67399
CCOB-2, Center of MASW/Refraction Array	37.25819	-121.67371
CCOB-2, Southeast End of MASW/Refraction Array	37.25796	-121.67343
HVSR Sensor 450	37.25895	-121.67315
HVSR Sensor 453	37.25842	-121.67419
HVSR Sensor 507	37.25900	-121.67383
NC.CCOB Seismic Station	37.25898	-121.67313

Notes: 1) WGS84 Coordinate System (decimal degrees)
2) Survey accuracy is estimated at 1 to 2 m.

Results:

V_S Model for MASW Array CCOB-1

Depth to Top of Layer (m)	Layer Thickness (m)	S-Wave Velocity (m/s)	Inferred P-Wave Velocity (m/s)	Assumed Poisson's Ratio	Assumed Density (g/cm^3)
0	1.5	256	478	0.300	1.8
1.5	2	339	634	0.300	1.8
3.5	3.5	412	770	0.300	1.9
7	4	538	2000	0.461	2.0
11	5	473	2000	0.47	2.0
16	6	383	2000	0.481	2.0
22	8	450	2000	0.473	2.0
30	>10	661	2000	0.439	2.1

Notes: 1) Saturated zone, with V_P of about 2,000 m/s, constrained at a depth of about 7 m based on seismic refraction survey.
2) Depth of investigation is about 40 m.
3) Bottom layer is a half space.

V_S Model for MASW Array CCOB-2

Depth to Top of Layer (m)	Layer Thickness (m)	S-Wave Velocity (m/s)	Inferred P-Wave Velocity (m/s)	Assumed Poisson's Ratio	Assumed Density (g/cm^3)
0	1.5	230	430	0.300	1.8
1.5	2.5	343	642	0.300	1.8
4	4	470	880	0.300	1.9
8	4	489	2000	0.468	2.0
12	5	367	2000	0.483	2.0
17	6	337	2000	0.485	2.0
23	7	417	2000	0.477	2.0
30	>10	609	2000	0.449	2.1

Notes: 1) Saturated zone, with V_P of about 2,000 m/s, constrained at a depth of about 8 m based on seismic refraction survey.
2) Depth of investigation is about 40 m.
3) Bottom layer is a half space.

Observations/Discussion:

- HVSR plots are generally similar at frequencies below 6 Hz. There is a possible broad, low amplitude HVSR peak in the 0.4 to 0.8 Hz range with maxima at about 0.7 Hz.
- P-wave seismic refraction and MASW data were acquired along two arrays (CCOB-1 and CCOB-2) aligned approximately orthogonal and parallel to the mapped strike of geologic bedding in the site vicinity. S-wave seismic refraction and MALW data were also acquired along array CCOB-2, in case needed for site characterization.
- The S-wave refraction and MALW data were not needed for site characterization and, therefore, were not reduced and modeled. Due to relatively low S-wave velocities at the site, the hammer sources used for MALW data acquisition probably did not generate sufficient low frequency energy to image to 30 m depth. S-wave seismic refraction and MALW data were, however, reviewed and indicate that S-wave velocity does not exceed 500 m/s in the upper 20 m.
- Based on review of S-wave seismic refraction and MASW and MALW Rayleigh and Love wave dispersion data, it is clear that a shallow high velocity layer in the P-wave seismic refraction data is associated with saturated sediments. Therefore, only one of the P-wave seismic refraction lines (CCOB-1) was modeled. Seismic refraction first arrival data for array CCOB-2 were reviewed with the saturated zone interpreted at an average depth of about 8 m.

- The P-wave refraction data for array CCOB-1 were modeled using a tomographic inversion routine with a layer-based starting model. The seismic refraction model was extended to far offset shot locations to extend depth of investigation. A larger geophone spacing is usually preferred for extending depth of investigation when applying tomographic inversion routines.
- The P-wave seismic refraction survey design allowed P-wave velocity to be imaged to a maximum depth of about 15 m. The seismic refraction model shows that P-wave velocity is about 400 to 600 m/s at the surface and between 900 and 1,000 m/s between a depth of 2 and 5 m. P-wave velocity increases abruptly from 1,400 to 1,800 m/s in the 5 to 9 m depth range in what is interpreted as the top of the saturated zone. P-wave velocity exceeds 2,000 m/s below a depth of 9 to 11 m.
- The seismic refraction model indicates that there is some lateral velocity variation above the saturated zone, particularly lower velocity surficial sediments at the southwest end of the array.
- The seismic refraction/MASW arrays CCOB-1 and CCOB-2 were oriented approximately orthogonal and parallel to the strike of the geologic bedding, respectively. S-wave velocities are relatively low at this site and the sediments likely behave more as a soil than rock. Therefore, steep dip of the bedding may have limited impact on surface wave measurements, except that lateral velocity variation could be more significant beneath the array oriented orthogonal to strike.
- Noise conditions at the site were not sufficient for application of passive surface wave techniques.
- Both Rayleigh wave and Love wave data were acquired at the site, but it was only necessary to reduce the Rayleigh wave data at this time.
- The minimum wavelength Rayleigh wave phase velocity data extracted from the 48-channel MASW arrays was about 12 and 9 m, for arrays CCOB-1 and CCOB-2, respectively. Reducing data from smaller hammer sources using a limited offset receiver array (i.e. less active geophones) allowed for extraction of surface wave dispersion data to a minimum wavelength of about 4 m for both arrays CCOB-1 and CCOB-2.
- A maximum 80 to 90 m wavelength Rayleigh wave was extracted from the MASW data by slightly relaxing the near field criteria typically applied during this investigation. The maximum wavelength Rayleigh wave was set equal to 1.25 times the source to midpoint of receiver array distance.
- There is about 30 and 80 m/s of scatter in Rayleigh wave dispersion data, likely the result of lateral velocity variation.
- A representative dispersion curve was generated for each MASW data set using a moving average, polynomial curve fitting routine and used for modeling.
- The signature of the Rayleigh wave dispersion curves for both arrays CCOB-1 and CCOB-2 dictate that a velocity inversion may occur at the site. This is plausible given that the sediments consist of clay and desiccation driven hardening can cause V_S to increase as the degree of saturation decreases. It would, therefore, not be unexpected for V_S to be slightly higher above the historic water table at this site.
- The MASW data were modeled using the fundamental mode assumption (2-D solution in the WinSASW software package, which is equivalent to fundamental mode for most V_S model types, but also has limited capability of accounting for dominant higher modes at high frequencies/small wavelengths associated with high velocity surface layers). The

resulting V_S models were evaluated to confirm that the fundamental mode has the highest amplitude at all frequencies and that potential modal superposition will have only minor influence on the resulting models.

- Surface wave depth of investigation is about 40 m based on the half of maximum wavelength criteria.
- V_{S30} is 418 and 381 m/s for MASW arrays CCOB-1 and CCOB-2, respectively, averaging 400 m/s.
- Average S-wave velocity between 1 m (assumed sensor depth) and 31 m is 433 and 395 m/s for arrays CCOB-1 and CCOB-2, respectively, averaging 414 m/s.

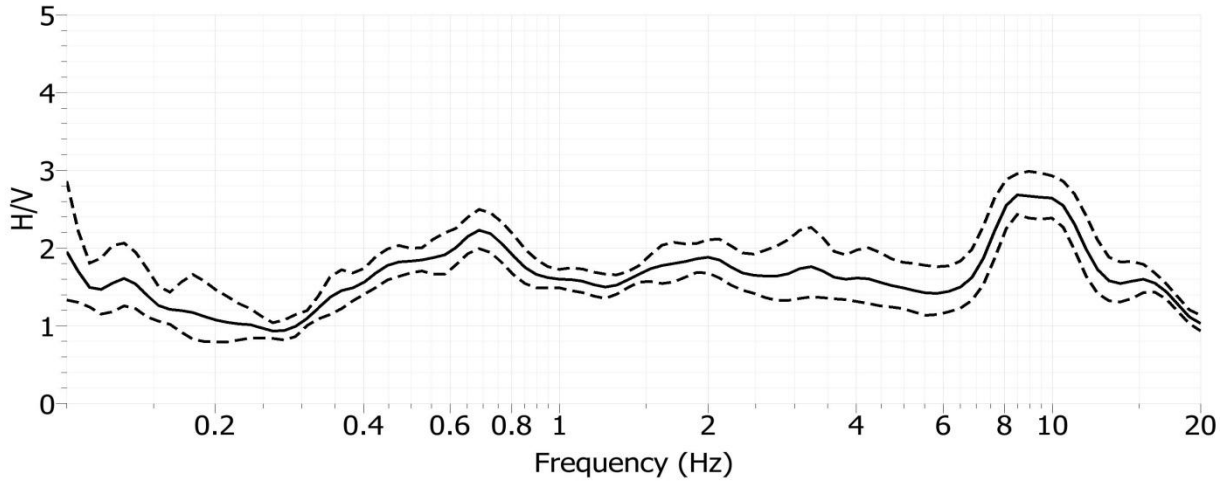

Site NC.CCOB, H/V Spectral Ratio, Array CCOB-1, Sensor 453

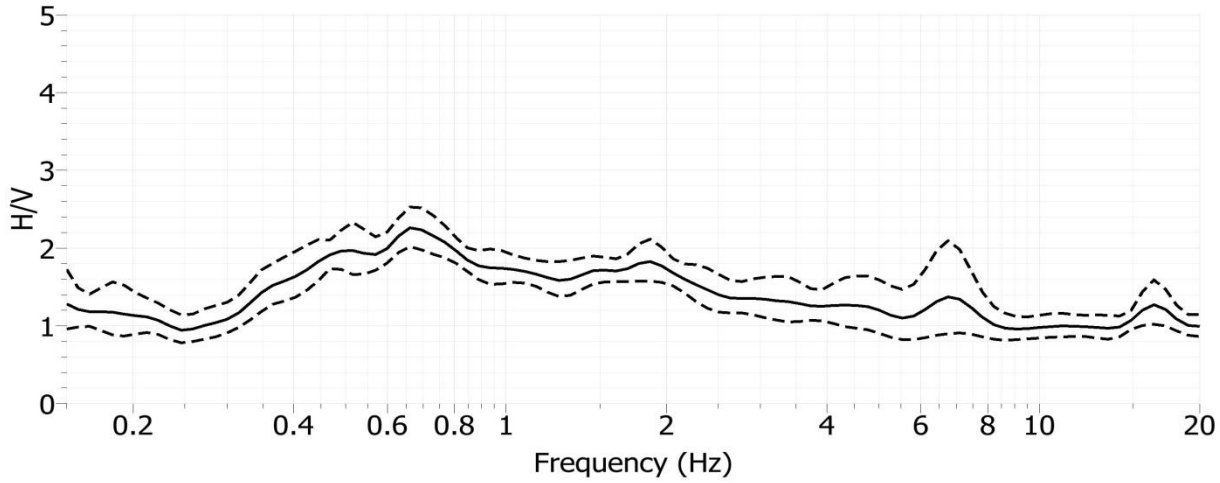

Site NC.CCOB, H/V Spectral Ratio, Array CCOB-1, Sensor 507

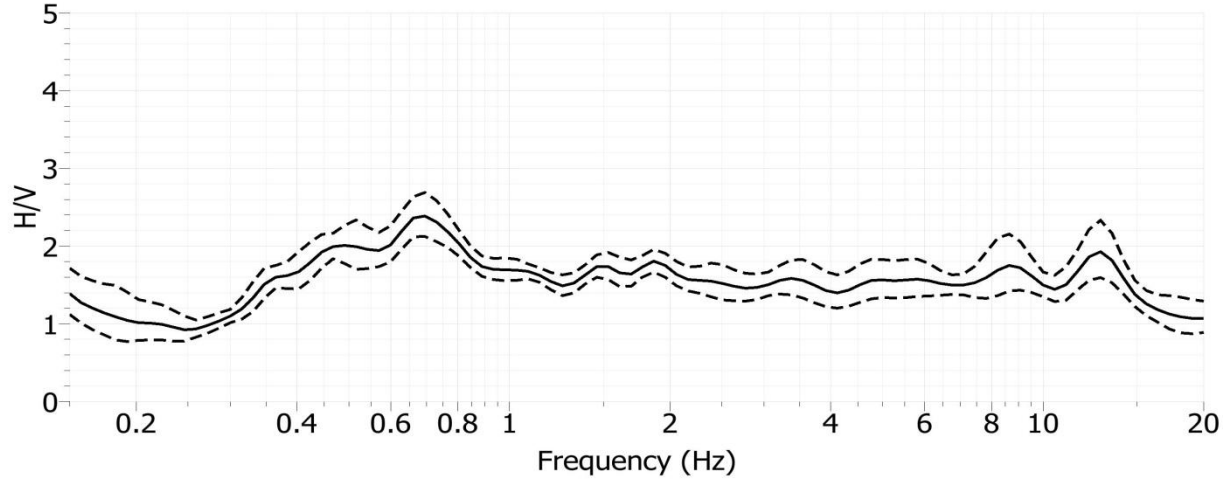

Site NC.CCOB, H/V Spectral Ratio, Near Seismic Station, Sensor 450

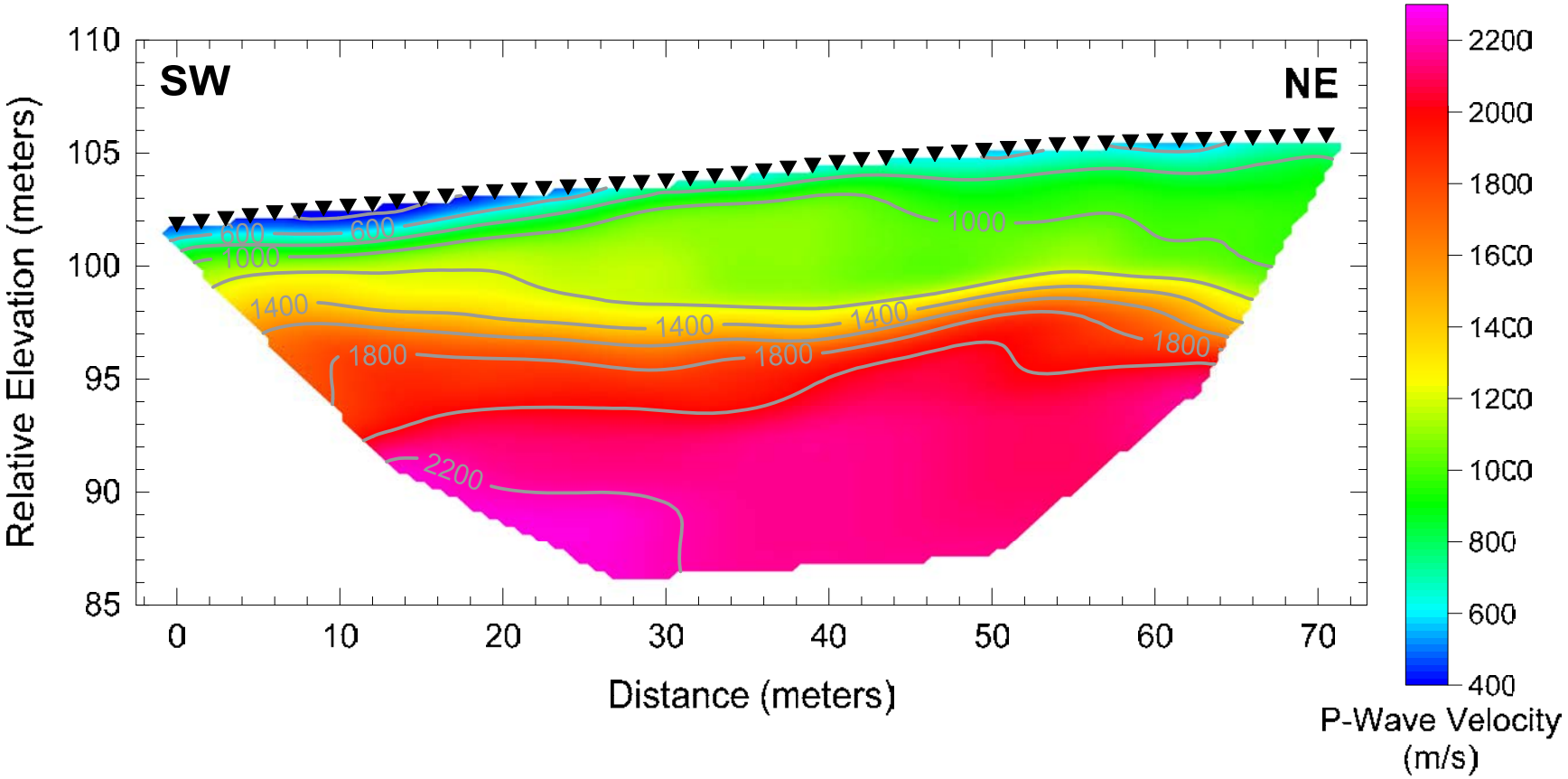

Array CCOB-1 – Tomographic Seismic Refraction Model utilizing Layer Based Starting Model

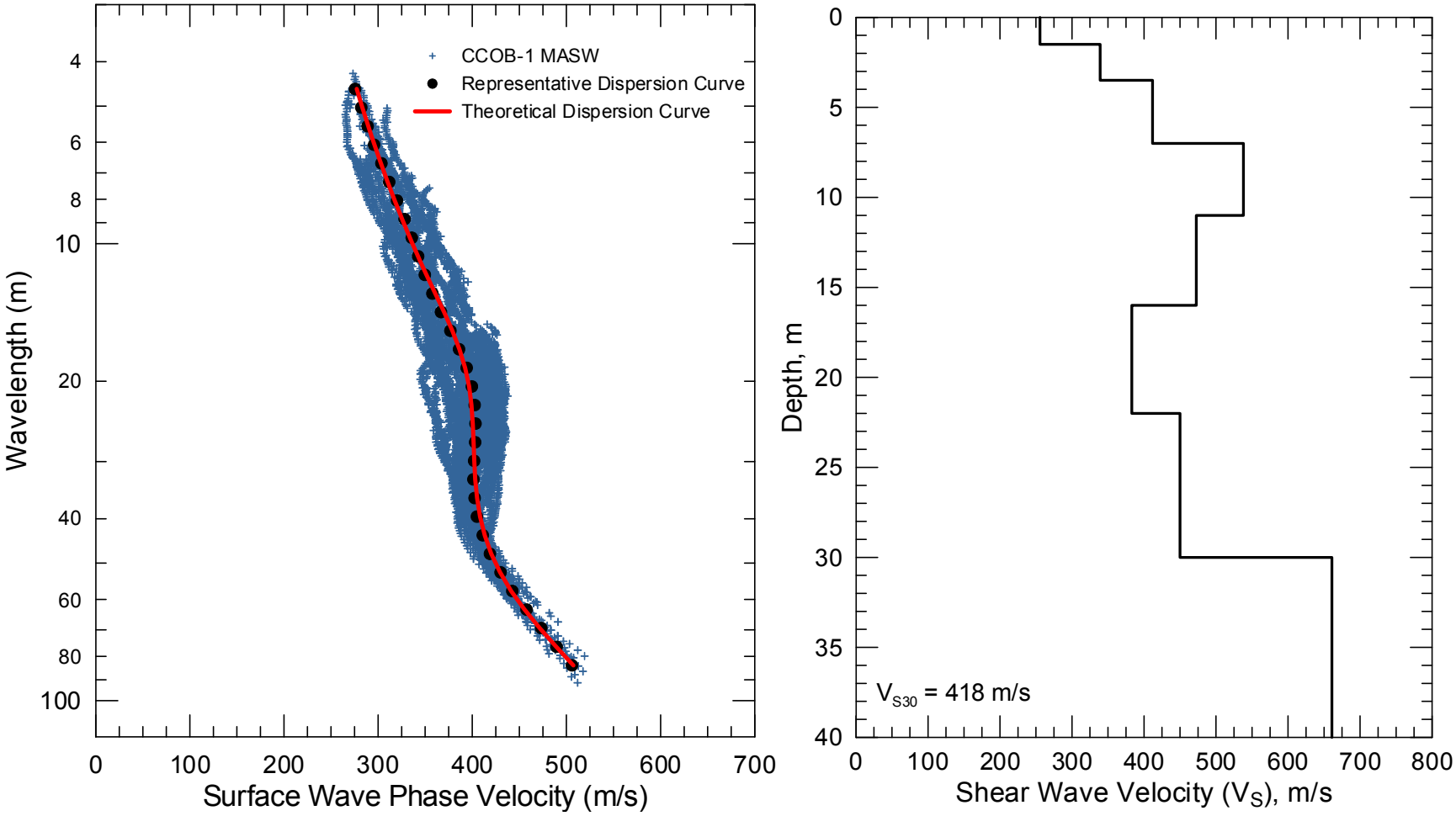

NC.CCOB - Field, representative and inverted theoretical surface wave dispersion data (left) and associated V_S model (right) for MASW (Rayleigh wave) array CCOB-1.

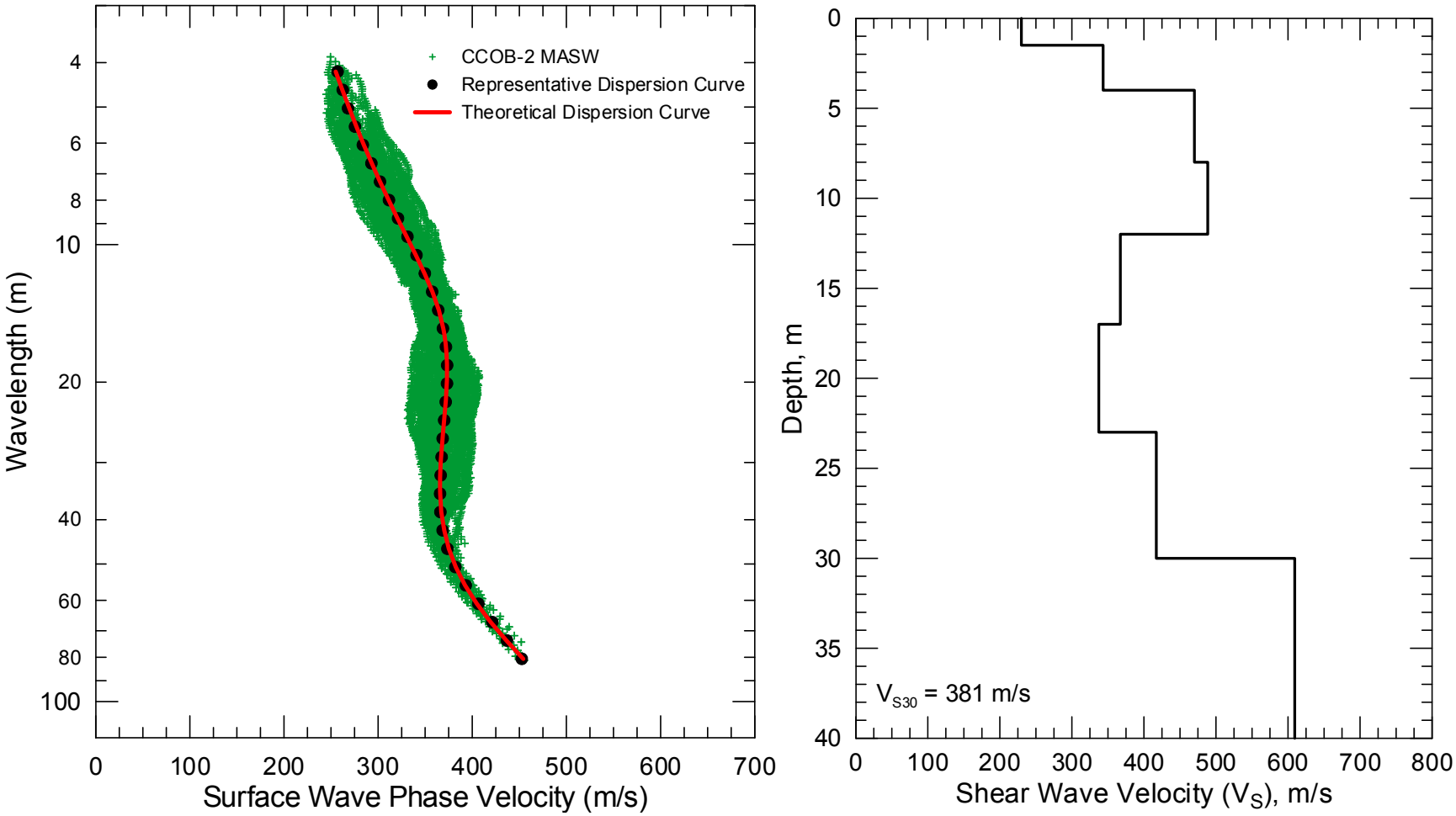

NC.CCOB - Field, representative and inverted theoretical surface wave dispersion data (left) and associated V_S model (right) for MASW (Rayleigh wave) array CCOB-2.

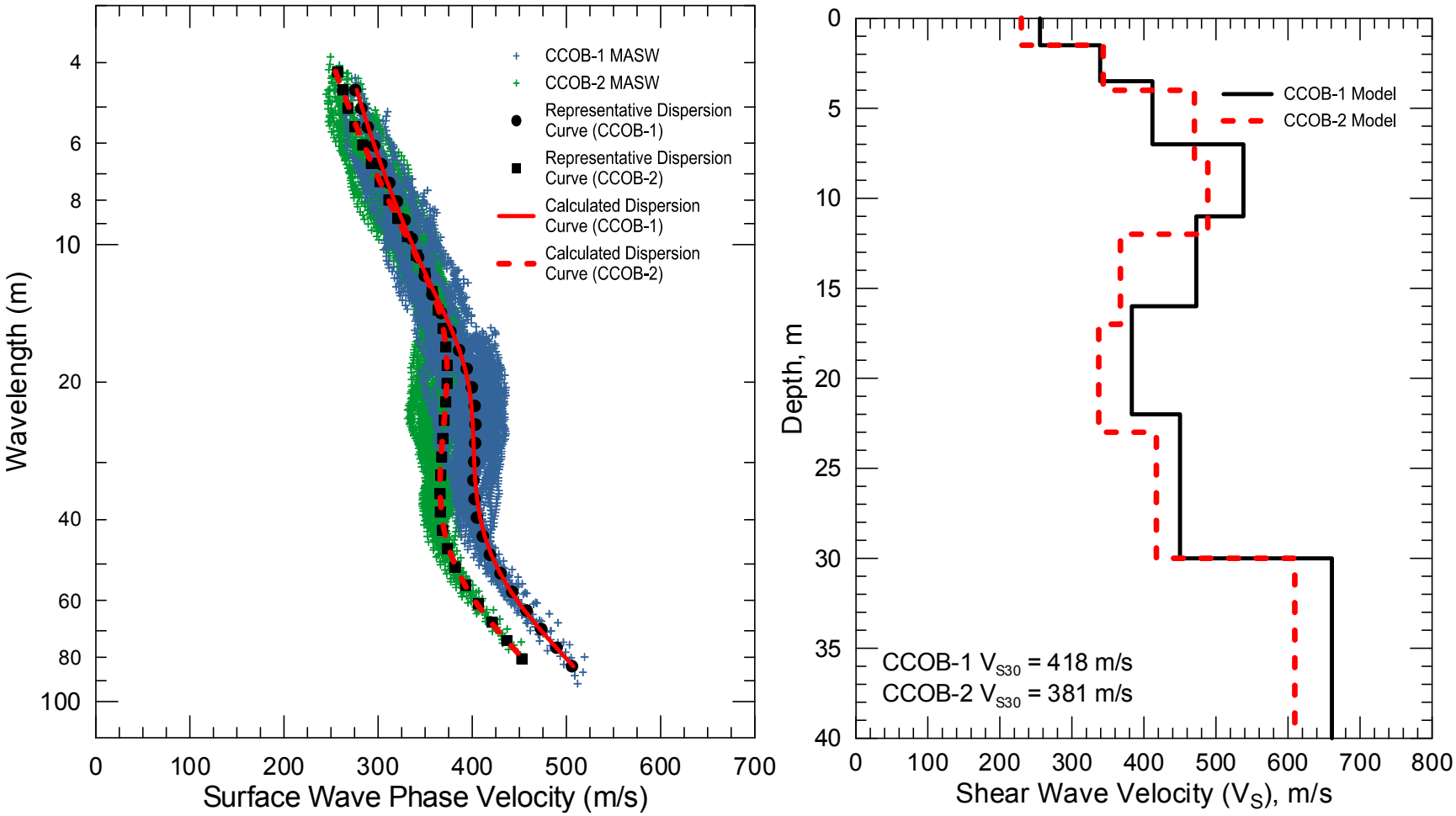

NC.CCOB - Field, representative and inverted theoretical surface wave dispersion data (left) and associated V_S model (right) for MASW (Rayleigh wave) arrays CCOB-1 and CCOB-2.

Site NC.CHR

Location: Mt. Hamilton Road, Santa Clara County, California

Latitude: 37.37289 **Longitude:** -121.76887
(Station coordinates provided by USGS, WGS84 coordinate system)

V_{S30} (measured): 471 m/s

V_{S30} (adjusted to more accurately reflect seismic station conditions): 471 m/s (no adjustment necessary).

NEHRP Site Class: C

Geomatrix Code: IMB

Geologic Conditions/Observations: Seismic station located on the Tertiary (Miocene) Briones Formation, a marine sandstone. The sandstone unit is overturned and has dips of about 55 to 65 degrees to the northeast in the site vicinity. The Hayward Fault is located about 1.6 km to the southwest.

Site Conditions: Rural site. Rolling hills in site vicinity. Test area located along a ridge orientated subparallel to the strike of the sandstone unit. There is about a 2 m topographic depression in the center of the seismic line.

Geophysical Methods Utilized: HVSR, Seismic Refraction, MASW

Geophysical Testing Arrays:

1. Array CHR-1 (48 channel MASW and P-wave seismic refraction array utilizing 4.5 Hz vertical geophones spaced 1.5 m apart for a length of 70.5 m, forward and reverse shot locations with multiple source offsets and source types and multiple interior shot locations).
2. Three HVSR measurement locations: two distributed along array CHR-1 and one adjacent to the seismic station.

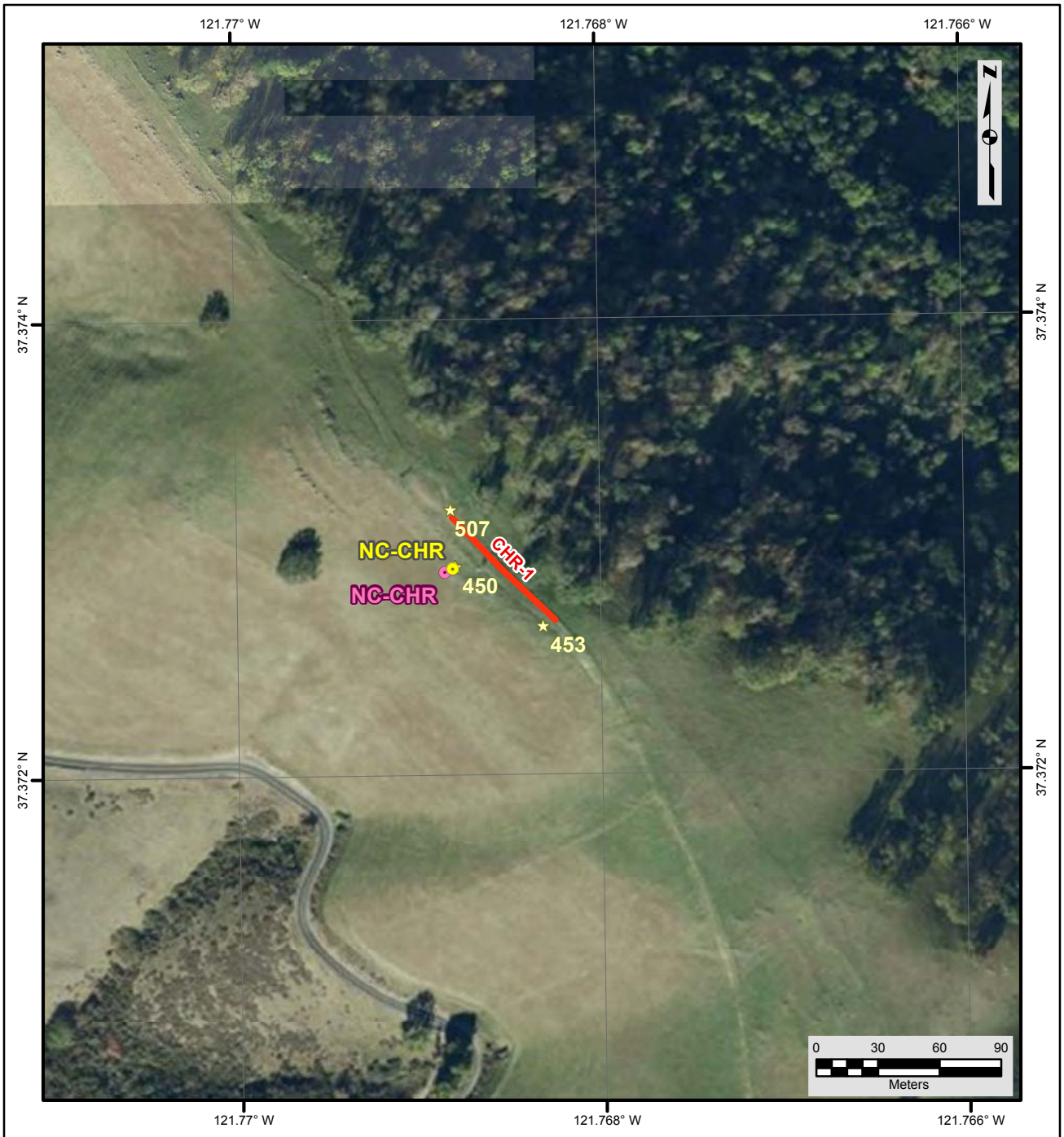

Legend

- Seismic Station - Approximate Surveyed Location
- Seismic Station - Approximate Location of Record
- H/V Spectral Ratio Location
- MASW and Seismic Refraction Array

NOTES:
1. WGS 1984 COORDINATE SYSTEM
2. Image Source: ESRI, i-cubed, USDA FSA, USGS, AEX, GeoEye, Getmapping, Aerogrid, IGP

File Name: NC-CHR-I

Date: 10/6/2011

USGS science for a changing world

GEOVision geophysical services

RECOVERY.GOV

SITE MAP
NC•CHR

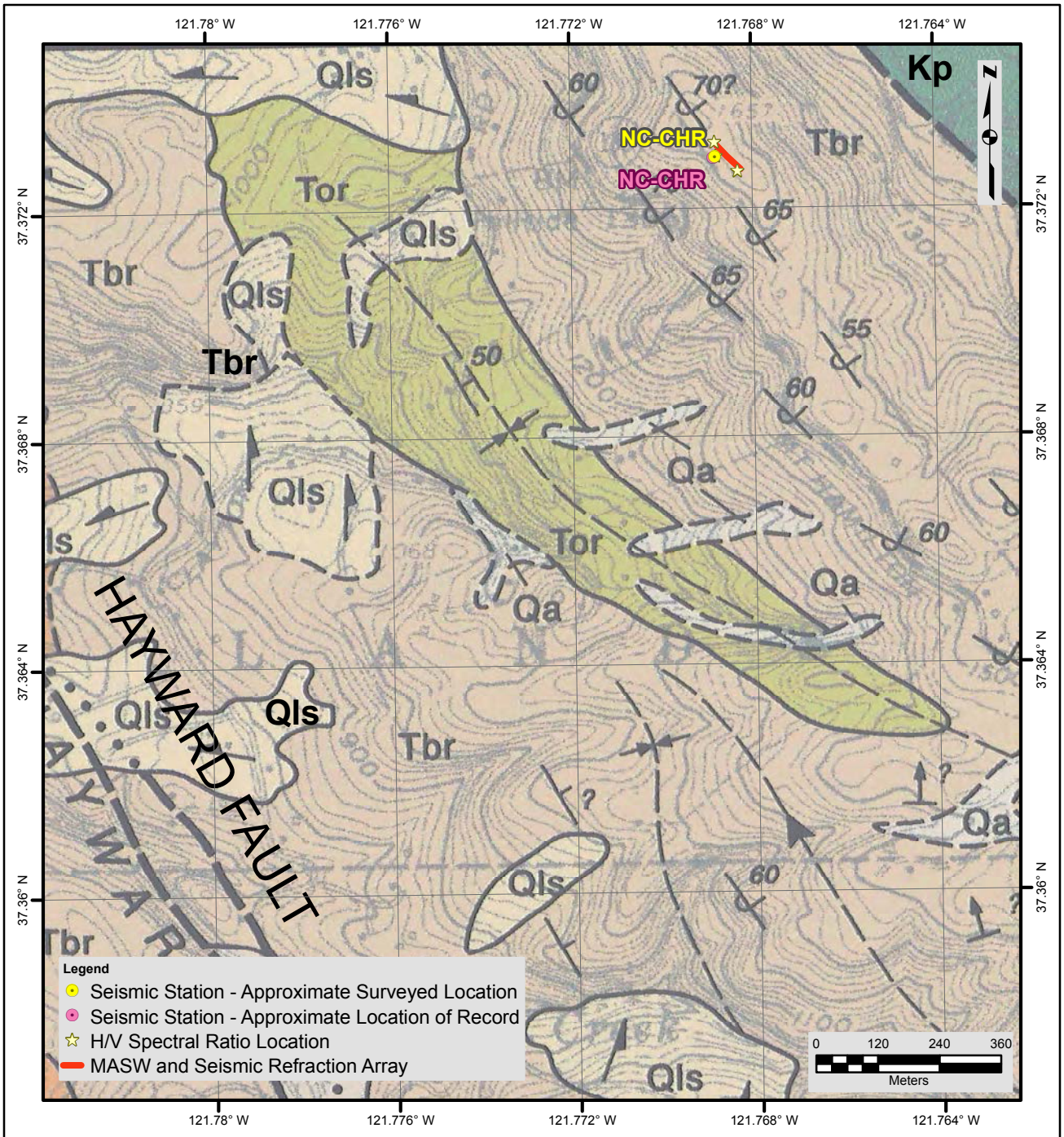

Description of Geologic Map Units

Qa = Quaternary (Holocene) alluvial gravel, sand and clay of valley areas and fans
Qls = Quaternary (Pleistocene - Holocene) landslide rubble
Tor = Tertiary (Miocene - Pliocene) Orinda Formation, weakly lithified sandstone and pebble conglomerate, terrestrial
Tbr = Tertiary (Miocene) Briones Formation, marine, lithified sandstone
Kp = Mesozoic (Upper Cretaceous) Panoche Formation, clay shale or mudstone, bedded, lithified

NOTES:
1. WGS 1984 COORDINATE SYSTEM
2. Geologic Map of the San Jose East Quadrangle, Santa Clara County, California by Thomas W. Dibblee, Jr., 2005
3. See site map for details of geophysical survey

File Name: NC-CHR

Date: 10/6/2011

USGS science for a changing world

GEOVision geophysical services

GEOLOGIC MAP
NC•CHR

RECOVERY.GOV

Looking at HVSR sensors 450 (Trillium) and Tromino ENGR and NC.CHR seismic station

NC.CHR seismic station

Looking southeast along array CHR-1

Seismic refraction and MASW data acquisition

Looking northwest along array CHR-1

Location of Geophysical Testing Arrays:

Location	Latitude	Longitude
CHR-1, Northwest End of MASW/Refraction Array	37.37313	-121.76883
CHR-1, Center of MASW/Refraction Array	37.37290	-121.76856
CHR-1, Southeast End of MASW/Refraction Array	37.37268	-121.76826
HVSR Sensor 450	37.37292	-121.76881
HVSR Sensor 453	37.37265	-121.76833
HVSR Sensor 507	37.37317	-121.76884
NC.CHR Seismic Station	37.37291	-121.76883

Notes: 1) WGS84 Coordinate System (decimal degrees)
2) Survey accuracy is estimated at 1 to 2 m.

Results:

V_S Model 1 (Northwest Energy Source Locations)

Depth to Top of Layer (m)	Layer Thickness (m)	S-Wave Velocity (m/s)	Inferred P-Wave Velocity (m/s)	Assumed Poisson's Ratio	Assumed Density (g/cm^3)
0	1	188	351	0.3	1.7
1	1.5	264	494	0.3	1.7
2.5	5	385	720	0.3	1.8
7.5	6	462	864	0.3	1.9
13.5	7	503	940	0.3	1.9
20.5	8	666	1246	0.3	2.1
28.5	>6.5	777	1455	0.3	2.1

Notes: 1) Data modeled assuming dispersion curve is the fundamental mode.
2) Depth of investigation is about 35m.
3) Bottom layer is a half space.

V_S Model 2(Southeast Energy Source Locations)

Depth to Top of Layer (m)	Layer Thickness (m)	S-Wave Velocity (m/s)	Inferred P-Wave Velocity (m/s)	Assumed Poisson's Ratio	Assumed Density (g/cm^3)
0	1	183	342	0.3	1.7
1	1.5	267	500	0.3	1.7
2.5	5	337	630	0.3	1.8
7.5	6	476	891	0.3	1.9
13.5	7	605	1131	0.3	2.0
20.5	8	749	1402	0.3	2.1
28.5	>6.5	898	1680	0.3	2.1

Notes: 1) Data modeled assuming dispersion curve is the fundamental mode.
2) Depth of investigation is about 35 m.
3) Bottom layer is a half space.

Observations/Discussion:

- There are no distinct peaks in the HVSR data.
- The P-wave seismic refraction data quality is very good; however, given the steeply dipping beds in the site vicinity the presence of out of plane refractors cannot be refuted.
- The P-wave seismic refraction data collected along array CHR-1 were modeled using a tomographic inversion routine with both a smooth velocity gradient and layer based starting model. The starting models were extended to far offset shot locations to extend depth of investigation.
- The seismic refraction survey design allowed P-wave velocity structure to be imaged to a maximum depth of about 20 m. The tomographic inversion of the seismic refraction data using layer based and smooth velocity gradient starting models yielded similar final models. The seismic refraction models show that P-wave velocity is about 300 to 600 m/s at the surface, increasing to 1,000 m/s at a depth of 2 to 6 m and exceeding 1,200 m/s at a depth below 8 to 14 m.
- The seismic refraction models indicate that there is some lateral velocity variation at this site; most significantly a slight thickening of a low velocity surficial sediment layer in the central portion of the line and higher velocity sediments at depth beneath the northwest end of the line.
- Noise conditions at the site were not sufficient for application of passive surface wave techniques.
- Compilation of a Rayleigh wave dispersion curve was complicated by lateral velocity variation, both near surface and at depth. There was clear divergence of the phase velocities at long wavelengths (low frequencies) generated from offend source locations at the northwest and southeast ends of the array. Additionally, source locations in the center of the array yielded lower phase velocities at small wavelengths (high frequencies), which is consistent with the seismic refraction models. Therefore, the MASW data were modeled by developing two dispersion curves: one from interior and

northwest source locations and the other from southeast and interior source locations. Both dispersion curves were supplemented at small wavelengths by SASW analysis of selected MASW receiver pairs from the source locations at the respective ends of the array. Source locations in the central portion of the array were not utilized for analysis for reasons discussed above.

- There is about 60 m/s scatter in final MASW dispersion curves selected for modeling, likely the result of lateral velocity variation.
- The minimum wavelength surface wave phase velocity data extracted from the 48-channel MASW array is about 22 m for source locations off the northwest end of the array and 25 m for source locations off the southeast end of the array. Data reduction using seismic records from smaller hammer sources and a limited offset receiver array (i.e. less active geophones) allowed extraction of surface wave dispersion data to a minimum wavelength of about 4 m.
- A representative dispersion curve was generated for each MASW data set using a moving average, polynomial curve fitting routine and used for modeling.
- The V_S model developed for the Rayleigh wave dispersion curve developed from source locations at the southeast end of array CNR-1 (Model 2) has about 15% higher S-wave velocity below a depth of 13.5 m than that from the northwest source locations (Model 1). There is, however, only a 4% difference in V_{S30} between the two models.
- Surface wave depth of investigation is about 35 m based on half of maximum wavelength criteria.
- The inferred P-wave velocities in the surface wave models are generally lower than those in the seismic refraction models. The sandstone unit has steep dip at this site and the seismic refraction model could overestimate velocity structure immediately beneath the array if first arrival data consists of out of plane refractors from higher velocity sandstone layers adjacent to the line.
- V_{S30} is 462 m/s for Model 1 and 480 m/s for Model 2, averaging 471 m/s (Site Class C).
- The S-wave velocity models derived from the surface wave testing are believed to be representative of average subsurface velocity structure. However, geology at the site is complex with steeply dipping bedding. The seismic line was oriented subparallel to strike and surface topography did not allow acquisition of data perpendicular to strike. In such geologic conditions, weathering must play a significant role in near surface velocity structure for surface wave techniques to be effective.
- V_{S30} estimated from the central portion of the P-wave seismic refraction model with an assumed Poisson's ratio of 0.333 is 526 m/s, about 11 % higher than that estimated from the surface wave sounding. Of course, Poisson's ratio is not known for the sandstone unit and the seismic refraction model could be impacted by out of plane refractors. Additionally, more research is needed to determine whether surface wave models are representative of average velocity structure in cases of significant lateral velocity variation.
- Site characterization of this site would have benefited from an S-wave seismic refraction survey to further constrain subsurface S-wave velocity structure.

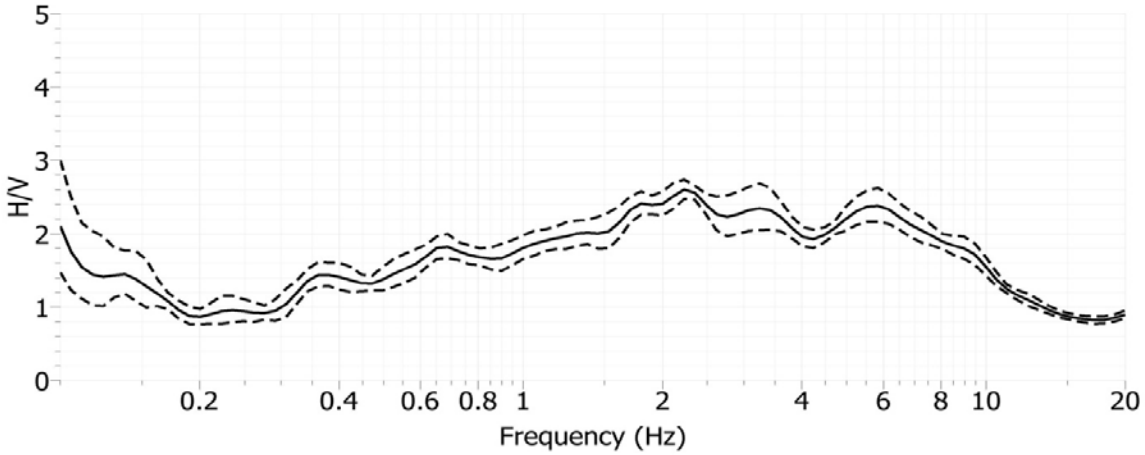

Site NC.CHR, H/V Spectral Ratio, Array CHR-1, Sensor 507

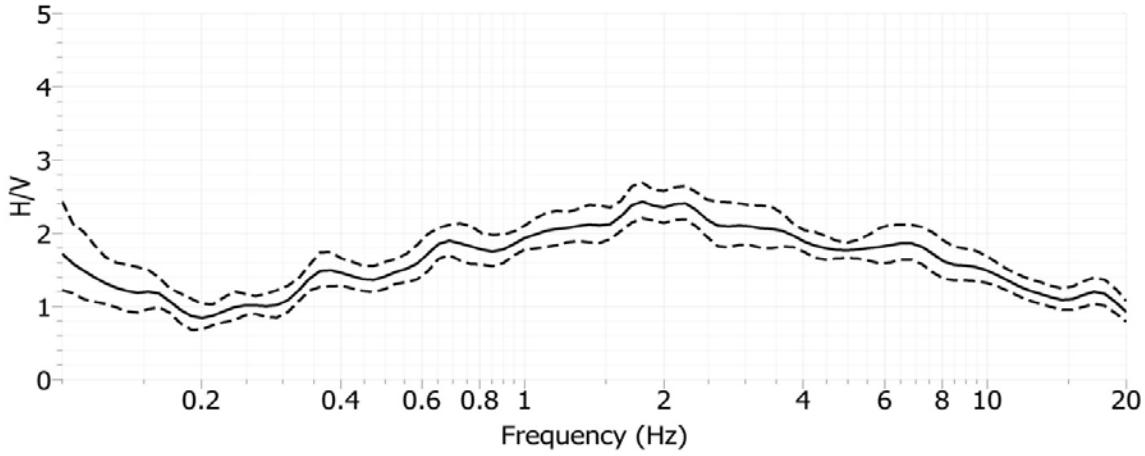

Site NC.CHR, H/V Spectral Ratio, Near Seismic Station, Sensor 450

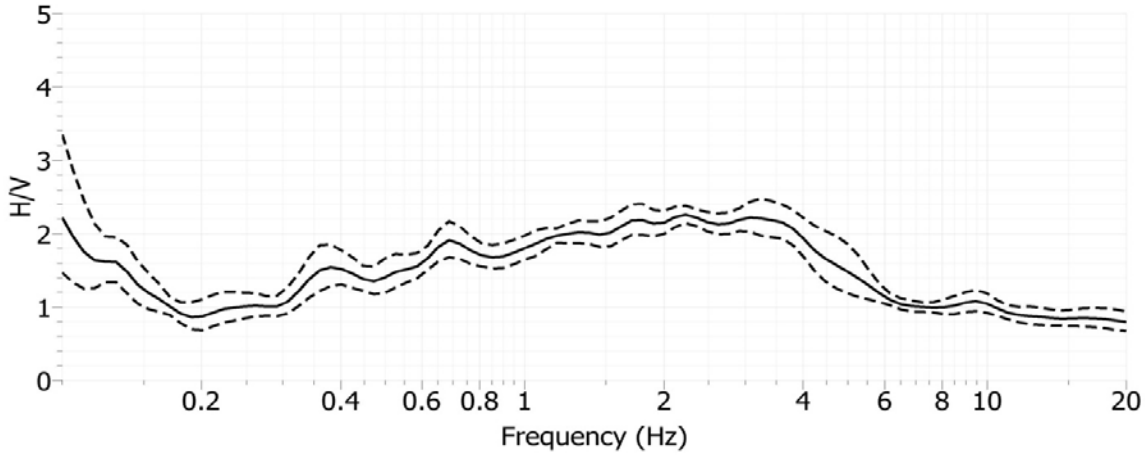

Site NC.CHR, H/V Spectral Ratio, Array CHR-1, Sensor 453

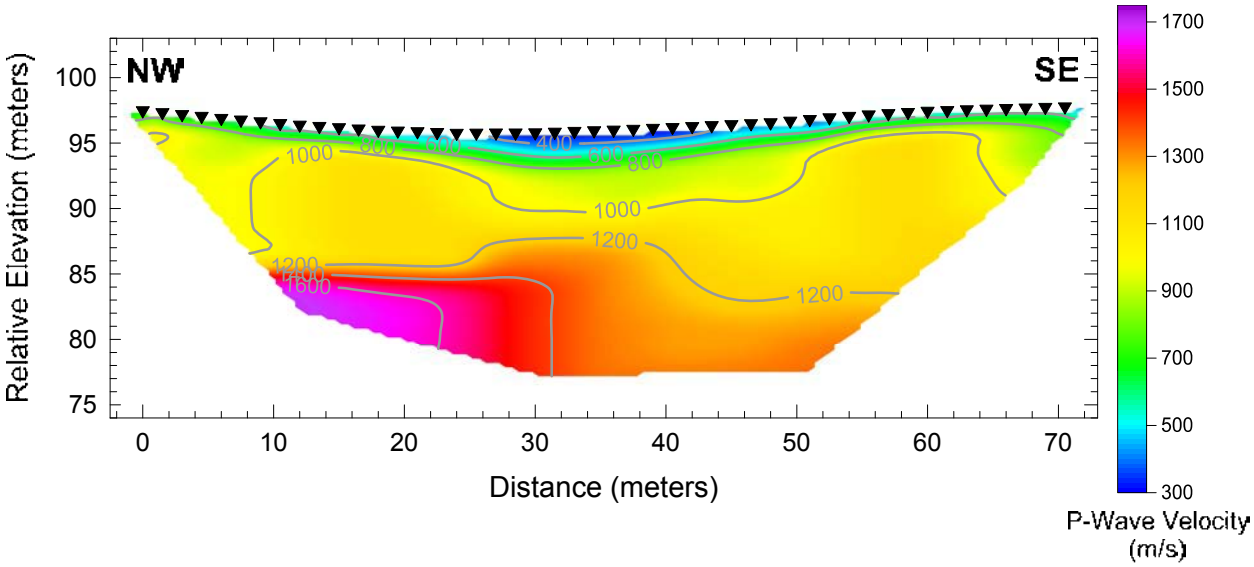

Array CHR-1 – P-wave Tomographic Seismic Refraction Model utilizing Layer Based Starting Model

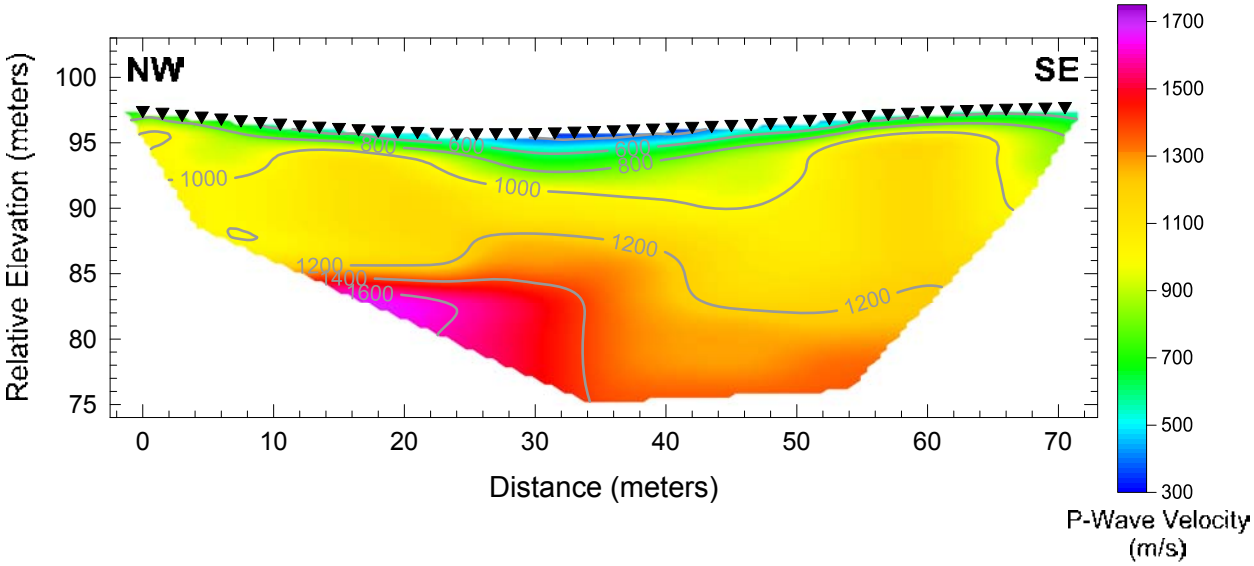

Array CHR-1 – P-wave Tomographic Seismic Refraction Model utilizing Smooth Velocity Gradient Starting Model

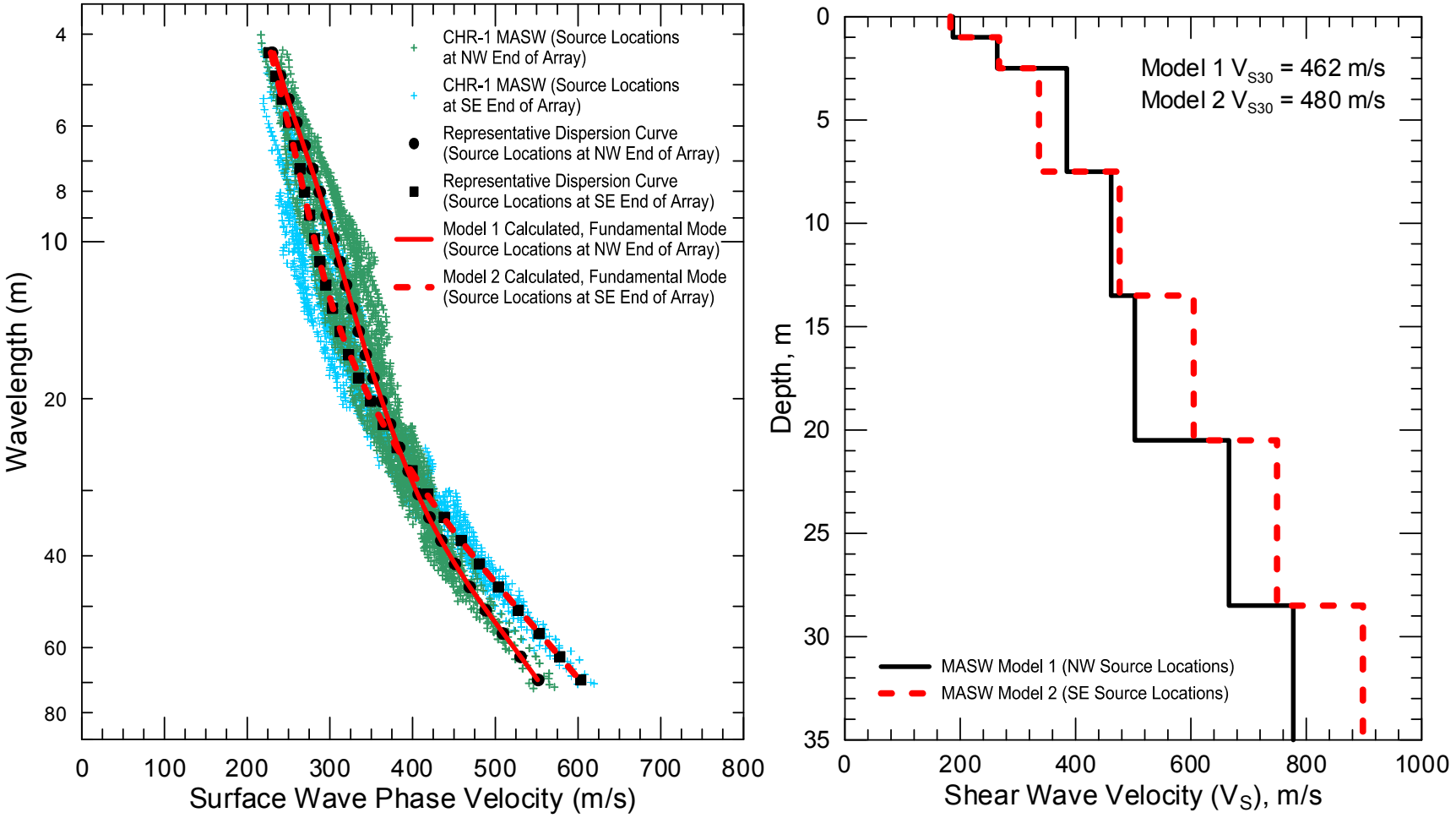

NC.CHR - Field, representative and inverted theoretical Rayleigh wave dispersion data (left) and associated V_S models (right)

Site NC.CNI

Location: Niles Canyon, Alameda County, California

Latitude: 37.60791 **Longitude:** -121.96442
(Approximate station coordinates from site survey, WGS84 coordinate system)

V_{S30} (measured): 517 m/s

V_{S30} (adjusted to more accurately reflect seismic station conditions): 584 m/s (average S-wave velocity between 1 and 31 m adjusting for sensor likely being located beneath residual soil layer).

NEHRP Site Class: C

Geomatrix Code: IKB

Geologic Conditions/Observations: Seismic station located on geologic unit mapped as Mesozoic (Cretaceous) Oakland Sandstone. The mapped location of the Sheridan Creek Fault is about 100 m northeast of the seismic station. Bedding attitudes are not plotted on the geologic map; however, visible outcrops on the site map indicate that bedding has a southeast to northwest strike and probable steep dip.

Site Conditions: Rural site located on gently rolling hills. Ground surface elevation decreases about 3.5 m to the southwest along the 70.5 m long MASW and seismic refraction array.

Geophysical Methods Utilized: HVSR, P- and S-wave Seismic Refraction, MASW (Rayleigh Wave) and MALW (Love Wave)

Geophysical Testing Arrays:

1. Array CNI-1 (48 channel MASW, MALW and P- and S-wave seismic refraction array utilizing 4.5 Hz vertical or horizontal geophones spaced 1.5 m apart for a length of 70.5 m, forward and reverse shot locations with multiple source offsets and source types and multiple interior shot locations).
2. Three HVSR measurement locations distributed along array CNI-1.

Legend

- Seismic Station - Approximate Surveyed Location
- Seismic Station - Approximate Location of Record
- H/V Spectral Ratio Location
- MASW and Seismic Refraction Array (S- and P-wave)

NOTES:
1. WGS 1984 COORDINATE SYSTEM
2. Image Source: ESRI, i-cubed, USDA FSA, USGS, AEX, GeoEye, Getmapping, Aerogrid, IGP

File Name: NC-CNI-I

Date: 11/3/2011

USGS science for a changing world

GEOVision geophysical services

SITE MAP
NC•CNI

RECOVERY.GOV

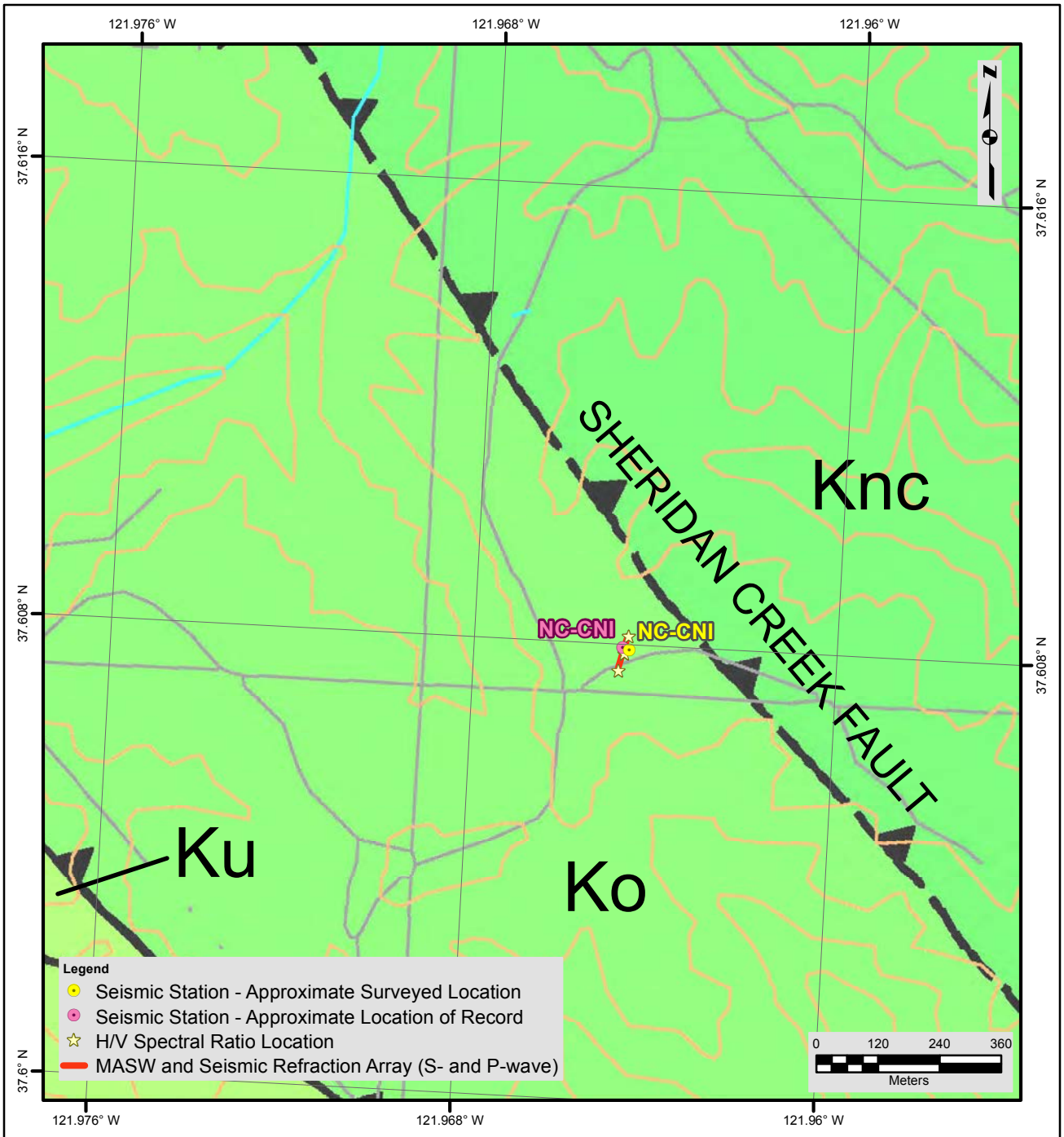

Description of Geologic Map Units

Ko = Mesozoic (Cretaceous) Oakland Sandstone
Ku = Mesozoic (Cretaceous) undivided sandstone and siltstone
Knc = Mesozoic (Cretaceous) sandstone and shale of Niles Canyon area

NOTES:
1. WGS 1984 COORDINATE SYSTEM
2. Geologic Map of the Hayward Fault Zone, by R.W. Graymer, D.L. Jones, and E.E. Brabb, 1995
3. See site map for details of geophysical survey

File Name: NC-CNI

Date: 11/3/2011

USGS science for a changing world

GEOVision geophysical services

RECOVERY.GOV

GEOLOGIC MAP
NC•CNI

Seismic station NC.CNI

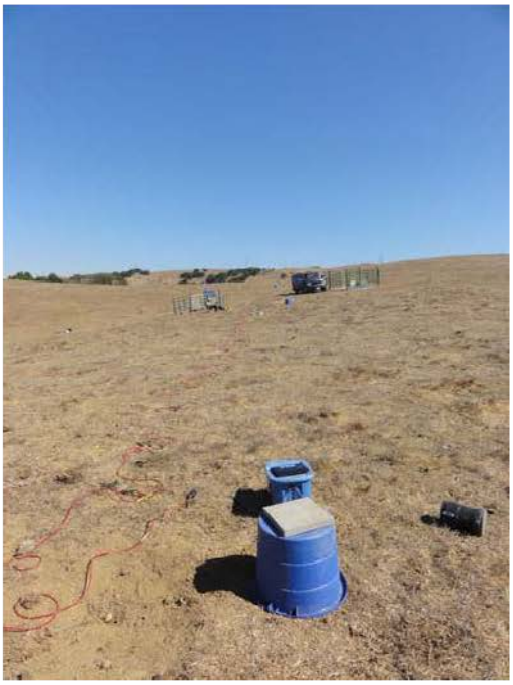

Looking northeast along array CNI-1
and at HVSR sensor 507

MASW and P-wave seismic refraction data
acquisition along array CNI-1

Looking southwest along array CNI-1
and at HVSR sensor 450

S-wave seismic refraction/Love wave MASW
data acquisition

Location of Geophysical Testing Arrays:

Location	Latitude	Longitude
CNI-1, Southwest End of MASW/Seismic Refraction Array	37.60754	-121.96465
CNI-1, Center of MASW/Seismic Refraction Array	37.60785	-121.96456
CNI-1, Northeast End of MASW/Seismic Refraction Array	37.60815	-121.96446
HVSR Sensor 450	37.60815	-121.96444
HVSR Sensor 453	37.60784	-121.96452
HVSR Sensor 507	37.60754	-121.96463
NC.CNI Seismic Station	37.60791	-121.96442

Notes: 1) WGS84 Coordinate System (decimal degrees)
2) Survey accuracy is estimated at 1 to 2 m.

Results:

V_S Model 1 (MASW - Rayleigh wave)

Depth to Top of Layer (m)	Layer Thickness (m)	S-Wave Velocity (m/s)	Inferred P-Wave Velocity (m/s)	Assumed Poisson's Ratio	Assumed Density (g/cm^3)
0	1.5	156	291	0.300	1.8
1.5	2.5	329	616	0.300	1.9
4	5.5	690	1291	0.300	2.0
9.5	5.5	569	1064	0.300	2.0
15	8	526	2400	0.475	2.1
23	>12	873	2400	0.424	2.2

Notes: 1) Saturated zone, with V_P of about 2,400 m/s, constrained at a depth of about 15 m based on seismic refraction survey.
2) Depth of investigation is about 35 m.
3) Bottom layer is a half space.

V_S Model 2 (MASW, better agreement with Love wave model)

Depth to Top of Layer (m)	Layer Thickness (m)	S-Wave Velocity (m/s)	Inferred P-Wave Velocity (m/s)	Assumed Poisson's Ratio	Assumed Density (g/cm^3)
0	0.75	91	169	0.300	1.8
0.75	3.25	454	850	0.300	1.9
4	5.5	486	910	0.300	2.0
9.5	5.5	541	1012	0.300	2.0
15	8	556	2400	0.472	2.1
23	>12	863	2400	0.426	2.2

Notes: 1) Saturated zone, with V_P of about 2,400 m/s, constrained at a depth of about 15 m based on seismic refraction survey.
2) Depth of investigation is about 35 m.
3) Bottom layer is a half space.

V_S Model (MALW - Love Wave)

Depth to Top of Layer (m)	Layer Thickness (m)	S-Wave Velocity (m/s)	Assumed Density (g/cm^3)
0	0.6	102	1.8
0.6	3.4	403	1.9
4	5.5	533	2.0
9.5	5.5	540	2.0
15	8	580	2.1
23	12	870	2.2

Notes: 1) Depth of investigation is about 30 m.
2) Bottom layer is a half space.
3) Half space velocity not well resolved.

Observations/Discussion:

- HVSR plots are generally similar at frequencies below 6 Hz, but have different peaks in the 6 to 20 Hz range. The sources of the high frequency HVSR peaks are uncertain, but peaks occur at different frequencies on the two horizontal channels.
- The P- and S-wave refraction data for array CNI-1 were modeled using a tomographic inversion routine with a layer-based starting model. The seismic refraction models were extended to far offset shot locations to extend depth of investigation. A larger geophone spacing is preferred for extending depth of investigation, when applying tomographic inversion routines.

- The P-wave first arrival data were picked to a greater degree of accuracy than the S-wave first arrival because a larger energy source was used for P-wave data acquisition and weak P-wave refraction events often occur before the S-waves in S-wave seismic records. Much of the uncertainty in picking the S-wave first arrival occurs at receiver locations relatively close to the source.
- The P-wave seismic refraction survey design allowed P-wave velocity to be imaged to a maximum depth of about 20 m. The seismic refraction model shows that P-wave velocity is about 450 m/s at the surface and between 800 and 1,200 between a depth of 1.5 and 14 m. P-wave velocity increases abruptly to greater than 1,800 to 2,400 m/s below a depth of 15 m.
- The S-wave seismic refraction survey design allowed S-wave velocity to be imaged to a maximum depth of about 15 m. The seismic refraction model shows that S-wave velocity is less than 200 m/s at the surface, increases to 500 m/s at a depth of 2 to 5 m and is slightly greater than 600 m/s below a depth of 7 to 11 m.
- The S-wave seismic refraction model indicates that the high velocity layer below a depth of 15 m on the P-wave seismic refraction model is likely associated with saturated sandstone.
- The seismic refraction models, particularly the P-wave model, indicate that there is some lateral velocity variation at this site. P-wave velocities below a depth of about 2 m and above the saturated zone are typically in the 900 to 1,050 m/s range beneath the southwest half of the array and between 1,100 and 1,200 beneath the northeast half of the array. S-wave velocities are also slightly higher beneath the northeast half of the line.
- The seismic refraction/MASW array was orientated at about a 45 to 60 degree angle to the strike of the geologic bedding in order for the array to follow the ridge upon which the seismic station is located and minimize topographic variation along the line. The geologic bedding may have very steep dip at this site (not measured) and weathering would need to control velocity structure for surface wave techniques to be effective. In such geologic conditions, it may be preferred to orient the seismic line parallel to strike or acquire seismic data along profiles both parallel to and perpendicular to strike. Acquisition of seismic data along profiles parallel to strike can also be problematic if, for example, the seismic line is located along the contact of layers with differing velocity or if relatively thin dipping layers have significantly different velocity. A seismic line orientated parallel to strike and next to the seismic station is possible at this site, but the line would have had more topographic variation than the selected line orientation.
- Noise conditions at the site were not sufficient for application of passive surface wave techniques.
- Both MASW (Rayleigh wave) and MALW (Love wave) data were acquired at the site.
- The minimum wavelength Rayleigh wave phase velocity data extracted from the 48-channel MASW array was about 12 m. Reducing data from smaller hammer sources using a limited offset receiver array (i.e. less active geophones) allowed for extraction of surface wave dispersion data to a minimum wavelength of about 3 m. The minimum wavelength Love wave phase velocity data extracted from the 48-channel MALW array was about 9 m. Reducing data using a limited offset receiver array (i.e. less active geophones) allowed for extraction of surface wave dispersion data to a minimum wavelength of about 2 m.

- A maximum 80 m wavelength was extracted from the Rayleigh and Love wave data using a source location 30 m from the near geophone. This wavelength occurs at a frequency of about 8 Hz in the Love wave dispersion data and 9 Hz in the Rayleigh wave dispersion data.
- There is about 80 and 50 m/s of scatter in Rayleigh and Love wave dispersion data, respectively. This scatter is in part due to lateral velocity variation caused by differential weathering of near surface sedimentary rock and variable thickness of a thin residual soil layer. Scatter in the Rayleigh and Love wave dispersion data indicates that there may be as much as 10% of variability in V_{S30} along the seismic line. Such variability may be the norm for many rock sites.
- A representative dispersion curve was generated for the MASW and MALW data sets using a moving average, polynomial curve fitting routine and used for modeling.
- Rayleigh wave based methods have been applied to engineering scale investigations for a much longer period of time than Love wave techniques. Although journal articles on Love wave techniques have become more prevalent in the last several years, applied research on topics such as near-field effects and resulting survey design based wavelength limitations, minimum wavelength required to image to a depth of 30 m, source frequency limitations, etc., have yet to be published.
- Love wave phase velocities are typically slightly higher than Rayleigh wave phase velocities at high frequencies and lower at low frequencies. Therefore, it would appear that lower frequency Love wave data, relative to Rayleigh wave dispersion data, is required to image to a given depth. This could be a significant problem if Love wave data acquisition is limited to a hammer and traction plank source.
- The minimum Rayleigh wave wavelength required to develop a V_S model to 30 m depth is 60 m. Forward modeling indicates that a Love wave wavelength as high as 90 m, may be required to image to 30 m depth. Therefore, with only a sledge hammer and traction plank energy source, MALW investigation to a depth of 30 m is likely limited to high velocity sites. In fact, the unavailability of cost effective, low frequency S-wave energy sources will be a limiting factor in the application of Love wave techniques to 30 m soundings at low velocity sites. Passive Love wave techniques need to be further explored.
- Two V_S models are presented for the Rayleigh wave dispersion data. Model 1 has the lowest RMS error, achieved by allowing a velocity inversion in the model. This model does not agree with the seismic refraction models or the Love wave dispersion data. Model 2 has higher RMS error, but is in much better agreement with the refraction models and Love wave dispersion data.
- A single V_S model is presented for the Love wave dispersion data. As discussed above, this model is most similar to Rayleigh wave Model 2. Rayleigh and Love wave methods will not generate the same V_S models if sediments and rock are anisotropic. Joint inversion of Rayleigh and Love wave dispersion curves should be explored further, but the inversion routines must allow for a certain degree of anisotropy.
- Surface wave depth of investigation is about 35 m for the Rayleigh wave models and 30 m for the Love wave model.
- The V_S models derived from the Rayleigh and Love wave dispersion data are generally consistent with the seismic refraction models, although velocities are slightly lower in the surface wave models.

- The S-wave velocity models derived from the surface wave testing are believed to be representative of average subsurface velocity structure. However, geology at the site is complex, with dipping bedding, and the seismic line was oriented at a high angle to strike to minimize topographic variation along the line. In such conditions, weathering must play a significant role in near surface velocity structure for surface wave techniques to be effective. It is difficult to predict the effect of dipping beds on the surface wave dispersion data, but severe lateral velocity variation is an obvious possibility in such conditions. A line parallel to strike would demonstrate if shallow S-wave velocity structure is primarily controlled by weathering at the site. Of course, acquisition of surface wave data parallel to strike can also pose potential problems.
- V_{S30} is 517 m/s for Rayleigh wave Model 1 and 505 m/s for Rayleigh wave Model 2 (Site Class C). Model 2 is considered most representative of site conditions based on seismic refraction and Love wave dispersion data.
- V_{S30} is 529 m/s for the Love wave V_S model (Site Class C).
- Average V_{S30} (Love wave model and Rayleigh wave Model 2) is 517 m/s.
- Average S-wave velocity between 1 m (assumed sensor depth) and 31 m is 568 m/s for Rayleigh wave Model 1, 580 m/s for Rayleigh wave Model 2 and 589 m/s for the Love wave model.

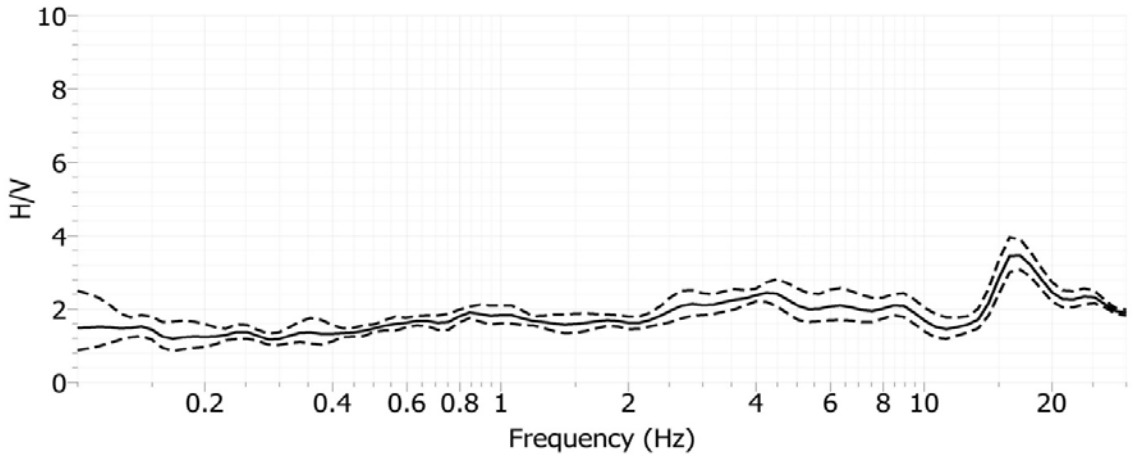

Site CI.CNI, H/V Spectral Ratio, Array CNI-1, Sensor 450

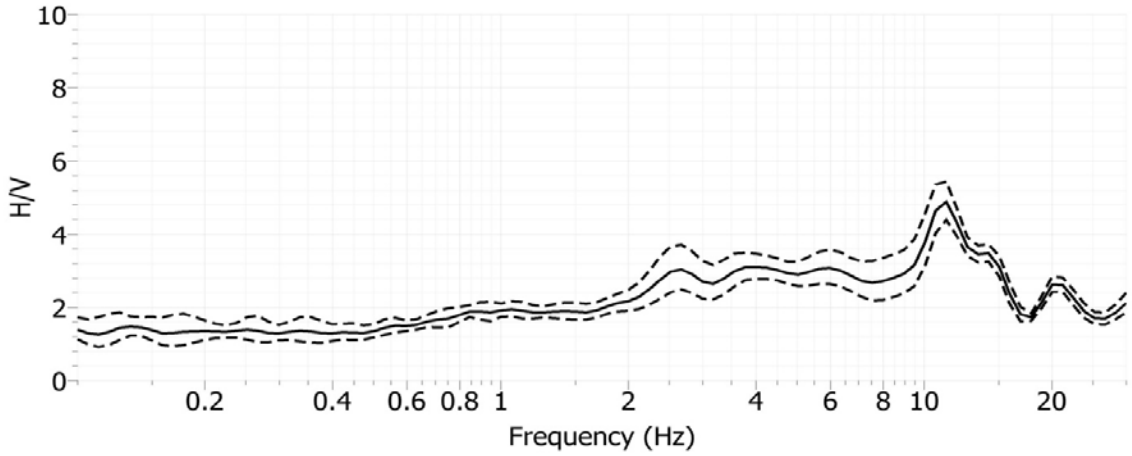

Site CI.CNI, H/V Spectral Ratio, Array CNI-1, Sensor 453

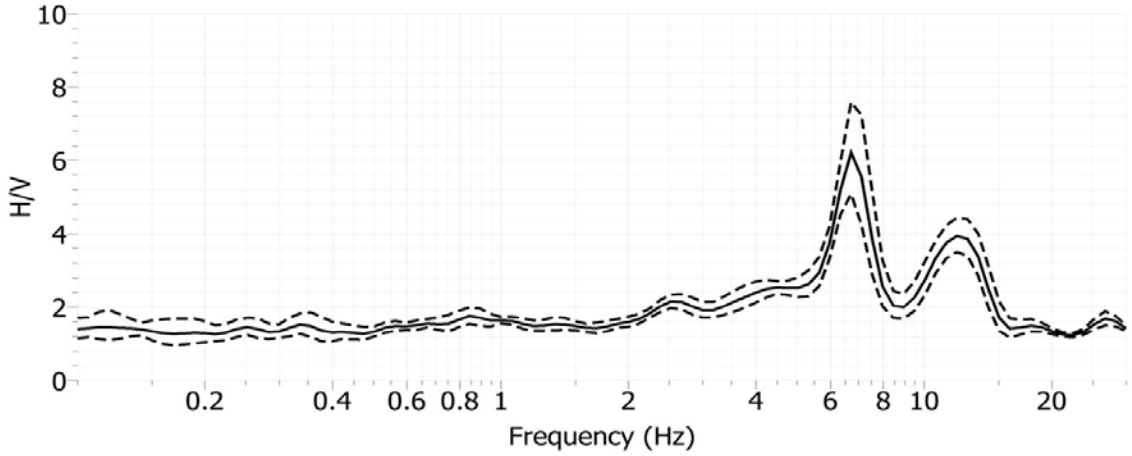

Site CI.CNI, H/V Spectral Ratio, Array CNI-1, Sensor 507

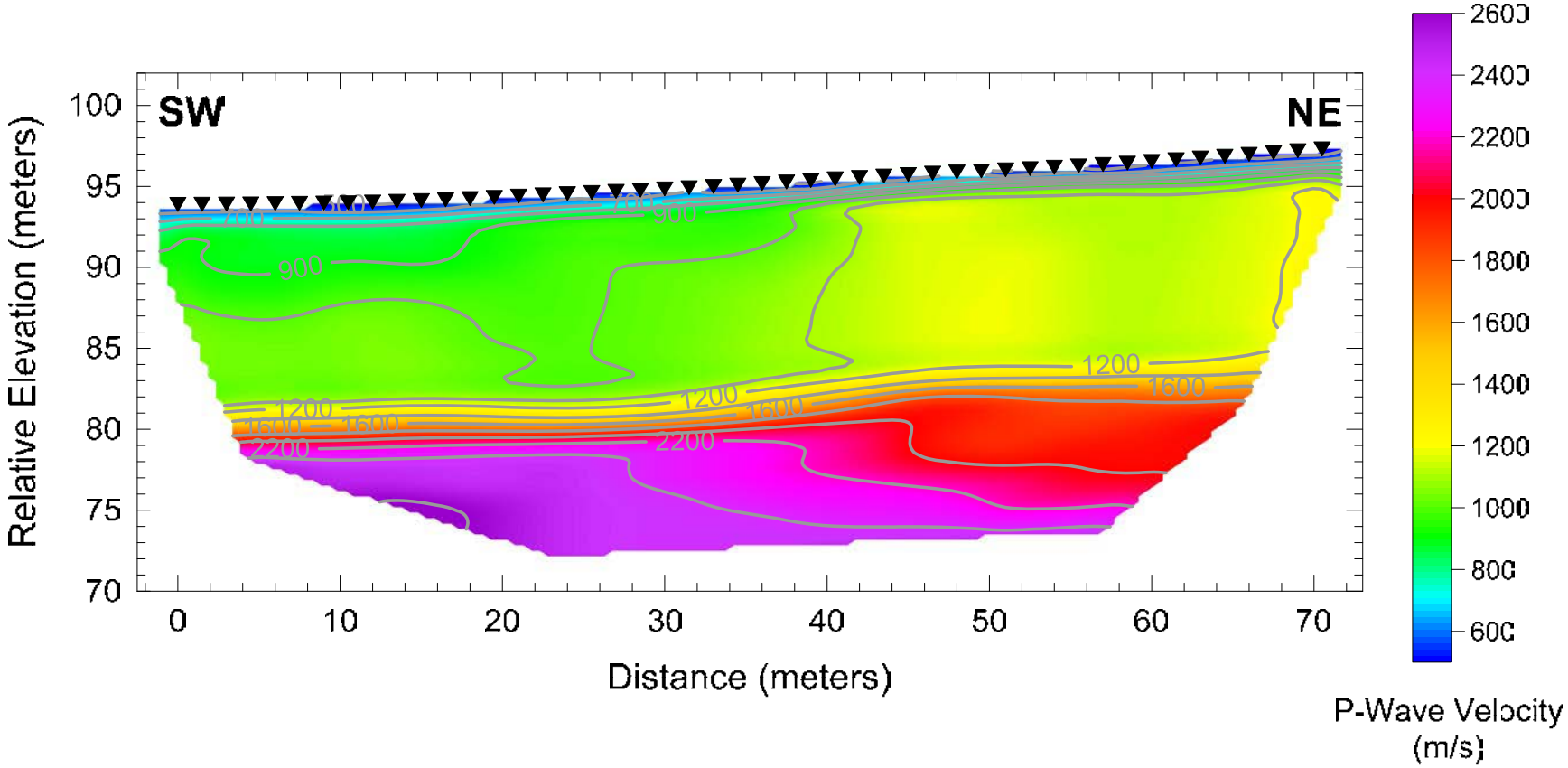

Array CNI-1 – P-wave tomographic seismic refraction model utilizing layer based starting model

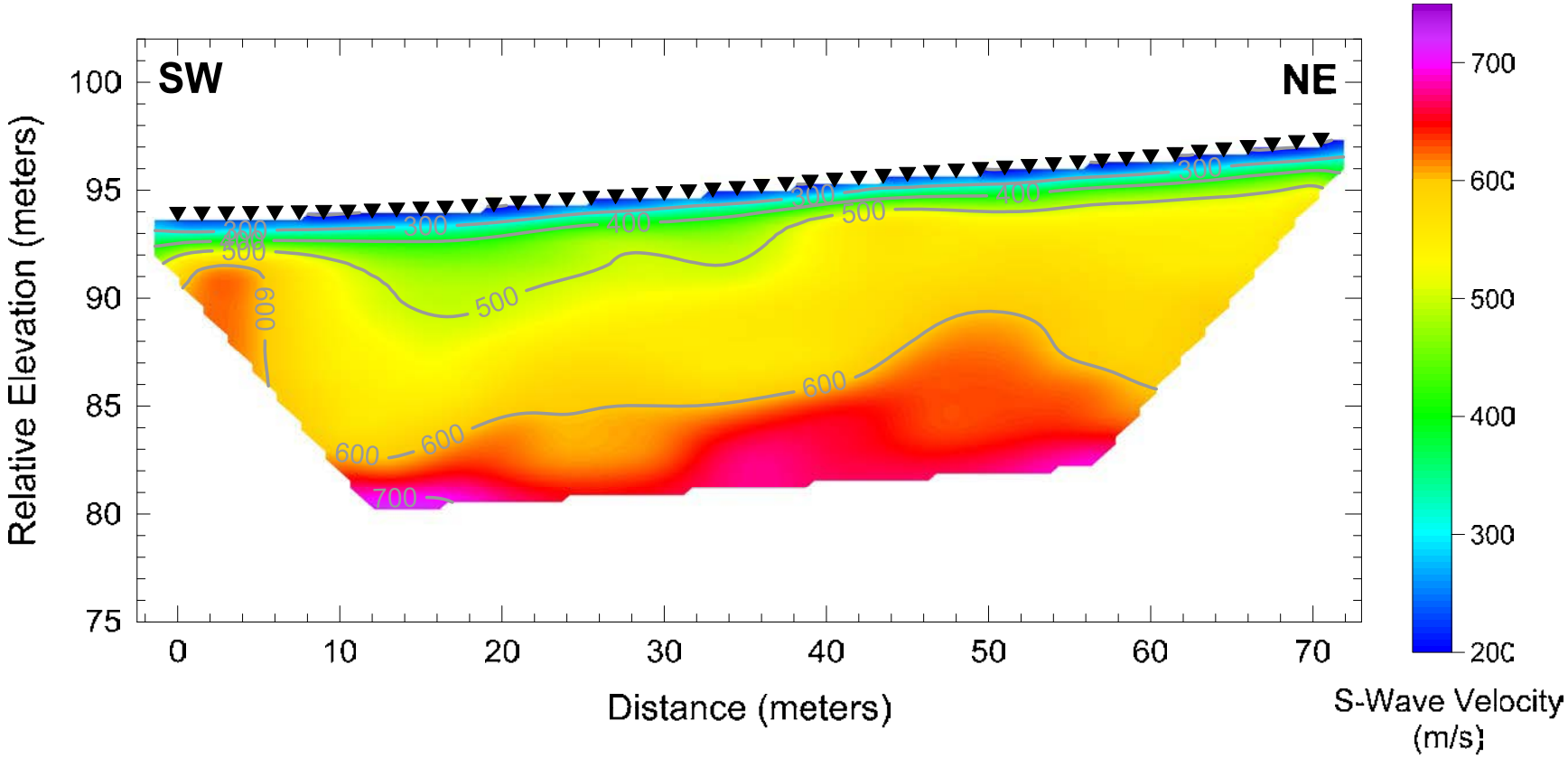

Array CNI-1 – S-wave tomographic seismic refraction model utilizing layer based starting model

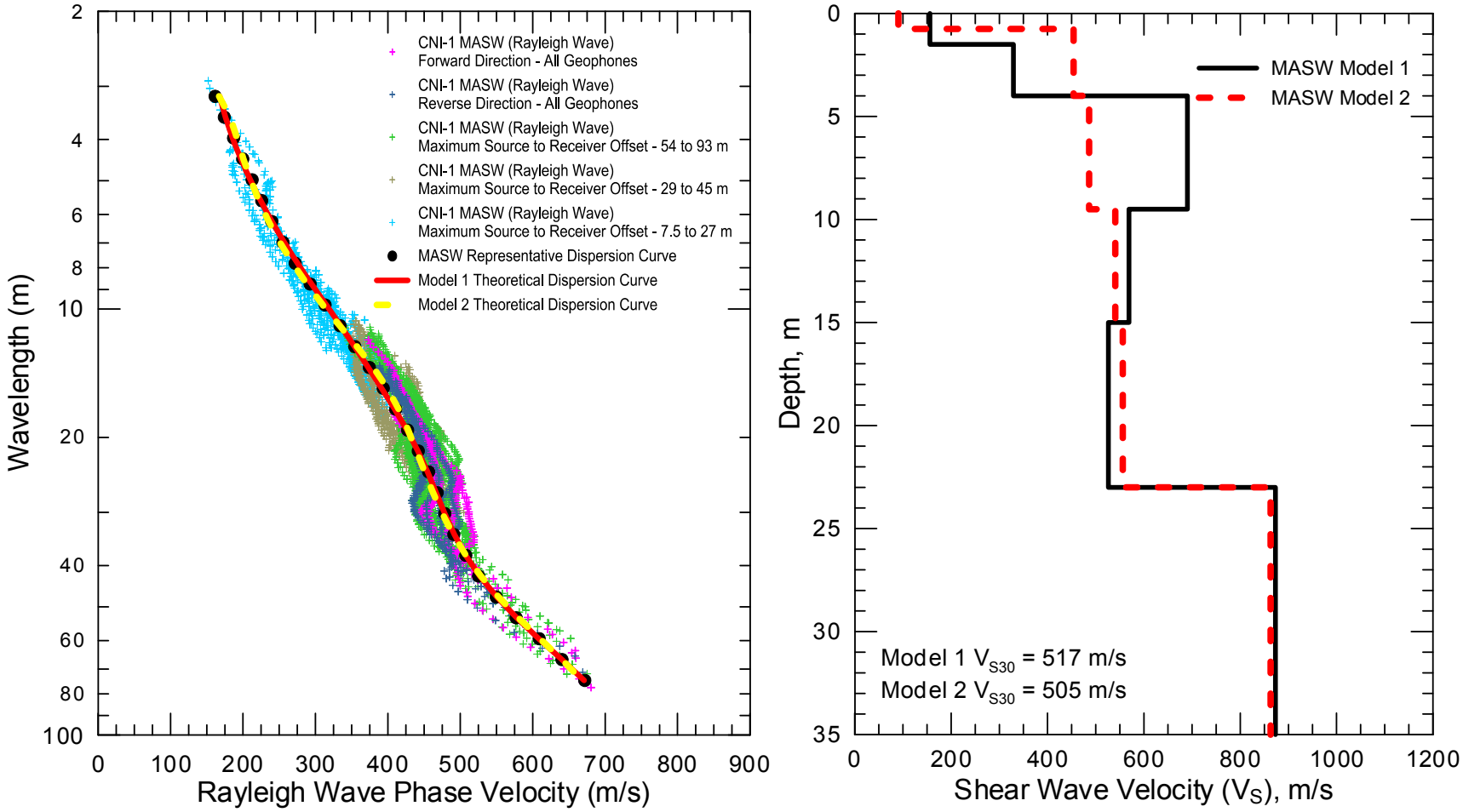

NC.CNI - Field, representative and inverted theoretical surface wave dispersion data (left) and associated V_S model (right) for Rayleigh wave data. The plot of Rayleigh wave dispersion data demonstrates the strategy utilized to extract phase velocity data over a wide wavelength/frequency range. Model 1 has the lowest RMS error, but is not realistic based on the S-wave seismic refraction model. Model 2 has slightly higher RMS error, but is most consistent with the V_S model developed from the Love wave dispersion data.

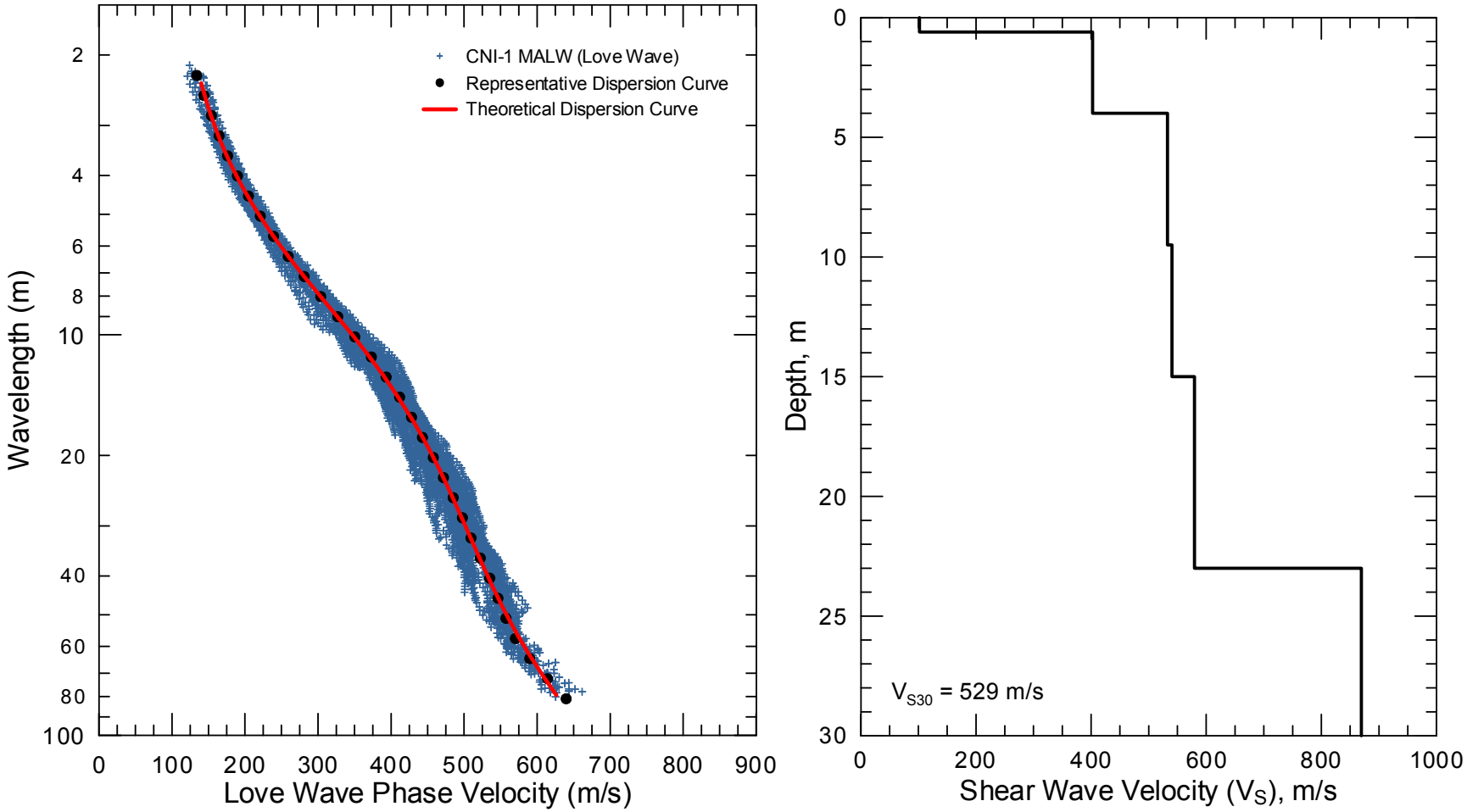

NC.CNI - Field, representative and inverted theoretical surface wave dispersion data (left) and associated V_S model (right) for Love wave data

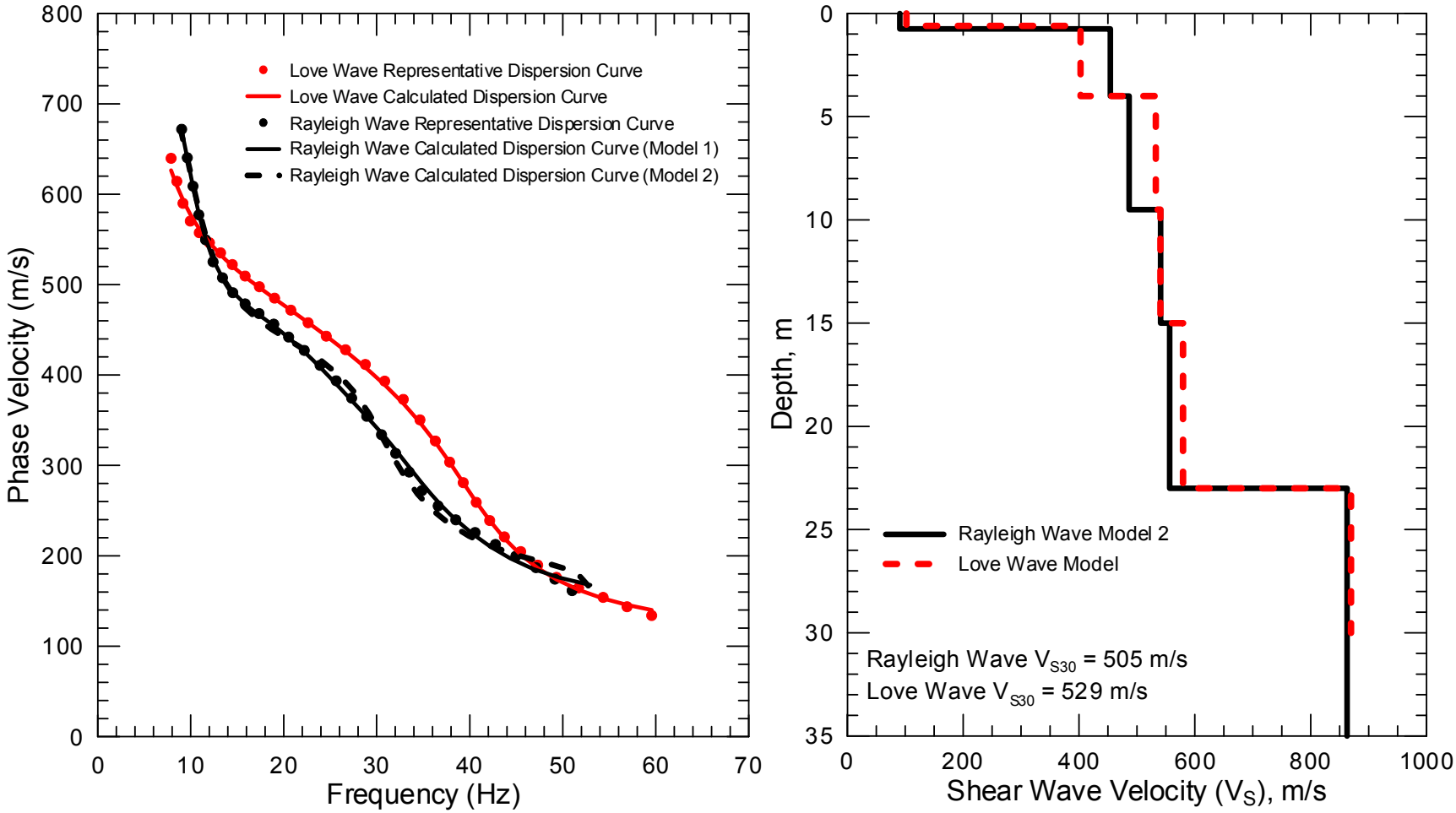

NC.CNI - Comparison of V_S models resulting from inversion of Rayleigh and Love wave dispersion curves

Site NC.CSL

Location: San Leandro Hills, Alameda County, California

Latitude: 37.72410 **Longitude:** -122.11927

(Station coordinates modified based on field GPS survey, WGS84 coordinate system)

V_{S30} (measured): 378 m/s

V_{S30} (adjusted to more accurately reflect seismic station conditions): 391 m/s (average S-wave velocity between 1 and 31 m adjusting for inferred sensor depth)

NEHRP Site Class: C

Geomatrix Code: IVB/IVC

Geologic Conditions/Observations: Site located on geologic unit mapped as Mesozoic (Jurassic) Arc Volcanics. The Chabot and Hayward Faults are located about 0.6 and 1 km northeast and southwest of the seismic station, respectively.

Site Conditions: Rural site. Hilly terraced topography in site vicinity. MASW array located on parts of three terraces with an approximate 5 m decrease in elevation to the southeast along the 70.5 m long array. There were no alternate test locations in the immediate vicinity of the seismic station.

Geophysical Methods Utilized: HVSR, MASW, Seismic Refraction

Geophysical Testing Arrays:

1. Array CSL-1 (48 channel MASW and P-wave seismic refraction array utilizing 4.5 Hz vertical geophones spaced 1.5 m apart for a length of 70.5 m, forward and reverse shot locations with multiple source offsets and source types and multiple interior shots).
2. Three HVSR measurement locations: two distributed along array CSL-1 and the other near the seismic station.

Legend

- Seismic Station - Approximate Surveyed Location
- Seismic Station - Approximate Location of Record
- H/V Spectral Ratio Location
- MASW and Seismic Refraction Array

NOTES:
1. WGS 1984 COORDINATE SYSTEM
2. Image Source: (c) Microsoft Corporation and its data suppliers

File Name: NC-CSL-I

Date: 2/7/2013

USGS science for a changing world

GEOVision geophysical services

RECOVERY.GOV

SITE MAP
NC•CSL

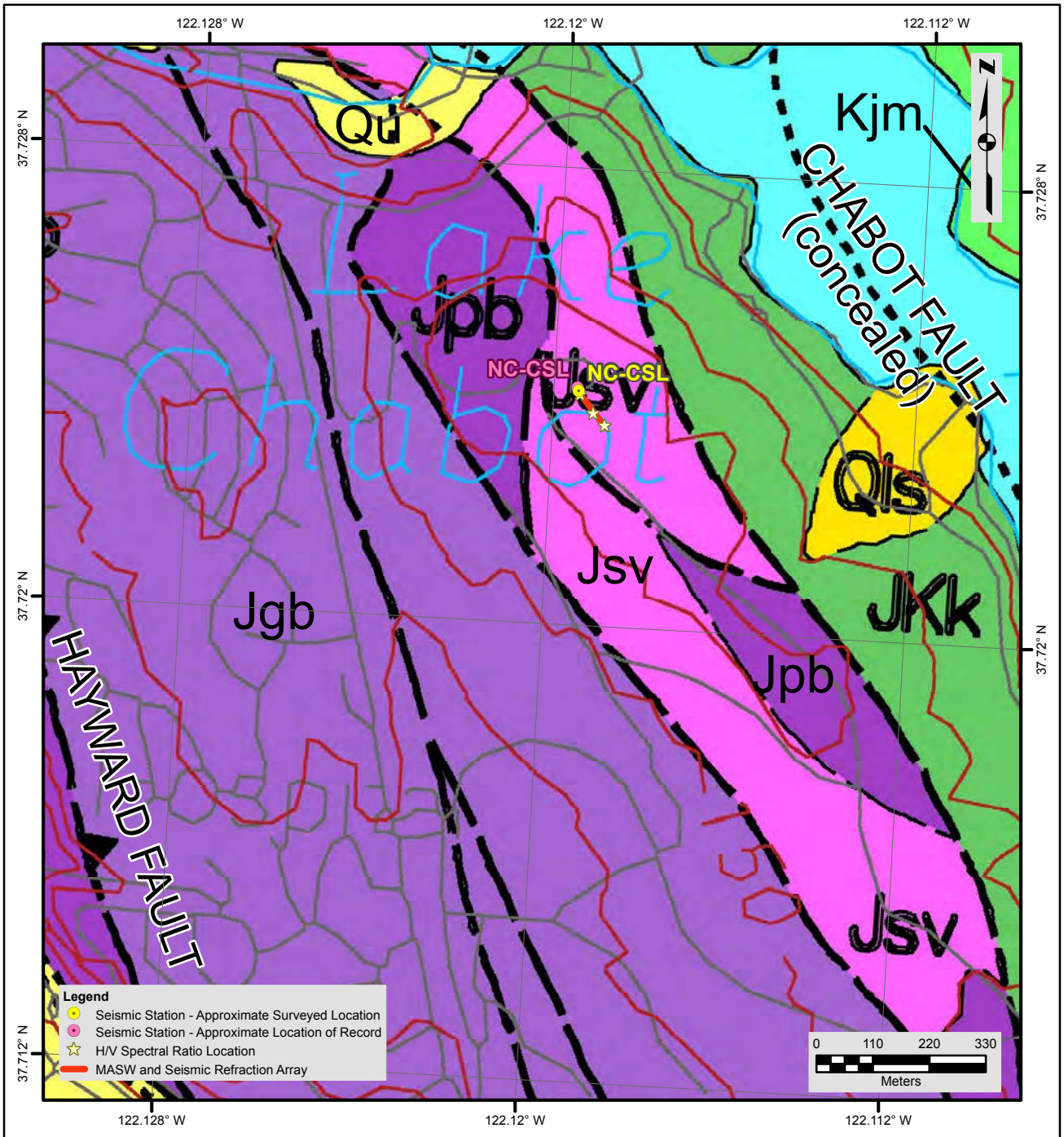

Description of Geologic Map Units

Qls = Quaternary (Holocene) landslide deposits
Qu = Quaternary (Holocene) undivided deposits
Kjm = Mesozoic (Cretaceous) Great Valley Sequence; Joaquin Miller Formation
JKk = Mesozoic (Jurassic to Cretaceous) Great Valley Sequence; Knoxville Formation; conglomerate and volcanogenic conglomerate
Jsv = Mesozoic (Jurassic) Arc Volcanics; keratophyre
Jpb = Mesozoic (Jurassic) Coast Range Ophiolite; pillow basalt and basalt
Jgb = Mesozoic (Jurassic) Coast Range Ophiolite; gabbro and diabase

NOTES:
1. WGS 1984 COORDINATE SYSTEM
2. Geologic Map of the Hayward fault zone, by R.W. Graymer, D.L. Jones, and E.E. Brabb, 1995
3. See site map for details of geophysical survey

USGS science for a changing world
GEOVision geophysical services

GEOLOGIC MAP
NC•CSL

File Name: NC-CSL
Date: 2/7/2013

NC.CSL seismic station

Looking north towards seismic station and HVSR sensor TRO-1 (Tromino ENGR)

Looking southeast along array CSL-1

Looking northwest along array CSL-1. Note terraced topography that could not be avoided.

Looking northwest at the northwestern end of array CSL-1 and towards seismic station

Location of Geophysical Testing Arrays:

Location	Latitude	Longitude
CSL-1, Northwest End of MASW/Refraction Array	37.72398	-122.11916
CSL-1, Center of MASW/Refraction Array	37.72374	-122.11890
CSL-1, Southeast End of MASW/Refraction Array	37.72349	-122.11865
HVSR Sensor Tromino 1 (TRO-1)	37.72405	-122.11923
HVSR Sensor Tromino 2 (TRO-2)	37.72373	-122.11892
HVSR Sensor Tromino 3 (TRO-3)	37.72352	-122.11865
NC.CSL Seismic Station	37.72410	-122.11927

Notes: 1) WGS84 Coordinate System (decimal degrees)
2) Survey accuracy is estimated at 1 to 2 m.

Results:

V_S Model

Depth to Top of Layer (m)	Layer Thickness (m)	S-Wave Velocity (m/s)	Inferred P-Wave Velocity (m/s)	Inferred Poisson's Ratio	Inferred Density (g/cm^3)
0	1	221	414	0.3	1.7
1	1.5	264	494	0.3	1.8
2.5	2.5	286	536	0.3	1.8
5	8	360	673	0.3	1.9
13	8	387	724	0.3	1.9
21	>9	514	961	0.3	2.0

Notes: 1) Depth of investigation is about 30 m.
2) Bottom layer is a half space.

Observations/Discussion:

- HVSR plots are similar at all measurement locations below a frequency of about 20 Hz, validating the 1-D velocity structure assumption.
- There is a distinct HVSR peak in the 1.5 to 2.5 Hz range, which indicates that there is a significant increase in S-wave velocity at a depth on the order of 40 to 60 m (based on estimated V_{S30} discussed below and quarter wavelength approximation).
- P-wave refraction data is quite noisy at this site and there was difficulty accurately interpreting first arrivals in asphalt covered portions of the line. Preliminary refraction models did not achieve sufficient depth of investigation to be of use and, therefore, a P-wave seismic refraction model is not presented. The seismic refraction did reveal, however, that there may be significant lateral velocity variation with near surface sediments/weathered rock having higher velocity to the northwest.
- Noise conditions at the site were not sufficient to apply passive surface wave techniques.
- Only some off-end shot locations could be accessed with the accelerated weight drop energy source. The furthest off-end shot locations could only be accessed with a 20 lb sledge hammer energy source. Rayleigh wave phase velocity data with wavelengths greater than 60 m (frequency of about 6.5 Hz) were, therefore, not extracted from 20-lb hammer shot records.
- The minimum wavelength surface wave phase velocity data extracted from the 48-channel MASW arrays is about 12 m. Data reduction using seismic records from smaller hammer sources and a limited offset receiver array (i.e. less active geophones) allowed extraction of surface wave dispersion data to a minimum wavelength of about 2.5 m.
- There is significant scatter in the surface wave dispersion data, resulting from lateral velocity variation. Even after selective use of individual dispersion curves that are coherent with those from off-end shot locations using a full 48 channel receiver array there is still up to about 50 m/s scatter in the dispersion data.
- A representative dispersion curve was generated for the surface wave data set using a moving average, polynomial curve fitting routine. This representative dispersion curve was used for data modeling.
- Review of seismic refraction data revealed no evidence of saturated sediments/weathered rock in the upper 25 m.
- Surface wave depth of investigation is about 30 m based on half of maximum wavelength criteria.
- V_{S30} is 378 m/s (NEHRP Site Class C/D).
- Average S-wave velocity between 1 m (inferred sensor depth) and 31 m is 391 m/s (NEHRP Site Class C).
- Given that the seismic refraction data indicated that near surface sediments have higher velocity at the northwest end of the line, the site can be considered NEHRP Site Class C.
- Based on scatter in the surface wave dispersion data, there is likely at least 7.5% variation is the presented V_{S30} in the immediate site vicinity.

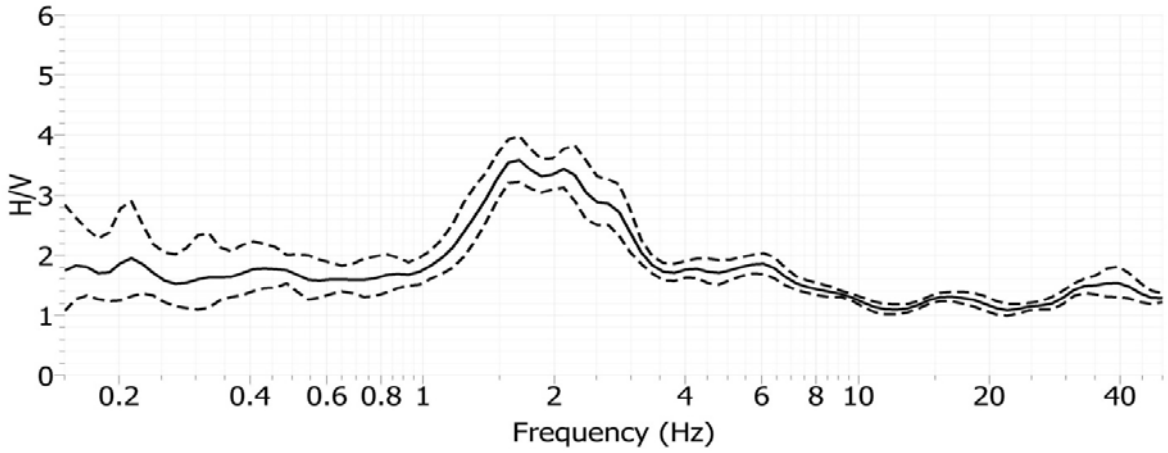

Site NC.CSL, H/V Spectral Ratio, Near Seismic Station, Sensor TRO-1

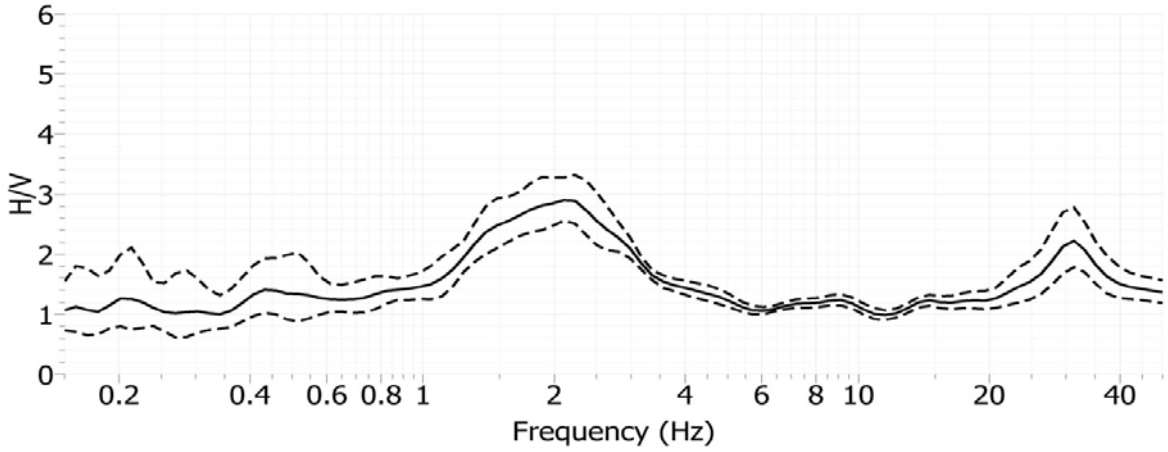

Site NC.CSL, H/V Spectral Ratio, Array CSL-1, Sensor TRO-2

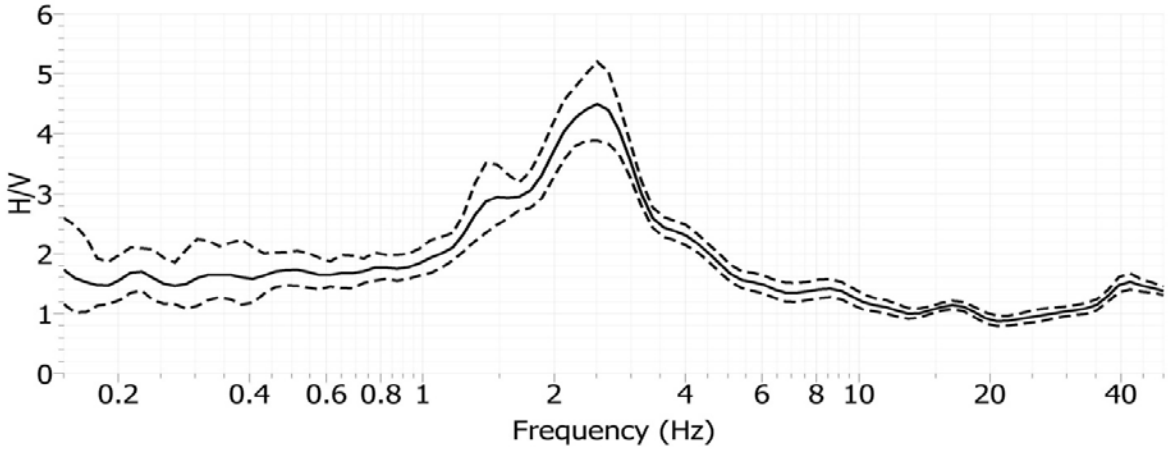

Site NC.CSL, H/V Spectral Ratio, Array CSL-1, Sensor TRO-3

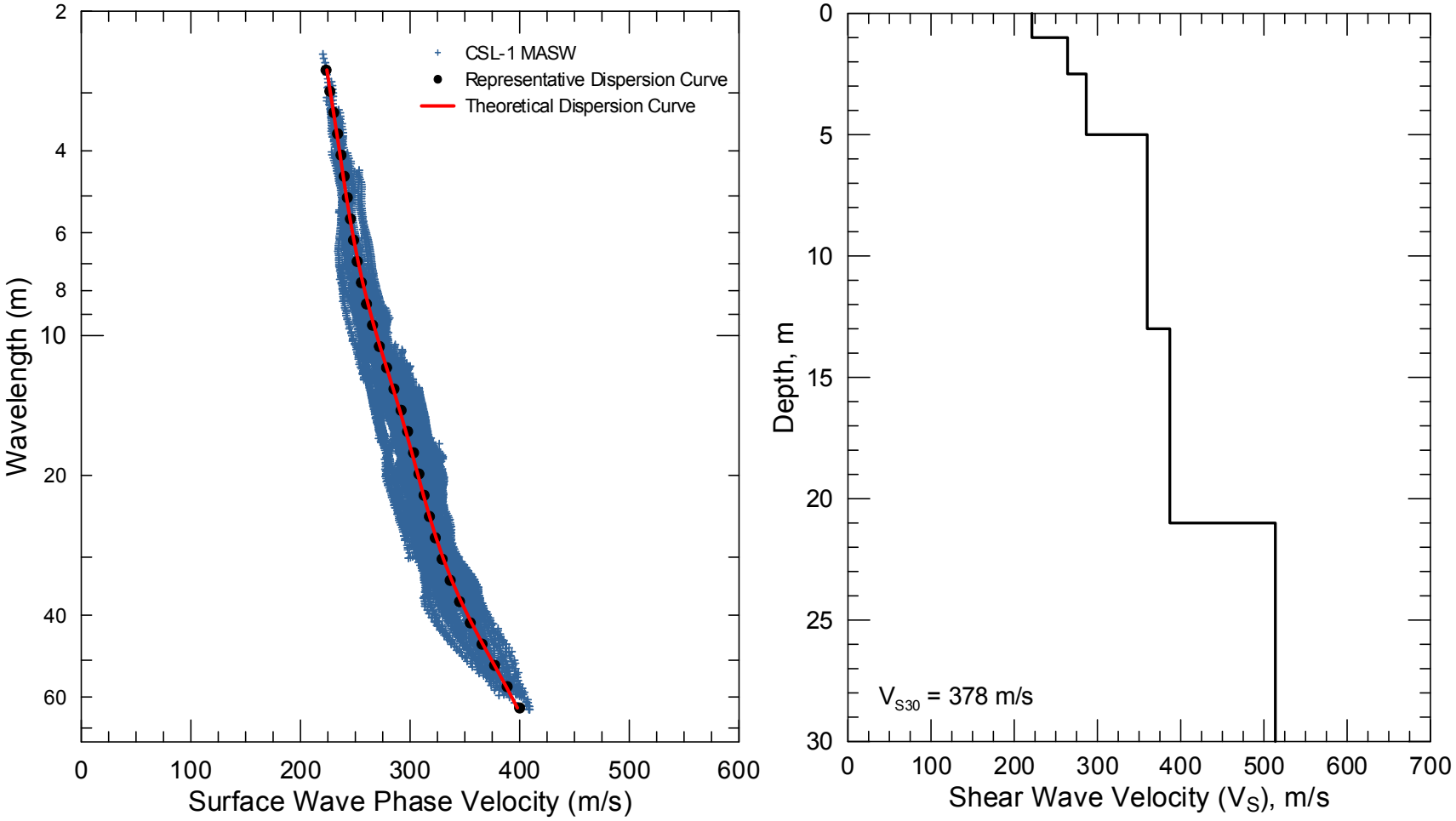

NC.CSL - Field, representative and inverted theoretical surface wave dispersion data (left) and associated V_S model (right)

Site NC.HCAB

Location: Canada Road, Santa Clara County, California

Former Location Latitude: 37.02537 **Former Location Longitude:** -121.48453
(Station coordinates provided by USGS, WGS84 coordinate system).

Current Location Latitude: 37.02533 **Current Location Longitude:** -121.48476
(Station coordinates modified based on site GPS survey and are in WGS84 coordinate system).

V_{S30} (measured): 646 m/s

V_{S30} (adjusted to more accurately reflect seismic station conditions): 671 m/s (average S-wave velocity between 1 and 31 m adjusting for assumed 1 m sensor depth of the former station location). No adjustment necessary for the current station location.

NEHRP Site Class: C

Geomatrix Code: IEB/ILB

Geologic Conditions/Observations: Seismic station located on geologic unit mapped as Tertiary (Paleocene-Eocene) clay shale or mudstone. Bedding dips about 45 to 50 degrees to the northeast in the immediate site vicinity.

Site Conditions: Rural site located on gently rolling hills. Ground surface elevation decreases about 4.5 m to northwest along 70.5 m long MASW and seismic refraction array.

Geophysical Methods Utilized: HVSR, Seismic Refraction, MASW

Geophysical Testing Arrays:

1. Array HCAB-1 (48 channel MASW and P-wave seismic refraction array utilizing 4.5 Hz vertical geophones spaced 1.5 m apart for a length of 70.5 m, forward and reverse shot locations with multiple source offsets and source types and multiple interior shot locations).
2. Three HVSR measurement locations distributed along array HCAB-1.

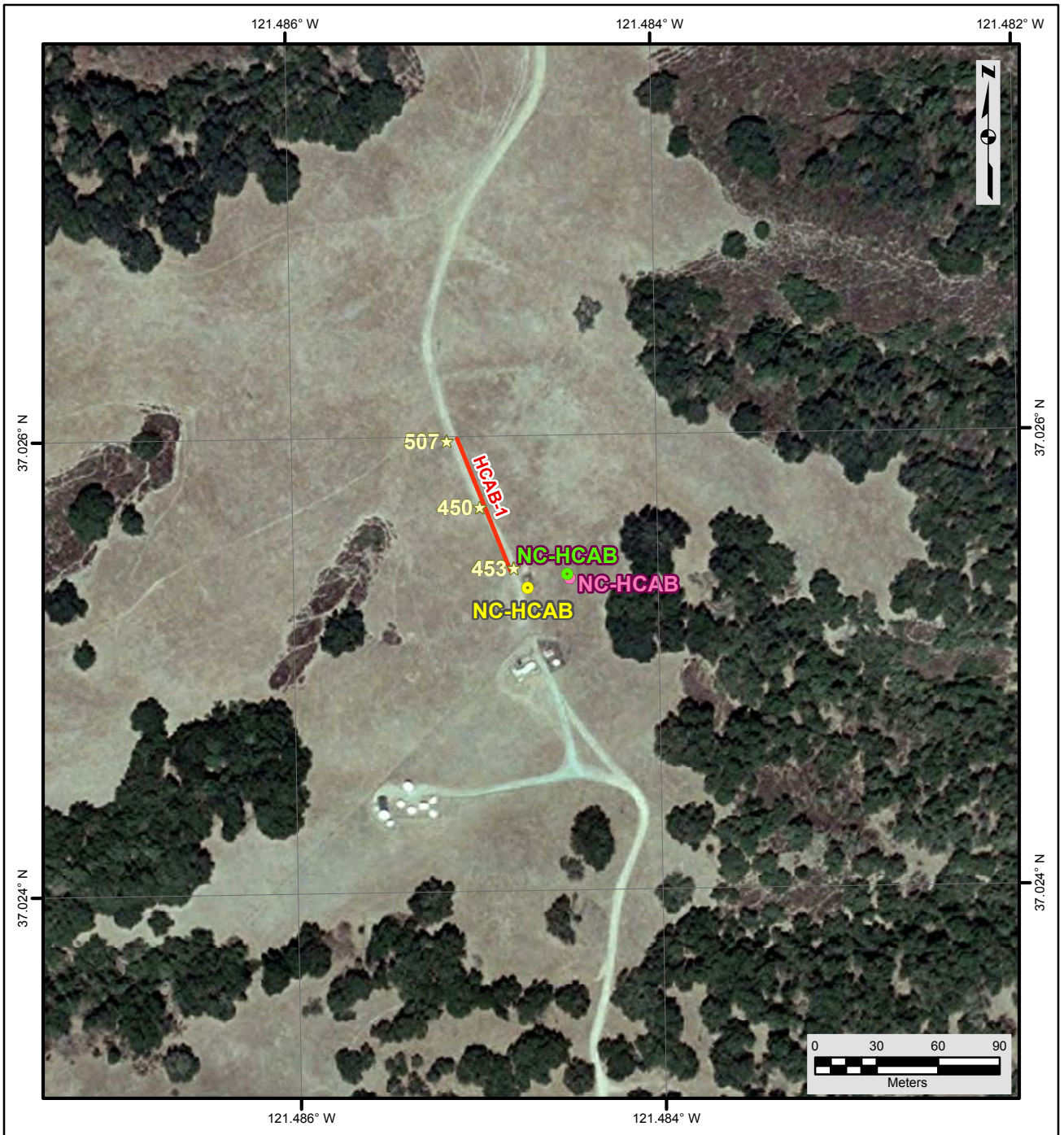

Legend

- Seismic Station - Approximate Surveyed Current Location
- Seismic Station - Approximate Surveyed Former Location
- Seismic Station - Approximate Location of Record
- H/V Spectral Ratio Location
- MASW and Seismic Refraction Array

NOTES:
1. WGS 1984 COORDINATE SYSTEM
2. Image Source: ESRI, i-cubed, USDA FSA, USGS, AEX, GeoEye, Getmapping, Aerogrid, IGP

File Name: NC-HCAB-I

Date: 10/17/2011

USGS science for a changing world

GEOVision geophysical services

RECOVERY.GOV

SITE MAP
NC•HCAB

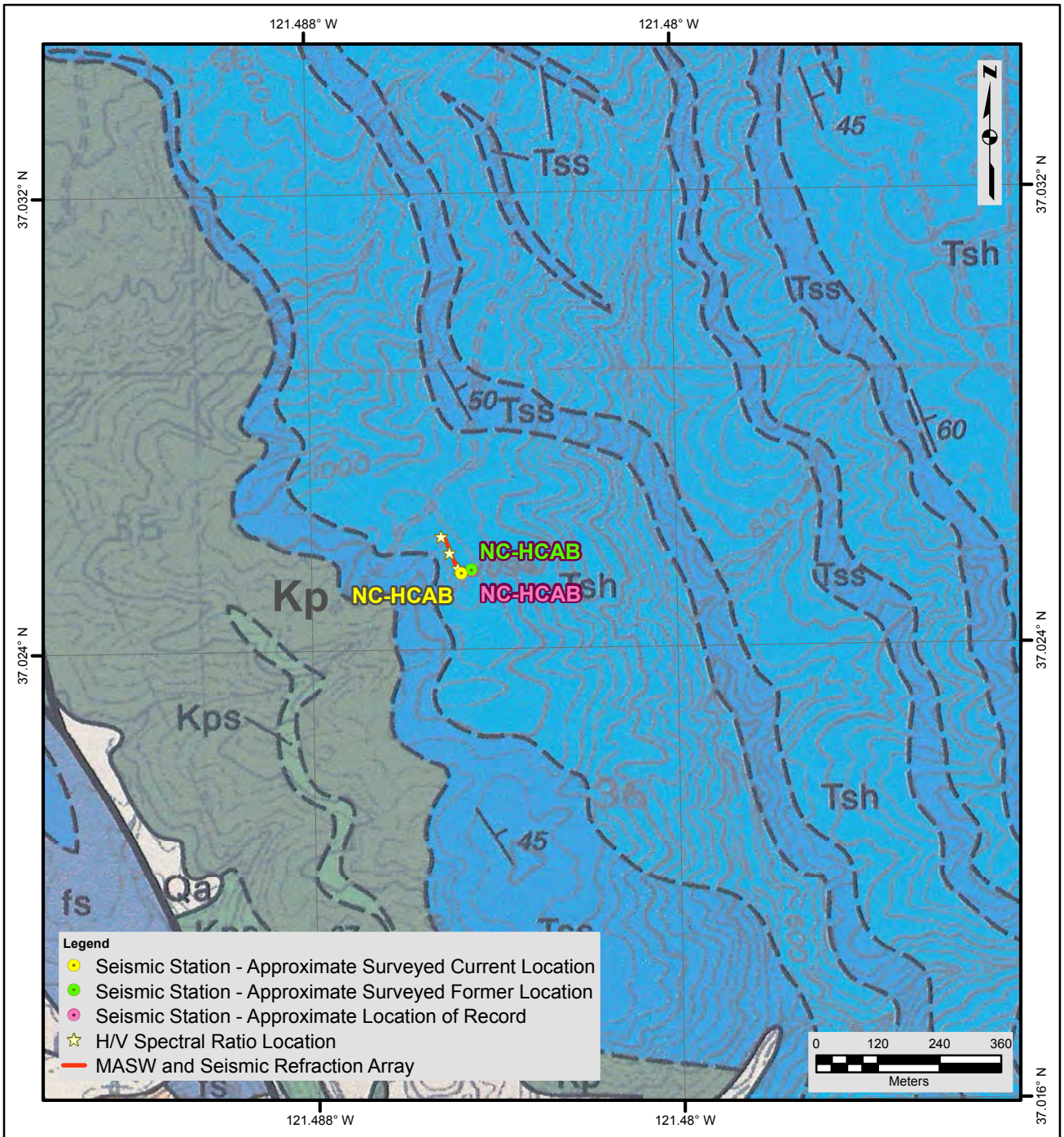

Description of Geologic Map Units

Qa = Quaternary (Holocene) gravel and sand of Coyote Creek channel
Qls = Quaternary (Pleistocene or Holocene) landslide rubble derived from rocks upslope
Qoa = Quaternary (Pleistocene) dissected older alluvial gravel and sand
Tsh = Tertiary (Paleocene-Eocene) clay shale or mudstone, micaceous
Tss = Tertiary (Paleocene-Eocene) sandstone, fine to medium grained, bedded, arkosic, occurs as basal layer and thin layers throughout Tsh
Kp = Mesozoic (Late Cretaceous) Panoche Formation; clay shale or claystone, bedded, micaceous, argillaceous
Kps = Mesozoic (Late Cretaceous) Panoche Formation; sandstone, bedded, hard, fine to med-grained, arkosic

NOTES:
1. WGS 1984 COORDINATE SYSTEM
2. Geologic Map of the Gilroy Hot Springs Quadrangle, Santa Clara County, California by Thomas W. Dibblee, Jr., 2007
3. See site map for details of geophysical survey

File Name: NC-HCAB

Date: 10/17/2011

USGS science for a changing world

GEOVision geophysical services

GEOLOGIC MAP
NC•HCAB

RECOVERY.GOV

Looking west at former seismic station location and small shed currently housing seismic station

Looking southeast towards HVSR sensor 453 and shed currently housing seismic station

Looking northeast along array HCAB-1

P-wave seismic refraction data acquisition

MASW data acquisition using accelerated weight drop energy source

Location of Geophysical Testing Arrays:

Location	Latitude	Longitude
HCAB-1, Southeast End of MASW/Refraction Array	37.02541	-121.48485
HCAB-1, Center of MASW/Refraction Array	37.02570	-121.48499
HCAB-1, Northwest End of MASW/Refraction Array	37.02599	-121.48514
HVSR Sensor 450	37.02569	-121.48502
HVSR Sensor 453	37.02542	-121.48483
HVSR Sensor 507	37.02598	-121.48519
NC.HCAB Seismic Station - Current Location	37.02533	-121.48476
NC.HCAB Seismic Station - Former Location	37.02539	-121.48454

Notes: 1) WGS84 Coordinate System (decimal degrees)
2) Survey accuracy is estimated at 1 to 2 m.

Results:

V_S Model 1

Depth to Top of Layer (m)	Layer Thickness (m)	S-Wave Velocity (m/s)	Inferred P-Wave Velocity (m/s)	Assumed Poisson's Ratio	Assumed Density (g/cm^3)
0	2.5	373	698	0.3	1.9
2.5	4.5	588	1099	0.3	2.0
7	15	645	1206	0.3	2.0
22	>8	977	1827	0.3	2.0

Notes: 1) Depth of investigation is about 30 m.
2) Bottom layer is a half space.

V_S Model 2

Depth to Top of Layer (m)	Layer Thickness (m)	S-Wave Velocity (m/s)	Inferred P-Wave Velocity (m/s)	Assumed Poisson's Ratio	Assumed Density (g/cm^3)
0	2.5	378	707	0.3	1.9
2.5	3.5	574	1074	0.3	2.0
6	5	637	1192	0.3	2.0
11	7	640	1197	0.3	2.0
18	11	750	1402	0.3	2.1
29	>1	1120	2095	0.3	2.1

Notes: 1) Depth of investigation is about 30 m.
2) Bottom layer is a half space.

Observations/Discussion:

- Field observations indicate that the seismic station was moved from the former location into a very small structure.
- There are subtle differences between the HVSR plots, although the plots have similar general characteristics.
- There are no clear high amplitude HVSR peaks, but there are multiple, low amplitude peaks (or elevated HVSR response) at frequencies above 3 Hz. All HVSR plots have elevated HVSR response over the 3.5 to 6 Hz range, and several peaks at higher frequencies. HVSR sensor has a high amplitude peak at about 11.5 Hz that could correlate to much lower amplitude peaks in the 11 to 13 Hz range at sensors 450 and 453.
- The seismic refraction/MASW array was orientated almost parallel to strike of the geologic bedding, which dips on the order of 45 to 50 degrees to the northeast. It should be noted that although the seismic station sits on Tertiary clay shale or mudstone, dipping about 45 to 50 degrees to the northeast, a possibly higher velocity Tertiary sandstone unit is mapped as outcropping 30 m, or more, west of the array. Surficial geology was not confirmed in the field due to residual soil cover.
- The P-wave refraction data for array HCAB-1 was modeled using a tomographic inversion routine with a smooth velocity gradient starting model. The seismic refraction model was extended to far offset shot locations to increase depth on investigation. A longer receiver array is preferred for extending depth of investigation, but at the expense of the efficiency in combining seismic refraction and MASW data acquisition along the shorter array.
- The seismic refraction model indicates that there is significant lateral P-wave velocity variation in the upper 15 m with a thickening sequence of lower velocity sediments to the southeast. The most significant lateral velocity variation occurs in the southeastern most 20 m of the seismic profile. P-wave velocity is about 750 to 1,000 m/s at the surface, increasing to 1,200 m/s at a depth of about 1 to 11 m, 1,400 m/s at a depth of about 1 to 15 m and is over 1,800 m/s below a depth of about 16 to 20 m.
- Noise conditions at the site were not sufficient for application of passive surface wave techniques.
- MASW data reduction was complicated by the lateral velocity variation at the site with a localized zone of lower velocity sedimentary rock at the southeast end of the array. Therefore, only limited use was made of offend shot locations and interior seismic refraction shot locations from the southeast end of the line. An alternate MASW array could yield better data assuming that lateral velocity variation can be avoided.
- The minimum wavelength surface wave phase velocity data extracted from the 48-channel MASW array was about 12 m. Reducing data from smaller hammer sources using a limited offset receiver array (i.e. less active geophones) allowed extraction of surface wave dispersion data to a minimum wavelength of about 6.5 m.
- There is about 50 m/s scatter MASW dispersion data, which is in part due to lateral velocity variation discussed above.
- A representative dispersion curve was generated for the MASW data set using a moving average, polynomial curve fitting routine and used for modeling.
- Two V_S models were generated for the surface wave dispersion data: a model with a minimal number of layers resulting in a large impedance contrast at 22 m depth (Model

1) and a model with an intermediate velocity layer resulting in the large impedance contrast occurring at greater depth (Model 2). Such non-uniqueness is typical of the inversion of surface geophysical data. V_{S30} is relatively insensitive to non-uniqueness in the S-wave velocity models.

- Surface wave depth of investigation is about 30 m based on half of maximum wavelength criteria.
- The inferred P-wave velocities in surface wave model, based on an assumed Poisson's ratio of 0.3 and modeled S-wave velocity, are generally consistent with the P-wave refraction model in the upper 10 to 15 m but slightly low below 15 m depth. Model 1 is in better agreement with the P-wave refraction model at depth.
- V_{S30} is 655 for Model 1 and 637 m/s Model 2, averaging 646 m/s (Site Class C).
- Average S-wave velocity between 1 m (assumed sensor depth at former location) and 31 m is 679 m/s for Model 1 and 662 m/s for Model 2, averaging 671 m/s. This average velocity is not applicable to the current seismic station location, which is on the surface in a small shed.
- V_{S30} may vary by as much as 10% over small areas at this site due to lateral velocity variation, but not enough to change the NEHRP Site Class.

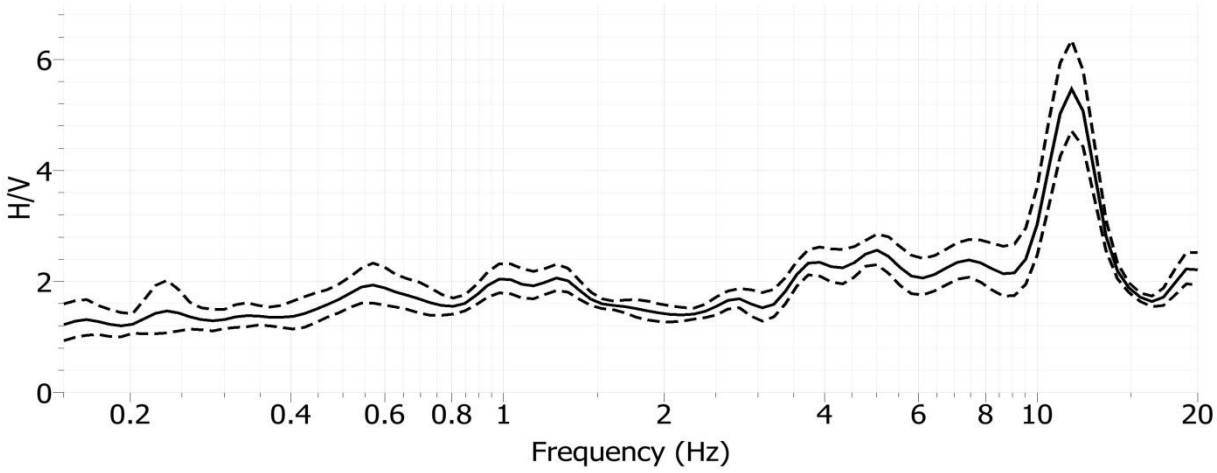

Site NC.HCAB, H/V Spectral Ratio, Array HCAB-1, Sensor 507

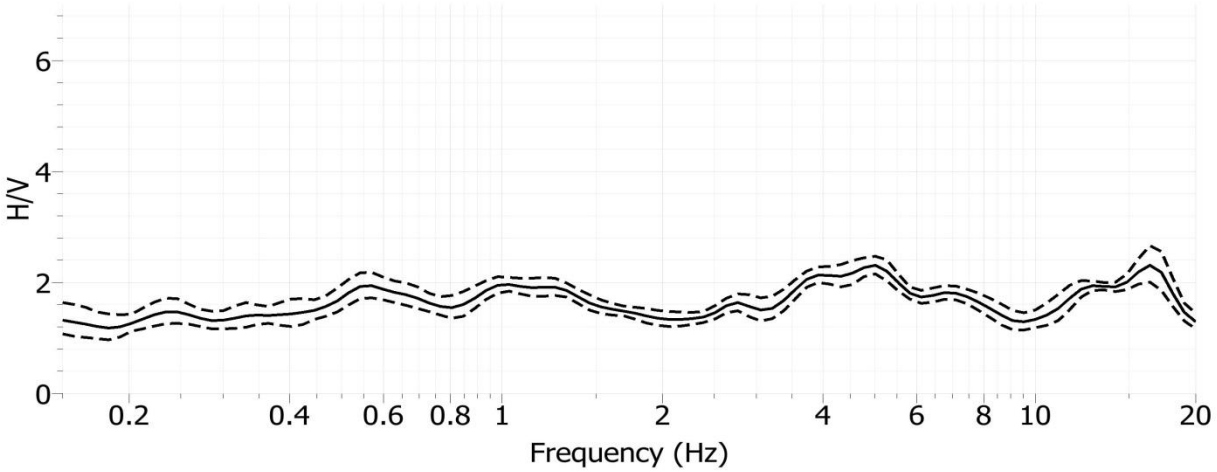

Site NC.HCAB, H/V Spectral Ratio, Array HCAB-1, Sensor 450

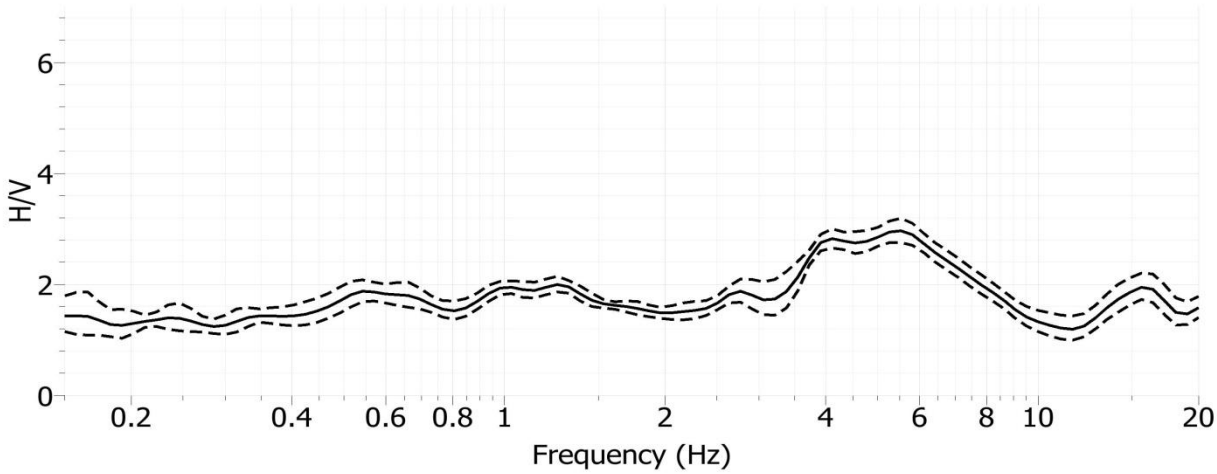

Site NC.HCAB, H/V Spectral Ratio, Array HCAB-1, Sensor 453

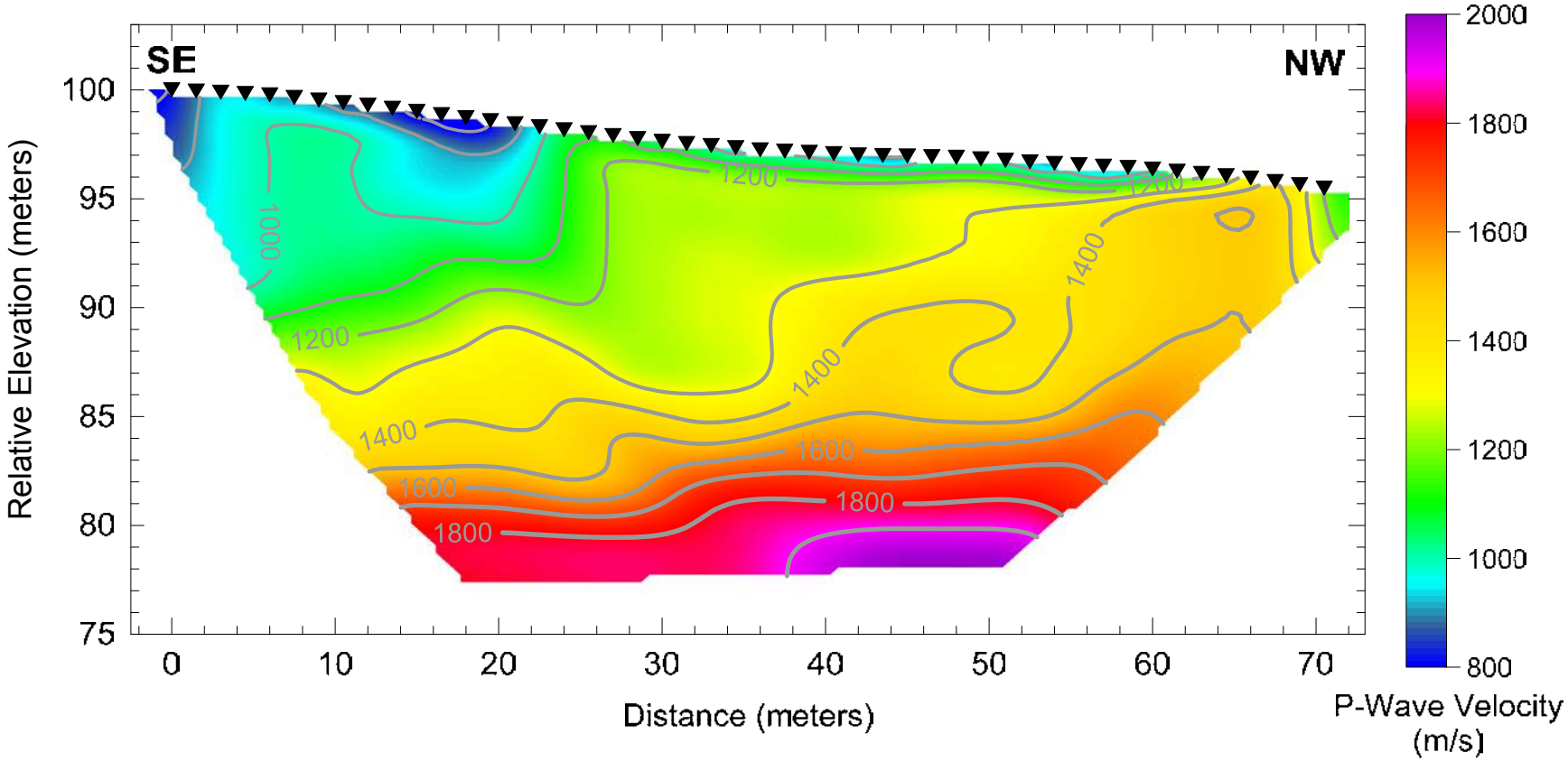

Array HCAB-1 – Tomographic seismic refraction model utilizing smooth velocity gradient starting model

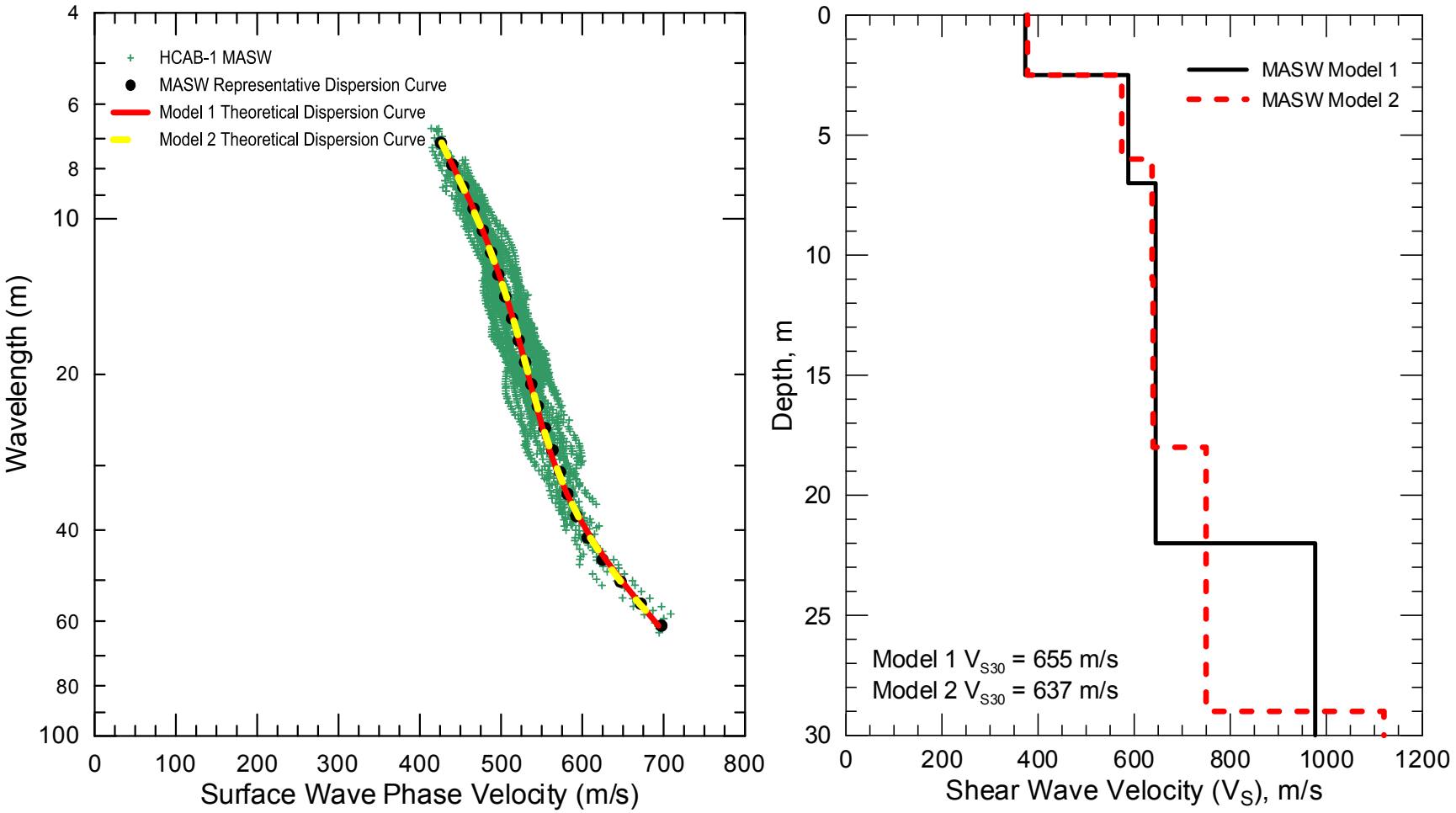

NC.HCAB - Field, representative and inverted theoretical surface wave dispersion data (left) and associated V_S model (right)

Site NC.JBMB

Location: Black Mountain, Santa Clara County, California

Latitude: 37.31861 **Longitude:** -122.15314
(Station coordinates provided by USGS, WGS84 coordinate system)

V_{S30} (measured): 584 m/s

V_{S30} (adjusted to more accurately reflect seismic station conditions): 637 m/s (average S-wave velocity between 1 and 31 m adjusting for sensor depth and sensor not being placed on loose soil).

NEHRP Site Class: C

Geomatrix Code: IFB

Geologic Conditions/Observations: Seismic station located at the mapped contact of the Mesozoic (Jurassic and Cretaceous) Franciscan Assemblage greenstone and greywacke sandstone units. Geologic map(s) indicate that bedding dips about 15 to 50 degrees to the northeast in the immediate site vicinity. The Pilarcitos Fault is located about 1 km southwest of the site.

Site Conditions: Rural site located on gently rolling hills. There is 5 to 9 m of elevation variation along the 70.5 m long seismic refraction and surface wave arrays.

Geophysical Methods Utilized: HVSR, Seismic Refraction (P- and S-wave), MASW (Rayleigh wave), MALW (Love wave)

Geophysical Testing Arrays:

1. Array JBMB-1 (48 channel MASW and P-wave seismic refraction array utilizing 4.5 Hz vertical geophones spaced 1.5 m apart for a length of 70.5 m, forward and reverse shot locations with multiple source offsets and source types (hammers only) and multiple interior shot locations).
2. Array JBMB-1 (48 channel MALW and S-wave seismic refraction array utilizing 4.5 Hz horizontal geophones space 1.5 m apart for a length of 70.5 m, coincident with P-wave and MASW array of same name).
3. Array JBMB-2 (48 channel MASW and P-wave seismic refraction array utilizing 4.5 Hz vertical geophones spaced 1.5 m apart for a length of 70.5 m, forward and reverse shot locations with multiple source offsets and source types (hammers only) and multiple interior shot locations).

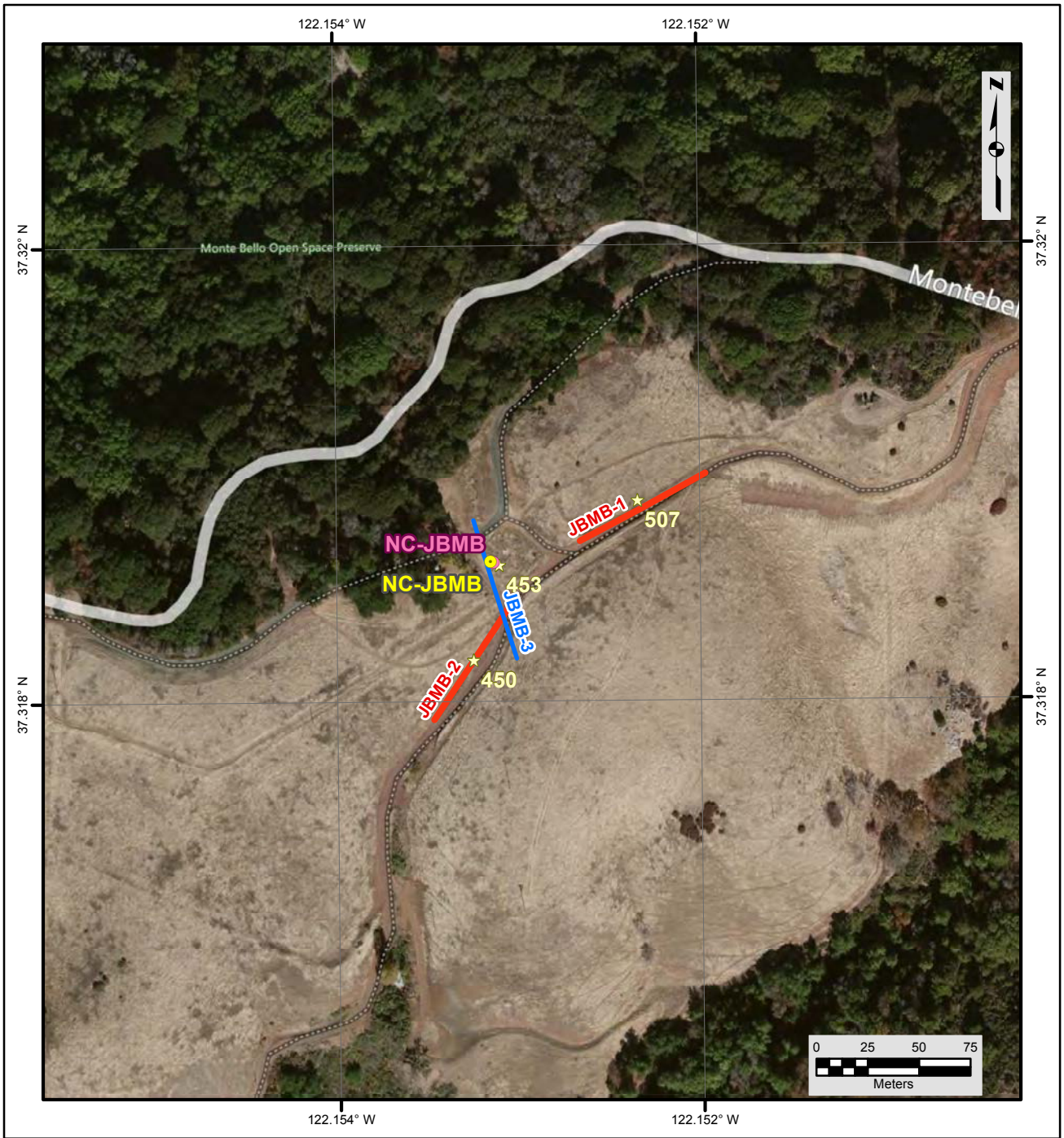

Legend

- Seismic Station - Approximate Surveyed Location
- Seismic Station - Approximate Location of Record
- H/V Spectral Ratio Location
- MASW and Seismic Refraction Array (P-wave)
- MASW and Seismic Refraction Array (P- and S-wave)

NOTES:
1. WGS 1984 COORDINATE SYSTEM
2. Image Source: (c) Microsoft Corporation and its data suppliers

File Name: NC-JBMB-I

Date: 5/7/2012

USGS science for a changing world

GEOVision geophysical services

RECOVERY.GOV

SITE MAP
NC•JBMB

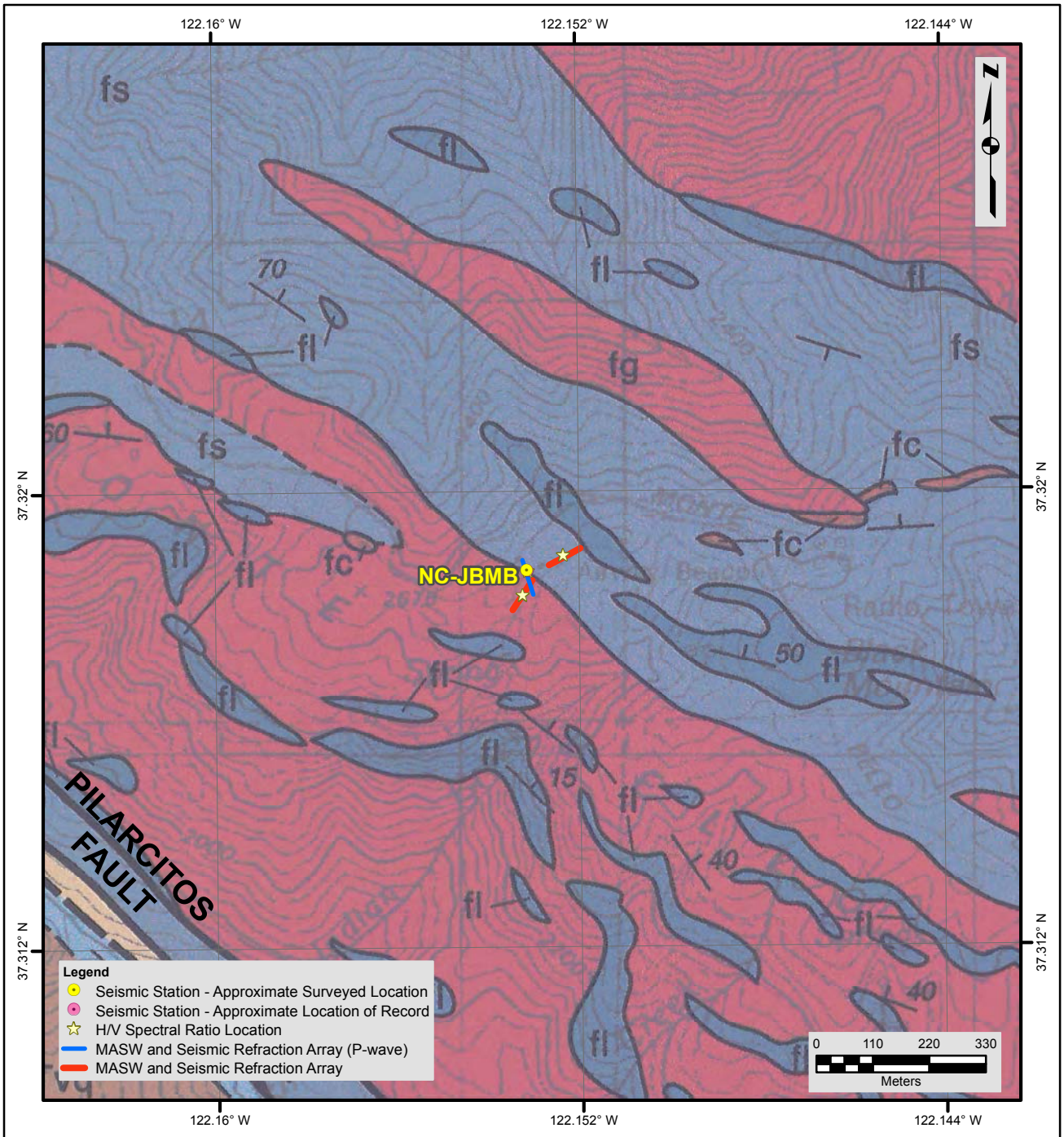

Description of Geologic Map Units

fg = Mesozoic (Jurassic and Cretaceous) Franciscan Assemblage; greenstone, massive, amorphous, locally brecciated, intertongued with fs
fs = Mesozoic (jurassic and Cretaceous) Franciscan Assemblage; greywacke sandstone or metagreywacke, hard, fine grained, massive to bedded, fractured, includes melange
fc = Mesozoic (Jurassic and Cretaceous) Franciscan Assemblage; chert or metachert, thin bedded, contorted, locally jasperized
fl = Mesozoic (Jurassic and Cretaceous) Franciscan Assemblage; limestone, hard, massive to bedded, very fine grained, occurs as lenses

NOTES:
1. WGS 1984 COORDINATE SYSTEM
2. Geologic Map of the Mindego Hill Quadrangle San Mateo, Santa Clara and Santa Cruz Counties, California by Thomas W. Dibblee, Jr., 2007
3. See site map for details of geophysical survey

USGS science for a changing world

GEOVision geophysical services

GEOLOGIC MAP
NC•JBMB

RECOVERY.GOV

File Name: NC-JBMB

Date: 5/7/2012

Looking east towards seismic station NC.JBMB and location of array JBMB-1 along road

NC.JBMB seismic station

Looking southwest along array JBMB-1

Looking northwest along array JBMB-2

Looking southeast along array JBMB-3

4. Array JBMB-2 (48 channel MALW and S-wave seismic refraction array utilizing 4.5 Hz horizontal geophones space 1.5 m apart for a length of 70.5 m, coincident with P-wave and MASW array of same name).
5. Array JBMB-3 (48 channel MASW and P-wave seismic refraction array utilizing 4.5 Hz vertical geophones spaced 1.5 m apart for a length of 70.5 m, forward and reverse shot locations with multiple source offsets and source types (hammers only) and multiple interior shot locations).
6. Three HVSR measurement locations: one near the center of array JBMB-1, one near the center of array JBMB-2 and the other adjacent to the seismic station.

Location of Geophysical Testing Arrays:

Location	Latitude	Longitude
JBMB-1, Southwest End of MASW/Refraction Array	37.31870	-122.15266
JBMB-1, Center of MASW/Refraction Array	37.31884	-122.15233
JBMB-1, Northeast End of MASW/Refraction Array	37.31900	-122.15197
JBMB-2, Southwest End of MASW/Refraction Array	37.31792	-122.15347
JBMB-2, Center of MASW/Refraction Array	37.31818	-122.15325
JBMB-2, Northeast End of MASW/Refraction Array	37.31844	-122.15304
JBMB-3, Northwest End of MASW/Refraction Array	37.31879	-122.15325
JBMB-3, Center of MASW/Refraction Array	37.31849	-122.15313
JBMB-3, Southeast End of MASW/Refraction Array	37.31819	-122.15302
HVSR Sensor 450	37.31817	-122.15323
HVSR Sensor 453	37.31860	-122.15312
HVSR Sensor 507	37.31888	-122.15235
NC.JBMB Seismic Station	37.31861	-122.15316

Notes: 1) WGS84 Coordinate System (decimal degrees)

2) Survey accuracy is estimated at 1 to 2 m.

Results:

Array JBMB-1 V_S Model (Rayleigh wave)

Depth to Top of Layer (m)	Layer Thickness (m)	S-Wave Velocity (m/s)	Inferred P-Wave Velocity (m/s)	Assumed Poisson's Ratio	Assumed Density (g/cm^3)
0	1	185	347	0.300	1.70
1	1.5	252	472	0.300	1.70
2.5	2.5	357	668	0.300	1.80
5	4	417	780	0.300	1.90
9	5	448	2500	0.483	1.90
14	7	484	2500	0.481	2.00
21	7	590	2500	0.471	2.05
28	>7	779	2500	0.446	2.10

Notes: 1) Saturated zone, with V_P of about 2,500 m/s, constrained at a depth of about 9 m based on seismic refraction survey.
2) Depth of investigation is about 35 m.
3) Bottom layer is a half space.

Array JBMB-2 V_S Model (Love wave)

Depth to Top of Layer (m)	Layer Thickness (m)	S-Wave Velocity (m/s)	Inferred P-Wave Velocity (m/s)	Assumed Poisson's Ratio	Assumed Density (g/cm^3)
0	1	182	340	0.300	1.70
1	1.5	237	443	0.300	1.80
2.5	2.5	464	868	0.300	2.00
5	4	548	1026	0.300	2.00
9	4	639	2750	0.471	2.10
13	8	789	2750	0.455	2.20
21	>9	857	2750	0.446	2.20

Notes: 1) Saturated zone, with V_P of about 2,750 m/s, constrained at a depth of about 9 m based on seismic refraction survey.
2) Depth of investigation is about 30 m.
3) Bottom layer is a half space.

Observations/Discussion:

- The seismic station is located at the mapped contact of Franciscan greenstone and greywacke units, which are locally dipping to the northeast. Due to soil cover, the geologic contact could not verified in the field. Therefore, during the first site visit, P-wave seismic refraction and MASW data were acquired along two arrays (JBMB-1 and JBMB-2), each located on one of the mapped geologic units. The two seismic refraction arrays are oriented almost orthogonal to the strike of the geologic bedding. Array JBMB-1 is located on the mapped greywacke sandstone and array JBMB-2 is located on the mapped greenstone unit. Preliminary review of the surface wave data indicated that velocity structure beneath the two arrays was significantly different and that reliable Rayleigh wave phase velocity data could not be extracted from array JBMB-2. Therefore, the site was revisited and S-wave refraction and MALW data acquired along arrays JBMB-1 and JBMB-2. To determine the geologic unit that the seismic station sits on, P-wave seismic refraction and MASW data were acquired along array JBMB-3, located as close as possible to the seismic station and oriented almost orthogonal to arrays JBMB-1 and JBMB-2.
- There are no clear high amplitude HVSR peaks by which to assess lateral velocity variation.
- The P-wave refraction data for arrays JBMB-1, JBMB-2 and JBMB-3 were modeled using a tomographic inversion routine with a layer based starting model. The seismic refraction models were extended to far offset shot locations to extend depth of investigation. S-wave seismic refraction data acquired along arrays JBMB-1 and JBMB-2 have not been modeled at this time as it was not considered necessary for site characterization. S-wave seismic refraction data were reviewed to confirm that S-wave velocity structure was different beneath the two arrays. The maximum V_S in the upper 20 m was found to be on the order of 550 to 600 m/s for array JBMB-1 and 750 to 850 m/s for array JBMB-2.
- The seismic refraction survey design allowed P-wave velocity to be imaged to a maximum depth of about 17 to 20 m. The P-wave refraction models for arrays JBMB-1 to JBMB-3 all have a thin, low velocity sediment layer at the surface with P-wave velocity in the 250 to 500 m/s range and variable thickness. All of the seismic refraction models have P-wave velocity between 2,000 and 3,000 m/s at depths below 7 to 11 m. Based on review of the S-wave seismic refraction records and surface wave data, it is clear that P-wave velocities over 1,600 to 2,000 m/s are associated with saturated Franciscan rocks. The saturated greywacke beneath array JBMB-1 has lower P-wave velocity than the saturated greenstone beneath array JBMB-2. The saturated Franciscan Assemblage rocks beneath array JBMB-3 have intermediate P-wave velocities, similar to those at the northwestern end of array JBMB-2 where the two arrays intersect. The biggest difference in P-wave velocity between arrays JBMB-1 and JBMB-2 is associated with the unsaturated rock. The weathered greywacke sandstone unit beneath array JBMB-1 has P-wave velocity of about 800 m/s at a depth of 1 to 3 m, increasing with depth to a maximum velocity of about 1,000 m/s above the saturated zone. The weathered greenstone unit beneath array JBMB-2 has P-wave velocity of about 800 m/s at a depth of 1 to 3 m, increasing with depth to a maximum velocity of about 1,400 m/s above the saturated zone. Array JBMB-3 is most similar to array JBMB-2, with P-wave

velocity of 800 m/s at a depth of 1.5 to 2.5 m, increasing with depth to a maximum velocity of about 1,400 m/s above the saturated zone.

- All of the P-wave seismic refraction models have near surface lateral velocity variation; most significantly a variable thickness, low velocity sediment layer overlying higher velocity weathered sedimentary rock.
- The P-wave seismic refraction models are not particularly useful for characterizing S-wave velocity structure because of the relatively shallow saturated zone. The seismic refraction models do, however, indicate that arrays JBMB-2 and JBMB-3 have similar near surface velocity structure and are most representative of velocity structure beneath the seismic station.
- The seismic refraction/surface arrays JBMB-1 and JBMB-2 were orientated almost perpendicular to the strike of the geologic bedding, which dips on the order of 15 to 50 degrees to the northeast. For surface waves methods to be effective in such environments, the dipping beds need to have similar seismic velocity with near surface velocities a function of weathering rather than lithology. Often it is not possible to align arrays parallel to strike because of topography. Array JBMB-3 is closer to being aligned parallel to strike.
- Noise conditions at the site were not sufficient for application of passive surface wave techniques.
- Both the MASW and MALW data acquired along array JBMB-1 were of good quality. Interpretation of velocity structure beneath this array is limited to analysis of the MASW data at this time. Interpretation of MASW data collected along arrays JBMB-2 and JBMB-3 appeared to be significantly impacted by dominant higher modes at low frequencies and we do not believe that a reliable V_S model could be developed from this data. The preliminary Rayleigh wave dispersion data reduced from array JBMB-3 were more similar to that from array JBMB-2 than that from array JBMB-1. The MALW data collected along array JBMB-2 were off much better quality than the MASW data without the concern of dominant higher modes, at least with the velocity structure beneath the array. Therefore, Love wave dispersion data from array JBMB-2 were used to characterize V_S structure beneath the array. Based on the seismic refraction models and inspection of Rayleigh wave phase velocity data, array JBMB-2 is considered more representative of seismic station conditions than array JBMB-1.
- Array JBMB-1 MASW data reduction was complicated by dominant higher modes at high frequencies. However, the fundamental mode was recovered at high frequencies (small wavelengths) using limited offset range receiver gathers. The largest energy source utilized for data acquisition consisted of a 20 lb hammer and, therefore, the lowest frequency Rayleigh wave phase velocity data extracted from the seismic records was restricted to 7.5 to 8 Hz, equivalent to a wavelength of about 80 m.
- The array JBMB-2 MALW data reduction was uncomplicated, but Love wave dispersion data were noisy at low frequencies, resulting in more scatter. High frequency Love wave dispersion data were extracted from the northwestern half of the array where there is a thicker sequence of low velocity sediments overlying weathered rock. This portion of the array is also closest to the seismic station.
- The minimum wavelength surface wave phase velocity data extracted from the 48-channel MASW array (JBMB-1) was about 20 m. Reducing data from smaller hammer

sources using a limited offset receiver array (i.e. less active geophones) allowed for extraction of surface wave dispersion data to a minimum wavelength of about 3.5 m.

- The minimum wavelength surface wave phase velocity data extracted from the 48-channel MALW array (JBMB-2) was about 23 m. Reducing data from smaller hammer sources using a limited offset receiver array (i.e. less active geophones) allowed for extraction of surface wave dispersion data to a minimum wavelength of about 2 m.
- The maximum wavelength Rayleigh wave phase velocity data extracted from a particular source-receiver gather combination was set equal to the lesser of 80 m or 1.25 times the distance from the source to midpoint of the receiver array.
- The maximum wavelength Love wave phase velocity data extracted from a particular source-receiver gather combination was set equal to the lesser of 90 m or 1.25 times the distance from the source to midpoint of the receiver array.
- There is nominally about 50 m/s of scatter in array JBMB-1 MASW dispersion data and 50 to 100 m/s scatter in the array JBMB-2 MALW dispersion data resulting from near surface lateral velocity variation. The Love wave dispersion data from array JBMB-2 were particularly noisy at long wavelengths, resulting in additional scatter, and no attempt was made to extract dispersion data at wavelengths greater than 90 m.
- Representative dispersion curve was generated for the array JBMB-1 MASW and array JBMB-2 MALW data sets using a moving average, polynomial curve fitting routine and used for modeling.
- Surface wave depth of investigation is about 35 m for MASW array JBMB-1 based on half of maximum wavelength criteria. Surface wave depth of investigation is about 30 m for MALW array JBMB-2 based on one third of maximum wavelength.
- The depth of the saturated zone was constrained at an approximate depth of 9 m in the surface wave models for arrays JBMB-1 and JBMB-2, based on the seismic refraction models. The P-wave velocity of saturated sedimentary rock was constrained at 2,500 and 2,750 m/s for arrays JBMB-1 and JBMB-2, respectively. It should be noted, that P-wave velocity and Poisson's ratio are not needed for modeling of Love wave dispersion data.
- V_{S30} is 441 and 584 m/s for arrays JBMB-1 and JBMB-2, respectively (NEHRP Site Class C).
- Average S-wave velocity between 1 and 31 m, to account for assumed sensor depth and the sensor not being placed on loose surficial soils, is 470 and 637 m/s for arrays JBMB-1 and JBMB-2, respectively.
- The V_S model for array JBMB-2 is considered most representative of the velocity structure at the seismic station. The seismic station is, however, located near the mapped geologic contact of Franciscan greenstone and greywacke sandstone units and V_{S30} appears to vary by more than 30% between the two geologic units.

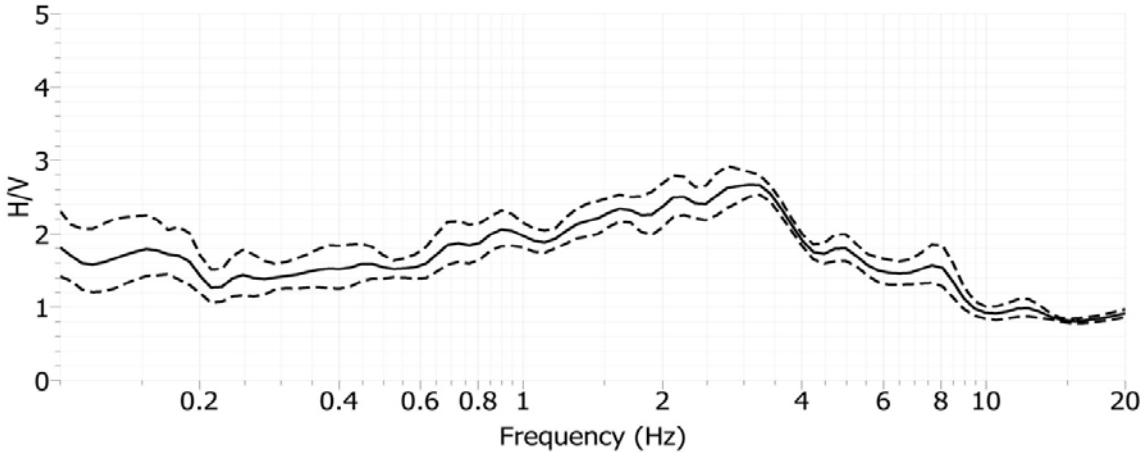

Site NC.JBMB, H/V Spectral Ratio, Array JBMB-1, Sensor 507

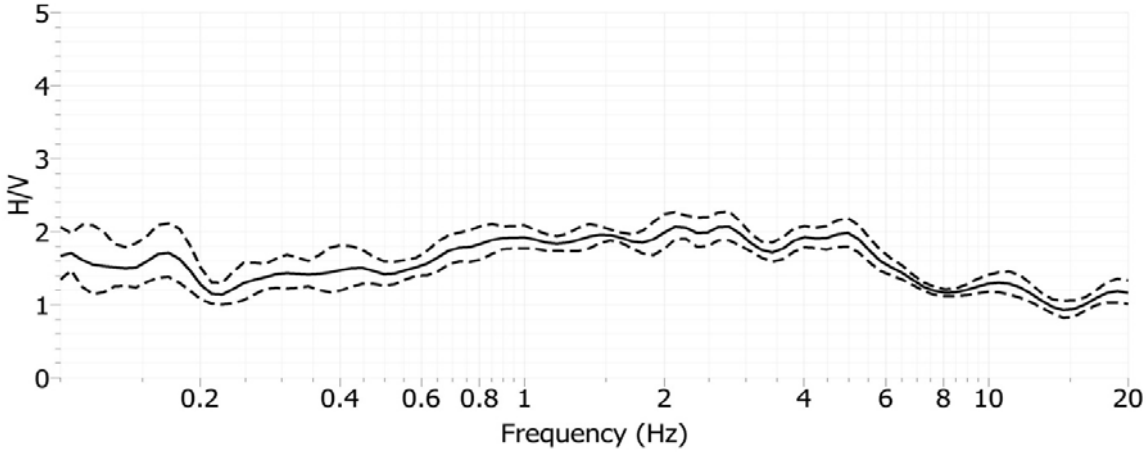

Site NC.JBMB, H/V Spectral Ratio, Near Seismic Station, Sensor 453

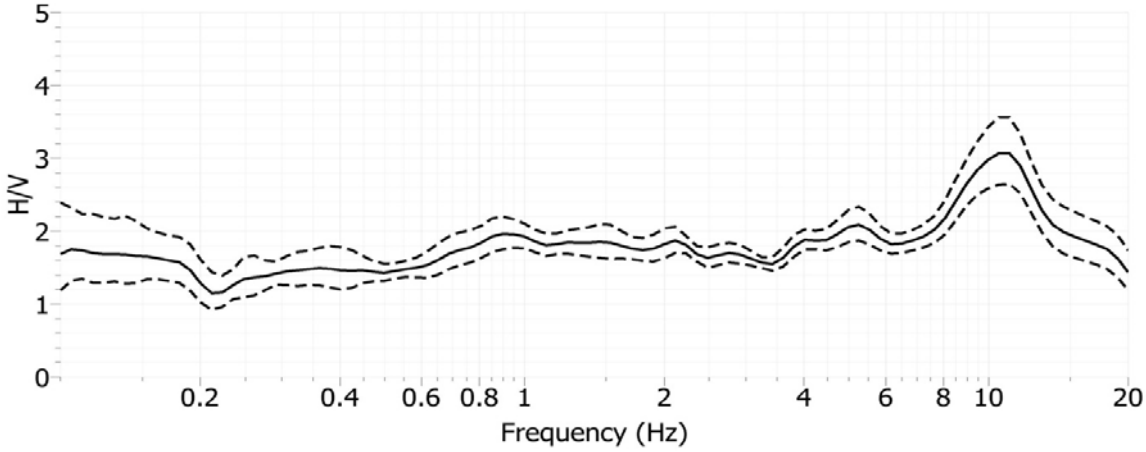

Site NC.JBMB, H/V Spectral Ratio, Array JBMB-2, Sensor 450

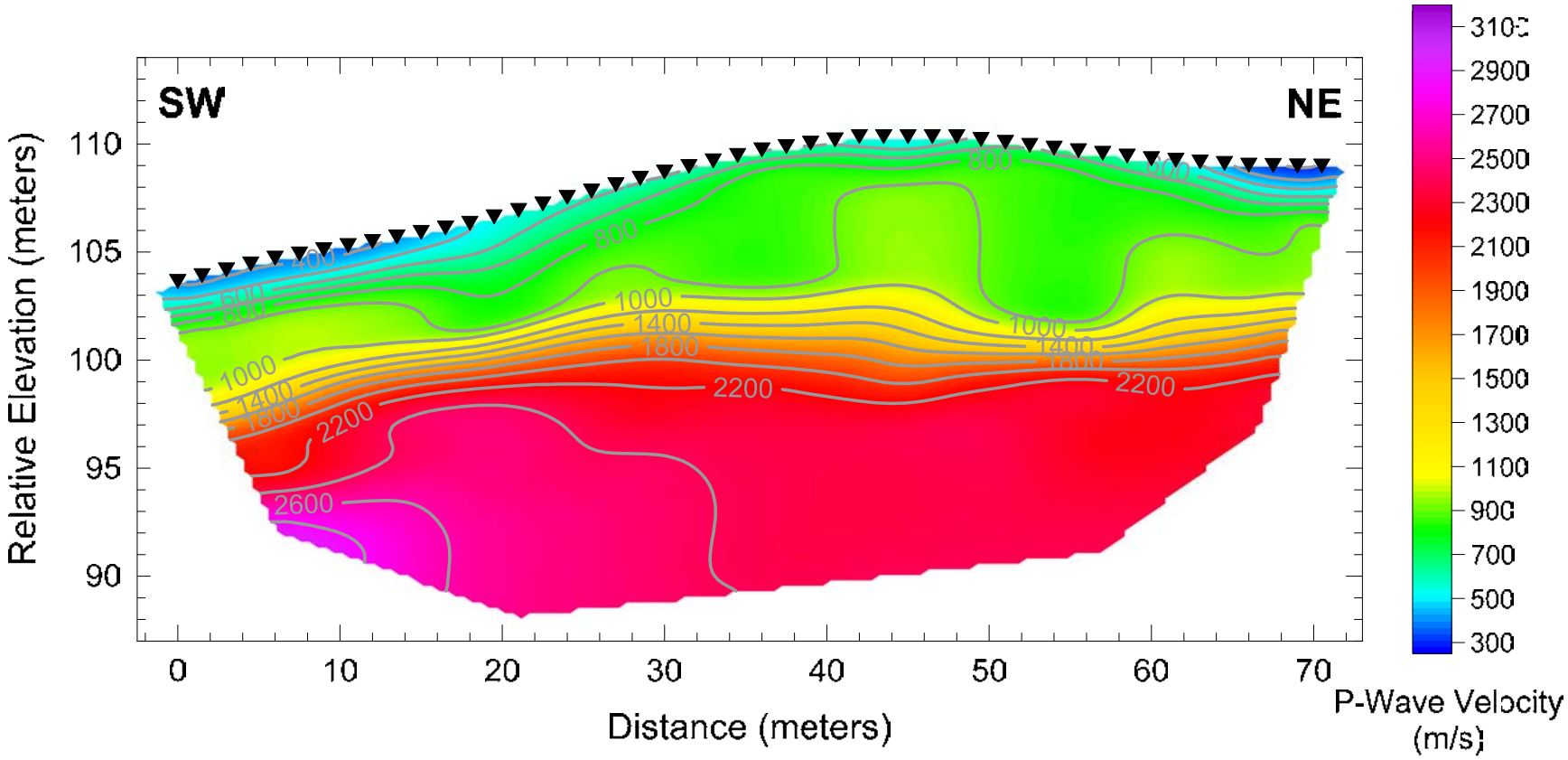

Array JBMB-1 – P-wave tomographic seismic refraction model developed using a layer based starting model

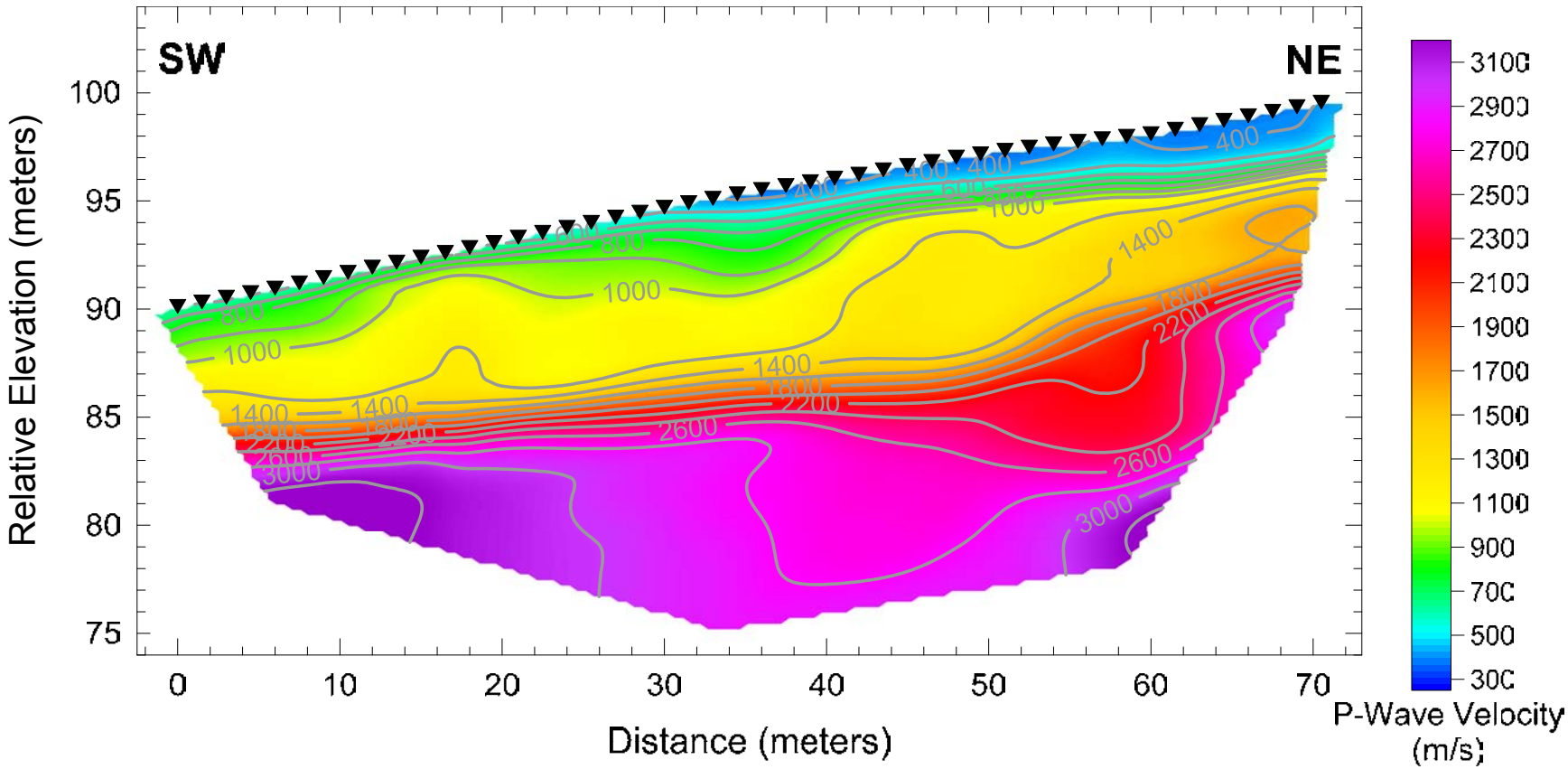

Array JBMB-2 – P-wave tomographic seismic refraction model developed using a layer based starting model

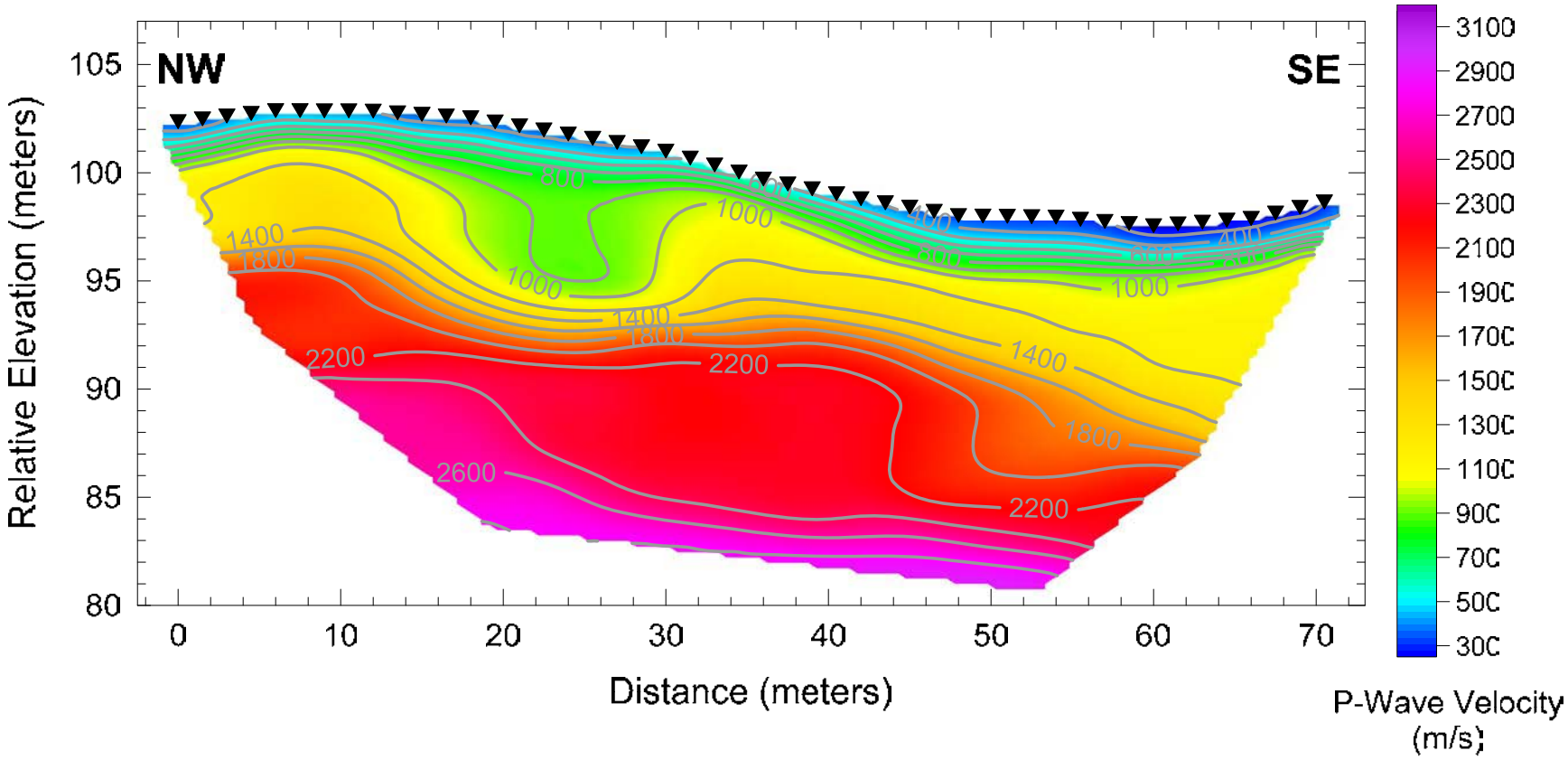

Array JBMB-3 – P-wave tomographic seismic refraction model developed using a layer based starting model

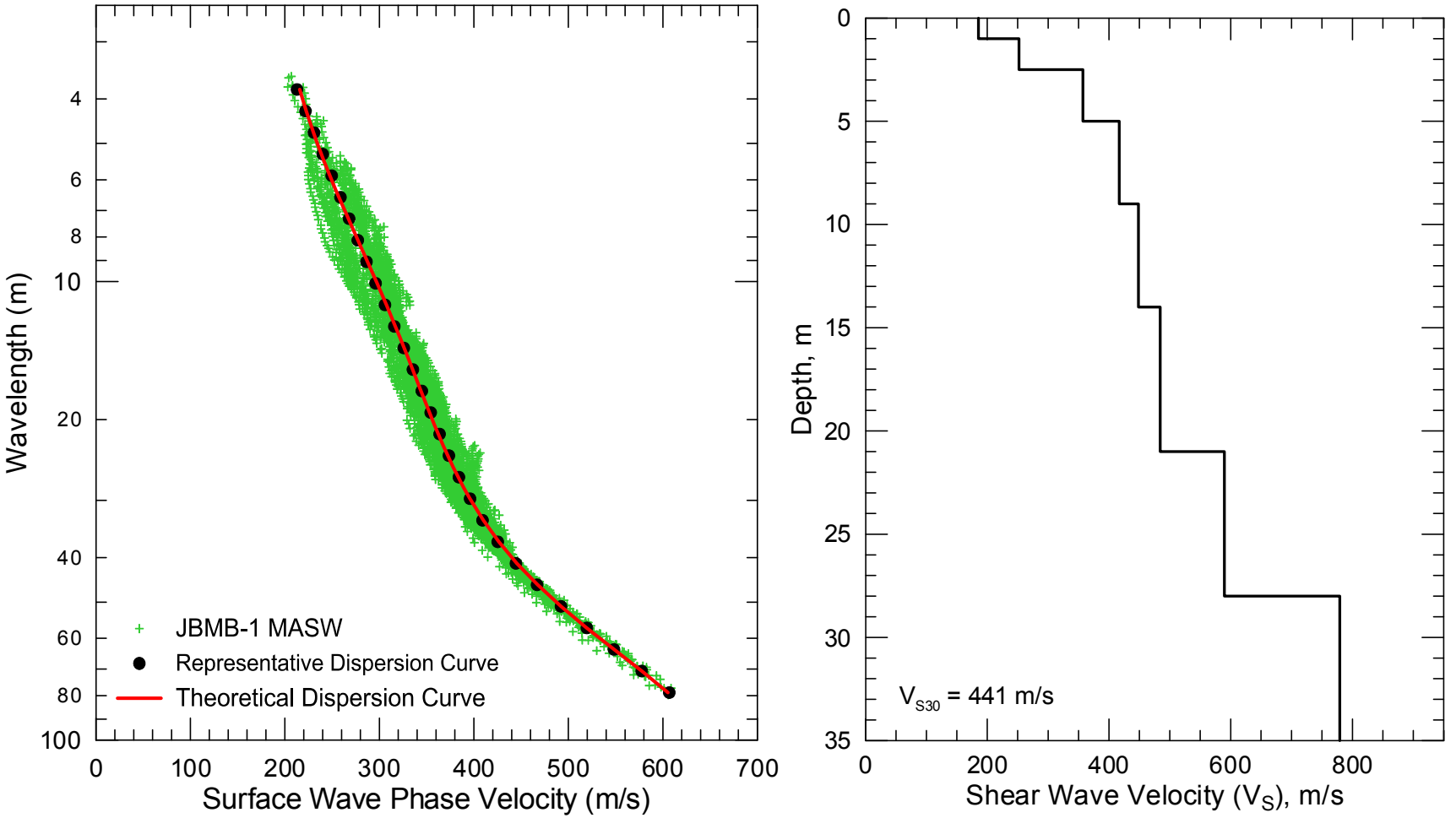

NC.JBMB - Field, representative and inverted theoretical surface wave dispersion data (left) and associated V_S model (right) for Array JBMB-1 MASW (Rayleigh wave) data

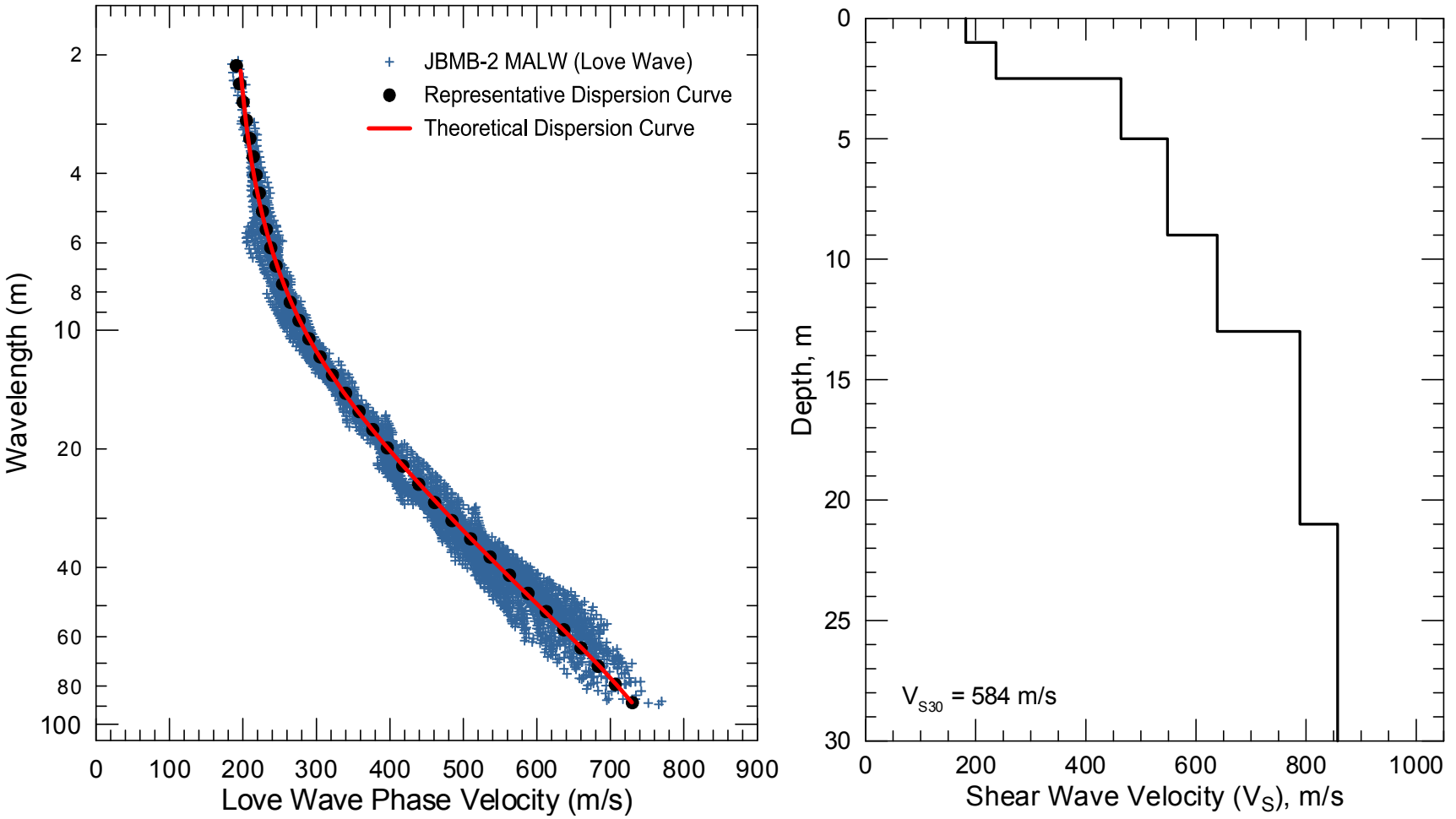

NC.JBMB - Field, representative and inverted theoretical surface wave dispersion data (left) and associated V_S model (right) for Array JBMB-2 MALW (Love wave) data

Site NC.JBNB

Location: Ben Lomond Mountain, Santa Cruz County, California

Latitude: 37.12043 **Longitude:** -122.15520
(Station coordinates provided by USGS, WGS84 coordinate system)

V_{S30} (measured): 760 m/s

V_{S30} (adjusted to more accurately reflect seismic station conditions): 942 (average S-wave velocity between 1.5 and 31.5 m adjusting for seismic station being located on weathered rock) or 842 m/s (V_{S30} estimated by replacing V_S in upper 1.5 m with V_S of underlying unit to account for the seismic sensor being placed on rock).

NEHRP Site Class: B (after adjusting for seismic station conditions)

Geomatrix Code: IGA

Geologic Conditions/Observations: Seismic station located on Mesozoic (Cretaceous) granitic rock (quartz diorite to granodiorite).

Site Conditions: Rural site. Test area located on a plateau on top of Ben Lomond Mountain. There is only about 2.5 m of elevation variation along the 70.5 m long seismic line. The seismic station is located at the edge of the plateau where topography falls off relatively steeply to the northeast.

Geophysical Methods Utilized: HVSR, Seismic Refraction (P- and S-wave), MASW (Rayleigh wave), MALW (Love wave)

Geophysical Testing Arrays:

1. Array JBNB-1 (48 channel MASW and P-wave seismic refraction array utilizing 4.5 Hz vertical geophones spaced 1.5 m apart for a length of 70.5 m, forward and reverse shot locations with multiple source offsets and source types and multiple interior shot locations).
2. Array JBNB-1 (48 channel MALW and S-wave seismic refraction array utilizing 10 Hz horizontal geophones spaced 1.5 m apart for a length of 70.5 m, forward and reverse shot locations with multiple source offsets and multiple interior shot locations). Coincident with P-wave refraction/MASW array of same name.
3. Three HVSR measurement locations: two distributed along array JBNB-1 and the other adjacent to the seismic station.

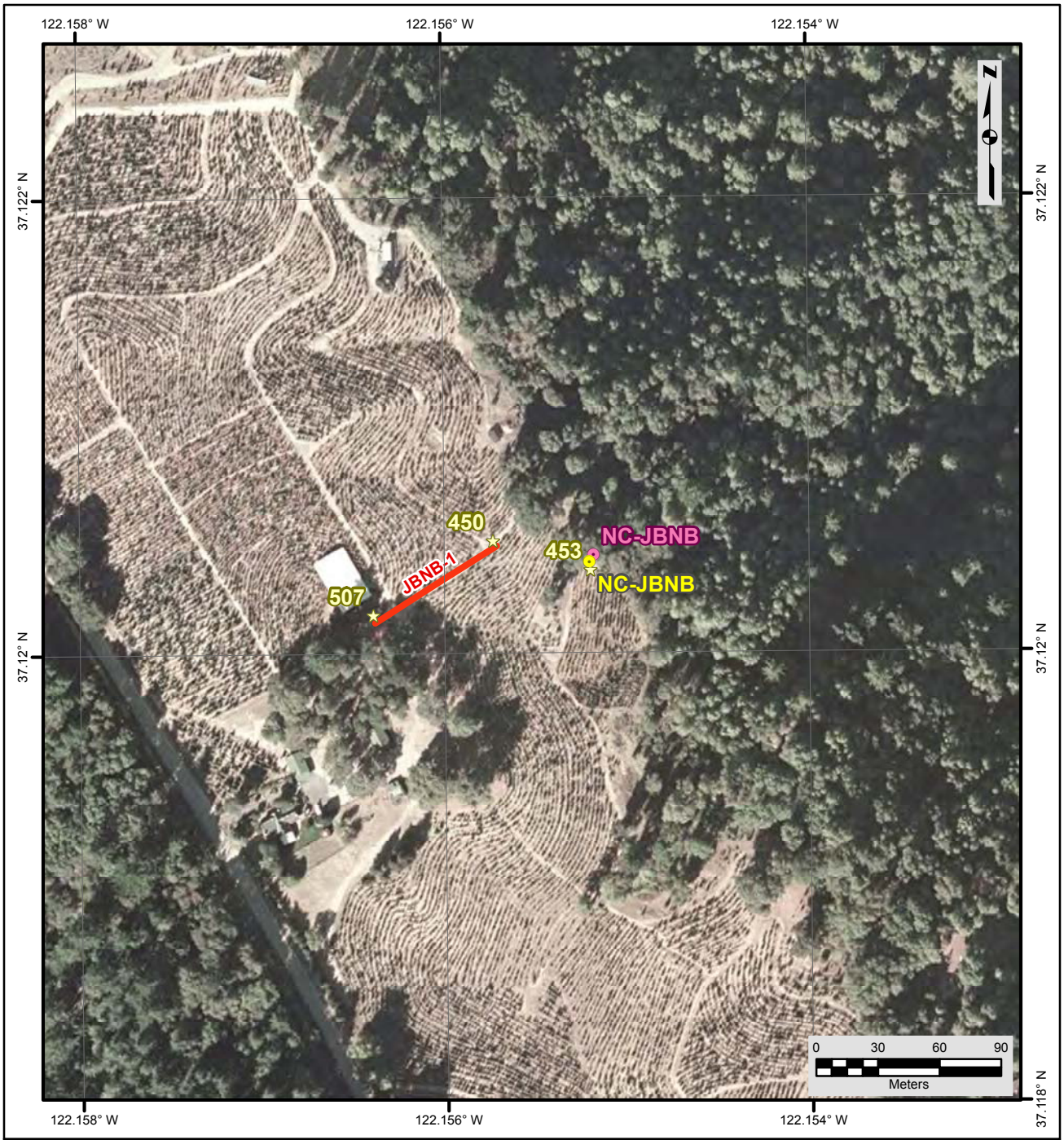

Legend

- Seismic Station - Approximate Surveyed Location
- Seismic Station - Approximate Location of Record
- H/V Spectral Ratio Location
- MASW and Seismic Refraction Array (S- and P-wave)

NOTES:
1. WGS 1984 COORDINATE SYSTEM
2. Image Source: ESRI, i-cubed, USDA FSA, USGS, AEX, GeoEye, Getmapping, Aerogrid, IGP

File Name: NC-JBNB-I

Date: 10/20/2011

USGS science for a changing world

GEOVision geophysical services

RECOVERY.GOV

SITE MAP
NC•JBNB

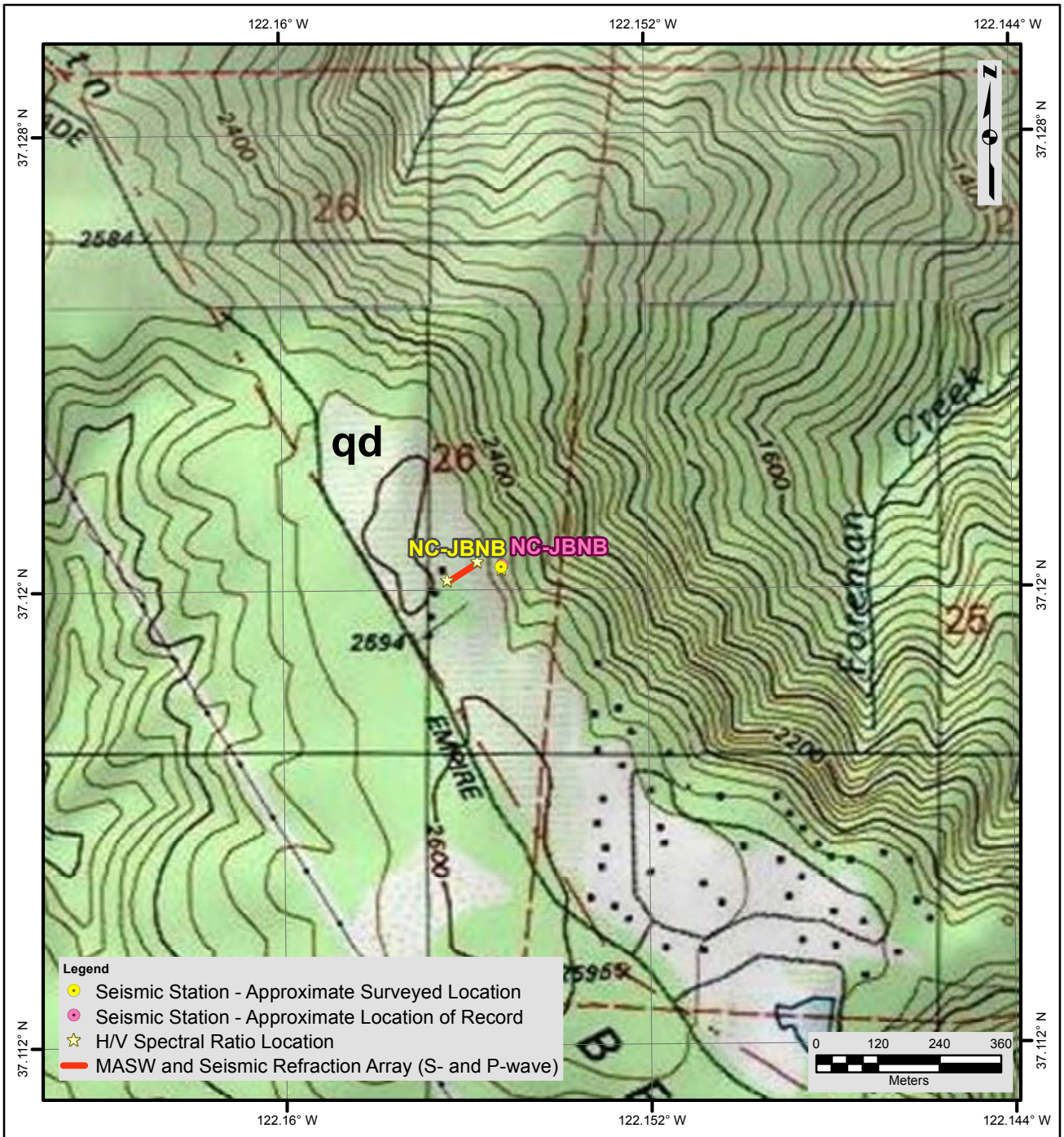

Description of Geologic Map Units

qd = Mesozoic (Cretaceous) quartz diorite to granodiorite

NOTES:
1. WGS 1984 COORDINATE SYSTEM
2. Geologic Map of Santa Cruz County, California compiled by Earl E. Brabb, 1989
3. See site map for details of geophysical survey

File Name: NC-JBNB

Date: 10/20/2011

USGS science for a changing world

GEOVision geophysical services

GEOLOGIC MAP
NC•JBNB

NC.JBNB seismic station

Seismic station NC.JBNB located on rock outcrop

Looking southwest along array JBNB-1 and at HVSR sensor 450

Looking northeast along array JBNB-1

Looking southwest from center of array JBNB-1

Location of Geophysical Testing Arrays:

Location	Latitude	Longitude
JBNB-1, Southwest End of MASW/Refraction Array	37.12014	-122.15640
JBNB-1, Center of MASW and Refraction Array	37.12031	-122.15606
JBNB-1, Northeast End of MASW/Refraction Array	37.12047	-122.15573
HVSR Sensor 450	37.12049	-122.15575
HVSR Sensor 453	37.12036	-122.15522
HVSR Sensor 507	37.12017	-122.15641
NC.JBNB Seismic Station	37.12040	-122.15522

Notes: 1) WGS84 Coordinate System (decimal degrees)
2) Survey accuracy is estimated at 2 to 3 m.

Results:

V_S Model from MALW (Love Wave) Sounding

Depth to Top of Layer (m)	Layer Thickness (m)	S-Wave Velocity (m/s)	Inferred P-Wave Velocity (m/s)	Assumed Poisson's Ratio	Assumed Density (g/cm^3)
0	1	140	263	0.3	1.7
1	1.5	306	571	0.3	1.8
2.5	2.5	343	642	0.3	1.8
5	4	1042	1947	0.3	2.1
9	7	1229	2298	0.3	2.2
16	>14	1319	2469	0.3	2.2

Notes: 1) Depth of investigation is about 30 m.
2) Bottom layer is a half space.

Average V_S Model from Central Portion of S-wave Refraction Line (Layered Starting Model)

Depth to Top of Layer (m)	Layer Thickness (m)	S-Wave Velocity (m/s)
0.00	0.52	190
0.52	1.03	203
1.55	1.03	322
2.58	1.03	412
3.61	1.03	477
4.64	1.03	529
5.67	1.03	538
6.70	2.16	866
8.86	2.16	1352
11.03	2.16	1517
13.19	2.16	1582
15.36	2.16	1626
17.52	2.16	1713
19.69	2.16	1726
21.85	Half Space	1746

Average V_S Model from Central Portion of S-wave Refraction Line (Smooth Starting Model)

Depth to Top of Layer (m)	Layer Thickness (m)	S-Wave Velocity (m/s)
0.00	0.52	184
0.52	1.03	227
1.55	1.03	300
2.58	1.03	399
3.61	1.03	473
4.64	1.03	580
5.67	1.03	692
6.70	2.16	869
8.86	2.16	1177
11.03	2.16	1402
13.19	2.16	1598
15.36	2.16	1655
17.52	2.16	1735
19.69	2.16	1786
21.85	2.16	1825
24.02	2.16	1868
26.18	2.16	1904
28.35	Half Space	1904

Average V_P and Estimated V_S Models from Central Portion of P-wave Seismic Refraction Line (Layered Starting Model)

Depth to Top of Layer (m)	Layer Thickness (m)	P-Wave Velocity (m/s)	Estimated S-Wave Velocity (m/s)			
			Poisson's Ratio = 0.25	Poisson's Ratio = 0.30	Poisson's Ratio = 0.3333	Poisson's Ratio = 0.35
0.00	0.52	306	177	164	153	147
0.52	1.03	338	195	181	169	162
1.55	1.03	572	330	306	286	275
2.58	1.03	653	377	349	327	314
3.61	1.03	743	429	397	372	357
4.64	1.03	783	452	419	392	376
5.67	1.03	813	470	435	407	391
6.70	2.16	911	526	487	456	438
8.86	2.16	2192	1266	1172	1096	1053
11.03	2.16	2614	1509	1397	1307	1256
13.19	2.16	2824	1631	1510	1412	1357
15.36	2.16	3153	1821	1686	1577	1515
17.52	2.16	3255	1879	1740	1627	1564
19.69	2.16	3317	1915	1773	1659	1594
21.85	2.16	3396	1960	1815	1698	1631
24.02	2.16	3445	1989	1842	1723	1655
26.18	Half Space	3511	2027	1876	1755	1686

Average V_P and Estimated V_S Models from Central Portion of P-wave Seismic Refraction Line (Smooth Velocity Gradient Starting Model)

Depth to Top of Layer (m)	Layer Thickness (m)	P-Wave Velocity (m/s)	Estimated S-Wave Velocity (m/s)			
			Poisson's Ratio = 0.25	Poisson's Ratio = 0.30	Poisson's Ratio = 0.3333	Poisson's Ratio = 0.35
0.00	0.52	293	169	157	147	141
0.52	1.03	385	222	206	192	185
1.55	1.03	500	289	267	250	240
2.58	1.03	658	380	352	329	316
3.61	1.03	753	435	402	376	362
4.64	1.03	864	499	462	432	415
5.67	1.03	994	574	531	497	477
6.70	2.16	1203	695	643	602	578
8.86	2.16	1685	973	900	842	809
11.03	2.16	2202	1271	1177	1101	1058
13.19	2.16	2457	1419	1313	1229	1180
15.36	2.16	3012	1739	1610	1506	1447
17.52	2.16	3211	1854	1716	1605	1542
19.69	2.16	3505	2023	1873	1752	1684
21.85	2.16	3577	2065	1912	1788	1718
24.02	2.16	3622	2091	1936	1811	1740
26.18	2.16	3656	2111	1954	1828	1756
28.35	Half Space	3714	2144	1985	1857	1784

Observations/Discussion:

- There are no clear peaks in the HVSR data, although there may be weak HVSR peaks in the 8 to 12 and 21 to 25 Hz range.
- Field observations indicated that the MASW (Rayleigh wave) technique was not effective at this site due to the thin layer of low velocity sediments overlying high velocity rock and/or lateral variability of the subsurface velocity structure. Therefore, both P- and S-wave seismic refraction surveys were conducted and MALW (Love wave) data acquired.
- The P- and S-wave seismic refraction data for array JBNB-1 were modeled using a tomographic inversion routine with both layer-based and smooth velocity gradient starting models. The seismic refraction models were extended to far offset shot locations to extend depth of investigation. It should be noted that a larger geophone spacing, rather than the utilization of far offset shot locations, is preferred for extending depth of investigation, when applying tomographic inversion routines. However, the seismic refraction data were acquired in conjunction with surface wave data, where a shorter array length is preferred.
- Both the P- and S-wave seismic refraction data sets are of very good quality. The P-wave first arrival data were picked to a greater degree of accuracy than the S-wave first arrival data because the S-wave is not typically the first energy on a seismic record, even when using a horizontal traction plank as an energy source. The air wave arrives before the direct soil arrival in many of the P-wave seismic records and an attempt was made to pick the direct arrival after the air wave, which was not too difficult with this data set.
- Tomographic inversion of the P-wave first arrival data utilizing layered and smooth starting models yielded similar V_P models. The P-wave seismic refraction survey design allowed P-wave velocity to be imaged to a maximum depth of about 25 m. The seismic refraction models indicate that P-wave velocity is about 250 to 400 m/s at the surface and increases to 750 m/s at a depth of 2 to 6 m, 1,000 m/s at a depth of 5 to 8 m and over 3,000 m/s at a depth of 10 to 20 m. The maximum P-wave velocity in the models is in the 3,500 to 3,750 m/s range; although it was possible to model the seismic refraction data with a maximum P-wave velocity of 3,000 m/s with only a small increase in RMS error. P-wave velocity, is however, expected in increase gradually with depth as the degree of weathering decreases.
- Tomographic inversion of the S-wave first arrival data utilizing layered and smooth starting models yielded similar V_S models and the models show similar velocity structure as the V_P models. The S-wave seismic refraction survey design allowed S-wave velocity to be imaged to a maximum depth of about 25 m. The seismic refraction models indicate that S-wave velocity is about 150 to 250 m/s at the surface and increases to 400 m/s at a depth of 1 to 5 m, 600 m/s at a depth of 4 to 6 m, 1,000 m/s at a depth of 6 to 10 m and over 1,600 m/s at a depth of 9 to 22 m. The maximum S-wave velocity in the models was in the 1,900 to 2,000 m/s range; although it was possible to model the seismic refraction data with a maximum S-wave velocity of 1,600 m/s with only a small increase in RMS error. S-wave velocity, is however, expected in increase gradually with depth as the degree of weathering decreases.
- Although the P- and S-wave seismic refraction models reveal similar velocity structure, they are not in particularly good agreement in the 2 to 12 m depth range. Below 12 m depth, the models indicate that Poisson's ratio is on the order of 0.3, which is realistic for weathered rock. Above 12 m, either Poisson's ratio is significantly lower than 0.3 or

there is error in picking first arrivals in the S-wave seismic data, which contributes to error in the model.

- Longer seismic refraction lines would have been preferred to image to 30 m depth and more accurately constrain the high seismic velocities. There was sufficient space at the site for a 130 to 141 m long refraction line with no offend shot locations.
- There is lateral velocity variation at the site, particularly at depth where the zone of lower velocity weathered rock thickens to the northeast.
- V_{S30} was estimated between 25.5 and 51 m on the S-wave refraction model that used a layered starting model, by projecting the velocity at 22 m depth to 30 m depth. Over this interval, V_{S30} ranges from about 778 to 945 m/s, about a 21% variation over a 25 m distance on the array where much of the lateral velocity variation occurs. An average V_S model was developed over the 25.5 to 52 m distance interval by averaging the slowness of each model cell at a particular depth and average V_{S30} was determined to be 859 m/s. Setting the maximum velocity to 1,600 m/s during modeling has minimal effect on V_{S30}, changing the V_{S30} range to 764 to 947 m/s and average V_{S30} to 851 m/s. Average V_S between 1.5 and 31.5 m is 1,063 m/s. V_{S30} calculated after replacing the V_S of the sediments in the upper 1.5 m with that of the underlying layer is 939 m/s.
- V_{S30} was estimated between 25.5 and 51 m on the S-wave refraction model that used a smooth velocity gradient starting model, by projecting the velocity at 28 m depth to 30 m depth. Over this interval, V_{S30} ranges from about 809 to 963 m/s, about a 19% variation over a 25 m distance. An average V_S model was developed over the 25.5 to 52 m distance interval by averaging the slowness of each model cell at a particular depth and average V_{S30} was determined to be 878 m/s. Average V_S between 1.5 and 31.5 m is 1,079 m/s. V_{S30} calculated after replacing the V_S of the sediments in the upper 1.5 m with that of the underlying layer is 938 m/s.
- V_{P30} between 25.5 and 51 m varies from about 1,266 to 1,524 m/s, a 20% variation, and averages 1,402 m/s on the P-wave velocity model developed using a layered starting model. Estimating V_{S30} from V_{P30} assuming constant Poisson's ratio in the range of 0.25 to 0.35 results in V_{S30} in the 809 to 673 m/s range. This large variation in potential V_{S30} demonstrates the risks in attempting to estimate V_{S30} from P-wave velocity data, even with a realistic estimate of Poisson's ratio and this approach should only be used as a last resort.
- V_{P30} between 25.5 and 51 m varies from about 1,314 to 1,552 m/s, an 18% variation, and averages 1,438 m/s on the P-wave velocity model developed using a smooth velocity starting model. Estimating V_{S30} from V_{P30} assuming constant Poisson's ratio in the range of 0.25 to 0.35 results in V_{S30} in the 830 to 691 m/s range.
- Noise conditions at the site were not sufficient for application of passive surface wave techniques.
- MASW (Rayleigh wave) data quality is poor due to the high velocity shallow rock and lateral velocity variation and were not reduced. MALW (Love wave) data was of better quality than the MASW data and were, therefore, reduced and modeled. It is difficult to predict the effect of the significant lateral velocity variation (20% or larger variation in V_{S30} beneath the array) on the resulting surface wave model.
- The minimum wavelength surface wave phase velocity data extracted from the 48-channel MALW array is about 14 m. Data reduction using seismic records from smaller

hammer sources and a limited offset receiver array (i.e. less active geophones) allowed extraction of surface wave dispersion data to a minimum wavelength of about 2.5 m.

- There is nominally about 50 to 100 m/s scatter in MALW dispersion data likely due to the effects of lateral velocity variation, even after selective use of MALW dispersion data.
- A representative dispersion curve was generated for the MALW data set using a moving average, polynomial curve fitting routine and used for modeling.
- Surface wave depth of investigation is assumed to be about 30 m. It does appear as though the MALW technique required longer wavelength Love wave phase velocity data to image to 30 m depth than the Rayleigh wave technique requires. The maximum wavelength Love wave phase velocity used for modeling was about 80 m, which may still not be enough to image to 30 m depth. A 60 m wavelength is the minimum wavelength Rayleigh wave phase velocity required to image to 30 m depth.
- V_{S30} from the MALW V_S model is 760 m/s (Site Class B).
- Average S-wave velocity between 1.5 m and 31.5 m from the MALW V_S model, to account for seismic sensor being located on rock 942 m/s (Site Class B). Alternatively, V_{S30} calculated after replacing the V_S of the material in the upper 1.5 m with that immediately below, again to account for the seismic station being placed on rock, is 842 m/s (Site Class B).
- V_{S30} and adjusted V_{S30} estimated from the P-wave seismic refraction models and an assumed constant Poisson's ratio of 0.3 is very similar to that estimated from the MALW sounding.
- V_{S30} and adjusted V_{S30} estimated from the S-wave seismic refraction models are about 12 to 15% higher than those from the MALW sounding. V_{S30} from the MALW sounding is similar to the lowest V_{S30} in the 25.5 to 51 m distance range on the S-wave refraction model. The predicted V_{S30} from the S-wave refraction model is also higher than that estimated from the P-wave refraction model using a Poisson's ratio of 0.25. Because the P-wave first arrival data are more accurate than the S-wave first arrival data, there may be higher error in the S-wave refraction model. S-wave refraction data quality, however, was quite good, but interpretation is more difficult.
- The MALW model has higher V_S over the 5 to 9 m depth range and lower V_S at depths greater than 15 m than the V_S models estimated from the P- and S-wave refraction models. Models could have been generated for the P- and S-wave refraction data sets with maximum V_P and V_S or 3,000 m/s and 1,600 m/s, respectively, which is closer, but still higher, than the MALW V_S model at depth. It is possible that the MALW model reflects the lower velocities (thicker weathering profile) at the northeast end of the seismic line. A longer seismic refraction line would better constrain the bedrock velocities at depth.
- For site characterization purposes, we recommend using the S-wave velocity structure derived from the MALW model, which is conservative (low) relative to that estimated from the S-wave refraction model.

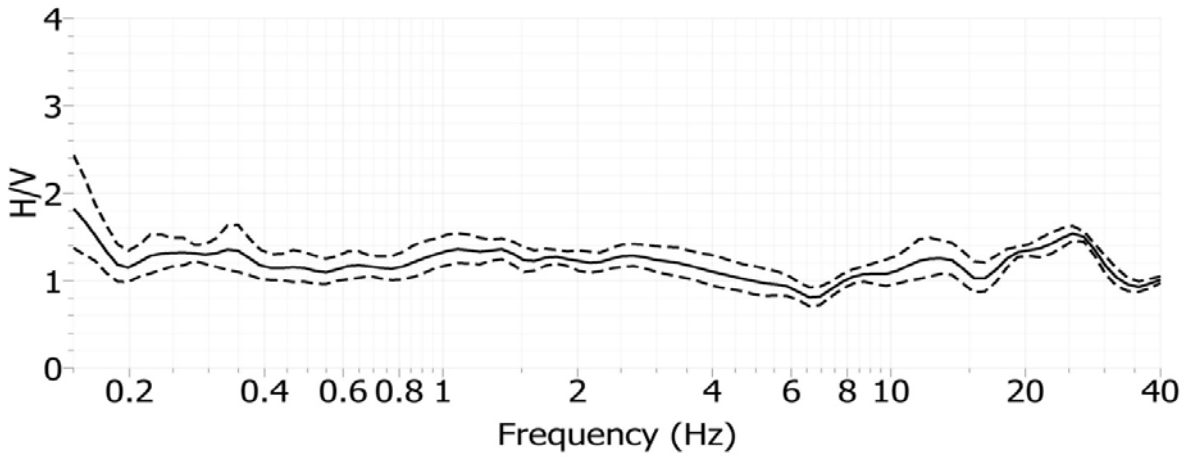

Site NC.JBNB, H/V Spectral Ratio, Array JBNB-1, Sensor 507

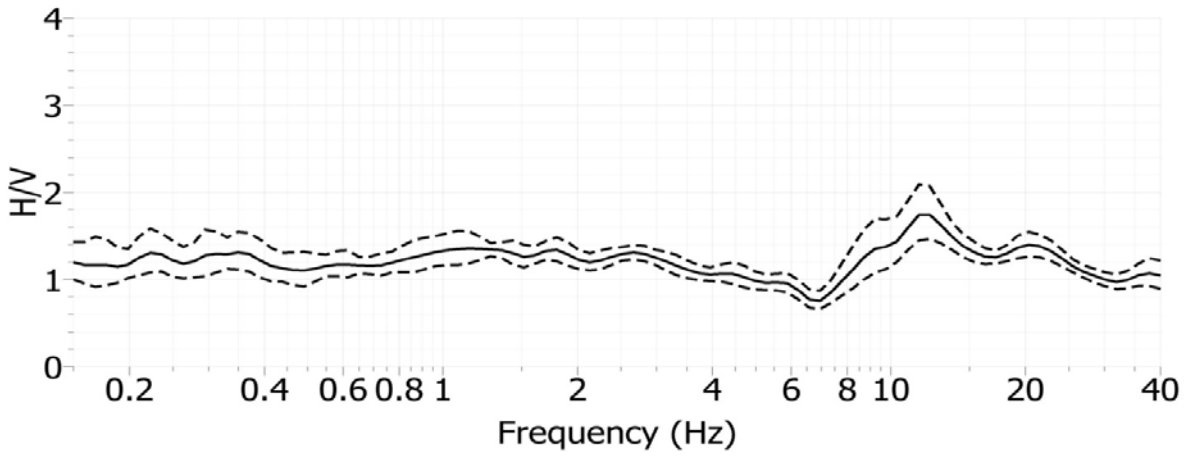

Site NC.JBNB, H/V Spectral Ratio, Array JBNB-1, Sensor 450

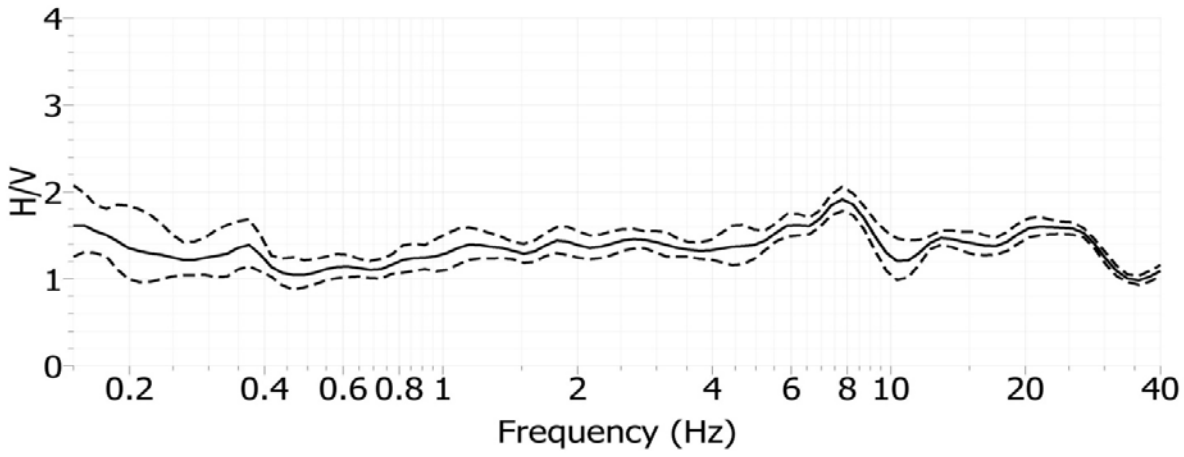

Site NC.JBNB, H/V Spectral Ratio, Near Seismic Station, Sensor 453

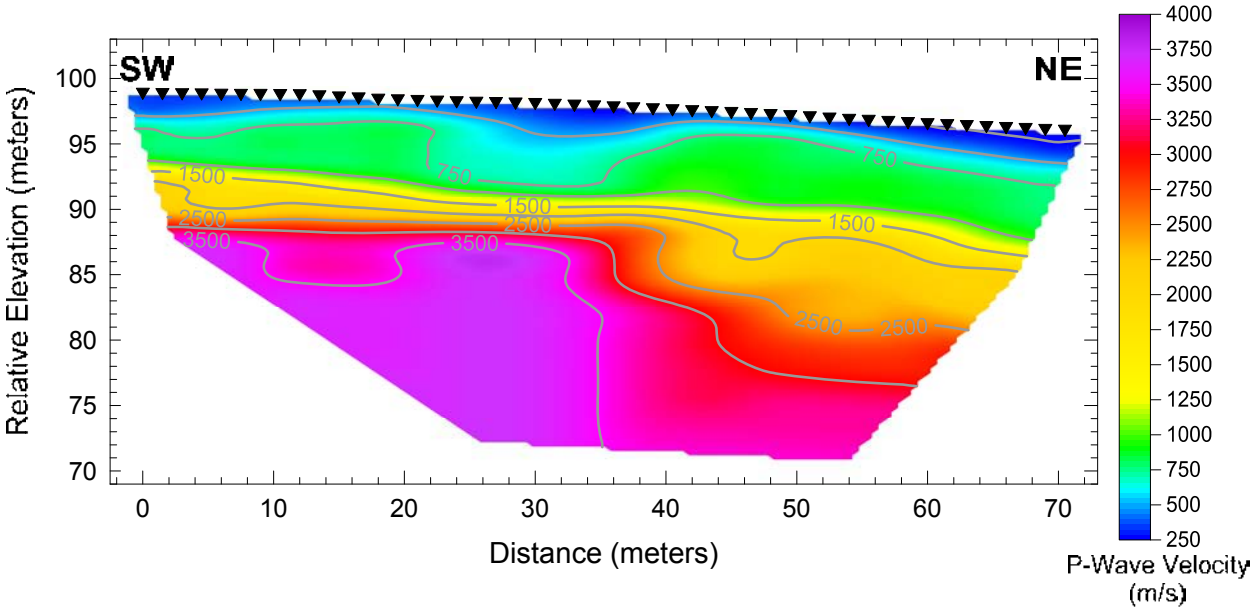

Array JBNB-1 – P-wave Tomographic Seismic Refraction Model utilizing Layer Based Starting Model

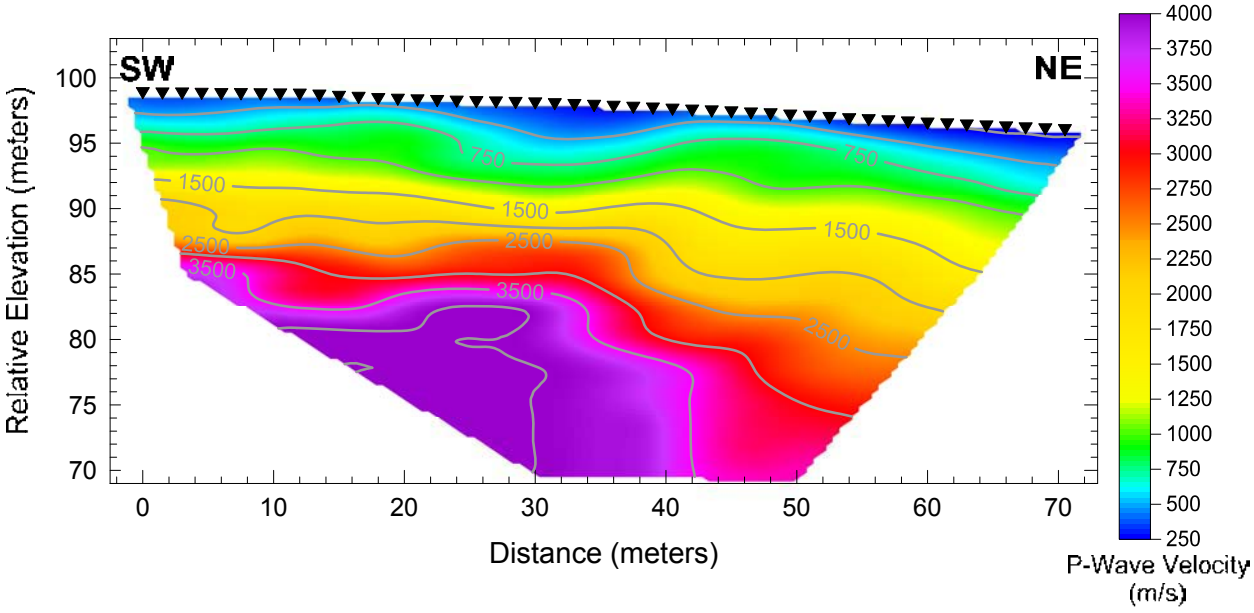

Array JBNB-1 – P-wave Tomographic Seismic Refraction Model utilizing Smooth Velocity Gradient Starting Model

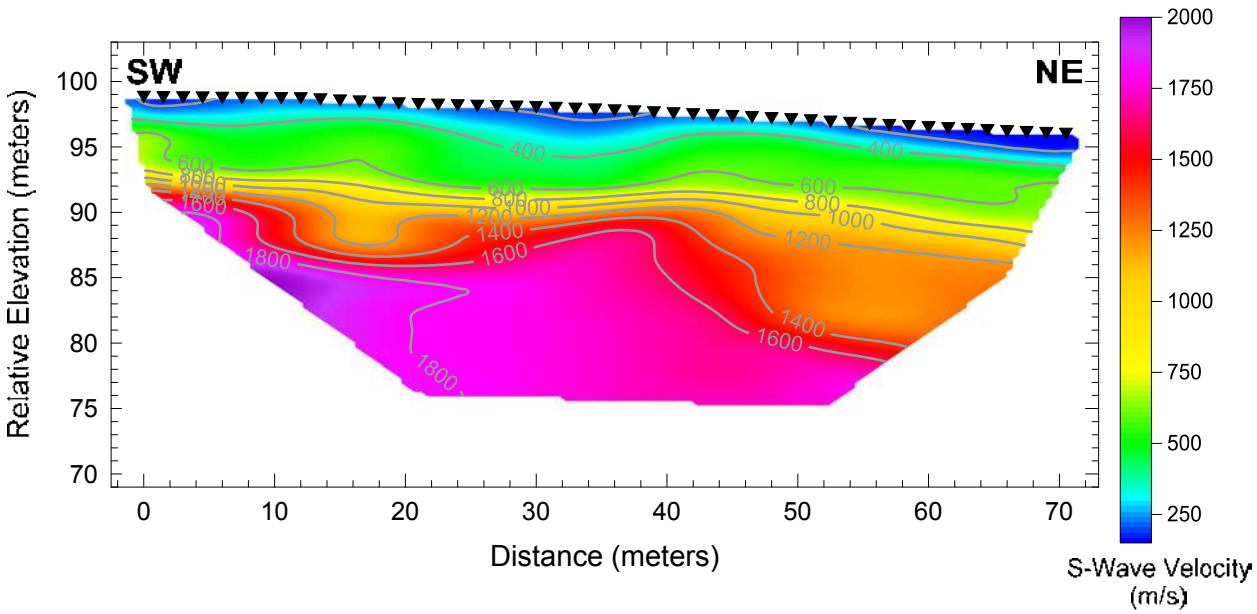

Array JBNB-1 – S-wave Tomographic Seismic Refraction Model utilizing Layer Based Starting Model

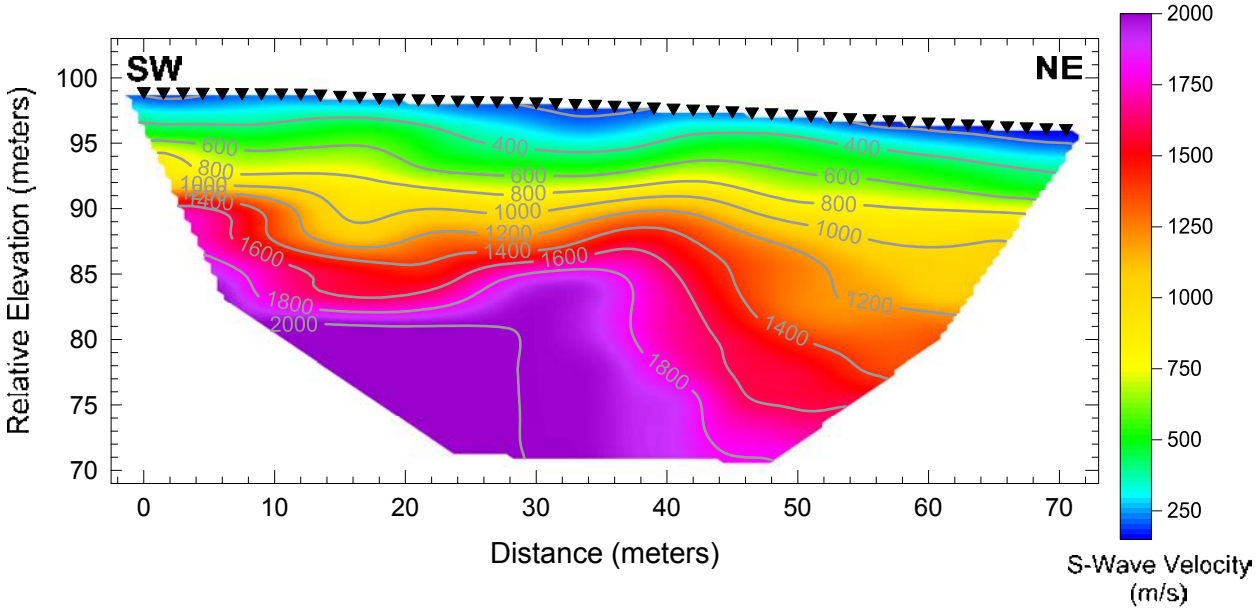

Array JBNB-1 – S-wave Tomographic Seismic Refraction Model utilizing Smooth Velocity Gradient Starting Model

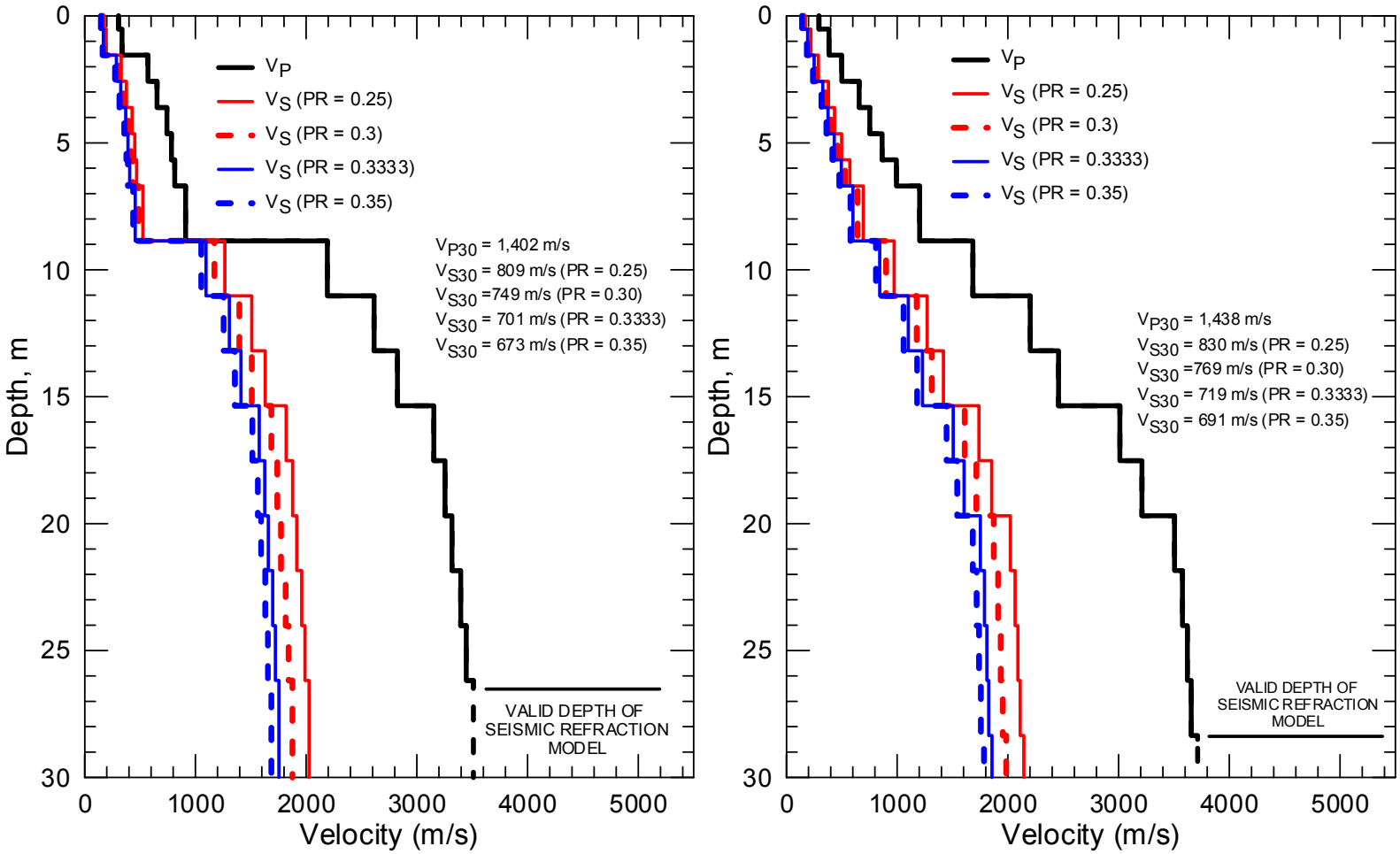

NC.JBNB – Average P-wave velocity structure and estimated S-wave velocity structure between a position of 25.5 and 51 m on the P-wave seismic refraction models for array JBNB-1 utilizing both layered (left) and smooth velocity gradient (right) starting models. Although the maximum seismic refraction depth of investigation is limited to about 26 to 28 m, P-wave velocity is very high at the bottom of the model and is not expected to increase significantly between the valid depth of investigation and 30 m. A longer seismic line would be preferred to both more accurately model the high P-wave velocities and to image to 30 m depth.

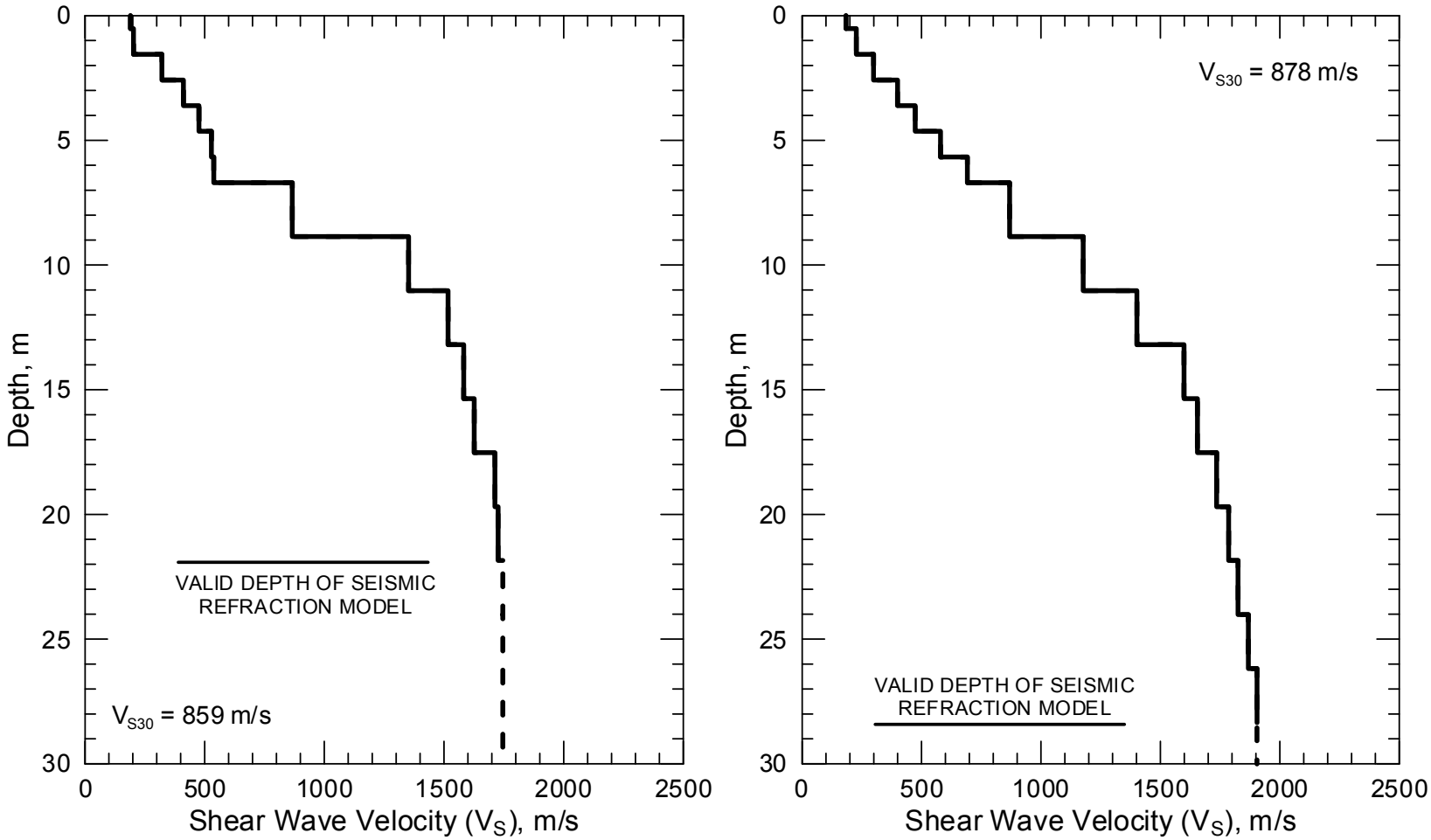

NC.JBNB – Average S-wave velocity structure between a position of 25.5 and 51 m on the S-wave seismic refraction models array JBNB-1 resulting from tomographic inversions that utilized a layered starting model (left) and smooth velocity gradient starting model (right). Although seismic refraction depth of investigation is limited to about 22 to 28 m, S-wave velocity is very high at the bottom of the model and not expected to increase significantly between the valid depth of exploration and 30 m. A longer seismic line would be preferred to both more accurately model the high S-wave velocities and to image to 30 m depth.

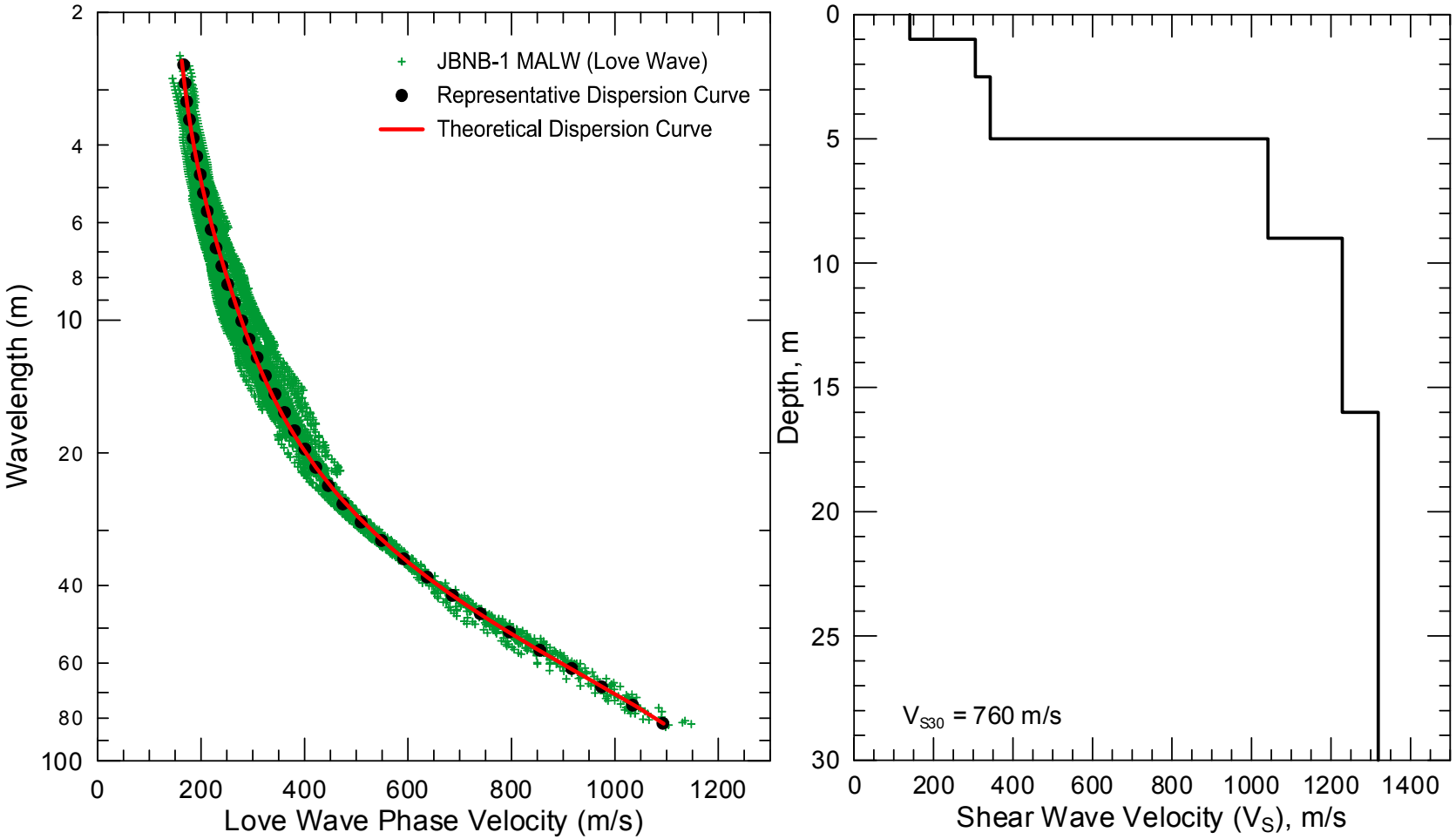

NC.JBNB - Field, representative and inverted theoretical surface wave dispersion data (left) and associated V_S model (right)

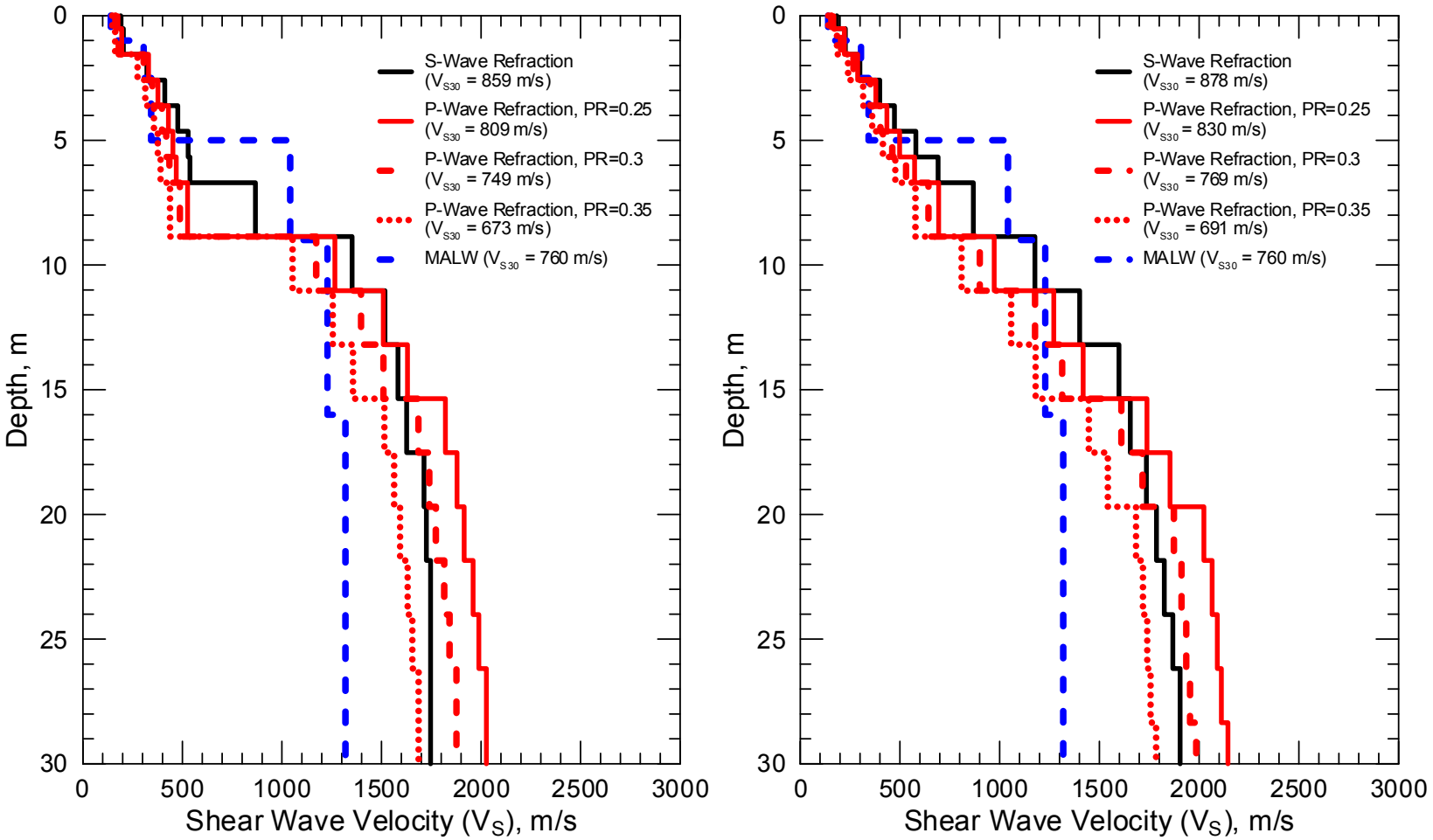

NC.JBNB – Comparison of S-wave velocity models derived from the MALW (Love wave), S-wave seismic refraction and P-wave seismic refraction surveys. Models on the left present seismic refraction models that utilized a layered starting model. Models on the right present seismic refraction models that utilized a smooth velocity gradient starting model.

Site NC.JELB

Location: Ellicott, Coastal Nursery, 117 Rancho Road, Watsonville, California

Latitude: 36.92742 **Longitude:** -121.82765
(Station coordinates modified based on field GPS survey, WGS84 coordinate system)

V_{S30} (measured): 323 m/s

V_{S30} (adjusted to more accurately reflect seismic station conditions): 323 m/s (no adjustment necessary).

NEHRP Site Class: D

Geomatrix Code: IQD

Geologic Conditions/Observations: Quaternary (Pleistocene) Aromas Sand deposits.

Site Conditions: Rural site. Test area located on relatively planar surface with elevation decreasing gently to the east and surrounded by hilly terrain.

Geophysical Methods Utilized: HVSR, MASW

Geophysical Testing Arrays:

1. Array JELB-1 (48 channel MASW array utilizing 4.5 Hz vertical geophones spaced 1.5 m apart for a length of 70.5 m, forward and reverse shot locations with multiple source offsets and source types and center shot location).
2. Three HVSR measurement locations; two distributed along JELB-1 and one near the seismic station.

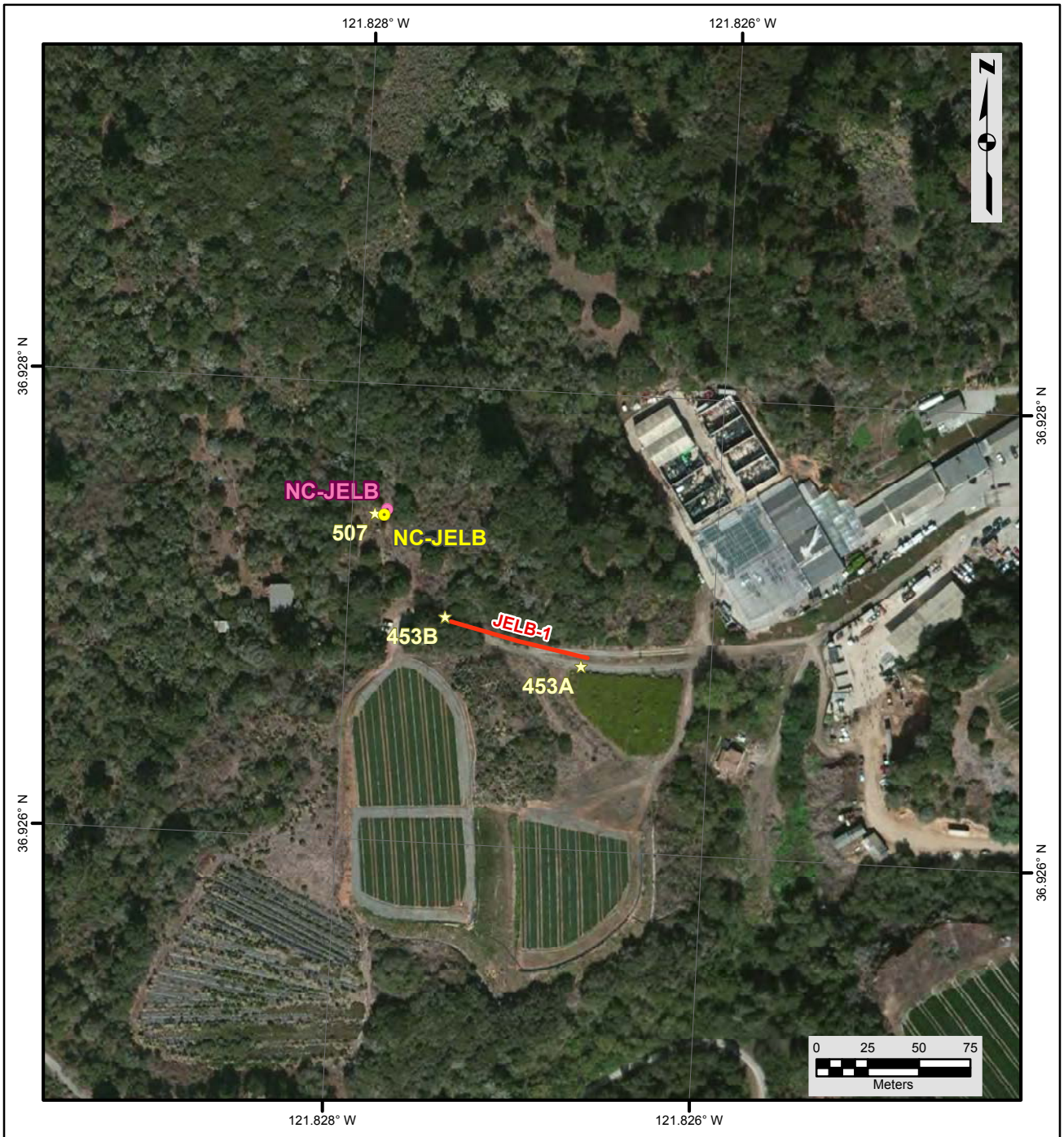

Legend

- Seismic Station - Approximate Surveyed Location
- Seismic Station - Approximate Location of Record
- H/V Spectral Ratio Location
- MASW Array

NOTES:
1. WGS 1984 COORDINATE SYSTEM
2. Image Source: ESRI, i-cubed, USDA FSA, USGS, AEX, GeoEye, Getmapping, Aerogrid, IGP

File Name: NC-JELB-I

Date: 2/7/2013

USGS science for a changing world

GEOVision geophysical services

RECOVERY.GOV

SITE MAP
NC•JELB

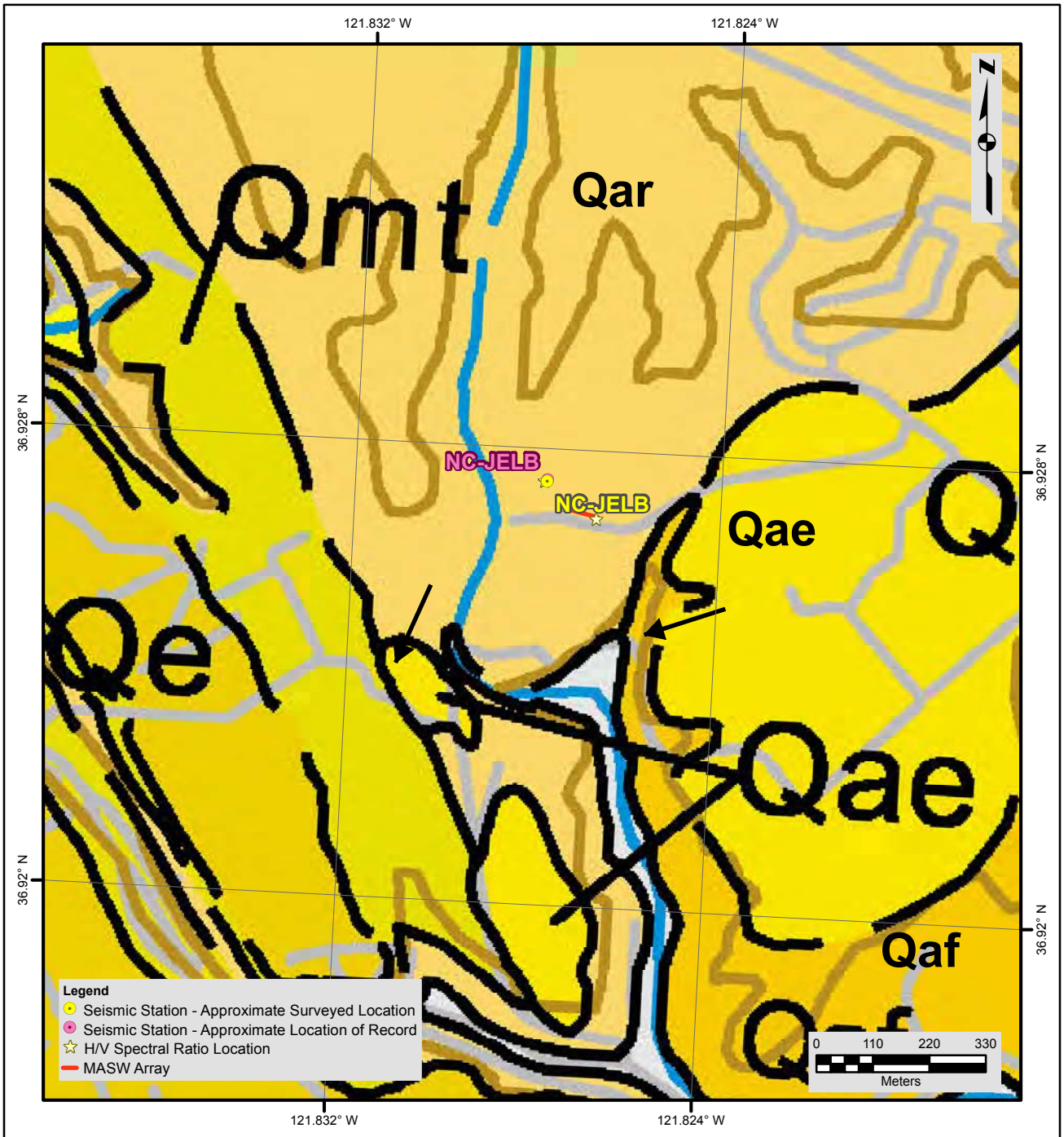

Description of Geologic Map Units

Qe = Quaternary (Holocene) eolian sand
Qmt = Quaternary (Pleistocene) marine terrace deposits, gravel, sand, silt and clay on wave cut surfaces
Qar = Quaternary (Pleistocene) Aromas Sand,clay, silt, sand and gravel, eolian and fluvial facies, undivided
Qae = Quaternary (Pleistocene) Aromas Sand, eolian facies, clay, silt, sand and gravel
Qaf = Quaternary (Pleistocene) Aromas Sand, fluvial facies, clay, silt, sand and gravel

NOTES:
1. WGS 1984 COORDINATE SYSTEM
2. Geologic Map of the Monterey 30'x60' Quadrangle and Adjacent Areas, California, compiled by David L. Wagner, H. Gary Greene, George J. Saucedo and Cynthia L. Pridmore, 2002
3. See site map for details of geophysical survey

File Name: NC-JELB

Date: 2/7/2013

USGS science for a changing world

GEOVision geophysical services

GEOLOGIC MAP
NC•JELB

RECOVERY.GOV

Looking south towards NC.JELB seismic station

HVSR sensor 289 and Tromino near NC.JELB seismic station

Looking southeast toward MASW array JELB-1 from NC.JELB seismic station

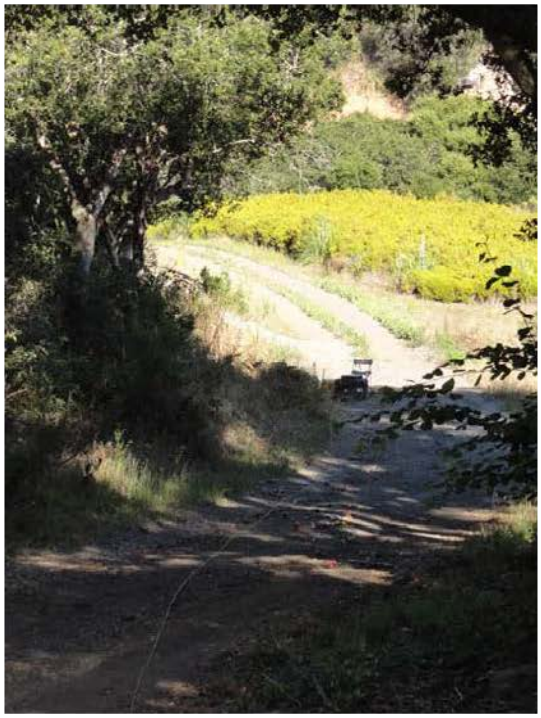

Looking east towards center of MASW array JELB-1

MASW data acquisition along array JELB-1 using 3lb hammer

Location of Geophysical Testing Arrays:

Location	Latitude	Longitude
JELB-1, West end of Array	36.92697	-121.82726
JELB-1, Center of Array	36.92690	-121.82689
JELB-1, East end of Array	36.92684	-121.82651
HVSR Sensor 507	36.92743	-121.82771
HVSR Sensor 453A	36.92681	-121.82654
HVSR Sensor 453B	36.92699	-121.82730
NC-JELB Seismic Station	36.92742	-121.82765

Notes: 1) WGS84 Coordinate System (decimal degrees)

2) Survey accuracy is estimated at 1 to 2 m.

Results:

V_S Model

Depth to Top of Layer (m)	Layer Thickness (m)	S-Wave Velocity (m/s)	Inferred P-Wave Velocity (m/s)	Assumed Poisson's Ratio	Assumed Density (g/cm^3)
0	1	201	377	0.300	1.9
1	1.5	227	425	0.300	1.9
2.5	2	283	529	0.300	1.9
4.5	10.5	326	611	0.300	1.9
15	10	322	1500	0.476	2.0
25	>5	453	1600	0.457	2.0

Observations/Discussion:

- HVSR data are almost identical at every station below a frequency of about 8 Hz, validating the 1-D velocity assumption.
- There is a clear, high amplitude HVSR peak at a frequency of about 0.26 Hz which would be associated with a large impedance contrast (e.g. bedrock) at great depth.
- Noise conditions at the site were not sufficient to apply passive surface wave techniques.
- Based on interactive, horizontal layer-based analysis of seismic refraction first arrival data, P-wave velocity structure in the upper 15 to 20 m consists of a 1.5 to 2.5 m layer with P-wave velocity in the 375 to 425 m/s range, underlain by sediments with a P-wave velocity in the 525 to 575 m/s range to a depth of about 13 to 22 m, which may be underlain by saturated sediments. The potential saturated sediment unit appears to be dipping (i.e. different apparent velocities of about 1,800 and 1,100 m/s on the forward and reverse off-end shot locations) or, alternatively, there is lateral velocity variation in the overlying sediments. There was not sufficient space at the site for the off-end shots required to more accurately characterize the possible saturated sediment unit. A high amplitude reflection also occurs from the possible water table.
- There is about 25 m/s scatter in the MASW dispersion data, which may be partially associated with lateral velocity variation.
- A representative dispersion curve was generated for the combined MASW data set using a moving average, polynomial curve fitting routine and used for modeling.
- Water table depth constrained to about 15 m based on seismic refraction analysis discussed above (1,500 to 1,600 m/s V_P for saturated sediments).
- Surface wave depth of investigation is about 30 m based on half of maximum wavelength criteria.
- The inferred P-wave velocities in surface wave model, based on an assumed Poisson's ratio of 0.3 and modeled S-wave velocity, are consistent with simplified P-wave refraction model.
- V_{S30} is 323 m/s (Site Class D).

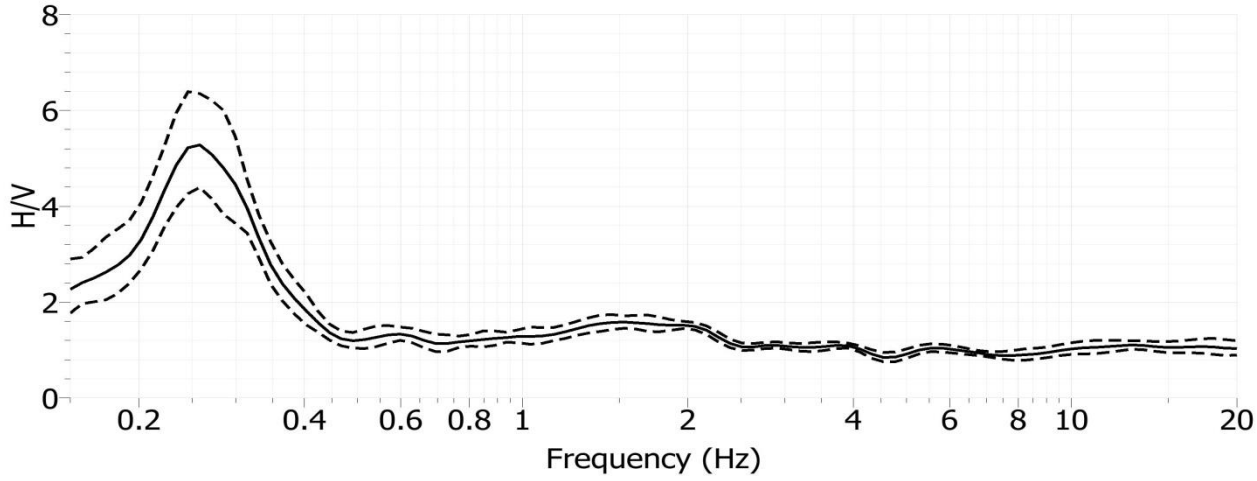

Site NC.JELB, H/V Spectral Ratio, Near Seismic Station, Sensor 507

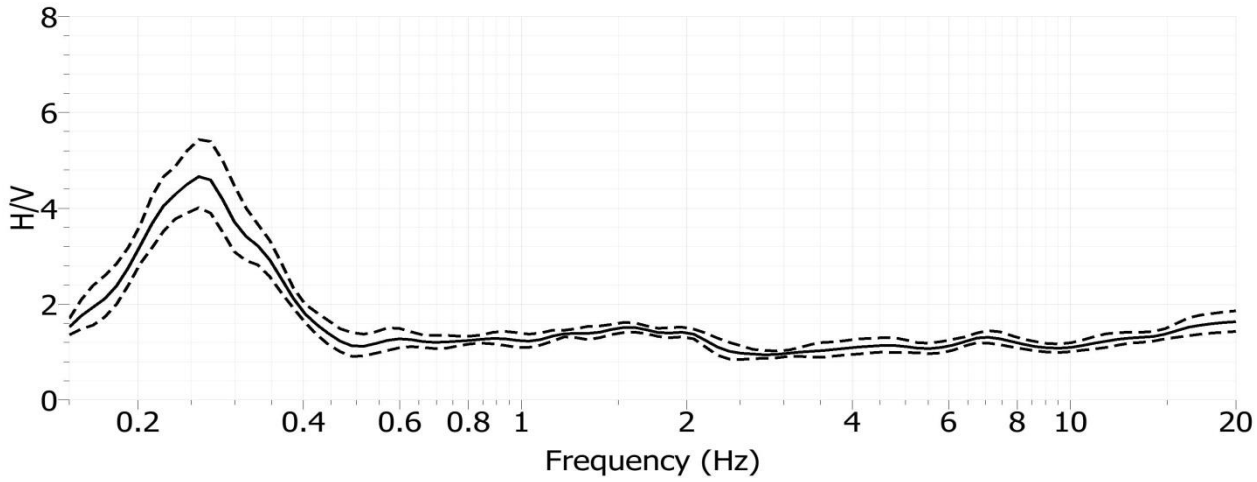

Site NC.JELB, H/V Spectral Ratio, Array JELB-1, Sensor 453B

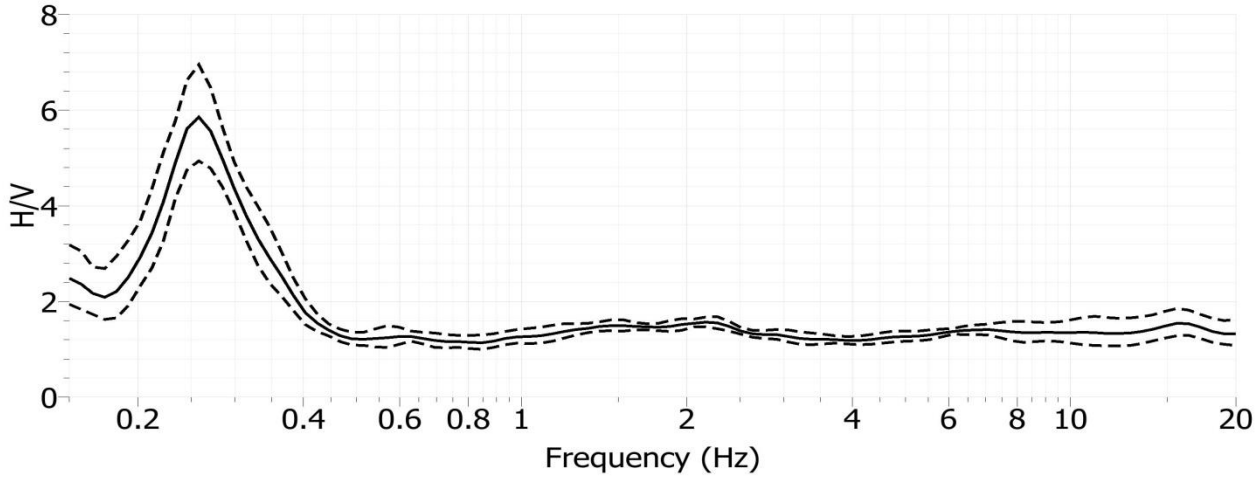

Site NC.JELB, H/V Spectral Ratio, Array JELB-1, Sensor 453A

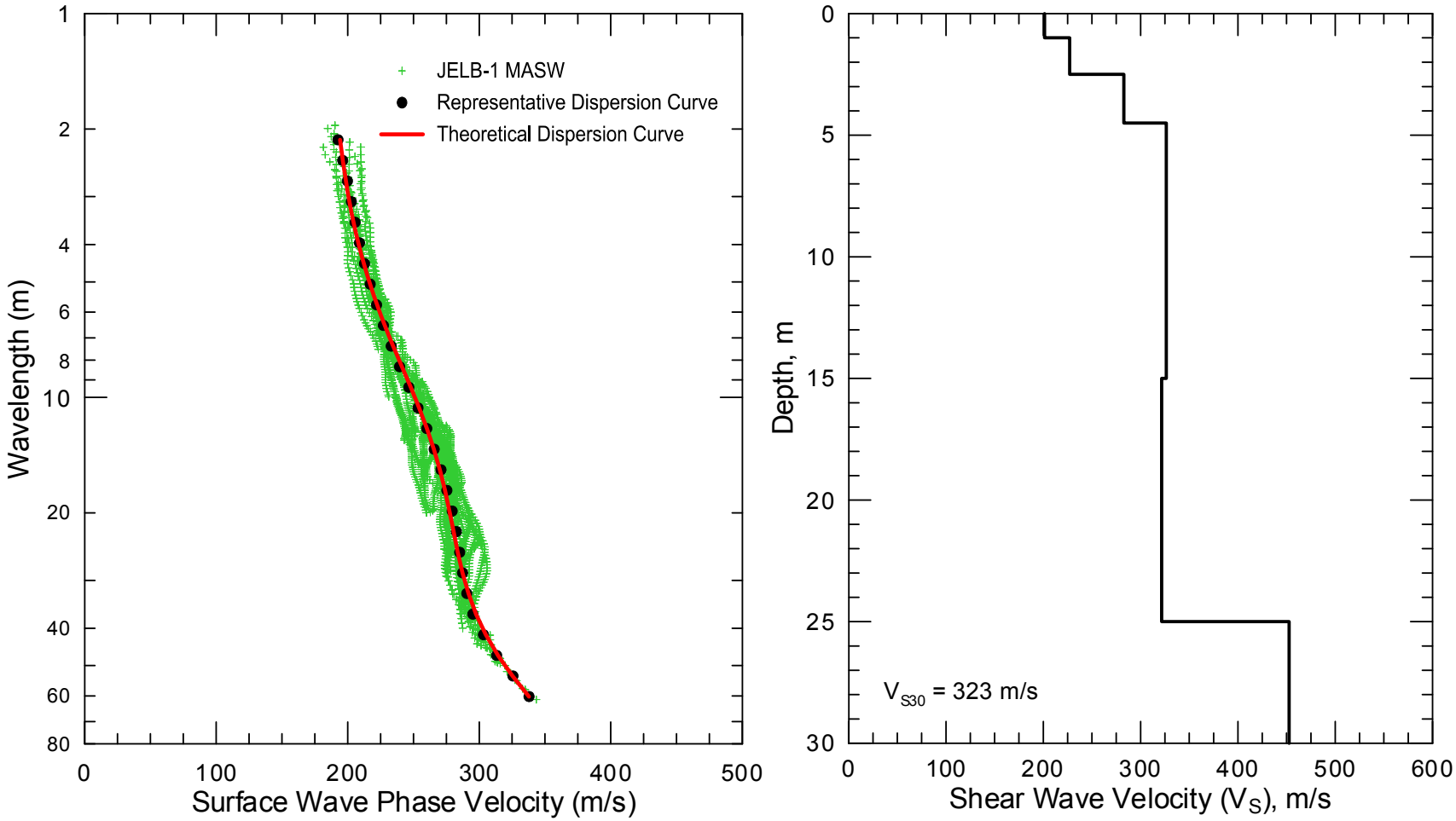

NC.JELB - Field, representative and inverted theoretical surface wave dispersion data (left) and associated V_S model (right)

Site NC.JFP

Location: Foothills Park, Santa Clara County, California

Latitude: 37.36045 **Longitude:** -122.18986
(Station coordinates provided by USGS, WGS84 coordinate system)

V_{S30} (measured): 437 m/s

V_{S30} (adjusted to more accurately reflect seismic station conditions): 456 m/s (average S-wave velocity between 0.5 and 30.5 m to account for assumed seismic sensor depth).

NEHRP Site Class: C

Geomatrix Code: IFB

Geologic Conditions/Observations: Seismic station located on geologic unit mapped as Mesozoic (Jurassic and Cretaceous) Franciscan Assemblage, greenstone unit. The San Andreas Fault Zone is located about 1 km southwest of the site and the Adobe Creek fault is located about 0.4 km northeast of the site.

Site Conditions: Rural site located on the ridge of a hill. Undulating, hilly topography in the site vicinity. There is about a 6 m increase in ground surface elevation to the southwest along the 117.5 m long array JFP-2.

Geophysical Methods Utilized: HVSR, Seismic Refraction (P- and S-wave), MASW (Rayleigh Wave) and MALW (Love Wave)

Geophysical Testing Arrays:

1. Array JFP-1 (48 channel MASW and P-wave seismic refraction array utilizing 4.5 Hz vertical geophones spaced 1.5 m apart for a length of 70.5 m, forward and reverse shot locations with multiple source offsets and source types (hammers only) and multiple interior shot locations).
2. Array JFP-2 (48 channel P and S-wave seismic refraction, MASW and MALW array utilizing 4.5 Hz vertical/horizontal geophones spaced 2.5 m apart for a length of 117.5 m, forward and reverse shot locations with multiple source offsets and source types and multiple interior shot locations).
3. Three HVSR measurement locations: two along array JFP-1 and the other near the seismic station.

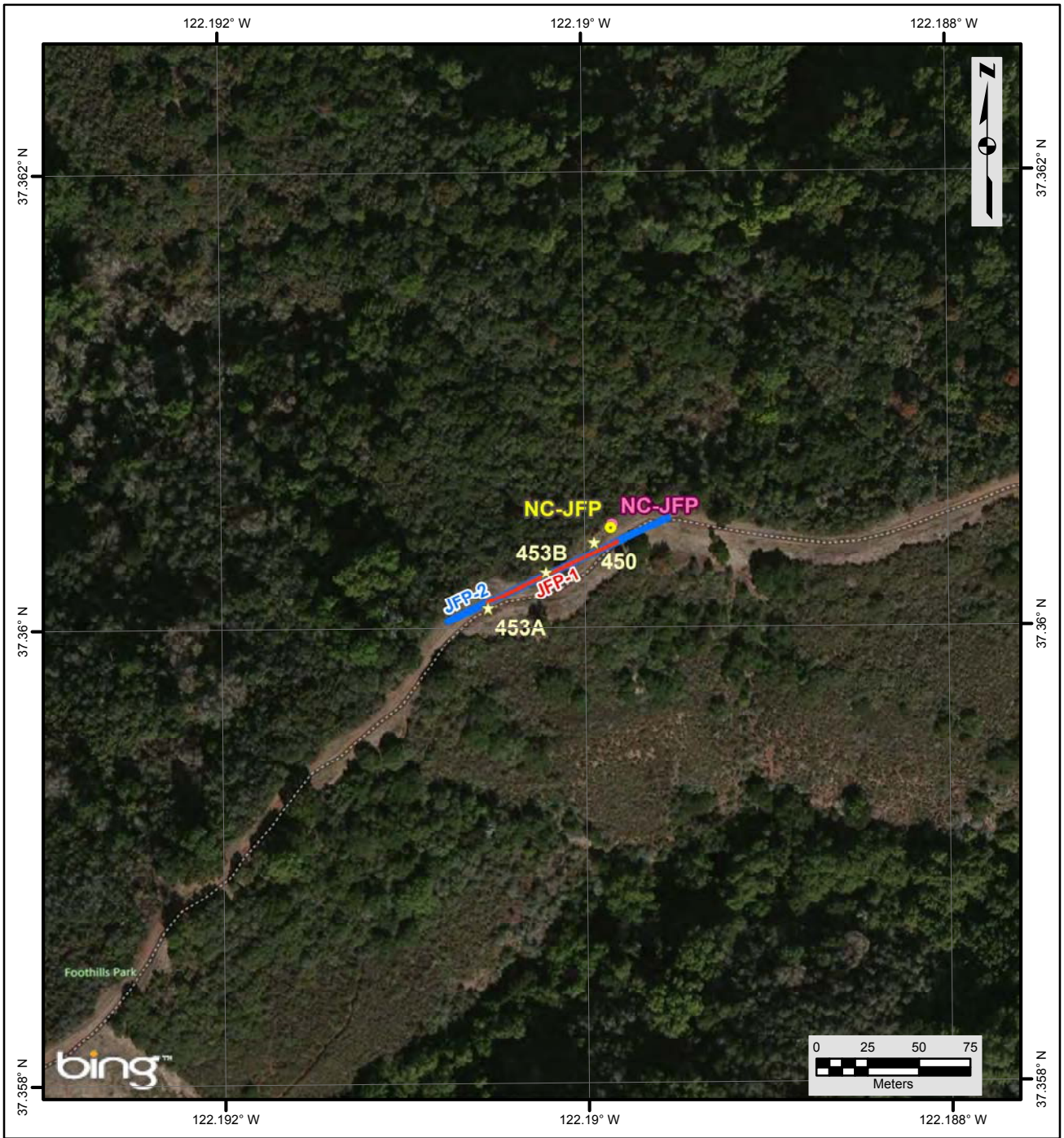

Legend

- Seismic Station - Approximate Surveyed Location
- Seismic Station - Approximate Location of Record
- H/V Spectral Ratio Location
- MASW and Seismic Refraction Array
- MASW and Seismic Refraction Array (P- and S-wave)

NOTES:
1. WGS 1984 COORDINATE SYSTEM
2. Image Source: (c) Microsoft Corporation and its data suppliers

File Name: NC-JFP-I

Date: 10/11/2012

USGS science for a changing world

GEOVision geophysical services

RECOVERY.GOV

SITE MAP
NC•JFP

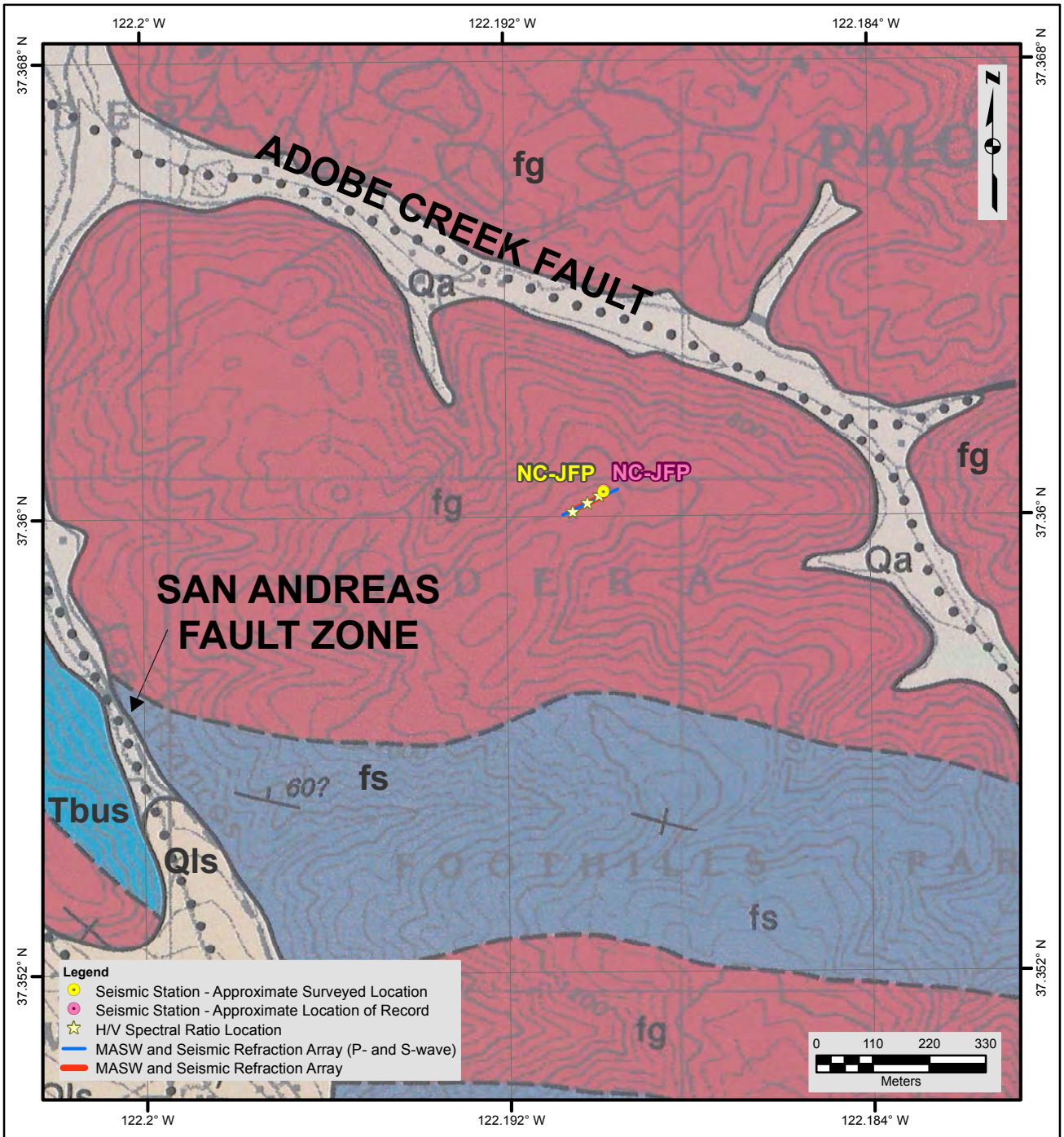

Description of Geologic Map Units

Qa = Quaternary (Holocene) alluvial gravel, sand and clay of valley areas
Qls = Quaternary (Pleistocene to Holocene) landslide rubble
Tbus = Tertiary (Eocene) Butano Formation; sandstone, lithified, massive, hard
fg = Mesozoic (Jurassic and Cretaceous) Franciscan Assemblage; greenstone, massive, amorphous, locally brecciated, interstratified with fs
fs = Mesozoic (Jurassic and Cretaceous) Franciscan Assemblage; graywacke sandstone or metagraywacke, hard, coherent but fractured, massive to bedded

NOTES:
1. WGS 1984 COORDINATE SYSTEM
2. Geologic Map of the Mindego Hill Quadrangle San Mateo, Santa Clara and Santa Cruz Counties, California by Thomas W. Dibblee, Jr., 2007
3. See site map for details of geophysical survey

USGS science for a changing world

GEOVision geophysical services

GEOLOGIC MAP
NC•JFP

RECOVERY.GOV

File Name: NC-JFP

Date: 10/11/2012

NC.JFP seismic station

Looking northeast along array JFP-1 and at HVSR sensor 453A

Looking southwest along array JFP-1

Looking northeast along S-wave seismic refraction and MALW array JFP-2

Looking northeast along array JFP-2 towards seismic station

Location of Geophysical Testing Arrays:

Location	Latitude	Longitude
JFP-1, Southwest End of MASW/Refraction Array	37.36011	-122.19055
JFP-1, Center of MASW/Refraction Array	37.36021	-122.19023
JFP-1, Northeast End of MASW/Refraction Array	37.36037	-122.18983
JFP-2, Southwest End of MASW/Refraction Array	37.36001	-122.19081
JFP-2, Center of MASW/Refraction Array	37.36024	-122.19021
JFP-2, Northeast End of MASW/Refraction Array	37.36046	-122.18961
HVSR Sensor 450	37.36037	-122.18996
HVSR Sensor 453A	37.36008	-122.19054
HVSR Sensor 453B	37.36024	-122.19022
NC.JFP Seismic Station	37.36044	-122.18987

Notes: 1) WGS84 Coordinate System (decimal degrees)
2) Survey accuracy is estimated at 1 to 2 m.

Results:

V_S Model (MALW Array)

Depth to Top of Layer (m)	Layer Thickness (m)	S-Wave Velocity (m/s)	Inferred P-Wave Velocity (m/s)	Assumed Poisson's Ratio	Assumed Density (g/cm^3)
0	0.5	140	262	0.3	1.7
0.5	1.5	237	443	0.3	1.8
2	3	239	448	0.3	1.8
5	5	374	700	0.3	1.9
10	7	501	937	0.3	2.0
17	8	634	1187	0.3	2.1
25	>5	793	1483	0.3	2.1

Notes: 1) Depth of investigation is about 30 to 35 m.
2) Bottom layer is a half space.
3) Half space V_S not well resolved.

Average V_P and Estimated V_S Models from Central Portion of P-wave Seismic Refraction Line

Depth to Top of Layer (m)	Layer Thickness (m)	P-Wave Velocity (m/s)	Estimated S-Wave Velocity (m/s)				
			Poisson's Ratio = 0.25	Poisson's Ratio = 0.3	Poisson's Ratio = 0.35	Poisson's Ratio = 0.4	Poisson's Ratio = 0.45
0.00	0.55	289	167	154	139	118	87
0.55	1.10	497	287	266	239	203	150
1.65	1.10	546	315	292	262	223	165
2.75	1.10	586	338	313	281	239	177
3.85	1.10	656	379	351	315	268	198
4.95	1.10	733	423	392	352	299	221
6.05	1.10	803	464	429	386	328	242
7.15	2.31	899	519	480	432	367	271
9.46	2.31	1079	623	577	518	440	325
11.77	2.31	1135	656	607	545	464	342
14.08	2.31	1240	716	663	596	506	374
16.39	2.31	1382	798	739	664	564	417
18.70	2.31	1632	942	872	784	666	492
21.01	2.31	1666	962	891	801	680	502
23.32	2.31	1683	972	900	808	687	507
25.63	Half Space	1708	986	913	820	697	515

Observations/Discussion:

- Field testing was conducted at this site on two occasions. During the first site visit on 7/7/11, P-wave seismic refraction and MASW data were acquired along the 70.5 m long array JFP-1. HVSR data were also acquired at this time. After preliminary review of the data, it was determined that the MASW interpretation could be very difficult due to lateral velocity variation and possible dominant higher modes. Therefore, P- and S-wave seismic refraction and MALW data were acquired along the 117.5 m long array JFP-2 on 11/15 and 11/16/2011. Because the site is located in a county park, testing was required to be conducted along the dirt road next to the seismic station. There were no alternate test locations in close proximity to the seismic station.
- The HVSR plots at the three measurement locations are similar. There are no high amplitude HVSR peaks; however, there is a weak, but inconclusive peak in the 4.5 to 5 Hz range at each of the measurement locations.
- The P-wave first arrival data were of good quality. The air wave arrives before the direct soil arrival on some P-wave refraction shot records and picking the later arrival was occasionally problematic. Lateral velocity variation is clearly evident on many of the seismic records; however, there were no alternate test locations in close proximity to the seismic station. S-wave seismic refraction data quality is not considered good enough to

model at this time; however, it was possible to reduce and model MALW data. S-wave seismic refraction does seem to indicate, however, that the saturated zone is not present in the upper 30 m.

- The P-wave refraction data for array JFP-2 were modeled using a tomographic inversion routine with a smooth velocity gradient starting model. Seismic refraction data collected along array JFP-1 were not modeled as the array is collocated with array JFP-2.
- The P-wave seismic refraction survey design for array JFP-2 allowed P-wave velocity to be imaged to a maximum depth of about 25 m. P-wave velocity is about 250 to 450 m/s at the surface, increasing to 1,000 m/s at a depth of 8 to 14 m and over 1,500 m/s at a depth of about 10 to 22 m. The maximum P-wave velocity in the seismic refraction model is 1,800 m/s. A P-wave velocity of 1,800 m/s could be associated with saturated sediments/soft rock or harder, unsaturated rock. Although not modeled, the S-wave seismic refraction seems to indicate that the rock is not saturated.
- There is significant lateral velocity variation beneath the seismic line, which likely contributed to MASW data being too difficult to analyze and complicated MALW interpretation.
- The average P-wave velocity of the upper 30 m (V_{P30}) was estimated between 30 and 87.5 m on the P-wave refraction model for array JFP-2. V_{P30} ranges from about 933 to 1,072 m/s over this interval; a 14% variation. V_{P30} is similar towards each end of the array and lower in the central portion of the array.
- An average V_P model was developed over the 30 to 87.5 m distance interval by horizontally averaging the travel time of each model cell and cell thickness and average V_{P30} was determined to be 1,014 m/s. Assuming constant Poisson's ratios of 0.25, 0.3, 0.35 and 0.4 would result in an estimated V_{S30} of 586, 542, 487 and 414 m/s, respectively. Bedrock is not expected to be saturated in the upper 30 m, therefore, Poisson's ratio in the 0.3 to 0.35 range is probable.
- Noise conditions at the site were not sufficient for application of passive surface wave techniques.
- Review of Rayleigh wave (MASW) data indicated that analysis would be very difficult due to the lateral velocity variation and possible dominant higher modes on some seismic records. Although not modeled, the MASW data were screened to determine the approximate range for the Rayleigh wave phase velocity at a wavelength of 40 m (V_{R40}). V_{R40} was typically found to vary from about 400 to 525 m/s. The Brown, et al. (2000) relationship between V_{R40} and V_{S30} would, therefore, indicate that V_{S30} could be in the 418 to 549 m/s range, which is consistent with the P-wave seismic refraction data for realistic Poisson's ratio in the 0.3 to 0.4 range.
- The Love wave (MALW) data also suffered from lateral velocity variation, but dominant higher modes were not an issue. Therefore, the MALW data collected along array JFP-2 were used for site characterization.
- There is significant scatter in the MALW dispersion data at wavelengths less than 35 m, which is due to the lateral velocity variation observed in the seismic refraction models. There is much less lateral velocity variation at longer wavelengths, but this is primarily due to the use of longer receiver arrays to generate the long wavelength Love wave dispersion data. However, the fact that long wavelength Love wave data from forward and reverse shot location does not diverge at long wavelengths seems to indicate that the lateral velocity variation at depth averages out over long distances rather than the velocity

structure having an effective dip. Small wavelength Love wave dispersion data extracted from limited offset receiver arrays and source locations at the southwest end of the array appear to be more consistent with longer wavelength phase velocity data. Several interior source locations in the central portion of the array yielded lower phase velocities at small wavelengths and are likely associated with the lower near surface P-wave velocities between 55 and 85 m on the seismic refraction model. Small wavelength Love wave dispersion data extracted from source locations at the northeast end of the array typically had higher phase velocities, possibly due to the higher near surface velocities in the vicinity of 30 m on the P-wave seismic refraction model. Only small wavelength Love wave dispersion data that tied into longer wavelength dispersion data were used to develop a V_S model. This dispersion curve consisted of all dispersion data extracted from source locations at both ends of the array with receiver gathers of at least 36 geophones, small wavelength Love wave dispersion data from limited offset receiver gathers associated with source locations at the southwest end of the array, and small wavelength Love wave dispersion data from interior source locations that was consistent with the above.

- There is about 40 to 50 m/s scatter in the final dispersion curve selected for modeling; whereas there was up to about 150 m/s scatter at small wavelengths in the complete Love wave phase velocity data set.
- The maximum wavelength extracted from the MALW data was set equal to the lesser of 110 m or 1.4 times the distance between the source and center of receiver array. There is little information available on near field effects in MALW data, but as the particle motion is orthogonal to direction of propagation, near field effects may be less that typically observed for Rayleigh waves. The real limitation of the MALW technique, relative to the MASW technique, is the unavailability of cost effective low frequency energy sources and that longer wavelengths (lower frequencies) appear to be required to image to a specific depth.
- The minimum wavelength surface wave phase velocity data extracted from the 48-channel MALW array is about 22 m. Data reduction using limited maximum offset receiver arrays (i.e. less active geophones) allowed extraction of surface wave dispersion data to a minimum wavelength of about 2.5 m.
- A representative dispersion curve was generated for the final edited MALW data set using a moving average, polynomial curve fitting routine and used for modeling.
- Although the minimum wavelength in the Love wave dispersion data is 2.5 m, a thin 0.5 m thick low velocity layer was permitted in the V_S model based on the seismic refraction model. Under normal conditions, a 2.5 m minimum wavelength would dictate a nominal 1 m thickness of the surface layer in the model.
- Surface wave depth of investigation is about 30 to 35 m based on a third of maximum wavelength. It appears that longer wavelength Love wave phase velocity data are needed to image to 30 m than for Rayleigh waves.
- V_{S30} derived from the Love wave V_S model is 437 m/s (NEHRP Site Class C).
- The average S-wave velocity between 0.5 and 30.5 m, to account for assumed sensor depth and the fact that the sensor is not placed on loose sediments, is 456 m/s (NEHRP Site Class C).
- V_{S30} derived from the Love wave V_S model is consistent with that derived from the estimated S-wave velocity model derived from the average P-wave refraction model and

an assumed constant Poisson's ratio of between 0.35 and 0.4. Poisson's ratio of 0.35 to 0.4 would seem a little high and the possibility should be considered that the MALW Vs model is trending towards the lower velocities beneath the array. The MALW V_S model is consistent with the lower values of V_{S30} estimated from V_{R40} observed in the MASW data. It is possible that the higher values of V_{R40} are associated with dispersion data affected by higher modes, in which case the MASW and MALW data would be consistent. It should also be noted that selective use of small wavelength Love wave dispersion data has skewed the resulting V_S model to lower near surface velocities. More research is needed on the effects of lateral velocity variation on V_S models developed using surface wave techniques.

- Based on P-wave seismic refraction data, there is likely a minimum of 15% variation in V_{S30} in the vicinity of the seismic station. The MALW V_S model may reflect the lower bound of V_{S30} in the site vicinity. Regardless of lateral velocity variation, V_{S30} in the vicinity of the seismic station is in low to intermediate velocity range within NEHRP Site Class C.
- The weak HVSR peak in the 4.5 to 5.5 Hz range is consistent with the top of the higher velocity rock in the seismic refraction and MALW models at depths on the order of 15 to 22 m.
- The seismic refraction technique (both P- and S-wave) has been shown to be effective at mapping lateral velocity variation and could be used to identify areas where velocity structure is relatively 1-D in nature. Testing could be conducted along shorter MASW, MALW or SASW arrays in such areas to obtain more valid V_S models.

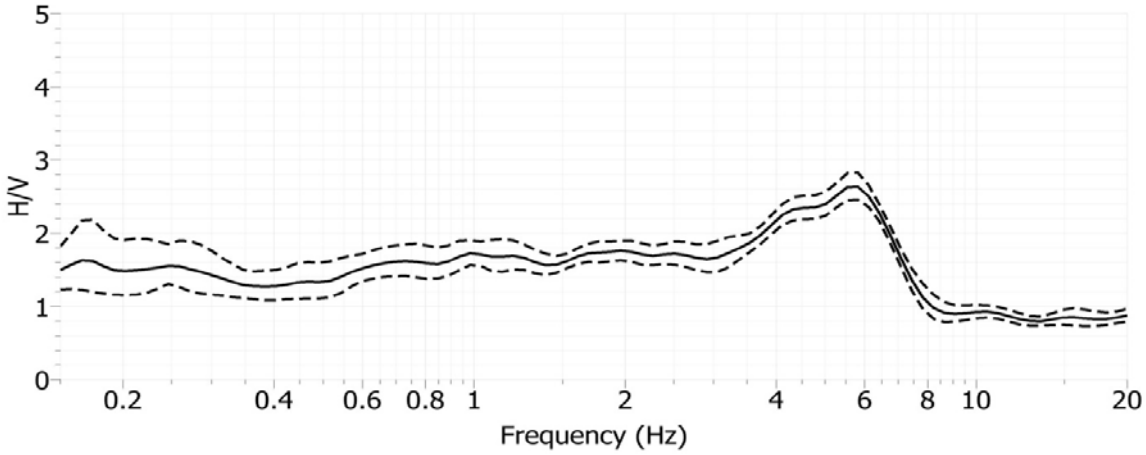

Site NC.JFP, H/V Spectral Ratio, Array JFP-1, Sensor 453A

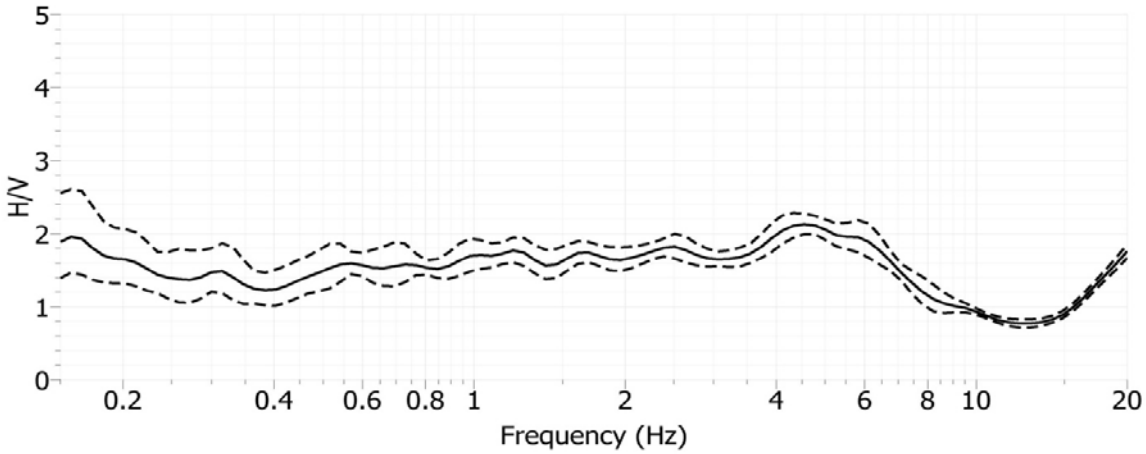

Site NC.JFP, H/V Spectral Ratio, Array JFP-1, Sensor 453B

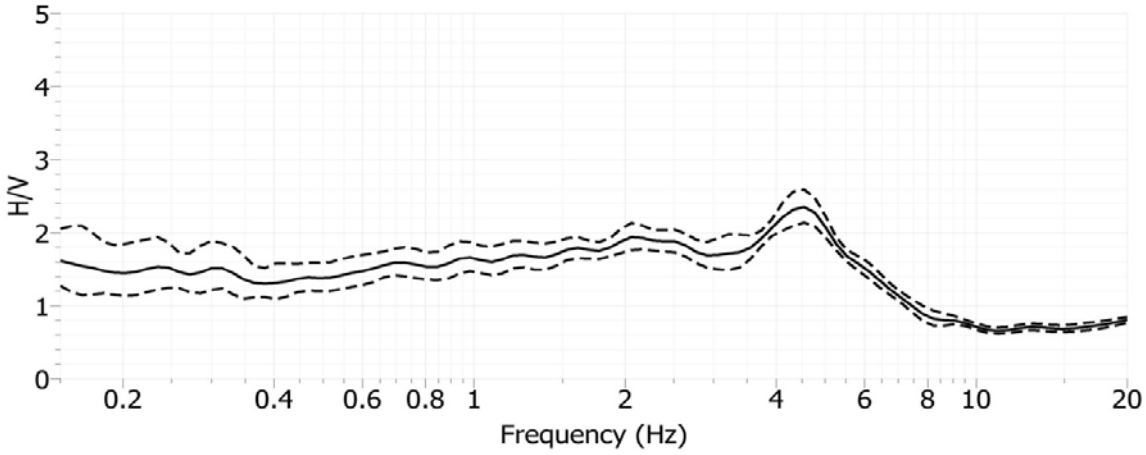

Site NC.JFP, H/V Spectral Ratio, Near Seismic Station, Sensor 450

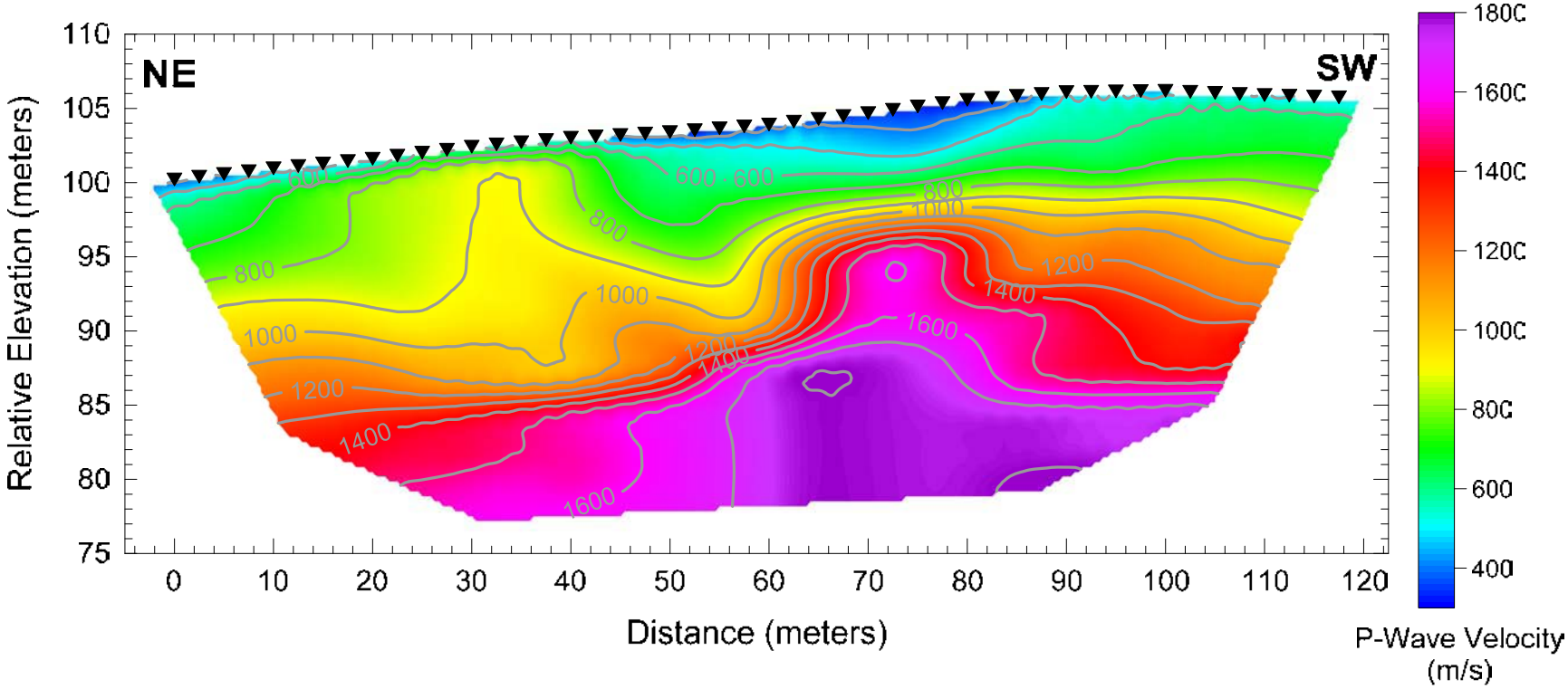

Array JFP-2 – Tomographic seismic refraction model developed using a smooth velocity gradient starting model

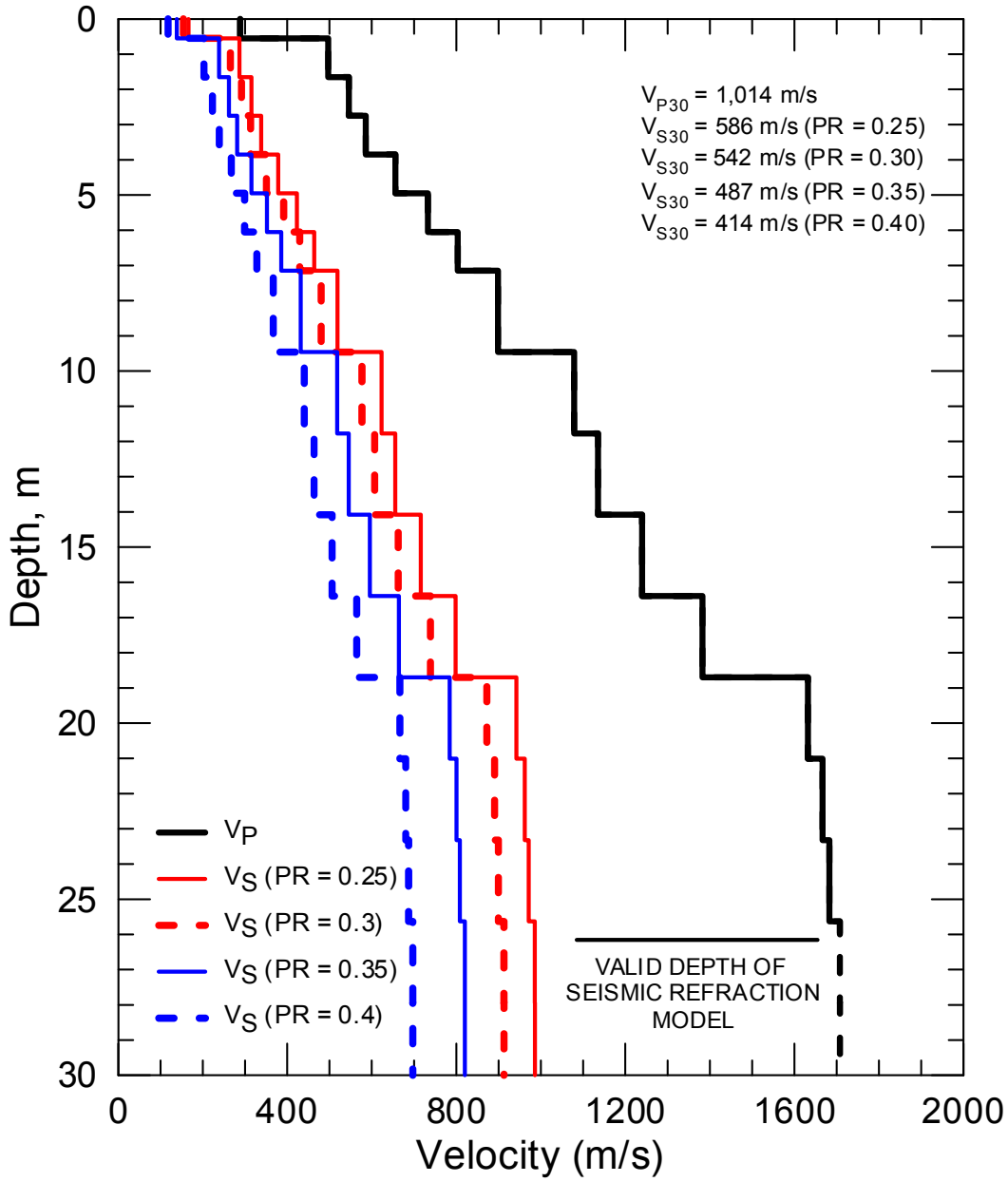

NC.JFP – Average P-wave velocity and estimated S-wave velocity between 30 and 87.5 m on P-wave seismic refraction array JFP-2

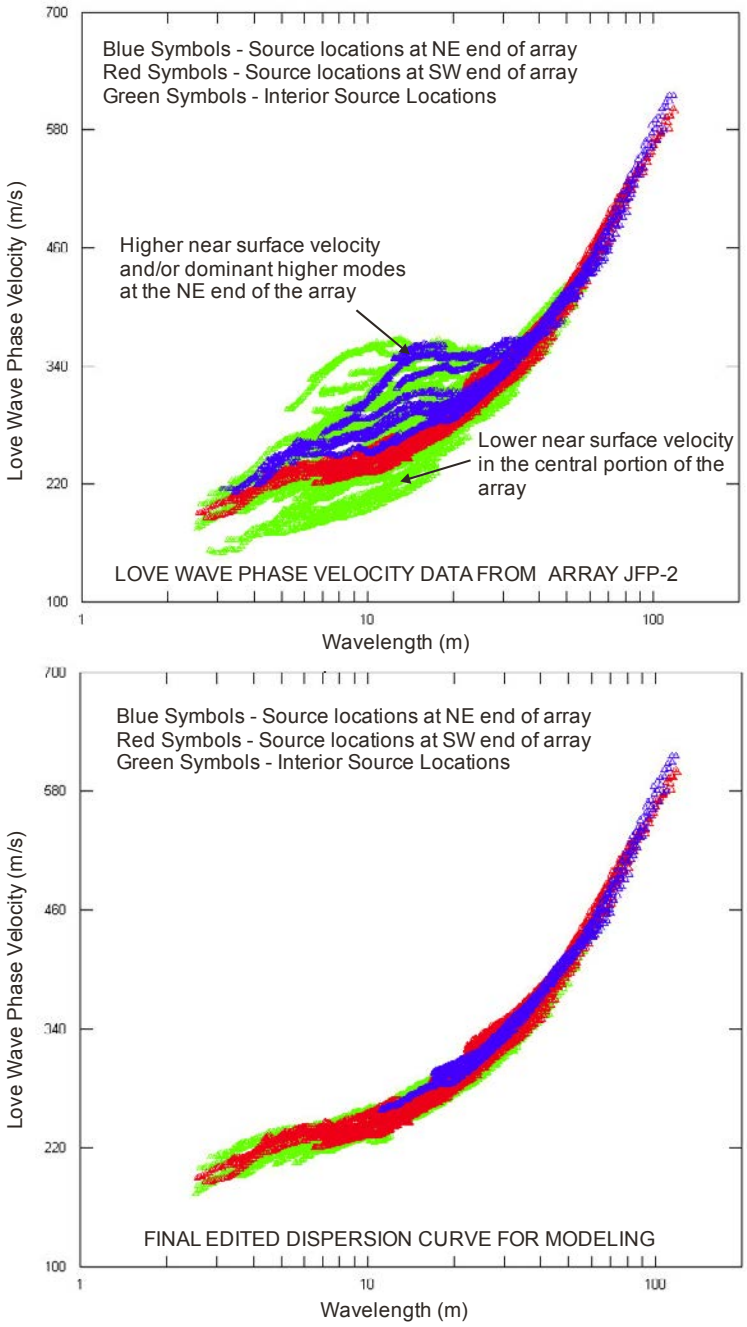

NC.JFP – MALW dispersion data from array JFP-2 illustrating the effects of near surface lateral velocity variation and/or dominant higher modes (top) and the final dispersion curve selected for modeling (bottom). The significant scatter in the Love wave dispersion data occurs at wavelengths less than 35 m. The final dispersion curve consisted of small wavelength dispersion data from small offset range receiver gathers with source locations at the southwest end of the array supplemented by dispersion data from interior seismic refraction source locations and long wavelength dispersion data from large offset range receiver gathers with source locations at both ends of the array.

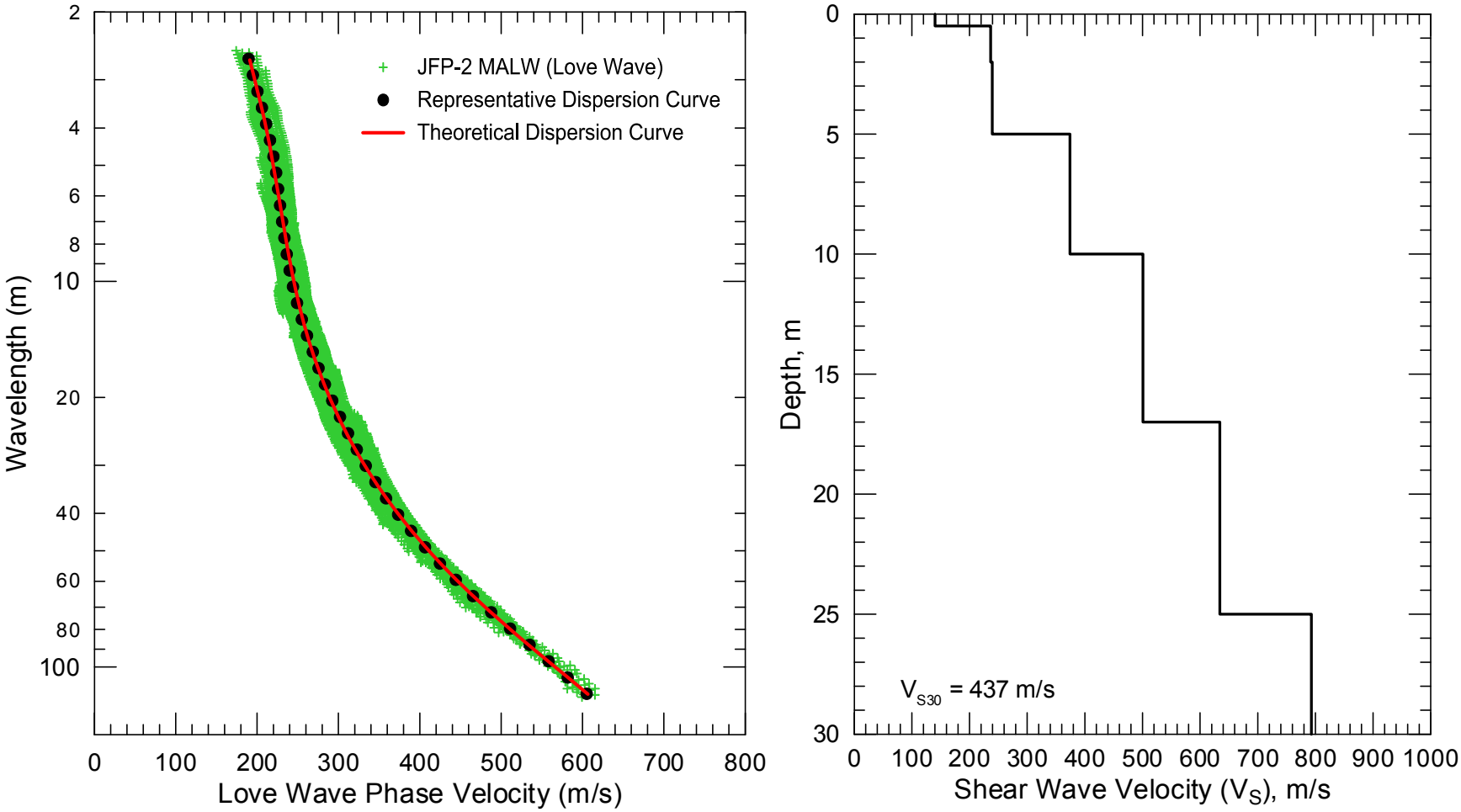

NC.JFP - Field, representative and inverted theoretical Love wave dispersion data (left) and associated V_S model (right)

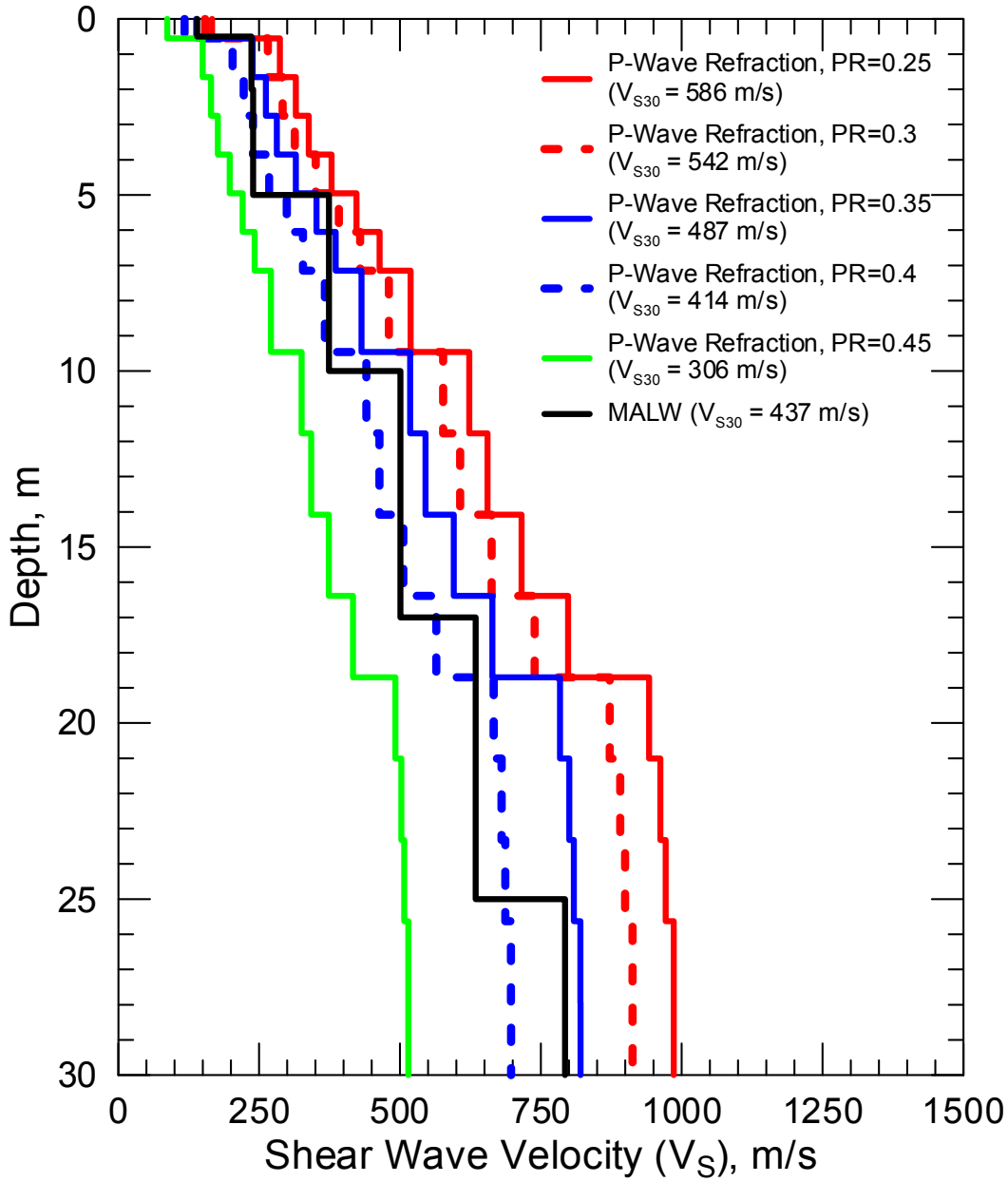

NC.JFP – Comparison of S-wave velocity models derived from the MALW sounding and the average V_P model from the P-wave seismic refraction survey. The MALW V_S model is most consistent with the S-wave velocities derived from the average V_P model using constant Poisson's ratio in the 0.35 to 0.4 range. These values of Poisson's ratio seem a little high and the possibility should be considered that the MALW V_S model is trending towards the lower velocities beneath the array.

Site NC.JLAB

Location: Laurel Hill, Santa Clara County, California

Latitude: 37.15432 **Longitude:** -121.73467
(Station coordinates provided by USGS, WGS84 coordinate system)

V_{S30} (measured): 477 m/s

V_{S30} (adjusted to more accurately reflect seismic station conditions): 559 m/s (average S-wave velocity between 0.75 and 30.75 m to account for assumed sensor depth and the sensor not being placed on loose surficial soils).

NEHRP Site Class: C

Geomatrix Code: IFB

Geologic Conditions/Observations: Seismic station located Mesozoic (Jurassic and Cretaceous) Franciscan Assemblage consisting of a mélange of mostly claystone and greywacke.

Site Conditions: Rural site. Undulating, hilly topography in site vicinity. Seismic station located near the top of Laurel Hill. Geophysical testing conducted along the top of the ridge with about 7 m of elevation variation along the 70.5 m long array.

Geophysical Methods Utilized: HVSR, Seismic Refraction (P- and S-wave), MASW(Rayleigh wave), MALW (Love wave)

Geophysical Testing Arrays:

1. Array JLAB-1 (48 channel P- and S-wave seismic refraction, MASW and MALW array utilizing 4.5 Hz vertical and 10 Hz horizontal geophones spaced 1.5 m apart for a length of 70.5 m, forward and reverse shot locations with multiple source offsets and source types and multiple interior shot locations).
2. Three HVSR measurement locations: two distributed along array JLAB-1 and the other near the seismic station.

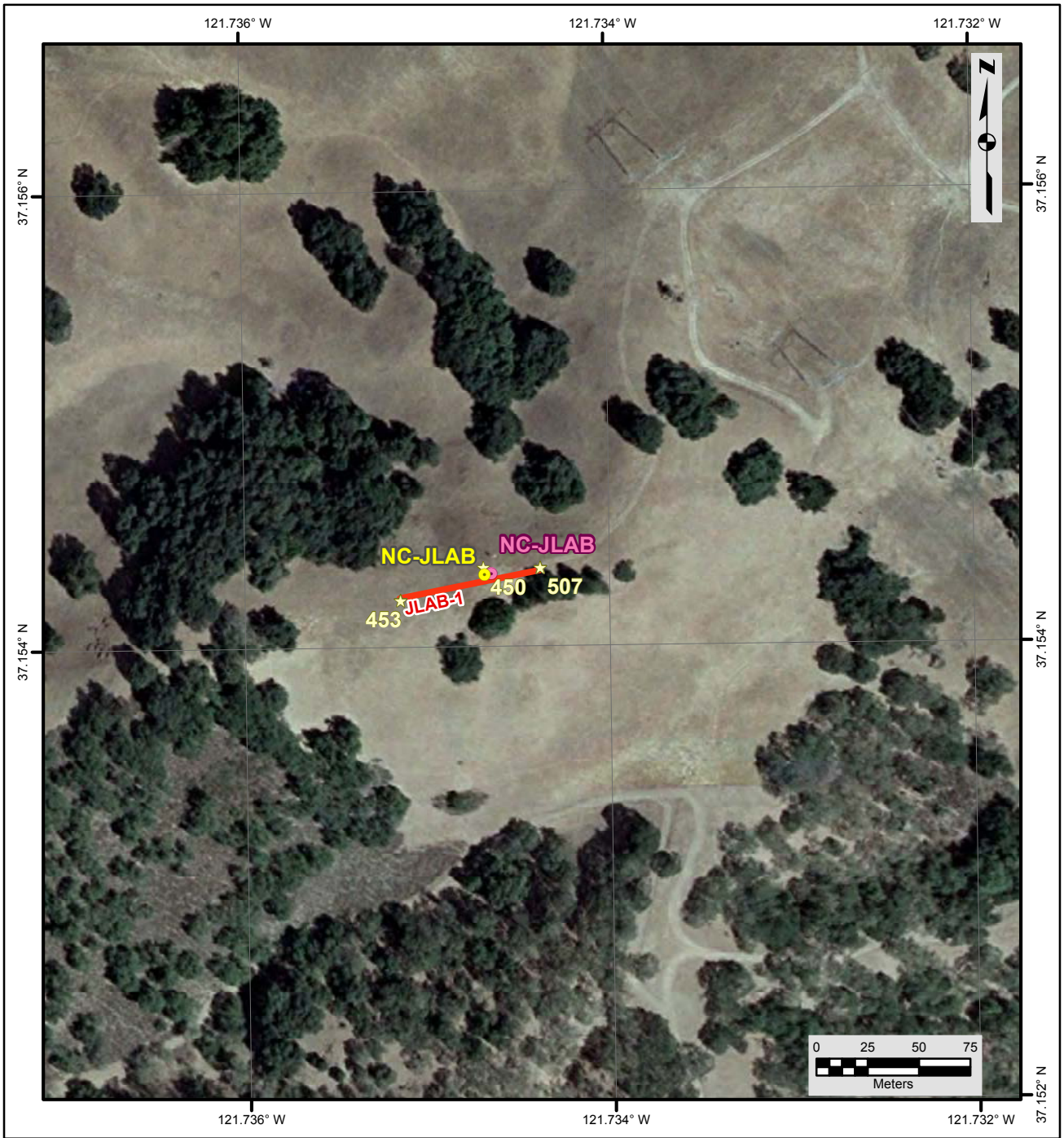

Legend

- Seismic Station - Approximate Surveyed Location
- Seismic Station - Approximate Location of Record
- H/V Spectral Ratio Location
- MASW and Seismic Refraction Array (S- and P-wave)

NOTES:
1. WGS 1984 COORDINATE SYSTEM
2. Image Source: ESRI, i-cubed, USDA FSA, USGS, AEX, GeoEye, Getmapping, Aerogrid, IGP

File Name: NC-JLAB-I

Date: 2/7/2013

USGS science for a changing world

GEOVision geophysical services

RECOVERY.GOV

SITE MAP
NC•JLAB

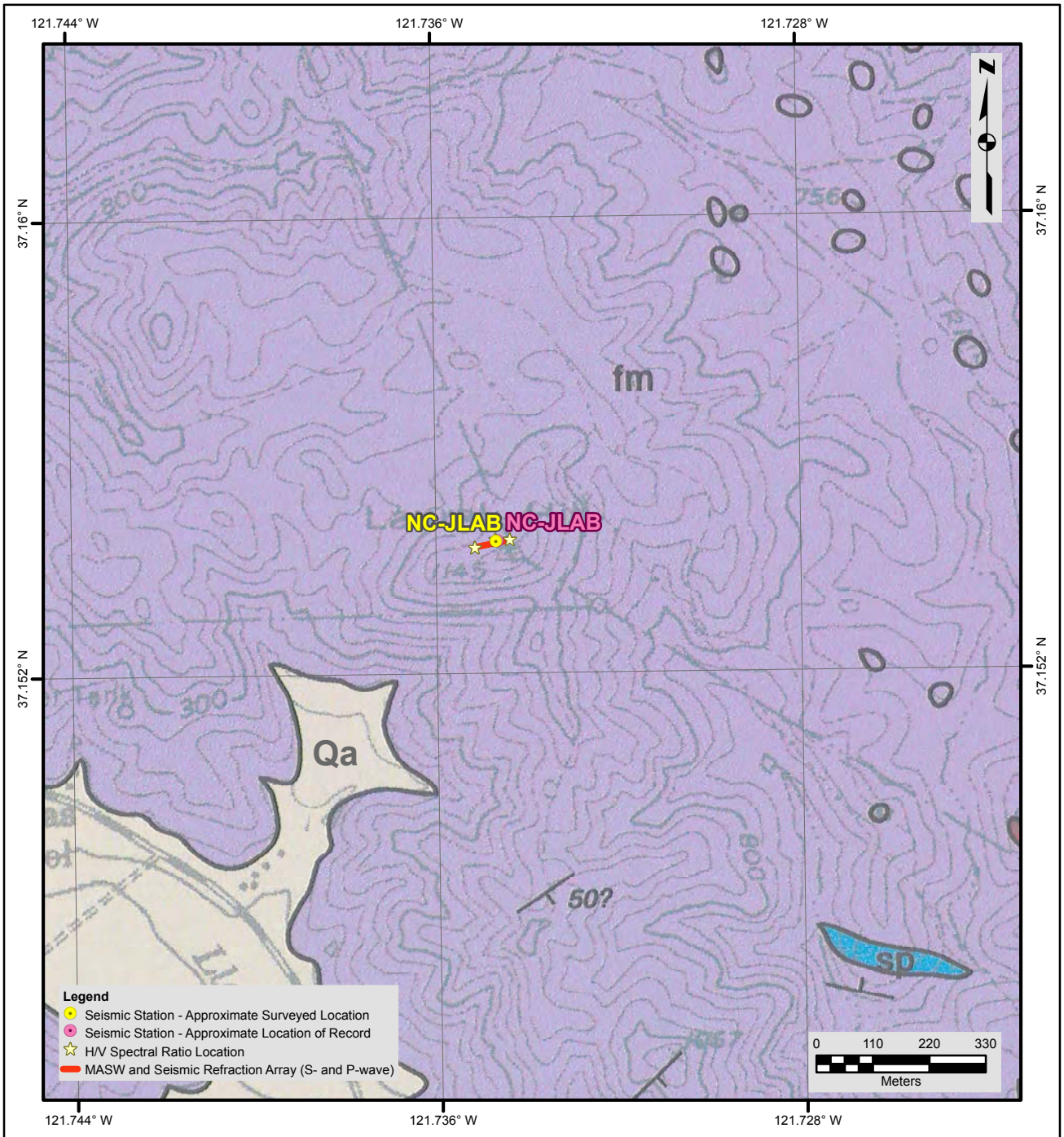

Description of Geologic Map Units

Qa = Quaternary (Holocene) alluvial gravel, sand and clay of valleys
sp = Mesozoic (Jurassic and Cretaceous) Coast Range Ophiolite Complex; serpentinite, amorphous, massive, fractured and slickensided
fm = Mesozoic (Jurassic and Cretaceous) Franciscan Assemblage; melange of mostly claystone and graywacke to metagraywacke, massive, fine grained, hard but fractured, brecciated and sheared

NOTES:
1. WGS 1984 COORDINATE SYSTEM
2. Geologic Map of the Morgan Hill Quadrangle, Santa Clara County, California by Thomas W. Dibblee, Jr., 2005
3. See site map for details of geophysical survey

USGS science for a changing world

GEOVision geophysical services

RECOVERY.GOV

GEOLOGIC MAP
NC•JLAB

File Name: NC-JLAB

Date: 2/7/2013

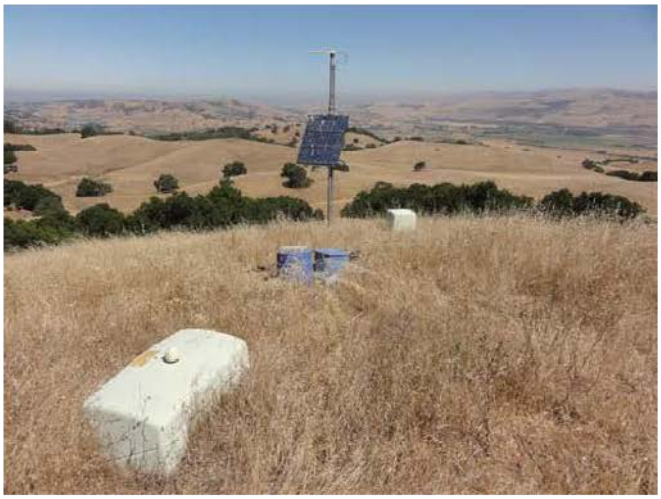

Looking north at NC.JLAB seismic station

Looking west towards HVSR sensor 507 and seismic station

Looking east along P-wave seismic refraction and MASW array JLAB-1

Accelerated weight drop energy source used for P-wave seismic refraction and MASW data acquisition

Looking west along S-wave seismic refraction and MALW array JLAB-1

Location of Geophysical Testing Arrays:

Location	Latitude	Longitude
JLAB-1, Southwest End of MASW/Refraction Array	37.15422	-121.73517
JLAB-1, Center of MASW/Refraction Array	37.15427	-121.73479
JLAB-1, Northeast End of MASW/Refraction Array	37.15433	-121.73440
HVSR Sensor 450	37.15434	-121.73471
HVSR Sensor 453	37.15421	-121.73517
HVSR Sensor 507	37.15434	-121.73440
NC.JLAB Seismic Station	37.15432	-121.73471

Notes: 1) WGS84 Coordinate System (decimal degrees)
2) Survey accuracy is estimated at 1 to 2 m.

Results:

V_S Model (MASW Sounding)

Depth to Top of Layer (m)	Layer Thickness (m)	S-Wave Velocity (m/s)	Inferred P-Wave Velocity (m/s)	Assumed Poisson's Ratio	Assumed Density (g/cm^3)
0	0.75	75	140	0.3	1.70
0.75	2.5	315	589	0.3	1.90
3.25	4.25	422	789	0.3	2.00
7.5	5	479	896	0.3	2.00
12.5	9.5	615	1151	0.3	2.10
22	>8	892	1668	0.3	2.15

Notes: 1) Depth of investigation is about 30 m.
2) Bottom layer is a half space.
3) Half space velocity not well constrained.

Average V_P and Estimated V_S Models from Central Portion of P-wave Seismic Refraction Line

Depth to Top of Layer (m)	Layer Thickness (m)	P-Wave Velocity (m/s)	Estimated S-Wave Velocity (m/s)			
			Poisson's Ratio = 0.25	Poisson's Ratio = 0.3	Poisson's Ratio = 0.35	Poisson's Ratio = 0.4
0.00	0.53	257	148	137	123	105
0.53	1.05	634	366	339	305	259
1.58	1.05	718	414	384	345	293
2.63	1.05	766	442	410	368	313
3.69	1.05	768	443	410	369	313
4.74	1.05	774	447	414	372	316
5.80	1.05	783	452	419	376	320
6.85	2.21	817	472	437	393	334
9.06	2.21	827	478	442	397	338
11.27	2.21	846	489	452	407	346
13.49	2.21	877	507	469	421	358
15.70	2.21	939	542	502	451	383
17.91	2.21	1059	611	566	509	432
20.13	2.21	1225	707	655	589	500
22.34	2.21	1352	781	723	650	552
24.55	2.21	1503	868	803	722	614
26.76	Half Space	1601	924	856	769	653

Observations/Discussion:

- HVSR data are generally similar at the three measurement locations. There is a high frequency HVSR peak that increases in frequency from west to east. This HVSR peak varies from 6.5 to 7 Hz at sensor location 453, 8.5 Hz at sensor location 450 and possibly 9 Hz at sensor location 507, although the peak is weak and inconclusive at this location. These HVSR peaks would tend to indicate that either a geologic contact shallows to the east and/or the average S-wave velocity of the sediments overlying this structure is increasing to the east. The source of the high frequency microtremor energy at this rural site is not clear.
- Both P- and S-wave seismic refraction and MASW and MALW data were acquired at this site because field review of MASW data indicated that MASW interpretation could be difficult. Unfortunately, at the time of this investigation, only 10 Hz horizontal geophones were available for MALW data acquisition, which ultimately limited the use of the technique at this site.
- The possibility cannot be discounted that the first arrival data along a segment of the P-wave seismic refraction line are associated with an out of plane refractor or thin high velocity layer because the amplitude of the head wave rapidly attenuates with distance from the source. If a high velocity layer or out of plane refractor affects the seismic refraction data, then there is a possibility that depths to deeper structures would be overestimated.
- No attempt has been made to model the S-wave seismic refraction data at this time. There is strong P-wave energy before the S-wave arrivals in the seismic records and opposite polarity sources (hammer blows from each side of the S-wave plank) do not result in clear polarity reversal on the S-wave seismic records. Therefore, picking of S-wave first arrivals would be limited to use of an S-wave stacked section (subtracting the opposite polarity records to reduce P-wave energy and enhance S-wave energy). S-wave seismic records were, however, reviewed and indicate that S-wave velocities in the 500 to 650 m/s range are plausible at relatively shallow depth.
- The P-wave seismic refraction data for array JLAB-1 were modeled using a tomographic inversion routine with a smooth velocity gradient starting model. The P-wave seismic refraction model was extended to far offset shot locations to extend depth of investigation. It should be noted that a larger geophone spacing, rather than the utilization of far offset shot locations, is preferred for extending depth of investigation, when applying tomographic inversion routines. However, the seismic refraction data were acquired in conjunction with surface wave data, where a shorter array length is preferred.
- The P-wave seismic refraction survey design allowed P-wave velocity to be imaged to a depth of over 25 m. The seismic refraction model indicates that P-wave velocity is about 300 to 400 m/s at the surface and increases to 700 m/s at a depth of 1 to 6 m, 1,000 m/s at a depth of 12 to 21 m and over 1,600 m/s at a depth of 22 m, or greater. The possibility cannot be discounted that P-wave velocities over 1,600 m/s are associated with saturated soft rock.
- The seismic refraction survey indicates that there is lateral velocity variation at the site, as is the norm for rock sites. There is a very thin, nominal 0.5 to 1 m thick, residual soil layer overlying weathered rock. This layer may have its greatest thickness and lowest velocity towards the northeast end of the array. The southwest end of the array appears

to have higher velocity soft rock near the surface, although the possibility that these velocities are artificially high due to a high velocity layer or out of plane refractor cannot be discounted.

- The seismic refraction model, which shows higher velocity, although possibly saturated, soft rock at shallower depth and higher velocity near surface sediments/rock at the southwest end of the array, is not consistent with the HVSR observations. There may be higher than normal error in the seismic refraction model due to potential influence of a high velocity layer/zone or out of plane refractor on the model. The source of microtremor energy for the high frequency HVSR peaks is uncertain. If the noise source were, for example, wind blowing trees in close proximity to the sensor locations, then the results may not be valid.
- The average P-wave velocity of the upper 30 m (V_{P30}) was estimated between 16.5 and 46.5 m on the P-wave refraction model, where depth of investigation is greatest. V_{P30} generally decreases to the northeast and ranges from about 815 to 1,049 m/s over the 21 to 46.5 m position interval, a 25% variation. This apparent lateral velocity variation may be greater than actually occurs if the refraction model is impacted in areas by the occurrence of a high velocity layer or out of plane refractor. Additionally, if the soft rock is saturated below depths of 22 m, the lateral velocity variation in S-wave velocity structure would be slightly less. Regardless of the complexities at the site, P-wave velocity structure can still be used to validate S-wave velocity structure resulting from surface wave testing.
- An average V_P model was developed over the 16.5 to 46.5 m distance interval by horizontally averaging the travel time of each model cell, or slowness if cell thickness is relatively uniform, and cell thickness and average V_{P30} were determined to be 922 m/s. Assuming constant Poisson's ratios of 0.25, 0.3, 0.35 and 0.4 would result in an estimated V_{S30} of 532, 493, 443 and 376 m/s, respectively.
- Noise conditions at the site were not sufficient for application of passive surface wave techniques.
- The seismic refraction model indicates that there is a very thin layer of low velocity sediments overlying soft, weathered rock. This is a very common occurrence at sites in this part of California and can be quite problematic for surface wave testing using Rayleigh wave methods. This type of velocity structure will often excite a dominant first higher mode over a wide, intermediate frequency range, depending upon the thickness of the surface layer and velocity contrast with the underlying layer. Further compounding the problem is that the surface layer invariably has variable thickness and seismic velocity. In many cases, the fundamental mode is dominant at low frequencies (large wavelengths) and an accurate estimate of V_{S30} can still be made. By attempting to extract Rayleigh wave phase velocity data from multiple source locations and variable receiver arrays, it is often possible to recover the fundamental mode at high frequencies, although lateral velocity variation may result in significant scatter in the Rayleigh wave phase velocity data. Love wave techniques typically perform better in this type of environment because the fundamental mode is dominant and, therefore, should be available, if needed.
- MALW (Love wave) data were acquired at this site but, unfortunately, only 10 Hz horizontal geophones were available at the time of the field investigation. At the time, Love wave techniques were typically being applied to shallow, high velocity rock sites and the need for this technique at some soft rock sites with a thin soil layer was just

becoming apparent. Because of the relatively low S-wave velocity at this site, Love waves would need to be generated and recorded to a frequency on the order of 5 Hz to image to 30 m depth, which is beyond the capability of 10-Hz geophones and pushing the capability of a hammer and plank energy source. One disadvantage of Love wave techniques is the absence of cost effective, low frequency energy sources. Costly vibratory sources may be the best means of generating coherent low frequency Love wave energy. Although of better quality than the Rayleigh wave data, Love wave data collected at this site were not modeled due to insufficient low frequency energy. Love wave phase velocity could not be accurately extracted at wavelengths between 60 and 90 m, which is required to image to 30 m depth. Love wave data were, however, inspected and confirm that there is likely a thin, low velocity layer at the surface. Additionally, Love wave data indicates that V_{S30} may be in the 425 to 500 m/s range based on 400 to 475 m/s phase velocities at wavelengths of 40 to 60 m.

- MASW data reduction was complicated by dominant higher modes on some seismic records and possible significant lateral velocity variation. It was difficult extracting dispersion data from 48 channel receiver gathers at source locations offset from the northeast end of the array. Better success was obtained using receiver arrays of 42 geophones or less. It was also not possible to extract long wavelength dispersion data from the source locations offset 20 and 30 m from the near geophone on the southwest end of the array. Dominant higher modes at high frequencies also made it difficult to extract small wavelength dispersion data, although it was possible to extract Rayleigh wave phase velocity data to a wavelength as low as 4 m, using limited offset receiver arrays from some seismic records. Lateral velocity variation is such that multi-mode modeling of the MASW data is not applicable and there also appears to be a strong source location dependence of the energy of the higher modes.
- The minimum wavelength surface wave phase velocity data extracted from the 48-channel MASW array is about 13 m. Data reduction using seismic records from smaller hammer sources and a limited offset receiver array (i.e. less active geophones) allowed extraction of surface wave dispersion data to a minimum wavelength of about 4 m.
- There is nominally about 50 to 75 m/s scatter in MASW dispersion data, likely due to the effects of lateral velocity variation.
- The Rayleigh wave phase velocity at 40 m wavelength (V_{R40}) is in the 470 to 525 m/s range which would result in an estimated V_{S30} of 491 to 549 m/s, based on the Brown, et al., 2000 relationship, assuming that the dispersion curve at 40 m wavelength is the fundamental mode, which is likely the case.
- A representative dispersion curve was generated for the MASW data set using a moving average, polynomial curve fitting routine and used for modeling.
- Although a minimum Rayleigh wave wavelength of only 4 m was obtained from the MASW data, a 0.75 m thick low velocity layer was permitted in the V_S model based on observations in the seismic refraction data and review of the MALW data.
- Surface wave depth of investigation is about 30 m based on the one half of maximum wavelength criteria.
- There is good agreement between the average V_S models calculated from the P-wave seismic refraction model assuming constant values of Poisson's ratio in the 0.25 to 0.35 range and the V_S model resulting from inversion of the Rayleigh wave phase velocity data, especially in the upper 13 m. Below a depth of 13 m, the MASW V_S model

overestimates S-wave velocity relative to the seismic refraction model. The velocity of the half space in the MASW V_S model is not well constrained and, if superposition of the fundamental and first higher modes occurs at long wavelengths, the half space velocity would be overestimated using the fundamental mode assumption. The seismic refraction model does, however, support S-wave velocities of over 800 m/s at 30 m depth, providing the rock is not saturated at this depth. S-wave seismic refraction and MALW data are both inconclusive as to where S-wave velocity exceeds 650 m/s at depth. Because V_{S30} is heavily weighted towards the lower velocity near surface sediments, increased uncertainly in S-wave velocity structure at depth does not significantly affect V_{S30}.

- V_{S30} from the MASW V_S model is 477 m/s (NEHRP Site Class C).
- V_{S30} estimated from the MASW sounding is consistent with that determined from the average P-wave refraction model using a constant Poisson's ratio in the realistic 0.3 to 0.35 range. Review of Love wave phase velocity data also supports V_{S30} being in the 400 to 500 m/s range.
- Average S-wave velocity between a depth of 0.75 and 30.75 m, to account for assumed seismic sensor depth and the fact that the sensor is not placed on loose surficial soil, is 559 m/s (NEHRP Site Class C).
- For site characterization purposes, the use of the MASW V_S model is recommended. There may be more than 10% variation in V_{S30} in the immediate site vicinity based on the seismic refraction model. Although data reduction and analysis was somewhat challenging at this site, V_{S30} determined from the MASW (Rayleigh wave) sounding is consistent with the P-wave seismic refraction model and review of Love wave data.
- A more accurate V_S model would likely be developed from MALW (Love wave) data acquired using 4.5 Hz geophones and an energy source capable of generating coherent Love wave energy in the 5 Hz range.

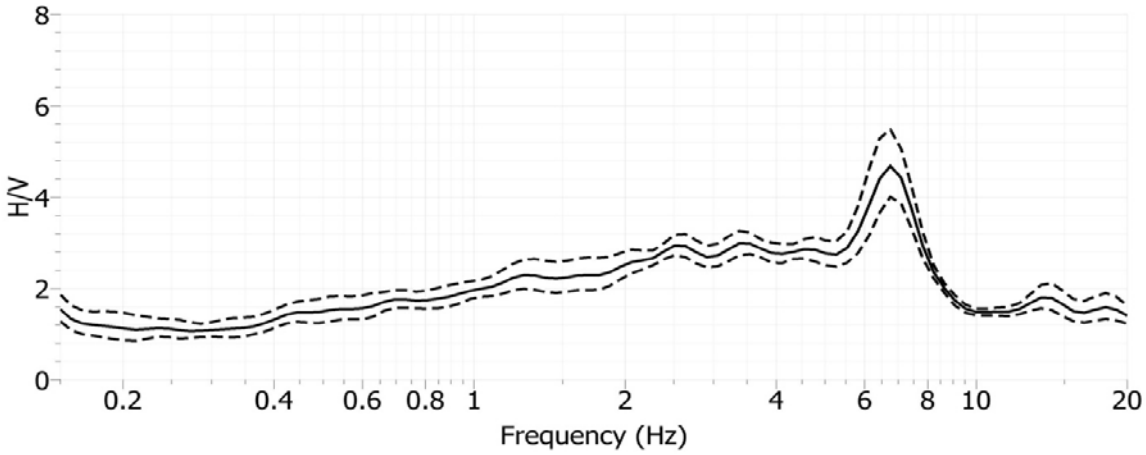

Site NC.JLAB, H/V Spectral Ratio, Array JLAB-1, Sensor 453

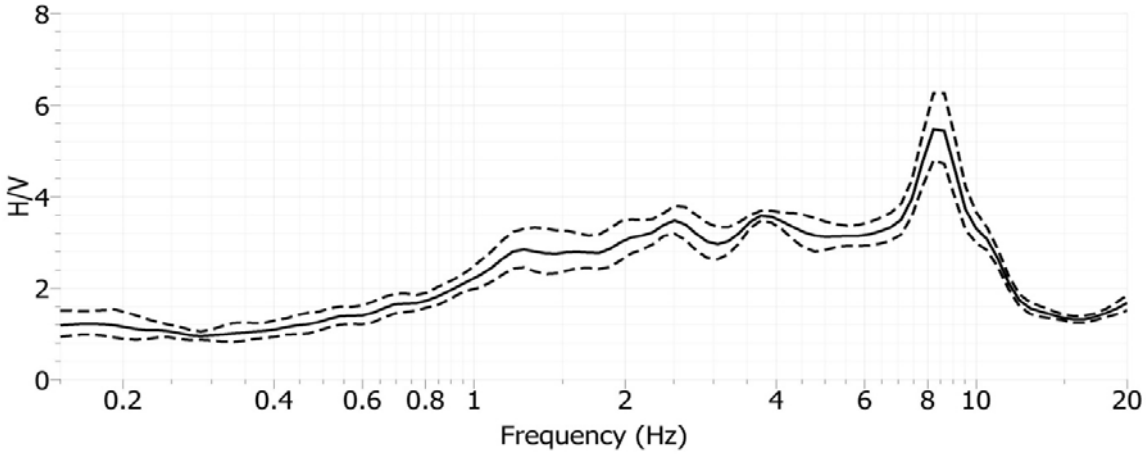

Site NC.JLAB, H/V Spectral Ratio, Near Seismic Station, Sensor 450

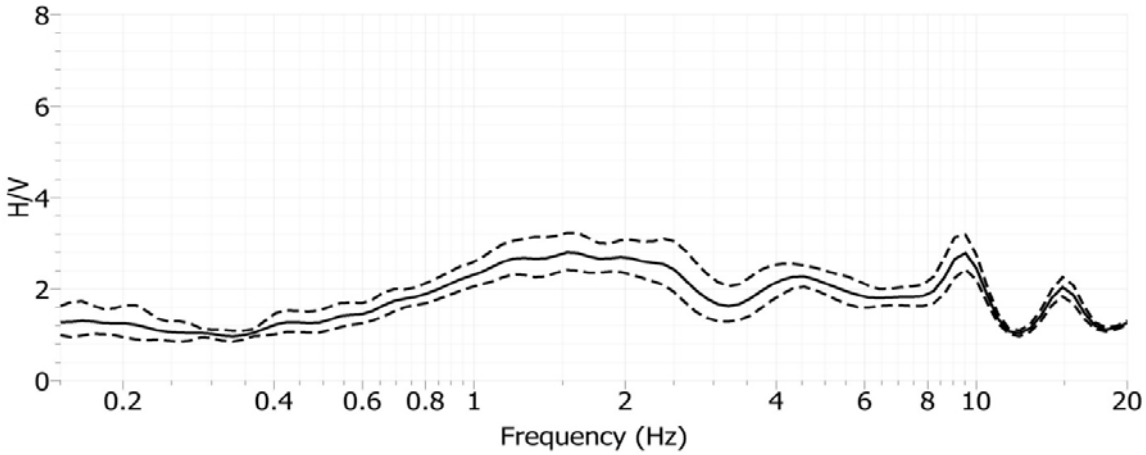

Site NC.JLAB, H/V Spectral Ratio, Array JLAB-1, Sensor 507

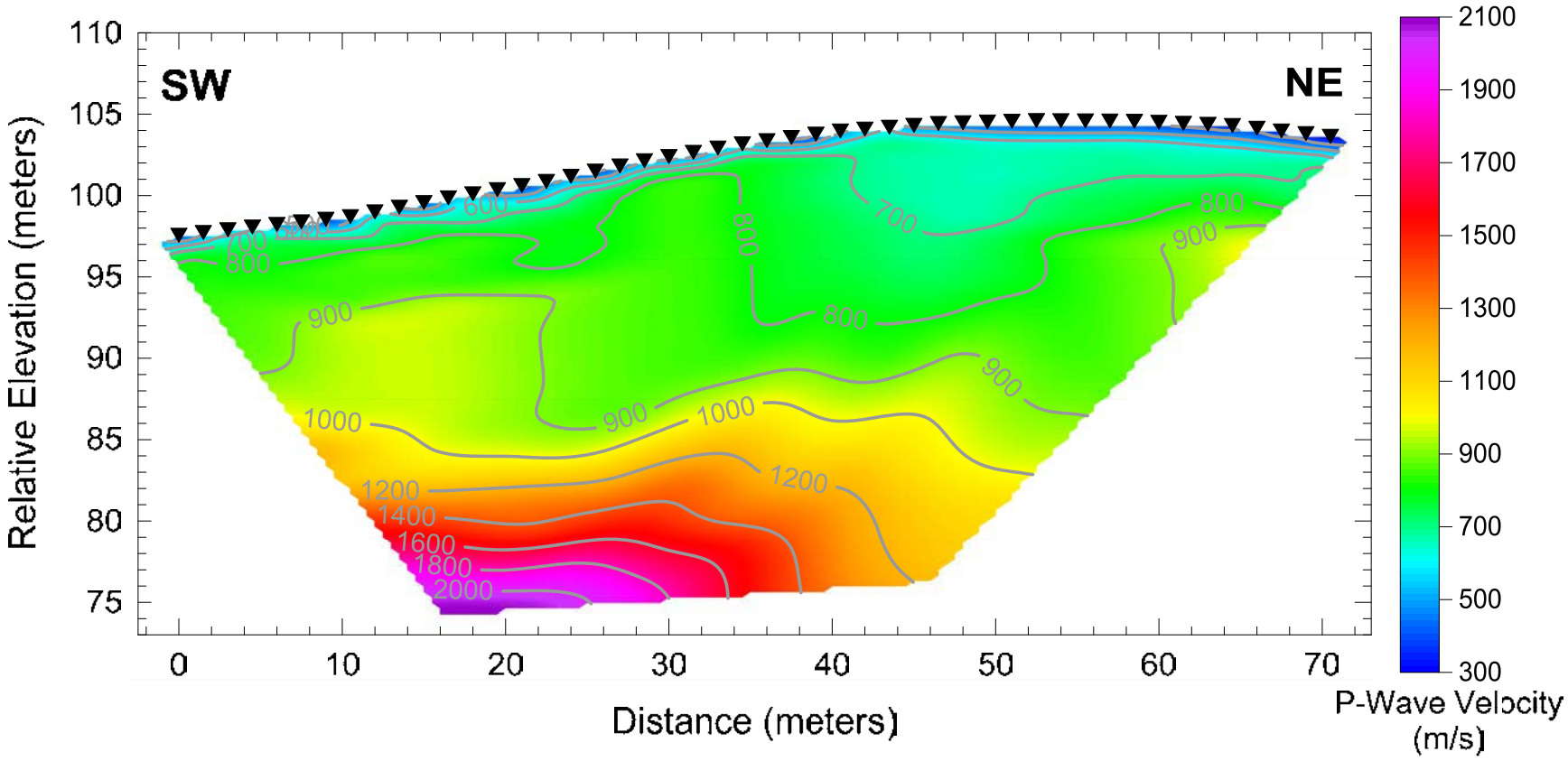

Array JLAB-1 – P-wave tomographic seismic refraction model developed utilizing a smooth velocity gradient starting model

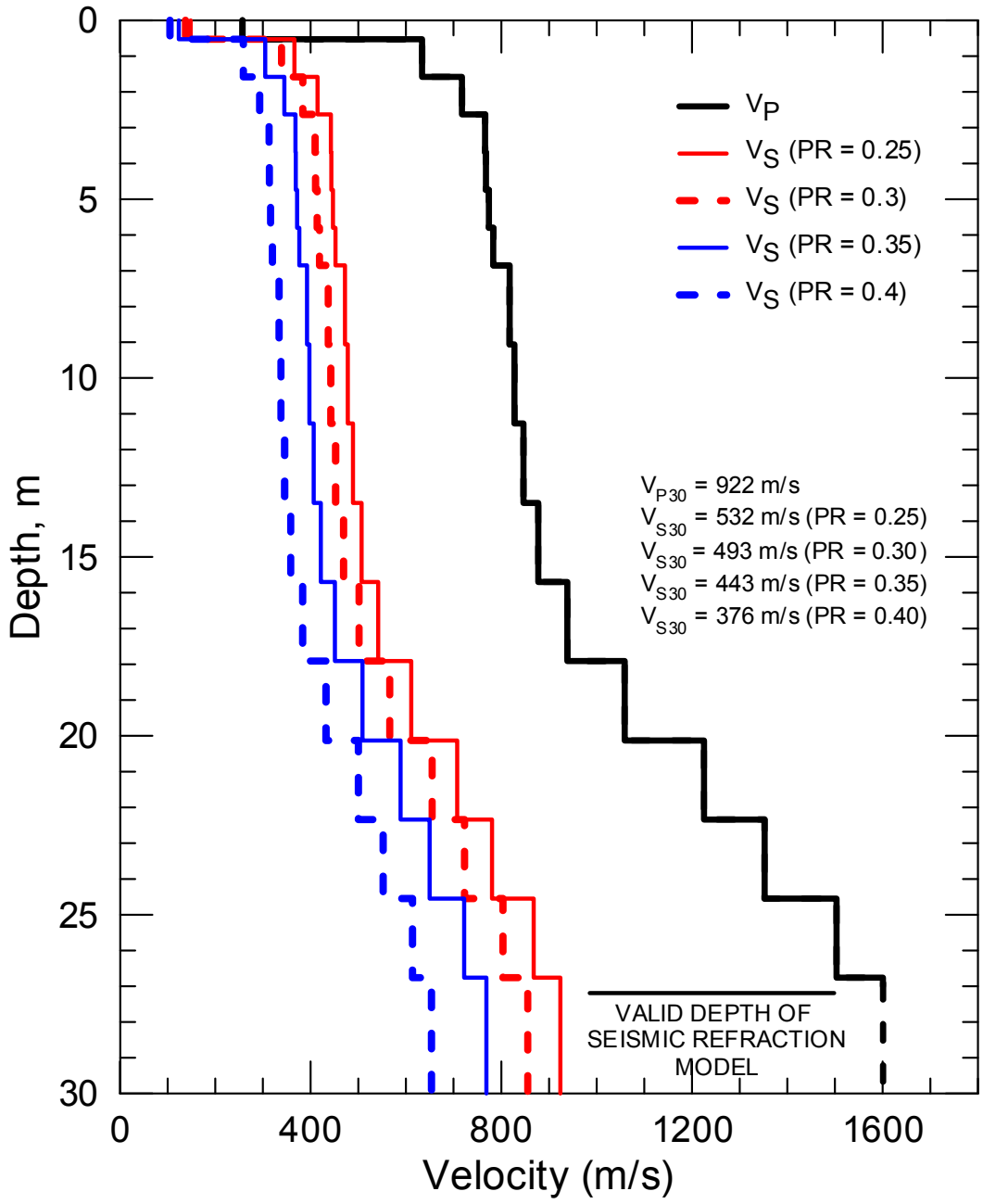

NC.JLAB – Average P-wave velocity structure and estimated S-wave velocity structure between a position of 16.5 and 46.5 m on the P-wave seismic refraction model for array JLAB-1.

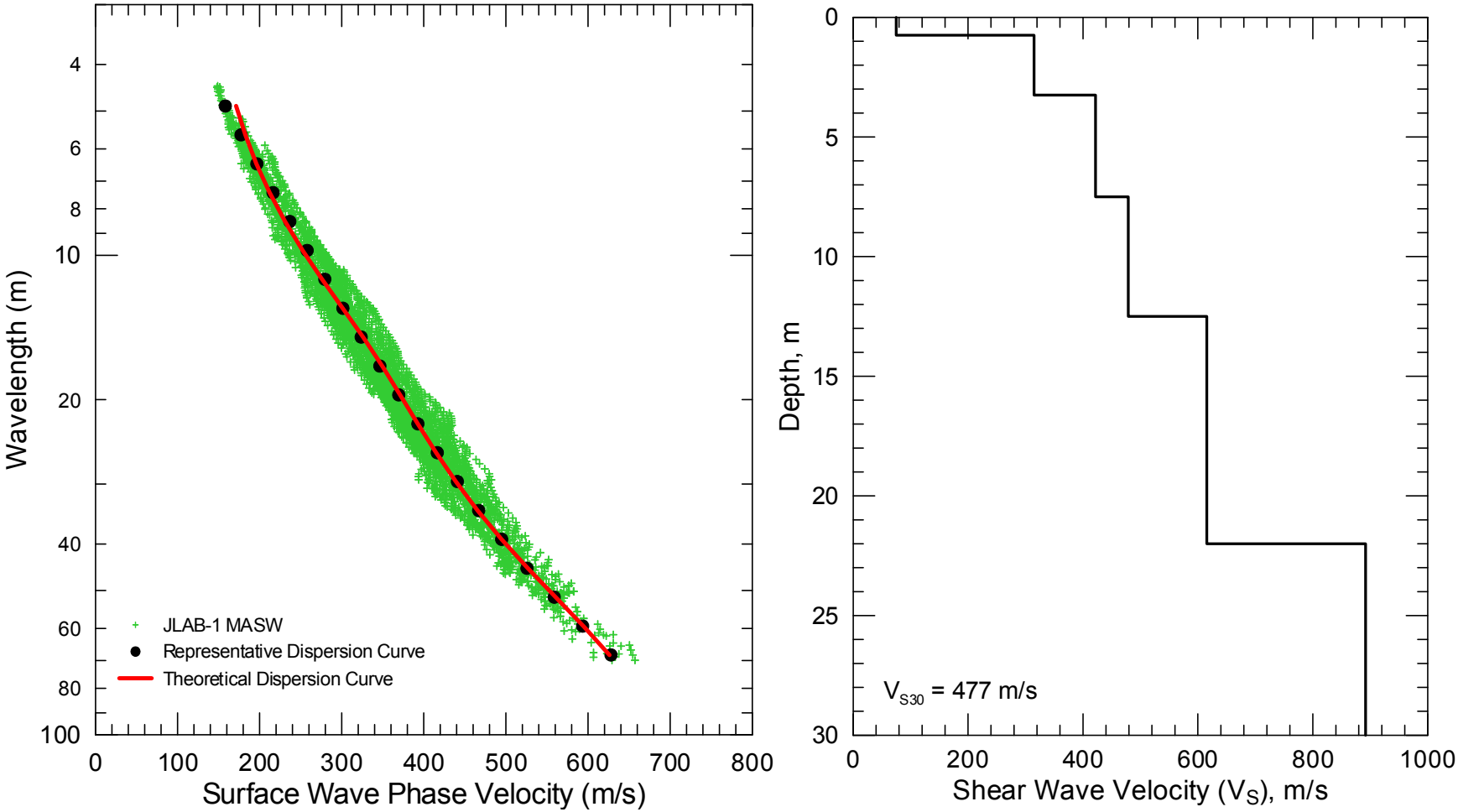

NC.JLAB - Field, representative and inverted theoretical surface wave dispersion data (left) and associated V_S model (right)

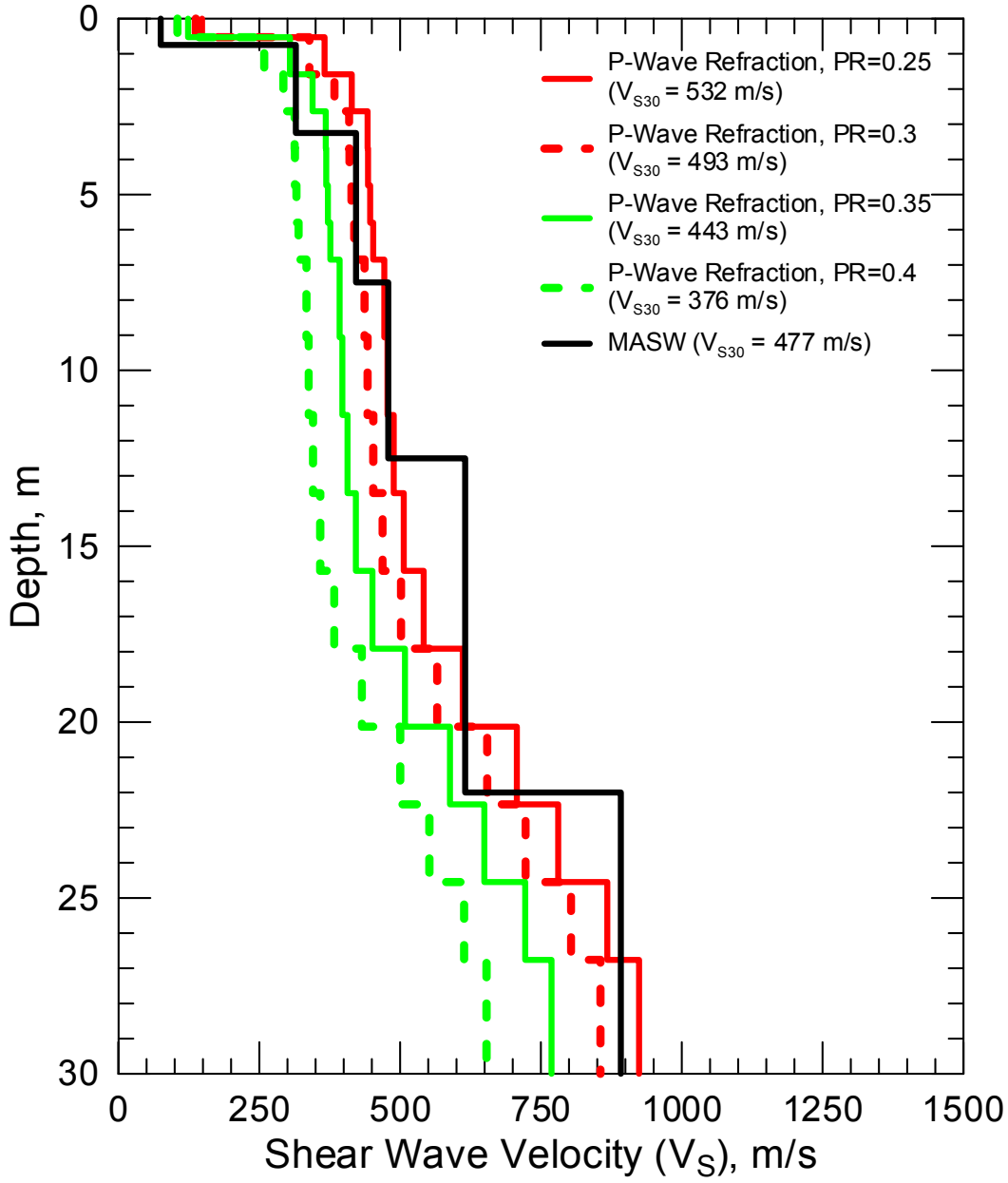

NC.JLAB – Comparison of S-wave velocity models derived from the MASW sounding and the average V_P model from the P-wave seismic refraction surveys. The MASW V_S model slightly overestimates V_S at depths below 13 m relative to the average seismic refraction model. There is, however, 25% variation in V_{P30} beneath the central portion of the seismic line and the MASW V_S model could be skewed towards the higher velocities at shallower depth to the southwest. V_{S30} estimated from the MASW array is in good agreement with that estimated from the P-wave seismic refraction model with constant Poisson's ratio in the 0.3 to 0.35 range.

Site NC.JSFB

Location: Stanford Telescope, Santa Clara County, California

Latitude: 37.40372 **Longitude:** -122.17596
(Station coordinates provided by USGS, WGS84 coordinate system)

V_{S30} (measured): 432 m/s

V_{S30} (adjusted to more accurately reflect seismic station conditions): 463 m/s (average S-wave velocity between 1 and 31 m adjusting for assumed 1 m sensor depth).

NEHRP Site Class: C

Geomatrix Code: IMB

Geologic Conditions/Observations: Seismic station located on geologic unit mapped as Tertiary (Miocene) Monterey Formation. Bedding dips about 15 to 20 degrees to the southwest in the immediate site vicinity.

Site Conditions: Rural site located on gently rolling hills with nearby telecommunication facilities. Ground surface elevation decreases about 6 m to the southwest along the 70.5 m long MASW and seismic refraction array.

Geophysical Methods Utilized: HVSR, Seismic Refraction, MASW

Geophysical Testing Arrays:

1. Array JSFB-1 (48 channel MASW and P-wave seismic refraction array utilizing 4.5 Hz vertical geophones spaced 1.5 m apart for a length of 70.5 m, forward and reverse shot locations with multiple source offsets and source types and multiple interior shot locations).
2. Three HVSR measurement locations; two distributed along array JSFB-1 and one adjacent to the seismic station. HVSR measurements were also made with a Tromino ENGY near the seismic station.

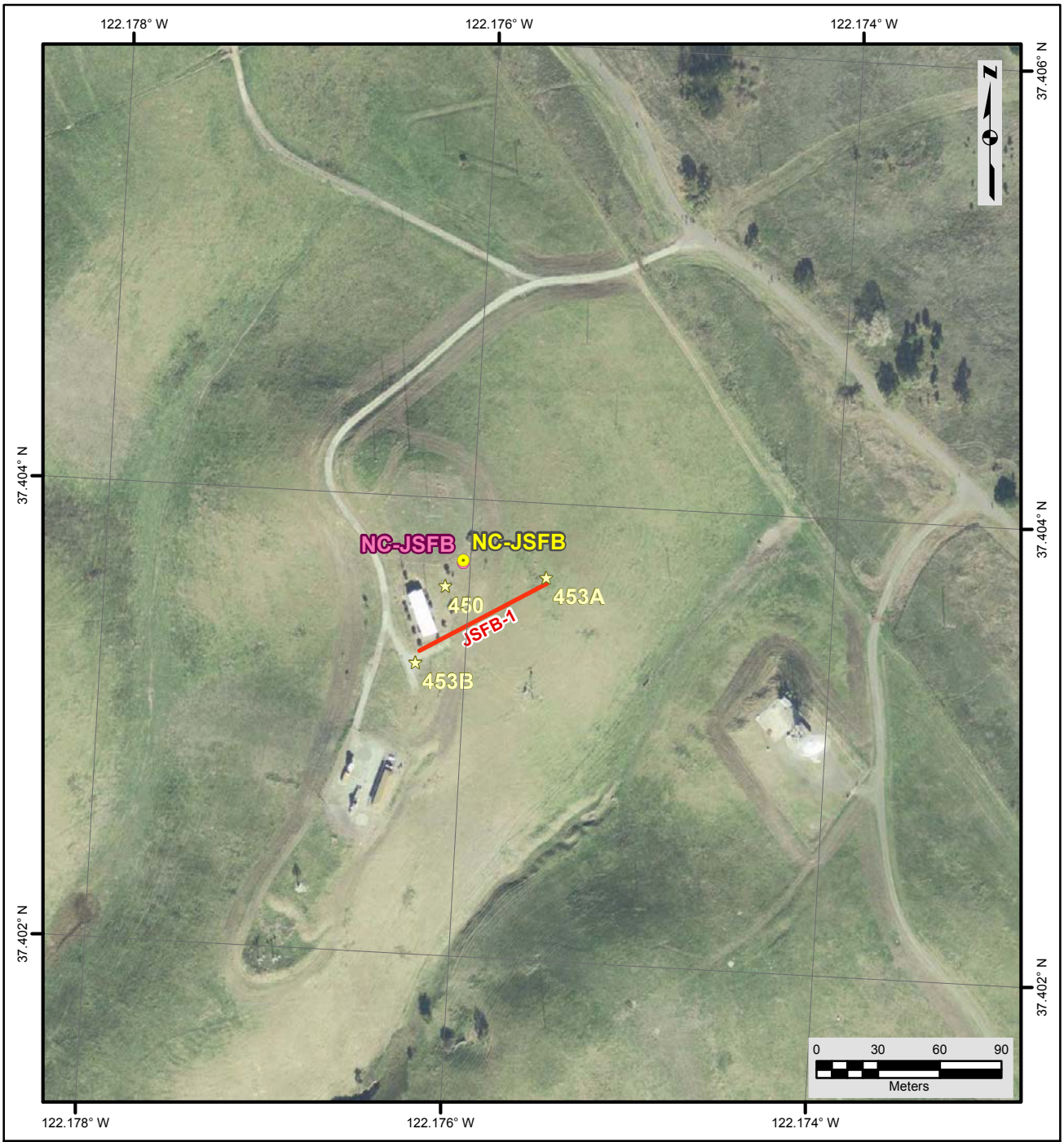

Legend

- Seismic Station - Approximate Surveyed Location
- Seismic Station - Approximate Location of Record
- H/V Spectral Ratio Location
- MASW and Seismic Refraction Array

NOTES:
1. WGS 1984 COORDINATE SYSTEM
2. Image Source: ESRI, i-cubed, USDA FSA, USGS, AEX, GeoEye, Getmapping, Aerogrid, IGP

File Name: NC-JSFB-I

Date: 10/18/2011

USGS science for a changing world

GEOVision geophysical services

RECOVERY.GOV

SITE MAP
NC•JSFB

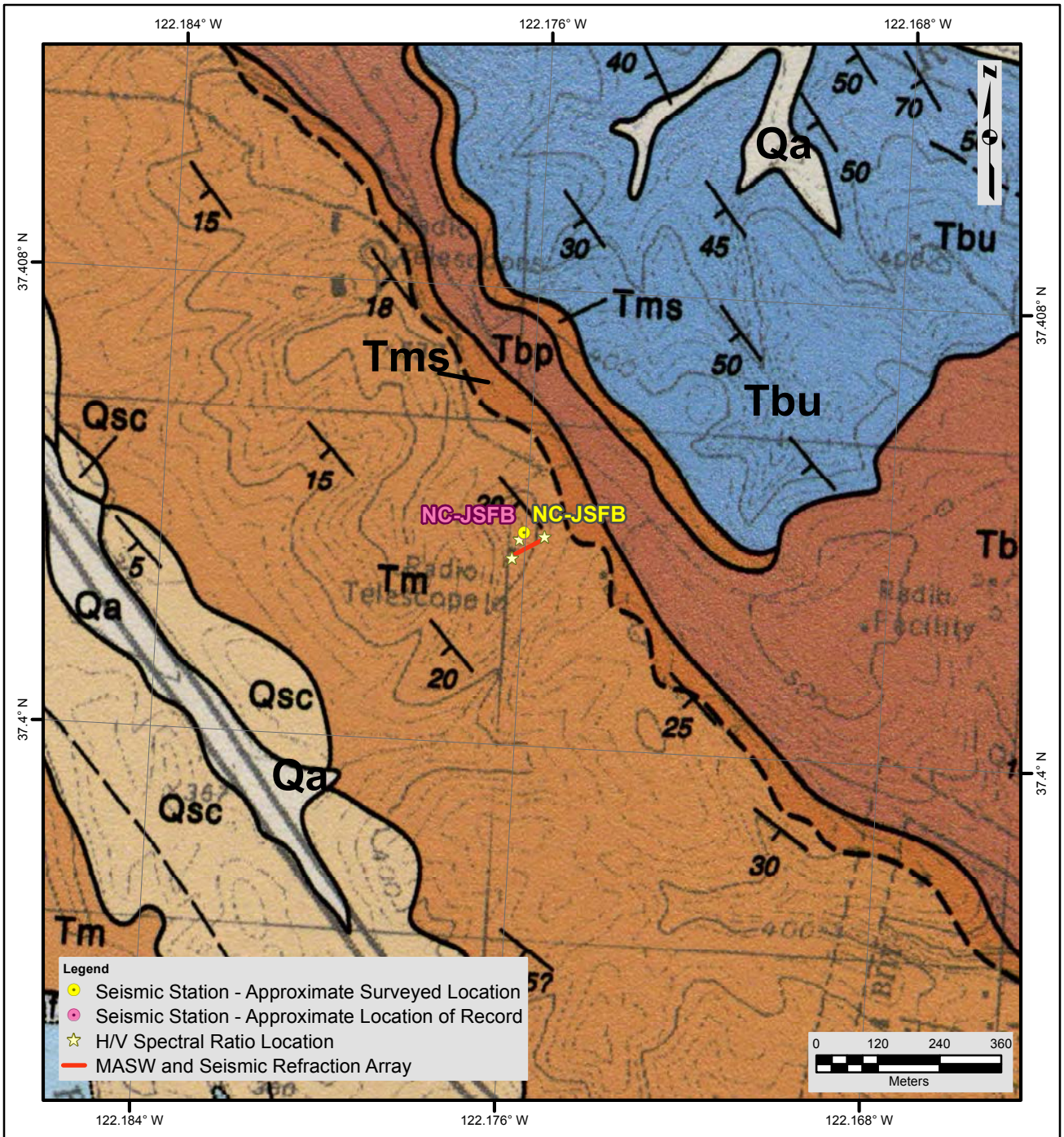

Description of Geologic Map Units

Qa = Quaternary (Holocene) alluvial gravel, sand, silt and clay
Qsc = Quaternary (Pleistocene/Pliocene) Santa Clara Formation; gravel/conglomerate, sandstone and mudstone, cobble, pebble and boulder conglomerate of chert, greenstone, graywacke, schist, serpentinite and limestone in a sandy matrix
Tm = Tertiary (Miocene) Monterey Formation; siliceous shale, with chert, diatomaceous mudstone, minor siltstone, sandstone, hard to semi-silaceous shale and conglomerate
Tbp = Tertiary (Miocene) Page Mill Basalt; basalt flows and agglomerate, massive, finely crystalline, dense to vesicular
Tms = Tertiary (Miocene) Matadero Sandstone; sandstone, mostly fine grained, massive to poorly bedded, soft
Tbu = Tertiary (Eocene) Butano Formation; sandstone, massive, hard, some micaceous shale and lenses of pebble-cobble conglomerate

NOTES:
1. WGS 1984 COORDINATE SYSTEM
2. Geologic Map of the Palo Alto and Mountain View Quadrangles Alameda, San Mateo, and Santa Clara Counties, California by Thomas W. Dibblee, Jr., 2007
3. See site map for details of geophysical survey

File Name: NC-JSFB

Date: 9/16/2011

USGS science for a changing world

GEOVision geophysical services

RECOVERY.GOV

GEOLOGIC MAP
NC•JSFB

NC.JSFB seismic station

Looking northeast along MASW and seismic refraction array JSFB-1

Seismic refraction data acquisition

Tromino ENGR seismic sensor also used for an HVSR measurement

Looking north towards HVSR sensor 453 and NC.JSFB seismic station

Location of Geophysical Testing Arrays:

Location	Latitude	Longitude
JSFB-1, Southwest End of MASW/Refraction Array	37.40333	-122.17617
JSFB-1, Center of MASW/Refraction Array	37.40349	-122.17584
JSFB-1, Northeast End of MASW/Refraction Array	37.40365	-122.17549
HVSR Sensor 450	37.40362	-122.17605
HVSR Sensor 453A	37.40368	-122.17550
HVSR Sensor 453B	37.40328	-122.17619
HVSR Sensor Tromino ENGY	37.40372	-122.17597
NC.JSFB Seismic Station	37.40373	-122.17596

Notes: 1) WGS84 Coordinate System (decimal degrees)
2) Survey accuracy is estimated at 1 to 2 m

Results:

V_S Model

Depth to Top of Layer (m)	Layer Thickness (m)	S-Wave Velocity (m/s)	Inferred P-Wave Velocity (m/s)	Assumed Poisson's Ratio	Assumed Density (g/cm^3)
0	0.75	136	255	0.3	1.8
0.75	1.25	269	502	0.3	1.9
2	3	382	714	0.3	1.9
5	4	442	827	0.3	2.0
9	6	454	850	0.3	2.0
15	8	474	886	0.3	2.0
23	10	566	1060	0.3	2.1
33	>7	708	1324	0.3	2.1

Notes: 1) Depth of investigation is about 40 m.
2) Bottom layer is a half space.

Observations/Discussion:

- HVSR plots are very similar at every station, especially HVSR sensors 453a and 450, validating the 1-D velocity assumption.
- There are no clear high amplitude HVSR peaks, although there is a possible weak peak in the 0.2 to 0.3 Hz range. Noise at frequencies less than 0.2 Hz makes it difficult to accurately resolve this peak, which, if real, is associated with very deep geologic structure. It is unclear what effects dipping and folded geologic layers may have on HVSR response.
- HVSR data were also recorded with a Tromino ENGY, which was located adjacent to the Nanometrics Trillium Compact sensor 450. Both HVSR sensors yielded similar results. Although not designed to measure at frequencies less than 0.3 Hz, the Tromino data supports the potential, weak HVSR peak in the 0.2 to 0.3 Hz range.
- The P-wave refraction data for array JSFB-1 were modeled using a tomographic inversion routine with a smooth velocity gradient starting model. The seismic refraction model was extended to far offset shot locations to extend depth of investigation.
- Picking of seismic refraction first arrival data was complicated in some areas by possible out of plane refractors or low amplitude first arrivals from thin, relatively high velocity layers.
- The seismic refraction survey design allowed P-wave velocity to be imaged to a maximum depth of about 20 m. Without extension of the model to far offset shot locations, the effective depth of investigation is about 15 m. The seismic refraction model shows that P-wave velocity is about 400 to 600 m/s at the surface, increasing to 700 to 900 m/s at a depth of 1 to 10 m, 1,000 to 1,200 m/s at a depth of 15 to 20 m and greater than 1,400 m/s at a depth below 20 m.
- Extending the model to far offset shot locations allowed the model to be extended to a greater depth, revealing layers with P-wave velocity on the order of 1,400 to 1,600 m/s at nominal depths of 20 m to 23 m. It should be noted that a longer receiver array would be required to accurately image velocity structure at these depths; however, the far offset shot locations do support P-wave velocity continuing to increase with depth below 15 m.
- The seismic refraction model indicates that there is lateral velocity variation at this site, with higher P-wave velocities at shallower depth near the southwest end and center of the line.
- The seismic refraction/MASW array was orientated almost perpendicular to the strike of the geologic bedding, which dips on the order of 15 to 20 degrees in a southerly direction. The seismic refraction model appears to indicate that the velocity structure is a function of the weathering rather than the dip of the layers, suggesting that a surface wave sounding will generate a representative velocity model even though the seismic line is not parallel to strike.
- Noise conditions at the site were not sufficient for application of passive surface wave techniques.

- The minimum wavelength surface wave phase velocity data extracted from the 48-channel MASW array was about 10 m. Reducing data from smaller hammer sources using a limited offset receiver array (i.e. less active geophones) allowed for extraction of surface wave dispersion data to a minimum wavelength of about 5.5 m. MASW analysis of a limited group of receivers and SASW analysis of selected receiver pairs from the 3 lb hammer shot located at -1.5 m allowed for extraction of phase velocity data to a wavelength of about 1.3 m.
- A large number of limited offset MASW receiver arrays from shot locations near the center of the array and, to a lesser degree, the southwest end of the array, yielded lower phase velocities over a wide wavelength range less than 30 m. These data were not used during modeling as they did not tie in very well with phase velocity data extracted using the full receiver array. Forward modeling indicated that these lower phase velocities are associated with a minor thickening of the thin, low velocity residual soil layer and that an increase of the thickness of this layer from 1 m to 2 m can have a significant effect on surface wave dispersion data to wavelengths up to 30 m, but affects V_{S30} by less than 10%.
- There is about 40 m/s of scatter in MASW dispersion data, particularly at wavelengths below 30 m, which is in part due to lateral velocity variation caused by differential weathering of near surface sedimentary rock and variable thickness of a thin residual soil layer. Scatter in MASW dispersion data is less than 25 m/s at wavelengths greater than 40 m.
- A representative dispersion curve was generated for the MASW data set using a moving average, polynomial curve fitting routine and used for modeling.
- Surface wave depth of investigation is about 40 m based on half of maximum wavelength criteria.
- The inferred P-wave velocities in the surface wave model, based on an assumed Poisson's ratio of 0.3 and modeled S-wave velocity, are consistent with the P-wave refraction model in the upper 15 m. Below a depth of 15 m, the surface wave model inferred P-wave velocities are lower than the P-wave velocities on the seismic refraction model. This may be due to saturation of the Monterey Formation at depth resulting in a higher Poisson's ratio.
- Synthetic HVSR modeling, using the surface wave V_S model, indicates that an HVSR peak is not expected at this site at frequencies below 20 Hz, validating the absence of an HVSR peak in the field measurements.
- The S-wave velocity model derived from the surface wave testing is believed to be representative of average subsurface velocity structure. However, geology at the site is complex, with dipping bedding, and the seismic line was oriented perpendicular to strike. It is difficult to predict the effect of dipping beds on surface wave dispersion data. A line parallel to strike would demonstrate if shallow S-wave velocity structure is primarily controlled by weathering at the site.
- V_{S30} is 432 m/s (Site Class C).
- Average S-wave velocity between 1 m (assumed sensor depth) and 31 m is 463 m/s.

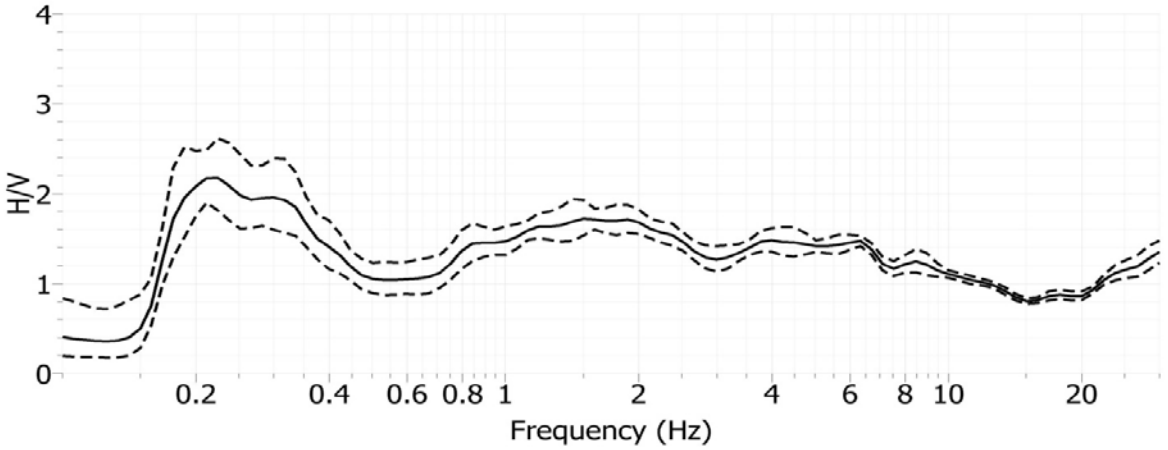

Site NC.JSFB, H/V Spectral Ratio, Array JSFB-1, Sensor 453B

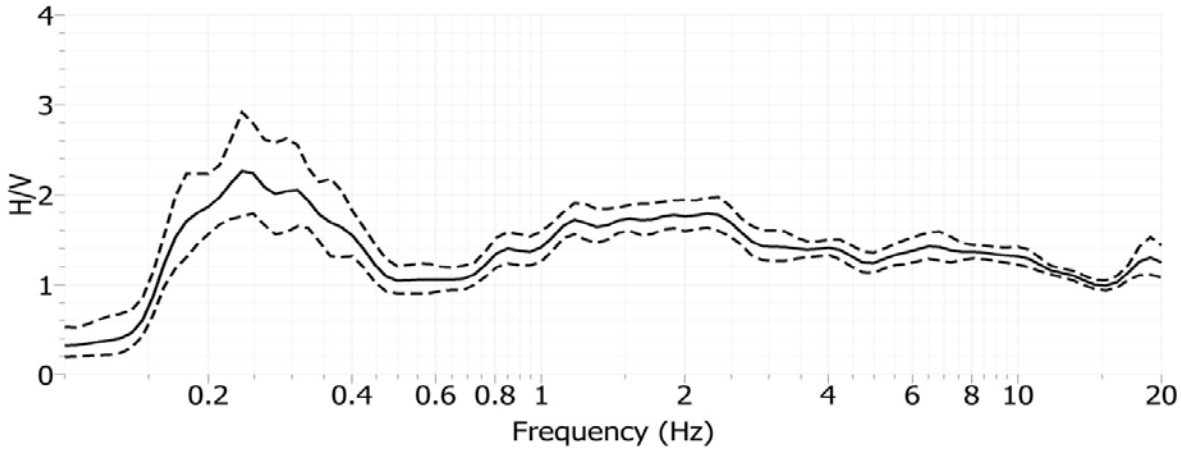

Site NC.JSFB, H/V Spectral Ratio, Near Seismic Station, Sensor 450

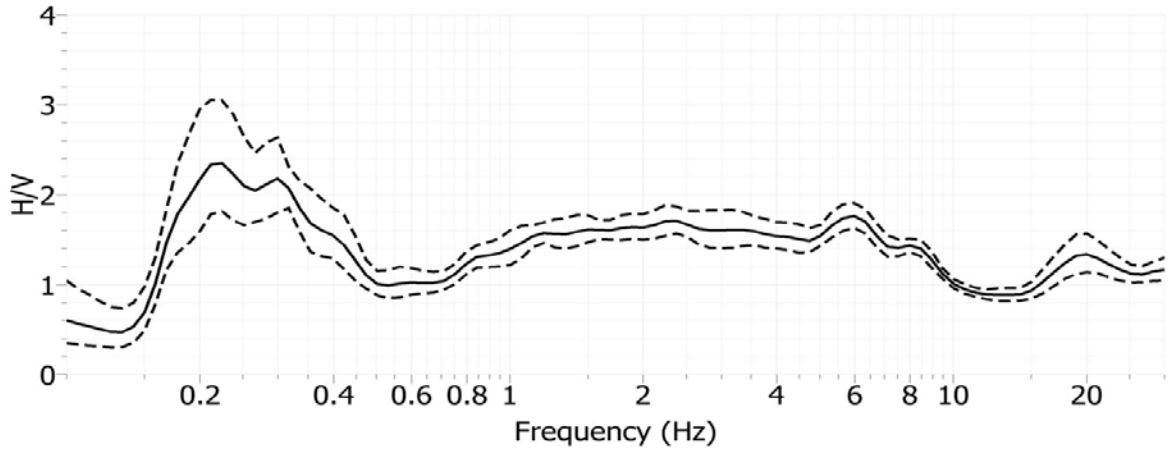

Site NC.JSFB, H/V Spectral Ratio, Array JSFB-1, Sensor 453A

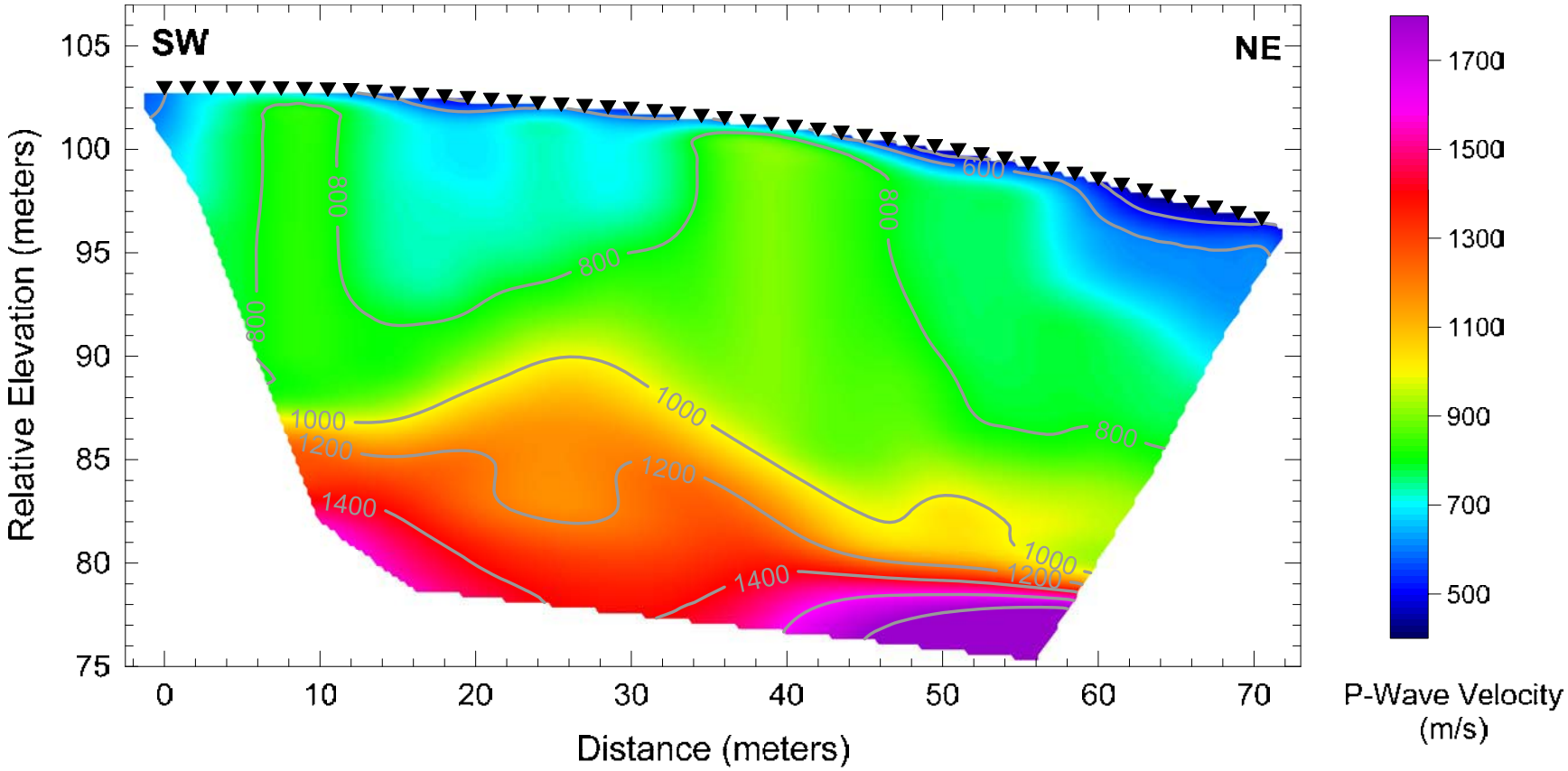

Array JSFB-1 – Tomographic seismic refraction model utilizing smooth velocity gradient starting model

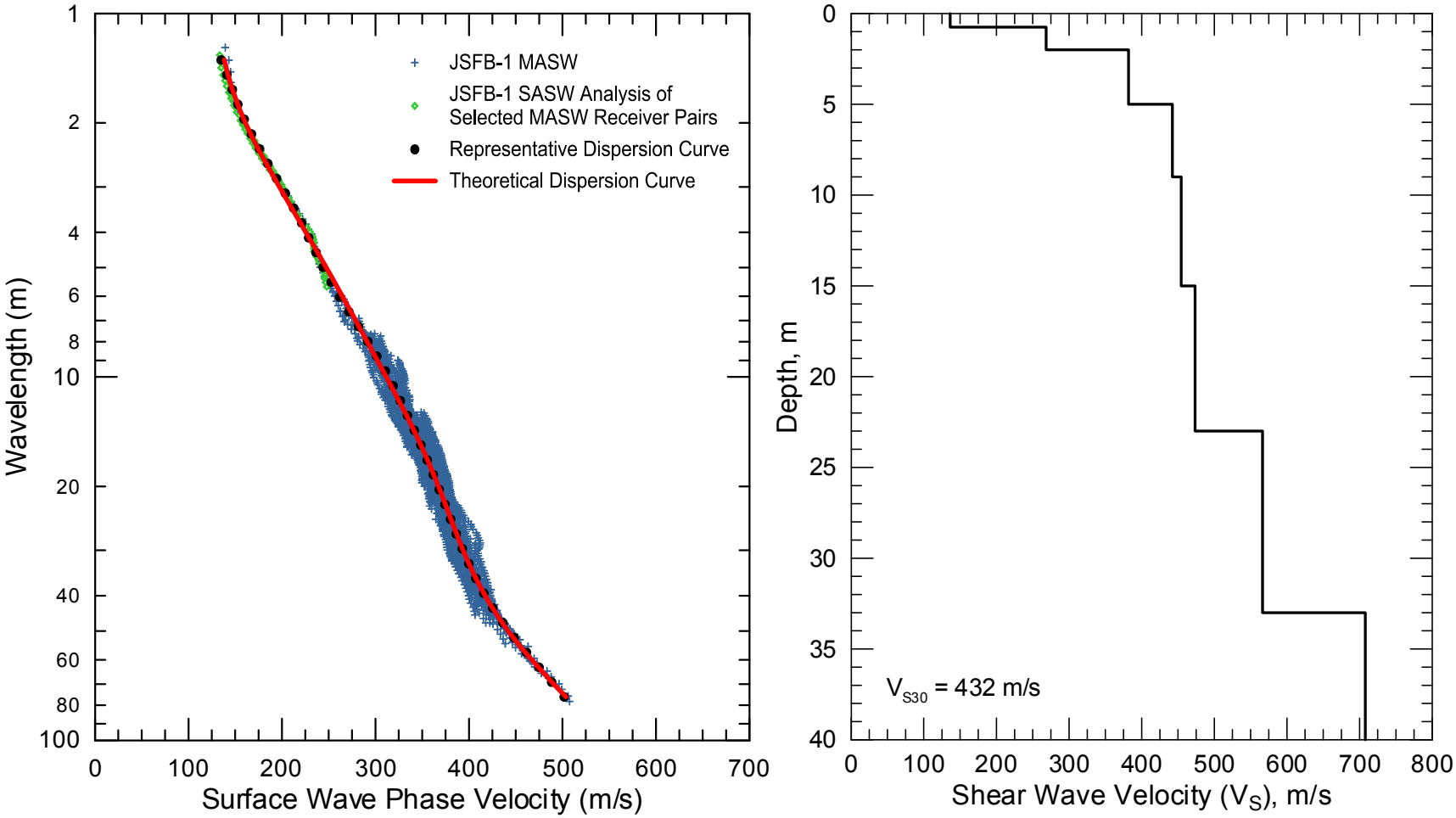

NC.JSFB - Field, representative and inverted theoretical surface wave dispersion data (left) and associated V_S model (right)

Site NC.JSGB

Location: Saratoga Golf Course, Saratoga, Santa Clara County, California

Latitude: 37.28395 **Longitude:** -122.05026
(Station coordinates modified based on field GPS survey, WGS84 coordinate system)

V_{S30} (measured): 376 m/s

V_{S30} (adjusted to more accurately reflect seismic station conditions): 400 m/s (average S-wave velocity between 1 and 31 m to account for assumed sensor depth).

NEHRP Site Class: C

Geomatrix Code: IQD

Geologic Conditions/Observations: Site located on geologic unit mapped as Quaternary (Pleistocene) Santa Clara Formation.

Site Conditions: Rural site next to golf course. Seismic station located on the edge of a hill. There was only one feasible test location on the Santa Clara Formation near the seismic station.

Geophysical Methods Utilized: HVSR, MASW

Geophysical Testing Arrays:

1. Array JSGB-1 (48 channel MASW array utilizing 4.5 Hz vertical geophones spaced 1.25 m apart for a length of 58.75 m, forward and reverse shot locations with multiple source offsets and source types and multiple interior shots).
2. Three HVSR measurement locations: two along array JSGB-1 and the other next to the seismic station.

Legend

- Seismic Station - Approximate Surveyed Location
- Seismic Station - Approximate Location of Record
- H/V Spectral Ratio Location
- MASW and Seismic Refraction Array

NOTES:
1. WGS 1984 COORDINATE SYSTEM
2. Image Source: ESRI, i-cubed, USDA FSA, USGS, AEX, GeoEye, Getmapping, Aerogrid, IGP

File Name: NC-JSGB-I

Date: 3/21/2012

USGS science for a changing world

GEOVision geophysical services

RECOVERY.GOV

SITE MAP
NC•JSGB

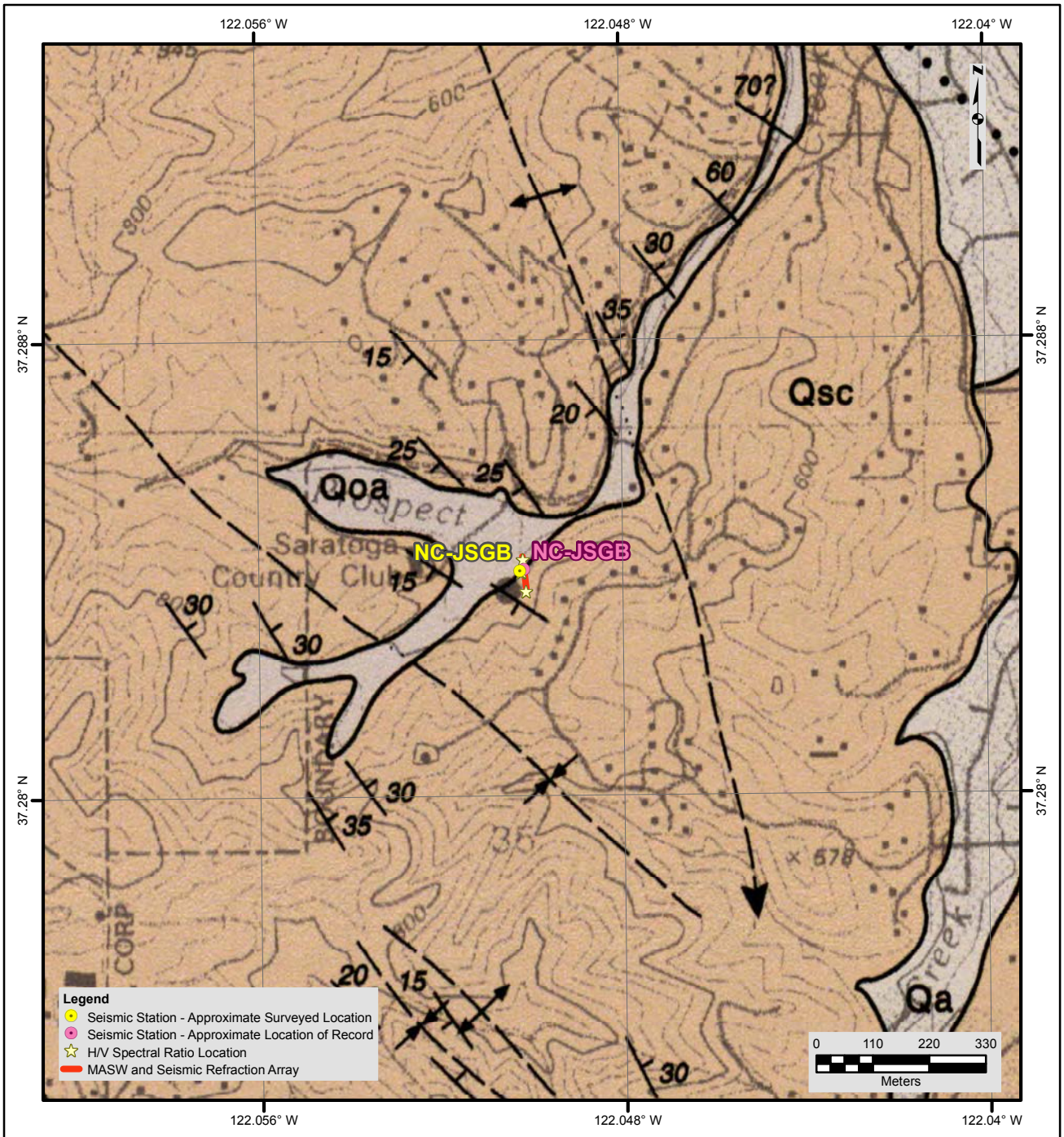

Description of Geologic Map Units

Qoa = Quaternary (Pleistocene) older alluvial terrace gravel, sand and clay
Qsc = Quaternary (Pleistocene) Santa Clara Formation; gravel/conglomerate, sandstone, and mudstone; claystone and siltstone; cobble, pebble and boulder conglomerate of chert, greenstone, graywacke, schist, serpentinite and limestone in a sandy matrix

NOTES:
1. WGS 1984 COORDINATE SYSTEM
2. Geologic Map of the Cupertino and San Jose West Quadrangles, Santa Clara and Santa Cruz Counties, California by Thomas W. Dibblee, Jr., 2007
3. See site map for details of geophysical survey

File Name: NC-JSGB

Date: 3/21/2012

USGS science for a changing world

GEOVision geophysical services

GEOLOGIC MAP
NC•JSGB

RECOVERY.GOV

Looking northwest towards seismic station NC.JSGB and HVSR sensor 453

Looking south along array JSGB-1 towards seismic station

Looking north towards center of array JSGB-1 and seismic station

Looking south along array JSGB-1. The array is partially located on the side of a hill which is not desirable for surface wave data acquisition

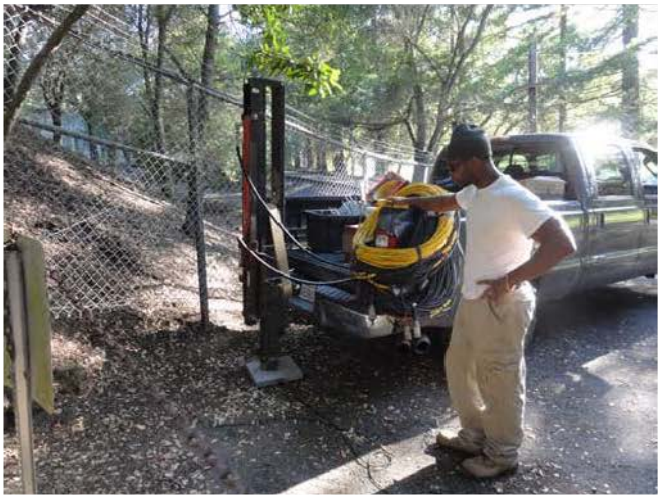

Only several source locations were accessible to the accelerated weight drop energy source

Location of Geophysical Testing Arrays:

Location	Latitude	Longitude
JSGB-1, South End of MASW Array	37.28362	-122.05012
JSGB-1, North End of MASW Array	37.28420	-122.05020
HVSR Sensor 450	37.28358	-122.05012
HVSR Sensor 453	37.28392	-122.05024
HVSR Sensor 507	37.28414	-122.05019
NC.JSGB Seismic Station	37.28395	-122.05026

Notes: 1) WGS84 Coordinate System (decimal degrees)
2) Survey accuracy is estimated at 2 to 3 m.

Results:

V_S Model

Depth to Top of Layer (m)	Layer Thickness (m)	S-Wave Velocity (m/s)	Inferred P-Wave Velocity (m/s)	Inferred Poisson's Ratio	Inferred Density (g/cm^3)
0	1	149	279	0.3	1.70
1	2	232	433	0.3	1.75
3	2	309	578	0.3	1.80
5	21	417	1800	0.472	1.90
26	>4	518	1800	0.455	2.00

Notes: 1) Saturated zone with V_P = 1,800 m/s fixed at a depth of 5 m based on review of limited seismic refraction first arrival data.
2) Depth of investigation is about 30 m.
3) Bottom layer is a half space.

Observations/Discussion:

- The seismic station is located adjacent to a water tank sitting on a pad cut into the side of a hill comprised of Santa Clara Formation. There was only one feasible test location near the seismic station, a trail adjacent to the seismic station. Parts of this trail were cut into the side of the hill, which is not ideal for surface wave data acquisition.
- HVSR plots at the three measurement locations are very similar. There are multiple low amplitude HVSR peaks at about 0.3, 0.95 and 12 to 14 Hz.
- P-wave seismic refraction data were not acquired at this soil site; however, MASW seismic records were reviewed to determine general P-wave velocity structure. Surficial sediments have a P-wave velocity on the order of 400 m/s. P-wave velocity increases to

about 1,800 m/s at a depth on the order of 2 to 5 m. The 1,800 m/s refractor is expected to be associated with the water table or a zone or perched water.

- Although the HVSR plots are relatively uniform, there is significant evidence of near surface lateral velocity variation evident in the seismic records. This complicated MASW data reduction and resulted in significant scatter in the surface wave dispersion curve. It also appeared difficult to clearly identify the fundamental mode in some of the MASW data. Significant effort was required to extract coherent dispersion data over the 13 to 21 m wavelength range. Given the degree of lateral velocity variation and apparent complex wave propagation, analysis would have benefited from the additional interior shot locations generally acquired during seismic refraction surveys, but not acquired at this site. To supplement the MASW dispersion data, SASW data reduction techniques were applied to the time history data from selected MASW receiver pairs for source locations at both ends of the array. These data were consistent with the MASW data and, therefore, combined with the MASW data for modeling.
- The near field wavelength criteria generally applied during this investigation was relaxed somewhat with no obvious near field effects, which typically result in lower phase velocities, observed in the Rayleigh wave phase velocity data selected for modeling. Additionally, as only one side of the array was accessible to the accelerated weight drop energy source, the maximum wavelength Rayleigh wave was restricted to about 62 m. This is equivalent to a frequency of 7 Hz, the lowest frequency we are generally comfortable generating with a 20 lb sledge hammer energy source.
- The minimum wavelength surface wave phase velocity data extracted from the 48-channel MASW array is about 26 m. Data reduction using seismic records from smaller hammer sources and a limited offset receiver array (i.e. less active geophones) allowed extraction of surface wave dispersion data to a minimum wavelength of about 1.5 m.
- There is nominally about 60 m/s scatter in the MASW dispersion data selected for modeling likely due to lateral velocity variation.
- A representative dispersion curve was generated for the MASW data set using a moving average, polynomial curve fitting routine and used for modeling.
- The saturated zone with an estimated P-wave velocity of 1,800 m/s was fixed at a depth of 5 m during data modeling.
- Layer thickness in the V_S model was used to limit velocity inversions in the model as a velocity inversion does not appear warranted based on geologic conditions.
- Surface wave depth of investigation is about 30 m based on half of maximum wavelength criteria.
- V_{S30} is 376 m/s (NEHRP Site Class C/D).
- Average S-wave velocity between 1 m (assumed sensor depth) and 31 m is 400 m/s (NEHRP Site Class C).

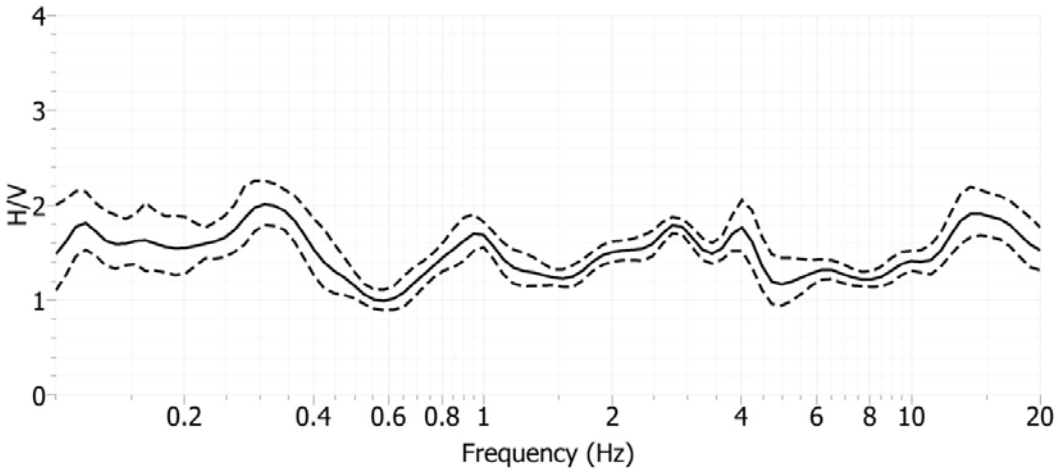

Site NC.JSGB, H/V Spectral Ratio, Array JSGB-1, Sensor 507

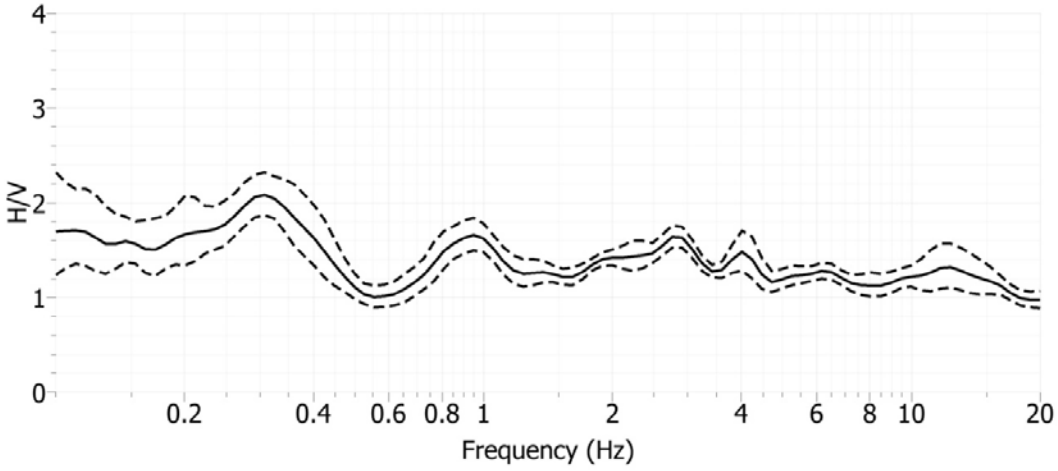

Site NC.JSGB, H/V Spectral Ratio, Near Seismic Station, Sensor 453

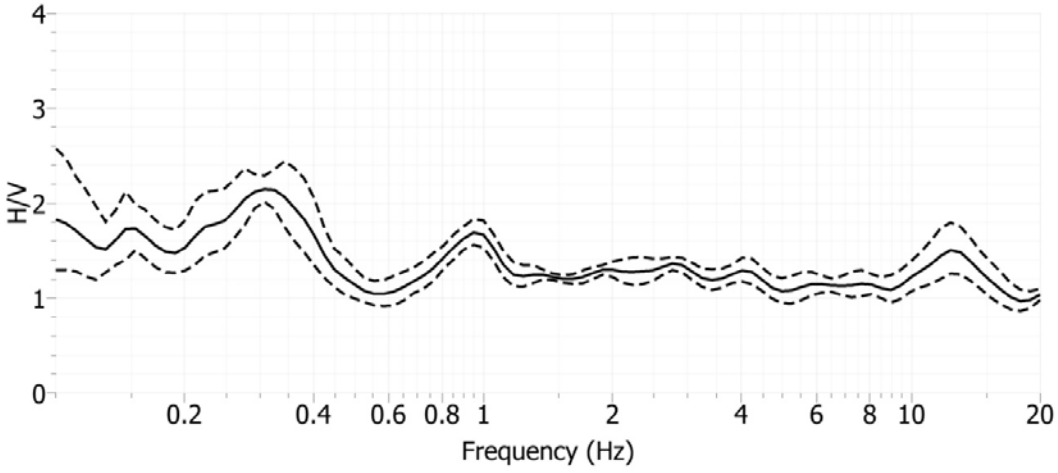

Site NC.JSGB, H/V Spectral Ratio, Array JSGB-1, Sensor 450

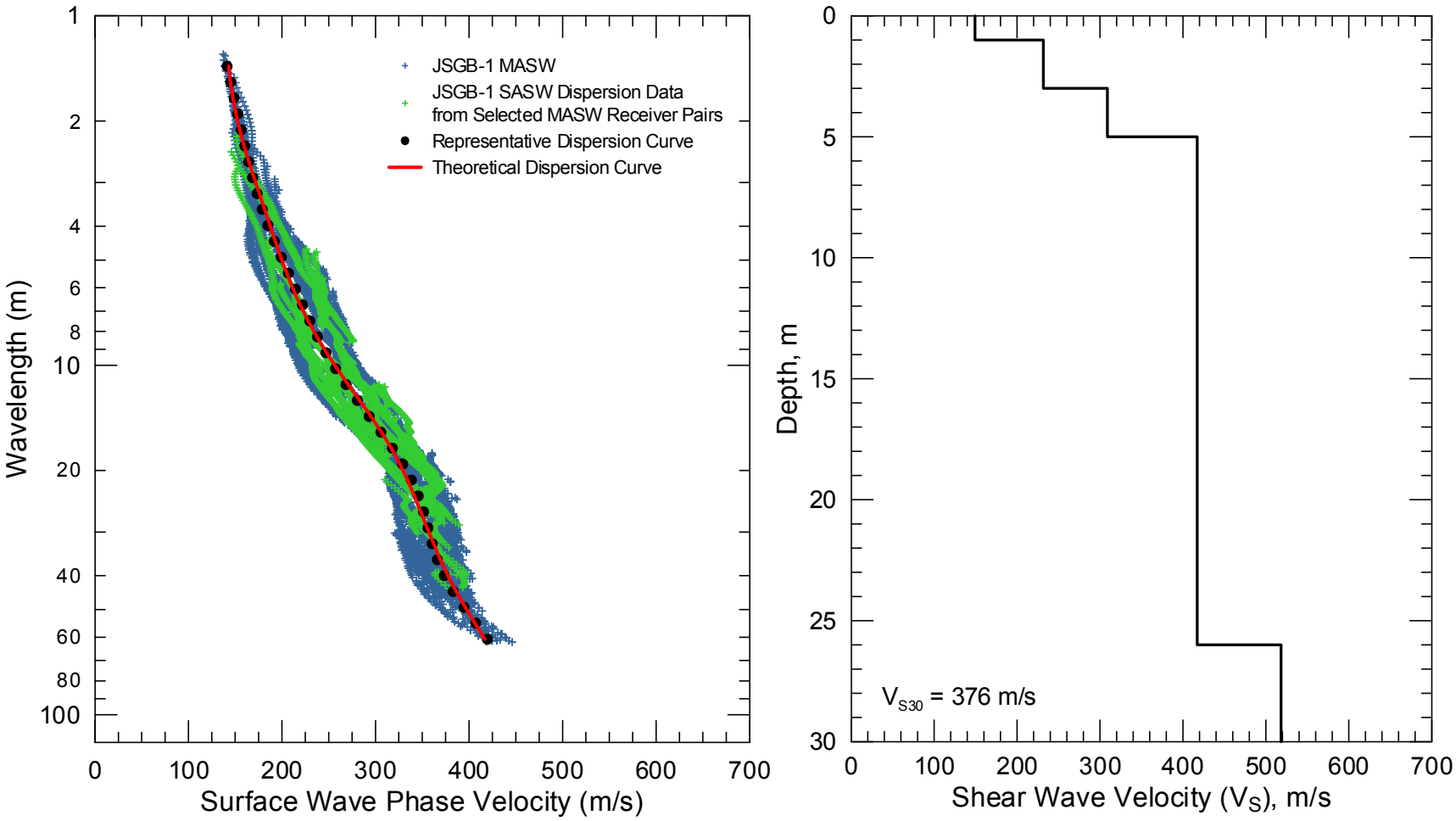

NC.JSGB - Field, representative and inverted theoretical surface wave dispersion data (left) and associated V_S model (right)

Site NC.MBS1

Location: Big Spring, Mono County, California

Latitude: 37.76099 **Longitude:** -118.94467
(Station coordinates based on site GPS survey, WGS84 coordinate system)

V_{S30} (measured): 740 m/s

V_{S30} (adjusted to more accurately reflect seismic station conditions): 833 m/s (average S-wave velocity between 1 and 31 m adjusting for assumed 1 m sensor depth).

NEHRP Site Class: C/B

Geomatrix Code: IGA

Geologic Conditions/Observations: Seismic station located on geologic unit mapped as Mesozoic (Jurassic) granitic rocks.

Site Conditions: Rural site. Undulating (hilly) topography in site vicinity. Seismic station located at the toe of slope of a bedrock outcrop.

Geophysical Methods Utilized: HVSR, Seismic Refraction (P- and S-wave), MASW (Rayleigh Wave), MALW (Love Wave)

Geophysical Testing Arrays:

1. Array MBS1-1 (48 channel MASW and P-wave seismic refraction array utilizing 4.5 Hz vertical geophones spaced 2 m apart for a length of 94 m, forward and reverse shot locations with multiple source offsets and source types and multiple interior shot locations).
2. Array MBS1-2 (24 channel P-wave seismic refraction array utilizing 4.5 Hz vertical geophones spaced 3 m apart for a length of 69 m, forward and reverse shot locations and multiple interior shot locations and 48 channel S-wave seismic refraction array utilizing 4.5 Hz horizontal geophones space 1.5 m apart for a length of 70.5 m).
3. Array MBS1-3 (48 channel MASW and P-wave seismic refraction array utilizing 4.5 Hz vertical geophones spaced 1.5 m apart for a length of 70.5 m, forward and reverse shot locations with multiple source offsets and source types and multiple interior shot locations).
4. Array MBS1-4 (48 channel MALW and S-wave seismic refraction array utilizing 4.5 Hz horizontal geophones spaced 1 m apart for a length of 47 m). Located along array MBS1-3 with origin located 10 m southeast of the origin of array MBS1-3.

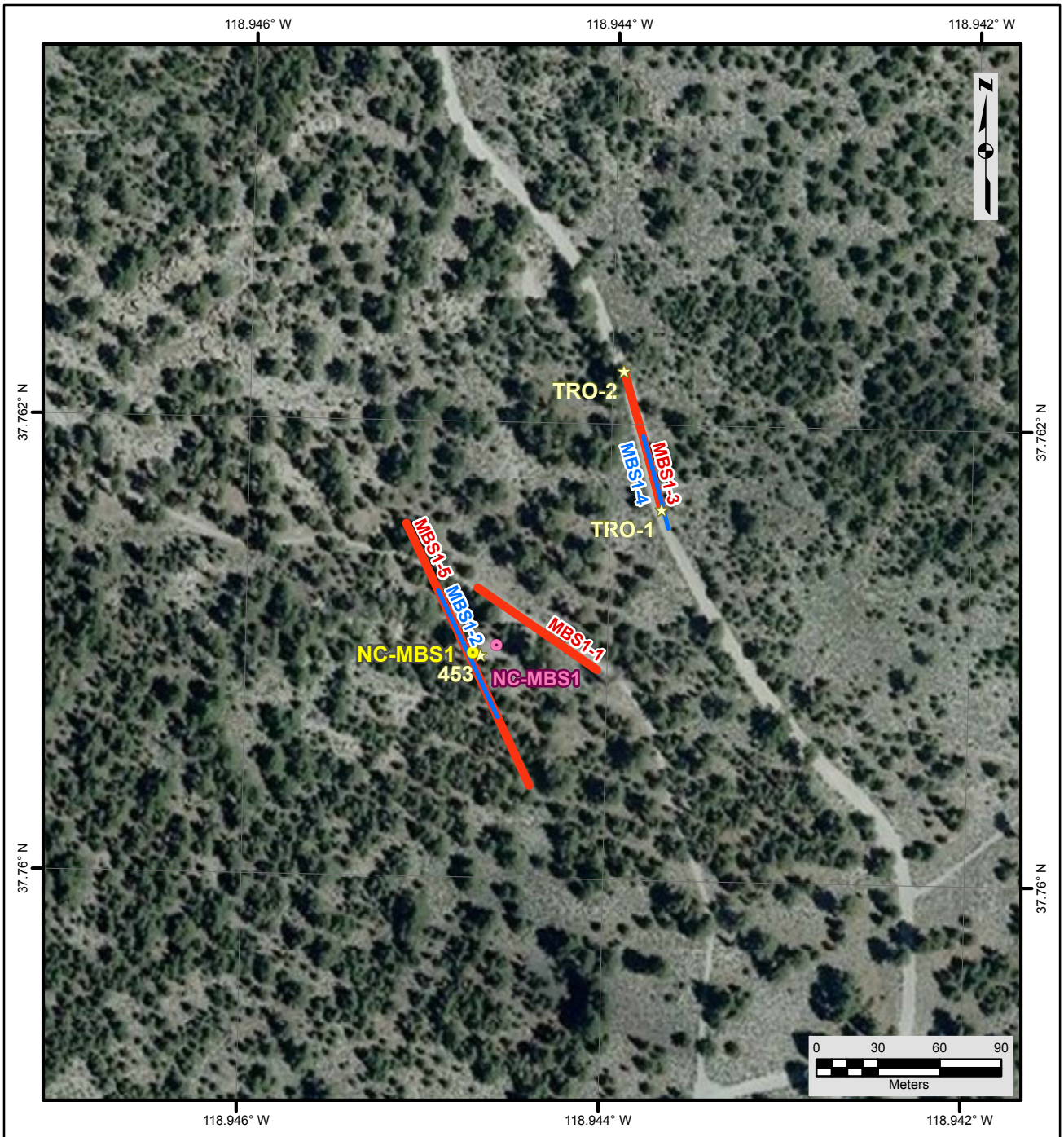

Legend

- Seismic Station - Approximate Surveyed Location
- Seismic Station - Approximate Location of Record
- H/V Spectral Ratio Location
- MASW and Seismic Refraction Array (P- and/or S-wave)
- MASW and Seismic Refraction Array

NOTES:
1. WGS 1984 COORDINATE SYSTEM
2. Image Source: ESRI, i-cubed, USDA FSA, USGS, AEX, GeoEye, Getmapping, Aerogrid, IGP

File Name: NC-MBS1-I

Date: 5/10/2012

USGS science for a changing world

GEOVision geophysical services

RECOVERY.GOV

SITE MAP
NC•MBS1

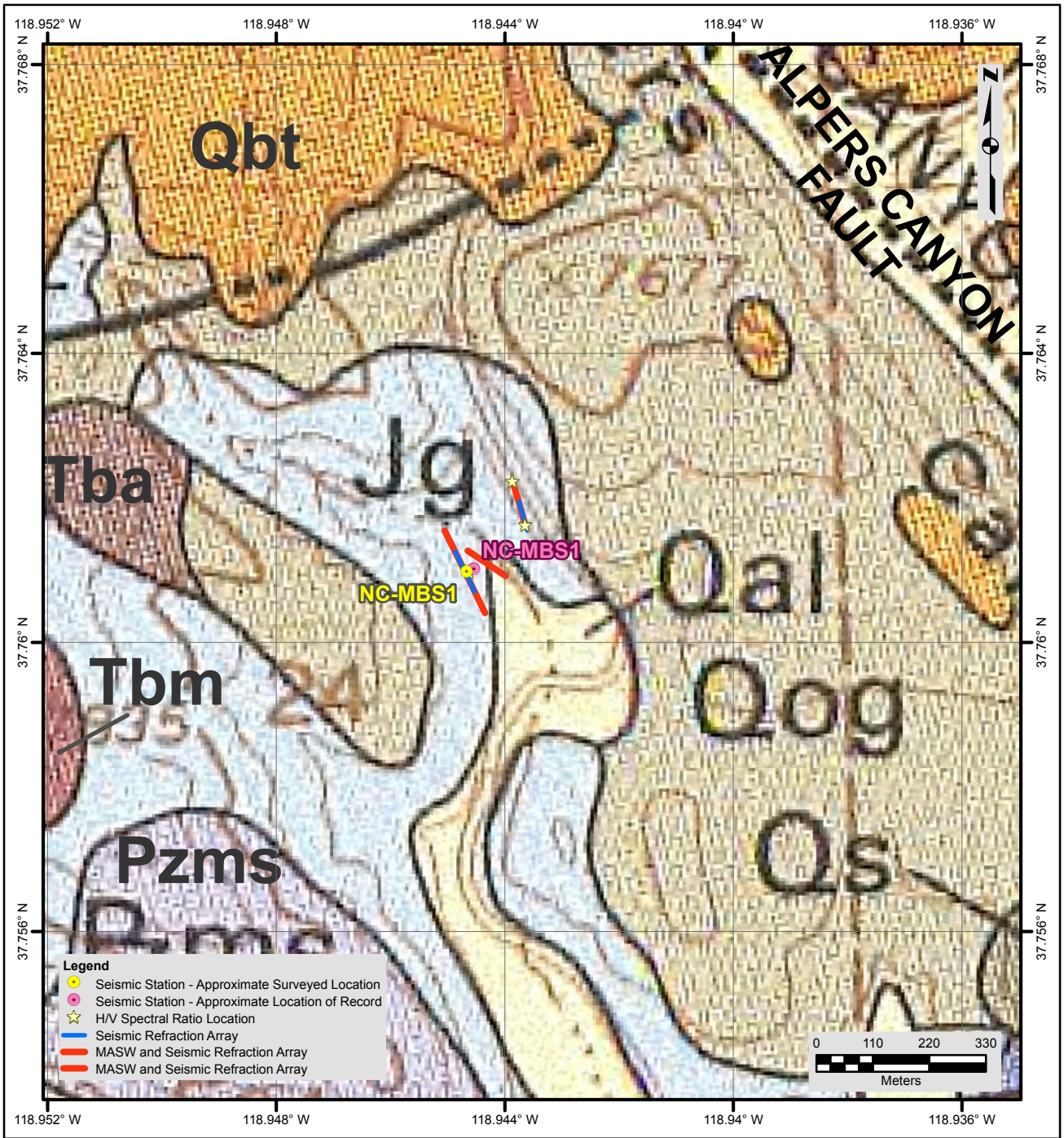

Description of Geologic Map Units

Qal = Quaternary (Holocene) younger alluvium, unconsolidated silt, sand and gravel
Qog = Quaternary (Pleistocene) older gravel deposits, coarse gravels
Qbt = Quaternary (Pleistocene) Bishop Tuff, nonwelded to densely welded rhyolite ash-flow tuff
Tbm = Tertiary (Pliocene) quartz latite of Bald Mountain
Tba = Tertiary (Pliocene) trachybasaltic and trachyandesitic lavas
Jg = Mesozoic (Jurassic) granitic rocks mapped as granite of Casa Diablo Mountain
Pzms = Paleozoic (Odovician to Permian) metasedimentary rocks

NOTES:
1. WGS 1984 COORDINATE SYSTEM
2. Geologic Map of Long Valley Caldera, Mono-Inyo Craters Volcanic Chain, and Vicinity, Eastern California, by Roy A. Bailey, 1989
3. See site map for details of geophysical survey

File Name: NC-MBS1

Date: 3/29/2012

USGS science for a changing world

GEOVision geophysical services

RECOVERY.GOV

GEOLOGIC MAP
NC•MBS1

Looking northwest along array MBS1-1

Looking east at NC.MBS1 seismic station

Looking southeast along array MBS1-2

Looking northwest along arrays MBS1-3 and MBS1-4

Looking southeast towards center of P-wave refraction array MBS1-5

5. Array MBS1-5 (48 channel P-wave seismic refraction array utilizing 4.5 Hz vertical geophones spaced 3 m apart for a length of 141 m, forward and reverse shot locations and multiple interior shot locations). Coincident with Array MBS1-2.
6. Three HVSR measurement locations: two distributed along array MBS1-3 and one adjacent to the seismic station.

Location of Geophysical Testing Arrays:

Location	Latitude	Longitude
MBS1-1, Northwest End of MASW/Refraction Array	37.76131	-118.94489
MBS1-1, Center of MASW/Refraction Array	37.76114	-118.94439
MBS1-1, Southeast End of MASW/Refraction Array	37.76092	-118.94398
MBS1-2, Northwest End of 24 Channel MASW/Refraction Array	37.76125	-118.94488
MBS1-2, Center of 24 Channel MASW/Refraction Array	37.76097	-118.94468
MBS1-2, Southeast End of 24 Channel MASW/Refraction Array	37.76074	-118.94457
MBS1-2, Northwest End of 48 Channel MALW/Refraction Array	37.76071	-118.94453
MBS1-2, Center of 48 Channel MALW/Refraction Array	37.76098	-118.94469
MBS1-2, Southeast End of 48 Channel MALW/Refraction Array	37.76125	-118.94487
MBS1-3, Southeast End of MASW/Refraction Array	37.76163	-118.94364
MBS1-3, Center of MASW/Refraction Array	37.76193	-118.94375
MBS1-3, Northwest End of MASW/Refraction Array	37.76223	-118.94387
MBS1-4, Southeast End of MALW/Refraction Array	37.76155	-118.94360
MBS1-4, Center of MALW/Refraction Array	37.76175	-118.94368
MBS1-4, Northwest End of MALW/Refraction Array	37.76195	-118.94375
MBS1-5, Southeast End of P-wave Refraction Array	37.76040	-118.94436
MBS1-5, Center of P-wave Refraction Array	37.76098	-118.94469
MBS1-5, Northwest End of P-wave Refraction Array	37.76154	-118.94505
HVSR Sensor 453	37.76098	-118.94463
HVSR Sensor Tromino ENGY (TRO-1)	37.76163	-118.94364
HVSR Sensor Tromino ENGY (TRO-2)	37.76223	-118.94387
NC.MBS1 Seismic Station	37.76099	-118.94467

Notes: 1) WGS84 Coordinate System (decimal degrees)

2) Survey accuracy is estimated at 2 to 4 m.

Results:

Average V_P Model and Estimated V_S Models between 51 and 99 m on P-wave Seismic Refraction Array MBS1-5

Depth to Top of Layer (m)	Layer Thickness (m)	P-Wave Velocity (m/s)	Estimated S-Wave Velocity (m/s)			
			Poisson's Ratio = 0.25	Poisson's Ratio = 0.3	Poisson's Ratio = 0.35	Poisson's Ratio = 0.4
0.00	0.48	254	146	136	122	104
0.48	0.97	348	201	186	167	142
1.45	0.97	402	232	215	193	164
2.42	0.97	412	238	220	198	168
3.39	0.97	729	421	389	350	297
4.36	0.97	982	567	525	472	401
5.32	0.97	1204	695	644	579	492
6.29	2.03	1297	749	693	623	530
8.32	2.03	1386	800	741	666	566
10.36	2.03	1532	884	819	736	625
12.39	2.03	1851	1069	989	889	756
14.42	2.03	1883	1087	1006	904	769
16.46	2.03	1927	1112	1030	926	787
18.49	2.03	1996	1152	1067	959	815
20.52	2.03	2216	1280	1185	1065	905
22.55	2.03	2260	1305	1208	1086	923
24.59	2.03	2285	1319	1221	1098	933
26.62	Half Space	2413	1393	1290	1159	985

Average V_P Model and Estimated V_S Models between 51 and 75 m on P-wave Seismic Refraction Array MBS1-5

Depth to Top of Layer (m)	Layer Thickness (m)	P-Wave Velocity (m/s)	Estimated S-Wave Velocity (m/s)			
			Poisson's Ratio = 0.25	Poisson's Ratio = 0.3	Poisson's Ratio = 0.35	Poisson's Ratio = 0.4
0.00	0.49	289	167	155	139	118
0.49	0.97	438	253	234	210	179
1.46	0.97	537	310	287	258	219
2.43	0.97	557	322	298	268	227
3.40	0.97	1335	771	714	641	545
4.37	0.97	1354	782	724	651	553
5.34	0.97	1419	819	758	682	579
6.32	2.04	1494	862	798	718	610
8.36	2.04	1628	940	870	782	665
10.40	2.04	1737	1003	928	834	709
12.44	2.04	1852	1069	990	890	756
14.48	2.04	1889	1091	1010	908	771
16.52	2.04	1962	1133	1049	943	801
18.56	2.04	2066	1193	1104	992	843
20.60	2.04	2237	1292	1196	1075	913
22.64	2.04	2248	1298	1202	1080	918
24.68	2.04	2272	1312	1214	1091	927
26.72	Half Space	2385	1377	1275	1146	974

Observations/Discussion:

- Multiple attempts were made to characterize this site with the site being visited on 8/21/10, 10/28/11 and 11/10/11. During the first site visit on 8/21/10, seismic refraction and MASW data were acquired along the 96 m long array MBS1-1 and 69 m long array MBS1-2. Array MBS1-2 was located adjacent to the seismic station, at the toe of slope of a bedrock outcrop, and was not expected to yield surface wave dispersion data. HVSR data were also acquired at the site, but were not of sufficient quality for modeling as adequate field procedures for acquisition of high quality HVSR data using Nanometrics Trillium Compact seismometers were still under development. Therefore, the site was revisited on 10/28/11 when HVSR data were acquired with both a Nanometrics Trillium Compact and Micromed Tromino ENGY and an attempt was made to acquire surface wave data at an alternate test location. P-wave seismic refraction and MASW data were acquired along the 70.5 m long array MBS1-3 and S-wave refraction and MALW data were acquired along to 47 m long array MBS1-4. The origin of array MBS1-4 was offset 10 m to the southeast of array MBS1-3 and the length of the array was reduced to avoid significant lateral velocity variation observed during acquisition of the seismic data along

array MBS1-3. Review of the seismic data collected along arrays MBS1-3 and MBS1-4 revealed that the arrays did not yield useful surface wave dispersion data. Therefore, the site was revisited a final time on 11/10/11 when P-wave refraction array MBS1-2 was replaced with the 141 m long P-wave refraction array MBS1-5 and S-wave refraction data were acquired along array MBS1-2.

- HVSR data were acquired adjacent to the seismic station, near the center of arrays MBS1-2 and MBS1-5, using a Nanometrics Trillium Compact seismograph. HVSR data were also acquired near the southeast and northwest ends of array MDPB-3 using a Micromed Tromino ENGY. There are no low frequency peaks in the HVSR data that might be expected for a rock site. There is a peak at 20 Hz in the HVSR data collected adjacent to the seismic station. If this peak has a geologic source, then it would be related to a couple meters of low velocity sediments overlying bedrock. There are no conclusive HVSR peaks in the HVSR data collected along array MBS1-3.
- It was not possible to extract surface wave dispersion data of sufficient reliability to characterize S-wave velocity structure from any of the multiple seismic arrays acquired at this site. The primary reason for failure of surface wave techniques at this site is the highly variable weathering of the granitic rocks as evidenced by seismic refraction models presented below.
- P-wave seismic refraction data were interpreted for arrays MBS1-1, MBS1-3 and MBS1-5. The longer array MBS1-5 replaces the shorter and coincidently located array MBS1-2. P-wave seismic refraction data collected along array MBS1-5, approximately centered at the seismic station, were of the best quality. The highly variable weathering of bedrock in the vicinity of arrays MBS1-1 and MBS1-3 was such that out of plane refractors may have occurred as first arrivals on some seismic records. These arrays were, however, processed to demonstrate the lateral velocity variation at the site and range of bedrock P-wave velocity.
- S-wave refraction data were acquired along array MBS1-2, approximately centered at the seismic station, and array MBS1-4, coincident with the southeastern half of array MBS1-3. First arrival data could not be accurately interpreted from array MBS1-2 seismic refraction data due to probable converted waves occurring as high amplitude first arrivals on some of the seismic records. S-wave seismic refraction data collected along array MBS1-4 were of better quality. This data was modeled to determine nominal S-wave velocity for bedrock in the site vicinity, but should not be used for site characterization because the array is located about 110 m from the seismic station and there is significant lateral velocity variation evident in all refraction models.
- The P-wave refraction data for array MBS1-1 were modeled using a tomographic inversion routine with a layer based starting model. The seismic refraction model was extended to far offset shot locations to extend depth of investigation. The seismic refraction survey design allowed P-wave velocity to be imaged to a maximum depth of about 20 m. The seismic refraction model indicates that there is about 3 to 9 m of sediments with P-wave velocity between 250 and 400 m/s overlying weathered bedrock with P-wave velocity between about 750 and 2,000 m/s. There is significant lateral velocity variation beneath this array due to variable thickness of the sediments overlying bedrock and differential weathering of the bedrock unit. Surface wave data of sufficient quality to model subsurface S-wave velocity structure could not be recovered from this array.

- The P-wave refraction data for array MBS1-3 were modeled using a tomographic inversion routine with a smooth velocity gradient starting model. Data quality was such that the seismic refraction model was not extended to offend shot locations. The seismic refraction survey design allowed P-wave velocity to be imaged to a maximum depth of about 15 m. The seismic array was located on weathered rock and the velocity model indicates that there is significant lateral velocity variation with P-wave velocity ranging from about 500 to 2,250 m/s. The obvious lateral velocity variation limited the use of surface wave data from the array.
- The S-wave refraction data for array MBS1-4 were modeled using a tomographic inversion routine with a layer based starting model. As with array MBS1-3, data quality was not particularly good possibly due to the complex velocity structure. The seismic refraction model was extended to limited offend shot locations to extend depth of investigation. The origin on array MBS1-4 was offset 10 m southeast of the origin of array MBS1-3 (i.e. position of 20 m on array MBS1-4 equals 10 m on array MBS1-3, etc.). The seismic refraction survey design allowed S-wave velocity to be imaged to a maximum depth of about 10 m. Relatively high S-wave velocity between 10 and 20 m and at 40 m on array MBS1-4 correspond to the localized high P-wave velocity zones at 0 to 10 m and 30 m on the P-wave model for array MBS1-3. Data quality is not good enough to warrant using the P- and S-wave refraction models to accurately estimate Poisson's ratio. It is, however, clear that S-wave velocity in the 900 to 1,000 m/s can be expected for weathered bedrock in the site vicinity.
- The P-wave seismic refraction data for array MBS1-5 were modeled using a tomographic inversion routine with a layer-based starting model. The model was extended to off-end shot locations to extend depth of investigation. The depth of investigation was about 28 m. The seismic refraction model indicates that there is about 1 to 4 m of sediments with P-wave velocity in the 250 to 350 m/s range overlying weathered bedrock with P-wave velocity increasing with depth from about 650 m/s to over 2,000 m/s at a depth of about 8 to 19 m. The maximum P-wave velocity in the model is about 2,450 m/s. P-wave velocities of weathered bedrock beneath array MBS1-5 are generally slightly higher than beneath arrays MBS1-1 and MBS1-3. The seismic station is located adjacent to a position of about 69 m on the seismic array. The P-wave refraction data collected along array MBS1-5 is used for site characterization. Reliable S-wave refraction data were not obtained from the coincident, but shorter array MBS1-2.
- The average P-wave velocity of the upper 30 m (V_{P30}) was estimated between 51 and 99 m on the array MBS1-5 refraction model, where depth of investigation is greatest. V_{P30} ranges from about 963 to 1,541 m/s over this interval; a significant 47% variation related to variable sediment thickness and variable weathering of the granitic rocks. An average V_P model was developed over the 51 to 99 m distance interval by horizontally averaging the travel time of each model cell and cell thickness and average V_{P30} was determined to be 1,181 m/s. Assuming constant Poisson's ratios of 0.25, 0.3, 0.35 and 0.4 would result in an estimated V_{S30} of 685, 634, 570 and 484 m/s, respectively. The average V_P between 1 and 31 m, to account to assumed seismic sensor depth, is 1,345 m/s. Assuming constant Poisson's ratios of 0.25, 0.3, 0.35 and 0.4 would result in estimated average V_S between 1 and 31 m (adjusted V_{S30}) of 776, 719, 646 and 549 m/s, respectively.
- The seismic station is located adjacent to a portion of array MBS1-5 with higher near surface P-wave velocity. Therefore, to more accurately reflect seismic station conditions,

the average P-wave velocity of the upper 30 m (V_{P30}) was estimated between 51 and 75 m on the array MBS1-5 refraction model. V_{P30} ranges from about 1,095 to 1,541 m/s over this interval; a 32% variation. An average V_P model was developed over the 51 to 75 m distance interval by horizontally averaging the travel time of each model cell and cell thickness and average V_{P30} was determined to be 1,384 m/s. Assuming constant Poisson's ratios of 0.25, 0.3, 0.35 and 0.4 would result in an estimated V_{S30} of 799, 740, 665 and 565 m/s, respectively. The average V_P between 1 and 31 m, to account to assumed seismic sensor depth, is 1,559 m/s. Assuming constant Poisson's ratios of 0.25, 0.3, 0.35 and 0.4 would result in estimated average V_S between 1 and 31 m (adjusted V_{S30}) of 900, 833, 749 and 636 m/s, respectively.

- An average Poisson's ratio of 0.3 is considered reasonable for weathered granitic rock. A Poisson's ratio of 0.3 yields estimated S-wave velocity of 800 to 1,100 m/s between depths of about 5 and 16 m in the two average V_P models for array MBS1-5, discussed above, which is consistent with the S-wave velocities observed in the V_S model for S-wave refraction array MBS1-4.
- The average V_P model between 51 and 75 m on array MBS1-5 is considered most representative of seismic station conditions. Estimated V_{S30}, using a constant Poisson's ratio of 0.3 is 740 m/s (NEHRP Site Class C) and adjusted V_{S30} (1 to 31 m) is 833 m/s (NEHRP Site Class B).
- Given the significant lateral velocity variation in the site vicinity, requiring that S-wave velocity structure be estimated from P-wave seismic refraction models using an assumed Poisson's ratio of 0.3, we recommend that this site be further characterized by borehole and geophysical logging.
- Even though site characterization was complicated, all areas in the site vicinity with soil cover will definitely fall into the NEHRP Site Class C category. Exposed bedrock will fall into the NEHRP Site Class C or B depending on the local weathering profile.

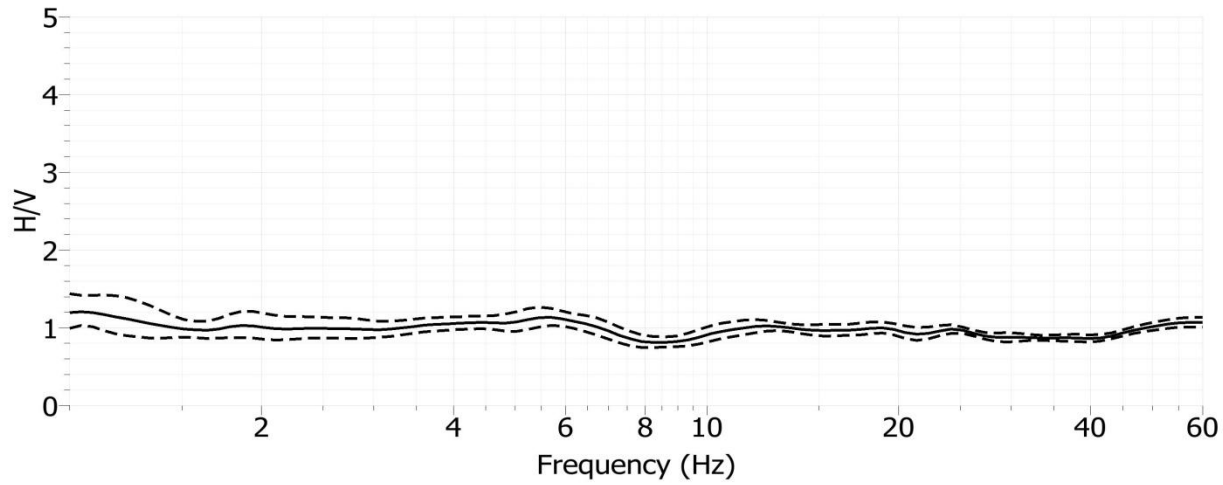

Site NC-MBS1, H/V Spectral Ratio, Array MBS1-3, Sensor TRO-2

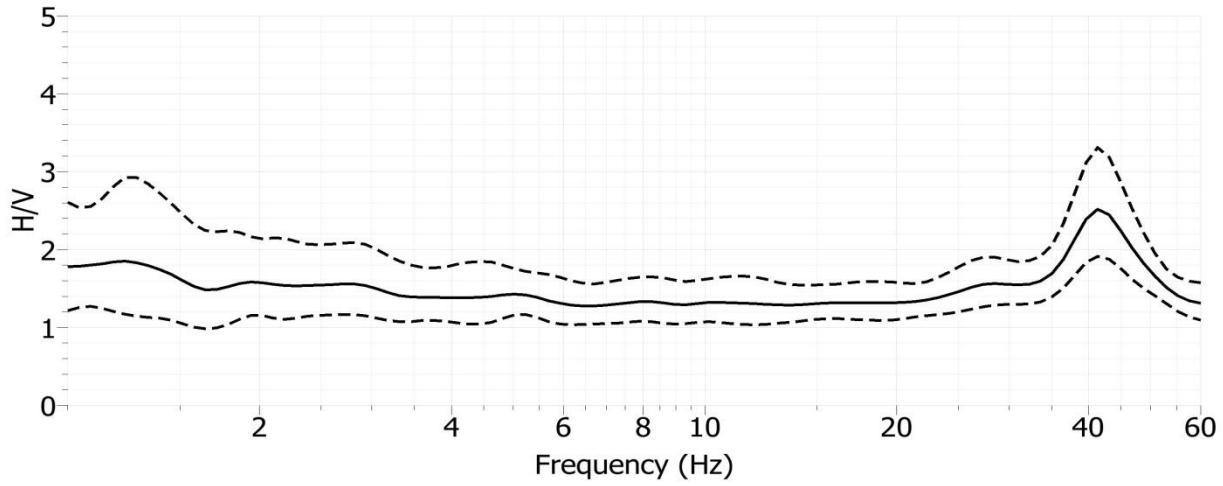

Site NC-MBS1, H/V Spectral Ratio, Array MBS1-3, Sensor TRO-1

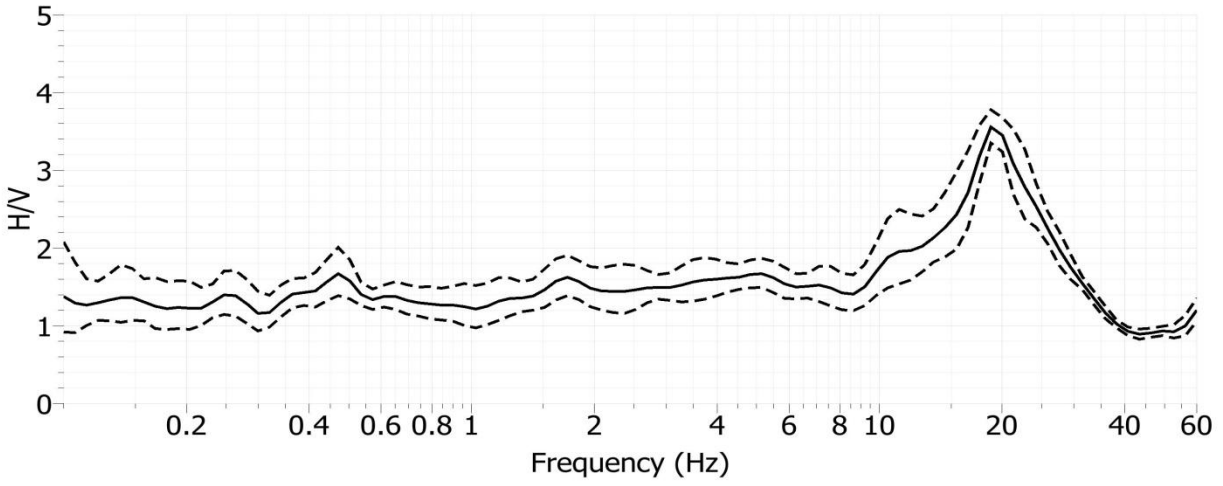

Site NC-MBS1, H/V Spectral Ratio, Near Seismic Station, Sensor 453

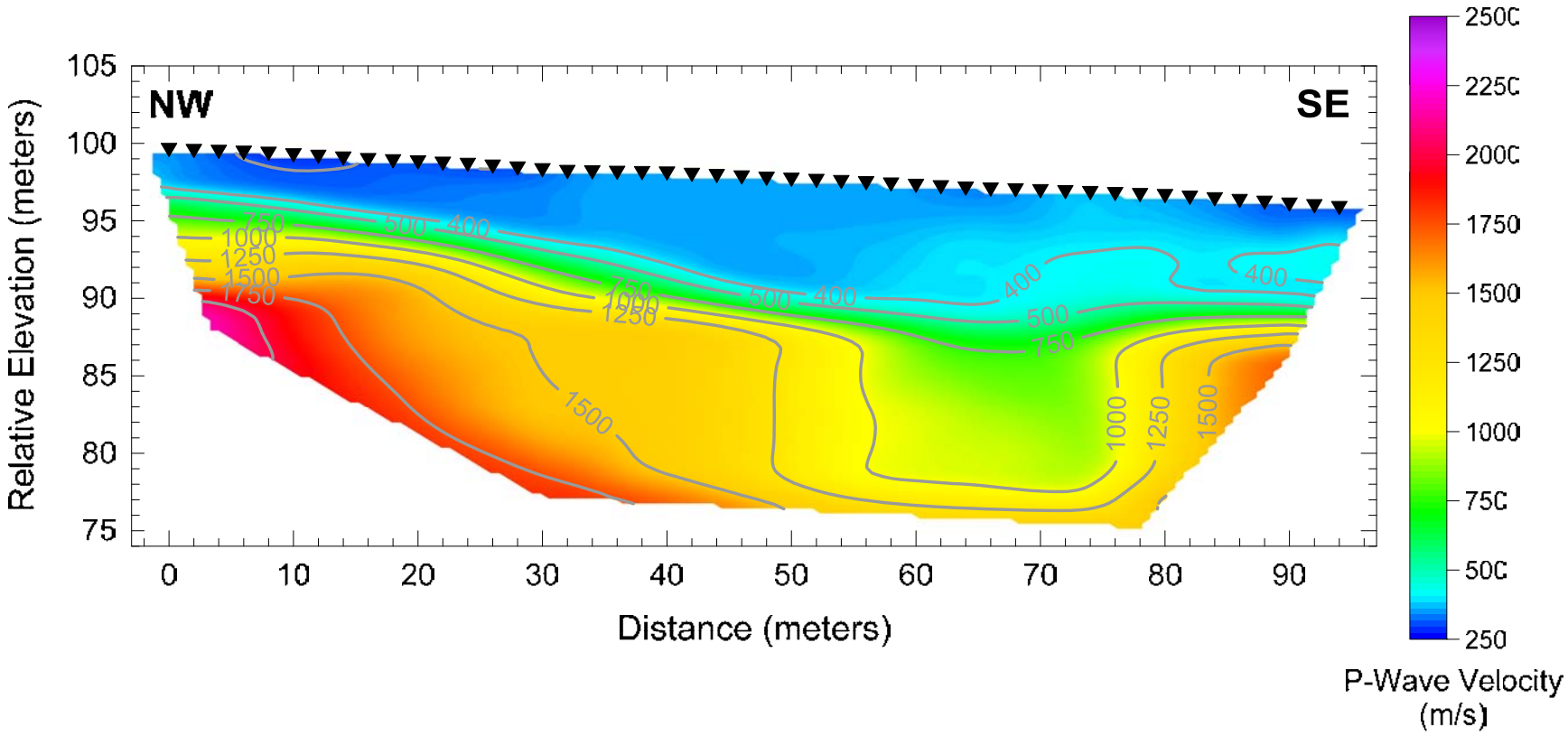

Array MBS1-1 – P-wave tomographic seismic refraction model developed using a layer based starting model

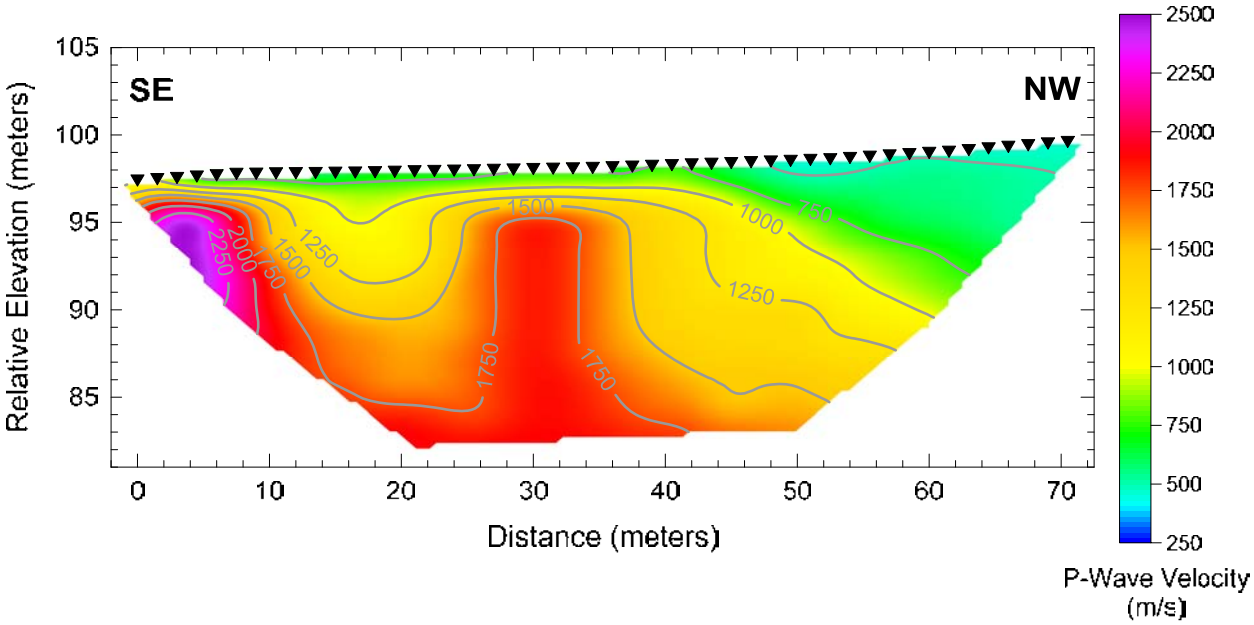

Array MBS1-3 – P-wave tomographic seismic refraction model developed using a smooth velocity gradient starting model

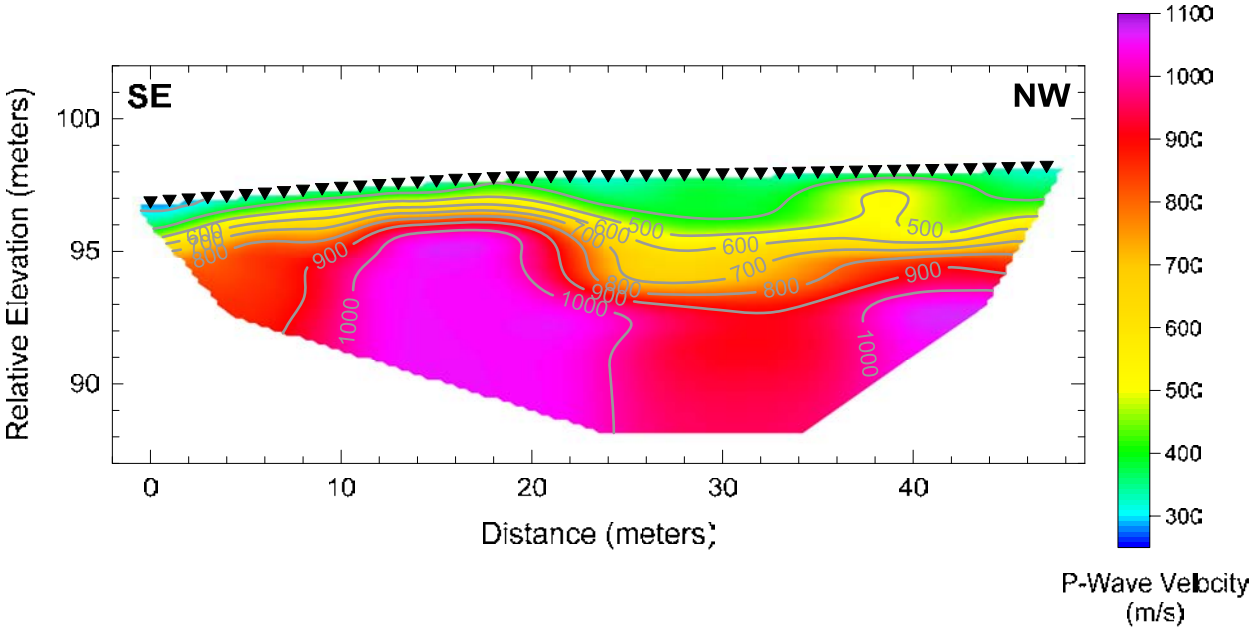

Array MBS1-4 – S-wave tomographic seismic refraction model developed using a layer based starting model (Array MBS1-4 is offset 10 m to the southeast from Array MBS1-3)

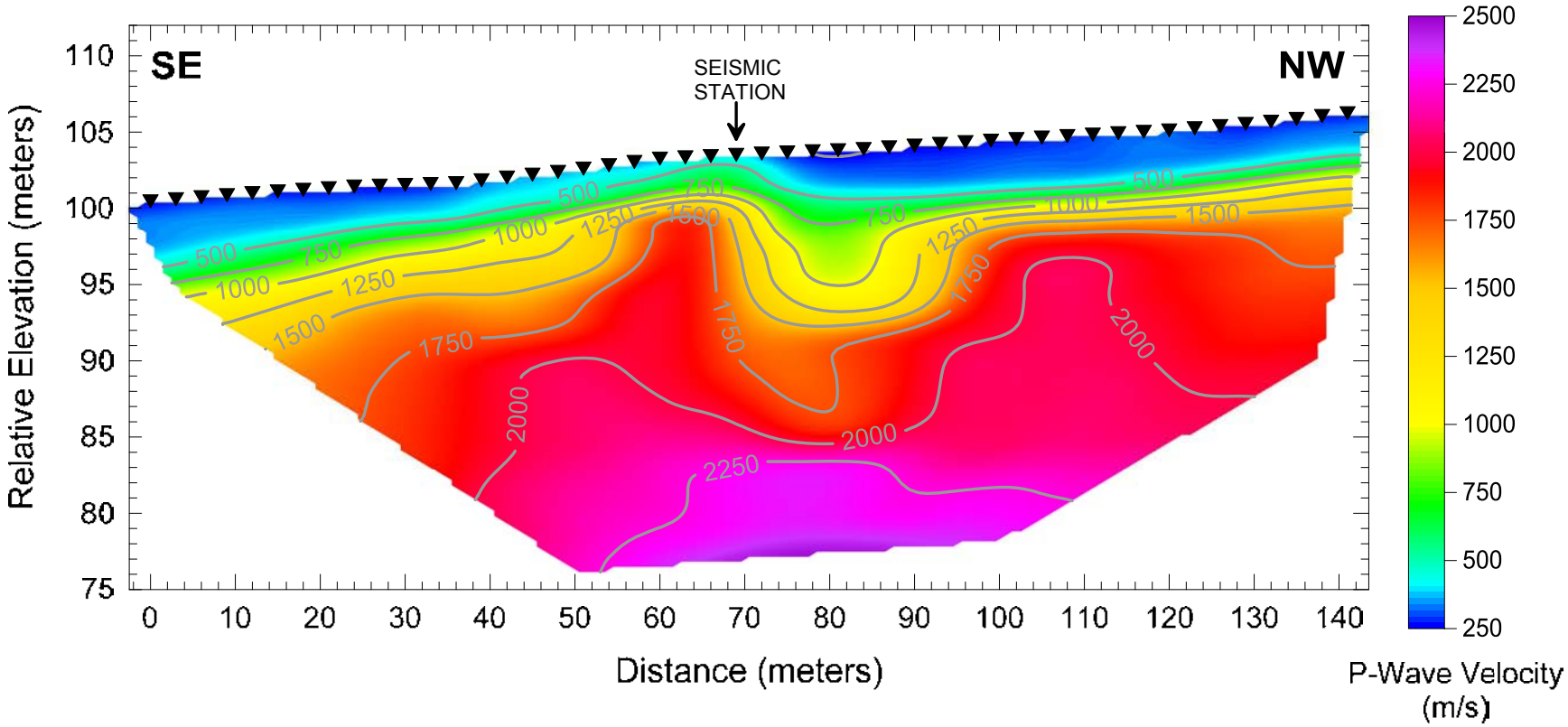

Array MBS1-5 – P-wave tomographic seismic refraction model developed using a layer based starting model

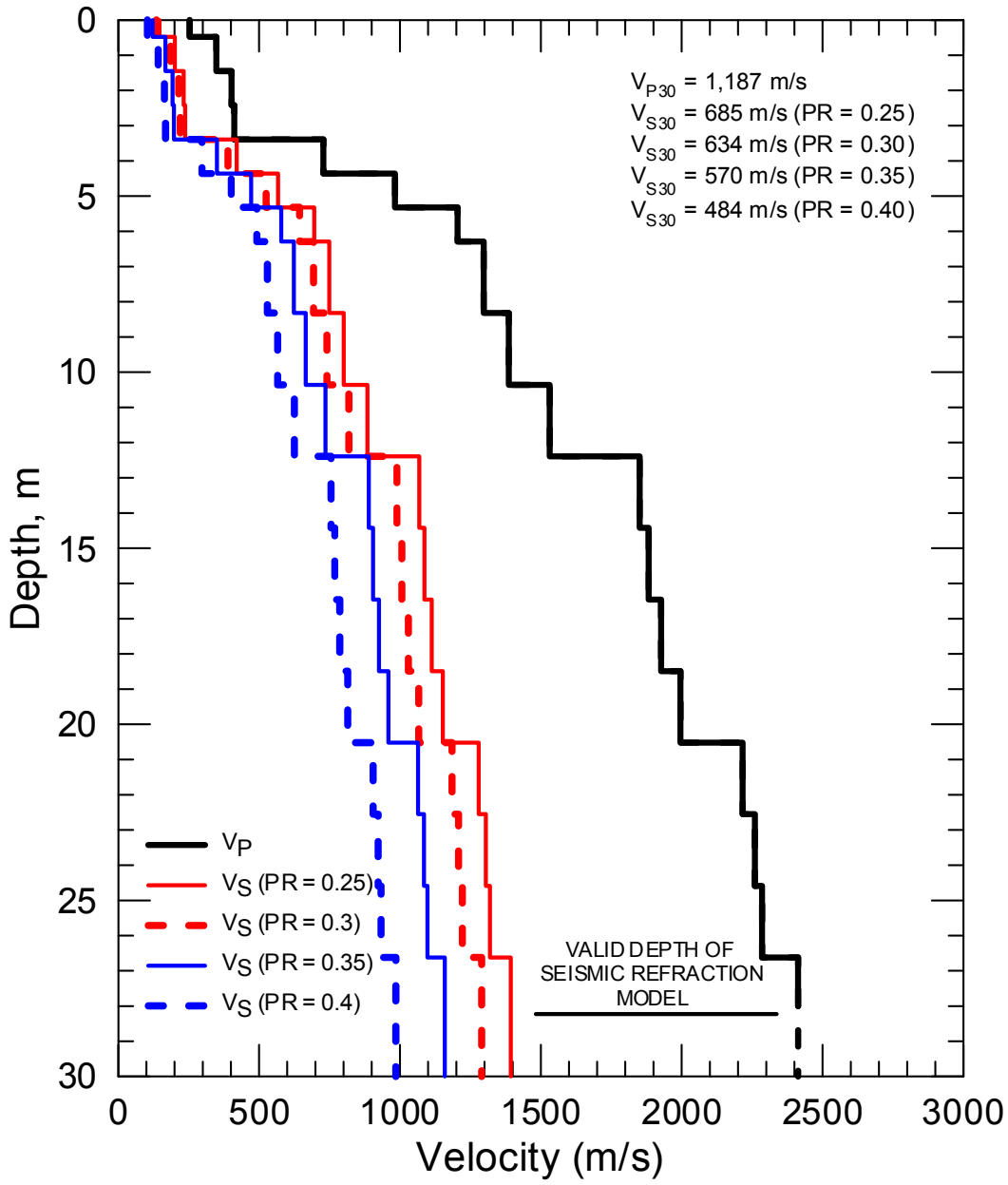

NC.MBS1 – Average P-wave velocity structure and estimated S-wave velocity structure between a position of 51 and 99 m on the P-wave seismic refraction model for array MBS1-5

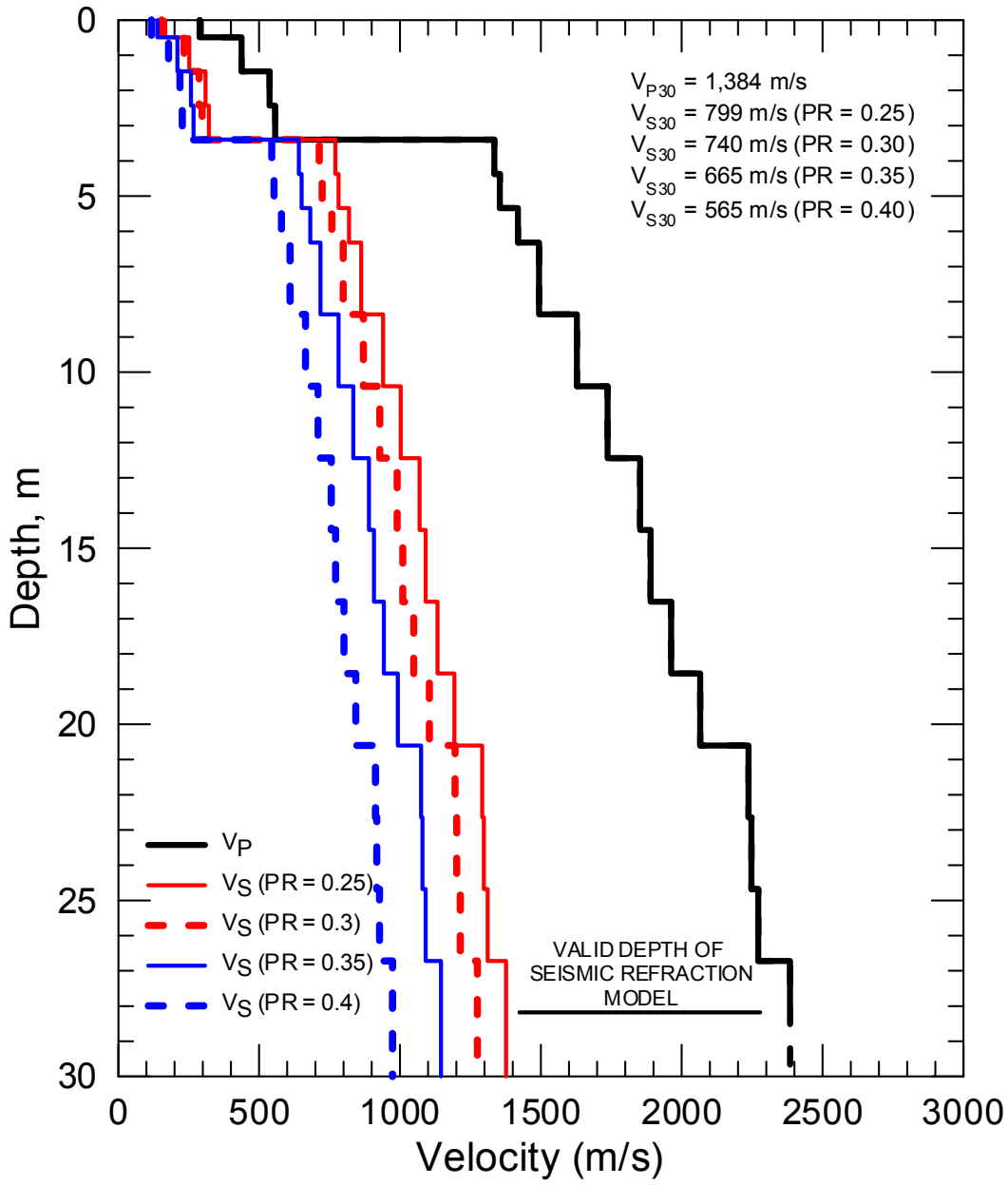

NC.MBS1 – Average P-wave velocity structure and estimated S-wave velocity structure between a position of 51 and 75 m on the P-wave seismic refraction model for array MBS1-5

Site NC.MDPB

Location: Devils Postpile, Mammoth, California

Latitude: 37.63227 **Longitude:** -119.07935
(Station coordinates provided by USGS, WGS84 coordinate system)

V_{S30} (measured): 580 m/s

V_{S30} (adjusted to more accurately reflect seismic station conditions): 706 m/s (average S-wave velocity between 1 and 31 m adjusting for assumed 1 m sensor depth).

NEHRP Site Class: C

Geomatrix Code: IVA

Geologic Conditions/Observations: Seismic station located on geologic unit mapped as Quaternary (Pleistocene) andesite. Cretaceous granitic rocks outcrop within 350 m of the seismic station and underlie the andesite unit.

Site Conditions: Rural site. Hilly, undulating topography in site vicinity. Seismic station located on top of small hill.

Geophysical Methods Utilized: HVSR, Seismic Refraction, MASW

Geophysical Testing Arrays:

1. Array MDPB-1 - 48 channel MASW and P-wave seismic refraction array utilizing 4.5 Hz vertical geophones spaced 1.5 m apart for a length of 70.5 m, forward and reverse shot locations with multiple source offsets and source types and multiple interior shot locations.
2. Array MDPB-2 - 24 channel MASW and P-wave seismic refraction array utilizing 4.5 Hz vertical geophones spaced 2 m apart for a length of 46 m, forward and reverse shot locations with multiple source offsets and source types (hammers only) and multiple interior shot locations. Array MDPB-2 is replaced by array MDPB-3.
3. Array MDPB-3 - 48 channel MASW and P-wave seismic refraction array utilizing 4.5 Hz vertical geophones spaced 1 m apart for a length of 47 m, forward and reverse shot locations with multiple source offsets and source types (hammers only) and multiple interior shot locations. Origin of array MDPB-3 is located 9 m southeast of the origin of array MDPB-2.
4. Three HVSR measurement locations: one along array MDPB-1, one along array MDPB-3 and one adjacent to the seismic station near array MDPB-3.

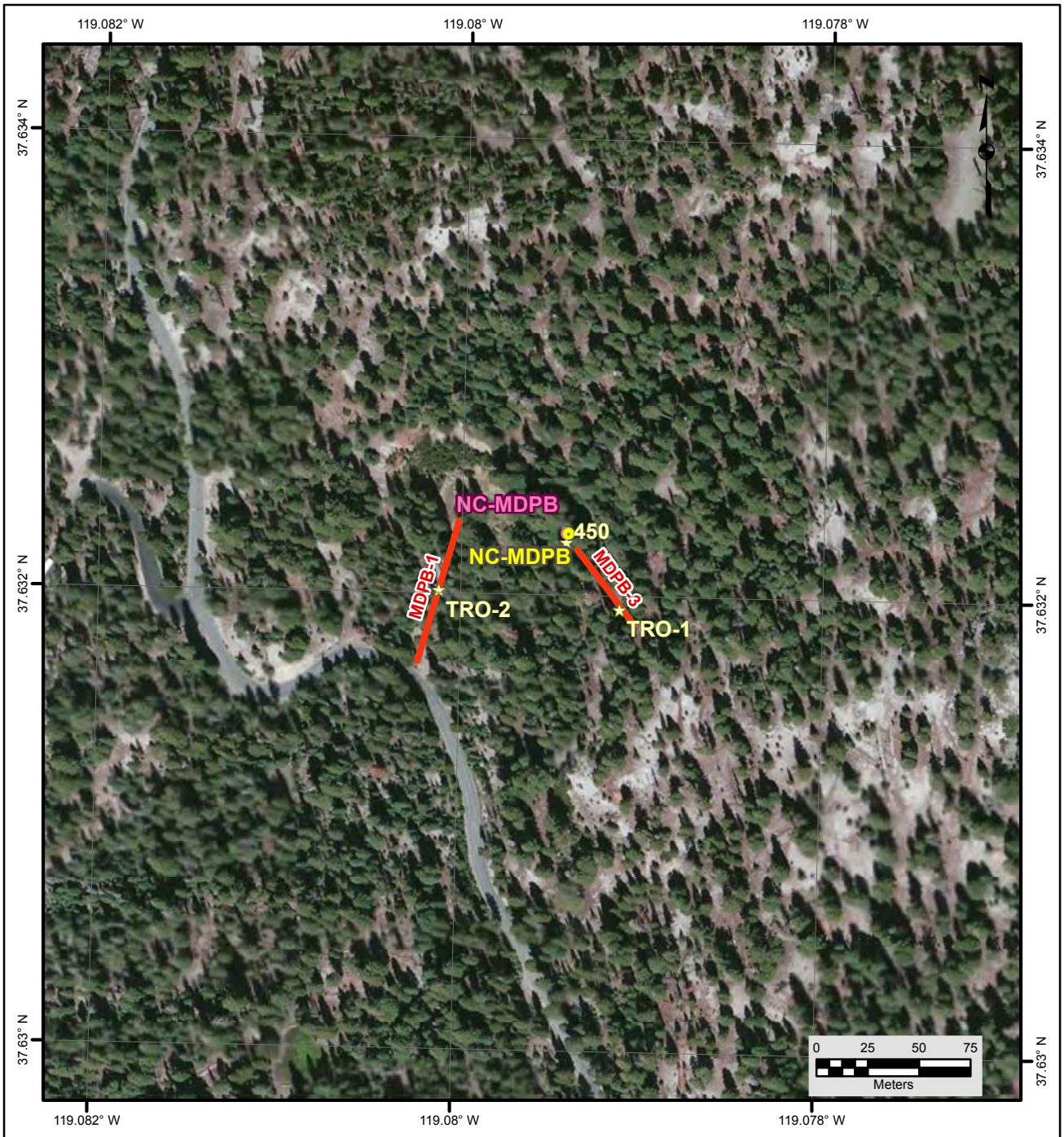

Legend

- Seismic Station - Approximate Surveyed Location
- Seismic Station - Approximate Location of Record
- H/V Spectral Ratio Location
- MASW and Seismic Refraction Array

NOTES:
1. WGS 1984 COORDINATE SYSTEM
2. Image Source: (c) Microsoft Corporation and its data suppliers

File Name: NC-MDPB-I

Date: 2/9/2012

USGS science for a changing world

GEOVision geophysical services

RECOVERY.GOV

SITE MAP
NC•MDPB

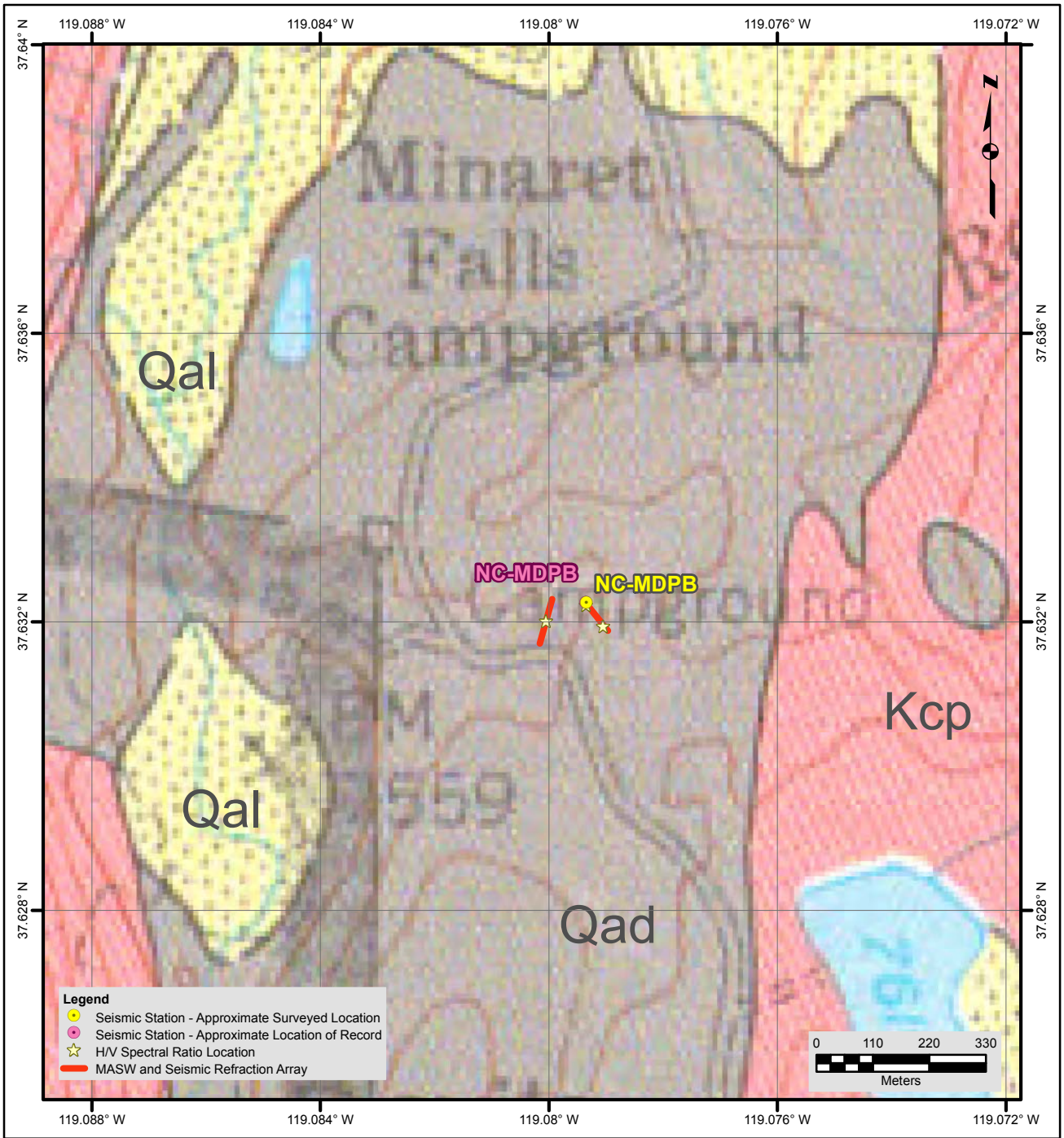

Description of Geologic Map Units

Qal = Quaternary (Holocene) alluvial and colluvial deposits, valley fill
Qad =Quaternary (Pleistocene) andesite of the Devils Postpile
Kcp = Cretaceous granitic rocks similar to the Cathedral Peak Granite

NOTES:
1. WGS 1984 COORDINATE SYSTEM
2. Geologic Map of the Devil's Postpile Quadrangle, Sierra Nevada, California by N. King Huber and C. Dean Rinehart, 1965
3. See site map for details of geophysical survey

File Name: NC-MDPB

Date: 2/9/2012

USGS science for a changing world

GEOVision geophysical services

GEOLOGIC MAP
NC•MDPB

RECOVERY.GOV

Looking at HVSR sensor 453 and seismic station

HVSR sensor 453 placed in deep hole due to loose surficial sediments

Looking northwest along array MDPB-3

Looking northeast along array MDPB-1

MASW data acquisition on array MDPB-3

Location of Geophysical Testing Arrays:

Location	Latitude	Longitude
MDPB-1, Southwest End of MASW/Refraction Array	37.63170	-119.08016
MDPB-1, Center of MASW/Refraction Array	37.63201	-119.08004
MDPB-1, Northeast End of MASW/Refraction Array	37.63232	-119.07995
MDPB-3, Northwest End of MASW/Refraction Array	37.63220	-119.07929
MDPB-3, Center of MASW/Refraction Array	37.63204	-119.07913
MDPB-3, Southeast End of MASW/Refraction Array	37.63188	-119.07920
HVSR Sensor 453 (Nanometrics Trillium Compact)	37.63223	-119.07935
HVSR Sensor Tromino ENGY (TRO-1)	37.63194	-119.07905
HVSR Sensor Tromino ENGY (TRO-2)	37.63201	-119.08005
NC.MDPB Seismic Station	37.63227	-119.07934

Notes: 1) WGS84 Coordinate System (decimal degrees)
2) Survey accuracy is estimated at 2 to 3 m.

Results:

V_S Model

Depth to Top of Layer (m)	Layer Thickness (m)	S-Wave Velocity (m/s)	Inferred P-Wave Velocity (m/s)	Assumed Poisson's Ratio	Assumed Density (g/cm^3)
0	0.5	67	125	0.300	1.60
0.5	0.5	167	312	0.300	1.70
1	16	628	1176	0.300	2.10
17	>13	823	1539	0.300	2.15

Notes: 1) Depth of investigation is about 30 m.
2) Bottom layer is a half space.

Observations/Discussion:

- This site was visited on 8/22/10 and 10/27/11. During the first site visit on 8/22/10, seismic refraction and MASW data were acquired along the 48 channel array MDPB-1 and 24 channel array MDPB-2. HVSR data were also acquired at the site, but were not useable as adequate field procedures were yet to be developed for acquisition of high quality HVSR data using Nanometrics Trillium Compact seismometers. Review of the MASW data revealed that useful MASW data were not acquired along array MDPB-2 and it was hoped that better data could be acquired using a 48 channel array rather than a

24 channel array. The seismic refraction data indicated that the velocity structure beneath array MDPB-1 was not representative of the seismic station and, therefore, this array could not be used for site characterization. Therefore, the site was revisited on 10/27/11 when HVSR data were acquired with both a Nanometrics Trillium Compact and Micromed Tromino ENGY and array MDPB-2 was replaced with array MDPB-3. Array MDPB-3 has the same orientation as array MDPB-2, but the origin of the array is located 9 m southeast of the origin of array MDPB-2.

- HVSR data were acquired adjacent to the seismic station, near the northwest end of array MDPB-3, using a Nanometrics Trillium Compact seismograph. HVSR data were also acquired near the southeast end of array MDPB-3 and center of array MDPB-1 using a Micromed Tromino ENGY. The HVSR measurements made with the Trillium Compact and Tromino ENGY along array MDPB-3 are quite different. The HVSR measurements made with the Trillium (sensor 453) show a weak HVSR peak at 4 Hz; whereas, there are no peaks on the HVSR data acquired with the Tromino (sensor TRO-1). The 4 Hz HVSR peak is primarily controlled by a single horizontal component and is, therefore, questionable. Interestingly, the Tromino also has stronger response on one of the two horizontal sensors. Assuming that the 4 Hz HVSR peak has a geologic source, there are two possible explanations for the different response between the Trillium and Tromino: sensor coupling and sensor sensitivity. The Trillium is usually deployed in a deeper hole than the Tromino and the aluminum cradle for the Trillium sensor may allow better sensor coupling to the ground. Additionally, the site is considered a very low noise environment and it is possible that the Trillium Compact has better sensitivity than the Tromino. It should be noted that both sensors have yielded similar high frequency HVSR response at numerous sites with higher noise levels; however, it appears that more investigation is needed into the source of variable HVSR response at low noise sites. HVSR data acquired at the center of array MDPB-1 using the Tromino also have no significant HVSR peaks, although there is a weak peak at about 4 Hz.
- P-wave seismic refraction data quality was excellent along array MDPB-1, but not very good along array MDPB-3. The first arrival data were very weak along array MDPB-3 due to the highly fractured rock and there were also possible out of plane refractors. There was also not very coherent surface wave energy in the seismic data collected along MDPB-3.
- The P-wave refraction data for arrays MDPB-1 and MDPB-3 were modeled using a tomographic inversion routine with a layer based starting model. The seismic refraction models were extended to far offset shot locations to extend depth of investigation.
- The seismic refraction survey design for array MDPB-1 allowed P-wave velocity to be imaged to a maximum depth of about 15 m. The seismic refraction model shows a thin layer of sediments overlying weathered rock. P-wave velocity is about 300 to 400 m/s at the surface, increasing to 1,200 m/s at a depth of 2 to 3 m, 2,000 m/s at a depth of 5 to 13 m and 2,400 m/s at a depth 6 m to greater than 15 m. There is lateral velocity variation beneath the array with a thinner zone of sediments and thicker sequence of more weathered (lower velocity) rock beneath the southwestern portion of the array.
- The seismic refraction survey design for array MDPB-3 allowed P-wave velocity to be imaged to a maximum depth of about 10 m. The seismic refraction model shows a thin layer of sediments/decomposed rock overlying intensely weathered rock. P-wave velocity is about 300 to 400 m/s at the surface, increasing to 600 m/s at a depth of 1 to 2

m and 1,200 m/s at a depth of 2 to 5 m. Maximum P-wave velocities in the model are in the 1,400 to 1,600 m/s range at a depth of 4 m, or more. There is some lateral velocity variation beneath the array with slightly variable thickness of the surficial sediment layer and variable weathered rock velocity. P-wave velocity beneath array MDPB-3 is generally lower than beneath array MDPB-1. However, ground surface elevation is about 10 m higher in the vicinity of array MDPB-3.

- Noise conditions at the site were not sufficient for application of passive surface wave techniques.
- Surface wave data collected along array MDPB-1 were not analyzed as the array is not considered representative of the seismic station. Due to the shallow, abrupt increase in seismic velocity, the MALW (Love wave) technique would likely perform better along array MDPB-1.
- Reduction of MASW data collected along array MDPB-3 was difficult due to the thin layer of low velocity residual soil overlying rock, lateral velocity variation and probable significant scattering of surface wave energy. It was, however, possible to develop a relatively coherent dispersion curve for modeling, although small wavelength Rayleigh wave phase velocity data are only representative of a portion of the line and only about 70% of the picked dispersion curve files were used for analysis.
- The minimum wavelength surface wave phase velocity data extracted from the 48-channel MASW array was about 18 m. Reducing data from smaller hammer sources using a limited offset receiver array (i.e. less active geophones) allowed for extraction of surface wave dispersion data to a minimum wavelength of about 3.5 m.
- Near field criteria typically applied during this investigation had to be significantly relaxed of obtain the required 60 m wavelength Rayleigh wave phase velocity data to image to 30 m depth.
- There is about 50 to 80 m/s of scatter in MASW dispersion data selected for analysis (that which formed the most coherent dispersion curve) likely due to lateral velocity variation caused by differential weathering of near surface weathered rock and variable thickness of a thin residual soil layer.
- A representative dispersion curve was generated for the MASW data set using a moving average, polynomial curve fitting routine and used for modeling.
- During inversion of the Rayleigh wave dispersion curve, only a minimal number of layers were used in the V_S model to limit the occurrence of unrealistic velocity inversions.
- Surface wave depth of investigation is about 30 m based on half of maximum wavelength criteria.
- The inferred P-wave velocities in the surface wave model, based on an assumed Poisson's ratio of 0.3 and modeled S-wave velocity, are generally consistent with the P-wave refraction model in the upper 10 m.
- V_{S30} is 580 m/s (Site Class C).
- Average S-wave velocity between 1 m (assumed sensor depth) and 31 m is 706 m/s.

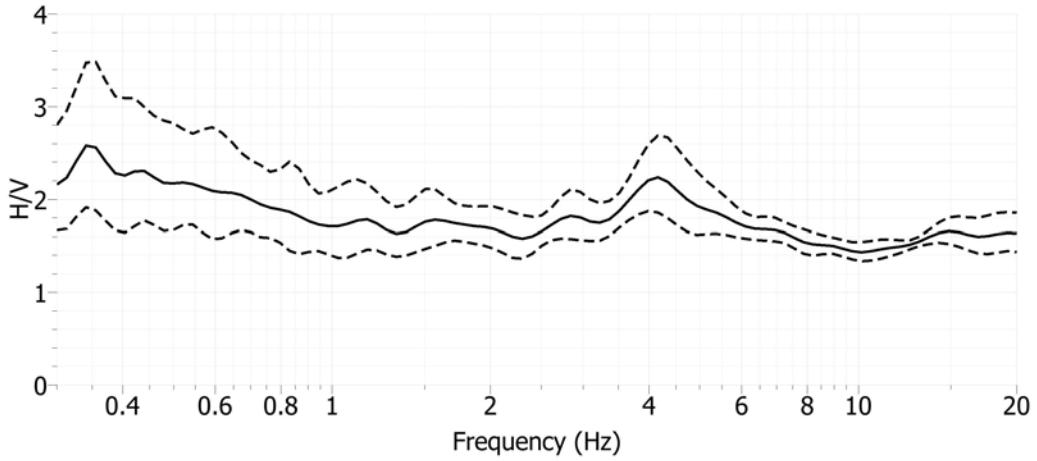

Site NC.MDPB, H/V Spectral Ratio, Array MDPB-1, Sensor TRO-2

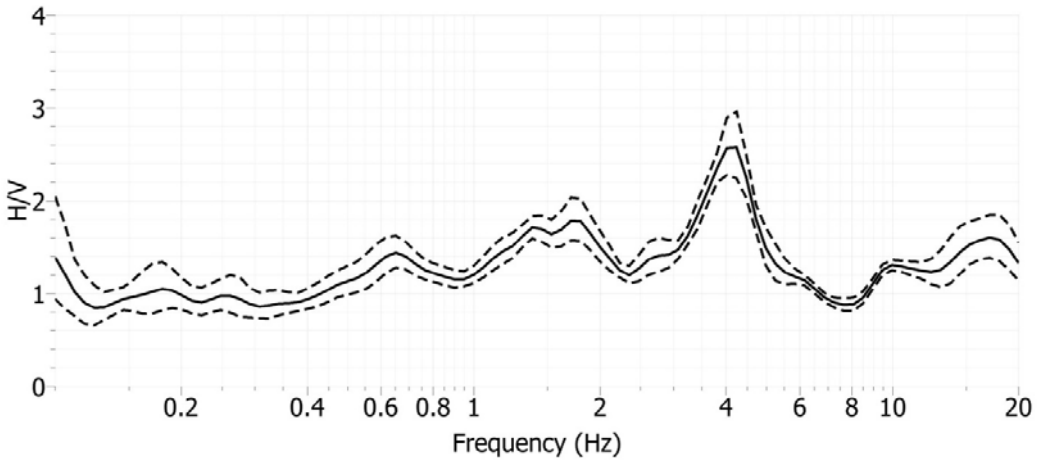

Site NC.MDPB, H/V Spectral Ratio, Near Seismic Station, Sensor 453

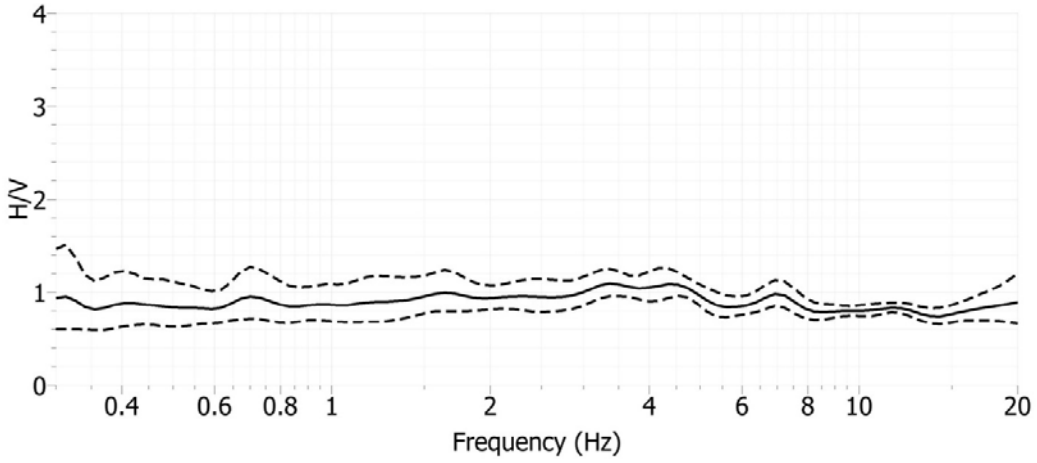

Site NC.MDPB, H/V Spectral Ratio, Array MDPB-3, Sensor TRO-1

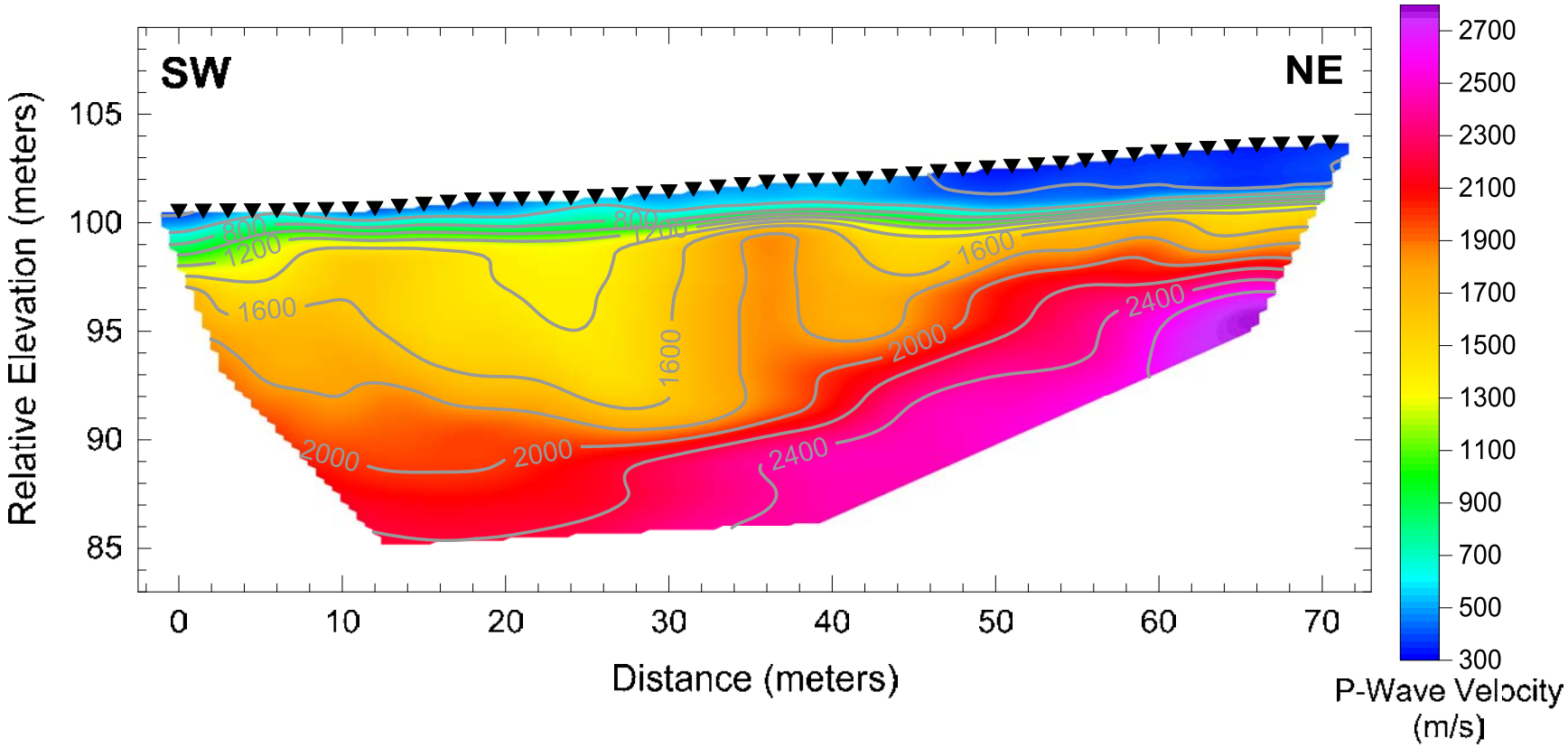

Array MDPB-1 – P-wave tomographic seismic refraction model developed utilizing a layer based starting model

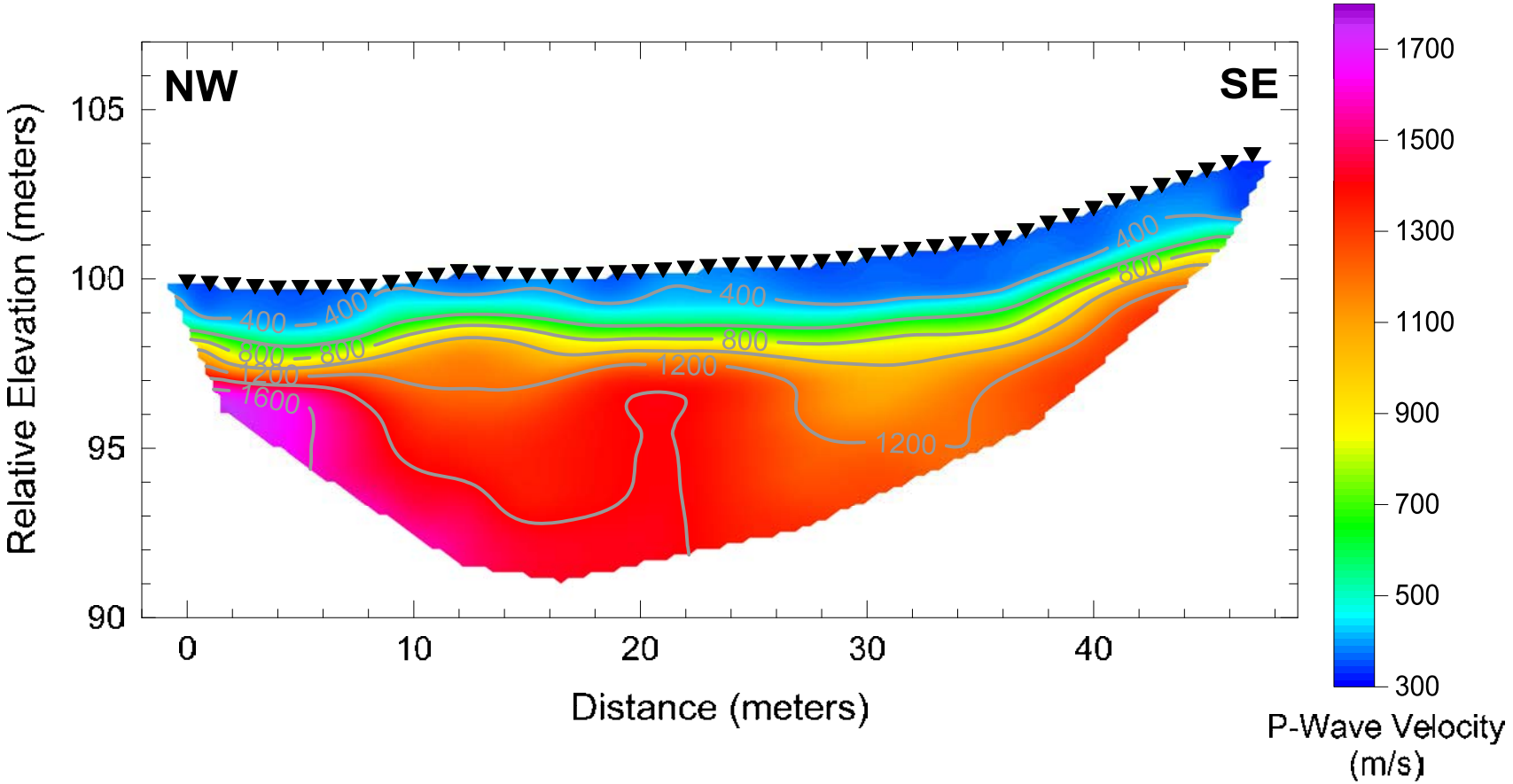

Array MDPB-3– P-wave tomographic seismic refraction model developed utilizing a layer based starting model

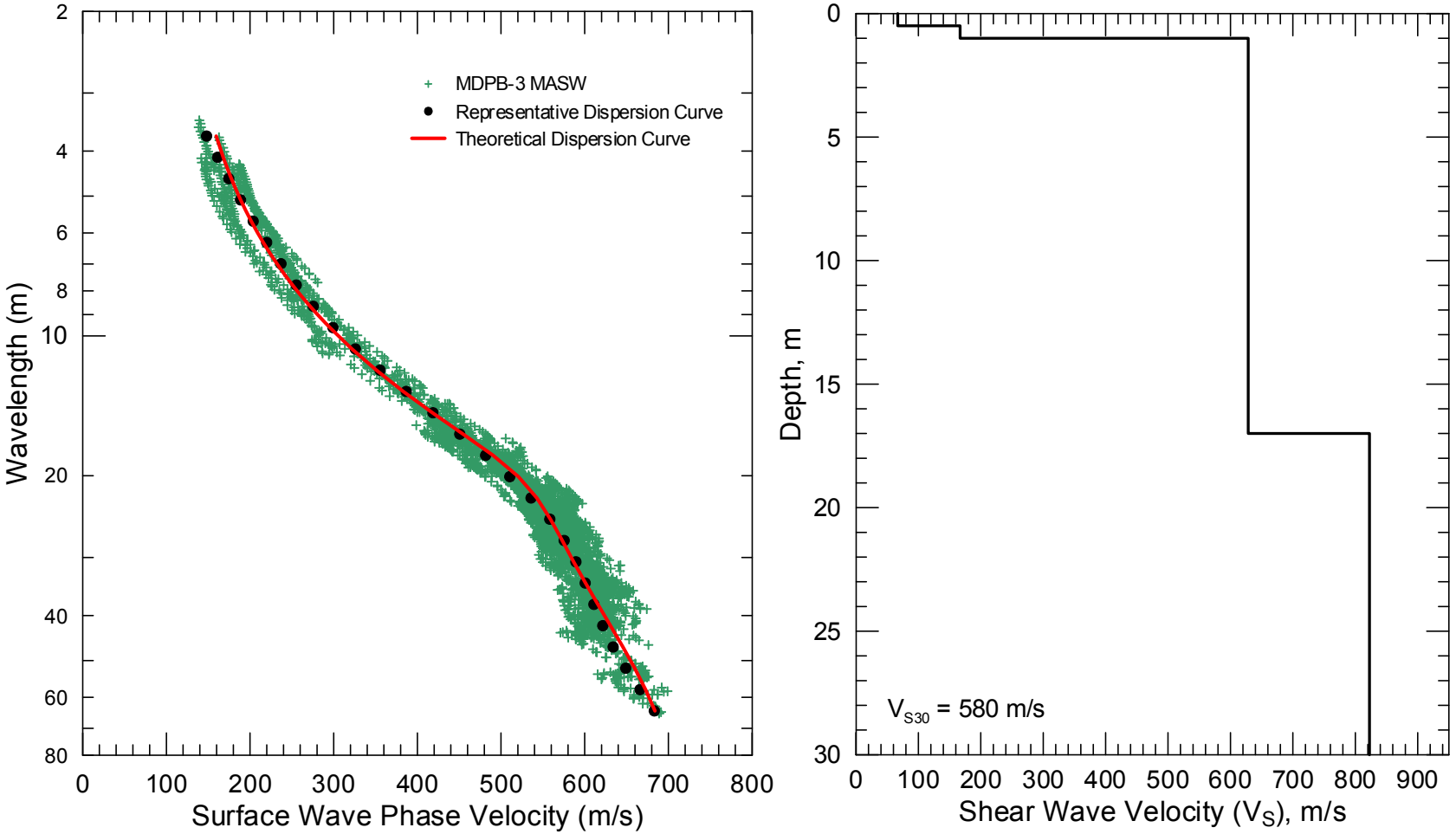

NC.MDPB - Field, representative and inverted theoretical surface wave dispersion data (left) and associated V_S model (right) for Array MDPB-3

Site NC.MMLB

Location: Mammoth Lakes Knolls, Mammoth Lakes, California

Latitude: 37.65909 **Longitude:** -118.97907
(Station coordinates provided by USGS, WGS84 coordinate system)

V_{S30} (measured): 317 m/s

V_{S30} (adjusted to more accurately reflect seismic station conditions): 317 m/s (no adjustment necessary).

NEHRP Site Class: D

Geomatrix Code: IVD

Geologic Conditions/Observations: Seismic station located on Quaternary (Pleistocene) rhyolite of Mammoth Knolls.

Site Conditions: Rural site. Seismic station located on mountain top. Gentle to steep topography in site vicinity. Approximately 3 m of elevation variation along the 70.5 m MASW array with topography falling off more abruptly beyond the ends of the array.

Geophysical Methods Utilized: HVSR, Seismic Refraction, MASW

Geophysical Testing Arrays:

1. Array MMLB-1 (48 channel MASW and P-wave seismic refraction array utilizing 4.5 Hz vertical geophones spaced 1.5 m apart for a length of 70.5 m, forward and reverse shot locations with multiple source offsets and source types and multiple interior shot locations).
2. Three HVSR measurement locations: two distributed along array MMLB-1 and one near the seismic station. One HVSR measurement made using a Nanometrics Trillium and the other two using a Tromino ENGY.

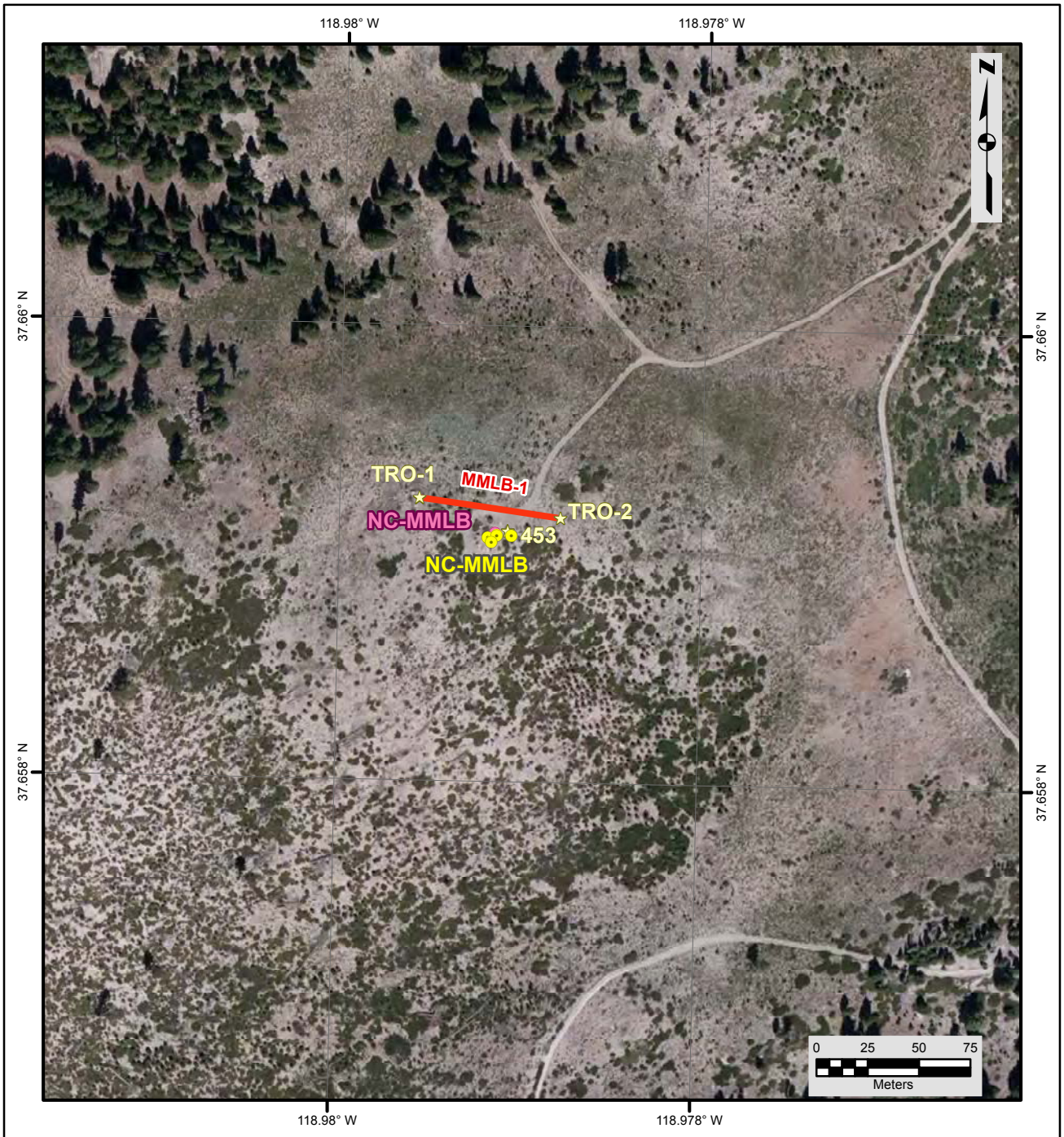

Legend

- Seismic Station - Surveyed Location
- Seismic Station - Location of Record
- H/V Spectral Ratio Location
- MASW, SASW & Seismic Refraction Array

NOTES:
1. WGS 1984 COORDINATE SYSTEM
2. Image Source: ESRI, i-cubed, USDA FSA, USGS, AEX, GeoEye, Getmapping, Aerogrid, IGP

File Name: NC-MMLB-1

Date: 2/7/2013

USGS science for a changing world

GEOVision geophysical services

RECOVERY.GOV

SITE MAP
NC•MMLB

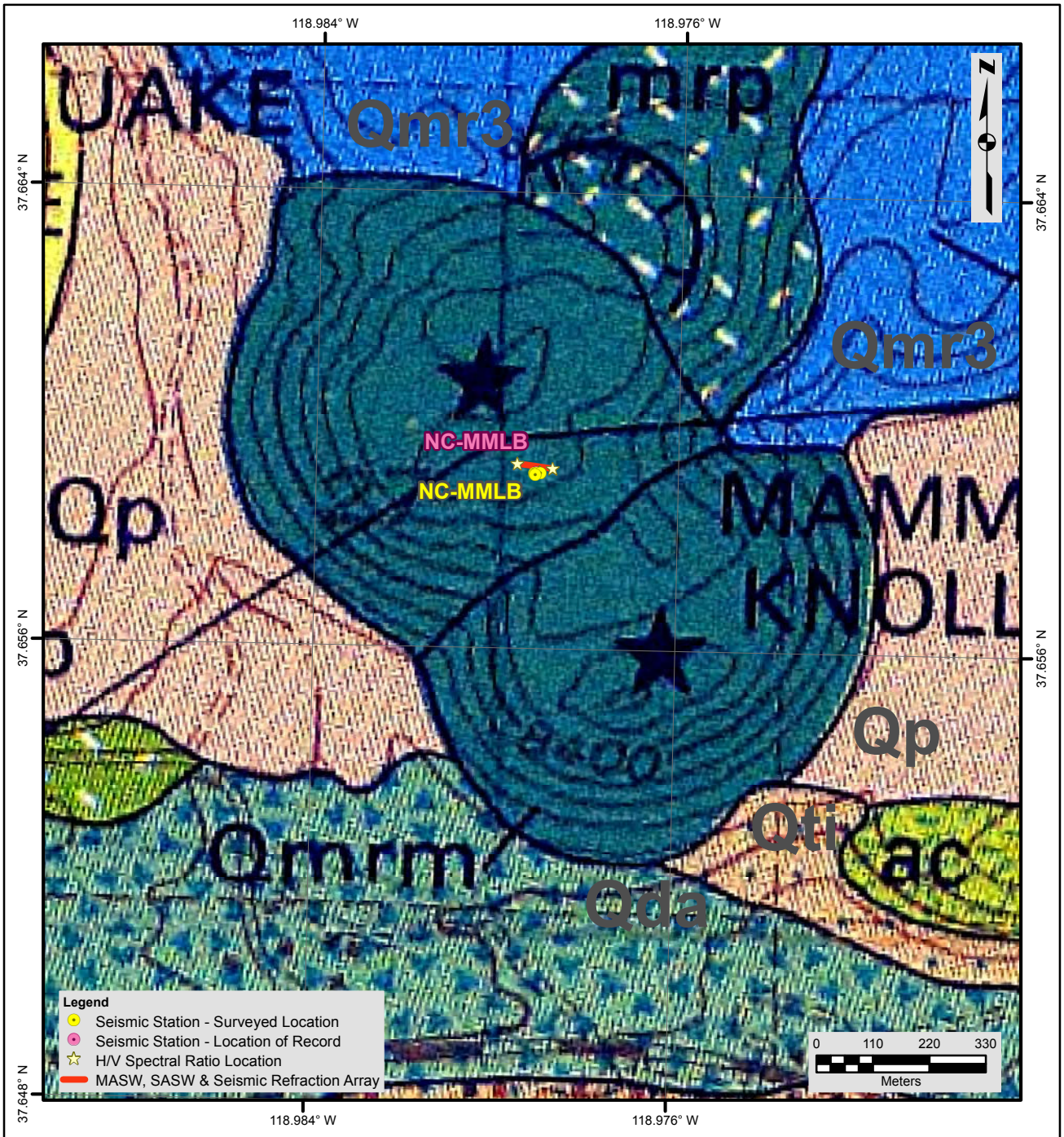

Description of Geologic Map Units

Qp = Quaternary (Pleistocene and Holocene) pyroclastic fall deposits, rhyolite ash and pumice lapilli
Qda = Quaternary (Pleistocene) debris-avalanche deposits, coarse cobbles and boulders in sandy matrix, mostly hornblende-biotite quartz latite
Qti = Quaternary (Pleistocene) Tioga Till, sharp moraine crests, granitic boulders
Qmrm = Quaternary (Pleistocene) porphorytic, high-silica rhyolite of Mammoth Knolls
mrp = Quaternary (Pleistocene) crudely bedded near-vent pyroclastic rhyolite breccia
Qmr3 = Quaternary (Pleistocene) hornblende-biotite rhyolite
ac = Quaternary (Pleistocene) trachyandesitic cinder

NOTES:
1. WGS 1984 COORDINATE SYSTEM
2. Geologic Map of Long Valley Caldera, Mono-Inyo Craters Volcanic Chain, and Vicinity, Eastern California by Roy A. Bailey, 1989
3. See site map for details of geophysical survey

USGS science for a changing world

GEOVision geophysical services

GEOLOGIC MAP
NC•MMLB

File Name: NC-MMLB

Date: 2/7/2013

NC.MMLB seismic station

Looking north towards center of array MMLB-1 from seismic station

Looking southeast towards center of array MMLB-1 and seismic station

Looking southwest towards seismic station from eastern end of array MMLB-1

MASW and seismic refraction data acquisition

Location of Geophysical Testing Array(s):

Location	Latitude	Longitude
MMLB-1, West End of MASW/Refraction Array	37.65924	-118.97949
MMLB-1, Center of MASW/Refraction Array	37.65920	-118.97910
MMLB-1, East End of MASW/Refraction Array	37.65916	-118.97871
HVSR Sensor Tromino ENGY (TRO-1)	37.65924	-118.97949
HVSR Sensor Tromino ENGY (TRO-2)	37.65916	-118.97871
HVSR Sensor 453	37.65910	-118.97900
NC.MMLB Seismic Station	37.65907	-118.97911
NC.MMLB Seismic Station	37.65908	-118.97906
NC.MMLB Seismic Station	37.65908	-118.97898
NC.MMLB Seismic Station	37.65905	-118.97909

Notes: 1) WGS84 Coordinate System (decimal degrees)
2) Survey accuracy is estimated at 1 to 2 m.

Results:

V_S Model

Depth to Top of Layer (m)	Layer Thickness (m)	S-Wave Velocity (m/s)	Inferred P-Wave Velocity (m/s)	Assumed Poisson's Ratio	Assumed Density (g/cm^3)
0	1	145	271	0.3	1.7
1	2	193	361	0.3	1.7
3	3	236	442	0.3	1.8
6	4	295	553	0.3	1.8
10	5	324	605	0.3	1.8
15	6	376	704	0.3	1.9
21	7	441	825	0.3	2.0
28	>2	513	960	0.3	2.0

Notes: 1) Depth of investigation is about 30m.
2) Bottom layer is a half space.

Observations/Discussion:

- Geophysical testing at this site was originally conducted on 8/19/10. HVSR data were not of acceptable quality due to gusting winds and poor sensor coupling. The site was therefore revisited on 10/29/11 with HVSR data acquisition repeated and additional source locations occupied on the MASW and seismic refraction array MMLB-1.

- The HVSR curves are different indicating that there may be lateral velocity variation at this site. All HVSR plots have a low amplitude peak in the 2 to 3 Hz range, but differ at other frequencies. HVSR sensor 453 (Nanometrics Trillium) has HVSR peaks at about 1.3 and 2.3 Hz. HVSR sensor TRO-1 has a peak at about 2.9 Hz and slightly elevated HVSR response to a frequency of 15 Hz. HVSR sensor TRO-2 has a peak at about 2.7 Hz. The possibility cannot be discounted that the Tromino does not respond to the 1.3 Hz peak detected by the Trillium due to reduced sensor sensitivity and low noise levels.
- The P-wave refraction data collected along array MMLB-1 were modeled using a tomographic inversion routine with both a smooth velocity gradient and layered starting model. The seismic refraction model was extended to some far offset shot locations to extend depth of investigation.
- The P-wave velocity of the near surface sediments is less than that of the air wave, making picking of first arrival data at small source offsets difficult.
- The seismic refraction survey design allowed P-wave velocity to be imaged to a maximum depth of about 15 to 20 m. Both seismic refraction models are similar and show that P-wave velocity is about 300 to 400 m/s at the surface, increasing to 500 m/s at a nominal depth of 11 to 16 m and 650 m/s at a nominal depth of 15 to 21 m. P-wave velocity appears to exceed 700 m/s at depths below 20 m. P-wave velocity is higher at shallower depth than described above at the westernmost end of the array.
- The seismic refraction model indicates that there is some lateral velocity variation at the site with higher P-wave velocities at shallower depth at the west end of the line. There were no reasonable alternate test locations at the site in close proximity to the seismic station.
- Noise conditions at the site were not sufficient for application of passive surface wave techniques.
- It was only possible to utilize the accelerated weight drop energy source at several shot locations at the eastern end of the array. Rayleigh wave phase velocity data at frequencies less than 7 Hz (wavelength of about 40 m) were not extracted from data acquired using the 20 lb hammer energy source.
- The minimum wavelength surface wave phase velocity data extracted from the 48-channel MASW array was about 8 m. Data reduction using seismic records from smaller hammer sources and a limited offset receiver array (i.e. less active geophones) allowed extraction of surface wave dispersion data to a minimum wavelength of about 2 m.
- There is about 40 to 50 m/s scatter in the MASW dispersion data, which is likely due, in part, to lateral velocity variation.
- A representative dispersion curve was generated for the MASW data set using a moving average, polynomial curve fitting routine and used for modeling.
- Surface wave depth of investigation is about 30 m based on half of maximum wavelength criteria.
- The inferred P-wave velocities in the surface wave model, assuming a Poisson's ratio of 0.3, are generally consistent with the average velocity structure in the seismic refraction model, especially considering unknown Poisson's ratio.
- V_{S30} is 317 m/s (Site Class C).

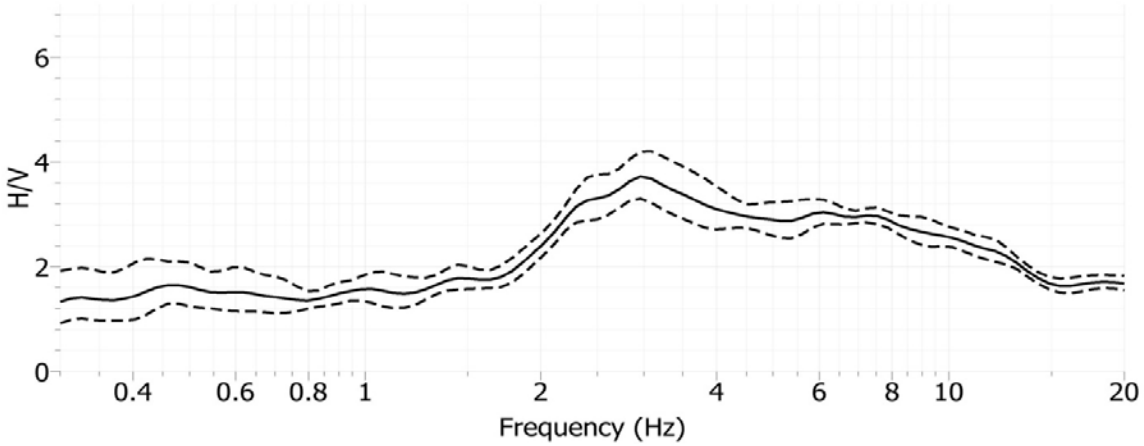

Site NC.MMLB, H/V Spectral Ratio, Array MMLB-1, Sensor TRO-1

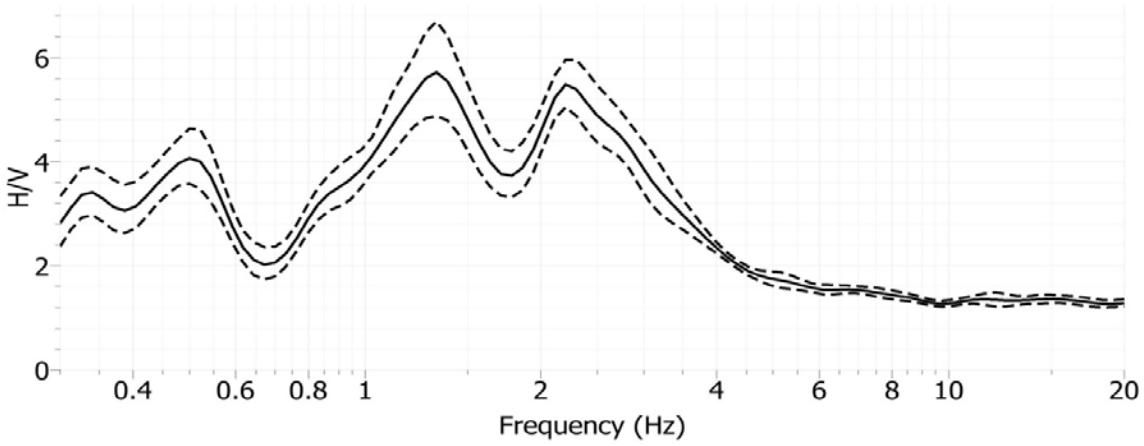

Site NC.MMLB, H/V Spectral Ratio, Near Seismic Station, Sensor 453

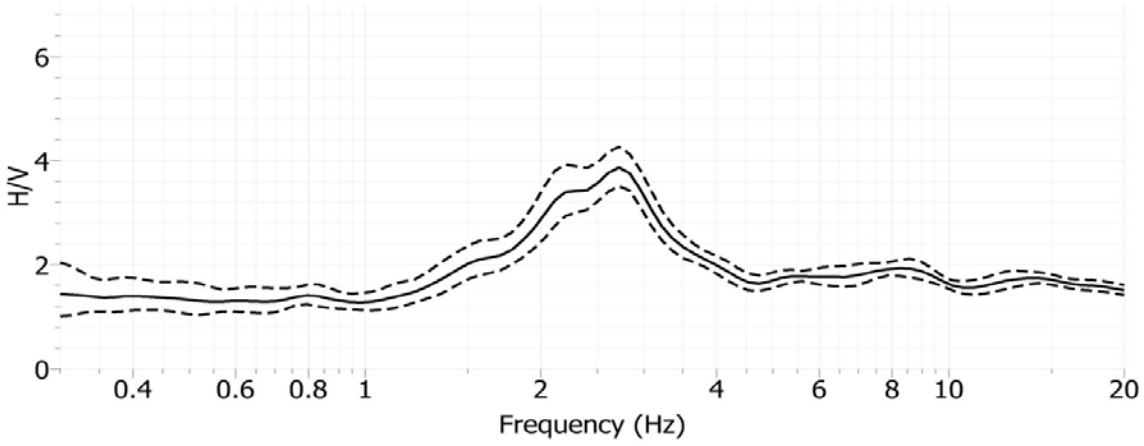

Site NC.MMLB, H/V Spectral Ratio, Array MMLB-1, Sensor TRO-2

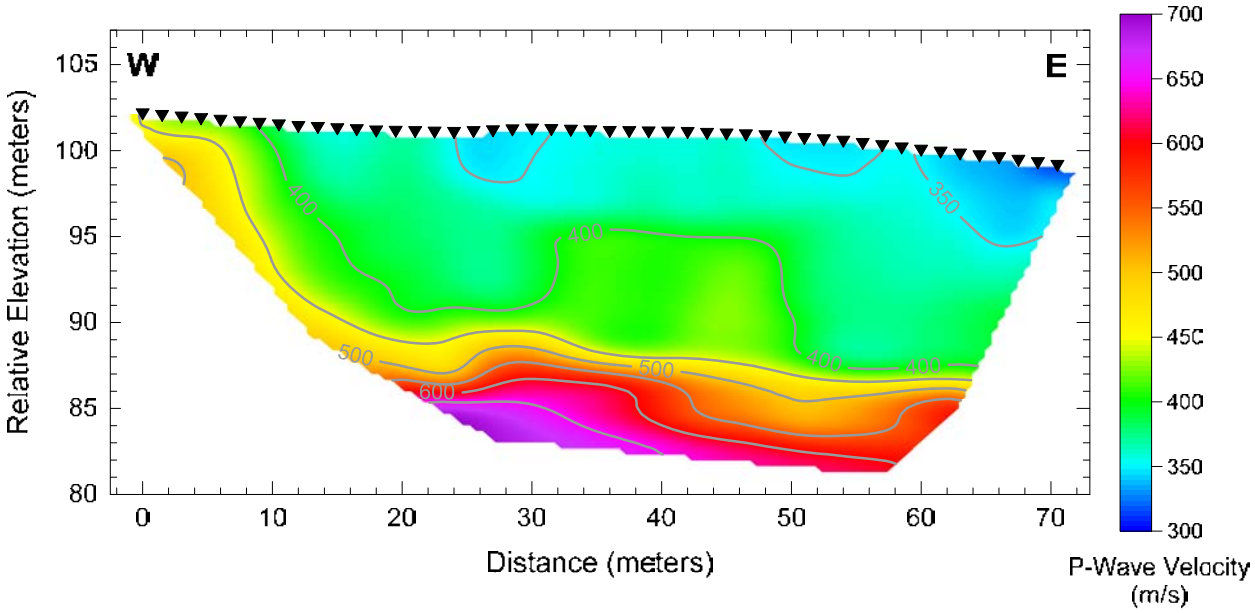

Array MMLB-1 – Tomographic Seismic Refraction Model utilizing Layer Based Starting Model

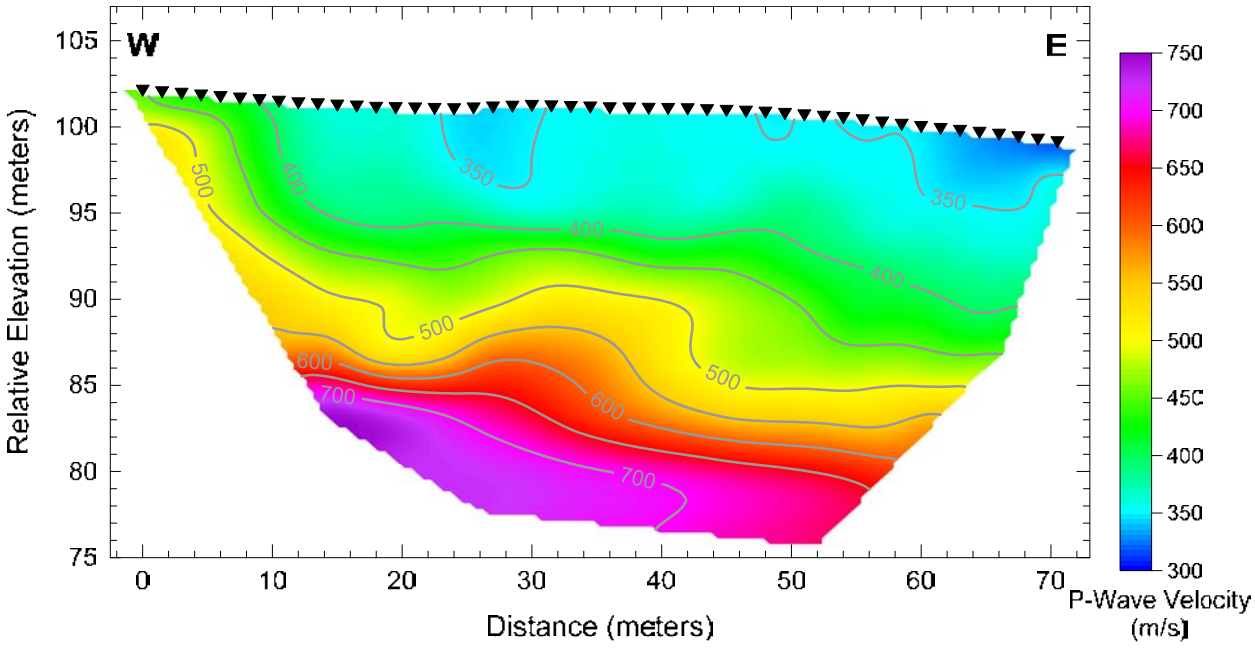

Array MMLB-1 – Tomographic Seismic Refraction Model utilizing Smooth Velocity Gradient Starting Model

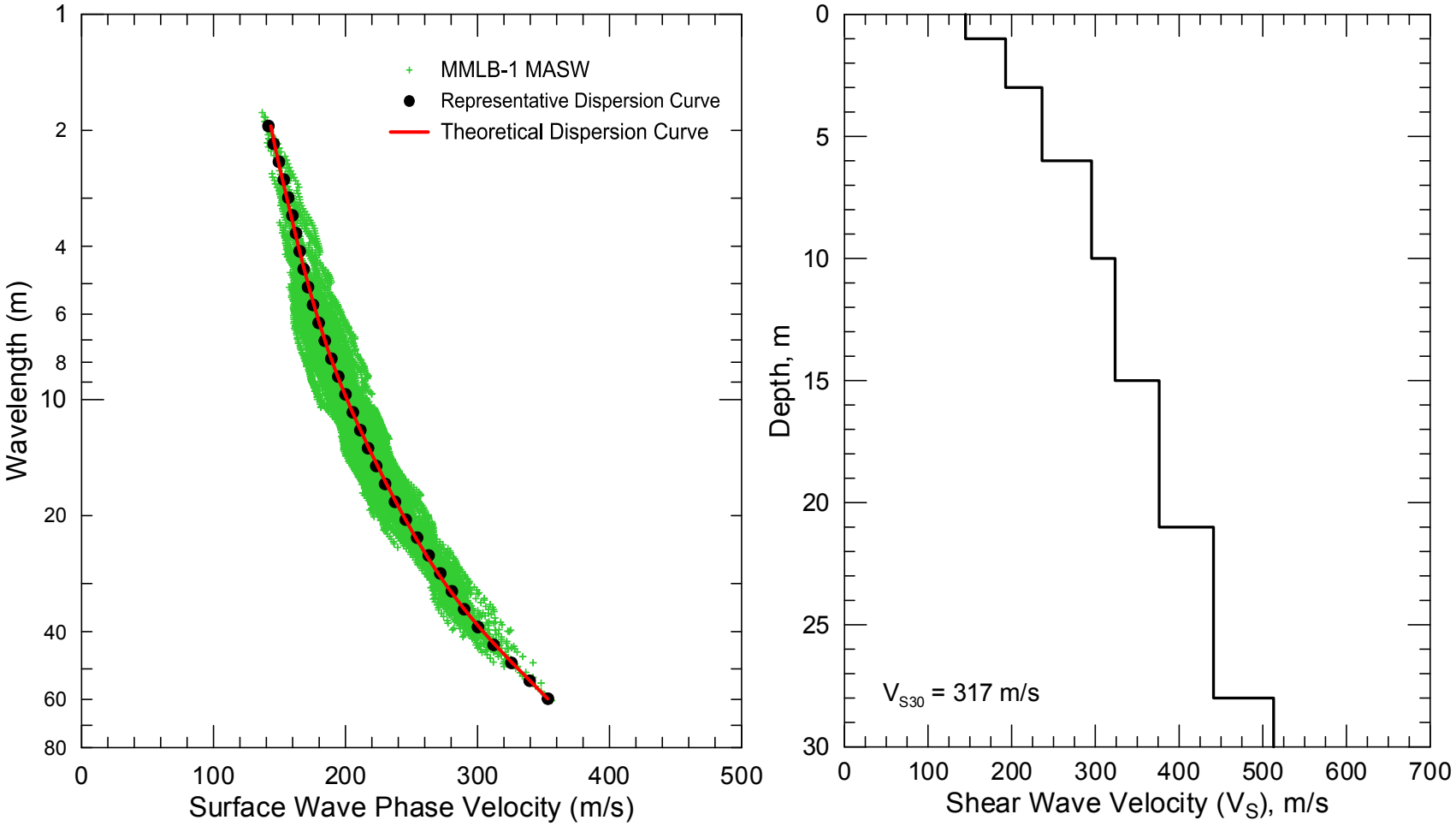

NC.MMLB- Field, representative and inverted theoretical surface wave dispersion data (left) and associated V_S model (right)

Site NC.MMX1

Location: MotoCross Track near Mammoth Lakes, Mono County, California

Latitude: 37.61711 **Longitude:** -118.95976
(Station coordinates provided by USGS, WGS84 coordinate system)

V_{S30} (measured): 565 m/s

V_{S30} (adjusted to more accurately reflect seismic station conditions): 687 m/s (average S-wave velocity of the upper 30 m of rock to account for sensor being placed on rock).

NEHRP Site Class: C

Geomatrix Code: IZA

Geologic Conditions/Observations: Seismic station located on geologic unit mapped as Paleozoic metasedimentary rocks. Cretaceous granodiorite and quartz monzonite also outcrop in the site vicinity.

Site Conditions: Rural site located at the base of a mountain. Steep mountainous topography south of the seismic station and relatively flat to undulating topography in meadow north of seismic station.

Geophysical Methods Utilized: HVSR, Seismic Refraction (P- and S-wave), MASW (Rayleigh Wave), MALW (Love Wave)

Geophysical Testing Arrays:

1. Array MMX1-1 (48 channel MASW and P-wave seismic refraction array utilizing 4.5 Hz vertical geophones spaced 1.5 m apart for a length of 70.5 m, forward and reverse shot locations with multiple source offsets and source types and multiple interior shot locations).
2. Array MMX1-2 (48 channel MASW and P-wave seismic refraction array utilizing 4.5 Hz vertical geophones spaced 1.5 m apart for a length of 70.5 m, forward and reverse shot locations with multiple source offsets and source types and multiple interior shot locations and a 48 channel MALW and S-wave seismic refraction array utilizing 4.5 Hz horizontal geophones spaced 1.5 m apart for a length of 70.5 m).
3. Array MMX1-4 (48 channel P-wave seismic refraction array utilizing 4.5 Hz vertical geophones spaced 3 m apart for a length of 141 m, forward and reverse shot locations and multiple interior shot locations).
4. Three HVSR measurement locations: two distributed along array MMX1-2 and one adjacent to the seismic station.

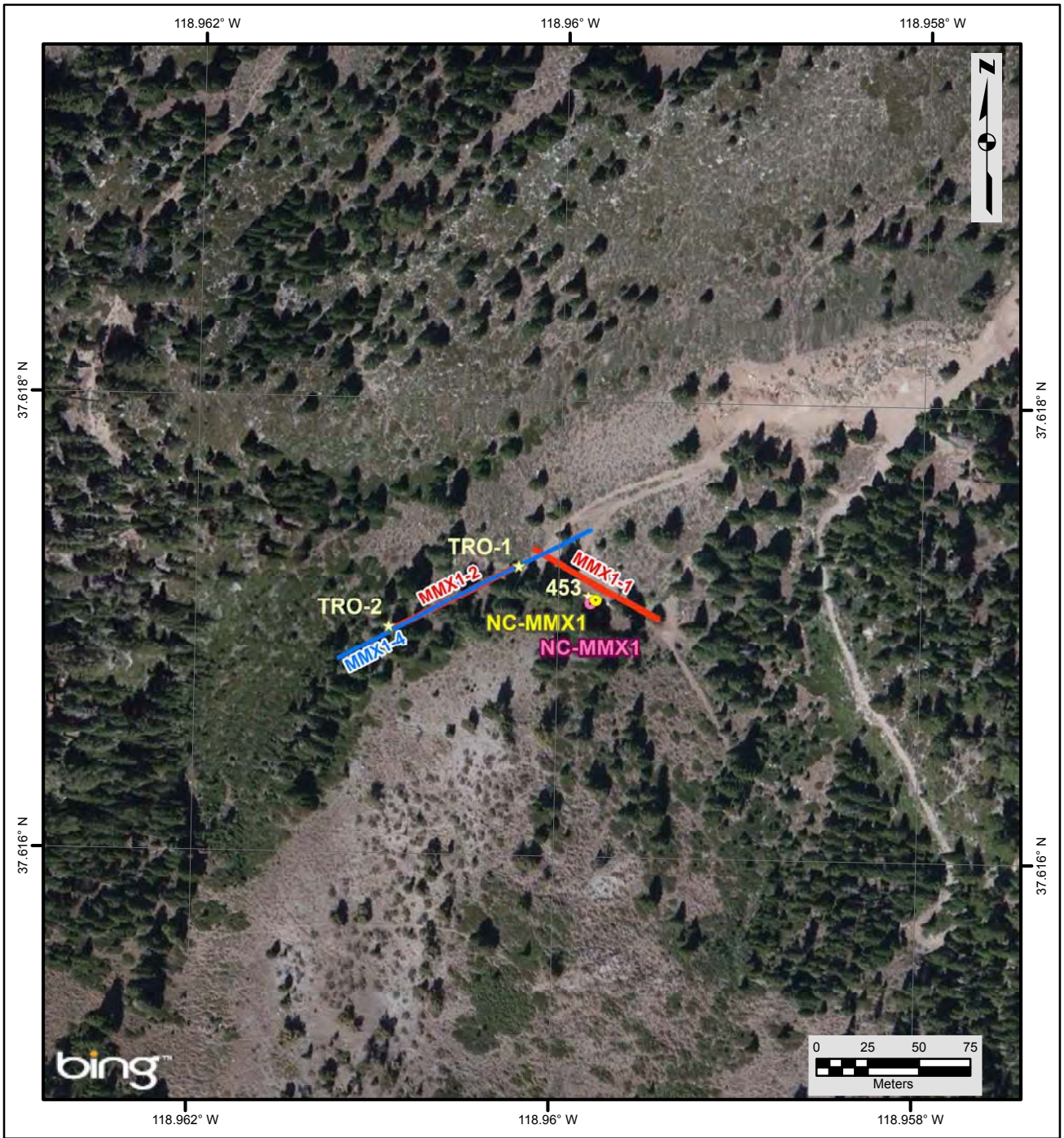

Legend

- Seismic Station - Approximate Surveyed Location
- Seismic Station - Approximate Location of Record
- H/V Spectral Ratio Location
- Seismic Refraction Array
- MASW and/or Seismic Refraction Array

NOTES:
1. WGS 1984 COORDINATE SYSTEM
2. Image Source: (c) Microsoft Corporation and its data suppliers

File Name: NC-MMX1-I

Date: 2/7/2013

USGS science for a changing world

GEOVision geophysical services

RECOVERY.GOV

SITE MAP
NC•MMX1

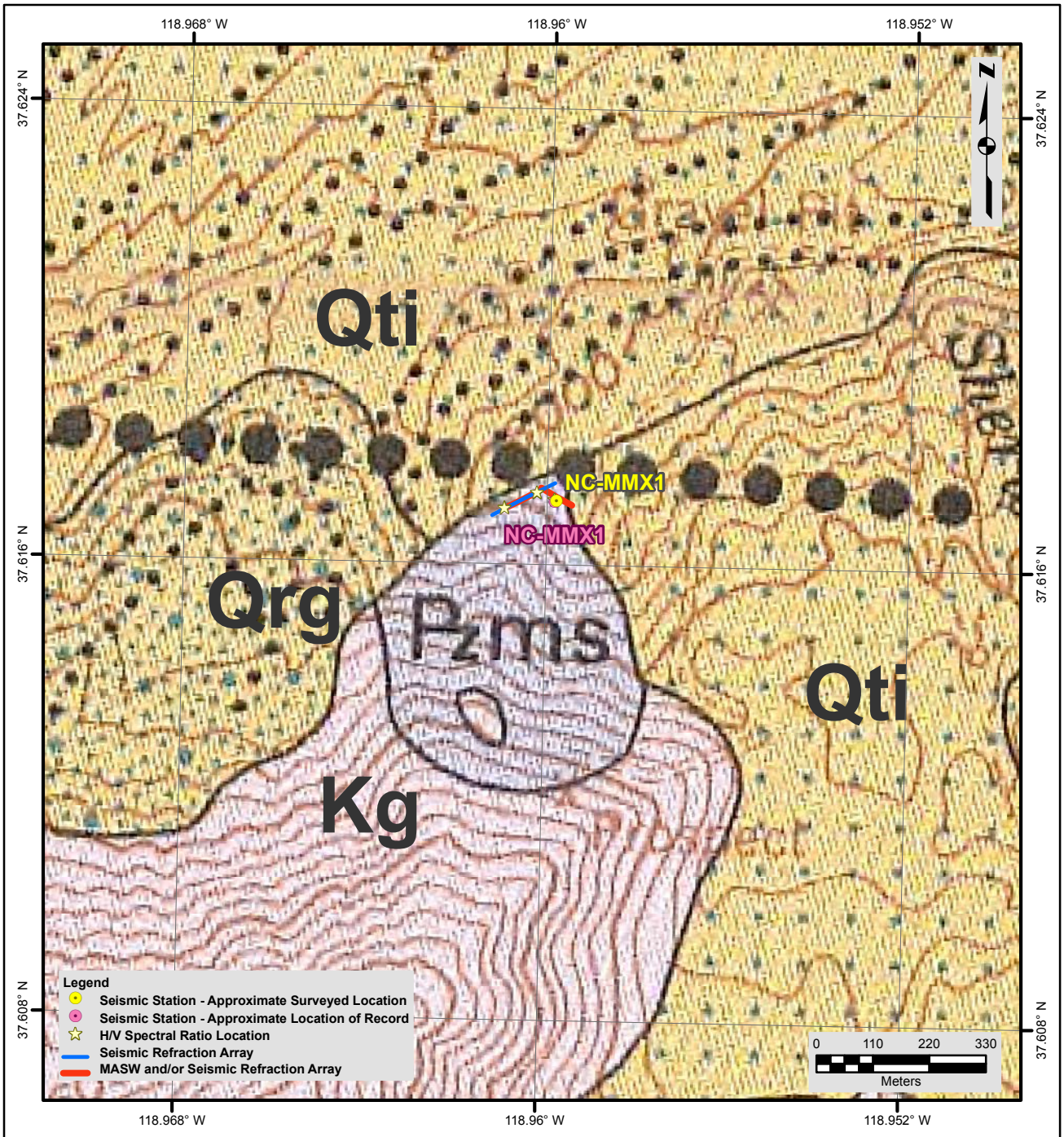

Description of Geologic Map Units

Qrg = Quaternary (Holocene) rock glacier; coarse angular rock debris with ice, neoglacial deposits
Qti = Quaternary (Pleistocene) Tioga Till; sharp-crested moraines with little surface weathering
Kg = Cretaceous granodiorite, quartz monzonite similar to the Cathedral Peak Granite
Pzms = Paleozoic Metasedimentary rocks

NOTES:
1. WGS 1984 COORDINATE SYSTEM
2. Geologic Map of Long Valley Caldera, Mono-Inyo Craters Volcanic Chain and Vicinity, Eastern California by Roy A. Bailey, 1989
3. See site map for details of geophysical survey

File Name: NC-MMX1

Date: 4/12/2012

USGS science for a changing world

GEOVision geophysical services

RECOVERY.GOV

GEOLOGIC MAP
NC•MMX1

NC.MMX1 seismic Station

Looking southwest along array MMX1-2 and at HVSR sensor TRO-1

Looking southeast along array MMX1-1

Looking northeast along P-wave seismic refraction array MMX1-4

S-wave seismic refraction data acquisition along array MMX1-2

Location of Geophysical Testing Arrays:

Location	Latitude	Longitude
MMX1-1, Northwest End of MASW/Refraction Array	37.61734	-118.96007
MMX1-1, Center of MASW/Refraction Array	37.61720	-118.95975
MMX1-1, Southeast End of MASW/Refraction Array	37.61705	-118.95939
MMX1-2, Southwest End of MASW/Refraction Array	37.61698	-118.96086
MMX1-2, Center of MASW/Refraction Array	37.61712	-118.96051
MMX1-2, Northeast End of MASW/Refraction Array	37.61727	-118.96016
MMX1-4, Southwest End of Refraction Array	37.61685	-118.96114
MMX1-4 Center of Refraction Array	37.61715	-118.96046
MMX1-4, Northeast End of Refraction Array	37.61743	-118.95977
HVSR Sensor Tromino ENGY (TRO-1)	37.61727	-118.96016
HVSR Sensor Tromino ENGY (TRO-2)	37.61700	-118.96087
HVSR Sensor 453	37.61714	-118.95977
NC.MMX1 Seismic Station	37.61712	-118.95973

Notes: 1) WGS84 Coordinate System (decimal degrees)

2) Survey accuracy is estimated at 2 to 3 m.

Results:

Average V_P Model and Estimated V_S Models from Central Portion of P-wave Seismic Refraction Array MMX1-1

Depth to Top of Layer (m)	Layer Thickness (m)	P-Wave Velocity (m/s)	Estimated S-Wave Velocity (m/s)			
			Poisson's Ratio = 0.25	Poisson's Ratio = 0.3	Poisson's Ratio = 0.35	Poisson's Ratio = 0.4
0.00	0.40	338	195	180	162	138
0.40	0.79	360	208	193	173	147
1.19	0.79	385	223	206	185	157
1.99	0.79	388	224	207	186	158
2.78	0.79	391	225	209	188	159
3.58	0.79	626	361	334	301	255
4.37	0.79	897	518	479	431	366
5.17	1.67	950	548	508	456	388
6.84	1.67	987	570	527	474	403
8.50	1.67	1053	608	563	506	430
10.17	1.67	1055	609	564	507	431
11.84	1.67	1056	610	564	507	431
13.51	1.67	1087	628	581	522	444
15.18	Half Space	1152	665	616	553	470

Average V_S Model from Central Portion of S-wave Seismic Refraction Array MMX1-2

Depth to Top of Layer (m)	Layer Thickness (m)	S-Wave Velocity (m/s)
0.00	0.42	108
0.42	0.84	186
1.26	0.84	257
2.10	0.84	340
2.95	0.84	424
3.79	0.84	513
4.63	0.84	524
5.47	1.77	554
7.24	1.77	605
9.01	1.77	668
10.78	1.77	718
12.54	1.77	813
14.31	1.77	847
16.08	1.77	975
17.85	1.77	1000
19.62	Half Space	1040

Average V_P Model and Estimated V_S Models from Central Portion of P-wave Seismic Refraction Array MMX1-4

Depth to Top of Layer (m)	Layer Thickness (m)	P-Wave Velocity (m/s)	Estimated S-Wave Velocity (m/s)			
			Poisson's Ratio = 0.25	Poisson's Ratio = 0.3	Poisson's Ratio = 0.35	Poisson's Ratio = 0.4
0.00	0.53	203	117	109	98	83
0.53	1.06	331	191	177	159	135
1.59	1.06	545	315	291	262	222
2.65	1.06	679	392	363	326	277
3.71	1.06	787	454	421	378	321
4.77	1.06	935	540	500	449	382
5.83	1.06	998	576	533	479	407
6.89	2.23	1137	656	608	546	464
9.12	2.23	1277	737	682	613	521
11.35	2.23	1385	800	740	665	565
13.57	2.23	1429	825	764	686	583
15.80	2.23	1524	880	815	732	622
18.03	2.23	1618	934	865	777	660
20.25	2.23	1688	974	902	811	689
22.48	2.23	1730	999	925	831	706
24.71	Half Space	1774	1024	948	852	724

Observations/Discussion:

- Seismic station NC.MMX1 is located at the toe of an outcrop of metasedimentary rock. The seismic sensor is located in a vault 1 to 2 m deep and likely rests on rock. Seismic stations located at the toe of a bedrock outcrop have proven the most difficult to characterize. Surface wave techniques cannot be expected to be effective because the bedrock surface will be dipping beneath an array located parallel to the toe of slope. Acquiring surface wave data along an array some distance from the bedrock outcrop is not an option because bedrock velocity becomes very difficult to accurately characterize using surface wave techniques when even only several meters of sediments overly rock. The most success characterizing this type of site has been with S-wave refraction surveys conducted along the toe of slope. If S-wave seismic refraction interpretation becomes difficult or inaccurate due to P-wave interference, out of plane refractors, or converted waves, then P-wave wave seismic refraction surveys may be the only means by which to characterize the site. Alternatively, an S-wave seismic refraction survey located some distance from the outcrop may be more effective, although the weathering profile in rock located beneath several meters, or more, of sediments may differ from that beneath the exposed outcrop.

- This site was visited on two occasions to attempt site characterization. During the first site visit on 8/20/10, P-wave seismic refraction and MASW data were acquired along the 70.5 m long array MMX1-1 parallel to and about 8 m from the outcrop and seismic station. Preliminary data reduction revealed that the MASW survey was not successful and that the P-wave refraction depth of investigation was not great enough to image to 30 m depth. Therefore, the site was visited again on 10/26/11 during which time arrays MMX1-2 and MMX1-4 were completed. Arrays MMX1-2 and MMX1-4 were located along the toe of slope of the bedrock outcrop in an area where there was space for a longer array. MASW, MALW and S-wave seismic refraction data were acquired along the 70.5 m long array MMX1-2 and P-wave seismic refraction data were acquired along the 141 m long array MMX1-4.
- There are no distinct high amplitude HVSR peaks at the three measurement stations. HVSR sensors TRO-1 and TRO2, however, have a potential, weak HVSR peak at about 5.5 Hz. The significance of this HVSR peak is not clear given the very shallow bedrock and dipping bedrock surface.
- Several attempts were made to acquire surface wave data at this site: MASW data acquisition along arrays MMX1-1 and MMX1-2 and MALW data acquisition along array MMX1-2. MASW data were not considered useful. The MALW data were slightly better; however, dispersion data were generally noisy at long wavelengths and Love wave phase velocity could not be extracted to a long enough wavelength to image to 30 m depth. Additionally, with the bedrock surface dipping beneath the array, there is a strong possibility that the Love wave dispersion data contains artifacts and is not valid. Site characterization was, therefore, limited to the analysis of P-wave seismic refraction data collected along arrays MMX1-1 and MMX1-4 and S-wave seismic refraction data collected along array MMX1-2.
- The P-wave seismic refraction data for array MMX1-1 were modeled using a tomographic inversion routine with a layer-based starting model. The model was extended to off-end shot locations to extend depth of investigation. The depth of investigation was about 16 m. The seismic refraction model indicates that there is about 3.5 m of sediments with P-wave velocity in the 250 to 400 m/s range overlying weathered bedrock with P-wave velocity increasing with depth from about 650 m/s to over 1,150 m/s at a depth of about 15 m.
- The average P-wave velocity of the upper 30 m (V_{P30}) was estimated between 24 and 48 m on the array MMX1-1 refraction model, where depth of investigation is greatest, by projecting the velocity at 16 m depth to 30 m depth. V_P likely increases with depth below a depth of 16 m and any estimation of V_{P30} or V_{S30} from this data set will most likely be underestimated. V_{P30} ranges from about 846 to 916 m/s over this interval; an 8% variation. An average V_P model was developed over the 24 to 48 m distance interval by horizontally averaging the travel time of each model cell and cell thickness and average V_{P30} was determined to be 875 m/s. Assuming constant Poisson's ratios of 0.25, 0.3, 0.35 and 0.4 would result in an estimated V_{S30} of 505, 468, 420 and 357 m/s, respectively. The seismic station most likely rests on rock, and V_{S30} is adjusted for seismic station conditions by determining the average V_S between 3.6 m (the top of rock) and 33.6 m. The average V_P between 3.6 and 33.6 m is 1,077 m/s. Assuming constant Poisson's ratios of 0.25, 0.3, 0.35 and 0.4 would result in an estimated average V_S between 3.6 and 33.6 m (adjusted V_{S30}) of 622, 576, 517 and 440 m/s, respectively.

Bedrock is not expected to be saturated in the upper 30 m, therefore, a realistic estimate of Poisson's ratio would be about 0.3. Estimated adjusted V_{S30} for an assumed Poisson's ratio of 0.3, which is 576 m/s, likely presents the lower bound for the site as this model underestimates V_{P30} due to the limited 16 m depth of investigation.

- The P-wave seismic refraction data for array MMX1-4 were modeled using a tomographic inversion routine with a smooth velocity gradient starting model. The depth of investigation was about 26 m. The seismic refraction model indicates that there is up to 1.6 m of sediments with P-wave velocity in the 250 to 400 m/s range overlying weathered bedrock with P-wave velocity increasing with depth from about 550 m/s to over 1,500 m/s at a depth of about 7 to 18 m. The maximum P-wave velocity in the model is about 1,800 m/s and the highest velocity bedrock becomes shallower to the southwest.
- The average V_{P30} was estimated between 54 and 111 m on the array MMX1-4 refraction model, where depth of investigation is greatest, by projecting the velocity at 26 m depth to 30 m depth. V_{P30} ranges from about 1,034 to 1,103 m/s over this interval; a 6% variation. V_{P30} is likely higher than 1,103 m/s southwest of 54 m and may be slightly lower than 1,034 northeast of 111 m. Estimated V_{P30} is higher than that estimated for array MMX1-1, primarily due to thinner sediment cover and greater depth of investigation. An average V_P model was developed over the 54 to 111 m distance interval by horizontally averaging the travel time of each model cell and cell thickness and average V_{P30} was determined to be 1,065 m/s. Assuming constant Poisson's ratios of 0.25, 0.3, 0.35 and 0.4 would result in an estimated V_{S30} of 615, 569, 512 and 435 m/s, respectively. The seismic station most likely rests on rock, and V_{S30} is adjusted for seismic station conditions by determining the average V_S between 1.6 m (the top of rock) and 31.6 m. The average V_P between 1.6 and 31.6 m is 1,291 m/s. Assuming constant Poisson's ratios of 0.25, 0.3, 0.35 and 0.4 would result in an estimated average V_S between 1.6 and 31.6 m (adjusted V_{S30}) of 745, 690, 620 and 527 m/s, respectively.
- The P-wave velocity structure at a position of 111 m is located at a position closest to array MMX1-1. P-wave velocity between a depth of 7 and 16 m is about 15% higher at a position of 111 m on array MMX1-4 than on array MMX1-1. V_{P30} at a position of 111 m is 1,042 m/s and V_{S30} and adjusted V_{S30} (1.6 to 31.6 m) are 557 and 651 m/s, respectively, for an assumed constant Poisson's ratio of 0.3. To more accurately estimate V_{S30} beneath array MMX1-1, the velocity structure below a depth of 18 m at a position of 111 m on array MMX1-4 was inserted into the average V_P model for array MMX1-1. This resulted in an increase in average V_{P30} for array MMX1-1 to 964 m/s and an increase in V_{S30} and adjusted V_{S30} (3.6 to 33.6 m) to 515 and 679 m/s, respectively, for an assumed constant Poisson's ratio of 0.3.
- The S-wave refraction data for array MMX1-2 were modeled using a tomographic inversion routine with a smooth velocity gradient starting model. The seismic refraction model was extended to limited far offset shot locations to extend depth of investigation. S-wave first arrival data were very difficult to accurately pick due to strong P-wave interference, probable higher velocity converted waves and possible out of plane refractors. The resulting S-wave refraction model is, therefore, not considered as accurate as the P-wave velocity models and should not be used alone for site characterization.

- The array MMX1-2 S-wave seismic refraction survey design allowed S-wave velocity to be imaged to a maximum depth of about 20 m. The seismic refraction model indicates that S-wave velocity is about 100 to 200 m/s at the surface and increases to over 400 m/s at a depth of 2.5 to 4 m, 600 m/s at a depth of 5 to 9 m, 800 m/s at a depth of about 9 to 14 and over 1,000 m/s at a depth of 12 to 19 m.
- V_{S30} was estimated between 15 and 36 m on the S-wave refraction model, where depth of investigation is greatest, by projecting the velocity at 20 m depth to 30 m depth. We believe that S-wave velocity is overestimated at 20 m depth due to issues with possible converted waves and it is unlikely that velocity gets any higher between 20 and 30 m. Over this interval V_{S30} ranges from about 603 to 644 m/s, a 7% variation.
- An average V_S model was developed over the 15 to 36 m distance interval by horizontally averaging the travel time of each model cell and cell thickness and average V_{S30} was determined to be 619 m/s. The average V_S between 1.3 and 31.3 m (adjusted V_{S30}) to account for the seismic station resting on rock is 727 m/s.
- As previously mentioned, interpretation of the S-wave seismic refraction data was very difficult. Comparison of the average S-wave refraction velocity model to estimated V_S from the average V_P model for array MMX1-4 for constant Poisson's ratios of 0.25, 0.3 and 0.35 indicates that above 16 m the S-wave refraction model is consistent with the P-wave refraction model for Poisson's ratio in the 0.25 to 0.3 range. Below a depth of 16 m, the S-wave refraction model yields higher V_S. Picking of S-wave first arrivals was extremely difficult at long offsets, and we believe that the S-wave refraction model overestimates V_S at depths below 16 m due to interference from P-wave energy and converted waves. Given the uncertainty in the S-wave velocity model from the S-wave seismic refraction survey (i.e. possible overestimated velocity at depth), the V_{S30} and adjusted V_{S30} estimates should be considered the upper bound for the site.
- In summary, V_{S30} estimates are 515 m/s for P-wave refraction array MMX1-1 with velocity structure below 18 m from a position of 111 m on array MMX1-4 and an assumed Poisson's ratio of 0.3; 569 m/s from the average V_P model for array MMX1-4 and assumed constant Poisson's ratio of 0.3; 557 m/s from the V_P model at a position of 111 m on array MMX1-4 and an assumed constant Poisson's ratio of 0.3 (closest point on array MMX1-4 to the seismic station and array MMX1-1) and 619 m/s from the average V_S model for S-wave refraction array MMX1-2. The average V_{S30} of the above four estimates is 565 m/s.
- In summary, adjusted V_{S30} (the average V_S estimates for the upper 30 m of weathered rock) are 679 m/s for P-wave refraction array MMX1-1 with velocity structure below 18 m from a position of 111 m on array MMX1-4 and an assumed Poisson's ratio of 0.3; 690 m/s from the average V_P model for array MMX1-4 and assumed constant Poisson's ratio of 0.3; 651 m/s from the V_P model at a position of 111 m on array MMX1-4 and an assumed constant Poisson's ratio of 0.3 (closest point on array MMX1-4 to the seismic station and array MMX1-1) and 727 m/s from the average V_S model for S-wave refraction array MMX1-2. The average adjusted V_{S30} of the above four estimates is 687 m/s.
- For the purpose of site characterization, we average the four V_{S30} and adjusted V_{S30} estimates made above and calculated from the S-wave seismic refraction model and P-wave refraction models using an assumed constant Poisson's ratio of 0.3.

- In conclusion, V_{S30} averages about 565 m/s (NEHRP Site Class C) and, more importantly, adjusted V_{S30} (average V_S of the upper 30 m of weathered rock) averages about 687 m/s (NEHRP Site Class C).
- Although there is some uncertainty in V_{S30} and adjusted V_{S30} at this site, there is only about 11% variation in adjusted V_{S30} between four averaged estimates. Adjusted V_{S30} is clearly in the upper velocity range of NEHRP Site Class C and there is no evidence that the site could fall into the NEHRP Site Class B velocity range.

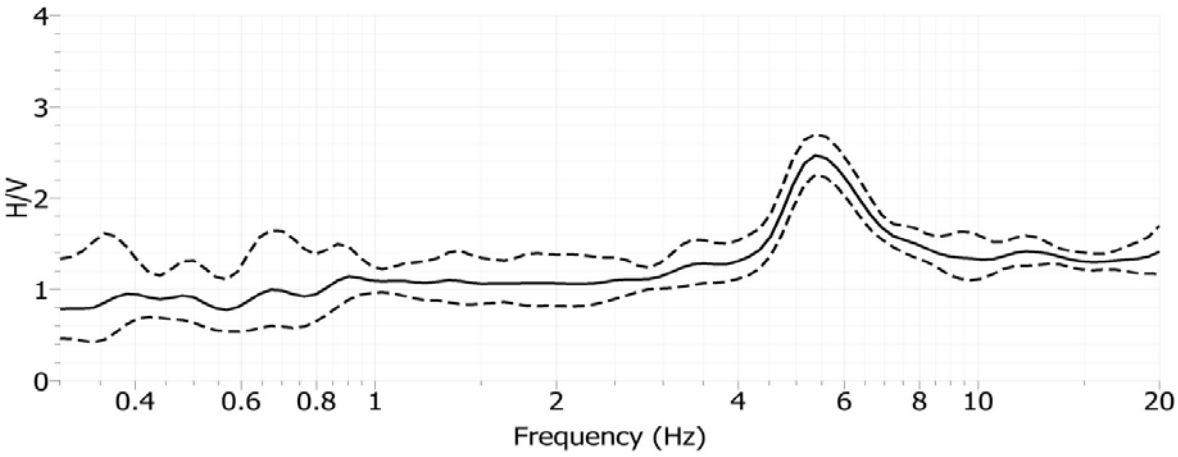

Site NC.MMX1, H/V Spectral Ratio, Array MMX1-1, Sensor TRO-2

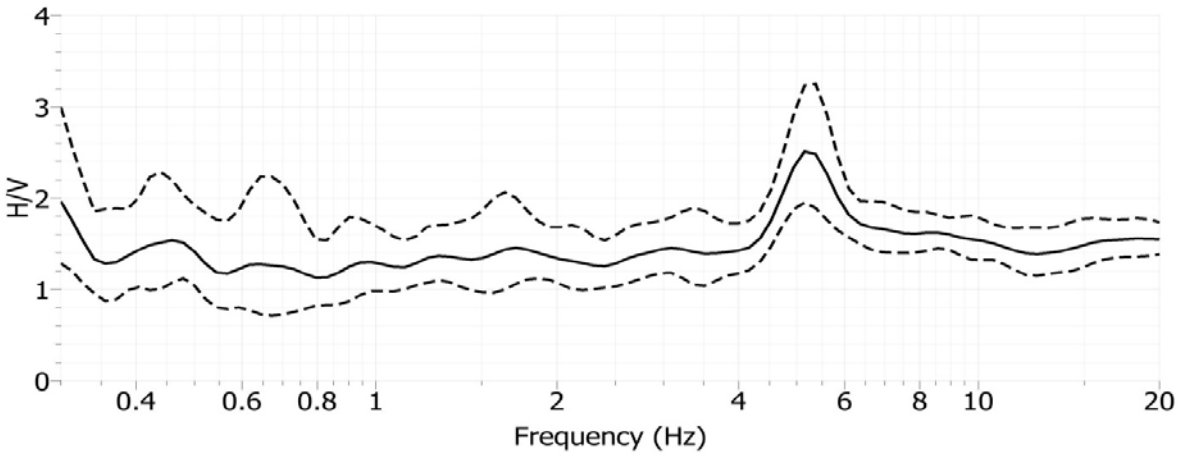

Site NC.MMX1, H/V Spectral Ratio, Array MMX1-1, Sensor TRO-1

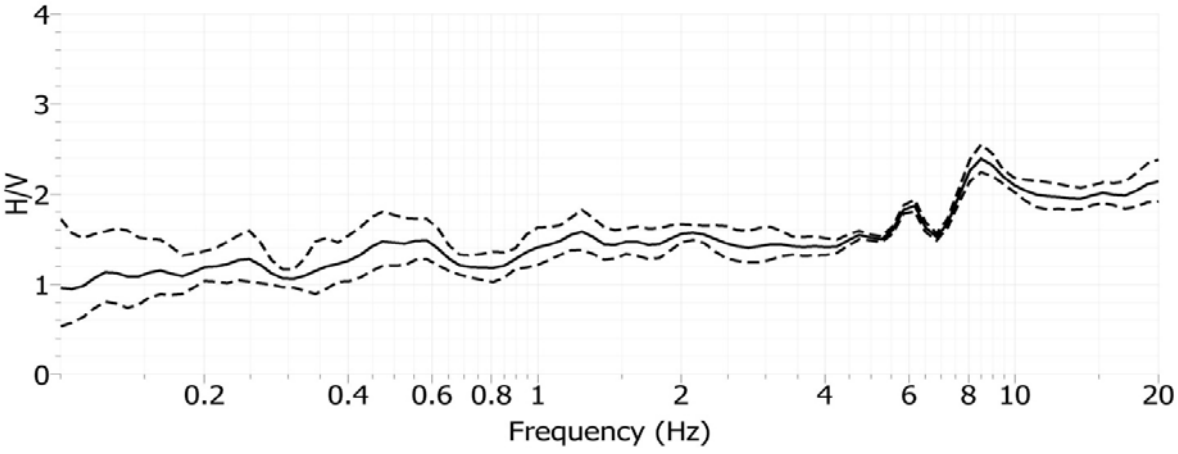

Site NC.MMX1, H/V Spectral Ratio, Near Seismic Station, Sensor 453

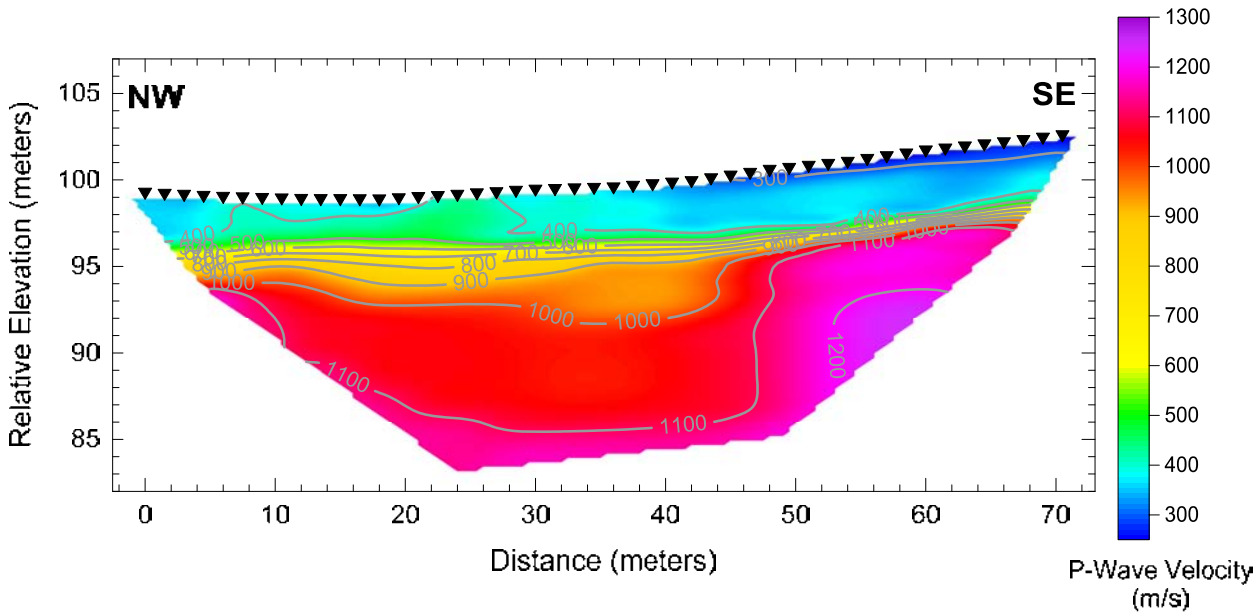

Array MMX1-1 – P-wave Tomographic Seismic Refraction Model Developed using a Layer Based Starting Model

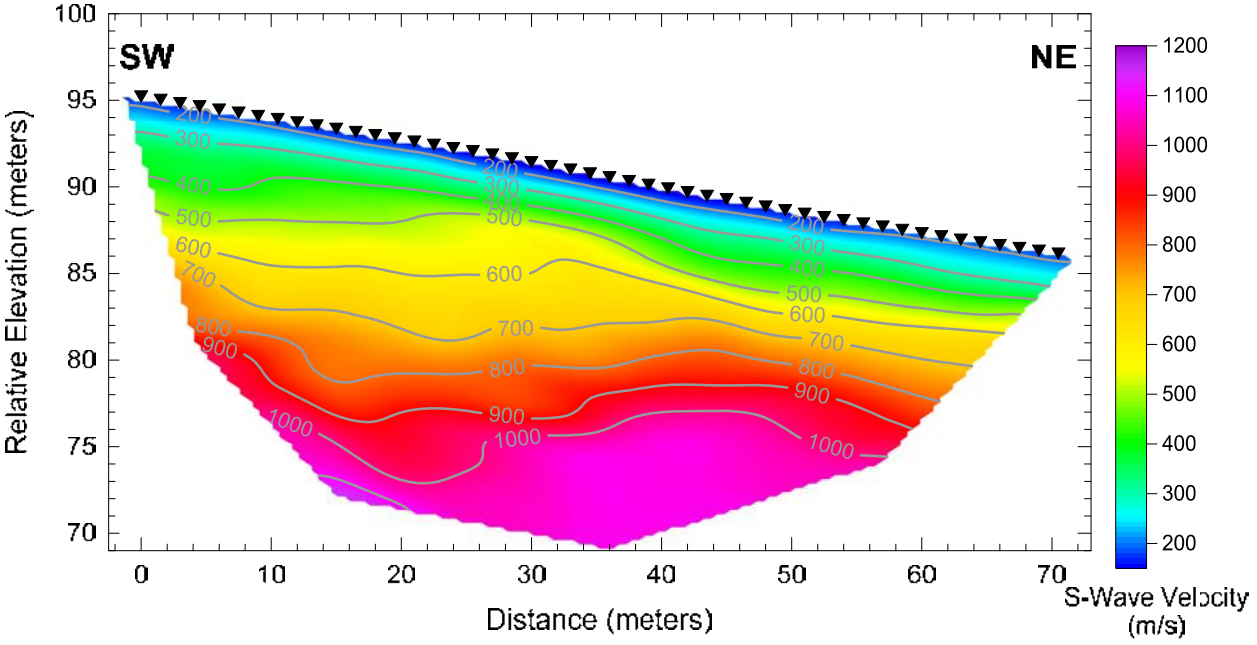

Array MMX1-2 – S-wave Tomographic Seismic Refraction Model Developed using a Smooth Velocity Gradient Starting Model

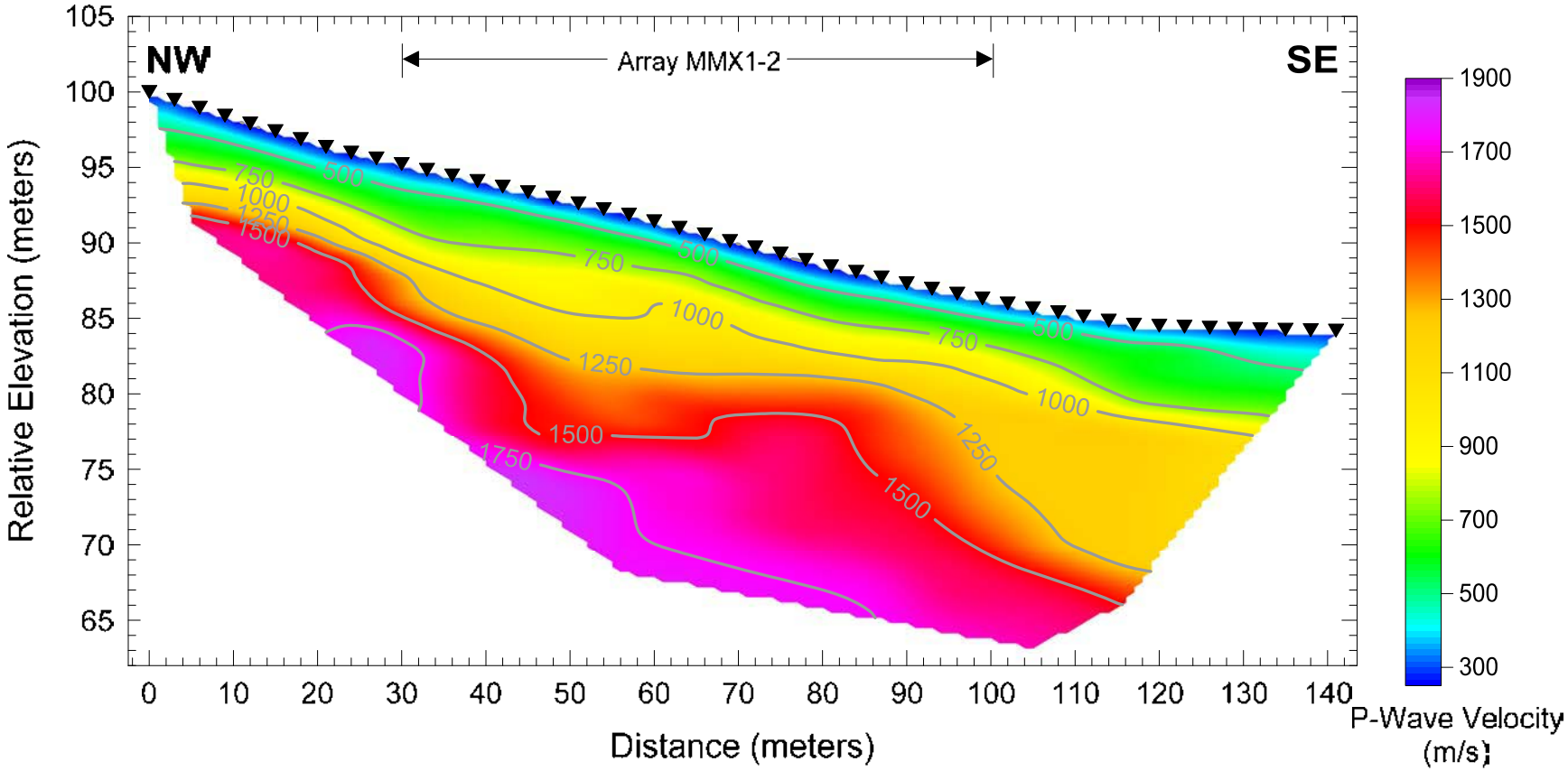

Array MMX1-4 – P-wave Tomographic Seismic Refraction Model Developed using a Smooth Velocity Gradient Starting Model

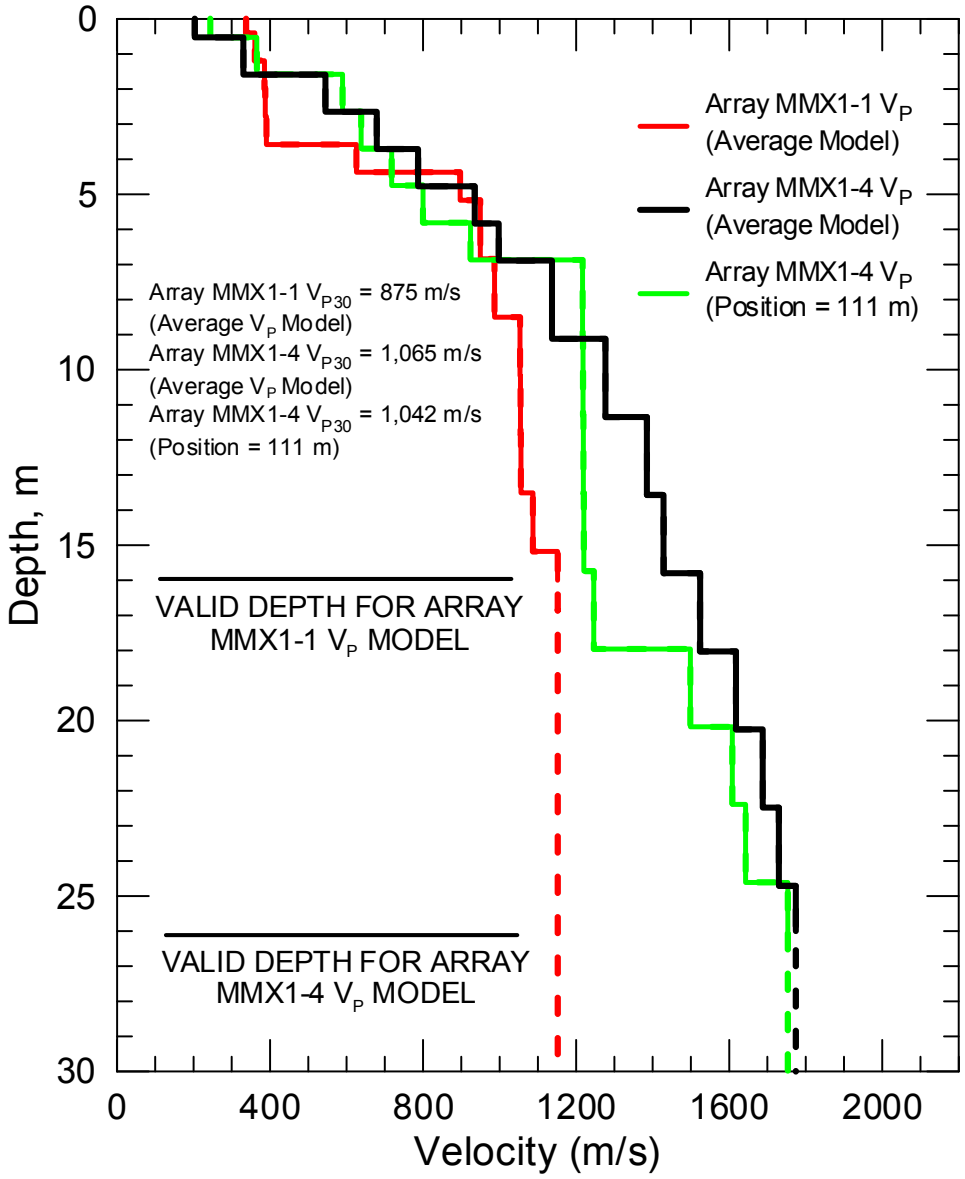

NC.MMX1 – Average V_P models between 24 and 48 m on array MMX1-1 and between 54 and 111 m on array MMX1-4 and the V_P model at a position of 111 m on array MMX1-4. There is a thicker sequence of sediments beneath array MMX1-1, which is located about 8 m from the toe of slope, compared to array MMX1-4, which is located along the toe of slope. The seismic station is located at the toe of slope near the center of array MMX1-1 with the seismic sensor likely placed on weathered rock. Bedrock velocities are higher at depths below 7 m on array MMX1-4, even at a position of 111 m, which is closest to array MMX1-1. Depth of investigation along array MMX1-1 is only about 16 m and this model will underestimate V_{P30} because bedrock velocity likely increases with depth below 16 m. On the other hand, array MMX1-4 may overestimate V_{P30} beneath the seismic station because bedrock velocity may be slightly higher beneath this array.

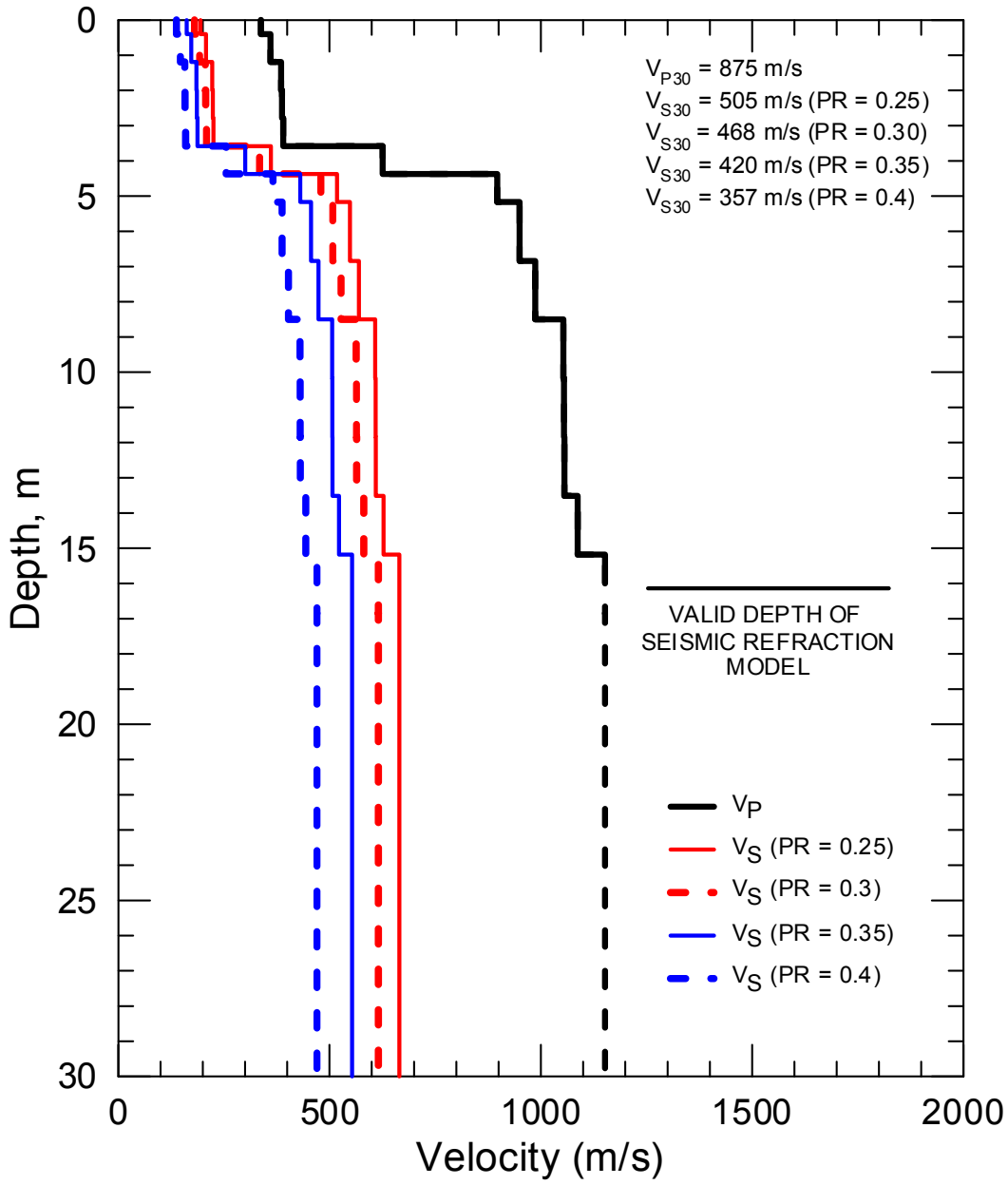

NC.MMX1 – Average P-wave velocity structure and estimated S-wave velocity structure between a position of 24 and 48 m on the P-wave seismic refraction model for array MMX1-1 developed using a layered starting model. The maximum seismic refraction depth of investigation is limited to about 16 m and P-wave velocity is expected to gradually increase with depth below 16 m, therefore, V_{P30} is likely underestimated.

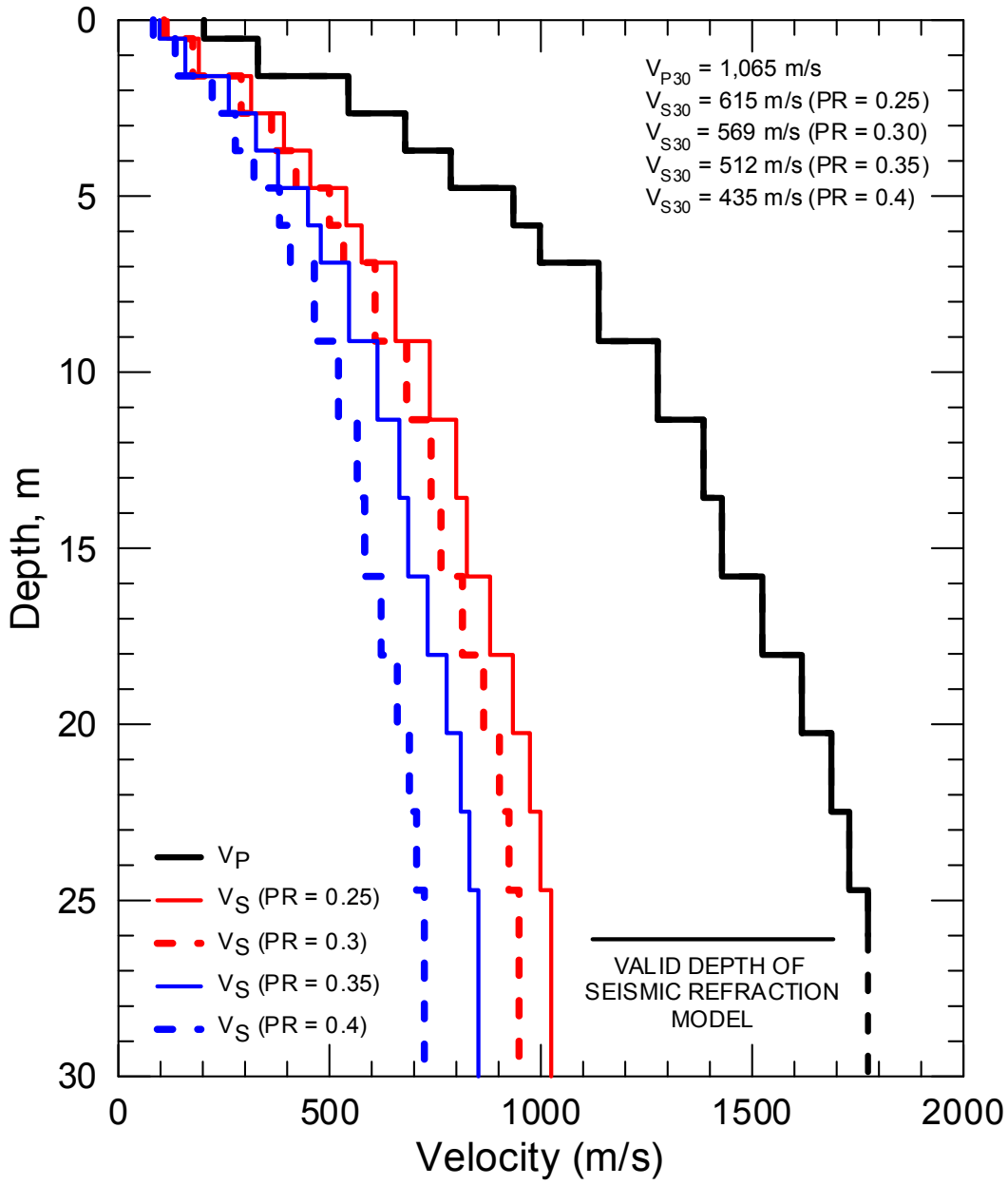

NC.MMX1 – Average P-wave velocity structure and estimated S-wave velocity structure between a position of 54 and 111 m on the P-wave seismic refraction model for array MMX1-4 developed using a smooth velocity gradient starting model.

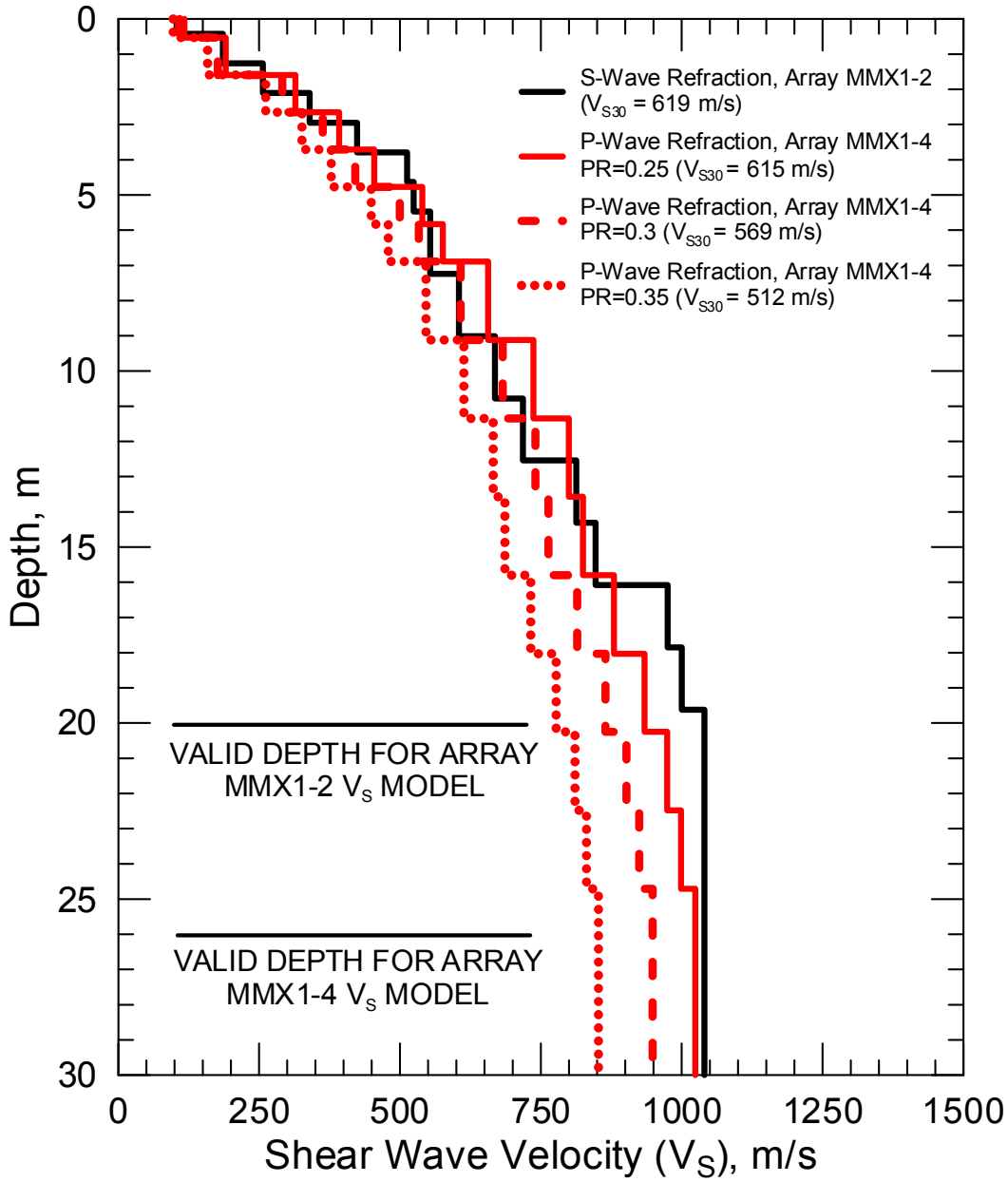

NC.MMX1 – Comparison of S-wave velocity models derived from the S-wave seismic refraction survey along array MMX1-2 and P-wave seismic refraction survey along array MMX1-4. S-wave wave velocity is estimated from the average P-wave velocity model between 54 and 111 m on array MMX1-4, assuming constant Poisson's ratio of 0.25, 0.3 and 0.35. The S-wave seismic refraction data were difficult to interpret due to strong P-wave energy, possible converted waves and poor polarity reversal on some shot records. The S-wave refraction model is likely reliable in the upper 15 m, but appears to overestimate V_S at greater depths, possibly because it was very difficult to interpret first arrival data at long offsets.

Site NC.PAGB

Location: Antelope Grade, San Luis Obispo County, California

Latitude: 35.73065 **Longitude:** -120.24986
(Station coordinates provided by USGS, WGS84 coordinate system)

V_{S30} (measured): 473 m/s

V_{S30} (adjusted to more accurately reflect seismic station conditions): 510 m/s (average S-wave velocity between 1 and 31 m adjusting for assumed sensor depth and sensor likely being placed on serpentinite).

NEHRP Site Class: C

Geomatrix Code: IJB

Geologic Conditions/Observations: Seismic station located on geologic unit mapped as Mesozoic (Jurassic) serpentinite.

Site Conditions: Rural site located on gently rolling hills. Ground surface elevation increases about 4 to 4.5 to the southeast along the 70.5 m long MASW and seismic refraction arrays PAGB-1 and PAGB-2.

Geophysical Methods Utilized: HVSR, P- and S-wave Seismic Refraction, MASW (Rayleigh wave) and MALW (Love wave)

Geophysical Testing Arrays:

1. Array PAGB-1 (48 channel MASW, MALW and P- and S-wave seismic refraction array utilizing 4.5 Hz vertical or 10 Hz horizontal geophones spaced 1.5 m apart for a length of 70.5 m, forward and reverse shot locations with multiple source offsets and source types and multiple interior shot locations).
2. Array PAGB-2 (48 channel MASW, MALW and P- and S-wave seismic refraction array utilizing 4.5 Hz vertical or horizontal geophones spaced 1.5 m apart for a length of 70.5 m, forward and reverse shot locations with multiple source offsets and source types and multiple interior shot locations).
3. Three HVSR measurement locations distributed along array PAGB-1.

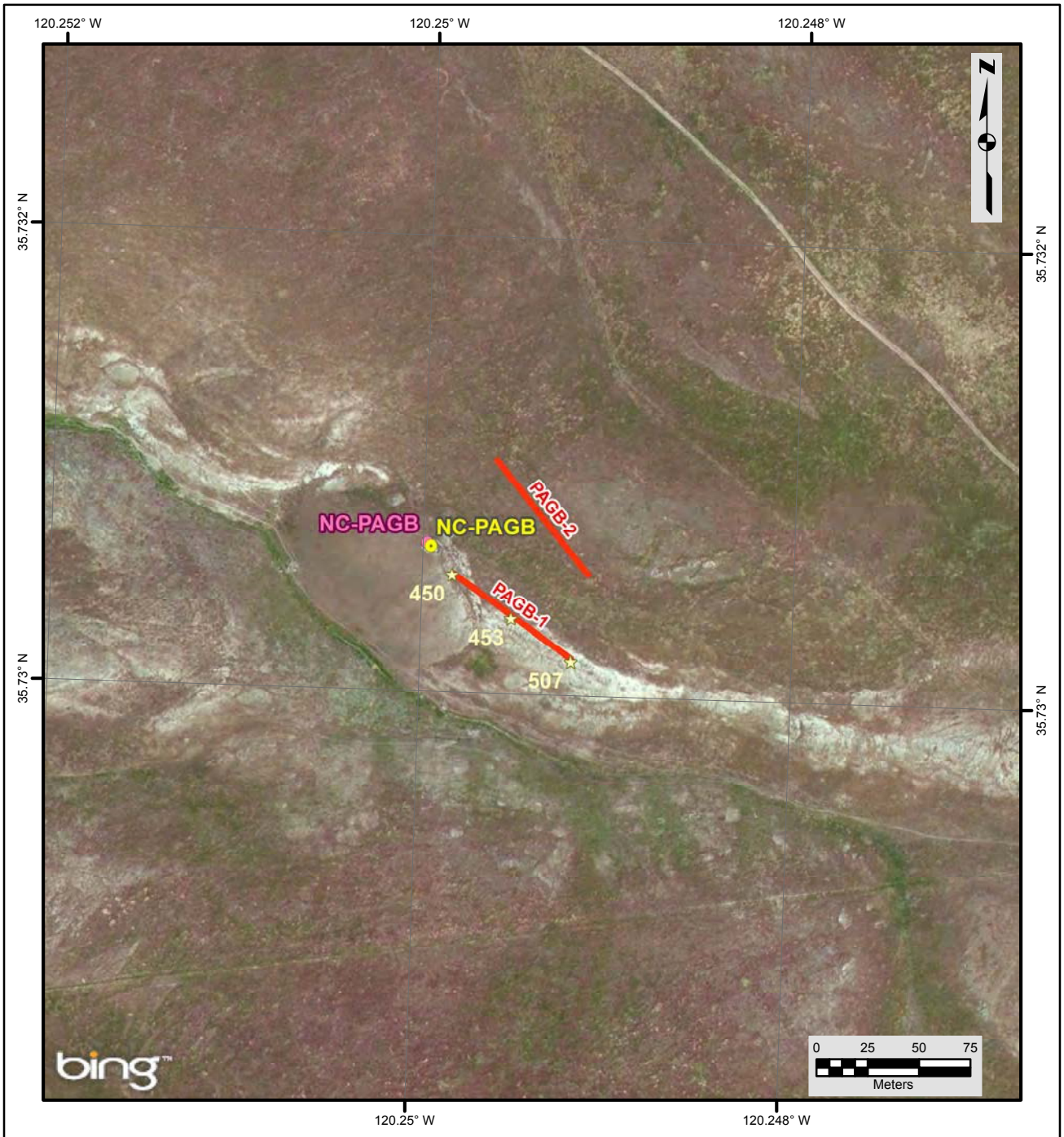

Legend

- Seismic Station - Approximate Surveyed Location
- Seismic Station - Approximate Location of Record
- H/V Spectral Ratio Location
- MASW and Seismic Refraction Array

NOTES:
1. WGS 1984 COORDINATE SYSTEM
2. Image Source: (c) Microsoft Corporation and its data suppliers

File Name: NC-PAGB-I

Date: 2/7/2013

USGS science for a changing world

GEOVision geophysical services

RECOVERY.GOV

SITE MAP
NC•PAGB

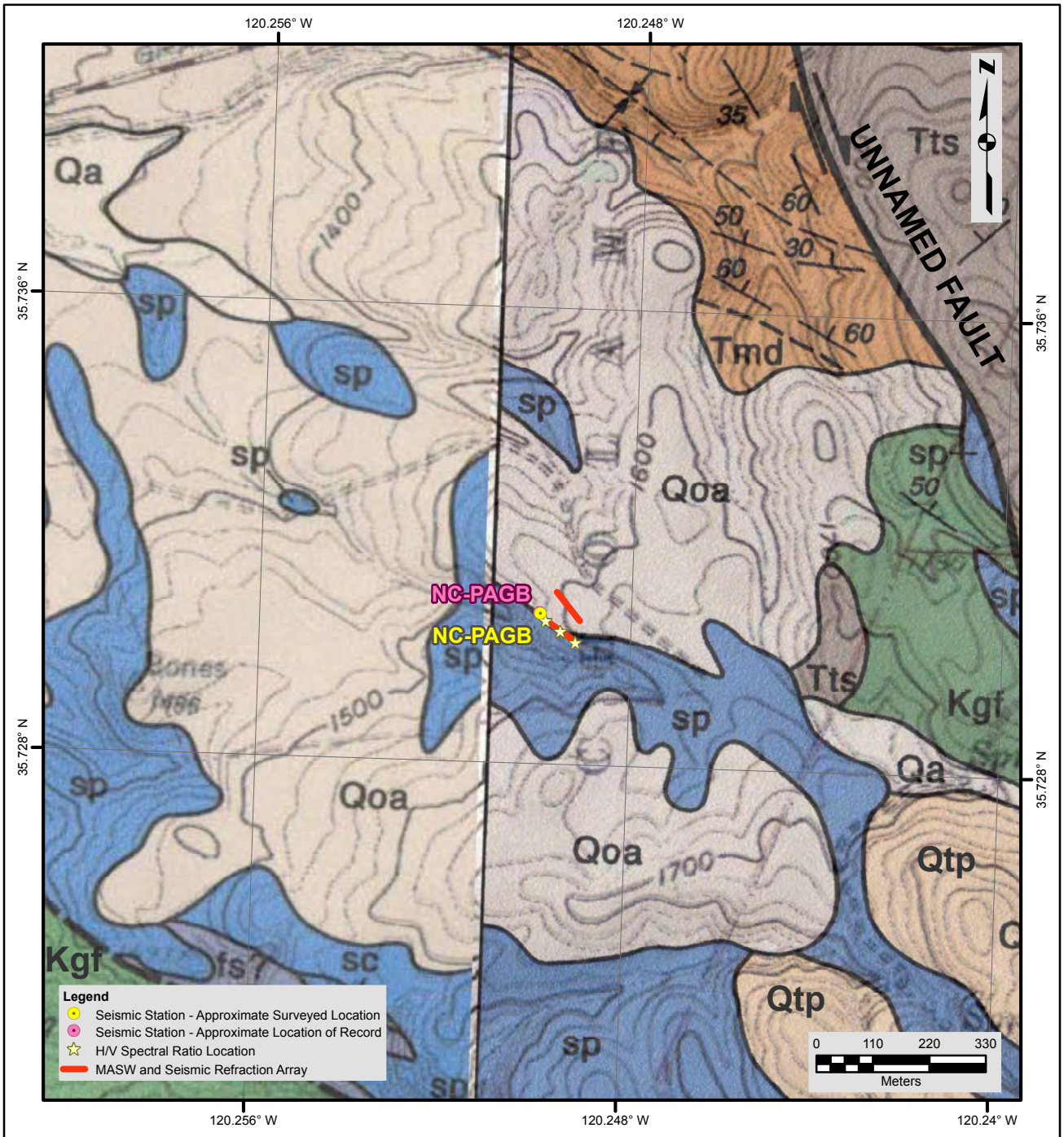

Description of Geologic Map Units

Qa = Quaternary (Holocene) alluvial gravel, sand and clay of valley areas
Qoa = Quaternary (Pleistocene) alluvial fan gravel of shale and sandstone detritus
QTp = Quaternary (Pleistocene to Latest Pliocene) Paso Robles Formation; weakly indurated alluvial pebble gravel of shale and sandstone detritus
Tmd = Tertiary (Miocene) Monterey Shale; Devilwater Shale Member, clay shale, silty, crumbly
Tts = Tertiary (Lower Miocene) Temblor Formation; marine clastic, lithified sandstone, some clay shale, undivided
Kgf = Mesozoic (Cretaceous) Gravelly Flat Formation; lithified clay shale, interbeds of graywacke sandstone
sp = Mesozoic (Jurassic) serpentinite, sheared, slickensided
fs = Late Mesozoic Franciscan Assemblage; graywacke sandstone, hard, massive, severely fractured, brecciated

NOTES:
1. WGS 1984 COORDINATE SYSTEM
2. Geologic Map of the Orchard Peak and Cholame Quadrangles, San Luis Obispo, Monterey and Kern Counties, California by Thomas W. Dibblee, Jr., 2005
3. See site map for details of geophysical survey

USGS science for a changing world

GEOVision geophysical services

GEOLOGIC MAP
NC•PAGB

File Name: NC-PAGB

Date: 2/7/2013

Seismic Station NC.PAGB. Note serpentinite outcrop adjacent to seismic station

Looking northwest along array PAGB-1 and at HVSR sensor 507

S-wave seismic refraction and MALW data acquisition along array PAGB-1

Looking northwest towards seismic station and at the northwest end of array PAGB-1 and at HVSR sensor 450

Looking west towards seismic station and at array PAGB-2

Location of Geophysical Testing Arrays:

Location	Latitude	Longitude
PAGB-1, Northwest End of MASW/Refraction array	35.73052	-120.24971
PAGB-1, Center of MASW/Refraction Array	35.73034	-120.24939
PAGB-1, Southeast End of MASW/Refraction Array	35.73016	-120.24907
PAGB-2, Northwest End of MASW/Refraction Array	35.73102	-120.24950
PAGB-2, Center of MASW/Refraction Array	35.73078	-120.24925
PAGB-2, Southeast End of MASW/Refraction Array	35.73053	-120.24899
HVSR Sensor 450	35.73051	-120.24972
HVSR Sensor 453	35.73033	-120.24940
HVSR Sensor 507	35.73015	-120.24907
NC.PAGB Seismic Station	35.73064	-120.24984

Notes: 1) WGS84 Coordinate System (decimal degrees)
2) Survey accuracy is estimated at 1 to 2 m.

Results:

Array PAGB-1 V_S Model (Love wave MALW)

Depth to Top of Layer (m)	Layer Thickness (m)	S-Wave Velocity (m/s)	Inferred P-Wave Velocity (m/s)	Assumed Poisson's Ratio	Assumed Density (g/cm^3)
0	1	170	319	0.300	1.8
1	3	346	648	0.300	1.9
4	4	403	753	0.300	1.9
8	5	424	2000	0.477	2.0
13	5	480	2000	0.469	2.0
18	8	682	2000	0.434	2.1
26	>4	790	2000	0.408	2.1

Notes: 1) Saturated zone, with V_P of about 2,000 m/s, constrained at a depth of about 8 m based on seismic refraction survey. Note that V_P and Poisson's ratio has no affect on Love wave V_S model, but shown but shown for consistency.
2) Depth of investigation is about 30 m.
3) Bottom layer is a half space.
4) Half space velocity not well constrained.

Array PAGB-2 V_S Model (Rayleigh Wave MASW)

Depth to Top of Layer (m)	Layer Thickness (m)	S-Wave Velocity (m/s)	Inferred P-Wave Velocity (m/s)	Assumed Poisson's Ratio	Assumed Density (g/cm^3)
0	1	131	244	0.300	1.7
1	2	201	375	0.300	1.8
3	4	260	486	0.300	1.8
7	8	267	499	0.300	1.8
15	8	427	2000	0.476	2.0
23	>12	610	2200	0.458	2.1

Notes: 1) Saturated zone, with V_P of about 2,000 to 2,200 m/s, constrained at a depth of about 15 m based on seismic refraction survey.
2) Depth of investigation is about 35 m.
2) Bottom layer is a half space.

Observations/Discussion:

- This site is located near the edge of two geologic maps and there is a discrepancy in the geologic units on the two maps. The geologic map on which the seismic station is located indicates that the seismic station is located at the edge of an outcrop of Jurassic serpentinite with serpentinite located south of the seismic station and Pleistocene old alluvium located north of the seismic station. The adjacent geologic map indicates that some of the area mapped as old alluvium could be serpentinite.
- Field investigations were conducted at this site on two occasions. Initially, P- and S-wave seismic refraction, MASW and MALW data were acquired along array PAGB-1, located on the edge of the mapped serpentinite outcrop. Preliminary review of the data indicated that data quality was significantly degraded by lateral velocity variation and possible higher modes in the Rayleigh wave data. Therefore, P- and S-wave seismic refraction, MASW and MALW data were acquired at a later data on array PAGB-2, located about 40 to 50 m northeast of the seismic station on mapped old alluvium. Serpentinite does not outcrop along array PAGB-2, but was expected to be relatively shallow. As will be discussed below, S-wave velocity is much lower in the vicinity of array PAGB-2 indicating that the serpentinite significantly deepens to the northeast and this array should not be used for the purpose of site characterization. Arrays PAGB-1 and PAGB-2 are orientated subparallel to regional geologic trends (faulting, geologic strike) in the site vicinity.
- HVSR sensors had to be coupled to the ground by using plaster to set an aluminum cradle in a shallow hole. There is no distinct HVSR peak occurring at similar frequency at all of the measurements stations. The HVSR data for sensor 507 has a peak at about 9.5 Hz and elevated HVSR response at frequencies between 1 and 8 Hz. HVSR sensors 453 and 507 do not have elevated HVSR response over the 1 to 8 Hz frequency rate and,

therefore, the elevated HVSR response could be associated with sensor placement. Additionally, HVSR sensors 453 and 507 do not have a strong peak at 9.5 Hz, but may have weak peaks at 6.5 and 8 Hz, respectively. The different high frequency HVSR response at the site indicates that there is likely lateral velocity variation beneath array PAGB-1. There were no feasible alternate test locations on mapped serpentinite in close proximity to the seismic station.

- Only P-wave seismic refraction data have been interpreted at this time. There is possible evidence of high velocity layers or out of plane refractors beneath some segments of the seismic lines, which are expected to complicate surface wave interpretation. Based on review of S-wave seismic refraction data and surface wave data, it appears that the sediments/rock are saturated at shallow depth. Therefore, the primary use of P-wave seismic refraction data at this site is to determine approximate depth to groundwater for surface wave modeling.
- The P-wave refraction data for arrays PAGB-1 and PAGB-2 were modeled using a tomographic inversion routine with a layered starting model. The seismic refraction models were extended to far offset shot locations to extend depth of investigation.
- The P-wave seismic refraction survey design allowed P-wave velocity to be imaged to a maximum depth of about 20 to 25 m. The seismic refraction model for array PAGB-1 shows that P-wave velocity is about 400 to 700 m/s at the surface and increases from about 1,000 to 1,600 m/s over the 7 to 11 m depth interval at what is expected to be the top of the saturated zone. The maximum P-wave velocity in the model is about 2,400 m/s. The seismic refraction model for array PAGB-2 shows that P-wave velocity is about 300 to 400 m/s at the surface and increases to 600 m/s at a depth of about 6 to 9 m and over 1,600 m/s at a depth of 12 to 16 m. Based on review of S-wave seismic refraction and surface wave data, P-wave velocities over 1,600 m/s are expected to be associated with saturated, weathered sedimentary rock at this site. The maximum P-wave velocity in the model is about 2,400 m/s.
- There is a significant difference in the P-wave velocity models between arrays PAGB-1 and PAGB-2. Near surface velocities are much higher beneath array PAGB-1 where the weathered serpentinite bedrock is located at or near the surface. Low near surface velocities beneath array PAGB-2 appear to be associated with a thick sequence of alluvium overlying the serpentinite unit. The saturated zone is also about 6 m deeper beneath array PAGB-2 as this array is located at higher ground surface elevation. The velocity structure beneath array PAGB-1 should be considered representative of seismic station conditions. Array PAGB-2 should not be used to characterize the seismic station.
- Noise conditions at the site were not sufficient for application of passive surface wave techniques.
- Both MASW (Rayleigh wave) and MALW (Love wave) data were acquired along arrays PAGB-1 and PAGB-2. Only 10 Hz horizontal geophones were available for MALW data acquisition on array PAGB-1, whereas 4.5 Hz horizontal geophones were available for array PAGB-2.
- It was not possible to develop a coherent dispersion curve from the Rayleigh wave phase velocity data along array PAGB-1. Lateral velocity variation and dominant higher modes appeared to be a significant issue with this data set. In fact, source locations at various offsets from each end of the array often yielded significantly different dispersion curves

at long wavelengths. V_{R40} ranges from about 400 to 525 m/s, although the higher velocities may be associated with dominant higher modes or modal superposition.

- MALW (Love wave) data along array PAGB-1 were generally better than the Rayleigh wave data, although there was still significant scatter in the phase velocity dispersion data due to lateral velocity variation. It was necessary to pick Love wave dispersion data to a frequency of about 6 to 7 Hz to obtain the 90 m wavelength necessary to develop a V_S model to 30 m depth. The use of 4.5 Hz horizontal geophones and a better low frequency energy source may have yielded more reliable results. The Love wave dispersion data for array PAGB-1 is consistent with the Rayleigh wave data.
- The MASW (Rayleigh wave) data was the better data set at array PAGB-2. S-wave velocities are significantly lower beneath this array, likely due to a thick sequence of alluvium overlying the serpentinite, and it was not possible to extract Love wave phase velocity to long enough wavelength to image to 30 m depth.
- The minimum wavelength Love wave phase velocity data extracted from the 48-channel MALW array PAGB-1 was about 12 m. Reducing data from smaller hammer sources using a limited offset receiver array (i.e. less active geophones) allowed for extraction of surface wave dispersion data to a minimum wavelength of about 4 m. The minimum wavelength Rayleigh wave phase velocity data extracted from the 48-channel MASW array PAGB-2 was about 22 m. Reducing data using a limited offset receiver array (i.e. less active geophones) allowed for extraction of surface wave dispersion data to a minimum wavelength of about 2.5 m.
- There is about 30 and 80 m/s of scatter in Rayleigh and Love wave dispersion data, respectively. This scatter is in part due to lateral velocity variation caused by differential weathering of near surface sedimentary rock (array PAGB-1) and variable thickness of the alluvium layer (array PAGB-2).
- A representative dispersion curve was generated for the Rayleigh and Love wave MASW data sets using a moving average, polynomial curve fitting routine and used for modeling.
- Based on the seismic refraction models, saturated sediments with V_P of 2,000 m/s, or greater, were constrained at a depth of 8 m beneath array PAGB-1 and 15 m beneath array PAGB-2. This is consistent with array PAGB-2 being located at higher elevation than array PAGB-1. The actual elevation difference between the two arrays was not measured but may be on the order of 6 m.
- Surface wave depth of investigation is about 30 m for the array PAGB-1 Love wave model and 35 m for the array PAGB-2 Rayleigh wave models.
- Both the seismic refraction and surface wave V_S models indicate that velocity structure is much different beneath arrays PAGB-1 and PAGB-2. Array PAGB-2 appears to have a relatively thick sequence of low velocity alluvium overlying the serpentinite unit. The seismic refraction data for array PAGB-2 indicates that higher velocity weathered serpentinite (P-wave velocity of greater than 600 m/s) may be as shallow as 6 to 9 m, although velocity structure at these depths may be somewhat skewed by the underlying saturated zone. The surface wave V_S model indicates that the higher velocity weathered rock may be deeper (between 7 and 15 m).
- Scatter in the Love wave dispersion data is such that the half space velocity is not well resolved in the V_S model for array PAGB-1; however, V_{S30} is likely much better constrained. Based on scatter in the dispersion data variations in V_{S30} of 10% beneath the array would not be unexpected.

- V_{S30} is 473 m/s for array PAGB-1 (NEHRP Site Class C), based on analysis of Love wave dispersion data. Array PAGB-1 is considered most representative of conditions at the seismic station.
- Average S-wave velocity between 1 m (assumed sensor depth) and 31 m is 510 m/s for array PAGB-1.
- V_{S30} is 322 m/s for array PAGB-2 (NEHRP Site Class D), based on analysis of Rayleigh wave dispersion data. Array PAGB-2 is not considered representative of conditions at the seismic station.
- Average S-wave velocity between 1 m (assumed sensor depth) and 31 m is 344 m/s for array PAGB-2.
- Although arrays PAGB-1 and PAGB-2 are only 40 to 50 m apart, there is a very large difference in velocity structure and V_{S30} beneath the two arrays. Array PAGB-2 appears to have a relatively thick sequence of alluvium overlying serpentinite, whereas the serpentinite unit is at or near the surface in the immediate vicinity of array PAGB-1.
- The V_S model from array PAGB-1 should be used for purpose of site characterization; however, it should be recognized that there is significant lateral velocity variation in the site vicinity.

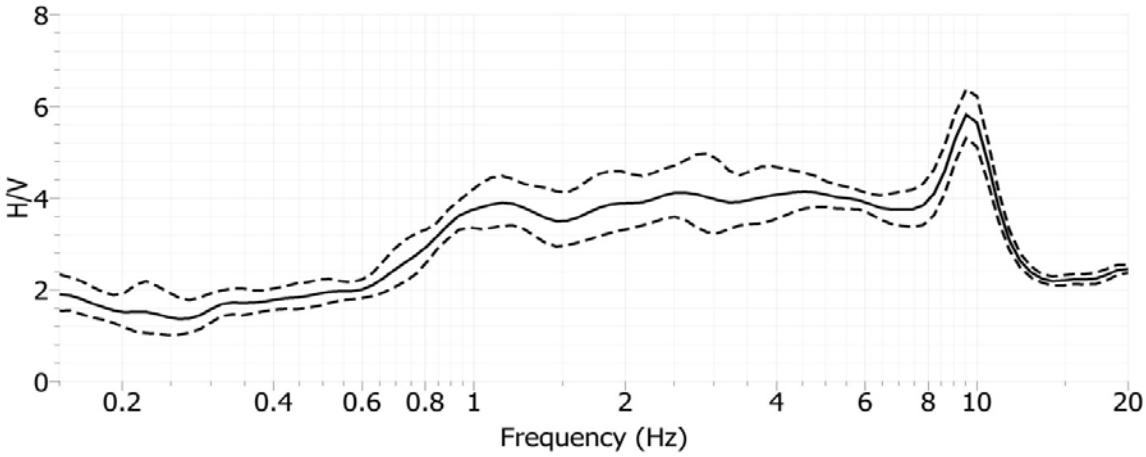

Site NC.PAGB, H/V Spectral Ratio, Array PAGB-1, Sensor 450

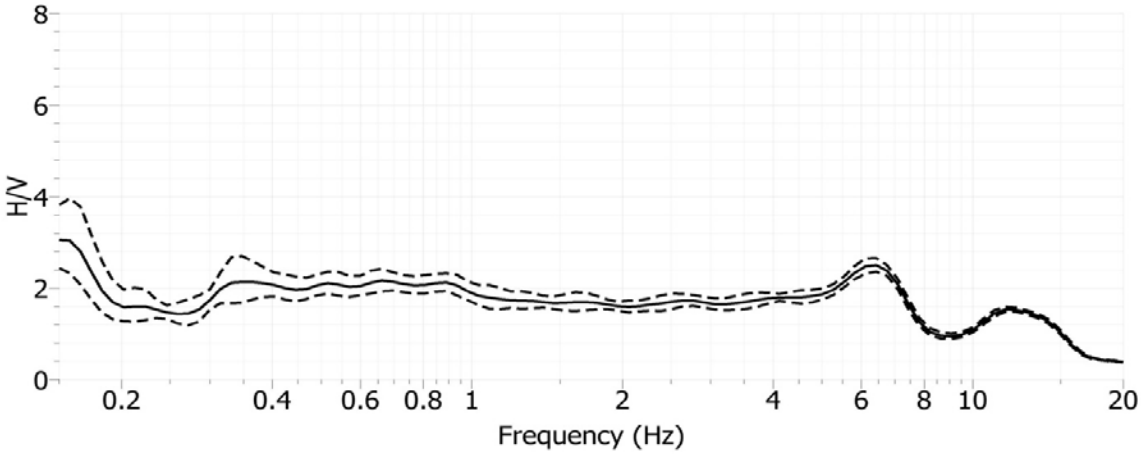

Site NC.PAGB, H/V Spectral Ratio, Array PAGB-1, Sensor 453

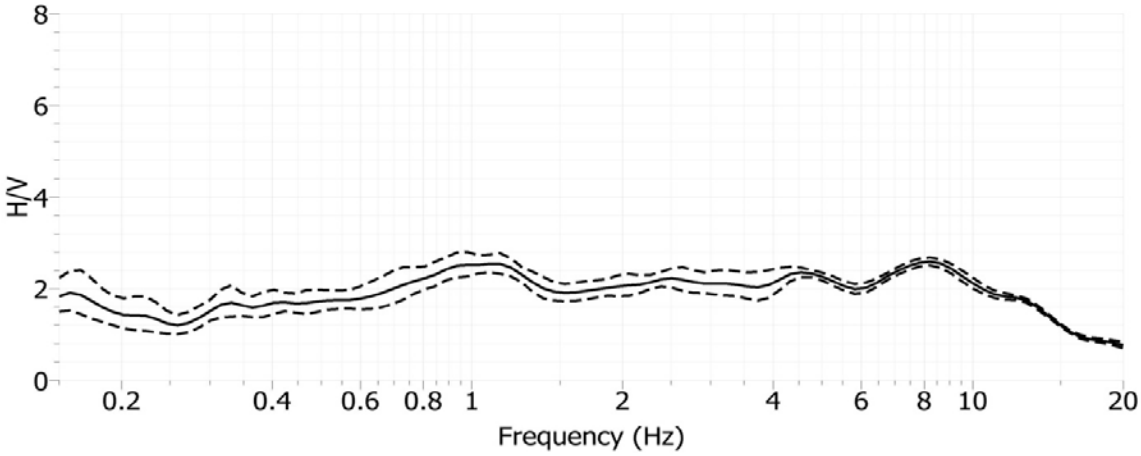

Site NC.PAGB, H/V Spectral Ratio, Array PAGB-1, Sensor 507

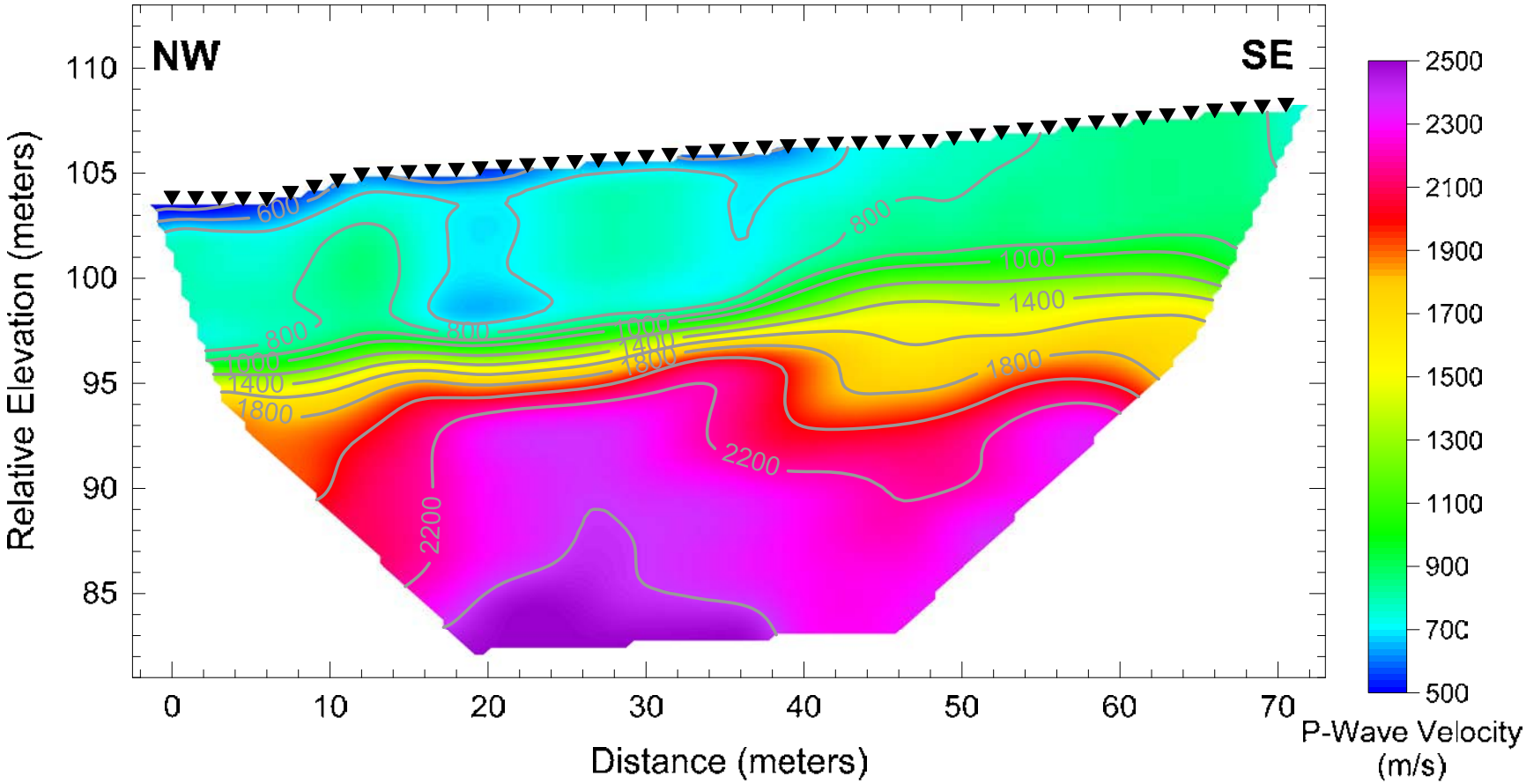

Array PAGB-1 – P-wave Tomographic seismic refraction model developed using a layer-based starting model

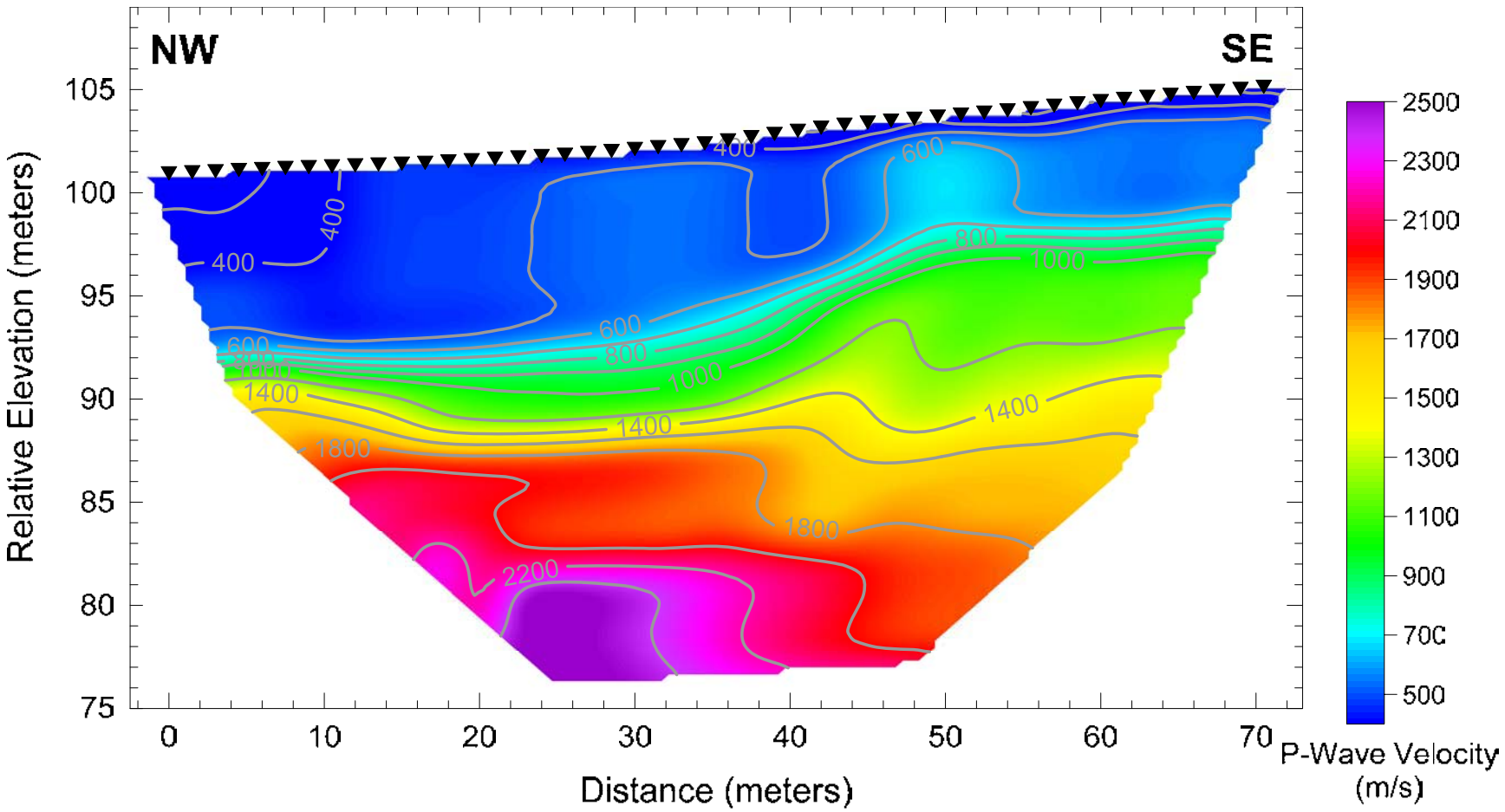

Array PAGB-2 – P-wave Tomographic seismic refraction model developed using a layer-based starting model

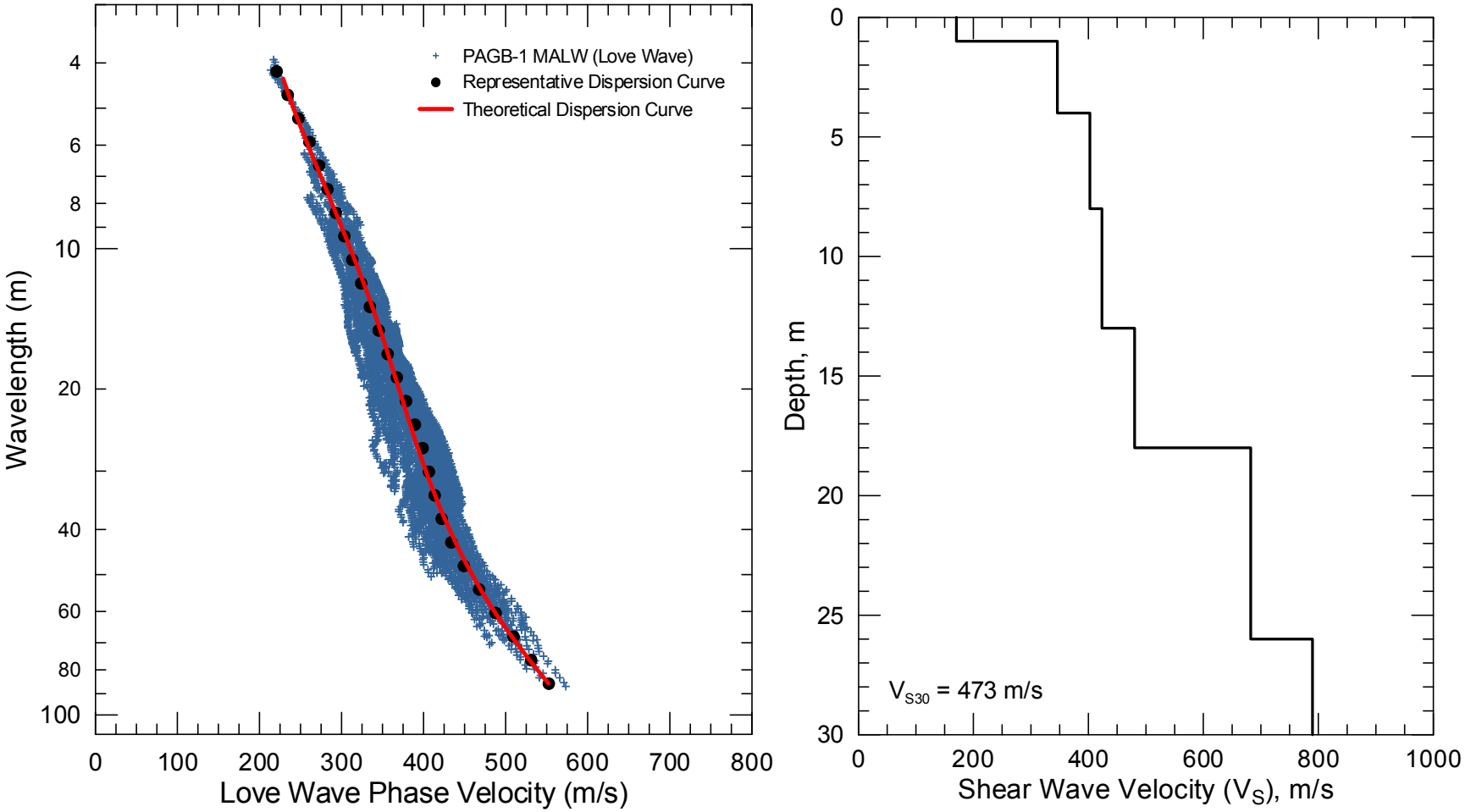

NC.PAGB - Field, representative and inverted theoretical surface wave dispersion data (left) and associated V_S model (right) for Love wave data collected along array PAGB-1

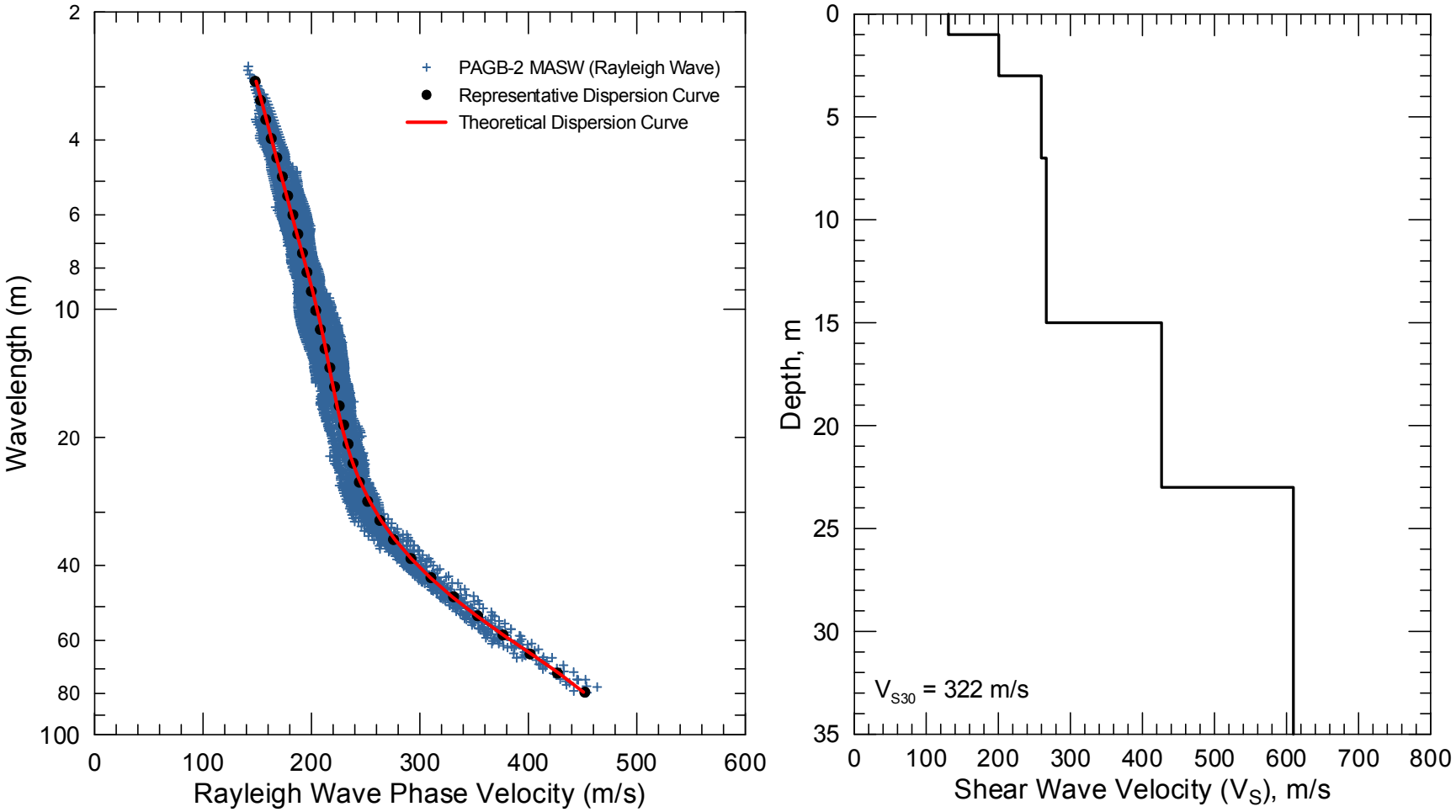

NC.PAGB - Field, representative and inverted theoretical surface wave dispersion data (left) and associated V_S model (right) for Rayleigh wave data collected along array PAGB-2

Site NC.PHOB

Location: Hog Canyon #3, Ranchita Canyon Road, Parkfield, California

Latitude: 35.86661 **Longitude:** -120.47960
(Station coordinates provided by USGS, WGS84 coordinate system)

V_{S30} (measured): 376 m/s

V_{S30} (adjusted to more accurately reflect seismic station conditions): 404 m/s (average S-wave velocity between 1 and 31 m adjusting for 1 m assumed sensor depth).

NEHRP Site Class: C

Geomatrix Code: IQD/IPD

Geologic Conditions/Observations: Quaternary (Pleistocene) and Tertiary (Pliocene) alluvial conglomerate (Paso Robles Formation).

Site Conditions: Rural site with no noise from traffic. Test area located on a relatively flat hill top, near communication towers, with gentle to steep slopes to the sides.

Geophysical Methods Utilized: HVSR, MASW, SASW

Geophysical Testing Arrays:

1. Array PHOB-1 (48 channel MASW array utilizing 4.5 Hz vertical geophones spaced 1.5 m apart for a length of 70.5 m, forward and reverse shot locations with multiple source offsets and source types and center shot location).
2. Array PHOB-1 (SASW array centered at the midpoint of and aligned along the MASW array with the same name. SASW data acquired using common center point geometry, 4.5 and 1 Hz geophones, 2 to 40 m receiver spacing, and forward and reversed shot locations)
3. Three HVSR measurement locations distributed along array PHOB-1.

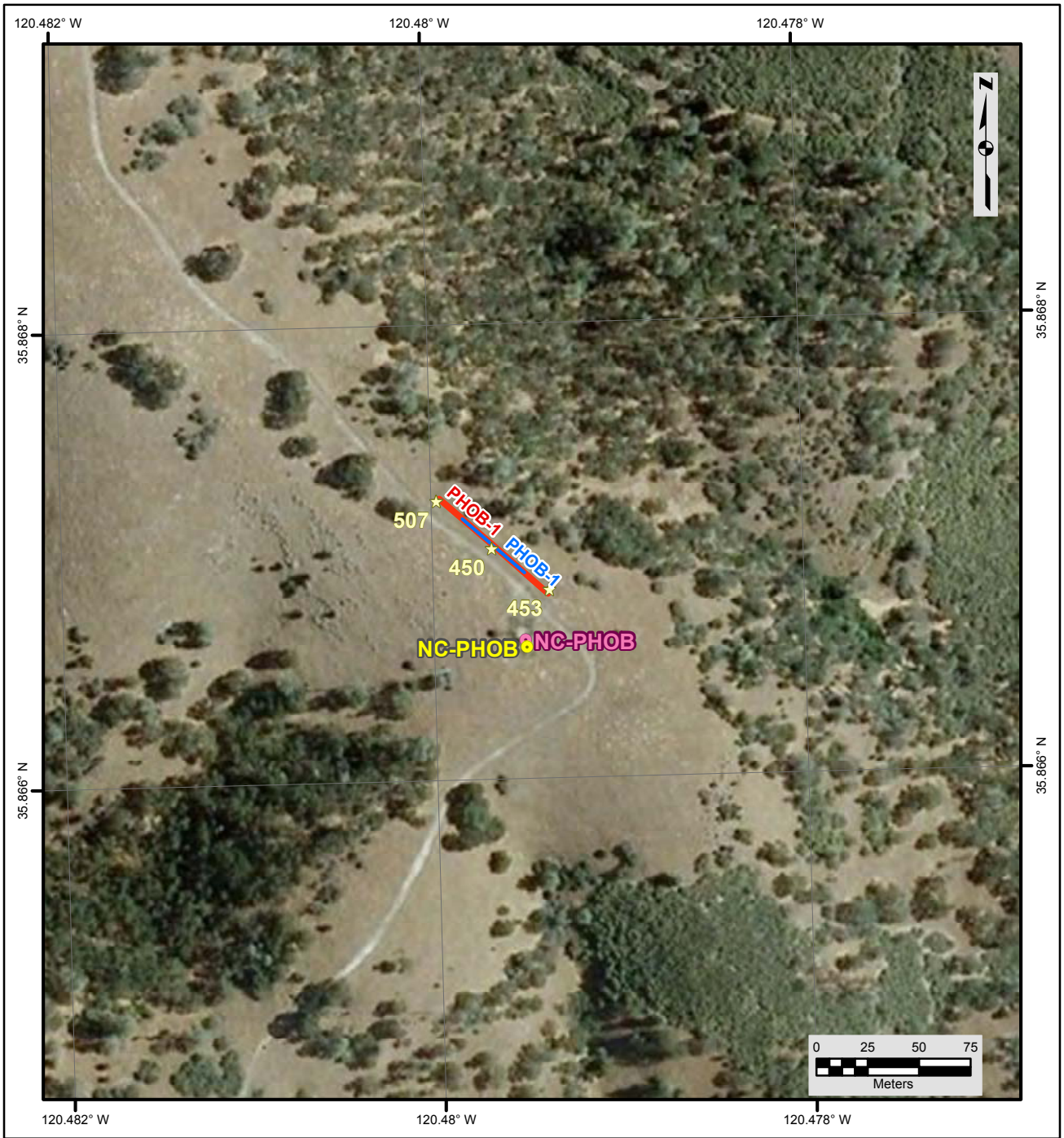

Legend

- Seismic Station - Approximate Surveyed Location
- Seismic Station - Approximate Location of Record
- H/V Spectral Ratio Location
- SASW Array
- MASW and Refraction Array

NOTES:
1. WGS 1984 COORDINATE SYSTEM
2. Image Source: ESRI, i-cubed, USDA FSA, USGS, AEX, GeoEye, Getmapping, Aerogrid, IGP

File Name: NC-PHOB-I

Date: 11/15/2012

USGS science for a changing world

GEOVision geophysical services

RECOVERY.GOV

SITE MAP
NC•PHOB

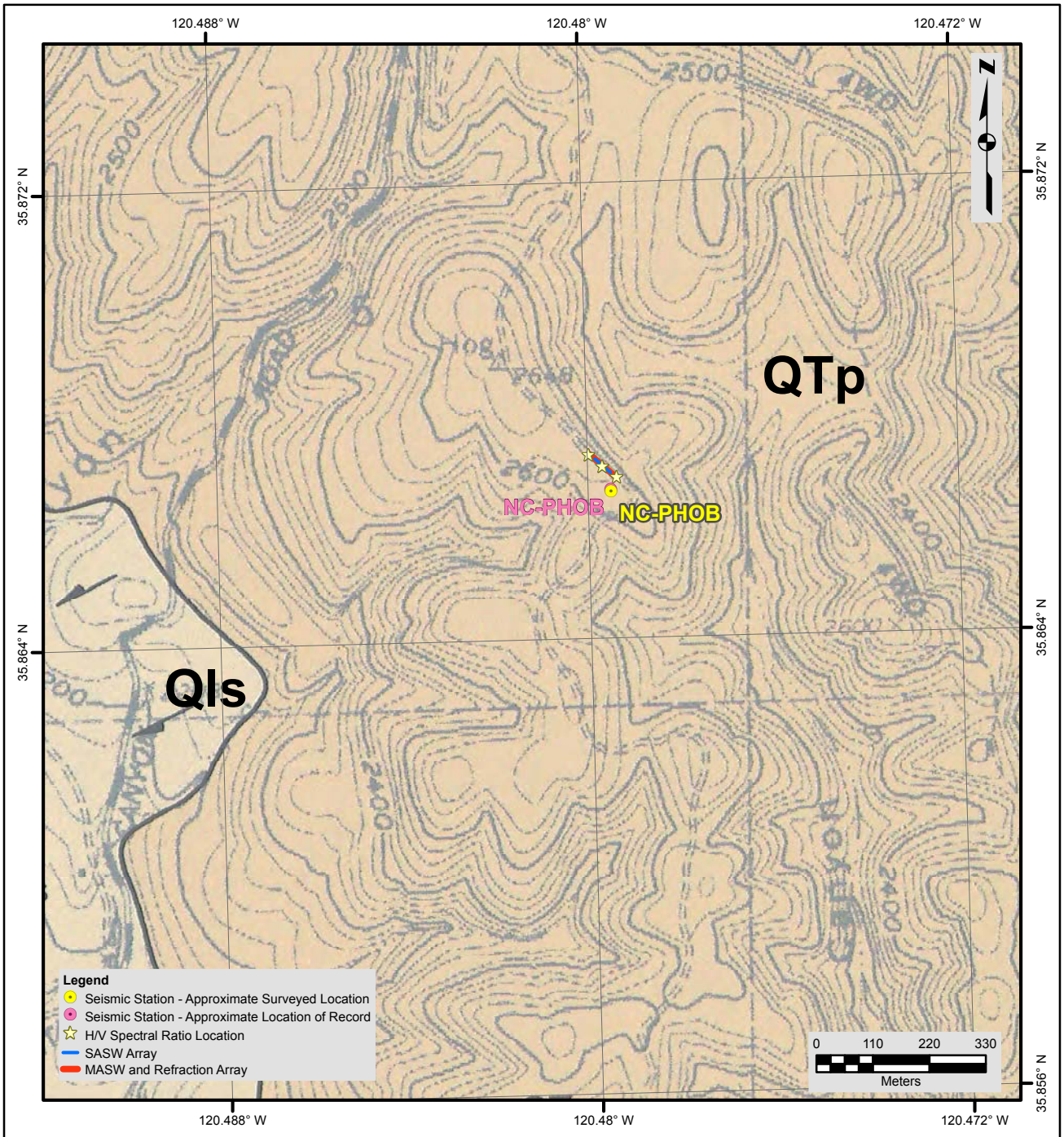

Description of Geologic Map Units

Qls = Quaternary (Holocene) rubble derived from rocks upslope
QTp = Quaternary (Pliocene to Pleistocene) Paso Robles Formation; sand and gravel

NOTES:
1. WGS 1984 COORDINATE SYSTEM
2. Geologic Map of the Cholame Quadrangle, San Luis Obispo and Monterey Counties, California by Thomas W. Dibblee, Jr., 2005
3. See site map for details of geophysical survey

File Name: NC-PHOB

Date: 2/7/2013

USGS science for a changing world

GEOVision geophysical services

GEOLOGIC MAP
NC•PHOB

RECOVERY.GOV

Looking southeast along MASW array PHOB-1 and towards location of NC.PHOB seismic

Looking south towards HVSR sensor 453 and location of NC.PHOB seismic station

MASW and seismic refraction data acquisition along array PHOB-1 using sledge hammer

SASW testing along array PHOB-1

Looking southeast along SASW array PHOB-1

Location of Geophysical Testing Arrays:

Location	Latitude	Longitude
PHOB-1, Northwest end of MASW Array	35.86724	-120.48005
PHOB-1, Center of SASW and MASW Array	35.86703	-120.47976
PHOB-1, Southeast end of MASW Array	35.86681	-120.47947
HVSR Sensor 450	35.86701	-120.47977
HVSR Sensor 453	35.86683	-120.47947
HVSR Sensor 507	35.86723	-120.48006
NC.PHOB Seismic Station	35.86658	-120.47959

Notes: 1) WGS84 Coordinate System (decimal degrees)
2) Survey accuracy is estimated at 1 to 2 m

Results:

V_S Model

Depth to Top of Layer (m)	Layer Thickness (m)	S-Wave Velocity (m/s)	Inferred P-Wave Velocity (m/s)	Assumed Poisson's Ratio	Assumed Density (g/cm^3)
0	1	131	245	0.3	1.8
1	2	289	540	0.3	1.9
3	3	359	672	0.3	1.9
6	6	371	694	0.3	1.9
12	8	426	796	0.3	1.9
20	10	455	851	0.3	2.0
30	>5	501	937	0.3	2.0

Observations/Discussion:

- HVSR data are generally very similar at every station below a frequency of 8 Hz, validating the 1-D velocity assumption. The HVSR plot for sensor 453 exhibits a small trough at 3 Hz that is not present at the other sensor locations. Other than this feature, the HVSR plots are effectively identical.
- There is a clear HVSR peak at about 0.34 Hz which would be associated with a large impedance contrast at great depth.
- Noise conditions at the site were not sufficient to apply passive surface wave techniques.
- Based on inspection of seismic refraction first arrival data, P-wave velocity in the upper 15 m is typically in the 675 to 725 m/s range, except for a very thin lower velocity layer at the surface.
- Water table located at a depth of greater than 30 m based on seismic refraction survey design and absence of a water table refractor.
- Surface wave dispersion data from SASW and MASW datasets are in excellent agreement at this site. There is, however, sufficient near surface lateral velocity variation at the site where selected use of limited offset range MASW data from the near offset and center shot locations was required for MASW and SASW dispersion data to be in such good agreement at small wavelengths (high frequencies).
- Representative dispersion curves were generated for each surface wave data set using a moving average, polynomial curve fitting routine. These individual representative dispersion curves were combined and a representative dispersion curve generated for the combined data set for data modeling.
- Surface wave depth of investigation is about 35 m based on half of maximum wavelength criteria.
- The inferred P-wave velocities in the surface wave model, based on an assumed Poisson's ratio of 0.3, and modeled S-wave velocity are reasonably consistent with simplified P-wave refraction model.
- V_{S30} is 376 m/s (Site Class C).
- Average S-wave velocity between 1 m (assumed sensor depth) and 31 m is 404 m/s.

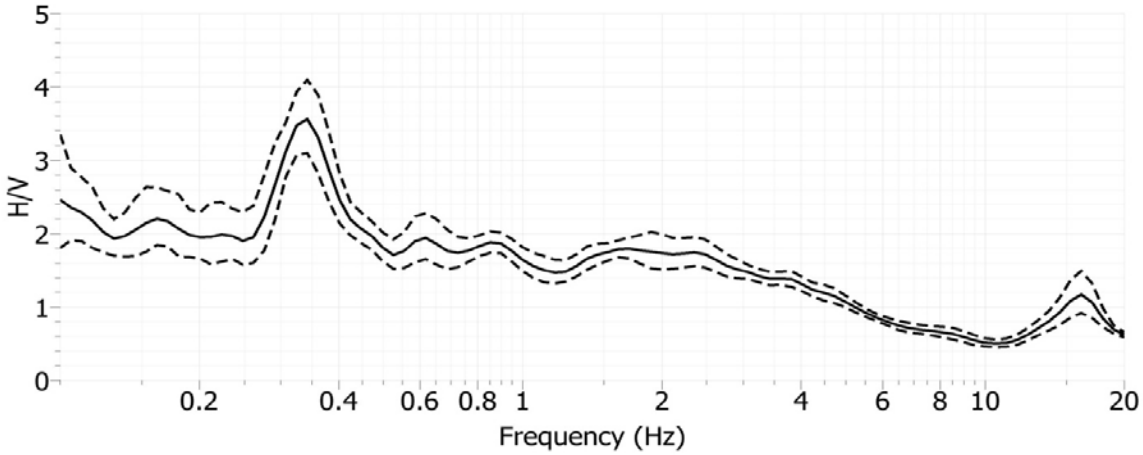

Site NC.PHOB, H/V Spectral Ratio, Array PHOB-1, Sensor 507

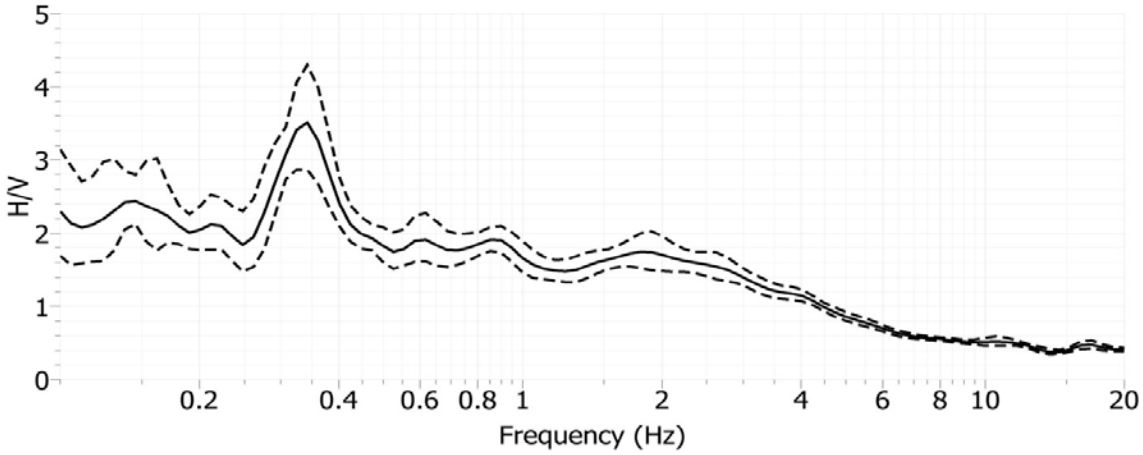

Site NC.PHOB, H/V Spectral Ratio, Array PHOB-1, Sensor 450

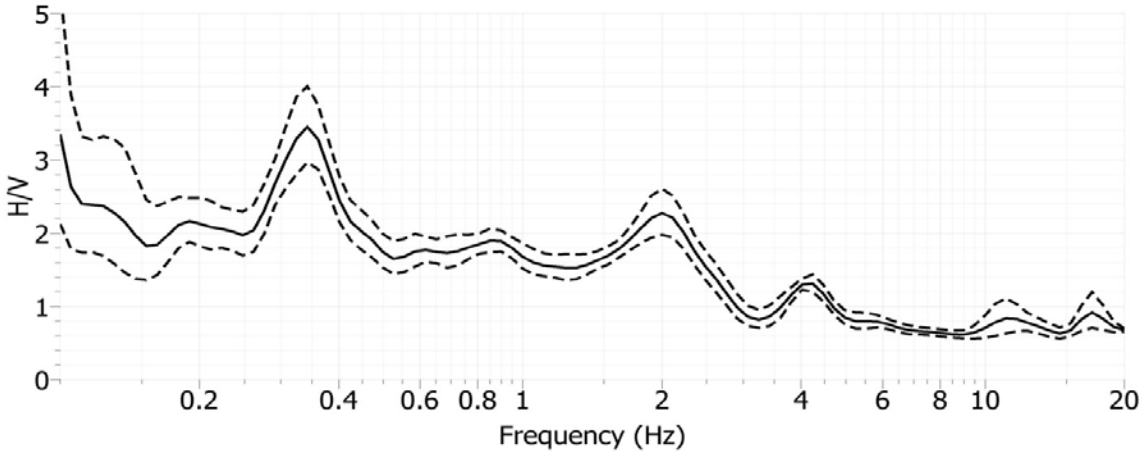

Site NC.PHOB, H/V Spectral Ratio, Array PHOB-1, Sensor 453

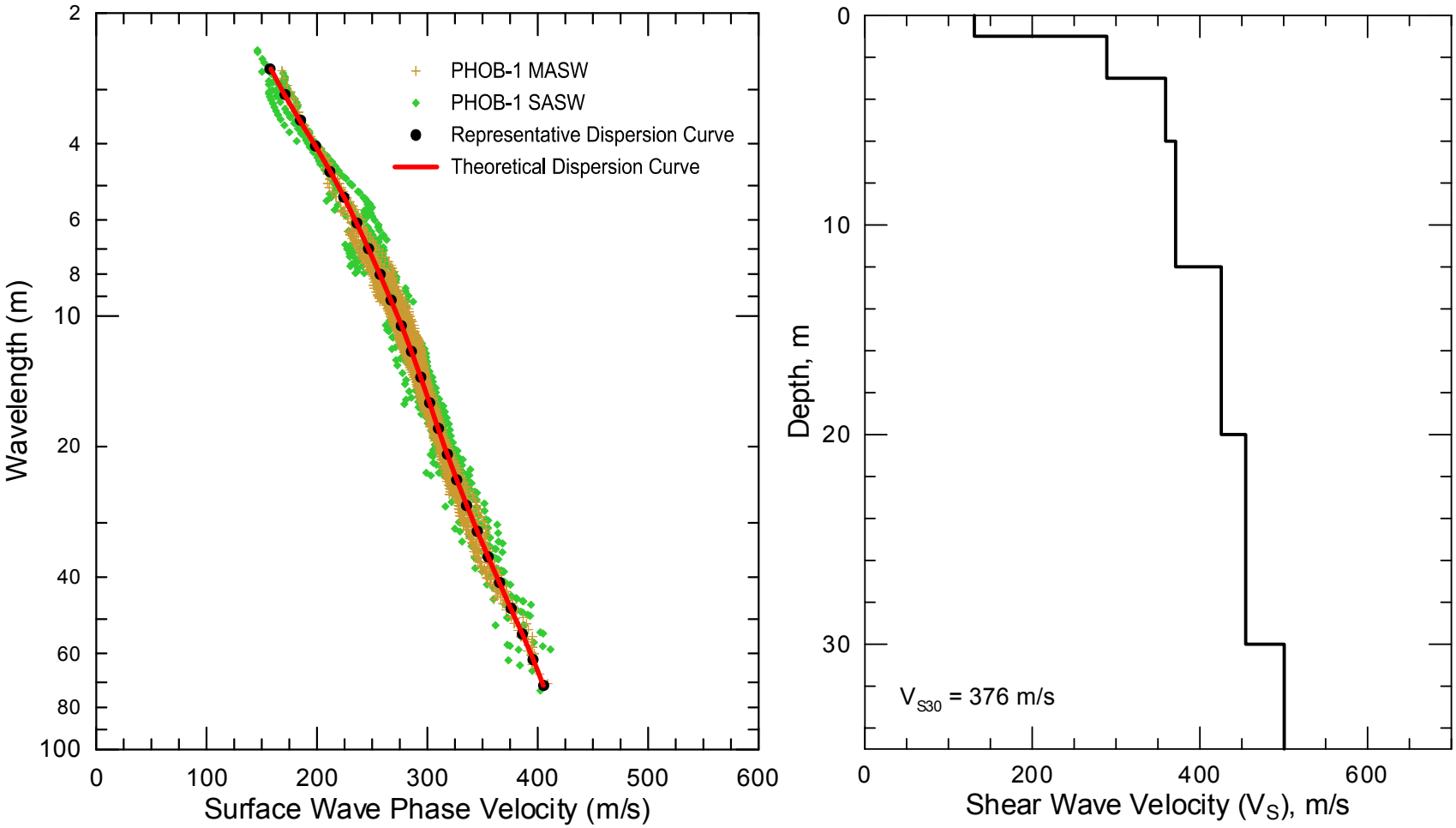

NC.PHOB - Field, representative and inverted theoretical surface wave dispersion data (left) and associated V_S model (right)

Site NC.PHSB

Location: Hesperia #3, Bryson-Hesperia Road, Bradley, California

Latitude: 35.82402 **Longitude:** -121.05396
(Station coordinates modified based on field GPS survey, WGS84 coordinate system)

V_{S30} (measured): 422 m/s

V_{S30} (adjusted to more accurately reflect seismic station conditions): 422 m/s (no adjustment necessary).

NEHRP Site Class: C

Geomatrix Code: IMB

Geologic Conditions/Observations: Seismic station located on Tertiary (Miocene) Vaqueros Sandstone, a massive, arkosic and moderately lithified unit. The sandstone unit dips about 15 to 30 degrees to the northeast in the site vicinity.

Site Conditions: Rural site. Seismic station located on a hilltop. Relatively flat topography in close proximity to test area. Steep, undulating topography in site vicinity.

Geophysical Methods Utilized: HVSR, Seismic Refraction, MASW

Geophysical Testing Arrays:

1. Array PHSB-1 (48 channel MASW and P-wave seismic refraction array utilizing 4.5 Hz vertical geophones spaced 1.5 m apart for a length of 70.5 m, forward and reverse shot locations with multiple source offsets and source types (hammers only) and multiple interior shot locations).
2. Three HVSR measurement locations; two distributed along array PHSB-1 and the other adjacent to the seismic station.

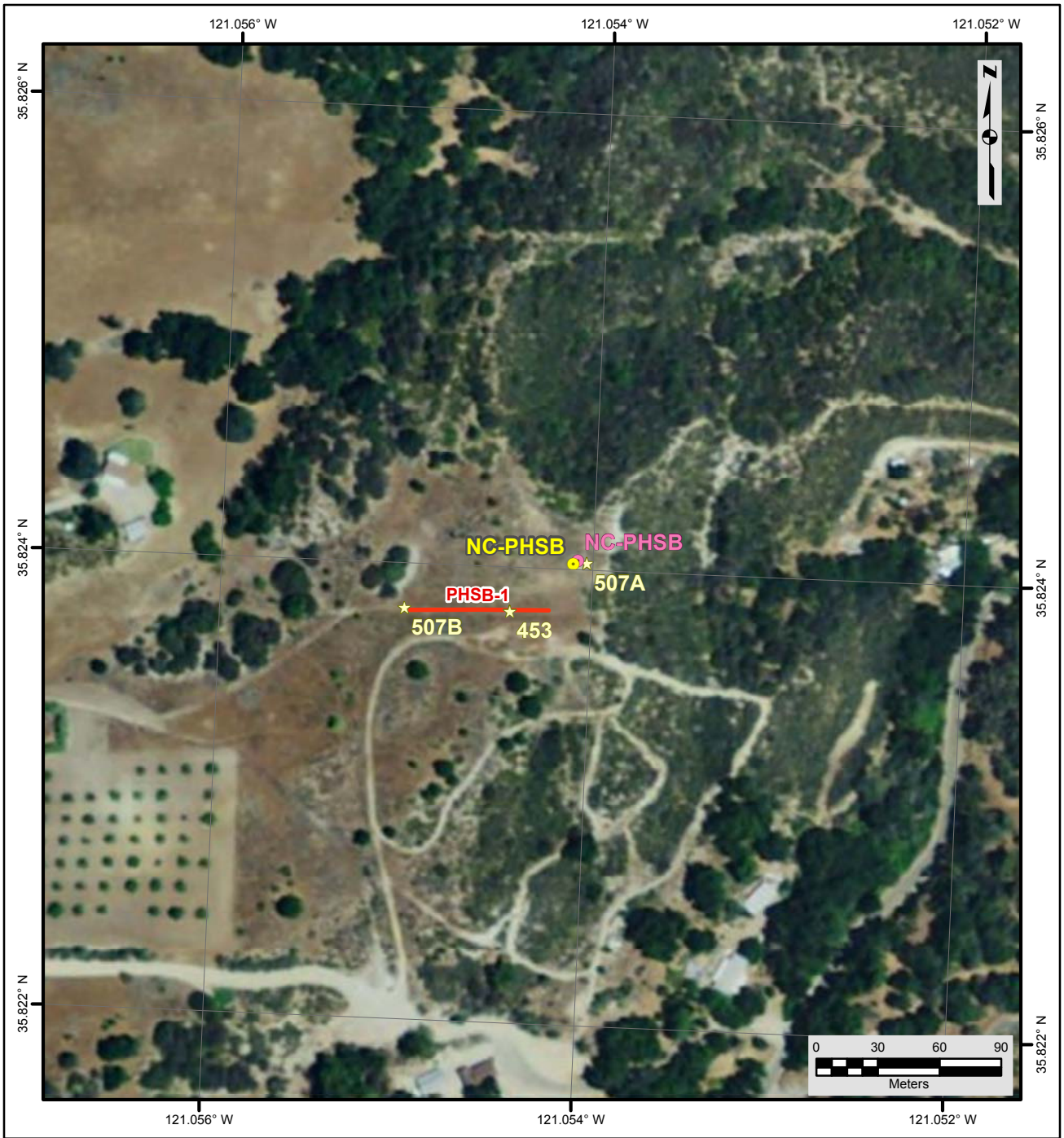

Legend

- Seismic Station - Approximate Surveyed Location
- Seismic Station - Approximate Location of Record
- H/V Spectral Ratio Location
- MASW and Seismic Refraction Array

NOTES:
1. WGS 1984 COORDINATE SYSTEM
2. Image Source: ESRI, i-cubed, USDA FSA, USGS, AEX, GeoEye, Getmapping, Aerogrid, IGP

File Name: NC-PHSB-I

Date: 9/22/2011

USGS science for a changing world

GEOVision geophysical services

RECOVERY.GOV

SITE MAP
NC•PHSB

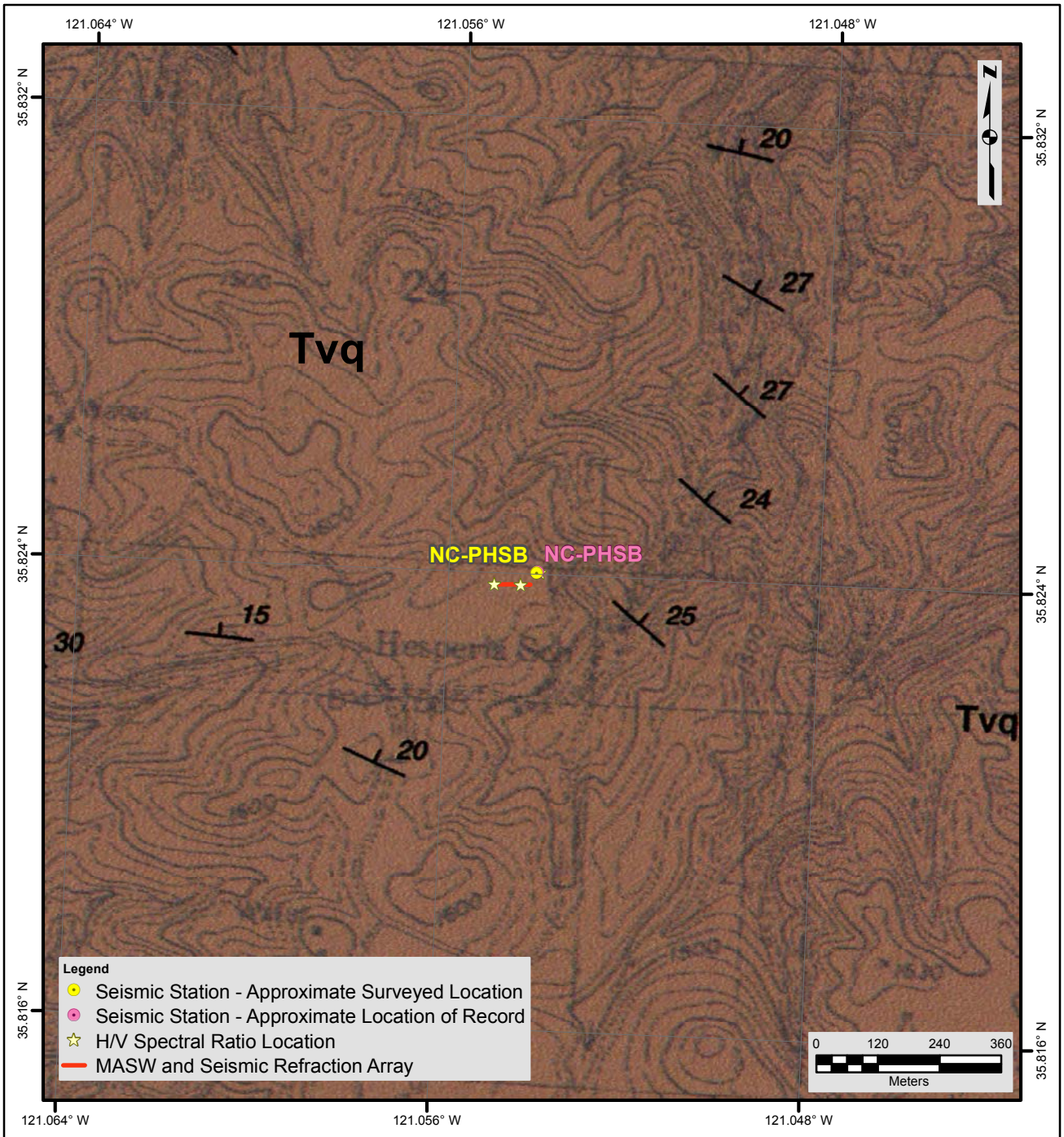

Description of Geologic Map Units

Tvq = Tertiary (Miocene) Vaqueros Sandstone; moderately lithified, semi-friable, thick bedded to massive, medium to coarse grained, locally cross-bedded, arkosic, locally fossiliferous

NOTES:
1. WGS 1984 COORDINATE SYSTEM
2. Geologic Map of the Bryson Quadrangle, Monterey & San Luis Obispo Counties, California by Thomas W. Dibblee, Jr., 2006
3. See site map for details of geophysical survey

File Name: NC-PHSB

Date: 9/16/2011

USGS science for a changing world

GEOVision geophysical services

GEOLOGIC MAP
NC•PHSB

RECOVERY.GOV

Looking west along array PHSB-1 and at HVSR sensor 453

Looking west towards NC.PHSB seismic station from HVSR sensor 507A

Looking east along array PHSB-1

Looking east along array PHSB-1

Data acquisition along array PHSB-1

Location of Geophysical Testing Arrays:

Location	Latitude	Longitude
PHSB-1, West End of Array	35.82379	-121.05484
PHSB-1, Center of Array	35.82381	-121.05445
PHSB-1, East End of Array	35.82382	-121.05408
HVSR Sensor 453	35.82381	-121.05429
HVSR Sensor 507B	35.82380	-121.05485
HVSR Sensor 507A	35.82403	-121.05388
NC.PHSB Seismic Station	35.82402	-121.05396

Notes: 1) WGS84 Coordinate System (decimal degrees)
2) Survey accuracy is estimated at 1 to 2 m

Results:

V_S Model

Depth to Top of Layer (m)	Layer Thickness (m)	S-Wave Velocity (m/s)	Inferred P-Wave Velocity (m/s)	Inferred Poisson's Ratio	Inferred Density (g/cm^3)
0	1	137	256	0.3	1.8
1	2	210	393	0.3	1.9
3	3	359	671	0.3	2.0
6	4	405	757	0.3	2.0
10	5	490	916	0.3	2.1
15	7	539	1008	0.3	2.1
22	9	626	1171	0.3	2.2
31	>4	796	1490	0.3	2.2

Notes: 1) Depth of investigation is about 35 m.
2) Bottom layer is a half space.

Observations/Discussion:

- The HVSR plots are very similar at all of the measurement locations, validating the 1-D velocity structure assumption.
- There are no significant HVSR peaks, but maybe a very weak peak at about 0.4 Hz and a trough at 0.2 Hz.
- Two models were generated for the seismic refraction data using tomographic inversion; one using a layer based starting model and the other using a smooth velocity gradient starting model. Resulting P-wave velocity models are very similar with V_P increasing with depth from 350 m/s near the surface to 700 m/s at a depth of 2 to 4 m, reaching

1,000 m/s at a depth of 3 to 13 m and exceeding 1,600 m/s by a depth of 8 to 23 m. Higher velocity sandstone occurs at shallower depth between 5 and 35 m along the profile and may be associated with the dipping rock units.

- The P-wave seismic refraction survey indicates that there is some lateral velocity variation at the site.
- Seismic refraction depth of investigation was extended by extending the models to off-end sources. A longer array without off-end sources would have been preferred to extend P-wave depth of investigation, but was not practical because the energy source was limited to a 20 lb sledge hammer.
- Based on array length, the seismic refraction models are probably most accurate to depths of 15 to 20 m.
- Noise conditions at the site were not sufficient for application of passive surface wave techniques.
- There is some scatter in the MASW dispersion data, possibly associated with lateral velocity variation, as supported by the seismic refraction model.
- A representative dispersion curve was generated for the MASW data set using a moving average, polynomial curve fitting routine and used for modeling.
- P-wave velocities in surface wave model, based on an assumed Poisson's ratio of 0.3, are generally consistent with P-wave velocities in seismic refraction models in the upper 20 m. A slightly higher Poisson's ratio of 0.33 to 0.35 may fit slightly better. The surface wave model most closely fits the portion the seismic refraction model where higher velocities are deepest. The lowest layer in the surface wave model, V_S of about 796 m/s at a depth of 31 m, likely corresponds to P-wave velocities of 1,600 m/s and greater in the seismic refraction model. The seismic refraction models show P-wave velocity greater than 1,600 m/s at a maximum depth of 23 m, significantly shallower than the surface wave model. The seismic refraction survey, however, was not designed to accurately image velocity structure at depths below about 20 m.
- The surface wave velocity model appears to represent velocity structure over the portions of the seismic refraction model where higher velocities are deepest. Based on the seismic refraction survey, there may be areas in the vicinity of the seismic station there S-wave velocities and V_{S30} are higher than those from the surface wave model, unless the high velocity zone in the seismic refraction models is representative of a localized inclusion rather than a higher velocity dipping layer.
- Surface wave depth of investigation is about 35 m based on half of maximum wavelength criteria.
- V_{S30} is 422 m/s (Site Class C).
- Average S-wave velocity between 2 m and 32 m is 485 m/s.
- Average S-wave velocity between 1 m and 31 m is 459 m/s.

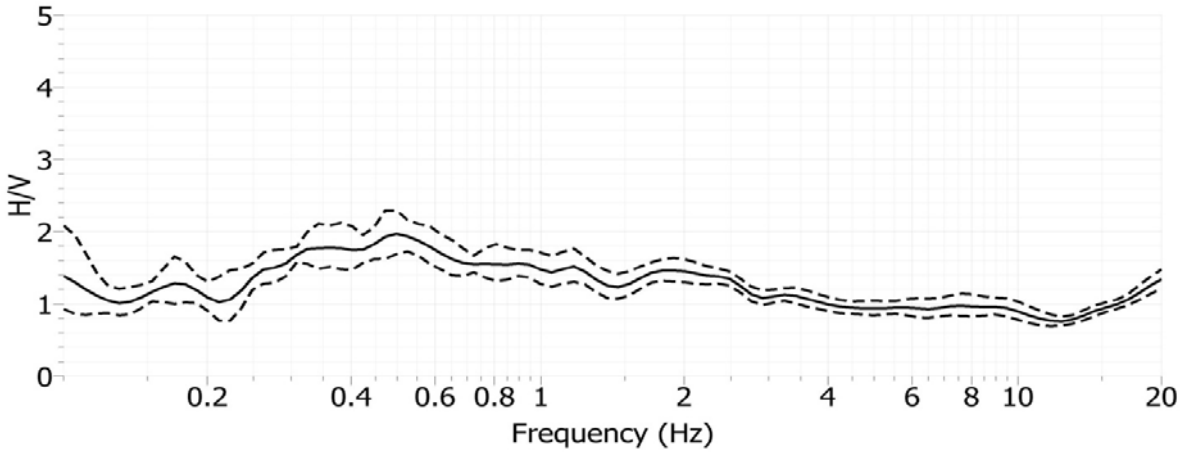

Site NC.PHSB, H/V Spectral Ratio, Array PHSB-1, Sensor 507B

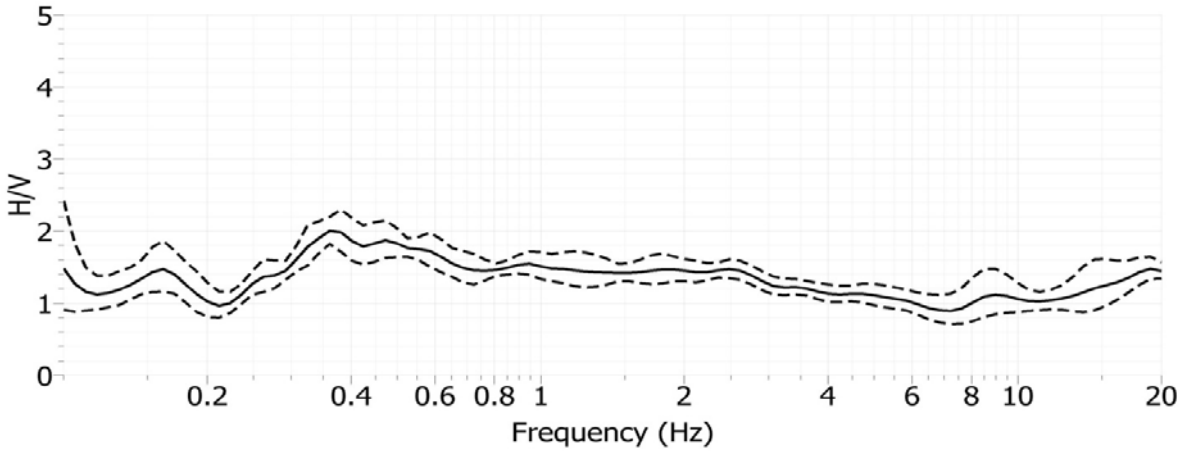

Site NC.PHSB, H/V Spectral Ratio, Array PHSB-1, Sensor 453

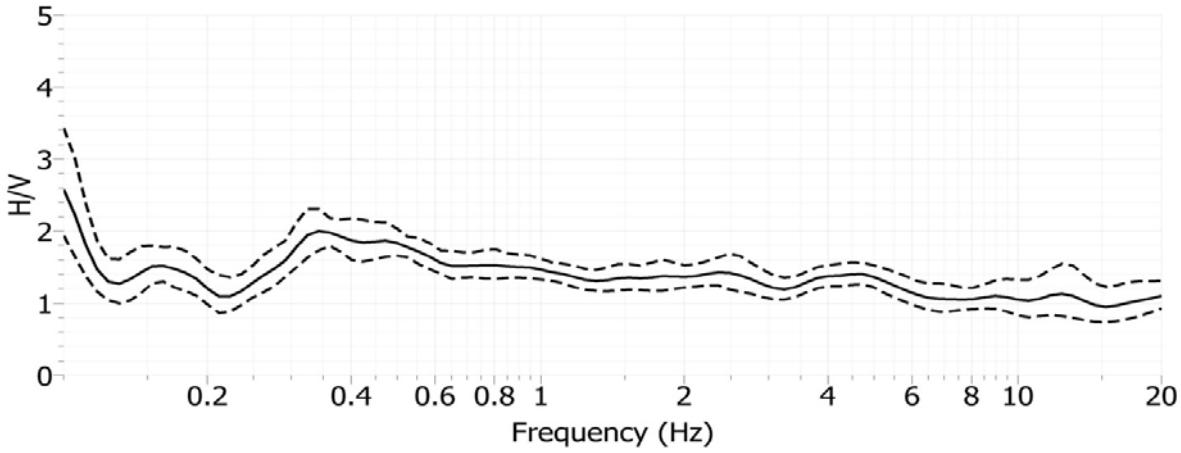

Site NC.PHSB, H/V Spectral Ratio, Near Seismic Station, Sensor 507A

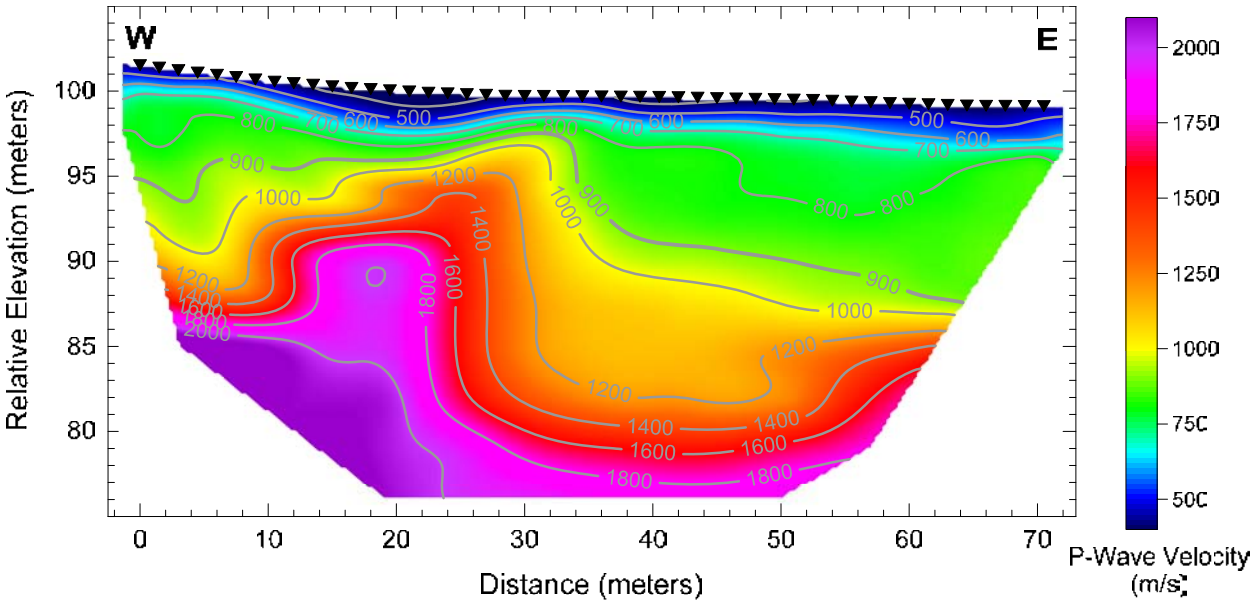

Array PHSB-1 – Tomographic seismic refraction model developed utilizing a layer based starting model

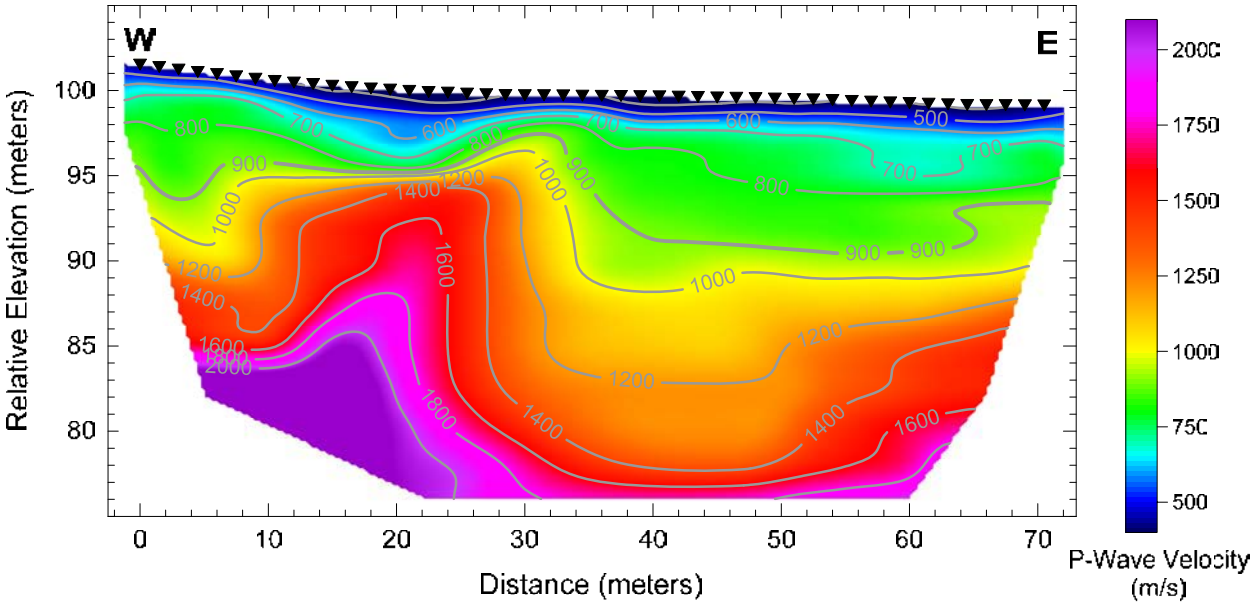

Array PHSB-1 – Tomographic seismic refraction model developed utilizing a smooth velocity gradient starting model

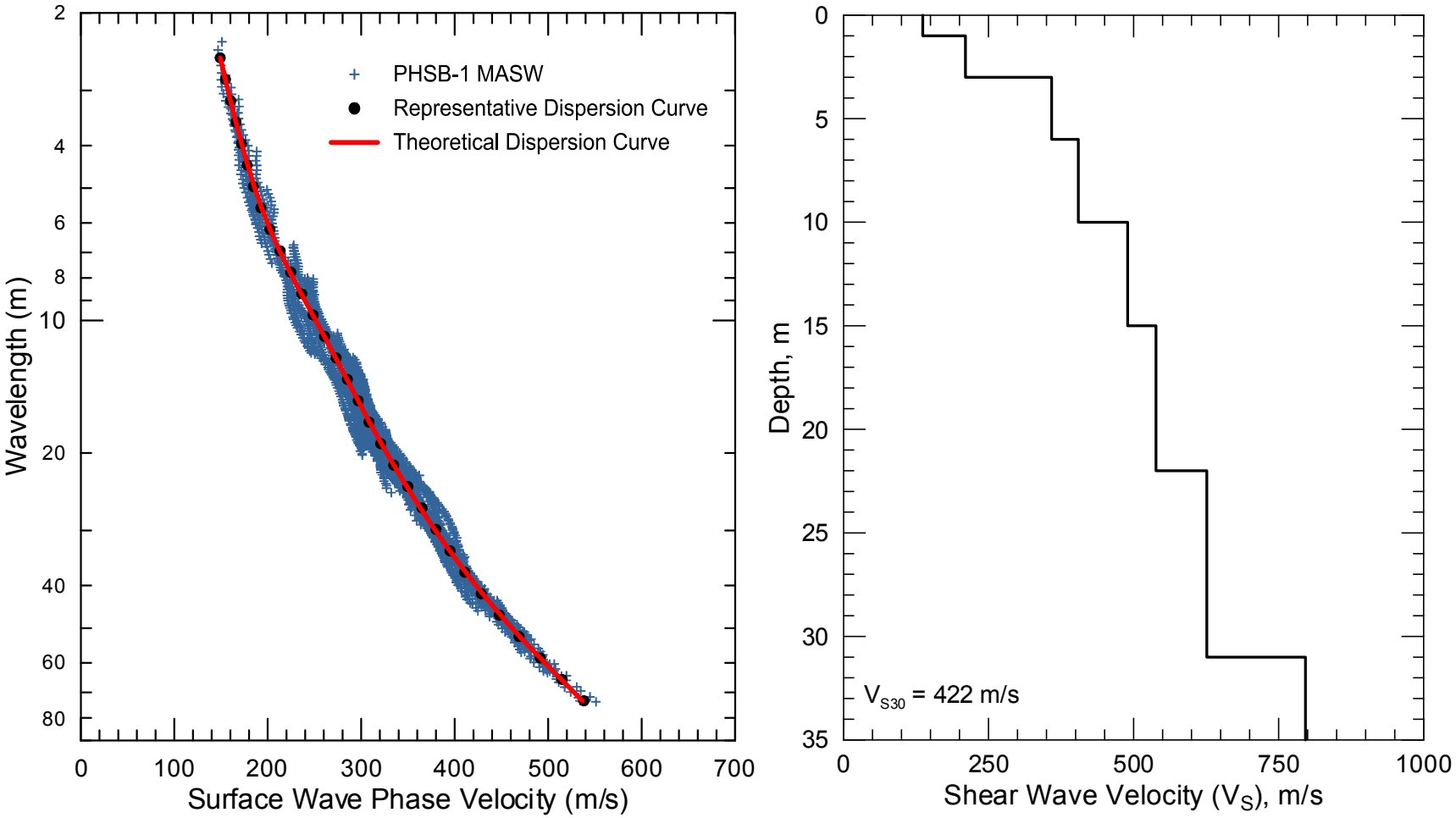

NC.PHSB - Field, representative and inverted theoretical surface wave dispersion data (left) and associated V_S model (right)

Site NC.PMPB

Location: Monarch Peak, Monterey County, California

Latitude: 36.21590 **Longitude:** -120.80126
(Station coordinates provided by USGS, WGS84 coordinate system)

V_{S30} (measured): 308 m/s

V_{S30} (adjusted to more accurately reflect seismic station conditions): 308 m/s (no adjustment necessary).

NEHRP Site Class: D

Geomatrix Code: IFD

Geologic Conditions/Observations: Seismic station located on geologic unit mapped as Mesozoic (Jurassic and Cretaceous) Franciscan Assemblage. Bedding dips on the order of 25 degrees to the northeast in the immediate site vicinity. The San Andreas Fault is located about 225 m northeast of the seismic station.

Site Conditions: Rural site located on gently rolling hills. Test area located on top of ridge with ground surface elevation decreasing about 1.5 m to the southeast along the 70.5 m long MASW and seismic refraction array.

Geophysical Methods Utilized: HVSR, Seismic Refraction (P- and S-wave), MASW (Rayleigh Wave) and MALW (Love Wave)

Geophysical Testing Arrays:

1. Array PMPB-1 (48 channel MASW and P-wave seismic refraction array utilizing 4.5 Hz vertical geophones spaced 1.5 m apart for a length of 70.5 m, forward and reverse shot locations with multiple source offsets and source types and multiple interior shot locations).
2. Array PMPB-1 (48 channel MALW and S-wave seismic refraction array utilizing 10 Hz horizontal geophones spaced 1.5 m apart for a length of 70.5 m, forward and reverse shot locations with multiple source offsets and multiple interior shot locations). Coincident with P-wave array of same name.
3. Three HVSR measurement locations distributed along array PMPB-1.

Legend

- Seismic Station - Approximate Surveyed Location
- Seismic Station - Approximate Location of Record
- H/V Spectral Ratio Location
- MASW and Seismic Refraction Array (P- and S-wave)

NOTES:
1. WGS 1984 COORDINATE SYSTEM
2. Image Source: ESRI, i-cubed, USDA FSA, USGS, AEX, GeoEye, Getmapping, Aerogrid, IGP

File Name: NC-PMPB-I

Date: 11/15/2012

USGS science for a changing world

GEOVision geophysical services

RECOVERY.GOV

SITE MAP
NC•PMPB

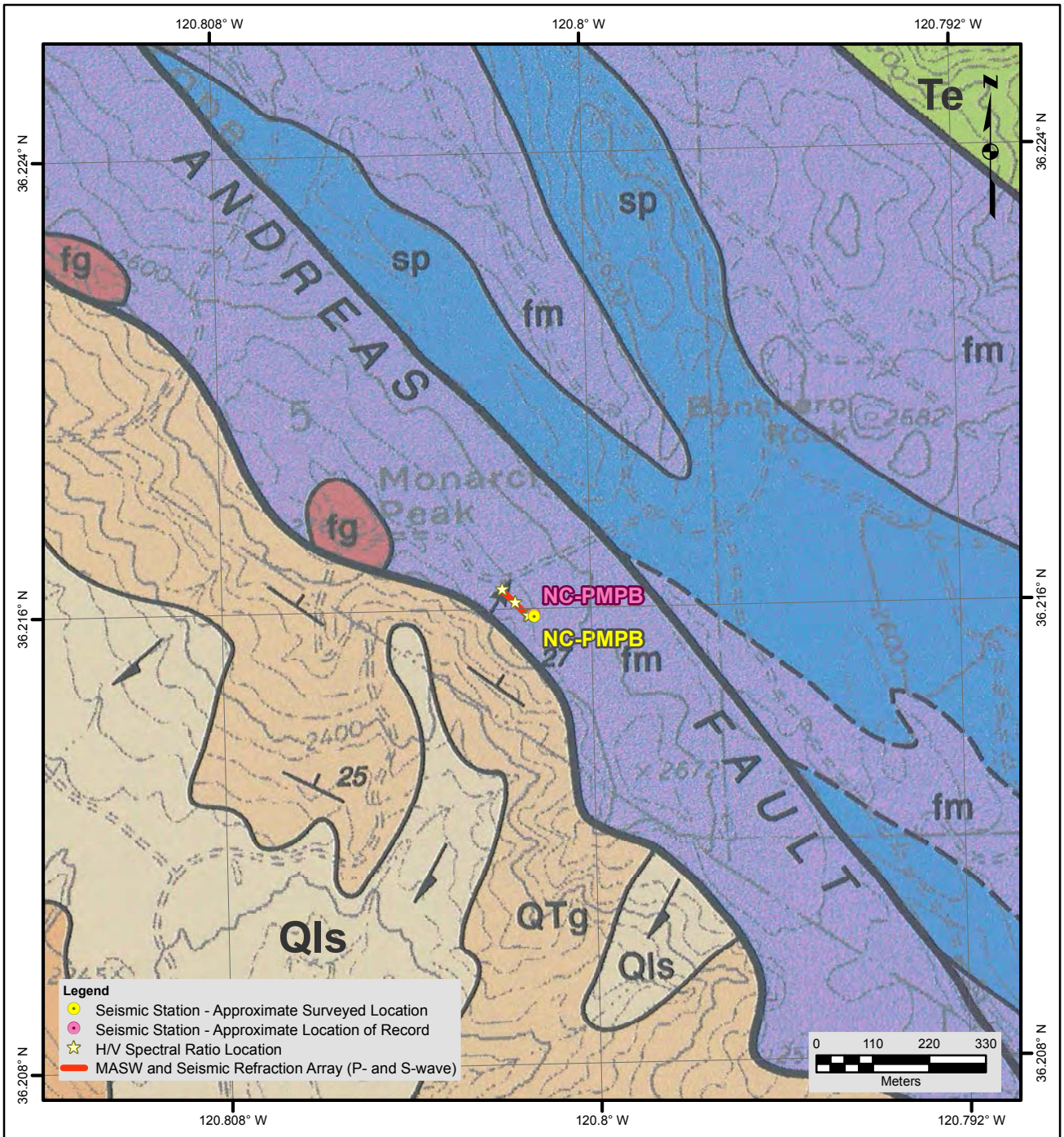

Description of Geologic Map Units

Qls = Quaternary (Pleistocene) landslide debris
QTg = Tertiary-Quaternary (Pliocene-Pleistocene) Paso Robles Formation; conglomerate and clay
Te = Tertiary (Pliocene to Upper Miocene) Etchegoin Formation; shallow marine clastic, moderately lithified sandstone, medium to locally coarse-grained to gritty or pebbly, arkosic, locally fossiliferous with small clam shells, minor interbes of siltstone/claystone
sp = Mesozoic (Jurassic and Cretaceous) serpentinite, massive, composed of amorphous antigorite with magnetite, pervasively sheared and slickensided
fg = Mesozoic (Jurassic and Cretaceous) Franciscan Assemblage; greenstone, massive, hard, aphanitic, carbonate veins
fm = Mesozoic (Jurassic and Cretaceous) Franciscan Assemblage; melange of graywacke, greenstone, chert and blueschist

NOTES:
1. WGS 1984 COORDINATE SYSTEM
2. Geologic Map of the Monarch Peak Quadrangle, Monterey and San Benito Counties, California by Thomas W. Dibblee, Jr., 2007
3. See site map for details of geophysical survey

File Name: NC-PMPB

Date: 1/5/2012

USGS science for a changing world

GEOVision geophysical services

GEOLOGIC MAP
NC•PMPB

RECOVERY.GOV

Looking at HVSR sensor 453 and NC.PMPB seismic station

Looking southeast along array PMPB-1 and at HVSR sensor 507

Looking northwest along array PMPB-1

S-wave seismic refraction and Love wave (MALW) data acquisition

P-wave seismic refraction and MASW data acquisition

Location of Geophysical Testing Arrays:

Location	Latitude	Longitude
PMPB-1, Northwest End of MASW/Refraction Array	36.21634	-120.80196
PMPB-1, Center of MASW/Refraction Array	36.21611	-120.80169
PMPB-1, Southeast End of MASW/Refraction Array	36.21588	-120.80142
HVSR Sensor 450	36.21612	-120.80166
HVSR Sensor 453	36.21589	-120.80140
HVSR Sensor 507	36.21636	-120.80194
NC.PMPB Seismic Station	36.21586	-120.80126

Notes: 1) WGS84 Coordinate System (decimal degrees)
2) Survey accuracy is estimated at 1 to 2 m

Results:

V_S Model

Depth to Top of Layer (m)	Layer Thickness (m)	S-Wave Velocity (m/s)	Inferred P-Wave Velocity (m/s)	Assumed Poisson's Ratio	Assumed Density (g/cm^3)
0	0.6	77	144	0.3	1.7
0.6	3.4	190	355	0.3	1.7
4	3.5	250	467	0.3	1.8
7.5	4.5	315	2000	0.5	1.9
12	6	342	2000	0.5	1.9
18	7	427	2000	0.5	2.0
25	>5	529	2000	0.5	2.0

Notes: 1) Depth of investigation is about 30 m.
2) Bottom layer is a half space.

Observations/Discussion:

- HVSR plots are generally very similar at every station at frequencies below about 12 Hz, validating the 1-D velocity assumption. HVSR data for sensor 450 is more noisy than that at the other sensors. HVSR data were also acquired with a Tromino ENGY adjacent to Trillium sensor 453 and has similar response.
- There are no distinct high amplitude HVSR peaks at lower frequencies, although there is an elevated HVSR response over the 1.5 to 10 Hz range with possible weak peaks in the 2 to 2.5 Hz and 8 Hz ranges. It is unclear what effects dipping and folded geologic layers may have on HVSR response.

- The P-wave refraction data for array PMPB-1 were not modeled because the saturated zone appears to be located at shallow depth. Inspection of the P-wave first arrival data revealed a 1.5 to 3 m thick layer of low velocity sediments with P-wave velocity of about 350 to 375 m/s, underlain by sediments/weathered rock with P-wave velocity of about 750 to 800 m/s. The saturated zone with P-wave velocity of about 2,000 m/s was determined to be located at an approximate depth of 7.5 m.
- The S-wave refraction data were not modeled at this time, although inspection of the S-wave seismic records revealed that the maximum S-wave velocity in the seismic data, limited to a depth of investigation of about 20 m, is about 400 m/s.
- The seismic testing array was located on a dirt road along the top of a ridge and is subparallel (within 30 degrees) to the strike of the geologic bedding, which dips on the order of 25 degrees in a northeasterly direction.
- Noise conditions at the site were not sufficient for application of passive surface wave techniques.
- Review of Rayleigh wave (MASW) data indicated that higher modes were dominant over a wide frequency range. The source of dominant higher mode energy Rayleigh wave data is not clear. Dominant higher modes were not, however, a significant issue in Love wave (MALW) data. Therefore, modeling of Love wave, rather than Rayleigh wave, phase velocity data was conducted at this site. It should be noted, however, that the Love wave data were acquired using 10 Hz horizontal geophones and a hammer/traction plank energy source. To develop a V_S model to 30 m depth it was necessary to pick Love wave phase velocity data to a frequency of about 5 Hz, which is below the natural frequency of the geophone and pushing the limits of the energy source. Consideration should be given to reacquiring the Love wave data with 4.5 Hz geophones. A lower frequency energy source would also be beneficial.
- The minimum wavelength Love wave phase velocity data extracted from the 48-channel MASW array was about 9 m. Reducing data from smaller hammer sources using a limited offset receiver array (i.e. less active geophones) allowed for extraction of surface wave dispersion data to a minimum wavelength of about 4 m.
- There is about 25 m/s of scatter in MALW dispersion data, which is in part due to lateral velocity variation caused by differential weathering of near surface sedimentary rock and variable thickness of a thin residual soil layer.
- A representative dispersion curve was generated for the MALW data set using a moving average, polynomial curve fitting routine and used for modeling.
- Surface wave depth of investigation is about 30 m based on half of maximum wavelength criteria.
- The S-wave velocity model derived from the surface wave testing is believed to be representative of average subsurface velocity structure. However, geology at the site is complex, with dipping bedding, and the seismic line was oriented about 30 degrees from geologic strike. It is difficult to predict the effect of dipping beds on surface wave dispersion data; however, near surface velocities are more indicative of sediments rather than rock, in which case the dipping bedding may not be so significant.
- V_{S30} is 308 m/s (Site Class D).

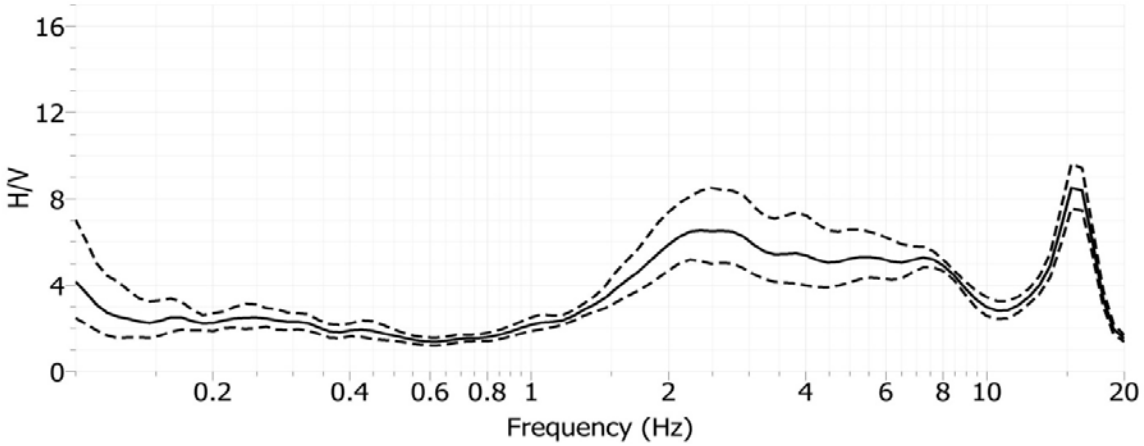

Site NC.PMPB, H/V Spectral Ratio, Array PMPB-1, Sensor 507

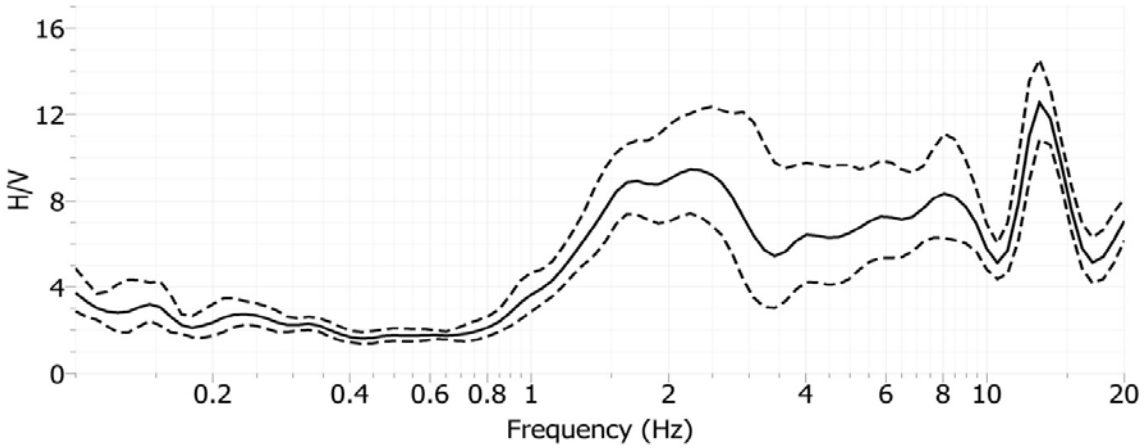

Site NC.PMPB, H/V Spectral Ratio, Array PMPB-1, Sensor 450

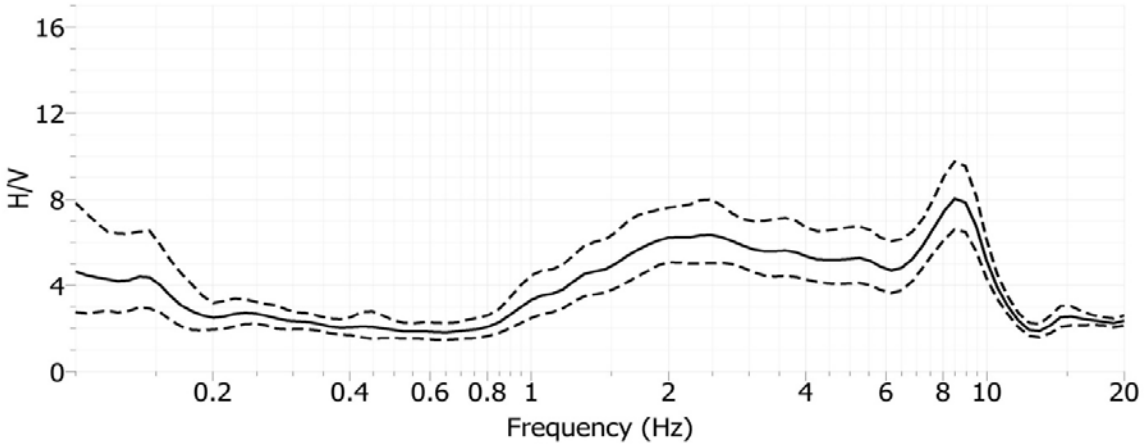

Site NC.PMPB, H/V Spectral Ratio, Array PMPB-1, Sensor 453

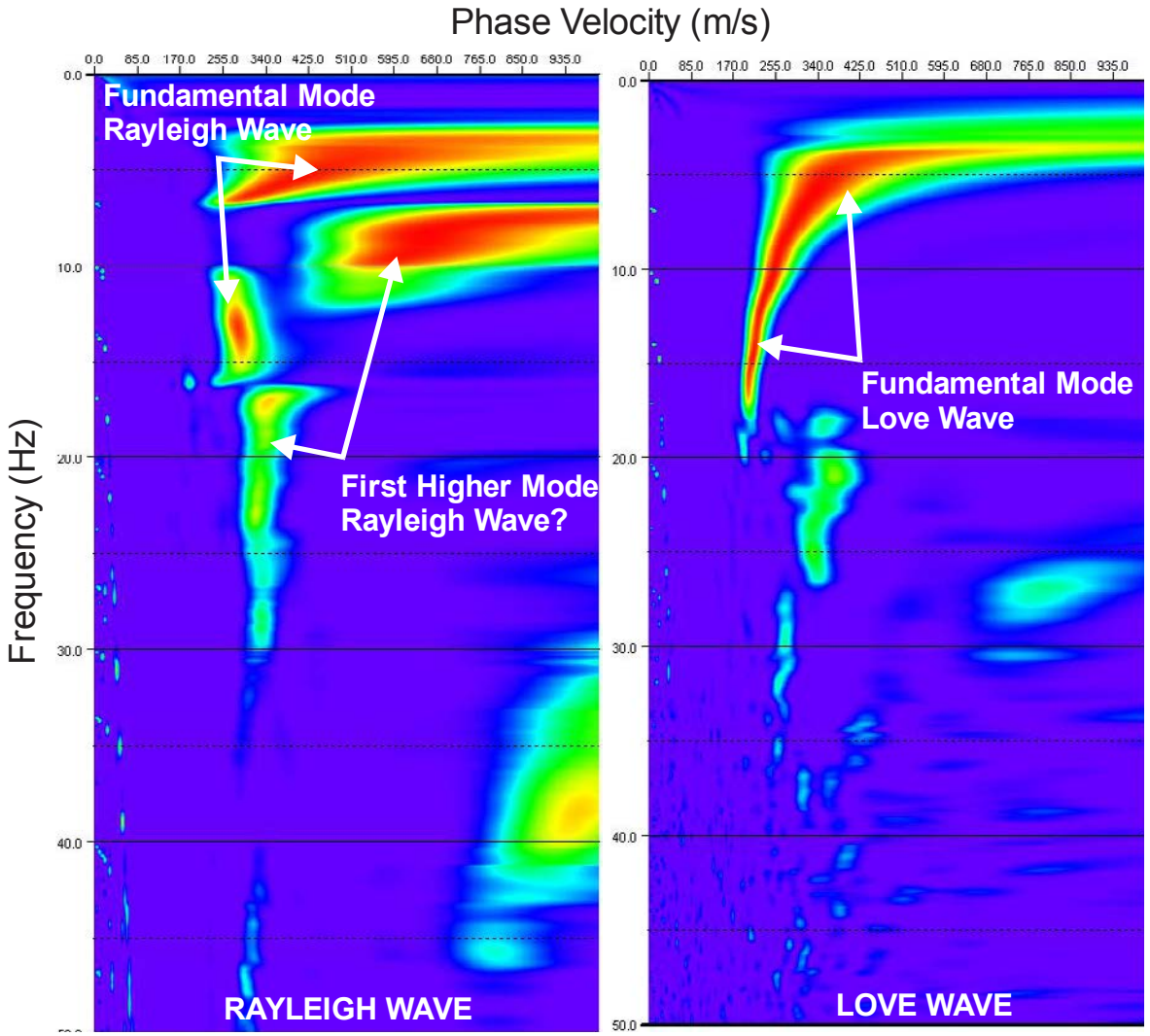

Array PMPB-1 – Comparison of Rayleigh and Love wave overtone images demonstrating dominant higher mode energy in the Rayleigh wave data.

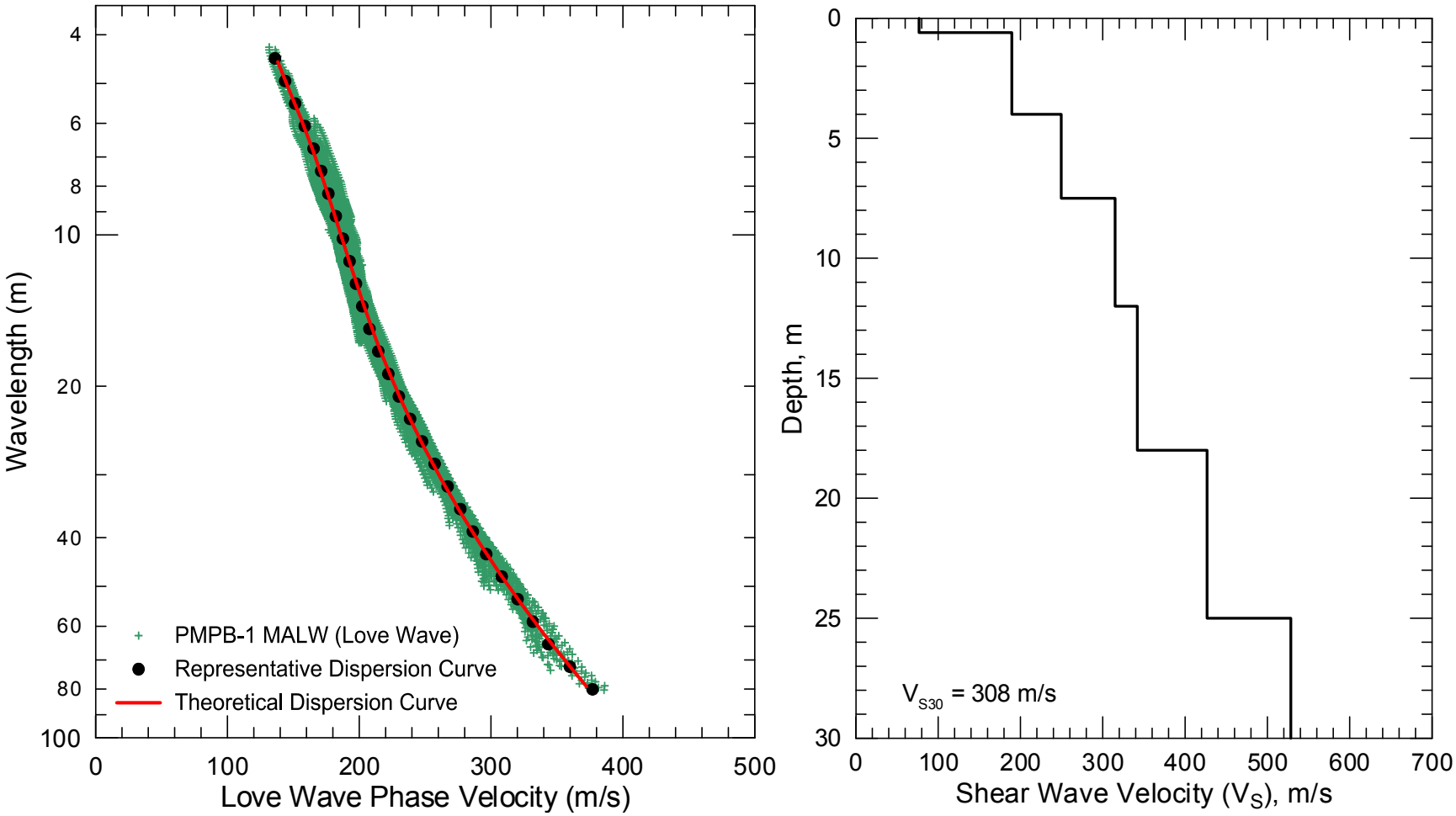

NC.PMPB - Field, representative and inverted theoretical surface wave dispersion data (left) and associated V_S model (right)

Site NC.PSM

Location: Smith Mountain, Monterey County, California

Latitude: 36.06880 **Longitude:** -120.59618
(Station coordinates provided by USGS, WGS84 coordinate system)

V_{S30} (measured): 560 m/s ±15% (additional geophysical testing needed to refine)

V_{S30} (adjusted to more accurately reflect seismic station conditions): 620 m/s ±15% potential error (V_P < 700 m/s in seismic refraction model replaced with velocity of underlying layer to account for seismic station being located on weathered rock).

NEHRP Site Class: C

Geomatrix Code: IMB/IMA

Geologic Conditions/Observations: Seismic station located on geologic unit mapped as Tertiary (Miocene) Monterey Shale.

Site Conditions: Rural site. Hilly topography in site vicinity. Seismic station located on outcrop of weathered rock on a ridge top. Test area is located along a dirt road cut into the side of the bedrock ridge with mapped landslide deposits immediately to the east. There is about a 9 m increase in elevation to the northeast along the 70.5 m MASW and seismic refraction array.

Geophysical Methods Utilized: HVSR, Seismic Refraction, MASW

Geophysical Testing Arrays:

1. Array PSM-1 (48 channel MASW and P-wave seismic refraction array utilizing 4.5 Hz vertical geophones spaced 1.5 m apart for a length of 70.5 m, forward and reverse shot locations with multiple source offsets and source types and multiple interior shot locations).
2. Three HVSR measurement locations: one at each end of array PSM-1 and the other adjacent to the seismic station.

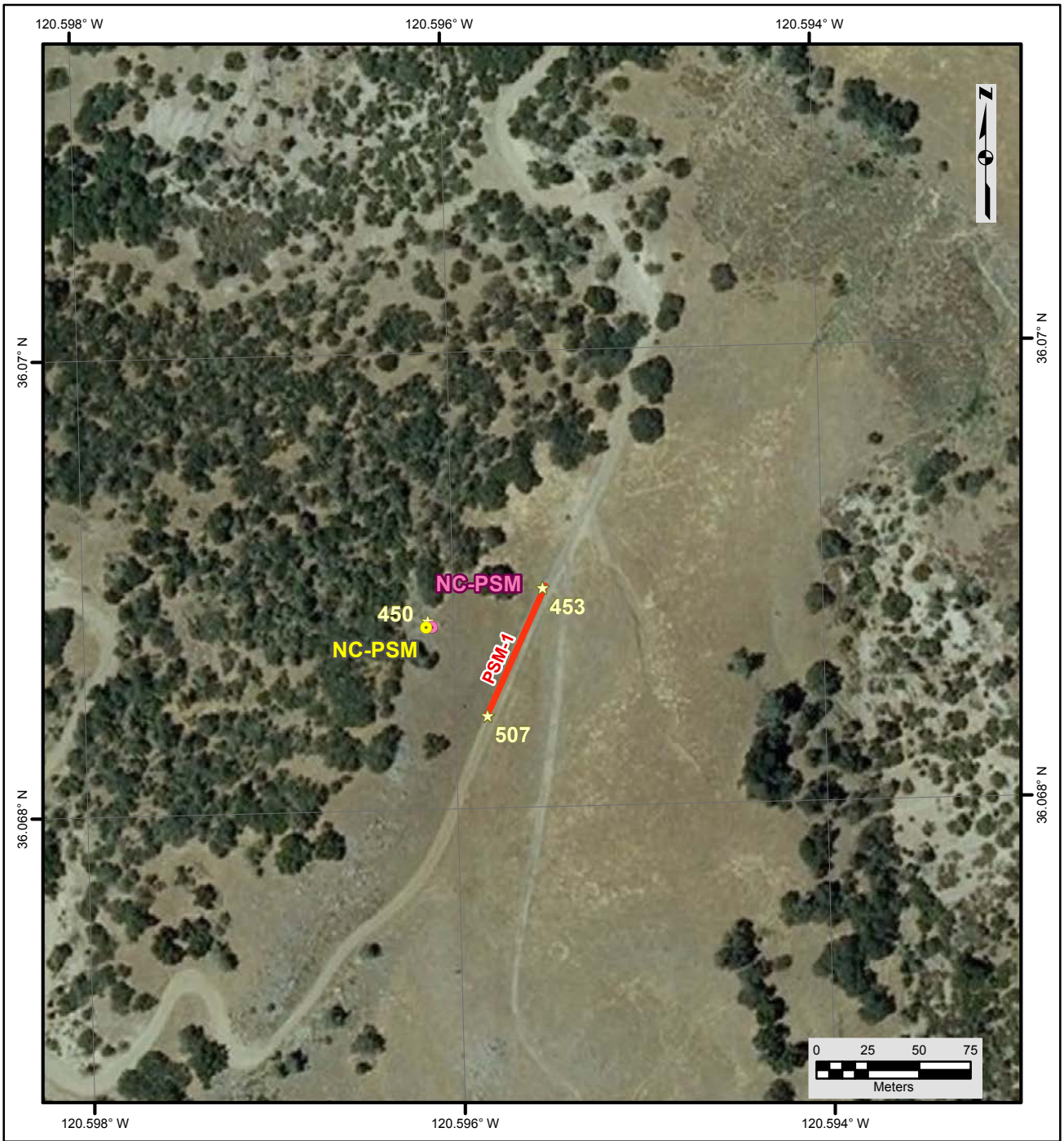

Legend

- Seismic Station - Approximate Surveyed Location
- Seismic Station - Approximate Location of Record
- H/V Spectral Ratio Location
- MASW and Seismic Refraction Array

NOTES:
1. WGS 1984 COORDINATE SYSTEM
2. Image Source: ESRI, i-cubed, USDA FSA, USGS, AEX, GeoEye, Getmapping, Aerogrid, IGP

File Name: NC-PSM-I

Date: 3/23/2012

USGS science for a changing world

GEOVision geophysical services

SITE MAP
NC•PSM

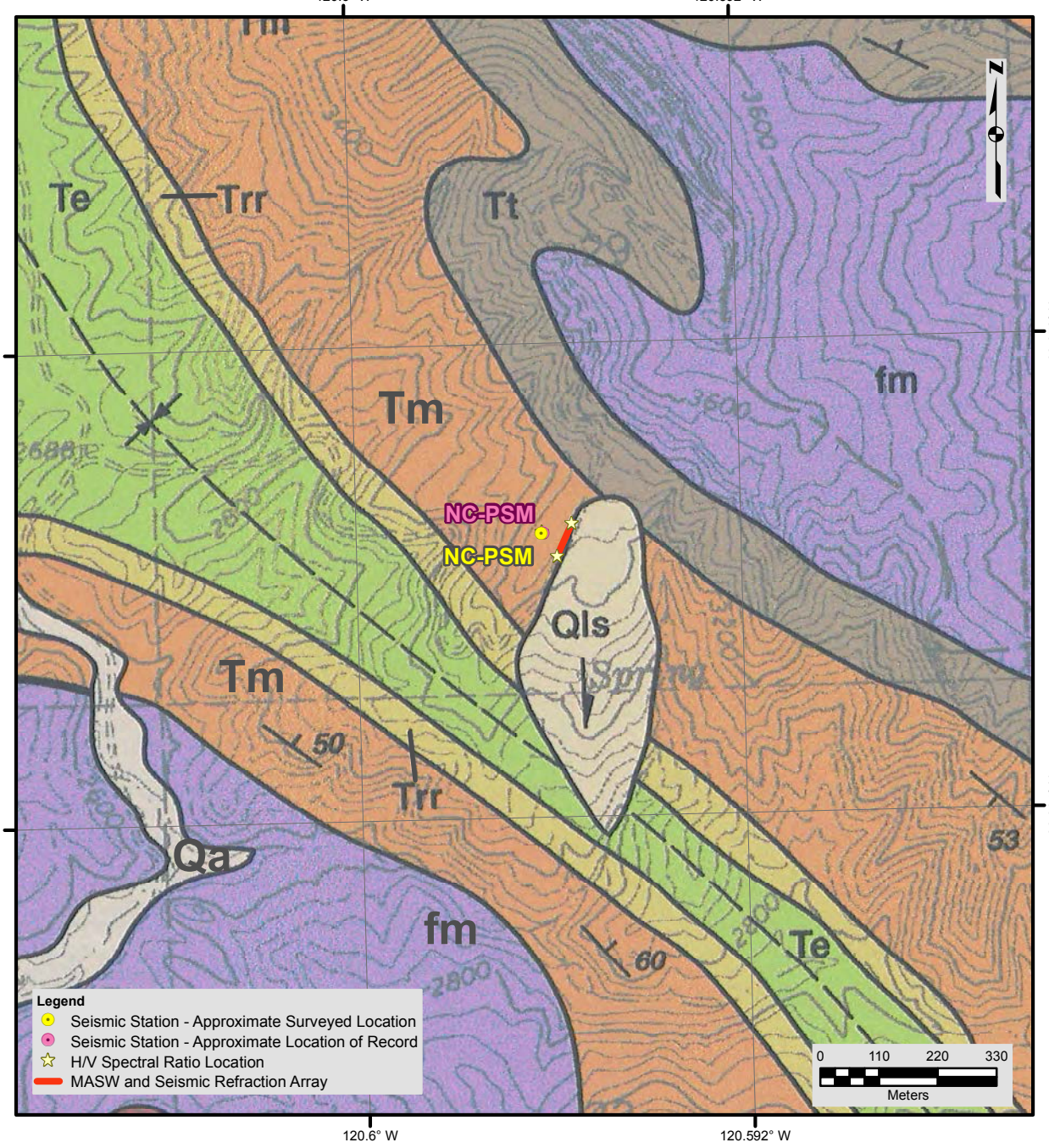

Description of Geologic Map Units

Qa = Quaternary (Holocene) alluvial gravel and sand of flood plains
Qls = Quaternary (Pleistocene to Holocene) landslide rubble
Te = Tertiary (Pliocene) Etchegoin Formation; shallow marine clastic, sandstone
Tm = Tertiary (Miocene) Monterey Shale; marine biogenetic, siliceous shale
Trr = Tertiary (Miocene) Reef Ridge Shale; marine clastic, clay shale
Tt = Tertiary (Miocene) Temblor Sandstone; marine clastic, sandstone
fm = Mesozoic (Jurassic - Cretaceous) Franciscan Assemblage; submetamorphosed eugeosynclinal marine sedimentary and mafic volcanic rocks, melange of fragments

NOTES:
1. WGS 1984 COORDINATE SYSTEM
2. Geologic Map of the Smith Mountain Quadrangle, Monterey and Fresno Counties, California by Thomas W. Dibblee, Jr., 2006
3. See site map for details of geophysical survey

USGS science for a changing world
GEOVision geophysical services

GEOLOGIC MAP
NC•PSM

File Name: NC-PSM
Date: 3/21/2012

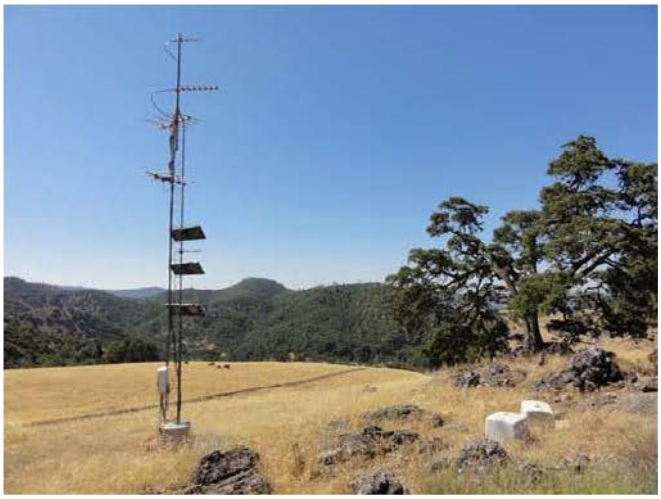

Seismic station NC.PSM located on weathered rock

Looking southeast from seismic station NC.PSM towards location of array PSM-1

Looking southwest towards seismic station and at northeast end of array PSM-1 and HVSR sensor 453

Looking northeast along array PSM-1

Looking southwest along array PSM-1

Location of Geophysical Testing Arrays:

Location	Latitude	Longitude
PSM-1, Southwest End of MASW/Refraction Array	36.06840	-120.59590
PSM-1, Center of MASW/Refraction Array	36.06869	-120.59573
PSM-1, Northeast End of MASW/Refraction Array	36.06897	-120.59556
HVSR Sensor 450	36.06883	-120.59620
HVSR Sensor 453	36.06896	-120.59558
HVSR Sensor 507	36.06840	-120.59589
NC.PSM Seismic Station	36.06880	-120.59621

Notes: 1) WGS84 Coordinate System (decimal degrees)
2) Survey accuracy is estimated at 1 to 2 m.

Results:

V_S Model for MASW Array (not representative of seismic station conditions)

Depth to Top of Layer (m)	Layer Thickness (m)	S-Wave Velocity (m/s)	Inferred P-Wave Velocity (m/s)	Assumed Poisson's Ratio	Assumed Density (g/cm^3)
0	1	113	212	0.300	1.6
1	1.5	158	296	0.300	1.7
2.5	2.5	205	384	0.300	1.7
5	5	302	564	0.300	1.8
10	7	400	747	0.300	1.9
17	9	512	1800	0.456	2.0
26	>4	621	1900	0.440	2.1

Notes: 1) Saturated zone with V_P in the 1,800 to 1,900 m/s range constrained at average depth of 17 m based on seismic refraction model. However, the presence of saturated sedimentary rock is not conclusive.
2) Depth of investigation is about 30 m.
3) Bottom layer is a half space.

Average V_P and Estimated V_S Models from Central Portion of P-wave Seismic Refraction Line

Depth to Top of Layer (m)	Layer Thickness (m)	P-Wave Velocity (m/s)	Estimated S-Wave Velocity (m/s)				
			Poisson's Ratio = 0.25	Poisson's Ratio = 0.3	Poisson's Ratio = 0.35	Poisson's Ratio = 0.4	Poisson's Ratio = 0.45
0.00	0.51	227	131	121	109	93	68
0.51	1.02	453	261	242	218	185	137
1.53	1.02	584	337	312	281	239	176
2.55	1.02	685	396	366	329	280	207
3.56	1.02	765	442	409	367	312	231
4.58	1.02	804	464	430	386	328	242
5.60	1.02	820	473	438	394	335	247
6.62	2.14	995	574	532	478	406	300
8.76	2.14	1049	606	561	504	428	316
10.90	2.14	1273	735	680	611	520	384
13.04	2.14	1540	889	823	740	629	464
15.17	2.14	1584	915	847	761	647	478
17.31	2.14	1699	981	908	816	694	512
19.45	2.14	1811	1046	968	870	739	546
21.59	2.14	1816	1048	971	872	741	547
23.73	Half Space	1838	1061	982	883	750	554

Average V_P Model and V_S Model Estimated Using Variable Poisson's Ratio from Central Portion of P-wave Seismic Refraction Line

Depth to Top of Layer (m)	Layer Thickness (m)	P-Wave Velocity (m/s)	Estimated S-wave Velocity (m/s)	Inferred Poisson's Ratio
0.00	0.51	227	121	0.300
0.51	1.02	453	242	0.300
1.53	1.02	584	292	0.333
2.55	1.02	685	343	0.333
3.56	1.02	765	367	0.350
4.58	1.02	804	386	0.350
5.60	1.02	820	394	0.350
6.62	2.14	995	478	0.350
8.76	2.14	1049	504	0.350
10.90	2.14	1273	520	0.400
13.04	2.14	1540	556	0.425
15.17	2.14	1584	572	0.425
17.31	2.14	1699	614	0.425
19.45	2.14	1811	654	0.425
21.59	2.14	1816	656	0.425
23.73	Half Space	1838	664	0.425

V_P and Estimated V_S Models from a Position of 25.5 m on the P-wave Seismic Refraction Model (Highest V_{P30} in the Central Portion of the Line)

Depth to Top of Layer (m)	Layer Thickness (m)	P-Wave Velocity (m/s)	Estimated S-Wave Velocity (m/s)				
			Poisson's Ratio = 0.25	Poisson's Ratio = 0.3	Poisson's Ratio = 0.35	Poisson's Ratio = 0.4	Poisson's Ratio = 0.45
0.00	0.51	241	139	129	116	98	73
0.51	1.02	483	279	258	232	197	146
1.53	1.02	752	434	402	361	307	227
2.55	1.02	1158	669	619	556	473	349
3.56	1.02	1225	707	655	588	500	369
4.58	1.02	1416	818	757	680	578	427
5.60	1.02	1433	827	766	688	585	432
6.62	2.14	1436	829	768	690	586	433
8.76	2.14	1460	843	780	701	596	440
10.90	2.14	1572	908	840	755	642	474
13.03	2.14	1679	969	897	806	685	506
15.17	2.14	1683	972	900	809	687	508
17.31	2.14	1813	1047	969	871	740	547
19.45	2.14	1814	1047	970	871	741	547
21.59	2.14	1816	1049	971	872	741	548
23.73	Half Space	1891	1092	1011	908	772	570

V_P Model and V_S Model Estimated Using Variable Poisson's Ratio from a Position of 25.5 m on the P-wave Seismic Refraction Model (Highest V_{P30} in the Central Portion of the Line)

Depth to Top of Layer (m)	Layer Thickness (m)	P-Wave Velocity (m/s)	Estimated S-wave Velocity (m/s)	Inferred Poisson's Ratio
0.00	0.51	241	129	0.300
0.51	1.02	483	258	0.300
1.53	1.02	752	376	0.333
2.55	1.02	1158	579	0.333
3.56	1.02	1225	588	0.350
4.58	1.02	1416	633	0.375
5.60	1.02	1433	641	0.375
6.62	2.14	1436	642	0.375
8.76	2.14	1460	653	0.375
10.90	2.14	1572	668	0.390
13.03	2.14	1679	685	0.400
15.17	2.14	1683	687	0.400
17.31	2.14	1813	740	0.400
19.45	2.14	1814	741	0.400
21.59	2.14	1816	741	0.400
23.73	Half Space	1891	772	0.400

V_P and Estimated V_S Models from a Position of 51 m on the P-wave Seismic Refraction Model (Lowest V_{P30} in the Central Portion of the Line)

Depth to Top of Layer (m)	Layer Thickness (m)	P-Wave Velocity (m/s)	Estimated S-Wave Velocity (m/s)				
			Poisson's Ratio = 0.25	Poisson's Ratio = 0.3	Poisson's Ratio = 0.35	Poisson's Ratio = 0.4	Poisson's Ratio = 0.45
0.00	0.51	233	135	125	112	95	70
0.51	1.02	440	254	235	211	180	133
1.53	1.02	467	269	249	224	190	141
2.55	1.02	476	275	254	229	194	143
3.57	1.02	500	289	267	240	204	151
4.59	1.02	534	308	285	256	218	161
5.61	1.02	554	320	296	266	226	167
6.62	2.14	707	408	378	340	289	213
8.76	2.14	782	451	418	375	319	236
10.91	2.14	1017	587	544	489	415	307
13.05	2.14	1209	698	646	581	493	364
15.19	2.14	1266	731	677	608	517	382
17.33	2.14	1290	745	689	620	527	389
19.47	2.14	1734	1001	927	833	708	523
21.61	2.14	1774	1024	948	852	724	535
23.75	Half Space	1782	1029	952	856	727	537

V_P Model and V_S Model Estimated Using Variable Poisson's Ratio from a Position of 51 m on the P-wave Seismic Refraction Model (Lowest V_{P30} in the Central Portion of the Line)

Depth to Top of Layer (m)	Layer Thickness (m)	P-Wave Velocity (m/s)	Estimated S-wave Velocity (m/s)	Inferred Poisson's Ratio
0.00	0.51	233	125	0.300
0.51	1.02	440	235	0.300
1.53	1.02	467	233	0.333
2.55	1.02	476	238	0.333
3.57	1.02	500	240	0.350
4.59	1.02	534	256	0.350
5.61	1.02	554	266	0.350
6.62	2.14	707	340	0.350
8.76	2.14	782	375	0.350
10.91	2.14	1017	489	0.350
13.05	2.14	1209	581	0.350
15.19	2.14	1266	608	0.350
17.33	2.14	1290	620	0.350
19.47	2.14	1734	626	0.425
21.61	2.14	1774	641	0.425
23.75	Half Space	1782	643	0.425

Observations/Discussion:

- The seismic station is located on a ridge with outcropping rock mapped as Miocene Monterey Formation. The seismic line was located along a dirt road cut into the side of the ridge, less than 50 m from the seismic station, as this was the only location that permitted access with a truck mounted weight drop source. The seismic line is located on mapped Monterey Formation, but at the edge of a Holocene landslide. As will be discussed below, the velocity structure beneath at least part of the seismic line does not appear to be representative of the seismic station and additional geophysical testing should be considered.
- There are no distinct, high amplitude HVSR peaks. The HVSR curves are, however, quite similar at frequencies below 3 Hz, where there is slightly elevated HVSR response between 0.9 and 2 Hz.
- The P-wave seismic refraction data for array PSM-1 were modeled using a tomographic inversion routine with a smooth velocity gradient starting model. The P-wave seismic refraction model was extended to far offset shot locations to extend depth of investigation. It should be noted that a larger geophone spacing, rather than the utilization of far offset shot locations, is preferred for extending depth of investigation, when applying tomographic inversion routines. However, the seismic refraction data were acquired in conjunction with surface wave data, where a shorter array length is preferred.
- The P-wave seismic refraction survey design allowed P-wave velocity to be imaged to a maximum depth of about 24 m. The seismic refraction model indicates that P-wave velocity is about 200 to 250 m/s at the surface and increases to 400 to 450 m/s at a nominal depth of 0.5 m, 1,000 m/s at a depth of 2 to 14 m, 1,400 m/s at a depth of 5 to 19 m, and over 1,800 m/s at a depth of 13 to 20 m. The maximum P-wave velocity in the central portion of the model, where depth of investigation is greatest, is about 1,900 m/s. Although not conclusive, P-wave velocities greater than 1,600 m/s could be associated with saturated, weathered rock. P-wave velocities in the 1,600 to 1,800 m/s range occur at relatively uniform elevation, providing some support for the presence of saturated rock.
- The seismic refraction survey indicates that there is significant lateral velocity variation at the site with thicker sequence of lower velocity sediments and weathered rock beneath the northeastern half of the line and an elevated zone of higher velocity weathered rock beneath the southwest to central portion of the seismic line.
- The average P-wave velocity of the upper 30 m (V_{P30}) was estimated between 22.5 and 51 m on the P-wave refraction model, where depth of investigation is greatest. To estimate V_{P30} the P-wave velocity at a depth of 24 m, nominal depth of investigation, was projected to 30 m depth. V_{P30} ranges from about 894 to 1,337 m/s between a position of 22.5 to 51 m, a 39% variation. The highest and lowest estimated V_{P30} over this distance interval occurs at a position of 25.5 and 51 m, respectively. V_{P30} is expected to be lower than the maximum southwest of 22.5 m and close to the minimum northeast of 51 m.
- An average V_P model was developed over the 22.5 to 51 m distance interval by horizontally averaging the travel time of each model cell and cell thickness and average V_{P30} was determined to be 1,103 m/s. Assuming constant Poisson's ratios of 0.25, 0.3, 0.35, 0.4 and 0.45 would result in an estimated V_{S30} of 637, 590, 530, 450 and 333 m/s, respectively. Poisson's ratio of 0.4 to 0.45 is likely only applicable to saturated rock, which, if present, occurs at a depth greater than 13 m. Therefore, estimated V_{S30} based

on constant Poisson's ratios of 0.4 to 0.45 are expected to underestimate V_{S30}. Likewise, if rock is saturated at a depth between 13 and 20 m, V_{S30} estimated using constant Poisson's ratio lower than 0.35 are expected to overestimate V_{S30}.

- The lowest value of V_{P30} over the 22.5 to 51 m distance interval is 894 m/s and occurs at a position of 51 m. Assuming constant Poisson's ratios of 0.25, 0.3, 0.35, 0.4 and 0.45 would result in an estimated V_{S30} of 516, 478, 429, 365 and 270 m/s, respectively. This portion of the seismic line has a thicker sequence of low velocity sediments, likely associated with the adjacent landslide, and is not representative of the seismic station, which sits on weathered rock.
- The highest value of V_{P30} over the 22.5 to 51 m distance interval is 1,338 m/s and occurs at a position of 25.5 m. Assuming constant Poisson's ratios of 0.25, 0.3, 0.35, 0.4 and 0.45 would result in an estimated V_{S30} of 772, 715, 643, 546 and 403 m/s, respectively. This portion of the seismic line has the highest velocity near surface rock and may be most representative of seismic station conditions. However, because of the large degree of lateral velocity variation at the site, geophysical testing is required in closer proximity to the seismic station to accurately constrain velocity structure at the seismic station.
- Noise conditions at the site were not sufficient for application of passive surface wave techniques.
- MASW (Rayleigh wave) data collected along array PSM-1 are not expected to be viable due to the significant lateral velocity variation beneath the array. However, an attempt was made to reduce and model the MASW data. As expected, it was very difficult to reduce the MASW data due to the lateral velocity variation. Almost all small wavelength/high frequency Rayleigh wave dispersion data originates from source locations in the northeastern half of the array where there is thicker, low velocity sediment cover. Therefore, near surface velocity structure is definitely biased towards the lower velocities at the northeast end of the array. Dominant higher modes were prevalent at high frequencies on seismic records associated with source locations at the southwestern portion of the array. There was also difficulty extracting long wavelength dispersion data using far offset source locations and the full 48 channel receiver array. As expected, dispersion curves from source locations at each end of the array diverged at long wavelengths. The maximum wavelength surface wave data extracted from source locations at the southwest end of the array was about 65 m. Longer wavelength dispersion data with the expected higher phase velocity was obtained from source locations at the northeast end of the array. However, these dispersion data were cut to a maximum wavelength of 65 m to avoid bias. It should be noted, that the Yoon and Rix (2005) near field criteria, which establishes the maximum wavelength as the source to midpoint of the receiver array distance would result in a maximum wavelength of about 65 m based on the survey design. For most source locations the maximum wavelength established using this criteria was relaxed by up to 25%. Ideally, an alternate location would have been identified for site characterization, although significant 2-D velocity variation may be the norm in the immediate site vicinity.
- The minimum wavelength surface wave phase velocity data extracted from the 48-channel MASW array is about 25 m, although minimum wavelength was significantly greater for many of the source locations offset more that 10 m from the near geophone. Data reduction using seismic records from smaller hammer sources and a limited offset receiver array (i.e. less active geophones) allowed extraction of surface wave dispersion

data to a minimum wavelength of about 2.5 m, most of this data originating from receiver arrays in the northeast portion of the array.

- There is nominally about 40 m/s scatter in MASW dispersion data selected for modeling, likely due to the effects of lateral velocity variation.
- A representative dispersion curve was generated for the MASW data set using a moving average, polynomial curve fitting routine and used for modeling.
- Saturated weathered rock with V_P in the 1,800 to 1,900 m/s range was fixed at a depth of 17 m, the average depth to the 1,800 m/s contour on the seismic refraction model. Because of the unknown affect of the lateral velocity variation of the MASW V_S model, it is not possible to conclusively state that the weathered rock is saturated without S-wave refraction data.
- Surface wave depth of investigation is about 30 m based on one half of maximum wavelength criteria.
- The only estimated V_S structure from the P-wave seismic refraction model that the MASW V_S model is consistent with is the refraction model at 51 m, where V_{P30} is lowest. This is consistent with the fact that much of the higher frequency surface wave dispersion data resulted from source locations and receiver arrays in the northeast half of the array. Additionally, the MASW V_S model requires high Poisson's ratio (i.e. saturated weathered rock) below a depth of 15 to 17 m for fit the refraction model.
- V_{S30} from the MASW V_S model is 339 m/s (NEHRP Site Class D/C).
- V_{S30} from the MASW V_S model, after replacing the S-wave velocity of the sediments in the upper 10 m ($V_S < 350$ m/s) with that of the underling layer to account for the seismic station being located on weathered rock, is 451 m/s (NEHRP Site Class C).
- The MASW V_S model significantly underestimated V_S relative to the average and highest V_{P30} seismic refraction models. These models are considered more characteristic of seismic station conditions and, therefore, the MASW V_S model should not be used for site characterization purposes.
- Accurate site characterization cannot be made with geophysical data available at this time. The MASW V_S model is not considered representative of seismic station velocity structure. The possibility of saturated weathered rock adds significant error to estimating S-wave velocity structure using P-wave velocity and an assumed constant Poisson's ratio. However, until additional data becomes available, the P-wave refraction models were explored to determine feasible ranges of V_{S30} and to determine NEHRP Site Class. It is also important to note that the seismic station is located on rock; whereas, there is some variable thickness residual soil and/or landslide deposits overlying rock beneath array PSM-1. To adjust V_{S30} to approximate seismic station conditions, weathered rock was assumed to have a minimum P-wave velocity of 700 m/s and all P-wave velocities in the models less than 700 m/s were replaced with the velocity of the underlying layer. P-wave velocity was then converted to S-wave velocity using both assumed constant and variable Poisson's ratio models as outlined below.

- A constant Poisson's ratio of 0.35 was first assumed in assessing the P-wave refraction model. This is probably somewhat conservative for unsaturated shale, but will compensate for the possibility of higher Poisson's ratio saturated rock at depth. Estimated V_{S30} for a constant Poisson's ratio of 0.35 is 530, 643 and 429 for the average V_P model, V_P model at 25.5 m with the high V_{P30} and V_P model at 51 m with low V_{P30}, respectively. Adjusted V_{S30} for a constant Poisson's ratio of 0.35 is 597, 712 and 509 for the average V_P model, V_P model at 25.5 m with the high V_{P30} and V_P model at 51 m with low V_{P30}, respectively. The upper 3.5, 1.5 and 6.6 m of these models were replaced with the velocity of the underlying material, respectively. The low value is most likely not representative of the seismic station and can be discounted. Therefore, V_{S30} and adjusted V_{S30} likely fall between 530 and 643 m/s and 597 and 712 m/s, respectively.
- The second approach for exploring the possible range of V_{S30} from the P-wave seismic refraction model was to use a variable Poisson's ratio. Poisson's ratio of 0.3 to 0.35 were used for unsaturated sediments and weathered rock and Poisson's ratio of 0.4 to 0.425 were used for possible saturated weathered rock (V_P > 1,500 m/s). Poisson's ratio was allowed to gradually increase from inferred unsaturated to saturated rock to ensure that V_S increased with depth, a reasonable assumption. The V_P model at 25.5 m with the highest V_{P30} required higher Poisson's ratio for the unsaturated zone and lower Poisson's ratio for the inferred saturated zone to avoid velocity inversions. Estimated V_{S30} for a variable Poisson's ratio (models are presented in tabular and graphical form) is 478, 599 and 413 for the average V_P model, V_P model at 25.5 m with the high V_{P30} and V_P model at 51 m with low V_{P30}, respectively. Adjusted V_{S30} for a variable Poisson's ratio is 521, 648 and 476 for the average V_P model, V_P model at 25.5 m with the high V_{P30} and V_P model at 51 m with low V_{P30}, respectively. The upper 3.5, 1.5 and 6.6 m of these models were replaced with the velocity of the underlying material, respectively. The low value is most likely not representative of the seismic station and can be discounted. Therefore, V_{S30} and adjusted V_{S30} likely fall between 478 and 599 m/s and 521 and 648 m/s, respectively.
- Based on the two approaches outlined above, V_{S30} may range from about 478 to 643 m/s, averaging 563 m/s with a potential 15% error. Adjusted V_{S30} may range from about 521 to 712 m/s, averaging 617 m/s with a potential 15% error.
- For the purpose of approximate site characterization, we recommend that the ranges of estimated V_{S30} from the P-wave seismic refraction models be utilized until additional geophysical testing can be conducted. Therefore, at this time V_{S30} and adjusted V_{S30} are approximated at 560 and 620 m/s, respectively, both with about 15% error (NEHRP Site Class C). Both of these values have been rounded to the nearest 10 m/s.
- Although there is significant error in V_{S30} at this site, the site appears to clearly fall into the middle of the NEHRP Site Class C range. Only adjusted V_{S30} from the estimated V_S model at a position of 25.5 m (highest V_{P30}) with constant Poisson's ratio of 0.3, or less, exceeds 760 m/s, as required for Site Class B.

- Additional geophysical testing at this site is required to more accurately determine S-wave velocity structure at this seismic station. There is significant topographic variation and only localized outcrops of Monterey Formation in the site vicinity. Options for additional testing follow and should consider P- and S-wave refraction, MASW (Raleigh wave) and MALW (Love wave) techniques, as applicable. The array could be moved about 40 m to the southwest to avoid the low velocity zone beneath the northeastern half of the array, although there is steeper topography perpendicular to the array in this area and there is no guarantee that the velocity structure in this area is characteristic of the seismic station. It may be possible to place an array on the ridge top slightly west of the seismic station. There may be significant topographic variation along such an array limiting geophysical testing to P-wave S-wave seismic refraction techniques. Finally, P- and S-wave seismic refraction data could be acquired along an array oriented perpendicular to the ridge and centered adjacent to the seismic station. There would be too much topographic variation along such an array for surface wave techniques to be applicable.

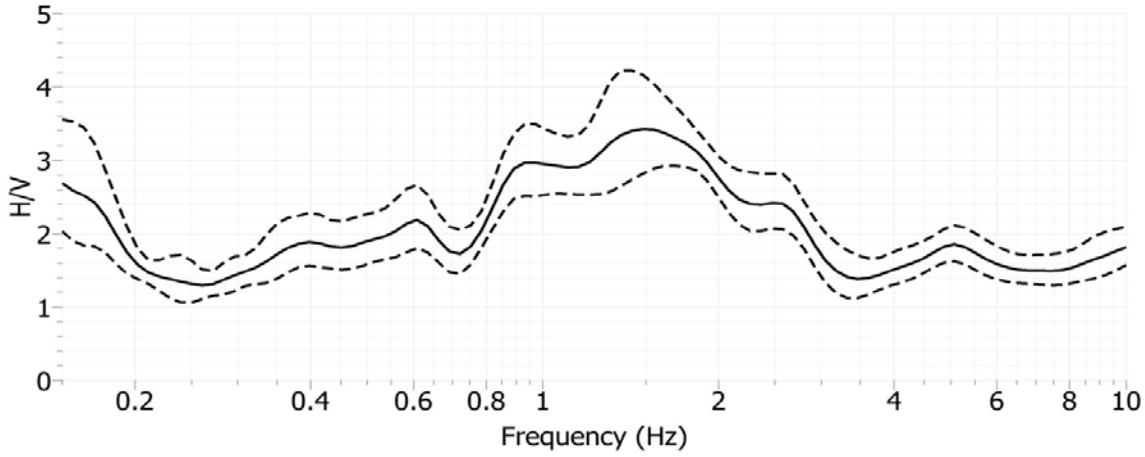

Site NC.PSM, H/V Spectral Ratio, Array PSM-1, Sensor 453

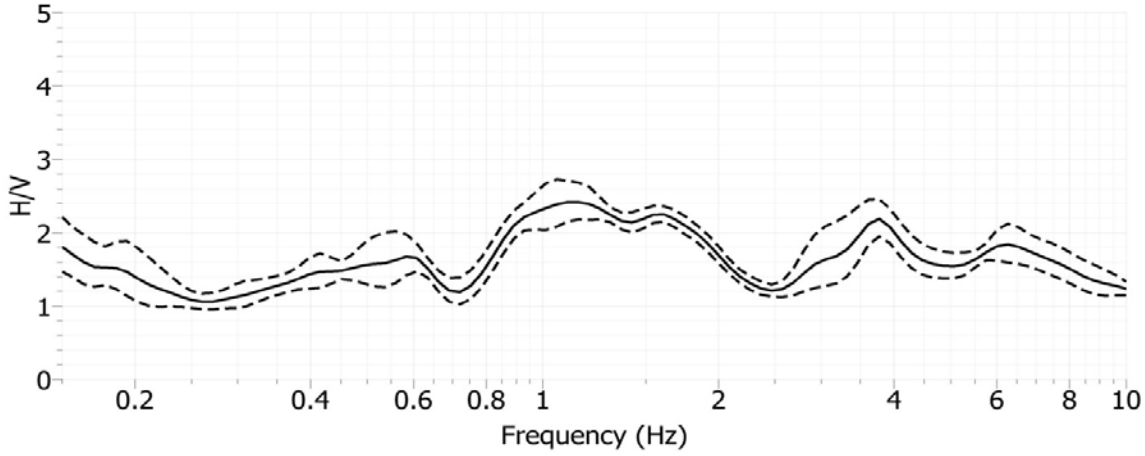

Site NC.PSM, H/V Spectral Ratio, Near Seismic Station, Sensor 450

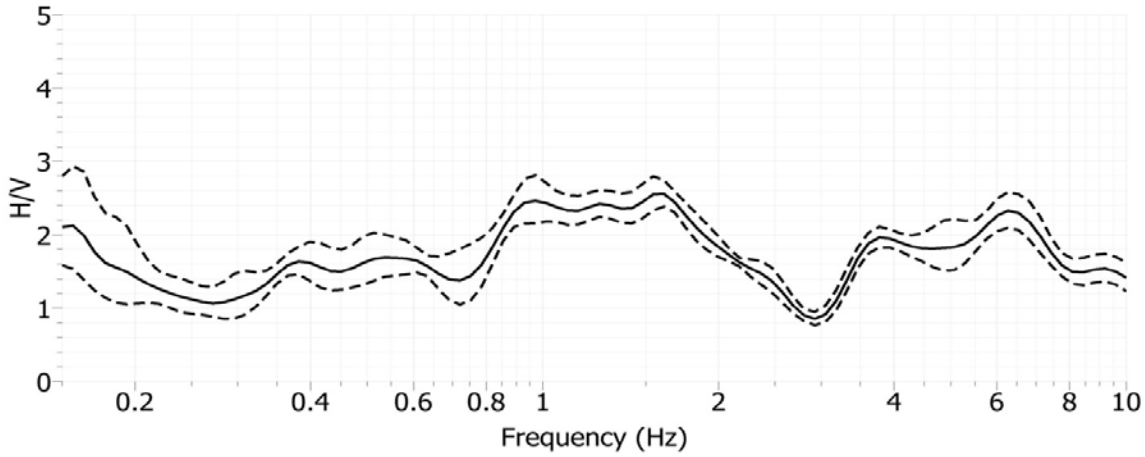

Site NC.PSM, H/V Spectral Ratio, Array PSM-1, Sensor 507

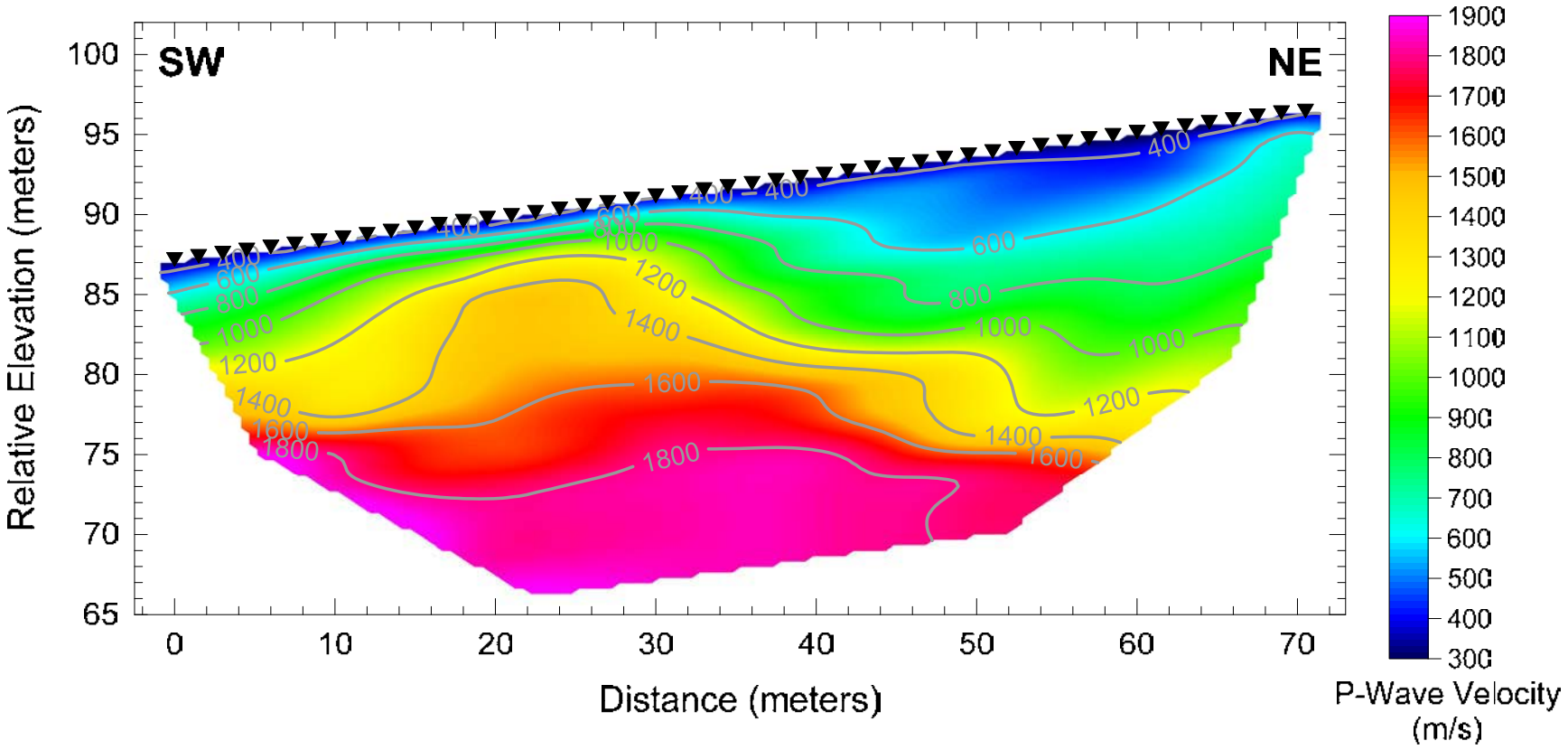

Array PSM-1 – Tomographic seismic refraction model developed using a smooth velocity gradient starting model

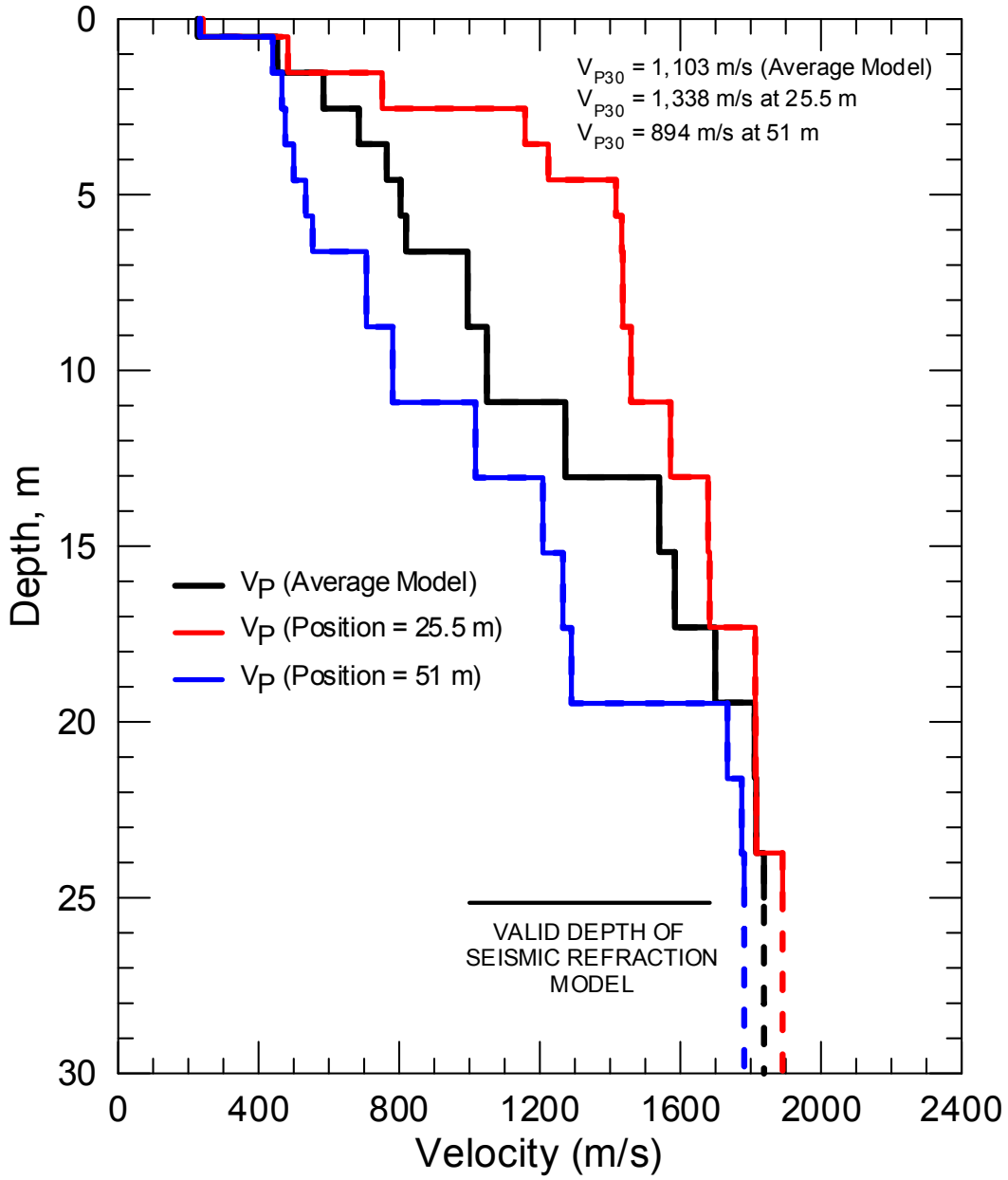

NC.PSM – Average P-wave velocity structure between 22.5 and 51m on P-wave seismic refraction array PSM-1 and the P-wave velocity structure at 25.5 m (maximum V_{P30} over the 22.5 to 51 m interval) and 512 m (minimum V_{P30} over 22.5 to 51 m interval). P-wave velocity is not well constrained below a depth of 25 m and computations are made assuming that velocity is constant below this depth. There is about 40% variation in V_{P30} beneath the array and, therefore, the array is not suitable for surface wave testing. Additionally, although located within 50 m of the seismic station, only the velocity structure beneath the southwestern portion of the array appears consistent with expected seismic station conditions.

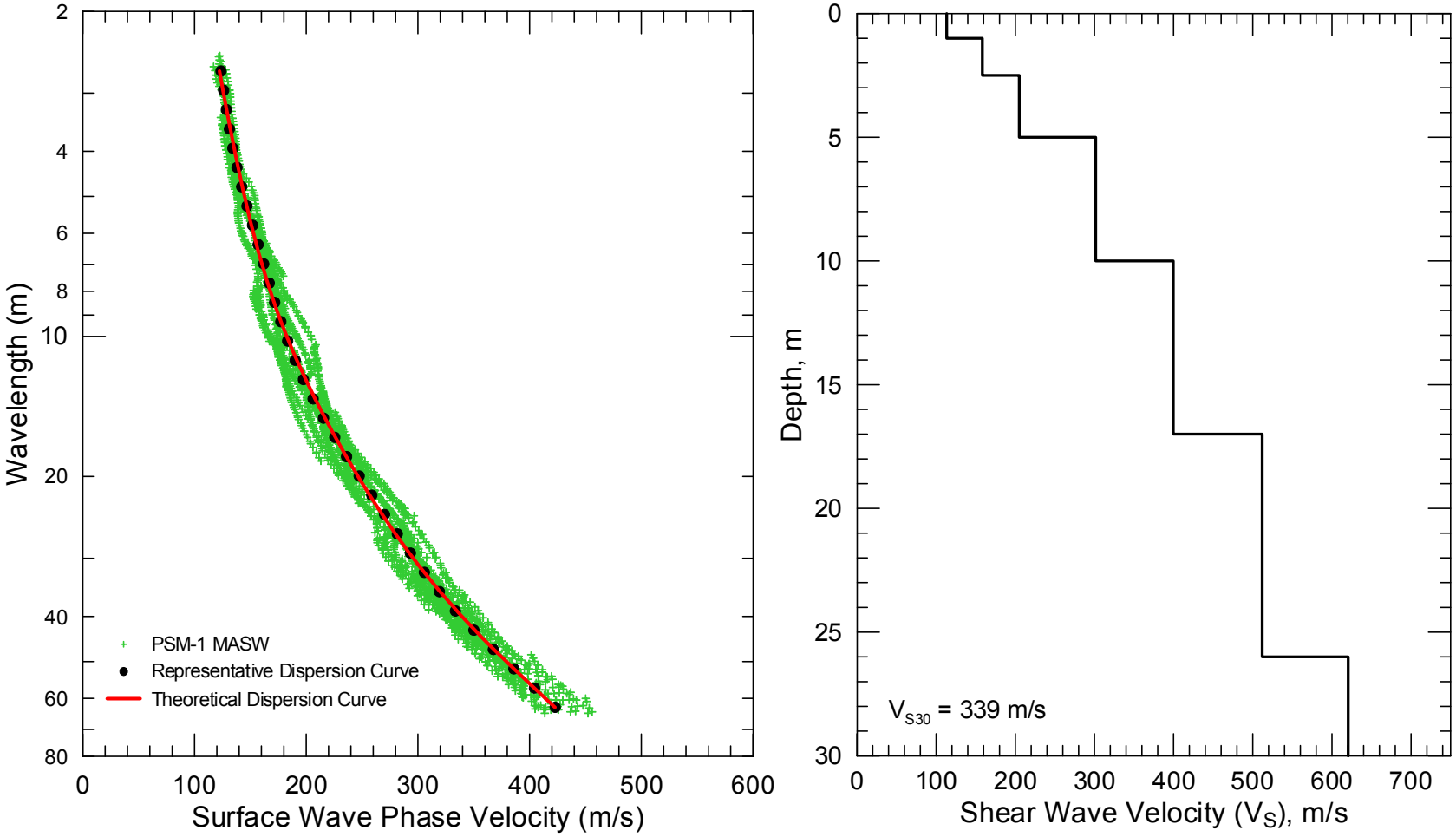

NC.PSM - Field, representative and inverted theoretical surface wave dispersion data (left) and associated V_S model (right)

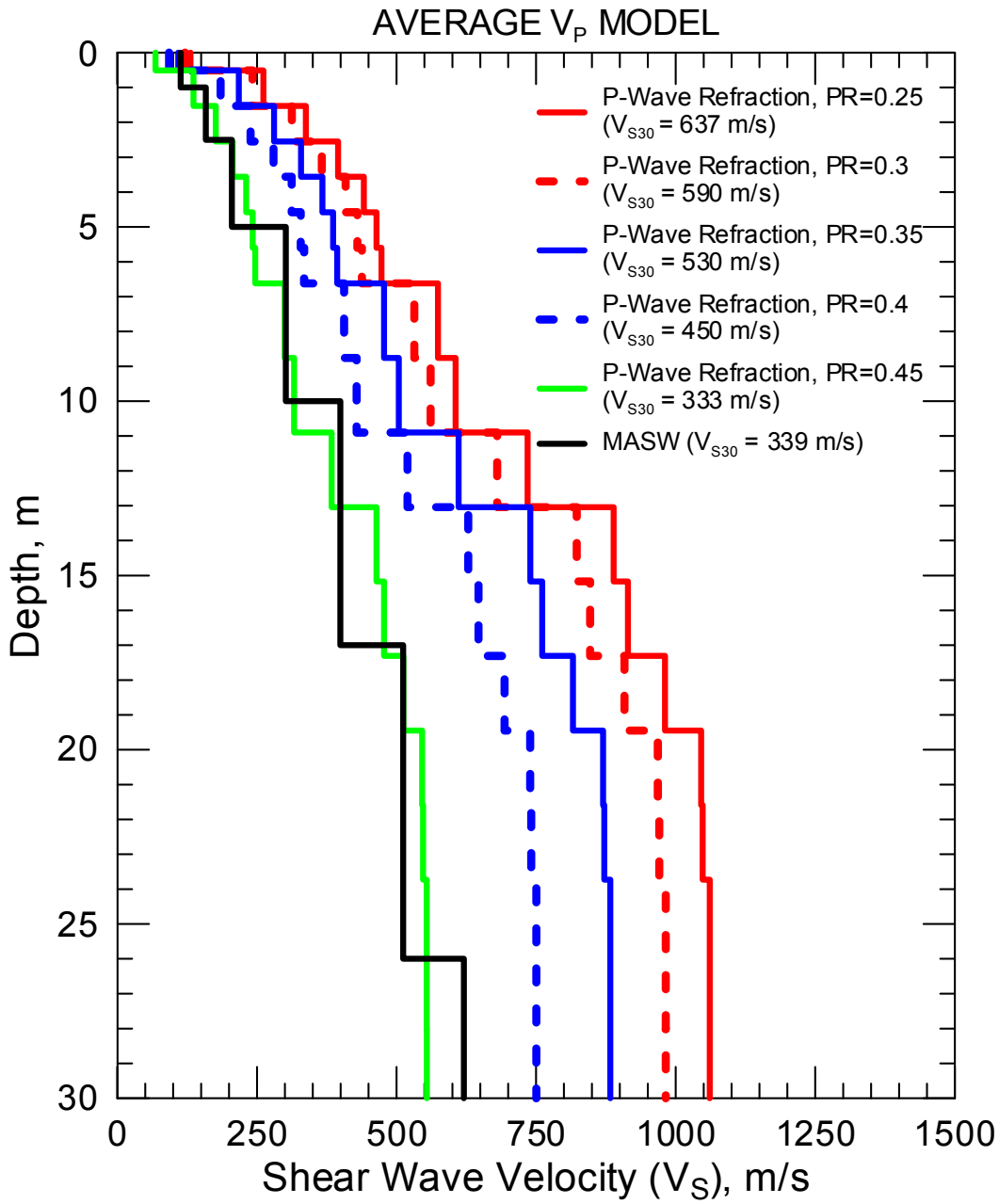

NC.PSM – Comparison of S-wave velocity models derived from the MASW sounding and the average V_P model from the P-wave seismic refraction surveys. The MASW V_S model significantly underestimates V_S relative to the average seismic refraction model. The lateral velocity variation is such that the MASW V_S model should not be considered valid. The MASW V_S model may indicate that bedrock is saturated at depth resulting in high Poisson's ratio, but is not conclusive.

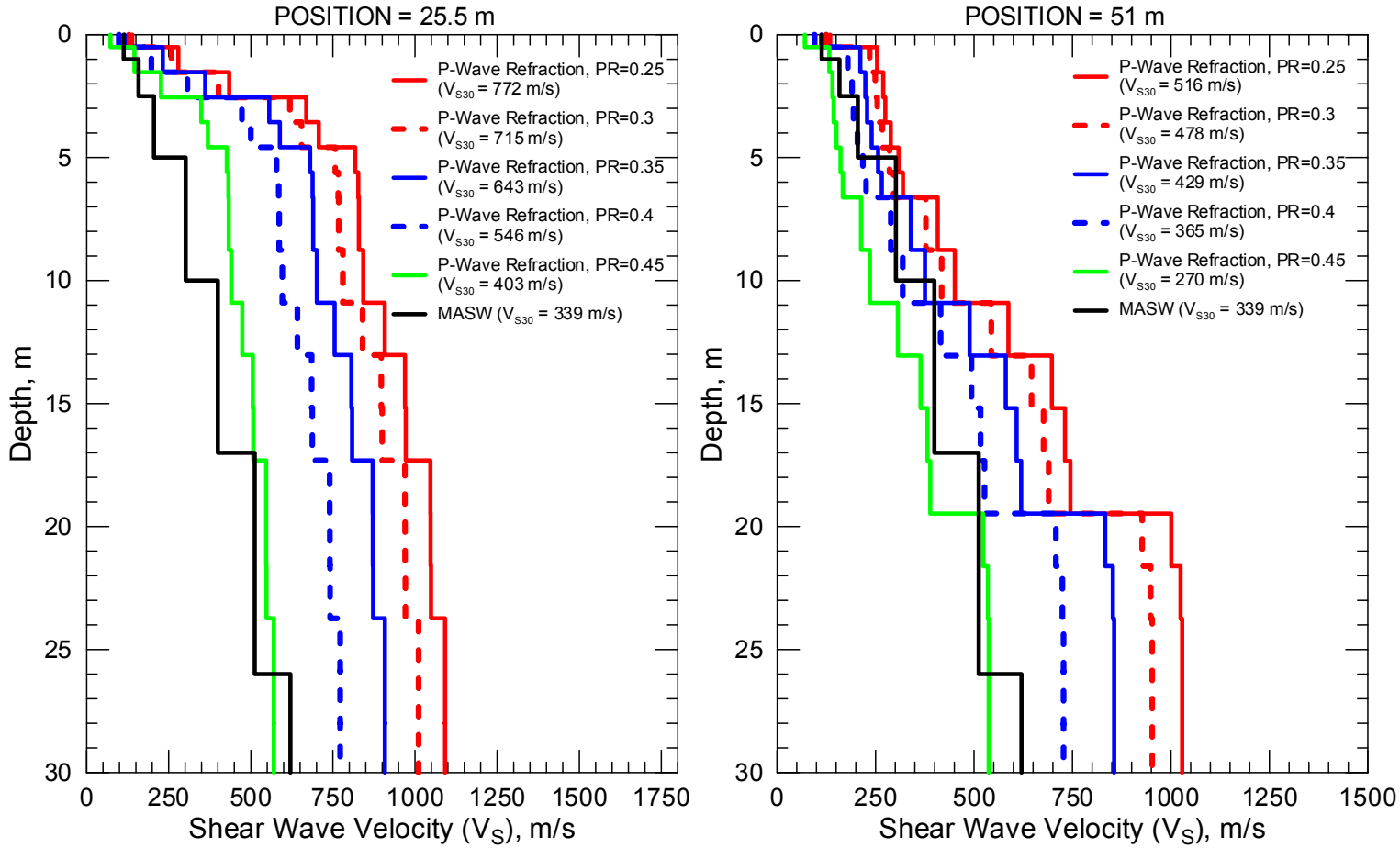

NC.PSM – Comparison of the V_S model derived from the MASW data and the estimated V_S models derived from the P-wave seismic refraction survey at locations over the 22.5 to 51 m distance interval with the highest and lowest V_{P30}. The figures on the left and right present estimated V_S from the seismic refraction V_P model at a position of 25.5 m (highest V_{P30}) and 51 m (lowest V_{P30}), respectively. The MASW V_S model significantly underestimates V_S relative to the highest V_{P30} seismic refraction model, but is in better agreement with the seismic refraction model at 51 m, assuming that the bedrock is saturated below a depth of 20 m. The lateral velocity variation is such that the MASW V_S model should not be considered reliable and is only used, at most, to determine realistic ranges of Poisson's ratio to estimate V_S from the P-wave refraction model at a position of 22.5 m, which is considered more representative of seismic station.

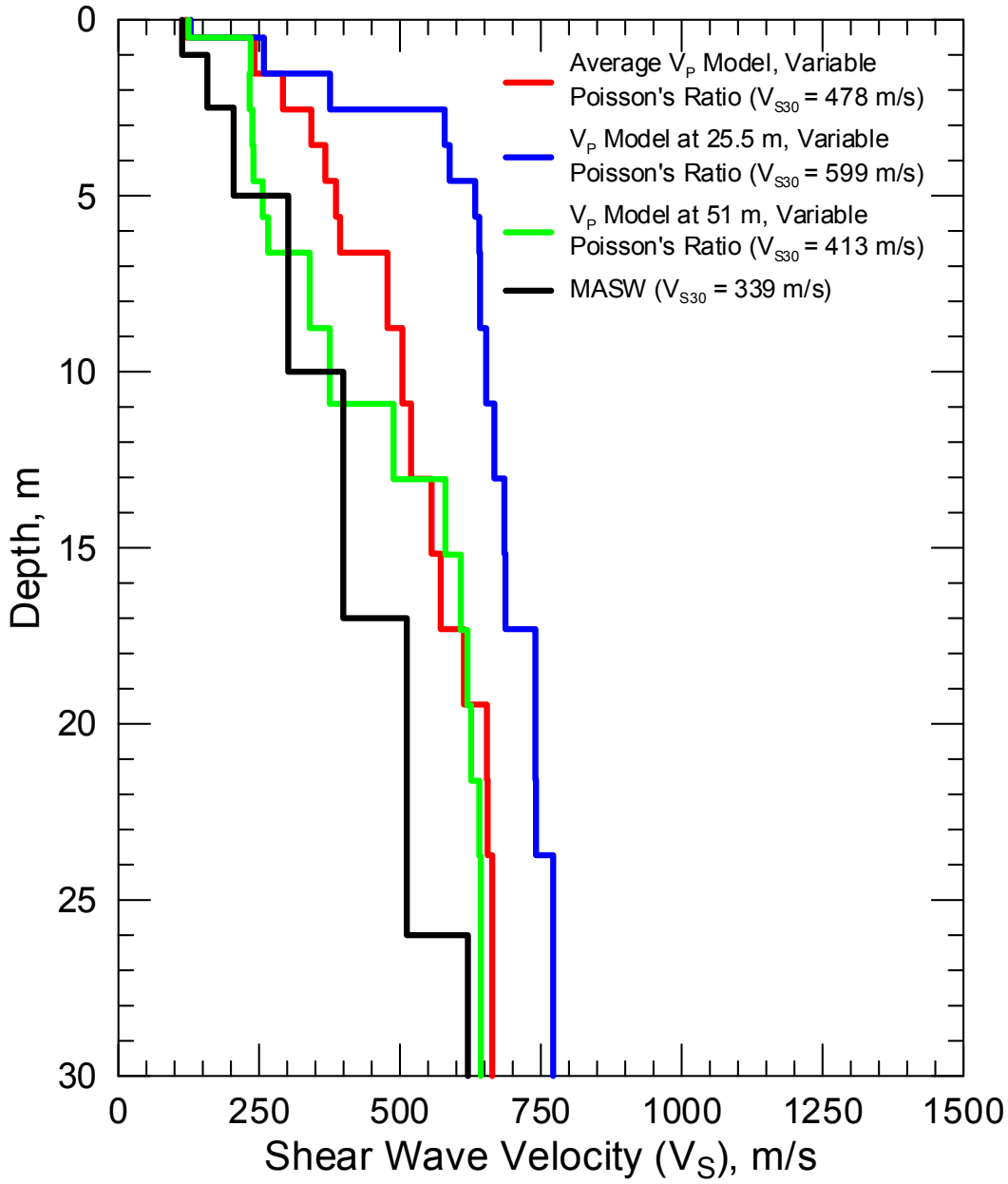

NC.PSM – Comparison of the V_S model derived from the MASW data and the estimated V_S models derived from the P-wave seismic refraction survey using variable Poisson's ratio. These models are also provided in tabular form. None of the models estimated from the seismic refraction V_P model are in good agreement with the MASW V_S model. The MASW V_S model is not considered valid due to severe lateral velocity variation and is not representative of seismic station conditions. The V_S model estimated from the seismic refraction V_P model at 51 m would be in better agreement with the MASW V_S model if a Poisson's ratio of 0.45 rather than 0.425 was used for inferred saturated rock. However, given the uncertainty in the MASW data at this site, a successfully implemented S-wave refraction survey would be required to confirm that weathered rock at depth is saturated.

Site NM.BLO

Location: University of Indiana, Bloomington, Monroe County, Indiana

Latitude: 39.17190 **Longitude:** -86.52220
(Station coordinates provided by USGS, WGS84 coordinate system)

V_{S30} (measured): 1,202 m/s (based on average V_S model from S-wave seismic refraction array BLO-3, ±5% due to expected lateral velocity variation and/or error).

V_{S30} (adjusted to more accurately reflect seismic station conditions): 2,317 m/s (approximate average V_S of the upper 30 m of rock based on S-wave seismic refraction model for array BLO-3 to account for seismic sensor being located on an isolated concrete pier anchored on bedrock, ±5% due to expected lateral velocity variation and/or error).

NEHRP Site Class: B (based on V_{S30}), A (based on the more appropriate adjusted V_{S30})

Geomatrix Code: DZA

Geologic Conditions/Observations: Seismic station located on geologic unit mapped as Paleozoic (Mississippian) Sanders Group, which consists of a fine-grained dolomite, limestone and calcarenites with minor chert, siltstone and shale.

Site Conditions: Suburban site located on the University of Indiana campus in Bloomington, Indiana. Relatively flat terrain in site vicinity.

Geophysical Methods Utilized: HVSR, Seismic Refraction (P- and S-wave), MASW (Rayleigh wave), MALW (Love Wave)

Geophysical Testing Arrays:

1. Array BLO-1 (48 channel MASW, MALW and P- and S-wave seismic refraction array utilizing 4.5 Hz vertical/horizontal geophones spaced 1.5 m apart for a length of 70.5 m, forward and reverse shot locations with multiple source offsets and source types and multiple interior shot locations).
2. Array BLO-2 (48 channel MALW and S-wave seismic refraction array utilizing 4.5 Hz horizontal geophones spaced 1.5 m apart for a length of 70.5 m with multiple off-end and interior source locations).
3. Array BLO-3 (48 channel P and S-wave seismic refraction array utilizing 4.5 Hz vertical/horizontal geophones spaced 3 m apart for a length of 141 m, forward and reverse shot locations and multiple interior shot locations).
4. Seven HVSR measurement locations: three distributed along array BLO-1, three distributed along array BLO-2 and one adjacent to the seismic station.

Legend

- Seismic Station - Approximate Location of Record
- H/V Spectral Ratio Location
- MALW and Seismic Refraction Array (S-wave)
- Seismic Refraction Array (S- and P-wave)
- MASW and Seismic Refraction Array (S- and P-wave)

NOTES:
1. WGS 1984 COORDINATE SYSTEM
2. Image Source: (c) Microsoft Corporation and its data suppliers

File Name: NM-BLO-I

Date: 6/17/2012

USGS science for a changing world

GEOVision geophysical services

SITE MAP
NM•BLO

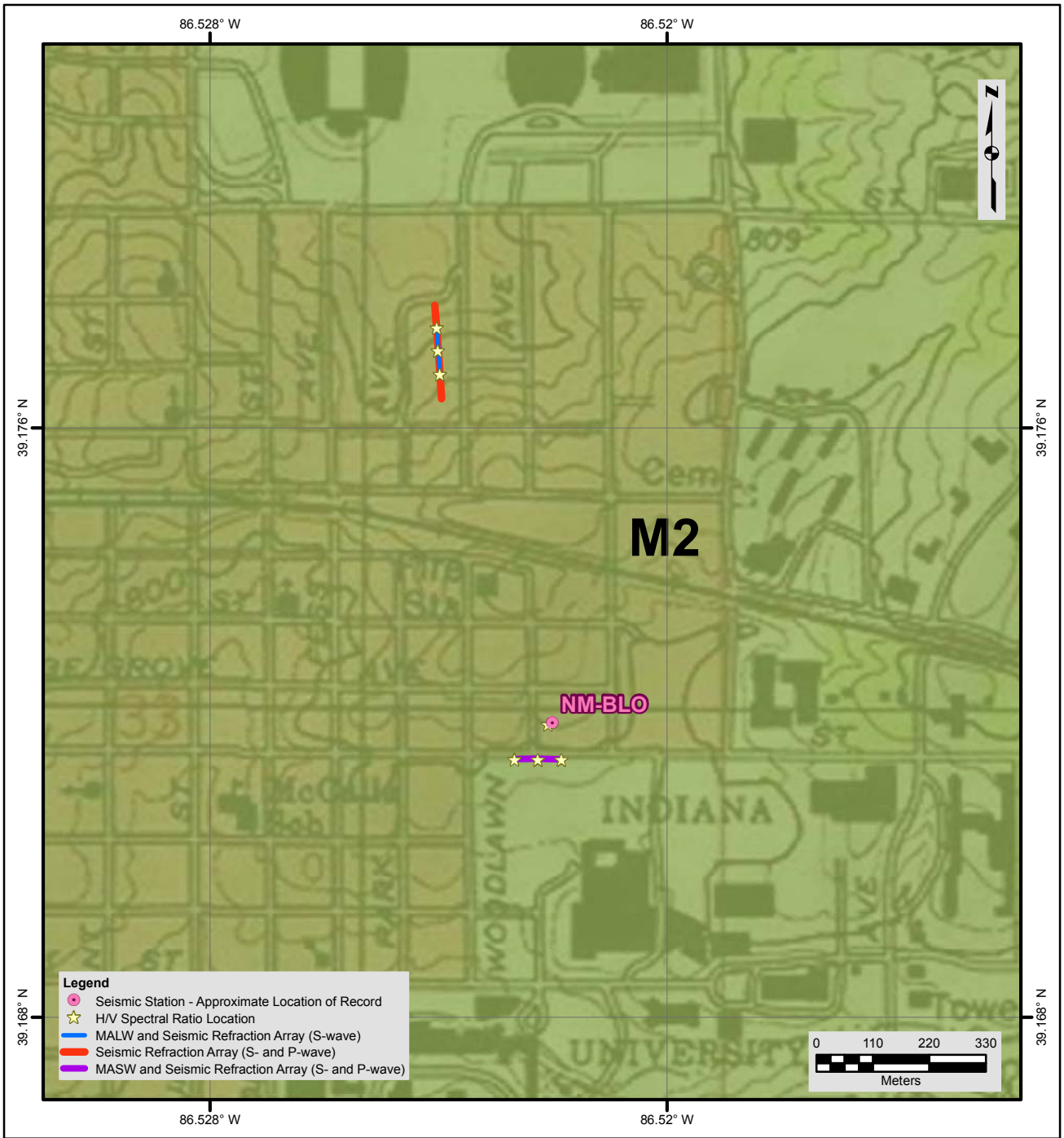

Description of Geologic Map Units

M2 = Paleozoic (Mississippian) Sanders Group; fine-grained dolomite and limestone and calcarenites, with minor chert, siltstone and shale

NOTES:
1. WGS 1984 COORDINATE SYSTEM
2. Indiana Geological Survey Miscellaneous Map 48
3. See site map for details of geophysical survey

File Name: NM-BLO

Date: 4/12/2012

USGS science for a changing world

GEOVision geophysical services

GEOLOGIC MAP
NM•BLO

RECOVERY.GOV

Seismic Station NM.BLO

HVSR measurements on array BLO-1
using a Micromed Tromino ENGR

Looking northeast towards building housing
seismic station from array BLO-1

Looking north along array BLO-2

Looking west along array BLO-1

Location of Geophysical Testing Arrays:

Location	Latitude	Longitude
BLO-1, West End of MASW/Refraction Array	39.17151	-86.52265
BLO-1, Center of MASW/Refraction Array	39.17151	-86.52224
BLO-1, East End of MASW/Refraction Array	39.17150	-86.52185
BLO-2, South End of Seismic Refraction Array	39.17672	-86.52397
BLO-2, Center of Seismic Refraction Array	39.17704	-86.52401
BLO-2, North End of Seismic Refraction Array	39.17736	-86.52404
BLO-3, South End of Seismic Refraction Array	39.17639	-86.52397
BLO-3, Center of Seismic Refraction Array	39.17703	-86.52401
BLO-3, North End of Seismic Refraction Array	39.17766	-86.52406
HVSR Sensor 453 (Nanometrics Trillium Compact)	39.17149	-86.52226
HVSR Sensor Tromino ENGY (TRO-2)	39.17150	-86.52267
HVSR Sensor Tromino ENGY (TRO-1)	39.17149	-86.52185
HVSR Sensor Tromino ENGY (TRO-3)	39.17197	-86.52208
HVSR Sensor Tromino ENGY (TRO-1A)	39.17672	-86.52397
HVSR Sensor Tromino ENGY (TRO-2A)	39.17704	-86.52401
HVSR Sensor Tromino ENGY (TRO-3A)	39.17736	-86.52404

Notes: 1) WGS84 Coordinate System (decimal degrees)

2) Survey accuracy is estimated at 1 to 2 m.

3) HVSR Sensor TRO-3 located inside building and coordinates are estimated.

Results:

Average V_S Model from Central Portion of S-wave Seismic Refraction Array BLO-3

Depth to Top of Layer (m)	Layer Thickness (m)	S-Wave Velocity (m/s)
0.00	0.49	207
0.49	0.99	267
1.48	0.99	272
2.47	0.99	277
3.46	0.99	959
4.45	0.99	1473
5.44	0.99	1563
6.42	2.08	1754
8.50	2.08	2135
10.57	2.08	2485
12.65	2.08	2628
14.72	2.08	2702
16.80	2.08	2727
18.88	2.08	2739
20.95	Half Space	2761

Observations/Discussion:

- The seismic station is located on the ground floor of a building on an isolated concrete pier that is anchored into bedrock. Therefore, the S-wave velocity of the bedrock unit is of primary interest. All possible test locations in the site vicinity have several meters of soil overlying bedrock, which complicates site characterization.
- The field investigation was conducted at this site on two occasions. On 10/9/2011, MASW, MALW, P- and S-wave seismic refraction, and HVSR data were acquired along the 70.5 m long array BLO-1, located near the building housing the seismic station. This array was located in a grass covered area next to a road and was the only permitted and accessible test location in close proximity to the seismic station. There was traffic noise during data acquisition and the possibility of utilities near the test area could not be discounted. Because of the very thin soil cover overlying high velocity bedrock, surface wave techniques were not expected to be effective at accurately characterizing the S-wave velocity of the rock. It was, therefore, critical that high quality S-wave seismic refraction data be acquired to map the rock velocity. P-wave seismic refraction data quality was degraded slightly by traffic noise and the bedrock refracted arrival was very weak. It was, however, possible to generate a P-wave refraction model for this data set

although a longer array would have been preferred to more accurately constrain the high P-wave velocity of the bedrock. S-wave refraction data collected along this array were much too noisy to be utilized for site characterization. HVSR data collected along array BLO-1 confirmed that bedrock was very shallow. In an attempt to acquire better quality S-wave seismic refraction data, the site was revisited on 2/12/12. Geophysical testing was conducted in a field about 600 m from the seismic station. The bedrock appears relatively unweathered and moving a large distance away from the seismic station did not seem problematic. S-wave seismic refraction and MALW data were acquired along the 70.5 m long array BLO-2 and P- and S-wave seismic refraction data were acquired along the 141 m long array BLO-3 during this site visit. HVSR measurements were also made along array BLO-2.

- Three HVSR measurements were made along array BLO-1; two with a Micromed Tromino ENGY and the other with a Nanometrics Trillium Compact. The HVSR measurements at the three locations have a high amplitude HVSR peak in the 24.5 to 26 Hz range, indicating that the bedrock is only a couple meters deep (assumed average Vs of 200 m/s for the sediments and 25 Hz HVSR peak result in 2 m bedrock depth using the quarter wavelength approximation). Interestingly, the HVSR data collected with the Trillium has a slightly higher amplitude HVSR peak. An additional HVSR measurement was made with the Tromino on the concrete block that the seismic station sits on. This HVSR plot is not presented as the only HVSR peak is near the Nyquist frequency of 64 Hz (128 Hz sample rate) and may be associated with 60 Hz electrical noise. As the concrete block sits on high velocity rock, an HVSR peak is not expected at the seismic station.
- Three HVSR measurements were made along array BLO-2 using the Tromino. An HVSR peak of 18 to 22.5 Hz (frequency increasing from north to south) occurs at the three measurement locations, indicating the bedrock is slightly deeper beneath array BLO-2 than beneath array BLO-1, assuming similar soil velocity. The amplitude of the HVSR peaks along array BLO-2 are also lower than those along array BLO-1. This may be associated with the partially frozen ground during testing along array BLO-2, as the impedance contrast between the sediments and rock is not expected to be significantly difference between the two arrays.
- The P-wave seismic refraction data for array BLO-1 and the P- and S-wave seismic refraction data for array BLO-3 were modeled using a tomographic inversion routine with two layer starting model developed using the time-term method. The resulting tomographic inversion, therefore, retains the characteristics of the starting model (steep rather than gradual velocity gradient at the top of bedrock), but allows for possible adjustment for weathering in the uppermost bedrock zone.
- The P-wave first arrival data associated with the high velocity bedrock refractor for both arrays BLO-1 and BLO-3 were very weak, complicating accurate picking of the first arrival data. The bedrock refractor was generally easier to pick on the S-wave seismic refraction records and there was good polarity reversal between the opposite direction S-wave shots. However, we do not believe that the soil S-wave velocity could be accurately constrained in the S-wave refraction data due to possible earlier arriving P-wave energy. Fortunately, we are only concerned with determining the S-wave velocity of the bedrock at this site. If accurate bedrock depth was required, then S-wave velocity

of the sediments would have been constrained using surface wave data and constrained in the refraction model.

- The P-wave seismic refraction survey design for arrays BLO-1 and BLO-3 allowed P-wave velocity to be imaged to a maximum depth of about 13 and 17 m, respectively. The P-wave velocity of the sediments overlying rock is better constrained in the P-wave velocity model for the shorter array BLO-1. As discussed previously, the P-wave first arrival was very weak in both data sets, which will result in larger error in modeled velocity structure. Both velocity models are similar, exhibiting a thin low velocity soil layer over high velocity bedrock with some weathering in the uppermost bedrock. Bedrock P-wave velocities may exceed 5,000 m/s at depths on the order of 5 to 12 m. Bedrock velocities as high as 5,800 m/s occur in the model for array BLO-3; however, this data set can be modeled with a maximum P-wave velocity of 5,000 m/s with minimum change in RMS error. Seismic refraction data acquired at a location with slightly deeper rock may yield a stronger bedrock first arrival data and more accurate estimates of P-wave velocity of the rock.
- The S-wave seismic refraction survey design for array BLO-3 allowed S-wave velocity to be imaged to a maximum depth of about 20 m. The S-wave velocity of the thin soil layer could not be accurately constrained and resulting bedrock depth should only be considered approximate. Bedrock depth was not a target of this investigation and, if it was, soil velocity would have been constrained using surface wave data. The seismic refraction model indicates that S-wave velocity is about 200 m/s at the surface and increases to over 1,000 m/s at a depth of about 3.5 m and over 2,500 m/s at a depth of about 9 to 13 m. The maximum S-wave velocities in the model are about 2,800 m/s. The S-wave velocity of the soil layer may be slightly overestimated with bedrock depth being closer to 2 to 3 m beneath array BLO-3. The bedrock first arrival was much stronger in the S-wave seismic refraction data and could be picked to a reasonable degree of accuracy.
- V_{S30} was estimated between 43 and 142 m on the S-wave refraction model, where depth of investigation is greatest, by projecting the velocity at 20 m depth to 30 m depth. S-wave velocity is very high at a depth of 20 m and not expected to increase significantly between 20 and 30 m. Over this interval V_{S30} ranges from about 1,162 to 1,251 m/s, a 7% variation.
- An average V_S model was developed over the 43 to 142 m distance interval by horizontally averaging the travel time of each model cell and cell thickness and average V_{S30} was determined to be 1,202 m/s. V_{S30} is significantly impacted by the thin, low velocity soil layer overlying rock. Because the seismic station is coupled to rock via a concrete pier, the average S-wave velocity of the upper 30 m of rock is of primary interest. The average V_S between 3.5 and 33.5 m, to account for the seismic sensor being coupled to rock, is 2,317 m/s. To address possible errors in the estimated V_S of bedrock, V_{S30} was also estimated assuming a maximum V_S of 2,500 m/s for bedrock and by also assuming that the V_S of the half space is 3,000 m/s. A maximum V_S of 2,500 m/s for bedrock would change V_{S30} to 2,195 m/s, a 5% reduction. Increasing V_S of the half space to 3,000 m/s would change V_{S30} to 2,384 m/s, a 3% increase.
- Geologic conditions at the site (i.e. very shallow high velocity rock) were not conducive to successful application of passive surface wave techniques.

- Surface wave techniques were not expected to be effective at this site due to the thin soil layer overlying high velocity bedrock. Additionally, surface wave techniques were not expected to be able to accurately estimate V_S of the shallow bedrock unit. MASW (Rayleigh wave) and MALW (Love wave) data were collected along array BLO-1 and generally found to not be useful. MALW data were collected along array BLO-2. These data were of much better quality than that acquired along array BLO-1 and could be used to estimate bedrock depth and the V_S of the sediments overlying bedrock; neither of which was of interest at this site. Given the shallow depth to bedrock, better MALW data would be obtained along a shorter array to minimize the effects of variable bedrock depth. MALW collected along BLO-2 were not reduced and modeled as we believe that the S-wave seismic refraction data provide a more accurate estimate of the S-wave velocity of bedrock in this geologic environment.
- For the purpose of site characterization, we recommend using the average S-wave velocity structure of the bedrock between 43 and 142 m on the S-wave seismic refraction model for array BLO-3.
- In summary, V_{S30} beneath the central portion of S-wave seismic refraction array BLO-3 is 1,202 m/s (NEHRP Site Class B). HVSR data indicates that bedrock is about 20% shallower in the vicinity of array BLO-1, which would increase V_{S30} by about 10%. V_{S30} of the bedrock unit (average V_S between 3.5 and 33.5 m in the S-wave refraction model for array BLO-3) is 2,317 m/s (NEHRP Site Class A).
- The seismic refraction technique is not capable of detecting velocity inversions; therefore, review of available geologic data from the area is recommended to confirm that geologic layers that may have lower seismic velocities are not present in the upper 30 m.

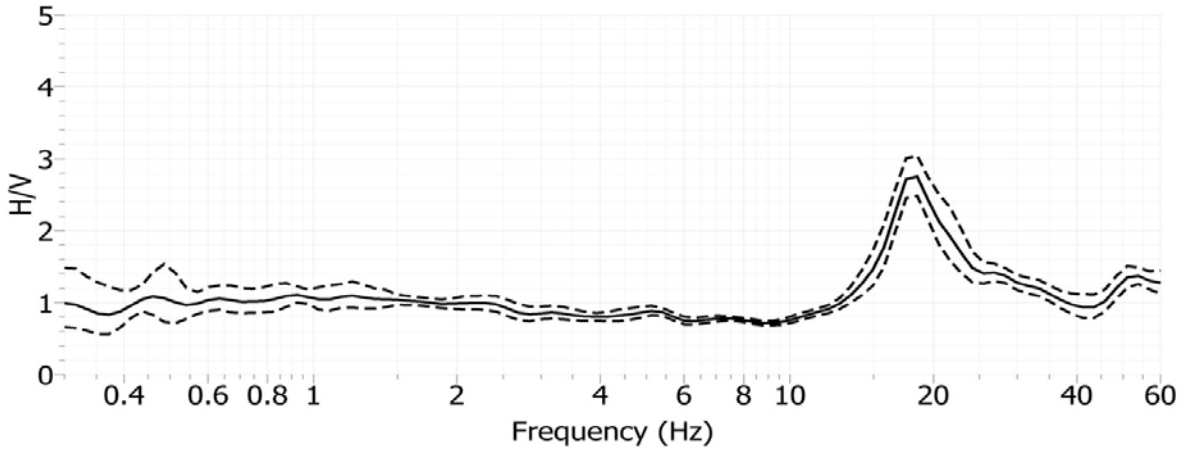

Site NM.BLO, H/V Spectral Ratio, Array BLO-2, SensorTRO-3A

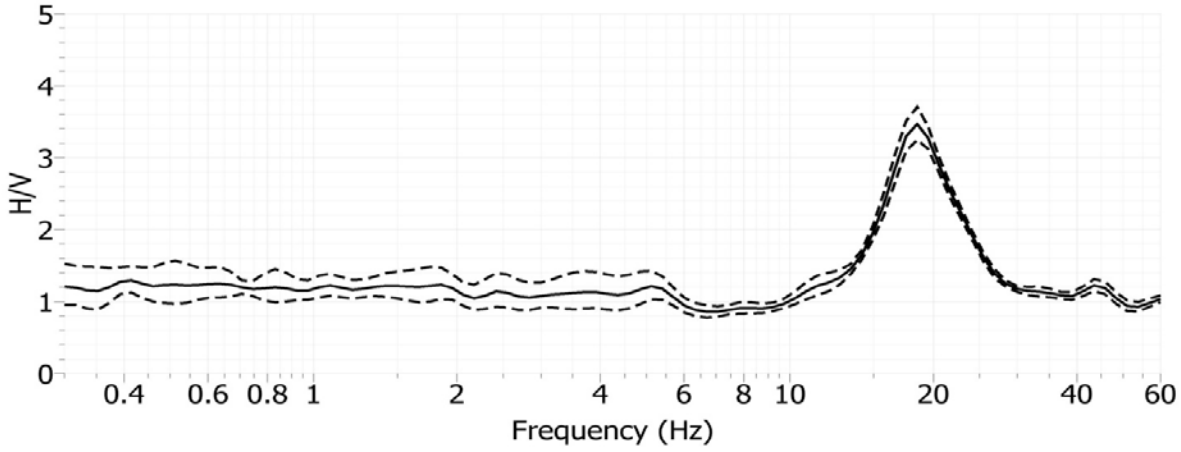

Site NM.BLO, H/V Spectral Ratio, Array BLO-2, Sensor TRO-2A

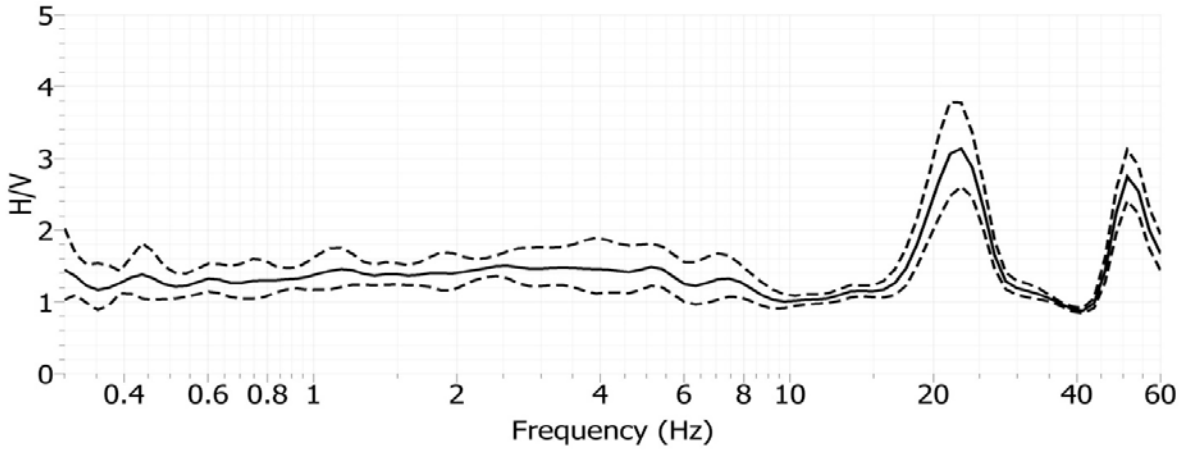

Site NM.BLO, H/V Spectral Ratio, Array BLO-2, Sensor TRO-1A

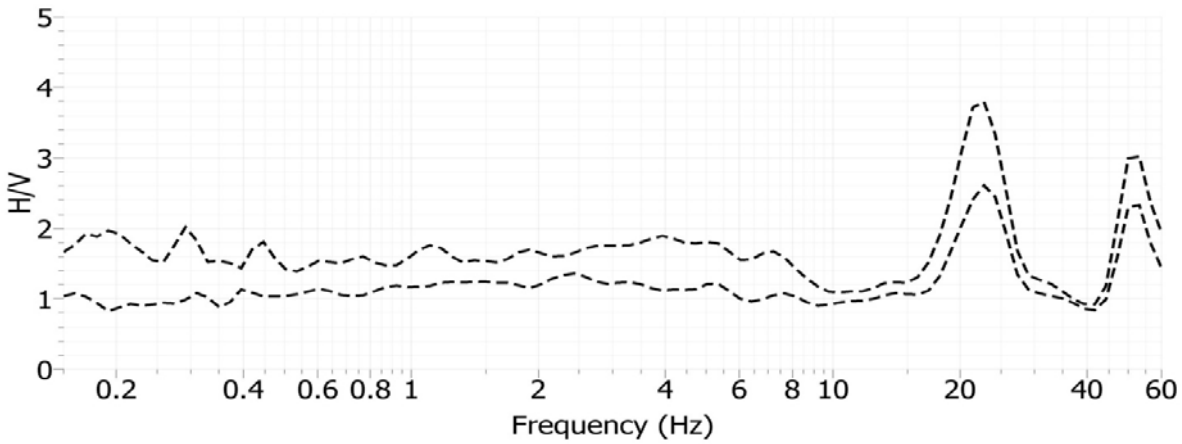

Site NM.BLO, H/V Spectral Ratio, Near Seismic Station, Sensor TRO-3

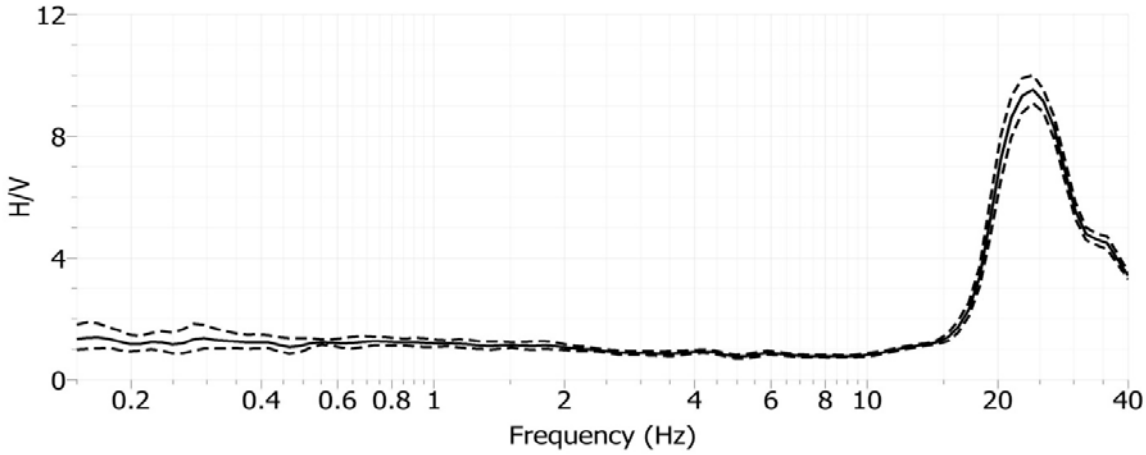

Site NM.BLO, H/V Spectral Ratio, Array BLO-1, Sensor TRO-2

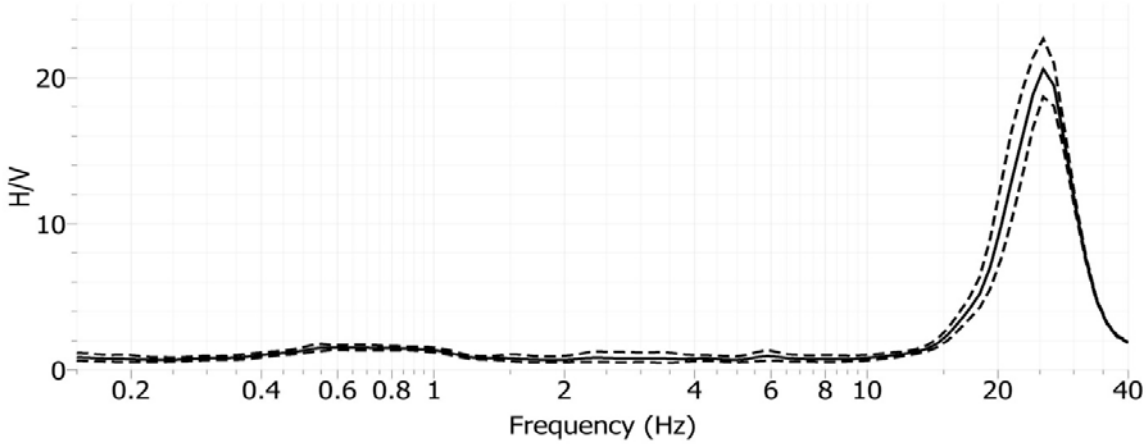

Site NM.BLO, H/V Spectral Ratio, Array BLO-1, Sensor 453

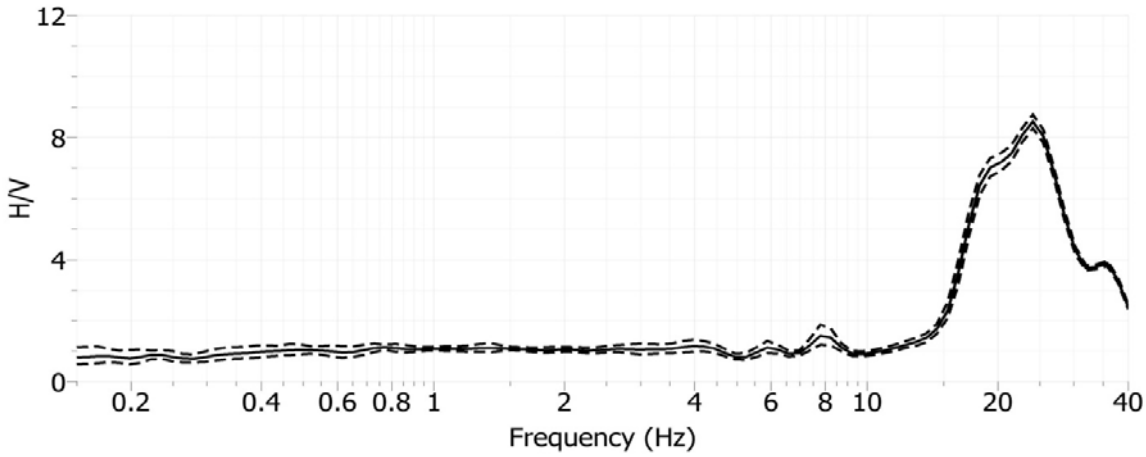

Site NM.BLO, H/V Spectral Ratio, Array BLO-1, Sensor TRO-1

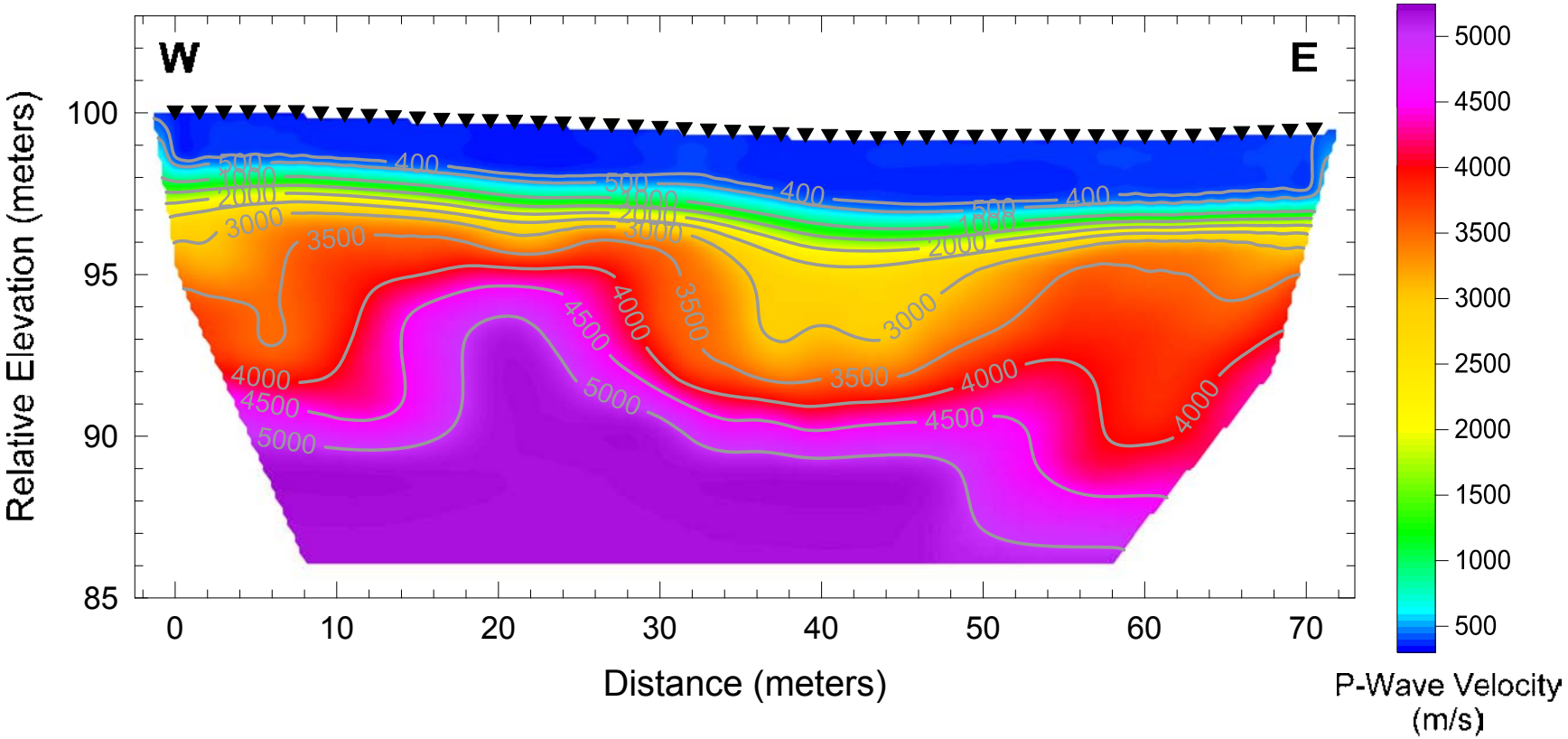

Array BLO-1 – P-wave Tomographic Seismic Refraction Model Developed using a Layer-Based Starting Model

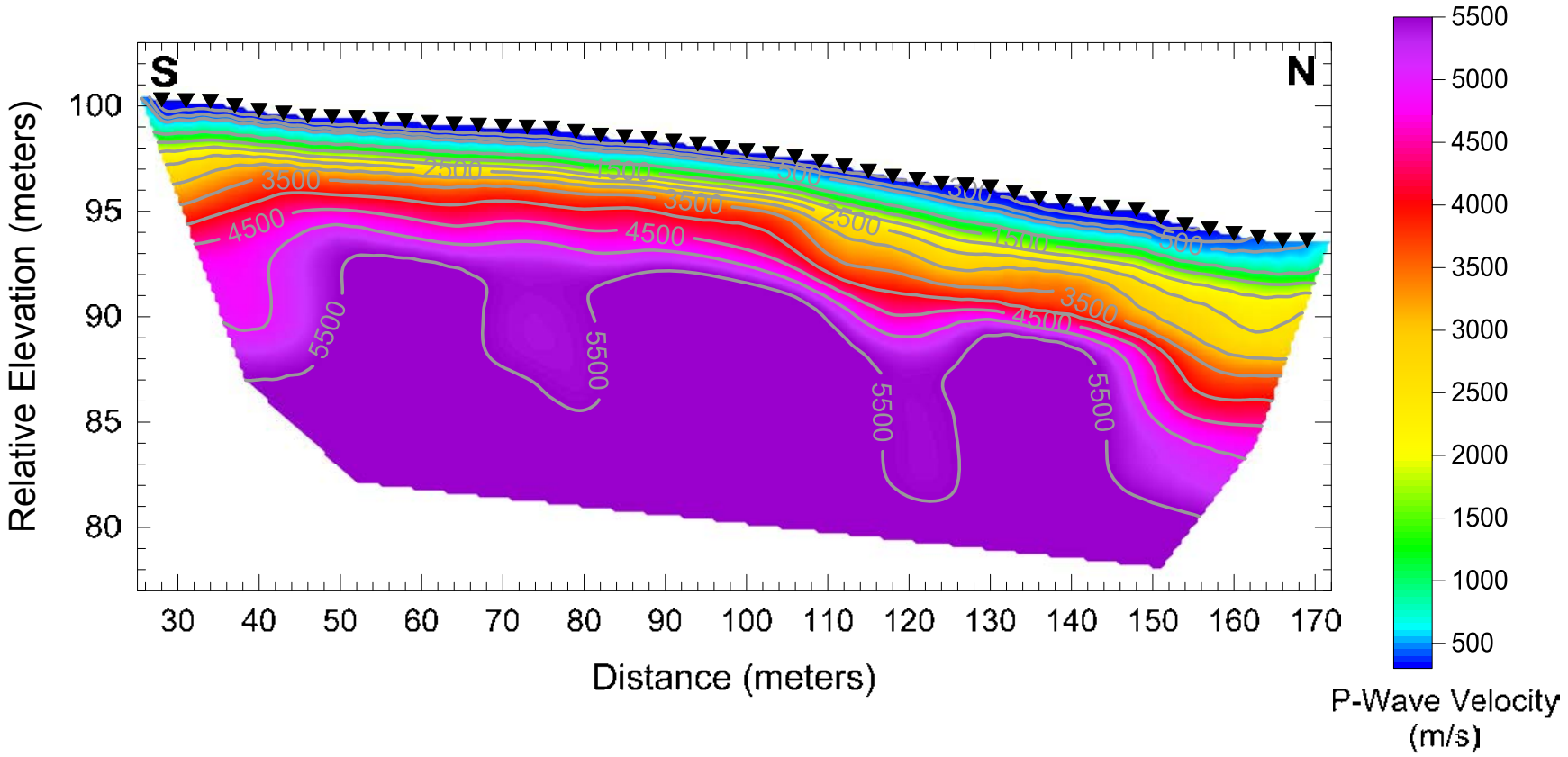

Array BLO-3 – P-wave Tomographic Seismic Refraction Model Developed using a Layer-Based Starting Model

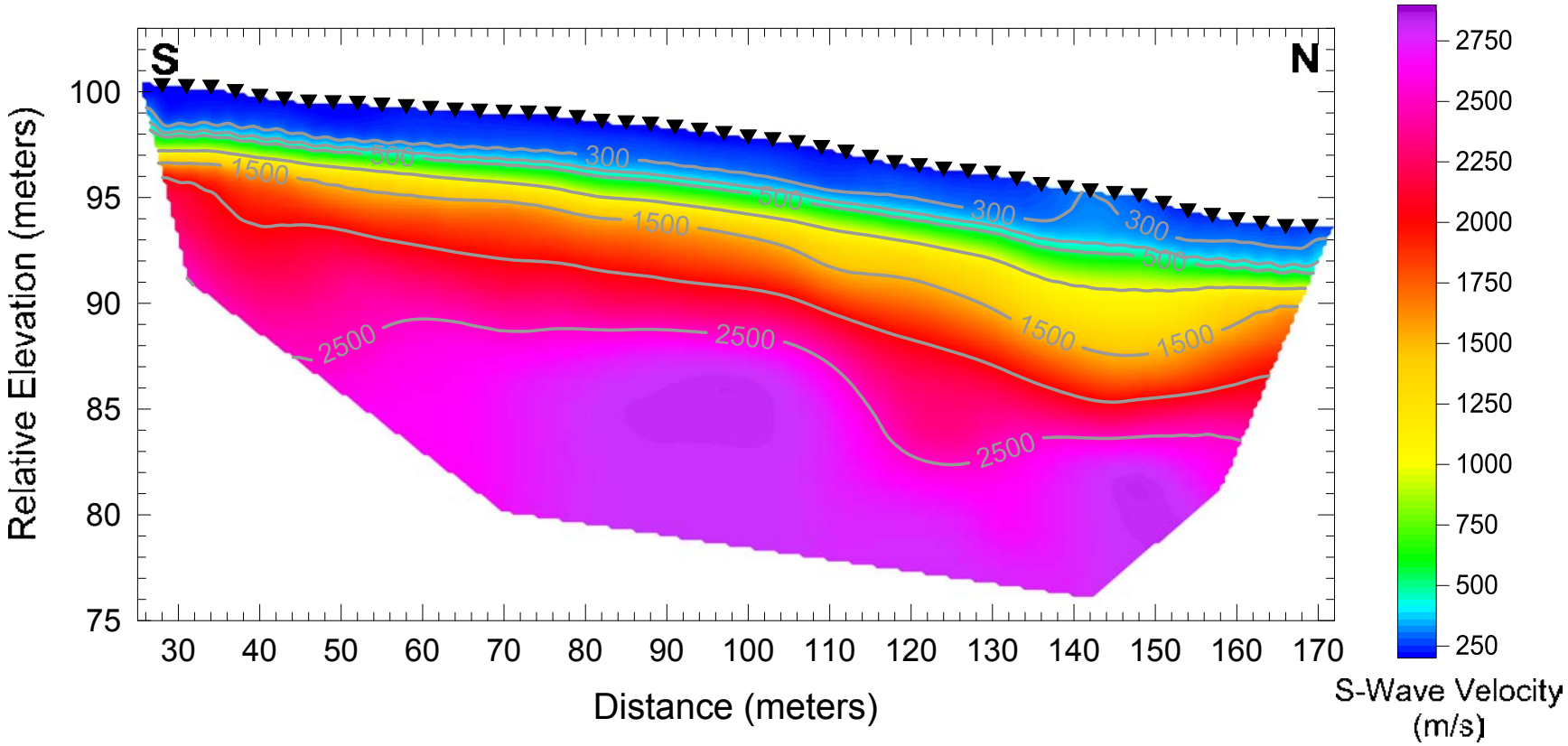

Array BLO-3 – S-wave Tomographic Seismic Refraction Model Developed using a Layer-Based Starting Model

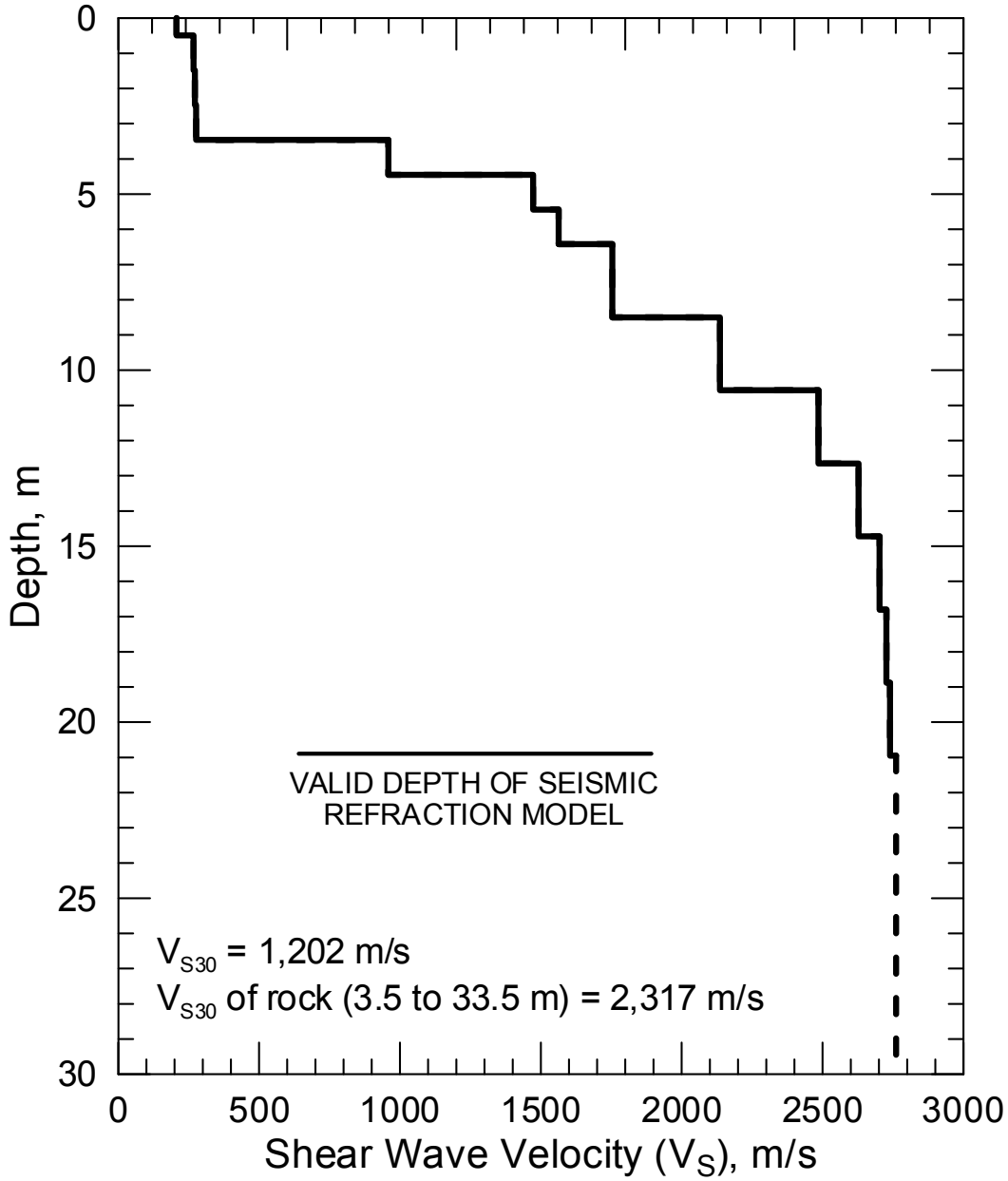

NM.BLO – Average S-wave velocity structure between 43 and 142 m on S-wave seismic refraction array BLO-3. Although seismic refraction depth of investigation is limited to about 20 m, S-wave velocity is very high at 20 m depth and not expected to increase significantly between 20 and 30 m.

Site NM.JCMO

Location: Jefferson College, Hillsboro, Missouri

Latitude: 38.25749 **Longitude:** -90.55847
(Station coordinates provided by USGS, WGS84 coordinate system)

V_{S30} (measured): 768 m/s (approximate ±15% variation along array JCMO-1 with V_{S30} at the seismic station likely being slightly lower than the average value presented, based on HVSR peak frequency).

V_{S30} (adjusted to more accurately reflect seismic station conditions): 902 m/s (average S-wave velocity between 1 and 31 m adjusting for assumed 1 m sensor depth. Approximate ±15% variation along array JCMO-1 with adjusted V_{S30} at the seismic station likely being slightly lower than the average value presented, based on HVSR peak frequency).

NEHRP Site Class: B

Geomatrix Code: LZA

Geologic Conditions/Observations: Seismic station located on a thin soil layer overlying a geologic unit mapped as Paleozoic (Ordovician) Jefferson City Dolomite.

Site Conditions: Suburban site located on gently rolling hills with nearby college dormitories. Testing location was along the side of a road where ground surface elevation decreases about 2 m to the northeast along the 70.5 m long MASW and seismic refraction array.

Geophysical Methods Utilized: HVSR, Seismic Refraction (P- and S-wave), MASW (Rayleigh Wave), MALW (Love Wave)

Geophysical Testing Arrays:

1. Array JCMO-1 (48 channel MASW and P-wave seismic refraction array utilizing 4.5 Hz vertical geophones spaced 1.5 m apart for a length of 70.5 m, forward and reverse shot locations with multiple source offsets and source types and multiple interior shot locations).
2. Array JCMO-1 (48 channel S-wave seismic refraction array utilizing 4.5 Hz horizontal geophones spaced 1.5 m apart for a length of 70.5 m, coincident with P-wave seismic refraction and MASW array of same name).
3. Four HVSR measurement locations: three distributed along array JCMO-1 and one adjacent to the seismic station.

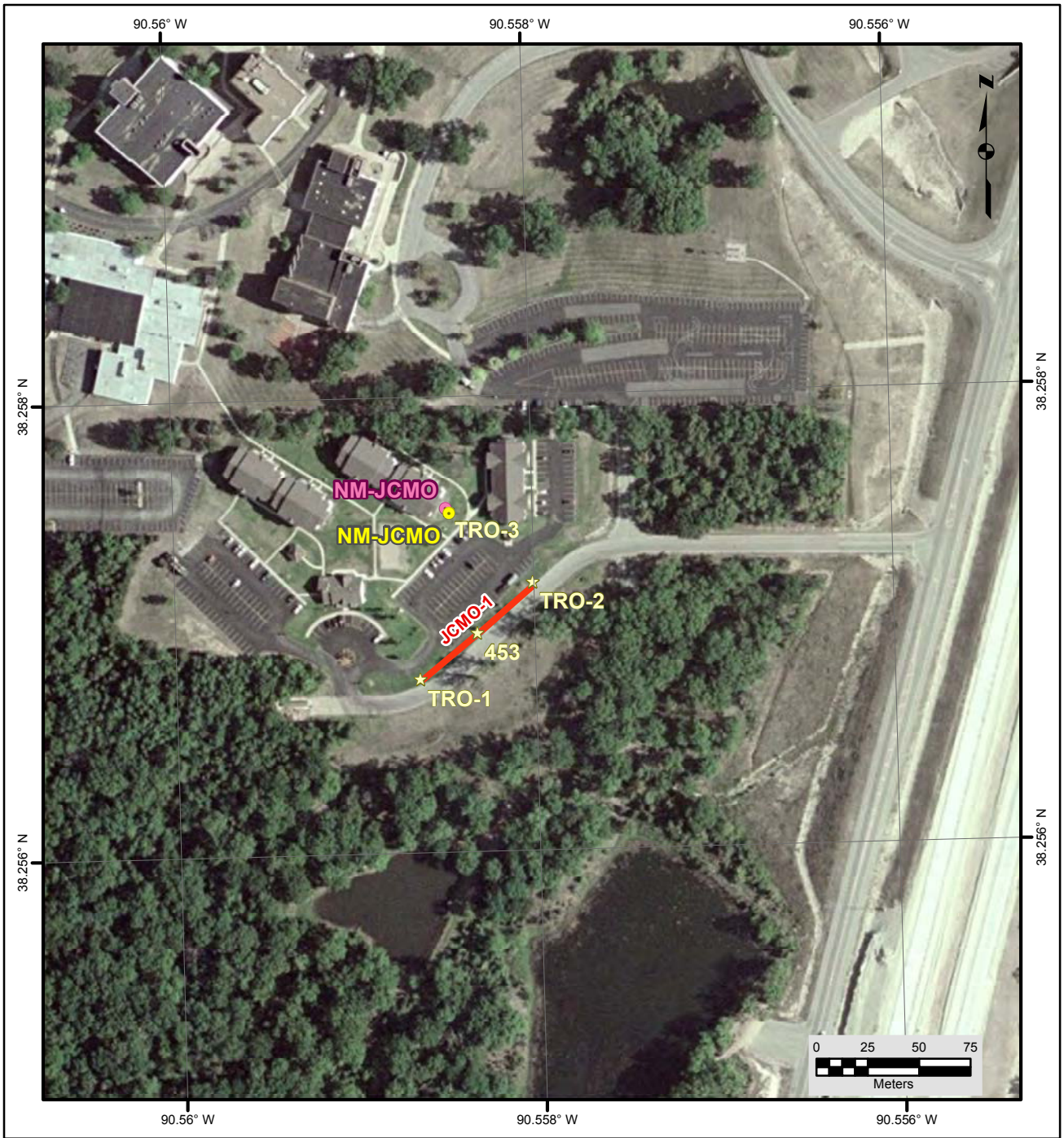

Legend

- Seismic Station - Approximate Surveyed Location
- Seismic Station - Approximate Location of Record
- H/V Spectral Ratio Location
- MASW and Seismic Refraction Array

NOTES:
1. WGS 1984 COORDINATE SYSTEM
2. Image Source: ESRI, i-cubed, USDA FSA, USGS, AEX, GeoEye, Getmapping, Aerogrid, IGP

File Name: NM-JCMO-I

Date: 5/10/2012

USGS science for a changing world

GEOVision geophysical services

RECOVERY.GOV

SITE MAP
NM•JCMO

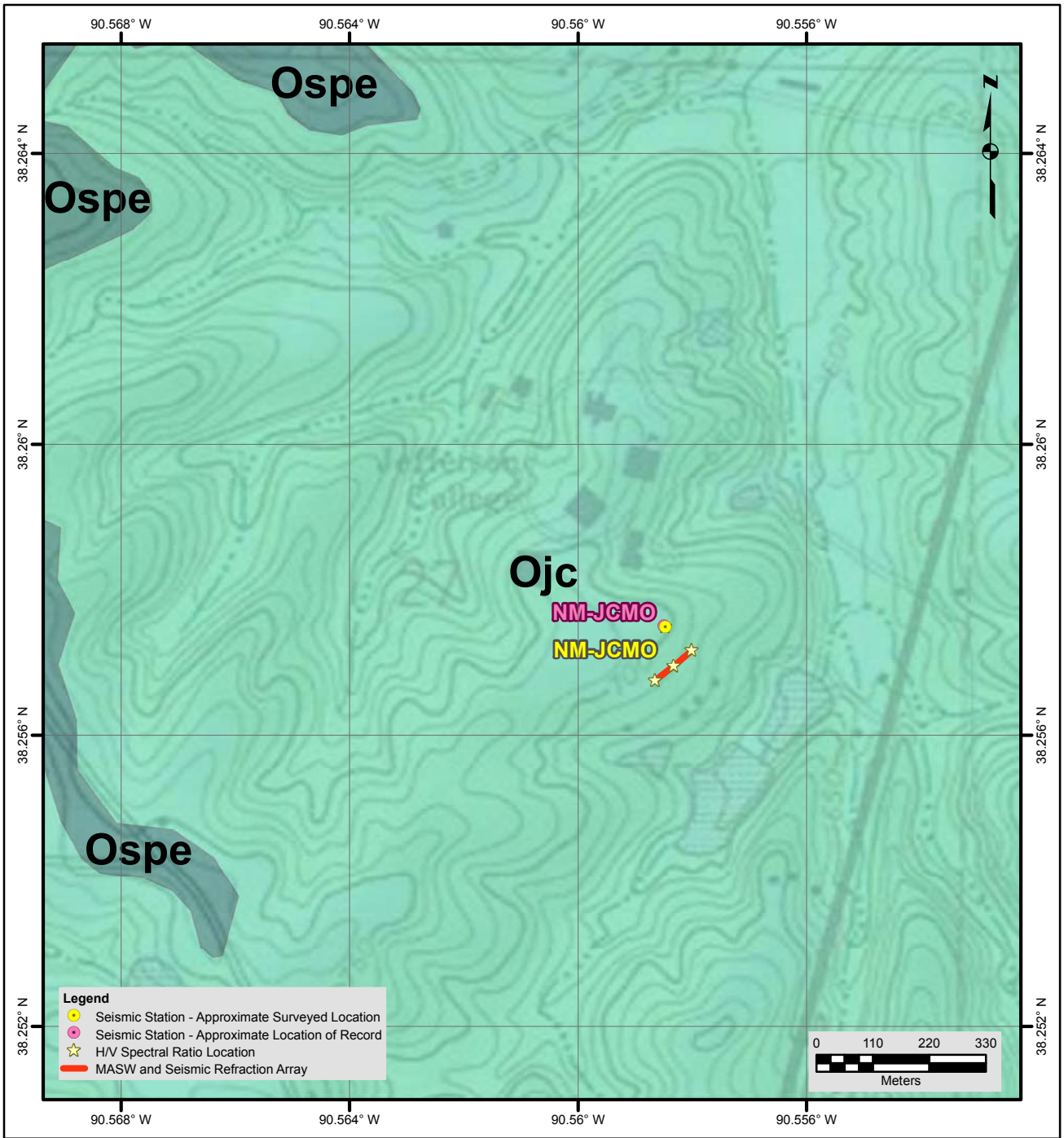

Description of Geologic Map Units

Ospe = Paleozoic (Early to Middle Ordovician) Everton Formation; dolomite with interbedded limestone and sandstone
Ojc = Paleozoic (Early Ordovician) Jefferson City Dolomite; fine crystalline, silty, cherty dolomite, and oolitic chert with local sandstone beds

NOTES:
1. WGS 1984 COORDINATE SYSTEM
2. Geologic Map of Missouri
Bruce R. Johnson and Beth Leveritch, 1998,
M.A. Middendorf 2003
3. See site map for details of geophysical survey

File Name: NM-JCMO

Date: 5/10/2012

USGS science for a changing world

GEOVision geophysical services

GEOLOGIC MAP
NM•JCMO

RECOVERY.GOV

NM.JCMO seismic station (in front of building)

NM.JCMO seismic station and HVSR sensor location TRO-3

Looking northeast along array JCMO-1 and at HVSR station TRO-1 (seismic station adjacent to building at top left)

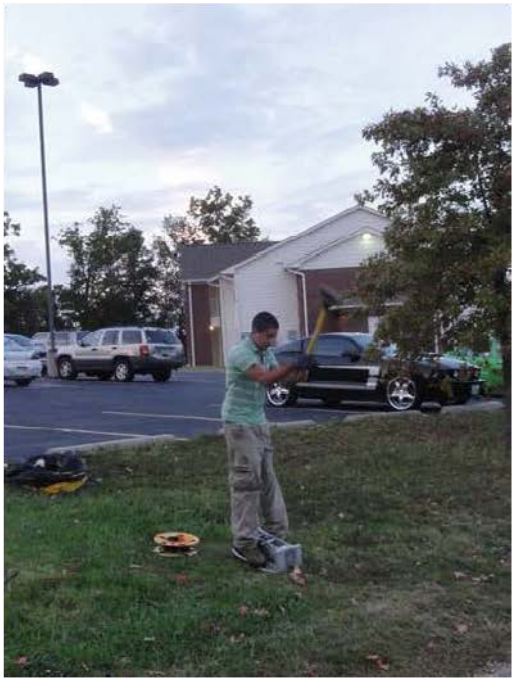

S-wave seismic refraction and MALW data acquisition on array JCMO-1

Looking southwest along array JCMO-1

Location of Geophysical Testing Arrays:

Location	Latitude	Longitude
JCMO-1, Southwest End of MASW/Refraction Array	38.25676	-90.55864
JCMO-1, Northeast End of MASW/Refraction Array	38.25716	-90.55802
HVSR Sensor TRO-1 (Micromed Tromino ENGY)	38.25676	-90.55865
HVSR Sensor TRO-2 (Micromed Tromino ENGY)	38.25718	-90.55801
HVSR Sensor TRO-3 (Micromed Tromino ENGY)	38.25750	-90.55848
HVSR Sensor 453 (Nanometrics Trillium Compact)	38.25696	-90.55833
NM.JCMO Seismic Station	38.25749	-90.55847

Notes: 1) WGS84 Coordinate System (decimal degrees)
2) Survey accuracy is estimated at 1 to 2 m

Results:

MALW V_S Model 1 (Average Dispersion Curve)

Depth to Top of Layer (m)	Layer Thickness (m)	S-Wave Velocity (m/s)	Inferred P-Wave Velocity (m/s)	Inferred Poisson's Ratio	Inferred Density (g/cm^3)
0	0.5	115	215	0.3	1.60
0.5	1.5	245	459	0.3	1.70
2	2	286	536	0.3	1.80
4	3	775	1449	0.3	2.10
7	4	946	1769	0.3	2.15
11	5	1136	2125	0.3	2.20
16	6	1342	2510	0.3	2.30
22	>8	1724	3225	0.3	2.40

Notes: 1) Depth of investigation is about 30 m.
2) Bottom layer is a half space.

MALW V_S Model 2 (Lower Envelope of Dispersion Curve)

Depth to Top of Layer (m)	Layer Thickness (m)	S-Wave Velocity (m/s)	Inferred P-Wave Velocity (m/s)	Inferred Poisson's Ratio	Inferred Density (g/cm^3)
0	0.5	112	209	0.3	1.60
0.5	2	252	471	0.3	1.70
2.5	2	283	529	0.3	1.80
4.5	3.5	797	1490	0.3	2.10
8	4	908	1698	0.3	2.15
12	5	1002	1875	0.3	2.20
17	7	1071	2005	0.3	2.20
24	>6	1381	2584	0.3	2.30

Notes: 1) Depth of investigation is about 30 m.
2) Bottom layer is a half space.

MALW V_S Model 3 (Upper Envelope of Dispersion Curve)

Depth to Top of Layer (m)	Layer Thickness (m)	S-Wave Velocity (m/s)	Inferred P-Wave Velocity (m/s)	Inferred Poisson's Ratio	Inferred Density (g/cm^3)
0.0	0.5	119	223	0.3	1.60
0.5	1.5	225	420	0.3	1.70
2.0	1.5	315	589	0.3	1.80
3.5	3.0	687	1284	0.3	2.10
6.5	4.0	920	1721	0.3	2.15
10.5	5.0	1518	2839	0.3	2.25
15.5	6.0	2066	3864	0.3	2.40
21.5	>8.5	2406	4499	0.3	2.50

Notes: 1) Depth of investigation is about 30 m.
2) Bottom layer is a half space.

Observations/Discussion:

- Array JCMO-1 located about 50 m southeast of the seismic station. Both P- and S-wave seismic refraction, MASW and MALW data were acquired along array JCMO-1. P- and S-wave seismic refraction data are of very poor quality, due to combination of noise and complex velocity structure, and reliable interpretations of the seismic refraction data could not be made. Preliminary modeling of the seismic refraction data did, however, indicate that there is significant lateral velocity variation beneath the array with P- and S-

wave velocities possibly exceeding 4,000 and 2,000 m/s at depth, respectively. Potential alternate locations with sufficient space for testing are located much further from the seismic station and generally have different ground surface elevation. At a minimum, it should be possible to acquire good quality S-wave refraction and MALW data in an area with more 1-D geologic structure. However, given the degree of lateral velocity variation beneath array JCMO-1, velocity structure from distant test locations could not be correlated to the seismic station unless multiple testing locations demonstrate that the lateral velocity variation is limited to the area around array JCMO-1. The HVSR technique could be used to locate an area with similar HVSR response to the seismic station; however, it would still be possible that the bedrock has different velocity structure. If significant lateral velocity variation is typical of the site, then a borehole velocity log adjacent to the seismic station would be the only way to accurately determine velocity structure beneath the seismic station.

- Three HVSR measurements were made with a Micromed Tromino ENGY: one at each end of array JCMO-1 and one near the seismic station. An HVSR measurement was also made in the center of array JCMO-1 using a Nanometrics Trillium Compact.
- HVSR data are significantly different at all measurement locations due to lateral velocity variation. The frequency of the HVSR peak at measurement locations on array JCMO-1 decreases to the northeast from a high amplitude peak at 19 Hz at sensor location TRO-1 (southwest end of the array), intermediate amplitude peak at 14 Hz at sensor location 453 (center of array) and weak peak(s) in the 5 to 8 Hz range at sensor location TRO-2 (northeast end of array). This is consistent with bedrock deepening to the northeast. The amplitude of the peaks may also indicate that bedrock is more weathered, resulting in lower seismic velocity, to the northeast. There is a weak HVSR peak at about 10 Hz adjacent to the seismic station, which could indicate that velocity structure at the seismic station, or at least bedrock depth, is most similar to the area between the center and northeast ends of array JCMO-1.
- Reliable seismic refraction models could not be developed; however, seismic refraction data does confirm that there is significant lateral velocity variation, with bedrock being slightly deeper and more weathered beneath the northeastern portion of array JCMO-1.
- Noise and geologic conditions at the site were not sufficient for application of passive surface wave techniques.
- Both MASW and MALW data were acquired along array JCMO-1. Due to the shallow high velocity bedrock there were significant issues with dominant higher modes and lateral velocity variation in the MASW data and, therefore, the MASW data were not modeled. MALW data were of much better quality than the MASW data, with dominant higher mode Love waves not appearing to be an issue. There is, however, significant scatter in the Love wave dispersion data, particularly at long wavelengths/low frequencies.
- The maximum wavelength Love wave phase velocity data extracted from the data set was typically set equal to the lesser of 90 m or 1.6 to 2 times the distance from the source to midpoint of the active receiver array. Some near field effects may occur at long wavelengths, although it should be noted that the lower and upper envelopes of the long wavelength dispersion data originate from source receiver combinations with the largest distance from the source to midpoint of the receiver array and it is clear that the scatter in the dispersion data is not attributed to near field effects.

- The minimum wavelength surface wave phase velocity data extracted from the 48-channel MALW array was about 7 m, although only source locations offset from the southwest end of the array yield Love wave dispersion data over a wide frequency/wavelength range. Reducing data from smaller hammer sources using a limited offset receiver array (i.e. less active geophones) allowed for extraction of Love wave dispersion data to a minimum wavelength of about 1.5 m.
- There is significant scatter in Love wave dispersion data, particularly at long wavelengths where there is about 250 to 375 m/s of scatter. Source locations at the southwest end of the array and large offset receiver gathers (36 to 48 channels) and receiver gathers limited to the northeastern half of the array yield the lowest Love wave phase velocities at long wavelengths. The scatter in the dispersion data is so extreme that a single V_S model that accurately represents subsurface velocity structure cannot be developed. Rather a range of models that may represent subsurface velocity structure are developed.
- A representative dispersion curve was generated for the MASW data set using a moving average, polynomial curve fitting routine and used for modeling.
- Dispersion curve segments defining the lower and upper envelope of the dispersion curve at long wavelengths were also combined and a representative dispersion curve developed for each.
- Because of the significant lateral velocity variation beneath array JCMO-1, three models were developed for the MALW data set to explore the variation in V_{S30}. Model 1 fits the representative dispersion curve and is, therefore, considered the average V_S model for the array. Models 2 and 3 fit the lower and upper envelopes of the Love wave dispersion data, respectively.
- Surface wave depth of investigation is about 30 m based on one-third of the maximum wavelength criteria.
- V_{S30} is 768, 680 and 880 m/s for MASW V_S Models 1 (average), 2 (lower envelope) and 3 (upper envelope), respectively (NEHRP Site Class C to B).
- Average S-wave velocity between 1 m (assumed sensor depth) and 31 m is 902, 781 and 1,068 m/s for MALW V_S Models 1 to 3, respectively (NEHRP Site Class B).
- For the purpose of site characterization, we recommend using MALW V_S Model 1, the V_S model developed from the average representative dispersion curve. Based on the HVSR peak near the seismic station and the HVSR peaks along array JCMO-1, V_{S30} at the seismic station may be slightly lower than that from Model 1; however, adjusted V_{S30} at the seismic station is clearly in the NEHRP Site Class B velocity range.
- In summary, V_{S30} is estimated to be about 768 m/s (NEHRP Site Class B) and adjusted V_{S30} is 902 m/s (NEHRP Site Class B).
- Given the apparent lateral velocity variation in the site vicinity, a borehole velocity log would be required to accurately determine V_{S30} at the seismic station. There is not sufficient space for a long MALW array next to the seismic station location; however, MALW or Love wave SASW data acquisition along a short array in the available space would improve correlation of velocity structure at the seismic station to that along array JCMO-1.

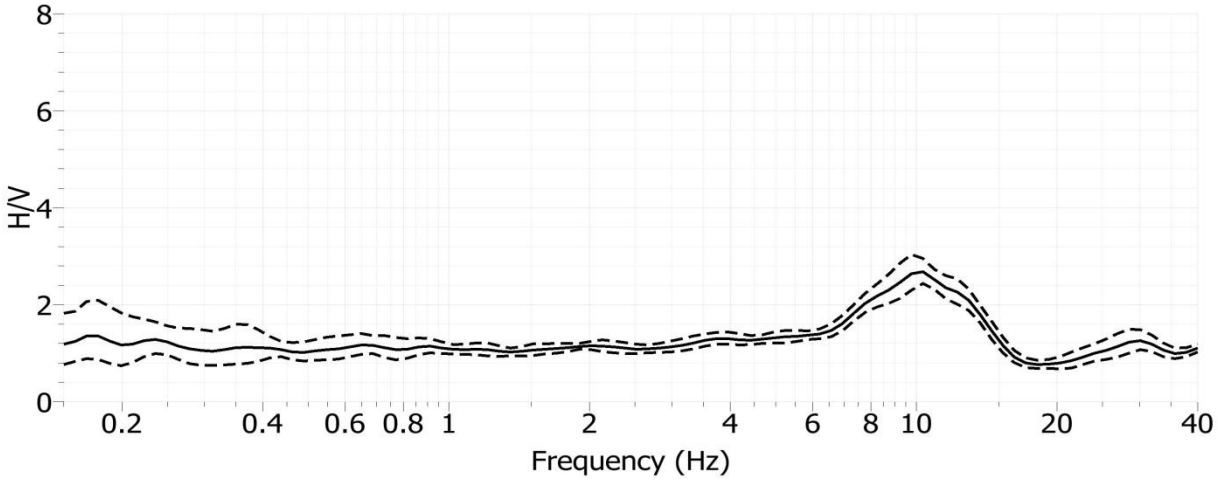

Site NM.JCMO, H/V Spectral Ratio, Near Seismic Station, Sensor TRO-3

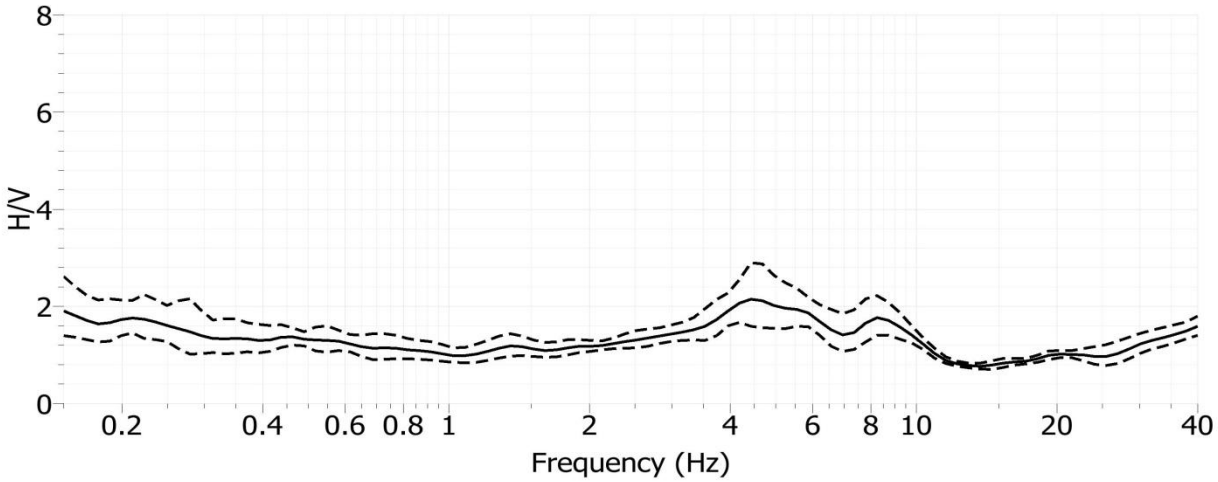

Site NM.JCMO, H/V Spectral Ratio, Array JCMO-1, Sensor TRO-2

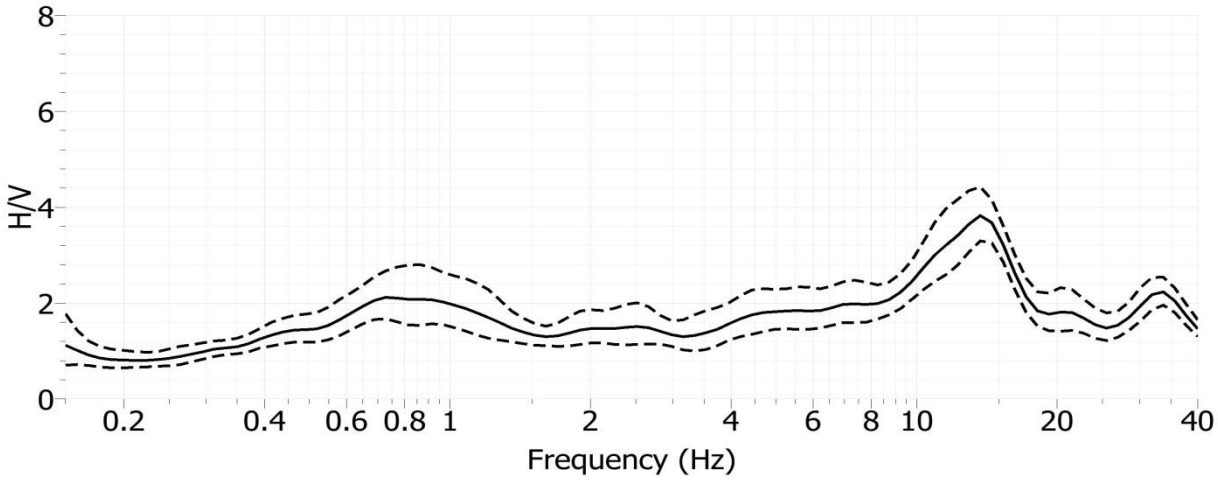

Site NM.JCMO, H/V Spectral Ratio, Array JCMO-1, Sensor 453

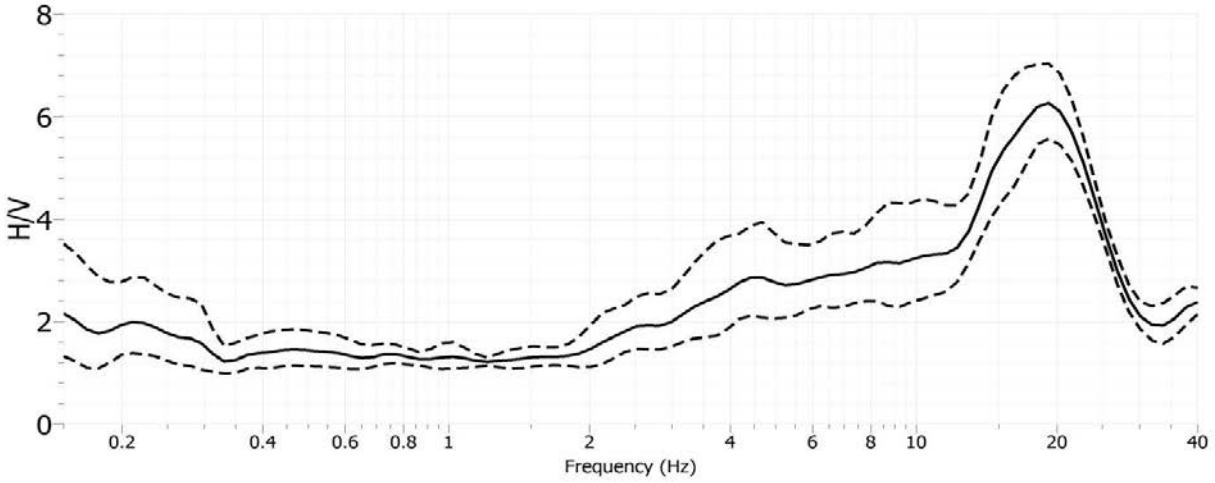

Site NM.JCMO, H/V Spectral Ratio, Array JCMO -1, Sensor TRO-1

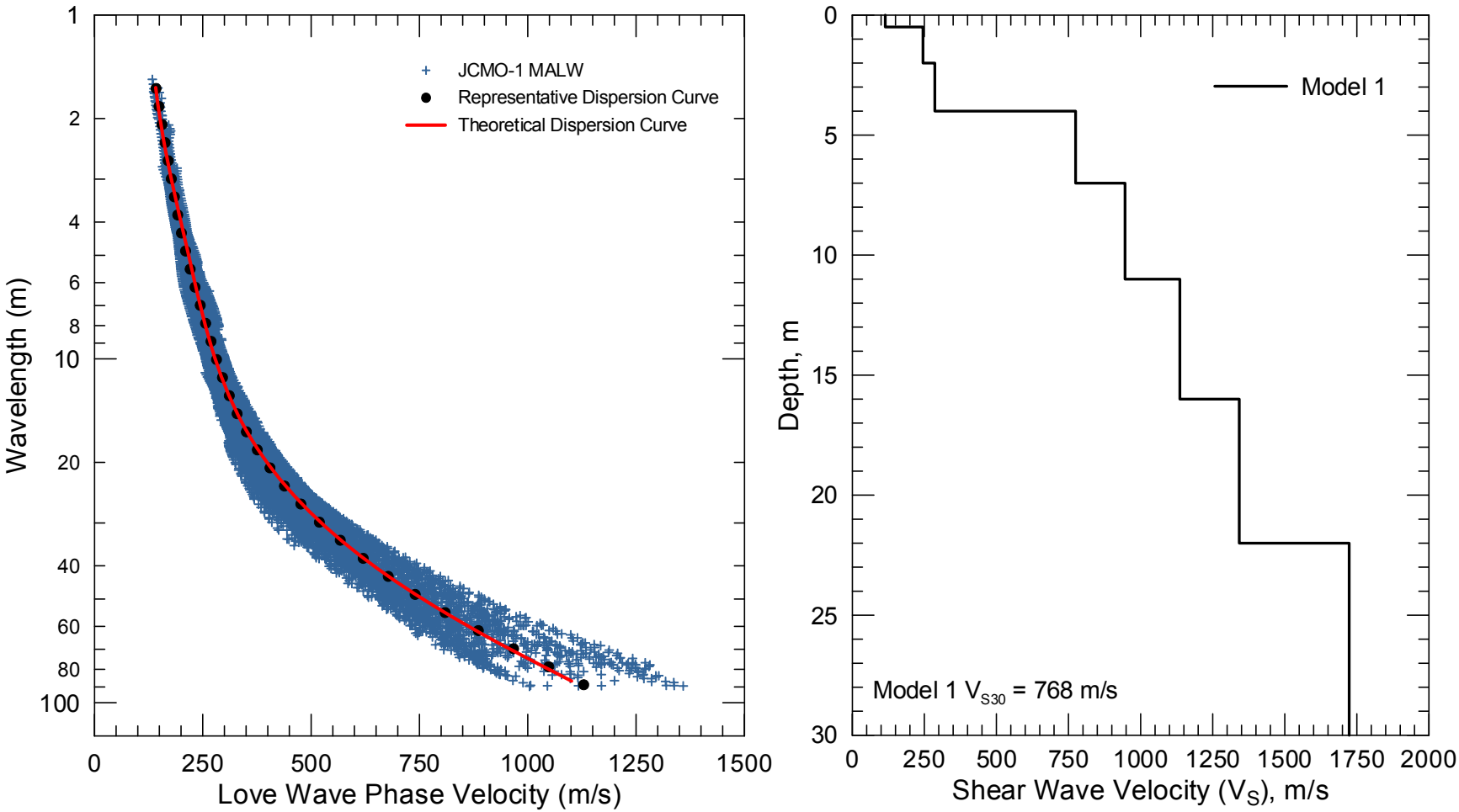

NM.JCMO - Field, representative and inverted theoretical Love wave dispersion data (left) and associated V_S model (right)

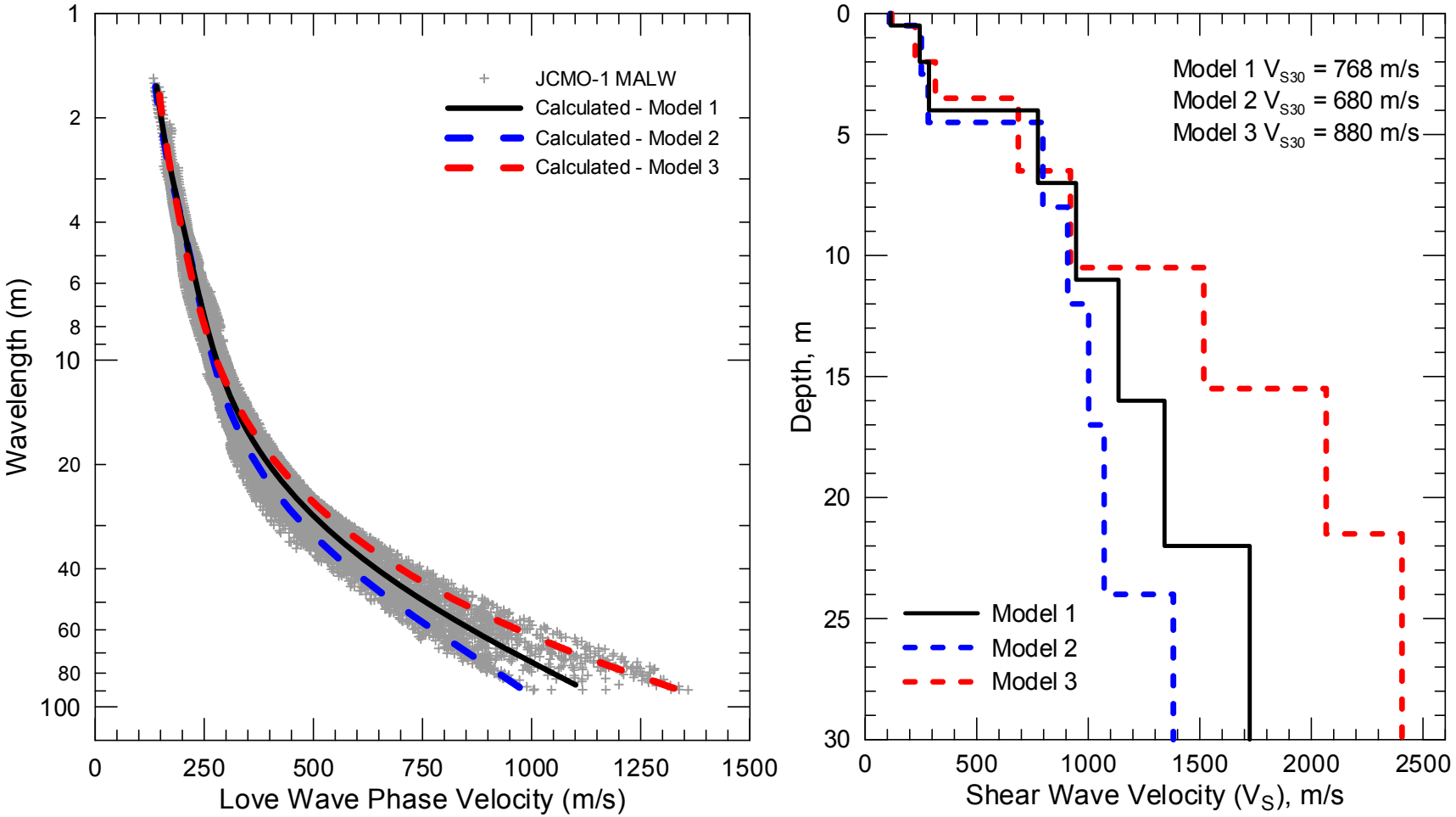

NM.JCMO – Field and calculated Love wave dispersion data (left) and associated V_S models (right) fitting average (Model 1), lower envelope (Model 2) and upper envelope (Model 3) Love wave dispersion data. There is significant lateral velocity variation beneath the surface wave array.

Site NM.PIOH

Location: Edison Community College, Piqua, Ohio

Latitude: 40.15802 **Longitude:** -84.21151
(Station coordinates modified based on observation of the seismic station location in photographs located at http://www.eas.slu.edu/eqc/eqc_netinfo/PIOH/images and identification of approximate station location on Google Earth)

V_{S30} (measured): 416 m/s

V_{S30} (adjusted to more accurately reflect seismic station conditions): 447 m/s (average S-wave velocity between 1 and 31 m to account for assumed sensor depth).

NEHRP Site Class: C

Geomatrix Code: IZB

Geologic Conditions/Observations: Site located on geologic unit mapped as Paleozoic (Ordovician) interbedded shale, limestone and dolomite. A surficial soil layer overlies rock.

Site Conditions: Suburban site located on college campus. Relatively flat terrain in immediate site vicinity.

Geophysical Methods Utilized: HVSR, MASW, Seismic Refraction

Geophysical Testing Arrays:

1. Array PIOH-1 (48 channel MASW and seismic refraction array utilizing 4.5 Hz vertical geophones spaced 1.5 m apart for a length of 70.5 m, forward and reverse shot locations with multiple source offsets and source types and multiple interior shots).
2. Three HVSR measurement locations distributed along array PIOH-1.

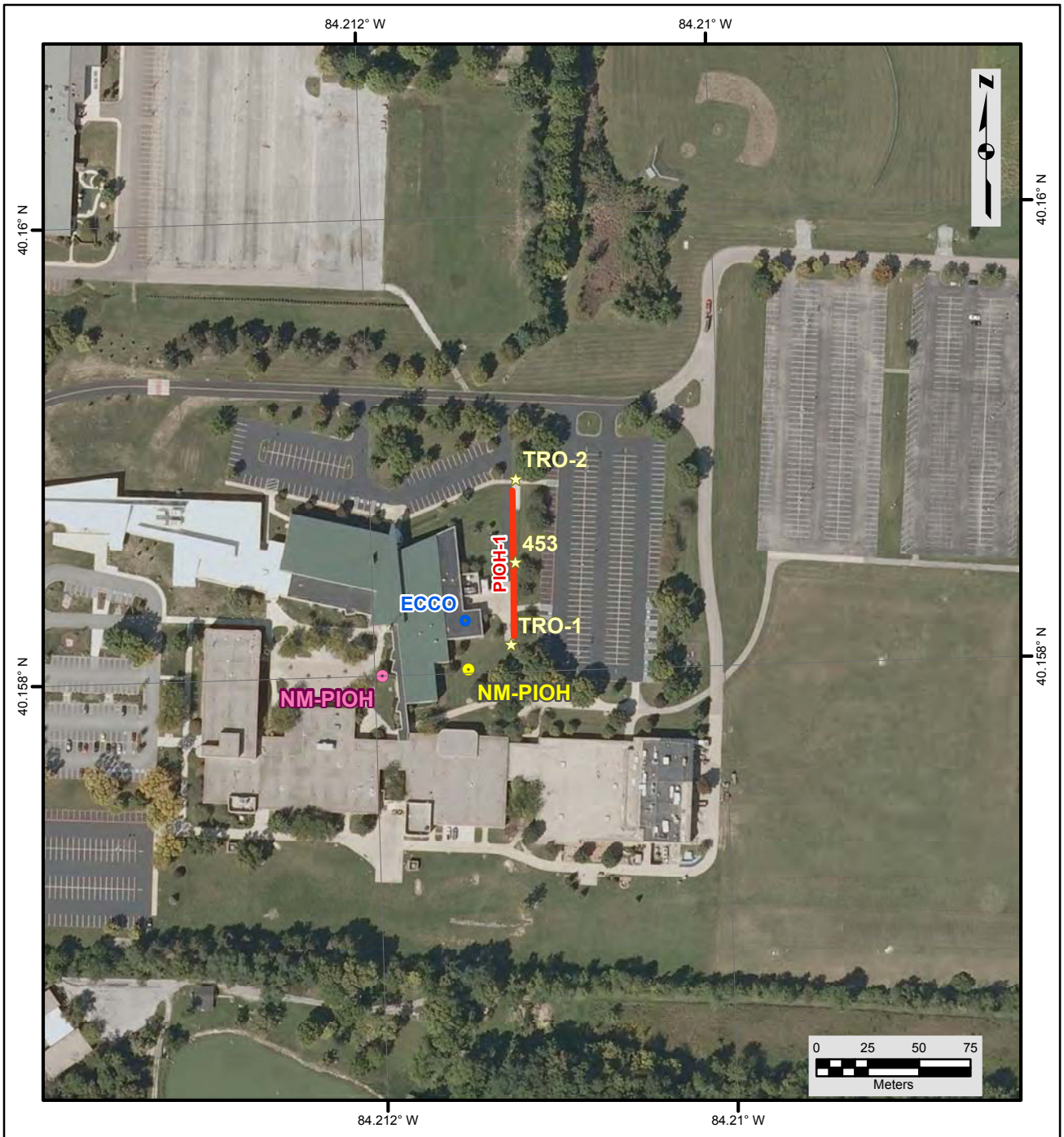

Legend

- Seismic Station - Approximate Surveyed Location
- Seismic Station - Approximate Location of Record
- OhioSeis Network Station - Approximate Surveyed Location
- H/V Spectral Ratio Location
- MASW and Seismic Refraction Array

NOTES:
1. WGS 1984 COORDINATE SYSTEM
2. Image Source: ESRI, i-cubed, USDA FSA, USGS, AEX, GeoEye, Getmapping, Aerogrid, IGP

File Name: NM-PIOH-I

Date: 4/5/2012

USGS science for a changing world

GEOVision geophysical services

RECOVERY.GOV

SITE MAP
NM•PIOH

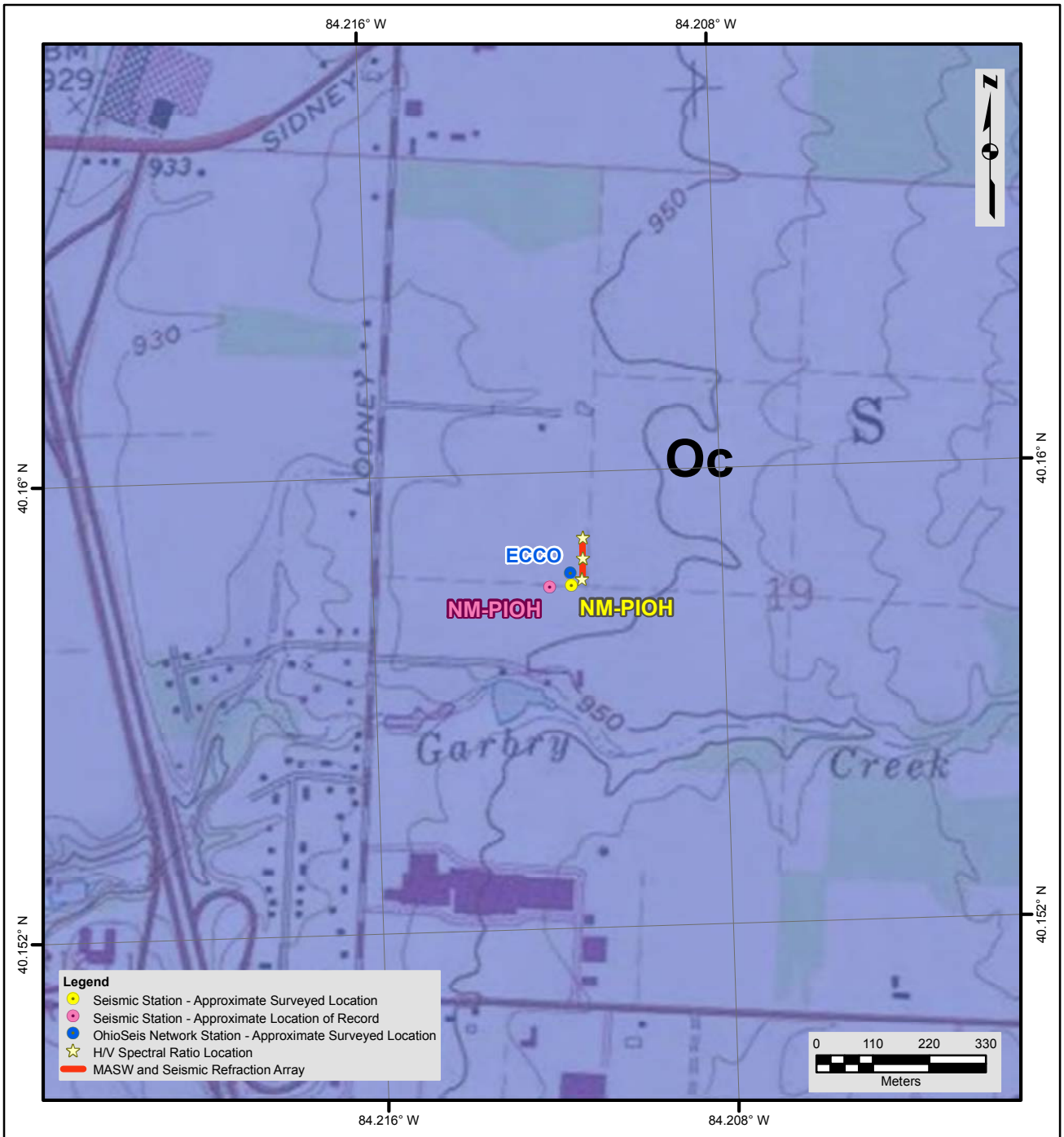

Description of Geologic Map Units

Oc = Paleozoic (Ordovician) interbedded shale, limestone and dolomite

NOTES:
1. WGS 1984 COORDINATE SYSTEM
2. Bedrock Geologic Map of Ohio
Ohio Division of Geological Survey Map BG-1, Version 6.0
compilation by E. R. Slucher, E. M. Swinford, G. E. Larsen
GIS by D. M. Powers, 2006
3. See site map for details of geophysical survey

File Name: NM-PIOH

Date: 4/5/2012

USGS science for a changing world

GEOVision geophysical services

GEOLOGIC MAP
NM•PIOH

RECOVERY.GOV

NM.PIOH seismic station
(http://www.eas.slu.edu/eqc/eqc_netinfo/PIOH/images)

NM.PIOH seismic recording system and
OhioSeis Network seismic station ECCO

Looking southwest towards center of array PIOH-1
and location of seismic station

Looking northwest towards seismic
station location from source location
offset from south end of array PIOH-1

Looking north along array PIOH-1

Location of Geophysical Testing Arrays:

Location	Latitude	Longitude
PIOH-1, South End of MASW/Refraction Array	40.15816	-84.21124
PIOH-1, Center of MASW/Refraction Array	40.15848	-84.21123
PIOH-1, North End of MASW/Refraction Array	40.15879	-84.21123
HVSR Sensor TRO-1 (Micromed Tromino ENGY)	40.15812	-84.21126
HVSR Sensor TRO-2 (Micromed Tromino ENGY)	40.15885	-84.21120
HVSR Sensor 453 (Nanometrics Trillium Compact)	40.15848	-84.21122
NM.PIOH Seismic Station	40.15802	-84.21151

Notes: 1) WGS84 Coordinate System (decimal degrees)
2) Survey accuracy is estimated at 1 to 2 m.
3) Seismic station coordinates not surveyed but approximated based on field observation.

Results:

V_S Model

Depth to Top of Layer (m)	Layer Thickness (m)	S-Wave Velocity (m/s)	Inferred P-Wave Velocity (m/s)	Assumed Poisson's Ratio	Assumed Density (g/cm^3)
0	2.5	159	298	0.3	1.80
2.5	5.5	323	1800	0.483	1.90
8	7	447	1850	0.469	2.00
15	8	567	1900	0.451	2.05
23	10	732	2000	0.423	2.10
33	>2	903	2100	0.386	2.15

Notes: 1) Saturated zone with V_P = 1,800 to 2,100 m/s fixed at a depth of 2.5 m based on review of seismic refraction first arrival data.
2) Depth of investigation is about 35 m.
3) Bottom layer is a half space.
4) Half space velocity not well resolved.

Observations/Discussion:

- The actual seismic station location was not photographed or surveyed in the field as the field crew was directed to the NM.PIOH recording system and Ohio Seismic Network station ECCO. However, the seismic station could be relatively accurately located on aerial imagery on Google Earth using seismic station photographs from the web site *http://www.eas.slu.edu/eqc/eqc_netinfo/PIOH/images* as a guide.
- Three HVSR measurements were made at the site: two with a Micromed Tromino ENGY and the other with a Nanometrics Trillium Compact. HVSR plots at the three measurement locations are similar with a clear peak at 1.3 to 1.5 Hz. The HVSR amplitudes and peak frequency are, however, slightly different between the measurements made with the Tromino and Trillium. The Trillium has a HVSR peak at about 1.3 Hz relative to 1.5 Hz for the Tromino and the Trillium has a HVSR peak amplitude of about 5 relative to 2 for the Tromino. The Trillium Compact is a much lower frequency seismometer and is expected to perform better than the Tromino at low frequencies. Although we expect that the difference in HVSR data are associated with instrumentation, the possibility cannot be discounted that sensor coupling and/or lateral velocity variation also play a role.
- P-wave seismic refraction data were not modeled as the only refractor in the seismic records appeared to be a shallow water table. Seismic refraction data were, however, inspected and the saturated zone, with V_P between 1,800 and 2,100 m/s, was interpreted at a depth of 2.5 to 3.5 m.
- There is very good reflectivity in the MASW seismic records with multiple reflectors in the upper 100 m, or more.
- Noise conditions at the site did not appear adequate for successful application of passive surface wave techniques.
- The maximum wavelength extracted from a specific receiver gather was generally set to the lesser of 71 m or 1.25 times the distance from the source to midpoint of receiver gather. This is slightly more aggressive than the Yoon and Rix (2009) near field criteria. The maximum wavelength was established at 71 m because the scatter in the dispersion data associated with lateral velocity variation, near field effects, body wave effects, noise, etc. appeared to increase significantly at greater wavelengths.
- The minimum wavelength Rayleigh wave phase velocity data extracted from the 48-channel MASW array is about 9 m. Data reduction using seismic records from smaller hammer sources and a limited offset receiver array (i.e. less active geophones) allowed extraction of surface wave dispersion data to a minimum wavelength of about 1.5 m.
- There is nominally about 50 m/s scatter in the Rayleigh wave dispersion data likely due in part to lateral velocity variation.
- A representative dispersion curve was generated for the MASW data set using a moving average, polynomial curve fitting routine and used for modeling.
- The saturated zone with estimated P-wave velocity increasing with depth from 1,800 to 2,100 m/s was fixed at a depth of 2.5 m during data modeling.
- Surface wave depth of investigation is about 35 m based on one-half of maximum wavelength criteria.
- The surface wave data was modeled using the fundamental mode assumption. Subsequent evaluation of the V_S model indicated that the first higher mode would at most

have a minimal effect on measured phase velocity at only the longest measured wavelengths.

- The surface wave model shows a thin, low velocity layer up to 2.5 m thick, overlying weathered bedrock with V_S gradually increasing with depth. The surface wave V_S model indicates that near surface bedrock is very weathered at this site.
- V_{S30} is 416 m/s (NEHRP Site Class C).
- The average S-wave velocity between 1 and 31 m, to account for assumed sensor depth, is 447 m/s (NEHRP Site Class C).
- Using the quarter wavelength approximation, the geologic contact associated with the 1.3 Hz HVSR peak is located at a minimum depth of about 80 m assuming that V_{S30} represents the average V_S of the geologic units overlying the contact. V_S is expected to gradually increase below 30 m depth and, therefore, the geologic contact associated with the HVSR peak is probably greater than 100 m deep.

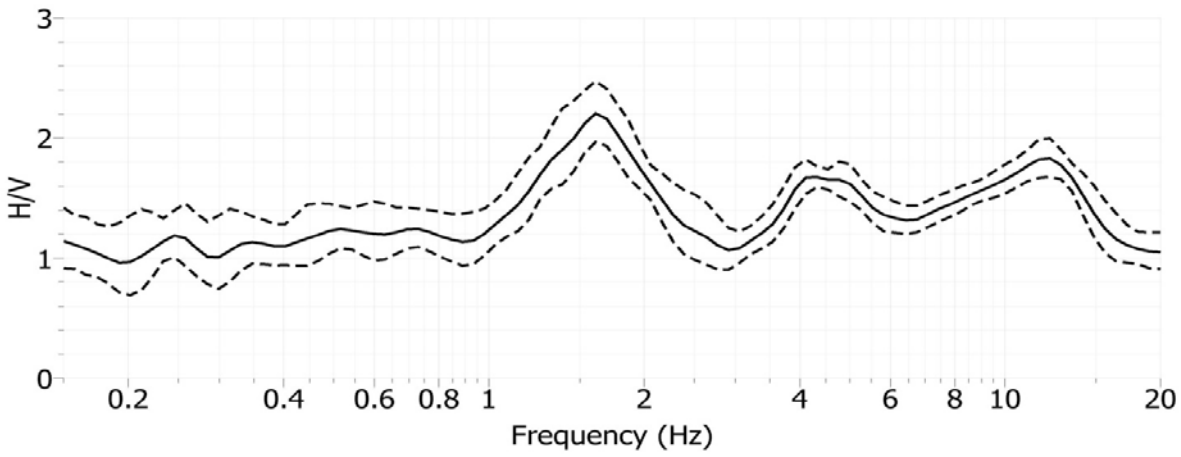

Site NM.PIOH, H/V Spectral Ratio, Array PIOH-1, Sensor TRO-2

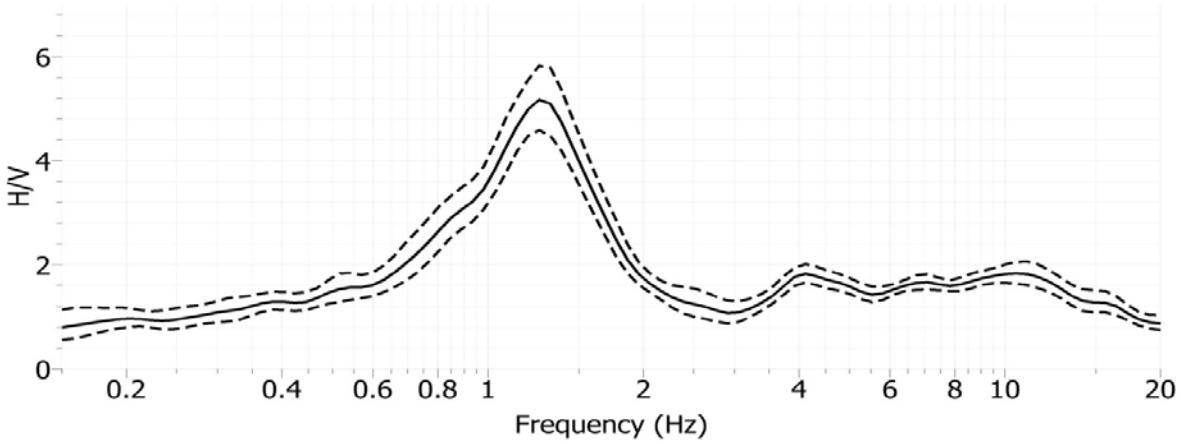

Site NM.PIOH, H/V Spectral Ratio, Array PIOH-1, Sensor 453

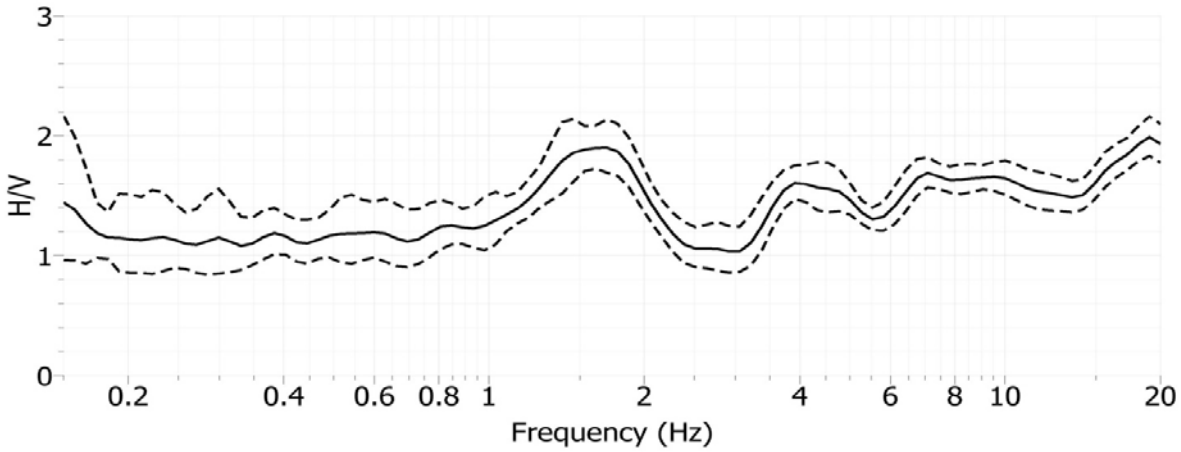

Site NM.PIOH, H/V Spectral Ratio, Array PIOH-1, Sensor TRO-1

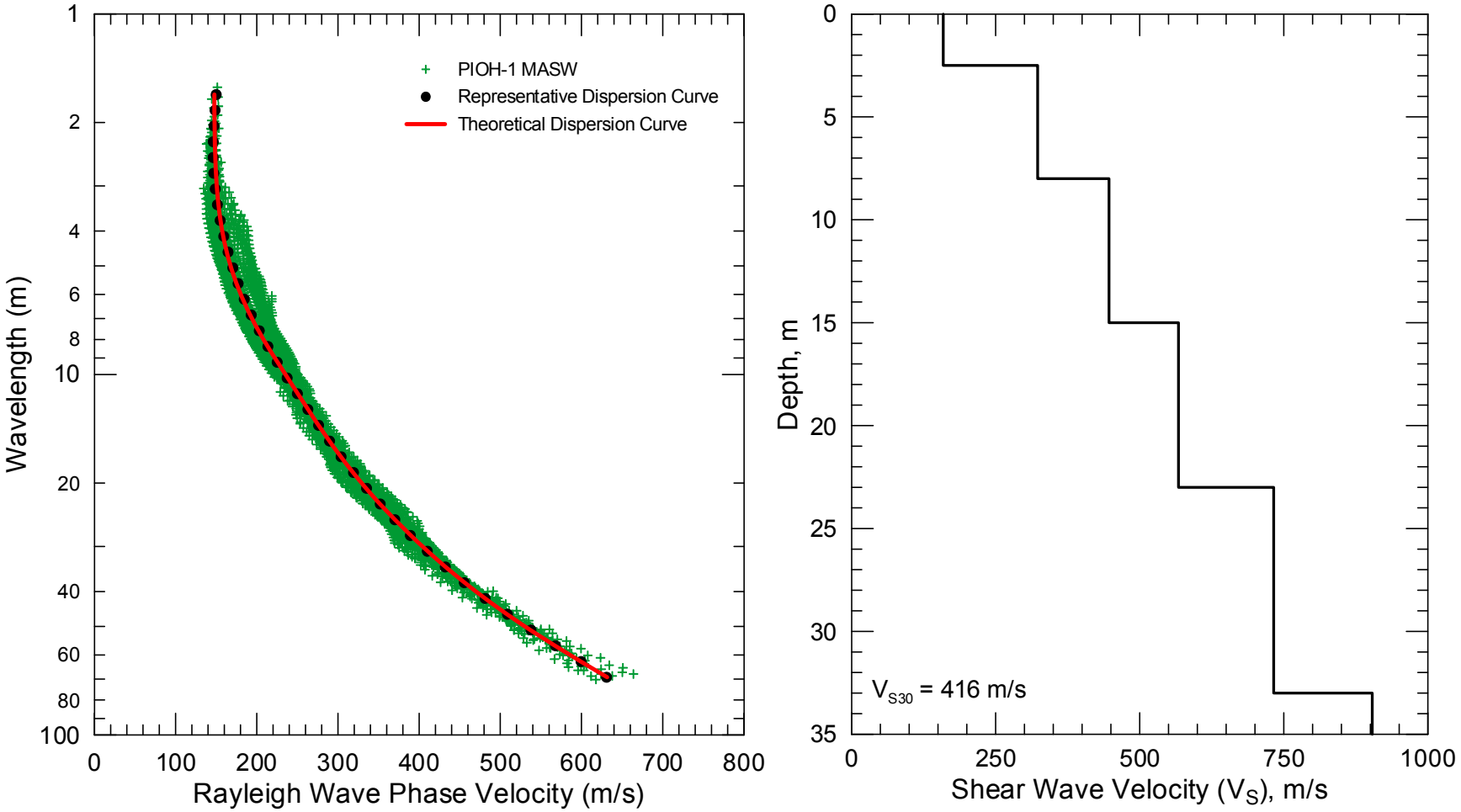

NM.PIOH - Field, representative and inverted theoretical surface wave dispersion data (left) and associated V_S model

Site PG.DCD

Location: Diablo Creek, Diablo Canyon Power Plant, San Luis Obispo County, California

Latitude: 35.22132 **Longitude:** -120.84669
(Station coordinates based on site GPS survey, WGS84 coordinate system)

V_{S30} (measured): 517 m/s

V_{S30} (adjusted to more accurately reflect seismic station conditions): 687 to 841 m/s. The average S-wave velocity between 3 and 33 m and 4 and 34 m, attempting to adjust for the seismic station being located on weathered rock), is 687 and 739 m/s, respectively. V_{S30} estimated by replacing V_S in upper 7 m (low velocity sediments) with V_S of underlying unit to account for the seismic sensor being placed on rock is 841 m/s.

NEHRP Site Class: C (based on V_{S30}), C/B (after adjusting for seismic station conditions)

Geomatrix Code: IVA

Geologic Conditions/Observations: Seismic station located on mapped Tertiary (Lower Miocene) marine pyroclastic volcanic rocks.

Site Conditions: Rural site. Test area located in a narrow canyon with steep topography to the sides. Ground surface elevation increases about 15 m to the northeast along the 70.5 m long seismic line. The seismic line is about 3 to 6 m from the bedrock outcrop and there is expected to be several meters of alluvium overlying bedrock beneath the seismic line. The seismic station is located on the west side of the canyon on weathered rock.

Geophysical Methods Utilized: HVSR, Seismic Refraction (P- and S-wave), MASW (Rayleigh wave), MALW (Love wave)

Geophysical Testing Arrays:

1. Array DCD-1 (48 channel MASW and P-wave seismic refraction array utilizing 4.5 Hz vertical geophones spaced 1.5 m apart for a length of 70.5 m, forward and reverse shot locations with multiple source offsets and source types and multiple interior shot locations).
2. Array DCD-1 (48 channel MALW and S-wave seismic refraction array utilizing 10 Hz horizontal geophones spaced 1.5 m apart for a length of 70.5 m, forward and reverse shot locations with multiple source offsets and multiple interior shot locations). Coincident with P-wave refraction/MASW array of same name.
3. Three HVSR measurement locations distributed along array DCD-1.

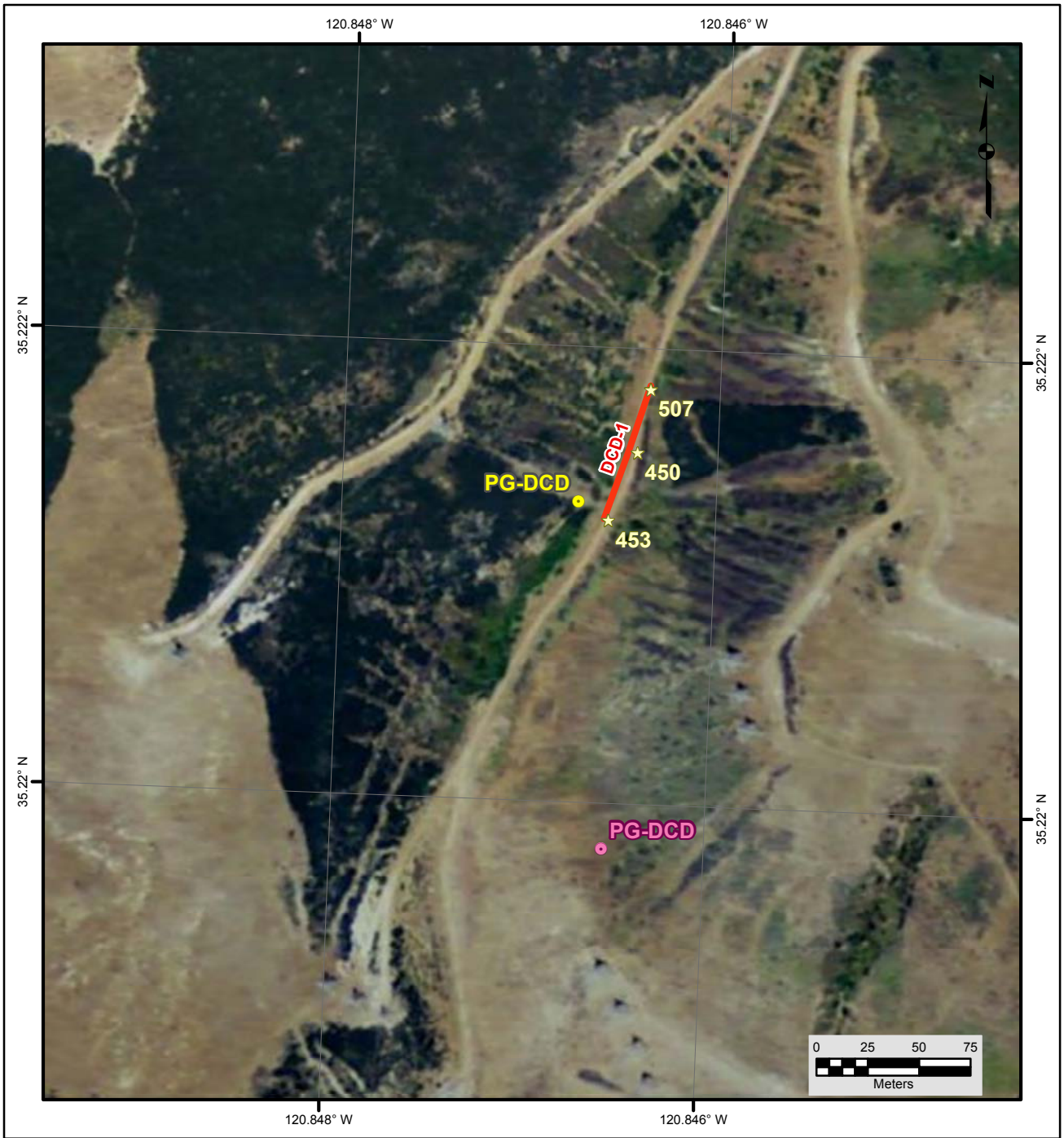

Legend

- Seismic Station - Approximate Surveyed Location
- Seismic Station - Approximate Location of Record
- H/V Spectral Ratio Location
- MASW and Seismic Refraction Array (P- and S-wave)

NOTES:
1. WGS 1984 COORDINATE SYSTEM
2. Image Source: ESRI, i-cubed, USDA FSA, USGS, AEX, GeoEye, Getmapping, Aerogrid, IGP

File Name: PG-DCD-I

Date: 1/19/2012

USGS science for a changing world

GEOVision geophysical services

RECOVERY.GOV

SITE MAP
PG•DCD

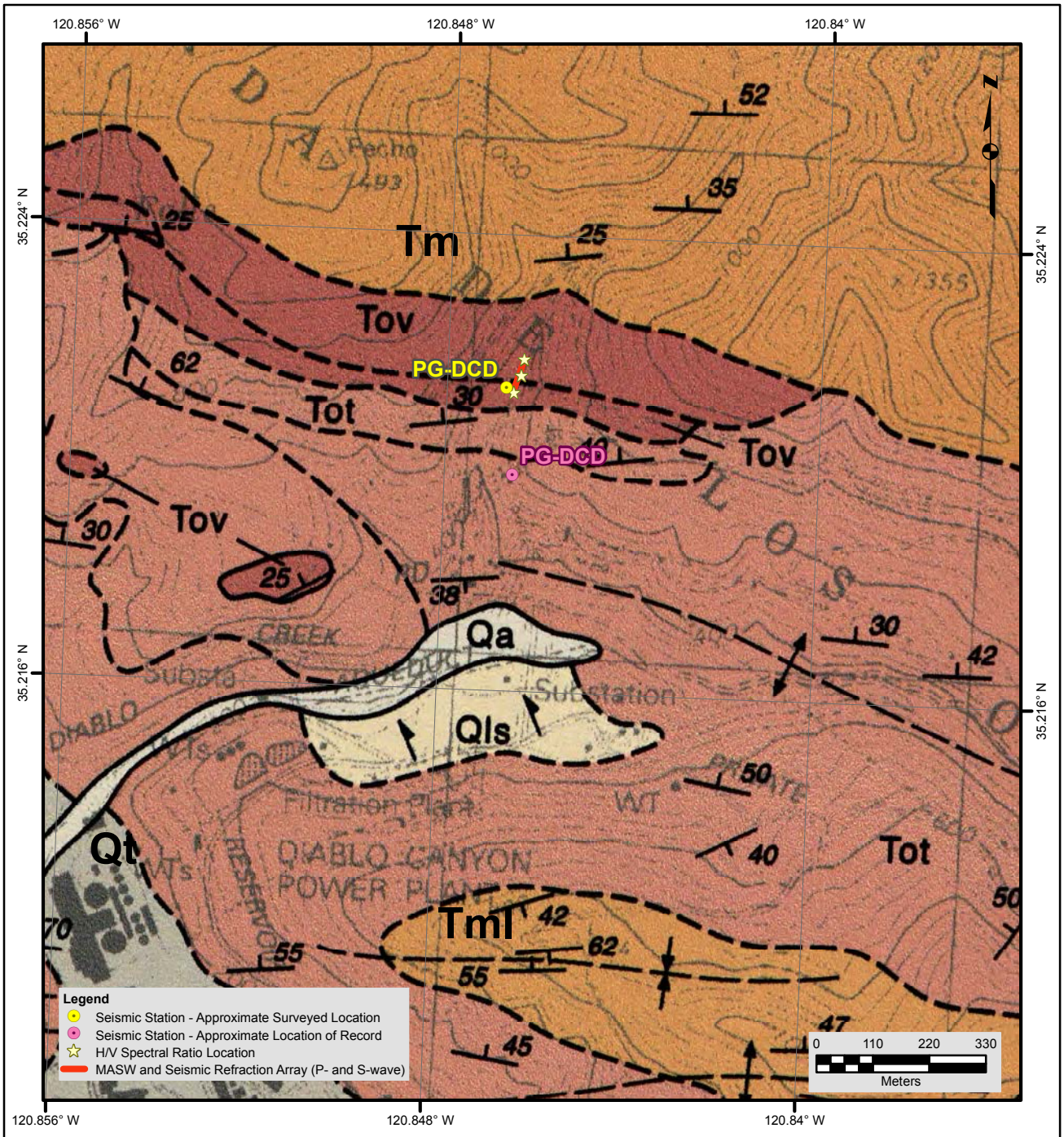

Description of Geologic Map Units

Qa = Quaternary (Holocene) alluvial gravel, sand and clay of valley areas and stream channels
Qt = Quaternary (Holocene) unconsolidated sand, silt, clay and gravel of marine terrace deposits
Qls = Quaternary (Pleistocene) landslide rubble
Tm = Tertiary (Upper Miocene) Monterey Formation; platy siliceous shale, cherty
Tml = Tertiary (Middle Miocene) lower part of Monterey Formation; Point Sal Formation; semi-siliceous shale
Tot = Tertiary (Lower Miocene) marine pyroclastic tuff, fine-grained, massive; includes tuff breccia with small clasts of pumice and perlite
Tov = Tertiary (Lower Miocene) marine pyroclastic volcanic rocks, mostly basalt but some andesitic rock

NOTES:
1. WGS 1984 COORDINATE SYSTEM
2. Geologic Map of the Port San Luis Quadrangle, San Luis Obispo County, California by Thomas W. Dibblee, Jr., 2006
3. See site map for details of geophysical survey

USGS science for a changing world

GEOVision geophysical services

GEOLOGIC MAP
PG•DCD

File Name: PG-DCD

Date: 1/19/2012

PG.DCD seismic station

Looking southwest along array DCD-1 from HVSR sensor 507

P-wave seismic refraction and MASW data acquisition using accelerated weight drop energy source

PG.DCD seismic station

S-wave seismic refraction and MALW data acquisition

Location of Geophysical Testing Arrays:

Location	Latitude	Longitude
DCD-1, Southwest End of MASW/Refraction Array	35.22125	-120.84655
DCD-1, Center of MASW/Refraction Array	35.22154	-120.84644
DCD-1, Northeast End of MASW/Refraction Array	35.22184	-120.84633
HVSR Sensor 450	35.22154	-120.84638
HVSR Sensor 453	35.22124	-120.84653
HVSR Sensor 507	35.22182	-120.84633
PG.DCD Seismic Station	35.22132	-120.84669

Notes: 1) WGS84 Coordinate System (decimal degrees)
2) Survey accuracy is estimated at 1 to 2 m.

Results:

V_S Model from MALW (Love Wave) Sounding

Depth to Top of Layer (m)	Layer Thickness (m)	S-Wave Velocity (m/s)	Inferred P-Wave Velocity (m/s)	Assumed Poisson's Ratio	Assumed Density (g/cm^3)
0	1	145	271	0.3	1.7
1	2	197	368	0.3	1.7
3	4	253	474	0.3	1.8
7	4	665	1245	0.3	2.1
11	5	871	1631	0.3	2.1
16	7	991	1855	0.3	2.2
23	>7	1107	2071	0.3	2.2

Notes: 1) Depth of investigation is about 30 m.
2) Model which best fits the seismic refraction model.
3) Bottom layer is a half space.

Average V_P and Estimated V_S Models from Central Portion of P-wave Seismic Refraction Line (Layered Starting Model)

Depth to Top of Layer (m)	Layer Thickness (m)	P-Wave Velocity (m/s)	Estimated S-Wave Velocity (m/s)			
			Poisson's Ratio = 0.25	Poisson's Ratio = 0.30	Poisson's Ratio = 0.3333	Poisson's Ratio = 0.35
0.00	0.41	248	143	133	124	119
0.41	0.82	341	197	182	170	164
1.22	0.82	404	233	216	202	194
2.04	0.82	409	236	218	204	196
2.86	0.82	410	237	219	205	197
3.67	0.82	412	238	220	206	198
4.49	0.82	413	239	221	207	199
5.30	1.71	567	327	303	283	272
7.02	1.71	1215	702	650	608	584
8.73	1.71	1296	748	692	648	622
10.44	1.71	1379	796	737	690	663
12.16	1.71	1518	876	811	759	729
13.87	1.71	1752	1012	937	876	842
15.58	1.71	1851	1069	989	925	889
17.29	1.71	2050	1183	1096	1025	985
19.01	1.71	2074	1198	1109	1037	996
20.72	Half Space	2075	1198	1109	1037	997

Observations/Discussion:

- The HVSR plots are very similar validating the 1D velocity structure assumption. There is a high amplitude HVSR peak in the 6.5 to 7.5 Hz range, which is likely associated with the shallow bedrock surface. There is inconclusive evidence of additional low frequency HVSR peaks at 0.4 Hz and possibly at lower frequency.
- Field observations indicated that the MASW (Rayleigh wave) technique was not going to be effective at this site due to the thin layer of low velocity sediments overlying high velocity rock and/or lateral variability of the subsurface velocity structure. Therefore, both P- and S-wave seismic refraction surveys were conducted and MALW (Love wave) data acquired.
- S-wave seismic refraction data quality was not very good due to probably P-wave interference and, therefore, no attempt was made to model the S-wave seismic refraction data. However, MALW (Love wave) data quality was good and was, therefore, modeled.
- P-wave seismic refraction data quality was good. However, the air wave arrives before the direct soil arrival in many of the P-wave seismic records and an attempt was made to

pick the direct arrival after the air wave, which was not too difficult with this data set. Picking the higher velocity air wave would only have resulted in bedrock depth increasing by about a meter.

- The P-wave seismic refraction data for array DCD-1 were modeled using a tomographic inversion routine with a layer-based starting model. The seismic refraction model was extended to far offset shot locations to extend depth of investigation. It should be noted that a larger geophone spacing, rather than the utilization of far offset shot locations, is preferred for extending depth of investigation, when applying tomographic inversion routines. However, the seismic refraction data were acquired in conjunction with surface wave data, where a shorter array length is preferred.
- The layer based starting model showed bedrock in the 6 to 8 m depth range.
- The P-wave seismic refraction survey design allowed P-wave velocity to be imaged to a maximum depth of about 20 to 25 m. The seismic refraction model indicates that P-wave velocity is about 250 to 350 m/s at the surface and increases to 750 m/s at a depth of 6 to 8 m, 1,500 m/s at a depth of 10 to 13 m and over 2,000 m/s at a depth of about 14 to 17 m. The maximum P-wave velocity in the model is about 2,250.
- As mentioned previously, longer seismic refraction lines would have been preferred to image to 30 m depth and more accurately constrain the high seismic velocities. There was sufficient space at the site for a 130 to 141 m long refraction line with no offend shot locations.
- Although there is about 15 m of elevation variation along the seismic line, the seismic refraction model indicates that subsurface velocity structure is subparallel to the ground surface and, therefore, surface wave techniques should still be effective.
- V_{P30} was estimated between 30 and 54 m on the P-wave refraction model by projecting the velocity at 22 m depth to 30 m depth. Over this interval, V_{P30} ranges from about 941 to 1,030 m/s, about a 9% variation over a 24 m segment of the array. An average V_P model was developed over the 30 to 54 m distance interval by averaging the slowness of each model cell at a particular depth and average V_{P30} was determined to be 995 m/s.
- Estimating V_{S30} from V_{P30} assuming constant Poisson's ratio in the range of 0.25 to 0.35 results in V_{S30} in the 574 to 478 m/s range. This large variation in potential V_{S30} demonstrates the risks in attempting to estimate V_{S30} from P-wave velocity data, even with a realistic estimate of Poisson's ratio and this approach should only be used as a last resort.
- Noise conditions at the site were not sufficient for application of passive surface wave techniques.
- MASW (Rayleigh wave) data quality is poor due to the high velocity shallow rock and was not reduced. MALW (Love wave) data were of significantly better quality than the MASW data and was, therefore, reduced and modeled.
- The minimum wavelength surface wave phase velocity data extracted from the 48-channel MALW array is about 5 m. Data reduction using seismic records from smaller hammer sources and a limited offset receiver array (i.e. less active geophones) allowed extraction of surface wave dispersion data to a minimum wavelength of about 2.5 m.
- There is nominally about 25 m/s scatter in MALW dispersion data, likely due to the effects of minor lateral velocity variation at the site.
- A representative dispersion curve was generated for the MALW data set using a moving average, polynomial curve fitting routine and used for modeling.

- Surface wave depth of investigation is estimated to be about 30 m.
- Several V_S models were generated from the Love wave phase velocity dispersion curve to demonstrate nonuniqueness. These models have higher velocity rock in the 6.5 to 9 m depth range, which is consistent with the 6 to 8 m bedrock depths imaged in the seismic refraction data. The models also illustrate that bedrock can be modeled with an increase in velocity with depth or with constant velocity. As expected V_{S30} is similar for all of the models, varying from 514 to 530 m/s. Generally, V_{S30} increases with increasing depth to bedrock because the modeled bedrock velocity increases with increasing bedrock depth.
- The equivalent V_S models from the Love wave data were compared to the seismic refraction model and the V_S model with bedrock depth at 7 m and increasing velocity with depth in the bedrock was found to be in the best agreement with the seismic refraction model. It should be noted that MALW V_S models with bedrock depth in the 8 to 8.5 m range have slightly better RMS errors than the other models. Although V_{S30} is not sensitive to bedrock depth, adjustments to the V_{S30} estimate to account for placement of the seismic station on weathered rock are very sensitive to the model.
- V_{S30} from the final MALW V_S model is 518 m/s (Site Class C).
- Estimated V_{S30} after replacing the V_S of the 7 m of sediments with the velocity of the underlying layer is 841 m/s (Site Class B).
- Average S-wave velocity between 3 m and 33 m and 4 and 34 m, an alternate attempt to adjust for seismic station conditions, is 687 and 739 m/s, respectively (Site Class C and C/B).
- V_{S30} estimated from the P-wave seismic refraction models and an assumed constant Poisson's ratio of 0.3 to 0.333 is very similar to that estimated from the MALW sounding. In fact, the V_S models estimated from the P-wave seismic refraction survey and the final V_S model from the MALW sounding are in excellent agreement.
- As mentioned previously, adjusted V_{S30} has significant variability between the equivalent MALW V_S models. Replacing the sediment velocity (6.5 to 9 m sediment thickness) with the velocity of the uppermost bedrock unit results in an adjusted V_{S30} ranging from 782 to 1,078 m/s, increasing with increasing bedrock depth. Average V_S between 3 and 33 m ranges from 670 to 730 m/s. Average V_S between 4 and 34 m ranges from 718 to 776 m/s.
- Although it is not possible to conduct a 30 m deep surface wave sounding immediately adjacent to the seismic station, it may be possible to acquire seismic data along a very short array (10 to 20 m) to determine the near surface weathering profile in rock and better adjust the models above for actual seismic station conditions. Such testing would have to be conducted at a time when the poison oak is not present in the site vicinity.

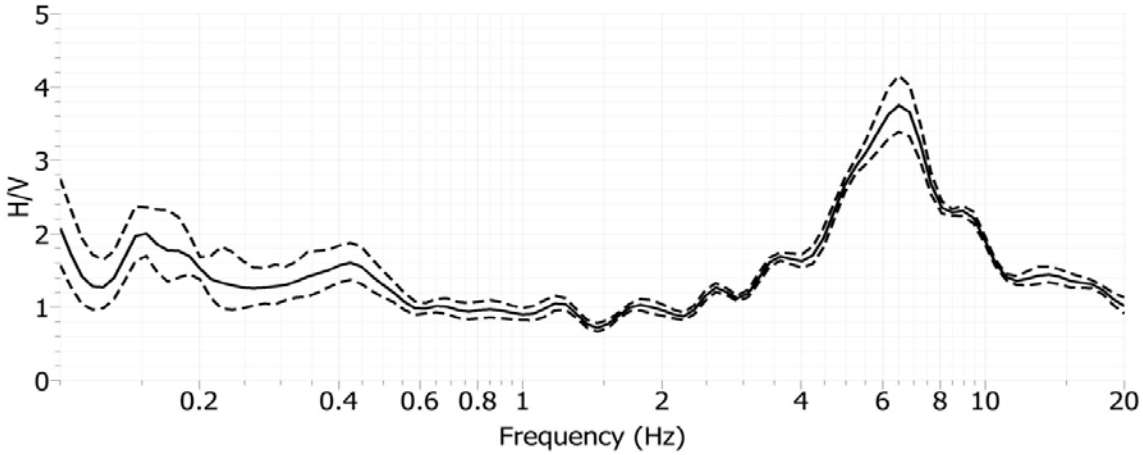

Site PG.DCD, H/V Spectral Ratio, Array DCD-1, Sensor 507

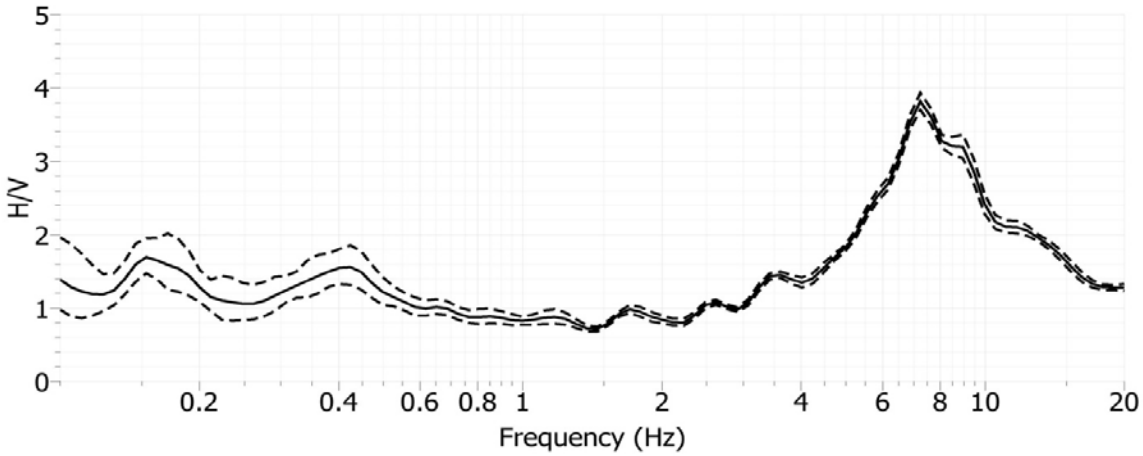

Site PG.DCD, H/V Spectral Ratio, Array DCD-1, Sensor 450

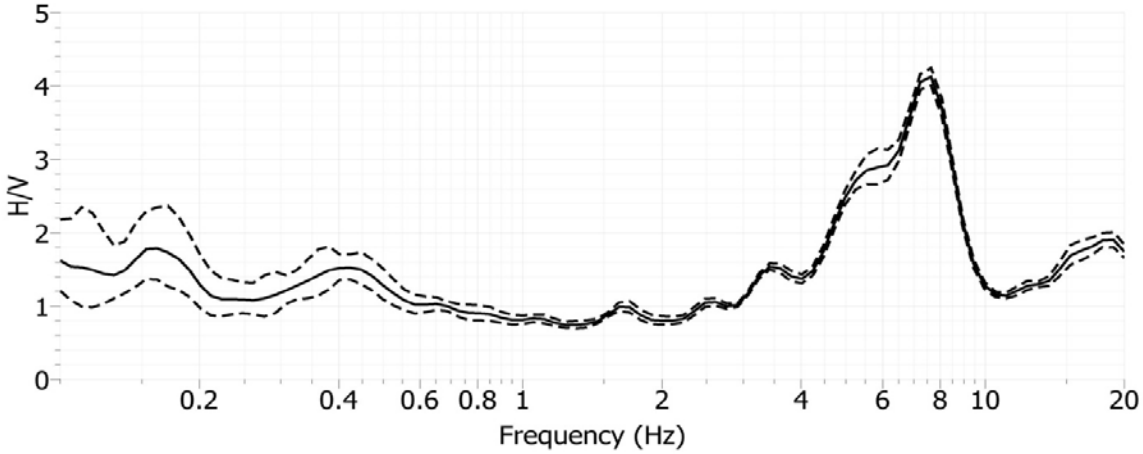

Site PG.DCD, H/V Spectral Ratio, Array DCD-1, Sensor 453

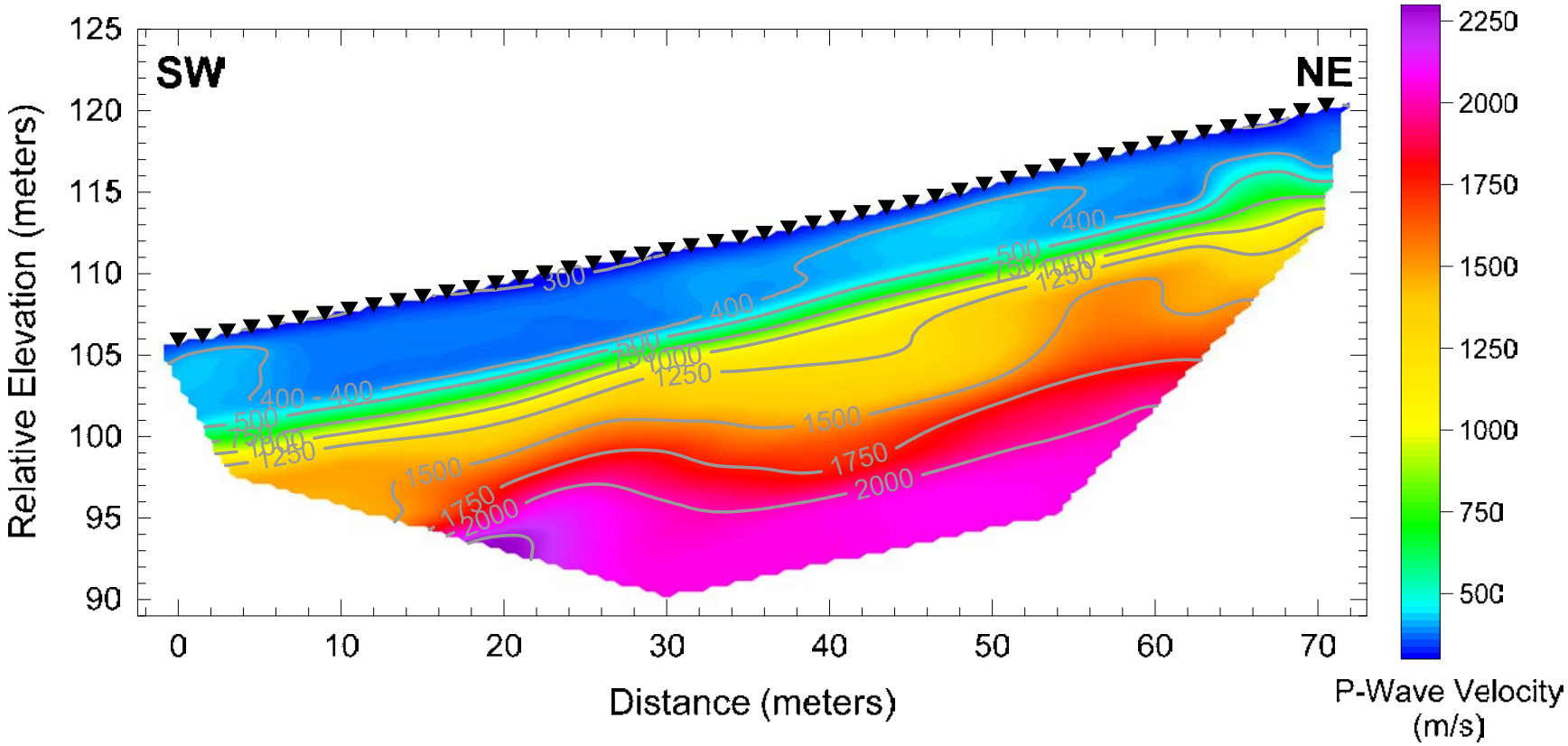

Array DCD-1 – P-wave Tomographic Seismic Refraction Model utilizing Layer Based Starting Model

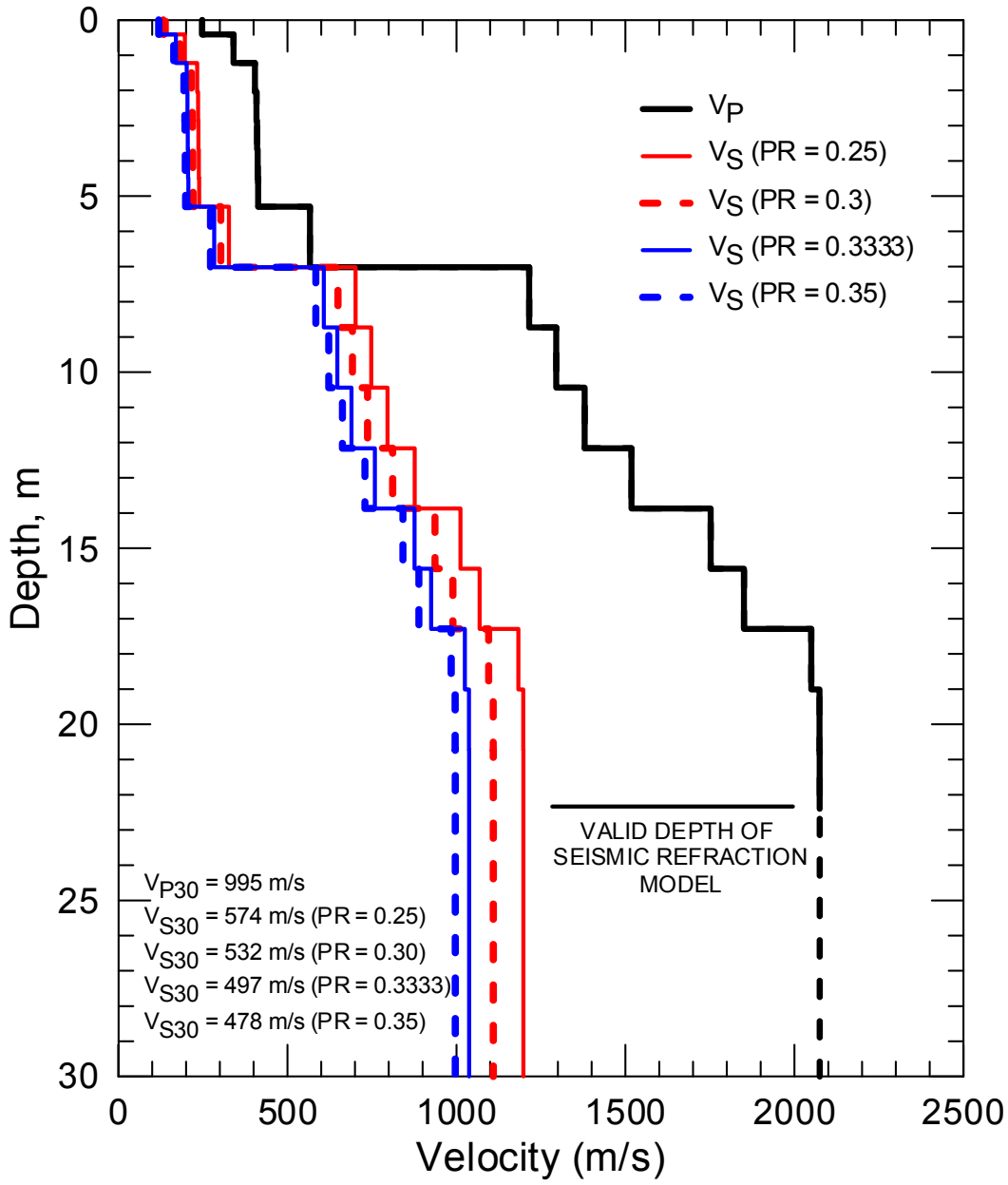

PG.DCD – Average P-wave velocity structure and estimated S-wave velocity structure between a position of 30 and 54 m on the P-wave seismic refraction model for array DCD-1 utilizing a layered starting model. P-wave velocity is assumed to be constant below a depth of 24 m, the estimated maximum depth of investigation.

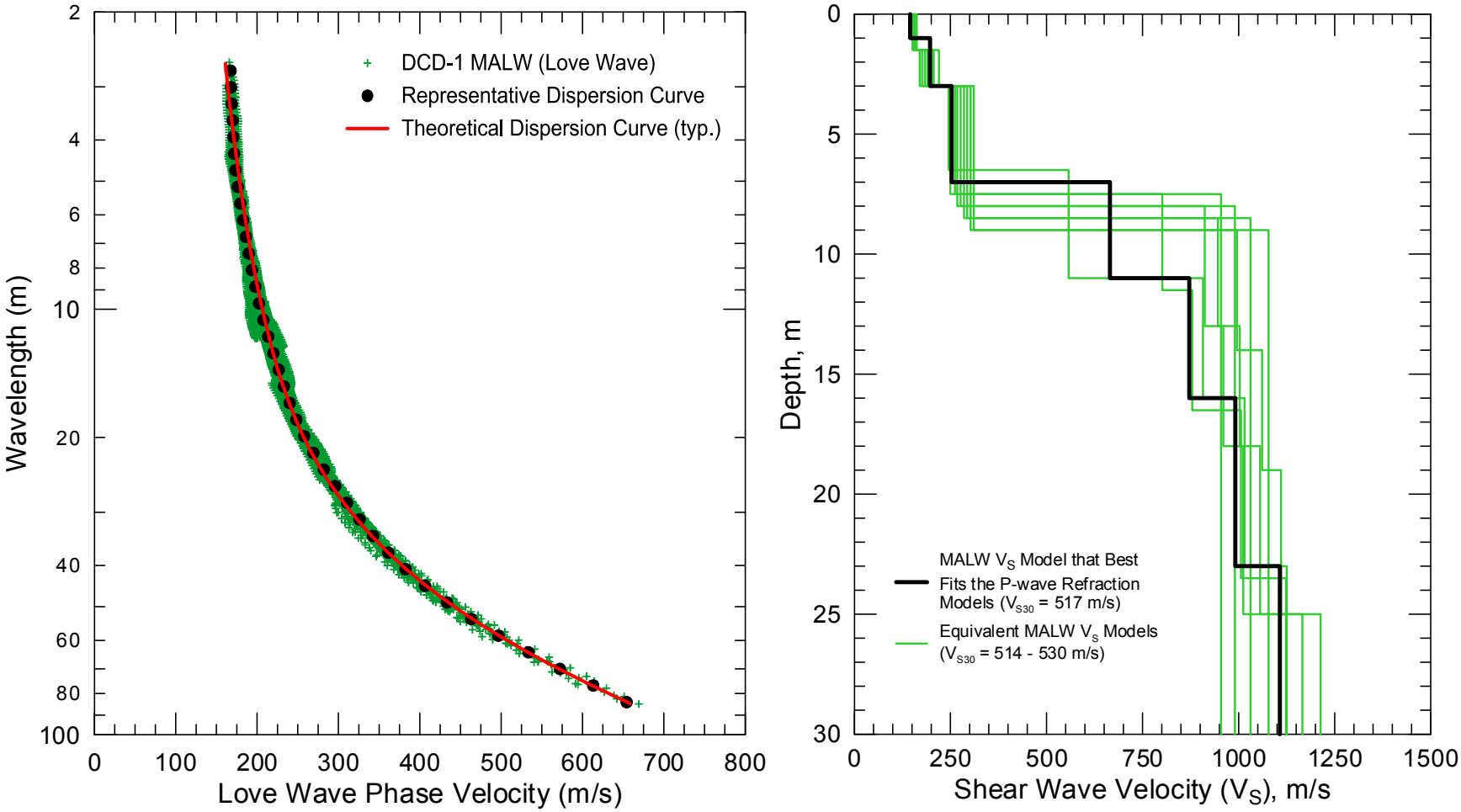

PG.DCD - Field, representative and inverted theoretical surface wave dispersion data (left) and associated equivalent V_S models (right)

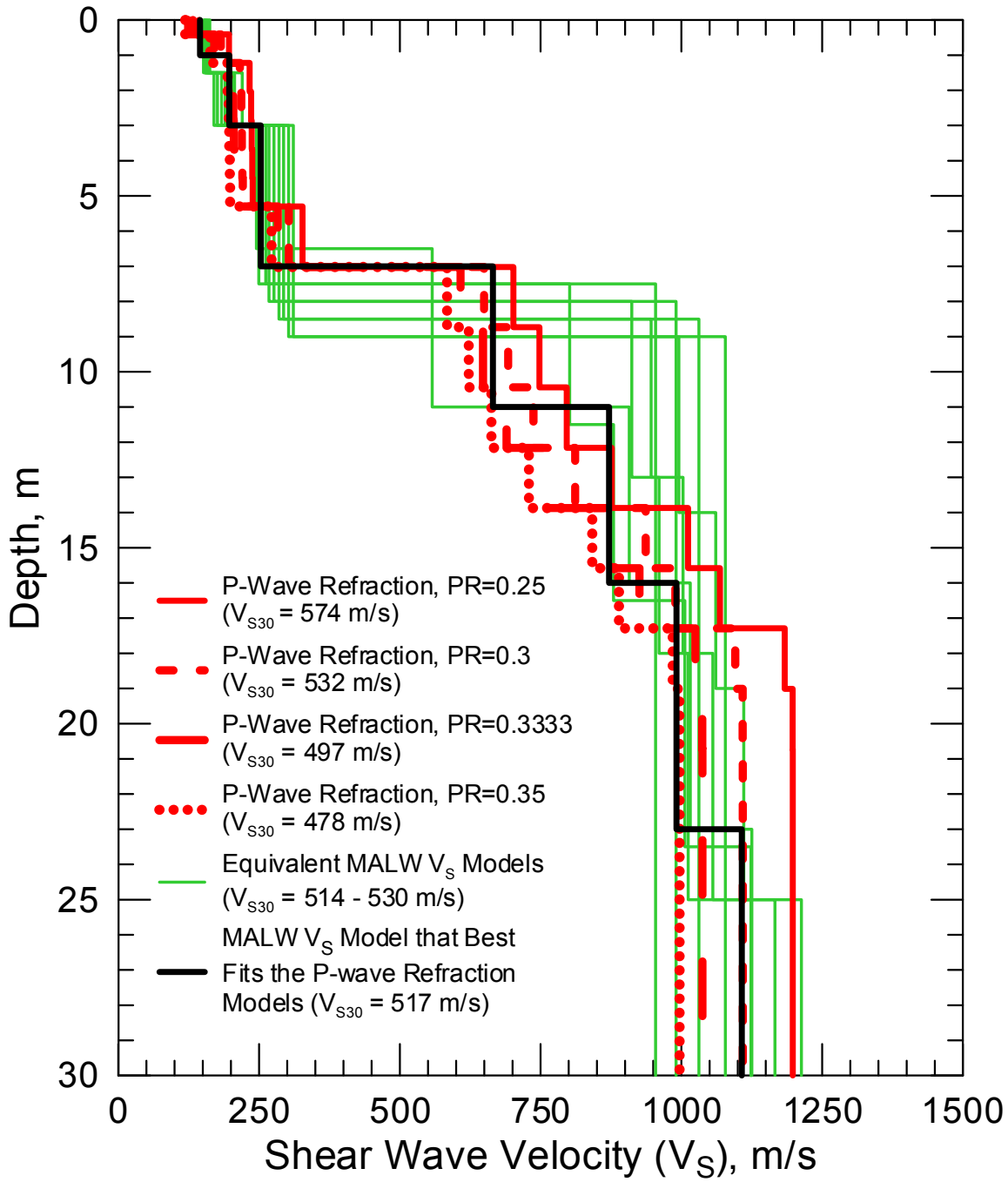

PG.DCD – Comparison of S-wave velocity models derived from the MALW (Love wave) and P-wave seismic refraction surveys. The V_S models estimated from the P-wave seismic refraction survey were used to determine the most appropriate V_S model from the MALW sounding.

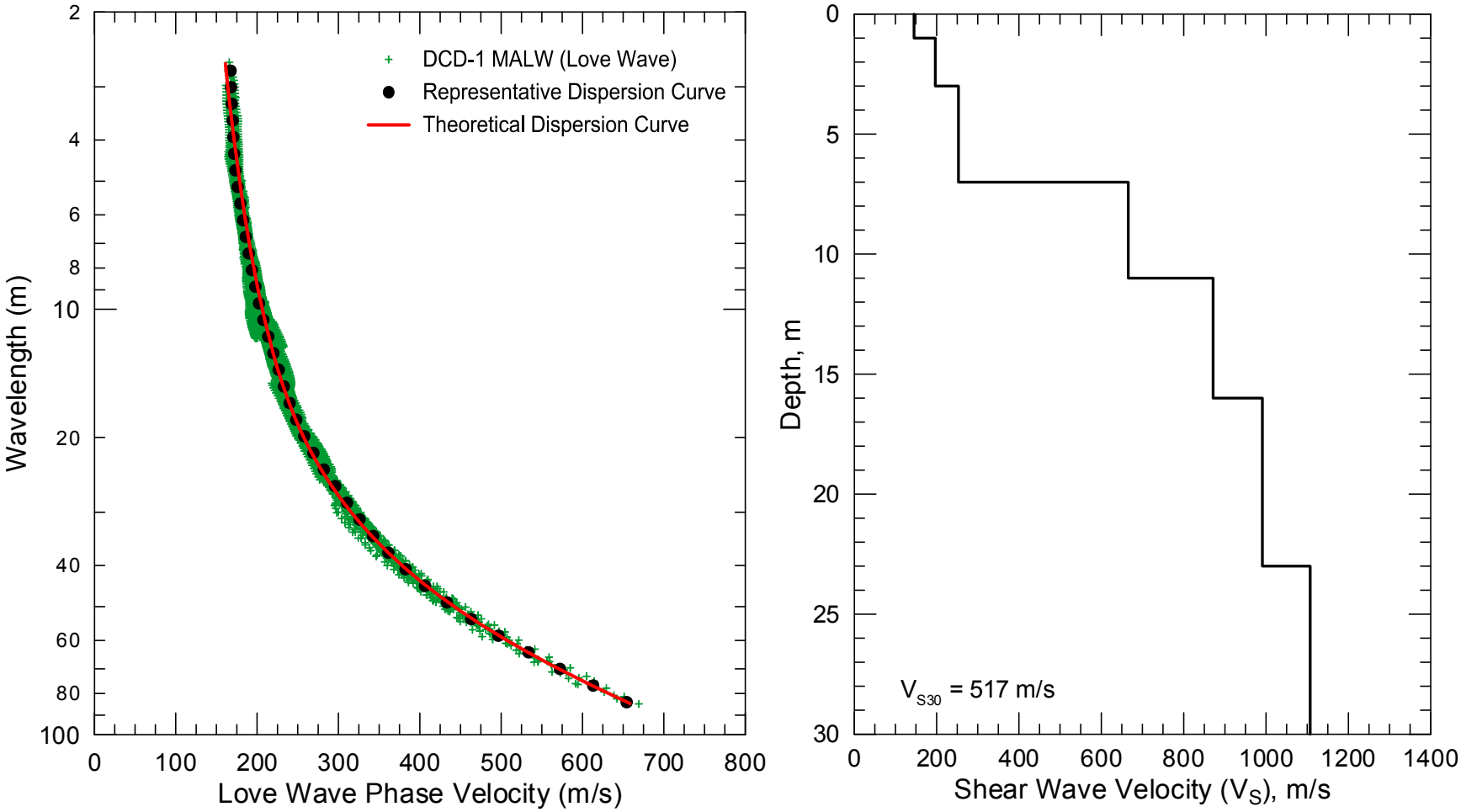

PG.DCD - Field, representative and inverted theoretical surface wave dispersion data (left) and associated V_S model (right)

Site PG.SHD

Location: San Luis Hill, Diablo Canyon Power Plant, San Luis Obispo County, California

Latitude: 35.16898 **Longitude:** -120.76319
(Station coordinates based on site GPS survey, WGS84 coordinate system)

V_{S30} (measured): 818 m/s

V_{S30} (adjusted to more accurately reflect seismic station conditions): 935 m/s (average S-wave velocity between 0.5 and 30.5 m adjusting for assumed 1 m sensor depth).

NEHRP Site Class: B

Geomatrix Code: IKA

Geologic Conditions/Observations: Seismic station located on geologic unit mapped as Mesozoic (Cretaceous) Atascadero Formation, a hard sandstone. The geologic map indicates that bedding dips about 30 to 45 degrees to the southwest in the immediate site vicinity.

Site Conditions: Rural site located near the top of San Luis Hill. Undulating (hilly) topography in site vicinity. Seismic testing arrays located on relatively planar surfaces.

Geophysical Methods Utilized: HVSR, Seismic Refraction (P- and S-wave), MASW (Rayleigh wave), MALW (Love wave)

Geophysical Testing Arrays:

1. Array SHD-1 (48 channel MASW and P-wave seismic refraction array utilizing 4.5 Hz vertical geophones spaced 1.5 m apart for a length of 70.5 m, forward and reverse shot locations with multiple source offsets and source types and multiple interior shot locations.
2. Array SHD-1 (48 channel MALW and S-wave seismic refraction array utilizing 10 Hz horizontal geophones spaced 1.5 m apart for a length of 70.5 m, forward and reverse shot locations with multiple source offsets and multiple interior shot locations). Same location as P-wave refraction/MASW array of same name.
3. Array SHD-2 (48 channel MASW and P-wave seismic refraction array utilizing 4.5 Hz vertical geophones spaced 1.5 m apart for a length of 70.5 m, forward and reverse shot locations with multiple source offsets and source types and multiple interior shot locations).
4. Three HVSR measurement locations: two distributed along array SHD-1 and one adjacent to the seismic station.

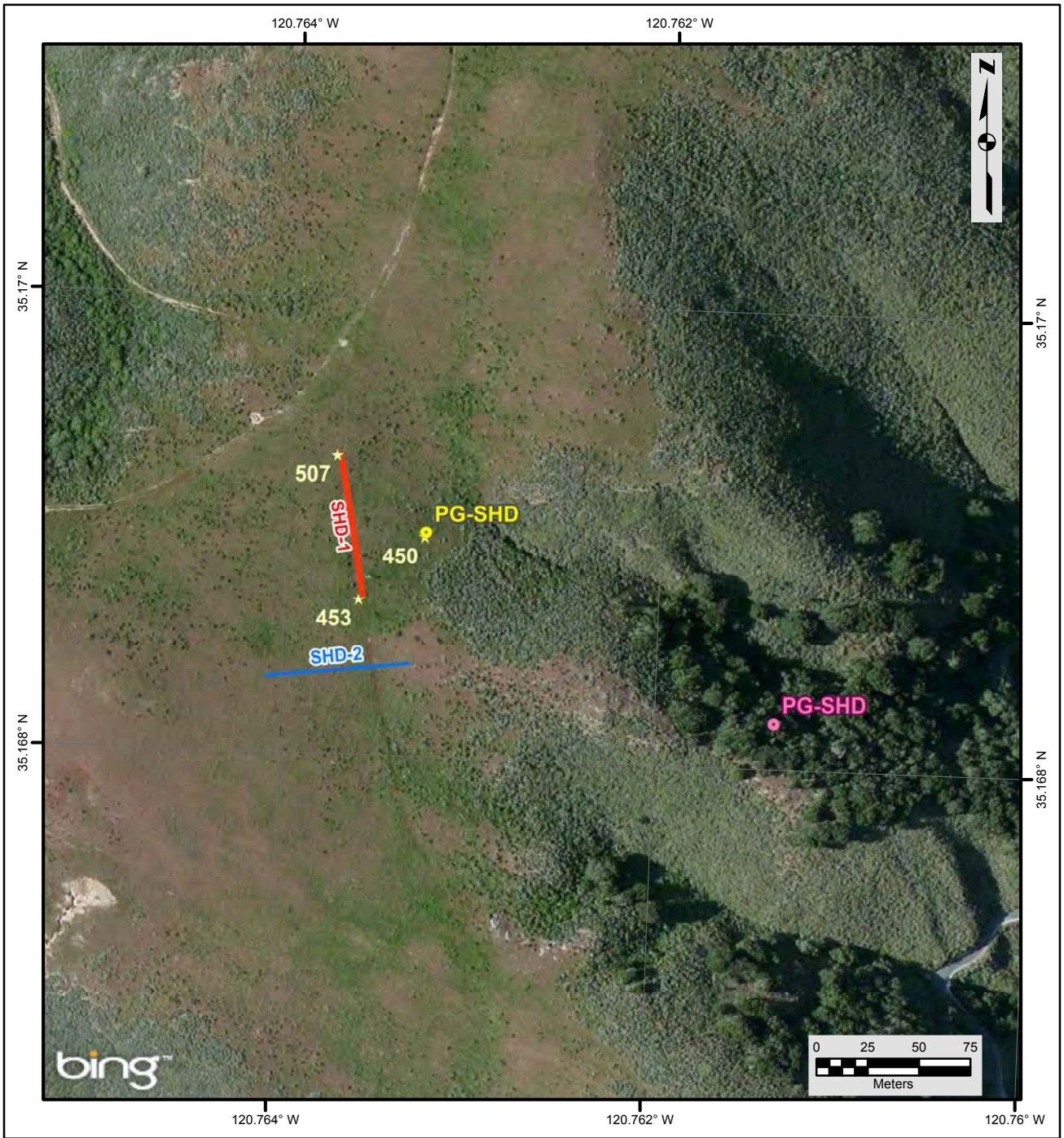

Legend

- Seismic Station - Approximate Surveyed Location
- Seismic Station - Approximate Location of Record
- H/V Spectral Ratio Location
- MASW and Seismic Refraction Array (P- and S-wave)
- MASW and Seismic Refraction Array

NOTES:
1. WGS 1984 COORDINATE SYSTEM
2. Image Source: (c) Microsoft Corporation and its data suppliers

File Name: PG-SHD-I

Date: 2/7/2013

USGS science for a changing world

GEOVision geophysical services

RECOVERY.GOV

SITE MAP
PG•SHD

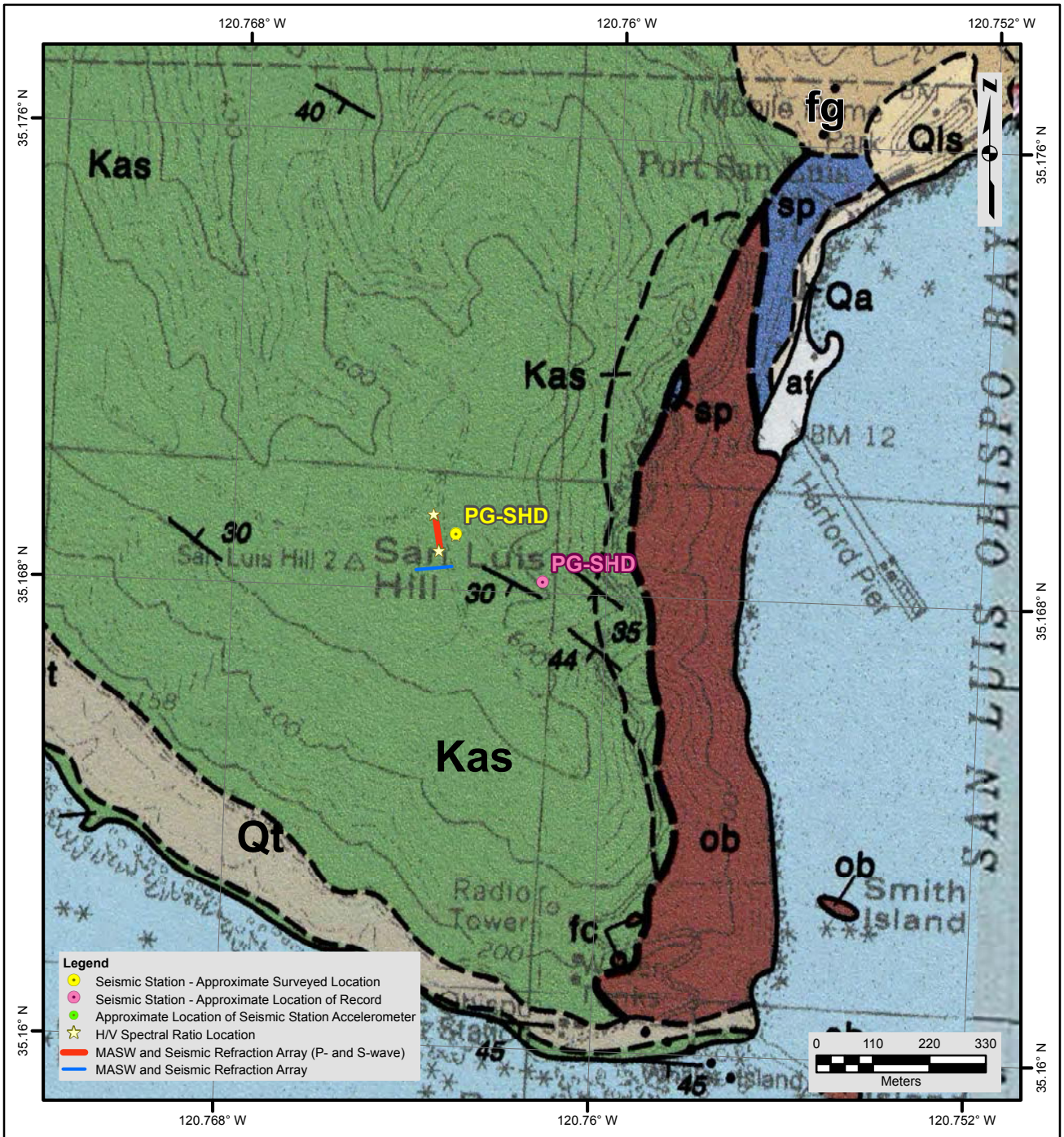

Description of Geologic Map Units

af = Quaternary (Holocene) artificial fill
Qa = Quaternary (Holocene) alluvial gravel, sand and clay of valley areas and stream channels
Qt = Quaternary (Holocene) unconsolidated sand, silt, clay and gravel of marine terrace deposits
Qls = Quaternary (Pleistocene) landslide rubble
Kas = Mesozoic (Cretaceous) Atascadero Formation; sandstone, hard, arkosic, micaceous
sp = Mesozoic (Jurassic & Cretaceous) serpentine; massive amorphous
ob = Mesozoic (Jurassic & Cretaceous) diabase, fine-grained, massive
fg = Mesozoic (Jurassic & Cretaceous) Franciscan Assemblage; greenstone, massive, aphanitic

NOTES:
1. WGS 1984 COORDINATE SYSTEM
2. Geologic Map of the Port San Luis Quadrangle, San Luis Obispo County, California by Thomas W. Dibblee, Jr., 2006
3. See site map for details of geophysical survey

USGS science for a changing world

GEOVision geophysical services

GEOLOGIC MAP
PG•SHD

File Name: PG-SHD

Date: 2/7/2013

Looking at PG.SHD seismic station and HVSR sensor 450

Looking north along array SHD-1

Looking south towards center of array SHD-1

S-wave seismic refraction acquisition along array SHD-1

Looking east along array SHD-2

Location of Geophysical Testing Arrays:

Location	Latitude	Longitude
SHD-1, South End of MASW/Seismic Refraction Array	35.16869	-120.76352
SHD-1, Center of MASW/Seismic Refraction Array	35.16900	-120.76359
SHD-1, North End of MASW/Seismic Refraction Array	35.16931	-120.76366
SHD-2, West End of MASW/Seismic Refraction Array	35.16833	-120.76402
SHD-2, Center of MASW/Seismic Refraction Array	35.16837	-120.76364
SHD-2, East End of MASW/Seismic Refraction Array	35.16841	-120.76326
HVSR Sensor 450	35.16896	-120.76320
HVSR Sensor 453	35.16868	-120.76354
HVSR Sensor 507	35.16931	-120.76368
PG.SHD Seismic Station (Seismometers)	35.16898	-120.76319
PG.SHD Seismic Station (Accelerometer)	35.16886	-120.76335

Notes: 1) WGS84 Coordinate System (decimal degrees)
2) Survey accuracy is estimated at 1 to 2 m

Results:

V_S Model (MASW Array SHD-1)

Depth to Top of Layer (m)	Layer Thickness (m)	S-Wave Velocity (m/s)	Inferred P-Wave Velocity (m/s)	Assumed Poisson's Ratio	Assumed Density (g/cm^3)
0	0.65	97	194	0.333	1.60
0.65	1.6	436	873	0.333	1.90
2.25	3.25	713	1425	0.333	2.10
5.5	7	870	1740	0.333	2.10
12.5	7	1087	2174	0.333	2.15
19.5	9	1241	2483	0.333	2.20
28.5	>6.5	1448	2897	0.333	2.20

Notes: 1) Depth of investigation is about 35 m.
2) Bottom layer is a half space.

V_S Model (MALW Array SHD-1)

Depth to Top of Layer (m)	Layer Thickness (m)	S-Wave Velocity (m/s)	Inferred P-Wave Velocity (m/s)	Assumed Poisson's Ratio	Assumed Density (g/cm^3)
0	0.5	104	208	0.333	1.60
0.5	1.75	390	780	0.333	1.90
2.25	2.25	747	1495	0.333	2.10
4.5	6	893	1785	0.333	2.10
10.5	8	1044	2088	0.333	2.15
18.5	>11.5	1273	2547	0.333	2.20

Notes: 1) Depth of investigation is about 30 m.
2) Poisson's ratio and P-wave velocity do not influence model.
3) Bottom layer is a half space.

Average V_P Model and Estimated V_S Models from Central Portion of P-wave Seismic Refraction Array SHD-1

Depth to Top of Layer (m)	Layer Thickness (m)	P-Wave Velocity (m/s)	Estimated S-Wave Velocity (m/s)			
			Poisson's Ratio = 0.25	Poisson's Ratio = 0.3	Poisson's Ratio = 0.35	Poisson's Ratio = 0.4
0.00	0.51	352	203	188	169	144
0.51	1.02	737	425	394	354	301
1.53	1.02	1365	788	730	656	557
2.55	1.02	1594	920	852	766	651
3.56	1.02	1670	964	893	802	682
4.58	1.02	1911	1103	1022	918	780
5.60	1.02	1930	1114	1032	927	788
6.62	2.14	2054	1186	1098	987	839
8.76	2.14	2111	1219	1129	1014	862
10.89	2.14	2179	1258	1165	1047	889
13.03	2.14	2242	1295	1199	1077	915
15.17	2.14	2566	1482	1372	1233	1048
17.31	2.14	2604	1503	1392	1251	1063
19.45	2.14	2749	1587	1470	1321	1122
21.58	2.14	2810	1622	1502	1350	1147
23.72	Half Space	2932	1693	1567	1408	1197

Average V_P Model and Estimated V_S Models from Central Portion of P-wave Seismic Refraction Array SHD-2

Depth to Top of Layer (m)	Layer Thickness (m)	P-Wave Velocity (m/s)	Estimated S-Wave Velocity (m/s)			
			Poisson's Ratio = 0.25	Poisson's Ratio = 0.3	Poisson's Ratio = 0.35	Poisson's Ratio = 0.4
0.00	0.49	313	181	167	150	128
0.49	0.97	628	363	336	302	256
1.46	0.97	1082	625	578	520	442
2.44	0.97	1291	745	690	620	527
3.41	0.97	1461	844	781	702	596
4.38	0.97	1624	938	868	780	663
5.36	0.97	1658	957	886	796	677
6.33	2.05	1734	1001	927	833	708
8.38	2.05	1822	1052	974	875	744
10.42	2.05	2032	1173	1086	976	830
12.47	2.05	2096	1210	1120	1007	856
14.51	2.05	2222	1283	1188	1067	907
16.56	2.05	2249	1299	1202	1081	918
18.60	2.05	2653	1532	1418	1275	1083
20.65	Half Space	3041	1755	1625	1461	1241

Observations/Discussion:

- During acquisition of MASW data along array SHD-1 the observation was made that higher mode Rayleigh waves were dominant at high frequencies/small wavelengths. Therefore, S-wave refraction and MALW data were also acquired along the array. Additionally, MASW and P-wave seismic refraction data were acquired along an orthogonal array (SHD-2) to confirm that issues with higher mode Rayleigh wave data were not localized to array SHD-1 and evaluate lateral velocity variation. Arrays SHD-1 and SHD-2 are not aligned parallel or orthogonal to the mapped strike of the geologic bedding. An array aligned parallel to strike and located in close proximity to the seismic station would have introduced undesired topographic variation and would not have had vehicular access. It would, however, be possible to locate an array parallel to strike at greater distance from the seismic station.
- HVSR plots are very similar at every station at frequencies lower than 10 Hz. HVSR sensor locations 450 and 507 have a high amplitude peak in the 14 to 15 Hz range. This peak results from only one of the horizontal channels and may not have a geologic

source. All HVSR measurements have elevated response over the 1.5 to 15 Hz range, but no distinct peaks.

- The P-wave refraction data for arrays SHD-1 and SHD-2 were modeled using a tomographic inversion routine with a smooth velocity gradient starting model. The seismic refraction models were extended to far offset shot locations to extend depth of investigation. Ideally, the seismic refraction data would have been acquired along a longer array; however, the seismic refraction data was acquired in conjunction with MASW/MALW data, which benefit from a shorter array.
- The S-wave seismic refraction data acquired along array SHD-1 have not been analyzed to date. S-wave refraction data were reviewed, and it is clear that S-wave velocity exceeds 1,100 m/s beneath the array.
- The P-wave seismic refraction survey design for array SHD-1 allowed P-wave velocity to be imaged to a maximum depth of about 25 m. The seismic refraction model indicates that P-wave velocity is about 300 to 400 m/s at the surface, increasing to over 1,000 m/s at a depth of 1 to 2 m, 2,000 m/s at a depth of 5 to 7 m and over 2,500 m/s at a depth of 10 to 15 m. The maximum P-wave velocity in the model is about 3,000 m/s at a depth of 24 m, or more. The observed S-wave velocity of over 1,100 in the S-wave seismic records would indicate that bedrock is not saturated, at least in the upper 24 m.
- The average P-wave velocity of the upper 30 m (V_{P30}) was estimated between 24 and 48 m on the P-wave refraction model for array SHD-1, where depth of investigation is greatest. To estimate V_{P30} the P-wave velocity at a depth of 25 m, nominal depth of investigation, was projected to 30 m depth. V_{P30} ranges from about 1,901 to 2,045 m/s over the 24 to 48 m position interval, a 7% variation. An average V_P model was developed over the 24 to 48 m distance interval by horizontally averaging the travel time of each model cell and cell thickness and average V_{P30} was determined to be 1,973 m/s. Assuming constant Poisson's ratios of 0.25, 0.3, 0.35 and 0.4 would result in an estimated V_{S30} of 1,139, 1,055, 948 and 806 m/s, respectively. The average V_S between 0.5 and 30.5 m to account for assumed sensor depth is 1,244, 1,151, 1,035, and 879 m/s for constant Poisson's ratio of 0.25, 0.3, 0.35 and 0.4, respectively. Poisson's ratio in the 0.3 to 0.35 range is realistic for an unsaturated sandstone unit.
- The P-wave seismic refraction survey design for array SHD-2 allowed P-wave velocity to be imaged to a maximum depth of about 22 m. The seismic refraction model indicates that P-wave velocity is about 275 to 375 m/s at the surface and increases to over 1,000 m/s at a depth of 1 to 2 m, 2,000 m/s at a depth of 4 to 13 m and over 3,000 m/s at a depth of 19 to 21 m.
- The average P-wave velocity of the upper 30 m (V_{P30}) was estimated between 24 and 48 m on the P-wave refraction model for array SHD-2, where depth of investigation is greatest. To estimate V_{P30} the P-wave velocity at a depth of 22 m, nominal depth of investigation, was projected to 30 m depth. V_{P30} ranges from about 1,697 to 2,049 m/s over the 24 to 48 m position interval, a 19% variation. An average V_P model was developed over the 24 to 48 m distance interval by horizontally averaging the travel time of each model cell and cell thickness and average V_{P30} was determined to be 1,810 m/s. Assuming constant Poisson's ratios of 0.25, 0.3, 0.35 and 0.4 would result in an estimated V_{S30} of 1,045, 967, 869 and 739 m/s, respectively. The average V_S between 0.5 and 30.5 m to account for assumed sensor depth is 1,141, 1,056, 949, and 807 m/s for constant

Poisson's ratio of 0.25, 0.3, 0.35 and 0.4, respectively. Poisson's ratio in the 0.3 to 0.35 range is realistic for an unsaturated sandstone unit.

- The P-wave seismic refraction models for arrays SHD-1 and SHD-2 have slight differences. Array SHD-1 generally has higher P-wave velocity at depth less than 19 m but lower velocity at greater depths. Array SHD-2 has more lateral velocity variation than array SHD-1 with 19% variation in V_{P30} in the central 24 m of the array compared to 7% variation in V_{P30} for array SHD-1over the same distance interval. The maximum V_{P30} in the central portion of the seismic lines is similar for both arrays; however, the minimum V_{P30} is about 11% less for array SHD-2. The average V_{P30} over the 24 to 48 m distance interval on the two arrays is about 8% lower for array SHD-2, indicating that V_{S30} will also be lower beneath array SHD-2.
- Noise conditions at the site were not sufficient for application of passive surface wave techniques.
- Both of the MASW (Rayleigh wave) and MALW (Love wave) data acquired along array SHD-1, located closest to the seismic station, were reduced and modeled. MASW data acquired along array SHD-2 was reduced, but not modeled, as the data quality is not as good as that for array SHD-1 and the array is located further from the seismic station. Review of the Rayleigh wave phase velocity data extracted from array SHD-2 does support V_{S30} being lower than at array SHD-1, as indicated by the seismic refraction models.
- Reduction of the MASW and MALW data collected along array SHD-1 was challenging. The presence of a very thin low velocity layer overlying much higher velocity weathered sandstone, as evident in the seismic refraction models, excited a dominant higher mode at frequencies greater than about 30 Hz. Only by use of limited offset receiver gathers associated with interior and off-end source locations could small wavelength (<15 m) fundamental mode Rayleigh wave phase velocity data be extracted from the MASW data set. Love wave dispersion data only appeared to be reliable at frequencies higher than 13 Hz.
- The minimum wavelength Rayleigh wave phase velocity data extracted from the 48-channel MASW array was about 25 m, due to a dominant first higher mode at high frequencies. Reducing data from smaller hammer sources using a limited offset receiver array (i.e. less active geophones) allowed for extraction of surface wave dispersion data to a minimum wavelength of about 3.5 m. The minimum wavelength Love wave phase velocity data extracted from the 48-channel MALW array was about 14 m. Reducing data using a limited offset receiver array (i.e. less active geophones) allowed for extraction of surface wave dispersion data to a minimum wavelength of about 2 m.
- Surface wave dispersion data was extracted from the MASW and MALW seismic records to a maximum wavelength of 100 and 90 m, respectively. The near field criteria typically applied to MASW data was relaxed somewhat and the maximum wavelength was set equal to the minimum of 100 m or 1.4 times the distance from the source to midpoint of the active receiver array.
- There is about 100 to 150 m/s of scatter in Rayleigh and Love wave dispersion data. This scatter is in part due to lateral velocity variation and indicates there may be over 10% variability in V_{S30} along the array. Such lateral velocity variation is the norm for many rock sites.

- A representative dispersion curve was generated for the Rayleigh and Love wave MASW data sets using a moving average, polynomial curve fitting routine and used for modeling.
- Surface wave depth of investigation is about 35 m for the Rayleigh wave model and 30 m for the Love wave model, based on one half to one third the maximum wavelength.
- The V_S models derived from the Rayleigh and Love wave dispersion data are generally consistent with one another, but yield lower estimates of V_{S30} than the average P-wave seismic refraction model with nominal Poisson's ratio in the 0.3 to 0.35 range. Poisson's ratio would need to be in the 0.35 to 0.4 range, which appears high for unsaturated sandstone for the seismic refraction model to be consistent with the surface wave models.
- A thin (0.5 to 0.65 m thick), low velocity surface layer, which is supported by the seismic refraction model, was inserted into the MASW and MALW V_S models even though the minimum wavelength dispersion data extracted from the MASW and MALW data sets was 3.5 and 2 m, respectively. This layer is what appears to excite a dominant first higher mode in the Rayleigh wave dispersion data at high frequencies. The velocity and thickness of this layer is not well constrained. This will not significantly affect V_{S30}, but may have a larger influence on adjustments to V_{S30} for seismic sensor depth.
- The S-wave velocity models derived from the surface wave testing are believed to be representative of average subsurface velocity structure. However, geology at the site is complex, with dipping bedding, and the seismic lines were oriented at a high angle to strike to minimize topographic variation along the lines. In such conditions, weathering must play a significant role in near surface velocity structure for surface wave techniques to be effective. It is difficult to predict the effect of dipping beds on the surface wave dispersion data, but severe lateral velocity variation is an obvious possibility in such conditions. The seismic refraction model for array SHD-1 indicates that geologic dip does not have a significant effect on velocity structure beneath the array.
- For the purpose of site characterization, we recommend using the average velocity structure of the Rayleigh wave and Love wave V_S models. V_{S30} may vary by about 5 to 10% beneath the array due to lateral velocity variation.
- V_{S30} is 795 and 840 m/s for the Rayleigh and Love wave V_S models, respectively, averaging 818 m/s (NEHRP Site Class B).
- Average S-wave velocity between 0.5 m (approximate sensor depth) and 30.5 m is 912 and 958 m/s for the Rayleigh and Love wave V_S models, respectively, averaging 935 m/s (NEHRP Site Class B).

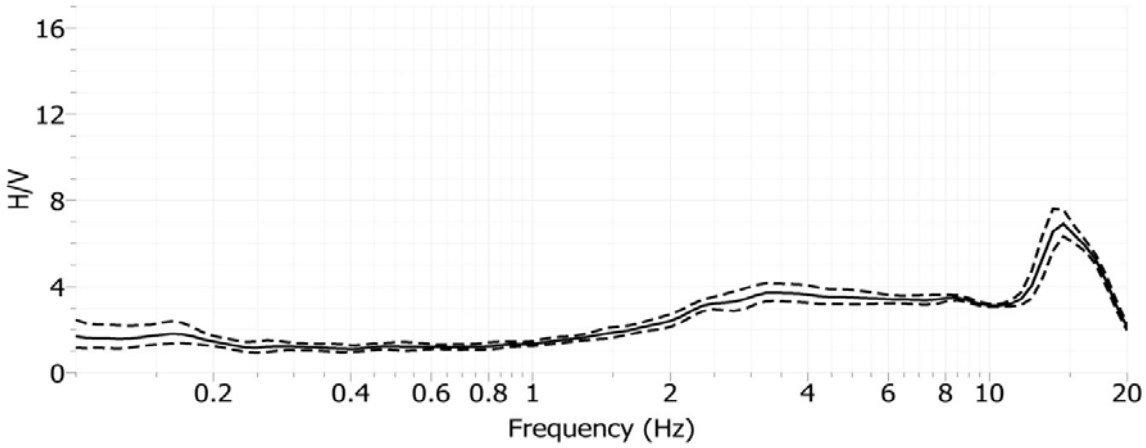

Site PG.SHD, H/V Spectral Ratio, Array SHD-1, Sensor 507

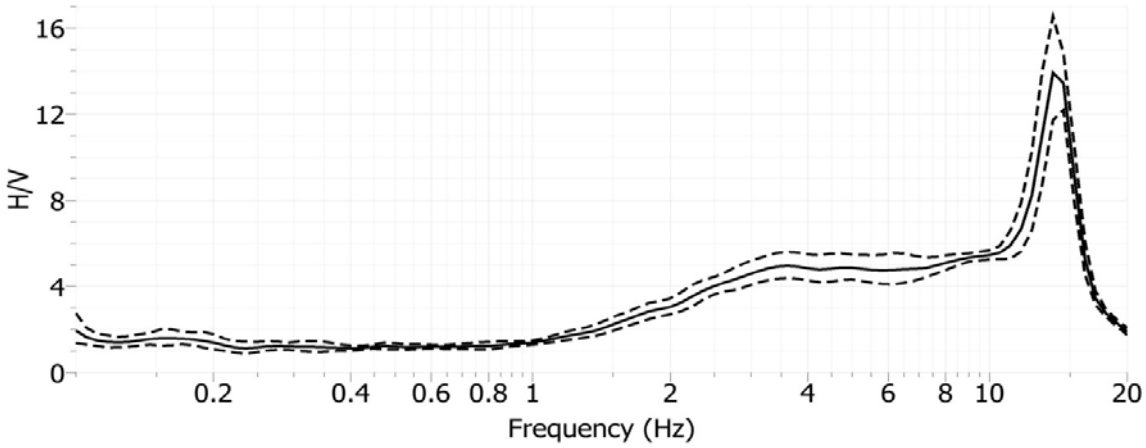

Site PG.SHD, H/V Spectral Ratio, Near Seismic Station, Sensor 450

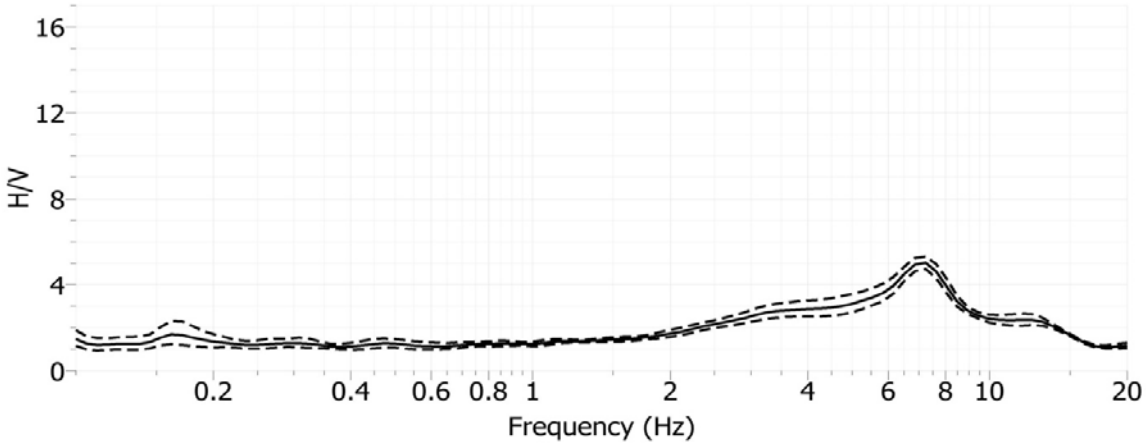

Site PG.SHD, H/V Spectral Ratio, Array SHD-1, Sensor 453

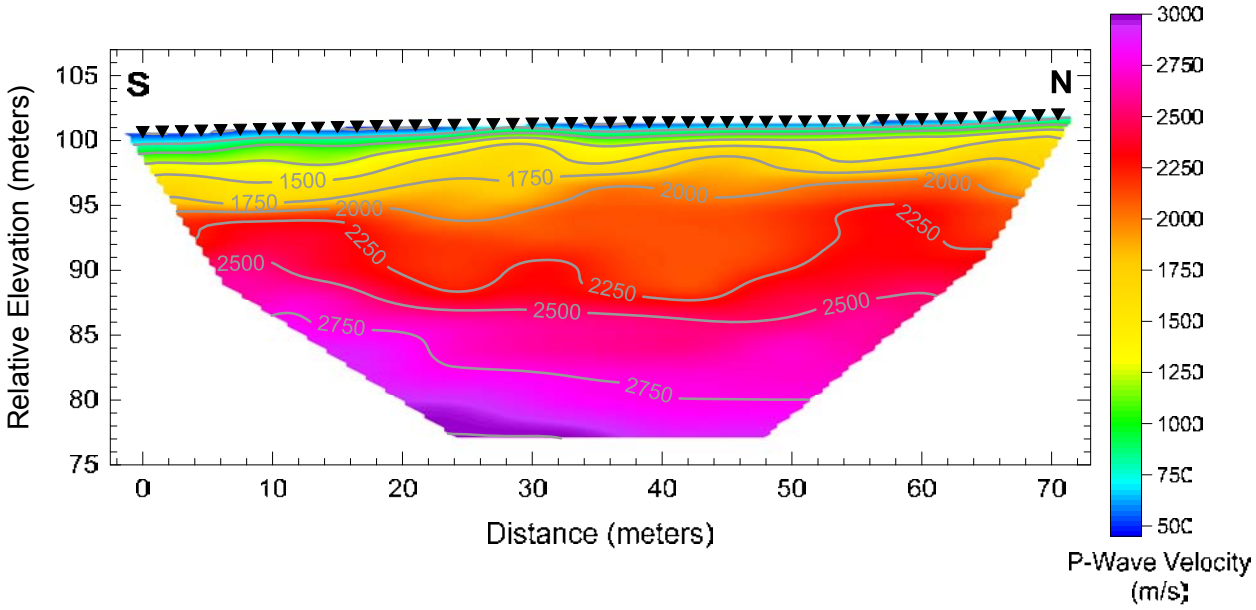

Array SHD-1 – P-wave Tomographic Seismic Refraction Model Developed using a Smooth Velocity Gradient Starting Model

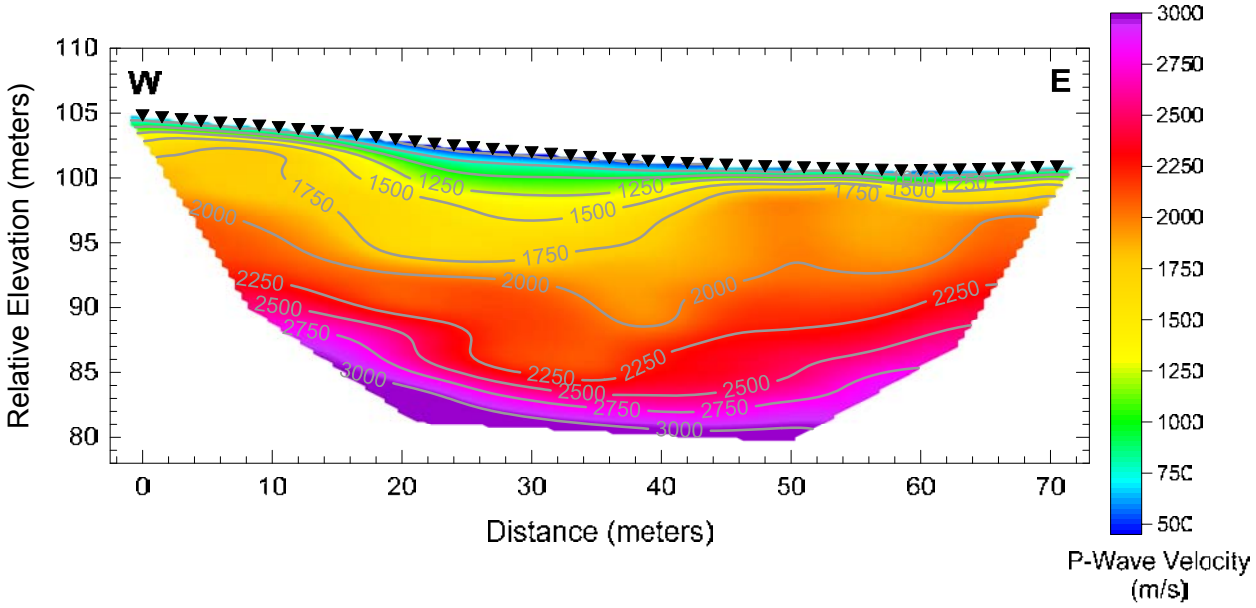

Array SHD-2 – P-wave Tomographic Seismic Refraction Model Developed using a Smooth Velocity Gradient Starting Model

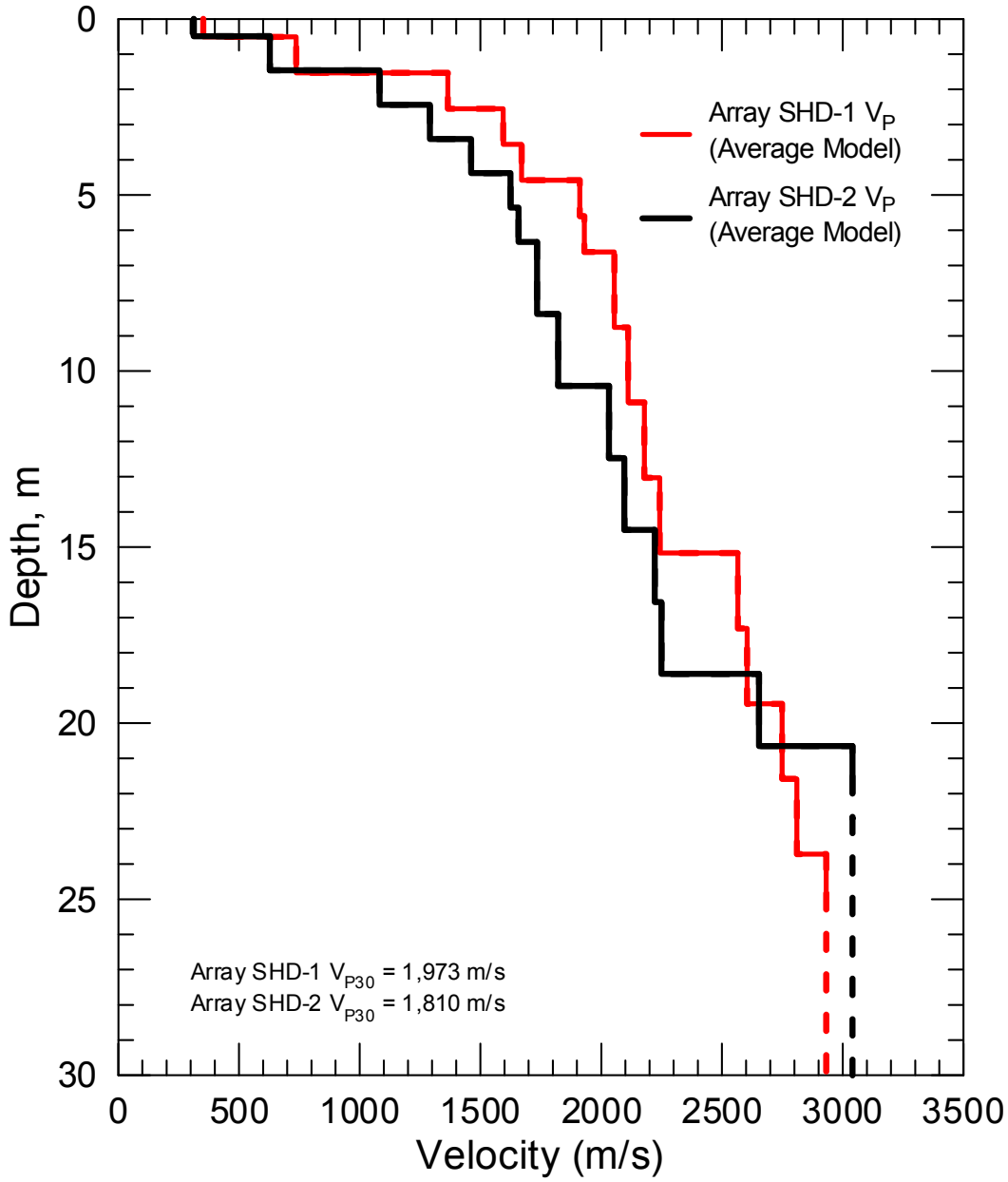

PG.SHD – Average V_P models between 24 and 48 m on arrays SHD-1 and SHD-2. Depth of investigation was limited to about 22 to 25 m and the models were extrapolated to 30 m depth. There is an 8% variation in V_{P30} along the central 24 m segment of the two arrays.

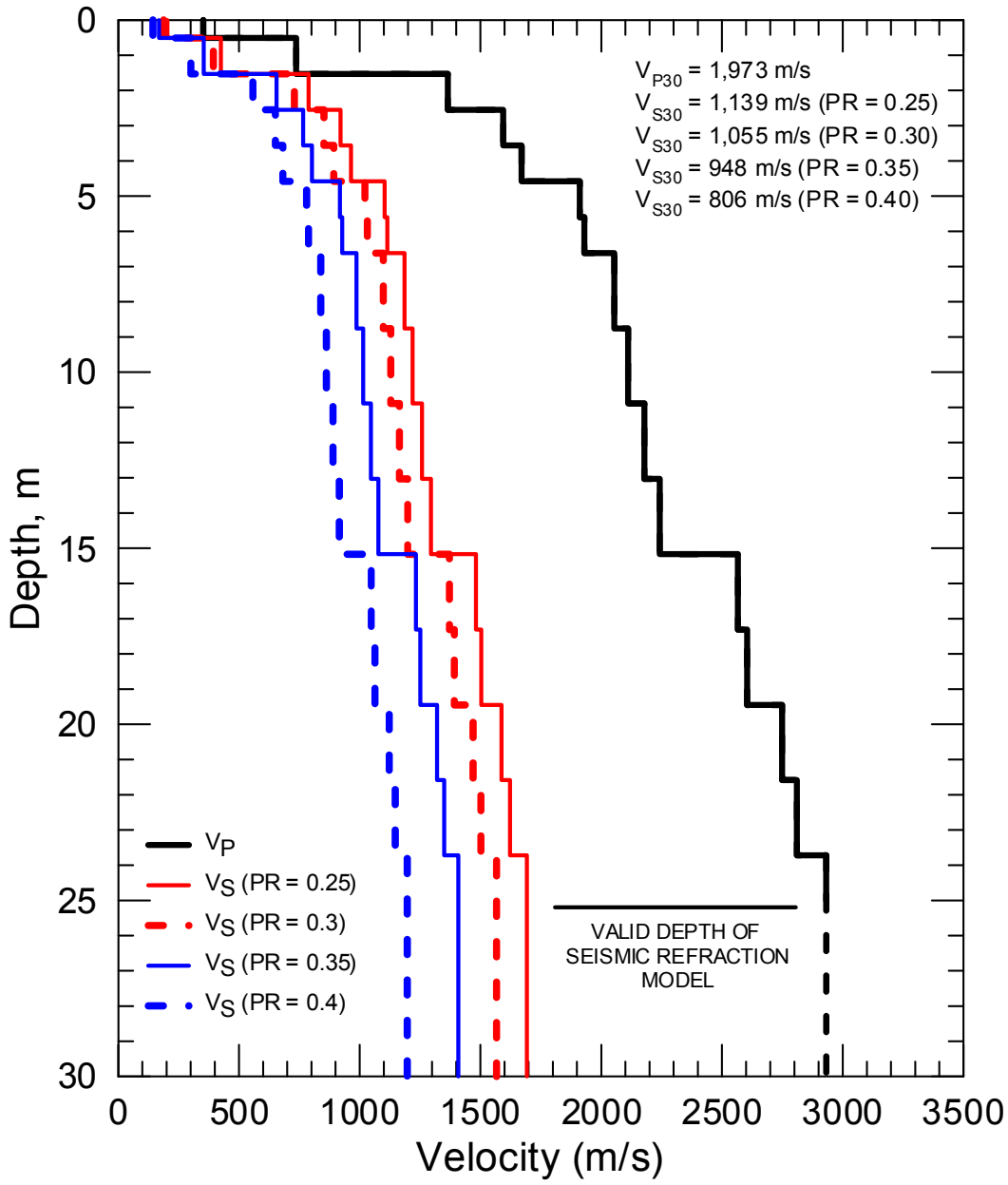

PG.SHD – Average P-wave velocity structure and estimated S-wave velocity structure between a position of 24 and 48 m on the P-wave seismic refraction model for array SHD-1. The maximum seismic refraction depth of investigation is limited to about 25 m; however, P-wave velocity is not expected to significantly increase with depth between 25 and 30 m.

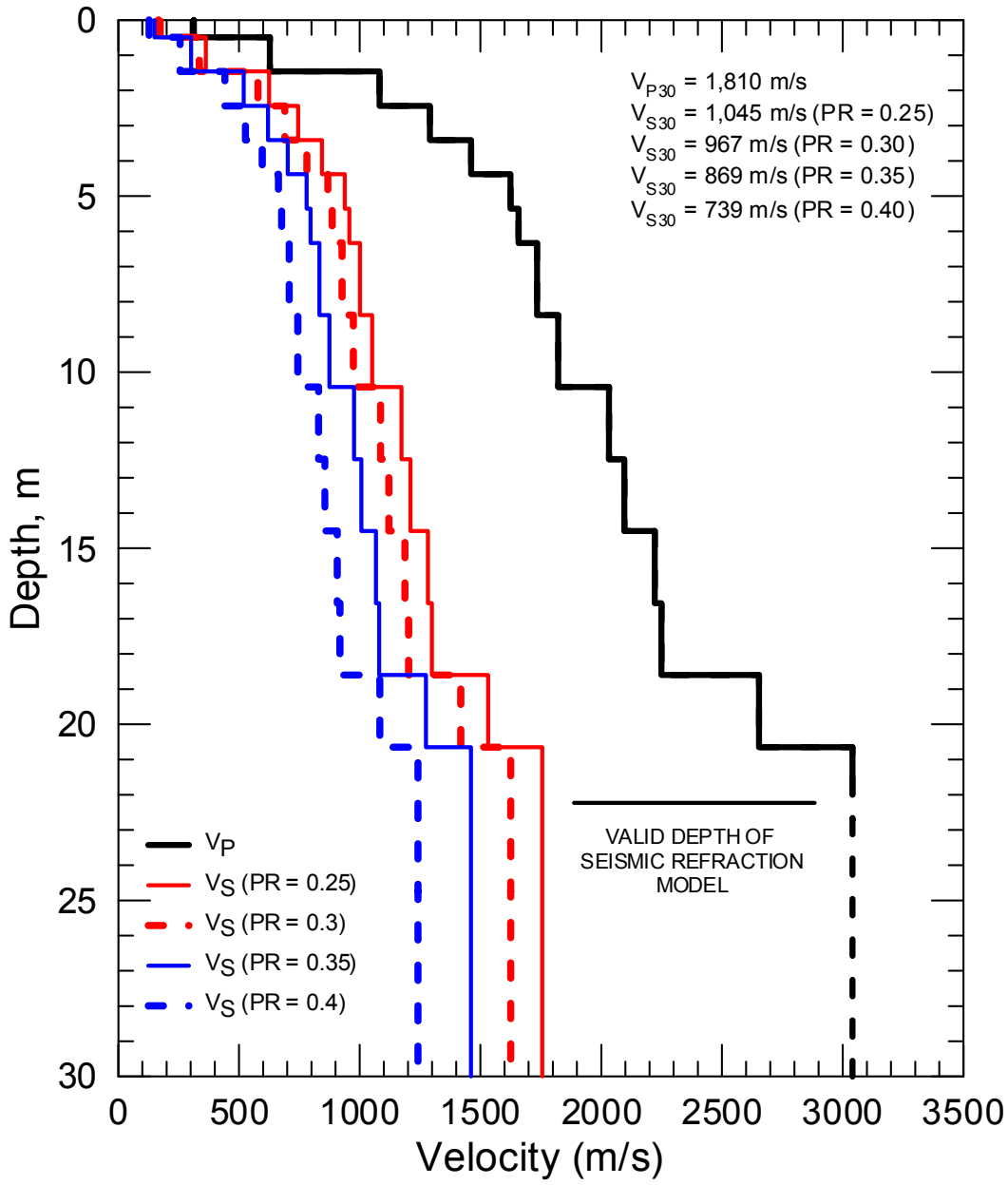

PG.SHD – Average P-wave velocity structure and estimated S-wave velocity structure between a position of 24 and 48 m on the P-wave seismic refraction model for array SHD-1. The maximum seismic refraction depth of investigation is limited to about 22 m; however, P-wave velocity is not expected to significantly increase with depth between 22 and 30 m.

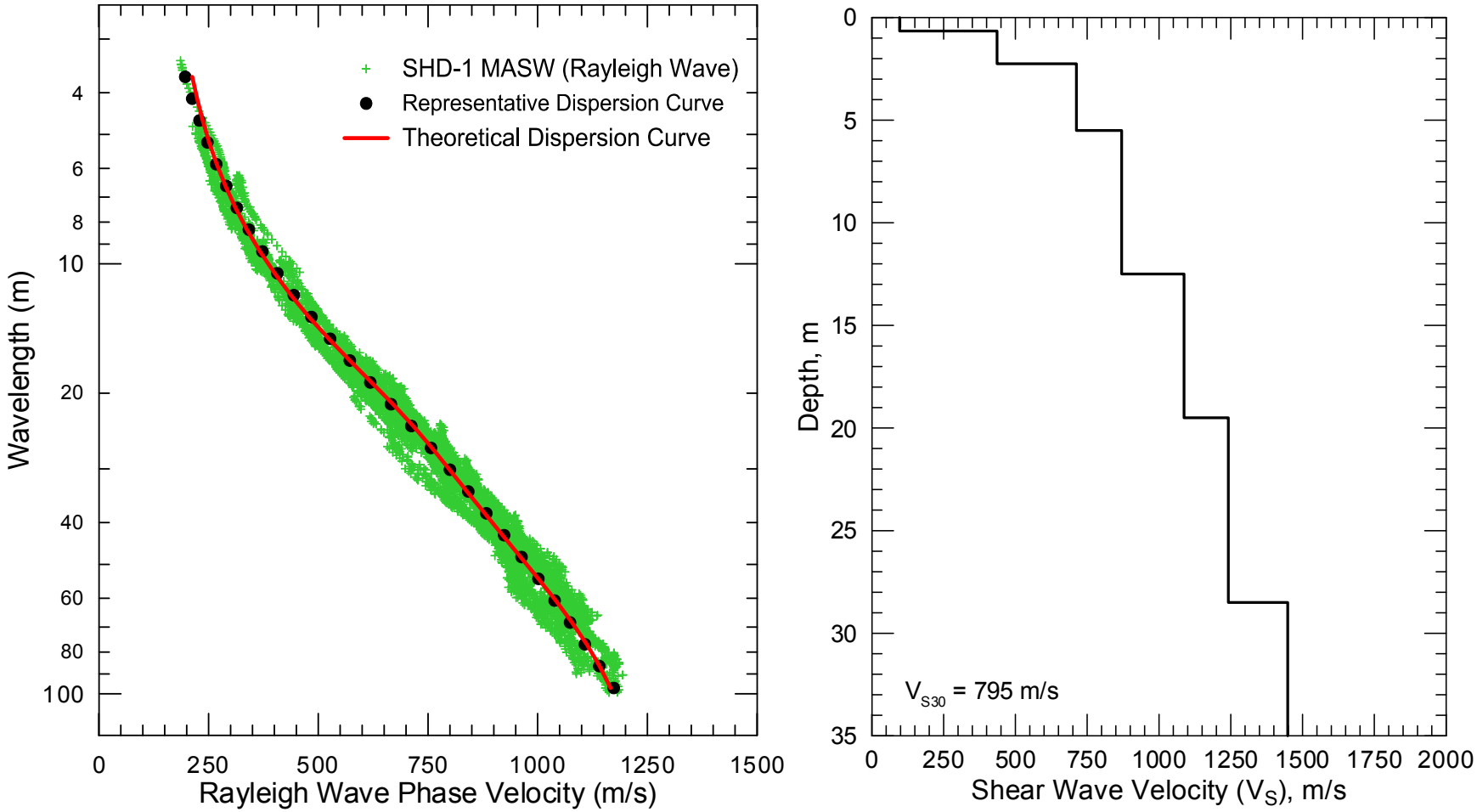

PG.SHD - Field, representative and inverted theoretical Rayleigh wave dispersion data (left) and associated V_S model (right) from MASW array SHD-1

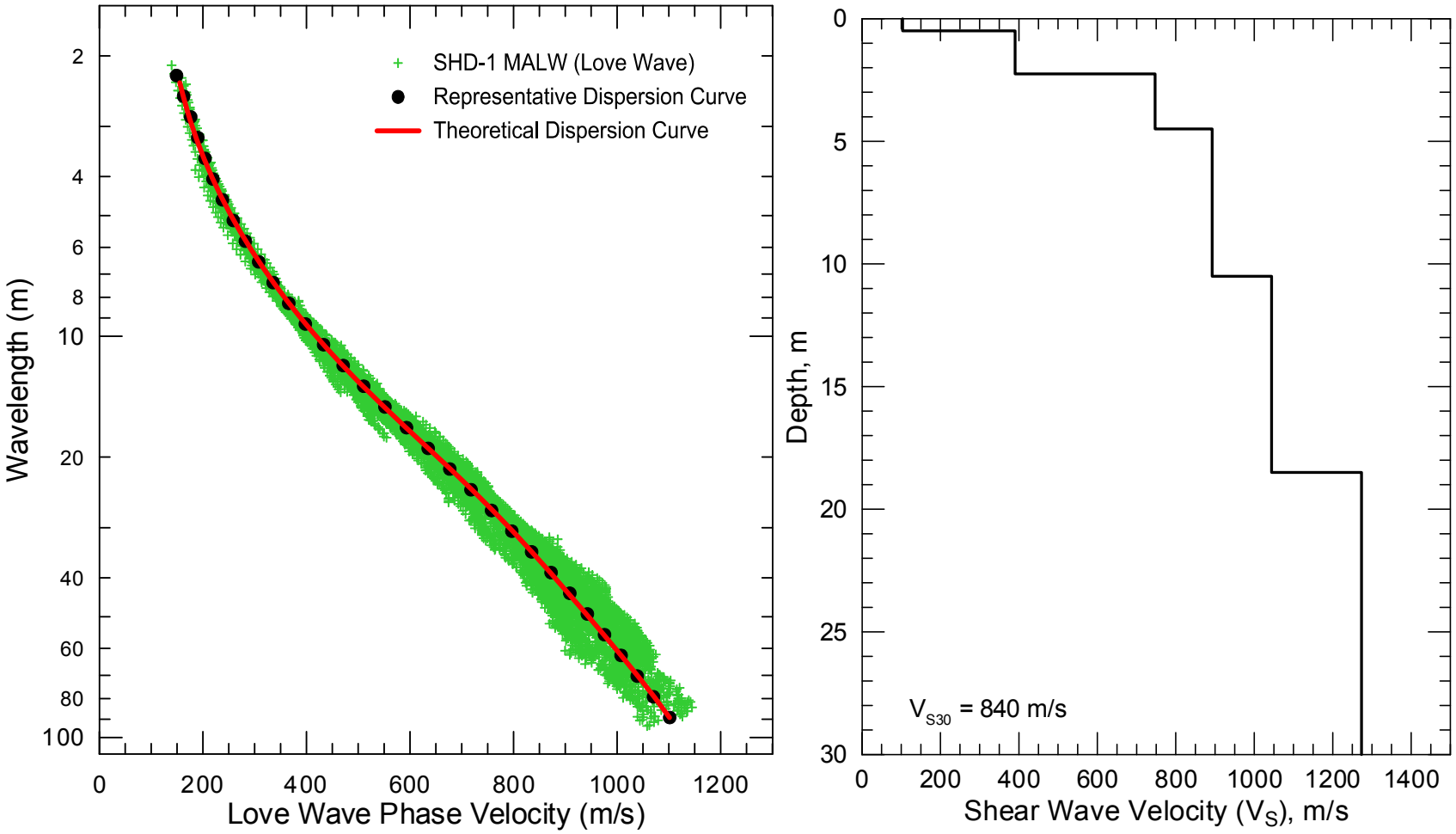

PG.SHD - Field, representative and inverted theoretical Love wave dispersion data (left) and associated V_S model (right) from MALW array SHD-1

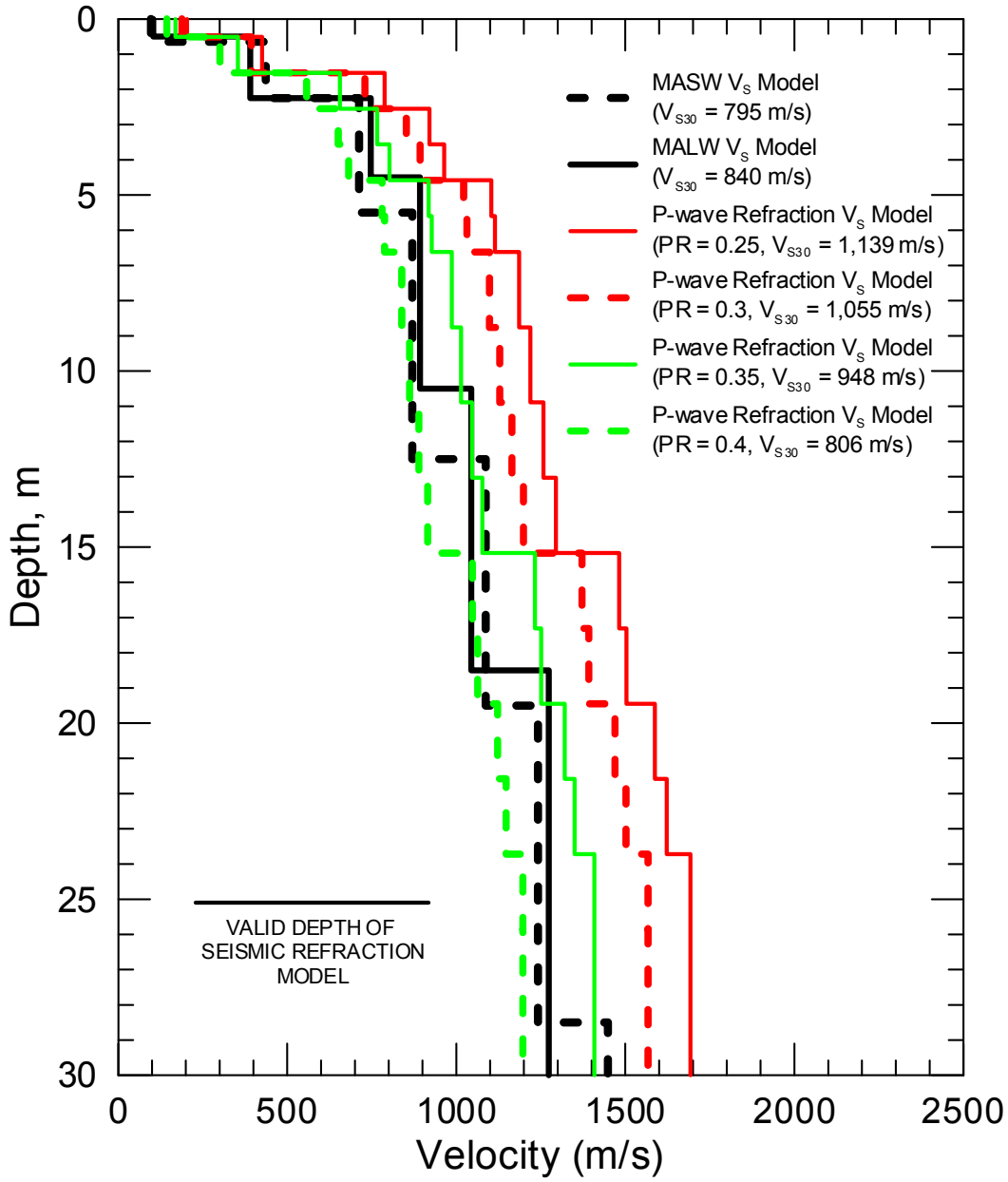

PG.SHD – Comparison of S-wave velocity models derived from the MASW, MALW and P-wave seismic refraction survey along array SHD-1. S-wave wave velocity is estimated from the average P-wave velocity model between 24 and 48 m on array SHD-1, assuming constant Poisson's ratio of 0.25, 0.3, 0.35 and 0.4. The V_S models resulting from inversion of Rayleigh and Love wave phase velocity data are relatively consistent. However, the V_S models derived from the surface wave data yield lower estimates of V_{S30} than from the P-wave refraction model with nominal Poisson's ratio in the 0.3 to 0.35 range. For the seismic refraction model to be consistent with the surface wave models Poisson's ratio would have to be in the 0.35 to 0.4 range, which would seem high for unsaturated sandstone. Potentially, the average seismic refraction model between 24 and 48 m on array SHD-1 is not representative of average velocity structure below the 70.5 m long array.

Site PG.VPD

Location: PG&E Diablo Canyon, Valencia Peak, San Luis Obispo County, California

Latitude: 35.23979 **Longitude:** -120.86951
(Station coordinates modified based on field GPS survey, WGS84 coordinate system)

V_{S30} (measured): 262 m/s

V_{S30} (adjusted to more accurately reflect seismic station conditions): 262 m/s (no adjustment necessary).

NEHRP Site Class: D

Geomatrix Code: IMD

Geologic Conditions/Observations: Seismic station located on Tertiary (Miocene) Monterey Formation, primarily consisting of shale.

Site Conditions: Rural site. Rolling topography in site vicinity. Seismic station located on top of a ridge of intensely weathered shale. Seismic line located on relatively planar surface with a 3.5 m decrease in surface elevation to east along 70.5 m long seismic line. The seismic station is about 4 to 5 m lower in elevation than the seismic line.

Geophysical Methods Utilized: HVSR, Seismic Refraction, MASW

Geophysical Testing Arrays:

1. Array VPD-1 (48 channel MASW and P-wave seismic refraction array utilizing 4.5 Hz vertical geophones spaced 1.5 m apart for a length of 70.5 m, forward and reverse shot locations with multiple source offsets and source types (AWD only used where possible) and multiple interior shot locations).
2. Three HVSR measurement locations distributed along array VPD-1.

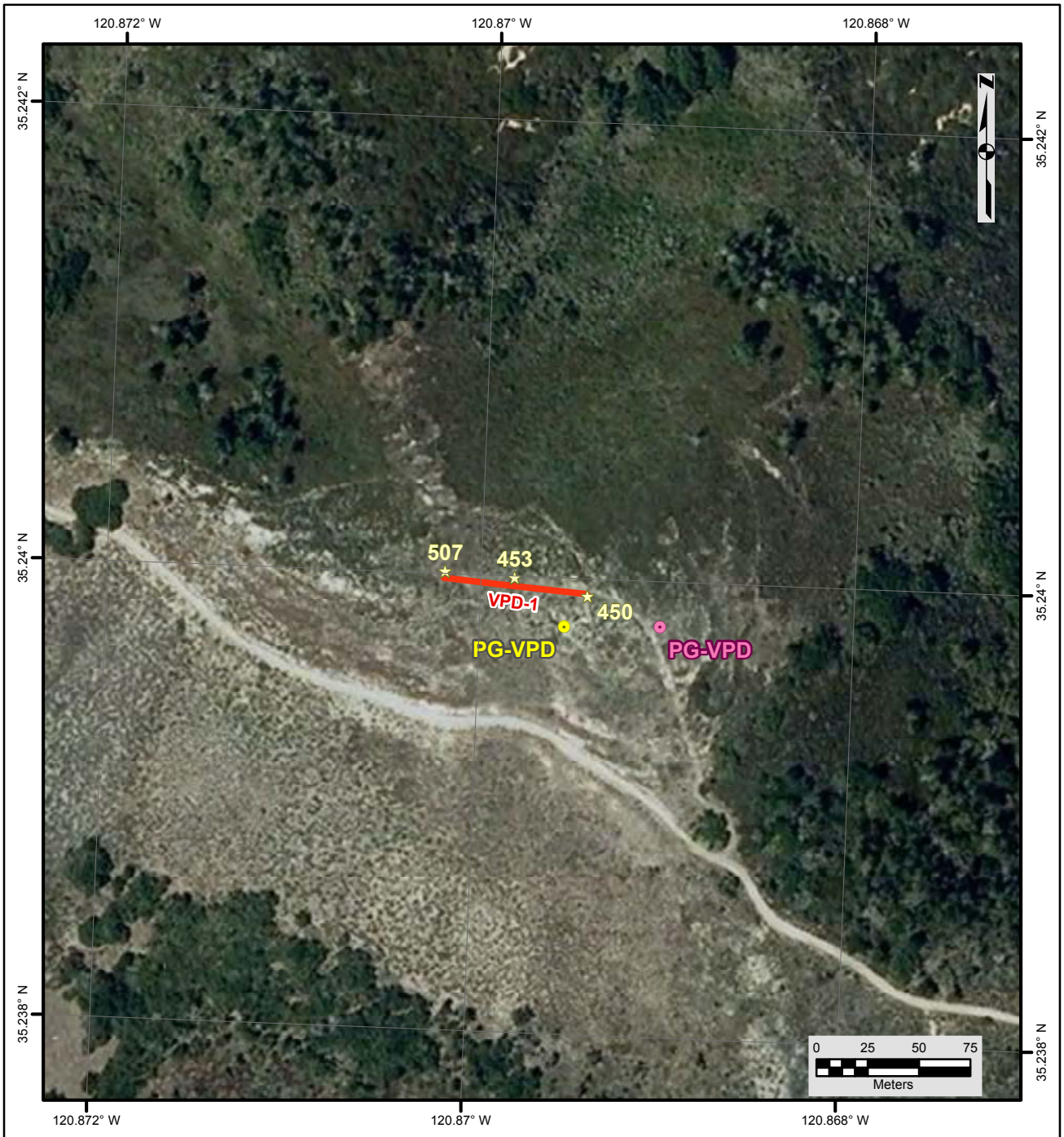

Legend

- Seismic Station - Approximate Surveyed Location
- Seismic Station - Approximate Location of Record
- H/V Spectral Ratio Location
- MASW and Seismic Refraction Array

NOTES:
1. WGS 1984 COORDINATE SYSTEM
2. Image Source: ESRI, i-cubed, USDA FSA, USGS, AEX, GeoEye, Getmapping, Aerogrid, IGP

File Name: PG-VPD-I

Date: 11/15/2012

USGS science for a changing world

GEOVision geophysical services

RECOVERY.GOV

SITE MAP
PG•VPD

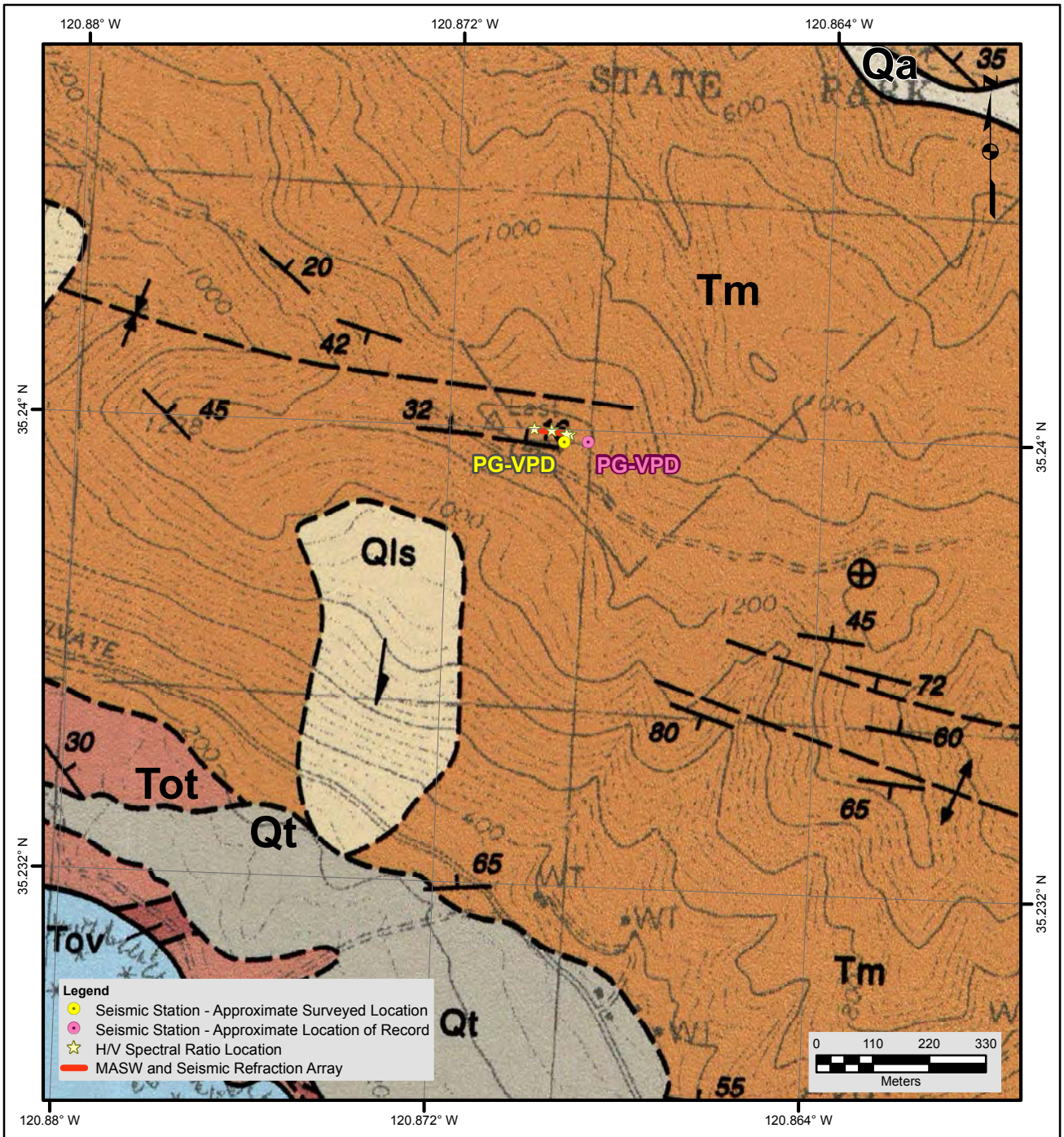

Description of Geologic Map Units

Qa = Quaternary (Holocene) alluvial gravel, sand and clay of valley areas and stream channels
Qt = Quaternary (Holocene) unconsolidated sand, silt, clay and gravel of marine terrace deposits
Qls = Quaternary (Pleistocene) landslide rubble
Tm = Tertiary (Upper Miocene) Monterey Formation; thin-bedded, platy siliceous shale, cherty
Tot = Tertiary (Lower Miocene) Obispo Formation; marine pyroclastic tuff, fine-grained, massive; includes tuff breccia with small clasts of pumice and perlite
Tov = Tertiary (Lower Miocene) Obispo Formation; marine pyroclastic volcanic rocks, mostly basalt but some andesitic rock

NOTES:
1. WGS 1984 COORDINATE SYSTEM
2. Geologic Map of the Port San Luis Quadrangle, San Luis Obispo County, California by Thomas W. Dibblee, Jr., 2006
3. See site map for details of geophysical survey

File Name: PG-VPD

Date: 1/5/2012

USGS science for a changing world

GEOVision geophysical services

GEOLOGIC MAP
PG•VPD

RECOVERY.GOV

Looking east along array VPD-1 and at HVSR sensor 507

Looking at PG.VPD seismic station towards east end of array VPD-1

Looking west along array VPD-1 and at HVSR sensor 450

P-wave seismic refraction and MASW data acquisition

MASW data acquisition using accelerated weight drop energy source

Location of Geophysical Testing Arrays:

Location	Latitude	Longitude
VPD-1, Northwest End of MASW/Refraction Array	35.23998	-120.87017
VPD-1, Center of MASW/Refraction Array	35.23996	-120.86978
VPD-1, Southeast End of MASW/Refraction Array	35.23993	-120.86940
HVSR Sensor 450	35.23992	-120.86939
HVSR Sensor 453	35.23999	-120.86979
HVSR Sensor 507	35.24001	-120.87016
PG.VPD Seismic Station	35.23979	-120.86951
PG.VPD Seismic Station Accelerometer	35.23981	-120.86947

Notes: 1) WGS84 Coordinate System (decimal degrees)
2) Survey accuracy is estimated at 1 to 2 m.

Results:

V_S Model

Depth to Top of Layer (m)	Layer Thickness (m)	S-Wave Velocity (m/s)	Inferred P-Wave Velocity (m/s)	Assumed Poisson's Ratio	Assumed Density (g/cm^3)
0	1	138	258	0.3	1.7
1	2	216	404	0.3	1.8
3	3	246	461	0.3	1.8
6	6	258	484	0.3	1.8
12	11	261	487	0.3	1.8
23	>7	347	649	0.3	1.9

Notes: 1) Depth of investigation is about 30 m.
2) Bottom layer is a half space.

Observations/Discussion:

- The HVSR curves are very similar at frequencies below 4 Hz and have some minor differences at higher frequencies, possibly due to lateral velocity variation in near surface sediments.
- There is a HVSR peak in the 0.8 to 0.9 Hz range at each measurement location.
- The P-wave refraction data for array VPD-1 were modeled using a tomographic inversion routine with a smooth velocity gradient starting model. The seismic refraction model was extended to far offset shot locations to extend depth of investigation.
- The seismic refraction survey design allowed P-wave velocity to be imaged to a maximum depth of about 15 m. The seismic refraction model shows that P-wave velocity is about 300 to 400 m/s at the surface and increases to about 550 m/s at a depth of 2 to 14 m. These low P-wave velocities indicate that the Tertiary Monterey Formation is intensely weathered in the near surface.
- The seismic refraction model indicates that there is lateral velocity variation at the site with low velocity sediments thickening to the east.
- Noise conditions at the site were not sufficient for application of passive surface wave techniques.
- The minimum wavelength surface wave phase velocity data extracted from the 48-channel MASW array is about 6 m. Data reduction using seismic records from smaller hammer sources and a limited offset receiver array (i.e. less active geophones) allowed extraction of surface wave dispersion data to a minimum wavelength of about 3 m.
- A maximum wavelength of 45 m was extracted from MASW data collected with a 20 lb hammer source. This is equivalent to a frequency of slightly less than 6 Hz, which is still pushing the envelope for a hammer energy source. Fortunately, one end of the MASW line was accessible to the accelerated weight drop source, whereby more reliable long wavelength surface wave dispersion data could be obtained.
- There is significant scatter in the MASW dispersion data, as expected based on the lateral velocity variation in the seismic refraction model. A coherent surface wave dispersion curve, thought to be most representative of conditions at the east end of the array near the seismic station, was developed using only about two-thirds of the reduced phase velocity data. There remains about 30 to 40 m/s scatter in this dispersion curve due to lateral velocity variation.
- A representative dispersion curve was generated for the MASW data set using a moving average, polynomial curve fitting routine and used for modeling.
- Surface wave depth of investigation is about 30 m based on half of maximum wavelength criteria.
- The inferred P-wave velocities in the surface wave model are generally consistent with the velocity structure at the eastern end of the seismic refraction model, especially considering unknown Poisson's ratio. P-wave velocity is, however, slightly higher below a depth of about 10 m in the seismic refraction model.
- V_{S30} is 262 m/s (Site Class D).

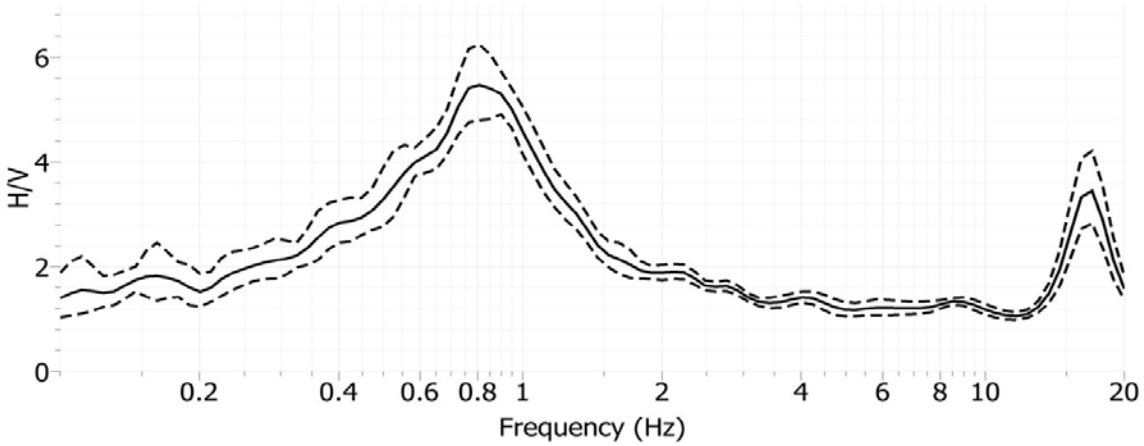

Site CI.VPD, H/V Spectral Ratio, Array VPD-1, Sensor 507

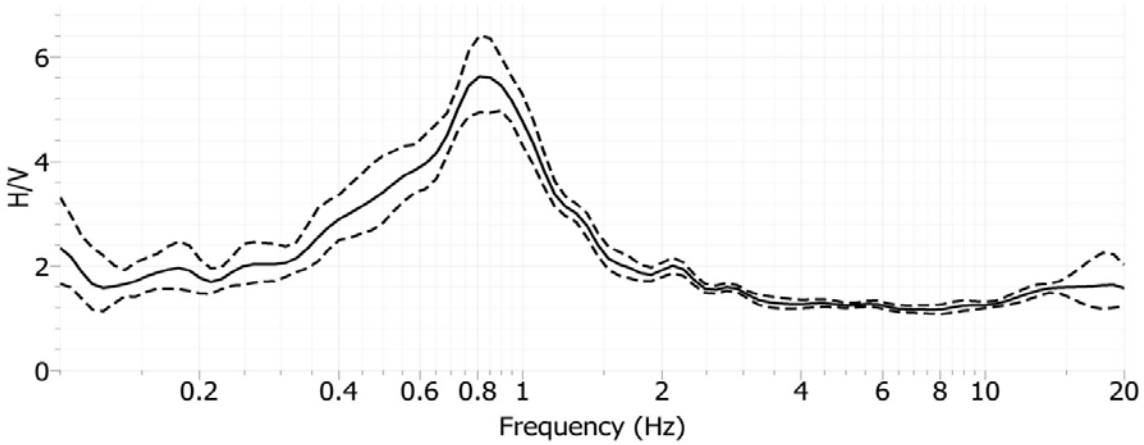

Site CI.VPD, H/V Spectral Ratio, Array VPD-1, Sensor 453

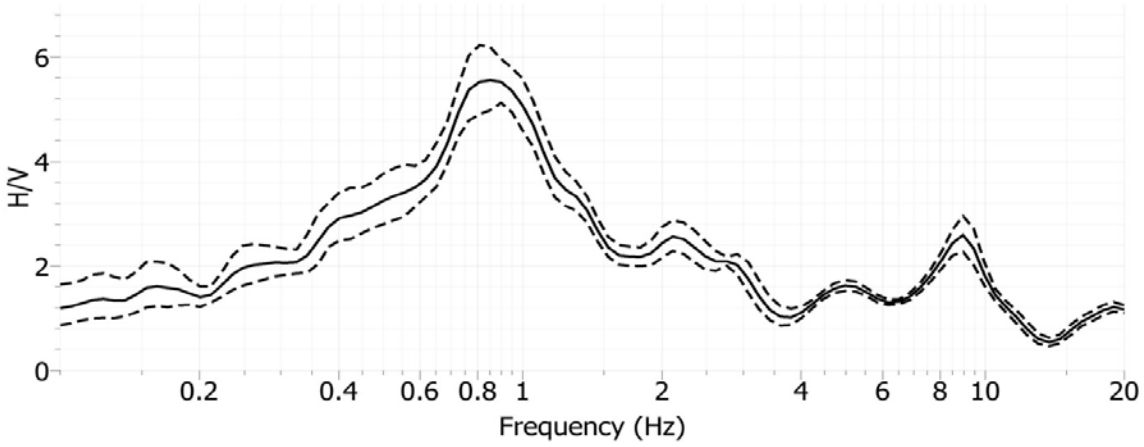

Site CI.VPD, H/V Spectral Ratio, Array VPD-1, Sensor 450

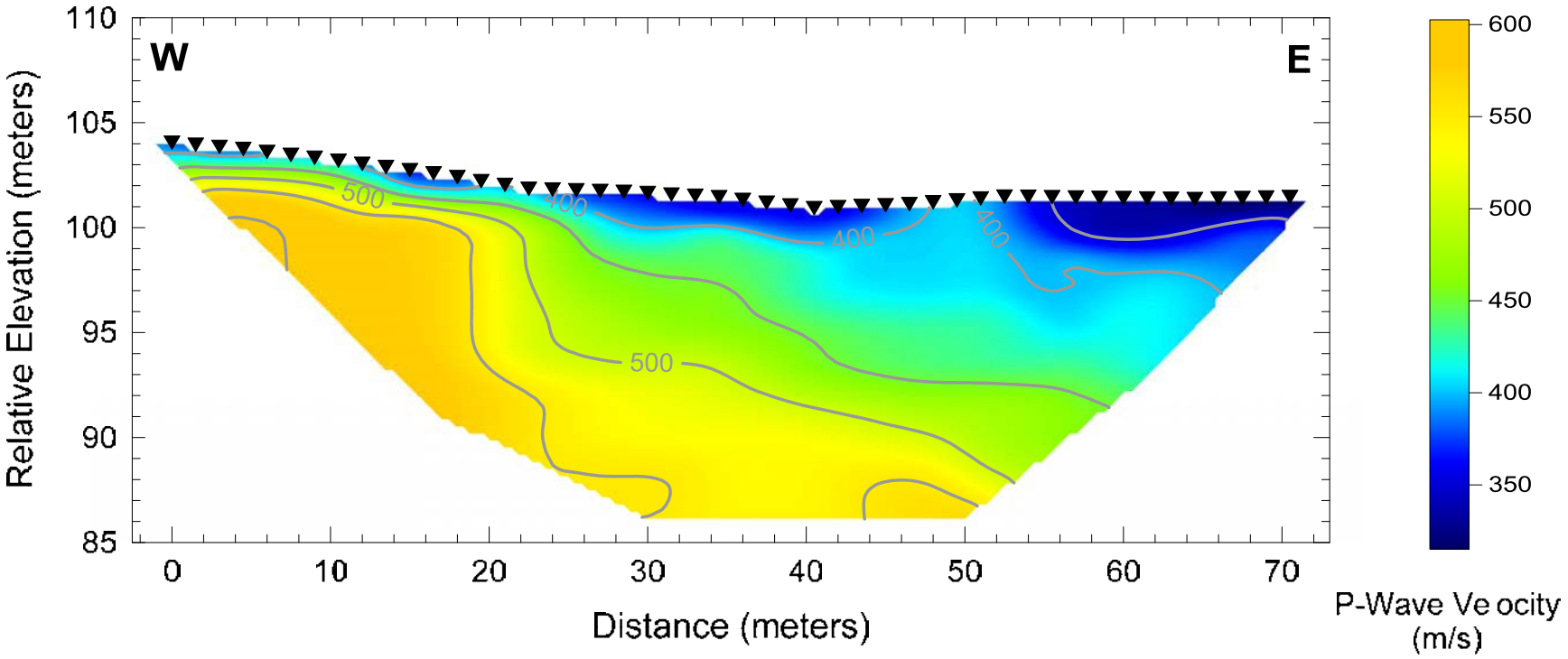

Array VPD-1 – Tomographic seismic refraction model utilizing smooth velocity gradient starting model

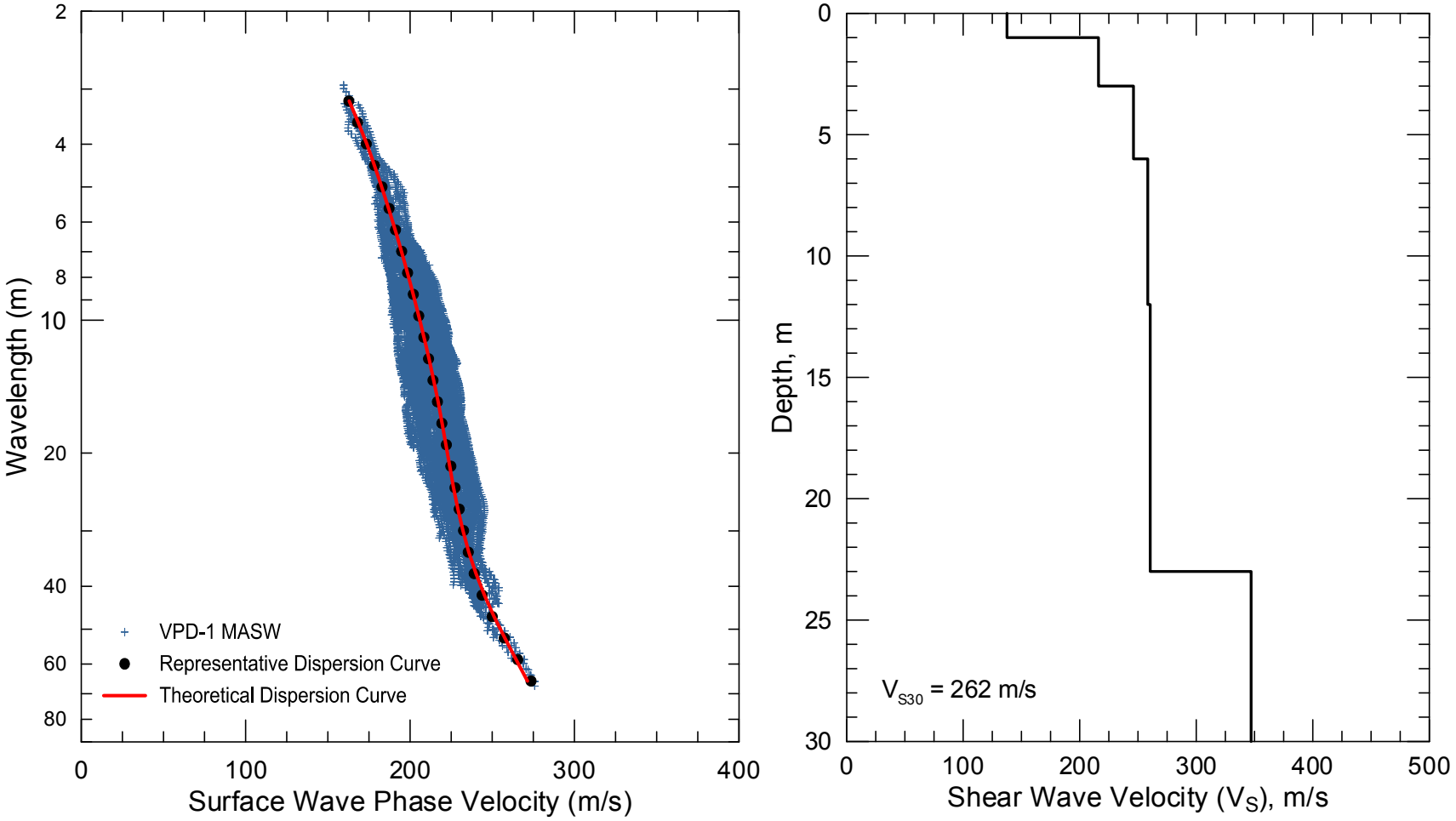

PG.VPD - Field, representative and inverted theoretical surface wave dispersion data (left) and associated V_S model (right)

Site US.ACSO

Location: Alum Creek State Park, Delaware, Ohio

Latitude: 40.23228 **Longitude:** -82.98202
(Station coordinates from field survey, WGS84 coordinate system)

V_{S30} (measured): 460 m/s (Refer to addendum for final recommended V_S models and V_{S30})

V_{S30} (adjusted to more accurately reflect seismic station conditions): 500 m/s (average S-wave velocity between 1 and 31 m adjusting for assumed 1 m sensor depth).

NEHRP Site Class: C

Geomatrix Code: IZB

Geologic Conditions/Observations: Bedrock geology in site vicinity mapped as Paleozoic (Upper Devonian) shale, siltstone and very fine-grained sandstone. Field observations indicate that a sediment layer of unknown thickness overlies the sedimentary rock.

Site Conditions: Rural site. Undulating topography in site vicinity. Test area located in a field with relatively flat topography near an Ohio State Geological Survey building.

Geophysical Methods Utilized: HVSR, Seismic Refraction (P-wave), MASW (Rayleigh wave)

Geophysical Testing Arrays:

1. Array ACSO-1 (48 channel MASW array, utilizing 4.5 Hz vertical geophones spaced 1.5 m apart for a length of 70.5 m, forward and reverse shot locations with multiple source offsets and source types and multiple interior shot locations).
2. Array ACSO-2 (48 channel P-wave seismic refraction array, with same orientation as array ACSO-1 and origin located 27 m northwest of the end of array ACSO-1, utilizing 4.5 Hz vertical geophones spaced 3 m apart for a length of 141 m, forward and reverse shot locations with multiple source offsets and source types and multiple interior shot locations).
3. Four HVSR measurement locations: three distributed along array ACSO-1 and the other near the seismic station.

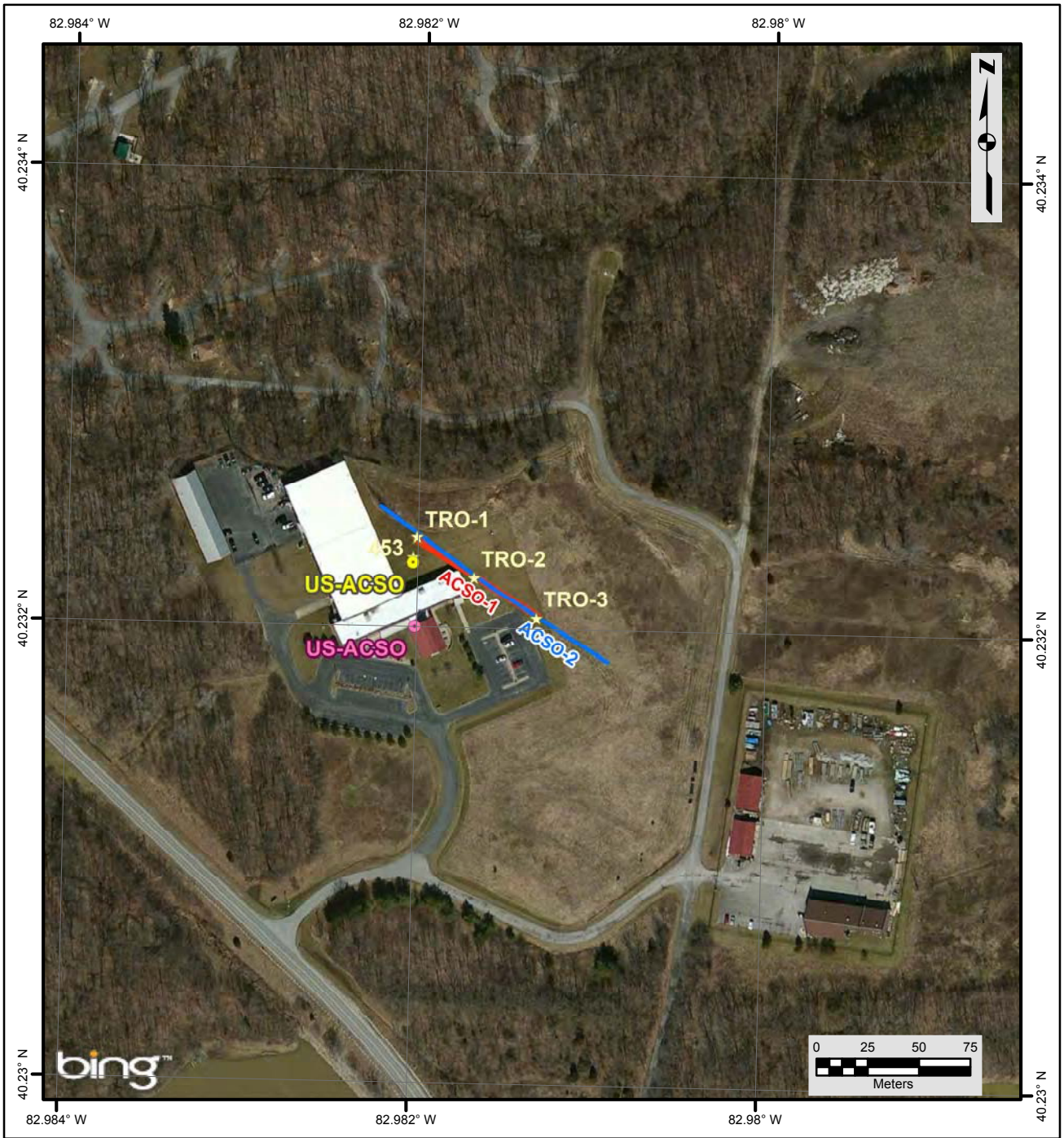

Legend

- Seismic Station - Approximate Surveyed Location
- Seismic Station - Approximate Location of Record
- H/V Spectral Ratio Location
- P-wave Seismic Refraction and MASW Array
- MASW Array

NOTES:
1. WGS 1984 COORDINATE SYSTEM
2. Image Source: (c) Microsoft Corporation and its data suppliers

File Name: US-ACSO-I

Date: 2/7/2013

USGS science for a changing world

GEOVision geophysical services

RECOVERY.GOV

SITE MAP
US•ACSO

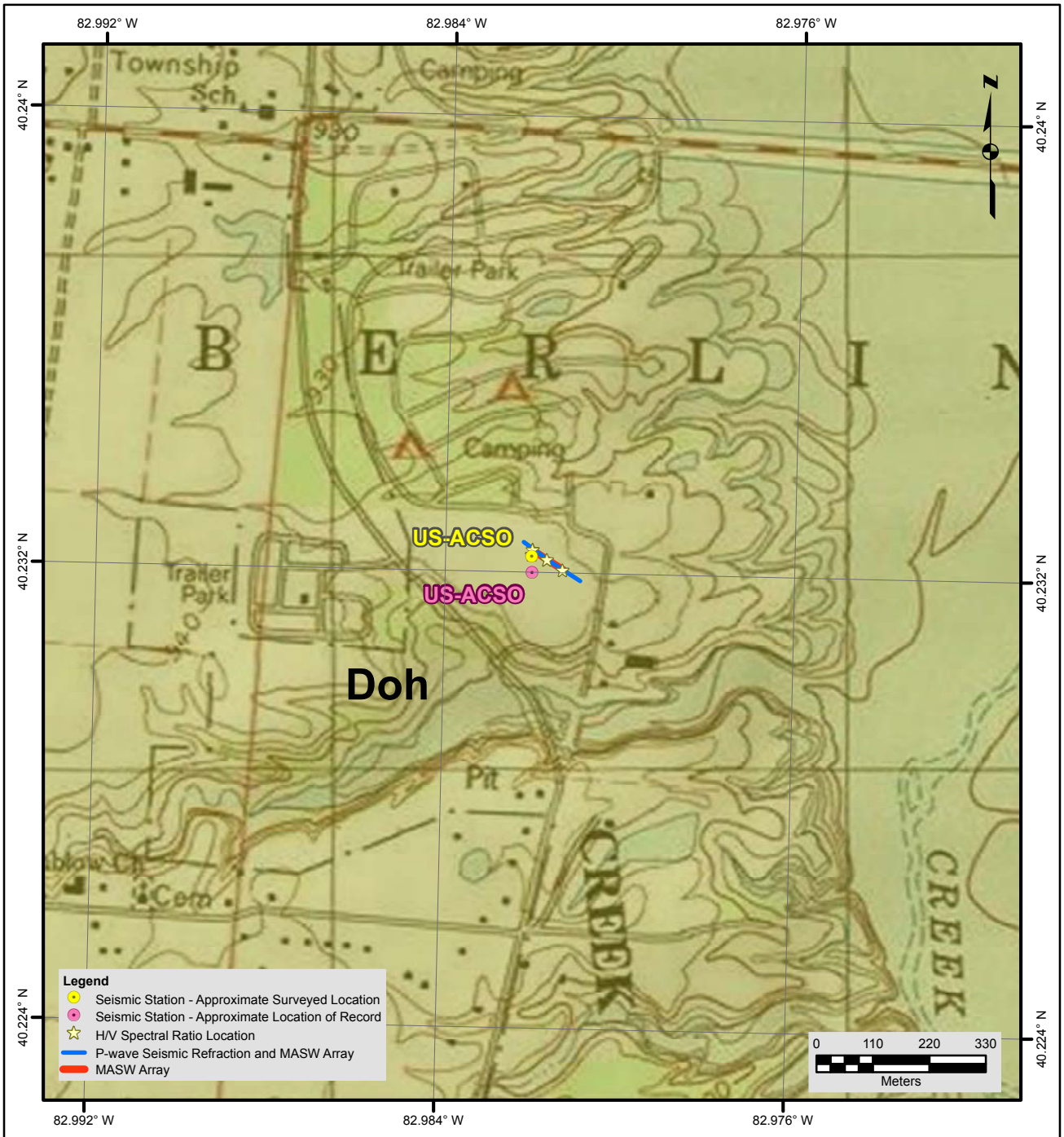

Description of Geologic Map Units

Doh = Paleozoic (Upper Devonian) shale, siltstone, very fine-grained sandstone, carbonaceous, calcareous concretions common in lower portion

NOTES:
1. WGS 1984 COORDINATE SYSTEM
2. Bedrock Geologic Map of Ohio
Ohio Division of Geological Survey Map BG-1, Version 6.0
compilation by E. R. Slucher, E. M. Swinford, G. E. Larsen
GIS by D. M. Powers, 2006
3. See site map for details of geophysical survey

File Name: US-ACSO

Date: 2/7/2013

USGS science for a changing world

GEOVision geophysical services

GEOLOGIC MAP
US•ACSO

RECOVERY.GOV

Looking northeast towards seismic station US.ACSO and MASW array ACSO-1

Looking northwest along MASW array ACSO-1

Looking northwest at off-end shot location on MASW array ACSO-1 and at the seismic station

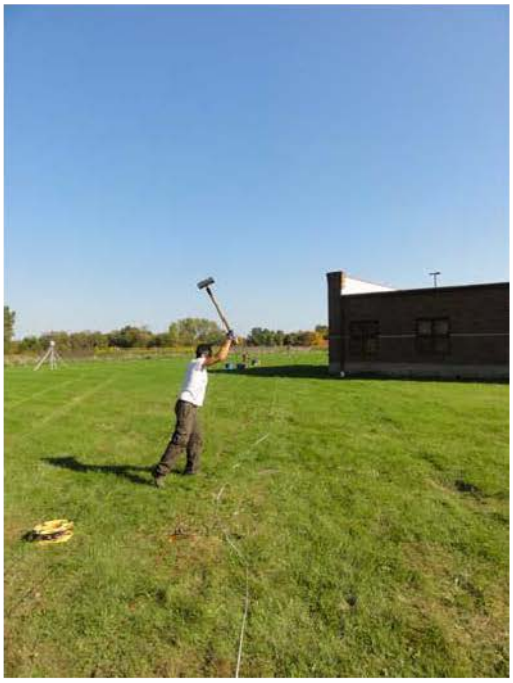

Looking southeast along P-wave seismic refraction array ACSO-2

HVSR sensor placed in a shallow hole

Location of Geophysical Testing Arrays:

Location	Latitude	Longitude
ACSO-1, Northwest End of MASW Array	40.23238	-82.98200
ACSO-1, Center of MASW Array	40.23222	-82.98165
ACSO-1, Southeast End of MASW Passive Array	40.23205	-82.98130
ACSO-2, Northwest End of P-wave Seismic Refraction Array	40.23252	-82.98221
ACSO-2, Center of P-wave Seismic Refraction Array	40.23219	-82.98160
ACSO-2, Southeast End of P-wave Seismic Refraction Array	40.23186	-82.98089
HVSR Sensor TRO-1 (Tromino ENGY)	40.23239	-82.98199
HVSR Sensor TRO-2 (Tromino ENGY)	40.23222	-82.98166
HVSR Sensor TRO-3 (Tromino ENGY)	40.23204	-82.98130
HVSR Sensor 453 (Nanometrics Trillium Compact)	40.23230	-82.98202
US.ACSO Seismic Station	40.23228	-82.98202

Notes: 1) WGS84 Coordinate System (decimal degrees)
2) Survey accuracy is estimated at 1 to 2 m.

Results: (Refer to addendum for final recommended V_S models)

V_S Model 1FM (Near Surface Velocity Structure Representative of Southeast Portion of Array, Fundamental Mode Assumption)

Depth to Top of Layer (m)	Layer Thickness (m)	S-Wave Velocity (m/s)	Inferred P-Wave Velocity (m/s)	Assumed Poisson's Ratio	Assumed Density (g/cm^3)
0	1.25	110	206	0.300	1.70
1.25	2.75	228	426	0.300	1.80
4	3	420	785	0.300	1.90
7	3	675	1500	0.373	2.10
10	15	917	2250	0.400	2.10
25	>10	974	3000	0.441	2.15

Notes: 1) Saturated sediments/rock with V_P of 1,500 to 3,000 fixed at a depth of 6 to 7 m based on seismic refraction models.
2) Depth of investigation is about 35 m.
3) Bottom layer is a half space.
4) V_{S30} = 531 m/s.

V_S Model 1AM (Near Surface Velocity Structure Representative of Southeast Portion of Array, Average Mode Assumption)

Depth to Top of Layer (m)	Layer Thickness (m)	S-Wave Velocity (m/s)	Inferred P-Wave Velocity (m/s)	Assumed Poisson's Ratio	Assumed Density (g/cm^3)
0	1.5	127	234	0.292	1.70
1.5	1.5	183	345	0.306	1.80
3	3	331	610	0.291	1.90
6	4	406	1500	0.461	2.00
10	6	532	2000	0.462	2.00
16	8	646	2500	0.464	2.10
24	>11	935	3000	0.446	2.15

Notes: 1) Saturated sediments/rock with V_P of 1,500 to 3,000 fixed at a depth of 6 to 7 m based on seismic refraction models.
2) Depth of investigation is about 35 m.
3) Bottom layer is a half space.
4) V_{S30} = 435 m/s.

V_S Model 1G3 (Near Surface Velocity Structure Representative of Southeast Portion of Array, 3-D Global Inversion in WinSASW Software Package)

Depth to Top of Layer (m)	Layer Thickness (m)	S-Wave Velocity (m/s)	Inferred P-Wave Velocity (m/s)	Assumed Poisson's Ratio	Assumed Density (g/cm^3)
0	1.5	117	218	0.300	1.70
1.5	1.5	196	367	0.300	1.80
3	3	299	559	0.300	1.85
6	4	409	1500	0.460	2.00
10	6	511	2000	0.465	2.00
16	9	652	2500	0.464	2.10
25	>10	985	3000	0.440	2.15

Notes: 1) Saturated sediments/rock with V_P of 1,500 to 3,000 fixed at a depth of 6 to 7 m based on seismic refraction models.
2) Depth of investigation is about 35 m.
3) Bottom layer is a half space.
4) V_{S30} = 423 m/s.

V_S Model 2FM (Near Surface Velocity Structure Representative of Northwest Portion of Array, Fundamental Mode Assumption)

Depth to Top of Layer (m)	Layer Thickness (m)	S-Wave Velocity (m/s)	Inferred P-Wave Velocity (m/s)	Assumed Poisson's Ratio	Assumed Density (g/cm^3)
0	1.5	196	367	0.300	1.70
1.5	1.5	279	522	0.300	1.80
3	3	325	607	0.300	1.85
6	4	448	1500	0.451	2.00
10	6	551	2000	0.459	2.00
16	8	611	2500	0.468	2.10
24	>11	1030	3000	0.433	2.15

Notes: 1) Saturated sediments/rock with V_P of 1,500 to 3,000 fixed at a depth of 6 to 7 m based on seismic refraction models.
2) Depth of investigation is about 35 m.
3) Bottom layer is a half space.
4) V_{S30} = 492 m/s.

V_S Model 2AM (Near Surface Velocity Structure Representative of Northwest Portion of Array, Average Mode Assumption)

Depth to Top of Layer (m)	Layer Thickness (m)	S-Wave Velocity (m/s)	Inferred P-Wave Velocity (m/s)	Assumed Poisson's Ratio	Assumed Density (g/cm^3)
0	1.5	201	379	0.303	1.70
1.5	1.5	265	499	0.305	1.80
3	3	326	611	0.302	1.85
6	4	431	1500	0.455	2.00
10	6	534	2000	0.462	2.00
16	8	634	2500	0.466	2.10
24	>11	935	3000	0.446	2.15

Notes: 1) Saturated sediments/rock with V_P of 1,500 to 3,000 fixed at a depth of 6 to 7 m based on seismic refraction models.
2) Depth of investigation is about 35 m.
3) Bottom layer is a half space.
4) V_{S30} = 485 m/s.

Observations/Discussion:

- Seismic testing was conducted at the only location on the subject property where a long enough array could be established. This required that the array pass near the corner of a building, which is not ideal; however, the building does not have a basement. The array may, however, pass from the building pad to softer undisturbed soils, which would introduce near surface lateral velocity variation. Alternate testing locations would require moving further from the seismic station, possibly along a dirt road in the site vicinity. During acquisition of the 70.5 m long MASW array ACSO-1, the observation was made that a longer line would be beneficial for P-wave seismic refraction data acquisition. Therefore, P-wave seismic refraction data was also acquired along the 141 m long array ACSO-2, which has the same orientation and overlaps array ACSO-1.
- HVSR data were acquired at three locations along array ACSO-1 using a Micromed Tromino ENGY and at an additional location next to the seismic station using a Nanometrics Trillium Compact. The HVSR curves are very similar at all measurement locations with a broad HVSR peak in the 4 to 6 Hz range.
- P-wave seismic refraction data quality was excellent. The P-wave seismic refraction data for array ACSO-2 were modeled using a tomographic inversion routine with both layer-based and smooth velocity gradient starting models. The P-wave seismic refraction survey design allowed P-wave velocity to be imaged to a depth of about 30 m, or greater.
- The seismic refraction models indicate that P-wave velocity is about 200 to 350 m/s at the surface and increases to 1,000 m/s at a depth of 3 to 6 m, 1,500 m/s at a depth of 7 to 9 m, 2,000 m/s at a depth of 11 to 15 m and over 3,000 m/s at a depth of about 23 to 28 m. The maximum P-wave velocity in the seismic refraction model that utilized a smooth velocity gradient starting model is about 3,750 m/s. However, the seismic refraction data can be modeled without P-wave velocity significantly exceeding 3,000 m/s, as shown in the seismic refraction model developed utilizing a layer based starting model.
- The saturated zone is expected to be relatively shallow at this site. Review of the seismic refraction travel time data and the seismic refraction models indicates that the saturated zone may be as shallow as 4 m or as deep as 7 m. The saturated zone contact is somewhat unclear because of the possibility of shallow, high velocity sedimentary rock. It should be noted that the seismic saturated zone is not always precisely correlated with the water table as P-wave velocity does not increase to over the P-wave velocity of water until over about 99% of the pore space is filled with water.
- The seismic refraction survey indicates that there is some lateral velocity variation, particularly a slight thickening of a low velocity unsaturated sediment layer to the southeast. It is important to note that the near surface velocity structure is not well resolved due to the 3 m geophone spacing. A shorter seismic array with smaller geophone spacing would better resolve velocity structure in the upper couple meters. However, review of seismic records from array ACSO-1 confirms the near surface lateral velocity variation. The observed near surface velocity variation is expected to give rise to different high frequency/small wavelength surface wave dispersion data from source locations at each end of MASW array ACSO-1. The seismic record for the center shot location on array ACSO-1 clearly shows lateral velocity variation in surface wave propagation.
- The average P-wave velocity of the upper 30 m (V_{P30}) was estimated between 36 and 105 m, where depth of investigation is greatest, on the P-wave refraction model developed

using a layer-based starting model. V_{P30} ranges from about 1,247 to 1,513 m/s between a position of 36 to 105 m, a 20% variation. V_{P30} is highest at a position of 36 m, near the northwest end of MASW array ACSO-1, and lowest at a position of 99 m, near the southeast end of array ACSO-1.

- An average V_P model was developed over the 36 to 105 m distance interval by horizontally averaging the travel time of each model cell and cell thickness and average V_{P30} was determined to be 1,345 m/s. Assuming a constant Poisson's ratio of 0.25, 0.3, 0.35, 0.4 and 0.45 would result in an estimated V_{S30} of 776, 719, 646, 549 and 405 m/s, respectively. Because shallow sediments and bedrock are saturated, Poisson's ratio is expected to be highly variable and, therefore, the P-wave refraction models are not particularly useful for validating the S-wave velocity models developed from the MASW data.
- The seismic model developed using a smooth velocity gradient starting model, yielded a similar range of V_{P30} of 1,272 to 1,498 m/s over the 36 to 105 m distance interval of array ACSO-2. Because of the similarities in the two seismic refraction models, only the seismic refraction model developed using a layered starting model was used for correlation with the surface wave models.
- Noise conditions at the site were not sufficient for application of passive surface wave techniques.
- MASW (Rayleigh wave) data reduction was complicated by near surface lateral velocity variation and probable dominant first higher mode energy. As shown in an attached figure, two dispersion curves were picked from the MASW data collected along array ACSO-1. These dispersion curves are similar at wavelengths greater than 30 m, but diverge at smaller wavelengths. Typically, the different dispersion curves at small wavelengths (high frequency) are attributed to lateral velocity variation, especially if supported by seismic refraction models as is the case at this site. However, dominant higher modes may also be problematic at this site. The lowest small wavelength Rayleigh wave phase velocity data originates from limited offset range receiver gathers in the southeast half of the array and source locations offset from the southeast end of the array and in the center of the array. It was challenging to extract this dispersion data indicating that the lower velocity, near surface sediments are very localized or that the first higher mode is generally dominant at high frequencies. It has been observed at other sites that, in some cases, the first higher mode can be dominant over a wide frequency range when there is a very thin low velocity layer overlying much higher velocity sediments/rock. It was much more difficult interpreting small wavelength dispersion data from receiver gathers limited to the northwest half of the array with northwest offset and center source locations. As mentioned earlier, Rayleigh wave phase velocity data from these source locations and limited offset range receiver gathers is higher at wavelengths smaller than 30 m than that associated with the other half of the array. Long wavelength Rayleigh wave phase velocity data extracted from source locations at both ends of the array and receiver gathers consisting of at least 30 geophones tie into both small wavelength dispersion curve segments at wavelengths greater than 30 m, but at small wavelengths only ties into the higher phase velocity dispersion data. Interpreted first higher mode from receiver gathers in the SE half of the array tie into the dispersion data interpreted from 30 to 48 channel receiver gathers and source locations at both ends of the array and the small wavelength dispersion data from receiver gathers in the NW half

of the array. This may be a coincidence or indicate that the first higher mode is dominant over a wide frequency range for many source locations. SASW analysis of selected receiver pairs with source locations at the southeast and center of the array was performed to validate the lower phase velocity MASW dispersion curve. SASW analysis was limited to attempting to identify the fundamental mode, at least at high frequencies, and the resulting dispersion curve is identical to that resulting from MASW analysis. It should be noted that the smallest wavelength dispersion data resulted from a single, small offset pair of receivers and both the near offset southeast and center source locations. It was also generally difficult extracting the small wavelength dispersion data. The similarity in the lower phase velocity dispersion curve extracted by both MASW and SASW data analysis indicates that SASW inversion strategies (i.e. 3-D global inversion) could be applicable to modeling the MASW dispersion curve. SASW analysis using source locations at the northeast end of the array was not completed, but was much more difficult, indicating that dominant higher modes could be an issue at this end of the array.

- Two dispersion curves representing the lower and upper (not including definitive first higher mode data) are selected for modeling. V_S models resulting from the lower and upper phase velocity dispersion curves are referred to as Models 1 and 2, respectively. The possibility must be considered that the higher phase velocity dispersion curve is associated with the first higher mode rather than the fundamental mode. However, lateral velocity observed in both seismic refraction and surface wave data may support this dispersion curve being associated with the fundamental mode. Although, only the lower small wavelength phase velocity data appears to be conclusively associated with the fundamental model. In the lower phase velocity dispersion curve, the possibility cannot be discounted that the fundamental mode jumps to the first higher mode or modal superposition occurs at long wavelengths.
- To minimize near field effects, the maximum wavelength was set to the smaller of 80 m or 1.25 times the distance between the source and center of the active receiver array for this data set.
- The minimum wavelength surface wave phase velocity data extracted from the data set is about 2.5 m for the lower phase velocity dispersion curve and 4.5 m for the higher phase velocity dispersion curve.
- There is nominally about 20 to 60 m/s scatter in MASW dispersion data associated with the two dispersion curves.
- A representative dispersion curve was generated for each MASW data set using a moving average, polynomial curve fitting routine and used for modeling.
- V_{R40} is in the 495 to 535 m/s range which would result in an estimated V_{S30} of 517 to 559 m/s, based on the Brown, et al., 2000 relationship, assuming that the dispersion curve at 40 m wavelength is the fundamental mode. From experience, these V_{S30} estimates may be slightly high (~5%) due to the shallow saturated zone at the site. This V_{S30} estimate is only intended as a guide to check the inverted V_S model or to be used at sites with complex velocity structure when a dispersion curve cannot be developed over sufficient frequency range for modeling. V_{S30} would be lower if the dispersion curve were associated with the first higher mode or if modal superposition occurs at low frequencies.
- The lower phase velocity dispersion curve (Model 1) were modeled using the fundamental mode assumption (2-D solution in the WinSASW software package, which is approximately equivalent to fundamental mode), average mode assumption (observed

dispersion curve consists of the average of all modes based on relative amplitude of each mode estimated for a plane Rayleigh wave) using the Seisimager software module WaveEq developed by Oyo Corporation and the 3-D global inversion option in the WinSASW software package (cylindrical point load source, two receivers, source to near receiver distance equal to two wavelengths, receiver spacing equal to two wavelengths). The average mode assumption is an attempt to deal with modal superposition that may occur at low frequencies due to lack of resolution partially associated with finite receiver array length. However, the analytical method used to estimate the relative energy of each mode assumes a far-field, plane Rayleigh wave and does not consider source-receiver geometry and is optimally suited for the modeling of passive surface wave data. It is well documented that source-receiver geometry affects the energy in higher modes and, therefore, the average mode assumption may not always be accurate. However, modeling of average mode may result in a more accurate model than incorrectly assuming that the dispersion curve is fundamental mode, especially if only the lowest frequency portion of the dispersion curve is affected by modal superposition. The 3-D global inversion option in the WinSASW software package is also an attempt to deal with modal superposition and the effects of body waves. However, this modeling routine is designed to model SASW data acquired with a pair of receivers and is not generally considered applicable to MASW data, but was applied at this site because SASW analysis of MASW shot gather receiver pairs yielded the same dispersion curve.

- Calculated Rayleigh wave phase velocity modes for fundamental mode V_S Model 1FM (lower, small wavelength/higher frequency Rayleigh wave phase velocity data reflecting near surface velocity structure beneath southeastern portion of array ACSO-1) indicates that this model should excite a dominant higher mode at frequencies below 20 Hz. Additionally, S-wave velocity at depth is not consistent with the P-wave seismic refraction model, assuming that the subsurface rock is saturated with Poisson's ratio on the order of 0.45. Therefore, we conclude that the Model 1FM V_S model is not representative of subsurface velocity structure.
- Calculated Rayleigh wave phase velocity modes for average mode V_S Model 1AM indicates that the representative dispersion may be associated with the fundamental mode above 24 Hz, first higher mode below 18 Hz with mode mixing between 18 and 24 Hz. A multi-mode inversion of the dispersion data, assuming fundamental mode about 24 Hz and first higher mode below 18 Hz, would yield a very similar V_S model. The average mode (Model 1AM) and 3-D global inversion (Model 1G3) models are very similar at this site.
- Calculated Rayleigh wave phase velocity modes for fundamental mode for V_S Model 2FM (higher, small wavelength/higher frequency Rayleigh wave phase velocity data possibly reflecting near surface velocity structure beneath northwestern portion of array ACSO-1) indicates that the fundamental mode should be dominant over a wide frequency range. The average mode assumption only results in small adjustments to the V_S structure (Model 2AM), particularly the velocity of the half space. The possibility should not be discounted that the dispersion curve associated with Model 2 is the first higher mode rather than fundamental mode. However, Models 1AM and 2AM are almost identical below a depth of 3 m, indicating that they may both be most representative of subsurface velocity structure. Of course, for these models to be correct, the long

wavelength dispersion data would in one case represent the first higher mode and the other case the fundamental mode, which would be a highly unlikely coincidence.

- MASW V_S Model 1AM compares reasonably favorably with S-wave velocity structure estimated from the P-wave velocity structure at a position of 99 m on array ACSO-2 using assumed Poisson's ratio of 0.35 for depths less than 4.7 m (unsaturated sediments) and 0.45 for depths greater than 4.7 m (saturated sediments). MASW V_S Model 2AM compares reasonably favorably with S-wave velocity structure estimated from the P-wave velocity structure at a position of 36 m on array ACSO-2 using assumed Poisson's ratio of 0.35 for depths less than 3.3 m (unsaturated sediments) and 0.45 for depths greater than 3.3 m (saturated sediments). Therefore, S-wave velocity structure from Models 1AM and 2AM are considered representative of subsurface velocity structure at the site. Although there is uncertainty in the V_S models associated with lateral velocity variation and a possible dominant higher mode, the uncertainty does not appear to significantly impact estimated V_{S30}.
- Surface wave depth of investigation is about 35 m based on the one half to one third of maximum wavelength criteria.
- The HVSR peak at this site averages about 5 Hz. Modeling HVSR response from Vs models 1AM and 2AM results in slightly higher frequency estimated HVSR peaks. Using the quarter wavelength approximation to estimate the HVSR peak associated with the high velocity half space results in slightly lower frequency estimated HVSR peaks. Joint inversion of the HVSR data and Rayleigh wave velocity dispersion curve may result in more accurate V_S models, assuming the effects of near surface lateral velocity variation can be overcome. Joint inversion of HVSR and Love wave dispersion data may be more applicable at this site because the velocity structure at this site will not excite a dominant higher mode Love wave at long wavelengths.
- V_{S30} is 531, 435, and 423 for the Model 1 fundamental mode (Model 1FM), average mode (Model 1AM) and 3-D global inversion (Model 1G3) surface wave models, respectively (NEHRP Site Class C). We do not believe that the fundamental mode V_S model is representative of subsurface velocity structure at this site. The average mode and 3-D global inversion V_S models are very similar, but recommend use of the average mode V_S model (Model 1AM) to represent subsurface velocity structure.
- Average S-wave velocity between 1 and 31 m, to account for assumed 1 m sensor depth, is 619, 482 and 473 m/s for the Model 1 fundamental mode, average mode and 3-D global inversion surface wave models, respectively. We recommend that the adjusted V_{S30} from the average mode V_S model (Model 1AM) be used for site characterization.
- V_{S30} is 492 and 485 for the Model 2 fundamental mode (Model 2FM) and average mode (Model 2AM) surface wave models, respectively (NEHRP Site Class C). The Vs models are very similar, but recommend use of the average mode V_S model (Model 2AM) to represent subsurface velocity structure.
- Average S-wave velocity between 1 and 31 m, to account for assumed 1 m sensor depth, is 527 and 517 m/s for the Models 2FM and 2AM, respectively. We recommend that the adjusted V_{S30} from the average mode V_S model (Model 2AM) be used for site characterization. As previously mentioned, there is a possibility that the dispersion curve used to develop Models 2FM and 2AM consists of the first higher mode at all frequencies. In this case, both Models 2FM and 2AM will overestimate V_{S30}.

- The average V_{S30} of Models 1AM and 2AM, 460 m/s, is recommended for the purpose of site characterization.
- The average adjusted V_{S30}, between 1 and 31 m, of Models 1AM and 2AM, 500 m/s, is recommended for the purpose of site characterization.
- Although the average V_{S30} between Models 1AM and 2AM is recommended for the purpose of site characterization, the possibility should be considered that only Model 1AM is valid at this site.
- There is uncertainty in the V_S models at this site, related to lateral velocity variation and uncertainty in which Rayleigh wave modes are dominant. If the dispersion curves are actually representative of the fundamental mode then V_{S30} would be at most 15% higher than that presented. Acquisition of S-wave seismic refraction and MALW (Love wave) data is recommended to better constrain/validate subsurface velocity structure. Lateral velocity variation would still affect MALW data, but at this site the uncertainty introduced by possible higher modes would not be an issue with Love wave dispersion data. Regardless of the uncertainly with data modeling at this site, V_{S30} clearly falls into the low to intermediate NEHRP Site Class C velocity range.

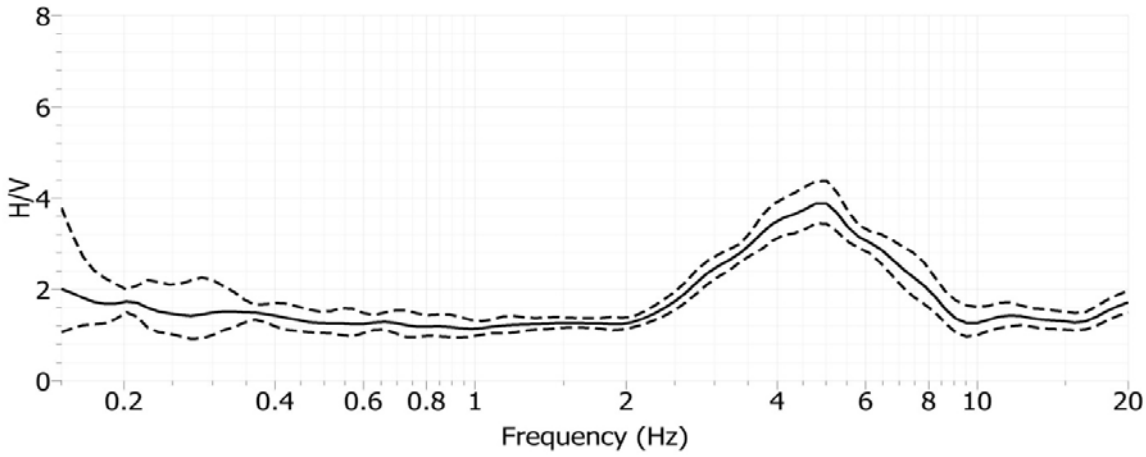

Site US.ACSO, H/V Spectral Ratio, Array ACSO-1, Sensor TRO-1

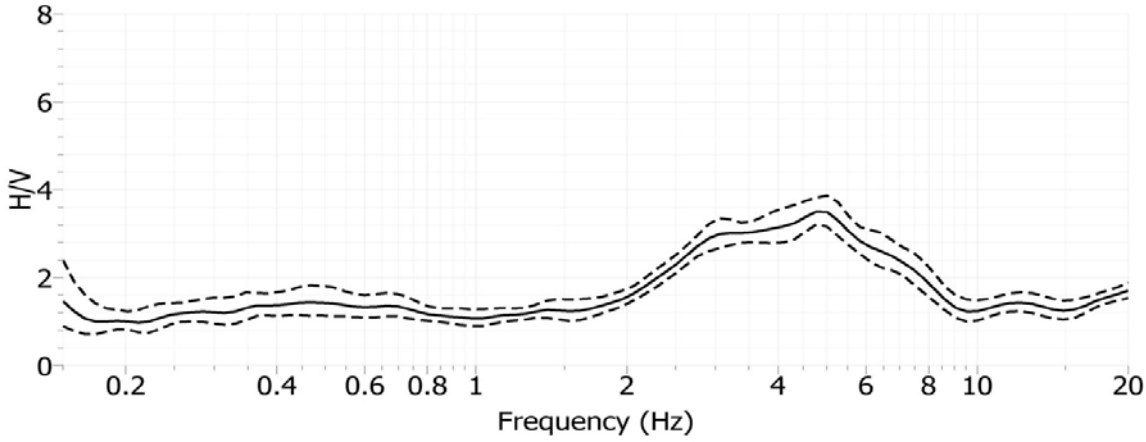

Site US.ACSO, H/V Spectral Ratio, Seismic Station, Sensor 453

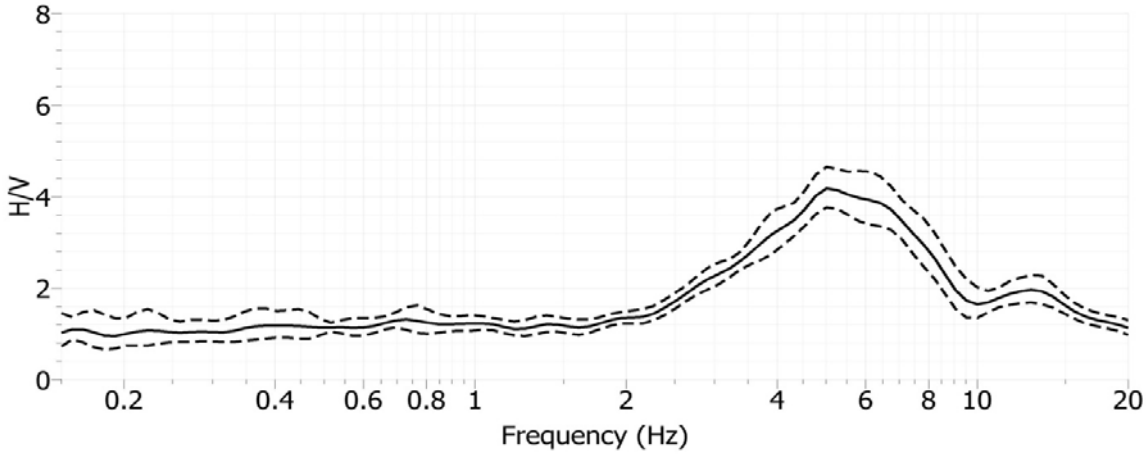

Site US.ACSO, H/V Spectral Ratio, Array ACSO-1, TRO-2

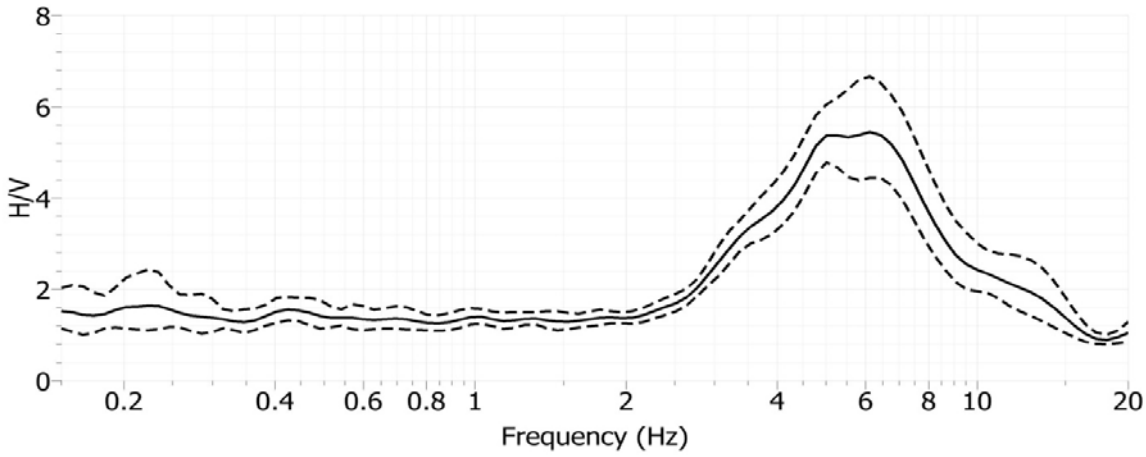

Site US.ACSO, H/V Spectral Ratio, Array ACSO-1, Sensor TRO-3

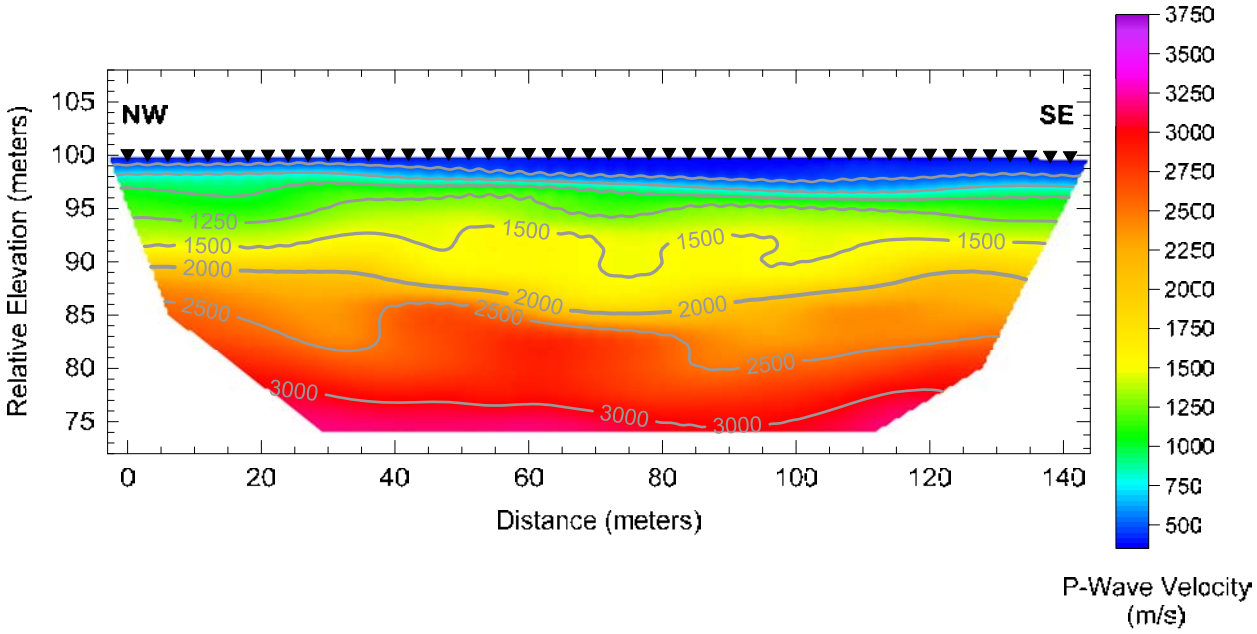

Array ACSO-2 – P-wave Tomographic Seismic Refraction Model Developed using a Layer Based Starting Model

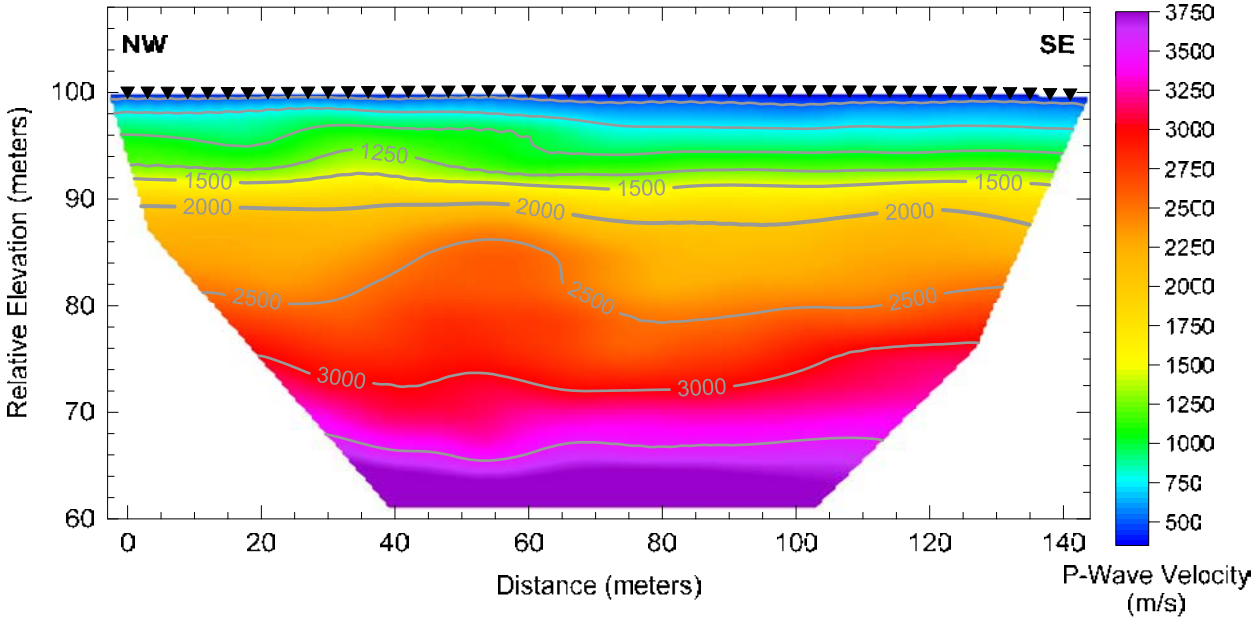

Array ACSO-2 – P-wave Tomographic Seismic Refraction Model Developed using a Smooth Velocity Gradient Starting Model

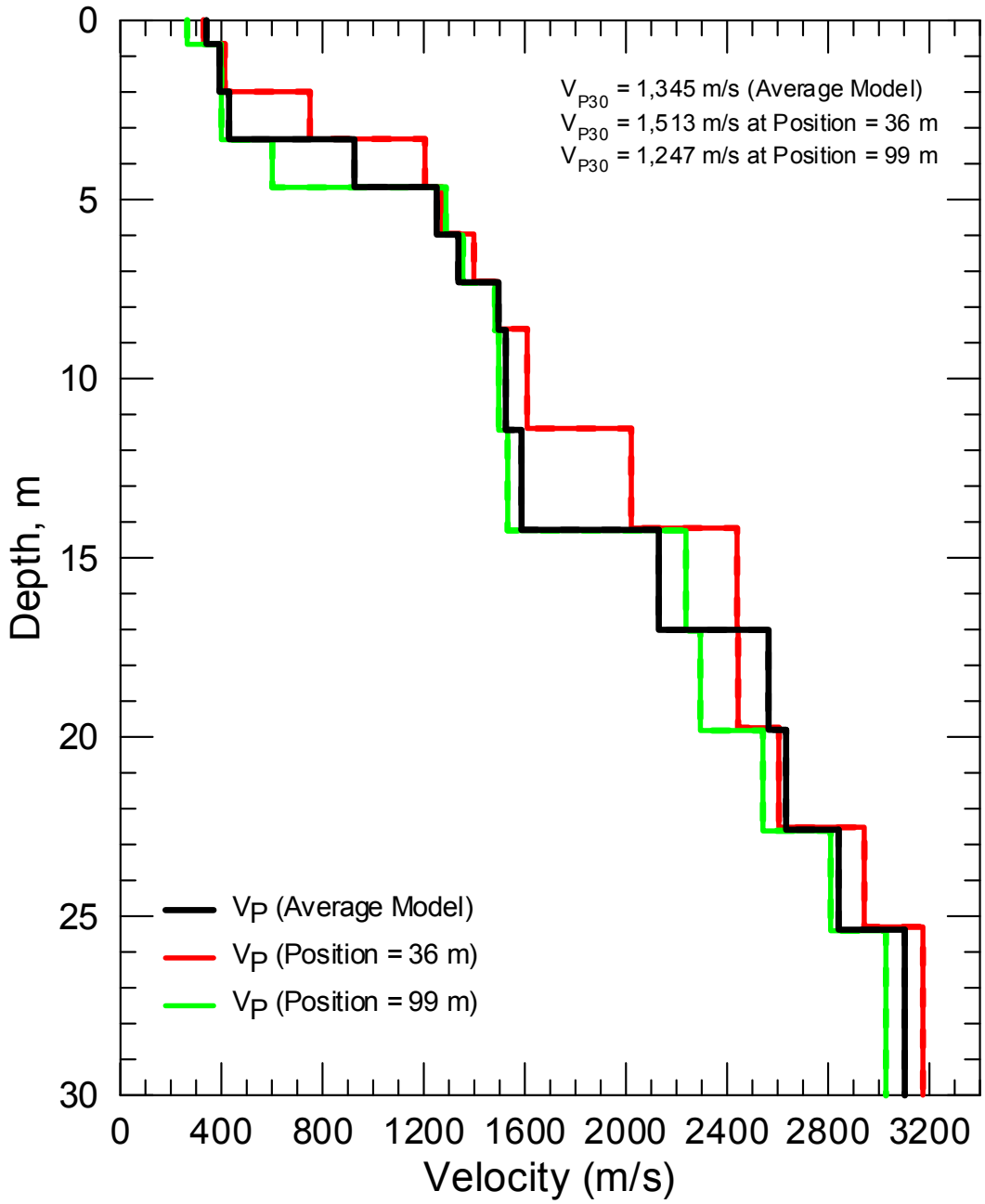

US.ACSO – Average P-wave velocity structure between a position of 36 and 105 m on the P-wave seismic refraction model for array ACSO-2 developed by tomographic inversion with a layer based starting model and the P-wave velocity structure at positions of 36 m (maximum V_{P30} and near the northeast end of MASW array ACSO-1) and 99 m (minimum V_{P30} and near the southwest end of MASW array ACSO-1). There is a 20% difference in V_{P30} between the velocity model at a position of 36 m and that at 99 m, primarily due to lateral velocity variation in the upper 5 m. Part, but not all, of the lateral velocity variation may be due to variable depth to the saturated zone, which will not impact S-wave velocity.

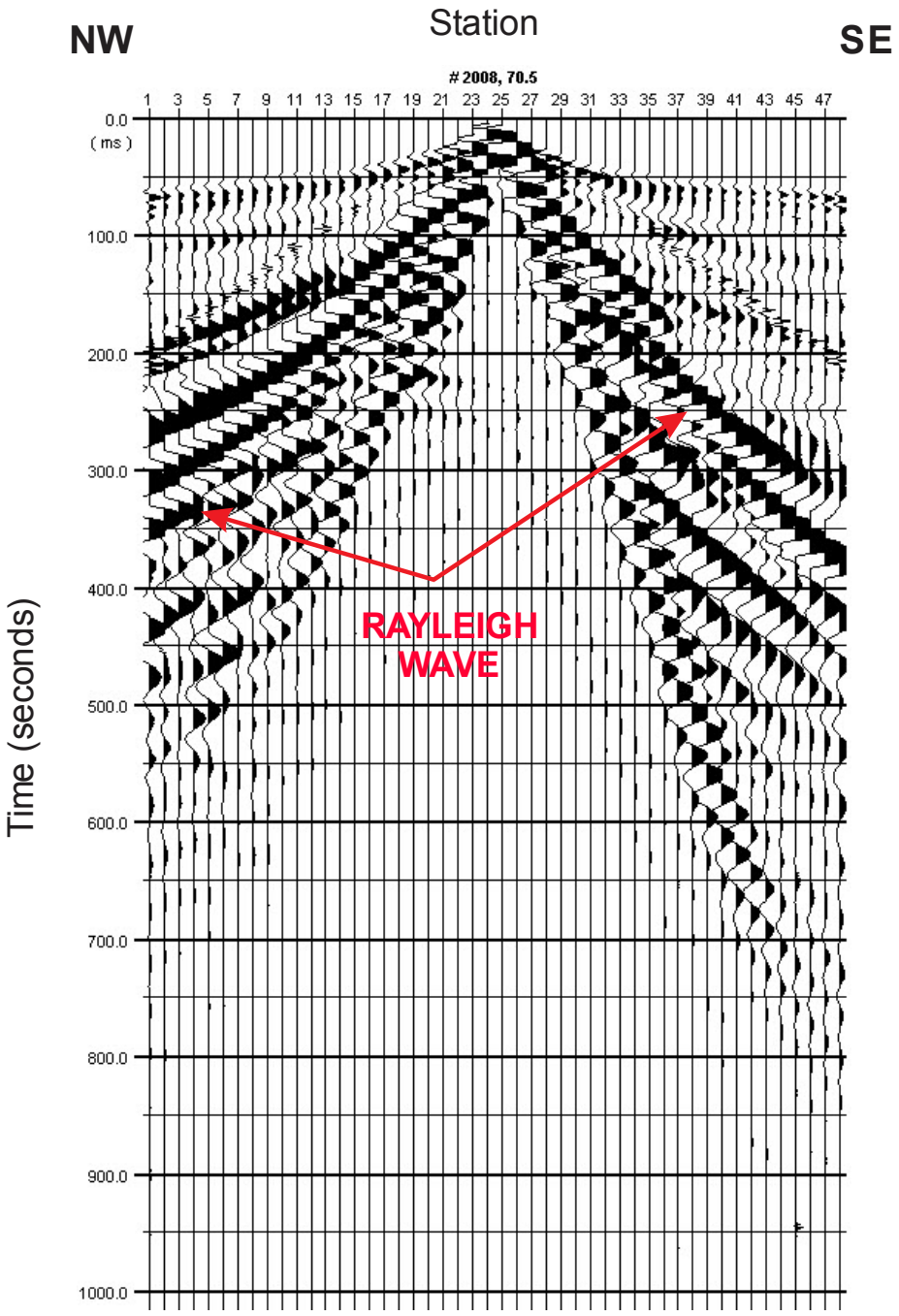

US.ACSO – Seismic record from center shot location of array ACSO-1 illustrating the effects of near surface lateral velocity variation. There is a distinct difference in the velocity of surface wave energy propagating in the forward (southeast) and reverse (northwest) directions on the seismic record. Lateral velocity variation should always be avoided; however, at this site there were limited options for geophysical testing in close proximity to the seismic station and on the subject property.

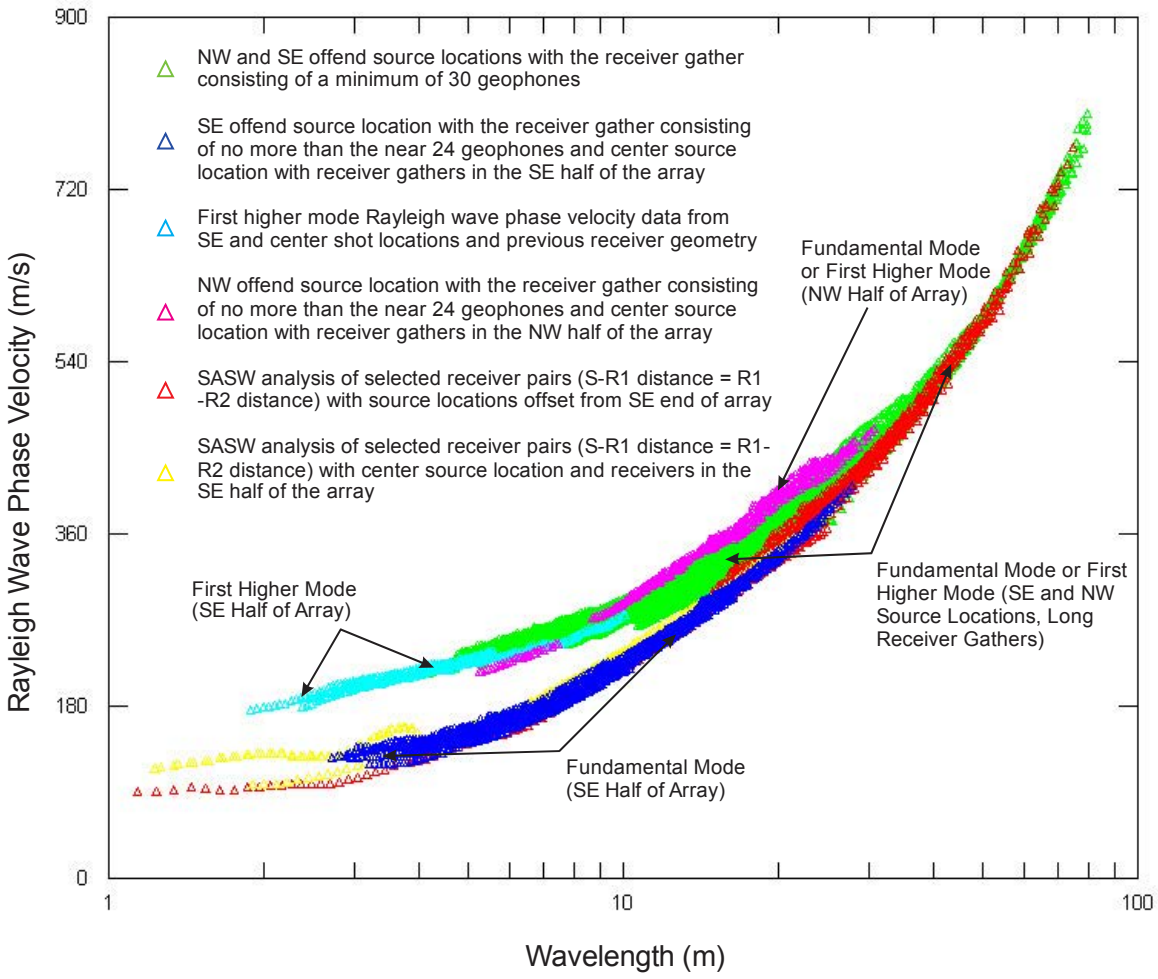

US.ACSO – MASW (Rayleigh wave) dispersion data from array ACSO-1. Interpretation is complicated by the effects of near surface lateral velocity variation and a possible dominant first higher mode. Small wavelength dispersion data from receiver gathers in the SE and NE halves of the array diverge at wavelengths less than 30 m. Interpreted first higher mode from receiver gathers in the SE half of the array tie into the dispersion data interpreted from 30 to 48 channel receiver gathers and source locations at both ends of the array and the small wavelength dispersion data from receiver gathers in the NW half of the array. This may be a coincidence or indicate that the first higher mode is dominant over a wide frequency range for many source locations. Two dispersion curves representing the lower and upper (not including definitive first higher mode data) are selected for modeling, although only the lower envelope may represent the fundamental mode at small wavelengths (high frequencies). The fundamental mode may jump to the first higher mode or modal superposition may occur at long wavelengths. SASW analysis of selected receiver pairs with SE source locations and the center source location validate the lower MASW dispersion curve. These data are not used for modeling because they are considered redundant. MALW (Love wave) data acquisition is recommended at this site as the fundamental mode should be dominant at low frequencies (long wavelengths).

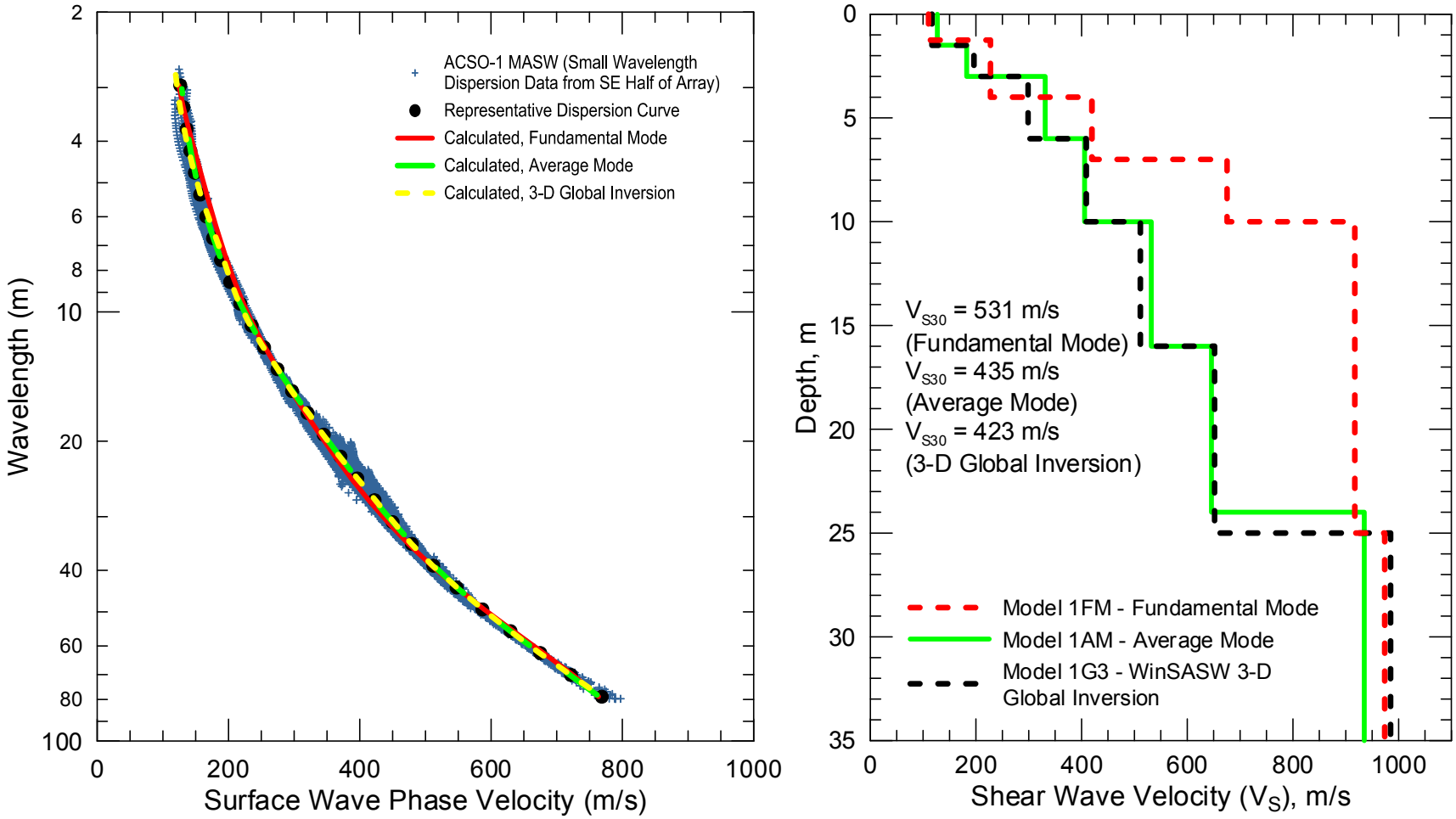

US.ACSO - Field, representative and inverted theoretical surface wave dispersion data (left) and associated V_S models (right) for fundamental and average mode assumption and 3-D global inversion of Rayleigh wave phase velocity data interpreted as being representative of near surface velocity structure beneath the southeast half of the array (Model 1).

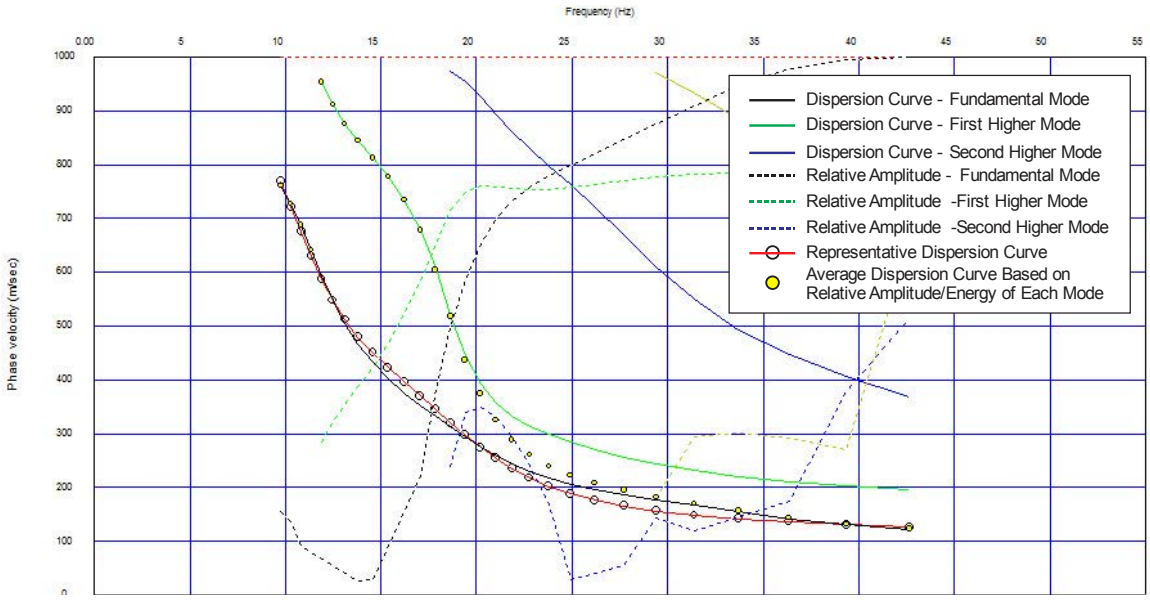

Calculated Rayleigh wave phase velocity modes for fundamental mode for V_S Model 1FM (lower small wavelength/higher frequency Rayleigh wave phase velocity data reflecting near surface velocity structure beneath southeastern portion of array ACSO-1) demonstrating that this model should excite a dominant higher mode at frequencies below 20 Hz. As is evident, it was difficult fitting a fundamental mode dispersion curve to the representative dispersion curve. It should be noted, however, that the analytical routine used to estimate the amplitudes of the higher modes does not include the source location and makes a plane wave assumption.

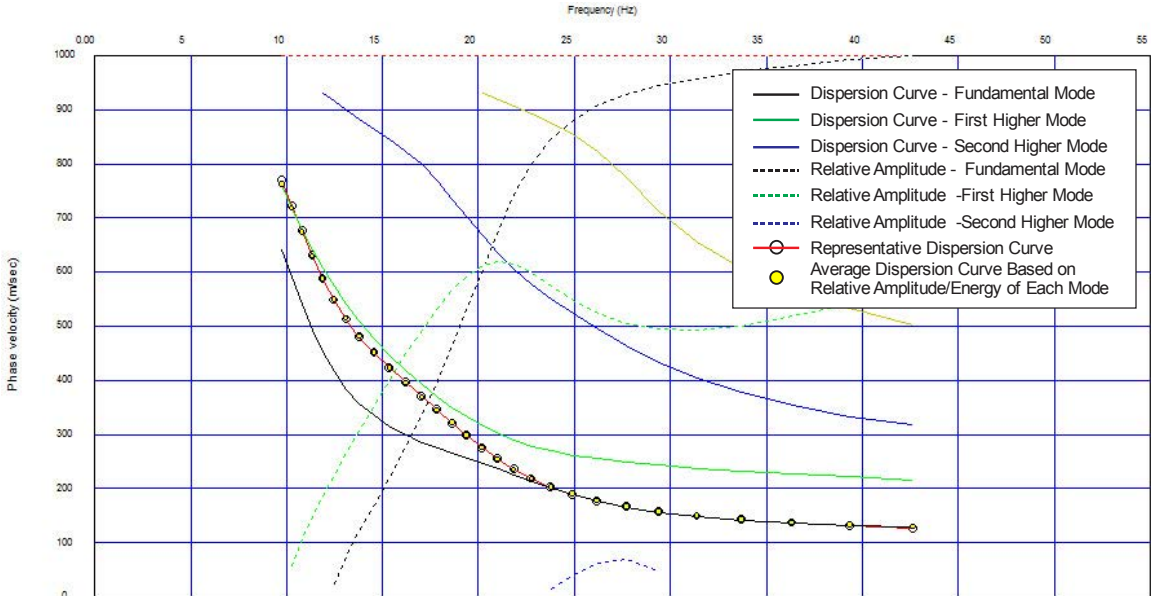

Calculated Rayleigh wave phase velocity modes for V_S Model 1AM developed using the average mode assumption in an attempt to account for possible modal superposition (mode mixing) at low frequencies. The V_S model is very similar to what would have been derived with a multi-mode inversion assuming fundamental mode above 24 Hz and first higher mode below 18 Hz.

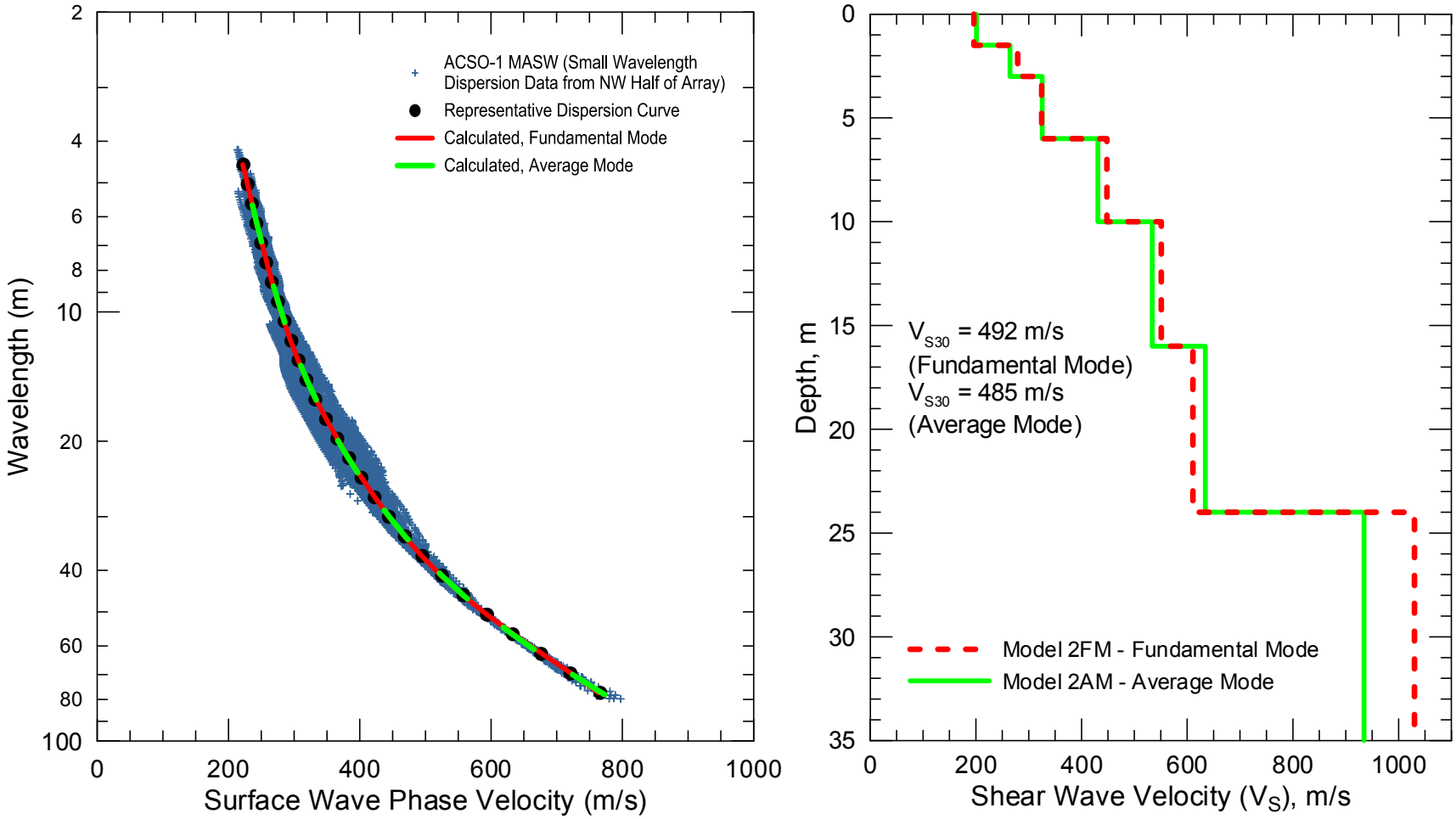

US.ACSO - Field, representative and inverted theoretical surface wave dispersion data (left) and associated V_S models (right) for fundamental and average mode assumption of Rayleigh wave phase velocity data interpreted as being representative of near surface velocity structure beneath the northwest half of the array (Model 2). There is a distinct possibility that this dispersion curve is associated with the first higher mode rather than the fundamental mode. Interestingly, however, the V_S models are very similar to the average mode V_S Model 1AM.

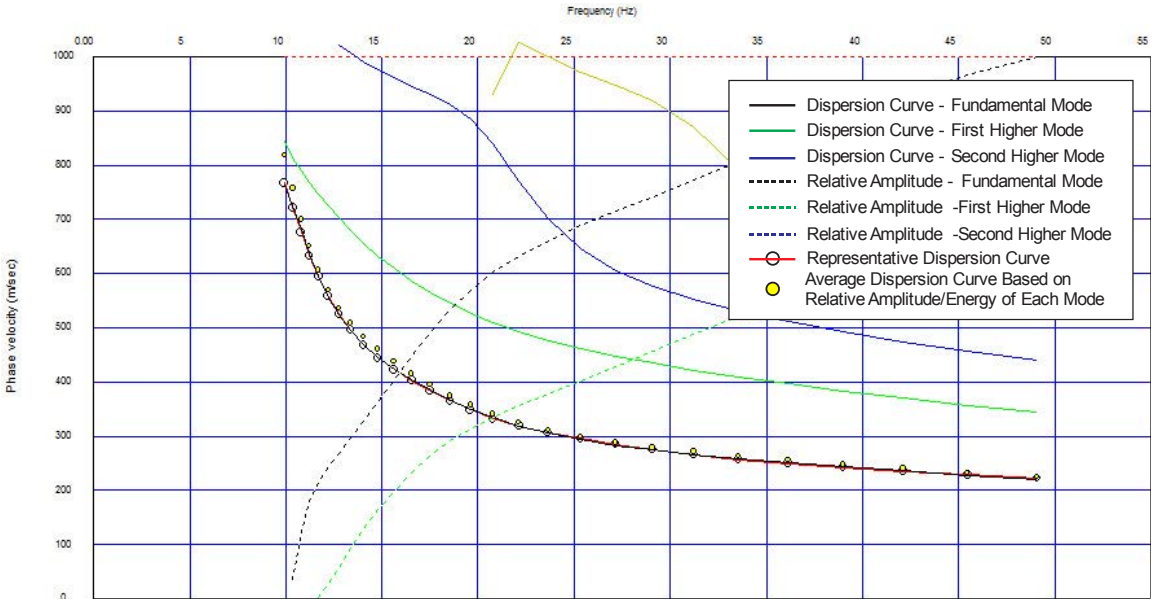

Calculated Rayleigh wave phase velocity modes for fundamental mode for V_S Model 2FM (Higher small wavelength/higher frequency Rayleigh wave phase velocity data possibly reflecting near surface velocity structure beneath northwestern portion of array ACSO-1). With this V_S model the fundamental mode is generally dominant at all frequencies and the dispersion curve is reasonably accurately modeled using the fundamental mode assumption. The problem, or course, is that the long wavelength portion of the dispersion curve cannot be both fundamental mode, as in this case, and first higher mode as for Model 1AM. There is a possibility that the Model 2 representative dispersion curve represents the first higher mode.

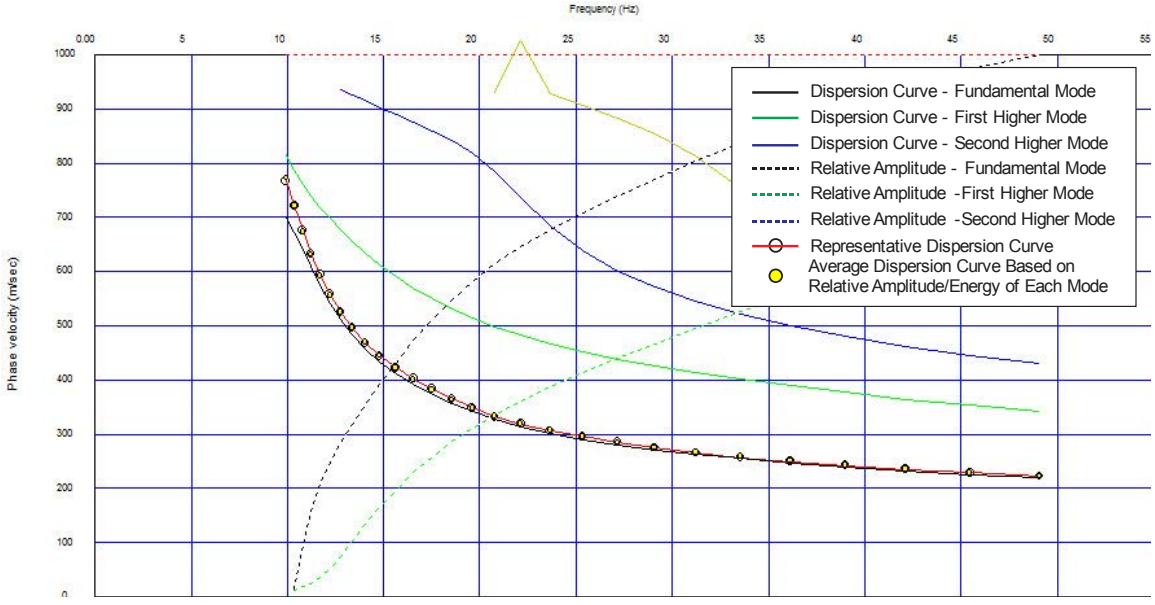

Calculated Rayleigh wave phase velocity modes for V_S Model 2AM developed using the average mode assumption in an attempt to account for possible modal superposition (mode mixing) at low frequencies. The V_S model is only slightly different to that derived with fundamental mode inversion.

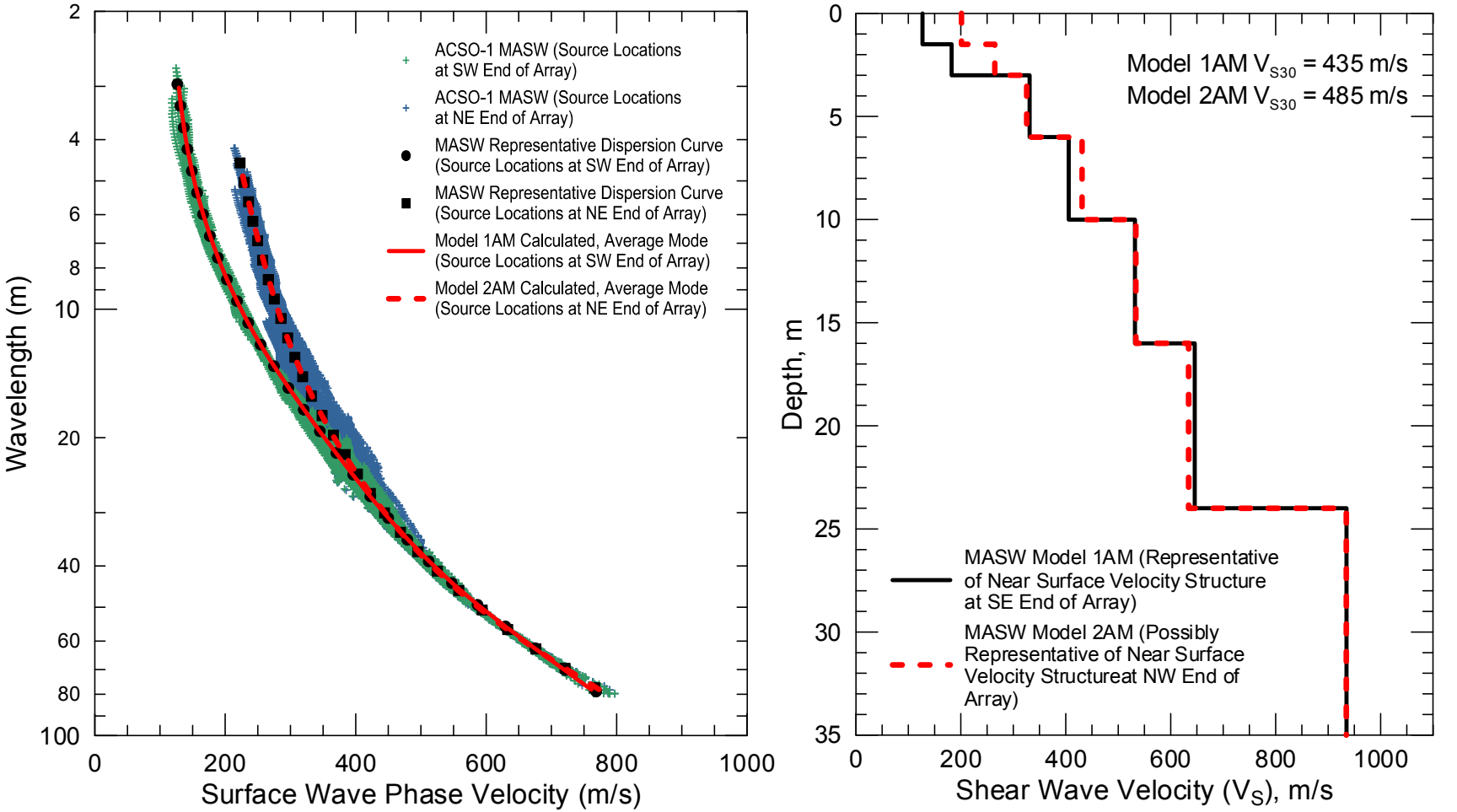

US.ACSO - Field, representative and inverted theoretical surface wave dispersion data (left) and associated V_S models (right) for average mode assumption of Rayleigh wave phase velocity. Models 1AM and 2AM represent near surface velocity structure beneath the southeast and northwest portions of array ACSO-1, respectively. Interestingly, the V_S models are almost identical below a depth of 3 m. However, the dispersion curve for Model 1AM effectively represents the fundamental mode at small wavelengths and the first higher mode at long wavelengths; whereas, the dispersion curve for Model 2AM generally represents the fundamental mode. The long wavelength portion of the dispersion curve cannot be associated with both the fundamental mode and first higher mode.

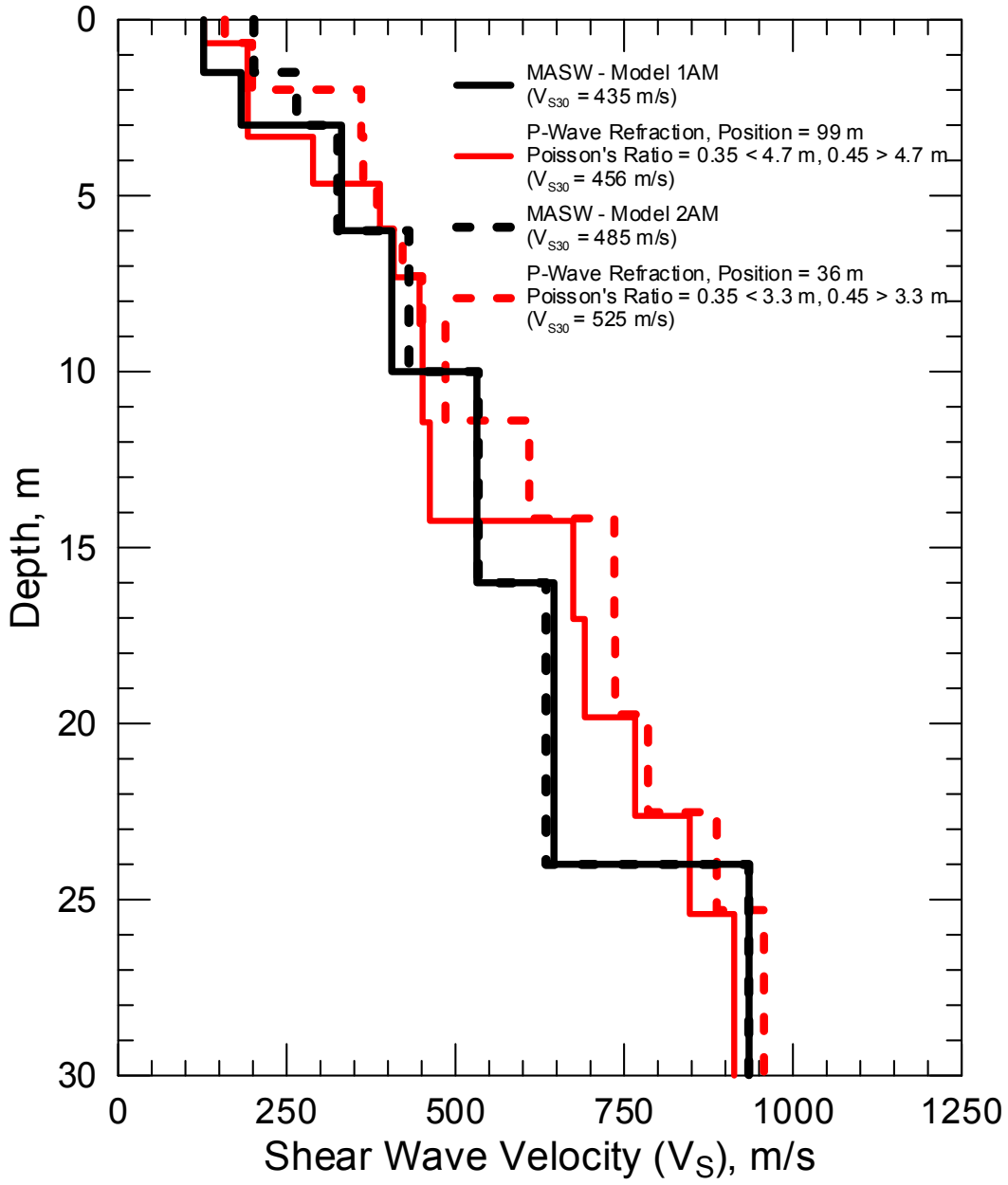

US.ACSO – Comparison of S-wave velocity models derived from the MASW data and estimated from the P-wave seismic refraction model. MASW Model 1AM, derived from dispersion data thought to reflect the near surface velocity structure beneath the southwestern portion of array ACSO-1 using the average mode assumption, is compared to S-wave velocity structure estimated from the P-wave velocity structure at a position of 99 m on array ACSO-2 using assumed Poisson's ratio of 0.35 for depths less than 4.7 m (unsaturated sediments) and 0.45 for depths greater than 4.7 m (saturated sediments). MASW Model 2AM, derived from dispersion data thought to reflect the near surface velocity structure beneath the northeastern portion of array ACSO-1 using the average mode assumption, is compared to S-wave velocity structure estimated from the P-wave velocity structure at a position of 36 m on array ACSO-2 using assumed Poisson's ratio of 0.35 for depths less than 3.3 m (unsaturated sediments) and 0.45 for depths greater than 3.3 m (saturated sediments).

Addendum - Site US.ACSO

Location: Alum Creek State Park, Delaware, Ohio

Latitude: 40.23228 **Longitude:** -82.98202
(Station coordinates from field survey, WGS84 coordinate system)

Final Recommended V_{S30} (measured): 417 m/s

V_{S30} (adjusted to more accurately reflect seismic station conditions): 467 m/s (average S-wave velocity between 1 and 31 m adjusting for assumed 1 m sensor depth).

NEHRP Site Class: C

Geomatrix Code: IZB

Geologic Conditions/Observations: Bedrock geology in site vicinity mapped as Paleozoic (Upper Devonian) shale, siltstone and very fine-grained sandstone. Field observations indicate that a sediment layer of unknown thickness overlies the sedimentary rock.

Site Conditions: Rural site. Undulating topography in site vicinity. Test area located in a field with relatively flat topography near an Ohio State Geological Survey building.

Additional Geophysical Methods Utilized: Seismic Refraction (S-wave), MALW (Love wave)

Additional Geophysical Testing Arrays:

1. Array ACSO-1 (48 channel S-wave seismic refraction and MALW array, utilizing 4.5 Hz horizontal geophones spaced 1.5 m apart for a length of 70.5 m, forward and reverse shot locations with multiple source offsets and multiple interior shot locations). The array is coincident with the MASW array of the same name.

Location of Geophysical Testing Arrays: (See original site report)

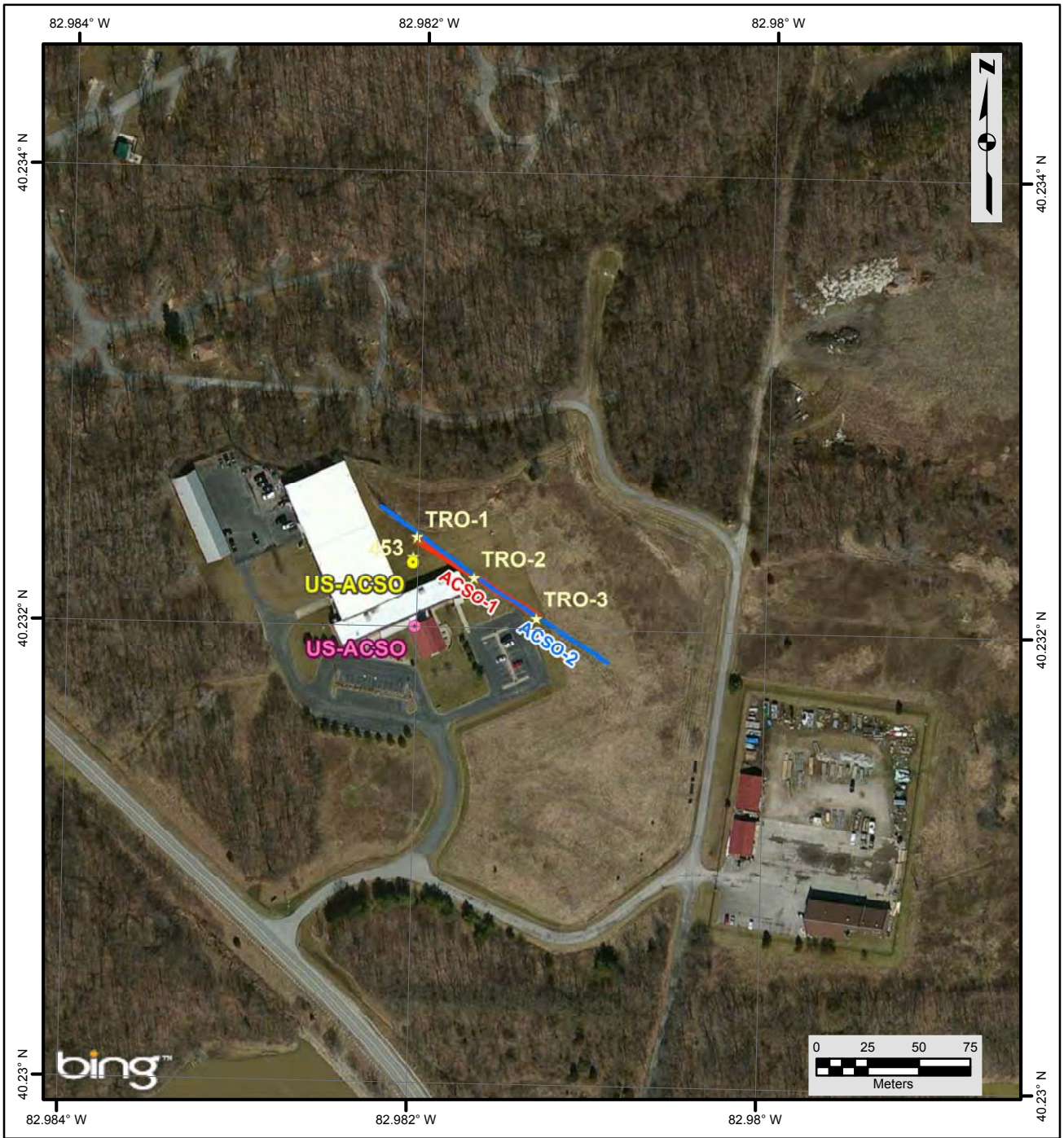

Legend

- Seismic Station - Approximate Surveyed Location
- Seismic Station - Approximate Location of Record
- H/V Spectral Ratio Location
- MASW and Seismic Refraction Array (P- and S-wave)
- MASW and Seismic Refraction Array (P-wave)

NOTES:
1. WGS 1984 COORDINATE SYSTEM
2. Image Source: (c) Microsoft Corporation and its data suppliers

File Name: US-ACSO-I-2

Date: 2/7/2013

USGS science for a changing world

GEOVision geophysical services

RECOVERY.GOV

SITE MAP
US•ACSO

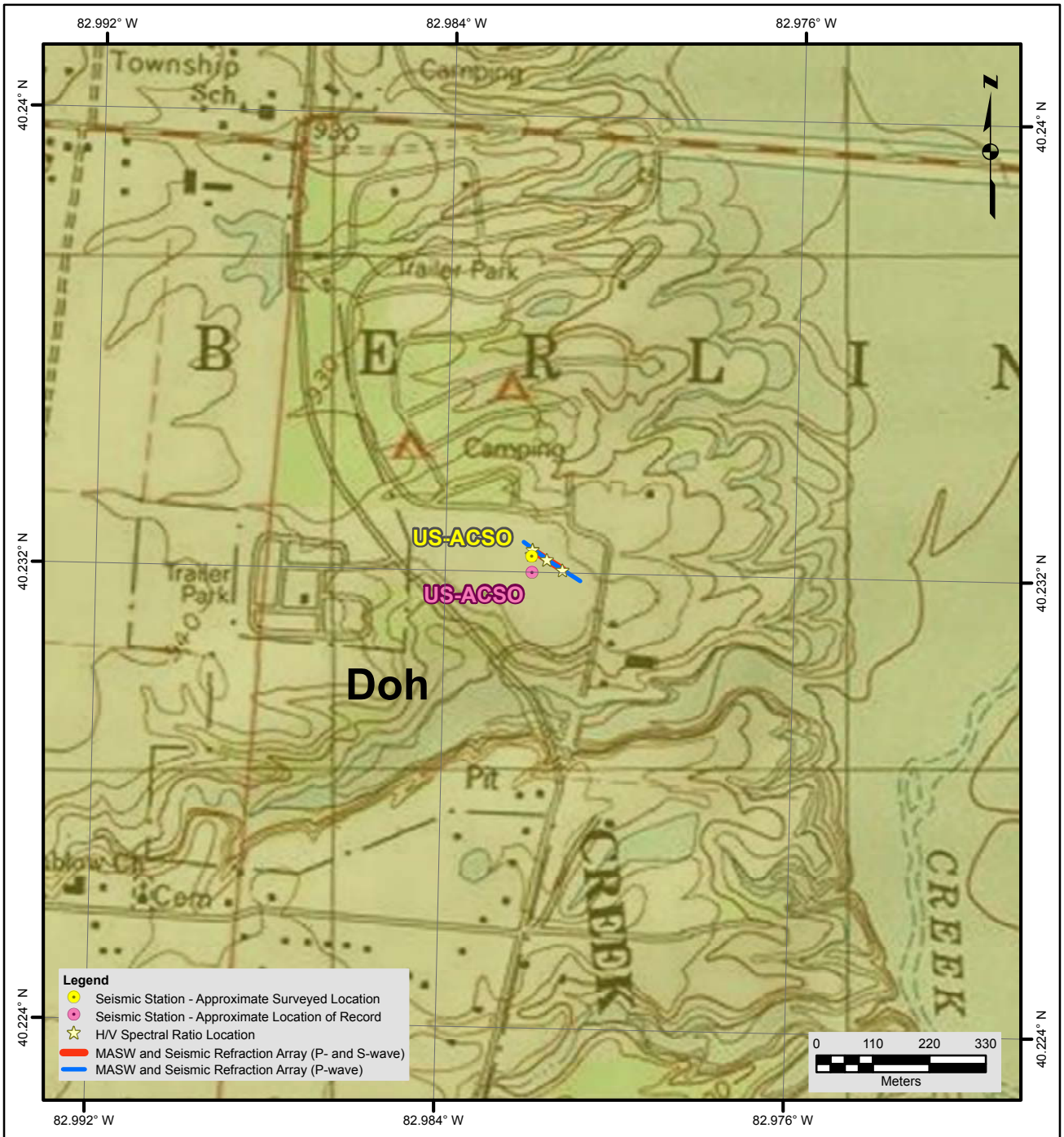

Description of Geologic Map Units

Doh = Paleozoic (Upper Devonian) shale, siltstone, very fine-grained sandstone, carbonaceous, calcareous concretions common in lower portion

NOTES:
1. WGS 1984 COORDINATE SYSTEM
2. Bedrock Geologic Map of Ohio
Ohio Division of Geological Survey Map BG-1, Version 6.0
compilation by E. R. Slucher, E. M. Swinford, G. E. Larsen
GIS by D. M. Powers, 2006
3. See site map for details of geophysical survey

File Name: US-ACSO-2

Date: 1/3/2013

USGS science for a changing world

GEOVision geophysical services

GEOLOGIC MAP
US•ACSO

RECOVERY.GOV

Looking southwest towards seismic station US.ACSO and MALW array ACSO-1

Looking northwest along S-wave refraction and MALW array ACSO-1

Looking southeast at off-end shot location on S-wave seismic refraction and MALW array ACSO-1

Looking southeast along array ACSO-1

Hammer-impact, aluminum S-wave seismic source used to acquire S-wave refraction and MALW data

Results:

Final V_S Model from MASW (Rayleigh wave) Dispersion Data Modeled as Average/Effective Mode (Near Surface Velocity Structure Representative of Southeast Portion of Array)

Depth to Top of Layer (m)	Layer Thickness (m)	S-Wave Velocity (m/s)	Inferred P-Wave Velocity (m/s)	Assumed Poisson's Ratio	Assumed Density (g/cm^3)
0	1.5	127	237	0.301	1.70
1.5	1.5	183	342	0.300	1.75
3	3	338	632	0.300	1.85
6	4	392	1785	0.475	1.95
10	6	539	2078	0.464	2.05
16	13	644	2289	0.457	2.10
29	>6	1190	3381	0.429	2.30

Notes: 1) Saturated sediments/rock with V_P of 1,500 to 3,500 fixed at a depth of 6 m based on P-wave seismic refraction models.
2) Depth of investigation is about 35 m.
3) Bottom layer is a half space.
4) V_{S30} = 421 m/s.

Final V_S Model from MALW (Love wave) Dispersion Data Modeled as Fundamental Mode

Depth to Top of Layer (m)	Layer Thickness (m)	S-Wave Velocity (m/s)	Inferred P-Wave Velocity (m/s)	Assumed Poisson's Ratio	Assumed Density (g/cm^3)
0	0.75	95	178	0.300	1.70
0.75	2	180	337	0.300	1.75
2.75	3.25	299	558	0.300	1.80
6	4	425	1851	0.472	1.95
10	19	584	2168	0.461	2.05
29	>1	1220	3440	0.428	2.30

Notes: 1) Saturated sediments/rock with V_P of 1,500 to 3,500 fixed at a depth of 6 m based on P-wave seismic refraction models, but no effect on inversion of Love wave dispersion data.
2) Depth of investigation is about 30 m.
3) Bottom layer is a half space.
4) V_{S30} = 413 m/s.

Average V_S Model from Central Portion of S-wave Seismic Refraction Array ACSO-1

Depth to Top of Layer (m)	Layer Thickness (m)	S-Wave Velocity (m/s)
0.00	0.62	114
0.62	1.23	152
1.85	1.23	266
3.09	1.23	277
4.32	1.23	310
5.55	1.23	417
6.79	1.23	427
8.02	2.59	475
10.61	2.59	557
13.20	2.59	643
15.80	2.59	726
18.39	2.59	743
20.98	2.59	750
23.57	2.59	756
26.16	2.59	759
28.75	2.59	1585
31.34	2.59	1644
33.94	Half Space	1782

Observations/Discussion:

- Analysis of MASW (Rayleigh wave) data acquired at US.ACSO (see original data report) indicated that the first higher mode Rayleigh wave was dominant at low frequencies (large wavelengths) requiring a multi-mode or effective mode inversion of the dispersion curve. To test the accuracy of the resulting models and estimates of V_{S30}, MALW (Love wave) and S-wave seismic refraction data were acquired along the same array used for MASW data acquisition (Array ACSO-1) on 6/30/12. These data were acquired at no cost while a field crew was in route to a different project site and, unfortunately, there was not time to acquire S-wave refraction and MALW data along the longer array ACSO-2 that was used for P-wave seismic refraction analysis. In retrospect, given the site velocity structure, the S-wave refraction survey would have strongly benefited from data acquisition along the longer array ACSO-2.
- S-wave seismic refraction data quality was excellent. The S-wave seismic refraction data for array ACSO-1 were modeled using a tomographic inversion routine with both layer-based and smooth velocity gradient starting models. Several seismic refraction models were developed using different starting models to investigate nonuniqueness in seismic refraction modeling with a single model selected for the purpose of site characterization. The seismic refraction model was extended to far-offset shot locations to extend maximum depth of investigation to 30 m, or more. There is a significant increase in S-

wave velocity at the site at a depth on the order of 25 to 30 m, or more, and the velocity of this layer would have been much better constrained using a longer array.

- After data modeling, horizontal position in the S-wave seismic refraction model for array ACSO-1 was shifted by 27 m so that positions are the same as the P-wave refraction model for array ACSO-2 (see original site report).
- The seismic refraction model selected for the purpose of site characterization utilized a user-defined layered starting model resulting from interactive, horizontal layer based analysis of the seismic refraction first arrival data. This seismic refraction model indicates that S-wave velocity is about 100 m/s at the surface and increases to over 200 m/s at a depth of 0.5 to 2 m, over 400 m/s at a depth of 5 to 6 m, over 700 m/s at a depth of 15 to 18 m and over 1,500 m/s at a depth of about 28 to 31 m. The depth and velocity of the high velocity layer would likely be better constrained using a longer seismic refraction line. Additionally, bedrock geology at the site is mapped as consisting of interbedded shale, siltstone and sandstone and there is a strong possibility that velocity inversions occur within the bedrock unit.
- The average S-wave velocity of the upper 30 m (V_{S30}) was estimated between 48 and 78 m on the S-wave refraction model, where depth of investigation is greatest. Over this interval, V_{S30} ranges from about 456 to 482 m/s, a 6% variation. An average V_S model was developed over the 48 to 78 m distance interval by horizontally averaging the travel time of each model cell and cell thickness and average V_{S30} was determined to be 463 m/s.
- The seismic refraction model indicates that there is some minor lateral velocity variation beneath array ACSO-1, especially near the surface.
- To investigate nonuniqueness in seismic refraction models, six additional models were developed using different layered starting models, primarily by adjusting the depth to the high velocity layer near the base of the model, and using a smooth velocity gradient starting model. These models have the high velocity unit at depths ranging from about 21 to 34 m and all of the models have similar RMS error. All of the models indicate that V_S likely exceeds 1,600 m/s at depth, although the possibility cannot be discounted that velocity inversions occur beneath this higher velocity layer. Average V_S models were developed over the 48 to 78 m distance interval for each of these models and are presented. V_{S30} varies from 463 to 474 on the seven V_S models, all of which have similar RMS errors, indicating that time averaged velocity is not significantly affected by the nonuniqueness.
- Love wave data were acquired using 4.5 Hz horizontal geophones and a hammer-impact S-wave energy source, developed by Seth Haines at USGS. Love wave phase velocity data were reduced to frequencies as low as 6 Hz at this site, possibly near the low frequency limit of the energy source.
- To minimize near field effects, the maximum wavelength Love wave data extracted from the data set for array ACSO-1 was set equal to the lesser of 100 m or 1.5 times the distance between the source and midpoint of the active receiver array. A 100 m wavelength Love wave occurs at an average frequency of about 6 Hz.
- Review of both Rayleigh and Love wave dispersion data at frequencies lower than used for modeling indicates that V_S exceeds 1,200 m/s at depths below the surface wave depth of investigation.

- The minimum wavelength Love wave phase velocity data extracted from the 48-channel MALW array ACSO-1 was about 4 m. Reducing data using limited offset receiver arrays (i.e. less active geophones) allowed for extraction of surface wave dispersion data to a minimum wavelength of about 1.5 m.
- There is nominally about 40 to 70 m/s of scatter in MALW dispersion data, which is likely in part related to lateral velocity variation. The Love wave phase velocity data from source locations at the northwest and southeast ends of the array diverge over a wide frequency range due to the lateral velocity variation.
- The Love wave dispersion data indicates that the Rayleigh wave dispersion data associated with Model 2 in the original site report is most likely associated with the first higher mode and, therefore, the Model 2 V_S model, which was developed assuming that the dispersion curve consisted of the effective mode, is not valid. The Model 1 V_S model, developed using the average/effective mode assumption, in the original site report is valid; however, alternate V_S models have been developed for the Rayleigh wave phase velocity data during the current investigation.
- A representative dispersion curve was generated for the MALW data set using a moving average, polynomial curve fitting routine and used for modeling. Additional representative dispersion curves were developed for the lower and upper envelopes of the Love wave dispersion data to investigate lateral velocity variation.
- Love wave depth of investigation is about 30 m based on one third of the maximum wavelength (100 m); whereas, Rayleigh wave depth of investigation is about 35 m based on one-half of the maximum Rayleigh wavelength (80 m).
- Multiple V_S models were developed for the Rayleigh and Love wave dispersion data to illustrate the nonuniqueness inherent in the inversion process. Typically only the depth to and/or thickness of layers below a depth of 14 m were adjusted to specifically explore the nonuniqueness in depth to the high velocity half space. Nonuniqueness is quite extreme at this site as there appears to be a significant increase in velocity near the maximum depth of investigation. Investigation to greater depth using a longer receiver array and lower frequency energy sources would slightly improve the nonuniqueness in the V_S models, particularly in the velocity of the half space. The S-wave seismic refraction models appear to have slightly less nonuniqueness than the surface wave models.
- The V_S model(s) resulting from average/effective mode modeling of the Rayleigh wave dispersion data appear to excite a dominant fundamental mode at wavelengths less that 11 m and dominant first higher mode at wavelengths greater than 18 m. V_S models were developed for the Love wave dispersion data using a fundamental mode inversion algorithm.
- For the purpose of site characterization we select V_S models with depth to the high velocity bedrock unit at 29 m, slightly greater than the intermediate depth to rock in the equivalent surface wave and seismic refraction V_S models. Additionally, high velocity bedrock in the 28 to 32 m depth range with velocity greater than 1,100 m/s is required to model an HVSR peak in the observed 5 to 6 Hz frequency range. It should be noted, however, that the quarter wavelength approximation results in much lower predicted fundamental frequency for the V_S models with high velocity bedrock in the 28 to 32 m depth range. The quarter wavelength approximation, however, assumes a homogeneous layer over a half space, which does not closely reflect the velocity structure at this site.

- The V_S of the half space located at a depth of 29 m is not well resolved in the Love wave dispersion data as the half space is located near the depth of investigation. A lower frequency energy source and longer array would be required to more accurately resolve the velocity of the half space.
- The V_S models developed from average/effective mode inversion of the Rayleigh wave dispersion data and fundamental mode inversion of the Love wave dispersion data are relatively similar with the small differences possibly explained by anisotropy.
- V_{S30} for the representative Rayleigh wave and Love wave V_S models is 421 and 413 m/s, respectively (NEHRP Site Class C).
- The average V_S between 1 and 31 m to account for approximate sensor depth (adjusted V_{S30}) is 467 m/s for both the MASW and MALW V_S models selected for the purpose of site characterization (NEHRP Site Class C).
- The velocity structure at this site is such that significant nonuniqueness is observed in the V_S models developed from inversion of the Rayleigh and Love wave dispersion data, yet V_{S30} only ranges from 420 to 438 m/s in the equivalent Rayleigh wave V_S models, 410 to 433 m/s in the equivalent Love wave V_S models with variable bedrock depth and 411 to 428 m/s in the equivalent Love wave V_S models with high velocity rock at 29 m depth. Therefore, the variation in V_{S30} associated with nonuniqueness is only about 5% at the site with the V_S models selected for site characterization having V_{S30} near the lower end of the range.
- V_S models developed for the lower and upper envelope of the Love wave dispersion data have V_{S30} of 399 and 432 m/s, respectively, an 8% variation.
- The S-wave refraction model is consistent with the Rayleigh and Love wave V_S models at depths below 15 m, but has higher V_S at greater depths resulting in an estimated V_{S30} about 10% higher than that developed from the surface wave models. In sedimentary rock environments, it is not unusual for the seismic refraction model to overestimate velocity structure because the seismic refraction technique cannot detect velocity inversions that often occur. Velocity inversions can only be detected in body wave data if there is excellent reflectivity and subhorizontal layering. Therefore, the possibility should always be considered that seismic refraction V_S models overestimate V_{S30} in sediment and sedimentary rock environments. Even in cases where velocity inversions are too thin to be detected, surface wave models will more accurately reflect average velocity structure in such environments.
- For the purpose of site characterization, we recommend using the representative S-wave velocity models developed from the MASW (Rayleigh wave) and MALW (Love wave) data collected along array ACSO-1. These V_S models supersede the V_S models presented in the original site report. Lateral velocity variation and nonuniqueness is such that V_{S30} should be considered to vary by as much as ±5%.

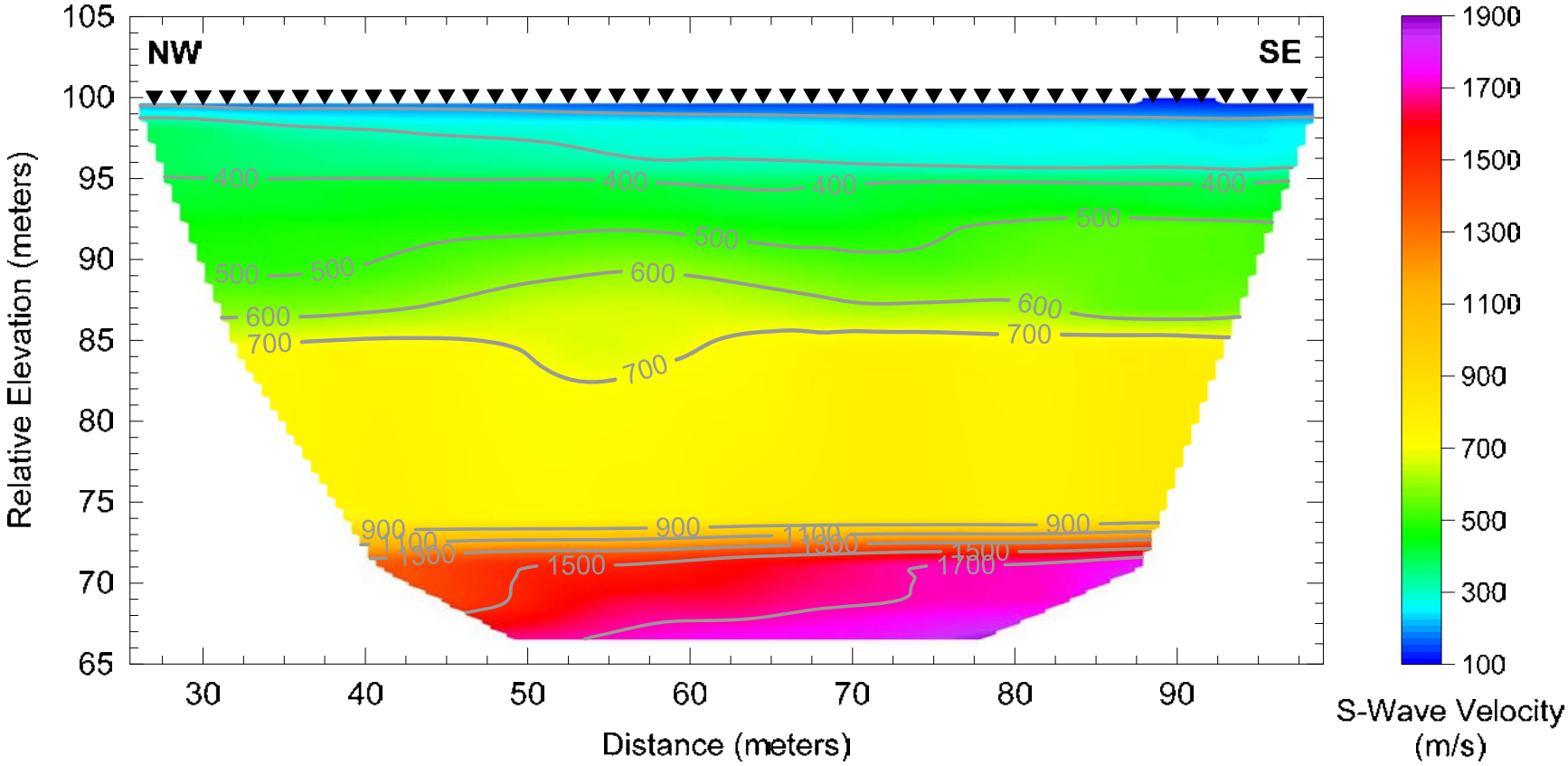

Array ACSO-1 – S-wave Tomographic Seismic Refraction Model Developed using a Layer Based Starting Model

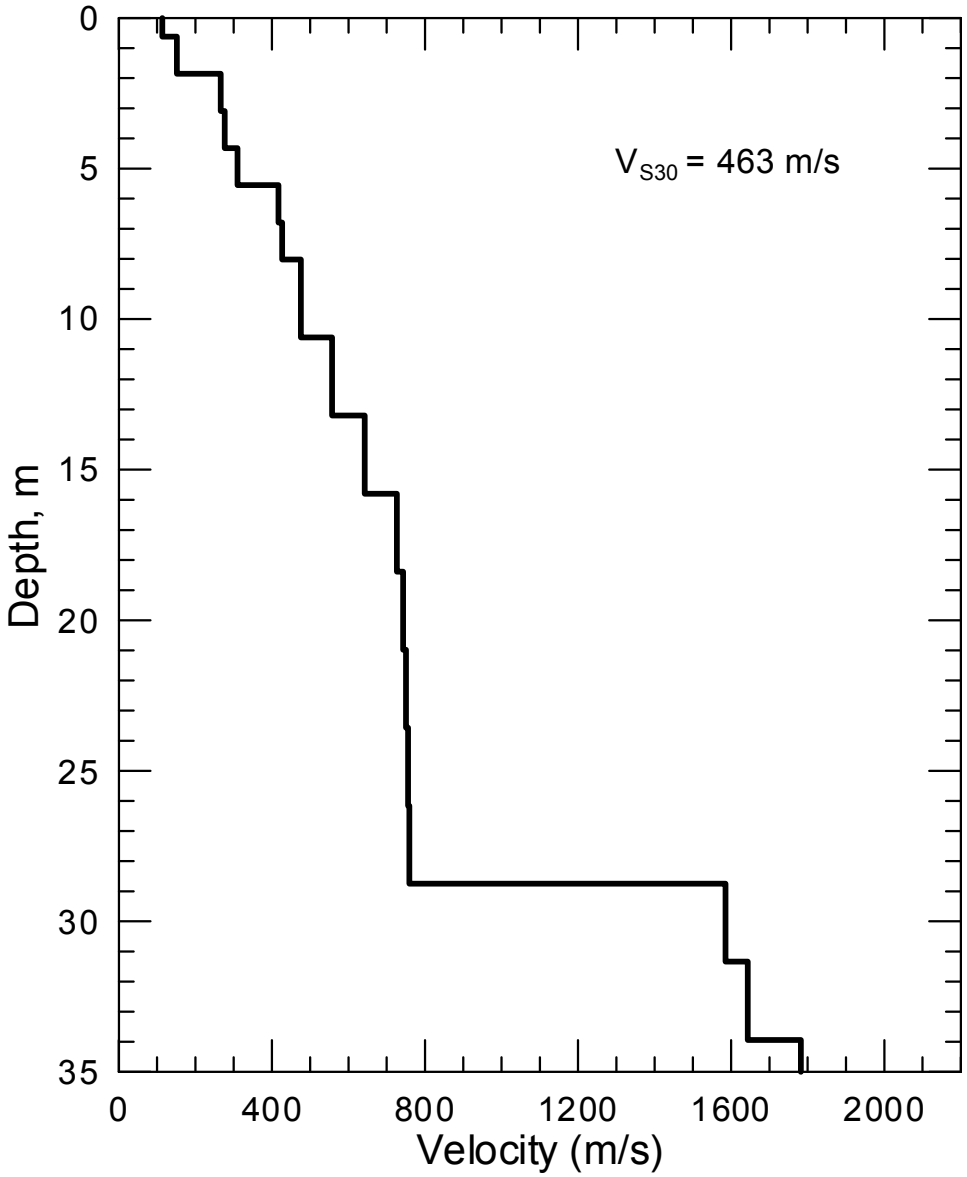

US.ACSO – Average S-wave velocity structure between a position of 48 and 78 m on the S-wave seismic refraction model for array ACSO-1 used for the purpose of site characterization and presented earlier. The model was developed by tomographic inversion with a simple layered starting model developed by interactive, horizontal layer-based analysis of the seismic refraction records. There is a 6% difference in V_{S30} between a position of 48 and 78 m due to lateral velocity variation in the upper 5 m.

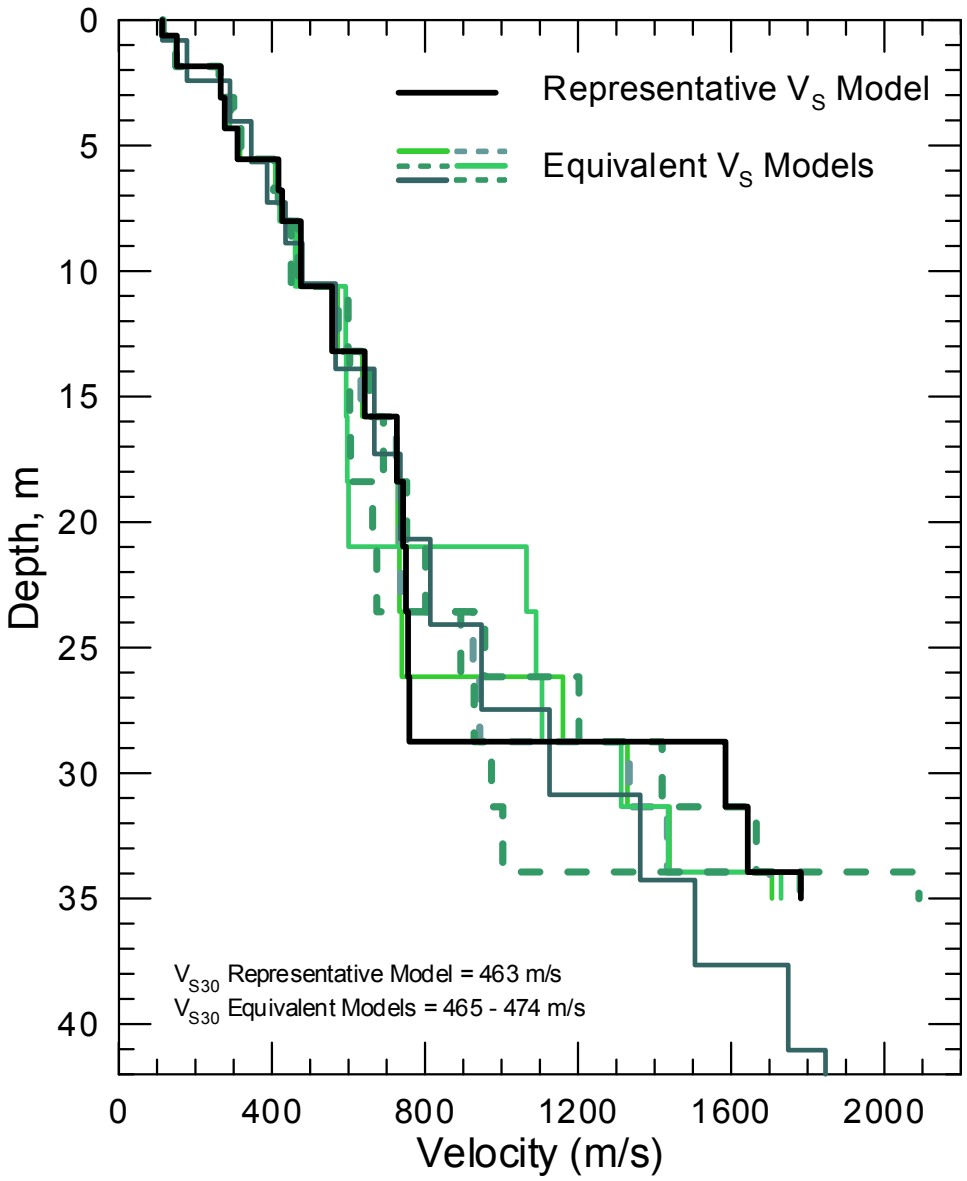

US.ACSO – Average S-wave velocity structure between a position of 48 and 78 m on several seismic refraction models developed for array ACSO-1 using different layer-based starting models and a smooth velocity gradient starting model. All of the models have similar RMS error and this figure demonstrates the nonuniqueness inherent in modeling of seismic refraction data. There is very little variation in V_{S30} between the equivalent V_S models. Array ACSO-1 is not of sufficient length to accurately model the high velocity layer below a depth of 25 m; however, all of the equivalent models indicate that V_S likely exceeds 1,600 m/s at depth. Bedrock at the site is sedimentary in composition and it is likely that velocity inversions occur within the higher velocity rock, in which case the seismic refraction models may overestimate velocities and V_{S30}.

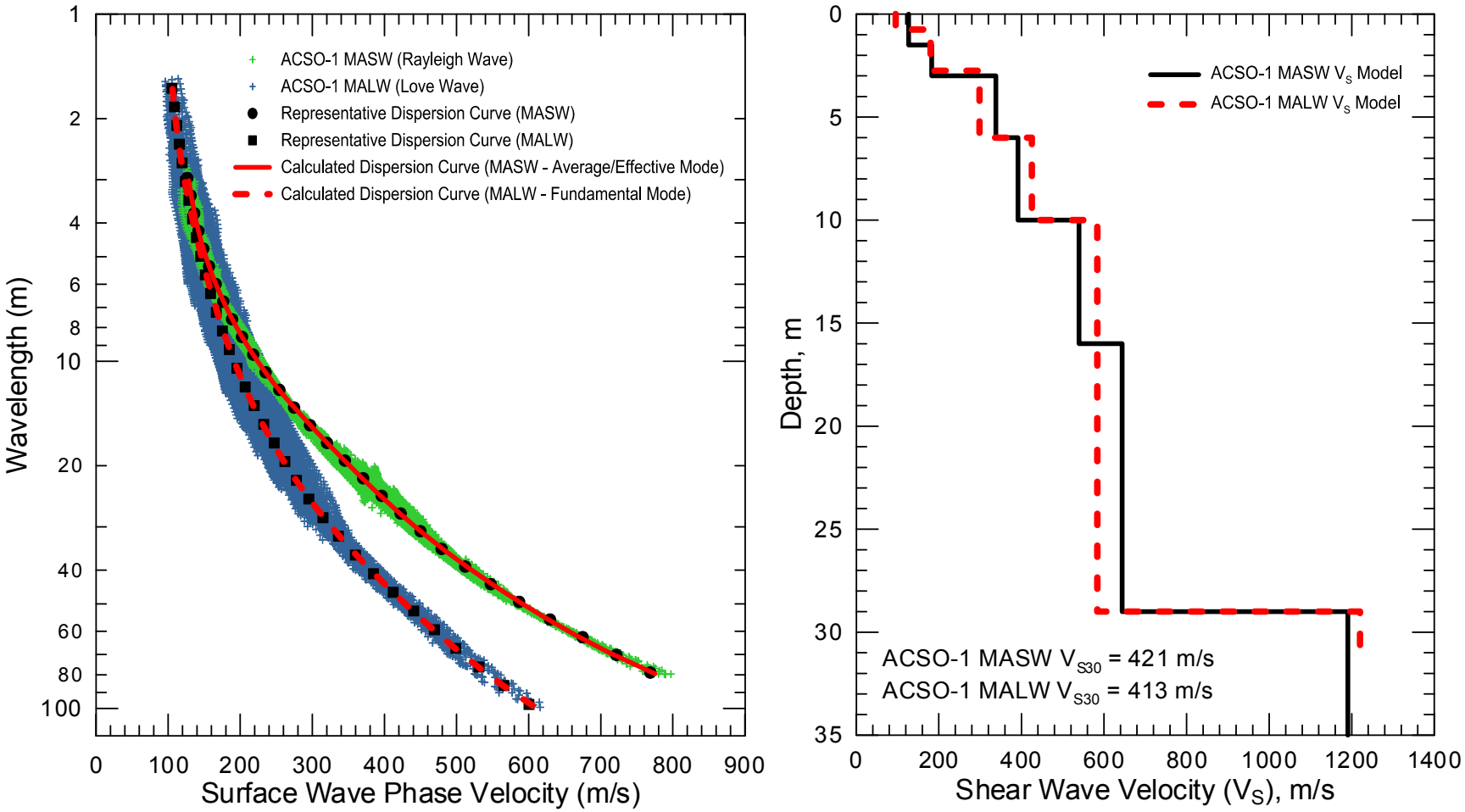

US.ACSO - Field, representative and calculated surface wave dispersion data (left) and associated V_S models (right) for MASW (Rayleigh wave) and MALW (Love wave) dispersion data. The Rayleigh wave dispersion curve is primarily derived from seismic records associated with source locations at the southeast end of the array and was modeled as the average/effective mode, which effectively modeled wavelengths less than 12 m as the fundamental mode and wavelengths greater than 18 m as the first higher mode. Seismic records with source locations at the northwest end of the array yielded Rayleigh wave dispersion data that appear to be associated with the first higher mode. The Love wave dispersion curve was modeled as the fundamental mode.

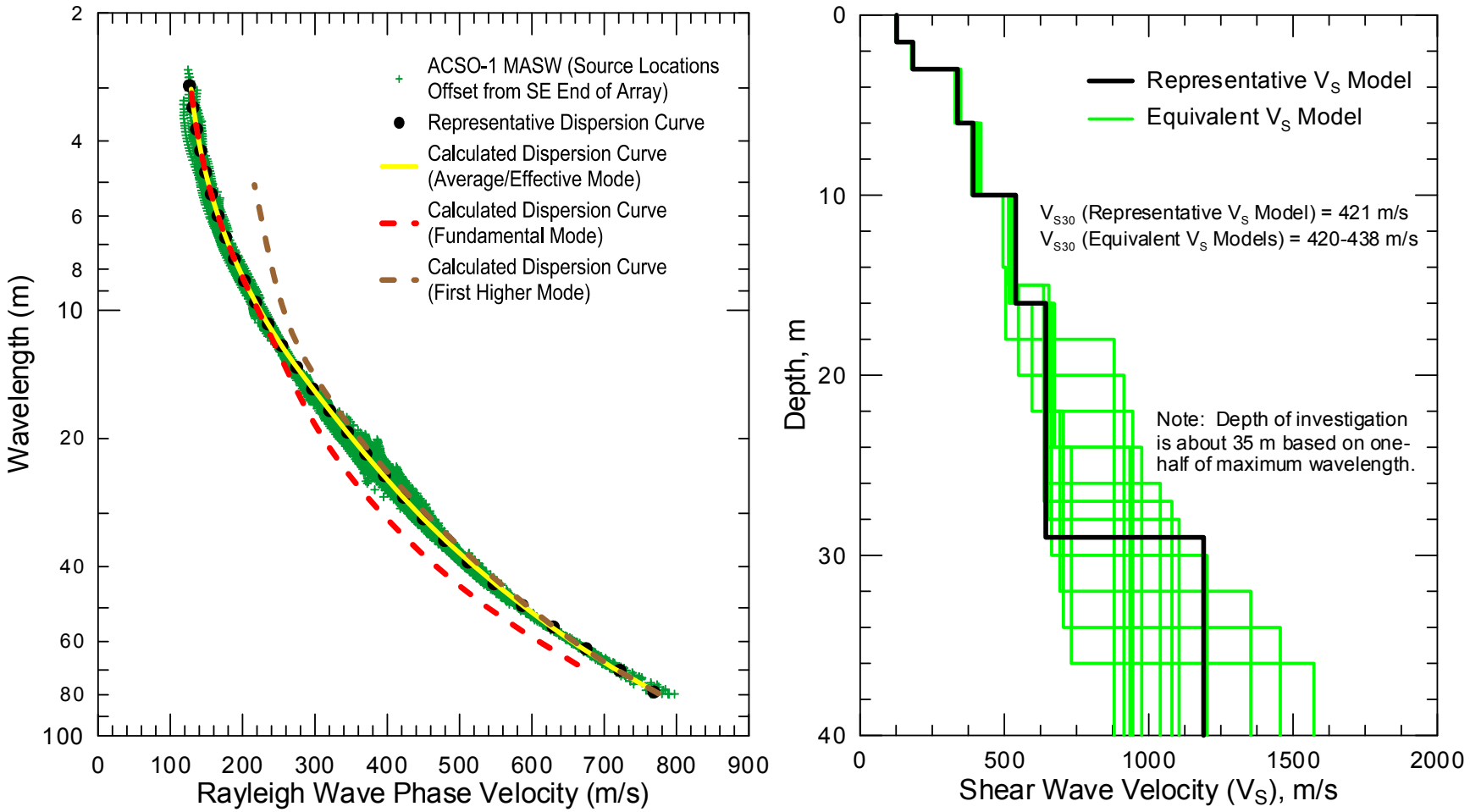

US.ACSO - Field, representative and calculated surface wave dispersion data (left) and associated equivalent V_S models (right) for Rayleigh wave phase velocity data interpreted as being representative of near surface velocity structure beneath the southeast half of the array and modeled as the average/effective mode. The calculated fundamental, average and first higher mode dispersion curves for the representative V_S model are plotted above. Multiple equivalent V_S models are presented to demonstrate the nonuniqueness inherent in the inversion of surface wave data, which is much more problematic when there is an abrupt increase in velocity at depth. Although the depth and V_S of the half space are poorly constrained in the models, V_{S30} varies by less than 5%.

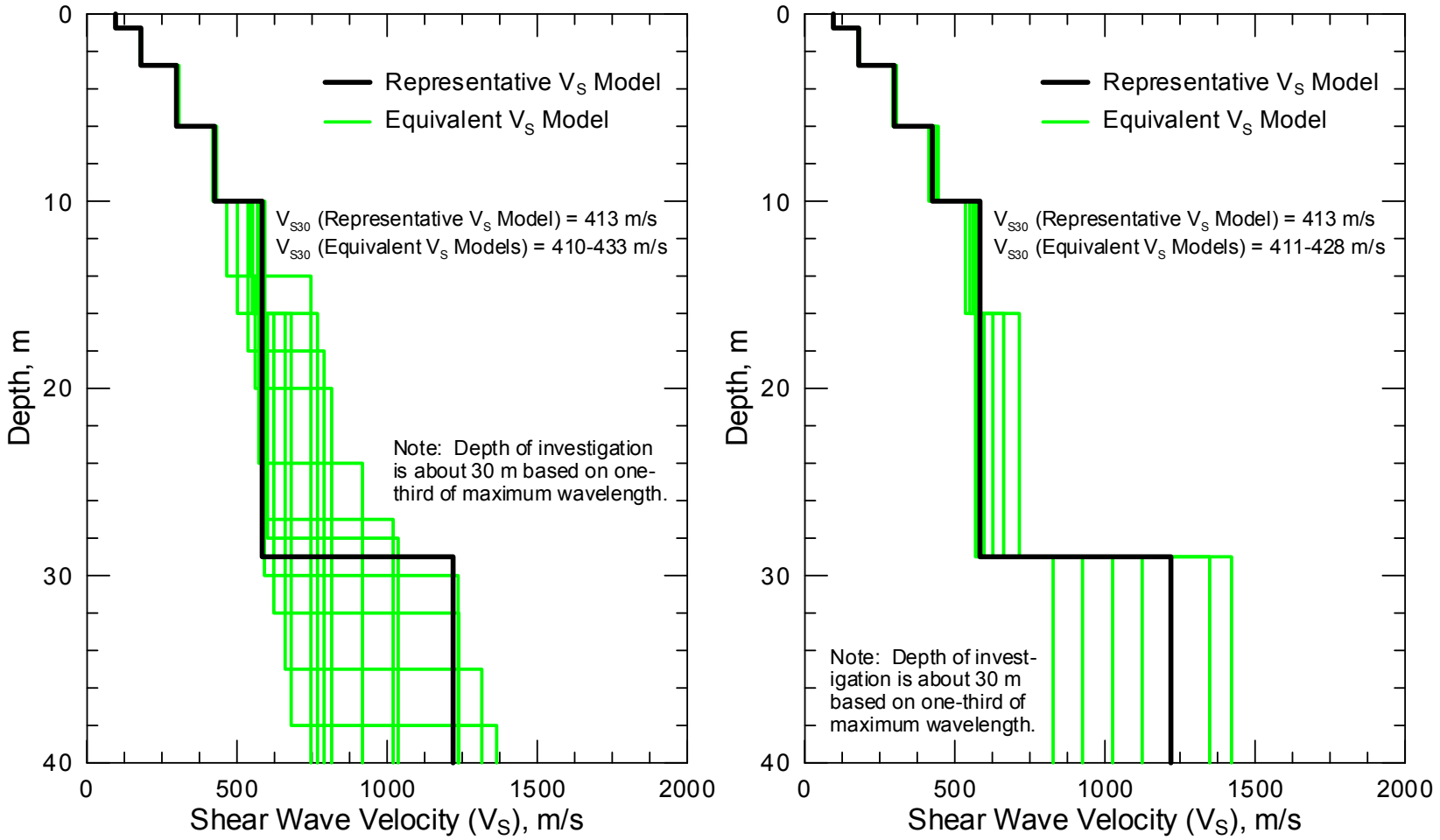

US.ACSO - Equivalent V_S models for Love wave phase velocity data inverted as the fundamental mode, demonstrating the nonuniqueness inherent in the inversion of surface wave data, which is much more problematic when there is an abrupt increase in velocity at depth. The models on the left, which yield calculated dispersion curves with RMS errors in the 1.5 to 2.1 m/s range, demonstrate that the depth and V_S of the half space is poorly constrained. The models on the right, which yield calculated dispersion curves with RMS errors in the 1.6 to 2.7 m/s range, demonstrate that the velocity of the half space at 29 m depth is poorly constrained as the interface is located near the maximum depth of investigation. Although the depth and V_S of the half space are poorly constrained in the models, V_{S30} only varies by about 5%.

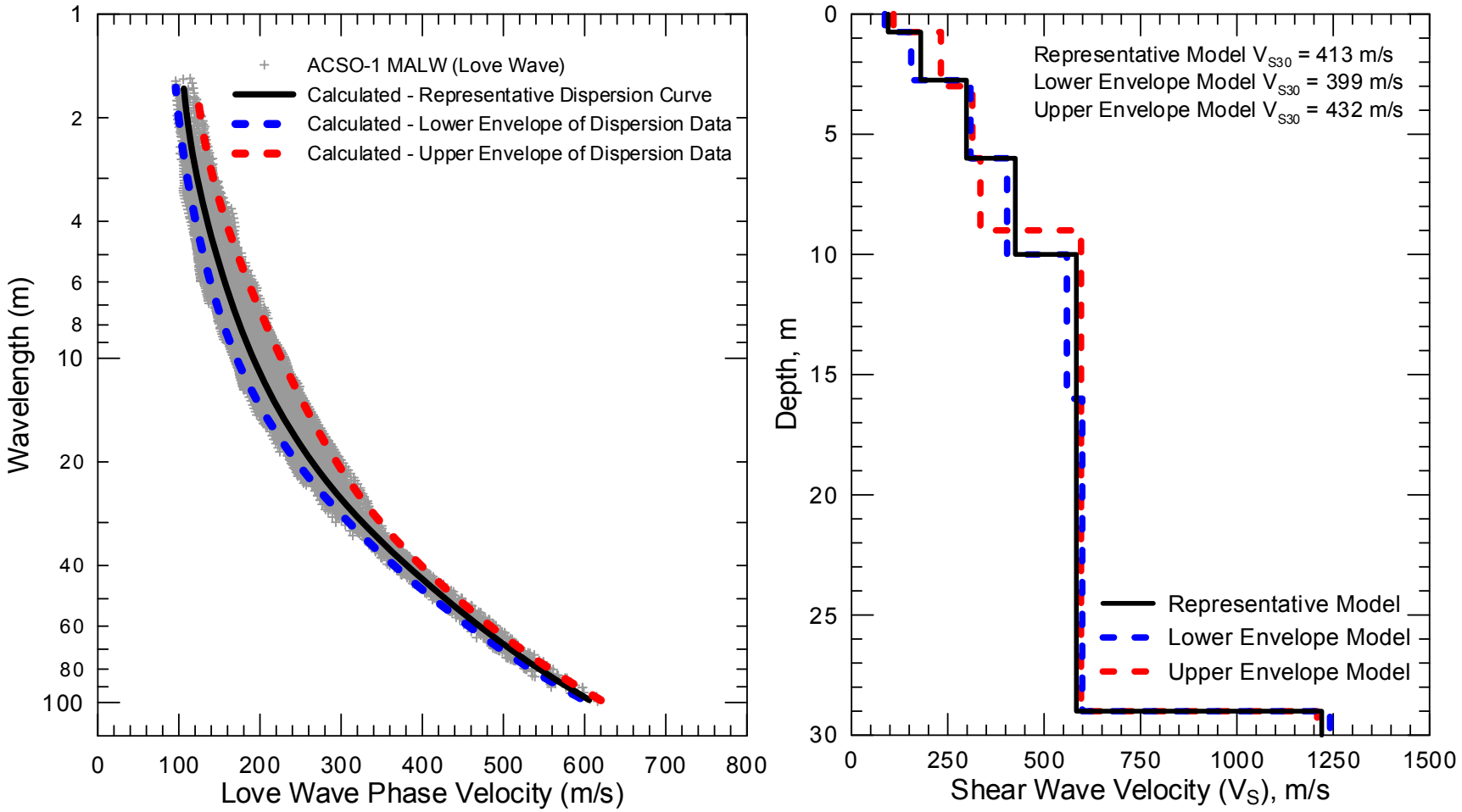

US.ACSO – Field and calculated Love wave dispersion data (left) and associated V_S models (right) fitting the representative average, lower envelope and upper envelope of the Love wave dispersion data. Although there is significant scatter in the Love wave dispersion data at wavelengths less than 40 m, there is only about an 8% variation in V_{S30} between the lower and upper envelope V_S models.

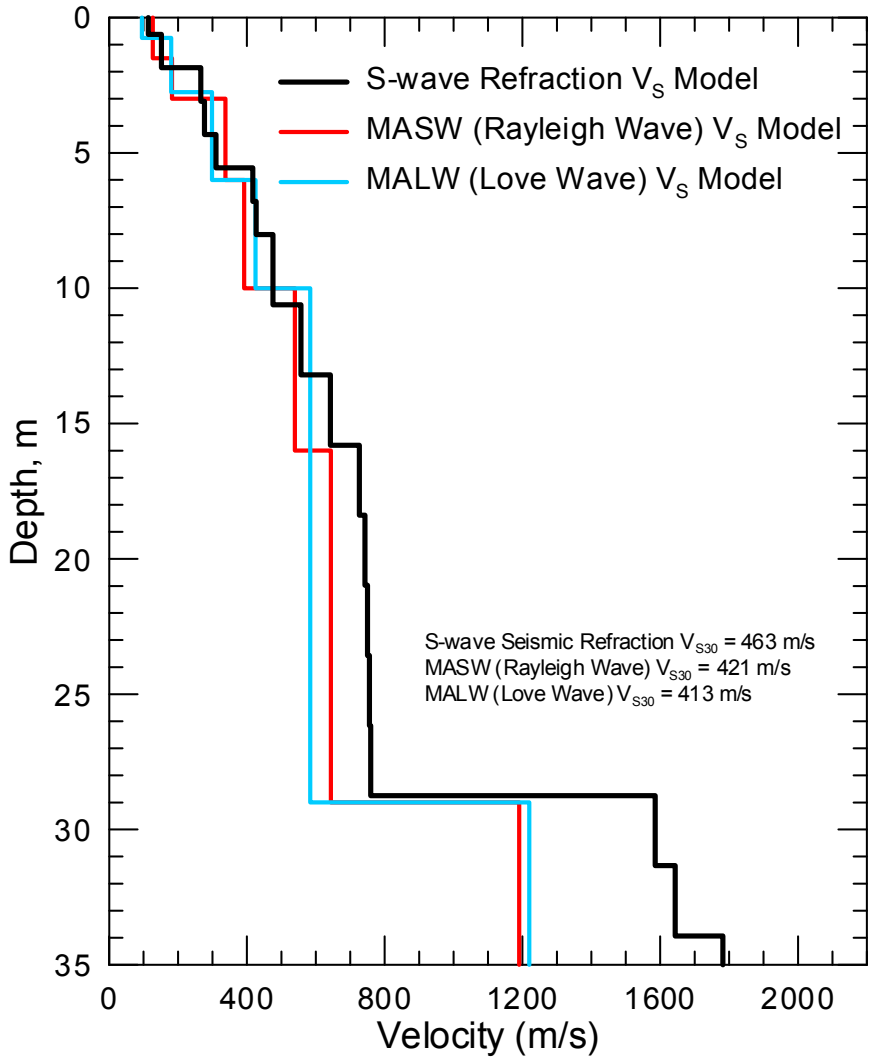

US.ACSO – Comparison of S-wave velocity models, used for the purpose of site characterization, developed from the MASW (Rayleigh wave), MALW (Love wave) and S-wave seismic refraction data. The Rayleigh wave, Love wave and seismic refraction models are relatively similar in the upper 15 m. Below a depth of 15 m, the S-wave refraction model overestimates V_S relative to the surface wave V_S models, particularly the high velocity layer below a depth of 29 m. The high velocity layer is not well constrained in the surface wave models as the layer occurs near the inferred maximum depth of investigation. Additionally, the seismic refraction array is of insufficient length to accurately constrain the velocity of the high velocity layer, although review of the seismic refraction data clearly indicates that V_S of this layer exceeds 1,600 m/s. Bedrock geology at this site consists of alternating sandstone, shale and siltstone and there is a strong possibility that lower velocity rock underlies the high velocity unit, which is somewhat supported by the lower modeled V_S in the surface wave models. V_{S30} estimated from the average S-wave refraction model is about 10% higher than that estimated from the surface wave models. It is not unusual for seismic refraction models to overestimate V_{S30} in sedimentary rock environments as the models do not reflect the effects of velocity inversions that are often present.